Wed. May 29, 2019

[J] Poster | U (Union)：Union

10:45 AM - 12:15 PM JST | 1:45 AM - 3:15 AM UTC | Poster Hall International Exhibition Hall8, Makuhari Messe_1

[U-04] Capture the fast process in Earth and planetary science

convener:Takashi Yoshino(Institute for Planetary Materials, Okayama University), Yoshinori Tange(Japan Synchrotron Radiation Research Institute)

[U04-P01] Present status of time resolved measurement using X-ray absorption spectroscopy at SPring-8

*Kiyofumi Nitta[1], Oki Sekizawa[1], Kazuo Kato[1], Hitoshi Osawa[1] (1.Japan Synchrotron Radiation Research Institute)

[U04-P02] Ultrafast time-resolved XFEL diffraction study on shock-compressed corundum

*Yoshinori Tange[1] (1.Japan Synchrotron Radiation Research Institute)

[J] Poster | U (Union)：Union

5:15 PM - 6:30 PM JST | 8:15 AM - 9:30 AM UTC | Poster Hall International Exhibition Hall8, Makuhari Messe_1

[U-04] Capture the fast process in Earth and planetary science

convener:Takashi Yoshino(Institute for Planetary Materials, Okayama University), Yoshinori Tange(Japan Synchrotron Radiation Research Institute)

[U04-P01] Present status of time resolved measurement using X-ray absorption spectroscopy at SPring-8

*Kiyofumi Nitta[1], Oki Sekizawa[1], Kazuo Kato[1], Hitoshi Osawa[1] (1.Japan Synchrotron Radiation Research Institute)

[U04-P02] Ultrafast time-resolved XFEL diffraction study on shock-compressed corundum

*Yoshinori Tange[1] (1.Japan Synchrotron Radiation Research Institute)

[J] Oral | U (Union)：Union

1:45 PM - 3:15 PM JST | 4:45 AM - 6:15 AM UTC | 103 1F

[U-04] Capture the fast process in Earth and planetary science

convener:Takashi Yoshino(Institute for Planetary Materials, Okayama University), Yoshinori Tange(Japan Synchrotron Radiation Research Institute), Chairperson:Takashi Yoshino(Okayama University), Yoshio Kono(愛媛大学地球深部ダイナミクスセンター), Yoshinori Tange

1:48 PM - 2:00 PM JST | 4:48 AM - 5:00 AM UTC

[U04-01] Toward organization of a new field on fast process in Earth and planetary science

★Invited Papers

*Takashi Yoshino[1] (1.Institute for Planetary Materials, Okayama University)

2:00 PM - 2:15 PM JST | 5:00 AM - 5:15 AM UTC

[U04-02] Fractal particle size distribution of pulverized fault rocks and dynamic fragmentation of rocks

★Invited Papers

*Jun Muto[1], Osamu Nishikawa[2], Hiroyuki Nagahama[1] (1.Department of Earth Sciences, Tohoku University, 2.Graduate School of Engineering and Resource Sciences, Akita University)

2:15 PM - 2:30 PM JST | 5:15 AM - 5:30 AM UTC

[U04-03] Universal aspects of acceleration process toward unstable fast rupture

★Invited Papers

*Takahiro Hatano[1] (1.Earthquake Research Institute, University of Tokyo)

2:30 PM - 2:45 PM JST | 5:30 AM - 5:45 AM UTC

[U04-04] Semi-brittle flow in dunite and harzburgite at upper mantle pressures

★Invited Papers

*Tomohiro Ohuchi[1], Xinglin Lei[2], Yuji Higo[3], Yoshinori Tange[3] (1.Geodynamics Research Center, Ehime University, 2.National Institute of Advanced Industrial Science and Technology, 3.Japan Synchrotron Radiation Research Institute)

2:45 PM - 3:00 PM JST | 5:45 AM - 6:00 AM UTC

[U04-05] A mechanism of magma fracturing revealed by in-situ X-ray imaging and diffraction

★Invited Papers

*Satoshi Okumura[1], Kentaro Uesugi[2], Tatsuya Sakamaki[1], Akio Goto[3] (1.Division of Earth and Planetary Materials Science, Department of Earth Science, Graduate School of Science, Tohoku University, 2.SPring-8/JASRI, 3.Center for Northeast Asian Studies, Tohoku University)

3:00 PM - 3:15 PM JST | 6:00 AM - 6:15 AM UTC

[U04-06] Estimation of physical parameters of volcanic eruptions based on analysis of eruptive products –Toward understanding of eruption dynamics–

★Invited Papers

*Fukashi Maeno[1] (1.Earthquake Research Institute, University of Tokyo)

[J] Oral | U (Union)：Union

3:30 PM - 5:00 PM JST | 6:30 AM - 8:00 AM UTC | 103 1F

[U-04] Capture the fast process in Earth and planetary science

convener:Takashi Yoshino(Institute for Planetary Materials, Okayama University), Yoshinori Tange(Japan Synchrotron Radiation Research Institute), Chairperson:Takashi Yoshino(Okayama University), Yoshio Kono(愛媛大学地球深部ダイナミクスセンター), Yoshinori Tange

3:30 PM - 3:45 PM JST | 6:30 AM - 6:45 AM UTC

[U04-07] Chemical reaction processes bridge between asteroid Ryugu and early evolution of Earth

★Invited Papers

*Seiji Sugita[1,3], Hideharu Kuwahara[2], Kosuke Kurosawa[3] (1.Department of Earth and Planetary Science, Graduate School of Science Sciece, The University of Tokyo, 2.Ehime University, 3.Chiba Institute of Technology)

3:45 PM - 4:00 PM JST | 6:45 AM - 7:00 AM UTC

[U04-08] Time-resolved synchrotron X-ray observations of mineral transformations under static pressures: applications to non-equilibrium behaviors in shocked meteorites

★Invited Papers

*Tomoaki Kubo[1], Masaaki Miyahara[2] (1.Kyushu University, 2.Hiroshima University)

4:00 PM - 4:15 PM JST | 7:00 AM - 7:15 AM UTC

[U04-09] Ultrafast pump-probe experiemnts for planetary materials using high-power lasers and XFEL

★Invited Papers

*Norimasa Ozaki[1] (1.Osaka University)

4:15 PM - 4:30 PM JST | 7:15 AM - 7:30 AM UTC

[U04-10] Tracking dynamical phenomena with X-ray free-electron lasers

★Invited Papers

*Tetsuo Katayama[1] (1.Japan Synchrotron Radiation Research Institute)

4:30 PM - 4:45 PM JST | 7:30 AM - 7:45 AM UTC

[U04-11] High speed measurement with synchrotron radiation X-ray.

★Invited Papers

*Kentaro Uesugi[1] (1.Japan Synchrotron Radiation Research Institute)

4:45 PM - 4:58 PM JST | 7:45 AM - 7:58 AM UTC

[U04-12] Recent advances in high-pressure synchrotron X-ray experiments on magmas under pressure at the beamline 16-BM-B in Advanced Photon Source

★Invited Papers

*Yoshio Kono[1] (1.Geodynamics Research Center, Ehime University)

[J] Oral | U (Union)：Union

10:45 AM - 12:15 PM JST | 1:45 AM - 3:15 AM UTC | Convention Hall A 2F

[U-07] How JpGU will manage environment and disaster from the impacts of unforeseen geo-hazards

convener:Koji Okumura(Graduate School of Letters, Hiroshima University), Jun Matsumoto(Deaprtment of Geography, Tokyo Metropolitan University), Daisaku Kawabata(Institute of Geology and Geoinformation, Geological Survey of Japan, AIST), Masaki Matsushima(Department of Earth and Planetary Sciences, School of Science, Tokyo Institute of Technology), Chairperson:Daisaku Kawabata, Koji Okumura(Hiroshima University)

10:45 AM - 10:55 AM JST | 1:45 AM - 1:55 AM UTC

[U07-01] Seismotectonic environments and landscape as keys to mitigate the impacts from unexpected hazards

*Koji Okumura[1] (1.Graduate School of Letters, Hiroshima University)

10:55 AM - 11:10 AM JST | 1:55 AM - 2:10 AM UTC

[U07-02] Activities related with the eruption at Kusatsu-Shiranesan (Motoshiranesan) volcano on 23 Jan,2018 - Focusing on JMA's activities -

*Junichi Miyamura[1] (1.Japan Meteorological Agency)

11:10 AM - 11:25 AM JST | 2:10 AM - 2:25 AM UTC

[U07-03] Correspondences to society events at emergency disaster – In case of the Annual Meeting of the Geological Society of Japan -

*Matsuda Hiroki[1,2] (1.Kumamoto University, 2.the Geological Society of Japan)

11:25 AM - 11:40 AM JST | 2:25 AM - 2:40 AM UTC

[U07-04] Aftershock and microtremor array observation around the source area of the 2018 Hokkaido Eastern Iburi earthquake

*Masayuki Yoshimi[1], Kahori Iiyama[2], Hitoshi Morikawa[2], Hiroyuki Goto[3] (1.Geological Survey of Japan, AIST, 2.Tokyo Institute of Technology, 3.DPRI, Kyoto Univ.)

11:40 AM - 11:55 AM JST | 2:40 AM - 2:55 AM UTC

[U07-05] Effect of non-linear site response on earthquake hazard map

*Takao Kagawa[1] (1.Tottori University Graduate School of Engineering)

11:55 AM - 12:10 PM JST | 2:55 AM - 3:10 AM UTC

[U07-06] Evolution of catastrofic landslides due to rapid valley incision and filling since Last Glacial Age in central Nepal Himalayas

★Invited Papers

*Hiroshi YAGI[1] (1.Faculty of Art, Science and Education, Yamagata University)

[E] Poster | P (Space and Planetary Sciences)：P-PS Planetary Sciences

10:45 AM - 12:15 PM JST | 1:45 AM - 3:15 AM UTC | Poster Hall International Exhibition Hall8, Makuhari Messe_2

[P-PS02] Regolith Science

convener:Koji Wada(Planetary Exploration Research Center, Chiba Institute of Technology), Akiko Nakamura(Graduate School of Science, Kobe University), Patrick Michel(Observatoire De La Cote D'Azur), Kevin John Walsh(Southwest Research Institute Boulder)

[PPS02-P01] Abrasion experiments of mineral and meteorite grains: Dependence of particle size and vibration rate on abrasion rate and its application to Itokawa and lunar regolith particles.

*Hirotaka Yamaguchi[1], Akira Tsuchiyama[1], Akiko Nakamura[2] (1.National University Corporation, Kyoto University, 2.National University Corporation,Kobe University)

[PPS02-P02] Measurements of adhesive force of meteorite powders using centrifugal method

*Yuuya Nagaashi[1], Akiko Nakamura[1] (1.Kobe University)

[PPS02-P03] Laboratory impact penetration experiments conducted at simulated reduced gravity

*Akiko Nakamura[1], Kana Morizono[2], Yuuya Nagaashi[1] (1.Graduate School of Science, Kobe University, 2.Faculty of Science, Kobe University)

[PPS02-P04] MARAUDERS: Using instrumented nano-impactors to probe the icy properties of Lunar permanently shadowed regions

*Ronald Ballouz[1], Sarah T Crites[2], Naoya Ozaki[2], Shun Arahata[3], Nicola Baresi[2], Ralf Bolden, Onur Celik[4,2], Yu Himeno[3], Lucie Riu[2], Kevin J Walsh[5] (1.Lunar and Planetary Lab, University of Arizona, Tucson, AZ, USA, 2.Institute of Space and Astronautical Science, Sagamihara, Japan, 3.University of Tokyo, Tokyo, Japan, 4.Sokendai Graduate University, Japan, 5.Southwest Research Institute, Boulder, CO, USA)

[PPS02-P05] Surface size-frequency distribution of accumulating boulders using discrete element simulations of spherical particles in 3D

*Hiroshi Kikuchi[1], Hideaki Miyamoto[1] (1.The University of Tokyo)

[PPS02-P06] Experimental Study to Determine the Best Compression Ratio of High-Resolution Images of Small Bodies for the Martian Moons eXploration (MMX) Mission

*Yuta Shimizu[1], Hiroaki Kamiyoshihara[1], Takafumi Niihara[1], Hideaki Miyamoto[1] (1.University of Tokyo)

[E] Poster | P (Space and Planetary Sciences)：P-PS Planetary Sciences

5:15 PM - 6:30 PM JST | 8:15 AM - 9:30 AM UTC | Poster Hall International Exhibition Hall8, Makuhari Messe_2

[P-PS02] Regolith Science

convener:Koji Wada(Planetary Exploration Research Center, Chiba Institute of Technology), Akiko Nakamura(Graduate School of Science, Kobe University), Patrick Michel(Observatoire De La Cote D'Azur), Kevin John Walsh(Southwest Research Institute Boulder)

[PPS02-P01] Abrasion experiments of mineral and meteorite grains: Dependence of particle size and vibration rate on abrasion rate and its application to Itokawa and lunar regolith particles.

*Hirotaka Yamaguchi[1], Akira Tsuchiyama[1], Akiko Nakamura[2] (1.National University Corporation, Kyoto University, 2.National University Corporation,Kobe University)

[PPS02-P02] Measurements of adhesive force of meteorite powders using centrifugal method

*Yuuya Nagaashi[1], Akiko Nakamura[1] (1.Kobe University)

[PPS02-P03] Laboratory impact penetration experiments conducted at simulated reduced gravity

*Akiko Nakamura[1], Kana Morizono[2], Yuuya Nagaashi[1] (1.Graduate School of Science, Kobe University, 2.Faculty of Science, Kobe University)

[PPS02-P04] MARAUDERS: Using instrumented nano-impactors to probe the icy properties of Lunar permanently shadowed regions

*Ronald Ballouz[1], Sarah T Crites[2], Naoya Ozaki[2], Shun Arahata[3], Nicola Baresi[2], Ralf Bolden, Onur Celik[4,2], Yu Himeno[3], Lucie Riu[2], Kevin J Walsh[5] (1.Lunar and Planetary Lab, University of Arizona, Tucson, AZ, USA, 2.Institute of Space and Astronautical Science, Sagamihara, Japan, 3.University of Tokyo, Tokyo, Japan, 4.Sokendai Graduate University, Japan, 5.Southwest Research Institute, Boulder, CO, USA)

[PPS02-P05] Surface size-frequency distribution of accumulating boulders using discrete element simulations of spherical particles in 3D

*Hiroshi Kikuchi[1], Hideaki Miyamoto[1] (1.The University of Tokyo)

[PPS02-P06] Experimental Study to Determine the Best Compression Ratio of High-Resolution Images of Small Bodies for the Martian Moons eXploration (MMX) Mission

*Yuta Shimizu[1], Hiroaki Kamiyoshihara[1], Takafumi Niihara[1], Hideaki Miyamoto[1] (1.University of Tokyo)

[E] Oral | P (Space and Planetary Sciences)：P-PS Planetary Sciences

1:45 PM - 3:15 PM JST | 4:45 AM - 6:15 AM UTC | A01 TOKYO BAY MAKUHARI HALL

[P-PS02] Regolith Science

convener:Koji Wada(Planetary Exploration Research Center, Chiba Institute of Technology), Akiko Nakamura(Graduate School of Science, Kobe University), Patrick Michel(Observatoire De La Cote D'Azur), Kevin John Walsh(Southwest Research Institute Boulder), Chairperson:Koji Wada(Planetary Exploration Research Center, Chiba Institute of Technology)

1:45 PM - 2:00 PM JST | 4:45 AM - 5:00 AM UTC

[PPS02-01] Moganite in a lunar meteorite as a trace of H_2O ice in the lunar regolith

★Invited Papers

*Masahiro KAYAMA[1] (1.Tohoku University)

2:00 PM - 2:15 PM JST | 5:00 AM - 5:15 AM UTC

[PPS02-02] Simulating the Lunar Soil: a Japanese Lunar Soil Simulant FJS-1 and Its Properties

★Invited Papers

*Naohiro Uyama[1], Hiroshi Kanamori[1], Shigeru Aoki[1] (1.Shimizu Corporation)

2:15 PM - 2:30 PM JST | 5:15 AM - 5:30 AM UTC

[PPS02-03] Experimental estimation of regolith scattering behavior when a space lander touches on a planetary body

★Invited Papers

*Mitsuhisa Baba[1], Ronald Louis Ballouz[2], Masatsugu Otsuki[1] (1.Japan Aerospace Exploration Agency, 2.The University of Arizona)

2:30 PM - 2:45 PM JST | 5:30 AM - 5:45 AM UTC

[PPS02-04] Ray systems in granular cratering

*Tapan Sabuwala[1], Christian Butcher[1], Gustavo Gioia[1], Pinaki Chakraborty[1] (1.Okinawa Institute of Science and Technology Graduate University)

2:45 PM - 3:00 PM JST | 5:45 AM - 6:00 AM UTC

[PPS02-05] Scaling of oblique impact cratering onto inclined granular layer

Shinta Takizawa[1], *Hiroaki Katsuragi[1] (1.Graduate School of Environmental Studies, Nagoya University)

3:00 PM - 3:15 PM JST | 6:00 AM - 6:15 AM UTC

[PPS02-06] Experimental study on gravitational effects on crater size formed by low-velocity impacts into granular media

*Masato Kiuchi[1], Akiko M Nakamura[2], Koji Wada[3] (1.Japan aerospace exploration agency, Institute of space and astronautical science, 2.Department of Planetology, Kobe University, 3.Planetary Exploration Research Center, Chiba Institute of Technology)

[E] Oral | P (Space and Planetary Sciences)：P-PS Planetary Sciences

3:30 PM - 5:00 PM JST | 6:30 AM - 8:00 AM UTC | A01 TOKYO BAY MAKUHARI HALL

[P-PS02] Regolith Science

convener:Koji Wada(Planetary Exploration Research Center, Chiba Institute of Technology), Akiko Nakamura(Graduate School of Science, Kobe University), Patrick Michel(Observatoire De La Cote D'Azur), Kevin John Walsh(Southwest Research Institute Boulder), Chairperson:Akiko Nakamura(Graduate School of Science, Kobe University)

3:30 PM - 3:45 PM JST | 6:30 AM - 6:45 AM UTC

[PPS02-07] Impact Ejecta Environment of an Eccentric Asteroid: 3200 Phaethon

*Jamey Szalay[1], Peter Pokorny[2], Mihaly Horanyi[3], Diego Janches[2], Menelaos Sarantos[2], Ralf Srama[4] (1.Princeton University, 2.NASA/GSFC, 3.University of Colorado Boulder, 4.University of Stuttgart)

3:45 PM - 4:00 PM JST | 6:45 AM - 7:00 AM UTC

[PPS02-08] On the Detection of an Ejecta Dust Cloud Around Asteroid (3200) Phaethon by the DESTINY$^+$ Dust Analyzer

*Hiroshi Kimura[1], Masanori Kobayashi[1], Koji Wada[1], Tomoko Arai[1], Hiroki Senshu[1], Masateru Ishiguro[2], Hidekazu Hanayama[3], Ko Ishibashi[1], Takayuki Hirai[1], Fumi Yoshida[1], Peng Hong[1] (1.Planetary Exploration Research Center, 2.Seoul National University, 3.Ishigakijima Astronomical Observatory)

4:00 PM - 4:15 PM JST | 7:00 AM - 7:15 AM UTC

[PPS02-09] Close-up thermal and optical observation of asteroid Ryugu

★Invited Papers

*Naoya Sakatani[1], Tatsuaki Okada[1], Satoshi Tanaka[1], Hiroki Senshu[2], Yuri Shimaki[1], Takehiko Arai[3], Toru Kouyama[5], Hirohide Demura[6], Kentaro Suko[6], Tomohiko Sekiguchi[4], Jun Takita[15], Tetsuya Fukuhara[4], Makoto Taguchi[4], Thomas Müller[7], Axel Hargermann[8], Jens Biele[9], Matthias Grott[9], Marco Delbo[10], Seiji Sugita[13], Rie Honda[12], Tomokatsu Morota[11], Manabu Yamada[2], Shingo Kameda[4], ERI TATSUMI[13], Yasuhiro Yokota[1], Hidehiko Suzuki[14], Chikatoshi Honda[6], Kazunori Ogawa[16], Masahiko Hayakawa[1], Moe Matsuoka[1], Yuichiro Cho[13], Hirotaka Sawada[1] (1.Institute of Space and Astronautical Science, Japan Aerospace Exploration Agency, 2.Chiba Institute of Technology, 3.Ashikaga University, 4.Rikkyo University, 5.National Institute of Advanced Industrial Science and Technology, 6.University of Aizu, 7.Max-Planck Institute for Extraterrestrial Physics, 8.University of Stirling, 9.German Aerospace Center, 10.Observatoire de la Côte d'Azur, CNRS, 11.Nagoya University, 12.Kochi University, 13.University of Tokyo, 14.Meiji University, 15.Hokkaido University for Education, 16.Kobe University)

4:15 PM - 4:30 PM JST | 7:15 AM - 7:30 AM UTC

[PPS02-10] In-Situ Investigation of Asteroid (162173) Ryugu by the Hayabusa2 MASCOT Lander

★Invited Papers

*Hajime Yano[1], Tra-Mi Ho[2], Ralf Jaumann[3], Jean-Pierre Bibring[4], Karl-Heinz Glassmeier[5], Matthias Grott[3], David Hercik[5], Jens Biele[6], Maximilian Hamm[3], Nicole Schmitz[3], Stefanus Schröder[3], Katharina Otto[3], Christian Krause[6], Laurence Lorda[7], Aurelie Moussi-Soffys[7], Cedric Pilorget[4], Vincent Hamm[4], Lucie Riu[1], Tatsuaki Okada[1], Naoya Sakatani[1], Josef Reill[8], Kaname Sasaki[2], Markus Schlotterer[2], Yuichi Tsuda[1], Stephan Ulamec[6], Friederike Wolff[8], Patrick Michel[9], Marco Delbo[9], Kazunori Ogawa[10], Hiroki Senshu[11], Tetsuo Yoshimitsu[1], Frank Preusker[3], Frank Scholten[3], Stephan Elgner[3], Stefano Mottola[3], Ekkehard Kührt[3], Takanao Saiki[1], Yuya Mimasu[1] (1.Institute of Space and Astronautical Science, Japan Aerospace Exploration Agency, Sagamihara, Japan, , 2.German Aerospace Center DLR Bremen, Bremen, Germany, 3.German Aerospace Center, Berlin, Germany, 4.Univ. de Paris Sud-Orsay, IAS, Orsay, France, 5.TU Braunschweig, Braunschweig, Germany, 6.German Aerospace Center DLR Cologne, Cologne, Germany, 7.National Centre for Space Studies, CNES, Toulouse, France, 8.German Aerospace Center, DLR, Oberpfaffenhofen, Germany, 9.Université Côte d'Azur, Observatoire de la Côte d'Azur, CNRS, Laboratoire Lagrange, Nice, France, 10.Department of Planetology, Graduate School of Science, Kobe University, Kobe, Japan, 11.Planetary Exploration Research Center, Chiba Institute of Technology, Narashino, Japan)

4:30 PM - 4:45 PM JST | 7:30 AM - 7:45 AM UTC

[PPS02-11] Evidence of Mass Movement and Boulder Transport on Bennu from NASA's OSIRIS-REx Space Mission

★Invited Papers

*Erica R Jawin[1], Kevin J Walsh[2], Tim McCoy[1], Harold C Connolly[3], Dante S Lauretta[4], Ron L Ballouz[4], Jamie L Molaro[5], Olivier S Barnouin[6], Mike Nolan[4] (1.Smithsonian National Institute, Washington, DC, USA, 2.Southwest Research Institute, Boulder, CO, USA, 3.Dept. of Geology, Rowan University, Glassboro, NJ, USA, 4.Lunar and

Planetary Laboratory, University of Arizona, Tucson, AZ, USA , 5.Planetary Science Institute, Tucson, AZ, USA, 6.The Applied Physics Laboratory, Johns Hopkins University, Laurel, MD, USA)

4:45 PM - 5:00 PM JST | 7:45 AM - 8:00 AM UTC

[PPS02-12] Resurfacing processes on small asteroids constrained by crater size distributions on Ryugu, Itokawa, and Eros

*Naofumi Takaki[1], Yuichiro Cho[1], Tomokatsu Morota[3], ERI TATSUMI[1], Kazuo Yoshioka[1], Hirotaka Sawada[5], yokota yasuhiro[2,5], Naoya Sakatani[5], Masahiko Hayakawa[5], Moe Matsuoka[5], Rie Honda[2], Shingo Kameda[4], Manabu Yamada[6], Toru Kouyama[8], Hidehiko Suzuki[10], Chikatoshi Honda[7], Kazunori Ogawa[9], Hideaki Miyamoto[1], Olivier Barnouin[11], Patrick Michel[12], Carolyn Ernst[11], Seiji Sugita[1,6] (1.University of Tokyo, 2.Kochi University, 3.Nagoya University, 4.Rikkyo University, 5.JAXA, 6.Chiba Institute of Technology, Planetary Exploration Res. Center, 7.University of Aizu, 8.AIST, 9.Kobe University, 10.Meiji University, 11.Johns Hopkins University Applied Physics Laboratory, 12.Nice Observatory)

[E] Oral | P (Space and Planetary Sciences)：P-PS Planetary Sciences

9:00 AM - 10:30 AM JST | 12:00 AM - 1:30 AM UTC | A01 TOKYO BAY MAKUHARI HALL

[P-PS03] Solar System Small Bodies: A New Frontier Arising Hayabusa 2, OSIRIS-REx and Other Projects

convener:Masateru Ishiguro(Department of Physics and Astronomy, Seoul National University), Taishi Nakamoto(Tokyo Institute of Technology), Masanao Abe(Institute of Space and Astronautical Science, Japan Aerospace Exploration Agency), Olivier S Barnouin(Johns Hopkins University Applied Physics Laboratory), Chairperson:Taishi Nakamoto(Tokyo Institute of Technology)

9:00 AM - 9:15 AM JST | 12:00 AM - 12:15 AM UTC

[PPS03-19] The shape of Bennu: Implications for internal structure.

★Invited Papers

*Olivier S Barnouin[1], Micheal G. Daly[2], Eric E Palmer[3], Robert W Gaskell[3], John R. Weirich[3], Catherine L Johnson[4], Manar Al Asad[4], James H Roberts[1], Mark E. Perry[1], Hannah C.M. Sursorney[4], R. Terik Daly[1], Edward B. Bierhaus[5], Jeff A Seabrook[2], Raymond C. Espiritu[1], A. Hari Nair[1], Lilian Nguyen[1], Gregory A Neumann[6], Carolyn M Ernst[1], William V Boynton[7], Micheal C. Nolan[7], Coralie D. Adams[9], Micheal C. Moreau[6], Bashar Rizk[7], Christian Drouet D'Aubigny[7], Erica R. Jawin[8], Kevin J Walsh[10], Patrick Michel[11], Stephen R. Schwartz[7], Ronald L. Ballouz[7], Erwan M Mazarico[6], Daniel J. Scheeres[12], Jay W. McMahon[12], W Bottke[10], Seiji Sugita[13], Naru Hirata[14], Noayuki Hirata[15], Sei-ichiro Watanbe[16], Keara N. Burke[7], Daniella N. DellaGuistina[7], Carinna A. Bennet[7], Dante Lauretta[7] (1.Johns Hopkins University Applied Physics Laboratory, 2.The Centre for Research in Earth and Space Science, York University, Toronto, Ontario, Canada., 3.Planetary Science Institute, Tucson, AZ, USA, 4.Department of Earth, Ocean and Atmospheric Sciences, University of British Columbia, Vancouver, Canada., 5.Lockheed Martin Space Systems Company, Denver, CO, USA., 6.NASA Goddard Space Flight Center, Greenbelt, MD, USA., 7.Lunar Planetary Laboratory, University of Arizona, Tucson, AZ, USA., 8.Smithsonian Institution National Museum of Natural History, Washington, DC, USA., 9.KinetX Aerospace, Inc. Simi Valley, CA, USA, 10.Southwest Research Institute, Boulder, CO, USA., 11.Université Côte d'Azur, Observatoire de la Côte d'Azur, CNRS, Laboratoire Lagrange, Nice, France., 12.Department of Aerospace Engineering Sciences, University of Colorado, Boulder, CO, USA., 13.University of Tokyo, Tokyo, Japan., 14.Aizu University, Aizu-Wakamatsu, Japan., 15.Kobe University, Kobe, Japan., 16.Nagoya University, Nagoya, Japan.)

9:15 AM - 9:30 AM JST | 12:15 AM - 12:30 AM UTC

[PPS03-20] Global Geology of Bennu from NASA's OSIRIS-REx Space Mission

★Invited Papers

*Erica R Jawin[1], Kevin J Walsh[2], Tim McCoy[1], Harold C Connolly[3], Dante S Lauretta[4], Ron L Ballouz[4], Olivier S Barnouin[5], C Beddingfield[6], Carina A Bennett[4], Edward B Bierhaus[7], Keara N Burke[4], Ben Clark[8], Michael G Daly[9], Marco Delbo[10], Daniella DellaGiustina[4], Jason P Dworkin[11], Christine Hartzell[12], John Marshall[6], Patrick Michel[10], Jamie L. Molaro[13], Mike Nolan[4], Maurizio Pajola[14], Mark Perry[5], Bashar Rizk[4], Scott Sandford[15], Dan J Scheeres[16], Stephen R Schwartz[4], David Trang[17] (1.Smithsonian National Institute, Washington, DC, USA, 2.Southwest Research Institute, Boulder, CO, USA, 3.Dept. of Geology, Rowan University, Glassboro, NJ, USA, 4.Lunar and Planetary Laboratory, University of Arizona, Tucson, AZ, USA , 5.The Applied Physics Laboratory, Johns Hopkins University, Laurel, MD, USA, 6.SETI Institute, Mountain View, CA, USA, 7.Lockheed Martin Space Systems Company, USA, 8.Space Science Institute, Boulder CO, USA, 9.York University, Canada, 10.Laboratoire Lagrange, Université Côte d'Azur, Observatoire de la Côte d'Azur, CNRS, Laboratoire Lagrange, Nice, France, 11.NASA Goddard Space Flight Center, Greenbelt, MD, USA, 12.Department of Aerospace Engineering, University of Maryland, College Park MD, USA, 13.Planetary Science Institute, Tucson, AZ, USA, 14.INAF - Astronomical Observatory of Padova, Italy, 15.NASA Ames Research Center, USA, 16.Dept. of Aerospace Engineering Sciences, University of Colorado, Boulder, CO, USA, 17.HIGP/University of Hawaii at Manoa, USA)

9:30 AM - 9:45 AM JST | 12:30 AM - 12:45 AM UTC

[PPS03-21] Modeling surface mobility mechanisms on a top-shaped near-Earth asteroid

★Invited Papers

*Ronald Ballouz[1], Nicola Baresi[2], Olivier S Barnouin[3], Carina A Bennet[1], Edward B Bierhaus[4], Keara N Burke[1], Harold C Connolly[5], Sarah T Crites[2], Daniella DellaGiustitna[1], Erica Jawin[6], Dante S Lauretta[1], Patrick Michel[7], Derek C Richardson[8], Dan J Scheeres[9], Stephen Schwartz[1], Seiji Sugita[10], Eri Tatsumi[10], Florian Thuillet[7], Kevin Walsh[11] (1.Lunar and Planetary Lab, University of Arizona, Tucson, AZ, USA, 2.Institute of Space and Astronautical Science, Sagamihara, Japan, 3.The Applied Physics Laboratory, Johns Hopkins University, Laurel, MD, USA, 4.Lockheed Martin, Boulder, CO, USA, 5.Department of Geology, Rowan University, Glassboro, NJ, USA, 6.Smithsonian National Museum of Natural History, Washington, DC, USA, 7.UCA-OCA-CNRS, Lagrange Laboratory, Nice, France, 8.Dept. of Astronomy, University of Maryland, College Park, MD, USA, 9.Dept. of Aerospace Engineering Sciences, University of Colorado, Boulder, CO, USA, 10.University of Tokyo, Tokyo, Japan, 11.Southwest Research Institute, Boulder, CO, USA)

9:45 AM - 10:00 AM JST | 12:45 AM - 1:00 AM UTC

[PPS03-22] **Visualization and Analysis of Solar System Small Bodies with NASA's Solar System Treks Project**

*Brian Hamilton Day[1], Emily Law[2] (1.NASA Solar System Exploration Research Virtual Institute, NASA Ames Research Center, 2.NASA Jet Propulsion Laboratory, California Institute of Technology)

10:00 AM - 10:15 AM JST | 1:00 AM - 1:15 AM UTC

[PPS03-23] Density Distribution within Small Solar System Bodies Based on Smooth Terrain Shape: Asteroid 25143 Itokawa and Comet 67P/Churyumov-Gerasimenko

*Masanori Kanamaru[1], Sho Sasaki[1], Mark Wieczorek[2] (1.Osaka University, 2.Côte d'Azur Observatory)

10:15 AM - 10:30 AM JST | 1:15 AM - 1:30 AM UTC

[PPS03-24] Low temperature hydration experiments of cometary analog materials towards the Comet Astrobiology Exploration Sample Return (CAESAR) mission

*Aki Takigawa[1,4], Yuki Kimura[1], Yoshihiro Furukawa[2], Tomoki Nakamura[3] (1.Graduate School of Science, Kyoto University, 2.Institute of Low Temperature Science, 3.Graduate School of Science, Tohoku University, 4.The Hakubi Center for Advanced Research)

[E] Oral | P (Space and Planetary Sciences)：P-PS Planetary Sciences

10:45 AM - 12:15 PM JST | 1:45 AM - 3:15 AM UTC | A01 TOKYO BAY MAKUHARI HALL

[P-PS03] Solar System Small Bodies: A New Frontier Arising Hayabusa 2, OSIRIS-REx and Other Projects

convener:Masateru Ishiguro(Department of Physics and Astronomy, Seoul National University), Taishi Nakamoto(Tokyo Institute of Technology), Masanao Abe(Institute of Space and Astronautical Science, Japan Aerospace Exploration Agency), Olivier S Barnouin(Johns Hopkins University Applied Physics Laboratory), Chairperson:Masateru Ishiguro(Seoul National University)

10:45 AM - 11:00 AM JST | 1:45 AM - 2:00 AM UTC

[PPS03-25] Overview and current status of DESTINY$^+$ mission

★Invited Papers

*Tomoko Arai[1], Masanori Kobayashi[1], Ko Ishibashi[1], Fumi Yoshida[1], Hiroshi Kimura[1], Takayuki Hirai[1], Hong Peng[1], Manabu Yamada[1], Hiroki Senshu[1], Koji Wada[1], Ralf Srama[2], Harald Kruger[3], Jun-ichi Watanabe[4], Takashi Ito[4], Masateru Ishiguro[5], Tomoki Nakamura[6], Hikaru Yabuta[7], Shogo Tachibana[8], Takashi Mikouchi[8], Shinsuke Abe[9], Katsuhito Ohtsuka[10], Seitaro Urakawa[11], Keiko Nakamura-Messenger[12], Mutsumi Komatsu[13], Shingo Kameda[14], Masato Kagitani[6], Naru Hirata[15], Hirohide Demura[15], Sho Sasaki[16], Takahiro Hiroi[17], Goro Komatsu[18], Hidehiro Kaneda[19], Takaya Inamori[19], Takaya Okamoto[20], Toshifumi Yanagisawa[20], Makoto Yoshikawa[20], Hajime Yano[20], Tatsuaki Okada[20], Takahiro Iwata[20], Takafumi Ootsubo[20], Yasuhiro Kawakatsu[20], Hiroyuki Toyota[20], Kazutaka Nishiyama[20], Takeshi Takashima[20] (1.Planetary Exploration Research Center, Chiba Institute of Technology, 2.University of Stuttgart, 3.Max Planck Institute, 4.National Astronomical Observatory of Japan , 5.Seoul National Universtiy, 6.Tohoku University, 7.Hiroshima University, 8.The University of Tokyo, 9.Nihon University, 10.Tokyo Meteor Network, 11.Japan Spaceguard Association, 12.NASA , 13.The Graduate University for Advanced Studies, 14.Rikkyo University, 15.Aizu University, 16.Osaka University, 17.Brown University, 18.D'Annunzio University, 19.Nagoya University, 20.JAXA)

11:00 AM - 11:15 AM JST | 2:00 AM - 2:15 AM UTC

[PPS03-26] Observational campaign of (3200) Phaethon and (155140) 2005UD in 2017-2018

*Fumi Yoshida[1], Tomoko Arai[1], Ko Ishibashi[1], Peng Hong[1], Ryo Ishimaru[1], DESTINY+ International observation collaborators (1.Planetary Exploration Research Center, Chiba Institute of Technology)

11:15 AM - 11:30 AM JST | 2:15 AM - 2:30 AM UTC

[PPS03-27] Rotationally-resolved spectroscopic observations of Phaethon - 2005 UD, and their fragments detected by lunar impact flashes.

*Shinsuke Abe[1], Nicholas Moskovitz[2], Fumi Yoshida[3], Katsutoshi Ohtsuka[4], Ito Takashi[5], Ryota Fuse[1], Masahisa Yanagisawa[6], Ryuhei Yamada[7] (1.Department of Aerospace Engineering, College of Science and Technology, Nihon University, 2.Lowell Observatory, 3.Planetary Exploration Research Center, Chiba Institute of Technology, 4.Tokyo Meteor Network, 5.National Astronomical Observatory of Japan, 6.The University of Electro-Communications, 7.The University of Aizu, Department of Computer Science and Engineering)

11:30 AM - 11:45 AM JST | 2:30 AM - 2:45 AM UTC

[PPS03-28] Thermal Radiation Pressure Force on Regolith Particles of Atmosphereless Bodies

*Yoonsoo P. Bach[1], Masateru Ishiguro[1] (1.Department of Physics and Astronomy, Seoul National University)

11:45 AM - 12:00 PM JST | 2:45 AM - 3:00 AM UTC

[PPS03-29] A kilometre-sized Kuiper belt object revealed by OASES stellar occultation observations

*Ko Arimatsu[1,2], Kohji Tsumura[3], Fumihiko Usui[4], Shinnaka Yoshiharu[5], Kohei Ichikawa[3,6,7], Takafumi Ootsubo[8], Takayuki Kotani[2,9], Takehiko Wada[8], Koichi Nagase[8], Jun-ichi Watanabe[2] (1.Astronomical Observatory, Graduate School of Science, Kyoto University, 2.National Astronomical Observatory of Japan, 3.Frontier Research Institute for Interdisciplinary Science, Tohoku University, 4.Center for Planetary Science, Graduate School of Science, Kobe University, 5.Laboratory of Infrared High-resolution Spectroscopy, Koyama Astronomical Observatory, Kyoto Sangyo University, 6.Department of Astronomy, Columbia University, 7.Department of Physics and Astronomy, University of Texas at San Antonio, 8.Department of Space Astronomy and Astrophysics, Institute of Space and Astronautical Science, Japan Aerospace Exploration Agency, 9.Astrobiology Center, National Institutes of Natural Sciences)

12:00 PM - 12:15 PM JST | 3:00 AM - 3:15 AM UTC

[PPS03-30] AKARI/IRC near-infrared asteroid spectroscopic survey: AcuA-spec

*Fumihiko Usui[1], Sunao Hasegawa[2], Takafumi Ootsubo[2], Takashi Onaka[3,4] (1.Kobe University, 2.ISAS/JAXA, 3.The University of Tokyo, 4.Meisei University)

[E] Poster | P (Space and Planetary Sciences)：P-PS Planetary Sciences

3:30 PM - 5:00 PM JST | 6:30 AM - 8:00 AM UTC | Poster Hall International Exhibition Hall8, Makuhari Messe_1

[P-PS03] Solar System Small Bodies: A New Frontier Arising Hayabusa 2, OSIRIS-REx and Other Projects

convener:Masateru Ishiguro(Department of Physics and Astronomy, Seoul National University), Taishi Nakamoto(Tokyo Institute of Technology), Masanao Abe(Institute of Space and Astronautical Science, Japan Aerospace Exploration Agency), Olivier S Barnouin(Johns Hopkins University Applied Physics Laboratory)

[PPS03-P01] Impact experiments on low strength coarse-grained regolith simulating surface materials on asteroid Ryugu

*Yuya Yamamoto[1], Masahiko Arakawa[1], Minami Yasui[1], Sunao Hasegawa[2], Ryo Sugimura[1] (1.Graduate School of Science, Kobe University, 2.ISAS, JAXA)

[PPS03-P02] Reflectance estimation of asteroid Ryugu using MASCOT

*Marika Ishida[1], Koto Amano[1], Keiichi Moroi[1], ERI TATSUMI[2], Tra-Mi Ho[10], Shingo Kameda[1], Seiji Sugita[2], Rie Honda[3], Tomokatsu Morota[4], yokota yasuhiro[5], Toru Kouyama[6], Hidehiko Suzuki[7], Manabu Yamada[8], Naoya Sakatani[5], Chikatoshi Honda[9], Masahiko Hayakawa[5], Kazuo Yoshioka[2], Moe Matsuoka[5], Yuichiro Cho[2], Hirotaka Sawada[5] (1.Rikkyo Univ., 2.Univ. of Tokyo, 3.Kochi Univ., 4.Nagoya Univ., 5.JAXA/ISAS, 6.AIST, 7.Meiji Univ., 8.Chiba Inst. Tech, 9.Univ. of Aizu, 10.DLR)

[PPS03-P03] Flyby observation of Asteroid (3200) Phaethon by DESTINY$^+$ onboard cameras

*Ko Ishibashi[1], Shingo Kameda[2], Masato Kagitani[3], Peng Hong[1], Manabu Yamada[1], Osamu Okudaira[1], Tomoko Arai[1], Fumi Yoshida[1], Shunsuke Sato[4], Takahiro Ishimaru[4], Takaya Okamoto[4], Takahiro Iwata[4], Tatsuaki Okada[4], Takeshi Takashima[4] (1.Chiba Institute of Technology, 2.Rikkyo University, 3.Tohoku Universtiy, 4.Japan Aerospace Exploration Agency)

[PPS03-P04] Polarimetric Study of Asteroids in Comet-Like Orbits (ACOs)

*Jooyeon Geem[1], Masateru Ishiguro[1], Yoonsoo P. Bach[1], Daisuke Kuroda[2], Hiroyuki Naito[3], Hidekazu Hanayama[4], yoonyoung kim[10], Yuna G. Kwon[1], Sunho Jin[1], Tomohiko Sekiguchi[5], Ryo Okazaki[5], Jeremie J. Vaubaillon[6], Masataka Imai[7], Tatsuharu Oono[8], Yuki Futamuts[8], Seiko Takagi[8], Mitsuteru Sato[8], Kiyoshi Kuramoto[8], Makoto Watanabe[9] (1.Astronomy program, Dept of Physics and Astronomy, Seoul National University, 2.Okayama Observatory, Kyoto University, 3.Nayoro Observatory, 4.Ishigakijima Astronomical Observatory, National Astronomical Observatory of Japan, 5.Hokkaido University of Education, 6.Observatoire de Paris, I.M.C.C.E., 7.National Institute of Advanced Industrial Science and Technology, 8.Department of Cosmosciences, Graduate School of Science, Hokkaido University, 9.Department of Applied Physics, Okayama University of Science, 10.Max Planck Institute for Solar System Research)

[PPS03-P05] Dynamical lifetime of the Oort Cloud new comets under planetary perturbation

*Ito Takashi[1], Arika Higuchi[1] (1.National Astronomical Observatory of Japan)

[PPS03-P06] Thermal Infrared Imaging of C-type Asteroid 162173 Ryugu with Porous Surfaces

*Tatsuaki Okada[1,2], Tetsuya Fukuhara[3], Satoshi Tanaka[1], Makoto Taguchi[3], Takehiko Arai[4], Naoya Sakatani[1], Yuri Shimaki[1], Hiroki Senshu[5], Yoshiko Ogawa[6], Hirohide Demura[6], Kentaro Suko[6], Kohei Kitazato[6], Toru Kouyama[7], Tomohiko Sekiguchi[8], Jun Takita[9], Sunao Hasegawa[1], Tsuneo Matsunaga[10], Takehiko Wada[1], Takeshi Imamura[2], Jorn Helbert[11], Thomas G. Mueller[12], Axel Hagermann[13], Jens Biele[11], Matthias Grott[11], Maximiliam Hamm[11], Marco Delbo[14], Yukio Yamamoto[1], Naru Hirata[6], Naoyuki Hirata[15], Fuyuto Terui[1], Takanao Saiki[1], Satoru Nakazawa[1], Makoto Yoshikawa[1], Sei-ichiro WATANABE[1,16], Yuichi Tuda[1] (1.Institute of Space and Astronautical Science, Japan Aerospace Exploration Agency, 2.University of Tokyo, 3.Rikkyo University, 4.Ashikaga University, 5.Chiba Institute of Technology, 6.University of Aizu, 7.National Institute of Advanced Industrial Science and Technology, 8.Hokkaido University of Education, 9.Hokkaido Kitami-Hokuto High School, 10.National Institute for Environmental Studies, 11.German Aerospace Center, 12.Max-Planck Institute for Extraterrestrial Physics, 13.University of Stirling, 14.Observatoire de la Côte d'Azur, 15.Kobe University, 16.Nagoya University)

[PPS03-P07] Data Release of Asteroid 162173 Ryugu by Observation of Thermal Infrared Imager onboard Hayabusa2

*Takehiko Arai[1], Hirohide Demura[2], Toru Kouyama[7], Naoya Sakatani[3], Kentaro Suko[2], Yuri Shimaki[3], Hiroki Senshu[5], Tomohiko Sekiguchi[6], Yoshiko Ogawa[2], Sunao Hasegawa[3], Takehiko Wada[3], Takeshi Imamura[10], Tsuneo Matsunaga[9], Jun Takita[8], Kohei Kitazato[2], Makoto Taguchi[4], Tetsuya Fukuhara[4], Satoshi Tanaka[3], Tatsuaki Okada[3] (1.Ashikaga University, 2.The University of Aizu, 3.Japan Aerospace Exploration Agency (JAXA), 4.Rikkyo University,

5.Chiba Institute of Technology, 6.Hokkaido University of Education, 7.National Institute of Advanced Industrial Science and Technology (AIST), 8.Hokkaido Kitami Hokuto High School, 9.National Institute for Environmental Studies (NIES), 10.The University of Tokyo)

[PPS03-P08] Multi-mission capability of HARMONICS

*Shintaro Tsunoda[1], Hirohide Demura[1], Naru Hirata[1] (1.The University of Aizu)

[PPS03-P09] New interface of verification for calibration and conversion in HEAT : Hayabusa2 Exploration Assistant for TIR

*Tatsuro Kobayashi[1], Kentaro Suko[1], Hirohide Demura[1], Yoshiko Ogawa[1], Takehiko Arai[2], Naoya Sakatani[3], Tatsuaki Okada[3], Satoshi Tanaka[3], Tetsuya Fukuhara[4] (1.The University of Aizu, 2.Ashikaga University, 3.Institute of Space and Astronautical Science, Japan Aerospace Exploration Agency, 4.Rikkyo University)

[PPS03-P10] **Dust particle evolution of a near-Earth object 252P/LINEAR from near-infrared polarimetric observations in 2016**

*Yuna G Kwon[1], Masateru Ishiguro[1], Jungmi Kwon[2], Daisuke Kuroda[3], Myungshin Im[1], Changsu Choi[1], Motohide Tamura[4], Takahiro Nagayama[5], Nobuyuki Kawai[6], Jun-ichi Watanabe[7] (1.Seoul National Univ., 2.ISAS/Japan Aerospace Exploration Agency, 3.Okayama Astrophysical Observatory, 4.The Univ. of Tokyo, 5.Kagoshima Univ., 6.Tokyo Institute of Technology, 7.National Astronomical Observatory of Japan)

[PPS03-P11] **Performance Evaluation of TRIPOL on the 61-cm Telescope at Seoul National University for Polarimetric Observations of Solar System Small Bodies**

*Sunho Jin[1], Masateru Ishiguro[1], Yuna G Kwon[1], Jooyeon Geem[1], Yoonsoo P. Bach[1], Jinguk Seo[1], Hiroshi Sasago[2], Shuji Sato[3] (1.Seoul National University, 2.Sasago Co.,Ltd, 3.Nagoya University)

[PPS03-P12] Smart Interface of HEAT: Hayabusa2 Exploration Assistant for TIR

*Kentaro Suko[1], Tatsuro Kobayashi[1], Hirohide Demura[1], Takehiko Arai[2], Naoya Sakatani[3], Tatsuaki Okada[3], Satoshi Tanaka[3], Tetsuya Fukuhara[4] (1.The University of Aizu, 2.Ashikaga University, 3.Institute of Space and Astronautical Science, Japan Aerospace Exploration Agency, 4.Rikkyo University)

[PPS03-P13] Experimental Study on Collision Crater Formed on Bulge Geography

*Yusaku Yokota[1], Yuya Yamamoto[2], Minami Yasui[2], Masahiko Arakawa[2] (1.Faculty of Science, Kobe University, 2.Graduate School of Science, Kobe University)

[PPS03-P14] Initial analysis plan of soluble organic compounds for the Hayabusa2 sample from asteroid Ryugu

*Hiroshi Naraoka[1], Yoshinori Takano[2], Jason P. Dworkin[3], SOM Analysis Team (1.Department of Earth and Planetary Sciences, Research Center for Planetary Trace Organic Compounds, Kyushu University, 2.Japan Agency for Marine-Earth Science and Technology, 3.Astrochemistry Laboratory NASA Goddard Space Flight Center, Greenbelt, MD 20771 USA)

[PPS03-P15] Radar and optical simultaneous observations of faint meteors with MU radar and Tomo-e Gozen

*Ryou Ohsawa[1], Akira Hirota[2], Shinsuke Abe[2], Daniel Kastinen[3], Kero Johan[3], yasunori Fujiwara[4], Takuji Nakamura[5], Shigeyuki Sako[1], Yuto Kojima[1], Jun-ichi Watanabe[6] (1.Institute of Astronomy, Graduate School of Science, The University of Tokyo, 2.Department of Aerospace Engineering, College of Science & Technology, Nihon University, 3.Swedish Institute of Space Physics, 4.SOKENDAI (The Graduate University for Advanced Studies), 5.National Institute of Polar Research, 6.National Astronomical Observatory of Japan)

[PPS03-P16] Global distribution and spectral characteristics of bright spots on asteroid Ryugu

*Masanori Suemitsu[1], Tomokatsu Morota[1], Rie Honda[2], Singo Kameda[15], Eri Tatsumi[3], Manabu Yamada[4], Naoya Sakatani[5], Toru Kouyama[6], Yokota Yasuhiro[7], Yuichiro Cho[8], Hidehiko Suzuki[9], Masahiko Hayakawa[10], Moe Matsuoka[10], Chikatoshi Honda[11], Tatsuhiro Michikami[12], Kazuo Yoshioka[13], Kazunori Ogawa[14], Hirotaka Sawada[5], Seiji Sugita[3] (1.Graduate School of Environmental Studies, Nagoya University, 2.Department of Science and Technology, System of Natural Science, Kochi Unicversity, 3.Graduate School of Earth and Planetary Science, Tokyo Unicversity, 4.Planetary Exploration Reserch Center, Chiba Institute of Technology, 5.Institute of Space and Astoronautical Science, Japan Aerospace Exploration Agency, 6.National Institute of Advanced Industrial Science and Technology, 7.Kochi University, 8.Department of Earth and Planetary Science, Tokyo University, 9.Depertment of physics, Meiji University , 10.Department of Solar System Science, Institute of Space and Astoronautical Science, Japan Aerospace Exploration Agency, 11.Aizu University, 12.Faculty of Engineering, Kindai University, 13.Graduate School of frontier Science, Tokyo University, 14.Kobe University, 15.Rikkyo University)

[PPS03-P17] Polarimetry of (155140) 2005 UD: the Dynamical Association with (3200) Phaethon

*Masateru Ishiguro[1], Jooyeon Geem[1], Hiroyuki Naito[2], Yoonsoo P. Bach[1], Daisuke Kuroda[3], Tatsuharu Ono[4], Seiko Takagi[4], Mitsuteru Sato[4], Kiyoshi Kuramoto[4], Tomohiko Sekiguchi[5], Masataka Imai[6], Makoto Watanabe[7], Katsuhito Ohtsuka[8], Sunao Hasegawa[9], Takashi Ito[10], Fumi Yoshida[11], Tomoko Arai[11] (1.Department of Physics and Astronomy, Seoul National University, 2.Nayoro Observatory, 3.Okayama Observatory, Kyoto University, 4.Department of Cosmosciences, Graduate School of Science, Hokkaido University, 5.Hokkaido University of Education, 6.National Institute of Advanced Industrial Science and Technology, 7.Department of Applied Physics, Okayama University of Science, 8.Tokyo Meteor Network, 9.Japan Aerospace Exploration Agency, 10.National Astronomical Observatory of Japan, 11.Planetary Exploration Research Center, Chiba Institute of Technology)

[PPS03-P18] **Follow-up observations for AKARI/IRC near-infrared asteroid spectroscopic survey (AcuA-spec)**

*Sunao Hasegawa[1], Daisuke KURODA[2], Kenshi YANAGISAWA[3], Fumihiko Usui[4] (1.Japan Aerospace Exploration Agency, 2.Kyoto University, 3.National Astronomical Observatory of Japan, 4.Kobe University)

[PPS03-P19] Amino acids on witness coupons collected from the ISAS/JAXA curation facility for the assessment and quality control of the Hayabusa2 sampling procedure

*Haruna Sugahara[1,2], Yoshinori Takano[1], Yuzuru Karouji[3], Kazuya Kumagai[4], Toru Yada[3], Naohiko Ohkouchi[1], Masanao Abe[3], Hayabusa2 project team (1.Japan Agency for Marine-Earth Science and Technology (JAMSTEC), 2. Institut de Chimie de Nice, Universite Cote dAzur, 3.Japan Aerospace Exploration Agency (JAXA), 4.Marine Works Japan Ltd.)

[PPS03-P20] Hayabusa2 orbit determination using c5++ software

*Keiko Yamamoto[1], Toshimichi Otsubo[2], Koji Matsumoto[1], Hirotomo Noda[1], Noriyuki Namiki[1], Hiroki Senshu[3], Takahide Mizuno[4], Naoko Ogawa[4], Go Ono[4], Yuya Mimasu[4], Kent Yoshikawa[4], Tadateru Takahashi[4], Yuto Takei[4], Atsushi Fujii[4], Fuyuto Terui[4], Takanao Saiki[4], Satoru Nakazawa[4], Makoto Yoshikawa[4], Yuichi Tsuda[4] (1.National Astronomical Observatory of Japan, 2.Hitotsubashi University, 3.Chiba Institute of Technology, 4.Japan Aerospace Exploration Agency)

[PPS03-P21] **Landing Site Selection for Hayabusa2: Scientific Evaluation of the Candidate Sites on Asteroid (162173) Ryugu**

*Hikaru Yabuta[1], Sei-ichiro WATANABE[2], Tomoki Nakamura[3], Naru Hirata[4], Seiji Sugita[5], Tatsuaki Okada[6], Kohei Kitazato[4], Yoshiaki Ishihara[7], Tomokatsu Morota[2], Naoya Sakatani[6], Koji Matsumoto[8], Koji Wada[9], Shogo Tachibana[5], Mutsumi Komatsu[10], ERI TATSUMI[5], Moe Matsuoka[6], Chikatoshi Honda[4], Takahiro Hiroi[11], Hiroki Senshu[9], Rie Honda[12], Yasuhiro Yokota[6], Rina Noguchi[6], Yuri Shimaki[6], Deborah Lorin Domingue[13], Lucille Le Corre[13], Antonella Barucci[14], Ernest Palomba[15], Shota Kikuchi[6], Akira Miura[6], Tomohiro Yamaguchi[6], Yukio Yamamoto[6], Takanao Saiki[6], Satoshi Tanaka[6], Makoto Yoshikawa[6], Yuichi Tsuda[6] (1.Hiroshima University, Department of Earth and Planetary Systems Science, 2.Nagoya University, 3.Tohoku University, 4.University of Aizu, 5.The University of Tokyo, 6.ISAS/JAXA, 7.NIES, 8.NAOJ, 9.Chiba Institute of Technology, Planetary Exploration Research Center (PERC), 10.Sokendai, 11.Brown University, 12.Kochi University, 13.Planetary Science Institute, USA, 14.Observatoire Paris-Site de Meudon, LESIA, France, 15.INAF-IAPS, Italy.)

[PPS03-P22] Visible Photometric, Spectroscopic and Polarimetric observations of an inactive comet, P/2016 BA14 with the 1.6m Pirka Telescope

*Ryo Yamagata[1], Tomohiko Sekiguchi[1], Ryo Okazaki[1], Kazuya Doi[1], Daisuke Kuroda[2], Masateru Ishiguro[3], Hiroyuki Naito[4] (1.Hokkaido University of Education, 2.Kyoto University, 3.Seoul National University, 4.Nayoro Observatory)

[PPS03-P23] **Polycyclic aromatic hydrocarbons and aliphatic hydrocarbons in Jbilet Winselwan carbonaceous chondrite : Attempt to evaluate the thermal metamorphism degree on the parent body**

Hiroki Kato[1], *Hikaru Yabuta[1] (1.Hiroshima University, Department of Earth and Planetary Systems Science)

[PPS03-P24] Disk-Resolved Photometry Analysis of the Asteroid Ryugu Images Obtained by Hayabusa2 Visible Camera ONC

*yokota yasuhiro[1,2], Rie Honda[1], ERI TATSUMI[3], Deborah Domingue[4], Stefanus E. Schroeder[5], Moe Matsuoka[2], Seiji Sugita[3], Tomokatsu Morota[6], Shingo Kameda[7], Toru Kouyama[8], Hidehiko Suzuki[9], Manabu Yamada[10], Naoya Sakatani[2], Chikatoshi Honda[11], Masahiko Hayakawa[2], Kazuo Yoshioka[3], Yuichiro Cho[3], Hirotaka Sawada[2] (1.Kochi University, 2.ISAS/JAXA, 3.Univ. of Tokyo, 4.Planetary Science Institute, 5.DLR, 6.Nagoya Univ., 7.Rikkyo Univ., 8.AIST, 9.Meiji Univ., 10.Chiba Institute od Technology, 11.Aizu Univ.)

[E] Poster | P (Space and Planetary Sciences)：P-PS Planetary Sciences

5:15 PM - 6:30 PM JST | 8:15 AM - 9:30 AM UTC | Poster Hall International Exhibition Hall8, Makuhari Messe_3

[P-PS03] Solar System Small Bodies: A New Frontier Arising Hayabusa 2, OSIRIS-REx and Other Projects

convener:Masateru Ishiguro(Department of Physics and Astronomy, Seoul National University), Taishi Nakamoto(Tokyo Institute of Technology), Masanao Abe(Institute of Space and Astronautical Science, Japan Aerospace Exploration Agency), Olivier S Barnouin(Johns Hopkins University Applied Physics Laboratory)

[PPS03-P01] Impact experiments on low strength coarse-grained regolith simulating surface materials on asteroid Ryugu

*Yuya Yamamoto[1], Masahiko Arakawa[1], Minami Yasui[1], Sunao Hasegawa[2], Ryo Sugimura[1] (1.Graduate School of Science, Kobe University, 2.ISAS, JAXA)

[PPS03-P02] Reflectance estimation of asteroid Ryugu using MASCOT

*Marika Ishida[1], Koto Amano[1], Keiichi Moroi[1], ERI TATSUMI[2], Tra-Mi Ho[10], Shingo Kameda[1], Seiji Sugita[2], Rie Honda[3], Tomokatsu Morota[4], yokota yasuhiro[5], Toru Kouyama[6], Hidehiko Suzuki[7], Manabu Yamada[8], Naoya Sakatani[5], Chikatoshi Honda[9], Masahiko Hayakawa[5], Kazuo Yoshioka[2], Moe Matsuoka[5], Yuichiro Cho[2], Hirotaka Sawada[5] (1.Rikkyo Univ., 2.Univ. of Tokyo, 3.Kochi Univ., 4.Nagoya Univ., 5.JAXA/ISAS, 6.AIST, 7.Meiji Univ., 8.Chiba Inst. Tech, 9.Univ. of Aizu, 10.DLR)

[PPS03-P03] Flyby observation of Asteroid (3200) Phaethon by DESTINY$^+$ onboard cameras

*Ko Ishibashi[1], Shingo Kameda[2], Masato Kagitani[3], Peng Hong[1], Manabu Yamada[1], Osamu Okudaira[1], Tomoko Arai[1], Fumi Yoshida[1], Shunsuke Sato[4], Takahiro Ishimaru[4], Takaya Okamoto[4], Takahiro Iwata[4], Tatsuaki Okada[4], Takeshi Takashima[4] (1.Chiba Institute of Technology, 2.Rikkyo University, 3.Tohoku Universtiy, 4.Japan Aerospace Exploration Agency)

[PPS03-P04] Polarimetric Study of Asteroids in Comet-Like Orbits (ACOs)

*Jooyeon Geem[1], Masateru Ishiguro[1], Yoonsoo P. Bach[1], Daisuke Kuroda[2], Hiroyuki Naito[3], Hidekazu Hanayama[4], yoonyoung kim[10], Yuna G. Kwon[1], Sunho Jin[1], Tomohiko Sekiguchi[5], Ryo Okazaki[5], Jeremie J. Vaubaillon[6], Masataka Imai[7], Tatsuharu Oono[8], Yuki Futamuts[8], Seiko Takagi[8], Mitsuteru Sato[8], Kiyoshi Kuramoto[8], Makoto Watanabe[9] (1.Astronomy program, Dept of Physics and Astronomy, Seoul National University, 2.Okayama Observatory, Kyoto University, 3.Nayoro Observatory, 4.Ishigakijima Astronomical Observatory, National Astronomical Observatory of Japan, 5.Hokkaido University of Education, 6.Observatoire de Paris, I.M.C.C.E., 7.National Institute of Advanced Industrial Science and Technology, 8.Department of Cosmosciences, Graduate School of Science, Hokkaido University, 9.Department of Applied Physics, Okayama University of Science, 10.Max Planck Institute for Solar System Research)

[PPS03-P05] Dynamical lifetime of the Oort Cloud new comets under planetary perturbation

*Ito Takashi[1], Arika Higuchi[1] (1.National Astronomical Observatory of Japan)

[PPS03-P06] Thermal Infrared Imaging of C-type Asteroid 162173 Ryugu with Porous Surfaces

*Tatsuaki Okada[1,2], Tetsuya Fukuhara[3], Satoshi Tanaka[1], Makoto Taguchi[3], Takehiko Arai[4], Naoya Sakatani[1], Yuri Shimaki[1], Hiroki Senshu[5], Yoshiko Ogawa[6], Hirohide Demura[6], Kentaro Suko[6], Kohei Kitazato[6], Toru Kouyama[7], Tomohiko Sekiguchi[8], Jun Takita[9], Sunao Hasegawa[1], Tsuneo Matsunaga[10], Takehiko Wada[1], Takeshi Imamura[2], Jorn Helbert[11], Thomas G. Mueller[12], Axel Hagermann[13], Jens Biele[11], Matthias Grott[11], Maximiliam Hamm[11], Marco Delbo[14], Yukio Yamamoto[1], Naru Hirata[6], Naoyuki Hirata[15], Fuyuto Terui[1], Takanao Saiki[1], Satoru Nakazawa[1], Makoto Yoshikawa[1], Sei-ichiro WATANABE[1,16], Yuichi Tuda[1] (1.Institute of Space and Astronautical Science, Japan Aerospace Exploration Agency, 2.University of Tokyo, 3.Rikkyo University, 4.Ashikaga University, 5.Chiba Institute of Technology, 6.University of Aizu, 7.National Institute of Advanced Industrial Science and Technology, 8.Hokkaido University of Education, 9.Hokkaido Kitami-Hokuto High School, 10.National Institute for Environmental Studies, 11.German Aerospace Center, 12.Max-Planck Institute for Extraterrestrial Physics, 13.University of Stirling, 14.Observatoire de la Côte d'Azur, 15.Kobe University, 16.Nagoya University)

[PPS03-P07] Data Release of Asteroid 162173 Ryugu by Observation of Thermal Infrared Imager onboard Hayabusa2

*Takehiko Arai[1], Hirohide Demura[2], Toru Kouyama[7], Naoya Sakatani[3], Kentaro Suko[2], Yuri Shimaki[3], Hiroki Senshu[5], Tomohiko Sekiguchi[6], Yoshiko Ogawa[2], Sunao Hasegawa[3], Takehiko Wada[3], Takeshi Imamura[10], Tsuneo Matsunaga[9], Jun Takita[8], Kohei Kitazato[2], Makoto Taguchi[4], Tetsuya Fukuhara[4], Satoshi Tanaka[3], Tatsuaki Okada[3] (1.Ashikaga University, 2.The University of Aizu, 3.Japan Aerospace Exploration Agency (JAXA), 4.Rikkyo University,

5.Chiba Institute of Technology, 6.Hokkaido University of Education, 7.National Institute of Advanced Industrial Science and Technology (AIST), 8.Hokkaido Kitami Hokuto High School, 9.National Institute for Environmental Studies (NIES), 10.The University of Tokyo)

[PPS03-P08] Multi-mission capability of HARMONICS

*Shintaro Tsunoda[1], Hirohide Demura[1], Naru Hirata[1] (1.The University of Aizu)

[PPS03-P09] New interface of verification for calibration and conversion in HEAT : Hayabusa2 Exploration Assistant for TIR

*Tatsuro Kobayashi[1], Kentaro Suko[1], Hirohide Demura[1], Yoshiko Ogawa[1], Takehiko Arai[2], Naoya Sakatani[3], Tatsuaki Okada[3], Satoshi Tanaka[3], Tetsuya Fukuhara[4] (1.The University of Aizu, 2.Ashikaga University, 3.Institute of Space and Astronautical Science, Japan Aerospace Exploration Agency, 4.Rikkyo University)

[PPS03-P10] **Dust particle evolution of a near-Earth object 252P/LINEAR from near-infrared polarimetric observations in 2016**

*Yuna G Kwon[1], Masateru Ishiguro[1], Jungmi Kwon[2], Daisuke Kuroda[3], Myungshin Im[1], Changsu Choi[1], Motohide Tamura[4], Takahiro Nagayama[5], Nobuyuki Kawai[6], Jun-ichi Watanabe[7] (1.Seoul National Univ., 2.ISAS/Japan Aerospace Exploration Agency, 3.Okayama Astrophysical Observatory, 4.The Univ. of Tokyo, 5.Kagoshima Univ., 6.Tokyo Institute of Technology, 7.National Astronomical Observatory of Japan)

[PPS03-P11] **Performance Evaluation of TRIPOL on the 61-cm Telescope at Seoul National University for Polarimetric Observations of Solar System Small Bodies**

*Sunho Jin[1], Masateru Ishiguro[1], Yuna G Kwon[1], Jooyeon Geem[1], Yoonsoo P. Bach[1], Jinguk Seo[1], Hiroshi Sasago[2], Shuji Sato[3] (1.Seoul National University, 2.Sasago Co.,Ltd, 3.Nagoya University)

[PPS03-P12] Smart Interface of HEAT: Hayabusa2 Exploration Assistant for TIR

*Kentaro Suko[1], Tatsuro Kobayashi[1], Hirohide Demura[1], Takehiko Arai[2], Naoya Sakatani[3], Tatsuaki Okada[3], Satoshi Tanaka[3], Tetsuya Fukuhara[4] (1.The University of Aizu, 2.Ashikaga University, 3.Institute of Space and Astronautical Science, Japan Aerospace Exploration Agency, 4.Rikkyo University)

[PPS03-P13] Experimental Study on Collision Crater Formed on Bulge Geography

*Yusaku Yokota[1], Yuya Yamamoto[2], Minami Yasui[2], Masahiko Arakawa[2] (1.Faculty of Science, Kobe University, 2.Graduate School of Science, Kobe University)

[PPS03-P14] Initial analysis plan of soluble organic compounds for the Hayabusa2 sample from asteroid Ryugu

*Hiroshi Naraoka[1], Yoshinori Takano[2], Jason P. Dworkin[3], SOM Analysis Team (1.Department of Earth and Planetary Sciences, Research Center for Planetary Trace Organic Compounds, Kyushu University, 2.Japan Agency for Marine-Earth Science and Technology, 3.Astrochemistry Laboratory NASA Goddard Space Flight Center, Greenbelt, MD 20771 USA)

[PPS03-P15] Radar and optical simultaneous observations of faint meteors with MU radar and Tomo-e Gozen

*Ryou Ohsawa[1], Akira Hirota[2], Shinsuke Abe[2], Daniel Kastinen[3], Kero Johan[3], yasunori Fujiwara[4], Takuji Nakamura[5], Shigeyuki Sako[1], Yuto Kojima[1], Jun-ichi Watanabe[6] (1.Institute of Astronomy, Graduate School of Science, The University of Tokyo, 2.Department of Aerospace Engineering, College of Science & Technology, Nihon University, 3.Swedish Institute of Space Physics, 4.SOKENDAI (The Graduate University for Advanced Studies), 5.National Institute of Polar Research, 6.National Astronomical Observatory of Japan)

[PPS03-P16] Global distribution and spectral characteristics of bright spots on asteroid Ryugu

*Masanori Suemitsu[1], Tomokatsu Morota[1], Rie Honda[2], Singo Kameda[15], Eri Tatsumi[3], Manabu Yamada[4], Naoya Sakatani[5], Toru Kouyama[6], Yokota Yasuhiro[7], Yuichiro Cho[8], Hidehiko Suzuki[9], Masahiko Hayakawa[10], Moe Matsuoka[10], Chikatoshi Honda[11], Tatsuhiro Michikami[12], Kazuo Yoshioka[13], Kazunori Ogawa[14], Hirotaka Sawada[5], Seiji Sugita[3] (1.Graduate School of Environmental Studies, Nagoya University, 2.Department of Science and Technology, System of Natural Science, Kochi Unicversity, 3.Graduate School of Earth and Planetary Science, Tokyo Unicversity, 4.Planetary Exploration Reserch Center, Chiba Institute of Technology, 5.Institute of Space and Astoronautical Science, Japan Aerospace Exploration Agency, 6.National Institute of Advanced Industrial Science and Technology, 7.Kochi University, 8.Department of Earth and Planetary Science, Tokyo University, 9.Depertment of physics, Meiji University , 10.Department of Solar System Science, Institute of Space and Astoronautical Science, Japan Aerospace Exploration Agency, 11.Aizu University, 12.Faculty of Engineering, Kindai University, 13.Graduate School of frontier Science, Tokyo University, 14.Kobe University, 15.Rikkyo University)

[PPS03-P17] Polarimetry of (155140) 2005 UD: the Dynamical Association with (3200) Phaethon

*Masateru Ishiguro[1], Jooyeon Geem[1], Hiroyuki Naito[2], Yoonsoo P. Bach[1], Daisuke Kuroda[3], Tatsuharu Ono[4], Seiko Takagi[4], Mitsuteru Sato[4], Kiyoshi Kuramoto[4], Tomohiko Sekiguchi[5], Masataka Imai[6], Makoto Watanabe[7], Katsuhito Ohtsuka[8], Sunao Hasegawa[9], Takashi Ito[10], Fumi Yoshida[11], Tomoko Arai[11] (1.Department of Physics and Astronomy, Seoul National University, 2.Nayoro Observatory, 3.Okayama Observatory, Kyoto University, 4.Department of Cosmosciences, Graduate School of Science, Hokkaido University, 5.Hokkaido University of Education, 6.National Institute of Advanced Industrial Science and Technology, 7.Department of Applied Physics, Okayama University of Science, 8.Tokyo Meteor Network, 9.Japan Aerospace Exploration Agency, 10.National Astronomical Observatory of Japan, 11.Planetary Exploration Research Center, Chiba Institute of Technology)

[PPS03-P18] **Follow-up observations for AKARI/IRC near-infrared asteroid spectroscopic survey (AcuA-spec)**

*Sunao Hasegawa[1], Daisuke KURODA[2], Kenshi YANAGISAWA[3], Fumihiko Usui[4] (1.Japan Aerospace Exploration Agency, 2.Kyoto University, 3.National Astronomical Observatory of Japan, 4.Kobe University)

[PPS03-P19] Amino acids on witness coupons collected from the ISAS/JAXA curation facility for the assessment and quality control of the Hayabusa2 sampling procedure

*Haruna Sugahara[1,2], Yoshinori Takano[1], Yuzuru Karouji[3], Kazuya Kumagai[4], Toru Yada[3], Naohiko Ohkouchi[1], Masanao Abe[3], Hayabusa2 project team (1.Japan Agency for Marine-Earth Science and Technology (JAMSTEC), 2. Institut de Chimie de Nice, Universite Cote dAzur, 3.Japan Aerospace Exploration Agency (JAXA), 4.Marine Works Japan Ltd.)

[PPS03-P20] Hayabusa2 orbit determination using c5++ software

*Keiko Yamamoto[1], Toshimichi Otsubo[2], Koji Matsumoto[1], Hirotomo Noda[1], Noriyuki Namiki[1], Hiroki Senshu[3], Takahide Mizuno[4], Naoko Ogawa[4], Go Ono[4], Yuya Mimasu[4], Kent Yoshikawa[4], Tadateru Takahashi[4], Yuto Takei[4], Atsushi Fujii[4], Fuyuto Terui[4], Takanao Saiki[4], Satoru Nakazawa[4], Makoto Yoshikawa[4], Yuichi Tsuda[4] (1.National Astronomical Observatory of Japan, 2.Hitotsubashi University, 3.Chiba Institute of Technology, 4.Japan Aerospace Exploration Agency)

[PPS03-P21] **Landing Site Selection for Hayabusa2: Scientific Evaluation of the Candidate Sites on Asteroid (162173) Ryugu**

*Hikaru Yabuta[1], Sei-ichiro WATANABE[2], Tomoki Nakamura[3], Naru Hirata[4], Seiji Sugita[5], Tatsuaki Okada[6], Kohei Kitazato[4], Yoshiaki Ishihara[7], Tomokatsu Morota[2], Naoya Sakatani[6], Koji Matsumoto[8], Koji Wada[9], Shogo Tachibana[5], Mutsumi Komatsu[10], ERI TATSUMI[5], Moe Matsuoka[6], Chikatoshi Honda[4], Takahiro Hiroi[11], Hiroki Senshu[9], Rie Honda[12], Yasuhiro Yokota[6], Rina Noguchi[6], Yuri Shimaki[6], Deborah Lorin Domingue[13], Lucille Le Corre[13], Antonella Barucci[14], Ernest Palomba[15], Shota Kikuchi[6], Akira Miura[6], Tomohiro Yamaguchi[6], Yukio Yamamoto[6], Takanao Saiki[6], Satoshi Tanaka[6], Makoto Yoshikawa[6], Yuichi Tsuda[6] (1.Hiroshima University, Department of Earth and Planetary Systems Science, 2.Nagoya University, 3.Tohoku University, 4.University of Aizu, 5.The University of Tokyo, 6.ISAS/JAXA, 7.NIES, 8.NAOJ, 9.Chiba Institute of Technology, Planetary Exploration Research Center (PERC), 10.Sokendai, 11.Brown University, 12.Kochi University, 13.Planetary Science Institute, USA, 14.Observatoire Paris-Site de Meudon, LESIA, France, 15.INAF-IAPS, Italy.)

[PPS03-P22] Visible Photometric, Spectroscopic and Polarimetric observations of an inactive comet, P/2016 BA14 with the 1.6m Pirka Telescope

*Ryo Yamagata[1], Tomohiko Sekiguchi[1], Ryo Okazaki[1], Kazuya Doi[1], Daisuke Kuroda[2], Masateru Ishiguro[3], Hiroyuki Naito[4] (1.Hokkaido University of Education, 2.Kyoto University, 3.Seoul National University, 4.Nayoro Observatory)

[PPS03-P23] **Polycyclic aromatic hydrocarbons and aliphatic hydrocarbons in Jbilet Winselwan carbonaceous chondrite : Attempt to evaluate the thermal metamorphism degree on the parent body**

Hiroki Kato[1], *Hikaru Yabuta[1] (1.Hiroshima University, Department of Earth and Planetary Systems Science)

[PPS03-P24] Disk-Resolved Photometry Analysis of the Asteroid Ryugu Images Obtained by Hayabusa2 Visible Camera ONC

*yokota yasuhiro[1,2], Rie Honda[1], ERI TATSUMI[3], Deborah Domingue[4], Stefanus E. Schroeder[5], Moe Matsuoka[2], Seiji Sugita[3], Tomokatsu Morota[6], Shingo Kameda[7], Toru Kouyama[8], Hidehiko Suzuki[9], Manabu Yamada[10], Naoya Sakatani[2], Chikatoshi Honda[11], Masahiko Hayakawa[2], Kazuo Yoshioka[3], Yuichiro Cho[3], Hirotaka Sawada[2] (1.Kochi University, 2.ISAS/JAXA, 3.Univ. of Tokyo, 4.Planetary Science Institute, 5.DLR, 6.Nagoya Univ., 7.Rikkyo Univ., 8.AIST, 9.Meiji Univ., 10.Chiba Institute od Technology, 11.Aizu Univ.)

[E] Poster | P (Space and Planetary Sciences)：P-EM Solar-Terrestrial Sciences, Space Electromagnetism & Space Environment

10:45 AM - 12:15 PM JST | 1:45 AM - 3:15 AM UTC | Poster Hall International Exhibition Hall8, Makuhari Messe_3

[P-EM09] Vertical coupling in the atmosphere and Ionosphere

convener:Huixin Liu(Earth and Planetary Science Division, Kyushu University SERC, Kyushu University), Loren Chang(Institute of Space Science, National Central University), Yuichi Otsuka(Institute for Space-Earth Environmental Research, Nagoya University)

[PEM09-P01] Local-time Variabilities of SABER CO_2 in the Mesosphere and Lower Thermosphere Region

*Cornelius Csar Jude Salinas[1], Loren Chang[1], Danie Liang[2], Jia Yue[3], Liying Qian[4], Quan Gan[5], James Russel III[3], Martin G Mlynczak[6] (1.Institute of Space Science, National Central University, 2.Institute of Earth Science, Academia Sinica, 3.Department of Atmospheric Sciences, Hampton University, 4.High Altitude Observatory, National Center for Atmospheric Research, 5.Department of Physics and Astronomy, Clemson University, 6.NASA Langley Research Center)

[PEM09-P02] Enhanced dynamo electric field as a possible cause of ionosphere disturbance before Large Earthquake

*Koichiro Oyama[1,2,3] (1.Institute of Plasma and Space Sciences,National Cheng Kung Univ., Taiwan, 2.International Ceneter for Space Weather Sudy and Education, Kyushu Univ.,, 3.CoLtd. Asia Space Environment Research Consortium, Japan)

[PEM09-P03] Morphology of E1 and E2 Kelvin waves from ECMWF reanalysis

*Chen-Jeih Pan[1], Wei-Sheng Chen[1], Uma Das[2] (1.Institute of Space Science, National Central University, 2.Department of Physics, Indian Institute of Information Technology, Kalyani, India)

[PEM09-P04] Impact of strong ENSO on TEC activity disturbed by ultra-fast Kelvin waves

*Wei-Sheng Chen[1], C.J. Pan[1], Uma Das[2], Chian-Chiau Lin[3] (1.Institute of Space Science, National Central University, Taiwan, 2.Department of Physics, Indian Institute of Information Technology, Kalyani, India, 3.Environmental Research and Information Center, Chang Jung Christian University, Taiwan)

[PEM09-P05] Observation and simulation of propagation of coseismic infrasound to the ionosphere

*Jaroslav Chum[1] (1.Institute of Atmospheric Physics of the Czech Academy of Sciences)

[PEM09-P06] Solar wind influence on tropical cyclones mediated by atmospheric gravity waves

*Paul Prikryl[1,2], Iurii Cherniak[3], Irina Zakharenkova[4,5], James M. Weygand[6], Bharat S. R. Kunduri[7] (1.Physics Department, University of New Brunswick, Fredericton, NB, Canada, 2.Geomagnetic Laboratory, Natural Resources Canada, Ottawa, ON, Canada, 3.COSMIC Program Office, University Corporation for Atmospheric Research, Boulder, CO, USA, 4.West Department of IZMIRAN, Kaliningrad, Russia, 5.University of Warmia and Mazury in Olsztyn, Poland, 6.Earth Planetary and Space Sciences, University of California, Los Angeles, CA, USA, 7.Bradley Dept. of Electrical and Computer Engineering, Virginia Tech, Blacksburg, VA, USA)

[PEM09-P07] VIPIR ionospheric observations in Japan

*Takuya Tsugawa[1], Hideo Maeno[1], Michi Nishioka[1], Takumi Kondo[1], Mamoru Ishii[1] (1.National Institute of Information and Communications Technology)

[PEM09-P08] Simulation Results and Performance Analysis of Phase Velocity Spectral Analysis Software (M-Transform) for Airglow Imaging Data

*Septi Perwitasari[1], Takuji Nakamura[2], Masaru Kogure[2], Yoshihiro Tomikawa[2], Mitsumu K. Ejiri[2] (1.LAPAN, 2.NIPR)

[PEM09-P09] Comparisons of Co-incident Ionospheric Plasma Observations Between FORMOSAT-5/AIP and Millstone Hill Incoherent Scatter Radar

*Yi-Wun Chen[1], Chi-Kuang Chao[1] (1.Graduate Institute of Space Science, National Central University, Taiwan)

[PEM09-P10] Sub-ionospheric effects of volcano eruptions using VLF/LF standard radio waves

*Kei Maruyama[1], Hiroyo Ohya[1], Fuminori Tsuchiya[2], Kenro Nozaki[5], Kozo Yamashita[3], Yukihiro Takahashi[4], Hiroyuki Nakata[1], Toshiaki Takano[1] (1.Chiba University, 2.Tohoku University, 3.Ashikaga University, 4.Hokkaido University, 5.National Institute of Information and Communications Technology)

[PEM09-P11] Observations of ionospheric and mesospheric wave structures by a low-cost airglow imaging system

*Keisuke Hosokawa[1], Nanami Kusuyama[1], Yuta Hozumi[1], Kohei Takami[1], Susumu Saito[2], Yasunobu Ogawa[3], Mamoru Ishii[4], Yuichi Otsuka[5], Takuya Tsugawa[4] (1.University of Electro-Communications, 2.ENRI, 3.NIPR, 4.NICT, 5.ISEE, Nagoya University)

[PEM09-P12] Analysis of characteristics of ionospheric parameters, Sq index and neutral winds over Taiwan

*Yu-Jung Chuo[1] (1.Department of Information Technology, Ling Tung University)

[PEM09-P13] Statistical study on daytime Es observed by ground-ionosonde and RO-COSMIC in magnetic Equator region in 2010

*Zheng Wang [1,2], Huixin Liu[1] (1.Department of Earth and Planetary Sciences, School of Science, Kyushu University, Japan. , 2.National Space Science Center, Chinese Academy of Sciences, China.)

[PEM09-P14] The statistical study of the growth rates of Medium-Scale Traveling Ionospheric Disturbances observed with GPS-TEC

*Takafumi Ikeda[1], Akinori Saito[1], Takuya Tsugawa[2], Hiroyuki Shinagawa[2] (1.Department of Geophysics, Graduate School of Science, Kyoto University, 2.National Institutes of Information and Communications Technology)

[PEM09-P15] Comparison of Gravity Wave Activity in the Mesosphere Observed by OH Airglow Imagers and MF Radars over the Antarctic (Syowa & Davis).

*Masaru Kogure[1], Takuji Nakamura[1,2], Yoshihiro Tomikawa[1,2], Mitsumu K. Ejiri[1,2], Takanori Nishiyama[2,1], Masaki Tsutsumi[1,2], Michael J. Taylor[3], Yucheng Zhao[3], P.-Dominique Pautet[3], Damian Murphy[4] (1.National Institute of Polar Research, 2.Department of Polar Science, Sokendai, 3.Physics Department, Utah State University, 4.Australian Antarctic Division)

[E] Poster | P (Space and Planetary Sciences)：P-EM Solar-Terrestrial Sciences, Space Electromagnetism & Space Environment

5:15 PM - 6:30 PM JST | 8:15 AM - 9:30 AM UTC | Poster Hall International Exhibition Hall8, Makuhari Messe_4

[P-EM09] Vertical coupling in the atmosphere and Ionosphere

convener:Huixin Liu(Earth and Planetary Science Division, Kyushu University SERC, Kyushu University), Loren Chang(Institute of Space Science, National Central University), Yuichi Otsuka(Institute for Space-Earth Environmental Research, Nagoya University)

[PEM09-P01] Local-time Variabilities of SABER CO_2 in the Mesosphere and Lower Thermosphere Region

*Cornelius Csar Jude Salinas[1], Loren Chang[1], Danie Liang[2], Jia Yue[3], Liying Qian[4], Quan Gan[5], James Russel III[3], Martin G Mlynczak[6] (1.Institute of Space Science, National Central University, 2.Institute of Earth Science, Academia Sinica, 3.Department of Atmospheric Sciences, Hampton University, 4.High Altitude Observatory, National Center for Atmospheric Research, 5.Department of Physics and Astronomy, Clemson University, 6.NASA Langley Research Center)

[PEM09-P02] Enhanced dynamo electric field as a possible cause of ionosphere disturbance before Large Earthquake

*Koichiro Oyama[1,2,3] (1.Institute of Plasma and Space Sciences,National Cheng Kung Univ., Taiwan, 2.International Ceneter for Space Weather Sudy and Education, Kyushu Univ.,, 3.CoLtd. Asia Space Environment Research Consortium, Japan)

[PEM09-P03] Morphology of E1 and E2 Kelvin waves from ECMWF reanalysis

*Chen-Jeih Pan[1], Wei-Sheng Chen[1], Uma Das[2] (1.Institute of Space Science, National Central University, 2.Department of Physics, Indian Institute of Information Technology, Kalyani, India)

[PEM09-P04] Impact of strong ENSO on TEC activity disturbed by ultra-fast Kelvin waves

*Wei-Sheng Chen[1], C.J. Pan[1], Uma Das[2], Chian-Chiau Lin[3] (1.Institute of Space Science, National Central University, Taiwan, 2.Department of Physics, Indian Institute of Information Technology, Kalyani, India, 3.Environmental Research and Information Center, Chang Jung Christian University, Taiwan)

[PEM09-P05] Observation and simulation of propagation of coseismic infrasound to the ionosphere

*Jaroslav Chum[1] (1.Institute of Atmospheric Physics of the Czech Academy of Sciences)

[PEM09-P06] Solar wind influence on tropical cyclones mediated by atmospheric gravity waves

*Paul Prikryl[1,2], Iurii Cherniak[3], Irina Zakharenkova[4,5], James M. Weygand[6], Bharat S. R. Kunduri[7] (1.Physics Department, University of New Brunswick, Fredericton, NB, Canada, 2.Geomagnetic Laboratory, Natural Resources Canada, Ottawa, ON, Canada, 3.COSMIC Program Office, University Corporation for Atmospheric Research, Boulder, CO, USA, 4.West Department of IZMIRAN, Kaliningrad, Russia, 5.University of Warmia and Mazury in Olsztyn, Poland, 6.Earth Planetary and Space Sciences, University of California, Los Angeles, CA, USA, 7.Bradley Dept. of Electrical and Computer Engineering, Virginia Tech, Blacksburg, VA, USA)

[PEM09-P07] VIPIR ionospheric observations in Japan

*Takuya Tsugawa[1], Hideo Maeno[1], Michi Nishioka[1], Takumi Kondo[1], Mamoru Ishii[1] (1.National Institute of Information and Communications Technology)

[PEM09-P08] Simulation Results and Performance Analysis of Phase Velocity Spectral Analysis Software (M-Transform) for Airglow Imaging Data

*Septi Perwitasari[1], Takuji Nakamura[2], Masaru Kogure[2], Yoshihiro Tomikawa[2], Mitsumu K. Ejiri[2] (1.LAPAN, 2.NIPR)

[PEM09-P09] Comparisons of Co-incident Ionospheric Plasma Observations Between FORMOSAT-5/AIP and Millstone Hill Incoherent Scatter Radar

*Yi-Wun Chen[1], Chi-Kuang Chao[1] (1.Graduate Institute of Space Science, National Central University, Taiwan)

[PEM09-P10] Sub-ionospheric effects of volcano eruptions using VLF/LF standard radio waves

*Kei Maruyama[1], Hiroyo Ohya[1], Fuminori Tsuchiya[2], Kenro Nozaki[5], Kozo Yamashita[3], Yukihiro Takahashi[4], Hiroyuki Nakata[1], Toshiaki Takano[1] (1.Chiba University, 2.Tohoku University, 3.Ashikaga University, 4.Hokkaido University, 5.National Institute of Information and Communications Technology)

[PEM09-P11] Observations of ionospheric and mesospheric wave structures by a low-cost airglow imaging system

*Keisuke Hosokawa[1], Nanami Kusuyama[1], Yuta Hozumi[1], Kohei Takami[1], Susumu Saito[2], Yasunobu Ogawa[3], Mamoru Ishii[4], Yuichi Otsuka[5], Takuya Tsugawa[4] (1.University of Electro-Communications, 2.ENRI, 3.NIPR, 4.NICT, 5.ISEE, Nagoya University)

[PEM09-P12] Analysis of characteristics of ionospheric parameters, Sq index and neutral winds over Taiwan

*Yu-Jung Chuo[1] (1.Department of Information Technology, Ling Tung University)

[PEM09-P13] Statistical study on daytime Es observed by ground-ionosonde and RO-COSMIC in magnetic Equator region in 2010

*Zheng Wang [1,2], Huixin Liu[1] (1.Department of Earth and Planetary Sciences, School of Science, Kyushu University, Japan. , 2.National Space Science Center, Chinese Academy of Sciences, China.)

[PEM09-P14] The statistical study of the growth rates of Medium-Scale Traveling Ionospheric Disturbances observed with GPS-TEC

*Takafumi Ikeda[1], Akinori Saito[1], Takuya Tsugawa[2], Hiroyuki Shinagawa[2] (1.Department of Geophysics, Graduate School of Science, Kyoto University, 2.National Institutes of Information and Communications Technology)

[PEM09-P15] Comparison of Gravity Wave Activity in the Mesosphere Observed by OH Airglow Imagers and MF Radars over the Antarctic (Syowa & Davis).

*Masaru Kogure[1], Takuji Nakamura[1,2], Yoshihiro Tomikawa[1,2], Mitsumu K. Ejiri[1,2], Takanori Nishiyama[2,1], Masaki Tsutsumi[1,2], Michael J. Taylor[3], Yucheng Zhao[3], P.-Dominique Pautet[3], Damian Murphy[4] (1.National Institute of Polar Research, 2.Department of Polar Science, Sokendai, 3.Physics Department, Utah State University, 4.Australian Antarctic Division)

[E] Oral | P (Space and Planetary Sciences)：P-EM Solar-Terrestrial Sciences, Space Electromagnetism & Space Environment

1:45 PM - 3:15 PM JST | 4:45 AM - 6:15 AM UTC | A03 TOKYO BAY MAKUHARI HALL

[P-EM09] Vertical coupling in the atmosphere and Ionosphere

convener:Huixin Liu(Earth and Planetary Science Division, Kyushu University SERC, Kyushu University), Loren Chang(Institute of Space Science, National Central University), Yuichi Otsuka(Institute for Space-Earth Environmental Research, Nagoya University), Chairperson:Patrick Espy(Norwegian University of Science and Technology), Astrid Maute(National Center for Atmospheric Research, US)

1:45 PM - 2:05 PM JST | 4:45 AM - 5:05 AM UTC

[PEM09-01] **Vertical Coupling from the Atmosphere to Geospace at Arrival Heights in Antarctica**

★Invited Papers

*Xinzhao Chu[1] (1.University of Colorado Boulder)

2:05 PM - 2:20 PM JST | 5:05 AM - 5:20 AM UTC

[PEM09-02] Vertical structure of terdiurnal tides in the Antarctic MLT region: 15 years observation over Syowa

*Huixin Liu[1], Masaki Tsutsumi[2], Hanli Liu[3] (1.Earth and Planetary Science Division, Kyushu University, Japan, 2.National Institute for Polar Research, Japan, 3.National Center for Atmospheric Research, US)

2:20 PM - 2:35 PM JST | 5:20 AM - 5:35 AM UTC

[PEM09-03] **3D Investigation of gravity waves propagation by Continuous Doppler sounding**

*Jaroslav Chum[1], Katerina Podolska[1] (1.Institute of Atmospheric Physics of the Czech Academy of Sciences)

2:35 PM - 2:55 PM JST | 5:35 AM - 5:55 AM UTC

[PEM09-04] **Observations of MLT dynamics using meteor radars and meteor radar networks**

★Invited Papers

*Gunter Stober[1], Vivien Matthias[2], Sven Wilhelm[1], Dimitry Pokhotelov[1], Alexander Kozlovsky[3], Evgenia Belova[4], Johan Kero[4], Chris Hall[5], Masaki Tsutsumi[6] (1.Leibniz Institute of Atmospheric Physics, 2.Potsdam Institute for Climate Impact Research, Earth System Analysis - Research Domain 1, Potsdam, Germany, 3.Sodankylä Geophysical Observatory, Sodankylä, FIN-99600, Finland, 4.Swedish Institute of Space Physics, Box 812, 98128 Kiruna, Sweden, 5.Tromsø Geophysical Observatory UiT-the Arctic University of Norway, Tromsø, Norway, 6.National Institute of Polar Research, Tokyo, Japan)

2:55 PM - 3:15 PM JST | 5:55 AM - 6:15 AM UTC

[PEM09-05] Ionospheric Variability Associated with the Quasi-6-day Planetary Wave

★Invited Papers

*Yosuke Yamazaki[1] (1.GFZ German Research Centre for Geosciences)

[E] Oral | P (Space and Planetary Sciences)：P-EM Solar-Terrestrial Sciences, Space Electromagnetism & Space Environment

3:30 PM - 5:00 PM JST | 6:30 AM - 8:00 AM UTC | A03 TOKYO BAY MAKUHARI HALL

[P-EM09] Vertical coupling in the atmosphere and Ionosphere

convener:Huixin Liu(Earth and Planetary Science Division, Kyushu University SERC, Kyushu University), Loren Chang(Institute of Space Science, National Central University), Yuichi Otsuka(Institute for Space-Earth Environmental Research, Nagoya University), Chairperson:Yuichi Otsuka, Yosuke Yosuke Yamazaki(GFZ Potsdam, Germany)

3:30 PM - 3:50 PM JST | 6:30 AM - 6:50 AM UTC

[PEM09-06] Results of FORMOSAT-3/COSMIC to the most recent developments on FORMOSAT-7/COSMIC-2

★Invited Papers

*JANN-YENQ Liu[1] (1.Center for Astronautical Physics and Engineering; Graduate Institute of Space Science, National Central University, Taiwan)

3:50 PM - 4:05 PM JST | 6:50 AM - 7:05 AM UTC

[PEM09-07] A morphological study on the relationship between electron density fluctuations and magnetic fluctuations observed by low altitude satellites in low and middle latitudes

*Toshihiko Iyemori[1], Tadashi Aoyama[1], Yoshihiro Yokoyama[1] (1.Kyoto University)

4:05 PM - 4:25 PM JST | 7:05 AM - 7:25 AM UTC

[PEM09-08] Observations of the Thermosphere and Ionosphere by the NASA GOLD Mission

★Invited Papers

*Stanley C Solomon[1], Alan G. Burns[1], Richard W. Eastes[2], William E. McClintock[2] (1.National Center for Atmospheric Research, 2.University of Colorado)

4:25 PM - 4:40 PM JST | 7:25 AM - 7:40 AM UTC

[PEM09-09] Temporal and spatial evolutions of storm enhanced density in the mid- and low-latitude regions as seen in the variation of global total electron content

*Atsuki Shinbori[1], Takuya Sori[1], Yuichi Otsuka[1], Takuya Tsugawa[2], Michi Nishioka[2] (1.Institute for Space-Earth Environment Research (ISEE), Nagoya University, 2.National Institute of Information and Communications Technology (NICT))

4:40 PM - 4:55 PM JST | 7:40 AM - 7:55 AM UTC

[PEM09-10] **Tidal Forcing Effects on the Zonal Variation of Solstice Equatorial Plasma Bubbles**

*Loren Chang[1], Jude Salinas[1], Yi-Chung Chiu[1], Pei-yun Chiu[1], Charles Lin[2] (1.Institute of Space Science and Engineering, Center for Astronautical Physics and Engineering, National Central University, Taiwan, 2.Department of Earth Science, National Cheng Kung University, Taiwan)

[E] Poster | P (Space and Planetary Sciences)：P-EM Solar-Terrestrial Sciences, Space Electromagnetism & Space Environment

1:45 PM - 3:15 PM JST | 4:45 AM - 6:15 AM UTC | Poster Hall International Exhibition Hall8, Makuhari Messe_1

[P-EM11] Dynamics of Magnetosphere and Ionosphere

convener:Aoi Nakamizo(Applied Electromagnetic Research Institute, National Institute of Information and Communications Technology), Mitsunori Ozaki(Faculty of Electrical and Computer Engineering, Institute of Science and Engineering, Kanazawa University), Akiko Fujimoto(Kyushu Institute of Technology), Tomoaki Hori(Institute for Space-Earth Environmental Research, Nagoya University)

[PEM11-P01] Effects of Inclination/Rotation of Earth's Magnetic Axis on Magnetosphere Simulated by Global MHD Model

*Aoi Nakamizo[1] (1.Applied Electromagnetic Research Institute, National Institute of Information and Communications Technology)

[PEM11-P02] Asymmetric deformation of the magnetosphere under low-density solar wind

*Masaki N Nishino[1,2], Yoshifumi Saito[2], Kazuo Shiokawa[1], Masaki Fujimoto[2] (1.Institute for Space-Earth Environmental Research, Nagoya University, 2.JAXA/ISAS)

[PEM11-P03] New perspectives on coupling processes in solar-terrestrial system obtained by comprehensive data analysis

*Yoshimasa Tanaka[1], Norio Umemura[2], Shuji Abe[3], Satoru UeNo[4], Masahito Nose[2], Yumi Nakagawa[5] (1.National Institute of Polar Research, 2.Institute for Space-Earth Environmental Research, Nagoya University, 3.International Center for Space Weather Science and Education, 4.Kwasan & Hida Observatories, School of Science, Kyoto University, 5.Ibaraki University)

[PEM11-P04] The interaction between the magnetosphere-ionosphere compound system and the magnetic field topology

*Shigeru Fujita[1], Takashi Tanaka[2], Masakazu Watanabe[2] (1.Meteorological College, Japan Meteorological Agency/ Nationa Institute of Polar Research, 2.Kyushu University)

[PEM11-P05] Effects of the dipole tilt and the interplanetary magnetic field Bx component on the dawn-dusk and interhemispheric asymmetries of the interchange convection cycle

*Masakazu Watanabe[1,2], Takashi Tanaka[2], Shigeru Fujita[3,4] (1.Graduate School of Science, Kyushu University, 2.International Center for Space Weather Science and Education, Kyushu University, 3.Meteorological College, 4.National Institute of Polar Research)

[PEM11-P06] Transient polar ionospheric convection response to negative dynamic pressure pulse

*Jianjun Liu[1] (1.Polar Research Institute of China)

[PEM11-P07] An active ionosphere: a new perspective of field line dipolarization

*Osuke Saka[1] (1.Office Geophysik)

[PEM11-P08] Toward the automatic identification of FLR signals in the SuperDARN data by using the gradient method

*Hideaki Kawano[1,2], Akira Sessai Yukimatu[3,4], Nozomu Nishitani[5], Yoshimasa Tanaka[3,4], Satoko Saita[6], Tomoaki Hori[5] (1.Dept. Earth Planet. Sci., Kyushu Univ., 2.ICSWSE, Kyushu University, 3.National Institute of Polar Research, 4.SOKENDAI, 5.ISEE, Nagoya University, 6.Kitakyushu College)

[PEM11-P09] A statistical study of Pi2 pulsations observed in the upper ionosphere using Swarm magnetic field data

*Park Jaehee[1], Khan-Hyuk Kim[1], Junga Hwang[2] (1.School of Space Research, Kyung Hee University, Gyeonggi, South Korea, 2.Korea Astronomy and Space Science Institute, Daejeon,South Korea)

[PEM11-P10] Study on the global distribution characteristics of Pc 1-2 geomagnetic pulsation with the 10Hz data of the MAGDAS system

*Taisei Kabasawa[1], Akimasa Yoshikawa[1], Teiji Uozumi[1], Akiko Fujimoto[1], Shuji Abe[1] (1.Kyushu University)

[PEM11-P11] In-situ Observations of Reconnection Separatrix Regions in the near-Earth Magnetotail

*Mizuho Araki[1], Masahiro Hoshino[1], Kunihiro Keika[1], Yoshifumi Saito[2] (1.Graduate School of Science, The University of Tokyo, 2.Institude of Space and Astronautical Science)

[PEM11-P12] Flow speed dependence of ion temperature, electron temperature, and their ratio in the near-Earth magnetotail reconnection region

*Kaori Watanabe[1], Masahiro Hoshino[1], Kunihiro Keika[1], Yoshifumi Saito[2], Naritoshi Kitamura[1] (1.Univ. of Tokyo, 2.ISAS/JAXA)

[PEM11-P13] **Examining Minimum Cyclotron Resonant Electron Energy of EMIC Waves with MMS**

*Si Liu[1] (1.Changsha University of Science and Technology)

[PEM11-P14] Small scale whistler mode waves near the magnetic field intensity minimum in the magnetosheath

*Naritoshi Kitamura[1], Takanobu Amano[1], Yoshiharu Omura[2], Satoko Nakamura[2], Chika Umegaki[1], Scott A Boardsen[3,4], Narges Ahmadi[5], Robert E Ergun[5], Olivier Le Contel[6], Per-Arne Lindqvist[7], Yoshifumi Saito[8], Shoichiro Yokota[9], Daniel J Gershman[3], Barbara L Giles[3], Thomas E Moore[3], William R Paterson[3], Craig J Pollock[10], Christopher T Russell[11], Robert J Strangeway[11], James L Burch[12] (1.Department of Earth and Planetary Science, Graduate School of Science, The University of Tokyo, 2.Research Institute for Sustainable Humanosphere, Kyoto University, 3.NASA Goddard Space Flight Center, 4.University of Maryland, 5.Laboratory for Atmospheric and Space Physics, University of Colorado, 6.Laboratoire de Physique des Plasmas, UMR7648 CNRS/Ecole Polytechnique/UPMC/Université Paris-Sud/Observatoire de Paris, 7.Royal Institute of Technology, 8.Institute of Space and Astronautical Science, Japan Aerospace Exploration Agency, 9.Department of Earth and Space Science, Graduate School of Science, Osaka University, 10.Denali Scientific, 11.Institute of Geophysics and Planetary Physics, University of California, Los Angeles, 12.Southwest Research Institute)

[PEM11-P15] Spatial characteristics of the internal modulation of pulsating aurora: multi-point high-speed optical observations in Scandinavia

*Yuki Kawamura[1], Keisuke Hosokawa[1], Shin-ichiro Oyama[2,3], Yoshizumi Miyoshi[2], Yasunobu Ogawa[3], Satoshi Kurita[2], Satoshi Ebukuro[1], Ryoichi Fujii[4] (1.Department of Communication Engineering and Informatics, University of Electro-Communications, 2.Institute for Space-Earth Environmental Research, Nagoya University, 3.National Institute of Polar Research, 4.Research Organization of Information and Systems)

[PEM11-P16] **Large-scale characteristics of pulsating aurora periodicities:multi-point high-speed optical observations in Scandinavia**

*Satoshi Ebukuro[1], Keisuke Hosokawa[1], Shin-ichiro Oyama[2,3,5], Yoshizumi Miyoshi[2], Yasunobu Ogawa[3], Satoshi Kurita[2], Yuki Kawamura[1], Ryoichi Fujii[4] (1.Department of Communication Engineering and Informatics, University of Electro-Communications, 2.Institute for Space-Earth Environmental Research, Nagoya University, 3.National Institute of Polar Research, 4.Research Organization of Information and Systems, 5.University of Oulu)

[PEM11-P17] Variations of cosmic noise absorption (CNA) by energetic electron precipitation (EEP) and changes of the auroral morphology

*Miyamoto Taishiro[1], Shin-ichiro Oyama[1,4,5], Yasunobu Ogawa[2], Keisuke Hosokawa[3], Satoshi Kurita[1], Yoshizumi Miyoshi[1], Ryuho Kataoka[2], Hiroshi Miyaoka[2], Tero Raita[4] (1. Institute for Space-Earth Environmental Research,Nagoya University, 2.National Institute of Polar Research, 3.Department of Communication Engineering and Informatics, University of Electro-Communications, 4.Sodankylä Geophysical Observatory, University of Oulu, 5.Ionosphere Research Unit, University of Oulu)

[PEM11-P18] Spatiotemporal characteristics on the source region of flash aurora using ray tracing analysis

*Tomohiro Inoue[1], Mitsunori Ozaki[1], Yoshitaka Goto[1], Satoshi Yagitani[1], Yoshiya Kasahara[1], Kazuo Shiokawa[2], Yoshizumi Miyoshi[2], Ryuho Kataoka[3], Yusuke Ebihara[4] (1.Kanazawa University , 2.Nagoya University, 3.National Institute of Polar Research, 4.Kyoto University)

[PEM11-P19] Molecular ion supply mechanisms from the low-altitude ionosphere to magnetosphere observed by EISCAT and Arase(ERG)

*Masayoshi Takada[1], Kanako Seki[1], Yasunobu Ogawa[2], Kunihiro Keika[3], Satoshi Kasahara[4], Shoichiro Yokota[5], Tomoaki Hori[7], Kazushi Asamura[6], Yoshizumi Miyoshi[7] (1.Graduate School of Science, Tokyo University, 2.National Institute of Polar Research, 3.Department of Earth and Planetary Science, Graduate School of Science, Tokyo University, 4.The University of Tokyo, 5.Graduate School of Science, Osaka University, 6.Institute of Space and Astronautical Science, Japan Aerospace Exploration Agency, 7.Institute for Space-Earth Environmental Research, Nagoya University)

[PEM11-P20] Optical and radar observation of the dynamic auroral forms

*Yunosuke Nagafusa[1], Tima Sergienko[2], Satoshi Taguchi[1], Urban Braendstroem[2], Masatoshi Yamauchi[2] (1.Graduate School of Science, Kyoto University, 2.Swedish Institute of Space Physics, Kiruna)

[PEM11-P21] Observations of MF/HF auroral radio emissions at three ground-based stations

*Yuka Sato[1], Atsushi Kumamoto[2], Yuto Katoh[2], Akira Kadokura[3,4], Yasunobu Ogawa[3,4], Atsuki Shinbori[5] (1.Nippon Institute of Technology (NIT), 2.Graduate School of Science, Tohoku University, 3.National Institute of Polar Research (NIPR), 4.The Graduate University for Advanced Studies, 5.Institute for Space-Earth Environmental Research (ISEE), Nagoya University)

[PEM11-P22] **Ionospheric F-region Drift Measurements Derived from DPS-4D at Zhongshan Station, Antarctic**

*Xiangcai Chen[1] (1.Polar Research Institute of China)

[PEM11-P23] PARM-HEP Observation of Precipitating High Energy Electrons over Pulsating Aurora

*Taku Namekawa[1], Takefumi Mitani[2], Kazushi Asamura[2], Yoshifumi Saito[2] (1.Department of Earth and Planetary Science, Graduate school of Science, The University of Tokyo, 2.Institute of Space and Astronautical Science, Japan Aerospace Exploration Agency)

[PEM11-P24] Development of the medium-energy electron detector with hemispherical field-of-view and the flight test in the PARM (Pulsating AuRora and Microburst) mission

*Shin Sugo[1], Oya Kawashima[1], Kazushi Asamura[2], Reiko Nomura[3], Yasunobu Ogawa[4], Keisuke Hosokawa[5], Yoshizumi Miyoshi[6], Takefumi Mitani[2], Taku Namekawa[1,2], Takeshi Sakanoi[7], Mizuki Fukizawa[7], Naoshi Yagi[7], Satoshi Kasahara[1] (1.The University of Tokyo, 2.Institute of Space and Astronautical Science, Japan Aerospace Exploration Agency, 3.National Astronomical Observatory of Japan, 4.National Institute of Polar Research, 5.The University of Electro-Communications, 6.Institute for Space-Earth Environmental Research, Nagoya University, 7.Tohoku University)

[PEM11-P25] Auroral substorm onset in satellite-based global images and ground-based all-sky images

*Akimasa Ieda[1], Kirsti Kauristie[2], Yukitoshi Nishimura[3], Yukinaga Miyashita[4], Harald U Frey[5], Liisa Juusola[2], Daniel Whiter[6], Masahito Nose[7], Matthew O Fillingim[5], Farideh Honary[8], Neil C Rogers[8], Yoshizumi Miyoshi[1], Shinobu Machida[1] (1.Institute for Space-Earth Environmental Research, Nagoya University, 2.Finnish Meteorological Institute, 3.Boston university, 4.Korea Astronomy and Space Science Institute, 5.University of California Berkeley, 6.University of Southampton, 7.Graduate School of Science, Kyoto University, 8.Lancaster University)

[PEM11-P26] Automatic Classification of Auroral images using optical flow feature

*Naoto Kashiwagi[1], Akiko Fujimoto[1], Terumasa Tokunaga[1], Yoshizumi Miyoshi[2], Yasunobu Ogawa[3], Keisuke Hosokawa[4] (1.Kyushu Institute of Technology, 2.Nagoya University, 3.National Institute of Polar Research, 4.The University of Electro-Communications)

[PEM11-P27] Fine-scale visualization of aurora in a wide area using color digital camera images from the International Space Station

*Sota Nanjo[1], Yuta Hozumi[1], Keisuke Hosokawa[1] (1.The University of Electro-Communications)

[PEM11-P28] Geospace Imaging via the soft X-ray imager: GEO-X mission

*Yoshizumi Miyoshi[1], Yuichiro Ezoe[2], Satoshi Kasahara[3], Yosuke Matsumoto[4], Kumi Ishikawa[5], Ryuho Kataoka[6], Hiroki Ito[1], Daiki Ishi[2], Masaki Numazawa[2], Atsushi Yamazaki[5], Hiroshi Hasegawa[5], Masaki Fujimoto[5], Kazuhisa Mitsuda[5] (1.Institute for Space-Earth Environmental Research, Nagoya University, 2.Tokyo Metropolitan University, 3.University of Tokyo, 4.Chiba University, 5.ISAS/JAXA, 6.NIPR)

[E] Poster | P (Space and Planetary Sciences)：P-EM Solar-Terrestrial Sciences, Space Electromagnetism & Space Environment

5:15 PM - 6:30 PM JST | 8:15 AM - 9:30 AM UTC | Poster Hall International Exhibition Hall8, Makuhari Messe_5

[P-EM11] Dynamics of Magnetosphere and Ionosphere

convener:Aoi Nakamizo(Applied Electromagnetic Research Institute, National Institute of Information and Communications Technology), Mitsunori Ozaki(Faculty of Electrical and Computer Engineering, Institute of Science and Engineering, Kanazawa University), Akiko Fujimoto(Kyushu Institute of Technology), Tomoaki Hori(Institute for Space-Earth Environmental Research, Nagoya University)

[PEM11-P01] Effects of Inclination/Rotation of Earth's Magnetic Axis on Magnetosphere Simulated by Global MHD Model

*Aoi Nakamizo[1] (1.Applied Electromagnetic Research Institute, National Institute of Information and Communications Technology)

[PEM11-P02] Asymmetric deformation of the magnetosphere under low-density solar wind

*Masaki N Nishino[1,2], Yoshifumi Saito[2], Kazuo Shiokawa[1], Masaki Fujimoto[2] (1.Institute for Space-Earth Environmental Research, Nagoya University, 2.JAXA/ISAS)

[PEM11-P03] New perspectives on coupling processes in solar-terrestrial system obtained by comprehensive data analysis

*Yoshimasa Tanaka[1], Norio Umemura[2], Shuji Abe[3], Satoru UeNo[4], Masahito Nose[2], Yumi Nakagawa[5] (1.National Institute of Polar Research, 2.Institute for Space-Earth Environmental Research, Nagoya University, 3.International Center for Space Weather Science and Education, 4.Kwasan & Hida Observatories, School of Science, Kyoto University, 5.Ibaraki University)

[PEM11-P04] The interaction between the magnetosphere-ionosphere compound system and the magnetic field topology

*Shigeru Fujita[1], Takashi Tanaka[2], Masakazu Watanabe[2] (1.Meteorological College, Japan Meteorological Agency/ Nationa Institute of Polar Research, 2.Kyushu University)

[PEM11-P05] Effects of the dipole tilt and the interplanetary magnetic field Bx component on the dawn-dusk and interhemispheric asymmetries of the interchange convection cycle

*Masakazu Watanabe[1,2], Takashi Tanaka[2], Shigeru Fujita[3,4] (1.Graduate School of Science, Kyushu University, 2.International Center for Space Weather Science and Education, Kyushu University, 3.Meteorological College, 4.National Institute of Polar Research)

[PEM11-P06] Transient polar ionospheric convection response to negative dynamic pressure pulse

*Jianjun Liu[1] (1.Polar Research Institute of China)

[PEM11-P07] An active ionosphere: a new perspective of field line dipolarization

*Osuke Saka[1] (1.Office Geophysik)

[PEM11-P08] Toward the automatic identification of FLR signals in the SuperDARN data by using the gradient method

*Hideaki Kawano[1,2], Akira Sessai Yukimatu[3,4], Nozomu Nishitani[5], Yoshimasa Tanaka[3,4], Satoko Saita[6], Tomoaki Hori[5] (1.Dept. Earth Planet. Sci., Kyushu Univ., 2.ICSWSE, Kyushu University, 3.National Institute of Polar Research, 4.SOKENDAI, 5.ISEE, Nagoya University, 6.Kitakyushu College)

[PEM11-P09] A statistical study of Pi2 pulsations observed in the upper ionosphere using Swarm magnetic field data

*Park Jaehee[1], Khan-Hyuk Kim[1], Junga Hwang[2] (1.School of Space Research, Kyung Hee University, Gyeonggi, South Korea, 2.Korea Astronomy and Space Science Institute, Daejeon,South Korea)

[PEM11-P10] Study on the global distribution characteristics of Pc 1-2 geomagnetic pulsation with the 10Hz data of the MAGDAS system

*Taisei Kabasawa[1], Akimasa Yoshikawa[1], Teiji Uozumi[1], Akiko Fujimoto[1], Shuji Abe[1] (1.Kyushu University)

[PEM11-P11] In-situ Observations of Reconnection Separatrix Regions in the near-Earth Magnetotail

*Mizuho Araki[1], Masahiro Hoshino[1], Kunihiro Keika[1], Yoshifumi Saito[2] (1.Graduate School of Science, The University of Tokyo, 2.Institude of Space and Astronautical Science)

[PEM11-P12] Flow speed dependence of ion temperature, electron temperature, and their ratio in the near-Earth magnetotail reconnection region

*Kaori Watanabe[1], Masahiro Hoshino[1], Kunihiro Keika[1], Yoshifumi Saito[2], Naritoshi Kitamura[1] (1.Univ. of Tokyo, 2.ISAS/JAXA)

[PEM11-P13] **Examining Minimum Cyclotron Resonant Electron Energy of EMIC Waves with MMS**

*Si Liu[1] (1.Changsha University of Science and Technology)

[PEM11-P14] Small scale whistler mode waves near the magnetic field intensity minimum in the magnetosheath

*Naritoshi Kitamura[1], Takanobu Amano[1], Yoshiharu Omura[2], Satoko Nakamura[2], Chika Umegaki[1], Scott A Boardsen[3,4], Narges Ahmadi[5], Robert E Ergun[5], Olivier Le Contel[6], Per-Arne Lindqvist[7], Yoshifumi Saito[8], Shoichiro Yokota[9], Daniel J Gershman[3], Barbara L Giles[3], Thomas E Moore[3], William R Paterson[3], Craig J Pollock[10], Christopher T Russell[11], Robert J Strangeway[11], James L Burch[12] (1.Department of Earth and Planetary Science, Graduate School of Science, The University of Tokyo, 2.Research Institute for Sustainable Humanosphere, Kyoto University, 3.NASA Goddard Space Flight Center, 4.University of Maryland, 5.Laboratory for Atmospheric and Space Physics, University of Colorado, 6.Laboratoire de Physique des Plasmas, UMR7648 CNRS/Ecole Polytechnique/UPMC/Université Paris-Sud/Observatoire de Paris, 7.Royal Institute of Technology, 8.Institute of Space and Astronautical Science, Japan Aerospace Exploration Agency, 9.Department of Earth and Space Science, Graduate School of Science, Osaka University, 10.Denali Scientific, 11.Institute of Geophysics and Planetary Physics, University of California, Los Angeles, 12.Southwest Research Institute)

[PEM11-P15] Spatial characteristics of the internal modulation of pulsating aurora: multi-point high-speed optical observations in Scandinavia

*Yuki Kawamura[1], Keisuke Hosokawa[1], Shin-ichiro Oyama[2,3], Yoshizumi Miyoshi[2], Yasunobu Ogawa[3], Satoshi Kurita[2], Satoshi Ebukuro[1], Ryoichi Fujii[4] (1.Department of Communication Engineering and Informatics, University of Electro-Communications, 2.Institute for Space-Earth Environmental Research, Nagoya University, 3.National Institute of Polar Research, 4.Research Organization of Information and Systems)

[PEM11-P16] **Large-scale characteristics of pulsating aurora periodicities:multi-point high-speed optical observations in Scandinavia**

*Satoshi Ebukuro[1], Keisuke Hosokawa[1], Shin-ichiro Oyama[2,3,5], Yoshizumi Miyoshi[2], Yasunobu Ogawa[3], Satoshi Kurita[2], Yuki Kawamura[1], Ryoichi Fujii[4] (1.Department of Communication Engineering and Informatics, University of Electro-Communications, 2.Institute for Space-Earth Environmental Research, Nagoya University, 3.National Institute of Polar Research, 4.Research Organization of Information and Systems, 5.University of Oulu)

[PEM11-P17] Variations of cosmic noise absorption (CNA) by energetic electron precipitation (EEP) and changes of the auroral morphology

*Miyamoto Taishiro[1], Shin-ichiro Oyama[1,4,5], Yasunobu Ogawa[2], Keisuke Hosokawa[3], Satoshi Kurita[1], Yoshizumi Miyoshi[1], Ryuho Kataoka[2], Hiroshi Miyaoka[2], Tero Raita[4] (1. Institute for Space-Earth Environmental Research,Nagoya University, 2.National Institute of Polar Research, 3.Department of Communication Engineering and Informatics, University of Electro-Communications, 4.Sodankylä Geophysical Observatory, University of Oulu, 5.Ionosphere Research Unit, University of Oulu)

[PEM11-P18] Spatiotemporal characteristics on the source region of flash aurora using ray tracing analysis

*Tomohiro Inoue[1], Mitsunori Ozaki[1], Yoshitaka Goto[1], Satoshi Yagitani[1], Yoshiya Kasahara[1], Kazuo Shiokawa[2], Yoshizumi Miyoshi[2], Ryuho Kataoka[3], Yusuke Ebihara[4] (1.Kanazawa University , 2.Nagoya University, 3.National Institute of Polar Research, 4.Kyoto University)

[PEM11-P19] Molecular ion supply mechanisms from the low-altitude ionosphere to magnetosphere observed by EISCAT and Arase(ERG)

*Masayoshi Takada[1], Kanako Seki[1], Yasunobu Ogawa[2], Kunihiro Keika[3], Satoshi Kasahara[4], Shoichiro Yokota[5], Tomoaki Hori[7], Kazushi Asamura[6], Yoshizumi Miyoshi[7] (1.Graduate School of Science, Tokyo University, 2.National Institute of Polar Research, 3.Department of Earth and Planetary Science, Graduate School of Science, Tokyo University, 4.The University of Tokyo, 5.Graduate School of Science, Osaka University, 6.Institute of Space and Astronautical Science, Japan Aerospace Exploration Agency, 7.Institute for Space-Earth Environmental Research, Nagoya University)

[PEM11-P20] Optical and radar observation of the dynamic auroral forms

*Yunosuke Nagafusa[1], Tima Sergienko[2], Satoshi Taguchi[1], Urban Braendstroem[2], Masatoshi Yamauchi[2] (1.Graduate School of Science, Kyoto University, 2.Swedish Institute of Space Physics, Kiruna)

[PEM11-P21] Observations of MF/HF auroral radio emissions at three ground-based stations

*Yuka Sato[1], Atsushi Kumamoto[2], Yuto Katoh[2], Akira Kadokura[3,4], Yasunobu Ogawa[3,4], Atsuki Shinbori[5] (1.Nippon Institute of Technology (NIT), 2.Graduate School of Science, Tohoku University, 3.National Institute of Polar Research (NIPR), 4.The Graduate University for Advanced Studies, 5.Institute for Space-Earth Environmental Research (ISEE), Nagoya University)

[PEM11-P22] **Ionospheric F-region Drift Measurements Derived from DPS-4D at Zhongshan Station, Antarctic**

*Xiangcai Chen[1] (1.Polar Research Institute of China)

[PEM11-P23] PARM-HEP Observation of Precipitating High Energy Electrons over Pulsating Aurora

*Taku Namekawa[1], Takefumi Mitani[2], Kazushi Asamura[2], Yoshifumi Saito[2] (1.Department of Earth and Planetary Science, Graduate school of Science, The University of Tokyo, 2.Institute of Space and Astronautical Science, Japan Aerospace Exploration Agency)

[PEM11-P24] Development of the medium-energy electron detector with hemispherical field-of-view and the flight test in the PARM (Pulsating AuRora and Microburst) mission

*Shin Sugo[1], Oya Kawashima[1], Kazushi Asamura[2], Reiko Nomura[3], Yasunobu Ogawa[4], Keisuke Hosokawa[5], Yoshizumi Miyoshi[6], Takefumi Mitani[2], Taku Namekawa[1,2], Takeshi Sakanoi[7], Mizuki Fukizawa[7], Naoshi Yagi[7], Satoshi Kasahara[1] (1.The University of Tokyo, 2.Institute of Space and Astronautical Science, Japan Aerospace Exploration Agency, 3.National Astronomical Observatory of Japan, 4.National Institute of Polar Research, 5.The University of Electro-Communications, 6.Institute for Space-Earth Environmental Research, Nagoya University, 7.Tohoku University)

[PEM11-P25] Auroral substorm onset in satellite-based global images and ground-based all-sky images

*Akimasa Ieda[1], Kirsti Kauristie[2], Yukitoshi Nishimura[3], Yukinaga Miyashita[4], Harald U Frey[5], Liisa Juusola[2], Daniel Whiter[6], Masahito Nose[7], Matthew O Fillingim[5], Farideh Honary[8], Neil C Rogers[8], Yoshizumi Miyoshi[1], Shinobu Machida[1] (1.Institute for Space-Earth Environmental Research, Nagoya University, 2.Finnish Meteorological Institute, 3.Boston university, 4.Korea Astronomy and Space Science Institute, 5.University of California Berkeley, 6.University of Southampton, 7.Graduate School of Science, Kyoto University, 8.Lancaster University)

[PEM11-P26] Automatic Classification of Auroral images using optical flow feature

*Naoto Kashiwagi[1], Akiko Fujimoto[1], Terumasa Tokunaga[1], Yoshizumi Miyoshi[2], Yasunobu Ogawa[3], Keisuke Hosokawa[4] (1.Kyushu Institute of Technology, 2.Nagoya University, 3.National Institute of Polar Research, 4.The University of Electro-Communications)

[PEM11-P27] Fine-scale visualization of aurora in a wide area using color digital camera images from the International Space Station

*Sota Nanjo[1], Yuta Hozumi[1], Keisuke Hosokawa[1] (1.The University of Electro-Communications)

[PEM11-P28] Geospace Imaging via the soft X-ray imager: GEO-X mission

*Yoshizumi Miyoshi[1], Yuichiro Ezoe[2], Satoshi Kasahara[3], Yosuke Matsumoto[4], Kumi Ishikawa[5], Ryuho Kataoka[6], Hiroki Ito[1], Daiki Ishi[2], Masaki Numazawa[2], Atsushi Yamazaki[5], Hiroshi Hasegawa[5], Masaki Fujimoto[5], Kazuhisa Mitsuda[5] (1.Institute for Space-Earth Environmental Research, Nagoya University, 2.Tokyo Metropolitan University, 3.University of Tokyo, 4.Chiba University, 5.ISAS/JAXA, 6.NIPR)

[E] Oral | P (Space and Planetary Sciences)：P-EM Solar-Terrestrial Sciences, Space Electromagnetism & Space Environment

3:30 PM - 5:00 PM JST | 6:30 AM - 8:00 AM UTC | A04 TOKYO BAY MAKUHARI HALL

[P-EM11] Dynamics of Magnetosphere and Ionosphere

convener:Aoi Nakamizo(Applied Electromagnetic Research Institute, National Institute of Information and Communications Technology), Mitsunori Ozaki(Faculty of Electrical and Computer Engineering, Institute of Science and Engineering, Kanazawa University), Akiko Fujimoto(Kyushu Institute of Technology), Tomoaki Hori(Institute for Space-Earth Environmental Research, Nagoya University), Chairperson:Hiroshi Hasegawa(Institute of Space and Astronautical Science, JAXA)

3:30 PM - 3:45 PM JST | 6:30 AM - 6:45 AM UTC

[PEM11-01] **A Case Study Based on Ground Observations of the Conjugate Ionospheric Response to Interplanetary Shock in Polar Regions**

*He Fang[1], Zejun HU[1], Hongqiao HU[1] (1.Polar Research Institute of China)

3:45 PM - 4:00 PM JST | 6:45 AM - 7:00 AM UTC

[PEM11-02] **Effects of Solar Illumination on the Auroral Electrojet Intensity**

*Shinichi Ohtani[1], Jesper W Gjerloev[1] (1.The Johns Hopkins University Applied Physics Laboratory)

4:00 PM - 4:15 PM JST | 7:00 AM - 7:15 AM UTC

[PEM11-03] Quasi-persistent multiple mesoscale field-aligned currents in the duskside auroral oval

*Yoshihiro Yokoyama[1], Satoshi Taguchi[1], Toshihiko Iyemori[2], Keisuke Hosokawa[3] (1.Department of Geophysics, Graduate School of Science, Kyoto University, 2.Kyoto University, 3.Department of Communication Engineering and Informatics, University of Electro-Communications)

4:15 PM - 4:30 PM JST | 7:15 AM - 7:30 AM UTC

[PEM11-04] Generation of dispersive Alfvenic turbulence in magnetosphere-ionosphere feedback coupling

*Tomo-Hiko Watanabe[1], Masatoshi Kaneyama[1], Shinya Maeyama[1] (1.Graduate School of Science, Nagoya University)

4:30 PM - 4:45 PM JST | 7:30 AM - 7:45 AM UTC

[PEM11-05] Aspects of simulating magnetosphere-ionosphere coupling via field-aligned current

*Astrid I Maute[1], Arthur D Richmond[1], Gang Lu[1] (1.High Altitude Observatory, National Center for Atmospheric Research, Boulder CO, 80301, USA)

4:45 PM - 5:00 PM JST | 7:45 AM - 8:00 AM UTC

[PEM11-06] **Revisiting the energy conversion process of Birkeland current generation**

*Akimasa Yoshikawa[1] (1.Department of Earth and Planetary Sciences, Kyushu University)

[E] Oral | P (Space and Planetary Sciences)：P-EM Solar-Terrestrial Sciences, Space Electromagnetism & Space Environment

9:00 AM - 10:30 AM JST | 12:00 AM - 1:30 AM UTC | A04 TOKYO BAY MAKUHARI HALL

[P-EM13] Inner magnetosphere: Recent understanding and new insights

convener:Yusuke Ebihara(Research Institute for Sustainable Humanosphere, Kyoto University), Danny Summers(Memorial University of Newfoundland), Yoshizumi Miyoshi(Institute for Space-Earth Environmental Research, Nagoya University), Shinji Saito(Graduate School of Science, Nagoya University), Chairperson:Shinji Saito(ISEE, Nagoya University), Yusuke Ebihara(RISH, Kyoto University)

9:00 AM - 9:15 AM JST | 12:00 AM - 12:15 AM UTC

[PEM13-11] Nonlinear Damping of Oblique Whistler Mode Waves Via Landau Resonance

*Yikai HSIEH[1], Yoshiharu Omura[1] (1.Reserach Institute for Sustainable Humanosphere, Kyoto University)

9:15 AM - 9:30 AM JST | 12:15 AM - 12:30 AM UTC

[PEM13-12] Instantaneous Frequency Analysis on Nonlinear EMIC Emissions: Arase Observation

*Masafumi Shoji[1], Yoshizumi Miyoshi[1], Yoshiharu Omura[2], Lynn M Kistler[1,3], Yasumasa Kasaba[4], Shoya Matsuda[5], Yoshiya Kasahara[6], Ayako Matsuoka[5], Reiko Nomura[7], Keigo Ishisaka[8], Atsushi Kumamoto[4], Fuminori Tsuchiya[4], Satoshi Yagitani[6], Mariko Teramoto[1], Kazushi Asamura[5], Takeshi Takashima[5], Iku Shinohara[5] (1.Institute for Space-Earth Environmental Research, Nagoya University, 2.Research Institute for Sustainable Humanosphere, Kyoto University, 3.Institute for the Study of Earth Oceans and Space, University of New Hampshire, 4.Tohoku University, 5.Institute of Space and Astronautical Science, 6.Kanazawa University, 7.National Astronomical Observatory of Japan, 8.Toyama Prefecture University)

9:30 AM - 9:45 AM JST | 12:30 AM - 12:45 AM UTC

[PEM13-13] Rapid Precipitation by EMIC Rising-tone Emissions of Relativistic Electrons Observed by the Van Allen Probes Mission

*Satoko Nakamura[1], Yoshiharu Omura[1], Craig Kletzing[2], Daniel Baker[3] (1.Research Institute for Sustainable Humanosphere, Kyoto University., 2.Department of Physics and Astronomy University of Iowa , 3.The Laboratory for Atmospheric and Space Physics (LASP) at the University of Colorado)

9:45 AM - 10:00 AM JST | 12:45 AM - 1:00 AM UTC

[PEM13-14] Plasmaspheric EMIC waves excited through mode conversion from equatorial noise under existence of M/Q=2 ions

*Yoshizumi Miyoshi[1], Shoya Matsuda[2], Satoshi Kurita[1], koji nomura[1], Kunihiro Keika[3], Masafumi Shoji[1], Naritoshi Kitamura[3], Yoshiya Kasahara[4], Ayako Matsuoka[2], Iku Shinohara[2], Kazuo Shiokawa[1], Shinobu Machida[1], Ondrej Santolik[5], Scott Boardsen[6], Richard Horne[7], Wygant John[8] (1.Institute for Space-Earth Environmental Research, Nagoya University, 2.JAXA, 3.University of Tokyo, 4.Kanazawa University, 5.CAS, 6.NASA, 7.British Antarctic Survey, 8.University of Minnesota)

10:00 AM - 10:15 AM JST | 1:00 AM - 1:15 AM UTC

[PEM13-15] Generation Mechanism of Non-thermal Continuum Radiation

*Yoshiharu Omura[1], Miroslav Horky[1,2] (1.Reserach Institute for Sustainable Humanosphere, Kyoto University, 2.Department of Space Physics, Institute of Atmospheric Physics, Czech Academy of Sciences)

10:15 AM - 10:30 AM JST | 1:15 AM - 1:30 AM UTC

[PEM13-16] Influence of kappa distributions on the sweep rate of whistler mode chorus waves

*Danny Summers[1] (1.Memorial University of Newfoundland)

[E] Oral | P (Space and Planetary Sciences)：P-EM Solar-Terrestrial Sciences, Space Electromagnetism & Space Environment

10:45 AM - 12:15 PM JST | 1:45 AM - 3:15 AM UTC | A04 TOKYO BAY MAKUHARI HALL

[P-EM13] Inner magnetosphere: Recent understanding and new insights

convener:Yusuke Ebihara(Research Institute for Sustainable Humanosphere, Kyoto University), Danny Summers(Memorial University of Newfoundland), Yoshizumi Miyoshi(Institute for Space-Earth Environmental Research, Nagoya University), Shinji Saito(Graduate School of Science, Nagoya University), Chairperson:Yusuke Ebihara(RISH, Kyoto University), Shinji Saito(ISEE, Nagoya University)

10:45 AM - 11:05 AM JST | 1:45 AM - 2:05 AM UTC

[PEM13-17] The Impacts of Substorms on the Ring Current

★Invited Papers

*Jasmine Kaur Sandhu[1], I. J. Rae[1], M. Gkioulidou[2], C. Forsyth[1], G. D. Reeves[3], M. P. Freeman[4], K. R. Murphy[5], M.-T. Walach[6], H. E. Spence[7] (1.Mullard Space Science Laboratory, University College London, UK., 2.Applied Physics Laboratory, John Hopkins University, USA., 3.Los Alamos National Laboratory, USA., 4.British Antarctic Survey, UK., 5.University of Maryland, USA., 6.Lancaster University, UK., 7.University of New Hampshire, USA.)

11:05 AM - 11:25 AM JST | 2:05 AM - 2:25 AM UTC

[PEM13-18] Dipolarization in the Inner Magnetosphere: Comparison between Geosynchronous Orbit and Further Inside

★Invited Papers

*Shinichi Ohtani[1], Tetsuo Motoba[1], Matina Gkioulidou[1], Kazue Takahashi[1] (1.The Johns Hopkins University Applied Physics Laboratory)

11:25 AM - 11:40 AM JST | 2:25 AM - 2:40 AM UTC

[PEM13-19] Substorm-associated particle injection near/at geosynchronous orbit: Observations from ERG and GOES

*Tzu-Fang Chang[1,2], Chio-Zong Cheng[2], Sunny Wing-Yee Tam[2], Chih-Yu Chiang[2], Yoshizumi Miyoshi[1], Tomoaki Hori[1], Takefumi Mitani[3], Takeshi Takashima[3], Ayako Matsuoka[3], Mariko Teramoto[1], Iku Shinohara[3] (1.Institute for Space-Earth Environmental Research, Nagoya University, Japan, 2.Institute of Space and Plasma Sciences, National Cheng Kung University, Tainan, Taiwan, 3.Institute of Space and Astronautical Science, Japan Aerospace Exploration Agency, Japan)

11:40 AM - 11:55 AM JST | 2:40 AM - 2:55 AM UTC

[PEM13-20] Substorm -like energetic electron injection observed at the plasma sheet boundary in the inner magnetosphere

*Iku Shinohara[1], Nagai Tsugunobu[1], Takefumi Mitani[1], Nana Higashio[2], Satoshi Kasahara[3], Yoichi Kazama[4], Shiang-Yu Wang[4], Sunny Tam[5], Ayako Matsuoka[1], Kazushi Asamura[1], Shoichiro Yokota[6], Takeshi Takashima[1], Yoshizumi Miyoshi[7] (1.Japan Aerospace Exploration Agency/Institute of Space and Astronautical Science, 2.Japan Aerospace Exploration Agency, 3.The University of Tokyo, 4.Academia Sinica/Institute of Astronomy and Astrophysics, 5.National Cheng Kung University, 6.Osaka University, 7.Nagoya University/Institute for Space-Earth Einvironment Research)

11:55 AM - 12:10 PM JST | 2:55 AM - 3:10 AM UTC

[PEM13-21] Magnetic field disturbances associated with the magnetic dipolarization observed by Arase (ERG) in the inner magnetosphere

*Ayako Matsuoka[1], Masahito Nose[2], Yoshizumi Miyoshi[2], Iku Shinohara[1], Mariko Teramoto[2], Reiko Nomura[3], Akiko Fujimoto[4], Yoshimasa Tanaka[5], Manabu Shinohara[6], Yoshiya Kasahara[7], Yasumasa Kasaba[8], Keigo Ishisaka[9], Shoya Matsuda[1], Masafumi Shoji[2], Tomoko Nakagawa[10], Yoichi Kazama[11], Shiang-Yu Wang[11], Satoshi Kasahara[12], Shoichiro Yokota[13], Takefumi Mitani[1] (1.Institute of Space and Astronautical Science, Japan Aerospace Exploration Agency, 2.Institute for Space-Earth Environmental Research, Nagoya University, 3.RISE, National Astronomical Observatory of Japan, 4.School of Computer Science and Systems Engineering, Kyushu Institute of Technology, 5.National Institute of Polar Research, 6.National Institute of Technology, Kagoshima College, 7.Information Media Center, Kanazawa University, 8.Planetary Plasma and Atmospheric Research Center, Tohoku University, 9.Faculty of Engineering, Toyama Prefectural University, 10.Faculty of Engineering, Tohoku Institute of Technology, 11.Academia Sinica Institute of Astronomy and Astrophysics, 12.School of Science, The University of Tokyo, 13.School of Science, Osaka University)

[E] Oral | P (Space and Planetary Sciences)：P-EM Solar-Terrestrial Sciences, Space Electromagnetism & Space Environment

1:45 PM - 3:15 PM JST | 4:45 AM - 6:15 AM UTC | A04 TOKYO BAY MAKUHARI HALL

[P-EM13] Inner magnetosphere: Recent understanding and new insights

convener:Yusuke Ebihara(Research Institute for Sustainable Humanosphere, Kyoto University), Danny Summers(Memorial University of Newfoundland), Yoshizumi Miyoshi(Institute for Space-Earth Environmental Research, Nagoya University), Shinji Saito(Graduate School of Science, Nagoya University), Chairperson:Yoshizumi Miyoshi(ISEE, Nagoya University), Yusuke Ebihara(RISH, Kyoto University)

1:45 PM - 2:05 PM JST | 4:45 AM - 5:05 AM UTC

[PEM13-22] Statistical Property of Long Lasting Poloidal Pc 4-5 Waves and Relation with Particle Dynamics in the Inner Magnetosphere: Van Allen Probes Observations

★Invited Papers

*Kazuhiro Yamamoto[1], Masahito Nose[2], Kunihiro Keika[3], Charles W. Smith[4], Robert J. MacDowall[5], Donald G. Mitchell[6], Hyomin Kim[7], John Wygant[8] (1.Graduate School of Science, Kyoto University, 2.Institute for Space-Earth Environmental Research, Nagoya University, 3.Graduate School of Science, the University of Tokyo, 4.Institute for the Study of Earth, Oceans, and Space, University of New Hampshire, 5.Solar System Exploration Division, Goddard Space Flight Center, 6.The Johns Hopkins University Applied Physics Laboratory, 7.Center for Solar Terrestrial Research, New Jersey Institute of Technology, 8.School of Physics and Astronomy, University of Minnesota)

2:05 PM - 2:25 PM JST | 5:05 AM - 5:25 AM UTC

[PEM13-23] Subauroral Polarization Streams: Indication of Magnetosphere–Ionosphere Coupling

★Invited Papers

*Fei He[1,2,3], Xiao-Xin Zhang[4], Wenbin Wang[5], Zhonghua Yao[1,2,3], Yong Wei[1,2,3], Zhi-Peng Ren[1,2,3], Xinan Yue[1,2,3], Weixing Wan[1,2,3] (1.Institute of Geology & Geophysics, CAS, 2.Institutions of Earth Science, CAS, 3.College of Earth and Planetary Sciences, UCAS, 4.National Center for Space Weather, CMA, 5.High Altitude Observatory, NCAR)

2:25 PM - 2:40 PM JST | 5:25 AM - 5:40 AM UTC

[PEM13-24] Simultaneous Arase-ground observations of a purple and green auroral arc

*Kazuo Shiokawa[1], Masahito Nose[1], Satoshi Tsuchiya[1], Yuki Takagi[1], Shun Imajo[1], Yoshimasa Tanaka[2], Yoshizumi Miyoshi[1], Keisuke Hosokawa[3], Yoichi Kazama[4], Shiang-Yu Wang[4], Sunny W.Y. Tam[4], Kazushi Asamura[5], Satoshi Kasahara[6], Shoichiro Yokota[7], Tomoaki Hori[1], Kunihiro Keika[6], Ayako Matsuoka[5] (1.Institute for Space-Earth Environmental Research, Nagoya University, 2.National Institute of Polar Research, 3.The University of Electro-Communications, 4.National Cheng Kung University, 5.Institute of Space and Astronautical Science, Japan Aerospace Exploration Agency, 6.University of Tokyo, 7.Osaka University)

2:40 PM - 2:55 PM JST | 5:40 AM - 5:55 AM UTC

[PEM13-25] Multiple Satellite Observations of Oxygen Torus in the Inner Magnetosphere

*Masahito Nose[1], Ayako Matsuoka[2], Atsushi Kumamoto[3], Yoshiya Kasahara[4], J Goldstein[5,6], Mariko Teramoto[1], Fuminori Tsuchiya[3], Shoya Matsuda[2], Masafumi Shoji[1], Shun Imajo[1], Oimatsu Satoshi[7], Kazuhiro Yamamoto[7], Yuki Obana[8], Reiko Nomura[9], Akiko Fujimoto[10], Iku Shinohara[2], Yoshizumi Miyoshi[1], W S Kurth[11], C A Kletzing[11], C W Smith[12], R J MacDowall[13] (1.Institute for Space-Earth Environmental Research, Nagoya University, 2.Institute of Space and Astronautical Science, Japan Aerospace Exploration Agency, 3.Graduate School of Science, Tohoku University, 4.Information Media Center, Kanazawa University, 5.Space Science and Engineering Division, Southwest Research Institute, 6.University of Texas at San Antonio, 7.Graduate School of Science, Kyoto University, 8.Faculty of Engineering, Osaka Electro-Communication University, 9.National Astronomical Observatory of Japan, 10.Kyushu Institute of Technology, 11.Department of Physics and Astronomy, University of Iowa, 12.Institute for the Study of Earth, Oceans, and Space, University of New Hampshire, 13.Solar System Exploration Division, Goddard Space Flight Center)

2:55 PM - 3:10 PM JST | 5:55 AM - 6:10 AM UTC

[PEM13-26] Study of characteristics of storm-time Pc5 ULF waves excited by the drift-bounce resonance with ring current ions based on the global drift-kinetic simulation

*Tomotsugu Yamakawa[1], Kanako Seki[1], Takanobu Amano[1], Yoshizumi Miyoshi[2], Naoko Takahashi[1] (1.Department of Earth and Planetary Science, School of Science, The University of Tokyo, 2.ISEE, Nagoya University)

[E] Poster | P (Space and Planetary Sciences)：P-EM Solar-Terrestrial Sciences, Space Electromagnetism & Space Environment

3:30 PM - 5:00 PM JST | 6:30 AM - 8:00 AM UTC | Poster Hall International Exhibition Hall8, Makuhari Messe_2

[P-EM13] Inner magnetosphere: Recent understanding and new insights

convener:Yusuke Ebihara(Research Institute for Sustainable Humanosphere, Kyoto University), Danny Summers(Memorial University of Newfoundland), Yoshizumi Miyoshi(Institute for Space-Earth Environmental Research, Nagoya University), Shinji Saito(Graduate School of Science, Nagoya University)

[PEM13-P01] Evaluation of wave normal and Poynting vector analyses for whistler mode waves observed by the waveform capture (WFC) on board the Arase

*Yoshiya Kasahara[1], Satoshi Ikarashi[1], Hiroyuki Nishizawa[1], Shoya Matsuda[2], Fuminori Tsuchiya[3], Atsushi Kumamoto[3], Yasumasa Kasaba[3], Mitsunori Ozaki[1], Ayako Matsuoka[2] (1.Kanazawa University, 2.ISAS/JAXA, 3.Tohoku University)

[PEM13-P02] Calibration of electric fields dedicated to the measurement of the S-WPIA of the Arase Satellite

*Miki Jumpei[1], Hirotsugu Kojima[2], Yuto Katoh[3], Shoya Matsuda[4], Yoshiya Kasahara[5], Mitsuru Hikishima[4], Satoshi Kurita[6], Masahiro Kitahara[3], Satoshi Kasahara[7], Yoshizumi Miyoshi[6], Atsushi Kumamoto[3], Ayako Matsuoka[4], Shoichiro Yokota[8], Tomoaki Hori[6], Kunihiro Keika[7] (1.Space Radio Engineering Laboratory, Division of Electrical Engineering, Kyoto University Graduated School, 2.Research Institute for Sustainable Humanosphere, Kyoto University, 3.Graduate School of Science and Faculty of Science, Tohoku University, 4.Institute of Space and Astronautical Science, JAXA, 5.Information Media Center, Kanazawa University, 6.Institute for Space-Earth Environmental Research, Nagoya University, 7.School of Science, The University of Tokyo, 8.School of Science, Osaka University)

[PEM13-P03] Enhancement of whistler-mode chorus in association with Pc 4-5 ULF waves and related variation of high energy electrons

*Atsuhiro Ono[1], Yuto Katoh[1], Atsushi Kumamoto[1], Fuminori Tsuchiya[1], Mariko Teramoto[2], Yoshiya Kasahara[3], Shoya Matsuda[4], Ayako Matsuoka[4], Takefumi Mitani[4], Tomoaki Hori[2], Satoshi Kasahara[5], Shoichiro Yokota[6], Kunihiro Keika[5], Yoshizumi Miyoshi[2], Iku Shinohara[4] (1.Tohoku University, 2.Nagoya University, 3.Kanazawa University, 4.ISAS/JAXA, 5.The University of Tokyo, 6.Osaka University)

[PEM13-P04] Sudden enhancements of electron cyclotron harmonic waves observed by the Arase satellite

*Shinjo Airi[1], Hirotsugu Kojima[1], Yoshiya Kasahara[2], Yoichi Kazama[3], Hideyuki Usui[4], Yoshizumi Miyoshi[5], Yasumasa Kasaba[6], Shoya Matsuda[7], Tomoaki Hori[5], S. -Y. Wang[8], Sunny W.Y. Tam[9], Atsushi Kumamoto[10], Ayako Matsuoka[11] (1.Research institute for sustainable humanosphere, Kyoto University, 2.Information Media Center, Kanazawa University, 3.ASIAA, 4.Graduate school of system informatics Kobe University, 5.Institute for Space-Earth Environmental Research, Nagoya University, 6.Planetary Plasma and Atmospheric Research Center, Tohoku University, 7.Institute of Space and Astronautical Science/Japan Aerospace Exploration Agency, 8.ASIAA, Taiwan, 9.ISAPS, NCKU, Taiwan, 10.Department of Geophysics, Graduate School of Science, Tohoku University, 11.Research Division for Space Plasma, Institute of Space and Astronautical Science, Japan Aerospace Exploration Agency)

[PEM13-P05] Correlation between pulsating aurora and electrostatic electron cyclotron harmonic waves obtained from coordinated Arase and ground data

*Mizuki Fukizawa[1], Takeshi Sakanoi[1], Yoshizumi Miyoshi[2], Keisuke Hosokawa[3], Yoichi Kazama[4], Yoshiya Kasahara[5], Shoya Matsuda[6], Ayako Matsuoka[7], Wang Shiang-Yu[4], Sunny Wing-Yee Tam[8], Ryuho Kataoka[9] (1.Planetary Plasma and Atmospheric Research Center, Graduate School of Science, Tohoku University, 2.Institute for Space-Earth Environmental Research, Nagoya University, 3.Department of Communication Engineering and Informatics, University of Electro-Communications, 4.Academia Sinica Institute of Astronomy and Astrophysics, 5.Information Media Center, Kanazawa University, 6.Institute of Space and Astronautical Science/Japan Aerospace Exploration Agency, 7.Research Division for Space Plasma, Institute of Space and Astronautical Science, Japan Aerospace Exploration Agency, 8.Institute of Space and Plasma Sciences, College of Sciences, National Cheng Kung University , 9.National Institute of Polar Research)

[PEM13-P06] Automatic determination of Upper Hybrid Resonance Frequencies by Convolutional Neural Network.

*Shoya Matsuda[1], Tatsuhito Hasegawa[2], Atsushi Kumamoto[3], Fuminori Tsuchiya[3], Yoshiya Kasahara[4], Yoshizumi Miyoshi[5], Yasumasa Kasaba[3], Ayako Matsuoka[1] (1.Institute of Space and Astronautical Science/Japan Aerospace Exploration Agency, 2.University of Fukui, 3.Tohoku University, 4.Kanazawa University, 5.ISEE, Nagoya University)

[PEM13-P07] Amplitude dependence of whistler wave motion on electron scattering process

*Yoshiki Ito[1], Yoshizumi Miyoshi[1], Shinji Saito[1] (1.Nagoya University, ISEE)

[PEM13-P08] Two-dimensional simulation of whistler mode wave packets interacting with energetic electrons

*Takeshi Nogi[1], Yoshiharu Omura[1] (1.Reserch Institute for Sustainable Humanosphere, Kyoto University)

[PEM13-P09] Relativistic electron acceleration by whistler-mode chorus waves in 1D, 2D, and 3D magnetic field models.

*Keita Takahashi[1], Yoshiharu Omura[1], Yikai HSIEH[1], Danny Summers[2] (1.Research Institute for Sustainable Humanosphere, Kyoto University , 2.Department of Mathematics and Statistics, Memorial University of Newfoundland)

[PEM13-P10] Study of global spatio-temporal development of magnetospheric ELF/VLF waves for the 26-30 March 2017 storm based on ground and satellite observations and the RAM simulations

*Yuhei Takeshita[1], Kazuo Shiokawa[1], Yoshizumi Miyoshi[1], Mitsunori Ozaki[2], Yoshiya Kasahara[2], Martine Connors[3], Jyrki Manninen[4], Craig Kletzing[5], Vania Jordanova[6] (1.Nagoya University, Institute for Space-Earth Environmental Resarch, 2.Kanazawa University, 3.Athabasca University, 4.Sodankylä Geophysical Observatory, 5.The University of Iowa, 6.Los Alamos National Laboratory)

[PEM13-P11] Flux decrease of outer radiation belt electrons associated with solar wind pressure pulse: A Code coupling simulation of GEMSIS-RB and GEMSIS-GM

*Ito Hiroki[1], Yoshizumi Miyoshi[1], Shinji Saito[2], Yosuke Matsumoto[3], Takanobu Amano[4] (1.Institute for Space-Earth Environmental Research, Nagoya University, 2. Graduate School of Science, Nagoya University, 3. Graduate School of Science, Chiba University, 4.Department of Earth and Planetary Science, University of Tokyo)

[PEM13-P12] Non-diffusive response of outer belt electrons on interplanetary shock

Takuma Toishi[1], *Yusuke Ebihara[1], Takashi Tanaka[2] (1.Research Institute for Sustainable Humanosphere, Kyoto University, 2.Kyushu University)

[PEM13-P13] PARM: Initial result of the auroral camera on the G-CHASER (RockSat-XN) rocket and status of the development of auroral cameras for the LAMP rocket experiment

*Naoshi Yagi[1], Takeshi Sakanoi[1], Fukizawa Mizuki[1], Kazushi Asamura[2], Yoshizumi Miyoshi[3], Keisuke Hosokawa[4], Genki Ishizawa[5] (1.Planetary Plasma and Atmospheric Research Center, Graduate School of Science, Tohoku University, 2.Institute of Space and Astronautical Science, Japan Aerospace Exploration Agency, 3.Institute for Space-Earth Environmental Research, Nagoya University, 4.Department of Communication Engineering and Informatics, University of Electro-Communications, 5.Space & terrestrial plasma pyhsics)

[PEM13-P14] First simultaneous observation of a SAR arc at subauroral latitudes using a ground all-sky camera and the Arase satellite in the inner magnetosphere

*Yudai Inaba[1], Kazuo Shiokawa[1], Shin-ichiro Oyama[1,8,9], Yuichi Otsuka[1], Atsuki Shinbori[1], Yoichi Kazama[2], Shiang-Yu Wang[2], Sunny W. Y. Tam[2], Shoichiro Yokota[3], Satoshi Kasahara[4], Kunihiro Keika[4], Tomoaki Hori[1], Ayako Matsuoka[5], Yoshiya Kasahara[6], Atsushi Kumamoto[7], Yasumasa Kasaba[7], Yoshizumi Miyoshi[1], Iku Shinohara[5], Arto Oksanen[10] (1.Institute for Space-Earth Environmental Research, 2.Academia Sinica, 3.Osaka Univ, 4.Tokyo Univ, 5.JAXA, 6.Kanazawa University, 7.Tohoku University, 8.University of Oulu, Finland, 9.National Institute of Polar Research, 10.Jyväskylän Sirius ry, Finland)

[PEM13-P15] Pi2 pulsations observed by the Arase satellite inside and outside the plasmapause

*Mariko Teramoto[1], Ayako Matsuoka[2], Reiko Nomura[5], Yoshiya Kasahara[3], Yasumasa Kasaba[4], Atsushi Kumamoto[4], Fuminori Tsuchiya[4], Shoya Matsuda[2], Masahito Nose[1], Masafumi Shoji[1], Yasunori Tsugawa[1], Shun Imajo[1], Yoshizumi Miyoshi[1], Iku Shinohara[2] (1.Institute for Space-Earth Environmental Research Nagoya University, 2.Institute of Space and Astronautical Science, Japan Aerospace eXploration Agency, 3.Kanazawa University, 4.Tohoku University, 5.National Astronomical Observatory of Japan)

[PEM13-P16] An extreme erosion of the plasmasphere during the 7–10 September 2017 storm

*Yuki Obana[1], Naomi Maruyama[2,3], Atsuki Shinbori[4], Kumiko K. Hashimoto[5], Mariangel Fedrizzi[2,3], Masahito Nose[4], Yuichi Otsuka[4], Nozomu Nishitani[4], Tomoaki Hori[4], Atsushi Kumamoto[6], Fuminori Tsuchiya[6], Shoya Matsuda[7], Ayako Matsuoka[7], Yoshiya Kasahara[8], Akimasa Yoshikawa[9], Yoshizumi Miyoshi[4], Iku Shinohara[7] (1.Osaka Electro-Communication University, 2.University of Colorado Boulder, 3.NOAA Space Weather Prediction Center, 4.Nagoya

University, 5.Kibi International University, 6.Tohoku University, 7.Japan Aerospace Exploration Agency, 8.Kanazawa University, 9.Kyushu University)

[PEM13-P17] Relative contribution of ULF and chorus waves to the radiation belt variation: Comparison between multi-point observations and BATSRUS + CRCM simulation

*Naoko Takahashi[1], Kanako Seki[1], Mei-Ching Fok[2], Yihua Zheng[2], Yoshizumi Miyoshi[3], David Hartley[4], Ayako Matsuoka[5], Yoshiya Kasahara[6], Yasumasa Kasaba[7], Nana Higashio[8] (1.Graduate School of Science, University of Tokyo, 2.NASA Goddard Space Flight Center, 3.Institute for Space-Earth Environmental Research, Nagoya University, 4.Department of Physics and Astronomy, University of Iowa, 5.Institute of Space and Astronautical Science, Japan Aerospace Exploration Agency, 6.Information Media Center, Kanazawa University, 7.Planetary Plasma and Atmospheric Research Center, Tohoku University, 8.Japan Aerospace Exploration Agency)

[PEM13-P18] Modulation of the D-region ionosphere by Pc5 waves observed by VLF/LF standard radio waves

*Miyashita Takuya[1], Hiroyo Ohya[1], Fuminori Tsuchiya[2], Hiroyuki Nakata[1], Toshiaki Takano[1], Kazuo Shiokawa[3], Yoshizumi Miyoshi[3] (1.Chiba University, 2.Tohoku University, 3.Nagoya University)

[PEM13-P19] Oxygen-proton differences in ion energies dominating plasma pressure: Dependence on storm phases and solar wind drivers

*Kunihiro Keika[1], Satoshi Kasahara[1], Shoichiro Yokota[2], Masahiro Hoshino[1], Kanako Seki[1], Masahito Nose[3], Yoshizumi Miyoshi[3], Iku Shinohara[4] (1.Graduate School of Science, The University of Tokyo , 2.Graduate School of Science, Osaka University, 3.Institute for Space-Earth Environmental Research, Nagoya University, 4.Institute of Space and Astronautical Science, Japan Aerospace Exploration Agency)

[PEM13-P20] Mass dependence of penetration depth of multi-energy ions in the inner magnetosphere during magnetic storms: Arase observations

*Ryosuke Fujii[1], Yoshizumi Miyoshi[1], Masafumi Shoji[1], Kazushi Asamura[2], Lynn Kistler[1,8], Vania Jordanova[9], Tomoaki Hori[1], Satoshi Kurita[1], Mariko Teramoto[1], Yasunori Tsugawa[1], Yoshiya Kasahara[3], Yasumasa Kasaba[4], Atsushi Kumamoto[5], Fuminori Tsuchiya[4], Shoichiro Yokota[6], Kunihiro Keika[7], Ayako Matsuoka[2], Iku Shinohara[2] (1.Institute for Space-Earth Environmental Research, Nagoya University, 2.Institute of Space and Astronautical Science, Japan Aerospace Exploration Agency, 3.Information Media Center, Kanazawa University, 4.Planetary Plasma and Atmospheric Research Center, Tohoku University, 5.Department of Geophysics, Graduate School of Science, Tohoku University, 6.Graduate School of Science, Osaka University, 7.Department of Earth and Planetary Science, Graduate School of Science, The University of Tokyo, 8.University of New Hampshire, 9.Los Alamos National Laboratory)

[PEM13-P21] Relativistic Acceleration of Energetic Protons by Electromagnetic Ion Cyclotron Waves in the Jovian Magnetosphere

*Tomohiro Sekine[1], Yoshiharu Omura[1], Danny Summers[2], Yikai HSIEH[1], Satoko Nakamura[1] (1.Reserach Institute for Sustainable Humanosphere, Kyoto University, 2.Memorial University of Newfoundland)

[PEM13-P22] Statistical study of IPDP type EMIC wave-related electron precipitation at subauroral latitude

*Asuka Hirai[1], Fuminori Tsuchiya[1], Takahiro Obara[1], Yasumasa Kasaba[1], Yuto Katoh[2], Hiroaki Misawa[1], Kazuo Shiokawa[3], Yoshizumi Miyoshi[3], Satoshi Kurita[3], Martin G Connors[4] (1.Planetary Plasma and Atmospheric Research Center, Graduate School of Science, Tohoku Univ. , 2.Department of Geophysics, Graduate School of Science, Tohoku University, 3.Institute for Space-Earth Environmental Research, Nagoya University, 4.Athabasca University)

[PEM13-P23] Meridional distributions of proton plasma and pressure-driven currents in the nightside inner magnetosphere: Arase observations

*Shun Imajo[1], Masahito Nose[1], Satoshi Kasahara[2], Shoichiro Yokota[3], Ayako Matsuoka[4], Kunihiro Keika[2], Tomoaki Hori[1], Mariko Teramoto[1], Kazuhiro Yamamoto[5], Oimatsu Satoshi[5], Reiko Nomura[6], Akiko Fujimoto[7], Iku Shinohara[4], Yoshizumi Miyoshi[1] (1.Institute for Space-Earth Environmental Research, Nagoya University, 2.Graduate School of Science, The University of Tokyo, 3.Graduate School of Science, Osaka University, 4.Institute of Space and Astronautical Science, Japan Aerospace Exploration Agency, 5.Graduate School of Science, Kyoto University, 6.National Astronomical Observatory of Japan, 7.Kyushu Institute of Technology)

[PEM13-P24] Space Weather Effects on Energetic Proton Flux Response in South Atlantic Anomaly

*Kirolosse Mina GIRGIS[1,2], Tohru Hada[1], Shuichi Matsukiyo[1] (1.Earth System Science and Technology (ESST) Department, Interdisciplinary Graduate School of Engineering Sciences (IGSES), Kyushu University, Japan, 2.Aerospace Engineering Department, Faculty of Engineering, Cairo University, Egypt)

[PEM13-P25] Solar-cycle variations of >30 keV electron flux enhancements under the inner radiation belt

*ALLA SUVOROVA[1] (1.National Central University)

[PEM13-P26] Energy spectra variations of high energy electrons in the inner magnetosphere observed by HEP/XEP on ARASE and SEDA-e on HIMAWARI

*Takeshi Takashima[1], Takefumi Mitani[1], Nana Higashio[2], Tsutomu Nagatsuma[3] (1. ISAS/JAXA, 2.Research and Development Directorate/JAXA, 3.NiCT)

[PEM13-P27] Inter-channel calibration of the high-energy electron experiments (HEP) instrument onboard the Arase satellite

*Tomoaki Hori[1], Takefumi Mitani[2], Takeshi Takashima[2], Park Inchun[1], Satoshi Kurita[1], Mariko Teramoto[1], Nana Higashio[3], Satoshi Kasahara[4], Shoichiro Yokota[5], Yoshizumi Miyoshi[1], Iku Shinohara[2] (1.Institute for Space-Earth Environmental Research, Nagoya University, 2.Japan Aerospace Exploration Agency, Institute of Space and Astronautical Science, 3.Japan Aerospace Exploration Agency, 4.Graduate School of Science, The University of Tokyo, 5.Graduate School of Science, Osaka University)

[PEM13-P28] Particle simulation for calibrating the HEP data onboard the ARASE satellite

*PARK INCHUN[1], Yoshizumi Miyoshi[1], Takefumi Mitani[2], Tomoaki Hori[1], Satoshi Kurita[1], Mariko Teramoto[1], Takeshi Takashima[2], Nana Higashio[3], Iku Shinohara[2] (1.Nagoya University Institute for Space-Earth Environmental Research, 2.Japan Aerospace Exploration Agency Institute of Space and Astronautical Science , 3.Japan Aerospace Exploration Agency)

[PEM13-P29] Geant4 model calculation and energetic particle observation with HEP/Arase in the inner radiation belt

*Honoka Toda[1], Wataru Miyake[1], Takefumi Mitani[3], Takeshi Takashima[3], Yoshizumi Miyoshi[2], PARK INCHUN[2], Tomoaki Hori[2] (1.Tokai University, 2.ISEE/Nagoya University, 3.ISAS/JAXA)

[PEM13-P30] Validation of High-energy electron detector simulator for the HEP instruments onboard Arase

*Takefumi Mitani[1], PARK INCHUN[2], Tomoaki Hori[2], Taku Namekawa[1,3], Kazushi Asamura[1], Takeshi Takashima[1], Satoshi Kasahara[3], Satoshi Kurita[2], Mariko Teramoto[2], Nana Higashio[1], Yoshizumi Miyoshi[2], Iku Shinohara[1] (1.Japan Aerospace Exploration Agency, Institute of Space and Astronautical Science, 2.Institute for Space-Earth Environmental Research, Nagoya Univ., 3.The university of Tokyo)

[E] Poster | P (Space and Planetary Sciences)：P-EM Solar-Terrestrial Sciences, Space Electromagnetism & Space Environment

5:15 PM - 6:30 PM JST | 8:15 AM - 9:30 AM UTC | Poster Hall International Exhibition Hall8, Makuhari Messe_6

[P-EM13] Inner magnetosphere: Recent understanding and new insights

convener:Yusuke Ebihara(Research Institute for Sustainable Humanosphere, Kyoto University), Danny Summers(Memorial University of Newfoundland), Yoshizumi Miyoshi(Institute for Space-Earth Environmental Research, Nagoya University), Shinji Saito(Graduate School of Science, Nagoya University)

[PEM13-P01] Evaluation of wave normal and Poynting vector analyses for whistler mode waves observed by the waveform capture (WFC) on board the Arase

*Yoshiya Kasahara[1], Satoshi Ikarashi[1], Hiroyuki Nishizawa[1], Shoya Matsuda[2], Fuminori Tsuchiya[3], Atsushi Kumamoto[3], Yasumasa Kasaba[3], Mitsunori Ozaki[1], Ayako Matsuoka[2] (1.Kanazawa University, 2.ISAS/JAXA, 3.Tohoku University)

[PEM13-P02] Calibration of electric fields dedicated to the measurement of the S-WPIA of the Arase Satellite

*Miki Jumpei[1], Hirotsugu Kojima[2], Yuto Katoh[3], Shoya Matsuda[4], Yoshiya Kasahara[5], Mitsuru Hikishima[4], Satoshi Kurita[6], Masahiro Kitahara[3], Satoshi Kasahara[7], Yoshizumi Miyoshi[6], Atsushi Kumamoto[3], Ayako Matsuoka[4], Shoichiro Yokota[8], Tomoaki Hori[6], Kunihiro Keika[7] (1.Space Radio Engineering Laboratory, Division of Electrical Engineering, Kyoto University Graduated School, 2.Research Institute for Sustainable Humanosphere, Kyoto University, 3.Graduate School of Science and Faculty of Science, Tohoku University, 4.Institute of Space and Astronautical Science, JAXA, 5.Information Media Center, Kanazawa University, 6.Institute for Space-Earth Environmental Research, Nagoya University, 7.School of Science, The University of Tokyo, 8.School of Science, Osaka University)

[PEM13-P03] Enhancement of whistler-mode chorus in association with Pc 4-5 ULF waves and related variation of high energy electrons

*Atsuhiro Ono[1], Yuto Katoh[1], Atsushi Kumamoto[1], Fuminori Tsuchiya[1], Mariko Teramoto[2], Yoshiya Kasahara[3], Shoya Matsuda[4], Ayako Matsuoka[4], Takefumi Mitani[4], Tomoaki Hori[2], Satoshi Kasahara[5], Shoichiro Yokota[6], Kunihiro Keika[5], Yoshizumi Miyoshi[2], Iku Shinohara[4] (1.Tohoku University, 2.Nagoya University, 3.Kanazawa University, 4.ISAS/JAXA, 5.The University of Tokyo, 6.Osaka University)

[PEM13-P04] Sudden enhancements of electron cyclotron harmonic waves observed by the Arase satellite

*Shinjo Airi[1], Hirotsugu Kojima[1], Yoshiya Kasahara[2], Yoichi Kazama[3], Hideyuki Usui[4], Yoshizumi Miyoshi[5], Yasumasa Kasaba[6], Shoya Matsuda[7], Tomoaki Hori[5], S. -Y. Wang[8], Sunny W.Y. Tam[9], Atsushi Kumamoto[10], Ayako Matsuoka[11] (1.Research institute for sustainable humanosphere, Kyoto University, 2.Information Media Center, Kanazawa University, 3.ASIAA, 4.Graduate school of system informatics Kobe University, 5.Institute for Space-Earth Environmental Research, Nagoya University, 6.Planetary Plasma and Atmospheric Research Center, Tohoku University, 7.Institute of Space and Astronautical Science/Japan Aerospace Exploration Agency, 8.ASIAA, Taiwan, 9.ISAPS, NCKU, Taiwan, 10.Department of Geophysics, Graduate School of Science, Tohoku University, 11.Research Division for Space Plasma, Institute of Space and Astronautical Science, Japan Aerospace Exploration Agency)

[PEM13-P05] Correlation between pulsating aurora and electrostatic electron cyclotron harmonic waves obtained from coordinated Arase and ground data

*Mizuki Fukizawa[1], Takeshi Sakanoi[1], Yoshizumi Miyoshi[2], Keisuke Hosokawa[3], Yoichi Kazama[4], Yoshiya Kasahara[5], Shoya Matsuda[6], Ayako Matsuoka[7], Wang Shiang-Yu[4], Sunny Wing-Yee Tam[8], Ryuho Kataoka[9] (1.Planetary Plasma and Atmospheric Research Center, Graduate School of Science, Tohoku University, 2.Institute for Space-Earth Environmental Research, Nagoya University, 3.Department of Communication Engineering and Informatics, University of Electro-Communications, 4.Academia Sinica Institute of Astronomy and Astrophysics, 5.Information Media Center, Kanazawa University, 6.Institute of Space and Astronautical Science/Japan Aerospace Exploration Agency, 7.Research Division for Space Plasma, Institute of Space and Astronautical Science, Japan Aerospace Exploration Agency, 8.Institute of Space and Plasma Sciences, College of Sciences, National Cheng Kung University , 9.National Institute of Polar Research)

[PEM13-P06] Automatic determination of Upper Hybrid Resonance Frequencies by Convolutional Neural Network.

*Shoya Matsuda[1], Tatsuhito Hasegawa[2], Atsushi Kumamoto[3], Fuminori Tsuchiya[3], Yoshiya Kasahara[4], Yoshizumi Miyoshi[5], Yasumasa Kasaba[3], Ayako Matsuoka[1] (1.Institute of Space and Astronautical Science/Japan Aerospace Exploration Agency, 2.University of Fukui, 3.Tohoku University, 4.Kanazawa University, 5.ISEE, Nagoya University)

[PEM13-P07] Amplitude dependence of whistler wave motion on electron scattering process

*Yoshiki Ito[1], Yoshizumi Miyoshi[1], Shinji Saito[1] (1.Nagoya University, ISEE)

[PEM13-P08] Two-dimensional simulation of whistler mode wave packets interacting with energetic electrons

*Takeshi Nogi[1], Yoshiharu Omura[1] (1.Reserch Institute for Sustainable Humanosphere, Kyoto University)

[PEM13-P09] Relativistic electron acceleration by whistler-mode chorus waves in 1D, 2D, and 3D magnetic field models.

*Keita Takahashi[1], Yoshiharu Omura[1], Yikai HSIEH[1], Danny Summers[2] (1.Research Institute for Sustainable Humanosphere, Kyoto University , 2.Department of Mathematics and Statistics, Memorial University of Newfoundland)

[PEM13-P10] Study of global spatio-temporal development of magnetospheric ELF/VLF waves for the 26-30 March 2017 storm based on ground and satellite observations and the RAM simulations

*Yuhei Takeshita[1], Kazuo Shiokawa[1], Yoshizumi Miyoshi[1], Mitsunori Ozaki[2], Yoshiya Kasahara[2], Martine Connors[3], Jyrki Manninen[4], Craig Kletzing[5], Vania Jordanova[6] (1.Nagoya University, Institute for Space-Earth Environmental Resarch, 2.Kanazawa University, 3.Athabasca University, 4.Sodankylä Geophysical Observatory, 5.The University of Iowa, 6.Los Alamos National Laboratory)

[PEM13-P11] Flux decrease of outer radiation belt electrons associated with solar wind pressure pulse: A Code coupling simulation of GEMSIS-RB and GEMSIS-GM

*Ito Hiroki[1], Yoshizumi Miyoshi[1], Shinji Saito[2], Yosuke Matsumoto[3], Takanobu Amano[4] (1.Institute for Space-Earth Environmental Research, Nagoya University, 2. Graduate School of Science, Nagoya University, 3. Graduate School of Science, Chiba University, 4.Department of Earth and Planetary Science, University of Tokyo)

[PEM13-P12] Non-diffusive response of outer belt electrons on interplanetary shock

Takuma Toishi[1], *Yusuke Ebihara[1], Takashi Tanaka[2] (1.Research Institute for Sustainable Humanosphere, Kyoto University, 2.Kyushu University)

[PEM13-P13] PARM: Initial result of the auroral camera on the G-CHASER (RockSat-XN) rocket and status of the development of auroral cameras for the LAMP rocket experiment

*Naoshi Yagi[1], Takeshi Sakanoi[1], Fukizawa Mizuki[1], Kazushi Asamura[2], Yoshizumi Miyoshi[3], Keisuke Hosokawa[4], Genki Ishizawa[5] (1.Planetary Plasma and Atmospheric Research Center, Graduate School of Science, Tohoku University, 2.Institute of Space and Astronautical Science, Japan Aerospace Exploration Agency, 3.Institute for Space-Earth Environmental Research, Nagoya University, 4.Department of Communication Engineering and Informatics, University of Electro-Communications, 5.Space & terrestrial plasma pyhsics)

[PEM13-P14] First simultaneous observation of a SAR arc at subauroral latitudes using a ground all-sky camera and the Arase satellite in the inner magnetosphere

*Yudai Inaba[1], Kazuo Shiokawa[1], Shin-ichiro Oyama[1,8,9], Yuichi Otsuka[1], Atsuki Shinbori[1], Yoichi Kazama[2], Shiang-Yu Wang[2], Sunny W. Y. Tam[2], Shoichiro Yokota[3], Satoshi Kasahara[4], Kunihiro Keika[4], Tomoaki Hori[1], Ayako Matsuoka[5], Yoshiya Kasahara[6], Atsushi Kumamoto[7], Yasumasa Kasaba[7], Yoshizumi Miyoshi[1], Iku Shinohara[5], Arto Oksanen[10] (1.Institute for Space-Earth Environmental Research, 2.Academia Sinica, 3.Osaka Univ, 4.Tokyo Univ, 5.JAXA, 6.Kanazawa University, 7.Tohoku University, 8.University of Oulu, Finland, 9.National Institute of Polar Research, 10.Jyväskylän Sirius ry, Finland)

[PEM13-P15] Pi2 pulsations observed by the Arase satellite inside and outside the plasmapause

*Mariko Teramoto[1], Ayako Matsuoka[2], Reiko Nomura[5], Yoshiya Kasahara[3], Yasumasa Kasaba[4], Atsushi Kumamoto[4], Fuminori Tsuchiya[4], Shoya Matsuda[2], Masahito Nose[1], Masafumi Shoji[1], Yasunori Tsugawa[1], Shun Imajo[1], Yoshizumi Miyoshi[1], Iku Shinohara[2] (1.Institute for Space-Earth Environmental Research Nagoya University, 2.Institute of Space and Astronautical Science, Japan Aerospace eXploration Agency, 3.Kanazawa University, 4.Tohoku University, 5.National Astronomical Observatory of Japan)

[PEM13-P16] An extreme erosion of the plasmasphere during the 7–10 September 2017 storm

*Yuki Obana[1], Naomi Maruyama[2,3], Atsuki Shinbori[4], Kumiko K. Hashimoto[5], Mariangel Fedrizzi[2,3], Masahito Nose[4], Yuichi Otsuka[4], Nozomu Nishitani[4], Tomoaki Hori[4], Atsushi Kumamoto[6], Fuminori Tsuchiya[6], Shoya Matsuda[7], Ayako Matsuoka[7], Yoshiya Kasahara[8], Akimasa Yoshikawa[9], Yoshizumi Miyoshi[4], Iku Shinohara[7] (1.Osaka Electro-Communication University, 2.University of Colorado Boulder, 3.NOAA Space Weather Prediction Center, 4.Nagoya

University, 5.Kibi International University, 6.Tohoku University, 7.Japan Aerospace Exploration Agency, 8.Kanazawa University, 9.Kyushu University)

[PEM13-P17] Relative contribution of ULF and chorus waves to the radiation belt variation: Comparison between multi-point observations and BATSRUS + CRCM simulation

*Naoko Takahashi[1], Kanako Seki[1], Mei-Ching Fok[2], Yihua Zheng[2], Yoshizumi Miyoshi[3], David Hartley[4], Ayako Matsuoka[5], Yoshiya Kasahara[6], Yasumasa Kasaba[7], Nana Higashio[8] (1.Graduate School of Science, University of Tokyo, 2.NASA Goddard Space Flight Center, 3.Institute for Space-Earth Environmental Research, Nagoya University, 4.Department of Physics and Astronomy, University of Iowa, 5.Institute of Space and Astronautical Science, Japan Aerospace Exploration Agency, 6.Information Media Center, Kanazawa University, 7.Planetary Plasma and Atmospheric Research Center, Tohoku University, 8.Japan Aerospace Exploration Agency)

[PEM13-P18] Modulation of the D-region ionosphere by Pc5 waves observed by VLF/LF standard radio waves

*Miyashita Takuya[1], Hiroyo Ohya[1], Fuminori Tsuchiya[2], Hiroyuki Nakata[1], Toshiaki Takano[1], Kazuo Shiokawa[3], Yoshizumi Miyoshi[3] (1.Chiba University, 2.Tohoku University, 3.Nagoya University)

[PEM13-P19] Oxygen-proton differences in ion energies dominating plasma pressure: Dependence on storm phases and solar wind drivers

*Kunihiro Keika[1], Satoshi Kasahara[1], Shoichiro Yokota[2], Masahiro Hoshino[1], Kanako Seki[1], Masahito Nose[3], Yoshizumi Miyoshi[3], Iku Shinohara[4] (1.Graduate School of Science, The University of Tokyo , 2.Graduate School of Science, Osaka University, 3.Institute for Space-Earth Environmental Research, Nagoya University, 4.Institute of Space and Astronautical Science, Japan Aerospace Exploration Agency)

[PEM13-P20] Mass dependence of penetration depth of multi-energy ions in the inner magnetosphere during magnetic storms: Arase observations

*Ryosuke Fujii[1], Yoshizumi Miyoshi[1], Masafumi Shoji[1], Kazushi Asamura[2], Lynn Kistler[1,8], Vania Jordanova[9], Tomoaki Hori[1], Satoshi Kurita[1], Mariko Teramoto[1], Yasunori Tsugawa[1], Yoshiya Kasahara[3], Yasumasa Kasaba[4], Atsushi Kumamoto[5], Fuminori Tsuchiya[4], Shoichiro Yokota[6], Kunihiro Keika[7], Ayako Matsuoka[2], Iku Shinohara[2] (1.Institute for Space-Earth Environmental Research, Nagoya University, 2.Institute of Space and Astronautical Science, Japan Aerospace Exploration Agency, 3.Information Media Center, Kanazawa University, 4.Planetary Plasma and Atmospheric Research Center, Tohoku University, 5.Department of Geophysics, Graduate School of Science, Tohoku University, 6.Graduate School of Science, Osaka University, 7.Department of Earth and Planetary Science, Graduate School of Science, The University of Tokyo, 8.University of New Hampshire, 9.Los Alamos National Laboratory)

[PEM13-P21] Relativistic Acceleration of Energetic Protons by Electromagnetic Ion Cyclotron Waves in the Jovian Magnetosphere

*Tomohiro Sekine[1], Yoshiharu Omura[1], Danny Summers[2], Yikai HSIEH[1], Satoko Nakamura[1] (1.Reserach Institute for Sustainable Humanosphere, Kyoto University, 2.Memorial University of Newfoundland)

[PEM13-P22] Statistical study of IPDP type EMIC wave-related electron precipitation at subauroral latitude

*Asuka Hirai[1], Fuminori Tsuchiya[1], Takahiro Obara[1], Yasumasa Kasaba[1], Yuto Katoh[2], Hiroaki Misawa[1], Kazuo Shiokawa[3], Yoshizumi Miyoshi[3], Satoshi Kurita[3], Martin G Connors[4] (1.Planetary Plasma and Atmospheric Research Center, Graduate School of Science, Tohoku Univ. , 2.Department of Geophysics, Graduate School of Science, Tohoku University, 3.Institute for Space-Earth Environmental Research, Nagoya University, 4.Athabasca University)

[PEM13-P23] Meridional distributions of proton plasma and pressure-driven currents in the nightside inner magnetosphere: Arase observations

*Shun Imajo[1], Masahito Nose[1], Satoshi Kasahara[2], Shoichiro Yokota[3], Ayako Matsuoka[4], Kunihiro Keika[2], Tomoaki Hori[1], Mariko Teramoto[1], Kazuhiro Yamamoto[5], Oimatsu Satoshi[5], Reiko Nomura[6], Akiko Fujimoto[7], Iku Shinohara[4], Yoshizumi Miyoshi[1] (1.Institute for Space-Earth Environmental Research, Nagoya University, 2.Graduate School of Science, The University of Tokyo, 3.Graduate School of Science, Osaka University, 4.Institute of Space and Astronautical Science, Japan Aerospace Exploration Agency, 5.Graduate School of Science, Kyoto University, 6.National Astronomical Observatory of Japan, 7.Kyushu Institute of Technology)

[PEM13-P24] Space Weather Effects on Energetic Proton Flux Response in South Atlantic Anomaly

*Kirolosse Mina GIRGIS[1,2], Tohru Hada[1], Shuichi Matsukiyo[1] (1.Earth System Science and Technology (ESST) Department, Interdisciplinary Graduate School of Engineering Sciences (IGSES), Kyushu University, Japan, 2.Aerospace Engineering Department, Faculty of Engineering, Cairo University, Egypt)

[PEM13-P25] Solar-cycle variations of >30 keV electron flux enhancements under the inner radiation belt

*ALLA SUVOROVA[1] (1.National Central University)

[PEM13-P26] Energy spectra variations of high energy electrons in the inner magnetosphere observed by HEP/XEP on ARASE and SEDA-e on HIMAWARI

*Takeshi Takashima[1], Takefumi Mitani[1], Nana Higashio[2], Tsutomu Nagatsuma[3] (1. ISAS/JAXA, 2.Research and Development Directorate/JAXA, 3.NiCT)

[PEM13-P27] Inter-channel calibration of the high-energy electron experiments (HEP) instrument onboard the Arase satellite

*Tomoaki Hori[1], Takefumi Mitani[2], Takeshi Takashima[2], Park Inchun[1], Satoshi Kurita[1], Mariko Teramoto[1], Nana Higashio[3], Satoshi Kasahara[4], Shoichiro Yokota[5], Yoshizumi Miyoshi[1], Iku Shinohara[2] (1.Institute for Space-Earth Environmental Research, Nagoya University, 2.Japan Aerospace Exploration Agency, Institute of Space and Astronautical Science, 3.Japan Aerospace Exploration Agency, 4.Graduate School of Science, The University of Tokyo, 5.Graduate School of Science, Osaka University)

[PEM13-P28] Particle simulation for calibrating the HEP data onboard the ARASE satellite

*PARK INCHUN[1], Yoshizumi Miyoshi[1], Takefumi Mitani[2], Tomoaki Hori[1], Satoshi Kurita[1], Mariko Teramoto[1], Takeshi Takashima[2], Nana Higashio[3], Iku Shinohara[2] (1.Nagoya University Institute for Space-Earth Environmental Research, 2.Japan Aerospace Exploration Agency Institute of Space and Astronautical Science , 3.Japan Aerospace Exploration Agency)

[PEM13-P29] Geant4 model calculation and energetic particle observation with HEP/Arase in the inner radiation belt

*Honoka Toda[1], Wataru Miyake[1], Takefumi Mitani[3], Takeshi Takashima[3], Yoshizumi Miyoshi[2], PARK INCHUN[2], Tomoaki Hori[2] (1.Tokai University, 2.ISEE/Nagoya University, 3.ISAS/JAXA)

[PEM13-P30] Validation of High-energy electron detector simulator for the HEP instruments onboard Arase

*Takefumi Mitani[1], PARK INCHUN[2], Tomoaki Hori[2], Taku Namekawa[1,3], Kazushi Asamura[1], Takeshi Takashima[1], Satoshi Kasahara[3], Satoshi Kurita[2], Mariko Teramoto[2], Nana Higashio[1], Yoshizumi Miyoshi[2], Iku Shinohara[1] (1.Japan Aerospace Exploration Agency, Institute of Space and Astronautical Science, 2.Institute for Space-Earth Environmental Research, Nagoya Univ., 3.The university of Tokyo)

[J] Oral | P (Space and Planetary Sciences)：P-EM Solar-Terrestrial Sciences, Space Electromagnetism & Space Environment

9:00 AM - 10:30 AM JST | 12:00 AM - 1:30 AM UTC | A03 TOKYO BAY MAKUHARI HALL

[P-EM16] Physics and Chemistry in the Atmosphere and Ionosphere

convener:Yuichi Otsuka(Institute for Space-Earth Environmental Research, Nagoya University), Takuya Tsugawa(National Institute of Information and Communications Technology), Seiji Kawamura(National Institute of Information and Communications Technology), Chairperson:Mitsumu Ejiri(国立極地研究所), Yuichi Otsuka

9:00 AM - 9:15 AM JST | 12:00 AM - 12:15 AM UTC

[PEM16-01] The model study of ionospheric variations during the solar eclipse event by assimulating the GNSS TEC observations

*Chia-Hung Chen[1], Charles Lin[1], Tomoko Matsuo[2] (1.Department of Earth Sciences, National Cheng Kung University, 2.Department of Aerospace Engineering Sciences, University of Colorado at Boulder, CO)

9:15 AM - 9:30 AM JST | 12:15 AM - 12:30 AM UTC

[PEM16-02] Characteristics of mesoscale thermospheric-ionospheric dynamics associated with heating in the auroral region

*Tomokazu Oigawa[1], Hiroyuki Shinagawa[2], Satoshi Taguchi[1] (1.Department of Geophysics, Graduate School of Science, Kyoto University, 2.National Institute of Information and Communications Technology)

9:30 AM - 9:45 AM JST | 12:30 AM - 12:45 AM UTC

[PEM16-03] Spatial distribution of the polar thermospheric wind acceleration and importance of the 2D measurement

*Shin-ichiro Oyama[1,2,3], Anita Aikio[2], Mark G Conde[4], Heikki Vanhamaki[2], Ilkka Virtanen[2], Thomas Ulich[5], Urban Brandstrom[6], Pekka Verronen[7], Monika Andersson[7], Niilo Kalakoski[7], Lassi Roininen[8], Sari Lasanen[8], Abiyot Workayehu[2], Kazuo Shiokawa[1], Heqiucen XU[1], Mamoru Ishii[9], Masafumi Hirahara[1], Takeshi Sakanoi[10], Masato Kagitani[10], Juha Sorri[5], Tomi Teppo[5], Yoshimasa Tanaka[3], Christopher Fallen[4], Brenton J Watkins[4], Mikko Orispaa[5], Yasunobu Ogawa[3], Lei Cai[11], Esa Turunen[5], Kirsti Kauristie[7], Takuo T. Tsuda[12], Junichi Kurihara[13] (1.Institute for Space-Earth Environmental Research, Nagoya University, Japan, 2.University of Oulu, Finland, 3.National Institute of Polar Research, Japan, 4.Geophysical Institute, University of Alaska Fairbanks, US, 5.Sodankyla Geophysical Observatory, University of Oulu, Finland, 6.The Swedish Institute of Space Physics (IRF), Sweden, 7.Finnish Meteorological Institute, Finland, 8.Lappeenranta-Lahti University of Technology, Finland, 9.National Institute of Information and Communications Technology, Japan, 10.Tohoku University, Japan, 11.KTH Royal Institute of Technology, Sweden, 12.The University of Electro-Communications, 13.Hokkaido University)

9:45 AM - 10:00 AM JST | 12:45 AM - 1:00 AM UTC

[PEM16-04] Analysis of the thermospheric neutral wind vector using observed images of *Trimethylaluminium* (*C6H18Al2*) released from sounding rocket in the upper atmosphere

*Yuki Otsuka[1], Masa-yuki Yamamoto[1], Hiroaki Saito[1] (1.Kochi University of Technology)

10:00 AM - 10:15 AM JST | 1:00 AM - 1:15 AM UTC

[PEM16-05] Establishment of real-time analysis method in a new HRO interferometer system and operation test of comprehensive meteor observation

*Takumi Sato[1], Seiya Takeda[2], Masa-yuki Yamamoto[1] (1.KOCHI UNIVERSITY OF TECHNOLOGY, 2.Inc.Bascule)

10:15 AM - 10:30 AM JST | 1:15 AM - 1:30 AM UTC

[PEM16-06] Solar flare effects of the D-region ionosphere using daytime tweek atmospherics

*Kodai Yamanobe[1], Hiroyo Ohya[2], Hiroyuki Nakata[2], Toshiaki Takano[2], Kazuo Shiokawa[3] (1.Graduate School of Science and Engineering, Chiba University , 2.Graduate School of Science and Engineering, Chiba University, 3.Institute for Space-Earth Environmental Research, Nagoya University)

[J] Oral | P (Space and Planetary Sciences)：P-EM Solar-Terrestrial Sciences, Space Electromagnetism & Space Environment

10:45 AM - 12:15 PM JST | 1:45 AM - 3:15 AM UTC | A03 TOKYO BAY MAKUHARI HALL

[P-EM16] Physics and Chemistry in the Atmosphere and Ionosphere

convener:Yuichi Otsuka(Institute for Space-Earth Environmental Research, Nagoya University), Takuya Tsugawa(National Institute of Information and Communications Technology), Seiji Kawamura(National Institute of Information and Communications Technology), Chairperson:Yuichi Otsuka, Mitsumu Ejiri(国立極地研究所)

10:45 AM - 11:00 AM JST | 1:45 AM - 2:00 AM UTC

[PEM16-07] Toward a detection of sporadic-E episodes by ALOS2 ScaSAR InSAR

*Masato Furuya[1], Jun Maeda[2], Kosuke Heki[1] (1.Department of Earth and Planetary Sciences Hokkaido University, 2.Hokkaido University Library)

11:00 AM - 11:15 AM JST | 2:00 AM - 2:15 AM UTC

[PEM16-08] Vertical fine structure and time evolution of plasma irregularities in the E_s layer, observed by a high resolution Ca^+ lidar

*Mitsumu K. Ejiri[1,2], Takuji Nakamura[1,2], Takuo T. Tsuda[3], Takanori Nishiyama[1,2], Makoto Abo[4], Toru Takahashi[1], Katsuhiko Tsuno[5], Takuya Kawahara[6], Takayo Ogawa[5], Satoshi Wada[5] (1.National Institute of Polar Research, 2.SOKENDAI (Department of Polar Science, The Graduate University for Advanced Studies), 3.The University of Electro-Communications, 4.Tokyo Metropolitan University, 5.RIKEN, RAP, 6.Shinshu University Faculty of Engineering)

11:15 AM - 11:30 AM JST | 2:15 AM - 2:30 AM UTC

[PEM16-09] Study of Effects of Stratospheric Sudden Warming on Medium-Scale Traveling Ionospheric Disturbances Using Total Electron Content Data Obtained from World-Wide GPS Receiver Networks

*Yuichi Otsuka[1], Atsuki Shinbori[1], Prayitno Abadi[2], Takuya Tsugawa[3], Michi Nishioka[3] (1.Institute for Space-Earth Environmental Research, Nagoya University, 2.LAPAN, 3.National Institute of Information and Communications Technology)

11:30 AM - 11:45 AM JST | 2:30 AM - 2:45 AM UTC

[PEM16-10] Tsunami-generated ionospheric currents inferred from geomagnetic observations at ground level: Case for the 2011 Tohoku Earthquake

*Takuto Minami[1], Masashi Kamogawa[2], Tsutomu Ogawa[1], Makoto Uyeshima[1], Toru Mogi[3], Hiroshi Ichihara[4] (1.Earthquake Research Institute,The University of Tokyo, 2.Department of Physics, Tokyo Gakugei University, 3.Graduate School of Engineering, Hokkaido University, 4.Graduate School of Environmental Studies, Nagoya University)

11:45 AM - 12:00 PM JST | 2:45 AM - 3:00 AM UTC

[PEM16-11] Relationship between the magnitude of Sakurajima eruptions and the disturbance of GPS-TEC

*Kiyoto Shoji[1], Hiroyuki Nakata[1], Toshiaki Takano[1], Hiroyo Ohya[1], Takuya Tsugawa[2], Michi Nishioka[2] (1.Graduate School of Science and Engineering, Chiba University, 2.National Institute of Information and Communications Technology)

12:00 PM - 12:15 PM JST | 3:00 AM - 3:15 AM UTC

[PEM16-12] Water vapor estimation using digital terrestriall broadcasting waves - Simultaneous observation with microwave radiometer -

*Hiroshi HANADO[1], Seiji Kawamura[1], Hironori Iwai[1], Shinsuke Satoh[1], Katsuhiro Nakagawa[1], Takuya Tajiri[2], Narihiro Orikasa[2], Yoshinori Shoji[2], Kentaro Araki[2], Hiromu Seko[2] (1.National Institute of Information and Communications Technology, 2.Meteorological Research Institute)

[J] Oral | P (Space and Planetary Sciences)：P-EM Solar-Terrestrial Sciences, Space Electromagnetism & Space Environment

1:45 PM - 3:15 PM JST | 4:45 AM - 6:15 AM UTC | 201A 2F

[P-EM18] Heliosphere and Interplanetary Space

convener:Ken Tsubouchi(University of Electro-Communications), Masaki N Nishino(Japan Aerospace Exploration Agency, Institute of Space and Astronautical Science), Yasuhiro Nariyuki(Faculty of Human Development, University of Toyama), Kazumasa Iwai(Institute for Space?Earth Environmental Research (ISEE), Nagoya University), Chairperson:Yasuhiro Nariyuki, Kazumasa Iwai

1:45 PM - 2:00 PM JST | 4:45 AM - 5:00 AM UTC

[PEM18-01] Problems in determining structures of interplanetary magnetic flux ropes

*Katsuhide Marubashi[1], Yuki Kubo[1], Nobuhiko Nishimura[2], Munetoshi Tokumaru[2], Nada Al-Haddad[3] (1.National Institute of Information and Communications Technology , 2.ISEE, Nagoya University, 3.IACS, Catholic University of America)

2:00 PM - 2:15 PM JST | 5:00 AM - 5:15 AM UTC

[PEM18-02] Validation of estimated interplanetary flux rope axial direction using internal plasma motions: benchmark test

*Nobuhiko Nishimura[1], Munetoshi Tokumaru[1], Katsuhide Marubashi[2] (1.Institute for Space Earth Environmental Research, 2.National Institute of Information and Communications Technology)

2:15 PM - 2:30 PM JST | 5:15 AM - 5:30 AM UTC

[PEM18-03] Effect of line-of-sight integration on locations of coronal mass ejection in the sky projection map of interplanetary scintillation observations

*Munetoshi Tokumaru[1], Ken'ichi Fujiki[1], Kazumasa Iwai[1] (1.Institute for Space-Earth Environmental Research, Nagoya University)

2:30 PM - 2:45 PM JST | 5:30 AM - 5:45 AM UTC

[PEM18-04] Estimation of spatial structure of whistler mode wave packets in Earth’s bow shock by multiple spacecraft analysis

*Chika Umegaki[1], Takanobu Amano[1], Naritoshi Kitamura[1] (1.The university of tokyo)

2:45 PM - 3:00 PM JST | 5:45 AM - 6:00 AM UTC

[PEM18-05] Experimental Test for Stochastic Shock Drift Acceleration Theory

*Takanobu Amano[1], Takuma Katou[1], Naritoshi Kitamura[1], Mitsuo Oka[2], Yosuke Matsumoto[3], Masahiro Hoshino[1] (1.Department of Earth and Planetary Science, University of Tokyo, 2.Space Sciences Laboratory, University of California, Berkeley, 3.Department of Physics, Chiba University)

3:00 PM - 3:15 PM JST | 6:00 AM - 6:15 AM UTC

[PEM18-06] Radial structure of heliospheric boundary region

*Shuichi Matsukiyo[1], Gary P. Zank[2], Haruichi Washimi[3], Tohru Hada[1] (1.Faculty of Engineering Sciences, Kyushu University, 2.The Center for Space Plasma and Aeronomic Research, University of Alabama in Huntsville, 3.International Center for Space Weather Science and Education, Kyushu University)

[J] Poster | P (Space and Planetary Sciences)：P-EM Solar-Terrestrial Sciences, Space Electromagnetism & Space Environment

3:30 PM - 5:00 PM JST | 6:30 AM - 8:00 AM UTC | Poster Hall International Exhibition Hall8, Makuhari Messe_3

[P-EM18] Heliosphere and Interplanetary Space

convener:Ken Tsubouchi(University of Electro-Communications), Masaki N Nishino(Japan Aerospace Exploration Agency, Institute of Space and Astronautical Science), Yasuhiro Nariyuki(Faculty of Human Development, University of Toyama), Kazumasa Iwai(Institute for Space?Earth Environmental Research (ISEE), Nagoya University)

[PEM18-P01] Study of the contribution of electric field to the acceleration of cometary ions around comet 67P/Churyumov-Gerasimenko

*Kazuki Yamagishi[1], Yuto Katoh[1], Tomoki Kimura[1], Atsushi Kumamoto[1] (1.Department of Geophysics, Graduate School of Science, Tohoku University)

[PEM18-P02] Energy conversion process at the lunar wake boundary

*Tomoko Nakagawa[1], Hideo Tsunakawa[2], Yoshifumi Saito[3] (1.Information and Communication Engineering, Tohoku Institute of Technology, 2.Department of Earth and Planetary Sciences, School of Science, Tokyo Institute of Technology , 3.JAXA,ISAS)

[PEM18-P03] Electron acceleration at quasi-perpendicular collisionless shock: One-dimensional PIC simulation

*Fumiko Otsuka[1], Shuichi Matsukiyo[2], Mitsuo Oka[3] (1.NIT, Kurume College, 2.ESST, Kyushu Univ., 3.UC Berkeley)

[PEM18-P04] 4-season's optical observation of neutral helium distribution in interplanetary space by Hisaki

*Atsushi Yamazaki[1], Go Murakami[1], Kazuo Yoshioka[2], Tomoki Kimura[3], Fuminori Tsuchiya[4], Masato Kagitani[4], Takeshi Sakanoi[4], Naoki Terada[5], Yasumasa Kasaba[4], Ichiro Yoshikawa[6], Hisaki (SPRINT-A) Project team (1.Japan Aerospace Exploration Agency, Institute of Space and Astronautical Science , 2.The University of Tokyo, Graduate School of Frontier Sciences, 3.Tohoku University, 4.Tohoku University, Planetary Plasma and Atmospheric Research Center , 5.Tohoku University, Graduate School of Sciense, 6.The University of Tokyo)

[PEM18-P05] Structural variations in the pickup ion density associated with magnetic reconnection at the heliopause

*Ken Tsubouchi[1] (1.University of Electro-Communications)

[J] Poster | P (Space and Planetary Sciences)：P-EM Solar-Terrestrial Sciences, Space Electromagnetism & Space Environment

5:15 PM - 6:30 PM JST | 8:15 AM - 9:30 AM UTC | Poster Hall International Exhibition Hall8, Makuhari Messe_7

[P-EM18] Heliosphere and Interplanetary Space

convener:Ken Tsubouchi(University of Electro-Communications), Masaki N Nishino(Japan Aerospace Exploration Agency, Institute of Space and Astronautical Science), Yasuhiro Nariyuki(Faculty of Human Development, University of Toyama), Kazumasa Iwai(Institute for Space?Earth Environmental Research (ISEE), Nagoya University)

[PEM18-P01] Study of the contribution of electric field to the acceleration of cometary ions around comet 67P/Churyumov-Gerasimenko

*Kazuki Yamagishi[1], Yuto Katoh[1], Tomoki Kimura[1], Atsushi Kumamoto[1] (1.Department of Geophysics, Graduate School of Science, Tohoku University)

[PEM18-P02] Energy conversion process at the lunar wake boundary

*Tomoko Nakagawa[1], Hideo Tsunakawa[2], Yoshifumi Saito[3] (1.Information and Communication Engineering, Tohoku Institute of Technology, 2.Department of Earth and Planetary Sciences, School of Science, Tokyo Institute of Technology , 3.JAXA,ISAS)

[PEM18-P03] Electron acceleration at quasi-perpendicular collisionless shock: One-dimensional PIC simulation

*Fumiko Otsuka[1], Shuichi Matsukiyo[2], Mitsuo Oka[3] (1.NIT, Kurume College, 2.ESST, Kyushu Univ., 3.UC Berkeley)

[PEM18-P04] 4-season's optical observation of neutral helium distribution in interplanetary space by Hisaki

*Atsushi Yamazaki[1], Go Murakami[1], Kazuo Yoshioka[2], Tomoki Kimura[3], Fuminori Tsuchiya[4], Masato Kagitani[4], Takeshi Sakanoi[4], Naoki Terada[5], Yasumasa Kasaba[4], Ichiro Yoshikawa[6], Hisaki (SPRINT-A) Project team (1.Japan Aerospace Exploration Agency, Institute of Space and Astronautical Science , 2.The University of Tokyo, Graduate School of Frontier Sciences, 3.Tohoku University, 4.Tohoku University, Planetary Plasma and Atmospheric Research Center , 5.Tohoku University, Graduate School of Sciense, 6.The University of Tokyo)

[PEM18-P05] Structural variations in the pickup ion density associated with magnetic reconnection at the heliopause

*Ken Tsubouchi[1] (1.University of Electro-Communications)

[J] Oral | P (Space and Planetary Sciences)：P-CG Complex & General

9:00 AM - 10:30 AM JST | 12:00 AM - 1:30 AM UTC | 105 1F

[P-CG24] New Developments of Planetary Sciences with ALMA

convener:Takayuki Muto(Division of Liberal Arts, Kogakuin University), Munetake Momose(The College of Science, Ibaraki University), Hideo Sagawa(Faculty of Science, Kyoto Sangyo University), Masumi Shimojo(National Astronomical Observatory of Japan), Chairperson:Takayuki Muto

9:00 AM - 9:15 AM JST | 12:00 AM - 12:15 AM UTC

[PCG24-01] Understanding solar atmosphere by ALMA observations

★Invited Papers

*Tomoko Kawate[1], Takenori J Okamoto[2], Kazumasa Iwai[3], Satoshi Masuda[3], Masumi Shimojo[2] (1.Institute of Space and Astronautical Science, Japan Aerospace Exploration Agency, 2.National Astronomical Observatory of Japan, 3.Nagoya University)

9:15 AM - 9:30 AM JST | 12:15 AM - 12:30 AM UTC

[PCG24-02] **Multi-thermal structures in a spicule observed with ALMA, IRIS, and AIA/SDO**

*Masumi Shimojo[1], Tomoko Kawate[2], Takenori Okamoto[1], Takaaki Yokoyama[3] (1.National Astronomical Observatory of Japan, 2. Institute of Space and Astronautical Science , 3.University of Tokyo)

9:30 AM - 9:45 AM JST | 12:30 AM - 12:45 AM UTC

[PCG24-03] Observing the 2018 global dust storm on Mars with ALMA

Shohei Aoki[2], *Hideo Sagawa[1], Kazi Rigl[3], Geronimo L. Villanueva[4], Bill Dent[5], Hiroyuki Maezawa[6], Severine Robert[2], Hiromu Nakagawa[7], Frank Daerden[2], Takeshi Kuroda[8], Marco Giuranna[10], Kazuya Saigo[9], Michael J. Mumma[4], Yasumasa Kasaba[7], Ann Carine Vandaele[2] (1.Kyoto Sangyo University, 2.Royal Belgian Institute for Space Aeronomy, 3.Italian ALMA Regional Centre, INAF-Istituto di Radioastronomia, 4.NASA Goddard Space Flight Center, USA, 5.ESO ALMA, Chile, 6.Osaka Prefecture University, 7.Tohoku University, 8.NICT Big Data Integration Research Center, 9.NAOJ Chile Observatory, 10.Istituto di Astrofisica e Planetologia Spaziali, Italy)

9:45 AM - 10:00 AM JST | 12:45 AM - 1:00 AM UTC

[PCG24-04] Atmospheric observation of submillimeter wave and the thermal evolution of ice giants

★Invited Papers

*Kenji Kurosaki[1], Masahiro Ikoma[2] (1.Department of Physics, Nagoya University , 2.Department of Earth and Planetary Science, Graduate School of Science, The University of Tokyo)

10:00 AM - 10:30 AM JST | 1:00 AM - 1:30 AM UTC

[PCG24-05] Planetary-system formation revealed with ALMA

★Invited Papers

*Misato Fukagawa[1] (1.National Astronomical Observatory of Japan)

[J] Oral | P (Space and Planetary Sciences)：P-CG Complex & General

10:45 AM - 12:15 PM JST | 1:45 AM - 3:15 AM UTC | 105 1F

[P-CG24] New Developments of Planetary Sciences with ALMA

convener:Takayuki Muto(Division of Liberal Arts, Kogakuin University), Munetake Momose(The College of Science, Ibaraki University), Hideo Sagawa(Faculty of Science, Kyoto Sangyo University), Masumi Shimojo(National Astronomical Observatory of Japan), Chairperson:Munetake MOMOSE(Ibaraki University)

10:45 AM - 11:00 AM JST | 1:45 AM - 2:00 AM UTC

[PCG24-06] Probing dust aggregate structure in protoplanetary disks by millimeter-wave polarization

*Ryo Tazaki[1], Hidekazu Tanaka[1], Takayuki Muto[2], Akimasa Kataoka[3], Satoshi Okuzumi[4] (1.Tohoku University, 2.Kogakuin University, 3.NAOJ, 4.Tokyo Institute of Technology)

11:00 AM - 11:15 AM JST | 2:00 AM - 2:15 AM UTC

[PCG24-07] A CONSTRAINT ON THE AMOUNT OF HYDROGEN FROM THE CO CHEMISTRY IN DEBRIS DISKS

*Hiroshi Kobayashi[1], Kazunari Iwasaki[2,4], Aya Higuchi[3] (1.Department of Physics, Nagoya University, 2.NAOJ, 3.RIKEN, 4.Osaka University)

11:15 AM - 11:30 AM JST | 2:15 AM - 2:30 AM UTC

[PCG24-08] Structure of the protoplanetary disk around V1094 Sco obtained from dust continuum emission and SED

*Sanemichi Takahashi[1,2], Takayuki Muto[1], Takashi Tsukagoshi[2], Jun Hashimoto[2] (1.Kogakuin University, 2.NAOJ)

11:30 AM - 11:45 AM JST | 2:30 AM - 2:45 AM UTC

[PCG24-09] The Synthetic ALMA Multiband Analysis of the Dust Properties of the TW Hya Protoplanetary Disk

*Seongjoong Kim[1], Hideko Nomura[1], Takashi Tsukagoshi[2], Ryohei Kawabe[2,3,4], Takayuki Muto[5] (1.Department of Earth and Planetary Sciences, Tokyo Institute of Technology, 2.National Astronomical Observatory of Japan, 3.The Graduate University for Advanced Studies (SOKENDAI), 4.Department of Astronomy, School of Science, University of Tokyo, 5.Division of Liberal Arts, Kogakuin University)

11:45 AM - 12:00 PM JST | 2:45 AM - 3:00 AM UTC

[PCG24-10] Dust evolution in the protoplanetary disk around TW Hya

*Takayuki Matsuura[1], Satoshi Okuzumi[1] (1.Tokyo Institute of Technology)

12:00 PM - 12:15 PM JST | 3:00 AM - 3:15 AM UTC

[PCG24-11] Discovery of a localized excess in the millimeter emission of the protoplanetary disk around TW Hya

*Takashi Tsukagoshi[1], Takayuki Muto[2], Hideko Nomura[3], Ryohei Kawabe[1,4,5], Kazuhiro Kanagawa[9], Satoshi Okuzumi[3], Shigeru Ida[10], Catherine Walsh[6], Tom J Millar[7], Sanemichi Takahashi[2,1], Jun Hashimoto[8], Taichi Uyama[5], Motohide Tamura[5,8] (1.Division of Radio Astronomy, National Astronomical Observatory of Japan, 2.Division of Liberal Arts, Kogakuin University, 3.Department of Earth and Planetary Sciences, Tokyo Institute of Technology, 4.The Graduate University for Adnvanced Studies, 5.School of Science, University of Tokyo, 6.School of Physics and Astronomy, University of Leeds, 7.Astrophysics Research Centre, Queen's University Belfast, 8.Astrobiology Center, National Institutes of Natural Sciences, 9.Research Center for the Early Universe, University of Tokyo, 10.Earth-Life Science Institute, Tokyo Institute of Technology)

[J] Poster | P (Space and Planetary Sciences)：P-CG Complex & General

3:30 PM - 5:00 PM JST | 6:30 AM - 8:00 AM UTC | Poster Hall International Exhibition Hall8, Makuhari Messe_4

[P-CG24] New Developments of Planetary Sciences with ALMA

convener:Takayuki Muto(Division of Liberal Arts, Kogakuin University), Munetake Momose(The College of Science, Ibaraki University), Hideo Sagawa(Faculty of Science, Kyoto Sangyo University), Masumi Shimojo(National Astronomical Observatory of Japan)

[PCG24-P01] Nitrogen isotopic fractionation on Titan atmosphere: An analysis of ALMA archive data

*Hideo Sagawa[1], Takahiro Iino[2], Takashi Tsukagoshi[3] (1.Kyoto Sangyo University, 2.Tokyo University of Agriculture and Technology, 3.National Astronomical Observatory of Japan)

[PCG24-P02] Investigating the gas-to-dust ratio in the protoplanetary disk of HD 142527

*Soon Kang-Lou[1], Munetake Momose[1], Takayuki Muto[2], Takashi Tsukagoshi[3], Akimasa Kataoka[3], Tomoyuki Hanawa[4], Misato Fukagawa[3], Kazuya Saigo[3], Hiroshi Shibai[5] (1.Ibaraki University, 2.Kogakuin University, 3.National Astronomical Observatory of Japan, 4.Chiba University, 5.Osaka University)

[PCG24-P03] Super-resolution Imaging of the Protoplanetary Disk HD 142527 Using Sparse Modeling

*Masayuki Yamaguchi[1,2], Kazunori Akiyama[3,2], Akimasa Kataoka[2,6], Takashi Tsukagoshi[2], Takayuki Muto[4], Shiro Ikeda[5], Misato Fukagawa[2], Mareki Honma[2,6], Ryohei Kawabe[2,1,6] (1.The University of Tokyo, 2.National Astronomical Observatory of Japan, 3.Massachusetts Institute of Technology, Haystack Observatory, 4.Kogakuin University, 5.The Institute of Statistical Mathematics, 6. Graduate University for Advanced Studies)

[PCG24-P04] Detail Structures of Dust Disk around T-Tauri star RY Tau in ALMA High-Spatial Resolution Imaging

*Mihoko Konishi[1,2], Jun Hashimoto[1,2], Hauyu Liu[3], Ruobing Dong[4], Takayuki Muto[5] (1.Astrobiology Center, National Institute of Natural Science, 2.National Astronomical Observatory of Japan, 3.Institute of Astronomy and Astrophysics, Academia Sinica, 4.University of Victoria, 5.Kogakuin University)

[PCG24-P05] Possible inclined inner protoplanetary disk

*Jun Hashimoto[1], Mihoko Konishi[1], Taichi Uyama[2], Christian Ginski[3], Matthias Samland[4] (1.AstroBiology Center, National Institutes of Natural Sciences, 2.University of Tokyo, 3.University of Amsterdam, 4.Max Planck Institute for Astronomy)

[PCG24-P06] Search for the Inner Disk Structures in "Transitional" Disks

*Takayuki Muto[1], Jun Hashimoto[2], Takashi Tsukagoshi[3], Mihoko Konishi[3], Tomoyuki Kudo[3] (1.Division of Liberal Arts, Kogakuin University, 2.Astrobiology Center, 3.NAOJ)

[J] Poster | P (Space and Planetary Sciences)：P-CG Complex & General

5:15 PM - 6:30 PM JST | 8:15 AM - 9:30 AM UTC | Poster Hall International Exhibition Hall8, Makuhari Messe_8

[P-CG24] New Developments of Planetary Sciences with ALMA

convener:Takayuki Muto(Division of Liberal Arts, Kogakuin University), Munetake Momose(The College of Science, Ibaraki University), Hideo Sagawa(Faculty of Science, Kyoto Sangyo University), Masumi Shimojo(National Astronomical Observatory of Japan)

[PCG24-P01] Nitrogen isotopic fractionation on Titan atmosphere: An analysis of ALMA archive data

*Hideo Sagawa[1], Takahiro Iino[2], Takashi Tsukagoshi[3] (1.Kyoto Sangyo University, 2.Tokyo University of Agriculture and Technology, 3.National Astronomical Observatory of Japan)

[PCG24-P02] Investigating the gas-to-dust ratio in the protoplanetary disk of HD 142527

*Soon Kang-Lou[1], Munetake Momose[1], Takayuki Muto[2], Takashi Tsukagoshi[3], Akimasa Kataoka[3], Tomoyuki Hanawa[4], Misato Fukagawa[3], Kazuya Saigo[3], Hiroshi Shibai[5] (1.Ibaraki University, 2.Kogakuin University, 3.National Astronomical Observatory of Japan, 4.Chiba University, 5.Osaka University)

[PCG24-P03] Super-resolution Imaging of the Protoplanetary Disk HD 142527 Using Sparse Modeling

*Masayuki Yamaguchi[1,2], Kazunori Akiyama[3,2], Akimasa Kataoka[2,6], Takashi Tsukagoshi[2], Takayuki Muto[4], Shiro Ikeda[5], Misato Fukagawa[2], Mareki Honma[2,6], Ryohei Kawabe[2,1,6] (1.The University of Tokyo, 2.National Astronomical Observatory of Japan, 3.Massachusetts Institute of Technology, Haystack Observatory, 4.Kogakuin University, 5.The Institute of Statistical Mathematics, 6. Graduate University for Advanced Studies)

[PCG24-P04] Detail Structures of Dust Disk around T-Tauri star RY Tau in ALMA High-Spatial Resolution Imaging

*Mihoko Konishi[1,2], Jun Hashimoto[1,2], Hauyu Liu[3], Ruobing Dong[4], Takayuki Muto[5] (1.Astrobiology Center, National Institute of Natural Science, 2.National Astronomical Observatory of Japan, 3.Institute of Astronomy and Astrophysics, Academia Sinica, 4.University of Victoria, 5.Kogakuin University)

[PCG24-P05] Possible inclined inner protoplanetary disk

*Jun Hashimoto[1], Mihoko Konishi[1], Taichi Uyama[2], Christian Ginski[3], Matthias Samland[4] (1.AstroBiology Center, National Institutes of Natural Sciences, 2.University of Tokyo, 3.University of Amsterdam, 4.Max Planck Institute for Astronomy)

[PCG24-P06] Search for the Inner Disk Structures in "Transitional" Disks

*Takayuki Muto[1], Jun Hashimoto[2], Takashi Tsukagoshi[3], Mihoko Konishi[3], Tomoyuki Kudo[3] (1.Division of Liberal Arts, Kogakuin University, 2.Astrobiology Center, 3.NAOJ)

[E] Oral | A (Atmospheric and Hydrospheric Sciences)：A-AS Atmospheric Sciences, Meteorology & Atmospheric Environment

9:00 AM - 10:30 AM JST | 12:00 AM - 1:30 AM UTC | 104 1F

[A-AS01] High performance computing for next generation weather, climate, and environmental sc iences

convener:Hiromu Seko(Meteorological Research Institute), Takemasa Miyoshi(RIKEN), Chihiro Kodama(Japan Agency for Marine-Earth Science and Technology), Masayuki Takigawa(Japan Agency for Marine-Earth Science and Technology), Chairperson:Hiromu Seko(Meteorological Research Institute), Chihiro Kodama(Japan Agency for Marine-Earth Science and Technology)

9:00 AM - 9:15 AM JST | 12:00 AM - 12:15 AM UTC

[AAS01-01] Data Assimilation Studies using Big Observation Data in the Projects of Post K and BDA

*Hiromu Seko[1], Masaru Kunii[2], Yohei Sawada[1], Kozo Okamoto[1], Sho Yokota[1], Kosuke Ito[3], Kazuki Shimoji[2] (1.Meteorological Research Institute, 2.Japan Meteorological Agency, 3.University of the Ryukyus)

9:15 AM - 9:30 AM JST | 12:15 AM - 12:30 AM UTC

[AAS01-02] **High-resolution Numerical Weather Simulation with a Large Domain for Extreme Heavy Rainfall Events**

*Tsutao OIZUMI[1,2], Kazuo Saito[4,3], le duc[1], Junshi Ito[3] (1.Japan Agency for Marine-Earth Science and Technology, 2.Meteorological Research Institute, 3.The Atmosphere and Ocean Research Institute, 4.Japan Meteorological Business Support Center)

9:30 AM - 9:45 AM JST | 12:30 AM - 12:45 AM UTC

[AAS01-03] A Numerical Case Study on a Tornado that Formed in a Quasi Linear Convective System

★Invited Papers

*Eigo Tochimoto[1], Hiroshi Niino[1] (1.Atmosphere and Ocean Research Institute, The University of Tokyo)

9:45 AM - 10:00 AM JST | 12:45 AM - 1:00 AM UTC

[AAS01-04] Improving the observation operator for Phased Array Weather Radar in the SCALE-LETKF system

*Arata Amemiya[1], Takumi Honda[1], Takemasa Miyoshi[1] (1.RIKEN Center for Computational Science)

10:00 AM - 10:15 AM JST | 1:00 AM - 1:15 AM UTC

[AAS01-05] Data assimilation and forecast experiments for the record-breaking rainfall event in Japan in July 2018 with NICAM-LETKF at 112-km and 28-km resolution

*Koji Terasaki[1], Takemasa Miyoshi[1] (1.RIKEN Center for Computational Science)

10:15 AM - 10:30 AM JST | 1:15 AM - 1:30 AM UTC

[AAS01-06] Model Parameter Estimation with Data Assimilation Using NICAM-LETKF

★Invited Papers

*Shunji Kotsuki[1], Yousuke Sato[2], Koji Terasaki[1], Hasashi Yashiro[1], Hirofumi Tomita[1], Masaki Satoh[3], Takemasa Miyoshi[1] (1.RIKEN Center for Computational Science, 2.Graduate School of Engineering, Nagoya University, 3.Atmosphere and Ocean Research Institute, the University of Tokyo)

[E] Oral | A (Atmospheric and Hydrospheric Sciences)：A-AS Atmospheric Sciences, Meteorology & Atmospheric Environment

10:45 AM - 12:15 PM JST | 1:45 AM - 3:15 AM UTC | 104 1F

[A-AS01] High performance computing for next generation weather, climate, and environmental sc iences

convener:Hiromu Seko(Meteorological Research Institute), Takemasa Miyoshi(RIKEN), Chihiro Kodama(Japan Agency for Marine-Earth Science and Technology), Masayuki Takigawa(Japan Agency for Marine-Earth Science and Technology), Chairperson:Masayuki Takigawa(Japan Agency for Marine-Earth Science and Technology), Takemasa Miyoshi(RIKEN Advanced Institute for Computational Science)

10:45 AM - 11:00 AM JST | 1:45 AM - 2:00 AM UTC

[AAS01-07] 3D debris flow simulations by using smoothed particle hydrodynamics (SPH) method

*Shoji Ueta[1], Natsuki Hosono[2], Yosuke Alexandre Yamashiki[1] (1.Kyoto University, 2.JAMSTEC)

11:00 AM - 11:15 AM JST | 2:00 AM - 2:15 AM UTC

[AAS01-08] **Regional atmospheric data assimilation coupled with an ocean mixed layer model: a case of typhoon Soudelor (2015)**

*Kohei Takatama[1], Takumi Honda[1], Takemasa Miyoshi[1] (1.RIKEN)

11:15 AM - 11:30 AM JST | 2:15 AM - 2:30 AM UTC

[AAS01-09] Effective Radiative Forcing and Climate Response to Short-Lived Climate Pollutants Under Different Scenarios

Hua Zhang[1], *Bing Xie[1], Zhili Wang[1] (1.China Meteorological Administration)

11:30 AM - 11:45 AM JST | 2:30 AM - 2:45 AM UTC

[AAS01-10] **The NICAM–SPRINTARS simulation of the long-range transport of black carbon using the K computer**

★Invited Papers

*Yousuke Yamashita[1], Masayuki Takigawa[1], Daisuke Goto[2], Hisashi Yashiro[3], Masaki Satoh[4,1], Yugo Kanaya[1], Fumikazu Taketani[1], Takuma Miyakawa[1] (1.Japan Agency for Marine-Earth Science and Technology, 2.National Institute for Environmental Studies, 3.RIKEN Advanced Institute for Computational Science (AICS), 4.Atmosphere and Ocean Research Institute, The University of Tokyo)

11:45 AM - 12:00 PM JST | 2:45 AM - 3:00 AM UTC

[AAS01-11] High-resolution, ensemble simulations of intense tropical cyclones and their stochasticity during the El Niños of 1997 and 2015

*Yohei Yamada[1], Chihiro Kodama[1], Masaki Satoh[1,2], Masuo Nakano[1], Tomoe Nasuno[1], Masato Sugi[3] (1.Japan Agency for Marine-Earth Science and Technology, 2.Atmosphere and Ocean Research Institute, The university of Tokyo, 3.Meteorological Research Institute, Japan Meteorological Agency)

12:00 PM - 12:15 PM JST | 3:00 AM - 3:15 AM UTC

[AAS01-12] **NICAM results of the project DYAMOND for global storm-resolving model intercomparison**

★Invited Papers

*Masaki Satoh[1], Ryosuke Shibuya[2], Chihiro Kodama[2] (1.Atmosphere and Ocean Research Institute, The University of Tokyo, 2.JAMSTEC)

[E] Poster | A (Atmospheric and Hydrospheric Sciences)：A-AS Atmospheric Sciences, Meteorology & Atmospheric Environment

3:30 PM - 5:00 PM JST | 6:30 AM - 8:00 AM UTC | Poster Hall International Exhibition Hall8, Makuhari Messe_5

[A-AS01] High performance computing for next generation weather, climate, and environmental sc iences

convener:Hiromu Seko(Meteorological Research Institute), Takemasa Miyoshi(RIKEN), Chihiro Kodama(Japan Agency for Marine-Earth Science and Technology), Masayuki Takigawa(Japan Agency for Marine-Earth Science and Technology)

[AAS01-P01] **Categorized correction forecast for accumulative precipitation of heavy rainfall processes based on optimal probability (OPPF) in medium-extended-range forecast time**

*Ruoyun Niu[1] (1.National Meteorological Center)

[AAS01-P02] **Characteristics of temporal and spatial distribution of regional rainstorm processes to the east of 95°E in China during 1981-2015**

*Ruoyun Niu[1], Couhua Liu[1] (1.National Meteorological Center)

[AAS01-P03] Near-real-time SCALE-LETKF forecasts of the record breaking rainfall in Japan in July 2018

*Takumi Honda[1], Guo-Yuan Lien[2,1], Takemasa Miyoshi[1] (1.RIKEN Center for Computational Science, 2.Central Weather Bureau)

[AAS01-P04] An objective Frontal Analysis Techniques and Application in Model Verification

*couhua liu[1] (1.National Meteorology Centre of China Meteorological Administration)

[AAS01-P05] Assimilating every 30-second phased array weather radar data in a torrential rainfall event on July 6, 2018 around Kobe city

*Yasumitsu Maejima[1], Shigenori Otsuka[1], Takemasa Miyoshi[1,2] (1.RIKEN Center for Computational Science, 2.University of Maryland, College Park)

[AAS01-P06] The impact of range sidelobes from phased array weather radar observations to short-range convective forecasts

*James David Taylor[1], Guo-Yuan Lien[1], Shinsuke Satoh[2], Takemasa Miyoshi[1] (1.RIKEN Research center for computational science, 2.NICT National Institute of Information and Communications Technology)

[AAS01-P07] Development of Hydro-debris 2D model for larger area

*Yosuke Alexandre Yamashiki[1], Tsutao OIZUMI[2], Bruno Ribeiro[1], Ryusuke Kuroki[1] (1.Earth & Planetary Water Resources Assessment Laboratory Graduate School of Advanced Integrated Studies in Human Survivability Kyoto University, 2.Japan Association of Marine-Earth Science and Tecnology)

[AAS01-P08] **Research on the application of an improved terrain-following vertical coordinates on GRAPES model**

*chao li[1] (1.NWPC.CMA)

[AAS01-P09] Development of a parallel spherical harmonic transform library: design and performance

*Fuyuki SAITO[1] (1.Japan Agency for Marine-Earth Science and Technology)

[AAS01-P10] Global data assimilation of multi-species satellite measurements for atmospheric chemistry analysis

*Takashi Sekiya[1], Kazuyuki Miyazaki[2,1], Koji Ogochi[1], Kengo Sudo[3,1], Masayuki Takigawa[1] (1.Japan Agency for Marine-Earth Science and Technology, 2.Jet Propulsion Laboratory/California Institute for Technology, 3.Graduate School of Environmental Studies, Nagoya University)

[AAS01-P11] The sensitivity to WRF shortwave radiation parameterizations in prediction of global horizontal irradiance for investigating interactions of atmosphere with croplands

*Ankur Srivastava[1], Sarita Kumari[1], Rajkumar Dhakar[2] (1.Indian Institute of Technology Delhi, 2.Indian Agriculture Research Institute)

[AAS01-P12] The development of an atmospheric aerosol/chemistry–climate model, BCC_AGCM_CUACE2.0, and simulated effective radiative forcing of nitrate aerosols

*QI AN[1,2,4], Hua Zhang[2], Zhili Wang[2], Yi Liu[1,4], Bing Xie[3], Qianxia Liu[3], Zaizhi Wang[3], Sunling Gong[2] (1.LAGEO, IAP, CAS, 2.LaSW, CAMS, 3.NCC,CMA, 4.UCAS)

[AAS01-P13] **Impacts of different types and intensities of El Niño events on winter aerosols over China**

*Xiaochao Yu[1,2], Zhili Wang[2,1], Hua Zhang[2], Shuyun Zhao[3] (1.Collaborative Innovation Center on Forecast and Evaluation of Meteorological Disasters, Nanjing University of Information Science and Technology, Nanjing, 210044, China, 2.State Key Laboratory of Severe Weather and Key Laboratory of Atmospheric Chemistry of CMA, Chinese Academy of Meteorological Sciences, Beijing, 100081, China., 3.National Climate Center, China Meteorological Administration, Beijing, 100081, China)

[AAS01-P14] High Cloud Annual Variation and Its Responses to Global Warming in the NICAM AMIP Experiment

*Ying-Wen Chen[1], Masaki Satoh[1,2], Chihiro Kodama[2], Akira Noda[2], Yohei Yamada[2] (1.Atmospheric and Ocean Research Institute, The University of Tokyo , 2.Japan Agency for Marine-Earth Science and Technology)

[AAS01-P15] Improvements in Simulating the Relationship between ENSO and East Asian Summer Rainfall in the CMIP5 Models

*Yuanhai FU[1], Riyu Lu[1] (1.IAP, CAS)

[E] Poster | A (Atmospheric and Hydrospheric Sciences)：A-AS Atmospheric Sciences, Meteorology & Atmospheric Environment

5:15 PM - 6:30 PM JST | 8:15 AM - 9:30 AM UTC | Poster Hall International Exhibition Hall8, Makuhari Messe_9

[A-AS01] High performance computing for next generation weather, climate, and environmental sc iences

convener:Hiromu Seko(Meteorological Research Institute), Takemasa Miyoshi(RIKEN), Chihiro Kodama(Japan Agency for Marine-Earth Science and Technology), Masayuki Takigawa(Japan Agency for Marine-Earth Science and Technology)

[AAS01-P01] **Categorized correction forecast for accumulative precipitation of heavy rainfall processes based on optimal probability (OPPF) in medium-extended-range forecast time**

*Ruoyun Niu[1] (1.National Meteorological Center)

[AAS01-P02] **Characteristics of temporal and spatial distribution of regional rainstorm processes to the east of 95°E in China during 1981-2015**

*Ruoyun Niu[1], Couhua Liu[1] (1.National Meteorological Center)

[AAS01-P03] Near-real-time SCALE-LETKF forecasts of the record breaking rainfall in Japan in July 2018

*Takumi Honda[1], Guo-Yuan Lien[2,1], Takemasa Miyoshi[1] (1.RIKEN Center for Computational Science, 2.Central Weather Bureau)

[AAS01-P04] An objective Frontal Analysis Techniques and Application in Model Verification

*couhua liu[1] (1.National Meteorology Centre of China Meteorological Administration)

[AAS01-P05] Assimilating every 30-second phased array weather radar data in a torrential rainfall event on July 6, 2018 around Kobe city

*Yasumitsu Maejima[1], Shigenori Otsuka[1], Takemasa Miyoshi[1,2] (1.RIKEN Center for Computational Science, 2.University of Maryland, College Park)

[AAS01-P06] The impact of range sidelobes from phased array weather radar observations to short-range convective forecasts

*James David Taylor[1], Guo-Yuan Lien[1], Shinsuke Satoh[2], Takemasa Miyoshi[1] (1.RIKEN Research center for computational science, 2.NICT National Institute of Information and Communications Technology)

[AAS01-P07] Development of Hydro-debris 2D model for larger area

*Yosuke Alexandre Yamashiki[1], Tsutao OIZUMI[2], Bruno Ribeiro[1], Ryusuke Kuroki[1] (1.Earth & Planetary Water Resources Assessment Laboratory Graduate School of Advanced Integrated Studies in Human Survivability Kyoto University, 2.Japan Association of Marine-Earth Science and Tecnology)

[AAS01-P08] **Research on the application of an improved terrain-following vertical coordinates on GRAPES model**

*chao li[1] (1.NWPC.CMA)

[AAS01-P09] Development of a parallel spherical harmonic transform library: design and performance

*Fuyuki SAITO[1] (1.Japan Agency for Marine-Earth Science and Technology)

[AAS01-P10] Global data assimilation of multi-species satellite measurements for atmospheric chemistry analysis

*Takashi Sekiya[1], Kazuyuki Miyazaki[2,1], Koji Ogochi[1], Kengo Sudo[3,1], Masayuki Takigawa[1] (1.Japan Agency for Marine-Earth Science and Technology, 2.Jet Propulsion Laboratory/California Institute for Technology, 3.Graduate School of Environmental Studies, Nagoya University)

[AAS01-P11] The sensitivity to WRF shortwave radiation parameterizations in prediction of global horizontal irradiance for investigating interactions of atmosphere with croplands

*Ankur Srivastava[1], Sarita Kumari[1], Rajkumar Dhakar[2] (1.Indian Institute of Technology Delhi, 2.Indian Agriculture Research Institute)

[AAS01-P12] The development of an atmospheric aerosol/chemistry–climate model, BCC_AGCM_CUACE2.0, and simulated effective radiative forcing of nitrate aerosols

*QI AN[1,2,4], Hua Zhang[2], Zhili Wang[2], Yi Liu[1,4], Bing Xie[3], Qianxia Liu[3], Zaizhi Wang[3], Sunling Gong[2] (1.LAGEO, IAP, CAS, 2.LaSW, CAMS, 3.NCC,CMA, 4.UCAS)

[AAS01-P13] **Impacts of different types and intensities of El Niño events on winter aerosols over China**

*Xiaochao Yu[1,2], Zhili Wang[2,1], Hua Zhang[2], Shuyun Zhao[3] (1.Collaborative Innovation Center on Forecast and Evaluation of Meteorological Disasters, Nanjing University of Information Science and Technology, Nanjing, 210044, China, 2.State Key Laboratory of Severe Weather and Key Laboratory of Atmospheric Chemistry of CMA, Chinese Academy of Meteorological Sciences, Beijing, 100081, China., 3.National Climate Center, China Meteorological Administration, Beijing, 100081, China)

[AAS01-P14] High Cloud Annual Variation and Its Responses to Global Warming in the NICAM AMIP Experiment

*Ying-Wen Chen[1], Masaki Satoh[1,2], Chihiro Kodama[2], Akira Noda[2], Yohei Yamada[2] (1.Atmospheric and Ocean Research Institute, The University of Tokyo , 2.Japan Agency for Marine-Earth Science and Technology)

[AAS01-P15] Improvements in Simulating the Relationship between ENSO and East Asian Summer Rainfall in the CMIP5 Models

*Yuanhai FU[1], Riyu Lu[1] (1.IAP, CAS)

[J] Oral | A (Atmospheric and Hydrospheric Sciences)：A-AS Atmospheric Sciences, Meteorology & Atmospheric Environment

9:00 AM - 10:30 AM JST | 12:00 AM - 1:30 AM UTC | 102 1F

[A-AS04] Atmospheric Chemistry

convener:Tomoki Nakayama(Graduate School of Fisheries and Environmental Sciences, Nagasaki University), Yoko Iwamoto(Graduate School of Biosphere Science, Hiroshima University), Sakae Toyoda(Department of Chemical Science and Engineering, Tokyo Institute of Technology), Nawo Eguchi(Kyushu University), Chairperson:Fumiko Nakagawa(名古屋大学)

9:00 AM - 9:30 AM JST | 12:00 AM - 12:30 AM UTC

[AAS04-01] Reconstruction and fluctuation mechanism of past aerosols preserved in ice cores

★Invited Papers

*Iizuka Yoshinori[1], Ryu Uemura[2], Koji Fujita[3], Shohei Hattori[4], Osamu Seki[1], Naga Oshima[5], Hiroshi Ohno[6], Sumito Matoba[1] (1.Institite of Low Temperature Science, Hokkaido University, 2.Department of Chemistry, Biology, and Marine Science, Faculty of Science, University of the Ryukyus, 3.Graduate School of Environmental Studies, Nagoya University, 4.Department of Chemical Science and Engineering, School of Materials and Chemical Technology, Tokyo Institute of Technology,, 5.Meteorological Research Institute, 6.Kitami Institute of Technology)

9:30 AM - 9:45 AM JST | 12:30 AM - 12:45 AM UTC

[AAS04-02] The 60 years history of atmospheric formation pathways responsible for sulfate based on triple oxygen isotopic composition of sulfate preserved in SE-Dome ice core

*Shohei Hattori[1], Iizuka Yoshinori[2], Koji Fujita[3], Ryu Uemura[4], Sakiko Ishino[1], Naga Oshima[5], Nozomi Suzuki[1], Sumito Matoba[2], Asuka Tsuruta[1], Joel Savarino[6], Naohiro Yoshida[1] (1.Department of Chemical Science and Engineering, School of Materials and Chemical Technology, Tokyo Institute of Technology, 2.Institute of Low Temperature Science, Hokkaido University, 3.Graduate School of Environmental Studies, Nagoya University, Nagoya, Japan., 4.Department of Chemistry, Biology, and Marine Science, Faculty of Science, University of the Ryukyus, 5.Meteorological Research Institute, 6.Institut des Geoscience de l'Environnement, Universite Grenoble Alpes/CNRS)

9:45 AM - 10:00 AM JST | 12:45 AM - 1:00 AM UTC

[AAS04-03] Estimation of high sulfate aerosol sources in 2012 spring at Cape Hedo, Okinawa

*Syuichi Itahashi[1], Shiro Hatakeyama[2], Kojiro Shimada[3], Akinori Takami[4] (1.Central Research Institute of Electric Power Industry, 2.Center for Environmental Science in SaitamaCenter for Environmental Science in Saitama, 3.School of Creative Science and Engineering, Waseda University, 4.National Institute for Environmental Studies)

10:00 AM - 10:15 AM JST | 1:00 AM - 1:15 AM UTC

[AAS04-04] Isotopic constrains on sources and formation pathways of atmospheric nitrate in Mt. Everest

*Kun Wang[1,2,4], Shohei Hattori[2], Shichang Kang[1,3,4], Mang Lin[2], Naohiro Yoshida[2,5] (1.Northwest Institute of Eco-Environment and Resources, Chinese Academy of Sciences , 2.Department of Chemical Science and Engineering, School of Materials and Chemical Technology, Tokyo Institute of Technology, 3.CAS Center for Excellence in Tibetan Plateau Earth Sciences, 4.University of Chinese Academy of Sciences, 5. Earth-Life Science Institute, Tokyo Institute of Technology)

10:15 AM - 10:30 AM JST | 1:15 AM - 1:30 AM UTC

[AAS04-05] Development of a large volume sampling system for measuring stable isotope analysis of carbonyl sulfide and field observation

*Kazuki Kamezaki[1], Shohei Hattori[1], Naohiro Yoshida[1,2] (1.Department of Chemical Science and Engineering, School of Materials and Chemical Technology, Tokyo Institute of Technology, 4259 Nagatsuta-cho, Midori-ku, Yokohama, Kanagawa 226-8502, Japan, 2.Earth-Life Science Institute, Tokyo Institute of Technology, 2-12-1-IE-1 Ookayama, Meguro-ku, Tokyo 152-8550, Japan)

[J] Oral | A (Atmospheric and Hydrospheric Sciences)：A-AS Atmospheric Sciences, Meteorology & Atmospheric Environment

1:45 PM - 3:15 PM JST | 4:45 AM - 6:15 AM UTC | 102 1F

[A-AS04] Atmospheric Chemistry

convener:Tomoki Nakayama(Graduate School of Fisheries and Environmental Sciences, Nagasaki University), Yoko Iwamoto(Graduate School of Biosphere Science, Hiroshima University), Sakae Toyoda(Department of Chemical Science and Engineering, Tokyo Institute of Technology), Nawo Eguchi(Kyushu University), Chairperson:Takashi Maki(気象研究所)

1:45 PM - 2:00 PM JST | 4:45 AM - 5:00 AM UTC

[AAS04-06] Observations of aerosol optical properties by sky radiometers at SKYNET Southeast and South Asian sites

*Al Mashroor Fatmi[1], Hitoshi Irie[1], Hossain Mohammed Syedul Hoque[1], Alessandro Damiani[1], Pradeep Khatri[2], Tamio Takamura[1], Thanawat Jurupongsaku[3], Govindan Pandithurai[4] (1.Center for Environmental Remote Sensing Chiba University , 2.Tohoku University, 3.Chulalongkorn University, 4.Indian Institute of Tropical Metereology)

2:00 PM - 2:15 PM JST | 5:00 AM - 5:15 AM UTC

[AAS04-07] Analysis of factors causing variations in the absorption Ångström exponent of aerosols in Japan using skyradiometers

*Kodai Yamaguchi[1], Hitoshi Irie[1], Pradeep Khatri[2], Toshihiko Takemura[3], Hirokazu Yamamoto[4] (1.Chiba University, 2.Tohoku University, 3.Kyushu University, 4.National Institute of Advanced Industrial Science and Technology)

2:15 PM - 2:30 PM JST | 5:15 AM - 5:30 AM UTC

[AAS04-08] Sources of atmospheric black carbon and related carbonaceous components at Rishiri Island, Japan

*Chunmao Zhu[1], Yugo Kanaya[1], Hisayuki Yoshikawa[2], Tomohisa Irino[2], Osamu Seki[2], Yasunori Tohjima[3] (1.Japan Agency for Marine-Earth Science and Technology, 2.Hokkaido University, 3.National Institute for Environmental Studies)

2:30 PM - 2:45 PM JST | 5:30 AM - 5:45 AM UTC

[AAS04-09] Black Carbon and Inorganic Aerosols in Snowpack over the Arctic

*Tatsuhiro Mori[1], Kumiko Goto-Azuma[2,3], Yutaka Kondo[2], Yoshimi Ogawa-Tsukagawa[2], Kazuhiko Miura[1], Motohiro Hirabayashi[2], Naga Oshima[4], Makoto Koike[5], Kaarle Kupiainen[6], Nobuhiro Moteki[5], Sho Ohata[7], Sinha Puna Ram[8], Konosuke Sugiura[9], Teruo Aoki[10], Martin Schneebeli[11], Konrad Steffen[11], Atsushi Sato[12], Akane Tsushima[13], Vladimir Makarov[14], Satoshi Omiya[15,16], Atsuko Sugimoto[17], Shinya Takano[17] (1.Tokyo University of Science, 2.National Institute of Polar Research, 3.The Graduate University for Advanced Studies, 4.Meteorological Research Institute, 5.Depertment of Earth and Planetary Science, Graduate School of Science, The University of Tokyo, 6.Environmental Protection Department Ministry of the Environment, 7.Institute for Space–Earth Environmental Research (ISEE), Nagoya University, 8.Department of Space Indian Space Research Organization, 9.University of Toyama, 10.Okayama University, 11.WSL Institute for Snow and Avalanche Research, 12.former Snow and Ice Research Center, 13.Reserach Institute for Humanity and Nature, 14.Melnikov's Permafrost Institute, 15.Institute of Low Temperature Science, Hokkaido University, 16.Civil Engineering Research Institute for Cold Region, 17.Graduate School of Environmental Science, Hokkaido University)

2:45 PM - 3:00 PM JST | 5:45 AM - 6:00 AM UTC

[AAS04-10] The single-particle extinction and scattering method for online characterization of submicron particles: Principles and applications to aerosol research

*Nobuhiro Moteki[1] (1.The Univerisity of Tokyo)

3:00 PM - 3:15 PM JST | 6:00 AM - 6:15 AM UTC

[AAS04-11] High spatial resolution vehicular emissions inventory for China using VEIN model

*Sergio Ibarra Espinosa[1], Xuelei Zhang[1], Aijun Xiu[1], Edmilson Dias de Freitas[2] (1.Research Group of Regional Atmospheric Environment, Northeast Institute of Geography and Agroecology, Chinese Academy of Sciences, P. R. China, 2.Department of Atmospheric Sciences, University of São Paulo, Brazil.)

[J] Oral | A (Atmospheric and Hydrospheric Sciences)：A-AS Atmospheric Sciences, Meteorology & Atmospheric Environment

3:30 PM - 5:00 PM JST | 6:30 AM - 8:00 AM UTC | 102 1F

[A-AS04] Atmospheric Chemistry

convener:Tomoki Nakayama(Graduate School of Fisheries and Environmental Sciences, Nagasaki University), Yoko Iwamoto(Graduate School of Biosphere Science, Hiroshima University), Sakae Toyoda(Department of Chemical Science and Engineering, Tokyo Institute of Technology), Nawo Eguchi(Kyushu University), Chairperson:Kentaro Ishijima(気象研究所)

3:30 PM - 4:00 PM JST | 6:30 AM - 7:00 AM UTC

[AAS04-12] Effect of land use change on GHG fluxes of tropical peat forests in Borneo island

★Invited Papers

*Ryuichi Hirata[1], Habura Borjigin[1], Tomohiro Shiraishi[1], Takashi Hirano[2], Lulie Melling[3] (1.National Institute for Environmental Studies, 2.Hokkaido University, 3.Sarawak Tropical Peat Research Institute)

4:00 PM - 4:30 PM JST | 7:00 AM - 7:30 AM UTC

[AAS04-13] Remote sensing of carbon assimilation function of terrestrial ecosystem by Earth-observation satellite

★Invited Papers

*Hibiki M Noda[1], Yukio Yoshida[1], Haruki Oshio[1], Tomoki Kiyono[1], Tatsuya Miyauchi[1], Tsuneo Matsunaga[1] (1.NIES National Institute of Environmental Studies)

4:30 PM - 4:45 PM JST | 7:30 AM - 7:45 AM UTC

[AAS04-14] Analysis of the carbon dioxide in the upper troposphere and lower stratosphere by the data from GOSAT TANSO-FTS TIR

*Nawo Eguchi[1], Akihiro Honda[1], Naoko Saitoh[2], Yosuke Niwa[3] (1.Kyushu University, 2.Chiba University, 3.National Institute for Environmental Studies)

4:45 PM - 5:00 PM JST | 7:45 AM - 8:00 AM UTC

[AAS04-15] Seasonal and interannual variations of the Atmospheric Potential Oxygen over the Western North Pacific observed by using a cargo aircraft C-130H

*Shigeyuki Ishidoya[1], Kazuhiro Tsuboi[2], Yosuke Niwa[3], Shohei Murayama[1], Hidekazu Matsueda[2], Yousuke Sawa[2], Nobuyuki Aoki[1], Kentaro Ishijima[2], Kentaro Kozumi[4], Genta Umezawa[4], Kazuya Yukita[4], Shigeharu Nishida[4], Megumi Yamamoto[4] (1.National Institute of Advanced Industrial Science and Technology (AIST), 2.Meteorological Research Institute, 3.National Institute for Environmental Studies, 4.Japan Meteorological Agency)

[J] Oral | A (Atmospheric and Hydrospheric Sciences)：A-AS Atmospheric Sciences, Meteorology & Atmospheric Environment

9:00 AM - 10:30 AM JST | 12:00 AM - 1:30 AM UTC | 201B 2F

[A-AS05] Stratosphere-troposphere Processes And their Role in Climate

convener:Yoshio Kawatani(Japan Agency for Marine-Earth Science and Technology), Shingo Watanabe(Japan Agency for Marine-Earth Science and Technology), Takashi Sekiya(Japan Agency for Marine-Earth Science and Technology), Kaoru Sato(Department of Earth and Planetary Science, Graduate School of Science, The University of Tokyo), Chairperson:Watanabe Shingo(海洋研究開発機構)

9:10 AM - 9:40 AM JST | 12:10 AM - 12:40 AM UTC

[AAS05-01] Turbulent kinetic energy dissipation rates depending on the polar vortex and on synoptic-scale disturbances in the UTLS region in the Antarctic

★Invited Papers

*Masashi Kohma[1], Kaoru Sato[1], Koji Nishimura[2], Masaki Tsutsumi[2] (1.Department of Earth and Planet Science, Graduate School of Science, The University of Tokyo, 2.National Institute of Polar Research and The Graduate University for Advanced Studies (SOKENDAI))

9:40 AM - 9:55 AM JST | 12:40 AM - 12:55 AM UTC

[AAS05-02] Momentum budget of semiannual oscillation around the tropical stratopause

*Yoshihiro Tomikawa[1,2], V. Lynn Harvey[3], John A. Knox[4], Masatomo Fujiwara[5] (1.National Institute of Polar Research, 2.SOKENDAI, 3.University of Colorado Boulder, 4.University of Georgia, 5.Hokkaido University)

9:55 AM - 10:10 AM JST | 12:55 AM - 1:10 AM UTC

[AAS05-03] A study on sources of gravity waves that reach the summer stratosphere and mesosphere based on high-resolution radiosonde data

*Haruka Okui[1], Masashi Kohma[1], Kaoru Sato[1] (1.Department of Earth and Planetary Science, Graduate School of Science, The University of Tokyo)

10:10 AM - 10:25 AM JST | 1:10 AM - 1:25 AM UTC

[AAS05-04] Stratospheric initial conditions provide seasonal predictability of the North Atlantic and Arctic Oscillations

*Yu Nie[1], Adam Scaife[2,3], Hong-Li Ren[1,4], Ruth Comer[2], Martin Andrews[2] (1.Laboratory for Climate Studies, National Climate Center, China Meteorological Administration, Beijing, China, 2.Met Office Hadley Centre, Exeter, UK, 3.College of Engineering, Mathematics and Physical Sciences, University of Exeter, Exeter, UK, 4.Department of Atmospheric Science, School of Environmental Studies, China University of Geoscience, Wuhan, China)

[J] Oral | A (Atmospheric and Hydrospheric Sciences)：A-AS Atmospheric Sciences, Meteorology & Atmospheric Environment

10:45 AM - 12:15 PM JST | 1:45 AM - 3:15 AM UTC | 201B 2F

[A-AS05] Stratosphere-troposphere Processes And their Role in Climate

convener:Yoshio Kawatani(Japan Agency for Marine-Earth Science and Technology), Shingo Watanabe(Japan Agency for Marine-Earth Science and Technology), Takashi Sekiya(Japan Agency for Marine-Earth Science and Technology), Kaoru Sato(Department of Earth and Planetary Science, Graduate School of Science, The University of Tokyo), Chairperson:Takashi Sekiya

10:45 AM - 11:15 AM JST | 1:45 AM - 2:15 AM UTC

[AAS05-05] Transport of trace gases into the extratropical upper troposphere/lower stratosphere

★Invited Papers

*Yoichi Inai[1], Ryo Fujita[2,1], Toshinobu Machida[3], Hidekazu Matsueda[4], Yousuke Sawa[4], Kazuhiro Tsuboi[4], Keiichi Katsumata[3,5], Shinji Morimoto[1], Shuji Aoki[1], Takakiyo Nakazawa[1] (1.Tohoku Univ., 2.Imperial College London, 3.NIES, 4.MRI, 5.Takachiho Chem. Industrial)

11:15 AM - 11:30 AM JST | 2:15 AM - 2:30 AM UTC

[AAS05-06] Possible impacts of stratospheric ozone on circulation changes in the tropical tropposphere following a stratospheric sudden warming event

*Makoto Deushi[1] (1.Department of Atmospheric Environment and Applied Meteorology, Meteorological Research Institute)

11:30 AM - 11:45 AM JST | 2:30 AM - 2:45 AM UTC

[AAS05-07] **Stratosphere-troposphere exchange of ozone and carbon monoxide over the northern Pacific Ocean in northern winter using two chemical reanalysis data sets**

*Haosen Xi[1], Masatomo Fujiwara[1], Kazuyuki Miyazaki[2] (1.Graduate School of Environmental Science, Hokkaido University, 2.NASA Jet Propulsion Laboratory, California Institute of Technology, USA)

11:45 AM - 12:00 PM JST | 2:45 AM - 3:00 AM UTC

[AAS05-08] **Inter-comparison of Upper Air Temperature in China between Satellite MSU and Radiosonde Datasts**

*Yanjun GUO[1], Cheng-zhi Zou[2], Panmao Zhai[3], Guofu Wang[1] (1.National Climate Center(NCC), China Meteorological Administration(CMA) , 2.Center for Satellite Applications and Research, NOAA/NESDIS, 3.Chinese Academy of Meteorolgical Sciences (CAMS), China Meteorological Administration (CMA))

12:00 PM - 12:15 PM JST | 3:00 AM - 3:15 AM UTC

[AAS05-09] Environmental Characterization of the Atmosphere Using WACCM-X

*Rose Tseng[1], Michelle Kanipe[1], Brian Urbancic[1], Robert Tournay[1], Omar Nava[1], Daniel Emmons[1], Robert Loper[1], Charlton Lewis[1] (1.Air Force Institute of Technology)

[J] Oral | A (Atmospheric and Hydrospheric Sciences)：A-AS Atmospheric Sciences, Meteorology & Atmospheric Environment

1:45 PM - 3:15 PM JST | 4:45 AM - 6:15 AM UTC | 201B 2F

[A-AS05] Stratosphere-troposphere Processes And their Role in Climate

convener:Yoshio Kawatani(Japan Agency for Marine-Earth Science and Technology), Shingo Watanabe(Japan Agency for Marine-Earth Science and Technology), Takashi Sekiya(Japan Agency for Marine-Earth Science and Technology), Kaoru Sato(Department of Earth and Planetary Science, Graduate School of Science, The University of Tokyo), Chairperson:Yoshio Kawatani

1:45 PM - 2:15 PM JST | 4:45 AM - 5:15 AM UTC

[AAS05-10] Diagnostics of a WN2-type major sudden stratospheric warming event in February 2018 using a new three-dimensional wave activity flux

★Invited Papers

*Yayoi Harada[1], Kaoru Sato[2], Takenari Kinoshita[3], Ryosuke Yasui[2], Toshihiko Hirooka[4], Hiroaki Naoe[1] (1.Meteorological Research Institute, 2.Department of Earth and Planetary Science, Graduate School of Science, The University of Tokyo, 3.Japan Agency for Marine-Earth Science and Technology, 4.Department of Earth and Planetary Sciences, Kyushu University)

2:15 PM - 2:45 PM JST | 5:15 AM - 5:45 AM UTC

[AAS05-11] Response of the Southern Hemisphere atmosphere to the QBO from winter to early summer

★Invited Papers

*Yousuke Yamashita[1], Hiroaki Naoe[2], Makoto Inoue[3], Masaaki Takahashi[4] (1.Japan Agency for Marine-Earth Science and Technology, 2.Meteorological Research Institute, 3.Akita Prefectural University, 4.National Institute for Environmental Studies)

2:45 PM - 3:00 PM JST | 5:45 AM - 6:00 AM UTC

[AAS05-12] Influence of QBO-like Oscillation on Tropical Convective Systems in a Three-Dimensional Minimal Model Framework of the Stratosphere-Troposphere Coupled System

*Shigeo Yoden[1], Hai Bui[2], Takahiro Banno[1] (1.Division of Earth and Planetary Sciences, Graduate School of Science, Kyoto University, 2.Geophysical Institute, University of Bergen)

3:00 PM - 3:15 PM JST | 6:00 AM - 6:15 AM UTC

[AAS05-13] Downward Propagation of Planetary Wave Packets from the Stratosphere to the Troposphere During Northern Hemisphere Winter

*Matsuyama Yuya[1], Toshihiko Hirooka[2] (1.Department of Earth and Planetary Sciences, Graduate School of Science, Kyushu University, 2.Department of Earth and Planetary Sciences, Faculty of Science, Kyushu University)

[J] Poster | A (Atmospheric and Hydrospheric Sciences)：A-AS Atmospheric Sciences, Meteorology & Atmospheric Environment

3:30 PM - 5:00 PM JST | 6:30 AM - 8:00 AM UTC | Poster Hall International Exhibition Hall8, Makuhari Messe_6

[A-AS05] Stratosphere-troposphere Processes And their Role in Climate

convener:Yoshio Kawatani(Japan Agency for Marine-Earth Science and Technology), Shingo Watanabe(Japan Agency for Marine-Earth Science and Technology), Takashi Sekiya(Japan Agency for Marine-Earth Science and Technology), Kaoru Sato(Department of Earth and Planetary Science, Graduate School of Science, The University of Tokyo)

[AAS05-P01] **An advanced impact of Arctic stratospheric ozone changes on spring precipitation in China**

*Fei Xie[1] (1.Beijing Normal University)

[AAS05-P02] Global Cooling System installed on the beach by means of Artificial Convection and Artificial Rain

*Murakami Hideyo[1] (1.Ii Ecology Development)

[AAS05-P03] Stratospheric front-like temperature structure and gravity wave activity during a stratospheric sudden warming event in 2016

*Yukari Sumi[1], Kaoru Sato[1] (1.University of Tokyo)

[AAS05-P04] The effects of a well-resolved stratosphere on the simulated boreal winter circulation in a climate model

*Yoshio Kawatani[1], Kevin Hamilton[2], Lesley J. Gray[3], Scott M. Osprey[3], Shingo Watanabe[1], Yousuke Yamashita[1] (1.Japan Agency for Marine-Earth Science and Technology, 2.International Pacific Research Center, University of Hawaii, 3.Atmospheric, Oceanic and Planetary Physics, Department of Physics, University of Oxford)

[AAS05-P05] On the relation between three-dimensional wave activity flux and pseudo momentum without using intrinsic phase velocities

★Invited Papers

*Takenari Kinoshita[1] (1.Japan Agency for Marine-Earth Science and Technology)

[AAS05-P06] Hindcasts of the 2016 Disruption of the Stratospheric Quasi-biennial Oscillation

*Shingo Watanabe[1], Kevin Hamilton[2], Scott Osprey[3], Yoshio Kawatani[1], Eriko Nishimoto (1.Japan Agency for Marine-Earth Science and Technology, 2.International Pacific Research Center, University of Hawaii at Manoa, 3.NCAS-Climate, University of Oxford)

[AAS05-P07] Selection bias of quasi-fixed-point observations in the ExUTLS and its impact on the seasonal record

*Yoichi Inai[1], Toshinobu Machida[2], Hidekazu Matsueda[3], Yousuke Sawa[3], Kazuhiro Tsuboi[3], Keiichi Katsumata[2,4], Shinji Morimoto[1], Shuji Aoki[1], Takakiyo Nakazawa[1], Ryo Fujita[5,1] (1.Tohoku Univ., 2.NIES, 3.MRI, 4.Takachiho Chem. Industrial, 5.Imperial College London)

[AAS05-P08] Varying Rossby Wave Trains from the Developing to Decaying Period of the Upper Atmospheric Heat Source over the Tibetan Plateau in Boreal Summer

*Chuandong Zhu[1,2], Rongcai Ren[1] (1.Institute of Atmospheric Physics, Chinese Academy of Sciences, 2.University of Chinese Academy of Sciences)

[AAS05-P09] **Equilibrium Climate Responses of the East Asian Summer Monsoon to Various Anthropogenic Aerosol Species**

*Qiuyan Wang[2,1], Zhili Wang[1,2], Hua Zhang[3,2] (1.State Key Laboratory of Severe Weather & Key Laboratory of Atmospheric Chemistry of CMA, Chinese Academy of Meteorological Sciences, Beijing, 2.Collaborative Innovation Center on Forecast and Evaluation of Meteorological Disasters, Nanjing University of Information Science and Technology, Nanjing, 3.Laboratory for Climate Studies, National Climate Center, China Meteorological Administration, Beijing)

[AAS05-P10] Analysis of specific energy in zonal currents focusing on the analogy between jet stream and open channel flow

*Yoshikazu Kitano[1], Tomohito J. Yamada[2] (1.Central Research Institute of Electric Power Industry, 2.Faculty of Engineering, Hokkaido University)

[AAS05-P11] Analysis of the ozone reduction event over the southern tip of South America in November 2009

*Hideharu Akiyoshi[1], Masanao Kadowaki[2], Haruna Nakamura[3], Takafumi Sugita[1], Toshihiko Hirooka[4], Yayoi Harada[5], Akira Mizuno[6] (1.National Institute for Environmental Studies, 2.Japan Atomic Energy Agency, 3.Fujitsu FIP Corporation, 4.Department of Earth and Planetary Sciences, Kyushu University, 5.Meteorological Research Institute, 6.Institute for Space-Earth Environmental Research, Nagoya University)

[AAS05-P12] **Analysis of relatively low ozone in Arctic spring during the QBO-westerly and solar-minimum years**

*Yousuke Yamashita[1,2], Hideharu Akiyoshi[2], Masaaki Takahashi[2] (1.Japan Agency for Marine-Earth Science and Technology, 2.National Institute for Environmental Studies)

[AAS05-P13] Evaluation of ozone in the upper troposphere and lower stratosphere derived from multi-species satellite data assimilation

*Takashi Sekiya[1], Kazuyuki Miyazaki[2,1], Koji Ogochi[1], Kengo Sudo[3,1], Masayuki Takigawa[1] (1.Japan Agency for Marine-Earth Science and Technology, 2.Jet Propulsion Laboratory/California Institute for Technology, 3.Graduate School of Environmental Studies, Nagoya University)

[AAS05-P14] Characteristics of Initial Perturbation of JMA GEPS during Sudden Stratospheric Warmings

★Invited Papers

*Shunsuke Noguchi[1,2] (1.Japan Agency for Marine-Earth Science and Technology, 2.Meteorological Research institute, Japan Meteorological Agency)

[J] Poster | A (Atmospheric and Hydrospheric Sciences)：A-AS Atmospheric Sciences, Meteorology & Atmospheric Environment

5:15 PM - 6:30 PM JST | 8:15 AM - 9:30 AM UTC | Poster Hall International Exhibition Hall8, Makuhari Messe_10

[A-AS05] Stratosphere-troposphere Processes And their Role in Climate

convener:Yoshio Kawatani(Japan Agency for Marine-Earth Science and Technology), Shingo Watanabe(Japan Agency for Marine-Earth Science and Technology), Takashi Sekiya(Japan Agency for Marine-Earth Science and Technology), Kaoru Sato(Department of Earth and Planetary Science, Graduate School of Science, The University of Tokyo)

[AAS05-P01] **An advanced impact of Arctic stratospheric ozone changes on spring precipitation in China**

*Fei Xie[1] (1.Beijing Normal University)

[AAS05-P02] Global Cooling System installed on the beach by means of Artificial Convection and Artificial Rain

*Murakami Hideyo[1] (1.Ii Ecology Development)

[AAS05-P03] Stratospheric front-like temperature structure and gravity wave activity during a stratospheric sudden warming event in 2016

*Yukari Sumi[1], Kaoru Sato[1] (1.University of Tokyo)

[AAS05-P04] The effects of a well-resolved stratosphere on the simulated boreal winter circulation in a climate model

*Yoshio Kawatani[1], Kevin Hamilton[2], Lesley J. Gray[3], Scott M. Osprey[3], Shingo Watanabe[1], Yousuke Yamashita[1] (1.Japan Agency for Marine-Earth Science and Technology, 2.International Pacific Research Center, University of Hawaii, 3.Atmospheric, Oceanic and Planetary Physics, Department of Physics, University of Oxford)

[AAS05-P05] On the relation between three-dimensional wave activity flux and pseudo momentum without using intrinsic phase velocities

★Invited Papers

*Takenari Kinoshita[1] (1.Japan Agency for Marine-Earth Science and Technology)

[AAS05-P06] Hindcasts of the 2016 Disruption of the Stratospheric Quasi-biennial Oscillation

*Shingo Watanabe[1], Kevin Hamilton[2], Scott Osprey[3], Yoshio Kawatani[1], Eriko Nishimoto (1.Japan Agency for Marine-Earth Science and Technology, 2.International Pacific Research Center, University of Hawaii at Manoa, 3.NCAS-Climate, University of Oxford)

[AAS05-P07] Selection bias of quasi-fixed-point observations in the ExUTLS and its impact on the seasonal record

*Yoichi Inai[1], Toshinobu Machida[2], Hidekazu Matsueda[3], Yousuke Sawa[3], Kazuhiro Tsuboi[3], Keiichi Katsumata[2,4], Shinji Morimoto[1], Shuji Aoki[1], Takakiyo Nakazawa[1], Ryo Fujita[5,1] (1.Tohoku Univ., 2.NIES, 3.MRI, 4.Takachiho Chem. Industrial, 5.Imperial College London)

[AAS05-P08] Varying Rossby Wave Trains from the Developing to Decaying Period of the Upper Atmospheric Heat Source over the Tibetan Plateau in Boreal Summer

*Chuandong Zhu[1,2], Rongcai Ren[1] (1.Institute of Atmospheric Physics, Chinese Academy of Sciences, 2.University of Chinese Academy of Sciences)

[AAS05-P09] **Equilibrium Climate Responses of the East Asian Summer Monsoon to Various Anthropogenic Aerosol Species**

*Qiuyan Wang[2,1], Zhili Wang[1,2], Hua Zhang[3,2] (1.State Key Laboratory of Severe Weather & Key Laboratory of Atmospheric Chemistry of CMA, Chinese Academy of Meteorological Sciences, Beijing, 2.Collaborative Innovation Center on Forecast and Evaluation of Meteorological Disasters, Nanjing University of Information Science and Technology, Nanjing, 3.Laboratory for Climate Studies, National Climate Center, China Meteorological Administration, Beijing)

[AAS05-P10] Analysis of specific energy in zonal currents focusing on the analogy between jet stream and open channel flow

*Yoshikazu Kitano[1], Tomohito J. Yamada[2] (1.Central Research Institute of Electric Power Industry, 2.Faculty of Engineering, Hokkaido University)

[AAS05-P11] Analysis of the ozone reduction event over the southern tip of South America in November 2009

*Hideharu Akiyoshi[1], Masanao Kadowaki[2], Haruna Nakamura[3], Takafumi Sugita[1], Toshihiko Hirooka[4], Yayoi Harada[5], Akira Mizuno[6] (1.National Institute for Environmental Studies, 2.Japan Atomic Energy Agency, 3.Fujitsu FIP Corporation, 4.Department of Earth and Planetary Sciences, Kyushu University, 5.Meteorological Research Institute, 6.Institute for Space-Earth Environmental Research, Nagoya University)

[AAS05-P12] **Analysis of relatively low ozone in Arctic spring during the QBO-westerly and solar-minimum years**

*Yousuke Yamashita[1,2], Hideharu Akiyoshi[2], Masaaki Takahashi[2] (1.Japan Agency for Marine-Earth Science and Technology, 2.National Institute for Environmental Studies)

[AAS05-P13] Evaluation of ozone in the upper troposphere and lower stratosphere derived from multi-species satellite data assimilation

*Takashi Sekiya[1], Kazuyuki Miyazaki[2,1], Koji Ogochi[1], Kengo Sudo[3,1], Masayuki Takigawa[1] (1.Japan Agency for Marine-Earth Science and Technology, 2.Jet Propulsion Laboratory/California Institute for Technology, 3.Graduate School of Environmental Studies, Nagoya University)

[AAS05-P14] Characteristics of Initial Perturbation of JMA GEPS during Sudden Stratospheric Warmings

★Invited Papers

*Shunsuke Noguchi[1,2] (1.Japan Agency for Marine-Earth Science and Technology, 2.Meteorological Research institute, Japan Meteorological Agency)

[E] Poster | A (Atmospheric and Hydrospheric Sciences)：A-OS Ocean Sciences & Ocean Environment

10:45 AM - 12:15 PM JST | 1:45 AM - 3:15 AM UTC | Poster Hall International Exhibition Hall8, Makuhari Messe_4

[A-OS08] ECS-Kuroshio and Ryukyu Current System -Observation, modeling and theory-

convener:Hirohiko Nakamura(Kagoshima University, Faculy of Fisheries), Xiao-Hua Zhu(Second Institute of Oceanography)

[AOS08-P01] **Impact of the mesosacle eddies on the western boundary current over the entire western North Pacific**

*Kako Shinichiro[1], Hirohiko Nakamura[2] (1.Graduate School of Science and Engineering, Kagoshima University, 2.Faculty of Fisheries, Kagoshima University)

[AOS08-P02] Glider observations of interleaving layers in the Kuroshio

*Sen Jan[1], Shih-Hong Wang[1], Kai-Chieh Yang[1], Yiing Jang Yang[1], Ming-Huei Chang[1] (1.Institute of Oceanography, National Taiwan Univ.)

[AOS08-P03] Bottom Pressure in the East China Sea -Observation and modeling

*Hua Zheng[1], Xiao-Hua Zhu[1], Hirohiko Nakamura[2], Jae-Hun Park[3], Chanhyung Jeon[4], Ruixiang Zhao[1], Ayako Nishina[2], Chuanzheng Zhang[1], Hanna Na[5], Ze-Nan Zhu[1], Hong Sik Min[6] (1.Second Institute of Oceanography, Ministry of Natural Resources, China, 2.Faculty of Fisheries, Kagoshima University, Kagoshima, Japan, 3.Department of Ocean Sciences, Inha University, Incheon, South Kore, 4.Department of Marine Science and Biological Engineering, Inha University, Incheon, Korea, 5.School of Earth and Environmental Sciences, Seoul National University, Seoul, Korea, 6.Ocean Circulation and Climate Research Center, Korea Institute of Ocean Science and Technology, Busan, Korea)

[AOS08-P04] A numerical study on the dynamics of seasonal velocity variation in the East China Sea

*ZHENLONG ZHANG[1], Nakamura Hirohiko[1], Xiao-Hua Zhu[2] (1.Kagoshima University, 2.Ministry of Natural Resources, CHINA.)

[AOS08-P05] Temporal and spatial velocity variations over the Kuroshio Extension, Kuroshio and Ryukyu Current System in 1982-2014

*YUXIANG QIAO[1], Hirohiko Nakamura[2], AYAKO NISHINA[2] (1.Kagoshima University, Graduate School of Fisheries, 2.Kagoshima University, Faculty of Fishries)

[AOS08-P06] Characteristics of water in the southern Okinawa Trough.

*Ayako Nishina[1], Hirohiko Nakamura[1], Jae-Hun Park[2], Xiao-Hua Zhu[3], Hong Sik Min[4], Hanna Na[5] (1.Kagoshima University, 2.Inha University, 3.Second Institute of Oceanography, 4.Korea Institute of Ocean Science and Technology, 5.Seoul National University)

[E] Poster | A (Atmospheric and Hydrospheric Sciences)：A-OS Ocean Sciences & Ocean Environment

5:15 PM - 6:30 PM JST | 8:15 AM - 9:30 AM UTC | Poster Hall International Exhibition Hall8, Makuhari Messe_11

[A-OS08] ECS-Kuroshio and Ryukyu Current System -Observation, modeling and theory-

convener:Hirohiko Nakamura(Kagoshima University, Faculy of Fisheries), Xiao-Hua Zhu(Second Institute of Oceanography)

[AOS08-P01] Impact of the mesosacle eddies on the western boundary current over the entire western North Pacific

*Kako Shinichiro[1], Hirohiko Nakamura[2] (1.Graduate School of Science and Engineering, Kagoshima University, 2.Faculty of Fisheries, Kagoshima University)

[AOS08-P02] Glider observations of interleaving layers in the Kuroshio

*Sen Jan[1], Shih-Hong Wang[1], Kai-Chieh Yang[1], Yiing Jang Yang[1], Ming-Huei Chang[1] (1.Institute of Oceanography, National Taiwan Univ.)

[AOS08-P03] Bottom Pressure in the East China Sea -Observation and modeling

*Hua Zheng[1], Xiao-Hua Zhu[1], Hirohiko Nakamura[2], Jae-Hun Park[3], Chanhyung Jeon[4], Ruixiang Zhao[1], Ayako Nishina[2], Chuanzheng Zhang[1], Hanna Na[5], Ze-Nan Zhu[1], Hong Sik Min[6] (1.Second Institute of Oceanography, Ministry of Natural Resources, China, 2.Faculty of Fisheries, Kagoshima University, Kagoshima, Japan, 3.Department of Ocean Sciences, Inha University, Incheon, South Kore, 4.Department of Marine Science and Biological Engineering, Inha University, Incheon, Korea, 5.School of Earth and Environmental Sciences, Seoul National University, Seoul, Korea, 6.Ocean Circulation and Climate Research Center, Korea Institute of Ocean Science and Technology, Busan, Korea)

[AOS08-P04] A numerical study on the dynamics of seasonal velocity variation in the East China Sea

*ZHENLONG ZHANG[1], Nakamura Hirohiko[1], Xiao-Hua Zhu[2] (1.Kagoshima University, 2.Ministry of Natural Resources, CHINA.)

[AOS08-P05] Temporal and spatial velocity variations over the Kuroshio Extension, Kuroshio and Ryukyu Current System in 1982-2014

*YUXIANG QIAO[1], Hirohiko Nakamura[2], AYAKO NISHINA[2] (1.Kagoshima University, Graduate School of Fisheries, 2.Kagoshima University, Faculty of Fishries)

[AOS08-P06] Characteristics of water in the southern Okinawa Trough.

*Ayako Nishina[1], Hirohiko Nakamura[1], Jae-Hun Park[2], Xiao-Hua Zhu[3], Hong Sik Min[4], Hanna Na[5] (1.Kagoshima University, 2.Inha University, 3.Second Institute of Oceanography, 4.Korea Institute of Ocean Science and Technology, 5.Seoul National University)

[E] Oral | A (Atmospheric and Hydrospheric Sciences)：A-OS Ocean Sciences & Ocean Environment

1:45 PM - 3:15 PM JST | 4:45 AM - 6:15 AM UTC | 105 1F

[A-OS08] ECS-Kuroshio and Ryukyu Current System -Observation, modeling and theory-

convener:Hirohiko Nakamura(Kagoshima University, Faculy of Fisheries), Xiao-Hua Zhu(Second Institute of Oceanography), Chairperson:Hirohiko Nakamura(Kagoshima University), Jae-Hun Park(Inha University)

1:50 PM - 2:10 PM JST | 4:50 AM - 5:10 AM UTC

[AOS08-01] Downstream Evolution of the Kuroshio Velocity Structure and Transport

★Invited Papers

*Magdalena Andres[1], Sen Jan[2] (1.Woods Hole Oceanographic Institution, 2.National Taiwan University)

2:10 PM - 2:25 PM JST | 5:10 AM - 5:25 AM UTC

[AOS08-02] **Non-seasonal variability of the Kuroshio shelf intrusion and its associated changes in the ocean environment over the East China Sea during 1993-2017**

*Jiwon Kang[1], Hanna Na[1] (1.School of Earth and Environmental Sciences, Seoul National University, Republic of Korea)

2:25 PM - 2:40 PM JST | 5:25 AM - 5:40 AM UTC

[AOS08-03] The temporal and spatial variability of the Kuroshio in the East China Sea and its associated mechanisms

*Yanzhou Wei[1] (1.State Key Laboratory of Satellite Ocean Environment Dynamics, Second Institute of Oceanography, Ministry of Natural Resources, Hangzhou, China)

2:40 PM - 2:55 PM JST | 5:40 AM - 5:55 AM UTC

[AOS08-04] The Joint Kuroshio–Ryukyu Current System Study and a rapid report about mooring observations southeast of Miyakojima

*Xiao-Hua Zhu[1], Hirohiko Nakamura[2], Jae-Hun Park[3], Ruixiang Zhao[1], Ayako Nishina[2], Chuanzheng Zhang[1], Chanhyung Jeon[4], Hanna Na[5], Ze-Nan Zhu[1], Hong Sik Min[6] (1.State Key Laboratory of Satellite Ocean Environment Dynamics, Second Institute of Oceanography, Ministry of Natural Resources, Hangzhou, China, 2.Faculty of Fisheries, Kagoshima University, Kagoshima, Japan, 3.Department of Ocean Sciences, Inha University, Incheon, South Korea, 4.Department of Marine Science and Biological Engineering, Inha University, Incheon, Korea, 5.School of Earth and Environmental Sciences, Seoul National University, Seoul, Korea, 6.Ocean Circulation and Climate Research Center, Korea Institute of Ocean Science and Technology, Busan, Korea)

2:55 PM - 3:10 PM JST | 5:55 AM - 6:10 AM UTC

[AOS08-05] Relationship of the Kuroshio with the current fields in the East China Sea from observations and model results

*Hong Sik Min[1], Chorong Hwang[1], Dong Guk Kim[1], Hirohiko Nakamura[2], Ayako Nishina[2], Xiao-Hua Zhu[3], Jae-Hun Park[4], Chanhyung Jeon[4], Hanna Na[5], Naoki Hirose[6] (1.Korea Institute of Ocean Science & Technology, 2.Kagoshima University, 3.Second Institute of Oceanography, 4.Inha University, 5.Seoul National University, 6.Kyushu University)

[E] Oral | A (Atmospheric and Hydrospheric Sciences)：A-OS Ocean Sciences & Ocean Environment

3:30 PM - 5:00 PM JST | 6:30 AM - 8:00 AM UTC | 105 1F

[A-OS08] ECS-Kuroshio and Ryukyu Current System -Observation, modeling and theory-

convener:Hirohiko Nakamura(Kagoshima University, Faculy of Fisheries), Xiao-Hua Zhu(Second Institute of Oceanography), Chairperson:Jae-Hun Park(Inha University), Hirohiko Nakamura(Kagoshima University)

3:35 PM - 3:55 PM JST | 6:35 AM - 6:55 AM UTC

[AOS08-06] Separating Small-Scale Oceanic Internal Waves and Vortical Motions

★Invited Papers

*Ren-Chieh Lien[1] (1.University of Washington, Seattle, WA, USA)

3:55 PM - 4:10 PM JST | 6:55 AM - 7:10 AM UTC

[AOS08-07] Structure and variability of the Kuroshio current in the Tokara Strait

*Zhao-Jun Liu[1], Hirohiko Nakamura[2], Xiao-Hua Zhu[1], Ayako Nishina[2], Xinyu Guo[3], Menghong Dong[1] (1.Second Institute of Oceanography, China, 2.Kagoshima University, Japan, 3.Ehime University, Japan)

4:10 PM - 4:25 PM JST | 7:10 AM - 7:25 AM UTC

[AOS08-08] **Near-inertial waves advected by the Kuroshio from observation and simulation**

*CHANHYUNG JEON[1], Jae-Hun Park[1], Hirohiko Nakamura[2], Ayako Nishina[2], Xiao-Hua Zhu[3], Dong Guk Kim[4], Hong Sik Min[4], Sok Kuh Kang[4], Hanna Na[5], Naoki Hirose[6], Youngseok Choi[1] (1.Inha University, 2.Kagoshima University, 3.Second Institute of Oceanography, 4.Korea Institute of Ocean Science and Technology, 5.Seoul National University, 6.Kyushu University)

4:25 PM - 4:40 PM JST | 7:25 AM - 7:40 AM UTC

[AOS08-09] Turbulent mixing and near-inertial internal waves induced by the Kuroshio over seamounts in the Tokara Strait

*Takeyoshi Nagai[1], Daisuke Hasegawa[2], Eisuke Tsutsumi[3], Hirohiko Nakamura[4], Ayako Nishina[4], Tomoharu Senjyu[3], Takahiro Endoh[3], Takeshi Matsuno[3], Ryuichiro Inoue[5], Amit Tandon[6] (1.Department of Ocean Sciences, Tokyo University of Marine Science and Technology, 2.Tohoku National Fisheries Research Institute, Japan Fisheries Research and Education Agency, 3.Kyushu University, Research Institute for Applied Mechanics, 4.Faculty of Fisheries Kagoshima University, 5.Ocean Circulation Research Group, Japan Agency for Marine-Earth Science and Technology, 6.Mechanical Engineering Department & SMAST, University of Massachusetts Dartmouth)

4:40 PM - 4:55 PM JST | 7:40 AM - 7:55 AM UTC

[AOS08-10] Microstructure and mooring observations of enhanced mixing in the Kerama Gap

*Ryuichiro Inoue[1], Hirohiko Nakamura[2], Takahiro Tanaka[3], Shinzou Fujio[4], Daigo Yanagimoto[4], Ichiro Yasuda[4] (1.Japan Agency for Marine-Earth Science and Technology, 2.Kagoshima University, Faculy of Fisheries, 3.Tohoku National Fisheries Research Institute, Japan Fisheries Research and Education Agency, 4.The University of Tokyo, Atmosphere and Ocean Research Institute)

[E] Oral | A (Atmospheric and Hydrospheric Sciences)：A-OS Ocean Sciences & Ocean Environment

9:00 AM - 10:30 AM JST | 12:00 AM - 1:30 AM UTC | 301A 3F

[A-OS11] Continental-Oceanic Mutual Interaction: Planetary scale Material Circulation

convener:Yosuke Alexandre Yamashiki(Earth & Planetary Water Resources Assessment Laboratory Graduate School of Advanced Integrated Studies in Human Survivability Kyoto University), Yukio Masumoto(Graduate School of Science, The University of Tokyo), Swadhin Behera(Climate Variation Predictability and Applicability Research Group, Application Laboratory, JAMSTEC, 3173-25 Showa-machi, Yokohama 236-0001), Takanori Sasaki(Department of Astronomy, Kyoto University), Chairperson:Yukio Masumoto, Behera Swadhin(JAMSTEC)

9:00 AM - 9:15 AM JST | 12:00 AM - 12:15 AM UTC

[AOS11-01] Explorations and current understandings for subsurface ocean of icy bodies

★Invited Papers

*Jun Kimura[1] (1.Osaka University)

9:15 AM - 9:30 AM JST | 12:15 AM - 12:30 AM UTC

[AOS11-02] **Climate predictability for societal applications including AI/ML**

*Swadhin Behera[1], Manali Pal[2], J.V. Ratnam[1], Rajib Maity[2], Takeshi Doi[1], Yushi Morioka[1], Masami Nonaka[1] (1.Application Laboratory, JAMSTEC, 3173-25 Showa-machi, Yokohama 236-0001, 2.Indian Institute of Technology, Kharagpur, India)

9:30 AM - 9:45 AM JST | 12:30 AM - 12:45 AM UTC

[AOS11-03] Re-entry of giant-impact fragments and early evolution of the Earth's ocean

*Takanori Sasaki[1] (1.Department of Astronomy, Kyoto University)

9:45 AM - 10:00 AM JST | 12:45 AM - 1:00 AM UTC

[AOS11-04] Modeling of Extreme Freshwater Discharge and influence from Japanese First-Class Rivers to Coastal zones

*Ryusuke Kuroki, Yosuke Alexandre Yamashiki[1], Sergey Varlamov[2], Yasumasa Miyazawa[2], Racault Fanny Marie[3], Hoshin Vijai Gupta[4] (1.Kyoto University, 2.Application Laboratory, Japan Agency for Marine-Earth Science and Technology, Japan, 3.Plymouth Marine Laboratory, Plymouth, United Kingdom, 4.University of Arizona)

10:00 AM - 10:15 AM JST | 1:00 AM - 1:15 AM UTC

[AOS11-05] Establishment of new curriculum at Biosphere 2

*Kenji Miki[1], Takao Doi[2], Yosuke Yamashiki[3], Masahiro Terada[2] (1.Kyoto University Graduate School of Agriculture, 2.Kyoto University Unit of Synergetic Studies for Space, 3.Graduate School of Advanced Integrated Studies in Human Survivability)

10:15 AM - 10:30 AM JST | 1:15 AM - 1:30 AM UTC

[AOS11-06] Development of the highly precise high-speed photometry technique with the photometer mounted with PIRKA telescope

*Nami Kimura[1] (1.Hokkaido University)

[E] Oral | A (Atmospheric and Hydrospheric Sciences)：A-OS Ocean Sciences & Ocean Environment

10:45 AM - 12:15 PM JST | 1:45 AM - 3:15 AM UTC | 301A 3F

[A-OS11] Continental-Oceanic Mutual Interaction: Planetary scale Material Circulation

convener:Yosuke Alexandre Yamashiki(Earth & Planetary Water Resources Assessment Laboratory Graduate School of Advanced Integrated Studies in Human Survivability Kyoto University), Yukio Masumoto(Graduate School of Science, The University of Tokyo), Swadhin Behera(Climate Variation Predictability and Applicability Research Group, Application Laboratory, JAMSTEC, 3173-25 Showa-machi, Yokohama 236-0001), Takanori Sasaki(Department of Astronomy, Kyoto University), Chairperson:Yosuke Yamashiki(GSAIS Kyoto University), Takanori Sasaki(Department of Astronomy, Kyoto University)

10:45 AM - 11:00 AM JST | 1:45 AM - 2:00 AM UTC

[AOS11-07] **The Drivers of early Archean Earth's Hydrology: Resolving the Faint Young Sun's Paradox**

★Invited Papers

*Vladimir Airapetian[1], Guillaume Gronoff[2], Michael Way[3], Meng Jin[4] (1.NASA Goddard Space Flight Center/SEEC and American University, 2.NASA LaRC/SSAI, 3.NASA GISS/SEEC, 4.SETI)

11:00 AM - 11:15 AM JST | 2:00 AM - 2:15 AM UTC

[AOS11-08] Experimental study on elementary hydrological process of rainfall in a forested continental hinterland

*Shigeki Murakami[1] (1.Kyushu Research Cente, Forestry and Forest Products Research Institute)

11:15 AM - 11:30 AM JST | 2:15 AM - 2:30 AM UTC

[AOS11-09] Radiological Assessment of Martian and Terrestrial Surface during Young Sun

*Yosuke Alexandre Yamashiki[1], Hiroyuki Maehara[6], Yuta Notsu[3], Tatsuhiko Sato[2], Airapetian Vladimir[7], Shota Notsu[3], Ryusuke Kuroki[1], keiya murashima[5], Hiroaki Sato[4], Hina Bando[5], Kosuke Namekata[3], Takanori Sasaki[3], Scott Thomas[8], Nogami Daisaku[3], Kazunari Shibata[9] (1.Earth & Planetary Water Resources Assessment Laboratory Graduate School of Advanced Integrated Studies in Human Survivability Kyoto University, 2.Japan Atomic Energy Agency, 3.Graduate School of Science, Kyoto University, 4.School of Engineering, 5.School of Science, 6.National Astronomical Observatory of Japan, 7.NASA / Goddard Space Flight Center, 8.University of Bristol , 9.Kwasan Astronomical Observatory, Kyoto University)

11:30 AM - 11:45 AM JST | 2:30 AM - 2:45 AM UTC

[AOS11-10] **Evaluation of scintillator detection materials for application within environmental radiation monitoring**

*Peter George Martin[1], D. Connor[1], M. Lowden[1], T. B. Scott[1] (1.School of Physics, University of Bristol, Bristol, UK)

11:45 AM - 12:00 PM JST | 2:45 AM - 3:00 AM UTC

[AOS11-11] The important factors for future human space activity in terms of space medicine

*Masahiro Terada[1], Yosuke Yamashiki[1], Kenji Miki[1], Satoko Tsujihiro[1], Takao Doi[1] (1.Kyoto University, Unit of Synergetic Studies for Space)

12:00 PM - 12:15 PM JST | 3:00 AM - 3:15 AM UTC

[AOS11-12] Storm Surge Response to Freshwater Outflow from Typhoons on the Ibaraki Coast

*Josko Troselj[1], Nobuhito Mori[1] (1.Coastal Engineering Laboratory, Disaster Prevention Research Institute, Kyoto University)

[E] Poster | A (Atmospheric and Hydrospheric Sciences)：A-OS Ocean Sciences & Ocean Environment

3:30 PM - 5:00 PM JST | 6:30 AM - 8:00 AM UTC | Poster Hall International Exhibition Hall8, Makuhari Messe_7

[A-OS11] Continental-Oceanic Mutual Interaction: Planetary scale Material Circulation

convener:Yosuke Alexandre Yamashiki(Earth & Planetary Water Resources Assessment Laboratory Graduate School of Advanced Integrated Studies in Human Survivability Kyoto University), Yukio Masumoto(Graduate School of Science, The University of Tokyo), Swadhin Behera(Climate Variation Predictability and Applicability Research Group, Application Laboratory, JAMSTEC, 3173-25 Showa-machi, Yokohama 236-0001), Takanori Sasaki(Department of Astronomy, Kyoto University)

[AOS11-P01] Remote Sensing of Chlorophyll-a and Submerged Aquatic Vegetation for a Freshwater Lake in Japan

*Shweta Yadav[1], Yamashiki Yosuke[1], Junichi Susaki[1], Kanako Ishikawa[2] (1.Kyoto University, 2.Lake Biwa Environmental Research Institute)

[AOS11-P02] Hydrological and Debris-flow simulation of Martian Surface in Hesperian & early Amazonian epoch

*Hiroaki Sato[2], Yosuke Alexandre Yamashiki[1], Ryusuke Kuroki[1], Hideaki Miyamoto[3], Ryodo Hemmi[3] (1.Earth & Planetary Water Resources Assessment Laboratory Graduate School of Advanced Integrated Studies in Human Survivability Kyoto University, 2.Faculty of Engineering, Kyoto University, 3.Graduate School of Engineering, The University of Tokyo)

[AOS11-P03] Global Lakes & reservoirs Repository and their application for terrestrial surface environment

*Yosuke Alexandre Yamashiki[1], Ryusuke Kuroki[1], Botong Gao[1], Hina Bando[2], Fuka Takagi[3], Shweta Yadav[4] (1.Earth & Planetary Water Resources Assessment Laboratory Graduate School of Advanced Integrated Studies in Human Survivability Kyoto University, 2.Faculty of Science, Kyoto University, 3.Faculty of Agriculture, Kyoto University, 4.Educational Unit for Studies on Connectivity of Hills, Humans and Ocean, Kyoto University)

[AOS11-P04] Numerical simulation of Tidal Heating using SPH and its application to inner sea formation

*keiya murashima[1], Yosuke Alexandre Yamashiki[1], Natsuki Hosono[2] (1.Kyoto University, 2.Japan Agency for Marine-Earth Science and Technology)

[E] Poster | A (Atmospheric and Hydrospheric Sciences)：A-OS Ocean Sciences & Ocean Environment

5:15 PM - 6:30 PM JST | 8:15 AM - 9:30 AM UTC | Poster Hall International Exhibition Hall8, Makuhari Messe_12

[A-OS11] Continental-Oceanic Mutual Interaction: Planetary scale Material Circulation

convener:Yosuke Alexandre Yamashiki(Earth & Planetary Water Resources Assessment Laboratory Graduate School of Advanced Integrated Studies in Human Survivability Kyoto University), Yukio Masumoto(Graduate School of Science, The University of Tokyo), Swadhin Behera(Climate Variation Predictability and Applicability Research Group, Application Laboratory, JAMSTEC, 3173-25 Showa-machi, Yokohama 236-0001), Takanori Sasaki(Department of Astronomy, Kyoto University)

[AOS11-P01] **Remote Sensing of Chlorophyll-a and Submerged Aquatic Vegetation for a Freshwater Lake in Japan**

*Shweta Yadav[1], Yamashiki Yosuke[1], Junichi Susaki[1], Kanako Ishikawa[2] (1.Kyoto University, 2.Lake Biwa Environmental Research Institute)

[AOS11-P02] Hydrological and Debris-flow simulation of Martian Surface in Hesperian & early Amazonian epoch

*Hiroaki Sato[2], Yosuke Alexandre Yamashiki[1], Ryusuke Kuroki[1], Hideaki Miyamoto[3], Ryodo Hemmi[3] (1.Earth & Planetary Water Resources Assessment Laboratory Graduate School of Advanced Integrated Studies in Human Survivability Kyoto University, 2.Faculty of Engineering, Kyoto University, 3.Graduate School of Engineering, The University of Tokyo)

[AOS11-P03] Global Lakes & reservoirs Repository and their application for terrestrial surface environment

*Yosuke Alexandre Yamashiki[1], Ryusuke Kuroki[1], Botong Gao[1], Hina Bando[2], Fuka Takagi[3], Shweta Yadav[4] (1.Earth & Planetary Water Resources Assessment Laboratory Graduate School of Advanced Integrated Studies in Human Survivability Kyoto University, 2.Faculty of Science, Kyoto University, 3.Faculty of Agriculture, Kyoto University, 4.Educational Unit for Studies on Connectivity of Hills, Humans and Ocean, Kyoto University)

[AOS11-P04] Numerical simulation of Tidal Heating using SPH and its application to inner sea formation

*keiya murashima[1], Yosuke Alexandre Yamashiki[1], Natsuki Hosono[2] (1.Kyoto University, 2.Japan Agency for Marine-Earth Science and Technology)

[J] Poster | A (Atmospheric and Hydrospheric Sciences)：A-OS Ocean Sciences & Ocean Environment

10:45 AM - 12:15 PM JST | 1:45 AM - 3:15 AM UTC | Poster Hall International Exhibition Hall8, Makuhari Messe_5

[A-OS14] Coastal physical processes associated with mixing, eddies, internal waves

convener:Eiji Masunaga(Ibaraki University), Taira Nagai(Graduate School of Science, The University of Tokyo), TSUTSUMI EISUKE(Atmosphere and Ocean Research Institute, The University of Tokyo)

[AOS14-P01] **Development of methods and systems for vertical mixing and observations (OMIX-A01-1)**

*Ichiro Yasuda[1], Koenjong Lee[1], Shinzo Fujio[1], Daigo Yanagimoto[1], Maki Nagasawa[1], Yusuke Kawaguchi[1], Eitarou Oka[1], Shuo Zhai[1], Shino Kimura[1], Ryuichiro Inoue[2], Daisuke Hasegawa[3], Takahiro Tanaka[3], Masao Ishii[4], Toshiya Nakano[4], Yasutaka Goto[4] (1.Atmosphere and Ocean Research Institute, The University of Tokyo, 2.Japan Agency of Marine-Earth Science and Technology, 3.Fisheries Research Agency, 4.Japan Meteorological Agency)

[AOS14-P02] **Observation of enhanced nonlinear interactions after the passage of typhoon in the western South China Sea**

*gui ying Chen, chang rong Liang, xiao dong Shang

[AOS14-P03] Investigating vertical mixing in estuarine pycnocline: a case study in the Ariake Sea, Japan

*Takeshi Matsuno[1], Eisuke Tsutsumi[1] (1.Kyushu University)

[AOS14-P04] Possibility of interactions between the coastal and offshore branch of Tsushima Warm Current over the submarine canyon in the Sea of Japan.

*Yosuke Igeta[1], Alexander Yankovsky [2], Mizuki Kuga[1], Naoki Hirose[3], Kenichi Fukudome[4] (1.Japan Sea National Fishseries Research Institute, 2.University of South Carolina, 3.RIAM Kyushu Univ., 4.National Institute of Technology, Toyama College)

[J] Poster | A (Atmospheric and Hydrospheric Sciences)：A-OS Ocean Sciences & Ocean Environment

5:15 PM - 6:30 PM JST | 8:15 AM - 9:30 AM UTC | Poster Hall International Exhibition Hall8, Makuhari Messe_13

[A-OS14] Coastal physical processes associated with mixing, eddies, internal waves

convener:Eiji Masunaga(Ibaraki University), Taira Nagai(Graduate School of Science, The University of Tokyo), TSUTSUMI EISUKE(Atmosphere and Ocean Research Institute, The University of Tokyo)

[AOS14-P01] Development of methods and systems for vertical mixing and observations (OMIX-A01-1)

*Ichiro Yasuda[1], Koenjong Lee[1], Shinzo Fujio[1], Daigo Yanagimoto[1], Maki Nagasawa[1], Yusuke Kawaguchi[1], Eitarou Oka[1], Shuo Zhai[1], Shino Kimura[1], Ryuichiro Inoue[2], Daisuke Hasegawa[3], Takahiro Tanaka[3], Masao Ishii[4], Toshiya Nakano[4], Yasutaka Goto[4] (1.Atmosphere and Ocean Research Institute, The University of Tokyo, 2.Japan Agency of Marine-Earth Science and Technology, 3.Fisheries Research Agency, 4.Japan Meteorological Agency)

[AOS14-P02] Observation of enhanced nonlinear interactions after the passage of typhoon in the western South China Sea

*gui ying Chen, chang rong Liang, xiao dong Shang

[AOS14-P03] Investigating vertical mixing in estuarine pycnocline: a case study in the Ariake Sea, Japan

*Takeshi Matsuno[1], Eisuke Tsutsumi[1] (1.Kyushu University)

[AOS14-P04] Possibility of interactions between the coastal and offshore branch of Tsushima Warm Current over the submarine canyon in the Sea of Japan.

*Yosuke Igeta[1], Alexander Yankovsky [2], Mizuki Kuga[1], Naoki Hirose[3], Kenichi Fukudome[4] (1.Japan Sea National Fishseries Research Institute, 2.University of South Carolina, 3.RIAM Kyushu Univ., 4.National Institute of Technology, Toyama College)

[J] Oral | A (Atmospheric and Hydrospheric Sciences)：A-OS Ocean Sciences & Ocean Environment

1:45 PM - 3:15 PM JST | 4:45 AM - 6:15 AM UTC | 301A 3F

[A-OS14] Coastal physical processes associated with mixing, eddies, internal waves

convener:Eiji Masunaga(Ibaraki University), Taira Nagai(Graduate School of Science, The University of Tokyo), TSUTSUMI EISUKE(Atmosphere and Ocean Research Institute, The University of Tokyo), Chairperson:Eiji Masunaga, Eisuke Tsutsumi

1:45 PM - 2:00 PM JST | 4:45 AM - 5:00 AM UTC

[AOS14-01] The cooling of sea surface temperature in the southern Indonesian Seas due to a combination of the Ekman transport and tidal mixing in narrow straits

*Taira Nagai[1], Toshiyuki Hibiya[1] (1.Graduate School of Science, The University of Tokyo)

2:00 PM - 2:15 PM JST | 5:00 AM - 5:15 AM UTC

[AOS14-02] A reanalysis of regional circulations in the Southern South China Sea using a HYCOM-ROMS downscaling ocean model

*Naru Takaura[1], Yusuke Uchiyama[1], Nizamani Zafarullah[2], Akihiko Nakayama[2] (1.Kobe Univ, 2.Tunku Abdul Rahman University)

2:15 PM - 2:30 PM JST | 5:15 AM - 5:30 AM UTC

[AOS14-03] Nutrient and phytoplankton dynamics in the continental slope region of the East China Sea associated with the Kuroshio frontal eddy

*Naoki Yoshie[1], Anri Kabe[1], Kazuki Ohgi[1], Eisuke Tsutsumi[2], Shigenobu Takeda[3], Joji Ishizaka[4], Xinyu Guo[1] (1.Center for Marine Environmental Studies, Ehime University, 2.Research Institute for Applied Mechanics, Kyushu University, 3.Faculty of Fisheries, Nagasaki University, 4.Institute for Space-Earth Environmental Research, Nagoya University)

2:30 PM - 2:45 PM JST | 5:30 AM - 5:45 AM UTC

[AOS14-04] Dissipation and transport due to internal tides generated by multiple submarine canyons

*Qiang Li[1], Xianzhong Mao[1], Ran Liao[1] (1.Tsinghua University)

2:45 PM - 3:00 PM JST | 5:45 AM - 6:00 AM UTC

[AOS14-05] Measurement of Physical structure in Kasumigaura using high resolution tow-yo instrument

*Daiki Asaoka[1], Eiji Masunaga[1], Shunsuke Komuro[2], Shunichi Matsumoto[2], Masahiko Ono[3], Hiroaki Banba[3] (1.Ibaraki University, 2.Ibaraki Kasumigaura Environmental Science Center, 3.Ministry of Land, Infrastructure, Transport and Tourism)

3:00 PM - 3:15 PM JST | 6:00 AM - 6:15 AM UTC

[AOS14-06] Mixing and baroclinic structure in a stratified shallow lake, Lake Kasumigaura, Japan

*Eiji Masunaga[1], Daiki Asaoka[1], Shunsuke Komuro[2], Shunichi Matsumoto[2], Masahiko Ono[3], Hiroaki Banba[3] (1.Ibaraki University, 2.Ibaraki Kasumigaura Environmental Science Center, 3.Ministry of Land, Infrastructure, Transport and Tourism)

[J] Oral | A (Atmospheric and Hydrospheric Sciences)：A-OS Ocean Sciences & Ocean Environment

3:30 PM - 5:00 PM JST | 6:30 AM - 8:00 AM UTC | 301A 3F

[A-OS14] Coastal physical processes associated with mixing, eddies, internal waves

convener:Eiji Masunaga(Ibaraki University), Taira Nagai(Graduate School of Science, The University of Tokyo), TSUTSUMI EISUKE(Atmosphere and Ocean Research Institute, The University of Tokyo), Chairperson:Eiji Masunaga, Taira Nagai

3:30 PM - 3:45 PM JST | 6:30 AM - 6:45 AM UTC

[AOS14-07] Turbulent mixing and vertical nitrate flux in the Bungo Channel, Japan

*TSUTSUMI EISUKE[1], Naoki Yoshie[2], Takashi Mano[3], Kanda Taisei[3], Naoki Fujii[4], Xinyu Guo[2] (1.Research Institute for Applied Mechanics, Kyushu University, 2.Center for Marine Environmental Studies, Ehime Univeristy, 3.Graduate School for Science and Engineering, Ehime University, 4.Faculty of Agriculture, Saga Univerisity)

3:45 PM - 4:00 PM JST | 6:45 AM - 7:00 AM UTC

[AOS14-08] Numerical Analysis of Submerged Turbulent Buoyant Jet in River Mouth

*Yen-Chen Mou[1], Gene You[1], Chih-Chieh Young[2] (1.National Taiwan University, 2.National Taiwan Ocean University)

4:00 PM - 4:15 PM JST | 7:00 AM - 7:15 AM UTC

[AOS14-09] Implementing regional downscaling capability in the STEAMER radionuclide dispersion prediction system based on multi-nested ROMS model

*Kamidaira Yuki[1], Hideyuki Kawamura[1], Takuya Kobayashi[1], Yusuke Uchiyama[2] (1.Japan Atomic Energy Agency, 2.Kobe University)

4:15 PM - 4:30 PM JST | 7:15 AM - 7:30 AM UTC

[AOS14-10] Transport processes around the Izu-chain islands investigated with a Lagrangian particle tracking model

*Waku Kimura[1], Eiji Masunaga[1], Taichi Kosako[2], Yusuke Uchiyama[3] (1.Ibaraki University, 2.Port and Airport Research Institute, 3.Kobe University)

4:30 PM - 4:45 PM JST | 7:30 AM - 7:45 AM UTC

[AOS14-11] Fates and dynamical roles of pinch-off mesoscale eddies originated from the Kuroshio Extension Jet

*Yusuke Uchiyama[1], Nobue Okada[1], Changming Dong[2] (1.Graduate School of Engineering, Kobe University, 2.Nanjing University of Information Science & Technology)

[E] Oral | A (Atmospheric and Hydrospheric Sciences)：A-HW Hydrology & Water Environment

3:30 PM - 5:00 PM JST | 6:30 AM - 8:00 AM UTC | 201B 2F

[A-HW22] Materials transport and nutrient cycles in watersheds; from headwaters to coastal seas

convener:Masahiro Kobayashi(Forestry and Forest Products Research Institute), Seiko Yoshikawa(Institute for Agro-environmental Sciences, National Agriculture and Food Research Organization), Jun Yasumoto(University of the Ryukyus, Faculty of Agriculuture), Adina Paytan(University of California Santa Cruz), Chairperson:Noboru Okuda(Research Institute for Humanity and Nature)

3:40 PM - 4:00 PM JST | 6:40 AM - 7:00 AM UTC

[AHW22-01] **Coral Skeleton $\delta^{15}N$ as a Tracer of Historic Nutrient Loading to a Coral Reef in Maui, Hawaii**

★Invited Papers

*Adina Paytan[1] (1.University of California Santa Cruz)

4:00 PM - 4:15 PM JST | 7:00 AM - 7:15 AM UTC

[AHW22-02] **The Use of Ammonium and Trace Metals in Identifying Low Redox Environment Zone at Indonesian Coastal Alluvial Groundwater**

*Anna Fadliah Rusydi[1,4], Mitsuyo - Saito[2], Seiichiro - Ioka[3], Shin-ichi - Onodera[1] (1.Graduate School of Integrated Arts and Sciences, Hiroshima University, Japan, 2.Graduate School of Environmental and Life Sciences, Okayama University, Japan, 3.Institute of Regional Innovation, Hirosaki University, Japan, 4.Research Center for Geotechnology, Indonesian Institute of Sciences, Indonesia)

4:15 PM - 4:30 PM JST | 7:15 AM - 7:30 AM UTC

[AHW22-03] Spatial and temporal variation in submarine groundwater discharge (SGD) on a beach scale in a temperate coastal island: a multi-tracer approach

*Mitsuyo Saito[1], Shin-ichi Onodera[2], Yusuke Tomozawa[2], Kazuyoshi Asai[3] (1.Graduate School of Environmental and Life Science, Okayama University, 2.Graduate School of Integrated Arts and Sciences, Hiroshima University, 3.Geo Science Laboratory)

4:30 PM - 4:45 PM JST | 7:30 AM - 7:45 AM UTC

[AHW22-04] **Phosphorus discharge via groundwater into the lake, based on lacustrine groundwater discharge (LGD) and alluvial plain sediment**

*Shin-ichi Onodera[1], Mitsuyo Saito[2], Guangzhe Jin[3], Anna Fadliah Rusydi[1], Yusuke Tomozawa[1], Kunyang Wang[1], Syuhei Ban[4], Noboru Okuda[5] (1.Graduate School of Integrated and Arts Sciences, Hiroshima University, 2. Graduate School of Environmental and Life Science, Okayama University, 3.Guangdong Ocean University, 4.The University of Shiga Prefecture, 5.Research Institute for Humanity and Nature)

4:45 PM - 5:00 PM JST | 7:45 AM - 8:00 AM UTC

[AHW22-05] **Geochemical controls and health implications of water chemistry in Benoue River Basin, North Cameroon: Insights from Major ions**

*Sharon Bih Kimbi[1,2], Wilson Y Fantong[3], Samuel N Ayonghe[2], Robert Kringel[4], Shin-ichi Onodera[1] (1.Graduate School of Integrate Arts and Sciences, Hiroshima University, 2.Department of Environmental Science, Faculty of science, University of Buea, 3.Institute of Mining and Geological Research (IRGM), 4.Federal Institute for Geoscience and Natural Resources Bundesanstalt fur Geowissenschaften und Rohstoffe (BGR) PRESS NO & SW)

[E] Oral | A (Atmospheric and Hydrospheric Sciences)：A-HW Hydrology & Water Environment

9:00 AM - 10:30 AM JST | 12:00 AM - 1:30 AM UTC | 103 1F

[A-HW23] Hydrology & Water Environment

convener:Isao Machida(Geological Survey of Japan), Dai Yamazaki(Institute of Industrial Sciences, The University of Tokyo), Takeshi Hayashi(Faculty of Education and Human Studies, Akita University), Keisuke Fukushi(Institute of Nature & Environmental Technology, Kanazawa University), Chairperson:Takeshi Hayashi(Faculty of Education and Human Studies, Akita University)

9:00 AM - 9:15 AM JST | 12:00 AM - 12:15 AM UTC

[AHW23-12] Drought Analysis based on Copulas and Poisson Process

*Pei-Yu Wu[1], Gene Jiing-yun You[1] (1.National Taiwan University, Department of Civil Engineering)

9:15 AM - 9:30 AM JST | 12:15 AM - 12:30 AM UTC

[AHW23-13] **Snow melt dynamics in snowfall dominated mountain regions in Shonai**

*Alexander Brandt[1,3], Muhammad Fraz Ismail[2], Larry Maximo Lopez Caceres[1], Wolfgang Bogacki[2] (1.Yamagata University, 2.Hochschule Koblenz, 3.UGAS)

9:30 AM - 9:45 AM JST | 12:30 AM - 12:45 AM UTC

[AHW23-14] Study on transport of particulate organic matter in a small river with forest and paddy filed by using carbon isotopes ($\delta^{13}C$ and $\Delta^{14}C$)

*Seiya Nagao[1], Ryunosuke Tahara[2], Shinya Ochiai[1], Akiko Goto[3], Takashi Hasegawa[3] (1.Institute of Nature and Environmental Technology, Kanazawa University, 2.Graduate School of Natural Science and Technology, Kanazawa University, 3.Institute of Science and Engineering, Kanazawa University)

9:45 AM - 10:00 AM JST | 12:45 AM - 1:00 AM UTC

[AHW23-15] **Sources of Shallow Groundwater Salinity in the Ganges Delta of Bangladesh**

*Masudur Rahman[1,2], Tomochika Tokunaga[1] (1.Department of Environment Systems, Graduate School of Frontier Sciences, The University of Tokyo, 5-1-5, Kashiwa-no-ha, Kashiwa-shi, Chiba 277-8563, Japan, 2.Environmental Science Discipline, Life Science School, Khulna University, Khulna 9208, Bangladesh)

10:00 AM - 10:15 AM JST | 1:00 AM - 1:15 AM UTC

[AHW23-16] **Groundwater chemistry in the Gunii Khooloi basin, Southern Gobi Region of Mongolia using multivariate analysis**

*Batdemberel BAYANZUL[1,2], Isao Machida[3], Kengo Nakamura[2], Noriaki Watanabe[2], Takeshi Komai[2] (1.School of Geology and Mining Engineering, Mongolian University of Science and Technology, 2.Graduate School of Environmental Studies, Tohoku University, 3.Groundwater research group, Advanced Industrial Science and Technology)

10:15 AM - 10:30 AM JST | 1:15 AM - 1:30 AM UTC

[AHW23-17] **Temporal observation of molybdenum concentrations in rivers from Erdenet mining area, Mongolia**

*Solongo Tsetsgee[1], Keisuke Fukushi[1], Altansukh Ochir[2], Takahashi Yoshio[3], Ariuntungalag Yunden[2], Enkhjin Odgerel[2], Noriko Hasebe[1] (1.Kanazawa University, 2.National University of Mongolia, 3.The University of Toyko)

[E] Oral | A (Atmospheric and Hydrospheric Sciences)：A-HW Hydrology & Water Environment

10:45 AM - 12:15 PM JST | 1:45 AM - 3:15 AM UTC | 103 1F

[A-HW23] Hydrology & Water Environment

convener:Isao Machida(Geological Survey of Japan), Dai Yamazaki(Institute of Industrial Sciences, The University of Tokyo), Takeshi Hayashi(Faculty of Education and Human Studies, Akita University), Keisuke Fukushi(Institute of Nature & Environmental Technology, Kanazawa University), Chairperson:Keisuke Fukushi

10:45 AM - 11:05 AM JST | 1:45 AM - 2:05 AM UTC

[AHW23-18] Solid-water interaction of Mn and As near the bottom of Lake Biwa. –Implications for the spatio-temporal change of these elements for past 40 years-

★Invited Papers

*TAKAAKI ITAI[1], SACHIKA NATORI[1] (1.Department of Earth and Planetary Science, The University of Tokyo)

11:05 AM - 11:20 AM JST | 2:05 AM - 2:20 AM UTC

[AHW23-19] **Sources, pathways and treatment of contaminants in surface water: Applicability in developing countries**

*Mst. Shamsun Nahar[1] (1.Earth Consultant Co. Ltd, Toyama, Japan)

11:20 AM - 11:35 AM JST | 2:20 AM - 2:35 AM UTC

[AHW23-20] **Numerical simulations (COMSOL) of γ-Fe_2O_3 nanohybrids for transport (3D) and arsenic removal in homogeneous porous media**

*Ajay Kumar[1], Himanshu Joshi[1], Anil Kumar[1] (1.INDIAN INSTITUTE OF TECHNOLOGY ROORKEE, INDIA)

11:35 AM - 11:50 AM JST | 2:35 AM - 2:50 AM UTC

[AHW23-21] **Transport processes of suspended solids in the Kumaki River inferred from atmospheric radionuclides**

*Shinya Ochiai[1], Ryunosuke Tahara[2], Tetsuya Matsunaka[1], Seiya Nagao[1] (1.Institute of Nature and Environmental Technology, Kanazawa University, 2.Graduate School of Natural Science and Technology, Kanazawa University)

11:50 AM - 12:05 PM JST | 2:50 AM - 3:05 AM UTC

[AHW23-22] Using tritium in Japanese precipitation for tritium-tracer transit time studies across Asia

*Maksym Gusyev[1], Yoshito Kikumori[1], Terumasa Nishihara[2], Takeshi Hayashi[3], Kimpei Ichiyanagi[4], Naofumi Akata[5], Tomoki Oda[6], Uwe Morgenstern[7], Michael Stewart[7] (1.International Centre for Water Hazard and Risk Management (ICHARM), Public Works Research Institute (PWRI), 2.Civil Engineering Research Institute for Cold Region, PWRI, 3.Akita University, 4.Kumamoto University, 5.National Institute for Fusion Science (NIFS), 6.University of Tokyo, 7.GNS Science, New Zealand)

[E] Poster | A (Atmospheric and Hydrospheric Sciences)：A-HW Hydrology & Water Environment

3:30 PM - 5:00 PM JST | 6:30 AM - 8:00 AM UTC | Poster Hall International Exhibition Hall8, Makuhari Messe_8

[A-HW23] Hydrology & Water Environment

convener:Isao Machida(Geological Survey of Japan), Dai Yamazaki(Institute of Industrial Sciences, The University of Tokyo), Takeshi Hayashi(Faculty of Education and Human Studies, Akita University), Keisuke Fukushi(Institute of Nature & Environmental Technology, Kanazawa University)

[AHW23-P01] **A multiobjective risk management model for real-time reservoir flood control operation**

*Juan Chen[1,2], Ping-An Zhong[2], XinYu Wan[2], Yu Zhang[2] (1.College of Earth Sciences and Engineering, Hohai University, 2.College of Hydrology and Water Resources, Hohai University)

[AHW23-P02] **Assessment of the Flow Regime of Roanoke River due to Climatic and Anthropogenic Activities**

*Rahul Kumar Singh[1], Dr. Manoj Kumar Jain[1] (1.Indian Institute of Technology, Roorkee, India)

[AHW23-P03] Predictive Analysis of Climate, Water, Health and the Environment Nexus

*Abhishek [1], Deepika [2] (1.Technical University Dresden, GERMANY, 2.BPS Government Medical College for Women, Sonepat, INDIA)

[AHW23-P05] Severe droughts provide huge fuel for widespread wildfires in California in USA

*Linghua Qiu[1], Ji Chen[1], Haiyun Shi[2], Liqun Sun[3], Jun Niu[4] (1.the University of Hong Kong, 2.Southern University of Science and Technology, 3.Shenzhen Institutes of Advanced Technology, Chinese Academy of Sciences, 4.China Agricultural University)

[AHW23-P06] A comprehensive evaluation of MODIS-based water use efficiency with global eddy covariance flux data and a process model

*Shanshan YANG[1,2], Jiahua ZHANG[1], Sha ZHANG[1,2], Jingwen WANG[1,2], Yun BAI[1,2], Fengmei YAO[2], Huadong GUO[1] (1.Institute of Remote Sensing and Digital Earth, Chinese Academy of Sciences, 2.University of Chinese Academy of Sciences, Beijing, China)

[AHW23-P07] Impact of variability and anisotropy in the correlation decay distance for precipitation spatial interpolation in China

*yingxian zhang[1] (1.National Climate Center, China Meteorological Administration)

[AHW23-P08] New Record-Breaking Frequency of Annual Maximum Daily Precipitation of 58 stations in the whole Japan, an increasing of extreme values.

*Chhay Ngorn SEANG[1], Tomohito YAMADA[1] (1.Hokkaido University)

[AHW23-P09] Quantifying stemflow to better express its ecohydrological significance

*Shin'ichi Iida[1], Darryl E. Carlye-Moses[2], Sonja Germer[3], Pilar Llorens[4], Beate Michalzik[5], Kazuki Nanko[1], Alexander Tischer[5], Delphis F. Levia[6] (1.Department of Disaster Prevention, Meteorology and Hydrology, Forestry and Forest Products Research Institute, 2.Department of Geography and Environmental Studies, Thompson Rivers University, Kamloops, British Columbia, Canada, 3.Department of Bioengineering, Leibniz Institute for Agricultural Engineering and Bioeconomy, Potsdam, Germany, 4.Institute of Environmental Assessment and Water Research (IDAEA-CSIC), Barcelona, Spain, 5.Soil Science, Institute of Geography, Friedrich Schiller University Jena, Jena, Germany, 6.Department of Geography and Department of Plant and Soil Sciences, University of Delaware, Newark, DE, USA)

[AHW23-P10] **Hydraulic analysis of overland flow caused by temporally varying rainfall**

*PING-CHENG HSIEH[1], Ming-Chang Wu[1] (1.National Chung Hsing University)

[AHW23-P11] A comparative Study on Water Environment of Isolated Islands - Focusing on Islands in Nagasaki Prefecture - (3)

*Go Yamaki[1], Koji Kodera[2], Kazuki Asami[1], Yoshihiro IGARI[1], Masaki Horiuchi[1] (1.Grad. Student, Hosei Univ., 2.Dep. of Geography, Hosei Univ.)

[AHW23-P12] **Water environment around Kusatsu-Shirane volcano and consideration of the effect of eruption in January 2018**

*Igari Yoshihiro[1], Koji Kodera[2], Kazuki Asami[1] (1.Grad.Student,Hosei Univ., 2.Dep.of Geography Hosei Univ.)

[AHW23-P13] Re-consideration of discharge rate of spring water in Lake Ezu, Kumamoto

*Kimpei Ichiyanagi[1], Kiyoshi Ide[1], Jun Shimada[1], Tsutomu Ichikawa[2] (1.Kumamoto University, 2.Tokai University)

[AHW23-P14] **Evaluating the efficacy of hydrologically and hydrodynamically driven methods of e-flow assessment for Upper Godavari River Basin, India**

*GAURAV KALIDAS PAKHALE[1], Jyoti Punjahari Nale[2], Ashvin Kumar Gosain[3], Rakesh Khosa[3] (1.PhD Research Scholar, Civil Engineering Department, Indian Institute of Technology, Delhi, 2.Project Advisor, IEWP, GIZ India, New Delhi, India, 3.Professor, Civil Engineering Department, Indian Institute of Technology, Delhi)

[AHW23-P15] Presence of pharmaceutical compounds in freshwater lakes and their impact on phytoplankton

*Nandakumar Kanavillil[1], Cassandra Fligg[1], Sreekumari Kurissery[1] (1.Lakehead University, Canada)

[AHW23-P16] **Novel approximate solutions for solute transport due to injections: considering the scale-dependent dispersion and non-integer flow dimension**

*Ye-Chen Lin[1], Hund-Der Yeh[1] (1.National Chiao Tung Univ.)

[AHW23-P17] Experimemtal study on the residual saturation of Porous Media using Pore Doublets Micromodel

*Chun-Wei Peng[1] (1.Taiwan National Chiao Tung University)

[AHW23-P18] Assessment of Synergy between Biomedical Waste and Shallow Groundwater Pollution

*Deepika [1], Abhishek [2] (1.BPS Government Medical College for Women, Sonepat, INDIA, 2.Technical University Dresden, GERMANY)

[AHW23-P19] Erosion and transport processes of earth surface materials in a reservoir-catchment system inferred from atmospheric radionuclides ^{7}Be and ^{210}Pb

*Mikiya Tsuruoka[1], Shinya Ochiai[2], Atsushi Matsuki[2], Seiya Nagao[2] (1.Graduate School of Natural Science and Technology, Kanazawa University, 2.Institute of Nature and Environmental Technology, Kanazawa University)

[AHW23-P20] Fluctuation of groundwater level in a sloping unconfined aquifer due to time varying recharge

*Ming-Chang Wu[1], Ping-Cheng Hsieh[1] (1.National Chung Hsing University)

[AHW23-P21] **Effect of cutoff wall on recharge water storage volume**

*Pei-hsun Tsai[1], Jung-hsing Tai[1] (1.Chaoyang University of Technology)

[AHW23-P22] **Studying Operation Parameters on Flat-Plate Membrane Bioreactor for Sewage Treatment**

*Jen Hung Chiu[1], Wen Chin Chen[1] (1.Studying Operation Parameters on Flat-Plate Membrane Bioreactor for Sewage Treatment)

[AHW23-P23] **Mine-water quality at a tertiary coalfield in India: Characterisation and treatment using novel polyvinyl alcohol (PVA) gel bioreactor**

*Aparna Dutta[1], Sudipta Sarkar[1] (1.Indian Institute of Technology Roorkee)

[E] Poster | A (Atmospheric and Hydrospheric Sciences)：A-HW Hydrology & Water Environment

5:15 PM - 6:30 PM JST | 8:15 AM - 9:30 AM UTC | Poster Hall International Exhibition Hall8, Makuhari Messe_14

[A-HW23] Hydrology & Water Environment

convener:Isao Machida(Geological Survey of Japan), Dai Yamazaki(Institute of Industrial Sciences, The University of Tokyo), Takeshi Hayashi(Faculty of Education and Human Studies, Akita University), Keisuke Fukushi(Institute of Nature & Environmental Technology, Kanazawa University)

[AHW23-P01] **A multiobjective risk management model for real-time reservoir flood control operation**

*Juan Chen[1,2], Ping-An Zhong[2], XinYu Wan[2], Yu Zhang[2] (1.College of Earth Sciences and Engineering, Hohai University, 2.College of Hydrology and Water Resources, Hohai University)

[AHW23-P02] **Assessment of the Flow Regime of Roanoke River due to Climatic and Anthropogenic Activities**

*Rahul Kumar Singh[1], Dr. Manoj Kumar Jain[1] (1.Indian Institute of Technology, Roorkee, India)

[AHW23-P03] Predictive Analysis of Climate, Water, Health and the Environment Nexus

*Abhishek [1], Deepika [2] (1.Technical University Dresden, GERMANY, 2.BPS Government Medical College for Women, Sonepat, INDIA)

[AHW23-P05] Severe droughts provide huge fuel for widespread wildfires in California in USA

*Linghua Qiu[1], Ji Chen[1], Haiyun Shi[2], Liqun Sun[3], Jun Niu[4] (1.the University of Hong Kong, 2.Southern University of Science and Technology, 3.Shenzhen Institutes of Advanced Technology, Chinese Academy of Sciences, 4.China Agricultural University)

[AHW23-P06] A comprehensive evaluation of MODIS-based water use efficiency with global eddy covariance flux data and a process model

*Shanshan YANG[1,2], Jiahua ZHANG[1], Sha ZHANG[1,2], Jingwen WANG[1,2], Yun BAI[1,2], Fengmei YAO[2], Huadong GUO[1] (1.Institute of Remote Sensing and Digital Earth, Chinese Academy of Sciences, 2.University of Chinese Academy of Sciences, Beijing, China)

[AHW23-P07] Impact of variability and anisotropy in the correlation decay distance for precipitation spatial interpolation in China

*yingxian zhang[1] (1.National Climate Center, China Meteorological Administration)

[AHW23-P08] New Record-Breaking Frequency of Annual Maximum Daily Precipitation of 58 stations in the whole Japan, an increasing of extreme values.

*Chhay Ngorn SEANG[1], Tomohito YAMADA[1] (1.Hokkaido University)

[AHW23-P09] Quantifying stemflow to better express its ecohydrological significance

*Shin'ichi Iida[1], Darryl E. Carlye-Moses[2], Sonja Germer[3], Pilar Llorens[4], Beate Michalzik[5], Kazuki Nanko[1], Alexander Tischer[5], Delphis F. Levia[6] (1.Department of Disaster Prevention, Meteorology and Hydrology, Forestry and Forest Products Research Institute, 2.Department of Geography and Environmental Studies, Thompson Rivers University, Kamloops, British Columbia, Canada, 3.Department of Bioengineering, Leibniz Institute for Agricultural Engineering and Bioeconomy, Potsdam, Germany, 4.Institute of Environmental Assessment and Water Research (IDAEA-CSIC), Barcelona, Spain, 5.Soil Science, Institute of Geography, Friedrich Schiller University Jena, Jena, Germany, 6.Department of Geography and Department of Plant and Soil Sciences, University of Delaware, Newark, DE, USA)

[AHW23-P10] **Hydraulic analysis of overland flow caused by temporally varying rainfall**

*PING-CHENG HSIEH[1], Ming-Chang Wu[1] (1.National Chung Hsing University)

[AHW23-P11] A comparative Study on Water Environment of Isolated Islands - Focusing on Islands in Nagasaki Prefecture - (3)

*Go Yamaki[1], Koji Kodera[2], Kazuki Asami[1], Yoshihiro IGARI[1], Masaki Horiuchi[1] (1.Grad. Student, Hosei Univ., 2.Dep. of Geography, Hosei Univ.)

[AHW23-P12] **Water environment around Kusatsu-Shirane volcano and consideration of the effect of eruption in January 2018**

*Igari Yoshihiro[1], Koji Kodera[2], Kazuki Asami[1] (1.Grad.Student,Hosei Univ., 2.Dep.of Geography Hosei Univ.)

[AHW23-P13] Re-consideration of discharge rate of spring water in Lake Ezu, Kumamoto

*Kimpei Ichiyanagi[1], Kiyoshi Ide[1], Jun Shimada[1], Tsutomu Ichikawa[2] (1.Kumamoto University, 2.Tokai University)

[AHW23-P14] **Evaluating the efficacy of hydrologically and hydrodynamically driven methods of e-flow assessment for Upper Godavari River Basin, India**

*GAURAV KALIDAS PAKHALE[1], Jyoti Punjahari Nale[2], Ashvin Kumar Gosain[3], Rakesh Khosa[3] (1.PhD Research Scholar, Civil Engineering Department, Indian Institute of Technology, Delhi, 2.Project Advisor, IEWP, GIZ India, New Delhi, India, 3.Professor, Civil Engineering Department, Indian Institute of Technology, Delhi)

[AHW23-P15] Presence of pharmaceutical compounds in freshwater lakes and their impact on phytoplankton

*Nandakumar Kanavillil[1], Cassandra Fligg[1], Sreekumari Kurissery[1] (1.Lakehead University, Canada)

[AHW23-P16] **Novel approximate solutions for solute transport due to injections: considering the scale-dependent dispersion and non-integer flow dimension**

*Ye-Chen Lin[1], Hund-Der Yeh[1] (1.National Chiao Tung Univ.)

[AHW23-P17] Experimemtal study on the residual saturation of Porous Media using Pore Doublets Micromodel

*Chun-Wei Peng[1] (1.Taiwan National Chiao Tung University)

[AHW23-P18] Assessment of Synergy between Biomedical Waste and Shallow Groundwater Pollution

*Deepika [1], Abhishek [2] (1.BPS Government Medical College for Women, Sonepat, INDIA, 2.Technical University Dresden, GERMANY)

[AHW23-P19] Erosion and transport processes of earth surface materials in a reservoir-catchment system inferred from atmospheric radionuclides ^{7}Be and ^{210}Pb

*Mikiya Tsuruoka[1], Shinya Ochiai[2], Atsushi Matsuki[2], Seiya Nagao[2] (1.Graduate School of Natural Science and Technology, Kanazawa University, 2.Institute of Nature and Environmental Technology, Kanazawa University)

[AHW23-P20] Fluctuation of groundwater level in a sloping unconfined aquifer due to time varying recharge

*Ming-Chang Wu[1], Ping-Cheng Hsieh[1] (1.National Chung Hsing University)

[AHW23-P21] **Effect of cutoff wall on recharge water storage volume**

*Pei-hsun Tsai[1], Jung-hsing Tai[1] (1.Chaoyang University of Technology)

[AHW23-P22] **Studying Operation Parameters on Flat-Plate Membrane Bioreactor for Sewage Treatment**

*Jen Hung Chiu[1], Wen Chin Chen[1] (1.Studying Operation Parameters on Flat-Plate Membrane Bioreactor for Sewage Treatment)

[AHW23-P23] **Mine-water quality at a tertiary coalfield in India: Characterisation and treatment using novel polyvinyl alcohol (PVA) gel bioreactor**

*Aparna Dutta[1], Sudipta Sarkar[1] (1.Indian Institute of Technology Roorkee)

[J] Oral | A (Atmospheric and Hydrospheric Sciences)：A-CC Cryospheric Sciences & Cold District Environment

9:00 AM - 10:30 AM JST | 12:00 AM - 1:30 AM UTC | 303 3F

[A-CC27] Glaciology

convener:Takayuki Nuimura(Tokyo Denki University), Ishikawa Mamoru(Hokkaido University), Kzutaka Tateyama(National University Corporation Kitami Institute of Technology), Hiroto Nagai(Waseda Univ., School of Education), Chairperson:Hiroto Nagai(Japan Aerospace Exploration Agency)

9:00 AM - 9:15 AM JST | 12:00 AM - 12:15 AM UTC

[ACC27-01] The early validation results of the GCOM-C/SGLI cryosphere standard product

★Invited Papers

*Rigen Shimada[1], Masahiro Hori[1], Teruo Aoki[2,3], Tomonori Tanikawa[2], Sumito Matoba[4], Masashi Niwano[2], Knut Stamnes[5], Wei Li[5], Nan Chen[5] (1.Japan Aerospace Exploration Agency, 2.Meteorological Research Institute, 3.Okayama University, 4.Institute of Low Temperature Science, Hokkaido University, 5.Stevens Institute of Technology)

9:15 AM - 9:30 AM JST | 12:15 AM - 12:30 AM UTC

[ACC27-02] Overview of the cryospheric variables derived from GCOM-C/SGLI observations: The first-year results

★Invited Papers

*Masahiro Hori[1], Teruo Aoki[2,4], Knut Stamnes[3], Wei Li[3], Nan Chen[3], Rigen Shimada[1], Tomonori Tanikawa[4], Masashi Niwano[4] (1.Earth Observation Reseacrh Center, Japan Aerospace Exploration Agency, 2.Okayama University, 3.Stevens Institute of Technology, 4.Meteorological Research Institute)

9:30 AM - 9:45 AM JST | 12:30 AM - 12:45 AM UTC

[ACC27-03] Relationships between PASAR-2 backscatter amplitude changes and snow depths

*Hiroto Nagai[1], Satoru Yamaguchi[2], Katsuya Yamashita[2], Mayumi Kashima[3] (1.Waseda University, School of Education, 2. National Research Institute for Earth Science and Disaster Resilience, 3.Esri Japan Corporation)

9:45 AM - 10:00 AM JST | 12:45 AM - 1:00 AM UTC

[ACC27-04] Breaking-off of hanging glaciers at Mt. Langtang-Lirung in Nepal

Honami Watanabe[2], *Chiyuki Narama[1], Yoshitaka Mori[2], Katsuhisa Kawashima[3] (1.Niigata University, Program of Field Research in the Environmental Sciences, 2.Graduate School of Science and Technology, Niigata University, 3.Research Institute for Natural Hazards & Disaster Recovery, Niigata University)

10:00 AM - 10:15 AM JST | 1:00 AM - 1:15 AM UTC

[ACC27-05] Spatial distribution of ice cliff in the Trakarding glacier, Nepal Himalaya

*Yota Sato[1], Koji Fujita[1], Hiroshi Inoue[2], Sojiro Sunako[1], Akiko Sakai[1], Akane Tsushima[1], Evgeny Podolskiy[3,4], Etienne Berthier[5], Rijan Kayastha[6] (1.Graduate School of Environmental Studies, Nagoya University, 2.National Research Institute for Earth Science and Disaster Resilience, 3.Arctic Research Center, Hokkaido University, 4.Global Station for Arctic Research, Global Institution for Collaborative Research and Education, Hokkaido University, 5.Centre National de la Recherche Scientifique, 6.School of Science, Kathmandu University)

10:15 AM - 10:30 AM JST | 1:15 AM - 1:30 AM UTC

[ACC27-06] Quantify the range of projections of future changes in glacier mass caused by differences among observed past climate datasets

*Megumi Watanabe[1], Aki Yanagawa[2], Yukiko Hirabayashi[3], Satoshi Watanabe[4], Shinjiro Kanae[1] (1.Tokyo Institute of Technology, 2.Meisei University, 3.Shibaura Institute of Technology, 4.The University of Tokyo)

[J] Oral | A (Atmospheric and Hydrospheric Sciences)：A-CC Cryospheric Sciences & Cold District Environment

10:45 AM - 12:15 PM JST | 1:45 AM - 3:15 AM UTC | 303 3F

[A-CC27] Glaciology

convener:Takayuki Nuimura(Tokyo Denki University), Ishikawa Mamoru(Hokkaido University), Kzutaka Tateyama(National University Corporation Kitami Institute of Technology), Hiroto Nagai(Waseda Univ., School of Education), Chairperson:Takayuki Nuimura(Chiba Institute of Science)

10:45 AM - 11:00 AM JST | 1:45 AM - 2:00 AM UTC

[ACC27-07] Preliminary analysis result of the Handheld Integrating Sphere Snow Grain Sizer (HISSGraS)

*Teruo Aoki[1,2,3], Masashi Niwano[2], Satoru Yamaguchi[4], Sumito Matoba[5], Tomonori Tanikawa[2], Masahiro Hori[6], Rigen Shimada[6], Akihiro Hachikubo[7] (1.The Graduate School of Natural Science and Technology, Okayama University, 2.Meteorological Research Institute, Japan Meteorological Agency, 3.National Institute of Polar Research, 4.National Research Institute for Earth Science and Disaster Resilience, 5.Institute of Low Temperature Sciences, Hokkaido University, 6.Earth Observation Research Center, Japan Aerospace Exploration Agency, 7.Kitami Institute of Technology)

11:00 AM - 11:15 AM JST | 2:00 AM - 2:15 AM UTC

[ACC27-08] Experimental study on compaction process of highly porous ice: Implications for density change of icy regolith layer on icy bodies

Minami Yabe[1], *Minami Yasui[1], Masahiko Arakawa[1] (1.Department of Planetology, Graduate School of Science, Kobe University)

11:15 AM - 11:30 AM JST | 2:15 AM - 2:30 AM UTC

[ACC27-09] **Effect of snow impurities on the radiation budget and snow melting observed at Sapporo during 10 winter seasons**

*Yoichiro Hirozawa[1], Teruo Aoki[1,2], Masashi Niwano[2], Sumito Matoba[3], Yuji Kodama[4], Tomonori Tanikawa[2] (1.Okayama University, Graduate School of Natural Science and Technology, 2.Meteorological Research Institute, 3.Institute of Low Temperature Science, Hokkaido University, 4.National Institute of Polar Research)

[J] Poster | A (Atmospheric and Hydrospheric Sciences)：A-CC Cryospheric Sciences & Cold District Environment

3:30 PM - 5:00 PM JST | 6:30 AM - 8:00 AM UTC | Poster Hall International Exhibition Hall8, Makuhari Messe_9

[A-CC27] Glaciology

convener:Takayuki Nuimura(Tokyo Denki University), Ishikawa Mamoru(Hokkaido University), Kzutaka Tateyama(National University Corporation Kitami Institute of Technology), Hiroto Nagai(Waseda Univ., School of Education)

[ACC27-P01] Recent surface changes of rock glaciers in Tien Shan Mountains

*Hideyuki Takadama[1], Narama Chiyuki[2], Tsutomu Yamanokuchi[3], Takeo Tadono[4] (1.Graduate school of Science and Technology, Niigata university, 2.Department of Science, Niigata University , 3.RESTEC, 4.JAXA)

[ACC27-P02] Verification of AMSR-2 sea ice concentration and utilization of ship navigation in the Arctic Ocean

*Nodoka Ono[1] (1.Earth Observation Research Center, Japan Aerospace Exploration Agency)

[ACC27-P03] Ice thickness and flow of the perennial snow patch at Karamatsu-sawa in Hida mountain range

*Kenshiro Arie[1], Chiyuki Narama[2], Kotaro FUKUI[3], Hajime IIDA[3] (1.Graduate School of Science and Technology, Niigata University, 2.Faculty of Science, Niigata University, 3.Tateyama Caldera Sabo Museum)

[ACC27-P04] Meltwater discharge from Wilkes Basin, East Antarctica at around 4.2 ka revealed from Beryllium-10 analysis of marine sediments

*Bethany Behrens[1,2], Yosuke Miyairi[1], Adam Sproson[1], Masako Yamane[3], Yusuke Yokoyama[1,2,4,5] (1.Atmosphere and Ocean Research Institute, University of Tokyo, 5-1-5 Kashiwanoha, Kashiwa, Chiba 277-8564, Japan, 2.Graduate Program on Environmental Science, University of Tokyo, Komaba, Meguro, Tokyo 153-0041, Japan, 3.Institute for Space-Earth Environmental Research, Nagoya University, Furocho, Chikusa, Nagoya, Aichi, 464-8601, Japan, 4.Japan Agency for Marine-Earth Science and Technology (JAMSTEC), Natsushimacho, Yokosuka, Kanagawa Prefecture 237-0061, Japan, 5.Department of Earth and Planetary Science, Graduate School of Science, University of Tokyo, Hongo, Bunkyo, Tokyo 113-8654, Japan)

[ACC27-P05] Daily variation of supraglacial lakes in the southern Inylchek Glacier

*Naoki Sakurai[1], Chiyuki Narama[2], Hiroshi Inoue[3], Muhammed Esenamanov[4], Zarylbek Usekov[4] (1.Niigata University, 2. Niigata University Department of Science, 3.National Research Institute for Earth Science and Disaster Prevention, 4.Central Asian Institute for Applied Geosciences)

[ACC27-P06] Historical development of Spillway Lake on Ngozompa Glacier, Nepal

*Mohan Bahadur Chand[1], Teiji Watanabe[2], Yusuki Kobayashi[1] (1.Graduate School of Environmental Science, Hokkaido University, 2.Faculty of Environmental Earth Science, Hokkaido University)

[ACC27-P07] Feature analysis of the spectral of snow, ice, and water in Lake Suwa using MODIS data

*Tomohiro Nakazawa[1], Takashi Nonaka[2], Keishi Iwashita[2] (1.Department of Civil Engineering, College of Industrial Technology, Nihon University , 2.College of Industrial Technology, Nihon University)

[J] Poster | A (Atmospheric and Hydrospheric Sciences)：A-CC Cryospheric Sciences & Cold District Environment

5:15 PM - 6:30 PM JST | 8:15 AM - 9:30 AM UTC | Poster Hall International Exhibition Hall8, Makuhari Messe_15

[A-CC27] Glaciology

convener:Takayuki Nuimura(Tokyo Denki University), Ishikawa Mamoru(Hokkaido University), Kzutaka Tateyama(National University Corporation Kitami Institute of Technology), Hiroto Nagai(Waseda Univ., School of Education)

[ACC27-P01] Recent surface changes of rock glaciers in Tien Shan Mountains

*Hideyuki Takadama[1], Narama Chiyuki[2], Tsutomu Yamanokuchi[3], Takeo Tadono[4] (1.Graduate school of Science and Technology, Niigata university, 2.Department of Science, Niigata University , 3.RESTEC, 4.JAXA)

[ACC27-P02] Verification of AMSR-2 sea ice concentration and utilization of ship navigation in the Arctic Ocean

*Nodoka Ono[1] (1.Earth Observation Research Center, Japan Aerospace Exploration Agency)

[ACC27-P03] Ice thickness and flow of the perennial snow patch at Karamatsu-sawa in Hida mountain range

*Kenshiro Arie[1], Chiyuki Narama[2], Kotaro FUKUI[3], Hajime IIDA[3] (1.Graduate School of Science and Technology, Niigata University, 2.Faculty of Science, Niigata University, 3.Tateyama Caldera Sabo Museum)

[ACC27-P04] Meltwater discharge from Wilkes Basin, East Antarctica at around 4.2 ka revealed from Beryllium-10 analysis of marine sediments

*Bethany Behrens[1,2], Yosuke Miyairi[1], Adam Sproson[1], Masako Yamane[3], Yusuke Yokoyama[1,2,4,5] (1.Atmosphere and Ocean Research Institute, University of Tokyo, 5-1-5 Kashiwanoha, Kashiwa, Chiba 277-8564, Japan, 2.Graduate Program on Environmental Science, University of Tokyo, Komaba, Meguro, Tokyo 153-0041, Japan, 3.Institute for Space-Earth Environmental Research, Nagoya University, Furocho, Chikusa, Nagoya, Aichi, 464-8601, Japan, 4.Japan Agency for Marine-Earth Science and Technology (JAMSTEC), Natsushimacho, Yokosuka, Kanagawa Prefecture 237-0061, Japan, 5.Department of Earth and Planetary Science, Graduate School of Science, University of Tokyo, Hongo, Bunkyo, Tokyo 113-8654, Japan)

[ACC27-P05] Daily variation of supraglacial lakes in the southern Inylchek Glacier

*Naoki Sakurai[1], Chiyuki Narama[2], Hiroshi Inoue[3], Muhammed Esenamanov[4], Zarylbek Usekov[4] (1.Niigata University, 2. Niigata University Department of Science, 3.National Research Institute for Earth Science and Disaster Prevention, 4.Central Asian Institute for Applied Geosciences)

[ACC27-P06] Historical development of Spillway Lake on Ngozompa Glacier, Nepal

*Mohan Bahadur Chand[1], Teiji Watanabe[2], Yusuki Kobayashi[1] (1.Graduate School of Environmental Science, Hokkaido University, 2.Faculty of Environmental Earth Science, Hokkaido University)

[ACC27-P07] Feature analysis of the spectral of snow, ice, and water in Lake Suwa using MODIS data

*Tomohiro Nakazawa[1], Takashi Nonaka[2], Keishi Iwashita[2] (1.Department of Civil Engineering, College of Industrial Technology, Nihon University , 2.College of Industrial Technology, Nihon University)

[E] Oral | A (Atmospheric and Hydrospheric Sciences)：A-CG Complex & General

3:30 PM - 5:00 PM JST | 6:30 AM - 8:00 AM UTC | 302 3F

[A-CG34] Satellite Earth Environment Observation

convener:Riko Oki(Japan Aerospace Exploration Agency), Yoshiaki HONDA(Center for Environmental Remote Sensing, Chiba University), Yukari Takayabu(Atmosphere and Ocean Research Institute, the University of Tokyo), Tsuneo Matsunaga(Center for Global Environmental Research and Satellite Observation Center, National Institute for Environmental Studies), Chairperson:Misako Kachi(Earth Observation Research Center, Japan Aerospace Exploration Agency)

3:30 PM - 3:45 PM JST | 6:30 AM - 6:45 AM UTC

[ACG34-01] Current Status and Future Plan of the Global Change Observation Mission - Water (GCOM-W) and Advanced Microwave Scanning Radiometer 2 (AMSR2)

*Misako Kachi[1], Takashi Maeda[1], Nodoka Ono[1], Hideyuki Fujii[1], Marehito Kasahara[1], Naoto Ebuchi[1,2] (1.Earth Observation Research Center, Japan Aerospace Exploration Agency, 2.Institute of Low Temperature Science, Hokkaido University)

3:45 PM - 4:00 PM JST | 6:45 AM - 7:00 AM UTC

[ACG34-02] Testing and Evaluation for JPSS-1 Algorithms using Algorithm Development Library Block 2.1

*Bigyani Das[1,2], Weizhong Chen[1,2], Thomas S King[1,2], Walter Wolf[2] (1.IMSG, 2.STAR/NESDIS/NOAA)

4:00 PM - 4:15 PM JST | 7:00 AM - 7:15 AM UTC

[ACG34-03] Remote Sensing of Atmospheric and Surface Properties using Hyperspectral satellite Sensors

*Xu Liu[1] (1.NASA Langley Research Center)

4:15 PM - 4:30 PM JST | 7:15 AM - 7:30 AM UTC

[ACG34-04] **RADIOMETRIC UNIFORMITY AND STABILITY OF GROUND SITE CHARACTERIZATION FOR INSAT-3D**

*Shailesh Parihar[1], R. Bhatla[1], A. K. Mitra[2] (1.Banaras Hindu University, Varanasi, India, 2.India Meteorological Department, New Delhi, India)

4:30 PM - 4:45 PM JST | 7:30 AM - 7:45 AM UTC

[ACG34-05] Vicarious calibration activities of ASTER Thermal Infrared Radiometer (TIR) for Earth environmental observation

*Satoru Yamamoto[1], Hideyuki Tonooka[2], Soushi Kato[3], Kazuki Ayuzawa[2], Tsuneo Matsunaga[4] (1.Japan Space Systems, 2.Ibaraki University, 3.Remote Sensing Technology Center of Japan, 4.National Institute for Environmental Studies)

4:45 PM - 5:00 PM JST | 7:45 AM - 8:00 AM UTC

[ACG34-06] **Overview of Vegetation Lidar MOLI**

★Invited Papers

*Haruhisa Shimoda[1], Toshiyoshi Kimura[2], Rei Mituhashi [2], Junpei Muruoka [2], Daisuke Sakaizawa[2], Tadashi Imai [2], Kazuhiro Asai[3] (1.Tokai University, 2.JAXA, 3.Tohoku Institute of Technology)

[E] Poster | A (Atmospheric and Hydrospheric Sciences)：A-CG Complex & General

10:45 AM - 12:15 PM JST | 1:45 AM - 3:15 AM UTC | Poster Hall International Exhibition Hall8, Makuhari Messe_6

[A-CG35] Projection and detection of global environmental change

convener:Michio Kawamiya(Japan Agency for Marine-Earth Science and Technology), Hiroaki Tatebe(Japan Agency for Marine-Earth Science and Technology), Kaoru Tachiiri(Japan Agency for Marine-Earth Science and Technology)

[ACG35-P01] **World Regionalization of Climate Change (1961–2010)**

*Shao Sun[1,2], Peijun Shi[2,3,4], Daoyi Gong[2], Tao Zhou[2] (1.National Climate Center, China Meteorological Administration, Beijing 100081, China, 2.State Key Laboratory of Earth Surface Processes and Resource Ecology, Beijing Normal University, Beijing 100875, China, 3.Key Laboratory of Environmental Change and Natural Disaster of Ministry of Education, Beijing Normal University, Beijing 100875, China, 4.Academy of Disaster Reduction and Emergency Management, Ministry of Civil Affairs & Ministry of Education, Beijing 100875, China)

[ACG35-P02] Quantifying and identifying future climate signal, noise, and internal variability at finer temporal scales

*Jongho Kim[1], Manh Van Doi[1] (1.University of Ulsan)

[ACG35-P03] Basic evaluation of MIROC6 and current status of CMIP6 experiments

*Hiroaki Tatebe[1] (1.Japan Agency for Marine-Earth Science and Technology)

[ACG35-P04] **Synchronized increase of extreme cold and warm events in China during the recent global warming slowdown**

*Xiubao Sun[1,3], Chunzai Wang[1], Guoyu Ren[2,3], Panfeng Zhang[2] (1.State Key Laboratory of Tropical Oceanography (LTO), South China Sea Institute of Oceanology(SCSIO), Chinese Academy of Sciences (CAS), 2.Department of Atmospheric Science, School of Environmental Studies, China University of Geosciences (CUG), 3.Laboratory for Climate Studies, National Climate Center (NCC), China Meteorological Administration (CMA))

[ACG35-P05] Quantification of thermodynamical and dynamical contributions to the anthropogenic influences on tropical cyclone rainfall extremes

*Cheng-Ta Chen[1], Shih-How Lo[1], Chung-Chieh Wang[1], Kazuhisa Tsuboki[2] (1.Department of Earth Sciences, National Taiwan Normal University, 2.Hydrospheric-Atmospheric Research Center, Nagoya University)

[ACG35-P06] **Temporal Evolution of the Long-Term Distributional Biases of Climate Models as a Parameter for the Regional Evaluation of the Simulation of Climate Change**

*Martin Gomez-Garcia[1], Akiko Matsumura[1], Shiro Hishinuma[1], Daikichi Ogawada[1] (1.Nippon Koei Co. Ltd., Reasearch and Development Center)

[ACG35-P07] A global simulation of bioenergy crop yield

*Zhipin Ai[1], Naota Hanasaki[1] (1.National Institute for Environmental Studies)

[ACG35-P08] Integrated Research Program for Advancing Climate Models - Theme B: national research program in Japan on earth system modeling

*Michio Kawamiya[1], Tomohiro Hajima[1], Kaoru Tachiiri[1], Jun'ichi Tsutsui[2], Tokuta Yokohata[3], Takashi Arakawa[4], Takahiro Inoue[4] (1.Japan Agency for Marine-Earth Science and Technology, 2.Central Research Institute of Electric Power Industry, 3.National Institute for Environmental Studies, 4.Research Organization for Information Science and Technology)

[ACG35-P09] Towards probabilistic climate projections based on the CMIP6 multi-model ensemble

*Junichi Tsutsui[1] (1.Central Research Institute of Electric Power Industry)

[ACG35-P10] Effect on the earth system of realizing 1.5 degree climate target by overshooting after reaching 2 degree level

*Kaoru Tachiiri[1], Herran Diego Silva[2], Xuanming Su[1], Michio Kawamiya[1] (1.Japan Agency for Marine-Earth Science and Technology, 2.Institute for Global Environmental Strategies)

[ACG35-P11] **Historical regional and sectoral contributions to climate change**

*Xuanming Su[1], Kaoru Tachiiri[1], Katsumasa TANAKA[2], Michio Watanabe[1] (1.Japan Agency for Marine-Earth Science and Technology, 2.National Institute for Environmental Studies)

[ACG35-P12] **Future projection of global climate, water, food, bio-energy, and land investigated with MIROC-INTEG: a global bio-geophysical land surface model with human components**

*Tokuta Yokohata[1], Yusuke Satoh[1], Tsuguki Kinoshita[2], Gen Sakurai[3], Yadu Pokhrel[4], Akihiko Ito[1], Etsushi Kato[5], Masashi Okada[1], Naota Hanasaki[1], Tomoko Nitta[6], Seita Emori[1] (1.National Institute for Environmental Studies, 2.Ibaraki University, 3.National Agriculture and Food Research Organization, 4.Michigan State University, 5.The Institute of Applied Energy, 6.University of Tokyo)

[ACG35-P13] **Downscaling a global agricultural land use model to country level for national SSP analysis**

*Wenchao Wu[1], Tomoko Hasegawa[1], Kiyoshi Takahashi[1], Shinichiro Fujimori[2] (1.National Institute for Environmental Studies, 2.Kyoto Univ.)

[ACG35-P14] Extreme Events and Emergent Trends in Marine Ecosystem Stressors under a historical/RCP8.5 Climate Change Pathway

*Keith Bradley Rodgers[1,2], Sarah Schlunegger[3], Richard Slater[3], Burke Hales[4], Axel Timmermann[1,2] (1.IBS Center for Climate Physics, Busan, South Korea, 2.Pusan National University, Busan, South Korea, 3.AOS Program, Princeton University, Princeton NJ, USA, 4.College of Ocean and Atmospheric Sciences, Oregon State Universitym, Corvallis, OR, USA)

[E] Poster | A (Atmospheric and Hydrospheric Sciences)：A-CG Complex & General

5:15 PM - 6:30 PM JST | 8:15 AM - 9:30 AM UTC | Poster Hall International Exhibition Hall8, Makuhari Messe_16

[A-CG35] Projection and detection of global environmental change

convener:Michio Kawamiya(Japan Agency for Marine-Earth Science and Technology), Hiroaki Tatebe(Japan Agency for Marine-Earth Science and Technology), Kaoru Tachiiri(Japan Agency for Marine-Earth Science and Technology)

[ACG35-P01] **World Regionalization of Climate Change (1961–2010)**

*Shao Sun[1,2], Peijun Shi[2,3,4], Daoyi Gong[2], Tao Zhou[2] (1.National Climate Center, China Meteorological Administration, Beijing 100081, China, 2.State Key Laboratory of Earth Surface Processes and Resource Ecology, Beijing Normal University, Beijing 100875, China, 3.Key Laboratory of Environmental Change and Natural Disaster of Ministry of Education, Beijing Normal University, Beijing 100875, China, 4.Academy of Disaster Reduction and Emergency Management, Ministry of Civil Affairs & Ministry of Education, Beijing 100875, China)

[ACG35-P02] Quantifying and identifying future climate signal, noise, and internal variability at finer temporal scales

*Jongho Kim[1], Manh Van Doi[1] (1.University of Ulsan)

[ACG35-P03] Basic evaluation of MIROC6 and current status of CMIP6 experiments

*Hiroaki Tatebe[1] (1.Japan Agency for Marine-Earth Science and Technology)

[ACG35-P04] **Synchronized increase of extreme cold and warm events in China during the recent global warming slowdown**

*Xiubao Sun[1,3], Chunzai Wang[1], Guoyu Ren[2,3], Panfeng Zhang[2] (1.State Key Laboratory of Tropical Oceanography (LTO), South China Sea Institute of Oceanology(SCSIO), Chinese Academy of Sciences (CAS), 2.Department of Atmospheric Science, School of Environmental Studies, China University of Geosciences (CUG), 3.Laboratory for Climate Studies, National Climate Center (NCC), China Meteorological Administration (CMA))

[ACG35-P05] Quantification of thermodynamical and dynamical contributions to the anthropogenic influences on tropical cyclone rainfall extremes

*Cheng-Ta Chen[1], Shih-How Lo[1], Chung-Chieh Wang[1], Kazuhisa Tsuboki[2] (1.Department of Earth Sciences, National Taiwan Normal University, 2.Hydrospheric-Atmospheric Research Center, Nagoya University)

[ACG35-P06] **Temporal Evolution of the Long-Term Distributional Biases of Climate Models as a Parameter for the Regional Evaluation of the Simulation of Climate Change**

*Martin Gomez-Garcia[1], Akiko Matsumura[1], Shiro Hishinuma[1], Daikichi Ogawada[1] (1.Nippon Koei Co. Ltd., Reasearch and Development Center)

[ACG35-P07] A global simulation of bioenergy crop yield

*Zhipin Ai[1], Naota Hanasaki[1] (1.National Institute for Environmental Studies)

[ACG35-P08] Integrated Research Program for Advancing Climate Models - Theme B: national research program in Japan on earth system modeling

*Michio Kawamiya[1], Tomohiro Hajima[1], Kaoru Tachiiri[1], Jun'ichi Tsutsui[2], Tokuta Yokohata[3], Takashi Arakawa[4], Takahiro Inoue[4] (1.Japan Agency for Marine-Earth Science and Technology, 2.Central Research Institute of Electric Power Industry, 3.National Institute for Environmental Studies, 4.Research Organization for Information Science and Technology)

[ACG35-P09] Towards probabilistic climate projections based on the CMIP6 multi-model ensemble

*Junichi Tsutsui[1] (1.Central Research Institute of Electric Power Industry)

[ACG35-P10] Effect on the earth system of realizing 1.5 degree climate target by overshooting after reaching 2 degree level

*Kaoru Tachiiri[1], Herran Diego Silva[2], Xuanming Su[1], Michio Kawamiya[1] (1.Japan Agency for Marine-Earth Science and Technology, 2.Institute for Global Environmental Strategies)

[ACG35-P11] **Historical regional and sectoral contributions to climate change**

*Xuanming Su[1], Kaoru Tachiiri[1], Katsumasa TANAKA[2], Michio Watanabe[1] (1.Japan Agency for Marine-Earth Science and Technology, 2.National Institute for Environmental Studies)

[ACG35-P12] **Future projection of global climate, water, food, bio-energy, and land investigated with MIROC-INTEG: a global bio-geophysical land surface model with human components**

*Tokuta Yokohata[1], Yusuke Satoh[1], Tsuguki Kinoshita[2], Gen Sakurai[3], Yadu Pokhrel[4], Akihiko Ito[1], Etsushi Kato[5], Masashi Okada[1], Naota Hanasaki[1], Tomoko Nitta[6], Seita Emori[1] (1.National Institute for Environmental Studies, 2.Ibaraki University, 3.National Agriculture and Food Research Organization, 4.Michigan State University, 5.The Institute of Applied Energy, 6.University of Tokyo)

[ACG35-P13] **Downscaling a global agricultural land use model to country level for national SSP analysis**

*Wenchao Wu[1], Tomoko Hasegawa[1], Kiyoshi Takahashi[1], Shinichiro Fujimori[2] (1.National Institute for Environmental Studies, 2.Kyoto Univ.)

[ACG35-P14] Extreme Events and Emergent Trends in Marine Ecosystem Stressors under a historical/RCP8.5 Climate Change Pathway

*Keith Bradley Rodgers[1,2], Sarah Schlunegger[3], Richard Slater[3], Burke Hales[4], Axel Timmermann[1,2] (1.IBS Center for Climate Physics, Busan, South Korea, 2.Pusan National University, Busan, South Korea, 3.AOS Program, Princeton University, Princeton NJ, USA, 4.College of Ocean and Atmospheric Sciences, Oregon State Universitym, Corvallis, OR, USA)

[E] Oral | A (Atmospheric and Hydrospheric Sciences)：A-CG Complex & General

1:45 PM - 3:15 PM JST | 4:45 AM - 6:15 AM UTC | 303 3F

[A-CG35] Projection and detection of global environmental change

convener:Michio Kawamiya(Japan Agency for Marine-Earth Science and Technology), Hiroaki Tatebe(Japan Agency for Marine-Earth Science and Technology), Kaoru Tachiiri(Japan Agency for Marine-Earth Science and Technology), Chairperson:Hiroaki Tatebe

1:45 PM - 2:00 PM JST | 4:45 AM - 5:00 AM UTC

[ACG35-01] **Sour and anoxic Sea of Japan in the near future**

*Chen-Tung Arthur Chen[1], Hon-Kit Lui[1], Masao Ishii[2] (1.National Sun Yat Sen University, 2.Japan Meteorological Agency)

2:00 PM - 2:15 PM JST | 5:00 AM - 5:15 AM UTC

[ACG35-02] **Decadal predictions of the variable ocean carbon uptake**

★Invited Papers

*Hongmei Li[1], Tatiana Ilyina[1], Wolfgang A. Müller[1,2], Peter Landschützer[1] (1.Max Planck Institute for Meteorology, Bundesstraße 53, 20146 Hamburg, Germany, 2.Deutscher Wetterdienst, Bernhard-Nocht-Straße 76, 20359 Hamburg, Germany)

2:15 PM - 2:30 PM JST | 5:15 AM - 5:30 AM UTC

[ACG35-03] Air-sea CO_2 flux variations in the tropical Pacific simulated with two ESMs embedded an ocean data assimilation system

*Michio Watanabe[1], Hiroaki Tatebe[1], Hiroshi Koyama[1], Tomohiro Hajima[1], Masahiro Watanabe[2], Michio Kawamiya[1] (1.Japan Agency for Marine-Earth Science and Technology, 2.Atmosphere and Ocean Research Institute, the University of Tokyo)

2:30 PM - 2:45 PM JST | 5:30 AM - 5:45 AM UTC

[ACG35-04] **A Study of Decadal Ocean Deoxygenation and Heat Uptake from a suite of OMIP Simulations**

*Yohei Takano[1], Jerry Tjiputra[2], Jörg Schwinger[2], Matthias Gröger[3], Sarah Berthet[4], Roland Séférian[4], Andrew Yool[5], Julien Palmieri[5], Michio Watanabe[6], Irene Stemmler[1], Tatiana Ilyina[1] (1.Max Planck Institute for Meteorology, 2.Norwegian Research Centre, 3.Swedish Meteorological and Hydrological Institute, 4.Centre National de Recherche Météorologique, Unite mixte de recherche 3589 Météo-France/CNRS, 5. National Oceanography Centre, 6.Japan Agency for Marine-Earth Science and Technology)

2:45 PM - 3:00 PM JST | 5:45 AM - 6:00 AM UTC

[ACG35-05] **Role of large-scale environmental variability in changing storm climate**

*Nilima Aditya Natoo[1] (1.University of Bremen, Germany)

3:00 PM - 3:15 PM JST | 6:00 AM - 6:15 AM UTC

[ACG35-06] The forced response of the climate system: The case of climatic teleconnections

*Tamas Bodai[1], Matyas Herein[2], Gabor Drotos[3] (1.University of Reading, 2.Eotvos University Budapest, 3.Universitat de les Illes Balears)

[E] Oral | A (Atmospheric and Hydrospheric Sciences)：A-CG Complex & General

3:30 PM - 5:00 PM JST | 6:30 AM - 8:00 AM UTC | 303 3F

[A-CG35] Projection and detection of global environmental change

convener:Michio Kawamiya(Japan Agency for Marine-Earth Science and Technology), Hiroaki Tatebe(Japan Agency for Marine-Earth Science and Technology), Kaoru Tachiiri(Japan Agency for Marine-Earth Science and Technology), Chairperson:Kaoru Tachiiri(Japan Agency for Marine-Earth Science and Technology), Michio Kawamiya(JAMSTEC)

3:30 PM - 3:45 PM JST | 6:30 AM - 6:45 AM UTC

[ACG35-07] Guiding Mother Earth: taking stock of progress to a long-term temperature goal

★Invited Papers

*Myles Robert Allen[1] (1.Environmental Change Institute, School of Geography and the Environment and Department of Physics, University of Oxford)

3:45 PM - 4:00 PM JST | 6:45 AM - 7:00 AM UTC

[ACG35-08] **Uneven distributions of four hazard indicators of climate change with the Paris Agreement's goals**

*Hideo Shiogama[1] (1.Center for Global Environmental Research, National Institute for Environmental Studies)

4:00 PM - 4:15 PM JST | 7:00 AM - 7:15 AM UTC

[ACG35-09] Understanding the centennial-scale human-natural interactions using an integrated terrestrial model MIROC-INTEG under ISIMIP2 project

*Yusuke Satoh[1], Julien Boulange[1], Naota Hanasaki[1], Kumiko Takata[1], Yadu Pokhrel[3], Ted Veldkamp[2,4], Peter Burek[2], Tokuta Yokohata[1] (1.National Institute for Environmental Studies, 2.International Institute for Applied Systems Analysis, 3.Department of Civil and Environmental Engineering, Michigan State University, 4.Institute for Environmental Studies (IVM), VU Amsterdam)

4:15 PM - 4:30 PM JST | 7:15 AM - 7:30 AM UTC

[ACG35-10] Radiative forcing of the physiological CO_2 response

*Victor Brovkin[1], Veronika Gayler[1], Sonia I Seneviratne[2], Pierre Gentine[3] (1.Max Planck Institute for Meteorology, Hamburg, Germany, 2.ETH, Institute for Atmospheric and Climate Science, Zurich, Switzerland, 3.Columbia University, Earth and Environmental Engineering, New York, USA)

4:30 PM - 4:45 PM JST | 7:30 AM - 7:45 AM UTC

[ACG35-11] Progress of MIROC-ES2 simulations in CMIP6 and the analysis of the biogeochemical feedbacks

*Tomohiro Hajima[1], Shingo Watanabe[1], Michio Kawamiya[1], Kaoru Tachiiri[1], Hiroaki Tatebe[1], Akihiko Ito[2], Kumiko TAKATA[2], Michio Watanabe[1], Maki Noguchi[1], Akitomo Yamamoto[1], Akinori Ito[1], Manabu Abe[1], Rumi Ohgaito[1], Dai Yamazaki[3] (1.Japan Agency for Marine-Earth Science and Technology, 2.National Institute for Environmental Studies, 3.Institute of Industrial Science, the University of Tokyo)

4:45 PM - 5:00 PM JST | 7:45 AM - 8:00 AM UTC

[ACG35-12] The impact of long-term historical warming on the global terrestrial gross primary production

*Irina Melnikova[1], Takahiro Sasai[1] (1.Tohoku University)

[J] Oral | A (Atmospheric and Hydrospheric Sciences)：A-CG Complex & General

10:45 AM - 12:15 PM JST | 1:45 AM - 3:15 AM UTC | 102 1F

[A-CG42] Biogeochemical linkages between the surface ocean and atmosphere

convener:Yuzo Miyazaki(Institute of Low Temperature Science, Hokkaido University), Jun Nishioka(Hokkaido University, Institute of low temperature sciences), Koji Suzuki(Hokkaido University), Yoko Iwamoto(Graduate School of Biosphere Science, Hiroshima University), Chairperson:Yuzo Miyazaki(Institute of low temperature science, Hokkaido University), Jun Nishioka(Institute of low temperature science, Hokkaido University)

10:45 AM - 11:00 AM JST | 1:45 AM - 2:00 AM UTC

[ACG42-01] Production of bromoform in sea ice and emission to the atmosphere

*Daiki Nomura[1], Atsushi Ooki[1], Ellen Damm[2], Gerhard Dieckmann[2], Bruno Delille[3], Markus Frey[4], Mats Granskog[5], Klaus Meiners[6,7], Anna Silyakova[8], Takeshi Tamura[9], Jean-Louis Tison[10], Youhei Yamashita[11] (1.Faculty of Fisheries Sciences, Hokkaido University, 2.Alfred Wegener Institute for Polar and Marine Research, Bremerhaven, Germany, 3.Université de Liège, Liège, Belgium., 4.British Antarctic Survey, Cambridge, United Kingdom., 5.Norwegian Polar Institute, Tromsø, Norway., 6.Antarctic Climate andEcosystems Cooperative Research Centre, University of Tasmania, Hobart, Australia., 7.Australian Antarctic Division, Kingston, Australia., 8.Centre for Arctic Gas Hydrate, Environment and Climate, Tromsø, Norway., 9.National Institute of Polar Research, Tokyo, Japan., 10.Université Libre de Bruxelles, Bruxelles, Belgium., 11.Graduate School of Environmental Sceince, Hokkaido University, Sapporo, Japan.)

11:00 AM - 11:15 AM JST | 2:00 AM - 2:15 AM UTC

[ACG42-02] Accumulation processes of trace metals into arctic sea ice: distribution of Fe, Mn and Cd associated with ice structure

*La Kenya Evans[1], Jun Nishioka[1] (1.Institute of Low Temperature Sciences, Hokkaido University)

11:15 AM - 11:30 AM JST | 2:15 AM - 2:30 AM UTC

[ACG42-03] Is halogen chemistry responsible for low ozone levels observed over western Pacific equatorial region? - From observations on R/V Mirai

*Yugo Kanaya[1], Kazuyuki Miyazaki[1], Fumikazu Taketani[1], Takuma Miyakawa[1], Hisahiro Takashima[1,2], Yuichi Komazaki[1], Xiaole PAN[3,1], Saki Kato[2], Kengo Sudo[4,1] (1.Research and Development Center for Global Change, Japan Agency for Marine-Earth Science and Technology, 2.Fukuoka University, 3.Institute of Atmospheric Physics, Chinese Academy of Sciences, China, 4.Nagoya University)

11:30 AM - 11:45 AM JST | 2:30 AM - 2:45 AM UTC

[ACG42-04] Very low $\delta^{15}N$ of atmospheric nitrate found in the earstern equatorial Pacific and its implication to dynamic nitrogen recycle between ocean and lower atmosphere

*Shohei Hattori[1], Kazuki Kamezaki[1], Yoko Iwamoto[2], Sakiko Ishino[1], Mitsuo Uematsu[3], Kazuhiko Miura[4], Naohiro Yoshida[1] (1.Department of Chemical Science and Engineering, School of Materials and Chemical Technology, Tokyo Institute of Technology, 2.Hiroshima University, 3.University of Tokyo, 4.Tokyo University of Science)

11:45 AM - 12:00 PM JST | 2:45 AM - 3:00 AM UTC

[ACG42-05] Origin of water-soluble organic nitrogen in marine atmospheric aerosols in the subtropical North Pacific

*Tsukasa Dobashi[1,2], Yuzo Miyazaki[1], Eri Tachibana[1], Yoko Iwamoto[3], Kazutaka Takahashi[4], Sachiko Horii[4], Shu-Kuan Wong[5], Koji Hamasaki[5] (1.Institute of Low Temperature Science, Hokkaido Univ., 2.Graduate School of Env. Sci., Hokkaido Univ., 3.Graduate School of Biosphere Science, Hiroshima Univ., 4.Graduate School of Agricultural and Life Sciences, Univ. of Tokyo, 5.Atmosphere and Ocean Research Institute, Univ. of Tokyo)

12:00 PM - 12:15 PM JST | 3:00 AM - 3:15 AM UTC

[ACG42-06] Impacts of ammonia on gas-particle partition and AWC during the 2016 APHH-Beijing campaign: inducing effects of nitrate ammonium

*baozhu Ge[1], Xiaobin Xu[2], Zhiqiang Ma[3], Xiaole PAN[1], Zhe WANG[1,4], Weili Lin[5], Bin Ouyang[6], Danhui Xu[1], James Lee[7], Mei Zheng[8], Dongsheng Ji[1], Yele Sun[1], Huabin Dong[8], Freya Anne Squires[7], Pingqing Fu[1], Zifa Wang[1] (1.State Key Laboratory of Atmospheric Boundary Layer Physics and Atmospheric Chemistry, Institute of Atmospheric Physics, Chinese Academy of Sciences, Beijing 100029, China, 2.State Key Laboratory of Severe Weather & Key Laboratory for Atmospheric Chemistry of China Meteorological Administration, Chinese Academy of Meteorological Sciences, Beijing 100081, China, 3.Institute of Urban Meteorology, China Meteorological Administration, Beijing, China, 4.Research Institute for Applied Mechanics (RIAM), Kyushu University, Fukuoka, Japan, 5.College of Life and Environmental Sciences, Minzu University of China, Beijing 100081, China, 6.Lancaster Environment Centre,

Lancaster University, Lancaster, LA1 4YQ, UK, 7.National Centre for Atmospheric Science Department of Chemistry, University of York, York, YO10 5DD, UK, 8.State Key Joint Laboratory of Environmental Simulation and Pollution Control, College of Environmental Sciences and Engineering, Peking University, Beijing, 100871, China)

[J] Poster | A (Atmospheric and Hydrospheric Sciences)：A-CG Complex & General

3:30 PM - 5:00 PM JST | 6:30 AM - 8:00 AM UTC | Poster Hall International Exhibition Hall8, Makuhari Messe_10

[A-CG42] Biogeochemical linkages between the surface ocean and atmosphere

convener:Yuzo Miyazaki(Institute of Low Temperature Science, Hokkaido University), Jun Nishioka(Hokkaido University, Institute of low temperature sciences), Koji Suzuki(Hokkaido University), Yoko Iwamoto(Graduate School of Biosphere Science, Hiroshima University)

[ACG42-P01] Mixing States of Aged Black Carbon Collected over the Western North Pacific Ocean

*Momoka Yoshizue[1], Masahiro Momoi[1], Kouji Adachi[2], Masanori Yabuki[3], Tatsuhiro Mori[1], Akiho Suizu[4], Shinichi Kodama[1,4], Kazuhiko Miura[1], Mitsuo Uematsu[4] (1.Tokyo University of Science, 2.Meteorological Research Institute, 3.Kyoto University, 4.The University of Tokyo)

[ACG42-P02] Influence of Deposition of Atmospheric Inorganic Nitrogen Compounds to Marine Ecosystem at Bay of Bengal

*Fumikazu Taketani[1], Maki Noguchi Aita[1], Kazuyo Yamaji[1,2], Takashi Sekiya[1], Kohei Ikeda[3], Taketo Hashioka[1], Makio Honda[1], Kazuhiko Matsumoto[1], Yugo Kanaya[1] (1.Japan Agency for Marine-Earth Science and Technology, 2.Kobe University, 3.National Institute for Environmental Studies)

[ACG42-P03] Carbon isotopic characterization of organic aerosols in tropical marine atmosphere at the Maïdo high-altitude observatory, Reunion Island

Sharmine Akter Simu[1], *Yuzo Miyazaki[1], OCTAVE Science Team (1.Institute of Low Temperature Science, Hokkaido University)

[J] Poster | A (Atmospheric and Hydrospheric Sciences)：A-CG Complex & General

5:15 PM - 6:30 PM JST | 8:15 AM - 9:30 AM UTC | Poster Hall International Exhibition Hall8, Makuhari Messe_17

[A-CG42] Biogeochemical linkages between the surface ocean and atmosphere

convener:Yuzo Miyazaki(Institute of Low Temperature Science, Hokkaido University), Jun Nishioka(Hokkaido University, Institute of low temperature sciences), Koji Suzuki(Hokkaido University), Yoko Iwamoto(Graduate School of Biosphere Science, Hiroshima University)

[ACG42-P01] Mixing States of Aged Black Carbon Collected over the Western North Pacific Ocean

*Momoka Yoshizue[1], Masahiro Momoi[1], Kouji Adachi[2], Masanori Yabuki[3], Tatsuhiro Mori[1], Akiho Suizu[4], Shinichi Kodama[1,4], Kazuhiko Miura[1], Mitsuo Uematsu[4] (1.Tokyo University of Science, 2.Meteorological Research Institute, 3.Kyoto University, 4.The University of Tokyo)

[ACG42-P02] Influence of Deposition of Atmospheric Inorganic Nitrogen Compounds to Marine Ecosystem at Bay of Bengal

*Fumikazu Taketani[1], Maki Noguchi Aita[1], Kazuyo Yamaji[1,2], Takashi Sekiya[1], Kohei Ikeda[3], Taketo Hashioka[1], Makio Honda[1], Kazuhiko Matsumoto[1], Yugo Kanaya[1] (1.Japan Agency for Marine-Earth Science and Technology, 2.Kobe University, 3.National Institute for Environmental Studies)

[ACG42-P03] Carbon isotopic characterization of organic aerosols in tropical marine atmosphere at the Maïdo high-altitude observatory, Reunion Island

Sharmine Akter Simu[1], *Yuzo Miyazaki[1], OCTAVE Science Team (1.Institute of Low Temperature Science, Hokkaido University)

[E] Oral | H (Human Geosciences)：H-GM Geomorphology

1:45 PM - 3:15 PM JST | 4:45 AM - 6:15 AM UTC | 101 1F

[H-GM03] Geomorphology

convener:Tsuyoshi Hattanji(Faculty of Life and Environmental Sciences, University of Tsukuba), Masayuki Seto(Fukushima Future Center for Regional Revitalization, Fukushima University), Chairperson:Thomas Parkner, Tsuyoshi Hattanji

1:45 PM - 2:00 PM JST | 4:45 AM - 5:00 AM UTC

[HGM03-01] Surface structure as a control for gully complex development in the Mackey`s block, North Island, New Zealand

*Thomas Parkner[1] (1.University of Tsukuba, Graduate School of Life and Environmental Sciences)

2:00 PM - 2:15 PM JST | 5:00 AM - 5:15 AM UTC

[HGM03-02] Model Linking Landslides and River Evolution of Incisional Channel Created by River Erosion

*Chia-Ting Kao[1], Gene Jiing-yun You[1] (1.National Taiwan University)

2:15 PM - 2:30 PM JST | 5:15 AM - 5:30 AM UTC

[HGM03-03] **A semi-automated method for extracting channels and channel profiles from LiDAR-derived digital elevation models**

*Pinliang Dong[1] (1.University of North Texas)

2:30 PM - 2:45 PM JST | 5:30 AM - 5:45 AM UTC

[HGM03-04] Laboratory experiments on the landform development

*Shunji Ouchi[1] (1.Faculty of Science and Engineering, Chuo University)

2:45 PM - 3:00 PM JST | 5:45 AM - 6:00 AM UTC

[HGM03-05] Characteristics of lake sediment from southern part of Mongolia and comparison to meteorological data

*Uyangaa Udaanjargal[1], Noriko Hasebe[1], Keisuke Fukushi[1], Tanaka Yukiya[2], Davaadorj Davaasuren[4], Makoto Sambo[1], Baasansuren Gankhurel[1], Nagayoshi Katsuta[3], Shinya Ochiai[1], Tuvshin Gerelmaa[4] (1.Kanazawa University, 2.Kyunghee University, 3.Gifu University, 4.National University of Mongolia)

3:00 PM - 3:15 PM JST | 6:00 AM - 6:15 AM UTC

[HGM03-06] **Evaluation of geomorphological changes on Kujukuri beach based on UAV SfM**

*Mergen Kungaa[1], Toshihiko Sugai[1], Natsuki Sasaki[1], Taiga Kimori[1], Taro Funatsu (1.Tokyo University, Graduate School of Frontier Sciences, Department of Natural Environmental Studies)

[E] Poster | H (Human Geosciences)：H-GM Geomorphology

3:30 PM - 5:00 PM JST | 6:30 AM - 8:00 AM UTC | Poster Hall International Exhibition Hall8, Makuhari Messe_11

[H-GM03] Geomorphology

convener:Tsuyoshi Hattanji(Faculty of Life and Environmental Sciences, University of Tsukuba), Masayuki Seto(Fukushima Future Center for Regional Revitalization, Fukushima University)

[HGM03-P01] Honeycomb Weathering (Tafoni) of Sandstone and Environmental Factors in Yonaguni Island, Okinawa Prefecture, Japan

*Takayuki Ogata[1] (1.Disaster Prevention Research Center for Island Regions, University of the Ryukyus)

[HGM03-P02] Colluvial deposits in first-order streams and channel head migration by shallow landslides: Case study in granitic basins, Asaminami, Hiroshima, Japan

*Tsuyoshi Hattanji[1], Ryuya Kodama[2], Takahisa Furuichi[3], Shoji Doshida[4], Yasushi Tanaka[5] (1.Faculty of Life and Environmental Sciences, University of Tsukuba, 2.former College of Geoscience, University of Tsukuba, 3.Hokkaido University, 4.National Research Institute of Fire and Disaster, 5.Komazawa University)

[HGM03-P03] Rock restrictions on topographical features of rivers: model experiment

*Yuta Takase[1], Noritaka Endo[1] (1.Kanazawa University)

[HGM03-P04] Stream power incision model and the stage of topographic equilibrium, using physical experiments

*Imamura Akihiro[1], Noritaka Endo[1] (1.Kanazawa University)

[HGM03-P05] Downstream variation in gravel size of the Tenjin River system

*Kazuaki Hori[1], Kazuya Yonehara[1] (1.Department of Geography, Graduate School of Environmental Studies, Nagoya University)

[HGM03-P06] Talus slope development in the time of deglaciation: a case study of the Rev Valley, SW Spitsbergen

*Krzysztof Senderak[1], Marta Kondracka[1], Bogdan Gądek[1] (1.Faculty of Earth Sciences, University of Silesia)

[HGM03-P07] **Distribution of Large Benthic Foraminifers in one of Majuro's Conservation Areas – Drenmeo Island**

*Benedict Yamamura[1], Kazuhiko Fujita[2], Melba White[3], Kyotak Ishiguro[3], Hironobu Kan[1] (1.Kyushu University, Integrated Sciences for Global Society - Research Center for Coastal Seafloor , 2.Department of Physics and Earth Sciences, University of the Ryukyus, 3.Marshall Islands Marine Resources Authority)

[HGM03-P08] Luminescence chronology of fluvial and marine records from subsurface sediment cores: An insight into the geomorphic evolution of Kaveri delta, India

*kartika goswami[1], Anbarasu Kumaresan[2], Sivakumar Krishnan[2], Senthil K. Sadasivam[2], Manoj Kumar Jaiswal[1] (1.Department of Earth Sciences, Indian Institute of Science Education and Reserach Kolkata, 2.National College Tiruchirappalli, India)

[E] Poster | H (Human Geosciences)：H-GM Geomorphology

5:15 PM - 6:30 PM JST | 8:15 AM - 9:30 AM UTC | Poster Hall International Exhibition Hall8, Makuhari Messe_18

[H-GM03] Geomorphology

convener:Tsuyoshi Hattanji(Faculty of Life and Environmental Sciences, University of Tsukuba), Masayuki Seto(Fukushima Future Center for Regional Revitalization, Fukushima University)

[HGM03-P01] Honeycomb Weathering (Tafoni) of Sandstone and Environmental Factors in Yonaguni Island, Okinawa Prefecture, Japan

*Takayuki Ogata[1] (1.Disaster Prevention Research Center for Island Regions, University of the Ryukyus)

[HGM03-P02] Colluvial deposits in first-order streams and channel head migration by shallow landslides: Case study in granitic basins, Asaminami, Hiroshima, Japan

*Tsuyoshi Hattanji[1], Ryuya Kodama[2], Takahisa Furuichi[3], Shoji Doshida[4], Yasushi Tanaka[5] (1.Faculty of Life and Environmental Sciences, University of Tsukuba, 2.former College of Geoscience, University of Tsukuba, 3.Hokkaido University, 4.National Research Institute of Fire and Disaster, 5.Komazawa University)

[HGM03-P03] Rock restrictions on topographical features of rivers: model experiment

*Yuta Takase[1], Noritaka Endo[1] (1.Kanazawa University)

[HGM03-P04] Stream power incision model and the stage of topographic equilibrium, using physical experiments

*Imamura Akihiro[1], Noritaka Endo[1] (1.Kanazawa University)

[HGM03-P05] Downstream variation in gravel size of the Tenjin River system

*Kazuaki Hori[1], Kazuya Yonehara[1] (1.Department of Geography, Graduate School of Environmental Studies, Nagoya University)

[HGM03-P06] Talus slope development in the time of deglaciation: a case study of the Rev Valley, SW Spitsbergen

*Krzysztof Senderak[1], Marta Kondracka[1], Bogdan Gądek[1] (1.Faculty of Earth Sciences, University of Silesia)

[HGM03-P07] **Distribution of Large Benthic Foraminifers in one of Majuro's Conservation Areas – Drenmeo Island**

*Benedict Yamamura[1], Kazuhiko Fujita[2], Melba White[3], Kyotak Ishiguro[3], Hironobu Kan[1] (1.Kyushu University, Integrated Sciences for Global Society - Research Center for Coastal Seafloor , 2.Department of Physics and Earth Sciences, University of the Ryukyus, 3.Marshall Islands Marine Resources Authority)

[HGM03-P08] Luminescence chronology of fluvial and marine records from subsurface sediment cores: An insight into the geomorphic evolution of Kaveri delta, India

*kartika goswami[1], Anbarasu Kumaresan[2], Sivakumar Krishnan[2], Senthil K. Sadasivam[2], Manoj Kumar Jaiswal[1] (1.Department of Earth Sciences, Indian Institute of Science Education and Reserach Kolkata, 2.National College Tiruchirappalli, India)

[J] Oral | H (Human Geosciences)：H-GM Geomorphology

9:00 AM - 10:30 AM JST | 12:00 AM - 1:30 AM UTC | 101 1F

[H-GM04] Geomorphology

convener:Tsuyoshi Hattanji(Faculty of Life and Environmental Sciences, University of Tsukuba), Masayuki Seto(Fukushima Future Center for Regional Revitalization, Fukushima University), Chairperson:Tsuyoshi Hattanji

9:00 AM - 9:15 AM JST | 12:00 AM - 12:15 AM UTC

[HGM04-01] Salt weathering in humidity-change environments: a laboratory experiment

*Masato Sato[1], Tsuyoshi Hattanji[2] (1.Graduate School of Life and environmental Sciences, University of Tsukuba, 2.Faculty of Life and Environmental Sciences, University of Tsukuba)

9:15 AM - 9:30 AM JST | 12:15 AM - 12:30 AM UTC

[HGM04-02] Verification a new control device of blown sand transport rate by wind tunnel experiments

*Yoshinori Kodama[1], Riko Saikusa[2] (1.Faculty of Agriculture, 2.Faculty of Regional Sciences)

9:30 AM - 9:45 AM JST | 12:30 AM - 12:45 AM UTC

[HGM04-03] Bedrock landslides, river blockage, and barrier-lake outburst as general geomorphic processes in high-relief mountainous landscape: an example from the Marshyangdi River, central Nepal

*Yuki Matsushi[1], Hiroshi YAGI[2], Hiroyuki Matsuzaki[3] (1.Disaster Prevention Research Institute, Kyoto University, 2.Department of Education, Art and Science, Yamagata University, 3.icro Analysis Laboratory, Tandem Accelerator, The University of Tokyo)

9:45 AM - 10:00 AM JST | 12:45 AM - 1:00 AM UTC

[HGM04-04] Influence of lithology on production and transport of soils on hillslopes underlain by granite and hornfels

*Takuma Watakabe[1], Yuki Matsushi[2], Hiroyuki Matsuzaki[3] (1.Graduate School of Science, Kyoto University, 2.Disaster Prevention Research Institute, Kyoto University, 3.The University Museum, The University of Tokyo)

10:00 AM - 10:15 AM JST | 1:00 AM - 1:15 AM UTC

[HGM04-05] Characterization of the vertical unsaturated flow for an integrated prediction of the storm runoff response and landslide initiation on a hillslope

*Makoto Tani[1], Yuki Matsushi[2], Takahiro Sayama[2], Nagahiro Kojima[3] (1.University of Human Environments, 2.Disaster Prevention Research Institute, Kyoto University, 3.Lake Biwa Environmental Research Institute)

[J] Oral | H (Human Geosciences)：H-GM Geomorphology

10:45 AM - 12:15 PM JST | 1:45 AM - 3:15 AM UTC | 101 1F

[H-GM04] Geomorphology

convener:Tsuyoshi Hattanji(Faculty of Life and Environmental Sciences, University of Tsukuba), Masayuki Seto(Fukushima Future Center for Regional Revitalization, Fukushima University), Chairperson:Masayuki Seto, Hiroshi Shimazu

10:45 AM - 11:00 AM JST | 1:45 AM - 2:00 AM UTC

[HGM04-06] The landform and flood characteristics of the Iron Gate on the ancient road from Samarkand to Bamian, south Uzbekistan

*Hiroshi Shimazu[1] (1.Department of Geography, Faculty of Geo-Environmental Science, Rissho University)

11:00 AM - 11:15 AM JST | 2:00 AM - 2:15 AM UTC

[HGM04-07] OSL dating of sediment core in Olgoi lake, Mongolia

*Yudai Igarashi[1], Noriko Hasebe[1], Nagayoshi Katsuta[2], Hitoshi Hasegawa[3], Davaadorj Davaasuren[4], Yukiya Tanaka[5], Uyangaa Udaanjargal[1], Keisuke Fukushi[1], Ichinnorov Niiden[6] (1.Kanazawa University, 2.Gihu University, 3.Kochi University, 4.National University of Mongolia, 5.Kyunghee University, 6.Mongolian Academy of Science)

11:15 AM - 11:30 AM JST | 2:15 AM - 2:30 AM UTC

[HGM04-08] Paleo Lake level change in southern part of Mongolia

*Noriko Hasebe[1], Makoto Sambo[2], Uyangaa Udaanjargal[2,3], Shuukaaz Ganbat[3], Keisuke Fukushi[1], Yukiya Tanaka[4], Davaadorj Davaasuren[3] (1.Institute of Nature and Environmental Technology, Kanazawa University, 2.Department of Earth Sciences, Kanazawa University, 3.National University of Mongolia, 4.Kyunghee University)

11:30 AM - 11:45 AM JST | 2:30 AM - 2:45 AM UTC

[HGM04-09] Numerical modeling of wave propagation on the coral reef based on high resolution 3D topography

*Kenta Minamidate[1], Kazuhisa Goto[2], Masashi Watanabe[3,4], Volker Roeber[5,6], Ken Toguchi[7], Masami Sannoh[8], Yosuke Nakashima[9], Hironobu Kan[10] (1.Graduate School of Science, Tohoku University, 2.International Research Institute of Disaster Science (IRIDeS), Tohoku University, 3.Graduate School of Engineering, Tohoku University, 4.Graduate School of Science and Engineering, Chuo University, 5.Hawaii University, 6.Université de Pau et des Pays de l'Adour, 7.Ryukyu University, 8.Mikuniya Corporation, 9.NIT, Ariake College, 10.Graduate School of Integrated Sciences for Global Society, Kyushu University)

11:45 AM - 12:00 PM JST | 2:45 AM - 3:00 AM UTC

[HGM04-10] Coastal Seafloor Geomorphology: launching of a new field and perspectives

*Hironobu Kan[1], Nobuyuki Hori[2], Tatsuro Nakai[3], Yusuke Yokoyama[4], Kazuhiko Fujita[5], Hitoshi Hasegawa[3], Yosuke Nakashima[6], Kensaku Urata[1], Atsushi Suzuki[7], Masayuki Nagao[7], Kazuhisa Goto[8] (1.Graduate School of Integrated Sciences for Global Society, Kyushu University, 2.Emeritus Professor, Department of Geography, Tokyo Metropolitan University, 3.Department of Geography and Environmental Studies, Kokushikan University, 4.AORI, University of Tokyo, 5.Department of Physics and Earth Sciences, Faculty of Science, University of the Ryukyus, 6.National Institute of Technology, Ariake College, 7.Research Institute of Geology and Geoinformation, AIST, 8.IRIDeS, Tohoku University)

[J] Poster | H (Human Geosciences)：H-GM Geomorphology

3:30 PM - 5:00 PM JST | 6:30 AM - 8:00 AM UTC | Poster Hall International Exhibition Hall8, Makuhari Messe_12

[H-GM04] Geomorphology

convener:Tsuyoshi Hattanji(Faculty of Life and Environmental Sciences, University of Tsukuba), Masayuki Seto(Fukushima Future Center for Regional Revitalization, Fukushima University)

[HGM04-P01] Automatic landform classification using Self-Organizing Map (SOM) by geomorphological features calculated from DEM

*Ito Yoshiki[1], Yoshiya Oda[1], Toshifumi Matsuoka[2] (1.Tokyo Metropolitan University, 2.Fukada Geological Institute)

[HGM04-P02] **Functionalization of the Average Erosion of Drainage Basin Using DEM**

*Rei Yamanaka[1], Tatsuto Aoki[1] (1.Kanazawa University)

[HGM04-P03] The Movement of Sediment and Development of Gullies Inside of Landslide area

*Yasuhiro Horikawa[1], Tatsuto Aoki[2] (1.Tsukuba University, 2.Kanazawa University)

[HGM04-P04] Detailed topographic survey of valley head in hill by terrestrial laser scanning

*KIYOSHI SAIJO[1], Takahisa Furuichi[2], Asaka Konno[3] (1.Miyagi University of Education, 2.Graduate School of Agriculture, Hokkaido University, 3.Tokoha University)

[HGM04-P05] Preliminary application of electrical resistivity tomography to estimate subsurface structure of unchanneled valley: A case at granitic hillslope near Mt. Tsukuba, Japan

*Naoyuki Yoshihara[1], Tsuyoshi Hattanji[2] (1.Graduate School of Life and Environmental Sciences, University of Tsukuba, 2.Faculty of Life and Environmental Sciences, University of Tsukuba)

[HGM04-P06] Estimating distribution of soil thickness in doline from electrical resistivity tomography:A case study in the Akiyoshi-dai Karst Plateau, Japan

*Naoya Hiramoto[1], Tsuyoshi Hattanji[2] (1.Graduate School of Life and Environmental Sciences, University of Tsukuba, 2.Faculty of Life and Environmental Sciences, University of Tsukuba)

[HGM04-P07] Occurrence and origin of potholes developed on the eastern slope of Miharayama in Hachijojima, Izu Islands, Tokyo Prefecture, Japan

*Takashi Ishibashi[1], Tomoaki Mastumi[2], Ren Higuchi[2], Yuki Yamatmoto[2], Keigo Shimada[2], Hirotomo Morimoto[2], Tsutomu Shimada[3], Kenji Asakura[4] (1.Masutomi Museum of Geocience, 2.Ritsumeikan University Explorers Club, 3.Pothole Survey Team, 4.Kyoto University Graduate School of Science)

[HGM04-P08] Temporal and spatial changes of sediment supply processes from tributaries since the last glacial period in the upper valleys of the Tama and Ara rivers, central Japan

*Takayuki Takahashi[1], Toshihiko Sugai[1] (1.Graduate School of Frontier Sciences, The University of Tokyo)

[HGM04-P09] Landform evolution and active tectonics in the eastern part of Oiso Hills inferred by characteristics of gravels composing Kissawa Formation, Japan

*Masahiro Muraki[1], Toshihiko Sugai[1] (1.Graduate School of Frontier Science, The University of Tokyo)

[HGM04-P10] Sediment movement and collapse of bank protections by a series of large flood events at the Sendai River, Tottori, southwest Japan

*Yoshinori Kodama[1], Kento Takemoto[2] (1.Faculty of Agriculture, 2.Hyogo Prefecture)

[HGM04-P11] Channel incision history with knickpoint retreat in the Kushira River after the deposition of Ata pyroclastic flow, Osumi Peninsula, Kyushu, Japan

*Shintaro Takanami[1] (1.Meiji University)

[HGM04-P12] **Implications of the distribution of marine terraces and submerged terraces in Japanese Island**

*Tetsuya Komatsu[1], Hiura Yuki[1], Takayuki Takahashi[2], Taro Funatsu[2], Masahiro Muraki[2], Taiga Kimori[2], Toshihiko Sugai[2] (1.Japan Atomic Energy Agency, 2.Graduate School of Frontier Sciences, The University of Tokyo)

[HGM04-P13] Marine erosional landforms along the southern coast of Yonaguni Island, Ryukyus

*Hayate Kimura[1], Kensaku Urata[2], HASEGAWA Hitoshi[3], Toshihiko Ichihara[4], Atsushi Suzuki[5], Nobuyuki Hori[6], Hironobu Kan[2] (1.Graduate school of integrated sciences for global society, 2.Graduate School of Integrated Sciences for Global Society, Kyushu University, 3.Kokushikan University, 4.Sedimentary Environments Research, 5.Geological Survey of Japan National Institute of Advanced Industrial Science and Technology (AIST), 6.Department of Geography, Nara University)

[HGM04-P14] Seafloor topography of Amami Sumiyo Bay -Visualization of Seafloor derived from multibeam bathymetric survey-

*Miho Tanaka[1], Ken Toguchi[2], Nobuyuki Hori[3], Hayate Kimura[4], Yukihiko Imai[5], Yosuke Nakashima[6], Yayoi Najima[7], Hironobu Kan[8] (1.Graduate School of Integrated Sciences for Global Society, 2.University of the Ryukyus, 3.Tokyo Metropolitan University, 4.School of Engineering, Kyushu University, 5.Faculty of science, Okayama University, 6.National Institute of Technology, Ariake College, 7.The Graduate University for Advanced Studies, 8.Kyushu University)

[J] Poster | H (Human Geosciences)：H-GM Geomorphology

5:15 PM - 6:30 PM JST | 8:15 AM - 9:30 AM UTC | Poster Hall International Exhibition Hall8, Makuhari Messe_19

[H-GM04] Geomorphology

convener:Tsuyoshi Hattanji(Faculty of Life and Environmental Sciences, University of Tsukuba), Masayuki Seto(Fukushima Future Center for Regional Revitalization, Fukushima University)

[HGM04-P01] Automatic landform classification using Self-Organizing Map (SOM) by geomorphological features calculated from DEM

*Ito Yoshiki[1], Yoshiya Oda[1], Toshifumi Matsuoka[2] (1.Tokyo Metropolitan University, 2.Fukada Geological Institute)

[HGM04-P02] **Functionalization of the Average Erosion of Drainage Basin Using DEM**

*Rei Yamanaka[1], Tatsuto Aoki[1] (1.Kanazawa University)

[HGM04-P03] The Movement of Sediment and Development of Gullies Inside of Landslide area

*Yasuhiro Horikawa[1], Tatsuto Aoki[2] (1.Tsukuba University, 2.Kanazawa University)

[HGM04-P04] Detailed topographic survey of valley head in hill by terrestrial laser scanning

*KIYOSHI SAIJO[1], Takahisa Furuichi[2], Asaka Konno[3] (1.Miyagi University of Education, 2.Graduate School of Agriculture, Hokkaido University, 3.Tokoha University)

[HGM04-P05] Preliminary application of electrical resistivity tomography to estimate subsurface structure of unchanneled valley: A case at granitic hillslope near Mt. Tsukuba, Japan

*Naoyuki Yoshihara[1], Tsuyoshi Hattanji[2] (1.Graduate School of Life and Environmental Sciences, University of Tsukuba, 2.Faculty of Life and Environmental Sciences, University of Tsukuba)

[HGM04-P06] Estimating distribution of soil thickness in doline from electrical resistivity tomography:A case study in the Akiyoshi-dai Karst Plateau, Japan

*Naoya Hiramoto[1], Tsuyoshi Hattanji[2] (1.Graduate School of Life and Environmental Sciences, University of Tsukuba, 2.Faculty of Life and Environmental Sciences, University of Tsukuba)

[HGM04-P07] Occurrence and origin of potholes developed on the eastern slope of Miharayama in Hachijojima, Izu Islands, Tokyo Prefecture, Japan

*Takashi Ishibashi[1], Tomoaki Mastumi[2], Ren Higuchi[2], Yuki Yamatmoto[2], Keigo Shimada[2], Hirotomo Morimoto[2], Tsutomu Shimada[3], Kenji Asakura[4] (1.Masutomi Museum of Geocience, 2.Ritsumeikan University Explorers Club, 3.Pothole Survey Team, 4.Kyoto University Graduate School of Science)

[HGM04-P08] Temporal and spatial changes of sediment supply processes from tributaries since the last glacial period in the upper valleys of the Tama and Ara rivers, central Japan

*Takayuki Takahashi[1], Toshihiko Sugai[1] (1.Graduate School of Frontier Sciences, The University of Tokyo)

[HGM04-P09] Landform evolution and active tectonics in the eastern part of Oiso Hills inferred by characteristics of gravels composing Kissawa Formation, Japan

*Masahiro Muraki[1], Toshihiko Sugai[1] (1.Graduate School of Frontier Science, The University of Tokyo)

[HGM04-P10] Sediment movement and collapse of bank protections by a series of large flood events at the Sendai River, Tottori, southwest Japan

*Yoshinori Kodama[1], Kento Takemoto[2] (1.Faculty of Agriculture, 2.Hyogo Prefecture)

[HGM04-P11] Channel incision history with knickpoint retreat in the Kushira River after the deposition of Ata pyroclastic flow, Osumi Peninsula, Kyushu, Japan

*Shintaro Takanami[1] (1.Meiji University)

[HGM04-P12] **Implications of the distribution of marine terraces and submerged terraces in Japanese Island**

*Tetsuya Komatsu[1], Hiura Yuki[1], Takayuki Takahashi[2], Taro Funatsu[2], Masahiro Muraki[2], Taiga Kimori[2], Toshihiko Sugai[2] (1.Japan Atomic Energy Agency, 2.Graduate School of Frontier Sciences, The University of Tokyo)

[HGM04-P13] Marine erosional landforms along the southern coast of Yonaguni Island, Ryukyus

*Hayate Kimura[1], Kensaku Urata[2], HASEGAWA Hitoshi[3], Toshihiko Ichihara[4], Atsushi Suzuki[5], Nobuyuki Hori[6], Hironobu Kan[2] (1.Graduate school of integrated sciences for global society, 2.Graduate School of Integrated Sciences for Global Society, Kyushu University, 3.Kokushikan University, 4.Sedimentary Environments Research, 5.Geological Survey of Japan National Institute of Advanced Industrial Science and Technology (AIST), 6.Department of Geography, Nara University)

[HGM04-P14] Seafloor topography of Amami Sumiyo Bay -Visualization of Seafloor derived from multibeam bathymetric survey-

*Miho Tanaka[1], Ken Toguchi[2], Nobuyuki Hori[3], Hayate Kimura[4], Yukihiko Imai[5], Yosuke Nakashima[6], Yayoi Najima[7], Hironobu Kan[8] (1.Graduate School of Integrated Sciences for Global Society, 2.University of the Ryukyus, 3.Tokyo Metropolitan University, 4.School of Engineering, Kyushu University, 5.Faculty of science, Okayama University, 6.National Institute of Technology, Ariake College, 7.The Graduate University for Advanced Studies, 8.Kyushu University)

[J] Oral | H (Human Geosciences)：H-SC Social Earth Sciences & Civil/Urban System Sciences

9:00 AM - 10:30 AM JST | 12:00 AM - 1:30 AM UTC | 301B 3F

[H-SC07] CCUS (Carbon Dioxide Capture, Utilization, and Storage) for Climate Mitigation

convener:Masao Sorai(Institute for Geo-Resources and Environment, National Institute of Advanced Industrial Science and Technology), Ziqiu Xue(Research Institute of Innovative Tech for the Earth), Masaatsu Aichi(Graduate School of Frontier Sciences, University of Tokyo), Chairperson:Masao Sorai(National Institute of Advanced Industrial Science and Technology)

9:00 AM - 9:15 AM JST | 12:00 AM - 12:15 AM UTC

[HSC07-01] Numerical simulation of variational pore pressure response to ocean tidal loading during CO2 injection

*Toshifumi Akaki[1], Hajime Yamamoto[1] (1.Taisei Corporation)

9:15 AM - 9:30 AM JST | 12:15 AM - 12:30 AM UTC

[HSC07-02] Relationship between rock deformation and permeability evolution during fracturing in rocks for CCUS technology

*Takashi Fujii[1], Xinglin Lei[1], Masao Sorai[1] (1.National Institute of Advanced Industrial Science and Technology)

9:30 AM - 9:45 AM JST | 12:30 AM - 12:45 AM UTC

[HSC07-03] Comparison of Optical Fiber Sensing Technique and Strain Gauge in a Measurement of Rock Deformation Caused by Chemical Osmosis

*Shogo Hirota[1], Tomochika Tokunaga[1], Ziqiu Xue[2], Hyuck Park[2] (1.Department of Environmental Systems, Graduate School of Frontier Science, the University of Tokyo, 2.Research Institute of Innovative Technology for the Earth)

9:45 AM - 10:00 AM JST | 12:45 AM - 1:00 AM UTC

[HSC07-04] Experiment of precipitation of salt for dry-out condition caused by CO_2 storage in saline aquifer

*Hayato Morigaki[1,2], Masaatsu Aichi[1] (1.University of Tokyo, 2.Toshiba Energy Systems & Solution Corporation)

10:00 AM - 10:15 AM JST | 1:00 AM - 1:15 AM UTC

[HSC07-05] Thermodynamic Approach to Wettability of CO_2/Brine/Mineral System by Augmented Young Laplace Equation

*Masashige Shiga[1,2], Masao Sorai[1], Masaatsu Aichi[2], Hiromi Honda[2] (1.AIST, 2.The University of Tokyo)

10:15 AM - 10:30 AM JST | 1:15 AM - 1:30 AM UTC

[HSC07-06] A proposal of CO2 underground storage using hydrate

*Takaomi Tobase[1] (1.Electric Power Development Co., Ltd.)

[J] Oral | H (Human Geosciences)：H-SC Social Earth Sciences & Civil/Urban System Sciences

10:45 AM - 12:15 PM JST | 1:45 AM - 3:15 AM UTC | 301B 3F

[H-SC07] CCUS (Carbon Dioxide Capture, Utilization, and Storage) for Climate Mitigation

convener:Masao Sorai(Institute for Geo-Resources and Environment, National Institute of Advanced Industrial Science and Technology), Ziqiu Xue(Research Institute of Innovative Tech for the Earth), Masaatsu Aichi(Graduate School of Frontier Sciences, University of Tokyo), Chairperson:Ziqiu Xue(Research Institute of Innovative Technology for the Earth)

10:45 AM - 11:00 AM JST | 1:45 AM - 2:00 AM UTC

[HSC07-07] CO_2 behavior simulation using large scale geological model

*Yuuki Shigeoka[1], Haruki Nishiyama[1], Hiroshi Kinoto[1], Takaomi Tobase[2], Takahiro Nakajima[3], Ziqiu Xue[3] (1.JP Business Survice Corporation, 2.Electric Power Development Co., Ltd., 3.Research Institute of Innovative Technology for the Earth)

11:00 AM - 11:15 AM JST | 2:00 AM - 2:15 AM UTC

[HSC07-08] **Monitoring hydromechanical responses in aquifer by distributed fiber-optic strain sensing: From lab to field**

*Yi Zhang[1,2], Ziqiu Xue[1,2], Tsutomu Hashimoto[1,2], Hyuck Park[1,2] (1.Geological Carbon dioxide Storage Technology Research Association, 2.Research Institute of Innovative Tech for the Earth)

11:15 AM - 11:30 AM JST | 2:15 AM - 2:30 AM UTC

[HSC07-09] **Field Testing of Hybrid Brillouin-Rayleigh Distributed Sensing System for Subsurface Water Injection Monitoring**

*Yankun Sun[1,2], Ziqiu Xue[1,2], Tsutomu Hashimoto[1,2], Xinglin Lei[3], Yi Zhang[1,2] (1.Geological Carbon Dioxide Storage Technology Research Association, 2.Research Institute of Innovative Technology for the Earth, 3.National Institute of Advanced Industrial Science and Technology)

11:30 AM - 11:45 AM JST | 2:30 AM - 2:45 AM UTC

[HSC07-10] Gravity monitoring using superconducting gravimeters near the seashore at the Tomakomai CCS demonstration site

*Hiroki Goto[1,2], Mituhiko Sugihara[1,2], Hiroshi Ikeda[3], Yuji Nishi[1,2], Tsuneo Ishido[1,2], Masao Sorai[1,2] (1.Geological Carbon Dioxide Storage Technology Research Association, 2.National Institute of Advanced Industrial Science and Technology, 3.University of Tsukuba)

11:45 AM - 12:00 PM JST | 2:45 AM - 3:00 AM UTC

[HSC07-11] Pilot test for microbubble CO_2 injection to reservoir in oil field - Test planning and preparation -

*Kazunori Nakagawa[1], Ryo Ueda[1], Masanori Nakano[1], Ziqiu Xue[2] (1.Japan Petroleum Exploration Co., Ltd., 2.Research Institute of Innovative Technology for the Earth)

12:00 PM - 12:15 PM JST | 3:00 AM - 3:15 AM UTC

[HSC07-12] Mechanisms inducing anomalously high pCO_2 without CO_2 leakage in coastal environment

*Yuji Watanabe[1,2], Keisuke Uchimoto[1,2], Makoto Nishimura[1,2], Saeko Mito[1,2], Ziqiu Xue[1,2] (1.Geological CO2 Storage Technology Research Association, 2.RITE)

[J] Poster | H (Human Geosciences)：H-SC Social Earth Sciences & Civil/Urban System Sciences

3:30 PM - 5:00 PM JST | 6:30 AM - 8:00 AM UTC | Poster Hall International Exhibition Hall8, Makuhari Messe_13

[H-SC07] CCUS (Carbon Dioxide Capture, Utilization, and Storage) for Climate Mitigation

convener:Masao Sorai(Institute for Geo-Resources and Environment, National Institute of Advanced Industrial Science and Technology), Ziqiu Xue(Research Institute of Innovative Tech for the Earth), Masaatsu Aichi(Graduate School of Frontier Sciences, University of Tokyo)

[HSC07-P01] Evaluation of seismic event location accuracy of Tomakomai CO2 injection site: a numerical simulation case study

*Luchen Wang[1], Takahiro Nakajima[1], Ziqiu Xue[1] (1.RITE, Research Institute of Innovative Technology for the Earth)

[HSC07-P02] Technical Challenges of Machine Learning Approach for Porosity Estimation in Nagaoka CCS site

*Takayuki Miyoshi[1], Takahiro Nakajima[1], Ziqiu Xue[1] (1.Research Institute of Innovative Technology for the Earth)

[HSC07-P03] Utilization of wave attenuation in time-lapse sonic logging data to evaluate the effect of super-critical CO_2 in the reservoir

*Takahiro Nakajima[2,1], Luchen Wang[2,1], Ziqiu Xue[2,1] (1.Research Institute of Innovative Technology for the Earth, 2.Geological Carbon Dioxide Storage Technology Research Association)

[HSC07-P04] **Geological sequestration in saline carbonate formations: CO_2-brine-rock interaction**

*Shachi Shachi[1], Brijesh Kumar Yadav[1], Mohammad Azizur Rahman[2], Mayur Pal[3] (1.Indian Institute of Technology Roorkee, 2.Texas A&M University Qatar, 3.North Oil Company, Qatar)

[HSC07-P05] **Changes in sealing performance of artificial caprocks caused by carbonate reactions**

*Masao Sorai[1] (1.Geological Survey of Japan, National Institute of Advanced Industrial Science and Technology)

[HSC07-P06] **CO_2 migration characteristics of microbubble and conventional sequestration in Berea sandstone revealed by X-ray CT imaging**

*Hongyu Zhai[1,2], Yi Zhang[1,2], Hyuck Park[1,2], Ziqiu Xue[1,2] (1.Geological Carbon dioxide Storage Technology Research Association,9-2, Kizugawadai, Kizugawa Shi, Kyoto, 6190292 Japan, 2.Research Institute of Innovative Technology for the Earth (RITE),9-2, Kizugawadai, Kizugawa Shi, Kyoto, 6190292 Japan)

[HSC07-P07] Strain detection by optical fiber for CO_2 injected core specimen

*Hyuck Park[1], Yankun Sun[1], Ziqiu Xue[1] (1.Research Institute of Innovative Technology for the Earth)

[HSC07-P08] Bed deformation measured by distributed optical fiber and its sedimentological interpretation: alternated sandstone and mudstone aquifer, Boso Peninsula, Japan

*Takuma Ito[1,2], Tsutomu Hashimoto[1,2], Ziqiu Xue[1,2] (1.Research Institute of Innovative Technology for the Earth, 2.Geological Carbon Dioxide Storage Technology Research Association)

[HSC07-P09] How many data are necessary to make a suitable threshold for anomalous pCO_2 owing to CO_2 leakage?

*Keisuke Uchimoto[1,2], Yuji Watanabe[1,2], Makoto Nishimura[1,2], Ziqiu Xue[1,2] (1.Geological Carbon dioxide Storage Technology Research Association , 2.Research Institute of Innovative Technology for the Earth)

[J] Poster | H (Human Geosciences)：H-SC Social Earth Sciences & Civil/Urban System Sciences

5:15 PM - 6:30 PM JST | 8:15 AM - 9:30 AM UTC | Poster Hall International Exhibition Hall8, Makuhari Messe_20

[H-SC07] CCUS (Carbon Dioxide Capture, Utilization, and Storage) for Climate Mitigation

convener:Masao Sorai(Institute for Geo-Resources and Environment, National Institute of Advanced Industrial Science and Technology), Ziqiu Xue(Research Institute of Innovative Tech for the Earth), Masaatsu Aichi(Graduate School of Frontier Sciences, University of Tokyo)

[HSC07-P01] Evaluation of seismic event location accuracy of Tomakomai CO2 injection site: a numerical simulation case study

*Luchen Wang[1], Takahiro Nakajima[1], Ziqiu Xue[1] (1.RITE, Research Institute of Innovative Technology for the Earth)

[HSC07-P02] Technical Challenges of Machine Learning Approach for Porosity Estimation in Nagaoka CCS site

*Takayuki Miyoshi[1], Takahiro Nakajima[1], Ziqiu Xue[1] (1.Research Institute of Innovative Technology for the Earth)

[HSC07-P03] Utilization of wave attenuation in time-lapse sonic logging data to evaluate the effect of super-critical CO_2 in the reservoir

*Takahiro Nakajima[2,1], Luchen Wang[2,1], Ziqiu Xue[2,1] (1.Research Institute of Innovative Technology for the Earth, 2.Geological Carbon Dioxide Storage Technology Research Association)

[HSC07-P04] **Geological sequestration in saline carbonate formations: CO_2-brine-rock interaction**

*Shachi Shachi[1], Brijesh Kumar Yadav[1], Mohammad Azizur Rahman[2], Mayur Pal[3] (1.Indian Institute of Technology Roorkee, 2.Texas A&M University Qatar, 3.North Oil Company, Qatar)

[HSC07-P05] **Changes in sealing performance of artificial caprocks caused by carbonate reactions**

*Masao Sorai[1] (1.Geological Survey of Japan, National Institute of Advanced Industrial Science and Technology)

[HSC07-P06] **CO_2 migration characteristics of microbubble and conventional sequestration in Berea sandstone revealed by X-ray CT imaging**

*Hongyu Zhai[1,2], Yi Zhang[1,2], Hyuck Park[1,2], Ziqiu Xue[1,2] (1.Geological Carbon dioxide Storage Technology Research Association,9-2, Kizugawadai, Kizugawa Shi, Kyoto, 6190292 Japan, 2.Research Institute of Innovative Technology for the Earth (RITE),9-2, Kizugawadai, Kizugawa Shi, Kyoto, 6190292 Japan)

[HSC07-P07] Strain detection by optical fiber for CO_2 injected core specimen

*Hyuck Park[1], Yankun Sun[1], Ziqiu Xue[1] (1.Research Institute of Innovative Technology for the Earth)

[HSC07-P08] Bed deformation measured by distributed optical fiber and its sedimentological interpretation: alternated sandstone and mudstone aquifer, Boso Peninsula, Japan

*Takuma Ito[1,2], Tsutomu Hashimoto[1,2], Ziqiu Xue[1,2] (1.Research Institute of Innovative Technology for the Earth, 2.Geological Carbon Dioxide Storage Technology Research Association)

[HSC07-P09] How many data are necessary to make a suitable threshold for anomalous pCO_2 owing to CO_2 leakage?

*Keisuke Uchimoto[1,2], Yuji Watanabe[1,2], Makoto Nishimura[1,2], Ziqiu Xue[1,2] (1.Geological Carbon dioxide Storage Technology Research Association , 2.Research Institute of Innovative Technology for the Earth)

[E] Oral | H (Human Geosciences)：H-DS Disaster geosciences

9:00 AM - 10:30 AM JST | 12:00 AM - 1:30 AM UTC | 304 3F

[H-DS10] Natural hazards impacts on human society, economics and technological systems

convener:ELENA PETROVA(Lomonosov Moscow State University, Faculty of Geography), Hajime Matsushima(Research Faculty of Agriculture, Hokkaido University), Chairperson:Elena Petrova, Hajime Matsushima

9:00 AM - 9:15 AM JST | 12:00 AM - 12:15 AM UTC

[HDS10-01] People's lives utilizing coastal dunes ecosystem service

★Invited Papers

*Kaneko Korehisa[1] (1.Hokuso Creature Association)

9:15 AM - 9:30 AM JST | 12:15 AM - 12:30 AM UTC

[HDS10-02] Survey on the Impact of Sea wall on the Vegetation of Coastal sand dune

*XIANGMEI ZHONG[1], Hajime Matsushima[2], Akira Suzuki[3], Yoshihiko Hirabuki[4], Kouji Kimura[5] (1.Graduate school of Agriculture, Hokkaido University, 2.Research Faculty of Agriculture, Hokkaido University, 3.Kita-no-satohama Hana-no-kanehashi Network, 4.Faculty of Liberal Arts, Tohoku Gakuin University, 5.Snow Brand Seed Co., Ltd.)

9:30 AM - 9:45 AM JST | 12:30 AM - 12:45 AM UTC

[HDS10-03] Greening on the seawall: challenge to conversion from gray to green infrastructure.

★Invited Papers

*Hajime Matsushima[1], Akira Suzuki[2], Kouji Kimura[4], Xiangmei Zhong[5], Yoshihiko Hirabuki[3] (1.Research Faculty of Agriculture, Hokkaido University, 2.Kita-no-satohama Hana-no-kakehashi Network, 3.Faculty of Liberal Arts, Tohoku Gakuin University, 4.Snow Brand Seed Co., Ltd., 5.Graduate school of Agriculture, Hokkaido University)

9:45 AM - 10:00 AM JST | 12:45 AM - 1:00 AM UTC

[HDS10-04] Distribution Characteristics of Informal Green Space and Its Extension of perspective into Green Infrastructure

*minseo kim[1], Katsunori Furuya[1] (1.Chiba University Graduate School of Horticulture)

10:00 AM - 10:15 AM JST | 1:00 AM - 1:15 AM UTC

[HDS10-05] DISASTER ANALYSIS OF LIGHTNING STRIKE DENSITY BASED ON LANDFORM FOR REDUCING VICTIMS IN WONOSOBO, INDONESIA

*Astry Zulky Permatasari[1], Gagad Nur Ridho[1], Yan Abdi Rahmanu[1], Emilya Nurjani[1] (1.Gadjah Mada University)

10:15 AM - 10:30 AM JST | 1:15 AM - 1:30 AM UTC

[HDS10-06] Development of Cost Competitive Unmanned Aerial Vehicle for Search and Rescue

*Aditya Keshav Natoo

[E] Poster | H (Human Geosciences)：H-DS Disaster geosciences

10:45 AM - 12:15 PM JST | 1:45 AM - 3:15 AM UTC | Poster Hall International Exhibition Hall8, Makuhari Messe_7

[H-DS10] Natural hazards impacts on human society, economics and technological systems

convener:ELENA PETROVA(Lomonosov Moscow State University, Faculty of Geography), Hajime Matsushima(Research Faculty of Agriculture, Hokkaido University)

[HDS10-P01] **The 2018 Activity of Kamchatka Volcanoes and Danger to Aviation**

*Olga Girina[1], Dmitry Melnikov[1], Alexander Manevich[1], Anton Nuzhdaev[1], Elena Petrova[2] (1.Institute of Volcanology and Seismology, Far East Division, Russian Academy of Sciences, 2.M.V. Lomonosov Moscow State University)

[HDS10-P02] Planning Methodology on the Effective Use of Green Infrastructure for Disaster Risk Reduction

★Invited Papers

*Keita Aragane[1], Satoshi Funakubo[1] (1.National Institute for Land Infrastructure Management)

[HDS10-P03] EMERGENCY CALL PATTERN IN PETROZAVODSK

*Boris Zalmanovich Belashev[1], Natalia Vladimirovna Krutskikh[1], Anna Aleksandrovna Gerasimova[1] (1.Karelian research center of Russian academy of science)

[HDS10-P04] IDENTIFYING “REGIMES” IN THE TIME SEQUENCES OF PROCESSES

*Boris Zalmanovich Belashev[1] (1.Karelian research center of Russian academy of science)

[HDS10-P05] **Investigation of status and demand on public service of earthquake disaster mitigation in China**

*Lina Dong[1], Weiping Lian[1], Weitao Chen[1] (1.Development Research Center, China Earthquake Administration)

[HDS10-P06] Analysis of Eco-DRR and Ecological Services using InVEST at the Disaster Areas of Kumamoto Earthquake

*Minghui Tang[1], Naoko Fujita[1] (1.Kyushu University)

[HDS10-P07] Transformation as praxis: Exploring socially just and transdisciplinary pathways to sustainability in marginal environments (TAPESTRY)

*Nobuhito Ohte[1], Lyla Mehta[2], Synne Movik[3], Devanathan Parthasarathy[4] (1.Department of Social Informatics, Graduate School of Informatics, Kyoto University, 2.Institute of Development Studies at the University of Sussex, 3.Department of Urban and Regional Planning, Norwegian University of Life Sciences, 4.Department of Humanities and Social Sciences, Indian Institute of Technology)

[HDS10-P08] Study for the Establishment of the Design for Disaster prevention through the survey of Recognition of tsunami disaster prevention from the viewpoint of green infrastructure in the coastal area of Kyushu-Pacific region.

*Shanshan Xu[1], Naoko Fujita[1], Minghui Tang[1] (1.Kyushu University)

[HDS10-P09] Design for Green Infrastructure: Analysis of Landscape change in the Kumamoto earthquake area

★Invited Papers

*Naoko Fujita[1] (1.Kyushu University)

[E] Poster | H (Human Geosciences)：H-DS Disaster geosciences

5:15 PM - 6:30 PM JST | 8:15 AM - 9:30 AM UTC | Poster Hall International Exhibition Hall8, Makuhari Messe_21

[H-DS10] Natural hazards impacts on human society, economics and technological systems

convener:ELENA PETROVA(Lomonosov Moscow State University, Faculty of Geography), Hajime Matsushima(Research Faculty of Agriculture, Hokkaido University)

[HDS10-P01] **The 2018 Activity of Kamchatka Volcanoes and Danger to Aviation**

*Olga Girina[1], Dmitry Melnikov[1], Alexander Manevich[1], Anton Nuzhdaev[1], Elena Petrova[2] (1.Institute of Volcanology and Seismology, Far East Division, Russian Academy of Sciences, 2.M.V. Lomonosov Moscow State University)

[HDS10-P02] Planning Methodology on the Effective Use of Green Infrastructure for Disaster Risk Reduction

★Invited Papers

*Keita Aragane[1], Satoshi Funakubo[1] (1.National Institute for Land Infrastructure Management)

[HDS10-P03] EMERGENCY CALL PATTERN IN PETROZAVODSK

*Boris Zalmanovich Belashev[1], Natalia Vladimirovna Krutskikh[1], Anna Aleksandrovna Gerasimova[1] (1.Karelian research center of Russian academy of science)

[HDS10-P04] IDENTIFYING “REGIMES” IN THE TIME SEQUENCES OF PROCESSES

*Boris Zalmanovich Belashev[1] (1.Karelian research center of Russian academy of science)

[HDS10-P05] **Investigation of status and demand on public service of earthquake disaster mitigation in China**

*Lina Dong[1], Weiping Lian[1], Weitao Chen[1] (1.Development Research Center, China Earthquake Administration)

[HDS10-P06] Analysis of Eco-DRR and Ecological Services using InVEST at the Disaster Areas of Kumamoto Earthquake

*Minghui Tang[1], Naoko Fujita[1] (1.Kyushu University)

[HDS10-P07] Transformation as praxis: Exploring socially just and transdisciplinary pathways to sustainability in marginal environments (TAPESTRY)

*Nobuhito Ohte[1], Lyla Mehta[2], Synne Movik[3], Devanathan Parthasarathy[4] (1.Department of Social Informatics, Graduate School of Informatics, Kyoto University, 2.Institute of Development Studies at the University of Sussex, 3.Department of Urban and Regional Planning, Norwegian University of Life Sciences, 4.Department of Humanities and Social Sciences, Indian Institute of Technology)

[HDS10-P08] Study for the Establishment of the Design for Disaster prevention through the survey of Recognition of tsunami disaster prevention from the viewpoint of green infrastructure in the coastal area of Kyushu-Pacific region.

*Shanshan Xu[1], Naoko Fujita[1], Minghui Tang[1] (1.Kyushu University)

[HDS10-P09] Design for Green Infrastructure: Analysis of Landscape change in the Kumamoto earthquake area

★Invited Papers

*Naoko Fujita[1] (1.Kyushu University)

[E] Oral | H (Human Geosciences)：H-DS Disaster geosciences

1:45 PM - 3:15 PM JST | 4:45 AM - 6:15 AM UTC | 301B 3F

[H-DS10] Natural hazards impacts on human society, economics and technological systems

convener:ELENA PETROVA(Lomonosov Moscow State University, Faculty of Geography), Hajime Matsushima(Research Faculty of Agriculture, Hokkaido University), Chairperson:Hajime Matsushima, Elena Petrova

1:45 PM - 2:00 PM JST | 4:45 AM - 5:00 AM UTC

[HDS10-07] **Seasonal variations of atmospheric hazard impacts on infrastructure**

★Invited Papers

*ELENA PETROVA[1] (1.Lomonosov Moscow State University, Faculty of Geography)

2:00 PM - 2:15 PM JST | 5:00 AM - 5:15 AM UTC

[HDS10-08] Assessment of water supply function and measures for chemical release accidents triggered by major earthquakes

*Lisa Ito[1], Toyohiko Nakakubo[2], Naoya Kojima[1], Akihiro Tokai[1] (1.Graduate School of Engineering, Osaka University, 2.Faculty of Core Research, Ochanomizu University)

2:15 PM - 2:30 PM JST | 5:15 AM - 5:30 AM UTC

[HDS10-09] Development of disaster risk management plan of a thermal power plant: Spearheading the paradigm shift from disaster management to disaster risk management of NATECH in India

*Repaul Kanji[1], Madan Mohan Rout[2], Ankur Srivastava[3] (1.Gujarat Institute of Disaster Management, Gandhinagar, Gujarat, India, 2.Institute of Seismological Research, Gandhinagar, India, 3.Indian Institute of Technology Delhi, India)

2:30 PM - 2:45 PM JST | 5:30 AM - 5:45 AM UTC

[HDS10-10] **Applying Transfer Learning to Improve Machine Learning Impact Model at Extremes**

*Peter Lawrence Watson[1], Manos Anagnostou[1], David Wanik[1] (1.University of Connecticut)

2:45 PM - 3:00 PM JST | 5:45 AM - 6:00 AM UTC

[HDS10-11] rescEU, the European Union Civil Protection System UCPM and the future role of Geosciences in natural disaster reduction

*Andreas Nikolaus Kueppers[1] (1.GFZ - Deutsches Geoforschungszentrum - Helmholtz Zentrum Potsdam)

3:00 PM - 3:15 PM JST | 6:00 AM - 6:15 AM UTC

[HDS10-12] The Probability of Satellite Anomalies by a Disastrous Solar Flare

*Daikichi SEKI[1,2,3] (1.Graduate School of Advanced Integrated Studies in Human Survivability, Kyoto University, 2.Centre for the Study of Existential Risk, University of Cambridge, 3.Astronomical Observatory, Kyoto University)

[E] Oral | H (Human Geosciences)：H-DS Disaster geosciences

3:30 PM - 5:00 PM JST | 6:30 AM - 8:00 AM UTC | 301B 3F

[H-DS10] Natural hazards impacts on human society, economics and technological systems

convener:ELENA PETROVA(Lomonosov Moscow State University, Faculty of Geography), Hajime Matsushima(Research Faculty of Agriculture, Hokkaido University), Chairperson:Elena Petrova, Hajime Matsushima

3:30 PM - 3:50 PM JST | 6:30 AM - 6:50 AM UTC

[HDS10-13] Management and Maintenance for Disaster prevention park in Tokyo Metropolitan Government

★Invited Papers

*Masayshi Kikuchi[1] (1.Tokyo Metropolitan Park Association)

3:50 PM - 4:05 PM JST | 6:50 AM - 7:05 AM UTC

[HDS10-14] Rebuilding Tourism after the Great East Japan Earthquake and Examining Post-Disaster Tourism in Kamaishi City

*Satoshi Sasaki[1], Kiyotatsu Yamamoto[2], Kaoruko Sasaki[3] (1.Iwate University, 2.The University of Tokyo, 3.Hokkaido University)

4:05 PM - 4:20 PM JST | 7:05 AM - 7:20 AM UTC

[HDS10-15] Population Change in Ishinomaki City, Miyagi Prefecture, with a Focus on the Area around the Earthquake Ruins

*Ryo Nishisaka[1], Katsunori Furuya[1] (1.Chiba University)

4:20 PM - 4:35 PM JST | 7:20 AM - 7:35 AM UTC

[HDS10-16] The Way of Seeing the Atomic Bomb Dome and the Relationship with Viewers' Attributes

*yasuhara arisa[1], Kiyotatsu Yamamoto[1], Akio Shimomura[1] (1.Graduate School of Agricultural and Life Sciences, The University of Tokyo)

4:35 PM - 4:50 PM JST | 7:35 AM - 7:50 AM UTC

[HDS10-17] Flood Disaster Risk Analysis at Ratnapura in Sri Lanka

*Tsuchida Ryo[1], Kaoru Takara[1] (1.Graduate School of Advanced Integrated Studies in Human Survivability, Kyoto University)

[J] Oral | H (Human Geosciences)：H-DS Disaster geosciences

9:00 AM - 10:30 AM JST | 12:00 AM - 1:30 AM UTC | Convention Hall B 2F

[H-DS13] Tsunami and Tsunami Forecast

convener:Naotaka YAMAMOTO CHIKASADA(National Research Institute for Earth Science and Disaster Resilience), Hiroaki Tsushima(Japan Meteorological Agency), Tatsuya Kubota(National Research Institute for Earth Science and Disaster Resilience), Chairperson:Masaaki Minami(気象研究所), Naotaka Chikasada(National Res. Inst. for Earth Science and Disaster Resilience)

9:00 AM - 9:15 AM JST | 12:00 AM - 12:15 AM UTC

[HDS13-07] Functions of Real-time Tsunami Inundation Forecast System Using S-net Pressure Data

*Wataru Suzuki[1], Naotaka YAMAMOTO CHIKASADA[1], Takayuki Miyoshi[1], Shin Aoi[1] (1.National Research Institute for Earth Science and Disaster Resilience)

9:15 AM - 9:30 AM JST | 12:15 AM - 12:30 AM UTC

[HDS13-08] Improvement of Real-time Tsunami Forecast System for Outer-rise Earthquake

*Naotaka YAMAMOTO CHIKASADA[1], Toshitaka Baba[2] (1.NIED, 2.Tokushima University)

9:30 AM - 9:45 AM JST | 12:30 AM - 12:45 AM UTC

[HDS13-09] Maximum tsunami height prediction using Ocean-Bottom Pressure Values based on Gaussian Process Regression

*Kotaro Takahashi[1], Kenjiro Kashiwabara[1], Yasuhiko Igarashi[1,2], Toshitaka Baba[3], Takane Hori[4], Masato Okada[1] (1.Graduate School of Frontier Sciences, The University of Tokyo, 2.Japan Science and Technology Agency PRESTO, 3.Institute of Technology and Science, The University of Tokushima, 4.Research and Development Center for Earthquake and Tsunami, Japan Agency for Marine-Earth Science and Technology)

9:45 AM - 10:00 AM JST | 12:45 AM - 1:00 AM UTC

[HDS13-10] Improvement for Finite-Difference Formula of Non-Linear Longwave Equations to Express Tsunami Decay

*Masaaki MINAMI[1] (1.Meteorological Research Institute)

10:00 AM - 10:15 AM JST | 1:00 AM - 1:15 AM UTC

[HDS13-11] **Real time tsunami inundation forecast method developed for Central America Region**

*Yuichiro Tanioka[1], Ulbert Gleb Grillo[2], Greyving Jose Argrello[2], Amilcar Cabrera[2] (1.Hokkaido University, Institute of Seismology and Volcanology, 2.Nicaraguan Institute of Territorial Studies, Nicaragua)

10:15 AM - 10:30 AM JST | 1:15 AM - 1:30 AM UTC

[HDS13-12] Near-fault observations of an offshore earthquake by DONET: Comparison of ocean bottom pressure gauges and strong-motion accelerometers

*Ayumu Mizutani[1], Kiyoshi Yomogida[1] (1.Natural History Science, Graduate School of Science, Hokkaido University, Earth and Planetary Dynamics)

[J] Oral | H (Human Geosciences)：H-DS Disaster geosciences

10:45 AM - 12:15 PM JST | 1:45 AM - 3:15 AM UTC | Convention Hall B 2F

[H-DS13] Tsunami and Tsunami Forecast

convener:Naotaka YAMAMOTO CHIKASADA(National Research Institute for Earth Science and Disaster Resilience), Hiroaki Tsushima(Japan Meteorological Agency), Tatsuya Kubota(National Research Institute for Earth Science and Disaster Resilience), Chairperson:Kentaro Imai, Toshitaka Baba(Graduate School of Science and Technology, Tokushima University)

10:45 AM - 11:00 AM JST | 1:45 AM - 2:00 AM UTC

[HDS13-13] **Investigation of variation in multiple tsunami inundation modelling**

*Yoshinori Shigihara[1], Kentaro Imai[2], Hiroyuki Iwase[3], Koji Kawasaki[4], Makoto Nemoto[5], Toshitaka Baba[6], Naotaka YAMAMOTO CHIKASADA[7], Yu Chida[8], Taro Arikawa[9] (1.Department of Civil and Environmental Engineering, National Dedense Academy, 2.Japan Agency for Marine-Earth Science and Technology, 3.Ecoh Corporation, 4.Hydro Technology Institute, Co., Ltd., 5.OYO Corporation, 6.Graduate School of Science and Technology, Tokushima University, 7.National Research Institute for Earth Science and Disaster Resilience, 8.Port and Airport Research Institute, 9.Civil and Environmental Engineering, Faculty of Science and Engineering, Chuo University)

11:00 AM - 11:15 AM JST | 2:00 AM - 2:15 AM UTC

[HDS13-14] **Numerical Modeling of Tsunami Inundation in Urban Area using Sub-Grid Scale Drag Force Model**

*Nobuki Fukui[1], Nobuhito Mori[2] (1.Graduate School of Engineering, Kyoto University, 2.Disaster Prevention Research Institute, Kyoto University)

11:15 AM - 11:30 AM JST | 2:15 AM - 2:30 AM UTC

[HDS13-15] Numerical experiment of tsunami deposits related to fault parameters by sediment transport model

*Ako YAMAMOTO[1], Tomoyuki Takahashi[2], Kenji Harada[3] (1.Forest of Research and Management Organization Forestry and Forest Products Research Institute, 2.Kansai University, 3.Shizuoka University)

11:30 AM - 11:45 AM JST | 2:30 AM - 2:45 AM UTC

[HDS13-16] Evaluation of potential impact of tsunami-induced sediment transport in Kochi Prefecture during the Nankai Trough megathrust earthquake and tsunami

*Kei Yamashita[1], Daisuke Sugawara[2], Shuji Seto[1], Taro Arikawa[3], Tomoyuki Takahashi[4], Fumihiko Imamura[1] (1.International Research Institute of Disaster Science, Tohoku University, 2.Museum of Natural and Environmental History, Shizuoka, 3.Faculty of Science and Engineering , Chuo University, 4.Faculty of Societal Safety Sciences, Kansai University)

11:45 AM - 12:00 PM JST | 2:45 AM - 3:00 AM UTC

[HDS13-17] Tsunami damage of the Keicho Earthquake of February 3rd, 1605 on the coasts of Tokai, Shikoku, and Kyushu Districts

*Yoshinobu Tsuji[1], Kentaro Imai[2], Yuuichi Ebina[3], Hiroyuki Iwase[4], Ryoko Oobayashi[2] (1.Shimanto City, 2.JAMSTEC, 3.IRIDeS, 4.Ecoh co. LTD)

12:00 PM - 12:15 PM JST | 3:00 AM - 3:15 AM UTC

[HDS13-18] Re-examination of tsunami heights distribution during the 1854 Ansei Tokai Earthquake

*Kentaro Imai[1], ebina yuichi[2], Yoshinobu Tsuji[3], Hiroyuki Iwase[4], Takane Hori[1], Narumi Takahashi[1,5], Takashi Furumura[6] (1.Japan Agency for Marine-Earth Science and Technology, 2.International Research Institute of Disaster Science, 3.Shimanto City, 4.ECOH CORPORATION, 5.National Research Institute for Earth Science and Disaster Resilience, 6.Earthquake Research Institute The University of Tokyo)

[J] Oral | H (Human Geosciences)：H-RE Resource and Engineering Geology

10:45 AM - 12:15 PM JST | 1:45 AM - 3:15 AM UTC | 106 1F

[H-RE16] Resource Geology

convener:Tsubasa Otake(Division of Sustainable Resources Engineering, Faculty of Engineering, Hokkaido University), Daisuke Araoka(Geological Survey of Japan, National Institute of Advanced Industrial Science and Technology), Ryohei Takahashi(Graduate School of International Resource Sciences, Akita University), Tatsuo Nozaki(Research and Development Center for Submarine Resources, Japan Agency for Marine-Earth Science and Technology), Chairperson:Tsubasa Otake(Faculty of Engineering, Hokkaido University), Daisuke Araoka

10:45 AM - 11:15 AM JST | 1:45 AM - 2:15 AM UTC

[HRE16-01] The role of water in the concentration of Cr

★Invited Papers

*Shoji Arai[1] (1.Department of Earth Sciences, Faculty of Science, Kanazawa University)

11:15 AM - 11:30 AM JST | 2:15 AM - 2:30 AM UTC

[HRE16-02] Mineralogical Features of Silver-Bearing Minerals in Chimney Ore from Myojinsho Caldera, Myojin Knoll and Bayonnaise Knoll Seafloor Hydrothermal Area, Izu-Bonin Arc

Shinji Kawaguchi[1], *Kotaro Yonezu[1], Thomas Tindell[1], Jun-ichiro Ishibashi[2], Tatsuo Nozaki[3], Yoko Ohtomo[4], Koichiro Watanabe[1] (1.Deaprtment of Earth Resources Engineering, Faculty of Engineering, Kyushu University, 2.Department of Earth and Planetary Sciences, Faculty of Sciences, Kyushu University, 3.Research and Development Center for Submarine Resources, Japan Agency for Marine-Earth Science and Technology, 4.Faculty of Engineering, Hokkaido University)

11:30 AM - 11:45 AM JST | 2:30 AM - 2:45 AM UTC

[HRE16-03] Organic matters and acid-sulfate alteration in Itomuka Mine, Hokkaido, Japan: implications for the transportation and deposition mechanisms of mercury

*Takuya Echigo[1], Mitsuyoshi Kimata[2], Masahiro Shimizu[2] (1.Graduate School of International Resource Sciences, Akita University, 2.Graduate School of Life and Environmental Sciences, University of Tsukuba)

11:45 AM - 12:00 PM JST | 2:45 AM - 3:00 AM UTC

[HRE16-04] **Significances of 12 Ma manganese ores in the Hokuroku district, Akita: unique Mn accumulation and interaction with organic matter during submarine hydrothermal activities**

*Yuya Tsukamoto[1], Takeshi Kakegawa[1] (1.Tohoku Univ.)

12:00 PM - 12:15 PM JST | 3:00 AM - 3:15 AM UTC

[HRE16-05] Microbial communities around ca. 2.7 Ga submarine hydrothermal fields at the Potterdoal deposit in Abitibi Greenstone Belt, Canada

*Takeru Osato[1], Akizumi Ishida[1], Takeshi Kakegawa[1] (1.Tohoku University)

[J] Oral | H (Human Geosciences)：H-RE Resource and Engineering Geology

1:45 PM - 3:15 PM JST | 4:45 AM - 6:15 AM UTC | 106 1F

[H-RE16] Resource Geology

convener:Tsubasa Otake(Division of Sustainable Resources Engineering, Faculty of Engineering, Hokkaido University), Daisuke Araoka(Geological Survey of Japan, National Institute of Advanced Industrial Science and Technology), Ryohei Takahashi(Graduate School of International Resource Sciences, Akita University), Tatsuo Nozaki(Research and Development Center for Submarine Resources, Japan Agency for Marine-Earth Science and Technology), Chairperson:Tatsuo Nozaki(JAMSTEC), Ryohei Takahashi(Faculty of International Resource Sciences, Akita University)

1:45 PM - 2:15 PM JST | 4:45 AM - 5:15 AM UTC

[HRE16-06] Development of nano-fabrication and high-resolution electron microscopy techniques: their possible applications to resource geology

★Invited Papers

*Naotaka Tomioka[1], Satoko Motai[1], Yu Kodama[2], Motoo Ito[1] (1.Kochi Institute for Core Sample Research, Japan Agency for Marine-Earth Science and Technology, 2.Marine Works Japan)

2:15 PM - 2:30 PM JST | 5:15 AM - 5:30 AM UTC

[HRE16-07] Microscopic study on rare earth elements in ion-adsorption type ore of China

*Hiroki Mukai[1], Yoshiaki Kon[1], Kenzo Sanematsu[1], Yoshio Takahashi[2], Motoo Ito[3] (1.National Institute of Advanced Industrial Science and Technology, 2.Graduate School of Science, the University of Tokyo, 3.Kochi Institute for Core Sample Research JAMSTEC)

2:30 PM - 2:45 PM JST | 5:30 AM - 5:45 AM UTC

[HRE16-08] Geochemical features of “invisible gold” in pyrites from the Akeshi and Kasuga deposits, Kagoshima, Japan

*Mizuki Ishida[1], Rurik Romeo[2,3], Mathieu Leisen[2,3], Junji Torimoto[4], Tatsuo Nozaki[4,5,6,7], Kazutaka Yasukawa[1,6], Koichiro Fujinaga[6,1], Kentaro Nakamura[1], Martin Reich[2,3], Yasuhiro Kato[1,6,5] (1.Department of Systems Innovation, School of Engineering, The University of Tokyo, 2.Department of Geology and Andean Geothermal Center of Excellence (CEGA), FCFM, 3.Millennium Nucleus for Metal Tracing Along Subduction, FCFM, Universidad de Chile, FCFM, 4.Japan Agency for Marine-Earth Science and Technology (JAMSTEC), 5.Frontier Research Center for Energy and Resources, School of Engineering, The University of Tokyo, 6.Ocean Resources Research Center for Next Generation, Chiba Institute of Technology, 7.Department of Planetology, Graduate School of Science, Kobe University)

2:45 PM - 3:00 PM JST | 5:45 AM - 6:00 AM UTC

[HRE16-09] Hydrothermal Mineral Assemblage of the Southwest Prospect, in the Vicinity Sto. Tomas II (Philex) Porphyry Cu-Au Deposit, Baguio District, Philippines

*Avriel Venis Literal Cirineo[1], Akira Imai[2], Ryohei Takahashi[1], Noel C. Oliveros[3], Redempta P. Baluda[3], Victor B. Maglambayan[3], Roy Ronald C. Luis[3], Maria Lourdes M. Faustino[3] (1.Graduate School of International Resource Sciences, Akita University, 2.Faculty of Engineering, Kyushu University, 3.Philex Mining Corporation)

3:00 PM - 3:15 PM JST | 6:00 AM - 6:15 AM UTC

[HRE16-10] Characteristics and genesis of weathering REE deposits

★Invited Papers

*Kenzo Sanematsu[1] (1.Mineral Resource Research Group, Institute for Geo-Resources and Environment, Geological Survey of Japan, National Institute of Advanced Industrial Science and Technology)

[J] Poster | H (Human Geosciences)：H-RE Resource and Engineering Geology

3:30 PM - 5:00 PM JST | 6:30 AM - 8:00 AM UTC | Poster Hall International Exhibition Hall8, Makuhari Messe_14

[H-RE16] Resource Geology

convener:Tsubasa Otake(Division of Sustainable Resources Engineering, Faculty of Engineering, Hokkaido University), Daisuke Araoka(Geological Survey of Japan, National Institute of Advanced Industrial Science and Technology), Ryohei Takahashi(Graduate School of International Resource Sciences, Akita University), Tatsuo Nozaki(Research and Development Center for Submarine Resources, Japan Agency for Marine-Earth Science and Technology)

[HRE16-P01] Mineral Chemistry and Petrogenesis of the Mazua Ultramafic Massif, Northern Mozambique: Constraints on the Associated Fe-Ti Oxides Deposit

*David Augusto Bene Unganai[1], Akira Imai[2], Ryohei Takahashi[1], Daud Liace Jamal[3], Takashi Hoshide[1] (1.Akita University, 2.Kyushu University, 3.Eduardo Mondlane University)

[HRE16-P02] **Ni-Cu-PGM Mineralisation in the Bastard Reef and Merensky Reef of the Flatreef section, Turfspruit Farm, Northern Limb, Bushveld Igneous Complex, South Africa.**

*MOKHIRI MALESELA MAKHAFOLA[1], Tsubasa Otake[1], Tsutomu Sato[1], Danie Grobler[2] (1.Hokkaido University, 2.Ivanplats Pty. Ltd)

[HRE16-P03] Characteristics of Porphyry Copper-Gold Mineralization in the Grasberg Mine, Papua, Indonesia

*Kanehiko Kawasaki[1], Kotaro Yonezu[2], Reza Al Furqan[3], Benny Bensaman[4], Mega Fatimah Rosana[4] (1.Kyushu University Facurity of Engineering, 2.Deaprtment of Earth Resources Engineering, Faculty of Engineering, Kyushu University, 3.PT Freeport Indonesia, 4.Department of Geology, Padjadjaran University)

[HRE16-P04] Formation of Ni-bearing minerals during chemical weathering of ultramafic rocks in Myanmar

*Ayaka Murofushi[1], Akane Ito[1], Tsubasa Otake[2], Kenzo Sanematsu[3], Kyaw Zay Ya[1,4], Tsutomu Sato[2] (1.Graduate school of Engineering, Hokkaido University, 2.Facility of Engineering, Hokkaido University, 3.Geological Survey of Japan, National Institute of Advanced Industrial Science and Technology, 4.Department of Geological Survey and Mineral Exploration)

[HRE16-P05] Geological Characteristics and Mineralogy of the Makorungo and Nalia Gold Prospects, Northeastern Mozambique

*Manuel Augusto Manuel Nopeia[1], Ryohei Takahashi[1], Akira Imai[2], Daud Liace Jamal[3] (1.Akita University, 2.Kyushu University, 3.Eduardo Mondlane University)

[HRE16-P06] Geochemical features of the Hishikari epithermal gold deposit based on simultaneous multi-element analysis

*Sota Nishida[1], Mizuki Ishida[1], Kazutaka Yasukawa[1,2], Kentaro Nakamura[1], Koichiro Fujinaga[2,1], Yasuhiro Kato[3,1,2] (1.Department of Systems Innovation, School of Engineering, The University of Tokyo, 2.Ocean Resources Research Center for Next Generation, Chiba Institute of Technology, 3.Frontier Research Center for Energy and Resources, School of Engineering, The University of Tokyo)

[HRE16-P07] Transformation of ore minerals and their geochemical signatures in submarine hydrothermal ore deposits in Izena Hole, Okinawa Trough

*IKESHIMA TAKURO[1], Tsubasa Otake[1], Tsutomu Sato[1], Akane Ito[1], Shuji Ono[1], Jun-ichiro Ishibashi[2], Tatsuo Nozaki[3], Hidenori Kumagai[3], Lena Maeda[3] (1.Hokkaido University, 2.Kyushu University, 3.Japan Agency for Marine-Earth Science and Technology (JAMSTEC))

[HRE16-P08] Geochemical behavior of heavy metals during wastewater treatment in Chingola Stream of the Zambia Copperbelt

*Cryton Phiri[1], Daiki Shimazui[2], Tsutomu Sato[2], Tsubasa Otake[2] (1.University of Zambia, 2.Hokkaido University)

[J] Poster | H (Human Geosciences)：H-RE Resource and Engineering Geology

5:15 PM - 6:30 PM JST | 8:15 AM - 9:30 AM UTC | Poster Hall International Exhibition Hall8, Makuhari Messe_22

[H-RE16] Resource Geology

convener:Tsubasa Otake(Division of Sustainable Resources Engineering, Faculty of Engineering, Hokkaido University), Daisuke Araoka(Geological Survey of Japan, National Institute of Advanced Industrial Science and Technology), Ryohei Takahashi(Graduate School of International Resource Sciences, Akita University), Tatsuo Nozaki(Research and Development Center for Submarine Resources, Japan Agency for Marine-Earth Science and Technology)

[HRE16-P01] Mineral Chemistry and Petrogenesis of the Mazua Ultramafic Massif, Northern Mozambique: Constraints on the Associated Fe-Ti Oxides Deposit

*David Augusto Bene Unganai[1], Akira Imai[2], Ryohei Takahashi[1], Daud Liace Jamal[3], Takashi Hoshide[1] (1.Akita University, 2.Kyushu University, 3.Eduardo Mondlane University)

[HRE16-P02] **Ni-Cu-PGM Mineralisation in the Bastard Reef and Merensky Reef of the Flatreef section, Turfspruit Farm, Northern Limb, Bushveld Igneous Complex, South Africa.**

*MOKHIRI MALESELA MAKHAFOLA[1], Tsubasa Otake[1], Tsutomu Sato[1], Danie Grobler[2] (1.Hokkaido University, 2.Ivanplats Pty. Ltd)

[HRE16-P03] Characteristics of Porphyry Copper-Gold Mineralization in the Grasberg Mine, Papua, Indonesia

*Kanehiko Kawasaki[1], Kotaro Yonezu[2], Reza Al Furqan[3], Benny Bensaman[4], Mega Fatimah Rosana[4] (1.Kyushu University Facurity of Engineering, 2.Deaprtment of Earth Resources Engineering, Faculty of Engineering, Kyushu University, 3.PT Freeport Indonesia, 4.Department of Geology, Padjadjaran University)

[HRE16-P04] Formation of Ni-bearing minerals during chemical weathering of ultramafic rocks in Myanmar

*Ayaka Murofushi[1], Akane Ito[1], Tsubasa Otake[2], Kenzo Sanematsu[3], Kyaw Zay Ya[1,4], Tsutomu Sato[2] (1.Graduate school of Engineering, Hokkaido University, 2.Facility of Engineering, Hokkaido University, 3.Geological Survey of Japan, National Institute of Advanced Industrial Science and Technology, 4.Department of Geological Survey and Mineral Exploration)

[HRE16-P05] Geological Characteristics and Mineralogy of the Makorungo and Nalia Gold Prospects, Northeastern Mozambique

*Manuel Augusto Manuel Nopeia[1], Ryohei Takahashi[1], Akira Imai[2], Daud Liace Jamal[3] (1.Akita University, 2.Kyushu University, 3.Eduardo Mondlane University)

[HRE16-P06] Geochemical features of the Hishikari epithermal gold deposit based on simultaneous multi-element analysis

*Sota Nishida[1], Mizuki Ishida[1], Kazutaka Yasukawa[1,2], Kentaro Nakamura[1], Koichiro Fujinaga[2,1], Yasuhiro Kato[3,1,2] (1.Department of Systems Innovation, School of Engineering, The University of Tokyo, 2.Ocean Resources Research Center for Next Generation, Chiba Institute of Technology, 3.Frontier Research Center for Energy and Resources, School of Engineering, The University of Tokyo)

[HRE16-P07] Transformation of ore minerals and their geochemical signatures in submarine hydrothermal ore deposits in Izena Hole, Okinawa Trough

*IKESHIMA TAKURO[1], Tsubasa Otake[1], Tsutomu Sato[1], Akane Ito[1], Shuji Ono[1], Jun-ichiro Ishibashi[2], Tatsuo Nozaki[3], Hidenori Kumagai[3], Lena Maeda[3] (1.Hokkaido University, 2.Kyushu University, 3.Japan Agency for Marine-Earth Science and Technology (JAMSTEC))

[HRE16-P08] Geochemical behavior of heavy metals during wastewater treatment in Chingola Stream of the Zambia Copperbelt

*Cryton Phiri[1], Daiki Shimazui[2], Tsutomu Sato[2], Tsubasa Otake[2] (1.University of Zambia, 2.Hokkaido University)

[E] Poster | H (Human Geosciences)：H-TT Technology & Techniques

1:45 PM - 3:15 PM JST | 4:45 AM - 6:15 AM UTC | Poster Hall International Exhibition Hall8, Makuhari Messe_2

[H-TT21] Non-destructive techniques applied to stone cultural heritage

convener:Chiaki T. Oguchi(Institute for Environmental Science and Technology, Graduate School of Science and Engineering, Saitama University), Celine Elise Thomachot-Schneider(Groupe d'etude des environnements naturels, anthropiques et archeologiques - Universite de Reims-Champagne-Ardenne (France)), Wonsuh Song(Waseda University), Miguel Gomez-Heras(Universidad Autonoma de Madrid)

[HTT21-P01] **Comparison and Analysis of GNSS-RTK Combined with 3D LiDAR Technology on Monument Maintenance Project**

*Lih-Shinn Hwang[1], Chien-Hua Chiu[1], Chien-Wen Wang[1], Hsiao-Hung Chen[1] (1.National Defense Univ.)

[HTT21-P02] Non-destructive field measurement for investigation of deteriorated parts of an artificial cave

Kaisei Sakane[1], *Chiaki T. Oguchi[1], Yasuhiko TAMURA[2] (1.Institute for Environmental Science and Technology, Graduate School of Science and Engineering, Saitama University, 2.The Exective Committee for the Preservation of Taya Cavern)

[HTT21-P03] Ultra-portable thermal cameras for moisture detection

*Miguel Gomez-Heras[1], Laura Lopez-Gonzalez[2], Maria Teresa Gil-Muñoz[3] (1.Universidad Autonoma de Madrid, 2.Artfabrik, 3.Universidad Complutense de Madrid)

[HTT21-P04] A laboratory experiment on stone decay by combination of salt and ice crystallization

*Masato Sato[1], Tsuyoshi Hattanji[2] (1.Graduate School of Life and environmental Sciences, 2.Faculty of Life and EnvironmentalSciences, University of Tsukuba)

[HTT21-P05] Study of the micro-climatic monitoring on the Saint-Remi Basilica (Rheims, France)

*Emilie Huby[1], Celine Elise Thomachot-Schneider[1], Patricia Vazquez[1], Gilles Fronteau[1] (1.Universite de Reims-Champagne-Ardenne)

[E] Poster | H (Human Geosciences)：H-TT Technology & Techniques

5:15 PM - 6:30 PM JST | 8:15 AM - 9:30 AM UTC | Poster Hall International Exhibition Hall8, Makuhari Messe_23

[H-TT21] Non-destructive techniques applied to stone cultural heritage

convener:Chiaki T. Oguchi(Institute for Environmental Science and Technology, Graduate School of Science and Engineering, Saitama University), Celine Elise Thomachot-Schneider(Groupe d'etude des environnements naturels, anthropiques et archeologiques - Universite de Reims-Champagne-Ardenne (France)), Wonsuh Song(Waseda University), Miguel Gomez-Heras(Universidad Autonoma de Madrid)

[HTT21-P01] **Comparison and Analysis of GNSS-RTK Combined with 3D LiDAR Technology on Monument Maintenance Project**

*Lih-Shinn Hwang[1], Chien-Hua Chiu[1], Chien-Wen Wang[1], Hsiao-Hung Chen[1] (1.National Defense Univ.)

[HTT21-P02] Non-destructive field measurement for investigation of deteriorated parts of an artificial cave

Kaisei Sakane[1], *Chiaki T. Oguchi[1], Yasuhiko TAMURA[2] (1.Institute for Environmental Science and Technology, Graduate School of Science and Engineering, Saitama University, 2.The Exective Committee for the Preservation of Taya Cavern)

[HTT21-P03] Ultra-portable thermal cameras for moisture detection

*Miguel Gomez-Heras[1], Laura Lopez-Gonzalez[2], Maria Teresa Gil-Muñoz[3] (1.Universidad Autonoma de Madrid, 2.Artfabrik, 3.Universidad Complutense de Madrid)

[HTT21-P04] A laboratory experiment on stone decay by combination of salt and ice crystallization

*Masato Sato[1], Tsuyoshi Hattanji[2] (1.Graduate School of Life and environmental Sciences, 2.Faculty of Life and EnvironmentalSciences, University of Tsukuba)

[HTT21-P05] Study of the micro-climatic monitoring on the Saint-Remi Basilica (Rheims, France)

*Emilie Huby[1], Celine Elise Thomachot-Schneider[1], Patricia Vazquez[1], Gilles Fronteau[1] (1.Universite de Reims-Champagne-Ardenne)

[E] Oral | H (Human Geosciences)：H-TT Technology & Techniques

3:30 PM - 5:00 PM JST | 6:30 AM - 8:00 AM UTC | 101 1F

[H-TT21] Non-destructive techniques applied to stone cultural heritage

convener:Chiaki T. Oguchi(Institute for Environmental Science and Technology, Graduate School of Science and Engineering, Saitama University), Celine Elise Thomachot-Schneider(Groupe d'etude des environnements naturels, anthropiques et archeologiques - Universite de Reims-Champagne-Ardenne (France)), Wonsuh Song(Waseda University), Miguel Gomez-Heras(Universidad Autonoma de Madrid), Chairperson:Wonsuh Song, Chiaki Oguchi

3:30 PM - 3:45 PM JST | 6:30 AM - 6:45 AM UTC

[HTT21-01] Study on creation of 3D model by SfM photogrammetry: An example of Taya Cave

Kisara Shimizu[1], *Chiaki T. Oguchi[1], Yasuhiko TAMURA[2], Yuichi S. Hayakawa[3], Takuro Ogura[4], OGATA KEISUKE[5] (1.Institute for Environmental Science and Technology, Graduate School of Science and Engineering, Saitama University, 2.The Exective Committee for the Preservation of Taya Cavern, 3.Faculty of Environmental Earth Science, Hokkaido University, 4.Graduate School of Frontier Sciences, The University of Tokyo, 5.Tsurumi University)

3:45 PM - 4:00 PM JST | 6:45 AM - 7:00 AM UTC

[HTT21-02] **TLS measurement data and 3D printing of an artificial cave for geotechnical and educational applications**

*Yuichi S. Hayakawa[1,2], Takuro Ogura[4,5], Yasuhiko Tamura[2], Chiaki T. Oguchi[3], Kisara Shimizu[3] (1.Faculty of Environmental Earth Science, Hokkaido University, 2.Center for Spatial Information Science, The University of Tokyo, 3.Saitama University, 4.Graduate School of Frontier Science, The University of Tokyo, 5.Graduate School of Environmental Science, Hokkaido University)

4:00 PM - 4:15 PM JST | 7:00 AM - 7:15 AM UTC

[HTT21-03] Conservation restoration of the world heritage of Okinawa Prefecture, Sonohyan-utaki Ishimon - Situation after 30 years since filling with mortar and applying silicone resin.

*Wonsuh Song[1], Tadateru Nishiura[2], Chiaki T. Oguchi[3] (1.Waseda University, 2.Kokushika Univeristy, 3.Saitama University)

4:15 PM - 4:30 PM JST | 7:15 AM - 7:30 AM UTC

[HTT21-04] Application of portable XRF analysis for provenance of seabed worked stone in coastal are of Kochi Prefecture

★Invited Papers

*Wataru Tanikawa[1], Go-Ichiro Uramoto[2], Masafumi MURAYAMA[2], Yohei Hamada[1], Yuhji Yamamoto[2], Osamu Tadai[3] (1.Japan Agency for Marine-Earth Science and Technology, Kochi Instutute for Core Sample Research, 2.Kochi University, Center for Advanced Marine Core Research, 3.Marine Works Japan LTD.)

4:30 PM - 4:45 PM JST | 7:30 AM - 7:45 AM UTC

[HTT21-05] pXRF analyses on Assyrain sculptures

★Invited Papers

*Ryo Anma[1], Ki-Cheol Shin[2], Chikako Watanabe[3], Akihiro Tuji[4] (1.Graduate School of Technology, Industrial and Social Sciences, Tokushima University, 2.Research Institute for Humanity and Nature, 3.Faculty of International Studies, Osaka Gakuin University, 4.National Museum of Nature and Science)

4:45 PM - 5:00 PM JST | 7:45 AM - 8:00 AM UTC

[HTT21-06] Discussion

*Chiaki T. Oguchi[1] (1.Institute for Environmental Science and Technology, Graduate School of Science and Engineering, Saitama University)

[E] Poster | H (Human Geosciences)：H-CG Complex & General

3:30 PM - 5:00 PM JST | 6:30 AM - 8:00 AM UTC | Poster Hall International Exhibition Hall8, Makuhari Messe_15

[H-CG25] International Comparison of Landscape Appreciation

convener:Anastasia Petrova(Institute of Oriental Studies of the Russian Academy of Sciences), yoji aoki(Open University of Japan)

[HCG25-P01] **The Globally Important Agricultural Heritage of Aso from the perspective of landscape and its supporting systems**

*REIKO MACHIDA[1] (1.TOKYO UNIVERSITY OF AGRICULTURE)

[HCG25-P02] **Hazardous natural phenomena and weather conditions appreciation in Russian landscape painting**

*ELENA PETROVA[1] (1.Lomonosov Moscow State University, Faculty of Geography)

[HCG25-P03] Trends of evaluation items to landscape appreciation until 2017 in the English journals

*yoji aoki[1], keisuke mukagai[2], Anastasia Petrova[3] (1.Open University of Japan, 2.Nagano University, 3.Institute of Oriental Studies, Russian Academy of Sciences)

[E] Poster | H (Human Geosciences)：H-CG Complex & General

5:15 PM - 6:30 PM JST | 8:15 AM - 9:30 AM UTC | Poster Hall International Exhibition Hall8, Makuhari Messe_24

[H-CG25] International Comparison of Landscape Appreciation

convener:Anastasia Petrova(Institute of Oriental Studies of the Russian Academy of Sciences), yoji aoki(Open University of Japan)

[HCG25-P01] **The Globally Important Agricultural Heritage of Aso from the perspective of landscape and its supporting systems**

*REIKO MACHIDA[1] (1.TOKYO UNIVERSITY OF AGRICULTURE)

[HCG25-P02] **Hazardous natural phenomena and weather conditions appreciation in Russian landscape painting**

*ELENA PETROVA[1] (1.Lomonosov Moscow State University, Faculty of Geography)

[HCG25-P03] Trends of evaluation items to landscape appreciation until 2017 in the English journals

*yoji aoki[1], keisuke mukagai[2], Anastasia Petrova[3] (1.Open University of Japan, 2.Nagano University, 3.Institute of Oriental Studies, Russian Academy of Sciences)

[J] Poster | S (Solid Earth Sciences)：S-SS Seismology

1:45 PM - 3:15 PM JST | 4:45 AM - 6:15 AM UTC | Poster Hall International Exhibition Hall8, Makuhari Messe_3

[S-SS09] Earthquake prediction and forecast

convener:Masayuki Obayashi(Japan Agency for Marine-Earth Science and Technology), Toshitaka Baba(Graduate School of Science and Technology, Tokushima University)

[SSS09-P01] A method to ditect seismic precursors

*Kozo Takahashi

[SSS09-P02] Difference of foreshock characteristics between real data and synthetic ETAS catalogs: through the application of an empirical earthquake forecast model based on foreshocks

*Fuyuki Hirose[1], Koji Tamaribuchi[1], Kenji Maeda[2] (1.Seismology and Tsunami Research Department, Meteorological Research Institute, 2.Seismology and Volcanology Department, Japan Meteorological Agency)

[SSS09-P03] The increase in missing waveform images of the F-net broadband seismograph network preceding the 2011 Tohoku earthquake (2)

*Yoshiki SUE[1] (1.none)

[SSS09-P04] On the *b*-value of the OBS seismic observation around the Suruga Bay Senoumi

*Taiyo Sotani[1], Hisatoshi Baba[4], Takahito Nishimiya[2], Nakao Nagisa[1], Toshiyasu Nagao[3] (1.Toukai Univrsity, 2.Meteorological Research Institute, Japan Meteorological Agency, 3.Institute of Oceanic Research and development, Tokai University, 4.Department of Marine and Earth Science, Tokai University)

[SSS09-P05] Trial Result of Long-term Occurrence Probabilities with The Moderate Repeating Earthquakes Using The Lognormal Distribution Model with Bayesian Approach

*Masayuki Tanaka[1] (1.Meteorological Research Institute)

[SSS09-P06] **Structural heterogeneity under the 2018 Mw6.6 Eastern Iburi earthquake in Hokkaido, Japan and its implications for rupture initiations**

*ZHI WANG[1] (1.Key Laboratory of Marginal Sea Geology at South China Sea Institute of Oceanology of CAS of China)

[J] Poster | S (Solid Earth Sciences)：S-SS Seismology

5:15 PM - 6:30 PM JST | 8:15 AM - 9:30 AM UTC | Poster Hall International Exhibition Hall8, Makuhari Messe_25

[S-SS09] Earthquake prediction and forecast

convener:Masayuki Obayashi(Japan Agency for Marine-Earth Science and Technology), Toshitaka Baba(Graduate School of Science and Technology, Tokushima University)

[SSS09-P01] A method to ditect seismic precursors

*Kozo Takahashi

[SSS09-P02] Difference of foreshock characteristics between real data and synthetic ETAS catalogs: through the application of an empirical earthquake forecast model based on foreshocks

*Fuyuki Hirose[1], Koji Tamaribuchi[1], Kenji Maeda[2] (1.Seismology and Tsunami Research Department, Meteorological Research Institute, 2.Seismology and Volcanology Department, Japan Meteorological Agency)

[SSS09-P03] The increase in missing waveform images of the F-net broadband seismograph network preceding the 2011 Tohoku earthquake (2)

*Yoshiki SUE[1] (1.none)

[SSS09-P04] On the *b*-value of the OBS seismic observation around the Suruga Bay Senoumi

*Taiyo Sotani[1], Hisatoshi Baba[4], Takahito Nishimiya[2], Nakao Nagisa[1], Toshiyasu Nagao[3] (1.Toukai Univrsity, 2.Meteorological Research Institute, Japan Meteorological Agency, 3.Institute of Oceanic Research and development, Tokai University, 4.Department of Marine and Earth Science, Tokai University)

[SSS09-P05] Trial Result of Long-term Occurrence Probabilities with The Moderate Repeating Earthquakes Using The Lognormal Distribution Model with Bayesian Approach

*Masayuki Tanaka[1] (1.Meteorological Research Institute)

[SSS09-P06] **Structural heterogeneity under the 2018 Mw6.6 Eastern Iburi earthquake in Hokkaido, Japan and its implications for rupture initiations**

*ZHI WANG[1] (1.Key Laboratory of Marginal Sea Geology at South China Sea Institute of Oceanology of CAS of China)

[J] Oral | S (Solid Earth Sciences)：S-SS Seismology

3:30 PM - 5:00 PM JST | 6:30 AM - 8:00 AM UTC | A05 TOKYO BAY MAKUHARI HALL

[S-SS09] Earthquake prediction and forecast

convener:Masayuki Obayashi(Japan Agency for Marine-Earth Science and Technology), Toshitaka Baba(Graduate School of Science and Technology, Tokushima University), Chairperson:Sumio Yoshikawa(気象研究所), Mamoru Kato(Graduate School of Human and Environmental Studies Kyoto University)

3:30 PM - 3:45 PM JST | 6:30 AM - 6:45 AM UTC

[SSS09-01] **Objective evaluationof precursory seismic quiescence and activation phenomenon in wide area**

*Sumio Yoshikawa[1] (1.Meteorological Research Institute)

3:45 PM - 4:00 PM JST | 6:45 AM - 7:00 AM UTC

[SSS09-02] Long-term Probability of a Great Earthquake along the Kurile Trench, Hokkaido Japan (2)

*Masajiro Imoto[1], Morilkawa Nobuyuki[1], Fujiwara Hiroyuki[1] (1.National Research Institute for Earth Science and Disaster Resilience)

4:00 PM - 4:15 PM JST | 7:00 AM - 7:15 AM UTC

[SSS09-03] Parallel and Focused Increase Trends in Time Series (M-T Diagram) of Earthquake Occurrences

*Satoshi Hashimoto[1] (1.none)

4:15 PM - 4:30 PM JST | 7:15 AM - 7:30 AM UTC

[SSS09-04] Revisiting a simple method for short-term earthquake probabilities derived from past Seismicity

*Mamoru Kato[1] (1.Graduate School of Human and Environmental Studies Kyoto University)

4:30 PM - 4:45 PM JST | 7:30 AM - 7:45 AM UTC

[SSS09-05] Recent anomalous groundwater temperature and water level changes at the frontier land zone of Nanki region for impending great earthquakes at the Nankai trough

*Tameshige Tsukuda[1] (1.none)

4:45 PM - 5:00 PM JST | 7:45 AM - 8:00 AM UTC

[SSS09-06] What happen on the East Japan Megaquake; answer to sufferers

*Nobuaki Niitsuma[1] (1.Institute of Geosciences,Shizuoka University)

[J] Oral | S (Solid Earth Sciences)：S-SS Seismology

9:00 AM - 10:30 AM JST | 12:00 AM - 1:30 AM UTC | A05 TOKYO BAY MAKUHARI HALL

[S-SS14] Fault Rheology and Earthquake Physics

convener:Keishi Okazaki(Japan Agency for Marine-Earth Science and Technology), Hideki Mukoyoshi(Department of Geoscience Interdisciplinary Graduate School of Science and Engineering, Shimane University), Hiroyuki Noda(Kyoto University, Disaster Prevention Research Institute), Keisuke Yoshida(Tohoku University), Chairperson:Hideki Mukoyoshi, Shunya Kaneki(Osaka University)

9:00 AM - 9:15 AM JST | 12:00 AM - 12:15 AM UTC

[SSS14-07] Effect of slickenside on the crustal strength

*Jun-ichi Ando[1], Takayoshi Nagaoka[1], Naotaka Tomioka[2], Hiroyuki Kagi[3], Kaushik Das[1] (1.Department of Earth and Planetary Systems Science, Hiroshima University, 2.Kochi Institute for core sample research, Japan Agency for Marine-Earth Science and Technology, 3.Geochemical Research Center, Graduate School of Science, University of Tokyo)

9:15 AM - 9:30 AM JST | 12:15 AM - 12:30 AM UTC

[SSS14-08] Dehydroxylation kinetics of clay minerals and its application to friction heating along an imbricate thrust in an accretionary prism

★Invited Papers

*Hirokazu Masumoto[1], Jun Kameda[1] (1.Faculty of Science, Hokkaido University)

9:30 AM - 9:45 AM JST | 12:30 AM - 12:45 AM UTC

[SSS14-09] Origin of frictional melt in the Jurassic accretionary complex of the Mino Belt on the basis of trace element and isotope analysis

*Chizuru Ozawa[1], Tsuyoshi Ishikawa[2], Kohtaro Ujiie[1] (1.University of Tsukuba, 2.JAMSTEC)

9:45 AM - 10:00 AM JST | 12:45 AM - 1:00 AM UTC

[SSS14-10] Geochemical constraint on the origin of albite-bearing black fault rocks in the Kodiak accretionary complex

*Tsuyoshi Ishikawa[1], Asuka Yamaguchi[2] (1.Kochi Institute for Core Sample Research, Japan Agency for Marine-Earth Science and Technology, 2.AORI, The University of Tokyo)

10:00 AM - 10:15 AM JST | 1:00 AM - 1:15 AM UTC

[SSS14-11] Importance of initial maturity and reaction kinetics on maturation of carbonaceous material and its implications for thermal maturity as a proxy for temperature in estimation of coseismic slip parameters

*Shunya Kaneki[1], Ichiba Tatsuya[1], Shuhei Yamashita[1], Tetsuro Hirono[1] (1.Graduate School of Science, Osaka University)

10:15 AM - 10:30 AM JST | 1:15 AM - 1:30 AM UTC

[SSS14-12] Experimental investigation of cumulative effect on thermal maturation of carbonaceous material as a proxy for earthquake slip

*Tetsuro Hirono[1], Yuhtaro Shimamura[1], Shunya Kaneki[2] (1.Department of Earth and Space Science, Graduate School of Science, Osaka University, 2.Disaster Prevention Research Institute, Kyoto University)

[J] Oral | S (Solid Earth Sciences)：S-SS Seismology

10:45 AM - 12:15 PM JST | 1:45 AM - 3:15 AM UTC | A05 TOKYO BAY MAKUHARI HALL

[S-SS14] Fault Rheology and Earthquake Physics

convener:Keishi Okazaki(Japan Agency for Marine-Earth Science and Technology), Hideki Mukoyoshi(Department of Geoscience Interdisciplinary Graduate School of Science and Engineering, Shimane University), Hiroyuki Noda(Kyoto University, Disaster Prevention Research Institute), Keisuke Yoshida(Tohoku University), Chairperson:Hiroyuki Noda(DPRI, Kyoto University), Keishi Okazaki(JAMSTEC)

10:45 AM - 11:00 AM JST | 1:45 AM - 2:00 AM UTC

[SSS14-13] **Fault rheology at the depth limits of the seismogenic zone**

★Invited Papers

*Berend Antonie Verberne[1] (1.Geological Survey of Japan, National Institute of Industrial Science and Technology)

11:00 AM - 11:15 AM JST | 2:00 AM - 2:15 AM UTC

[SSS14-14] Fault models revisited based on friction to flow law

*Toshihiko Shimamoto[1] (1.State Key Laboratory of Earthquake Dynamics, Institute of Geology, China Earthquake Administration)

11:15 AM - 11:30 AM JST | 2:15 AM - 2:30 AM UTC

[SSS14-15] Timing of Earthquakes on Intraplate Active Faults Subjected to Stress Perturbation by Megathrust Earthquakes: Insights from Earthquake Sequence Simulation

*Hiroyuki Noda[1] (1.Kyoto University, Disaster Prevention Research Institute)

11:30 AM - 11:45 AM JST | 2:30 AM - 2:45 AM UTC

[SSS14-16] Physics of earthquake triggering: effect of stress perturbation to slip acceleration

★Invited Papers

*Takahiro Hatano[1] (1.Earthquake Research Institute, University of Tokyo)

11:45 AM - 12:00 PM JST | 2:45 AM - 3:00 AM UTC

[SSS14-17] Foreshock activities controlled by slip rate on a 4-meter-long laboratory fault

*Futoshi Yamashita[1], Eiichi Fukuyama[1], Shiqing Xu[1] (1.National Research Institute for Earth Science and Disaster Resilience)

12:00 PM - 12:15 PM JST | 3:00 AM - 3:15 AM UTC

[SSS14-18] Supersonic propagation of slow slip rupture during rock friction experiments

*Eiichi Fukuyama[1], Futoshi Yamashita[1], Shiqing Xu[1] (1.National Research Institute for Earth Science and Disaster Resilience)

[J] Oral | S (Solid Earth Sciences)：S-SS Seismology

1:45 PM - 3:15 PM JST | 4:45 AM - 6:15 AM UTC | A05 TOKYO BAY MAKUHARI HALL

[S-SS14] Fault Rheology and Earthquake Physics

convener:Keishi Okazaki(Japan Agency for Marine-Earth Science and Technology), Hideki Mukoyoshi(Department of Geoscience Interdisciplinary Graduate School of Science and Engineering, Shimane University), Hiroyuki Noda(Kyoto University, Disaster Prevention Research Institute), Keisuke Yoshida(Tohoku University), Chairperson:Hiroyuki Noda(DPRI, Kyoto University), Keisuke Yoshida(東北大学大学院理学研究科 地球物理学専攻)

1:45 PM - 2:00 PM JST | 4:45 AM - 5:00 AM UTC

[SSS14-19] The role of fault damage zone in the supershear rupture of the 2018 Mw 7.5 Palu earthquake

*Lingsen Meng[1], Han Bao[1], Jean-Paul Ampuero[2], Eric Fielding[3], Cunren Liang[4], Christopher Milliner [3], Tian Feng[1], Hui Huang[1] (1.University of California Los Angeles, 2.Université Côte d'Azur and IRD, 3.Jet Propulsion Laboratory , 4.California Institute of Technology)

2:00 PM - 2:15 PM JST | 5:00 AM - 5:15 AM UTC

[SSS14-20] The role of curvature in earthquake mechanics

*Pierre Romanet[1], Daisuke Sato[2], Ryosuke Ando[1] (1.Earth and Planetary Science Department, University of Tokyo, 2.Disaster Prevention Research Institute, Kyoto University)

2:15 PM - 2:30 PM JST | 5:15 AM - 5:30 AM UTC

[SSS14-21] **Heterogeneous source modelling by the fully dynamic simulations of earthquake cycles on a strike-slip fault and scaling relations.**

*Percy Galvez[1,5], Anatoly Petukhin[2], Paul Somerville[3], Ken Miyakoshi[2], Kojiro Irikura[4] (1.KAUST University, Saudi Arabia, 2.Geo-Research Institute, Osaka Japan, 3.AECOM, Los Angeles, USA., 4.Aichi Institute of Technology, Japan, 5.ETH Zurich, Switzerland)

2:30 PM - 2:45 PM JST | 5:30 AM - 5:45 AM UTC

[SSS14-22] **Strain energy released by an earthquake: Contributions of random slip fluctuations**

*Tatsuhiko Saito[1], Akemi Noda[1] (1.National Research Institute for Earth Science and Disaster Resilience)

2:45 PM - 3:00 PM JST | 5:45 AM - 6:00 AM UTC

[SSS14-23] The change in the elastic strain energy due to the 1992 Landers earthquake and triggering mechanisms of aftershock activity

*Toshiko Terakawa[1], Mitsuhiro Matsu'ura[2], Akemi Noda[3] (1.Graduate School of Environmental Studies, Nagoya University, 2.Institute of Statistical Mathematics, 3.National Research Institute for Earth Science and Disaster Resilience)

3:00 PM - 3:15 PM JST | 6:00 AM - 6:15 AM UTC

[SSS14-24] Toward understanding generation mechanism of crustal earthquakes based on accumulation/release of elastic strain energy

★Invited Papers

*Akemi Noda[1] (1.National Research Institute for Earth Science and Disaster Resilience)

[J] Poster | S (Solid Earth Sciences)：S-SS Seismology

3:30 PM - 5:00 PM JST | 6:30 AM - 8:00 AM UTC | Poster Hall International Exhibition Hall8, Makuhari Messe_16

[S-SS14] Fault Rheology and Earthquake Physics

convener:Keishi Okazaki(Japan Agency for Marine-Earth Science and Technology), Hideki Mukoyoshi(Department of Geoscience Interdisciplinary Graduate School of Science and Engineering, Shimane University), Hiroyuki Noda(Kyoto University, Disaster Prevention Research Institute), Keisuke Yoshida(Tohoku University)

[SSS14-P01] Measurement of shear-wave polarization anisotropy in crack-bearing Aji granite during shear experiment

*Jinki Tanaka[1], Ikuo Katayama[1] (1.Hiroshima University)

[SSS14-P02] Effects of talc content on frictional properties of quartz gouge

Risako Shirahige[1], Inori Tatara[1], *Ken-ichi Hirauchi[1], Takato Takemura[2] (1.Department of Geosciences, Faculty of Science, Shizuoka University, 2.Department of Earth and Environmental Sciences, College of Humanities and Sciences, Nihon University)

[SSS14-P03] Mechanism controlling the frictional strength of quartz rocks at intermediate slip rates

*Kyuichi Kanagawa[1], Asuka Sugita[2], Miki Takahashi[3], Michiyo Sawai[1] (1.School of Science, Chiba University, 2.Faculty of Science, Chiba University, 3.Research Institute of Earthquake and Volcano Geology, Geological Survey of Japan)

[SSS14-P04] **Evolution of hydraulic and frictional properties of incoming hemipelagic sediments during diagenetic reactions**

*Keishi Okazaki[1], Ikuo Katayama[2], Asuka Yamaguchi[3] (1.Japan Agency for Marine-Earth Science and Technology, 2.Dept. of Earth & Planetary Systems Science, Hiroshima University, 3.AORI, the University of Tokyo)

[SSS14-P05] Contrasting silica precipitation via flash vaporization and fluid flow and possible effects on fault properties

*Takamasa Niibe[1], Atsushi Okamoto[1], Takashi Amagai[2], Noriyoshi Tsuchiya[1] (1.Graduate School of Environmental Studies, Tohoku University, 2.Japan Oil, Gas and Metals National Corporation)

[SSS14-P06] Temporal variations of reflected and transmitted wave during a slide-hold-slide experiment on a biaxial friction testing machine

*Miyuu Uemura[1], Yoshihiro Ito[2], Ikuo Katayama[3] (1.Kyoto University, 2.Disaster Prevention Research Institute, Kyoto University, 3.Department of Earth and Planetary Systems Science, Hiroshima University)

[SSS14-P07] Monitoring stress-induced changes of laboratory fault by ultrasonic coda wavesMonitoring stress-induced changes of laboratory fault by ultrasonic coda waves

*Fan XIE[1], Yaqiong REN[1] (1.Institute of Geophysics, China Earthquake Administration)

[SSS14-P08] Longer duration of meta-instability stage of laboratory earthquakes on a 1.5m granite fault

*yaqiong Ren[1] (1.Institute of Geophysics, China Earthquake Administration)

[SSS14-P09] Estimation of the frictional heat and the amount of wall rock incorporation by thermal fracturing during an earthquake: An example from the pseudotachylyte in Jurassic accretionary complex

*Ayaka Nagate[1], Kohtaro Ujiie[1] (1.University of Tsukuba)

[SSS14-P10] Porosity variation of fault rocks accompanied the Median Tectonic Line in Shikoku, southwestern Japan

*Michiharu Ikeda[1], Takeshi Tsuji[2], Tomohiro Tsuji[1], Kozo Onishi[3], Naoki Nishizaka[3] (1.Shikoku Research Institute Incorporated, 2.Kyushu University, 3.Shikoku Electric Power Company, Incorporated)

[SSS14-P11] Characteristics of inactive section of the Median Tectonic Line from drillcore samples in Shikoku, southwestern Japan

*Hideto Uchida[1], Michiharu Ikeda[1], Takeshi Tsuji[2], Kozo Onishi[3], Naoki Nishizaka[3] (1.Department of Civil Engineering, Shikoku Research Institute incorporated, 2.Department of Earth Resources Engineering, Kyusyu University, 3.Shikoku Electronic Power)

[SSS14-P12] Surface and internal textures of clasts in incohesive fault rocks and their significance

*Tetsuhiro Togo[1], Toshihiko Shimamoto[2], Michiyo Sawai[3] (1.THE EARTH, 2.Institute of Geology, China Earthquake Administration, 3.Chiba Univ.)

[SSS14-P13] **Fault Displacement Assessment of Surface-rupturing Earthquakes for Nuclear Installations and the use of Physics-based Rupture Models**

*Luis Angel Dalguer[1], Yoshimitsu Fukushima[2] (1.3Q-Lab GmbH, 2.International Atomic Energy Agency)

[SSS14-P14] Dynamic rupture simulation for seismic hazard assessment: Application to the Futagawa and Hinagu fault zones (Part 2)

*Yuko Kase[1] (1.Geological Survey of Japan, AIST)

[SSS14-P15] Quantification of gaps between slip-length scaling law of earthquakes and stick-slip experiments.

*Shinichi Oba[1], Yuta Mitsui[2] (1.Graduate School of Science and Tecnology, Shizuoka University, 2.Faculty of Science, Shizuoka University)

[SSS14-P16] Effect of Wear Process on Earthquake Recurrence

*Jeen-Hwa Wang[1] (1.Academia Sinica)

[SSS14-P17] On the Mechanical Relation between Individual Interaction and Collective Behavior of Multiple Fault Sets Subjected to Quasi-Static Loading

*Koji Uenishi[1,2], Yuki Fukuda[2], Nobuki Kame[3] (1.Department of Advanced Energy, The University of Tokyo, 2.Department of Aeronautics and Astronautics, The University of Tokyo, 3.Earthquake Research Institute, The University of Tokyo)

[SSS14-P18] Inelastic deformation in a region of the transient and forced extensional horizontal crustal strain

*Takao Eguchi, Yasuyuki Iwase[1] (1.National Defense Academy, Japan)

[SSS14-P19] Representation Theorem and Green's Function (3) - - Strain, Stress, and Density Perturbation Fields due to a Point Source Using 2nd Derivative of Green's Function in an Unbounded Homogeneous Isotropic Elastic Medium - -

*Masaya Kimura[1], Nobuki Kame[1] (1.Earthquake Research Institute,The University of Tokyo)

[SSS14-P20] Development of a method of visualization of abrupt changes in slip-rate and rupture velocity toward better understanding of high-frequency radiation on a fault.

*Takahiro ayukai[1], Yuji Yagi[2], Ryo Okuwaki[3], Keita Kayano[3], Kousuke Shimizu[3] (1.School of Life and Environmental Sciences, University of Tsukuba, 2.Graduate School of Life and Environmental Sciences, University of Tsukuba, Tsukuba, 3.Graduate School of Life and Environmental Sciences, University of Tsukuba)

[SSS14-P21] Issues in earthquake-source-inversion analysis, evaluated through singular value decomposition

*Keita Kayano[1], Yuji Yagi[1], Ryo Okuwaki[1], Kousuke Shimizu[1] (1.Tsukuba University)

[SSS14-P22] **Source process of recent M6-class inland earthquakes in Japan**

*Ritsuya Shibata[1], Naofumi Aso[1], Junichi Nakajima[1], Satoshi Ide[2] (1.Department of Earth and Planetary Sciences, Tokyo Institute of Technology, 2.Department of Earth and Planetary Science, University of Tokyo)

[SSS14-P23] Expected slip direction on assumed fault planes of large earthquakes inferred from stress field after the 2016 Kumamoto earthquake sequence, in central Kyushu, Japan

*Ayaho Mitsuoka[1], Satoshi Matsumoto[2], Azusa Shito[2], Hiroshi Shimizu[2], Group for urgent joint seismic observation of the 2016 Kumamoto earthquake (1.Department of Earth and Planetary Sciences, Graduate School of Science, Kyushu University, 2.Institute of Seismology and Volcanology, Faculty of Sciences, Kyushu University)

[SSS14-P24] Spaciotemporal change of source parameters of repeaters due to the 2011 Tohoku-Oki earthquake

*Kazuya Tateiwa[1], Tomomi Okada[1], Toshio Kono[1], Naoki Uchida[1] (1.Research Center for Prediction of Earthquakes and Volcanic Eruptions, Graduate School of Science, Tohoku University)

[SSS14-P25] Slip distributions and relation of slip-rate and shear stress for the Boso slow slip events

*Takuma Kobayashi[1], Toshinori Sato[2] (1.Graduate School of Science and Engineering, Chiba University, 2.Graduate School of Science, Chiba University)

[SSS14-P26] Repeating inland earthquakes in northern Ibaraki Prefecture activated after the 2011 Tohoku-Oki earthquake

Ryo Takahashi[1], *Keisuke Yoshida[1], Akira Hasegawa[1], Toru Matsuzawa[1] (1.Tohoku University)

[J] Poster | S (Solid Earth Sciences)：S-SS Seismology

5:15 PM - 6:30 PM JST | 8:15 AM - 9:30 AM UTC | Poster Hall International Exhibition Hall8, Makuhari Messe_26

[S-SS14] Fault Rheology and Earthquake Physics

convener:Keishi Okazaki(Japan Agency for Marine-Earth Science and Technology), Hideki Mukoyoshi(Department of Geoscience Interdisciplinary Graduate School of Science and Engineering, Shimane University), Hiroyuki Noda(Kyoto University, Disaster Prevention Research Institute), Keisuke Yoshida(Tohoku University)

[SSS14-P01] Measurement of shear-wave polarization anisotropy in crack-bearing Aji granite during shear experiment

*Jinki Tanaka[1], Ikuo Katayama[1] (1.Hiroshima University)

[SSS14-P02] Effects of talc content on frictional properties of quartz gouge

Risako Shirahige[1], Inori Tatara[1], *Ken-ichi Hirauchi[1], Takato Takemura[2] (1.Department of Geosciences, Faculty of Science, Shizuoka University, 2.Department of Earth and Environmental Sciences, College of Humanities and Sciences, Nihon University)

[SSS14-P03] Mechanism controlling the frictional strength of quartz rocks at intermediate slip rates

*Kyuichi Kanagawa[1], Asuka Sugita[2], Miki Takahashi[3], Michiyo Sawai[1] (1.School of Science, Chiba University, 2.Faculty of Science, Chiba University, 3.Research Institute of Earthquake and Volcano Geology, Geological Survey of Japan)

[SSS14-P04] **Evolution of hydraulic and frictional properties of incoming hemipelagic sediments during diagenetic reactions**

*Keishi Okazaki[1], Ikuo Katayama[2], Asuka Yamaguchi[3] (1.Japan Agency for Marine-Earth Science and Technology, 2.Dept. of Earth & Planetary Systems Science, Hiroshima University, 3.AORI, the University of Tokyo)

[SSS14-P05] Contrasting silica precipitation via flash vaporization and fluid flow and possible effects on fault properties

*Takamasa Niibe[1], Atsushi Okamoto[1], Takashi Amagai[2], Noriyoshi Tsuchiya[1] (1.Graduate School of Environmental Studies, Tohoku University, 2.Japan Oil, Gas and Metals National Corporation)

[SSS14-P06] Temporal variations of reflected and transmitted wave during a slide-hold-slide experiment on a biaxial friction testing machine

*Miyuu Uemura[1], Yoshihiro Ito[2], Ikuo Katayama[3] (1.Kyoto University, 2.Disaster Prevention Research Institute, Kyoto University, 3.Department of Earth and Planetary Systems Science, Hiroshima University)

[SSS14-P07] Monitoring stress-induced changes of laboratory fault by ultrasonic coda wavesMonitoring stress-induced changes of laboratory fault by ultrasonic coda waves

*Fan XIE[1], Yaqiong REN[1] (1.Institute of Geophysics, China Earthquake Administration)

[SSS14-P08] Longer duration of meta-instability stage of laboratory earthquakes on a 1.5m granite fault

*yaqiong Ren[1] (1.Institute of Geophysics, China Earthquake Administration)

[SSS14-P09] Estimation of the frictional heat and the amount of wall rock incorporation by thermal fracturing during an earthquake: An example from the pseudotachylyte in Jurassic accretionary complex

*Ayaka Nagate[1], Kohtaro Ujiie[1] (1.University of Tsukuba)

[SSS14-P10] Porosity variation of fault rocks accompanied the Median Tectonic Line in Shikoku, southwestern Japan

*Michiharu Ikeda[1], Takeshi Tsuji[2], Tomohiro Tsuji[1], Kozo Onishi[3], Naoki Nishizaka[3] (1.Shikoku Research Institute Incorporated, 2.Kyushu University, 3.Shikoku Electric Power Company, Incorporated)

[SSS14-P11] Characteristics of inactive section of the Median Tectonic Line from drillcore samples in Shikoku, southwestern Japan

*Hideto Uchida[1], Michiharu Ikeda[1], Takeshi Tsuji[2], Kozo Onishi[3], Naoki Nishizaka[3] (1.Department of Civil Engineering, Shikoku Research Institute incorporated, 2.Department of Earth Resources Engineering, Kyusyu University, 3.Shikoku Electronic Power)

[SSS14-P12] Surface and internal textures of clasts in incohesive fault rocks and their significance

*Tetsuhiro Togo[1], Toshihiko Shimamoto[2], Michiyo Sawai[3] (1.THE EARTH, 2.Institute of Geology, China Earthquake Administration, 3.Chiba Univ.)

[SSS14-P13] **Fault Displacement Assessment of Surface-rupturing Earthquakes for Nuclear Installations and the use of Physics-based Rupture Models**

*Luis Angel Dalguer[1], Yoshimitsu Fukushima[2] (1.3Q-Lab GmbH, 2.International Atomic Energy Agency)

[SSS14-P14] Dynamic rupture simulation for seismic hazard assessment: Application to the Futagawa and Hinagu fault zones (Part 2)

*Yuko Kase[1] (1.Geological Survey of Japan, AIST)

[SSS14-P15] Quantification of gaps between slip-length scaling law of earthquakes and stick-slip experiments.

*Shinichi Oba[1], Yuta Mitsui[2] (1.Graduate School of Science and Tecnology, Shizuoka University, 2.Faculty of Science, Shizuoka University)

[SSS14-P16] Effect of Wear Process on Earthquake Recurrence

*Jeen-Hwa Wang[1] (1.Academia Sinica)

[SSS14-P17] On the Mechanical Relation between Individual Interaction and Collective Behavior of Multiple Fault Sets Subjected to Quasi-Static Loading

*Koji Uenishi[1,2], Yuki Fukuda[2], Nobuki Kame[3] (1.Department of Advanced Energy, The University of Tokyo, 2.Department of Aeronautics and Astronautics, The University of Tokyo, 3.Earthquake Research Institute, The University of Tokyo)

[SSS14-P18] Inelastic deformation in a region of the transient and forced extensional horizontal crustal strain

*Takao Eguchi, Yasuyuki Iwase[1] (1.National Defense Academy, Japan)

[SSS14-P19] Representation Theorem and Green's Function (3) - - Strain, Stress, and Density Perturbation Fields due to a Point Source Using 2nd Derivative of Green's Function in an Unbounded Homogeneous Isotropic Elastic Medium - -

*Masaya Kimura[1], Nobuki Kame[1] (1.Earthquake Research Institute,The University of Tokyo)

[SSS14-P20] Development of a method of visualization of abrupt changes in slip-rate and rupture velocity toward better understanding of high-frequency radiation on a fault.

*Takahiro ayukai[1], Yuji Yagi[2], Ryo Okuwaki[3], Keita Kayano[3], Kousuke Shimizu[3] (1.School of Life and Environmental Sciences, University of Tsukuba, 2.Graduate School of Life and Environmental Sciences, University of Tsukuba, Tsukuba, 3.Graduate School of Life and Environmental Sciences, University of Tsukuba)

[SSS14-P21] Issues in earthquake-source-inversion analysis, evaluated through singular value decomposition

*Keita Kayano[1], Yuji Yagi[1], Ryo Okuwaki[1], Kousuke Shimizu[1] (1.Tsukuba University)

[SSS14-P22] **Source process of recent M6-class inland earthquakes in Japan**

*Ritsuya Shibata[1], Naofumi Aso[1], Junichi Nakajima[1], Satoshi Ide[2] (1.Department of Earth and Planetary Sciences, Tokyo Institute of Technology, 2.Department of Earth and Planetary Science, University of Tokyo)

[SSS14-P23] Expected slip direction on assumed fault planes of large earthquakes inferred from stress field after the 2016 Kumamoto earthquake sequence, in central Kyushu, Japan

*Ayaho Mitsuoka[1], Satoshi Matsumoto[2], Azusa Shito[2], Hiroshi Shimizu[2], Group for urgent joint seismic observation of the 2016 Kumamoto earthquake (1.Department of Earth and Planetary Sciences, Graduate School of Science, Kyushu University, 2.Institute of Seismology and Volcanology, Faculty of Sciences, Kyushu University)

[SSS14-P24] Spaciotemporal change of source parameters of repeaters due to the 2011 Tohoku-Oki earthquake

*Kazuya Tateiwa[1], Tomomi Okada[1], Toshio Kono[1], Naoki Uchida[1] (1.Research Center for Prediction of Earthquakes and Volcanic Eruptions, Graduate School of Science, Tohoku University)

[SSS14-P25] Slip distributions and relation of slip-rate and shear stress for the Boso slow slip events

*Takuma Kobayashi[1], Toshinori Sato[2] (1.Graduate School of Science and Engineering, Chiba University, 2.Graduate School of Science, Chiba University)

[SSS14-P26] Repeating inland earthquakes in northern Ibaraki Prefecture activated after the 2011 Tohoku-Oki earthquake

Ryo Takahashi[1], *Keisuke Yoshida[1], Akira Hasegawa[1], Toru Matsuzawa[1] (1.Tohoku University)

[J] Oral | S (Solid Earth Sciences)：S-SS Seismology

9:00 AM - 10:30 AM JST | 12:00 AM - 1:30 AM UTC | A02 TOKYO BAY MAKUHARI HALL

[S-SS15] Active faults and paleoseismology

convener:Mamoru Koarai(Earth Science course, College of Science, Ibaraki University), Takashi OGAMI(National Institute of Advanced Industrial Science and Technology), Ryosuke Doke(Hot Springs Research Institute of Kanagawa Prefecture), Hisao Kondo(Geological Survey of Japan, National Institute of Advanced Industrial Science and Technology), Chairperson:Takashi Azuma(AIST), Mamoru KOARAI(Ibaraki University)

9:15 AM - 9:30 AM JST | 12:15 AM - 12:30 AM UTC

[SSS15-05] Paleoseismological survey on the Shibetsu fault zone in the eastern part of Hokkaido, Japan

*Takashi Azuma[1], Daisuke Hirouchi[2], Koji Okumura[3], Kaoru Taniguchi[4], Masashi Omata[4], Yorihide Kohriya[4] (1.National Institute of Advanced Industrial Science and Technology, 2.Shinshu University, 3.Hiroshima University, 4.Pasco CORPORATION)

9:30 AM - 9:45 AM JST | 12:30 AM - 12:45 AM UTC

[SSS15-06] Deformation of marine terrace surfaces associated with active Rokkasho fault in southern Shimokita peninsula, northern Japan

*Mitsuhisa Watanabe[1] (1.Faculty of Sociology, Toyo University)

9:45 AM - 10:00 AM JST | 12:45 AM - 1:00 AM UTC

[SSS15-07] **Vertical crustal movement during the past 600 years in the Kikai Island, deduced from the height distribution and ages of coral microatolls**

*Masanobu Shishikura[1], Hideaki Maemoku[2], Tomoo Echigo[3], Yuichi Namegaya[1], Tatsuya Ishiyama[4], Ryo Kinjo[2], Naoto Inoue[3] (1.Institute of Earthquake and Volcano Geology, National Institute of Advanced Industrial Science and Technology, 2.Hosei University, 3.Geo-Reserch Institute, 4.Earthquake Research Institute, University of Tokyo)

10:00 AM - 10:15 AM JST | 1:00 AM - 1:15 AM UTC

[SSS15-08] Variation of coseismic fault displacements on multiple seismic cycles at a site: An example from the Kamishiro fault, Itoigawa-Shizuoka Tectonic Line active fault system, central Japan

*Naoya Takahashi[1], Shinji Toda[2] (1.Graduate school of Science, Department of Earth Science, Tohoku University, 2.International Research Institute of Disaster Science, Tohoku University)

10:15 AM - 10:30 AM JST | 1:15 AM - 1:30 AM UTC

[SSS15-09] High-resolution shear-wave seismic reflection surveys across the Kamishiro fault, Itoigawa-Shizuoka Tectonic Line active fault system, central Japan

*Naoki IKEGUCHI[1], Nobuhisa Matsuta[2], Kyoko Kagohara[3], Shinsuke Okada[4], Daisuke Hirouchi[5], Tatsuya Ishiyama[1], Katsuya Noda[6], Hiroshi Sato[1] (1.Earthquake Resarch Institute University of Tokyo, 2.Graduate School of Education, Okayama University, 3.Faculty of Education, Yamaguchi University, 4.Graduate school of Science, Tohoku University, 5.Faculty of Education, Shinshu University, 6.GEOSYS Inc.)

[J] Oral | S (Solid Earth Sciences)：S-SS Seismology

10:45 AM - 12:15 PM JST | 1:45 AM - 3:15 AM UTC | A02 TOKYO BAY MAKUHARI HALL

[S-SS15] Active faults and paleoseismology

convener:Mamoru Koarai(Earth Science course, College of Science, Ibaraki University), Takashi OGAMI(National Institute of Advanced Industrial Science and Technology), Ryosuke Doke(Hot Springs Research Institute of Kanagawa Prefecture), Hisao Kondo(Geological Survey of Japan, National Institute of Advanced Industrial Science and Technology), Chairperson:HISAO KONDO(Geological Survey of Japan, National Institute of Advanced Industrial Science and Technology), Nobuhiko Sugito(Hosei University)

10:45 AM - 11:00 AM JST | 1:45 AM - 2:00 AM UTC

[SSS15-10] Paleoseismic investigations on the un-ruptured section during the 2014 earthquake along the Kamishiro fault, ISTL active fault zone, Central Japan

*Hisao Kondo[1], Hideki Kurosawa[2], Yoko Hirakura[2], Keita Takada[3], Kohei Abe[2], Miwako Ito[2], Atsuo Igarashi[3], Tetsuya Ikeda[3], Atsushi Miwa[2] (1.Geological Survey of Japan, National Institute of Advanced Industrial Science and Technology, 2.OYO Cooperation, 3.Fukken Co., Ltd)

11:00 AM - 11:15 AM JST | 2:00 AM - 2:15 AM UTC

[SSS15-11] P-wave seismic reflection profiling across the northern central ISTL active fault system, central Japan

*Haruo Kimura[1], Hisao Kondo[2], Yasuhiko Akinaga[3], Shigeru Okamoto[3], Masaki Suehiro[3] (1.Central Research Institute of Electric Power Industry, 2.Geological Survey of Japan, AIST, 3.Hanshin Consultants Co., Ltd.)

11:15 AM - 11:30 AM JST | 2:15 AM - 2:30 AM UTC

[SSS15-12] History of interplate earthquakes along the Sagami Trough from uplifted coasts in the Boso Peninsula

*Junki Komori[1], Masanobu Shishikura[2], Ryosuke Ando[1] (1.The University of Tokyo, 2.The National Institute of Advanced Industrial Science and Technology)

11:30 AM - 11:45 AM JST | 2:30 AM - 2:45 AM UTC

[SSS15-13] Inferring location and activity of the Iriyamase fault, the Fujikawa-kako fault zone, based on boring core sample analyses and physical fault model

*Namiki Ryo[1], Ryosuke Ando[1], Masanobu Shishikura[2] (1.The University of Toyko, 2.National Institute of Advanced Industrial Science and Technology)

11:45 AM - 12:00 PM JST | 2:45 AM - 3:00 AM UTC

[SSS15-14] **Coastal submergence events identified by fossil diatoms and plant macrofossils at Ukishima-ga-hara adjacent to the Suruga Trough (eastern Nankai Trough), central Japan**

*Yuki Sawai[1], Arata Momohara[2], DAN MATSUMOTO[1], Yumi Shimada[1,3] (1.Geological Survey of Japan, AIST, 2.Chiba University, 3.University of Tsukuba)

[J] Oral | S (Solid Earth Sciences)：S-SS Seismology

1:45 PM - 3:15 PM JST | 4:45 AM - 6:15 AM UTC | A02 TOKYO BAY MAKUHARI HALL

[S-SS15] Active faults and paleoseismology

convener:Mamoru Koarai(Earth Science course, College of Science, Ibaraki University), Takashi OGAMI(National Institute of Advanced Industrial Science and Technology), Ryosuke Doke(Hot Springs Research Institute of Kanagawa Prefecture), Hisao Kondo(Geological Survey of Japan, National Institute of Advanced Industrial Science and Technology), Chairperson:Takashi Ogami(AIST), Koji Okumura(Hiroshima University)

1:45 PM - 2:00 PM JST | 4:45 AM - 5:00 AM UTC

[SSS15-15] Shallow structures and tectonic geomorphology of active blind thrusts imaged by new hi-resolution seismic reflection profiling, Hokkaido, Northern Japan

*Tatsuya Ishiyama[1], Naoko Kato[1], Hiroshi Sato[1], Taro Koike[2], Katsuya Noda[2] (1.Earthquake Research Institute, University of Tokyo, 2.Geosys, Inc.)

2:00 PM - 2:15 PM JST | 5:00 AM - 5:15 AM UTC

[SSS15-16] Paleo-seismological survey on the Idenokuchi fault, Nishihara village, Kumamoto prefecture

*Daisuke Ishimura[1], Hiroyuki Tsutsumi[2], Naoya Takahashi[3], Ryuhei Oda[1], Jun Matsukaze[1], Heitaro Kaneda[4], Motoya Kobayashi[4], Yasuhiro Kumahara[5], Makoto Kobayashi[6], Toshihiko Ichihara[7] (1.Department of Geography, Tokyo Metropolitan University, 2.Department of Environmental Systems Science, Faculty of Science and Engineering, Doshisha University, 3.Department of EarthScience, Tohoku University, 4.Graduate School of Science, Chiba University, 5.Graduate School of Education, Hiroshima University, 6.Research Center for Volcanic Hazards and Their Mitigation, Tokyo Metropolitan University, 7.Sedimentary Environments Research)

2:15 PM - 2:30 PM JST | 5:15 AM - 5:30 AM UTC

[SSS15-17] Paleoseismic investigations of the Hinagu fault zone, Kumamoto, Japan: Preliminary result of trenching survey at Yatsushiro city

*Yukari Miyashita[1], Takashi Azuma[1], Yusuke Komine[2], Masao Kametaka[2], Midori Kishiyama[2] (1.Institute of Earthquake and Volcano Geology, Geological Survey of Japan, National Institute of Advanced Industrial Science and Technology, 2.Dia Consultants Co. Ltd.)

2:30 PM - 2:45 PM JST | 5:30 AM - 5:45 AM UTC

[SSS15-18] Seismic trenching on offshore part of the Hinagu Fault Zone, Kyushu, Japan −3D structure and paleo-seismicity of offshore dextral strike-slip fault

*Takashi OGAMI[1], Shintaro Abe[2], Kenjiro Mukaiyama[3], Shigeyuki Suda[4] (1.Geological Survey of Japan, AIST, 2.ADEP, 3.Kawasaki Geological Engineering Co. Ltd., 4.JGI Inc.)

2:45 PM - 3:00 PM JST | 5:45 AM - 6:00 AM UTC

[SSS15-19] Conductivity Structure models of large and small slip regions at the 2016 Kumamoto earthquake sequence

*Satoru Yamaguchi[1], Yuto Yamanaka[2], Akira Mimura[1], Kazuki Fkue[1], Daigo Furukawa[1], Tada-nori Goto[3], Hisatoshi Koji[3], Sota Kawaguchi[3], Koki Aizawa[4], Shinichi Takakura[5] (1.Department of Geosciences, Graduate School of Science, Osaka City University, 2.Faculty of Science, Osaka City University, 3.Department of Urban Management, Graduate School of Engineering, Kyoto University, 4.Institute of Seismology and Volcanology, Kyushu University, 5. Geological Survey of Japan, National Institute of Advanced Industrial Science and Technology)

3:00 PM - 3:15 PM JST | 6:00 AM - 6:15 AM UTC

[SSS15-20] The Timing and Extent of the Last Surface Rupture Event on the Himalayan Frontal Thrust in Central Nepal around Butwal

*Koji Okumura[1], Soma Nath Sapkota[2], Prakash Pokhrel[2], Hisao Kondo[4], Takuya Furuhashi[3] (1.Graduate School of Letters, Hiroshima University, 2.Department of Mines and Geology, 3.Taiheiyo Cement Corporation, 4.Geological Survey of Japan, AIST)

[J] Oral | S (Solid Earth Sciences)：S-SS Seismology

3:30 PM - 5:00 PM JST | 6:30 AM - 8:00 AM UTC | A02 TOKYO BAY MAKUHARI HALL

[S-SS15] Active faults and paleoseismology

convener:Mamoru Koarai(Earth Science course, College of Science, Ibaraki University), Takashi OGAMI(National Institute of Advanced Industrial Science and Technology), Ryosuke Doke(Hot Springs Research Institute of Kanagawa Prefecture), Hisao Kondo(Geological Survey of Japan, National Institute of Advanced Industrial Science and Technology), Chairperson:Ryosuke Doke(Hot Springs Research Institute of Kanagawa Prefecture), Mamoru KOARAI(Ibaraki University)

3:30 PM - 4:00 PM JST | 6:30 AM - 7:00 AM UTC

[SSS15-21] Linear surface ruptures detected by SAR - - *the Kumamoto earthquake, the Northern Osaka earthquake and the Hokkaido Eastern Iburi earthquake*

★Invited Papers

*Satoshi Fujiwara[1], Hiroshi Une[1], Takayuki Nakano[1], Hiroshi Yarai[1], Tomokazu Kobayashi[1], Yu Morishita[1] (1.GSI of Japan)

4:00 PM - 4:15 PM JST | 7:00 AM - 7:15 AM UTC

[SSS15-22] Acquisition of micro-landforms in the forest using small UAV-LiDAR: An example from surface rupture of the 2008 Iwate-Miyagi Nairiku, Japan, earthquake

*Asaka Konno[1], Taro Suzuki[2], Shinji Toda[1] (1.International Research Institute of Disaster Science, Tohoku University, 2.Waseda University)

4:15 PM - 4:30 PM JST | 7:15 AM - 7:30 AM UTC

[SSS15-23] **Bayesian Inference and Forecast on Renewal Processes for Recurrent Earthquakes with Uncertain Occurrence Times**

*Shunichi Nomura[1], Yosihiko Ogata[1] (1.The Institute of Statistical Mathematics)

4:30 PM - 4:45 PM JST | 7:30 AM - 7:45 AM UTC

[SSS15-24] **Slip rate of the Chaman fault: estimates based on ^{10}Be exposure dating for offset geomorphic surfaces in Afghanistan**

*Zakeria Shnizai[1], Yuki Matsushi[2], Hiroyuki Tsutsumi[1] (1.Doshisha University, 2.Kyoto University)

[J] Oral | S (Solid Earth Sciences)：S-SS Seismology

1:45 PM - 3:15 PM JST | 4:45 AM - 6:15 AM UTC | A08 TOKYO BAY MAKUHARI HALL

[S-SS17] Seismic evidence of volcanic roots

convener:Naofumi Aso(Tokyo Institute of Technology), Yohei Yukutake(Hot Springs Research Institute of Kanagawa Prefecture), Chairperson:Naofumi Aso, Yohei Yukutake

1:45 PM - 2:00 PM JST | 4:45 AM - 5:00 AM UTC

[SSS17-01] Spectral characteristics of deep low frequency earthquakes at Mount Fuji

★Invited Papers

*Motoo Ukawa[1] (1.Nihon University)

2:00 PM - 2:15 PM JST | 5:00 AM - 5:15 AM UTC

[SSS17-02] Deep low-frequency earthquakes corresponding to the 2011 and 2018 eruptions in Kirishima volcano

*Ryo Kurihara[1], Kazushige Obara[1], Akiko Takeo[1], Yusaku Tanaka[1] (1.Earthquake Research Institute, The University of Tokyo)

2:15 PM - 2:30 PM JST | 5:15 AM - 5:30 AM UTC

[SSS17-03] Origin of long-duration of deep low-frequency earthquakes and activity of shallow low-frequency earthquakes beneath northeastern Japan

*Masahiro Kosuga[1], Taichi Haruyama[1], Yuki Matsuno[2], Iori Narita[2], Takuto Maeda[1] (1.Graduate School of Science and Technology, Hirosaki University, 2.Faculty of Science and Technology, Hirosaki University)

2:30 PM - 2:45 PM JST | 5:30 AM - 5:45 AM UTC

[SSS17-04] Deep low-frequency earthquakes, tomography and magmatic system beneath active volcanoes

★Invited Papers

*Dapeng Zhao[1] (1.Department of Geophysics, Tohoku University)

2:45 PM - 3:00 PM JST | 5:45 AM - 6:00 AM UTC

[SSS17-05] Seismic imaging of deep structure beneath active volcanoes

*Junichi Nakajima[1] (1.Department of Earth and Planetary Sciences, Tokyo Institute of Technology)

3:00 PM - 3:15 PM JST | 6:00 AM - 6:15 AM UTC

[SSS17-06] Deep low-frequency volcanic earthquakes and their implication for deep crustal processes in the magmatic arc

*Haruhisa Nakamichi[1] (1.Sakurajima Volcano Research Center, Disaster Prevention Research Institute, Kyoto University)

[J] Poster | S (Solid Earth Sciences)：S-SS Seismology

3:30 PM - 5:00 PM JST | 6:30 AM - 8:00 AM UTC | Poster Hall International Exhibition Hall8, Makuhari Messe_17

[S-SS17] Seismic evidence of volcanic roots

convener:Naofumi Aso(Tokyo Institute of Technology), Yohei Yukutake(Hot Springs Research Institute of Kanagawa Prefecture)

[SSS17-P01] S-wave reflectors beneath the earthquake swarm in the Yonezawa-Kitakata area, NE Japan

*Manami Suzuki [1], Akiko Hasemi[1], Tomomi Okada[1], Toru Matsuzawa[1], Norihito Umino[1], Takashi Nakayama[1], Noriko Tsumura[2], Tadashi Yamashina[3], Group for the aftershock observations of the 2011 off the Pacific of Tohoku Earthquake (1.Research Center for Prediction of Earthquakes and Volcanic Eruptions, Graduate School of Science, Tohoku University, 2.Graduate School of Science, Chiba University, 3.Faculty of Science and Technology, Kochi University)

[SSS17-P02] Imaging of the magma pathway beneath Kirishima volcanoes by seismic interferometry

*Yutaka Nagaoka[1], Kiwamu Nishida[2], Yosuke Aoki[2], Minoru Takeo[2], Takahiro Ohkura[3], Shin Yoshikawa[3] (1.Volcanology Research Department, Meteorological Research Institute, 2.Earthquake Research Institute, The University of Tokyo, 3.Aso Volcanological Laboratory, Institute for Geothermal Sciences, Graduate School of Science, Kyoto University)

[SSS17-P03] Finite element three-dimensional seismic waveform calculations of volcanic deep low frequency earthquake including true topographic effects of Hakone volcano

*Lina Yamaya[1], Kimihiro Mochizuki[1], Tsuyoshi Ichimura[1], Kohei Fujita[1], Takeshi Akuhara[1], Takane Hori[2], Ryou Honda[3], Yohei Yukutake[3] (1.Earthquake Research Institute, Univ. of Tokyo, 2.JAMSTEC, 3.Hot Springs Research Institute of Kanagawa)

[SSS17-P04] Magma transport system beneath Hakone volcano inferred from deep low frequency earthquakes

*Yohei Yukutake[1], Yuki Abe[1] (1.Hot Springs Research Institute of Kanagawa Prefecture)

[SSS17-P05] Hypocenter and waveform characteristics of deep low-frequency earthquakes beneath Zao volcano

*Takuma Ikegaya[1], Mare Yamamoto[1] (1.Graduate School of Science, Tohoku University)

[SSS17-P06] Mechanisms transition of LFEs beneath Zao volcano due to the stress change induced by the 2011 Tohoku earthquake

*Genki Oikawa[1], Naofumi Aso[1], Junichi Nakajima[1], Toru Matsuzawa[2] (1.Tokyo Institute of Technology, 2.Tohoku University)

[SSS17-P07] Magma/gas intrusion process of Shinmoedake Eruption in 2017 suggested by volcanic tremors location with ASL method

Shoya Imamura[1], *Makoto OKUBO[2] (1.Faculty of Science, Kochi University, 2.Natural Science Cluster, Kochi University)

[SSS17-P08] Source depth estimation of a magmatic inflation in 2008-2010 at Mt. Fuji, Japan, based on sparsity-promoting L1 inversion of GNSS data

*Yuta Mitsui[1], Takahiro Kato[2] (1.Department of Geosciences, Shizuoka University, 2.formerly at Department of Geosciences, Shizuoka University)

[J] Poster | S (Solid Earth Sciences)：S-SS Seismology

5:15 PM - 6:30 PM JST | 8:15 AM - 9:30 AM UTC | Poster Hall International Exhibition Hall8, Makuhari Messe_27

[S-SS17] Seismic evidence of volcanic roots

convener:Naofumi Aso(Tokyo Institute of Technology), Yohei Yukutake(Hot Springs Research Institute of Kanagawa Prefecture)

[SSS17-P01] S-wave reflectors beneath the earthquake swarm in the Yonezawa-Kitakata area, NE Japan

*Manami Suzuki [1], Akiko Hasemi[1], Tomomi Okada[1], Toru Matsuzawa[1], Norihito Umino[1], Takashi Nakayama[1], Noriko Tsumura[2], Tadashi Yamashina[3], Group for the aftershock observations of the 2011 off the Pacific of Tohoku Earthquake (1.Research Center for Prediction of Earthquakes and Volcanic Eruptions, Graduate School of Science, Tohoku University, 2.Graduate School of Science, Chiba University, 3.Faculty of Science and Technology, Kochi University)

[SSS17-P02] Imaging of the magma pathway beneath Kirishima volcanoes by seismic interferometry

*Yutaka Nagaoka[1], Kiwamu Nishida[2], Yosuke Aoki[2], Minoru Takeo[2], Takahiro Ohkura[3], Shin Yoshikawa[3] (1.Volcanology Research Department, Meteorological Research Institute, 2.Earthquake Research Institute, The University of Tokyo, 3.Aso Volcanological Laboratory, Institute for Geothermal Sciences, Graduate School of Science, Kyoto University)

[SSS17-P03] Finite element three-dimensional seismic waveform calculations of volcanic deep low frequency earthquake including true topographic effects of Hakone volcano

*Lina Yamaya[1], Kimihiro Mochizuki[1], Tsuyoshi Ichimura[1], Kohei Fujita[1], Takeshi Akuhara[1], Takane Hori[2], Ryou Honda[3], Yohei Yukutake[3] (1.Earthquake Research Institute, Univ. of Tokyo, 2.JAMSTEC, 3.Hot Springs Research Institute of Kanagawa)

[SSS17-P04] Magma transport system beneath Hakone volcano inferred from deep low frequency earthquakes

*Yohei Yukutake[1], Yuki Abe[1] (1.Hot Springs Research Institute of Kanagawa Prefecture)

[SSS17-P05] Hypocenter and waveform characteristics of deep low-frequency earthquakes beneath Zao volcano

*Takuma Ikegaya[1], Mare Yamamoto[1] (1.Graduate School of Science, Tohoku University)

[SSS17-P06] Mechanisms transition of LFEs beneath Zao volcano due to the stress change induced by the 2011 Tohoku earthquake

*Genki Oikawa[1], Naofumi Aso[1], Junichi Nakajima[1], Toru Matsuzawa[2] (1.Tokyo Institute of Technology, 2.Tohoku University)

[SSS17-P07] Magma/gas intrusion process of Shinmoedake Eruption in 2017 suggested by volcanic tremors location with ASL method

Shoya Imamura[1], *Makoto OKUBO[2] (1.Faculty of Science, Kochi University, 2.Natural Science Cluster, Kochi University)

[SSS17-P08] Source depth estimation of a magmatic inflation in 2008-2010 at Mt. Fuji, Japan, based on sparsity-promoting L1 inversion of GNSS data

*Yuta Mitsui[1], Takahiro Kato[2] (1.Department of Geosciences, Shizuoka University, 2.formerly at Department of Geosciences, Shizuoka University)

[E] Poster | S (Solid Earth Sciences)：S-IT Science of the Earth's Interior & Techtonophysics

10:45 AM - 12:15 PM JST | 1:45 AM - 3:15 AM UTC | Poster Hall International Exhibition Hall8, Makuhari Messe_8

[S-IT26] New perspectives on the geodynamics of East Asia

convener:Timothy B Byrne(University of Connecticut), Asuka Yamaguchi(Atomosphere and Ocean Research Institute, The University of Tokyo), Jonny Wu(University of Houston), Kyoko Okino(Atmosphere and Ocean Research Institute, The University of Tokyo)

[SIT26-P01] Geochemical characteristics of effusive rocks (greenstones) in the Hidaka Belt, Hokkaido, Japan

*Toru Yamasaki[1], Futoshi Nanayama[1] (1.Geol. Survey of Japan (AIST))

[SIT26-P02] Large gas reservoir in continental back-arc basin, revealed by automatic seismic velocity analysis in the Okinawa Trough

*Kota Mukumoto[1], Takeshi Tsuji[1], Andri Hendriyana[1] (1.Kyushu University)

[SIT26-P03] Characterize coseismic deformation of Mw 7.5 Palu earthquake in a triple junction in Sulawesi, Indonesia

*MIN-CHIEN TSAI[1], Ying-Hui Yang[2], Chun-Ying Chiu[3], Jyr-Ching Hu[3] (1.Seismological center, Central Weather Bureau, Taipei, Taiwan, R.O.C., 2.School of Civil Engineering and Architecture, Southwest Petroleum University, Chengdu, China, 3.Department of Geosciences, National Taiwan University, Taipei, Taiwan, R.O.C.)

[E] Poster | S (Solid Earth Sciences)：S-IT Science of the Earth's Interior & Techtonophysics

5:15 PM - 6:30 PM JST | 8:15 AM - 9:30 AM UTC | Poster Hall International Exhibition Hall8, Makuhari Messe_28

[S-IT26] New perspectives on the geodynamics of East Asia

convener:Timothy B Byrne(University of Connecticut), Asuka Yamaguchi(Atomosphere and Ocean Research Institute, The University of Tokyo), Jonny Wu(University of Houston), Kyoko Okino(Atmosphere and Ocean Research Institute, The University of Tokyo)

[SIT26-P01] Geochemical characteristics of effusive rocks (greenstones) in the Hidaka Belt, Hokkaido, Japan

*Toru Yamasaki[1], Futoshi Nanayama[1] (1.Geol. Survey of Japan (AIST))

[SIT26-P02] Large gas reservoir in continental back-arc basin, revealed by automatic seismic velocity analysis in the Okinawa Trough

*Kota Mukumoto[1], Takeshi Tsuji[1], Andri Hendriyana[1] (1.Kyushu University)

[SIT26-P03] Characterize coseismic deformation of Mw 7.5 Palu earthquake in a triple junction in Sulawesi, Indonesia

*MIN-CHIEN TSAI[1], Ying-Hui Yang[2], Chun-Ying Chiu[3], Jyr-Ching Hu[3] (1.Seismological center, Central Weather Bureau, Taipei, Taiwan, R.O.C., 2.School of Civil Engineering and Architecture, Southwest Petroleum University, Chengdu, China, 3.Department of Geosciences, National Taiwan University, Taipei, Taiwan, R.O.C.)

[E] Oral | S (Solid Earth Sciences)：S-IT Science of the Earth's Interior & Techtonophysics

1:45 PM - 3:15 PM JST | 4:45 AM - 6:15 AM UTC | A09 TOKYO BAY MAKUHARI HALL

[S-IT26] New perspectives on the geodynamics of East Asia

convener:Timothy B Byrne(University of Connecticut), Asuka Yamaguchi(Atomosphere and Ocean Research Institute, The University of Tokyo), Jonny Wu(University of Houston), Kyoko Okino(Atmosphere and Ocean Research Institute, The University of Tokyo), Chairperson:Jonny Wu, Okino Kyoko

1:45 PM - 2:00 PM JST | 4:45 AM - 5:00 AM UTC

[SIT26-01] How to solve controversies in Cenozoic tectonics in western Pacific margin

*Gaku Kimura[1] (1.Tokyo University of Marine Science and Technology)

2:00 PM - 2:15 PM JST | 5:00 AM - 5:15 AM UTC

[SIT26-02] Plio-Pleistocene plate interactions associated the Philippine Sea Plate

*Timothy B Byrne[1], Gaku Kimura[3], Jonny Wu[2] (1.University of Connecticut, 2.University of Houston, 3.Tokyo University of Science and Technology)

2:15 PM - 2:30 PM JST | 5:15 AM - 5:30 AM UTC

[SIT26-03] A regional mylonite zone between the Mesozoic metamorphic basement and the subducted Miocene covered schists in eastern Range of Taiwan: A possible Plio-Pleistocene transform fault between Eurasia and the Philippine Sea plate

*Gong-Ruei Ho[1], Jian-Cheng Lee[1], Timothy B Byrne[2], En-Chao Yeh[3] (1.Institute of Earth Sciences, Academia Sinica, 2.Department of Geography, University of Connecticut, 3.Department of Earth Sciences, National Taiwan Normal University)

2:30 PM - 2:45 PM JST | 5:30 AM - 5:45 AM UTC

[SIT26-04] **Coeval exhumation or subduction channel extrusion of the high pressure Yuli belt? Insights from the Shoufeng fault in eastern Taiwan**

*Jian-Cheng Lee[1,5], Gong-Ruei Ho[1,5], Timothy B Byrne[2], Yuan Hsi Lee[3,5], En-Chao Yeh[4,5] (1.Academia Sinica, 2.Univerity of Connecticut, 3.National Chung Cheng University, 4.National Taiwan Normal University, 5.The Yuli Exhumation Study team (YES Team))

2:45 PM - 3:00 PM JST | 5:45 AM - 6:00 AM UTC

[SIT26-05] Metamorphic temperature variation across the Yuli belt: a clue about exhumation of high-pressure rocks?

*Chin-Ho Tsai[1], Chih-Ying Yeh[1], Yui Kouketsu[2], Masaki Enami[3] (1.Department of Natural Resources & Environmental Studies, National Dong Hwa Univ., 2.Department of Earth & Planetary Sciences, Nagoya Univ., 3.Institute for Space-Earth Environmental Research, Nagoya Univ.)

3:00 PM - 3:15 PM JST | 6:00 AM - 6:15 AM UTC

[SIT26-06] **Thermal state, slab metamorphism and interface seismicity in Mariana based on 3-D modeling**

*Yingfeng Ji[1,2,3], Shoichi Yoshioka[3,4] (1.Center of Excellence in Tibetan Plateau Earth Science, Chinese Academy of Sciences, 2.Key laboratory of continental collision and plateau uplift, Institute of Tibetan Plateau, Chinese Academy of Sciences, 3.Research Center for Urban Safety and Security, Kobe University, 4.Graduate School of Science, Kobe University)

[E] Oral | S (Solid Earth Sciences)：S-IT Science of the Earth's Interior & Techtonophysics

3:30 PM - 5:00 PM JST | 6:30 AM - 8:00 AM UTC | A09 TOKYO BAY MAKUHARI HALL

[S-IT26] New perspectives on the geodynamics of East Asia

convener:Timothy B Byrne(University of Connecticut), Asuka Yamaguchi(Atomosphere and Ocean Research Institute, The University of Tokyo), Jonny Wu(University of Houston), Kyoko Okino(Atmosphere and Ocean Research Institute, The University of Tokyo), Chairperson:Asuka Yamaguchi(Atomosphere and Ocean Research Institute, The University of Tokyo), Tim Byrne

3:30 PM - 3:45 PM JST | 6:30 AM - 6:45 AM UTC

[SIT26-07] **A tomography-led plate reconstruction of NE Asia during the late Cretaceous**

*Jonny Wu[1], Yi-An Lin[1], Nicolas Flament[2], Tsung-Jui Wu[1], Yiduo Liu[1] (1.University of Houston, 2.University of Wollongong)

3:45 PM - 4:00 PM JST | 6:45 AM - 7:00 AM UTC

[SIT26-08] Geodynamic models of late Mesozoic intraoceanic subduction offshore NE Asia caused by growing Izanagi plate

*Lorenzo Colli[1], Jonny Wu[1], Yi-An Lin[1] (1.University of Houston)

4:00 PM - 4:15 PM JST | 7:00 AM - 7:15 AM UTC

[SIT26-09] **Early Cretaceous to Paleocene magmatism in the Sikhote-Alin area and their implications for Paleo-Pacific plate subduction and continental evolution**

*Tsung-Jui Wu[1], Jonny Wu[1], Igor Alexandrov[2], Thomas Lapen[1] (1.Department of Earth and Atmospheric sciences, University of Houston, Houston, U.S., 2.Far East Geological Institute, Russian Academy of Sciences, Vladivostok, Russia)

4:15 PM - 4:30 PM JST | 7:15 AM - 7:30 AM UTC

[SIT26-10] Processes of subduction initiation revealed by P-T paths of amphibolite and blueschist tectonic blocks in serpentinite mélange: An example from the Kamuikotan high-P/T metamorphic rocks in Hokkaido, northern Japan

*Toru Takeshita[1], Ayumi S. Okamoto, Wonji Shin[1], Mizuho Ando[1] (1.Department of Natural History Sciences, Graduate School of Science, Hokkaido University)

4:30 PM - 4:50 PM JST | 7:30 AM - 7:50 AM UTC

[SIT26-11] Metamorphism in the Sanbagawa belt of SW Japan as a record of subduction processes

★Invited Papers

*Simon Richard Wallis[1] (1.University of Tokyo)

4:50 PM - 5:00 PM JST | 7:50 AM - 8:00 AM UTC

[SIT26-12] Subduction and exhumation of the high pressure metamorphic rocks: What we know and what we need to know.

*Timothy B Byrne[1] (1.University of Connecticut)

[J] Oral | S (Solid Earth Sciences)：S-MP Mineralogy & Petrology

9:00 AM - 10:30 AM JST | 12:00 AM - 1:30 AM UTC | A08 TOKYO BAY MAKUHARI HALL

[S-MP32] Deformed rocks, Metamorphic rocks and Tectonics

convener:Yumiko Harigane(Geological Survey of Japan, National Institute of Advanced Industrial Science and Technology (AIST)), Yoshihiro Nakamura(Geological Survey of Japan, National Institute of Advanced Industrial Science and Technology), Chairperson:Yoshihiro Nakamura(産総研), Yumiko Harigane(産総研)

9:00 AM - 9:15 AM JST | 12:00 AM - 12:15 AM UTC

[SMP32-01] Argon release mechanism of deformed phengite

*Tetsumaru Itaya[1] (1.Engineering Geology Center, Hiruzen Institute for Geology and Chronology)

9:15 AM - 9:30 AM JST | 12:15 AM - 12:30 AM UTC

[SMP32-02] Detrital zircons from a traverse along the Asemi River (Sanbagawa Metamorphic Belt, Shikoku, Japan): U-Pb geochronology and Hf isotopic composition

*Ulrich Knittel[1], Shigeyuki Suzuki[2], Monika Walia[3], Juan-Hsi Lee[4], Hao-Yang Lee[5] (1.RWTH Aachen University, 2.Okayama University, 3.Nat. Taiwan University , 4.Chung Cheng University, 5.Academia Sinica)

9:30 AM - 9:45 AM JST | 12:30 AM - 12:45 AM UTC

[SMP32-03] Tectonic process of the Sanbagawa eclogite: zircon U–Pb and REE composition analyses

*Shogo Aoki[1], Kazumasa Aoki[2], Tatsuki Tsujimori[3], Yuta Tsuchiya[1], Daichi Kato[2] (1.Department of Biosphere-Geosphere Science, Okayama University of Science, 2.Department of Applied Science, Okayama University of Science, 3.Center for Northeast Asian Studies, Tohoku University)

9:45 AM - 10:00 AM JST | 12:45 AM - 1:00 AM UTC

[SMP32-04] Petrological implications of a new occurrence of retrogressed eclogite from the Sanbagawa belt of southwest Japan

*Tomoki Taguchi[1], Shunsuke Endo[2], Yohei Igami[1,3], Akira Miyake[1] (1.Graduate School of Science, Kyoto University, 2.Interdisciplinary Faculty of Science and Engineering, Shimane University, 3.Institute of Materials and Systems for Sustainability, Nagoya University)

10:00 AM - 10:15 AM JST | 1:00 AM - 1:15 AM UTC

[SMP32-05] *P-T* estimations of Kashio mylonite in Oshika, Nagano, Japan: Constraints on the amalgamation of Ryoke and Sambagawa belts

*Yoshihiro Nakamura[1], Yutaka Takahasi[1], Tohru Danhara[2], Hideki Iwano[2], Takehumi Hirata[3] (1.Geological Survey of Japan, National Institute of Advanced Industrial Science and Technology, 2.Kyoto Fission-Track Co., Ltd., 3.Geochemical Research Center, The University of Tokyo)

10:15 AM - 10:30 AM JST | 1:15 AM - 1:30 AM UTC

[SMP32-06] Static phenomena retained by garnet during exhumation of metamorphic rocks

*Masaki Enami[1], Yui Kouketsu[2] (1.Institute for Space–Earth Environmental Research, Nagoya University, 2. Nagoya University)

[J] Oral | S (Solid Earth Sciences)：S-MP Mineralogy & Petrology

10:45 AM - 12:15 PM JST | 1:45 AM - 3:15 AM UTC | A08 TOKYO BAY MAKUHARI HALL

[S-MP32] Deformed rocks, Metamorphic rocks and Tectonics

convener:Yumiko Harigane(Geological Survey of Japan, National Institute of Advanced Industrial Science and Technology (AIST)), Yoshihiro Nakamura(Geological Survey of Japan, National Institute of Advanced Industrial Science and Technology), Chairperson:Tomoki Taguchi(京都大学　大学院理学研究科), Kenta Yoshida(JAMSTEC)

10:45 AM - 11:00 AM JST | 1:45 AM - 2:00 AM UTC

[SMP32-07] Garnet zoning suggesting the correlation between the Higo and Abukuma metamorphic rocks

*Tadao Nishiyama[1], Yuto Wakida[1] (1.Department of Earth and Environmental Sciences, School of Science, Graduate School of Science and Technology, Kumamoto University)

11:00 AM - 11:15 AM JST | 2:00 AM - 2:15 AM UTC

[SMP32-08] $FeAlO_3$ phase at ultrahigh-temperature metamorphic conditions: Evidences from the sillimanite—Fe_2O_3 and sillimanite—Fe_3O_4 systems at 9 kbar and 1050 °C

*Toshisuke Kawasaki[1], Tatsuro Adachi[2], Hiroaki Ohfuji[1], Yasuhito Osanai[2] (1.Ehime University, 2.Kyushu University)

11:15 AM - 11:30 AM JST | 2:15 AM - 2:30 AM UTC

[SMP32-09] **Halogens in nanogranitoids entrapped during granulite facies to ultrahigh-temperature metamorphism in the lower crust**

*Fumiko Higashino[1], Tetsuo Kawakami[2] (1. Graduate School of Environmental Studies, Tohoku University, 2.Graduate School of Science, Kyoto University)

11:30 AM - 11:45 AM JST | 2:30 AM - 2:45 AM UTC

[SMP32-10] Significance of high-Ti biotite and anatectic conditions of paragneiss in the Oki-Dogo Island, Japan

Hiroshi Yoshida[1], *Shunsuke Endo[1], Mai Fujiwara[1], Atsushi Kamei[1] (1.Department of Earth Science, Interdisciplinary Faculty of Science and Engineering, Shimane University)

11:45 AM - 12:00 PM JST | 2:45 AM - 3:00 AM UTC

[SMP32-11] Eclogite-to-granulite transition in the Ufipa Complex (Tanzania): the time-lag between collision and the granulitization

*Morita Isamu[1], Tatsuki Tsujimori[1], Nelson Boniface[2], Shogo Aoki[3], Kazumasa Aoki[3] (1.Tohoku University, 2.University of Dar es Salaam, 3.Okayama University of Science)

12:00 PM - 12:15 PM JST | 3:00 AM - 3:15 AM UTC

[SMP32-12] **Switching of metamorphic growth kinetics due to volume fraction of metamorphic fluid**

*Kazuhiro Miyazaki[1] (1.Orogenic Processes Research Group, Institute of Geology and Geoinformation, Geological Survey of Japan/National Institute of Advanced Industrial Science and Technology)

[J] Poster | S (Solid Earth Sciences)：S-MP Mineralogy & Petrology

1:45 PM - 3:15 PM JST | 4:45 AM - 6:15 AM UTC | Poster Hall International Exhibition Hall8, Makuhari Messe_4

[S-MP32] Deformed rocks, Metamorphic rocks and Tectonics

convener:Yumiko Harigane(Geological Survey of Japan, National Institute of Advanced Industrial Science and Technology (AIST)), Yoshihiro Nakamura(Geological Survey of Japan, National Institute of Advanced Industrial Science and Technology)

[SMP32-P01] Pressure-temperature estimates of the Lützow-Holm Complex utilizing distributions of trace elements and inclusions in garnet porphyroblasts in pelitic gneisses

*Kota Suzuki[1], Tetsuo Kawakami[1], Yohei Igami[2] (1.Department of Geology and Mineralogy, Graduate School of Science, Kyoto University, 2.Institute of Materials and Systems for Sustainability, Nagoya University)

[SMP32-P02] Microstructures and pressure-temperature condition in pelitic gneisses from the Lützow-Holm Complex at Akarui Point, East Antarctica

*Hayato Yodoya[1], Takeshi Ikeda[2] (1.Department of Earth and Planetary Sciences, Graduate School of Scinece, Kyushu University, 2.Department of Earth and Planetary Sciences, Faculty of School of Scinece, Kyushu University)

[SMP32-P03] Long-lived (>90 Myr) granulite-facies metamorphism in the Trivandrum Block, southern India.

*Hikaru Kadowaki[1], Toshiaki Tsunogae[2], Santosh M.[3], Shaji E.[4], Yusuke Takamura[5], Yukiyasu Tsutsumi[6] (1.College of Geoscience, Graduate School of Life and Environmental Sciences, University of Tsukuba, 2.Faculty of Life and Environmental Sciences, University of Tsukuba, 3.School of Earth Sciences and Resources, China University of Geosciences Beijing, 4.Department of Geology, University of Kerala, 5. Doctoral Program in Earth Evolution Sciences, Graduate School of Life and Environmental Sciences, University of Tsukuba, 6.Department of Geology and Paleontology, National Museum of Nature and Science)

[SMP32-P04] Dislocation microstructures in garnet: Thermal effect during deeper crustal seismic slip in orogen-boundary shear zone

*Kaushik Das[1], Naotaka Tomioka[2], Proloy Ganguly[3], Jun-ichi Ando[1], Gautam Ghosh[3], Sankar Bose[3] (1.Hiroshima University, 2.Kochi Institute for Core Sample Research, JAMSTEC, 3.Presidency University, India)

[SMP32-P05] U-Pb zircon ages of migmatitic rocks from the Ryoke belt in the Mikawa and eastern Sanuki areas

*Keiichi Kazuratachi[1], Tetsuo Kawakami[1], Etienne Skrzypek[1], Shuhei Sakata[2], Takafumi Hirata[3] (1.Kyoto University, 2.Gakushuin University, 3.The University of Tokyo)

[SMP32-P06] Structural geology of Hidaka metamorphic belt in the Mt.Nozuka area, Hokkaido, Japan - Growth and formation process of the Cenozoic continental crust by island arc/arc join and its mechanism-

*Moeko Kanno[1], Tsuyoshi Toyoshima[2] (1.Graduate school of Science and Technology, Niigata University , 2.Department of Geology,Faculty of Science,Niigata University)

[SMP32-P07] THE PRESSURE-TEMPERATURE PATH AND MINERAL ASSEMBLAGE OF THE KHONICHIIN OVOO AREA, SOUTHEASTERN MONGOLIA.

*Undarmaa Batsaikhan[1], Noriyoshi Tsuchiya[1], Masaoki Uno[1], Yukio Isozaki[2], Uyanga Bold[2], OTGONBAYAR DANDAR[1], Hikaru Sawada[2] (1.Graduate School of Environmental Studies, Tohoku University, 2.Graduate School of Arts and Sciences the University of Tokyo)

[SMP32-P08] **Pressure-temperature conditions of contact metamorphism in Nokita area, Itoshima Peninsula, northwest Kyushu**

*Takeshi Ikeda[1], Kento Ota[2] (1.Department of Earth and Planetary Sciences,Faculty of Scinece, Kyushu University, 2.Department of Earth and Planetary Sciences,Graduate School of Scinece, Kyushu University)

[SMP32-P09] Evidence of Partial Melting of Migmatitic Felsic Gneiss from Nagasaki Metamorphic Complex in Amakusa-Shimoshima, western Kyushu, Japan

*Yuki Mori[1], Takeshi Ikeda[2], Kazuhiro Miyazaki[3] (1.Department of Earth and Planetary Sciences, Graduate School of Sciences, Kyushu University, 2.Department of Earth and Planetary Sciences, Faculty of Sciences, Kyushu University, 3.Research Institute of Geology and Geoinformation, Geological Survey of Japan, National Institute of Advanced Industrial Science and Technology)

[SMP32-P10] **Microstructural Analysis of Quartz grains in Monomineralic and Polyphase domains: A case study from Main Central Thrust (MCT) Zone Mylonites, western Himalaya, India**

*Shivaji Saha[1], Toru Takeshita[1], Subhajit Ghosh[2], Hari Bahadur Srivastava[3] (1.Department of Natural History Sciences, Hokkaido University, 2.Earthquake Research Institute, The University of Tokyo, 3.Department of Geology, Banaras Hindu University)

[SMP32-P11] **Tectono-thermal evolution of the Main Central Thrust (MCT) zone rocks of the Himalayan Crystalline Complex (*HCC*), Darjeeling-Sikkim Himalaya**

*Subhajit Ghosh[1,2], Santanu Bose[2,3], Nibir Mandal[4], Arijit Laik[2] (1.Earthquake Research Institute, The University of Tokyo, 1-1-1 Yayoi, Bunkyo-Ku, Tokyo 113-0032, 2.Department of Geology, University of Calcutta, 35, Ballygunge Circular Road, Kolkata 700019, India, 3.Department of Geology, Presidency University, 86/1 College Street, Kolkata 700073, India, 4.Department of Geological Sciences, Jadavpur University, Kolkata 700032, India)

[SMP32-P12] Thermal structure and deformation history of the low-grade Sanbagawa belt in the central of Kii Peninsula and tectonic implications

*Ken Yamaoka[1,2], Simon Wallis[1], Hiroshi Mori[2] (1.University of Tokyo, 2.Shinshu University)

[SMP32-P13] Antigorite Raman spectrum: a case study in Shiraga region of the central Shikoku, Sanbagawa metamorphic belt, SW Japan

*Kota Ando[1], Yui Kouketsu[1], Katsuyoshi Michibayashi[1] (1.Nagoya University)

[SMP32-P14] A fluid inclusion study from the late Paleozoic retrograde eclogite from the Yunotani Valley of the Omi area, Hida-Gaien Belt, Japan

*Yuzuki Shinji[1], Tatsuki Tsujimori[1], Tatsuhiko Kawamoto[2] (1.Tohoku University, 2.Shizuoka University)

[SMP32-P15] Development of reaction-induced stress and permeability in MgO-H_2O system

*Hisamu Kasahara[1], Masaoki Uno[1], Atsushi Okamoto[1], Noriyoshi Tsuchiya[1] (1.Graduate School of Environmental Studies, Tohoku University)

[SMP32-P16] Crystal orientation analysis of olivine in ultra-mylonite using TKD method: progress in spatial resolution from EBSD

*Yohei Igami[1], Katsuyoshi Michibayashi[2], Kakihata Yuki[2], Yui Kouketsu[2] (1.Institute of Materials and Systems for Sustainability, Nagoya University, 2.Graduate School of Environmental Studies, Nagoya University)

[SMP32-P17] Elucidation of effective diffusion coefficient along grain boundaries by hydrothermal experiment using low porosity rocks

*Naoki Sugisawa[1], Masaoki Uno[1], Noriyoshi Tsuchiya[1] (1.Graduate school of environmental studies Tohoku university)

[SMP32-P18] **Seismic slipping events recorded in a fault gouge zone: evidence from the Nojima Fault drill holes, SW Japan**

*Aiming Lin[1], Takafumi Nishiwaki[1] (1.Department of Geophysics, Graduate School of Science, Kyoto University)

[SMP32-P19] Evolution of fluid chemistry during basalt-water and basalt-seawater interactions revealed by hydrothermal flow-through experiments

*Yusuke Netsu[1], Atsushi Okamoto[1], Nobuo Hirano[1], Masaoki Uno[1], Noriyoshi Tsuchiya[1] (1.Tohoku University, Graduate School of Environment Studies)

[SMP32-P20] **3D microstructural analyses of fault rocks using CT and μCT scanning techniques**

*Bingcheng Liu[1], Aiming Lin[1], Takafumi Nishiwaki[1] (1.Kyoto University)

[SMP32-P21] **Dissolution kinetics of forsterite olivine at >200 °C: implication for the kinetics of serpentinization.**

*Ryosuke Oyanagi[1], Tatsu Kuwatani[1], Katsuhiko Suzuki[1] (1.Japan Agency for Marine-Earth Science and Technology)

[J] Poster | S (Solid Earth Sciences)：S-MP Mineralogy & Petrology

5:15 PM - 6:30 PM JST | 8:15 AM - 9:30 AM UTC | Poster Hall International Exhibition Hall8, Makuhari Messe_29

[S-MP32] Deformed rocks, Metamorphic rocks and Tectonics

convener:Yumiko Harigane(Geological Survey of Japan, National Institute of Advanced Industrial Science and Technology (AIST)), Yoshihiro Nakamura(Geological Survey of Japan, National Institute of Advanced Industrial Science and Technology)

[SMP32-P01] Pressure-temperature estimates of the Lützow-Holm Complex utilizing distributions of trace elements and inclusions in garnet porphyroblasts in pelitic gneisses

*Kota Suzuki[1], Tetsuo Kawakami[1], Yohei Igami[2] (1.Department of Geology and Mineralogy, Graduate School of Science, Kyoto University, 2.Institute of Materials and Systems for Sustainability, Nagoya University)

[SMP32-P02] Microstructures and pressure-temperature condition in pelitic gneisses from the Lützow-Holm Complex at Akarui Point, East Antarctica

*Hayato Yodoya[1], Takeshi Ikeda[2] (1.Department of Earth and Planetary Sciences, Graduate School of Scinece, Kyushu University, 2.Department of Earth and Planetary Sciences, Faculty of School of Scinece, Kyushu University)

[SMP32-P03] Long-lived (>90 Myr) granulite-facies metamorphism in the Trivandrum Block, southern India.

*Hikaru Kadowaki[1], Toshiaki Tsunogae[2], Santosh M.[3], Shaji E.[4], Yusuke Takamura[5], Yukiyasu Tsutsumi[6] (1.College of Geoscience, Graduate School of Life and Environmental Sciences, University of Tsukuba, 2.Faculty of Life and Environmental Sciences, University of Tsukuba, 3.School of Earth Sciences and Resources, China University of Geosciences Beijing, 4.Department of Geology, University of Kerala, 5. Doctoral Program in Earth Evolution Sciences, Graduate School of Life and Environmental Sciences, University of Tsukuba, 6.Department of Geology and Paleontology, National Museum of Nature and Science)

[SMP32-P04] Dislocation microstructures in garnet: Thermal effect during deeper crustal seismic slip in orogen-boundary shear zone

*Kaushik Das[1], Naotaka Tomioka[2], Proloy Ganguly[3], Jun-ichi Ando[1], Gautam Ghosh[3], Sankar Bose[3] (1.Hiroshima University, 2.Kochi Institute for Core Sample Research, JAMSTEC, 3.Presidency University, India)

[SMP32-P05] U-Pb zircon ages of migmatitic rocks from the Ryoke belt in the Mikawa and eastern Sanuki areas

*Keiichi Kazuratachi[1], Tetsuo Kawakami[1], Etienne Skrzypek[1], Shuhei Sakata[2], Takafumi Hirata[3] (1.Kyoto University, 2.Gakushuin University, 3.The University of Tokyo)

[SMP32-P06] Structural geology of Hidaka metamorphic belt in the Mt.Nozuka area, Hokkaido, Japan - Growth and formation process of the Cenozoic continental crust by island arc/arc join and its mechanism-

*Moeko Kanno[1], Tsuyoshi Toyoshima[2] (1.Graduate school of Science and Technology, Niigata University , 2.Department of Geology,Faculty of Science,Niigata University)

[SMP32-P07] THE PRESSURE-TEMPERATURE PATH AND MINERAL ASSEMBLAGE OF THE KHONICHIIN OVOO AREA, SOUTHEASTERN MONGOLIA.

*Undarmaa Batsaikhan[1], Noriyoshi Tsuchiya[1], Masaoki Uno[1], Yukio Isozaki[2], Uyanga Bold[2], OTGONBAYAR DANDAR[1], Hikaru Sawada[2] (1.Graduate School of Environmental Studies, Tohoku University, 2.Graduate School of Arts and Sciences the University of Tokyo)

[SMP32-P08] **Pressure-temperature conditions of contact metamorphism in Nokita area, Itoshima Peninsula, northwest Kyushu**

*Takeshi Ikeda[1], Kento Ota[2] (1.Department of Earth and Planetary Sciences,Faculty of Scinece, Kyushu University, 2.Department of Earth and Planetary Sciences,Graduate School of Scinece, Kyushu University)

[SMP32-P09] Evidence of Partial Melting of Migmatitic Felsic Gneiss from Nagasaki Metamorphic Complex in Amakusa-Shimoshima, western Kyushu, Japan

*Yuki Mori[1], Takeshi Ikeda[2], Kazuhiro Miyazaki[3] (1.Department of Earth and Planetary Sciences, Graduate School of Sciences, Kyushu University, 2.Department of Earth and Planetary Sciences, Faculty of Sciences, Kyushu University, 3.Research Institute of Geology and Geoinformation, Geological Survey of Japan, National Institute of Advanced Industrial Science and Technology)

[SMP32-P10] **Microstructural Analysis of Quartz grains in Monomineralic and Polyphase domains: A case study from Main Central Thrust (MCT) Zone Mylonites, western Himalaya, India**

*Shivaji Saha[1], Toru Takeshita[1], Subhajit Ghosh[2], Hari Bahadur Srivastava[3] (1.Department of Natural History Sciences, Hokkaido University, 2.Earthquake Research Institute, The University of Tokyo, 3.Department of Geology, Banaras Hindu University)

[SMP32-P11] **Tectono-thermal evolution of the Main Central Thrust (MCT) zone rocks of the Himalayan Crystalline Complex (*HCC*), Darjeeling-Sikkim Himalaya**

*Subhajit Ghosh[1,2], Santanu Bose[2,3], Nibir Mandal[4], Arijit Laik[2] (1.Earthquake Research Institute, The University of Tokyo, 1-1-1 Yayoi, Bunkyo-Ku, Tokyo 113-0032, 2.Department of Geology, University of Calcutta, 35, Ballygunge Circular Road, Kolkata 700019, India, 3.Department of Geology, Presidency University, 86/1 College Street, Kolkata 700073, India, 4.Department of Geological Sciences, Jadavpur University, Kolkata 700032, India)

[SMP32-P12] Thermal structure and deformation history of the low-grade Sanbagawa belt in the central of Kii Peninsula and tectonic implications

*Ken Yamaoka[1,2], Simon Wallis[1], Hiroshi Mori[2] (1.University of Tokyo, 2.Shinshu University)

[SMP32-P13] Antigorite Raman spectrum: a case study in Shiraga region of the central Shikoku, Sanbagawa metamorphic belt, SW Japan

*Kota Ando[1], Yui Kouketsu[1], Katsuyoshi Michibayashi[1] (1.Nagoya University)

[SMP32-P14] A fluid inclusion study from the late Paleozoic retrograde eclogite from the Yunotani Valley of the Omi area, Hida-Gaien Belt, Japan

*Yuzuki Shinji[1], Tatsuki Tsujimori[1], Tatsuhiko Kawamoto[2] (1.Tohoku University, 2.Shizuoka University)

[SMP32-P15] Development of reaction-induced stress and permeability in MgO-H_2O system

*Hisamu Kasahara[1], Masaoki Uno[1], Atsushi Okamoto[1], Noriyoshi Tsuchiya[1] (1.Graduate School of Environmental Studies, Tohoku University)

[SMP32-P16] Crystal orientation analysis of olivine in ultra-mylonite using TKD method: progress in spatial resolution from EBSD

*Yohei Igami[1], Katsuyoshi Michibayashi[2], Kakihata Yuki[2], Yui Kouketsu[2] (1.Institute of Materials and Systems for Sustainability, Nagoya University, 2.Graduate School of Environmental Studies, Nagoya University)

[SMP32-P17] Elucidation of effective diffusion coefficient along grain boundaries by hydrothermal experiment using low porosity rocks

*Naoki Sugisawa[1], Masaoki Uno[1], Noriyoshi Tsuchiya[1] (1.Graduate school of environmental studies Tohoku university)

[SMP32-P18] **Seismic slipping events recorded in a fault gouge zone: evidence from the Nojima Fault drill holes, SW Japan**

*Aiming Lin[1], Takafumi Nishiwaki[1] (1.Department of Geophysics, Graduate School of Science, Kyoto University)

[SMP32-P19] Evolution of fluid chemistry during basalt-water and basalt-seawater interactions revealed by hydrothermal flow-through experiments

*Yusuke Netsu[1], Atsushi Okamoto[1], Nobuo Hirano[1], Masaoki Uno[1], Noriyoshi Tsuchiya[1] (1.Tohoku University, Graduate School of Environment Studies)

[SMP32-P20] **3D microstructural analyses of fault rocks using CT and μCT scanning techniques**

*Bingcheng Liu[1], Aiming Lin[1], Takafumi Nishiwaki[1] (1.Kyoto University)

[SMP32-P21] **Dissolution kinetics of forsterite olivine at >200 °C: implication for the kinetics of serpentinization.**

*Ryosuke Oyanagi[1], Tatsu Kuwatani[1], Katsuhiko Suzuki[1] (1.Japan Agency for Marine-Earth Science and Technology)

[J] Oral | S (Solid Earth Sciences)：S-MP Mineralogy & Petrology

3:30 PM - 5:00 PM JST | 6:30 AM - 8:00 AM UTC | A08 TOKYO BAY MAKUHARI HALL

[S-MP32] Deformed rocks, Metamorphic rocks and Tectonics

convener:Yumiko Harigane(Geological Survey of Japan, National Institute of Advanced Industrial Science and Technology (AIST)), Yoshihiro Nakamura(Geological Survey of Japan, National Institute of Advanced Industrial Science and Technology), Chairperson:Shunsuke Endo(島根大学 総合理工学部 地球科学科), Ryosuke Oyanagi(国立研究開発法人 海洋研究開発機構 地球内部物質循環研究分野)

3:30 PM - 3:45 PM JST | 6:30 AM - 6:45 AM UTC

[SMP32-13] Early Paleozoic subduction-zone metamorphism in Japan: A geochronological reappraisal of Kitomyo Schists

*Shota Matsunaga [1], Tatsuki Tsujimori[1], Atsushi MIYASHITA[2], Shogo Aoki[3], Kazumasa Aoki[3] (1.Tohoku University, 2.Seikei University, 3. Okayama University of Science)

3:45 PM - 4:00 PM JST | 6:45 AM - 7:00 AM UTC

[SMP32-14] Dating a 'princess': U–Pb age determination of 'nunakawaite' (strontio-orthojoaquinite)

*Tatsuki Tsujimori[1], Tomomi Hara[1], Yuzuki Shinji[1], Tomohiro Ishizaka[1], Hiroshi Miyajima[2], Jun-Ichi Kimura[3], Shogo Aoki[4], Kazumasa Aoki[4] (1.Tohoku University, 2.Fossa Magna Museum, 3.JAMSTEC, 4.Okayama University of Science)

4:00 PM - 4:15 PM JST | 7:00 AM - 7:15 AM UTC

[SMP32-15] Modeling of the progressive evolution of subducting slab composition by sparse modeling

*Kenta Yoshida[1], Tatsu Kuwatani[1,2], Kenta Ueki[1], Ryosuke Oyanagi[1], Shotaro Akaho[3] (1.Japan Agency for Marine-earth Science and Technology (JAMSTEC), 2.PRESTO, Japan Science and Technology Agency, 3.National Institute of Advanced Industrial Science and Technology (AIST))

4:15 PM - 4:30 PM JST | 7:15 AM - 7:30 AM UTC

[SMP32-16] Bayesian statistical evaluation method for detrital zircon geochronology: Applications

*Tan Furukawa[1], Tatsuki Tsujimori[2], Shogo Aoki[3], Kazumasa Aoki[4] (1.Tohoku University, Department of Earth Science, 2.Tohoku University, 3.Faculty of Biosphere-Geosphere Science, Okayama University of Science, 4.Department of Applied Science Okayama University of Science)

4:30 PM - 4:45 PM JST | 7:30 AM - 7:45 AM UTC

[SMP32-17] 3D structural analysis using X-ray Computed Tomography technique: a case study for fault rocks from the Nojima Fault, southwest Japan

*Takafumi Nishiwaki[1], Aiming Lin[1], Bingcheng Liu[1] (1.Kyoto University)

4:45 PM - 5:00 PM JST | 7:45 AM - 8:00 AM UTC

[SMP32-18] High- and low-stress subduction zones recognized in the rock record

*Kazuhiko Ishii[1], Simon Richard Wallis[2] (1.Department of Physical Science, Graduate School of Sciences, Osaka Prefecture University, 2.Department of Earth and Planetary Science, Faculty of Science, The University of Tokyo)

[J] Oral | S (Solid Earth Sciences)：S-MP Mineralogy & Petrology

9:00 AM - 10:30 AM JST | 12:00 AM - 1:30 AM UTC | A07 TOKYO BAY MAKUHARI HALL

[S-MP33] Physics and Chemistry of Minerals

convener:Seiji Kamada(Frontier Research Institute for Interdisciplinary Sciences, Tohoku University), Masahiro KAYAMA(Department of Earth and Planetary Material Sciences, Faculty of Science, Tohoku University), Chairperson:Seiji Kamada(FRIS, Tohoku Univ.)

9:00 AM - 9:15 AM JST | 12:00 AM - 12:15 AM UTC

[SMP33-01] High-temperature Raman spectroscopic study of CO_2-containing melanophlogite

*Masami Kanzaki[1] (1.Institute for Planetary Matereials, Okayama University)

9:15 AM - 9:30 AM JST | 12:15 AM - 12:30 AM UTC

[SMP33-02] Synthesis of barium carbonate with calcite structure and rotational disorder of carbonate ions

*Hiroyuki Kagi[1], Ayaka Saito[1], Kazuki Komatsu[1], Jun Kawano[2] (1.Geochemical Research Center, Graduate School of Science, University of Tokyo, 2.Fuculty of Science, Hokkaido University)

9:30 AM - 9:45 AM JST | 12:30 AM - 12:45 AM UTC

[SMP33-03] In-situ Raman spectroscopy of ε-FeOOH under high pressures

*Osamu Ikeda[1], Tatsuya Sakamaki[1], Akio Suzuki[1] (1.Department of Earth Science, Graduate School of Science, Tohoku University)

9:45 AM - 10:00 AM JST | 12:45 AM - 1:00 AM UTC

[SMP33-04] **Strong hydrogen-bond generation in dense hydrous magnesium silicate phase E observed by single-crystal neutron diffraction**

*Narangoo Purevjav[1], Takuo Okuchi[1], Christina Hoffmann[2] (1.Institute for Planetary Materials, Okayama University, 2.Neutron Scattering Division, Neutron Sciences Directorate, Oak Ridge National Laboratory)

10:00 AM - 10:15 AM JST | 1:00 AM - 1:15 AM UTC

[SMP33-05] **Water partitioning between upper mantle minerals and melts**

*Dmitry Bondar[1], Hongzhan Fei[1], Tony Withers[1], Tomoo Katsura[1] (1.Bayerisches Geoinstitut, University of Bayreuth, 95440 Bayreuth, Germany)

10:15 AM - 10:30 AM JST | 1:15 AM - 1:30 AM UTC

[SMP33-06] Drop-solution enthalpy measurement of $MgSiO_3$ majorite

*Hiroshi Kojitani[1], Masamichi Noda[2], Toru Inoue[2,3], Masaki Akaogi[1] (1.Department of Chemistry, Faculty of Science, Gakushuin University, 2.GRC, Ehime University, 3.Dept. of Earth and Planetary systems Science, Hiroshima University)

[J] Oral | S (Solid Earth Sciences)：S-MP Mineralogy & Petrology

10:45 AM - 12:15 PM JST | 1:45 AM - 3:15 AM UTC | A07 TOKYO BAY MAKUHARI HALL

[S-MP33] Physics and Chemistry of Minerals

convener:Seiji Kamada(Frontier Research Institute for Interdisciplinary Sciences, Tohoku University), Masahiro KAYAMA(Department of Earth and Planetary Material Sciences, Faculty of Science, Tohoku University), Chairperson:Masahiro Kayama(東北大学)

10:45 AM - 11:00 AM JST | 1:45 AM - 2:00 AM UTC

[SMP33-07] High-pressure phase transitions of minerals in the system MgO-TiO_2

*Masaki Akaogi[1], Tetsuya Fujimura[1], Shunto Arai[1], Masaki Okano[1], Hiroshi Kojitani[1] (1.Department of Chemistry, Faculty of Science, Gakushuin University)

11:00 AM - 11:15 AM JST | 2:00 AM - 2:15 AM UTC

[SMP33-08] Phase change process of iron sulfide nanoparticle from amorphous to crystalline with grain growth

*Yoshinari Sano[1], Atsushi Kyono[2], Yasuhiro Yoneda[3], Gen-ichiro Yamamoto[1] (1.Graduate School of Life and Environmental Sciences, University of Tsukuba, 2.Faculty of Life and Environmental Sciences, University of Tsukuba, 3.Japan Atomic Energy Agency)

11:15 AM - 11:30 AM JST | 2:15 AM - 2:30 AM UTC

[SMP33-09] Texture formation in quenching of Fe-S-O micro melt spherules

*Hiroshi Isobe[1] (1.Department of Earth and Environmental Sciences, Faculty of Advanced Science and Technology, Kumamoto University)

11:30 AM - 11:45 AM JST | 2:30 AM - 2:45 AM UTC

[SMP33-10] Development of a software for electron diffraction simulation based on dynamical theory and its application to mineralogy

*Yusuke Seto[1], Masahiro Ohtuka[3], Akira Miyake[2] (1.Graduate School of Science, Kobe University, 2.Graduate School of Science, Kyoto University, 3.Graduate School of Technology, Nagoya University)

11:45 AM - 12:15 PM JST | 2:45 AM - 3:15 AM UTC

[SMP33-11] Site occupation analysis for cation in minerals by analytical electron microscopy: application of TEM-ALCHEMI for earth and planetary science

★Invited Papers

*Yohei Igami[1], Shunsuke Muto[1], Masahiro Ohtsuka[3], Akira Miyake[2], Takahiro Kuribayashi[4], Shoichi Toh[5] (1.Institute of Materials and Systems for Sustainability, Nagoya University, 2.Graduate School of Science, Kyoto University, 3.Graduate School of Engineering, Nagoya University, 4.Graduate School of Science, Tohoku University, 5.Faculty of Science, Fukuoka University)

[J] Oral | S (Solid Earth Sciences)：S-MP Mineralogy & Petrology

1:45 PM - 3:15 PM JST | 4:45 AM - 6:15 AM UTC | A07 TOKYO BAY MAKUHARI HALL

[S-MP33] Physics and Chemistry of Minerals

convener:Seiji Kamada(Frontier Research Institute for Interdisciplinary Sciences, Tohoku University), Masahiro KAYAMA(Department of Earth and Planetary Material Sciences, Faculty of Science, Tohoku University), Chairperson:Fumiya Noritake(Materials Science, Faculty of Engineering, Graduate Faculty of Interdisciplinary Research, UNIVERSITY OF YAMANASHI), Seiji Kamada(FRIS, Tohoku Univ.)

1:45 PM - 2:15 PM JST | 4:45 AM - 5:15 AM UTC

[SMP33-12] Molecular Dynamics Study of Soret Effect in Silicate Liquids

★Invited Papers

*Fumiya Noritake[1] (1.Graduate Faculty of interdisciplinary Research, University of Yamanashi)

2:15 PM - 2:30 PM JST | 5:15 AM - 5:30 AM UTC

[SMP33-13] Seebeck coefficient of olivine: Implausible Mercury's thermoelectric dynamo

*Hitoshi Gomi[1], Takashi Yoshino[1], Akira Yoneda[1] (1.Okayama University)

2:30 PM - 2:45 PM JST | 5:30 AM - 5:45 AM UTC

[SMP33-14] Density measurement of liquid gallium using externally heated diamond anvil cell

*Ryo Tsuruoka[1], Hidenori Terasaki[1], Seiji Kamada[2], Iori Yamada[1], Fumiya Maeda[3], Tadashi Kondo[1], Satoru Urakawa[4], Naohisa Hirao[5], Akihiko Machida[6] (1.Department of Earth and Space Science, Graduate School of Science Osaka University, 2.Frontier Research Institute for Interdisciplinary Sciences, Tohoku University, 3.Department of Earth and Planetary Materials Science, Graduate School of Science, Tohoku University, 4.Department of Earth Science, Okayama University, 5.Japan Synchrotron Radiation Research Institute, 6.National Institutes for Quantum and Radiological Science and Technology)

2:45 PM - 3:00 PM JST | 5:45 AM - 6:00 AM UTC

[SMP33-15] Density measurements of crystalline Fe and amorphous materials at high pressure

*Seiji Kamada[1,2], Hidenori Terasaki[3], Yusaku Takubo[3], Ryo Tsuruoka[3], Fumiya Maeda[2], Rui Yamada[1], Saori Kawaguchi[4], Naohisa Hirao[4], Akihiko Machida[5] (1.Frontier Research Institute for Interdisciplinary Sciences, Tohoku University, 2.Department of Earth Science, Graduate School of Science, Tohoku University, 3.Department of Earth and Space Science, Graduate School of Science, Osaka University, 4.JASRI, 5.QST)

3:00 PM - 3:15 PM JST | 6:00 AM - 6:15 AM UTC

[SMP33-16] DAC-GHz ultrasonic P wave velocity measurement on KCl and natural olivine

*Akira Yoneda[1], Shinichiro Kobayashi[2], Seiji Kamada[3] (1.Institute for planetary materials, Okayama University, 2.Department of Earth Science, Graduate school of Science, Tohoku Univ., 3.Frontier Research Institute for Interdisciplinary Sciences, Tohoku Univ.)

[J] Poster | S (Solid Earth Sciences)：S-MP Mineralogy & Petrology

3:30 PM - 5:00 PM JST | 6:30 AM - 8:00 AM UTC | Poster Hall International Exhibition Hall8, Makuhari Messe_18

[S-MP33] Physics and Chemistry of Minerals

convener:Seiji Kamada(Frontier Research Institute for Interdisciplinary Sciences, Tohoku University), Masahiro KAYAMA(Department of Earth and Planetary Material Sciences, Faculty of Science, Tohoku University)

[SMP33-P01] Raman spectroscopy of seifertite

*Masahiro KAYAMA[1], Eiji Ohtani[1], Masaaki Miyahara[2], Shohei Kaneko[1], Toshimori Sekine[3], Shin Ozawa[1], Naohisa Hirao[4] (1.Tohoku University, 2.Hiroshima University, 3.HPSTAR, 4.Japan Synchrotron Radiation Research Institute)

[SMP33-P02] Microtexture and crystallization process of impact diamonds

*Hiroaki Ohfuji[1], Motosuke Nakaya[1] (1.Geodynamics Research Center, Ehime University)

[SMP33-P03] **Metamorphic temperature analysis of H chondrites: Using revised Lindsley's pyroxene thermometer**

*Ryo Uehara[1], Yoshihiro Kuwahara[1], Kazuhiko Shimada[1], Yoshihiro Nakamuta[1], Seiichiro Uehara[1], Tatsuro Adachi[1] (1.Kyushu university)

[SMP33-P04] The occurrence combinations of Zeolites at Chichijima, Ogasawara Islands

Michiharu Ito[1], *Yuki Inoue[1], Mana Yasui[2], Atsushi Yamazaki[2], Hiroshi Hagiya[1] (1. Tokyo City University, 2.Waseda research institute for science and engineering)

[SMP33-P05] Title: Single-crystal X-ray diffraction study of mirabilite ($Na_2SO_4 \cdot 10H_2O$) from 213 to 303 K

*Ryutaro Ikeda[1] (1.University of tsukuba)

[SMP33-P06] Elastic constants of single-crystal topaz studied via sphere-resonance method

*Kako Aradachi[1], Tohru Watanabe[1], Morihisa Hamada[2] (1.University of Toyama, 2.JAMSTEC)

[SMP33-P07] Verification of damage by polishing of sheet-like minerals

*Yui Kouketsu[1], Kota Ando[1], Katsuyoshi Michibayashi[1] (1.Department of Earth & Planetary Sciences, Graduate School of Environmental Studies, Nagoya University)

[SMP33-P08] Description of Zebra Rock and the pattern formation model

*Kaoru Yoshimura[1], Atsushi Toramaru[2], Mie Ichihara[3], Takaaki Noguchi[4], Toru Matsumoto[5] (1.Department of Earth and Planetary Science, Graduate School of Science, Kyushu University, 2.Department of Earth and Planetary Sciences, Faculty of Sciences, Kyushu University, 3.Earthquake Research Institute, University of Tokyu, 4.Department of Arts and Science, Kyushu University, 5.Japan Aerospace Exploration Agency/ Institute of Space and Astronautical Science)

[SMP33-P09] Thermal conductivity anomaly of (Mg,Fe)CO_3 solid solution across the spin transition

*Keng-Hsien Chao[1], Wen-Pin Hsieh[1,2] (1.Institute of Earth Sciences, Academia Sinica, Taiwan, 2.Department of Geosciences, National Taiwan University, Taiwan)

[SMP33-P10] **Melting experiments in the $MgSiO_3$ – SiO_2 system under high pressures**

*Takuya Moriguti[1], Akira Yoneda[1], Eiji Ito[1] (1.Institute for Planetary Materials, Okayama University)

[SMP33-P11] Melting relations of the Fe-Ni-S-C system and the formation of superdeep diamonds

*Yu Itami[1], Satoru Urakawa[1] (1.Okayama University)

[SMP33-P12] Effect of ammonia on the stability of methane hydrate under high-pressure and high-temperature

*Hirokazu Kadobayashi[1], Hisako Hirai[2], Hiroaki Ohfuji[1], Hideaki Kawamura[1], Michika Ohtake[3], Yoshitaka Yamamoto[3] (1.Geodynamics Research Center, Ehime University, 2.Department of Environment System, Faculty of Geo-environmental Science, Rissho University, 3.National Institute of Advanced Industrial Science and Technology)

[SMP33-P13] Study on magnetite-maghemite-hematite transformation

*Ibuki Kinebuchi[1], Atsushi Kyono[1], Yoshinari Sano[1] (1.University of Tsukuba)

[SMP33-P14] The Effects of Temperature and Pressure on Hydromagnesite

*Gen-ichiro Yamamoto[1], Atsushi Kyono[1], Jun Abe[2], Takanori Hattori[3], Yoshitaka Matsushita[4], Yasuhiro Yoneda[3] (1.University of Tsukuba, 2.CROSS, 3.JAEA, 4.NIMS)

[SMP33-P15] Synthesis and crystal structure of Mg-bearing Fe_9O_{11}: New insight in the complexity of Fe-Mg oxides at conditions of the deep upper mantle

*Takayuki Ishii[1], Uenver-Thiele Laura[2], Alan B Woodland[2], Edith Alig[3], Tiziana Boffa Ballaran[1] (1.Bavarian Research Institute, University of Bayreuth, 2.Institut für Geowissenschaften, Goethe-Universität Frankfurt, 3.Institut für Anorganische und Analytische Chemie, Goethe-Universität Frankfurt)

[SMP33-P16] **Changes in specific surface area and morphology of kaolin group minerals with pressure treatment**

*Soyeon Kwon[1], Yongjae Lee[1] (1.YONSEI University)

[J] Poster | S (Solid Earth Sciences)：S-MP Mineralogy & Petrology

5:15 PM - 6:30 PM JST | 8:15 AM - 9:30 AM UTC | Poster Hall International Exhibition Hall8, Makuhari Messe_30

[S-MP33] Physics and Chemistry of Minerals

convener:Seiji Kamada(Frontier Research Institute for Interdisciplinary Sciences, Tohoku University), Masahiro KAYAMA(Department of Earth and Planetary Material Sciences, Faculty of Science, Tohoku University)

[SMP33-P01] Raman spectroscopy of seifertite

*Masahiro KAYAMA[1], Eiji Ohtani[1], Masaaki Miyahara[2], Shohei Kaneko[1], Toshimori Sekine[3], Shin Ozawa[1], Naohisa Hirao[4] (1.Tohoku University, 2.Hiroshima University, 3.HPSTAR, 4.Japan Synchrotron Radiation Research Institute)

[SMP33-P02] Microtexture and crystallization process of impact diamonds

*Hiroaki Ohfuji[1], Motosuke Nakaya[1] (1.Geodynamics Research Center, Ehime University)

[SMP33-P03] **Metamorphic temperature analysis of H chondrites: Using revised Lindsley's pyroxene thermometer**

*Ryo Uehara[1], Yoshihiro Kuwahara[1], Kazuhiko Shimada[1], Yoshihiro Nakamuta[1], Seiichiro Uehara[1], Tatsuro Adachi[1] (1.Kyushu university)

[SMP33-P04] The occurrence combinations of Zeolites at Chichijima, Ogasawara Islands

Michiharu Ito[1], *Yuki Inoue[1], Mana Yasui[2], Atsushi Yamazaki[2], Hiroshi Hagiya[1] (1. Tokyo City University, 2.Waseda research institute for science and engineering)

[SMP33-P05] Title: Single-crystal X-ray diffraction study of mirabilite ($Na_2SO_4 \cdot 10H_2O$) from 213 to 303 K

*Ryutaro Ikeda[1] (1.University of tsukuba)

[SMP33-P06] Elastic constants of single-crystal topaz studied via sphere-resonance method

*Kako Aradachi[1], Tohru Watanabe[1], Morihisa Hamada[2] (1.University of Toyama, 2.JAMSTEC)

[SMP33-P07] Verification of damage by polishing of sheet-like minerals

*Yui Kouketsu[1], Kota Ando[1], Katsuyoshi Michibayashi[1] (1.Department of Earth & Planetary Sciences, Graduate School of Environmental Studies, Nagoya University)

[SMP33-P08] Description of Zebra Rock and the pattern formation model

*Kaoru Yoshimura[1], Atsushi Toramaru[2], Mie Ichihara[3], Takaaki Noguchi[4], Toru Matsumoto[5] (1.Department of Earth and Planetary Science, Graduate School of Science, Kyushu University, 2.Department of Earth and Planetary Sciences, Faculty of Sciences, Kyushu University, 3.Earthquake Research Institute, University of Tokyu, 4.Department of Arts and Science, Kyushu University, 5.Japan Aerospace Exploration Agency/ Institute of Space and Astronautical Science)

[SMP33-P09] Thermal conductivity anomaly of $(Mg,Fe)CO_3$ solid solution across the spin transition

*Keng-Hsien Chao[1], Wen-Pin Hsieh[1,2] (1.Institute of Earth Sciences, Academia Sinica, Taiwan, 2.Department of Geosciences, National Taiwan University, Taiwan)

[SMP33-P10] **Melting experiments in the $MgSiO_3$ – SiO_2 system under high pressures**

*Takuya Moriguti[1], Akira Yoneda[1], Eiji Ito[1] (1.Institute for Planetary Materials, Okayama University)

[SMP33-P11] Melting relations of the Fe-Ni-S-C system and the formation of superdeep diamonds

*Yu Itami[1], Satoru Urakawa[1] (1.Okayama University)

[SMP33-P12] Effect of ammonia on the stability of methane hydrate under high-pressure and high-temperature

*Hirokazu Kadobayashi[1], Hisako Hirai[2], Hiroaki Ohfuji[1], Hideaki Kawamura[1], Michika Ohtake[3], Yoshitaka Yamamoto[3] (1.Geodynamics Research Center, Ehime University, 2.Department of Environment System, Faculty of Geo-environmental Science, Rissho University, 3.National Institute of Advanced Industrial Science and Technology)

[SMP33-P13] Study on magnetite-maghemite-hematite transformation

*Ibuki Kinebuchi[1], Atsushi Kyono[1], Yoshinari Sano[1] (1.University of Tsukuba)

[SMP33-P14] The Effects of Temperature and Pressure on Hydromagnesite

*Gen-ichiro Yamamoto[1], Atsushi Kyono[1], Jun Abe[2], Takanori Hattori[3], Yoshitaka Matsushita[4], Yasuhiro Yoneda[3] (1.University of Tsukuba, 2.CROSS, 3.JAEA, 4.NIMS)

[SMP33-P15] Synthesis and crystal structure of Mg-bearing Fe_9O_{11}: New insight in the complexity of Fe-Mg oxides at conditions of the deep upper mantle

*Takayuki Ishii[1], Uenver-Thiele Laura[2], Alan B Woodland[2], Edith Alig[3], Tiziana Boffa Ballaran[1] (1.Bavarian Research Institute, University of Bayreuth, 2.Institut für Geowissenschaften, Goethe-Universität Frankfurt, 3.Institut für Anorganische und Analytische Chemie, Goethe-Universität Frankfurt)

[SMP33-P16] **Changes in specific surface area and morphology of kaolin group minerals with pressure treatment**

*Soyeon Kwon[1], Yongjae Lee[1] (1.YONSEI University)

[E] Poster | S (Solid Earth Sciences)：S-GC Geochemistry

10:45 AM - 12:15 PM JST | 1:45 AM - 3:15 AM UTC | Poster Hall International Exhibition Hall8, Makuhari Messe_9

[S-GC40] Volatile Cycles in the Deep Earth - from Subduction Zone to Hot Spot

convener:Hirochika Sumino(Department of Basic Science, Graduate School of Arts and Sciences, The University of Tokyo), Takeshi Hanyu(Japan Agency for Marine-Earth Science and Technology, Department of Solid Earth Geochemistry), Yuji Sano(Division of Ocean and Earth Systems, Atmosphere and Ocean Research Institute, University of Tokyo), Gray E Bebout(Lehigh University)

[SGC40-P01] Continental growth models demystified

*Jun Korenaga[1] (1.Department of Geology and Geophysics, Yale University)

[SGC40-P02] Mass-independent sulfur isotope signature from the 2.7 Ga Belingwe komatiite: Recycling of crustal material in Archean

*Yusuke Kubota[1], Yuichiro Ueno[1,2,3], Kenji Shimizu[3], Fumihiro Matsuura[2], Akira Ishikawa[1,3] (1.Department of Earth and Planetary Sciences, Tokyo Institute of Technology, 2.Earth-Life Science Institute, Tokyo Institute of Technology, 3.Japan Agency for Marine-Earth Science and Technology (JAMSTEC))

[SGC40-P03] Determination of halogens in some standard materials using the neutron irradiation noble gas mass spectrometric technique

*Hirochika Sumino[1], Masahiro Kobayashi[2], Takehiko Saito[3], Keisuke Nagao[3] (1.Department of Basic Science, Graduate School of Arts and Sciences, The University of Tokyo, 2.Tokyo Metropolitan Industrial Technology Research Institute, 3.Geochemical Research Center, Graduate School of Science, University of Tokyo)

[SGC40-P04] FTIR spectroscopy and noble gas mass spectrometry for a single olivine grain

*Sota Niki[1], Hirochika Sumino[2], Masahiro Kobayashi[3], Hiroyuki Kagi[1], Takafumi Hirata[1], Chris J. Ballentine[4] (1.Geochemical Research Center, Grad. School of Science, Univ. of Tokyo, 2.Dept. of Basic Science, Grad. School of Arts and Sciences, Univ. of Tokyo, 3.Tokyo Metropolitan Industrial Technology Research Institute, 4.Dept. of Earth Sciences, Univ. of Oxford)

[SGC40-P05] New halogen incorporation mechanism in serpentine group minerals: Crystal chemical consideration

*Masami Kanzaki[1] (1.Institute for Planetary Matereials, Okayama University)

[SGC40-P06] Mineralogical and geochemical characteristics of cuttings from Taketomi hot spring

*Noriyuki Shingaki[1], Tomohiro Toki[1], Syogo Oshima[2], Masaaki chinen[3], Arito Sakaguchi[4], Naoto Takahata[5], Yuji Sano[5], Shirai Kotaro[5], Kentaro Tanaka[5] (1.University of the Ryukyus , 2.West Japan Engineering Consultants, Inc., 3.MicroRange, 4.Faculty of Science, Yamaguchi University, 5.Atmosphere and Ocean Research Institute, The University of Tokyo)

[SGC40-P07] Variation of helium isotope compositions at Lake Mashu

*Takanori Kagoshima[1], Yuji Sano[1], Atsushi Tanaka[2] (1.Atmosphere and Ocean Research Institute, University of Tokyo, 2.National Institute for Environmental Studies)

[SGC40-P08] Helium isotopes in Tachibana Bay and Shimabara Bay, Nagasaki

*Ma. Teresa Escobar[1], Yama Tomonaga[2], Hajime Obata[1], Shigenobu Takeda[3], Naoto Takahata[1], Yuji Sano[1] (1.Atmosphere and Ocean Research Institute, University of Tokyo, Kashiwanoha, Kashiwa, Chiba, Japan, 2.Eawag,, Swiss Federal Institute of Aquatic Science and Technology, Department of Water Resources and Drinking Water, Überlandstrasse 133 CH-8600 ,Dübendorf, Switzerland, 3.Graduate School of Fisheries and Environmental Sciences, Nagasaki University, Nagasaki, Japan)

[E] Poster | S (Solid Earth Sciences)：S-GC Geochemistry

5:15 PM - 6:30 PM JST | 8:15 AM - 9:30 AM UTC | Poster Hall International Exhibition Hall8, Makuhari Messe_31

[S-GC40] Volatile Cycles in the Deep Earth - from Subduction Zone to Hot Spot

convener:Hirochika Sumino(Department of Basic Science, Graduate School of Arts and Sciences, The University of Tokyo), Takeshi Hanyu(Japan Agency for Marine-Earth Science and Technology, Department of Solid Earth Geochemistry), Yuji Sano(Division of Ocean and Earth Systems, Atmosphere and Ocean Research Institute, University of Tokyo), Gray E Bebout(Lehigh University)

[SGC40-P01] Continental growth models demystified

*Jun Korenaga[1] (1.Department of Geology and Geophysics, Yale University)

[SGC40-P02] Mass-independent sulfur isotope signature from the 2.7 Ga Belingwe komatiite: Recycling of crustal material in Archean

*Yusuke Kubota[1], Yuichiro Ueno[1,2,3], Kenji Shimizu[3], Fumihiro Matsuura[2], Akira Ishikawa[1,3] (1.Department of Earth and Planetary Sciences, Tokyo Institute of Technology, 2.Earth-Life Science Institute, Tokyo Institute of Technology, 3.Japan Agency for Marine-Earth Science and Technology (JAMSTEC))

[SGC40-P03] Determination of halogens in some standard materials using the neutron irradiation noble gas mass spectrometric technique

*Hirochika Sumino[1], Masahiro Kobayashi[2], Takehiko Saito[3], Keisuke Nagao[3] (1.Department of Basic Science, Graduate School of Arts and Sciences, The University of Tokyo, 2.Tokyo Metropolitan Industrial Technology Research Institute, 3.Geochemical Research Center, Graduate School of Science, University of Tokyo)

[SGC40-P04] FTIR spectroscopy and noble gas mass spectrometry for a single olivine grain

*Sota Niki[1], Hirochika Sumino[2], Masahiro Kobayashi[3], Hiroyuki Kagi[1], Takafumi Hirata[1], Chris J. Ballentine[4] (1.Geochemical Research Center, Grad. School of Science, Univ. of Tokyo, 2.Dept. of Basic Science, Grad. School of Arts and Sciences, Univ. of Tokyo, 3.Tokyo Metropolitan Industrial Technology Research Institute, 4.Dept. of Earth Sciences, Univ. of Oxford)

[SGC40-P05] New halogen incorporation mechanism in serpentine group minerals: Crystal chemical consideration

*Masami Kanzaki[1] (1.Institute for Planetary Matereials, Okayama University)

[SGC40-P06] Mineralogical and geochemical characteristics of cuttings from Taketomi hot spring

*Noriyuki Shingaki[1], Tomohiro Toki[1], Syogo Oshima[2], Masaaki chinen[3], Arito Sakaguchi[4], Naoto Takahata[5], Yuji Sano[5], Shirai Kotaro[5], Kentaro Tanaka[5] (1.University of the Ryukyus , 2.West Japan Engineering Consultants, Inc., 3.MicroRange, 4.Faculty of Science, Yamaguchi University, 5.Atmosphere and Ocean Research Institute, The University of Tokyo)

[SGC40-P07] Variation of helium isotope compositions at Lake Mashu

*Takanori Kagoshima[1], Yuji Sano[1], Atsushi Tanaka[2] (1.Atmosphere and Ocean Research Institute, University of Tokyo, 2.National Institute for Environmental Studies)

[SGC40-P08] Helium isotopes in Tachibana Bay and Shimabara Bay, Nagasaki

*Ma. Teresa Escobar[1], Yama Tomonaga[2], Hajime Obata[1], Shigenobu Takeda[3], Naoto Takahata[1], Yuji Sano[1] (1.Atmosphere and Ocean Research Institute, University of Tokyo, Kashiwanoha, Kashiwa, Chiba, Japan, 2.Eawag,, Swiss Federal Institute of Aquatic Science and Technology, Department of Water Resources and Drinking Water, Überlandstrasse 133 CH-8600 ,Dübendorf, Switzerland, 3.Graduate School of Fisheries and Environmental Sciences, Nagasaki University, Nagasaki, Japan)

[E] Oral | S (Solid Earth Sciences)：S-GC Geochemistry

1:45 PM - 3:15 PM JST | 4:45 AM - 6:15 AM UTC | A10 TOKYO BAY MAKUHARI HALL

[S-GC40] Volatile Cycles in the Deep Earth - from Subduction Zone to Hot Spot

convener:Hirochika Sumino(Department of Basic Science, Graduate School of Arts and Sciences, The University of Tokyo), Takeshi Hanyu(Japan Agency for Marine-Earth Science and Technology, Department of Solid Earth Geochemistry), Yuji Sano(Division of Ocean and Earth Systems, Atmosphere and Ocean Research Institute, University of Tokyo), Gray E Bebout(Lehigh University), Chairperson:Takeshi Hanyu, Gray Bebout(Lehigh University), Yuji Sano, Hirochika Sumino

1:45 PM - 2:15 PM JST | 4:45 AM - 5:15 AM UTC

[SGC40-01] Continental growth, crustal recycling, and global water cycle

★Invited Papers

*Jun Korenaga[1] (1.Department of Geology and Geophysics, Yale University)

2:15 PM - 2:30 PM JST | 5:15 AM - 5:30 AM UTC

[SGC40-02] Role of volatiles in magma genesis of ascending mantle plume

*Eiichi Takahashi[1], Jintuan Wang[1], Li Li[1] (1.Guangzhou Institute of Geochemistry, Chinese Academy of Science)

2:30 PM - 2:45 PM JST | 5:30 AM - 5:45 AM UTC

[SGC40-03] DH partitioning experiment among high-pressure polymorph of olivine

*Asami Sano-Furukawa[1], Shoichi Itoh[2], Toru Inoue[3], Masamichi Noda[3] (1.J-PARC center, Japan Atomic Energy Agency, 2.Kyoto University, 3.Hiroshima University)

2:45 PM - 3:00 PM JST | 5:45 AM - 6:00 AM UTC

[SGC40-04] **Formation of Fe-rich volatile-bearing phases in the deep lower mantle and the implications for deep Earth volatile cycles**

*Li Zhang[1], Hongsheng Yuan[1], Eiji Ohtani[2], Lianjie Man[1], Duck Young Kim[1], Dmitry Popov[3], Yue Meng[3], Eran Greenberg[4], Vitali Prakapenka[4] (1.Center for High Pressure Science and Technology Advanced Research (HPSTAR), 2.Department of Earth Science, Graduate School of Science, Tohoku University, 3.HPCAT, X-ray Science Division, Argonne National Laboratory, 4.GeoSoilEnviroCARS, University of Chicago)

3:00 PM - 3:15 PM JST | 6:00 AM - 6:15 AM UTC

[SGC40-05] Estimation of the origin of Pitcairn Island OIB by Independent Component Analysis

*Takahiro Ozawa[1], Hikaru Iwamori[1,2,3], Takeshi Hanyu[2], Morihisa Hamada[2], Kenji Shimizu[4], Ushikubo Takayuki[4], Jun-Ichi Kimura[2], Q. Chang[2], Hitomi Nakamura[5], Motoo Ito[4] (1.Tokyo Institute of Tokyo, 2.Geochemical Evolution Research Program, Japan Agency for Marine-Earth Science and Technology, 3.Earthquake Research Institute, The University Tokyo, 4.Kochi Core Center, Japan Agency for Marine-Earth Science and Technology, 5.Geological Survey of Japan, National Institute of Advanced Industrial Science and Technology)

[E] Oral | S (Solid Earth Sciences)：S-GC Geochemistry

3:30 PM - 5:00 PM JST | 6:30 AM - 8:00 AM UTC | A10 TOKYO BAY MAKUHARI HALL

[S-GC40] Volatile Cycles in the Deep Earth - from Subduction Zone to Hot Spot

convener:Hirochika Sumino(Department of Basic Science, Graduate School of Arts and Sciences, The University of Tokyo), Takeshi Hanyu(Japan Agency for Marine-Earth Science and Technology, Department of Solid Earth Geochemistry), Yuji Sano(Division of Ocean and Earth Systems, Atmosphere and Ocean Research Institute, University of Tokyo), Gray E Bebout(Lehigh University), Chairperson:Takeshi Hanyu, Gray Bebout(Lehigh University), Yuji Sano, Hirochika Sumino

3:30 PM - 4:00 PM JST | 6:30 AM - 7:00 AM UTC

[SGC40-06] Tracing recycled volatiles in MORB with halogens

★Invited Papers

*Ray Burgess[1], Lorraine Ruzie-Hamilton[1], Patricia Clay[1], Bastian Joachim[2], Christopher Ballentine[3] (1.School of Earth and Environmental Sciences, University of Manchester, Manchester, M13 9PL UK, 2.Institute for Mineralogy and Petrography, University of Innsbruck, Innrain, 52A-6020, Innsbruck, Austria, 3.Department of Earth Sciences, University of Oxford, South Parks Road, Oxford, OX1 3AN UK)

4:00 PM - 4:15 PM JST | 7:00 AM - 7:15 AM UTC

[SGC40-07] Volatile composition in ocean island basalts

*Takeshi Hanyu[1] (1.Japan Agency for Marine-Earth Science and Technology, Department of Solid Earth Geochemistry)

4:15 PM - 4:30 PM JST | 7:15 AM - 7:30 AM UTC

[SGC40-08] Halogen heterogeneity in the subcontinental lithospheric mantle

*Hirochika Sumino[1], Masahiro Kobayashi[2], Ray Burgess[3], Chris J Ballentine[4] (1.Department of Basic Science, Graduate School of Arts and Sciences, University of Tokyo, 2.Tokyo Metropolitan Industrial Technology Research Institute, 3.School of Earth and Environmental Sciences, University of Manchester, 4.Department of Earth Sciences, University of Oxford)

4:30 PM - 4:45 PM JST | 7:30 AM - 7:45 AM UTC

[SGC40-09] Efficiency of Deep Carbon Subduction: Input, Metamorphic Records, and Bearing on Estimated Sources of Arc Volcanic Gases

*Gray E Bebout[1,2], Gabe S Epstein[2], Brian M House[3] (1.Institute for Planetary Materials, Okayama University, 2.Lehigh University, 3.University of California, San Diego)

4:45 PM - 5:00 PM JST | 7:45 AM - 8:00 AM UTC

[SGC40-10] Helium isotope variations in subduction-type volcanic hydrothermal systems

*Yuji Sano[1], Takanori Kagoshima[1], Naoto Takahata[1], Tetsuji Onoue[2], Tomo Shibata[3], Tobias P Fischer[4] (1.Division of Ocean and Earth Systems, Atmosphere and Ocean Research Institute, University of Tokyo, 2.Department of Earth and Environmental Sciences, Kumamoto University, 3.Institute for Geothermal Sciences, Kyoto University, 4.Department of Earth and Planetary Sciences, University of New Mexico)

[J] Poster | S (Solid Earth Sciences)：S-GC Geochemistry

3:30 PM - 5:00 PM JST | 6:30 AM - 8:00 AM UTC | Poster Hall International Exhibition Hall8, Makuhari Messe_19

[S-GC41] Solid Earth Geochemistry, Cosmochemistry

convener:Gen Shimoda(Geological Survey of Japan, AIST), Katsuhiko Suzuki(Research and Development Center for Submarine Resources, Japan Agency for Marine-Earth Science and Technology), Katsuyuki Yamashita(Graduate School of Natural Science and Technology, Okayama University), Akira Ishikawa(Department of Earth and Planetary Sciences, Tokyo Institute of Technology)

[SGC41-P01] Experimental and Simulation Study on the Migration Rule of Arsenic in the Soil of Surface Karst Zone in Southwest China

*bin zeng[1] (1.China University of Geosciences)

[SGC41-P02] H_2 production and CO_2 storage during peridotite serpentinization under CO_2-rich hydrothermal conditions: Influence of pyroxene

*Jiajie Wang[1], Noriaki Watanabe[1], Atsushi Okamoto[1], Kengo Nakamura[1], Takeshi Komai[1] (1.Tohoku Univ.)

[SGC41-P03] **Age determination of spherical carbonate concretions by Sr isotope stratigraphy**

*Yoshihiro Asahara[1], Hidekazu Yoshida[2], Koshi Yamamoto[1], Nagayoshi Katsuta[3], Masayo Minami[4], Richard Metcalfe[5] (1.Graduate School of Environmental Studies, Nagoya University, 2.Material Research Section, Nagoya University, University Museum, 3.Faculty of Education, Gifu University, 4.Institute for Space-Earth Environmental Research, Nagoya University, 5.Quintessa UK)

[SGC41-P04] Origin of mantle xenoliths from Kaula Island, Hawaii:Constrains from Os isotope and highly siderophile element compositions

*Ryo Fujita[1], Akira Ishikawa[1], Tetsuya Yokoyama[1], Michael O Garcia[2] (1.Tokyo Institute of Technology, 2.University of Hawaii)

[SGC41-P05] Petrological and Geochemical features of Miocene adakitic volcanic rocks in eastern part of Hokuriku region, SW Japan

*Watanabe Syun[1], Toshiro Takahashi[1] (1.Niigata university)

[SGC41-P06] Trace element and isotopic characteristics of high Nb basalts from Kyushu arc and back arc

*Bidisha Dey[1], Tomoyuki Shibata[1] (1.Department of Earth and Planetary Systems Science, Hiroshima University)

[SGC41-P07] Evaluation of digestion methods for Molybdenum concentration analysis for geological materials

Yu Mutsushika[1], *Akira Ishikawa[1], Tetsuya Yokoyama[1] (1.Department of Earth and Planetary Sciences, Tokyo Institute of Technology)

[SGC41-P08] *fs*LA-ICPMS analysis of XRF glass beads

*Q. Chang[1], T. Sato[2], J.-I. Kimura[1] (1.Dept. Solid Earth Geochem., JAMSTEC, 2.R&D Center for Ocean Drilling Sci., JAMSTEC)

[J] Poster | S (Solid Earth Sciences)：S-GC Geochemistry

5:15 PM - 6:30 PM JST | 8:15 AM - 9:30 AM UTC | Poster Hall International Exhibition Hall8, Makuhari Messe_32

[S-GC41] Solid Earth Geochemistry, Cosmochemistry

convener:Gen Shimoda(Geological Survey of Japan, AIST), Katsuhiko Suzuki(Research and Development Center for Submarine Resources, Japan Agency for Marine-Earth Science and Technology), Katsuyuki Yamashita(Graduate School of Natural Science and Technology, Okayama University), Akira Ishikawa(Department of Earth and Planetary Sciences, Tokyo Institute of Technology)

[SGC41-P01] Experimental and Simulation Study on the Migration Rule of Arsenic in the Soil of Surface Karst Zone in Southwest China

*bin zeng[1] (1.China University of Geosciences)

[SGC41-P02] H_2 production and CO_2 storage during peridotite serpentinization under CO_2-rich hydrothermal conditions: Influence of pyroxene

*Jiajie Wang[1], Noriaki Watanabe[1], Atsushi Okamoto[1], Kengo Nakamura[1], Takeshi Komai[1] (1.Tohoku Univ.)

[SGC41-P03] **Age determination of spherical carbonate concretions by Sr isotope stratigraphy**

*Yoshihiro Asahara[1], Hidekazu Yoshida[2], Koshi Yamamoto[1], Nagayoshi Katsuta[3], Masayo Minami[4], Richard Metcalfe[5] (1.Graduate School of Environmental Studies, Nagoya University, 2.Material Research Section, Nagoya University, University Museum, 3.Faculty of Education, Gifu University, 4.Institute for Space-Earth Environmental Research, Nagoya University, 5.Quintessa UK)

[SGC41-P04] Origin of mantle xenoliths from Kaula Island, Hawaii:Constrains from Os isotope and highly siderophile element compositions

*Ryo Fujita[1], Akira Ishikawa[1], Tetsuya Yokoyama[1], Michael O Garcia[2] (1.Tokyo Institute of Technology, 2.University of Hawaii)

[SGC41-P05] Petrological and Geochemical features of Miocene adakitic volcanic rocks in eastern part of Hokuriku region, SW Japan

*Watanabe Syun[1], Toshiro Takahashi[1] (1.Niigata university)

[SGC41-P06] Trace element and isotopic characteristics of high Nb basalts from Kyushu arc and back arc

*Bidisha Dey[1], Tomoyuki Shibata[1] (1.Department of Earth and Planetary Systems Science, Hiroshima University)

[SGC41-P07] Evaluation of digestion methods for Molybdenum concentration analysis for geological materials

Yu Mutsushika[1], *Akira Ishikawa[1], Tetsuya Yokoyama[1] (1.Department of Earth and Planetary Sciences, Tokyo Institute of Technology)

[SGC41-P08] *fs*LA-ICPMS analysis of XRF glass beads

*Q. Chang[1], T. Sato[2], J.-I. Kimura[1] (1.Dept. Solid Earth Geochem., JAMSTEC, 2.R&D Center for Ocean Drilling Sci., JAMSTEC)

[J] Oral | S (Solid Earth Sciences)：S-VC Volcanology

10:45 AM - 12:15 PM JST | 1:45 AM - 3:15 AM UTC | IC 2F

[S-VC38] Active Volcanism

convener:Yuta Maeda(Nagoya University), Takahiro Miwa(National research institute for earth science and disaster prevention), Takeshi Nishimura(Department of Geophysics, Graduate School of Science, Tohoku University), Chairperson:Nobukazu Seama, Tetsuo Matsuno

10:45 AM - 11:00 AM JST | 1:45 AM - 2:00 AM UTC

[SVC38-30] Summary of Kikai submarine caldera researches conducted by KOBEC (Kobe Ocean-Bottom Exploration Center)

*Nobukazu Seama[1,2], Tetsuo Matsuno[2,1], Koji Kiyosugi[3,2], Satoshi Shimizu[2], Reina Nakaoka[2], Keiko Suzuki-Kamata[2,1], Yasutomo Seto[1], Mamoru Sano[2], Yuiko Morita[4], Hikaru Iwamaru[2], Haruhisa Morozumi[2], Misaki Horiuchi[1], Kimihiro Nishimura[1], Hiroshi Ichihara[5], Kazuki Hayashi[1], Toki Hirose[1], Katsuya Kaneko[1,2], Hiroto Yamaguchi[4], Yuki Okizono[4], Hiroko Sugioka[1,2], Kazuo Nakahigashi[6,2], Yojiro Yamamoto[7], Tatsuya KODA[2], Shuichi Kodaira[7,2], Yoshiyuki Tatsumi[2,1], Scientific party of T/S Fukae-maru Kikai caldera research cruises (1.Department of Planetology, Graduate School of Science, Kobe University, 2.Kobe Ocean Bottom Exploration Center, Kobe University, 3.Organization of Advanced Science and Technology, Kobe University, 4.Department of Planetology, Faculty of Science, Kobe University, 5.Graduate school of environmental studies, Nagoya University, 6.Tokyo University of Marine Science and Technology, 7.Japan Agency for Marine-Earth Science and Technology)

11:00 AM - 11:15 AM JST | 2:00 AM - 2:15 AM UTC

[SVC38-31] Distribution of submarine pyroclastic-flow deposits of Akahoya eruption, Kikai caldera

*Satoshi Shimizu[1,2], Nobukazu Seama[3,1], Reina NAKAOKA[1], Tetsuo Matsuno[1,3], Koji Kiyosugi[5], Hikaru Iwamaru[1,2], Mamoru Sano[1,2], Kimihiro Nishimura[3], Keiko Suzuki-Kamata[1,3], Katsuya Kaneko[3], hiroto yamaguchi[4], Misaki Horiuchi[3], Toki Hirose[3], Kazuki Hayashi[3], Yoshiyuki Tatsumi[1,3] (1.Ocean Bottom Exploraiton Center, Kobe University, 2.Nippon Marine Enterprises, Ltd., 3.Department of Planetology, Graduate School of Science, Kobe University, 4.Department of Planetology, Faculty of Science, Kobe University, 5.Organization of Advanced Science and Technology, Kobe University)

11:15 AM - 11:30 AM JST | 2:15 AM - 2:30 AM UTC

[SVC38-32] Identification of submarine volcanic ash around the Kikai caldera with the Koya pyroclastic flow deposit inferred from glass composition

*Reina NAKAOKA[1], Keiko Suzuki-Kamata[1,2], Satoshi Shimizu[1], Yoshiyuki Tatsumi[1,2], Katsuya Kaneko[2,1], Koji Kiyosugi[3,1], Nobukazu Seama[2,1], Tetsuo Matsuno[1,2], Kimihiro Nishimura[2], Kazuki Hayashi[2] (1.Kobe Ocean-Bottom Exploration Center, Kobe University, 2.Department of Planetology, Graduate School ofScience, Kobe University, 3.Organization of Advanced Science and Technology, Kobe University)

11:30 AM - 11:45 AM JST | 2:30 AM - 2:45 AM UTC

[SVC38-33] Preliminary report of the sea floor survey by a remotely operated vehicle (ROV) at the Kikai caldera, SW Japan

*Koji Kiyosugi[1], Keiko Suzuki-Kamata[2], Haruhisa Morozumi[2,4], Yoshiyuki Tatsumi[2], Katsuya Kaneko[3], Reina NAKAOKA[2], Mamoru Sano[2], Satoshi Shimizu[2], Hikaru Iwamaru[2], Nobukazu Seama[3], Tetsuo Matsuno[2], Kimihiro Nishimura[3], Kazuki Hayashi[3], Misaki Horiuchi[3] (1.Organization for Advanced and Integrated Research, Kobe University, 2.Kobe Ocean-Bottom Exploration Center, Kobe University, 3.Department of Planetology, Graduate School of Science, Kobe University, 4.Japan Oil, Gas and Metals National Corporation)

11:45 AM - 12:00 PM JST | 2:45 AM - 3:00 AM UTC

[SVC38-34] Seismic activity beneath Kikai Caldera by using Ocean Bottom Observation

*Yasutomo Seto[1], Hiroko Sugioka[2], Yojiro Yamamoto[3], Tsutomu Takahashi[4] (1.Department of Planetology, Graduate School of Science, Kobe University, 2.Department of Planetology, Kobe University, 3.Japan Agency for Marine-Earth Science and Technology, 4.Research and Developement Center for Earthquake and Tsunami, Japan Agency for Marine-Earth Science and Technology)

12:00 PM - 12:15 PM JST | 3:00 AM - 3:15 AM UTC

[SVC38-35] An investigation of three-dimensional electrical resistivity structure under Kikai Caldera

*Tetsuo Matsuno[1,2], Toki Hirose[2], Yuuki Okizono[3], Nobukazu Seama[2,1], Hiroshi Ichihara[4], Hiroko Sugioka[2,1], Yoshiyuki Tatsumi[1,2] (1.Kobe Ocean Bottom Exploration Center, Kobe University, 2.Department of Planetology, Graduate School of Science, Kobe University, 3.Department of Planetology, Faculty of Science, Kobe University, 4.Graduate school of environmental studies, Nagoya University)

[J] Oral | S (Solid Earth Sciences)：S-VC Volcanology

1:45 PM - 3:15 PM JST | 4:45 AM - 6:15 AM UTC | IC 2F

[S-VC38] Active Volcanism

convener:Yuta Maeda(Nagoya University), Takahiro Miwa(National research institute for earth science and disaster prevention), Takeshi Nishimura(Department of Geophysics, Graduate School of Science, Tohoku University), Chairperson:Takeshi Ohba, Akihiko Terada

1:45 PM - 2:00 PM JST | 4:45 AM - 5:00 AM UTC

[SVC38-36] Time variation in the chemical and isotopic composition of fumarolic gases at Hakone volcano Japan

*Takeshi Ohba[1], Muga Yaguchi[2], Kana NISHINO[1], Nozomi Numanami[1], Yasushi DAITA[3], Urumu Tsunogai[4], Masanori Ito[4], Chiho Sukigara[4] (1.Department of chemistry, School of Science, Tokia University, 2.Meteorological Research Institute, JMA, 3.Kanagawa Environmental Research Center, 4.Nagoya University Graduate School of Environmental Studies)

2:00 PM - 2:15 PM JST | 5:00 AM - 5:15 AM UTC

[SVC38-37] Chemical and isotopic composition of volcanic gases at Mt Kirishima Iwoyama, Japan

*Takeshi Ohba[1], Muga Yaguchi[2], Kotaro Toyama[3], Hirochika Sumino[3], Urumu Tsunogai[4], Masanori Ito[4], Ryo Shingubara[4] (1.Department of chemistry, School of Science, Tokia University, 2.Meteorological Research Institute, 3.The University of Tokyo Graduate School of Arts and Sciences Department of Basic Science, 4.Nagoya University Graduate School of Environmental Studies)

2:15 PM - 2:30 PM JST | 5:15 AM - 5:30 AM UTC

[SVC38-38] Temporal and spatial variations of helium isotope ratios in volcanic gases in Kirishima volcanic group, Japan

*Kotaro Toyama[1], Hirochika Sumino[1], Kaori Kawana[1], Takeshi Ohba[2], Muga Yaguchi[3], Yoshihide Akiyama[1], Koki Aizawa[4], Kaori Tsukamoto[4] (1.Department of Basic Science, Graduate School of Arts and Sciences, The University of Tokyo, 2.Department of chemistry, School of Science, Tokia University, 3.Meteorological Research Institute, 4.Institute of Seismology and Volcanology, Faculty of Science, Kyushu University)

2:30 PM - 2:45 PM JST | 5:30 AM - 5:45 AM UTC

[SVC38-39] Emission regions of gaseous elemental mercury around Yugama crater lake at Kusatsu-Shirane volcano, Japan

*Akihiko Terada[1], Noriaki Mizutani[1] (1.Volcanic Fluid Research Center, Faculty of Science, Tokyo Institute of Technology)

2:45 PM - 3:00 PM JST | 5:45 AM - 6:00 AM UTC

[SVC38-40] Magnetotelluric images of Kusatsu-Shirane volcano, revisited by 3-D modeling with tetrahedral elements considered topography effect

*Kuo Hsuan Tseng[1], Yasuo Ogawa[1], Nurhassan .[2], Sabri Bulent Tank[3], Akihiko Terada[1], Wataru Kanda[1], Masato Fukai[1] (1.Tokyo Institute of Technology, 2.Bandung Institute of Technology, Indonesia, 3.Bogazici University, Turkey)

3:00 PM - 3:15 PM JST | 6:00 AM - 6:15 AM UTC

[SVC38-41] Magma conduit and associated hydrothermal systems of Aso volcano as revealed by broadband magnetotelluric data

*Nobuo Matsushima[1], Mitsuru Utsugi[2], Shinichi Takakura[1], Tadashi Yamasaki[1], Maki Hata[3], Takeshi Hashimoto[4], Makoto Uyeshima[3] (1.Geological Survey of Japan,AIST, 2.Kyoto University, 3.The University of Tokyo, 4.Hokkaido University)

[E] Oral | S (Solid Earth Sciences)：S-CG Complex & General

9:00 AM - 10:30 AM JST | 12:00 AM - 1:30 AM UTC | IC 2F

[S-CG48] Science of slow earthquakes: Toward unified understandings of whole earthquake process

convener:Satoshi Ide(Department of Earth an Planetary Science, University of Tokyo), Hitoshi Hirose(Research Center for Urban Safety and Security, Kobe University), Kohtaro Ujiie(Graduate School of Life and Environmental Sciences, University of Tsukuba), Takahiro Hatano(Earthquake Research Institute, University of Tokyo), Chairperson:Hitoshi Hirose, Yoshiyuki Tanaka

9:00 AM - 9:30 AM JST | 12:00 AM - 12:30 AM UTC

[SCG48-01] Variability of the space-time evolution of slow slip events off the Boso Peninsula, central Japan, from 1996 to 2018

★Invited Papers

*Jun'ichi Fukuda[1] (1.Earthquake Research Institute, University of Tokyo)

9:30 AM - 9:45 AM JST | 12:30 AM - 12:45 AM UTC

[SCG48-02] Cumulative slip distribution of short-term slow slip events in the western Shikoku area, southwest Japan based on tilt change measurements

*Hitoshi Hirose[1,2], Wakako Tamura[2], Takeshi Kimura[3] (1.Research Center for Urban Safety and Security, Kobe University, 2.Graduate School of Science, Kobe University, 3.National Research Institute for Earth Science and Disaster Resilience)

9:45 AM - 10:00 AM JST | 12:45 AM - 1:00 AM UTC

[SCG48-03] Shallow undersea SSEs off the western Japan monitored by the GNSS-A

*Yusuke Yokota[1], Tadashi Ishikawa[2] (1.Institute of Industrial Science, The University of Tokyo, 2.Hydrographic and Oceanographic department, Japan Coast Guard)

10:00 AM - 10:15 AM JST | 1:00 AM - 1:15 AM UTC

[SCG48-04] Co- and Post-seismic deformation due to the 2016 moderate earthquake sequence at the Chaman fault

*Fumiko Matsumoto[1], Masato Furuya[1] (1.Hokkaido University)

10:15 AM - 10:30 AM JST | 1:15 AM - 1:30 AM UTC

[SCG48-05] An attempt to quantify transient fluid flow during slow slip event using GNSS and gravity data-1st report

*Yusuke Umemiya[1], Yoshiyuki Tanaka[1] (1.The University of Tokyo)

[E] Poster | S (Solid Earth Sciences)：S-CG Complex & General

10:45 AM - 12:15 PM JST | 1:45 AM - 3:15 AM UTC | Poster Hall International Exhibition Hall8, Makuhari Messe_10

[S-CG48] Science of slow earthquakes: Toward unified understandings of whole earthquake process

convener:Satoshi Ide(Department of Earth an Planetary Science, University of Tokyo), Hitoshi Hirose(Research Center for Urban Safety and Security, Kobe University), Kohtaro Ujiie(Graduate School of Life and Environmental Sciences, University of Tsukuba), Takahiro Hatano(Earthquake Research Institute, University of Tokyo)

[SCG48-P01] Off the Kii Peninsula Shallow Low Frequency Earthquake in 2004 revealed by Ocean Bottom Seismometer

*Koji Tamaribuchi[1], Akio Kobayashi[1], Takahito Nishimiya[1], Satoshi Annoura[2] (1.Meteorological Research Institute, 2.Japan Meteorological Agency)

[SCG48-P02] The development of pressure vessel on gouges for rock deformation at seismic rates under water-saturated conditions

*Wei-Ting Lin[1], Li-Wei Kuo[1], Wen-Jie Wu[1], Jia-Jyun Dong[1], Yi-Hung Huang[2] (1.National Central University, 2.MATSUKI HYDRAULIC INDUSTRIAL CO. LTD)

[SCG48-P03] Spatial variations of shallow very low-frequency earthquake activity along the Nankai Trough based on CMT inversion using the 3D heterogeneous model

*Shunsuke Takemura[1], Takanori Matsuzawa[1], Akemi Noda[1], Takashi Tonegawa[2], Youichi Asano[1], Takeshi Kimura[1], Katsuhiko Shiomi[1] (1.National Research Institute for Earth Science and Disaster Resilience, 2.Japan Agency for Marine-Earth Science and Technology)

[SCG48-P04] Evaluation of Magnitude and Characteristics of Seismicity of Low Frequency Earthquakes in Parkfield

*Miki Aso[1,3], Naofumi Aso[2], Satoshi Ide[1] (1.Department of Earth and Planetary Science, The University of Tokyo, 2.Tokyo Institute of Technology, School of Science, 3.OYO RMS Corporation)

[SCG48-P05] Tectonic tremor catalog in the Tohoku-Hokkaido-Oki region using S-net

*Satoshi Ide[1], Tomoaki Nishikawa[2], Takanori Matsuzawa[3], Kazuaki Ohta[2], Naoki Uchida[4], Takuya NISHIMURA[2] (1.Department of Earth an Planetary Science, University of Tokyo, 2.Disaster Prevention Research Institute, Kyoto University, 3.National Research Institute for Earth Science and Disaster Resilience, 4.Graduate School of Science and International Research Institute of Disaster Science, Tohoku University)

[SCG48-P06] Spontaneous Slow Slip and Runaway Slip in Laboratory

*Miki Takahashi[1] (1.Institute of Earthquake and Volcano Geology, Geological Survey of Japan, AIST)

[SCG48-P07] Hydration and amorphization of quartz rocks during high-velocity frictional sliding: An examination of fault gouge from friction experiments of synthetic quartz

*Yuko Onoe[1], Hirotaka Iida[2], Akito Tsutsumi[1], Aki Takigawa[1] (1.Graduate School of Science, Kyoto University, 2.Geothermal Engineering Co., Ltd.)

[SCG48-P08] Constraining S Wave Velocity of the Source Region of Shallow Very Low-Frequency Earthquakes

*Takeshi Akuhara[1], Takashi Tonegawa[2] (1.Earthquake Research Institute, The University of Tokyo, 2.Research and Development center for Earthquake and Tsunami, Japan Agency for Marine-Earth Science and Technology)

[SCG48-P09] Quantitative relationship between aseismic slip propagation speed and frictional properties

*Keisuke Ariyoshi[1], Jean-Paul Ampuero[2,3], Roland Burgmann[4], Toru Matsuzawa[5], Akira Hasegawa[5], Ryota Hino[5], Takane Hori[1] (1.Japan Agency for Marine-Earth Science and Technology, 2.Université Côte d'Azur, 3.California Institute of Technology, 4.University of California, Berkeley, 5.Graduate School of Science, Tohoku University)

[SCG48-P10] Comprehensive detection of very low frequency earthquakes off the Pacific coasts of Hokkaido and Tohoku, northeastern Japan

*Satoru Baba[1], Akiko Takeo[1], Kazushige Obara[1], Takanori Matsuzawa[2], Takuto Maeda[3] (1.Earthquake Research Institute, University of Tokyo, 2.National Research Institute for Earth Science and Disaster Resilience, 3.Graduate School of Science and Technology, Hirosaki University)

[SCG48-P11] **Spatio-temporal evolution of long- and short-term slow slip events in the Tokai region, central Japan estimated from a very dense GNSS network, during 1997-2017**

*Hiromu Sakaue[1], Takuya NISHIMURA[2], Jun'ichi Fukuda[3], Teruyuki Kato[4] (1.Graduate School of Science, Kyoto University, 2.Disaster Prevention Research Institute Kyoto University, 3.Earthquake Research Institute,The University of Tokyo, 4.Hot Springs Research Institute of Kanagawa Prefecture)

[SCG48-P12] Broadband excitation of acoustic emission in granular stick-slip : experiments and spectral analyses

*Hidekazu Fukumizu[1], Ikuro Sumita[2] (1.Earth and Environmental Science Course, Division of Natural System, Graduate school of Natural Science and Technology, Kanazawa University, 2.School of Geosciences and Civil Engineering, Kanazawa University)

[SCG48-P13] Episodic tremor and slip silently invades strongly locked megathrust in the Nankai Trough

*Masayuki Kano[1], Aitaro Kato[2], Kazushige Obara[2] (1.Graduate school of science, Tohoku University, 2.Earthquake Research Institute, The University of Tokyo)

[SCG48-P14] Spatial distribution of the electrical resistivity beneath western part of Shikoku Island where long-term SSE events have repeatedly occurred

*Makoto Uyeshima[1], Maki Hata[1], Hiroshi Ichihara[2], Ryokei Yoshimura[3], Koki Aizawa[4] (1.Earthquake Research Institute, The University of Tokyo, 2.Graduate School of Environmental Studies, Nagoya University, 3.Disaster Prevention Research Institute, Kyoto University, 4.Institute of Seismology and Volcanology, Faculty of Sciences, Kyushu University)

[SCG48-P15] Variations of scaling relationships for shallow tremor observed along the Nankai trough

*Masaru Nakano[1], Suguru Yabe[1] (1.Japan Agency for Marine-Earth Science and Technology)

[SCG48-P16] Low-frequency earthquakes triggered by teleseismic surface waves by Ryukyu subduction zone.

Ayumi Kinjo[1], *Mamoru Nakamura[1] (1.Faculty of Science, University of the Ryukyus)

[SCG48-P17] Detection of small surface displacement accompanying deep low-frequency tremor in Shikoku region, southwest Japan

*Yutaro Okada[1], Takao Tabei[2] (1.Faculty of Science, Kochi University, 2.Faculty of Science and Technology, Kochi University)

[SCG48-P18] Long-term temporal change in crustal resistivity beneath western Shikoku

*Futoshi Yamashita[1], Yoshimori Honkura[1] (1.National Research Institute for Earth Science and Disaster Resilience)

[SCG48-P19] Slow decay of postseismic deformation compared with aftershocks following the 2011 Tohoku-oki Earthquake

*Yuta Mitsui[1], Shunsuke Morikami[2] (1.Department of Geosciences, Shizuoka University, 2.Formerly at Graduate School of Science and Technology, Shizuoka University)

[SCG48-P20] Serpentinite dehydration in subduction shear zones formed at source depths of slow earthquakes

*Yasushi Mori[1], Miki Shigeno[1], Kohtaro Ujiie[2], Kazuya Noro[2], Tadao Nishiyama[3] (1.Kitakyushu Museum of Natural History and Human History, 2.University of Tsukuba, 3.Kumamoto University)

[SCG48-P21] Earthquake swarms following very low-frequency earthquakes in the central Ryukyu Trench

*Mamoru Nakamura[1] (1.Faculty of Science, University of the Ryukyus)

[SCG48-P22] Seismic imaging in the central Nankai trough, off Shionomisaki to Kii channel

*Yasuyuki Nakamura[1], Shuichi Kodaira[1], Tetsuo No[1], Yuka Kaiho[1], Gou Fujie[1], Seiichi Miura[1], Kazuya Shiraishi[1] (1.Japan Agency for Marine Earth Science and Technology)

[SCG48-P23] Attempt to Detect Intra-plate SSEs Based on F3 Solution of GEONET

*Yusaku Tanaka[1] (1.Earthquake Research Institute)

[SCG48-P24] A new hydrothermal, low to high speed rotary-shearing apparatus: Reproduction of slow/megathrust earthquakes in laboratory

*Takehiro Hirose[1], Wataru Tanikawa[1], Yohei Hamada[1], Keishi Okazaki[1] (1.Kochi Institute for Core Sample Research, Japan Agency for Marine-Earth Science and Technology)

[SCG48-P25] Very low-frequency earthquakes in western Shikoku remotely triggered by the 2016 Mw5.9 off-Kii Peninsula earthquake

*Masatoshi Miyazawa[1] (1.Disaster Prevention Research Institute, Kyoto University)

[SCG48-P26] **Underground structure around source region of slow earthquakes in western Shikoku obtained by receiver function analysis**

Akira Hikita[1], Aitaro Kato[1], *Kazushige Obara[1], Akiko Takeo[1], Takeshi Akuhara[1] (1.Earthquake Research Institute, The University of Tokyo)

[SCG48-P27] Hypocenter determination of deep low frequency tremors beneath the Kii Peninsula by backprojection of seismic array data

*Kodai Sagae[1], Hisashi Nakahara[1], Takeshi Nishimura[1], Kazutoshi Imanishi[2] (1.Graduate School of Science,Tohoku University, 2.National Institute of Advanced Industrial Science and Technology (AIST))

[SCG48-P28] Triggered tremors and stress perturbations due to surface waves

*Ryohei Ikeda[1], Naoki Suda[1] (1.Hiroshima University)

[SCG48-P29] Numerical modeling of long- and shallow slow slip events including shallow region in Hyuganada and western Nankai, Japan

*Takanori Matsuzawa[1], Bunichiro Shibazaki[2] (1.National Research Institute for Earth Science and Disaster Resilience, 2.Building Research Institute)

[SCG48-P30] Further evidence for the influence of a subducting-ridge on the spatial strain accumulation and release pattern in the shallow eastern Nankai Trough, based on VLFE distribution

*Akiko Toh[1], Chen Wan-Jou [2], Doug Dreger[3], Wu-Cheng Chi[2], Satoshi Ide[1] (1.University of Tokyo, 2.Institute of Earth Sciences, Academia Sinica, 3.UC Berkeley)

[SCG48-P31] Evidence for semi-brittle flow in mantle-wedge serpentinites under high pore fluid pressure and their implications for deep low frequency earthquakes

Kengo Kataoka[1], Yurina Nagata[1], *Ken-ichi Hirauchi[1], Ryosuke Oyanagi[2], Atsushi Okamoto[3], Katsuyoshi Michibayashi[4] (1.Department of Geosciences, Faculty of Science, Shizuoka University, 2.Japan Agency for Marine-Earth Science and Technology, 3.Graduate School of Environmental studies, Tohoku University, 4.Department of Earth and Planetary Sciences, Nagoya University)

[SCG48-P32] Spatial distribution of slow slip events off the Boso peninsula from 1996 to 2018 under sparsity constraints

*Ryoko Nakata[1], Hideitsu Hino[2], Tatsu Kuwatani[3,4], Takahiro Akiyama[5], Shoichi Yoshioka[6], Masato Okada[7], Takane Hori[1] (1.Japan Agency for Marine-Earth Science and Technology, 2.The Institute of Statistical Mathematics, 3.Department of Solid Earth Geochemistry, Japan Agency for Marine-Earth Science and Technology, 4.PRESTO, Japan Science and Technology Agency, 5.Graduate School of Science, Kobe University, 6.Research Center for Urban Safety and Security, Kobe University, 7.Graduate School of Frontier Sciences, The University of Tokyo)

[SCG48-P33] Marine electromagnetic observations around a slow earthquake region in the western Nankai trough

*Hiroshi Ichihara[1], Tada-nori Goto[2], Tetsuo Matsuno[3], Noriko Tada[4], Shinya Sato[2] (1.Earthquake and Volcano Research Center, Nagoya University, 2.Graduate School of Engineering, Kyoto University, 3.Ocean Bottom Exploration Center, Kobe University, 4.JAMSTEC)

[SCG48-P34] Dynamics of precipitating injection fronts inside of structured medium

*Yutaka Sumino[1], Shunsuke Tanaka[1], Miyuki Kunihiro[1] (1.Tokyo University of Science)

[SCG48-P35] Permeability changes of simulated low permeable fault rocks induced by intermediate velocity friction test

*Wataru Tanikawa[1] (1.Japan Agency for Marine-Earth Science and Technology, Kochi Instutute for Core Sample Research)

[SCG48-P36] Modified relation between the coupling and tremor rates around the Shikoku region

*Tadafumi Ochi[1] (1.Institute of Earthquake and Volcano Geology, Geological Survey of Japan, The National Institute of Advanced Industrial Science and Technology)

[SCG48-P37] Spatiotemporal distribution of regular and very low-frequency earthquakes in the northern part of the Ryukyu subduction zone

*Youichi Asano[1], Kazuhiko Goto[2], Hiroshi Yakiwara[3], Shuichiro Hirano[3] (1.National Research Institute for Earth Science and Disaster Resilience, 2.Association for the development of earthquake prediction, 3.Nansei-toko Observatory for Earthquakes and Volcanoes, Kagoshima University)

[SCG48-P38] Possible tectonic tremor activities near the VLFE epicenters in the Sanriku-Oki region in 2011

*Hidenobu Takahashi[1], Ryota Hino[1], Yusaku Ohta[1], Naoki Uchida[1], Syuichi Suzuki[1], Masanao Shinohara[2], Takanori Matsuzawa[3] (1.Graduate school of Science Tohoku University , 2.Earthquake Research Institute, University of Tokyo, 3.National Research Institute for Earth Science and Disaster Resilience)

[SCG48-P39] Heterogeneous structure around a region of slow earthquake activity off Ibaraki prefecture along the Japan Trench

*Kimihiro Mochizuki[1], Tomoaki Yamada[1], Masanao Shinohara[1], Ryota Hino[2], Ryosuke Azuma[2], Yoshihiro Ito[3], Yoshio Murai[4], Kenji Uehira[5], Toshinori Sato[6] (1.ERI, Univ. of Tokyo, 2.Graduate School of Science, Tohoku Univ., 3.DPRI, Kyoto Univ., 4.Faculty of Science, Hokkaido Univ., 5.NIED, 6.Graduate School of Science, Chiba Univ.)

[SCG48-P40] Shallow low-frequency tremor triggered by nearby moderate earthquakes off Sanriku

*Sachiko Tanaka[1], Takanori Matsuzawa[1], Youichi Asano[1] (1.National Research Institute for Earth Science and Disaster Resilience)

[SCG48-P41] Slow slip events in the Bungo Channel over 15 years as inferred from GNSS data (1996-2011)

Takatoshi Yokoi[1], *SHINICHI MIYAZAKI[1], Hiromu Sakaue[1], Jun'ichi Fukuda[2] (1.Graduate School of Science, Kyoto University, 2.Earthquake Research Institute, The University of Tokyo)

[SCG48-P42] Investigations of sensor orientation and a possibility of detecting crustal deformation based on accelerometer records of S-net

*Ryota Takagi[1], Naoki Uchida[1], Takashi NAKAYAMA[1], Ryosuke Azuma[1], Akira Ishigami[1], Tomomi Okada[1], Yusaku Ohta[1], Ryota Hino[1] (1.Research Center for Prediction of Earthquakes and Volcanic Eruptions, Graduate School of Science, Tohoku University)

[SCG48-P43] Spatiotemporal variation of released seismic energy from shallow low-frequency tremor in Hyuga-nada, revealed by ocean bottom seismological observation

*Yusuke Yamashita[1], Saki Watanabe[2], Tomoaki Yamada[3], Masanao Shinohara[3], Takeshi Matsushima[2] (1.Disaster Prevention Research Institute, Kyoto University, 2.Institute of Seismology and Volcanology, Kyushu University, 3.Earthquake Research Institute, The University of Tokyo)

[SCG48-P44] Unified description of fast and slow earthquakes using velocity strengthening patches

*So Ozawa[1], Takahiro Hatano[1] (1.Earthquake Research Institute, the University of Tokyo)

[SCG48-P45] The b-value of the earthquake swarm activities accompanied by the Boso slow slip events

*Yuki Noda[1], Hitoshi Hirose[2,1] (1.Department of Planetology, Faculty of Science, Kobe University , 2.Research Center for Urban Safety and Security, Kobe University)

[SCG48-P46] **Three-dimensional thermal modeling associated with subduction of the Philippine Sea plate at the Ryukyu Trench, and its relation to the occurrence of interplate seismic events**

*Nobuaki Suenaga[1], Shoichi Yoshioka[2,1], Yinfeng Ji[3] (1.Graduate School of Science, Kobe University, Japan, 2.Research Center for Urban Safety and Security, Kobe University, Japan, 3.Chinese Academy of Science, Beijin, China)

[E] Poster | S (Solid Earth Sciences)：S-CG Complex & General

5:15 PM - 6:30 PM JST | 8:15 AM - 9:30 AM UTC | Poster Hall International Exhibition Hall8, Makuhari Messe_33

[S-CG48] Science of slow earthquakes: Toward unified understandings of whole earthquake process

convener:Satoshi Ide(Department of Earth an Planetary Science, University of Tokyo), Hitoshi Hirose(Research Center for Urban Safety and Security, Kobe University), Kohtaro Ujiie(Graduate School of Life and Environmental Sciences, University of Tsukuba), Takahiro Hatano(Earthquake Research Institute, University of Tokyo)

[SCG48-P01] Off the Kii Peninsula Shallow Low Frequency Earthquake in 2004 revealed by Ocean Bottom Seismometer

*Koji Tamaribuchi[1], Akio Kobayashi[1], Takahito Nishimiya[1], Satoshi Annoura[2] (1.Meteorological Research Institute, 2.Japan Meteorological Agency)

[SCG48-P02] The development of pressure vessel on gouges for rock deformation at seismic rates under water-saturated conditions

*Wei-Ting Lin[1], Li-Wei Kuo[1], Wen-Jie Wu[1], Jia-Jyun Dong[1], Yi-Hung Huang[2] (1.National Central University, 2.MATSUKI HYDRAULIC INDUSTRIAL CO. LTD)

[SCG48-P03] Spatial variations of shallow very low-frequency earthquake activity along the Nankai Trough based on CMT inversion using the 3D heterogeneous model

*Shunsuke Takemura[1], Takanori Matsuzawa[1], Akemi Noda[1], Takashi Tonegawa[2], Youichi Asano[1], Takeshi Kimura[1], Katsuhiko Shiomi[1] (1.National Research Institute for Earth Science and Disaster Resilience, 2.Japan Agency for Marine-Earth Science and Technology)

[SCG48-P04] Evaluation of Magnitude and Characteristics of Seismicity of Low Frequency Earthquakes in Parkfield

*Miki Aso[1,3], Naofumi Aso[2], Satoshi Ide[1] (1.Department of Earth and Planetary Science, The University of Tokyo, 2.Tokyo Institute of Technology, School of Science, 3.OYO RMS Corporation)

[SCG48-P05] Tectonic tremor catalog in the Tohoku-Hokkaido-Oki region using S-net

*Satoshi Ide[1], Tomoaki Nishikawa[2], Takanori Matsuzawa[3], Kazuaki Ohta[2], Naoki Uchida[4], Takuya NISHIMURA[2] (1.Department of Earth an Planetary Science, University of Tokyo, 2.Disaster Prevention Research Institute, Kyoto University, 3.National Research Institute for Earth Science and Disaster Resilience, 4.Graduate School of Science and International Research Institute of Disaster Science, Tohoku University)

[SCG48-P06] **Spontaneous Slow Slip and Runaway Slip in Laboratory**

*Miki Takahashi[1] (1.Institute of Earthquake and Volcano Geology, Geological Survey of Japan, AIST)

[SCG48-P07] Hydration and amorphization of quartz rocks during high-velocity frictional sliding: An examination of fault gouge from friction experiments of synthetic quartz

*Yuko Onoe[1], Hirotaka Iida[2], Akito Tsutsumi[1], Aki Takigawa[1] (1.Graduate School of Science, Kyoto University, 2.Geothermal Engineering Co., Ltd.)

[SCG48-P08] Constraining S Wave Velocity of the Source Region of Shallow Very Low-Frequency Earthquakes

*Takeshi Akuhara[1], Takashi Tonegawa[2] (1.Earthquake Research Institute, The University of Tokyo, 2.Research and Development center for Earthquake and Tsunami, Japan Agency for Marine-Earth Science and Technology)

[SCG48-P09] **Quantitative relationship between aseismic slip propagation speed and frictional properties**

*Keisuke Ariyoshi[1], Jean-Paul Ampuero[2,3], Roland Burgmann[4], Toru Matsuzawa[5], Akira Hasegawa[5], Ryota Hino[5], Takane Hori[1] (1.Japan Agency for Marine-Earth Science and Technology, 2.Université Côte d'Azur, 3.California Institute of Technology, 4.University of California, Berkeley, 5.Graduate School of Science, Tohoku University)

[SCG48-P10] Comprehensive detection of very low frequency earthquakes off the Pacific coasts of Hokkaido and Tohoku, northeastern Japan

*Satoru Baba[1], Akiko Takeo[1], Kazushige Obara[1], Takanori Matsuzawa[2], Takuto Maeda[3] (1.Earthquake Research Institute, University of Tokyo, 2.National Research Institute for Earth Science and Disaster Resilience, 3.Graduate School of Science and Technology, Hirosaki University)

[SCG48-P11] **Spatio-temporal evolution of long- and short-term slow slip events in the Tokai region, central Japan estimated from a very dense GNSS network, during 1997-2017**

*Hiromu Sakaue[1], Takuya NISHIMURA[2], Jun'ichi Fukuda[3], Teruyuki Kato[4] (1.Graduate School of Science, Kyoto University, 2.Disaster Prevention Research Institute Kyoto University, 3.Earthquake Research Institute,The University of Tokyo, 4.Hot Springs Research Institute of Kanagawa Prefecture)

[SCG48-P12] Broadband excitation of acoustic emission in granular stick-slip : experiments and spectral analyses

*Hidekazu Fukumizu[1], Ikuro Sumita[2] (1.Earth and Environmental Science Course, Division of Natural System, Graduate school of Natural Science and Technology, Kanazawa University, 2.School of Geosciences and Civil Engineering, Kanazawa University)

[SCG48-P13] Episodic tremor and slip silently invades strongly locked megathrust in the Nankai Trough

*Masayuki Kano[1], Aitaro Kato[2], Kazushige Obara[2] (1.Graduate school of science, Tohoku University, 2.Earthquake Research Institute, The University of Tokyo)

[SCG48-P14] Spatial distribution of the electrical resistivity beneath western part of Shikoku Island where long-term SSE events have repeatedly occurred

*Makoto Uyeshima[1], Maki Hata[1], Hiroshi Ichihara[2], Ryokei Yoshimura[3], Koki Aizawa[4] (1.Earthquake Research Institute, The University of Tokyo, 2.Graduate School of Environmental Studies, Nagoya University, 3.Disaster Prevention Research Institute, Kyoto University, 4.Institute of Seismology and Volcanology, Faculty of Sciences, Kyushu University)

[SCG48-P15] Variations of scaling relationships for shallow tremor observed along the Nankai trough

*Masaru Nakano[1], Suguru Yabe[1] (1.Japan Agency for Marine-Earth Science and Technology)

[SCG48-P16] Low-frequency earthquakes triggered by teleseismic surface waves by Ryukyu subduction zone.

Ayumi Kinjo[1], *Mamoru Nakamura[1] (1.Faculty of Science, University of the Ryukyus)

[SCG48-P17] Detection of small surface displacement accompanying deep low-frequency tremor in Shikoku region, southwest Japan

*Yutaro Okada[1], Takao Tabei[2] (1.Faculty of Science, Kochi University, 2.Faculty of Science and Technology, Kochi University)

[SCG48-P18] Long-term temporal change in crustal resistivity beneath western Shikoku

*Futoshi Yamashita[1], Yoshimori Honkura[1] (1.National Research Institute for Earth Science and Disaster Resilience)

[SCG48-P19] Slow decay of postseismic deformation compared with aftershocks following the 2011 Tohoku-oki Earthquake

*Yuta Mitsui[1], Shunsuke Morikami[2] (1.Department of Geosciences, Shizuoka University, 2.Formerly at Graduate School of Science and Technology, Shizuoka University)

[SCG48-P20] Serpentinite dehydration in subduction shear zones formed at source depths of slow earthquakes

*Yasushi Mori[1], Miki Shigeno[1], Kohtaro Ujiie[2], Kazuya Noro[2], Tadao Nishiyama[3] (1.Kitakyushu Museum of Natural History and Human History, 2.University of Tsukuba, 3.Kumamoto University)

[SCG48-P21] Earthquake swarms following very low-frequency earthquakes in the central Ryukyu Trench

*Mamoru Nakamura[1] (1.Faculty of Science, University of the Ryukyus)

[SCG48-P22] Seismic imaging in the central Nankai trough, off Shionomisaki to Kii channel

*Yasuyuki Nakamura[1], Shuichi Kodaira[1], Tetsuo No[1], Yuka Kaiho[1], Gou Fujie[1], Seiichi Miura[1], Kazuya Shiraishi[1] (1.Japan Agency for Marine Earth Science and Technology)

[SCG48-P23] Attempt to Detect Intra-plate SSEs Based on F3 Solution of GEONET

*Yusaku Tanaka[1] (1.Earthquake Research Institute)

[SCG48-P24] A new hydrothermal, low to high speed rotary-shearing apparatus: Reproduction of slow/megathrust earthquakes in laboratory

*Takehiro Hirose[1], Wataru Tanikawa[1], Yohei Hamada[1], Keishi Okazaki[1] (1.Kochi Institute for Core Sample Research, Japan Agency for Marine-Earth Science and Technology)

[SCG48-P25] Very low-frequency earthquakes in western Shikoku remotely triggered by the 2016 Mw5.9 off-Kii Peninsula earthquake

*Masatoshi Miyazawa[1] (1.Disaster Prevention Research Institute, Kyoto University)

[SCG48-P26] **Underground structure around source region of slow earthquakes in western Shikoku obtained by receiver function analysis**

Akira Hikita[1], Aitaro Kato[1], *Kazushige Obara[1], Akiko Takeo[1], Takeshi Akuhara[1] (1.Earthquake Research Institute, The University of Tokyo)

[SCG48-P27] Hypocenter determination of deep low frequency tremors beneath the Kii Peninsula by backprojection of seismic array data

*Kodai Sagae[1], Hisashi Nakahara[1], Takeshi Nishimura[1], Kazutoshi Imanishi[2] (1.Graduate School of Science,Tohoku University, 2.National Institute of Advanced Industrial Science and Technology (AIST))

[SCG48-P28] Triggered tremors and stress perturbations due to surface waves

*Ryohei Ikeda[1], Naoki Suda[1] (1.Hiroshima University)

[SCG48-P29] Numerical modeling of long- and shallow slow slip events including shallow region in Hyuganada and western Nankai, Japan

*Takanori Matsuzawa[1], Bunichiro Shibazaki[2] (1.National Research Institute for Earth Science and Disaster Resilience, 2.Building Research Institute)

[SCG48-P30] Further evidence for the influence of a subducting-ridge on the spatial strain accumulation and release pattern in the shallow eastern Nankai Trough, based on VLFE distribution

*Akiko Toh[1], Chen Wan-Jou [2], Doug Dreger[3], Wu-Cheng Chi[2], Satoshi Ide[1] (1.University of Tokyo, 2.Institute of Earth Sciences, Academia Sinica, 3.UC Berkeley)

[SCG48-P31] Evidence for semi-brittle flow in mantle-wedge serpentinites under high pore fluid pressure and their implications for deep low frequency earthquakes

Kengo Kataoka[1], Yurina Nagata[1], *Ken-ichi Hirauchi[1], Ryosuke Oyanagi[2], Atsushi Okamoto[3], Katsuyoshi Michibayashi[4] (1.Department of Geosciences, Faculty of Science, Shizuoka University, 2.Japan Agency for Marine-Earth Science and Technology, 3.Graduate School of Environmental studies, Tohoku University, 4.Department of Earth and Planetary Sciences, Nagoya University)

[SCG48-P32] Spatial distribution of slow slip events off the Boso peninsula from 1996 to 2018 under sparsity constraints

*Ryoko Nakata[1], Hideitsu Hino[2], Tatsu Kuwatani[3,4], Takahiro Akiyama[5], Shoichi Yoshioka[6], Masato Okada[7], Takane Hori[1] (1.Japan Agency for Marine-Earth Science and Technology, 2.The Institute of Statistical Mathematics, 3.Department of Solid Earth Geochemistry, Japan Agency for Marine-Earth Science and Technology, 4.PRESTO, Japan Science and Technology Agency, 5.Graduate School of Science, Kobe University, 6.Research Center for Urban Safety and Security, Kobe University, 7.Graduate School of Frontier Sciences, The University of Tokyo)

[SCG48-P33] Marine electromagnetic observations around a slow earthquake region in the western Nankai trough

*Hiroshi Ichihara[1], Tada-nori Goto[2], Tetsuo Matsuno[3], Noriko Tada[4], Shinya Sato[2] (1.Earthquake and Volcano Research Center, Nagoya University, 2.Graduate School of Engineering, Kyoto University, 3.Ocean Bottom Exploration Center, Kobe University, 4.JAMSTEC)

[SCG48-P34] Dynamics of precipitating injection fronts inside of structured medium

*Yutaka Sumino[1], Shunsuke Tanaka[1], Miyuki Kunihiro[1] (1.Tokyo University of Science)

[SCG48-P35] Permeability changes of simulated low permeable fault rocks induced by intermediate velocity friction test

*Wataru Tanikawa[1] (1.Japan Agency for Marine-Earth Science and Technology, Kochi Instutute for Core Sample Research)

[SCG48-P36] Modified relation between the coupling and tremor rates around the Shikoku region

*Tadafumi Ochi[1] (1.Institute of Earthquake and Volcano Geology, Geological Survey of Japan, The National Institute of Advanced Industrial Science and Technology)

[SCG48-P37] Spatiotemporal distribution of regular and very low-frequency earthquakes in the northern part of the Ryukyu subduction zone

*Youichi Asano[1], Kazuhiko Goto[2], Hiroshi Yakiwara[3], Shuichiro Hirano[3] (1.National Research Institute for Earth Science and Disaster Resilience, 2.Association for the development of earthquake prediction, 3.Nansei-toko Observatory for Earthquakes and Volcanoes, Kagoshima University)

[SCG48-P38] Possible tectonic tremor activities near the VLFE epicenters in the Sanriku-Oki region in 2011

*Hidenobu Takahashi[1], Ryota Hino[1], Yusaku Ohta[1], Naoki Uchida[1], Syuichi Suzuki[1], Masanao Shinohara[2], Takanori Matsuzawa[3] (1.Graduate school of Science Tohoku University , 2.Earthquake Research Institute, University of Tokyo, 3.National Research Institute for Earth Science and Disaster Resilience)

[SCG48-P39] Heterogeneous structure around a region of slow earthquake activity off Ibaraki prefecture along the Japan Trench

*Kimihiro Mochizuki[1], Tomoaki Yamada[1], Masanao Shinohara[1], Ryota Hino[2], Ryosuke Azuma[2], Yoshihiro Ito[3], Yoshio Murai[4], Kenji Uehira[5], Toshinori Sato[6] (1.ERI, Univ. of Tokyo, 2.Graduate School of Science, Tohoku Univ., 3.DPRI, Kyoto Univ., 4.Faculty of Science, Hokkaido Univ., 5.NIED, 6.Graduate School of Science, Chiba Univ.)

[SCG48-P40] Shallow low-frequency tremor triggered by nearby moderate earthquakes off Sanriku

*Sachiko Tanaka[1], Takanori Matsuzawa[1], Youichi Asano[1] (1.National Research Institute for Earth Science and Disaster Resilience)

[SCG48-P41] Slow slip events in the Bungo Channel over 15 years as inferred from GNSS data (1996-2011)

Takatoshi Yokoi[1], *SHINICHI MIYAZAKI[1], Hiromu Sakaue[1], Jun'ichi Fukuda[2] (1.Graduate School of Science, Kyoto University, 2.Earthquake Research Institute, The University of Tokyo)

[SCG48-P42] Investigations of sensor orientation and a possibility of detecting crustal deformation based on accelerometer records of S-net

*Ryota Takagi[1], Naoki Uchida[1], Takashi NAKAYAMA[1], Ryosuke Azuma[1], Akira Ishigami[1], Tomomi Okada[1], Yusaku Ohta[1], Ryota Hino[1] (1.Research Center for Prediction of Earthquakes and Volcanic Eruptions, Graduate School of Science, Tohoku University)

[SCG48-P43] Spatiotemporal variation of released seismic energy from shallow low-frequency tremor in Hyuga-nada, revealed by ocean bottom seismological observation

*Yusuke Yamashita[1], Saki Watanabe[2], Tomoaki Yamada[3], Masanao Shinohara[3], Takeshi Matsushima[2] (1.Disaster Prevention Research Institute, Kyoto University, 2.Institute of Seismology and Volcanology, Kyushu University, 3.Earthquake Research Institute, The University of Tokyo)

[SCG48-P44] Unified description of fast and slow earthquakes using velocity strengthening patches

*So Ozawa[1], Takahiro Hatano[1] (1.Earthquake Research Institute, the University of Tokyo)

[SCG48-P45] The b-value of the earthquake swarm activities accompanied by the Boso slow slip events

*Yuki Noda[1], Hitoshi Hirose[2,1] (1.Department of Planetology, Faculty of Science, Kobe University , 2.Research Center for Urban Safety and Security, Kobe University)

[SCG48-P46] **Three-dimensional thermal modeling associated with subduction of the Philippine Sea plate at the Ryukyu Trench, and its relation to the occurrence of interplate seismic events**

*Nobuaki Suenaga[1], Shoichi Yoshioka[2,1], Yinfeng Ji[3] (1.Graduate School of Science, Kobe University, Japan, 2.Research Center for Urban Safety and Security, Kobe University, Japan, 3.Chinese Academy of Science, Beijin, China)

[E] Oral | S (Solid Earth Sciences)：S-CG Complex & General

1:45 PM - 3:15 PM JST | 4:45 AM - 6:15 AM UTC | Convention Hall A 2F

[S-CG48] Science of slow earthquakes: Toward unified understandings of whole earthquake process

convener:Satoshi Ide(Department of Earth an Planetary Science, University of Tokyo), Hitoshi Hirose(Research Center for Urban Safety and Security, Kobe University), Kohtaro Ujiie(Graduate School of Life and Environmental Sciences, University of Tsukuba), Takahiro Hatano(Earthquake Research Institute, University of Tokyo), Chairperson:Kazushige Obara(Earthquake Research Institute, University of Tokyo), Aitaro Kato(Earthquake Research Institute, University of Tokyo)

1:45 PM - 2:00 PM JST | 4:45 AM - 5:00 AM UTC

[SCG48-06] Interplay between long-term SSE and ETS facilitated by different underground environment

*Kazushige Obara[1] (1.Earthquake Research Institute, The University of Tokyo)

2:00 PM - 2:15 PM JST | 5:00 AM - 5:15 AM UTC

[SCG48-07] **Determination of sVLFE epicenters around the subducted Kyushu-Palau Ridge from coda interferometry**

*Takashi Tonegawa[1], Yusuke Yamashita[2], Aki Ito[1], Masanao Shinohara[3], Daisuke Suetsugu[1], Tsutomu Takahashi[1], Yasushi Ishihara[1], Shuichi Kodaira[1], Yoshiyuki Kaneda[4] (1.JAMSTEC, 2.DPRI, Kyoto University, 3.ERI, The University of Tokyo, 4.Kagawa University)

2:15 PM - 2:30 PM JST | 5:15 AM - 5:30 AM UTC

[SCG48-08] Detection of slow earthquakes in the microseism frequency band (0.05–1.0 Hz) by large-scale waveform stacking

*Koki Masuda[1], Satoshi Ide[1], Kazuaki Ohta[2] (1.Department of Earth an Planetary Science, University of Tokyo, 2.Disaster Prevention Research Institute, Kyoto University)

2:30 PM - 2:45 PM JST | 5:30 AM - 5:45 AM UTC

[SCG48-09] Source characteristics of low-frequency earthquakes in Nankai subduction zone inferred from analysis of large event dataset

*Natalia Poiata[1], Mariano Supino[1,2], Gaetano Festa[2], Jean-Pierre Vilotte[1], Kazushige Obara[3] (1.Institut de Physique du Globe de Paris, 2.Università degli Studi di Napoli “ Federico II ”, Napoli, Italy, 3.Earthquake Research Institute, University of Tokyo, Japan)

2:45 PM - 3:00 PM JST | 5:45 AM - 6:00 AM UTC

[SCG48-10] **High-frequency radiation prior to semi-volcanic low-frequency earthquake in Eastern Shimane, SW Japan, illuminated by “0.1 manten” Hyper Dense Seismic Observation**

*Aitaro Kato[1], Shin'ichi Sakai[1], Satoshi Matsumoto[2], Yoshihisa Iio[3] (1.Earthquake Research Institute, the University of Tokyo, 2.Kyushu University, 3.Kyoto University)

3:00 PM - 3:15 PM JST | 6:00 AM - 6:15 AM UTC

[SCG48-11] Variation of Focal Mechanisms of Low Frequency Earthquakes in Parkfield

*Miki Aso[1,3], Naofumi Aso[2], Satoshi Ide[1] (1.Department of Earth and Planetary Science, The University of Tokyo, 2.Tokyo Institute of Technology, School of Science , 3.OYO RMS Corporation)

[E] Oral | S (Solid Earth Sciences)：S-CG Complex & General

3:30 PM - 5:00 PM JST | 6:30 AM - 8:00 AM UTC | Convention Hall A 2F

[S-CG48] Science of slow earthquakes: Toward unified understandings of whole earthquake process

convener:Satoshi Ide(Department of Earth an Planetary Science, University of Tokyo), Hitoshi Hirose(Research Center for Urban Safety and Security, Kobe University), Kohtaro Ujiie(Graduate School of Life and Environmental Sciences, University of Tsukuba), Takahiro Hatano(Earthquake Research Institute, University of Tokyo), Chairperson:Satoshi Ide(Graduate School of Science, University of Tokyo), Kazuaki Ohta

3:30 PM - 4:00 PM JST | 6:30 AM - 7:00 AM UTC

[SCG48-12] Mapping seismic data to slow slip using machine learning

★Invited Papers

*Bertrand Rouet-Leduc[1], Claudia Hulbert[2], Ian McBrearty[1], Paul Johnson[1] (1.Los Alamos National Laboratory, USA, 2.Ecole Normale Superieure, France)

4:00 PM - 4:15 PM JST | 7:00 AM - 7:15 AM UTC

[SCG48-13] Revealing the slow earthquake activity in the Japan Trench and its relation to the 2011 Tohoku-Oki earthquake

*Tomoaki Nishikawa[1], Takanori Matsuzawa[2], Kazuaki Ohta[1], Naoki Uchida[3], Takuya NISHIMURA[1], Satoshi Ide[4] (1.Disaster Prevention Research Institute, Kyoto University, 2.National Research Institute for Earth Science and Disaster Resilience, 3.Graduate School of Science, Tohoku University, 4.Graduate School of Science, The University of Tokyo)

4:15 PM - 4:30 PM JST | 7:15 AM - 7:30 AM UTC

[SCG48-14] Tremor and slow slip associated with afterslip of the 2011 Tohoku earthquake

*Kazuaki Ohta[1], Yoshihiro Ito[1], Ryota Hino[2], Shukei Ohyanagi[1], Takanori Matsuzawa[3], Masanao Shinohara[4], Hajime Shiobara[4] (1.Disaster Prevention Research Institute, Kyoto University, 2.Graduate School of Science, Tohoku University, 3.National Research Institute for Earth Science and Disaster Resilience, 4.Earthquake Research Institute, the University of Tokyo)

4:30 PM - 4:45 PM JST | 7:30 AM - 7:45 AM UTC

[SCG48-15] High definition imaging of the Japan Trench by OBS Array of Arrays: Does shallow tectonic tremor occur in the plate interface?

*Shukei Ohyanagi[1], Kazuaki Ohta[2], Yoshihiro Ito[2], Ryota Hino[3], Yusaku Ohta[3], Ryosuke Azuma[3], Masanao Shinohara[4], Kimihiro Mochizuki[4], Toshinori Sato[5], Yoshio Murai[6] (1.Kyoto University, Graduate School of Science, 2.Kyoto University, Disaster Prevention Research Institute, 3.Tohoku University, 4.Tokyo University, Earthquake Research Institute, 5.Chiba University, 6.Hokkaido University)

4:45 PM - 5:00 PM JST | 7:45 AM - 8:00 AM UTC

[SCG48-16] The activity of small repeating earthquakes after the 2011 Tohoku-oki earthquake: an examination based on the S-net and land networks

*Naoki Uchida[1], Ryota Takagi[1], Satoshi Hirahara[1], Takashi NAKAYAMA[1], Toru Matsuzawa[1], Sachiko Tanaka[2], Youichi Asano[2] (1.Research Center for Prediction of Earthquakes and Volcanic Eruptions Graduate School of Science, Tohoku University, 2.National Research Institute for Earth Science and Disaster Resilience)

[J] Oral | S (Solid Earth Sciences)：S-CG Complex & General

9:00 AM - 10:30 AM JST | 12:00 AM - 1:30 AM UTC | A09 TOKYO BAY MAKUHARI HALL

[S-CG57] Structure and evolution of Japanese islands - Formation of island arc systems and earthquake cycles

convener:Hiroshi Sato(Earthquake Prediction Research Center, Earthquake Research Institute, The University of Tokyo), Masanao Shinohara(Earthquake Research Institute, University of Tokyo), Masahiro Ishikawa(Graduate School of Environment and Information Sciences Yokohama National University), Makoto MATSUBARA(National Research Institute for Earth Science and Disaster Resilience), Chairperson:Masanao Shinohara(Earthquake Research Institute, The University of Tokyo), Tatsuya Ishiyama(Earthquake Research Institute, University of Tokyo)

9:00 AM - 9:15 AM JST | 12:00 AM - 12:15 AM UTC

[SCG57-01] Recent Earthquake Activity in Northern Hokkaido, Japan

Cancelled

*Tetsuo Takanami[1,2] (1.Carnegie Institution for Science, 2.Hokkaido Research Center of Geology)

9:15 AM - 9:30 AM JST | 12:15 AM - 12:30 AM UTC

[SCG57-02] Seismic constraints on the crustal structure off the southwestern coast of Hokkaido, Japan Sea

*Tetsuo No[1], Takeshi Sato[1], Shuichi Kodaira[1], Hiroshi Sato[2], Tatsuya Ishiyama[2] (1.JAMSTEC, 2.ERI, University of Tokyo)

9:30 AM - 9:45 AM JST | 12:30 AM - 12:45 AM UTC

[SCG57-03] Deep seismic reflection profiling across the Oshima Peninsula, SW Hokkaido, Japan

*Hiroshi Sato[1], Tatsuya Ishiyama[1], Naoko Kato[1], Hidehiko Shimizu[2], Takeshi Sato[3], Shinji Kawasaki[2], Tetsuo No[3], Shuichi Kodaira[3], Seiichi Miura[3] (1.Earthquake Research Institute, The University of Tokyo, 2.JGI Inc, 3.Japan Agency for Marine-Earth Acience and Technology)

9:45 AM - 10:00 AM JST | 12:45 AM - 1:00 AM UTC

[SCG57-04] Crustal deformation and stress accumulation on source faults around Hokkaido, Japan, due to coupling at the Kuril trench

*Akinori Hashima[1], Hiroshi Sato[1], Tatsuya Ishiyama[1], Andrew M. Freed[2] (1.Earthquake Research Institute, The University of Tokyo, 2.Purdue University)

10:00 AM - 10:15 AM JST | 1:00 AM - 1:15 AM UTC

[SCG57-05] Structural Heterogeneity in and around the Source Region of the 2018 Hokkaido Eastern Iburi Earthquake, Central Hokkaido, Japan

*Takaya Iwasaki[1], Noriko Tsumura[2], Tanio Ito[3], Kazunori Arita[4], Makoto Matsubara[5], Hiroshi Sato[1], Eiji Kurashimo[1], Naoshi Hirata[1], Susumu Abe[6], Katsuya Noda[7], Akira Fujiwara[8], Shinsuke Kikuchi[9], Kazuko Suzuki[10] (1.Eathquake Research Institute, the University of Tokyo, 2.Graduate School of Science, Chiba University, 3.Association for the Development of Earthquake Prediction, 4.Hokkaido Research Center of Geology, 5.National Research Institute for Earth Science and Disaster Resilience, 6.JAPEX, 7.GEOSYS Inc., 8.JOGMEC, 9.JGI Inc., 10.Schlumberger Ltd.)

10:15 AM - 10:30 AM JST | 1:15 AM - 1:30 AM UTC

[SCG57-06] Electrical resistivity distribution around the middle axis of Hokkaido Island: constraint for tectonics of ultra-mafic rocks

*Hiroshi Ichihara[1], Toru Mogi[1], Yusuke Yamaya[2] (1.Earthquake and Volcano Research Center, Nagoya University, 2.AIST)

[J] Oral | S (Solid Earth Sciences)：S-CG Complex & General

10:45 AM - 12:15 PM JST | 1:45 AM - 3:15 AM UTC | A09 TOKYO BAY MAKUHARI HALL

[S-CG57] Structure and evolution of Japanese islands - Formation of island arc systems and earthquake cycles

convener:Hiroshi Sato(Earthquake Prediction Research Center, Earthquake Research Institute, The University of Tokyo), Masanao Shinohara(Earthquake Research Institute, University of Tokyo), Masahiro Ishikawa(Graduate School of Environment and Information Sciences Yokohama National University), Makoto MATSUBARA(National Research Institute for Earth Science and Disaster Resilience), Chairperson:Hiroshi Sato(Earthquake Research Institute, Tokyo University), Masahiro Ishikawa(Yokohama National University)

10:45 AM - 11:00 AM JST | 1:45 AM - 2:00 AM UTC

[SCG57-07] Three-dimensional seismic velocity structure beneath and around Japanese Islands including beneath the Pacific Ocean using NIED S-net data

*Makoto MATSUBARA[1], Hiroshi Sato[2], Kenji Uehira[1], Masashi Mochizuki[4], Toshihiko Kanazawa[5], Narumi Takahashi[1], Kensuke Suzuki[3], Shinichiro Kamiya[1] (1.National Research Institute for Earth Science and Disaster Resilience, 2.Earthquake Research Institute, the University of Tokyo, 3.Japan Agency for Marine-Earth Science and Technology, 4.Ministry of Education, Culture, Sports, Science and Technology, Japan , 5.Association for the Development of Earthquake Prediction)

11:00 AM - 11:15 AM JST | 2:00 AM - 2:15 AM UTC

[SCG57-08] Spatio-temporal extent of Cretaceous fore-arc basin in Japan

*Yukio Isozaki[1], Ryo Hasegawa[1], Yukiyasu Tsutsumi[1] (1.Department of Earth Science and Astronomy, Multi-disciplinary Sciences - General Systems Studies, Graduate School of Arts and Sciences, The University of Tokyo)

11:15 AM - 11:30 AM JST | 2:15 AM - 2:30 AM UTC

[SCG57-09] Geotectonic identities of dismembered ancient fore-arc clastics: U-Pb dating of detrital zircons in Cretaceous-Paleogene shallow marine/fluvial sandstones sporadically found in Kanto, central Japan

*Ryo Hasegawa[1], Yukio Isozaki[1], Yukiyasu Tsutsumi[2] (1.Department of Earth Science and Astronomy, The University of Tokyo, 2.Department of Geology and Paleontology, National Museum of Nature and Science)

11:30 AM - 11:45 AM JST | 2:30 AM - 2:45 AM UTC

[SCG57-10] Laboratory Measurements of Vp, Vs and Vp/Vs for polycrystalline labradorite up to 800°C and 1GPa

*Satoko Honda[1], Masahiro Ishikawa[1] (1.Graduate School of Environment and Information Sciences, Yokohama National University)

11:45 AM - 12:00 PM JST | 2:45 AM - 3:00 AM UTC

[SCG57-11] Shallow to deeper structures of the Median Tectonic Line active fault system in Shikoku illuminated by new hi-resolution seismic reflection profiling, southwest Japan

*Tatsuya Ishiyama[1], Naoko Kato[1], Shin Koshiya[2], Hiroshi Sato[1], Makoto MATSUBARA[3], Tomoko Elizabeth Yano[3], Taro Koike[4], Katsuya Noda[4] (1.Earthquake Research Institute, University of Tokyo, 2.Department of Civil and Environmental Engineering, Faculty of Science and Engineering, Iwate University, 3.National Research Institute for Earth Science and Disaster Resilience, 4.Geosys, Inc.)

12:00 PM - 12:15 PM JST | 3:00 AM - 3:15 AM UTC

[SCG57-12] **Cenozoic evolution of the Tsushima Strait and the Fukue Basin, southern Sea of Japan: an interplay of tectonics, palaeo-environment, and volcanism**

*Johan S. Claringbould[1], Hiroshi Sato[1], Tatsuya Ishiyama[1], Anne Van Horne[1,2], Shinji Kawasaki[3], Susume Abe[4] (1.Earthquake Research Institute, The University of Tokyo, 2.Department of Geology and Geophysics, University of Wyoming, 3.JGI, Inc., 4.JAPEX)

[J] Poster | S (Solid Earth Sciences)：S-CG Complex & General

3:30 PM - 5:00 PM JST | 6:30 AM - 8:00 AM UTC | Poster Hall International Exhibition Hall8, Makuhari Messe_20

[S-CG57] Structure and evolution of Japanese islands - Formation of island arc systems and earthquake cycles

convener:Hiroshi Sato(Earthquake Prediction Research Center, Earthquake Research Institute, The University of Tokyo), Masanao Shinohara(Earthquake Research Institute, University of Tokyo), Masahiro Ishikawa(Graduate School of Environment and Information Sciences Yokohama National University), Makoto MATSUBARA(National Research Institute for Earth Science and Disaster Resilience)

[SCG57-P01] Crustal structure from the Japan Sea back-arc basin to the margin off SW Hokkaido deduced from the seismic survey

*Takeshi Sato[1], Tetsuo No[1], Shuichi Kodaira[1], Seiichi Miura[1], Tatsuya Ishiyama[2], Hiroshi Sato[2] (1.Research and Development Center for Earthquake and Tsunami, Japan Agency for Marine-Earth Science and Technology, 2.ERI, Univ. of Tokyo)

[SCG57-P02] Three-dimensional plate geometry model from the Nankai to the Ryukyu subduction zone

*Ayako Nakanishi[1], Tsutomu Takahashi[1], Yojiro Yamamoto[1], Mikiya Yamashita[1], Minako KATSUYAMA[1], Seiichi Miura[1], Narumi Takahashi[3,1], Hiromi Kamata[1], Shuichi Kodaira[1], Yoshiyuki Kaneda[2,1] (1.Japan Agency for Marine-Earth Science and Technology, 2.Kagawa University, 3.National Research Institute for Earth Science and Disaster Resilience)

[SCG57-P03] Trace elements and Sr-Nd-Hf-Pb isotopic composition of Miocene Tomari volcanic rocks, Shimokita Peninsula, Aomori, NE Japan

*Masataka Aizawa[1], Mitsuru Inaba[2], Satoshi Okamura[3,4], Ryuichi Shinjo[5] (1.Graduate School of Engineering and Sience, University of Ryukyus, 2.GeoPuck Association, 3.Hokkaido Education University, 4.Hokkaido Soil Research Co-op., 5.Faculty of Science, University of Ryukyus)

[SCG57-P04] Acceleration of oceanic plate following megathrust earthquakes

*Mohammad Yuzariyadi[1], Kosuke Heki[1] (1.Hokkaido University)

[SCG57-P05] 3D velocity model in the region of Nankai Trough

*Minako KATSUYAMA[1], Ayako Nakanishi[1], Rei Arai[1], Shigeyoshi Tanaka[1], Narumi Takahashi[2], Hiromi Kamata[1], Yoshiyuki Kaneda[3] (1.Japan Agency for Marine-Earth Science and Technology, 2.National Research Institute for Earth Science and Disaster Resilience, 3.Kagawa University)

[SCG57-P06] Depth of seismogenic layer at the 2018 North Osaka and the 2018 Hokkaido Eastern Iburi earthquake sites

*Tomoko Elizabeth Yano[1], Makoto MATSUBARA[1] (1.National Research Institute of Earth Science and Disaster Prevention)

[SCG57-P07] Seismic reflection profiling across the Median Tectonic Line (MTL) active fault system in Ehime and Tokushima Prefectures

*Naoko Kato[1], Tatsuya Ishiyama[1], Hiroshi Sato[1], Shin Koshiya[2], Taro Koike[3], Katsuya Noda[3] (1.Earthquake Research Institute,University of Tokyo, 2.Faculty of science and engineering, Iwate University, 3.Geosys, Inc.)

[J] Poster | S (Solid Earth Sciences)：S-CG Complex & General

5:15 PM - 6:30 PM JST | 8:15 AM - 9:30 AM UTC | Poster Hall International Exhibition Hall8, Makuhari Messe_34

[S-CG57] Structure and evolution of Japanese islands - Formation of island arc systems and earthquake cycles

convener:Hiroshi Sato(Earthquake Prediction Research Center, Earthquake Research Institute, The University of Tokyo), Masanao Shinohara(Earthquake Research Institute, University of Tokyo), Masahiro Ishikawa(Graduate School of Environment and Information Sciences Yokohama National University), Makoto MATSUBARA(National Research Institute for Earth Science and Disaster Resilience)

[SCG57-P01] Crustal structure from the Japan Sea back-arc basin to the margin off SW Hokkaido deduced from the seismic survey

*Takeshi Sato[1], Tetsuo No[1], Shuichi Kodaira[1], Seiichi Miura[1], Tatsuya Ishiyama[2], Hiroshi Sato[2] (1.Research and Development Center for Earthquake and Tsunami, Japan Agency for Marine-Earth Science and Technology, 2.ERI, Univ. of Tokyo)

[SCG57-P02] Three-dimensional plate geometry model from the Nankai to the Ryukyu subduction zone

*Ayako Nakanishi[1], Tsutomu Takahashi[1], Yojiro Yamamoto[1], Mikiya Yamashita[1], Minako KATSUYAMA[1], Seiichi Miura[1], Narumi Takahashi[3,1], Hiromi Kamata[1], Shuichi Kodaira[1], Yoshiyuki Kaneda[2,1] (1.Japan Agency for Marine-Earth Science and Technology, 2.Kagawa University, 3.National Research Institute for Earth Science and Disaster Resilience)

[SCG57-P03] Trace elements and Sr-Nd-Hf-Pb isotopic composition of Miocene Tomari volcanic rocks, Shimokita Peninsula, Aomori, NE Japan

*Masataka Aizawa[1], Mitsuru Inaba[2], Satoshi Okamura[3,4], Ryuichi Shinjo[5] (1.Graduate School of Engineering and Sience, University of Ryukyus, 2.GeoPuck Association, 3.Hokkaido Education University, 4.Hokkaido Soil Research Co-op., 5.Faculty of Science, University of Ryukyus)

[SCG57-P04] Acceleration of oceanic plate following megathrust earthquakes

*Mohammad Yuzariyadi[1], Kosuke Heki[1] (1.Hokkaido University)

[SCG57-P05] 3D velocity model in the region of Nankai Trough

*Minako KATSUYAMA[1], Ayako Nakanishi[1], Rei Arai[1], Shigeyoshi Tanaka[1], Narumi Takahashi[2], Hiromi Kamata[1], Yoshiyuki Kaneda[3] (1.Japan Agency for Marine-Earth Science and Technology, 2.National Research Institute for Earth Science and Disaster Resilience, 3.Kagawa University)

[SCG57-P06] Depth of seismogenic layer at the 2018 North Osaka and the 2018 Hokkaido Eastern Iburi earthquake sites

*Tomoko Elizabeth Yano[1], Makoto MATSUBARA[1] (1.National Research Institute of Earth Science and Disaster Prevention)

[SCG57-P07] Seismic reflection profiling across the Median Tectonic Line (MTL) active fault system in Ehime and Tokushima Prefectures

*Naoko Kato[1], Tatsuya Ishiyama[1], Hiroshi Sato[1], Shin Koshiya[2], Taro Koike[3], Katsuya Noda[3] (1.Earthquake Research Institute,University of Tokyo, 2.Faculty of science and engineering, Iwate University, 3.Geosys, Inc.)

[J] Oral | B (Biogeosciences)：B-CG Complex & General

9:00 AM - 10:30 AM JST | 12:00 AM - 1:30 AM UTC | 201A 2F

[B-CG07] Decoding the history of Earth: From Hadean to the present

convener:Tsuyoshi Komiya(Department of Earth Science & Astronomy Graduate School of Arts and Sciences The University of Tokyo), Yasuhiro Kato(Department of Systems Innovation, Graduate School of Engineering, University of Tokyo), Katsuhiko Suzuki(Research and Development Center for Submarine Resources, Japan Agency for Marine-Earth Science and Technology), Chairperson:Tomohiko Sato(Earth-Life Science Institute, Tokyo Institute of Technology)

9:00 AM - 9:15 AM JST | 12:00 AM - 12:15 AM UTC

[BCG07-01] Iron-oxidizing bacteria and stromatolites in the Ediacaran hydrothermal carbonate

*Akihiro Kano[1], Aya Miyazaki[1], Jumpei Yoshioka[1], Ibtissam Chraiki[2], Abdelhafed Barzouk[2], Nasrrddine Youbi[2,3], Hassan Admou[2], Moulay Ahmed Boumehdi[2,3], Lhou Maacha[4], Hsaine Baoutoul[4], Ismail Bouskri[4] (1.Graduate School of Science, The University of Tokyo, 2.Department of Geology, Faculty of Sciences-Semlalia, Cadi Ayyad University, 3.Instituto Dom Luiz, Faculdade de Ciências, Universidade de Lisboa, 4.Managem-ONA Group)

9:15 AM - 9:30 AM JST | 12:15 AM - 12:30 AM UTC

[BCG07-02] Carbonate carbon isotope stratigraphy of the Paleoproterozoic Francevillian Group in Gabon

★Invited Papers

*Tomohiko Sato[1], Yusuke Sawaki[2], Hisashi Asanuma[2], Hisahiro Ueda[1], Shigenori Maruyama[1] (1.Tokyo Institute of Technology, 2.The University of Tokyo)

9:30 AM - 9:45 AM JST | 12:30 AM - 12:45 AM UTC

[BCG07-03] The redox condition of late Paleoproterozoic shallow marine environment: The Cape Smith Belt, Canada

*Kento Motomura[1], Shoichi Kiyokawa[1], Minoru Ikehara[2], Takashi Sano[4], Kentaro Tanaka[3], Tsubasa Miki[3], Yuji Sano[3] (1.Kyushu University, 2.Kochi University, 3.University of Tokyo, 4.National Museum of Nature and Science)

9:45 AM - 10:00 AM JST | 12:45 AM - 1:00 AM UTC

[BCG07-04] Paleovegetation changes reconstructed by terrestrial plant biomarker analyses in the sediments deposited across the Cenomanian/Turonian boundary in the Tomamae area, Hokkaido, Japan

*Masashi A. Ikeda[1], Ken Sawada[2], Takuto Ando[3], Hideto Nakamura[4], Reishi Takashima[5], Hiroshi Nishi[5] (1.Graduate School of Science, Hokkaido University, 2.Department of Earth and Planetary Sciences, Faculty of Science, Hokkaido University, 3.Arctic Research Center, Hokkaido University, 4.Faculty of Science, Osaka City University, 5.The Center for Academic Resources and Archives, The Tohoku University Museum, Tohoku University)

10:00 AM - 10:15 AM JST | 1:00 AM - 1:15 AM UTC

[BCG07-05] A general overview of the research progress on REY-rich mud

*Yasuhiro Kato[1,2], Kentaro Nakamura[1], Koichiro Fujinaga[2,1], Kazutaka Yasukawa[1,2], Yutaro Takaya[3,1,2], Junichiro Ohta[2,1], Erika Tanaka[1], Kazuhide Mimura[1], Koichi Iijima[4,1], Shiki Machida[2,1], Tatsuo Nozaki[4,1,2,5], Jun-Ichi Kimura[4], Hikaru Iwamori[1,4,6] (1.The University of Tokyo, 2.ORCeNG, Chiba Institute of Technology, 3.Waseda University, 4.JAMSTEC, 5.Kobe University, 6.Tokyo Institute of Technology)

10:15 AM - 10:30 AM JST | 1:15 AM - 1:30 AM UTC

[BCG07-06] A cold and alkaline Hadean ocean caused by impact ejecta weathering

*Shintaro Kadoya[1], David C Catling[1] (1.University of Washington)

[J] Oral | B (Biogeosciences) : B-CG Complex & General

10:45 AM - 12:15 PM JST | 1:45 AM - 3:15 AM UTC | 201A 2F

[B-CG07] Decoding the history of Earth: From Hadean to the present

convener:Tsuyoshi Komiya(Department of Earth Science & Astronomy Graduate School of Arts and Sciences The University of Tokyo), Yasuhiro Kato(Department of Systems Innovation, Graduate School of Engineering, University of Tokyo), Katsuhiko Suzuki(Research and Development Center for Submarine Resources, Japan Agency for Marine-Earth Science and Technology), Chairperson:Satoshi Yoshida(Department of Earth Science & Astronomy, Graduate School of Arts and Sciences, The University of Tokyo)

10:45 AM - 11:00 AM JST | 1:45 AM - 2:00 AM UTC

[BCG07-07] **Impact-induced magmatism on early Earth**

*Hiroshi Ohmoto[1], Uschi M. Graham[2], Yuya Tsukamoto[3], Yumiko Watanabe[3], Takeshi Kakegawa[3], Hiroshi Hamasaki[4], Andrew Chorney[5], Katherine Crispin[1], Zi-Kui Liu[1] (1.The Pennsylvania State University, 2.Univ. of Kentucky, 3.Tohoku Univ., 4.Tokyo Gas, 5.Temple Univ.)

11:00 AM - 11:15 AM JST | 2:00 AM - 2:15 AM UTC

[BCG07-08] An evaluation of impact dating for shocked zircons with planar features (PFs) in the Vredefort dome by LA-ICP-MS multi-spot analysis

*Shinji Yamamoto[1], Taiga Kato[1] (1.Graduate School of Environment and Information Sciences, Yohohama National University)

11:15 AM - 11:30 AM JST | 2:15 AM - 2:30 AM UTC

[BCG07-09] **Application of acid-washing to trace element and tungsten isotope analyses of Eoarchean rocks from the Isua Supracrustal Belt**

★Invited Papers

*Hatsuki Enomoto[1], Tsuyoshi Iizuka[1], Yoshitaka Homma[1] (1.Department of Earth and Planetary Science, Graduate School of Science, The University of Tokyo)

11:30 AM - 11:45 AM JST | 2:30 AM - 2:45 AM UTC

[BCG07-10] Limited primary production in the early Archean oceans and its biogeochemical consequenses

★Invited Papers

*Kazumi Ozaki[1] (1.Toho University)

11:45 AM - 12:00 PM JST | 2:45 AM - 3:00 AM UTC

[BCG07-11] Behaviors of carbon cycle system and inevitability of the hot climate in the Archean Earth

★Invited Papers

*Yasuto Watanabe[1], Eiichi Tajika[1], Kazumi Ozaki[2], Peng Hong[3] (1.The University of Tokyo, 2.Toho University, 3.Chiba Institute of Technology)

12:00 PM - 12:15 PM JST | 3:00 AM - 3:15 AM UTC

[BCG07-12] Occurrence and chemical composition of metamorphic carbonate rocks in the Isua supracrustal belt, West Greenland: Implications for the origin of carbonate rocks and compositions of the Eoarchean seawater.

*Yoshida Satoshi[1], Kazutaka Yasukawa[2], Yasuhiro Kato[2], Yusuke Sawaki[3], Tsuyoshi Komiya[3] (1.Department of Earth & Planetary Science, Graduate School of Science, The University of Tokyo, 2.Department of Systems Innovation, Graduate School of Engineering, University of Tokyo, 3.Department of Earth Science & Astronomy Graduate School of Arts and Sciences, The University of Tokyo)

[J] Poster | B (Biogeosciences)：B-CG Complex & General

3:30 PM - 5:00 PM JST | 6:30 AM - 8:00 AM UTC | Poster Hall International Exhibition Hall8, Makuhari Messe_21

[B-CG07] Decoding the history of Earth: From Hadean to the present

convener:Tsuyoshi Komiya(Department of Earth Science & Astronomy Graduate School of Arts and Sciences The University of Tokyo), Yasuhiro Kato(Department of Systems Innovation, Graduate School of Engineering, University of Tokyo), Katsuhiko Suzuki(Research and Development Center for Submarine Resources, Japan Agency for Marine-Earth Science and Technology)

[BCG07-P01] Geology of the Eoarchean Nuvvuagittuq supracrustal belt, northeastern Canada: Reappraisal of Protoliths and ages of the sedimentary rocks

*Tsuyoshi Komiya[1], Shinji Yamamoto[2], Hiroki Uehara[1], Yoshida Satoshi[1], Aoi Murakami[1], Yuki Ishihara[1] (1.Department of Earth Science & Astronomy Graduate School of Arts and Sciences The University of Tokyo, 2.Graduate School of Environment and Information Sciences, Yohohama National University)

[BCG07-P02] Behavior of phosphorus during hydrothermal alteration of basalt under CO_2-rich condition

*Aoi Murakami[1], Yusuke Sawaki[2], Hisahiro Ueda[3], Yuji Orihashi[4], Shiki Machida[5], Tsuyoshi Komiya[2] (1.Department of Earth and Planetary Science, Graduate School of Science, The University of Tokyo, 2.The University of Tokyo, 3.Tokyo Institute of Technology, 4.Hirosaki University, 5.Chiba Institute of Technology)

[BCG07-P03] Origin of chromitites in the Akulleq terrane, southern West Greenland

*Kanta Takahashi[1], Tomoaki Morishita[1], Juan Miguel Ramirez Guotana[1], Kenichiro Tani[2], Yumiko Harigane[3], Ikuya Nishio[1], Kristoffer Szilas[4], Akihiro Tamura[1] (1.Kanazawa University, 2.Department of Geology and Paleontology, National Museum of Nature and Science, 3.Geological Survey of Japan, National Institute of Advanced Industrial Science and Technology (AIST), 4.University of Copenhagen)

[BCG07-P04] Metamorphic P–T condition of the Inyoni shear zone rocks in the Barberton Greenstone Belt, South Africa and its significance

*Daichi Kato[1], Kazumasa Aoki[1], Yuta Tsuchiya[2], Shogo Aoki[2], Tsuyoshi Komiya[3] (1.Department of Applied Science,Okayama University of Science, 2.Department of Biosphere-Geosphere Science,Okayama University of Science, 3.Department of Earth Science and Astronomy,University of Tokyo)

[BCG07-P05] Discovery of possible traces of asteroid impact within the fossil-bearing carbonaceous chert from the 3.4 Ga Strelley Pool Formation, Pilbara Craton of Western Australia - a preliminary study

*Kenichirio Sugitani[1], Ryoko Senda[3], Tsuyoshi Iizuka[2], Simon Wallis[2] (1.Nagoya University, 2.The University of Tokyo, 3.Kyushu University)

[BCG07-P06] High-resolution stable isotopes and chemical analyses on laminations of the early Proterozoic stromatolite

Yuta Miyanishi[1], Kazuki Takamura[1], *Nagayoshi Katsuta[1], Maki Morimoto[1], ATSUSHI YASUDA[2], Shin-ichi Kawakami[3] (1.Faculty of Education, Gifu University, 2.Earthquake Research Institute, University of Tokyo, 3.Faculty of Education, Gifu Shotoku Gakuen University)

[BCG07-P07] Biogeochemical dynamics in during the Great Oxidation Event constrained by a biogeochemical cycle model

*Yuna Miura[1], Kazumi Ozaki[1] (1.Toho University)

[BCG07-P08] Composition of seawater before the Sturtian Snowball Earth estimated by the occurrence of late Tonian evaporitic magnesite

*Aya Miyazaki[1], Akihiro Kano[1], Fumito Shiraishi[2] (1.Department of Earth and Planetary Science, The University of Tokyo, 2.Department of Earth and Planetary Systen Sciences, Hiroshima University)

[BCG07-P09] Geochemical characteristics of black shales in the Japanese accretionary complex across the Permian-Triassic boundary extracted by independent component analysis

*Moei Yano[1], Kazutaka Yasukawa[1,3], Koichiro Fujinaga[3,2], Kentaro Nakamura[1], Yasuhiro Kato[2,1,3] (1.Department of Systems Innvation, School of Engineering, The University of Tokyo, 2.Frontier Research Center for Energy and Resources, School of Engineering, The University of Tokyo, 3.Ocean Resources Research Center for Next Generation, Chiba Institute of Technology)

[BCG07-P10] The Distribution of the Ejecta Deposit derived from Australasian Tektite Event: Implication for the Location of the Impact

*Toshihiro Tada[1], Ryuji Tada[1,2], Paul Carling[3], Wickanet Songtham[4], Le Xuan Thuyen[5], Yu Chang, Eiichi Tajika[1]
(1.Department of Earth and Planetary Science, 2.Yunnan University, 3.Geography and Environment, University of Southampton, 4.Northeastern Research institute of Petrified Wood and Mineral Resources, Nakhon Ratchasima Rajabhat University, 5.Ho Chi Minh City University of Science)

[BCG07-P11] Tectonic-sedimentation reconstruction of Neoproterozoic metavolcanic sequences; the El-Dabbah area, Central Eastern Desert, Egypt

*Shoichi Kiyokawa[1], TAISHI SUZUKI[1], Maher Dawoud[3], El-Hasan Mohamed[3], Kenji Horie[2], Mami Takehara[2]
(1.Department of Earth and Planetary Sciences Faculty of sciences, Kyuushu University, 2.National Institute of Polar Research, 3.Department of Geology, Faculty of Science, Menoufiya University,)

[J] Poster | B (Biogeosciences)：B-CG Complex & General

5:15 PM - 6:30 PM JST | 8:15 AM - 9:30 AM UTC | Poster Hall International Exhibition Hall8, Makuhari Messe_35

[B-CG07] Decoding the history of Earth: From Hadean to the present

convener:Tsuyoshi Komiya(Department of Earth Science & Astronomy Graduate School of Arts and Sciences The University of Tokyo), Yasuhiro Kato(Department of Systems Innovation, Graduate School of Engineering, University of Tokyo), Katsuhiko Suzuki(Research and Development Center for Submarine Resources, Japan Agency for Marine-Earth Science and Technology)

[BCG07-P01] Geology of the Eoarchean Nuvvuagittuq supracrustal belt, northeastern Canada: Reappraisal of Protoliths and ages of the sedimentary rocks

*Tsuyoshi Komiya[1], Shinji Yamamoto[2], Hiroki Uehara[1], Yoshida Satoshi[1], Aoi Murakami[1], Yuki Ishihara[1] (1.Department of Earth Science & Astronomy Graduate School of Arts and Sciences The University of Tokyo, 2.Graduate School of Environment and Information Sciences, Yohohama National University)

[BCG07-P02] Behavior of phosphorus during hydrothermal alteration of basalt under CO_2-rich condition

*Aoi Murakami[1], Yusuke Sawaki[2], Hisahiro Ueda[3], Yuji Orihashi[4], Shiki Machida[5], Tsuyoshi Komiya[2] (1.Department of Earth and Planetary Science, Graduate School of Science, The University of Tokyo, 2.The University of Tokyo, 3.Tokyo Institute of Technology, 4.Hirosaki University, 5.Chiba Institute of Technology)

[BCG07-P03] Origin of chromitites in the Akulleq terrane, southern West Greenland

*Kanta Takahashi[1], Tomoaki Morishita[1], Juan Miguel Ramirez Guotana[1], Kenichiro Tani[2], Yumiko Harigane[3], Ikuya Nishio[1], Kristoffer Szilas[4], Akihiro Tamura[1] (1.Kanazawa University, 2.Department of Geology and Paleontology, National Museum of Nature and Science, 3.Geological Survey of Japan, National Institute of Advanced Industrial Science and Technology (AIST), 4.University of Copenhagen)

[BCG07-P04] Metamorphic P–T condition of the Inyoni shear zone rocks in the Barberton Greenstone Belt, South Africa and its significance

*Daichi Kato[1], Kazumasa Aoki[1], Yuta Tsuchiya[2], Shogo Aoki[2], Tsuyoshi Komiya[3] (1.Department of Applied Science,Okayama University of Science, 2.Department of Biosphere-Geosphere Science,Okayama University of Science, 3.Department of Earth Science and Astronomy,University of Tokyo)

[BCG07-P05] Discovery of possible traces of asteroid impact within the fossil-bearing carbonaceous chert from the 3.4 Ga Strelley Pool Formation, Pilbara Craton of Western Australia - a preliminary study

*Kenichirio Sugitani[1], Ryoko Senda[3], Tsuyoshi Iizuka[2], Simon Wallis[2] (1.Nagoya University, 2.The University of Tokyo, 3.Kyushu University)

[BCG07-P06] High-resolution stable isotopes and chemical analyses on laminations of the early Proterozoic stromatolite

Yuta Miyanishi[1], Kazuki Takamura[1], *Nagayoshi Katsuta[1], Maki Morimoto[1], ATSUSHI YASUDA[2], Shin-ichi Kawakami[3] (1.Faculty of Education, Gifu University, 2.Earthquake Research Institute, University of Tokyo, 3.Faculty of Education, Gifu Shotoku Gakuen University)

[BCG07-P07] Biogeochemical dynamics in during the Great Oxidation Event constrained by a biogeochemical cycle model

*Yuna Miura[1], Kazumi Ozaki[1] (1.Toho University)

[BCG07-P08] Composition of seawater before the Sturtian Snowball Earth estimated by the occurrence of late Tonian evaporitic magnesite

*Aya Miyazaki[1], Akihiro Kano[1], Fumito Shiraishi[2] (1.Department of Earth and Planetary Science, The University of Tokyo, 2.Department of Earth and Planetary Systen Sciences, Hiroshima University)

[BCG07-P09] Geochemical characteristics of black shales in the Japanese accretionary complex across the Permian-Triassic boundary extracted by independent component analysis

*Moei Yano[1], Kazutaka Yasukawa[1,3], Koichiro Fujinaga[3,2], Kentaro Nakamura[1], Yasuhiro Kato[2,1,3] (1.Department of Systems Innvation, School of Engineering, The University of Tokyo, 2.Frontier Research Center for Energy and Resources, School of Engineering, The University of Tokyo, 3.Ocean Resources Research Center for Next Generation, Chiba Institute of Technology)

[BCG07-P10] The Distribution of the Ejecta Deposit derived from Australasian Tektite Event: Implication for the Location of the Impact

*Toshihiro Tada[1], Ryuji Tada[1,2], Paul Carling[3], Wickanet Songtham[4], Le Xuan Thuyen[5], Yu Chang, Eiichi Tajika[1] (1.Department of Earth and Planetary Science, 2.Yunnan University, 3.Geography and Environment, University of Southampton, 4.Northeastern Research institute of Petrified Wood and Mineral Resources, Nakhon Ratchasima Rajabhat University, 5.Ho Chi Minh City University of Science)

[BCG07-P11] Tectonic-sedimentation reconstruction of Neoproterozoic metavolcanic sequences; the El-Dabbah area, Central Eastern Desert, Egypt

*Shoichi Kiyokawa[1], TAISHI SUZUKI[1], Maher Dawoud[3], El-Hasan Mohamed[3], Kenji Horie[2], Mami Takehara[2] (1.Department of Earth and Planetary Sciences Faculty of sciences, Kyuushu University, 2.National Institute of Polar Research, 3.Department of Geology, Faculty of Science, Menoufiya University,)

[E] Oral | M (Multidisciplinary and Interdisciplinary)：M-IS Intersection

3:30 PM - 5:00 PM JST | 6:30 AM - 8:00 AM UTC | 201A 2F

[M-IS07] Astrobiology

convener:Hikaru Yabuta(Hiroshima University, Department of Earth and Planetary Systems Science), Seiji Sugita(Department of Earth and Planetary Science, Graduate School of Science Sciece, The University of Tokyo), Misato Fukagawa(National Astronomical Observatory of Japan), Fujishima Kosuke(Tokyo Institute of Technology, Earth-Life Science Institute), Chairperson:Misato Fukagawa(名古屋大学大学院 理学研究科), Kosuke Fujishima(ELSI 地球生命研究所)

3:35 PM - 3:50 PM JST | 6:35 AM - 6:50 AM UTC

[MIS07-01] METEOROID AND DEBRIS IMPACT FLUX IN LOW EARTH ORBIT WITNESSED BY THE TANPOPO CAPTURE PANELS ONBOARD THE ISS IN 2015-2017

*Hajime Yano[1], K. Yamamoto[2], E. Minakami[2], M. Eitel[1,3], S. Sasaki[4], J. Imani[5], K. Okudaira[6], M. Higashide[7], E. Imai[8], Y. Kawaguchi[9], Yoko Kebukawa[10], H. Mita[11], M. Nishi[12], T. Noguchi[13], Makoto Tabata[14], A. Tsuchiyama[12], Hikaru Yabuta[15], K. Arai[8], H. Hashimoto[1], Kensei Kobayashi[10], A. Yamagishi[16] (1.Institute of Space and Astronautical Science, Japan Aerospace Exploration Agency, 2.Hosei University, 3.University of Stuttgart, 4.Tokyo University of Technology, 5.Yuki Seimitsu, Co. Ltd., 6.University of Aizu, 7.JAXA/Aerospace Research and Development Directorate, 8.Nagaoka University of Technology, 9.Chiba Institute of Technology, 10.Yokohama National University, 11.Fukuoka Institute of Technology, 12.Kyoto University, 13.Kyushu University, 14.Chiba University, 15.Hiroshima University, 16.Tokyo University of Pharmacy and Life Science)

3:50 PM - 4:10 PM JST | 6:50 AM - 7:10 AM UTC

[MIS07-02] Growth and transport of dust, ice, and organics in the inner part of protoplanetary disks

★Invited Papers

*Satoshi Okuzumi[1] (1.Department of Earth and Planetary Sciences, Tokyo Institute of Technology)

4:10 PM - 4:25 PM JST | 7:10 AM - 7:25 AM UTC

[MIS07-03] Model Prediction of Complex Organic Molecules in Protoplanetary Disks

*Hideko Nomura[1], Catherine Walsh[2], Tom J. Millar[3] (1.Department of Earth and Planetary Sciences, Tokyo Institute of Technology, 2.School of Physics and Astronomy, University of Leeds, 3.School of Mathematics and Physics, Queen’s University Belfast)

4:25 PM - 4:40 PM JST | 7:25 AM - 7:40 AM UTC

[MIS07-04] Abiotic synthesis of organic matters in environments simulating asteroids and the catalytic effect of minerals on amino acid formation

*Walaa Elmasry[1], Yoko Kebukawa[1], Kensei Kobayashi[1] (1.Yokohama National University)

4:40 PM - 4:55 PM JST | 7:40 AM - 7:55 AM UTC

[MIS07-05] Peptide Formation from amino acid precursors under simulated submarine hydrothermal environments

*Kensei Kobayashi[1], Keisuke Naito[1], Koki Naito[1], Soushi Kuramoto[1], Ei-ichi Imai[2], MITA Hajime[3], Yoko Kebukawa[1] (1.Yokohama National University, 2.Nagaoka University of Technology, 3.Fukuoka Institute of Technology)

[J] Oral | M (Multidisciplinary and Interdisciplinary)：M-IS Intersection

10:45 AM - 12:15 PM JST | 1:45 AM - 3:15 AM UTC | 304 3F

[M-IS19] Paleoclimatology and paleoceanography

convener:Yusuke Okazaki(Department of Earth and Planetary Sciences, Graduate School of Science, Kyushu University), Akira Oka(Atmosphere and Ocean Research Institute, The University of Tokyo), Michinobu Kuwae(Center for Marine Environmental Studies), Hitoshi Hasegawa(Faculty of Science and Technology, Kochi University), Chairperson:Yusuke Okazaki

10:45 AM - 11:00 AM JST | 1:45 AM - 2:00 AM UTC

[MIS19-01] Development of Longitudinal dunes under the Pangean atmospheric circulation

*Hiroki Shozaki[1], Hitoshi Hasegawa[2] (1.Faculty of Science, Kochi University, 2.Faculty of Science and Technology, Kochi University)

11:00 AM - 11:15 AM JST | 2:00 AM - 2:15 AM UTC

[MIS19-02] Response of primary producers in the ocean anoxic events during the Cretaceous

*Haga Mayuko[1], Eiichi Tajika[1], Kazumi Ozaki[2] (1.The University of Tokyo, 2.Toho University)

11:15 AM - 11:30 AM JST | 2:15 AM - 2:30 AM UTC

[MIS19-03] The linkage between desertification and tectonism inferred from the provenance change of the terrestrial sediments in the Tarim basin

*Aki Sakuma[1], Ryuji Tada[1], Tomohiro Yoshida[1], Hitoshi Hasegawa[2], Naomi Sugiura[1], Akinori Karasuda[1], Ke WANG[1], Hongbo Zheng[3] (1.Department of Earth and Planetary Science, School of Science, the University of Tokyo, 2.Faculty of Science and Technology, Kochi University, 3.School of Resource Environment and Earth Science, Yunnan University)

11:30 AM - 11:45 AM JST | 2:30 AM - 2:45 AM UTC

[MIS19-04] Paleoceanographic reconstruction in the northwestern Pacific during MIS 19 using ultra-high temporal resolution oxygen isotope profiles and planktonic foraminiferal assemblage

*Yuki Haneda[1], Nanako Yokokawa[1], Makoto Okada[1], Hiroki Hayashi[2], Yoshimi Kubota[3], Yusuke Suganuma[4] (1.College of Science, Ibaraki University, 2.Interdisciplinary Factulty of Science and Engineering, Shimane University, 3.National Museum of Nature and Science, 4.National Institute of Polar Research)

11:45 AM - 12:00 PM JST | 2:45 AM - 3:00 AM UTC

[MIS19-05] Paleoclimate reconstruction using fossil pollen analyses from a sedimentary sequence around the Matuyama-Brunhes polarity transition in the Chiba composite section

*Makoto Okada[1], Hitomi Takizawa[1], Yuki Haneda[2], Yusuke Suganuma[3,4], Quentin Simon[5] (1.Department of Earth Sciences, College of Science, Ibaraki University, 2.Graduate school of Science and Technology, Ibaraki University, 3.National Institute of Polar Research, 4.Graduate University for Advanced Studies, 5.Aix-Marseille University)

12:00 PM - 12:15 PM JST | 3:00 AM - 3:15 AM UTC

[MIS19-06] Reconstruction of vertical thermal structure in the western Pacific warm pool over the last 1 Myr

*Fumito Mizuno[1], Takuya Sagawa[2], Keisuke Mukaida[3], Yoshimi Kubota[4], Toshitsugu Yamazaki[5], Junichiro Kuroda[5] (1.Graduate School of Natural Science and Technology. Kanazawa University, 2.Institute of Science & Engineering. Kanazawa University, 3.Collage of Science & Engineering. Kanazawa University, 4.National Museum of Nature & Science, 5.Atmosphere and Ocean Research Institute. The University of Tokyo)

[J] Oral | M (Multidisciplinary and Interdisciplinary)：M-IS Intersection

1:45 PM - 3:15 PM JST | 4:45 AM - 6:15 AM UTC | 304 3F

[M-IS19] Paleoclimatology and paleoceanography

convener:Yusuke Okazaki(Department of Earth and Planetary Sciences, Graduate School of Science, Kyushu University), Akira Oka(Atmosphere and Ocean Research Institute, The University of Tokyo), Michinobu Kuwae(Center for Marine Environmental Studies), Hitoshi Hasegawa(Faculty of Science and Technology, Kochi University), Chairperson:Michinobu Kuwae(愛媛大学沿岸環境科学研究センター)

1:45 PM - 2:00 PM JST | 4:45 AM - 5:00 AM UTC

[MIS19-07] Future perspective on the response of marine calcifiers to “evil twins” of climate change due to increased PCO2

*Hodaka Kawahata[1] (1.Atmosphere Ocean Research Institute, the University of Tokyo)

2:00 PM - 2:22 PM JST | 5:00 AM - 5:22 AM UTC

[MIS19-08] Reconstruction of seawater pH and atmospheric CO_2 concentration based on boron isotopic composition of biogenic calcium carbonate

★Invited Papers

*Kaoru Kubota[1] (1.Kochi Institute for Core Sample Research, JAMSTEC)

2:22 PM - 2:37 PM JST | 5:22 AM - 5:37 AM UTC

[MIS19-09] A 70 years changes of the Java Sea surface condition based on geochemical analyses of a coral core

*Ai Genda[1], Atsushi Suzuki[2], Toyoho Ishimura[3], Minoru Ikehara[4], Mayuri Inoue[1] (1.Graduate School of National Science and Technology, Okayama University, 2.Geological Survey of Japan Natinal Institute of Advanced Industrial Science and Technology, 3.National Institute of Technology, Ibaraki College, 4.Center for Advanced Marine Core Research, Kochi University)

2:37 PM - 2:52 PM JST | 5:37 AM - 5:52 AM UTC

[MIS19-10] Reconstruction of paleoenvironments in the western Pacific for the last 220 years

Mutsumi Chihara[1], Ayaka Fukushima[2], Minoru Ikehara[3], Hodaka Kawahata[2], Atsushi Suzuki[4], *Mayuri Inoue[1] (1.Department of Earth Sciences, Okayama University, 2.Atmosphere and Ocean Research Institute, the University of Tokyo, 3.Center for Advanced Marine Core Research, Kochi University, 4.Geological Survey of Japan, AIST)

2:52 PM - 3:15 PM JST | 5:52 AM - 6:15 AM UTC

[MIS19-11] Ocean deoxygenation from the Last Glacial Maximum to the future global warming: inshight from model simulations

★Invited Papers

*Akitomo Yamamoto[1], Ayako Abe-Ouchi[2,1], Rumi Ohgaito[1], Akinori Ito[1], Masahito Shigemitsu[1], Yasuhiro Yamanaka[3], Akira Oka[2] (1.Japan Agency for Marine-Earth Science and TechnologyAtmosphere and Ocean Research Institute, 2.Atmosphere and Ocean Research Institute, The University of Tokyo, 3. Faculty of Environmental Earth Science, Hokkaido University)

[J] Oral | M (Multidisciplinary and Interdisciplinary)：M-IS Intersection

3:30 PM - 5:00 PM JST | 6:30 AM - 8:00 AM UTC | 304 3F

[M-IS19] Paleoclimatology and paleoceanography

convener:Yusuke Okazaki(Department of Earth and Planetary Sciences, Graduate School of Science, Kyushu University), Akira Oka(Atmosphere and Ocean Research Institute, The University of Tokyo), Michinobu Kuwae(Center for Marine Environmental Studies), Hitoshi Hasegawa(Faculty of Science and Technology, Kochi University), Chairperson:Akira Oka

3:30 PM - 3:52 PM JST | 6:30 AM - 6:52 AM UTC

[MIS19-12] Extraction of high-quality ^{14}C data from terrestrial sediments containing pollen fossils

★Invited Papers

*Takayuki Omori[1], Keitaro Yamada[2], Ikuko Kitaba[2], Takeshi Nakagawa[2] (1.The University Museum, The University of Tokyo, 2.Research Centre for Palaeoclimatology, Ritsumeikan University)

3:52 PM - 4:07 PM JST | 6:52 AM - 7:07 AM UTC

[MIS19-13] Oxygen isotope fluctuations of pollen fossils from Lake Suigetsu, Japan

*Keitaro Yamada[1], Takayuki Omori[2], Ikuko Kitaba[1], Takeshi Nakagawa[1] (1.Research Organization of Science and Technology, Ritsumeikan University, 2.The University museum, The University of Tokyo)

4:07 PM - 4:22 PM JST | 7:07 AM - 7:22 AM UTC

[MIS19-14] Reconstruction of lake-level changes during the last glaciation based on fossil diatom record in Lake Biwa

*Takashi Suzuki[1], Yoshio Inouchi[2], Keisuke Otsuka[1], Kaoru Kawakami[3] (1.Graduate School of Human Science, Waseda University, 2.Faculty of Human Sciences, Waseda University, 3.Graduate School of Environmental Science, Hokkaido University)

4:22 PM - 4:45 PM JST | 7:22 AM - 7:45 AM UTC

[MIS19-15] An estimation of microplatcis sedimentation flux in a coastal sea

★Invited Papers

*Hirofumi Hinata[1], Michinobu Kuwae[1], Issei Masumoto[1], Hayato Kawamata[1] (1.Ehime University)

4:45 PM - 5:00 PM JST | 7:45 AM - 8:00 AM UTC

[MIS19-16] Beppu Bay sediments: Potential palaeoenvironmental archives for a candidate auxiliary stratotype for Anthropocene-Holocene boundary

*Michinobu Kuwae[1], Yoshiaki Suzuki[2] (1.Center for Marine Environmental Studies, Ehime Univ., 2.Department of Eearth Scieces, Fuculty of Education and Integrated Arts and Sciences, Waseda Univ.)

[J] Poster | M (Multidisciplinary and Interdisciplinary)：M-IS Intersection

1:45 PM - 3:15 PM JST | 4:45 AM - 6:15 AM UTC | Poster Hall International Exhibition Hall8, Makuhari Messe_5

[M-IS22] Electromagnetic phenomena associated with seismic and volcanic activities

convener:Tetsuya Kodama(Research Unit I, Research and Development Directorate, Japan Space Exploration Agency), Toshiyasu Nagao(Institute of Oceanic Research and development, Tokai University)

[MIS22-P01] Ionospheric TEC changes immediately before large earthquakes: Derivation of the standard curve and discussion on the physical mechanisms

*Yuki Takasaka [1], Kosuke Heki[1] (1.Department of Earth and Planetary Science, Faculty of Science, Hokkaido University)

[MIS22-P02] Examination of ionospheric disturbances at different altitudes associated with Tohoku earthquake using HF Doppler sounding

*Natsuki Ono[1], Hiroyuki Nakata[1], Hiroyo Ohya[1], Toshiaki Takano[1], Ichiro Tomizawa[2], Keisuke Hosokawa[2], Takuya Tsugawa[3], Michi Nishioka[3] (1.Department of Electrical and Electronic Engineering, Graduate School of Science and Engineering, Chiba University, 2.The University of Electro-Communications, 3.NICT)

[MIS22-P03] **Electromagnetic observation addressed to the short-term earthquake prediction research in VLF band**

*Toshiyasu Nagao[1], Jun Izutsu[2], Masashi Kamogawa[3], Yoshiaki Orihara[1], Shigeki Sugiura[4], Hitoshi Kondo[4] (1.Institute of Oceanic Research and development, Tokai University, 2.Intl. Digital Earth Applied Sci. Res. Ctr, Chubu Inst. for Advanced Studies, Chubu Univ., 3.Department of Physics, Tokyo Gakugei University, 4.Genesis Research Institute, Inc.)

[MIS22-P04] ELF electric field intensity at the time of VLF precursor in the DEMETER data

*Masashi Kamogawa[1], Tetsuya Kodama[2], Toshiyasu Nagao[3] (1.Department of Physics, Tokyo Gakugei University, 2.Japan Space Exploration Agency, 3.Tokai University)

[J] Poster | M (Multidisciplinary and Interdisciplinary)：M-IS Intersection

5:15 PM - 6:30 PM JST | 8:15 AM - 9:30 AM UTC | Poster Hall International Exhibition Hall8, Makuhari Messe_36

[M-IS22] Electromagnetic phenomena associated with seismic and volcanic activities

convener:Tetsuya Kodama(Research Unit I, Research and Development Directorate, Japan Space Exploration Agency), Toshiyasu Nagao(Institute of Oceanic Research and development, Tokai University)

[MIS22-P01] Ionospheric TEC changes immediately before large earthquakes: Derivation of the standard curve and discussion on the physical mechanisms

*Yuki Takasaka [1], Kosuke Heki[1] (1.Department of Earth and Planetary Science, Faculty of Science, Hokkaido University)

[MIS22-P02] Examination of ionospheric disturbances at different altitudes associated with Tohoku earthquake using HF Doppler sounding

*Natsuki Ono[1], Hiroyuki Nakata[1], Hiroyo Ohya[1], Toshiaki Takano[1], Ichiro Tomizawa[2], Keisuke Hosokawa[2], Takuya Tsugawa[3], Michi Nishioka[3] (1.Department of Electrical and Electronic Engineering, Graduate School of Science and Engineering, Chiba University, 2.The University of Electro-Communications, 3.NICT)

[MIS22-P03] **Electromagnetic observation addressed to the short-term earthquake prediction research in VLF band**

*Toshiyasu Nagao[1], Jun Izutsu[2], Masashi Kamogawa[3], Yoshiaki Orihara[1], Shigeki Sugiura[4], Hitoshi Kondo[4] (1.Institute of Oceanic Research and development, Tokai University, 2.Intl. Digital Earth Applied Sci. Res. Ctr, Chubu Inst. for Advanced Studies, Chubu Univ., 3.Department of Physics, Tokyo Gakugei University, 4.Genesis Research Institute, Inc.)

[MIS22-P04] ELF electric field intensity at the time of VLF precursor in the DEMETER data

*Masashi Kamogawa[1], Tetsuya Kodama[2], Toshiyasu Nagao[3] (1.Department of Physics, Tokyo Gakugei University, 2.Japan Space Exploration Agency, 3.Tokai University)

[J] Oral | M (Multidisciplinary and Interdisciplinary)：M-IS Intersection

3:30 PM - 5:00 PM JST | 6:30 AM - 8:00 AM UTC | A07 TOKYO BAY MAKUHARI HALL

[M-IS22] Electromagnetic phenomena associated with seismic and volcanic activities

convener:Tetsuya Kodama(Research Unit I, Research and Development Directorate, Japan Space Exploration Agency), Toshiyasu Nagao(Institute of Oceanic Research and development, Tokai University), Chairperson:Tetsuya Kodama, Toshiyasu Nagao

3:30 PM - 3:45 PM JST | 6:30 AM - 6:45 AM UTC

[MIS22-01] Stress-induced charges in gabbro at high temperature

*Chihiro Yamanaka[1], Daiki Maezono[1] (1.Graduate School of Science, Osaka University)

3:45 PM - 4:00 PM JST | 6:45 AM - 7:00 AM UTC

[MIS22-02] Evaluation of ULF seismo-magnetic precursor phenomena at Kakioka, Japan over 1983 – 2018 by using SEA and Molchan's error diagram

*Katsumi Hattori[1], Kei Takahashi[2], Peng Han[3] (1.Department of Earth Sciences, Graduate School of Science, Chiba University, 2.Department of Earth Sciences, Faculty of Science, Chiba University, 3.Southern University of Science and Technology, China)

4:00 PM - 4:15 PM JST | 7:00 AM - 7:15 AM UTC

[MIS22-03] On the tsunami and electromagnetic pulses appeared abound 10min. after the 2011 Tohoku earthquake

*Yuji Enomoto[1], Tsuneaki Yamabe[1], Shigeki Sugiura[2], Hitoshi Kondo[2] (1.Shinshu Univeristy, Ueda Campus Fii, 2.Genesis Reserach Institute, Inc.)

4:15 PM - 4:30 PM JST | 7:15 AM - 7:30 AM UTC

[MIS22-04] Reinvestigation of correlation between groundwater anomalies and earthquakes carried out by an amateur network in Japan

*Yoshiaki Orihara[1], Masashi Kamogawa[2], Toshiyasu Nagao[1] (1.Institute of Oceanic Research and Development, Tokai University, 2.Dpt. of Phys., Tokyo Gakugei Univ.)

4:30 PM - 4:45 PM JST | 7:30 AM - 7:45 AM UTC

[MIS22-05] Participation Report of S-Booster 2018

*Tetsuya Kodama[1] (1.Research Unit I, Research and Development Directorate, Japan Space Exploration Agency)

4:45 PM - 5:00 PM JST | 7:45 AM - 8:00 AM UTC

[MIS22-06] The future direction of EMSEV, IUGG International Working Group

*Toshiyasu Nagao[1] (1.Institute of Oceanic Research and development, Tokai University)

[E] Poster | M (Multidisciplinary and Interdisciplinary)：M-GI General Geosciences, Information Geosciences & Simulations

10:45 AM - 12:15 PM JST | 1:45 AM - 3:15 AM UTC | Poster Hall International Exhibition Hall8, Makuhari Messe_11

[M-GI30] Data assimilation: A fundamental approach in geosciences

convener:Shin ya Nakano(The Institute of Statistical Mathematics), Yosuke Fujii(Meteorological Research Institute, Japan Meteorological Agency), SHINICHI MIYAZAKI(Graduate School of Science, Kyoto University), Takemasa Miyoshi(RIKEN)

[MGI30-P01] Superposition of atmospheric states using information redundancy for Numerical Weather Prediction

*Toshiyuki Ishibashi[1] (1.Meteorological Research Institute/Japan Meteorological Agency)

[MGI30-P02] **Numerical Weather Prediction Experiments using a Coupled Atmosphere-Ocean Data Assimilation System in JMA/MRI** (3)

*Toshiyuki Ishibashi[1], Takeshi Iriguchi[1], Yosuke Fujii[1], Tamaki Yasuda[1], Yuhei Takaya[1], Naoki Saito[1], Toshikazu Onogi[1] (1.Meteorological Research Institute/Japan Meteorological Agency)

[MGI30-P03] **Accurate estimation of posterior error covariance in a 4D-Var inverse analysis**

*Yosuke Niwa[1,2], Yosuke Fujii[2,3] (1.National Institute for Environmental Studies, 2.Meteorological Research Institute, Japan Meteorological Agency, 3.The Institute of Statistical Mathematics)

[MGI30-P04] Assimilation CO_2 concentration data in the Kanto region using AIST-MM model and for the estimation of CO_2 emissions

*Yutaka Arai[1], Ryoichi Imasu[1], Hiroaki Kondo[2], Yosuke Niwa[3] (1.Atmosphere and Ocean Research Institute, The University of Tokyo, 2.National Institute of Advanced Industrial Science and Technology, 3.National Institute for Environmental Studies, Independent Administrative Institutions)

[MGI30-P05] **Application of data assimilation method on parameter estimation of flow and nutrient behavior in watershed model**

*Yosuke Horie[1] (1.Nippon Koei Co., Ltd.)

[MGI30-P06] Bayesian inference of grain growth prediction via multi-phase-field models

*Shin-ichi Ito[1], Hiromichi Nagao[1], Takashi Kurokawa[1], Tadashi Kasuya[1], Junya Inoue[1] (1.The University of Tokyo)

[MGI30-P07] GNSS data assimilation for the Bungo channel Long-term SSEs using Ensemble Kalman Filter (EnKF)

*Megumi Fujita[1], Takuya NISHIMURA[2], Kazuro Hirahara[3], SHINICHI MIYAZAKI[1] (1.Graduate School of Science , Kyoto University, 2.Disaster Prevention Research Institute, Kyoto University, 3.Institute of Education, Research and Regional Cooperation for crisis Management Shikoku, Kagawa University)

[MGI30-P08] A data assimilation library with Python for parallel computing

*Shin ya Nakano[1], Yuya Ariyoshi[2], Tomoyuki Higuchi[1] (1.The Institute of Statistical Mathematics, 2.Faculty of Engineering, Nippon Bunri University)

[E] Poster | M (Multidisciplinary and Interdisciplinary)：M-GI General Geosciences, Information Geosciences & Simulations

5:15 PM - 6:30 PM JST | 8:15 AM - 9:30 AM UTC | Poster Hall International Exhibition Hall8, Makuhari Messe_37

[M-GI30] Data assimilation: A fundamental approach in geosciences

convener:Shin ya Nakano(The Institute of Statistical Mathematics), Yosuke Fujii(Meteorological Research Institute, Japan Meteorological Agency), SHINICHI MIYAZAKI(Graduate School of Science, Kyoto University), Takemasa Miyoshi(RIKEN)

[MGI30-P01] Superposition of atmospheric states using information redundancy for Numerical Weather Prediction

*Toshiyuki Ishibashi[1] (1.Meteorological Research Institute/Japan Meteorological Agency)

[MGI30-P02] **Numerical Weather Prediction Experiments using a Coupled Atmosphere-Ocean Data Assimilation System in JMA/MRI** (3)

*Toshiyuki Ishibashi[1], Takeshi Iriguchi[1], Yosuke Fujii[1], Tamaki Yasuda[1], Yuhei Takaya[1], Naoki Saito[1], Toshikazu Onogi[1] (1.Meteorological Research Institute/Japan Meteorological Agency)

[MGI30-P03] **Accurate estimation of posterior error covariance in a 4D-Var inverse analysis**

*Yosuke Niwa[1,2], Yosuke Fujii[2,3] (1.National Institute for Environmental Studies, 2.Meteorological Research Institute, Japan Meteorological Agency, 3.The Institute of Statistical Mathematics)

[MGI30-P04] Assimilation CO_2 concentration data in the Kanto region using AIST-MM model and for the estimation of CO_2 emissions

*Yutaka Arai[1], Ryoichi Imasu[1], Hiroaki Kondo[2], Yosuke Niwa[3] (1.Atmosphere and Ocean Research Institute, The University of Tokyo, 2.National Institute of Advanced Industrial Science and Technology, 3.National Institute for Environmental Studies, Independent Administrative Institutions)

[MGI30-P05] **Application of data assimilation method on parameter estimation of flow and nutrient behavior in watershed model**

*Yosuke Horie[1] (1.Nippon Koei Co., Ltd.)

[MGI30-P06] Bayesian inference of grain growth prediction via multi-phase-field models

*Shin-ichi Ito[1], Hiromichi Nagao[1], Takashi Kurokawa[1], Tadashi Kasuya[1], Junya Inoue[1] (1.The University of Tokyo)

[MGI30-P07] GNSS data assimilation for the Bungo channel Long-term SSEs using Ensemble Kalman Filter (EnKF)

*Megumi Fujita[1], Takuya NISHIMURA[2], Kazuro Hirahara[3], SHINICHI MIYAZAKI[1] (1.Graduate School of Science , Kyoto University, 2.Disaster Prevention Research Institute, Kyoto University, 3.Institute of Education, Research and Regional Cooperation for crisis Management Shikoku, Kagawa University)

[MGI30-P08] A data assimilation library with Python for parallel computing

*Shin ya Nakano[1], Yuya Ariyoshi[2], Tomoyuki Higuchi[1] (1.The Institute of Statistical Mathematics, 2.Faculty of Engineering, Nippon Bunri University)

[E] Oral | M (Multidisciplinary and Interdisciplinary)：M-GI General Geosciences, Information Geosciences & Simulations

1:45 PM - 3:15 PM JST | 4:45 AM - 6:15 AM UTC | 104 1F

[M-GI30] Data assimilation: A fundamental approach in geosciences

convener:Shin ya Nakano(The Institute of Statistical Mathematics), Yosuke Fujii(Meteorological Research Institute, Japan Meteorological Agency), SHINICHI MIYAZAKI(Graduate School of Science, Kyoto University), Takemasa Miyoshi(RIKEN), Chairperson:Takemasa Miyoshi(RIKEN Advanced Institute for Computational Science), Shin'ya Nakano(情報・システム研究機構 統計数理研究所)

1:45 PM - 2:00 PM JST | 4:45 AM - 5:00 AM UTC

[MGI30-01] Recent progresses and applications of geomagnetic data assimilation

★Invited Papers

*Julien Aubert[1], Vincent Lesur[1], Alexandre Fournier[1], Gauthier Hulot[1] (1.Institut de Physique du Globe de Paris, France)

2:00 PM - 2:15 PM JST | 5:00 AM - 5:15 AM UTC

[MGI30-02] Accounting for non-locality of vertical error correlation within ETKF through eigen-spectral localization

★Invited Papers

*Daisuke Hotta[1] (1.Meteorological Research Institute, Japan Meteorological Agency)

2:15 PM - 2:30 PM JST | 5:15 AM - 5:30 AM UTC

[MGI30-03] Data assimilation experiments with MODIS LAI observations and the dynamic global vegetation model SEIB-DGVM over Siberia

★Invited Papers

*Hazuki Arakida[1], Shunji Kotsuki[1], Shigenori Otsuka[1], Yohei Sawada[1,2], Takemasa Miyoshi[1] (1.RIKEN Center for Computational Science, 2.Meteorological Research Institute)

2:30 PM - 2:45 PM JST | 5:30 AM - 5:45 AM UTC

[MGI30-04] Inversion of the ocean vertical diffusivity from steady-state tracer distributions by using an adjoint method

★Invited Papers

*Akira Oka[1] (1.Atmosphere and Ocean Research Institute, The University of Tokyo)

2:45 PM - 3:00 PM JST | 5:45 AM - 6:00 AM UTC

[MGI30-05] Nonlinear data assimilation with 4DEnVar using iterative weather forecast model

*Sho Yokota[1], Ko Koizumi[1], Masaru Kunii[2,1], Kosuke Ito[3,1] (1.Meteorological Research Institute, Japan Meteorological Agency, 2.Numerical Prediction Division, Forecast Department, Japan Meteorological Agency, 3.University of the Ryukyus)

3:00 PM - 3:15 PM JST | 6:00 AM - 6:15 AM UTC

[MGI30-06] Development of Data Assimilation System for Atmospheric Density to Improve Satellite's Orbit Prediction Accuracy

*Hiroshi Kato[1], Hideaki Hinagawa[1], Kyohei Akiyama[1], Yuki Akiyama[1], Masaya Nakano[2], Daichi Obinata[2], Shinichi Nakamura[1] (1.Japan Aerospace Exploration Agency, 2.FUJITSU LIMITED)

[E] Oral | M (Multidisciplinary and Interdisciplinary)：M-GI General Geosciences, Information Geosciences & Simulations

3:30 PM - 5:00 PM JST | 6:30 AM - 8:00 AM UTC | 104 1F

[M-GI30] Data assimilation: A fundamental approach in geosciences

convener:Shin ya Nakano(The Institute of Statistical Mathematics), Yosuke Fujii(Meteorological Research Institute, Japan Meteorological Agency), SHINICHI MIYAZAKI(Graduate School of Science, Kyoto University), Takemasa Miyoshi(RIKEN), Chairperson:Shinichi Miyazaki(Kyoto University), Yosuke Fujii

3:30 PM - 3:45 PM JST | 6:30 AM - 6:45 AM UTC

[MGI30-07] An LETKF-based ocean reanalysis for the Asia-Oceania region using Himawari-8 SSTs and SMOS/SMAP SSS

★Invited Papers

*Shun Ohishi[1], Tsutomu Hihara[2], Hidenori AIKI[1], Joji Ishizaka[1], Yasumasa Miyazawa[2], Misako Kachi[3] (1.Nagoya University, 2.JAMSTEC, 3.JAXA)

3:45 PM - 4:00 PM JST | 6:45 AM - 7:00 AM UTC

[MGI30-08] Validation of JCOPE-T DA ocean assimilation product

*Tsutomu Hihara[1], Sergey Varlamov[1], Yasumasa Miyazawa[1], Toru Miyama[1], Misako Kachi[2], Hiroshi Murakami[2] (1.Japan Agency for Marine-Earth Science and Technology, 2.Japan Aerospace Exploration Agency)

4:00 PM - 4:15 PM JST | 7:00 AM - 7:15 AM UTC

[MGI30-09] **Do surface lateral flows matter for land data assimilation?: Implication for hyper-resolution land modeling and observation**

*Yohei Sawada[1] (1.Meteorological Research Institute)

4:15 PM - 4:30 PM JST | 7:15 AM - 7:30 AM UTC

[MGI30-10] Geodynamo data assimilation for candidate models of IGRF13-SV from Japan team

*Takuto Minami[1], Shin ya Nakano[2], Futoshi Takahashi[3], Masaki Matsushima[4], Hisayoshi Shimizu[1], Hiroaki TOH[5] (1.Ocean Hemisphere Research Institute, Earthquake Research Institute,The University of Tokyo, 2.The Institute of Statistical Mathematics, 3.Faculty of Science, Kyushu University, 4.School of Science, Tokyo Institute of Technology, 5.Graduate School of Science, Kyoto University)

4:30 PM - 4:45 PM JST | 7:30 AM - 7:45 AM UTC

[MGI30-11] A pilot study of geomagnetic data assimilation into a geodynamo model

*Shin ya Nakano[1], Takuto Minami[2], Futoshi Takahashi[3], Masaki Matsushima[4], Hiroaki TOH[5], Hisayoshi Shimizu[2] (1.The Institute of Statistical Mathematics, 2.Earthquake Research Institute, the University of Tokyo, 3.Faculty of Science, Kyushu University, 4.School of Science, Tokyo Institute of Technology, 5.Data Analysis Center for Geomagnetism and Space Magnetism, Graduate School of Science, Kyoto University)

4:45 PM - 5:00 PM JST | 7:45 AM - 8:00 AM UTC

[MGI30-12] Bayesian parameter estimation of a physics-based model of postseismic crustal deformation

★Invited Papers

*Jun'ichi Fukuda[1], Kaj Johnson[2] (1.Earthquake Research Institute, University of Tokyo, 2.Department of Earth and Atmospheric Sciences, Indiana University)

[J] Poster | M (Multidisciplinary and Interdisciplinary)：M-GI General Geosciences, Information Geosciences & Simulations

3:30 PM - 5:00 PM JST | 6:30 AM - 8:00 AM UTC | Poster Hall International Exhibition Hall8, Makuhari Messe_22

[M-GI36] Social media and earth and planetary sciences

convener:Kazuo Amano(Department of Environmental Sciences,Ibaraki University), Takashi Oguchi(Center for Spatial Information Science, The University of Tokyo), Masaki Ito(Institute of Industrial Science, the University of Tokyo), Kayoko Yamamoto(University of Elctro-Communications)

[MGI36-P01] Research and Development on Chatbot for Disaster Response

*Hiroki Azuma[1], Masatsugu Hangyo[2], Kiyonori Ohtake[3] (1.National Research Institute for Earth Science and Disaster Resilience, 2.Weathernews Inc., 3.National Institute of Information and Communications Technology)

[MGI36-P02] Collaboration between NIPR image platform service and social media

*Takeshi Terui[1], Yasuyuki Minamiyama[2], Masaki Hidano[3] (1.National Institute of Polar Research, 2.Tokyo Foundation for Policy Research, 3.Info Lounge Corporation)

[MGI36-P03] Twitter account of the Association of Japanese Geographers: History of establishment and operation

*Takashi Oguchi[1], Yuichiro Nishimura[2], Daichi Kohmoto[3], Atsuko Niina[4], Hitoshi Saito[5] (1.Center for Spatial Information Science, The University of Tokyo, 2.Division of Humanities and Social Sciences, Nara Women's University, 3.Nara University of Education, 4.Izu Peninsula Geopark Promotion Council, 5.College of Economics, Kanto Gakuin University)

[MGI36-P04] Utilization of SNS for the North-Ibaraki Geopark Plan after canceling the certification of JGC

*Kazuo Amano[1], Jun Hosoi[2] (1.The Institute of Natural Sciences, College of Humanities and Sciences, Nihon Univ., 2.Institute of Geology and Geoinformation, Geological Survey of Japan, AIST)

[J] Poster | M (Multidisciplinary and Interdisciplinary)：M-GI General Geosciences, Information Geosciences & Simulations

5:15 PM - 6:30 PM JST | 8:15 AM - 9:30 AM UTC | Poster Hall International Exhibition Hall8, Makuhari Messe_38

[M-GI36] Social media and earth and planetary sciences

convener:Kazuo Amano(Department of Environmental Sciences,Ibaraki University), Takashi Oguchi(Center for Spatial Information Science, The University of Tokyo), Masaki Ito(Institute of Industrial Science, the University of Tokyo), Kayoko Yamamoto(University of Elctro-Communications)

[MGI36-P01] Research and Development on Chatbot for Disaster Response

*Hiroki Azuma[1], Masatsugu Hangyo[2], Kiyonori Ohtake[3] (1.National Research Institute for Earth Science and Disaster Resilience, 2.Weathernews Inc., 3.National Institute of Information and Communications Technology)

[MGI36-P02] Collaboration between NIPR image platform service and social media

*Takeshi Terui[1], Yasuyuki Minamiyama[2], Masaki Hidano[3] (1.National Institute of Polar Research, 2.Tokyo Foundation for Policy Research, 3.Info Lounge Corporation)

[MGI36-P03] Twitter account of the Association of Japanese Geographers: History of establishment and operation

*Takashi Oguchi[1], Yuichiro Nishimura[2], Daichi Kohmoto[3], Atsuko Niina[4], Hitoshi Saito[5] (1.Center for Spatial Information Science, The University of Tokyo, 2.Division of Humanities and Social Sciences, Nara Women's University, 3.Nara University of Education, 4.Izu Peninsula Geopark Promotion Council, 5.College of Economics, Kanto Gakuin University)

[MGI36-P04] Utilization of SNS for the North-Ibaraki Geopark Plan after canceling the certification of JGC

*Kazuo Amano[1], Jun Hosoi[2] (1.The Institute of Natural Sciences, College of Humanities and Sciences, Nihon Univ., 2.Institute of Geology and Geoinformation, Geological Survey of Japan, AIST)

[J] Oral | M (Multidisciplinary and Interdisciplinary)：M-SD Space Development & Earth Observation from Space

9:00 AM - 10:30 AM JST | 12:00 AM - 1:30 AM UTC | 302 3F

[M-SD44] Future Missions of Satellite Earth Observation

convener:Yoshiaki HONDA(Center for Environmental Remote Sensing, Chiba University), Yukari Takayabu(Atmosphere and Ocean Research Institute, the University of Tokyo), Shinichi Sobue(Japan Aerospace Exploration Agency), Yuki Kaneko(Japan Aerospace Exploration Agency), Chairperson:Yoshiaki Honda

9:05 AM - 9:20 AM JST | 12:05 AM - 12:20 AM UTC

[MSD44-01] Experimental platform for design and advance evaluation of frequent satellite observations to innovate weather, ocean and land surface predictions

*Takemasa Miyoshi[1], Shunji Kotsuki[1], Koji Terasaki[1], Shigenori Otsuka[1], Takumi Honda[1], Atsushi Okazaki[1], Kohei Takatama[1] (1.RIKEN)

9:20 AM - 9:35 AM JST | 12:20 AM - 12:35 AM UTC

[MSD44-02] Technology demonstration mission for next generation precipitation observation radars

*Tomoo Ushio[1], Toshio Iguchi[2], Kenji Nakamura[4], Kinji Furukawa[3], Riko Oki[3], Daisuke Jodoi[3] (1.Tokyo Metropolitan University, 2.NICT, 3.JAXA, 4.Dokkyo University)

9:35 AM - 9:50 AM JST | 12:35 AM - 12:50 AM UTC

[MSD44-03] Mission of creating base maps as public infrastructures for disaster and monitoring

*ISHITSUKA Naoki[1] (1.The Remote Sensing Society of Japan)

9:50 AM - 10:05 AM JST | 12:50 AM - 1:05 AM UTC

[MSD44-04] Aerosol monitoring, forecasting and estimate of its impacts with multispectral imager data

*Keiya Yumimoto[1,2], Takashi Maki[2], Taichu Y Tanaka[2], Thomas Sekiyama[2], Toshihiko Takemura[1] (1.Kyushu University, 2.Meteorological Research Institute)

10:05 AM - 10:20 AM JST | 1:05 AM - 1:20 AM UTC

[MSD44-05] Global aerosol and cloud observation by space-borne multi-wavelength polarization high-spectral-resolution lidar

*Tomoaki Nishizawa[1], Hajime Okamoto[2], Syoken Ishii[3], Yoshitaka Jin[1] (1.National Institute for Environmental Studies, 2.Kyushu University, 3.National Institute of Information and Communication Technology)

[J] Oral | M (Multidisciplinary and Interdisciplinary)：M-SD Space Development & Earth Observation from Space

10:45 AM - 12:15 PM JST | 1:45 AM - 3:15 AM UTC | 302 3F

[M-SD44] Future Missions of Satellite Earth Observation

convener:Yoshiaki HONDA(Center for Environmental Remote Sensing, Chiba University), Yukari Takayabu(Atmosphere and Ocean Research Institute, the University of Tokyo), Shinichi Sobue(Japan Aerospace Exploration Agency), Yuki Kaneko(Japan Aerospace Exploration Agency), Chairperson:Kazuhiro Asai(東北工業大学), Toshiyoshi Kimura(宇宙航空研究開発機構)

10:45 AM - 11:00 AM JST | 1:45 AM - 2:00 AM UTC

[MSD44-06] Dual-Doppler-velocity-mission using cloud radar and lidar

*Okamoto Hajime[1], Kentaroh Suzuki[2], Tomoaki Nishizawa[3], Shoken Ishii[4] (1.Kyushu University, 2.The university of Tokyo, 3.National Instuitute for Environmental Studies, 4.National Institute of Information and Communications Technology)

11:00 AM - 11:15 AM JST | 2:00 AM - 2:15 AM UTC

[MSD44-07] Global wind profiling with space-based Doppler wind lidar for improvement of numerical weather prediction

*Shoken Ishii[1], Kozo Okaoto[2,1], Takuji Kubota[3], Atsushi Sato[4,1], Daisuke Sakaizaw[3], Tomoaki Nishizawa[5], Ayako Matsumoto[6], Tetsuya Tugami[6], Toshiyuki Ishibashi[2], Taichu Y Tanaka[2], Philippe Baron[1], Makoto Aoki[1], Riko Oki[3], Masaki Satoh[7], Toshiki Iwasaki[8] (1.National Institute of Information and Communications Technology, 2.JMA/MRI, 3.JAXA, 4.TIT, 5.NIES, 6.ANA, 7.University of Tokyo, 8.Tohoku University)

11:15 AM - 11:30 AM JST | 2:15 AM - 2:30 AM UTC

[MSD44-08] Technology demonstration of space-borne water vapor DIAL

*Makoto Abo[1], Chikao Nagasawa[1], Yasukuni Shibata[1], Osamu Uchino[2], Takashi Shibata[3] (1.Graduate School of System Design, Tokyo Metropolitan University, 2.National Institute for Environmental Studies, 3.Nagoya University)

11:30 AM - 12:00 PM JST | 2:30 AM - 3:00 AM UTC

[MSD44-09] Short presentation of poster session

*Yoshiaki HONDA[1] (1.Center for Environmental Remote Sensing, Chiba University)

[J] Oral | M (Multidisciplinary and Interdisciplinary)：M-SD Space Development & Earth Observation from Space

1:45 PM - 3:15 PM JST | 4:45 AM - 6:15 AM UTC | 302 3F

[M-SD44] Future Missions of Satellite Earth Observation

convener:Yoshiaki HONDA(Center for Environmental Remote Sensing, Chiba University), Yukari Takayabu(Atmosphere and Ocean Research Institute, the University of Tokyo), Shinichi Sobue(Japan Aerospace Exploration Agency), Yuki Kaneko(Japan Aerospace Exploration Agency), Chairperson:Riko Oki(宇宙航空研究開発機構)

1:45 PM - 2:00 PM JST | 4:45 AM - 5:00 AM UTC

[MSD44-10] **Himawari-8/9 follow-on satellites program**

*BESSHO Kotaro[1] (1.Japan Meteorological Agency)

2:00 PM - 2:15 PM JST | 5:00 AM - 5:15 AM UTC

[MSD44-11] Impact assessment of hyperspectral infrared sounders toward Himawari-8/9 follow-on satellites

*Kozo OKAMOTO[1], Hiromi Owada[2], Masahiro Kazumori[2], Michiko Otsuka[1], Yoshifumi Ota[2], Naotaka Uekiyo[1], Hiromu Seko[1], Akiyoshi Ando[2], Ryo Yoshida[2], Hiroshi Ishimoto[1], Masahiro Hayashi[1], Haruma Ishida[3], Yoshiaki Sato[2], Hiroshi Kunimatsu[2], Kotaro Bessho[2], Hironobu Yokota[2] (1.Meteorological Research Institute, 2.Japan Meteolological Agency, 3.Meteorological Satellite Center)

2:15 PM - 2:30 PM JST | 5:15 AM - 5:30 AM UTC

[MSD44-12] Observation system simulation experiments for a hyperspectral infrared sounder onboard geostationary satellite

*HIROMI OWADA[1], Kozo OKAMOTO[2], Masahiro Kazumori[1], NAOTAKA UEKIYO[2], Hiroshi Ishimoto[2], Masahiro Hayashi[2] (1.Japan Meteorological Agency, 2.Meteorological Research Institute)

2:30 PM - 2:45 PM JST | 5:30 AM - 5:45 AM UTC

[MSD44-13] Realization of pseudo high frequency high resolution observation by geostationary satellite and orbiting satellite combined observation

*Yoshiaki HONDA[1] (1.Center for Environmental Remote Sensing, Chiba University)

2:45 PM - 3:00 PM JST | 5:45 AM - 6:00 AM UTC

[MSD44-14] **Geostationary Optical Earth Observation Satellite**

*Kazuo Oki[1], Toshiyoshi Kimura[2], Tadahito Mizutani[2], Takeo Tadono[2] (1.The University of Tokyo, 2.JAXA)

[J] Poster | M (Multidisciplinary and Interdisciplinary)：M-SD Space Development & Earth Observation from Space

5:15 PM - 6:30 PM JST | 8:15 AM - 9:30 AM UTC | Poster Hall International Exhibition Hall8, Makuhari Messe_39

[M-SD44] Future Missions of Satellite Earth Observation

convener:Yoshiaki HONDA(Center for Environmental Remote Sensing, Chiba University), Yukari Takayabu(Atmosphere and Ocean Research Institute, the University of Tokyo), Shinichi Sobue(Japan Aerospace Exploration Agency), Yuki Kaneko(Japan Aerospace Exploration Agency)

[MSD44-P01] Monitoring climate variability and global water cycle and understanding their mechanisms (AMSR3)

*Hirohiko Masunaga[1], Naoto Ebuchi[2], Takeshi Tamura[3], Kei Yoshimura[4], Kazumasa Aonashi[5], Masahiro Kazumori[6], Katsuya Saitoh[7] (1.Nagoya University, 2.Hokkaido University, 3.National Institute of Polar Research, 4.University of Tokyo, 5.Meteorological Research Institute, 6.Japan Meteorological Agency, 7.Japan Fisheries Information Service Center)

[MSD44-P02] Precipitation Measuring Mission by Active Sensors

*Nobuhiro Takahashi[1], Yukari Takayabu[2], Kinji Furukawa[3], Riko Oki[3], Kosuke Yamamoto[3], Yuki Kaneko[3] (1.Institute for Space-Earth Environmental Research, Nagoya University, 2.The Atmosphere and Ocean Research Institute (AORI) , 3.The Japan Aerospace Exploration Agency (JAXA))

[MSD44-P03] Asian Small Precipitation Radar Constellation (ASPRC)

*Kinji Furukawa[1], Toshiaki Ogawa[2], Riko Oki[1], Takuji Kubota[1], Moeka Yamaji[1] (1.Japan Aerospace Exploration Agency, 2.NEC Corporation)

[MSD44-P04] In-orbit Payload Demonstration of Circularly Polarized SAR

*Josaphat Tetuko Sri Sumantyo[1], Kuze Hiroaki[1], Nobuyoshi Imura[1] (1.Center for Environmental Remote Sensing, Chiba University)

[MSD44-P05] Global wind measurement system using Doppler Wind Lidar and Imaging FTS

*Okamoto Hajime[1], Toshiyoshi Kimura[2], Daisuke Sakaizawa[2], Shoken Ishii[3] (1.Kyushu University, 2.Japan Aerospace Exploration Agency, 3.National Institute of Information and Communications Technology)

[MSD44-P06] Mission regarding monitoring and elucidation of global environmental change (global radiation forcing and ecological change that affect global warming)

*Yoshiaki HONDA[1], Teruo AOKI[2], Takashi NAKAJIMA[3], Mitsuhiro TORATANI[4] (1.Center for Environmental Remote Sensing, Chiba University, 2.Graduate School of Natural Science and Technology, Okayama University, 3.Tokai University, Research & Information Center, 4.Tokai University, Earth and Environmental Systems)

[MSD44-P07] Proposal of satellite for observing large point sources of carbon dioxide

*Hirofumi Ohyama[1], Tsuneo Matsunaga[1], Isamu Morino[1], Yukio Yoshida[1], Makoto Saito[1] (1.National Institute for Environmental Studies)

[MSD44-P08] Earth's health diagnosis - Imaging spectrometer of SLCP for early verification of global warming countermeasure effect, and understanding of status of air pollution -

*YASUKO KASAI[1], Yugo Kanaya[2], Hiroshi Tanimoto[3], JSAC Satellite team[4] (1.NICT, 2.JAMSTEC, 3.NIES, 4.JSAC)

[MSD44-P09] Spaceborne Vegetation lidar (MOLI)

*Kazuhiro Asai[1], Yasumasa Hirata[2], Gen Takao[2], Haruhisa Shimoda[3], Yoshiaki HONDA[4], Koji Kajiwara[4], Yoshio Awaya[5], Junichi Susaki[9], Takahiro Endo[6], Tsuneo Matsunaga[7], Yoshito Sawada[7], Nobuo Sugimoto[7], Tomoaki Nishizawa[7], Kohei Mizutani[8], Shoken Ishii[8], Toshiyoshi Kimura[10], Tadashi Imai[10], Masato Hayashi[10], Daisuke Sakaizawa[10], Jyunpei Murooka[10], Rei Mituhashi[10] (1.Tohoku Institute of Technology, 2.Forestry and Forest Products Research Institute, 3.Tokai University, 4.Chiba University, 5.Gifu University, 6.The Remote Sensing Technology Center of Japan, 7.National Institute for Environmental Research, 8.National Institute of Information and Communications Technology, 9.Kyoto University, 10.Japan Aerospace Exploration Agency)

[MSD44-P10] Estimation of forest resources by a dual-wavelength imaging LiDAR system

*Ryuichi Hirata[1], Yoshito Sawada[1], Masato Hayashi[2], Hideki Saito[3], Tomoaki Takahashi[3], Tsuneo Matsunaga[1] (1.National Institute for Environmental Studies, 2.Japan Aerospace eXploration Agency, 3.Forestry and Forest Products Research Institute)

[MSD44-P11] Development of new satellite to monitor SIF and PRI of terrestrial vegetation with high spatial and wavelength resolutions

*Hibiki M Noda[1], Kenji Omasa[2], Kouki Hikosaka[3], Kazuhito Ichii[4], Hideki Kobayashi[5], Tomomichi Kato[6], Hiroyuki Muraoka[7] (1.NIES National Institute of Environmental Studies, 2.University of Tokyo, 3.Tohoku University, 4.Chiba University, 5.JAMSTEC, 6.Hokkaido University, 7.Gifu University)

[MSD44-P12] Satellite Observation of the Whole Atmosphere - Superconducting Submillimeter-Wave Limb-Emission Sounder (SMILES-2)

*Masato Shiotani[1], Akinori Saito[1], Takatoshi Sakazaki[1], Satoshi Ochiai[2], Philippe Baron[2], Toshiyuki Nishibori[3], Makoto Suzuki[3], Takumi Abe[3], Hiroyuki Maezawa[4], Shin-ichiro Oyama[5,6,7] (1.Kyoto University, 2.National Institute of Information and Communications Technology, 3.Japan Aerospace Exploration Agency, 4.Osaka Prefecture University, 5.Nagoya University, 6.University of Oulu, 7.National Institute of Polar Research)

[MSD44-P13] Simulation studies for Superconducting Submillimeter-Wave Limb-Emission Sounder-2 (SMILES-2)

*Philippe Baron[1], Satoshi Ochiai[1], Donal Murtagh[5], Hideo Sagawa[2], Akinori Saito[3], Masato Shiotani[3], Makoto Suzuki[4] (1.National Institute of Information and Communications Technology, 2.Kyoto Sangyo University, 3.Kyoto University, 4.Japan Aerospace Exploration Agency, 5.Chalmers University of Technology, Sweden)

[MSD44-P14] Feasibility of Superconducting Submillimeter-Wave Limb-Emission Sounder (SMILES-2) on an M-class satellite

*Satoshi Ochiai[1], Philippe Baron[1], Yoshihisa Irimajiri[1], Toshiyuki Nishibori[2], Makoto Suzuki[2], Yoshinori Uzawa[3], Hiroyuki Maezawa[4], Takeshi Manabe[4], Akinori Saito[5], Masato Shiotani[5] (1.National Institute of Information and Communications Technology, 2.Japan Aerospace Exploration Agency, 3.National Astronomical Observatory of Japan, 4.Osaka Prefecture University, 5.Kyoto University)

[E] Poster | M (Multidisciplinary and Interdisciplinary)：M-TT Technology & Techniques

1:45 PM - 3:15 PM JST | 4:45 AM - 6:15 AM UTC | Poster Hall International Exhibition Hall8, Makuhari Messe_6

[M-TT45] Cryoseismology - a new proxy for detecting surface environmental variations of the Earth -

convener:Genti Toyokuni(Research Center for Prediction of Earthquakes and Volcanic Eruptions, Graduate School of Science, Tohoku University), Masaki Kanao(National Institute of Polar Research), Seiji Tsuboi(JAMSTEC, Center for Earth Information Science and Technology)

[MTT45-P01] Application of neural network and theoretical seismograms as training data to locate ice quakes

*Seiji Tsuboi[1], DAISUKE SUGIYAMA[1] (1.JAMSTEC, Center for Earth Information Science and Technology)

[MTT45-P02] **P-wave tomography beneath Greenland**

*Takaya Matsuno[1], Genti Toyokuni[1], Dapeng Zhao[1] (1.Research Center for Prediction of Earthquakes and Volcanic Eruptions, Graduate School of Science, Tohoku University)

[MTT45-P03] **Seismic observations in Greenland by a joint USA and Japanese GLISN team (2011–2018)**

*Genti Toyokuni[1], Masaki Kanao[2], Seiji Tsuboi[3], Yoko Tono[4] (1.RCPEVE, Tohoku Univ., 2.NIPR, 3.JAMSTEC, 4.ERI, Univ. Tokyo)

[E] Poster | M (Multidisciplinary and Interdisciplinary)：M-TT Technology & Techniques

5:15 PM - 6:30 PM JST | 8:15 AM - 9:30 AM UTC | Poster Hall International Exhibition Hall8, Makuhari Messe_40

[M-TT45] Cryoseismology - a new proxy for detecting surface environmental variations of the Earth -

convener:Genti Toyokuni(Research Center for Prediction of Earthquakes and Volcanic Eruptions, Graduate School of Science, Tohoku University), Masaki Kanao(National Institute of Polar Research), Seiji Tsuboi(JAMSTEC, Center for Earth Information Science and Technology)

[MTT45-P01] Application of neural network and theoretical seismograms as training data to locate ice quakes

*Seiji Tsuboi[1], DAISUKE SUGIYAMA[1] (1.JAMSTEC, Center for Earth Information Science and Technology)

[MTT45-P02] **P-wave tomography beneath Greenland**

*Takaya Matsuno[1], Genti Toyokuni[1], Dapeng Zhao[1] (1.Research Center for Prediction of Earthquakes and Volcanic Eruptions, Graduate School of Science, Tohoku University)

[MTT45-P03] **Seismic observations in Greenland by a joint USA and Japanese GLISN team (2011–2018)**

*Genti Toyokuni[1], Masaki Kanao[2], Seiji Tsuboi[3], Yoko Tono[4] (1.RCPEVE, Tohoku Univ., 2.NIPR, 3.JAMSTEC, 4.ERI, Univ. Tokyo)

[J] Poster | U (Union) : Union

Wed. May 29, 2019 10:45 AM - 12:15 PM JST | Wed. May 29, 2019 1:45 AM - 3:15 AM UTC | Poster Hall International Exhibition Hall8, Makuhari Messe_1

[U-04] Capture the fast process in Earth and planetary science

convener:Takashi Yoshino(Institute for Planetary Materials, Okayama University), Yoshinori Tange(Japan Synchrotron Radiation Research Institute)

Phenomena such as destruction, eruption and collision are catastrophic phenomena, which is different from geological phenomena like mantle convection. However, global phenomena such as meteorite collisions characterised by extinction of dinosaurs were caused not only by long-term fluctuations but also by such a dramatic high-speed phenomenon. It is also important to understand the high-speed dynamics in order to consider evolution of the Earth and disaster prevention. Now it has become possible to capture fast phenomena from femtosecond to several minutes scale under the extreme condition with progress of synchrotron radiation technology. The purpose of this session is that comprehensively understand high-speed dynamics from many methods such as material science / observation / numerical model.

[U04-P01] Present status of time resolved measurement using X-ray absorption spectroscopy at SPring-8

*Kiyofumi Nitta[1], Oki Sekizawa[1], Kazuo Kato[1], Hitoshi Osawa[1] (1.Japan Synchrotron Radiation Research Institute)

[U04-P02] Ultrafast time-resolved XFEL diffraction study on shock-compressed corundum

*Yoshinori Tange[1] (1.Japan Synchrotron Radiation Research Institute)

Present status of time resolved measurement using X-ray absorption spectroscopy at SPring-8

*Kiyofumi Nitta[1], Oki Sekizawa[1], Kazuo Kato[1], Hitoshi Osawa[1]

1. Japan Synchrotron Radiation Research Institute

X-ray Absorption Fine Structure (XAFS) is powerful tool to investigate electric structure and local structure around X-ray absorption atom. Time resolved XAFS measurement developed from appearance of synchrotron radiation and have been applied to many fields. For example, time-resolved XAFS is applied for the catalytic reaction at the in-situ condition and give us the information about how the chemical reaction progresses. We will introduce three representative time-resolved XAFS measurement.

(Super) Quick XAFS (QXAFS),
In QXAFS, the monochromator sweeps quickly (or oscillates at high frequency in Super QXAFS) and it measures the incident X-ray and transmission/fluorescence X-ray intensity continuously. The time resolution depends on the sweep speed of monochromator and the flux of X-ray. The fastest time-resolution of QXAFS in SPring-8 is 800 μs/spectrum which using galvano motor driven monochromator and very compact Si channel-cut crystal without cooling system.

Energy Dispersive XAFS (DXAFS)
DXAFS is a method of measuring the XAFS spectrum by one-shot acquisition. DXAFS measurement is done by converting the energy of X rays into position information using a polychromator and monitoring the position and intensity using a position sensitive detector. So DXAFS has higher time-resolution than QXAFS and the time-resolution is about few ms as usual.

Pump-probe XAFS
Pump-probe XAFS is a method that uses bunch structures of synchrotron radiation. X-ray from the synchrotron facility has a time width. For example at SPring-8, the time width of each X-ray is about 50ps and interval between each X-ray is about 100nsec. Pump-probe XAFS use such time-structure and achieve high time-resolution. However, this method can only apply for repeated reactions.

Keywords: X-ray Absorption Spectroscopy, time-resolved, synchrtron

©2019. Japan Geoscience Union. All Right Reserved.

Ultrafast time-resolved XFEL diffraction study on shock-compressed corundum

*Yoshinori Tange[1]

1. Japan Synchrotron Radiation Research Institute

X-ray Free Electron Lasers (XFEL) allow us ultrafast observations due to its quite short X-ray exposure time of <10 fs (10^{-14} s) with extremely high peak brilliance of >10^{30} photons/sec·mm^2·mrad^2·0.1%b.w., which corresponds to 10^9-times higher compared to synchrotron radiation X-rays made by undulators in third-generation radiation facility such as SPring-8 in general. These extremely-intense and ultrashort-pulsed X-ray flash lamps made it possible to probe samples before the samples are damaged by external forces, conditions, and also XFEL itself.

In an XFEL facility SACLA, constructed at next to SPring-8, laser-driven shock-compression experiments are available with a high-power long-pulse laser system installed by Dr. N. Ozaki' s group and the Photon Pioneers Center in Osaka university. Using the high-power laser system (Nd:YAG, 532 nm, Hamamatsu Photonics K.K.) with the maximum energy of 50 J and pulse width of <10 ns (10^{-8} s), now we are able to reproduce ultrahigh-pressure and ultrahigh-temperature conditions to 1000 GPa (1 TPa) and >10,000 K regime. Here we show a result of in situ observation of shock-compressed polycrystalline corundum utilizing the high-power ns-pulsed pump laser with fs-pulsed intense probe X-ray based on pump-probe techniques.

The pump-probe measurements were carried out varying delay times of XFEL-probe exposure after flashing pump laser to generate shock wave on the surface of targets, which were composed of polypropylene ablator and corundum sample. After series of the pump-probe measurements, pseudo time-resolved profiles were obtained as a function of elapsed time after shock wave arrival to the sample through the ablator. As a result of the pump-probe laser-shock experiments, elastic/plastic compression, uniaxial/quasi-hydrostatic compression, and dynamic recrystallization were observed during shock-wave propagation in the corundum sample with the passing time in the maximum time-resolution of 0.2 ns. In the presentation, we will show the experimental setups and features of XRD profiles of the shock-compressed material in detail.

Keywords: ultrafast measurement, XFEL, shock compression, corundum

©2019. Japan Geoscience Union. All Right Reserved.

[J] Poster | U (Union) : Union

Wed. May 29, 2019 5:15 PM - 6:30 PM JST | Wed. May 29, 2019 8:15 AM - 9:30 AM UTC | Poster Hall International Exhibition Hall8, Makuhari Messe_1

[U-04] Capture the fast process in Earth and planetary science

convener:Takashi Yoshino(Institute for Planetary Materials, Okayama University), Yoshinori Tange(Japan Synchrotron Radiation Research Institute)

Phenomena such as destruction, eruption and collision are catastrophic phenomena, which is different from geological phenomena like mantle convection. However, global phenomena such as meteorite collisions characterised by extinction of dinosaurs were caused not only by long-term fluctuations but also by such a dramatic high-speed phenomenon. It is also important to understand the high-speed dynamics in order to consider evolution of the Earth and disaster prevention. Now it has become possible to capture fast phenomena from femtosecond to several minutes scale under the extreme condition with progress of synchrotron radiation technology. The purpose of this session is that comprehensively understand high-speed dynamics from many methods such as material science / observation / numerical model.

[U04-P01] Present status of time resolved measurement using X-ray absorption spectroscopy at SPring-8

*Kiyofumi Nitta[1], Oki Sekizawa[1], Kazuo Kato[1], Hitoshi Osawa[1] (1.Japan Synchrotron Radiation Research Institute)

[U04-P02] Ultrafast time-resolved XFEL diffraction study on shock-compressed corundum

*Yoshinori Tange[1] (1.Japan Synchrotron Radiation Research Institute)

Present status of time resolved measurement using X-ray absorption spectroscopy at SPring-8

*Kiyofumi Nitta[1], Oki Sekizawa[1], Kazuo Kato[1], Hitoshi Osawa[1]

1. Japan Synchrotron Radiation Research Institute

X-ray Absorption Fine Structure (XAFS) is powerful tool to investigate electric structure and local structure around X-ray absorption atom. Time resolved XAFS measurement developed from appearance of synchrotron radiation and have been applied to many fields. For example, time-resolved XAFS is applied for the catalytic reaction at the in-situ condition and give us the information about how the chemical reaction progresses. We will introduce three representative time-resolved XAFS measurement.

(Super) Quick XAFS (QXAFS),
In QXAFS, the monochromator sweeps quickly (or oscillates at high frequency in Super QXAFS) and it measures the incident X-ray and transmission/fluorescence X-ray intensity continuously. The time resolution depends on the sweep speed of monochromator and the flux of X-ray. The fastest time-resolution of QXAFS in SPring-8 is 800 μs/spectrum which using galvano motor driven monochromator and very compact Si channel-cut crystal without cooling system.

Energy Dispersive XAFS (DXAFS)
DXAFS is a method of measuring the XAFS spectrum by one-shot acquisition. DXAFS measurement is done by converting the energy of X rays into position information using a polychromator and monitoring the position and intensity using a position sensitive detector. So DXAFS has higher time-resolution than QXAFS and the time-resolution is about few ms as usual.

Pump-probe XAFS
Pump-probe XAFS is a method that uses bunch structures of synchrotron radiation. X-ray from the synchrotron facility has a time width. For example at SPring-8, the time width of each X-ray is about 50ps and interval between each X-ray is about 100nsec. Pump-probe XAFS use such time-structure and achieve high time-resolution. However, this method can only apply for repeated reactions.

Keywords: X-ray Absorption Spectroscopy, time-resolved, synchrtron

©2019. Japan Geoscience Union. All Right Reserved.

Ultrafast time-resolved XFEL diffraction study on shock-compressed corundum

*Yoshinori Tange[1]

1. Japan Synchrotron Radiation Research Institute

X-ray Free Electron Lasers (XFEL) allow us ultrafast observations due to its quite short X-ray exposure time of <10 fs (10^{-14} s) with extremely high peak brilliance of >10^{30} photons/sec·mm^2·mrad^2·0.1%b.w., which corresponds to 10^9-times higher compared to synchrotron radiation X-rays made by undulators in third-generation radiation facility such as SPring-8 in general. These extremely-intense and ultrashort-pulsed X-ray flash lamps made it possible to probe samples before the samples are damaged by external forces, conditions, and also XFEL itself.

In an XFEL facility SACLA, constructed at next to SPring-8, laser-driven shock-compression experiments are available with a high-power long-pulse laser system installed by Dr. N. Ozaki' s group and the Photon Pioneers Center in Osaka university. Using the high-power laser system (Nd:YAG, 532 nm, Hamamatsu Photonics K.K.) with the maximum energy of 50 J and pulse width of <10 ns (10^{-8} s), now we are able to reproduce ultrahigh-pressure and ultrahigh-temperature conditions to 1000 GPa (1 TPa) and >10,000 K regime. Here we show a result of in situ observation of shock-compressed polycrystalline corundum utilizing the high-power ns-pulsed pump laser with fs-pulsed intense probe X-ray based on pump-probe techniques.

The pump-probe measurements were carried out varying delay times of XFEL-probe exposure after flashing pump laser to generate shock wave on the surface of targets, which were composed of polypropylene ablator and corundum sample. After series of the pump-probe measurements, pseudo time-resolved profiles were obtained as a function of elapsed time after shock wave arrival to the sample through the ablator. As a result of the pump-probe laser-shock experiments, elastic/plastic compression, uniaxial/quasi-hydrostatic compression, and dynamic recrystallization were observed during shock-wave propagation in the corundum sample with the passing time in the maximum time-resolution of 0.2 ns. In the presentation, we will show the experimental setups and features of XRD profiles of the shock-compressed material in detail.

Keywords: ultrafast measurement, XFEL, shock compression, corundum

©2019. Japan Geoscience Union. All Right Reserved.

[J] Oral | U (Union)：Union

Wed. May 29, 2019 1:45 PM - 3:15 PM JST | Wed. May 29, 2019 4:45 AM - 6:15 AM UTC | 103 1F

[U-04] Capture the fast process in Earth and planetary science

convener:Takashi Yoshino(Institute for Planetary Materials, Okayama University), Yoshinori Tange(Japan Synchrotron Radiation Research Institute), Chairperson:Takashi Yoshino(Okayama University), Yoshio Kono(愛媛大学地球深部ダイナミクスセンター), Yoshinori Tange

Phenomena such as destruction, eruption and collision are catastrophic phenomena, which is different from geological phenomena like mantle convection. However, global phenomena such as meteorite collisions characterised by extinction of dinosaurs were caused not only by long-term fluctuations but also by such a dramatic high-speed phenomenon. It is also important to understand the high-speed dynamics in order to consider evolution of the Earth and disaster prevention. Now it has become possible to capture fast phenomena from femtosecond to several minutes scale under the extreme condition with progress of synchrotron radiation technology. The purpose of this session is that comprehensively understand high-speed dynamics from many methods such as material science / observation / numerical model.

1:45 PM - 1:48 PM JST | 4:45 AM - 4:48 AM UTC

Introduction

1:48 PM - 2:00 PM JST | 4:48 AM - 5:00 AM UTC

[U04-01] Toward organization of a new field on fast process in Earth and planetary science

★Invited Papers

*Takashi Yoshino[1] (1.Institute for Planetary Materials, Okayama University)

2:00 PM - 2:15 PM JST | 5:00 AM - 5:15 AM UTC

[U04-02] Fractal particle size distribution of pulverized fault rocks and dynamic fragmentation of rocks

★Invited Papers

*Jun Muto[1], Osamu Nishikawa[2], Hiroyuki Nagahama[1] (1.Department of Earth Sciences, Tohoku University, 2.Graduate School of Engineering and Resource Sciences, Akita University)

2:15 PM - 2:30 PM JST | 5:15 AM - 5:30 AM UTC

[U04-03] Universal aspects of acceleration process toward unstable fast rupture

★Invited Papers

*Takahiro Hatano[1] (1.Earthquake Research Institute, University of Tokyo)

2:30 PM - 2:45 PM JST | 5:30 AM - 5:45 AM UTC

[U04-04] Semi-brittle flow in dunite and harzburgite at upper mantle pressures

★Invited Papers

*Tomohiro Ohuchi[1], Xinglin Lei[2], Yuji Higo[3], Yoshinori Tange[3] (1.Geodynamics Research Center, Ehime University, 2.National Institute of Advanced Industrial Science and Technology, 3.Japan Synchrotron Radiation Research Institute)

2:45 PM - 3:00 PM JST | 5:45 AM - 6:00 AM UTC

[U04-05] A mechanism of magma fracturing revealed by in-situ X-ray imaging and diffraction

★Invited Papers

*Satoshi Okumura[1], Kentaro Uesugi[2], Tatsuya Sakamaki[1], Akio Goto[3] (1.Division of Earth and Planetary Materials Science, Department of Earth Science, Graduate School of Science, Tohoku University, 2.SPring-8/JASRI, 3.Center for Northeast Asian Studies, Tohoku University)

3:00 PM - 3:15 PM JST | 6:00 AM - 6:15 AM UTC

[U04-06] Estimation of physical parameters of volcanic eruptions based on analysis of eruptive products –Toward understanding of eruption dynamics–

★Invited Papers

*Fukashi Maeno[1] (1.Earthquake Research Institute, University of Tokyo)

Toward organization of a new field on fast process in Earth and planetary science

*Takashi Yoshino[1]

1. Institute for Planetary Materials, Okayama University

In the evolution of the Earth and the planet, it is necessary to consider that the event occurred on a short scale, which is different from the evolution on the geological time scale, gives a global impact on the evolution of the planetary scale and its surface environment.In order to understand such events, it is indispensable to understand high-speed processes such as destructive processes as typified by seismic activity, eruption processes in volcanic activities, and huge meteorite collision processes. Since these phenomena are events that can occur anytime even now, it is also an important research topic in terms of disaster prevention. In this presentation, we propose to combine the research on the elementary processes of these phenomena and the research on the influence of these phenomena from various types of research fields, and aim to construct an interdisciplinary research organization.
In recent years, with the progress of measurement experiment technology in large synchrotron radiation facility and X-ray free electron laser facility, It has been possible to detect the short time scale catastrophic phenomenon occurring in extreme environments in a wide range time interval extending from several minutes ($> 10^2$ s) to femtosecond (10^{-15} s). Studies combining synchrotron radiation with high pressure experiments is shifting from the observation of static processes to monitoring of dynamic processes such as deformation, attenuation, and destruction. It is becoming possible to capture phenomena on the millisecond scale.Situations are being developed that can detect the high-speed process. In studies using X-ray free electron laser, a situation where the collision process can be tracked in detail at 100 picosecond scale has been realized during impact compression experiment using high intensity laser. Furthermore, in the field of computer science using supercomputers, the progress of high-speed process reproduction experiments has been remarkable, and it is time to be able to oversee seamless research on capturing high-speed processes from atomic scale to huge meteorite collision.Research on high-speed processes has been studied independently in each event, but there are many aspects that common phenomena in the method of grasping the high-speed process and its elementary process are common. This session was planned with the goal of forming a research network that can efficiently operate "knowledge" by incorporating numerous methods such as material science, geophysical observation and numerical model. By establishing and utilizing this network, it is expected that we will comprehensively understand the high speed dynamics in Earth and planetary science, and at the same time obtain new knowledge about the impact on the global scale and cause a new paradigm shift.

Keywords: high speed process, failure, collision, eruption

©2019. Japan Geoscience Union. All Right Reserved.

Fractal particle size distribution of pulverized fault rocks and dynamic fragmentation of rocks

*Jun Muto[1], Osamu Nishikawa[2], Hiroyuki Nagahama[1]

1. Department of Earth Sciences, Tohoku University, 2. Graduate School of Engineering and Resource Sciences, Akita University

Earthquake is a catastrophic phenomenon caused by the rapid slip on fault. Development of high-speed rotary shear apparatus enables us to conduct friction experiments of various rocks at seismic slip rates to investigate dynamic fault behaviors [1]. The nominal strain rate at the seismic slip reaches 100 /s under the slip rate of 1 m/s occurring across the 1 cm width of the slip zone. On the other hand, the field observations along large-scale strike-slip faults reported the peculiar fault rocks with in-situ shattered microstructures [2]. The rocks are called pulverized fault rocks and characterized by a lack of shear deformation and intense fragmentation. These intensive damage zones have been suggested to form dynamically during earthquake rupture propagation. Theoretical calculation of the rupture propagation predicts much higher strain-rate deformation exceeding 10000 /s near the rupture tip [3]. However, because such high strain rate can be achieved only along the very close to the tip, several models have also been proposed to explain the wide distribution (~ 100 m from the fault core) of the pulverized rocks along the fault [2,4,5]. From the microstructural analysis of pulverized rocks, we reported the measurements of size distributions of fractured particles [6]. Fragments in those rocks in both fault zones show a fractal size (power-law) distribution down to the micron scale. Fractal dimensions of fragments, dependent on mineral types, reaches 2.92 near the fault cores. The value exceeds a theoretical upper fractal limit of confined comminution (~2.58 [7]) and experimentally created gouges by high-speed friction experiment (~2.6 [8]). Fractal dimensions close to 3.0 have been reported in high-speed impact loading experiments. The observed fractal properties imply that pulverization is likely to have occurred by a dynamic stress pulse with instantaneous volumetric expansion, possibly during seismic rupture propagation similar to impact loading. The obtained results from fractal properties of the pulverized rocks are consistent with laboratory experiments for dynamic fragmentation of rocks using Split-Hopkinson Pressure Bar (SHPB or Kolsky Bar) apparatus [5, 9]. SHPB is a loading apparatus that transmits planar elastic compressive waves into a sample under strain rates of 10 ~ 1000/s. Using the apparatus, Doan and Gary [5] clearly showed that the high strain rate exceeds 150 /s is required to cause pulverization of granite. Moreover, from the analysis of grain size distribution of fragments created by SHPB experiments of fine-grained novaculite, Barber and Griffith [9] showed that energy dissipation by fragmentation is not trivial than previously considered (10 % to as much as 40 %). According to dynamic fragmentation model by Hild [10], strength of rocks in multiple fragmentation regime dramatically increases with strain rate. This implies that the significant strain-rate hardening accompanying pulverization may be the responsible for the significant energy sink of the earthquake [9]. In the presentation, we review the dynamic fragmentation phenomena based on field evidence, theoretical models and laboratory experiments using SHPB apparatus to shed light on the dynamic fault behavior.

References: [1] Di Toro, G. et al. (2011), Nature, 471, 494-498. [2] Dor, O. et al. (2006) EPSL, 245, 642-654. [3] Reches, Z., Dewers, T. A. (2005) EPSL, 235, 361-374. [4] Ben-Zion, Y., Shi, Z.Q. (2005) EPSL, 236, 486-496. [5] Doan, M. L., Gary, G. (2009) Nature Geosci., 2, 709-712. [6] Muto, J., Nakatani, T., Nishikawa, O., Nagahama, H. (2015) GRL, 42, 3811–3819, doi:10.1002/2015GL064026. [7] Sammis, C. et al. (1987) Pageoph, 125, 777-812. [8] Stünitz, H. et al. (2010) JSG, 32, 59-69. [9] Barber, T., Griffith, W.

©2019. Japan Geoscience Union. All Right Reserved.

A. (2017) Phil. Trans. R. Soc. A, 375, 20160002. [10] Hild, F. et al. (2003) Rev. Franco. Gen. Civ., 7, 973-1003.

Keywords: Pulverized rocks, Dynamic fragmentation, Split-Hopkinson Pressure Bar Apparatus, Fractal, Earthquake rupture propagation

©2019. Japan Geoscience Union. All Right Reserved.

Universal aspects of acceleration process toward unstable fast rupture

*Takahiro Hatano[1]

1. Earthquake Research Institute, University of Tokyo

In this talk, we will elaborate the acceleration process of unstable slip on a model of earthquake fault. based on an empirical friction law that has been verified in the lab scale, it is shown that slip velocity increases in a power law manner resembling the inverse Omori law. This acceleration process has been known empirically, and is derivable theoretically for a class of simple systems. We will show that this power-law acceleration is realized in a wider class of systems including non-planer faults and random brittle media. Analysis on a mean-field model indicates saddle node bifurcation is responsible for the power law behavior.

Keywords: earthquake, slip nucleation, precursory phenomena

©2019. Japan Geoscience Union. All Right Reserved.

Semi-brittle flow in dunite and harzburgite at upper mantle pressures

*Tomohiro Ohuchi[1], Xinglin Lei[2], Yuji Higo[3], Yoshinori Tange[3]

1. Geodynamics Research Center, Ehime University, 2. National Institute of Advanced Industrial Science and Technology, 3. Japan Synchrotron Radiation Research Institute

The mechanism of intraslab earthquakes (> 40 km depth) is fundamentally different from those of shallower ones. This is because the frictional strength is much higher and fracture process associates ductile flow (i.e., semi-brittle flow) at deeper parts. The location of the double seismic zone in the subducting Pacific slab corresponds to the main dehydration field in the pressure-temperature diagram of the hydrous peridotite (Omori et al., 2002). The cause of intraslab seismicity at intermediate depths has been attributed to breakdown of hydrous minerals such as serpentinite (e.g., Ferrand et al., 2017) and lawsonite (Okazaki et al., 2016) because it causes unstable fault slip or shear localization. However, the role of aqueous fluid in fracturing at high pressures is still unclear.

To evaluate the effect of water on semi-brittle behavior of dunite and harzburgite, we conducted in-situ uniaxial deformation experiments on as-is/water-saturated dunite and harzburgite at pressures 1-3 GPa and temperatures 670-1250 K with a constant displacement rate using a deformation-DIA apparatus. Pressure, stress, and strain were measured in situ by using x-ray diffraction patterns and radiographs. Radiographs were taken at each several minutes in most of deformation experiments, though radiographs were continuously taken (each 5 seconds) during a deformation run (at 2 GPa and 860 K). Acoustic emissions (AEs) were also recorded continuously on six sensors, and three-dimensional AE source location were determined.

Formation of throughgoing faults was observed in water-saturated dunite and harzburgite at 860 K and lower temperatures. Fault slip rate is between 3E-5 and 4E-4 s^{-1} which are comparable to the background strain rate just before a faulting (1E-5 and 3E-4 s^{-1}), showing that shear localization is ineffective under water-saturated conditions. Addition of the aqueous fluid resulted in the reduction in the number of AE events in the faulted sample (i.e., aseismic faulting). A high time-resolution strain monitoring revealed that fault slip rate fluctuate within several ten seconds (i.e., stick-slip phenomena). Because the high time-resolution strain monitoring is a preliminary experiment, the relationship between stick-slip phenomena and aqueous fluid is unclear. We will investigate that point in near future.

Keywords: water, semi-brittle flow, faulting

©2019. Japan Geoscience Union. All Right Reserved.

A mechanism of magma fracturing revealed by in-situ X-ray imaging and diffraction

*Satoshi Okumura[1], Kentaro Uesugi[2], Tatsuya Sakamaki[1], Akio Goto[3]

1. Division of Earth and Planetary Materials Science, Department of Earth Science, Graduate School of Science, Tohoku University, 2. SPring-8/JASRI, 3. Center for Northeast Asian Studies, Tohoku University

Explosive volcanism is one of the most spectacular phenomena on Earth. Explosive volcanism is characterized by the vigorous release of magma fragments and volcanic gases to the surface. In such cases, the magma is the continuum in the crust but becomes fragmented during its ascent. In particular, brittle fragmentation of silicic (relatively SiO2-rich) magma results in explosive eruptions. Therefore, the cause of brittle fragmentation of magma determines whether the eruption will be explosive or effusive.

The viscoelasticity of magma and the relaxation timescale of its structure are currently thought to control fragmentation (Dingwell, 1996 Science). Under rapid deformation rates, magma exhibits elastic behaviour, while viscous magma behaviour is dominant when the deformation rate is slow. Fiber elongation experiments for magmas clearly demonstrate the transition from viscous elongation to brittle fracturing with increased elongation rates. This transition is empirically formulated and can be applied to the modelling of volcanic eruptions (Gonnermann and Manga, 2003 Nature). In contrast, the atomic- to nano-scale structure of melt across this transition is poorly understood. For example, magma exhibits shear thinning (viscosity decreases as shear rate increases) behaviour when the shear rate is close to the conditions at which magma fracturing occurs. No explanation for the relationship between shear thinning and brittle fracturing has yet been proposed. Understanding the atomic- to nano-scale structures across viscous to brittle transition will provide important information for clarifying the mechanism of magma fragmentation. We have investigated magma fracturing by using in-situ X-ray imaging and diffraction techniques. Some preliminary results of our work will be introduced in this presentation.

Keywords: Volcanic eruption, Magma, Fracturing, X-ray imaging, X-ray diffraction

©2019. Japan Geoscience Union. All Right Reserved.

Estimation of physical parameters of volcanic eruptions based on analysis of eruptive products –Toward understanding of eruption dynamics–

*Fukashi Maeno[1]

1. Earthquake Research Institute, University of Tokyo

'Volume' and 'mass discharge rate' of volcanic eruptions are fundamental parameters in understanding the spatiotemporal scale of magma accumulation and migration in the shallow crust and the type and nature of the surface phenomena accompanying the eruption. 'Volume' of one volcanic eruption is the most fundamental physical parameter for determining the scale of the eruption. Its mid- to long-term transition is related to the accumulation process of magma and the frequency of the eruption, as well as the entire volcanic activity. On the other hand, 'discharge rate' of magma is closely related to magma ascending process, and it is a parameter that controls diversity and transition of eruption styles, eruption intensity, and plume height, etc. The elucidation of 'volume' and 'discharge rate' of magma (physical parameter of eruption) is a key in understanding various volcanic phenomena occurring in the crust and the earth surface as the magma rises. The improvement of the estimation accuracy is indispensable to promote the understanding of the causes of diversity of volcanic activities and eruption phenomena, and the magma reservoir-conduit system. Also the magma discharge rate, which is one of the factors that dominates the diversity of the eruption, greatly influences the characteristics of the eruptive products caused by magma ascent and decompression such as the microstructure and texture, and the chemical composition heterogeneity. The elucidation of the relationship between such physical parameters of eruption and the characteristics of the products may enhance the understanding of volcanic eruptions. On the other hand, in recent eruptions, by comparing ejecta/deposit data with various remote observation data from the ground and satellites, it is possible to grasp the process from magma extrusion to deposition at high resolution. The knowledge obtained therefrom is expected to be an important constraint in the reconstruction of past volcanic events. Estimation of the eruption physical parameters is important not only for understanding the dynamics of volcanic eruption but also for predicting volcanic disasters and future eruptions. In this presentation, we will introduce the estimation of physical parameters of eruption in recent volcanic eruptions and the past gigantic caldera-forming eruptions and also describe the issues.

Keywords: volcanic eruption, eruptive volume, discharge rate, physical parameter

©2019. Japan Geoscience Union. All Right Reserved.

[J] Oral | U (Union)：Union

Wed. May 29, 2019 3:30 PM - 5:00 PM JST | Wed. May 29, 2019 6:30 AM - 8:00 AM UTC | 103 1F

[U-04] Capture the fast process in Earth and planetary science

convener:Takashi Yoshino(Institute for Planetary Materials, Okayama University), Yoshinori Tange(Japan Synchrotron Radiation Research Institute), Chairperson:Takashi Yoshino(Okayama University), Yoshio Kono(愛媛大学地球深部ダイナミクスセンター), Yoshinori Tange

Phenomena such as destruction, eruption and collision are catastrophic phenomena, which is different from geological phenomena like mantle convection. However, global phenomena such as meteorite collisions characterised by extinction of dinosaurs were caused not only by long-term fluctuations but also by such a dramatic high-speed phenomenon. It is also important to understand the high-speed dynamics in order to consider evolution of the Earth and disaster prevention. Now it has become possible to capture fast phenomena from femtosecond to several minutes scale under the extreme condition with progress of synchrotron radiation technology. The purpose of this session is that comprehensively understand high-speed dynamics from many methods such as material science / observation / numerical model.

3:30 PM - 3:45 PM JST | 6:30 AM - 6:45 AM UTC

[U04-07] Chemical reaction processes bridge between asteroid Ryugu and early evolution of Earth

★Invited Papers

*Seiji Sugita[1,3], Hideharu Kuwahara[2], Kosuke Kurosawa[3] (1.Department of Earth and Planetary Science, Graduate School of Science Sciece, The University of Tokyo, 2.Ehime University, 3.Chiba Institute of Technology)

3:45 PM - 4:00 PM JST | 6:45 AM - 7:00 AM UTC

[U04-08] Time-resolved synchrotron X-ray observations of mineral transformations under static pressures: applications to non-equilibrium behaviors in shocked meteorites

★Invited Papers

*Tomoaki Kubo[1], Masaaki Miyahara[2] (1.Kyushu University, 2.Hiroshima University)

4:00 PM - 4:15 PM JST | 7:00 AM - 7:15 AM UTC

[U04-09] Ultrafast pump-probe experiemnts for planetary materials using high-power lasers and XFEL

★Invited Papers

*Norimasa Ozaki[1] (1.Osaka University)

4:15 PM - 4:30 PM JST | 7:15 AM - 7:30 AM UTC

[U04-10] Tracking dynamical phenomena with X-ray free-electron lasers

★Invited Papers

*Tetsuo Katayama[1] (1.Japan Synchrotron Radiation Research Institute)

4:30 PM - 4:45 PM JST | 7:30 AM - 7:45 AM UTC

[U04-11] High speed measurement with synchrotron radiation X-ray.

★Invited Papers

*Kentaro Uesugi[1] (1.Japan Synchrotron Radiation Research Institute)

4:45 PM - 4:58 PM JST | 7:45 AM - 7:58 AM UTC

[U04-12] Recent advances in high-pressure synchrotron X-ray experiments on magmas under pressure at the beamline 16-BM-B in Advanced Photon Source

★Invited Papers

*Yoshio Kono[1] (1.Geodynamics Research Center, Ehime University)

4:58 PM - 5:00 PM JST | 7:58 AM - 8:00 AM UTC

Discussion

Chemical reaction processes bridge between asteroid Ryugu and early evolution of Earth

*Seiji Sugita[1,3], Hideharu Kuwahara[2], Kosuke Kurosawa[3]

1. Department of Earth and Planetary Science, Graduate School of Science Sciece, The University of Tokyo, 2. Ehime University, 3. Chiba Institute of Technology

JAXA's Hayabusa2 has arrived at asteroid Ryugu and is uncovering many new aspects of the primitive asteroid, such as extremly low albedo (4.5+/- 0.1%), flat spectra (Cb type), young resurfacing age (<10^6 yr for the top 1 m layer), high boulder number dentity (x2 of Itokawa) and low abundance of hydrated minerals. These pieces of information is very importance for understanding the early evolution of inner solar system and Earth's surface environment. In particular, what happens upon hypervelocity impacts of such bodies is important for understading the atmospheric chemistry of early Earth. In this study, we review atmospheric entry processes, high-temperature chemistry processes, and discuss the implications of recent results on asteroid missions, such as Hayabusa2 and OSIRIS-REx, for Earth's early evolution.

Keywords: Asteroid missions, Hypervelocity impacts, Impact vapor clouds, Atmospheric entry physics

©2019. Japan Geoscience Union. All Right Reserved.

Time-resolved synchrotron X-ray observations of mineral transformations under static pressures: applications to non-equilibrium behaviors in shocked meteorites

*Tomoaki Kubo[1], Masaaki Miyahara[2]

1. Kyushu University, 2. Hiroshima University

High-pressure transformations occur on timescales of ~0.01 to a few seconds in shocked meteorites. Reactions in such short timescales often remain incomplete and/or metastable state, which is usually problematic for the interpretation, but can be good information for shock durations if the kinetics is experimentally known. Here we present some experimental results on curious kinetic behaviors in seifertite and lingunite, those presences in shocked meteorites have been difficult to explain based on phase equilibrium. A conventional method combining multi-anvil high-pressure apparatus with synchrotron white X-ray was routinely used to observe non-equilibrium behaviors and their kinetics in minerals at pressures up to ~30 GPa by collecting time-resolved X-ray diffraction data every 10 sec with energy dispersive method. By using this system, we found that seifertite and lingunite are metastably formed at high pressures from silica and plagioclase, respectively. The problematic presence of these phases in shocked meteorites can be reasonably explained as metastable phases. Extrapolations of kinetic data obtained to shorter timescales at higher temperatures of shock events uniquely constrain the critical shock durations and the size of the impactor. Similar strategy has also been applied to the back-transformation recorded in shocked meteorites. Time-resolved X-ray observations have revealed that some high-pressure phases such as bridgmanite and lingunite do not directly transform to their low-pressure phases, but through the amorphous state. This may explain the presence of amorphous phases with enstatite and plagioclase compositions in shocked meteorites. Our studies demonstrate that the conventional 10-second time-resolved synchrotron X-ray observations under static pressures capture the critical processes of solid-state reactions during shock events. On the other hand, crystallization of high-pressure phases from shock-induced melt is another important process to be solved. Improvement of the system with better time resolution and grain observations by 2D detector are required to detect the rapid melt crystallization processes.

©2019. Japan Geoscience Union. All Right Reserved.

Ultrafast pump-probe experiemnts for planetary materials using high-power lasers and XFEL

*Norimasa Ozaki[1]

1. Osaka University

Materials at high pressures and temperatures are of great current interest for warm dense matter (WDM) physics, planetary sciences, and inertial fusion energy research. At the high-energy density (HED) conditions, the micro-structures of material significantly influence the behavior and properties. Ultra-short X-ray pulse, *i.e.*, X-ray free electron laser (XFEL), is a unique and powerful tool to directly observe a structure and to reveal the time scale of the structural change under the dynamic high pressures. Here we present recent experimental results on shock-compressed planetary materials using high-power laser and XFEL.

©2019. Japan Geoscience Union. All Right Reserved.

Tracking dynamical phenomena with X-ray free-electron lasers

*Tetsuo Katayama[1]

1. Japan Synchrotron Radiation Research Institute

X-ray free-electron lasers (XFELs) provide brilliant X-ray pulses with femtosecond duration and are utilized to track dynamics, which is difficult to capture using synchrotron radiation. In the femtosecond time domain, one can achieve "molecular movie"[1-3] with an atomic spatio-temporal resolution by combining XFEL and synchronized optical laser pulses. On the other hand, in the nanosecond time domain, XFELs are utilized to observe irreversible dynamic processes[4,5] with the single-shot measurement scheme that can not be performed with synchrotron radiation.
In this presentation, I will talk XFEL properties and research examples at SACLA to discuss the XFEL potentials in Earth and planetary science.

1. T. Katayama *et al.*, submitted.
2. K. H. Kim *et al.*, *Nature* **518**, 385-389 (2015).
3. T. Katayama *et al.*, *Struct. Dyn.* **3**, 034301 (2016).
4. K. H. Kim *et al.*, *Science* **358**, 1589-1593 (2017).
5. E. Nango *et al.*, *Science* **354**, 1552-1557 (2016).

Keywords: X-ray free-electron laser, dynamics

©2019. Japan Geoscience Union. All Right Reserved.

High speed measurement with synchrotron radiation X-ray.

*Kentaro Uesugi[1]

1. Japan Synchrotron Radiation Research Institute

X-ray is suitable for a probe for investigation of materials inside because of its deep penetration depth. For examples, X-ray transmission images show the internal structure of materials, the X-ray energy spectrums show the chemical characteristics and mineral phase of the materials can be obtained from X-ray diffraction.

Synchrotron radiation X-ray has continuum spectrum and is highly collimated basically. Therefore, the X-ray condition such as energy, beam size and intensity could be tuned for the purpose of the measurement and materials. A lot of insertion devices such as in-vacuum type undulator have been installed in a storage ring of third-generation synchrotron radiation facility to obtain ultra-high flux density (photons / sec / mm^2) or brilliance (photons / sec / mm^2 / $(mrad)^2$ / 0.1%b.w.) X-ray at the sample. The highest brilliance of X-ray is about 10^9 time higher than the laboratory-based X-ray source. The high brilliant X-ray enable us to do ultra-high speed, spatial resolution and energy resolution measurement comparing to laboratory-based system.
At the SPring-8 the following experiments could be possible, X-ray imaging with more than 1kHz frame rate (liquid flow), X-ray diffraction with several kHz (insect flapping) and dispersive XAFS with 100Hz. These are essential technique for capturing various non-equilibrium or dynamic phenomena. At the conference, some examples of high speed measurement will be shown.

Keywords: Synchrotron radiation X-ray, High speed measurement, X-ray imaging

©2019. Japan Geoscience Union. All Right Reserved.

Recent advances in high-pressure synchrotron X-ray experiments on magmas under pressure at the beamline 16-BM-B in Advanced Photon Source

*Yoshio Kono[1]

1. Geodynamics Research Center, Ehime University

High-pressure synchrotron X-ray experiments using large volume press is one of the most useful tools to investigate structure and properties of Earth’ s materials under high pressure and high temperature conditions. However, in contrast to extensive studies on high-pressure mineralogy and mineral physics, experimental investigation of structure and properties of magmas under pressure has been limited, due to experimental difficulties. In the past decade, new developments in high-pressure experiments, particularly combined with synchrotron X-ray techniques, have advanced the study of magmas under pressure. The new experiments have revealed significant changes to the structure and physical properties of magmas under pressure. In this talk, I will introduce recent advances in high-pressure synchrotron X-ray experiments for studying magmas at high pressures, developed at the beamline 16-BM-B, HPCAT in Advanced Photon Source, USA.

Keywords: High pressure, Magma, Synchrotron X-ray

©2019. Japan Geoscience Union. All Right Reserved.

[J] Oral | U (Union)：Union

Wed. May 29, 2019 10:45 AM - 12:15 PM JST | Wed. May 29, 2019 1:45 AM - 3:15 AM UTC | Convention Hall A 2F

[U-07] How JpGU will manage environment and disaster from the impacts of unforeseen geo-hazards

convener:Koji Okumura(Graduate School of Letters, Hiroshima University), Jun Matsumoto(Deaprtment of Geography, Tokyo Metropolitan University), Daisaku Kawabata(Institute of Geology and Geoinformation, Geological Survey of Japan, AIST), Masaki Matsushima(Department of Earth and Planetary Sciences, School of Science, Tokyo Institute of Technology), Chairperson:Daisaku Kawabata, Koji Okumura(Hiroshima University)

Japan Geoscience Union has established the Environment and Disaster Coping Committee in 2008 to cope with various environmental and natural hazard issues. Those issues are among the most urgent and important geoscientific issues for the society. The enormous extent and severity of the disasters caused by the 2011 Tohoku earthquake and tsunamis urged collaboration of many scientific associations to know the effects of the extreme natural hazards. A number of severe meteorological, volcanic, and earthquake hazards demanded interdisciplinary collaboration to respond to the emergencies. The occurrence and consequence of severe disasters were clearly controlled by the combined effect of environments and hazards. In this session, we share our activities related with recent unforseen disasters, and discuss how Japan Geoscience Union sets up the framework to enhance the real cooperation among scientific associations to prepare the impacts of unexpected hazards.

10:45 AM - 10:55 AM JST | 1:45 AM - 1:55 AM UTC

[U07-01] Seismotectonic environments and landscape as keys to mitigate the impacts from unexpected hazards

*Koji Okumura[1] (1.Graduate School of Letters, Hiroshima University)

10:55 AM - 11:10 AM JST | 1:55 AM - 2:10 AM UTC

[U07-02] Activities related with the eruption at Kusatsu-Shiranesan (Motoshiranesan) volcano on 23 Jan,2018 - Focusing on JMA's activities -

*Junichi Miyamura[1] (1.Japan Meteorological Agency)

11:10 AM - 11:25 AM JST | 2:10 AM - 2:25 AM UTC

[U07-03] Correspondences to society events at emergency disaster – In case of the Annual Meeting of the Geological Society of Japan -

*Matsuda Hiroki[1,2] (1.Kumamoto University, 2.the Geological Society of Japan)

11:25 AM - 11:40 AM JST | 2:25 AM - 2:40 AM UTC

[U07-04] Aftershock and microtremor array observation around the source area of the 2018 Hokkaido Eastern Iburi earthquake

*Masayuki Yoshimi[1], Kahori Iiyama[2], Hitoshi Morikawa[2], Hiroyuki Goto[3] (1.Geological Survey of Japan, AIST, 2.Tokyo Institute of Technology, 3.DPRI, Kyoto Univ.)

11:40 AM - 11:55 AM JST | 2:40 AM - 2:55 AM UTC

[U07-05] Effect of non-linear site response on earthquake hazard map

*Takao Kagawa[1] (1.Tottori University Graduate School of Engineering)

11:55 AM - 12:10 PM JST | 2:55 AM - 3:10 AM UTC

[U07-06] Evolution of catastrofic landslides due to rapid valley incision and filling since Last Glacial Age in central Nepal Himalayas

★Invited Papers

*Hiroshi YAGI[1] (1.Faculty of Art, Science and Education, Yamagata University)

12:10 PM - 12:15 PM JST | 3:10 AM - 3:15 AM UTC
Discussion

Seismotectonic environments and landscape as keys to mitigate the impacts from unexpected hazards

*Koji Okumura[1]

1. Graduate School of Letters, Hiroshima University

Even if we know little about the hazards that may occur at certain location, the geologic envieonments and landscape may tell us the risks. They are seismotectonic enveironments and landscapes. Since people contact with geologic and geomorphic environments and landscapes very often, they will be useful keys to understand the risks from natural hazards in that location. The environments and landscapes of the 2018 June 16 Osaka-hokub earthquakes and 2018 September 6 Hokkaido Iburi Tobu earthquakes will be discussed.

Keywords: seismotectonics, geology, geomorphology

©2019. Japan Geoscience Union. All Right Reserved.

Activities related with the eruption at Kusatsu-Shiranesan (Motoshiranesan) volcano on 23 Jan,2018 - Focusing on JMA’s activities -

*Junichi Miyamura[1]

1. Japan Meteorological Agency

Japan is one of the world's leading volcanic country with 111 active volcanoes, and so many volcanic disasters have been repeated. But after the early 20th century, no large eruptions occurred and volcanic activity in Japan has been quiet.
On the other hand, the eruption at Ontakesan volcano on 2014 sacrificed many mountaineers who were near the crater and caused the greatest volcanic disaster after the war. One of the features of eruptive disasters is that even a small eruption could lead to a great disaster if encountered near the crater. In the latest case, the eruption at Kusatsu-Shiranesan volcano on January 23, 2018 suddenly occurred at Motoshiranesan where there was no record of historical eruption and caused human damage at the ski resort near the eruption point.
The Volcanological Society of Japan was established as the world's first academic conference on volcanoes in 1932 and re-established as a specified nonprofit corporation in 2002 for the purpose of advance and disseminate volcanology and related science. The institution to which the member belongs is not only universities and research institutes, but also local municipalities, disaster prevention organizations, high schools and geological consultants. Recently, in order to lead to the reduction of volcanic disaster by volcanology research, we also focus on public awareness raising, such as opening lectures and symposiums targeting the general public.
In this presentation, we will introduce the activities related with the 2018 Motoshiranesan eruption by each institution, mainly on the correspondence of Japan Meteorological Agency.

Keywords: The Volcanological Society of Japan, The 2018 Motoshiranesan Eruption, Japan Meteorological Agency, Support for Activities of Volcanic Disaster Mitigation

©2019. Japan Geoscience Union. All Right Reserved.

Correspondences to society events at emergency disaster –In case of the Annual Meeting of the Geological Society of Japan -

*Matsuda Hiroki[1,2]

1. Kumamoto University, 2. the Geological Society of Japan

We, the Geological Society of Japan, had the misfortune to be hit by emergency disasters during the Annual Meeting last two years. Consequently, we had no choice but to cancel a part of the Meeting. In this presentation, the circumstances and our treatments in those emergencies will be introduced.

Keywords: correspondence at emergency disaster, typhoon, earthquake, the Geological Society of Japan

©2019. Japan Geoscience Union. All Right Reserved.

Aftershock and microtremor array observation around the source area of the 2018 Hokkaido Eastern Iburi earthquake

*Masayuki Yoshimi[1], Kahori Iiyama[2], Hitoshi Morikawa[2], Hiroyuki Goto[3]

1. Geological Survey of Japan, AIST, 2. Tokyo Institute of Technology, 3. DPRI, Kyoto Univ.

The 2018 Hokkaido Eastern Iburi earthquake (Mw 6.6, depth=37 km) is a shallow to moderate depth earthquake. Strong ground motions were widely observed around the source area and in the Ishikari-Yufutsu sedimentary basin, culminated with the maximum seismic intensity VII of the JMA scale at JMA Atsuma seismic station. Waveforms with clear velocity pulse, having 1 to 3 dominant period, were observed along the west of the source area: K-NET Mukawa (HKD126), JMA Atsuma, KiK-net Atsuma (IBUH03), and Atsuma city hall. Velocity response spectra of these pulse waveforms are comparable to that of the Takatori station record, located close to the heavy damage area, during the 1995 Kobe earthquake. Therefore, we need to resolve the reason why such strong ground motions were developed during the 2018 earthquake although the magnitude was moderate (Mw 6.6) and focal depth was not shallow.

Four seismic station, where the strong pulse waveform was observed, are commonly located along the basin edge of the Yufutsu sedimentary basin. The subsurface velocity structure around the source area is considered to responsible for producing the ground motions. Thus, we conducted temporal observation of aftershocks and microtremor array measurements around the source area to investigate spatial variation of the site amplification and subsurface velocity structure. We deployed 14 temporal seismic station during 16th-21st Sep., 2018 to record around 20 aftershocks with magnitude larger than M2. We also conducted microtremor array survey at 13 locations with array aperture of several to 30 meters. Site amplification and subsurface velocity structures will be shown.

Keywords: The 2018 Hokkaido Eastern Iburi earthquake, strong ground motion, aftershock observation, microtremor array survey, subsurface velocity structure, site amplification

©2019. Japan Geoscience Union. All Right Reserved.

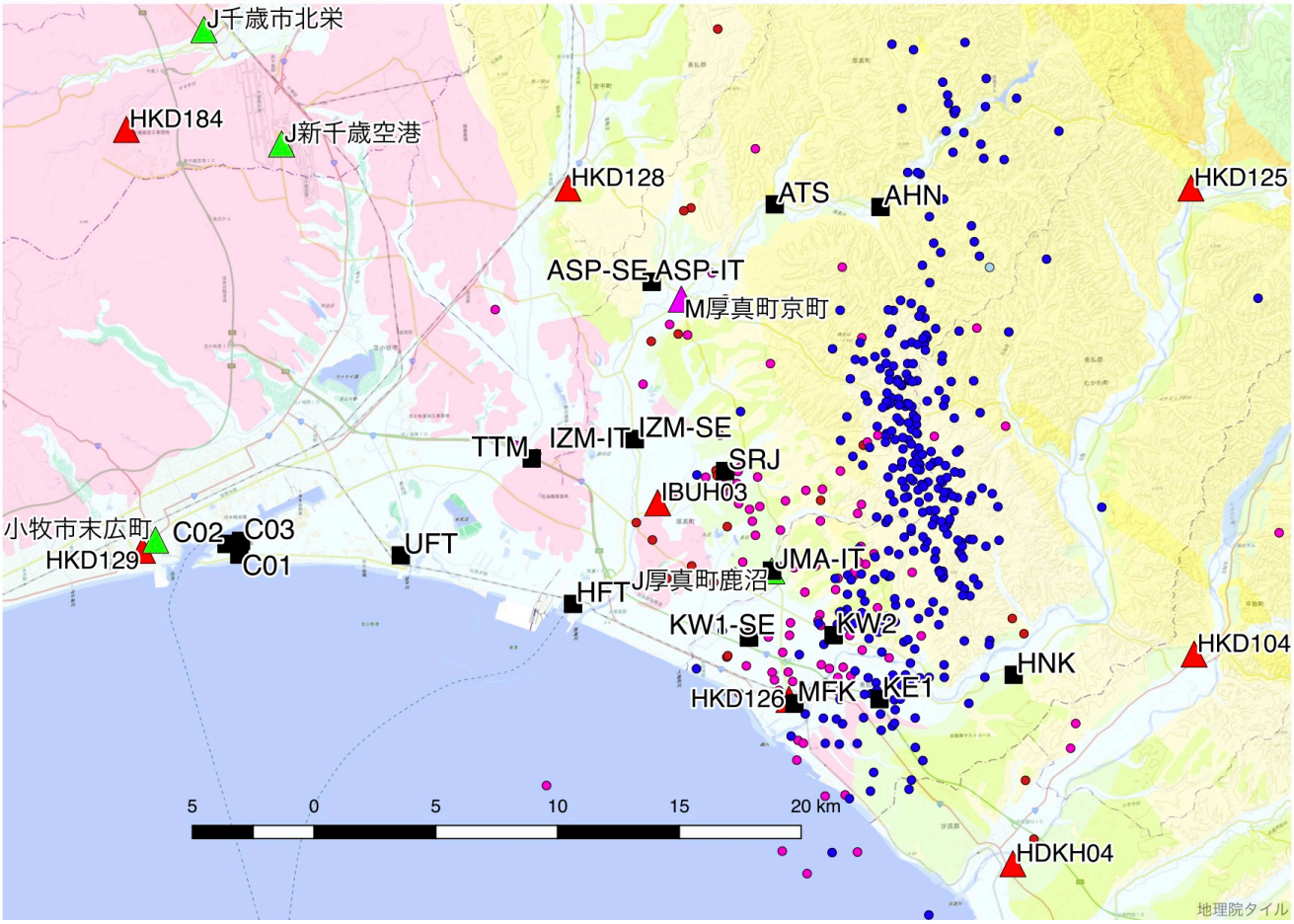

©2019. Japan Geoscience Union. All Right Reserved.

Effect of non-linear site response on earthquake hazard map

*Takao Kagawa[1]

1. Tottori University Graduate School of Engineering

Various earthquake hazard maps are published by country and municipalities in Japan. It is better to consider non-linear site response for the hazard maps, however, simple frequency independent amplification of ground motion is frequently adopted. The site responses are generally evaluated from the data of microtremor or stationary earthquake observations; i.e. weak motion, therefore rigidity reduction and damping increase under strong ground motion are not considered in the responses. It is suspected that prolonged predominant period by non-linear site response and synchronized prolongation of residential natural period cause heavy building damages by the 2016 Kumamoto earthquake. It is also suspected that non-linear site response was one of triggers of slope failures and fill ground disaster through the 2018 Hokkaido eastern Iburi earthquake. The non-linear site response is an important issue to consider earthquake disaster by strong ground motion and also ground disaster.

Seismological community has noticed the effect from 1990s, however, evaluation methodology; i.e. program SHAKE, has been proposed in 1970s in engineering community. Latest methodologies have been introduced for modeling subsurface structures in seismological community such as microtremor survey, seismic interferometry, diffuse wave field theory and so on. Joint study across research fields beyond earth and planetary science is required for providing further realistic earthquake hazard map.

Keywords: Non-linear site response, Earthquake hazard map, Joint study across research fields

©2019. Japan Geoscience Union. All Right Reserved.

Evolution of catastrofic landslides due to rapid valley incision and filling since Last Glacial Age in central Nepal Himalayas

*Hiroshi YAGI[1]

1. Faculty of Art, Science and Education, Yamagata University

There remain higher landslides located on the upper slope of inner gorge, that was formed due to sever valley incision before 20k in the Last Glacial Age.

Sever valley incision caused destabilization of valley slope and the consequent valley filling stabilized the valley slope again. Present landslides are caused by re-incision of the filling of the Last Glacial Age.

Keywords: Nepal Lessor Himalaya, rapid valley incision & valley filling, destabilization of valley slope, inner gorge, last glacial age

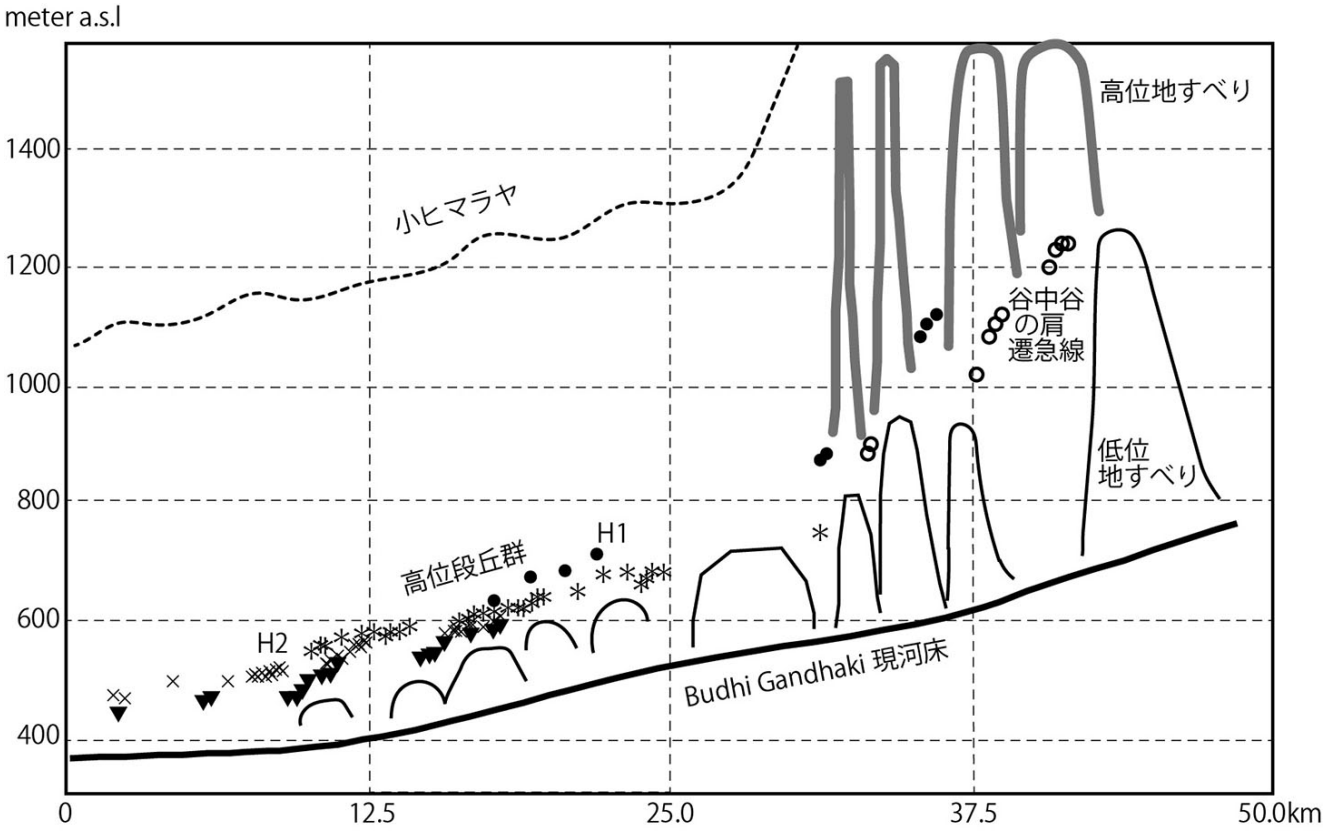

©2019. Japan Geoscience Union. All Right Reserved.

[E] Poster | P (Space and Planetary Sciences)：P-PS Planetary Sciences

Wed. May 29, 2019 10:45 AM - 12:15 PM JST | Wed. May 29, 2019 1:45 AM - 3:15 AM UTC | Poster Hall International Exhibition Hall8, Makuhari Messe_2

[P-PS02] Regolith Science

convener:Koji Wada(Planetary Exploration Research Center, Chiba Institute of Technology), Akiko Nakamura(Graduate School of Science, Kobe University), Patrick Michel(Observatoire De La Cote D'Azur), Kevin John Walsh(Southwest Research Institute Boulder)

Recent planetary explorations have revealed that almost all solid bodies in the solar system are covered with small particles, called regolith. The surface geology, especially regolith behavior on the surfaces of solid bodies, becomes increasingly more important as represented by Hayabusa mission and other on-going and planned sample-return missions such as Hayabusa2, OSIRIS-REx, and MMX.

For fully understanding the regolith science, it is required to know and compare the regolith conditions on various celestial bodies, from asteroids to planets, with various methods.

Therefore, this session welcomes broad topics related to regolith on various celestial bodies, such as asteroids, comets, the Moon, the martian moons, Mars, etc. Papers on the formation, evolution, and alteration processes of regolith particles and regolith systems on the surface of planetary bodies, remote and in-situ observational results and techniques, analyses and results of returned samples, and laboratory, numerical, and theoretical studies on the fundamental physical and chemical processes are all welcome.

Note that what we call regolith is not just fine grains: all kinds of materials (more or less loose) that lie on the surface, from cobbles to finer grains, are our targets.

[PPS02-P01] Abrasion experiments of mineral and meteorite grains: Dependence of particle size and vibration rate on abrasion rate and its application to Itokawa and lunar regolith particles.

*Hirotaka Yamaguchi[1], Akira Tsuchiyama[1], Akiko Nakamura[2] (1.National University Corporation, Kyoto University, 2.National University Corporation,Kobe University)

[PPS02-P02] Measurements of adhesive force of meteorite powders using centrifugal method

*Yuuya Nagaashi[1], Akiko Nakamura[1] (1.Kobe University)

[PPS02-P03] Laboratory impact penetration experiments conducted at simulated reduced gravity

*Akiko Nakamura[1], Kana Morizono[2], Yuuya Nagaashi[1] (1.Graduate School of Science, Kobe University, 2.Faculty of Science, Kobe University)

[PPS02-P04] MARAUDERS: Using instrumented nano-impactors to probe the icy properties of Lunar permanently shadowed regions

*Ronald Ballouz[1], Sarah T Crites[2], Naoya Ozaki[2], Shun Arahata[3], Nicola Baresi[2], Ralf Bolden, Onur Celik[4,2], Yu Himeno[3], Lucie Riu[2], Kevin J Walsh[5] (1.Lunar and Planetary Lab, University of Arizona, Tucson, AZ, USA, 2.Institute of Space and Astronautical Science, Sagamihara, Japan, 3.University of Tokyo, Tokyo, Japan, 4.Sokendai Graduate University, Japan, 5.Southwest Research Institute, Boulder, CO, USA)

[PPS02-P05] Surface size-frequency distribution of accumulating boulders using discrete element simulations of spherical particles in 3D

*Hiroshi Kikuchi[1], Hideaki Miyamoto[1] (1.The University of Tokyo)

[PPS02-P06] Experimental Study to Determine the Best Compression Ratio of High-Resolution Images of Small Bodies for the Martian Moons eXploration (MMX) Mission

*Yuta Shimizu[1], Hiroaki Kamiyoshihara[1], Takafumi Niihara[1], Hideaki Miyamoto[1] (1.University of Tokyo)

Abrasion experiments of mineral and meteorite grains: Dependence of particle size and vibration rate on abrasion rate and its application to Itokawa and lunar regolith particles.

*Hirotaka Yamaguchi[1], Akira Tsuchiyama[1], Akiko Nakamura[2]

1. National University Corporation, Kyoto University, 2. National University Corporation,Kobe University

Rounded edges were found in some regolith particles collected from asteroid Itokawa [1] and Moon [2]. These particles should be formed by mechanical abrasion [1]. Seismic-induced grain motion by micrometeoroid impacts [1] and YORP effect [3] were proposed for the abrasion process on Itokawa. However, it is not clear how these processes actually work on the surfaces of the airless celestial bodies.

In order to understand detailed process of the abrasion, our research group have carried out abrasion experiments using mineral, rock and meteorite grains (grain size: 1-2 mm) [4]. Samples used were quartz, olivine, corundum, marble, L5 chondrite meteorite (Sayh al Uhaymir 001) and CM chondrite meteorite (Murchison). These particles were put into a vessel of 10 mL with the filling ratio of ~50 % and the sample was vibrated with the rate from 1000 to 3000 rpm using a multi-beads-shocker (YASUIKIKAI Co.). The proportion of powder (<250 μm) produced by vibration at first 1 min., ΔP_1, was adopted as the measure of abrasion and its dependence of the vibration rate and the sample strength was examined. However, the particle size used in the experiments (1-2 mm) is larger than Itokawa particles (< a few hundred μm). In addition, the vibration rates used in the experiments are larger than those estimated for Itokawa(~100 rpm) and Moon (~700 rpm) by considering the maximum seismic acceleration due to micrometeoroidimpacts onto their surface [5]. In the present study, therefore, we conducted new experiments with different parameters such as particle size and vibration rate using the same experimental procedure as [4]. In the present experiments, we used quartz grains for examining the effect of packing ratio in the vessel (Exp-1), particle size (Exp-2), mixing ratio of large and small particles (Exp-3). The effect of lower vibration rate (100 - 1000 rpm) was examined using olivine and basalt as well as quartz (Exp-4). Experiments using basalt at higher vibration rates were also made.

We obtained following results. Exp-1: $\Delta P_1$was constant in a wide range of the filling rate except for the filling rate of 2/3, where ΔP_1showed a peak value. Exp-2: $\Delta P_1$is proportional to the particle size. Exp-3: When the proportion of large particles is larger than 25%, $\Delta P_1$is almost constant and the same as $\Delta P_1$for the large particles. Exp-4: In the previous experiments, ΔP_1increases with the vibration rate with the power of 1.1-2.9 for large vibration rates (>~1000 rpm) [4] while the power becomes smaller (0.67-0.77) for smaller vibration rates (<~1000 rpm). This result shows that the abrasion mode changed at ~1000 rpm. In order to understand abrasion modes, SEM observation of powder particles produced in the abrasion experiments were also made. It was found that chipping of particle edges occurred at low vibration rate (~100 rpm) and the proportion of gradual wearing on the whole particle surface gradually increased as the vibration rate increased.

We estimated the amount of abrasion of Itokawa and lunar regolith particles in a regolith layer by impact based on the present experiments. ΔP_1values of basalt at 100 and 700 rpm, which corresponding to Itokawa and Moon [4], are ~0.1 %and ~1 %, respectively (Exp-4). If we consider the size of Itokawa and Moon particle (~100 μm), ΔP_1on Itokawa and Moon should be ~0.01%and ~0.1%, respectively(Exp-2). These values are larger than those estimated from the previous experiments [4] by the order of about 1.

©2019. Japan Geoscience Union. All Right Reserved.

The present results suggest that abrasion is possible on the Moon and may occur on Itokawa as well.

[1] Tsuchiyama et al. 2011. Science, 333, 1125-1128.

[2] Sakurama et al. 2016. JpGU, Abstract, PPS03-13.

[3] Connolly et al. 2015. Earth Planet and Space, 67: 12.

[4] Tsuchiyama et al. 2018. LPSC, Abstract 1844.

[5] Yasui et al. 2015. Icarus, 260: 320-331.

©2019. Japan Geoscience Union. All Right Reserved.

Measurements of adhesive force of meteorite powders using centrifugal method

*Yuuya Nagaashi[1], Akiko Nakamura[1]

1. Kobe University

Introduction: Layer of fine particles in the laboratory shows fluffy structure owing to interparticle force (e.g., Kiuchi and Nakamura, 2014). On small bodies, interparticle forces are thought to be dominant compared to gravitational force for small particles. Fast rotators spin in excess of what gravity alone could hold together were shown to be explained by cohesive force between constituent particles (Sánchez & Scheeres, 2016). Measurements of cohesive force between micron-size spherical silica particles using an atomic force microscope cantilever (Heim et al., 1999) showed that the results agree with predictions of the JKR model (Johnson et al., 1971). On the other hand, measurements of cohesive force between 50 or 100 μm glass beads and a glass plate using centrifugal method showed that the results are by several orders of magnitude smaller than predictions of the JKR theory (Nagaashi et al., 2018). In addition, it was also shown that ~ 70 μm irregularly-shaped silica and alumina grains have the range of adhesive force similar to the glass beads, indicating that the adhesive force of the spherical and the irregular particles used in the measurement is dependent not on the macroscopic shape but on the microscopic surface roughness. However, it is not clear whether the adhesive force of the particles that actually form the asteroids is similar to those of silica grains. Measurements of adhesive force of meteorite powders will bring important knowledge of adhesive force of the asteroid-forming particles for understanding physical processes occurring on asteroids.

Experimental method: In this study, we used centrifugal method as in our previous study (Nagaashi et al., 2018) in order to measure cohesive or adhesive force between a particle and a plate. This method can directly measure the cohesive or adhesive force of many particles at the same time, which enables us to statistically analyze the results. Additionally, it can also deal with irregularly shaped particles. The measurements were conducted for carbonaceous chondrite (CV3: Allende, CM2: Murchison), ordinary chondrite (LL3.5: NWA 539, LL5: NWA 1794, LL6: NWA 542), and Eucrite (Millbillillie) powders of median diameter ~ 50 μm. We discretely increased the centrifugal acceleration from 10g to 5000g (g: the Earth's gravitational acceleration) and took optical microscope images of the same location of the plate before and after applying centrifugal force at each centrifugal acceleration. We determined the range of centrifugal acceleration within which the particle separated from the plate based on the microscope images and estimated the cohesive or adhesive force between the particle and the plate. More detail description of the procedure is described in Nagaashi et al. (2018).

Results: As compared with the JKR adhesion force $F_{ad} = 3\pi\gamma R$ (γ: surface energy, R: reduced radius of particle) for a spherical particle of silica composition, we calculated the effective surface energy of particles which reproduces the measurement value, and compared the results of each type of meteorite powders. Similar to the previous results described in the above (Nagaashi et al., 2018), the measurements of meteorite powders showed a wide range of adhesive force distributions over several orders of magnitude for all measured meteorite types. In addition, we found that the effective surface energy of Allende and Murchison meteorite particles were several times smaller than those for the particles of the other meteorite types. There is no difference in the axial ratio of each type of meteorite powders, and therefore this is likely due to differences in material composition or micro-topography of the particles.

©2019. Japan Geoscience Union. All Right Reserved.

©2019. Japan Geoscience Union. All Right Reserved.

Laboratory impact penetration experiments conducted at simulated reduced gravity

*Akiko Nakamura[1], Kana Morizono[2], Yuuya Nagaashi[1]

1. Graduate School of Science, Kobe University, 2. Faculty of Science, Kobe University

Small bodies are covered with a layer of regolith made up of particles of various sizes. It is important to understand the interactions that occur with surface regolith when a spacecraft lands on or when a block secondarily collide with the regolith layer at low velocity. Penetration depth of an impactor in granular layer was investigated under Earth’ s gravity and an empirical relationship between the drop height and penetration depth was shown to reproduce the experimental results for various granular materials (Uehara et al., 2013). Deceleration of spherical impactor in granular layer was experimentally and theoretically investigated and deceleration formulae were proposed (Katsuragi and Durian 2007, Nakamura et al., 2013; Katsuragi and Durian 2013). On the other hand, interactions of spheres with simulated regolith have been studied at reduced gravity and micro-gravity conditions (Murdoch et al., 2016; Brisset et al., 2018). However, more data of penetration depth of impactor are required to establish quantitative understanding of the penetration process in regolith under low gravity.

We conducted laboratory low-velocity impact experiments of a sphere into granular layer at reduced gravity. Impactor was a glass sphere with a diameter of 16.7 mm and granular layer consisted of glass beads with a diameter of 1 mm. The glass beads were packed in a bucket having a diameter of 15 cm and a depth of 15 cm. The bucket was hung with three constant load springs. The bucket was fixed with two electromagnets, and when the electromagnet was switched off, it dropped vertically downward with the gravity reduced. The simulated reduced gravity level was monitored by an accelerometer placed in a bucket and found to be on average 0.26 G. A plastic straw with horizontal line drawing was glued to the glass sphere. The glass sphere collided with the glass bead layer at a relative velocity between 2 and 4 ms $^{-1}$. The penetration process of the glass sphere with the straw was imaged at 240 fps by a camera attached to the bucket. The final depth of the glass sphere was found to be systematically deeper than the depth found in the experiment conducted at 1 G.

Keywords: regolith, low gravity, impact

©2019. Japan Geoscience Union. All Right Reserved.

MARAUDERS: Using instrumented nano-impactors to probe the icy properties of Lunar permanently shadowed regions

*Ronald Ballouz[1], Sarah T Crites[2], Naoya Ozaki[2], Shun Arahata[3], Nicola Baresi[2], Ralf Bolden, Onur Celik[4,2], Yu Himeno[3], Lucie Riu[2], Kevin J Walsh[5]

1. Lunar and Planetary Lab, University of Arizona, Tucson, AZ, USA, 2. Institute of Space and Astronautical Science, Sagamihara, Japan, 3. University of Tokyo, Tokyo, Japan, 4. Sokendai Graduate University, Japan, 5. Southwest Research Institute, Boulder, CO, USA

The Mini lAndeRs And boUncers Deployed for Exploration and Regolith Science (MARAUDERS) is a small satellite concept that aims to characterize the surface and volatile properties of regolith in permanently shadowed regions (PSRs) around the Moon's poles. Large PSRs are cold enough to trap scientifically and economically valuable volatiles such as water ice. However, despite ongoing studies, the distribution, abundance, and physical phase of volatiles at the Moon's poles remains elusive [1]. *In-situ* measurements are required to conclusively determine the geotechnical and physical properties of lunar polar volatiles. To address these needs, the MARAUDERS team is currently developing a technique using instrumented nano-impactors to determine the mechanical properties of regolith at the impact point.

Small spacecraft equipped with penetrators or inertial measurement units (IMU) can characterize the strength and structure of the planetary surface that they impact. Early space exploration used penetrometers to determine the surface properties of the Moon and Mars before the arrival of astronauts and rovers. In recent decades, spacecraft equipped with IMUs characterized the surface of Titan [1], and determined the sub-surface stratification of ice and rock on the comet 67P/C-G [2]. While this technique is unable to relay the detailed mineralogical and elemental composition at the impact point, it obtains a first-order structural knowledge of potentially hazardous surfaces and sub-surfaces that cannot be obtained through remote sensing. This is highly relevant for PSRs due to extreme environmental conditions such as the lack of solar illumination, cold temperatures, and challenging communications.

Here, we present preliminary analysis on the instrument capabilities based on the potential deployment scenarios to PSRs, and the possible mechanical properties of the regolith found within these regions (Fig. 1). We present a computational study of the varying response of an instrumented impactor impacting regolith with variable i) water ice content (0-10%), ii) impactor speeds (50-250 m/s], and iii) impact angles (45-90˚), using a discrete element method code [4]. Furthermore, we analyse the ejecta properties and resulting crater morphology in order to gain a better understanding of impact processes on icy bodies. Our next steps will be to conduct laboratory impact experiments using prototypes of our instrumented impactors to calibrate the impact response on lunar simulant with variable water-ice content.

References:

1. Lorenz, R. et al. (1994) Meas. Sci. Technol. 5, 1033-1041

2. Biele, J. et al. (2016), Science, 349, 6247.

3. Holsapple, K.A. (1994) LPSC 25, 559.

©2019. Japan Geoscience Union. All Right Reserved.

4. Richardson, D.C. et al. (2011) Icarus, 212, 427–437.

Acknowledgements:

This material is based upon work supported by ISAS/JAXA’s start-up fund for international collaborations, the Aerospace Project Research Associate Program, and the International Top Young Fellow Program.

Keywords: Moon, Permanently Shadowed Regions, Volatiles, Regolith Characterization

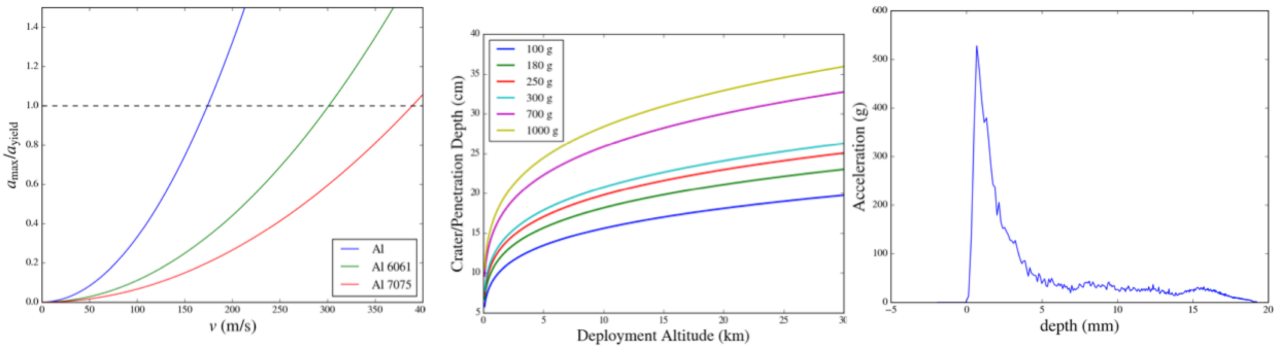

Fig. 1. Preliminary analysis showing shock tolerance, penetration depth, and instrument response for different instrument designs and impact speeds. Left: Maximum shock tolerance before material failure for three different aluminum alloy instrument housings. An Al-7075 housing can withstand impact speeds greater than 350 m/s. Middle: Penetrations depths for a 250 m/s impact for different impactor masses (100 - 1000 grams). For a nominal impactor mass of 180 g, a deployment from 15 km from the lunar surface results in a penetration depth of < 20 cm (based on [3]). Right: Simulated response of a 180 g impactor using a particle dynamics simulation.

©2019. Japan Geoscience Union. All Right Reserved.

Surface size-frequency distribution of accumulating boulders using discrete element simulations of spherical particles in 3D

*Hiroshi Kikuchi[1], Hideaki Miyamoto[1]

1. The University of Tokyo

Several spacecraft have revealed new detail about small bodies such as asteroids, comets, and small satellites. Images from Hayabusa, Hayabusa2, and OSIRIS-REx showed more boulders on the surfaces than originally expected. Owing to the high resolution at which images were taken, a number of boulders could often be observed in clusters. In future explorations, because we expect to observe more cases of boulder-rich surfaces, the characterization of the size-frequency distribution (SFD) will be important especially for the missions involving a lander such as MMX. Basically, measuring the SFD of boulders on a surface is expected to represent that of the interior. However, considering that surface boulders can hide the underlying boulder, it is not clear that the SFD in a volume can adequately be represented by its surface. Therefore, in this work, we focus on how accumulating boulders with a known SFD appear from above.
In order to compare the SFD on a surface with that of a volume, the initial SFD has to be known. For the initial study, numerical simulations are convenient, because they can easily prepare the suitable conditions. In the previous studies, spherical boulders were randomly distributed in three-dimensional space, and only those on the surface were automatically extracted and measured (Tancredi et al., 2015). It was found that the particle distribution on the surface well reproduces the overall particle distribution. We consider that there is room for improvement in the arrangement of particles and the measurement of particles. Thus, we implement a three-dimensional discrete element method using rigid spherical particles to simulate the accumulation of a boulder-rich regolith. We then measure particles one by one manually when viewed from above the surface. For initial conditions, we set the size and the number of boulders randomly as specified by the power law index of -3. During a simulation, particles are not initially adjacent to each other and are instead dropped from the height of 30 m above the 54 x 54 m planar surface. The total number of particles is changed from 3000 to 7000 in 1000 increments. After the simulation, the size and number of the particles are measured manually when viewing the surface from the vertical direction. Then we refer to Clauset et al. (2009) for fitting and evaluating the data using the p-value metric.
We find that the power law index of the SFD is low when the number of particles is 3000. This may be because the larger particles are not buried in the smaller particles, resulting in only the number of smaller particles being reduced when viewed from above. When the total number is 4000 or more in a volume and p-value is high, the surface power law index from the multiple simulations is consistent with the specified value of -3 for some cases.
The SFD observed on the surface corresponds to the SFD in the interior of the body for the following conditions: the thickness of the deposited particles is larger than the largest particle and the p-value is high. For more detailed analyses, investigating the effects of the number of simulations, the complicated shapes of boulders, and parameter studies are needed. In addition, for a deeper understanding of the problem, experiments in a similar condition to the airless bodies using simulated regolith particles such as UTPS-TB and UTPS-IB (Miyamoto et al., 2018) are also required.

Keywords: Discrete element method, Boulder size-frequency distribution, Interior of small bodies

©2019. Japan Geoscience Union. All Right Reserved.

Experimental Study to Determine the Best Compression Ratio of High-Resolution Images of Small Bodies for the Martian Moons eXploration (MMX) Mission

*Yuta Shimizu[1], Hiroaki Kamiyoshihara[1], Takafumi Niihara[1], Hideaki Miyamoto[1]

1. University of Tokyo

Data transmission rate becomes one of the biggest limiting factors in space explorations; technological advance in increasing pixel numbers of camera images dominates the improvement of the data transmission rate. Yet, high demand exists for high-resolution images especially in geological studies, and thus there is a tradeoff between the spatial resolutions (or pixel numbers) and the number of images to be transmitted to Earth. The telecommunications issue is critical for Martian Moons eXploration (MMX) mission that explore either/both Phobos and Deimos and return samples. Especially, timely transmission of high-resolution images is required for the selection of sampling site both in terms of scientific impacts and of the landing safety. The highest image resolution of the current camera configuration is as good as several tens of centimeters per pixel and the size of image is 3296 x 2472 pixels, which means 7 color (3 bands) images can be up to 1 GB if no compression is considered. During the landing phase, such large data have to be sent at the limited bitrate (< 32 kbps) to select landing and sampling sites, while the landing duration is about 4 hours. Thus, considering the best compression scheme of images is a big issue for landing operation. Lossy compression can significantly reduce the sizes of images, though images can be scientifically worthless when compressed too much. The best compression ratio should make the sizes of images as small as possible without losing scientific importance.

Here, we develop a method of rapidly determining the best compression ratio of high-resolution images of the surface of small bodies. For preparing the image studied in this research, we take an experimental scheme, where we develop a simulated Phobos surface by using a high-quality simulant of Phobos regolith (UTPS-TB) and take simulated images of the surface of Phobos in somehow similar condition with the camera of the MMX mission. The images are compressed by JPEG2000, which is planned to be used in MMX mission, and the influence of the compression is analyzed by objective methods such as Structural SIMilarity (SSIM) and entropy of image. The results shows that they are able to rapidly detect the exact ratio, in which the quality of the images started to be diminished.

Moreover, by defining scientific value of images as detectability of rock gravel on the surface of celestial bodies and showing that the loss of scientific value can be expressed by the change in the value of slope of Cumulative Size-Frequency Distribution (CSFD) of gravel, we carefully confirm whether the decrease in the image quality is truly connected with the loss of scientific information such as for landing operations and conclude that those objective methods can determine the best compression ratio. By using those methods, the spacecraft can autonomously complete the process of finding the best compression ratio, compressing images and sending it to the ground within a few minutes even if it has only a limited transmission rate.

Keywords: the best compression ratio, Cumulative Size-Frequency Distribution (CSFD), Martian Moons eXploration (MMX)

©2019. Japan Geoscience Union. All Right Reserved.

[E] Poster | P (Space and Planetary Sciences)：P-PS Planetary Sciences

Wed. May 29, 2019 5:15 PM - 6:30 PM JST | Wed. May 29, 2019 8:15 AM - 9:30 AM UTC | Poster Hall International Exhibition Hall8, Makuhari Messe_2

[P-PS02] Regolith Science

convener:Koji Wada(Planetary Exploration Research Center, Chiba Institute of Technology), Akiko Nakamura(Graduate School of Science, Kobe University), Patrick Michel(Observatoire De La Cote D'Azur), Kevin John Walsh(Southwest Research Institute Boulder)

Recent planetary explorations have revealed that almost all solid bodies in the solar system are covered with small particles, called regolith. The surface geology, especially regolith behavior on the surfaces of solid bodies, becomes increasingly more important as represented by Hayabusa mission and other on-going and planned sample-return missions such as Hayabusa2, OSIRIS-REx, and MMX.

For fully understanding the regolith science, it is required to know and compare the regolith conditions on various celestial bodies, from asteroids to planets, with various methods.

Therefore, this session welcomes broad topics related to regolith on various celestial bodies, such as asteroids, comets, the Moon, the martian moons, Mars, etc. Papers on the formation, evolution, and alteration processes of regolith particles and regolith systems on the surface of planetary bodies, remote and in-situ observational results and techniques, analyses and results of returned samples, and laboratory, numerical, and theoretical studies on the fundamental physical and chemical processes are all welcome.

Note that what we call regolith is not just fine grains: all kinds of materials (more or less loose) that lie on the surface, from cobbles to finer grains, are our targets.

[PPS02-P01] Abrasion experiments of mineral and meteorite grains: Dependence of particle size and vibration rate on abrasion rate and its application to Itokawa and lunar regolith particles.

*Hirotaka Yamaguchi[1], Akira Tsuchiyama[1], Akiko Nakamura[2] (1.National University Corporation, Kyoto University, 2.National University Corporation,Kobe University)

[PPS02-P02] Measurements of adhesive force of meteorite powders using centrifugal method

*Yuuya Nagaashi[1], Akiko Nakamura[1] (1.Kobe University)

[PPS02-P03] Laboratory impact penetration experiments conducted at simulated reduced gravity

*Akiko Nakamura[1], Kana Morizono[2], Yuuya Nagaashi[1] (1.Graduate School of Science, Kobe University, 2.Faculty of Science, Kobe University)

[PPS02-P04] MARAUDERS: Using instrumented nano-impactors to probe the icy properties of Lunar permanently shadowed regions

*Ronald Ballouz[1], Sarah T Crites[2], Naoya Ozaki[2], Shun Arahata[3], Nicola Baresi[2], Ralf Bolden, Onur Celik[4,2], Yu Himeno[3], Lucie Riu[2], Kevin J Walsh[5] (1.Lunar and Planetary Lab, University of Arizona, Tucson, AZ, USA, 2.Institute of Space and Astronautical Science, Sagamihara, Japan, 3.University of Tokyo, Tokyo, Japan, 4.Sokendai Graduate University, Japan, 5.Southwest Research Institute, Boulder, CO, USA)

[PPS02-P05] Surface size-frequency distribution of accumulating boulders using discrete element simulations of spherical particles in 3D

*Hiroshi Kikuchi[1], Hideaki Miyamoto[1] (1.The University of Tokyo)

[PPS02-P06] Experimental Study to Determine the Best Compression Ratio of High-Resolution Images of Small Bodies for the Martian Moons eXploration (MMX) Mission

*Yuta Shimizu[1], Hiroaki Kamiyoshihara[1], Takafumi Niihara[1], Hideaki Miyamoto[1] (1.University of Tokyo)

Abrasion experiments of mineral and meteorite grains: Dependence of particle size and vibration rate on abrasion rate and its application to Itokawa and lunar regolith particles.

*Hirotaka Yamaguchi[1], Akira Tsuchiyama[1], Akiko Nakamura[2]

1. National University Corporation, Kyoto University, 2. National University Corporation,Kobe University

Rounded edges were found in some regolith particles collected from asteroid Itokawa [1] and Moon [2]. These particles should be formed by mechanical abrasion [1]. Seismic-induced grain motion by micrometeoroid impacts [1] and YORP effect [3] were proposed for the abrasion process on Itokawa. However, it is not clear how these processes actually work on the surfaces of the airless celestial bodies.

In order to understand detailed process of the abrasion, our research group have carried out abrasion experiments using mineral, rock and meteorite grains (grain size: 1-2 mm) [4]. Samples used were quartz, olivine, corundum, marble, L5 chondrite meteorite (Sayh al Uhaymir 001) and CM chondrite meteorite (Murchison). These particles were put into a vessel of 10 mL with the filling ratio of ~50 % and the sample was vibrated with the rate from 1000 to 3000 rpm using a multi-beads-shocker (YASUIKIKAI Co.). The proportion of powder (<250 μm) produced by vibration at first 1 min., ΔP_1, was adopted as the measure of abrasion and its dependence of the vibration rate and the sample strength was examined. However, the particle size used in the experiments (1-2 mm) is larger than Itokawa particles (< a few hundred μm). In addition, the vibration rates used in the experiments are larger than those estimated for Itokawa(~100 rpm) and Moon (~700 rpm) by considering the maximum seismic acceleration due to micrometeoroidimpacts onto their surface [5]. In the present study, therefore, we conducted new experiments with different parameters such as particle size and vibration rate using the same experimental procedure as [4]. In the present experiments, we used quartz grains for examining the effect of packing ratio in the vessel (Exp-1), particle size (Exp-2), mixing ratio of large and small particles (Exp-3). The effect of lower vibration rate (100 - 1000 rpm) was examined using olivine and basalt as well as quartz (Exp-4). Experiments using basalt at higher vibration rates were also made.

We obtained following results. Exp-1: $\Delta P_1$was constant in a wide range of the filling rate except for the filling rate of 2/3, where ΔP_1showed a peak value. Exp-2: $\Delta P_1$is proportional to the particle size. Exp-3: When the proportion of large particles is larger than 25%, $\Delta P_1$is almost constant and the same as $\Delta P_1$for the large particles. Exp-4: In the previous experiments, ΔP_1increases with the vibration rate with the power of 1.1-2.9 for large vibration rates (>~1000 rpm) [4] while the power becomes smaller (0.67-0.77) for smaller vibration rates (<~1000 rpm). This result shows that the abrasion mode changed at ~1000 rpm. In order to understand abrasion modes, SEM observation of powder particles produced in the abrasion experiments were also made. It was found that chipping of particle edges occurred at low vibration rate (~100 rpm) and the proportion of gradual wearing on the whole particle surface gradually increased as the vibration rate increased.

We estimated the amount of abrasion of Itokawa and lunar regolith particles in a regolith layer by impact based on the present experiments. ΔP_1values of basalt at 100 and 700 rpm, which corresponding to Itokawa and Moon [4], are ~0.1 %and ~1 %, respectively (Exp-4). If we consider the size of Itokawa and Moon particle (~100 μm), ΔP_1on Itokawa and Moon should be ~0.01%and ~0.1%, respectively(Exp-2). These values are larger than those estimated from the previous experiments [4] by the order of about 1.

©2019. Japan Geoscience Union. All Right Reserved.

The present results suggest that abrasion is possible on the Moon and may occur on Itokawa as well.

[1] Tsuchiyama et al. 2011. Science, 333, 1125-1128.

[2] Sakurama et al. 2016. JpGU, Abstract, PPS03-13.

[3] Connolly et al. 2015. Earth Planet and Space, 67: 12.

[4] Tsuchiyama et al. 2018. LPSC, Abstract 1844.

[5] Yasui et al. 2015. Icarus, 260: 320-331.

©2019. Japan Geoscience Union. All Right Reserved.

Measurements of adhesive force of meteorite powders using centrifugal method

*Yuuya Nagaashi[1], Akiko Nakamura[1]

1. Kobe University

Introduction: Layer of fine particles in the laboratory shows fluffy structure owing to interparticle force (e.g., Kiuchi and Nakamura, 2014). On small bodies, interparticle forces are thought to be dominant compared to gravitational force for small particles. Fast rotators spin in excess of what gravity alone could hold together were shown to be explained by cohesive force between constituent particles (Sánchez & Scheeres, 2016). Measurements of cohesive force between micron-size spherical silica particles using an atomic force microscope cantilever (Heim et al., 1999) showed that the results agree with predictions of the JKR model (Johnson et al., 1971). On the other hand, measurements of cohesive force between 50 or 100 μm glass beads and a glass plate using centrifugal method showed that the results are by several orders of magnitude smaller than predictions of the JKR theory (Nagaashi et al., 2018). In addition, it was also shown that ~ 70 μm irregularly-shaped silica and alumina grains have the range of adhesive force similar to the glass beads, indicating that the adhesive force of the spherical and the irregular particles used in the measurement is dependent not on the macroscopic shape but on the microscopic surface roughness. However, it is not clear whether the adhesive force of the particles that actually form the asteroids is similar to those of silica grains. Measurements of adhesive force of meteorite powders will bring important knowledge of adhesive force of the asteroid-forming particles for understanding physical processes occurring on asteroids.

Experimental method: In this study, we used centrifugal method as in our previous study (Nagaashi et al., 2018) in order to measure cohesive or adhesive force between a particle and a plate. This method can directly measure the cohesive or adhesive force of many particles at the same time, which enables us to statistically analyze the results. Additionally, it can also deal with irregularly shaped particles. The measurements were conducted for carbonaceous chondrite (CV3: Allende, CM2: Murchison), ordinary chondrite (LL3.5: NWA 539, LL5: NWA 1794, LL6: NWA 542), and Eucrite (Millbillillie) powders of median diameter ~ 50 μm. We discretely increased the centrifugal acceleration from 10g to 5000g (g: the Earth's gravitational acceleration) and took optical microscope images of the same location of the plate before and after applying centrifugal force at each centrifugal acceleration. We determined the range of centrifugal acceleration within which the particle separated from the plate based on the microscope images and estimated the cohesive or adhesive force between the particle and the plate. More detail description of the procedure is described in Nagaashi et al. (2018).

Results: As compared with the JKR adhesion force $F_{ad} = 3\pi\gamma R$ (γ: surface energy, R: reduced radius of particle) for a spherical particle of silica composition, we calculated the effective surface energy of particles which reproduces the measurement value, and compared the results of each type of meteorite powders. Similar to the previous results described in the above (Nagaashi et al., 2018), the measurements of meteorite powders showed a wide range of adhesive force distributions over several orders of magnitude for all measured meteorite types. In addition, we found that the effective surface energy of Allende and Murchison meteorite particles were several times smaller than those for the particles of the other meteorite types. There is no difference in the axial ratio of each type of meteorite powders, and therefore this is likely due to differences in material composition or micro-topography of the particles.

©2019. Japan Geoscience Union. All Right Reserved.

©2019. Japan Geoscience Union. All Right Reserved.

Laboratory impact penetration experiments conducted at simulated reduced gravity

*Akiko Nakamura[1], Kana Morizono[2], Yuuya Nagaashi[1]

1. Graduate School of Science, Kobe University, 2. Faculty of Science, Kobe University

Small bodies are covered with a layer of regolith made up of particles of various sizes. It is important to understand the interactions that occur with surface regolith when a spacecraft lands on or when a block secondarily collide with the regolith layer at low velocity. Penetration depth of an impactor in granular layer was investigated under Earth’ s gravity and an empirical relationship between the drop height and penetration depth was shown to reproduce the experimental results for various granular materials (Uehara et al., 2013). Deceleration of spherical impactor in granular layer was experimentally and theoretically investigated and deceleration formulae were proposed (Katsuragi and Durian 2007, Nakamura et al., 2013; Katsuragi and Durian 2013). On the other hand, interactions of spheres with simulated regolith have been studied at reduced gravity and micro-gravity conditions (Murdoch et al., 2016; Brisset et al., 2018). However, more data of penetration depth of impactor are required to establish quantitative understanding of the penetration process in regolith under low gravity.

We conducted laboratory low-velocity impact experiments of a sphere into granular layer at reduced gravity. Impactor was a glass sphere with a diameter of 16.7 mm and granular layer consisted of glass beads with a diameter of 1 mm. The glass beads were packed in a bucket having a diameter of 15 cm and a depth of 15 cm. The bucket was hung with three constant load springs. The bucket was fixed with two electromagnets, and when the electromagnet was switched off, it dropped vertically downward with the gravity reduced. The simulated reduced gravity level was monitored by an accelerometer placed in a bucket and found to be on average 0.26 G. A plastic straw with horizontal line drawing was glued to the glass sphere. The glass sphere collided with the glass bead layer at a relative velocity between 2 and 4 ms $^{-1}$. The penetration process of the glass sphere with the straw was imaged at 240 fps by a camera attached to the bucket. The final depth of the glass sphere was found to be systematically deeper than the depth found in the experiment conducted at 1 G.

Keywords: regolith, low gravity, impact

©2019. Japan Geoscience Union. All Right Reserved.

MARAUDERS: Using instrumented nano-impactors to probe the icy properties of Lunar permanently shadowed regions

*Ronald Ballouz[1], Sarah T Crites[2], Naoya Ozaki[2], Shun Arahata[3], Nicola Baresi[2], Ralf Bolden, Onur Celik[4,2], Yu Himeno[3], Lucie Riu[2], Kevin J Walsh[5]

1. Lunar and Planetary Lab, University of Arizona, Tucson, AZ, USA, 2. Institute of Space and Astronautical Science, Sagamihara, Japan, 3. University of Tokyo, Tokyo, Japan, 4. Sokendai Graduate University, Japan, 5. Southwest Research Institute, Boulder, CO, USA

The Mini lAndeRs And boUncers Deployed for Exploration and Regolith Science (MARAUDERS) is a small satellite concept that aims to characterize the surface and volatile properties of regolith in permanently shadowed regions (PSRs) around the Moon's poles. Large PSRs are cold enough to trap scientifically and economically valuable volatiles such as water ice. However, despite ongoing studies, the distribution, abundance, and physical phase of volatiles at the Moon's poles remains elusive [1]. *In-situ* measurements are required to conclusively determine the geotechnical and physical properties of lunar polar volatiles. To address these needs, the MARAUDERS team is currently developing a technique using instrumented nano-impactors to determine the mechanical properties of regolith at the impact point.

Small spacecraft equipped with penetrators or inertial measurement units (IMU) can characterize the strength and structure of the planetary surface that they impact. Early space exploration used penetrometers to determine the surface properties of the Moon and Mars before the arrival of astronauts and rovers. In recent decades, spacecraft equipped with IMUs characterized the surface of Titan [1], and determined the sub-surface stratification of ice and rock on the comet 67P/C-G [2]. While this technique is unable to relay the detailed mineralogical and elemental composition at the impact point, it obtains a first-order structural knowledge of potentially hazardous surfaces and sub-surfaces that cannot be obtained through remote sensing. This is highly relevant for PSRs due to extreme environmental conditions such as the lack of solar illumination, cold temperatures, and challenging communications.

Here, we present preliminary analysis on the instrument capabilities based on the potential deployment scenarios to PSRs, and the possible mechanical properties of the regolith found within these regions (Fig. 1). We present a computational study of the varying response of an instrumented impactor impacting regolith with variable i) water ice content (0-10%), ii) impactor speeds (50-250 m/s], and iii) impact angles (45-90˚), using a discrete element method code [4]. Furthermore, we analyse the ejecta properties and resulting crater morphology in order to gain a better understanding of impact processes on icy bodies. Our next steps will be to conduct laboratory impact experiments using prototypes of our instrumented impactors to calibrate the impact response on lunar simulant with variable water-ice content.

References:

1. Lorenz, R. et al. (1994) Meas. Sci. Technol. 5, 1033-1041

2. Biele, J. et al. (2016), Science, 349, 6247.

3. Holsapple, K.A. (1994) LPSC 25, 559.

©2019. Japan Geoscience Union. All Right Reserved.

4. Richardson, D.C. et al. (2011) Icarus, 212, 427–437.

Acknowledgements:

This material is based upon work supported by ISAS/JAXA’s start-up fund for international collaborations, the Aerospace Project Research Associate Program, and the International Top Young Fellow Program.

Keywords: Moon, Permanently Shadowed Regions, Volatiles, Regolith Characterization

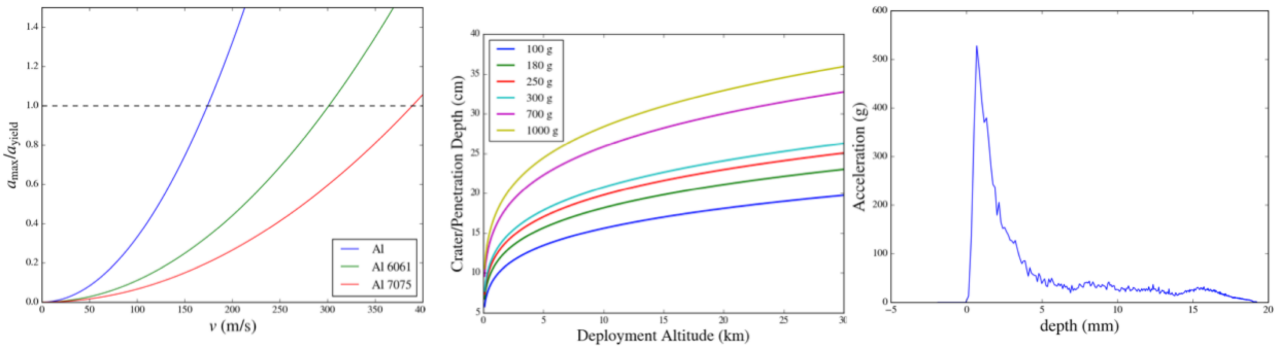

Fig. 1. Preliminary analysis showing shock tolerance, penetration depth, and instrument response for different instrument designs and impact speeds. Left: Maximum shock tolerance before material failure for three different aluminum alloy instrument housings. An Al-7075 housing can withstand impact speeds greater than 350 m/s. Middle: Penetrations depths for a 250 m/s impact for different impactor masses (100 - 1000 grams). For a nominal impactor mass of 180 g, a deployment from 15 km from the lunar surface results in a penetration depth of < 20 cm (based on [3]). Right: Simulated response of a 180 g impactor using a particle dynamics simulation.

©2019. Japan Geoscience Union. All Right Reserved.

Surface size-frequency distribution of accumulating boulders using discrete element simulations of spherical particles in 3D

*Hiroshi Kikuchi[1], Hideaki Miyamoto[1]

1. The University of Tokyo

Several spacecraft have revealed new detail about small bodies such as asteroids, comets, and small satellites. Images from Hayabusa, Hayabusa2, and OSIRIS-REx showed more boulders on the surfaces than originally expected. Owing to the high resolution at which images were taken, a number of boulders could often be observed in clusters. In future explorations, because we expect to observe more cases of boulder-rich surfaces, the characterization of the size-frequency distribution (SFD) will be important especially for the missions involving a lander such as MMX. Basically, measuring the SFD of boulders on a surface is expected to represent that of the interior. However, considering that surface boulders can hide the underlying boulder, it is not clear that the SFD in a volume can adequately be represented by its surface. Therefore, in this work, we focus on how accumulating boulders with a known SFD appear from above.
In order to compare the SFD on a surface with that of a volume, the initial SFD has to be known. For the initial study, numerical simulations are convenient, because they can easily prepare the suitable conditions. In the previous studies, spherical boulders were randomly distributed in three-dimensional space, and only those on the surface were automatically extracted and measured (Tancredi et al., 2015). It was found that the particle distribution on the surface well reproduces the overall particle distribution. We consider that there is room for improvement in the arrangement of particles and the measurement of particles. Thus, we implement a three-dimensional discrete element method using rigid spherical particles to simulate the accumulation of a boulder-rich regolith. We then measure particles one by one manually when viewed from above the surface. For initial conditions, we set the size and the number of boulders randomly as specified by the power law index of -3. During a simulation, particles are not initially adjacent to each other and are instead dropped from the height of 30 m above the 54 x 54 m planar surface. The total number of particles is changed from 3000 to 7000 in 1000 increments. After the simulation, the size and number of the particles are measured manually when viewing the surface from the vertical direction. Then we refer to Clauset et al. (2009) for fitting and evaluating the data using the p-value metric.
We find that the power law index of the SFD is low when the number of particles is 3000. This may be because the larger particles are not buried in the smaller particles, resulting in only the number of smaller particles being reduced when viewed from above. When the total number is 4000 or more in a volume and p-value is high, the surface power law index from the multiple simulations is consistent with the specified value of -3 for some cases.
The SFD observed on the surface corresponds to the SFD in the interior of the body for the following conditions: the thickness of the deposited particles is larger than the largest particle and the p-value is high. For more detailed analyses, investigating the effects of the number of simulations, the complicated shapes of boulders, and parameter studies are needed. In addition, for a deeper understanding of the problem, experiments in a similar condition to the airless bodies using simulated regolith particles such as UTPS-TB and UTPS-IB (Miyamoto et al., 2018) are also required.

Keywords: Discrete element method, Boulder size-frequency distribution, Interior of small bodies

©2019. Japan Geoscience Union. All Right Reserved.

Experimental Study to Determine the Best Compression Ratio of High-Resolution Images of Small Bodies for the Martian Moons eXploration (MMX) Mission

*Yuta Shimizu[1], Hiroaki Kamiyoshihara[1], Takafumi Niihara[1], Hideaki Miyamoto[1]

1. University of Tokyo

Data transmission rate becomes one of the biggest limiting factors in space explorations; technological advance in increasing pixel numbers of camera images dominates the improvement of the data transmission rate. Yet, high demand exists for high-resolution images especially in geological studies, and thus there is a tradeoff between the spatial resolutions (or pixel numbers) and the number of images to be transmitted to Earth. The telecommunications issue is critical for Martian Moons eXploration (MMX) mission that explore either/both Phobos and Deimos and return samples. Especially, timely transmission of high-resolution images is required for the selection of sampling site both in terms of scientific impacts and of the landing safety. The highest image resolution of the current camera configuration is as good as several tens of centimeters per pixel and the size of image is 3296 x 2472 pixels, which means 7 color (3 bands) images can be up to 1 GB if no compression is considered. During the landing phase, such large data have to be sent at the limited bitrate (< 32 kbps) to select landing and sampling sites, while the landing duration is about 4 hours. Thus, considering the best compression scheme of images is a big issue for landing operation. Lossy compression can significantly reduce the sizes of images, though images can be scientifically worthless when compressed too much. The best compression ratio should make the sizes of images as small as possible without losing scientific importance.

Here, we develop a method of rapidly determining the best compression ratio of high-resolution images of the surface of small bodies. For preparing the image studied in this research, we take an experimental scheme, where we develop a simulated Phobos surface by using a high-quality simulant of Phobos regolith (UTPS-TB) and take simulated images of the surface of Phobos in somehow similar condition with the camera of the MMX mission. The images are compressed by JPEG2000, which is planned to be used in MMX mission, and the influence of the compression is analyzed by objective methods such as Structural SIMilarity (SSIM) and entropy of image. The results shows that they are able to rapidly detect the exact ratio, in which the quality of the images started to be diminished.

Moreover, by defining scientific value of images as detectability of rock gravel on the surface of celestial bodies and showing that the loss of scientific value can be expressed by the change in the value of slope of Cumulative Size-Frequency Distribution (CSFD) of gravel, we carefully confirm whether the decrease in the image quality is truly connected with the loss of scientific information such as for landing operations and conclude that those objective methods can determine the best compression ratio. By using those methods, the spacecraft can autonomously complete the process of finding the best compression ratio, compressing images and sending it to the ground within a few minutes even if it has only a limited transmission rate.

Keywords: the best compression ratio, Cumulative Size-Frequency Distribution (CSFD), Martian Moons eXploration (MMX)

©2019. Japan Geoscience Union. All Right Reserved.

[E] Oral | P (Space and Planetary Sciences)：P-PS Planetary Sciences

Wed. May 29, 2019 1:45 PM - 3:15 PM JST | Wed. May 29, 2019 4:45 AM - 6:15 AM UTC | A01 TOKYO BAY MAKUHARI HALL

[P-PS02] Regolith Science

convener:Koji Wada(Planetary Exploration Research Center, Chiba Institute of Technology), Akiko Nakamura(Graduate School of Science, Kobe University), Patrick Michel(Observatoire De La Cote D'Azur), Kevin John Walsh(Southwest Research Institute Boulder), Chairperson:Koji Wada(Planetary Exploration Research Center, Chiba Institute of Technology)

Recent planetary explorations have revealed that almost all solid bodies in the solar system are covered with small particles, called regolith. The surface geology, especially regolith behavior on the surfaces of solid bodies, becomes increasingly more important as represented by Hayabusa mission and other on-going and planned sample-return missions such as Hayabusa2, OSIRIS-REx, and MMX.

For fully understanding the regolith science, it is required to know and compare the regolith conditions on various celestial bodies, from asteroids to planets, with various methods.

Therefore, this session welcomes broad topics related to regolith on various celestial bodies, such as asteroids, comets, the Moon, the martian moons, Mars, etc. Papers on the formation, evolution, and alteration processes of regolith particles and regolith systems on the surface of planetary bodies, remote and in-situ observational results and techniques, analyses and results of returned samples, and laboratory, numerical, and theoretical studies on the fundamental physical and chemical processes are all welcome.

Note that what we call regolith is not just fine grains: all kinds of materials (more or less loose) that lie on the surface, from cobbles to finer grains, are our targets.

1:45 PM - 2:00 PM JST | 4:45 AM - 5:00 AM UTC

[PPS02-01] Moganite in a lunar meteorite as a trace of H_2O ice in the lunar regolith

★Invited Papers

*Masahiro KAYAMA[1] (1.Tohoku University)

2:00 PM - 2:15 PM JST | 5:00 AM - 5:15 AM UTC

[PPS02-02] Simulating the Lunar Soil: a Japanese Lunar Soil Simulant FJS-1 and Its Properties

★Invited Papers

*Naohiro Uyama[1], Hiroshi Kanamori[1], Shigeru Aoki[1] (1.Shimizu Corporation)

2:15 PM - 2:30 PM JST | 5:15 AM - 5:30 AM UTC

[PPS02-03] Experimental estimation of regolith scattering behavior when a space lander touches on a planetary body

★Invited Papers

*Mitsuhisa Baba[1], Ronald Louis Ballouz[2], Masatsugu Otsuki[1] (1.Japan Aerospace Exploration Agency, 2.The University of Arizona)

2:30 PM - 2:45 PM JST | 5:30 AM - 5:45 AM UTC

[PPS02-04] Ray systems in granular cratering

*Tapan Sabuwala[1], Christian Butcher[1], Gustavo Gioia[1], Pinaki Chakraborty[1] (1.Okinawa Institute of Science and Technology Graduate University)

2:45 PM - 3:00 PM JST | 5:45 AM - 6:00 AM UTC

[PPS02-05] Scaling of oblique impact cratering onto inclined granular layer

Shinta Takizawa[1], *Hiroaki Katsuragi[1] (1.Graduate School of Environmental Studies, Nagoya University)

3:00 PM - 3:15 PM JST | 6:00 AM - 6:15 AM UTC

[PPS02-06] Experimental study on gravitational effects on crater size formed by low-velocity impacts into granular media

*Masato Kiuchi[1], Akiko M Nakamura[2], Koji Wada[3] (1.Japan aerospace exploration agency, Institute of space and astronautical science, 2.Department of Planetology, Kobe University, 3.Planetary Exploration

Research Center, Chiba Institute of Technology)

Moganite in a lunar meteorite as a trace of H_2O ice in the lunar regolith

*Masahiro KAYAMA[1]

1. Tohoku University

A large amount of H_2O ice has been observed on the regolith surface near the lunar poles by remote sensing spacecraft. However, only sparse evidence for H_2O ice beneath the top few millimeters of the regolith exists because neutron spectrometers cannot distinguish forms of H and near-infrared spectrometers are only sensitive to the optical surface. Furthermore, traces of H_2O ice have not yet been found from the lunar samples. Here, 13 different lunar meteorites with various lithologies have been investigated using micro-Raman spectrometry, electron microscopy, and synchrotron angle-dispersive x-ray diffraction (SR-XRD) to find a trace of H_2O ice in the subsurface. Consequently, moganite has been discovered from the KREEP (high potassium, rare-earth element, and phosphorous)-like gabbroic-basaltic brecciated meteorite NWA 2727 that may originate from the local crater sites within the Procellarum terranes.

Moganite (monoclinic SiO_2 phase that belongs to the *I2/a* space group) coexisting with coesite and stishovite (high-pressure SiO_2 polymorphs) was discovered only in NWA2727 by the micro-Raman spectrometry. NWA 2727 is mainly composed of gabbroic and basaltic clasts containing their breccia matrix, where only the breccia matrix contain moganite-bearing silica micrograins (2 to 13 mm in radius) between the constituent minerals (olivine, pyroxene and plagioclase). The SR-XRD analyses of these silica micrograins in the breccia matrix indicate a characteristic diffraction pattern that is in good agreement with the structure of moganite. However, no moganite was discovered from the basaltic and gabbroic clasts of NWA 2727 as well as in the other lunar meteorites selected here. Transmission electron microscopy of the silica micrograins demonstrates the aggregates of numerous euhedral or subhedral moganite nanoparticles (average radius of 4.5 nm).

Moganite was discovered in only one of those 13 samples. If terrestrial weathering had produced moganite in the lunar meteorites, there should be moganite present in all the samples, especially lunar meteorites fell to Earth around the same time (NWA 2977, 3333, and 6950 as measured here), but this was not the case. Furthermore, many previous researches on natural occurrences and laboratory experiments conclude that moganite is restricted to formation by precipitating from alkaline silicic acid (H_4SiO_4) water under high-pressure consolidation at >100 MPa, which is distinctly different environment from the desert that NWA 2727 found. A part of the moganite had changed into the coesite and stishovite, indicating their formation through heavy impact collisions on the Moon. These facts confirm our theory that it could not have formed in the desert.

Formation of lunar moganite can be interpreted based on the present and previous works as follows. Alkaline water-bearing carbonaceous chondrite collisions delivered abundant alkaline water to the lunar surface at <2.67 Ga. After the collisions, the delivered water was captured as fluid inside the breccia during the shock-induced consolidation. On the sunlit surface, lunar moganite precipitated from this captured alkaline water. Simultaneously, such captured water got cold-trapped at the lunar regolith in the subsurface and may still remain as ice underneath the local crater sites within the Procellarum terranes. Lunar moganite coexists with coesite and stishovite, thereby implying that a trace of the subsurface water ice was brought from the Moon by the recent impact at <1–30 Ma. Our moganite-precipitation simulation

©2019. Japan Geoscience Union. All Right Reserved.

modeling concludes a subsurface H_2O concentration higher than the estimated bulk content of 0.6 wt % is expected to still remain as ice. This value is in excellent agreement with the concentrations of H_2O ice on the poles by remote sensing spacecraft observation. Thus, the subsurface is expected to be the abundant and available water resource for future lunar explorations.

Keywords: Moganite, Lunar meteorite, H2O ice, Regolith

©2019. Japan Geoscience Union. All Right Reserved.

Simulating the Lunar Soil: a Japanese Lunar Soil Simulant FJS-1 and Its Properties

*Naohiro Uyama[1], Hiroshi Kanamori[1], Shigeru Aoki[1]

1. Shimizu Corporation

Going back to the Moon is a world-wide trend of space exploration based on the international cooperation as the Global Exploration Roadmap (GER3) stated. JAXA also proposed future human exploration missions around 2030 within the international cooperation. All scenarios have their bases on the scientific observation that a plenty of water (hydrogen) is trapped in the polar regions, especially inside the craters of permanent shadow. In order to investigate those water and other existing volatiles, however, many engineering challenges wait for human and robotic missions even only from the view of lunar soil, such as traversing the soft soil, drilling and/or excavating the soil, and handling the soil for desired sample collections and scientific processes, and more for the in-situ resource utilization and human missions. Thus, the ground tests prior to launches are of great importance to increase the possibility of mission success.

In order to offer opportunities for the community to perform ground tests, we have manufactured a lunar soil simulant, called FJS-1. The investigation of FJS-1 shows that many properties of FJS-1 lies close to the data collected from Apollo samples. For instance, the particle size distribution lies below 2 [mm]; the median particle size is between 70 and 75 [micro-m]; the shear strength, i.e. cohesion c, is 0 to 10 [kN/m2]; and the internal friction angle, phi, is 30 to 50 [deg]. The chemical composition is also close to Apollo samples with slight difference that FJS-1 contains more ferric oxide and Alkaline components than Apollo samples.

In addition to the basic properties, we started investigating the strength of frozen lunar soil using FJS-1. Determining the optimized configuration of a sampler such as a drill or an excavator needs the information of actual lunar soil; however, nobody knows the actual state, in other words, the ground truth of lunar water/ice yet. We therefore decided to investigate the strength of frozen soil, utilizing FJS-1, for the future use for drill or excavator designs. The qualitative observation from our first experiment is that the frozen FJS-1 at temperature below 0 [degC] became slightly loose when FJS-1 contained 0.5 to 1.0 [wt%] of water, and that the strength drastically increased above 2 [wt%]. We will conduct more experiments to collect a set of frozen soil strength to offer the estimates of the strength of lunar soil for future lunar exploration missions.

Keywords: Lunar soil, Soil simulant, FJS-1, Soil simulant properties, Frozen soil

©2019. Japan Geoscience Union. All Right Reserved.

Experimental estimation of regolith scattering behavior when a space lander touches on a planetary body

*Mitsuhisa Baba[1], Ronald Louis Ballouz[2], Masatsugu Otsuki[1]

1. Japan Aerospace Exploration Agency, 2. The University of Arizona

A planetary lander, which needs to land on and lift up from a planetary surface, needs to be concerned with levitated regolith. Regolith scattered by the landing foot pad might attach to or damage on-board instruments, such as the spacecraft’ s camera suite. To design the landing probe, it is necessary to estimate the expected area of the regolith that the probe may scatter. Here we show an experimental approach that was developed to study the behavior of scattered regolith under a vacuum environment. For the probe design, it is necessary to precisely measure the initial ejection angle, ejection velocity, and the amount of regolith that the landing foot pad scatters.

In order to characterize scattered-particle behavior, drop tests in a large vacuum chamber were conducted. A cylindrical mass projectile, mimicking the lander foot pad, fell freely from various heights in the vacuum chamber. The mass lands in a sandbox filled with silica sand and forms a crater with scattered sand particles. During silica sand scattering, a high-speed camera detected particle highlighted by a line laser. Initial ejection velocities and the ejection angles were estimated by processing the images of the impact site, captured by the high-speed camera.

The result of our study revealed that the ejection angle of scattered grains is not sensitive to the impact kinetic energy of the projectile. Our results are consistent with previous studies that showed a similar relationship between impact kinetic energy and ejection angle, but for lower impact energies. Moreover, we find that for impact speeds of ~ 4 m/s, the initial ejection velocity of a majority of the silica sand particle is distributed around 1 m/s.

Our experimental approach can be applied to various kinds of planetary regolith, such as Phobos simulant for the Martian Moons eXploration(MMX). These results help us to understand how to determine the optimal design conditions for a landing probe. Further studies that account for the effect of microgravity and changes to the bulk density and porosity of the regolith need to be undertaken based on drop tower test and numerical simulation.

Keywords: Regolith, Laboratory Experiment, Landing Gear

©2019. Japan Geoscience Union. All Right Reserved.

Ray systems in granular cratering

*Tapan Sabuwala[1], Christian Butcher[1], Gustavo Gioia[1], Pinaki Chakraborty[1]

1. Okinawa Institute of Science and Technology Graduate University

In classical experiments of granular cratering, a ball dropped on a smooth bed of grains ends up within a crater surrounded by a uniform blanket of ejecta. We show that such a uniform blanket of ejecta changes to a ray system, or set of radial streaks of ejecta, where the surface of the granular bed includes undulations. By carrying out numerous experiments and computational simulations thereof, we ascertain that the number of rays in a ray system $\propto D/\lambda$, where D is the diameter of the ball and λ the wavelength of the undulations. Further, we show that the ejecta in a ray system originates from valleys located in a narrow annulus of diameter D with center at the site of impact. The impacting ball creates a hemispherical shockwave, whose interaction with the surficial valleys engenders the ray system. Our findings may help shed light on the enigmatic ray systems that ring many impact craters on the Moon and other planetary bodies.

Keywords: impact crater, crater rays, granular cratering

©2019. Japan Geoscience Union. All Right Reserved.

Scaling of oblique impact cratering onto inclined granular layer

Shinta Takizawa[1], *Hiroaki Katsuragi[1]

1. Graduate School of Environmental Studies, Nagoya University

Empirical (Pi-group) scaling laws for craters created on an inclined granular layer by an oblique impact of a spherical projectile were experimentally obtained. In the experiment, inclination angle and incident angle were systematically (and independently) varied in the ranges of 0 to 33 degree and 10 to 170 degree, respectively. A spherical projectile (diameter 6 mm) was impacted onto a surface of inclined granular layer with an impact speed 10 - 100 m/s. Two high-speed cameras and laser profilometry system were used to measure the impact speed, angle, and final crater shape. From the experimental results, we found following behaviors. When the incident angle is small, almost symmetric craters were observed. However, the collapse of the upper crater wall was triggered when the inclination angle is large enough. The scale of the collapse grows as the inclination angle is increased. In addition, the crater volume strongly depends on inclination angle. By combining these experimental findings, we developed the empirical scaling for crater dimensions and aspect ratios. The obtained scaling is consistent with previous works on the normal impact to horizontal granular surface with high impact speed. We also discuss a possible way to evaluate the impact conditions from the actual astronomical impact craters.

Keywords: oblique impact , inclined granular layer

©2019. Japan Geoscience Union. All Right Reserved.

Experimental study on gravitational effects on crater size formed by low-velocity impacts into granular media

*Masato Kiuchi[1], Akiko M Nakamura[2], Koji Wada[3]

1. Japan aerospace exploration agency, Institute of space and astronautical science, 2. Department of Planetology, Kobe University, 3. Planetary Exploration Research Center, Chiba Institute of Technology

Craters on regolith surface can be formed at various impact velocities. When secondary craters form on the surface of small bodies, such as asteroids and comets, the impactors have very low-velocities of several m s^{-1} or less due to the small escape velocity of the bodies. These secondary collisions can increase the number of small craters on the surface and will affect the surface topography of small bodies. Therefore, it is important to investigate low-velocity impacts on granular materials that simulate regolith particles to understand the low-velocity cratering process on the surface of small bodies.

Low-velocity impact experiments with velocities in the range of several m s^{-1} and granular targets have been conducted to investigate crater size and develop empirical relationships between impact conditions and crater size under 1 G (e.g., Uehara et al., 2003; Walsh et al., 2003). However, it was found that the impact velocity dependence of crater diameter was inconsistent between the hypervelocity impact experiments conducted at low and high-gravity conditions (Gault and Wedekind, 1977; Schmidt and Housen, 1987) and the low-velocity impact experiments conducted under 1 G (Kiuchi et al., 2018, JpGU meeting).

We collected data of crater diameter on granular materials with impact velocities ranging from 1 to 4.6 m s^{-1} under a gravity range of 0.20 to 1 G to investigate the effects of gravity on crater diameter using a drop system developed for reduced gravity impact experiments (Kiuchi and Nakamura, 2015 JPGU meeting). Most of our experiments were conducted under 10^5 Pa for comparison with the low-velocity experiments under 1 G reported in previous studies, but we also conducted several experiments under 7 Pa according to the atmosphere-less condition of small bodies.

This time we newly organized our experimental results in which the gravity was changed using the atmospheric pressure dependence. As a result, the exponent values of gravity became close to that obtained by the high-velocity experiment (Gault and Wedekind, 1977). We compared our results with high-velocity experiments reported in previous studies. Our results for the glass projectile and the sand target almost agreed with the previous high-velocity crater-size scaling- law (Housen and Holsapple, 2011) when the atmospheric effect was taken into account, but the crater diameter for the steel projectile and the sand target was lower than that for the glass projectile. This result shows that the crater-size scaling- law obtained for high-velocity impact can be applied to low-velocity impacts of several m s^{-1} under reduced pressure when the density ratio of the projectile to the target is close to unity. The same scaling applies over a very wide range of impact velocities.

Keywords: Impact experiments at low-velocity, Gravitational effects on crater size

©2019. Japan Geoscience Union. All Right Reserved.

[E] Oral | P (Space and Planetary Sciences)：P-PS Planetary Sciences

Wed. May 29, 2019 3:30 PM - 5:00 PM JST | Wed. May 29, 2019 6:30 AM - 8:00 AM UTC | A01 TOKYO BAY MAKUHARI HALL

[P-PS02] Regolith Science

convener:Koji Wada(Planetary Exploration Research Center, Chiba Institute of Technology), Akiko Nakamura(Graduate School of Science, Kobe University), Patrick Michel(Observatoire De La Cote D'Azur), Kevin John Walsh(Southwest Research Institute Boulder), Chairperson:Akiko Nakamura(Graduate School of Science, Kobe University)

Recent planetary explorations have revealed that almost all solid bodies in the solar system are covered with small particles, called regolith. The surface geology, especially regolith behavior on the surfaces of solid bodies, becomes increasingly more important as represented by Hayabusa mission and other on-going and planned sample-return missions such as Hayabusa2, OSIRIS-REx, and MMX.

For fully understanding the regolith science, it is required to know and compare the regolith conditions on various celestial bodies, from asteroids to planets, with various methods.

Therefore, this session welcomes broad topics related to regolith on various celestial bodies, such as asteroids, comets, the Moon, the martian moons, Mars, etc. Papers on the formation, evolution, and alteration processes of regolith particles and regolith systems on the surface of planetary bodies, remote and in-situ observational results and techniques, analyses and results of returned samples, and laboratory, numerical, and theoretical studies on the fundamental physical and chemical processes are all welcome.

Note that what we call regolith is not just fine grains: all kinds of materials (more or less loose) that lie on the surface, from cobbles to finer grains, are our targets.

3:30 PM - 3:45 PM JST | 6:30 AM - 6:45 AM UTC

[PPS02-07] **Impact Ejecta Environment of an Eccentric Asteroid: 3200 Phaethon**

*Jamey Szalay[1], Peter Pokorny[2], Mihaly Horanyi[3], Diego Janches[2], Menelaos Sarantos[2], Ralf Srama[4] (1.Princeton University, 2.NASA/GSFC, 3.University of Colorado Boulder, 4.University of Stuttgart)

3:45 PM - 4:00 PM JST | 6:45 AM - 7:00 AM UTC

[PPS02-08] On the Detection of an Ejecta Dust Cloud Around Asteroid (3200) Phaethon by the DESTINY$^+$ Dust Analyzer

*Hiroshi Kimura[1], Masanori Kobayashi[1], Koji Wada[1], Tomoko Arai[1], Hiroki Senshu[1], Masateru Ishiguro[2], Hidekazu Hanayama[3], Ko Ishibashi[1], Takayuki Hirai[1], Fumi Yoshida[1], Peng Hong[1] (1.Planetary Exploration Research Center, 2.Seoul National University, 3.Ishigakijima Astronomical Observatory)

4:00 PM - 4:15 PM JST | 7:00 AM - 7:15 AM UTC

[PPS02-09] Close-up thermal and optical observation of asteroid Ryugu

★Invited Papers

*Naoya Sakatani[1], Tatsuaki Okada[1], Satoshi Tanaka[1], Hiroki Senshu[2], Yuri Shimaki[1], Takehiko Arai[3], Toru Kouyama[5], Hirohide Demura[6], Kentaro Suko[6], Tomohiko Sekiguchi[4], Jun Takita[15], Tetsuya Fukuhara[4], Makoto Taguchi[4], Thomas Müller[7], Axel Hargermann[8], Jens Biele[9], Matthias Grott[9], Marco Delbo[10], Seiji Sugita[13], Rie Honda[12], Tomokatsu Morota[11], Manabu Yamada[2], Shingo Kameda[4], ERI TATSUMI[13], Yasuhiro Yokota[1], Hidehiko Suzuki[14], Chikatoshi Honda[6], Kazunori Ogawa[16], Masahiko Hayakawa[1], Moe Matsuoka[1], Yuichiro Cho[13], Hirotaka Sawada[1] (1.Institute of Space and Astronautical Science, Japan Aerospace Exploration Agency, 2.Chiba Institute of Technology, 3.Ashikaga University, 4.Rikkyo University, 5.National Institute of Advanced Industrial Science and Technology, 6.University of Aizu, 7.Max-Planck Institute for Extraterrestrial Physics, 8.University of Stirling, 9.German Aerospace Center, 10.Observatoire de la Côte d'Azur, CNRS, 11.Nagoya University, 12.Kochi University, 13.University of Tokyo, 14.Meiji University, 15.Hokkaido University for Education, 16.Kobe University)

4:15 PM - 4:30 PM JST | 7:15 AM - 7:30 AM UTC

[PPS02-10] **In-Situ Investigation of Asteroid (162173) Ryugu by the Hayabusa2 MASCOT Lander**

★Invited Papers

*Hajime Yano[1], Tra-Mi Ho[2], Ralf Jaumann[3], Jean-Pierre Bibring[4], Karl-Heinz Glassmeier[5], Matthias Grott[3], David Hercik[5], Jens Biele[6], Maximilian Hamm[3], Nicole Schmitz[3], Stefanus Schröder[3], Katharina Otto[3], Christian Krause[6], Laurence Lorda[7], Aurelie Moussi-Soffys[7], Cedric Pilorget[4], Vincent Hamm[4], Lucie Riu[1], Tatsuaki Okada[1], Naoya Sakatani[1], Josef Reill[8], Kaname Sasaki[2], Markus Schlotterer[2], Yuichi Tsuda[1], Stephan Ulamec[6], Friederike Wolff[8], Patrick Michel[9], Marco Delbo[9], Kazunori Ogawa[10], Hiroki Senshu[11], Tetsuo Yoshimitsu[1], Frank Preusker[3], Frank Scholten[3], Stephan Elgner[3], Stefano Mottola[3], Ekkehard Kührt[3], Takanao Saiki[1], Yuya Mimasu[1] (1.Institute of Space and Astronautical Science, Japan Aerospace Exploration Agency, Sagamihara, Japan, , 2.German Aerospace Center DLR Bremen, Bremen, Germany, 3.German Aerospace Center, Berlin, Germany, 4.Univ. de Paris Sud-Orsay, IAS, Orsay, France, 5.TU Braunschweig, Braunschweig, Germany, 6.German Aerospace Center DLR Cologne, Cologne, Germany, 7.National Centre for Space Studies, CNES, Toulouse, France, 8.German Aerospace Center, DLR, Oberpfaffenhofen, Germany, 9.Université Côte d'Azur, Observatoire de la Côte d'Azur, CNRS, Laboratoire Lagrange, Nice, France, 10.Department of Planetology, Graduate School of Science, Kobe University, Kobe, Japan, 11.Planetary Exploration Research Center, Chiba Institute of Technology, Narashino, Japan)

4:30 PM - 4:45 PM JST | 7:30 AM - 7:45 AM UTC

[PPS02-11] Evidence of Mass Movement and Boulder Transport on Bennu from NASA's OSIRIS-REx Space Mission

★Invited Papers

*Erica R Jawin[1], Kevin J Walsh[2], Tim McCoy[1], Harold C Connolly[3], Dante S Lauretta[4], Ron L Ballouz[4], Jamie L Molaro[5], Olivier S Barnouin[6], Mike Nolan[4] (1.Smithsonian National Institute, Washington, DC, USA, 2.Southwest Research Institute, Boulder, CO, USA, 3.Dept. of Geology, Rowan University, Glassboro, NJ, USA, 4.Lunar and Planetary Laboratory, University of Arizona, Tucson, AZ, USA , 5.Planetary Science Institute, Tucson, AZ, USA, 6.The Applied Physics Laboratory, Johns Hopkins University, Laurel, MD, USA)

4:45 PM - 5:00 PM JST | 7:45 AM - 8:00 AM UTC

[PPS02-12] Resurfacing processes on small asteroids constrained by crater size distributions on Ryugu, Itokawa, and Eros

*Naofumi Takaki[1], Yuichiro Cho[1], Tomokatsu Morota[3], ERI TATSUMI[1], Kazuo Yoshioka[1], Hirotaka Sawada[5], yokota yasuhiro[2,5], Naoya Sakatani[5], Masahiko Hayakawa[5], Moe Matsuoka[5], Rie Honda[2], Shingo Kameda[4], Manabu Yamada[6], Toru Kouyama[8], Hidehiko Suzuki[10], Chikatoshi Honda[7], Kazunori Ogawa[9], Hideaki Miyamoto[1], Olivier Barnouin[11], Patrick Michel[12], Carolyn Ernst[11], Seiji Sugita[1,6] (1.University of Tokyo, 2.Kochi University, 3.Nagoya University, 4.Rikkyo University, 5.JAXA, 6.Chiba Institute of Technology, Planetary Exploration Res. Center, 7.University of Aizu, 8.AIST, 9.Kobe University, 10.Meiji University, 11.Johns Hopkins University Applied Physics Laboratory, 12.Nice Observatory)

Impact Ejecta Environment of an Eccentric Asteroid: 3200 Phaethon

*Jamey Szalay[1], Peter Pokorny[2], Mihaly Horanyi[3], Diego Janches[2], Menelaos Sarantos[2], Ralf Srama[4]

1. Princeton University, 2. NASA/GSFC, 3. University of Colorado Boulder, 4. University of Stuttgart

Airless regolith bodies in the solar system are continually bombarded by meteoroids, modifying their surfaces and sustaining impact ejecta clouds. While large bodies like the Moon retain a significant fraction of ejected regolith, small asteroids shed this material into the interplanetary dust complex. Measurements of the lunar impact ejecta cloud found it was sustained by the known sporadic meteoroid sources. Here, we extend lunar ejecta measurements using a model of the meteoroid environment at 1 au to investigate the structure of an ejecta cloud at an eccentric airless body, asteroid 3200 Phaethon: the target of JAXA’ s DESTINY+ mission.

Due to Phaethon's large eccentricity, Phaethon's peak ejecta density at 1 au is approximately 30 times higher compared to a body in a circular orbit at 1 au, largely due to enhanced ejecta production from meteoroids shed from Jupiter Family Comets. Such asymmetric ejecta production suggests Phaethon experiences significantly different meteoroid-specific space weathering processes than a body with a similar semi-major axis on a circular orbit. We estimate impact ejecta processes at Phaethon shed approximately 1 ton per year, which is not sufficient to appreciably contribute to the Geminids meteoroid complex, yet provides ample ejecta densities to measure with an in-situ dust detector aboard DESTINY+. These results suggest eccentric asteroids shed more material than those on near-circular orbits, and are suitable candidates for in-situ dust detection and chemical characterization due to their amplified asymmetric ejecta production.

In this presentation, we will summarize recent efforts to constrain the evolution and ejection of asteroid regolith for 3200 Phaethon. We will present predicted impact counts for a dust detector on close flybys of Phaethon in preparation for JAXA’ s DESTINY+ mission and discuss how such measurements would provide critical insight into Phaethon’ s origin and evolution in a manner unique to dust detection data.

Keywords: Ejecta, Meteoroids, Regolith

©2019. Japan Geoscience Union. All Right Reserved.

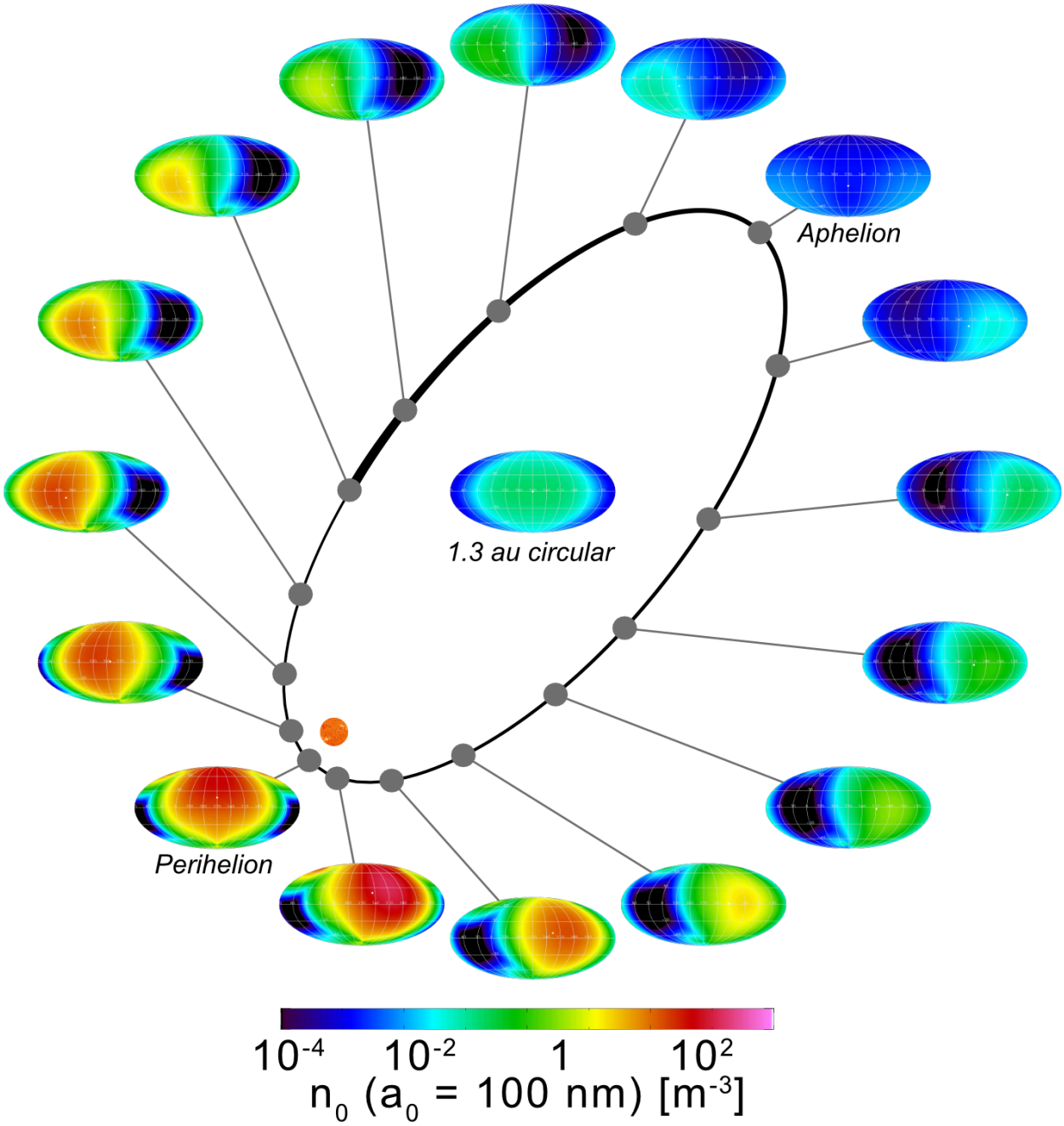

©2019. Japan Geoscience Union. All Right Reserved.

On the Detection of an Ejecta Dust Cloud Around Asteroid (3200) Phaethon by the DESTINY$^+$ Dust Analyzer

*Hiroshi Kimura[1], Masanori Kobayashi[1], Koji Wada[1], Tomoko Arai[1], Hiroki Senshu[1], Masateru Ishiguro[2], Hidekazu Hanayama[3], Ko Ishibashi[1], Takayuki Hirai[1], Fumi Yoshida[1], Peng Hong[1]

1. Planetary Exploration Research Center, 2. Seoul National University, 3. Ishigakijima Astronomical Observatory

We will provide the most recent report on the detectability of an ejecta cloud around Asteroid (3200) Phaethon by the DESTINY$^+$ Dust Analyzer (DDA), based on a model of dust dynamics in the cloud. We demonstrate that solar radiation pressure plays a vital role in shaping the spatial distribution of dust particles in Phaethon's ejecta cloud, because small particles, albeit the majority, are expelled from the sunward direction. We find that the DDA will have an opportunity of detecting dust particles in the ejecta cloud of Phaethon during a flyby, depending on the closest approach to the asteroid, heliocentric distance, and the initial velocity of ejecta. There are no hazard from impacts of 100 μm-sized ejecta particles that potentially could make tiny holes on the surface of the spacecraft during a flyby.

Keywords: Asteroid (3200) Phaethon, ejecta dust cloud, DESTINY+

©2019. Japan Geoscience Union. All Right Reserved.

Close-up thermal and optical observation of asteroid Ryugu

*Naoya Sakatani[1], Tatsuaki Okada[1], Satoshi Tanaka[1], Hiroki Senshu[2], Yuri Shimaki[1], Takehiko Arai[3], Toru Kouyama[5], Hirohide Demura[6], Kentaro Suko[6], Tomohiko Sekiguchi[4], Jun Takita[15], Tetsuya Fukuhara[4], Makoto Taguchi[4], Thomas Müller[7], Axel Hargermann[8], Jens Biele[9], Matthias Grott[9], Marco Delbo[10], Seiji Sugita[13], Rie Honda[12], Tomokatsu Morota[11], Manabu Yamada[2], Shingo Kameda[4], ERI TATSUMI[13], Yasuhiro Yokota[1], Hidehiko Suzuki[14], Chikatoshi Honda[6], Kazunori Ogawa[16], Masahiko Hayakawa[1], Moe Matsuoka[1], Yuichiro Cho[13], Hirotaka Sawada[1]

1. Institute of Space and Astronautical Science, Japan Aerospace Exploration Agency, 2. Chiba Institute of Technology, 3. Ashikaga University, 4. Rikkyo University, 5. National Institute of Advanced Industrial Science and Technology, 6. University of Aizu, 7. Max-Planck Institute for Extraterrestrial Physics, 8. University of Stirling, 9. German Aerospace Center, 10. Observatoire de la Côte d'Azur, CNRS, 11. Nagoya University, 12. Kochi University, 13. University of Tokyo, 14. Meiji University, 15. Hokkaido University for Education, 16. Kobe University

In 2018, the Hayabusa2 spacecraft successfully carried out four descend operations toward Ryugu’s surface. During these operations, we acquired highly resolved optical and thermal images from altitudes below several hundred meters, using Hayabusa2’s Optical Navigation Camera (ONC-T) and Thermal Infrared Imager (TIR), respectively. Close-up thermal images by TIR indicate thermophysical properties of the surface materials and its regional difference, which cannot be resolved by higher altitude observations (e.g., home-position observations from 20 km altitude). The temperature depends mainly on the thermal inertia of the observed medium; higher thermal inertia materials have lower daytime temperatures. Optical images by ONC-T show detailed physical conditions of the surface materials, such as particle size distribution of pebbles, surface morphology of small boulders and craters. At the spacecraft altitude of 100 m, for example, TIR and ONC-T have pixel resolutions of 8.9 cm/pix and 1.1 cm/pix, respectively. In this study, we report on a comparison of TIR and ONC images, especially for boulders and craters.

BOULDERS: TIR close-up observations showed various boulders with different daytime temperatures, or different thermal inertia. Typical thermal inertia of boulders is about 300 J m^{-2} K^{-1} $s^{-0.5}$, but there are a few boulders with thermal inertia up to 1000 J m^{-2} K^{-1} $s^{-0.5}$. The thermal inertia of rocks is mainly controlled by porosity, and porous rock has lower thermal inertia. Therefore, TIR observations show that the porosity of boulders is variable. Furthermore, boulders with high thermal inertia (low porosity) observed by ONC-T were found to be relatively brighter and had a smooth surface. Such variation in porosity, optical brightness, and surface morphology of boulders on Ryugu’s surface might reflect the degree of thermal metamorphism (depth of the source) in the parent body. If the constituents of Ryugu originate from variable depths inside the parent body, this supports the idea of a rubble pile formation of Ryugu after the catastrophic disruption of the parent body. This will place important constraints on the thermal evolution of the parent body.

CRATERS: During the MINERVA descend operations at 21st Sep., we acquired highly resolved images of two craters with diameter of less than 35 m by TIR, but both craters exhibit different thermal characteristics. One crater has a hot spot close to the center of crater, where the thermal inertia is estimated to be less than 150 J m^{-2} K^{-1} $s^{-0.5}$. On the other hand, there seems to be no hot spot in the other crater. The difference in thermophysical properties between these craters might be attributed to formation age or original surface conditions. Our finding of a hot spot with low thermal inertia indicates the presence of a fine-particle deposit in the crater and regolith generation related to the cratering process on this low-gravity asteroid.

©2019. Japan Geoscience Union. All Right Reserved.

©2019. Japan Geoscience Union. All Right Reserved.

In-Situ Investigation of Asteroid (162173) Ryugu by the Hayabusa2 MASCOT Lander

*Hajime Yano[1], Tra-Mi Ho[2], Ralf Jaumann[3], Jean-Pierre Bibring[4], Karl-Heinz Glassmeier[5], Matthias Grott[3], David Hercik[5], Jens Biele[6], Maximilian Hamm[3], Nicole Schmitz[3], Stefanus Schröder[3], Katharina Otto[3], Christian Krause[6], Laurence Lorda[7], Aurelie Moussi-Soffys[7], Cedric Pilorget[4], Vincent Hamm[4], Lucie Riu[1], Tatsuaki Okada[1], Naoya Sakatani[1], Josef Reill[8], Kaname Sasaki[2], Markus Schlotterer[2], Yuichi Tsuda[1], Stephan Ulamec[6], Friederike Wolff[8], Patrick Michel[9], Marco Delbo[9], Kazunori Ogawa[10], Hiroki Senshu[11], Tetsuo Yoshimitsu[1], Frank Preusker[3], Frank Scholten[3], Stephan Elgner[3], Stefano Mottola[3], Ekkehard Kührt[3], Takanao Saiki[1], Yuya Mimasu[1]

1. Institute of Space and Astronautical Science, Japan Aerospace Exploration Agency, Sagamihara, Japan, , 2. German Aerospace Center DLR Bremen, Bremen, Germany, 3. German Aerospace Center, Berlin, Germany, 4. Univ. de Paris Sud-Orsay, IAS, Orsay, France, 5. TU Braunschweig, Braunschweig, Germany, 6. German Aerospace Center DLR Cologne, Cologne, Germany, 7. National Centre for Space Studies, CNES, Toulouse, France, 8. German Aerospace Center, DLR, Oberpfaffenhofen, Germany, 9. Université Côte d’Azur, Observatoire de la Côte d'Azur, CNRS, Laboratoire Lagrange, Nice, France, 10. Department of Planetology, Graduate School of Science, Kobe University, Kobe, Japan, 11. Planetary Exploration Research Center, Chiba Institute of Technology, Narashino, Japan

After a journey of almost four years to the C-type asteroid (162173) Ryugu, the MASCOT lander of the Hayabusa2 mission was delivered to the asteroid’s surface on October 3rd in 2018 and successfully performed in situ investigations. MASCOT was released from the mother spacecraft at an altitude of 41 m and came to rest on the surface at a site located at 22.31±0.05°S, 317.16±0.05°E. MASCOT observed the surface for a full day-night cycle using its four science instruments until batteries ran out after 17h and 7min. The payload consisting of a wide angle camera (MASCAM), an imaging IR spectrometer (MicrOmega), a multi-channel radiometer (MARA), and a magnetometer (MasMAG) provided a wealth of data which helped to characterize the asteroid’s surface down to millimeter scale. MasCAM images revealed a surface dominated by rocks and boulders without showing fine-grained material. Boulders appeared either bright with smooth faces and sharp edges or dark with cauliflower-like crumbly surfaces. Inclusions observed in high-resolution images showed that rocks had strong similarities with carbonaceous chondrites. Temperatures of a ~60 cm diameter rock that have been measured in situ, were found to be consistent with a thermal inertia of 282(+93, -35) J m^{-2} K^{-1} $s^{-1/2}$, much lower than anticipated when compared to samples in our meteorite collections. This indicated that rocks on Ryugu were highly porous and likely very friable. The remnant magnetization of Ryugu's surface material on scales larger than 1 m was estimated to be lower than $3 \cdot 10^{-6}$ Am^2/kg (the measurement limit of MasMAG). A preliminary analysis of the induction effect in Ryugu caused by the variation in the solar wind magnetic field revealed significantly high electrical conductivity (of the order 1 S/m).

Keywords: Ryugu, Hayabusa2, Asteroid Surface, Lander, Carbonaceous Chondrites, High Porosity

©2019. Japan Geoscience Union. All Right Reserved.

Evidence of Mass Movement and Boulder Transport on Bennu from NASA's OSIRIS-REx Space Mission

*Erica R Jawin[1], Kevin J Walsh[2], Tim McCoy[1], Harold C Connolly[3], Dante S Lauretta[4], Ron L Ballouz[4], Jamie L Molaro[5], Olivier S Barnouin[6], Mike Nolan[4]

1. Smithsonian National Institute, Washington, DC, USA, 2. Southwest Research Institute, Boulder, CO, USA, 3. Dept. of Geology, Rowan University, Glassboro, NJ, USA, 4. Lunar and Planetary Laboratory, University of Arizona, Tucson, AZ, USA , 5. Planetary Science Institute, Tucson, AZ, USA, 6. The Applied Physics Laboratory, Johns Hopkins University, Laurel, MD, USA

The near-Earth Asteroid (101955) Bennu is currently being studied by the NASA OSIRIS-REx mission. This small, top-shaped asteroid has evidence of a diverse suite of geologic units, including impact craters, linear features, and abundant boulders at a range of sizes, geometric albedos, and morphologies. The surface of the asteroid appears to be old; however localized evidence of mass movement has been detected in various locations that suggests the surface is dynamic. The abundance of boulders on the surface varies widely with location, with concentrations of boulders located in local topographic lows (e.g. the interior of candidate impact craters, between linear ridges), suggesting that boulders travelled across the surface to result in these concentrations. Several locations that are abundant in boulders show evidence of imbrication in the local downslope direction, but evidence of imbrication is more localized than on other asteroids such as Itokawa. Evidence of mass movement at smaller particles sizes is also evident by burial of boulders: evidence of largescale W-E movement of material and burial of rocks has been identified, as well as pileup of boulders at locations downslope of scarps. In addition, the largest boulder on Bennu (~95 m diameter) appears to be partly buried, with a portion of the boulder of unknown size remaining in the subsurface. This boulder has an exposed face that extends vertically off the surface by ~20 m, suggesting that several tens of meters of finer-grained material could have accumulated to bury part of the boulder. The direction that material would have traveled to bury this boulder follows the regional slopes. As a comparison, the second largest boulder on Bennu (~50 m diameter) that is nearby albeit at a slightly higher latitude (45 S latitude, versus the buried boulder at 25 S latitude) is not buried –rather, this boulder appears to be perched on the surface. The variation in very large boulder burial suggests the surface of Bennu has potentially experienced large-scale material transport.

Keywords: OSIRIS-REx, Bennu, Mass-movement, Asteroid, Regolith

©2019. Japan Geoscience Union. All Right Reserved.

Resurfacing processes on small asteroids constrained by crater size distributions on Ryugu, Itokawa, and Eros

*Naofumi Takaki[1], Yuichiro Cho[1], Tomokatsu Morota[3], ERI TATSUMI[1], Kazuo Yoshioka[1], Hirotaka Sawada[5], yokota yasuhiro[2,5], Naoya Sakatani[5], Masahiko Hayakawa[5], Moe Matsuoka[5], Rie Honda[2], Shingo Kameda[4], Manabu Yamada[6], Toru Kouyama[8], Hidehiko Suzuki[10], Chikatoshi Honda[7], Kazunori Ogawa[9], Hideaki Miyamoto[1], Olivier Barnouin[11], Patrick Michel[12], Carolyn Ernst[11], Seiji Sugita[1,6]

1. University of Tokyo, 2. Kochi University, 3. Nagoya University, 4. Rikkyo University, 5. JAXA, 6. Chiba Institute of Technology, Planetary Exploration Res. Center, 7. University of Aizu, 8. AIST, 9. Kobe University, 10. Meiji University, 11. Johns Hopkins University Applied Physics Laboratory, 12. Nice Observatory

Recent ion irradiation experiments in laboratories suggest that space weathering may take place very rapidly [1], but telescopic observations of asteroids support much slower space weathering [2]. The spectral rejuvenation process on asteroid surfaces may hold a key for bridging the gap between the two opposite conclusions [3]. However, the nature of the spectral rejuvenation process has not been understood well yet. One approach for understanding the spectral rejuvenation process is to constrain the depth-age relation of surface layers on asteroids. In fact, imaging observations by Hayabusa2 revealed that smaller craters are highly depleted on the surface of the asteroid Ryugu [4], strongly suggesting that resurfacing is acting efficiently on near-surface layers. This depletion was already observed on Eros and Itokawa [5]. In this study, we analyze this depletion in small craters to constrain the resurfacing mechanism on small asteroids, such as Ryugu, Itokawa, and Eros. More specifically, we estimate the resurfacing age of Ryugu, Itokawa and Eros based on crater counting and crater production functions. Then we compare the analysis results with theoretical models for resurfacing mechanisms on such small asteroids.

Crater retention age can be estimated by using both the crater size frequency distribution (CSFD) and the crater production function (CPF). The CSFD on Ryugu shows that the large craters distribution (≧100m in diameter) is close to saturation level, but the number density of small craters (~10 m) is reduced by a factor of 100 [4]. Similar depletion in small craters is also observed on Itokawa [5]. We calculated crater retention ages for different size craters and derived the relation between crater retention ages and excavation depth of craters.

The CPFs on Ryugu, Itokawa, and Eros are estimated based on a classical main belt collisional evolution model and a scaling relation for crater formation. We used a scaling relation including armoring effect [6] for Ryugu and Itokawa to account for the high abundance of boulders on them. In this analysis, we used larger craters than ~10m in diameter. Finally, we derived the relation between crater retention age, t, and depth, d, of crater, $t \sim d^a$, where a is found to be 1.8±0.4 on Ryugu, 1.1±0.3 on Itokawa, and 1.9±0.3 on Eros, respectively. If crater degradation is controlled by a diffusion process, the relation between crater retention age t is proportional to the square of crater depth d, i.e., $t \sim d^2$. Ryugu's and Eros's power-law indices (a ~1.8-1.9) are consistent with diffusion (a = 2), which is not the case of Itokawa's power-law index. However, Itokawa's power-law index a increase to 1.9 if we include smaller craters than ~10m in

©2019. Japan Geoscience Union. All Right Reserved.

diameter in this analysis. This value is consistent with diffusion (a = 2). Actually, Michel et al. 2009 suggests that the depletion of small craters on Itokawa is reproduced by a seismic shaking model without taking an armoring effect into account [7]. The efficiency of an armoring effect for small craters on asteroids is uncertain, but an armoring effect may change the interpretation of CSFDs. In order to understand crater scaling for smaller craters, Small Carry-on Impactor (SCI) experiment on Hayabusa2 is important.

[1] Lantz+2018, Icarus, **302**, 10–17

[2] Lazzarin+2009 AA, **498**, 307-311

[3] Shestopalov+2013, Icarus, **225**, 781-798

[4] Sugita+2019, Science in revision

[5] Hirata+2009, Icarus, **200**, 486-502

[6] Tatsumi & Sugita 2018, Icarus, **300**, 227-248

[7] Michel+2009, Icarus, **200**, 503-513

Keywords: asteroid, crater, resurfacing, Ryugu, Itokawa, Hayabusa2

©2019. Japan Geoscience Union. All Right Reserved.

[E] Oral | P (Space and Planetary Sciences)：P-PS Planetary Sciences

Wed. May 29, 2019 9:00 AM - 10:30 AM JST | Wed. May 29, 2019 12:00 AM - 1:30 AM UTC | A01 TOKYO BAY MAKUHARI HALL

[P-PS03] Solar System Small Bodies: A New Frontier Arising Hayabusa 2, OSIRIS-REx and Other Projects

convener:Masateru Ishiguro(Department of Physics and Astronomy, Seoul National University), Taishi Nakamoto(Tokyo Institute of Technology), Masanao Abe(Institute of Space and Astronautical Science, Japan Aerospace Exploration Agency), Olivier S Barnouin(Johns Hopkins University Applied Physics Laboratory), Chairperson:Taishi Nakamoto(Tokyo Institute of Technology)

In June 2018, the Hayabusa 2 spacecraft arrived at the target asteroid Ryugu after three and half years journey. In addition, another spacecraft, OSIRIS-REx will soon arrive at its destination Bennu. With these arrivals, the solar system research is about to enter a new era. We have organized this small bodies session since 2012 and had a broad range of discussions from viewpoints of laboratory experiments, observations, space explorations, theoretical modeling, and sample analyses. In particular, this time, we aim to hold this session to bring the latest research on solar system small bodies, focusing on the initial results of Hayabusa 2 and OSIRIS-REx. Presentations in the related fields other than these two asteroidal missions are also welcomed.

9:00 AM - 9:15 AM JST | 12:00 AM - 12:15 AM UTC

[PPS03-19] The shape of Bennu: Implications for internal structure.

★Invited Papers

*Olivier S Barnouin[1], Micheal G. Daly[2], Eric E Palmer[3], Robert W Gaskell[3], John R. Weirich[3], Catherine L Johnson[4], Manar Al Asad[4], James H Roberts[1], Mark E. Perry[1], Hannah C.M. Sursorney[4], R. Terik Daly[1], Edward B. Bierhaus[5], Jeff A Seabrook[2], Raymond C. Espiritu[1], A. Hari Nair[1], Lilian Nguyen[1], Gregory A Neumann[6], Carolyn M Ernst[1], William V Boynton[7], Micheal C. Nolan[7], Coralie D. Adams[9], Micheal C. Moreau[6], Bashar Rizk[7], Christian Drouet D'Aubigny[7], Erica R. Jawin[8], Kevin J Walsh[10], Patrick Michel[11], Stephen R. Schwartz[7], Ronald L. Ballouz[7], Erwan M Mazarico[6], Daniel J. Scheeres[12], Jay W. McMahon[12], W Bottke[10], Seiji Sugita[13], Naru Hirata[14], Noayuki Hirata[15], Sei-ichiro Watanbe[16], Keara N. Burke[7], Daniella N. DellaGuistina[7], Carinna A. Bennet[7], Dante Lauretta[7] (1.Johns Hopkins University Applied Physics Laboratory, 2.The Centre for Research in Earth and Space Science, York University, Toronto, Ontario, Canada., 3.Planetary Science Institute, Tucson, AZ, USA, 4.Department of Earth, Ocean and Atmospheric Sciences, University of British Columbia, Vancouver, Canada., 5.Lockheed Martin Space Systems Company, Denver, CO, USA., 6.NASA Goddard Space Flight Center, Greenbelt, MD, USA., 7.Lunar Planetary Laboratory, University of Arizona, Tucson, AZ, USA., 8.Smithsonian Institution National Museum of Natural History, Washington, DC, USA., 9.KinetX Aerospace, Inc. Simi Valley, CA, USA, 10.Southwest Research Institute, Boulder, CO, USA., 11.Université Côte d'Azur, Observatoire de la Côte d'Azur, CNRS, Laboratoire Lagrange, Nice, France., 12.Department of Aerospace Engineering Sciences, University of Colorado, Boulder, CO, USA., 13.University of Tokyo, Tokyo, Japan., 14.Aizu University, Aizu-Wakamatsu, Japan., 15.Kobe University, Kobe, Japan., 16.Nagoya University, Nagoya, Japan.)

9:15 AM - 9:30 AM JST | 12:15 AM - 12:30 AM UTC

[PPS03-20] Global Geology of Bennu from NASA's OSIRIS-REx Space Mission

★Invited Papers

*Erica R Jawin[1], Kevin J Walsh[2], Tim McCoy[1], Harold C Connolly[3], Dante S Lauretta[4], Ron L Ballouz[4], Olivier S Barnouin[5], C Beddingfield[6], Carina A Bennett[4], Edward B Bierhaus[7], Keara N Burke[4], Ben Clark[8], Michael G Daly[9], Marco Delbo[10], Daniella DellaGiustina[4], Jason P Dworkin[11], Christine Hartzell[12], John Marshall[6], Patrick Michel[10], Jamie L. Molaro[13], Mike Nolan[4], Maurizio Pajola[14], Mark Perry[5], Bashar Rizk[4], Scott Sandford[15], Dan J Scheeres[16], Stephen R Schwartz[4], David Trang[17] (1.Smithsonian National Institute, Washington, DC, USA, 2.Southwest Research Institute, Boulder, CO, USA, 3.Dept. of Geology, Rowan University, Glassboro, NJ, USA, 4.Lunar and Planetary Laboratory, University of Arizona, Tucson, AZ, USA , 5.The Applied Physics Laboratory, Johns Hopkins University, Laurel, MD, USA, 6.SETI Institute, Mountain View, CA, USA, 7.Lockheed Martin Space Systems Company, USA, 8.Space Science Institute, Boulder CO, USA, 9.York University, Canada, 10.Laboratoire Lagrange, Université Côte d'Azur, Observatoire

de la Côte d'Azur, CNRS, Laboratoire Lagrange, Nice, France, 11.NASA Goddard Space Flight Center, Greenbelt, MD, USA, 12.Department of Aerospace Engineering, University of Maryland, College Park MD, USA, 13.Planetary Science Institute, Tucson, AZ, USA, 14.INAF - Astronomical Observatory of Padova, Italy, 15.NASA Ames Research Center, USA, 16.Dept. of Aerospace Engineering Sciences, University of Colorado, Boulder, CO, USA, 17.HIGP/University of Hawaii at Manoa, USA)

9:30 AM - 9:45 AM JST | 12:30 AM - 12:45 AM UTC

[PPS03-21] Modeling surface mobility mechanisms on a top-shaped near-Earth asteroid

★Invited Papers

*Ronald Ballouz[1], Nicola Baresi[2], Olivier S Barnouin[3], Carina A Bennet[1], Edward B Bierhaus[4], Keara N Burke[1], Harold C Connolly[5], Sarah T Crites[2], Daniella DellaGiustitna[1], Erica Jawin[6], Dante S Lauretta[1], Patrick Michel[7], Derek C Richardson[8], Dan J Scheeres[9], Stephen Schwartz[1], Seiji Sugita[10], Eri Tatsumi[10], Florian Thuillet[7], Kevin Walsh[11] (1.Lunar and Planetary Lab, University of Arizona, Tucson, AZ, USA, 2.Institute of Space and Astronautical Science, Sagamihara, Japan, 3.The Applied Physics Laboratory, Johns Hopkins University, Laurel, MD, USA, 4.Lockheed Martin, Boulder, CO, USA, 5.Department of Geology, Rowan University, Glassboro, NJ, USA, 6.Smithsonian National Museum of Natural History, Washington, DC, USA, 7.UCA-OCA-CNRS, Lagrange Laboratory, Nice, France, 8.Dept. of Astronomy, University of Maryland, College Park, MD, USA, 9.Dept. of Aerospace Engineering Sciences, University of Colorado, Boulder, CO, USA, 10.University of Tokyo, Tokyo, Japan, 11.Southwest Research Institute, Boulder, CO, USA)

9:45 AM - 10:00 AM JST | 12:45 AM - 1:00 AM UTC

[PPS03-22] **Visualization and Analysis of Solar System Small Bodies with NASA's Solar System Treks Project**

*Brian Hamilton Day[1], Emily Law[2] (1.NASA Solar System Exploration Research Virtual Institute, NASA Ames Research Center, 2.NASA Jet Propulsion Laboratory, California Institute of Technology)

10:00 AM - 10:15 AM JST | 1:00 AM - 1:15 AM UTC

[PPS03-23] Density Distribution within Small Solar System Bodies Based on Smooth Terrain Shape: Asteroid 25143 Itokawa and Comet 67P/Churyumov-Gerasimenko

*Masanori Kanamaru[1], Sho Sasaki[1], Mark Wieczorek[2] (1.Osaka University, 2.Côte d'Azur Observatory)

10:15 AM - 10:30 AM JST | 1:15 AM - 1:30 AM UTC

[PPS03-24] Low temperature hydration experiments of cometary analog materials towards the Comet Astrobiology Exploration Sample Return (CAESAR) mission

*Aki Takigawa[1,4], Yuki Kimura[1], Yoshihiro Furukawa[2], Tomoki Nakamura[3] (1.Graduate School of Science, Kyoto University, 2.Institute of Low Temperature Science, 3.Graduate School of Science, Tohoku University, 4.The Hakubi Center for Advanced Research)

The shape of Bennu: Implications for internal structure.

*Olivier S Barnouin[1], Micheal G. Daly[2], Eric E Palmer[3], Robert W Gaskell[3], John R. Weirich[3], Catherine L Johnson[4], Manar Al Asad[4], James H Roberts[1], Mark E. Perry[1], Hannah C.M. Sursorney[4], R. Terik Daly[1], Edward B. Bierhaus[5], Jeff A Seabrook[2], Raymond C. Espiritu[1], A. Hari Nair[1], Lilian Nguyen[1], Gregory A Neumann[6], Carolyn M Ernst[1], William V Boynton[7], Micheal C. Nolan[7], Coralie D. Adams[9], Micheal C. Moreau[6], Bashar Rizk[7], Christian Drouet D'Aubigny[7], Erica R. Jawin[8], Kevin J Walsh[10], Patrick Michel[11], Stephen R. Schwartz[7], Ronald L. Ballouz[7], Erwan M Mazarico[6], Daniel J. Scheeres[12], Jay W. McMahon[12], W Bottke[10], Seiji Sugita[13], Naru Hirata[14], Noayuki Hirata[15], Sei-ichiro Watanbe[16], Keara N. Burke[7], Daniella N. DellaGuistina[7], Carinna A. Bennet[7], Dante Lauretta[7]

1. Johns Hopkins University Applied Physics Laboratory, 2. The Centre for Research in Earth and Space Science, York University, Toronto, Ontario, Canada., 3. Planetary Science Institute, Tucson, AZ, USA, 4. Department of Earth, Ocean and Atmospheric Sciences, University of British Columbia, Vancouver, Canada., 5. Lockheed Martin Space Systems Company, Denver, CO, USA., 6. NASA Goddard Space Flight Center, Greenbelt, MD, USA., 7. Lunar Planetary Laboratory, University of Arizona, Tucson, AZ, USA., 8. Smithsonian Institution National Museum of Natural History, Washington, DC, USA., 9. KinetX Aerospace, Inc. Simi Valley, CA, USA, 10. Southwest Research Institute, Boulder, CO, USA., 11. Université Côte d’Azur, Observatoire de la Côte d’Azur, CNRS, Laboratoire Lagrange, Nice, France., 12. Department of Aerospace Engineering Sciences, University of Colorado, Boulder, CO, USA., 13. University of Tokyo, Tokyo, Japan., 14. Aizu University, Aizu-Wakamatsu, Japan., 15. Kobe University, Kobe, Japan., 16. Nagoya University, Nagoya, Japan.

Introduction: We used data collected by the Origins, Spectral Interpretation, Resource Identification, and Security–Regolith Explorer (OSIRIS-REx) spacecraft since November 1, 2018 to develop a global digital terrain model (DTM) of Bennu. The DTM is developed from images collected by the OSIRIS-REx Camera Suite using stereophotoclinometry (SPC). We validated the DTM independently using limb data and by the identification of keypoints between actual images and synthetic images rendered from the DTM. The results are also compared to an independent model derived from range measurements collected by the OSIRIS-REx Laser Altimeter (OLA). While developing the global model, we also refine the pole orientation and rotational state of the asteroid. The characteristics of the resulting global digital terrain model provide constraints on the factors responsible for the origin and evolution of Bennu’s shape and surface.

Digital Terrain Model Construction from Imaging: About 1500 OCAMS images with ground sample distance ranging from 30 to 200 m were used to develop the global DTM of Bennu. We used distant limb data of Bennu to construct an initial DTM of Bennu. Then a combination of geometric stereo data and surface lighting conditions (or photoclinometry) modeled small patches (or maplets) of terrain across the asteroid. Geometric stereo typically defines the location of the center of each maplet, while the surface tilts across the maplet are estimated by best fitting the brightness variations of images that contain some portion of the maplet. These maplets are then combined to build a global model. The model increases in detail, accuracy, and precision as higher-resolution images and images with different viewing conditions are incorporated.

©2019. Japan Geoscience Union. All Right Reserved.

Digital Terrain Model Construction from Laser Altimetry: We collated several six-hour linear scans obtained by OLA during orbit around Bennu to make an independent shape model of Bennu at a resolution equivalent to the one derived from imaging. This DTM is improved relative to the SPC-derived model because OLA better resolves the heights, and extent of 1 to 3m boulders across the surface of the asteroid.

Bennu’ s Geomorphological and Structural Properties: The evaluation of the both models shows that the average size of the asteroid is 490.06 ±0.16 m.

The model shows the presence of several features:
-An equatorial ridge that is muted, and is diamond-shaped when viewed from the pole;
-Topographic north-south ridges that extend in some instances from pole to pole. The ridges influence the distribution of boulders, which are frequently concentrated between the ridges;
-Large craters that influence some of the attributes of the shape, primarily along the equator;
-A few large protruding boulders >40 m in diameter and >10 m high, mostly in the southern hemisphere;
-Grooves, scarps, and troughs that in some instances extend several 10s to 100s of meters, with depths ranging from 2–10 m.

Conclusion: The initial shape characteristics suggest that Bennu has some interior stiffness. Considering past modeling efforts investigating deformation due to spin-up, the lack of a circular equatorial ridge with a pronounced bulge, and the presence of high standing north-south ridges indicate that in spite of an abundance of evidence for material moving towards the equator, Bennu has interior structure that resists deformation.

Keywords: (101955) Bennu, Asteroids, OSIRIS-REx mission

©2019. Japan Geoscience Union. All Right Reserved.

Global Geology of Bennu from NASA's OSIRIS-REx Space Mission

*Erica R Jawin[1], Kevin J Walsh[2], Tim McCoy[1], Harold C Connolly[3], Dante S Lauretta[4], Ron L Ballouz[4], Olivier S Barnouin[5], C Beddingfield[6], Carina A Bennett[4], Edward B Bierhaus[7], Keara N Burke[4], Ben Clark[8], Michael G Daly[9], Marco Delbo[10], Daniella DellaGiustina[4], Jason P Dworkin[11], Christine Hartzell[12], John Marshall[6], Patrick Michel[10], Jamie L. Molaro[13], Mike Nolan[4], Maurizio Pajola[14], Mark Perry[5], Bashar Rizk[4], Scott Sandford[15], Dan J Scheeres[16], Stephen R Schwartz[4], David Trang[17]

1. Smithsonian National Institute, Washington, DC, USA, 2. Southwest Research Institute, Boulder, CO, USA, 3. Dept. of Geology, Rowan University, Glassboro, NJ, USA, 4. Lunar and Planetary Laboratory, University of Arizona, Tucson, AZ, USA , 5. The Applied Physics Laboratory, Johns Hopkins University, Laurel, MD, USA, 6. SETI Institute, Mountain View, CA, USA, 7. Lockheed Martin Space Systems Company, USA, 8. Space Science Institute, Boulder CO, USA, 9. York University, Canada, 10. Laboratoire Lagrange, Université Côte d’Azur, Observatoire de la Côte d’Azur, CNRS, Laboratoire Lagrange, Nice, France, 11. NASA Goddard Space Flight Center, Greenbelt, MD, USA, 12. Department of Aerospace Engineering, University of Maryland, College Park MD, USA, 13. Planetary Science Institute, Tucson, AZ, USA, 14. INAF - Astronomical Observatory of Padova, Italy, 15. NASA Ames Research Center, USA, 16. Dept. of Aerospace Engineering Sciences, University of Colorado, Boulder, CO, USA, 17. HIGP/University of Hawaii at Manoa, USA

NASA’s OSIRIS-REx sample return mission has been observing the near-Earth Asteroid (101955) Bennu since December 2018 and will be collecting a sample of the surface in the summer of 2020, to be returned to Earth in 2023. Preliminary and ongoing observations have yielded much information about Bennu’s formation, evolution, and ongoing geologic activity. Here we report on the global geology of Bennu based on analyses of images combined with shape, mass, and slope measurements. Initial results suggest that Bennu is a rubble-pile asteroid, formed from a parent body that was collisionally disrupted and reaccumulated. The asteroid has a “top” shape which is spherical with an equatorial bulge, similar to other near-Earth asteroids including Ryugu as observed by the Hayabusa2 sample return space mission. Candidate impact craters have been observed at a range of diameters between ~10-150 m across the surface of Bennu, leading to a crater retention age of 100 million to 1 billion years. An apparent concentration of large crater candidates at low latitudes suggest that the equatorial ridge is stratigraphically old, and may have formed early in Bennu’s history or been inherited from the reaccumulation event which created the asteroid. Several linear features have been identified on Bennu, the largest of which are topographic highs that extend longitudinally from the northern polar regions to the equator. Boulders are concentrated between several of these linear ridges, as well as in the interior of large candidate craters. Boulders on Bennu appear to be geologically diverse. Boulder sizes range from < 3 m to ~95 m in diameter with large variations in geometric albedo, morphology, degree of burial, and state of degradation. Fractured boulders have been identified with various numbers, orientations, and widths of fractures. Distinct clasts within several boulders indicate they may be breccias, while piles of boulders may represent disaggregated polymict or brecciated boulders. Current imaging resolution cannot resolve centimeter-sized particles, so direct detections of regolith or other sub-cm sized particles have not been made. However, several small candidate craters (< 20 m diameter) have a significant lack of boulders relative to the surrounding terrain, and additional datasets suggest the presence of a component of fine-grained particles. Improved image resolution will aid in the identification of regolith deposits on Bennu.

Keywords: OSIRIS-REx, Bennu, Asteroid, Geology

©2019. Japan Geoscience Union. All Right Reserved.

©2019. Japan Geoscience Union. All Right Reserved.

Modeling surface mobility mechanisms on a top-shaped near-Earth asteroid

*Ronald Ballouz[1], Nicola Baresi[2], Olivier S Barnouin[3], Carina A Bennet[1], Edward B Bierhaus[4], Keara N Burke[1], Harold C Connolly[5], Sarah T Crites[2], Daniella DellaGiustitna[1], Erica Jawin[6], Dante S Lauretta[1], Patrick Michel[7], Derek C Richardson[8], Dan J Scheeres[9], Stephen Schwartz[1], Seiji Sugita[10], Eri Tatsumi[10], Florian Thuillet[7], Kevin Walsh[11]

1. Lunar and Planetary Lab, University of Arizona, Tucson, AZ, USA, 2. Institute of Space and Astronautical Science, Sagamihara, Japan, 3. The Applied Physics Laboratory, Johns Hopkins University, Laurel, MD, USA, 4. Lockheed Martin, Boulder, CO, USA, 5. Department of Geology, Rowan University, Glassboro, NJ, USA, 6. Smithsonian National Museum of Natural History, Washington, DC, USA, 7. UCA-OCA-CNRS, Lagrange Laboratory, Nice, France, 8. Dept. of Astronomy, University of Maryland, College Park, MD, USA, 9. Dept. of Aerospace Engineering Sciences, University of Colorado, Boulder, CO, USA, 10. University of Tokyo, Tokyo, Japan, 11. Southwest Research Institute, Boulder, CO, USA

The advent of near-Earth asteroid (NEA) encounters with spacecraft has provided a view of planetary surfaces evolving on the smallest objects yet explored. The arrival of OSIRIS-REx and Hayabusa2 at their target asteroids (101955) Bennu, with average diameter (d) = 0.49 km, and (162173) Ryugu (d = 0.90 km), revealed cratered top-shaped worlds with signs of surface mobility [1, 2]. Compared to larger planetary bodies, Bennu and Ryugu’s small sizes and gravities challenge the conventional understanding of surface modification mechanisms, such as the redistribution of boulders on the surface or the erasure of craters.

On the larger NEA (433) Eros (d = 16.8 km), boulders were spatially correlated with impact craters, which degrade through impact-induced seismic shaking [3]. However, our poor understanding of rubble-pile interiors [4], combined with processes that operate more efficiently on smaller NEAs (such as thermal re-radiation torques, i.e., the YORP effect [5]), introduces new complexities to understanding surface mobility on Bennu and Ryugu.

Here, we first present evidence of a dynamic surface on Bennu and Ryugu. Then, we present an analysis of the dynamical processes that may dominate the surface modification of small top-shaped NEAs. We model the redistribution of material on the surface due to different input energy sources: i) impact-induced seismic shaking, ii) YORP spin-up, iii) impact cratering, and iv) planetary encounters. We use a combination of techniques that allows us to approach the problem at multiple length and time scales. The first step models the global effect of the energy sources using analytical techniques. In the second step, we model the fine grain scale interactions in a microgravity environment in short timescales using a particle dynamics code [6,7]. Finally, we propagate the accumulated effect of the fine-scale interactions by integrating individual surface modifications over the typical timescale of each individual process. The results are used to assess which of the above listed mechanisms are the most effective at transforming small NEA surfaces.

References:

1. Walsh et al. 2019, Nature Geoscience, Accepted.

2. Sugita et al. 2019, Science, Accepted.

©2019. Japan Geoscience Union. All Right Reserved.

3. Richardson, J.E. et al. (2005) Icarus, 179, 324–349.

4. Scheeres, D.J. et al. (2015) in Asteroids IV (eds. Michel, DeMeo, & Bottke), pp. 745–766.

5. Bottke, W.F. et al. (2006) Annual Reviews of E&PS, 34, 157–191.

6. Richardson, D.C. et al. (2011) Icarus, 212, 427–437.

7. Schwartz, S.R. et al. (2012) Granular Matter, 14, 363–380.

Acknowledgements:

This material is based upon work supported by NASA under Contract NNM10AA11C issued through the New Frontiers Program and from Grant no. 80NSSC18K0226 as part of The OSIRIS-REx Participating Scientist Program. P.M. and F.T. P.M. acknowledge funding support from the French space agency CNES and from Academies of Excellence: Complex systems and Space, environment, risk, and resilience, part of the IDEX JEDI of the Université Côte d’Azur.

Keywords: Near Earth Asteroids, OSIRIS-REx, Hayabusa2

©2019. Japan Geoscience Union. All Right Reserved.

Visualization and Analysis of Solar System Small Bodies with NASA's Solar System Treks Project

*Brian Hamilton Day[1], Emily Law[2]

1. NASA Solar System Exploration Research Virtual Institute, NASA Ames Research Center, 2. NASA Jet Propulsion Laboratory, California Institute of Technology

In its investigations of Vesta and Ceres, NASA's Dawn mission has returned spectacular data detailing the surfaces of these two prominent small bodies in our Solar System's asteroid belt. In order to greatly facilitate dissemination, visualization, and analysis of this data, and public understanding of the mission, the Dawn mission has partnered with NASA's Solar System Treks Project (SSTP). SSTP has recently released an update to the Vesta Trek online portal (https://trek.nasa.gov/vesta/) and has released a new Ceres Trek portal (https://trek.nasa.gov/ceres/).

This presentation will showcase the use of the Ceres Trek and Vesta Trek portals and demonstrate how they can be used to visualize and analyze particularly interesting landforms such as the pitted terrain on Vesta and relic cryovolcanoes on Ceres. We will also demonstrate the new VR capability that has been added to the portals, allowing users to generate their own virtual reality flyovers for any user-defined paths along the bodies' surfaces. In addition to highlighting the portals for Ceres and Vesta, the presentation will preview additional portals being planned/developed for other small bodies. NASA and JAXA have requested the development of a portal for the asteroid Ryugu to facilitate dissemination, visualization, and analysis of data from Japan's Hayabusa2 mission, and a portal for Mars' moon Phobos in support of mission planning for Japan's MMX mission. We are also planning a portal for the asteroid Bennu with data from the OSIRIS-Rex mission.

All of these products are efforts in the NASA Solar System Treks Project (SSTP), available at https://trek.nasa.gov. NASA's Solar System Trek online portals provide web-based suites of interactive data visualization and analysis tools to enable mission planners, planetary scientists, students, and the general public to access mapped data products from past and current missions for a growing number of planetary bodies including the Moon, Mars, Vesta, etc. These portals are being used for site selection and analysis by NASA and a number of its international partners, supporting upcoming missions. In addition to demonstrating the capabilities of selected portals in this presentation, we will solicit input from the community for ideas for future enhancements to the portals.

Keywords: Ceres, Vesta

©2019. Japan Geoscience Union. All Right Reserved.

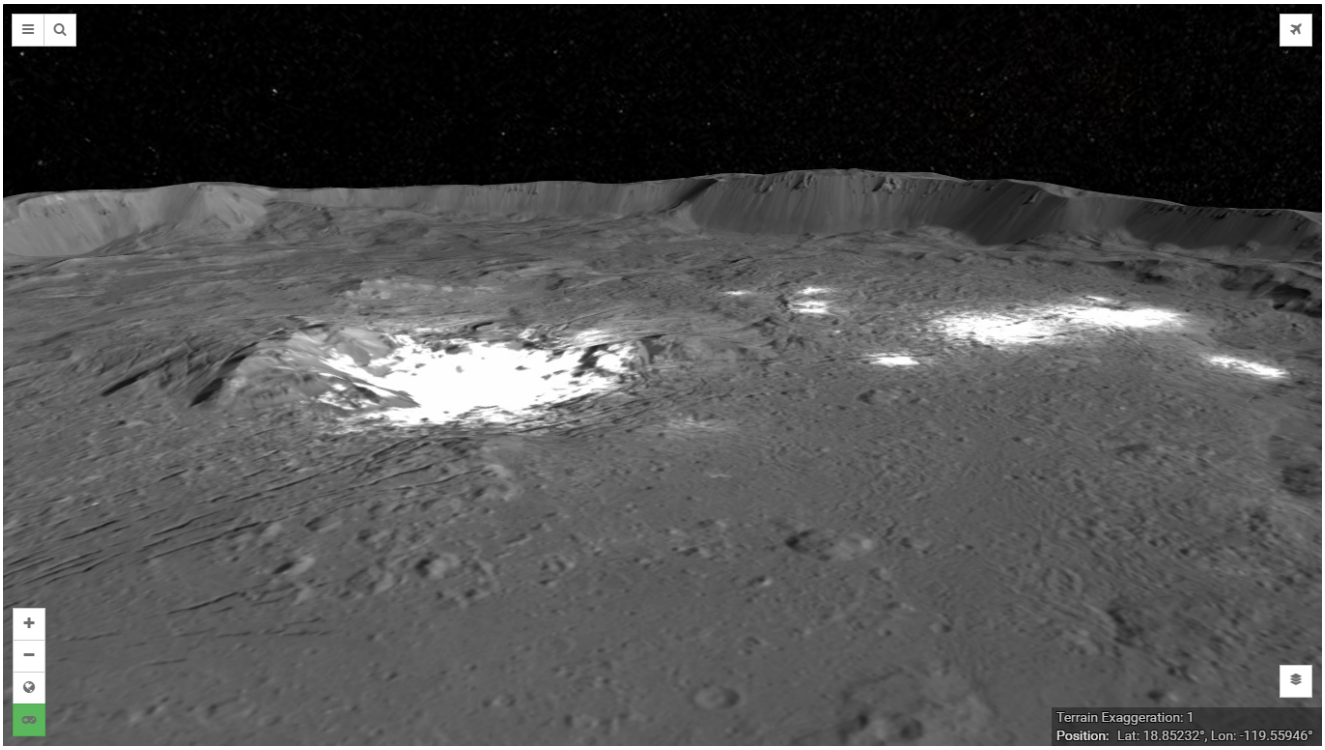

©2019. Japan Geoscience Union. All Right Reserved.

Density Distribution within Small Solar System Bodies Based on Smooth Terrain Shape: Asteroid 25143 Itokawa and Comet 67P/Churyumov-Gerasimenko

*Masanori Kanamaru[1], Sho Sasaki[1], Mark Wieczorek[2]

1. Osaka University, 2. Côte d'Azur Observatory

Small solar system bodies are the remnants of the early stage of the solar system formation. Shapes and interior structures of small bodies tell us about how they formed and evolved. Particularly, the interior density distribution of small bodies is an important clue for better understanding of planetesimal collisions and subsequent accumulation processes. However, we have much less information about their interiors than their surface properties, partly because it is difficult to measure the exterior gravity precisely in a small body mission. We have investigated a method to estimate density distribution within a small body based on combining spacecraft imagery and the simulated gravity field on the surface of the small body (Kanamaru and Sasaki, 2019; Kanamaru, Sasaki and Wieczorek, in prep.).

If a small body possesses loose regolith sufficiently, over geologic time, impact-induced seismic shaking or cometary activity may have triggered mass movement from a high standing region to a low standing region (Richardson and Bowling, 2014). Our inversion of density distribution assumes that a very flat region on a small body, which is covered with fine gravels and associated with the low standing area in gravitational potential, might approximate an equi-potential surface. Therefore, the inversion processes include (1) mapping a smooth terrain on a 3D shape model of the small body using the Small Body Mapping Tool, and (2) computing dynamic elevations above a reference potential surface given ununiform density distribution (as shown in the upper left panel in Figure). As a criteria for mapping the smooth terrain, we also used a surface roughness defined as the standard deviation of the dynamic elevations within a circle of a specific scale (upper right panel in Figure). The misfit between the smooth terrains and the equi-potential surface is characterized by the standard deviation of the surface elevations within the flat region. On the above assumption of the topographic erosion process, the minimum misfit gives a best fitting density. We applied this method to asteroid Itokawa and comet 67P/Churyumov-Gerasimenko to investigate whether each of their lobes has a different density from the other or not.

There exists three major smooth terrains on Itokawa, named MUSES-C Regio, Sagamihara Regio and Uchinoura Regio. Given different densities to the two lobes of Itokawa (the head and body), the misfit for the smooth terrains is minimized where the head of Itokawa has a higher density than the mean bulk density. Based on the consideration of the systematic errors that arise from the uncertainty of the shape model itself and the calculation error of the gravity field, the allowable range of the head density is estimated to be 2,450 (2,220-2,670) kg/m^3 in contrast to the body density of 1,930 (1,976-1,879) kg/m^3 . Such a great contrast in density between the two lobes is consistent with the independent estimate of the center-of-mass/center-of-figure offset of Itokawa based on the YORP spin-up observation (Lowry et al., 2014).

The comet nucleus of 67P also has a smooth terrain called Hapi, which is likely to be covered with particles falling from other regions. In the density inversion for the two lobes of 67P, the head and body (see the middle left panel in Figure), the best fitting density of the head is similar to the mean bulk density unlike the case of Itokawa (lower panel in Figure). This result indicates a global scaled homogeneity of

©2019. Japan Geoscience Union. All Right Reserved.

67P, which is consistent with the gravity measurement by Patzold et al. (2016). If the bi-lobed shape of the comet was formed by a sub-catastrophic disruption of its parent body and merger of two main fragments (Jutzi and Benz, 2017), it is possible for the two lobes to have the same density.

Keywords: Small solar system body, Asteroid 25143 Itokawa, Comet 67P/Churyumov-Gerasimenko, Interior density distribution, Gravity field

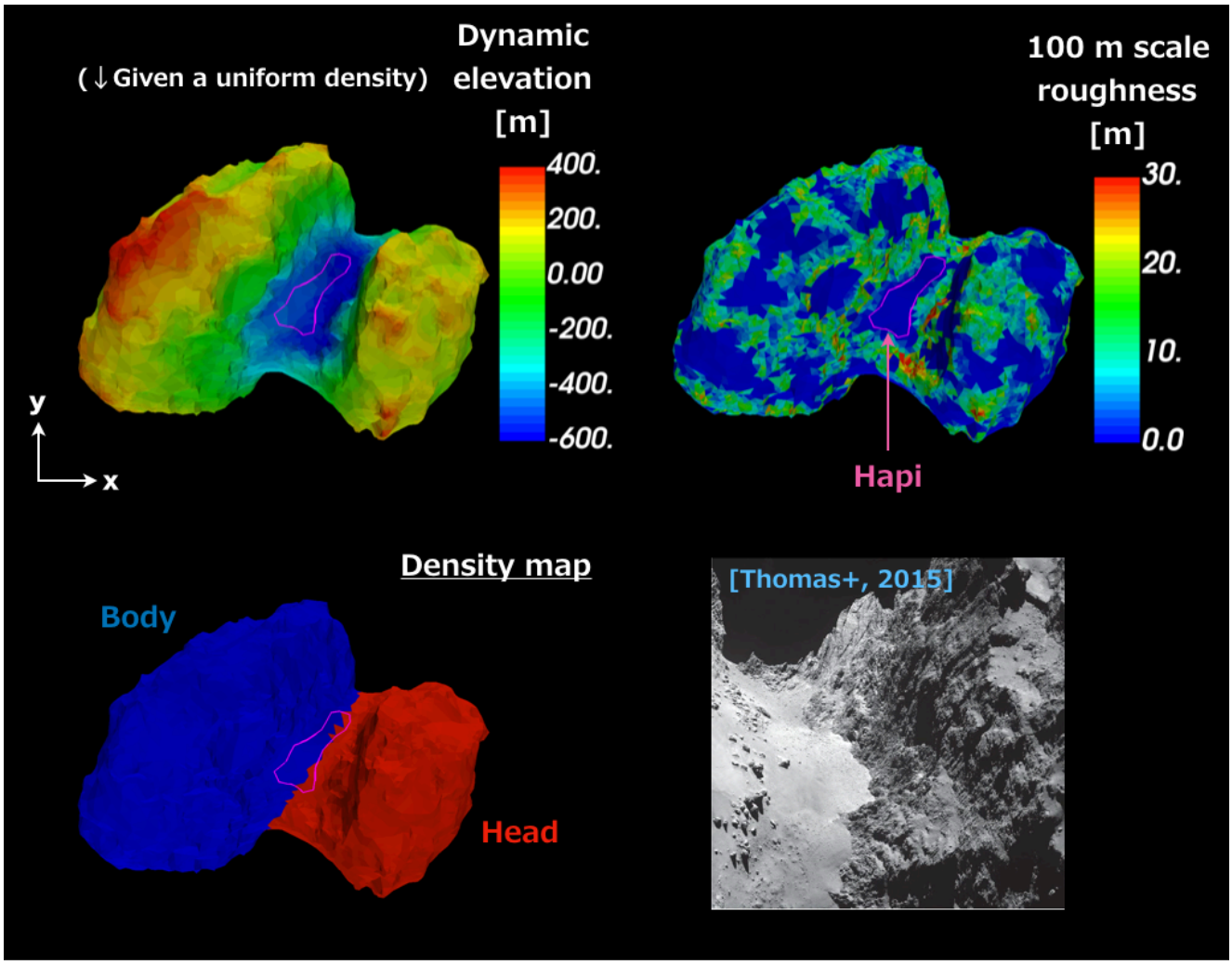

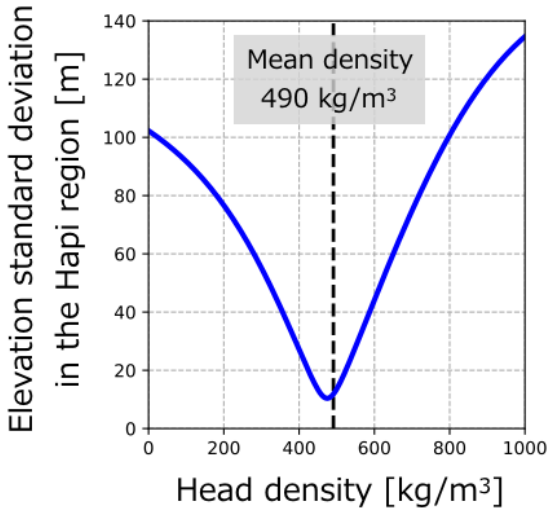

©2019. Japan Geoscience Union. All Right Reserved.

Low temperature hydration experiments of cometary analog materials towards the Comet Astrobiology Exploration Sample Return (CAESAR) mission

*Aki Takigawa[1,4], Yuki Kimura[1], Yoshihiro Furukawa[2], Tomoki Nakamura[3]

1. Graduate School of Science, Kyoto University, 2. Institute of Low Temperature Science, 3. Graduate School of Science, Tohoku University, 4. The Hakubi Center for Advanced Research

The Comet Astrobiology Exploration Sample Return (CAESAR) mission is a final candidate for selection as the fourth mission in NASA’s New Frontiers Program. CAESARaims to acquire and return to Earth for laboratory analysis a minimum of 80 g of surface material from the nucleus of comet 67P/Churyumov-Gerasimenko (67P) (Squyres et al. 2018).Near-infrared spectra of a short-period comet 67P taken by the spectrometer onboard Rosseta spacecraft also indicate the absence of phyllosilicates in this comet (Capaccioni et al. 2015). In order to return anhydrated samples from 67P, optimal conditions for sampling should be determined because cometary dust particles especially amorphous silicates are highly reactive. Hydration process of anhydrous crystalline silicates such as olivine is already well-characterized, whereas reaction of water vapor or ice with amorphous silicates and organic matters at temperatures below H_2O freezing points has been poorly understood. In this study, we performed incubation experiments of amorphous silicates and organic matters under low temperature conditions with ice or vapor of D_2O/NH_3.

Amorphous silicate nanoparticles with three different chemical compositions and textures (S1, S2, and S3), and commercial glycine and ribose powder were used in the experiments. S1 is composed of ~100 nm particles having $MgSi_2O_5$composition prepared with sol-gel processing. S2 and S3 are condensates from high temperature gases. S2 is amorphous Mg_2SiO_4nanoparticles of ~80 nm in size synthesized in a Radio Frequency plasma system (Koike et al. 2010). S3 is 30-100 nm sized amorphous silicate with Mg/Si~0.93 embedded with metallic Fe-Ni particles condensed from a high temperature vapor of the CI chondritic ratios of Mg, Al, Ca, Fe, and Nito Si in an induction thermal plasma system (Kim et al. 2017).

Two types of ice were used in the experiments to evaluate the effects of corrosive gases in 67P; (A) Pure D_2O ice (99.90% purity) and (B) Mixture D_2O ice with 0.3% H_2O and 0.15% NH_3. Experiments with different ices were performed in different vacuum containers placed in a cryogenic box. About 5 mg of three silicate and glycine samples were put in different open-top glass bottles (2 ml). Approximately 50 mg of chipped ice fragments were put in the glass bottles and directly contact with the silicate and glycine samples. Roughly ~500 mg of the same ice fragments were put in the vacuum containers as a vapor source. The temperature of the cryogenic box sets at -17 or -27˚C. The samples were exposed with saturated vapor of ices for 10-120 days. As a comparison, exposure experiments of amorphous silicate samples (S1, S2, and S3) to H_2O vapor were also conducted at 25 and 50˚C for 10 days.

The exposed silicate samples were analyzed with a powder X-ray diffraction (XRD, Rigaku SmartLab) and Fourier-transform infrared spectroscopy (FT-IR; JASCO MFT-680, Thermo Nicolet iS5). The recovery rate of glycine (i.e., molar ratio of recovered glycine over starting glycine) and ribose were obtained by liquid chromatography tandem mass spectrometer (LC/MSMS; Shimadzu LCMS-8040).

No clear change of the XRD patterns and FT-IR spectra for S1, S2, and S3 was confirmed after the

©2019. Japan Geoscience Union. All Right Reserved.

experiments for <120 days at -17 and -27˚C. The recovery of glycine exposed to D_2O ice and NH_3 -containing D_2O ice for 10 days was 108±8 mol% and 105±8 mol%, respectively. The recovery of ribose exposed to D_2O ice and NH_3-containing D_2O ice for 10 days was 108±12 mol% and 105±12 mol%, respectively. Bicause the ice sublimation timescale is very short at the exoerimental temperatures, the present results indicate that cometary silicates at <-20˚C in comets are pristine even if they have high surface to volume ratio and amorphous structures as GEMS grains in anhydrous CP-IDPs.

Keywords: comet, space exploration, hydration experiment

©2019. Japan Geoscience Union. All Right Reserved.

[E] Oral | P (Space and Planetary Sciences)：P-PS Planetary Sciences

Wed. May 29, 2019 10:45 AM - 12:15 PM JST | Wed. May 29, 2019 1:45 AM - 3:15 AM UTC | A01 TOKYO BAY MAKUHARI HALL

[P-PS03] Solar System Small Bodies: A New Frontier Arising Hayabusa 2, OSIRIS-REx and Other Projects

convener:Masateru Ishiguro(Department of Physics and Astronomy, Seoul National University), Taishi Nakamoto(Tokyo Institute of Technology), Masanao Abe(Institute of Space and Astronautical Science, Japan Aerospace Exploration Agency), Olivier S Barnouin(Johns Hopkins University Applied Physics Laboratory), Chairperson:Masateru Ishiguro(Seoul National University)

In June 2018, the Hayabusa 2 spacecraft arrived at the target asteroid Ryugu after three and half years journey. In addition, another spacecraft, OSIRIS-REx will soon arrive at its destination Bennu. With these arrivals, the solar system research is about to enter a new era. We have organized this small bodies session since 2012 and had a broad range of discussions from viewpoints of laboratory experiments, observations, space explorations, theoretical modeling, and sample analyses. In particular, this time, we aim to hold this session to bring the latest research on solar system small bodies, focusing on the initial results of Hayabusa 2 and OSIRIS-REx. Presentations in the related fields other than these two asteroidal missions are also welcomed.

10:45 AM - 11:00 AM JST | 1:45 AM - 2:00 AM UTC

[PPS03-25] Overview and current status of DESTINY$^+$ mission

★Invited Papers

*Tomoko Arai[1], Masanori Kobayashi[1], Ko Ishibashi[1], Fumi Yoshida[1], Hiroshi Kimura[1], Takayuki Hirai[1], Hong Peng[1], Manabu Yamada[1], Hiroki Senshu[1], Koji Wada[1], Ralf Srama[2], Harald Kruger[3], Jun-ichi Watanabe[4], Takashi Ito[4], Masateru Ishiguro[5], Tomoki Nakamura[6], Hikaru Yabuta[7], Shogo Tachibana[8], Takashi Mikouchi[8], Shinsuke Abe[9], Katsuhito Ohtsuka[10], Seitaro Urakawa[11], Keiko Nakamura-Messenger[12], Mutsumi Komatsu[13], Shingo Kameda[14], Masato Kagitani[6], Naru Hirata[15], Hirohide Demura[15], Sho Sasaki[16], Takahiro Hiroi[17], Goro Komatsu[18], Hidehiro Kaneda[19], Takaya Inamori[19], Takaya Okamoto[20], Toshifumi Yanagisawa[20], Makoto Yoshikawa[20], Hajime Yano[20], Tatsuaki Okada[20], Takahiro Iwata[20], Takafumi Ootsubo[20], Yasuhiro Kawakatsu[20], Hiroyuki Toyota[20], Kazutaka Nishiyama[20], Takeshi Takashima[20] (1.Planetary Exploration Research Center, Chiba Institute of Technology, 2.University of Stuttgart, 3.Max Planck Institute, 4.National Astronomical Observatory of Japan , 5.Seoul National Universtiy, 6.Tohoku University, 7.Hiroshima University, 8.The University of Tokyo, 9.Nihon University, 10.Tokyo Meteor Network, 11.Japan Spaceguard Association, 12.NASA , 13.The Graduate University for Advanced Studies, 14.Rikkyo University, 15.Aizu University, 16.Osaka University, 17.Brown University, 18.D'Annunzio University, 19.Nagoya University, 20.JAXA)

11:00 AM - 11:15 AM JST | 2:00 AM - 2:15 AM UTC

[PPS03-26] Observational campaign of (3200) Phaethon and (155140) 2005UD in 2017-2018

*Fumi Yoshida[1], Tomoko Arai[1], Ko Ishibashi[1], Peng Hong[1], Ryo Ishimaru[1], DESTINY+ International observation collaborators (1.Planetary Exploration Research Center, Chiba Institute of Technology)

11:15 AM - 11:30 AM JST | 2:15 AM - 2:30 AM UTC

[PPS03-27] Rotationally-resolved spectroscopic observations of Phaethon - 2005 UD, and their fragments detected by lunar impact flashes.

*Shinsuke Abe[1], Nicholas Moskovitz[2], Fumi Yoshida[3], Katsutoshi Ohtsuka[4], Ito Takashi[5], Ryota Fuse[1], Masahisa Yanagisawa[6], Ryuhei Yamada[7] (1.Department of Aerospace Engineering, College of Science and Technology, Nihon University, 2.Lowell Observatory, 3.Planetary Exploration Research Center, Chiba Institute of Technology, 4.Tokyo Meteor Network, 5.National Astronomical Observatory of Japan, 6.The University of Electro-Communications, 7.The University of Aizu, Department of Computer Science and Engineering)

11:30 AM - 11:45 AM JST | 2:30 AM - 2:45 AM UTC

[PPS03-28] Thermal Radiation Pressure Force on Regolith Particles of Atmosphereless Bodies

*Yoonsoo P. Bach[1], Masateru Ishiguro[1] (1.Department of Physics and Astronomy, Seoul National University)

11:45 AM - 12:00 PM JST | 2:45 AM - 3:00 AM UTC

[PPS03-29] A kilometre-sized Kuiper belt object revealed by OASES stellar occultation observations

*Ko Arimatsu[1,2], Kohji Tsumura[3], Fumihiko Usui[4], Shinnaka Yoshiharu[5], Kohei Ichikawa[3,6,7], Takafumi Ootsubo[8], Takayuki Kotani[2,9], Takehiko Wada[8], Koichi Nagase[8], Jun-ichi Watanabe[2] (1.Astronomical Observatory, Graduate School of Science, Kyoto University, 2.National Astronomical Observatory of Japan, 3.Frontier Research Institute for Interdisciplinary Science, Tohoku University, 4.Center for Planetary Science, Graduate School of Science, Kobe University, 5.Laboratory of Infrared High-resolution Spectroscopy, Koyama Astronomical Observatory, Kyoto Sangyo University, 6.Department of Astronomy, Columbia University, 7.Department of Physics and Astronomy, University of Texas at San Antonio, 8.Department of Space Astronomy and Astrophysics, Institute of Space and Astronautical Science, Japan Aerospace Exploration Agency, 9.Astrobiology Center, National Institutes of Natural Sciences)

12:00 PM - 12:15 PM JST | 3:00 AM - 3:15 AM UTC

[PPS03-30] AKARI/IRC near-infrared asteroid spectroscopic survey: AcuA-spec

*Fumihiko Usui[1], Sunao Hasegawa[2], Takafumi Ootsubo[2], Takashi Onaka[3,4] (1.Kobe University, 2.ISAS/JAXA, 3.The University of Tokyo, 4.Meisei University)

Overview and current status of DESTINY^{+} mission

*Tomoko Arai[1], Masanori Kobayashi[1], Ko Ishibashi[1], Fumi Yoshida[1], Hiroshi Kimura[1], Takayuki Hirai[1], Hong Peng[1], Manabu Yamada[1], Hiroki Senshu[1], Koji Wada[1], Ralf Srama[2], Harald Kruger[3], Jun-ichi Watanabe[4], Takashi Ito[4], Masateru Ishiguro[5], Tomoki Nakamura[6], Hikaru Yabuta[7], Shogo Tachibana[8], Takashi Mikouchi[8], Shinsuke Abe[9], Katsuhito Ohtsuka[10], Seitaro Urakawa[11], Keiko Nakamura-Messenger[12], Mutsumi Komatsu[13], Shingo Kameda[14], Masato Kagitani[6], Naru Hirata[15], Hirohide Demura[15], Sho Sasaki[16], Takahiro Hiroi[17], Goro Komatsu[18], Hidehiro Kaneda[19], Takaya Inamori[19], Takaya Okamoto[20], Toshifumi Yanagisawa[20], Makoto Yoshikawa[20], Hajime Yano[20], Tatsuaki Okada[20], Takahiro Iwata[20], Takafumi Ootsubo[20], Yasuhiro Kawakatsu[20], Hiroyuki Toyota[20], Kazutaka Nishiyama[20], Takeshi Takashima[20]

1. Planetary Exploration Research Center, Chiba Institute of Technology, 2. University of Stuttgart, 3. Max Planck Institute, 4. National Astronomical Observatory of Japan , 5. Seoul National Universtiy, 6. Tohoku University, 7. Hiroshima University, 8. The University of Tokyo, 9. Nihon University, 10. Tokyo Meteor Network, 11. Japan Spaceguard Association, 12. NASA , 13. The Graduate University for Advanced Studies, 14. Rikkyo University, 15. Aizu University, 16. Osaka University, 17. Brown University, 18. D'Annunzio University, 19. Nagoya University, 20. JAXA

DESTINY^{+} (Demonstration and Experiment of Space Technology for INterplanetary voYage, Phaethon fLyby and dUst Science) was selected in 2017 as a mission for JAXA/ISAS small-class program. It is a joint mission of technology demonstration and scientific observation. It will test high performance electric propelled vehicle technology and high-speed flyby of asteroid (3200) Phaethon and possibly asteroid 2005UD, which a break-up body from Phaethon as an extended mission. Engineering challenges include an up-close encounter at a distance of 500 km from Phaethon with radio-optical hybrid navigation guidance and control, and autonomous imaging based on optical information for target tracking during a high-speed flyby of 33km/sec. The science goal is to understand the nature and origin of cosmic dust brought onto the Earth, in the context of exogenous contribution of carbon and organics for possible prebiotic seeds of the terrestrial life. Phaethon is a parent body of Geminid meteor shower, and thus a known source to periodically provide dust to the Earth, via the dust stream. The science objectives are two folded: (1) in-situ analyses of velocity, arrival direction, mass and chemical composition of interplanetary and interstellar dust particles around 1 au, the dust trail, and nearby Phaethon, and (2) flyby imaging of Phaethon to study its geology, for understanding dust ejection mechanism of active asteroid and the surface compositional variation. High-spatial-resolution images of less than 5 meter per pixel are obtained with Telescopic camera (TCAP), and VIS-NIR spectral images of less than 100 meter per pixel are taken with multiband camera (MCAP). Mass, speed, arrival direction and chemical composition for each dust particle are analyzed with dust analyzer (DDA). Here, we present an overview and the current status of DESTINY^{+} mission.

Keywords: DESTINY+, Phaethon, Flyby, Geminid meteor shower, IDP

©2019. Japan Geoscience Union. All Right Reserved.

Observational campaign of (3200) Phaethon and (155140) 2005UD in 2017-2018

*Fumi Yoshida[1], Tomoko Arai[1], Ko Ishibashi[1], Peng Hong[1], Ryo Ishimaru[1], DESTINY+ International observation collaborators

1. Planetary Exploration Research Center, Chiba Institute of Technology

(3200) Phaethon is the flyby target and (155140) 2005UD is a second flyby candidate of the DESTINY+ mission. Each asteroid approached to the Earth and became bright in 2017-2018. We utilize this opportunity and organized an observation campaign for both asteroids with international collaborators. The following people participated to the observational campaign : F. Yoshida, R. Ishimaru, K. Ishibashi, P. Hong, T. Arai (PERC/ChiTech), R. Okazaki, T. Sekiguchi, H. Naito, M. Imai, T. Ono (Hokkaido University of Education), S. Urakawa (Japan Spaceguard Association, Bisei Spaceguard Center), Y. Shinnaka (Kyoto Sanyo Univ.), T. Tanigawa (Sumoto high school), T. Yanagisawa, H. Kurosaki (JAXA), S. Abe, R. Kato (Nihon Univ.), N. Natira, T. Nishiumi (Univ. of Tokyo), M. Ishiguro (Seoul National University), M.-J. Kim, Y.-J. Choi, H.-K. Moon (KASI), D.-H. Kim, H.-J. Lee, S.-M. Lee (Chungbuk National University), Zhong-Yi Lin (Institute of Astronomy, National Central University), Xiaobin Wang (Yunnan Observatories, CAS), A. Serebryanskiy, M. Krugov, I. Reva (Fesenkov Astrophysical Institute), O. Burkhonov, E. Kamoliddin (UBAI), A. Peyrot, J-P. Teng (Les Makes Observatory), Y. Krugly (Institute of Astronomy of V.N. Karazin Kharkiv National University), I. M. Volkov (SAI MSU, INASAN), I. V. Nikolenko, S. I. Barabanov (INASAN), M. Kaplan, O. Erece (Akdeniz university), A. Sonka, S. Anghel (Astronomical Institute of Romanian Academy, Bucharest University), M. Birlan, F. Vachier, J. Berthier (Observatoire de Paris, IMCCE, CNRS), A. Klotz (CNRS-OMP-IRAP), P. Thierry (Auragne Observatory), O. Ivanova, M. Husarik (Astronomical Institute of the Slovak Academy of Sciences), E. Kuznetsov, D. Glamazda, G. Kaiser, E. Koren, V. Krushinsky, A. Popov, A. Shagabutdinov, Y. Vibe (Ural Federal University), M. Lazzarin, V. Petropoulou, I. Bertini, F. La Forgia (University of Padova), E. Palomba, E. D'aversa, A. Migliorini (INAF-IAPS), J. Vaubaillon (Observatoire de Paris), T. G. Wilson (University College London, Isaac Newton Group), O. Vaduvescu (Isaac Newton Group, Instituto de Astrofísica de Canarias), M. Popescu, Julia de Leon (Instituto de Astrofísica de Canarias), V. Lorenzi (Fundación Galileo Galilei - INAF, Instituto de Astrofísica de Canarias), M. Granvik (University of Helsinki / Luleå University of Technology), A. Penttilä (University of Helsinki), K. O. Muinonen (University of Helsinki / National Land Survey of Finland), T. Kareta, V. Reddy, D. S. Lauretta, B. Sharkey, C. Hergenrother (LPL, University of Arizona), J. A. Sanchez (PSI), T. Linder (Astronomical Research Institute), O. Kuhn, A. Conrad (Large Binocular Telescope Observatory), N. Moskovitz (Lowell Observatory), J. Masiero, A. Mainzer, L. Benner, M. Brozovic, S. Naidu, J. Giorgini (NASA JPL), E.L. Wright, D. Jewitt (UCLA), P. Taylor, E. Rivera-Valentin, S. Bhiravarasu, B. Aponte-Hernandez (Lunar and Planetary Institute), S. Marshall, F. Venditti, A. Virkki, L. Zambrano-Marin (Arecibo Observatory & University of Central Florida), C. R. Sanchez-Vahamonde (University of Western Ontario) (in the order from east to west in Fig.1).

Most of results obtained from the campaign were presented in IDP2019, which was held at Tokyo Skytree Town Campus of CIT, Japan, on February 12-14, 2019 (Fig. 2). So far, for both asteroids, rotation period, average colors, absolute magnitudes, spectra (0.4-2.5 μm) were obtained by photometry and spectroscopy during this observation campaign. Radar observation were done for Phaethon, and polarimetric observations were done for both asteroids. As preliminary results, the following properties were reported. Rotation periods: 5.2 hr (or 7.85 hr) for 2005UD, 3.6hr for Phaethon. Average colors : B-V=0.71, V-R=0.37, V-I=0.32 for 2005UD, B-V=0.73, V-R=0.36 for Phaethon. Absolute magnitude is 17.25 mag for 2005UD. No significant variation of rotationally resolved VIS-NIR spectra were seen for

©2019. Japan Geoscience Union. All Right Reserved.

both asteroids. However, a slight variation of visual spectra of Phaethon taken in 2017 was reported. Both asteroids are in C-complex. Interestingly, in the NIR spectra, both asteroids show totally different spectra each other: concave-up and blue for Phaethon, linear and red for 2005UD. The results from polarimetric observation show both asteroids are very similar. As for Phaethon, rotational variation in polarization was reported. Lightcurve observations revealed Phethon has top shape. Radar observation estimated the Phaethon's diameter is about 6km, and revealed no coma, no satellite. Possible craters (D>1km below 30 deg latitude, D=1.5km near equator), 600m wide dark spot (likely a flattened region) were discovered.

Keywords: Asteroids, (3200) Phaethon, (155140) 2005UD

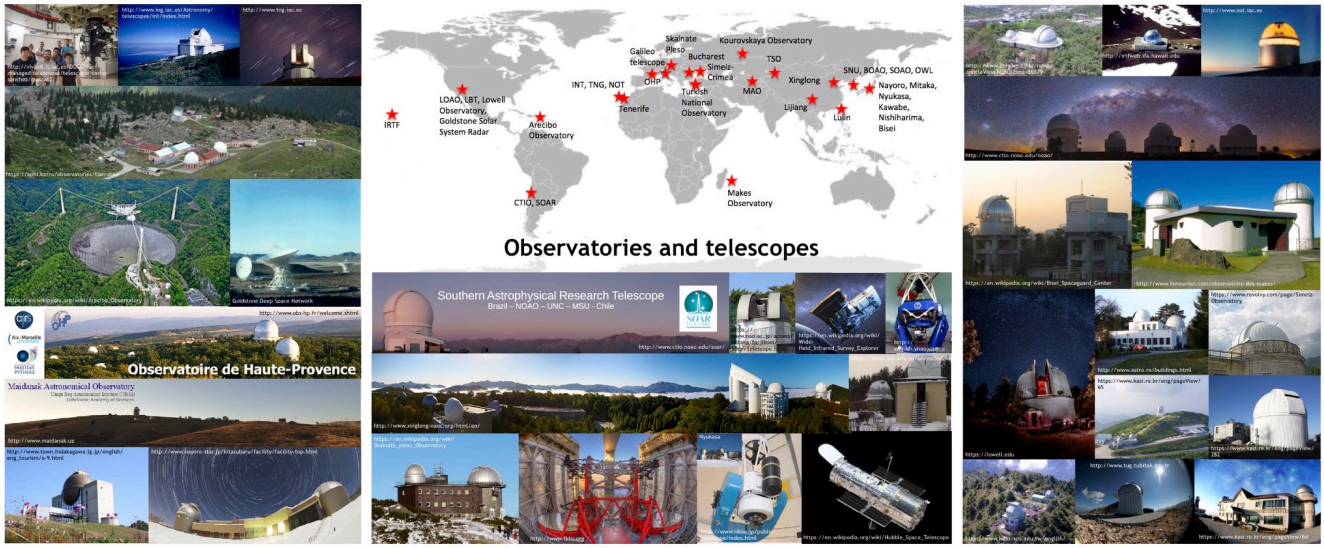

Fig1. Observatories and telescopes participating to the observation campaign of Phaethon and 2005UD in 2017 and 2018.

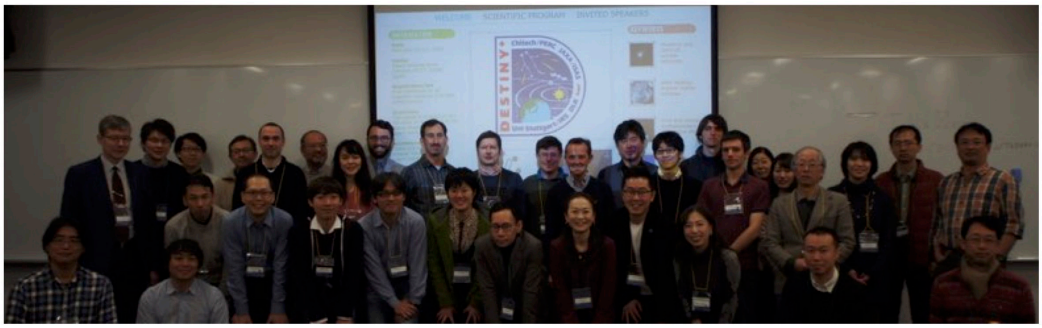

Fig2. IDP2019 held at Tokyo Skytree Town Campus of CIT, Chiba, Japan, on February 12–14, 2019.

©2019. Japan Geoscience Union. All Right Reserved.

Rotationally-resolved spectroscopic observations of Phaethon - 2005 UD, and their fragments detected by lunar impact flashes.

*Shinsuke Abe[1], Nicholas Moskovitz[2], Fumi Yoshida[3], Katsutoshi Ohtsuka[4], Ito Takashi[5], Ryota Fuse[1], Masahisa Yanagisawa[6], Ryuhei Yamada[7]

1. Department of Aerospace Engineering, College of Science and Technology, Nihon University, 2. Lowell Observatory, 3. Planetary Exploration Research Center, Chiba Institute of Technology, 4. Tokyo Meteor Network, 5. National Astronomical Observatory of Japan, 6. The University of Electro-Communications, 7. The University of Aizu, Department of Computer Science and Engineering

3200 Phaethon is an Apollo type near-Earth asteroid (NEA) categorized as a B-type asteroid which has been associated with the most intense meteor shower, Geminids. Cometary activity of Phaethon has been observed during its perihelion passage, ~0.140 AU, that motivates us to do direct exploration by the spacecraft, DESTINY+. It is also suggested that (155140) 2005 UD is a break-up pair of Phaethon because of dynamically similarity and same B-type spectrum type which is only ~5 % in NEA population. We examined the spectral properties of this asteroid pair to find the surface heterogeneity. Rotationally-resolved spectroscopic observations of Phaethon were carried out using 1.0-m telescopes at Lulin/Taiwan, and Kawabe/Wakayama, observatories in 2007 and 2017 apparitions, respectively. While Rotationally-resolved spectroscopic observation of 2005 UD was performed by using 4.1-m SOAR telescope at Cerro Tololo, Chili in 2018. It is presumably revealed that the surface heterogeneity, C-type like red slope surface area, of Phaethon was clearly seen from 2017 data, while no-existing surface heterogeneity was observed for 2005 UD.

When a meteoroid impacts the moon at several 10s of km/s, a brilliant flash at the point of impact can be observed as a flash in visible and near-infrared light. Lunar impact monitoring has a great advantage to detect large meteoroids in the mass range between 10s of grams and few kilograms corresponding to centimeters and tens of centimeters, which is as a bridge between visual meteors and small asteroids. We observed lunar impact flashes during Geminids maximum in 2018. 11 events were simultaneously detected from 2 locations at Nihon university and UEC, suggesting existence of relativity large fragments, several cm to several tens of cm in diameter, in the Geminid meteor stream.

In order to understand the Phaethon-Geminid stream Complex (PGC), ground-based telescopic observations of Geminids meteoroids and its parent splitting-bodies will be presented.

Keywords: Asteroids, Comets, Meteoroids, Lunar impact flash

©2019. Japan Geoscience Union. All Right Reserved.

Thermal Radiation Pressure Force on Regolith Particles of Atmosphereless Bodies

*Yoonsoo P. Bach[1], Masateru Ishiguro[1]

1. Department of Physics and Astronomy, Seoul National University

It is suggested that thermal fracture near the perihelion is a possible mechanism to produce the dust trail of the near-Earth asteroid, (3200) Phaethon (Jewitt and Li, 2013, ApJ 771, L36). For this scenario to be true, generated dust particles should have been ejected from the surface before its next apparition to show the detectable activities (Li and Jewitt, 2013, ApJ, 145, 154). It is, however, not well understood how these particles were escalated from the regolith against the asteroid's gravity. In this study, we hypothesize that the thermal radiation pressure around the perihelion passage would exert substantial force on dust grains to be lifted up and contributes the dust tail formation with further help of solar radiation pressure. As a result, we find that roughly ~1-10 micron size dust grains can be ejected from Phaethon by the mechanism, while a detailed model of gravitational field is required for accurate range of the particle sizes. Our idea is not necessarily limited to Phaethon case, but is applicable to any atmosphereless bodies. We will explain how the thermal radiation pressure is effective at different distances from the sun.

Keywords: asteroids, regolith, thermal radiation

©2019. Japan Geoscience Union. All Right Reserved.

A kilometre-sized Kuiper belt object revealed by OASES stellar occultation observations

*Ko Arimatsu[1,2], Kohji Tsumura[3], Fumihiko Usui[4], Shinnaka Yoshiharu[5], Kohei Ichikawa[3,6,7], Takafumi Ootsubo[8], Takayuki Kotani[2,9], Takehiko Wada[8], Koichi Nagase[8], Jun-ichi Watanabe[2]

1. Astronomical Observatory, Graduate School of Science, Kyoto University, 2. National Astronomical Observatory of Japan, 3. Frontier Research Institute for Interdisciplinary Science, Tohoku University, 4. Center for Planetary Science, Graduate School of Science, Kobe University, 5. Laboratory of Infrared High-resolution Spectroscopy, Koyama Astronomical Observatory, Kyoto Sangyo University, 6. Department of Astronomy, Columbia University, 7. Department of Physics and Astronomy, University of Texas at San Antonio, 8. Department of Space Astronomy and Astrophysics, Institute of Space and Astronautical Science, Japan Aerospace Exploration Agency, 9. Astrobiology Center, National Institutes of Natural Sciences

We will report the first detection of a single stellar occultation event candidate by a kilometer-sized (radius= 1-10 km) Kuiper belt object (KBO). Since the kilometer-sized KBOs are too faint to be detected directly, the monitoring of stellar occultation events is one possible way to discover them. With the aim of detecting the stellar occultation events, we launched an optical observation project named Organized Autotelescopes for Serendipitous Event Survey (OASES). We installed two low-cost OASES observation systems in different positions on the rooftop of the Miyako open-air school on Miyako Island, Miyakojima-shi, Okinawa Prefecture, Japan, and monitored up to 2000 stars simultaneously with a sampling cadence of 15.4Hz. In the 60-hour dataset obtained with the two-year OASES observations, we discovered one occultation candidate event by a KBO with a radius of approximately 1.3 km. Our present detection yields a surface number density of KBOs with radii exceeding 1.2 km is approximately 6×10^5 deg^{-2}. This surface number density favors a theoretical size distribution model with an excess signature at a radius of 1–2 km. The present results suggest that planetesimals before their runaway growth phase grew into kilometer-sized objects in the primordial outer Solar System and remain as one of the major populations in the present-day Kuiper belt.

Keywords: trans-Neptunian objects, Kuiper belt , ground based observations by optical telescopes

©2019. Japan Geoscience Union. All Right Reserved.

AKARI/IRC near-infrared asteroid spectroscopic survey: AcuA-spec

*Fumihiko Usui[1], Sunao Hasegawa[2], Takafumi Ootsubo[2], Takashi Onaka[3,4]

1. Kobe University, 2. ISAS/JAXA, 3. The University of Tokyo, 4. Meisei University

Water is found in various forms in our solar system and is one of the most important ingredients in the origin of life. It provides evidence for the evolution of the solar system, especially its thermal history. Hydrated minerals are formed in environments where anhydrous rock and liquid water exist together, resulting from aqueous alteration. Because hydrated minerals are stable even above the sublimation temperature of water ice, they become an important reservoir to trace the water present in the history of the solar system unless they were reset by a temperature change after formation. Asteroids are considered to record the initial conditions of our solar nebula of 4.6 Ga ago. To explore the existence of water in the present solar system, it is indispensable to investigate the presence of hydrated minerals and water ice on various types of asteroids. Hydrated minerals and water ice exhibit diagnostic absorption features in the so-called 3 micron band (approximately 2.5-3.5 micron wavelength range). Many spectroscopic surveys have been conducted in the 3 micron band using ground-based observatories, which are severely affected by telluric absorption at around 2.8 micron. Space-borne observations, free from the effect, therefore, offer an excellent opportunity to study and identify the mineral species in asteroids.

The Infrared Camera (IRC) on board the AKARI satellite has a unique spectroscopic capability covering 2.5-5 microns continuously with a spectral resolution of R~100, which provides valuable data thanks to its high sensitivity and unique wavelength coverage. We conducted a spectroscopic survey of asteroids in the 3 micron band using IRC. In the warm mission period of AKARI, 147 pointed observations were performed for 66 asteroids in the grism mode in 2.5-5 microns. According to our observations, it is found that most C-complex asteroids, especially all Ch-, Cgh-, B-, and Cb-type asteroids, have obvious absorption features in the reflectance spectra at around 2.75 micron, which is attributed to OH-stretch in hydrated minerals. The peak wavelength of the 2.7 micron band feature is concentrated at around 2.75 micron: in particular, there is a correlation between the peak wavelength and the band depth among 13 C-complex asteroids. This trend can be understood in terms of the process where hydrated minerals are being heated up and gradually losing water, that is, the dehydration process.

In this talk, we present the spectroscopic survey of asteroids with AKARI for detecting the 2.7 micron absorption features and discuss scenarios for the formation and evolution of C-complex asteroids.

Keywords: asteroids, hydrated minerals, near-infrared spectroscopy

©2019. Japan Geoscience Union. All Right Reserved.

[E] Poster | P (Space and Planetary Sciences)：P-PS Planetary Sciences

Wed. May 29, 2019 3:30 PM - 5:00 PM JST | Wed. May 29, 2019 6:30 AM - 8:00 AM UTC | Poster Hall International Exhibition Hall8, Makuhari Messe_1

[P-PS03] Solar System Small Bodies: A New Frontier Arising Hayabusa 2, OSIRIS-REx and Other Projects

convener:Masateru Ishiguro(Department of Physics and Astronomy, Seoul National University), Taishi Nakamoto(Tokyo Institute of Technology), Masanao Abe(Institute of Space and Astronautical Science, Japan Aerospace Exploration Agency), Olivier S Barnouin(Johns Hopkins University Applied Physics Laboratory)

In June 2018, the Hayabusa 2 spacecraft arrived at the target asteroid Ryugu after three and half years journey. In addition, another spacecraft, OSIRIS-REx will soon arrive at its destination Bennu. With these arrivals, the solar system research is about to enter a new era. We have organized this small bodies session since 2012 and had a broad range of discussions from viewpoints of laboratory experiments, observations, space explorations, theoretical modeling, and sample analyses. In particular, this time, we aim to hold this session to bring the latest research on solar system small bodies, focusing on the initial results of Hayabusa 2 and OSIRIS-REx. Presentations in the related fields other than these two asteroidal missions are also welcomed.

[PPS03-P01] Impact experiments on low strength coarse-grained regolith simulating surface materials on asteroid Ryugu

*Yuya Yamamoto[1], Masahiko Arakawa[1], Minami Yasui[1], Sunao Hasegawa[2], Ryo Sugimura[1] (1.Graduate School of Science, Kobe University, 2.ISAS, JAXA)

[PPS03-P02] Reflectance estimation of asteroid Ryugu using MASCOT

*Marika Ishida[1], Koto Amano[1], Keiichi Moroi[1], ERI TATSUMI[2], Tra-Mi Ho[10], Shingo Kameda[1], Seiji Sugita[2], Rie Honda[3], Tomokatsu Morota[4], yokota yasuhiro[5], Toru Kouyama[6], Hidehiko Suzuki[7], Manabu Yamada[8], Naoya Sakatani[5], Chikatoshi Honda[9], Masahiko Hayakawa[5], Kazuo Yoshioka[2], Moe Matsuoka[5], Yuichiro Cho[2], Hirotaka Sawada[5] (1.Rikkyo Univ., 2.Univ. of Tokyo, 3.Kochi Univ., 4.Nagoya Univ., 5.JAXA/ISAS, 6.AIST, 7.Meiji Univ., 8.Chiba Inst. Tech, 9.Univ. of Aizu, 10.DLR)

[PPS03-P03] Flyby observation of Asteroid (3200) Phaethon by DESTINY$^+$ onboard cameras

*Ko Ishibashi[1], Shingo Kameda[2], Masato Kagitani[3], Peng Hong[1], Manabu Yamada[1], Osamu Okudaira[1], Tomoko Arai[1], Fumi Yoshida[1], Shunsuke Sato[4], Takahiro Ishimaru[4], Takaya Okamoto[4], Takahiro Iwata[4], Tatsuaki Okada[4], Takeshi Takashima[4] (1.Chiba Institute of Technology, 2.Rikkyo University, 3.Tohoku Universtiy, 4.Japan Aerospace Exploration Agency)

[PPS03-P04] Polarimetric Study of Asteroids in Comet-Like Orbits (ACOs)

*Jooyeon Geem[1], Masateru Ishiguro[1], Yoonsoo P. Bach[1], Daisuke Kuroda[2], Hiroyuki Naito[3], Hidekazu Hanayama[4], yoonyoung kim[10], Yuna G. Kwon[1], Sunho Jin[1], Tomohiko Sekiguchi[5], Ryo Okazaki[5], Jeremie J. Vaubaillon[6], Masataka Imai[7], Tatsuharu Oono[8], Yuki Futamuts[8], Seiko Takagi[8], Mitsuteru Sato[8], Kiyoshi Kuramoto[8], Makoto Watanabe[9] (1.Astronomy program, Dept of Physics and Astronomy, Seoul National University, 2.Okayama Observatory, Kyoto University, 3.Nayoro Observatory, 4.Ishigakijima Astronomical Observatory, National Astronomical Observatory of Japan, 5.Hokkaido University of Education, 6.Observatoire de Paris, I.M.C.C.E., 7.National Institute of Advanced Industrial Science and Technology, 8.Department of Cosmosciences, Graduate School of Science, Hokkaido University, 9.Department of Applied Physics, Okayama University of Science, 10.Max Planck Institute for Solar System Research)

[PPS03-P05] Dynamical lifetime of the Oort Cloud new comets under planetary perturbation

*Ito Takashi[1], Arika Higuchi[1] (1.National Astronomical Observatory of Japan)

[PPS03-P06] Thermal Infrared Imaging of C-type Asteroid 162173 Ryugu with Porous Surfaces

*Tatsuaki Okada[1,2], Tetsuya Fukuhara[3], Satoshi Tanaka[1], Makoto Taguchi[3], Takehiko Arai[4], Naoya Sakatani[1], Yuri Shimaki[1], Hiroki Senshu[5], Yoshiko Ogawa[6], Hirohide Demura[6], Kentaro Suko[6], Kohei Kitazato[6], Toru Kouyama[7], Tomohiko Sekiguchi[8], Jun Takita[9], Sunao Hasegawa[1], Tsuneo Matsunaga[10], Takehiko Wada[1], Takeshi Imamura[2], Jorn Helbert[11], Thomas G. Mueller[12], Axel Hagermann[13], Jens Biele[11], Matthias Grott[11], Maximiliam Hamm[11], Marco Delbo[14], Yukio Yamamoto[1], Naru Hirata[6], Naoyuki Hirata[15], Fuyuto Terui[1], Takanao Saiki[1], Satoru Nakazawa[1], Makoto Yoshikawa[1], Sei-ichiro WATANABE[1,16], Yuichi Tuda[1] (1.Institute of Space and Astronautical Science, Japan Aerospace Exploration Agency, 2.University of Tokyo, 3.Rikkyo University, 4.Ashikaga University, 5.Chiba Institute of Technology, 6.University of Aizu, 7.National Institute of Advanced Industrial Science and Technology, 8.Hokkaido University of Education, 9.Hokkaido Kitami-Hokuto High School, 10.National Institute for Environmental Studies, 11.German Aerospace Center, 12.Max-Planck Institute for Extraterrestrial Physics, 13.University of Stirling, 14.Observatoire de la Côte d'Azur, 15.Kobe University, 16.Nagoya University)

[PPS03-P07] Data Release of Asteroid 162173 Ryugu by Observation of Thermal Infrared Imager onboard Hayabusa2

*Takehiko Arai[1], Hirohide Demura[2], Toru Kouyama[7], Naoya Sakatani[3], Kentaro Suko[2], Yuri Shimaki[3], Hiroki Senshu[5], Tomohiko Sekiguchi[6], Yoshiko Ogawa[2], Sunao Hasegawa[3], Takehiko Wada[3], Takeshi Imamura[10], Tsuneo Matsunaga[9], Jun Takita[8], Kohei Kitazato[2], Makoto Taguchi[4], Tetsuya Fukuhara[4], Satoshi Tanaka[3], Tatsuaki Okada[3] (1.Ashikaga University, 2.The University of Aizu, 3.Japan Aerospace Exploration Agency (JAXA), 4.Rikkyo University, 5.Chiba Institute of Technology, 6.Hokkaido University of Education, 7.National Institute of Advanced Industrial Science and Technology (AIST), 8.Hokkaido Kitami Hokuto High School, 9.National Institute for Environmental Studies (NIES), 10.The University of Tokyo)

[PPS03-P08] Multi-mission capability of HARMONICS

*Shintaro Tsunoda[1], Hirohide Demura[1], Naru Hirata[1] (1.The University of Aizu)

[PPS03-P09] New interface of verification for calibration and conversion in HEAT : Hayabusa2 Exploration Assistant for TIR

*Tatsuro Kobayashi[1], Kentaro Suko[1], Hirohide Demura[1], Yoshiko Ogawa[1], Takehiko Arai[2], Naoya Sakatani[3], Tatsuaki Okada[3], Satoshi Tanaka[3], Tetsuya Fukuhara[4] (1.The University of Aizu, 2.Ashikaga University, 3.Institute of Space and Astronautical Science, Japan Aerospace Exploration Agency, 4.Rikkyo University)

[PPS03-P10] **Dust particle evolution of a near-Earth object 252P/LINEAR from near-infrared polarimetric observations in 2016**

*Yuna G Kwon[1], Masateru Ishiguro[1], Jungmi Kwon[2], Daisuke Kuroda[3], Myungshin Im[1], Changsu Choi[1], Motohide Tamura[4], Takahiro Nagayama[5], Nobuyuki Kawai[6], Jun-ichi Watanabe[7] (1.Seoul National Univ., 2.ISAS/Japan Aerospace Exploration Agency, 3.Okayama Astrophysical Observatory, 4.The Univ. of Tokyo, 5.Kagoshima Univ., 6.Tokyo Institute of Technology, 7.National Astronomical Observatory of Japan)

[PPS03-P11] **Performance Evaluation of TRIPOL on the 61-cm Telescope at Seoul National University for Polarimetric Observations of Solar System Small Bodies**

*Sunho Jin[1], Masateru Ishiguro[1], Yuna G Kwon[1], Jooyeon Geem[1], Yoonsoo P. Bach[1], Jinguk Seo[1], Hiroshi Sasago[2], Shuji Sato[3] (1.Seoul National University, 2.Sasago Co.,Ltd, 3.Nagoya University)

[PPS03-P12] Smart Interface of HEAT: Hayabusa2 Exploration Assistant for TIR

*Kentaro Suko[1], Tatsuro Kobayashi[1], Hirohide Demura[1], Takehiko Arai[2], Naoya Sakatani[3], Tatsuaki Okada[3], Satoshi Tanaka[3], Tetsuya Fukuhara[4] (1.The University of Aizu, 2.Ashikaga University, 3.Institute of Space and Astronautical Science, Japan Aerospace Exploration Agency, 4.Rikkyo University)

[PPS03-P13] Experimental Study on Collision Crater Formed on Bulge Geography

*Yusaku Yokota[1], Yuya Yamamoto[2], Minami Yasui[2], Masahiko Arakawa[2] (1.Faculty of Science, Kobe University, 2.Graduate School of Science, Kobe University)

[PPS03-P14] Initial analysis plan of soluble organic compounds for the Hayabusa2 sample from asteroid Ryugu

*Hiroshi Naraoka[1], Yoshinori Takano[2], Jason P. Dworkin[3], SOM Analysis Team (1.Department of Earth and Planetary Sciences, Research Center for Planetary Trace Organic Compounds, Kyushu University, 2.Japan Agency for Marine-Earth Science and Technology, 3.Astrochemistry Laboratory NASA Goddard Space Flight Center, Greenbelt, MD 20771 USA)

[PPS03-P15] Radar and optical simultaneous observations of faint meteors with MU radar and Tomo-e Gozen

*Ryou Ohsawa[1], Akira Hirota[2], Shinsuke Abe[2], Daniel Kastinen[3], Kero Johan[3], yasunori Fujiwara[4], Takuji Nakamura[5], Shigeyuki Sako[1], Yuto Kojima[1], Jun-ichi Watanabe[6] (1.Institute of Astronomy, Graduate School of Science, The University of Tokyo, 2.Department of Aerospace Engineering, College of Science & Technology, Nihon University, 3.Swedish Institute of Space Physics, 4.SOKENDAI (The Graduate University for Advanced Studies), 5.National Institute of Polar Research, 6.National Astronomical Observatory of Japan)

[PPS03-P16] Global distribution and spectral characteristics of bright spots on asteroid Ryugu

*Masanori Suemitsu[1], Tomokatsu Morota[1], Rie Honda[2], Singo Kameda[15], Eri Tatsumi[3], Manabu Yamada[4], Naoya Sakatani[5], Toru Kouyama[6], Yokota Yasuhiro[7], Yuichiro Cho[8], Hidehiko Suzuki[9], Masahiko Hayakawa[10], Moe Matsuoka[10], Chikatoshi Honda[11], Tatsuhiro Michikami[12], Kazuo Yoshioka[13], Kazunori Ogawa[14], Hirotaka Sawada[5], Seiji Sugita[3] (1.Graduate School of Environmental Studies, Nagoya University, 2.Department of Science and Technology, System of Natural Science, Kochi Unicversity, 3.Graduate School of Earth and Planetary Science, Tokyo Unicversity, 4.Planetary Exploration Reserch Center, Chiba Institute of Technology, 5.Institute of Space and Astoronautical Science, Japan Aerospace Exploration Agency, 6.National Institute of Advanced Industrial Science and Technology, 7.Kochi University, 8.Department of Earth and Planetary Science, Tokyo University, 9.Depertment of physics, Meiji University , 10.Department of Solar System Science, Institute of Space and Astoronautical Science, Japan Aerospace Exploration Agency, 11.Aizu University, 12.Faculty of Engineering, Kindai University, 13.Graduate School of frontier Science, Tokyo University, 14.Kobe University, 15.Rikkyo University)

[PPS03-P17] Polarimetry of (155140) 2005 UD: the Dynamical Association with (3200) Phaethon

*Masateru Ishiguro[1], Jooyeon Geem[1], Hiroyuki Naito[2], Yoonsoo P. Bach[1], Daisuke Kuroda[3], Tatsuharu Ono[4], Seiko Takagi[4], Mitsuteru Sato[4], Kiyoshi Kuramoto[4], Tomohiko Sekiguchi[5], Masataka Imai[6], Makoto Watanabe[7], Katsuhito Ohtsuka[8], Sunao Hasegawa[9], Takashi Ito[10], Fumi Yoshida[11], Tomoko Arai[11] (1.Department of Physics and Astronomy, Seoul National University, 2.Nayoro Observatory, 3.Okayama Observatory, Kyoto University, 4.Department of Cosmosciences, Graduate School of Science, Hokkaido University, 5.Hokkaido University of Education, 6.National Institute of Advanced Industrial Science and Technology, 7.Department of Applied Physics, Okayama University of Science, 8.Tokyo Meteor Network, 9.Japan Aerospace Exploration Agency, 10.National Astronomical Observatory of Japan, 11.Planetary Exploration Research Center, Chiba Institute of Technology)

[PPS03-P18] **Follow-up observations for AKARI/IRC near-infrared asteroid spectroscopic survey (AcuA-spec)**

*Sunao Hasegawa[1], Daisuke KURODA[2], Kenshi YANAGISAWA[3], Fumihiko Usui[4] (1.Japan Aerospace Exploration Agency, 2.Kyoto University, 3.National Astronomical Observatory of Japan, 4.Kobe University)

[PPS03-P19] Amino acids on witness coupons collected from the ISAS/JAXA curation facility for the assessment and quality control of the Hayabusa2 sampling procedure

*Haruna Sugahara[1,2], Yoshinori Takano[1], Yuzuru Karouji[3], Kazuya Kumagai[4], Toru Yada[3], Naohiko Ohkouchi[1], Masanao Abe[3], Hayabusa2 project team (1.Japan Agency for Marine-Earth Science and Technology (JAMSTEC), 2. Institut de Chimie de Nice, Universite Cote dAzur, 3.Japan Aerospace Exploration Agency (JAXA), 4.Marine Works Japan Ltd.)

[PPS03-P20] Hayabusa2 orbit determination using c5++ software

*Keiko Yamamoto[1], Toshimichi Otsubo[2], Koji Matsumoto[1], Hirotomo Noda[1], Noriyuki Namiki[1], Hiroki Senshu[3], Takahide Mizuno[4], Naoko Ogawa[4], Go Ono[4], Yuya Mimasu[4], Kent Yoshikawa[4], Tadateru Takahashi[4], Yuto Takei[4], Atsushi Fujii[4], Fuyuto Terui[4], Takanao Saiki[4], Satoru Nakazawa[4], Makoto Yoshikawa[4], Yuichi Tsuda[4] (1.National Astronomical Observatory of Japan, 2.Hitotsubashi University, 3.Chiba Institute of Technology, 4.Japan Aerospace Exploration Agency)

[PPS03-P21] **Landing Site Selection for Hayabusa2: Scientific Evaluation of the Candidate Sites on Asteroid (162173) Ryugu**

*Hikaru Yabuta[1], Sei-ichiro WATANABE[2], Tomoki Nakamura[3], Naru Hirata[4], Seiji Sugita[5], Tatsuaki Okada[6], Kohei Kitazato[4], Yoshiaki Ishihara[7], Tomokatsu Morota[2], Naoya Sakatani[6], Koji Matsumoto[8], Koji Wada[9], Shogo Tachibana[5], Mutsumi Komatsu[10], ERI TATSUMI[5], Moe Matsuoka[6], Chikatoshi Honda[4], Takahiro Hiroi[11], Hiroki Senshu[9], Rie Honda[12], Yasuhiro Yokota[6], Rina Noguchi[6], Yuri Shimaki[6], Deborah Lorin Domingue[13], Lucille Le Corre[13], Antonella Barucci[14], Ernest Palomba[15], Shota Kikuchi[6], Akira Miura[6], Tomohiro Yamaguchi[6], Yukio Yamamoto[6], Takanao Saiki[6], Satoshi Tanaka[6], Makoto Yoshikawa[6], Yuichi Tsuda[6] (1.Hiroshima University, Department of Earth and Planetary Systems Science, 2.Nagoya University, 3.Tohoku University, 4.University of Aizu, 5.The University of Tokyo, 6.ISAS/JAXA, 7.NIES, 8.NAOJ, 9.Chiba Institute of Technology, Planetary Exploration Research Center (PERC), 10.Sokendai, 11.Brown University, 12.Kochi University, 13.Planetary Science Institute, USA, 14.Observatoire Paris-Site de Meudon, LESIA, France, 15.INAF-IAPS, Italy.)

[PPS03-P22] Visible Photometric, Spectroscopic and Polarimetric observations of an inactive comet, P/2016 BA14 with the 1.6m Pirka Telescope

*Ryo Yamagata[1], Tomohiko Sekiguchi[1], Ryo Okazaki[1], Kazuya Doi[1], Daisuke Kuroda[2], Masateru Ishiguro[3], Hiroyuki Naito[4] (1.Hokkaido University of Education, 2.Kyoto University, 3.Seoul National University, 4.Nayoro Observatory)

[PPS03-P23] **Polycyclic aromatic hydrocarbons and aliphatic hydrocarbons in Jbilet Winselwan carbonaceous chondrite : Attempt to evaluate the thermal metamorphism degree on the parent body**

Hiroki Kato[1], *Hikaru Yabuta[1] (1.Hiroshima University, Department of Earth and Planetary Systems Science)

[PPS03-P24] Disk-Resolved Photometry Analysis of the Asteroid Ryugu Images Obtained by Hayabusa2 Visible Camera ONC

*yokota yasuhiro[1,2], Rie Honda[1], ERI TATSUMI[3], Deborah Domingue[4], Stefanus E. Schroeder[5], Moe Matsuoka[2], Seiji Sugita[3], Tomokatsu Morota[6], Shingo Kameda[7], Toru Kouyama[8], Hidehiko Suzuki[9], Manabu Yamada[10], Naoya Sakatani[2], Chikatoshi Honda[11], Masahiko Hayakawa[2], Kazuo Yoshioka[3], Yuichiro Cho[3], Hirotaka Sawada[2] (1.Kochi University, 2.ISAS/JAXA, 3.Univ. of Tokyo, 4.Planetary Science Institute, 5.DLR, 6.Nagoya Univ., 7.Rikkyo Univ., 8.AIST, 9.Meiji Univ., 10.Chiba Institute od Technology, 11.Aizu Univ.)

Impact experiments on low strength coarse-grained regolith simulating surface materials on asteroid Ryugu

*Yuya Yamamoto[1], Masahiko Arakawa[1], Minami Yasui[1], Sunao Hasegawa[2], Ryo Sugimura[1]

1. Graduate School of Science, Kobe University, 2. ISAS, JAXA

Impact cratering is one of the most important physical processes, then we study crater scaling laws and impact induced seismic waves in order to elucidate various flow processes on asteroids caused by impacts. The conventional crater scaling laws are categorized into two regions according to the controlling physics for the crater growth: they are gravity and material strength. A crater formed on regolith layer is surely controlled by the gravity, however when the regolith layer was filled with coarse particles with low mechanical strength, then the several coarse grains might be disrupted to consume the Ek. Thus, the crater size could be affected by the disruptions of the coarse grains. We speculate that not only the gravity but also the grain strength could affect the final crater size. Then, we made cratering experiments by using the target made of weak particles, and studied the effects of the particle strength on the crater scaling law and the impact induced seismic wave.

Experiments: Cratering experiments were conducted by using a gas gun set at Kobe University and ISAS. Granular targets were prepared by using weathered tuff granules with the size of 1 to 4mm (small particle) and the size of 1 to 4cm (large particle). The crush strength of these tuff particles was measured to be about 60 kPa. A spherical projectile with the size of 3mm which is made of iron, zirconia, alumina, glass, and nylon) was lunched at the impact velocity from 40 to 200m/s, and a spherical Al projectile with the size of 2mm was impacted at the impact velocity from 1.2 to 4.5km/s, then these two types of the projectile were impacted on the target surface at the normal direction. Impact cratering process and ejecta curtain growth were observed by a high-speed camera at 10^3-10^5 fps, and the video images were used to analyze ejecta particles to reconstruct the trajectories. After the shot, the crater morphology was recorded and the diameter and the depth were measured. Impact induced seismic waves were measured by using 3 accelerometers (specific frequency is 30kHz) set at different positions from the impact point, and a data logger was used to record the seismic data through charge amplifiers (data acquisition rate is 100kHz) connecting to the accelerometer.

Results: The crater size was found to increase with the projectile kinetic energy (Ek) at lower than 0.14J and at higher than 0.63J, so that the crater size was almost constant among them, and more the crater size obtained at very high Ek was almost on the extrapolated line from the relationship given by the low Ek data. The pi-scaling law was used to construct the relationship between normalized radius (πR) and normalized gravity (π2), and πR at small π2 was found to be rather smaller than that obtained for sand and glass beads targets, and more πR at large π2 was found to be consistent with that for sand and glass beads. More detail analysis tells us that all the data separated into two trends with large offset according to the impact velocity and the projectile material. This offset might be caused by the disruption of several tuff particles. The ejection velocities of each tuff particle were so scattered, then the distinctive relationship between initial position of particle and the ejection velocity was not derived in the low velocity range. The propagation velocity of the impact induced seismic wave was about 30 m/s, and it is 1/3 of that for glass beads. Furthermore, we found that the relationship between the maximum acceleration and the distance from the impact point was about 1/10 of that obtained for glass beads: the seismic wave in the tuff granules attenuated so quickly compared to the glass beads. But, when the distance is normalized by the crater radius, these relationships almost consistent each other, so that the

©2019. Japan Geoscience Union. All Right Reserved.

normalized distance could be a good parameter for the scaling of the acceleration of seismic wave.

Keywords: impact cratering experiment, low strength, impact-induced seismic shaking, crater scaling law

©2019. Japan Geoscience Union. All Right Reserved.

Reflectance estimation of asteroid Ryugu using MASCOT

*Marika Ishida[1], Koto Amano[1], Keiichi Moroi[1], ERI TATSUMI[2], Tra-Mi Ho[10], Shingo Kameda[1], Seiji Sugita[2], Rie Honda[3], Tomokatsu Morota[4], yokota yasuhiro[5], Toru Kouyama[6], Hidehiko Suzuki[7], Manabu Yamada[8], Naoya Sakatani[5], Chikatoshi Honda[9], Masahiko Hayakawa[5], Kazuo Yoshioka[2], Moe Matsuoka[5], Yuichiro Cho[2], Hirotaka Sawada[5]

1. Rikkyo Univ., 2. Univ. of Tokyo, 3. Kochi Univ., 4. Nagoya Univ., 5. JAXA/ISAS, 6. AIST, 7. Meiji Univ., 8. Chiba Inst. Tech, 9. Univ. of Aizu, 10. DLR

Hayabusa2 is a sample-return mission for the C-type asteroid 162173 Ryugu. Hayabusa2 arrived at Ryugu on 27 June 2018, and various observations are still being conducted. Hayabusa2 performs multiband spectral observation by employing the optical navigation camera telescope (ONC-T)and can thereby obtain spectral map of Ryugu, which enables the study of material distribution and degree of space weathering of Ryugu. However, the sensitivity of ONC-T has been previously calibrated by incorporating the inflight data of stars with significant uncertainty. Hence, the authors aim to estimate the reflectance of Ryugu by employing Mobile Asteroid Surface Scout (MASCOT).
MASCOT comprises four instruments (MASCAM, MicrOmega, MARA, and MASMAG) that are employed for analyzing the soil of Ryugu. The upper side of the MASCOT landeris coated with white paint, and its spectral image was captured by ONC-T after its release from Hayabusa2 to Ryugu. The authors conducted on-ground reflectance measurement of a white plate whose white paint is identical to that of MASCOT. Hence, the primary objective of the proposed study is to estimate the reflectance of Ryugu by comparing MASCOT’ s white side’ s spectrum captured by ONC-T with the on-ground reflectance measurement of the white plate that has identical paint as MASCOT, and thus evaluate the validity.

Keywords: Hayabusa2, ONC-T, MASCOT

©2019. Japan Geoscience Union. All Right Reserved.

Flyby observation of Asteroid (3200) Phaethon by DESTINY$^+$ onboard cameras

*Ko Ishibashi[1], Shingo Kameda[2], Masato Kagitani[3], Peng Hong[1], Manabu Yamada[1], Osamu Okudaira[1], Tomoko Arai[1], Fumi Yoshida[1], Shunsuke Sato[4], Takahiro Ishimaru[4], Takaya Okamoto[4], Takahiro Iwata[4], Tatsuaki Okada[4], Takeshi Takashima[4]

1. Chiba Institute of Technology, 2. Rikkyo University, 3. Tohoku Universtiy, 4. Japan Aerospace Exploration Agency

DESTINY$^+$ (Demonstration and Experiment of Space Technology for INterplanetary voYage, Phaethon fLy-by and dUst Science) is a mission proposed for JAXA/ISAS Epsilon class small program, currently in the pre-project phase (Phase-A) with a launch targeted for 2023. DESTINY$^+$ is a joint mission of technology demonstration and scientific observation. The near-Earth asteroid (3200) Phaethon, the flyby target, is known as a parent body of the Geminid meteor shower, the size of which is approximately 5 to 6 km in diameter.

In this mission, spatially resolved images of Phaethon will be taken by two onboard cameras, the Telescopic CAmera for Phaethon (TCAP) and the Multiband CAmera for Phaethon (MCAP) during the flyby, in order to understand the nature of a meteor shower's parent body, which is one of the sources of interplanetary dust particles that are thought to be an important transport medium of organic matter to the Earth. The spacecraft flybys Phaethon with a relative speed of 30 to 40 km/s. Despite such a high flyby speed, the cameras are required to take un-blurred images of Phaethon.

The main purposes of the DESTINY$^+$ flyby observation of Phaethon is to understand the geology of a parent body of a meteor shower, and in particular constrain the dust ejection mechanisms from active (i.e., dust-ejecting) asteroids. The specific objectives of the camera observation are taking images for (1) obtaining the light curve of Phaethon in order to estimate the rotational period, (2) measuring the outline shape of Phaeton, (3) making a 3D shape model of Phaethon, (4) observing the surface geological features of Phaethon including dust ejection features, and (5) observing the surface material distribution of Phaethon. The observations (1) to (4) will be conducted by TCAP, and (5) by MCAP.

TCAP is a telescopic panchromatic camera for high spatial resolution imaging of the surface of Phaethon and have a rotational mirror for asteroid tracking during flyby. The rotational mirror can change the direction of the line of sight from 0 deg to 180 deg. This enables to observe Phaethon throughout the flyby with wide solar phase angles, which is extremely important to image and understand the surfaces of planetary bodies because the solar phase angle affects significantly the appearance of geological features in taken images.

MCAP is a multiband camera, the wavelengths of which are 400, 480, 550, 700, 850, and 950 nm (480 and 950 nm are optional bands) and has multiple optical systems and sensors in order to take all band images simultaneously. This is because there is not enough time to take each band image in turn with changing bandpass filters using such as a filter wheel in this high speed flyby mission. MCAP does not have a tracking mirror due to the weight limitation, and the line of sight of MCAP is fixed to the spacecraft with 40 deg off the relative velocity vector of the spacecraft.

We will explain the flyby imaging sequence of DESTINY$^+$, and show the conceptual designs of TCAP and MCAP.

©2019. Japan Geoscience Union. All Right Reserved.

Keywords: Phaethon, DESTINY+, Flyby, Camera

©2019. Japan Geoscience Union. All Right Reserved.

Polarimetric Study of Asteroids in Comet-Like Orbits (ACOs)

*Jooyeon Geem[1], Masateru Ishiguro[1], Yoonsoo P. Bach[1], Daisuke Kuroda[2], Hiroyuki Naito[3], Hidekazu Hanayama[4], yoonyoung kim[10], Yuna G. Kwon[1], Sunho Jin[1], Tomohiko Sekiguchi[5], Ryo Okazaki[5], Jeremie J. Vaubaillon[6], Masataka Imai[7], Tatsuharu Oono[8], Yuki Futamuts[8], Seiko Takagi[8], Mitsuteru Sato[8], Kiyoshi Kuramoto[8], Makoto Watanabe[9]

1. Astronomy program, Dept of Physics and Astronomy, Seoul National University, 2. Okayama Observatory, Kyoto University, 3. Nayoro Observatory, 4. Ishigakijima Astronomical Observatory, National Astronomical Observatory of Japan, 5. Hokkaido University of Education, 6. Observatoire de Paris, I.M.C.C.E., 7. National Institute of Advanced Industrial Science and Technology, 8. Department of Cosmosciences, Graduate School of Science, Hokkaido University, 9. Department of Applied Physics, Okayama University of Science, 10. Max Planck Institute for Solar System Research

It is important to determine the taxonomic types of small bodies in the solar system and further to study the spatial distribution of the planetary system. Among the small bodies, it is considered that there should be dormant comets that have lost a significant fraction of volatile materials in their subsurface layers. As a result, they are unable to produce any detectable coma and recognized as asteroids. It has been challenging to find out such dormant comet population from a list of known asteroids because of the asteroidal appearances. There are several attempts to find the dormant comet nuclei from asteroidal catalogs, for example, by using their reflectance spectra or orbital elements. However, little has been studied via polarimetry.
We conduct a polarimetric study of three candidates of dormant comet nuclei, (331471) 1984 QY1, (3552) Don Quixote and (944) Hidalgo, by using the 1.6-m Pirka Telescope at the Nayoro observatory (operated by Hokkaido University, Japan). We chose these asteroids in comet-like orbits (ACOs) based on the orbital elements (i.e., the Tisserand parameter with respect to Jupiter $T_J < 3$). We found that 1984 QY1 has a polarimetric albedo (geometric albedo determined via polarimetry) $p_V = 0.16 \pm 0.06$ while both Don Quixote and Hidalgo have Rc-band polarimetric albedo $p_R < 0.05$. Based on the polarimetric result together with a dynamical analysis, we conjectured that 1984 QY1 could be an S-type asteroid transported into the current orbit via 3:1 mean motion resonance with Jupiter. From the previous spectroscopic study, Don Quixote and Hidalgo are classified into D-type taxonomic group, which are typical of comet nuclei. In this presentation, we will introduce our polarimetric observations of ACOs and emphasize that polarimetry is a powerful tool for discriminating the asteroidal and cometary origins.

Keywords: Polarimetry, Asteroid

©2019. Japan Geoscience Union. All Right Reserved.

Dynamical lifetime of the Oort Cloud new comets under planetary perturbation

*Ito Takashi[1], Arika Higuchi[1]

1. National Astronomical Observatory of Japan

Nearly isotropic comets with very long orbital period are supposed to come from the Oort Cloud. Recent observational and theoretical studies have greatly revealed the dynamical nature of this cloud and its evolutionally history, but many issues are yet to be known. Our goal is to trace the dynamical evolution of the Oort Cloud new comets (OCNCs) produced by evolving comet cloud, hopefully estimating the fraction of OCNCs embedded in the current populations of the solar system small bodies. We combine two models to follow the dynamical evolution of OCNCs beginning from their production until their ejection out of the solar system, obtaining statistics of the dynamical lifetime of OCNCs: The first model is a semi-analytical one about the OCNC production in an evolving comet cloud under the perturbation of the galactic tide and stellar encounters. The second model numerically deals with planetary perturbation over OCNCs' dynamics in planetary region. The main results of the present study are: (1) Typical dynamical lifetime of OCNCs in our models turned out to be O(10^7) years. Once entering into the planetary region, most OCNCs stay there just for this timespan, then get ejected out of the solar system on hyperbolic orbits. (2) While averaged orbital inclination of OCNCs is small, the so-called "planet barrier" works rather effectively, preventing some OCNCs from penetrating into the terrestrial planetary region.

Keywords: Oort Cloud, comet, orbital dynamics

©2019. Japan Geoscience Union. All Right Reserved.

Thermal Infrared Imaging of C-type Asteroid 162173 Ryugu with Porous Surfaces

*Tatsuaki Okada[1,2], Tetsuya Fukuhara[3], Satoshi Tanaka[1], Makoto Taguchi[3], Takehiko Arai[4], Naoya Sakatani[1], Yuri Shimaki[1], Hiroki Senshu[5], Yoshiko Ogawa[6], Hirohide Demura[6], Kentaro Suko[6], Kohei Kitazato[6], Toru Kouyama[7], Tomohiko Sekiguchi[8], Jun Takita[9], Sunao Hasegawa[1], Tsuneo Matsunaga[10], Takehiko Wada[1], Takeshi Imamura[2], Jorn Helbert[11], Thomas G. Mueller[12], Axel Hagermann[13], Jens Biele[11], Matthias Grott[11], Maximiliam Hamm[11], Marco Delbo[14], Yukio Yamamoto[1], Naru Hirata[6], Naoyuki Hirata[15], Fuyuto Terui[1], Takanao Saiki[1], Satoru Nakazawa[1], Makoto Yoshikawa[1], Sei-ichiro WATANABE[1,16], Yuichi Tuda[1]

1. Institute of Space and Astronautical Science, Japan Aerospace Exploration Agency, 2. University of Tokyo, 3. Rikkyo University, 4. Ashikaga University, 5. Chiba Institute of Technology, 6. University of Aizu, 7. National Institute of Advanced Industrial Science and Technology, 8. Hokkaido University of Education, 9. Hokkaido Kitami-Hokuto High School, 10. National Institute for Environmental Studies, 11. German Aerospace Center, 12. Max-Planck Institute for Extraterrestrial Physics, 13. University of Stirling, 14. Observatoire de la Côte d'Azur, 15. Kobe University, 16. Nagoya University

Thermal images from global to close-up scales taken by the Thermal Infrared Imager TIR [1] on Hayabusa2 [2] have revealed thermophysical properties of the C-type Near-Earth Asteroid 162173 Ryugu. On 27 June 2018, Hayabusa2 arrived at Ryugu and started remote sensing to characterize the nature of the asteroid and find the proper landing sites. *In situ* surface experiments were conducted using the robotic landers Minerva-II and Mascot [3]. *In situ* radiometry was conducted by MARA on MASCOT during a day-night cycle to derive the thermal inertia of a single boulder [4]. Ground-based observations [5] have been informed that the averaged thermal inertia of the asteroid is from 150 to 300 [tiu = J m^{-2} $s^{-0.5}$ K^{-1}] [5,6], corresponding to the surface covered with cm-sized granules.

TIR is the same design as the LIR on Akatsuki Venus climate orbiter [6], with 8 to 12 μm wavelength range, 328 x 248 effective pixels, and the FOV and IFOV of 16.7˚ x 12.7˚ and 0.051˚ per pixel, respectively. The first image of Ryugu detected by TIR was a point source on 6 June 2018, as was previously predicted [7]. Disc-resolved thermal images of Ryugu was taken from the HP on 30 June. The surface temperature was measured at 300 to 370K at about 1AU from the Sun, and gradually decreased with the solar distance. Comparison of the results with modeling [8] shows that the surface of Ryugu is not like fine regolith nor base rocks. Most of large boulders on Ryugu show temperatures almost the same as the surrounding surfaces. Diurnal temperature profiles of Ryugu are rather flatter than expected for a smooth terrain. Apparent thermal inertia is ~300 tiu or larger, but probably lower than the value when the surface roughness is considered. All these facts are consistent with a very rough and porous surface with low porosity (~35 ±10 %) [9] and the surrounding surface is dominated by porous rocks larger than several centimeters. Macro porosity should be 30 to 50 % to account for the bulk density of Ryugu ~1200 kg m^{-3}.

During the descent operations for the release of landers and the touchdowns for sample collection, TIR has taken close-up thermal images of the local sites, continually from the altitude of 500 m until the start of final descent at 10 or 20 m altitude. Close-up thermal images show the surface physical state and a variety of boulders. Most of the boulders in close-up images have temperatures similar to the surroundings but with more variety. A small number of boulders are remarkably colder than the surroundings, indicating dense rocks with lower porosity.

©2019. Japan Geoscience Union. All Right Reserved.

These facts indicate that Ryugu is probably a rubble pile of loosely-bound porous rocks, which might originate from the outer layer of parent body where compaction did not occur effectively, while the dense boulders might originate the compacted center region of parent body or from the different parent body. A different composition (e.g., organic rich materials) cannot be ruled out so far to account for such a low thermal inertia (and low density) of Ryugu.

Acknowledgments: The authors appreciate all the members of the Hayabusa2 Project and supporting staff for their technical assistance and scientific discussions. This research is partly supported by the JSPS KAKENHI No. J26287108, No. J17H06459 (Aqua Planetology), and the Core-to-Core program “International Network of Planetary Sciences”. MDB acknowledges support from CNES.

References: [1] Okada T. et al. (2017) *SSR.,* 208, 255-286. [2] Tsuda Y. et al. (2013) *Acta. Astronautica, 91* , 356-362. [3] Ho T.M. et al. (2017) *SSR.,* 208, 255-286. [4] Grott, M. et al. (2019), submitted to Nature. [5] Mueller T.G. et al. (2016) Astronon. Astrophys., doi:10.1051/0004-6361/201629143. [6] Fukuhara T. et al. (2011) *EPS,* 63, 1009-1018. [7] Okada T. et al. (2018) *PSS., 158, 46-52.* [8] Takita J., et al. SSR, 2018, 287-315. [9] Okada T. (2016) *LPSC.*, 47, #1457.

Keywords: Hayabsua2, Thermal Infrared Imager, Thermal Inertia

©2019. Japan Geoscience Union. All Right Reserved.

Data Release of Asteroid 162173 Ryugu by Observation of Thermal Infrared Imager onboard Hayabusa2

*Takehiko Arai[1], Hirohide Demura[2], Toru Kouyama[7], Naoya Sakatani[3], Kentaro Suko[2], Yuri Shimaki[3], Hiroki Senshu[5], Tomohiko Sekiguchi[6], Yoshiko Ogawa[2], Sunao Hasegawa[3], Takehiko Wada[3], Takeshi Imamura[10], Tsuneo Matsunaga[9], Jun Takita[8], Kohei Kitazato[2], Makoto Taguchi[4], Tetsuya Fukuhara[4], Satoshi Tanaka[3], Tatsuaki Okada[3]

1. Ashikaga University, 2. The University of Aizu, 3. Japan Aerospace Exploration Agency (JAXA), 4. Rikkyo University, 5. Chiba Institute of Technology, 6. Hokkaido University of Education, 7. National Institute of Advanced Industrial Science and Technology (AIST), 8. Hokkaido Kitami Hokuto High School, 9. National Institute for Environmental Studies (NIES), 10. The University of Tokyo

The thermal infrared imager (TIR) onboard the Hayabusa2 spacecraft performed thermography of the asteroid 162173 Ryugu through in-situ observations from 2018 to 2019. The primary purpose of TIR is to determine the global thermophysical properties of the asteroid and to reveal the evolutional history such as physical properties of the coalesced bodies, orbital changes due to radiation force, and the thermal evolution. This study introduces observed data of TIR and public data for scientists. The data are released by JAXA data archives (DARTS) and NASA PDS.

Keywords: Hayabusa2, Thermal Infrared Imager, Asteroid Ryugu

©2019. Japan Geoscience Union. All Right Reserved.

Multi-mission capability of HARMONICS

*Shintaro Tsunoda[1], Hirohide Demura[1], Naru Hirata[1]

1. The University of Aizu

This research has updated HARMONICS from a viewpoint of multi-mission capability, such as the Martian satellite exploration mission MMX in 2020s. Newly additional function is Switching on the shape model interface.
Bird view and visualization of FOV is important in robotics control. This technology is also used for deep space explorer missions.
HARMONICS is visualization tool of FOV(Field Of View) of scientific instruments and spacecraft’s position for HAYABUSA mission. The software has been updated by University of Aizu students of the past. The original HARMONICS had been developed by Nemoto(2006). GUI of HARMONICS had been replaced GUI library from GKT to Qt and added new functions, such as interactive modification of input mission plan by Ueno+(2017). The software had been add FOV frustum function by Aoki(2017). HARMONICS has tried to manage data for each project based on preference file in 2018.
HARMONICS should improved scalability to be compatible for ongoing mission. HARMONICS had been used to decide shutter chance by Camera Science Team in the asteroid Itokawa rendezvous of HAYABUSA. This software has not used in the asteroid Ryugu rendezvous of HAYABUSA2. The proven software should be use for future ongoing missions other than HAYABUSA. This research is development to HARMONICS adapt to ongoing missions.
I separated the designation of the data set from the source code and clarified the part edited by the user and the part edited by the developer.
HARMONICS has the function to switch and display data of different missions by this research. When users extend HARMONICS for multiple missions, users don’t need edit source code. User needs only kernel and the shape model of spacecraft and target asteroid. User do not need tough coding. User can use easily HARMONICS by editing preference file and kernel.

Keywords: Hayabusa2, Ryugu, Software, visualization

©2019. Japan Geoscience Union. All Right Reserved.

New interface of verification for calibration and conversion in HEAT : Hayabusa2 Exploration Assistant for TIR

*Tatsuro Kobayashi[1], Kentaro Suko[1], Hirohide Demura[1], Yoshiko Ogawa[1], Takehiko Arai[2], Naoya Sakatani[3], Tatsuaki Okada[3], Satoshi Tanaka[3], Tetsuya Fukuhara[4]

1. The University of Aizu, 2. Ashikaga University, 3. Institute of Space and Astronautical Science, Japan Aerospace Exploration Agency, 4. Rikkyo University

Hayabusa2 is an ongoing mission for sample return from the asteroid Ryugu.
Candidates of sampling sites are selected based on surface mapping by optical instruments such as Thermal Camera (TIR). TIR observes surface infrared radiation from the asteroid. A software package peculiar to TIR is HEAT: Hayabusa2 Exploration Assistant for TIR. The software has four functions; Database for ground tests, calibration of flight data based on the ground tests, conversion from raw data to temperature one, and analysis for verifying the calibration and conversion. The converted data products are divided into some levels: Lv1 Raw data [DN], Lv2a Temperature [K], Lv2b is Brightness [W/m2], and higher thermal model with VTK format [K]. This research implements new interface of verification for calibration and conversion based on hearing and survey for requirements from TIR science team. The environment of implementation is following tool. OS: macOS Mojave 10.14.2. Computing language: C++, OpenGL. Frameworks: Qt5.4. Tools: Fits, Qt creator, SPICE toolkit, Visualization Toolkit, QcustomPlot, Xcode10.1.

Keywords: Hayabusa2, Software, Ryugu, Calibration

©2019. Japan Geoscience Union. All Right Reserved.

Dust particle evolution of a near-Earth object 252P/LINEAR from near-infrared polarimetric observations in 2016

*Yuna G Kwon[1], Masateru Ishiguro[1], Jungmi Kwon[2], Daisuke Kuroda[3], Myungshin Im[1], Changsu Choi[1], Motohide Tamura[4], Takahiro Nagayama[5], Nobuyuki Kawai[6], Jun-ichi Watanabe[7]

1. Seoul National Univ., 2. ISAS/Japan Aerospace Exploration Agency, 3. Okayama Astrophysical Observatory, 4. The Univ. of Tokyo, 5. Kagoshima Univ., 6. Tokyo Institute of Technology, 7. National Astronomical Observatory of Japan

Comets, one of the least-altered leftovers from the early solar system, have probably preserved the primitive structure inside, whereas their surfaces become differentiated from initial states after repetitive orbital revolutions around the sun. Resurfacing makes the surface drier and more consolidated than the bulk nuclei, creating inert refractory dust layer (so-called “dust mantle”). Near-Infrared (NIR) polarimetry is theoretically expected to maximize the contrast of the porosity between inner fresh and evolved dust particles, by harboring more dust constituents in the single wavelength than the optical, and thus intensifying electromagnetic interference in dust agglomerates. Despite the advantage, only few studies have been conducted in this approach at multiple observation epochs. Herein, we present our new multi-band NIR polarimetric (1.25—2.25 microns) study of near-Earth object 252P/LINEAR over 12 days near perihelion; alongside broadband optical photometric (0.48—0.80 microns) data over four months in 2016 and a subsidiary dynamical simulation over 1000 year backward in time. 252P/LINEAR drew attention due to (1) its close approach to the Earth (~0.036 au on 2016 March 16), (2) its possible pairing to a comet P/2016 BA14 (PanSTARRS), and (3) its very low activity level despite its relatively young dynamical age. In this study, we detected two discontinuous brightness enhancements of 252P/LINEAR, particularly, the former of which accompanied a significant increase of NIR polarization degree of the comet (by ~13 % at most) with unusual blue polarimetric color. We will discuss the most probable scenario of the observed results, together with the orbital evolution of the comet and a dynamical association with its pair.

Keywords: Comet, Near-earth object, Polarimetry, Dust

©2019. Japan Geoscience Union. All Right Reserved.

Performance Evaluation of TRIPOL on the 61-cm Telescope at Seoul National University for Polarimetric Observations of Solar System Small Bodies

*Sunho Jin[1], Masateru Ishiguro[1], Yuna G Kwon[1], Jooyeon Geem[1], Yoonsoo P. Bach[1], Jinguk Seo[1], Hiroshi Sasago[2], Shuji Sato[3]

1. Seoul National University, 2. Sasago Co.,Ltd, 3. Nagoya University

Polarimetry of solar system small bodies is a powerful technique for investigating their physical properties, such as albedos, particle sizes, and porosities of these bodies. Observational opportunities arise sometimes suddenly, that is, just after unforeseeable activations of comets and discoveries of near-miss asteroids. Here, we introduce our activity to install the polarimetric instrument, TRIPOL (Triple-Range Imager and POLarimeter) on the 61-cm telescope (a Ritchey-Chretien reflector with f/7.0) at the Center for Astronomy and Space Science, Seoul National University, and report an observational result of three comets. This combination provides an 8.0’ ´8.0’ field of view and pixel resolution of 0.94” pixel^{-1}. Throughout photometric observations, we determined the limiting magnitudes (defined as magnitudes for S/N=5) of 15.17±0.06 (g’-band), 15.68±0.01 (r’-band), 16.24±0.03 (I’-band), respectively, with total 240-seconds exposure (four 60-seconds exposure images, each was taken at different rotation angle for the half-wave plate). We also found that the instrumental polarizations are negligibly small, that is, -0.32±0.04% (g’-band), -0.36±0.05% (r’-band) and -0.21±0.04% (I’-band), while the polarization efficiencies are large enough to maximize the performance, that is, 97.52±0.03% (g’-band), 98.83±0.02% (r’-band) and 99.15±0.02% (I’-band).

With this instrument, we conducted polarimetric observations of three Jupiter-family comets, 21P/Giacobini-Zinner, 38P/Stephan-Oterma, and 46P/Wirtanen on a trial basis. It is known from a recent study that the polarization degrees of cometary dust particles are significantly influenced by gas emissions [1] With multiband data taken with TRIPOL, we eliminated an influence of gas contaminations and found that the dust polarization degrees of these three comets coincide with those of so-called ‘dust-rich comets’. From this result, we conjecture that the polarimetric property of Jupiter-family comets is broadly homogeneous, unlike asteroids. We plan to describe our future plan using the polarimetric system.

[1] Kwon, Y. G. et al. Astronomical Journal, 154, 4, 173, 2017

Keywords: Comet, Instrument, Polarimetry

©2019. Japan Geoscience Union. All Right Reserved.

Smart Interface of HEAT: Hayabusa2 Exploration Assistant for TIR

*Kentaro Suko[1], Tatsuro Kobayashi[1], Hirohide Demura[1], Takehiko Arai[2], Naoya Sakatani[3], Tatsuaki Okada[3], Satoshi Tanaka[3], Tetsuya Fukuhara[4]

1. The University of Aizu, 2. Ashikaga University, 3. Institute of Space and Astronautical Science, Japan Aerospace Exploration Agency, 4. Rikkyo University

The Hayabusa2 project is a sample return mission to the asteroid Ryugu. It was launched on Dec. 3, 2014, and it has been at Ryugu since June 27, 2018. Hayabusa2 has optical instrument called Thermal Infrared Imager (TIR). These main functions are to know natures of the asteroid and to select the candidate of safe landing sites for sampling based on thermos-physical properties of the surface. TIR records infrared radiation from the target as a digital number (DN). The infrared signal is affected by sensor-surrounding objects; lens, shutter, package, and case. TIR requires consideration about this effect when converts DN images to temperature one. This study improved conversion system to increase conversion efficiency.

Hayabusa2 TIR Science Team has developed an analysis supporting tool called Hayabusa2 Exploration Assistant for TIR (HEAT). HEAT is used to search TIR data interactively, display TIR images, and visualize thermal models. We receive TIR raw images (Product Level 1) from ISAS/JAXA and convert them to brightness temperature images (Level 2a) and radiance images (Level 2b) using HEAT at Univ. of Aizu. The converted images are provided to the Hayabusa2 project data server.

This part introduces a concept model. The spectral radiance emitted from a blackbody B(λ ,T) (W s r-1m-2) is given by the Planck function based on wavelength λ (m) and temperature T(K) as follows:

$$B(\lambda,T) = (2hc2/\lambda 5)^* (1/(\exp(\lambda kBT)-1))$$

H = 6.63*1034 (m2 kg s-2 s-1) is the Planck constant, c=2.9972*108(ms-1) is the speed of light, and KB= 1.38*10-23 (m2 kg s-2K-1) is the Boltzmann constant. The observed radiance L(T) (W sr−1 m−2) is as follows:

$$L(T)= \varepsilon \int BR(\lambda)d\lambda$$

ε is the spectral thermal emissivity, and R(λ) is the response function such as the detection efficiency of the bolometer, the measured transmittance of optics including the band-pass filter and the germanium lens. The calibration formula with two regressed parameters A and B is written as follows:

$$DN=A * L(T) + B$$

The converted temperatures of the Moon were lower than expected because each pixel did not cover the sunlit area entirely or due to roughness effect of the cratered terrain. TIR has been observing Ryugu in approach and rendezvous phases. The altitudes of TIR observations during the rendezvous phase range from 20 km to less than 10 m. This study has processed about 3000 Ryugu images observed by TIR since June 2018.

©2019. Japan Geoscience Union. All Right Reserved.

This study improved conversion system. Previous conversion system converts a TIR image one by one, but current conversion system converts TIR images in selected directory at once.

Keywords: Hayabusa2, TIR, HEAT, Software

©2019. Japan Geoscience Union. All Right Reserved.

Experimental Study on Collision Crater Formed on Bulge Geography

*Yusaku Yokota[1], Yuya Yamamoto[2], Minami Yasui[2], Masahiko Arakawa[2]

1. Faculty of Science, Kobe University, 2. Graduate School of Science, Kobe University

An equatorial bulge was found on the surface of asteroid Ryugu and Bennu by recent spacecrafts of Hayabusa2 and OSIRIS-Rex, and ridge structures with various scales originated by geological activities have been recognized on icy satellites. Impact craters are dominant geological features on solid planets such as asteroids and satellites, and a crater rim are also recognized as a ridge or bulge with a circular shape. These bulges and ridges are shown to be erased with time because small scale impacts excavate and disrupt these topographies. It is well known that old craters gradually degraded by small impacts to get blurred and could be completely erased. We can expect the similar degradation process on large bulges and ridge structures, so that the life time of these structures by small impacts is a good indicator of the formation age of these structure by geologic activities. So far, the effect of small impacts on the degradation is estimated by using the results on the flat surface, but actually the surface of the bulge is curved and there is a summit on the bulge. Therefore, if we estimate the life time of the bulge structure, we should consider the effect of the topography such as a summit and curvature. Then, the impacts on the bulge structure was studied to clarify how the bulge structure affected the crater formation efficiency. In this study, we suppose the bulge made from regolith and boulders, such as an equatorial bulge of Ryugu and assume the crater formation process dominated by not the strength but the gravity.

We prepared a triangular prism target to simulate the bilge structure, and set it like that the base of this prism is rectangle, then it looks triangle when we look it at the horizontal direction, and we can look at the linear summit from the top view. Quartz sands with the size of 100μm was used to build the target and the angle of repose for this quartz sand is about 30 degree. The slope of the prism was measured from the base, and we set the angle from 20 to 30 degree. The quartz sands were filled into a transparent water tank with the depth of 20 cm to prepare the bulge structure. Impact experiments were conducted by using a vertical type gas gun, and the water tank was set in the chamber to evacuate below 1000 Pa. A alumina sphere projectile with the size of 3mm was launched at the velocity from 70 to 200 m/s, and it was impacted on the bulge in the vertical direction: the impact angle measured from the target surface was about 60 degree when the slope was 30 degree. The distance from the impact pint to the summit (deviation distance, d_d) was changed from 0 to 20mm.

We found that the crater shape strongly depended on the d_d, so the crater shape was an ellipsoid when the impact point was near the summit. Th major axis appeared along the linear summit and the minor axis appeared across the summit. The aspect ratio of the major axis to the minor axis gradually changed toward 1 with the increase of d_d. Moreover, the aspect ratio becomes large at the same d_d when the impact velocity increased. The major axis of the ellipsoid crater formed on the bulge was slightly larger than the crater diameter formed on the flat surface, and the slope angle might affect the size of the ellipsoid because we found that the crater formed on the slope of 30 degree was systematically larger than that formed on the slope of 20 degree. We also observed an asymmetric ejecta curtain from the impact point on the bulge, moreover the ejecta curtain was notice to be deformed so much at the impact point near the summit because of the effect of curvature of the bulge on the crater flow.

Angle of repose, Impact crater, Bulge and ridge structure, Ejecta curtain

©2019. Japan Geoscience Union. All Right Reserved.

©2019. Japan Geoscience Union. All Right Reserved.

Initial analysis plan of soluble organic compounds for the Hayabusa2 sample from asteroid Ryugu

*Hiroshi Naraoka[1], Yoshinori Takano[2], Jason P. Dworkin[3], SOM Analysis Team

1. Department of Earth and Planetary Sciences, Research Center for Planetary Trace Organic Compounds, Kyushu University, 2. Japan Agency for Marine-Earth Science and Technology, 3. Astrochemistry Laboratory NASA Goddard Space Flight Center, Greenbelt, MD 20771 USA

The spectra of asteroid 162173 Ryugu taken by Near-Infrared Spectrometer (NIRS3) onboard Hayabusa2 are nearly featureless and consistent with carbonaceous chondrites (Matsuoka et al., 2018). The Hayabusa2 spacecraft will collect surface samples of Ryugu and deliver to the Earth during late 2020. The initial analysis of the Ryugu samples will focus on (1) detailed chemical and mineralogical characterization of the samples and (2) understanding the history of Ryugu and the Solar System in order to maximize the scientific achievement of the project and (3) to prove the scientific potential of the samples to the community for the analytical opportunity (Tachibana et al., 2014). We have organized an international team, consisting of 24 members currently, for the initial analysis of soluble organic matter (SOM) for the returned samples.
The primitive asteroidal materials are expected to contain diverse and complex (e.g. elemental, structural, and optical) organic matter all at low concentrations. The occurrence of SOM will provide clues to the origins of organic compounds as well as prebiotic molecules of potential relevance to origins of life on Earth and possibly elsewhere in the Solar System. We propose the comprehensive SOM analyses to reveal the chemical evolution of Ryugu using high-sensitive and high-resolution analytical methods as follows:

1) High-resolution mass spectrometry (HRMS) of various solvent extracts with electrospray ionization (ESI) coupled with or without nano-liquid chromatography.
2) Enantiomerically resolved amino acid analysis using high-resolution column chromatography with high-sensitive fluorescence spectroscopy coupled with HRMS.
3) *In situ* organic compound analysis and molecular imaging using desorption electrospray ionization (DESI) and/or direct analysis in real time (DART) equipped with HRMS.
4) Spatial resolution imaging of organic compounds using time of flight-secondary ion mass spectrometry (ToF-SIMS; Naraoka et al., 2015).

In addition, if the sample is available, we will also perform the following additional analyses:

5) Compound-specific isotope analysis using gas chromatography/combustion or pyrolysis /isotope ratio mass spectrometry (GC/C or pyrolysis/IRMS).
6) Bulk chemical and isotopic analysis of organic matter (C, H, N and S) using nano-EA/IRMS system and laser-tunable FT-IR spectroscopy.

Depending to the sample size available to the initial analysis, we will perform preliminary analytical tests using 30 mg, 10 mg, and 1 mg samples of the Murchison meteorite (CM2, positive SOM-rich), Yamato 793321 meteorite (heated CM2, positive SOM-depleted), and baked serpentine (negative SOM-depleted) as well as procedural blank. The analytical protocol will be discussed in the meeting.

< References >
Tachibana, S. et al. (2014) Hayabusa2: Scientific importance of samples returned from C-type near-Earth

©2019. Japan Geoscience Union. All Right Reserved.

asteroid (162173) 1999 JU3. Geochemical Journal. 48. 571-581. 10.2343/geochemj.2.0350.
Matsuoka, M. et al. (2018) Spectral comparison between asteroid (162173) Ryugu and carbonaceous meteorites. American Astronomical Society, DPS meeting #50.
Naraoka, H. et al. (2015) ToF-SIMS analysis of carbonaceous particles in the sample catcher of the Hayabusa spacecraft. Earth, Planets and Space, 67:67. DOI 10.1186/s40623-015-0224-0.
Naraoka, H. and Hashiguchi, M. (2018) *In situ* organic compound analysis on a meteorite surface by desorption electrospray ionization coupled with an Orbitrap mass spectrometer. Rapid Commun. Mass Spectrom. 32, 959-964.

Keywords: Hayabusa2, Ryugu, Carbonaceous Asteroid, Soluble Organic Matter

©2019. Japan Geoscience Union. All Right Reserved.

Radar and optical simultaneous observations of faint meteors with MU radar and Tomo-e Gozen

*Ryou Ohsawa[1], Akira Hirota[2], Shinsuke Abe[2], Daniel Kastinen[3], Kero Johan[3], yasunori Fujiwara[4], Takuji Nakamura[5], Shigeyuki Sako[1], Yuto Kojima[1], Jun-ichi Watanabe[6]

1. Institute of Astronomy, Graduate School of Science, The University of Tokyo, 2. Department of Aerospace Engineering, College of Science & Technology, Nihon University, 3. Swedish Institute of Space Physics, 4. SOKENDAI (The Graduate University for Advanced Studies), 5. National Institute of Polar Research, 6. National Astronomical Observatory of Japan

The Earth is surrounded by small dust grains produced by comets and asteroids. Tons of such grains plunge into the Earth's atmosphere hourly. Part of their kinetic energy excites and ionizes the surrounding atmosphere, which is observed as a meteor phenomenon. A simultaneous radar and optical observation is promising to constrain the motion and mass of a meteor at a time. We launched a project to observe faint meteors with Middle and Upper Atmosphere Radar (MU radar) and a wide-field CMOS mosaic camera Tomo-e Gozen installed on the 105 cm Kiso Schmidt telescope. The observations were carried out in 18--21, April, 2018. From tons of the detected meteors, the simultaneous detections were extracted in terms of the times, loci, and directions of the meteors. Finally, we identified the 894 meteor events simultaneously detected in the both sites. The optical brightness of the simultaneous meteors ranged from about 3--11 mag. in the V-band, which is about 5 magnitude fainter than in previous studies. We confirmed a clear correlation between the meteor brightnesses and the radar cross sections.

Keywords: meteor, interplanetary dust

©2019. Japan Geoscience Union. All Right Reserved.

Global distribution and spectral characteristics of bright spots on asteroid Ryugu

*Masanori Suemitsu[1], Tomokatsu Morota[1], Rie Honda[2], Singo Kameda[15], Eri Tatsumi[3], Manabu Yamada[4], Naoya Sakatani[5], Toru Kouyama[6], Yokota Yasuhiro[7], Yuichiro Cho[8], Hidehiko Suzuki[9], Masahiko Hayakawa[10], Moe Matsuoka[10], Chikatoshi Honda[11], Tatsuhiro Michikami[12], Kazuo Yoshioka[13], Kazunori Ogawa[14], Hirotaka Sawada[5], Seiji Sugita[3]

1. Graduate School of Environmental Studies, Nagoya University, 2. Department of Science and Technology, System of Natural Science, Kochi Unicversity, 3. Graduate School of Earth and Planetary Science, Tokyo Unicversity, 4. Planetary Exploration Reserch Center, Chiba Institute of Technology, 5. Institute of Space and Astoronautical Science, Japan Aerospace Exploration Agency, 6. National Institute of Advanced Industrial Science and Technology, 7. Kochi University, 8. Department of Earth and Planetary Science, Tokyo University, 9. Depertment of physics, Meiji University , 10. Department of Solar System Science, Institute of Space and Astoronautical Science, Japan Aerospace Exploration Agency, 11. Aizu University, 12. Faculty of Engineering, Kindai University, 13. Graduate School of frontier Science, Tokyo University, 14. Kobe University, 15. Rikkyo University

On June 27, 2018, the asteroid explorer Hayabusa2 arrived at the target C-type asteroid 162173 Ryugu. The telescopic optical navigation camera (ONC-T) on-board Hayabusa2 has acquired the multiband image data for the entire surface of Ryugu with spatial resolutions better than 2 m/pixel. These data show that the Ryugu surface has the very low surface reflectance, flat spectra, and its spatial homogeneity [Sugita et al. 2019]. However, more detailed observations on Ryugu have revealed that many boulders exhibit different spectral properties and that a number of spots with distinctively brighter than the surroundings [Sugita et al. 2019]. Although larger boulders have been analyzed to show that they form two distinctive spectral trends, no substantial spectral analyses on bright spots have been conducted. Determining whether or not these bright spots are one of the materials that originate from the parent body of Ryugu is important to understand the differentiation and geologic processes on the parent body. In this study, in order to understand origins of the bright spots, we investigated spectral characteristics of the bright spots and compared those of the boulders on Ryugu. We used the ONC-T multiband images obtained in Box-A (20 km altitude) and mid-altitude (5 km altitude) operations.

We found seven meter-sized bright spots that have radiance factor 1.3 to 2.0 times higher than that of the surrounding area. The spectra of these bright spots were classified into two types, one being a flat spectrum type and another being a convex spectrum type. The former type has spectrum similar to but flatter and brighter than the mean spectra of the whole Ryugu and boulders, suggesting that the bright spots originate from parent body of Ryugu. The latter type has spectrum similar to those of S-type asteroids, suggesting their exogenous origin.

Keywords: asteroids, Ryugu, bright spot, spectrum, boulder

©2019. Japan Geoscience Union. All Right Reserved.

Polarimetry of (155140) 2005 UD: the Dynamical Association with (3200) Phaethon

*Masateru Ishiguro[1], Jooyeon Geem[1], Hiroyuki Naito[2], Yoonsoo P. Bach[1], Daisuke Kuroda[3], Tatsuharu Ono[4], Seiko Takagi[4], Mitsuteru Sato[4], Kiyoshi Kuramoto[4], Tomohiko Sekiguchi[5], Masataka Imai[6], Makoto Watanabe[7], Katsuhito Ohtsuka[8], Sunao Hasegawa[9], Takashi Ito[10], Fumi Yoshida[11], Tomoko Arai[11]

1. Department of Physics and Astronomy, Seoul National University, 2. Nayoro Observatory, 3. Okayama Observatory, Kyoto University, 4. Department of Cosmosciences, Graduate School of Science, Hokkaido University, 5. Hokkaido University of Education, 6. National Institute of Advanced Industrial Science and Technology, 7. Department of Applied Physics, Okayama University of Science, 8. Tokyo Meteor Network, 9. Japan Aerospace Exploration Agency, 10. National Astronomical Observatory of Japan, 11. Planetary Exploration Research Center, Chiba Institute of Technology

An Apollo-type near--Earth asteroid, (155140) 2005 UD, is considered as a possible fragment from (3200) Phaethon, suggesting that Phaethon precursor body might undergo a catastrophic disruption in the past. Here we present our new observational evidence for supporting these two are common origin. We thus conducted a polarimetric observation in 2018 September-October and found that 2005 UD exhibited a polarimetric property significantly different from those of major taxonomic classes of NEAs (i.e., S- and C-type) but similar to that of Phaethon at a wide range of the solar phase angles. Using the polarimetric data, we derived the geometric albedo of ~0.1. In addition, we made a photometric observation at the opposition (the zero phase angle), and determined the mean absolute magnitude of 17.2, the synodic rotational period 5.23 hr, and the effective diameter 1.5 km in combination with the derived geometric albedo. From these evidence, we found that the Phaethon precursor body might have lost more than a few percents of the mass via a disruption if 2005 UD was indeed ejected from the Phaethon precursor.

Keywords: Asteroids, Space Mission (Destiny+)

©2019. Japan Geoscience Union. All Right Reserved.

Follow-up observations for AKARI/IRC near-infrared asteroid spectroscopic survey (AcuA-spec)

*Sunao Hasegawa[1], Daisuke KURODA[2], Kenshi YANAGISAWA[3], Fumihiko Usui[4]

1. Japan Aerospace Exploration Agency, 2. Kyoto University, 3. National Astronomical Observatory of Japan, 4. Kobe University

In the range from 1 to 2.5 μm, we made the spectroscopic observations of the AcuA-spec asteroids (Hasegawa et al. 2017, PASJ, 69, 9), whose spectra were obtained in continuous covered between 2.5 and 5.0 μm by NIR/IRC/AKARI (Usui et al. 2019, PASJ, 71, 1). Candidates of AcuA-spec asteroids were selected from only main-belt asteroids classified based on visible spectrophotometric and spectroscopic observations (Tholen 1984, PhD thesis, Arizona University; Bus & Binzel 2002, Icarus, 158, 146; Lazzaro et al. 2004, Icarus, 172, 179). About 200 classified asteroids were raised as observational candidates. Spectroscopic observations for 65 AcuA-spec asteroids which were selected among the AcuA-spec candidate catalogue in taking account of signal-noise ratio and target opportunity by AKARI were executed.
Section work of the AcuA-spec candidate catalogue was done around 2005, yet there were not many spectroscopic observations of asteroids in the near-infrared wavelength range. As a result of survey of published paper for near-infrared spectroscopic observations of asteroids, howevwer, it was found that spectroscopic observations in the near-infrared region of 1–2.5 μm for most AcuA-spec asteroids are performed except for several asteroids.
If data in near-infrared wavelength range of the lacked AcuA-spec asteroids were acquired, all AcuA-spec asteroids will have 0.35–5 μm of data available. Obtaining continuous reflectance of asteroids is essential data to compare with those such as meteorites. Based on the Bus-DeMeo taxonomy (DeMeo et al. 2009, Icarus, 202, 160), we conducted classification of all AcuA-spec asteroids using published and our observational data.

Keywords: asteroids, spectroscopy

©2019. Japan Geoscience Union. All Right Reserved.

Amino acids on witness coupons collected from the ISAS/JAXA curation facility for the assessment and quality control of the Hayabusa2 sampling procedure

*Haruna Sugahara[1,2], Yoshinori Takano[1], Yuzuru Karouji[3], Kazuya Kumagai[4], Toru Yada[3], Naohiko Ohkouchi[1], Masanao Abe[3], Hayabusa2 project team

1. Japan Agency for Marine-Earth Science and Technology (JAMSTEC), 2. Institut de Chimie de Nice, Universite Cote dAzur, 3. Japan Aerospace Exploration Agency (JAXA), 4. Marine Works Japan Ltd.

The Hayabusa2 spacecraft is visiting a near-Earth carbonaceous type (C-type) asteroid, 162173 Ryugu, and planning to return the pristine samples to the Earth. C-type asteroids are considered to be related with carbonaceous chondrites that are enriched in organic and volatile materials. The one of the scientific goals of Hayabusa2 mission is to understand the origin and evolution of organic materials through interactions with water and minerals in the early solar system [e.g., 1]. Thus, the characterization of organic materials in the returned sample has great importance for this purpose. However, the analysis of small quantities of extraterrestrial organic materials in the returned samples requires a great care to avoid the introduction of terrestrial contaminants and any artifact materials to the pristine samples. Thus, the assessment of the degrees of the terrestrial contaminants to the samples as well as the comprehensive and specific managements to minimize the terrestrial contamination throughout the mission is essential.

The purpose of the study is to investigate the potential terrestrial organic contamination in a clean chamber for the Hayabusa2 returned samples in an Institute of Space and Astronautical Science/Japan Aerospace Exploration Agency (ISAS/JAXA) curation room [2-4]. As the indicator of the terrestrial organic contaminants, we selected amino acids that ubiquitously exist in the terrestrial environments and are also the target molecules in the Hayabusa2 mission. In the study, we used witness coupons made of aluminum foil to collect the contaminants in the clean chamber. The witness coupons were collected at different exposure times, ranging from 1 day to 1 month to examine the accumulation rate of the contaminants. After the collection, amino acids on the witness coupons were extracted in hot water, hydrolysed with HCl, and then converted to *N*-pivaloyl isopropyl (Pv/iPr) ester derivatives for gas chromatographic (GC) analysis [5].

On the witness coupons, eight terrestrially common amino acids (glycine, alanine, valine, leucine, isoleucine, proline, aspartic acid and glutamic acid) were detected and seven of them, except valine due to the under quantification limit, were quantified. Among them, glycine was the most abundant species with the highest concentration of 10 pmol/cm^2. A time-dependent profile of the four major amino acids (glycine, alanine, aspartic acid and glutamic acid) showed the increasing trend between 1 to 7 days. The average accumulation rates are 1.2 pmol/cm^2/day for glycine, 0.6 pmol/cm^2/day for alanine, 0.1 pmol/cm^2/day for aspartic acid and 0.2 pmol/cm^2/day for glutamic acid. The species and the concentrations of amino acids on our witness coupons are similar to those reported by the National Aeronautics and Space Administration/Johnson Space Center (NASA/JSC) OSIRIS-REx team [6]. Thus, the quality control against terrestrial contaminants in ISAS/JAXA curation facility is at the same quantitative level as in their facility. This inter-laboratory evaluation [7] about the terrestrial organic contamination will provide important information for the curation procedure of the Hayabusa2-returned samples.

©2019. Japan Geoscience Union. All Right Reserved.

References: [1] Tachibana S. et al. (2014) Geochem. J., 48, 571-587. doi: 10.2343/geochemj.2.0350. [2] Yada T. et al. (2014) Meteorit. Planet. Sci., 49, 135-153. doi: 10.1111/maps.12027. [3] Sawada H. et al. (2017) Space Sci. Rev. 208, 81–106. doi: 10.1007/s11214-017-0338-8. [4] Okazaki R. et al. (2017) Space Sci. Rev. 208, 107–124. doi: 10.1007/s11214-016-0289-5. [5] Chikaraishi Y. et al. (2010) in *Earth, Life, Isotopes*, Kyoto Univ. Press, pp.367-386. [6] Dworkin et al. (2018) Space Sci. Rev. 214, 9. doi: 10.1007/s11214-017-0439-4. [7] Sugahara et al. (2018) Earth, Planets Space, 70, 194. doi: 10.1186/s40623-018-0965-7.

Keywords: Amino acid, Hayabusa2, Curation, Witness coupons, Quality control

©2019. Japan Geoscience Union. All Right Reserved.

Hayabusa2 orbit determination using c5++ software

*Keiko Yamamoto[1], Toshimichi Otsubo[2], Koji Matsumoto[1], Hirotomo Noda[1], Noriyuki Namiki[1], Hiroki Senshu[3], Takahide Mizuno[4], Naoko Ogawa[4], Go Ono[4], Yuya Mimasu[4], Kent Yoshikawa[4], Tadateru Takahashi[4], Yuto Takei[4], Atsushi Fujii[4], Fuyuto Terui[4], Takanao Saiki[4], Satoru Nakazawa[4], Makoto Yoshikawa[4], Yuichi Tsuda[4]

1. National Astronomical Observatory of Japan, 2. Hitotsubashi University, 3. Chiba Institute of Technology, 4. Japan Aerospace Exploration Agency

Hayabusa2 arrived at the target asteroid Ryugu in June 2018 and is currently conducting remote sensing observations with various onboard instruments. So far, we have improved orbit determination software c5++, originally developed for the analysis of satellite laser ranging (SLR) data of the Earth, so that it can be used for the analysis of laser ranging data between Hayabusa2 and Ryugu obtained by Hayabusa2 LIDAR. Then we used it for the estimation of Hayabusa2 trajectory and the GM value of Ryugu. However, in the case of Hayabusa2, it is difficult to determine all of the 6 components of the initial state vector precisely if only LIDAR range data was used, and the simultaneously estimated GM value also had large uncertainty. To overcome this problem, in addition to LIDAR ranging data, we used Automated-Image-Tracking (AIT) data obtained by wide-angle optical navigation camera (ONC-W1) for the estimation of Hayabusa2 trajectory. In principle, LIDAR data gives information on the radial direction and AIT data give the ones on the across and along track directions. Thus, both data sets are complementary and help to improve the precision of the trajectory estimation. For this purpose, we improved c5 ++ so that it can deal with AIT data as observation data. In the presentation, we will show the results of trajectory and GM estimations using LIDAR and AIT data, and show how much the precision and accuracy are improved compared to the case using LIDAR data only.

Keywords: Hayabusa2, Orbit Determination, Ryugu

©2019. Japan Geoscience Union. All Right Reserved.

Landing Site Selection for Hayabusa2: Scientific Evaluation of the Candidate Sites on Asteroid (162173) Ryugu

*Hikaru Yabuta[1], Sei-ichiro WATANABE[2], Tomoki Nakamura[3], Naru Hirata[4], Seiji Sugita[5], Tatsuaki Okada[6], Kohei Kitazato[4], Yoshiaki Ishihara[7], Tomokatsu Morota[2], Naoya Sakatani[6], Koji Matsumoto[8], Koji Wada[9], Shogo Tachibana[5], Mutsumi Komatsu[10], ERI TATSUMI[5], Moe Matsuoka[6], Chikatoshi Honda[4], Takahiro Hiroi[11], Hiroki Senshu[9], Rie Honda[12], Yasuhiro Yokota[6], Rina Noguchi[6], Yuri Shimaki[6], Deborah Lorin Domingue[13], Lucille Le Corre[13], Antonella Barucci[14], Ernest Palomba[15], Shota Kikuchi[6], Akira Miura[6], Tomohiro Yamaguchi[6], Yukio Yamamoto[6], Takanao Saiki[6], Satoshi Tanaka[6], Makoto Yoshikawa[6], Yuichi Tsuda[6]

1. Hiroshima University, Department of Earth and Planetary Systems Science, 2. Nagoya University, 3. Tohoku University, 4. University of Aizu, 5. The University of Tokyo, 6. ISAS/JAXA, 7. NIES, 8. NAOJ, 9. Chiba Institute of Technology, Planetary Exploration Research Center (PERC), 10. Sokendai, 11. Brown University, 12. Kochi University, 13. Planetary Science Institute, USA, 14. Observatoire Paris-Site de Meudon, LESIA, France, 15. INAF-IAPS, Italy.

On June 27, 2018, JAXA’s Hayabusa2 spacecraft arrived at its target C-type asteroid Ryugu. Immediately after arrival, remote-sensing observations were carried out with the Optical Navigation Camera (ONC), the Near Infrared Spectrometer (NIRS3), the Thermal Infrared Imager (TIR), and the Laser Altimeter (LIDAR). Based on data from this suite of instruments, we carried out the landing site selection for the first touch-down (TD1). Since the mission aims to understand i) the origin and chemical evolution of the solar system and ii) the formation process and structure of the asteroid, we have set the most scientifically valuable TD1 site as the least altered region where water and/or carbon are potentially abundant.

Landing candidate sites were first selected by engineering evaluation for operational safety followed by scientific evaluations based on criteria such as science and samplability for the most interesting sites. The process was repeated using the observations from the altitudes of 20 km, 6 km, and 5 km.

Scientific evaluations of the landing site candidates were conducted based on the data products from ONC, NIRS3, TIR, and LIDAR. The shape modeling team produced two different shape models. ONC produced multiband images and reflectance spectra, as well as maps of spectral indices and X-means clustering analysis. Measurements of boulder size-frequency and Hapke parameters in the candidate landing areas were examined. NIRS3 produced four types of spectral feature maps. TIR provided maps of maximum temperature from the October 22, 2018 TD1 practice operations, apparent thermal inertia, and typical grain size determinations. LIDAR provided time series ranging data, topography, and corrected spacecraft trajectory.

Engineering evaluation: The possible landing site candidates were selected from the engineering safety score map evaluated based on the sub-Earth distance, local solar angle, local slope and elevation maximum difference. Thermal prediction results for TD1 were obtained by TIR. Temperatures of each site are < 350 K, confirming the safe conditions. The regions that satisfied all the conditions were, L05, L07, L08, L12, M01, M03 and M04.

Scientific evaluation:
1) Boulders. Based on the distribution of boulders with a diameter larger than 3 m for each potential landing site, regions L07, L08, and M04 show smaller percentages of boulder coverage than other areas, and are regarded as safer sites for landing.

©2019. Japan Geoscience Union. All Right Reserved.

2) Geology. Ryugu exhibits a variety of topographic features and geologic settings. From a scientific perspective, it is of interest to be able to study various materials representing the evolution of Ryugu.
3) Hydrous minerals. The NIR spectral properties are nearly homogeneous across Ryugu’ s surface, especially between the candidate sites. The near-infrared reflectance spectra of Ryugu is similar to experimentally heated Murchison meteorite at 400˚C.
4) Carbon contents. It is likely that visible reflectance at 0.55 μm (R(0.55)) is influenced mostly by carbon content. R(0.55) is almost homogeneous across the surface with a low value, regardless of the candidate sites.
5) Secondary processes. Although the surface of Ryugu is almost homogeneous at the macro scale in the map of spectral slope from 0.48 to 0.86 μm, a slight heterogeneity is observed across the candidate regions. L-regions are relatively bluish and M-regions are reddish. Considering that spectral reddening is observed by laser irradiation of dehydrated carbonaceous chondrites, L regions are probably less altered and preferable for sampling.

In the total evaluation, L08, L07 and M04 were selected as the TD1 candidates on August 17, 2018. In September 2018, many boulders > 50 cm were additionally found for the sites during the rehearsal of TD1. Thus, the originally scheduled TD1 in October was postponed. Further search for a flat and safe site continued, and L08-E1 was determined as the TD1 site. The TD1 will be scheduled on Feb 22, 2019.

Keywords: Hayabusa2, Landing Site Selection

©2019. Japan Geoscience Union. All Right Reserved.

Visible Photometric, Spectroscopic and Polarimetric observations of an inactive comet, P/2016 BA14 with the 1.6m Pirka Telescope

*Ryo Yamagata[1], Tomohiko Sekiguchi[1], Ryo Okazaki[1], Kazuya Doi[1], Daisuke Kuroda[2], Masateru Ishiguro[3], Hiroyuki Naito[4]

1. Hokkaido University of Education, 2. Kyoto University, 3. Seoul National University, 4. Nayoro Observatory

We performed photometric, spectroscopic and polarimetric observations of an inactive comet, P/2016 BA14 with the 1.6m Pirka Telescope, Hokkaido.

P/2016 BA14 (a=3.02 au, e=0.67, i=18.9 deg.) was discovered as an unusual asteroid with a cometary orbit by the PANSTAARS on 2016 January 21.Since Knight et al. 2016 detected its cometary tail when the object close to sun(r=1.018au). It was classified into a Jupiter Family Comets. It can be regarded as a bare nucleus invisible coma because very weak comet activity that is different from general comet. There is a remarkable similarity between the orbits of 252P/LINEAR (a=3.05au, e=0.67, i=10.4deg) and P/2016 BA14. Jupiter Tisserand parameter is 252P/LINEAR and that of P/2016 BA14 are 2.82. P/2016 BA14 and 252P/LINEAR is division comet that is originally same comet (Jian-Yang.2017).

In this study, surface reflection properties of P/2016 BA14 classify D-type asteroids (Bus-DeMeo taxonomy) from result of visible spectroscopy (435-820nm). Color of surface is little red as D-type asteroid, but very blue as comet nucleus from result of BVRI photometry. The linear polarization Pr=10.46.±0.11% (α=46°) is in close accord with that of D-type asteroids and comet nucleus.

Keywords: P/2016 BA14, Photometric, Spectroscopic, Polarimetric, D-type

©2019. Japan Geoscience Union. All Right Reserved.

Polycyclic aromatic hydrocarbons and aliphatic hydrocarbons in Jbilet Winselwan carbonaceous chondrite : Attempt to evaluate the thermal metamorphism degree on the parent body

Hiroki Kato[1], *Hikaru Yabuta[1]

1. Hiroshima University, Department of Earth and Planetary Systems Science

Introduction: On June 27, 2018, Hayabusa2 spacecraft arrived at the C-type asteroid Ryugu. The surface of Ryugu has been thought to have experienced dehydration at least partially, according to the grand-based observation (Vilas et al. 2008; Hiroi et al. 1993). Therefore, it is important to investigate the chemical compositions of dehydrated carbonaceous CM chondrites for understanding the surface process of asteroid Ryugu. Although the extents of thermal metamorphism of CM chondrites have been evaluated by mineralogical compositions (e.g., Nakamura et al. 2006) and elemental and molecular compositions of insoluble organic matter (IOM) (e.g., Naraoka et al. 2004; Yabuta et al. 2005), the estimated temperature varies widely. On the other hand, soluble organic molecules from the dehydrated CM chondrites have not been quantified or below detection (e.g. Shimoyama et al. 1989), and there has been no study which evaluated thermal metamorphism based on the compositions of soluble organic molecules. Therefore, in this study, we analyzed aliphatic hydrocarbons and polycyclic aromatic hydrocarbons (PAHs) in Jbilet Winselwan CM chondrite, which is a dehydrated CM chondrite (Zolensky et al 2016) and show similar reflectance spectrum to that of asteroid Ryugu (Kameda et al. 2015), for precise evaluation of parent body thermal metamorphism. The relative abundances of the hydrocarbons were compared with those of Murray meteorite, which is a primitive CM chondrite.

Samples and Methods: Powdered samples of Jbilet Winselwan meteorite and Murray meteorite (0.2 - 0.4g) were extracted with dichloromethane/methanol (9:1) by sonication. The extracts were applied to a silica gel column. From the column, aliphatic hydrocarbons were eluated with hexane and then PAHs were eluated with dichloromethane. The hexane and dichloromethane eluates were concentrated to 100 μl individually under a nitrogen flow for analysis by a gas chromatography coupled with mass spectrometry (GC-MS). Identification and quantification of compounds were made by comparison of peak retention times on mass chromatograms and mass spectra, and peak areas, respectively, with those of standard compounds. For compounds without standard compounds, identification was made by comparison of mass spectra with library data.

Results and discussion: Total concentration of *n*-alkanes from Jbilet Winselwan meteorite (1.85 μg/g meteorite) was 40 times lower than those from Murray meteorite (80.7 μg/g meteorite). Relative abundances of short-chain *n*-alkanes (C_{15}-C_{16}) were dominant in Jbilet Winselwan meteorite, while those of long-chain *n*-alkanes (C_{17}-C_{21}) were dominant in Murray meteorite. This difference implies that short-chain *n*-alkanes were resulted from cracking of long-chain *n*-alkanes and/or IOM during thermal metamorphism of the parent body of Jbilet Winselwan meteorite. Total concentration of PAHs from Jbilet Winselwan meteorite (0.05 μg/ meteorite) was 1000 times lower than those from Murray meteorite (62.0 μg/g meteorite). Dimethylnaphthalene, fluorine, phenanthrene, pyrene, fluoranthene, methylbiphenyl (0.003-0.039 μg/g meteorite) were identified, while low molecular weight PAHs, such as naphthalene, methylnaphthalene, and acenaphthene, were not detected. The results suggest that PAHs with high volatility in Jbilet Winselwan meteorite were lost or involved in further aromatization during thermal metamorphism. Distributions of dimethylnaphthalene and methylbiphenyl isomers in Jbilet Winselwan

©2019. Japan Geoscience Union. All Right Reserved.

and Murray meteorites were similar, respectively, which indicates that the parent body of Jbilet Winselwan meteorite experienced relatively mild thermal metamorphism.

Keywords: Jbilet Winselwan meteorite, Soluble organic molecules, Dehydration

©2019. Japan Geoscience Union. All Right Reserved.

Disk-Resolved Photometry Analysis of the Asteroid Ryugu Images Obtained by Hayabusa2 Visible Camera ONC

*yokota yasuhiro[1,2], Rie Honda[1], ERI TATSUMI[3], Deborah Domingue[4], Stefanus E. Schroeder[5], Moe Matsuoka[2], Seiji Sugita[3], Tomokatsu Morota[6], Shingo Kameda[7], Toru Kouyama[8], Hidehiko Suzuki[9], Manabu Yamada[10], Naoya Sakatani[2], Chikatoshi Honda[11], Masahiko Hayakawa[2], Kazuo Yoshioka[3], Yuichiro Cho[3], Hirotaka Sawada[2]

1. Kochi University, 2. ISAS/JAXA, 3. Univ. of Tokyo, 4. Planetary Science Institute, 5. DLR, 6. Nagoya Univ., 7. Rikkyo Univ., 8. AIST, 9. Meiji Univ., 10. Chiba Institute od Technology, 11. Aizu Univ.

Since June 2018, the Optical Navigation Camera (ONC) onboard Hayabusa2, has observed the C-type asteroid 162173 Ryugu at a distance below 20 km. ONC-T and ONC-W1 are used for surface imaging operations, and their images allow us to investigate the disk-resolved photometric properties of the surface. A narrow-angle camera ONC-T has 7 broad-band filters ranging in wavelength from 0.39–0.95 μm. ONC-W1 is a wide-angle (> 65˚) pan-chromatic camera mainly used for optical navigation during cruise and low-altitude (< 20km) operations. We are proceeding the analysis of both dataset, ONC-T and ONC-W1.

Since Hayabusa2’s position is nominally fixed on the line connecting Ryugu and the Earth, the available solar phase angle range by ONC-T changes seasonally with the orbits of Earth and Ryugu around the sun. Therefore, we are collecting a large number of ONC-T images over a long period of time to cover a wide phase angle range.

ONC-W1 data has a strong point that it covers a wide phase angle range within a single frame during the descent operations, because of its wide field of view. One of our current challenges is deriving a precise viewing geometries (incidence angle, emission angle, and phase angle) at each pixel. Additionally, comparison of the absolute brightness value (radiance factor) with ONC-T is an ongoing issue.

Keywords: Asteroid, Photometry, Ryugu, Hayabusa2

©2019. Japan Geoscience Union. All Right Reserved.

[E] Poster | P (Space and Planetary Sciences)：P-PS Planetary Sciences

Wed. May 29, 2019 5:15 PM - 6:30 PM JST | Wed. May 29, 2019 8:15 AM - 9:30 AM UTC | Poster Hall International Exhibition Hall8, Makuhari Messe_3

[P-PS03] Solar System Small Bodies: A New Frontier Arising Hayabusa 2, OSIRIS-REx and Other Projects

convener:Masateru Ishiguro(Department of Physics and Astronomy, Seoul National University), Taishi Nakamoto(Tokyo Institute of Technology), Masanao Abe(Institute of Space and Astronautical Science, Japan Aerospace Exploration Agency), Olivier S Barnouin(Johns Hopkins University Applied Physics Laboratory)

In June 2018, the Hayabusa 2 spacecraft arrived at the target asteroid Ryugu after three and half years journey. In addition, another spacecraft, OSIRIS-REx will soon arrive at its destination Bennu. With these arrivals, the solar system research is about to enter a new era. We have organized this small bodies session since 2012 and had a broad range of discussions from viewpoints of laboratory experiments, observations, space explorations, theoretical modeling, and sample analyses. In particular, this time, we aim to hold this session to bring the latest research on solar system small bodies, focusing on the initial results of Hayabusa 2 and OSIRIS-REx. Presentations in the related fields other than these two asteroidal missions are also welcomed.

[PPS03-P01] Impact experiments on low strength coarse-grained regolith simulating surface materials on asteroid Ryugu

*Yuya Yamamoto[1], Masahiko Arakawa[1], Minami Yasui[1], Sunao Hasegawa[2], Ryo Sugimura[1] (1.Graduate School of Science, Kobe University, 2.ISAS, JAXA)

[PPS03-P02] Reflectance estimation of asteroid Ryugu using MASCOT

*Marika Ishida[1], Koto Amano[1], Keiichi Moroi[1], ERI TATSUMI[2], Tra-Mi Ho[10], Shingo Kameda[1], Seiji Sugita[2], Rie Honda[3], Tomokatsu Morota[4], yokota yasuhiro[5], Toru Kouyama[6], Hidehiko Suzuki[7], Manabu Yamada[8], Naoya Sakatani[5], Chikatoshi Honda[9], Masahiko Hayakawa[5], Kazuo Yoshioka[2], Moe Matsuoka[5], Yuichiro Cho[2], Hirotaka Sawada[5] (1.Rikkyo Univ., 2.Univ. of Tokyo, 3.Kochi Univ., 4.Nagoya Univ., 5.JAXA/ISAS, 6.AIST, 7.Meiji Univ., 8.Chiba Inst. Tech, 9.Univ. of Aizu, 10.DLR)

[PPS03-P03] Flyby observation of Asteroid (3200) Phaethon by DESTINY$^+$ onboard cameras

*Ko Ishibashi[1], Shingo Kameda[2], Masato Kagitani[3], Peng Hong[1], Manabu Yamada[1], Osamu Okudaira[1], Tomoko Arai[1], Fumi Yoshida[1], Shunsuke Sato[4], Takahiro Ishimaru[4], Takaya Okamoto[4], Takahiro Iwata[4], Tatsuaki Okada[4], Takeshi Takashima[4] (1.Chiba Institute of Technology, 2.Rikkyo University, 3.Tohoku Universtiy, 4.Japan Aerospace Exploration Agency)

[PPS03-P04] Polarimetric Study of Asteroids in Comet-Like Orbits (ACOs)

*Jooyeon Geem[1], Masateru Ishiguro[1], Yoonsoo P. Bach[1], Daisuke Kuroda[2], Hiroyuki Naito[3], Hidekazu Hanayama[4], yoonyoung kim[10], Yuna G. Kwon[1], Sunho Jin[1], Tomohiko Sekiguchi[5], Ryo Okazaki[5], Jeremie J. Vaubaillon[6], Masataka Imai[7], Tatsuharu Oono[8], Yuki Futamuts[8], Seiko Takagi[8], Mitsuteru Sato[8], Kiyoshi Kuramoto[8], Makoto Watanabe[9] (1.Astronomy program, Dept of Physics and Astronomy, Seoul National University, 2.Okayama Observatory, Kyoto University, 3.Nayoro Observatory, 4.Ishigakijima Astronomical Observatory, National Astronomical Observatory of Japan, 5.Hokkaido University of Education, 6.Observatoire de Paris, I.M.C.C.E., 7.National Institute of Advanced Industrial Science and Technology, 8.Department of Cosmosciences, Graduate School of Science, Hokkaido University, 9.Department of Applied Physics, Okayama University of Science, 10.Max Planck Institute for Solar System Research)

[PPS03-P05] Dynamical lifetime of the Oort Cloud new comets under planetary perturbation

*Ito Takashi[1], Arika Higuchi[1] (1.National Astronomical Observatory of Japan)

[PPS03-P06] Thermal Infrared Imaging of C-type Asteroid 162173 Ryugu with Porous Surfaces

*Tatsuaki Okada[1,2], Tetsuya Fukuhara[3], Satoshi Tanaka[1], Makoto Taguchi[3], Takehiko Arai[4], Naoya Sakatani[1], Yuri Shimaki[1], Hiroki Senshu[5], Yoshiko Ogawa[6], Hirohide Demura[6], Kentaro Suko[6], Kohei Kitazato[6], Toru Kouyama[7], Tomohiko Sekiguchi[8], Jun Takita[9], Sunao Hasegawa[1], Tsuneo Matsunaga[10], Takehiko Wada[1], Takeshi Imamura[2], Jorn Helbert[11], Thomas G. Mueller[12], Axel Hagermann[13], Jens Biele[11], Matthias Grott[11], Maximiliam Hamm[11], Marco Delbo[14], Yukio Yamamoto[1], Naru Hirata[6], Naoyuki Hirata[15], Fuyuto Terui[1], Takanao Saiki[1], Satoru Nakazawa[1], Makoto Yoshikawa[1], Sei-ichiro WATANABE[1,16], Yuichi Tuda[1] (1.Institute of Space and Astronautical Science, Japan Aerospace Exploration Agency, 2.University of Tokyo, 3.Rikkyo University, 4.Ashikaga University, 5.Chiba Institute of Technology, 6.University of Aizu, 7.National Institute of Advanced Industrial Science and Technology, 8.Hokkaido University of Education, 9.Hokkaido Kitami-Hokuto High School, 10.National Institute for Environmental Studies, 11.German Aerospace Center, 12.Max-Planck Institute for Extraterrestrial Physics, 13.University of Stirling, 14.Observatoire de la Côte d'Azur, 15.Kobe University, 16.Nagoya University)

[PPS03-P07] Data Release of Asteroid 162173 Ryugu by Observation of Thermal Infrared Imager onboard Hayabusa2

*Takehiko Arai[1], Hirohide Demura[2], Toru Kouyama[7], Naoya Sakatani[3], Kentaro Suko[2], Yuri Shimaki[3], Hiroki Senshu[5], Tomohiko Sekiguchi[6], Yoshiko Ogawa[2], Sunao Hasegawa[3], Takehiko Wada[3], Takeshi Imamura[10], Tsuneo Matsunaga[9], Jun Takita[8], Kohei Kitazato[2], Makoto Taguchi[4], Tetsuya Fukuhara[4], Satoshi Tanaka[3], Tatsuaki Okada[3] (1.Ashikaga University, 2.The University of Aizu, 3.Japan Aerospace Exploration Agency (JAXA), 4.Rikkyo University, 5.Chiba Institute of Technology, 6.Hokkaido University of Education, 7.National Institute of Advanced Industrial Science and Technology (AIST), 8.Hokkaido Kitami Hokuto High School, 9.National Institute for Environmental Studies (NIES), 10.The University of Tokyo)

[PPS03-P08] Multi-mission capability of HARMONICS

*Shintaro Tsunoda[1], Hirohide Demura[1], Naru Hirata[1] (1.The University of Aizu)

[PPS03-P09] New interface of verification for calibration and conversion in HEAT : Hayabusa2 Exploration Assistant for TIR

*Tatsuro Kobayashi[1], Kentaro Suko[1], Hirohide Demura[1], Yoshiko Ogawa[1], Takehiko Arai[2], Naoya Sakatani[3], Tatsuaki Okada[3], Satoshi Tanaka[3], Tetsuya Fukuhara[4] (1.The University of Aizu, 2.Ashikaga University, 3.Institute of Space and Astronautical Science, Japan Aerospace Exploration Agency, 4.Rikkyo University)

[PPS03-P10] **Dust particle evolution of a near-Earth object 252P/LINEAR from near-infrared polarimetric observations in 2016**

*Yuna G Kwon[1], Masateru Ishiguro[1], Jungmi Kwon[2], Daisuke Kuroda[3], Myungshin Im[1], Changsu Choi[1], Motohide Tamura[4], Takahiro Nagayama[5], Nobuyuki Kawai[6], Jun-ichi Watanabe[7] (1.Seoul National Univ., 2.ISAS/Japan Aerospace Exploration Agency, 3.Okayama Astrophysical Observatory, 4.The Univ. of Tokyo, 5.Kagoshima Univ., 6.Tokyo Institute of Technology, 7.National Astronomical Observatory of Japan)

[PPS03-P11] **Performance Evaluation of TRIPOL on the 61-cm Telescope at Seoul National University for Polarimetric Observations of Solar System Small Bodies**

*Sunho Jin[1], Masateru Ishiguro[1], Yuna G Kwon[1], Jooyeon Geem[1], Yoonsoo P. Bach[1], Jinguk Seo[1], Hiroshi Sasago[2], Shuji Sato[3] (1.Seoul National University, 2.Sasago Co.,Ltd, 3.Nagoya University)

[PPS03-P12] Smart Interface of HEAT: Hayabusa2 Exploration Assistant for TIR

*Kentaro Suko[1], Tatsuro Kobayashi[1], Hirohide Demura[1], Takehiko Arai[2], Naoya Sakatani[3], Tatsuaki Okada[3], Satoshi Tanaka[3], Tetsuya Fukuhara[4] (1.The University of Aizu, 2.Ashikaga University, 3.Institute of Space and Astronautical Science, Japan Aerospace Exploration Agency, 4.Rikkyo University)

[PPS03-P13] Experimental Study on Collision Crater Formed on Bulge Geography

*Yusaku Yokota[1], Yuya Yamamoto[2], Minami Yasui[2], Masahiko Arakawa[2] (1.Faculty of Science, Kobe University, 2.Graduate School of Science, Kobe University)

[PPS03-P14] Initial analysis plan of soluble organic compounds for the Hayabusa2 sample from asteroid Ryugu

*Hiroshi Naraoka[1], Yoshinori Takano[2], Jason P. Dworkin[3], SOM Analysis Team (1.Department of Earth and Planetary Sciences, Research Center for Planetary Trace Organic Compounds, Kyushu University, 2.Japan Agency for Marine-Earth Science and Technology, 3.Astrochemistry Laboratory NASA Goddard Space Flight Center, Greenbelt, MD 20771 USA)

[PPS03-P15] Radar and optical simultaneous observations of faint meteors with MU radar and Tomo-e Gozen

*Ryou Ohsawa[1], Akira Hirota[2], Shinsuke Abe[2], Daniel Kastinen[3], Kero Johan[3], yasunori Fujiwara[4], Takuji Nakamura[5], Shigeyuki Sako[1], Yuto Kojima[1], Jun-ichi Watanabe[6] (1.Institute of Astronomy, Graduate School of Science, The University of Tokyo, 2.Department of Aerospace Engineering, College of Science & Technology, Nihon University, 3.Swedish Institute of Space Physics, 4.SOKENDAI (The Graduate University for Advanced Studies), 5.National Institute of Polar Research, 6.National Astronomical Observatory of Japan)

[PPS03-P16] Global distribution and spectral characteristics of bright spots on asteroid Ryugu

*Masanori Suemitsu[1], Tomokatsu Morota[1], Rie Honda[2], Singo Kameda[15], Eri Tatsumi[3], Manabu Yamada[4], Naoya Sakatani[5], Toru Kouyama[6], Yokota Yasuhiro[7], Yuichiro Cho[8], Hidehiko Suzuki[9], Masahiko Hayakawa[10], Moe Matsuoka[10], Chikatoshi Honda[11], Tatsuhiro Michikami[12], Kazuo Yoshioka[13], Kazunori Ogawa[14], Hirotaka Sawada[5], Seiji Sugita[3] (1.Graduate School of Environmental Studies, Nagoya University, 2.Department of Science and Technology, System of Natural Science, Kochi Unicversity, 3.Graduate School of Earth and Planetary Science, Tokyo Unicversity, 4.Planetary Exploration Reserch Center, Chiba Institute of Technology, 5.Institute of Space and Astoronautical Science, Japan Aerospace Exploration Agency, 6.National Institute of Advanced Industrial Science and Technology, 7.Kochi University, 8.Department of Earth and Planetary Science, Tokyo University, 9.Depertment of physics, Meiji University , 10.Department of Solar System Science, Institute of Space and Astoronautical Science, Japan Aerospace Exploration Agency, 11.Aizu University, 12.Faculty of Engineering, Kindai University, 13.Graduate School of frontier Science, Tokyo University, 14.Kobe University, 15.Rikkyo University)

[PPS03-P17] Polarimetry of (155140) 2005 UD: the Dynamical Association with (3200) Phaethon

*Masateru Ishiguro[1], Jooyeon Geem[1], Hiroyuki Naito[2], Yoonsoo P. Bach[1], Daisuke Kuroda[3], Tatsuharu Ono[4], Seiko Takagi[4], Mitsuteru Sato[4], Kiyoshi Kuramoto[4], Tomohiko Sekiguchi[5], Masataka Imai[6], Makoto Watanabe[7], Katsuhito Ohtsuka[8], Sunao Hasegawa[9], Takashi Ito[10], Fumi Yoshida[11], Tomoko Arai[11] (1.Department of Physics and Astronomy, Seoul National University, 2.Nayoro Observatory, 3.Okayama Observatory, Kyoto University, 4.Department of Cosmosciences, Graduate School of Science, Hokkaido University, 5.Hokkaido University of Education, 6.National Institute of Advanced Industrial Science and Technology, 7.Department of Applied Physics, Okayama University of Science, 8.Tokyo Meteor Network, 9.Japan Aerospace Exploration Agency, 10.National Astronomical Observatory of Japan, 11.Planetary Exploration Research Center, Chiba Institute of Technology)

[PPS03-P18] **Follow-up observations for AKARI/IRC near-infrared asteroid spectroscopic survey (AcuA-spec)**

*Sunao Hasegawa[1], Daisuke KURODA[2], Kenshi YANAGISAWA[3], Fumihiko Usui[4] (1.Japan Aerospace Exploration Agency, 2.Kyoto University, 3.National Astronomical Observatory of Japan, 4.Kobe University)

[PPS03-P19] Amino acids on witness coupons collected from the ISAS/JAXA curation facility for the assessment and quality control of the Hayabusa2 sampling procedure

*Haruna Sugahara[1,2], Yoshinori Takano[1], Yuzuru Karouji[3], Kazuya Kumagai[4], Toru Yada[3], Naohiko Ohkouchi[1], Masanao Abe[3], Hayabusa2 project team (1.Japan Agency for Marine-Earth Science and Technology (JAMSTEC), 2. Institut de Chimie de Nice, Universite Cote dAzur, 3.Japan Aerospace Exploration Agency (JAXA), 4.Marine Works Japan Ltd.)

[PPS03-P20] Hayabusa2 orbit determination using c5++ software

*Keiko Yamamoto[1], Toshimichi Otsubo[2], Koji Matsumoto[1], Hirotomo Noda[1], Noriyuki Namiki[1], Hiroki Senshu[3], Takahide Mizuno[4], Naoko Ogawa[4], Go Ono[4], Yuya Mimasu[4], Kent Yoshikawa[4], Tadateru Takahashi[4], Yuto Takei[4], Atsushi Fujii[4], Fuyuto Terui[4], Takanao Saiki[4], Satoru Nakazawa[4], Makoto Yoshikawa[4], Yuichi Tsuda[4] (1.National Astronomical Observatory of Japan, 2.Hitotsubashi University, 3.Chiba Institute of Technology, 4.Japan Aerospace Exploration Agency)

[PPS03-P21] **Landing Site Selection for Hayabusa2: Scientific Evaluation of the Candidate Sites on Asteroid (162173) Ryugu**

*Hikaru Yabuta[1], Sei-ichiro WATANABE[2], Tomoki Nakamura[3], Naru Hirata[4], Seiji Sugita[5], Tatsuaki Okada[6], Kohei Kitazato[4], Yoshiaki Ishihara[7], Tomokatsu Morota[2], Naoya Sakatani[6], Koji Matsumoto[8], Koji Wada[9], Shogo Tachibana[5], Mutsumi Komatsu[10], ERI TATSUMI[5], Moe Matsuoka[6], Chikatoshi Honda[4], Takahiro Hiroi[11], Hiroki Senshu[9], Rie Honda[12], Yasuhiro Yokota[6], Rina Noguchi[6], Yuri Shimaki[6], Deborah Lorin Domingue[13], Lucille Le Corre[13], Antonella Barucci[14], Ernest Palomba[15], Shota Kikuchi[6], Akira Miura[6], Tomohiro Yamaguchi[6], Yukio Yamamoto[6], Takanao Saiki[6], Satoshi Tanaka[6], Makoto Yoshikawa[6], Yuichi Tsuda[6] (1.Hiroshima University, Department of Earth and Planetary Systems Science, 2.Nagoya University, 3.Tohoku University, 4.University of Aizu, 5.The University of Tokyo, 6.ISAS/JAXA, 7.NIES, 8.NAOJ, 9.Chiba Institute of Technology, Planetary Exploration Research Center (PERC), 10.Sokendai, 11.Brown University, 12.Kochi University, 13.Planetary Science Institute, USA, 14.Observatoire Paris-Site de Meudon, LESIA, France, 15.INAF-IAPS, Italy.)

[PPS03-P22] Visible Photometric, Spectroscopic and Polarimetric observations of an inactive comet, P/2016 BA14 with the 1.6m Pirka Telescope

*Ryo Yamagata[1], Tomohiko Sekiguchi[1], Ryo Okazaki[1], Kazuya Doi[1], Daisuke Kuroda[2], Masateru Ishiguro[3], Hiroyuki Naito[4] (1.Hokkaido University of Education, 2.Kyoto University, 3.Seoul National University, 4.Nayoro Observatory)

[PPS03-P23] **Polycyclic aromatic hydrocarbons and aliphatic hydrocarbons in Jbilet Winselwan carbonaceous chondrite : Attempt to evaluate the thermal metamorphism degree on the parent body**

Hiroki Kato[1], *Hikaru Yabuta[1] (1.Hiroshima University, Department of Earth and Planetary Systems Science)

[PPS03-P24] Disk-Resolved Photometry Analysis of the Asteroid Ryugu Images Obtained by Hayabusa2 Visible Camera ONC

*yokota yasuhiro[1,2], Rie Honda[1], ERI TATSUMI[3], Deborah Domingue[4], Stefanus E. Schroeder[5], Moe Matsuoka[2], Seiji Sugita[3], Tomokatsu Morota[6], Shingo Kameda[7], Toru Kouyama[8], Hidehiko Suzuki[9], Manabu Yamada[10], Naoya Sakatani[2], Chikatoshi Honda[11], Masahiko Hayakawa[2], Kazuo Yoshioka[3], Yuichiro Cho[3], Hirotaka Sawada[2] (1.Kochi University, 2.ISAS/JAXA, 3.Univ. of Tokyo, 4.Planetary Science Institute, 5.DLR, 6.Nagoya Univ., 7.Rikkyo Univ., 8.AIST, 9.Meiji Univ., 10.Chiba Institute od Technology, 11.Aizu Univ.)

Impact experiments on low strength coarse-grained regolith simulating surface materials on asteroid Ryugu

*Yuya Yamamoto[1], Masahiko Arakawa[1], Minami Yasui[1], Sunao Hasegawa[2], Ryo Sugimura[1]

1. Graduate School of Science, Kobe University, 2. ISAS, JAXA

Impact cratering is one of the most important physical processes, then we study crater scaling laws and impact induced seismic waves in order to elucidate various flow processes on asteroids caused by impacts. The conventional crater scaling laws are categorized into two regions according to the controlling physics for the crater growth: they are gravity and material strength. A crater formed on regolith layer is surely controlled by the gravity, however when the regolith layer was filled with coarse particles with low mechanical strength, then the several coarse grains might be disrupted to consume the Ek. Thus, the crater size could be affected by the disruptions of the coarse grains. We speculate that not only the gravity but also the grain strength could affect the final crater size. Then, we made cratering experiments by using the target made of weak particles, and studied the effects of the particle strength on the crater scaling law and the impact induced seismic wave.

Experiments: Cratering experiments were conducted by using a gas gun set at Kobe University and ISAS. Granular targets were prepared by using weathered tuff granules with the size of 1 to 4mm (small particle) and the size of 1 to 4cm (large particle). The crush strength of these tuff particles was measured to be about 60 kPa. A spherical projectile with the size of 3mm which is made of iron, zirconia, alumina, glass, and nylon) was lunched at the impact velocity from 40 to 200m/s, and a spherical Al projectile with the size of 2mm was impacted at the impact velocity from 1.2 to 4.5km/s, then these two types of the projectile were impacted on the target surface at the normal direction. Impact cratering process and ejecta curtain growth were observed by a high-speed camera at 10^3-10^5 fps, and the video images were used to analyze ejecta particles to reconstruct the trajectories. After the shot, the crater morphology was recorded and the diameter and the depth were measured. Impact induced seismic waves were measured by using 3 accelerometers (specific frequency is 30kHz) set at different positions from the impact point, and a data logger was used to record the seismic data through charge amplifiers (data acquisition rate is 100kHz) connecting to the accelerometer.

Results: The crater size was found to increase with the projectile kinetic energy (Ek) at lower than 0.14J and at higher than 0.63J, so that the crater size was almost constant among them, and more the crater size obtained at very high Ek was almost on the extrapolated line from the relationship given by the low Ek data. The pi-scaling law was used to construct the relationship between normalized radius (πR) and normalized gravity (π2), and πR at small π2 was found to be rather smaller than that obtained for sand and glass beads targets, and more πR at large π2 was found to be consistent with that for sand and glass beads. More detail analysis tells us that all the data separated into two trends with large offset according to the impact velocity and the projectile material. This offset might be caused by the disruption of several tuff particles. The ejection velocities of each tuff particle were so scattered, then the distinctive relationship between initial position of particle and the ejection velocity was not derived in the low velocity range. The propagation velocity of the impact induced seismic wave was about 30 m/s, and it is 1/3 of that for glass beads. Furthermore, we found that the relationship between the maximum acceleration and the distance from the impact point was about 1/10 of that obtained for glass beads: the seismic wave in the tuff granules attenuated so quickly compared to the glass beads. But, when the distance is normalized by the crater radius, these relationships almost consistent each other, so that the

©2019. Japan Geoscience Union. All Right Reserved.

normalized distance could be a good parameter for the scaling of the acceleration of seismic wave.

Keywords: impact cratering experiment, low strength, impact-induced seismic shaking, crater scaling law

©2019. Japan Geoscience Union. All Right Reserved.

Reflectance estimation of asteroid Ryugu using MASCOT

*Marika Ishida[1], Koto Amano[1], Keiichi Moroi[1], ERI TATSUMI[2], Tra-Mi Ho[10], Shingo Kameda[1], Seiji Sugita[2], Rie Honda[3], Tomokatsu Morota[4], yokota yasuhiro[5], Toru Kouyama[6], Hidehiko Suzuki[7], Manabu Yamada[8], Naoya Sakatani[5], Chikatoshi Honda[9], Masahiko Hayakawa[5], Kazuo Yoshioka[2], Moe Matsuoka[5], Yuichiro Cho[2], Hirotaka Sawada[5]

1. Rikkyo Univ., 2. Univ. of Tokyo, 3. Kochi Univ., 4. Nagoya Univ., 5. JAXA/ISAS, 6. AIST, 7. Meiji Univ., 8. Chiba Inst. Tech, 9. Univ. of Aizu, 10. DLR

Hayabusa2 is a sample-return mission for the C-type asteroid 162173 Ryugu. Hayabusa2 arrived at Ryugu on 27 June 2018, and various observations are still being conducted. Hayabusa2 performs multiband spectral observation by employing the optical navigation camera telescope (ONC-T)and can thereby obtain spectral map of Ryugu, which enables the study of material distribution and degree of space weathering of Ryugu. However, the sensitivity of ONC-T has been previously calibrated by incorporating the inflight data of stars with significant uncertainty. Hence, the authors aim to estimate the reflectance of Ryugu by employing Mobile Asteroid Surface Scout (MASCOT).
MASCOT comprises four instruments (MASCAM, MicrOmega, MARA, and MASMAG) that are employed for analyzing the soil of Ryugu. The upper side of the MASCOT landeris coated with white paint, and its spectral image was captured by ONC-T after its release from Hayabusa2 to Ryugu. The authors conducted on-ground reflectance measurement of a white plate whose white paint is identical to that of MASCOT. Hence, the primary objective of the proposed study is to estimate the reflectance of Ryugu by comparing MASCOT’ s white side’ s spectrum captured by ONC-T with the on-ground reflectance measurement of the white plate that has identical paint as MASCOT, and thus evaluate the validity.

Keywords: Hayabusa2, ONC-T, MASCOT

©2019. Japan Geoscience Union. All Right Reserved.

Flyby observation of Asteroid (3200) Phaethon by DESTINY$^+$ onboard cameras

*Ko Ishibashi[1], Shingo Kameda[2], Masato Kagitani[3], Peng Hong[1], Manabu Yamada[1], Osamu Okudaira[1], Tomoko Arai[1], Fumi Yoshida[1], Shunsuke Sato[4], Takahiro Ishimaru[4], Takaya Okamoto[4], Takahiro Iwata[4], Tatsuaki Okada[4], Takeshi Takashima[4]

1. Chiba Institute of Technology, 2. Rikkyo University, 3. Tohoku Universtiy, 4. Japan Aerospace Exploration Agency

DESTINY$^+$ (Demonstration and Experiment of Space Technology for INterplanetary voYage, Phaethon fLy-by and dUst Science) is a mission proposed for JAXA/ISAS Epsilon class small program, currently in the pre-project phase (Phase-A) with a launch targeted for 2023. DESTINY$^+$ is a joint mission of technology demonstration and scientific observation. The near-Earth asteroid (3200) Phaethon, the flyby target, is known as a parent body of the Geminid meteor shower, the size of which is approximately 5 to 6 km in diameter.

In this mission, spatially resolved images of Phaethon will be taken by two onboard cameras, the Telescopic CAmera for Phaethon (TCAP) and the Multiband CAmera for Phaethon (MCAP) during the flyby, in order to understand the nature of a meteor shower's parent body, which is one of the sources of interplanetary dust particles that are thought to be an important transport medium of organic matter to the Earth. The spacecraft flybys Phaethon with a relative speed of 30 to 40 km/s. Despite such a high flyby speed, the cameras are required to take un-blurred images of Phaethon.

The main purposes of the DESTINY$^+$ flyby observation of Phaethon is to understand the geology of a parent body of a meteor shower, and in particular constrain the dust ejection mechanisms from active (i.e., dust-ejecting) asteroids. The specific objectives of the camera observation are taking images for (1) obtaining the light curve of Phaethon in order to estimate the rotational period, (2) measuring the outline shape of Phaeton, (3) making a 3D shape model of Phaethon, (4) observing the surface geological features of Phaethon including dust ejection features, and (5) observing the surface material distribution of Phaethon. The observations (1) to (4) will be conducted by TCAP, and (5) by MCAP.

TCAP is a telescopic panchromatic camera for high spatial resolution imaging of the surface of Phaethon and have a rotational mirror for asteroid tracking during flyby. The rotational mirror can change the direction of the line of sight from 0 deg to 180 deg. This enables to observe Phaethon throughout the flyby with wide solar phase angles, which is extremely important to image and understand the surfaces of planetary bodies because the solar phase angle affects significantly the appearance of geological features in taken images.

MCAP is a multiband camera, the wavelengths of which are 400, 480, 550, 700, 850, and 950 nm (480 and 950 nm are optional bands) and has multiple optical systems and sensors in order to take all band images simultaneously. This is because there is not enough time to take each band image in turn with changing bandpass filters using such as a filter wheel in this high speed flyby mission. MCAP does not have a tracking mirror due to the weight limitation, and the line of sight of MCAP is fixed to the spacecraft with 40 deg off the relative velocity vector of the spacecraft.

We will explain the flyby imaging sequence of DESTINY$^+$, and show the conceptual designs of TCAP and MCAP.

©2019. Japan Geoscience Union. All Right Reserved.

Keywords: Phaethon, DESTINY+, Flyby, Camera

©2019. Japan Geoscience Union. All Right Reserved.

Polarimetric Study of Asteroids in Comet-Like Orbits (ACOs)

*Jooyeon Geem[1], Masateru Ishiguro[1], Yoonsoo P. Bach[1], Daisuke Kuroda[2], Hiroyuki Naito[3], Hidekazu Hanayama[4], yoonyoung kim[10], Yuna G. Kwon[1], Sunho Jin[1], Tomohiko Sekiguchi[5], Ryo Okazaki[5], Jeremie J. Vaubaillon[6], Masataka Imai[7], Tatsuharu Oono[8], Yuki Futamuts[8], Seiko Takagi[8], Mitsuteru Sato[8], Kiyoshi Kuramoto[8], Makoto Watanabe[9]

1. Astronomy program, Dept of Physics and Astronomy, Seoul National University, 2. Okayama Observatory, Kyoto University, 3. Nayoro Observatory, 4. Ishigakijima Astronomical Observatory, National Astronomical Observatory of Japan, 5. Hokkaido University of Education, 6. Observatoire de Paris, I.M.C.C.E., 7. National Institute of Advanced Industrial Science and Technology, 8. Department of Cosmosciences, Graduate School of Science, Hokkaido University, 9. Department of Applied Physics, Okayama University of Science, 10. Max Planck Institute for Solar System Research

It is important to determine the taxonomic types of small bodies in the solar system and further to study the spatial distribution of the planetary system. Among the small bodies, it is considered that there should be dormant comets that have lost a significant fraction of volatile materials in their subsurface layers. As a result, they are unable to produce any detectable coma and recognized as asteroids. It has been challenging to find out such dormant comet population from a list of known asteroids because of the asteroidal appearances. There are several attempts to find the dormant comet nuclei from asteroidal catalogs, for example, by using their reflectance spectra or orbital elements. However, little has been studied via polarimetry.
We conduct a polarimetric study of three candidates of dormant comet nuclei, (331471) 1984 QY1, (3552) Don Quixote and (944) Hidalgo, by using the 1.6-m Pirka Telescope at the Nayoro observatory (operated by Hokkaido University, Japan). We chose these asteroids in comet-like orbits (ACOs) based on the orbital elements (i.e., the Tisserand parameter with respect to Jupiter $T_J < 3$). We found that 1984 QY1 has a polarimetric albedo (geometric albedo determined via polarimetry) $p_V = 0.16 \pm 0.06$ while both Don Quixote and Hidalgo have Rc-band polarimetric albedo $p_R < 0.05$. Based on the polarimetric result together with a dynamical analysis, we conjectured that 1984 QY1 could be an S-type asteroid transported into the current orbit via 3:1 mean motion resonance with Jupiter. From the previous spectroscopic study, Don Quixote and Hidalgo are classified into D-type taxonomic group, which are typical of comet nuclei. In this presentation, we will introduce our polarimetric observations of ACOs and emphasize that polarimetry is a powerful tool for discriminating the asteroidal and cometary origins.

Keywords: Polarimetry, Asteroid

©2019. Japan Geoscience Union. All Right Reserved.

Dynamical lifetime of the Oort Cloud new comets under planetary perturbation

*Ito Takashi[1], Arika Higuchi[1]

1. National Astronomical Observatory of Japan

Nearly isotropic comets with very long orbital period are supposed to come from the Oort Cloud. Recent observational and theoretical studies have greatly revealed the dynamical nature of this cloud and its evolutionally history, but many issues are yet to be known. Our goal is to trace the dynamical evolution of the Oort Cloud new comets (OCNCs) produced by evolving comet cloud, hopefully estimating the fraction of OCNCs embedded in the current populations of the solar system small bodies. We combine two models to follow the dynamical evolution of OCNCs beginning from their production until their ejection out of the solar system, obtaining statistics of the dynamical lifetime of OCNCs: The first model is a semi-analytical one about the OCNC production in an evolving comet cloud under the perturbation of the galactic tide and stellar encounters. The second model numerically deals with planetary perturbation over OCNCs' dynamics in planetary region. The main results of the present study are: (1) Typical dynamical lifetime of OCNCs in our models turned out to be O(10^7) years. Once entering into the planetary region, most OCNCs stay there just for this timespan, then get ejected out of the solar system on hyperbolic orbits. (2) While averaged orbital inclination of OCNCs is small, the so-called "planet barrier" works rather effectively, preventing some OCNCs from penetrating into the terrestrial planetary region.

Keywords: Oort Cloud, comet, orbital dynamics

©2019. Japan Geoscience Union. All Right Reserved.

Thermal Infrared Imaging of C-type Asteroid 162173 Ryugu with Porous Surfaces

*Tatsuaki Okada[1,2], Tetsuya Fukuhara[3], Satoshi Tanaka[1], Makoto Taguchi[3], Takehiko Arai[4], Naoya Sakatani[1], Yuri Shimaki[1], Hiroki Senshu[5], Yoshiko Ogawa[6], Hirohide Demura[6], Kentaro Suko[6], Kohei Kitazato[6], Toru Kouyama[7], Tomohiko Sekiguchi[8], Jun Takita[9], Sunao Hasegawa[1], Tsuneo Matsunaga[10], Takehiko Wada[1], Takeshi Imamura[2], Jorn Helbert[11], Thomas G. Mueller[12], Axel Hagermann[13], Jens Biele[11], Matthias Grott[11], Maximiliam Hamm[11], Marco Delbo[14], Yukio Yamamoto[1], Naru Hirata[6], Naoyuki Hirata[15], Fuyuto Terui[1], Takanao Saiki[1], Satoru Nakazawa[1], Makoto Yoshikawa[1], Sei-ichiro WATANABE[1,16], Yuichi Tuda[1]

1. Institute of Space and Astronautical Science, Japan Aerospace Exploration Agency, 2. University of Tokyo, 3. Rikkyo University, 4. Ashikaga University, 5. Chiba Institute of Technology, 6. University of Aizu, 7. National Institute of Advanced Industrial Science and Technology, 8. Hokkaido University of Education, 9. Hokkaido Kitami-Hokuto High School, 10. National Institute for Environmental Studies, 11. German Aerospace Center, 12. Max-Planck Institute for Extraterrestrial Physics, 13. University of Stirling, 14. Observatoire de la Côte d'Azur, 15. Kobe University, 16. Nagoya University

Thermal images from global to close-up scales taken by the Thermal Infrared Imager TIR [1] on Hayabusa2 [2] have revealed thermophysical properties of the C-type Near-Earth Asteroid 162173 Ryugu. On 27 June 2018, Hayabusa2 arrived at Ryugu and started remote sensing to characterize the nature of the asteroid and find the proper landing sites. *In situ* surface experiments were conducted using the robotic landers Minerva-II and Mascot [3]. *In situ* radiometry was conducted by MARA on MASCOT during a day-night cycle to derive the thermal inertia of a single boulder [4]. Ground-based observations [5] have been informed that the averaged thermal inertia of the asteroid is from 150 to 300 [tiu = J m^{-2} $s^{-0.5}$ K^{-1}] [5,6], corresponding to the surface covered with cm-sized granules.

TIR is the same design as the LIR on Akatsuki Venus climate orbiter [6], with 8 to 12 μm wavelength range, 328 x 248 effective pixels, and the FOV and IFOV of 16.7˚ x 12.7˚ and 0.051˚ per pixel, respectively. The first image of Ryugu detected by TIR was a point source on 6 June 2018, as was previously predicted [7]. Disc-resolved thermal images of Ryugu was taken from the HP on 30 June. The surface temperature was measured at 300 to 370K at about 1AU from the Sun, and gradually decreased with the solar distance. Comparison of the results with modeling [8] shows that the surface of Ryugu is not like fine regolith nor base rocks. Most of large boulders on Ryugu show temperatures almost the same as the surrounding surfaces. Diurnal temperature profiles of Ryugu are rather flatter than expected for a smooth terrain. Apparent thermal inertia is ~300 tiu or larger, but probably lower than the value when the surface roughness is considered. All these facts are consistent with a very rough and porous surface with low porosity (~35 ±10 %) [9] and the surrounding surface is dominated by porous rocks larger than several centimeters. Macro porosity should be 30 to 50 % to account for the bulk density of Ryugu ~1200 kg m^{-3}.

During the descent operations for the release of landers and the touchdowns for sample collection, TIR has taken close-up thermal images of the local sites, continually from the altitude of 500 m until the start of final descent at 10 or 20 m altitude. Close-up thermal images show the surface physical state and a variety of boulders. Most of the boulders in close-up images have temperatures similar to the surroundings but with more variety. A small number of boulders are remarkably colder than the surroundings, indicating dense rocks with lower porosity.

©2019. Japan Geoscience Union. All Right Reserved.

These facts indicate that Ryugu is probably a rubble pile of loosely-bound porous rocks, which might originate from the outer layer of parent body where compaction did not occur effectively, while the dense boulders might originate the compacted center region of parent body or from the different parent body. A different composition (e.g., organic rich materials) cannot be ruled out so far to account for such a low thermal inertia (and low density) of Ryugu.

Acknowledgments: The authors appreciate all the members of the Hayabusa2 Project and supporting staff for their technical assistance and scientific discussions. This research is partly supported by the JSPS KAKENHI No. J26287108, No. J17H06459 (Aqua Planetology), and the Core-to-Core program “International Network of Planetary Sciences”. MDB acknowledges support from CNES.

References: [1] Okada T. et al. (2017) *SSR.,* 208, 255-286. [2] Tsuda Y. et al. (2013) *Acta. Astronautica, 91* , 356-362. [3] Ho T.M. et al. (2017) *SSR.,* 208, 255-286. [4] Grott, M. et al. (2019), submitted to Nature. [5] Mueller T.G. et al. (2016) Astronon. Astrophys., doi:10.1051/0004-6361/201629143. [6] Fukuhara T. et al. (2011) *EPS,* 63, 1009-1018. [7] Okada T. et al. (2018) *PSS., 158, 46-52.* [8] Takita J., et al. SSR, 2018, 287-315. [9] Okada T. (2016) *LPSC.*, 47, #1457.

Keywords: Hayabsua2, Thermal Infrared Imager, Thermal Inertia

©2019. Japan Geoscience Union. All Right Reserved.

Data Release of Asteroid 162173 Ryugu by Observation of Thermal Infrared Imager onboard Hayabusa2

*Takehiko Arai[1], Hirohide Demura[2], Toru Kouyama[7], Naoya Sakatani[3], Kentaro Suko[2], Yuri Shimaki[3], Hiroki Senshu[5], Tomohiko Sekiguchi[6], Yoshiko Ogawa[2], Sunao Hasegawa[3], Takehiko Wada[3], Takeshi Imamura[10], Tsuneo Matsunaga[9], Jun Takita[8], Kohei Kitazato[2], Makoto Taguchi[4], Tetsuya Fukuhara[4], Satoshi Tanaka[3], Tatsuaki Okada[3]

1. Ashikaga University, 2. The University of Aizu, 3. Japan Aerospace Exploration Agency (JAXA), 4. Rikkyo University, 5. Chiba Institute of Technology, 6. Hokkaido University of Education, 7. National Institute of Advanced Industrial Science and Technology (AIST), 8. Hokkaido Kitami Hokuto High School, 9. National Institute for Environmental Studies (NIES), 10. The University of Tokyo

The thermal infrared imager (TIR) onboard the Hayabusa2 spacecraft performed thermography of the asteroid 162173 Ryugu through in-situ observations from 2018 to 2019. The primary purpose of TIR is to determine the global thermophysical properties of the asteroid and to reveal the evolutional history such as physical properties of the coalesced bodies, orbital changes due to radiation force, and the thermal evolution. This study introduces observed data of TIR and public data for scientists. The data are released by JAXA data archives (DARTS) and NASA PDS.

Keywords: Hayabusa2, Thermal Infrared Imager, Asteroid Ryugu

©2019. Japan Geoscience Union. All Right Reserved.

Multi-mission capability of HARMONICS

*Shintaro Tsunoda[1], Hirohide Demura[1], Naru Hirata[1]

1. The University of Aizu

This research has updated HARMONICS from a viewpoint of multi-mission capability, such as the Martian satellite exploration mission MMX in 2020s. Newly additional function is Switching on the shape model interface.
Bird view and visualization of FOV is important in robotics control. This technology is also used for deep space explorer missions.
HARMONICS is visualization tool of FOV(Field Of View) of scientific instruments and spacecraft’s position for HAYABUSA mission. The software has been updated by University of Aizu students of the past. The original HARMONICS had been developed by Nemoto(2006). GUI of HARMONICS had been replaced GUI library from GKT to Qt and added new functions, such as interactive modification of input mission plan by Ueno+(2017). The software had been add FOV frustum function by Aoki(2017). HARMONICS has tried to manage data for each project based on preference file in 2018.
HARMONICS should improved scalability to be compatible for ongoing mission. HARMONICS had been used to decide shutter chance by Camera Science Team in the asteroid Itokawa rendezvous of HAYABUSA. This software has not used in the asteroid Ryugu rendezvous of HAYABUSA2. The proven software should be use for future ongoing missions other than HAYABUSA. This research is development to HARMONICS adapt to ongoing missions.
I separated the designation of the data set from the source code and clarified the part edited by the user and the part edited by the developer.
HARMONICS has the function to switch and display data of different missions by this research. When users extend HARMONICS for multiple missions, users don’t need edit source code. User needs only kernel and the shape model of spacecraft and target asteroid. User do not need tough coding. User can use easily HARMONICS by editing preference file and kernel.

Keywords: Hayabusa2, Ryugu, Software, visualization

©2019. Japan Geoscience Union. All Right Reserved.

New interface of verification for calibration and conversion in HEAT : Hayabusa2 Exploration Assistant for TIR

*Tatsuro Kobayashi[1], Kentaro Suko[1], Hirohide Demura[1], Yoshiko Ogawa[1], Takehiko Arai[2], Naoya Sakatani[3], Tatsuaki Okada[3], Satoshi Tanaka[3], Tetsuya Fukuhara[4]

1. The University of Aizu, 2. Ashikaga University, 3. Institute of Space and Astronautical Science, Japan Aerospace Exploration Agency, 4. Rikkyo University

Hayabusa2 is an ongoing mission for sample return from the asteroid Ryugu.
Candidates of sampling sites are selected based on surface mapping by optical instruments such as Thermal Camera (TIR). TIR observes surface infrared radiation from the asteroid. A software package peculiar to TIR is HEAT: Hayabusa2 Exploration Assistant for TIR. The software has four functions; Database for ground tests, calibration of flight data based on the ground tests, conversion from raw data to temperature one, and analysis for verifying the calibration and conversion. The converted data products are divided into some levels: Lv1 Raw data [DN], Lv2a Temperature [K], Lv2b is Brightness [W/m2], and higher thermal model with VTK format [K]. This research implements new interface of verification for calibration and conversion based on hearing and survey for requirements from TIR science team. The environment of implementation is following tool. OS: macOS Mojave 10.14.2. Computing language: C++, OpenGL. Frameworks: Qt5.4. Tools: Fits, Qt creator, SPICE toolkit, Visualization Toolkit, QcustomPlot, Xcode10.1.

Keywords: Hayabusa2, Software, Ryugu, Calibration

©2019. Japan Geoscience Union. All Right Reserved.

Dust particle evolution of a near-Earth object 252P/LINEAR from near-infrared polarimetric observations in 2016

*Yuna G Kwon[1], Masateru Ishiguro[1], Jungmi Kwon[2], Daisuke Kuroda[3], Myungshin Im[1], Changsu Choi[1], Motohide Tamura[4], Takahiro Nagayama[5], Nobuyuki Kawai[6], Jun-ichi Watanabe[7]

1. Seoul National Univ., 2. ISAS/Japan Aerospace Exploration Agency, 3. Okayama Astrophysical Observatory, 4. The Univ. of Tokyo, 5. Kagoshima Univ., 6. Tokyo Institute of Technology, 7. National Astronomical Observatory of Japan

Comets, one of the least-altered leftovers from the early solar system, have probably preserved the primitive structure inside, whereas their surfaces become differentiated from initial states after repetitive orbital revolutions around the sun. Resurfacing makes the surface drier and more consolidated than the bulk nuclei, creating inert refractory dust layer (so-called “dust mantle”). Near-Infrared (NIR) polarimetry is theoretically expected to maximize the contrast of the porosity between inner fresh and evolved dust particles, by harboring more dust constituents in the single wavelength than the optical, and thus intensifying electromagnetic interference in dust agglomerates. Despite the advantage, only few studies have been conducted in this approach at multiple observation epochs. Herein, we present our new multi-band NIR polarimetric (1.25—2.25 microns) study of near-Earth object 252P/LINEAR over 12 days near perihelion; alongside broadband optical photometric (0.48—0.80 microns) data over four months in 2016 and a subsidiary dynamical simulation over 1000 year backward in time. 252P/LINEAR drew attention due to (1) its close approach to the Earth (~0.036 au on 2016 March 16), (2) its possible pairing to a comet P/2016 BA14 (PanSTARRS), and (3) its very low activity level despite its relatively young dynamical age. In this study, we detected two discontinuous brightness enhancements of 252P/LINEAR, particularly, the former of which accompanied a significant increase of NIR polarization degree of the comet (by ~13 % at most) with unusual blue polarimetric color. We will discuss the most probable scenario of the observed results, together with the orbital evolution of the comet and a dynamical association with its pair.

Keywords: Comet, Near-earth object, Polarimetry, Dust

©2019. Japan Geoscience Union. All Right Reserved.

Performance Evaluation of TRIPOL on the 61-cm Telescope at Seoul National University for Polarimetric Observations of Solar System Small Bodies

*Sunho Jin[1], Masateru Ishiguro[1], Yuna G Kwon[1], Jooyeon Geem[1], Yoonsoo P. Bach[1], Jinguk Seo[1], Hiroshi Sasago[2], Shuji Sato[3]

1. Seoul National University, 2. Sasago Co.,Ltd, 3. Nagoya University

Polarimetry of solar system small bodies is a powerful technique for investigating their physical properties, such as albedos, particle sizes, and porosities of these bodies. Observational opportunities arise sometimes suddenly, that is, just after unforeseeable activations of comets and discoveries of near-miss asteroids. Here, we introduce our activity to install the polarimetric instrument, TRIPOL (Triple-Range Imager and POLarimeter) on the 61-cm telescope (a Ritchey-Chretien reflector with f/7.0) at the Center for Astronomy and Space Science, Seoul National University, and report an observational result of three comets. This combination provides an 8.0’ ´8.0’ field of view and pixel resolution of 0.94” pixel^{-1}. Throughout photometric observations, we determined the limiting magnitudes (defined as magnitudes for S/N=5) of 15.17±0.06 (g’-band), 15.68±0.01 (r’-band), 16.24±0.03 (I’-band), respectively, with total 240-seconds exposure (four 60-seconds exposure images, each was taken at different rotation angle for the half-wave plate). We also found that the instrumental polarizations are negligibly small, that is, -0.32±0.04% (g’-band), -0.36±0.05% (r’-band) and -0.21±0.04% (I’-band), while the polarization efficiencies are large enough to maximize the performance, that is, 97.52±0.03% (g’-band), 98.83±0.02% (r’-band) and 99.15±0.02% (I’-band).

With this instrument, we conducted polarimetric observations of three Jupiter-family comets, 21P/Giacobini-Zinner, 38P/Stephan-Oterma, and 46P/Wirtanen on a trial basis. It is known from a recent study that the polarization degrees of cometary dust particles are significantly influenced by gas emissions [1] With multiband data taken with TRIPOL, we eliminated an influence of gas contaminations and found that the dust polarization degrees of these three comets coincide with those of so-called ‘dust-rich comets’. From this result, we conjecture that the polarimetric property of Jupiter-family comets is broadly homogeneous, unlike asteroids. We plan to describe our future plan using the polarimetric system.

[1] Kwon, Y. G. et al. Astronomical Journal, 154, 4, 173, 2017

Keywords: Comet, Instrument, Polarimetry

©2019. Japan Geoscience Union. All Right Reserved.

Smart Interface of HEAT: Hayabusa2 Exploration Assistant for TIR

*Kentaro Suko[1], Tatsuro Kobayashi[1], Hirohide Demura[1], Takehiko Arai[2], Naoya Sakatani[3], Tatsuaki Okada[3], Satoshi Tanaka[3], Tetsuya Fukuhara[4]

1. The University of Aizu, 2. Ashikaga University, 3. Institute of Space and Astronautical Science, Japan Aerospace Exploration Agency, 4. Rikkyo University

The Hayabusa2 project is a sample return mission to the asteroid Ryugu. It was launched on Dec. 3, 2014, and it has been at Ryugu since June 27, 2018. Hayabusa2 has optical instrument called Thermal Infrared Imager (TIR). These main functions are to know natures of the asteroid and to select the candidate of safe landing sites for sampling based on thermos-physical properties of the surface. TIR records infrared radiation from the target as a digital number (DN). The infrared signal is affected by sensor-surrounding objects; lens, shutter, package, and case. TIR requires consideration about this effect when converts DN images to temperature one. This study improved conversion system to increase conversion efficiency.

Hayabusa2 TIR Science Team has developed an analysis supporting tool called Hayabusa2 Exploration Assistant for TIR (HEAT). HEAT is used to search TIR data interactively, display TIR images, and visualize thermal models. We receive TIR raw images (Product Level 1) from ISAS/JAXA and convert them to brightness temperature images (Level 2a) and radiance images (Level 2b) using HEAT at Univ. of Aizu. The converted images are provided to the Hayabusa2 project data server.

This part introduces a concept model. The spectral radiance emitted from a blackbody B(λ ,T) (W s r-1m-2) is given by the Planck function based on wavelength λ (m) and temperature T(K) as follows:

$$B(\lambda,T) = (2hc2/\lambda 5)^* (1/(\exp(\lambda kBT)-1))$$

H = 6.63*1034 (m2 kg s-2 s-1) is the Planck constant, c=2.9972*108(ms-1) is the speed of light, and KB= 1.38*10-23 (m2 kg s-2K-1) is the Boltzmann constant. The observed radiance L(T) (W sr−1 m−2) is as follows:

$$L(T)= \varepsilon \int BR(\lambda)d\lambda$$

ε is the spectral thermal emissivity, and R(λ) is the response function such as the detection efficiency of the bolometer, the measured transmittance of optics including the band-pass filter and the germanium lens. The calibration formula with two regressed parameters A and B is written as follows:

$$DN=A * L(T) + B$$

The converted temperatures of the Moon were lower than expected because each pixel did not cover the sunlit area entirely or due to roughness effect of the cratered terrain. TIR has been observing Ryugu in approach and rendezvous phases. The altitudes of TIR observations during the rendezvous phase range from 20 km to less than 10 m. This study has processed about 3000 Ryugu images observed by TIR since June 2018.

©2019. Japan Geoscience Union. All Right Reserved.

This study improved conversion system. Previous conversion system converts a TIR image one by one, but current conversion system converts TIR images in selected directory at once.

Keywords: Hayabusa2, TIR, HEAT, Software

©2019. Japan Geoscience Union. All Right Reserved.

Experimental Study on Collision Crater Formed on Bulge Geography

*Yusaku Yokota[1], Yuya Yamamoto[2], Minami Yasui[2], Masahiko Arakawa[2]

1. Faculty of Science, Kobe University, 2. Graduate School of Science, Kobe University

An equatorial bulge was found on the surface of asteroid Ryugu and Bennu by recent spacecrafts of Hayabusa2 and OSIRIS-Rex, and ridge structures with various scales originated by geological activities have been recognized on icy satellites. Impact craters are dominant geological features on solid planets such as asteroids and satellites, and a crater rim are also recognized as a ridge or bulge with a circular shape. These bulges and ridges are shown to be erased with time because small scale impacts excavate and disrupt these topographies. It is well known that old craters gradually degraded by small impacts to get blurred and could be completely erased. We can expect the similar degradation process on large bulges and ridge structures, so that the life time of these structures by small impacts is a good indicator of the formation age of these structure by geologic activities. So far, the effect of small impacts on the degradation is estimated by using the results on the flat surface, but actually the surface of the bulge is curved and there is a summit on the bulge. Therefore, if we estimate the life time of the bulge structure, we should consider the effect of the topography such as a summit and curvature. Then, the impacts on the bulge structure was studied to clarify how the bulge structure affected the crater formation efficiency. In this study, we suppose the bulge made from regolith and boulders, such as an equatorial bulge of Ryugu and assume the crater formation process dominated by not the strength but the gravity.

We prepared a triangular prism target to simulate the bilge structure, and set it like that the base of this prism is rectangle, then it looks triangle when we look it at the horizontal direction, and we can look at the linear summit from the top view. Quartz sands with the size of 100μm was used to build the target and the angle of repose for this quartz sand is about 30 degree. The slope of the prism was measured from the base, and we set the angle from 20 to 30 degree. The quartz sands were filled into a transparent water tank with the depth of 20 cm to prepare the bulge structure. Impact experiments were conducted by using a vertical type gas gun, and the water tank was set in the chamber to evacuate below 1000 Pa. A alumina sphere projectile with the size of 3mm was launched at the velocity from 70 to 200 m/s, and it was impacted on the bulge in the vertical direction: the impact angle measured from the target surface was about 60 degree when the slope was 30 degree. The distance from the impact pint to the summit (deviation distance, d_d) was changed from 0 to 20mm.

We found that the crater shape strongly depended on the d_d, so the crater shape was an ellipsoid when the impact point was near the summit. Th major axis appeared along the linear summit and the minor axis appeared across the summit. The aspect ratio of the major axis to the minor axis gradually changed toward 1 with the increase of d_d. Moreover, the aspect ratio becomes large at the same d_d when the impact velocity increased. The major axis of the ellipsoid crater formed on the bulge was slightly larger than the crater diameter formed on the flat surface, and the slope angle might affect the size of the ellipsoid because we found that the crater formed on the slope of 30 degree was systematically larger than that formed on the slope of 20 degree. We also observed an asymmetric ejecta curtain from the impact point on the bulge, moreover the ejecta curtain was notice to be deformed so much at the impact point near the summit because of the effect of curvature of the bulge on the crater flow.

Angle of repose, Impact crater, Bulge and ridge structure, Ejecta curtain

©2019. Japan Geoscience Union. All Right Reserved.

©2019. Japan Geoscience Union. All Right Reserved.

Initial analysis plan of soluble organic compounds for the Hayabusa2 sample from asteroid Ryugu

*Hiroshi Naraoka[1], Yoshinori Takano[2], Jason P. Dworkin[3], SOM Analysis Team

1. Department of Earth and Planetary Sciences, Research Center for Planetary Trace Organic Compounds, Kyushu University, 2. Japan Agency for Marine-Earth Science and Technology, 3. Astrochemistry Laboratory NASA Goddard Space Flight Center, Greenbelt, MD 20771 USA

The spectra of asteroid 162173 Ryugu taken by Near-Infrared Spectrometer (NIRS3) onboard Hayabusa2 are nearly featureless and consistent with carbonaceous chondrites (Matsuoka et al., 2018). The Hayabusa2 spacecraft will collect surface samples of Ryugu and deliver to the Earth during late 2020. The initial analysis of the Ryugu samples will focus on (1) detailed chemical and mineralogical characterization of the samples and (2) understanding the history of Ryugu and the Solar System in order to maximize the scientific achievement of the project and (3) to prove the scientific potential of the samples to the community for the analytical opportunity (Tachibana et al., 2014). We have organized an international team, consisting of 24 members currently, for the initial analysis of soluble organic matter (SOM) for the returned samples.
The primitive asteroidal materials are expected to contain diverse and complex (e.g. elemental, structural, and optical) organic matter all at low concentrations. The occurrence of SOM will provide clues to the origins of organic compounds as well as prebiotic molecules of potential relevance to origins of life on Earth and possibly elsewhere in the Solar System. We propose the comprehensive SOM analyses to reveal the chemical evolution of Ryugu using high-sensitive and high-resolution analytical methods as follows:

1) High-resolution mass spectrometry (HRMS) of various solvent extracts with electrospray ionization (ESI) coupled with or without nano-liquid chromatography.
2) Enantiomerically resolved amino acid analysis using high-resolution column chromatography with high-sensitive fluorescence spectroscopy coupled with HRMS.
3) *In situ* organic compound analysis and molecular imaging using desorption electrospray ionization (DESI) and/or direct analysis in real time (DART) equipped with HRMS.
4) Spatial resolution imaging of organic compounds using time of flight-secondary ion mass spectrometry (ToF-SIMS; Naraoka et al., 2015).

In addition, if the sample is available, we will also perform the following additional analyses:

5) Compound-specific isotope analysis using gas chromatography/combustion or pyrolysis /isotope ratio mass spectrometry (GC/C or pyrolysis/IRMS).
6) Bulk chemical and isotopic analysis of organic matter (C, H, N and S) using nano-EA/IRMS system and laser-tunable FT-IR spectroscopy.

Depending to the sample size available to the initial analysis, we will perform preliminary analytical tests using 30 mg, 10 mg, and 1 mg samples of the Murchison meteorite (CM2, positive SOM-rich), Yamato 793321 meteorite (heated CM2, positive SOM-depleted), and baked serpentine (negative SOM-depleted) as well as procedural blank. The analytical protocol will be discussed in the meeting.

< References >
Tachibana, S. et al. (2014) Hayabusa2: Scientific importance of samples returned from C-type near-Earth

©2019. Japan Geoscience Union. All Right Reserved.

asteroid (162173) 1999 JU3. Geochemical Journal. 48. 571-581. 10.2343/geochemj.2.0350.
Matsuoka, M. et al. (2018) Spectral comparison between asteroid (162173) Ryugu and carbonaceous meteorites. American Astronomical Society, DPS meeting #50.
Naraoka, H. et al. (2015) ToF-SIMS analysis of carbonaceous particles in the sample catcher of the Hayabusa spacecraft. Earth, Planets and Space, 67:67. DOI 10.1186/s40623-015-0224-0.
Naraoka, H. and Hashiguchi, M. (2018) *In situ* organic compound analysis on a meteorite surface by desorption electrospray ionization coupled with an Orbitrap mass spectrometer. Rapid Commun. Mass Spectrom. 32, 959-964.

Keywords: Hayabusa2, Ryugu, Carbonaceous Asteroid, Soluble Organic Matter

©2019. Japan Geoscience Union. All Right Reserved.

Radar and optical simultaneous observations of faint meteors with MU radar and Tomo-e Gozen

*Ryou Ohsawa[1], Akira Hirota[2], Shinsuke Abe[2], Daniel Kastinen[3], Kero Johan[3], yasunori Fujiwara[4], Takuji Nakamura[5], Shigeyuki Sako[1], Yuto Kojima[1], Jun-ichi Watanabe[6]

1. Institute of Astronomy, Graduate School of Science, The University of Tokyo, 2. Department of Aerospace Engineering, College of Science & Technology, Nihon University, 3. Swedish Institute of Space Physics, 4. SOKENDAI (The Graduate University for Advanced Studies), 5. National Institute of Polar Research, 6. National Astronomical Observatory of Japan

The Earth is surrounded by small dust grains produced by comets and asteroids. Tons of such grains plunge into the Earth's atmosphere hourly. Part of their kinetic energy excites and ionizes the surrounding atmosphere, which is observed as a meteor phenomenon. A simultaneous radar and optical observation is promising to constrain the motion and mass of a meteor at a time. We launched a project to observe faint meteors with Middle and Upper Atmosphere Radar (MU radar) and a wide-field CMOS mosaic camera Tomo-e Gozen installed on the 105 cm Kiso Schmidt telescope. The observations were carried out in 18--21, April, 2018. From tons of the detected meteors, the simultaneous detections were extracted in terms of the times, loci, and directions of the meteors. Finally, we identified the 894 meteor events simultaneously detected in the both sites. The optical brightness of the simultaneous meteors ranged from about 3--11 mag. in the V-band, which is about 5 magnitude fainter than in previous studies. We confirmed a clear correlation between the meteor brightnesses and the radar cross sections.

Keywords: meteor, interplanetary dust

©2019. Japan Geoscience Union. All Right Reserved.

Global distribution and spectral characteristics of bright spots on asteroid Ryugu

*Masanori Suemitsu[1], Tomokatsu Morota[1], Rie Honda[2], Singo Kameda[15], Eri Tatsumi[3], Manabu Yamada[4], Naoya Sakatani[5], Toru Kouyama[6], Yokota Yasuhiro[7], Yuichiro Cho[8], Hidehiko Suzuki[9], Masahiko Hayakawa[10], Moe Matsuoka[10], Chikatoshi Honda[11], Tatsuhiro Michikami[12], Kazuo Yoshioka[13], Kazunori Ogawa[14], Hirotaka Sawada[5], Seiji Sugita[3]

1. Graduate School of Environmental Studies, Nagoya University, 2. Department of Science and Technology, System of Natural Science, Kochi Unicversity, 3. Graduate School of Earth and Planetary Science, Tokyo Unicversity, 4. Planetary Exploration Reserch Center, Chiba Institute of Technology, 5. Institute of Space and Astoronautical Science, Japan Aerospace Exploration Agency, 6. National Institute of Advanced Industrial Science and Technology, 7. Kochi University, 8. Department of Earth and Planetary Science, Tokyo University, 9. Depertment of physics, Meiji University , 10. Department of Solar System Science, Institute of Space and Astoronautical Science, Japan Aerospace Exploration Agency, 11. Aizu University, 12. Faculty of Engineering, Kindai University, 13. Graduate School of frontier Science, Tokyo University, 14. Kobe University, 15. Rikkyo University

On June 27, 2018, the asteroid explorer Hayabusa2 arrived at the target C-type asteroid 162173 Ryugu. The telescopic optical navigation camera (ONC-T) on-board Hayabusa2 has acquired the multiband image data for the entire surface of Ryugu with spatial resolutions better than 2 m/pixel. These data show that the Ryugu surface has the very low surface reflectance, flat spectra, and its spatial homogeneity [Sugita et al. 2019]. However, more detailed observations on Ryugu have revealed that many boulders exhibit different spectral properties and that a number of spots with distinctively brighter than the surroundings [Sugita et al. 2019]. Although larger boulders have been analyzed to show that they form two distinctive spectral trends, no substantial spectral analyses on bright spots have been conducted. Determining whether or not these bright spots are one of the materials that originate from the parent body of Ryugu is important to understand the differentiation and geologic processes on the parent body. In this study, in order to understand origins of the bright spots, we investigated spectral characteristics of the bright spots and compared those of the boulders on Ryugu. We used the ONC-T multiband images obtained in Box-A (20 km altitude) and mid-altitude (5 km altitude) operations.

We found seven meter-sized bright spots that have radiance factor 1.3 to 2.0 times higher than that of the surrounding area. The spectra of these bright spots were classified into two types, one being a flat spectrum type and another being a convex spectrum type. The former type has spectrum similar to but flatter and brighter than the mean spectra of the whole Ryugu and boulders, suggesting that the bright spots originate from parent body of Ryugu. The latter type has spectrum similar to those of S-type asteroids, suggesting their exogenous origin.

Keywords: asteroids, Ryugu, bright spot, spectrum, boulder

©2019. Japan Geoscience Union. All Right Reserved.

Polarimetry of (155140) 2005 UD: the Dynamical Association with (3200) Phaethon

*Masateru Ishiguro[1], Jooyeon Geem[1], Hiroyuki Naito[2], Yoonsoo P. Bach[1], Daisuke Kuroda[3], Tatsuharu Ono[4], Seiko Takagi[4], Mitsuteru Sato[4], Kiyoshi Kuramoto[4], Tomohiko Sekiguchi[5], Masataka Imai[6], Makoto Watanabe[7], Katsuhito Ohtsuka[8], Sunao Hasegawa[9], Takashi Ito[10], Fumi Yoshida[11], Tomoko Arai[11]

1. Department of Physics and Astronomy, Seoul National University, 2. Nayoro Observatory, 3. Okayama Observatory, Kyoto University, 4. Department of Cosmosciences, Graduate School of Science, Hokkaido University, 5. Hokkaido University of Education, 6. National Institute of Advanced Industrial Science and Technology, 7. Department of Applied Physics, Okayama University of Science, 8. Tokyo Meteor Network, 9. Japan Aerospace Exploration Agency, 10. National Astronomical Observatory of Japan, 11. Planetary Exploration Research Center, Chiba Institute of Technology

An Apollo-type near--Earth asteroid, (155140) 2005 UD, is considered as a possible fragment from (3200) Phaethon, suggesting that Phaethon precursor body might undergo a catastrophic disruption in the past. Here we present our new observational evidence for supporting these two are common origin. We thus conducted a polarimetric observation in 2018 September-October and found that 2005 UD exhibited a polarimetric property significantly different from those of major taxonomic classes of NEAs (i.e., S- and C-type) but similar to that of Phaethon at a wide range of the solar phase angles. Using the polarimetric data, we derived the geometric albedo of ~0.1. In addition, we made a photometric observation at the opposition (the zero phase angle), and determined the mean absolute magnitude of 17.2, the synodic rotational period 5.23 hr, and the effective diameter 1.5 km in combination with the derived geometric albedo. From these evidence, we found that the Phaethon precursor body might have lost more than a few percents of the mass via a disruption if 2005 UD was indeed ejected from the Phaethon precursor.

Keywords: Asteroids, Space Mission (Destiny+)

©2019. Japan Geoscience Union. All Right Reserved.

Follow-up observations for AKARI/IRC near-infrared asteroid spectroscopic survey (AcuA-spec)

*Sunao Hasegawa[1], Daisuke KURODA[2], Kenshi YANAGISAWA[3], Fumihiko Usui[4]

1. Japan Aerospace Exploration Agency, 2. Kyoto University, 3. National Astronomical Observatory of Japan, 4. Kobe University

In the range from 1 to 2.5 μm, we made the spectroscopic observations of the AcuA-spec asteroids (Hasegawa et al. 2017, PASJ, 69, 9), whose spectra were obtained in continuous covered between 2.5 and 5.0 μm by NIR/IRC/AKARI (Usui et al. 2019, PASJ, 71, 1). Candidates of AcuA-spec asteroids were selected from only main-belt asteroids classified based on visible spectrophotometric and spectroscopic observations (Tholen 1984, PhD thesis, Arizona University; Bus & Binzel 2002, Icarus, 158, 146; Lazzaro et al. 2004, Icarus, 172, 179). About 200 classified asteroids were raised as observational candidates. Spectroscopic observations for 65 AcuA-spec asteroids which were selected among the AcuA-spec candidate catalogue in taking account of signal-noise ratio and target opportunity by AKARI were executed.
Section work of the AcuA-spec candidate catalogue was done around 2005, yet there were not many spectroscopic observations of asteroids in the near-infrared wavelength range. As a result of survey of published paper for near-infrared spectroscopic observations of asteroids, howevwer, it was found that spectroscopic observations in the near-infrared region of 1–2.5 μm for most AcuA-spec asteroids are performed except for several asteroids.
If data in near-infrared wavelength range of the lacked AcuA-spec asteroids were acquired, all AcuA-spec asteroids will have 0.35–5 μm of data available. Obtaining continuous reflectance of asteroids is essential data to compare with those such as meteorites. Based on the Bus-DeMeo taxonomy (DeMeo et al. 2009, Icarus, 202, 160), we conducted classification of all AcuA-spec asteroids using published and our observational data.

Keywords: asteroids, spectroscopy

©2019. Japan Geoscience Union. All Right Reserved.

Amino acids on witness coupons collected from the ISAS/JAXA curation facility for the assessment and quality control of the Hayabusa2 sampling procedure

*Haruna Sugahara[1,2], Yoshinori Takano[1], Yuzuru Karouji[3], Kazuya Kumagai[4], Toru Yada[3], Naohiko Ohkouchi[1], Masanao Abe[3], Hayabusa2 project team

1. Japan Agency for Marine-Earth Science and Technology (JAMSTEC), 2. Institut de Chimie de Nice, Universite Cote dAzur, 3. Japan Aerospace Exploration Agency (JAXA), 4. Marine Works Japan Ltd.

The Hayabusa2 spacecraft is visiting a near-Earth carbonaceous type (C-type) asteroid, 162173 Ryugu, and planning to return the pristine samples to the Earth. C-type asteroids are considered to be related with carbonaceous chondrites that are enriched in organic and volatile materials. The one of the scientific goals of Hayabusa2 mission is to understand the origin and evolution of organic materials through interactions with water and minerals in the early solar system [e.g., 1]. Thus, the characterization of organic materials in the returned sample has great importance for this purpose. However, the analysis of small quantities of extraterrestrial organic materials in the returned samples requires a great care to avoid the introduction of terrestrial contaminants and any artifact materials to the pristine samples. Thus, the assessment of the degrees of the terrestrial contaminants to the samples as well as the comprehensive and specific managements to minimize the terrestrial contamination throughout the mission is essential.

The purpose of the study is to investigate the potential terrestrial organic contamination in a clean chamber for the Hayabusa2 returned samples in an Institute of Space and Astronautical Science/Japan Aerospace Exploration Agency (ISAS/JAXA) curation room [2-4]. As the indicator of the terrestrial organic contaminants, we selected amino acids that ubiquitously exist in the terrestrial environments and are also the target molecules in the Hayabusa2 mission. In the study, we used witness coupons made of aluminum foil to collect the contaminants in the clean chamber. The witness coupons were collected at different exposure times, ranging from 1 day to 1 month to examine the accumulation rate of the contaminants. After the collection, amino acids on the witness coupons were extracted in hot water, hydrolysed with HCl, and then converted to *N*-pivaloyl isopropyl (Pv/iPr) ester derivatives for gas chromatographic (GC) analysis [5].

On the witness coupons, eight terrestrially common amino acids (glycine, alanine, valine, leucine, isoleucine, proline, aspartic acid and glutamic acid) were detected and seven of them, except valine due to the under quantification limit, were quantified. Among them, glycine was the most abundant species with the highest concentration of 10 pmol/cm^2. A time-dependent profile of the four major amino acids (glycine, alanine, aspartic acid and glutamic acid) showed the increasing trend between 1 to 7 days. The average accumulation rates are 1.2 pmol/cm^2/day for glycine, 0.6 pmol/cm^2/day for alanine, 0.1 pmol/cm^2/day for aspartic acid and 0.2 pmol/cm^2/day for glutamic acid. The species and the concentrations of amino acids on our witness coupons are similar to those reported by the National Aeronautics and Space Administration/Johnson Space Center (NASA/JSC) OSIRIS-REx team [6]. Thus, the quality control against terrestrial contaminants in ISAS/JAXA curation facility is at the same quantitative level as in their facility. This inter-laboratory evaluation [7] about the terrestrial organic contamination will provide important information for the curation procedure of the Hayabusa2-returned samples.

©2019. Japan Geoscience Union. All Right Reserved.

References: [1] Tachibana S. et al. (2014) Geochem. J., 48, 571-587. doi: 10.2343/geochemj.2.0350. [2] Yada T. et al. (2014) Meteorit. Planet. Sci., 49, 135-153. doi: 10.1111/maps.12027. [3] Sawada H. et al. (2017) Space Sci. Rev. 208, 81–106. doi: 10.1007/s11214-017-0338-8. [4] Okazaki R. et al. (2017) Space Sci. Rev. 208, 107–124. doi: 10.1007/s11214-016-0289-5. [5] Chikaraishi Y. et al. (2010) in *Earth, Life, Isotopes*, Kyoto Univ. Press, pp.367-386. [6] Dworkin et al. (2018) Space Sci. Rev. 214, 9. doi: 10.1007/s11214-017-0439-4. [7] Sugahara et al. (2018) Earth, Planets Space, 70, 194. doi: 10.1186/s40623-018-0965-7.

Keywords: Amino acid, Hayabusa2, Curation, Witness coupons, Quality control

©2019. Japan Geoscience Union. All Right Reserved.

Hayabusa2 orbit determination using c5++ software

*Keiko Yamamoto[1], Toshimichi Otsubo[2], Koji Matsumoto[1], Hirotomo Noda[1], Noriyuki Namiki[1], Hiroki Senshu[3], Takahide Mizuno[4], Naoko Ogawa[4], Go Ono[4], Yuya Mimasu[4], Kent Yoshikawa[4], Tadateru Takahashi[4], Yuto Takei[4], Atsushi Fujii[4], Fuyuto Terui[4], Takanao Saiki[4], Satoru Nakazawa[4], Makoto Yoshikawa[4], Yuichi Tsuda[4]

1. National Astronomical Observatory of Japan, 2. Hitotsubashi University, 3. Chiba Institute of Technology, 4. Japan Aerospace Exploration Agency

Hayabusa2 arrived at the target asteroid Ryugu in June 2018 and is currently conducting remote sensing observations with various onboard instruments. So far, we have improved orbit determination software c5++, originally developed for the analysis of satellite laser ranging (SLR) data of the Earth, so that it can be used for the analysis of laser ranging data between Hayabusa2 and Ryugu obtained by Hayabusa2 LIDAR. Then we used it for the estimation of Hayabusa2 trajectory and the GM value of Ryugu. However, in the case of Hayabusa2, it is difficult to determine all of the 6 components of the initial state vector precisely if only LIDAR range data was used, and the simultaneously estimated GM value also had large uncertainty. To overcome this problem, in addition to LIDAR ranging data, we used Automated-Image-Tracking (AIT) data obtained by wide-angle optical navigation camera (ONC-W1) for the estimation of Hayabusa2 trajectory. In principle, LIDAR data gives information on the radial direction and AIT data give the ones on the across and along track directions. Thus, both data sets are complementary and help to improve the precision of the trajectory estimation. For this purpose, we improved c5 ++ so that it can deal with AIT data as observation data. In the presentation, we will show the results of trajectory and GM estimations using LIDAR and AIT data, and show how much the precision and accuracy are improved compared to the case using LIDAR data only.

Keywords: Hayabusa2, Orbit Determination, Ryugu

©2019. Japan Geoscience Union. All Right Reserved.

Landing Site Selection for Hayabusa2: Scientific Evaluation of the Candidate Sites on Asteroid (162173) Ryugu

*Hikaru Yabuta[1], Sei-ichiro WATANABE[2], Tomoki Nakamura[3], Naru Hirata[4], Seiji Sugita[5], Tatsuaki Okada[6], Kohei Kitazato[4], Yoshiaki Ishihara[7], Tomokatsu Morota[2], Naoya Sakatani[6], Koji Matsumoto[8], Koji Wada[9], Shogo Tachibana[5], Mutsumi Komatsu[10], ERI TATSUMI[5], Moe Matsuoka[6], Chikatoshi Honda[4], Takahiro Hiroi[11], Hiroki Senshu[9], Rie Honda[12], Yasuhiro Yokota[6], Rina Noguchi[6], Yuri Shimaki[6], Deborah Lorin Domingue[13], Lucille Le Corre[13], Antonella Barucci[14], Ernest Palomba[15], Shota Kikuchi[6], Akira Miura[6], Tomohiro Yamaguchi[6], Yukio Yamamoto[6], Takanao Saiki[6], Satoshi Tanaka[6], Makoto Yoshikawa[6], Yuichi Tsuda[6]

1. Hiroshima University, Department of Earth and Planetary Systems Science, 2. Nagoya University, 3. Tohoku University, 4. University of Aizu, 5. The University of Tokyo, 6. ISAS/JAXA, 7. NIES, 8. NAOJ, 9. Chiba Institute of Technology, Planetary Exploration Research Center (PERC), 10. Sokendai, 11. Brown University, 12. Kochi University, 13. Planetary Science Institute, USA, 14. Observatoire Paris-Site de Meudon, LESIA, France, 15. INAF-IAPS, Italy.

On June 27, 2018, JAXA’s Hayabusa2 spacecraft arrived at its target C-type asteroid Ryugu. Immediately after arrival, remote-sensing observations were carried out with the Optical Navigation Camera (ONC), the Near Infrared Spectrometer (NIRS3), the Thermal Infrared Imager (TIR), and the Laser Altimeter (LIDAR). Based on data from this suite of instruments, we carried out the landing site selection for the first touch-down (TD1). Since the mission aims to understand i) the origin and chemical evolution of the solar system and ii) the formation process and structure of the asteroid, we have set the most scientifically valuable TD1 site as the least altered region where water and/or carbon are potentially abundant.

Landing candidate sites were first selected by engineering evaluation for operational safety followed by scientific evaluations based on criteria such as science and samplability for the most interesting sites. The process was repeated using the observations from the altitudes of 20 km, 6 km, and 5 km.

Scientific evaluations of the landing site candidates were conducted based on the data products from ONC, NIRS3, TIR, and LIDAR. The shape modeling team produced two different shape models. ONC produced multiband images and reflectance spectra, as well as maps of spectral indices and X-means clustering analysis. Measurements of boulder size-frequency and Hapke parameters in the candidate landing areas were examined. NIRS3 produced four types of spectral feature maps. TIR provided maps of maximum temperature from the October 22, 2018 TD1 practice operations, apparent thermal inertia, and typical grain size determinations. LIDAR provided time series ranging data, topography, and corrected spacecraft trajectory.

Engineering evaluation: The possible landing site candidates were selected from the engineering safety score map evaluated based on the sub-Earth distance, local solar angle, local slope and elevation maximum difference. Thermal prediction results for TD1 were obtained by TIR. Temperatures of each site are < 350 K, confirming the safe conditions. The regions that satisfied all the conditions were, L05, L07, L08, L12, M01, M03 and M04.

Scientific evaluation:
1) Boulders. Based on the distribution of boulders with a diameter larger than 3 m for each potential landing site, regions L07, L08, and M04 show smaller percentages of boulder coverage than other areas, and are regarded as safer sites for landing.

©2019. Japan Geoscience Union. All Right Reserved.

2) Geology. Ryugu exhibits a variety of topographic features and geologic settings. From a scientific perspective, it is of interest to be able to study various materials representing the evolution of Ryugu.
3) Hydrous minerals. The NIR spectral properties are nearly homogeneous across Ryugu’ s surface, especially between the candidate sites. The near-infrared reflectance spectra of Ryugu is similar to experimentally heated Murchison meteorite at 400˚C.
4) Carbon contents. It is likely that visible reflectance at 0.55 μm (R(0.55)) is influenced mostly by carbon content. R(0.55) is almost homogeneous across the surface with a low value, regardless of the candidate sites.
5) Secondary processes. Although the surface of Ryugu is almost homogeneous at the macro scale in the map of spectral slope from 0.48 to 0.86 μm, a slight heterogeneity is observed across the candidate regions. L-regions are relatively bluish and M-regions are reddish. Considering that spectral reddening is observed by laser irradiation of dehydrated carbonaceous chondrites, L regions are probably less altered and preferable for sampling.

In the total evaluation, L08, L07 and M04 were selected as the TD1 candidates on August 17, 2018. In September 2018, many boulders > 50 cm were additionally found for the sites during the rehearsal of TD1. Thus, the originally scheduled TD1 in October was postponed. Further search for a flat and safe site continued, and L08-E1 was determined as the TD1 site. The TD1 will be scheduled on Feb 22, 2019.

Keywords: Hayabusa2, Landing Site Selection

©2019. Japan Geoscience Union. All Right Reserved.

Visible Photometric, Spectroscopic and Polarimetric observations of an inactive comet, P/2016 BA14 with the 1.6m Pirka Telescope

*Ryo Yamagata[1], Tomohiko Sekiguchi[1], Ryo Okazaki[1], Kazuya Doi[1], Daisuke Kuroda[2], Masateru Ishiguro[3], Hiroyuki Naito[4]

1. Hokkaido University of Education, 2. Kyoto University, 3. Seoul National University, 4. Nayoro Observatory

We performed photometric, spectroscopic and polarimetric observations of an inactive comet, P/2016 BA14 with the 1.6m Pirka Telescope, Hokkaido.

P/2016 BA14 (a=3.02 au, e=0.67, i=18.9 deg.) was discovered as an unusual asteroid with a cometary orbit by the PANSTAARS on 2016 January 21.Since Knight et al. 2016 detected its cometary tail when the object close to sun(r=1.018au). It was classified into a Jupiter Family Comets. It can be regarded as a bare nucleus invisible coma because very weak comet activity that is different from general comet. There is a remarkable similarity between the orbits of 252P/LINEAR (a=3.05au, e=0.67, i=10.4deg) and P/2016 BA14. Jupiter Tisserand parameter is 252P/LINEAR and that of P/2016 BA14 are 2.82. P/2016 BA14 and 252P/LINEAR is division comet that is originally same comet (Jian-Yang.2017).

In this study, surface reflection properties of P/2016 BA14 classify D-type asteroids (Bus-DeMeo taxonomy) from result of visible spectroscopy (435-820nm). Color of surface is little red as D-type asteroid, but very blue as comet nucleus from result of BVRI photometry. The linear polarization Pr=10.46.±0.11% (α=46°) is in close accord with that of D-type asteroids and comet nucleus.

Keywords: P/2016 BA14, Photometric, Spectroscopic, Polarimetric, D-type

©2019. Japan Geoscience Union. All Right Reserved.

Polycyclic aromatic hydrocarbons and aliphatic hydrocarbons in Jbilet Winselwan carbonaceous chondrite : Attempt to evaluate the thermal metamorphism degree on the parent body

Hiroki Kato[1], *Hikaru Yabuta[1]

1. Hiroshima University, Department of Earth and Planetary Systems Science

Introduction: On June 27, 2018, Hayabusa2 spacecraft arrived at the C-type asteroid Ryugu. The surface of Ryugu has been thought to have experienced dehydration at least partially, according to the grand-based observation (Vilas et al. 2008; Hiroi et al. 1993). Therefore, it is important to investigate the chemical compositions of dehydrated carbonaceous CM chondrites for understanding the surface process of asteroid Ryugu. Although the extents of thermal metamorphism of CM chondrites have been evaluated by mineralogical compositions (e.g., Nakamura et al. 2006) and elemental and molecular compositions of insoluble organic matter (IOM) (e.g., Naraoka et al. 2004; Yabuta et al. 2005), the estimated temperature varies widely. On the other hand, soluble organic molecules from the dehydrated CM chondrites have not been quantified or below detection (e.g. Shimoyama et al. 1989), and there has been no study which evaluated thermal metamorphism based on the compositions of soluble organic molecules. Therefore, in this study, we analyzed aliphatic hydrocarbons and polycyclic aromatic hydrocarbons (PAHs) in Jbilet Winselwan CM chondrite, which is a dehydrated CM chondrite (Zolensky et al 2016) and show similar reflectance spectrum to that of asteroid Ryugu (Kameda et al. 2015), for precise evaluation of parent body thermal metamorphism. The relative abundances of the hydrocarbons were compared with those of Murray meteorite, which is a primitive CM chondrite.

Samples and Methods: Powdered samples of Jbilet Winselwan meteorite and Murray meteorite (0.2 - 0.4g) were extracted with dichloromethane/methanol (9:1) by sonication. The extracts were applied to a silica gel column. From the column, aliphatic hydrocarbons were eluated with hexane and then PAHs were eluated with dichloromethane. The hexane and dichloromethane eluates were concentrated to 100 μl individually under a nitrogen flow for analysis by a gas chromatography coupled with mass spectrometry (GC-MS). Identification and quantification of compounds were made by comparison of peak retention times on mass chromatograms and mass spectra, and peak areas, respectively, with those of standard compounds. For compounds without standard compounds, identification was made by comparison of mass spectra with library data.

Results and discussion: Total concentration of *n*-alkanes from Jbilet Winselwan meteorite (1.85 μg/g meteorite) was 40 times lower than those from Murray meteorite (80.7 μg/g meteorite). Relative abundances of short-chain *n*-alkanes (C_{15}-C_{16}) were dominant in Jbilet Winselwan meteorite, while those of long-chain *n*-alkanes (C_{17}-C_{21}) were dominant in Murray meteorite. This difference implies that short-chain *n*-alkanes were resulted from cracking of long-chain *n*-alkanes and/or IOM during thermal metamorphism of the parent body of Jbilet Winselwan meteorite. Total concentration of PAHs from Jbilet Winselwan meteorite (0.05 μg/ meteorite) was 1000 times lower than those from Murray meteorite (62.0 μg/g meteorite). Dimethylnaphthalene, fluorine, phenanthrene, pyrene, fluoranthene, methylbiphenyl (0.003-0.039 μg/g meteorite) were identified, while low molecular weight PAHs, such as naphthalene, methylnaphthalene, and acenaphthene, were not detected. The results suggest that PAHs with high volatility in Jbilet Winselwan meteorite were lost or involved in further aromatization during thermal metamorphism. Distributions of dimethylnaphthalene and methylbiphenyl isomers in Jbilet Winselwan

©2019. Japan Geoscience Union. All Right Reserved.

and Murray meteorites were similar, respectively, which indicates that the parent body of Jbilet Winselwan meteorite experienced relatively mild thermal metamorphism.

Keywords: Jbilet Winselwan meteorite, Soluble organic molecules, Dehydration

©2019. Japan Geoscience Union. All Right Reserved.

Disk-Resolved Photometry Analysis of the Asteroid Ryugu Images Obtained by Hayabusa2 Visible Camera ONC

*yokota yasuhiro[1,2], Rie Honda[1], ERI TATSUMI[3], Deborah Domingue[4], Stefanus E. Schroeder[5], Moe Matsuoka[2], Seiji Sugita[3], Tomokatsu Morota[6], Shingo Kameda[7], Toru Kouyama[8], Hidehiko Suzuki[9], Manabu Yamada[10], Naoya Sakatani[2], Chikatoshi Honda[11], Masahiko Hayakawa[2], Kazuo Yoshioka[3], Yuichiro Cho[3], Hirotaka Sawada[2]

1. Kochi University, 2. ISAS/JAXA, 3. Univ. of Tokyo, 4. Planetary Science Institute, 5. DLR, 6. Nagoya Univ., 7. Rikkyo Univ., 8. AIST, 9. Meiji Univ., 10. Chiba Institute od Technology, 11. Aizu Univ.

Since June 2018, the Optical Navigation Camera (ONC) onboard Hayabusa2, has observed the C-type asteroid 162173 Ryugu at a distance below 20 km. ONC-T and ONC-W1 are used for surface imaging operations, and their images allow us to investigate the disk-resolved photometric properties of the surface. A narrow-angle camera ONC-T has 7 broad-band filters ranging in wavelength from 0.39–0.95 μm. ONC-W1 is a wide-angle (> 65˚) pan-chromatic camera mainly used for optical navigation during cruise and low-altitude (< 20km) operations. We are proceeding the analysis of both dataset, ONC-T and ONC-W1.

Since Hayabusa2’s position is nominally fixed on the line connecting Ryugu and the Earth, the available solar phase angle range by ONC-T changes seasonally with the orbits of Earth and Ryugu around the sun. Therefore, we are collecting a large number of ONC-T images over a long period of time to cover a wide phase angle range.

ONC-W1 data has a strong point that it covers a wide phase angle range within a single frame during the descent operations, because of its wide field of view. One of our current challenges is deriving a precise viewing geometries (incidence angle, emission angle, and phase angle) at each pixel. Additionally, comparison of the absolute brightness value (radiance factor) with ONC-T is an ongoing issue.

Keywords: Asteroid, Photometry, Ryugu, Hayabusa2

©2019. Japan Geoscience Union. All Right Reserved.

[E] Poster | P (Space and Planetary Sciences)：P-EM Solar-Terrestrial Sciences, Space Electromagnetism & Space Environment

Wed. May 29, 2019 10:45 AM - 12:15 PM JST | Wed. May 29, 2019 1:45 AM - 3:15 AM UTC | Poster Hall International Exhibition Hall8, Makuhari Messe_3

[P-EM09] Vertical coupling in the atmosphere and Ionosphere

convener:Huixin Liu(Earth and Planetary Science Division, Kyushu University SERC, Kyushu University), Loren Chang(Institute of Space Science, National Central University), Yuichi Otsuka(Institute for Space-Earth Environmental Research, Nagoya University)

Vertical coupling mechanisms throughout the whole atmosphere are critical to understanding the near Earth space environment, as well as its sensitivity to the solar, geomagnetic, and atmospheric drivers. This international session focuses on physical/chemical processes occurring in the mesosphere, thermosphere, and ionosphere (MTI). Both quiet and disturbed states in response to lower atmospheric forcing or solar forcing are important for understanding the MTI system and its coupling to other regions. We invite presentations of observations and observational concepts with ground-based and/or space-borne instruments, theoretical studies, numerical simulations, and development of data analysis systems for various kinds of temporal and spatial variations in atmosphere-ionosphere coupled system.

[PEM09-P01] Local-time Variabilities of SABER CO_2 in the Mesosphere and Lower Thermosphere Region

*Cornelius Csar Jude Salinas[1], Loren Chang[1], Danie Liang[2], Jia Yue[3], Liying Qian[4], Quan Gan[5], James Russel III[3], Martin G Mlynczak[6] (1.Institute of Space Science, National Central University, 2.Institute of Earth Science, Academia Sinica, 3.Department of Atmospheric Sciences, Hampton University, 4.High Altitude Observatory, National Center for Atmospheric Research, 5.Department of Physics and Astronomy, Clemson University, 6.NASA Langley Research Center)

[PEM09-P02] Enhanced dynamo electric field as a possible cause of ionosphere disturbance before Large Earthquake

*Koichiro Oyama[1,2,3] (1.Institute of Plasma and Space Sciences,National Cheng Kung Univ., Taiwan, 2.International Ceneter for Space Weather Sudy and Education, Kyushu Univ.,, 3.CoLtd. Asia Space Environment Research Consortium, Japan)

[PEM09-P03] Morphology of E1 and E2 Kelvin waves from ECMWF reanalysis

*Chen-Jeih Pan[1], Wei-Sheng Chen[1], Uma Das[2] (1.Institute of Space Science, National Central University, 2.Department of Physics, Indian Institute of Information Technology, Kalyani, India)

[PEM09-P04] Impact of strong ENSO on TEC activity disturbed by ultra-fast Kelvin waves

*Wei-Sheng Chen[1], C.J. Pan[1], Uma Das[2], Chian-Chiau Lin[3] (1.Institute of Space Science, National Central University, Taiwan, 2.Department of Physics, Indian Institute of Information Technology, Kalyani, India, 3.Environmental Research and Information Center, Chang Jung Christian University, Taiwan)

[PEM09-P05] Observation and simulation of propagation of coseismic infrasound to the ionosphere

*Jaroslav Chum[1] (1.Institute of Atmospheric Physics of the Czech Academy of Sciences)

[PEM09-P06] Solar wind influence on tropical cyclones mediated by atmospheric gravity waves

*Paul Prikryl[1,2], Iurii Cherniak[3], Irina Zakharenkova[4,5], James M. Weygand[6], Bharat S. R. Kunduri[7] (1.Physics Department, University of New Brunswick, Fredericton, NB, Canada, 2.Geomagnetic Laboratory, Natural Resources Canada, Ottawa, ON, Canada, 3.COSMIC Program Office, University Corporation for Atmospheric Research, Boulder, CO, USA, 4.West Department of IZMIRAN, Kaliningrad, Russia, 5.University of Warmia and Mazury in Olsztyn, Poland, 6.Earth Planetary and Space Sciences, University of California, Los Angeles, CA, USA, 7.Bradley Dept. of Electrical and Computer Engineering, Virginia Tech, Blacksburg, VA, USA)

[PEM09-P07] VIPIR ionospheric observations in Japan

*Takuya Tsugawa[1], Hideo Maeno[1], Michi Nishioka[1], Takumi Kondo[1], Mamoru Ishii[1] (1.National Institute of Information and Communications Technology)

[PEM09-P08] Simulation Results and Performance Analysis of Phase Velocity Spectral Analysis Software (M-Transform) for Airglow Imaging Data

*Septi Perwitasari[1], Takuji Nakamura[2], Masaru Kogure[2], Yoshihiro Tomikawa[2], Mitsumu K. Ejiri[2] (1.LAPAN, 2.NIPR)

[PEM09-P09] Comparisons of Co-incident Ionospheric Plasma Observations Between FORMOSAT-5/AIP and Millstone Hill Incoherent Scatter Radar

*Yi-Wun Chen[1], Chi-Kuang Chao[1] (1.Graduate Institute of Space Science, National Central University, Taiwan)

[PEM09-P10] Sub-ionospheric effects of volcano eruptions using VLF/LF standard radio waves

*Kei Maruyama[1], Hiroyo Ohya[1], Fuminori Tsuchiya[2], Kenro Nozaki[5], Kozo Yamashita[3], Yukihiro Takahashi[4], Hiroyuki Nakata[1], Toshiaki Takano[1] (1.Chiba University, 2.Tohoku University, 3.Ashikaga University, 4.Hokkaido University, 5.National Institute of Information and Communications Technology)

[PEM09-P11] Observations of ionospheric and mesospheric wave structures by a low-cost airglow imaging system

*Keisuke Hosokawa[1], Nanami Kusuyama[1], Yuta Hozumi[1], Kohei Takami[1], Susumu Saito[2], Yasunobu Ogawa[3], Mamoru Ishii[4], Yuichi Otsuka[5], Takuya Tsugawa[4] (1.University of Electro-Communications, 2.ENRI, 3.NIPR, 4.NICT, 5.ISEE, Nagoya University)

[PEM09-P12] Analysis of characteristics of ionospheric parameters, Sq index and neutral winds over Taiwan

*Yu-Jung Chuo[1] (1.Department of Information Technology, Ling Tung University)

[PEM09-P13] Statistical study on daytime Es observed by ground-ionosonde and RO-COSMIC in magnetic Equator region in 2010

*Zheng Wang [1,2], Huixin Liu[1] (1.Department of Earth and Planetary Sciences, School of Science, Kyushu University, Japan. , 2.National Space Science Center, Chinese Academy of Sciences, China.)

[PEM09-P14] The statistical study of the growth rates of Medium-Scale Traveling Ionospheric Disturbances observed with GPS-TEC

*Takafumi Ikeda[1], Akinori Saito[1], Takuya Tsugawa[2], Hiroyuki Shinagawa[2] (1.Department of Geophysics, Graduate School of Science, Kyoto University, 2.National Institutes of Information and Communications Technology)

[PEM09-P15] Comparison of Gravity Wave Activity in the Mesosphere Observed by OH Airglow Imagers and MF Radars over the Antarctic (Syowa & Davis).

*Masaru Kogure[1], Takuji Nakamura[1,2], Yoshihiro Tomikawa[1,2], Mitsumu K. Ejiri[1,2], Takanori Nishiyama[2,1], Masaki Tsutsumi[1,2], Michael J. Taylor[3], Yucheng Zhao[3], P.-Dominique Pautet[3], Damian Murphy[4] (1.National Institute of Polar Research, 2.Department of Polar Science, Sokendai, 3.Physics Department, Utah State University, 4.Australian Antarctic Division)

Local-time Variabilities of SABER CO_2 in the Mesosphere and Lower Thermosphere Region

*Cornelius Csar Jude Salinas[1], Loren Chang[1], Danie Liang[2], Jia Yue[3], Liying Qian[4], Quan Gan[5], James Russel III[3], Martin G Mlynczak[6]

1. Institute of Space Science, National Central University, 2. Institute of Earth Science, Academia Sinica, 3. Department of Atmospheric Sciences, Hampton University, 4. High Altitude Observatory, National Center for Atmospheric Research, 5. Department of Physics and Astronomy, Clemson University, 6. NASA Langley Research Center

This work presents the local-time variabilities of CO_2 in the Mesosphere and Lower Thermosphere region (MLT region) as observed by the Sounding of the Atmosphere using Broadband Emission Radiometry (SABER) onboard the Thermosphere Ionosphere Mesosphere Energetics and Dynamics Satellite (TIMED Satellite). These are then compared to CO_2 as modeled by the Whole Atmosphere Community Climate Model –eXtended (WACCM-X). Also using WACCM-X, a tendency analysis using the continuity equation is done to explain the local-time variabilities of CO_2 in the MLT region. Finally, consequences of including a significant local-time variability in CO_2 when retrieving SABER temperature profiles are determined.

Keywords: Carbon Dioxide, Mesosphere and Lower Thermosphere Region, Tides

©2019. Japan Geoscience Union. All Right Reserved.

Enhanced dynamo electric field as a possible cause of ionosphere disturbance before Large Earthquake

*Koichiro Oyama[1,2,3]

1. Institute of Plasma and Space Sciences,National Cheng Kung Univ., Taiwan, 2. International Ceneter for Space Weather Sudy and Education, Kyushu Univ.,, 3. CoLtd. Asia Space Environment Research Consortium, Japan

Disturbance of ionosphere before large earthquakes has been very often reported. One of the possible disturbing drivers is electric field, which explains most of the ionosphere features we reported so far. However, the origin of the electric field is still in the darkness. One idea of electric field generation exists inside earth interior (Freund et a., 2006). We propose here that the electric field is dynamo field at the height of ≈100 km, which simply intensified before earthquake; intensified eastward (westward)electric field during daytime(nighttime). This idea explains satellite data (Oyama et al.,2008; Oyama et al.,2011; Ryu et al., 2014; Ryu et al., 2016; Oyama et al.,2016; Oyama et al., 2019).

Next question on the electric field generation is the mechanism which modifies the dynamo field. We speculate that modification of E field is a result of modification of neutral wind system, which is originally caused by internal gravity waves which propagate from below. Then again next question is on the origin of the internal gravity waves. The waves might be originally caused by the ground motion, and these waves which propagate upward might interact with planetary wave, and amplified. We show several side evidence of ground motions before earthquakes.

Keywords: Earthquake, Electric field, Ionosphere, Disturbance

©2019. Japan Geoscience Union. All Right Reserved.

Morphology of E1 and E2 Kelvin waves from ECMWF reanalysis

*Chen-Jeih Pan[1], Wei-Sheng Chen[1], Uma Das[2]

1. Institute of Space Science, National Central University, 2. Department of Physics, Indian Institute of Information Technology, Kalyani, India

Kelvin waves are planetary waves traveling eastwards and confined in the equatorial latitudes. The waves play an important role in middle atmosphere dynamics because they transfer energy and momentum from lower to higher altitudes, which contributes to the quasi-biennial oscillation (QBO) and further influences the global climate. Kelvin waves have been studied for many decades, and the most of studies were focused on the waves of wavenumber 1 (E1). On the other hand, the wavenumber-2 Kelvin waves (E2) are also an important part of Kelvin wave activities although their amplitude less than the E1. In this study, we analyzed the long-term European Centre for Medium-Range Weather Forecasts (ECMWF) reanalysis data and reported the morphology of E1 and E2 Kelvin waves in the stratospheric altitudes individually. The temperature from ECMWF reanalysis was used to extract the wave properties. Temperatures between latitudes of 10S and 10N were firstly gridded into the structure of day-altitude-longitude, and then subtract background (longitudinal means) to get equatorial temperature fluctuations. For each altitude, the two-dimensional fast Fourier transform was applied to each 96-day data segment and stepped forward in time by 1 day. The output spectra were then analyzed to get primary wave periods and amplitude variations. From spectra, the E1 amplitude is 1.5 to 2.0 times larger than the E2 in average. The E1 primary periods are 12 to 25 days and are restricted under the 20-km altitude. The periods of 8 to 14 days are the secondary group. They can propagate upward to the 40-km altitude. Regarding the E2, the primary periods are 7 to 12 days and are also restricted under the 20-km altitude. Its secondary group is the periods of 5 to 8 days, which also can propagate upward to the 40-km altitude. Furthermore, the altitude-time-amplitude variation show that the E2 waves are influenced strictly by the QBO westerly. Finally, the cross correlation between E1 and E2 show that the E1 and E2 have high correlation at altitudes close to the tropopause, which implies they are excited simultaneously.

Keywords: Kelvin waves, QBO

©2019. Japan Geoscience Union. All Right Reserved.

Impact of strong ENSO on TEC activity disturbed by ultra-fast Kelvin waves

*Wei-Sheng Chen[1], C.J. Pan[1], Uma Das[2], Chian-Chiau Lin[3]

1. Institute of Space Science, National Central University, Taiwan, 2. Department of Physics, Indian Institute of Information Technology, Kalyani, India, 3. Environmental Research and Information Center, Chang Jung Christian University, Taiwan

Ultra-fast Kelvin waves (UFKW) are a subclass of Kelvin waves that they have the shortest periods (2-5 days) and thus can propagate into the ionosphere. UFKW relate to ionospheric variations have been reported, which include ionospheric minimum virtual height (h'F), F2 maximum critical frequency (foF2), total electron content (TEC), S4 scintillations, etc. In the study, we analyzed the UFKW activities using SABER (Sounding of the Atmosphere using Broadband Emission Radiometry) temperatures and GIM (Global Ionospheric Maps) TEC from 2009 to 2011 to see how UFKW influence the ionosphere. The period 2009-2011 belongs to the strong ENSO period. Previous studies have shown that Kelvin waves were highly active in this period, especially in the early of 2010. Therefore, this study can implicitly reveal how the ionosphere responds to the ENSO. The wave signatures in SABER temperatures were extracted using the fast Fourier transform (FFT). Temperatures in the geographic equatorial latitudes were gridded into the day-altitude-longitude structure and then removed background to get temperature fluctuations. The two-dimensional FFT was applied to each 96-day data segment for each altitude and stepped forward in time by one day. Regarding TEC, the Lomb-Scargle periodogram was used to extract UFKW signatures. Because TEC has a strong local time variation and constrains by the geomagnetic configuration, TEC at 16 local time and low geomagnetic latitudes were selected. The background was removed firstly from the data and then fed TEC fluctuations into the Lomb-Scargle process, which also stepped forward in time by one day. The FFT and Lomb-Scargle process both outputted spectra, which revealed UFKW activities in the mesosphere and lower thermosphere (MLT) region (90-100 km) and the ionosphere (about 150-600 km). The results show that UFKW activities at two equatorial ionization anomalies (EIA) were almost identical, and both were higher than that at geomagnetic equator. Most of wave activities in the temperature field in the MLT region have corresponding activities in TEC. However, there are a lot of small amplitude activities only in TEC.

Keywords: ultra-fast Kelvin waves, ENSO, TEC

©2019. Japan Geoscience Union. All Right Reserved.

Observation and simulation of propagation of coseismic infrasound to the ionosphere

*Jaroslav Chum[1]

1. Institute of Atmospheric Physics of the Czech Academy of Sciences

Vertical motion of the ground surface caused by seismic waves generates acoustic waves that propagate nearly vertically upward owing to supersonic speed of seismic waves. As the air density decreases with height, the amplitude of acoustic waves increases to conserve the energy flux up to the altitudes where the air is so rarefied that it cannot sustain the propagation and the waves start dissipating. For distances up to about 1500 km from the epicenter of the strong earthquakes (M>7), the amplitude (oscillation velocity) of infrasound waves reaches significant values in the upper atmosphere. Consequently, the nonlinear phenomena start to play an important role. Spectral content of the wave packet is changed and the energy is transferred to lower frequencies, which can cause the formation of roughly bipolar N-shaped pulse. The simulation results are compared with observation for selected examples. It is also shown that only infrasound with periods larger than about 10 s (generated by long period seismic waves) can reach the ionospheric heights, namely the F layer where it can be easily detected.

Keywords: coseismic perturbation in the ionosphere, infrasound, nonlinear propagation

©2019. Japan Geoscience Union. All Right Reserved.

Solar wind influence on tropical cyclones mediated by atmospheric gravity waves

*Paul Prikryl[1,2], Iurii Cherniak[3], Irina Zakharenkova[4,5], James M. Weygand[6], Bharat S. R. Kunduri[7]

1. Physics Department, University of New Brunswick, Fredericton, NB, Canada, 2. Geomagnetic Laboratory, Natural Resources Canada, Ottawa, ON, Canada, 3. COSMIC Program Office, University Corporation for Atmospheric Research, Boulder, CO, USA, 4. West Department of IZMIRAN, Kaliningrad, Russia, 5. University of Warmia and Mazury in Olsztyn, Poland, 6. Earth Planetary and Space Sciences, University of California, Los Angeles, CA, USA, 7. Bradley Dept. of Electrical and Computer Engineering, Virginia Tech, Blacksburg, VA, USA

Solar wind coupling to the magnetosphere-ionosphere-atmosphere (MIA) system generates medium- and large-scale atmospheric gravity waves (AGWs) propagating globally from sources in the lower thermosphere at high latitudes. The AGWs propagate globally [1,2] upward and downward, are observed in the ionosphere as traveling ionospheric disturbances [3], can be ducted in lower atmosphere over long distances and reach troposphere. At the reflection point in the troposphere they can trigger moist instabilities to initiate convective bursts, with the latent heat release leading to intensification of storms [4]. In the follow-up studies [5,6,7] it was shown that explosive extratropical cyclones and rapid intensification of tropical cyclones tend to follow arrivals of solar wind high-speed streams (HSS) and/or interplanetary coronal mass ejections (ICMEs). The coupling of solar wind to MIA is most intense during the arrivals of co-rotating interaction regions (CIRs) and/or interplanetary shocks at the leading edges of HSSs and ICMEs when the amplitudes of aurorally-generated AGWs are largest. Ray tracing of AGWs in a model atmosphere show that they can reach tropical cyclones. Spiral gravity waves in typhoons were observed and simulated to propagate radially outward from the typhoon core [8]. The spectra of waves in surface pressure and surface wind measured by the Impacts of Typhoons on the Ocean in the Pacific (ITOP) buoy during the nearby passages of intense typhoons are similar to those of incoming aurorally-generated AGWs. It is suggested that the interaction of aurorally-generated gravity waves with the tropical cyclone vortex and the inner primary eyewall plays a role in the intensification process.

[1] Mayr H.G., et al., J. Geophys. Res., 89, 10929–10959, 1984.
[2] Prikryl P., et al., Ann. Geophys., 23, 401-417, 2005. doi:10.5194/angeo-23-401-2005
[3] Cherniak Iu., Zakharenkova I., Space Weather, 16, 2018. https://doi.org/10.1029/2018SW001869.
[4] Prikryl P., et al., Ann. Geophys. 27, 31–57, 2009. https://doi.org/10.5194/angeo-27-31-2009.
[5] Prikryl P., et al., J. Atmos. Sol.-Terr. Phys., 149, 219–231, 2016.
[6] Prikryl P., et al., J. Atmos. Sol.-Terr. Phys., 171, 94–110, 2018.
[7] Prikryl P., et al., J. Atmos. Sol.-Terr. Phys., 183, 36-60, https://doi.org/10.1016/j.jastp.2018.12.009.
[8] Nolan D.S., Zhang J.A., Geophys. Res. Lett., 44, 3924–3931, 2017. doi:10.1002/2017GL073572

Keywords: Solar wind-magnetosphere-ionosphere-atmosphere coupling, High-speed solar wind stream, Atmospheric gravity wave, Extratropical and tropical cyclones

©2019. Japan Geoscience Union. All Right Reserved.

VIPIR ionospheric observations in Japan

*Takuya Tsugawa[1], Hideo Maeno[1], Michi Nishioka[1], Takumi Kondo[1], Mamoru Ishii[1]

1. National Institute of Information and Communications Technology

National Institute of Information and Communications Technology (NICT) has observed ionosphere by ionosondes more than 70 years in Japan. At present, four ionosondes at Wakkanai (Sarobetsu), Kokubunji, Yamagawa, Okinawa (Ogimi) are automatically operated and controlled from Tokyo. Major ionospheric parameters such as foF2 and foEs are scaled from the ionograms automatically on a realtime basis and scaled manually for the final values. These scaled parameters are provided through our web site (http://wdc.nict.go.jp/IONO/). In 2017, we replaced the 10C ionosondes with Vertical Incidence Pulsed Ionospheric Radar 2 (VIPIR2) which can separate the O- and X-modes of ionospheric echoes which have improved the availability of automatic scaling of the ionogram. Our automatic scaling method has been improved using new O- and X-modes separated ionograms. As for future plans, we try to expand observation area by oblique sounding observations with VIPIRs in Japan and neighboring countries. We have also tried to detect arrival directions of ionospheric echo by using the 8ch receiving data as a interferometry. In this presentation, we will introduce current status and future plans of ionospheric observation in NICT.

Keywords: Ionosphere, Ionosonde, Space Weather

©2019. Japan Geoscience Union. All Right Reserved.

Simulation Results and Performance Analysis of Phase Velocity Spectral Analysis Software (M-Transform) for Airglow Imaging Data

*Septi Perwitasari[1], Takuji Nakamura[2], Masaru Kogure[2], Yoshihiro Tomikawa[2], Mitsumu K. Ejiri[2]

1. LAPAN, 2. NIPR

We have developed a user-friendly software based on *Matsuda et al.*, 2014's 3D-FFT method (M-Transform) for airglow data analysis as a function on Interactive Data Language (IDL). Input of this function is 3-D array of a time series of airglow image that have already been converted to geographical coordinate (*x*, *y*, *t*). The user can customize the wave parameters (e.g. horizontal wavelength (λ_h), wave period (τ), phase speed (*c*), image resolution in space (*dx*,*dy*) and time (*dt*)) in one-line command when executing the program, which depends on their analysis purpose. In order to exhibit this new function's performance and the characteristics/interpretation of the spectral analysis, we have run several test cases using artificial wave. The first case is artificial wave with constant speed (40 m/s) and different wave period (8, 15, 30 min) and horizontal wavelength. In second case, we applied Gaussian shape wave-packet with different FWHM (50, 100, 200 km). For the third test case, with a fixed wave packet size (100 km), we changed the wave packet duration (30, 60, 120 min). The results from the various simulations showed reasonable characteristics of the spectral analysis for different scenarios. We showed that the increase of wave period and horizontal wavelength lead to the wider spectrum with total power difference of ~10%. By changing the wave packet size, we showed that the bigger the wave packet size, the sharper and narrower the spectrum became with the total power increase 2x of the increase size of the wave packet. The result of changing the wave packet duration showed that the longer the duration of wave packet, the spectrum becomes sharper and the total power is proportional to the wave packet length. We also examined the aliasing and zero padding effect on the spectral analysis. In order to avoid the aliasing effect, it is recommended to set the period minimum to at least 2 x image interval (*dt*). More detailed analysis will be discussed during the presentation.

Keywords: Airglow, Gravity wave, Analysis software

©2019. Japan Geoscience Union. All Right Reserved.

Comparisons of Co-incident Ionospheric Plasma Observations Between FORMOSAT-5/AIP and Millstone Hill Incoherent Scatter Radar

*Yi-Wun Chen[1], Chi-Kuang Chao[1]

1. Graduate Institute of Space Science, National Central University, Taiwan

Advanced Ionospheric Probe (AIP) onboard FORMOSAT-5 satellite has routinely measured ionospheric plasma parameters, like ion concentration, velocity, and temperature in a sun-synchronous circular orbit at 720 km altitude along 2230 local-time sector since November 2017. AIP has found that the satellite has a much lower potential with respective to environmental plasma from measured current-voltage curves. A comparison study shall be performed to identify possible bias on the derived AIP parameters. Co-incident observations have been scheduled with Millstone Hill incoherent scatter radar during 30 January to 1 February 2019. In this poster, preliminary comparison results will be outlined and will be used to improve accuracy of the AIP measurement in the future.

Keywords: FORMOSAT-5, AIP, ionosphere

©2019. Japan Geoscience Union. All Right Reserved.

Sub-ionospheric effects of volcano eruptions using VLF/LF standard radio waves

*Kei Maruyama[1], Hiroyo Ohya[1], Fuminori Tsuchiya[2], Kenro Nozaki[5], Kozo Yamashita[3], Yukihiro Takahashi[4], Hiroyuki Nakata[1], Toshiaki Takano[1]

1. Chiba University, 2. Tohoku University, 3. Ashikaga University, 4. Hokkaido University, 5. National Institute of Information and Communications Technology

Several studies for the F-region ionosphere associated with volcano eruptions based on GPS-TEC data have been reported so far (e.g., Heki, 2006; Dautermann et al., 2009; Heki et al., 2010). These studies reported that acoustic waves excited by volcano eruptions reach up to the F-region ionosphere, and caused F-region perturbations. After eruption of the Kelud Volcano, Indonesia, in February 2014, acoustic resonance between the Earth’ s surface and lower thermosphere was reported based on TEC data and the seismic wave data (Nakashima et al., 2015). However, little studies on the D-region ionosphere associated with volcano eruptions have been reported. In this study, we investigate the D-region effects of eruptions of Sakurajima volcano (31.59N, 130.66E), Japan, at 04:11 UT on June 6, 2014, using intensity perturbation of VLF/LF transmitter signals. The VLF/LF propagation paths use in this study are JJY (JJY 60 kHz) - Tainan (TNN, Taiwan), and JJI (22.2 kHz) - TNN. Based on wavelet spectra, the perturbation of both transmitter signals had a frequency of 2-6 mHz during 04:12-04:30 UT after the eruptions (04:11 UT).We compared the perturbations with atmospheric pressure data obtained by an infrasonic meter observed by Sakurajima Volcano Research Center, Kyoto University, and seismic waves in the NIED F-net data (FUK, STM, and SBR) located close to the JJY-TNN path. The atmospheric pressure and vertical velocity of the seismic waves had the similar frequencies of 2-10 mHz during 04:12-04:47 UT. These similar frequencies suggest that the perturbations would be caused by acoustic resonance between the Earth's surface and lower thermosphere, or by acoustic and atmospheric gravity waves generated by volcanic eruptions. In the presentation, we will discuss the cause of the VLF/LF perturbations in more detail.

©2019. Japan Geoscience Union. All Right Reserved.

Observations of ionospheric and mesospheric wave structures by a low-cost airglow imaging system

*Keisuke Hosokawa[1], Nanami Kusuyama[1], Yuta Hozumi[1], Kohei Takami[1], Susumu Saito[2], Yasunobu Ogawa[3], Mamoru Ishii[4], Yuichi Otsuka[5], Takuya Tsugawa[4]

1. University of Electro-Communications, 2. ENRI, 3. NIPR, 4. NICT, 5. ISEE, Nagoya University

In the last two decades, all-sky airglow imagers with cooled CCD cameras have widely been used to observe large-scale wave structures in the F-region ionosphere, for example medium-scale traveling ionospheric disturbances (MSTIDs). Such wavy features are seen in the oxygen emission at 630.0 nm from altitudes slightly below the F-region peak. Similar optical observations of OH band emission have also enabled us to visualize atmospheric gravity waves at the mesospheric height. Deploying airglow imagers in multiple places is one of the cost-effective ways to visualize the large-scale structure of these wave structures at both the F-region ionosphere and mesosphere [e.g., Kubota et al., 2001; Suzuki et al., 2013]. However, ground-based airglow imagers equipped with a cooled CCD camera is still expensive; thus, it is rather difficult to deploy such systems in a wide area and carry out a network observation. To overcome this limitation, we recently developed a low-cost airglow imaging system (Low-Cost Airglow imaging System: LCAS) which consists of a small camera (WAT-910HX), fisheye lens and optical filter. We then confirmed its capability of imaging the spatial structure of polar cap patches and plasma bubble in the 630.0 nm emission from the F-region. But, still, it is unclarified if the system is also capable of detecting the two-dimensional structure of MSTIDs. On the night of May 12, 2018, we identified a weak wavy signature in the 630.0 nm airglow images from one of our LCAS stations in Ishigaki Island, Japan. The wave structure in the 630.0 nm images was smoothly connected to the structure of MSTIDs in the GPS-TEC data, which confirmed the ability of LCAS for detecting MSTIDs. We also identified smaller scale wave structures in the 630.0 nm images, showing characteristic concentric wave fronts. We speculate that gravity waves in the mesosphere were captured in the 630.0 nm images as a contamination of the OH airglow. This is mainly because we make use of an optical filter having 10 nm FWHM, which enables us to detect several spectral peaks of OH emission near the 630.0 nm oxygen emission. We have estimated the center of the concentric wave structures by using the curvature of the wave fronts, and then confirmed that active rain fall took place in a localized area close to the estimated center of the concentric waves. This result supports our hypothesis that the OH emission containing signatures of mesospheric gravity waves were detected in the 630.0 nm images. In summary, the 630.0 nm airglow observation of LCAS is able to observe MSTIDs and mesospheric gravity waves. This will allow us to monitor such wavy structures at two different altitudes by distributing the similar system in a wide area.

Keywords: Airglow, Traveling Ionospheric Disturbances

©2019. Japan Geoscience Union. All Right Reserved.

Analysis of characteristics of ionospheric parameters, Sq index and neutral winds over Taiwan

*Yu-Jung Chuo[1]

1. Department of Information Technology, Ling Tung University

In this paper, we examine the variation of thermospheric neutral winds and solar quiet (Sq) current of the geomagnetic fields for the equatorial ionospheric anomaly area (EIA) during the solar activity period in 1999. The thermospheric neutral winds are derived from the ionospheric F_2-layer peak height, hmF_2, by using the servo model method. The variability of the amplitude ofSq fields is derived from the ground geomagnetic fields in the components H and Z, respectively. Theresults of the current system show a same diurnal variation, which that peaks / valleys in the local noon time for Sq(H) / Sq(Z) in the low latitudes, respectively.The results also indicate a weak seasonal variation that peaks appear at the local summer of the Sq currents in H and Z components, respectively. The Sq current system is associated with the change of the equatorial electrojet (EEJ). Further, the variability is probably attributed to local thermospheric winds. The study also shows that the zonal and meridional components of the neutral winds at the EIA over Taiwan area. Furthermore, the study examines the variations of Sq(H), Sq(Z), neutral winds, and ionospheric parameters foE_s, NmF_2, and hmF_2during the disturbed geophysical conditions such as geomagnetic storm and earthquake. The result shows the variationsof ionospheric Sq(H), Sq(Z) and thermospheric neutral winds are different between the seismo-ionospheric and solar-terrestrial disturbed periods, even they lead the same decreasing electron density reaction in the ionosphere at the EIA over Taiwan area.

Keywords: Sq current, ionosphere, neutral winds

©2019. Japan Geoscience Union. All Right Reserved.

Statistical study on daytime Es observed by ground-ionosonde and RO-COSMIC in magnetic Equator region in 2010

*Zheng Wang [1,2], Huixin Liu[1]

1. Department of Earth and Planetary Sciences, School of Science, Kyushu University, Japan. , 2. National Space Science Center, Chinese Academy of Sciences, China.

Scintillations under 150 km height shown by radio occultation (RO) of COSMIC are considered to be associated with ionospheric sporadic E (Es) layer. In this paper, we make a Statistical study on daytime Es observed by ground-ionosonde at five stations in magnetic Equator region in 2010, and make a comparison with S4 index from RO-COSMIC within 6 degree of each station. The results show that: At each station the diurnal variation of foEs from ionosonde decrease a little around LT 0600 and then increase, having maximum around LT 1200, decrease around LT 1800 and then increase near LT 2000-2200; All the S4>=0.3 observations during daytime come from RO-COSMIC under 150 km height; The diurnal variation of S4 index under 150 km height from RO-COSMIC over each station has similar trend with that of foEs at the same station; S4 index over 150 km height from RO-COSMIC is only high during nighttime; For the stations at different longitudes, Es occurrences from ionosonde are positively associated with S4>=0.3 from RO-COSMIC. The comparison shows that the S4 index from RO-COSMIC could show some features of daytime Es layer in magnetic Equator region without the location limitation of ground stations.

Keywords: daytime ionospheric sporadic E, ground-ionosonde , radio occultation of COSMIC , magnetic Equator region

©2019. Japan Geoscience Union. All Right Reserved.

The statistical study of the growth rates of Medium-Scale Traveling Ionospheric Disturbances observed with GPS-TEC

*Takafumi Ikeda[1], Akinori Saito[1], Takuya Tsugawa[2], Hiroyuki Shinagawa[2]

1. Department of Geophysics, Graduate School of Science, Kyoto University, 2. National Institutes of Information and Communications Technology

We think two mechanism, E-F coupling and Perkins Instability, will relate to growth for nighttime-MSTID in mid-latitude [Tsunoda and Cosgrove., 2001 ; Perkins., 1973]. Linear growth rate of perturbation intensity of Pedersen conductivity expected from E-F coupling is around 15 minutes [Yokoyama et al., 2009], which is far shorter than one expected from Perkins Instability [Fukao and Kelley, 1991 ; Miller et al., 1997 ; Shiokawa et al., 2003]. However, Es layer’ s spatial and temporal scale is less than 100km and 15min [Maeda et al., 2013 ; S.Saito et al., 2007]. They are different from MSTID’ s ones, which are 200-400 km and around 2hours [Otsuka et al., 2011]. To decide which instability is responsible for growth of nighttime MSTID, the growth rate of MSTID was observationally determined with ground-based GPS network data.

We statistically investigated the growth rate of nighttime-MSTID in Japan in 2014 observed with GPS-TEC. The growth rate of nighttime -MSTID observed was 1.0 - 6.0 $\times 10^{-4}$ s^{-1} during 1800LT-2400LT in summer.Linear growth rate of Perkins instability in summer was 1.0 - 6.0 $\times 10^{-4}$ s^{-1} during 1800LT - 2400LT, so they were less than one of the E-F coupling instability. Also,Seasonal distribution of observed growth rate before midnight was similar to that of linear growth rate.U×B derived by GAIA model was high in spring - summer and seasonal distribution of U×B was similar to that of linear growth rate. Therefore, the growth of MSTID when propagating is not determined by E-F coupling instability but Perkins instability and neutral wind.

Keywords: MSTID, GPS-TEC, Ionosphere

©2019. Japan Geoscience Union. All Right Reserved.

Comparison of Gravity Wave Activity in the Mesosphere Observed by OH Airglow Imagers and MF Radars over the Antarctic (Syowa & Davis).

*Masaru Kogure[1], Takuji Nakamura[1,2], Yoshihiro Tomikawa[1,2], Mitsumu K. Ejiri[1,2], Takanori Nishiyama[2,1], Masaki Tsutsumi[1,2], Michael J. Taylor[3], Yucheng Zhao[3], P.-Dominique Pautet[3], Damian Murphy[4]

1. National Institute of Polar Research, 2. Department of Polar Science, Sokendai, 3. Physics Department, Utah State University, 4. Australian Antarctic Division

Gravity waves transport momentum and energy from the lower atmosphere to the upper atmosphere and drive the general circulation, which significantly changes the temperature in the middle atmosphere [Fritts and Alexander, 2003]. To understand this role quantitatively will improve the modern general circulation models [Garcia et al., 2017].

The polar night jet region is known to have high gravity-wave activity. However, sources of gravity waves, their propagation, and their spectra are poorly understood because of a lack of observations. In particular, little is known about the dependence of their characteristics on their spectra (i.e., wavenumber and frequency) and on interactions among waves with several wavenumbers and frequencies [Fritts and Alexander, 2003]. To understand these, our group has observed gravity waves at different sites over the Antarctic.

Observation techniques have limitations due to the breadth of the gravity wave spectrum and the target and physical parameter sensed by the observing system [Alexander et al., 1998]. In this study an OH imager and an MF radar are used. Both instruments cover the OH layer (~87 km altitude), but both cover quite different ranges of the wave spectrum. The OH imager can observe waves with shorter ground-based periods (8-60 min) and shorter horizontal wavelengths (2-100 km) [Matsuda et al., 2017]. On the other hand, the MF radar can observe waves with the longer ground-based periods (>~30 min). It also has a preference for the waves with longer horizontal wavelength because of its observational volume.

This study derives gravity-wave perturbations, over Syowa and Davis, from the OH imager data based on Matsuda et al. [2014] and the MF radar data based on Murphy et al. [2007], respectively. In this presentation, we would like to show the gravity wave activity, over Syowa and Davis, with the shorter horizontal wavelength (i.e., observed by the OH imagers) and with the longer horizontal wavelength (i.e., observed by the MF radars). The correlation and relationship between both wave activities will be discussed. Also, we would like to discuss the local variation of that relationship.

Keywords: Gravity Wave, Middle Atmosphere, OH Imager

©2019. Japan Geoscience Union. All Right Reserved.

[E] Poster | P (Space and Planetary Sciences)：P-EM Solar-Terrestrial Sciences, Space Electromagnetism & Space Environment

Wed. May 29, 2019 5:15 PM - 6:30 PM JST | Wed. May 29, 2019 8:15 AM - 9:30 AM UTC | Poster Hall International Exhibition Hall8, Makuhari Messe_4

[P-EM09] Vertical coupling in the atmosphere and Ionosphere

convener:Huixin Liu(Earth and Planetary Science Division, Kyushu University SERC, Kyushu University), Loren Chang(Institute of Space Science, National Central University), Yuichi Otsuka(Institute for Space-Earth Environmental Research, Nagoya University)

Vertical coupling mechanisms throughout the whole atmosphere are critical to understanding the near Earth space environment, as well as its sensitivity to the solar, geomagnetic, and atmospheric drivers. This international session focuses on physical/chemical processes occurring in the mesosphere, thermosphere, and ionosphere (MTI). Both quiet and disturbed states in response to lower atmospheric forcing or solar forcing are important for understanding the MTI system and its coupling to other regions. We invite presentations of observations and observational concepts with ground-based and/or space-borne instruments, theoretical studies, numerical simulations, and development of data analysis systems for various kinds of temporal and spatial variations in atmosphere-ionosphere coupled system.

[PEM09-P01] Local-time Variabilities of SABER CO_2 in the Mesosphere and Lower Thermosphere Region

*Cornelius Csar Jude Salinas[1], Loren Chang[1], Danie Liang[2], Jia Yue[3], Liying Qian[4], Quan Gan[5], James Russel III[3], Martin G Mlynczak[6] (1.Institute of Space Science, National Central University, 2.Institute of Earth Science, Academia Sinica, 3.Department of Atmospheric Sciences, Hampton University, 4.High Altitude Observatory, National Center for Atmospheric Research, 5.Department of Physics and Astronomy, Clemson University, 6.NASA Langley Research Center)

[PEM09-P02] Enhanced dynamo electric field as a possible cause of ionosphere disturbance before Large Earthquake

*Koichiro Oyama[1,2,3] (1.Institute of Plasma and Space Sciences,National Cheng Kung Univ., Taiwan, 2.International Ceneter for Space Weather Sudy and Education, Kyushu Univ.,, 3.CoLtd. Asia Space Environment Research Consortium, Japan)

[PEM09-P03] Morphology of E1 and E2 Kelvin waves from ECMWF reanalysis

*Chen-Jeih Pan[1], Wei-Sheng Chen[1], Uma Das[2] (1.Institute of Space Science, National Central University, 2.Department of Physics, Indian Institute of Information Technology, Kalyani, India)

[PEM09-P04] Impact of strong ENSO on TEC activity disturbed by ultra-fast Kelvin waves

*Wei-Sheng Chen[1], C.J. Pan[1], Uma Das[2], Chian-Chiau Lin[3] (1.Institute of Space Science, National Central University, Taiwan, 2.Department of Physics, Indian Institute of Information Technology, Kalyani, India, 3.Environmental Research and Information Center, Chang Jung Christian University, Taiwan)

[PEM09-P05] Observation and simulation of propagation of coseismic infrasound to the ionosphere

*Jaroslav Chum[1] (1.Institute of Atmospheric Physics of the Czech Academy of Sciences)

[PEM09-P06] Solar wind influence on tropical cyclones mediated by atmospheric gravity waves

*Paul Prikryl[1,2], Iurii Cherniak[3], Irina Zakharenkova[4,5], James M. Weygand[6], Bharat S. R. Kunduri[7] (1.Physics Department, University of New Brunswick, Fredericton, NB, Canada, 2.Geomagnetic Laboratory, Natural Resources Canada, Ottawa, ON, Canada, 3.COSMIC Program Office, University Corporation for Atmospheric Research, Boulder, CO, USA, 4.West Department of IZMIRAN, Kaliningrad, Russia, 5.University of Warmia and Mazury in Olsztyn, Poland, 6.Earth Planetary and Space Sciences, University of California, Los Angeles, CA, USA, 7.Bradley Dept. of Electrical and Computer Engineering, Virginia Tech, Blacksburg, VA, USA)

[PEM09-P07] VIPIR ionospheric observations in Japan

*Takuya Tsugawa[1], Hideo Maeno[1], Michi Nishioka[1], Takumi Kondo[1], Mamoru Ishii[1] (1.National Institute of Information and Communications Technology)

[PEM09-P08] Simulation Results and Performance Analysis of Phase Velocity Spectral Analysis Software (M-Transform) for Airglow Imaging Data

*Septi Perwitasari[1], Takuji Nakamura[2], Masaru Kogure[2], Yoshihiro Tomikawa[2], Mitsumu K. Ejiri[2] (1.LAPAN, 2.NIPR)

[PEM09-P09] Comparisons of Co-incident Ionospheric Plasma Observations Between FORMOSAT-5/AIP and Millstone Hill Incoherent Scatter Radar

*Yi-Wun Chen[1], Chi-Kuang Chao[1] (1.Graduate Institute of Space Science, National Central University, Taiwan)

[PEM09-P10] Sub-ionospheric effects of volcano eruptions using VLF/LF standard radio waves

*Kei Maruyama[1], Hiroyo Ohya[1], Fuminori Tsuchiya[2], Kenro Nozaki[5], Kozo Yamashita[3], Yukihiro Takahashi[4], Hiroyuki Nakata[1], Toshiaki Takano[1] (1.Chiba University, 2.Tohoku University, 3.Ashikaga University, 4.Hokkaido University, 5.National Institute of Information and Communications Technology)

[PEM09-P11] Observations of ionospheric and mesospheric wave structures by a low-cost airglow imaging system

*Keisuke Hosokawa[1], Nanami Kusuyama[1], Yuta Hozumi[1], Kohei Takami[1], Susumu Saito[2], Yasunobu Ogawa[3], Mamoru Ishii[4], Yuichi Otsuka[5], Takuya Tsugawa[4] (1.University of Electro-Communications, 2.ENRI, 3.NIPR, 4.NICT, 5.ISEE, Nagoya University)

[PEM09-P12] Analysis of characteristics of ionospheric parameters, Sq index and neutral winds over Taiwan

*Yu-Jung Chuo[1] (1.Department of Information Technology, Ling Tung University)

[PEM09-P13] Statistical study on daytime Es observed by ground-ionosonde and RO-COSMIC in magnetic Equator region in 2010

*Zheng Wang [1,2], Huixin Liu[1] (1.Department of Earth and Planetary Sciences, School of Science, Kyushu University, Japan. , 2.National Space Science Center, Chinese Academy of Sciences, China.)

[PEM09-P14] The statistical study of the growth rates of Medium-Scale Traveling Ionospheric Disturbances observed with GPS-TEC

*Takafumi Ikeda[1], Akinori Saito[1], Takuya Tsugawa[2], Hiroyuki Shinagawa[2] (1.Department of Geophysics, Graduate School of Science, Kyoto University, 2.National Institutes of Information and Communications Technology)

[PEM09-P15] Comparison of Gravity Wave Activity in the Mesosphere Observed by OH Airglow Imagers and MF Radars over the Antarctic (Syowa & Davis).

*Masaru Kogure[1], Takuji Nakamura[1,2], Yoshihiro Tomikawa[1,2], Mitsumu K. Ejiri[1,2], Takanori Nishiyama[2,1], Masaki Tsutsumi[1,2], Michael J. Taylor[3], Yucheng Zhao[3], P.-Dominique Pautet[3], Damian Murphy[4] (1.National Institute of Polar Research, 2.Department of Polar Science, Sokendai, 3.Physics Department, Utah State University, 4.Australian Antarctic Division)

Local-time Variabilities of SABER CO_2 in the Mesosphere and Lower Thermosphere Region

*Cornelius Csar Jude Salinas[1], Loren Chang[1], Danie Liang[2], Jia Yue[3], Liying Qian[4], Quan Gan[5], James Russel III[3], Martin G Mlynczak[6]

1. Institute of Space Science, National Central University, 2. Institute of Earth Science, Academia Sinica, 3. Department of Atmospheric Sciences, Hampton University, 4. High Altitude Observatory, National Center for Atmospheric Research, 5. Department of Physics and Astronomy, Clemson University, 6. NASA Langley Research Center

This work presents the local-time variabilities of CO_2 in the Mesosphere and Lower Thermosphere region (MLT region) as observed by the Sounding of the Atmosphere using Broadband Emission Radiometry (SABER) onboard the Thermosphere Ionosphere Mesosphere Energetics and Dynamics Satellite (TIMED Satellite). These are then compared to CO_2 as modeled by the Whole Atmosphere Community Climate Model –eXtended (WACCM-X). Also using WACCM-X, a tendency analysis using the continuity equation is done to explain the local-time variabilities of CO_2 in the MLT region. Finally, consequences of including a significant local-time variability in CO_2 when retrieving SABER temperature profiles are determined.

Keywords: Carbon Dioxide, Mesosphere and Lower Thermosphere Region, Tides

©2019. Japan Geoscience Union. All Right Reserved.

Enhanced dynamo electric field as a possible cause of ionosphere disturbance before Large Earthquake

*Koichiro Oyama[1,2,3]

1. Institute of Plasma and Space Sciences,National Cheng Kung Univ., Taiwan, 2. International Ceneter for Space Weather Sudy and Education, Kyushu Univ.,, 3. CoLtd. Asia Space Environment Research Consortium, Japan

Disturbance of ionosphere before large earthquakes has been very often reported. One of the possible disturbing drivers is electric field, which explains most of the ionosphere features we reported so far. However, the origin of the electric field is still in the darkness. One idea of electric field generation exists inside earth interior (Freund et a., 2006). We propose here that the electric field is dynamo field at the height of ≈100 km, which simply intensified before earthquake; intensified eastward (westward)electric field during daytime(nighttime). This idea explains satellite data (Oyama et al.,2008; Oyama et al.,2011; Ryu et al., 2014; Ryu et al., 2016; Oyama et al.,2016; Oyama et al., 2019).

Next question on the electric field generation is the mechanism which modifies the dynamo field. We speculate that modification of E field is a result of modification of neutral wind system, which is originally caused by internal gravity waves which propagate from below. Then again next question is on the origin of the internal gravity waves. The waves might be originally caused by the ground motion, and these waves which propagate upward might interact with planetary wave, and amplified. We show several side evidence of ground motions before earthquakes.

Keywords: Earthquake, Electric field, Ionosphere, Disturbance

©2019. Japan Geoscience Union. All Right Reserved.

Morphology of E1 and E2 Kelvin waves from ECMWF reanalysis

*Chen-Jeih Pan[1], Wei-Sheng Chen[1], Uma Das[2]

1. Institute of Space Science, National Central University, 2. Department of Physics, Indian Institute of Information Technology, Kalyani, India

Kelvin waves are planetary waves traveling eastwards and confined in the equatorial latitudes. The waves play an important role in middle atmosphere dynamics because they transfer energy and momentum from lower to higher altitudes, which contributes to the quasi-biennial oscillation (QBO) and further influences the global climate. Kelvin waves have been studied for many decades, and the most of studies were focused on the waves of wavenumber 1 (E1). On the other hand, the wavenumber-2 Kelvin waves (E2) are also an important part of Kelvin wave activities although their amplitude less than the E1. In this study, we analyzed the long-term European Centre for Medium-Range Weather Forecasts (ECMWF) reanalysis data and reported the morphology of E1 and E2 Kelvin waves in the stratospheric altitudes individually. The temperature from ECMWF reanalysis was used to extract the wave properties. Temperatures between latitudes of 10S and 10N were firstly gridded into the structure of day-altitude-longitude, and then subtract background (longitudinal means) to get equatorial temperature fluctuations. For each altitude, the two-dimensional fast Fourier transform was applied to each 96-day data segment and stepped forward in time by 1 day. The output spectra were then analyzed to get primary wave periods and amplitude variations. From spectra, the E1 amplitude is 1.5 to 2.0 times larger than the E2 in average. The E1 primary periods are 12 to 25 days and are restricted under the 20-km altitude. The periods of 8 to 14 days are the secondary group. They can propagate upward to the 40-km altitude. Regarding the E2, the primary periods are 7 to 12 days and are also restricted under the 20-km altitude. Its secondary group is the periods of 5 to 8 days, which also can propagate upward to the 40-km altitude. Furthermore, the altitude-time-amplitude variation show that the E2 waves are influenced strictly by the QBO westerly. Finally, the cross correlation between E1 and E2 show that the E1 and E2 have high correlation at altitudes close to the tropopause, which implies they are excited simultaneously.

Keywords: Kelvin waves, QBO

©2019. Japan Geoscience Union. All Right Reserved.

Impact of strong ENSO on TEC activity disturbed by ultra-fast Kelvin waves

*Wei-Sheng Chen[1], C.J. Pan[1], Uma Das[2], Chian-Chiau Lin[3]

1. Institute of Space Science, National Central University, Taiwan, 2. Department of Physics, Indian Institute of Information Technology, Kalyani, India, 3. Environmental Research and Information Center, Chang Jung Christian University, Taiwan

Ultra-fast Kelvin waves (UFKW) are a subclass of Kelvin waves that they have the shortest periods (2-5 days) and thus can propagate into the ionosphere. UFKW relate to ionospheric variations have been reported, which include ionospheric minimum virtual height (h'F), F2 maximum critical frequency (foF2), total electron content (TEC), S4 scintillations, etc. In the study, we analyzed the UFKW activities using SABER (Sounding of the Atmosphere using Broadband Emission Radiometry) temperatures and GIM (Global Ionospheric Maps) TEC from 2009 to 2011 to see how UFKW influence the ionosphere. The period 2009-2011 belongs to the strong ENSO period. Previous studies have shown that Kelvin waves were highly active in this period, especially in the early of 2010. Therefore, this study can implicitly reveal how the ionosphere responds to the ENSO. The wave signatures in SABER temperatures were extracted using the fast Fourier transform (FFT). Temperatures in the geographic equatorial latitudes were gridded into the day-altitude-longitude structure and then removed background to get temperature fluctuations. The two-dimensional FFT was applied to each 96-day data segment for each altitude and stepped forward in time by one day. Regarding TEC, the Lomb-Scargle periodogram was used to extract UFKW signatures. Because TEC has a strong local time variation and constrains by the geomagnetic configuration, TEC at 16 local time and low geomagnetic latitudes were selected. The background was removed firstly from the data and then fed TEC fluctuations into the Lomb-Scargle process, which also stepped forward in time by one day. The FFT and Lomb-Scargle process both outputted spectra, which revealed UFKW activities in the mesosphere and lower thermosphere (MLT) region (90-100 km) and the ionosphere (about 150-600 km). The results show that UFKW activities at two equatorial ionization anomalies (EIA) were almost identical, and both were higher than that at geomagnetic equator. Most of wave activities in the temperature field in the MLT region have corresponding activities in TEC. However, there are a lot of small amplitude activities only in TEC.

Keywords: ultra-fast Kelvin waves, ENSO, TEC

©2019. Japan Geoscience Union. All Right Reserved.

Observation and simulation of propagation of coseismic infrasound to the ionosphere

*Jaroslav Chum[1]

1. Institute of Atmospheric Physics of the Czech Academy of Sciences

Vertical motion of the ground surface caused by seismic waves generates acoustic waves that propagate nearly vertically upward owing to supersonic speed of seismic waves. As the air density decreases with height, the amplitude of acoustic waves increases to conserve the energy flux up to the altitudes where the air is so rarefied that it cannot sustain the propagation and the waves start dissipating. For distances up to about 1500 km from the epicenter of the strong earthquakes (M>7), the amplitude (oscillation velocity) of infrasound waves reaches significant values in the upper atmosphere. Consequently, the nonlinear phenomena start to play an important role. Spectral content of the wave packet is changed and the energy is transferred to lower frequencies, which can cause the formation of roughly bipolar N-shaped pulse. The simulation results are compared with observation for selected examples. It is also shown that only infrasound with periods larger than about 10 s (generated by long period seismic waves) can reach the ionospheric heights, namely the F layer where it can be easily detected.

Keywords: coseismic perturbation in the ionosphere, infrasound, nonlinear propagation

©2019. Japan Geoscience Union. All Right Reserved.

Solar wind influence on tropical cyclones mediated by atmospheric gravity waves

*Paul Prikryl[1,2], Iurii Cherniak[3], Irina Zakharenkova[4,5], James M. Weygand[6], Bharat S. R. Kunduri[7]

1. Physics Department, University of New Brunswick, Fredericton, NB, Canada, 2. Geomagnetic Laboratory, Natural Resources Canada, Ottawa, ON, Canada, 3. COSMIC Program Office, University Corporation for Atmospheric Research, Boulder, CO, USA, 4. West Department of IZMIRAN, Kaliningrad, Russia, 5. University of Warmia and Mazury in Olsztyn, Poland, 6. Earth Planetary and Space Sciences, University of California, Los Angeles, CA, USA, 7. Bradley Dept. of Electrical and Computer Engineering, Virginia Tech, Blacksburg, VA, USA

Solar wind coupling to the magnetosphere-ionosphere-atmosphere (MIA) system generates medium- and large-scale atmospheric gravity waves (AGWs) propagating globally from sources in the lower thermosphere at high latitudes. The AGWs propagate globally [1,2] upward and downward, are observed in the ionosphere as traveling ionospheric disturbances [3], can be ducted in lower atmosphere over long distances and reach troposphere. At the reflection point in the troposphere they can trigger moist instabilities to initiate convective bursts, with the latent heat release leading to intensification of storms [4]. In the follow-up studies [5,6,7] it was shown that explosive extratropical cyclones and rapid intensification of tropical cyclones tend to follow arrivals of solar wind high-speed streams (HSS) and/or interplanetary coronal mass ejections (ICMEs). The coupling of solar wind to MIA is most intense during the arrivals of co-rotating interaction regions (CIRs) and/or interplanetary shocks at the leading edges of HSSs and ICMEs when the amplitudes of aurorally-generated AGWs are largest. Ray tracing of AGWs in a model atmosphere show that they can reach tropical cyclones. Spiral gravity waves in typhoons were observed and simulated to propagate radially outward from the typhoon core [8]. The spectra of waves in surface pressure and surface wind measured by the Impacts of Typhoons on the Ocean in the Pacific (ITOP) buoy during the nearby passages of intense typhoons are similar to those of incoming aurorally-generated AGWs. It is suggested that the interaction of aurorally-generated gravity waves with the tropical cyclone vortex and the inner primary eyewall plays a role in the intensification process.

[1] Mayr H.G., et al., J. Geophys. Res., 89, 10929–10959, 1984.
[2] Prikryl P., et al., Ann. Geophys., 23, 401-417, 2005. doi:10.5194/angeo-23-401-2005
[3] Cherniak Iu., Zakharenkova I., Space Weather, 16, 2018. https://doi.org/10.1029/2018SW001869.
[4] Prikryl P., et al., Ann. Geophys. 27, 31–57, 2009. https://doi.org/10.5194/angeo-27-31-2009.
[5] Prikryl P., et al., J. Atmos. Sol.-Terr. Phys., 149, 219–231, 2016.
[6] Prikryl P., et al., J. Atmos. Sol.-Terr. Phys., 171, 94–110, 2018.
[7] Prikryl P., et al., J. Atmos. Sol.-Terr. Phys., 183, 36-60, https://doi.org/10.1016/j.jastp.2018.12.009.
[8] Nolan D.S., Zhang J.A., Geophys. Res. Lett., 44, 3924–3931, 2017. doi:10.1002/2017GL073572

Keywords: Solar wind-magnetosphere-ionosphere-atmosphere coupling, High-speed solar wind stream, Atmospheric gravity wave, Extratropical and tropical cyclones

©2019. Japan Geoscience Union. All Right Reserved.

VIPIR ionospheric observations in Japan

*Takuya Tsugawa[1], Hideo Maeno[1], Michi Nishioka[1], Takumi Kondo[1], Mamoru Ishii[1]

1. National Institute of Information and Communications Technology

National Institute of Information and Communications Technology (NICT) has observed ionosphere by ionosondes more than 70 years in Japan. At present, four ionosondes at Wakkanai (Sarobetsu), Kokubunji, Yamagawa, Okinawa (Ogimi) are automatically operated and controlled from Tokyo. Major ionospheric parameters such as foF2 and foEs are scaled from the ionograms automatically on a realtime basis and scaled manually for the final values. These scaled parameters are provided through our web site (http://wdc.nict.go.jp/IONO/). In 2017, we replaced the 10C ionosondes with Vertical Incidence Pulsed Ionospheric Radar 2 (VIPIR2) which can separate the O- and X-modes of ionospheric echoes which have improved the availability of automatic scaling of the ionogram. Our automatic scaling method has been improved using new O- and X-modes separated ionograms. As for future plans, we try to expand observation area by oblique sounding observations with VIPIRs in Japan and neighboring countries. We have also tried to detect arrival directions of ionospheric echo by using the 8ch receiving data as a interferometry. In this presentation, we will introduce current status and future plans of ionospheric observation in NICT.

Keywords: Ionosphere, Ionosonde, Space Weather

©2019. Japan Geoscience Union. All Right Reserved.

Simulation Results and Performance Analysis of Phase Velocity Spectral Analysis Software (M-Transform) for Airglow Imaging Data

*Septi Perwitasari[1], Takuji Nakamura[2], Masaru Kogure[2], Yoshihiro Tomikawa[2], Mitsumu K. Ejiri[2]

1. LAPAN, 2. NIPR

We have developed a user-friendly software based on *Matsuda et al.*, 2014's 3D-FFT method (M-Transform) for airglow data analysis as a function on Interactive Data Language (IDL). Input of this function is 3-D array of a time series of airglow image that have already been converted to geographical coordinate (*x*, *y*, *t*). The user can customize the wave parameters (e.g. horizontal wavelength (λ_h), wave period (τ), phase speed (*c*), image resolution in space (*dx*,*dy*) and time (*dt*)) in one-line command when executing the program, which depends on their analysis purpose. In order to exhibit this new function's performance and the characteristics/interpretation of the spectral analysis, we have run several test cases using artificial wave. The first case is artificial wave with constant speed (40 m/s) and different wave period (8, 15, 30 min) and horizontal wavelength. In second case, we applied Gaussian shape wave-packet with different FWHM (50, 100, 200 km). For the third test case, with a fixed wave packet size (100 km), we changed the wave packet duration (30, 60, 120 min). The results from the various simulations showed reasonable characteristics of the spectral analysis for different scenarios. We showed that the increase of wave period and horizontal wavelength lead to the wider spectrum with total power difference of ~10%. By changing the wave packet size, we showed that the bigger the wave packet size, the sharper and narrower the spectrum became with the total power increase 2x of the increase size of the wave packet. The result of changing the wave packet duration showed that the longer the duration of wave packet, the spectrum becomes sharper and the total power is proportional to the wave packet length. We also examined the aliasing and zero padding effect on the spectral analysis. In order to avoid the aliasing effect, it is recommended to set the period minimum to at least 2 x image interval (*dt*). More detailed analysis will be discussed during the presentation.

Keywords: Airglow, Gravity wave, Analysis software

©2019. Japan Geoscience Union. All Right Reserved.

Comparisons of Co-incident Ionospheric Plasma Observations Between FORMOSAT-5/AIP and Millstone Hill Incoherent Scatter Radar

*Yi-Wun Chen[1], Chi-Kuang Chao[1]

1. Graduate Institute of Space Science, National Central University, Taiwan

Advanced Ionospheric Probe (AIP) onboard FORMOSAT-5 satellite has routinely measured ionospheric plasma parameters, like ion concentration, velocity, and temperature in a sun-synchronous circular orbit at 720 km altitude along 2230 local-time sector since November 2017. AIP has found that the satellite has a much lower potential with respective to environmental plasma from measured current-voltage curves. A comparison study shall be performed to identify possible bias on the derived AIP parameters. Co-incident observations have been scheduled with Millstone Hill incoherent scatter radar during 30 January to 1 February 2019. In this poster, preliminary comparison results will be outlined and will be used to improve accuracy of the AIP measurement in the future.

Keywords: FORMOSAT-5, AIP, ionosphere

©2019. Japan Geoscience Union. All Right Reserved.

Sub-ionospheric effects of volcano eruptions using VLF/LF standard radio waves

*Kei Maruyama[1], Hiroyo Ohya[1], Fuminori Tsuchiya[2], Kenro Nozaki[5], Kozo Yamashita[3], Yukihiro Takahashi[4], Hiroyuki Nakata[1], Toshiaki Takano[1]

1. Chiba University, 2. Tohoku University, 3. Ashikaga University, 4. Hokkaido University, 5. National Institute of Information and Communications Technology

Several studies for the F-region ionosphere associated with volcano eruptions based on GPS-TEC data have been reported so far (e.g., Heki, 2006; Dautermann et al., 2009; Heki et al., 2010). These studies reported that acoustic waves excited by volcano eruptions reach up to the F-region ionosphere, and caused F-region perturbations. After eruption of the Kelud Volcano, Indonesia, in February 2014, acoustic resonance between the Earth’ s surface and lower thermosphere was reported based on TEC data and the seismic wave data (Nakashima et al., 2015). However, little studies on the D-region ionosphere associated with volcano eruptions have been reported. In this study, we investigate the D-region effects of eruptions of Sakurajima volcano (31.59N, 130.66E), Japan, at 04:11 UT on June 6, 2014, using intensity perturbation of VLF/LF transmitter signals. The VLF/LF propagation paths use in this study are JJY (JJY 60 kHz) - Tainan (TNN, Taiwan), and JJI (22.2 kHz) - TNN. Based on wavelet spectra, the perturbation of both transmitter signals had a frequency of 2-6 mHz during 04:12-04:30 UT after the eruptions (04:11 UT).We compared the perturbations with atmospheric pressure data obtained by an infrasonic meter observed by Sakurajima Volcano Research Center, Kyoto University, and seismic waves in the NIED F-net data (FUK, STM, and SBR) located close to the JJY-TNN path. The atmospheric pressure and vertical velocity of the seismic waves had the similar frequencies of 2-10 mHz during 04:12-04:47 UT. These similar frequencies suggest that the perturbations would be caused by acoustic resonance between the Earth's surface and lower thermosphere, or by acoustic and atmospheric gravity waves generated by volcanic eruptions. In the presentation, we will discuss the cause of the VLF/LF perturbations in more detail.

©2019. Japan Geoscience Union. All Right Reserved.

Observations of ionospheric and mesospheric wave structures by a low-cost airglow imaging system

*Keisuke Hosokawa[1], Nanami Kusuyama[1], Yuta Hozumi[1], Kohei Takami[1], Susumu Saito[2], Yasunobu Ogawa[3], Mamoru Ishii[4], Yuichi Otsuka[5], Takuya Tsugawa[4]

1. University of Electro-Communications, 2. ENRI, 3. NIPR, 4. NICT, 5. ISEE, Nagoya University

In the last two decades, all-sky airglow imagers with cooled CCD cameras have widely been used to observe large-scale wave structures in the F-region ionosphere, for example medium-scale traveling ionospheric disturbances (MSTIDs). Such wavy features are seen in the oxygen emission at 630.0 nm from altitudes slightly below the F-region peak. Similar optical observations of OH band emission have also enabled us to visualize atmospheric gravity waves at the mesospheric height. Deploying airglow imagers in multiple places is one of the cost-effective ways to visualize the large-scale structure of these wave structures at both the F-region ionosphere and mesosphere [e.g., Kubota et al., 2001; Suzuki et al., 2013]. However, ground-based airglow imagers equipped with a cooled CCD camera is still expensive; thus, it is rather difficult to deploy such systems in a wide area and carry out a network observation. To overcome this limitation, we recently developed a low-cost airglow imaging system (Low-Cost Airglow imaging System: LCAS) which consists of a small camera (WAT-910HX), fisheye lens and optical filter. We then confirmed its capability of imaging the spatial structure of polar cap patches and plasma bubble in the 630.0 nm emission from the F-region. But, still, it is unclarified if the system is also capable of detecting the two-dimensional structure of MSTIDs. On the night of May 12, 2018, we identified a weak wavy signature in the 630.0 nm airglow images from one of our LCAS stations in Ishigaki Island, Japan. The wave structure in the 630.0 nm images was smoothly connected to the structure of MSTIDs in the GPS-TEC data, which confirmed the ability of LCAS for detecting MSTIDs. We also identified smaller scale wave structures in the 630.0 nm images, showing characteristic concentric wave fronts. We speculate that gravity waves in the mesosphere were captured in the 630.0 nm images as a contamination of the OH airglow. This is mainly because we make use of an optical filter having 10 nm FWHM, which enables us to detect several spectral peaks of OH emission near the 630.0 nm oxygen emission. We have estimated the center of the concentric wave structures by using the curvature of the wave fronts, and then confirmed that active rain fall took place in a localized area close to the estimated center of the concentric waves. This result supports our hypothesis that the OH emission containing signatures of mesospheric gravity waves were detected in the 630.0 nm images. In summary, the 630.0 nm airglow observation of LCAS is able to observe MSTIDs and mesospheric gravity waves. This will allow us to monitor such wavy structures at two different altitudes by distributing the similar system in a wide area.

Keywords: Airglow, Traveling Ionospheric Disturbances

©2019. Japan Geoscience Union. All Right Reserved.

Analysis of characteristics of ionospheric parameters, Sq index and neutral winds over Taiwan

*Yu-Jung Chuo[1]

1. Department of Information Technology, Ling Tung University

In this paper, we examine the variation of thermospheric neutral winds and solar quiet (Sq) current of the geomagnetic fields for the equatorial ionospheric anomaly area (EIA) during the solar activity period in 1999. The thermospheric neutral winds are derived from the ionospheric F_2-layer peak height, hmF_2, by using the servo model method. The variability of the amplitude ofSq fields is derived from the ground geomagnetic fields in the components H and Z, respectively. Theresults of the current system show a same diurnal variation, which that peaks / valleys in the local noon time for Sq(H) / Sq(Z) in the low latitudes, respectively.The results also indicate a weak seasonal variation that peaks appear at the local summer of the Sq currents in H and Z components, respectively. The Sq current system is associated with the change of the equatorial electrojet (EEJ). Further, the variability is probably attributed to local thermospheric winds. The study also shows that the zonal and meridional components of the neutral winds at the EIA over Taiwan area. Furthermore, the study examines the variations of Sq(H), Sq(Z), neutral winds, and ionospheric parameters foE_s, NmF_2, and hmF_2during the disturbed geophysical conditions such as geomagnetic storm and earthquake. The result shows the variationsof ionospheric Sq(H), Sq(Z) and thermospheric neutral winds are different between the seismo-ionospheric and solar-terrestrial disturbed periods, even they lead the same decreasing electron density reaction in the ionosphere at the EIA over Taiwan area.

Keywords: Sq current, ionosphere, neutral winds

©2019. Japan Geoscience Union. All Right Reserved.

Statistical study on daytime Es observed by ground-ionosonde and RO-COSMIC in magnetic Equator region in 2010

*Zheng Wang [1,2], Huixin Liu[1]

1. Department of Earth and Planetary Sciences, School of Science, Kyushu University, Japan. , 2. National Space Science Center, Chinese Academy of Sciences, China.

Scintillations under 150 km height shown by radio occultation (RO) of COSMIC are considered to be associated with ionospheric sporadic E (Es) layer. In this paper, we make a Statistical study on daytime Es observed by ground-ionosonde at five stations in magnetic Equator region in 2010, and make a comparison with S4 index from RO-COSMIC within 6 degree of each station. The results show that: At each station the diurnal variation of foEs from ionosonde decrease a little around LT 0600 and then increase, having maximum around LT 1200, decrease around LT 1800 and then increase near LT 2000-2200; All the S4>=0.3 observations during daytime come from RO-COSMIC under 150 km height; The diurnal variation of S4 index under 150 km height from RO-COSMIC over each station has similar trend with that of foEs at the same station; S4 index over 150 km height from RO-COSMIC is only high during nighttime; For the stations at different longitudes, Es occurrences from ionosonde are positively associated with S4>=0.3 from RO-COSMIC. The comparison shows that the S4 index from RO-COSMIC could show some features of daytime Es layer in magnetic Equator region without the location limitation of ground stations.

Keywords: daytime ionospheric sporadic E, ground-ionosonde , radio occultation of COSMIC , magnetic Equator region

©2019. Japan Geoscience Union. All Right Reserved.

The statistical study of the growth rates of Medium-Scale Traveling Ionospheric Disturbances observed with GPS-TEC

*Takafumi Ikeda[1], Akinori Saito[1], Takuya Tsugawa[2], Hiroyuki Shinagawa[2]

1. Department of Geophysics, Graduate School of Science, Kyoto University, 2. National Institutes of Information and Communications Technology

We think two mechanism, E-F coupling and Perkins Instability, will relate to growth for nighttime-MSTID in mid-latitude [Tsunoda and Cosgrove., 2001 ; Perkins., 1973]. Linear growth rate of perturbation intensity of Pedersen conductivity expected from E-F coupling is around 15 minutes [Yokoyama et al., 2009], which is far shorter than one expected from Perkins Instability [Fukao and Kelley, 1991 ; Miller et al., 1997 ; Shiokawa et al., 2003]. However, Es layer’ s spatial and temporal scale is less than 100km and 15min [Maeda et al., 2013 ; S.Saito et al., 2007]. They are different from MSTID’ s ones, which are 200-400 km and around 2hours [Otsuka et al., 2011]. To decide which instability is responsible for growth of nighttime MSTID, the growth rate of MSTID was observationally determined with ground-based GPS network data.

We statistically investigated the growth rate of nighttime-MSTID in Japan in 2014 observed with GPS-TEC. The growth rate of nighttime -MSTID observed was 1.0 - 6.0 $\times 10^{-4}$ s^{-1} during 1800LT-2400LT in summer.Linear growth rate of Perkins instability in summer was 1.0 - 6.0 $\times 10^{-4}$ s^{-1} during 1800LT - 2400LT, so they were less than one of the E-F coupling instability. Also,Seasonal distribution of observed growth rate before midnight was similar to that of linear growth rate.U×B derived by GAIA model was high in spring - summer and seasonal distribution of U×B was similar to that of linear growth rate. Therefore, the growth of MSTID when propagating is not determined by E-F coupling instability but Perkins instability and neutral wind.

Keywords: MSTID, GPS-TEC, Ionosphere

©2019. Japan Geoscience Union. All Right Reserved.

Comparison of Gravity Wave Activity in the Mesosphere Observed by OH Airglow Imagers and MF Radars over the Antarctic (Syowa & Davis).

*Masaru Kogure[1], Takuji Nakamura[1,2], Yoshihiro Tomikawa[1,2], Mitsumu K. Ejiri[1,2], Takanori Nishiyama[2,1], Masaki Tsutsumi[1,2], Michael J. Taylor[3], Yucheng Zhao[3], P.-Dominique Pautet[3], Damian Murphy[4]

1. National Institute of Polar Research, 2. Department of Polar Science, Sokendai, 3. Physics Department, Utah State University, 4. Australian Antarctic Division

Gravity waves transport momentum and energy from the lower atmosphere to the upper atmosphere and drive the general circulation, which significantly changes the temperature in the middle atmosphere [Fritts and Alexander, 2003]. To understand this role quantitatively will improve the modern general circulation models [Garcia et al., 2017].

The polar night jet region is known to have high gravity-wave activity. However, sources of gravity waves, their propagation, and their spectra are poorly understood because of a lack of observations. In particular, little is known about the dependence of their characteristics on their spectra (i.e., wavenumber and frequency) and on interactions among waves with several wavenumbers and frequencies [Fritts and Alexander, 2003]. To understand these, our group has observed gravity waves at different sites over the Antarctic.

Observation techniques have limitations due to the breadth of the gravity wave spectrum and the target and physical parameter sensed by the observing system [Alexander et al., 1998]. In this study an OH imager and an MF radar are used. Both instruments cover the OH layer (~87 km altitude), but both cover quite different ranges of the wave spectrum. The OH imager can observe waves with shorter ground-based periods (8-60 min) and shorter horizontal wavelengths (2-100 km) [Matsuda et al., 2017]. On the other hand, the MF radar can observe waves with the longer ground-based periods (>~30 min). It also has a preference for the waves with longer horizontal wavelength because of its observational volume.

This study derives gravity-wave perturbations, over Syowa and Davis, from the OH imager data based on Matsuda et al. [2014] and the MF radar data based on Murphy et al. [2007], respectively. In this presentation, we would like to show the gravity wave activity, over Syowa and Davis, with the shorter horizontal wavelength (i.e., observed by the OH imagers) and with the longer horizontal wavelength (i.e., observed by the MF radars). The correlation and relationship between both wave activities will be discussed. Also, we would like to discuss the local variation of that relationship.

Keywords: Gravity Wave, Middle Atmosphere, OH Imager

©2019. Japan Geoscience Union. All Right Reserved.

[E] Oral | P (Space and Planetary Sciences)：P-EM Solar-Terrestrial Sciences, Space Electromagnetism & Space Environment

Wed. May 29, 2019 1:45 PM - 3:15 PM JST | Wed. May 29, 2019 4:45 AM - 6:15 AM UTC | A03 TOKYO BAY MAKUHARI HALL

[P-EM09] Vertical coupling in the atmosphere and Ionosphere

convener:Huixin Liu(Earth and Planetary Science Division, Kyushu University SERC, Kyushu University), Loren Chang(Institute of Space Science, National Central University), Yuichi Otsuka(Institute for Space-Earth Environmental Research, Nagoya University), Chairperson:Patrick Espy(Norwegian University of Science and Technology), Astrid Maute(National Center for Atmospheric Research, US)

Vertical coupling mechanisms throughout the whole atmosphere are critical to understanding the near Earth space environment, as well as its sensitivity to the solar, geomagnetic, and atmospheric drivers. This international session focuses on physical/chemical processes occurring in the mesosphere, thermosphere, and ionosphere (MTI). Both quiet and disturbed states in response to lower atmospheric forcing or solar forcing are important for understanding the MTI system and its coupling to other regions. We invite presentations of observations and observational concepts with ground-based and/or space-borne instruments, theoretical studies, numerical simulations, and development of data analysis systems for various kinds of temporal and spatial variations in atmosphere-ionosphere coupled system.

1:45 PM - 2:05 PM JST | 4:45 AM - 5:05 AM UTC

[PEM09-01] **Vertical Coupling from the Atmosphere to Geospace at Arrival Heights in Antarctica**

★Invited Papers

*Xinzhao Chu[1] (1.University of Colorado Boulder)

2:05 PM - 2:20 PM JST | 5:05 AM - 5:20 AM UTC

[PEM09-02] Vertical structure of terdiurnal tides in the Antarctic MLT region: 15 years observation over Syowa

*Huixin Liu[1], Masaki Tsutsumi[2], Hanli Liu[3] (1.Earth and Planetary Science Division, Kyushu University, Japan, 2.National Institute for Polar Research, Japan, 3.National Center for Atmospheric Research, US)

2:20 PM - 2:35 PM JST | 5:20 AM - 5:35 AM UTC

[PEM09-03] **3D Investigation of gravity waves propagation by Continuous Doppler sounding**

*Jaroslav Chum[1], Katerina Podolska[1] (1.Institute of Atmospheric Physics of the Czech Academy of Sciences)

2:35 PM - 2:55 PM JST | 5:35 AM - 5:55 AM UTC

[PEM09-04] **Observations of MLT dynamics using meteor radars and meteor radar networks**

★Invited Papers

*Gunter Stober[1], Vivien Matthias[2], Sven Wilhelm[1], Dimitry Pokhotelov[1], Alexander Kozlovsky[3], Evgenia Belova[4], Johan Kero[4], Chris Hall[5], Masaki Tsutsumi[6] (1.Leibniz Institute of Atmospheric Physics, 2.Potsdam Institute for Climate Impact Research, Earth System Analysis - Research Domain 1, Potsdam, Germany, 3.Sodankylä Geophysical Observatory, Sodankylä, FIN-99600, Finland, 4.Swedish Institute of Space Physics, Box 812, 98128 Kiruna, Sweden, 5.Tromsø Geophysical Observatory UiT-the Arctic University of Norway, Tromsø, Norway, 6.National Institute of Polar Research, Tokyo, Japan)

2:55 PM - 3:15 PM JST | 5:55 AM - 6:15 AM UTC

[PEM09-05] Ionospheric Variability Associated with the Quasi-6-day Planetary Wave

★Invited Papers

*Yosuke Yamazaki[1] (1.GFZ German Research Centre for Geosciences)

Vertical Coupling from the Atmosphere to Geospace at Arrival Heights in Antarctica

*Xinzhao Chu[1]

1. University of Colorado Boulder

The observational campaign with Fe Boltzmann and Na Doppler lidars has entered its 9th year at Arrival Heights near McMurdo (77.8S, 166.7E), Antarctica. The unique datasets have opened an exceptional window for exploration in the vertical coupling from the lower atmosphere to the thermosphere, and vertical coupling among the neutral atmosphere, ionosphere, and magnetosphere. Collaborating with theoreticians and modelers, we are attempting to establish a vertical picture of gravity waves in Antarctica from near the surface to the thermosphere, and a key concept is the secondary gravity wave generation initially hypothesized by Dr. Sharon Vadas. Combining observations with numerical modeling, we are also trying to understand how metal layers with cosmic dust origins are formed high in the thermosphere and ionosphere F-region via a complex atmosphere-ionosphere-magnetosphere (AIM) coupling and even correlating with solar wind activity. In this paper we will report a few studies that may be intriguing for advancing the understandings of vertical coupling from the atmosphere to the geospace at Arrival Heights that is a gravity-wave hotspot and by the edge of polar cap and auroral zone.

©2019. Japan Geoscience Union. All Right Reserved.

Vertical structure of terdiurnal tides in the Antarctic MLT region: 15 years observation over Syowa

*Huixin Liu[1], Masaki Tsutsumi[2], Hanli Liu[3]

1. Earth and Planetary Science Division, Kyushu University, Japan, 2. National Institute for Polar Research, Japan, 3. National Center for Atmospheric Research, US

The terdiurnal tide (TDT) in the Antarctica mesosphere and lower thermosphere (MLT) region is poorly known. In this study, we examine its characteristics using long-term neutral wind observations at Syowa (69S, 39E) between January 2004 and July 2018. The analysis reveals TDT being a significant tidal component in the Antarctica with distinct vertical structures and seasonal evolution. (1) It shows a prominent height-dependent seasonal variation, being in opposite phase above and below 94 km altitude, with peak amplitude in June –July at altitudes below 94 km, but in November –December above it. (2) The zonal wind component is 90 phase shifted from the meridional, with its amplitude of comparable or larger values than the meridional in all seasons except for November –December. (3) The vertical wavelength is shortest (50 –65 km) in local summer (Nov.–Jan.) and longes (80 –110 km) in local winter (Jun.–Aug.). Most of these features differ from those reported in the Arctic, indicating hemispheric asymmetry. Furthermore, the phase structure reveals a dominant upward propagating mode in local summer, but superposition of more than one mode in other seasons. Especially in local winter, a downward propagating mode above 95 km suggests Joule heating/ion drag as likely tidal sources from above, in addition to those from lower atmosphere. The nearly 15 years Syowa observations provide new constrains and benchmark for model simulations that seek to understan terdiurnal tidal forcing mechanisms in polar regions.

Keywords: Terdiurnal tide, Antarctica, vertical coupling

©2019. Japan Geoscience Union. All Right Reserved.

3D Investigation of gravity waves propagation by Continuous Doppler sounding

*Jaroslav Chum[1], Katerina Podolska[1]

1. Institute of Atmospheric Physics of the Czech Academy of Sciences

Multi-point continuous Doppler sounding is a useful tool to investigate short-time fluctuations in the ionosphere. We present analysis of GW propagation in the upper atmosphere and ionosphere in 3D. It is based on multi-point continuous Doppler sounding at three different frequencies; sounding radio waves of various frequencies reflect at different altitudes. The advantage of this analysis is information about the GW propagation in 3D and about the attenuation of wave power with height. The disadvantage is a relatively small number of events that can be analyzed as critical frequency of the ionosphere foF2 has to be larger than the highest sounding frequency and also significant cross-correlation between signals reflecting at different altitudes is necessary.

Keywords: atmospheric internal gravity waves, ionosphere , Doppler sounding, 3D analysis, Attenuation

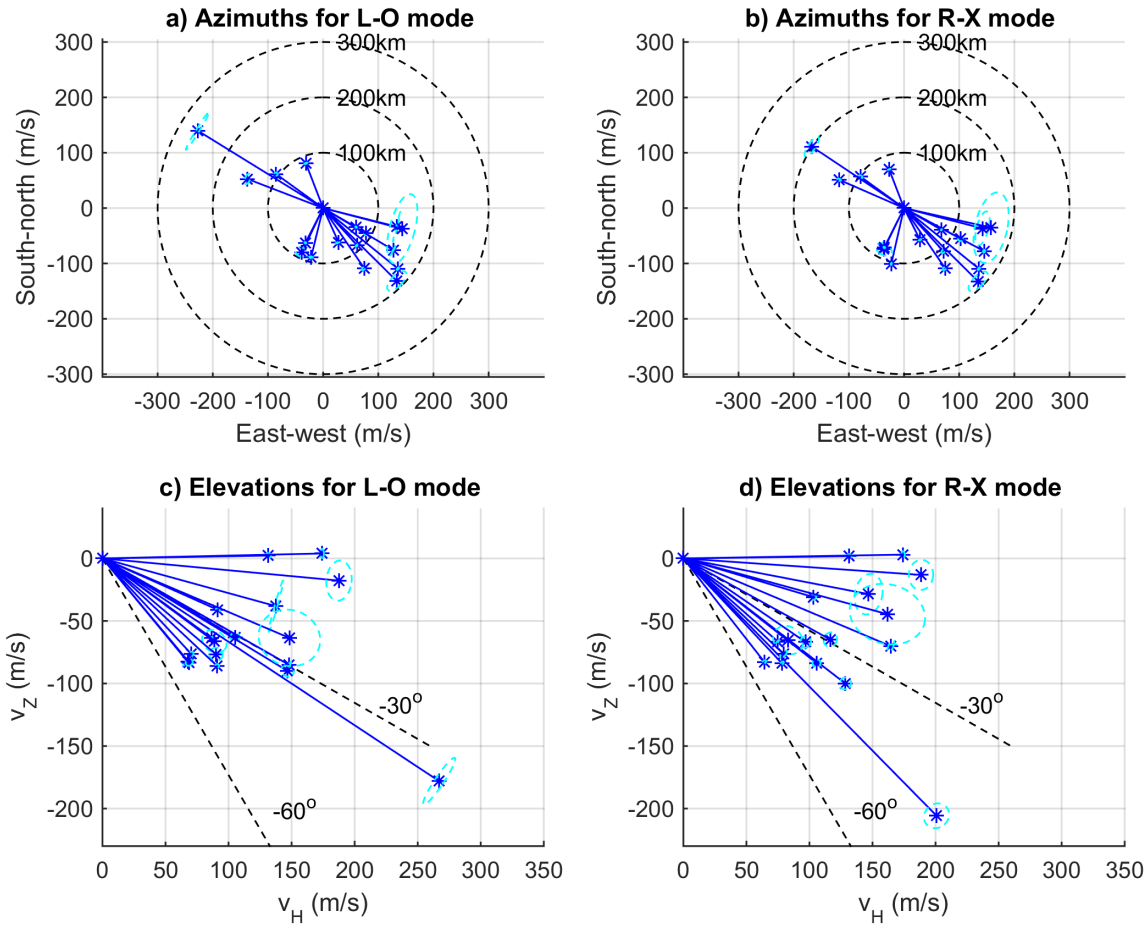

©2019. Japan Geoscience Union. All Right Reserved.

Observations of MLT dynamics using meteor radars and meteor radar networks

*Gunter Stober[1], Vivien Matthias[2], Sven Wilhelm[1], Dimitry Pokhotelov[1], Alexander Kozlovsky[3], Evgenia Belova[4], Johan Kero[4], Chris Hall[5], Masaki Tsutsumi[6]

1. Leibniz Institute of Atmospheric Physics, 2. Potsdam Institute for Climate Impact Research, Earth System Analysis - Research Domain 1, Potsdam, Germany, 3. Sodankylä Geophysical Observatory, Sodankylä, FIN-99600, Finland, 4. Swedish Institute of Space Physics, Box 812, 98128 Kiruna, Sweden, 5. Tromsø Geophysical Observatory UiT-the Arctic University of Norway, Tromsø, Norway, 6. National Institute of Polar Research, Tokyo, Japan

The winter 2015/16 was characterized by an unusually strong polar vortex with values up to 2 standard deviations guiding the mid-latitude planetary waves into the subtropical mesosphere. This exceptionally strong wave activity in the subtropical mesosphere led to a regionally reversed meridional temperature gradient resulting in a zonal wind reversal between 70 and 80 km at polar latitudes due to the thermal wind relation. This regional wind reversal changes the propagation conditions for waves propagating upward from the mesosphere into the thermosphere/ionosphere. The variability of the thermosphere/ionosphere is influenced by forcing from below and thus by gravity waves and atmospheric tides propagating upward from the mesosphere into the thermosphere.
To investigate the change in propagation characteristics of gravity waves and tides in the upper mesosphere/ lower thermosphere (MLT) during this unusual zonal wind reversal in winter 2015/16 we use data from a meteor radar network in Scandinavia. With this network we are able to apply tomographic wind field analysis obtaining horizontally resolved wind fields and horizontal wavelength spectra. Further, we are able to assess the spatial and temporal day-to-day variability of tides.

Keywords: meteor radar, horizontally resolved winds, planetary waves, atmospheric tides and gravity waves, vertical coupling

©2019. Japan Geoscience Union. All Right Reserved.

Ionospheric Variability Associated with the Quasi-6-day Planetary Wave

*Yosuke Yamazaki[1]

1. GFZ German Research Centre for Geosciences

The state of the ionosphere varies from day to day. This is partly due to atmospheric waves that propagate to the upper atmosphere from below. The present study investigates the ionospheric variability associated with the quasi-6-day wave (Q6DW), which is a westward-traveling planetary wave with zonal wave number s=1 and period around t=6d. First, the Q6DW effect on the equatorial ionospheric electric field is examined using the equatorial electrojet measurements from CHAMP and Swarm satellites, as well as ground-based magnetometer and radar observations. Case studies are presented where westward-propagating disturbances with s=1 and t~6d are observed in the daytime equatorial ionospheric electric field. Geopotential height measurements from the Aura satellite confirm the presence of the Q6DW in the lower thermosphere during those events. Next, the impact of the Q6DW on the equatorial ionization anomaly (EIA) is assessed using global maps of total electron content (TEC) from Global Positioning System data. It is shown that the amplitude of the Q6DW in TEC is largest at the EIA crest latitudes and its intra-annual variability closely follows the Q6DW variability in the lower thermosphere.

Keywords: ionosphere/thermosphere, quasi-6-day wave, equatorial region

©2019. Japan Geoscience Union. All Right Reserved.

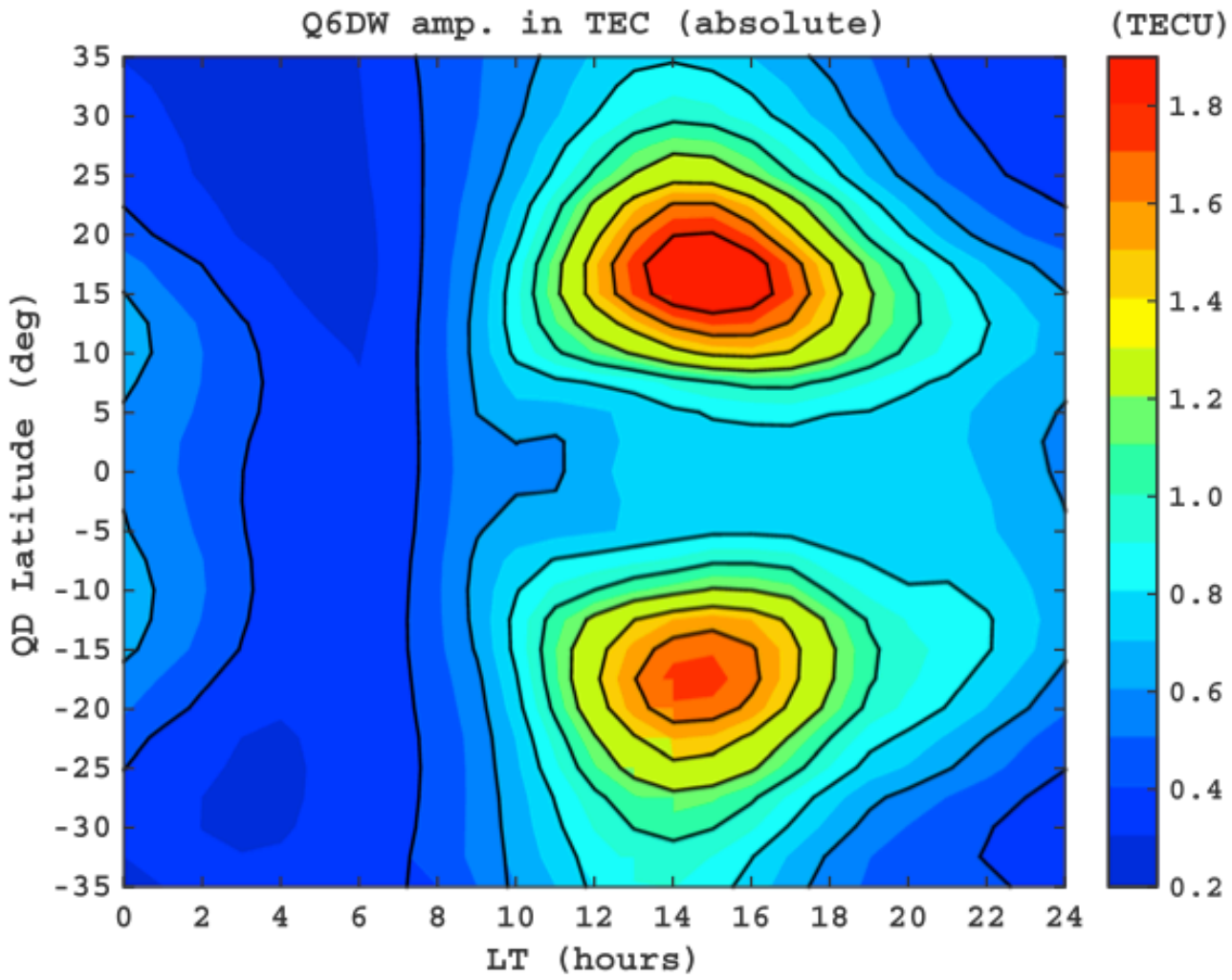

©2019. Japan Geoscience Union. All Right Reserved.

[E] Oral | P (Space and Planetary Sciences)：P-EM Solar-Terrestrial Sciences, Space Electromagnetism & Space Environment

Wed. May 29, 2019 3:30 PM - 5:00 PM JST | Wed. May 29, 2019 6:30 AM - 8:00 AM UTC | A03 TOKYO BAY MAKUHARI HALL

[P-EM09] Vertical coupling in the atmosphere and Ionosphere

convener:Huixin Liu(Earth and Planetary Science Division, Kyushu University SERC, Kyushu University), Loren Chang(Institute of Space Science, National Central University), Yuichi Otsuka(Institute for Space-Earth Environmental Research, Nagoya University), Chairperson:Yuichi Otsuka, Yosuke Yosuke Yamazaki(GFZ Potsdam, Germany)

Vertical coupling mechanisms throughout the whole atmosphere are critical to understanding the near Earth space environment, as well as its sensitivity to the solar, geomagnetic, and atmospheric drivers. This international session focuses on physical/chemical processes occurring in the mesosphere, thermosphere, and ionosphere (MTI). Both quiet and disturbed states in response to lower atmospheric forcing or solar forcing are important for understanding the MTI system and its coupling to other regions. We invite presentations of observations and observational concepts with ground-based and/or space-borne instruments, theoretical studies, numerical simulations, and development of data analysis systems for various kinds of temporal and spatial variations in atmosphere-ionosphere coupled system.

3:30 PM - 3:50 PM JST | 6:30 AM - 6:50 AM UTC

[PEM09-06] Results of FORMOSAT-3/COSMIC to the most recent developments on FORMOSAT-7/COSMIC-2

★Invited Papers

*JANN-YENQ Liu[1] (1.Center for Astronautical Physics and Engineering; Graduate Institute of Space Science, National Central University, Taiwan)

3:50 PM - 4:05 PM JST | 6:50 AM - 7:05 AM UTC

[PEM09-07] A morphological study on the relationship between electron density fluctuations and magnetic fluctuations observed by low altitude satellites in low and middle latitudes

*Toshihiko Iyemori[1], Tadashi Aoyama[1], Yoshihiro Yokoyama[1] (1.Kyoto University)

4:05 PM - 4:25 PM JST | 7:05 AM - 7:25 AM UTC

[PEM09-08] Observations of the Thermosphere and Ionosphere by the NASA GOLD Mission

★Invited Papers

*Stanley C Solomon[1], Alan G. Burns[1], Richard W. Eastes[2], William E. McClintock[2] (1.National Center for Atmospheric Research, 2.University of Colorado)

4:25 PM - 4:40 PM JST | 7:25 AM - 7:40 AM UTC

[PEM09-09] Temporal and spatial evolutions of storm enhanced density in the mid- and low-latitude regions as seen in the variation of global total electron content

*Atsuki Shinbori[1], Takuya Sori[1], Yuichi Otsuka[1], Takuya Tsugawa[2], Michi Nishioka[2] (1.Institute for Space-Earth Environment Research (ISEE), Nagoya University, 2.National Institute of Information and Communications Technology (NICT))

4:40 PM - 4:55 PM JST | 7:40 AM - 7:55 AM UTC

[PEM09-10] **Tidal Forcing Effects on the Zonal Variation of Solstice Equatorial Plasma Bubbles**

*Loren Chang[1], Jude Salinas[1], Yi-Chung Chiu[1], Pei-yun Chiu[1], Charles Lin[2] (1.Institute of Space Science and Engineering, Center for Astronautical Physics and Engineering, National Central University, Taiwan, 2.Department of Earth Science, National Cheng Kung University, Taiwan)

4:55 PM - 5:00 PM JST | 7:55 AM - 8:00 AM UTC

Discussion

Results of FORMOSAT-3/COSMIC to the most recent developments on FORMOSAT-7/COSMIC-2

*JANN-YENQ Liu[1]

1. Center for Astronautical Physics and Engineering; Graduate Institute of Space Science, National Central University, Taiwan

The FORMOSAT-3 Project is also named Constellation Observing System for Meteorology, Ionosphere and Climate (COSMIC), or FORMOSAT-3/COSMIC (F3/C) for short. The project is targeted to place six micro-satellites into six different orbits with 72-deg inclination at 700~800 kilometer above the earth ground. These satellites orbit around the earth to form a low-earth-orbit constellation that conduct radio occultation (RO) by receiving signals transmitted by the 24 US GPS satellites. The satellite observation covers the entire global ionosphere, providing over 2,500 global RO sounding data (electron density and S4 scintillation profiles) per day since 15 April 2006. This for the first time allows scientists observing the 3D ionospheric electron density structure and dynamics. Simultaneous F3/C RO observations and ground-based receiver measurements of International GNSS (global navigation satellite system) Service (IGS) further initiate constructing three different models for monitoring (near real-time), nowcasting (few minutes to hours), and forecasting (few hours to days) the ionospheric weather resulted from the space weather (solar disturbances, solar winds, magnetic storms, etc.); the atmospheric severe weathers (typhoons, fronts, volcano eruptions, etc.); and the lithosphere weather (earthquakes, tsunami, etc.). The monitoring model is combining the total electron content (TEC) or the GNSS satellite signal scintillations of F3/C and ground-based IGS observations to construct an advanced GIM (global ionospheric map) to report the ionospheric bias and develop L-band scintillation models for communication, positioning, and navigation applications. The nowcast model is a global 3D ionospheric data assimilation model based on the Gauss-Markov Kalman filter with an existing background model to assimilate the TEC observations from the ground-based IGS receivers and space-based F3/C to output the global electron density for coming few minutes to hours. On the other hand, to carry out a long-term forecast, the neutral compositions in the atmosphere should be taken into consideration. Therefore, to develop a forecast model assimilating the observations of F3/C and IGS ground-based receivers into a neutral-ion coupled model. Following the F3/C, FORMOSAT-7/COSMIC (F7/C2) consists of six small-satellites with 24-deg inclination and about 500 km altitude will be launched in 2019. The developed models with F7/C2 RO by receiving signals transmitted by the GPS/GLONASS satellites and IVM (ionospheric velocity meter) plasma measurements as well as ground-based IGS GNSS data shall significantly improve the space weather monitoring/nowcast/forecast in the near future.

Keywords: ionospheric space weather, FORMOSAT-3/COSMIC, FORMOSAT-7/COSMIC, Kalman filter

©2019. Japan Geoscience Union. All Right Reserved.

A morphological study on the relationship between electron density fluctuations and magnetic fluctuations observed by low altitude satellites in low and middle latitudes

*Toshihiko Iyemori[1], Tadashi Aoyama[1], Yoshihiro Yokoyama[1]

1. Kyoto University

Polar orbiting low-altitude satellites such as the Swarm satellites observe magnetic and electron density fluctuations in low and middle latitudes along satellite orbit. The magnetic fluctuations typically have the period about 10-30seconds along satellite orbit and they are mostly small-scale field-aligned current effects and named as 'magnetic ripples'. They are supposed to be generated in lower ionosphere by dynamo mechanism caused by neutral atmospheric waves from lower atmosphere. On the nightside, they still exist with smaller amplitude because of lower ionospheric conductivity. Plasma bubbles also exist on the nightside and they normally accompany magnetic fluctuations to keep pressure balance. If we trace down to the dynamo layer around 120km altitude from magnetic ripples and compare the electron density fluctuations, they correspond better than the correspondence on the orbit. This indicates vertical propagation of atmospheric waves which causes both magnetic ripples and electron density fluctuations. On the other hand, in well-developed plasma bubbles, plasma density fluctuation and magnetic fluctuation occur at the same location on the orbit. In this study, we present morphological relationship between the two phenomena. That is, we investigate how magnetic ripples relate to plasma bubbles.

Keywords: magnetic ripples, ionospheric electron density, plasma bubbles

©2019. Japan Geoscience Union. All Right Reserved.

Observations of the Thermosphere and Ionosphere by the NASA GOLD Mission

*Stanley C Solomon[1], Alan G. Burns[1], Richard W. Eastes[2], William E. McClintock[2]

1. National Center for Atmospheric Research, 2. University of Colorado

The new Global-scale Observations of the Limb and Disk (GOLD) mission is an imaging spectrograph deployed in geostationary orbit on the SES-14 communications satellite. GOLD measures airglow emitted by the Earth in the far-ultraviolet region of the spectrum from 132 to 164 nm, notably including the 135.6 nm doublet of atomic oxygen (O), and most of the LBH bands of molecular nitrogen (N_2). During the day, the ratios of the oxygen to nitrogen emissions indicate the relative column densities of O and N_2, and temperature can be inferred from the spectral shape of the LBH bands. During the night, radiative recombination emissions by the O doublet indicate the density of the ionosphere, particularly the equatorial ionization anomalies and the structured instabilities that form within them. GOLD also measures exospheric temperatures on the limb, it infers molecular oxygen densities from stellar occultations, and it can also see northern hemisphere aurora. SES-14 was launched in January 2018, the satellite achieved geostationary orbit in, and GOLD observations commenced in October. We will give an overview of the GOLD mission and show preliminary results from its first months of operations. Despite the recent quiet conditions with low solar activity, composition images reveal daily and seasonal variations, indicative of global vertical wind patterns. The equatorial ionization anomalies are seen to be surprisingly variable and dynamic, with instabilities forming on most nights, even at solar minimum. We will compare GOLD results with global general circulation models and airglow emissions modeling, and discuss how these data could be used in assimilation models of the upper atmosphere and ionosphere.

Keywords: Thermosphere, Ionosphere, Ultraviolet Imaging

©2019. Japan Geoscience Union. All Right Reserved.

Temporal and spatial evolutions of storm enhanced density in the mid- and low-latitude regions as seen in the variation of global total electron content

*Atsuki Shinbori[1], Takuya Sori[1], Yuichi Otsuka[1], Takuya Tsugawa[2], Michi Nishioka[2]

1. Institute for Space-Earth Environment Research (ISEE), Nagoya University, 2. National Institute of Information and Communications Technology (NICT)

The global electron density distribution in the ionosphere depends strongly on geographical latitude, longitude, and local time. The structure changes severely from the high-latitude to the equatorial regions associated with geomagnetic storms. The storm-time prominent ionospheric phenomena are tongue of ionization (TOI), storm-enhanced density (SED), and equatorial ionization anomaly (EIA). These phenomena are very dynamic because ionospheric electric fields and particle precipitation from the magnetosphere vary significantly during the development and decay of the geomagnetic storms. The generation mechanism of SED has been thought as local upward **E**x**B** drifts [e.g., Huang et al., 2005, Liu et al., 2016], westward plasma transportation from the nightside to the dayside by sub-auroral polarization stream (SAPS) [Foster et al., 2007], equatorward neutral winds [Anderson, 1976], and latitudinal expansion of the EIA [e.g., Kelley et al., 2004]. However, since such different mechanisms of the formation of SED have been proposed by many researchers, a comprehensive understanding of the cause of SED formation has not yet been done. In this study, we investigate the temporal and spatial evolutions of SED during the development and decay of geomagnetic storms using Global Navigation Satellite System (GNSS) Total Electron Content (TEC) data with high time and spatial resolutions, to identify the main mechanism responsible for SED. We also use solar wind data and geomagnetic indices to see the interplanetary condition and geomagnetic activity during geomagnetic storms. In the present analysis, we first calculate the average absolute TEC (ATEC) of 10 geomagnetically quiet days every month, referring to the list of quiet and disturbed days provided by GFZ. Next, we subtract the storm-time ATEC from the average ATEC and create global maps of the difference ATEC in geographical and geomagnetic coordinates. Several hours after the onset of the main phase of the geomagnetic storms, the enhanced TEC region with a narrow latitudinal width (5-10 degrees) appears at high latitudes (60-70 degrees in geomagnetic latitude (GMLAT)) of the afternoon sector (12-16 h, MLT: magnetic local time). The enhanced TEC region is located at a lower latitude of the equatorward wall of the midlatitude trough. As the geomagnetic storms grow, the enhanced TEC region expands to the nightside (~20 h, MLT) within a time scale of 20-30 minutes, and the region moves equatorward within several hours. After that, apart from the midlatitude enhanced TEC phenomena, another TEC enhancement takes place in the low-latitude region (15-30 degrees, GMLAT) on both sides of the dip equator. This observational fact cannot be explained by the latitudinal expansion of the EIA and westward transportation of a part of the higher latitude EIA by SAPS [Kelley et al., 2004; Foster et al., 2007]. As already proposed by Liu et al. [2016], the midlatitude enhanced TEC signature may be caused by upward **E**x**B** drifts that lift the ionosphere in the sunlit region to higher altitudes. In future study, we verify the effect of the localized **E**x**B** drifts on the formation of SED from a comparison between the global TEC and ionospheric plasma flow observed by the SuperDARN radars.

Keywords: Geomagnetic storm, Ionosphere, Storm enhanced density, Equatorial ionization anomaly, Midlatitude, Convection electric field

©2019. Japan Geoscience Union. All Right Reserved.

©2019. Japan Geoscience Union. All Right Reserved.

Tidal Forcing Effects on the Zonal Variation of Solstice Equatorial Plasma Bubbles

*Loren Chang[1], Jude Salinas[1], Yi-Chung Chiu[1], Pei-yun Chiu[1], Charles Lin[2]

1. Institute of Space Science and Engineering, Center for Astronautical Physics and Engineering, National Central University, Taiwan, 2. Department of Earth Science, National Cheng Kung University, Taiwan

Equatorial plasma bubbles are elongated plasma depletions that can occur in the nighttime ionospheric F region, causing scintillation in satellite navigation and communications signals, and manifesting in ionograms as spread F. Equatorial plasma bubbles are believed to be Rayleigh-Taylor instabilities seeded by vertically propagating gravity waves. A necessary pre-condition for plasma bubble formation is believed to be a threshold vertical ion drift from the E region, which is required to produce the vertical plasma gradients conducive to such an instability. Factors affecting the zonal and seasonal variation of equatorial plasma bubbles therefore include magnetic declination, as well as the strength of the equatorial electojet, and neutral winds in the lower thermosphere controlling vertical plasma drifts via the wind dynamo. In most longitude zones, the above factors result in elevated occurrence rates of equatorial plasma bubbles during the equinoxes. The notable exception is over the central Pacific and African sectors, where equatorial plasma bubble activity maximizes during solstice. As the zonal separation of the two sectors is roughly half the Earth’ s circumference, *Tsunoda et al.* (2015) hypothesized that the solstice maxima in these two sectors could be driven by a zonal wavenumber 2 atmospheric tidal component in the mesosphere and lower thermosphere (MLT). In this study, we find that the post-sunset electron density observed by FORMOSAT-3/COSMIC during the boreal summer does indeed exhibit a wave-2 zonal distribution in both the equatorial and northern mid latitude regions. The equatorial wave-2 is consistent with results expected from elevated vertical ion drift over the Central Pacific and African sectors, while the mid- latitude wave-2 is consistent with the Mid-Summer Nighttime Anomaly. Using COSMIC, the seasonal, longitudinal, and local time variation of ionospheric tidal and stationary planetary wave (SPW) components that produce zonal wavenumber 2 disturbances when viewed in a constant local time frame is examined. Numerical experiments are also carried out using the Thermosphere Ionosphere Electrodynamics General Circulation Model (TIE-GCM) to determine the effect of the aforementioned tidal and SPW components on vertical ion drift, showing a clear wave-2 modulation of vertical ion drift when subject to forcing from wave-2 atmospheric tidal components in the mesosphere and lower thermosphere. The aforementioned results are consistent with the solstice maxima hypothesis.

Keywords: Ionosphere, Scintillation, Tides

©2019. Japan Geoscience Union. All Right Reserved.

[E] Poster | P (Space and Planetary Sciences)：P-EM Solar-Terrestrial Sciences, Space Electromagnetism & Space Environment

Wed. May 29, 2019 1:45 PM - 3:15 PM JST | Wed. May 29, 2019 4:45 AM - 6:15 AM UTC | Poster Hall International Exhibition Hall8, Makuhari Messe_1

[P-EM11] Dynamics of Magnetosphere and Ionosphere

convener:Aoi Nakamizo(Applied Electromagnetic Research Institute, National Institute of Information and Communications Technology), Mitsunori Ozaki(Faculty of Electrical and Computer Engineering, Institute of Science and Engineering, Kanazawa University), Akiko Fujimoto(Kyushu Institute of Technology), Tomoaki Hori(Institute for Space-Earth Environmental Research, Nagoya University)

This session provides an opportunity to present recent results from satellite and ground-based observations and theoretical and simulation studies on the magnetosphere, ionosphere, and their coupling processes. We invite talks and posters discussing various phenomena related to the magnetosphere-ionosphere system: solar wind-magnetosphere interaction, magnetosphere-ionosphere convection, field-aligned current, magnetic storms/substorms, neutral-plasma interaction, ionospheric ion inflow and outflow, aurora phenomena, and so forth. Discussions on planetary and satellite ionosphere and magnetospheres, future missions and instrument developments are also welcome.

[PEM11-P01] Effects of Inclination/Rotation of Earth's Magnetic Axis on Magnetosphere Simulated by Global MHD Model

*Aoi Nakamizo[1] (1.Applied Electromagnetic Research Institute, National Institute of Information and Communications Technology)

[PEM11-P02] Asymmetric deformation of the magnetosphere under low-density solar wind

*Masaki N Nishino[1,2], Yoshifumi Saito[2], Kazuo Shiokawa[1], Masaki Fujimoto[2] (1.Institute for Space-Earth Environmental Research, Nagoya University, 2.JAXA/ISAS)

[PEM11-P03] New perspectives on coupling processes in solar-terrestrial system obtained by comprehensive data analysis

*Yoshimasa Tanaka[1], Norio Umemura[2], Shuji Abe[3], Satoru UeNo[4], Masahito Nose[2], Yumi Nakagawa[5] (1.National Institute of Polar Research, 2.Institute for Space-Earth Environmental Research, Nagoya University, 3.International Center for Space Weather Science and Education, 4.Kwasan & Hida Observatories, School of Science, Kyoto University, 5.Ibaraki University)

[PEM11-P04] The interaction between the magnetosphere-ionosphere compound system and the magnetic field topology

*Shigeru Fujita[1], Takashi Tanaka[2], Masakazu Watanabe[2] (1.Meteorological College, Japan Meteorological Agency/ Nationa Institute of Polar Research, 2.Kyushu University)

[PEM11-P05] Effects of the dipole tilt and the interplanetary magnetic field Bx component on the dawn-dusk and interhemispheric asymmetries of the interchange convection cycle

*Masakazu Watanabe[1,2], Takashi Tanaka[2], Shigeru Fujita[3,4] (1.Graduate School of Science, Kyushu University, 2.International Center for Space Weather Science and Education, Kyushu University, 3.Meteorological College, 4.National Institute of Polar Research)

[PEM11-P06] Transient polar ionospheric convection response to negative dynamic pressure pulse

*Jianjun Liu[1] (1.Polar Research Institute of China)

[PEM11-P07] An active ionosphere: a new perspective of field line dipolarization

*Osuke Saka[1] (1.Office Geophysik)

[PEM11-P08] Toward the automatic identification of FLR signals in the SuperDARN data by using the gradient method

*Hideaki Kawano[1,2], Akira Sessai Yukimatu[3,4], Nozomu Nishitani[5], Yoshimasa Tanaka[3,4], Satoko Saita[6], Tomoaki Hori[5] (1.Dept. Earth Planet. Sci., Kyushu Univ., 2.ICSWSE, Kyushu University, 3.National Institute of Polar Research, 4.SOKENDAI, 5.ISEE, Nagoya University, 6.Kitakyushu College)

[PEM11-P09] A statistical study of Pi2 pulsations observed in the upper ionosphere using Swarm magnetic field data

*Park Jaehee[1], Khan-Hyuk Kim[1], Junga Hwang[2] (1.School of Space Research, Kyung Hee University, Gyeonggi, South Korea, 2.Korea Astronomy and Space Science Institute, Daejeon,South Korea)

[PEM11-P10] Study on the global distribution characteristics of Pc 1-2 geomagnetic pulsation with the 10Hz data of the MAGDAS system

*Taisei Kabasawa[1], Akimasa Yoshikawa[1], Teiji Uozumi[1], Akiko Fujimoto[1], Shuji Abe[1] (1.Kyushu University)

[PEM11-P11] In-situ Observations of Reconnection Separatrix Regions in the near-Earth Magnetotail

*Mizuho Araki[1], Masahiro Hoshino[1], Kunihiro Keika[1], Yoshifumi Saito[2] (1.Graduate School of Science, The University of Tokyo, 2.Institude of Space and Astronautical Science)

[PEM11-P12] Flow speed dependence of ion temperature, electron temperature, and their ratio in the near-Earth magnetotail reconnection region

*Kaori Watanabe[1], Masahiro Hoshino[1], Kunihiro Keika[1], Yoshifumi Saito[2], Naritoshi Kitamura[1] (1.Univ. of Tokyo, 2.ISAS/JAXA)

[PEM11-P13] **Examining Minimum Cyclotron Resonant Electron Energy of EMIC Waves with MMS**

*Si Liu[1] (1.Changsha University of Science and Technology)

[PEM11-P14] Small scale whistler mode waves near the magnetic field intensity minimum in the magnetosheath

*Naritoshi Kitamura[1], Takanobu Amano[1], Yoshiharu Omura[2], Satoko Nakamura[2], Chika Umegaki[1], Scott A Boardsen[3,4], Narges Ahmadi[5], Robert E Ergun[5], Olivier Le Contel[6], Per-Arne Lindqvist[7], Yoshifumi Saito[8], Shoichiro Yokota[9], Daniel J Gershman[3], Barbara L Giles[3], Thomas E Moore[3], William R Paterson[3], Craig J Pollock[10], Christopher T Russell[11], Robert J Strangeway[11], James L Burch[12] (1.Department of Earth and Planetary Science, Graduate School of Science, The University of Tokyo, 2.Research Institute for Sustainable Humanosphere, Kyoto University, 3.NASA Goddard Space Flight Center, 4.University of Maryland, 5.Laboratory for Atmospheric and Space Physics, University of Colorado, 6.Laboratoire de Physique des Plasmas, UMR7648 CNRS/Ecole Polytechnique/UPMC/Université Paris-Sud/Observatoire de Paris, 7.Royal Institute of Technology, 8.Institute of Space and Astronautical Science, Japan Aerospace Exploration Agency, 9.Department of Earth and Space Science, Graduate School of Science, Osaka University, 10.Denali Scientific, 11.Institute of Geophysics and Planetary Physics, University of California, Los Angeles, 12.Southwest Research Institute)

[PEM11-P15] Spatial characteristics of the internal modulation of pulsating aurora: multi-point high-speed optical observations in Scandinavia

*Yuki Kawamura[1], Keisuke Hosokawa[1], Shin-ichiro Oyama[2,3], Yoshizumi Miyoshi[2], Yasunobu Ogawa[3], Satoshi Kurita[2], Satoshi Ebukuro[1], Ryoichi Fujii[4] (1.Department of Communication Engineering and Informatics, University of Electro-Communications, 2.Institute for Space-Earth Environmental Research, Nagoya University, 3.National Institute of Polar Research, 4.Research Organization of Information and Systems)

[PEM11-P16] **Large-scale characteristics of pulsating aurora periodicities:multi-point high-speed optical observations in Scandinavia**

*Satoshi Ebukuro[1], Keisuke Hosokawa[1], Shin-ichiro Oyama[2,3,5], Yoshizumi Miyoshi[2], Yasunobu Ogawa[3], Satoshi Kurita[2], Yuki Kawamura[1], Ryoichi Fujii[4] (1.Department of Communication Engineering and Informatics, University of Electro-Communications, 2.Institute for Space-Earth Environmental Research, Nagoya University, 3.National Institute of Polar Research, 4.Research Organization of Information and Systems, 5.University of Oulu)

[PEM11-P17] Variations of cosmic noise absorption (CNA) by energetic electron precipitation (EEP) and changes of the auroral morphology

*Miyamoto Taishiro[1], Shin-ichiro Oyama[1,4,5], Yasunobu Ogawa[2], Keisuke Hosokawa[3], Satoshi Kurita[1], Yoshizumi Miyoshi[1], Ryuho Kataoka[2], Hiroshi Miyaoka[2], Tero Raita[4] (1. Institute for Space-Earth Environmental Research,Nagoya University, 2.National Institute of Polar Research, 3.Department of Communication Engineering and Informatics, University of Electro-Communications, 4.Sodankylä Geophysical Observatory, University of Oulu, 5.Ionosphere Research Unit, University of Oulu)

[PEM11-P18] Spatiotemporal characteristics on the source region of flash aurora using ray tracing analysis

*Tomohiro Inoue[1], Mitsunori Ozaki[1], Yoshitaka Goto[1], Satoshi Yagitani[1], Yoshiya Kasahara[1], Kazuo Shiokawa[2], Yoshizumi Miyoshi[2], Ryuho Kataoka[3], Yusuke Ebihara[4] (1.Kanazawa University , 2.Nagoya University, 3.National Institute of Polar Research, 4.Kyoto University)

[PEM11-P19] Molecular ion supply mechanisms from the low-altitude ionosphere to magnetosphere observed by EISCAT and Arase(ERG)

*Masayoshi Takada[1], Kanako Seki[1], Yasunobu Ogawa[2], Kunihiro Keika[3], Satoshi Kasahara[4], Shoichiro Yokota[5], Tomoaki Hori[7], Kazushi Asamura[6], Yoshizumi Miyoshi[7] (1.Graduate School of Science, Tokyo University, 2.National Institute of Polar Research, 3.Department of Earth and Planetary Science, Graduate School of Science, Tokyo University, 4.The University of Tokyo, 5.Graduate School of Science, Osaka University, 6.Institute of Space and Astronautical Science, Japan Aerospace Exploration Agency, 7.Institute for Space-Earth Environmental Research, Nagoya University)

[PEM11-P20] Optical and radar observation of the dynamic auroral forms

*Yunosuke Nagafusa[1], Tima Sergienko[2], Satoshi Taguchi[1], Urban Braendstroem[2], Masatoshi Yamauchi[2] (1.Graduate School of Science, Kyoto University, 2.Swedish Institute of Space Physics, Kiruna)

[PEM11-P21] Observations of MF/HF auroral radio emissions at three ground-based stations

*Yuka Sato[1], Atsushi Kumamoto[2], Yuto Katoh[2], Akira Kadokura[3,4], Yasunobu Ogawa[3,4], Atsuki Shinbori[5] (1.Nippon Institute of Technology (NIT), 2.Graduate School of Science, Tohoku University, 3.National Institute of Polar Research (NIPR), 4.The Graduate University for Advanced Studies, 5.Institute for Space-Earth Environmental Research (ISEE), Nagoya University)

[PEM11-P22] **Ionospheric F-region Drift Measurements Derived from DPS-4D at Zhongshan Station, Antarctic**

*Xiangcai Chen[1] (1.Polar Research Institute of China)

[PEM11-P23] PARM-HEP Observation of Precipitating High Energy Electrons over Pulsating Aurora

*Taku Namekawa[1], Takefumi Mitani[2], Kazushi Asamura[2], Yoshifumi Saito[2] (1.Department of Earth and Planetary Science, Graduate school of Science, The University of Tokyo, 2.Institute of Space and Astronautical Science, Japan Aerospace Exploration Agency)

[PEM11-P24] Development of the medium-energy electron detector with hemispherical field-of-view and the flight test in the PARM (Pulsating AuRora and Microburst) mission

*Shin Sugo[1], Oya Kawashima[1], Kazushi Asamura[2], Reiko Nomura[3], Yasunobu Ogawa[4], Keisuke Hosokawa[5], Yoshizumi Miyoshi[6], Takefumi Mitani[2], Taku Namekawa[1,2], Takeshi Sakanoi[7], Mizuki Fukizawa[7], Naoshi Yagi[7], Satoshi Kasahara[1] (1.The University of Tokyo, 2.Institute of Space and Astronautical Science, Japan Aerospace Exploration Agency, 3.National Astronomical Observatory of Japan, 4.National Institute of Polar Research, 5.The University of Electro-Communications, 6.Institute for Space-Earth Environmental Research, Nagoya University, 7.Tohoku University)

[PEM11-P25] Auroral substorm onset in satellite-based global images and ground-based all-sky images

*Akimasa Ieda[1], Kirsti Kauristie[2], Yukitoshi Nishimura[3], Yukinaga Miyashita[4], Harald U Frey[5], Liisa Juusola[2], Daniel Whiter[6], Masahito Nose[7], Matthew O Fillingim[5], Farideh Honary[8], Neil C Rogers[8], Yoshizumi Miyoshi[1], Shinobu Machida[1] (1.Institute for Space-Earth Environmental Research, Nagoya University, 2.Finnish Meteorological Institute, 3.Boston university, 4.Korea Astronomy and Space Science Institute, 5.University of California Berkeley, 6.University of Southampton, 7.Graduate School of Science, Kyoto University, 8.Lancaster University)

[PEM11-P26] Automatic Classification of Auroral images using optical flow feature

*Naoto Kashiwagi[1], Akiko Fujimoto[1], Terumasa Tokunaga[1], Yoshizumi Miyoshi[2], Yasunobu Ogawa[3], Keisuke Hosokawa[4] (1.Kyushu Institute of Technology, 2.Nagoya University, 3.National Institute of Polar Research, 4.The University of Electro-Communications)

[PEM11-P27] Fine-scale visualization of aurora in a wide area using color digital camera images from the International Space Station

*Sota Nanjo[1], Yuta Hozumi[1], Keisuke Hosokawa[1] (1.The University of Electro-Communications)

[PEM11-P28] Geospace Imaging via the soft X-ray imager: GEO-X mission

*Yoshizumi Miyoshi[1], Yuichiro Ezoe[2], Satoshi Kasahara[3], Yosuke Matsumoto[4], Kumi Ishikawa[5], Ryuho Kataoka[6], Hiroki Ito[1], Daiki Ishi[2], Masaki Numazawa[2], Atsushi Yamazaki[5], Hiroshi Hasegawa[5], Masaki Fujimoto[5], Kazuhisa Mitsuda[5] (1.Institute for Space-Earth Environmental Research, Nagoya University, 2.Tokyo Metropolitan University, 3.University of Tokyo, 4.Chiba University, 5.ISAS/JAXA, 6.NIPR)

Effects of Inclination/Rotation of Earth’s Magnetic Axis on Magnetosphere Simulated by Global MHD Model

*Aoi Nakamizo[1]

1. Applied Electromagnetic Research Institute, National Institute of Information and Communications Technology

Recently, we have shown that the ionospheric Hall conductance distribution, owing to the polarization field generated by its nonuniformity, largely control the magnetospheric configuration and dynamics by using a global MHD model. The effects of the ionospheric conductance on the magnetosphere were also reported by previous studies based on other global models; for example, the current-voltage relationship in the solar wind-magnetosphere-ionosphere [Fedder and Lyon, 1987] and the plasma pressure distribution in the near-Earth region [Ridley et al., 2004]. These studies indicate that the ionospheric conductance is one of the most important settings in the global models to accurately simulate the magnetosphere.

On the other hand, in the development/improvement of the global MHD model in NICT, which was originally developed by Tanaka [1994] and Tanaka et al. [2010], introducing the inclination and rotation of Earth’s magnetic axis with respect to the rotation axis has been remained as one of the most difficult problems. In other words, in the present model, the precession between the magnetic axis and the rotation axis is not included. This means that the simulated magnetosphere will show a different structure and temporal development than the actual magnetosphere.

We, for the first time, equivalently introduce the precession by rotating the background conductance distribution due to solar illumination (i.e., depending on the geographic coordinate) with respect to the geomagnetic coordinate. (Improvement of the conductance setting in the auroral region is the next challenge.) In this paper, we will show how the simulated magnetosphere is changed by this improvement, focusing on the near-Earth plasma environment.

Keywords: M-I Coupling, Global MHD Simulation, Ionospheric Effect

©2019. Japan Geoscience Union. All Right Reserved.

Asymmetric deformation of the magnetosphere under low-density solar wind

*Masaki N Nishino[1,2], Yoshifumi Saito[2], Kazuo Shiokawa[1], Masaki Fujimoto[2]

1. Institute for Space-Earth Environmental Research, Nagoya University, 2. JAXA/ISAS

The density of the solar wind around the Earth's magnetosphere sometimes decreases to only several percent of the usual value, and such density extrema results in a significant reduction of dynamic pressure and Alfvenic Mach number of the solar wind flow. While simple expansion of the Earth's magnetosphere by the low dynamic pressure was assumed in previous studies, a global-MHD simulation study predicted a remarkable dawn-dusk asymmetry of the magnetosphere in shape under low-density solar wind and Parker-spiral IMF configuration. Here we present evidence of asymmetric deformation of the magnetosphere under low-density solar wind and Parker-spiral IMF conditions, based on several events of GEOTAIL observations. As predicted by the global-MHD simulation, the magnetosphere on the dawnside expands much further than the magnetopause location of simple (symmetric) expansion, while no significant expansion is detected in the dusk tail flank. Fast ion beams detected at the flank magnetopause suggest that magnetic reconnection frequently occurs due to the low-beta environment of the magnetosheath.

Keywords: Low density solar wind, Magnetosphere, Plasma transport

©2019. Japan Geoscience Union. All Right Reserved.

New perspectives on coupling processes in solar-terrestrial system obtained by comprehensive data analysis

*Yoshimasa Tanaka[1], Norio Umemura[2], Shuji Abe[3], Satoru UeNo[4], Masahito Nose[2], Yumi Nakagawa[5]

1. National Institute of Polar Research, 2. Institute for Space-Earth Environmental Research, Nagoya University, 3. International Center for Space Weather Science and Education, 4. Kwasan & Hida Observatories, School of Science, Kyoto University, 5. Ibaraki University

In the Earth’ s upper atmosphere above 60 km, including magnetosphere and ionosphere, various phenomena are generated by energy inputs from solar radiation (including solar wind) and atmospheric waves propagating from the lower atmosphere. Thus, comprehensive analysis of various kinds of satellite and ground-based observational data using advanced methods is required to understand physical mechanism of the phenomena. For such interdisciplinary studies, it is important to share data distributed across many universities and institutes and use advanced tools, such as metadata database for cross-searching a variety of datasets and analysis software for analyzing various types of data in an integrated fashion. In fact, many scientific papers on the upper atmosphere have recently been obtained by comprehensive analysis of various data with such analysis tools.
We present some examples of scientific results achieved by comprehensively analyzing data from multiple regions. These examples include the effect of solar coronal holes on the Earth’ s geomagnetic activity and the interaction between solar wind, magnetosphere, ionosphere and neutral atmosphere. The former study investigated long-term trends of coronal boles, solar wind parameters, and Earth’ s geomagnetic indices during two solar cycles. It showed the possibility that the solar wind speed and geomagnetic activities may be controlled by the size and latitudinal distribution of coronal holes. The latter analyzed multi-instrument data simultaneously obtained from interplanetary space, magnetosphere, and ionosphere and mesosphere in both northern and southern hemispheres. They newly found that the polar mesosphere is affected by relativistic electron precipitation caused by the interaction with magnetospheric plasma waves during the high-speed solar wind stream. These studies demonstrate that sharing and comprehensive analysis of long-term, multiple-sphere, and multi-instrument data using sophisticated tools are very effective to produce scientific outcomes. At present there are data gap areas in the Asia and African regions. Therefore, we believe that filling in the data gap by international collaborations could be a breakthrough for unsolved issues in the upper atmosphere.

Keywords: upper atmosphere, coupling between multiple regions, comprehensive analysis, long-term observational data

©2019. Japan Geoscience Union. All Right Reserved.

The interaction between the magnetosphere-ionosphere compound system and the magnetic field topology

*Shigeru Fujita[1], Takashi Tanaka[2], Masakazu Watanabe[2]

1. Meteorological College, Japan Meteorological Agency/ Nationa Institute of Polar Research, 2. Kyushu University

The steady convection in the magnetosphere-ionosphere coupling system is composed of the following self-consistent elementary processes; dynamo in the cusp-mantle region, the field-perpendicular current system in the magnetosphere, the field-aligned current system connecting the ionosphere, the ionospheric electric field, the magnetospheric convection corresponding to the ionospheric electric field, and the high plasma pressure distribution in the cusp region [Tanaka, 2007].

The energy of the convection is transported from the solar wind across the magnetopause where the magnetic field configures the null-separator structure. Since the magnetic field configuration of the null-separator structure is originally derived from the superposition of two scalar fields [Stern, 1973], say, the dipole field and the uniform field, the magnetic field of the null-separator would not have free energy necessary for plasma acceleration. However, the simulation reveals that the magnetic field has a tension force near the null point. Therefore, we need a mechanism that transports the energy to this region.

It is revealed from the simulation that the bow shock supplies the energy. Indeed, the current from the bow shock deforms the magnetic field of the null-separator structure. In addition, it is noted that the Chapman-Ferraro current also deforms the magnetic field configuration in the magnetopause. This fact indicates that the convection system in the magnetosphere contributes to deformation of the null-separator structure. That is to say, energy transport from the solar wind to the magnetosphere-ionosphere compound system is affected by the physical processes in the convection. Therefore, as a result of the interaction between the magnetosphere-ionosphere convection and the null-separator structure, the magnetosphere-ionosphere compound system can be extended to the solar wind-magnetosphere-ionosphere compound system.

References

T. Tanaka (2007), Magnetosphere-Ionosphere Convection as a Compound System, Space Sci Rev, 133, 1-72, DOI 10.1007/s11214-007-9168-4.

Stern, D. P. (1973), A study of the electric field in an open magnetospheric model, J. Geophys. Res., 78(31), 7292-7305, doi:10.1029/JA078i031p07292.

Keywords: global MHD simulation, compound system

©2019. Japan Geoscience Union. All Right Reserved.

Effects of the dipole tilt and the interplanetary magnetic field Bx component on the dawn-dusk and interhemispheric asymmetries of the interchange convection cycle

*Masakazu Watanabe[1,2], Takashi Tanaka[2], Shigeru Fujita[3,4]

1. Graduate School of Science, Kyushu University, 2. International Center for Space Weather Science and Education, Kyushu University, 3. Meteorological College, 4. National Institute of Polar Research

The interchange cycle is a mode of magnetic flux circulation that appears for periods of northward interplanetary magnetic field (IMF). It is made up of IMF-to-open reconnection in one hemisphere and open-to-closed reconnection in the other hemisphere. The two reconnection processes have the same topological nature in that the roles of the two reconnecting field lines interchange at the time of reconnection. The interchange cycle is characterized by reciprocation of open magnetic flux between the two hemispheres. One observable signature of the interchange cycle is an appearance of a reverse cell circulating in the closed field line region of the ionosphere, which is named the “reciprocal cell.” The reciprocal cell appears in the open-to-closed reconnection hemisphere, whereas in the opposite IMF-to-open reconnection hemisphere, there appears a lobe cell circulating exclusively on open field lines. For given (1) IMF By, (2) IMF Bx, and (3) dipole tilt conditions, two interchange cycles concur, one on the dawnside and the other on the duskside. For an ideal case, one can easily expect the mode of the interchange cycles to occur. For example, for the case of due northward IMF with significant dipole tilt, the twin reverse cells in the summer hemisphere are both lobe cells, while in the winter hemisphere the twin reverse cells are both reciprocal cells. For the general case, however, one cannot predict the mode of the interchange cycles without quantitative modeling. The purpose of this study is to examine how the presence of dipole tilt or IMF Bx alters the dawn-dusk and north-south pattern of the twin reverse cells. For this purpose, we perform numerical magnetohydrodynamic simulations using the REPPU (Reproduce Plasma Universe) code developed by T. Tanaka. In the presentation, we discuss the dipole tilt and IMF Bx effects revealed by the numerical modeling.

Keywords: ionospheric convection, interchange reconnection, reciprocal cell

©2019. Japan Geoscience Union. All Right Reserved.

Transient polar ionospheric convection response to negative dynamic pressure pulse

*Jianjun Liu[1]

1. Polar Research Institute of China

The response of the high latitude ionospheric convection to a sudden decrease in solar wind dynamic pressure provides a unique opportunity to investigate how the solar wind couples to the dayside magnetosphere and ionosphere. Here, the event shows three IMF components do not have prominent changes, but the solar wind plasma went down to near zero magnitude, which leads to very weak solar wind driving during northward IMF. However, ionospheric convection observed by SuperDARN radars showed enhanced plasma flow speed in the central polar cap region just after the negative pressure pulse arrival to the magnetosphere. Simultaneous convection map generated by SuperDARN measurement presents enlarged convection cell with obvious equatorward moving Heppner-Maynard boundary. It is noted that cross polar cap potential enhanced instantly and this enhanced feature continued almost 10 min. The distribution of total electron content (TEC) exhibited typical auroral oval signature especially on dayside ionosphere, TEC density in auroral oval showed a noticeable decrease after the arrival of the negative pressure pulse. Both ionospheric convection and TEC distribution reveal that negative pressure pulse impacts the magnetosphere-ionosphere coupling system directly and dramatically. Moreover, the TIEGCM model also showed an enhanced polar potential pattern.

Keywords: Dynamic pressure, Ionospheric convection, Auroral oval

©2019. Japan Geoscience Union. All Right Reserved.

An active ionosphere: a new perspective of field line dipolarization

*Osuke Saka[1]

1. Office Geophysik

Transient westward electric fields from the magnetosphere generate equatorward plasma drifts of the order of kilometers per second in the auroral ionosphere. This flow channel extends in north-south directions and is produced in the initial pulse of Pi2 pulsations associated with the filed line dipolarization. Drifts in the ionosphere of the order of kilometers per second that accumulated plasmas at the low latitude end of the flow channel are of such large degree that possible vertical transport effects (including precipitation) along the field lines may be ignored. We suggest that plasma compression in the ionosphere implemented the ionosphere to be active. Active ionosphere generates field-aligned currents to satisfy the quasi-neutrality of the ionosphere, ion acoustic wave for ion outflows and the inverted-V type electron precipitations in the topside ionosphere, and poleward expansion of auroras due to a nonlinear evolution of the ionosphere. We will study auroral expansion in this acoustic regime.

Keywords: Substorm, Auroral substorm, Ionosphere

©2019. Japan Geoscience Union. All Right Reserved.

Toward the automatic identification of FLR signals in the SuperDARN data by using the gradient method

*Hideaki Kawano[1,2], Akira Sessai Yukimatu[3,4], Nozomu Nishitani[5], Yoshimasa Tanaka[3,4], Satoko Saita[6], Tomoaki Hori[5]

1. Dept. Earth Planet. Sci., Kyushu Univ., 2. ICSWSE, Kyushu University, 3. National Institute of Polar Research, 4. SOKENDAI, 5. ISEE, Nagoya University, 6. Kitakyushu College

The FLR (Field Line Resonance) takes place where the frequency of an incoming wave matches the eigen-frequency of magnetospheric magnetic field lines, and excites the eigen-oscillation of the field lines. The FLR can be identified by using the unique manner of change in the amplitude and the phase of thus excited eigen-oscillation across the resonant point. That is, the amplitude is maximum at the resonant point, and the phase changes the most steeply across the resonance point. The FLR-generated eigen-oscillations can be identified in the ground magnetic field data and the ionospheric plasma velocity data. From thus identified eigen-frequency ("FLR frequency" below) one can estimate the magnetospheric plasma density along the field line which passes through the ground/ionospheric observation point.

In this study we use the SuperDARN radar data to identify FLR: For each radar beam from each SuperDARN radar, the velocity of the ionospheric plasma flow along the line of sight (VLOS) of the beam is obtained; we use the VLOS data to identify the FLR and estimate the magnetospheric plasma density. Unlike the ground magnetometer data, the SuperDARN data is two-dimensional, enabling two-dimensional estimates of the magnetospheric equatorial plasma density and magnetospheric region identification.

To achieve that, it is important to identify as many FLR events as possible. Overwrapping of non-FLR waves/perturbations hides FLR events. As a countermeasure to this problem, the so-called gradient method has been applied to the ground magnetometer data; this method cancels out the overwrapping signals by dividing the data from a magnetometer by the data from another magnetometer having an adequate latitudinal distance from the other. The division yields the amplitude ratio and the phase difference. The gradient method is effective since the FLR frequency tends to depend on the latitude more strongly than the overwrapping signals.

The gradient method is also applicable to the SuperDARN VLOS data. The field of view of each beam is divided into Range Gates (RGs below) having the same length along the beam. The identification number of the RGs increases with increasing distance from the radar. The VLOS is obtained for each RG. Thus, each RG can be regarded as a "virtual observatory."

As an initial study, we have selected an FLR event which was identified in the VLOS data of a radar (at Hankasalmi) without the use of the gradient method, selected a beam, and selected a few pairs of RGs of the beam. We then have manually applied the gradient method to the VLOS data of the above-selected RG pairs, and successfully identified the FLR. In more detail, the identification has been successful only for two paired RGs whose RG numbers differs by two. This suggest that, since the length of the RG, mapped to the meridional plane, was about 40km for this event, about 80km distance was the best (with the resolution of 40km) for this event. This distance reflects the resonance width, which is an important quantity reflecting the diffusion and dissipation of the FLR energy.

©2019. Japan Geoscience Union. All Right Reserved.

In order to identify as many FLR events as possible, it is also important to automatically identify the FLR events, since visual identification is time-consuming. The gradient method enables automatic identification more easily than analyses of VLOS itself, since the gradient method yields peaks in both the amplitude ratio and the phase difference. We have started making a program for automatic identification by applying the gradient method to VLOS; the version at the time of this abstract has successfully identified FLRs for all of the above-stated pairs of RGs.

©2019. Japan Geoscience Union. All Right Reserved.

A statistical study of Pi2 pulsations observed in the upper ionosphere using Swarm magnetic field data

*Park Jaehee[1], Khan-Hyuk Kim[1], Junga Hwang[2]

1. School of Space Research, Kyung Hee University, Gyeonggi, South Korea, 2. Korea Astronomy and Space Science Institute, Daejeon,South Korea

The properties of Pi2 pulsations observed in the upper ionosphere are studied using magnetic field data acquired by the Swarm-A spacecraft in low Earth orbit (LEO) and at the low-latitude Bohyun ground station (BOH, L = 1,3) for January 2014-Jun 2015. From time intervals when Swarm-A was on the nightside (magnetic local time (MLT) = 1800-0600 hrs) and the BOH station was near midnight (MLT = 2100-0300 hrs), we identified 623 Pi2 events in the horizontal H component of the BOH data. For each event we examine the coherence between the horizontal H component on the ground and the B_x (radial) azimuthal B_y (azimuthal), or B_z (compressional) components at Swarm-A. Out of 623 events, the B_x-H high coherence (> 0.7) events are ~6%, the B_y-H high coherence events are ~4%, and the B_z-H high coherence events are ~25%. The ground-satellite high coherence events occurred when the spacecraft was located within a magnetic latitude range of ±50°. Using the ground-satellite high coherence events, we examined the latitudinal structure of the relative amplitude and phase of the ionospheric Pi2 pulsations detected at Swarm-A. Confirming previous observations at LEO, we found that the ionospheric Pi2 pulsations are characterized by symmetric odd mode standing oscillations in the north-south direction, having a node for B_x oscillation and an antinode for B_z oscillation, respectively, at the equator. This indicates that the source of ionospheric Pi2 pulsations is the plasmaspheric resonance.

Keywords: Pi2 pulsations

©2019. Japan Geoscience Union. All Right Reserved.

Study on the global distribution characteristics of Pc 1-2 geomagnetic pulsation with the 10Hz data of the MAGDAS system

*Taisei Kabasawa[1], Akimasa Yoshikawa[1], Teiji Uozumi[1], Akiko Fujimoto[1], Shuji Abe[1]

1. Kyushu University

The magnetic field observed on the ground is affected by the space weather phenomena such as magnetic storms and auroral storms.

The Pc1 geomagnetic pulsation (frequency range of 0.2-5.0 seconds) activated mainly around a high-latitude region is understood as a phenomenon accompanied by the excitation of EMIC waves to cause the particle acceleration in the equatorial region of the magnetosphere. Also, it is well known that Pc1 waves propagate horizontally in the ionospheric at the F layer. However, it is not clarified about the global occurrence and propagation properties of Pc1 geomagnetic pulsation on the ground. Moreover, although induction magnetometers are used to observe the high-frequency magnetic field disturbance phenomenon like Pc1 and Pc2 (frequency range of 5.0-10.0 seconds) geomagnetic pulsation, the global observation network with induction magnetometers covering from high-latitude to low-latitude area and equator domain does not exist at this stage. On the other hand, although it is common to use Fluxgate magnetometers for the observation of global space weather phenomenon, it is considered to be unsuitable for analysis of the high-frequency Pc1-2 geomagnetic pulsation because its time accuracy is usually one second value.

The ground multipoint magnetic field observation network which Kyushu University has developed (MAGDAS-9 magnetometer) acquire a 250Hz sampling and 10Hz mean data. Also, it is the only geomagnetic observation network that can investigate the global aspects of Pc1-2 geomagnetic pulsation.

In this study, we investigated the global distribution of Pc1-2 pulsation from polar region to equatorial region with magnetic field data provided by MAGDAS and Dst/AE index provided by the WDC for Geomagnetism, Kyoto. As a result, when the substorm have occurred during a magnetic storm time, generation of Pc1-2 pulsation from high-latitude to middle-and-low latitude region and further arrival of Pc2 pulsation to the dip-equator are identified. The elucidation of occurrence characteristic of the Pc1-2 pulsation on the ground with the EMIC waves excitation is very important not only for space weather application to be able to monitor particle energization process via EMIC excitation but also the elucidation of the super global coupling process from inner magnetosphere to the global ionosphere from polar to equatorial region. In this presentation, we will report the preliminary results of observational analysis of Pc1-2 pulsation by using MAGDAS network. We also discuss the comprehensive approach for understanding global coupling process among inner magnetosphere and high-middle-low latitude to the equatorial region by using FM-CW radar data, PWING induction magnetometer data, and the geo-space environment data from the ERG satellite.

Keywords: Pc1-2 pulsation, EMIC waves, global coupling

©2019. Japan Geoscience Union. All Right Reserved.

In-situ Observations of Reconnection Separatrix Regions in the near-Earth Magnetotail

*Mizuho Araki[1], Masahiro Hoshino[1], Kunihiro Keika[1], Yoshifumi Saito[2]

1. Graduate School of Science, The University of Tokyo, 2. Institude of Space and Astronautical Science

Magnetic reconnection which converts magnetic energy into thermal and kinetic energy of plasmas is an important physical mechanism of plasma heating and acceleration. Particularly in the Petschek-type reconnection, plasma acceleration and heating in the slow-mode shocks formed at the separatrices must be taken into consideration. The structure of the slow-mode shocks in the distant tail of the Earth’s magnetosphere was investigated with in-situ observations made by the GEOTAIL satellite (Saito et.al, 1995). It is observationally suggested that about 10% of the plasma sheet boundary layer (PSBL) is slow-mode shocks. It is, however, not fully understood what determines this percentage and what is the difference in the ion and electron temperature changes between slow-mode shocks and others separatrix regions.
In this study, we utilized multi-spacecraft in-situ observations of separatrix regions at magnetic reconnection in the near-Earth magnetotail (GSM-X is between ~13 and ~25RE). We used data obtained from FPI (Fast Plasma Investigation) and FGM (Fluxgate Magnetometer) on board the MMS satellite from June 1, 2017to August 31, 2017. We examined occurrence locations, ion flow directions and velocity of ion flow in downstream regions of observed events. We also examined changes in ion and electron temperatures and the ion-to-electron temperature ratio.

We classified their events into 2 types according to plasma beta in the in-flow regions: below 0.1 or around 1. We term them “lobe reconnection” and “plasma sheet reconnection”, respectively. In the former type, plasmas in the in-flow regions are cold and tenuous. In the latter type, plasmas in the in-flow regions are hot and dense. In both types, we observed increases in ion and electron temperatures increase, but their characteristics are different. In the lobe reconnection, ion temperatures increase from several hundred eV to several keV. In the plasma sheet reconnection, ion temperatures also increase from about 1 keV to several keV. The increase rate of the electron temperature is less than one order of magnitude for both types, smaller than that of the ion temperature; the electron temperature increases up to at most 1 keV. The ion-to-electron temperature ratio in the out-flow regions in both types is about 5 for both types. We then examined changes of the ion-to-electron temperature ratio and found that the changes are consistent with the result reported by Wang et al. (2012).

In this presentation, we will show the results of separatrix crossing events (both lobe and plasma sheet reconnection events) that occur in 2017 and 2018. We will identify whether each of the separatrices is a slow shock or not and how the separatrix conditions affect ion and electron heating. These characteristics will provide insights into heating mechanisms and energy conversion through separatrix regions.

Reference:

Yoshifumi Saito, Toshifumi Mukai, Toshio Terasawa, Atsuhiro Nishida, Shinobu Machida, Masafumi Hirahara, Kiyoshi Maezawa, Susumu Kokubun, and Tatsundo Yamamoto, Slow-mode shocks in the magneto, J. Geophys. Res., 100, A12, 23,567, 1995

©2019. Japan Geoscience Union. All Right Reserved.

Chih-Ping Wang, Matina Gkioulidou, Larry R. Lyons and Vassilis Angelopoulos, Spatial distributions of ion to electron temperature ratio in the magnetosheath and plasma sheet, J. Geophys. Res., 117, A08215, 2012

Keywords: Magnetic Reconnection, MMS satellite, Earth's Magnetotail

©2019. Japan Geoscience Union. All Right Reserved.

Flow speed dependence of ion temperature, electron temperature, and their ratio in the near-Earth magnetotail reconnection region

*Kaori Watanabe[1], Masahiro Hoshino[1], Kunihiro Keika[1], Yoshifumi Saito[2], Naritoshi Kitamura[1]

1. Univ. of Tokyo, 2. ISAS/JAXA

Plasma in the Earth's magnetotail are heated up to 1-10 keV and stored in the plasma sheet. One of the heating or acceleration mechanisms is the magnetic reconnection. Heated or accelerated plasma are transported both earthward and tailward as fast flow with a speed of several hundred kilometers per second. However, what determines the partition among ion and electron thermal energy and kinetic energy is an unresolved problem. It has been reported that ion temperature T_i, electron temperature T_e, and their ratio T_i/T_e vary spatially and depend on the conditions of fast flows [Wang et al., 2012, Runov et al., 2018] but there are few studies which focus on macroscopic profiles of them in reconnection regions in the magnetotail.

In this study, we examine the relation between flow speed and average profiles of T_i, T_e, and T_i/T_e in the magnetotail reconnection region by using data obtained from FPI and FGM on board the MMS spacecraft. We use the observations for a period from May to August 2017 and take out the data in the region of $X_{GSM} < -15$ Re, -10 Re $< Y_{GSM} < 10$ Re, and beta > 0.1. We then divide them into different groups according to flow speed normalized by alfven speed and show B_z/B_{lobe}– B_x/B_{lobe} maps of T_i, T_e, and T_i/T_e of each group. The results show that ion temperature increase with increasing flow speed while electron temperature decrease. Ion temperature are hotter around the X-point. The structure of inflow and outflow regions is pronounced in the profile of electron temperature. T_i/T_e in inflow region are greater than in outflow region, which means that ion and electron temperatures become comparable by passing through the diffusion region. The results suggest that electron get less energy when more energy is partitioned into plasma kinetic energy. We will discuss about the profiles of anisotropy of plasma temperatures to know more details about the heating mechanisms.

Keywords: temperature ratio, flow, MMS

©2019. Japan Geoscience Union. All Right Reserved.

Examining Minimum Cyclotron Resonant Electron Energy of EMIC Waves with MMS

*Si Liu[1]

1. Changsha University of Science and Technology

Electromagnetic ion cyclotron (EMIC) waves can be in cyclotron resonance with relativistic electrons, causing relativistic electron precipitation. The four ideal Magnetospheric Multiscale (MMS) spacecraft provide great opportunity to directly calculate the wave vector ***k*** of EMIC waves by phase differencing technique and hence estimate the minimum resonant energy by the resonance condition. Deriving a simplified analytic solution, we find that the phase differencing method can still provide an estimate of the dominant wave number when a finite wave number spread or a finite frequency spread is present. Numerical calculations indicate that quasi-antiparallel propagation dominates the EMIC event on 20 November 2015, which is consistent with the FFT spectral analysis results. We also find that obtained wave vectors, roughly agreeing with the validity of cold plasma theory, might significantly vary from wave packet to wave packet. Moreover, minimum resonant electron energies gradually increase from 0.5 MeV to tens of MeV with a decreasing parallel componet of ***k***. Current results provide evidence that EMIC waves can be in resonance with the electrons of energies down to hundreds of keV. It further demonstrates that EMIC waves in a narrow frequency band can effectively interact with the relativistic electrons with a broad energy range.

Keywords: EMIC waves, minimum resonant electron energy, wave vector, phase differencing

©2019. Japan Geoscience Union. All Right Reserved.

Small scale whistler mode waves near the magnetic field intensity minimum in the magnetosheath

*Naritoshi Kitamura[1], Takanobu Amano[1], Yoshiharu Omura[2], Satoko Nakamura[2], Chika Umegaki[1], Scott A Boardsen[3,4], Narges Ahmadi[5], Robert E Ergun[5], Olivier Le Contel[6], Per-Arne Lindqvist[7], Yoshifumi Saito[8], Shoichiro Yokota[9], Daniel J Gershman[3], Barbara L Giles[3], Thomas E Moore[3], William R Paterson[3], Craig J Pollock[10], Christopher T Russell[11], Robert J Strangeway[11], James L Burch[12]

1. Department of Earth and Planetary Science, Graduate School of Science, The University of Tokyo, 2. Research Institute for Sustainable Humanosphere, Kyoto University, 3. NASA Goddard Space Flight Center, 4. University of Maryland, 5. Laboratory for Atmospheric and Space Physics, University of Colorado, 6. Laboratoire de Physique des Plasmas, UMR7648 CNRS/Ecole Polytechnique/UPMC/Université Paris-Sud/Observatoire de Paris, 7. Royal Institute of Technology, 8. Institute of Space and Astronautical Science, Japan Aerospace Exploration Agency, 9. Department of Earth and Space Science, Graduate School of Science, Osaka University, 10. Denali Scientific, 11. Institute of Geophysics and Planetary Physics, University of California, Los Angeles, 12. Southwest Research Institute

Wave-particle interactions are thought to play a crucial role in energy transfer in collisionless space plasmas in which the motion of charged particles is controlled by electromagnetic fields. In the terrestrial magnetosheath, intense whistler mode waves, called 'Lion roars', are often detected by spacecraft around minima of semi-periodic fluctuations of magnetic field intensity due to mirror mode structures and motion of the structures. It is expected that whistler mode waves are efficiently generated near a local minimum of magnetic field intensity due to the smallest cyclotron resonance velocity. We report the detailed characteristics of such whistler mode waves using the data obtained by the four MMS (Magnetospheric Multiscale) spacecraft. Because reversals of field-aligned component of Poynting flux around minima in mirror mode structures correspond to reversals of gradient of magnetic field intensity along the magnetic field, whistler mode events with reversals of the field-aligned component of Poynting flux are good candidates of observations of effective wave generation regions along field lines. Even in such events, phase difference and change of amplitude of whistler mode waves observed by the four spacecraft do not have a clear correlation in cases of ~40 km separation, which is much smaller than the spatial scale of magnetic field depression due to mirror mode structures and is even smaller than the local thermal ion gyro scale. This result indicates that the coherent whistler wave generation in mirror mode structures has very limited spatial scale across field lines and is probably affected by any electron scale process. A plane wave approximation can be usable only in a very small scale. Because some events in cases of ~7 km separation showed good correlation among four spacecraft, the typical scale of coherent whistler wave across field lines can be at least an order of 10 km in mirror mode structures in the terrestrial magnetosheath. The whistler mode waves observed by a spacecraft in a mirror mode structure are a cluster of waves from multiple spatially small sources.

Keywords: Whistler mode wave, Plasma wave, MMS spacecraft, Wave-particle interaction

©2019. Japan Geoscience Union. All Right Reserved.

Spatial characteristics of the internal modulation of pulsating aurora: multi-point high-speed optical observations in Scandinavia

*Yuki Kawamura[1], Keisuke Hosokawa[1], Shin-ichiro Oyama[2,3], Yoshizumi Miyoshi[2], Yasunobu Ogawa[3], Satoshi Kurita[2], Satoshi Ebukuro[1], Ryoichi Fujii[4]

1. Department of Communication Engineering and Informatics, University of Electro-Communications, 2. Institute for Space-Earth Environmental Research, Nagoya University, 3. National Institute of Polar Research, 4. Research Organization of Information and Systems

Pulsating aurora (PsA) is a kind of diffuse aurora which almost always appears in the morning side during the recovery phase of auroral substorm. PsA typically has two characteristic temporal variations. One is so-called main pulsation whose period ranges from a few to a few tens of seconds. The other is a few Hz brightness modulation (internal modulation) which is often seen during the ON time of the main pulsation. Previous studies have suggested that the temporal variation of PsA is characterized by wave-particle interaction between whistler-mode chorus waves and high energy electrons in the magnetosphere. Especially, it has been indicated that there is one to one correspondence between the amplitude variation of chorus waves and the luminosity modulation of PsA.
Recent studies revealed the occurrence distribution of the frequency of the internal modulation. However, there have been no studies which analyzed the spatial distribution of the internal modulation.

To reveal the spatial characteristics of the internal modulation, we need to perform a frequency analysis of the internal modulation by using data from high speed optical instruments having wide spatial coverage. For this purpose, we make use of highly sensitive EMCCD cameras which have been operated in Sodankylä and Kevo in Finland, Tromsø in Norway, and Tjautjas in Sweden. In these observations, all-sky images are taken with a sampling rate of 100 Hz, which is sufficient to identify temporal variations of the internal modulation.

In the frequency analysis, we have employed all-sky images taken on March 15, 2018 (00:00 –01:30 UT) in Sodankylä, Kevo, Tromsø, and Tjautjas. We computed the average frequency of the internal modulation from each pixel of the EMCCD cameras and derived the spatial distribution of their dominant frequencies. Regardless of the latitude, each pulsating patch was fluctuating at a similar frequency. We also derived the frequency spectrum of several pulsating patches existing at different positions in the north-south direction and found that those frequency spectrums of pulsating patches have peaks at about 3 Hz. These results indicate that the frequency of the internal modulation does not depend on the magnetic latitude, and the frequency of the internal modulation is collimated on 3 Hz.
In the presentation, we discuss why the frequency of the internal modulation concentrate on 3 Hz by taking into account the time of flight of PsA electrons.

Keywords: Pulsating aurora, Internal modulation

©2019. Japan Geoscience Union. All Right Reserved.

Large-scale characteristics of pulsating aurora periodicities: multi-point high-speed optical observations in Scandinavia

*Satoshi Ebukuro[1], Keisuke Hosokawa[1], Shin-ichiro Oyama[2,3,5], Yoshizumi Miyoshi[2], Yasunobu Ogawa[3], Satoshi Kurita[2], Yuki Kawamura[1], Ryoichi Fujii[4]

1. Department of Communication Engineering and Informatics, University of Electro-Communications, 2. Institute for Space-Earth Environmental Research, Nagoya University, 3. National Institute of Polar Research, 4. Research Organization of Information and Systems, 5. University of Oulu

It has been known that most of diffuse aurorae in the morning side are composed of luminous patches whose brightness modulates quasi-periodically. Such aurorae are termed as pulsating aurora (PsA) and have been studied extensively in the last decade. PsA patches have a scale size of a few hundreds of km and are usually observed during the late recovery phase of substorms. The entire temporal variation of PsA consists of two individual modulations: main pulsation and internal modulation. The periodicity of the main pulsation ranges from a few to a few tens of seconds and the internal modulation, showing a few Hz scintillating luminosity changes, is often embedded within the ON time of the main pulsation. Previous studies using satellites indicated one-to-one correlation between PsA and chorus wave near the equatorial plane of the magnetosphere, suggesting that ground-based observations of PsA can be used for mapping the activity of chorus in the magnetosphere in 2D fashion. In the past, the spatial characteristics of chorus wave have not visualized in detail because satellite observations only cover a single point in the magnetosphere. To overcome this limitation, we derive the spatial distribution of chorus waves by using ground-based optical observations of PsA and discuss the ambient parameters which characterize the nature of chorus.
For this purpose, we have employed data from electron multiplying charge-coupled device (EMCCD) cameras deployed at multiple sites in Scandinavia to derive the large-scale characteristics of PsA. EMCCD cameras have been operative in Kevo and Sodankyla in Finland, Tromsoe in Norway, and Tjautjas in Sweden and their temporal resolution is 100 Hz. We conducted a frequency analysis for a PsA event on March 28, 2017 (23:30 to 24:10 UT). During the event studied, there existed three different regions of PsA, regions A, B and C, showing different modulation periods. It was also found that the boundaries between these three regions were sharp. We derived the 2D frequency map by using data from all the available stations. As a result, it became clear that the higher latitude region (region C) showed faster internal modulation than the lower latitude region (region A). In addition, region B, which was sandwiched by regions A and C, did not show any internal modulations (i.e., main pulsation without internal modulation). In the presentation, we discuss why the three regions showed different modulation periods with sharp boundaries. In particular, we address what ambient conditions can control the absence of internal modulation in region B. We also derived similar frequency maps of chorus waves by tracing the PsA modulation with the Tsyganenko 04 magnetic field model, which could be used to estimate the spatial extent of chorus wave generation region.

Keywords: Pulsating aurora, Chorus wave, Main pulsation, Internal modulation

©2019. Japan Geoscience Union. All Right Reserved.

Variations of cosmic noise absorption (CNA) by energetic electron precipitation (EEP) and changes of the auroral morphology

*Miyamoto Taishiro[1], Shin-ichiro Oyama[1,4,5], Yasunobu Ogawa[2], Keisuke Hosokawa[3], Satoshi Kurita[1], Yoshizumi Miyoshi[1], Ryuho Kataoka[2], Hiroshi Miyaoka[2], Tero Raita[4]

1. Institute for Space-Earth Environmental Research,Nagoya University, 2. National Institute of Polar Research, 3. Department of Communication Engineering and Informatics, University of Electro-Communications, 4. Sodankylä Geophysical Observatory, University of Oulu, 5. Ionosphere Research Unit, University of Oulu

Temporal and spatial variations of aurora morphology in association with substorm have been studied for more than half a century. Various types of aurora are known, such as discrete arc emitting at relatively high intensity and elongating along the zonal direction, and diffuse aurora with darker but more widely spreading in the sky. Pulsating aurora, which is characterized by quasi-periodic oscillations in the emission intensity at periods of a few to tens seconds, and auroral patches observed embedding in the pulsating aurora tend to appear at the recovery phase of substorm, especially from midnight to dawn. It is known that these types of aurora are accompanied by energetic electron precipitation exceeding several hundreds keV. Elucidation of the causality to produce pulsating aurora and energetic electron precipitation is an important theme to understand relationships between the radiation belt and upper-middle atmosphere of the earth. Analyzing measurements from satellite observations (e.g., Arase) and ground-based optical/radio technique observations, the generation mechanism is thought to be mainly attributed to wave particle interactions due to plasma wave and electrons in the magnetosphere. In this study, we focus on relationships between auroral morphological changes, in particular spatiotemporal evolutions to patches and coinciding precipitations of the energetic electron.

Some previous studies have presented changes in morphology from pulsating aurora to patch structures [e.g., Shiokawa et al., 2014] and temporal variations of energetic electron precipitation [e.g., Hosokawa and Ogawa, 2015]. As mentioned above, the wave-particle interaction has been widely accepted with experimental evidences to support generation of pulsating aurora and energetic electron precipitation. However, our understanding has not yet reached its maturity of presenting spatiotemporal evolutions of auroral morphology and associated electron precipitation. Oyama et al. [2017] presented enhancements of CNA (cosmic noise absorption) coinciding with appearance of the patch structure but with only two events. Furthermore, due to measurements with intensive diagnostic instruments, the result was based on information of a part of the auroral ionosphere. In this study, we conducted observations to capture simultaneously time evolutions and spatial distributions of auroral morphology and energetic electron precipitation by utilizing a network of EMCCD (Electron Multiplying Charge Coupled Device) cameras and riometers deployed in Northern Europe.

This study will present three events (February 19-20, 2018, March 6-7, 2017, and March 29-30, 2017). On the way of all events, after substorm onsets twice near Northern Europe, another onset occurred again at more west side (near Iceland or Greenland area) but at dawn in the Northern Europe. In this study, we have focused on the aurora and CNA associated with the latter onset, and at that time, the aurora spatially and temporally shifted from diffuse to pulsation and patch structures. This suggests that substorm activities occurred in the distance can induce these auroral morphological changes seen in the Northern Europe. CNA at that time is characterized by gradual variations with time scale of several hours. This trend cannot be seen at substorm onset near the Northern Europe. Moreover, in the latitude distribution, the feature was confirmed that CNA increases at the latitude where patch structure is seen, and CNA keeps

©2019. Japan Geoscience Union. All Right Reserved.

constant value at the latitude where patch structure is not seen. In the presentation, based on these observations, we will discuss physical mechanisms to cause changes in the auroral morphology and energetic electron precipitation, which can be seen as increases of CNA.

Keywords: Ionosphere, Aurora, Energetic Electron Precipitation (EEP)

©2019. Japan Geoscience Union. All Right Reserved.

Spatiotemporal characteristics on the source region of flash aurora using ray tracing analysis

*Tomohiro Inoue[1], Mitsunori Ozaki[1], Yoshitaka Goto[1], Satoshi Yagitani[1], Yoshiya Kasahara[1], Kazuo Shiokawa[2], Yoshizumi Miyoshi[2], Ryuho Kataoka[3], Yusuke Ebihara[4]

1. Kanazawa University , 2. Nagoya University, 3. National Institute of Polar Research, 4. Kyoto University

Whistler mode waves cause precipitation of high-energy electrons via wave-particle interactions in the magnetosphere. The scattered particles precipitate to the ground along the geomagnetic field line. Then, flush aurora, which is a rapid (less than 1 s) auroral phenomenon, is happened. Flash aurora is important for understanding the spatial evolution of wave-particle interaction region in the magnetosphere. We observed the mainly southward spread of flush aurora. In order to understand the spatial-time variation of wave-particle interaction region, we analyze the propagation effects of whistler mode waves near the magnetic equator region using ray tracing analysis. We calculated the ray paths of whistler mode waves (0.2 fce and 0.4 fce) near the magnetic equator (-10 to +10 degrees of geographic latitude), where fce is the electron cyclotron frequency at the magnetic equator. The initial ray paths put in the assumption of a spatial spread with the wave normal angles of tens of degrees along the magnetic field line at the magnetic equator (a point source). Then, we traced the magnetic field lines from the ray paths of whistler mode waves and estimated the precipitation area of electrons in the ionosphere using the IGRF model. The calculation results showed the precipitation area was not mainly spread southward, but evolved northward in the preliminary study.
In this presentation, we will present the spatiotemporal characteristics of flash aurora and the analysis results of ray tracing in detail.

Keywords: Flush aurora, Whistler mode wave, Ray tracing, Wave-particle interaction

©2019. Japan Geoscience Union. All Right Reserved.

Molecular ion supply mechanisms from the low-altitude ionosphere to magnetosphere observed by EISCAT and Arase(ERG)

*Masayoshi Takada[1], Kanako Seki[1], Yasunobu Ogawa[2], Kunihiro Keika[3], Satoshi Kasahara[4], Shoichiro Yokota[5], Tomoaki Hori[7], Kazushi Asamura[6], Yoshizumi Miyoshi[7]

1. Graduate School of Science, Tokyo University, 2. National Institute of Polar Research, 3. Department of Earth and Planetary Science, Graduate School of Science, Tokyo University, 4. The University of Tokyo, 5. Graduate School of Science, Osaka University, 6. Institute of Space and Astronautical Science, Japan Aerospace Exploration Agency, 7. Institute for Space-Earth Environmental Research, Nagoya University

Molecular ions ($O_2^+/NO^+/N_2^+$) in the magnetosphere have been observed during magnetic storms [Peterson et al., 1994; Klecker et al., 1986]. These molecular ions are considered to originate from the Earth’ s ionosphere. It is considered that they have been transported upward by some heating processes in the ionosphere. However, due to the larger mass than atomic ions (O^+), the molecular ions usually exist only in the low-altitude ionosphere below 300 km altitude. It is hence difficult to transport these molecular ions by overcoming loss by chemical reactions to the high-altitude ionosphere where the ion upflow and outflows usually take place [Peterson et al., 1994]. Therefore, it is necessary to reveal what mechanism causes molecular ion upflow during the magnetic storms. In this study, we aim at the observational assessments of the supply processes of the molecular ions from the low-altitude ionosphere to the magnetosphere based on conjugate observations by EISCAT radar and the Arase (ERG) satellite.

The EISCAT radar and the Arase (ERG) satellite have the conjunction event during the large magnetic storm with the minimum Dst of -124 nT on September 8, 2017. During the event, the Arase satellite was located in the dusk-side inner magnetosphere and observed molecular ions in the energy range of 12-180 keV/q. The EISCAT radar simultaneously observed the ion upflow (with the upward velocity of ~50-150 m/s) from the low-altitude ionosphere (~250-400 km) together with strong ion heating (>2000 K). The convective electric field was also enhanced by a factor of 2 in the same region. We estimated each term in the equation of motion for ions. The result indicates that the ion upflow reached stable equilibrium because the upward ion and electron pressure gradients are balanced with the downward gravitational force. It is suggested that the ion upflow can take place from the low-altitude ionosphere due to strong ion pressure gradient. We also estimated the flux decrease of molecular ions due to dissociative recombination. The flux decreased to ~1 % at 350 km compared with 280 km. The estimated upflow flux of molecular ions at 350 km is $>10^{10}$ m^{-2} s^{-1} . Comparison between distribution functions observed by Arase satellite and EISCAT radar suggests that acceleration by 3 orders of magnitudes is necessary during the outflow process. These results indicate that the strong ion frictional heating during magnetic storms enabled molecular ions to be transported upward from the low-altitude ionosphere and provide a source of molecular ion outflows into the magnetosphere.

Keywords: Molecular ion, EISCAT radar, Arase (ERG) satellite, Ion upflow, Ionospheric heating

©2019. Japan Geoscience Union. All Right Reserved.

Optical and radar observation of the dynamic auroral forms

*Yunosuke Nagafusa[1], Tima Sergienko[2], Satoshi Taguchi[1], Urban Braendstroem[2], Masatoshi Yamauchi[2]

1. Graduate School of Science, Kyoto University, 2. Swedish Institute of Space Physics, Kiruna

Ionosphere disturbances caused by the auroral electron precipitations are studied using auroral images taken by Auroral Large Imaging System (ALIS) and ionospheric parameters measured by EISCAT UHF radar that were conjugate with ALIS field-of-view. ALIS consists of several remote controlled stations located in northern Scandinavia, separated by approximately 50 km. Each station is equipped with a high-resolution CCD detector with 1024×1024 pixels, and a filter wheel with six positions for narrow-band interference filters. In this study we use the data obtained with the 557.7 nm filter, which show the auroral emission originated from the atomic oxygen. EISCAT UHF radar located in northern Norway near Tromsø operating in the BEATA program provides the ionospheric electron density, electron and ion temperatures, and ion velocity with the time resolution of 5 s and the spatial resolution of 1.5 km. The auroral images from the different ALIS stations were used for triangulation of the auroral forms in order to determine the aurora position in relation to the radar beam. For each auroral arc, the electron density, the electron and ion temperatures measured inside and in the vicinity of the auroral forms were analyzed with the aim of understanding the ionospheric response to the different types of auroral electron precipitations.

Keywords: aurora, ionospheric parameters, electron precipitations

©2019. Japan Geoscience Union. All Right Reserved.

Observations of MF/HF auroral radio emissions at three ground-based stations

*Yuka Sato[1], Atsushi Kumamoto[2], Yuto Katoh[2], Akira Kadokura[3,4], Yasunobu Ogawa[3,4], Atsuki Shinbori[5]

1. Nippon Institute of Technology (NIT), 2. Graduate School of Science, Tohoku University, 3. National Institute of Polar Research (NIPR), 4. The Graduate University for Advanced Studies, 5. Institute for Space-Earth Environmental Research (ISEE), Nagoya University

We started ground-based observations of MF/HF auroral radio emissions about 10 years ago at two stations (The Husafell Station, Iceland, September 2005; The Kjell Henriksen Observatory, Svalbard, September 2008) and found multiple unknown properties of MF/HF auroral radio emissions, e.g. polarization features [*Sato et al.*, 2008, 2015] and existence of a higher frequency component [*Sato et al.*, 2012]. To make a next siginificant step for a futher understanding of MF/HF auroral radio emissions, we installed a new dedicated instrumentation at the KAIRA (Kilpisjärvi Atmospheric Imaging Receiver Array) site in Kilpisjärvi, Finland (Latitude: 60.07 N, Longitude: 20.76 E) in the summer of 2018. It is a passive receiving system designed to realize a high-resolution spectral, interferometric and polarization measurements using 4 loop antennas and a software-defined radio (SDR) receiver. This SDR receiver can implement high-speed, flexible digital signal processing of RF signals and obtain high-resolution spectra pauselessly throughout the night in a wide frequency range up to 6 MHz. One of the main research subjects of this project is radio emission spontaneously emitted from aurora. There are long-known three types of MF/HF auroral radio emissions identified at ground level: auroral hiss, medium frequency burst (MFB), and auroral roar. Investigation into the generation of these emissions not only offers a tool of great promise for remote sensing of ionospheric plasma processes and parameters but also gives the foundation for understanding various radiation mechanisms that occur in planetary magnetospheres and plasma in space. In combination with the long-term continuous observations in Iceland and Svalbard and future EISCAT_3D experiments, observation with this new instrumentation will provide a first-time opportunity to reveal spatiotemporal variations of macro and fine structures of MF/HF auroral radio emissions associated with substorm evolution. In this presentation, we show detailed specification of this new instrumentation and some initial results.

Keywords: auroral phenomena, radio wave propagation, wave-particle interaction

©2019. Japan Geoscience Union. All Right Reserved.

Ionospheric F-region Drift Measurements Derived from DPS-4D at Zhongshan Station, Antarctic

*Xiangcai Chen[1]

1. Polar Research Institute of China

By means of high-frequency radio sounding, the ionospheric plasma drift can be measured by the Doppler frequency shift of signal. In this paper we analyze the ionospheric F-region plasma motion performed by Digisonde Portable Sounder (DPS-4D) at cusp latitude over Zhongshan Station in Antarctic. By restricting the echo arrival angle, and selecting the reflection height range at 175 –475 km, we present the variation of the F-region plasma drift measurements by setting limits on the Doppler frequency shift. Base on the 7.5 min interval Digisonde drift data from November 2011 to February 2012, we considered the variations of the plasma drift in F-region under the different geomagnetic activity (Kp) and magnetic local time, as well as it correlation with interplanetary magnetic field (IMF). The results indicate that properly restricting the Doppler frequency shift of the echo has a strong effect that contributes to the accurate and robust measurements of the ionospheric plasma drift. The mean value of horizontal drift mostly leveled off to about 600 m/s at altitude around of 230 km, while the field-aligned component of drift showed mean values of -25 m/s near pre-noon and +40 m/s during the night. These strong diurnal variations have dependence on the sign and strength of the IMF B_y and B_z components. It implies that the contraction and expansion of the polar cap with Kp and the convection in the proximity of the throat with different IMF conditions have a profound influence on the observed drift velocities.

Keywords: Digisonde DPS 4, Doppler frequency shift, remote sensing, polar ionosphere, plasma drift

©2019. Japan Geoscience Union. All Right Reserved.

PARM-HEP Observation of Precipitating High Energy Electrons over Pulsating Aurora

*Taku Namekawa[1], Takefumi Mitani[2], Kazushi Asamura[2], Yoshifumi Saito[2]

1. Department of Earth and Planetary Science, Graduate school of Science, The University of Tokyo, 2. Institute of Space and Astronautical Science, Japan Aerospace Exploration Agency

The phenomenon called microbursts that radiation belt particles precipitate to the Earth’ s atmosphere is thought to be largely related to the dissipation of high energy electrons in radiation belt. It is suggested that this phenomenon is caused by pitch angle scattering of the magnetospheric particles by plasma waves, which is a mechanism similar to the cause of the pulsating aurora observed in the Earth’ s polar region. There is a possibility that the origin of microburst can be clarified by proving simultaneous occurrence of microburst and pulsating aurora, but observational verification has not been made yet. For that purpose, we have developed a high-energy electron detector (HEP) for the observation of sub-relativistic - relativistic energy electrons that make up the microburst. HEP is designed to measure electrons between 300 keV and 2 MeV with energy resolution of 20% or less and with signal processing time of ~ 5 μs. Energy analysis is performed by the detection part of this instrument using SSD (Solid State Detector). Performance tests of this instrument are carried out using a sealed radiation source and a high energy electron beam line. This instrument is installed as one of the core instruments of the PARM instrument package developed for the simultaneous observation of the pulsating aurora and microburst by an international student sounding rocket experiment RockSat-XN and LAMP (Loss through Auroral Microburst Pulsation) sounding rocket experiment. We have succeeded in obtaining the flight data on 13 January 2019 from RockSat-XN sounding rocket experiment. In parallel, we are now preparing HEP analyzer for LAMP sounding rocket experiment. In this presentation, we will show the outline and observation results of RockSat-XN-HEP as well as the LAMP-HEP development status.

Keywords: Microburst, PARM, RockSat-XN, LAMP, Sounding rocket, Pulsating aurora

©2019. Japan Geoscience Union. All Right Reserved.

Development of the medium-energy electron detector with hemispherical field-of-view and the flight test in the PARM (Pulsating AuRora and Microburst) mission

*Shin Sugo[1], Oya Kawashima[1], Kazushi Asamura[2], Reiko Nomura[3], Yasunobu Ogawa[4], Keisuke Hosokawa[5], Yoshizumi Miyoshi[6], Takefumi Mitani[2], Taku Namekawa[1,2], Takeshi Sakanoi[7], Mizuki Fukizawa[7], Naoshi Yagi[7], Satoshi Kasahara[1]

1. The University of Tokyo, 2. Institute of Space and Astronautical Science, Japan Aerospace Exploration Agency, 3. National Astronomical Observatory of Japan, 4. National Institute of Polar Research, 5. The University of Electro-Communications, 6. Institute for Space-Earth Environmental Research, Nagoya University, 7. Tohoku University

Energetic electrons significantly affect ionospheric dynamics and the long-term evolution of surfaces and atmospheres of planets and moons. Since the energetic electron flux is not necessarily isotropic, it is important to cover the broad solid angle to quantitatively evaluate the effects on solar system bodies. With future planetary explorations in mind, we developed the medium-energy (20 - 100 keV) electron detector (MED) which can cover almost 2-pi steradian without the spacecraft spin. In order to test the performance of this analyzer in the relevant environment, we participated in the PARM mission, which aimed to measure electron precipitation using NASA’s sounding rocket RockSat-XN. In this presentation we report on MED observation results obtained through the flight on 13 January 2019.

©2019. Japan Geoscience Union. All Right Reserved.

Auroral substorm onset in satellite-based global images and ground-based all-sky images

*Akimasa Ieda[1], Kirsti Kauristie[2], Yukitoshi Nishimura[3], Yukinaga Miyashita[4], Harald U Frey[5], Liisa Juusola[2], Daniel Whiter[6], Masahito Nose[7], Matthew O Fillingim[5], Farideh Honary[8], Neil C Rogers[8], Yoshizumi Miyoshi[1], Shinobu Machida[1]

1. Institute for Space-Earth Environmental Research, Nagoya University, 2. Finnish Meteorological Institute, 3. Boston university, 4. Korea Astronomy and Space Science Institute, 5. University of California Berkeley, 6. University of Southampton, 7. Graduate School of Science, Kyoto University, 8. Lancaster University

Substorm onset has originally been defined as a longitudinally extended sudden auroral brightening (Akasofu initial brightening: AIB) followed a few minutes later by an auroral poleward expansion in ground-based all-sky images (ASIs). In contrast, such clearly marked two-stage development has not been evident in satellite-based global images (GIs). Instead, substorm onsets have been identified as localized sudden brightenings that expand immediately poleward.
To resolve these differences, optical substorm onset signatures in GIs and ASIs are compared in this study for a substorm that occurred on December 7, 1999. For this substorm, the Polar satellite ultraviolet global imager was operated with a fixed-filter (170 nm) mode, enabling a higher time resolution (37 s) than usual to resolve the possible two-stage development. These data were compared with 20-s resolution green-line (557.7 nm) ASIs at Muonio in Finland. The ASIs revealed the AIB at 2124:50 UT and the subsequent poleward expansion at 2127:50 UT, whereas the GIs revealed only an onset brightening that started at 2127:49 UT.
Thus, the onset in the GIs was delayed relative to the AIB and in fact agreed with the poleward expansion in the ASIs. The fact that the AIB was not evident in the GIs may be attributed to the limited spatial resolution of GIs for thin auroral arc brightenings. The implications of these results for the definition of substorm onset are discussed herein.

Keywords: substorm, auroral breakup, aurora

©2019. Japan Geoscience Union. All Right Reserved.

Original substorm onset (Akasofu 1964; 2010)

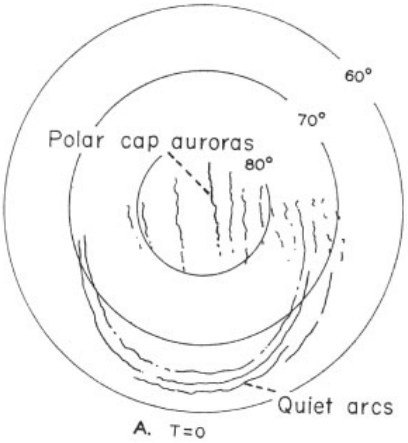

FIG. 2. THE DISTRIBUTION OF THE AURORAS DURING THE QUIET PHASE.

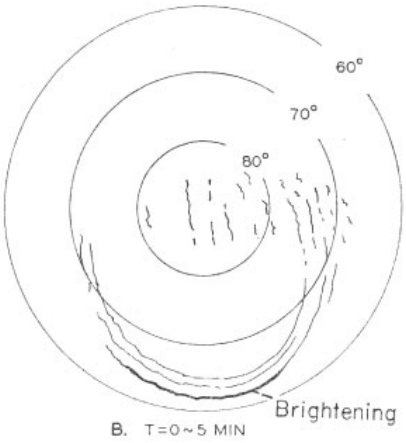

FIG. 3. AURORAS DURING THE EXPANSIVE PHASE (STAGE I).

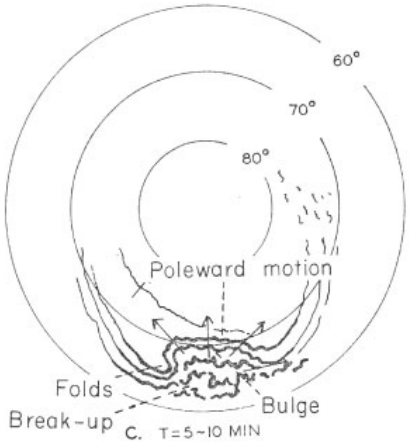

FIG. 4. AURORAS DURING THE EXPANSIVE PHASE (STAGE II).

a Time < 0
Before onset
Quiet arc

b T = 0 ~ 5 min
Expansion phase stage 1
Initial brightening
T = 0: Substorm onset

c T = 5 ~ 10 min
Expansion phase stage 2
Poleward expansion
(Auroral breakup)

Ground and satellite observations (Ieda et al. 2018: 10.1186/s40623-018-0843-3)

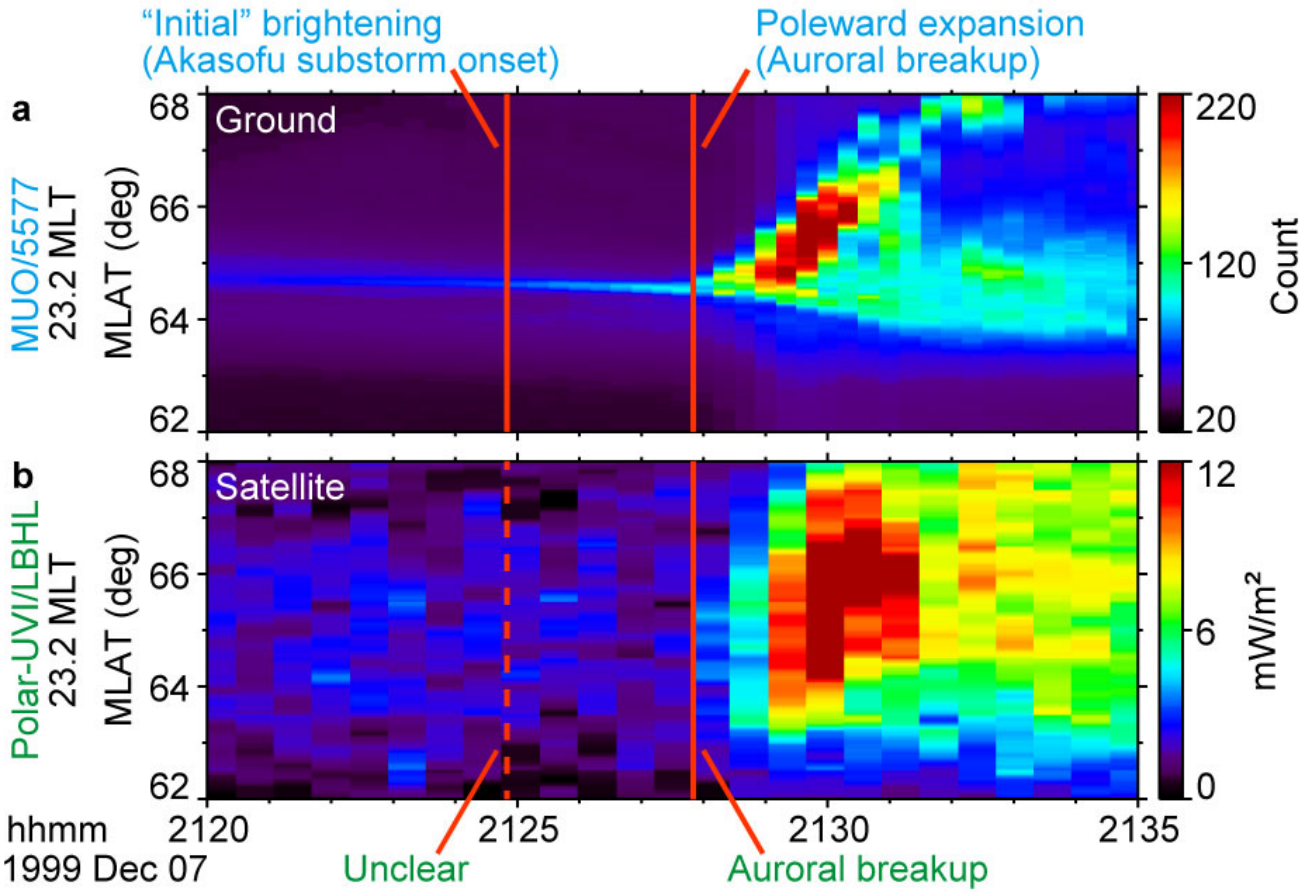

©2019. Japan Geoscience Union. All Right Reserved.

Automatic Classification of Auroral images using optical flow feature

*Naoto Kashiwagi[1], Akiko Fujimoto[1], Terumasa Tokunaga[1], Yoshizumi Miyoshi[2], Yasunobu Ogawa[3], Keisuke Hosokawa[4]

1. Kyushu Institute of Technology, 2. Nagoya University, 3. National Institute of Polar Research, 4. The University of Electro-Communications

The machine learning technique including the deep learning has been developed and the practical uses have increased on various field. On the study of auroral detection, the concern over the automatic image classification has risen using the approach of machine learning technique for the large statistical analysis of auroral images. The automatic auroral image classification has tried to use some techniques from computer vision, machine vision and pattern recognition. There are roughly two kinds of the selected feature: the color of image and the motion of aurora image sequences. The works based on the color feature of aurora image have been performed by Rao et al. (2014) and Tanaka et al. (2015). Rao et al. (2014) performed Support Vector Machines (SVM) classification with several local feature extraction techniques, and found that Scale Invariant Feature Transform (SIFT), OpponentSIFT, is the most effective feature for the automated classification of color aurora images. Tanaka et al. (2015) used the aurora area using the HSV model. They mentioned that it is difficult to classify the images including the diffuse aurora and cloud area. The color feature work well for the color auroral image, while the gray-scale (optically filtered) auroral images need other features on the automated classification. Blixt et al. (2006) applied the optical flow estimation to auroral image sequences. Their case study showed the useful tool for representing the motion of the aurora. In this study, we validate the optical flow estimation to extract the feature of auroral image, and automatically classify the large gray-scale auroral images using the machine learning with Convolution Neural Network (CNN). We use 63,486 gray-scale aurora images in total and use five categories for the preparation of supervised learning data, 1) aurora, 2) aurora and cloudy, 3) aurora and moon, 4) aurora, cloudy and moon, 5) noaurora. We perform the Hold-out and the Cross Validation to evaluate our classification performance. We obtained 98.58% of the classification accuracy based on Hold-out and 98.47% of the classification accuracy based on Cross Validation.

Keywords: Aurora, Optical flow, Convolution Neural Network

©2019. Japan Geoscience Union. All Right Reserved.

Fine-scale visualization of aurora in a wide area using color digital camera images from the International Space Station

*Sota Nanjo[1], Yuta Hozumi[1], Keisuke Hosokawa[1]

1. The University of Electro-Communications

Various ground-based and space-based imagers have been used to observe aurora borealis and australis. So far, however, it has been difficult to observe the detailed spatial structure of auroras in a wide area with sufficient spatial and temporal resolution. Since the photographs taken from the International Space Station (ISS) have sufficient spatial and temporal resolution, it is possible to visualize the fine-scale structures of aurora in a wide area. A calibration of imaging parameters of the photographs using star lights was proposed by a previous research. The accuracy in the timestamp was not guaranteed by the method based on the star lights because the position of the star lights in the image did not change with elapsed time. Thus, it is still difficult to use the mapped data for studying fast variations of aurora, for example pulsating aurora (PsA). Therefore, in this study, we calibrated the images from the ISS using city lights which change their apparent positions with elapsed time. In order to validate the calibration method using city light positions, we mapped two PsA events in the photographs to the geographical coordinate, and compared with those from ground-based all-sky imagers in Alaska and Canada. We found that the approximate shape of discrete aurora and the temporal variation of PsA derived from the ISS images are consistent with those from the ground-based observation. The accuracy in the timestamp is less than 0.5 sec and that in space in the direction perpendicular to the line of sight of the camera is within 5 km. In the presentation, we will also address how the mapped full-color images can be used for studies of PsA in the future work.

Keywords: aurora, ISS

©2019. Japan Geoscience Union. All Right Reserved.

PARM: Investigation of precipitating high-energy electrons into the auroral ionosphere with sounding rockets

*Kazushi Asamura[1], Yoshizumi Miyoshi[2], Keisuke Hosokawa[3], Takefumi Mitani[1], Taku Namekawa[1,5], Takeshi Sakanoi[4], Naoshi Yagi[4], Mizuki Fukizawa[4], Genki Ishizawa[4], Satoshi Kasahara[5], Shin Sugo[5], Oya Kawashima[5], Reiko Nomura[6], Masahito Nose[2], Mariko Teramoto[2], Yasunobu Ogawa[7], Shinji Saito[2], Ryoichi Fujii[8]

1. ISAS / JAXA, 2. ISEE, Nagoya University, 3. The University of Electro-Communications, 4. Tohoku University, 5. The University of Tokyo, 6. NAOJ / NINS, 7. NiPR / ROIS, 8. ROIS

Bursty precipitations of high-energy electrons into the polar ionopshere have been observed by low-altitude satellite, for example, SAMPEX and FIREBIRD II. These precipitations, called microburst, may contribute to the loss of the terrestrial radiation belt through the collisional energy loss with the dense, cold atmospheric particles. Recent numerical simulations successfully reproduce these microburst precipitations with a few Hz modulations by taking into account the pitch angle scattering with the whistler chorus elements at off-equator regions in the inner magnetosphere. Therefore, one can expect that the miscroburst precipitations have properties depending on auroral activities especially the pulsating auroras. In order to investigate the mechanisms of the microburst precipitations by in-situ observations, we are developing two instrument packages: PARM (Pulsating AuRora and Microbursts; already developed) and PARM-2 (being developed), both of which are designed suitable for sounding rocket experiments. PARM consists of four sensors; HEP (high-energy electron energy spectrometer), MED (medium-energy electron detector), AIC (auroral camera), and AFG (ASIC-based fluxgate magnetometer). PARM was onboard the NASA's RockSat-XN sounding rocket, and launched from Andoya, Norway at 09:13UT, Jan 13, 2019. On the other hand, PARM-2 is under development. It consists of HEP, two AICs, and MIM (magneto-impedance magnetometer). PARM-2 is to be onboard the NASA's LAMP sounding rocket which will fly from Poker Flat, Alaska in the period between the end of 2019 and the beginning of 2020.

We will present the overview of PARM missions including the initial results of RockSat-XN/PARM with ground-based observations and preparation status of LAMP/PARM-2.

Keywords: electron microburst precipitation, sounding rocket, pulsating aurora

©2019. Japan Geoscience Union. All Right Reserved.

[E] Poster | P (Space and Planetary Sciences)：P-EM Solar-Terrestrial Sciences, Space Electromagnetism & Space Environment

Wed. May 29, 2019 5:15 PM - 6:30 PM JST | Wed. May 29, 2019 8:15 AM - 9:30 AM UTC | Poster Hall International Exhibition Hall8, Makuhari Messe_5

[P-EM11] Dynamics of Magnetosphere and Ionosphere

convener:Aoi Nakamizo(Applied Electromagnetic Research Institute, National Institute of Information and Communications Technology), Mitsunori Ozaki(Faculty of Electrical and Computer Engineering, Institute of Science and Engineering, Kanazawa University), Akiko Fujimoto(Kyushu Institute of Technology), Tomoaki Hori(Institute for Space-Earth Environmental Research, Nagoya University)

This session provides an opportunity to present recent results from satellite and ground-based observations and theoretical and simulation studies on the magnetosphere, ionosphere, and their coupling processes. We invite talks and posters discussing various phenomena related to the magnetosphere-ionosphere system: solar wind-magnetosphere interaction, magnetosphere-ionosphere convection, field-aligned current, magnetic storms/substorms, neutral-plasma interaction, ionospheric ion inflow and outflow, aurora phenomena, and so forth. Discussions on planetary and satellite ionosphere and magnetospheres, future missions and instrument developments are also welcome.

[PEM11-P01] Effects of Inclination/Rotation of Earth's Magnetic Axis on Magnetosphere Simulated by Global MHD Model

*Aoi Nakamizo[1] (1.Applied Electromagnetic Research Institute, National Institute of Information and Communications Technology)

[PEM11-P02] Asymmetric deformation of the magnetosphere under low-density solar wind

*Masaki N Nishino[1,2], Yoshifumi Saito[2], Kazuo Shiokawa[1], Masaki Fujimoto[2] (1.Institute for Space-Earth Environmental Research, Nagoya University, 2.JAXA/ISAS)

[PEM11-P03] New perspectives on coupling processes in solar-terrestrial system obtained by comprehensive data analysis

*Yoshimasa Tanaka[1], Norio Umemura[2], Shuji Abe[3], Satoru UeNo[4], Masahito Nose[2], Yumi Nakagawa[5] (1.National Institute of Polar Research, 2.Institute for Space-Earth Environmental Research, Nagoya University, 3.International Center for Space Weather Science and Education, 4.Kwasan & Hida Observatories, School of Science, Kyoto University, 5.Ibaraki University)

[PEM11-P04] The interaction between the magnetosphere-ionosphere compound system and the magnetic field topology

*Shigeru Fujita[1], Takashi Tanaka[2], Masakazu Watanabe[2] (1.Meteorological College, Japan Meteorological Agency/ Nationa Institute of Polar Research, 2.Kyushu University)

[PEM11-P05] Effects of the dipole tilt and the interplanetary magnetic field Bx component on the dawn-dusk and interhemispheric asymmetries of the interchange convection cycle

*Masakazu Watanabe[1,2], Takashi Tanaka[2], Shigeru Fujita[3,4] (1.Graduate School of Science, Kyushu University, 2.International Center for Space Weather Science and Education, Kyushu University, 3.Meteorological College, 4.National Institute of Polar Research)

[PEM11-P06] Transient polar ionospheric convection response to negative dynamic pressure pulse

*Jianjun Liu[1] (1.Polar Research Institute of China)

[PEM11-P07] An active ionosphere: a new perspective of field line dipolarization

*Osuke Saka[1] (1.Office Geophysik)

[PEM11-P08] Toward the automatic identification of FLR signals in the SuperDARN data by using the gradient method

*Hideaki Kawano[1,2], Akira Sessai Yukimatu[3,4], Nozomu Nishitani[5], Yoshimasa Tanaka[3,4], Satoko Saita[6], Tomoaki Hori[5] (1.Dept. Earth Planet. Sci., Kyushu Univ., 2.ICSWSE, Kyushu University, 3.National Institute of Polar Research, 4.SOKENDAI, 5.ISEE, Nagoya University, 6.Kitakyushu College)

[PEM11-P09] A statistical study of Pi2 pulsations observed in the upper ionosphere using Swarm magnetic field data

*Park Jaehee[1], Khan-Hyuk Kim[1], Junga Hwang[2] (1.School of Space Research, Kyung Hee University, Gyeonggi, South Korea, 2.Korea Astronomy and Space Science Institute, Daejeon,South Korea)

[PEM11-P10] Study on the global distribution characteristics of Pc 1-2 geomagnetic pulsation with the 10Hz data of the MAGDAS system

*Taisei Kabasawa[1], Akimasa Yoshikawa[1], Teiji Uozumi[1], Akiko Fujimoto[1], Shuji Abe[1] (1.Kyushu University)

[PEM11-P11] In-situ Observations of Reconnection Separatrix Regions in the near-Earth Magnetotail

*Mizuho Araki[1], Masahiro Hoshino[1], Kunihiro Keika[1], Yoshifumi Saito[2] (1.Graduate School of Science, The University of Tokyo, 2.Institude of Space and Astronautical Science)

[PEM11-P12] Flow speed dependence of ion temperature, electron temperature, and their ratio in the near-Earth magnetotail reconnection region

*Kaori Watanabe[1], Masahiro Hoshino[1], Kunihiro Keika[1], Yoshifumi Saito[2], Naritoshi Kitamura[1] (1.Univ. of Tokyo, 2.ISAS/JAXA)

[PEM11-P13] **Examining Minimum Cyclotron Resonant Electron Energy of EMIC Waves with MMS**

*Si Liu[1] (1.Changsha University of Science and Technology)

[PEM11-P14] Small scale whistler mode waves near the magnetic field intensity minimum in the magnetosheath

*Naritoshi Kitamura[1], Takanobu Amano[1], Yoshiharu Omura[2], Satoko Nakamura[2], Chika Umegaki[1], Scott A Boardsen[3,4], Narges Ahmadi[5], Robert E Ergun[5], Olivier Le Contel[6], Per-Arne Lindqvist[7], Yoshifumi Saito[8], Shoichiro Yokota[9], Daniel J Gershman[3], Barbara L Giles[3], Thomas E Moore[3], William R Paterson[3], Craig J Pollock[10], Christopher T Russell[11], Robert J Strangeway[11], James L Burch[12] (1.Department of Earth and Planetary Science, Graduate School of Science, The University of Tokyo, 2.Research Institute for Sustainable Humanosphere, Kyoto University, 3.NASA Goddard Space Flight Center, 4.University of Maryland, 5.Laboratory for Atmospheric and Space Physics, University of Colorado, 6.Laboratoire de Physique des Plasmas, UMR7648 CNRS/Ecole Polytechnique/UPMC/Université Paris-Sud/Observatoire de Paris, 7.Royal Institute of Technology, 8.Institute of Space and Astronautical Science, Japan Aerospace Exploration Agency, 9.Department of Earth and Space Science, Graduate School of Science, Osaka University, 10.Denali Scientific, 11.Institute of Geophysics and Planetary Physics, University of California, Los Angeles, 12.Southwest Research Institute)

[PEM11-P15] Spatial characteristics of the internal modulation of pulsating aurora: multi-point high-speed optical observations in Scandinavia

*Yuki Kawamura[1], Keisuke Hosokawa[1], Shin-ichiro Oyama[2,3], Yoshizumi Miyoshi[2], Yasunobu Ogawa[3], Satoshi Kurita[2], Satoshi Ebukuro[1], Ryoichi Fujii[4] (1.Department of Communication Engineering and Informatics, University of Electro-Communications, 2.Institute for Space-Earth Environmental Research, Nagoya University, 3.National Institute of Polar Research, 4.Research Organization of Information and Systems)

[PEM11-P16] **Large-scale characteristics of pulsating aurora periodicities:multi-point high-speed optical observations in Scandinavia**

*Satoshi Ebukuro[1], Keisuke Hosokawa[1], Shin-ichiro Oyama[2,3,5], Yoshizumi Miyoshi[2], Yasunobu Ogawa[3], Satoshi Kurita[2], Yuki Kawamura[1], Ryoichi Fujii[4] (1.Department of Communication Engineering and Informatics, University of Electro-Communications, 2.Institute for Space-Earth Environmental Research, Nagoya University, 3.National Institute of Polar Research, 4.Research Organization of Information and Systems, 5.University of Oulu)

[PEM11-P17] Variations of cosmic noise absorption (CNA) by energetic electron precipitation (EEP) and changes of the auroral morphology

*Miyamoto Taishiro[1], Shin-ichiro Oyama[1,4,5], Yasunobu Ogawa[2], Keisuke Hosokawa[3], Satoshi Kurita[1], Yoshizumi Miyoshi[1], Ryuho Kataoka[2], Hiroshi Miyaoka[2], Tero Raita[4] (1. Institute for Space-Earth Environmental Research,Nagoya University, 2.National Institute of Polar Research, 3.Department of Communication Engineering and Informatics, University of Electro-Communications, 4.Sodankylä Geophysical Observatory, University of Oulu, 5.Ionosphere Research Unit, University of Oulu)

[PEM11-P18] Spatiotemporal characteristics on the source region of flash aurora using ray tracing analysis

*Tomohiro Inoue[1], Mitsunori Ozaki[1], Yoshitaka Goto[1], Satoshi Yagitani[1], Yoshiya Kasahara[1], Kazuo Shiokawa[2], Yoshizumi Miyoshi[2], Ryuho Kataoka[3], Yusuke Ebihara[4] (1.Kanazawa University , 2.Nagoya University, 3.National Institute of Polar Research, 4.Kyoto University)

[PEM11-P19] Molecular ion supply mechanisms from the low-altitude ionosphere to magnetosphere observed by EISCAT and Arase(ERG)

*Masayoshi Takada[1], Kanako Seki[1], Yasunobu Ogawa[2], Kunihiro Keika[3], Satoshi Kasahara[4], Shoichiro Yokota[5], Tomoaki Hori[7], Kazushi Asamura[6], Yoshizumi Miyoshi[7] (1.Graduate School of Science, Tokyo University, 2.National Institute of Polar Research, 3.Department of Earth and Planetary Science, Graduate School of Science, Tokyo University, 4.The University of Tokyo, 5.Graduate School of Science, Osaka University, 6.Institute of Space and Astronautical Science, Japan Aerospace Exploration Agency, 7.Institute for Space-Earth Environmental Research, Nagoya University)

[PEM11-P20] Optical and radar observation of the dynamic auroral forms

*Yunosuke Nagafusa[1], Tima Sergienko[2], Satoshi Taguchi[1], Urban Braendstroem[2], Masatoshi Yamauchi[2] (1.Graduate School of Science, Kyoto University, 2.Swedish Institute of Space Physics, Kiruna)

[PEM11-P21] Observations of MF/HF auroral radio emissions at three ground-based stations

*Yuka Sato[1], Atsushi Kumamoto[2], Yuto Katoh[2], Akira Kadokura[3,4], Yasunobu Ogawa[3,4], Atsuki Shinbori[5] (1.Nippon Institute of Technology (NIT), 2.Graduate School of Science, Tohoku University, 3.National Institute of Polar Research (NIPR), 4.The Graduate University for Advanced Studies, 5.Institute for Space-Earth Environmental Research (ISEE), Nagoya University)

[PEM11-P22] **Ionospheric F-region Drift Measurements Derived from DPS-4D at Zhongshan Station, Antarctic**

*Xiangcai Chen[1] (1.Polar Research Institute of China)

[PEM11-P23] PARM-HEP Observation of Precipitating High Energy Electrons over Pulsating Aurora

*Taku Namekawa[1], Takefumi Mitani[2], Kazushi Asamura[2], Yoshifumi Saito[2] (1.Department of Earth and Planetary Science, Graduate school of Science, The University of Tokyo, 2.Institute of Space and Astronautical Science, Japan Aerospace Exploration Agency)

[PEM11-P24] Development of the medium-energy electron detector with hemispherical field-of-view and the flight test in the PARM (Pulsating AuRora and Microburst) mission

*Shin Sugo[1], Oya Kawashima[1], Kazushi Asamura[2], Reiko Nomura[3], Yasunobu Ogawa[4], Keisuke Hosokawa[5], Yoshizumi Miyoshi[6], Takefumi Mitani[2], Taku Namekawa[1,2], Takeshi Sakanoi[7], Mizuki Fukizawa[7], Naoshi Yagi[7], Satoshi Kasahara[1] (1.The University of Tokyo, 2.Institute of Space and Astronautical Science, Japan Aerospace Exploration Agency, 3.National Astronomical Observatory of Japan, 4.National Institute of Polar Research, 5.The University of Electro-Communications, 6.Institute for Space-Earth Environmental Research, Nagoya University, 7.Tohoku University)

[PEM11-P25] Auroral substorm onset in satellite-based global images and ground-based all-sky images

*Akimasa Ieda[1], Kirsti Kauristie[2], Yukitoshi Nishimura[3], Yukinaga Miyashita[4], Harald U Frey[5], Liisa Juusola[2], Daniel Whiter[6], Masahito Nose[7], Matthew O Fillingim[5], Farideh Honary[8], Neil C Rogers[8], Yoshizumi Miyoshi[1], Shinobu Machida[1] (1.Institute for Space-Earth Environmental Research, Nagoya University, 2.Finnish Meteorological Institute, 3.Boston university, 4.Korea Astronomy and Space Science Institute, 5.University of California Berkeley, 6.University of Southampton, 7.Graduate School of Science, Kyoto University, 8.Lancaster University)

[PEM11-P26] Automatic Classification of Auroral images using optical flow feature

*Naoto Kashiwagi[1], Akiko Fujimoto[1], Terumasa Tokunaga[1], Yoshizumi Miyoshi[2], Yasunobu Ogawa[3], Keisuke Hosokawa[4] (1.Kyushu Institute of Technology, 2.Nagoya University, 3.National Institute of Polar Research, 4.The University of Electro-Communications)

[PEM11-P27] Fine-scale visualization of aurora in a wide area using color digital camera images from the International Space Station

*Sota Nanjo[1], Yuta Hozumi[1], Keisuke Hosokawa[1] (1.The University of Electro-Communications)

[PEM11-P28] Geospace Imaging via the soft X-ray imager: GEO-X mission

*Yoshizumi Miyoshi[1], Yuichiro Ezoe[2], Satoshi Kasahara[3], Yosuke Matsumoto[4], Kumi Ishikawa[5], Ryuho Kataoka[6], Hiroki Ito[1], Daiki Ishi[2], Masaki Numazawa[2], Atsushi Yamazaki[5], Hiroshi Hasegawa[5], Masaki Fujimoto[5], Kazuhisa Mitsuda[5] (1.Institute for Space-Earth Environmental Research, Nagoya University, 2.Tokyo Metropolitan University, 3.University of Tokyo, 4.Chiba University, 5.ISAS/JAXA, 6.NIPR)

Effects of Inclination/Rotation of Earth’s Magnetic Axis on Magnetosphere Simulated by Global MHD Model

*Aoi Nakamizo[1]

1. Applied Electromagnetic Research Institute, National Institute of Information and Communications Technology

Recently, we have shown that the ionospheric Hall conductance distribution, owing to the polarization field generated by its nonuniformity, largely control the magnetospheric configuration and dynamics by using a global MHD model. The effects of the ionospheric conductance on the magnetosphere were also reported by previous studies based on other global models; for example, the current-voltage relationship in the solar wind-magnetosphere-ionosphere [Fedder and Lyon, 1987] and the plasma pressure distribution in the near-Earth region [Ridley et al., 2004]. These studies indicate that the ionospheric conductance is one of the most important settings in the global models to accurately simulate the magnetosphere.

On the other hand, in the development/improvement of the global MHD model in NICT, which was originally developed by Tanaka [1994] and Tanaka et al. [2010], introducing the inclination and rotation of Earth’s magnetic axis with respect to the rotation axis has been remained as one of the most difficult problems. In other words, in the present model, the precession between the magnetic axis and the rotation axis is not included. This means that the simulated magnetosphere will show a different structure and temporal development than the actual magnetosphere.

We, for the first time, equivalently introduce the precession by rotating the background conductance distribution due to solar illumination (i.e., depending on the geographic coordinate) with respect to the geomagnetic coordinate. (Improvement of the conductance setting in the auroral region is the next challenge.) In this paper, we will show how the simulated magnetosphere is changed by this improvement, focusing on the near-Earth plasma environment.

Keywords: M-I Coupling, Global MHD Simulation, Ionospheric Effect

©2019. Japan Geoscience Union. All Right Reserved.

Asymmetric deformation of the magnetosphere under low-density solar wind

*Masaki N Nishino[1,2], Yoshifumi Saito[2], Kazuo Shiokawa[1], Masaki Fujimoto[2]

1. Institute for Space-Earth Environmental Research, Nagoya University, 2. JAXA/ISAS

The density of the solar wind around the Earth's magnetosphere sometimes decreases to only several percent of the usual value, and such density extrema results in a significant reduction of dynamic pressure and Alfvenic Mach number of the solar wind flow. While simple expansion of the Earth's magnetosphere by the low dynamic pressure was assumed in previous studies, a global-MHD simulation study predicted a remarkable dawn-dusk asymmetry of the magnetosphere in shape under low-density solar wind and Parker-spiral IMF configuration. Here we present evidence of asymmetric deformation of the magnetosphere under low-density solar wind and Parker-spiral IMF conditions, based on several events of GEOTAIL observations. As predicted by the global-MHD simulation, the magnetosphere on the dawnside expands much further than the magnetopause location of simple (symmetric) expansion, while no significant expansion is detected in the dusk tail flank. Fast ion beams detected at the flank magnetopause suggest that magnetic reconnection frequently occurs due to the low-beta environment of the magnetosheath.

Keywords: Low density solar wind, Magnetosphere, Plasma transport

©2019. Japan Geoscience Union. All Right Reserved.

New perspectives on coupling processes in solar-terrestrial system obtained by comprehensive data analysis

*Yoshimasa Tanaka[1], Norio Umemura[2], Shuji Abe[3], Satoru UeNo[4], Masahito Nose[2], Yumi Nakagawa[5]

1. National Institute of Polar Research, 2. Institute for Space-Earth Environmental Research, Nagoya University, 3. International Center for Space Weather Science and Education, 4. Kwasan & Hida Observatories, School of Science, Kyoto University, 5. Ibaraki University

In the Earth’ s upper atmosphere above 60 km, including magnetosphere and ionosphere, various phenomena are generated by energy inputs from solar radiation (including solar wind) and atmospheric waves propagating from the lower atmosphere. Thus, comprehensive analysis of various kinds of satellite and ground-based observational data using advanced methods is required to understand physical mechanism of the phenomena. For such interdisciplinary studies, it is important to share data distributed across many universities and institutes and use advanced tools, such as metadata database for cross-searching a variety of datasets and analysis software for analyzing various types of data in an integrated fashion. In fact, many scientific papers on the upper atmosphere have recently been obtained by comprehensive analysis of various data with such analysis tools.
We present some examples of scientific results achieved by comprehensively analyzing data from multiple regions. These examples include the effect of solar coronal holes on the Earth’ s geomagnetic activity and the interaction between solar wind, magnetosphere, ionosphere and neutral atmosphere. The former study investigated long-term trends of coronal boles, solar wind parameters, and Earth’ s geomagnetic indices during two solar cycles. It showed the possibility that the solar wind speed and geomagnetic activities may be controlled by the size and latitudinal distribution of coronal holes. The latter analyzed multi-instrument data simultaneously obtained from interplanetary space, magnetosphere, and ionosphere and mesosphere in both northern and southern hemispheres. They newly found that the polar mesosphere is affected by relativistic electron precipitation caused by the interaction with magnetospheric plasma waves during the high-speed solar wind stream. These studies demonstrate that sharing and comprehensive analysis of long-term, multiple-sphere, and multi-instrument data using sophisticated tools are very effective to produce scientific outcomes. At present there are data gap areas in the Asia and African regions. Therefore, we believe that filling in the data gap by international collaborations could be a breakthrough for unsolved issues in the upper atmosphere.

Keywords: upper atmosphere, coupling between multiple regions, comprehensive analysis, long-term observational data

©2019. Japan Geoscience Union. All Right Reserved.

The interaction between the magnetosphere-ionosphere compound system and the magnetic field topology

*Shigeru Fujita[1], Takashi Tanaka[2], Masakazu Watanabe[2]

1. Meteorological College, Japan Meteorological Agency/ Nationa Institute of Polar Research, 2. Kyushu University

The steady convection in the magnetosphere-ionosphere coupling system is composed of the following self-consistent elementary processes; dynamo in the cusp-mantle region, the field-perpendicular current system in the magnetosphere, the field-aligned current system connecting the ionosphere, the ionospheric electric field, the magnetospheric convection corresponding to the ionospheric electric field, and the high plasma pressure distribution in the cusp region [Tanaka, 2007].

The energy of the convection is transported from the solar wind across the magnetopause where the magnetic field configures the null-separator structure. Since the magnetic field configuration of the null-separator structure is originally derived from the superposition of two scalar fields [Stern, 1973], say, the dipole field and the uniform field, the magnetic field of the null-separator would not have free energy necessary for plasma acceleration. However, the simulation reveals that the magnetic field has a tension force near the null point. Therefore, we need a mechanism that transports the energy to this region.

It is revealed from the simulation that the bow shock supplies the energy. Indeed, the current from the bow shock deforms the magnetic field of the null-separator structure. In addition, it is noted that the Chapman-Ferraro current also deforms the magnetic field configuration in the magnetopause. This fact indicates that the convection system in the magnetosphere contributes to deformation of the null-separator structure. That is to say, energy transport from the solar wind to the magnetosphere-ionosphere compound system is affected by the physical processes in the convection. Therefore, as a result of the interaction between the magnetosphere-ionosphere convection and the null-separator structure, the magnetosphere-ionosphere compound system can be extended to the solar wind-magnetosphere-ionosphere compound system.

References

T. Tanaka (2007), Magnetosphere-Ionosphere Convection as a Compound System, Space Sci Rev, 133, 1-72, DOI 10.1007/s11214-007-9168-4.

Stern, D. P. (1973), A study of the electric field in an open magnetospheric model, J. Geophys. Res., 78(31), 7292-7305, doi:10.1029/JA078i031p07292.

Keywords: global MHD simulation, compound system

©2019. Japan Geoscience Union. All Right Reserved.

Effects of the dipole tilt and the interplanetary magnetic field Bx component on the dawn-dusk and interhemispheric asymmetries of the interchange convection cycle

*Masakazu Watanabe[1,2], Takashi Tanaka[2], Shigeru Fujita[3,4]

1. Graduate School of Science, Kyushu University, 2. International Center for Space Weather Science and Education, Kyushu University, 3. Meteorological College, 4. National Institute of Polar Research

The interchange cycle is a mode of magnetic flux circulation that appears for periods of northward interplanetary magnetic field (IMF). It is made up of IMF-to-open reconnection in one hemisphere and open-to-closed reconnection in the other hemisphere. The two reconnection processes have the same topological nature in that the roles of the two reconnecting field lines interchange at the time of reconnection. The interchange cycle is characterized by reciprocation of open magnetic flux between the two hemispheres. One observable signature of the interchange cycle is an appearance of a reverse cell circulating in the closed field line region of the ionosphere, which is named the “reciprocal cell.” The reciprocal cell appears in the open-to-closed reconnection hemisphere, whereas in the opposite IMF-to-open reconnection hemisphere, there appears a lobe cell circulating exclusively on open field lines. For given (1) IMF By, (2) IMF Bx, and (3) dipole tilt conditions, two interchange cycles concur, one on the dawnside and the other on the duskside. For an ideal case, one can easily expect the mode of the interchange cycles to occur. For example, for the case of due northward IMF with significant dipole tilt, the twin reverse cells in the summer hemisphere are both lobe cells, while in the winter hemisphere the twin reverse cells are both reciprocal cells. For the general case, however, one cannot predict the mode of the interchange cycles without quantitative modeling. The purpose of this study is to examine how the presence of dipole tilt or IMF Bx alters the dawn-dusk and north-south pattern of the twin reverse cells. For this purpose, we perform numerical magnetohydrodynamic simulations using the REPPU (Reproduce Plasma Universe) code developed by T. Tanaka. In the presentation, we discuss the dipole tilt and IMF Bx effects revealed by the numerical modeling.

Keywords: ionospheric convection, interchange reconnection, reciprocal cell

©2019. Japan Geoscience Union. All Right Reserved.

Transient polar ionospheric convection response to negative dynamic pressure pulse

*Jianjun Liu[1]

1. Polar Research Institute of China

The response of the high latitude ionospheric convection to a sudden decrease in solar wind dynamic pressure provides a unique opportunity to investigate how the solar wind couples to the dayside magnetosphere and ionosphere. Here, the event shows three IMF components do not have prominent changes, but the solar wind plasma went down to near zero magnitude, which leads to very weak solar wind driving during northward IMF. However, ionospheric convection observed by SuperDARN radars showed enhanced plasma flow speed in the central polar cap region just after the negative pressure pulse arrival to the magnetosphere. Simultaneous convection map generated by SuperDARN measurement presents enlarged convection cell with obvious equatorward moving Heppner-Maynard boundary. It is noted that cross polar cap potential enhanced instantly and this enhanced feature continued almost 10 min. The distribution of total electron content (TEC) exhibited typical auroral oval signature especially on dayside ionosphere, TEC density in auroral oval showed a noticeable decrease after the arrival of the negative pressure pulse. Both ionospheric convection and TEC distribution reveal that negative pressure pulse impacts the magnetosphere-ionosphere coupling system directly and dramatically. Moreover, the TIEGCM model also showed an enhanced polar potential pattern.

Keywords: Dynamic pressure, Ionospheric convection, Auroral oval

©2019. Japan Geoscience Union. All Right Reserved.

An active ionosphere: a new perspective of field line dipolarization

*Osuke Saka[1]

1. Office Geophysik

Transient westward electric fields from the magnetosphere generate equatorward plasma drifts of the order of kilometers per second in the auroral ionosphere. This flow channel extends in north-south directions and is produced in the initial pulse of Pi2 pulsations associated with the filed line dipolarization. Drifts in the ionosphere of the order of kilometers per second that accumulated plasmas at the low latitude end of the flow channel are of such large degree that possible vertical transport effects (including precipitation) along the field lines may be ignored. We suggest that plasma compression in the ionosphere implemented the ionosphere to be active. Active ionosphere generates field-aligned currents to satisfy the quasi-neutrality of the ionosphere, ion acoustic wave for ion outflows and the inverted-V type electron precipitations in the topside ionosphere, and poleward expansion of auroras due to a nonlinear evolution of the ionosphere. We will study auroral expansion in this acoustic regime.

Keywords: Substorm, Auroral substorm, Ionosphere

©2019. Japan Geoscience Union. All Right Reserved.

Toward the automatic identification of FLR signals in the SuperDARN data by using the gradient method

*Hideaki Kawano[1,2], Akira Sessai Yukimatu[3,4], Nozomu Nishitani[5], Yoshimasa Tanaka[3,4], Satoko Saita[6], Tomoaki Hori[5]

1. Dept. Earth Planet. Sci., Kyushu Univ., 2. ICSWSE, Kyushu University, 3. National Institute of Polar Research, 4. SOKENDAI, 5. ISEE, Nagoya University, 6. Kitakyushu College

The FLR (Field Line Resonance) takes place where the frequency of an incoming wave matches the eigen-frequency of magnetospheric magnetic field lines, and excites the eigen-oscillation of the field lines. The FLR can be identified by using the unique manner of change in the amplitude and the phase of thus excited eigen-oscillation across the resonant point. That is, the amplitude is maximum at the resonant point, and the phase changes the most steeply across the resonance point. The FLR-generated eigen-oscillations can be identified in the ground magnetic field data and the ionospheric plasma velocity data. From thus identified eigen-frequency ("FLR frequency" below) one can estimate the magnetospheric plasma density along the field line which passes through the ground/ionospheric observation point.

In this study we use the SuperDARN radar data to identify FLR: For each radar beam from each SuperDARN radar, the velocity of the ionospheric plasma flow along the line of sight (VLOS) of the beam is obtained; we use the VLOS data to identify the FLR and estimate the magnetospheric plasma density. Unlike the ground magnetometer data, the SuperDARN data is two-dimensional, enabling two-dimensional estimates of the magnetospheric equatorial plasma density and magnetospheric region identification.

To achieve that, it is important to identify as many FLR events as possible. Overwrapping of non-FLR waves/perturbations hides FLR events. As a countermeasure to this problem, the so-called gradient method has been applied to the ground magnetometer data; this method cancels out the overwrapping signals by dividing the data from a magnetometer by the data from another magnetometer having an adequate latitudinal distance from the other. The division yields the amplitude ratio and the phase difference. The gradient method is effective since the FLR frequency tends to depend on the latitude more strongly than the overwrapping signals.

The gradient method is also applicable to the SuperDARN VLOS data. The field of view of each beam is divided into Range Gates (RGs below) having the same length along the beam. The identification number of the RGs increases with increasing distance from the radar. The VLOS is obtained for each RG. Thus, each RG can be regarded as a "virtual observatory."

As an initial study, we have selected an FLR event which was identified in the VLOS data of a radar (at Hankasalmi) without the use of the gradient method, selected a beam, and selected a few pairs of RGs of the beam. We then have manually applied the gradient method to the VLOS data of the above-selected RG pairs, and successfully identified the FLR. In more detail, the identification has been successful only for two paired RGs whose RG numbers differs by two. This suggest that, since the length of the RG, mapped to the meridional plane, was about 40km for this event, about 80km distance was the best (with the resolution of 40km) for this event. This distance reflects the resonance width, which is an important quantity reflecting the diffusion and dissipation of the FLR energy.

©2019. Japan Geoscience Union. All Right Reserved.

In order to identify as many FLR events as possible, it is also important to automatically identify the FLR events, since visual identification is time-consuming. The gradient method enables automatic identification more easily than analyses of VLOS itself, since the gradient method yields peaks in both the amplitude ratio and the phase difference. We have started making a program for automatic identification by applying the gradient method to VLOS; the version at the time of this abstract has successfully identified FLRs for all of the above-stated pairs of RGs.

©2019. Japan Geoscience Union. All Right Reserved.

A statistical study of Pi2 pulsations observed in the upper ionosphere using Swarm magnetic field data

*Park Jaehee[1], Khan-Hyuk Kim[1], Junga Hwang[2]

1. School of Space Research, Kyung Hee University, Gyeonggi, South Korea, 2. Korea Astronomy and Space Science Institute, Daejeon,South Korea

The properties of Pi2 pulsations observed in the upper ionosphere are studied using magnetic field data acquired by the Swarm-A spacecraft in low Earth orbit (LEO) and at the low-latitude Bohyun ground station (BOH, L = 1,3) for January 2014-Jun 2015. From time intervals when Swarm-A was on the nightside (magnetic local time (MLT) = 1800-0600 hrs) and the BOH station was near midnight (MLT = 2100-0300 hrs), we identified 623 Pi2 events in the horizontal H component of the BOH data. For each event we examine the coherence between the horizontal H component on the ground and the B_x (radial) azimuthal B_y (azimuthal), or B_z (compressional) components at Swarm-A. Out of 623 events, the B_x-H high coherence (> 0.7) events are ~6%, the B_y-H high coherence events are ~4%, and the B_z-H high coherence events are ~25%. The ground-satellite high coherence events occurred when the spacecraft was located within a magnetic latitude range of ±50°. Using the ground-satellite high coherence events, we examined the latitudinal structure of the relative amplitude and phase of the ionospheric Pi2 pulsations detected at Swarm-A. Confirming previous observations at LEO, we found that the ionospheric Pi2 pulsations are characterized by symmetric odd mode standing oscillations in the north-south direction, having a node for B_x oscillation and an antinode for B_z oscillation, respectively, at the equator. This indicates that the source of ionospheric Pi2 pulsations is the plasmaspheric resonance.

Keywords: Pi2 pulsations

©2019. Japan Geoscience Union. All Right Reserved.

Study on the global distribution characteristics of Pc 1-2 geomagnetic pulsation with the 10Hz data of the MAGDAS system

*Taisei Kabasawa[1], Akimasa Yoshikawa[1], Teiji Uozumi[1], Akiko Fujimoto[1], Shuji Abe[1]

1. Kyushu University

The magnetic field observed on the ground is affected by the space weather phenomena such as magnetic storms and auroral storms.

The Pc1 geomagnetic pulsation (frequency range of 0.2-5.0 seconds) activated mainly around a high-latitude region is understood as a phenomenon accompanied by the excitation of EMIC waves to cause the particle acceleration in the equatorial region of the magnetosphere. Also, it is well known that Pc1 waves propagate horizontally in the ionospheric at the F layer. However, it is not clarified about the global occurrence and propagation properties of Pc1 geomagnetic pulsation on the ground. Moreover, although induction magnetometers are used to observe the high-frequency magnetic field disturbance phenomenon like Pc1 and Pc2 (frequency range of 5.0-10.0 seconds) geomagnetic pulsation, the global observation network with induction magnetometers covering from high-latitude to low-latitude area and equator domain does not exist at this stage. On the other hand, although it is common to use Fluxgate magnetometers for the observation of global space weather phenomenon, it is considered to be unsuitable for analysis of the high-frequency Pc1-2 geomagnetic pulsation because its time accuracy is usually one second value.

The ground multipoint magnetic field observation network which Kyushu University has developed (MAGDAS-9 magnetometer) acquire a 250Hz sampling and 10Hz mean data. Also, it is the only geomagnetic observation network that can investigate the global aspects of Pc1-2 geomagnetic pulsation.

In this study, we investigated the global distribution of Pc1-2 pulsation from polar region to equatorial region with magnetic field data provided by MAGDAS and Dst/AE index provided by the WDC for Geomagnetism, Kyoto. As a result, when the substorm have occurred during a magnetic storm time, generation of Pc1-2 pulsation from high-latitude to middle-and-low latitude region and further arrival of Pc2 pulsation to the dip-equator are identified. The elucidation of occurrence characteristic of the Pc1-2 pulsation on the ground with the EMIC waves excitation is very important not only for space weather application to be able to monitor particle energization process via EMIC excitation but also the elucidation of the super global coupling process from inner magnetosphere to the global ionosphere from polar to equatorial region. In this presentation, we will report the preliminary results of observational analysis of Pc1-2 pulsation by using MAGDAS network. We also discuss the comprehensive approach for understanding global coupling process among inner magnetosphere and high-middle-low latitude to the equatorial region by using FM-CW radar data, PWING induction magnetometer data, and the geo-space environment data from the ERG satellite.

Keywords: Pc1-2 pulsation, EMIC waves, global coupling

©2019. Japan Geoscience Union. All Right Reserved.

In-situ Observations of Reconnection Separatrix Regions in the near-Earth Magnetotail

*Mizuho Araki[1], Masahiro Hoshino[1], Kunihiro Keika[1], Yoshifumi Saito[2]

1. Graduate School of Science, The University of Tokyo, 2. Institude of Space and Astronautical Science

Magnetic reconnection which converts magnetic energy into thermal and kinetic energy of plasmas is an important physical mechanism of plasma heating and acceleration. Particularly in the Petschek-type reconnection, plasma acceleration and heating in the slow-mode shocks formed at the separatrices must be taken into consideration. The structure of the slow-mode shocks in the distant tail of the Earth’s magnetosphere was investigated with in-situ observations made by the GEOTAIL satellite (Saito et.al, 1995). It is observationally suggested that about 10% of the plasma sheet boundary layer (PSBL) is slow-mode shocks. It is, however, not fully understood what determines this percentage and what is the difference in the ion and electron temperature changes between slow-mode shocks and others separatrix regions.
In this study, we utilized multi-spacecraft in-situ observations of separatrix regions at magnetic reconnection in the near-Earth magnetotail (GSM-X is between ~13 and ~25RE). We used data obtained from FPI (Fast Plasma Investigation) and FGM (Fluxgate Magnetometer) on board the MMS satellite from June 1, 2017to August 31, 2017. We examined occurrence locations, ion flow directions and velocity of ion flow in downstream regions of observed events. We also examined changes in ion and electron temperatures and the ion-to-electron temperature ratio.

We classified their events into 2 types according to plasma beta in the in-flow regions: below 0.1 or around 1. We term them “lobe reconnection” and “plasma sheet reconnection”, respectively. In the former type, plasmas in the in-flow regions are cold and tenuous. In the latter type, plasmas in the in-flow regions are hot and dense. In both types, we observed increases in ion and electron temperatures increase, but their characteristics are different. In the lobe reconnection, ion temperatures increase from several hundred eV to several keV. In the plasma sheet reconnection, ion temperatures also increase from about 1 keV to several keV. The increase rate of the electron temperature is less than one order of magnitude for both types, smaller than that of the ion temperature; the electron temperature increases up to at most 1 keV. The ion-to-electron temperature ratio in the out-flow regions in both types is about 5 for both types. We then examined changes of the ion-to-electron temperature ratio and found that the changes are consistent with the result reported by Wang et al. (2012).

In this presentation, we will show the results of separatrix crossing events (both lobe and plasma sheet reconnection events) that occur in 2017 and 2018. We will identify whether each of the separatrices is a slow shock or not and how the separatrix conditions affect ion and electron heating. These characteristics will provide insights into heating mechanisms and energy conversion through separatrix regions.

Reference:

Yoshifumi Saito, Toshifumi Mukai, Toshio Terasawa, Atsuhiro Nishida, Shinobu Machida, Masafumi Hirahara, Kiyoshi Maezawa, Susumu Kokubun, and Tatsundo Yamamoto, Slow-mode shocks in the magneto, J. Geophys. Res., 100, A12, 23,567, 1995

©2019. Japan Geoscience Union. All Right Reserved.

Chih-Ping Wang, Matina Gkioulidou, Larry R. Lyons and Vassilis Angelopoulos, Spatial distributions of ion to electron temperature ratio in the magnetosheath and plasma sheet, J. Geophys. Res., 117, A08215, 2012

Keywords: Magnetic Reconnection, MMS satellite, Earth's Magnetotail

©2019. Japan Geoscience Union. All Right Reserved.

Flow speed dependence of ion temperature, electron temperature, and their ratio in the near-Earth magnetotail reconnection region

*Kaori Watanabe[1], Masahiro Hoshino[1], Kunihiro Keika[1], Yoshifumi Saito[2], Naritoshi Kitamura[1]

1. Univ. of Tokyo, 2. ISAS/JAXA

Plasma in the Earth's magnetotail are heated up to 1-10 keV and stored in the plasma sheet. One of the heating or acceleration mechanisms is the magnetic reconnection. Heated or accelerated plasma are transported both earthward and tailward as fast flow with a speed of several hundred kilometers per second. However, what determines the partition among ion and electron thermal energy and kinetic energy is an unresolved problem. It has been reported that ion temperature T_i, electron temperature T_e, and their ratio T_i/T_e vary spatially and depend on the conditions of fast flows [Wang et al., 2012, Runov et al., 2018] but there are few studies which focus on macroscopic profiles of them in reconnection regions in the magnetotail.

In this study, we examine the relation between flow speed and average profiles of T_i, T_e, and T_i/T_e in the magnetotail reconnection region by using data obtained from FPI and FGM on board the MMS spacecraft. We use the observations for a period from May to August 2017 and take out the data in the region of $X_{GSM} < -15$ Re, -10 Re $< Y_{GSM} < 10$ Re, and beta > 0.1. We then divide them into different groups according to flow speed normalized by alfven speed and show B_z/B_{lobe}– B_x/B_{lobe} maps of T_i, T_e, and T_i/T_e of each group. The results show that ion temperature increase with increasing flow speed while electron temperature decrease. Ion temperature are hotter around the X-point. The structure of inflow and outflow regions is pronounced in the profile of electron temperature. T_i/T_e in inflow region are greater than in outflow region, which means that ion and electron temperatures become comparable by passing through the diffusion region. The results suggest that electron get less energy when more energy is partitioned into plasma kinetic energy. We will discuss about the profiles of anisotropy of plasma temperatures to know more details about the heating mechanisms.

Keywords: temperature ratio, flow, MMS

©2019. Japan Geoscience Union. All Right Reserved.

Examining Minimum Cyclotron Resonant Electron Energy of EMIC Waves with MMS

*Si Liu[1]

1. Changsha University of Science and Technology

Electromagnetic ion cyclotron (EMIC) waves can be in cyclotron resonance with relativistic electrons, causing relativistic electron precipitation. The four ideal Magnetospheric Multiscale (MMS) spacecraft provide great opportunity to directly calculate the wave vector ***k*** of EMIC waves by phase differencing technique and hence estimate the minimum resonant energy by the resonance condition. Deriving a simplified analytic solution, we find that the phase differencing method can still provide an estimate of the dominant wave number when a finite wave number spread or a finite frequency spread is present. Numerical calculations indicate that quasi-antiparallel propagation dominates the EMIC event on 20 November 2015, which is consistent with the FFT spectral analysis results. We also find that obtained wave vectors, roughly agreeing with the validity of cold plasma theory, might significantly vary from wave packet to wave packet. Moreover, minimum resonant electron energies gradually increase from 0.5 MeV to tens of MeV with a decreasing parallel componet of ***k***. Current results provide evidence that EMIC waves can be in resonance with the electrons of energies down to hundreds of keV. It further demonstrates that EMIC waves in a narrow frequency band can effectively interact with the relativistic electrons with a broad energy range.

Keywords: EMIC waves, minimum resonant electron energy, wave vector, phase differencing

©2019. Japan Geoscience Union. All Right Reserved.

Small scale whistler mode waves near the magnetic field intensity minimum in the magnetosheath

*Naritoshi Kitamura[1], Takanobu Amano[1], Yoshiharu Omura[2], Satoko Nakamura[2], Chika Umegaki[1], Scott A Boardsen[3,4], Narges Ahmadi[5], Robert E Ergun[5], Olivier Le Contel[6], Per-Arne Lindqvist[7], Yoshifumi Saito[8], Shoichiro Yokota[9], Daniel J Gershman[3], Barbara L Giles[3], Thomas E Moore[3], William R Paterson[3], Craig J Pollock[10], Christopher T Russell[11], Robert J Strangeway[11], James L Burch[12]

1. Department of Earth and Planetary Science, Graduate School of Science, The University of Tokyo, 2. Research Institute for Sustainable Humanosphere, Kyoto University, 3. NASA Goddard Space Flight Center, 4. University of Maryland, 5. Laboratory for Atmospheric and Space Physics, University of Colorado, 6. Laboratoire de Physique des Plasmas, UMR7648 CNRS/Ecole Polytechnique/UPMC/Université Paris-Sud/Observatoire de Paris, 7. Royal Institute of Technology, 8. Institute of Space and Astronautical Science, Japan Aerospace Exploration Agency, 9. Department of Earth and Space Science, Graduate School of Science, Osaka University, 10. Denali Scientific, 11. Institute of Geophysics and Planetary Physics, University of California, Los Angeles, 12. Southwest Research Institute

Wave-particle interactions are thought to play a crucial role in energy transfer in collisionless space plasmas in which the motion of charged particles is controlled by electromagnetic fields. In the terrestrial magnetosheath, intense whistler mode waves, called 'Lion roars', are often detected by spacecraft around minima of semi-periodic fluctuations of magnetic field intensity due to mirror mode structures and motion of the structures. It is expected that whistler mode waves are efficiently generated near a local minimum of magnetic field intensity due to the smallest cyclotron resonance velocity. We report the detailed characteristics of such whistler mode waves using the data obtained by the four MMS (Magnetospheric Multiscale) spacecraft. Because reversals of field-aligned component of Poynting flux around minima in mirror mode structures correspond to reversals of gradient of magnetic field intensity along the magnetic field, whistler mode events with reversals of the field-aligned component of Poynting flux are good candidates of observations of effective wave generation regions along field lines. Even in such events, phase difference and change of amplitude of whistler mode waves observed by the four spacecraft do not have a clear correlation in cases of ~40 km separation, which is much smaller than the spatial scale of magnetic field depression due to mirror mode structures and is even smaller than the local thermal ion gyro scale. This result indicates that the coherent whistler wave generation in mirror mode structures has very limited spatial scale across field lines and is probably affected by any electron scale process. A plane wave approximation can be usable only in a very small scale. Because some events in cases of ~7 km separation showed good correlation among four spacecraft, the typical scale of coherent whistler wave across field lines can be at least an order of 10 km in mirror mode structures in the terrestrial magnetosheath. The whistler mode waves observed by a spacecraft in a mirror mode structure are a cluster of waves from multiple spatially small sources.

Keywords: Whistler mode wave, Plasma wave, MMS spacecraft, Wave-particle interaction

©2019. Japan Geoscience Union. All Right Reserved.

Spatial characteristics of the internal modulation of pulsating aurora: multi-point high-speed optical observations in Scandinavia

*Yuki Kawamura[1], Keisuke Hosokawa[1], Shin-ichiro Oyama[2,3], Yoshizumi Miyoshi[2], Yasunobu Ogawa[3], Satoshi Kurita[2], Satoshi Ebukuro[1], Ryoichi Fujii[4]

1. Department of Communication Engineering and Informatics, University of Electro-Communications, 2. Institute for Space-Earth Environmental Research, Nagoya University, 3. National Institute of Polar Research, 4. Research Organization of Information and Systems

Pulsating aurora (PsA) is a kind of diffuse aurora which almost always appears in the morning side during the recovery phase of auroral substorm. PsA typically has two characteristic temporal variations. One is so-called main pulsation whose period ranges from a few to a few tens of seconds. The other is a few Hz brightness modulation (internal modulation) which is often seen during the ON time of the main pulsation. Previous studies have suggested that the temporal variation of PsA is characterized by wave-particle interaction between whistler-mode chorus waves and high energy electrons in the magnetosphere. Especially, it has been indicated that there is one to one correspondence between the amplitude variation of chorus waves and the luminosity modulation of PsA.
Recent studies revealed the occurrence distribution of the frequency of the internal modulation. However, there have been no studies which analyzed the spatial distribution of the internal modulation.

To reveal the spatial characteristics of the internal modulation, we need to perform a frequency analysis of the internal modulation by using data from high speed optical instruments having wide spatial coverage. For this purpose, we make use of highly sensitive EMCCD cameras which have been operated in Sodankylä and Kevo in Finland, Tromsø in Norway, and Tjautjas in Sweden. In these observations, all-sky images are taken with a sampling rate of 100 Hz, which is sufficient to identify temporal variations of the internal modulation.

In the frequency analysis, we have employed all-sky images taken on March 15, 2018 (00:00 –01:30 UT) in Sodankylä, Kevo, Tromsø, and Tjautjas. We computed the average frequency of the internal modulation from each pixel of the EMCCD cameras and derived the spatial distribution of their dominant frequencies. Regardless of the latitude, each pulsating patch was fluctuating at a similar frequency. We also derived the frequency spectrum of several pulsating patches existing at different positions in the north-south direction and found that those frequency spectrums of pulsating patches have peaks at about 3 Hz. These results indicate that the frequency of the internal modulation does not depend on the magnetic latitude, and the frequency of the internal modulation is collimated on 3 Hz.
In the presentation, we discuss why the frequency of the internal modulation concentrate on 3 Hz by taking into account the time of flight of PsA electrons.

Keywords: Pulsating aurora, Internal modulation

©2019. Japan Geoscience Union. All Right Reserved.

Large-scale characteristics of pulsating aurora periodicities: multi-point high-speed optical observations in Scandinavia

*Satoshi Ebukuro[1], Keisuke Hosokawa[1], Shin-ichiro Oyama[2,3,5], Yoshizumi Miyoshi[2], Yasunobu Ogawa[3], Satoshi Kurita[2], Yuki Kawamura[1], Ryoichi Fujii[4]

1. Department of Communication Engineering and Informatics, University of Electro-Communications, 2. Institute for Space-Earth Environmental Research, Nagoya University, 3. National Institute of Polar Research, 4. Research Organization of Information and Systems, 5. University of Oulu

It has been known that most of diffuse aurorae in the morning side are composed of luminous patches whose brightness modulates quasi-periodically. Such aurorae are termed as pulsating aurora (PsA) and have been studied extensively in the last decade. PsA patches have a scale size of a few hundreds of km and are usually observed during the late recovery phase of substorms. The entire temporal variation of PsA consists of two individual modulations: main pulsation and internal modulation. The periodicity of the main pulsation ranges from a few to a few tens of seconds and the internal modulation, showing a few Hz scintillating luminosity changes, is often embedded within the ON time of the main pulsation. Previous studies using satellites indicated one-to-one correlation between PsA and chorus wave near the equatorial plane of the magnetosphere, suggesting that ground-based observations of PsA can be used for mapping the activity of chorus in the magnetosphere in 2D fashion. In the past, the spatial characteristics of chorus wave have not visualized in detail because satellite observations only cover a single point in the magnetosphere. To overcome this limitation, we derive the spatial distribution of chorus waves by using ground-based optical observations of PsA and discuss the ambient parameters which characterize the nature of chorus.
For this purpose, we have employed data from electron multiplying charge-coupled device (EMCCD) cameras deployed at multiple sites in Scandinavia to derive the large-scale characteristics of PsA. EMCCD cameras have been operative in Kevo and Sodankyla in Finland, Tromsoe in Norway, and Tjautjas in Sweden and their temporal resolution is 100 Hz. We conducted a frequency analysis for a PsA event on March 28, 2017 (23:30 to 24:10 UT). During the event studied, there existed three different regions of PsA, regions A, B and C, showing different modulation periods. It was also found that the boundaries between these three regions were sharp. We derived the 2D frequency map by using data from all the available stations. As a result, it became clear that the higher latitude region (region C) showed faster internal modulation than the lower latitude region (region A). In addition, region B, which was sandwiched by regions A and C, did not show any internal modulations (i.e., main pulsation without internal modulation). In the presentation, we discuss why the three regions showed different modulation periods with sharp boundaries. In particular, we address what ambient conditions can control the absence of internal modulation in region B. We also derived similar frequency maps of chorus waves by tracing the PsA modulation with the Tsyganenko 04 magnetic field model, which could be used to estimate the spatial extent of chorus wave generation region.

Keywords: Pulsating aurora, Chorus wave, Main pulsation, Internal modulation

©2019. Japan Geoscience Union. All Right Reserved.

Variations of cosmic noise absorption (CNA) by energetic electron precipitation (EEP) and changes of the auroral morphology

*Miyamoto Taishiro[1], Shin-ichiro Oyama[1,4,5], Yasunobu Ogawa[2], Keisuke Hosokawa[3], Satoshi Kurita[1], Yoshizumi Miyoshi[1], Ryuho Kataoka[2], Hiroshi Miyaoka[2], Tero Raita[4]

1. Institute for Space-Earth Environmental Research,Nagoya University, 2. National Institute of Polar Research, 3. Department of Communication Engineering and Informatics, University of Electro-Communications, 4. Sodankylä Geophysical Observatory, University of Oulu, 5. Ionosphere Research Unit, University of Oulu

Temporal and spatial variations of aurora morphology in association with substorm have been studied for more than half a century. Various types of aurora are known, such as discrete arc emitting at relatively high intensity and elongating along the zonal direction, and diffuse aurora with darker but more widely spreading in the sky. Pulsating aurora, which is characterized by quasi-periodic oscillations in the emission intensity at periods of a few to tens seconds, and auroral patches observed embedding in the pulsating aurora tend to appear at the recovery phase of substorm, especially from midnight to dawn. It is known that these types of aurora are accompanied by energetic electron precipitation exceeding several hundreds keV. Elucidation of the causality to produce pulsating aurora and energetic electron precipitation is an important theme to understand relationships between the radiation belt and upper-middle atmosphere of the earth. Analyzing measurements from satellite observations (e.g., Arase) and ground-based optical/radio technique observations, the generation mechanism is thought to be mainly attributed to wave particle interactions due to plasma wave and electrons in the magnetosphere. In this study, we focus on relationships between auroral morphological changes, in particular spatiotemporal evolutions to patches and coinciding precipitations of the energetic electron.

Some previous studies have presented changes in morphology from pulsating aurora to patch structures [e.g., Shiokawa et al., 2014] and temporal variations of energetic electron precipitation [e.g., Hosokawa and Ogawa, 2015]. As mentioned above, the wave-particle interaction has been widely accepted with experimental evidences to support generation of pulsating aurora and energetic electron precipitation. However, our understanding has not yet reached its maturity of presenting spatiotemporal evolutions of auroral morphology and associated electron precipitation. Oyama et al. [2017] presented enhancements of CNA (cosmic noise absorption) coinciding with appearance of the patch structure but with only two events. Furthermore, due to measurements with intensive diagnostic instruments, the result was based on information of a part of the auroral ionosphere. In this study, we conducted observations to capture simultaneously time evolutions and spatial distributions of auroral morphology and energetic electron precipitation by utilizing a network of EMCCD (Electron Multiplying Charge Coupled Device) cameras and riometers deployed in Northern Europe.

This study will present three events (February 19-20, 2018, March 6-7, 2017, and March 29-30, 2017). On the way of all events, after substorm onsets twice near Northern Europe, another onset occurred again at more west side (near Iceland or Greenland area) but at dawn in the Northern Europe. In this study, we have focused on the aurora and CNA associated with the latter onset, and at that time, the aurora spatially and temporally shifted from diffuse to pulsation and patch structures. This suggests that substorm activities occurred in the distance can induce these auroral morphological changes seen in the Northern Europe. CNA at that time is characterized by gradual variations with time scale of several hours. This trend cannot be seen at substorm onset near the Northern Europe. Moreover, in the latitude distribution, the feature was confirmed that CNA increases at the latitude where patch structure is seen, and CNA keeps

©2019. Japan Geoscience Union. All Right Reserved.

constant value at the latitude where patch structure is not seen. In the presentation, based on these observations, we will discuss physical mechanisms to cause changes in the auroral morphology and energetic electron precipitation, which can be seen as increases of CNA.

Keywords: Ionosphere, Aurora, Energetic Electron Precipitation (EEP)

©2019. Japan Geoscience Union. All Right Reserved.

Spatiotemporal characteristics on the source region of flash aurora using ray tracing analysis

*Tomohiro Inoue[1], Mitsunori Ozaki[1], Yoshitaka Goto[1], Satoshi Yagitani[1], Yoshiya Kasahara[1], Kazuo Shiokawa[2], Yoshizumi Miyoshi[2], Ryuho Kataoka[3], Yusuke Ebihara[4]

1. Kanazawa University , 2. Nagoya University, 3. National Institute of Polar Research, 4. Kyoto University

Whistler mode waves cause precipitation of high-energy electrons via wave-particle interactions in the magnetosphere. The scattered particles precipitate to the ground along the geomagnetic field line. Then, flush aurora, which is a rapid (less than 1 s) auroral phenomenon, is happened. Flash aurora is important for understanding the spatial evolution of wave-particle interaction region in the magnetosphere. We observed the mainly southward spread of flush aurora. In order to understand the spatial-time variation of wave-particle interaction region, we analyze the propagation effects of whistler mode waves near the magnetic equator region using ray tracing analysis. We calculated the ray paths of whistler mode waves (0.2 fce and 0.4 fce) near the magnetic equator (-10 to +10 degrees of geographic latitude), where fce is the electron cyclotron frequency at the magnetic equator. The initial ray paths put in the assumption of a spatial spread with the wave normal angles of tens of degrees along the magnetic field line at the magnetic equator (a point source). Then, we traced the magnetic field lines from the ray paths of whistler mode waves and estimated the precipitation area of electrons in the ionosphere using the IGRF model. The calculation results showed the precipitation area was not mainly spread southward, but evolved northward in the preliminary study.
In this presentation, we will present the spatiotemporal characteristics of flash aurora and the analysis results of ray tracing in detail.

Keywords: Flush aurora, Whistler mode wave, Ray tracing, Wave-particle interaction

©2019. Japan Geoscience Union. All Right Reserved.

Molecular ion supply mechanisms from the low-altitude ionosphere to magnetosphere observed by EISCAT and Arase(ERG)

*Masayoshi Takada[1], Kanako Seki[1], Yasunobu Ogawa[2], Kunihiro Keika[3], Satoshi Kasahara[4], Shoichiro Yokota[5], Tomoaki Hori[7], Kazushi Asamura[6], Yoshizumi Miyoshi[7]

1. Graduate School of Science, Tokyo University, 2. National Institute of Polar Research, 3. Department of Earth and Planetary Science, Graduate School of Science, Tokyo University, 4. The University of Tokyo, 5. Graduate School of Science, Osaka University, 6. Institute of Space and Astronautical Science, Japan Aerospace Exploration Agency, 7. Institute for Space-Earth Environmental Research, Nagoya University

Molecular ions ($O_2^+/NO^+/N_2^+$) in the magnetosphere have been observed during magnetic storms [Peterson et al., 1994; Klecker et al., 1986]. These molecular ions are considered to originate from the Earth’ s ionosphere. It is considered that they have been transported upward by some heating processes in the ionosphere. However, due to the larger mass than atomic ions (O^+), the molecular ions usually exist only in the low-altitude ionosphere below 300 km altitude. It is hence difficult to transport these molecular ions by overcoming loss by chemical reactions to the high-altitude ionosphere where the ion upflow and outflows usually take place [Peterson et al., 1994]. Therefore, it is necessary to reveal what mechanism causes molecular ion upflow during the magnetic storms. In this study, we aim at the observational assessments of the supply processes of the molecular ions from the low-altitude ionosphere to the magnetosphere based on conjugate observations by EISCAT radar and the Arase (ERG) satellite.

The EISCAT radar and the Arase (ERG) satellite have the conjunction event during the large magnetic storm with the minimum Dst of -124 nT on September 8, 2017. During the event, the Arase satellite was located in the dusk-side inner magnetosphere and observed molecular ions in the energy range of 12-180 keV/q. The EISCAT radar simultaneously observed the ion upflow (with the upward velocity of ~50-150 m/s) from the low-altitude ionosphere (~250-400 km) together with strong ion heating (>2000 K). The convective electric field was also enhanced by a factor of 2 in the same region. We estimated each term in the equation of motion for ions. The result indicates that the ion upflow reached stable equilibrium because the upward ion and electron pressure gradients are balanced with the downward gravitational force. It is suggested that the ion upflow can take place from the low-altitude ionosphere due to strong ion pressure gradient. We also estimated the flux decrease of molecular ions due to dissociative recombination. The flux decreased to ~1 % at 350 km compared with 280 km. The estimated upflow flux of molecular ions at 350 km is $>10^{10}$ m^{-2} s^{-1} . Comparison between distribution functions observed by Arase satellite and EISCAT radar suggests that acceleration by 3 orders of magnitudes is necessary during the outflow process. These results indicate that the strong ion frictional heating during magnetic storms enabled molecular ions to be transported upward from the low-altitude ionosphere and provide a source of molecular ion outflows into the magnetosphere.

Keywords: Molecular ion, EISCAT radar, Arase (ERG) satellite, Ion upflow, Ionospheric heating

©2019. Japan Geoscience Union. All Right Reserved.

Optical and radar observation of the dynamic auroral forms

*Yunosuke Nagafusa[1], Tima Sergienko[2], Satoshi Taguchi[1], Urban Braendstroem[2], Masatoshi Yamauchi[2]

1. Graduate School of Science, Kyoto University, 2. Swedish Institute of Space Physics, Kiruna

Ionosphere disturbances caused by the auroral electron precipitations are studied using auroral images taken by Auroral Large Imaging System (ALIS) and ionospheric parameters measured by EISCAT UHF radar that were conjugate with ALIS field-of-view. ALIS consists of several remote controlled stations located in northern Scandinavia, separated by approximately 50 km. Each station is equipped with a high-resolution CCD detector with 1024×1024 pixels, and a filter wheel with six positions for narrow-band interference filters. In this study we use the data obtained with the 557.7 nm filter, which show the auroral emission originated from the atomic oxygen. EISCAT UHF radar located in northern Norway near Tromsø operating in the BEATA program provides the ionospheric electron density, electron and ion temperatures, and ion velocity with the time resolution of 5 s and the spatial resolution of 1.5 km. The auroral images from the different ALIS stations were used for triangulation of the auroral forms in order to determine the aurora position in relation to the radar beam. For each auroral arc, the electron density, the electron and ion temperatures measured inside and in the vicinity of the auroral forms were analyzed with the aim of understanding the ionospheric response to the different types of auroral electron precipitations.

Keywords: aurora, ionospheric parameters, electron precipitations

©2019. Japan Geoscience Union. All Right Reserved.

Observations of MF/HF auroral radio emissions at three ground-based stations

*Yuka Sato[1], Atsushi Kumamoto[2], Yuto Katoh[2], Akira Kadokura[3,4], Yasunobu Ogawa[3,4], Atsuki Shinbori[5]

1. Nippon Institute of Technology (NIT), 2. Graduate School of Science, Tohoku University, 3. National Institute of Polar Research (NIPR), 4. The Graduate University for Advanced Studies, 5. Institute for Space-Earth Environmental Research (ISEE), Nagoya University

We started ground-based observations of MF/HF auroral radio emissions about 10 years ago at two stations (The Husafell Station, Iceland, September 2005; The Kjell Henriksen Observatory, Svalbard, September 2008) and found multiple unknown properties of MF/HF auroral radio emissions, e.g. polarization features [*Sato et al.*, 2008, 2015] and existence of a higher frequency component [*Sato et al.*, 2012]. To make a next siginificant step for a futher understanding of MF/HF auroral radio emissions, we installed a new dedicated instrumentation at the KAIRA (Kilpisjärvi Atmospheric Imaging Receiver Array) site in Kilpisjärvi, Finland (Latitude: 60.07 N, Longitude: 20.76 E) in the summer of 2018. It is a passive receiving system designed to realize a high-resolution spectral, interferometric and polarization measurements using 4 loop antennas and a software-defined radio (SDR) receiver. This SDR receiver can implement high-speed, flexible digital signal processing of RF signals and obtain high-resolution spectra pauselessly throughout the night in a wide frequency range up to 6 MHz. One of the main research subjects of this project is radio emission spontaneously emitted from aurora. There are long-known three types of MF/HF auroral radio emissions identified at ground level: auroral hiss, medium frequency burst (MFB), and auroral roar. Investigation into the generation of these emissions not only offers a tool of great promise for remote sensing of ionospheric plasma processes and parameters but also gives the foundation for understanding various radiation mechanisms that occur in planetary magnetospheres and plasma in space. In combination with the long-term continuous observations in Iceland and Svalbard and future EISCAT_3D experiments, observation with this new instrumentation will provide a first-time opportunity to reveal spatiotemporal variations of macro and fine structures of MF/HF auroral radio emissions associated with substorm evolution. In this presentation, we show detailed specification of this new instrumentation and some initial results.

Keywords: auroral phenomena, radio wave propagation, wave-particle interaction

©2019. Japan Geoscience Union. All Right Reserved.

Ionospheric F-region Drift Measurements Derived from DPS-4D at Zhongshan Station, Antarctic

*Xiangcai Chen[1]

1. Polar Research Institute of China

By means of high-frequency radio sounding, the ionospheric plasma drift can be measured by the Doppler frequency shift of signal. In this paper we analyze the ionospheric F-region plasma motion performed by Digisonde Portable Sounder (DPS-4D) at cusp latitude over Zhongshan Station in Antarctic. By restricting the echo arrival angle, and selecting the reflection height range at 175 –475 km, we present the variation of the F-region plasma drift measurements by setting limits on the Doppler frequency shift. Base on the 7.5 min interval Digisonde drift data from November 2011 to February 2012, we considered the variations of the plasma drift in F-region under the different geomagnetic activity (Kp) and magnetic local time, as well as it correlation with interplanetary magnetic field (IMF). The results indicate that properly restricting the Doppler frequency shift of the echo has a strong effect that contributes to the accurate and robust measurements of the ionospheric plasma drift. The mean value of horizontal drift mostly leveled off to about 600 m/s at altitude around of 230 km, while the field-aligned component of drift showed mean values of -25 m/s near pre-noon and +40 m/s during the night. These strong diurnal variations have dependence on the sign and strength of the IMF B_y and B_z components. It implies that the contraction and expansion of the polar cap with Kp and the convection in the proximity of the throat with different IMF conditions have a profound influence on the observed drift velocities.

Keywords: Digisonde DPS 4, Doppler frequency shift, remote sensing, polar ionosphere, plasma drift

©2019. Japan Geoscience Union. All Right Reserved.

PARM-HEP Observation of Precipitating High Energy Electrons over Pulsating Aurora

*Taku Namekawa[1], Takefumi Mitani[2], Kazushi Asamura[2], Yoshifumi Saito[2]

1. Department of Earth and Planetary Science, Graduate school of Science, The University of Tokyo, 2. Institute of Space and Astronautical Science, Japan Aerospace Exploration Agency

The phenomenon called microbursts that radiation belt particles precipitate to the Earth’ s atmosphere is thought to be largely related to the dissipation of high energy electrons in radiation belt. It is suggested that this phenomenon is caused by pitch angle scattering of the magnetospheric particles by plasma waves, which is a mechanism similar to the cause of the pulsating aurora observed in the Earth’ s polar region. There is a possibility that the origin of microburst can be clarified by proving simultaneous occurrence of microburst and pulsating aurora, but observational verification has not been made yet. For that purpose, we have developed a high-energy electron detector (HEP) for the observation of sub-relativistic - relativistic energy electrons that make up the microburst. HEP is designed to measure electrons between 300 keV and 2 MeV with energy resolution of 20% or less and with signal processing time of ~ 5 μs. Energy analysis is performed by the detection part of this instrument using SSD (Solid State Detector). Performance tests of this instrument are carried out using a sealed radiation source and a high energy electron beam line. This instrument is installed as one of the core instruments of the PARM instrument package developed for the simultaneous observation of the pulsating aurora and microburst by an international student sounding rocket experiment RockSat-XN and LAMP (Loss through Auroral Microburst Pulsation) sounding rocket experiment. We have succeeded in obtaining the flight data on 13 January 2019 from RockSat-XN sounding rocket experiment. In parallel, we are now preparing HEP analyzer for LAMP sounding rocket experiment. In this presentation, we will show the outline and observation results of RockSat-XN-HEP as well as the LAMP-HEP development status.

Keywords: Microburst, PARM, RockSat-XN, LAMP, Sounding rocket, Pulsating aurora

©2019. Japan Geoscience Union. All Right Reserved.

Development of the medium-energy electron detector with hemispherical field-of-view and the flight test in the PARM (Pulsating AuRora and Microburst) mission

*Shin Sugo[1], Oya Kawashima[1], Kazushi Asamura[2], Reiko Nomura[3], Yasunobu Ogawa[4], Keisuke Hosokawa[5], Yoshizumi Miyoshi[6], Takefumi Mitani[2], Taku Namekawa[1,2], Takeshi Sakanoi[7], Mizuki Fukizawa[7], Naoshi Yagi[7], Satoshi Kasahara[1]

1. The University of Tokyo, 2. Institute of Space and Astronautical Science, Japan Aerospace Exploration Agency, 3. National Astronomical Observatory of Japan, 4. National Institute of Polar Research, 5. The University of Electro-Communications, 6. Institute for Space-Earth Environmental Research, Nagoya University, 7. Tohoku University

Energetic electrons significantly affect ionospheric dynamics and the long-term evolution of surfaces and atmospheres of planets and moons. Since the energetic electron flux is not necessarily isotropic, it is important to cover the broad solid angle to quantitatively evaluate the effects on solar system bodies. With future planetary explorations in mind, we developed the medium-energy (20 - 100 keV) electron detector (MED) which can cover almost 2-pi steradian without the spacecraft spin. In order to test the performance of this analyzer in the relevant environment, we participated in the PARM mission, which aimed to measure electron precipitation using NASA’s sounding rocket RockSat-XN. In this presentation we report on MED observation results obtained through the flight on 13 January 2019.

©2019. Japan Geoscience Union. All Right Reserved.

Auroral substorm onset in satellite-based global images and ground-based all-sky images

*Akimasa Ieda[1], Kirsti Kauristie[2], Yukitoshi Nishimura[3], Yukinaga Miyashita[4], Harald U Frey[5], Liisa Juusola[2], Daniel Whiter[6], Masahito Nose[7], Matthew O Fillingim[5], Farideh Honary[8], Neil C Rogers[8], Yoshizumi Miyoshi[1], Shinobu Machida[1]

1. Institute for Space-Earth Environmental Research, Nagoya University, 2. Finnish Meteorological Institute, 3. Boston university, 4. Korea Astronomy and Space Science Institute, 5. University of California Berkeley, 6. University of Southampton, 7. Graduate School of Science, Kyoto University, 8. Lancaster University

Substorm onset has originally been defined as a longitudinally extended sudden auroral brightening (Akasofu initial brightening: AIB) followed a few minutes later by an auroral poleward expansion in ground-based all-sky images (ASIs). In contrast, such clearly marked two-stage development has not been evident in satellite-based global images (GIs). Instead, substorm onsets have been identified as localized sudden brightenings that expand immediately poleward.
To resolve these differences, optical substorm onset signatures in GIs and ASIs are compared in this study for a substorm that occurred on December 7, 1999. For this substorm, the Polar satellite ultraviolet global imager was operated with a fixed-filter (170 nm) mode, enabling a higher time resolution (37 s) than usual to resolve the possible two-stage development. These data were compared with 20-s resolution green-line (557.7 nm) ASIs at Muonio in Finland. The ASIs revealed the AIB at 2124:50 UT and the subsequent poleward expansion at 2127:50 UT, whereas the GIs revealed only an onset brightening that started at 2127:49 UT.
Thus, the onset in the GIs was delayed relative to the AIB and in fact agreed with the poleward expansion in the ASIs. The fact that the AIB was not evident in the GIs may be attributed to the limited spatial resolution of GIs for thin auroral arc brightenings. The implications of these results for the definition of substorm onset are discussed herein.

Keywords: substorm, auroral breakup, aurora

©2019. Japan Geoscience Union. All Right Reserved.

Original substorm onset (Akasofu 1964; 2010)

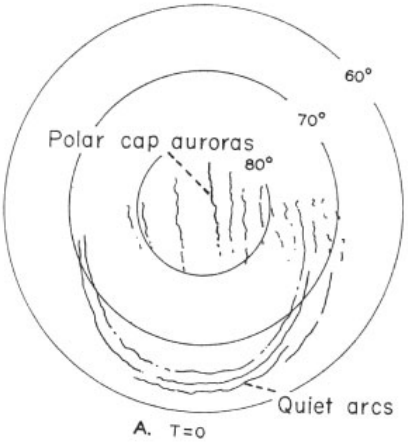

FIG. 2. THE DISTRIBUTION OF THE AURORAS DURING THE QUIET PHASE.

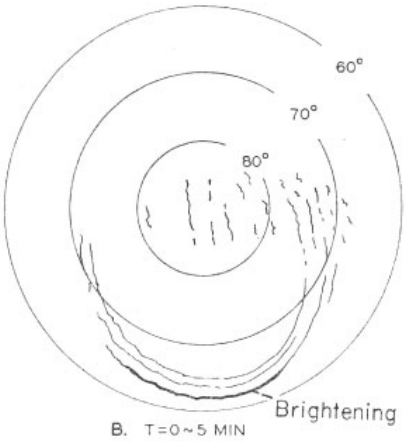

FIG. 3. AURORAS DURING THE EXPANSIVE PHASE (STAGE I).

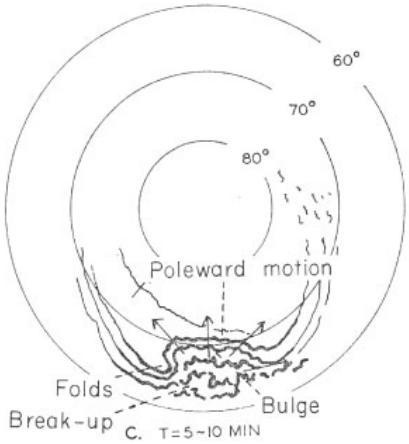

FIG. 4. AURORAS DURING THE EXPANSIVE PHASE (STAGE II).

a Time < 0
Before onset
Quiet arc

b T = 0 ~ 5 min
Expansion phase stage 1
Initial brightening
T = 0: Substorm onset

c T = 5 ~ 10 min
Expansion phase stage 2
Poleward expansion
(Auroral breakup)

Ground and satellite observations (Ieda et al. 2018: 10.1186/s40623-018-0843-3)

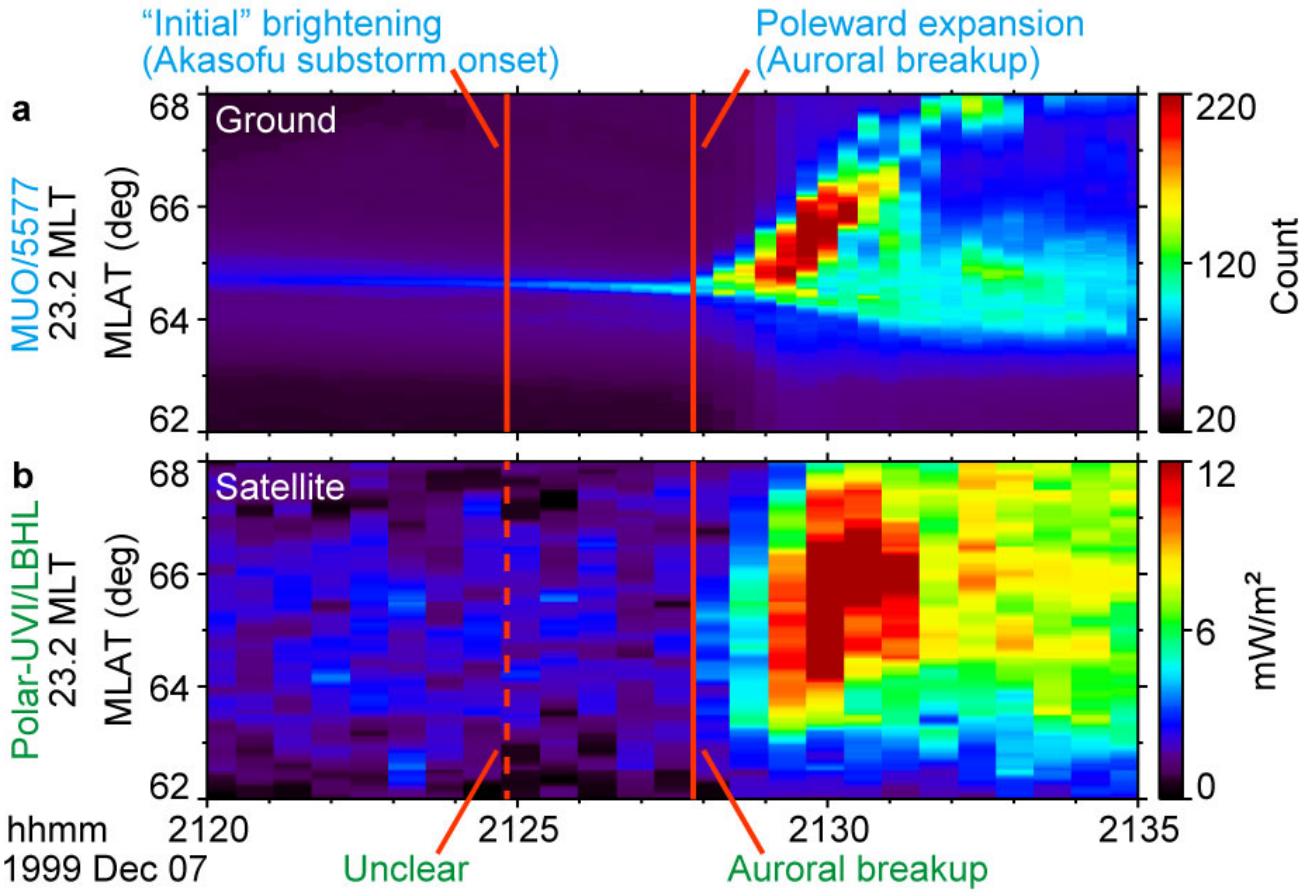

©2019. Japan Geoscience Union. All Right Reserved.

Automatic Classification of Auroral images using optical flow feature

*Naoto Kashiwagi[1], Akiko Fujimoto[1], Terumasa Tokunaga[1], Yoshizumi Miyoshi[2], Yasunobu Ogawa[3], Keisuke Hosokawa[4]

1. Kyushu Institute of Technology, 2. Nagoya University, 3. National Institute of Polar Research, 4. The University of Electro-Communications

The machine learning technique including the deep learning has been developed and the practical uses have increased on various field. On the study of auroral detection, the concern over the automatic image classification has risen using the approach of machine learning technique for the large statistical analysis of auroral images. The automatic auroral image classification has tried to use some techniques from computer vision, machine vision and pattern recognition. There are roughly two kinds of the selected feature: the color of image and the motion of aurora image sequences. The works based on the color feature of aurora image have been performed by Rao et al. (2014) and Tanaka et al. (2015). Rao et al. (2014) performed Support Vector Machines (SVM) classification with several local feature extraction techniques, and found that Scale Invariant Feature Transform (SIFT), OpponentSIFT, is the most effective feature for the automated classification of color aurora images. Tanaka et al. (2015) used the aurora area using the HSV model. They mentioned that it is difficult to classify the images including the diffuse aurora and cloud area. The color feature work well for the color auroral image, while the gray-scale (optically filtered) auroral images need other features on the automated classification. Blixt et al. (2006) applied the optical flow estimation to auroral image sequences. Their case study showed the useful tool for representing the motion of the aurora. In this study, we validate the optical flow estimation to extract the feature of auroral image, and automatically classify the large gray-scale auroral images using the machine learning with Convolution Neural Network (CNN). We use 63,486 gray-scale aurora images in total and use five categories for the preparation of supervised learning data, 1) aurora, 2) aurora and cloudy, 3) aurora and moon, 4) aurora, cloudy and moon, 5) noaurora. We perform the Hold-out and the Cross Validation to evaluate our classification performance. We obtained 98.58% of the classification accuracy based on Hold-out and 98.47% of the classification accuracy based on Cross Validation.

Keywords: Aurora, Optical flow, Convolution Neural Network

©2019. Japan Geoscience Union. All Right Reserved.

Fine-scale visualization of aurora in a wide area using color digital camera images from the International Space Station

*Sota Nanjo[1], Yuta Hozumi[1], Keisuke Hosokawa[1]

1. The University of Electro-Communications

Various ground-based and space-based imagers have been used to observe aurora borealis and australis. So far, however, it has been difficult to observe the detailed spatial structure of auroras in a wide area with sufficient spatial and temporal resolution. Since the photographs taken from the International Space Station (ISS) have sufficient spatial and temporal resolution, it is possible to visualize the fine-scale structures of aurora in a wide area. A calibration of imaging parameters of the photographs using star lights was proposed by a previous research. The accuracy in the timestamp was not guaranteed by the method based on the star lights because the position of the star lights in the image did not change with elapsed time. Thus, it is still difficult to use the mapped data for studying fast variations of aurora, for example pulsating aurora (PsA). Therefore, in this study, we calibrated the images from the ISS using city lights which change their apparent positions with elapsed time. In order to validate the calibration method using city light positions, we mapped two PsA events in the photographs to the geographical coordinate, and compared with those from ground-based all-sky imagers in Alaska and Canada. We found that the approximate shape of discrete aurora and the temporal variation of PsA derived from the ISS images are consistent with those from the ground-based observation. The accuracy in the timestamp is less than 0.5 sec and that in space in the direction perpendicular to the line of sight of the camera is within 5 km. In the presentation, we will also address how the mapped full-color images can be used for studies of PsA in the future work.

Keywords: aurora, ISS

©2019. Japan Geoscience Union. All Right Reserved.

PARM: Investigation of precipitating high-energy electrons into the auroral ionosphere with sounding rockets

*Kazushi Asamura[1], Yoshizumi Miyoshi[2], Keisuke Hosokawa[3], Takefumi Mitani[1], Taku Namekawa[1,5], Takeshi Sakanoi[4], Naoshi Yagi[4], Mizuki Fukizawa[4], Genki Ishizawa[4], Satoshi Kasahara[5], Shin Sugo[5], Oya Kawashima[5], Reiko Nomura[6], Masahito Nose[2], Mariko Teramoto[2], Yasunobu Ogawa[7], Shinji Saito[2], Ryoichi Fujii[8]

1. ISAS / JAXA, 2. ISEE, Nagoya University, 3. The University of Electro-Communications, 4. Tohoku University, 5. The University of Tokyo, 6. NAOJ / NINS, 7. NiPR / ROIS, 8. ROIS

Bursty precipitations of high-energy electrons into the polar ionopshere have been observed by low-altitude satellite, for example, SAMPEX and FIREBIRD II. These precipitations, called microburst, may contribute to the loss of the terrestrial radiation belt through the collisional energy loss with the dense, cold atmospheric particles. Recent numerical simulations successfully reproduce these microburst precipitations with a few Hz modulations by taking into account the pitch angle scattering with the whistler chorus elements at off-equator regions in the inner magnetosphere. Therefore, one can expect that the miscroburst precipitations have properties depending on auroral activities especially the pulsating auroras. In order to investigate the mechanisms of the microburst precipitations by in-situ observations, we are developing two instrument packages: PARM (Pulsating AuRora and Microbursts; already developed) and PARM-2 (being developed), both of which are designed suitable for sounding rocket experiments. PARM consists of four sensors; HEP (high-energy electron energy spectrometer), MED (medium-energy electron detector), AIC (auroral camera), and AFG (ASIC-based fluxgate magnetometer). PARM was onboard the NASA's RockSat-XN sounding rocket, and launched from Andoya, Norway at 09:13UT, Jan 13, 2019. On the other hand, PARM-2 is under development. It consists of HEP, two AICs, and MIM (magneto-impedance magnetometer). PARM-2 is to be onboard the NASA's LAMP sounding rocket which will fly from Poker Flat, Alaska in the period between the end of 2019 and the beginning of 2020.

We will present the overview of PARM missions including the initial results of RockSat-XN/PARM with ground-based observations and preparation status of LAMP/PARM-2.

Keywords: electron microburst precipitation, sounding rocket, pulsating aurora

©2019. Japan Geoscience Union. All Right Reserved.

[E] Oral | P (Space and Planetary Sciences)：P-EM Solar-Terrestrial Sciences, Space Electromagnetism & Space Environment

Wed. May 29, 2019 3:30 PM - 5:00 PM JST | Wed. May 29, 2019 6:30 AM - 8:00 AM UTC | A04 TOKYO BAY MAKUHARI HALL

[P-EM11] Dynamics of Magnetosphere and Ionosphere

convener:Aoi Nakamizo(Applied Electromagnetic Research Institute, National Institute of Information and Communications Technology), Mitsunori Ozaki(Faculty of Electrical and Computer Engineering, Institute of Science and Engineering, Kanazawa University), Akiko Fujimoto(Kyushu Institute of Technology), Tomoaki Hori(Institute for Space-Earth Environmental Research, Nagoya University), Chairperson:Hiroshi Hasegawa(Institute of Space and Astronautical Science, JAXA)

This session provides an opportunity to present recent results from satellite and ground-based observations and theoretical and simulation studies on the magnetosphere, ionosphere, and their coupling processes. We invite talks and posters discussing various phenomena related to the magnetosphere-ionosphere system: solar wind-magnetosphere interaction, magnetosphere-ionosphere convection, field-aligned current, magnetic storms/substorms, neutral-plasma interaction, ionospheric ion inflow and outflow, aurora phenomena, and so forth. Discussions on planetary and satellite ionosphere and magnetospheres, future missions and instrument developments are also welcome.

3:30 PM - 3:45 PM JST | 6:30 AM - 6:45 AM UTC

[PEM11-01] **A Case Study Based on Ground Observations of the Conjugate Ionospheric Response to Interplanetary Shock in Polar Regions**

*He Fang[1], Zejun HU[1], Hongqiao HU[1] (1.Polar Research Institute of China)

3:45 PM - 4:00 PM JST | 6:45 AM - 7:00 AM UTC

[PEM11-02] **Effects of Solar Illumination on the Auroral Electrojet Intensity**

*Shinichi Ohtani[1], Jesper W Gjerloev[1] (1.The Johns Hopkins University Applied Physics Laboratory)

4:00 PM - 4:15 PM JST | 7:00 AM - 7:15 AM UTC

[PEM11-03] Quasi-persistent multiple mesoscale field-aligned currents in the duskside auroral oval

*Yoshihiro Yokoyama[1], Satoshi Taguchi[1], Toshihiko Iyemori[2], Keisuke Hosokawa[3] (1.Department of Geophysics, Graduate School of Science, Kyoto University, 2.Kyoto University, 3.Department of Communication Engineering and Informatics, University of Electro-Communications)

4:15 PM - 4:30 PM JST | 7:15 AM - 7:30 AM UTC

[PEM11-04] Generation of dispersive Alfvenic turbulence in magnetosphere-ionosphere feedback coupling

*Tomo-Hiko Watanabe[1], Masatoshi Kaneyama[1], Shinya Maeyama[1] (1.Graduate School of Science, Nagoya University)

4:30 PM - 4:45 PM JST | 7:30 AM - 7:45 AM UTC

[PEM11-05] Aspects of simulating magnetosphere-ionosphere coupling via field-aligned current

*Astrid I Maute[1], Arthur D Richmond[1], Gang Lu[1] (1.High Altitude Observatory, National Center for Atmospheric Research, Boulder CO, 80301, USA)

4:45 PM - 5:00 PM JST | 7:45 AM - 8:00 AM UTC

[PEM11-06] **Revisiting the energy conversion process of Birkeland current generation**

*Akimasa Yoshikawa[1] (1.Department of Earth and Planetary Sciences, Kyushu University)

A Case Study Based on Ground Observations of the Conjugate Ionospheric Response to Interplanetary Shock in Polar Regions

*He Fang[1], Zejun HU[1], Hongqiao HU[1]

1. Polar Research Institute of China

This study uses data acquired by an imaging riometer, an ionosphere total electron content (TEC) monitor, and three specific wavelength auroral imagers at the conjugate Antarctic Zhongshan (ZHS) and Arctic Yellow River (YRS) stations to investigate the response of the polar ionosphere to a space weather event induced by solar flare activity on July 14, 2012. After the geomagnetic storm suddenly commenced and a magnetospheric substorm was triggered by the arrival of an interplanetary shock wave and its interaction with the magnetosphere at 18:10 UT, significantly enhanced auroral activity was observed by the auroral imagers at the ZHS. Meanwhile, the polar conjugate observation stations in the two hemispheres recorded notable growth of the two-dimensional cosmic noise adsorption and similar motion tendencies. According to our analysis and comparison of the ionospheric TEC data acquired by the conjugate stations, the TEC at both locations presented a considerable growth tendency after the interplanetary shock wave arrived, although the two stations experienced different sunlight conditions (polar night in the Antarctic region and polar day in the Arctic region). However, a comparison with high-frequency radar data demonstrated that different sources were responsible for the electron density enhancement of the ionosphere. In the Arctic polar day region, the increased electron density may have been caused by anti-sunward convection of the plasma irregularity, whereas in the Antarctic polar night region, the increased electron density may have been caused by energetic particle precipitation at the magnetospheric tail. Different physical processes might be the cause of the differential responses of the ionosphere at the two studied geomagnetic conjugate stations in the same solar activity event due to different local photoionization conditions.

Keywords: polar ionosphere, conjugate, substorm, response, irregularity

©2019. Japan Geoscience Union. All Right Reserved.

Effects of Solar Illumination on the Auroral Electrojet Intensity

*Shinichi Ohtani[1], Jesper W Gjerloev[1]

1. The Johns Hopkins University Applied Physics Laboratory

The present study investigates the dependence of the local auroral electrojet (AEJ) intensity on the solar illumination by statistically examining the northward geomagnetic disturbance in terms of the solar zenith angle (SZA) χ. It is found that on the day side, both westward and eastward electrojets (WEJ and EEJ) are more intense for smaller χ suggesting that the solar EUV-induced conductance is the dominant factor for the AEJ intensity. On the night side, in contrast, the χ dependence of the AEJ intensity, if sorted solely by the magnetic local time (MLT), is apparently different for stations at different longitudes and in different hemispheres. However, if additionally sorted by the dipole tilt angle ϕ, a consistent pattern emerges. It is therefore suggested that although ϕ and χ are correlated, the dipole tilt angle and SZA have physically different effects on the local AEJ intensity. The nightside AEJ, especially the WEJ, tends to be more intense for small $|\phi|$. Moreover, whereas the WEJ is statistically more intense when the ionosphere is dark, the EEJ is more intense when sunlit. The preference of the WEJ for the dark ionosphere extends widely in MLT from premidnight to dawn, and therefore, it cannot be linked exclusively with the substorms or be attributed to the previously proposed processes of the preferred auroral precipitation in the dark ionosphere. Instead, it may be explained at least morphologically in terms of the conductance enhancement due to the diffuse auroral precipitation, which is also prevalent from premidnight to dawn and is more intense in the dark hemisphere.

Keywords: Auroral electrojets, Solar illumination, Ionospheric conductance, Dipole tilt, Solar zenith angle, Diffuse aurora

©2019. Japan Geoscience Union. All Right Reserved.

Quasi-persistent multiple mesoscale field-aligned currents in the duskside auroral oval

*Yoshihiro Yokoyama[1], Satoshi Taguchi[1], Toshihiko Iyemori[2], Keisuke Hosokawa[3]

1. Department of Geophysics, Graduate School of Science, Kyoto University, 2. Kyoto University, 3. Department of Communication Engineering and Informatics, University of Electro-Communications

Within a large-scale field-aligned current, whose latitudinal width is a few hundred kilometers in the ionosphere, smaller-scale current structures are often embedded. Previous studies have shown that a mesoscale upward field-aligned current with widths of order 10 km generally agree with auroral arcs. However, we still do not understand how this relation forms. In this study, using multispacecraft Swarm data and aurora data from a ground-based all-sky imager at Longyearbyen, Svalbard, we have examined mesoscale features of the field-aligned current and auroral arcs in the duskside auroral oval. We focused on the situation when the large-scale Region 1 current diminishes so that mesoscale features can stand out. Through the cross-correlation analysis of the magnetic perturbations observed by Swarm A and Swarm C, we took events in which the observed magnetic perturbations represent the spatial structure of multiple pairs of upward/downward mesoscale field-aligned currents, not Alfven wave. Conjugate observations between Swarm satellites and the all-sky imager have shown that auroral arcs actually occur in the region of the upward field-aligned current. The result of the analysis of the all-sky image data obtained before and after the conjunction event has shown that the auroral arcs have quasi-persistent features, and also indicated when the auroral arcs appear and disappear. From these results, we discuss how the mesoscale field-aligned current can form.

Keywords: Field-aligned current, Postnoon aurora, Swarm satellites

©2019. Japan Geoscience Union. All Right Reserved.

Generation of dispersive Alfvenic turbulence in magnetosphere-ionosphere feedback coupling

*Tomo-Hiko Watanabe[1], Masatoshi Kaneyama[1], Shinya Maeyama[1]

1. Graduate School of Science, Nagoya University

Magnetosphere-ionosphere (M-I) feedback coupling is considered to provide possible explanations to self-excitatation of auroral arc structures with enhancements of the ionospheric density and the field-aligned current. Recent theoretical and numerical studies have revealed generation of Alfvenic turbulence in the nonlinear evolution of the feedback instability, following the Kelvin-Helmholtz instability accompanied with curl structures of the ionospheric density.
Our recent study has extented to include effects of the electron intertia in the magnetospheric dynamics, where the dispersive Alfven waves with the parallel electric field play a key role in the M-I coupling. The linear stability analysis incuding the electron inertia term has shown the stabilization effect while the mean parallel acceleration of electrons is self-consistently included in the model of auroral arc growth. Nonlinear simulations of the feedback instability have also demonstrated generation of the Alfvenic turbulence with finite parallel electric fields, where a power law energy spectra are obtained for the parallel and perpendicular wavenumbers. The physical picture of Alfvenic turbulence obtained in the persent study is consistent to FAST spacecraft observations of the dispersive Alfven waves and the electron acceleration in the Alfvenic aurora.

Keywords: aurora, magnetosphere-ionosphere coupling, turbulence, electron acceleration, Alfven waves

©2019. Japan Geoscience Union. All Right Reserved.

Aspects of simulating magnetosphere-ionosphere coupling via field-aligned current

*Astrid I Maute[1], Arthur D Richmond[1], Gang Lu[1]

1. High Altitude Observatory, National Center for Atmospheric Research, Boulder CO, 80301, USA

Magnetosphere-ionosphere (MI) coupling is crucial in modeling the thermosphere-ionosphere (TI) response to geomagnetic activity. In general circulation models (GCMs) the MI coupling is frequently realized by specifying the ion convection and auroral particle precipitation patterns from, e.g., empirical models or assimilative models. Using assimilative models, such as the Assimilative Model of Ionospheric Electrodynamics (AMIE), has the advantage that the ion convection and auroral particle precipitation patterns are self-consistent and based on available observations. However, assimilating data can be time consuming and requires expert knowledge, and therefore it is so far not the standard way of MI coupling in GCMs. With the availability of AMPERE data, there is an increased interest of employing field-aligned currents (FAC) in GCMs to represent the MI coupling. The FAC from AMPERE captures interhemispheric differences in the MI coupling not represented by empirical ion convection models. However, since GCMs mostly employ prescribed high latitude ion convection patterns little is known about differences in the TI response to high latitude forcing by prescribed FACs.

In this study, we will compare with the help of a simulated geomagnetic storm the different MI coupling methods, i.e., AMIE, empirical ion convection and AMPERE field-aligned current. We illustrate the sensitivity of the Joule heating and low latitude electric field with respect of the spatial distribution of the aurora and ion convection for the different cases. The influence of interhemispheric differences in the MI coupling on the middle and low latitude thermosphere-ionosphere system will be examined.

Keywords: Magnetosphere-ionosphere coupling via field-aligned current, Interhemispheric assymetries, Middle and low latitude effects

©2019. Japan Geoscience Union. All Right Reserved.

Revisiting the energy conversion process of Birkeland current generation

*Akimasa Yoshikawa[1]

1. Department of Earth and Planetary Sciences, Kyushu University

As shown by Vasyliunas [1970], the magnetospheric diamagnetic current has a finite divergece when it crosses the region with a finite B gradient and connects to the Field-Aligned Current (FAC). A pressure gradient force, the origin of the diamagnetic current in a force balance to the Ampere force, never twists plasma flow. While for the development of magnetic shear, which corresponds to FAC, combination of Ampere’ s law , Faraday’ s induction law and MHD Ohm’ s law require the gradient of plasma vortex along B-field. In other words, for the existence of a quasi-steady FAC in the MHD scheme, the plasma vorticity along the B-field is inevitably required.

Of course, for the development of plasma vorticity, we need a dynamical process that twists the plasma. What is the dynamical process that twists the plasma as FACs are generated due to the divergence of the diamagnetic current? A conventional answer to this question is a mode conversion between the compressional mode and the Alfven mode when the diamagnetic current is growing (in inductive process). However, in principle, the magnetosphere-ionosphere coupling system forms a dissipative structure in the open solar-terrestrial system. Therefore, even in a macroscopic quasi-steady system, the constant conversion from the thermal energy to the magnetic energy and the internal mode conversion from magnetic compression to the magnetic shear should continuously take place. In this sense, we need to revisit the dynamical process of FAC. In this presentation, we will discuss what is the dynamical process and what is the quasi-steady state of FACs in a dissipative structure of the open magnetosphere-ionosphere system.

Keywords: Birkeland Current, Magnetosphere-Ionosphere Coupling, Energy Conversion

©2019. Japan Geoscience Union. All Right Reserved.

[E] Oral | P (Space and Planetary Sciences)：P-EM Solar-Terrestrial Sciences, Space Electromagnetism & Space Environment

Wed. May 29, 2019 9:00 AM - 10:30 AM JST | Wed. May 29, 2019 12:00 AM - 1:30 AM UTC | A04 TOKYO BAY MAKUHARI HALL

[P-EM13] Inner magnetosphere: Recent understanding and new insights

convener:Yusuke Ebihara(Research Institute for Sustainable Humanosphere, Kyoto University), Danny Summers(Memorial University of Newfoundland), Yoshizumi Miyoshi(Institute for Space-Earth Environmental Research, Nagoya University), Shinji Saito(Graduate School of Science, Nagoya University), Chairperson:Shinji Saito(ISEE, Nagoya University), Yusuke Ebihara(RISH, Kyoto University)

The inner magnetosphere is characterized by the dominance of intrinsic dipolar Earth's magnetic field. The dipolar magnetic field traps charged particles, resulting in the formation of unique particle environment known as the plasmasphere, the ring current, and the radiation belt. The inner magnetosphere is always changing because of incoming energy from the outer magnetosphere and the ionosphere in the forms of particles and electromagnetic fields. In the inner magnetosphere, the particle energy is transferred to the field energy, and vice versa. The mutual coupling between particles and fields also makes the inner magnetosphere unique. The outgoing energy to these regions is also known to be significant, such as precipitation into the upper atmosphere and sub-auroral disturbances. A number of satellites (e.g., DMSP, NOAA, Geotail, Cluster, THEMIS, Van Allen Probes, MMS, and Arase), ground-based instruments (e.g., SuperDARN and EISCAT radars, magnetometers, and cameras), and numerical simulations (e.g., global particle simulation, PIC simulation, and hybrid simulation) have successfully surveyed the inner magnetosphere, which deepen our knowledge significantly. USAF DSX, UCLA Elfin and NASA CeRES will be launched soon, being expected to provide important information. We solicit papers describing recent results on the inner magnetosphere and/or its coupling with the other regions, including the ionosphere and the outer magnetosphere.

9:00 AM - 9:15 AM JST | 12:00 AM - 12:15 AM UTC

[PEM13-11] Nonlinear Damping of Oblique Whistler Mode Waves Via Landau Resonance

*Yikai HSIEH[1], Yoshiharu Omura[1] (1.Reserach Institute for Sustainable Humanosphere, Kyoto University)

9:15 AM - 9:30 AM JST | 12:15 AM - 12:30 AM UTC

[PEM13-12] Instantaneous Frequency Analysis on Nonlinear EMIC Emissions: Arase Observation

*Masafumi Shoji[1], Yoshizumi Miyoshi[1], Yoshiharu Omura[2], Lynn M Kistler[1,3], Yasumasa Kasaba[4], Shoya Matsuda[5], Yoshiya Kasahara[6], Ayako Matsuoka[5], Reiko Nomura[7], Keigo Ishisaka[8], Atsushi Kumamoto[4], Fuminori Tsuchiya[4], Satoshi Yagitani[6], Mariko Teramoto[1], Kazushi Asamura[5], Takeshi Takashima[5], Iku Shinohara[5] (1.Institute for Space-Earth Environmental Research, Nagoya University, 2.Research Institute for Sustainable Humanosphere, Kyoto University, 3.Institute for the Study of Earth Oceans and Space, University of New Hampshire, 4.Tohoku University, 5.Institute of Space and Astronautical Science, 6.Kanazawa University, 7.National Astronomical Observatory of Japan, 8.Toyama Prefecture University)

9:30 AM - 9:45 AM JST | 12:30 AM - 12:45 AM UTC

[PEM13-13] Rapid Precipitation by EMIC Rising-tone Emissions of Relativistic Electrons Observed by the Van Allen Probes Mission

*Satoko Nakamura[1], Yoshiharu Omura[1], Craig Kletzing[2], Daniel Baker[3] (1.Research Institute for Sustainable Humanosphere, Kyoto University., 2.Department of Physics and Astronomy University of Iowa , 3.The Laboratory for Atmospheric and Space Physics (LASP) at the University of Colorado)

9:45 AM - 10:00 AM JST | 12:45 AM - 1:00 AM UTC

[PEM13-14] Plasmaspheric EMIC waves excited through mode conversion from equatorial noise under existence of M/Q=2 ions

*Yoshizumi Miyoshi[1], Shoya Matsuda[2], Satoshi Kurita[1], koji nomura[1], Kunihiro Keika[3], Masafumi Shoji[1], Naritoshi Kitamura[3], Yoshiya Kasahara[4], Ayako Matsuoka[2], Iku Shinohara[2], Kazuo Shiokawa[1], Shinobu Machida[1], Ondrej Santolik[5], Scott Boardsen[6], Richard Horne[7], Wygant John[8] (1.Institute for Space-Earth

Environmental Research, Nagoya University, 2.JAXA, 3.University of Tokyo, 4.Kanazawa University, 5.CAS, 6.NASA, 7.British Antarctic Survey, 8.University of Minnesota)

10:00 AM - 10:15 AM JST | 1:00 AM - 1:15 AM UTC

[PEM13-15] Generation Mechanism of Non-thermal Continuum Radiation

*Yoshiharu Omura[1], Miroslav Horky[1,2] (1.Reserach Institute for Sustainable Humanosphere, Kyoto University, 2.Department of Space Physics, Institute of Atmospheric Physics, Czech Academy of Sciences)

10:15 AM - 10:30 AM JST | 1:15 AM - 1:30 AM UTC

[PEM13-16] Influence of kappa distributions on the sweep rate of whistler mode chorus waves

*Danny Summers[1] (1.Memorial University of Newfoundland)

Nonlinear Damping of Oblique Whistler Mode Waves Via Landau Resonance

*Yikai HSIEH[1], Yoshiharu Omura[1]

1. Reserach Institute for Sustainable Humanosphere, Kyoto University

Nonlinear trapping of electrons via Landau resonance is an important mechanism of oblique whistler mode wave-particle interactions. Electrons trapped by Landau resonance gain energies from waves. The Landau resonance velocity becomes very close to the group velocity of nearly parallel whistler mode waves at frequencies around half the electron gyrofrequency, resulting in a long interaction time and possible wave damping. We perform test particle simulations with parameters at L = 5 and a small wave normal angle 10 degrees to study the wave-particle interactions via the Landau resonance. Analyzing the wave electric fields and the resonant currents formed by electrons undergoing Landau and cyclotron resonances, we show that effective wave damping occurs near half the electron gyrofrequency. This nonlinear wave damping is contributed by Landau resonance rather than cyclotron resonance. Furthermore, we confirm that this damping is dominated by perpendicular components of the wave electric field and perpendicular resonant currents. The simulation results indicate that nonlinear damping via Landau resonance is one of the mechanisms dividing chorus emissions into the upper band and the lower band.

Keywords: whistler mode waves, wave-particle interaction, relativistic electrons, Landau resonance

©2019. Japan Geoscience Union. All Right Reserved.

Instantaneous Frequency Analysis on Nonlinear EMIC Emissions: Arase Observation

*Masafumi Shoji[1], Yoshizumi Miyoshi[1], Yoshiharu Omura[2], Lynn M Kistler[1,3], Yasumasa Kasaba[4], Shoya Matsuda[5], Yoshiya Kasahara[6], Ayako Matsuoka[5], Reiko Nomura[7], Keigo Ishisaka[8], Atsushi Kumamoto[4], Fuminori Tsuchiya[4], Satoshi Yagitani[6], Mariko Teramoto[1], Kazushi Asamura[5], Takeshi Takashima[5], Iku Shinohara[5]

1. Institute for Space-Earth Environmental Research, Nagoya University, 2. Research Institute for Sustainable Humanosphere, Kyoto University, 3. Institute for the Study of Earth Oceans and Space, University of New Hampshire, 4. Tohoku University, 5. Institute of Space and Astronautical Science, 6. Kanazawa University, 7. National Astronomical Observatory of Japan, 8. Toyama Prefecture University

In the inner magnetosphere, the Arase spacecraft has observed electromagnetic ion cyclotron (EMIC) emissions with both rising and falling frequencies. The instantaneous frequency analyses on the electromagnetic fields of the EMIC rising tone emission have been performed by the Hilbert-Huang transform. The time variation of the instantaneous frequency shows a good agreement with the nonlinear theory for the frequency evolutions. Rapid instantaneous frequency modulation is also found during the rising tone emission. We estimate the peak-to-peak time of the fluctuation in the frequency and find that the fluctuation is caused around a half of the particle trapping time. From the motion of the phase-bunched particle around the resonant velocity, it is expected that the nonlinear resonant current, which induces the falling frequency is formed in half the trapping time.

Keywords: nonlinear wave particle interaction, Arase spacecraft

©2019. Japan Geoscience Union. All Right Reserved.

Rapid Precipitation by EMIC Rising-tone Emissions of Relativistic Electrons Observed by the Van Allen Probes Mission

*Satoko Nakamura[1], Yoshiharu Omura[1], Craig Kletzing[2], Daniel Baker[3]

1. Research Institute for Sustainable Humanosphere, Kyoto University., 2. Department of Physics and Astronomy University of Iowa , 3. The Laboratory for Atmospheric and Space Physics (LASP) at the University of Colorado

On 23 February 2014, Van Allen Probes sensors observed quite strong electromagnetic ion cyclotron waves (EMIC) in the outer dayside magnetosphere. The maximum amplitude was more than 14 nT, comparable to 7 % of the magnitude of the ambient magnetic field. The EMIC waves consisted of a series of coherent rising tone emissions. Rising tones are excited sporadically by energetic protons. At the same time, the probes detected drastic fluctuations in fluxes of MeV electrons. It was found that the electron fluxes decreased by more than 30 % during the one minute following the observation of each EMIC rising tone emissions. Furthermore, it is concluded that the flux reduction is a non-adiabatic (irreversible) process since holes in the particle flux levels appear as drift echoes with energy dispersion. We examine the process of the electron pitch angle scattering by nonlinear wave trapping due to anomalous cyclotron resonance with EMIC rising tone emissions. The energy range of precipitated electrons corresponds to the presumed energy for the threshold amplitude for nonlinear wave trapping. This is the first report of rapid precipitation by this mechanism of relativistic electrons by EMIC rising tone emissions and their drift echoes in time observed by spacecraft.

©2019. Japan Geoscience Union. All Right Reserved.

Plasmaspheric EMIC waves excited through mode conversion from equatorial noise under existence of M/Q=2 ions

*Yoshizumi Miyoshi[1], Shoya Matsuda[2], Satoshi Kurita[1], koji nomura[1], Kunihiro Keika[3], Masafumi Shoji[1], Naritoshi Kitamura[3], Yoshiya Kasahara[4], Ayako Matsuoka[2], Iku Shinohara[2], Kazuo Shiokawa[1], Shinobu Machida[1], Ondrej Santolik[5], Scott Boardsen[6], Richard Horne[7], Wygant John[8]

1. Institute for Space-Earth Environmental Research, Nagoya University, 2. JAXA, 3. University of Tokyo, 4. Kanazawa University, 5. CAS, 6. NASA, 7. British Antarctic Survey, 8. University of Minnesota

Equatorial noise (EN, and referred to as magnetosonic mode waves) emissions are observed inside and outside the plasmapause and propagate across the magnetic field. In this study, we found the mode conversion from EN to EMIC waves in the plasmasphere using the plasma wave data from Van Allen Probes and Arase. When EN propagates into the earthward across the field line toward the Earth, EN splits into different waves modes; EN, and EMIC waves with the existence of M/Q=2 ions (deuteron or alpha particles) in the deep plasmasphere and the topside ionosphere. The oblique EMIC waves are excited through this mode conversion process, which are different characteristics of the propagation directions from EMIC waves generated from other processes. This mode conversion contributes to an origin of the plasmaspheric EMIC waves, especially at L<2.

Keywords: Arase, Plasmaspheric EMIC waves, M/Q=2 ions

©2019. Japan Geoscience Union. All Right Reserved.

Generation Mechanism of Non-thermal Continuum Radiation

*Yoshiharu Omura[1], Miroslav Horky[1,2]

1. Reserach Institute for Sustainable Humanosphere, Kyoto University, 2. Department of Space Physics, Institute of Atmospheric Physics, Czech Academy of Sciences

We study a possible nonlinear mechanism which could be responsible for generation of the non-thermal continuum radiation. We propose a theoretical model and perform numerical simulations using a 2-D electromagnetic particle code (KEMPO2) [1] to verify the mechanism [2]. In the simulation system, we have density gradient and ring beam electrons in the dense region as a source of electrostatic waves through ring-beam instability. These electrostatic waves cause non-gyrotropy of the ring velocity distribution which is necessary for generation of the harmonic waves. Velocity component V_y together with magnetic field B_z of the generated Z-mode waves creates Lorentz force in the x-direction (along the magnetic field). Hence, oscillating energetic electrons work as an anntenna emiting O-mode waves to the low density region. Electromagnetic O-mode waves are emitted at harmonics of the cyclotron frequency up to the maximal plasma frequency of the high density region, and they are observed as non-thermal continuum radiation in the low density region.

References:
[1] M. Horky, Y. Omura, and O. Santolik, Particle simulation of electromagnetic emissions from electrostatic instability driven by an electron ring beam on the density gradient, Physics of Plasmas 25, 042905, doi: 10.1063/1.5025912, 2018.
[2] M. Horky, and Y. Omura, Novel nonlinear mechanism of the generation of non-thermal continuum radiation, Physics of Plasmas 26, 2019.

Keywords: wave-particle interaction, nonlinear process, plasma_pause

©2019. Japan Geoscience Union. All Right Reserved.

Influence of kappa distributions on the sweep rate of whistler mode chorus waves

*Danny Summers[1]

1. Memorial University of Newfoundland

Kappa particle distributions typically possess a high-energy power-law tail characterized by a spectral index kappa. Here we consider the bi-kappa and kappa-loss-cone distributions. The influence of kappa distributions on the linear growth rate of whistler-mode waves is mediated by the electron anisotropy. The linear growth rate corresponding to kappa distributions (for kappa=2) exceeds that for a bi-Maxwellian distribution for electron anisotropies less than a critical value; for anisotropies greater than the critical value the opposite applies. The influence of kappa distributions on the threshold wave amplitude for nonlinear growth depends on the wave frequency, the electron anisotropy and the temperature of the (hot) energetic electrons that generate the waves. We construct time profiles of the amplitude and frequency of chorus wave elements for various sets of parameters. We examine how the sweep (chirp) rate of the waves depends on the kappa index. Nonlinear growth of whistler mode waves can be enhanced or inhibited by kappa distributions,dependent on the values of the parameters of the background plasma and the properties of the injected energetic electron population that generates the waves.

Keywords: kappa distributions, whistler mode waves, chorus sweep rates

©2019. Japan Geoscience Union. All Right Reserved.

[E] Oral | P (Space and Planetary Sciences)：P-EM Solar-Terrestrial Sciences, Space Electromagnetism & Space Environment

Wed. May 29, 2019 10:45 AM - 12:15 PM JST | Wed. May 29, 2019 1:45 AM - 3:15 AM UTC | A04 TOKYO BAY MAKUHARI HALL

[P-EM13] Inner magnetosphere: Recent understanding and new insights

convener:Yusuke Ebihara(Research Institute for Sustainable Humanosphere, Kyoto University), Danny Summers(Memorial University of Newfoundland), Yoshizumi Miyoshi(Institute for Space-Earth Environmental Research, Nagoya University), Shinji Saito(Graduate School of Science, Nagoya University), Chairperson:Yusuke Ebihara(RISH, Kyoto University), Shinji Saito(ISEE, Nagoya University)

The inner magnetosphere is characterized by the dominance of intrinsic dipolar Earth's magnetic field. The dipolar magnetic field traps charged particles, resulting in the formation of unique particle environment known as the plasmasphere, the ring current, and the radiation belt. The inner magnetosphere is always changing because of incoming energy from the outer magnetosphere and the ionosphere in the forms of particles and electromagnetic fields. In the inner magnetosphere, the particle energy is transferred to the field energy, and vice versa. The mutual coupling between particles and fields also makes the inner magnetosphere unique. The outgoing energy to these regions is also known to be significant, such as precipitation into the upper atmosphere and sub-auroral disturbances. A number of satellites (e.g., DMSP, NOAA, Geotail, Cluster, THEMIS, Van Allen Probes, MMS, and Arase), ground-based instruments (e.g., SuperDARN and EISCAT radars, magnetometers, and cameras), and numerical simulations (e.g., global particle simulation, PIC simulation, and hybrid simulation) have successfully surveyed the inner magnetosphere, which deepen our knowledge significantly. USAF DSX, UCLA Elfin and NASA CeRES will be launched soon, being expected to provide important information. We solicit papers describing recent results on the inner magnetosphere and/or its coupling with the other regions, including the ionosphere and the outer magnetosphere.

10:45 AM - 11:05 AM JST | 1:45 AM - 2:05 AM UTC

[PEM13-17] The Impacts of Substorms on the Ring Current

★Invited Papers

*Jasmine Kaur Sandhu[1], I. J. Rae[1], M. Gkioulidou[2], C. Forsyth[1], G. D. Reeves[3], M. P. Freeman[4], K. R. Murphy[5], M.-T. Walach[6], H. E. Spence[7] (1.Mullard Space Science Laboratory, University College London, UK., 2.Applied Physics Laboratory, John Hopkins University, USA., 3.Los Alamos National Laboratory, USA., 4.British Antarctic Survey, UK., 5.University of Maryland, USA., 6.Lancaster University, UK., 7.University of New Hampshire, USA.)

11:05 AM - 11:25 AM JST | 2:05 AM - 2:25 AM UTC

[PEM13-18] Dipolarization in the Inner Magnetosphere: Comparison between Geosynchronous Orbit and Further Inside

★Invited Papers

*Shinichi Ohtani[1], Tetsuo Motoba[1], Matina Gkioulidou[1], Kazue Takahashi[1] (1.The Johns Hopkins University Applied Physics Laboratory)

11:25 AM - 11:40 AM JST | 2:25 AM - 2:40 AM UTC

[PEM13-19] Substorm-associated particle injection near/at geosynchronous orbit: Observations from ERG and GOES

*Tzu-Fang Chang[1,2], Chio-Zong Cheng[2], Sunny Wing-Yee Tam[2], Chih-Yu Chiang[2], Yoshizumi Miyoshi[1], Tomoaki Hori[1], Takefumi Mitani[3], Takeshi Takashima[3], Ayako Matsuoka[3], Mariko Teramoto[1], Iku Shinohara[3] (1.Institute for Space-Earth Environmental Research, Nagoya University, Japan, 2.Institute of Space and Plasma Sciences, National Cheng Kung University, Tainan, Taiwan, 3.Institute of Space and Astronautical Science, Japan Aerospace Exploration Agency, Japan)

11:40 AM - 11:55 AM JST | 2:40 AM - 2:55 AM UTC

[PEM13-20] Substorm -like energetic electron injection observed at the plasma sheet boundary in the inner magnetosphere

*Iku Shinohara[1], Nagai Tsugunobu[1], Takefumi Mitani[1], Nana Higashio[2], Satoshi Kasahara[3], Yoichi Kazama[4], Shiang-Yu Wang[4], Sunny Tam[5], Ayako Matsuoka[1], Kazushi Asamura[1], Shoichiro Yokota[6], Takeshi Takashima[1], Yoshizumi Miyoshi[7] (1.Japan Aerospace Exploration Agency/Institute of Space and Astronautical Science, 2.Japan Aerospace Exploration Agency, 3.The University of Tokyo, 4.Academia Sinica/Institute of Astronomy and Astrophysics, 5.National Cheng Kung University, 6.Osaka University, 7.Nagoya University/Institute for Space-Earth Einvironment Research)

11:55 AM - 12:10 PM JST | 2:55 AM - 3:10 AM UTC

[PEM13-21] Magnetic field disturbances associated with the magnetic dipolarization observed by Arase (ERG) in the inner magnetosphere

*Ayako Matsuoka[1], Masahito Nose[2], Yoshizumi Miyoshi[2], Iku Shinohara[1], Mariko Teramoto[2], Reiko Nomura[3], Akiko Fujimoto[4], Yoshimasa Tanaka[5], Manabu Shinohara[6], Yoshiya Kasahara[7], Yasumasa Kasaba[8], Keigo Ishisaka[9], Shoya Matsuda[1], Masafumi Shoji[2], Tomoko Nakagawa[10], Yoichi Kazama[11], Shiang-Yu Wang[11], Satoshi Kasahara[12], Shoichiro Yokota[13], Takefumi Mitani[1] (1.Institute of Space and Astronautical Science, Japan Aerospace Exploration Agency, 2.Institute for Space-Earth Environmental Research, Nagoya University, 3.RISE, National Astronomical Observatory of Japan, 4.School of Computer Science and Systems Engineering, Kyushu Institute of Technology, 5.National Institute of Polar Research, 6.National Institute of Technology, Kagoshima College, 7.Information Media Center, Kanazawa University, 8.Planetary Plasma and Atmospheric Research Center, Tohoku University, 9.Faculty of Engineering, Toyama Prefectural University, 10.Faculty of Engineering, Tohoku Institute of Technology, 11.Academia Sinica Institute of Astronomy and Astrophysics, 12.School of Science, The University of Tokyo, 13.School of Science, Osaka University)

12:10 PM - 12:15 PM JST | 3:10 AM - 3:15 AM UTC

Discussion

The Impacts of Substorms on the Ring Current

*Jasmine Kaur Sandhu[1], I. J. Rae[1], M. Gkioulidou[2], C. Forsyth[1], G. D. Reeves[3], M. P. Freeman[4], K. R. Murphy[5], M.-T. Walach[6], H. E. Spence[7]

1. Mullard Space Science Laboratory, University College London, UK., 2. Applied Physics Laboratory, John Hopkins University, USA., 3. Los Alamos National Laboratory, USA., 4. British Antarctic Survey, UK., 5. University of Maryland, USA., 6. Lancaster University, UK., 7. University of New Hampshire, USA.

Substorms are a highly dynamic process that result in the global redistribution of energy within the magnetosphere. The occurrence of a substorm can provide the inner magnetosphere with hot ions and consequently intensify the ring current population. However, substorms are a highly variable phenomenon that can occur as an isolated event or as part of a sequence. In this study we determine the extent to which substorms enhance the ring current energy content and compare how the energy enhancement varies with substorm type.

Using ion observations (H^+, O^+, and He^+) from the RBSPICE and HOPE instruments onboard the Van Allen Probes, we quantify how the total ring current energy content changes during the substorm process. A statistical analysis demonstrates the impact of a typical substorm on the ring current region. We find that ~ 5% of the total energy released at substorm onset is transferred into the ring current population, and energises the ring current by 12% on average. The features of the energy enhancement correlate well with the expected properties of particle injections into the inner magnetosphere, and large enhancements in the O^+ contribution to the energy content suggest important compositional variations.

Analysis also reveals that the ring current response to substorms is strongly dependent upon the type of substorm activity. The results show that substorms followed by a series of successive substorms are associated with significantly different ring current conditions and enhancements compared to isolated substorms. We present clear magnitude and local time differences that illustrate the complexity and variability of the substorm-ring current coupling, along with an interpretation of the details of this relationship.

Keywords: Ring Current, Substorms, Van Allen Probes, Magnetosphere

©2019. Japan Geoscience Union. All Right Reserved.

Dipolarization in the Inner Magnetosphere: Comparison between Geosynchronous Orbit and Further Inside

*Shinichi Ohtani[1], Tetsuo Motoba[1], Matina Gkioulidou[1], Kazue Takahashi[1]

1. The Johns Hopkins University Applied Physics Laboratory

The present study addresses the current system associated with dipolarization in the inner magnetosphere. *Ohtani et al.* [2018] examined dipolarization events observed by the Van Allen Probes (RBSP) satellites within 5.8 R_E from Earth, and by statistically comparing signatures at nearby RBSP or GOES satellites, they found that dipolarization signatures are often highly correlated (c.c. > 0.8) within 1 hr in MLT and 1 R_E in R_{XY}, and the dipolarization region expands earthward as well as azimuthally. In the present study we use, as a reference, the GOES geosynchronous satellites instead, and we examine how the magnetic field at the RBSP position changes responding to sharp dipolarizations at geosynchronous orbit. As expected from the aforementioned result, the two spacecraft occasionally observe similar dipolarization signatures with some time delay. It is, however, also found that in some events the magnetic field changes far less systematically at the RBSP probes, and in other events it barely changes or changes very gradually even if the RBSP probes are located very close to the GOES location in longitude (DMLT = 0.0 ~ 0.5 hr in MLT). By examining such variability with respect to the radial distance and magnetic latitude of the RBSP probes, we address the spatial structure of the associated current system. We also examine the variation of particle fluxes at the RBSP probes for each type of the magnetic response, and discuss the result in terms of the enhancement of local plasma pressure and the formation of a R2-sense field-aligned current system, which we suggest coexists along with the conventional substorm wedge current system.

Reference:

Ohtani, S., Motoba, T., Gkioulidou, M., Takahashi, K., & Singer, H. J. (2018). Spatial development of the dipolarization region in the inner magnetosphere. Journal of Geophysical Research: Space Physics, 123, 5452–5463. https://doi.org/10.1029/2018JA025443.

Keywords: Dipolarization, Inner magnetosphere, Substorms, Field-aligned currents

©2019. Japan Geoscience Union. All Right Reserved.

Substorm-associated particle injection near/at geosynchronous orbit: Observations from ERG and GOES

*Tzu-Fang Chang[1,2], Chio-Zong Cheng[2], Sunny Wing-Yee Tam[2], Chih-Yu Chiang[2], Yoshizumi Miyoshi[1], Tomoaki Hori[1], Takefumi Mitani[3], Takeshi Takashima[3], Ayako Matsuoka[3], Mariko Teramoto[1], Iku Shinohara[3]

1. Institute for Space-Earth Environmental Research, Nagoya University, Japan, 2. Institute of Space and Plasma Sciences, National Cheng Kung University, Tainan, Taiwan, 3. Institute of Space and Astronautical Science, Japan Aerospace Exploration Agency, Japan

The injection of electrons during the substorm event, occurring on Apr. 5, 2017, was observed by the ERG (Arase), GOES-15 and GOES-13 spacecraft near/at geosynchronous orbit. The ERG satellite observed the nearly-dispersionless injection and the subsequent drift echoes while the GOES-15 and GOES-13 captured the drift echoes with dispersion. The multipoint observations provide constraints for us to simulate the substorm-associated injection. We improve an existing model in the literature to study the substorm injection event. Since the electron energies of interest are comparable to the rest mass energy, our work further provides the relativistic form of the previous model and employs a semi-empirical model instead of a dipole-based one in the previous study. Our simulations successfully reproduce the key features of the nearly-dispersionless injection and the drift echoes. The periods of drift echoes show a better fit to the spacecraft observations when relativistic effects are taken into account. The substorm-associated injection event can be better simulated by the further-developed model shown in this study.

Keywords: ERG, Arase, substorm injection, drift echoes, relativistic effects

©2019. Japan Geoscience Union. All Right Reserved.

Substorm -like energetic electron injection observed at the plasma sheet boundary in the inner magnetosphere

*Iku Shinohara[1], Nagai Tsugunobu[1], Takefumi Mitani[1], Nana Higashio[2], Satoshi Kasahara[3], Yoichi Kazama[4], Shiang-Yu Wang[4], Sunny Tam[5], Ayako Matsuoka[1], Kazushi Asamura[1], Shoichiro Yokota[6], Takeshi Takashima[1], Yoshizumi Miyoshi[7]

1. Japan Aerospace Exploration Agency/Institute of Space and Astronautical Science, 2. Japan Aerospace Exploration Agency, 3. The University of Tokyo, 4. Academia Sinica/Institute of Astronomy and Astrophysics, 5. National Cheng Kung University, 6. Osaka University, 7. Nagoya University/Institute for Space-Earth Einvironment Research

The Arase (ERG) satellite is possible to observe higher L-value plasma sheet close to the plasma sheet boundary because of its characteristic orbit, and, actually, Arase has observed several lobe entry events just outside of the outer radiation belt. In some of these events, we found that energetic electron bursts up to (sometimes, over) 300 keV appear at the plasma sheet boundary. The purpose of this study is to address where do the energetic electron bursts at higher latitude come from and what is the contribution of magnetotail reconnection and its associated acceleration process to the generation of the energetic electron bursts.

However, the observed energetic electron bursts look quite similar to typical dispersionless substorm injection events. If the observed electron bursts are due to the substorm injection, the observation cannot be explained by the standard understanding of the injection because (1) the injection occurs associated with local magnetic field dipolarizations in downstream of the magnetotail reconnection jets (in deep inside of the plasma sheet) and (2) energetic electrons observed at the plasma sheet boundary are thought to be directly accelerated from magnetotail reconnection sites. Since the pitch angle distribution of 100-200 keV electron shows enhancement both of parallel and perpendicular fluxes, the observed results suggest the coexistence of (1) and (2). In this presentation, we will discuss the physical meanings of the observed electron bursts. The discussion is important to address the relationship between magnetotail reconnection and injections, and the results might contribute to a better understanding of electron acceleration processes and energy input to the inner magnetosphere.

Keywords: plasma sheet boundary, electron acceleration

©2019. Japan Geoscience Union. All Right Reserved.

Magnetic field disturbances associated with the magnetic dipolarization observed by Arase (ERG) in the inner magnetosphere

*Ayako Matsuoka[1], Masahito Nose[2], Yoshizumi Miyoshi[2], Iku Shinohara[1], Mariko Teramoto[2], Reiko Nomura[3], Akiko Fujimoto[4], Yoshimasa Tanaka[5], Manabu Shinohara[6], Yoshiya Kasahara[7], Yasumasa Kasaba[8], Keigo Ishisaka[9], Shoya Matsuda[1], Masafumi Shoji[2], Tomoko Nakagawa[10], Yoichi Kazama[11], Shiang-Yu Wang[11], Satoshi Kasahara[12], Shoichiro Yokota[13], Takefumi Mitani[1]

1. Institute of Space and Astronautical Science, Japan Aerospace Exploration Agency, 2. Institute for Space-Earth Environmental Research, Nagoya University, 3. RISE, National Astronomical Observatory of Japan, 4. School of Computer Science and Systems Engineering, Kyushu Institute of Technology, 5. National Institute of Polar Research, 6. National Institute of Technology, Kagoshima College, 7. Information Media Center, Kanazawa University, 8. Planetary Plasma and Atmospheric Research Center, Tohoku University, 9. Faculty of Engineering, Toyama Prefectural University, 10. Faculty of Engineering, Tohoku Institute of Technology, 11. Academia Sinica Institute of Astronomy and Astrophysics, 12. School of Science, The University of Tokyo, 13. School of Science, Osaka University

The magneto-hydrodynamic waves propagating in the plasma sheet are recognized to transport substantial energies in the magnetosphere. We investigated magnetic field disturbances of the Alfven waves observed by the Arase spacecraft at about 5 earth-radii distance in the midnight. In the inner plasma sheet Alfven waves were often accompanied by the magnetic dipolarization.
We examined the magnetic disturbances in the plane perpendicular to the ambient magnetic field. In the two events examined in our study, the magnetic field disturbances were linearly polarized and the polarization direction gradually rotated 180 degrees in 200 seconds. It is well interpreted that Arase traversed a magnetic flux tube where torsional Alfven waves propagated. The change of the polarization direction reflected the change of observation location in the flux tube. Torsional-mode is significantly common and natural as the parallel-propagating Alfven wave. It is known that large-scale energy transfer and dissipation of the torsional Alfven waves take place on the solar surface.
Meanwhile, in the boundary plasma sheet adjacent to the lobe, the magnetic field disturbances were linearly polarized again and confined to the dawn-dusk direction. They are interpreted as plane Alfven waves having uniformity in the dawn-dusk direction and propagating obliquely. The kinetic effect of the Alfven waves has been often discussed in previous works in association with the auroral emission at the ionospheric altitude.

Keywords: Arase, magnetic field, dipolarization, Alfven wave

©2019. Japan Geoscience Union. All Right Reserved.

[E] Oral | P (Space and Planetary Sciences)：P-EM Solar-Terrestrial Sciences, Space Electromagnetism & Space Environment

Wed. May 29, 2019 1:45 PM - 3:15 PM JST | Wed. May 29, 2019 4:45 AM - 6:15 AM UTC | A04 TOKYO BAY MAKUHARI HALL

[P-EM13] Inner magnetosphere: Recent understanding and new insights

convener:Yusuke Ebihara(Research Institute for Sustainable Humanosphere, Kyoto University), Danny Summers(Memorial University of Newfoundland), Yoshizumi Miyoshi(Institute for Space-Earth Environmental Research, Nagoya University), Shinji Saito(Graduate School of Science, Nagoya University), Chairperson:Yoshizumi Miyoshi(ISEE, Nagoya University), Yusuke Ebihara(RISH, Kyoto University)

The inner magnetosphere is characterized by the dominance of intrinsic dipolar Earth's magnetic field. The dipolar magnetic field traps charged particles, resulting in the formation of unique particle environment known as the plasmasphere, the ring current, and the radiation belt. The inner magnetosphere is always changing because of incoming energy from the outer magnetosphere and the ionosphere in the forms of particles and electromagnetic fields. In the inner magnetosphere, the particle energy is transferred to the field energy, and vice versa. The mutual coupling between particles and fields also makes the inner magnetosphere unique. The outgoing energy to these regions is also known to be significant, such as precipitation into the upper atmosphere and sub-auroral disturbances. A number of satellites (e.g., DMSP, NOAA, Geotail, Cluster, THEMIS, Van Allen Probes, MMS, and Arase), ground-based instruments (e.g., SuperDARN and EISCAT radars, magnetometers, and cameras), and numerical simulations (e.g., global particle simulation, PIC simulation, and hybrid simulation) have successfully surveyed the inner magnetosphere, which deepen our knowledge significantly. USAF DSX, UCLA Elfin and NASA CeRES will be launched soon, being expected to provide important information. We solicit papers describing recent results on the inner magnetosphere and/or its coupling with the other regions, including the ionosphere and the outer magnetosphere.

1:45 PM - 2:05 PM JST | 4:45 AM - 5:05 AM UTC

[PEM13-22] Statistical Property of Long Lasting Poloidal Pc 4-5 Waves and Relation with Particle Dynamics in the Inner Magnetosphere: Van Allen Probes Observations

★Invited Papers

*Kazuhiro Yamamoto[1], Masahito Nose[2], Kunihiro Keika[3], Charles W. Smith[4], Robert J. MacDowall[5], Donald G. Mitchell[6], Hyomin Kim[7], John Wygant[8] (1.Graduate School of Science, Kyoto University, 2.Institute for Space-Earth Environmental Research, Nagoya University, 3.Graduate School of Science, the University of Tokyo, 4.Institute for the Study of Earth, Oceans, and Space, University of New Hampshire, 5.Solar System Exploration Division, Goddard Space Flight Center, 6.The Johns Hopkins University Applied Physics Laboratory, 7.Center for Solar Terrestrial Research, New Jersey Institute of Technology, 8.School of Physics and Astronomy, University of Minnesota)

2:05 PM - 2:25 PM JST | 5:05 AM - 5:25 AM UTC

[PEM13-23] Subauroral Polarization Streams: Indication of Magnetosphere–Ionosphere Coupling

★Invited Papers

*Fei He[1,2,3], Xiao-Xin Zhang[4], Wenbin Wang[5], Zhonghua Yao[1,2,3], Yong Wei[1,2,3], Zhi-Peng Ren[1,2,3], Xinan Yue[1,2,3], Weixing Wan[1,2,3] (1.Institute of Geology & Geophysics, CAS, 2.Institutions of Earth Science, CAS, 3.College of Earth and Planetary Sciences, UCAS, 4.National Center for Space Weather, CMA, 5.High Altitude Observatory, NCAR)

2:25 PM - 2:40 PM JST | 5:25 AM - 5:40 AM UTC

[PEM13-24] Simultaneous Arase-ground observations of a purple and green auroral arc

*Kazuo Shiokawa[1], Masahito Nose[1], Satoshi Tsuchiya[1], Yuki Takagi[1], Shun Imajo[1], Yoshimasa Tanaka[2], Yoshizumi Miyoshi[1], Keisuke Hosokawa[3], Yoichi Kazama[4], Shiang-Yu Wang[4], Sunny W.Y. Tam[4], Kazushi Asamura[5], Satoshi Kasahara[6], Shoichiro Yokota[7], Tomoaki Hori[1], Kunihiro Keika[6], Ayako Matsuoka[5] (1.Institute for Space-Earth Environmental Research, Nagoya University, 2.National Institute of Polar Research, 3.The University of Electro-Communications, 4.National Cheng Kung University, 5.Institute of

Space and Astronautical Science, Japan Aerospace Exploration Agency, 6.University of Tokyo, 7.Osaka University)

2:40 PM - 2:55 PM JST | 5:40 AM - 5:55 AM UTC

[PEM13-25] Multiple Satellite Observations of Oxygen Torus in the Inner Magnetosphere

*Masahito Nose[1], Ayako Matsuoka[2], Atsushi Kumamoto[3], Yoshiya Kasahara[4], J Goldstein[5,6], Mariko Teramoto[1], Fuminori Tsuchiya[3], Shoya Matsuda[2], Masafumi Shoji[1], Shun Imajo[1], Oimatsu Satoshi[7], Kazuhiro Yamamoto[7], Yuki Obana[8], Reiko Nomura[9], Akiko Fujimoto[10], Iku Shinohara[2], Yoshizumi Miyoshi[1], W S Kurth[11], C A Kletzing[11], C W Smith[12], R J MacDowall[13] (1.Institute for Space-Earth Environmental Research, Nagoya University, 2.Institute of Space and Astronautical Science, Japan Aerospace Exploration Agency, 3.Graduate School of Science, Tohoku University, 4.Information Media Center, Kanazawa University, 5.Space Science and Engineering Division, Southwest Research Institute, 6.University of Texas at San Antonio, 7.Graduate School of Science, Kyoto University, 8.Faculty of Engineering, Osaka Electro-Communication University, 9.National Astronomical Observatory of Japan, 10.Kyushu Institute of Technology, 11.Department of Physics and Astronomy, University of Iowa, 12.Institute for the Study of Earth, Oceans, and Space, University of New Hampshire, 13.Solar System Exploration Division, Goddard Space Flight Center)

2:55 PM - 3:10 PM JST | 5:55 AM - 6:10 AM UTC

[PEM13-26] Study of characteristics of storm-time Pc5 ULF waves excited by the drift-bounce resonance with ring current ions based on the global drift-kinetic simulation

*Tomotsugu Yamakawa[1], Kanako Seki[1], Takanobu Amano[1], Yoshizumi Miyoshi[2], Naoko Takahashi[1] (1.Department of Earth and Planetary Science, School of Science, The University of Tokyo, 2.ISEE, Nagoya University)

3:10 PM - 3:15 PM JST | 6:10 AM - 6:15 AM UTC

Discussion

Statistical Property of Long Lasting Poloidal Pc 4-5 Waves and Relation with Particle Dynamics in the Inner Magnetosphere: Van Allen Probes Observations

*Kazuhiro Yamamoto[1], Masahito Nose[2], Kunihiro Keika[3], Charles W. Smith[4], Robert J. MacDowall[5], Donald G. Mitchell[6], Hyomin Kim[7], John Wygant[8]

1. Graduate School of Science, Kyoto University, 2. Institute for Space-Earth Environmental Research, Nagoya University, 3. Graduate School of Science, the University of Tokyo, 4. Institute for the Study of Earth, Oceans, and Space, University of New Hampshire, 5. Solar System Exploration Division, Goddard Space Flight Center, 6. The Johns Hopkins University Applied Physics Laboratory, 7. Center for Solar Terrestrial Research, New Jersey Institute of Technology, 8. School of Physics and Astronomy, University of Minnesota

Poloidal ULF waves in the inner magnetosphere have been attracting many attentions because they can interact with plasma particles. A lot of event analysis of the drift-bounce resonance, the bounce resonance, and the drift resonance have been conducted (e.g., *Hughes et al.*, 1978; *Takahashi et al.*, 1990, 2018; *Liu et al.*, 2013; *Dai et al.*, 2013; *Min et al.*, 2017; *Oimatsu et al.*, 2018; *Rubtsov* et al., 2018). However, the statistical relation between the poloidal mode waves and particles is rarely reported, and the phase relation between poloidal oscillations and resonance particles is only studied by *Ren et al.* (2018).

To reveal the importance of a poloidal ULF wave in the dynamics of the inner magnetosphere, we statistically analyzed 91 events of the poloidal waves detected by Van Allen Probes with duration time larger than 2 hr, because significant wave particle interaction is expected for such long lasting waves. We calculated eigen-frequencies of the selected waves using the Tsyganenko 89 model (*Tsyganenko*, 1989), and found that most of them are second harmonic mode waves. The cross phase between the radial magnetic field and the azimuthal electric field also supports this result. Using the ion sounding technique (*Su et al.*, 1977; *Min et al.*, 2017; *Yamamoto et al.*, 2018), we estimated the azimuthal wave number (*m* number) for 47 events from RBSPICE observation. Most of the 47 events have m = -120 to -200 (i.e., westward propagation). These high-m waves can be excited by wave-particle interaction.

Relation between the high-m poloidal waves and the plasmasphere was investigated. When the poloidal waves were observed, cold electron density increased by a factor of ~2. When the electron density decreased to the original state, the poloidal waves disappeared. This implies that the poloidal waves are excited in the structured high electron density region like plasma plume. The scenario of wave excitation through bounce resonance proposed by *Liu et al.* (2013) can explain the density variations during wave appearance.

We will also discuss the variations of proton flux around resonance energy and evaluate the importance of poloidal ULF waves in the dynamics of the inner magnetosphere. During quiet period ($|Dst| < 10$ nT), the proton flux at energy of (0.3-1)W_{res} (W_{res}: resonance energy) was slightly smaller than that on the orbit just before the wave onset. The decrease of resonance particle flux may be caused by wave-particle interaction.

Keywords: poloidal ULF waves, ring current, plasmasphere, wave particle interaction, Van Allen Probes (RBSP)

©2019. Japan Geoscience Union. All Right Reserved.

©2019. Japan Geoscience Union. All Right Reserved.

Subauroral Polarization Streams: Indication of Magnetosphere–Ionosphere Coupling

*Fei He[1,2,3], Xiao-Xin Zhang[4], Wenbin Wang[5], Zhonghua Yao[1,2,3], Yong Wei[1,2,3], Zhi-Peng Ren[1,2,3], Xinan Yue[1,2,3], Weixing Wan[1,2,3]

1. Institute of Geology & Geophysics, CAS, 2. Institutions of Earth Science, CAS, 3. College of Earth and Planetary Sciences, UCAS, 4. National Center for Space Weather, CMA, 5. High Altitude Observatory, NCAR

Subauroral polarization streams, or SAPS, are narrow channels of strong westward ion flows in both the subauroral ionosphere and the conjugated inner magnetosphere in the nightside during geomagnetic storms and substorms. The SAPS are closely related with ionospheric conductivity and region–2 field–aligned currents. Many characteristics of SAPS have been determined from space–based measurements of electric fields and ion drifts in the ionosphere and the magnetosphere, and ground–based radar observations, such as the global occurrence based on the statistics of many individual event, long term variabilities, hemispheric asymmetries, electromagnetic wave structures, double peak signatures, and evolution patterns during intense storms and quiet time substorms. Multisatellite observations during a geomagnetic storm indicated that the SAPS were first initiated around the dusk sector and then expanded toward the midnight, moved to low latitudes and formed a wedge-shaped structure during the main phase. More recently, multisatellite observations during a severe storm revealed that strong oscillations occurred in the SAPS channel when IMF By changed from positive to negative. The SAPS oscillations were first observed in the pre–midnight sector and propagated towards the dusk sector. The oscillations may be related to the waves generated by the interaction between the fast–flowing energetic plasma sheet ions and the cold plasmasphere. The new features of SAPS provide new insights in to the coupling dynamics in the magnetosphere.

Keywords: SAPS, Large-scale structure, Oscillations, plasma sheet, storm

©2019. Japan Geoscience Union. All Right Reserved.

Simultaneous Arase-ground observations of a purple and green auroral arc

*Kazuo Shiokawa[1], Masahito Nose[1], Satoshi Tsuchiya[1], Yuki Takagi[1], Shun Imajo[1], Yoshimasa Tanaka[2], Yoshizumi Miyoshi[1], Keisuke Hosokawa[3], Yoichi Kazama[4], Shiang-Yu Wang[4], Sunny W.Y. Tam[4], Kazushi Asamura[5], Satoshi Kasahara[6], Shoichiro Yokota[7], Tomoaki Hori[1], Kunihiro Keika[6], Ayako Matsuoka[5]

1. Institute for Space-Earth Environmental Research, Nagoya University, 2. National Institute of Polar Research, 3. The University of Electro-Communications, 4. National Cheng Kung University, 5. Institute of Space and Astronautical Science, Japan Aerospace Exploration Agency, 6. University of Tokyo, 7. Osaka University

The purple auroral emission at a wavelength of 427.8nm is often caused by resonant scattering of sunlight by nitrogen molecular ions at the high-latitude part of auroral arcs, and can be a manifestation of ion upflow in the auroral ionosphere. We report the first particle observation for the source region of a purple/green auroral arc in the inner magnetosphere, which was made by the Arase satellite. The auroral arc appeared and expanded equatorward from ~0310 UT (midnight in local time) on September 11, 2018 at Nain, Canada, in association with the expansion phase of a substorm that occurred during the arrival of a corotating interaction region (CIR) in the solar wind. The auroral arc is characterized by purple and green emissions at the top and bottom parts, respectively, suggesting resonant-scattering of sunlight by auroral nitrogen molecular ions. Bi-directional field-aligned electrons with energies of ~keV were observed by the LEP-e onboard the Arase satellite during the arc crossing at L ~ 6.4, while source electrons become isotropic in the diffuse aurora afterwards. Electrons at energies of ~20 keV measured by the MEP-e of Arase also show a bi-directional (nearly) field-aligned distribution, while electron loss cone was identified at the arc crossing. The low-energy protons measured by LEP-i of Arase show time-pitch-angle dispersion from anti-earthward (180 degree) to earthward (0 degree) during the arc crossing. Based on these observations, we discuss physical mechanisms that cause these particle features and the observed purple/green auroral arc.

Keywords: purple auroral arc, simultaneous satellite-ground observation, field-aligned electron precipitation

©2019. Japan Geoscience Union. All Right Reserved.

Multiple Satellite Observations of Oxygen Torus in the Inner Magnetosphere

*Masahito Nose[1], Ayako Matsuoka[2], Atsushi Kumamoto[3], Yoshiya Kasahara[4], J Goldstein[5,6], Mariko Teramoto[1], Fuminori Tsuchiya[3], Shoya Matsuda[2], Masafumi Shoji[1], Shun Imajo[1], Oimatsu Satoshi[7], Kazuhiro Yamamoto[7], Yuki Obana[8], Reiko Nomura[9], Akiko Fujimoto[10], Iku Shinohara[2], Yoshizumi Miyoshi[1], W S Kurth[11], C A Kletzing[11], C W Smith[12], R J MacDowall[13]

1. Institute for Space-Earth Environmental Research, Nagoya University, 2. Institute of Space and Astronautical Science, Japan Aerospace Exploration Agency, 3. Graduate School of Science, Tohoku University, 4. Information Media Center, Kanazawa University, 5. Space Science and Engineering Division, Southwest Research Institute, 6. University of Texas at San Antonio, 7. Graduate School of Science, Kyoto University, 8. Faculty of Engineering, Osaka Electro-Communication University, 9. National Astronomical Observatory of Japan, 10. Kyushu Institute of Technology, 11. Department of Physics and Astronomy, University of Iowa, 12. Institute for the Study of Earth, Oceans, and Space, University of New Hampshire, 13. Solar System Exploration Division, Goddard Space Flight Center

A recent study employing the Arase and Van Allen Probes A satellites at different MLT revealed an event in which the inner magnetospheric O^+ density enhancement (know as the dense oxygen torus) does not extend over all MLT. Rather, the torus is skewed toward the dawn sector, being described more precisely as a crescent-shaped torus or a pinched torus [Nosé et al., 2018]. In the reported event of 24 April 2017, Arase flying in the morning sector detected an enhancement of the average plasma mass up to ~3.5 amu around *L*=4.9–5.2, while Van Allen Probe A flying in the afternoon sector observed no clear enhancements in the average plasma mass. In the present study, we focus on simultaneous observations of the magnetic field and plasma waves made by the Arase and Van Allen Probes A and B satellites on 12 September 2017. For this event the orbital configuration of the satellites is opposite to that in the study by Nosé et al. [2018]; that is, Arase is in the afternoon and the Van Allen Probes are in the morning. It is found that only Probe B observed a clear enhancement in the average plasma mass up to ~4 amu around *L*=3.5 and MLT=9.0 hr. This result demonstrates that the crescent-shaped O^+ torus is not a unique (single-event) occurrence, and thus may be a general feature of the density enhancement in the inner magnetosphere.

©2019. Japan Geoscience Union. All Right Reserved.

Study of characteristics of storm-time Pc5 ULF waves excited by the drift-bounce resonance with ring current ions based on the global drift-kinetic simulation

*Tomotsugu Yamakawa[1], Kanako Seki[1], Takanobu Amano[1], Yoshizumi Miyoshi[2], Naoko Takahashi[1]

1. Department of Earth and Planetary Science, School of Science, The University of Tokyo, 2. ISEE, Nagoya University

Storm-time Pc5 waves are electromagnetic fluctuations in the inner magnetosphere with the frequency of 1.67-6.67 mHz, and are considered to be generated by ring current ions associated with the injection from the magnetotail during substorms. The excitation mechanism and global distribution of Pc5 waves are keys to understand dynamic variation of the outer radiation belt, since Pc5 waves are considered to contribute to the radial diffusion of radiation belt electrons [e.g. Elkington et al., 2003]. Promising candidates of excitation mechanism of the storm-time Pc5 waves are the drift or drift-bounce resonance [Southwood, 1976]. Although previous spacecraft observations suggest the resonant excitation [e.g., Dai et al., 2013; Yeoman and Wright., 2001], there are other possibilities such as periodic pressure inhomogeneity formed by time-dependent injections. Theoretically, Yamakawa et al. [2019] confirmed the drift resonance excitation of storm-time Pc5 waves in 3D dipole structure based on the drift-kinetic simulation. However, in what kind of situation the drift resonance is switched to the drift-bounce resonance is far from understood.

In order to simulate the excitation of the storm-time Pc5 waves, we perform a kinetic simulation for ring current particles using GEMSIS-RC model [Amano et al., 2011], in which five-dimensional drift-kinetic equation for the phase space density (PSD) of ring current ions and Maxwell equations are solved self-consistently under assumption that the first adiabatic invariant is conserved. In order to simulate consequence of ion injection from the plasma sheet, we set a localized high-pressure region around midnight consisting of H+ ions. We compare two cases of the initial velocity distribution; the Maxwellian velocity distribution with the isotropic temperature of 16 keV (Case a) and the velocity distribution with the phase bunching in the southern hemisphere due to the bounce motion of ions in addition to the background Maxwellian distribution (Case b). For the Case b, we changed the strength of the initial phase bunching to investigate the conditions for drift-bounce resonance to be dominant.In Case a, the simulation results show the drift resonance excitation of both poloidal and toroidal mode waves in Pc5 frequency range in the dayside dusk sector. These waves are fundamental mode waves with azimuthal wave number m ~ - 20 propagating westward. Global distribution of the excited Pc5 waves indicates that they are excited where the local growth rate resultant from the positive PSD gradient in energy is positive. In Case b, excitation of the second harmonic poloidal-mode Pc4 ULF waves due to the drift-bounce resonance was identified in the dayside dusk sector in the strong bunching case. We will also report on characteristics of excited ULF waves and their dependence on the initial bunching strength of injected ions with a focus of the relative contribution of the drift and drift-bounce resonances.

References:

©2019. Japan Geoscience Union. All Right Reserved.

Amano et al., J. *Geophys. Res.*, vol.116, No.A2, 216, 2011.

Elkington et al., J. *Geophys*. Res., vol.108, No.A3, 1116, 2003.

Dai et al., *Geophys. Res. Lett.*, vol.40, No.16, 4127-4132, 2013.

Yeoman et al., *Ann. Geophys.*, vol.19, No.2, 159-170, 2001.

Southwood, J. *Geophys. Res.*, vol.81, No.19, 3340-3348, 1976.

Yamakawa et al., *Geophys. Res. Lett.*, in press, 2019.

Keywords: ring current, Pc5 ULF, drift-bounce resonance, drift-kinetic simulation, magnetic storm

©2019. Japan Geoscience Union. All Right Reserved.

[E] Poster | P (Space and Planetary Sciences)：P-EM Solar-Terrestrial Sciences, Space Electromagnetism & Space Environment

Wed. May 29, 2019 3:30 PM - 5:00 PM JST | Wed. May 29, 2019 6:30 AM - 8:00 AM UTC | Poster Hall International Exhibition Hall8, Makuhari Messe_2

[P-EM13] Inner magnetosphere: Recent understanding and new insights

convener:Yusuke Ebihara(Research Institute for Sustainable Humanosphere, Kyoto University), Danny Summers(Memorial University of Newfoundland), Yoshizumi Miyoshi(Institute for Space-Earth Environmental Research, Nagoya University), Shinji Saito(Graduate School of Science, Nagoya University)

The inner magnetosphere is characterized by the dominance of intrinsic dipolar Earth's magnetic field. The dipolar magnetic field traps charged particles, resulting in the formation of unique particle environment known as the plasmasphere, the ring current, and the radiation belt. The inner magnetosphere is always changing because of incoming energy from the outer magnetosphere and the ionosphere in the forms of particles and electromagnetic fields. In the inner magnetosphere, the particle energy is transferred to the field energy, and vice versa. The mutual coupling between particles and fields also makes the inner magnetosphere unique. The outgoing energy to these regions is also known to be significant, such as precipitation into the upper atmosphere and sub-auroral disturbances. A number of satellites (e.g., DMSP, NOAA, Geotail, Cluster, THEMIS, Van Allen Probes, MMS, and Arase), ground-based instruments (e.g., SuperDARN and EISCAT radars, magnetometers, and cameras), and numerical simulations (e.g., global particle simulation, PIC simulation, and hybrid simulation) have successfully surveyed the inner magnetosphere, which deepen our knowledge significantly. USAF DSX, UCLA Elfin and NASA CeRES will be launched soon, being expected to provide important information. We solicit papers describing recent results on the inner magnetosphere and/or its coupling with the other regions, including the ionosphere and the outer magnetosphere.

[PEM13-P01] Evaluation of wave normal and Poynting vector analyses for whistler mode waves observed by the waveform capture (WFC) on board the Arase

*Yoshiya Kasahara[1], Satoshi Ikarashi[1], Hiroyuki Nishizawa[1], Shoya Matsuda[2], Fuminori Tsuchiya[3], Atsushi Kumamoto[3], Yasumasa Kasaba[3], Mitsunori Ozaki[1], Ayako Matsuoka[2] (1.Kanazawa University, 2.ISAS/JAXA, 3.Tohoku University)

[PEM13-P02] Calibration of electric fields dedicated to the measurement of the S-WPIA of the Arase Satellite

*Miki Jumpei[1], Hirotsugu Kojima[2], Yuto Katoh[3], Shoya Matsuda[4], Yoshiya Kasahara[5], Mitsuru Hikishima[4], Satoshi Kurita[6], Masahiro Kitahara[3], Satoshi Kasahara[7], Yoshizumi Miyoshi[6], Atsushi Kumamoto[3], Ayako Matsuoka[4], Shoichiro Yokota[8], Tomoaki Hori[6], Kunihiro Keika[7] (1.Space Radio Engineering Laboratory, Division of Electrical Engineering, Kyoto University Graduated School, 2.Research Institute for Sustainable Humanosphere, Kyoto University, 3.Graduate School of Science and Faculty of Science, Tohoku University, 4.Institute of Space and Astronautical Science, JAXA, 5.Information Media Center, Kanazawa University, 6.Institute for Space-Earth Environmental Research, Nagoya University, 7.School of Science, The University of Tokyo, 8.School of Science, Osaka University)

[PEM13-P03] Enhancement of whistler-mode chorus in association with Pc 4-5 ULF waves and related variation of high energy electrons

*Atsuhiro Ono[1], Yuto Katoh[1], Atsushi Kumamoto[1], Fuminori Tsuchiya[1], Mariko Teramoto[2], Yoshiya Kasahara[3], Shoya Matsuda[4], Ayako Matsuoka[4], Takefumi Mitani[4], Tomoaki Hori[2], Satoshi Kasahara[5], Shoichiro Yokota[6], Kunihiro Keika[5], Yoshizumi Miyoshi[2], Iku Shinohara[4] (1.Tohoku University, 2.Nagoya University, 3.Kanazawa University, 4.ISAS/JAXA, 5.The University of Tokyo, 6.Osaka University)

[PEM13-P04] Sudden enhancements of electron cyclotron harmonic waves observed by the Arase satellite

*Shinjo Airi[1], Hirotsugu Kojima[1], Yoshiya Kasahara[2], Yoichi Kazama[3], Hideyuki Usui[4], Yoshizumi Miyoshi[5], Yasumasa Kasaba[6], Shoya Matsuda[7], Tomoaki Hori[5], S. -Y. Wang[8], Sunny W.Y. Tam[9], Atsushi

Kumamoto[10], Ayako Matsuoka[11] (1.Research institute for sustainable humanosphere, Kyoto University, 2.Information Media Center, Kanazawa University, 3.ASIAA, 4.Graduate school of system informatics Kobe University, 5.Institute for Space-Earth Environmental Research, Nagoya University, 6.Planetary Plasma and Atmospheric Research Center, Tohoku University, 7.Institute of Space and Astronautical Science/Japan Aerospace Exploration Agency, 8.ASIAA, Taiwan, 9.ISAPS, NCKU, Taiwan, 10.Department of Geophysics, Graduate School of Science, Tohoku University, 11.Research Division for Space Plasma, Institute of Space and Astronautical Science, Japan Aerospace Exploration Agency)

[PEM13-P05] Correlation between pulsating aurora and electrostatic electron cyclotron harmonic waves obtained from coordinated Arase and ground data

*Mizuki Fukizawa[1], Takeshi Sakanoi[1], Yoshizumi Miyoshi[2], Keisuke Hosokawa[3], Yoichi Kazama[4], Yoshiya Kasahara[5], Shoya Matsuda[6], Ayako Matsuoka[7], Wang Shiang-Yu[4], Sunny Wing-Yee Tam[8], Ryuho Kataoka[9] (1.Planetary Plasma and Atmospheric Research Center, Graduate School of Science, Tohoku University, 2.Institute for Space-Earth Environmental Research, Nagoya University, 3.Department of Communication Engineering and Informatics, University of Electro-Communications, 4.Academia Sinica Institute of Astronomy and Astrophysics, 5.Information Media Center, Kanazawa University, 6.Institute of Space and Astronautical Science/Japan Aerospace Exploration Agency, 7.Research Division for Space Plasma, Institute of Space and Astronautical Science, Japan Aerospace Exploration Agency, 8.Institute of Space and Plasma Sciences, College of Sciences, National Cheng Kung University , 9.National Institute of Polar Research)

[PEM13-P06] Automatic determination of Upper Hybrid Resonance Frequencies by Convolutional Neural Network.

*Shoya Matsuda[1], Tatsuhito Hasegawa[2], Atsushi Kumamoto[3], Fuminori Tsuchiya[3], Yoshiya Kasahara[4], Yoshizumi Miyoshi[5], Yasumasa Kasaba[3], Ayako Matsuoka[1] (1.Institute of Space and Astronautical Science/Japan Aerospace Exploration Agency, 2.University of Fukui, 3.Tohoku University, 4.Kanazawa University, 5.ISEE, Nagoya University)

[PEM13-P07] Amplitude dependence of whistler wave motion on electron scattering process

*Yoshiki Ito[1], Yoshizumi Miyoshi[1], Shinji Saito[1] (1.Nagoya University, ISEE)

[PEM13-P08] Two-dimensional simulation of whistler mode wave packets interacting with energetic electrons

*Takeshi Nogi[1], Yoshiharu Omura[1] (1.Reserch Institute for Sustainable Humanosphere, Kyoto University)

[PEM13-P09] Relativistic electron acceleration by whistler-mode chorus waves in 1D, 2D, and 3D magnetic field models.

*Keita Takahashi[1], Yoshiharu Omura[1], Yikai HSIEH[1], Danny Summers[2] (1.Research Institute for Sustainable Humanosphere, Kyoto University , 2.Department of Mathematics and Statistics, Memorial University of Newfoundland)

[PEM13-P10] Study of global spatio-temporal development of magnetospheric ELF/VLF waves for the 26-30 March 2017 storm based on ground and satellite observations and the RAM simulations

*Yuhei Takeshita[1], Kazuo Shiokawa[1], Yoshizumi Miyoshi[1], Mitsunori Ozaki[2], Yoshiya Kasahara[2], Martine Connors[3], Jyrki Manninen[4], Craig Kletzing[5], Vania Jordanova[6] (1.Nagoya University, Institute for Space-Earth Environmental Resarch, 2.Kanazawa University, 3.Athabasca University, 4.Sodankylä Geophysical Observatory, 5.The University of Iowa, 6.Los Alamos National Laboratory)

[PEM13-P11] Flux decrease of outer radiation belt electrons associated with solar wind pressure pulse: A Code coupling simulation of GEMSIS-RB and GEMSIS-GM

*Ito Hiroki[1], Yoshizumi Miyoshi[1], Shinji Saito[2], Yosuke Matsumoto[3], Takanobu Amano[4] (1.Institute for Space-Earth Environmental Research, Nagoya University, 2. Graduate School of Science, Nagoya

University, 3. Graduate School of Science, Chiba University, 4.Department of Earth and Planetary Science, University of Tokyo)

[PEM13-P12] Non-diffusive response of outer belt electrons on interplanetary shock

Takuma Toishi[1], *Yusuke Ebihara[1], Takashi Tanaka[2] (1.Research Institute for Sustainable Humanosphere, Kyoto University, 2.Kyushu University)

[PEM13-P13] PARM: Initial result of the auroral camera on the G-CHASER (RockSat-XN) rocket and status of the development of auroral cameras for the LAMP rocket experiment

*Naoshi Yagi[1], Takeshi Sakanoi[1], Fukizawa Mizuki[1], Kazushi Asamura[2], Yoshizumi Miyoshi[3], Keisuke Hosokawa[4], Genki Ishizawa[5] (1.Planetary Plasma and Atmospheric Research Center, Graduate School of Science, Tohoku University, 2.Institute of Space and Astronautical Science, Japan Aerospace Exploration Agency, 3.Institute for Space-Earth Environmental Research, Nagoya University, 4.Department of Communication Engineering and Informatics, University of Electro-Communications, 5.Space & terrestrial plasma pyhsics)

[PEM13-P14] First simultaneous observation of a SAR arc at subauroral latitudes using a ground all-sky camera and the Arase satellite in the inner magnetosphere

*Yudai Inaba[1], Kazuo Shiokawa[1], Shin-ichiro Oyama[1,8,9], Yuichi Otsuka[1], Atsuki Shinbori[1], Yoichi Kazama[2], Shiang-Yu Wang[2], Sunny W. Y. Tam[2], Shoichiro Yokota[3], Satoshi Kasahara[4], Kunihiro Keika[4], Tomoaki Hori[1], Ayako Matsuoka[5], Yoshiya Kasahara[6], Atsushi Kumamoto[7], Yasumasa Kasaba[7], Yoshizumi Miyoshi[1], Iku Shinohara[5], Arto Oksanen[10] (1.Institute for Space-Earth Environmental Research, 2.Academia Sinica, 3.Osaka Univ, 4.Tokyo Univ, 5.JAXA, 6.Kanazawa University, 7.Tohoku University, 8.University of Oulu, Finland, 9.National Institute of Polar Research, 10.Jyväskylän Sirius ry, Finland)

[PEM13-P15] Pi2 pulsations observed by the Arase satellite inside and outside the plasmapause

*Mariko Teramoto[1], Ayako Matsuoka[2], Reiko Nomura[5], Yoshiya Kasahara[3], Yasumasa Kasaba[4], Atsushi Kumamoto[4], Fuminori Tsuchiya[4], Shoya Matsuda[2], Masahito Nose[1], Masafumi Shoji[1], Yasunori Tsugawa[1], Shun Imajo[1], Yoshizumi Miyoshi[1], Iku Shinohara[2] (1.Institute for Space-Earth Environmental Research Nagoya University, 2.Institute of Space and Astronautical Science, Japan Aerospace eXploration Agency, 3.Kanazawa University, 4.Tohoku University, 5.National Astronomical Observatory of Japan)

[PEM13-P16] An extreme erosion of the plasmasphere during the 7–10 September 2017 storm

*Yuki Obana[1], Naomi Maruyama[2,3], Atsuki Shinbori[4], Kumiko K. Hashimoto[5], Mariangel Fedrizzi[2,3], Masahito Nose[4], Yuichi Otsuka[4], Nozomu Nishitani[4], Tomoaki Hori[4], Atsushi Kumamoto[6], Fuminori Tsuchiya[6], Shoya Matsuda[7], Ayako Matsuoka[7], Yoshiya Kasahara[8], Akimasa Yoshikawa[9], Yoshizumi Miyoshi[4], Iku Shinohara[7] (1.Osaka Electro-Communication University, 2.University of Colorado Boulder, 3.NOAA Space Weather Prediction Center, 4.Nagoya University, 5.Kibi International University, 6.Tohoku University, 7.Japan Aerospace Exploration Agency, 8.Kanazawa University, 9.Kyushu University)

[PEM13-P17] Relative contribution of ULF and chorus waves to the radiation belt variation: Comparison between multi-point observations and BATSRUS + CRCM simulation

*Naoko Takahashi[1], Kanako Seki[1], Mei-Ching Fok[2], Yihua Zheng[2], Yoshizumi Miyoshi[3], David Hartley[4], Ayako Matsuoka[5], Yoshiya Kasahara[6], Yasumasa Kasaba[7], Nana Higashio[8] (1.Graduate School of Science, University of Tokyo, 2.NASA Goddard Space Flight Center, 3.Institute for Space-Earth Environmental Research, Nagoya University, 4.Department of Physics and Astronomy, University of Iowa, 5.Institute of Space and Astronautical Science, Japan Aerospace Exploration Agency, 6.Information Media Center, Kanazawa University, 7.Planetary Plasma and Atmospheric Research Center, Tohoku University, 8.Japan Aerospace Exploration Agency)

[PEM13-P18] Modulation of the D-region ionosphere by Pc5 waves observed by VLF/LF standard radio waves

*Miyashita Takuya[1], Hiroyo Ohya[1], Fuminori Tsuchiya[2], Hiroyuki Nakata[1], Toshiaki Takano[1], Kazuo Shiokawa[3], Yoshizumi Miyoshi[3] (1.Chiba University, 2.Tohoku University, 3.Nagoya University)

[PEM13-P19] Oxygen-proton differences in ion energies dominating plasma pressure: Dependence on storm phases and solar wind drivers

*Kunihiro Keika[1], Satoshi Kasahara[1], Shoichiro Yokota[2], Masahiro Hoshino[1], Kanako Seki[1], Masahito Nose[3], Yoshizumi Miyoshi[3], Iku Shinohara[4] (1.Graduate School of Science, The University of Tokyo , 2.Graduate School of Science, Osaka University, 3.Institute for Space-Earth Environmental Research, Nagoya University, 4.Institute of Space and Astronautical Science, Japan Aerospace Exploration Agency)

[PEM13-P20] Mass dependence of penetration depth of multi-energy ions in the inner magnetosphere during magnetic storms: Arase observations

*Ryosuke Fujii[1], Yoshizumi Miyoshi[1], Masafumi Shoji[1], Kazushi Asamura[2], Lynn Kistler[1,8], Vania Jordanova[9], Tomoaki Hori[1], Satoshi Kurita[1], Mariko Teramoto[1], Yasunori Tsugawa[1], Yoshiya Kasahara[3], Yasumasa Kasaba[4], Atsushi Kumamoto[5], Fuminori Tsuchiya[4], Shoichiro Yokota[6], Kunihiro Keika[7], Ayako Matsuoka[2], Iku Shinohara[2] (1.Institute for Space-Earth Environmental Research, Nagoya University, 2.Institute of Space and Astronautical Science, Japan Aerospace Exploration Agency, 3.Information Media Center, Kanazawa University, 4.Planetary Plasma and Atmospheric Research Center, Tohoku University, 5.Department of Geophysics, Graduate School of Science, Tohoku University, 6.Graduate School of Science, Osaka University, 7.Department of Earth and Planetary Science, Graduate School of Science, The University of Tokyo, 8.University of New Hampshire, 9.Los Alamos National Laboratory)

[PEM13-P21] Relativistic Acceleration of Energetic Protons by Electromagnetic Ion Cyclotron Waves in the Jovian Magnetosphere

*Tomohiro Sekine[1], Yoshiharu Omura[1], Danny Summers[2], Yikai HSIEH[1], Satoko Nakamura[1] (1.Reserach Institute for Sustainable Humanosphere, Kyoto University, 2.Memorial University of Newfoundland)

[PEM13-P22] Statistical study of IPDP type EMIC wave-related electron precipitation at subauroral latitude

*Asuka Hirai[1], Fuminori Tsuchiya[1], Takahiro Obara[1], Yasumasa Kasaba[1], Yuto Katoh[2], Hiroaki Misawa[1], Kazuo Shiokawa[3], Yoshizumi Miyoshi[3], Satoshi Kurita[3], Martin G Connors[4] (1.Planetary Plasma and Atmospheric Research Center, Graduate School of Science, Tohoku Univ. , 2.Department of Geophysics, Graduate School of Science, Tohoku University, 3.Institute for Space-Earth Environmental Research, Nagoya University, 4.Athabasca University)

[PEM13-P23] Meridional distributions of proton plasma and pressure-driven currents in the nightside inner magnetosphere: Arase observations

*Shun Imajo[1], Masahito Nose[1], Satoshi Kasahara[2], Shoichiro Yokota[3], Ayako Matsuoka[4], Kunihiro Keika[2], Tomoaki Hori[1], Mariko Teramoto[1], Kazuhiro Yamamoto[5], Oimatsu Satoshi[5], Reiko Nomura[6], Akiko Fujimoto[7], Iku Shinohara[4], Yoshizumi Miyoshi[1] (1.Institute for Space-Earth Environmental Research, Nagoya University, 2.Graduate School of Science, The University of Tokyo, 3.Graduate School of Science, Osaka University, 4.Institute of Space and Astronautical Science, Japan Aerospace Exploration Agency, 5.Graduate School of Science, Kyoto University, 6.National Astronomical Observatory of Japan, 7.Kyushu Institute of Technology)

[PEM13-P24] Space Weather Effects on Energetic Proton Flux Response in South Atlantic Anomaly

*Kirolosse Mina GIRGIS[1,2], Tohru Hada[1], Shuichi Matsukiyo[1] (1.Earth System Science and Technology (ESST) Department, Interdisciplinary Graduate School of Engineering Sciences (IGSES), Kyushu University, Japan, 2.Aerospace Engineering Department, Faculty of Engineering, Cairo University, Egypt)

[PEM13-P25] Solar-cycle variations of >30 keV electron flux enhancements under the inner radiation belt

*ALLA SUVOROVA[1] (1.National Central University)

[PEM13-P26] Energy spectra variations of high energy electrons in the inner magnetosphere observed by HEP/XEP on ARASE and SEDA-e on HIMAWARI

*Takeshi Takashima[1], Takefumi Mitani[1], Nana Higashio[2], Tsutomu Nagatsuma[3] (1. ISAS/JAXA, 2.Research and Development Directorate/JAXA, 3.NiCT)

[PEM13-P27] Inter-channel calibration of the high-energy electron experiments (HEP) instrument onboard the Arase satellite

*Tomoaki Hori[1], Takefumi Mitani[2], Takeshi Takashima[2], Park Inchun[1], Satoshi Kurita[1], Mariko Teramoto[1], Nana Higashio[3], Satoshi Kasahara[4], Shoichiro Yokota[5], Yoshizumi Miyoshi[1], Iku Shinohara[2] (1.Institute for Space-Earth Environmental Research, Nagoya University, 2.Japan Aerospace Exploration Agency, Institute of Space and Astronautical Science, 3.Japan Aerospace Exploration Agency, 4.Graduate School of Science, The University of Tokyo, 5.Graduate School of Science, Osaka University)

[PEM13-P28] Particle simulation for calibrating the HEP data onboard the ARASE satellite

*PARK INCHUN[1], Yoshizumi Miyoshi[1], Takefumi Mitani[2], Tomoaki Hori[1], Satoshi Kurita[1], Mariko Teramoto[1], Takeshi Takashima[2], Nana Higashio[3], Iku Shinohara[2] (1.Nagoya University Institute for Space-Earth Environmental Research, 2.Japan Aerospace Exploration Agency Institute of Space and Astronautical Science , 3.Japan Aerospace Exploration Agency)

[PEM13-P29] Geant4 model calculation and energetic particle observation with HEP/Arase in the inner radiation belt

*Honoka Toda[1], Wataru Miyake[1], Takefumi Mitani[3], Takeshi Takashima[3], Yoshizumi Miyoshi[2], PARK INCHUN[2], Tomoaki Hori[2] (1.Tokai University, 2.ISEE/Nagoya University, 3.ISAS/JAXA)

[PEM13-P30] Validation of High-energy electron detector simulator for the HEP instruments onboard Arase

*Takefumi Mitani[1], PARK INCHUN[2], Tomoaki Hori[2], Taku Namekawa[1,3], Kazushi Asamura[1], Takeshi Takashima[1], Satoshi Kasahara[3], Satoshi Kurita[2], Mariko Teramoto[2], Nana Higashio[1], Yoshizumi Miyoshi[2], Iku Shinohara[1] (1.Japan Aerospace Exploration Agency, Institute of Space and Astronautical Science, 2.Institute for Space-Earth Environmental Research, Nagoya Univ., 3.The university of Tokyo)

Evaluation of wave normal and Poynting vector analyses for whistler mode waves observed by the waveform capture (WFC) on board the Arase

*Yoshiya Kasahara[1], Satoshi Ikarashi[1], Hiroyuki Nishizawa[1], Shoya Matsuda[2], Fuminori Tsuchiya[3], Atsushi Kumamoto[3], Yasumasa Kasaba[3], Mitsunori Ozaki[1], Ayako Matsuoka[2]

1. Kanazawa University, 2. ISAS/JAXA, 3. Tohoku University

The Plasma Wave Experiment (PWE) is one of scientific instruments on board the Arase (ERG) satellite to measure electric field from DC to 10 MHz and magnetic field from a few Hz to 100 kHz in the inner magnetosphere. It is well known that chorus wave, one of typical plasma waves in VLF range observed in the inner magnetosphere, is a plausible candidate that accelerates relativistic electrons in the radiation belt. Besides the chorus, the Arase has observed various kinds of plasma waves such as lightning whistlers and hiss waves. It is very important to study the propagation characteristics of these waves.

In the present paper, we developed a direction finding system applicable to whistler mode waves using the data from waveform capture (WFC), which is one of receivers covering the frequency range below 20kHz implemented in the PWE. The absolute directions of the wave normal and Poynting vectors were derived in the coordinate system referring the ambient magnetic field and geomagnetic meridian plane. We also estimated the Poynting vector theoretically using the derived wave normal vector, electron density and ambient magnetic field intensity to confirm the validity of the results from the observation data.

We demonstrated that the results were generally reliable, but further calibration is necessary for electric field to improve the accuracy of Poynting vector because the waveform of electric field is now calibrated under the assumptions of theoretical antenna capacitance in a vacuum and typical plasma impedance. In other words, we expect to be able to correct the calibration table for electric field measurements from the direction finding results.

In the presentation, we introduce some typical results which have been derived from the observation data of upper- and lower-band chorus, and lightning whistlers.

Keywords: Whistler mode wave, Waveform Capture, Direction finding, Plasma wave

©2019. Japan Geoscience Union. All Right Reserved.

Calibration of electric fields dedicated to the measurement of the S-WPIA of the Arase Satellite

*Miki Jumpei[1], Hirotsugu Kojima[2], Yuto Katoh[3], Shoya Matsuda[4], Yoshiya Kasahara[5], Mitsuru Hikishima[4], Satoshi Kurita[6], Masahiro Kitahara[3], Satoshi Kasahara[7], Yoshizumi Miyoshi[6], Atsushi Kumamoto[3], Ayako Matsuoka[4], Shoichiro Yokota[8], Tomoaki Hori[6], Kunihiro Keika[7]

1. Space Radio Engineering Laboratory, Division of Electrical Engineering, Kyoto University Graduated School, 2. Research Institute for Sustainable Humanosphere, Kyoto University, 3. Graduate School of Science and Faculty of Science, Tohoku University, 4. Institute of Space and Astronautical Science, JAXA, 5. Information Media Center, Kanazawa University, 6. Institute for Space-Earth Environmental Research, Nagoya University, 7. School of Science, The University of Tokyo, 8. School of Science, Osaka University

The outer radiation belt consists of high-energy electrons. They are strongly affected by geomagnetic activities in the relation to solar wind conditions. The important science target of the Arase mission is to clarify generation/loss mechanisms of relativistic electrons in the outer radiation belt. Wave-particle interactions are thought to be a plausible mechanism for generation/loss processes of relativistic electrons. S-WPIA (Software-type Wave-Particle Interaction Analyzer) is installed in the Arase satellite. The WPIA is a newly developed observation system that enables us to quantitatively understand the interaction between plasma waves and electrons. The WPIA has the capability to identify a relative phase angle of a plasma wave vector and a velocity vector of each detected particle. Since phase information of observed plasma waves is essential to the WPIA, precise calibrations of plasma wave data are important. While the calibration data for the magnetic field sensors are identical to those we obtained during the ground tests of the instruments, the calibration data for electric field sensors strongly depend on plasma parameters around the satellite. Furthermore, there are still unclear parameters at the inputs of preamplifiers relating to the connection with electric field sensors. The calibration for electric field data needs to be performed carefully consulting observation data after the launch.

The present paper focuses on the calibration of plasma wave data for the S-WPIA’s data processing. We picked up events including whistler-mode chorus emissions and lightning-whistler waves. They all are electromagnetic waves, so-called whistler mode waves. The amplitude ratios of their electric field and magnetic field components can be theoretically calculated referring to the Appleton-Hartlee equations. Poynting vectors of whistler mode waves can be also theoretically obtained. We compared the observation results of the picked up events with the theoretical ones. The results show the precise calibration for the magnetic field data have been made. On the other hand, the calibration for the electric field data should be further modified consulting plasma parameters and other uncertain parameters at the input of preamplifiers. In the present paper, we will discuss the improvement of the calibration for electric field data by correcting the calibration table to aim the precise S-WPIA data processing.

©2019. Japan Geoscience Union. All Right Reserved.

Enhancement of whistler-mode chorus in association with Pc 4-5 ULF waves and related variation of high energy electrons

*Atsuhiro Ono[1], Yuto Katoh[1], Atsushi Kumamoto[1], Fuminori Tsuchiya[1], Mariko Teramoto[2], Yoshiya Kasahara[3], Shoya Matsuda[4], Ayako Matsuoka[4], Takefumi Mitani[4], Tomoaki Hori[2], Satoshi Kasahara[5], Shoichiro Yokota[6], Kunihiro Keika[5], Yoshizumi Miyoshi[2], Iku Shinohara[4]

1. Tohoku University, 2. Nagoya University, 3. Kanazawa University, 4. ISAS/JAXA, 5. The University of Tokyo, 6. Osaka University

Whistler-mode chorus emissions play significant roles in the acceleration and loss of energetic electrons in the magnetosphere. One of the important factors which control periodic enhancement of chorus emissions is ULF (Ultra Low Frequency) waves. Previous studies reported that the compressional component of Pc4-5 ULF waves modulates the intensity of chorus waves [Li et al., 2011] and that the toroidal and poloidal components of Pc4-5 ULF waves as well [Jaynes et al., 2015]. Previous studies also suggested that enhancement of the temperature anisotropy of energetic electrons in the wave generation region should be required for the chorus generation. In order to understand the reported correspondence, in addition to the wave observation, we should examine simultaneously observed variations of the flux and the pitch angle distribution of energetic electrons.

In the present study, we investigate the relationship between chorus emissions and ULF waves using particle and electromagnetic field observations made by the Arase satellite. First, we analyze data observed by the Onboard Frequency Analyzer (OFA) of the Plasma Wave Experiment (PWE) and the Magnetic Field Experiment (MGF) during the campaign observation period of the Arase satellite with ground stations from March to April in 2017. As a result, we identified the simultaneous enhancement of chorus emissions and Pc4-5 ULF waves, which was dominated by the toroidal component, from 2130 to 2200 UT on March 27, 2017. The Arase satellite was located at the magnetic local time about 04:00, the magnetic latitude about -10 degrees, and the L-value about 6 during the event. We find that there is one-to-one correspondence between chorus emissions and the toroidal component of ULF waves; chorus emissions enhanced at the timings when the toroidal magnetic field component of ULF waves had a peak in the westward direction. The identified phase relationship is different from that reported by Jaynes et al. (2015), which isn't one-to-one correspondence. Next, we evaluate the resonance energy of the observed chorus emissions, using the ratio of the plasma frequency to the electron cyclotron frequency (f_p/f_{ce}) based on the upper-hybrid resonance frequency derived from the spectra observed by the High Frequency Analyzer (HFA) of PWE and the ambient magnetic field intensity observed by MGF. We find that f_p/f_{ce} is 3.3-3.4 during the event and that the resonance energy for whistler-mode waves in the frequency range of 0.1-0.2 f_{ce} is estimated to be about 100-400keV, which is larger than typical energies of resonating electrons observed in the inner magnetosphere. The estimated large resonant energy can be explained by the frequency range of the observed chorus emissions, approximately 0.1 - 0.2 f_{ce}, is relatively lower than that observed in typical cases.
We also analyze variations of the flux and the pitch angle distribution of energetic electrons during the event using data observed by the High-energy electron experiments (HEP) instrument onboard Arase. The result shows that both the flux and the pitch angle distribution of electrons in the kinetic energy range from 100 to 400 keV, which corresponds to the estimated resonance energy, did not fluctuate with the intensity variation of the chorus emissions and the ULF waves. In addition, we analyze the data observed by the Medium-energy particle experiments - electron analyzer (MEP-e) for energetic electrons in the energy range of 10-80 keV, lower than the estimated resonance energy. Then we identify the

©2019. Japan Geoscience Union. All Right Reserved.

corresponding variation of both the flux and the pitch angle distribution in the 40-60 keV energy range. One of the possible reasons why no significant variations were observed in the hundred keV range would be that the Arase satellite was located in the off-equatorial region during the event, and that the satellite was away from the wave generation region.

Keywords: ULF waves, chorus emissions

©2019. Japan Geoscience Union. All Right Reserved.

Sudden enhancements of electron cyclotron harmonic waves observed by the Arase satellite

*Shinjo Airi[1], Hirotsugu Kojima[1], Yoshiya Kasahara[2], Yoichi Kazama[3], Hideyuki Usui[4], Yoshizumi Miyoshi[5], Yasumasa Kasaba[6], Shoya Matsuda[7], Tomoaki Hori[5], S. -Y. Wang[8], Sunny W.Y. Tam[9], Atsushi Kumamoto[10], Ayako Matsuoka[11]

1. Research institute for sustainable humanosphere, Kyoto University, 2. Information Media Center, Kanazawa University, 3. ASIAA, 4. Graduate school of system informatics Kobe University, 5. Institute for Space-Earth Environmental Research, Nagoya University, 6. Planetary Plasma and Atmospheric Research Center, Tohoku University, 7. Institute of Space and Astronautical Science/Japan Aerospace Exploration Agency, 8. ASIAA, Taiwan, 9. ISAPS, NCKU, Taiwan, 10. Department of Geophysics, Graduate School of Science, Tohoku University, 11. Research Division for Space Plasma, Institute of Space and Astronautical Science, Japan Aerospace Exploration Agency

Electron cyclotron harmonic (ECH) waves are commonly observed in the low latitude region just outside the terrestrial plasmapause. They are purely electrostatic and their frequency spectra show harmonic structures. The harmonic structures are believed to depend on the temperature and density ratio between cold and hot background electrons. The Plasma Wave Experiment (PWE) onboard the Arase satellite has observed ECH waves since the start of its operation. The observed ECH waves are classified into two types. They are the diffuse ECH waves and the enhanced ECH waves. The diffuse ECH waves are weak and they appear as continuous emissions that last for more than a few minutes. The enhanced ECH waves are the sudden enhancements of the diffuse ECH in shorter periods. The present paper focuses on the enhanced ECH waves observed by the Arase satellite.

Kazama et al. (2018) introduced the event that the repeated enhancement of ECH waves is associated with density depletions near the plasmapause. They succeeded in revealing the good correlation of the enhancement of the ECH waves and the sudden decrease of the cold electrons with energies lower than the lowest energy limit of the particle detector. The observed electron features are clear in the relation to the enhancement of ECH waves, but the mechanism of the enhancement is still unclear. We searched for such events of the enhanced ECH waves and examined the correlation of wave intensities, spacecraft potentials and electron velocity distributions observed by the Arase satellite. Some of the events show the features similar to those of Kazama et al. (2018), but there are also many other events with no correlation between the enhancements of the ECH waves and the density depletions. In the present paper, we examine velocity distribution functions of electrons observed by the low-energy particle experiments-electron analyzer (LEPe) onboard Arase. Velocity distribution functions allow us to examine temperature anisotropies of electrons and calculate linear dispersion relations for the ECH waves. Once we get electron temperatures, resonance velocities are calculated. On the other hand, since the wavelength of the ECH waves is very short, the relation of the wavelength and the length of the Arase electric field sensors is also important in evaluating the time variations of the ECH wave intensity. We study the enhanced ECH waves in various viewpoints using wave and electron data observed by the Arase satellite and discuss the generation mechanism in the present paper.

©2019. Japan Geoscience Union. All Right Reserved.

Correlation between pulsating aurora and electrostatic electron cyclotron harmonic waves obtained from coordinated Arase and ground data

*Mizuki Fukizawa[1], Takeshi Sakanoi[1], Yoshizumi Miyoshi[2], Keisuke Hosokawa[3], Yoichi Kazama[4], Yoshiya Kasahara[5], Shoya Matsuda[6], Ayako Matsuoka[7], Wang Shiang-Yu[4], Sunny Wing-Yee Tam[8], Ryuho Kataoka[9]

1. Planetary Plasma and Atmospheric Research Center, Graduate School of Science, Tohoku University, 2. Institute for Space-Earth Environmental Research, Nagoya University, 3. Department of Communication Engineering and Informatics, University of Electro-Communications, 4. Academia Sinica Institute of Astronomy and Astrophysics, 5. Information Media Center, Kanazawa University, 6. Institute of Space and Astronautical Science/Japan Aerospace Exploration Agency, 7. Research Division for Space Plasma, Institute of Space and Astronautical Science, Japan Aerospace Exploration Agency, 8. Institute of Space and Plasma Sciences, College of Sciences, National Cheng Kung University , 9. National Institute of Polar Research

Pulsating auroras (PsAs) are thought to be generated by precipitating electrons scattered by lower-band chorus (LBC) waves near the magnetic equator through cyclotron resonance. Previous studies showed one-to-one correlation between LBC wave intensity observed by satellites near the magnetic equator and PsA intensity obtained by ground-based all-sky imager [e.g., Nishimura et al., Science, 2010, Nishimura et al., JGR, 2011]. In addition, electrostatic electron cyclotron harmonic (ECH) waves can also interact with magnetospheric electrons and scatter their pitch angle theoretically [e.g., Lyons, JGR, 1974]. However, characteristics of aurora caused by ECH are not understood. In our study, we report for the first time in the world that not only LBC but also ECH wave intensity has correlation with the PsA intensity using coordinated Arase and ground-based imager observations. The first campaign observations between the Arase satellite and ground-based optical imager were conducted in March 2017. A typical substorm occurred on 27 March 2017 and the ionospheric footprint of Arase traversed the field of view of all-sky imager at Sodankylä during 00:00–03:15 UT on 29 March 2017. Quasi-periodic LBC and ECH waves were observed by Arase near the magnetic equator and PsA was detected by the all-sky imager during 01:30–02:00 UT. We calculated the cross-correlation coefficients between auroral intensity and LBC or ECH wave intensity from 01:30 UT to 02:00 UT with a time window of every 2 minutes. The highest cross-correlation coefficient between auroral intensity and LBC wave intensity was 0.73 and that between auroral intensity and ECH wave intensity was 0.62 from 01:46 UT to 01:48 UT, and they were statistically significant. The period of auroral intensity which correlated with LBC intensity was shorter than 10 s and that correlated with ECH intensity was 10–20 s. We estimated the precipitating electron energy assuming that the time lag when the cross-correlation coefficient became the highest equals to the travel time of electrons from the modulated source region to the auroral emission height. We shifted the variation of auroral intensity against that of ECH or LBC wave intensity with a time step of 0.01 s using 100 Hz sampling image data taken by the all-sky imager. The estimated energy of precipitating electron interacted with LBC waves was ~20–67 keV and that interacted with ECH waves was ~3–4 keV. On the other hand, we independently estimated the cyclotron resonance energy of LBC and ECH waves from the Arase's observation data and geomagnetic field model by TS04 Model [Tsyganenko and Sitnov, JGR, 2005]. The estimated cyclotron resonance energy of LBC waves was ~30 keV. Although the cyclotron resonance energy of ECH waves could not be estimated because it was difficult to obtain the electron temperature and wave normal angle of ECH waves from Arase data, we suggest the cyclotron resonance energy of ECH waves to be a few keV with probable assumptions. From these results, we suggest that LBC waves interact with high energy electrons which cause auroral emission at lower altitudes, while ECH waves interact with

©2019. Japan Geoscience Union. All Right Reserved.

relatively low energy electrons which cause auroral emission at higher altitudes. These results were published in Fukizawa et al. [GRL, 2018].
To verify whether ECH waves indeed scatter the pitch angle of electrons, we compared ECH wave intensity with electron flux in the loss cone obtained with low-energy particle experiments-electron analyzer onboard Arase. We also give results of other coordinated observation events.

Keywords: pulsating aurora, ECH waves, wave-particle interaction

©2019. Japan Geoscience Union. All Right Reserved.

Automatic determination of Upper Hybrid Resonance Frequencies by Convolutional Neural Network.

*Shoya Matsuda[1], Tatsuhito Hasegawa[2], Atsushi Kumamoto[3], Fuminori Tsuchiya[3], Yoshiya Kasahara[4], Yoshizumi Miyoshi[5], Yasumasa Kasaba[3], Ayako Matsuoka[1]

1. Institute of Space and Astronautical Science/Japan Aerospace Exploration Agency, 2. University of Fukui, 3. Tohoku University, 4. Kanazawa University, 5. ISEE, Nagoya University

Electron number density is a key parameter for discussions of plasma wave generation/propagation, and wave-particle interaction in the inner magnetosphere. The High Frequency Analyzer (HFA) is a subsystem of Plasma Wave Experiment (PWE) aboard Arase [Kasahara et al. (2018), Kumamoto et al. (2018), Miyoshi et al. (2018)]. The HFA measures electric field spectra in a frequency range from 10 kHz to 10 MHz, which covers a typical frequency range of Upper Hybrid Resonance (UHR) frequency in the inner magnetosphere. Kumamoto et al. (2018) proposed the semiautomatic method for the identification of UHR frequency by computer and a human operator. However, it takes a enormous effort of a human operator.

We propose an automatic determination system of UHR frequency by machine learning. Machine learning is a technique in the field of artificial intelligence to give computers the ability to learn with data. In this study, we defined a task of UHR frequency determination as supervised regression that a computer estimates UHR frequencies using the dataset composed of electric field dynamic spectra with correct UHR frequency labels. We adopted Convolutional Neural Network (CNN) as a machine learning algorithm. In this study, we introduce our machine learning approach and initial results for determining UHR frequency from electric field spectra observed by PWE/HFA.

Keywords: Arase satellite, UHR frequency, Machine learning

©2019. Japan Geoscience Union. All Right Reserved.

Amplitude dependence of whistler wave motion on electron scattering process

*Yoshiki Ito[1], Yoshizumi Miyoshi[1], Shinji Saito[1]

1. Nagoya University, ISEE

Whistler mode chorus waves cause scattering and acceleration of energetic electrons in the inner magnetosphere. The interaction processes have been modeled as diffusive process. The pitch angle diffusion coefficients of the pitch angle scattering depend on the power of chorus waves, so that it is expected that the scattering rate also depends on the wave amplitude. On the other hand, several previous studies indicated that the Lorentz force by the wave magnetic field is larger than the mirror force if the wave amplitudes increase and the electron trajectories in the velocity space are different from the diffusive distributions. In this study, we investigate chorus wave amplitude dependence of electron scattering using the GEMSIS-RBW simulation code. The RBW simulation demonstrates generation of periodical rising-tone chorus waves propagating along a magnetic field line to higher latitudes, and calculates local pitch angle and energy change by the imposed waves on the field line. At small wave amplitudes, time variations of pitch angle and energy of electrons are similar to diffusive process. At large wave amplitudes, some electrons increase both pitch angle and energy at interaction with the first rising tone, and then they decrease these parameters at interaction with the second rising tone. The process in the first rising tone seems to be the phase trapping, while the process in the second rising tone seems to be dislocation. Therefore, nonlinear scattering processes, which are phase trapping and dislocations, occur during the interactions with periodical rising-tone chorus waves with large amplitudes, which are quite different from quasi-linear scattering process.

©2019. Japan Geoscience Union. All Right Reserved.

Two-dimensional simulation of whistler mode wave packets interacting with energetic electrons

*Takeshi Nogi[1], Yoshiharu Omura[1]

1. Reserch Institute for Sustainable Humanosphere, Kyoto University

We perform two-dimensional electromagnetic particle simulations to study basic characteristics of whistler-mode wave particle interaction involved in the generation and propagation processes of chorus emissions with wave normal angles oblique to the static magnetic field. We assume a simple periodic (x, y) system with the magnetic field taken in the x-direction. We find the linear phase of the instability is much affected by electrostatic thermal fluctuations. It is necessary to put many super-particles in a grid cell to suppress the thermal fluctuation. We next put an array of antennas perpendicular to the background magnetic field, and oscillate the antenna current to generate obliquely propagating waves. In addition to the nonlinear trapping of energetic electrons through the cyclotron resonance, another nonlinear trapping of electrons takes place through the Landau resonance. Structures of the nonlinear trapping potentials change with the varying frequency, affecting efficiency of energy transfer between the wave and energetic electrons. We study nonlinear evolution of the wave packet, and competing processes of both resonances in accelerating energetic electrons to higher energies.

©2019. Japan Geoscience Union. All Right Reserved.

Relativistic electron acceleration by whistler-mode chorus waves in 1D, 2D, and 3D magnetic field models.

*Keita Takahashi[1], Yoshiharu Omura[1], Yikai HSIEH[1], Danny Summers[2]

1. Research Institute for Sustainable Humanosphere, Kyoto University , 2. Department of Mathematics and Statistics, Memorial University of Newfoundland

We evaluate the acceleration efficiencies of relativistic electrons under a 1D, 2D, and 3D model magnetic fields. We perform test-particle simulations and analyze nonlinear trapping motions of resonant electrons in each model. As a chorus wave model, we assume that a chorus wave packet generated at the magnetic equator propagates along the magnetic field to higher latitudes. When we perform simulations with the whistler mode wave, the cyclotron resonance with energetic electrons occurs at the similar timing in each model. Although we find relativistic turning acceleration (RTA) [1] to take place in each model, acceleration efficiencies of resonant electrons are different in these models. In terms of the numerical Green's function[2], we find a clear difference in time evolution of the distribution function in energy and equatorial pitch angle. The energy gap between resonant electrons and non-resonant electrons in the 1D model is slightly different from those in the 2D and 3D models. The energy gap in the 3D model is the largest among the three magnetic field models. This difference is due to additional oscillations in the velocity phase space, which only occur in the 2D and 3D models. These oscillations occur because the magnitude of the magnetic field changes during one period of relativistic cyclotron motion, affecting the nonlinear trapping conditions of resonant electrons.

References:

[1] Y. Omura, N. Furuya, D. Summers, Relativistic turning acceleration of resonant electrons by coherent whistler-mode waves in a dipole magnetic field, Journal Geophysical Research, Vol. 112, A06236, doi:10.1029/2006JA012243, 2007.

[2] Y. Omura, Y. Miyashita, M. Yoshikawa, D. Summers, M. Hikishima, Y. Ebihara, and Y. Kubota (2015), Formation process of relativistic electron flux through interaction with chorus emissions in the Earth's inner magnetosphere, J. Geophys. Res. Space Physics, 120, 9545–9562, doi:10.1002/2015JA021563, 2015.

©2019. Japan Geoscience Union. All Right Reserved.

Study of global spatio-temporal development of magnetospheric ELF/VLF waves for the 26-30 March 2017 storm based on ground and satellite observations and the RAM simulations

*Yuhei Takeshita[1], Kazuo Shiokawa[1], Yoshizumi Miyoshi[1], Mitsunori Ozaki[2], Yoshiya Kasahara[2], Martine Connors[3], Jyrki Manninen[4], Craig Kletzing[5], Vania Jordanova[6]

1. Nagoya University, Institute for Space-Earth Environmental Resarch, 2. Kanazawa University, 3. Athabasca University, 4. Sodankylä Geophysical Observatory, 5. The University of Iowa, 6. Los Alamos National Laboratory

The magnetospheric ELF/VLF waves are plasma waves generated by energetic electrons from several keV to tens keV with temperature anisotropy at magnetospheric equatorial plane of the inner magnetosphere. These ELF/VLF waves with frequencies lower than local half gyro frequency (lower-band) can propagate to the ground along magnetic field line. It is also known that the ELF/VLF waves interact with electrons drifting longitudinally in the inner magnetosphere, and help accelerating them to relativistic energies. Takeshita et al. [SGEPSS, 2018] statistically investigated the longitudinal extent of the magnetospheric ELF/VLF waves using six ground-based stations for two months, and showed the average extent of the ELF/VLF waves as ~90 degrees in longitude. However, Jordanova et al. [JGR, 2010] investigated the global distribution of linear growth rate of whistler mode chorus waves using global ring current-atmosphere interactions model (RAM), and showed that the region of large linear growth rate can extend ~180 degrees in longitude during the geomagnetic storm of 22 April 2001.

In this study we investigate the spatio-temporal distibution of the source region of magnetospheric ELF/VLF waves based on ground and satellite observations during the geomagnetic storm period from 26-30 March 2017, and compare it with global distribution of non-linear waves proxy of whistler mode chorus waves obtained by the RAM simulation. In this preliminary simulation, the simple dipole field and the Volland-Stern electric field are used as ambient magnetic and electric fields. And we assumed simply the Maxwell distribution as an energy spectrum using the empirical model of Tsyganenko and Mukai [2003]. In order to evaluate the non-linear wave excitation, we have estimated the optimum amplitude and the threshold value indicated by Omura and Nunn [2011]. We investigated the existence of lower band chorus waves using ground based observations at Athabasca (ATH; 54.7N, 246.4E, MLAT: 61.3N), Kapuskasing (KAP; 49.4N, 277.8E, MLAT: 58.7N), Kannuslehto (KAN: 67.7N, 26.3E, MLAT: 64.5N) and satellite-based observations by ERG with an apogee in the pre-dawn sector and RBSP-A and RBSP-B with an apogees in the post-dusk sector. We found the magnetospheric ELF/VLF waves exist from 3 MLT to 12 MLT for most periods from main- to recovery-phases of the magnetic storm. However, the RAM simulation did not predict wave generation during recovery phase of the storm. We compare the simulation and the ground-satellite observation in detail, and calculate the over-estimate rate (the ratio of wave existence period on the simulation to no wave period on the observation) and under-estimate rate (the ratio of no wave period on the simulation to wave existence period on the observation). We found the over-estimate rate become high (0.2~0.9) and under-estimate rate become low (0~0.4) in the main phase of the storm. This indicates that the longitudinal size of chorus source region predicted by simulation is larger than the observed size at the main phase. We also found that the over-estimate rate becomes low (0~0.2) and under-estimate rate becomes high (~1) during the recovery phase of the storm. This indicates that the simulation does not reproduce the wave existence during the recovery phase of the storm. Looking into the MLT distribution, the simulation predicts the wave existence from dusk to the midnight sector, but the

©2019. Japan Geoscience Union. All Right Reserved.

waves were not observed in this local time sector during the main phase. In case of recovery phase, the simulation did not predict wave existence but the observation showed continuous wave existence from dawn to the noon sector.

Keywords: chorus, ERG satellite, ground based observation

©2019. Japan Geoscience Union. All Right Reserved.

Flux decrease of outer radiation belt electrons associated with solar wind pressure pulse: A Code coupling simulation of GEMSIS-RB and GEMSIS-GM

*Ito Hiroki[1], Yoshizumi Miyoshi[1], Shinji Saito[2], Yosuke Matsumoto[3], Takanobu Amano[4]

1. Institute for Space-Earth Environmental Research, Nagoya University, 2. Graduate School of Science, Nagoya University, 3. Graduate School of Science, Chiba University, 4. Department of Earth and Planetary Science, University of Tokyo

Relativistic electron flux of the outer radiation belt dynamically changes in response to solar wind variations. There exist several conditions to cause the flux drop-out of the outer belt electrons. The magnetopause shadowing (MPS) is one of the processes to cause the rapid loss of outer belt electrons (e.g.,Kim et al.,2008). In this study, we investigate how radiation belt electrons are lost through the MPS process with a code-coupling simulation using GEMSIS-RB test particle simulation code (Saito et al., 2010) and GEMSIS-GM global MHD magnetosphere simulation code (Matsumoto et al., 2010) by focusing the equatorial pitch angle and local time dependence. We calculate trajectories of electrons in electromagnetic fields calculated from GEMSIS-GM with initial L-shells from 6 to 11, initial energies from 1 MeV to 10 MeV, and initial pitch angles between 50 degrees and 90 degrees, using the relativistic guiding-center equation. The simulation consists of the following three phases associated with variations of the solar wind dynamic pressure; [i] The standoff distance of magnetopause at the subsolar point is 12 Re with the initial dynamic pressure of 1.0 nPa. [ii] The solar wind dynamic pressure becomes 2.5 nPa, and the magnetopause moves to 9 Re. [iii] The solar wind dynamic pressure decreases, so that the inflation of the magnetopause takes place and the standoff distance of the magnetopause is 10 Re. During phase [ii], the high-latitude reconnections occur at dawn-side firstly and many electrons escape from the magnetosphere to the interplanetary magnetic field along the field line in the dawn side. Subsequently, the high-latitude reconnections occur at the high-latitude in the dusk side. In phase [iii], the remained electrons in the magnetosphere escape into the interplanetary in both the dawn and dusk sides. The loss at the dusk-side is outward motion of the trapped electrons caused by the dawn-to-dusk electric fields associated with the inflation of the magnetosphere. The study showed detailed process of the electron escape into the interplanetary magnetic field and the electron escape occur in both enhancement/decrease of the dynamic pressure.

Keywords: Magnetopause Shadowing, global MHD magnetosphere simulation, test particle simulation

©2019. Japan Geoscience Union. All Right Reserved.

Non-diffusive response of outer belt electrons on interplanetary shock

Takuma Toishi[1], *Yusuke Ebihara[1], Takashi Tanaka[2]

1. Research Institute for Sustainable Humanosphere, Kyoto University, 2. Kyushu University

Test particle simulation is performed in the electric and magnetic fields given by a global magnetohydrodynamics (MHD) simulation. When an interplanetary shock strikes the magnetosphere, a compressional wave propagates tailward. Pre-existing relativistic electrons that are initially located at fixed radial distances are redistributed by the electric and magnetic fields associated with the compressional wave. When the electrons encounter the nightside, they undergo complicated paths under the complicated distribution of the electric and the magnetic fields. Consequently, a group of isolated electrons forms, suggesting non-diffusive response. We discuss the redistribution processes in terms of the magnetospheric processes.

Keywords: radiation belt, MHD simulation, Test particle simulation

©2019. Japan Geoscience Union. All Right Reserved.

PARM: Initial result of the auroral camera on the G-CHASER (RockSat-XN) rocket and status of the development of auroral cameras for the LAMP rocket experiment

*Naoshi Yagi[1], Takeshi Sakanoi[1], Fukizawa Mizuki[1], Kazushi Asamura[2], Yoshizumi Miyoshi[3], Keisuke Hosokawa[4], Genki Ishizawa[5]

1. Planetary Plasma and Atmospheric Research Center, Graduate School of Science, Tohoku University, 2. Institute of Space and Astronautical Science, Japan Aerospace Exploration Agency, 3. Institute for Space-Earth Environmental Research, Nagoya University, 4. Department of Communication Engineering and Informatics, University of Electro-Communications, 5. Space & terrestrial plasma pyhsics

We developed an Aurora Imaging Camera (AIC) for NASA’ s G-CHASER (RockSat-XN) sounding rocket launched on 13th January, 2019. In addition, LAMP sounding rocket scheduled to be launched from December 2019 to February 2020 to reveal the spatio-temporal relationship between PsA and relativistic electrons, namely microbursts. In this presentation, we report the development of AIC, the result f the G-CHASER (RockSat-XN) rocket, as well as the current status of LAMP rocket project.

On the G-CHASER rocket experiment, 7 scientific and educational instruments were provided from Japan, U.S., Norway and Puerto Rico. Japanese instrument, called PARM, consists of an intermediate energy (20 - 100 keV) electron detector MED, high energy (several hundred keV - 2 MeV) electron detector HEP, fluxgate magnetometer AFG, and auroral camera AIC. Concerning development of AIC, we carried out sensitivity calibration experiment, electrical function test, fabrications, focus adjustment and environmental (vibration, vacuum and thermal) tests from January to July 2018. AIC consists of detector unit AIC-S and power/data processing electric unit AIC-E. AIC-S consists of a CCD camera (Watec 910 HX), wide-angle lens (F-number: 1.6, focal length: 3.5 mm, field of view: 96.4˚x75˚) and a glass filter (RG665) that transmits light with a wavelength longer than 665 nm.

NASA decided to launch the G-CHASER rocket at 9:00UT on 13rd January 2019 from Andoya Space Center, Norway (69.3˚N, 16.0˚E in the geographic coordinate). At this time, the solar elevation was -4˚, hence twilight had been already started and the region above 15km was sunlit. AIC detected leak light from the rocket skirt until the separation of skirt at an altitude of 82.9km. From time variation of AIC data, rocket spin frequencies were estimated to be ~5Hz at ~20km altitude and ~1Hz at ~80km altitude. This is consistent with the modulation period of magnetic field data observed by AFG. Because AIC was designed to measure weak pulsating aurora with hundreds Rayleigh, the AIC data was saturated above 82.9km after separation of rocket in the sunlit region, and no aurora was observed.

We are also conducting the LAMP sounding rocket project whose PI is Dr. Sarah Jones in NASA/GSFC. This is scheduled to be launched at Poker Flat Research Range in Alaska in 2019 winter. Japanese PARM2 team will provide high energy (several hundred keV - 2 MeV) electron detector HEP, fluxgate magnetometer MIM, and auroral cameras AIC2. We concern AIC2 that consists of two cameras AIC2-S1/AIC2-S2 and power/data processing electric unit AIC2-E. AIC2-S1/S2 and AIC2-E will be installed on a despun platform to derotate rocket spin. AIC2-S1 measures N2 1stPG emission with a narrow FOV lens (F value: 0.95, focal length:17mm, field of view 27x27deg), and AIC-S2 measures OI 844.6nm emission with a wide-angle lens (F value:1.6, focal length:3.5 mm, diagonal field of view:120x120˚). AIC2-S1 will take fine structure of PsA in the region more than 100 x 100 km area around the magnetic footprint with a few kilometer resolution, while AIC2-S2 will obtain an altitude distribution of

©2019. Japan Geoscience Union. All Right Reserved.

PsA in the F-region as well as wide-range distribution of PsA. The characteristic energy of precipitating electron can be estimated from the ration of OI844.6 and N2 1stPG. The cameras are conducted by a single board computer NanoPi M4 via USB3.0 high speed interface. We confirmed to get frame sampling rate with approximately 10Hz with this system. Region-of-interest (ROI) of 3660 x 3660 pixel area is binned with 61x61pixels, and finally image data with 60 x 60 bin (16 bit/bin) is recorded at 10 Hz. The precise imaging and altitude distribution of PsA are obtained with AIC2 at two wavelengths with 10Hz sampling. The imaging data combined with precipitating electron data in the wide energy range enable us to investigate the relativistic electron precipitation in microbursts that is probably caused by chorus waves in the magnetosphere.

Keywords: auroral camera, rocket experiment

©2019. Japan Geoscience Union. All Right Reserved.

First simultaneous observation of a SAR arc at subauroral latitudes using a ground all-sky camera and the Arase satellite in the inner magnetosphere

*Yudai Inaba[1], Kazuo Shiokawa[1], Shin-ichiro Oyama[1,8,9], Yuichi Otsuka[1], Atsuki Shinbori[1], Yoichi Kazama[2], Shiang-Yu Wang[2], Sunny W. Y. Tam[2], Shoichiro Yokota[3], Satoshi Kasahara[4], Kunihiro Keika[4], Tomoaki Hori[1], Ayako Matsuoka[5], Yoshiya Kasahara[6], Atsushi Kumamoto[7], Yasumasa Kasaba[7], Yoshizumi Miyoshi[1], Iku Shinohara[5], Arto Oksanen[10]

1. Institute for Space-Earth Environmental Research, 2. Academia Sinica, 3. Osaka Univ, 4. Tokyo Univ, 5. JAXA, 6. Kanazawa University, 7. Tohoku University, 8. University of Oulu, Finland, 9. National Institute of Polar Research, 10. Jyväskylän Sirius ry, Finland

Stable Auroral Red (SAR) arc is characterized by a 630.0 nm emission observed at subauroral latitudes. The energy of precipitating electrons that cause the SAR arc emission is several electron volts (eV). Precipitation of low-energy electrons is expected to occur due to spatial overlap between the plasmasphere and the ring current, where high-energy (more than 10 keV) ring current ions heat low-energy (less than 1 eV) electrons in the plasmasphere. Simultaneous observations of SAR arcs using the ionospheric satellite and ground all-sky cameras have been already done [e.g., Foster et al., 1994]. However, there has been no reports on in-situ measurements of plasma and electromagnetic fields in the inner magnetosphere, where the plasmaspheric plasma is heated by the ring current. In this study, we report simultaneous observations of a SAR arc at 22:04 UT on March 28, 2017, by using an all-sky camera at Nyrola (62.34 N, 25.51 E, MLAT 59.4 N) at subauroral latitudes and the Arase satellite. We analyze the all-sky camera data and the satellite data of this event to investigate the generation mechanism of the SAR arc. We find interesting features in the electric field data and the energy flux of electrons observed by the electric field detector of the plasma wave experiment (EFD/PWE) and the low-energy particle experiments–electron analyzer (LEP-e), respectively, onboard the Arase satellite at the crossing of the SAR arc. A negative excursion of the Ez component of the electric field (GSE coordinate system) with an amplitude of ~2.4 mV/m was observed at the crossing time. The Bx component of the magnetic field (GSE coordinate system) was negative. Thus the direction of the E ×B drift is westward, which is consistent with the westward auroral motion observed in the SAR arc by the ground all-sky camera. At the SAR arc crossing, the energy flux of electrons below 100-eV electrons is slightly intensified. We will discuss these observations in relation to the proposed SAR-arc generation mechanisms.

Keywords: ERG, SAR arc, All-sky imager, Simultaneous observation

©2019. Japan Geoscience Union. All Right Reserved.

Pi2 pulsations observed by the Arase satellite inside and outside the plasmapause

*Mariko Teramoto[1], Ayako Matsuoka[2], Reiko Nomura[5], Yoshiya Kasahara[3], Yasumasa Kasaba[4], Atsushi Kumamoto[4], Fuminori Tsuchiya[4], Shoya Matsuda[2], Masahito Nose[1], Masafumi Shoji[1], Yasunori Tsugawa[1], Shun Imajo[1], Yoshizumi Miyoshi[1], Iku Shinohara[2]

1. Institute for Space-Earth Environmental Research Nagoya University, 2. Institute of Space and Astronautical Science, Japan Aerospace eXploration Agency, 3. Kanazawa University, 4. Tohoku University, 5. National Astronomical Observatory of Japan

The spatial structure of Pi2 pulsation relative to the plasmasphere has been studied using the magnetic and electric field observed from the equatorial orbiting satellite in the inner magnetosphere by Takahashi et al (2003; 1995). They showed that the nightside Pi2 pulsations in the inner magnetosphere, which have high coherence with those at low-latitude ground station, are dominated by the poloidal component (the radial and compressional components for the magnetic field and azimuthal component for the electric field). The amplitudes of the compressional magnetic field has maximum and azimuthal electric field and the compressional magnetic field have maximum and minimum in the vicinity of the plasmaspause, respectively. The phase of the azimuthal electric field relative to low-latitude Pi2 pulsations on ground is 90 degrees in the plasmasphere. Such radial profile of the amplitude and phase of Pi2 pulsations can be explained by a plasmaspheric cavity mode resonance. However, the latitudinal structure of Pi2 pulsations in the electric field has not been examined. We investigate the latitudinal characteristics of off-equatorial Pi2 pulsations on the nightside and their relation to the plasmapause using the magnetic field measured by the fluxgate magnetometer measured by the Magnetic Field Experiment (MGF), the electric field measured by the Electric field Detector (EFD), and electron density derived from the spectra measured by the High Frequency Analyzer (HFA) from the Arase satellite.

©2019. Japan Geoscience Union. All Right Reserved.

An extreme erosion of the plasmasphere during the 7–10 September 2017 storm

*Yuki Obana[1], Naomi Maruyama[2,3], Atsuki Shinbori[4], Kumiko K. Hashimoto[5], Mariangel Fedrizzi[2,3], Masahito Nose[4], Yuichi Otsuka[4], Nozomu Nishitani[4], Tomoaki Hori[4], Atsushi Kumamoto[6], Fuminori Tsuchiya[6], Shoya Matsuda[7], Ayako Matsuoka[7], Yoshiya Kasahara[8], Akimasa Yoshikawa[9], Yoshizumi Miyoshi[4], Iku Shinohara[7]

1. Osaka Electro-Communication University, 2. University of Colorado Boulder, 3. NOAA Space Weather Prediction Center, 4. Nagoya University, 5. Kibi International University, 6. Tohoku University, 7. Japan Aerospace Exploration Agency, 8. Kanazawa University, 9. Kyushu University

We report an extreme erosion of the plasmasphere arising from the September 2017 storm. The cold electron density is identified from the upper limit frequency of UHR waves observed by the HFA of the PWE instrument onboard the Arase spacecraft. The HFA provides the spectrograms of electric fields in a frequency range from 10 kHz to 10 MHz with an 8-sec time resolution (Kasahara et al., 2018; Kumamoto et al., 2018). Such wide frequency coverage allows observation of the UHR frequency even deep inside the plasmasphere.
The electron density profiles reveal that the plasmasphere was severely eroded during the recovery phase of the storm and the plasmapause was located at L~1.7 at 23 UT on 8 Sep 2017. This is the first report of such deep erosion of the plasmasphere (L_{PP}<2) with the in-situ observation of the electron density. The degree of the severity is much more than what is expected from the SYM-H minimum (−146 nT) of the event.
We further study absolute GNSS-TEC, ground-based magnetic field, the doppler velocity obtained from the SuperDARN Hokkaido Radars to investigate the location of the midlatitude ionospheric trough, the penetration of the convection electric field to the equator and middle latitudes, respectively. Our results suggest that the middle latitude electric field was penetrated from the high-latitude storm time convection for several hours. Futhermore, the Ionosphere-Plasmasphere-Electrodynamics (IPE) model (Sun et al., 2015; Maruyama et al., 2016) is used to understand the dynamics of the plasmasphere. The IPE results suggest that the middle latitude electric field penetrates from the high-latitude storm time convection that lasts for several hours can explain the degree of severity during the September 7-11 2017 storm.

Keywords: plasmasphere, innner magnetosphere, Magnetosphere-ionosphere coupling

©2019. Japan Geoscience Union. All Right Reserved.

Relative contribution of ULF and chorus waves to the radiation belt variation: Comparison between multi-point observations and BATSRUS + CRCM simulation

*Naoko Takahashi[1], Kanako Seki[1], Mei-Ching Fok[2], Yihua Zheng[2], Yoshizumi Miyoshi[3], David Hartley[4], Ayako Matsuoka[5], Yoshiya Kasahara[6], Yasumasa Kasaba[7], Nana Higashio[8]

1. Graduate School of Science, University of Tokyo, 2. NASA Goddard Space Flight Center, 3. Institute for Space-Earth Environmental Research, Nagoya University, 4. Department of Physics and Astronomy, University of Iowa, 5. Institute of Space and Astronautical Science, Japan Aerospace Exploration Agency, 6. Information Media Center, Kanazawa University, 7. Planetary Plasma and Atmospheric Research Center, Tohoku University, 8. Japan Aerospace Exploration Agency

Earth’ s radiation belt is the area where electrons with energies from hundreds of keV to several MeV are trapped. When, where, and how the radiation belt exhibits a dramatic variation during a magnetic storm is of global interest. The dynamic variation of the radiation belt is caused by various wave-particle interactions: (1) the radial diffusion of electrons driven by ultra-low-frequency (ULF) waves in Pc5 frequency ranges (1.6–6.7 mHz) and (2) the local acceleration caused by wave-particle interactions between whistler-mode chorus waves and radiation belt particles. Over the past decade, multi-point observations and numerical simulations have provided evidence to support above physical processes. However, it is debatable how much each wave contributes to the radiation belt variation during a magnetic storm. A few previous studies have quantitatively compared roles of local acceleration and radial transport by calculating diffusion coefficients, whereas the global context between the wave growth and the relativistic electron flux enhancement has not been extensively studied. To address these issues, the comprehensive study using multi-point observations and numerical simulations (not empirical models) makes essential and significant contributions.

We focus on the magnetic storm on 27-30 May 2017. This magnetic storm is triggered by coronal mass ejections and induces a clear interplanetary shock. Fortunately, several satellites are scattered in the inner magnetosphere and detect both ULF and chorus waves during this magnetic storm. Arase and Van Allen Probes also detect variations of relativistic electron fluxes associated with the Dst index variation. We examine L-value dependence of ULF and chorus wave powers and find the difference of wave activity during the recovery phase. The chorus wave activity is large during the early recovery phase, while the ULF wave activity is large during the late recovery phase. The difference of wave activity may contribute to the radial profile in the phase space density of relativistic electrons. To grasp the extent of individual wave contribution, we also perform the comprehensive ring current model (CRCM) coupled with Block-Adaptive-Tree Solar-Wind Roe-Type Upwind Scheme (BATSRUS) simulation. BATSRUS with CRCM well reproduces global characteristics of energetic electron fluxes and wave growth during this magnetic storm. We will further evaluate global distribution of simulated wave power comparing to the observation, and then discuss the temporal and spatial context between each wave growth and the radiation belt variation.

©2019. Japan Geoscience Union. All Right Reserved.

Modulation of the D-region ionosphere by Pc5 waves observed by VLF/LF standard radio waves

*Miyashita Takuya[1], Hiroyo Ohya[1], Fuminori Tsuchiya[2], Hiroyuki Nakata[1], Toshiaki Takano[1], Kazuo Shiokawa[3], Yoshizumi Miyoshi[3]

1. Chiba University, 2. Tohoku University, 3. Nagoya University

Ionospheric modulation due to ultra low frequency (ULF) Pc5 waves have been observed by GPS-total electron content (TEC), high frequency (HF) Doppler sounders, and SuperDARN HF radars [e.g., Pilipenko et al., 2014; Belakhovsky et al., 2016]. However, there are few reports for the modulation of the lower ionospheric associated with the ULF Pc5 waves using VLF/LF transmitter signals. In this study, we investigate the D-region signatures of the modulation due to the ULF Pc5 waves using a network of very low frequency (VLF)/low frequency (LF) standard radio waves. We show oscillations in intensities of the VLF/LF waves with a period of 4-6 minutes during substorms on 27 April, 2017. The transmitter signals from NAA (USA, 24.0 kHz, L = 2.88), NLK (USA, 24.8 kHz, L = 2.88), NDK (USA, 25.2 kHz, L = 2.98) and WWVB (USA, 60.0 kHz, L = 2.26) were observed by the receivers at ATH (Athabasca, L=4.31) and PKR (Poker Flat, L=5.95). The substorm occurred at 04:30 UT. Based on the wavelet analysis, we found that the intensities for the NDK-ATH and WWVB-ATH paths showed oscillations with a period of 4-6 minutes during the substorm growth phase (05:00-06:00 UT). Magnetic field variations observed by ground magnetometers around the NDK-ATH and WWVB-ATH paths also showed the same periodicity, which means that the variations in the VLF/LF intensities would be caused by Pc5 modulations. The magnetic field oscillations were observed in wide latitude range. The intensity of the oscillation was larger at high latitude magnetometers than those around the location of the NDK-ATH and WWVB-ATH path (mid-latitude). The Pc5 oscillations could be excited by solar wind because solar wind speed had similar period of the 4-6 minutes. In this presentation, we will discuss the cause of these VLF/LF oscillations.

Keywords: VLF/LF standard radio waves, Pc5, ULF

©2019. Japan Geoscience Union. All Right Reserved.

Oxygen-proton differences in ion energies dominating plasma pressure: Dependence on storm phases and solar wind drivers

*Kunihiro Keika[1], Satoshi Kasahara[1], Shoichiro Yokota[2], Masahiro Hoshino[1], Kanako Seki[1], Masahito Nose[3], Yoshizumi Miyoshi[3], Iku Shinohara[4]

1. Graduate School of Science, The University of Tokyo , 2. Graduate School of Science, Osaka University, 3. Institute for Space-Earth Environmental Research, Nagoya University, 4. Institute of Space and Astronautical Science, Japan Aerospace Exploration Agency

The ion pressure in the inner magnetosphere is generally dominated by protons with energies of a few to a few 100s keV. Oxygen ions of ionospheric origin, O+, can make a significant contribution to the ion pressure during geomagnetically active periods. Our previous study (Keika et al., 2018, GRL) examined the radial dependence of contributing energies, which we term an energy range that makes the dominant contribution to the plasma pressure, during the main phase of the six magnetic storms in Year 2017. We found clear oxygen-proton differences in the contributing energies in the outer part (L>5) of the ring current region. The contributing energies were higher for O+ than for H+. The results provided in situ evidence of the contribution from mass-dependent/selective acceleration processes to the energization of the outer part of the ring current.

The present study extends this analysis toward a larger database obtained from a longer period of magnetic storm times including the recovery phase. We also compare mass-dependent/selective energization between different solar wind drivers such as coronal mass ejections and corotational interaction regions. We primarily use data from the MEP-i (Medium-Energy Particle experiments - ion mass analyzer) on board the Arase spacecraft. MEP-i measures ions with energies of 10 to 180 keV/q and distinguishes between different ion species. Arase observed the nightside near-Earth magnetosphere (L<10) during 7 CME-driven and 7 CIR-driven storms with the Dst minimum of smaller than -50 nT in Years 2017 and 2018. The dependence on storm phases and solar wind drivers helps identify magnetospheric conditions favorable for mass-dependent/selective acceleration and in turn provides clues for understanding important physical mechanisms. Utilizing observations made by the MMS spacecraft in the near-Earth plasma sheet, we also compare oxygen-to-proton differences inside earthward bursty bulk flows with the Arase/MEP-i observations. The multi-spacecraft observations help better understand the temporal evolution of the mass-dependent/selective acceleration processes.

Keywords: Magnetic storms, Substorms, RIng current, Oxygen ions, Ion transport and acceleration

©2019. Japan Geoscience Union. All Right Reserved.

Mass dependence of penetration depth of multi-energy ions in the inner magnetosphere during magnetic storms: Arase observations

*Ryosuke Fujii[1], Yoshizumi Miyoshi[1], Masafumi Shoji[1], Kazushi Asamura[2], Lynn Kistler[1,8], Vania Jordanova[9], Tomoaki Hori[1], Satoshi Kurita[1], Mariko Teramoto[1], Yasunori Tsugawa[1], Yoshiya Kasahara[3], Yasumasa Kasaba[4], Atsushi Kumamoto[5], Fuminori Tsuchiya[4], Shoichiro Yokota[6], Kunihiro Keika[7], Ayako Matsuoka[2], Iku Shinohara[2]

1. Institute for Space-Earth Environmental Research, Nagoya University, 2. Institute of Space and Astronautical Science, Japan Aerospace Exploration Agency, 3. Information Media Center, Kanazawa University, 4. Planetary Plasma and Atmospheric Research Center, Tohoku University, 5. Department of Geophysics, Graduate School of Science, Tohoku University, 6. Graduate School of Science, Osaka University, 7. Department of Earth and Planetary Science, Graduate School of Science, The University of Tokyo, 8. University of New Hampshire, 9. Los Alamos National Laboratory

During magnetic storms, the ring current ions move toward the Earth, and the inner edge position of the ring current depends on the convection electric field. We investigate variations of the inner edge of the ring current ions, so-called, penetration depth, during magnetic storms using the ion measurements made by the Low-energy particle experiments-ion mass analyzer (LEP-i)/Medium-energy particle experiments-ion mass analyzer (MEP-i) instruments onboard the Arase satellite. The Arase satellite typically observes the earthward penetration of the ring current protons associated with the enhancement of the dawn-to-dusk electric field in the inner magnetosphere during the storm main phase. The plasmapause moves earthward during the main phase. On the other hand, the convection electric field decreases during the storm recovery phase in which the flux of ring current protons decreases. We identify that the penetration depth of protons depends on the minimum Dst index during the storms as well as the proton energy.

We also investigate the penetration depth of other ions, i.e., helium and oxygen ions. Because the life times of helium and oxygen ions due to charge exchange reaction for are longer than that of protons, it is expected that these ions can penetrate deeper than protons and temporal and spatial evolution can be observed clearly. We will also discuss the relation between the position of ring current inner edge and cross polar cap potential.

Keywords: The Arase satellite, Ring current, Ions

©2019. Japan Geoscience Union. All Right Reserved.

Relativistic Acceleration of Energetic Protons by Electromagnetic Ion Cyclotron Waves in the Jovian Magnetosphere

*Tomohiro Sekine[1], Yoshiharu Omura[1], Danny Summers[2], Yikai HSIEH[1], Satoko Nakamura[1]

1. Reserach Institute for Sustainable Humanosphere, Kyoto University, 2. Memorial University of Newfoundland

We perform test particle simulations of nonlinear interaction between energetic protons and EMIC waves. We assume a coherent EMIC waves that have a constant frequency and propagate parallel to the magnetic field. We find that protons can be trapped and accelerated by EMIC waves. We find a very efficient acceleration process of protons in which kinetic energy of protons increases while directions of parallel velocities reverses when we assume parameters in the Jovian magnetosphere. We notice that this phenomenon is very similar to the interaction process between relativistic electrons and whistler-mode waves, which is called Relativistic Turning Acceleration (RTA) [1]. In order to analyze the phenomena, we have developed nonlinear trapping theory of interaction between relativistic protons and EMIC waves. Next, we compare the theory and simulation results. We confirm that the results satisfy the conditions for RTA. Following the trajectories of many resonant protons, we obtain time evolution of the distribution function of relativistic protons as a function of energy and equatorial pitch angle based on the numerical Green’ s function method [2].

References:

[1] Y. Omura, N. Furuya, D. Summers, Relativistic turning acceleration of resonant electrons by coherent whistler-mode waves in a dipole magnetic field, Journal Geophysical Research, Vol. 112, A06236, doi:10.1029/2006JA012243, 2007.

[2] Y. Omura, Y. Miyashita, M. Yoshikawa, D. Summers, M. Hikishima, Y. Ebihara, and Y. Kubota (2015), Formation process of relativistic electron flux through interaction with chorus emissions in the Earth’ s inner magnetosphere, J. Geophys. Res. Space Physics, 120, 9545–9562, doi:10.1002/2015JA021563, 2015.

©2019. Japan Geoscience Union. All Right Reserved.

Statistical study of IPDP type EMIC wave-related electron precipitation at subauroral latitude

*Asuka Hirai[1], Fuminori Tsuchiya[1], Takahiro Obara[1], Yasumasa Kasaba[1], Yuto Katoh[2], Hiroaki Misawa[1], Kazuo Shiokawa[3], Yoshizumi Miyoshi[3], Satoshi Kurita[3], Martin G Connors[4]

1. Planetary Plasma and Atmospheric Research Center, Graduate School of Science, Tohoku Univ. , 2. Department of Geophysics, Graduate School of Science, Tohoku University, 3. Institute for Space-Earth Environmental Research, Nagoya University, 4. Athabasca University

The outer radiation belt electrons disappear during the main phase of geomagnetic storms. One of the loss mechanisms of electrons from the outer belt is precipitation into the atmosphere due to wave-particle interactions. Electromagnetic ion cyclotron (EMIC) waves are believed to be important plasma waves that contribute to the loss of the outer radiation belt due to pitch angle scattering. They can scatter relativistic and ultra-relativistic electrons. However, there are still questions left about the contribution of EMIC waves to the whole loss of radiation belt electrons and possible conditions favorable to pitch angle scattering.

EMIC waves mainly propagate along magnetic field lines and are observed on the ground as Pc1 geomagnetic pulsations. Intervals of pulsations of diminishing periods (IPDP) are Pc1/EMIC waves that are characterized by frequency rise from 0.1 to 1–2 Hz in a period of ~1 h, and often occur during substorms. Recent studies reported that IPDP are preferentially associated with relativistic electron precipitation. However, the statistical relation between IPDP waves and relativistic electron precipitation, and their physical mechanism, remain open issues.

We investigated differences in characteristics between IPDP and other types of Pc1 by using an induction magnetometer and VLF radio wave data that is a proxy of electron precipitations at subauroral latitude from 1 November 2016 to 30 June 2018. We used the induction magnetometer of PWING (study of dynamical variation of Particles and Waves in the INner magnetosphere using Ground-based network observations) at Athabasca, Canada (54.6˚N, 246.36˚E, L = 4.39). VLF radio waves propagate from transmitters to receivers in subionospheric waveguide. The modulations of VLF signals are detected as occurrence of sub-relativistic and relativistic electron (>100 keV) precipitation due to ionization changes in the lower ionosphere along the radio wave propagation path. VLF radio waves are transmitter from NDK, U.S. (46.367˚N, 261.467˚E, L =3.13) and NLK, U.S. (48.2˚N, 238.083˚E, L =2.84) and received at Athabasca. We selected EMIC wave events on the basis of the following criteria: (1) EMIC wave power is higher than 10^{-5} nT^2/Hz. (2) Duration of EMIC waves is longer than 20 min. (3) Interval between one EMIC wave event and the next one is longer than 30 min. Electron precipitation was identified as a decrease in amplitude of VLF signals from the quiet day curve (QDC). We counted as EMIC wave-driven electron precipitation if we detect temporal correspondence with EMIC waves. In this period, we found 950 EMIC wave events, and 87 of total EMIC wave events were IPDP events (9.2%). Local time dependence of EMIC waves shows that IPDP often occurs in the afternoon and evening sector, while other types of Pc1 occur in all local time range, but with a maximum in 12–16 MLT, which is consistent with previous studies. Simultaneous observation of the magnetometer and VLF radio waves were available for 286 days, and we found 163 EMIC wave events. 19 of 163 EMIC wave events were clearly associated with electron precipitation (12%). Among 19 electron precipitation events, 15 events were caused by IPDP (79%). Also, the electron precipitation events were observed in the evening sector with similar local time dependence to IPDP. This result suggests that IPDP is more likely to cause electron precipitation than other Pc1 wave types. In previous studies, IPDP occurs due to ion cyclotron instability of ring current ions in the evening sector, and favorable region for electron scattering by EMIC waves is high density duskside plasmapause

©2019. Japan Geoscience Union. All Right Reserved.

and plasmaspheric plume because dense plasma lowers minimum resonant energy of electrons. It is assumed that occurrence region of IPDP is coincident with the preferential region for MeV electron scattering by EMIC waves. For this reason, it is expected that IPDP type EMIC waves significantly cause relativistic electron precipitations in the duskside.

Keywords: EMIC waves, electron precipitation, subionospheric VLF radio waves

©2019. Japan Geoscience Union. All Right Reserved.

Meridional distributions of proton plasma and pressure-driven currents in the nightside inner magnetosphere: Arase observations

*Shun Imajo[1], Masahito Nose[1], Satoshi Kasahara[2], Shoichiro Yokota[3], Ayako Matsuoka[4], Kunihiro Keika[2], Tomoaki Hori[1], Mariko Teramoto[1], Kazuhiro Yamamoto[5], Oimatsu Satoshi[5], Reiko Nomura[6], Akiko Fujimoto[7], Iku Shinohara[4], Yoshizumi Miyoshi[1]

1. Institute for Space-Earth Environmental Research, Nagoya University, 2. Graduate School of Science, The University of Tokyo, 3. Graduate School of Science, Osaka University, 4. Institute of Space and Astronautical Science, Japan Aerospace Exploration Agency, 5. Graduate School of Science, Kyoto University, 6. National Astronomical Observatory of Japan, 7. Kyushu Institute of Technology

We examine the averaged meridional distributions of proton plasma parameters and pressure-driven currents in the nightside (20–04 h magnetic local time) ring current region during disturbed times (-80 < SYM-H* < -40 nT) using ion measurements covering energy range of 10–180 keV by the Arase satellite. Because the Arase satellite has a large inclination orbit of 31°, it covers the absolute value of magnetic latitude (|MLAT|) range of 0–40° and the radial distance of < 6 Re. We find that the plasma pressure decreases significantly with MLAT. The plasma pressure on the same L^* shell at 30°<|MLAT|<40° is about 10–60% of that at 0°<|MLAT|<10°, and the percentage of decrease is larger on lower L^* shells. The pressure anisotropy which is defined by the perpendicular pressure divided by the parallel pressure decreases with radial distance and shows a weak dependence on |MLAT|. The magnitude of the plasma beta at 30°<|MLAT|<40° is one or two order smaller than that at 0°<|MLAT|<10°. The relative plasma pressure distribution predicted from the magnetic strength and anisotropy is roughly consistent with the observed plasma pressure for L^*=3.5–5.5. The azimuthal pressure-gradient current derived from the plasma pressure distribution spreads over ~-20° |MLAT|, while the curvature current is limited in ~0–10° |MLAT|. We suggest that the latitudinal dependences should be taken into account when considering a temporal evolution of ring current particles from L distributions of successive orbits.

Keywords: meridional distributions, plasma pressure, pressure-driven currents, Arase satellite

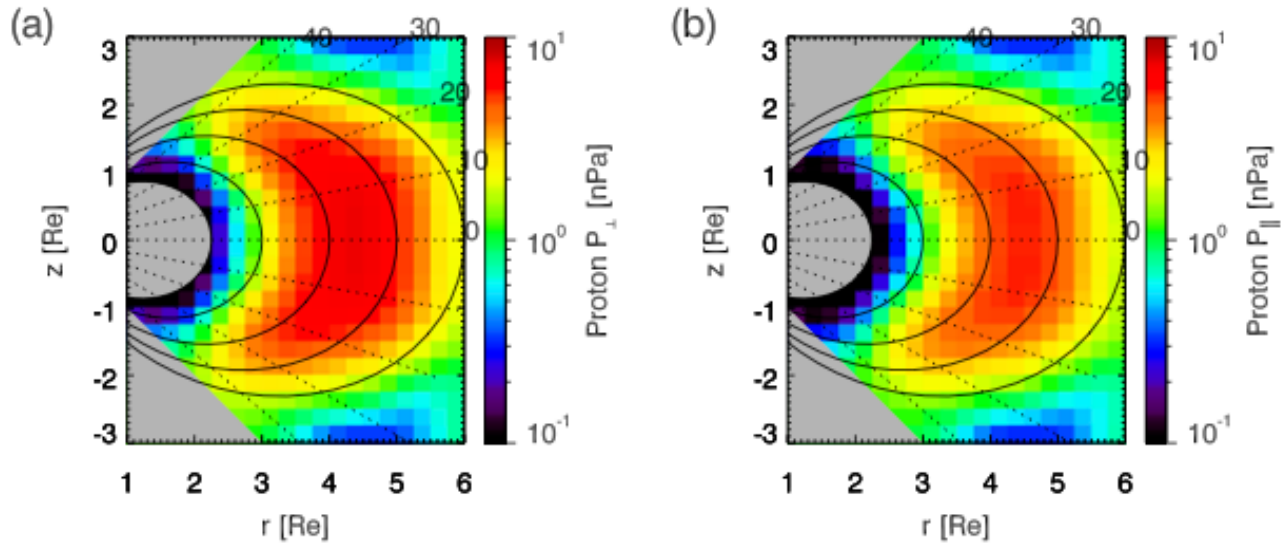

©2019. Japan Geoscience Union. All Right Reserved.

Space Weather Effects on Energetic Proton Flux Response in South Atlantic Anomaly

*Kirolosse Mina GIRGIS[1,2], Tohru Hada[1], Shuichi Matsukiyo[1]

1. Earth System Science and Technology (ESST) Department, Interdisciplinary Graduate School of Engineering Sciences (IGSES), Kyushu University, Japan, 2. Aerospace Engineering Department, Faculty of Engineering, Cairo University, Egypt

In this research, energetic proton flux in the inner radiation belt, is studied inside the South Atlantic Anomaly (SAA) by performing test particle simulations, where the background time-varying magnetic field is provided by Tsyganenko model, according to *Dst* index and altitudes. The objective of this investigation, is to estimate and forecast the additional radiation dose, occurring on spacecraft and human bodies, due to their passage inside the anomaly, and precisely, during intense solar storms. It was found that within minutes, proton flux in the SAA, penetrated deeper downward by about 200 km, when the *Dst* index is decreased (< -210 nT), and a after few more minutes, it was significantly reduced at all the altitudes; the last conclusion was confirmed by satellite observations.

Keywords: South Atlantic Anomaly, Space Weather, Dst Index, Radiation Dose, Proton Flux

©2019. Japan Geoscience Union. All Right Reserved.

Solar-cycle variations of >30 keV electron flux enhancements under the inner radiation belt

*ALLA SUVOROVA[1]

1. National Central University

Intense fluxes of 30-300 electrons can arise in the equatorial ionosphere outside the South Atlantic Anomaly. It was established that the electrons were injected from the inner radiation belt probably due to a mechanism of fast radial transport in the crossed electric and magnetic fields. Continuous monitoring of energetic particles at low heights of ~850 km with the MEPED instrument onboard the NOAA/POES satellites allowed compiling large statistics of the >30 keV electron enhancements from 1998 to 2018. We studied particle flux variations with geomagnetic activity and solar cycle. We found that geomagnetic activity measured by Dst and AE indices are not key factors of occurrence rate increase for electron injections, but influence on intensity of particles. The occurrence rate is controlled by auroral conductivity on the dayside and significantly enhanced during northern summer. Descending phase of solar cycle plays a major role in the occurrence rate increase.

Keywords: magnetosphere-ionosphere, energetic electrons, low latitudes, solar cycle

©2019. Japan Geoscience Union. All Right Reserved.

Energy spectra variations of high energy electrons in the inner magnetosphere observed by HEP/XEP on ARASE and SEDA-e on HIMAWARI

*Takeshi Takashima[1], Takefumi Mitani[1], Nana Higashio[2], Tsutomu Nagatsuma[3]

1. ISAS/JAXA, 2. Research and Development Directorate/JAXA, 3. NiCT

The relativistic electrons in the outer radiation belt were disappeared/increased and their energy spectra were changed dynamically in some storms observed by XEP/HEP onboard the ARASE spacecraft. In the same time, SEDA-e with energy range 200keV-4.5MeV for electron on board the HIMAWARI-8, Japanese weather satellite on GEO, observed increase of relativistic electron in different local time.
When comparing the energy spectra, there are times when the spectrum matches or does not match. It is also observed that the change in the slope of the energy spectrum differs with time. These phenomena are observed even when there are two satellites at the same local time.
We will report on energy spectra variations of high energy electrons including calibrations of differential flux between XEP and HEP and discuss comparisons with energy spectra between ARAE and HIMAWARI that observed each storm in different local time.

Keywords: relativistic electron, inner magnetosphere, ARASE

©2019. Japan Geoscience Union. All Right Reserved.

Inter-channel calibration of the high-energy electron experiments (HEP) instrument onboard the Arase satellite

*Tomoaki Hori[1], Takefumi Mitani[2], Takeshi Takashima[2], Park Inchun[1], Satoshi Kurita[1], Mariko Teramoto[1], Nana Higashio[3], Satoshi Kasahara[4], Shoichiro Yokota[5], Yoshizumi Miyoshi[1], Iku Shinohara[2]

1. Institute for Space-Earth Environmental Research, Nagoya University, 2. Japan Aerospace Exploration Agency, Institute of Space and Astronautical Science, 3. Japan Aerospace Exploration Agency, 4. Graduate School of Science, The University of Tokyo, 5. Graduate School of Science, Osaka University

An inter-channel comparison of electron fluxes measured by the HEP instrument onboard the Arase satellite is conducted with a focus on the apparent non-uniformity in detection efficiency and relative offset of the background flux level between the channels, which was partly reported previously. We extend the data set to cover the entire two-year period since the start of the regular observations. The flux ratio of different channels is sorted by the electron flux level of much higher energies that was simultaneously measured by the extremely high-energy electron experiment (XEP) instrument onboard Arase. The result shows that the HEP flux of all azimuthal channels is more or less affected by MeV electrons which are most likely to have penetrated into the instrument box and directly hit the detectors. However, it is also revealed that the non-uniform count distribution over the channels still remains even when the penetrating electrons are absent. We conduct a set of Geant-4 simulations to trace electrons with various energies and incident angles to the detector plane in order to give a quantitative interpretation for the resultant count distributions, in terms of the effects of penetrating electrons and obliquely-colliding incident electrons.

Keywords: Arase satellite, particle instrument, calibration

©2019. Japan Geoscience Union. All Right Reserved.

Particle simulation for calibrating the HEP data onboard the ARASE satellite

*PARK INCHUN[1], Yoshizumi Miyoshi[1], Takefumi Mitani[2], Tomoaki Hori[1], Satoshi Kurita[1], Mariko Teramoto[1], Takeshi Takashima[2], Nana Higashio[3], Iku Shinohara[2]

1. Nagoya University Institute for Space-Earth Environmental Research, 2. Japan Aerospace Exploration Agency Institute of Space and Astronautical Science , 3. Japan Aerospace Exploration Agency

Understanding the detailed characteristics of the HEP (High-Energy electron Experiment) instrument onboard the Arase satellite is crucial for data calibration. Due to difficulties of reproducing the severe radiation environment of the inner magnetosphere on the ground, computer simulation is the best method to understand instrument responses to the ambient radiation environment. Through Monte-Carlo simulations using the Geant4 tool, we have reconstructed the geometry of the HEP instrument and modeled the high-energy particle environment. Using the developed model, we have studied the efficiency of the detectors, the angular resolution, and the g-factors, which depend on the particle energy and the sensor channels. While the previous studies were based on a uni-direction simulation with electron pencil beams, this study adopted all the detector channels and energy bends of HEP thus resulting in more advanced simulations. Based on the results, we have made a new calibration table depending on the angle of incident particles. We have also estimated the g-factor which depends on the incident particle energy. The updated calibration table and g-factors are important for calibrating the HEP data as well as inter-calibrations with other particle instruments' data.

Keywords: ARASE, Geant4, HEP

©2019. Japan Geoscience Union. All Right Reserved.

Geant4 model calculation and energetic particle observation with HEP/Arase in the inner radiation belt

*Honoka Toda[1], Wataru Miyake[1], Takefumi Mitani[3], Takeshi Takashima[3], Yoshizumi Miyoshi[2], PARK INCHUN[2], Tomoaki Hori[2]

1. Tokai University, 2. ISEE/Nagoya University, 3. ISAS/JAXA

The high-energy electron experiments (HEP) instrument installed on the Arase is designed to observe energetic electrons of 70 keV to 2 MeV. The HEP registers high electron counts for the MeV energy range, not only in the outer belt but also in the inner belt, in MeV energy range. On the contrary, Van Allen Probes have hardly detected MeV electrons in the inner radiation belt. A probable interpretation is that the counts of HEP are caused due to contamination of high-energy protons. In order to verify this idea, we have modeled the HEP instrument a Geant4 simulation to determine the energy of penetrating protons. The result clearly shows that high-energy protons, it has become clear that high-energy protons of a few to a few tens of MeV can contribute to the apparent high counts of HEP. No instrument for measuring protons in this energy range is installed on the satellite. We will discuss the possibility of research on the spatial distribution and time variation of high-energy protons in the inner belt based on observation data from the HEP instrument.

Keywords: Arase, Proton Radiation Belt, HEP

©2019. Japan Geoscience Union. All Right Reserved.

Validation of High-energy electron detector simulator for the HEP instruments onboard Arase

*Takefumi Mitani[1], PARK INCHUN[2], Tomoaki Hori[2], Taku Namekawa[1,3], Kazushi Asamura[1], Takeshi Takashima[1], Satoshi Kasahara[3], Satoshi Kurita[2], Mariko Teramoto[2], Nana Higashio[1], Yoshizumi Miyoshi[2], Iku Shinohara[1]

1. Japan Aerospace Exploration Agency, Institute of Space and Astronautical Science, 2. Institute for Space-Earth Environmental Research, Nagoya Univ., 3. The university of Tokyo

The high-energy electron experiments (HEP) onboard the Arase satellite detects 70 keV-2 MeV electrons and generates a three-dimensional velocity distribution for these electrons in every period of the satellite's rotation. Electrons are detected by two instruments, namely, HEP-L and HEP-H, which differ in their geometric factor (G-factor) and range of energies they detect. HEP-L detects 70 keV–1 MeV electrons and its G-factor is 9.3 $\times 10^{-4}$ cm^2 sr at maximum, while HEP-H observes 0.7 MeV–2 MeV electrons and its G-factor is 9.3 $\times 10^{-3}$ cm^2 sr at maximum. The instruments utilize silicon strip detectors and application-specific integrated circuits to readout the incident charge signal from each strip.

In order to deduce the distribution of incident electrons from the direction and energy detections in orbit, we have developed a detector simulator using the Geant4 toolkit. Especially contamination due to high energy particles must be considered quantitatively. We have also been working on electron beam experiments using HEP detector modules which are almost the same as the flight model in order to compare detailed simulations and experimental data.

We will present a comparison between results from the electron beam experiments and those from the detector simulator. And we will discuss its influence on the interpretation of the observational data obtained in orbit.

Keywords: high-energy electron, Arase, Geant4

©2019. Japan Geoscience Union. All Right Reserved.

[E] Poster | P (Space and Planetary Sciences)：P-EM Solar-Terrestrial Sciences, Space Electromagnetism & Space Environment

Wed. May 29, 2019 5:15 PM - 6:30 PM JST | Wed. May 29, 2019 8:15 AM - 9:30 AM UTC | Poster Hall International Exhibition Hall8, Makuhari Messe_6

[P-EM13] Inner magnetosphere: Recent understanding and new insights

convener:Yusuke Ebihara(Research Institute for Sustainable Humanosphere, Kyoto University), Danny Summers(Memorial University of Newfoundland), Yoshizumi Miyoshi(Institute for Space-Earth Environmental Research, Nagoya University), Shinji Saito(Graduate School of Science, Nagoya University)

The inner magnetosphere is characterized by the dominance of intrinsic dipolar Earth's magnetic field. The dipolar magnetic field traps charged particles, resulting in the formation of unique particle environment known as the plasmasphere, the ring current, and the radiation belt. The inner magnetosphere is always changing because of incoming energy from the outer magnetosphere and the ionosphere in the forms of particles and electromagnetic fields. In the inner magnetosphere, the particle energy is transferred to the field energy, and vice versa. The mutual coupling between particles and fields also makes the inner magnetosphere unique. The outgoing energy to these regions is also known to be significant, such as precipitation into the upper atmosphere and sub-auroral disturbances. A number of satellites (e.g., DMSP, NOAA, Geotail, Cluster, THEMIS, Van Allen Probes, MMS, and Arase), ground-based instruments (e.g., SuperDARN and EISCAT radars, magnetometers, and cameras), and numerical simulations (e.g., global particle simulation, PIC simulation, and hybrid simulation) have successfully surveyed the inner magnetosphere, which deepen our knowledge significantly. USAF DSX, UCLA Elfin and NASA CeRES will be launched soon, being expected to provide important information. We solicit papers describing recent results on the inner magnetosphere and/or its coupling with the other regions, including the ionosphere and the outer magnetosphere.

[PEM13-P01] Evaluation of wave normal and Poynting vector analyses for whistler mode waves observed by the waveform capture (WFC) on board the Arase

*Yoshiya Kasahara[1], Satoshi Ikarashi[1], Hiroyuki Nishizawa[1], Shoya Matsuda[2], Fuminori Tsuchiya[3], Atsushi Kumamoto[3], Yasumasa Kasaba[3], Mitsunori Ozaki[1], Ayako Matsuoka[2] (1.Kanazawa University, 2.ISAS/JAXA, 3.Tohoku University)

[PEM13-P02] Calibration of electric fields dedicated to the measurement of the S-WPIA of the Arase Satellite

*Miki Jumpei[1], Hirotsugu Kojima[2], Yuto Katoh[3], Shoya Matsuda[4], Yoshiya Kasahara[5], Mitsuru Hikishima[4], Satoshi Kurita[6], Masahiro Kitahara[3], Satoshi Kasahara[7], Yoshizumi Miyoshi[6], Atsushi Kumamoto[3], Ayako Matsuoka[4], Shoichiro Yokota[8], Tomoaki Hori[6], Kunihiro Keika[7] (1.Space Radio Engineering Laboratory, Division of Electrical Engineering, Kyoto University Graduated School, 2.Research Institute for Sustainable Humanosphere, Kyoto University, 3.Graduate School of Science and Faculty of Science, Tohoku University, 4.Institute of Space and Astronautical Science, JAXA, 5.Information Media Center, Kanazawa University, 6.Institute for Space-Earth Environmental Research, Nagoya University, 7.School of Science, The University of Tokyo, 8.School of Science, Osaka University)

[PEM13-P03] Enhancement of whistler-mode chorus in association with Pc 4-5 ULF waves and related variation of high energy electrons

*Atsuhiro Ono[1], Yuto Katoh[1], Atsushi Kumamoto[1], Fuminori Tsuchiya[1], Mariko Teramoto[2], Yoshiya Kasahara[3], Shoya Matsuda[4], Ayako Matsuoka[4], Takefumi Mitani[4], Tomoaki Hori[2], Satoshi Kasahara[5], Shoichiro Yokota[6], Kunihiro Keika[5], Yoshizumi Miyoshi[2], Iku Shinohara[4] (1.Tohoku University, 2.Nagoya University, 3.Kanazawa University, 4.ISAS/JAXA, 5.The University of Tokyo, 6.Osaka University)

[PEM13-P04] Sudden enhancements of electron cyclotron harmonic waves observed by the Arase satellite

*Shinjo Airi[1], Hirotsugu Kojima[1], Yoshiya Kasahara[2], Yoichi Kazama[3], Hideyuki Usui[4], Yoshizumi Miyoshi[5], Yasumasa Kasaba[6], Shoya Matsuda[7], Tomoaki Hori[5], S. -Y. Wang[8], Sunny W.Y. Tam[9], Atsushi

Kumamoto[10], Ayako Matsuoka[11] (1.Research institute for sustainable humanosphere, Kyoto University, 2.Information Media Center, Kanazawa University, 3.ASIAA, 4.Graduate school of system informatics Kobe University, 5.Institute for Space-Earth Environmental Research, Nagoya University, 6.Planetary Plasma and Atmospheric Research Center, Tohoku University, 7.Institute of Space and Astronautical Science/Japan Aerospace Exploration Agency, 8.ASIAA, Taiwan, 9.ISAPS, NCKU, Taiwan, 10.Department of Geophysics, Graduate School of Science, Tohoku University, 11.Research Division for Space Plasma, Institute of Space and Astronautical Science, Japan Aerospace Exploration Agency)

[PEM13-P05] Correlation between pulsating aurora and electrostatic electron cyclotron harmonic waves obtained from coordinated Arase and ground data

*Mizuki Fukizawa[1], Takeshi Sakanoi[1], Yoshizumi Miyoshi[2], Keisuke Hosokawa[3], Yoichi Kazama[4], Yoshiya Kasahara[5], Shoya Matsuda[6], Ayako Matsuoka[7], Wang Shiang-Yu[4], Sunny Wing-Yee Tam[8], Ryuho Kataoka[9] (1.Planetary Plasma and Atmospheric Research Center, Graduate School of Science, Tohoku University, 2.Institute for Space-Earth Environmental Research, Nagoya University, 3.Department of Communication Engineering and Informatics, University of Electro-Communications, 4.Academia Sinica Institute of Astronomy and Astrophysics, 5.Information Media Center, Kanazawa University, 6.Institute of Space and Astronautical Science/Japan Aerospace Exploration Agency, 7.Research Division for Space Plasma, Institute of Space and Astronautical Science, Japan Aerospace Exploration Agency, 8.Institute of Space and Plasma Sciences, College of Sciences, National Cheng Kung University , 9.National Institute of Polar Research)

[PEM13-P06] Automatic determination of Upper Hybrid Resonance Frequencies by Convolutional Neural Network.

*Shoya Matsuda[1], Tatsuhito Hasegawa[2], Atsushi Kumamoto[3], Fuminori Tsuchiya[3], Yoshiya Kasahara[4], Yoshizumi Miyoshi[5], Yasumasa Kasaba[3], Ayako Matsuoka[1] (1.Institute of Space and Astronautical Science/Japan Aerospace Exploration Agency, 2.University of Fukui, 3.Tohoku University, 4.Kanazawa University, 5.ISEE, Nagoya University)

[PEM13-P07] Amplitude dependence of whistler wave motion on electron scattering process

*Yoshiki Ito[1], Yoshizumi Miyoshi[1], Shinji Saito[1] (1.Nagoya University, ISEE)

[PEM13-P08] Two-dimensional simulation of whistler mode wave packets interacting with energetic electrons

*Takeshi Nogi[1], Yoshiharu Omura[1] (1.Reserch Institute for Sustainable Humanosphere, Kyoto University)

[PEM13-P09] Relativistic electron acceleration by whistler-mode chorus waves in 1D, 2D, and 3D magnetic field models.

*Keita Takahashi[1], Yoshiharu Omura[1], Yikai HSIEH[1], Danny Summers[2] (1.Research Institute for Sustainable Humanosphere, Kyoto University , 2.Department of Mathematics and Statistics, Memorial University of Newfoundland)

[PEM13-P10] Study of global spatio-temporal development of magnetospheric ELF/VLF waves for the 26-30 March 2017 storm based on ground and satellite observations and the RAM simulations

*Yuhei Takeshita[1], Kazuo Shiokawa[1], Yoshizumi Miyoshi[1], Mitsunori Ozaki[2], Yoshiya Kasahara[2], Martine Connors[3], Jyrki Manninen[4], Craig Kletzing[5], Vania Jordanova[6] (1.Nagoya University, Institute for Space-Earth Environmental Resarch, 2.Kanazawa University, 3.Athabasca University, 4.Sodankylä Geophysical Observatory, 5.The University of Iowa, 6.Los Alamos National Laboratory)

[PEM13-P11] Flux decrease of outer radiation belt electrons associated with solar wind pressure pulse: A Code coupling simulation of GEMSIS-RB and GEMSIS-GM

*Ito Hiroki[1], Yoshizumi Miyoshi[1], Shinji Saito[2], Yosuke Matsumoto[3], Takanobu Amano[4] (1.Institute for Space-Earth Environmental Research, Nagoya University, 2. Graduate School of Science, Nagoya

University, 3. Graduate School of Science, Chiba University, 4.Department of Earth and Planetary Science, University of Tokyo)

[PEM13-P12] Non-diffusive response of outer belt electrons on interplanetary shock

Takuma Toishi[1], *Yusuke Ebihara[1], Takashi Tanaka[2] (1.Research Institute for Sustainable Humanosphere, Kyoto University, 2.Kyushu University)

[PEM13-P13] PARM: Initial result of the auroral camera on the G-CHASER (RockSat-XN) rocket and status of the development of auroral cameras for the LAMP rocket experiment

*Naoshi Yagi[1], Takeshi Sakanoi[1], Fukizawa Mizuki[1], Kazushi Asamura[2], Yoshizumi Miyoshi[3], Keisuke Hosokawa[4], Genki Ishizawa[5] (1.Planetary Plasma and Atmospheric Research Center, Graduate School of Science, Tohoku University, 2.Institute of Space and Astronautical Science, Japan Aerospace Exploration Agency, 3.Institute for Space-Earth Environmental Research, Nagoya University, 4.Department of Communication Engineering and Informatics, University of Electro-Communications, 5.Space & terrestrial plasma pyhsics)

[PEM13-P14] First simultaneous observation of a SAR arc at subauroral latitudes using a ground all-sky camera and the Arase satellite in the inner magnetosphere

*Yudai Inaba[1], Kazuo Shiokawa[1], Shin-ichiro Oyama[1,8,9], Yuichi Otsuka[1], Atsuki Shinbori[1], Yoichi Kazama[2], Shiang-Yu Wang[2], Sunny W. Y. Tam[2], Shoichiro Yokota[3], Satoshi Kasahara[4], Kunihiro Keika[4], Tomoaki Hori[1], Ayako Matsuoka[5], Yoshiya Kasahara[6], Atsushi Kumamoto[7], Yasumasa Kasaba[7], Yoshizumi Miyoshi[1], Iku Shinohara[5], Arto Oksanen[10] (1.Institute for Space-Earth Environmental Research, 2.Academia Sinica, 3.Osaka Univ, 4.Tokyo Univ, 5.JAXA, 6.Kanazawa University, 7.Tohoku University, 8.University of Oulu, Finland, 9.National Institute of Polar Research, 10.Jyväskylän Sirius ry, Finland)

[PEM13-P15] Pi2 pulsations observed by the Arase satellite inside and outside the plasmapause

*Mariko Teramoto[1], Ayako Matsuoka[2], Reiko Nomura[5], Yoshiya Kasahara[3], Yasumasa Kasaba[4], Atsushi Kumamoto[4], Fuminori Tsuchiya[4], Shoya Matsuda[2], Masahito Nose[1], Masafumi Shoji[1], Yasunori Tsugawa[1], Shun Imajo[1], Yoshizumi Miyoshi[1], Iku Shinohara[2] (1.Institute for Space-Earth Environmental Research Nagoya University, 2.Institute of Space and Astronautical Science, Japan Aerospace eXploration Agency, 3.Kanazawa University, 4.Tohoku University, 5.National Astronomical Observatory of Japan)

[PEM13-P16] An extreme erosion of the plasmasphere during the 7–10 September 2017 storm

*Yuki Obana[1], Naomi Maruyama[2,3], Atsuki Shinbori[4], Kumiko K. Hashimoto[5], Mariangel Fedrizzi[2,3], Masahito Nose[4], Yuichi Otsuka[4], Nozomu Nishitani[4], Tomoaki Hori[4], Atsushi Kumamoto[6], Fuminori Tsuchiya[6], Shoya Matsuda[7], Ayako Matsuoka[7], Yoshiya Kasahara[8], Akimasa Yoshikawa[9], Yoshizumi Miyoshi[4], Iku Shinohara[7] (1.Osaka Electro-Communication University, 2.University of Colorado Boulder, 3.NOAA Space Weather Prediction Center, 4.Nagoya University, 5.Kibi International University, 6.Tohoku University, 7.Japan Aerospace Exploration Agency, 8.Kanazawa University, 9.Kyushu University)

[PEM13-P17] Relative contribution of ULF and chorus waves to the radiation belt variation: Comparison between multi-point observations and BATSRUS + CRCM simulation

*Naoko Takahashi[1], Kanako Seki[1], Mei-Ching Fok[2], Yihua Zheng[2], Yoshizumi Miyoshi[3], David Hartley[4], Ayako Matsuoka[5], Yoshiya Kasahara[6], Yasumasa Kasaba[7], Nana Higashio[8] (1.Graduate School of Science, University of Tokyo, 2.NASA Goddard Space Flight Center, 3.Institute for Space-Earth Environmental Research, Nagoya University, 4.Department of Physics and Astronomy, University of Iowa, 5.Institute of Space and Astronautical Science, Japan Aerospace Exploration Agency, 6.Information Media Center, Kanazawa University, 7.Planetary Plasma and Atmospheric Research Center, Tohoku University, 8.Japan Aerospace Exploration Agency)

[PEM13-P18] Modulation of the D-region ionosphere by Pc5 waves observed by VLF/LF standard radio waves

*Miyashita Takuya[1], Hiroyo Ohya[1], Fuminori Tsuchiya[2], Hiroyuki Nakata[1], Toshiaki Takano[1], Kazuo Shiokawa[3], Yoshizumi Miyoshi[3] (1.Chiba University, 2.Tohoku University, 3.Nagoya University)

[PEM13-P19] Oxygen-proton differences in ion energies dominating plasma pressure: Dependence on storm phases and solar wind drivers

*Kunihiro Keika[1], Satoshi Kasahara[1], Shoichiro Yokota[2], Masahiro Hoshino[1], Kanako Seki[1], Masahito Nose[3], Yoshizumi Miyoshi[3], Iku Shinohara[4] (1.Graduate School of Science, The University of Tokyo , 2.Graduate School of Science, Osaka University, 3.Institute for Space-Earth Environmental Research, Nagoya University, 4.Institute of Space and Astronautical Science, Japan Aerospace Exploration Agency)

[PEM13-P20] Mass dependence of penetration depth of multi-energy ions in the inner magnetosphere during magnetic storms: Arase observations

*Ryosuke Fujii[1], Yoshizumi Miyoshi[1], Masafumi Shoji[1], Kazushi Asamura[2], Lynn Kistler[1,8], Vania Jordanova[9], Tomoaki Hori[1], Satoshi Kurita[1], Mariko Teramoto[1], Yasunori Tsugawa[1], Yoshiya Kasahara[3], Yasumasa Kasaba[4], Atsushi Kumamoto[5], Fuminori Tsuchiya[4], Shoichiro Yokota[6], Kunihiro Keika[7], Ayako Matsuoka[2], Iku Shinohara[2] (1.Institute for Space-Earth Environmental Research, Nagoya University, 2.Institute of Space and Astronautical Science, Japan Aerospace Exploration Agency, 3.Information Media Center, Kanazawa University, 4.Planetary Plasma and Atmospheric Research Center, Tohoku University, 5.Department of Geophysics, Graduate School of Science, Tohoku University, 6.Graduate School of Science, Osaka University, 7.Department of Earth and Planetary Science, Graduate School of Science, The University of Tokyo, 8.University of New Hampshire, 9.Los Alamos National Laboratory)

[PEM13-P21] Relativistic Acceleration of Energetic Protons by Electromagnetic Ion Cyclotron Waves in the Jovian Magnetosphere

*Tomohiro Sekine[1], Yoshiharu Omura[1], Danny Summers[2], Yikai HSIEH[1], Satoko Nakamura[1] (1.Reserach Institute for Sustainable Humanosphere, Kyoto University, 2.Memorial University of Newfoundland)

[PEM13-P22] Statistical study of IPDP type EMIC wave-related electron precipitation at subauroral latitude

*Asuka Hirai[1], Fuminori Tsuchiya[1], Takahiro Obara[1], Yasumasa Kasaba[1], Yuto Katoh[2], Hiroaki Misawa[1], Kazuo Shiokawa[3], Yoshizumi Miyoshi[3], Satoshi Kurita[3], Martin G Connors[4] (1.Planetary Plasma and Atmospheric Research Center, Graduate School of Science, Tohoku Univ. , 2.Department of Geophysics, Graduate School of Science, Tohoku University, 3.Institute for Space-Earth Environmental Research, Nagoya University, 4.Athabasca University)

[PEM13-P23] Meridional distributions of proton plasma and pressure-driven currents in the nightside inner magnetosphere: Arase observations

*Shun Imajo[1], Masahito Nose[1], Satoshi Kasahara[2], Shoichiro Yokota[3], Ayako Matsuoka[4], Kunihiro Keika[2], Tomoaki Hori[1], Mariko Teramoto[1], Kazuhiro Yamamoto[5], Oimatsu Satoshi[5], Reiko Nomura[6], Akiko Fujimoto[7], Iku Shinohara[4], Yoshizumi Miyoshi[1] (1.Institute for Space-Earth Environmental Research, Nagoya University, 2.Graduate School of Science, The University of Tokyo, 3.Graduate School of Science, Osaka University, 4.Institute of Space and Astronautical Science, Japan Aerospace Exploration Agency, 5.Graduate School of Science, Kyoto University, 6.National Astronomical Observatory of Japan, 7.Kyushu Institute of Technology)

[PEM13-P24] Space Weather Effects on Energetic Proton Flux Response in South Atlantic Anomaly

*Kirolosse Mina GIRGIS[1,2], Tohru Hada[1], Shuichi Matsukiyo[1] (1.Earth System Science and Technology (ESST) Department, Interdisciplinary Graduate School of Engineering Sciences (IGSES), Kyushu University, Japan, 2.Aerospace Engineering Department, Faculty of Engineering, Cairo University, Egypt)

[PEM13-P25] Solar-cycle variations of >30 keV electron flux enhancements under the inner radiation belt

*ALLA SUVOROVA[1] (1.National Central University)

[PEM13-P26] Energy spectra variations of high energy electrons in the inner magnetosphere observed by HEP/XEP on ARASE and SEDA-e on HIMAWARI

*Takeshi Takashima[1], Takefumi Mitani[1], Nana Higashio[2], Tsutomu Nagatsuma[3] (1. ISAS/JAXA, 2.Research and Development Directorate/JAXA, 3.NiCT)

[PEM13-P27] Inter-channel calibration of the high-energy electron experiments (HEP) instrument onboard the Arase satellite

*Tomoaki Hori[1], Takefumi Mitani[2], Takeshi Takashima[2], Park Inchun[1], Satoshi Kurita[1], Mariko Teramoto[1], Nana Higashio[3], Satoshi Kasahara[4], Shoichiro Yokota[5], Yoshizumi Miyoshi[1], Iku Shinohara[2] (1.Institute for Space-Earth Environmental Research, Nagoya University, 2.Japan Aerospace Exploration Agency, Institute of Space and Astronautical Science, 3.Japan Aerospace Exploration Agency, 4.Graduate School of Science, The University of Tokyo, 5.Graduate School of Science, Osaka University)

[PEM13-P28] Particle simulation for calibrating the HEP data onboard the ARASE satellite

*PARK INCHUN[1], Yoshizumi Miyoshi[1], Takefumi Mitani[2], Tomoaki Hori[1], Satoshi Kurita[1], Mariko Teramoto[1], Takeshi Takashima[2], Nana Higashio[3], Iku Shinohara[2] (1.Nagoya University Institute for Space-Earth Environmental Research, 2.Japan Aerospace Exploration Agency Institute of Space and Astronautical Science , 3.Japan Aerospace Exploration Agency)

[PEM13-P29] Geant4 model calculation and energetic particle observation with HEP/Arase in the inner radiation belt

*Honoka Toda[1], Wataru Miyake[1], Takefumi Mitani[3], Takeshi Takashima[3], Yoshizumi Miyoshi[2], PARK INCHUN[2], Tomoaki Hori[2] (1.Tokai University, 2.ISEE/Nagoya University, 3.ISAS/JAXA)

[PEM13-P30] Validation of High-energy electron detector simulator for the HEP instruments onboard Arase

*Takefumi Mitani[1], PARK INCHUN[2], Tomoaki Hori[2], Taku Namekawa[1,3], Kazushi Asamura[1], Takeshi Takashima[1], Satoshi Kasahara[3], Satoshi Kurita[2], Mariko Teramoto[2], Nana Higashio[1], Yoshizumi Miyoshi[2], Iku Shinohara[1] (1.Japan Aerospace Exploration Agency, Institute of Space and Astronautical Science, 2.Institute for Space-Earth Environmental Research, Nagoya Univ., 3.The university of Tokyo)

Evaluation of wave normal and Poynting vector analyses for whistler mode waves observed by the waveform capture (WFC) on board the Arase

*Yoshiya Kasahara[1], Satoshi Ikarashi[1], Hiroyuki Nishizawa[1], Shoya Matsuda[2], Fuminori Tsuchiya[3], Atsushi Kumamoto[3], Yasumasa Kasaba[3], Mitsunori Ozaki[1], Ayako Matsuoka[2]

1. Kanazawa University, 2. ISAS/JAXA, 3. Tohoku University

The Plasma Wave Experiment (PWE) is one of scientific instruments on board the Arase (ERG) satellite to measure electric field from DC to 10 MHz and magnetic field from a few Hz to 100 kHz in the inner magnetosphere. It is well known that chorus wave, one of typical plasma waves in VLF range observed in the inner magnetosphere, is a plausible candidate that accelerates relativistic electrons in the radiation belt. Besides the chorus, the Arase has observed various kinds of plasma waves such as lightning whistlers and hiss waves. It is very important to study the propagation characteristics of these waves.

In the present paper, we developed a direction finding system applicable to whistler mode waves using the data from waveform capture (WFC), which is one of receivers covering the frequency range below 20kHz implemented in the PWE. The absolute directions of the wave normal and Poynting vectors were derived in the coordinate system referring the ambient magnetic field and geomagnetic meridian plane. We also estimated the Poynting vector theoretically using the derived wave normal vector, electron density and ambient magnetic field intensity to confirm the validity of the results from the observation data.

We demonstrated that the results were generally reliable, but further calibration is necessary for electric field to improve the accuracy of Poynting vector because the waveform of electric field is now calibrated under the assumptions of theoretical antenna capacitance in a vacuum and typical plasma impedance. In other words, we expect to be able to correct the calibration table for electric field measurements from the direction finding results.

In the presentation, we introduce some typical results which have been derived from the observation data of upper- and lower-band chorus, and lightning whistlers.

Keywords: Whistler mode wave, Waveform Capture, Direction finding, Plasma wave

©2019. Japan Geoscience Union. All Right Reserved.

Calibration of electric fields dedicated to the measurement of the S-WPIA of the Arase Satellite

*Miki Jumpei[1], Hirotsugu Kojima[2], Yuto Katoh[3], Shoya Matsuda[4], Yoshiya Kasahara[5], Mitsuru Hikishima[4], Satoshi Kurita[6], Masahiro Kitahara[3], Satoshi Kasahara[7], Yoshizumi Miyoshi[6], Atsushi Kumamoto[3], Ayako Matsuoka[4], Shoichiro Yokota[8], Tomoaki Hori[6], Kunihiro Keika[7]

1. Space Radio Engineering Laboratory, Division of Electrical Engineering, Kyoto University Graduated School, 2. Research Institute for Sustainable Humanosphere, Kyoto University, 3. Graduate School of Science and Faculty of Science, Tohoku University, 4. Institute of Space and Astronautical Science, JAXA, 5. Information Media Center, Kanazawa University, 6. Institute for Space-Earth Environmental Research, Nagoya University, 7. School of Science, The University of Tokyo, 8. School of Science, Osaka University

The outer radiation belt consists of high-energy electrons. They are strongly affected by geomagnetic activities in the relation to solar wind conditions. The important science target of the Arase mission is to clarify generation/loss mechanisms of relativistic electrons in the outer radiation belt. Wave-particle interactions are thought to be a plausible mechanism for generation/loss processes of relativistic electrons. S-WPIA (Software-type Wave-Particle Interaction Analyzer) is installed in the Arase satellite. The WPIA is a newly developed observation system that enables us to quantitatively understand the interaction between plasma waves and electrons. The WPIA has the capability to identify a relative phase angle of a plasma wave vector and a velocity vector of each detected particle. Since phase information of observed plasma waves is essential to the WPIA, precise calibrations of plasma wave data are important. While the calibration data for the magnetic field sensors are identical to those we obtained during the ground tests of the instruments, the calibration data for electric field sensors strongly depend on plasma parameters around the satellite. Furthermore, there are still unclear parameters at the inputs of preamplifiers relating to the connection with electric field sensors. The calibration for electric field data needs to be performed carefully consulting observation data after the launch.

The present paper focuses on the calibration of plasma wave data for the S-WPIA’s data processing. We picked up events including whistler-mode chorus emissions and lightning-whistler waves. They all are electromagnetic waves, so-called whistler mode waves. The amplitude ratios of their electric field and magnetic field components can be theoretically calculated referring to the Appleton-Hartlee equations. Poynting vectors of whistler mode waves can be also theoretically obtained. We compared the observation results of the picked up events with the theoretical ones. The results show the precise calibration for the magnetic field data have been made. On the other hand, the calibration for the electric field data should be further modified consulting plasma parameters and other uncertain parameters at the input of preamplifiers. In the present paper, we will discuss the improvement of the calibration for electric field data by correcting the calibration table to aim the precise S-WPIA data processing.

©2019. Japan Geoscience Union. All Right Reserved.

Enhancement of whistler-mode chorus in association with Pc 4-5 ULF waves and related variation of high energy electrons

*Atsuhiro Ono[1], Yuto Katoh[1], Atsushi Kumamoto[1], Fuminori Tsuchiya[1], Mariko Teramoto[2], Yoshiya Kasahara[3], Shoya Matsuda[4], Ayako Matsuoka[4], Takefumi Mitani[4], Tomoaki Hori[2], Satoshi Kasahara[5], Shoichiro Yokota[6], Kunihiro Keika[5], Yoshizumi Miyoshi[2], Iku Shinohara[4]

1. Tohoku University, 2. Nagoya University, 3. Kanazawa University, 4. ISAS/JAXA, 5. The University of Tokyo, 6. Osaka University

Whistler-mode chorus emissions play significant roles in the acceleration and loss of energetic electrons in the magnetosphere. One of the important factors which control periodic enhancement of chorus emissions is ULF (Ultra Low Frequency) waves. Previous studies reported that the compressional component of Pc4-5 ULF waves modulates the intensity of chorus waves [Li et al., 2011] and that the toroidal and poloidal components of Pc4-5 ULF waves as well [Jaynes et al., 2015]. Previous studies also suggested that enhancement of the temperature anisotropy of energetic electrons in the wave generation region should be required for the chorus generation. In order to understand the reported correspondence, in addition to the wave observation, we should examine simultaneously observed variations of the flux and the pitch angle distribution of energetic electrons.

In the present study, we investigate the relationship between chorus emissions and ULF waves using particle and electromagnetic field observations made by the Arase satellite. First, we analyze data observed by the Onboard Frequency Analyzer (OFA) of the Plasma Wave Experiment (PWE) and the Magnetic Field Experiment (MGF) during the campaign observation period of the Arase satellite with ground stations from March to April in 2017. As a result, we identified the simultaneous enhancement of chorus emissions and Pc4-5 ULF waves, which was dominated by the toroidal component, from 2130 to 2200 UT on March 27, 2017. The Arase satellite was located at the magnetic local time about 04:00, the magnetic latitude about -10 degrees, and the L-value about 6 during the event. We find that there is one-to-one correspondence between chorus emissions and the toroidal component of ULF waves; chorus emissions enhanced at the timings when the toroidal magnetic field component of ULF waves had a peak in the westward direction. The identified phase relationship is different from that reported by Jaynes et al. (2015), which isn't one-to-one correspondence. Next, we evaluate the resonance energy of the observed chorus emissions, using the ratio of the plasma frequency to the electron cyclotron frequency (f_p/f_{ce}) based on the upper-hybrid resonance frequency derived from the spectra observed by the High Frequency Analyzer (HFA) of PWE and the ambient magnetic field intensity observed by MGF. We find that f_p/f_{ce} is 3.3-3.4 during the event and that the resonance energy for whistler-mode waves in the frequency range of 0.1-0.2 f_{ce} is estimated to be about 100-400keV, which is larger than typical energies of resonating electrons observed in the inner magnetosphere. The estimated large resonant energy can be explained by the frequency range of the observed chorus emissions, approximately 0.1 - 0.2 f_{ce}, is relatively lower than that observed in typical cases.
We also analyze variations of the flux and the pitch angle distribution of energetic electrons during the event using data observed by the High-energy electron experiments (HEP) instrument onboard Arase. The result shows that both the flux and the pitch angle distribution of electrons in the kinetic energy range from 100 to 400 keV, which corresponds to the estimated resonance energy, did not fluctuate with the intensity variation of the chorus emissions and the ULF waves. In addition, we analyze the data observed by the Medium-energy particle experiments - electron analyzer (MEP-e) for energetic electrons in the energy range of 10-80 keV, lower than the estimated resonance energy. Then we identify the

©2019. Japan Geoscience Union. All Right Reserved.

corresponding variation of both the flux and the pitch angle distribution in the 40-60 keV energy range. One of the possible reasons why no significant variations were observed in the hundred keV range would be that the Arase satellite was located in the off-equatorial region during the event, and that the satellite was away from the wave generation region.

Keywords: ULF waves, chorus emissions

©2019. Japan Geoscience Union. All Right Reserved.

Sudden enhancements of electron cyclotron harmonic waves observed by the Arase satellite

*Shinjo Airi[1], Hirotsugu Kojima[1], Yoshiya Kasahara[2], Yoichi Kazama[3], Hideyuki Usui[4], Yoshizumi Miyoshi[5], Yasumasa Kasaba[6], Shoya Matsuda[7], Tomoaki Hori[5], S. -Y. Wang[8], Sunny W.Y. Tam[9], Atsushi Kumamoto[10], Ayako Matsuoka[11]

1. Research institute for sustainable humanosphere, Kyoto University, 2. Information Media Center, Kanazawa University, 3. ASIAA, 4. Graduate school of system informatics Kobe University, 5. Institute for Space-Earth Environmental Research, Nagoya University, 6. Planetary Plasma and Atmospheric Research Center, Tohoku University, 7. Institute of Space and Astronautical Science/Japan Aerospace Exploration Agency, 8. ASIAA, Taiwan, 9. ISAPS, NCKU, Taiwan, 10. Department of Geophysics, Graduate School of Science, Tohoku University, 11. Research Division for Space Plasma, Institute of Space and Astronautical Science, Japan Aerospace Exploration Agency

Electron cyclotron harmonic (ECH) waves are commonly observed in the low latitude region just outside the terrestrial plasmapause. They are purely electrostatic and their frequency spectra show harmonic structures. The harmonic structures are believed to depend on the temperature and density ratio between cold and hot background electrons. The Plasma Wave Experiment (PWE) onboard the Arase satellite has observed ECH waves since the start of its operation. The observed ECH waves are classified into two types. They are the diffuse ECH waves and the enhanced ECH waves. The diffuse ECH waves are weak and they appear as continuous emissions that last for more than a few minutes. The enhanced ECH waves are the sudden enhancements of the diffuse ECH in shorter periods. The present paper focuses on the enhanced ECH waves observed by the Arase satellite.

Kazama et al. (2018) introduced the event that the repeated enhancement of ECH waves is associated with density depletions near the plasmapause. They succeeded in revealing the good correlation of the enhancement of the ECH waves and the sudden decrease of the cold electrons with energies lower than the lowest energy limit of the particle detector. The observed electron features are clear in the relation to the enhancement of ECH waves, but the mechanism of the enhancement is still unclear. We searched for such events of the enhanced ECH waves and examined the correlation of wave intensities, spacecraft potentials and electron velocity distributions observed by the Arase satellite. Some of the events show the features similar to those of Kazama et al. (2018), but there are also many other events with no correlation between the enhancements of the ECH waves and the density depletions. In the present paper, we examine velocity distribution functions of electrons observed by the low-energy particle experiments-electron analyzer (LEPe) onboard Arase. Velocity distribution functions allow us to examine temperature anisotropies of electrons and calculate linear dispersion relations for the ECH waves. Once we get electron temperatures, resonance velocities are calculated. On the other hand, since the wavelength of the ECH waves is very short, the relation of the wavelength and the length of the Arase electric field sensors is also important in evaluating the time variations of the ECH wave intensity. We study the enhanced ECH waves in various viewpoints using wave and electron data observed by the Arase satellite and discuss the generation mechanism in the present paper.

©2019. Japan Geoscience Union. All Right Reserved.

Correlation between pulsating aurora and electrostatic electron cyclotron harmonic waves obtained from coordinated Arase and ground data

*Mizuki Fukizawa[1], Takeshi Sakanoi[1], Yoshizumi Miyoshi[2], Keisuke Hosokawa[3], Yoichi Kazama[4], Yoshiya Kasahara[5], Shoya Matsuda[6], Ayako Matsuoka[7], Wang Shiang-Yu[4], Sunny Wing-Yee Tam[8], Ryuho Kataoka[9]

1. Planetary Plasma and Atmospheric Research Center, Graduate School of Science, Tohoku University, 2. Institute for Space-Earth Environmental Research, Nagoya University, 3. Department of Communication Engineering and Informatics, University of Electro-Communications, 4. Academia Sinica Institute of Astronomy and Astrophysics, 5. Information Media Center, Kanazawa University, 6. Institute of Space and Astronautical Science/Japan Aerospace Exploration Agency, 7. Research Division for Space Plasma, Institute of Space and Astronautical Science, Japan Aerospace Exploration Agency, 8. Institute of Space and Plasma Sciences, College of Sciences, National Cheng Kung University , 9. National Institute of Polar Research

Pulsating auroras (PsAs) are thought to be generated by precipitating electrons scattered by lower-band chorus (LBC) waves near the magnetic equator through cyclotron resonance. Previous studies showed one-to-one correlation between LBC wave intensity observed by satellites near the magnetic equator and PsA intensity obtained by ground-based all-sky imager [e.g., Nishimura et al., Science, 2010, Nishimura et al., JGR, 2011]. In addition, electrostatic electron cyclotron harmonic (ECH) waves can also interact with magnetospheric electrons and scatter their pitch angle theoretically [e.g., Lyons, JGR, 1974]. However, characteristics of aurora caused by ECH are not understood. In our study, we report for the first time in the world that not only LBC but also ECH wave intensity has correlation with the PsA intensity using coordinated Arase and ground-based imager observations. The first campaign observations between the Arase satellite and ground-based optical imager were conducted in March 2017. A typical substorm occurred on 27 March 2017 and the ionospheric footprint of Arase traversed the field of view of all-sky imager at Sodankylä during 00:00–03:15 UT on 29 March 2017. Quasi-periodic LBC and ECH waves were observed by Arase near the magnetic equator and PsA was detected by the all-sky imager during 01:30–02:00 UT. We calculated the cross-correlation coefficients between auroral intensity and LBC or ECH wave intensity from 01:30 UT to 02:00 UT with a time window of every 2 minutes. The highest cross-correlation coefficient between auroral intensity and LBC wave intensity was 0.73 and that between auroral intensity and ECH wave intensity was 0.62 from 01:46 UT to 01:48 UT, and they were statistically significant. The period of auroral intensity which correlated with LBC intensity was shorter than 10 s and that correlated with ECH intensity was 10–20 s. We estimated the precipitating electron energy assuming that the time lag when the cross-correlation coefficient became the highest equals to the travel time of electrons from the modulated source region to the auroral emission height. We shifted the variation of auroral intensity against that of ECH or LBC wave intensity with a time step of 0.01 s using 100 Hz sampling image data taken by the all-sky imager. The estimated energy of precipitating electron interacted with LBC waves was ~20–67 keV and that interacted with ECH waves was ~3–4 keV. On the other hand, we independently estimated the cyclotron resonance energy of LBC and ECH waves from the Arase's observation data and geomagnetic field model by TS04 Model [Tsyganenko and Sitnov, JGR, 2005]. The estimated cyclotron resonance energy of LBC waves was ~30 keV. Although the cyclotron resonance energy of ECH waves could not be estimated because it was difficult to obtain the electron temperature and wave normal angle of ECH waves from Arase data, we suggest the cyclotron resonance energy of ECH waves to be a few keV with probable assumptions. From these results, we suggest that LBC waves interact with high energy electrons which cause auroral emission at lower altitudes, while ECH waves interact with

©2019. Japan Geoscience Union. All Right Reserved.

relatively low energy electrons which cause auroral emission at higher altitudes. These results were published in Fukizawa et al. [GRL, 2018].
To verify whether ECH waves indeed scatter the pitch angle of electrons, we compared ECH wave intensity with electron flux in the loss cone obtained with low-energy particle experiments-electron analyzer onboard Arase. We also give results of other coordinated observation events.

Keywords: pulsating aurora, ECH waves, wave-particle interaction

©2019. Japan Geoscience Union. All Right Reserved.

Automatic determination of Upper Hybrid Resonance Frequencies by Convolutional Neural Network.

*Shoya Matsuda[1], Tatsuhito Hasegawa[2], Atsushi Kumamoto[3], Fuminori Tsuchiya[3], Yoshiya Kasahara[4], Yoshizumi Miyoshi[5], Yasumasa Kasaba[3], Ayako Matsuoka[1]

1. Institute of Space and Astronautical Science/Japan Aerospace Exploration Agency, 2. University of Fukui, 3. Tohoku University, 4. Kanazawa University, 5. ISEE, Nagoya University

Electron number density is a key parameter for discussions of plasma wave generation/propagation, and wave-particle interaction in the inner magnetosphere. The High Frequency Analyzer (HFA) is a subsystem of Plasma Wave Experiment (PWE) aboard Arase [Kasahara et al. (2018), Kumamoto et al. (2018), Miyoshi et al. (2018)]. The HFA measures electric field spectra in a frequency range from 10 kHz to 10 MHz, which covers a typical frequency range of Upper Hybrid Resonance (UHR) frequency in the inner magnetosphere. Kumamoto et al. (2018) proposed the semiautomatic method for the identification of UHR frequency by computer and a human operator. However, it takes a enormous effort of a human operator.

We propose an automatic determination system of UHR frequency by machine learning. Machine learning is a technique in the field of artificial intelligence to give computers the ability to learn with data. In this study, we defined a task of UHR frequency determination as supervised regression that a computer estimates UHR frequencies using the dataset composed of electric field dynamic spectra with correct UHR frequency labels. We adopted Convolutional Neural Network (CNN) as a machine learning algorithm. In this study, we introduce our machine learning approach and initial results for determining UHR frequency from electric field spectra observed by PWE/HFA.

Keywords: Arase satellite, UHR frequency, Machine learning

©2019. Japan Geoscience Union. All Right Reserved.

Amplitude dependence of whistler wave motion on electron scattering process

*Yoshiki Ito[1], Yoshizumi Miyoshi[1], Shinji Saito[1]

1. Nagoya University, ISEE

Whistler mode chorus waves cause scattering and acceleration of energetic electrons in the inner magnetosphere. The interaction processes have been modeled as diffusive process. The pitch angle diffusion coefficients of the pitch angle scattering depend on the power of chorus waves, so that it is expected that the scattering rate also depends on the wave amplitude. On the other hand, several previous studies indicated that the Lorentz force by the wave magnetic field is larger than the mirror force if the wave amplitudes increase and the electron trajectories in the velocity space are different from the diffusive distributions. In this study, we investigate chorus wave amplitude dependence of electron scattering using the GEMSIS-RBW simulation code. The RBW simulation demonstrates generation of periodical rising-tone chorus waves propagating along a magnetic field line to higher latitudes, and calculates local pitch angle and energy change by the imposed waves on the field line. At small wave amplitudes, time variations of pitch angle and energy of electrons are similar to diffusive process. At large wave amplitudes, some electrons increase both pitch angle and energy at interaction with the first rising tone, and then they decrease these parameters at interaction with the second rising tone. The process in the first rising tone seems to be the phase trapping, while the process in the second rising tone seems to be dislocation. Therefore, nonlinear scattering processes, which are phase trapping and dislocations, occur during the interactions with periodical rising-tone chorus waves with large amplitudes, which are quite different from quasi-linear scattering process.

©2019. Japan Geoscience Union. All Right Reserved.

Two-dimensional simulation of whistler mode wave packets interacting with energetic electrons

*Takeshi Nogi[1], Yoshiharu Omura[1]

1. Reserch Institute for Sustainable Humanosphere, Kyoto University

We perform two-dimensional electromagnetic particle simulations to study basic characteristics of whistler-mode wave particle interaction involved in the generation and propagation processes of chorus emissions with wave normal angles oblique to the static magnetic field. We assume a simple periodic (x, y) system with the magnetic field taken in the x-direction. We find the linear phase of the instability is much affected by electrostatic thermal fluctuations. It is necessary to put many super-particles in a grid cell to suppress the thermal fluctuation. We next put an array of antennas perpendicular to the background magnetic field, and oscillate the antenna current to generate obliquely propagating waves. In addition to the nonlinear trapping of energetic electrons through the cyclotron resonance, another nonlinear trapping of electrons takes place through the Landau resonance. Structures of the nonlinear trapping potentials change with the varying frequency, affecting efficiency of energy transfer between the wave and energetic electrons. We study nonlinear evolution of the wave packet, and competing processes of both resonances in accelerating energetic electrons to higher energies.

©2019. Japan Geoscience Union. All Right Reserved.

Relativistic electron acceleration by whistler-mode chorus waves in 1D, 2D, and 3D magnetic field models.

*Keita Takahashi[1], Yoshiharu Omura[1], Yikai HSIEH[1], Danny Summers[2]

1. Research Institute for Sustainable Humanosphere, Kyoto University , 2. Department of Mathematics and Statistics, Memorial University of Newfoundland

We evaluate the acceleration efficiencies of relativistic electrons under a 1D, 2D, and 3D model magnetic fields. We perform test-particle simulations and analyze nonlinear trapping motions of resonant electrons in each model. As a chorus wave model, we assume that a chorus wave packet generated at the magnetic equator propagates along the magnetic field to higher latitudes. When we perform simulations with the whistler mode wave, the cyclotron resonance with energetic electrons occurs at the similar timing in each model. Although we find relativistic turning acceleration (RTA) [1] to take place in each model, acceleration efficiencies of resonant electrons are different in these models. In terms of the numerical Green's function[2], we find a clear difference in time evolution of the distribution function in energy and equatorial pitch angle. The energy gap between resonant electrons and non-resonant electrons in the 1D model is slightly different from those in the 2D and 3D models. The energy gap in the 3D model is the largest among the three magnetic field models. This difference is due to additional oscillations in the velocity phase space, which only occur in the 2D and 3D models. These oscillations occur because the magnitude of the magnetic field changes during one period of relativistic cyclotron motion, affecting the nonlinear trapping conditions of resonant electrons.

References:

[1] Y. Omura, N. Furuya, D. Summers, Relativistic turning acceleration of resonant electrons by coherent whistler-mode waves in a dipole magnetic field, Journal Geophysical Research, Vol. 112, A06236, doi:10.1029/2006JA012243, 2007.

[2] Y. Omura, Y. Miyashita, M. Yoshikawa, D. Summers, M. Hikishima, Y. Ebihara, and Y. Kubota (2015), Formation process of relativistic electron flux through interaction with chorus emissions in the Earth's inner magnetosphere, J. Geophys. Res. Space Physics, 120, 9545–9562, doi:10.1002/2015JA021563, 2015.

©2019. Japan Geoscience Union. All Right Reserved.

Study of global spatio-temporal development of magnetospheric ELF/VLF waves for the 26-30 March 2017 storm based on ground and satellite observations and the RAM simulations

*Yuhei Takeshita[1], Kazuo Shiokawa[1], Yoshizumi Miyoshi[1], Mitsunori Ozaki[2], Yoshiya Kasahara[2], Martine Connors[3], Jyrki Manninen[4], Craig Kletzing[5], Vania Jordanova[6]

1. Nagoya University, Institute for Space-Earth Environmental Resarch, 2. Kanazawa University, 3. Athabasca University, 4. Sodankylä Geophysical Observatory, 5. The University of Iowa, 6. Los Alamos National Laboratory

The magnetospheric ELF/VLF waves are plasma waves generated by energetic electrons from several keV to tens keV with temperature anisotropy at magnetospheric equatorial plane of the inner magnetosphere. These ELF/VLF waves with frequencies lower than local half gyro frequency (lower-band) can propagate to the ground along magnetic field line. It is also known that the ELF/VLF waves interact with electrons drifting longitudinally in the inner magnetosphere, and help accelerating them to relativistic energies. Takeshita et al. [SGEPSS, 2018] statistically investigated the longitudinal extent of the magnetospheric ELF/VLF waves using six ground-based stations for two months, and showed the average extent of the ELF/VLF waves as ~90 degrees in longitude. However, Jordanova et al. [JGR, 2010] investigated the global distribution of linear growth rate of whistler mode chorus waves using global ring current-atmosphere interactions model (RAM), and showed that the region of large linear growth rate can extend ~180 degrees in longitude during the geomagnetic storm of 22 April 2001.

In this study we investigate the spatio-temporal distibution of the source region of magnetospheric ELF/VLF waves based on ground and satellite observations during the geomagnetic storm period from 26-30 March 2017, and compare it with global distribution of non-linear waves proxy of whistler mode chorus waves obtained by the RAM simulation. In this preliminary simulation, the simple dipole field and the Volland-Stern electric field are used as ambient magnetic and electric fields. And we assumed simply the Maxwell distribution as an energy spectrum using the empirical model of Tsyganenko and Mukai [2003]. In order to evaluate the non-linear wave excitation, we have estimated the optimum amplitude and the threshold value indicated by Omura and Nunn [2011]. We investigated the existence of lower band chorus waves using ground based observations at Athabasca (ATH; 54.7N, 246.4E, MLAT: 61.3N), Kapuskasing (KAP; 49.4N, 277.8E, MLAT: 58.7N), Kannuslehto (KAN: 67.7N, 26.3E, MLAT: 64.5N) and satellite-based observations by ERG with an apogee in the pre-dawn sector and RBSP-A and RBSP-B with an apogees in the post-dusk sector. We found the magnetospheric ELF/VLF waves exist from 3 MLT to 12 MLT for most periods from main- to recovery-phases of the magnetic storm. However, the RAM simulation did not predict wave generation during recovery phase of the storm. We compare the simulation and the ground-satellite observation in detail, and calculate the over-estimate rate (the ratio of wave existence period on the simulation to no wave period on the observation) and under-estimate rate (the ratio of no wave period on the simulation to wave existence period on the observation). We found the over-estimate rate become high (0.2~0.9) and under-estimate rate become low (0~0.4) in the main phase of the storm. This indicates that the longitudinal size of chorus source region predicted by simulation is larger than the observed size at the main phase. We also found that the over-estimate rate becomes low (0~0.2) and under-estimate rate becomes high (~1) during the recovery phase of the storm. This indicates that the simulation does not reproduce the wave existence during the recovery phase of the storm. Looking into the MLT distribution, the simulation predicts the wave existence from dusk to the midnight sector, but the

©2019. Japan Geoscience Union. All Right Reserved.

waves were not observed in this local time sector during the main phase. In case of recovery phase, the simulation did not predict wave existence but the observation showed continuous wave existence from dawn to the noon sector.

Keywords: chorus, ERG satellite, ground based observation

©2019. Japan Geoscience Union. All Right Reserved.

Flux decrease of outer radiation belt electrons associated with solar wind pressure pulse: A Code coupling simulation of GEMSIS-RB and GEMSIS-GM

*Ito Hiroki[1], Yoshizumi Miyoshi[1], Shinji Saito[2], Yosuke Matsumoto[3], Takanobu Amano[4]

1. Institute for Space-Earth Environmental Research, Nagoya University, 2. Graduate School of Science, Nagoya University, 3. Graduate School of Science, Chiba University, 4. Department of Earth and Planetary Science, University of Tokyo

Relativistic electron flux of the outer radiation belt dynamically changes in response to solar wind variations. There exist several conditions to cause the flux drop-out of the outer belt electrons. The magnetopause shadowing (MPS) is one of the processes to cause the rapid loss of outer belt electrons (e.g.,Kim et al.,2008). In this study, we investigate how radiation belt electrons are lost through the MPS process with a code-coupling simulation using GEMSIS-RB test particle simulation code (Saito et al., 2010) and GEMSIS-GM global MHD magnetosphere simulation code (Matsumoto et al., 2010) by focusing the equatorial pitch angle and local time dependence. We calculate trajectories of electrons in electromagnetic fields calculated from GEMSIS-GM with initial L-shells from 6 to 11, initial energies from 1 MeV to 10 MeV, and initial pitch angles between 50 degrees and 90 degrees, using the relativistic guiding-center equation. The simulation consists of the following three phases associated with variations of the solar wind dynamic pressure; [i] The standoff distance of magnetopause at the subsolar point is 12 Re with the initial dynamic pressure of 1.0 nPa. [ii] The solar wind dynamic pressure becomes 2.5 nPa, and the magnetopause moves to 9 Re. [iii] The solar wind dynamic pressure decreases, so that the inflation of the magnetopause takes place and the standoff distance of the magnetopause is 10 Re. During phase [ii], the high-latitude reconnections occur at dawn-side firstly and many electrons escape from the magnetosphere to the interplanetary magnetic field along the field line in the dawn side. Subsequently, the high-latitude reconnections occur at the high-latitude in the dusk side. In phase [iii], the remained electrons in the magnetosphere escape into the interplanetary in both the dawn and dusk sides. The loss at the dusk-side is outward motion of the trapped electrons caused by the dawn-to-dusk electric fields associated with the inflation of the magnetosphere. The study showed detailed process of the electron escape into the interplanetary magnetic field and the electron escape occur in both enhancement/decrease of the dynamic pressure.

Keywords: Magnetopause Shadowing, global MHD magnetosphere simulation, test particle simulation

©2019. Japan Geoscience Union. All Right Reserved.

Non-diffusive response of outer belt electrons on interplanetary shock

Takuma Toishi[1], *Yusuke Ebihara[1], Takashi Tanaka[2]

1. Research Institute for Sustainable Humanosphere, Kyoto University, 2. Kyushu University

Test particle simulation is performed in the electric and magnetic fields given by a global magnetohydrodynamics (MHD) simulation. When an interplanetary shock strikes the magnetosphere, a compressional wave propagates tailward. Pre-existing relativistic electrons that are initially located at fixed radial distances are redistributed by the electric and magnetic fields associated with the compressional wave. When the electrons encounter the nightside, they undergo complicated paths under the complicated distribution of the electric and the magnetic fields. Consequently, a group of isolated electrons forms, suggesting non-diffusive response. We discuss the redistribution processes in terms of the magnetospheric processes.

Keywords: radiation belt, MHD simulation, Test particle simulation

©2019. Japan Geoscience Union. All Right Reserved.

PARM: Initial result of the auroral camera on the G-CHASER (RockSat-XN) rocket and status of the development of auroral cameras for the LAMP rocket experiment

*Naoshi Yagi[1], Takeshi Sakanoi[1], Fukizawa Mizuki[1], Kazushi Asamura[2], Yoshizumi Miyoshi[3], Keisuke Hosokawa[4], Genki Ishizawa[5]

1. Planetary Plasma and Atmospheric Research Center, Graduate School of Science, Tohoku University, 2. Institute of Space and Astronautical Science, Japan Aerospace Exploration Agency, 3. Institute for Space-Earth Environmental Research, Nagoya University, 4. Department of Communication Engineering and Informatics, University of Electro-Communications, 5. Space & terrestrial plasma pyhsics

We developed an Aurora Imaging Camera (AIC) for NASA’ s G-CHASER (RockSat-XN) sounding rocket launched on 13th January, 2019. In addition, LAMP sounding rocket scheduled to be launched from December 2019 to February 2020 to reveal the spatio-temporal relationship between PsA and relativistic electrons, namely microbursts. In this presentation, we report the development of AIC, the result f the G-CHASER (RockSat-XN) rocket, as well as the current status of LAMP rocket project.

On the G-CHASER rocket experiment, 7 scientific and educational instruments were provided from Japan, U.S., Norway and Puerto Rico. Japanese instrument, called PARM, consists of an intermediate energy (20 - 100 keV) electron detector MED, high energy (several hundred keV - 2 MeV) electron detector HEP, fluxgate magnetometer AFG, and auroral camera AIC. Concerning development of AIC, we carried out sensitivity calibration experiment, electrical function test, fabrications, focus adjustment and environmental (vibration, vacuum and thermal) tests from January to July 2018. AIC consists of detector unit AIC-S and power/data processing electric unit AIC-E. AIC-S consists of a CCD camera (Watec 910 HX), wide-angle lens (F-number: 1.6, focal length: 3.5 mm, field of view: 96.4˚x75˚) and a glass filter (RG665) that transmits light with a wavelength longer than 665 nm.

NASA decided to launch the G-CHASER rocket at 9:00UT on 13rd January 2019 from Andoya Space Center, Norway (69.3˚N, 16.0˚E in the geographic coordinate). At this time, the solar elevation was -4˚, hence twilight had been already started and the region above 15km was sunlit. AIC detected leak light from the rocket skirt until the separation of skirt at an altitude of 82.9km. From time variation of AIC data, rocket spin frequencies were estimated to be ~5Hz at ~20km altitude and ~1Hz at ~80km altitude. This is consistent with the modulation period of magnetic field data observed by AFG. Because AIC was designed to measure weak pulsating aurora with hundreds Rayleigh, the AIC data was saturated above 82.9km after separation of rocket in the sunlit region, and no aurora was observed.

We are also conducting the LAMP sounding rocket project whose PI is Dr. Sarah Jones in NASA/GSFC. This is scheduled to be launched at Poker Flat Research Range in Alaska in 2019 winter. Japanese PARM2 team will provide high energy (several hundred keV - 2 MeV) electron detector HEP, fluxgate magnetometer MIM, and auroral cameras AIC2. We concern AIC2 that consists of two cameras AIC2-S1/AIC2-S2 and power/data processing electric unit AIC2-E. AIC2-S1/S2 and AIC2-E will be installed on a despun platform to derotate rocket spin. AIC2-S1 measures N2 1stPG emission with a narrow FOV lens (F value: 0.95, focal length:17mm, field of view 27x27deg), and AIC-S2 measures OI 844.6nm emission with a wide-angle lens (F value:1.6, focal length:3.5 mm, diagonal field of view:120x120˚). AIC2-S1 will take fine structure of PsA in the region more than 100 x 100 km area around the magnetic footprint with a few kilometer resolution, while AIC2-S2 will obtain an altitude distribution of

©2019. Japan Geoscience Union. All Right Reserved.

PsA in the F-region as well as wide-range distribution of PsA. The characteristic energy of precipitating electron can be estimated from the ration of OI844.6 and N2 1stPG. The cameras are conducted by a single board computer NanoPi M4 via USB3.0 high speed interface. We confirmed to get frame sampling rate with approximately 10Hz with this system. Region-of-interest (ROI) of 3660 x 3660 pixel area is binned with 61x61pixels, and finally image data with 60 x 60 bin (16 bit/bin) is recorded at 10 Hz. The precise imaging and altitude distribution of PsA are obtained with AIC2 at two wavelengths with 10Hz sampling. The imaging data combined with precipitating electron data in the wide energy range enable us to investigate the relativistic electron precipitation in microbursts that is probably caused by chorus waves in the magnetosphere.

Keywords: auroral camera, rocket experiment

©2019. Japan Geoscience Union. All Right Reserved.

First simultaneous observation of a SAR arc at subauroral latitudes using a ground all-sky camera and the Arase satellite in the inner magnetosphere

*Yudai Inaba[1], Kazuo Shiokawa[1], Shin-ichiro Oyama[1,8,9], Yuichi Otsuka[1], Atsuki Shinbori[1], Yoichi Kazama[2], Shiang-Yu Wang[2], Sunny W. Y. Tam[2], Shoichiro Yokota[3], Satoshi Kasahara[4], Kunihiro Keika[4], Tomoaki Hori[1], Ayako Matsuoka[5], Yoshiya Kasahara[6], Atsushi Kumamoto[7], Yasumasa Kasaba[7], Yoshizumi Miyoshi[1], Iku Shinohara[5], Arto Oksanen[10]

1. Institute for Space-Earth Environmental Research, 2. Academia Sinica, 3. Osaka Univ, 4. Tokyo Univ, 5. JAXA, 6. Kanazawa University, 7. Tohoku University, 8. University of Oulu, Finland, 9. National Institute of Polar Research, 10. Jyväskylän Sirius ry, Finland

Stable Auroral Red (SAR) arc is characterized by a 630.0 nm emission observed at subauroral latitudes. The energy of precipitating electrons that cause the SAR arc emission is several electron volts (eV). Precipitation of low-energy electrons is expected to occur due to spatial overlap between the plasmasphere and the ring current, where high-energy (more than 10 keV) ring current ions heat low-energy (less than 1 eV) electrons in the plasmasphere. Simultaneous observations of SAR arcs using the ionospheric satellite and ground all-sky cameras have been already done [e.g., Foster et al., 1994]. However, there has been no reports on in-situ measurements of plasma and electromagnetic fields in the inner magnetosphere, where the plasmaspheric plasma is heated by the ring current. In this study, we report simultaneous observations of a SAR arc at 22:04 UT on March 28, 2017, by using an all-sky camera at Nyrola (62.34 N, 25.51 E, MLAT 59.4 N) at subauroral latitudes and the Arase satellite. We analyze the all-sky camera data and the satellite data of this event to investigate the generation mechanism of the SAR arc. We find interesting features in the electric field data and the energy flux of electrons observed by the electric field detector of the plasma wave experiment (EFD/PWE) and the low-energy particle experiments–electron analyzer (LEP-e), respectively, onboard the Arase satellite at the crossing of the SAR arc. A negative excursion of the Ez component of the electric field (GSE coordinate system) with an amplitude of ~2.4 mV/m was observed at the crossing time. The Bx component of the magnetic field (GSE coordinate system) was negative. Thus the direction of the E ×B drift is westward, which is consistent with the westward auroral motion observed in the SAR arc by the ground all-sky camera. At the SAR arc crossing, the energy flux of electrons below 100-eV electrons is slightly intensified. We will discuss these observations in relation to the proposed SAR-arc generation mechanisms.

Keywords: ERG, SAR arc, All-sky imager, Simultaneous observation

©2019. Japan Geoscience Union. All Right Reserved.

Pi2 pulsations observed by the Arase satellite inside and outside the plasmapause

*Mariko Teramoto[1], Ayako Matsuoka[2], Reiko Nomura[5], Yoshiya Kasahara[3], Yasumasa Kasaba[4], Atsushi Kumamoto[4], Fuminori Tsuchiya[4], Shoya Matsuda[2], Masahito Nose[1], Masafumi Shoji[1], Yasunori Tsugawa[1], Shun Imajo[1], Yoshizumi Miyoshi[1], Iku Shinohara[2]

1. Institute for Space-Earth Environmental Research Nagoya University, 2. Institute of Space and Astronautical Science, Japan Aerospace eXploration Agency, 3. Kanazawa University, 4. Tohoku University, 5. National Astronomical Observatory of Japan

The spatial structure of Pi2 pulsation relative to the plasmasphere has been studied using the magnetic and electric field observed from the equatorial orbiting satellite in the inner magnetosphere by Takahashi et al (2003; 1995). They showed that the nightside Pi2 pulsations in the inner magnetosphere, which have high coherence with those at low-latitude ground station, are dominated by the poloidal component (the radial and compressional components for the magnetic field and azimuthal component for the electric field). The amplitudes of the compressional magnetic field has maximum and azimuthal electric field and the compressional magnetic field have maximum and minimum in the vicinity of the plasmaspause, respectively. The phase of the azimuthal electric field relative to low-latitude Pi2 pulsations on ground is 90 degrees in the plasmasphere. Such radial profile of the amplitude and phase of Pi2 pulsations can be explained by a plasmaspheric cavity mode resonance. However, the latitudinal structure of Pi2 pulsations in the electric field has not been examined. We investigate the latitudinal characteristics of off-equatorial Pi2 pulsations on the nightside and their relation to the plasmapause using the magnetic field measured by the fluxgate magnetometer measured by the Magnetic Field Experiment (MGF), the electric field measured by the Electric field Detector (EFD), and electron density derived from the spectra measured by the High Frequency Analyzer (HFA) from the Arase satellite.

©2019. Japan Geoscience Union. All Right Reserved.

An extreme erosion of the plasmasphere during the 7–10 September 2017 storm

*Yuki Obana[1], Naomi Maruyama[2,3], Atsuki Shinbori[4], Kumiko K. Hashimoto[5], Mariangel Fedrizzi[2,3], Masahito Nose[4], Yuichi Otsuka[4], Nozomu Nishitani[4], Tomoaki Hori[4], Atsushi Kumamoto[6], Fuminori Tsuchiya[6], Shoya Matsuda[7], Ayako Matsuoka[7], Yoshiya Kasahara[8], Akimasa Yoshikawa[9], Yoshizumi Miyoshi[4], Iku Shinohara[7]

1. Osaka Electro-Communication University, 2. University of Colorado Boulder, 3. NOAA Space Weather Prediction Center, 4. Nagoya University, 5. Kibi International University, 6. Tohoku University, 7. Japan Aerospace Exploration Agency, 8. Kanazawa University, 9. Kyushu University

We report an extreme erosion of the plasmasphere arising from the September 2017 storm. The cold electron density is identified from the upper limit frequency of UHR waves observed by the HFA of the PWE instrument onboard the Arase spacecraft. The HFA provides the spectrograms of electric fields in a frequency range from 10 kHz to 10 MHz with an 8-sec time resolution (Kasahara et al., 2018; Kumamoto et al., 2018). Such wide frequency coverage allows observation of the UHR frequency even deep inside the plasmasphere.
The electron density profiles reveal that the plasmasphere was severely eroded during the recovery phase of the storm and the plasmapause was located at L~1.7 at 23 UT on 8 Sep 2017. This is the first report of such deep erosion of the plasmasphere (L_{PP}<2) with the in-situ observation of the electron density. The degree of the severity is much more than what is expected from the SYM-H minimum (−146 nT) of the event.
We further study absolute GNSS-TEC, ground-based magnetic field, the doppler velocity obtained from the SuperDARN Hokkaido Radars to investigate the location of the midlatitude ionospheric trough, the penetration of the convection electric field to the equator and middle latitudes, respectively. Our results suggest that the middle latitude electric field was penetrated from the high-latitude storm time convection for several hours. Futhermore, the Ionosphere-Plasmasphere-Electrodynamics (IPE) model (Sun et al., 2015; Maruyama et al., 2016) is used to understand the dynamics of the plasmasphere. The IPE results suggest that the middle latitude electric field penetrates from the high-latitude storm time convection that lasts for several hours can explain the degree of severity during the September 7-11 2017 storm.

Keywords: plasmasphere, innner magnetosphere, Magnetosphere-ionosphere coupling

©2019. Japan Geoscience Union. All Right Reserved.

Relative contribution of ULF and chorus waves to the radiation belt variation: Comparison between multi-point observations and BATSRUS + CRCM simulation

*Naoko Takahashi[1], Kanako Seki[1], Mei-Ching Fok[2], Yihua Zheng[2], Yoshizumi Miyoshi[3], David Hartley[4], Ayako Matsuoka[5], Yoshiya Kasahara[6], Yasumasa Kasaba[7], Nana Higashio[8]

1. Graduate School of Science, University of Tokyo, 2. NASA Goddard Space Flight Center, 3. Institute for Space-Earth Environmental Research, Nagoya University, 4. Department of Physics and Astronomy, University of Iowa, 5. Institute of Space and Astronautical Science, Japan Aerospace Exploration Agency, 6. Information Media Center, Kanazawa University, 7. Planetary Plasma and Atmospheric Research Center, Tohoku University, 8. Japan Aerospace Exploration Agency

Earth’ s radiation belt is the area where electrons with energies from hundreds of keV to several MeV are trapped. When, where, and how the radiation belt exhibits a dramatic variation during a magnetic storm is of global interest. The dynamic variation of the radiation belt is caused by various wave-particle interactions: (1) the radial diffusion of electrons driven by ultra-low-frequency (ULF) waves in Pc5 frequency ranges (1.6–6.7 mHz) and (2) the local acceleration caused by wave-particle interactions between whistler-mode chorus waves and radiation belt particles. Over the past decade, multi-point observations and numerical simulations have provided evidence to support above physical processes. However, it is debatable how much each wave contributes to the radiation belt variation during a magnetic storm. A few previous studies have quantitatively compared roles of local acceleration and radial transport by calculating diffusion coefficients, whereas the global context between the wave growth and the relativistic electron flux enhancement has not been extensively studied. To address these issues, the comprehensive study using multi-point observations and numerical simulations (not empirical models) makes essential and significant contributions.

We focus on the magnetic storm on 27-30 May 2017. This magnetic storm is triggered by coronal mass ejections and induces a clear interplanetary shock. Fortunately, several satellites are scattered in the inner magnetosphere and detect both ULF and chorus waves during this magnetic storm. Arase and Van Allen Probes also detect variations of relativistic electron fluxes associated with the Dst index variation. We examine L-value dependence of ULF and chorus wave powers and find the difference of wave activity during the recovery phase. The chorus wave activity is large during the early recovery phase, while the ULF wave activity is large during the late recovery phase. The difference of wave activity may contribute to the radial profile in the phase space density of relativistic electrons. To grasp the extent of individual wave contribution, we also perform the comprehensive ring current model (CRCM) coupled with Block-Adaptive-Tree Solar-Wind Roe-Type Upwind Scheme (BATSRUS) simulation. BATSRUS with CRCM well reproduces global characteristics of energetic electron fluxes and wave growth during this magnetic storm. We will further evaluate global distribution of simulated wave power comparing to the observation, and then discuss the temporal and spatial context between each wave growth and the radiation belt variation.

©2019. Japan Geoscience Union. All Right Reserved.

Modulation of the D-region ionosphere by Pc5 waves observed by VLF/LF standard radio waves

*Miyashita Takuya[1], Hiroyo Ohya[1], Fuminori Tsuchiya[2], Hiroyuki Nakata[1], Toshiaki Takano[1], Kazuo Shiokawa[3], Yoshizumi Miyoshi[3]

1. Chiba University, 2. Tohoku University, 3. Nagoya University

Ionospheric modulation due to ultra low frequency (ULF) Pc5 waves have been observed by GPS-total electron content (TEC), high frequency (HF) Doppler sounders, and SuperDARN HF radars [e.g., Pilipenko et al., 2014; Belakhovsky et al., 2016]. However, there are few reports for the modulation of the lower ionospheric associated with the ULF Pc5 waves using VLF/LF transmitter signals. In this study, we investigate the D-region signatures of the modulation due to the ULF Pc5 waves using a network of very low frequency (VLF)/low frequency (LF) standard radio waves. We show oscillations in intensities of the VLF/LF waves with a period of 4-6 minutes during substorms on 27 April, 2017. The transmitter signals from NAA (USA, 24.0 kHz, L = 2.88), NLK (USA, 24.8 kHz, L = 2.88), NDK (USA, 25.2 kHz, L = 2.98) and WWVB (USA, 60.0 kHz, L = 2.26) were observed by the receivers at ATH (Athabasca, L=4.31) and PKR (Poker Flat, L=5.95). The substorm occurred at 04:30 UT. Based on the wavelet analysis, we found that the intensities for the NDK-ATH and WWVB-ATH paths showed oscillations with a period of 4-6 minutes during the substorm growth phase (05:00-06:00 UT). Magnetic field variations observed by ground magnetometers around the NDK-ATH and WWVB-ATH paths also showed the same periodicity, which means that the variations in the VLF/LF intensities would be caused by Pc5 modulations. The magnetic field oscillations were observed in wide latitude range. The intensity of the oscillation was larger at high latitude magnetometers than those around the location of the NDK-ATH and WWVB-ATH path (mid-latitude). The Pc5 oscillations could be excited by solar wind because solar wind speed had similar period of the 4-6 minutes. In this presentation, we will discuss the cause of these VLF/LF oscillations.

Keywords: VLF/LF standard radio waves, Pc5, ULF

©2019. Japan Geoscience Union. All Right Reserved.

Oxygen-proton differences in ion energies dominating plasma pressure: Dependence on storm phases and solar wind drivers

*Kunihiro Keika[1], Satoshi Kasahara[1], Shoichiro Yokota[2], Masahiro Hoshino[1], Kanako Seki[1], Masahito Nose[3], Yoshizumi Miyoshi[3], Iku Shinohara[4]

1. Graduate School of Science, The University of Tokyo , 2. Graduate School of Science, Osaka University, 3. Institute for Space-Earth Environmental Research, Nagoya University, 4. Institute of Space and Astronautical Science, Japan Aerospace Exploration Agency

The ion pressure in the inner magnetosphere is generally dominated by protons with energies of a few to a few 100s keV. Oxygen ions of ionospheric origin, O+, can make a significant contribution to the ion pressure during geomagnetically active periods. Our previous study (Keika et al., 2018, GRL) examined the radial dependence of contributing energies, which we term an energy range that makes the dominant contribution to the plasma pressure, during the main phase of the six magnetic storms in Year 2017. We found clear oxygen-proton differences in the contributing energies in the outer part (L>5) of the ring current region. The contributing energies were higher for O+ than for H+. The results provided in situ evidence of the contribution from mass-dependent/selective acceleration processes to the energization of the outer part of the ring current.

The present study extends this analysis toward a larger database obtained from a longer period of magnetic storm times including the recovery phase. We also compare mass-dependent/selective energization between different solar wind drivers such as coronal mass ejections and corotational interaction regions. We primarily use data from the MEP-i (Medium-Energy Particle experiments - ion mass analyzer) on board the Arase spacecraft. MEP-i measures ions with energies of 10 to 180 keV/q and distinguishes between different ion species. Arase observed the nightside near-Earth magnetosphere (L<10) during 7 CME-driven and 7 CIR-driven storms with the Dst minimum of smaller than -50 nT in Years 2017 and 2018. The dependence on storm phases and solar wind drivers helps identify magnetospheric conditions favorable for mass-dependent/selective acceleration and in turn provides clues for understanding important physical mechanisms. Utilizing observations made by the MMS spacecraft in the near-Earth plasma sheet, we also compare oxygen-to-proton differences inside earthward bursty bulk flows with the Arase/MEP-i observations. The multi-spacecraft observations help better understand the temporal evolution of the mass-dependent/selective acceleration processes.

Keywords: Magnetic storms, Substorms, RIng current, Oxygen ions, Ion transport and acceleration

©2019. Japan Geoscience Union. All Right Reserved.

Mass dependence of penetration depth of multi-energy ions in the inner magnetosphere during magnetic storms: Arase observations

*Ryosuke Fujii[1], Yoshizumi Miyoshi[1], Masafumi Shoji[1], Kazushi Asamura[2], Lynn Kistler[1,8], Vania Jordanova[9], Tomoaki Hori[1], Satoshi Kurita[1], Mariko Teramoto[1], Yasunori Tsugawa[1], Yoshiya Kasahara[3], Yasumasa Kasaba[4], Atsushi Kumamoto[5], Fuminori Tsuchiya[4], Shoichiro Yokota[6], Kunihiro Keika[7], Ayako Matsuoka[2], Iku Shinohara[2]

1. Institute for Space-Earth Environmental Research, Nagoya University, 2. Institute of Space and Astronautical Science, Japan Aerospace Exploration Agency, 3. Information Media Center, Kanazawa University, 4. Planetary Plasma and Atmospheric Research Center, Tohoku University, 5. Department of Geophysics, Graduate School of Science, Tohoku University, 6. Graduate School of Science, Osaka University, 7. Department of Earth and Planetary Science, Graduate School of Science, The University of Tokyo, 8. University of New Hampshire, 9. Los Alamos National Laboratory

During magnetic storms, the ring current ions move toward the Earth, and the inner edge position of the ring current depends on the convection electric field. We investigate variations of the inner edge of the ring current ions, so-called, penetration depth, during magnetic storms using the ion measurements made by the Low-energy particle experiments-ion mass analyzer (LEP-i)/Medium-energy particle experiments-ion mass analyzer (MEP-i) instruments onboard the Arase satellite. The Arase satellite typically observes the earthward penetration of the ring current protons associated with the enhancement of the dawn-to-dusk electric field in the inner magnetosphere during the storm main phase. The plasmapause moves earthward during the main phase. On the other hand, the convection electric field decreases during the storm recovery phase in which the flux of ring current protons decreases. We identify that the penetration depth of protons depends on the minimum Dst index during the storms as well as the proton energy.

We also investigate the penetration depth of other ions, i.e., helium and oxygen ions. Because the life times of helium and oxygen ions due to charge exchange reaction for are longer than that of protons, it is expected that these ions can penetrate deeper than protons and temporal and spatial evolution can be observed clearly. We will also discuss the relation between the position of ring current inner edge and cross polar cap potential.

Keywords: The Arase satellite, Ring current, Ions

©2019. Japan Geoscience Union. All Right Reserved.

Relativistic Acceleration of Energetic Protons by Electromagnetic Ion Cyclotron Waves in the Jovian Magnetosphere

*Tomohiro Sekine[1], Yoshiharu Omura[1], Danny Summers[2], Yikai HSIEH[1], Satoko Nakamura[1]

1. Reserach Institute for Sustainable Humanosphere, Kyoto University, 2. Memorial University of Newfoundland

We perform test particle simulations of nonlinear interaction between energetic protons and EMIC waves. We assume a coherent EMIC waves that have a constant frequency and propagate parallel to the magnetic field. We find that protons can be trapped and accelerated by EMIC waves. We find a very efficient acceleration process of protons in which kinetic energy of protons increases while directions of parallel velocities reverses when we assume parameters in the Jovian magnetosphere. We notice that this phenomenon is very similar to the interaction process between relativistic electrons and whistler-mode waves, which is called Relativistic Turning Acceleration (RTA) [1]. In order to analyze the phenomena, we have developed nonlinear trapping theory of interaction between relativistic protons and EMIC waves. Next, we compare the theory and simulation results. We confirm that the results satisfy the conditions for RTA. Following the trajectories of many resonant protons, we obtain time evolution of the distribution function of relativistic protons as a function of energy and equatorial pitch angle based on the numerical Green’ s function method [2].

References:

[1] Y. Omura, N. Furuya, D. Summers, Relativistic turning acceleration of resonant electrons by coherent whistler-mode waves in a dipole magnetic field, Journal Geophysical Research, Vol. 112, A06236, doi:10.1029/2006JA012243, 2007.

[2] Y. Omura, Y. Miyashita, M. Yoshikawa, D. Summers, M. Hikishima, Y. Ebihara, and Y. Kubota (2015), Formation process of relativistic electron flux through interaction with chorus emissions in the Earth’ s inner magnetosphere, J. Geophys. Res. Space Physics, 120, 9545–9562, doi:10.1002/2015JA021563, 2015.

©2019. Japan Geoscience Union. All Right Reserved.

Statistical study of IPDP type EMIC wave-related electron precipitation at subauroral latitude

*Asuka Hirai[1], Fuminori Tsuchiya[1], Takahiro Obara[1], Yasumasa Kasaba[1], Yuto Katoh[2], Hiroaki Misawa[1], Kazuo Shiokawa[3], Yoshizumi Miyoshi[3], Satoshi Kurita[3], Martin G Connors[4]

1. Planetary Plasma and Atmospheric Research Center, Graduate School of Science, Tohoku Univ. , 2. Department of Geophysics, Graduate School of Science, Tohoku University, 3. Institute for Space-Earth Environmental Research, Nagoya University, 4. Athabasca University

The outer radiation belt electrons disappear during the main phase of geomagnetic storms. One of the loss mechanisms of electrons from the outer belt is precipitation into the atmosphere due to wave-particle interactions. Electromagnetic ion cyclotron (EMIC) waves are believed to be important plasma waves that contribute to the loss of the outer radiation belt due to pitch angle scattering. They can scatter relativistic and ultra-relativistic electrons. However, there are still questions left about the contribution of EMIC waves to the whole loss of radiation belt electrons and possible conditions favorable to pitch angle scattering.

EMIC waves mainly propagate along magnetic field lines and are observed on the ground as Pc1 geomagnetic pulsations. Intervals of pulsations of diminishing periods (IPDP) are Pc1/EMIC waves that are characterized by frequency rise from 0.1 to 1–2 Hz in a period of ~1 h, and often occur during substorms. Recent studies reported that IPDP are preferentially associated with relativistic electron precipitation. However, the statistical relation between IPDP waves and relativistic electron precipitation, and their physical mechanism, remain open issues.

We investigated differences in characteristics between IPDP and other types of Pc1 by using an induction magnetometer and VLF radio wave data that is a proxy of electron precipitations at subauroral latitude from 1 November 2016 to 30 June 2018. We used the induction magnetometer of PWING (study of dynamical variation of Particles and Waves in the INner magnetosphere using Ground-based network observations) at Athabasca, Canada (54.6˚N, 246.36˚E, L = 4.39). VLF radio waves propagate from transmitters to receivers in subionospheric waveguide. The modulations of VLF signals are detected as occurrence of sub-relativistic and relativistic electron (>100 keV) precipitation due to ionization changes in the lower ionosphere along the radio wave propagation path. VLF radio waves are transmitter from NDK, U.S. (46.367˚N, 261.467˚E, L =3.13) and NLK, U.S. (48.2˚N, 238.083˚E, L =2.84) and received at Athabasca. We selected EMIC wave events on the basis of the following criteria: (1) EMIC wave power is higher than 10^{-5} nT^2/Hz. (2) Duration of EMIC waves is longer than 20 min. (3) Interval between one EMIC wave event and the next one is longer than 30 min. Electron precipitation was identified as a decrease in amplitude of VLF signals from the quiet day curve (QDC). We counted as EMIC wave-driven electron precipitation if we detect temporal correspondence with EMIC waves. In this period, we found 950 EMIC wave events, and 87 of total EMIC wave events were IPDP events (9.2%). Local time dependence of EMIC waves shows that IPDP often occurs in the afternoon and evening sector, while other types of Pc1 occur in all local time range, but with a maximum in 12–16 MLT, which is consistent with previous studies. Simultaneous observation of the magnetometer and VLF radio waves were available for 286 days, and we found 163 EMIC wave events. 19 of 163 EMIC wave events were clearly associated with electron precipitation (12%). Among 19 electron precipitation events, 15 events were caused by IPDP (79%). Also, the electron precipitation events were observed in the evening sector with similar local time dependence to IPDP. This result suggests that IPDP is more likely to cause electron precipitation than other Pc1 wave types. In previous studies, IPDP occurs due to ion cyclotron instability of ring current ions in the evening sector, and favorable region for electron scattering by EMIC waves is high density duskside plasmapause

©2019. Japan Geoscience Union. All Right Reserved.

and plasmaspheric plume because dense plasma lowers minimum resonant energy of electrons. It is assumed that occurrence region of IPDP is coincident with the preferential region for MeV electron scattering by EMIC waves. For this reason, it is expected that IPDP type EMIC waves significantly cause relativistic electron precipitations in the duskside.

Keywords: EMIC waves, electron precipitation, subionospheric VLF radio waves

©2019. Japan Geoscience Union. All Right Reserved.

Meridional distributions of proton plasma and pressure-driven currents in the nightside inner magnetosphere: Arase observations

*Shun Imajo[1], Masahito Nose[1], Satoshi Kasahara[2], Shoichiro Yokota[3], Ayako Matsuoka[4], Kunihiro Keika[2], Tomoaki Hori[1], Mariko Teramoto[1], Kazuhiro Yamamoto[5], Oimatsu Satoshi[5], Reiko Nomura[6], Akiko Fujimoto[7], Iku Shinohara[4], Yoshizumi Miyoshi[1]

1. Institute for Space-Earth Environmental Research, Nagoya University, 2. Graduate School of Science, The University of Tokyo, 3. Graduate School of Science, Osaka University, 4. Institute of Space and Astronautical Science, Japan Aerospace Exploration Agency, 5. Graduate School of Science, Kyoto University, 6. National Astronomical Observatory of Japan, 7. Kyushu Institute of Technology

We examine the averaged meridional distributions of proton plasma parameters and pressure-driven currents in the nightside (20–04 h magnetic local time) ring current region during disturbed times (-80 < SYM-H* < -40 nT) using ion measurements covering energy range of 10–180 keV by the Arase satellite. Because the Arase satellite has a large inclination orbit of 31°, it covers the absolute value of magnetic latitude (|MLAT|) range of 0–40° and the radial distance of < 6 Re. We find that the plasma pressure decreases significantly with MLAT. The plasma pressure on the same L^* shell at 30°<|MLAT|<40° is about 10–60% of that at 0°<|MLAT|<10°, and the percentage of decrease is larger on lower L^* shells. The pressure anisotropy which is defined by the perpendicular pressure divided by the parallel pressure decreases with radial distance and shows a weak dependence on |MLAT|. The magnitude of the plasma beta at 30°<|MLAT|<40° is one or two order smaller than that at 0°<|MLAT|<10°. The relative plasma pressure distribution predicted from the magnetic strength and anisotropy is roughly consistent with the observed plasma pressure for L^*=3.5–5.5. The azimuthal pressure-gradient current derived from the plasma pressure distribution spreads over ~-20° |MLAT|, while the curvature current is limited in ~0–10° |MLAT|. We suggest that the latitudinal dependences should be taken into account when considering a temporal evolution of ring current particles from L distributions of successive orbits.

Keywords: meridional distributions, plasma pressure, pressure-driven currents, Arase satellite

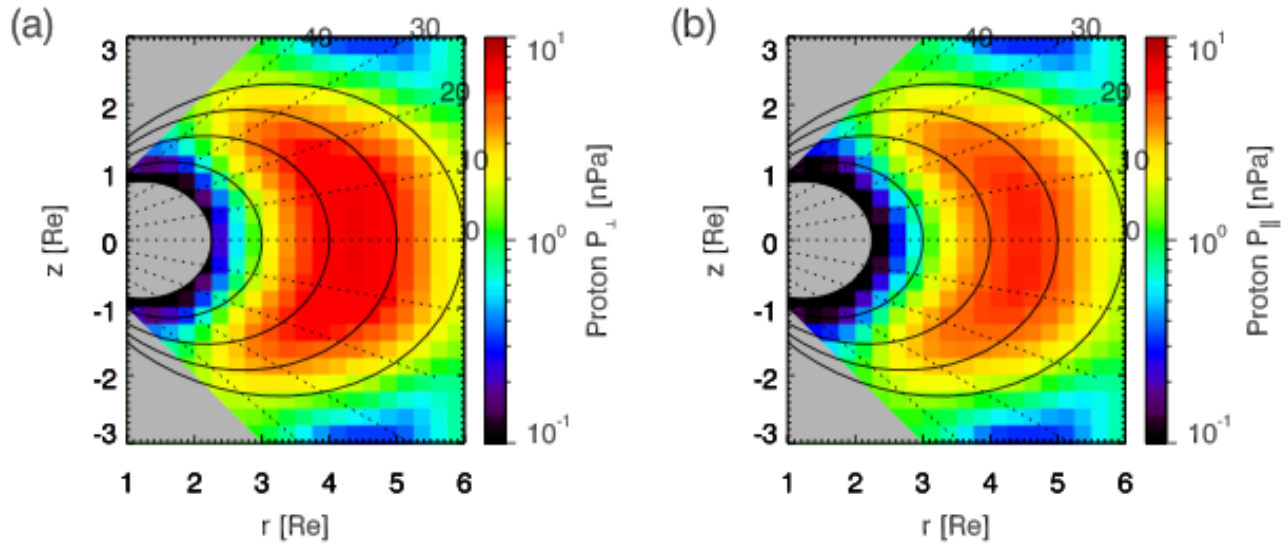

©2019. Japan Geoscience Union. All Right Reserved.

Space Weather Effects on Energetic Proton Flux Response in South Atlantic Anomaly

*Kirolosse Mina GIRGIS[1,2], Tohru Hada[1], Shuichi Matsukiyo[1]

1. Earth System Science and Technology (ESST) Department, Interdisciplinary Graduate School of Engineering Sciences (IGSES), Kyushu University, Japan, 2. Aerospace Engineering Department, Faculty of Engineering, Cairo University, Egypt

In this research, energetic proton flux in the inner radiation belt, is studied inside the South Atlantic Anomaly (SAA) by performing test particle simulations, where the background time-varying magnetic field is provided by Tsyganenko model, according to *Dst* index and altitudes. The objective of this investigation, is to estimate and forecast the additional radiation dose, occurring on spacecraft and human bodies, due to their passage inside the anomaly, and precisely, during intense solar storms. It was found that within minutes, proton flux in the SAA, penetrated deeper downward by about 200 km, when the *Dst* index is decreased (< -210 nT), and a after few more minutes, it was significantly reduced at all the altitudes; the last conclusion was confirmed by satellite observations.

Keywords: South Atlantic Anomaly, Space Weather, Dst Index, Radiation Dose, Proton Flux

©2019. Japan Geoscience Union. All Right Reserved.

Solar-cycle variations of >30 keV electron flux enhancements under the inner radiation belt

*ALLA SUVOROVA[1]

1. National Central University

Intense fluxes of 30-300 electrons can arise in the equatorial ionosphere outside the South Atlantic Anomaly. It was established that the electrons were injected from the inner radiation belt probably due to a mechanism of fast radial transport in the crossed electric and magnetic fields. Continuous monitoring of energetic particles at low heights of ~850 km with the MEPED instrument onboard the NOAA/POES satellites allowed compiling large statistics of the >30 keV electron enhancements from 1998 to 2018. We studied particle flux variations with geomagnetic activity and solar cycle. We found that geomagnetic activity measured by Dst and AE indices are not key factors of occurrence rate increase for electron injections, but influence on intensity of particles. The occurrence rate is controlled by auroral conductivity on the dayside and significantly enhanced during northern summer. Descending phase of solar cycle plays a major role in the occurrence rate increase.

Keywords: magnetosphere-ionosphere, energetic electrons, low latitudes, solar cycle

©2019. Japan Geoscience Union. All Right Reserved.

Energy spectra variations of high energy electrons in the inner magnetosphere observed by HEP/XEP on ARASE and SEDA-e on HIMAWARI

*Takeshi Takashima[1], Takefumi Mitani[1], Nana Higashio[2], Tsutomu Nagatsuma[3]

1. ISAS/JAXA, 2. Research and Development Directorate/JAXA, 3. NiCT

The relativistic electrons in the outer radiation belt were disappeared/increased and their energy spectra were changed dynamically in some storms observed by XEP/HEP onboard the ARASE spacecraft. In the same time, SEDA-e with energy range 200keV-4.5MeV for electron on board the HIMAWARI-8, Japanese weather satellite on GEO, observed increase of relativistic electron in different local time.
When comparing the energy spectra, there are times when the spectrum matches or does not match. It is also observed that the change in the slope of the energy spectrum differs with time. These phenomena are observed even when there are two satellites at the same local time.
We will report on energy spectra variations of high energy electrons including calibrations of differential flux between XEP and HEP and discuss comparisons with energy spectra between ARAE and HIMAWARI that observed each storm in different local time.

Keywords: relativistic electron, inner magnetosphere, ARASE

©2019. Japan Geoscience Union. All Right Reserved.

Inter-channel calibration of the high-energy electron experiments (HEP) instrument onboard the Arase satellite

*Tomoaki Hori[1], Takefumi Mitani[2], Takeshi Takashima[2], Park Inchun[1], Satoshi Kurita[1], Mariko Teramoto[1], Nana Higashio[3], Satoshi Kasahara[4], Shoichiro Yokota[5], Yoshizumi Miyoshi[1], Iku Shinohara[2]

1. Institute for Space-Earth Environmental Research, Nagoya University, 2. Japan Aerospace Exploration Agency, Institute of Space and Astronautical Science, 3. Japan Aerospace Exploration Agency, 4. Graduate School of Science, The University of Tokyo, 5. Graduate School of Science, Osaka University

An inter-channel comparison of electron fluxes measured by the HEP instrument onboard the Arase satellite is conducted with a focus on the apparent non-uniformity in detection efficiency and relative offset of the background flux level between the channels, which was partly reported previously. We extend the data set to cover the entire two-year period since the start of the regular observations. The flux ratio of different channels is sorted by the electron flux level of much higher energies that was simultaneously measured by the extremely high-energy electron experiment (XEP) instrument onboard Arase. The result shows that the HEP flux of all azimuthal channels is more or less affected by MeV electrons which are most likely to have penetrated into the instrument box and directly hit the detectors. However, it is also revealed that the non-uniform count distribution over the channels still remains even when the penetrating electrons are absent. We conduct a set of Geant-4 simulations to trace electrons with various energies and incident angles to the detector plane in order to give a quantitative interpretation for the resultant count distributions, in terms of the effects of penetrating electrons and obliquely-colliding incident electrons.

Keywords: Arase satellite, particle instrument, calibration

©2019. Japan Geoscience Union. All Right Reserved.

Particle simulation for calibrating the HEP data onboard the ARASE satellite

*PARK INCHUN[1], Yoshizumi Miyoshi[1], Takefumi Mitani[2], Tomoaki Hori[1], Satoshi Kurita[1], Mariko Teramoto[1], Takeshi Takashima[2], Nana Higashio[3], Iku Shinohara[2]

1. Nagoya University Institute for Space-Earth Environmental Research, 2. Japan Aerospace Exploration Agency Institute of Space and Astronautical Science , 3. Japan Aerospace Exploration Agency

Understanding the detailed characteristics of the HEP (High-Energy electron Experiment) instrument onboard the Arase satellite is crucial for data calibration. Due to difficulties of reproducing the severe radiation environment of the inner magnetosphere on the ground, computer simulation is the best method to understand instrument responses to the ambient radiation environment. Through Monte-Carlo simulations using the Geant4 tool, we have reconstructed the geometry of the HEP instrument and modeled the high-energy particle environment. Using the developed model, we have studied the efficiency of the detectors, the angular resolution, and the g-factors, which depend on the particle energy and the sensor channels. While the previous studies were based on a uni-direction simulation with electron pencil beams, this study adopted all the detector channels and energy bends of HEP thus resulting in more advanced simulations. Based on the results, we have made a new calibration table depending on the angle of incident particles. We have also estimated the g-factor which depends on the incident particle energy. The updated calibration table and g-factors are important for calibrating the HEP data as well as inter-calibrations with other particle instruments' data.

Keywords: ARASE, Geant4, HEP

©2019. Japan Geoscience Union. All Right Reserved.

Geant4 model calculation and energetic particle observation with HEP/Arase in the inner radiation belt

*Honoka Toda[1], Wataru Miyake[1], Takefumi Mitani[3], Takeshi Takashima[3], Yoshizumi Miyoshi[2], PARK INCHUN[2], Tomoaki Hori[2]

1. Tokai University, 2. ISEE/Nagoya University, 3. ISAS/JAXA

The high-energy electron experiments (HEP) instrument installed on the Arase is designed to observe energetic electrons of 70 keV to 2 MeV. The HEP registers high electron counts for the MeV energy range, not only in the outer belt but also in the inner belt, in MeV energy range. On the contrary, Van Allen Probes have hardly detected MeV electrons in the inner radiation belt. A probable interpretation is that the counts of HEP are caused due to contamination of high-energy protons. In order to verify this idea, we have modeled the HEP instrument a Geant4 simulation to determine the energy of penetrating protons. The result clearly shows that high-energy protons, it has become clear that high-energy protons of a few to a few tens of MeV can contribute to the apparent high counts of HEP. No instrument for measuring protons in this energy range is installed on the satellite. We will discuss the possibility of research on the spatial distribution and time variation of high-energy protons in the inner belt based on observation data from the HEP instrument.

Keywords: Arase, Proton Radiation Belt, HEP

©2019. Japan Geoscience Union. All Right Reserved.

Validation of High-energy electron detector simulator for the HEP instruments onboard Arase

*Takefumi Mitani[1], PARK INCHUN[2], Tomoaki Hori[2], Taku Namekawa[1,3], Kazushi Asamura[1], Takeshi Takashima[1], Satoshi Kasahara[3], Satoshi Kurita[2], Mariko Teramoto[2], Nana Higashio[1], Yoshizumi Miyoshi[2], Iku Shinohara[1]

1. Japan Aerospace Exploration Agency, Institute of Space and Astronautical Science, 2. Institute for Space-Earth Environmental Research, Nagoya Univ., 3. The university of Tokyo

The high-energy electron experiments (HEP) onboard the Arase satellite detects 70 keV-2 MeV electrons and generates a three-dimensional velocity distribution for these electrons in every period of the satellite's rotation. Electrons are detected by two instruments, namely, HEP-L and HEP-H, which differ in their geometric factor (G-factor) and range of energies they detect. HEP-L detects 70 keV–1 MeV electrons and its G-factor is 9.3 $\times 10^{-4}$ cm^2 sr at maximum, while HEP-H observes 0.7 MeV–2 MeV electrons and its G-factor is 9.3 $\times 10^{-3}$ cm^2 sr at maximum. The instruments utilize silicon strip detectors and application-specific integrated circuits to readout the incident charge signal from each strip.

In order to deduce the distribution of incident electrons from the direction and energy detections in orbit, we have developed a detector simulator using the Geant4 toolkit. Especially contamination due to high energy particles must be considered quantitatively. We have also been working on electron beam experiments using HEP detector modules which are almost the same as the flight model in order to compare detailed simulations and experimental data.

We will present a comparison between results from the electron beam experiments and those from the detector simulator. And we will discuss its influence on the interpretation of the observational data obtained in orbit.

Keywords: high-energy electron, Arase, Geant4

©2019. Japan Geoscience Union. All Right Reserved.

[J] Oral | P (Space and Planetary Sciences)：P-EM Solar-Terrestrial Sciences, Space Electromagnetism & Space Environment

Wed. May 29, 2019 9:00 AM - 10:30 AM JST | Wed. May 29, 2019 12:00 AM - 1:30 AM UTC | A03 TOKYO BAY MAKUHARI HALL

[P-EM16] Physics and Chemistry in the Atmosphere and Ionosphere

convener:Yuichi Otsuka(Institute for Space-Earth Environmental Research, Nagoya University), Takuya Tsugawa(National Institute of Information and Communications Technology), Seiji Kawamura(National Institute of Information and Communications Technology), Chairperson:Mitsumu Ejiri(国立極地研究所), Yuichi Otsuka

This session covers a broad scope of studies of physics and chemistry in the atmosphere and the ionosphere. Coupling processes between plasma and neutral species, and upward and downward coupling among lower/upper atmosphere, and ionosphere/mesosphere/thermosphere including magnetosphere are discussed. We solicit papers based on experiments with ground-based and/or space-borne instruments, theoretical studies, numerical simulations, and development of new observation techniques.

9:00 AM - 9:15 AM JST | 12:00 AM - 12:15 AM UTC

[PEM16-01] The model study of ionospheric variations during the solar eclipse event by assimulating the GNSS TEC observations

*Chia-Hung Chen[1], Charles Lin[1], Tomoko Matsuo[2] (1.Department of Earth Sciences, National Cheng Kung University, 2.Department of Aerospace Engineering Sciences, University of Colorado at Boulder, CO)

9:15 AM - 9:30 AM JST | 12:15 AM - 12:30 AM UTC

[PEM16-02] Characteristics of mesoscale thermospheric-ionospheric dynamics associated with heating in the auroral region

*Tomokazu Oigawa[1], Hiroyuki Shinagawa[2], Satoshi Taguchi[1] (1.Department of Geophysics, Graduate School of Science, Kyoto University, 2.National Institute of Information and Communications Technology)

9:30 AM - 9:45 AM JST | 12:30 AM - 12:45 AM UTC

[PEM16-03] Spatial distribution of the polar thermospheric wind acceleration and importance of the 2D measurement

*Shin-ichiro Oyama[1,2,3], Anita Aikio[2], Mark G Conde[4], Heikki Vanhamaki[2], Ilkka Virtanen[2], Thomas Ulich[5], Urban Brandstrom[6], Pekka Verronen[7], Monika Andersson[7], Niilo Kalakoski[7], Lassi Roininen[8], Sari Lasanen[8], Abiyot Workayehu[2], Kazuo Shiokawa[1], Heqiucen XU[1], Mamoru Ishii[9], Masafumi Hirahara[1], Takeshi Sakanoi[10], Masato Kagitani[10], Juha Sorri[5], Tomi Teppo[5], Yoshimasa Tanaka[3], Christopher Fallen[4], Brenton J Watkins[4], Mikko Orispaa[5], Yasunobu Ogawa[3], Lei Cai[11], Esa Turunen[5], Kirsti Kauristie[7], Takuo T. Tsuda[12], Junichi Kurihara[13] (1.Institute for Space-Earth Environmental Research, Nagoya University, Japan, 2.University of Oulu, Finland, 3.National Institute of Polar Research, Japan, 4.Geophysical Institute, University of Alaska Fairbanks, US, 5.Sodankyla Geophysical Observatory, University of Oulu, Finland, 6.The Swedish Institute of Space Physics (IRF), Sweden, 7.Finnish Meteorological Institute, Finland, 8.Lappeenranta-Lahti University of Technology, Finland, 9.National Institute of Information and Communications Technology, Japan, 10.Tohoku University, Japan, 11.KTH Royal Institute of Technology, Sweden, 12.The University of Electro-Communications, 13.Hokkaido University)

9:45 AM - 10:00 AM JST | 12:45 AM - 1:00 AM UTC

[PEM16-04] Analysis of the thermospheric neutral wind vector using observed images of *Trimethylaluminium* (*C6H18Al2*) released from sounding rocket in the upper atmosphere

*Yuki Otsuka[1], Masa-yuki Yamamoto[1], Hiroaki Saito[1] (1.Kochi University of Technology)

10:00 AM - 10:15 AM JST | 1:00 AM - 1:15 AM UTC

[PEM16-05] Establishment of real-time analysis method in a new HRO interferometer system and operation test of comprehensive meteor observation

*Takumi Sato[1], Seiya Takeda[2], Masa-yuki Yamamoto[1] (1.KOCHI UNIVERSITY OF TECHNOLOGY, 2.Inc.Bascule)

10:15 AM - 10:30 AM JST | 1:15 AM - 1:30 AM UTC

[PEM16-06] Solar flare effects of the D-region ionosphere using daytime tweek atmospherics

*Kodai Yamanobe[1], Hiroyo Ohya[2], Hiroyuki Nakata[2], Toshiaki Takano[2], Kazuo Shiokawa[3] (1.Graduate School of Science and Engineering, Chiba University , 2.Graduate School of Science and Engineering, Chiba University, 3.Institute for Space-Earth Environmental Research, Nagoya University)

The model study of ionospheric variations during the solar eclipse event by assimulating the GNSS TEC observations

*Chia-Hung Chen[1], Charles Lin[1], Tomoko Matsuo[2]

1. Department of Earth Sciences, National Cheng Kung University, 2. Department of Aerospace Engineering Sciences, University of Colorado at Boulder, CO

Using the physics-based thermosphere-ionosphere model (NCAR-TIEGCM) with an ensemble Kalman filter, this study reports the first data assimilative analysis of the ionosphere responses to the solar eclipse on 21 August 2017. The system, using a 2-minute assimilation cycle of data from ground-based GNSS observations, show dynamic variations of the equatorial ionization anomaly (EIA) due to the electrodynamic effects of the solar eclipse. Two major ionospheric responses are captured: (1) an early appearance of EIA at the westward boundary of moon shadow and (2) an enhanced EIA at lower latitudes and suppressed EIA at the higher latitudes. These eclipse-induced conjugate EIA variations are produced by an eastward electric field perturbation around magnetic equator and a westward electric field perturbation at the higher latitudes.

Keywords: Ionospheric data assimilation, solar eclipse, electric field perturbation

©2019. Japan Geoscience Union. All Right Reserved.

Characteristics of mesoscale thermospheric-ionospheric dynamics associated with heating in the auroral region

*Tomokazu Oigawa[1], Hiroyuki Shinagawa[2], Satoshi Taguchi[1]

1. Department of Geophysics, Graduate School of Science, Kyoto University, 2. National Institute of Information and Communications Technology

The thermosphere and ionosphere in the polar region have been studied for a long time. Recent results of the ground and satellite measurements have suggested that polar thermospheric and ionospheric dynamics are extremely complicated. In particular, in the auroral region, various processes, such as ion-neutral drag, Joule heating, heating and ionization by particle precipitation, chemical processes, diffusion, and atmospheric gravity waves, are strongly coupled. Previous observations have shown some characteristic mesoscale phenomena such as large vertical winds and significant increasing of mass density in the auroral region. It is considered that local heating plays an important role in such phenomena. However, we still have not quantitatively understood how such large vertical winds and significant increasing of mass density occur. In order to study the mesoscale thermospheric and ionospheric dynamics in the auroral region, a high-resolution numerical model including various physical and chemical processes is required. We will report on how the thermospheric and ionospheric dynamics change depending on the magnitude of the heating and the spatial structure of the heating region using a two-dimensional numerical model. In addition, interaction between the thermosphere and the ionosphere will be discussed.

Keywords: vertical neutral wind, neutral mass density, heating, auroral region, mesoscale, numerical simulation

©2019. Japan Geoscience Union. All Right Reserved.

Spatial distribution of the polar thermospheric wind acceleration and importance of the 2D measurement

*Shin-ichiro Oyama[1,2,3], Anita Aikio[2], Mark G Conde[4], Heikki Vanhamaki[2], Ilkka Virtanen[2], Thomas Ulich[5], Urban Brandstrom[6], Pekka Verronen[7], Monika Andersson[7], Niilo Kalakoski[7], Lassi Roininen[8], Sari Lasanen[8], Abiyot Workayehu[2], Kazuo Shiokawa[1], Heqiucen XU[1], Mamoru Ishii[9], Masafumi Hirahara[1], Takeshi Sakanoi[10], Masato Kagitani[10], Juha Sorri[5], Tomi Teppo[5], Yoshimasa Tanaka[3], Christopher Fallen[4], Brenton J Watkins[4], Mikko Orispaa[5], Yasunobu Ogawa[3], Lei Cai[11], Esa Turunen[5], Kirsti Kauristie[7], Takuo T. Tsuda[12], Junichi Kurihara[13]

1. Institute for Space-Earth Environmental Research, Nagoya University, Japan, 2. University of Oulu, Finland, 3. National Institute of Polar Research, Japan, 4. Geophysical Institute, University of Alaska Fairbanks, US, 5. Sodankyla Geophysical Observatory, University of Oulu, Finland, 6. The Swedish Institute of Space Physics (IRF), Sweden, 7. Finnish Meteorological Institute, Finland, 8. Lappeenranta-Lahti University of Technology, Finland, 9. National Institute of Information and Communications Technology, Japan, 10. Tohoku University, Japan, 11. KTH Royal Institute of Technology, Sweden, 12. The University of Electro-Communications, 13. Hokkaido University

Understanding the flow of energy and mass throughout the magnetosphere-ionosphere-thermosphere coupled system is a fundamental goal of solar-terrestrial physics. Since substantial energy accumulated in the substorm growth phase in the magnetospheric tail flows into the polar ionosphere immediately after the substorm onset, investigating the energy dissipation process at high latitudes around the time of substorm onset can contribute significantly to achieving that objective. The energy dissipation generates acceleration and heating of the ionosphere and thermosphere, but this might occur not only near aurora but also far from it by hundreds kilometers equatorward. We analyzed ionospheric and thermospheric measurements in the northern Scandinavian area (65-80 N) during periods of considerably low geomagnetic activity but with some aurorae above Svalbard (75-80 N). Thermospheric winds measured with a Fabry-Perot interferometer (FPI; 630.0 nm) at Tromsø, Norway (69.6 N) showed westward accelerations coinciding with auroral brightening at the Svalbard area at the dusk sector though the relative distance from Tromsø to the aurora was 200-500 km in some cases. Moving into the dawn sector with the earth’ s rotation, the acceleration direction turned to southeastward through stagnation area or period seen at magnetic local midnight. The acceleration pattern well represents thermospheric responses to the ionospheric convection, but of particular interest is its location, in which the thermospheric wind have been obtained at the sub-auroral region far from the main auroral oval. In this analysis, we cannot infer to horizontal patterns of the wind acceleration because we have only a point measurement from the Tromsø FPI. While this result suggests the importance of two-dimensional measurements of ionosphere and the thermosphere, we need a new configuration of the observation network to infer horizontal winds and accelerations. In this presentation, we will introduce “SDI-3D” project, which aims at developing 3 Scanning Doppler Imagers (SDIs) and deploying them at the same area as for the EISCAT_3D, which may start in operation in 2022.

Keywords: aurora, substorm, Thermosphere, Ionosphere

©2019. Japan Geoscience Union. All Right Reserved.

Analysis of the thermospheric neutral wind vector using observed images of *Trimethylaluminium* (*C6H18Al2*) released from sounding rocket in the upper atmosphere

*Yuki Otsuka[1], Masa-yuki Yamamoto[1], Hiroaki Saito[1]

1. Kochi University of Technology

Altitude profiles such as neutral atmospheric density and ionized atmospheric density in the thermosphere/ionosphere fluctuate by solar activity, season, day and night changes. These fluctuations with affecting on ground, communication with artificial satellites, and make affecting there orbits, but the detailed mechanism of occurrence has not been well understood. We have been conducting collaborative experiments with JAXA, NASA, etc. on inverstigating neutral atmospheric wind in the thermosphere/ionosphere, which is thought to play an important role in this mechanism.
In this research, the main objective is to calculate the neutral wind velocity in the thermosphere from the images of TMA observed in rocket experiment by JAXA conducted in July 2013.
JAXA conducted a rocket experiment in July 2013 to clarify the full picture of electromagnetic interaction and ionized/neutral atmosphere interaction acting on mid-latitude ionosphere. S-310-42 and S-520-27 sounding rocket were launched from Uchinoura Space Center(USC). Trimethylaluminum(TMA)was released in the former and lithium(Li) was released from the latter rocket into the upper atmosphere. Sequential optical observation of changes in these luminescent clouds was operated at each observation point and aircraft. Figure.1 shows the flight path of the aircraft/rockets in the experiment, the observation point, the emission region of TMA and Li, etc.
To calculate the wind speed, we use the images of TMA observed in July 2013 rocket experiment. I analyze the image sequence taken from the aircraft(Figure 2) and those images at USC(Figure 3)as a combination in which the TMA clouds are clearly seen and a long-time optical observations were performed. We use the method of Yokoyama(2011)and Kihara(2015)for caluculating of newtral wind speed.

Method by Yokoyama(2011)[1]
1 From the observed image, the central position of the cloud(TMA gas) is obtained from luminance information. Thereafter, the central axis of the TMA gas is obtained.
2 Choose one of the stars in the observed image as the center star. Also select ten stars around that.
3 Correct the distortion of the lens by using the X,Y coordinates of the stars(right ascension , declination) on the image.
4 Convert the coordinates of the obtained central axis are into celestial spherical coordinates. After that, it converts to earth coordinates using observation point information.
5 From the data of each observation point obtained by the above procedure, wind speed is calculated by using triangulation method.

Method by Kihara(2015)[2]
1 From the observed image, the central position of the cloud(TMA gas) is obtained from luminance information. Thereafter, the central axis of the TMA gas is obtained.
2 Correct distortion of the camera lens. After that, convert the coordinates on the image into the elevation and the azimuth angles.

©2019. Japan Geoscience Union. All Right Reserved.

3 After applying the correction, the difference information is obtained from two images of the same point at different times. Then, the wind speed is calculated from the difference information.

We carried ou extraction of central axis of a TMA cloud, extraction of stars on the images, conversion to elevation and azimuth angles, then derived an approximate wind speed profile. However, it is thought te error at the time of detecting the center axis of the TMA cloud and the conversion error at azimuth/elevation angles are influenced. In the future, it is also necessary to correct lens distortion, tilt of camera, and aircraft velocity and altitude changes.
In this presentation, we would like to introduce more precise caluculation method of neutral wind speed.
References
[1]Kihara Osaki, "Aircraft observation of lithium resonant scattered light emitted from the observational rocket into the super high-rise atmosphere and development of a daytime thermospheric neutral wind measurement method" 2004 Kochi University graduate special research report, 2015.
[2]Yokoyama Yuki, "Multipoint observation of resonant scattered light by rocket emission Li of S-520-23 and high precision analysis of thermospheric neutral wind" 2008 Kochi University of Technology graduate special research report, 2009.

Keywords: the thermospheric neutral wind, sounding rocket, Trimethylaluminium (C6H18Al2)

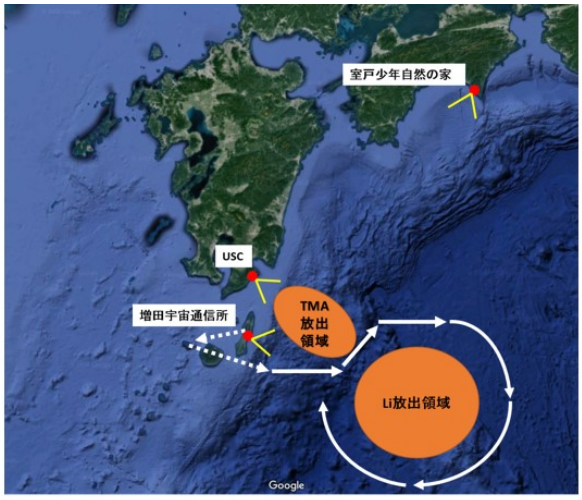

図1 Li、TMAの放出領域、航空機飛行経路、
地上観測点の位置関係

図2 航空機からの観測画像

図3 USCでの観測画像

©2019. Japan Geoscience Union. All Right Reserved.

Establishment of real-time analysis method in a new HRO interferometer system and operation test of comprehensive meteor observation

*Takumi Sato[1], Seiya Takeda[2], Masa-yuki Yamamoto[1]

1. KOCHI UNIVERSITY OF TECHNOLOGY, 2. Inc.Bascule

Meteors are natural phenomenon that dusts is space with several millimeters to several centimeters in diameter in outer space jump into and collide with upper atmosphere of the earth, vaporizing and getting hot because of adiabatic compression by aerodynamic heating with emitting light at the same time. At the moment, thermal energy by aerodynamic heating make molecules in the atmosphere ionize, with generating a large amount of plasma. This plasma makes a elongated dense-ionized column along the meteoric trajectory. Meteor radio observation is an observation method using scattered radio waves by free electrons in the ionized column. In this research, at Kochi University of Technology (KUT), we conducted Ham-band radio meteor observation (HRO) in forward scattering method using the 53.755 MHz VHF (amateur band) wave that is transmitted stably from Fukui Prefectural University.
The objective of this research is that we apply a new observation method and analyzing algorithm to KUT 5ch meteor radio interferometer and develop meteor research using 5 antennas of the meteor radio interferometer [1]. Because of the limited radio meteor observation in Japan, if we share accurate observation method and observation result with the other observers, we can contribute to the development of study on meteor science.
In this research, we conducted three methods (comprehensive meteor observation [1]) of the new HRO interferometer system (HRO interferometer system), optical observation, and infrasound observation.
In the HRO interferometer system, after the signal received at the antennas was demodulated in their receivers, with making input to an observation PC through an AD board, real-time processing by analysing software on the PC was performed. A group of data set triggered only when exceeding a threshold set in advance on the software are saved as a meteor echo. In the analysis of meteor plasma direction of each meteor with considering intrinsic phase difference, we calculated each phase difference in north-south and east-west directions with baseline length of 0.5 λ and 2.5 λ (λ is observation wavelength), after processing interference calculation among signals of multiple antennas using 5ch meteor radio interferometer [1].
In the optical observation, we used existing high sensitivity B/W CCD camera (WAT-100N) and color 4K camera (Sony, α6300) newly installed with a combination of UFOCaptureV2 and HD2 that are motion capture software. The observation data was analyzed from the information recorded by cameras by analyzing position, velocity, linearity of motion, etc. by using UFOAnalyzerV2 for data stored through UFOCaptureV2 and HD2.
In the infrasound observation, we conducted a unique meteor observation for such as large fireballs by using a group of infrasound sensors that can observe very low frequency sound of less than 20 Hz caused by large scale natural phenomena. It is possible to estimate energy scale of the meteor entry from obtained amplitude and period of the sound wave.
In order to determine the intrinsic phase shift, we searched for the observability of the same phenomenon for the comprehensive meteor observation data.
In this research, we obtained 2 meteor shower data from August 2018 to January 2019. Especially, in 2019 at Quadrantids, three candidates of the intrinsic phase shift was obtained by analysis of comprehensive meteor observation data, but we could not confirm the intrinsic phase shift.

©2019. Japan Geoscience Union. All Right Reserved.

As a result of this research, we obtained the candidate values necessary for accurate calculation of meteor plasma direction by the interferometer data processing. Due to lack of the observation data, we could not confirm the intrinsic phase shift, thus after checking the analyzing process, we will continue to use the system and obtain more data to establish the intrinsic phase shift and ensure the accuracy and reliability of the observation method.
We applied the new trial called real-time analyzing to KUT 5ch radio meteor interferometer with confirming the validity of the new receiver system, and obtained the candidate values of the intrinsic phase shift necessary for our future research. We shared a part of accurately obtained data on the web and a mailing lists, so as to contribute to the development of meteor science.

References
[1] Satoshi Mizumoto, “Calculation of meteor orbit by multiple-site radio observation and construction of a comprehensive meteor observation system”, Master thesis, 2017.

Keywords: Meteor, Ham-band radio meteor observation, Interferometer

©2019. Japan Geoscience Union. All Right Reserved.

Solar flare effects of the D-region ionosphere using daytime tweek atmospherics

*Kodai Yamanobe[1], Hiroyo Ohya[2], Hiroyuki Nakata[2], Toshiaki Takano[2], Kazuo Shiokawa[3]

1. Graduate School of Science and Engineering, Chiba University , 2. Graduate School of Science and Engineering, Chiba University, 3. Institute for Space-Earth Environmental Research, Nagoya University

It has been known that intensity and phase of very low frequency (VLF, 3-30 kHz)/low frequency (LF, 30-300 kHz) transmitter signals significantly change due to intense ionization by solar flares [e.g., Mitra, 1974; Thomson et al., 2005]. Santolik and Kolmasova [2017] showed daytime tweek atmospherics (1.5-10.0 kHz) did not become observal for two hours just after a solar flare of M2.2 class, which suggests large absorption due to the solar flare. However, there are little studies for tweeks during solar flares. In this study, we investigate solar flare effects of the D-region ionosphere using tweek atmospherics. We analyzed the daytime tweek atmospherics observed at Kagoshima (31.48N, 130.72E) and Moshiri (44.37N, 142.27E), Japan, during January-July, 2013. The sampling frequency is 20 kHz, and the VLF data were recorded for each two minuteat 20-22 and 50-52 minutes every hour. For two M1.4-class flares, the daytime tweeks were received about 30-40 minutes after the solar flares. For a M5.6-class flare, the daytime tweeks were not observed for about 4 hours after the solar flare. The tweek reflection height had a weak negative correlation (-0.38) with X-ray flux observed by the GOES-13/15 satellites, suggesting that electron density in the D-region ionosphere increased with increasing the X-ray flux.In the presentation, we will discuss the D-region ionization and propagation mechanism of the tweeks during solar flares in more detail.

©2019. Japan Geoscience Union. All Right Reserved.

[J] Oral | P (Space and Planetary Sciences)：P-EM Solar-Terrestrial Sciences, Space Electromagnetism & Space Environment

Wed. May 29, 2019 10:45 AM - 12:15 PM JST | Wed. May 29, 2019 1:45 AM - 3:15 AM UTC | A03 TOKYO BAY MAKUHARI HALL

[P-EM16] Physics and Chemistry in the Atmosphere and Ionosphere

convener:Yuichi Otsuka(Institute for Space-Earth Environmental Research, Nagoya University), Takuya Tsugawa(National Institute of Information and Communications Technology), Seiji Kawamura(National Institute of Information and Communications Technology), Chairperson:Yuichi Otsuka, Mitsumu Ejiri(国立極地研究所)

This session covers a broad scope of studies of physics and chemistry in the atmosphere and the ionosphere. Coupling processes between plasma and neutral species, and upward and downward coupling among lower/upper atmosphere, and ionosphere/mesosphere/thermosphere including magnetosphere are discussed. We solicit papers based on experiments with ground-based and/or space-borne instruments, theoretical studies, numerical simulations, and development of new observation techniques.

10:45 AM - 11:00 AM JST | 1:45 AM - 2:00 AM UTC

[PEM16-07] Toward a detection of sporadic-E episodes by ALOS2 ScaSAR InSAR

*Masato Furuya[1], Jun Maeda[2], Kosuke Heki[1] (1.Department of Earth and Planetary Sciences Hokkaido University, 2.Hokkaido University Library)

11:00 AM - 11:15 AM JST | 2:00 AM - 2:15 AM UTC

[PEM16-08] Vertical fine structure and time evolution of plasma irregularities in the E_s layer, observed by a high resolution Ca^+ lidar

*Mitsumu K. Ejiri[1,2], Takuji Nakamura[1,2], Takuo T. Tsuda[3], Takanori Nishiyama[1,2], Makoto Abo[4], Toru Takahashi[1], Katsuhiko Tsuno[5], Takuya Kawahara[6], Takayo Ogawa[5], Satoshi Wada[5] (1.National Institute of Polar Research, 2.SOKENDAI (Department of Polar Science, The Graduate University for Advanced Studies), 3.The University of Electro-Communications, 4.Tokyo Metropolitan University, 5.RIKEN, RAP, 6.Shinshu University Faculty of Engineering)

11:15 AM - 11:30 AM JST | 2:15 AM - 2:30 AM UTC

[PEM16-09] Study of Effects of Stratospheric Sudden Warming on Medium-Scale Traveling Ionospheric Disturbances Using Total Electron Content Data Obtained from World-Wide GPS Receiver Networks

*Yuichi Otsuka[1], Atsuki Shinbori[1], Prayitno Abadi[2], Takuya Tsugawa[3], Michi Nishioka[3] (1.Institute for Space-Earth Environmental Research, Nagoya University, 2.LAPAN, 3.National Institute of Information and Communications Technology)

11:30 AM - 11:45 AM JST | 2:30 AM - 2:45 AM UTC

[PEM16-10] Tsunami-generated ionospheric currents inferred from geomagnetic observations at ground level: Case for the 2011 Tohoku Earthquake

*Takuto Minami[1], Masashi Kamogawa[2], Tsutomu Ogawa[1], Makoto Uyeshima[1], Toru Mogi[3], Hiroshi Ichihara[4] (1.Earthquake Research Institute,The University of Tokyo, 2.Department of Physics, Tokyo Gakugei University, 3.Graduate School of Engineering, Hokkaido University, 4.Graduate School of Environmental Studies, Nagoya University)

11:45 AM - 12:00 PM JST | 2:45 AM - 3:00 AM UTC

[PEM16-11] Relationship between the magnitude of Sakurajima eruptions and the disturbance of GPS-TEC

*Kiyoto Shoji[1], Hiroyuki Nakata[1], Toshiaki Takano[1], Hiroyo Ohya[1], Takuya Tsugawa[2], Michi Nishioka[2] (1.Graduate School of Science and Engineering, Chiba University, 2.National Institute of Information and Communications Technology)

12:00 PM - 12:15 PM JST | 3:00 AM - 3:15 AM UTC

[PEM16-12] Water vapor estimation using digital terrestriall broadcasting waves - Simultaneous observation with microwave radiometer -

*Hiroshi HANADO[1], Seiji Kawamura[1], Hironori Iwai[1], Shinsuke Satoh[1], Katsuhiro Nakagawa[1], Takuya Tajiri[2], Narihiro Orikasa[2], Yoshinori Shoji[2], Kentaro Araki[2], Hiromu Seko[2] (1.National Institute of Information and Communications Technology, 2.Meteorological Research Institute)

Toward a detection of sporadic-E episodes by ALOS2 ScaSAR InSAR

*Masato Furuya[1], Jun Maeda[2], Kosuke Heki[1]

1. Department of Earth and Planetary Sciences Hokkaido University, 2. Hokkaido University Library

Maeda et al. (2016) and Furuya et al. (2017) reported their detections of sporadic-E (Es) episodes in Japan, using L-band interferometric synthetic aperture radar (InSAR). The SAR data images are acquired by Advanced Land Observation Satellite (ALOS) 1/2 launched by JAXA in 2006 and 2014, respectively. The high spatial resolution of InSAR data allow us to examine the detailed structure of Es episode, which will complement the high temporal resolution of GNSS TEC data. The previous two studies are based on stripmap-mode SAR images, which have higher spatial resolution but are limitted in terms of the observation swath-width (Maeda et al., 2016; Furuya et al., 2017). Although the stripmap-mode is the most standard SAR imaging mode, ScanSAR mode is also nearly operational nowadays, and can image the Earth with much wider swath-width by as much as 350 km; the standard stripmap-mode of SM1 for ALOS2 covers only 50 km. Although the ScanSAR mode is a bit worse in terms of the spatial resolution along radar range direction than the stripmap mode image, ScanSAR InSAR image can dramatically improve the observation coverage, and thus help detect both small-scale and large-scale structure of Es. We first check the data availability of ScanSAR images in Japan at any specific areas, and then check if any significant anomalies in either TEC or ROTI are observed via the database provided by NICT. We will report our preliminary results of ScanSAR InSAR imaging of Es in Japan.

Keywords: ionosphere, Sporadic-E, InSAR, ALOS2

©2019. Japan Geoscience Union. All Right Reserved.

Vertical fine structure and time evolution of plasma irregularities in the E_s layer, observed by a high resolution Ca^+ lidar

*Mitsumu K. Ejiri[1,2], Takuji Nakamura[1,2], Takuo T. Tsuda[3], Takanori Nishiyama[1,2], Makoto Abo[4], Toru Takahashi[1], Katsuhiko Tsuno[5], Takuya Kawahara[6], Takayo Ogawa[5], Satoshi Wada[5]

1. National Institute of Polar Research, 2. SOKENDAI (Department of Polar Science, The Graduate University for Advanced Studies), 3. The University of Electro-Communications, 4. Tokyo Metropolitan University, 5. RIKEN, RAP, 6. Shinshu University Faculty of Engineering

The vertical fine structures and the time evolution of plasma irregularities in the sporadic E (E_s) layer were observed via calcium ion (Ca^+) density measurements using a resonance scattering lidar with a high time-height resolution (5 s and 15 m) at Tachikawa (35.7˚N, 139.4˚E) on December 24, 2014. The observation successfully provided clearer fine structures of plasma irregularities, such as quasi-sinusoidal variation, localized clumps, “cats-eye” structures, and twist structures, in the sporadic Ca^+ (Ca^+_s) layers at around 100 km altitude. These fine structures suggested that the Kelvin-Helmholtz (K-H) instabilities occurred in the neutral atmosphere whose density changed temporarily or spatially. The maximum Ca^+ density in the Ca^+_s layer was two orders of magnitude smaller than the maximum electron density estimated from the critical frequency (f_oE_s) observed by the ionosonde at Kokubunji (35.7˚N, 139.5˚E) simultaneously. The correlation showed a strong positive correlation with a coefficient of 0.91. These results suggest that Ca^+ contributes forming the E_s layer as well as major metallic ions Fe^+ and Mg^+ in the lower thermosphere. Moreover, the formation of a new Ca^+_s layer at 110 km and the upward motions of the Ca^+_s layers at 100 km and 110 km were observed just after the sunrise time at the conjugation point and before the local sunrise. Although the presence or absence of a causal relationship with the sunrise time was not clear, a possible explanation for the formation and the upward motions of the Ca^+_s layers was the occurrence of strong eastward winds at around 100 km, rather than the enhancement of the eastward electric field.

Keywords: resonance scattering lidar, calcium ion density, sporadic E layer, fine structure, The mesosphere and lower thermosphere region

©2019. Japan Geoscience Union. All Right Reserved.

Study of Effects of Stratospheric Sudden Warming on Medium-Scale Traveling Ionospheric Disturbances Using Total Electron Content Data Obtained from World-Wide GPS Receiver Networks

*Yuichi Otsuka[1], Atsuki Shinbori[1], Prayitno Abadi[2], Takuya Tsugawa[3], Michi Nishioka[3]

1. Institute for Space-Earth Environmental Research, Nagoya University, 2. LAPAN, 3. National Institute of Information and Communications Technology

Medium-Scale Traveling Ionospheric Disturbances (MSTIDs) are wavy structures of the ionospheric plasma density with horizontal scale-size of hundreds of kilometers. In order to investigate effects of Stratosphere sudden warming (SSW) on MSTIDs, we have analyzed total electron content (TEC) data obtained from GPS receivers at different four longitudinal sectors (east Asia, Europe, and western and eastern America) before and after SSW that occurred on January 2009 and 2013. To obtain perturbation component of TEC, which could be caused by MSTID, we have subtracted 1-hour running average from the original TEC time series for each pair of satellites and receivers, and converted the slant to vertical TEC. We have defined MSTID activity as dI/I, where dI is the standard deviation of the perturbation component within 1 hour, and I is 1-hour average absolute vertical TEC. In this study, we applied the same method to the GPS-TEC data at mid-latitudes before and after major Stratospheric Sudden Warming (SSW) events that occurred on January 2009 and 2013. We have found that MSTID activity during daytime is high before SSW events and low after SSW events. On the other hand, the nighttime MSTID activity does not show such a difference between before and after SSW events. These results suggest difference of mechanisms generating MSTIDs between daytime and nighttime. The daytime MSTIDs could be caused by gravity waves propagating upward from below into the thermosphere. Recent simulations suggest that these gravity waves are secondary waves generated from dissipation of the primary waves in the MLT region. Miyoshi et al. (JGR, 2015) have reported that the generation of secondary gravity waves is more active when the strato-mesospheric jet is strong, and that the generation of secondary waves is inactive when the strato-mesospheric jet is attenuated or becomes westward. Consequently, low MSTID activity after January 24 could be caused by weaker generation of secondary gravity wave during weaker or westward strato-mesospheric jet. On the other hand, gravity waves propagating from below does not contribute to generation of MSTIDs during nighttime.

Keywords: GPS, TID, Stratospheric Sudden Warming

©2019. Japan Geoscience Union. All Right Reserved.

Tsunami-generated ionospheric currents inferred from geomagnetic observations at ground level: Case for the 2011 Tohoku Earthquake

*Takuto Minami[1], Masashi Kamogawa[2], Tsutomu Ogawa[1], Makoto Uyeshima[1], Toru Mogi[3], Hiroshi Ichihara[4]

1. Earthquake Research Institute,The University of Tokyo, 2. Department of Physics, Tokyo Gakugei University, 3. Graduate School of Engineering, Hokkaido University, 4. Graduate School of Environmental Studies, Nagoya University

It is known that large earthquakes cause atmospheric gravity/acoustic waves reaching the ionosphere and drive ionospheric dynamo currents at the altitude (e.g. Iyemori et al. 2005). Related phenomena were detected by observations of total electron content (TEC) (e.g. Tsugawa et al. 2011) and reported by numerical simulations (e.g. Kherani et al. 2013). However, the form of electric currents due to the coseismic ionospheric dynamo has never been revealed from the perspective of geomagnetic observations at ground level.

We investigated 1-min sampling magnetic data at nineteen on-land stations on the Japan Arc and at one ocean-bottom magnetometer ~200 km off the Tohoku, to reveal the form of coseismic electric currents in the ionosphere during the 2011 Tohoku earthquake (Mw 9.0). First, we subtracted the effects of non-seismic components of ionospheric and magnetospheric origins from the geomagnetic data, using magnetic transfer functions between the stations of interest along the Japan Arc and a reference site in China, Changchun. Second, we subtracted the oceanic dynamo effects due to the tsunami by a time-domain finite element simulation in the same manner as Minami et al. (2017). By rotating the coordinate system at each station to that consisting of radial and transverse axes in terms of the tsunami centre, we recognized a clear concentric propagation of a trough in the radial magnetic component with a phase velocity of ~ 1 km/sec and a trough amplitude of ~ 7 nT. This propagation happens in all the directions and the propagation velocity is almost the same as that of the slow coseismic ionospheric disturbances (CID) observed by TEC observations (e.g. Kakinami et al., 2013). The radial propagation of a trough in the radial component indicates presence of anti-clockwise electric currents in the ionosphere.

In the presentation, we report our analysis of the geomagnetic data at ground level and the inferred characteristics of the coseismic electric currents in the ionosphere. We also plan to show some results of spectral analyses of the propagation features involved in the geomagnetic data.

Keywords: tsunami, dynamo, magnetic observations, The 2011 Tohoku Earthquake

©2019. Japan Geoscience Union. All Right Reserved.

Relationship between the magnitude of Sakurajima eruptions and the disturbance of GPS-TEC

*Kiyoto Shoji[1], Hiroyuki Nakata[1], Toshiaki Takano[1], Hiroyo Ohya[1], Takuya Tsugawa[2], Michi Nishioka[2]

1. Graduate School of Science and Engineering, Chiba University, 2. National Institute of Information and Communications Technology

It is reported that ionospheric disturbances are caused by ground and atmospheric perturbations, e.g. earthquakes, typhoons and volcanic eruptions. Even though the volcanic eruptions excite the atmospheric waves, there is little reports of ionospheric disturbances caused by volcanic eruptions. Therefore, in this study, we analyzed the ionospheric disturbances caused by volcanic eruption using Total Electron Content (TEC) determined by GNSS system.
We analyzed TEC data observed in GNSS Earth Observation Network (GEONET) which is maintained by Geospatial Information Authority of Japan. We assumed that the ionospheric pierce points (IPP) are located at the altitude of 300 km. The 30-second TEC data are obtained in about 1200 points of GEONET. The mask angle is 30 degrees. We analyzed four events of Sakurajima eruptions (7:45 UT on Oct.-3-2009, 1:07 UT on Sep.-19-2012, 20:25 UT on Dec.-9-2012 and 20:21 UT on Feb.-12-2014). The magnitudes of the eruptions are estimated by the infrasound meter located at Higawa-Korimoto.
The TEC disturbances are larger in the larger magnitude of the events.
It is expected that the TEC disturbance is inversely correlated with the distance from the crater as the energy of the atmospheric wave spreads according to the distance from the crater. Examining the relationship between TEC disturbances and the distances of IPPs from the crater. There was an inverse correlation with the distance in one events out of four events. However, no correlation was found in the other three events. This may be due to the directions of the magnetic field and the wave normal of the disturbance to the GPS satellite-receiver. In order to correct these effect, we calculated two coupling coefficients of the directions of the atmospheric wave from the calculation results of the acoustic ray tracing the one is related to the direction of the magnetic field, and the other is to the direction between the transmitters (satellites) and GNSS receivers. After this connection, an inverse correlation between TEC disturbances and the distance from the crater was appeared in three events.
However, some data showed higher values than the expected values. In the IPPs where the corrected values are high, the correction coefficients are very small. Therefore, the cause of the high values is too effective correction.

Keywords: ionosphere, volcanic eruptions, Total Electron Content

©2019. Japan Geoscience Union. All Right Reserved.

Water vapor estimation using digital terrestriall broadcasting waves - Simultaneous observation with microwave radiometer -

*Hiroshi HANADO[1], Seiji Kawamura[1], Hironori Iwai[1], Shinsuke Satoh[1], Katsuhiro Nakagawa[1], Takuya Tajiri[2], Narihiro Orikasa[2], Yoshinori Shoji[2], Kentaro Araki[2], Hiromu Seko[2]

1. National Institute of Information and Communications Technology, 2. Meteorological Research Institute

1. Introduction

NICT is developing a method that can observe water vapor in a wide area and efficiently. Water vapor is an important quantity along with wind velocity and temperature in the weather prediction. Solid / liquid phase water in the atmosphere can be observed with weather radars, but water vapor, water in gas phase, can not be observed with radars. Water vapor observation methods in a wide area are limited. Currently, GPS / GNSS precipitable water observation which is used as water vapor data in a weather numerical model uses the delay amount of the L-band radio waves from the GPS / GNSS satellites. NICT have demonstrated that similar measurements are possible with the terrestrial digital broadcast wave in UHF [1]. The method is that using delay profile decorded from scattered pilot signals embedded in the terrestrial digital broadcast wave, the reflected wave scattered from the surrounding reflector, building or towers, is separated from the direct wave. By using phase difference between the reflected wave and direct one, the influence of the phase noise of the reference signal at the broadcast station / reception point is canceled, and the propagation delay of the UHF band radio wave is measured with accuracy of picosecond level.

2. Simultaneous observation with microwave radiometer

We installed a microwave radiometer and terrestrial digital broadcasting wave receiver on the roof of the Meteorological Research Institute, Tsukuba, in February 2017, and we are continuing long-term observation. The microwave radiometer is an instrument capable of observing the amount of water vapor accumulated in the vertical direction above the measurement point. On the other hand, water vapor observation by the terrestrial digital broadcast wave means the amount of water vapor along the horizontal direction near surface. These observation volumes are different in size and shape. Therefore, by combining the two sensors, complementary observation of the water vapor amount is expected. In terms of time resolution, the microwave radiometer is not so good as it directs the antenna beams in a plurality of directions and estimates from the received thermal noise powers. In the water vapor estimation by terrestrial digital reception, more than 50 samples are measured per second, and it has a rather high temporal resolution. In this presentation, we will compare the variation of water vapor observed by microwave radiometer and terrestrial digital broadcasting wave for about one and a half years, and introduce the analysis results focusing on the difference in characteristics.

Keywords: water vapor, digital terrestrial broadcasting wave, propagation delay

©2019. Japan Geoscience Union. All Right Reserved.

[J] Oral | P (Space and Planetary Sciences)：P-EM Solar-Terrestrial Sciences, Space Electromagnetism & Space Environment

Wed. May 29, 2019 1:45 PM - 3:15 PM JST | Wed. May 29, 2019 4:45 AM - 6:15 AM UTC | 201A 2F

[P-EM18] Heliosphere and Interplanetary Space

convener:Ken Tsubouchi(University of Electro-Communications), Masaki N Nishino(Japan Aerospace Exploration Agency, Institute of Space and Astronautical Science), Yasuhiro Nariyuki(Faculty of Human Development, University of Toyama), Kazumasa Iwai(Institute for Space?Earth Environmental Research (ISEE), Nagoya University), Chairperson:Yasuhiro Nariyuki, Kazumasa Iwai

This session aims to secure comprehensive insights into physical processes of plasmas and fields in the heliosphere. Presentations of the recent studies from any approaches (integrated observations/theoretical modeling/massive numerical simulation) are welcomed. Topics are not restricted to any specific issues: phenomenological studies on solar flares/CME/solar wind, and related fundamental physics problems such as shocks/waves/turbulence/particle transport and acceleration can be the main target, including heliospheric high-energy phenomena and their impact on the Earth's environment.

1:45 PM - 2:00 PM JST | 4:45 AM - 5:00 AM UTC

[PEM18-01] Problems in determining structures of interplanetary magnetic flux ropes

*Katsuhide Marubashi[1], Yuki Kubo[1], Nobuhiko Nishimura[2], Munetoshi Tokumaru[2], Nada Al-Haddad[3] (1.National Institute of Information and Communications Technology , 2.ISEE, Nagoya University, 3.IACS, Catholic University of America)

2:00 PM - 2:15 PM JST | 5:00 AM - 5:15 AM UTC

[PEM18-02] Validation of estimated interplanetary flux rope axial direction using internal plasma motions: benchmark test

*Nobuhiko Nishimura[1], Munetoshi Tokumaru[1], Katsuhide Marubashi[2] (1.Institute for Space Earth Environmental Research, 2.National Institute of Information and Communications Technology)

2:15 PM - 2:30 PM JST | 5:15 AM - 5:30 AM UTC

[PEM18-03] Effect of line-of-sight integration on locations of coronal mass ejection in the sky projection map of interplanetary scintillation observations

*Munetoshi Tokumaru[1], Ken'ichi Fujiki[1], Kazumasa Iwai[1] (1.Institute for Space-Earth Environmental Research, Nagoya University)

2:30 PM - 2:45 PM JST | 5:30 AM - 5:45 AM UTC

[PEM18-04] Estimation of spatial structure of whistler mode wave packets in Earth’s bow shock by multiple spacecraft analysis

*Chika Umegaki[1], Takanobu Amano[1], Naritoshi Kitamura[1] (1.The university of tokyo)

2:45 PM - 3:00 PM JST | 5:45 AM - 6:00 AM UTC

[PEM18-05] Experimental Test for Stochastic Shock Drift Acceleration Theory

*Takanobu Amano[1], Takuma Katou[1], Naritoshi Kitamura[1], Mitsuo Oka[2], Yosuke Matsumoto[3], Masahiro Hoshino[1] (1.Department of Earth and Planetary Science, University of Tokyo, 2.Space Sciences Laboratory, University of California, Berkeley, 3.Department of Physics, Chiba University)

3:00 PM - 3:15 PM JST | 6:00 AM - 6:15 AM UTC

[PEM18-06] Radial structure of heliospheric boundary region

*Shuichi Matsukiyo[1], Gary P. Zank[2], Haruichi Washimi[3], Tohru Hada[1] (1.Faculty of Engineering Sciences, Kyushu University, 2.The Center for Space Plasma and Aeronomic Research, University of Alabama in Huntsville, 3.International Center for Space Weather Science and Education, Kyushu University)

Problems in determining structures of interplanetary magnetic flux ropes

*Katsuhide Marubashi[1], Yuki Kubo[1], Nobuhiko Nishimura[2], Munetoshi Tokumaru[2], Nada Al-Haddad[3]

1. National Institute of Information and Communications Technology , 2. ISEE, Nagoya University, 3. IACS, Catholic University of America

The interplanetary magnetic flux ropes (IFRs) are ejected from the Sun to interplanetary space in association with the coronal mass ejections (CMEs). Their magnetic structure is an important research subject which provides information on the mechanism of CMEs. On the other hand, The IFRs often cause strong geomagnetic storms because of intense southward magnetic fields carried from the solar atmosphere. Thus, the IFRs have long been studied since they were discovered more than 30 years ago. It is the first step for such studies to determine the 3-D geometries and internal magnetic field structures of IFRs. We need to assume a physical model of the IFR and compare the model structure with observations. There are 2 representative analysis methods which are currently used along the line. They are: (1) a fitting method to models of force-free magnetic field configurations, and (2) a reconstruction method of magnetic field structures based on the Grad-Shafranov (GS) equation. Recently, Al-Haddad et al. (Solar Phys. 2018) examined the mutual agreement between the results from the two methods for 13 well-determined IFRs carefully selected. They found that the agreement is relatively good in only 6 cases, and thus concluded that the compatibility of different models with specific IFR structures must be taken into account.

The present study is an extension of the work by Al-Haddad et al. In the GS method, 2-D structure (essentially a cylindrical structure) is assumed, and the axis orientation is determined so that the symmetry condition is satisfied between inbound and outbound crossings of the IFR. If the IFR fields satisfy the force-free condition, the internal structures obtained by the 2 methods agree with each other. Actually, however, the GS method includes the effect of plasma pressure while the force-free model neglects the plasma pressure. This can cause the discrepancy between the two. With this idea in mind, we started to examine how the axis orientations deviate from each other. However, we encounter an unexpected problem, that is, it is not easy to point start and end times of an IFR from the observed data. Especially in the GS method, the selection of the IFR interval is strongly affected by the symmetry condition. In this presentation we show results of our trial to determine the axis orientation for many possible IFR intervals.

Keywords: interplanetary flux rope, force-free model, Grad-Shafranov equation

©2019. Japan Geoscience Union. All Right Reserved.

Validation of estimated interplanetary flux rope axial direction using internal plasma motions: benchmark test

*Nobuhiko Nishimura[1], Munetoshi Tokumaru[1], Katsuhide Marubashi[2]

1. Institute for Space Earth Environmental Research, 2. National Institute of Information and Communications Technology

Interplanetary flux rope (IFR) is a structure with helical magnetic field lines wrapping around a central axis to form a flux rope structure. Accurate estimation of this structure is important for improving the space weather forecasting and understanding the evolution of IFR. Local structures of IFRs have been investigated by many model fittings and reconstruction method. However, the outputs of these model fittings and reconstruction method are often different. The chirality and magnetic flux of corresponding flux rope at the Sun are often compared with those of IFR to check the validity of estimation of IFR properties, but it is questionable whether this consistency check guarantees the validity of IFR axis direction which is one of the important properties of IFR. In this study, we propose a method that validates IFR axial direction based on plasma motion. It is known that the radius of IFRs often expand or sometimes contract during the passage of IFR through a spacecraft and if the expansion or contraction exist, the direction of plasma motion in IFR may be perpendicular to IFR axis in the frame comoving with the IFR. This suggests that plasma velocity in IFR reflects the axial direction of IFR. We test the method for a well-investigated IFR event on May 21-22, 2007. The magnetic field structure of this event has already been investigated by Liu et al. (2008) using multi-spacecraft measurements at STEREO-B, ACE, Wind, and STEREO-A and other researches (e.g. Kilpua et al. 2009) which report similar axial directions to that of Liu et al. (2008). Herein, We consider that the axial direction determined by them is correct since Liu et al. (2008) found that output from reconstruction at STEREO-B agrees fairly well with the observations at ACE and Wind. We fit the cylindrical and toroidal IFR models (Marubashi et al. 2007) to this event and then apply our validation method proposed in this study to the outputs from the fittings. We checked whether the outputs with the correct axial direction are judged to be valid and vice versa. We find that the fitting result with correct axial direction is judged valid. However, our validation method also judged some fitting results with wrong axial direction to be valid. We need to improve our validation method to make it work well.

Keywords: interplanetary flux rope, interplanetary space, space weather

©2019. Japan Geoscience Union. All Right Reserved.

Effect of line-of-sight integration on locations of coronal mass ejection in the sky projection map of interplanetary scintillation observations

*Munetoshi Tokumaru[1], Ken'ichi Fujiki[1], Kazumasa Iwai[1]

1. Institute for Space-Earth Environmental Research, Nagoya University

The g-value derived from interplanetary scintillation (IPS) observations abruptly enhances when a high density (i.e. shocked) plasma associated with a coronal mass ejection (CME) intersects the line-of-sight (LOS). The plane-of-sky location of the line-of-sight, which shows the g-value enhancement, provide information of the radial distance of the CME-driven shock, and enables determination of the shock transit speed in the solar wind between the Sun and the Earth. It should be noted here that IPS measurements include an effect of the LOS integration, and the plane-of-sky location of g-value enhancements is affected significantly by this effect for some cases. The most significant bias is expected for an Earth-directed event. In this study, we investigated the dependence of the LOS integration effect on the radial distance, the angular width, and the non-uniform expansion for an Earth-directed CME. We made calculations of the sky projection map of g-value using the CME model (Tokumaru et al., 2003). As the result, we found that the plane-of-sky location of g-value enhancements tends to underestimate the actual distance of CME, and that this tendency is distinct in the region near the Sun, being less as the CME moves further from the Sun. This means that apparent acceleration is observed for an Earth directed CME propagating with a constant speed. The degree of this tendency is significant for a case with a small angular extent of CME and also for a case with the non-uniform expansion. Such apparent acceleration of CME near the Sun has seldom reported from IPS measurements for Earth-directed CMEs. This fact may suggest that the CME detected by IPS has a sufficiently large angular width, and hence that the acceleration effect is counterbalanced or overwhelmed by intrinsic deceleration of CME during propagation.

Keywords: interplanetary scintillation, solar wind, coronal mass ejection, space weather

©2019. Japan Geoscience Union. All Right Reserved.

Estimation of spatial structure of whistler mode wave packets in Earth's bow shock by multiple spacecraft analysis

*Chika Umegaki[1], Takanobu Amano[1], Naritoshi Kitamura[1]

1. The university of tokyo

There have been a lot of unresolved issues in the generation mechanism of nonthermal charged particles observed ubiquitously in space plasmas. The Fermi acceleration at a shock wave is one of the leading mechanisms for the nonthermal particle acceleration. In this mechanism, it is necessary to confine charged particles in the vicinity of the shock wave while charged particles are being accelerated, which requires pitch angle scattering due to wave-particle interactions. In the case of electrons, whistler mode waves are considered to play a major role in the pitch angle scattering. Whistler mode waves are electromagnetic waves that are right-hand circularly polarized with respect to the background magnetic field. They are thought to contribute to the scattering of electrons by interacting with counter-streaming electrons. In fact, there have been reports of coherent whistler mode waves propagating parallel to the magnetic field in the vicinity of the shock wave (Hull et al., 2012). Recently, it was found that such whistler mode waves are indeed resonantly interacting with suprathermal electrons (Oka et al., 2017). However, it has been known that the acceleration of electrons at the shock is rare, and the relation between whistler mode waves and electron scattering (or acceleration) efficiency has not yet been clarified. The applicability of the standard quasi-linear theory for the electron scattering efficiency by coherent whistler mode waves seen in the shock transition region is not understood very well. For this purpose, one has to identify the spatio-temporal scale of coherent whistler wave packets.
In this study, we aim to estimate the spatial scale of the coherent whistler mode waves around bow shock. For instance, by estimating the scale size of whistler mode wave packets in the direction perpendicular to the magnetic field, we may impose a limit for the energy of electrons being scattered by the wave. This is because gyroradii of electrons must be sufficiently smaller than the perpendicular size of wave packets otherwise the conventional cyclotron resonance theory should not be applicable. For this purpose, simultaneous observations by multiple spacecraft are necessary. In this study, we performed an analysis for high-frequency (~100 Hz) electromagnetic waves observed during bow shock crossings with enhanced energetic electron flux observed by NASA's MMS (Magnetospheric MultiScale) spacecraft.
In particular, we report results for the following two bow shock crossing events: 11:44 UT on October 7, 2015 (Event 1), and 10:29 UT on December 6, 2016 (Event 2). The spacecraft separation was 20 km and 7 km for the Event 1 and Event 2, and comparison between the two may enable us to estimate the scale size of whistler mode wave packets. We applied a band pass filter with for the frequency range 100-250 Hz (fce > 1 kHz) for Event 1, and 50-150 Hz (fce ~ 300 Hz) for Event 2 where prominent peaks were observed in the magnetic field power spectra. We confirmed that whistler mode waves appeared sporadically as wave packets with a short duration (50 - 100 ms). We used MVA (Minimum Variance Analysis) for determining the wave propagation direction. Note that we eliminated the 180-degree ambiguity by referring the Poynting vector direction. Also, we estimated the wavelength from the wave electric-to-magnetic field amplitude ratio using Faraday's law. The obtained wavelengths of the whistler mode waves were roughly 10 km. This indicates that the spacecraft separations were larger (smaller) than the wavelength for the Event 1 (2). By doing the same analysis for each spacecraft, we found that wave packets observed during Event 1 were almost always uncorrelated. On the other hand, both correlated and uncorrelated wave packets were found for Event 2. This suggests that the whistler mode wave packets have spatial scale of a few km. In this report, we will estimate the spatial scale sizes of wave packets in parallel and perpendicular to the magnetic field direction.

©2019. Japan Geoscience Union. All Right Reserved.

Keywords: whistler wave, MMS spacecraft

©2019. Japan Geoscience Union. All Right Reserved.

Experimental Test for Stochastic Shock Drift Acceleration Theory

*Takanobu Amano[1], Takuma Katou[1], Naritoshi Kitamura[1], Mitsuo Oka[2], Yosuke Matsumoto[3], Masahiro Hoshino[1]

1. Department of Earth and Planetary Science, University of Tokyo, 2. Space Sciences Laboratory, University of California, Berkeley, 3. Department of Physics, Chiba University

High-energy charged particles are ubiquitous in space. They have energies orders of magnitude higher than the thermal energy and often exhibit a power-law distribution in a wide energy range. The collisionless shock is one of the leading mechanisms that may produce such high-energy non-thermal particles. Indeed, radio, X-ray, and gamma-ray observations strongly suggest that shock waves associated with supernova remnants, pulsar winds, relativistic jets in active galactic nuclei and gamma-ray burst are accelerating relativistic electrons. On the other hand, in-situ observations in the heliosphere (at planetary bow shocks, or interplanetary shocks driven by coronal mass ejections) have shown that the acceleration of electrons is, in general, weak or even absent in many of the shock crossings.

We have recently proposed a theory for electron acceleration at shocks that may resolve the observational controversy. The theory referred to as stochastic shock drift acceleration (SSDA) assumes stochastic pitch-angle scattering during electrons are interacting with a collisionless shock. The energy gain comes from the gradient-B drift (due to the magnetic field compression in the shock transition layer) in the direction anti-parallel to the convection electric field and is not associated with the assumed scattering. The scattering is, however, essential to confine the accelerated electrons in the shock transition layer for a long time, because, otherwise they would quickly escape from the system. In other words, the theory assumes that the electron transport obeys the diffusion-convection equation with an energy gain term determined only by the magnetic field gradient. It successfully explains the formation of a power-law energy spectrum, with a maximum energy cut-off determined by the rate of pitch-angle scattering. We here present the result of an experimental test using NASA's MMS (Magnetospheric MultiScale) spacecraft observation of an Earth's bow shock crossing event on December 9, 2016.

In particular, we have checked the following points that are predicted by the theory: (1) exponential increase in energetic particle intensity toward downstream within the shock transition layer, (2) nearly isotropic pitch-angle distribution. We find that both are reasonably satisfied in a thin layer (~7 sec. or ~350 km assuming a shock propagation speed of ~50 km/s) within the shock transition region. The result is then used to estimate the rate of pitch-angle scattering as a function of energy. We find that the pitch-angle scattering rate increases as increasing the particle energy from just above the thermal energy up to a few keV, beyond which it saturates to a nearly constant value. We find that the observed maximum energy cut-off (~30 keV) in the electron energy spectrum is consistent with that predicted by the theory based on the observed pitch-angle scattering rate. All of these results strongly indicate that the observed non-thermal electrons are accelerated by the SSDA.

Keywords: shock, particle acceleration, non-thermal particle

©2019. Japan Geoscience Union. All Right Reserved.

Radial structure of heliospheric boundary region

*Shuichi Matsukiyo[1], Gary P. Zank[2], Haruichi Washimi[3], Tohru Hada[1]

1. Faculty of Engineering Sciences, Kyushu University, 2. The Center for Space Plasma and Aeronomic Research, University of Alabama in Huntsville, 3. International Center for Space Weather Science and Education, Kyushu University

The kinetic structure of the heliospheric boundaries is investigated using one-dimensional full PIC (Particle-In-Cell) simulations. Both the termination shock and the heliopause are simultaneously reproduced in the simulation. The spatial scale of the heliopause increases as the angle between the heliopause normal and local magnetic field (referred to as the normal angle, hereafter) becomes increasingly oblique. The VLISM region, out side the heliopause, contains compressible flucturations in both magnetic field and plasma density. The fluctuations are originated from the inner heliosheath, the region between the termination shock and the heliopause, pass the heliopause, and propagate away from it. The total pressure, including the plasma pressure and magnetic pressure, at the heliopause is not constant when the normal angle is oblique in contrast to predictions based on MHD theory. In the oblique case, the solar wind plasma and interstellar plasma are able to inter-penetrate by moving along the local magnetic field. Since their bulk velocities along the magnetic field differ from each other, the distributions overlap in phase space so that the effective local plasma pressure parallel to the magnetic field is enhanced. This results in an increase that resembles a hump in the density and parallel pressure of the local plasma, which is not seen in magnetic field.

Keywords: heliospheric boundaries, full particle-in-cell simulation

©2019. Japan Geoscience Union. All Right Reserved.

[J] Poster | P (Space and Planetary Sciences)：P-EM Solar-Terrestrial Sciences, Space Electromagnetism & Space Environment

Wed. May 29, 2019 3:30 PM - 5:00 PM JST | Wed. May 29, 2019 6:30 AM - 8:00 AM UTC | Poster Hall International Exhibition Hall8, Makuhari Messe_3

[P-EM18] Heliosphere and Interplanetary Space

convener:Ken Tsubouchi(University of Electro-Communications), Masaki N Nishino(Japan Aerospace Exploration Agency, Institute of Space and Astronautical Science), Yasuhiro Nariyuki(Faculty of Human Development, University of Toyama), Kazumasa Iwai(Institute for Space?Earth Environmental Research (ISEE), Nagoya University)

This session aims to secure comprehensive insights into physical processes of plasmas and fields in the heliosphere. Presentations of the recent studies from any approaches (integrated observations/theoretical modeling/massive numerical simulation) are welcomed. Topics are not restricted to any specific issues: phenomenological studies on solar flares/CME/solar wind, and related fundamental physics problems such as shocks/waves/turbulence/particle transport and acceleration can be the main target, including heliospheric high-energy phenomena and their impact on the Earth's environment.

[PEM18-P01] Study of the contribution of electric field to the acceleration of cometary ions around comet 67P/Churyumov-Gerasimenko

*Kazuki Yamagishi[1], Yuto Katoh[1], Tomoki Kimura[1], Atsushi Kumamoto[1] (1.Department of Geophysics, Graduate School of Science, Tohoku University)

[PEM18-P02] Energy conversion process at the lunar wake boundary

*Tomoko Nakagawa[1], Hideo Tsunakawa[2], Yoshifumi Saito[3] (1.Information and Communication Engineering, Tohoku Institute of Technology, 2.Department of Earth and Planetary Sciences, School of Science, Tokyo Institute of Technology , 3.JAXA,ISAS)

[PEM18-P03] Electron acceleration at quasi-perpendicular collisionless shock: One-dimensional PIC simulation

*Fumiko Otsuka[1], Shuichi Matsukiyo[2], Mitsuo Oka[3] (1.NIT, Kurume College, 2.ESST, Kyushu Univ., 3.UC Berkeley)

[PEM18-P04] 4-season's optical observation of neutral helium distribution in interplanetary space by Hisaki

*Atsushi Yamazaki[1], Go Murakami[1], Kazuo Yoshioka[2], Tomoki Kimura[3], Fuminori Tsuchiya[4], Masato Kagitani[4], Takeshi Sakanoi[4], Naoki Terada[5], Yasumasa Kasaba[4], Ichiro Yoshikawa[6], Hisaki (SPRINT-A) Project team (1.Japan Aerospace Exploration Agency, Institute of Space and Astronautical Science , 2.The University of Tokyo, Graduate School of Frontier Sciences, 3.Tohoku University, 4.Tohoku University, Planetary Plasma and Atmospheric Research Center , 5.Tohoku University, Graduate School of Sciense, 6.The University of Tokyo)

[PEM18-P05] Structural variations in the pickup ion density associated with magnetic reconnection at the heliopause

*Ken Tsubouchi[1] (1.University of Electro-Communications)

Study of the contribution of electric field to the acceleration of cometary ions around comet 67P/Churyumov-Gerasimenko

*Kazuki Yamagishi[1], Yuto Katoh[1], Tomoki Kimura[1], Atsushi Kumamoto[1]

1. Department of Geophysics, Graduate School of Science, Tohoku University

Comet is a small celestial object whose size is a few to tens of kilometers, consists mainly of water. Some water molecules sublimated from the cometary surface are ionized by the electron impact ionization and by the photoionization, and spread into space. Understanding the physics related to the motion of cometary ions serves important clues in discussion of the temporal/spatial scale of the molecular supply process from the celestial body to space, the transportation process of materials from the comet to other objects, and the atmospheric outflow process in small bodies.

Rosetta is a spacecraft launched by European Space Agency in 2004 and performed in situ observation around comet 67/P Churyumov-Gerasimenko during 2 years, from August 2014 to September 2016. Previous studies of observation results of Rosetta showed that cometary ions are accelerated radially from the comet nucleus (Behar et al., 2018). The motion of cometary ions has been studied under the influence of the electric field, which is the ambipolar electric field, the motional electric field, and the Hall electric field. Behar et al. (2018) suggested that the ambipolar electric field formed by the pressure gradient of electrons contributes to the acceleration of cometary ions around the comet. Although the diffusion and acceleration due to the electric field around the comet are important in understanding the motion of cometary ions, a quantitative evaluation has not been performed. In the present study, we quantitatively evaluate the contribution of the electric field to the acceleration of cometary ions in order to understand the acceleration process of cometary ions observed by Rosetta. We evaluate the acceleration process of cometary ions under the assumed electric field and compare the simulation results with the observation result of Rosetta.

First, we estimate the distribution of the electric field in the region within 1000 km from the comet nucleus. As a first step, we only consider the ambipolar electric field due to the spatial gradient of the pressure distribution of electrons around the comet nucleus, following the discussion of previous studies. We calculate the pressure distribution of electrons from the release rate of comet gas and the ionization rate, which are determined based on observation results, and assume that the electron temperature is 5eV. Next, we perform a test particle analysis to calculate the time evolution of the speed of an H_2O^+ cometary ion under the assumed electric field. We find that the cometary ion with the initial speed of 0.7 km/s is accelerated to 22.6 km/s at the distance of 1000 km from the nucleus. On the other hand, based on Rosetta's observation results, H_2O^+ ions are accelerated to 40 to 80 km/s in the region from 600 to 1000 km from the comet nucleus. We suggest that the acceleration by the ambipolar electric field alone is insufficient to explain the observation results. In this study, we also consider the motional electric field and discuss the contribution of the electric field to the acceleration of ions around the comet.

Keywords: comet, electric field, ion acceleration, interaction of solar wind with small objects

©2019. Japan Geoscience Union. All Right Reserved.

Energy conversion process at the lunar wake boundary

*Tomoko Nakagawa[1], Hideo Tsunakawa[2], Yoshifumi Saito[3]

1. Information and Communication Engineering, Tohoku Institute of Technology, 2. Department of Earth and Planetary Sciences, School of Science, Tokyo Institute of Technology , 3. JAXA,ISAS

At the lunar wake boundary, the solar wind ions are accelerated toward the center of the wake due to the pressure gradient, and produce vortex motion whose direction is consistent with the polarization of the magnetic fluctuations. The kinetic energy of the solar wind is converted into the electromagnetic energy and then field-aligned electric current.

Keywords: lunar wake, solar wind, vortex

©2019. Japan Geoscience Union. All Right Reserved.

Electron acceleration at quasi-perpendicular collisionless shock: One-dimensional PIC simulation

*Fumiko Otsuka[1], Shuichi Matsukiyo[2], Mitsuo Oka[3]

1. NIT, Kurume College, 2. ESST, Kyushu Univ., 3. UC Berkeley

A collisionless shock is thought to be an efficient accelerator of charged particles in space. At the quasi-perpendicular side of the earth's bow shock, non-thermal electrons are observed in-situ measurements. However, the electron acceleration process has not been unclear due to limited accuracies of instruments.Magnetospheric Multiscale (MMS) spacecraft launched on 2015 enables us to reveal the electron acceleration process in detail. The instruments measure the waves and particles with high time (millisecond) resolution and accuracy.

In this presentation, we perform one-dimensional particle-in-cell (PIC) simulation of a quasi-perpendicular collisionless shock and discuss electron acceleration at the shock, considering a direct comparison with MMS spacecraft data in mind. We will report the results of the runs with the Alfven Mach number 7, the shock angle (the angle between the background magnetic field and the shock normal) 70-80 degrees, and plasma beta 0.3-3, respectively. We evaluate electron distributions both in energy and pitch-angle, and upstream wave spectra, and discuss their temporal as well as spatial variations. Further, highly accelerated electrons are traced back to indentify their origin and acceleration process.

Keywords: electron acceleration, quasi-perpendicular shock, PIC simulation

©2019. Japan Geoscience Union. All Right Reserved.

4-season's optical observation of neutral helium distribution in interplanetary space by Hisaki

*Atsushi Yamazaki[1], Go Murakami[1], Kazuo Yoshioka[2], Tomoki Kimura[3], Fuminori Tsuchiya[4], Masato Kagitani[4], Takeshi Sakanoi[4], Naoki Terada[5], Yasumasa Kasaba[4], Ichiro Yoshikawa[6], Hisaki (SPRINT-A) Project team

1. Japan Aerospace Exploration Agency, Institute of Space and Astronautical Science , 2. The University of Tokyo, Graduate School of Frontier Sciences, 3. Tohoku University, 4. Tohoku University, Planetary Plasma and Atmospheric Research Center , 5. Tohoku University, Graduate School of Sciense, 6. The University of Tokyo

The Hisaki (SPRINT-A) satellite has a main scientific topic of the planetary magnetspheic physics and atmospheric evoluiton by long-term observations,
but also carried out an observation of helium atom resonance scattering from interplanetary space.
A material in the interstellar medium (ISM) travels into the heliosphere over the heliopause due to the relative velocity between the heliosphere
and interstellar gases. The helium atoms move into the neighboring from the sun without ionizing because of its high ionization energy.
The helium atoms are bent by sun gravity along the Keplerian orbit and forms a high density region on the down wind side, which is called helium
cone. The distribution of helium atoms in the helium cone can estimate the speed and direction of the interstellar wind, and the density and the
temperature of the helium atom in interstellar gases.
This study was carried out from the 1970s, but the interplanetary helium atoms observation is one of powerful tools to recognize the interstellar medium from inside the heliosphere.
The Hisaki satellite carried out the observaiont of the resonance scattering from inside the helium cone during November and December.
The interstellar parameters derived from The Hisaki's observation results of the helium cone four times in years of 2015 - 2018 are reported.

Keywords: EUV spectral observation, Interstellar wind and gas, Interplanetary neutral helium, HISAKI stellite

©2019. Japan Geoscience Union. All Right Reserved.

Structural variations in the pickup ion density associated with magnetic reconnection at the heliopause

*Ken Tsubouchi[1]

1. University of Electro-Communications

Pickup ions (PUIs) can be the probe for the physical processes occurring around the heliopause in the form of energetic neutral atoms (ENAs) after their charge-exchange with interstellar neutral particles. In this study, we focus on the nonstationarity of the heliopause, where the directional change in the magnetic field is approaching. This situation triggers the magnetic reconnection at the heliopause, resulting in the mixing of particles between the heliosphere and interstellar space. We have performed two-dimensional hybrid simulations to follow the PUI kinetics. It is confirmed that PUI in the outer heliosheath are gathered into the reconnection site accompanied with the coalescence of magnetic islands. We calculate the column density integrated across the heliopause, which will be associated with the ENA observations by IBEX. The properties of its spatial and temporal variations are compared with those from the case of Kelvin-Helmholtz instabilities along the heliopause. It will be useful for the identification of the heliopause environment by extracting these properties from the observational data.

©2019. Japan Geoscience Union. All Right Reserved.

[J] Poster | P (Space and Planetary Sciences)：P-EM Solar-Terrestrial Sciences, Space Electromagnetism & Space Environment

Wed. May 29, 2019 5:15 PM - 6:30 PM JST | Wed. May 29, 2019 8:15 AM - 9:30 AM UTC | Poster Hall International Exhibition Hall8, Makuhari Messe_7

[P-EM18] Heliosphere and Interplanetary Space

convener:Ken Tsubouchi(University of Electro-Communications), Masaki N Nishino(Japan Aerospace Exploration Agency, Institute of Space and Astronautical Science), Yasuhiro Nariyuki(Faculty of Human Development, University of Toyama), Kazumasa Iwai(Institute for Space?Earth Environmental Research (ISEE), Nagoya University)

This session aims to secure comprehensive insights into physical processes of plasmas and fields in the heliosphere. Presentations of the recent studies from any approaches (integrated observations/theoretical modeling/massive numerical simulation) are welcomed. Topics are not restricted to any specific issues: phenomenological studies on solar flares/CME/solar wind, and related fundamental physics problems such as shocks/waves/turbulence/particle transport and acceleration can be the main target, including heliospheric high-energy phenomena and their impact on the Earth's environment.

[PEM18-P01] Study of the contribution of electric field to the acceleration of cometary ions around comet 67P/Churyumov-Gerasimenko

*Kazuki Yamagishi[1], Yuto Katoh[1], Tomoki Kimura[1], Atsushi Kumamoto[1] (1.Department of Geophysics, Graduate School of Science, Tohoku University)

[PEM18-P02] Energy conversion process at the lunar wake boundary

*Tomoko Nakagawa[1], Hideo Tsunakawa[2], Yoshifumi Saito[3] (1.Information and Communication Engineering, Tohoku Institute of Technology, 2.Department of Earth and Planetary Sciences, School of Science, Tokyo Institute of Technology , 3.JAXA,ISAS)

[PEM18-P03] Electron acceleration at quasi-perpendicular collisionless shock: One-dimensional PIC simulation

*Fumiko Otsuka[1], Shuichi Matsukiyo[2], Mitsuo Oka[3] (1.NIT, Kurume College, 2.ESST, Kyushu Univ., 3.UC Berkeley)

[PEM18-P04] 4-season's optical observation of neutral helium distribution in interplanetary space by Hisaki

*Atsushi Yamazaki[1], Go Murakami[1], Kazuo Yoshioka[2], Tomoki Kimura[3], Fuminori Tsuchiya[4], Masato Kagitani[4], Takeshi Sakanoi[4], Naoki Terada[5], Yasumasa Kasaba[4], Ichiro Yoshikawa[6], Hisaki (SPRINT-A) Project team (1.Japan Aerospace Exploration Agency, Institute of Space and Astronautical Science , 2.The University of Tokyo, Graduate School of Frontier Sciences, 3.Tohoku University, 4.Tohoku University, Planetary Plasma and Atmospheric Research Center , 5.Tohoku University, Graduate School of Sciense, 6.The University of Tokyo)

[PEM18-P05] Structural variations in the pickup ion density associated with magnetic reconnection at the heliopause

*Ken Tsubouchi[1] (1.University of Electro-Communications)

Study of the contribution of electric field to the acceleration of cometary ions around comet 67P/Churyumov-Gerasimenko

*Kazuki Yamagishi[1], Yuto Katoh[1], Tomoki Kimura[1], Atsushi Kumamoto[1]

1. Department of Geophysics, Graduate School of Science, Tohoku University

Comet is a small celestial object whose size is a few to tens of kilometers, consists mainly of water. Some water molecules sublimated from the cometary surface are ionized by the electron impact ionization and by the photoionization, and spread into space. Understanding the physics related to the motion of cometary ions serves important clues in discussion of the temporal/spatial scale of the molecular supply process from the celestial body to space, the transportation process of materials from the comet to other objects, and the atmospheric outflow process in small bodies.

Rosetta is a spacecraft launched by European Space Agency in 2004 and performed in situ observation around comet 67/P Churyumov-Gerasimenko during 2 years, from August 2014 to September 2016. Previous studies of observation results of Rosetta showed that cometary ions are accelerated radially from the comet nucleus (Behar et al., 2018). The motion of cometary ions has been studied under the influence of the electric field, which is the ambipolar electric field, the motional electric field, and the Hall electric field. Behar et al. (2018) suggested that the ambipolar electric field formed by the pressure gradient of electrons contributes to the acceleration of cometary ions around the comet. Although the diffusion and acceleration due to the electric field around the comet are important in understanding the motion of cometary ions, a quantitative evaluation has not been performed. In the present study, we quantitatively evaluate the contribution of the electric field to the acceleration of cometary ions in order to understand the acceleration process of cometary ions observed by Rosetta. We evaluate the acceleration process of cometary ions under the assumed electric field and compare the simulation results with the observation result of Rosetta.

First, we estimate the distribution of the electric field in the region within 1000 km from the comet nucleus. As a first step, we only consider the ambipolar electric field due to the spatial gradient of the pressure distribution of electrons around the comet nucleus, following the discussion of previous studies. We calculate the pressure distribution of electrons from the release rate of comet gas and the ionization rate, which are determined based on observation results, and assume that the electron temperature is 5eV. Next, we perform a test particle analysis to calculate the time evolution of the speed of an H_2O^+ cometary ion under the assumed electric field. We find that the cometary ion with the initial speed of 0.7 km/s is accelerated to 22.6 km/s at the distance of 1000 km from the nucleus. On the other hand, based on Rosetta's observation results, H_2O^+ ions are accelerated to 40 to 80 km/s in the region from 600 to 1000 km from the comet nucleus. We suggest that the acceleration by the ambipolar electric field alone is insufficient to explain the observation results. In this study, we also consider the motional electric field and discuss the contribution of the electric field to the acceleration of ions around the comet.

Keywords: comet, electric field, ion acceleration, interaction of solar wind with small objects

©2019. Japan Geoscience Union. All Right Reserved.

Energy conversion process at the lunar wake boundary

*Tomoko Nakagawa[1], Hideo Tsunakawa[2], Yoshifumi Saito[3]

1. Information and Communication Engineering, Tohoku Institute of Technology, 2. Department of Earth and Planetary Sciences, School of Science, Tokyo Institute of Technology , 3. JAXA,ISAS

At the lunar wake boundary, the solar wind ions are accelerated toward the center of the wake due to the pressure gradient, and produce vortex motion whose direction is consistent with the polarization of the magnetic fluctuations. The kinetic energy of the solar wind is converted into the electromagnetic energy and then field-aligned electric current.

Keywords: lunar wake, solar wind, vortex

©2019. Japan Geoscience Union. All Right Reserved.

Electron acceleration at quasi-perpendicular collisionless shock: One-dimensional PIC simulation

*Fumiko Otsuka[1], Shuichi Matsukiyo[2], Mitsuo Oka[3]

1. NIT, Kurume College, 2. ESST, Kyushu Univ., 3. UC Berkeley

A collisionless shock is thought to be an efficient accelerator of charged particles in space. At the quasi-perpendicular side of the earth's bow shock, non-thermal electrons are observed in-situ measurements. However, the electron acceleration process has not been unclear due to limited accuracies of instruments.Magnetospheric Multiscale (MMS) spacecraft launched on 2015 enables us to reveal the electron acceleration process in detail. The instruments measure the waves and particles with high time (millisecond) resolution and accuracy.

In this presentation, we perform one-dimensional particle-in-cell (PIC) simulation of a quasi-perpendicular collisionless shock and discuss electron acceleration at the shock, considering a direct comparison with MMS spacecraft data in mind. We will report the results of the runs with the Alfven Mach number 7, the shock angle (the angle between the background magnetic field and the shock normal) 70-80 degrees, and plasma beta 0.3-3, respectively. We evaluate electron distributions both in energy and pitch-angle, and upstream wave spectra, and discuss their temporal as well as spatial variations. Further, highly accelerated electrons are traced back to indentify their origin and acceleration process.

Keywords: electron acceleration, quasi-perpendicular shock, PIC simulation

©2019. Japan Geoscience Union. All Right Reserved.

4-season's optical observation of neutral helium distribution in interplanetary space by Hisaki

*Atsushi Yamazaki[1], Go Murakami[1], Kazuo Yoshioka[2], Tomoki Kimura[3], Fuminori Tsuchiya[4], Masato Kagitani[4], Takeshi Sakanoi[4], Naoki Terada[5], Yasumasa Kasaba[4], Ichiro Yoshikawa[6], Hisaki (SPRINT-A) Project team

1. Japan Aerospace Exploration Agency, Institute of Space and Astronautical Science , 2. The University of Tokyo, Graduate School of Frontier Sciences, 3. Tohoku University, 4. Tohoku University, Planetary Plasma and Atmospheric Research Center , 5. Tohoku University, Graduate School of Sciense, 6. The University of Tokyo

The Hisaki (SPRINT-A) satellite has a main scientific topic of the planetary magnetspheic physics and atmospheric evoluiton by long-term observations,
but also carried out an observation of helium atom resonance scattering from interplanetary space.
A material in the interstellar medium (ISM) travels into the heliosphere over the heliopause due to the relative velocity between the heliosphere
and interstellar gases. The helium atoms move into the neighboring from the sun without ionizing because of its high ionization energy.
The helium atoms are bent by sun gravity along the Keplerian orbit and forms a high density region on the down wind side, which is called helium
cone. The distribution of helium atoms in the helium cone can estimate the speed and direction of the interstellar wind, and the density and the
temperature of the helium atom in interstellar gases.
This study was carried out from the 1970s, but the interplanetary helium atoms observation is one of powerful tools to recognize the interstellar medium from inside the heliosphere.
The Hisaki satellite carried out the observaiont of the resonance scattering from inside the helium cone during November and December.
The interstellar parameters derived from The Hisaki's observation results of the helium cone four times in years of 2015 - 2018 are reported.

Keywords: EUV spectral observation, Interstellar wind and gas, Interplanetary neutral helium, HISAKI stellite

©2019. Japan Geoscience Union. All Right Reserved.

Structural variations in the pickup ion density associated with magnetic reconnection at the heliopause

*Ken Tsubouchi[1]

1. University of Electro-Communications

Pickup ions (PUIs) can be the probe for the physical processes occurring around the heliopause in the form of energetic neutral atoms (ENAs) after their charge-exchange with interstellar neutral particles. In this study, we focus on the nonstationarity of the heliopause, where the directional change in the magnetic field is approaching. This situation triggers the magnetic reconnection at the heliopause, resulting in the mixing of particles between the heliosphere and interstellar space. We have performed two-dimensional hybrid simulations to follow the PUI kinetics. It is confirmed that PUI in the outer heliosheath are gathered into the reconnection site accompanied with the coalescence of magnetic islands. We calculate the column density integrated across the heliopause, which will be associated with the ENA observations by IBEX. The properties of its spatial and temporal variations are compared with those from the case of Kelvin-Helmholtz instabilities along the heliopause. It will be useful for the identification of the heliopause environment by extracting these properties from the observational data.

©2019. Japan Geoscience Union. All Right Reserved.

[J] Oral | P (Space and Planetary Sciences)：P-CG Complex & General

Wed. May 29, 2019 9:00 AM - 10:30 AM JST | Wed. May 29, 2019 12:00 AM - 1:30 AM UTC | 105 1F

[P-CG24] New Developments of Planetary Sciences with ALMA

convener:Takayuki Muto(Division of Liberal Arts, Kogakuin University), Munetake Momose(The College of Science, Ibaraki University), Hideo Sagawa(Faculty of Science, Kyoto Sangyo University), Masumi Shimojo(National Astronomical Observatory of Japan), Chairperson:Takayuki Muto

The Atacama Large Millimeter/Submillimeter Array (ALMA) starated its science operation in 2011, and long-baseline observations have become available since 2014. With its high sensitivity and resolution, ALMA has provided us with qualitatively new information on star and planet formation and small bodies in our Solar System. For example, in the observations of protoplanetary disks, ring-like structures have been commonly found and the structures with the scale of several-AU are discovered in several systems. In our solar system, 60km pixel-scale non-uniform brightness distribution and the rotation of the asteroid Juno are detected. Spatially-resolved thermal mapping of Europa icy surface enables us to search for thermal anomaly in possible plume source regions. As of Cycle 4, Solar observations are available, enabling us, for example, to determine the physical parameters of plasmoid quantitatively. In this session, we overview the latest results of ALMA observations in the field of planetary sciences. We also accept any theoretical and experimental works that are closely related to the observations and discuss the impact on the planetary science community.

9:00 AM - 9:15 AM JST | 12:00 AM - 12:15 AM UTC

[PCG24-01] Understanding solar atmosphere by ALMA observations

★Invited Papers

*Tomoko Kawate[1], Takenori J Okamoto[2], Kazumasa Iwai[3], Satoshi Masuda[3], Masumi Shimojo[2] (1.Institute of Space and Astronautical Science, Japan Aerospace Exploration Agency, 2.National Astronomical Observatory of Japan, 3.Nagoya University)

9:15 AM - 9:30 AM JST | 12:15 AM - 12:30 AM UTC

[PCG24-02] Multi-thermal structures in a spicule observed with ALMA, IRIS, and AIA/SDO

*Masumi Shimojo[1], Tomoko Kawate[2], Takenori Okamoto[1], Takaaki Yokoyama[3] (1.National Astronomical Observatory of Japan, 2. Institute of Space and Astronautical Science , 3.University of Tokyo)

9:30 AM - 9:45 AM JST | 12:30 AM - 12:45 AM UTC

[PCG24-03] Observing the 2018 global dust storm on Mars with ALMA

Shohei Aoki[2], *Hideo Sagawa[1], Kazi Rigl[3], Geronimo L. Villanueva[4], Bill Dent[5], Hiroyuki Maezawa[6], Severine Robert[2], Hiromu Nakagawa[7], Frank Daerden[2], Takeshi Kuroda[8], Marco Giuranna[10], Kazuya Saigo[9], Michael J. Mumma[4], Yasumasa Kasaba[7], Ann Carine Vandaele[2] (1.Kyoto Sangyo University, 2.Royal Belgian Institute for Space Aeronomy, 3.Italian ALMA Regional Centre, INAF-Istituto di Radioastronomia, 4.NASA Goddard Space Flight Center, USA, 5.ESO ALMA, Chile, 6.Osaka Prefecture University, 7.Tohoku University, 8.NICT Big Data Integration Research Center, 9.NAOJ Chile Observatory, 10.Istituto di Astrofisica e Planetologia Spaziali, Italy)

9:45 AM - 10:00 AM JST | 12:45 AM - 1:00 AM UTC

[PCG24-04] Atmospheric observation of submillimeter wave and the thermal evolution of ice giants

★Invited Papers

*Kenji Kurosaki[1], Masahiro Ikoma[2] (1.Department of Physics, Nagoya University , 2.Department of Earth and Planetary Science, Graduate School of Science, The University of Tokyo)

10:00 AM - 10:30 AM JST | 1:00 AM - 1:30 AM UTC

[PCG24-05] Planetary-system formation revealed with ALMA

★Invited Papers

*Misato Fukagawa[1] (1.National Astronomical Observatory of Japan)

Understanding solar atmosphere by ALMA observations

*Tomoko Kawate[1], Takenori J Okamoto[2], Kazumasa Iwai[3], Satoshi Masuda[3], Masumi Shimojo[2]

1. Institute of Space and Astronautical Science, Japan Aerospace Exploration Agency, 2. National Astronomical Observatory of Japan, 3. Nagoya University

ALMA started solar observations with Bands 3 and 6 from Cycle 4. Millimeter waves at 100 GHz (band 3) and 240 GHz (band6) are radiated by free-free emission in the chromosphere, and brightness temperatures are directly related with electron temperatures by the Planck function. Before ALMA, observations of the chromosphere are mainly performed by absorption lines from UV to near IR. These lines are formed under non-local thermodynamically equilibrium, and it is difficult to interpret brightness temperatures directly with electron temperatures. Thus, ALMA opens a new window for temperature diagnostics in the solar atmosphere.

Although intensities in millimeter wave in a quiet sun are directly related with electron temperatures, where these emissions come from is not well understood. Numerical and observational comparisons between millimeter waves and UV lines are performed in the past. However, temperature structures in the solar atmosphere are complex and full of varieties. We cannot simply estimate the formation region of millimeter waves from the case studies. In order to understand temperature structures in solar atmosphere by ALMA, it is crucial not only to compare between multiwavelength observations but also to understand radiative processes of millimeter waves and chromospheric lines in multiple regions in the solar atmosphere.

We analyze ALMA data of a plage region observed in Cycle 4. We compare the ALMA data with vector magnetic field in the photosphere by Hinode/SP, transition-region images and spectra by IRIS, and chromospheric and coronal images by SDO/AIA. As a result, velocities of a moving feature in a stripe structure in ALMA data correspond to sound speeds in the chromosphere, and it is reasonable to interpret that millimeter waves are emitted from the mid-chromosphere. However, we do not find the same structures between millimeter waves and chromospheric images. In this presentation, we review the preceding studies on the formation region of millimeter waves in the solar atmosphere, introduce the plage observation, compare with numerical simulation of radiative transfer of millimeter wave and chromospheric lines, and discuss what ALMA is looking in the solar atmosphere.

Keywords: Sun, radiative processes, chromosphere

©2019. Japan Geoscience Union. All Right Reserved.

Multi-thermal structures in a spicule observed with ALMA, IRIS, and AIA/SDO

*Masumi Shimojo[1], Tomoko Kawate[2], Takenori Okamoto[1], Takaaki Yokoyama[3]

1. National Astronomical Observatory of Japan, 2. Institute of Space and Astronautical Science , 3. University of Tokyo

A spicule is a key phenomenon for understanding the solar atmosphere. We succeeded in observing a large spicule with ALMA, IRIS, and AIA/SDO simultaneously, and report the details of the spicule in the paper. While an eruption of a blob-like structure shown in the 100 GHz images started just before appearing a spicule in the He II and Mg II images, a spicule seen in 100 GHz image itself began about one minute after beginning the spicule in the He II and Mg II images. The spicule in the 100 GHz images can be seen as an absorbing structure in the Fe XII images. The maximum height and width of the Mg II/He II spicule are larger than those of the 100 GHz/Fe XII spicule. The 100 GHz/Fe XII spicule is included in the Mg II/He II spicule and is located at the southern edge of the Mg II/He II spicule. The rising velocities of the spicule in the Mg II and He II image, and the erupted blob in the 100 GHz images are ~70 km/s. On the other hand, the rising velocity of the spicule in the 100 GHz and Fe XII images is ~40 km/s. Considering of the differences of the structures shown in the Mg II/He II and 100 GHz/Fe XII images, and the typical formation temperature of each band, the 100 GHz and Fe XII images show a cold and dense component of the spicule. The conclusion is consistent with the recently radiative MHD simulations, and we can explain why the 100 GHz spicule is delayed, shorter, and slower than the Mg II/He II spicule. The solar limb observations with ALMA are very few. Hence, it would be not accidentally that the blob-like eruptions are associated with both two large spicules observed with ALMA. The fact might suggest that large spicules included a cold and dense component is produced by magnetic reconnection that is induced by a plasmoid eruption, like a corona jet.

Keywords: Sun, Chromosphere, Millimeter wave, Jet, ALMA

©2019. Japan Geoscience Union. All Right Reserved.

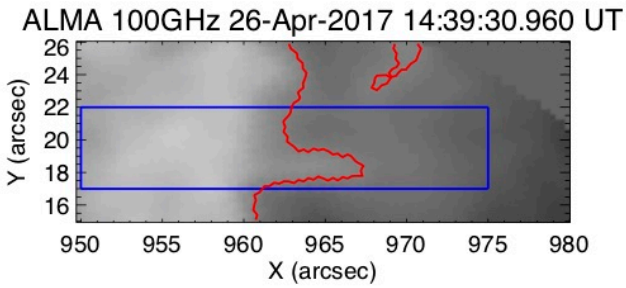

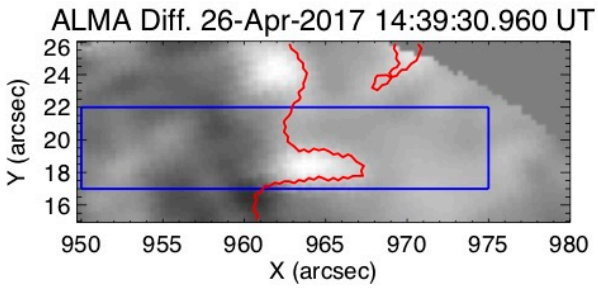

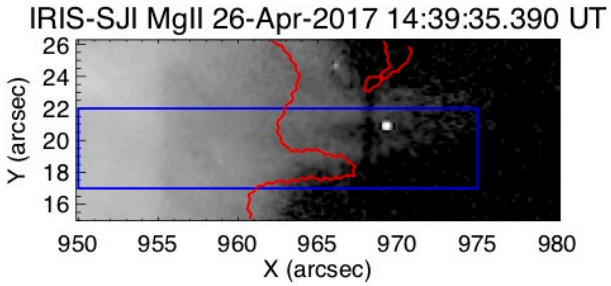

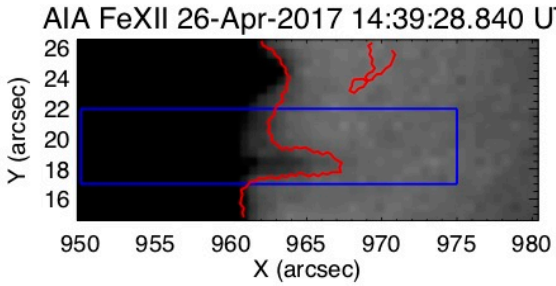

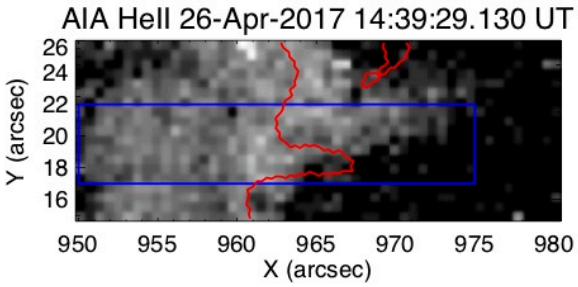

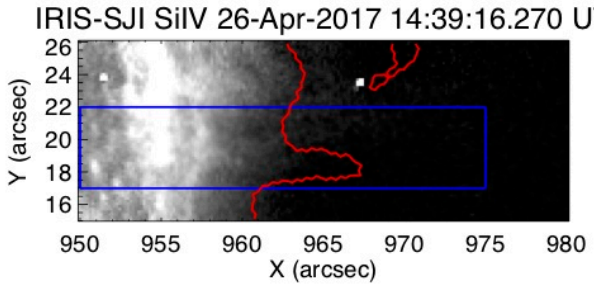

©2019. Japan Geoscience Union. All Right Reserved.

Observing the 2018 global dust storm on Mars with ALMA

Shohei Aoki[2], *Hideo Sagawa[1], Kazi Rigl[3], Geronimo L. Villanueva[4], Bill Dent[5], Hiroyuki Maezawa[6], Severine Robert[2], Hiromu Nakagawa[7], Frank Daerden[2], Takeshi Kuroda[8], Marco Giuranna[10], Kazuya Saigo[9], Michael J. Mumma[4], Yasumasa Kasaba[7], Ann Carine Vandaele[2]

1. Kyoto Sangyo University, 2. Royal Belgian Institute for Space Aeronomy, 3. Italian ALMA Regional Centre, INAF-Istituto di Radioastronomia, 4. NASA Goddard Space Flight Center, USA, 5. ESO ALMA, Chile, 6. Osaka Prefecture University, 7. Tohoku University, 8. NICT Big Data Integration Research Center, 9. NAOJ Chile Observatory, 10. Istituto di Astrofisica e Planetologia Spaziali, Italy

One of the most striking features in Martian atmosphere is a very large (planet-encircling) storm, "global dust storm". The storm lifts the dust particles from the surface into the air, where the dust particles block sunlight from reaching the surface. This brings a decrease of the surface temperature. In contrast, the thickened dust layer absorbs the radiation, and directly leads to heating the atmosphere. Such a drastic change in the thermal structure in the atmosphere induces significant modulation in the dynamics as well as in the composition.

Starting from the middle of June 2018, a global dust storm has occurred on Mars for the first time in the past 11 years. Taking this unique opportunity, we observed Mars with ALMA on 30 June 2018 and 16 July 2018 that correspond to active periods of the global dust storm.

Observing with submillimeter wavelength has a good advantage compared to other optical and infrared wavelengths, since the dust opacity becomes transparent at the submillimeter wave and the emission from deep inside the global dust storm can be detected. We used Band 5 (183 GHz) and 6 (220 and 230 GHz) on 30 June, and only Band 6 on 16 July. Band 6 measurements allow us to investigate maps of temperature vertical profiles and wind fields from the CO lines. Band 5 measurements enable us to investigate maps of water vapor vertical profiles. The preliminary results from these ALMA observations will be discussed in the presentation.

Keywords: Global dust storm, ALMA, Ground-based observation

©2019. Japan Geoscience Union. All Right Reserved.

Atmospheric observation of submillimeter wave and the thermal evolution of ice giants

*Kenji Kurosaki[1], Masahiro Ikoma[2]

1. Department of Physics, Nagoya University , 2. Department of Earth and Planetary Science, Graduate School of Science, The University of Tokyo

Our solar system has two ice giants: Uranus and Neptune. Voyager II explored Uranus in 1986 and Neptune in 1989 and observed the effective temperature and the gravitational moments that are important to understand the atmospheric and interior structure. Recently by use of ground telescope submillimeter absorption features are observed. Submillimeter observations showed that Uranus did not have remarkable feature while Neptune had absorption features of HCN and CO. That is, atmospheric structures are different between Uranus and Neptune. Since the amount of CO is related to the atmospheric O/H, the observation is expected to restrict the metal enrichment of ice giants. Moreover, the atmospheric structure affects the thermal evolution of the ice giants. In this talk, we focus on ice giants in our solar system.

Keywords: Ice giant, Atmosphere

©2019. Japan Geoscience Union. All Right Reserved.

Planetary-system formation revealed with ALMA

*Misato Fukagawa[1]

1. National Astronomical Observatory of Japan

I review the current understanding of planetary-system formation that has primarily been obtained from observations of protoplanetary disks, the birthplaces of planets, with the radio astronomical telescope, Atacama Large Millimeter/submillimeter Array (ALMA). High angular resolution is one of the most important observing capabilities to address planetary-system formation, given the spatial scale of the planetary systems including the Solar system (30 au to Neptune), and considering the distance to the nearest star forming regions (>100 pc) where we can observe young planet-forming disks. The resolution of ~5 au at least would be necessary to obtain the spatial distribution of disk material (various gas species, dust grains) which are ingredients of planets. ALMA is the interferometer consisting of multiple antennas, providing us the resolution of about 5 au recently. ALMA has provided at least 43 12-m antennas for recent observations, providing also high sensitivity and good image quality.

The ALMA observations have so far shown that (1) rings are common for protoplanetary disk and (2) the diversity in disk structure is still seen including spiral arms and strong non-axisymmetry. Rings and other disk structures often interpreted as the sign of planet-forming activity and these observations have stimulated theoretical study on how planetesimals (km-sized bodies) form and how planet formation proceeds in an entire region of the disk. The detection of various rare molecules including organic ones is another highlight. The emission from such molecules is quite faint and the detections were owing to the ALMA's high sensitivity. Other ALMA results include finding the possible new tool to probe grain growth using polarization, and detections of tenuous gas that may be produced by collisions of cometary or planetary bodies in more evolved debris disks. Those results also give us an insight on the fruitful future in comparative study with the distribution of various material in the Solar system.

Keywords: Exoplanets, Planet formation, ALMA, Astronomy

©2019. Japan Geoscience Union. All Right Reserved.

[J] Oral | P (Space and Planetary Sciences)：P-CG Complex & General

Wed. May 29, 2019 10:45 AM - 12:15 PM JST | Wed. May 29, 2019 1:45 AM - 3:15 AM UTC | 105 1F

[P-CG24] New Developments of Planetary Sciences with ALMA

convener:Takayuki Muto(Division of Liberal Arts, Kogakuin University), Munetake Momose(The College of Science, Ibaraki University), Hideo Sagawa(Faculty of Science, Kyoto Sangyo University), Masumi Shimojo(National Astronomical Observatory of Japan), Chairperson:Munetake MOMOSE(Ibaraki University)

The Atacama Large Millimeter/Submillimeter Array (ALMA) starated its science operation in 2011, and long-baseline observations have become available since 2014. With its high sensitivity and resolution, ALMA has provided us with qualitatively new information on star and planet formation and small bodies in our Solar System. For example, in the observations of protoplanetary disks, ring-like structures have been commonly found and the structures with the scale of several-AU are discovered in several systems. In our solar system, 60km pixel-scale non-uniform brightness distribution and the rotation of the asteroid Juno are detected. Spatially-resolved thermal mapping of Europa icy surface enables us to search for thermal anomaly in possible plume source regions. As of Cycle 4, Solar observations are available, enabling us, for example, to determine the physical parameters of plasmoid quantitatively. In this session, we overview the latest results of ALMA observations in the field of planetary sciences. We also accept any theoretical and experimental works that are closely related to the observations and discuss the impact on the planetary science community.

10:45 AM - 11:00 AM JST | 1:45 AM - 2:00 AM UTC

[PCG24-06] Probing dust aggregate structure in protoplanetary disks by millimeter-wave polarization

*Ryo Tazaki[1], Hidekazu Tanaka[1], Takayuki Muto[2], Akimasa Kataoka[3], Satoshi Okuzumi[4] (1.Tohoku University, 2.Kogakuin University, 3.NAOJ, 4.Tokyo Institute of Technology)

11:00 AM - 11:15 AM JST | 2:00 AM - 2:15 AM UTC

[PCG24-07] A CONSTRAINT ON THE AMOUNT OF HYDROGEN FROM THE CO CHEMISTRY IN DEBRIS DISKS

*Hiroshi Kobayashi[1], Kazunari Iwasaki[2,4], Aya Higuchi[3] (1.Department of Physics, Nagoya University, 2.NAOJ, 3.RIKEN, 4.Osaka University)

11:15 AM - 11:30 AM JST | 2:15 AM - 2:30 AM UTC

[PCG24-08] Structure of the protoplanetary disk around V1094 Sco obtained from dust continuum emission and SED

*Sanemichi Takahashi[1,2], Takayuki Muto[1], Takashi Tsukagoshi[2], Jun Hashimoto[2] (1.Kogakuin University, 2.NAOJ)

11:30 AM - 11:45 AM JST | 2:30 AM - 2:45 AM UTC

[PCG24-09] The Synthetic ALMA Multiband Analysis of the Dust Properties of the TW Hya Protoplanetary Disk

*Seongjoong Kim[1], Hideko Nomura[1], Takashi Tsukagoshi[2], Ryohei Kawabe[2,3,4], Takayuki Muto[5] (1.Department of Earth and Planetary Sciences, Tokyo Institute of Technology, 2.National Astronomical Observatory of Japan, 3.The Graduate University for Advanced Studies (SOKENDAI), 4.Department of Astronomy, School of Science, University of Tokyo, 5.Division of Liberal Arts, Kogakuin University)

11:45 AM - 12:00 PM JST | 2:45 AM - 3:00 AM UTC

[PCG24-10] Dust evolution in the protoplanetary disk around TW Hya

*Takayuki Matsuura[1], Satoshi Okuzumi[1] (1.Tokyo Institute of Technology)

12:00 PM - 12:15 PM JST | 3:00 AM - 3:15 AM UTC

[PCG24-11] Discovery of a localized excess in the millimeter emission of the protoplanetary disk around TW Hya

*Takashi Tsukagoshi[1], Takayuki Muto[2], Hideko Nomura[3], Ryohei Kawabe[1,4,5], Kazuhiro Kanagawa[9], Satoshi Okuzumi[3], Shigeru Ida[10], Catherine Walsh[6], Tom J Millar[7], Sanemichi Takahashi[2,1], Jun Hashimoto[8], Taichi Uyama[5], Motohide Tamura[5,8] (1.Division of Radio Astronomy, National Astronomical Observatory of Japan, 2.Division of Liberal Arts, Kogakuin University, 3.Department of Earth and Planetary Sciences, Tokyo Institute of Technology, 4.The Graduate University for Adnvanced Studies, 5.School of Science, University of Tokyo, 6.School of Physics and Astronomy, University of Leeds, 7.Astrophysics Research Centre, Queen's University Belfast, 8.Astrobiology Center, National Institutes of Natural Sciences, 9.Research Center for the Early Universe, University of Tokyo, 10.Earth-Life Science Institute, Tokyo Institute of Technology)

Probing dust aggregate structure in protoplanetary disks by millimeter-wave polarization

*Ryo Tazaki[1], Hidekazu Tanaka[1], Takayuki Muto[2], Akimasa Kataoka[3], Satoshi Okuzumi[4]

1. Tohoku University, 2. Kogakuin University, 3. NAOJ, 4. Tokyo Institute of Technology

Dust coagulation in protoplanetary disks is the first step of planetesimal formation and a pathway from dust aggregates to planetesimals remains unclear. Both laboratory and numerical studies have so far shown that the structure of a dust aggregate plays important roles in planetesimal formation. However, the aggregate structure has been poorly constrained by disk observations. Recently, ALMA opens a new window to observe (sub-)millimeter-wave polarization of disks, which is expected to provide additional constraints on dust aggregate properties. In this study, we perform 3D radiative transfer simulations in order to study how the structure of dust aggregates affects millimeter-wave polarization from disks. As a result, it is found that relatively compact particles are favorable to explain observed millimeter-wave scattering polarization of disks, whereas highly porous and fractal particles fail to explain the observations.

Keywords: Protoplanetary disks, Millimeter-wave polarization, Dust

©2019. Japan Geoscience Union. All Right Reserved.

A CONSTRAINT ON THE AMOUNT OF HYDROGEN FROM THE CO CHEMISTRY IN DEBRIS DISKS

*Hiroshi Kobayashi[1], Kazunari Iwasaki[2,4], Aya Higuchi[3]

1. Department of Physics, Nagoya University, 2. NAOJ, 3. RIKEN, 4. Osaka University

The faint CO gases in debris disks are easily dissolved into C by UV irradiation so that the ratio of C to CO may show the reformation rate of CO depending on the amount of underlying hydrogen molecules. We conduct radiative transfer calculations with chemical reactions for debris disks. We find the C/CO ratio is proportional to the far UV flux and the hydrogen nucleus number density. Using the deriving formula for the C/CO ratio, we give a constraint on the amount of hydrogen for debris disks around 49 Ceti with age ~ 40 Myr; the hydrogen nucleus density ~ 2x10^{-8} cm^{-3}. That implies that the debris disk contains tenuous gases caused by the depletion of a protoplanetary disk.

Keywords: Gas depletion in protoplanetar disks, Gaseous debris disks, planet formation

©2019. Japan Geoscience Union. All Right Reserved.

Structure of the protoplanetary disk around V1094 Sco obtained from dust continuum emission and SED

*Sanemichi Takahashi[1,2], Takayuki Muto[1], Takashi Tsukagoshi[2], Jun Hashimoto[2]

1. Kogakuin University, 2. NAOJ

Understanding the structure of protoplanetary disks is important for revealing the environment of planet formation. Recent ALMA observations have found that detailed structures are formed in protoplanetary disks. In this work, we investigate the structure of the protoplanetary disk around V1094 Sco. We performed numerical calculations of radiative transfer and compared the results with dust continuum emission obtained from ALMA Band 8 observations and SED. According to the dust continuum emission, we found that the disk consists of two regions, inner optically thick region (< 100 au) and outer optically thin region (> 100 au) . We also found that the results can reproduce the SED observations well when (1) disk inner edge is puffed up and the shadow is formed behind it and (2) the small grain (< 1 um) is depleted in the inner region.

Keywords: protoplanetary disks

©2019. Japan Geoscience Union. All Right Reserved.

The Synthetic ALMA Multiband Analysis of the Dust Properties of the TW Hya Protoplanetary Disk

*Seongjoong Kim[1], Hideko Nomura[1], Takashi Tsukagoshi[2], Ryohei Kawabe[2,3,4], Takayuki Muto[5]

1. Department of Earth and Planetary Sciences, Tokyo Institute of Technology, 2. National Astronomical Observatory of Japan, 3. The Graduate University for Advanced Studies (SOKENDAI), 4. Department of Astronomy, School of Science, University of Tokyo, 5. Division of Liberal Arts, Kogakuin University

Analyzing multiband observations of dust continuum emission is one of the useful tools to constrain dust properties which help us to understand the physical properties of the disks. We perform the synthetic ALMA multiband analysis to find the best ALMA band set for constraining the dust properties of the TW Hya protoplanetary disk. We find that the Band [10,6,3] set is the best set among the possible combinations of ALMA Band [3,4,5,6,7,8,9,10]. We also find two conditions for the good ALMA band sets providing narrow constraint ranges on dust properties; (1) Band 9 or 10 is included in the band set and (2) Enough frequency intervals between the bands. These are related with the conditions which give good constraints on dust properties: the combination of optically thick and thin bands are required, and large β (β is the power-law index of dust opacity, $\kappa_\nu \propto \nu^\beta$) and low dust temperature are preferable. To examine our synthetic analysis results, we apply the multiband analysis to ALMA archival data of the TW Hya disk at Band 4, 6, 7, and 9. Band [9,6,4] set provides the dust properties close to the model profile, while Band [7,6,4] set gives the dust properties deviating from the model at all radii with too broad constraint range to specify the accurate values of dust temperature, optical depth, and β. Since these features are expected by the synthetic multiband analysis, we confirm that the synthetic multiband analysis is well consistent with the results derived from real data.

Keywords: methods: observational, protoplanetary disks, stars: individual (TW Hydrae)

©2019. Japan Geoscience Union. All Right Reserved.

Dust evolution in the protoplanetary disk around TW Hya

*Takayuki Matsuura[1], Satoshi Okuzumi[1]

1. Tokyo Institute of Technology

Protoplanetary disks are places of planet formation. Therefore, researching construction and evolution of protoplanetary disks is important when we discuss planet formation. In particular, TW Hya is one of the best interesting stars to understand dust evolution in protoplanetary disks. It is a young star with a protoplanetary disk, and the disk has been observed at various wavelengths due to the good observation condition. Particularly, the latest high resolution imaging observation by ALMA revealed that the disk around TW Hya has gaps at 22 au and 37 au.
Various mechanisms of gap formation have been proposed. One of them is due to gravitational interaction between a planet and a disk. Accordingly, considering existence of planets, simulations on disk evolution are carried out. Those simulations show that dust is depleted and a gap forms at planetary orbit. However, the results of the simulations have different tendencies compared with the observation by ALMA, such as dust inside a gap is less than outside, and much dust accumulates on an outer edge of a gap.
Therefore, in this study, we aim to clarify what kind of physical characteristics the disk around TW Hya has in order to reproduce the dust distribution of TW Hya. For that, we simulate dust evolution in a disk and search for parameter ranges that reproduce the radial distribution of brightness temperature and spectral index obtained by ALMA. We assume that planets exist at 22 au and 37 au. We set the planet masses and the fragmentation velocity of dust to free parameters.
As the result, when the planet masses are 4—10 earth masses and the fragmentation velocity is 0.5 m s^{-1} , the simulation result reproduces observation by ALMA roughly. When we assume faster fragmentation velocity than the value that reproduce observation, dust is depleted inner the gap and more dust accumulates on the outer edge of the gap. When we assume heavier planets, more dust accumulates on the outer edge of the gaps and the contrasts of the gaps grow in excess. Thereby the observation is not reproduced.
The fragmentation velocity obtained in this study is slower than the value that has considered from a conventional growth theory of dust in disk. That suggests a possibility that monomers composing dust are large size of 10 μm or more(Wada et al.,2013), or monomers are covered by CO_2 ice(Musiolik et al.,2016). Additionally, the result suggests a possibility that planetesimals formed with the assumption different form scenario that dust coalesces into planetesimals.

Keywords: protoplanetary disk, TW Hya

©2019. Japan Geoscience Union. All Right Reserved.

Discovery of a localized excess in the millimeter emission of the protoplanetary disk around TW Hya

*Takashi Tsukagoshi[1], Takayuki Muto[2], Hideko Nomura[3], Ryohei Kawabe[1,4,5], Kazuhiro Kanagawa[9], Satoshi Okuzumi[3], Shigeru Ida[10], Catherine Walsh[6], Tom J Millar[7], Sanemichi Takahashi[2,1], Jun Hashimoto[8], Taichi Uyama[5], Motohide Tamura[5,8]

1. Division of Radio Astronomy, National Astronomical Observatory of Japan, 2. Division of Liberal Arts, Kogakuin University, 3. Department of Earth and Planetary Sciences, Tokyo Institute of Technology, 4. The Graduate University for Adnvanced Studies, 5. School of Science, University of Tokyo, 6. School of Physics and Astronomy, University of Leeds, 7. Astrophysics Research Centre, Queen's University Belfast, 8. Astrobiology Center, National Institutes of Natural Sciences, 9. Research Center for the Early Universe, University of Tokyo, 10. Earth-Life Science Institute, Tokyo Institute of Technology

Planets are formed from dust and gas in circumstellar disks around young stars.
Observations of dust and gas in circumstellar disks can provide fundamental information on planet formation processes, and high-resolution (sub-)millimeter imaging is now revealing the dust substructure likely generated by forming planets in disks.
Here we report the detection of an excess in dust continuum emission at 233 GHz (1.3 mm in wavelength) in the circumstellar disk around TW Hya, the closest such system to Earth, revealed through high-sensitivity observations with the Atacama Large Millimeter/submillimeter Array (ALMA).

We have carried out 3 au resolution continuum observations at 233 GHz (Band6) toward the protoplanetary disk (PPD) around TW Hya using ALMA in 2016 and 2017.
The sensitivity has been improved by a factor of 3 than that of our previous cycle 3 observations.
The overall structure is axisymmetric, and there are apparent gaps at 25 and 41 au as previously reported.
The most remarkable new finding is a few au scale excess emission at the south-west part of the PPD.
The excess emission is located at 52 au from the disk center and is 1.5 times brighter than the surrounding PPD.
The extracted emission after subtracting the axisymmetric PPD emission has a size of 4.4x1.0 au and a total flux density of 250 micro-Jy, corresponding to a dust mass of 0.03 earth masses.
Since the excess emission can also be marginally identified in the Band 7 image at almost the same position, the blob is unlikely a background source.
The excess emission can be explained by a massive CPD around a Neptune mass forming-planet or a dust clump accumulated in a small elongated vortex.

Keywords: Planet formation, Protoplanetary disk, ALMA

©2019. Japan Geoscience Union. All Right Reserved.

[J] Poster | P (Space and Planetary Sciences)：P-CG Complex & General

Wed. May 29, 2019 3:30 PM - 5:00 PM JST | Wed. May 29, 2019 6:30 AM - 8:00 AM UTC | Poster Hall International Exhibition Hall8, Makuhari Messe_4

[P-CG24] New Developments of Planetary Sciences with ALMA

convener:Takayuki Muto(Division of Liberal Arts, Kogakuin University), Munetake Momose(The College of Science, Ibaraki University), Hideo Sagawa(Faculty of Science, Kyoto Sangyo University), Masumi Shimojo(National Astronomical Observatory of Japan)

The Atacama Large Millimeter/Submillimeter Array (ALMA) starated its science operation in 2011, and long-baseline observations have become available since 2014. With its high sensitivity and resolution, ALMA has provided us with qualitatively new information on star and planet formation and small bodies in our Solar System. For example, in the observations of protoplanetary disks, ring-like structures have been commonly found and the structures with the scale of several-AU are discovered in several systems. In our solar system, 60km pixel-scale non-uniform brightness distribution and the rotation of the asteroid Juno are detected. Spatially-resolved thermal mapping of Europa icy surface enables us to search for thermal anomaly in possible plume source regions. As of Cycle 4, Solar observations are available, enabling us, for example, to determine the physical parameters of plasmoid quantitatively. In this session, we overview the latest results of ALMA observations in the field of planetary sciences. We also accept any theoretical and experimental works that are closely related to the observations and discuss the impact on the planetary science community.

[PCG24-P01] Nitrogen isotopic fractionation on Titan atmosphere: An analysis of ALMA archive data

*Hideo Sagawa[1], Takahiro Iino[2], Takashi Tsukagoshi[3] (1.Kyoto Sangyo University, 2.Tokyo University of Agriculture and Technology, 3.National Astronomical Observatory of Japan)

[PCG24-P02] Investigating the gas-to-dust ratio in the protoplanetary disk of HD 142527

*Soon Kang-Lou[1], Munetake Momose[1], Takayuki Muto[2], Takashi Tsukagoshi[3], Akimasa Kataoka[3], Tomoyuki Hanawa[4], Misato Fukagawa[3], Kazuya Saigo[3], Hiroshi Shibai[5] (1.Ibaraki University, 2.Kogakuin University, 3.National Astronomical Observatory of Japan, 4.Chiba University, 5.Osaka University)

[PCG24-P03] Super-resolution Imaging of the Protoplanetary Disk HD 142527 Using Sparse Modeling

*Masayuki Yamaguchi[1,2], Kazunori Akiyama[3,2], Akimasa Kataoka[2,6], Takashi Tsukagoshi[2], Takayuki Muto[4], Shiro Ikeda[5], Misato Fukagawa[2], Mareki Honma[2,6], Ryohei Kawabe[2,1,6] (1.The University of Tokyo, 2.National Astronomical Observatory of Japan, 3.Massachusetts Institute of Technology, Haystack Observatory, 4.Kogakuin University, 5.The Institute of Statistical Mathematics, 6. Graduate University for Advanced Studies)

[PCG24-P04] Detail Structures of Dust Disk around T-Tauri star RY Tau in ALMA High-Spatial Resolution Imaging

*Mihoko Konishi[1,2], Jun Hashimoto[1,2], Hauyu Liu[3], Ruobing Dong[4], Takayuki Muto[5] (1.Astrobiology Center, National Institute of Natural Science, 2.National Astronomical Observatory of Japan, 3.Institute of Astronomy and Astrophysics, Academia Sinica, 4.University of Victoria, 5.Kogakuin University)

[PCG24-P05] Possible inclined inner protoplanetary disk

*Jun Hashimoto[1], Mihoko Konishi[1], Taichi Uyama[2], Christian Ginski[3], Matthias Samland[4] (1.AstroBiology Center, National Institutes of Natural Sciences, 2.University of Tokyo, 3.University of Amsterdam, 4.Max Planck Institute for Astronomy)

[PCG24-P06] Search for the Inner Disk Structures in "Transitional" Disks

*Takayuki Muto[1], Jun Hashimoto[2], Takashi Tsukagoshi[3], Mihoko Konishi[3], Tomoyuki Kudo[3] (1.Division of Liberal Arts, Kogakuin University, 2.Astrobiology Center, 3.NAOJ)

Nitrogen isotopic fractionation on Titan atmosphere: An analysis of ALMA archive data

*Hideo Sagawa[1], Takahiro Iino[2], Takashi Tsukagoshi[3]

1. Kyoto Sangyo University, 2. Tokyo University of Agriculture and Technology, 3. National Astronomical Observatory of Japan

Observing isotopic fractionations of atmospheric molecules provides an important quantity to constrain physical and/or chemical processes that occur in the planetary atmosphere. Titan has a thick atmosphere mainly composed of nitrogen (N_2). It also contains many nitrogen-bearing compounds such as hydrogen cyanide (HCN), acetonitrile (CH_3CN), and cyanoacetylen (HC_3N), indicating the presence of a complex atmospheric chemistry among these nitriles. It is known that some of these nitriles have an isotopic fractionation that differs from the terrestrial values; for example, $^{14}N/^{15}N$ of HCN is 60 - 70 in Titan atmosphere whereas it is ~272 in the terrestrial atmosphere. Obtaining the $^{14}N/^{15}N$ values on other nitriles will help us to understand what is happening in Titan atmosphere.

Titan has been used as one of calibrator sources of ALMA observations, and therefore, not a few (> 900) data are stored in the ALMA archive. We surveyed all the Titan data in the ALMA archive, and extracted some data which were taken with sufficiently high spatial and spectral resolutions that can be endurable for scientific analyses. After careful investigation on the extracted data, we found one data set which contain the emission lines of the rotational transitions of $CH_3C^{14}N$ and $CH_3C^{15}N$.

By performing an inversion analysis using a radiative transfer model, we derived the nitrogen isotopic ratio on acetonitrile for the first time. Detail of the analysis will be presented in the meeting.

Keywords: Titan atmosphere, ALMA, isotopic fractionation

©2019. Japan Geoscience Union. All Right Reserved.

Investigating the gas-to-dust ratio in the protoplanetary disk of HD 142527

*Soon Kang-Lou[1], Munetake Momose[1], Takayuki Muto[2], Takashi Tsukagoshi[3], Akimasa Kataoka[3], Tomoyuki Hanawa[4], Misato Fukagawa[3], Kazuya Saigo[3], Hiroshi Shibai[5]

1. Ibaraki University, 2. Kogakuin University, 3. National Astronomical Observatory of Japan, 4. Chiba University, 5. Osaka University

We present the ALMA observations of the 98.5 GHz dust continuum and the ^{13}CO J = 1 −0 and C^{18}O J = 1 −0 line emission towards the protoplanetary disk of HD 142527. The 98.5 GHz continuum shows a strong azimuthal-asymmetric distribution similar to the previously reported 336 GHz continuum, and its peak emission at the dust concentrated northern region is optically thin at approximately 8 K. In every position angle, the peak brightness temperature of C^{18}O J = 1 −0 emission (≦ 25 K) is lower than that of the optically thick ^{13}CO J = 3 −2 (≈ 36 K), indicating that the C^{18}O is optically thin. We derive the gas and dust surface densities, Σ_g and Σ_d, of the disk of HD 142527 by using the ALMA Band 3 and Band 7 observations. In the analyses we assume the local thermodynamic equilibrium and the disk temperature to be the same as the peak brightness temperature of ^{13}CO J = 3 −2 with continuum emission. We successfully derived the gas-to-dust ratio G/D, defined as Σ_g/Σ_d, distribution across the disk. The ratio varies azimuthally, where it is ~3 and ~20 in the disk northern and southern regions, respectively. We also found that Σ_g varies approximately as $\propto \Sigma_d^{0.5}$, or equivalently G/D $\propto \Sigma_d^{-0.5}$. In addition, our results show that the peak Σ_d is located ahead of the peak Σ_g; if the latter correspond to a vortex of high gas pressure, the results indicate that the dust are trapped ahead of the vortex, which is predicted by theoretical studies.

Keywords: HD 142527, protoplanetary disk, gas-to-dust ratio

©2019. Japan Geoscience Union. All Right Reserved.

Super-resolution Imaging of the Protoplanetary Disk HD 142527 Using Sparse Modeling

*Masayuki Yamaguchi[1,2], Kazunori Akiyama[3,2], Akimasa Kataoka[2,6], Takashi Tsukagoshi[2], Takayuki Muto[4], Shiro Ikeda[5], Misato Fukagawa[2], Mareki Honma[2,6], Ryohei Kawabe[2,1,6]

1. The University of Tokyo, 2. National Astronomical Observatory of Japan, 3. Massachusetts Institute of Technology, Haystack Observatory, 4. Kogakuin University, 5. The Institute of Statistical Mathematics, 6. Graduate University for Advanced Studies

Recent Atacama Large Millimeter/submillimeter Array (ALMA) observations have provided new insights for planet formation process and simultaneously highlighted fundamental importance to pursue higher angular resolutions of observations to address opened questions. With the emphasis on improving the fidelity even at a super-resolution regime, many imaging techniques have been intensively developed in the last several years, which may provide substantial improvements in interferometric observations of protoplanetary disks. The CLEAN technique has been widely used, but recently, a new technique using the sparse modeling approach is suggested. This technique directly solves a set of undetermined equations and has been shown to behave better than the CLEAN technique based on mock observations with VLBI (Very Long Baseline Interferometry). However, it has never been applied to ALMA-like connected interferometers nor real observational data. In this work, for the first time, the sparse modeling technique is applied to observational data sets taken by ALMA. We evaluate the performance of the technique by comparing the resulting images with those derived by the CLEAN technique. We use two sets of ALMA archival data at Band 7 (~350GHz) for the protoplanetary disk around HD 142527. One is taken in the intermediate-baseline array configuration, and the other is in the longer-baseline array configuration. The image resolutions reconstructed from these data sets are different by a factor of ~ 3. With the two data sets independently taken by different array configurations, we show that SpM indeed achieves a higher fidelity than a multi-scale CLEAN technique, and provides consistent images from two data sets even beyond significant differences in angular resolutions by a factor ~ 3-4. Two SpM images consistently resolve radially and azimuthally asymmetric dust-grain emission of the outer disk, including a non-circular ridge shape well characterized by a simple logarithmic spiral. Resolved asymmetric structure of the outer disk provided by two SpM images may suggest complex gas kinematics near the inner-edge of the outer disk. Our results demonstrate that ongoing intensive developments of new imaging techniques will be ubiquitously beneficial to current and next-generation radio interferometers.

Keywords: Atacama Large Millimeter/submillimeter Array (ALMA), Radio Interferometer, Image Processing Techniques, Protoplanetary Disk, Planet Formation

©2019. Japan Geoscience Union. All Right Reserved.

Detail Structures of Dust Disk around T-Tauri star RY Tau in ALMA High-Spatial Resolution Imaging

*Mihoko Konishi[1,2], Jun Hashimoto[1,2], Hauyu Liu[3], Ruobing Dong[4], Takayuki Muto[5]

1. Astrobiology Center, National Institute of Natural Science, 2. National Astronomical Observatory of Japan, 3. Institute of Astronomy and Astrophysics, Academia Sinica, 4. University of Victoria, 5. Kogakuin University

RY Tau is categorized as a classical T-Tauri star with a mass of 2 solar mass and an age of 2 Myr (e.g., Calvet et al. 2004). The infrared excess indicates an existence of a protoplanetary disk around RY Tau (Furlan et al. 2009), and also the star is active predicted by jet detections (e.g., St-Onge & Bastien 2008). Previously, the disk imaged by the Combined Array for Research in Millimeter-wave Astronomy (CARMA) showed a cavity structure with a radius of about 0.1 arcsec in millimeter dust continuum (Isella et al. 2010), while no structures at >0.4 arcsec were detected in near infrared by Subaru Telescope (Takami et al. 2013). We investigated the visibilities of Atacama Large Millimeter/submillimeter Array (ALMA) archival data, and predicted other fine structures in RY Tau disk. Therefore, we observed with high spatial resolution.
Our observations (Project: 2017.1.01460.S, PI: J. Hashimoto) were conducted in October 2017 in Band 6 (~230 GHz, ~1.3mm). The total integration time was 5.14 minutes. We obtained three kinds of CO isotope (^{12}CO, ^{13}CO, and C^{18}O) as well as dust continuum. The CLEANed image had a beam size of 0.087×0.036 arcsec (PA: 30.7 degree) after the measurement set was calibrated by the code provided by ALMA. The dust emission from RY Tau disk could be detected (inclination: 65.9 degrees, position angle: 22.4 degrees) and the known cavity structure at 0.1 arcsec was clearly resolved. In addition, we confirmed a spatially-resolved gap structure at 0.35 arcsec and brightness asymmetry in the inner ring that were recently reported by Long et al. 2018. We then constructed a symmetric disk model (1 cavity + 1 gap) by comparing azimuthally-averaged visibilities, to investigate details of the gap structure. The best-fitted properties derived by Markov Chain Monte Carlo method showed that the gap is narrow and deep (width: 1.2 au, depth: 0.41). Although the inclination of RY Tau system is large (about 66 degrees), we could resolve the narrow and deep gap. It indicates that the scale height of RY Tau disk is small (< ~0.27 au). Dust might be settled down by some mechanisms such as low turbulence.
It should be noted that a distance of RY Tau measured by Gaia is largely different between Data Release 1 (170 pc) and 2 (440 pc). We found that it is high possibility of 178 pc based on the velocity distribution of ^{12}CO gas taken in our observation and previous ALMA data. In this abstract, a distance of 178 pc is employed for conversion.

Keywords: Protoplanetary Disk, Disk Structures, Dust Continuum

©2019. Japan Geoscience Union. All Right Reserved.

Possible inclined inner protoplanetary disk

*Jun Hashimoto[1], Mihoko Konishi[1], Taichi Uyama[2], Christian Ginski[3], Matthias Samland[4]

1. AstroBiology Center, National Institutes of Natural Sciences, 2. University of Tokyo, 3. University of Amsterdam, 4. Max Planck Institute for Astronomy

A young embedded planet in the protoplanetary disk is expected to interact with a parent disk. When the planet is inclined and massive enough (> 1 Jupiter mass), the disk-planet interaction theory predicts the disk inside the planetary orbit breaks from the outer disk. Such a misaligned inner disk can both warp gas velocity structures observed by ALMA and cast the shadows in the outer disk in the near-infrared image. By analyzing the position of the shadows in the outer disk, one can estimate the inclination of the inner disk relative to the outer disk. Furthermore such systems with shadows should be promising targets for searching young inclined planets in the disks, and would help understanding of planetary orbital evolution.

As a part of our survey in archival data obtained with VLT/SPHERE which is the high contrast instrument in near-infrared, we reduced LkHa 330. LkHa 330 is a T Tauri star with a mass of 2.2 solar mass and known to possess gap and spiral structures. By reducing VLT/SPHERE archival data at H band (1.6 micron), we found shadow structures at PA of 85 and 280 degree in the outer disk at 38 AU in radius. We also found a possible bright blob at PA of 160 degree with a separation of 23 AU from the central star. In the poster, we discuss the inclination of the inner disk by comparing our Monte Carlo radiative transfer calculations for the inclined disks and mention future ALMA proposal plan.

Keywords: protoplanetary disk

©2019. Japan Geoscience Union. All Right Reserved.

Search for the Inner Disk Structures in "Transitional" Disks

*Takayuki Muto[1], Jun Hashimoto[2], Takashi Tsukagoshi[3], Mihoko Konishi[3], Tomoyuki Kudo[3]

1. Division of Liberal Arts, Kogakuin University, 2. Astrobiology Center, 3. NAOJ

We present the ALMA archival search efforts for the discovery search for the inner disk structures in transitional disks. Transitional disks are the class of protoplanetary disks that have inner cavity. Recent discovery of the inner (a few AU scale) ring structures in the DM Tau disk (Kudo et al. 2018, ApJL, 868, L5) indicates that even if there is no detection of near infrared (NIR) excess in SED, the disk may still harbor an inner disk within a known large cavity structures. Such inner disk structures are important in understanding (extrasolar) planet formation since a few AU corresponds to the scale of the orbits of the planets within our Solar System.

A few AU region from the central star can be only probed by high resolution observations with ALMA. Such region is too cold to account for NIR excess while modest resolution (~0.2asec) radio observations can still not resolve the region at the typical distance (~140 pc) of protoplanetary disks.

We have conducted ALMA archival search for the potential transitional disk targets that may harbor inner disks. We present the methods of our search and possible candidates that deserve follow-up ALMA high resolution observations.

Keywords: Protoplanetary Disk, Radio Astronomy

©2019. Japan Geoscience Union. All Right Reserved.

[J] Poster | P (Space and Planetary Sciences)：P-CG Complex & General

Wed. May 29, 2019 5:15 PM - 6:30 PM JST | Wed. May 29, 2019 8:15 AM - 9:30 AM UTC | Poster Hall International Exhibition Hall8, Makuhari Messe_8

[P-CG24] New Developments of Planetary Sciences with ALMA

convener:Takayuki Muto(Division of Liberal Arts, Kogakuin University), Munetake Momose(The College of Science, Ibaraki University), Hideo Sagawa(Faculty of Science, Kyoto Sangyo University), Masumi Shimojo(National Astronomical Observatory of Japan)

The Atacama Large Millimeter/Submillimeter Array (ALMA) starated its science operation in 2011, and long-baseline observations have become available since 2014. With its high sensitivity and resolution, ALMA has provided us with qualitatively new information on star and planet formation and small bodies in our Solar System. For example, in the observations of protoplanetary disks, ring-like structures have been commonly found and the structures with the scale of several-AU are discovered in several systems. In our solar system, 60km pixel-scale non-uniform brightness distribution and the rotation of the asteroid Juno are detected. Spatially-resolved thermal mapping of Europa icy surface enables us to search for thermal anomaly in possible plume source regions. As of Cycle 4, Solar observations are available, enabling us, for example, to determine the physical parameters of plasmoid quantitatively. In this session, we overview the latest results of ALMA observations in the field of planetary sciences. We also accept any theoretical and experimental works that are closely related to the observations and discuss the impact on the planetary science community.

[PCG24-P01] Nitrogen isotopic fractionation on Titan atmosphere: An analysis of ALMA archive data

*Hideo Sagawa[1], Takahiro Iino[2], Takashi Tsukagoshi[3] (1.Kyoto Sangyo University, 2.Tokyo University of Agriculture and Technology, 3.National Astronomical Observatory of Japan)

[PCG24-P02] Investigating the gas-to-dust ratio in the protoplanetary disk of HD 142527

*Soon Kang-Lou[1], Munetake Momose[1], Takayuki Muto[2], Takashi Tsukagoshi[3], Akimasa Kataoka[3], Tomoyuki Hanawa[4], Misato Fukagawa[3], Kazuya Saigo[3], Hiroshi Shibai[5] (1.Ibaraki University, 2.Kogakuin University, 3.National Astronomical Observatory of Japan, 4.Chiba University, 5.Osaka University)

[PCG24-P03] Super-resolution Imaging of the Protoplanetary Disk HD 142527 Using Sparse Modeling

*Masayuki Yamaguchi[1,2], Kazunori Akiyama[3,2], Akimasa Kataoka[2,6], Takashi Tsukagoshi[2], Takayuki Muto[4], Shiro Ikeda[5], Misato Fukagawa[2], Mareki Honma[2,6], Ryohei Kawabe[2,1,6] (1.The University of Tokyo, 2.National Astronomical Observatory of Japan, 3.Massachusetts Institute of Technology, Haystack Observatory, 4.Kogakuin University, 5.The Institute of Statistical Mathematics, 6. Graduate University for Advanced Studies)

[PCG24-P04] Detail Structures of Dust Disk around T-Tauri star RY Tau in ALMA High-Spatial Resolution Imaging

*Mihoko Konishi[1,2], Jun Hashimoto[1,2], Hauyu Liu[3], Ruobing Dong[4], Takayuki Muto[5] (1.Astrobiology Center, National Institute of Natural Science, 2.National Astronomical Observatory of Japan, 3.Institute of Astronomy and Astrophysics, Academia Sinica, 4.University of Victoria, 5.Kogakuin University)

[PCG24-P05] Possible inclined inner protoplanetary disk

*Jun Hashimoto[1], Mihoko Konishi[1], Taichi Uyama[2], Christian Ginski[3], Matthias Samland[4] (1.AstroBiology Center, National Institutes of Natural Sciences, 2.University of Tokyo, 3.University of Amsterdam, 4.Max Planck Institute for Astronomy)

[PCG24-P06] Search for the Inner Disk Structures in "Transitional" Disks

*Takayuki Muto[1], Jun Hashimoto[2], Takashi Tsukagoshi[3], Mihoko Konishi[3], Tomoyuki Kudo[3] (1.Division of Liberal Arts, Kogakuin University, 2.Astrobiology Center, 3.NAOJ)

Nitrogen isotopic fractionation on Titan atmosphere: An analysis of ALMA archive data

*Hideo Sagawa[1], Takahiro Iino[2], Takashi Tsukagoshi[3]

1. Kyoto Sangyo University, 2. Tokyo University of Agriculture and Technology, 3. National Astronomical Observatory of Japan

Observing isotopic fractionations of atmospheric molecules provides an important quantity to constrain physical and/or chemical processes that occur in the planetary atmosphere. Titan has a thick atmosphere mainly composed of nitrogen (N_2). It also contains many nitrogen-bearing compounds such as hydrogen cyanide (HCN), acetonitrile (CH_3CN), and cyanoacetylen (HC_3N), indicating the presence of a complex atmospheric chemistry among these nitriles. It is known that some of these nitriles have an isotopic fractionation that differs from the terrestrial values; for example, $^{14}N/^{15}N$ of HCN is 60 - 70 in Titan atmosphere whereas it is ~272 in the terrestrial atmosphere. Obtaining the $^{14}N/^{15}N$ values on other nitriles will help us to understand what is happening in Titan atmosphere.

Titan has been used as one of calibrator sources of ALMA observations, and therefore, not a few (> 900) data are stored in the ALMA archive. We surveyed all the Titan data in the ALMA archive, and extracted some data which were taken with sufficiently high spatial and spectral resolutions that can be endurable for scientific analyses. After careful investigation on the extracted data, we found one data set which contain the emission lines of the rotational transitions of $CH_3C^{14}N$ and $CH_3C^{15}N$.

By performing an inversion analysis using a radiative transfer model, we derived the nitrogen isotopic ratio on acetonitrile for the first time. Detail of the analysis will be presented in the meeting.

Keywords: Titan atmosphere, ALMA, isotopic fractionation

©2019. Japan Geoscience Union. All Right Reserved.

Investigating the gas-to-dust ratio in the protoplanetary disk of HD 142527

*Soon Kang-Lou[1], Munetake Momose[1], Takayuki Muto[2], Takashi Tsukagoshi[3], Akimasa Kataoka[3], Tomoyuki Hanawa[4], Misato Fukagawa[3], Kazuya Saigo[3], Hiroshi Shibai[5]

1. Ibaraki University, 2. Kogakuin University, 3. National Astronomical Observatory of Japan, 4. Chiba University, 5. Osaka University

We present the ALMA observations of the 98.5 GHz dust continuum and the ^{13}CO J = 1 −0 and C^{18}O J = 1 −0 line emission towards the protoplanetary disk of HD 142527. The 98.5 GHz continuum shows a strong azimuthal-asymmetric distribution similar to the previously reported 336 GHz continuum, and its peak emission at the dust concentrated northern region is optically thin at approximately 8 K. In every position angle, the peak brightness temperature of C^{18}O J = 1 −0 emission (≦ 25 K) is lower than that of the optically thick ^{13}CO J = 3 −2 (≈ 36 K), indicating that the C^{18}O is optically thin. We derive the gas and dust surface densities, Σ_g and Σ_d, of the disk of HD 142527 by using the ALMA Band 3 and Band 7 observations. In the analyses we assume the local thermodynamic equilibrium and the disk temperature to be the same as the peak brightness temperature of ^{13}CO J = 3 −2 with continuum emission. We successfully derived the gas-to-dust ratio G/D, defined as Σ_g/Σ_d, distribution across the disk. The ratio varies azimuthally, where it is ~3 and ~20 in the disk northern and southern regions, respectively. We also found that Σ_g varies approximately as $\propto \Sigma_d^{0.5}$, or equivalently G/D $\propto \Sigma_d^{-0.5}$. In addition, our results show that the peak Σ_d is located ahead of the peak Σ_g; if the latter correspond to a vortex of high gas pressure, the results indicate that the dust are trapped ahead of the vortex, which is predicted by theoretical studies.

Keywords: HD 142527, protoplanetary disk, gas-to-dust ratio

©2019. Japan Geoscience Union. All Right Reserved.

Super-resolution Imaging of the Protoplanetary Disk HD 142527 Using Sparse Modeling

*Masayuki Yamaguchi[1,2], Kazunori Akiyama[3,2], Akimasa Kataoka[2,6], Takashi Tsukagoshi[2], Takayuki Muto[4], Shiro Ikeda[5], Misato Fukagawa[2], Mareki Honma[2,6], Ryohei Kawabe[2,1,6]

1. The University of Tokyo, 2. National Astronomical Observatory of Japan, 3. Massachusetts Institute of Technology, Haystack Observatory, 4. Kogakuin University, 5. The Institute of Statistical Mathematics, 6. Graduate University for Advanced Studies

Recent Atacama Large Millimeter/submillimeter Array (ALMA) observations have provided new insights for planet formation process and simultaneously highlighted fundamental importance to pursue higher angular resolutions of observations to address opened questions. With the emphasis on improving the fidelity even at a super-resolution regime, many imaging techniques have been intensively developed in the last several years, which may provide substantial improvements in interferometric observations of protoplanetary disks. The CLEAN technique has been widely used, but recently, a new technique using the sparse modeling approach is suggested. This technique directly solves a set of undetermined equations and has been shown to behave better than the CLEAN technique based on mock observations with VLBI (Very Long Baseline Interferometry). However, it has never been applied to ALMA-like connected interferometers nor real observational data. In this work, for the first time, the sparse modeling technique is applied to observational data sets taken by ALMA. We evaluate the performance of the technique by comparing the resulting images with those derived by the CLEAN technique. We use two sets of ALMA archival data at Band 7 (~350GHz) for the protoplanetary disk around HD 142527. One is taken in the intermediate-baseline array configuration, and the other is in the longer-baseline array configuration. The image resolutions reconstructed from these data sets are different by a factor of ~ 3. With the two data sets independently taken by different array configurations, we show that SpM indeed achieves a higher fidelity than a multi-scale CLEAN technique, and provides consistent images from two data sets even beyond significant differences in angular resolutions by a factor ~ 3-4. Two SpM images consistently resolve radially and azimuthally asymmetric dust-grain emission of the outer disk, including a non-circular ridge shape well characterized by a simple logarithmic spiral. Resolved asymmetric structure of the outer disk provided by two SpM images may suggest complex gas kinematics near the inner-edge of the outer disk. Our results demonstrate that ongoing intensive developments of new imaging techniques will be ubiquitously beneficial to current and next-generation radio interferometers.

Keywords: Atacama Large Millimeter/submillimeter Array (ALMA), Radio Interferometer, Image Processing Techniques, Protoplanetary Disk, Planet Formation

©2019. Japan Geoscience Union. All Right Reserved.

Detail Structures of Dust Disk around T-Tauri star RY Tau in ALMA High-Spatial Resolution Imaging

*Mihoko Konishi[1,2], Jun Hashimoto[1,2], Hauyu Liu[3], Ruobing Dong[4], Takayuki Muto[5]

1. Astrobiology Center, National Institute of Natural Science, 2. National Astronomical Observatory of Japan, 3. Institute of Astronomy and Astrophysics, Academia Sinica, 4. University of Victoria, 5. Kogakuin University

RY Tau is categorized as a classical T-Tauri star with a mass of 2 solar mass and an age of 2 Myr (e.g., Calvet et al. 2004). The infrared excess indicates an existence of a protoplanetary disk around RY Tau (Furlan et al. 2009), and also the star is active predicted by jet detections (e.g., St-Onge & Bastien 2008). Previously, the disk imaged by the Combined Array for Research in Millimeter-wave Astronomy (CARMA) showed a cavity structure with a radius of about 0.1 arcsec in millimeter dust continuum (Isella et al. 2010), while no structures at >0.4 arcsec were detected in near infrared by Subaru Telescope (Takami et al. 2013). We investigated the visibilities of Atacama Large Millimeter/submillimeter Array (ALMA) archival data, and predicted other fine structures in RY Tau disk. Therefore, we observed with high spatial resolution.
Our observations (Project: 2017.1.01460.S, PI: J. Hashimoto) were conducted in October 2017 in Band 6 (~230 GHz, ~1.3mm). The total integration time was 5.14 minutes. We obtained three kinds of CO isotope (^{12}CO, ^{13}CO, and C^{18}O) as well as dust continuum. The CLEANed image had a beam size of 0.087×0.036 arcsec (PA: 30.7 degree) after the measurement set was calibrated by the code provided by ALMA. The dust emission from RY Tau disk could be detected (inclination: 65.9 degrees, position angle: 22.4 degrees) and the known cavity structure at 0.1 arcsec was clearly resolved. In addition, we confirmed a spatially-resolved gap structure at 0.35 arcsec and brightness asymmetry in the inner ring that were recently reported by Long et al. 2018. We then constructed a symmetric disk model (1 cavity + 1 gap) by comparing azimuthally-averaged visibilities, to investigate details of the gap structure. The best-fitted properties derived by Markov Chain Monte Carlo method showed that the gap is narrow and deep (width: 1.2 au, depth: 0.41). Although the inclination of RY Tau system is large (about 66 degrees), we could resolve the narrow and deep gap. It indicates that the scale height of RY Tau disk is small (< ~0.27 au). Dust might be settled down by some mechanisms such as low turbulence.
It should be noted that a distance of RY Tau measured by Gaia is largely different between Data Release 1 (170 pc) and 2 (440 pc). We found that it is high possibility of 178 pc based on the velocity distribution of ^{12}CO gas taken in our observation and previous ALMA data. In this abstract, a distance of 178 pc is employed for conversion.

Keywords: Protoplanetary Disk, Disk Structures, Dust Continuum

©2019. Japan Geoscience Union. All Right Reserved.

Possible inclined inner protoplanetary disk

*Jun Hashimoto[1], Mihoko Konishi[1], Taichi Uyama[2], Christian Ginski[3], Matthias Samland[4]

1. AstroBiology Center, National Institutes of Natural Sciences, 2. University of Tokyo, 3. University of Amsterdam, 4. Max Planck Institute for Astronomy

A young embedded planet in the protoplanetary disk is expected to interact with a parent disk. When the planet is inclined and massive enough (> 1 Jupiter mass), the disk-planet interaction theory predicts the disk inside the planetary orbit breaks from the outer disk. Such a misaligned inner disk can both warp gas velocity structures observed by ALMA and cast the shadows in the outer disk in the near-infrared image. By analyzing the position of the shadows in the outer disk, one can estimate the inclination of the inner disk relative to the outer disk. Furthermore such systems with shadows should be promising targets for searching young inclined planets in the disks, and would help understanding of planetary orbital evolution.

As a part of our survey in archival data obtained with VLT/SPHERE which is the high contrast instrument in near-infrared, we reduced LkHa 330. LkHa 330 is a T Tauri star with a mass of 2.2 solar mass and known to possess gap and spiral structures. By reducing VLT/SPHERE archival data at H band (1.6 micron), we found shadow structures at PA of 85 and 280 degree in the outer disk at 38 AU in radius. We also found a possible bright blob at PA of 160 degree with a separation of 23 AU from the central star. In the poster, we discuss the inclination of the inner disk by comparing our Monte Carlo radiative transfer calculations for the inclined disks and mention future ALMA proposal plan.

Keywords: protoplanetary disk

©2019. Japan Geoscience Union. All Right Reserved.

Search for the Inner Disk Structures in "Transitional" Disks

*Takayuki Muto[1], Jun Hashimoto[2], Takashi Tsukagoshi[3], Mihoko Konishi[3], Tomoyuki Kudo[3]

1. Division of Liberal Arts, Kogakuin University, 2. Astrobiology Center, 3. NAOJ

We present the ALMA archival search efforts for the discovery search for the inner disk structures in transitional disks. Transitional disks are the class of protoplanetary disks that have inner cavity. Recent discovery of the inner (a few AU scale) ring structures in the DM Tau disk (Kudo et al. 2018, ApJL, 868, L5) indicates that even if there is no detection of near infrared (NIR) excess in SED, the disk may still harbor an inner disk within a known large cavity structures. Such inner disk structures are important in understanding (extrasolar) planet formation since a few AU corresponds to the scale of the orbits of the planets within our Solar System.

A few AU region from the central star can be only probed by high resolution observations with ALMA. Such region is too cold to account for NIR excess while modest resolution (~0.2asec) radio observations can still not resolve the region at the typical distance (~140 pc) of protoplanetary disks.

We have conducted ALMA archival search for the potential transitional disk targets that may harbor inner disks. We present the methods of our search and possible candidates that deserve follow-up ALMA high resolution observations.

Keywords: Protoplanetary Disk, Radio Astronomy

©2019. Japan Geoscience Union. All Right Reserved.

[E] Oral | A (Atmospheric and Hydrospheric Sciences)：A-AS Atmospheric Sciences, Meteorology & Atmospheric Environment

Wed. May 29, 2019 9:00 AM - 10:30 AM JST | Wed. May 29, 2019 12:00 AM - 1:30 AM UTC | 104 1F

[A-AS01] High performance computing for next generation weather, climate, and environmental sc iences

convener:Hiromu Seko(Meteorological Research Institute), Takemasa Miyoshi(RIKEN), Chihiro Kodama(Japan Agency for Marine-Earth Science and Technology), Masayuki Takigawa(Japan Agency for Marine-Earth Science and Technology), Chairperson:Hiromu Seko(Meteorological Research Institute), Chihiro Kodama(Japan Agency for Marine-Earth Science and Technology)

A lot of advanced simulation studies are being conducted by high performance supercomputers, such as K computer and Earth Simulator, in various fields including meteorology. The high performance supercomputers enable us to conduct numerical simulations and data assimilation of observation big-data (huge high-density and high-frequency data) with an order of magnitude higher resolutions and ensemble numbers than those with the previous supercomputers. In addition, the post-K computer will be available as a successor of K, and studies for the post-K computer are in progress. At this session, we comprehensively pick up the topics in the Atmospheric and Hydrospheric Sciences Sessions of the 2019 Union Meeting that comprise the atmospheric, oceanic and land sciences. This session aims to promote recent studies related to the issues on high performance computing in weather, climate, and environmental studies using the K computer and other supercomputers, and to enhance discussions on future directions of numerical simulations in meteorology.

9:00 AM - 9:15 AM JST | 12:00 AM - 12:15 AM UTC

[AAS01-01] Data Assimilation Studies using Big Observation Data in the Projects of Post K and BDA

*Hiromu Seko[1], Masaru Kunii[2], Yohei Sawada[1], Kozo Okamoto[1], Sho Yokota[1], Kosuke Ito[3], Kazuki Shimoji[2] (1.Meteorological Research Institute, 2.Japan Meteorological Agency, 3.University of the Ryukyus)

9:15 AM - 9:30 AM JST | 12:15 AM - 12:30 AM UTC

[AAS01-02] **High-resolution Numerical Weather Simulation with a Large Domain for Extreme Heavy Rainfall Events**

*Tsutao OIZUMI[1,2], Kazuo Saito[4,3], le duc[1], Junshi Ito[3] (1.Japan Agency for Marine-Earth Science and Technology, 2.Meteorological Research Institute, 3.The Atmosphere and Ocean Research Institute, 4.Japan Meteorological Business Support Center)

9:30 AM - 9:45 AM JST | 12:30 AM - 12:45 AM UTC

[AAS01-03] A Numerical Case Study on a Tornado that Formed in a Quasi Linear Convective System

★Invited Papers

*Eigo Tochimoto[1], Hiroshi Niino[1] (1.Atmosphere and Ocean Research Institute, The University of Tokyo)

9:45 AM - 10:00 AM JST | 12:45 AM - 1:00 AM UTC

[AAS01-04] Improving the observation operator for Phased Array Weather Radar in the SCALE-LETKF system

*Arata Amemiya[1], Takumi Honda[1], Takemasa Miyoshi[1] (1.RIKEN Center for Computational Science)

10:00 AM - 10:15 AM JST | 1:00 AM - 1:15 AM UTC

[AAS01-05] Data assimilation and forecast experiments for the record-breaking rainfall event in Japan in July 2018 with NICAM-LETKF at 112-km and 28-km resolution

*Koji Terasaki[1], Takemasa Miyoshi[1] (1.RIKEN Center for Computational Science)

10:15 AM - 10:30 AM JST | 1:15 AM - 1:30 AM UTC

[AAS01-06] Model Parameter Estimation with Data Assimilation Using NICAM-LETKF

★Invited Papers

*Shunji Kotsuki[1], Yousuke Sato[2], Koji Terasaki[1], Hasashi Yashiro[1], Hirofumi Tomita[1], Masaki Satoh[3], Takemasa Miyoshi[1] (1.RIKEN Center for Computational Science, 2.Graduate School of Engineering, Nagoya University, 3.Atmosphere and Ocean Research Institute, the University of Tokyo)

Data Assimilation Studies using Big Observation Data in the Projects of Post K and BDA

*Hiromu Seko[1], Masaru Kunii[2], Yohei Sawada[1], Kozo Okamoto[1], Sho Yokota[1], Kosuke Ito[3], Kazuki Shimoji[2]

1. Meteorological Research Institute, 2. Japan Meteorological Agency, 3. University of the Ryukyus

In the projects of 'Advancement of meteorological and global environmental predictions utilizing observational Big Data' of 'The post K computer development plan of the FLAGSHIP2020 Project' and 'Innovating "Big Data Assimilation" Technology for Revolutionizing Very-short-range Severe Weather Prediction', the data assimilation techniques including the coupling with the ocean model have been developed to improve the prediction accuracy of heavy rainfalls, typhoons and tornadoes, and to obtain the longer leading time (the time from the prediction to the occurrences of severe phenomena). The most of these studies were conducted by using the super computer 'K' and Big Observation Data. In this presentation, the impacts of rapid scan'atmospheric motion vector' and sea surface temperature of Himawari-8 on the Typhoon intensity and track predictions and on the rainfall predictions of heavy rainfalls, the assimilation results of all-sky radiance data in the convection scale prediction, and the reproduction of rainfall system that caused tornadoes by the data of Polarization radar and dense surface observation network will be presented.

Keywords: Data Assimilation, Big Observation Data

©2019. Japan Geoscience Union. All Right Reserved.

High-resolution Numerical Weather Simulation with a Large Domain for Extreme Heavy Rainfall Events

*Tsutao OIZUMI[1,2], Kazuo Saito[4,3], le duc[1], Junshi Ito[3]

1. Japan Agency for Marine-Earth Science and Technology, 2. Meteorological Research Institute, 3. The Atmosphere and Ocean Research Institute, 4. Japan Meteorological Business Support Center

In Japan, heavy rainfall occasionally causes disasters such as debris flows. For example, debris flows induced severe societal damages in Izu Oshima Island on 15-16 October 2013 and in Hiroshima City on 19-20 August 2014, western Japan on July 5th –8th 2018. To mitigate these disasters damage and evacuate residents in a timely fashion, an accurate numerical weather prediction (NWP) system is important.
In this study, we conducted an ultra-high resolution NWP simulations (grid spacing is 5 km to 150 m) with a large and small domain area to above heavy rainfall events. Several important model factors (grid spacing, PBL scheme model domain size) influencing heavy rainfall forecasting in NWP models were investigated. The model was an optimized version of the Japan Meteorological Agency Non-Hydrostatic Model for the supercomputer “K”.
The result showed the 2-km grid spacing models showed better precipitation performance than 5-km resolution models. And the 500-m resolution models showed better precipitation performance than 2-km grid spacing models. The 2-km and 500-m grid spacing models with the large model domain show better performance than those with the small domain. Overall, the results indicated that using a high-resolution model (500-m grid spacing) with the large model domain area provides an advantage for simulating heavy rain events.

Keywords: heavy rainfall, high resolution simulation, JMA-NHM

©2019. Japan Geoscience Union. All Right Reserved.

A Numerical Case Study on a Tornado that Formed in a Quasi Linear Convective System

*Eigo Tochimoto[1], Hiroshi Niino[1]

1. Atmosphere and Ocean Research Institute, The University of Tokyo

Tornadoes are mainly classified into three groups based on different types of convective systems: supercells, quasi-linear convective systems (QLCSs), and non-supercells. In the United States, it is estimated that 18% of all tornadoes are spawned by QLCSs. In Japan, although tornadoes associated QLCSs also occur and cause severe damages, the detailed features and formation mechanism of tornadoes have not been well under stood. Thus, we performed a high-resolution numerical simulation to reproduce and examine the formation process of a tornado that formed in a quasi linear convective system at Chiyoda-town, Ibaraki prefecture, Japan on 8 December 1992.

A quadruple-nested simulation using Japanese Meteorological Agency non-hydrostatic model was performed. A simulation with horizontal scale of 2km successfully reproduced the QLCS, which propagated eastward quickly and reached around Chiyoda-town at 0830 JST. A cold pool and its associated downdrafts existed behind the convection region with strong updrafts (>10m/s). A simulation with the finest horizontal scale of 50m successfully reproduced the tornado in the QLCS. The vertical vorticity and horizontal velocity exceeded 0.7 $s^{-1}$and 47m/s, respectively. At around 500m height, a low-level mesocyclone, which was accompanied by strong updrafts (>20m/s), formed and developed around the location of tornadogenesis. Near the surface, at 1 or 2 minutes before the tornadogenesis, strong rear-inflow jet (RIJ) accompanied by relatively cold air developed, and then tornado formed in the north of the RIJ. Thus, it is suggested that the RIJ play some roles in the formation and development of the tornado.

Keywords: Tornado, Convection

©2019. Japan Geoscience Union. All Right Reserved.

Improving the observation operator for Phased Array Weather Radar in the SCALE-LETKF system

*Arata Amemiya[1], Takumi Honda[1], Takemasa Miyoshi[1]

1. RIKEN Center for Computational Science

The observation operator of Phased Array Weather Radar (PAWR; Ushio et al. 2014; Yoshikawa et al. 2013) in the SCALE-LETKF data assimilation system (Lien et al., 2017) is revisited, and the impact of improving the observation operator on the analysis is examined.
Previous studies (Miyoshi et al., 2016, *IEEE*; Miyoshi et al., 2016, *BAMS*) have shown that the three-dimensional fine-scale structure of radar signals observed by PAWR can be successfully assimilated to produce a high-resolution analysis using a regional model SCALE-RM and the local ensemble transformed Kalman filter (LETKF). Forecasts using a high-resolution regional model from the analysis field has a potential to provide reliable precipitation forecasts for longer period of time than a simple nowcasting technique based on an advection scheme, since the explicit physical processes would allow us to capture the development of new convective cells. However, even with an analysis field incorporating such detailed observational data, accurate forecasting of localized convection systems is generally a challenging issue. In the previous studies mentioned above, there was a known problem that the area of strong radar echo calculated from the forecast field starts to expand unrealistically even within several minutes. Along with systematic model biases and imbalance, the observation operator could be the cause of this misrepresentation. Therefore, the observation operator of PAWR is revisited in this study.
The observation operator calculates equivalent radar reflectivity factor (Z_e [mm6/m3]) from hydrometeor mass density of each particle categories (W [g/m^2]). The cloud microphysics scheme in SCALE-RM (Tomita et al., 2008) is a 1-moment 6-caterogy scheme. They include 3 categories for precipitation particles, namely, rain, snow, and graupel. The relation between Z_e and each of W is obtained by an offline numerical calculation of Mie scattering and approximated in the form of an exponential function.
$Z_e = \alpha_r \exp(\beta_r) + \alpha_s \exp(\beta s) + \alpha_g \exp(\beta_g)$
Previous studies used values from a literature (Xue et al., 2009) for the coefficients. However, the coefficients used for graupel (α_g and β_g) has been originally calculated using assumptions about the particle size distribution different from those in SCALE-RM. In particular, a multiplicative factor of the particle size distribution of graupel in SCALE-RM is much smaller in their calculation ($N_0 = 3 \times 10^4$ m^{-4}) than that in SCALE-RM ($N_0 = 4 \times 10^6$ m^{-4}). This leads to an underestimation in sensitivity of graupel mass to observed radar reflectivity factor.
The new coefficients for graupel are chosen to be consistent with the SCALE-RM cloud microphysics scheme using the Joint-Simulator developed by Japan Aerospace Exploration Agency (JAXA). The results are $\alpha_g = 5.54 \times 10^3$, $\beta_g = 1.70$, where the original values from the literature are $\alpha_g = 8.18 \times 10^4$, $\beta_g = 1.50$.
The case study of PAWR assimilation on the localized short-duration heavy rain event on July 13, 2013 is performed again using the new coefficients and compared to previous results (Miyoshi et al., 2016, *IEEE*; Miyoshi et al., 2016, *BAMS*).
The results are shown in Fig. 1. With the new set of coefficients in PAWR observation operator, the evolution for the 30-minute forecast period is closer to the observation than that with the original coefficients. The rapidly-growing unrealistic spread of a large reflectivity area are significantly suppressed. The difference is also clear in the vertical profiles of area-averaged graupel mass. The rapid increase of graupel in the middle troposphere in the conventional forecast experiment implies the recovery from the imbalance by inconsistency between the observation operator and cloud microphysics scheme. The new coefficients lead to improve hte imbalance and provide physically more consistent analysis fields. To

©2019. Japan Geoscience Union. All Right Reserved.

further improve PAWR assimilation, this modification to the observation operator allows us to focus on other factors such as a model error treatment as the next step.

Keywords: Data Assimilation, Weather forecasting, Precipitation radar

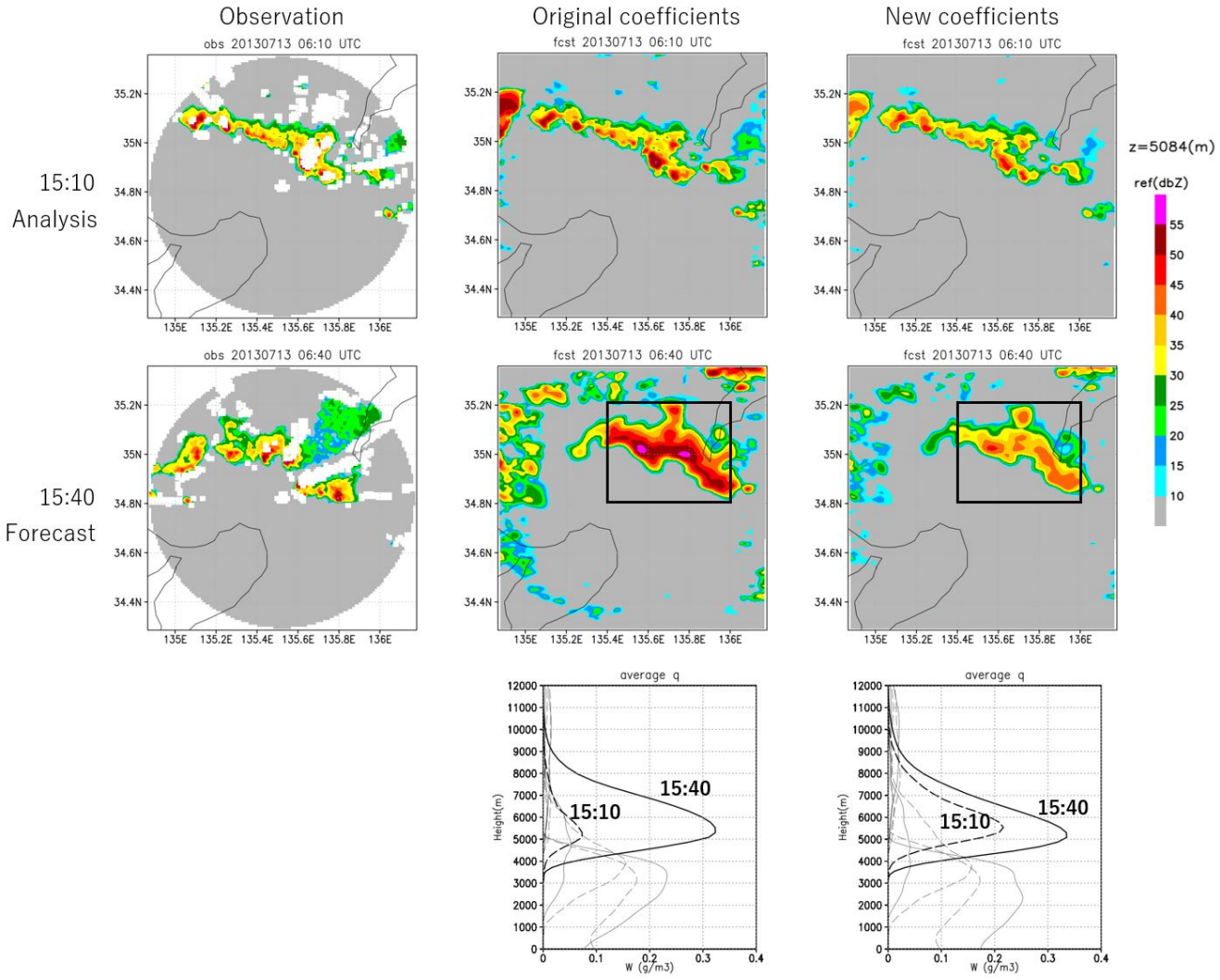

©2019. Japan Geoscience Union. All Right Reserved.

Data assimilation and forecast experiments for the record-breaking rainfall event in Japan in July 2018 with NICAM-LETKF at 112-km and 28-km resolution

*Koji Terasaki[1], Takemasa Miyoshi[1]

1. RIKEN Center for Computational Science

In July 2018, an active Baiu front caused record-breaking rainfalls and disasters in broad areas in western Japan. This study performs data assimilation and forecast experiments using the NICAM-LETKF system (Terasaki et al. 2015, Terasaki et al. 2017) at 112-km and 28-km resolution with 32 ensemble members. The computational efficiency is essential to run the high-resolution data assimilation cycle. Yashiro et al. (2016) developed a new NICAM-LETKF system to reduce the computational cost of the LETKF part by considering a throughput-aware framework. Data assimilation experiments are performed with conventional observations and advanced microwave sounding unit-A (AMSU-A) satellite radiances for one month starting at 0000 UTC 10 June 2018. Next, forecast experiments are initialized every day at 0000 UTC on 1-5 July 2018. The results show that the 28-km resolution experiment outperforms the 112-km resolution experiment for the location and intensity of the heavy rainfall, although the precipitation amount is significantly underestimated compared with the observation. The locations of the Pacific and Okhotsk highs determine the location of the Baiu front. The 112-km resolution may be too coarse to resolve these phenomena sufficiently.
More than a half of the computational time of the LETKF was occupied by file I/O in the previous NICAM-LETKF system. The new NICAM-LETKF system successfully accelerated by reducing the I/O time to be about 20% of the computational time of the LETKF.

Keywords: Data assimilation, Numerical weather prediction, NICAM-LETKF, Heavy rainfall

©2019. Japan Geoscience Union. All Right Reserved.

Model Parameter Estimation with Data Assimilation Using NICAM-LETKF

*Shunji Kotsuki[1], Yousuke Sato[2], Koji Terasaki[1], Hasashi Yashiro[1], Hirofumi Tomita[1], Masaki Satoh[3], Takemasa Miyoshi[1]

1. RIKEN Center for Computational Science, 2. Graduate School of Engineering, Nagoya University, 3. Atmosphere and Ocean Research Institute, the University of Tokyo

This study aims to improve forecasts of numerical weather prediction (NWP) models by optimizing model parameters with data assimilation. Kotsuki et al. (2018a, JGR) succeeded in improving global precipitation forecasts at 112-km-resolution NICAM (Nonhydrostatic ICosahedral Atmospheric Model) by estimating a parameter called B1 of Berry (1967)' s large-scale condensation scheme using satellite-observed precipitation data and the Local Ensemble Transform Kalman Filter (LETKF).

Extending the previous study, this study explores to improve the forecasts further using other satellite observations. This study estimates the parameter B1 as a global-constant parameter with cloud liquid water (CLW) data observed by GCOM-W/AMSR2. The parameter estimation successfully reduces excessive bias in CLW although precipitation forecasts are degraded. In addition, this study extends to estimate spatial distributions of the B1 parameter. The spatially-varying B1 parameter shows the best agreement to the spatial pattern of observed LWP. This presentation will include the most recent progress up to the time of the meeting.

Keywords: Model Parameter Estimation, Large Scale Condensation, Ensemble Kalman Filter, Liquid Water Path, Radiation Budget, NICAM-LETKF

©2019. Japan Geoscience Union. All Right Reserved.

[E] Oral | A (Atmospheric and Hydrospheric Sciences)：A-AS Atmospheric Sciences, Meteorology & Atmospheric Environment

Wed. May 29, 2019 10:45 AM - 12:15 PM JST | Wed. May 29, 2019 1:45 AM - 3:15 AM UTC | 104 1F

[A-AS01] High performance computing for next generation weather, climate, and environmental sc iences

convener:Hiromu Seko(Meteorological Research Institute), Takemasa Miyoshi(RIKEN), Chihiro Kodama(Japan Agency for Marine-Earth Science and Technology), Masayuki Takigawa(Japan Agency for Marine-Earth Science and Technology), Chairperson:Masayuki Takigawa(Japan Agency for Marine-Earth Science and Technology), Takemasa Miyoshi(RIKEN Advanced Institute for Computational Science)

A lot of advanced simulation studies are being conducted by high performance supercomputers, such as K computer and Earth Simulator, in various fields including meteorology. The high performance supercomputers enable us to conduct numerical simulations and data assimilation of observation big-data (huge high-density and high-frequency data) with an order of magnitude higher resolutions and ensemble numbers than those with the previous supercomputers. In addition, the post-K computer will be available as a successor of K, and studies for the post-K computer are in progress. At this session, we comprehensively pick up the topics in the Atmospheric and Hydrospheric Sciences Sessions of the 2019 Union Meeting that comprise the atmospheric, oceanic and land sciences. This session aims to promote recent studies related to the issues on high performance computing in weather, climate, and environmental studies using the K computer and other supercomputers, and to enhance discussions on future directions of numerical simulations in meteorology.

10:45 AM - 11:00 AM JST | 1:45 AM - 2:00 AM UTC

[AAS01-07] 3D debris flow simulations by using smoothed particle hydrodynamics (SPH) method

*Shoji Ueta[1], Natsuki Hosono[2], Yosuke Alexandre Yamashiki[1] (1.Kyoto University, 2.JAMSTEC)

11:00 AM - 11:15 AM JST | 2:00 AM - 2:15 AM UTC

[AAS01-08] **Regional atmospheric data assimilation coupled with an ocean mixed layer model: a case of typhoon Soudelor (2015)**

*Kohei Takatama[1], Takumi Honda[1], Takemasa Miyoshi[1] (1.RIKEN)

11:15 AM - 11:30 AM JST | 2:15 AM - 2:30 AM UTC

[AAS01-09] Effective Radiative Forcing and Climate Response to Short-Lived Climate Pollutants Under Different Scenarios

Hua Zhang[1], *Bing Xie[1], Zhili Wang[1] (1.China Meteorological Administration)

11:30 AM - 11:45 AM JST | 2:30 AM - 2:45 AM UTC

[AAS01-10] **The NICAM–SPRINTARS simulation of the long-range transport of black carbon using the K computer**

★Invited Papers

*Yousuke Yamashita[1], Masayuki Takigawa[1], Daisuke Goto[2], Hisashi Yashiro[3], Masaki Satoh[4,1], Yugo Kanaya[1], Fumikazu Taketani[1], Takuma Miyakawa[1] (1.Japan Agency for Marine-Earth Science and Technology, 2.National Institute for Environmental Studies, 3.RIKEN Advanced Institute for Computational Science (AICS), 4.Atmosphere and Ocean Research Institute, The University of Tokyo)

11:45 AM - 12:00 PM JST | 2:45 AM - 3:00 AM UTC

[AAS01-11] High-resolution, ensemble simulations of intense tropical cyclones and their stochasticity during the El Niños of 1997 and 2015

*Yohei Yamada[1], Chihiro Kodama[1], Masaki Satoh[1,2], Masuo Nakano[1], Tomoe Nasuno[1], Masato Sugi[3] (1.Japan Agency for Marine-Earth Science and Technology, 2.Atmosphere and Ocean Research Institute, The university of Tokyo, 3.Meteorological Research Institute, Japan Meteorological Agency)

12:00 PM - 12:15 PM JST | 3:00 AM - 3:15 AM UTC

[AAS01-12] **NICAM results of the project DYAMOND for global storm-resolving model intercomparison**

★Invited Papers

*Masaki Satoh[1], Ryosuke Shibuya[2], Chihiro Kodama[2] (1.Atmosphere and Ocean Research Institute, The University of Tokyo, 2.JAMSTEC)

3D debris flow simulations by using smoothed particle hydrodynamics (SPH) method

*Shoji Ueta[1], Natsuki Hosono[2], Yosuke Alexandre Yamashiki[1]

1. Kyoto University, 2. JAMSTEC

Yamashiki et al. (2012) and Yamashiki et al. (2013) perform laboratory experiments that represent a debris flow. We use smoothed particle hydrodynamics (SPH), Lagrangian numerical hydrodynamics method, and reproduce the experiments by 2D simulations. We find that water does not erode rock by using same size particles between water and rock, but that water can erode rock by using smaller size water particles than rock particle. We could extend this 2D simulation to 3D one and reproduce more realistic results.
Also, debris flows include not only rock and water but also mud. We developed a 3D SPH code that includes the solid-liquid mutual interaction with fully SPH manner to deal with multiphase flow well. We compare the results of the code with the results of a land slide experiment and some simulations in Igarashi et al. (2012) and find that we can get the results similar to those of experiments. We also try to perform more realistic debris flow simulationsin Hiroshima in 2014’s cases.

Keywords: debris flow, smoothed particle hydrodynamics

©2019. Japan Geoscience Union. All Right Reserved.

Regional atmospheric data assimilation coupled with an ocean mixed layer model: a case of typhoon Soudelor (2015)

*Kohei Takatama[1], Takumi Honda[1], Takemasa Miyoshi[1]

1. RIKEN

This study investigates the effect of atmosphere-ocean coupling in a regional atmospheric data assimilation system for a case of Typhoon Soudelor (2015). A simple ocean mixed layer model, known as the Price-Weller-Pinkel (PWP) model, has been implemented into a regional atmospheric data assimilation system SCALE-LETKF.

The results show that the PWP model produced reasonable sea surface temperature (SST) fields in response to the atmospheric flow, particularly, dropping SST associated with the typhoon’ s mixing the ocean upper layers. However, the analyzed track and intensity of the typhoon were not improved by coupling the PWP model. This can be explained by lower SSTs and by smaller ensemble spread of near surface atmospheric temperature. In the atmosphere-ocean coupling system, the stronger a typhoon, the cooler the SSTs via heat releases from the ocean surface and via vertical mixing of the upper ocean. These processes induce negative feedback for the typhoon development, so that the typhoon growth rates are suppressed (enhanced) in ensemble members with strong (weak) typhoon. This results in more similar typhoon intensities among ensemble members. Therefore, the coupled system reduces the ensemble spreads in the atmospheric fields associated with typhoon. The presentation will include the most up-to-date results at the time of the conference.

Keywords: Data Assimilation, Typhoon, Air-Sea Interaction

©2019. Japan Geoscience Union. All Right Reserved.

Effective Radiative Forcing and Climate Response to Short-Lived Climate Pollutants Under Different Scenarios

Hua Zhang[1], *Bing Xie[1], Zhili Wang[1]

1. China Meteorological Administration

We used an online aerosol-climate model (BCC_AGCM2.0_CUACE/Aero) to simulate effective radiative forcing and climate response to changes in the concentrations of short-lived climatic pollutants (SLCPs), including methane, tropospheric ozone, and black carbon, for the period 2010–2050 under Representative Concentration Pathway scenarios (RCPs) 8.5, 4.5, and 2.6. Under these three scenarios, the global annual mean effective radiative forcing were 0.1, 0.3, and 0.5 W m^{-2}, respectively. Under RCP 8.5, the change in SLCPs caused significant increases in surface air temperature (SAT) in middle and high latitudes of the Northern Hemisphere and significant decreases in precipitation in the Indian Peninsula and equatorial Pacific. Global mean SAT and precipitation increased by 0.13 K and 0.02 mm d^{-1}, respectively. The reduction in SLCPs from 2010 to 2050 under RCPs 4.5 and 2.6 led to significant decreases in SAT at high latitudes in the Northern Hemisphere. Precipitation increased slightly in most continental regions, and the Intertropical Convergence Zone moved southward under both of these mitigation scenarios. Global mean SAT decreased by 0.20 and 0.44 K, and global averaged precipitation decreased by 0.02 and 0.03 mm d^{-1}under RCPs 4.5 and 2.6, respectively.

Keywords: SLCP/SLCF, ERF, Climate response

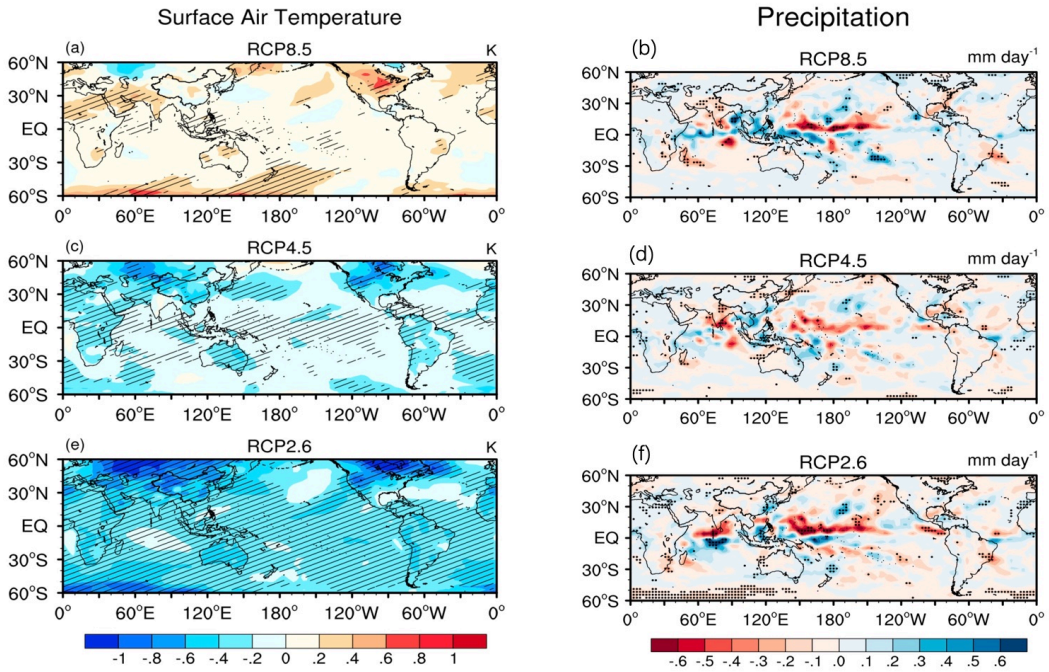

The spatial distribution of (left column) surface air temperature and (right column) precipitation resulting from changes of SLCPs, from 2010 to 2050, in (a and b) Representative Concentration Pathway 8.5 (RCP8.5), (c and d) RCP4.5, and (e and f) RCP2.6. The areas with “・” and “/” passed the 95% significance test.

©2019. Japan Geoscience Union. All Right Reserved.

The NICAM–SPRINTARS simulation of the long-range transport of black carbon using the K computer

*Yousuke Yamashita[1], Masayuki Takigawa[1], Daisuke Goto[2], Hisashi Yashiro[3], Masaki Satoh[4,1], Yugo Kanaya[1], Fumikazu Taketani[1], Takuma Miyakawa[1]

1. Japan Agency for Marine-Earth Science and Technology, 2. National Institute for Environmental Studies, 3. RIKEN Advanced Institute for Computational Science (AICS), 4. Atmosphere and Ocean Research Institute, The University of Tokyo

The Nonhydrostatic Icosahedral Atmospheric Model (NICAM)–SPRINTARS is the global aerosol transport model, which has been developed to calculate global aerosol transport and its influences on radiation and precipitation incorporated with the NICAM. The latest model is developed to include the forest fire emission with daily time-scales and has fine horizontal resolution with 56 km, which is capable of simulating fine scales transport processes of aerosols such as the accumulation of black carbon (BC) behind the cold front, and the wetdeposition process around the low-pressure system.
The large and continuous forest fire emission occurred around Lake Baikal of Siberia in September 2016. The observation of BC was performed from August to October by observational cruise of R/V Mirai (MR16-06) possessed by Japan Agency for Marine-Earth Science and Technology (JAMSTEC), and the maximum BC concentration was detected in 25–26 September around Aleutian Islands. These results imply the long-range transport of BC from Lake Baikal to Aleutian Islands, however, possibility of detection of anthropogenic BC emitted in Asia is not ruled out.
To analyze the origin and transport pathway of observed BC by R/V Mirai observation, we performed the experiments of the NICAM–SPRINTARS with anthropogenic and forest fire emission (Ant+Fire simulation) using the K computer. To estimate anthropogenic BC impact, the simulation without fire emission was performed (Ant simulation). Without fire emission, the BC concentration in 25–26 September is much smaller than observation, indicating small impact of anthropogenic BC on this event. In this event the BC is trapped behind the cold front and beyond the warm front to indicate high concentration peak (about 300 ng/m^3) of surface BC with sharp temporal change. This high concentration event is well simulated by the latest 56-km model, however, the low horizontal resolution experiments about 220-km show relatively low concentration peak (about 100–150 ng/m^3) with roughly temporal change.
We also estimate the BC transport to Arctic. The 56-km model simulation with Siberian forest fire emission (Ant+FireSb simulation) indicates a larger increase in Arctic column BC from 22 to 27 September than the Ant simulation, however, the 220-km model simulations indicate no significant difference of the Arctic column BC level to the Ant simulation.
These results indicate that one noticeable impact of latest model development is achieved by replacing the model’s horizontal resolution being 56-km, which is capable of simulating the fine structure of long-range BC transport to impact on the low human activity area such as Arctic and ocean.

Keywords: black carbon, aerosol transport model, K computer

©2019. Japan Geoscience Union. All Right Reserved.

High-resolution, ensemble simulations of intense tropical cyclones and their stochasticity during the El Niños of 1997 and 2015

*Yohei Yamada[1], Chihiro Kodama[1], Masaki Satoh[1,2], Masuo Nakano[1], Tomoe Nasuno[1], Masato Sugi[3]

1. Japan Agency for Marine-Earth Science and Technology, 2. Atmosphere and Ocean Research Institute, The university of Tokyo, 3. Meteorological Research Institute, Japan Meteorological Agency

Extreme El Niño events affect the number of intense tropical cyclones (ITCs) over the western North Pacific (e.g., Camargo and Sobel, 2005; Chan 2007). Extreme El Niño events were observed in 1997 and 2015. In the both years, the number of ITC were above normal in the western North Pacific. In order to clarify how, and to what extent, sea surface temperature (SST) anomaly distributions control the ITCs genesis, we conducted 50-member ensemble simulations for boreal summer in 1997 and 2015 using a global nonhydrostatic model called NICAM (Satoh et al. 2014) with a horizontal grid interval of 14 km. Clouds were explicitly calculated using a single-moment bulk microphysics scheme without cumulus convection scheme. The sea surface temperature was nudged toward observed SST data using a slab ocean model.

We found no robust control of ITCs by a prescribed SST distribution. These simulations showed that, even if the same SST was used as the boundary condition for each ensemble simulation, the number of ITCs varied substantially among members. This means that uncertainty remains large for seasonal forecasts of ITC activity. However, the ensemble simulations showed a clear relationship between the number of ITCs and their genesis locations in the western North Pacific. We compared environmental conditions between ensemble members. We found that the simulated numbers of ITCs in the western North Pacific were also closely related to the strength of the monsoon trough, which stochastically varies under given SST conditions. This indicates that reliable seasonal forecasting of ITCs depends on our ability to accurately reproduce the monsoon trough, whose strength is modulated mainly by internal atmospheric variability as well as SST.

Keywords: intense tropical cyclone, monsoon trough, El Niño, high resolution global nonhydrostatic model, ensemble simulation

©2019. Japan Geoscience Union. All Right Reserved.

NICAM results of the project DYAMOND for global storm-resolving model intercomparison

*Masaki Satoh[1], Ryosuke Shibuya[2], Chihiro Kodama[2]

1. Atmosphere and Ocean Research Institute, The University of Tokyo, 2. JAMSTEC

Project DYAMOND (DYnamics of the Atmospheric general circulation Modeled On Non-hydrostatic Domains; https://www.esiwace.eu/services/dyamond) describes a framework for the intercomparison of an emerging class of atmospheric circulations model that, through their resolution of the major modes of atmospheric heat transport, endeavor to represent the most important scales of the full three-dimensional fluid dynamics of the atmospheric circulation.

Nine models submitted simulations of the forty day intercomparison period. Eight of these employed a tiling of the sphere that was uniformly less than 5km. At these scales vertical accelerations that are non-hydrostatic become important, and convective storms in the tropics can be resolved by the underlying equations of motion. The models and some basic characteristics of their output are described in more detail, as is the availability and planned use of this output for future scientific study.

In this presentation, I will show some results of the DYAMOND simulations with NICAM and current status of DYAMOND with a list of possible participants, together with diagnostics considered.

Keywords: Global nonhydrostatic model, NICAM, DYAMOND, global storm-resolving model

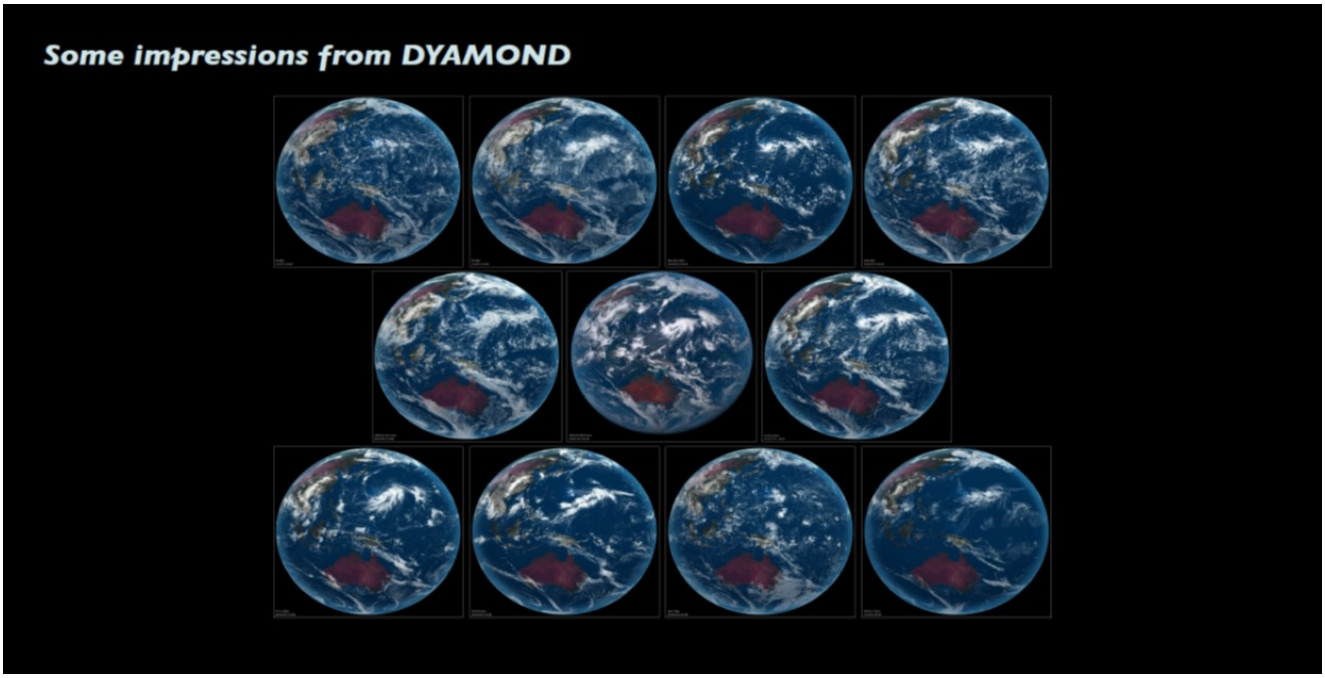

©2019. Japan Geoscience Union. All Right Reserved.

[E] Poster | A (Atmospheric and Hydrospheric Sciences)：A-AS Atmospheric Sciences, Meteorology & Atmospheric Environment

Wed. May 29, 2019 3:30 PM - 5:00 PM JST | Wed. May 29, 2019 6:30 AM - 8:00 AM UTC | Poster Hall International Exhibition Hall8, Makuhari Messe_5

[A-AS01] High performance computing for next generation weather, climate, and environmental sc iences

convener:Hiromu Seko(Meteorological Research Institute), Takemasa Miyoshi(RIKEN), Chihiro Kodama(Japan Agency for Marine-Earth Science and Technology), Masayuki Takigawa(Japan Agency for Marine-Earth Science and Technology)

A lot of advanced simulation studies are being conducted by high performance supercomputers, such as K computer and Earth Simulator, in various fields including meteorology. The high performance supercomputers enable us to conduct numerical simulations and data assimilation of observation big-data (huge high-density and high-frequency data) with an order of magnitude higher resolutions and ensemble numbers than those with the previous supercomputers. In addition, the post-K computer will be available as a successor of K, and studies for the post-K computer are in progress. At this session, we comprehensively pick up the topics in the Atmospheric and Hydrospheric Sciences Sessions of the 2019 Union Meeting that comprise the atmospheric, oceanic and land sciences. This session aims to promote recent studies related to the issues on high performance computing in weather, climate, and environmental studies using the K computer and other supercomputers, and to enhance discussions on future directions of numerical simulations in meteorology.

[AAS01-P01] **Categorized correction forecast for accumulative precipitation of heavy rainfall processes based on optimal probability (OPPF) in medium-extended-range forecast time**

*Ruoyun Niu[1] (1.National Meteorological Center)

[AAS01-P02] **Characteristics of temporal and spatial distribution of regional rainstorm processes to the east of 95°E in China during 1981-2015**

*Ruoyun Niu[1], Couhua Liu[1] (1.National Meteorological Center)

[AAS01-P03] Near-real-time SCALE-LETKF forecasts of the record breaking rainfall in Japan in July 2018

*Takumi Honda[1], Guo-Yuan Lien[2,1], Takemasa Miyoshi[1] (1.RIKEN Center for Computational Science, 2.Central Weather Bureau)

[AAS01-P04] An objective Frontal Analysis Techniques and Application in Model Verification

*couhua liu[1] (1.National Meteorology Centre of China Meteorological Administration)

[AAS01-P05] Assimilating every 30-second phased array weather radar data in a torrential rainfall event on July 6, 2018 around Kobe city

*Yasumitsu Maejima[1], Shigenori Otsuka[1], Takemasa Miyoshi[1,2] (1.RIKEN Center for Computational Science, 2.University of Maryland, College Park)

[AAS01-P06] The impact of range sidelobes from phased array weather radar observations to short-range convective forecasts

*James David Taylor[1], Guo-Yuan Lien[1], Shinsuke Satoh[2], Takemasa Miyoshi[1] (1.RIKEN Research center for computational science, 2.NICT National Institute of Information and Communications Technology)

[AAS01-P07] Development of Hydro-debris 2D model for larger area

*Yosuke Alexandre Yamashiki[1], Tsutao OIZUMI[2], Bruno Ribeiro[1], Ryusuke Kuroki[1] (1.Earth & Planetary Water Resources Assessment Laboratory Graduate School of Advanced Integrated Studies in Human Survivability Kyoto University, 2.Japan Association of Marine-Earth Science and Tecnology)

[AAS01-P08] **Research on the application of an improved terrain-following vertical coordinates on GRAPES model**

*chao li[1] (1.NWPC.CMA)

[AAS01-P09] Development of a parallel spherical harmonic transform library: design and performance

*Fuyuki SAITO[1] (1.Japan Agency for Marine-Earth Science and Technology)

[AAS01-P10] Global data assimilation of multi-species satellite measurements for atmospheric chemistry analysis

*Takashi Sekiya[1], Kazuyuki Miyazaki[2,1], Koji Ogochi[1], Kengo Sudo[3,1], Masayuki Takigawa[1] (1.Japan Agency for Marine-Earth Science and Technology, 2.Jet Propulsion Laboratory/California Institute for Technology, 3.Graduate School of Environmental Studies, Nagoya University)

[AAS01-P11] The sensitivity to WRF shortwave radiation parameterizations in prediction of global horizontal irradiance for investigating interactions of atmosphere with croplands

*Ankur Srivastava[1], Sarita Kumari[1], Rajkumar Dhakar[2] (1.Indian Institute of Technology Delhi, 2.Indian Agriculture Research Institute)

[AAS01-P12] The development of an atmospheric aerosol/chemistry–climate model, BCC_AGCM_CUACE2.0, and simulated effective radiative forcing of nitrate aerosols

*QI AN[1,2,4], Hua Zhang[2], Zhili Wang[2], Yi Liu[1,4], Bing Xie[3], Qianxia Liu[3], Zaizhi Wang[3], Sunling Gong[2] (1.LAGEO, IAP, CAS, 2.LaSW, CAMS, 3.NCC,CMA, 4.UCAS)

[AAS01-P13] **Impacts of different types and intensities of El Niño events on winter aerosols over China**

*Xiaochao Yu[1,2], Zhili Wang[2,1], Hua Zhang[2], Shuyun Zhao[3] (1.Collaborative Innovation Center on Forecast and Evaluation of Meteorological Disasters, Nanjing University of Information Science and Technology, Nanjing, 210044, China, 2.State Key Laboratory of Severe Weather and Key Laboratory of Atmospheric Chemistry of CMA, Chinese Academy of Meteorological Sciences, Beijing, 100081, China., 3.National Climate Center, China Meteorological Administration, Beijing, 100081, China)

[AAS01-P14] High Cloud Annual Variation and Its Responses to Global Warming in the NICAM AMIP Experiment

*Ying-Wen Chen[1], Masaki Satoh[1,2], Chihiro Kodama[2], Akira Noda[2], Yohei Yamada[2] (1.Atmospheric and Ocean Research Institute, The University of Tokyo , 2.Japan Agency for Marine-Earth Science and Technology)

[AAS01-P15] Improvements in Simulating the Relationship between ENSO and East Asian Summer Rainfall in the CMIP5 Models

*Yuanhai FU[1], Riyu Lu[1] (1.IAP, CAS)

Categorized correction forecast for accumulative precipitation of heavy rainfall processes based on optimal probability (OPPF) in medium-extended-range forecast time

*Ruoyun Niu[1]

1. National Meteorological Center

By taking the ensemble prediction data from ECMWF and the intensive observations of precipitation in China, the technology of categorized correction forecast for accumulative precipitation of heavy rainfall processes based on optimal probability(OPPF) is developed, and 3 calculation schemes of OPPF are designed according to overall technical route. Then the reforecast test are carried for the accumulative precipitation of 67 heavy rainfall processes from May to September during 1981 to 2015 in China, and the forecast performance of the 3 OPPFs against that of ensemble mean (EMPF) and control number (CTPF) is evaluated and contrasted. The results show that:(1) In the medium-extended-range (096-360h) forecast time, the performance of the 3 OPPFs are better than that of EMPF and CTPF for heavy precipitation forecast and clear-rain forecast. the performance of OPPF1 and OPPF2 is close to that of EMPF for Moderate precipitation and larger precipitation. OPPF3 produces the best performance among the 3 OPPFs. (2) There are obvious regional differences in forecast performances. TS of OPPF3 in southern China are higher than in northern China, and the performance of OPPF3 for heavy precipitation is better than that of EMPF in southern China. During 096-240h forecast time, the performance of OPPF3 for heavy precipitation is also better than that of EMPF in eastern part of Northeast China.

Keywords: optimal probability, accumulative precipitation of heavy precipitation processes, categorized correction forecast, comparative evaluation of forecast performance

©2019. Japan Geoscience Union. All Right Reserved.

Characteristics of temporal and spatial distribution of regional rainstorm processes to the east of 95ºE in China during 1981-2015

*Ruoyun Niu[1], Couhua Liu[1]

1. National Meteorological Center

The events of the regional rainstorm processes (RRP) to the east of 95ºE in China over 1981-2015 are constructed based on intensive daily observations of precipitation in China and NCEP/NCAR reanalysis data by means of subjective and objective analyses. Temporal and spatial characteristic distribution of RRP in China are further investigated using the methods of wavelet power spectrum, nine-point binomial smoothing and Ward cluster analysis. The main conclusions are as follows. (1) The annual average number of RRP to the east of 95ºE in China is nearly 30. RRP in the Yangtze-Huaihe River valley occur most frequently among the six subareas with an annual average number of about 19, followed by that in South China and the eastern part of Southwest China with the annual average number of RRP 10.5 and 5.8 times respectively. Annual average number of RRP are only about 1-3 times in other subareas. (2) The inter-annual and inter-decadal variations of the annual number of RRP exhibit distinct fluctuation characteristics. The inter-annual and inter-decadal fluctuating variation in the Yangtze-Huaihe River valley is the most consistent with that to the east of 95E in China. Moreover, the fluctuating variations have a significant positive correlation between South China and eastern part of Southwest China, and also between Northeast China and North China. The annual number of RRP over the east of 95E in China and its subareas demonstrates a periodic variation of 2-4a, and also shows a periodic variation of 6-10a in the Yangtze-Huaihe River valley and South China and eastern part of Northwest China, while a 13-17a oscillation can be found in North China.(3) On the whole, the occurrence frequency of RRP to the east of 95E in China is the most in summer (especially in July), the least in winter, and higher in spring than in autumn. The months when RRP occur most frequently are June and July in the Yangtze-Huaihe River valley and eastern part of Southwest China, and May and June in South China. RRP mainly appear in July and August in other subareas.(4) The distribution patterns of RRP to the east of 95E in China are divided into 7 types. The heavy precipitation areas for pattern Ⅰ-Ⅳ migrate northward step by step from South China and southern part of Yangtze River valley to Huanghuai Basin and eastern part of Sichuan Basin.The heavy precipitation areas of pattern Ⅴ-Ⅶ all are located at the Coastal region of Southeast China.

Keywords: Regional rainstorm processes, Method for distinguishing, Temporal and spatial distribution, Patterns of extremely regional rainstorm processes

©2019. Japan Geoscience Union. All Right Reserved.

Near-real-time SCALE-LETKF forecasts of the record breaking rainfall in Japan in July 2018

*Takumi Honda[1], Guo-Yuan Lien[2,1], Takemasa Miyoshi[1]

1. RIKEN Center for Computational Science, 2. Central Weather Bureau

In July 2018, a stationary precipitation band associated with the Baiu front induced a record breaking rainfall and caused catastrophic destruction in Japan. This event was successfully captured by the near-real-time (NRT) SCALE-LETKF system (Lien et al. 2017) consisting of the Scalable Computing for Advanced Library and Environment-Regional Model (SCALE-RM, Nishizawa et al. 2015; Sato et al. 2015) and the Local Ensemble Transform Kalman Filter (LETKF, Hunt et al. 2007; Miyoshi and Yamane 2007). This system has been continuously operated since 2015 with an 18-km mesh model domain and the ensemble size of 50. In the NRT SCALE-LETKF system, only conventional observations are assimilated every 6 hours. By conducting a series of 50-member ensemble forecasts from the 6-hourly SCALE-LETKF analyses, this study aims to investigate predictability of this torrential rainfall event and important factors that contributed to the heavy precipitation. In general, the NRT SCALE-LETKF system provides skillful ensemble forecasts of the rainfall a few days in advance. Interestingly, the forecast skill exhibits sudden improvement due to assimilating conventional observations at a single location far southwest from the peak accumulated rainfall location. Forecast differences and ensemble correlations suggest that an extratropical cyclone over the Sea of Japan and a low-level trough near Taiwan play important roles in determining the front location.

Keywords: Data assimilation, Numerical Weather Prediction

©2019. Japan Geoscience Union. All Right Reserved.

An objective Frontal Analysis Techniques and Application in Model Verification

*Couhua Liu[1]

1. National Meteorology Centre of China Meteorological Administration

This paper presents an objective Frontal analysis method based on pressure field for east Asia. Comparing to methods based on thermo-dynamical elements such as temperature, the method developed in this paper can avoid the complex affection from sea-land and landform. The method will be used to identification of fronts in analysis and prediction of ECMWF model all over 2015, and then model error of predicted fronts will be verification. The verification result show that, comparing to analysis field, the moving speed of fronts in prediction field of ECMWF model is slower and strength is weaker.

Keywords: front, model, verification

©2019. Japan Geoscience Union. All Right Reserved.

Assimilating every 30-second phased array weather radar data in a torrential rainfall event on July 6, 2018 around Kobe city

*Yasumitsu Maejima[1], Shigenori Otsuka[1], Takemasa Miyoshi[1,2]

1. RIKEN Center for Computational Science, 2. University of Maryland, College Park

To investigate the impact of every 30-second phased array weather radar (PAWR; Yoshikawa et al. 2013, Ushio et al. 2014) observation on a simulation of a severe rainfall event occurred on July 6, 2018 around Kobe city, we perform 30-second-update 100-m-mesh data assimilation (DA) experiments using the Local Ensemble Transform Kalman Filter with the Scalable Computing for Advanced Library and Environment regional numerical weather prediction model. Two experiments were performed: the test experiment with every 30-second PAWR observation (TEST), and the other without observation (NO-DA).

The TEST analysis shows intense rainfalls with detailed structure of active convection, better matching with the PAWR observation compared to NO-DA analysis. In the forecast experiment, the forecast initialized by the ensemble mean analysis of TEST is skillful for 20 minutes compared with NO-DA, although the skill is decreased rapidly. The results suggest that the PAWR DA have a potential to improve the numerical simulation for this torrential rainfall event.

Keywords: Data assimilation, Heavy rainfall forecast, High performance computing

©2019. Japan Geoscience Union. All Right Reserved.

The impact of range sidelobes from phased array weather radar observations to short-range convective forecasts

*James David Taylor[1], Guo-Yuan Lien[1], Shinsuke Satoh[2], Takemasa Miyoshi[1]

1. RIKEN Research center for computational science, 2. NICT National Institute of Information and Communications Technology

Range sidelobes are an erroneous feature of radar observations that are generated by the pulse compression process used to improve the range resolution of target echoes in high resolution radar systems. Phased array weather radar (PAWR) is an advanced radar system providing very dense observations of reflectivity and Doppler radial velocity at 100m range resolution for over 100 elevation angles every 30 seconds. The use of pulse compression in PAWR to provide very high range resolution data makes it subject to these types of errors, which can result in false echoes observed at other ranges.

In this study we investigate the impact of assimilating range sidelobes from PAWR observations to short-range convective forecasts. This happens frequently in the current QC algorithm, although we plan to improve the QC in the future. We employ the use of the SCALE-LETKF system which couples the Local Ensemble Transform Kalman Filter (LETKF) with the Scalable Computing for Advanced Library and Environment (SCALE)-RM model. We focus on a convective rainfall event in August 2016 that brought heavy, intense rainfall over Osaka. PAWRs located in Suita, Osaka and in Kobe well-captured the convective system over its life cycle but featured prominent range sidelobes as part of their observations. Here, observations from both radars are first used to identify the range sidelobes before performing a series of 30-second update cycling experiments using observations from the Suita PAWR both with and without range sidelobes within a high-resolution 100-m mesh. As well as investigating their impact on short-range forecasts, we aim to show how we can further the usefulness of having two sets of PAWR observations to observe the same convective system by using them to identify and remove range sidelobes and improve short-range forecasts of severe convective events through the assimilation of this data.

Keywords: LETKF, Assimilation, Forecasts, Convection, Sidelobes

©2019. Japan Geoscience Union. All Right Reserved.

Development of Hydro-debris 2D model for larger area

*Yosuke Alexandre Yamashiki[1], Tsutao OIZUMI[2], Bruno Ribeiro[1], Ryusuke Kuroki[1]

1. Earth & Planetary Water Resources Assessment Laboratory Graduate School of Advanced Integrated Studies in Human Survivability Kyoto University, 2. Japan Association of Marine-Earth Science and Tecnology

The Hydro-debris 2D model has been developed and applied for both larger and limited zones in the Hiroshima debris-flow disasters that occurred both in 2014 & 2018. The model application for hindcast for wider and limited areas with the same scheme is tested in order to obtain better and precise hindcast as well as a future forecast of rainfall-induced debris flow disasters by improving the geological classification module for the initiation of the debris flow. A universal algorithm for predicting the debris flow disasters solely by the initial geological boundary conditions and forecasted rainfall distribution may contribute to improving early warnings in this field.

Keywords: Debris flow, Hindcast

©2019. Japan Geoscience Union. All Right Reserved.

Research on the application of an improved terrain-following vertical coordinates on GRAPES model

*chao li[1]

1. NWPC.CMA

Errors caused by topographic feathers of the coordinate planes can be reduced with the Smoothed-level terrain-following coordinate(T-F coordinate for short). On higher layors,coordinate planes of T-F coordinate based on trigonometric function of cos (COS coordinate for short)are horizontal with almost none errors. However,on the lower layers,thickness between planes is too small to keep the model stability.At the same time,it will bring larger calculating errors which result in bad performance of the model.Considering all above,an improved COS coordinate is designed to average the thickness of COS coordinate planes.
Ideal and real case tests are conducted with the GRAPES_Meso model using the improved COS coordinate.The results of the tests indicate that:compared with the COS coordinate, the improved COS coordinate ,on one hand ,keep the planes horizontal on the higher layers ,on the other hand, lead the distribute of the coordinate planes more uniformity , which greatly reduced the errors on the lower layers;The coordinate can reproduce in general the mountain induced gravity waves in comparison to the analytic solution. However, the shapes,vertical structures and intensity of the waves are better simulated by the improved COS coordinate, in the lower levels where the COS coordinate didn’ t behave so better. In the one-month real case tests, the improved COS coordinate gives the better results in terms of smaller forecast bias and root mean square error, and higher anomaly correlation coefficients than the COS coordinate. In conclusion, the improved COS coordinate solves the calculation problems of the COS coordinate ,and improves the prediction ability.

Keywords: GRAPES Model, Terrain-following coordinate, Dynamic Core, Numerical Modelling

©2019. Japan Geoscience Union. All Right Reserved.

Development of a parallel spherical harmonic transform library: design and performance

*Fuyuki SAITO[1]

1. Japan Agency for Marine-Earth Science and Technology

The spherical harmonic transform (SHT) is a typical method to describe the dynamical core in climate models (e.g. MIROC). SHT is a combination of two transformation: a Fourier transformation in longitude and an associate Legendre transformation in latitude. Therefore, a simple way to introduce SHT in parallel computing is to apply domain decomposition in latitudes only, involving a relocation in latitudes before/after the Legendre transformation. However, the number of maximum processors is limited by the size of latitude dimension, which is an obstacle to more efficient computing. Recently the `physics' routines in a climate model have become more and more complex and expensive, thus the heavy computation significantly suffers from the limitation. A new (yet-another) library, Flageolet, has been developed to help parallel processing of SHT in particular for climate models like MIROC, to support more flexible domain decomposition, following the approach adopted in several 3D FFT libraries and also some climate models. As a continuation of last-year's presentation, which reports the design and performance of FFT part, those of SHT part as well as transposition part between FFT and ALT are reported in this study for various sizes of domain around T213 etc, examined on the Earth simulator.

Keywords: spherical harmonic transform

©2019. Japan Geoscience Union. All Right Reserved.

Global data assimilation of multi-species satellite measurements for atmospheric chemistry analysis

*Takashi Sekiya[1], Kazuyuki Miyazaki[2,1], Koji Ogochi[1], Kengo Sudo[3,1], Masayuki Takigawa[1]

1. Japan Agency for Marine-Earth Science and Technology, 2. Jet Propulsion Laboratory/California Institute for Technology, 3. Graduate School of Environmental Studies, Nagoya University

Information on tropospheric ozone and its precursors are important for human health, ecosystem, and climate studies. The combined use of satellite measurements of ozone and its precursors has great potential to provide comprehensive information on the tropospheric chemistry system on various spatial scales. In this study, we present the results of global data assimilation of multi-species measurements (O_3, NO_2, CO, HNO_3, and SO_2) from multi-satellite sensors (OMI, GOME-2, SCIAMACHY, MOPITT, TES, and MLS) using the ensemble Kalman filter approach (Miyazaki et al., 2015). We demonstrated that increasing horizontal resolution from 2.8 to 0.56 degree is necessary for capturing high concentrations of NO_2 in the megacities, whereas 1.1-degree resolution is more suitable for optimizing tropospheric chemistry system on regional and global scales considering the current computational resources (computational cost was larger by a factor of 10 at 0.56-dgree resolution than at 1.1-degree resolution). Using the data assimilation system at 1.1-degree resolution, we constructed an updated version of tropospheric chemistry reanalysis (TCR-2; Miyazaki et al., in prep.) data for 2005—2017, which provide valuable information on decadal changes in air pollutant concentrations and emissions. The estimated NO_x emissions were strongly increased from 2005 to 2011 (+37%/decade) and decreased from 2011 to 2017 (-37%/decade) in China, while the emissions exhibited decreasing trends in Europe (-11%/decade) and the United States (-27%/decade) and an increasing trend in India (+23%/decade) during 2005—2017. A post peta-scale supercomputer such as post-K computer will facilitate the data assimilation calculation to produce tropospheric chemistry reanalysis data at 0.56-degree resolution for air pollutions on a megacity scale globally in a consistent way, which will benefit future study of atmospheric environment on various spatial scales.

Keywords: Data assimilation, Atmospheric chemistry, Atmospheric environment

©2019. Japan Geoscience Union. All Right Reserved.

The sensitivity to WRF shortwave radiation parameterizations in prediction of global horizontal irradiance for investigating interactions of atmosphere with croplands

*Ankur Srivastava[1], Sarita Kumari[1], Rajkumar Dhakar[2]

1. Indian Institute of Technology Delhi, 2. Indian Agriculture Research Institute

The present study intends to evaluate the Advanced Research Weather Research Forecating (ARW) model performance in representing the observed global horizontal irradiance (GHI) measurements while using different shortwave radiation (SWR) parameterization schemes. Two cases are considered, first case is ‘clear sky condition’ which includes model simulation of a clear/ cloudless day and second case is ‘all sky condition’ which includes model simulations of a cloudy and a rainy day. The above two cases are formulated on the basis that amount of incoming SWR will be different in each case owing to the differences in atmospheric conditions.
For the mentioned instances dates of 23rd February, 9th January and 12th March of 2016, which are clear, cloudy and rainy days respectively, are chosen for WRF model simulation. The shortwave radiation schemes that were evaluated are: Dudhia, Community Atmosphere Model (CAM), the updated Rapid Radiative Transfer Model (RRTMG), the updated Goddard and the
Goddard Fluid Dynamics Laboratory (GFDL) schemes. The model generated predictions are verified against the GHI measurements at weather station of Indian Agriculture Research Institute (IARI), New Delhi.
All schemes perform better under ‘clear sky condition’ i.e. for clear/cloudless day. For both the cases Dudhia scheme performs best with Mean Bias (MB) of 62.84 Wm^{-2} for clear day, 86.44 Wm^{-2} for cloudy day and 89.44 Wm^{-2} for rainy day. All-inclusive, the model derived predictions are over estimated in all the schemes.

Keywords: global horizontal irradiance , parameterization, shortwave radiation

©2019. Japan Geoscience Union. All Right Reserved.

The development of an atmospheric aerosol/chemistry–climate model, BCC_AGCM_CUACE2.0, and simulated effective radiative forcing of nitrate aerosols

*QI AN[1,2,4], Hua Zhang[2], Zhili Wang[2], Yi Liu[1,4], Bing Xie[3], Qianxia Liu[3], Zaizhi Wang[3], Sunling Gong[2]

1. LAGEO, IAP, CAS, 2. LaSW, CAMS, 3. NCC,CMA, 4. UCAS

As important components of total anthropogenic aerosols, nitrate aerosols have large impacts on aerosol radiative forcing and climate at regional and seasonal scales, but few current climate models coupled nitrate chemical modules online. This study developed a next-generation atmospheric aerosol/chemistry–climate model, the BCC_AGCM_CUACE2.0. Then, the performance of the model for nitrate was evaluated, and the direct radiative forcing (DRF) and effective radiative forcing (ERF) due to nitrate were simulated for the present day (2010), near future (2030) and middle future (2050) under the Representative Concentration Pathway (RCP) 4.5, 6.0, and 8.5 scenarios relative to the pre-industrial era (1850). The model reproduced the distributions and seasonal changes in nitrate loading well and simulated surface concentrations matched observations in Europe and North America. Current global mean annual loading of nitrates was predicted to increase by 1.12 mg m^{-2} relative to 1850, with the largest increases occurring in East Asia (3.89 mg m^{-2}), Europe (3.6 mg m^{-2}), and South Asia (1.86 mg m^{-2}). The current global mean annual ERF of nitrates was −0.21 W m^{-2} relative to 1850. Due to global reductions in pollutant emissions, the nitrate ERF values were predicted to decrease to −0.17 and −0.20 W m^{-2} in 2030, −0.07 and −0.18 W m^{-2} in 2050 for RCP4.5 and 6.0 relative to 1850, respectively. Under RCP8.5, nitrate ERF values were −0.24 and −0.19 W m^{-2} in 2030 and 2050, respectively. Although global mean nitrate values showed a declining trend, future nitrate loading remained high in East Asia and South Asia.

Keywords: Effective radiative forcing, Nitrate

©2019. Japan Geoscience Union. All Right Reserved.

Impacts of different types and intensities of El Niño events on winter aerosols over China

*Xiaochao Yu[1,2], Zhili Wang[2,1], Hua Zhang[2], Shuyun Zhao[3]

1. Collaborative Innovation Center on Forecast and Evaluation of Meteorological Disasters, Nanjing University of Information Science and Technology, Nanjing, 210044, China, 2. State Key Laboratory of Severe Weather and Key Laboratory of Atmospheric Chemistry of CMA, Chinese Academy of Meteorological Sciences, Beijing, 100081, China., 3. National Climate Center, China Meteorological Administration, Beijing, 100081, China

El Niño is a strong signal of interannual climate variability. The occurrence of an El Niño event may have an important impact on atmospheric pollutant concentrations in China through changes to the regional climate. This study quantitatively examines the differences among the effects of different types and intensities of El Niño events on winter mean aerosol concentration and severe haze days in China. It is found that Central Pacific (CP) El Niño events lead to larger increases in the aerosol burden over southern China relative to the same intensity of Eastern Pacific (EP) events. For El Niño events of the same type but with different intensities, moderate events induce large increases in surface aerosol concentrations over the entire eastern China, while strong and weak events lead to obvious decreases in the surface aerosol concentration over northern China. These differences are mainly attributed to changes in atmospheric circulation, with the resulting changes in aerosol mass transport occurring in response to the different types of El Niño event. Except for moderate CP events, all kinds of El Niño events lead to an increase in severe haze days in winter over northern China. Strong and weak EP El Niño events and weak CP El Niño events lead to an increase in severe haze days in winter over southern China. A change in the south-north transport of aerosols caused by El Niño events also play a dominate role in changing the occurrence of winter haze days in China.

Keywords: Eastern Pacific El Niño, Central Pacific El Niño, aerosol concentration, severe haze day

©2019. Japan Geoscience Union. All Right Reserved.

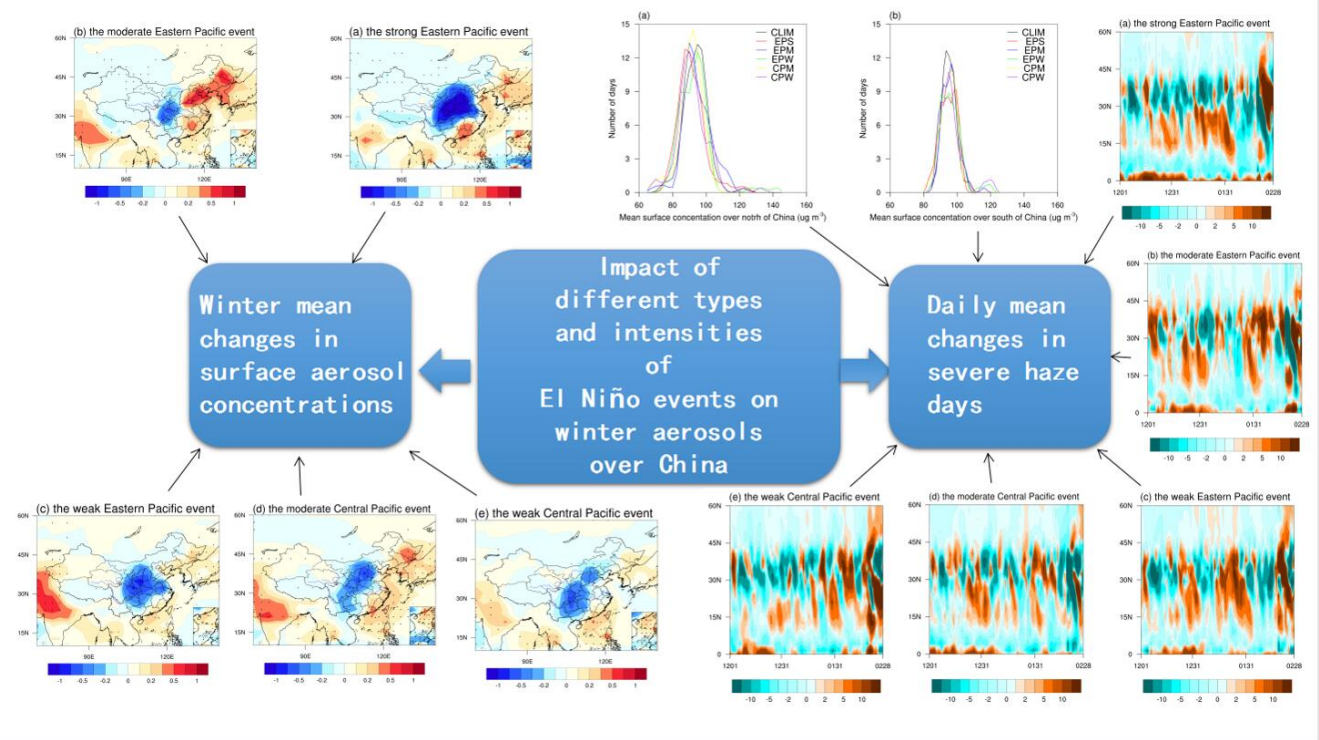

©2019. Japan Geoscience Union. All Right Reserved.

High Cloud Annual Variation and Its Responses to Global Warming in the NICAM AMIP Experiment

*Ying-Wen Chen[1], Masaki Satoh[1,2], Chihiro Kodama[2], Akira Noda[2], Yohei Yamada[2]

1. Atmospheric and Ocean Research Institute, The University of Tokyo , 2. Japan Agency for Marine-Earth Science and Technology

Uncertainties in climate sensitivity mainly come from the ambiguities in simulations of both high- and low-level clouds. The previous studies using NICAM’s short time simulation showed that the both the altitudes and amount of high clouds increase under the global warming condition, while other climate models show high cloud amount contrarily decreases.
Due to the progress in computer performance, long term climate simulation with $x < 20$ km becomes available. A pair of 25-year climate simulation (present and warming climate) with 14-km horizontal resolution (NICAM AMIP-like simulation, Kodama et al. 2015) has been performed by K computer. In this study, we analyze how the annual variation in high clouds is presented in the NICAM AMIP-like simulation. Satellite and in-situ data are used to investigate whether NICAM captures the observed responses of high clouds to the mean sea surface temperature (SST). Regressions between the high cloud amount variation and the SST variation is different with altitudes; positive regressions appear at altitudes above 100 hPa while negative regressions are found in altitudes below 100 hPa. The results are consistent with previous study based on observations (Zelinka and Hartmann 2011). Further analysis showed that the spatial pattern of high clouds is mainly associated with the El Nino response; as SST warmer, the high clouds shift in the eastern Pacific with higher. The increase of high clouds is associated with the increase of ice water content of cloud ice and snow. We argue that the response of high clouds to global warming is also explained by the change in the spatial distribution of the high clouds.

Keywords: Global Warming, Cloud-Resolving Model

©2019. Japan Geoscience Union. All Right Reserved.

Improvements in Simulating the Relationship between ENSO and East Asian Summer Rainfall in the CMIP5 Models

*Yuanhai FU[1], Riyu Lu[1]

1. IAP, CAS

There is a significant relationship between the preceding winter El Niño–Southern Oscillation (ENSO) and the subsequent East Asian summer rainfall (EASR), and this relationship is helpful for seasonal forecasting in East Asia. This study investigated the relationship between the preceding winter ENSO and EASR in the Coupled Model Intercomparison Project Phase 5 (CMIP5) models and compared the results with those from the CMIP3 models. In general, the CMIP5 models capture the ENSO–EASR relationship more realistically than the CMIP3 models. For instance, approximately two-thirds of the CMIP5 models capture the ENSO–EASR relationship, while less than one-third of the CMIP3 models capture the relationship. Further investigation suggests that the improvement could be attributed to simulating the physical processes of ENSO's impact on the EASR more realistically in the CMIP5 models, particularly the effect of ENSO on tropical Indian Ocean SST and the effect of Indian Ocean SST anomalies on the atmospheric convection over the Philippine Sea. However, there is large diversity in the ENSO–EASR relationship in the CMIP5 models, and most of the models underestimate the relationship. This underestimation comes from the underestimation of the physical processes, particularly from the underestimated impact of the atmospheric convection over the Philippine Sea on the EASR. The CMIP5 models that capture the ENSO–EASR relationship well/bad also show high/low skill in representing the physical processes.

Keywords: East Asian summer rainfall, ENSO, CMIP5 model

©2019. Japan Geoscience Union. All Right Reserved.

[E] Poster | A (Atmospheric and Hydrospheric Sciences)：A-AS Atmospheric Sciences, Meteorology & Atmospheric Environment

Wed. May 29, 2019 5:15 PM - 6:30 PM JST | Wed. May 29, 2019 8:15 AM - 9:30 AM UTC | Poster Hall International Exhibition Hall8, Makuhari Messe_9

[A-AS01] High performance computing for next generation weather, climate, and environmental sc iences

convener:Hiromu Seko(Meteorological Research Institute), Takemasa Miyoshi(RIKEN), Chihiro Kodama(Japan Agency for Marine-Earth Science and Technology), Masayuki Takigawa(Japan Agency for Marine-Earth Science and Technology)

A lot of advanced simulation studies are being conducted by high performance supercomputers, such as K computer and Earth Simulator, in various fields including meteorology. The high performance supercomputers enable us to conduct numerical simulations and data assimilation of observation big-data (huge high-density and high-frequency data) with an order of magnitude higher resolutions and ensemble numbers than those with the previous supercomputers. In addition, the post-K computer will be available as a successor of K, and studies for the post-K computer are in progress. At this session, we comprehensively pick up the topics in the Atmospheric and Hydrospheric Sciences Sessions of the 2019 Union Meeting that comprise the atmospheric, oceanic and land sciences. This session aims to promote recent studies related to the issues on high performance computing in weather, climate, and environmental studies using the K computer and other supercomputers, and to enhance discussions on future directions of numerical simulations in meteorology.

[AAS01-P01] **Categorized correction forecast for accumulative precipitation of heavy rainfall processes based on optimal probability (OPPF) in medium-extended-range forecast time**

*Ruoyun Niu[1] (1.National Meteorological Center)

[AAS01-P02] **Characteristics of temporal and spatial distribution of regional rainstorm processes to the east of 95°E in China during 1981-2015**

*Ruoyun Niu[1], Couhua Liu[1] (1.National Meteorological Center)

[AAS01-P03] Near-real-time SCALE-LETKF forecasts of the record breaking rainfall in Japan in July 2018

*Takumi Honda[1], Guo-Yuan Lien[2,1], Takemasa Miyoshi[1] (1.RIKEN Center for Computational Science, 2.Central Weather Bureau)

[AAS01-P04] An objective Frontal Analysis Techniques and Application in Model Verification

*couhua liu[1] (1.National Meteorology Centre of China Meteorological Administration)

[AAS01-P05] Assimilating every 30-second phased array weather radar data in a torrential rainfall event on July 6, 2018 around Kobe city

*Yasumitsu Maejima[1], Shigenori Otsuka[1], Takemasa Miyoshi[1,2] (1.RIKEN Center for Computational Science, 2.University of Maryland, College Park)

[AAS01-P06] The impact of range sidelobes from phased array weather radar observations to short-range convective forecasts

*James David Taylor[1], Guo-Yuan Lien[1], Shinsuke Satoh[2], Takemasa Miyoshi[1] (1.RIKEN Research center for computational science, 2.NICT National Institute of Information and Communications Technology)

[AAS01-P07] Development of Hydro-debris 2D model for larger area

*Yosuke Alexandre Yamashiki[1], Tsutao OIZUMI[2], Bruno Ribeiro[1], Ryusuke Kuroki[1] (1.Earth & Planetary Water Resources Assessment Laboratory Graduate School of Advanced Integrated Studies in Human Survivability Kyoto University, 2.Japan Association of Marine-Earth Science and Tecnology)

[AAS01-P08] **Research on the application of an improved terrain-following vertical coordinates on GRAPES model**

*chao li[1] (1.NWPC.CMA)

[AAS01-P09] Development of a parallel spherical harmonic transform library: design and performance

*Fuyuki SAITO[1] (1.Japan Agency for Marine-Earth Science and Technology)

[AAS01-P10] Global data assimilation of multi-species satellite measurements for atmospheric chemistry analysis

*Takashi Sekiya[1], Kazuyuki Miyazaki[2,1], Koji Ogochi[1], Kengo Sudo[3,1], Masayuki Takigawa[1] (1.Japan Agency for Marine-Earth Science and Technology, 2.Jet Propulsion Laboratory/California Institute for Technology, 3.Graduate School of Environmental Studies, Nagoya University)

[AAS01-P11] The sensitivity to WRF shortwave radiation parameterizations in prediction of global horizontal irradiance for investigating interactions of atmosphere with croplands

*Ankur Srivastava[1], Sarita Kumari[1], Rajkumar Dhakar[2] (1.Indian Institute of Technology Delhi, 2.Indian Agriculture Research Institute)

[AAS01-P12] The development of an atmospheric aerosol/chemistry–climate model, BCC_AGCM_CUACE2.0, and simulated effective radiative forcing of nitrate aerosols

*QI AN[1,2,4], Hua Zhang[2], Zhili Wang[2], Yi Liu[1,4], Bing Xie[3], Qianxia Liu[3], Zaizhi Wang[3], Sunling Gong[2] (1.LAGEO, IAP, CAS, 2.LaSW, CAMS, 3.NCC,CMA, 4.UCAS)

[AAS01-P13] **Impacts of different types and intensities of El Niño events on winter aerosols over China**

*Xiaochao Yu[1,2], Zhili Wang[2,1], Hua Zhang[2], Shuyun Zhao[3] (1.Collaborative Innovation Center on Forecast and Evaluation of Meteorological Disasters, Nanjing University of Information Science and Technology, Nanjing, 210044, China, 2.State Key Laboratory of Severe Weather and Key Laboratory of Atmospheric Chemistry of CMA, Chinese Academy of Meteorological Sciences, Beijing, 100081, China., 3.National Climate Center, China Meteorological Administration, Beijing, 100081, China)

[AAS01-P14] High Cloud Annual Variation and Its Responses to Global Warming in the NICAM AMIP Experiment

*Ying-Wen Chen[1], Masaki Satoh[1,2], Chihiro Kodama[2], Akira Noda[2], Yohei Yamada[2] (1.Atmospheric and Ocean Research Institute, The University of Tokyo , 2.Japan Agency for Marine-Earth Science and Technology)

[AAS01-P15] Improvements in Simulating the Relationship between ENSO and East Asian Summer Rainfall in the CMIP5 Models

*Yuanhai FU[1], Riyu Lu[1] (1.IAP, CAS)

Categorized correction forecast for accumulative precipitation of heavy rainfall processes based on optimal probability (OPPF) in medium-extended-range forecast time

*Ruoyun Niu[1]

1. National Meteorological Center

By taking the ensemble prediction data from ECMWF and the intensive observations of precipitation in China, the technology of categorized correction forecast for accumulative precipitation of heavy rainfall processes based on optimal probability(OPPF) is developed, and 3 calculation schemes of OPPF are designed according to overall technical route. Then the reforecast test are carried for the accumulative precipitation of 67 heavy rainfall processes from May to September during 1981 to 2015 in China, and the forecast performance of the 3 OPPFs against that of ensemble mean (EMPF) and control number (CTPF) is evaluated and contrasted. The results show that:(1) In the medium-extended-range (096-360h) forecast time, the performance of the 3 OPPFs are better than that of EMPF and CTPF for heavy precipitation forecast and clear-rain forecast. the performance of OPPF1 and OPPF2 is close to that of EMPF for Moderate precipitation and larger precipitation. OPPF3 produces the best performance among the 3 OPPFs. (2) There are obvious regional differences in forecast performances. TS of OPPF3 in southern China are higher than in northern China, and the performance of OPPF3 for heavy precipitation is better than that of EMPF in southern China. During 096-240h forecast time, the performance of OPPF3 for heavy precipitation is also better than that of EMPF in eastern part of Northeast China.

Keywords: optimal probability, accumulative precipitation of heavy precipitation processes, categorized correction forecast, comparative evaluation of forecast performance

©2019. Japan Geoscience Union. All Right Reserved.

Characteristics of temporal and spatial distribution of regional rainstorm processes to the east of 95ºE in China during 1981-2015

*Ruoyun Niu[1], Couhua Liu[1]

1. National Meteorological Center

The events of the regional rainstorm processes (RRP) to the east of 95ºE in China over 1981-2015 are constructed based on intensive daily observations of precipitation in China and NCEP/NCAR reanalysis data by means of subjective and objective analyses. Temporal and spatial characteristic distribution of RRP in China are further investigated using the methods of wavelet power spectrum, nine-point binomial smoothing and Ward cluster analysis. The main conclusions are as follows. (1) The annual average number of RRP to the east of 95ºE in China is nearly 30. RRP in the Yangtze-Huaihe River valley occur most frequently among the six subareas with an annual average number of about 19, followed by that in South China and the eastern part of Southwest China with the annual average number of RRP 10.5 and 5.8 times respectively. Annual average number of RRP are only about 1-3 times in other subareas. (2) The inter-annual and inter-decadal variations of the annual number of RRP exhibit distinct fluctuation characteristics. The inter-annual and inter-decadal fluctuating variation in the Yangtze-Huaihe River valley is the most consistent with that to the east of 95E in China. Moreover, the fluctuating variations have a significant positive correlation between South China and eastern part of Southwest China, and also between Northeast China and North China. The annual number of RRP over the east of 95E in China and its subareas demonstrates a periodic variation of 2-4a, and also shows a periodic variation of 6-10a in the Yangtze-Huaihe River valley and South China and eastern part of Northwest China, while a 13-17a oscillation can be found in North China.(3) On the whole, the occurrence frequency of RRP to the east of 95E in China is the most in summer (especially in July), the least in winter, and higher in spring than in autumn. The months when RRP occur most frequently are June and July in the Yangtze-Huaihe River valley and eastern part of Southwest China, and May and June in South China. RRP mainly appear in July and August in other subareas.(4) The distribution patterns of RRP to the east of 95E in China are divided into 7 types. The heavy precipitation areas for pattern Ⅰ-Ⅳ migrate northward step by step from South China and southern part of Yangtze River valley to Huanghuai Basin and eastern part of Sichuan Basin.The heavy precipitation areas of pattern Ⅴ-Ⅶ all are located at the Coastal region of Southeast China.

Keywords: Regional rainstorm processes, Method for distinguishing, Temporal and spatial distribution, Patterns of extremely regional rainstorm processes

©2019. Japan Geoscience Union. All Right Reserved.

Near-real-time SCALE-LETKF forecasts of the record breaking rainfall in Japan in July 2018

*Takumi Honda[1], Guo-Yuan Lien[2,1], Takemasa Miyoshi[1]

1. RIKEN Center for Computational Science, 2. Central Weather Bureau

In July 2018, a stationary precipitation band associated with the Baiu front induced a record breaking rainfall and caused catastrophic destruction in Japan. This event was successfully captured by the near-real-time (NRT) SCALE-LETKF system (Lien et al. 2017) consisting of the Scalable Computing for Advanced Library and Environment-Regional Model (SCALE-RM, Nishizawa et al. 2015; Sato et al. 2015) and the Local Ensemble Transform Kalman Filter (LETKF, Hunt et al. 2007; Miyoshi and Yamane 2007). This system has been continuously operated since 2015 with an 18-km mesh model domain and the ensemble size of 50. In the NRT SCALE-LETKF system, only conventional observations are assimilated every 6 hours. By conducting a series of 50-member ensemble forecasts from the 6-hourly SCALE-LETKF analyses, this study aims to investigate predictability of this torrential rainfall event and important factors that contributed to the heavy precipitation. In general, the NRT SCALE-LETKF system provides skillful ensemble forecasts of the rainfall a few days in advance. Interestingly, the forecast skill exhibits sudden improvement due to assimilating conventional observations at a single location far southwest from the peak accumulated rainfall location. Forecast differences and ensemble correlations suggest that an extratropical cyclone over the Sea of Japan and a low-level trough near Taiwan play important roles in determining the front location.

Keywords: Data assimilation, Numerical Weather Prediction

©2019. Japan Geoscience Union. All Right Reserved.

An objective Frontal Analysis Techniques and Application in Model Verification

*Couhua Liu[1]

1. National Meteorology Centre of China Meteorological Administration

This paper presents an objective Frontal analysis method based on pressure field for east Asia. Comparing to methods based on thermo-dynamical elements such as temperature, the method developed in this paper can avoid the complex affection from sea-land and landform. The method will be used to identification of fronts in analysis and prediction of ECMWF model all over 2015, and then model error of predicted fronts will be verification. The verification result show that, comparing to analysis field, the moving speed of fronts in prediction field of ECMWF model is slower and strength is weaker.

Keywords: front, model, verification

©2019. Japan Geoscience Union. All Right Reserved.

Assimilating every 30-second phased array weather radar data in a torrential rainfall event on July 6, 2018 around Kobe city

*Yasumitsu Maejima[1], Shigenori Otsuka[1], Takemasa Miyoshi[1,2]

1. RIKEN Center for Computational Science, 2. University of Maryland, College Park

To investigate the impact of every 30-second phased array weather radar (PAWR; Yoshikawa et al. 2013, Ushio et al. 2014) observation on a simulation of a severe rainfall event occurred on July 6, 2018 around Kobe city, we perform 30-second-update 100-m-mesh data assimilation (DA) experiments using the Local Ensemble Transform Kalman Filter with the Scalable Computing for Advanced Library and Environment regional numerical weather prediction model. Two experiments were performed: the test experiment with every 30-second PAWR observation (TEST), and the other without observation (NO-DA).

The TEST analysis shows intense rainfalls with detailed structure of active convection, better matching with the PAWR observation compared to NO-DA analysis. In the forecast experiment, the forecast initialized by the ensemble mean analysis of TEST is skillful for 20 minutes compared with NO-DA, although the skill is decreased rapidly. The results suggest that the PAWR DA have a potential to improve the numerical simulation for this torrential rainfall event.

Keywords: Data assimilation, Heavy rainfall forecast, High performance computing

©2019. Japan Geoscience Union. All Right Reserved.

The impact of range sidelobes from phased array weather radar observations to short-range convective forecasts

*James David Taylor[1], Guo-Yuan Lien[1], Shinsuke Satoh[2], Takemasa Miyoshi[1]

1. RIKEN Research center for computational science, 2. NICT National Institute of Information and Communications Technology

Range sidelobes are an erroneous feature of radar observations that are generated by the pulse compression process used to improve the range resolution of target echoes in high resolution radar systems. Phased array weather radar (PAWR) is an advanced radar system providing very dense observations of reflectivity and Doppler radial velocity at 100m range resolution for over 100 elevation angles every 30 seconds. The use of pulse compression in PAWR to provide very high range resolution data makes it subject to these types of errors, which can result in false echoes observed at other ranges.

In this study we investigate the impact of assimilating range sidelobes from PAWR observations to short-range convective forecasts. This happens frequently in the current QC algorithm, although we plan to improve the QC in the future. We employ the use of the SCALE-LETKF system which couples the Local Ensemble Transform Kalman Filter (LETKF) with the Scalable Computing for Advanced Library and Environment (SCALE)-RM model. We focus on a convective rainfall event in August 2016 that brought heavy, intense rainfall over Osaka. PAWRs located in Suita, Osaka and in Kobe well-captured the convective system over its life cycle but featured prominent range sidelobes as part of their observations. Here, observations from both radars are first used to identify the range sidelobes before performing a series of 30-second update cycling experiments using observations from the Suita PAWR both with and without range sidelobes within a high-resolution 100-m mesh. As well as investigating their impact on short-range forecasts, we aim to show how we can further the usefulness of having two sets of PAWR observations to observe the same convective system by using them to identify and remove range sidelobes and improve short-range forecasts of severe convective events through the assimilation of this data.

Keywords: LETKF, Assimilation, Forecasts, Convection, Sidelobes

©2019. Japan Geoscience Union. All Right Reserved.

Development of Hydro-debris 2D model for larger area

*Yosuke Alexandre Yamashiki[1], Tsutao OIZUMI[2], Bruno Ribeiro[1], Ryusuke Kuroki[1]

1. Earth & Planetary Water Resources Assessment Laboratory Graduate School of Advanced Integrated Studies in Human Survivability Kyoto University, 2. Japan Association of Marine-Earth Science and Tecnology

The Hydro-debris 2D model has been developed and applied for both larger and limited zones in the Hiroshima debris-flow disasters that occurred both in 2014 & 2018. The model application for hindcast for wider and limited areas with the same scheme is tested in order to obtain better and precise hindcast as well as a future forecast of rainfall-induced debris flow disasters by improving the geological classification module for the initiation of the debris flow. A universal algorithm for predicting the debris flow disasters solely by the initial geological boundary conditions and forecasted rainfall distribution may contribute to improving early warnings in this field.

Keywords: Debris flow, Hindcast

©2019. Japan Geoscience Union. All Right Reserved.

Research on the application of an improved terrain-following vertical coordinates on GRAPES model

*chao li[1]

1. NWPC.CMA

Errors caused by topographic feathers of the coordinate planes can be reduced with the Smoothed-level terrain-following coordinate(T-F coordinate for short). On higher layors,coordinate planes of T-F coordinate based on trigonometric function of cos (COS coordinate for short)are horizontal with almost none errors. However,on the lower layers,thickness between planes is too small to keep the model stability.At the same time,it will bring larger calculating errors which result in bad performance of the model.Considering all above,an improved COS coordinate is designed to average the thickness of COS coordinate planes.
Ideal and real case tests are conducted with the GRAPES_Meso model using the improved COS coordinate.The results of the tests indicate that:compared with the COS coordinate, the improved COS coordinate ,on one hand ,keep the planes horizontal on the higher layers ,on the other hand, lead the distribute of the coordinate planes more uniformity , which greatly reduced the errors on the lower layers;The coordinate can reproduce in general the mountain induced gravity waves in comparison to the analytic solution. However, the shapes,vertical structures and intensity of the waves are better simulated by the improved COS coordinate, in the lower levels where the COS coordinate didn’ t behave so better. In the one-month real case tests, the improved COS coordinate gives the better results in terms of smaller forecast bias and root mean square error, and higher anomaly correlation coefficients than the COS coordinate. In conclusion, the improved COS coordinate solves the calculation problems of the COS coordinate ,and improves the prediction ability.

Keywords: GRAPES Model, Terrain-following coordinate, Dynamic Core, Numerical Modelling

©2019. Japan Geoscience Union. All Right Reserved.

Development of a parallel spherical harmonic transform library: design and performance

*Fuyuki SAITO[1]

1. Japan Agency for Marine-Earth Science and Technology

The spherical harmonic transform (SHT) is a typical method to describe the dynamical core in climate models (e.g. MIROC). SHT is a combination of two transformation: a Fourier transformation in longitude and an associate Legendre transformation in latitude. Therefore, a simple way to introduce SHT in parallel computing is to apply domain decomposition in latitudes only, involving a relocation in latitudes before/after the Legendre transformation. However, the number of maximum processors is limited by the size of latitude dimension, which is an obstacle to more efficient computing. Recently the `physics' routines in a climate model have become more and more complex and expensive, thus the heavy computation significantly suffers from the limitation. A new (yet-another) library, Flageolet, has been developed to help parallel processing of SHT in particular for climate models like MIROC, to support more flexible domain decomposition, following the approach adopted in several 3D FFT libraries and also some climate models. As a continuation of last-year's presentation, which reports the design and performance of FFT part, those of SHT part as well as transposition part between FFT and ALT are reported in this study for various sizes of domain around T213 etc, examined on the Earth simulator.

Keywords: spherical harmonic transform

©2019. Japan Geoscience Union. All Right Reserved.

Global data assimilation of multi-species satellite measurements for atmospheric chemistry analysis

*Takashi Sekiya[1], Kazuyuki Miyazaki[2,1], Koji Ogochi[1], Kengo Sudo[3,1], Masayuki Takigawa[1]

1. Japan Agency for Marine-Earth Science and Technology, 2. Jet Propulsion Laboratory/California Institute for Technology, 3. Graduate School of Environmental Studies, Nagoya University

Information on tropospheric ozone and its precursors are important for human health, ecosystem, and climate studies. The combined use of satellite measurements of ozone and its precursors has great potential to provide comprehensive information on the tropospheric chemistry system on various spatial scales. In this study, we present the results of global data assimilation of multi-species measurements (O_3, NO_2, CO, HNO_3, and SO_2) from multi-satellite sensors (OMI, GOME-2, SCIAMACHY, MOPITT, TES, and MLS) using the ensemble Kalman filter approach (Miyazaki et al., 2015). We demonstrated that increasing horizontal resolution from 2.8 to 0.56 degree is necessary for capturing high concentrations of NO_2 in the megacities, whereas 1.1-degree resolution is more suitable for optimizing tropospheric chemistry system on regional and global scales considering the current computational resources (computational cost was larger by a factor of 10 at 0.56-dgree resolution than at 1.1-degree resolution). Using the data assimilation system at 1.1-degree resolution, we constructed an updated version of tropospheric chemistry reanalysis (TCR-2; Miyazaki et al., in prep.) data for 2005—2017, which provide valuable information on decadal changes in air pollutant concentrations and emissions. The estimated NO_x emissions were strongly increased from 2005 to 2011 (+37%/decade) and decreased from 2011 to 2017 (-37%/decade) in China, while the emissions exhibited decreasing trends in Europe (-11%/decade) and the United States (-27%/decade) and an increasing trend in India (+23%/decade) during 2005—2017. A post peta-scale supercomputer such as post-K computer will facilitate the data assimilation calculation to produce tropospheric chemistry reanalysis data at 0.56-degree resolution for air pollutions on a megacity scale globally in a consistent way, which will benefit future study of atmospheric environment on various spatial scales.

Keywords: Data assimilation, Atmospheric chemistry, Atmospheric environment

©2019. Japan Geoscience Union. All Right Reserved.

The sensitivity to WRF shortwave radiation parameterizations in prediction of global horizontal irradiance for investigating interactions of atmosphere with croplands

*Ankur Srivastava[1], Sarita Kumari[1], Rajkumar Dhakar[2]

1. Indian Institute of Technology Delhi, 2. Indian Agriculture Research Institute

The present study intends to evaluate the Advanced Research Weather Research Forecating (ARW) model performance in representing the observed global horizontal irradiance (GHI) measurements while using different shortwave radiation (SWR) parameterization schemes. Two cases are considered, first case is ‘clear sky condition’ which includes model simulation of a clear/ cloudless day and second case is ‘all sky condition’ which includes model simulations of a cloudy and a rainy day. The above two cases are formulated on the basis that amount of incoming SWR will be different in each case owing to the differences in atmospheric conditions.
For the mentioned instances dates of 23rd February, 9th January and 12th March of 2016, which are clear, cloudy and rainy days respectively, are chosen for WRF model simulation. The shortwave radiation schemes that were evaluated are: Dudhia, Community Atmosphere Model (CAM), the updated Rapid Radiative Transfer Model (RRTMG), the updated Goddard and the
Goddard Fluid Dynamics Laboratory (GFDL) schemes. The model generated predictions are verified against the GHI measurements at weather station of Indian Agriculture Research Institute (IARI), New Delhi.
All schemes perform better under ‘clear sky condition’ i.e. for clear/cloudless day. For both the cases Dudhia scheme performs best with Mean Bias (MB) of 62.84 Wm^{-2} for clear day, 86.44 Wm^{-2} for cloudy day and 89.44 Wm^{-2} for rainy day. All-inclusive, the model derived predictions are over estimated in all the schemes.

Keywords: global horizontal irradiance , parameterization, shortwave radiation

©2019. Japan Geoscience Union. All Right Reserved.

The development of an atmospheric aerosol/chemistry–climate model, BCC_AGCM_CUACE2.0, and simulated effective radiative forcing of nitrate aerosols

*QI AN[1,2,4], Hua Zhang[2], Zhili Wang[2], Yi Liu[1,4], Bing Xie[3], Qianxia Liu[3], Zaizhi Wang[3], Sunling Gong[2]

1. LAGEO, IAP, CAS, 2. LaSW, CAMS, 3. NCC,CMA, 4. UCAS

As important components of total anthropogenic aerosols, nitrate aerosols have large impacts on aerosol radiative forcing and climate at regional and seasonal scales, but few current climate models coupled nitrate chemical modules online. This study developed a next-generation atmospheric aerosol/chemistry–climate model, the BCC_AGCM_CUACE2.0. Then, the performance of the model for nitrate was evaluated, and the direct radiative forcing (DRF) and effective radiative forcing (ERF) due to nitrate were simulated for the present day (2010), near future (2030) and middle future (2050) under the Representative Concentration Pathway (RCP) 4.5, 6.0, and 8.5 scenarios relative to the pre-industrial era (1850). The model reproduced the distributions and seasonal changes in nitrate loading well and simulated surface concentrations matched observations in Europe and North America. Current global mean annual loading of nitrates was predicted to increase by 1.12 mg m^{-2} relative to 1850, with the largest increases occurring in East Asia (3.89 mg m^{-2}), Europe (3.6 mg m^{-2}), and South Asia (1.86 mg m^{-2}). The current global mean annual ERF of nitrates was −0.21 W m^{-2} relative to 1850. Due to global reductions in pollutant emissions, the nitrate ERF values were predicted to decrease to −0.17 and −0.20 W m^{-2} in 2030, −0.07 and −0.18 W m^{-2} in 2050 for RCP4.5 and 6.0 relative to 1850, respectively. Under RCP8.5, nitrate ERF values were −0.24 and −0.19 W m^{-2} in 2030 and 2050, respectively. Although global mean nitrate values showed a declining trend, future nitrate loading remained high in East Asia and South Asia.

Keywords: Effective radiative forcing, Nitrate

©2019. Japan Geoscience Union. All Right Reserved.

Impacts of different types and intensities of El Niño events on winter aerosols over China

*Xiaochao Yu[1,2], Zhili Wang[2,1], Hua Zhang[2], Shuyun Zhao[3]

1. Collaborative Innovation Center on Forecast and Evaluation of Meteorological Disasters, Nanjing University of Information Science and Technology, Nanjing, 210044, China, 2. State Key Laboratory of Severe Weather and Key Laboratory of Atmospheric Chemistry of CMA, Chinese Academy of Meteorological Sciences, Beijing, 100081, China., 3. National Climate Center, China Meteorological Administration, Beijing, 100081, China

El Niño is a strong signal of interannual climate variability. The occurrence of an El Niño event may have an important impact on atmospheric pollutant concentrations in China through changes to the regional climate. This study quantitatively examines the differences among the effects of different types and intensities of El Niño events on winter mean aerosol concentration and severe haze days in China. It is found that Central Pacific (CP) El Niño events lead to larger increases in the aerosol burden over southern China relative to the same intensity of Eastern Pacific (EP) events. For El Niño events of the same type but with different intensities, moderate events induce large increases in surface aerosol concentrations over the entire eastern China, while strong and weak events lead to obvious decreases in the surface aerosol concentration over northern China. These differences are mainly attributed to changes in atmospheric circulation, with the resulting changes in aerosol mass transport occurring in response to the different types of El Niño event. Except for moderate CP events, all kinds of El Niño events lead to an increase in severe haze days in winter over northern China. Strong and weak EP El Niño events and weak CP El Niño events lead to an increase in severe haze days in winter over southern China. A change in the south-north transport of aerosols caused by El Niño events also play a dominate role in changing the occurrence of winter haze days in China.

Keywords: Eastern Pacific El Niño, Central Pacific El Niño, aerosol concentration, severe haze day

©2019. Japan Geoscience Union. All Right Reserved.

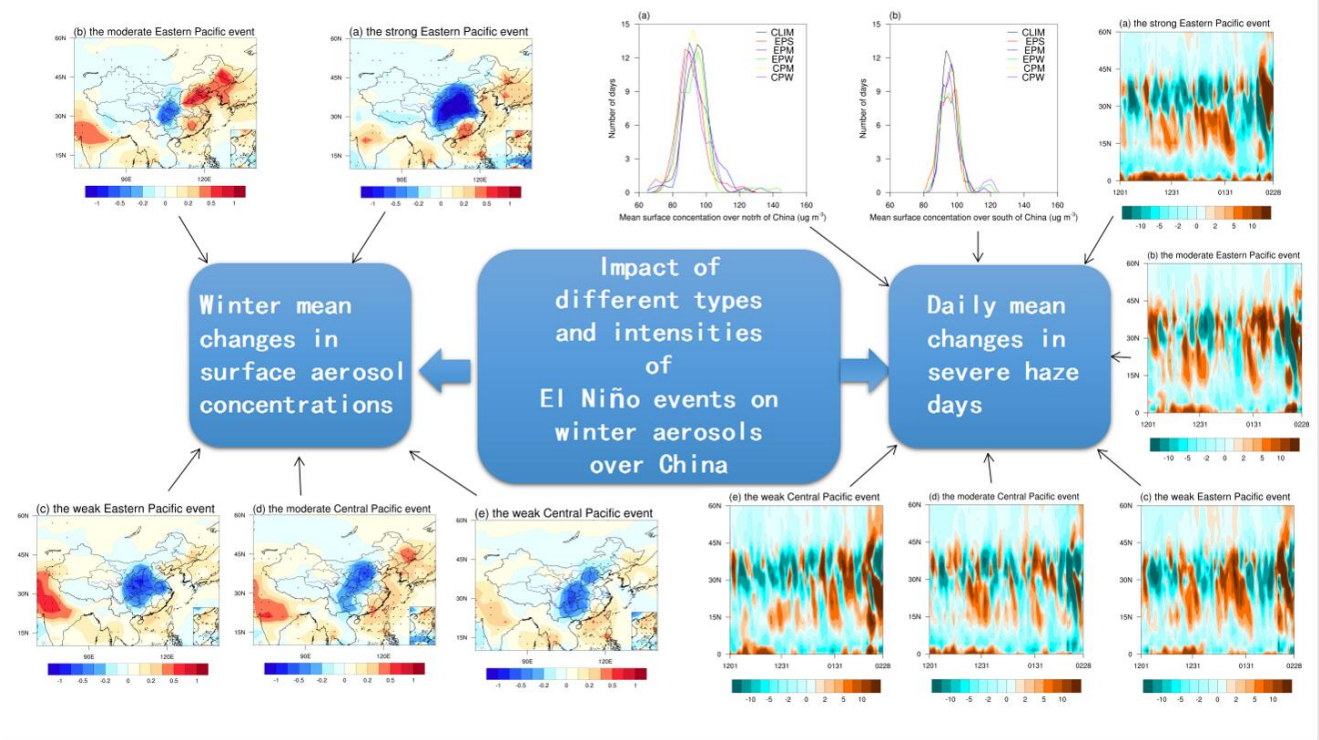

©2019. Japan Geoscience Union. All Right Reserved.

High Cloud Annual Variation and Its Responses to Global Warming in the NICAM AMIP Experiment

*Ying-Wen Chen[1], Masaki Satoh[1,2], Chihiro Kodama[2], Akira Noda[2], Yohei Yamada[2]

1. Atmospheric and Ocean Research Institute, The University of Tokyo , 2. Japan Agency for Marine-Earth Science and Technology

Uncertainties in climate sensitivity mainly come from the ambiguities in simulations of both high- and low-level clouds. The previous studies using NICAM’s short time simulation showed that the both the altitudes and amount of high clouds increase under the global warming condition, while other climate models show high cloud amount contrarily decreases.
Due to the progress in computer performance, long term climate simulation with $x < 20$ km becomes available. A pair of 25-year climate simulation (present and warming climate) with 14-km horizontal resolution (NICAM AMIP-like simulation, Kodama et al. 2015) has been performed by K computer. In this study, we analyze how the annual variation in high clouds is presented in the NICAM AMIP-like simulation. Satellite and in-situ data are used to investigate whether NICAM captures the observed responses of high clouds to the mean sea surface temperature (SST). Regressions between the high cloud amount variation and the SST variation is different with altitudes; positive regressions appear at altitudes above 100 hPa while negative regressions are found in altitudes below 100 hPa. The results are consistent with previous study based on observations (Zelinka and Hartmann 2011). Further analysis showed that the spatial pattern of high clouds is mainly associated with the El Nino response; as SST warmer, the high clouds shift in the eastern Pacific with higher. The increase of high clouds is associated with the increase of ice water content of cloud ice and snow. We argue that the response of high clouds to global warming is also explained by the change in the spatial distribution of the high clouds.

Keywords: Global Warming, Cloud-Resolving Model

©2019. Japan Geoscience Union. All Right Reserved.

Improvements in Simulating the Relationship between ENSO and East Asian Summer Rainfall in the CMIP5 Models

*Yuanhai FU[1], Riyu Lu[1]

1. IAP, CAS

There is a significant relationship between the preceding winter El Niño–Southern Oscillation (ENSO) and the subsequent East Asian summer rainfall (EASR), and this relationship is helpful for seasonal forecasting in East Asia. This study investigated the relationship between the preceding winter ENSO and EASR in the Coupled Model Intercomparison Project Phase 5 (CMIP5) models and compared the results with those from the CMIP3 models. In general, the CMIP5 models capture the ENSO–EASR relationship more realistically than the CMIP3 models. For instance, approximately two-thirds of the CMIP5 models capture the ENSO–EASR relationship, while less than one-third of the CMIP3 models capture the relationship. Further investigation suggests that the improvement could be attributed to simulating the physical processes of ENSO's impact on the EASR more realistically in the CMIP5 models, particularly the effect of ENSO on tropical Indian Ocean SST and the effect of Indian Ocean SST anomalies on the atmospheric convection over the Philippine Sea. However, there is large diversity in the ENSO–EASR relationship in the CMIP5 models, and most of the models underestimate the relationship. This underestimation comes from the underestimation of the physical processes, particularly from the underestimated impact of the atmospheric convection over the Philippine Sea on the EASR. The CMIP5 models that capture the ENSO–EASR relationship well/bad also show high/low skill in representing the physical processes.

Keywords: East Asian summer rainfall, ENSO, CMIP5 model

©2019. Japan Geoscience Union. All Right Reserved.

[J] Oral | A (Atmospheric and Hydrospheric Sciences)：A-AS Atmospheric Sciences, Meteorology & Atmospheric Environment

Wed. May 29, 2019 9:00 AM - 10:30 AM JST | Wed. May 29, 2019 12:00 AM - 1:30 AM UTC | 102 1F

[A-AS04] Atmospheric Chemistry

convener:Tomoki Nakayama(Graduate School of Fisheries and Environmental Sciences, Nagasaki University), Yoko Iwamoto(Graduate School of Biosphere Science, Hiroshima University), Sakae Toyoda(Department of Chemical Science and Engineering, Tokyo Institute of Technology), Nawo Eguchi(Kyushu University), Chairperson:Fumiko Nakagawa(名古屋大学)

This session provides a forum for the presentation of the broad spectrum of tropospheric and stratospheric chemistry, including various research topics (e.g., dynamical processes, air quality and climate), approaches (modeling, field measurements, remote sensing, and laboratory studies), and species (gas and aerosol). This session also provides an opportunity for discussing possible future collaboration with other research fields relevant to atmospheric chemistry. We strongly encourage authors to prepare presentation slides and a poster in English.

9:00 AM - 9:30 AM JST | 12:00 AM - 12:30 AM UTC

[AAS04-01] Reconstruction and fluctuation mechanism of past aerosols preserved in ice cores

★Invited Papers

*Iizuka Yoshinori[1], Ryu Uemura[2], Koji Fujita[3], Shohei Hattori[4], Osamu Seki[1], Naga Oshima[5], Hiroshi Ohno[6], Sumito Matoba[1] (1.Institite of Low Temperature Science, Hokkaido University, 2.Department of Chemistry, Biology, and Marine Science, Faculty of Science, University of the Ryukyus, 3.Graduate School of Environmental Studies, Nagoya University, 4.Department of Chemical Science and Engineering, School of Materials and Chemical Technology, Tokyo Institute of Technology,, 5.Meteorological Research Institute, 6.Kitami Institute of Technology)

9:30 AM - 9:45 AM JST | 12:30 AM - 12:45 AM UTC

[AAS04-02] The 60 years history of atmospheric formation pathways responsible for sulfate based on triple oxygen isotopic composition of sulfate preserved in SE-Dome ice core

*Shohei Hattori[1], Iizuka Yoshinori[2], Koji Fujita[3], Ryu Uemura[4], Sakiko Ishino[1], Naga Oshima[5], Nozomi Suzuki[1], Sumito Matoba[2], Asuka Tsuruta[1], Joel Savarino[6], Naohiro Yoshida[1] (1.Department of Chemical Science and Engineering, School of Materials and Chemical Technology, Tokyo Institute of Technology, 2.Institute of Low Temperature Science, Hokkaido University, 3.Graduate School of Environmental Studies, Nagoya University, Nagoya, Japan., 4.Department of Chemistry, Biology, and Marine Science, Faculty of Science, University of the Ryukyus, 5.Meteorological Research Institute, 6.Institut des Geoscience de l'Environnement, Universite Grenoble Alpes/CNRS)

9:45 AM - 10:00 AM JST | 12:45 AM - 1:00 AM UTC

[AAS04-03] Estimation of high sulfate aerosol sources in 2012 spring at Cape Hedo, Okinawa

*Syuichi Itahashi[1], Shiro Hatakeyama[2], Kojiro Shimada[3], Akinori Takami[4] (1.Central Research Institute of Electric Power Industry, 2.Center for Environmental Science in SaitamaCenter for Environmental Science in Saitama, 3.School of Creative Science and Engineering, Waseda University, 4.National Institute for Environmental Studies)

10:00 AM - 10:15 AM JST | 1:00 AM - 1:15 AM UTC

[AAS04-04] Isotopic constrains on sources and formation pathways of atmospheric nitrate in Mt. Everest

*Kun Wang[1,2,4], Shohei Hattori[2], Shichang Kang[1,3,4], Mang Lin[2], Naohiro Yoshida[2,5] (1.Northwest Institute of Eco-Environment and Resources, Chinese Academy of Sciences , 2.Department of Chemical Science and Engineering, School of Materials and Chemical Technology, Tokyo Institute of Technology, 3.CAS Center for Excellence in Tibetan Plateau Earth Sciences, 4.University of Chinese Academy of Sciences, 5. Earth-Life Science Institute, Tokyo Institute of Technology)

10:15 AM - 10:30 AM JST | 1:15 AM - 1:30 AM UTC

[AAS04-05] Development of a large volume sampling system for measuring stable isotope analysis of carbonyl sulfide and field observation

*Kazuki Kamezaki[1], Shohei Hattori[1], Naohiro Yoshida[1,2] (1.Department of Chemical Science and Engineering, School of Materials and Chemical Technology, Tokyo Institute of Technology, 4259 Nagatsuta-cho, Midori-ku, Yokohama, Kanagawa 226-8502, Japan, 2.Earth-Life Science Institute, Tokyo Institute of Technology, 2-12-1-IE-1 Ookayama, Meguro-ku, Tokyo 152-8550, Japan)

Reconstruction and fluctuation mechanism of past aerosols preserved in ice cores

*Iizuka Yoshinori[1], Ryu Uemura[2], Koji Fujita[3], Shohei Hattori[4], Osamu Seki[1], Naga Oshima[5], Hiroshi Ohno[6], Sumito Matoba[1]

1. Institite of Low Temperature Science, Hokkaido University, 2. Department of Chemistry, Biology, and Marine Science, Faculty of Science, University of the Ryukyus, 3. Graduate School of Environmental Studies, Nagoya University, 4. Department of Chemical Science and Engineering, School of Materials and Chemical Technology, Tokyo Institute of Technology,, 5. Meteorological Research Institute, 6. Kitami Institute of Technology

Ice cores can reconstruct past atmospheric environment. One of advantages for ice core archive is to reconstruct past gas and aerosols, which are important factors for evaluation of global warming. Antarctica and Greenland ice sheets have some ice domes (summit), where are useful sites for ice core drilling due to high elevation. Highland in the ice sheets can reconstruct wider emission area around the drilling sites.

At first, we will review some famous papers how reconstruct past aerosols from Antarctic dome ice cores. Antarctic dome cores can reconstruct recent 800 kyr BP, and aerosol fluctuation preserves in the cores along eight glacial-interglacial periods. Ice core community turns for obtain old ice archive in inland Antarctica (oldest ice project), so that Antarctic deep ice cores are one of topics for the ice core community.

Then, we will talk about our present project of Greenland SouthEastern Dome shallow ice core project (SE-Dome project). The SE-Dome has a huge accumulation rate (about 1.0 m water equivalent per year), where is about 4 time compared to ordinal Greenlandic dome ice cores, and 30 times to Antarctic ice cores. High accumulation dome has an advantage to reconstruct high-time resolution (e.g. seasonal scale) of recent epoch such as Anthropocene (AD 1750 to present). We obtained a 90 m ice core from the SE-Dome site in 2015, and then reconstructed aerosol fluctuations with seasonal scale from 1960 to 2014. As a result, sulfate flux responds to the decreasing trend of SOx emissions, but the nitrate flux does not follow the decrease in NOx. We have a plan in 2020 for next drilling of about 300 m ice core to reconstruct aerosol fluctuation with seasonal scale over the Anthropocene. We are looking for new joint studies using the ice core with members in the community of atmospheric chemistry.

Keywords: ice core, paleoenvironmental reconstruction, aerosol

©2019. Japan Geoscience Union. All Right Reserved.

The 60 years history of atmospheric formation pathways responsible for sulfate based on triple oxygen isotopic composition of sulfate preserved in SE-Dome ice core

*Shohei Hattori[1], Iizuka Yoshinori[2], Koji Fujita[3], Ryu Uemura[4], Sakiko Ishino[1], Naga Oshima[5], Nozomi Suzuki[1], Sumito Matoba[2], Asuka Tsuruta[1], Joel Savarino[6], Naohiro Yoshida[1]

1. Department of Chemical Science and Engineering, School of Materials and Chemical Technology, Tokyo Institute of Technology, 2. Institute of Low Temperature Science, Hokkaido University, 3. Graduate School of Environmental Studies, Nagoya University, Nagoya, Japan., 4. Department of Chemistry, Biology, and Marine Science, Faculty of Science, University of the Ryukyus, 5. Meteorological Research Institute, 6. Institut des Geoscience de l’Environnement, Universite Grenoble Alpes/CNRS

The atmospheric sulfate is important for both climate change and air quality; it influences radiation forcing and cloud’s lifetime, and accounts for major components in fine particulate matter mass in urban regions with affecting visibility and public health. The emitted SO_2 is oxidized by OH radicals in the gas-phase, but modeling studies suggest that the large proportions (~80%) of global sulfate production were occurred in the aqueous-phase. However, the treatment of aqueous-phase in cloud pH set in atmospheric chemistry-transport models had the largest impact for atmospheric sulfate concentrations. Due to the lack of critical understanding for the chemical processes responsible for sulfate production, it is difficult to predict future changes in [SO_4^{2-}] and its effects on climate and air quality.

To help address this, here we use mass-independent oxygen isotopic composition ($\Delta^{17}O$) of sulfate providing insight into past oxidation pathways responsible for sulfate formation. We present $\Delta^{17}O$ of SO_4^{2-} obtained from a 90.45 m depth ice core drilled at a high-elevation dome site in southeast Greenland called SE-Dome, covering the last 60 years. We found that $\Delta^{17}O$ of SO_4^{2-} with low during the 1960s-1970s and high in after the 2000s. This increase in $\Delta^{17}O$ of SO_4^{2-} indicates that sulfate formation pathways responsible for sulfate changed after 1960 to the present along with declining SO_2 emission. In the presentation, we will discuss the enhanced role of a oxidation processes contributing to increase $\Delta^{17}O$ of SO_4^{2-}, and its implication to the changes in atmospheric chemistry though the changes in anthropogenic activities. This provides insight into direct and indirect effects of anthropogenic activities to the air quality by changing sulfate formation pathways. These functions, so called “chemical feedback", should be considered for making efficient mitigation policy for climate change and air quality by controlling emission of anthropogenic pollutants.

Keywords: stable isotope, Sulfate, Triple oxygen isotopes, Chemical feedback

©2019. Japan Geoscience Union. All Right Reserved.

Estimation of high sulfate aerosol sources in 2012 spring at Cape Hedo, Okinawa

*Syuichi Itahashi[1], Shiro Hatakeyama[2], Kojiro Shimada[3], Akinori Takami[4]

1. Central Research Institute of Electric Power Industry, 2. Center for Environmental Science in SaitamaCenter for Environmental Science in Saitama, 3. School of Creative Science and Engineering, Waseda University, 4. National Institute for Environmental Studies

Air quality in Asia can cause regional-to-global environmental issues. Intensive observation campaigns approximately 1 week long have been conducted periodically from March 2010 to November 2015 at Cape Hedo, Okinawa, Japan. The period-averaged sulfate aerosol (SO_4^{2-}) concentrations for each campaign ranged from 0.34 to 6.97 $\mu g\ m^{-3}$, and the average concentration of all observations was 3.13 $\mu g\ m^{-3}$. The maximum daily mean concentrations surpassed 15 $\mu g\ m^{-3}$ in springtime 2012. The sources of this high SO_4^{2-} concentrations were estimated by using the air quality model with the tagged tracer method in this study. The main source of the high SO_4^{2-} concentrations in March was volcanoes and that in April was anthropogenic emissions from China. In March, the prevailing northerly wind transported a volcanic SO_2 plume with a low conversion ratio to Cape Hedo. The impacts of 15 volcanoes in Japan were estimated in this study, and a substantial impact of Sakurajima, which accounted for more SO_2 than anthropogenic emissions from Japan, was found. Throughout April, source apportionments from anthropogenic emissions from China were found; hence, the source was further divided into 31 provincial scales. Shandong and Jiangsu provinces, which are the first and seventh largest emission sources in China, were identified as important sources at Cape Hedo. These sources showed day-to-day variation, and the highest contribution from Shandong province was on April 23, whereas that from Jiangsu province was on April 22.

Keywords: Sulfate aerosol, Source contribution, Air quality model

©2019. Japan Geoscience Union. All Right Reserved.

Isotopic constrains on sources and formation pathways of atmospheric nitrate in Mt. Everest

*Kun Wang[1,2,4], Shohei Hattori[2], Shichang Kang[1,3,4], Mang Lin[2], Naohiro Yoshida[2,5]

1. Northwest Institute of Eco-Environment and Resources, Chinese Academy of Sciences , 2. Department of Chemical Science and Engineering, School of Materials and Chemical Technology, Tokyo Institute of Technology, 3. CAS Center for Excellence in Tibetan Plateau Earth Sciences, 4. University of Chinese Academy of Sciences, 5. Earth-Life Science Institute, Tokyo Institute of Technology

Studies on the sources and formation pathways of nitrate is crucial to better understand nitrogen cycle and atmospheric oxidation capacity. Tibetan Plateau (TP) and surroundings, referred to as the Third Pole and “Asia water tower”, contain the largest number of glaciers outside the polar regions and are largely experiencing shrinkage. A complete understanding on the source and formation mechanisms of atmospheric nitrate in the TP is important to indicate the impact of human activities on the environment and also crucial to investigate nitrogen cycle in glacier-hydrology systems of this region. Besides, it can supply information on interpreting ice core records to understand the past atmosphere chemistry. Here we collected aerosol samples from the Everest through pre-monsoon (April-May) and monsoon season (June-August) in 2018, and measured for the first time the isotopic compositions ($\delta^{15}N$, $\delta^{18}O$ and $\Delta^{17}O$) of nitrate in this region, allowing insights into their sources and potential formation mechanism. The results show that the seasonal variations in both $\delta^{15}N$ and $\Delta^{17}O$ values have a similar trends with maximum during pre-monsoon season and minimum during monsoon season. The relatively high values of $\delta^{15}N$ in pre-monsoon seasons, maybe indicate the enhanced contribution from fossil fuel combustions in South Asia which can be transported to our sampling sites across the Himalayas by the mountain/valley wind system. The $\Delta^{17}O$ (NO_3^-) value, which is dependent on both the $\Delta^{17}O$ (NO_2) value and the oxidation pathways (O_3 and OH) of NO_2 to NO_3^-, show that the O_3 oxidation pathway is dominant during pre-monsoon season, resulting in higher values of both $\delta^{18}O$ and $\Delta^{17}O$. In contrast, during monsoon season, formation involving HO_2/RO_2 radicals becomes important, producing lower values of $\delta^{18}O$ and $\Delta^{17}O$. To better understand the oxidation process of past atmosphere in the Everest region, observations of oxygen-17 excess of nitrate and sulfate in ice cores collected from this region in the future are recommended.

Keywords: Atmospheric nitrate, the Everest, Isotope, Aerosol, Oxidation pathways

©2019. Japan Geoscience Union. All Right Reserved.

Development of a large volume sampling system for measuring stable isotope analysis of carbonyl sulfide and field observation

*Kazuki Kamezaki[1], Shohei Hattori[1], Naohiro Yoshida[1,2]

1. Department of Chemical Science and Engineering, School of Materials and Chemical Technology, Tokyo Institute of Technology, 4259 Nagatsuta-cho, Midori-ku, Yokohama, Kanagawa 226-8502, Japan, 2. Earth-Life Science Institute, Tokyo Institute of Technology, 2-12-1-IE-1 Ookayama, Meguro-ku, Tokyo 152-8550, Japan

Carbonyl sulfide (OCS) is the most abundant sulfur-containing gas in the ambient atmosphere, with an average mixing ratio of 500 parts per trillion (ppt) by volume in the troposphere. OCS is suggested as a sulfur source of the stratospheric sulfate aerosols (SSA) which plays an important role for Earth of radiation budget and for ozone depletion. Moreover, since leaves consume OCS whenever they are assimilating CO_2 with same process but plant does not emit OCS to atmosphere by respiration, OCS provides a means to partition net ecosystem exchange into gross primary production (GPP) and respiration on land. Nevertheless, current figures for tropospheric OCS sources and sinks carry large uncertainties.

Isotope analysis is a useful tool to trace sources and transformations of trace gases. Very recently, Angert et al. (2019 Sci. Rep.) reported $d^{34}S$ value at Israel and Canary Island for tropospheric OCS using a gas chromatograph (GC)/multi collector-inductively coupled plasma mass spectrometer (MC-ICP-MS). For the measurement of sulfur isotope ratios of OCS in our laboratory, an online method measuring on a GC/isotope ratio (IR)-MS using S^+ fragmentation ions had been developed (Hattori et al., 2015). This method supports simple analysis of sulfur isotopic compositions of OCS over 8 nmol. However, application this method for atmospheric samples has yet to be done by this GC/IR-MS method, because of the large sample amounts that are necessary (i.e. 500 L of 500 pmol mol^{-1} OCS). Therefore, we developed a large volume air sampling system to apply S^+ IR-MS method for atmospheric samples and we observed $d^{34}S$ value in Suzukakedai campus at Yokohama (Kamezaki et al., 2019 Atmos. Meas. Tech.).

We will discuss the difference between the result of Angert et al. (2019) and our observation. Additionally, we also report the result in field campaign using our developed method.

Keywords: Carbonyl sulfide, Sulfur isotope, atmospheric trace components

©2019. Japan Geoscience Union. All Right Reserved.

[J] Oral | A (Atmospheric and Hydrospheric Sciences)：A-AS Atmospheric Sciences, Meteorology & Atmospheric Environment

Wed. May 29, 2019 1:45 PM - 3:15 PM JST | Wed. May 29, 2019 4:45 AM - 6:15 AM UTC | 102 1F

[A-AS04] Atmospheric Chemistry

convener:Tomoki Nakayama(Graduate School of Fisheries and Environmental Sciences, Nagasaki University), Yoko Iwamoto(Graduate School of Biosphere Science, Hiroshima University), Sakae Toyoda(Department of Chemical Science and Engineering, Tokyo Institute of Technology), Nawo Eguchi(Kyushu University), Chairperson:Takashi Maki(気象研究所)

This session provides a forum for the presentation of the broad spectrum of tropospheric and stratospheric chemistry, including various research topics (e.g., dynamical processes, air quality and climate), approaches (modeling, field measurements, remote sensing, and laboratory studies), and species (gas and aerosol). This session also provides an opportunity for discussing possible future collaboration with other research fields relevant to atmospheric chemistry. We strongly encourage authors to prepare presentation slides and a poster in English.

1:45 PM - 2:00 PM JST | 4:45 AM - 5:00 AM UTC

[AAS04-06] Observations of aerosol optical properties by sky radiometers at SKYNET Southeast and South Asian sites

*Al Mashroor Fatmi[1], Hitoshi Irie[1], Hossain Mohammed Syedul Hoque[1], Alessandro Damiani[1], Pradeep Khatri[2], Tamio Takamura[1], Thanawat Jurupongsaku[3], Govindan Pandithurai[4] (1.Center for Environmental Remote Sensing Chiba University , 2.Tohoku University, 3.Chulalongkorn University, 4.Indian Institute of Tropical Metereology)

2:00 PM - 2:15 PM JST | 5:00 AM - 5:15 AM UTC

[AAS04-07] Analysis of factors causing variations in the absorption Ångström exponent of aerosols in Japan using skyradiometers

*Kodai Yamaguchi[1], Hitoshi Irie[1], Pradeep Khatri[2], Toshihiko Takemura[3], Hirokazu Yamamoto[4] (1.Chiba University, 2.Tohoku University, 3.Kyushu University, 4.National Institute of Advanced Industrial Science and Technology)

2:15 PM - 2:30 PM JST | 5:15 AM - 5:30 AM UTC

[AAS04-08] Sources of atmospheric black carbon and related carbonaceous components at Rishiri Island, Japan

*Chunmao Zhu[1], Yugo Kanaya[1], Hisayuki Yoshikawa[2], Tomohisa Irino[2], Osamu Seki[2], Yasunori Tohjima[3] (1.Japan Agency for Marine-Earth Science and Technology, 2.Hokkaido University, 3.National Institute for Environmental Studies)

2:30 PM - 2:45 PM JST | 5:30 AM - 5:45 AM UTC

[AAS04-09] Black Carbon and Inorganic Aerosols in Snowpack over the Arctic

*Tatsuhiro Mori[1], Kumiko Goto-Azuma[2,3], Yutaka Kondo[2], Yoshimi Ogawa-Tsukagawa[2], Kazuhiko Miura[1], Motohiro Hirabayashi[2], Naga Oshima[4], Makoto Koike[5], Kaarle Kupiainen[6], Nobuhiro Moteki[5], Sho Ohata[7], Sinha Puna Ram[8], Konosuke Sugiura[9], Teruo Aoki[10], Martin Schneebeli[11], Konrad Steffen[11], Atsushi Sato[12], Akane Tsushima[13], Vladimir Makarov[14], Satoshi Omiya[15,16], Atsuko Sugimoto[17], Shinya Takano[17] (1.Tokyo University of Science, 2.National Institute of Polar Research, 3.The Graduate University for Advanced Studies, 4.Meteorological Research Institute, 5.Depertment of Earth and Planetary Science, Graduate School of Science, The University of Tokyo, 6.Environmental Protection Department Ministry of the Environment, 7.Institute for Space–Earth Environmental Research (ISEE), Nagoya University, 8.Department of Space Indian Space Research Organization, 9.University of Toyama, 10.Okayama University, 11.WSL Institute for Snow and Avalanche Research, 12.former Snow and Ice Research Center, 13.Reserach Institute for Humanity and Nature, 14.Melnikov's Permafrost Institute, 15.Institute of Low Temperature Science, Hokkaido University, 16.Civil Engineering Research Institute for Cold Region, 17.Graduate School of Environmental Science, Hokkaido University)

2:45 PM - 3:00 PM JST | 5:45 AM - 6:00 AM UTC

[AAS04-10] The single-particle extinction and scattering method for online characterization of submicron particles: Principles and applications to aerosol research

*Nobuhiro Moteki[1] (1.The Univerisity of Tokyo)

3:00 PM - 3:15 PM JST | 6:00 AM - 6:15 AM UTC

[AAS04-11] High spatial resolution vehicular emissions inventory for China using VEIN model

*Sergio Ibarra Espinosa[1], Xuelei Zhang[1], Aijun Xiu[1], Edmilson Dias de Freitas[2] (1.Research Group of Regional Atmospheric Environment, Northeast Institute of Geography and Agroecology, Chinese Academy of Sciences, P. R. China, 2.Department of Atmospheric Sciences, University of São Paulo, Brazil.)

Observations of aerosol optical properties by sky radiometers at SKYNET Southeast and South Asian sites

*Al Mashroor Fatmi[1], Hitoshi Irie[1], Hossain Mohammed Syedul Hoque[1], Alessandro Damiani[1], Pradeep Khatri[2], Tamio Takamura[1], Thanawat Jurupongsaku[3], Govindan Pandithurai[4]

1. Center for Environmental Remote Sensing Chiba University , 2. Tohoku University, 3. Chulalongkorn University, 4. Indian Institute of Tropical Metereology

Direct and scattered sunlight measurements using sky radiometers were performed at two SKYNET sites –Phimai (15.18˚N, 102.56˚E) in Thailand and New Delhi (28.63˚N, 77.17˚E) in India. Phimai is a rural site and during the dry season (January to April), the site is affected by biomass burning. New Delhi is an urban site and expected to be influenced by vehicular and industrial emissions and agricultural waste burning. Depending on the data availability, aerosol optical properties during the year 2012 and 2016 were analyzed for New Delhi and Phimai, respectively. During the dry season in 2016 at Phimai, enhanced aerosol absorption optical depth (AAOD) was observed corresponding to the influence of biomass burning. The wavelength dependence of AAOD was quantified using the absorption Ångström exponent (AAE). The mean AAE at Phimai during the dry season in 2016 was 1.5±0.2, indicating the presence of organic brown carbon aerosols. This was consistent with coincident multi-axis differential absorption spectroscopy measurements showing higher concentration of organic compounds (formaldehyde and glyoxal) during the dry season, corresponding to biomass burning. At New Delhi, the mean AAE values during winter (December ~ February) and monsoon season (June ~ August) were 1.51±0.23 and 0.88± 0.24, respectively. The higher AAE during winter indicates the significant injection of organic brown carbon, probably due to transportation of carbonaceous materials from agricultural waste burning from Northern India. Thus, deduction of AAE, retrieved through sky radiometers observations, is expected to be useful for better understanding the physical and optical properties of light absorbing organic aerosols.

©2019. Japan Geoscience Union. All Right Reserved.

Analysis of factors causing variations in the absorption Ångström exponent of aerosols in Japan using skyradiometers

*Kodai Yamaguchi[1], Hitoshi Irie[1], Pradeep Khatri[2], Toshihiko Takemura[3], Hirokazu Yamamoto[4]

1. Chiba University, 2. Tohoku University, 3. Kyushu University, 4. National Institute of Advanced Industrial Science and Technology

Aerosols have brought the most significant uncertainty in predicting future climate change. To reduce the uncertainty, it is essential to better understand the optical properties of aerosols. Organic aerosols and mineral dust, which are the main aerosols, have been considered to cause only a weak light absorption, and their radiative forcing has been negative in most climate models. However, recent laboratory experiments and observations indicated that there should be aerosols (such as brown carbon) causing a strong light absorption in particular in the ultraviolet-to-visible wavelength regions. Although the Absorption Ångström exponent (AAE) was used as a useful index for representing the wavelength dependence of such light absorption, its observation has been limited. Under this circumstance, we made long-term observations using skyradiometers of SKYNET at 6 sites in Japan (Chiba, Fukue, Kasuga, Miyakojima, Sendai, and Takayama). Using our newly developed analysis algorithm package (SR-CEReS), we retrieved AAE values for the 6 sites to investigate factors causing their variations. While the theoretical AAE value of black carbon is considered to be unity, our analysis shows that the annual averages of AAE were in the range from 1.15 to 1.51, indicating the presence of aerosols having strong light absorption in the ultraviolet-to-visible wavelength regions at all the 6 sites. Moreover, urban sites tended to show higher AAE values. We additionally analyzed nitrogen dioxide and sulfur dioxide concentration data taken by the Multi-Axis Differential Optical Absorption Spectroscopy (MAX-DOAS) observations, which were conducted simultaneously with the skyradiometer. Then, it was suggested that the AAE could be enhanced by emissions from ships, factories, or steelworks.

Keywords: Aerosol, Skyradiometer, Absorption Ångström exponent (AAE)

©2019. Japan Geoscience Union. All Right Reserved.

Sources of atmospheric black carbon and related carbonaceous components at Rishiri Island, Japan

*Chunmao Zhu[1], Yugo Kanaya[1], Hisayuki Yoshikawa[2], Tomohisa Irino[2], Osamu Seki[2], Yasunori Tohjima[3]

1. Japan Agency for Marine-Earth Science and Technology, 2. Hokkaido University, 3. National Institute for Environmental Studies

A field study was conducted to clarify sourcesof atmospheric black carbon and related carbonaceous components at Rishiri Island, Japan. We quantified equivalent black carbon (eBC) particle mass and the absorption Ångström exponent (AAE), atmospheric CO and CH_4, in addition to levoglucosan in total suspended particles, a typical tracer of biomass burning. Sixteen high eBC events were identified attributable to either anthropogenic sources or biomass burning in Siberia/China. These events were often accompanied by increases of co-emitted gases such as $CH_4$and CO. Specifically, we observed pollution events with elevated eBC, AAE, levoglucosan, and CH_4–CO slope in late July 2014, which were attributed to forest fires in Siberia by reference to the FLEXPART model footprint and fire hotspots. In autumn, drastic increases of eBC, AAE, and levoglucosan were observed, accompanied by an eBC–CO slope of >15 ng m^{-3}/ppb, resulting from long-range transport of emissions from extensive burning of crop residue on the Northeast China Plain. Other than the sources of fossil fuel combustion in China and forest fires in Siberia, we also report that pollution events in northern Japan are caused by crop residue burning in China. This study elucidated valuable information that will improve understanding of the effects of biomass burning in East Asia on atmospheric carbonaceous components.

Keywords: Aerosols, Biomass burning, Levoglucosan, Black carbon, FLEXPART

©2019. Japan Geoscience Union. All Right Reserved.

Black Carbon and Inorganic Aerosols in Snowpack over the Arctic

*Tatsuhiro Mori[1], Kumiko Goto-Azuma[2,3], Yutaka Kondo[2], Yoshimi Ogawa-Tsukagawa[2], Kazuhiko Miura[1], Motohiro Hirabayashi[2], Naga Oshima[4], Makoto Koike[5], Kaarle Kupiainen[6], Nobuhiro Moteki[5], Sho Ohata[7], Sinha Puna Ram[8], Konosuke Sugiura[9], Teruo Aoki[10], Martin Schneebeli[11], Konrad Steffen[11], Atsushi Sato[12], Akane Tsushima[13], Vladimir Makarov[14], Satoshi Omiya[15,16], Atsuko Sugimoto[17], Shinya Takano[17]

1. Tokyo University of Science, 2. National Institute of Polar Research, 3. The Graduate University for Advanced Studies, 4. Meteorological Research Institute, 5. Depertment of Earth and Planetary Science, Graduate School of Science, The University of Tokyo, 6. Environmental Protection Department Ministry of the Environment, 7. Institute for Space–Earth Environmental Research (ISEE), Nagoya University, 8. Department of Space Indian Space Research Organization, 9. University of Toyama, 10. Okayama University, 11. WSL Institute for Snow and Avalanche Research, 12. former Snow and Ice Research Center, 13. Reserach Institute for Humanity and Nature, 14. Melnikov’s Permafrost Institute, 15. Institute of Low Temperature Science, Hokkaido University, 16. Civil Engineering Research Institute for Cold Region, 17. Graduate School of Environmental Science, Hokkaido University

Black carbon (BC) deposited on snow lowers snow albedo, potentially contributing to the warming in the Arctic. The distributions of inorganic aerosols (ions), which contribute to direct and indirect aerosol effects, are also greatly influenced by deposition. It is critically important to measure the spatial distributions of BC and ions in snowpack in different regions of the Arctic to quantify these effects. Because accurate measurements of BC and ions in snowpack are very limited, we measured the mass concentrations of size-resolved BC (C_{MBC}) and ions in snowpack over Finland, Alaska, Siberia, Greenland, and Spitzbergen in early spring during the period of 2012 –2016 by using a single-particle soot photometer and ion chromatography, respectively. BC deposition amounts (DEP_{MBC}) during snow accumulation periods were derived from C_{MBC} and snow water equivalent (SWE). Detailed analyses have shown that the spatial distributions of the anthropogenic BC flux and topography strongly influenced the latitudinal variations of C_{MBC} and BC size distributions. The average size distributions of BC in snowpack shifted to smaller sizes with the decrease in C_{MBC}, likely due to an increase in the removal efficiency of BC with the increase in BC diameter during transport from major BC sources. The present C_{MBC} were much lower than previous C_{MBC} measured by using an Integrating Sphere/Integrating Sandwich spectrophotometer by a factor of about 13. The present accurate data of C_{MBC}, SWE, and DEP_{MBC} are very useful in constraining climate model to estimate the effect of BC on the climate of the Arctic.

Keywords: Black carbon, Wet deposition, Arctic

©2019. Japan Geoscience Union. All Right Reserved.

The single-particle extinction and scattering method for online characterization of submicron particles: Principles and applications to aerosol research

*Nobuhiro Moteki[1]

1. The Univerisity of Tokyo

We will introduce the single-particle extinction and scattering (SPES) method as a new fundamental tool for online measurements of submicron particles and its applications to aerosol research. The SPES method accurately determines the amplitude and phase of the forward-scattered wave from a single particle on the basis of the interference patterns between the scattered and the incident fields when the particle traverses a tightly-focused laser beam. The complex refractive index and volume of the detected particle can be estimated from the SPES data using our original data-processing algorithm. In the presentation, we will talk about the measurement principle, the theoretical framework of data analysis including the potential effects of particle shape, the performance tests, and some applications to black carbon and mineral particles.

Keywords: aerosol, dust, black carbon, biological particles, marine suspended particles, measurement technique

©2019. Japan Geoscience Union. All Right Reserved.

High spatial resolution vehicular emissions inventory for China using VEIN model

*Sergio Ibarra Espinosa[1], Xuelei Zhang[1], Aijun Xiu[1], Edmilson Dias de Freitas[2]

1. Research Group of Regional Atmospheric Environment, Northeast Institute of Geography and Agroecology, Chinese Academy of Sciences, P. R. China, 2. Department of Atmospheric Sciences, University of São Paulo, Brazil.

Vehicular emissions are an important source of pollution in China. These and other anthropocentric emissions, with poor meteorological conditions enhance critic episodes of high concentrations of air pollutants (Wang S. and Hao J., 2012). Environmental policies seeks to improve air quality by diminishing and cutting emissions, making the emissions characterization of crucial importance. Even more, air quality modelers needs emissions inventories as inputs, which usually suffer of limited temporal and spatial representation and over simplification. Under these circumstances, it is not expected good air quality simulations. I other words, garbage-in, garbage-out.

This study aims to improve the temporal and spatial representation of vehicular emissions. This will be achieve using the VEIN model (Ibarra-Espinosa *et al.,* 2017), initially with a top-down approach. The method and data is described as follows: stock vehicles will be obtained for 31 provinces (National Bureau of Statistics (NBS), 2016) considering vehicle survival pattern and average age of use of the fleet (HAO *et al*, 2011; Wang H. *et al*, 2012). NBS data is aggregated without discriminating taxis and motorcycles, therefore, the vehicular composition and activity will be obtained with the percentages of Wang H. *et* al, (2008): Passenger Cars (PC), Taxi, Motorcycle, Moped, Bus, Small Trucks, Medium Trucks and Heavy Trucks by type of fuel. Furthermore, we will divide traffic at peak and off peak hours and by Freeways, Arterial and residential roads, shown on Fig.1, in each province to obtain the representative speed in each case, based on the driving cycles obtained by Wang Q. *et al*, (2008). We will use Copert (Ntziachristos and Samaras, 2016) emissions factors inside VEIN correcting by chemical composition of fuel and deterioration factors. Cold starts and evaporative emissions will be obviously included. To ensure consistency with the emissions and fuel consumed on each province, activity will be calibrated in order that fuel consumption estimation or CO_2 estimations matches with statistics of automotive fuel sales or CO_2 emissions, depending on the availability of data. Top-down emissions will be spatially dis-aggregated by length of type of road from OpenStreetMap in each province as shown by Andrade *et al*, (2015).

Vehicular, Emissions, VEIN, China

REFERENCES

Andrade, M. D. F., Ynoue, R. Y., Freitas, E. D., Todesco, E., Vara Vela, A., Ibarra, S., ... & Carvalho, V. S. B. (2015). Air quality forecasting system for Southeastern Brazil. Frontiers in environmental Science, 3, 9.

Wang, S., & Hao, J. (2012). Air quality management in China: Issues, challenges, and options. Journal of

©2019. Japan Geoscience Union. All Right Reserved.

Environmental Sciences, 24(1), 2-13.

Hao, H., Wang, H., Ouyang, M., & Cheng, F. (2011). Vehicle survival patterns in China. Science China Technological Sciences, 54(3), 625-629.

Wang, H., Chen, C., Huang, C., & Fu, L. (2008). On-road vehicle emission inventory and its uncertainty analysis for Shanghai, China. Science of the Total Environment, 398(1-3), 60-67.

Wang, Q., Huo, H., He, K., Yao, Z., & Zhang, Q. (2008). Characterization of vehicle driving patterns and development of driving cycles in Chinese cities. Transportation research part D: Transport and Environment, 13(5), 289-297.

Ntziachristos, L. and Samaras, Z. (2016): EMEP/EEA emission inventory guidebook; Road Transport: Passenger cars, Light commercial trucks, Heavy-duty vehicles including buses and Motorcycles, European Environment Agency, Copenhagen.

Keywords: Vehicular emissions, VEIN, China

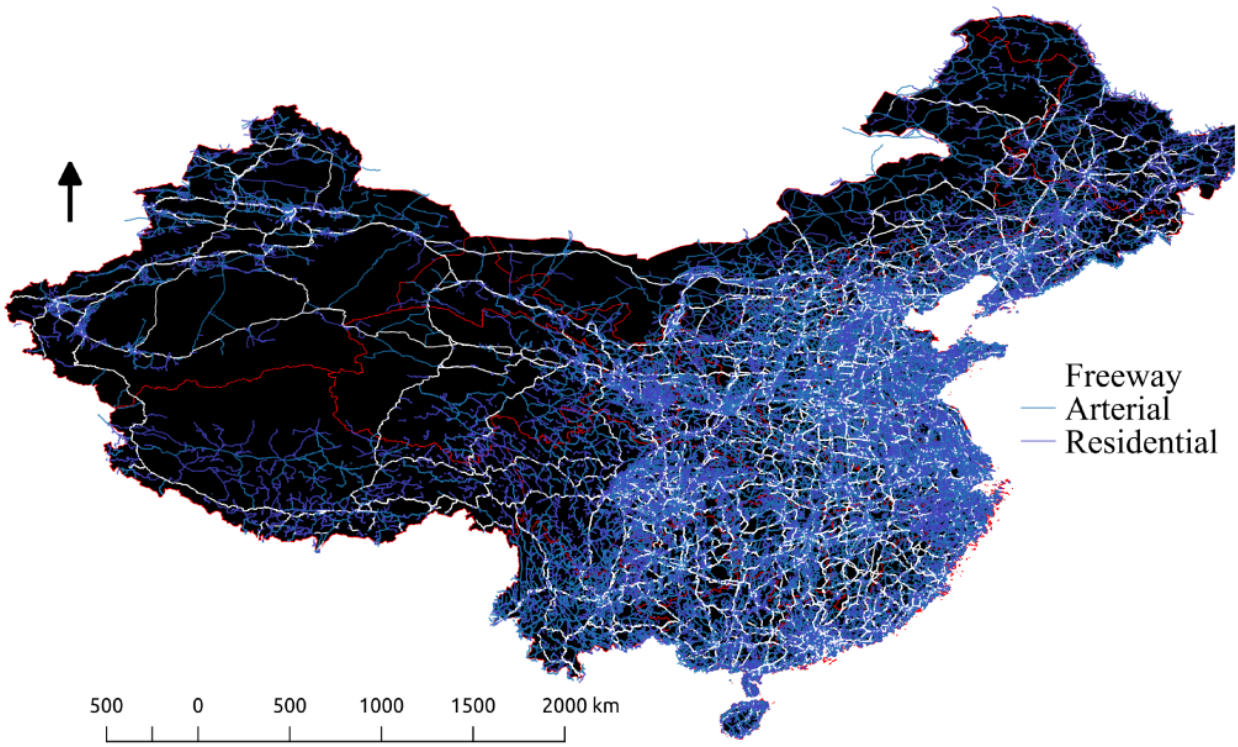

©2019. Japan Geoscience Union. All Right Reserved.

[J] Oral | A (Atmospheric and Hydrospheric Sciences)：A-AS Atmospheric Sciences, Meteorology & Atmospheric Environment

Wed. May 29, 2019 3:30 PM - 5:00 PM JST | Wed. May 29, 2019 6:30 AM - 8:00 AM UTC | 102 1F

[A-AS04] Atmospheric Chemistry

convener:Tomoki Nakayama(Graduate School of Fisheries and Environmental Sciences, Nagasaki University), Yoko Iwamoto(Graduate School of Biosphere Science, Hiroshima University), Sakae Toyoda(Department of Chemical Science and Engineering, Tokyo Institute of Technology), Nawo Eguchi(Kyushu University), Chairperson:Kentaro Ishijima(気象研究所)

This session provides a forum for the presentation of the broad spectrum of tropospheric and stratospheric chemistry, including various research topics (e.g., dynamical processes, air quality and climate), approaches (modeling, field measurements, remote sensing, and laboratory studies), and species (gas and aerosol). This session also provides an opportunity for discussing possible future collaboration with other research fields relevant to atmospheric chemistry. We strongly encourage authors to prepare presentation slides and a poster in English.

3:30 PM - 4:00 PM JST | 6:30 AM - 7:00 AM UTC

[AAS04-12] Effect of land use change on GHG fluxes of tropical peat forests in Borneo island

★Invited Papers

*Ryuichi Hirata[1], Habura Borjigin[1], Tomohiro Shiraishi[1], Takashi Hirano[2], Lulie Melling[3] (1.National Institute for Environmental Studies, 2.Hokkaido University, 3.Sarawak Tropical Peat Research Institute)

4:00 PM - 4:30 PM JST | 7:00 AM - 7:30 AM UTC

[AAS04-13] Remote sensing of carbon assimilation function of terrestrial ecosystem by Earth-observation satellite

★Invited Papers

*Hibiki M Noda[1], Yukio Yoshida[1], Haruki Oshio[1], Tomoki Kiyono[1], Tatsuya Miyauchi[1], Tsuneo Matsunaga[1] (1.NIES National Institute of Environmental Studies)

4:30 PM - 4:45 PM JST | 7:30 AM - 7:45 AM UTC

[AAS04-14] Analysis of the carbon dioxide in the upper troposphere and lower stratosphere by the data from GOSAT TANSO-FTS TIR

*Nawo Eguchi[1], Akihiro Honda[1], Naoko Saitoh[2], Yosuke Niwa[3] (1.Kyushu University, 2.Chiba University, 3.National Institute for Environmental Studies)

4:45 PM - 5:00 PM JST | 7:45 AM - 8:00 AM UTC

[AAS04-15] Seasonal and interannual variations of the Atmospheric Potential Oxygen over the Western North Pacific observed by using a cargo aircraft C-130H

*Shigeyuki Ishidoya[1], Kazuhiro Tsuboi[2], Yosuke Niwa[3], Shohei Murayama[1], Hidekazu Matsueda[2], Yousuke Sawa[2], Nobuyuki Aoki[1], Kentaro Ishijima[2], Kentaro Kozumi[4], Genta Umezawa[4], Kazuya Yukita[4], Shigeharu Nishida[4], Megumi Yamamoto[4] (1.National Institute of Advanced Industrial Science and Technology (AIST), 2.Meteorological Research Institute, 3.National Institute for Environmental Studies, 4.Japan Meteorological Agency)

Effect of land use change on GHG fluxes of tropical peat forests in Borneo island

*Ryuichi Hirata[1], Habura Borjigin[1], Tomohiro Shiraishi[1], Takashi Hirano[2], Lulie Melling[3]

1. National Institute for Environmental Studies, 2. Hokkaido University, 3. Sarawak Tropical Peat Research Institute

Borneo island, which is located in southeast Asia, has a rich forest and it store a huge carbon in biomass and soil. It is well known that peat, which is large carbon reservoir, widely spreads in the island. While tropical peat forest occupies only 0.25% of surface area on globe, it accounts 3% of soil organic carbon on earth. Tropical peat forest, in which forest grows on peat which depth from 1 to 10 m. Recently, the area of tropical peat forest is rapidly decreasing because of fire or plantation and has resulted in large carbon lost. Therefore, carbon management and control for tropical peat forest is very important with the objective of development, conservation and disaster prevention. In this study, we will introduce the studies to evaluate the effects of land use change on greenhouse gas fluxes of tropical peat lands from site scale to regional scale various methods i.e. flux observation of eddy covariance and chamber methods, remote sensing and numerical simulation under several projects.

Keywords: flux observation, remote sensing, model

©2019. Japan Geoscience Union. All Right Reserved.

Remote sensing of carbon assimilation function of terrestrial ecosystem by Earth-observation satellite

*Hibiki M Noda[1], Yukio Yoshida[1], Haruki Oshio[1], Tomoki Kiyono[1], Tatsuya Miyauchi[1], Tsuneo Matsunaga[1]

1. NIES National Institute of Environmental Studies

Since industrial evolution, global warming has progressed owing to increase of CO_2 emitted by human activities. To deal effectively with this issue by mitigation and adaptation, it is necessary to monitor emission and sequestration of GHGs with their underlying mechanisms including biogeochemical processes. Plant photosynthesis is one of the important factors to drive carbon cycling between atmosphere and biosphere. The terrestrial ecosystems assimilate about 30 % of anthropogenic CO_2 through photosynthesis. Since the photosynthetic process is quite sensitive to climatic conditions such as temperature, radiation and precipitation, there are still uncertainty in the estimation of photosynthetic production of regional to global scale. This uncertainty would be lager under climate change condition in near future. Thus, it is necessary to obtain the temporal dynamics of the photosynthetic production in large area.
Satellite remote sensing has been used to monitor the spatial and temporal dynamics of terrestrial ecosystems that are responsible for such photosynthetic CO_2 absorption. Such observation provides us with geographical information on the potential distribution of carbon sequestration by the aid of ecosystem models. In these years, advent of the spectroradiometer, which has high wavelength resolution, such as TANSO FTS on Greenhouse Gases Observing Satellite (GOSAT) enable us to observe solar-induced chlorophyll fluorescence (SIF) emitted from the terrestrial ecosystems. Since the chlorophyll fluorescence is emitted from photosynthetic process itself, SIF remote sensing is drawn considerable attention as a new technique to observe the photosynthetic activity of the vegetation. SIF has been measured by gas-measurement satellites, such as GOSAT, GOSAT-2, OCO-2 and GOME2 on MetOp A and B.
In this talk, we will introduce our previous and on-going studies about estimation of photosynthetic production of the terrestrial ecosystem. We also discuss about future perspective about SIF studies in GOSAT and GOSAT-2 projects.

Keywords: vegetation remote sensing, solar-induced chlorophyll fluorescence, GOSAT

©2019. Japan Geoscience Union. All Right Reserved.

Analysis of the carbon dioxide in the upper troposphere and lower stratosphere by the data from GOSAT TANSO-FTS TIR

*Nawo Eguchi[1], Akihiro Honda[1], Naoko Saitoh[2], Yosuke Niwa[3]

1. Kyushu University, 2. Chiba University, 3. National Institute for Environmental Studies

Stratospheric cooling was reported, it could be caused by increasing the carbon dioxide (CO_2), which is a major greenhouse gas. While, the concentration of CO_2 in the stratosphere is not well understood, nor are the exchange processes between the upper troposphere and lower stratosphere (UT/LS ; 250-100hPa). The present study investigated the intra-seasonal, seasonal and inter-annual variations of CO_2 to understand the CO_2 concentration at UT/LS and the Stratosphere and Troposphere exchange process.

We used the vertical profile data (Level 2) of CO_2 derived from thermal infrared (TIR) region (Band 4: 5.5 - 14.3 μm) of the Thermal And Near-infrared Sensor for carbon Observation (TANSO) - Fourier Transform spectrometer (FTS) on board Greenhouse gas Observing SATellite (GOSAT). The analysis period is four years from January 2010 to December 2013. We adapted the bias correction values derived from Saitoh et al. [AMT, 2016] which validated the TIR CO_2 profiles at UT/LS region with the Comprehensive Observation Network for TRace gases by AIrLiner (CONTRAIL). For reference, the atmospheric transport model, NIES-TM (ver.5) and the Nonhydrostatic Icosahedral Atmospheric Model (NICAM)–based Transport Model (TM) were used [Niwa et al., 2011; 2017].

The growth rate of CO_2 concentration at UT/LS were approximately 2 ppmv/year, which one at southern hemisphere were relatively larger than one at northern hemisphere. The seasonal variation of CO_2 concentration, showed that the maximum peak existed after a few month with respect to the peak at the middle or lower troposphere. The inter-annual variations were affected by the ENSO cycle; the higher (lower) CO_2 concentration at UT were seen during La Nina (Normal / El Nino) period. Finally, the intra-seasonal variation CO_2 concentration at UT/LS were associated with both the vertical and horizontal transportation due to the deep convection and the Asian monsoon anticyclonic circulation, respectively. To clarify the dynamics of CO_2 concentration on the time scale within the area and season within which we could not observe by aircraft observation or balloon observation, the results are used for verification of physicochemical process of global model and also for their development can do.

Keywords: greenhouse gases, stratosphere-troposphere exchange, GOSAT satellite

©2019. Japan Geoscience Union. All Right Reserved.

Seasonal and interannual variations of the Atmospheric Potential Oxygen over the Western North Pacific observed by using a cargo aircraft C-130H

*Shigeyuki Ishidoya[1], Kazuhiro Tsuboi[2], Yosuke Niwa[3], Shohei Murayama[1], Hidekazu Matsueda[2], Yousuke Sawa[2], Nobuyuki Aoki[1], Kentaro Ishijima[2], Kentaro Kozumi[4], Genta Umezawa[4], Kazuya Yukita[4], Shigeharu Nishida[4], Megumi Yamamoto[4]

1. National Institute of Advanced Industrial Science and Technology (AIST), 2. Meteorological Research Institute, 3. National Institute for Environmental Studies, 4. Japan Meteorological Agency

The cargo aircraft C-130H flies once per month from Atsugi Base (35.45˚N, 139.45˚E), Kanagawa, Japan, to Minamitorishima (MNM; 24.28˚N, 153.98˚E), and air samples are collected during the level flight (~6 km) and the descent portion at MNM. The air samples have been analyzed for $O_2/N_2$and Ar/N_2ratios and stable isotopic ratios of N_2, $O_2$and Ar since May 2012. The analysis indicated a significant artificial fractionation due to thermal diffusion during the air sample collection. Nevertheless we succeeded to correct the effects of the fractionation on the observed O_2/N_2ratio precisely by using the observed Ar/N_2 ratio (Ishidoya et al., 2014). The corrected O_2/N_2ratio showed a secular decrease accompanied by a prominent seasonal cycle. The average secular change rate of the mid-tropospheric corrected O_2/N_2ratio was found to be -25.2±0.5 per meg $yr^{-1}$for the period 2012 –2018, which agreed well with that observed at La Jolla, USA by Scripps O_2program (Keeling and Manning, 2014). As the uncertainty of the change rate, we considered the spatial difference of the rates and the stability of the O_2/N_2ratio of standard air.

The Atmospheric Potential Oxygen ($APO=O_2+1.1xCO_2$), calculated by using the corrected O_2/N_2ratio, also showed prominent seasonal cycles, and the amplitude of the mid-tropospheric seasonal APO cycle observed at 25.5˚N was found to be 55 and 31 % of those observed at 33.5˚N and the surface MNM (Ishidoya et al., 2017), respectively. On the other hand, the corresponding seasonal amplitude of CO_2at 25.5˚N was found to be 72 and 93 % of those at 33.5˚N and the surface MNM, respectively. An atmospheric transport model (Niwa et al., 2017) reproduced general features of the observed seasonal APO and CO_2cycles, and its tagged simulation suggested that the mid-tropospheric seasonal APO cycle in the northern low latitudes was reduced significantly by the anti-phase seasonal APO cycle from the southern hemisphere. The observed APO showed interannual variations superimposed on secular downward trends, and the temporal change rates take maxima from the end of 2014 to the beginning of the 2015 at the surface MNM and in the mid-troposphere at 29 –34 ˚N. A comparison between the observed and simulated interannual variations of APO suggested that an interannual variation of the atmospheric transport contributed about 30 % of the observed variation.

Acknowledgments

We thank the staff of Japan Meteorological Agency for their work to collect the air samples onboard a cargo aircraft C-130H. This study was partly supported by the JSPS KAKENHI Grant Number 15H02814, and the Global Environment Research Coordination System from the Ministry of the Environment, Japan.

©2019. Japan Geoscience Union. All Right Reserved.

References

Ishidoya, S. et al. (2014) New atmospheric O_2/N_2ratio measurements over the western North Pacific using a cargo aircraft C-130H, *SOLA*, **10**, 23-28.

Ishidoya, S. et al. (2017) Development of a continuous measurement system for atmospheric O_2/N_2ratio using a paramagnetic analyzer and its application in Minamitorishima Island, Japan, *SOLA*, **13**, 230-234.

Keeling, R. F., and A. C. Manning (2014) Studies of recent changes in atmospheric O_2content, in *Treatise on Geochemistry*,**5**, 2nd ed., pp. 385–404.

Niwa, Y. et al. (2017) A 4D-Var inversion system based on the icosahedral grid model (NICAM-TM 4D-Var v1.0) –Part 1: Offline forward and adjoint transport models, *Geosci. Model Dev.*, **10**, 1157-1174.

Keywords: Atmospheric Potential Oxygen (APO), aircraft observation

©2019. Japan Geoscience Union. All Right Reserved.

[J] Oral | A (Atmospheric and Hydrospheric Sciences)：A-AS Atmospheric Sciences, Meteorology & Atmospheric Environment

Wed. May 29, 2019 9:00 AM - 10:30 AM JST | Wed. May 29, 2019 12:00 AM - 1:30 AM UTC | 201B 2F

[A-AS05] Stratosphere-troposphere Processes And their Role in Climate

convener:Yoshio Kawatani(Japan Agency for Marine-Earth Science and Technology), Shingo Watanabe(Japan Agency for Marine-Earth Science and Technology), Takashi Sekiya(Japan Agency for Marine-Earth Science and Technology), Kaoru Sato(Department of Earth and Planetary Science, Graduate School of Science, The University of Tokyo), Chairperson:Watanabe Shingo(海洋研究開発機構)

The Stratosphere-troposphere Processes And their Role in Climate (SPARC) is one of the
major projects of the World Climate Research Programme (WCRP), and is characterized
by its focus on chemical and dynamical coupling in the stratosphere and troposphere. In
this session, we welcome presentations on various processes in the stratosphere and tro
posphere.

9:00 AM - 9:10 AM JST | 12:00 AM - 12:10 AM UTC

Introduction

9:10 AM - 9:40 AM JST | 12:10 AM - 12:40 AM UTC

[AAS05-01] Turbulent kinetic energy dissipation rates depending on the polar vortex and on synoptic-scale disturbances in the UTLS region in the Antarctic

★Invited Papers

*Masashi Kohma[1], Kaoru Sato[1], Koji Nishimura[2], Masaki Tsutsumi[2] (1.Department of Earth and Planet Science, Graduate School of Science, The University of Tokyo, 2.National Institute of Polar Research and The Graduate University for Advanced Studies (SOKENDAI))

9:40 AM - 9:55 AM JST | 12:40 AM - 12:55 AM UTC

[AAS05-02] Momentum budget of semiannual oscillation around the tropical stratopause

*Yoshihiro Tomikawa[1,2], V. Lynn Harvey[3], John A. Knox[4], Masatomo Fujiwara[5] (1.National Institute of Polar Research, 2.SOKENDAI, 3.University of Colorado Boulder, 4.University of Georgia, 5.Hokkaido University)

9:55 AM - 10:10 AM JST | 12:55 AM - 1:10 AM UTC

[AAS05-03] A study on sources of gravity waves that reach the summer stratosphere and mesosphere based on high-resolution radiosonde data

*Haruka Okui[1], Masashi Kohma[1], Kaoru Sato[1] (1.Department of Earth and Planetary Science, Graduate School of Science, The University of Tokyo)

10:10 AM - 10:25 AM JST | 1:10 AM - 1:25 AM UTC

[AAS05-04] Stratospheric initial conditions provide seasonal predictability of the North Atlantic and Arctic Oscillations

*Yu Nie[1], Adam Scaife[2,3], Hong-Li Ren[1,4], Ruth Comer[2], Martin Andrews[2] (1.Laboratory for Climate Studies, National Climate Center, China Meteorological Administration, Beijing, China, 2.Met Office Hadley Centre, Exeter, UK, 3.College of Engineering, Mathematics and Physical Sciences, University of Exeter, Exeter, UK, 4.Department of Atmospheric Science, School of Environmental Studies, China University of Geoscience, Wuhan, China)

10:25 AM - 10:30 AM JST | 1:25 AM - 1:30 AM UTC

Discussion

Turbulent kinetic energy dissipation rates depending on the polar vortex and on synoptic-scale disturbances in the UTLS region in the Antarctic

*Masashi Kohma[1], Kaoru Sato[1], Koji Nishimura[2], Masaki Tsutsumi[2]

1. Department of Earth and Planet Science, Graduate School of Science, The University of Tokyo, 2. National Institute of Polar Research and The Graduate University for Advanced Studies (SOKENDAI)

The turbulence kinetic energy dissipation rate (TKEDR) is a fundamental parameter describing atmospheric turbulence. Our previous study reported the first estimation of the TKEDR in the free atmosphere in the Antarctic from atmospheric radar measurements at Syowa Station, and showed that the TKEDR in the 10–15 km height range became large in May through October. This fact suggests that the seasonal evolution of polar vortex has impact on the TKEDR in the upper troposphere and lower stratosphere (UTLS). The present study investigates the dependence of the TKEDR on the relative location to the polar vortex and on each phase of synoptic scale disturbances during austral winter in the UTLS region using the radar measurements at Syowa Station. First, the TKEDR is obtained as a function of the relative distance from the edge of the polar vortex. The edge of the polar vortex was determined from Ertel’ s potential vorticity on 475-K isentropic surface (Nash et al., 1996). The result showed that the TKEDR is significantly large near the polar vortex edge compared to that outside and deep inside the polar vortex. Furthermore, it is clarified that the TKEDR largely depends on synoptic-scale PV perturbation around the tropopause (300-K isentropic surface).

Keywords: turbulent kinetic energy dissipation rate, polar vortex, atmospheric radar

©2019. Japan Geoscience Union. All Right Reserved.

Momentum budget of semiannual oscillation around the tropical stratopause

*Yoshihiro Tomikawa[1,2], V. Lynn Harvey[3], John A. Knox[4], Masatomo Fujiwara[5]

1. National Institute of Polar Research, 2. SOKENDAI, 3. University of Colorado Boulder, 4. University of Georgia, 5. Hokkaido University

Meteorological reanalysis data have been updated and improved in the past decade, which are pretty useful for climate and meteorological studies. Their comprehensive evaluation is going underway as the SPARC Reanalysis Intercomparison Project (S-RIP). This study reports the momentum budget of semiannual oscillation around the tropical stratopause for four kinds of the latest reanalysis data (i.e., MERRA, MERRA2, ERA-Interim, and JRA55) as a part of S-RIP. They showed that, while the westerly acceleration is primarily due to unresolved wave drag (i.e. gravity wave drag), the easterly acceleration is induced by momentum transport due to meridional circulation and resolved wave drag. This feature is consistent with previous studies based on simulation and observation. However, the contribution of unresolved wave drag is maximized in MERRA/MERRA2 later than in ERA-Interim/JRA55. We discuss the difference between the latest reanalyses and its impact on the tropical dynamics.

Keywords: stratopause, semiannual oscillation, reanalysis

©2019. Japan Geoscience Union. All Right Reserved.

A study on sources of gravity waves that reach the summer stratosphere and mesosphere based on high-resolution radiosonde data

*Haruka Okui[1], Masashi Kohma[1], Kaoru Sato[1]

1. Department of Earth and Planetary Science, Graduate School of Science, The University of Tokyo

Gravity waves (GWs) are mainly generated in the troposphere and play a crucial role in the momentum transport in the stratosphere and mesosphere. Several possible main sources of GWs are suggested by theoretical, numerical and observational studies; topography and jet-front systems in winter, and strong convection in summer (e.g. Sato *et al.*, 2009). In addition, theoretical work by Bühler *et al.* (1999) indicated that the Kelvin-Helmholtz (KH) shear instability can cause significant emission of GWs in summer. Having critical layers in the lower stratosphere, orographic waves hardly propagate into the summer stratosphere and mesosphere. On the other hand, most GWs emitted from the KH instability above the tropopausal jet do not encounter their critical layer and can reach the stratosphere and mesosphere. However, observational studies from this view point are insufficient. In this study, using high-resolution radiosonde data from 9 stations in Japan, the generation and propagation of GWs with short vertical wave length ($\leq$ 4 km) in the troposphere and lower stratosphere are investigated. The parameters describing the wave structure are estimated by a hodograph analysis. Drawing a comparison with GWs observed in winter, source and propagation characteristics of GWs in summer are highlighted. The latitude-height distribution of wave amplitudes and phase velocity characteristics suggests that orographic waves are not dominant in summer in contrast with those in winter. The vertical direction of wave energy propagation shows that summer GWs propagate upward and downward from the 10-15 km height region, where the occurrence frequency of the events with Richardson number (Ri) less than 0.25 (which is a necessary condition for the KH instability) is high. In addition, wave amplitudes in the lower stratosphere are relatively large above the peak of the occurrence frequency of $Ri < 0.25$, which is located around the latitude and height region of 30°N-35°N, 12-15 km. These results suggest that the KH instability is one of major sources of GWs in the summer stratosphere. The KH instability tends to occur when the vertical wind shear is large and the static stability is low. In summer, the vertical shear associated with the jet is stronger at higher latitudes and the static stability is lower at lower latitudes. The peak of occurrence frequency of $Ri < 0.25$ as mentioned above is situated at the middle latitudes inbetween. Therefore, it can be inferred that this region is climatologically important for shear-generated GWs which can reach the summer stratosphere.

Keywords: middle atmosphere, gravity waves

©2019. Japan Geoscience Union. All Right Reserved.

Stratospheric initial conditions provide seasonal predictability of the North Atlantic and Arctic Oscillations

*Yu Nie[1], Adam Scaife[2,3], Hong-Li Ren[1,4], Ruth Comer[2], Martin Andrews[2]

1. Laboratory for Climate Studies, National Climate Center, China Meteorological Administration, Beijing, China, 2. Met Office Hadley Centre, Exeter, UK, 3. College of Engineering, Mathematics and Physical Sciences, University of Exeter, Exeter, UK, 4. Department of Atmospheric Science, School of Environmental Studies, China University of Geoscience, Wuhan, China

The North Atlantic Oscillation (NAO), the regional manifestation of the Arctic Oscillation (AO), dominates winter climate variability in Europe and North America. Skilful seasonal forecasting of the winter NAO/AO has been demonstrated recently by dynamical prediction systems. However, the role of initial conditions in this predictability remains unknown. Using a latest generation seasonal forecasting system and reanalysis data, we show that the initial upper stratospheric zonal wind anomaly contributes to winter NAO/AO predictability through downward propagation of initial conditions. An initial polar westerly/easterly anomaly in the upper stratosphere propagates down to the troposphere in early winter, favoring a poleward/equatorward shift of the tropospheric mid-latitude jet. This tropospheric anomaly persists well into the late winter and induces the positive/negative phase of NAO/AO in the troposphere. Our results imply that good representation of stratospheric initial condition and stratosphere-troposphere coupling in models is important for winter climate prediction.

Keywords: Seasonal Prediction, Stratosphere, NAO/AO

©2019. Japan Geoscience Union. All Right Reserved.

[J] Oral | A (Atmospheric and Hydrospheric Sciences)：A-AS Atmospheric Sciences, Meteorology & Atmospheric Environment

Wed. May 29, 2019 10:45 AM - 12:15 PM JST | Wed. May 29, 2019 1:45 AM - 3:15 AM UTC | 201B 2F

[A-AS05] Stratosphere-troposphere Processes And their Role in Climate

convener:Yoshio Kawatani(Japan Agency for Marine-Earth Science and Technology), Shingo Watanabe(Japan Agency for Marine-Earth Science and Technology), Takashi Sekiya(Japan Agency for Marine-Earth Science and Technology), Kaoru Sato(Department of Earth and Planetary Science, Graduate School of Science, The University of Tokyo), Chairperson:Takashi Sekiya

The Stratosphere-troposphere Processes And their Role in Climate (SPARC) is one of the
major projects of the World Climate Research Programme (WCRP), and is characterized
by its focus on chemical and dynamical coupling in the stratosphere and troposphere. In
this session, we welcome presentations on various processes in the stratosphere and tro
posphere.

10:45 AM - 11:15 AM JST | 1:45 AM - 2:15 AM UTC

[AAS05-05] Transport of trace gases into the extratropical upper troposphere/lower stratosphere

★Invited Papers

*Yoichi Inai[1], Ryo Fujita[2,1], Toshinobu Machida[3], Hidekazu Matsueda[4], Yousuke Sawa[4], Kazuhiro Tsuboi[4], Keiichi Katsumata[3,5], Shinji Morimoto[1], Shuji Aoki[1], Takakiyo Nakazawa[1] (1.Tohoku Univ., 2.Imperial College London, 3.NIES, 4.MRI, 5.Takachiho Chem. Industrial)

11:15 AM - 11:30 AM JST | 2:15 AM - 2:30 AM UTC

[AAS05-06] Possible impacts of stratospheric ozone on circulation changes in the tropical tropposphere following a stratospheric sudden warming event

*Makoto Deushi[1] (1.Department of Atmospheric Environment and Applied Meteorology, Meteorological Research Institute)

11:30 AM - 11:45 AM JST | 2:30 AM - 2:45 AM UTC

[AAS05-07] **Stratosphere-troposphere exchange of ozone and carbon monoxide over the northern Pacific Ocean in northern winter using two chemical reanalysis data sets**

*Haosen Xi[1], Masatomo Fujiwara[1], Kazuyuki Miyazaki[2] (1.Graduate School of Environmental Science, Hokkaido University, 2.NASA Jet Propulsion Laboratory, California Institute of Technology, USA)

11:45 AM - 12:00 PM JST | 2:45 AM - 3:00 AM UTC

[AAS05-08] **Inter-comparison of Upper Air Temperature in China between Satellite MSU and Radiosonde Datasts**

*Yanjun GUO[1], Cheng-zhi Zou[2], Panmao Zhai[3], Guofu Wang[1] (1.National Climate Center(NCC), China Meteorological Administration(CMA) , 2.Center for Satellite Applications and Research, NOAA/NESDIS, 3.Chinese Academy of Meteorolgical Sciences (CAMS), China Meteorological Administration (CMA))

12:00 PM - 12:15 PM JST | 3:00 AM - 3:15 AM UTC

[AAS05-09] Environmental Characterization of the Atmosphere Using WACCM-X

*Rose Tseng[1], Michelle Kanipe[1], Brian Urbancic[1], Robert Tournay[1], Omar Nava[1], Daniel Emmons[1], Robert Loper[1], Charlton Lewis[1] (1.Air Force Institute of Technology)

Transport of trace gases into the extratropical upper troposphere/lower stratosphere

*Yoichi Inai[1], Ryo Fujita[2,1], Toshinobu Machida[3], Hidekazu Matsueda[4], Yousuke Sawa[4], Kazuhiro Tsuboi[4], Keiichi Katsumata[3,5], Shinji Morimoto[1], Shuji Aoki[1], Takakiyo Nakazawa[1]

1. Tohoku Univ., 2. Imperial College London, 3. NIES, 4. MRI, 5. Takachiho Chem. Industrial

To investigate the seasonal characteristics of chemical tracer distributions in the extratropical upper troposphere and lower stratosphere (ExUTLS) as well as stratosphere–troposphere exchange processes, origin fractions of air masses originating in the stratosphere, tropical troposphere, mid-latitude lower troposphere (LT), and high-latitude LT in the ExUTLS are estimated using 10-year backward trajectories calculated with European Centre For Medium-Range Weather Forecasts (ECMWF) ERA-Interim data as the meteorological input. Time-series of chemical tracers obtained from ground-based and airborne observations are incorporated into the trajectories, thus reconstructing spatiotemporal distributions of chemical tracers in the ExUTLS. The reconstructed tracer distributions are analysed with the origin fractions and the stratospheric age of air (AoA) estimated using the same backward trajectory. The reconstructed distributions of CO and CO_2 in the ExUTLS are affected primarily by tropospheric air masses because of the short chemical lifetime of the former and large seasonal variations in the troposphere of the latter. Distributions of CH_4, N_2O, and SF_6 are controlled primarily by seasonally varying air masses transported from the stratosphere. For CH_4 and N_2O distributions, their seasonally varying photochemical decay along the average pathway from the source region are particularly important. This study developed and demonstrated a unique and effective method to exploit the advantages of observational data in combination with trajectory analysis. This method provides a means to understand both air mass transport and chemical decay for photochemical active substances from a new perspective.

Keywords: Transport, Earth atmosphere, Trajectory analysis

©2019. Japan Geoscience Union. All Right Reserved.

Possible impacts of stratospheric ozone on circulation changes in the tropical troppposphere following a stratospheric sudden warming event

*Makoto Deushi[1]

1. Department of Atmospheric Environment and Applied Meteorology, Meteorological Research Institute

Many studies have shown that there are significant impacts of the stratospheric ozone on dynamical coupling between the stratosphere and troposphere (S-T) at middle and high latitudes, especially in the Southern hemisphere (e.g. Marshall *et al.*, JC, 2006; Thompson *et al.*, Nature Geo, 2011). In contrast, little attention has been given to role of the stratospheric ozone in modulating S-T dynamical coupling in the tropics (and sub-tropics) so far. Recently, there has been an increasing interest in the S-T dynamical coupling in the tropics because it has been recognized that this coupling has significant influences on moist convection and organized convective systems in the tropics (e.g. Son *et al.*, JC, 2017; Nishimoto and Yoden, JAS, 2017).
In this study, possible impacts of the stratospheric ozone on tropospheric circulation and precipitation in the tropical and sub-tropical regions were examined, focusing on a period of several months following a major stratospheric sudden warming (SSW) event. As a case study, the major SSW occurred in the winter of 2003/2004 was investigated. A set of ensemble re-forecasts was performed by using a chemistry-climate model (CCM) and an atmospheric general circulation model (AGCM) to elucidate radiative effects of the stratospheric ozone anomalies induced by the major SSW on the troposphere at low latitudes. The ensemble re-forecasts were conducted using the Lagged Averaged Forecasting (LAF) method with 60 ensemble members, where the initial-times were set just before the occurrence of the major SSW. The CCM resolves well full stratospheric and tropospheric chemistry processes, and considers online radiative feedbacks from the simulated atmospheric ozone. The CCM ensemble re-forecast was compared to the AGCM ensemble re-forecast in which climatological monthly mean ozone was forced. The CCM ensemble re-forecast reproduced well significant ozone decrease in the lower tropical stratosphere due to rapidly enhanced upward Brewer-Dobson circulation there after the major SSW. About two weeks after the occurrence of the major SSW, systematic differences with statistical significance between the two ensemble re-forecasts were simulated in the tropospheric circulation and precipitation especially in the northern tropics and sub-tropics. The northern cell of the Hadley circulation became stronger in the CCM ensemble re-forecast than in the AGCM one, with the larger amount of precipitation over the Intertropical Convergence Zone (ITCZ). To confirm these impacts of the stratospheric ozone on the (sub-) tropical troposphere, other major SSW events are also investigated.

Keywords: stratosphere-troposphere coupling, stratospheric ozone, tropical tropospheric circulation, stratospheric sudden warming

©2019. Japan Geoscience Union. All Right Reserved.

Stratosphere-troposphere exchange of ozone and carbon monoxide over the northern Pacific Ocean in northern winter using two chemical reanalysis data sets

*Haosen Xi[1], Masatomo Fujiwara[1], Kazuyuki Miyazaki[2]

1. Graduate School of Environmental Science, Hokkaido University, 2. NASA Jet Propulsion Laboratory, California Institute of Technology, USA

Stratosphere-troposphere exchange (STE) is one of the important factors that determine the distribution of constituents in the troposphere and stratosphere. Two-way airmass exchange between the lower stratosphere and the troposphere occurs in association with mid-latitude weather disturbances, with the net transport from the stratosphere to troposphere. In this study, we analyze the STE over the northern hemisphere Pacific Ocean in northern winter, focusing on transport of ozone and carbon monoxide (CO) using two chemical reanalysis data sets, the Tropospheric Chemical Reanalysis version 1 (TCR-1; Miyazaki et al., 2015) and the Monitoring Atmospheric Composition and Climate (MACC; Inness et al., 2013). The TCR-1 is a 10-year chemical reanalysis data set for the period from 2005 to 2014, while the MACC is for 2003 to 2012. Both reanalyses assimilate major satellite chemistry data during the respective periods. We calculate the amount of CO transported from the troposphere to stratosphere (TST) and ozone transported from the stratosphere to troposphere (STT) on the 350-K isentropic surface, by using 4 PVU potential vorticity to evaluate irreversible transport across the tropopause (e.g., Homeyer and Bowman, 2013). Results from the analysis of TCR-1 data are as follows. The amount of ozone transport per case maximizes in November and minimizes in February, and that in years 2005-2008 is significantly smaller than that in years 2009-2014 with the maximum in the 2010 winter (i.e., from November 2010 to March 2011). The amount of CO transport per case maximizes in March and minimizes in November, and that in years 2005-2009 is significantly larger than that in years 2010-2014 with the maximum in the 2009 winter. Results from MACC data are qualitatively similar. In the presentation we will also show the results with additional criteria for irreversibility by using trajectory calculations.

Keywords: ozone, carbon monoxide, stratosphere troposphere exchange

©2019. Japan Geoscience Union. All Right Reserved.

Inter-comparison of Upper Air Temperature in China between Satellite MSU and Radiosonde Datasts

*Yanjun GUO[1], Cheng-zhi Zou[2], Panmao Zhai[3], Guofu Wang[1]

1. National Climate Center(NCC), China Meteorological Administration(CMA) , 2. Center for Satellite Applications and Research, NOAA/NESDIS, 3. Chinese Academy of Meteorolgical Sciences (CAMS), China Meteorological Administration (CMA)

Reconciling upper-air temperature trends derived from radiosonde and satellite observations is a necessary step to confidently determine the global warming rate. This study examines the raw and homogenized radiosonde observations over China and compares them with layer-mean atmospheric temperatures derived from satellite microwave observations for the lower-troposphere (TLT), mid-troposphere (TMT), upper troposphere (TUT), and lower stratosphere (TLS) by three research groups. The comparisons are for averages over China, excluding Tibetan Plateau, and at individual stations where metadata contain information on radiosonde instrument changes. It is found that major differences between the satellite and radiosonde observations are related to artificial systematic changes. The radiosonde system updates in early 2000s over China caused significant discontinuities and led the radiosonde temperature trends to exhibit less warming in the middle and upper troposphere and more cooling in the lower stratosphere than the satellite temperatures. Homogenized radiosonde data have been further adjusted using shift-point adjustment approaches to match with satellite products for China average. The obtained trends during 1979-2015 from the re-adjusted radiosonde observation are respectively 0.203±0.066, 0.128±0.044, 0.034±0.039, and -0.329±0.135 K Decade^{-1} for TLT, TMT, TUT, and TLS equivalents. Compared to satellite trends, the re-adjusted radiosonde trends are within 0.01 K Decade^{-1} for TMT and TUT, and 0.054 K Decade^{-1} warmer for TLT and 0.051 K Decade^{-1} cooler for TLS. The results suggest that the use of satellite data as a reference are helpful in identifying and removing inhomogeneities of radiosonde temperatures over China and reconciling their trends to satellite microwave observations. Future efforts are to homogenize radiosonde temperatures at individual stations over China using similar approaches.

Keywords: upper air, temperature, satellite, radiosonde, China, trend

©2019. Japan Geoscience Union. All Right Reserved.

Inter-comparison of Upper Air Temperature in China between Satellite MSU and Radiosonde Datasets

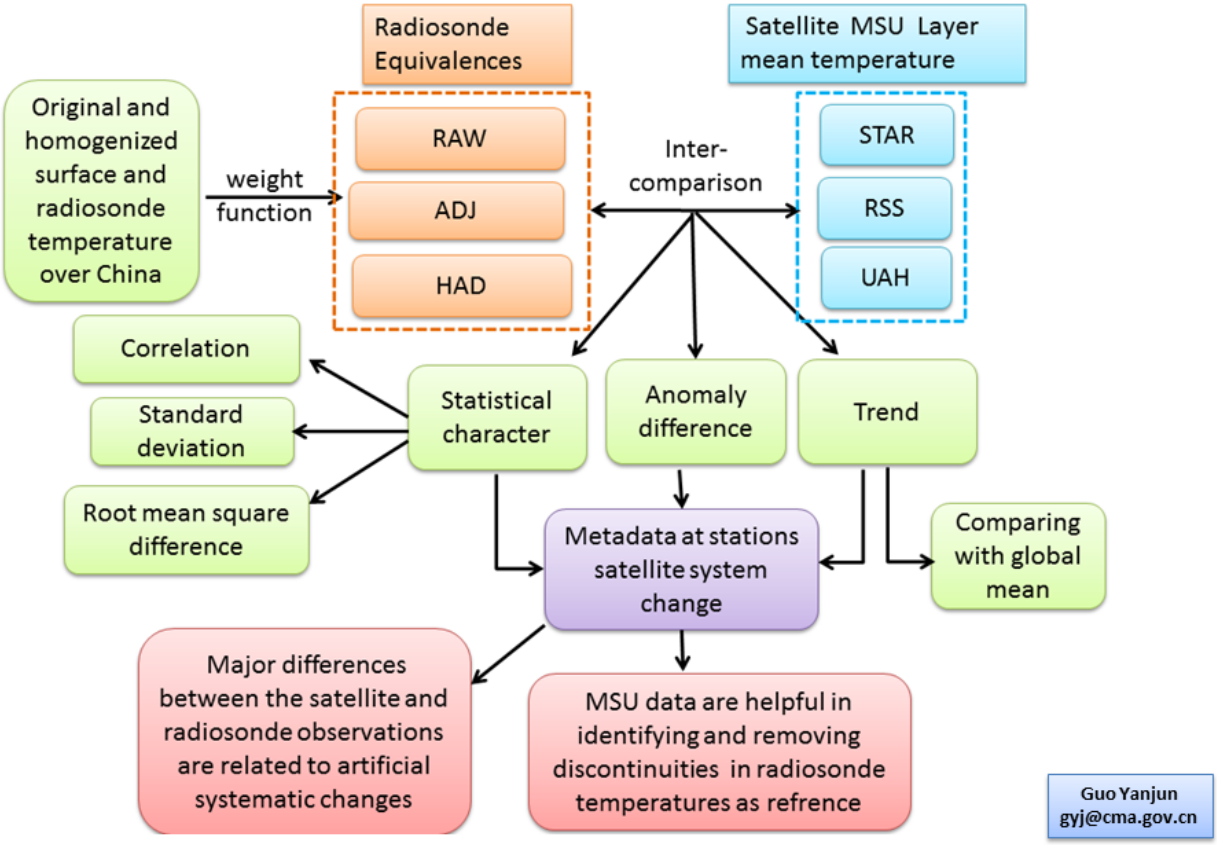

Guo Yanjun
gyj@cma.gov.cn

©2019. Japan Geoscience Union. All Right Reserved.

Environmental Characterization of the Atmosphere Using WACCM-X

*Rose Tseng[1], Michelle Kanipe[1], Brian Urbancic[1], Robert Tournay[1], Omar Nava[1], Daniel Emmons[1], Robert Loper[1], Charlton Lewis[1]

1. Air Force Institute of Technology

Researching the characteristics of the whole atmosphere can yield a variety of weather and climate understanding for the terrestrial and space environments. Of particular interest are the neutral species, wind, and temperature distributions from the surface to the middle atmosphere and across multiple latitudes. This is accomplished using data from the Whole Atmosphere Community Climate Model-Extended (WACCM-X) with the ionosphere, a model developed by inter-divisional collaboration at the University Corporation for Atmospheric Research. Presented here are the vertical profiles of neutral species, wind speed, and temperature of the troposphere and middle atmosphere up to 80 km. Preliminary results from a 10-year period show all three parameters vary temporally and spatially, particularly across latitudes and seasons. Ongoing work includes rigorous analysis, utilizing all years of WACCM-X data available.

Keywords: Whole Atmosphere, Climate

©2019. Japan Geoscience Union. All Right Reserved.

[J] Oral | A (Atmospheric and Hydrospheric Sciences)：A-AS Atmospheric Sciences, Meteorology & Atmospheric Environment

Wed. May 29, 2019 1:45 PM - 3:15 PM JST | Wed. May 29, 2019 4:45 AM - 6:15 AM UTC | 201B 2F

[A-AS05] Stratosphere-troposphere Processes And their Role in Climate

convener:Yoshio Kawatani(Japan Agency for Marine-Earth Science and Technology), Shingo Watanabe(Japan Agency for Marine-Earth Science and Technology), Takashi Sekiya(Japan Agency for Marine-Earth Science and Technology), Kaoru Sato(Department of Earth and Planetary Science, Graduate School of Science, The University of Tokyo), Chairperson:Yoshio Kawatani

The Stratosphere-troposphere Processes And their Role in Climate (SPARC) is one of the major projects of the World Climate Research Programme (WCRP), and is characterized by its focus on chemical and dynamical coupling in the stratosphere and troposphere. In this session, we welcome presentations on various processes in the stratosphere and tro posphere.

1:45 PM - 2:15 PM JST | 4:45 AM - 5:15 AM UTC

[AAS05-10] Diagnostics of a WN2-type major sudden stratospheric warming event in February 2018 using a new three-dimensional wave activity flux

★Invited Papers

*Yayoi Harada[1], Kaoru Sato[2], Takenari Kinoshita[3], Ryosuke Yasui[2], Toshihiko Hirooka[4], Hiroaki Naoe[1] (1.Meteorological Research Institute, 2.Department of Earth and Planetary Science, Graduate School of Science, The University of Tokyo, 3.Japan Agency for Marine-Earth Science and Technology, 4.Department of Earth and Planetary Sciences, Kyushu University)

2:15 PM - 2:45 PM JST | 5:15 AM - 5:45 AM UTC

[AAS05-11] Response of the Southern Hemisphere atmosphere to the QBO from winter to early summer

★Invited Papers

*Yousuke Yamashita[1], Hiroaki Naoe[2], Makoto Inoue[3], Masaaki Takahashi[4] (1.Japan Agency for Marine-Earth Science and Technology, 2.Meteorological Research Institute, 3.Akita Prefectural University, 4.National Institute for Environmental Studies)

2:45 PM - 3:00 PM JST | 5:45 AM - 6:00 AM UTC

[AAS05-12] Influence of QBO-like Oscillation on Tropical Convective Systems in a Three-Dimensional Minimal Model Framework of the Stratosphere-Troposphere Coupled System

*Shigeo Yoden[1], Hai Bui[2], Takahiro Banno[1] (1.Division of Earth and Planetary Sciences, Graduate School of Science, Kyoto University, 2.Geophysical Institute, University of Bergen)

3:00 PM - 3:15 PM JST | 6:00 AM - 6:15 AM UTC

[AAS05-13] Downward Propagation of Planetary Wave Packets from the Stratosphere to the Troposphere During Northern Hemisphere Winter

*Matsuyama Yuya[1], Toshihiko Hirooka[2] (1.Department of Earth and Planetary Sciences, Graduate School of Science, Kyushu University, 2.Department of Earth and Planetary Sciences, Faculty of Science, Kyushu University)

Diagnostics of a WN2-type major sudden stratospheric warming event in February 2018 using a new three-dimensional wave activity flux

*Yayoi Harada[1], Kaoru Sato[2], Takenari Kinoshita[3], Ryosuke Yasui[2], Toshihiko Hirooka[4], Hiroaki Naoe[1]

1. Meteorological Research Institute, 2. Department of Earth and Planetary Science, Graduate School of Science, The University of Tokyo, 3. Japan Agency for Marine-Earth Science and Technology, 4. Department of Earth and Planetary Sciences, Kyushu University

Observational features of atmospheric fields during a zonal wavenumber two (WN2) type major sudden stratospheric warming (MSSW) event that occurred in February 2018 (MSSW18) are analyzed using the Japanese 55-year Reanalysis, satellite measurements by a microwave limb sounder, and a new three-dimensional wave activity flux. MSSW18 was characterized by a clear polar vortex split, continuance of easterlies with remarkable double peaks, clear planetary-wave propagation in the easterly region of the upper stratosphere and extraordinary upward propagation of WN2 planetary waves from the upper troposphere whose peak was comparable to that during an MSSW event that occurred in January 2009 (MSSW09), although MSSW18 showed relatively modest warming, unclear disappearance of the stratopause and weak stratopause elevation compared to those during MSSW09. Further analyses revealed that wave packets propagated upward simultaneously in both the Eastern and Western Hemispheres. Those observed in the Eastern Hemisphere converged strongly at the western edge of the Aleutian High and most of them did not propagate into the upper stratosphere. The wave packets observed in the Western Hemisphere locally propagated into the upper stratosphere over North America despite the fact that easterlies were predominant there in the mature stage of MSSW18. Furthermore, our results revealed that the regions and levels of wave-packet attenuation corresponded well to the area of weak eastward phase tilt or the quasi-barotropic condition of smaller-scale waves during MSSW18, whereas during MSSW09 the westward phase tilts of smaller-scale waves were clearly visible in the upper stratosphere.

Keywords: Sudden stratospheric warming, Zonal wavenumber two, Wave activity flux

©2019. Japan Geoscience Union. All Right Reserved.

Response of the Southern Hemisphere atmosphere to the QBO from winter to early summer

*Yousuke Yamashita[1], Hiroaki Naoe[2], Makoto Inoue[3], Masaaki Takahashi[4]

1. Japan Agency for Marine-Earth Science and Technology, 2. Meteorological Research Institute, 3. Akita Prefectural University, 4. National Institute for Environmental Studies

The equatorial quasi-biennial oscillation (QBO) is dominant variability in the tropical stratosphere and is characterized by the oscillation of downward propagating easterly and westerly wind regimes. Several studies have examined possible linkages between the QBO and atmospheric circulations, such as the meridional circulation around tropics and the polar vortex intensity in the Northern Hemisphere (NH), which are related to the changes of waves and circulations in the stratosphere (e.g., Plumb and Bell 1982, Holton and Tan 1980). On the other hand, the mechanism by which the QBO modulates extratropical circulation over the Southern Hemisphere (SH) is poorly understood, as the various studies employed different height levels and metrics to define the phase of the QBO (e.g., Garcia and Solomon 1987; Baldwin and Dunkerton 1998; Naito 2002; Hitchman and Huesmann 2009). Previous studies employed composite analysis that possibly includes signals other than the response to the stratospheric QBO, such as the responses to solar cycle and El Niño-Southern Oscillation (ENSO). In this study, we examined the response of atmospheric circulation over the SH to the stratospheric QBO, using multiple linear regression analysis for the long-term Japanese 55-year Reanalysis (JRA-55) dataset to separate the influences of the QBO and other factors on the SH polar vortex. In addition to the terms of middle- and lower-stratospheric QBO, the multiple linear regression includes equivalent effective stratospheric chlorine (EESC), solar cycle, ENSO, and volcanic aerosol terms as explanatory variables. Analyses of the regression coefficients associated with both middle- and lower-stratospheric QBO suggest an influence on the SH polar vortex from SH winter through early summer in the seasonal evolution. One possible pathway is that the middle-stratospheric QBO results in the SH low latitudes stratospheric response through the QBO-induced mean meridional circulation, leading to a high-latitude response. This favors delayed downward evolution of the axis of SH polar vortex at high latitudes (around 60˚S) from August to November during the westerly phase of the QBO. Although this pathway is inconsistent with weakening of the SH polar vortex in August, the other possible pathway is unveiled from the detailed analysis. The other possible pathway involves the response to lower stratospheric QBO that induces the increase in upward propagation of planetary waves from the SH extratropical troposphere to stratosphere in August. This pathway is consistent with weakening of the SH polar vortex in August.

Keywords: quasi-biennial oscillation, Southern Hemisphere polar vortex, multiple linear regression

©2019. Japan Geoscience Union. All Right Reserved.

Influence of QBO-like Oscillation on Tropical Convective Systems in a Three-Dimensional Minimal Model Framework of the Stratosphere-Troposphere Coupled System

*Shigeo Yoden[1], Hai Bui[2], Takahiro Banno[1]

1. Division of Earth and Planetary Sciences, Graduate School of Science, Kyoto University, 2. Geophysical Institute, University of Bergen

We report on the three-dimensional minimal model of the stratosphere-troposphere coupled system that produces a self-sustained oscillation reminiscent of the quasi-biennial oscillation (QBO) in a radiative-moist convective quasi-equilibrium state. The computational domain is rectangular (640 km x 160 km, 5 km grid size; Bui et al., 2019), or square (100 km x 100 km, 1 km grid size), without Coriolis effects under doubly periodic boundary conditions. After initial transient time, a QBO-like oscillation with a period of about 300 days emerges in the stratosphere, both in the domain-averaged zonal wind and meridional wind (Figure-left). Synchronization of the zonal and meridional winds is characterized as an anti-clockwise rotation of a skewed spiral feature with height in the horizontal wind hodograph (Figure-right).

The QBO-like wind oscillation penetrates into the troposphere with large reduction of oscillation amplitude, and influences tropospheric temperature anomalies and precipitation with an irregular period of about 100 days. Heavy precipitation is associated with positive temperature anomalies. The simulation reveals three types of precipitation patterns; isolated quasi-stationary type clusters, fast-moving back-building type and squall-line type patterns. The quasi-stationary type is newly identified in the present three-dimensional model, and the zonal-height cross sections of the meridionally averaged clouds and relative humidity for this pattern show clear-sky areas without shallow clouds and with low humidity, whereas shallow clouds exist over the entire domain including non-precipitating areas with high humidity for the fast-moving back-building type or squall-line type patterns. Intermittent self-organization of convective systems into quasi-stationary type and transition back to the fast-moving back-building type or squall-line type are fundamental characteristics of self-aggregation in the three-dimensional minimal model framework.

Reference

Bui H., S. Yoden, and E. Nishimoto, 2019: QBO-like Oscillation in a Three-Dimensional Minimal Model Framework of the Stratosphere–Troposphere Coupled System. *SOLA*, **15**, 59–62.

©2019. Japan Geoscience Union. All Right Reserved.

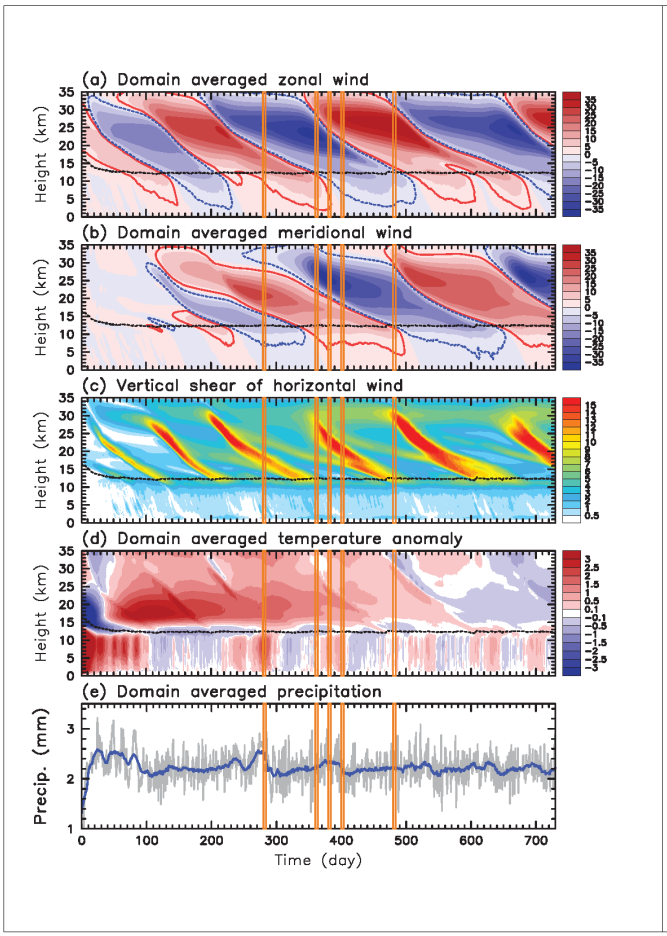

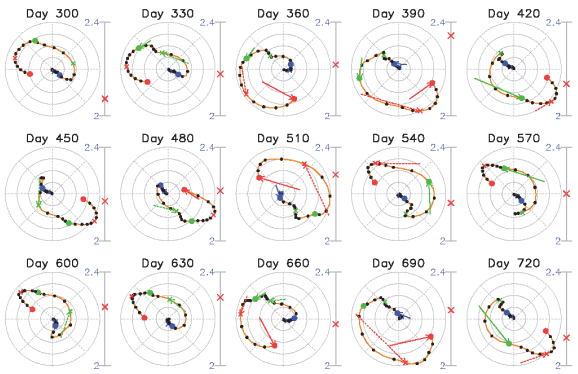

©2019. Japan Geoscience Union. All Right Reserved.

Downward Propagation of Planetary Wave Packets from the Stratosphere to the Troposphere During Northern Hemisphere Winter

*Matsuyama Yuya[1], Toshihiko Hirooka[2]

1. Department of Earth and Planetary Sciences, Graduate School of Science, Kyushu University, 2. Department of Earth and Planetary Sciences, Faculty of Science, Kyushu University

Downward propagation of planetary wave packets from the stratosphere to the troposphere is often observed during Northern Hemisphere winter and their influence on the tropospheric circulation has been also reported by various authors. Recent observational studies show that the downward propagation into the troposphere frequently occurs over the North America centered around 90W. Hence, we investigate the frequency distribution of downward propagation events of planetary wave packets and its relationship to the background field using the Japanese 55-year Reanalysis (JRA-55) data. We calculate Plumb’ s (1985) wave activity flux (WAF) and extract the downward propagation events over the analysis period (1958-2016) based on a specified criterion value for the vertical component of WAF at 30 hPa. Next, we investigate the longitudinal location of each downward propagation event and classify it into eight sectors of 45 degrees along the longitudinal circle to make a composite analysis of the classified events. Resultantly, around 500 events are extracted during the analysis period and it is found that about more than 80% of the events occurred in three sectors between 135W to 0E; these events are shown to be intimately related to the development of the Aleutian High in the stratosphere, which is located in the west of the downward propagation region. As for the other events, a developed anticyclone was also observed in the west of each downward propagation region.

Keywords: planetary wave packet, downward propagation, wave activity flux

©2019. Japan Geoscience Union. All Right Reserved.

[J] Poster | A (Atmospheric and Hydrospheric Sciences)：A-AS Atmospheric Sciences, Meteorology & Atmospheric Environment

Wed. May 29, 2019 3:30 PM - 5:00 PM JST | Wed. May 29, 2019 6:30 AM - 8:00 AM UTC | Poster Hall International Exhibition Hall8, Makuhari Messe_6

[A-AS05] Stratosphere-troposphere Processes And their Role in Climate

convener:Yoshio Kawatani(Japan Agency for Marine-Earth Science and Technology), Shingo Watanabe(Japan Agency for Marine-Earth Science and Technology), Takashi Sekiya(Japan Agency for Marine-Earth Science and Technology), Kaoru Sato(Department of Earth and Planetary Science, Graduate School of Science, The University of Tokyo)

The Stratosphere-troposphere Processes And their Role in Climate (SPARC) is one of the
major projects of the World Climate Research Programme (WCRP), and is characterized
by its focus on chemical and dynamical coupling in the stratosphere and troposphere. In
this session, we welcome presentations on various processes in the stratosphere and tro
posphere.

[AAS05-P01] An advanced impact of Arctic stratospheric ozone changes on spring precipitation in China

*Fei Xie[1] (1.Beijing Normal University)

[AAS05-P02] Global Cooling System installed on the beach by means of Artificial Convection and Artificial Rain

*Murakami Hideyo[1] (1.Ii Ecology Development)

[AAS05-P03] Stratospheric front-like temperature structure and gravity wave activity during a stratospheric sudden warming event in 2016

*Yukari Sumi[1], Kaoru Sato[1] (1.University of Tokyo)

[AAS05-P04] The effects of a well-resolved stratosphere on the simulated boreal winter circulation in a climate model

*Yoshio Kawatani[1], Kevin Hamilton[2], Lesley J. Gray[3], Scott M. Osprey[3], Shingo Watanabe[1], Yousuke Yamashita[1] (1.Japan Agency for Marine-Earth Science and Technology, 2.International Pacific Research Center, University of Hawaii, 3.Atmospheric, Oceanic and Planetary Physics, Department of Physics, University of Oxford)

[AAS05-P05] On the relation between three-dimensional wave activity flux and pseudo momentum without using intrinsic phase velocities

★Invited Papers

*Takenari Kinoshita[1] (1.Japan Agency for Marine-Earth Science and Technology)

[AAS05-P06] Hindcasts of the 2016 Disruption of the Stratospheric Quasi-biennial Oscillation

*Shingo Watanabe[1], Kevin Hamilton[2], Scott Osprey[3], Yoshio Kawatani[1], Eriko Nishimoto (1.Japan Agency for Marine-Earth Science and Technology, 2.International Pacific Research Center, University of Hawaii at Manoa, 3.NCAS-Climate, University of Oxford)

[AAS05-P07] Selection bias of quasi-fixed-point observations in the ExUTLS and its impact on the seasonal record

*Yoichi Inai[1], Toshinobu Machida[2], Hidekazu Matsueda[3], Yousuke Sawa[3], Kazuhiro Tsuboi[3], Keiichi Katsumata[2,4], Shinji Morimoto[1], Shuji Aoki[1], Takakiyo Nakazawa[1], Ryo Fujita[5,1] (1.Tohoku Univ., 2.NIES, 3.MRI, 4.Takachiho Chem. Industrial, 5.Imperial College London)

[AAS05-P08] Varying Rossby Wave Trains from the Developing to Decaying Period of the Upper Atmospheric Heat Source over the Tibetan Plateau in Boreal Summer

*Chuandong Zhu[1,2], Rongcai Ren[1] (1.Institute of Atmospheric Physics, Chinese Academy of Sciences, 2.University of Chinese Academy of Sciences)

[AAS05-P09] **Equilibrium Climate Responses of the East Asian Summer Monsoon to Various Anthropogenic Aerosol Species**

*Qiuyan Wang[2,1], Zhili Wang[1,2], Hua Zhang[3,2] (1.State Key Laboratory of Severe Weather & Key Laboratory of Atmospheric Chemistry of CMA, Chinese Academy of Meteorological Sciences, Beijing, 2.Collaborative Innovation Center on Forecast and Evaluation of Meteorological Disasters, Nanjing University of Information Science and Technology, Nanjing, 3.Laboratory for Climate Studies, National Climate Center, China Meteorological Administration, Beijing)

[AAS05-P10] Analysis of specific energy in zonal currents focusing on the analogy between jet stream and open channel flow

*Yoshikazu Kitano[1], Tomohito J. Yamada[2] (1.Central Research Institute of Electric Power Industry, 2.Faculty of Engineering, Hokkaido University)

[AAS05-P11] Analysis of the ozone reduction event over the southern tip of South America in November 2009

*Hideharu Akiyoshi[1], Masanao Kadowaki[2], Haruna Nakamura[3], Takafumi Sugita[1], Toshihiko Hirooka[4], Yayoi Harada[5], Akira Mizuno[6] (1.National Institute for Environmental Studies, 2.Japan Atomic Energy Agency, 3.Fujitsu FIP Corporation, 4.Department of Earth and Planetary Sciences, Kyushu University, 5.Meteorological Research Institute, 6.Institute for Space-Earth Environmental Research, Nagoya University)

[AAS05-P12] **Analysis of relatively low ozone in Arctic spring during the QBO-westerly and solar-minimum years**

*Yousuke Yamashita[1,2], Hideharu Akiyoshi[2], Masaaki Takahashi[2] (1.Japan Agency for Marine-Earth Science and Technology, 2.National Institute for Environmental Studies)

[AAS05-P13] Evaluation of ozone in the upper troposphere and lower stratosphere derived from multi-species satellite data assimilation

*Takashi Sekiya[1], Kazuyuki Miyazaki[2,1], Koji Ogochi[1], Kengo Sudo[3,1], Masayuki Takigawa[1] (1.Japan Agency for Marine-Earth Science and Technology, 2.Jet Propulsion Laboratory/California Institute for Technology, 3.Graduate School of Environmental Studies, Nagoya University)

[AAS05-P14] Characteristics of Initial Perturbation of JMA GEPS during Sudden Stratospheric Warmings

★Invited Papers

*Shunsuke Noguchi[1,2] (1.Japan Agency for Marine-Earth Science and Technology, 2.Meteorological Research institute, Japan Meteorological Agency)

An advanced impact of Arctic stratospheric ozone changes on spring precipitation in China

*Fei Xie[1]

1. Beijing Normal University

The effect of spring Arctic Stratospheric Ozone (ASO) changes on spring precipitation in China is analyzed using observations, reanalysis data, and the Whole Atmosphere Community Climate Model version 4 (WACCM4). We find that February–March mean ASO changes have a significant impact on April–May mean precipitation over the Loess Plateau and the middle–lower reaches of the Yangtze River—two important grain-producing regions with large populations. Changes in the polar vortex link the ASO to precipitation in China. Stratospheric circulation anomalies caused by ASO changes can propagate to the North Pacific. An increase in ASO leads to enhanced westerlies in the high and low latitudes of the North Pacific but weakened westerlies in the mid-latitudes of the North Pacific. The circulation anomalies over the North Pacific, forced by the increase of ASO, can extend westwards to East Asia, leading to an abnormal anticyclone in the East Asian upper and middle troposphere, and an abnormal cyclone in the lower troposphere. This enhances the warm and humid airstream from the Western Pacific to the Chinese mainland and strengthens upwelling over the Loess Plateau and the middle–lower reaches of the Yangtze River. These conditions enhance precipitation in central China during positive ASO anomaly events and reduce precipitation during negative events. The WACCM4 simulations support the results from our statistical analysis of observations and reanalysis data. Our results suggest that ASO variation can serve as a predictor of spring precipitation variation over the Loess Plateau and the middle–lower reaches of the Yangtze River.

Keywords: Arctic Stratospheric Ozone, Spring precipitation

©2019. Japan Geoscience Union. All Right Reserved.

Global Cooling System installed on the beach by means of Artificial Convection and Artificial Rain

*Murakami Hideyo[1]

1. Ii Ecology Development

In recent years the Earth is warming. The sun radiates sunlight energy and warms the Earth. The Earth reflects a part of sunlight energy to space and radiates infrared ray including latent heat energy to space. An amount of sunlight energy received by the earth is almost the same as an amount of energy sent out by the earth. The amount of sunlight energy is almost constant. On the other hand Greenhouse gas such as CO_2 decreases a ratio of a heat enrgy which air sent out to space to a heat enrgy which air radiates. Then global mean temperature is increasing and many severe climate events due to mean temperature increase happen. In the world many people study to decrease CO_2 accumulation in air and not to increase global mean temperature. However a useful system for decreasing CO_2 accumulation cannot be developed.

This paper studies Global Cooling System. Global Cooling System is composed of Artificial Convection Equipment (type II) and a control center. Global Cooling System can cancel mean temperature increase and cools the Earth, even if air has a lot of greenhouse gas and mean temperature increase is 2℃.

Artificial Convection Equipment looks like a large greenhouse, which is composed of 1 roof, 1 wall, 1 air inlet, 1 air outlet and 1 heater. Artificial Convection Equipment is installed on a tropical beach where it is hot and humidity (35℃, 26.2g kg^{-1}), and a sea breeze during daytime. The roof and the wall are made of transparent plastic sheet and there are the heater (black sheet) under the roof. The heater receives sunlight energy under the roof and changes sunlight energy to heat energy, and warms air inputted from the inlet and sends out heated air from the outlet. Heated air is lighter than circumstance air and is lifted up to the troposphere. The lifted air, which includes a lot of vapor, is cooled in the troposphere. Then vapor is cooled and is changed to artificial rain or snow in the troposphere. The artificial rain or snow falls down to the land. As a result Artificial Convection Equipment artificially makes convection between the beach surface and the troposphere, by transporting warmed air from the beach surface to the troposphere upward and bringing down artificial rain or snow with high altitude air downward. The lifted air sends out latent heat and sensing heat energy of circumstance air including vapor on the beach surface to space, and the artificial rain or snow with the high altitude air absorbs sensing heat and dissolution heat from circumstance air on the land, and cools the land surface too. Furthermore in a region where it is hot and small rain, a half amount of artificial rain is absorbed by plants. Plants vaporize it and absorbs latent heat from circumstance air. Then the earth is cooled by plants too.

This paper analyses Global Cooling System by means of Artificial Convection and Artificial Rain, and shows that mean temperature increase can be stop by Global Cooling System. A large scale of experiment is required to reconfirm a characteristics of Global Cooling System.

Keywords: global cooling, artificial convection, latent heat, artificial rain

©2019. Japan Geoscience Union. All Right Reserved.

Stratospheric front-like temperature structure and gravity wave activity during a stratospheric sudden warming event in 2016

*Yukari Sumi[1], Kaoru Sato[1]

1. University of Tokyo

A large-scale front-like temperature structure is observed in the Arctic stratosphere during a stratospheric sudden warming (SSW) event in 2016. As reported by previous studies, it is shown that a stratospheric front with a vertical scale of about 15 km is formed near the polar vortex edge and vertically tilts toward a colder region. Moreover, we found that the front is the strongest a few days prior to the major warming and that a local maximum of temperature appears in the exit region of a jet streak. These characteristics of the front are roughly common among other SSW events. However, it is not clear as to why the front-like structure is strengthened during the SSW event, which still needs more observational analysis. In the present study, the semi-geostrophic system is considered to better understand the frontogenesis in the stratosphere. Q-vector and frontogenesis function are computed by using MERRA-2 reanalysis data. Near the front region, the geostrophic and ageostrophic parts of the frontogenesis function have large negative and small positive values, respectively. Therefore, it is suggested that the weakening of the front due to geostrophic flow is dominant over the strengthening of the front due to ageostrophic flow. The ageostrophic part is further separated into horizontal and vertical components. The vertical component is positive and significantly larger than the horizontal component. This result implies that the frontogenetic effect of the ageostrophic motion mainly comes from the vertical motion, which seems to be different from the tropospheric front: convergence of the horizontal ageostrophic wind is dominant for the tropospheric front because the vertical motion is suppressed near the ground surface. In addition, gravity wave (GW) activity near the front is examined by using dry temperature data from FORMOSAT-3/COSMIC satellite. The vertical wavelength of the GW is estimated from 1D-Stockwell transform (S-transform) for the temperature data. The S-transform spectra have a peak around 4–7 km in the vertical range between 25 and 35 km where the stratospheric front is the strongest.

Keywords: stratosphere, stratospheric sudden warming

©2019. Japan Geoscience Union. All Right Reserved.

The effects of a well-resolved stratosphere on the simulated boreal winter circulation in a climate model

*Yoshio Kawatani[1], Kevin Hamilton[2], Lesley J. Gray[3], Scott M. Osprey[3], Shingo Watanabe[1], Yousuke Yamashita[1]

1. Japan Agency for Marine-Earth Science and Technology, 2. International Pacific Research Center, University of Hawaii, 3. Atmospheric, Oceanic and Planetary Physics, Department of Physics, University of Oxford

The impact of stratospheric representation is investigated using the Model for Interdisciplinary Research On Climate Atmospheric General Circulation Model (MIROC-AGCM) run with different model-lid heights and stratospheric vertical resolutions, but unchanged horizontal resolutions (~1.125°) and subgrid parameterizations. One hundred year integrations of the model were conducted using configurations with 34, 42, 72 and 168 vertical layers and model-lid heights of ~27 km (L34), 47 km (L42), 47 km (L72) and 100 km (L168). Analysis of the results focused on the Northern Hemisphere in winter. Compared with the L42 model, the L34 model produces a poorer simulation of the stratospheric Brewer-Dobson circulation (BDC) in the lower stratosphere, with weaker polar downwelling and accompanying cold pole and westerly jet biases. The westerly bias extends into the troposphere and even to the surface. The tropospheric westerlies and zone of baroclinic wave activity shift northward; surface pressure has negative (positive) biases in the high (mid) latitudes, with concomitant precipitation shifts. The L72/L168 models generate a Quasi-Biennial Oscillation (QBO) while the L34/42 models do not. The L168 model includes the mesosphere, and thus resolves the upper branch of the BDC. The L72 model simulates stronger polar downwelling associated with the BDC than does the L42 model. However, experiments with prescribed nudging of the tropical stratospheric winds suggest differences in the QBO representation cannot account for L72-L42 differences in the climatological polar night jet structure. The results show that the stratospheric vertical resolution and inclusion of the full middle atmosphere significantly affect tropospheric circulations.

Keywords: middle atmosphere

©2019. Japan Geoscience Union. All Right Reserved.

On the relation between three-dimensional wave activity flux and pseudo momentum without using intrinsic phase velocities

*Takenari Kinoshita[1]

1. Japan Agency for Marine-Earth Science and Technology

The middle-atmosphere general circulation is driven by various wave activities. The transformed Eulerian-Mean (TEM) are the useful tools to diagnose interaction between waves and mean state. The three-dimensional (3D) extension of TEM equations has been conducted since 1980s and the recent study uses the 3D wave activity flux for the analysis of special structure of Rossby wave activities during Stratospheric Sudden Warming. It was proved that divergence of wave activity flux corresponds to the time variation of pseudo momentum in the TEM equations (Eliassen-Palm relation). Also, this relation is proved in the 3D-TEM equations. However, the pseudo momentum used in the relation is defined as the wave energy divided by intrinsic phase velocities and is difficult to use in the data analysis. In this study, referring Double Impulse pseudo momentum of Aiki et al. (2015), the pseudo momentum without using intrinsic phase velocities are introduced and the relation between 3D wave activity flux divergence and time variation of pseudo momentum in the middle atmosphere is reported.

Keywords: wave activity flux, pseudo momentum

©2019. Japan Geoscience Union. All Right Reserved.

Hindcasts of the 2016 Disruption of the Stratospheric Quasi-biennial Oscillation

*Shingo Watanabe[1], Kevin Hamilton[2], Scott Osprey[3], Yoshio Kawatani[1], Eriko Nishimoto

1. Japan Agency for Marine-Earth Science and Technology, 2. International Pacific Research Center, University of Hawaii at Manoa, 3. NCAS-Climate, University of Oxford

In early 2016 the quasi-biennial oscillation in tropical stratospheric winds was disrupted by an anomalous easterly jet centered at ~40 hPa, a development that was completely missed by all operational extended range weather forecast systems. This event and its predictability are investigated through ensemble hindcasts using a global model notable for its sophisticated representation of the upper atmosphere. Key to prediction of this event is simulating the slowly evolving mean winds in the winter subtropics that provide a waveguide for Rossby waves propagating from the winter hemisphere. Its association to the strong El Nino condition in 2015 is also investigated by changing sea surface temperatures.

Keywords: quasi-biennial oscillation, Rossby wave, extended range hindcast

©2019. Japan Geoscience Union. All Right Reserved.

Selection bias of quasi-fixed-point observations in the ExUTLS and its impact on the seasonal record

*Yoichi Inai[1], Toshinobu Machida[2], Hidekazu Matsueda[3], Yousuke Sawa[3], Kazuhiro Tsuboi[3], Keiichi Katsumata[2,4], Shinji Morimoto[1], Shuji Aoki[1], Takakiyo Nakazawa[1], Ryo Fujita[5,1]

1. Tohoku Univ., 2. NIES, 3. MRI, 4. Takachiho Chem. Industrial, 5. Imperial College London

Fixed-point observations are essential for long-term monitoring of the atmospheric environment. However, some attention might be paid to the interpretation of seasonal variations appearing in the observational record, particularly for regions with large seasonal variations. In the extra-tropical upper troposphere/lower stratosphere (ExUTLS), the climatological tropopause height changes with season. This leads to a seasonal dependence of whether individual fixed-point observations are included in the stratosphere or the troposphere. In this study, using the reanalysis fields, quasi-fixed-point observations in the ExUTLS are simulated and categorized as being in the troposphere or stratosphere based on their position relative to the dynamic tropopause, to investigate seasonal tendencies of the categorization. The influence of these tendencies on seasonal variations of atmospheric composition in the categorized data is estimated. The seasonal cycles of CH_4, N_2O and SF_6 mixing ratios are found to change with the categorization method. In particular, the minimum values for these tropospheric tracers in observations categorized as stratospheric occur 1–2 months later than in uncategorized observations. This delay in stratospheric record is interpreted as the selection bias, that is, the air mass categorized as the stratospheric atmosphere biased to some specific meteorological situation due to the seasonal variation of ExUTLS meteorological field.

Keywords: Earth atmosphere, Observation

©2019. Japan Geoscience Union. All Right Reserved.

Varying Rossby Wave Trains from the Developing to Decaying Period of the Upper Atmospheric Heat Source over the Tibetan Plateau in Boreal Summer

*Chuandong Zhu[1,2], Rongcai Ren[1]

1. Institute of Atmospheric Physics, Chinese Academy of Sciences, 2. University of Chinese Academy of Sciences

This study demonstrates the two different Rossby wave train (RWT) patterns related to the developing/decaying upper atmospheric heat source over the Tibetan Plateau (TPUHS) in boreal summer. The results show that the summer TPUHS is dominated by quasi-biweekly variability, particularly from late July to mid-August when the subtropical jet steadily stays to the north of the TP. During the developing period of TPUHS events, the intensifying TPUHS corresponds to an anomalous upper-tropospheric high over the TP, which acts as the main source of a RWT that extends northeastward, via North China, the central Pacific and Alaska, to the northeastern Pacific region. This RWT breaks up while the anomalous high is temporarily replaced by an anomalous low due to the further deepened convective heating around the TPUHS peak. However, this anomalous low, though existing for only three to four days due to the counteracting dynamical effects of the persisting upper/lower divergence/convergence over the TP, acts as a new wave source to connect to an anomalous dynamical high over the Baikal region. Whilst the anomalous low is diminishing rapidly, this Baikal high becomes the main source of a new RWT, which develops eastward over the North Pacific region till around eight days after the TPUHS peak. Nevertheless, the anomaly centers along this decaying-TPUHS-related RWT mostly appear much weaker than those along the previous RWT. Therefore, their impacts on circulation and weather differ considerably from the developing to the decaying period of TPUHS events.

Keywords: Tibetan Plateau, upper atmospheric heat source, Rossby wave train, circulation and weather

©2019. Japan Geoscience Union. All Right Reserved.

Equilibrium Climate Responses of the East Asian Summer Monsoon to Various Anthropogenic Aerosol Species

*Qiuyan Wang[2,1], Zhili Wang[1,2], Hua Zhang[3,2]

1. State Key Laboratory of Severe Weather & Key Laboratory of Atmospheric Chemistry of CMA, Chinese Academy of Meteorological Sciences, Beijing, 2. Collaborative Innovation Center on Forecast and Evaluation of Meteorological Disasters, Nanjing University of Information Science and Technology, Nanjing, 3. Laboratory for Climate Studies, National Climate Center, China Meteorological Administration, Beijing

The equilibrium climate responses of the East Asian summer monsoon (EASM) to increases in various types of anthropogenic aerosol emissions, including sulfate, organic carbon (OC), and black carbon (BC), from 1850 to 2000 are studied using an aerosol-climate online model. The results show that various aerosol species have substantially different impacts on the EASM by changing the local sea-land surface thermal difference and atmospheric circulation. The increased sulfate leads to decrease in the surface thermal difference between the land and ocean, the southward shift of the East Asian subtropical jet (EASJ), and significant northerly wind anomalies at 850 hPa over eastern China and the ambient oceans, thus dampening the EASM markedly. Pronounced surface cooling appears and an anomalous anticyclone is formed over the oceans north of 30˚N due to the increase of OC. These cause slight increase in sea-land surface thermal difference and southerly flow anomalies to the west of the anticyclonic center, thereby strengthening the northern East Asian summer monsoon (NEASM). However, the increased OC decreases the sea-land surface thermal contrast over southern China, which weakens the southern East Asian summer monsoon (SEASM). The responses of summer 850 hPa winds and rainfall over the East Asian monsoon region (EAMR) to increase in BC are generally consistent with those to increase in OC. The increased BC leads to the strengthening of the NEASM north of 35˚N and slight weakening of the SEASM south of 35˚N. Also, the simulated responses of the EASM to increase in BC are not changed when BC emission is scaled up by five times its 2000 levels, but the intensities of responses are enhanced. Overall, the increase in sulfate primarily weakens the EASM, while the increases in BC and OC mitigate the weakening of the NEASM to some extent.

Keywords: EASM, various aerosol species, equilibrium climate response

©2019. Japan Geoscience Union. All Right Reserved.

Analysis of specific energy in zonal currents focusing on the analogy between jet stream and open channel flow

*Yoshikazu Kitano[1], Tomohito J. Yamada[2]

1. Central Research Institute of Electric Power Industry, 2. Faculty of Engineering, Hokkaido University

Atmospheric blocking is one of the important causes of meteorological extremes in mid-latitude, such as cold spells, heat waves and long-term heavy rainfalls. Rossby (1950) focused on dynamical analogies between the hydraulic jump in open channel flow and the atmospheric blocking in jet stream, and proposed a theoretical formula to explain the two dynamically possible states in zonal currents which are compatible with supercritical and subcritical flow in an open channel flow. Armi (1989) focused on the specific energy flux in zonal currents and showed that a dimensionless parameter, which is called Froude/Rossby number, is analogous to the Froude number of open channel flow. Kitano and Yamada (2017) extended these theories to realistic conditions in atmosphere and showed a relationship between typical blocking flow and specific energy flux in jet stream. In this study, we analyzed several blocking episodes using specific energy flux and found energetic signals over Japan and its surroundings before Pacific blocking occasions. These signals may contribute to prediction on blocking.

Keywords: atmospheric blocking, jet stream, open channel flow

©2019. Japan Geoscience Union. All Right Reserved.

Analysis of the ozone reduction event over the southern tip of South America in November 2009

*Hideharu Akiyoshi[1], Masanao Kadowaki[2], Haruna Nakamura[3], Takafumi Sugita[1], Toshihiko Hirooka[4], Yayoi Harada[5], Akira Mizuno[6]

1. National Institute for Environmental Studies, 2. Japan Atomic Energy Agency, 3. Fujitsu FIP Corporation, 4. Department of Earth and Planetary Sciences, Kyushu University, 5. Meteorological Research Institute, 6. Institute for Space-Earth Environmental Research, Nagoya University

A reduction of the total ozone over the southern tip of South America lasting 3 weeks occurred in November 2009. Analyses of the ERA-Interim reanalysis data and the total ozone observed by the OMI indicate that the total ozone reduction event was caused by a migration of the polar vortex toward the South American continent at the time of the vortex breakup. The vortex migration is associated with an enhanced wave flux from the troposphere at 120–150˚W and 50–60˚S to the west of the South American continent to the stratosphere over the southern part of the continent, which led to a large negative geopotential height anomaly in the lower stratosphere. In November, a blocking pattern was diagnosed from the 500 hPa geopotential height over the west of the South American continent. These results suggest a relation between the long-lasting reduction of the total ozone over the southern tip of South America and the blocking phenomenon in the troposphere of the Southern Hemisphere through wave propagation from the blocking region in 2009.

The total ozone, the geopotential height at 50 hPa and 500 hPa, the wave activity flux, the polar vortex migration and elongation, and the blocking pattern in the Southern Hemisphere November for 1979–2015 as well as 2009 were investigated. The results show that the relation between the blocking pattern in the troposphere and the large polar vortex migration and elongation in the stratosphere is also evident in November 1987, 1994, 1997, 2001, and 2011. Especially, in November 1994, 1997, and 2011, the blocking pattern and the polar vortex migration occurred near the South American continent.

These results indicate that the migration of the Antarctic polar vortex to the southern tip of South America in November occurred occasionally in the past. They also suggest that diagnosis of blocking pattern in the Southern Hemisphere troposphere may be useful for prediction of the direction of polar vortex migration in the stratosphere, and hence, prediction of high UV radiation risk over the southern tip of South America in early summer.

This research was supported by JST/JICA, SATREPS, the Environment Research and Technology Development Fund.

Keywords: ozone hole, South America, polar vortex, blocking, November 2009, ERA-Interim reanalysis data

©2019. Japan Geoscience Union. All Right Reserved.

Analysis of relatively low ozone in Arctic spring during the QBO-westerly and solar-minimum years

*Yousuke Yamashita[1,2], Hideharu Akiyoshi[2], Masaaki Takahashi[2]

1. Japan Agency for Marine-Earth Science and Technology, 2. National Institute for Environmental Studies

The equatorial quasi-biennial oscillation (QBO) and the 11-year solar cycle are known to cause year-to-year variability of the Northern Hemisphere (NH) polar vortex (e.g. Holton and Tan, 1980; Labitzke, 1987). Labitzke (1987) and several studies following her work have been used the four categories of the QBO and 11-year solar cycle, according to the westerly/easterly phase of the QBO (QBO-W/QBO-E) and the maximum/minimum phase of the 11-year solar cycle (S_{max}/ S_{min}). Camp and Tung (2007) suggested that the NH polar vortex is the most stable and the least perturbed state in late winter during the QBO-W/S_{min} years relative to the other three groups (QBO-W/S_{max}, QBO-E/S_{max}, and QBO-E/S_{min}), in agreement with the work of Labitzke and van Loon (1988). Their findings are in agreement with the smallest magnitude of the Arctic total ozone in QBO-W/S_{min} years among the four categories (Li and Tung 2014), because the ozone depletion is enhanced in the stable and cold polar vortex associated with an increase in chemical destruction through heterogeneous reactions on the Polar Stratospheric Clouds (PSCs). Since the Arctic ozone amount is related to the ozone transport as well as the chemical ozone destruction, the estimation of their influences is still challenging issue for understanding the small amount of the Arctic total ozone in March.

In this study, we analyze the Arctic ozone amount using TOMS/OMI observations, ERA-interim reanalysis data, and the outputs of a chemistry climate model (CCM) with REF-C1SD hindcast simulation, in which the model’s zonal/meridional wind and temperature are nudged toward those of the ERA-interim reanalysis data with a 6-hour interval. The anomaly from the average for all the years of 1979–2011 in the Arctic total ozone amount is calculated for QBO-W/S_{min} group in late winter. We estimate the amounts of ozone transport and chemical ozone destruction and their effects on the derived Arctic ozone anomaly for the QBO-W/S_{min} group with CCM outputs.

Result of the composite mean for QBO-W/S_{min} years shows negative anomaly (relatively small amount) of total ozone in February–March compared to the 1979–2011 average from the CCM output, in agreement with the satellite observation, reanalysis data. To distinguish the effect of chemical ozone destruction from that of ozone transport for the total ozone anomaly in February–March, we analyze the total ozone anomaly of the passive ozone tracer without any chemical change in the CCM. The negative anomalies of the passive ozone tracer have a similar distribution to that of chemically reactive ozone with similar magnitude, suggesting that the negative anomalies of total ozone are mainly caused by ozone transport.

The outputs of CCM are also analyzed for vertical profile of ozone concentration, which indicates negative anomaly of the Arctic ozone in the upper troposphere and the lower stratosphere for the QBO-W/S_{min} condition, the maximum anomaly of ozone partial column is located around 50–70 hPa. The partial column of the passive ozone tracer at these levels also shows negative anomalies, whilst their magnitudes are small, especially at 50 hPa in March. These results suggest the significant influence of ozone transport on the negative ozone anomaly in February–March, whilst the influence of chemistry is partially large at 50 hPa in March.

©2019. Japan Geoscience Union. All Right Reserved.

Keywords: stratospheric ozone, Northern Hemisphere polar vortex, chemistry climate mode

©2019. Japan Geoscience Union. All Right Reserved.

Evaluation of ozone in the upper troposphere and lower stratosphere derived from multi-species satellite data assimilation

*Takashi Sekiya[1], Kazuyuki Miyazaki[2,1], Koji Ogochi[1], Kengo Sudo[3,1], Masayuki Takigawa[1]

1. Japan Agency for Marine-Earth Science and Technology, 2. Jet Propulsion Laboratory/California Institute for Technology, 3. Graduate School of Environmental Studies, Nagoya University

Ozone (O_3) in the upper troposphere and lower stratosphere (UTLS) has a stronger greenhouse effect than in the lower troposphere. However, information on O_3 in the UTLS from observations with the global coverage is still limited. Multi-species satellite data assimilation of stratospheric O_3, and tropospheric O_3 and its precursors is expected to provide better constraints on O_3 in the UTLS, because O_3 in the UTLS is controlled by stratospheric O_3 intrusions, O_3 transport from middle and lower troposphere, and in-situ O_3 chemical production. In this study, we evaluate O_3 in the UTLS derived from the multi-species data assimilation with horizontal resolutions of 2.8, 1.1, and 0.56 degree using ozonesonde observations (not used for data assimilation) in April 2008. Assimilated data were obtained from the OMI, GOME-2, and SCIAMACHY for tropospheric NO_2 column, the TES for O_3 profile, the MOPITT for total CO column, the MLS for O_3 and HNO_3 profiles, and the OMI for total SO_2 column. At 200 hPa, 300 hPa, and 500 hPa, the data assimilation at 0.56-degree resolution reduced root mean square errors (RMSEs) against ozonesonde observations in the northern midlatitudes by 32%, 31%, and 13%, respectively, compared to the model simulation without data assimilation. The overall data assimilation performance for O_3 concentrations is not sensitive to horizontal resolution in the altitudes between 200 hPa and 500 hPa (i.e., the RMSEs were within 7% at all resolutions). Meanwhile, the data assimilation at 0.56-degree resolution improved agreements with ozonesonde observations at 300 hPa by up to 55% compared to 1.1- and 2.8-degree resolutions during a deep stratospheric intrusion episode at Trinidad Head (124˚W, 41˚N) through resolving small-scale transport processes. These results confirm that O_3 analyses derived from multi-species data assimilation are suitable for understanding spatial and temporal variations in O_3 in the UTLS and their controlling processes.

Keywords: Satellite data assimilation, Ozone, Atmospheric chemistry

©2019. Japan Geoscience Union. All Right Reserved.

Characteristics of Initial Perturbation of JMA GEPS during Sudden Stratospheric Warmings

*Shunsuke Noguchi[1,2]

1. Japan Agency for Marine-Earth Science and Technology, 2. Meteorological Research institute, Japan Meteorological Agency

In order to sophisticate the ensemble forecasting and data assimilation system of the whole atmosphere, it is necessary to accumulate the knowledge about the uncertainty of the analysis in the stratosphere and mesosphere, which is poor in comparison with that in the troposphere. Therefore, this study investigates characteristics of initial perturbation of the Japan Meteorological Agency (JMA) Global Ensemble Prediction System (GEPS), which has been replaced in March 2017.

By focusing on two Sudden Stratospheric Warming (SSW) events occurred in 2017-2018 and 2018-2019 winters, several aspects of the new JMA GEPS are revealed as follows: (1) There is large uncertainty above the upper stratosphere (which has not been reflected in the previous system). (2) The analysis ensemble spread increases and penetrates downward from the upper stratosphere during the onset period of both SSW events, though its precursory nature is not so evident as pointed by previous studies (e.g. Enomoto et al. 2010). (3) After SSW events, the analysis ensemble spread in the middle and upper stratosphere shrinks in association with the change of dominant physical processes. However, relatively large spreads, which may have implications for the stratosphere-troposphere coupling, are sometimes found in the lower stratosphere.

The quality of forecasts and analyses above the upper stratosphere would be inevitable from the artificial effect of sponge layers near the model top. Therefore, it is worth comparing or communicating with results of some high-top system to validate the appropriateness of above-mentioned aspects (e.g. (1)) and recognize limitations of current operational settings.

Keywords: Sudden Stratospheric Warming, Ensemble Prediction System

©2019. Japan Geoscience Union. All Right Reserved.

[J] Poster | A (Atmospheric and Hydrospheric Sciences)：A-AS Atmospheric Sciences, Meteorology & Atmospheric Environment

Wed. May 29, 2019 5:15 PM - 6:30 PM JST | Wed. May 29, 2019 8:15 AM - 9:30 AM UTC | Poster Hall International Exhibition Hall8, Makuhari Messe_10

[A-AS05] Stratosphere-troposphere Processes And their Role in Climate

convener:Yoshio Kawatani(Japan Agency for Marine-Earth Science and Technology), Shingo Watanabe(Japan Agency for Marine-Earth Science and Technology), Takashi Sekiya(Japan Agency for Marine-Earth Science and Technology), Kaoru Sato(Department of Earth and Planetary Science, Graduate School of Science, The University of Tokyo)

The Stratosphere-troposphere Processes And their Role in Climate (SPARC) is one of the
major projects of the World Climate Research Programme (WCRP), and is characterized
by its focus on chemical and dynamical coupling in the stratosphere and troposphere. In
this session, we welcome presentations on various processes in the stratosphere and tro
posphere.

[AAS05-P01] An advanced impact of Arctic stratospheric ozone changes on spring precipitation in China

*Fei Xie[1] (1.Beijing Normal University)

[AAS05-P02] Global Cooling System installed on the beach by means of Artificial Convection and Artificial Rain

*Murakami Hideyo[1] (1.Ii Ecology Development)

[AAS05-P03] Stratospheric front-like temperature structure and gravity wave activity during a stratospheric sudden warming event in 2016

*Yukari Sumi[1], Kaoru Sato[1] (1.University of Tokyo)

[AAS05-P04] The effects of a well-resolved stratosphere on the simulated boreal winter circulation in a climate model

*Yoshio Kawatani[1], Kevin Hamilton[2], Lesley J. Gray[3], Scott M. Osprey[3], Shingo Watanabe[1], Yousuke Yamashita[1] (1.Japan Agency for Marine-Earth Science and Technology, 2.International Pacific Research Center, University of Hawaii, 3.Atmospheric, Oceanic and Planetary Physics, Department of Physics, University of Oxford)

[AAS05-P05] On the relation between three-dimensional wave activity flux and pseudo momentum without using intrinsic phase velocities

★Invited Papers

*Takenari Kinoshita[1] (1.Japan Agency for Marine-Earth Science and Technology)

[AAS05-P06] Hindcasts of the 2016 Disruption of the Stratospheric Quasi-biennial Oscillation

*Shingo Watanabe[1], Kevin Hamilton[2], Scott Osprey[3], Yoshio Kawatani[1], Eriko Nishimoto (1.Japan Agency for Marine-Earth Science and Technology, 2.International Pacific Research Center, University of Hawaii at Manoa, 3.NCAS-Climate, University of Oxford)

[AAS05-P07] Selection bias of quasi-fixed-point observations in the ExUTLS and its impact on the seasonal record

*Yoichi Inai[1], Toshinobu Machida[2], Hidekazu Matsueda[3], Yousuke Sawa[3], Kazuhiro Tsuboi[3], Keiichi Katsumata[2,4], Shinji Morimoto[1], Shuji Aoki[1], Takakiyo Nakazawa[1], Ryo Fujita[5,1] (1.Tohoku Univ., 2.NIES, 3.MRI, 4.Takachiho Chem. Industrial, 5.Imperial College London)

[AAS05-P08] Varying Rossby Wave Trains from the Developing to Decaying Period of the Upper Atmospheric Heat Source over the Tibetan Plateau in Boreal Summer

*Chuandong Zhu[1,2], Rongcai Ren[1] (1.Institute of Atmospheric Physics, Chinese Academy of Sciences, 2.University of Chinese Academy of Sciences)

[AAS05-P09] **Equilibrium Climate Responses of the East Asian Summer Monsoon to Various Anthropogenic Aerosol Species**

*Qiuyan Wang[2,1], Zhili Wang[1,2], Hua Zhang[3,2] (1.State Key Laboratory of Severe Weather & Key Laboratory of Atmospheric Chemistry of CMA, Chinese Academy of Meteorological Sciences, Beijing, 2.Collaborative Innovation Center on Forecast and Evaluation of Meteorological Disasters, Nanjing University of Information Science and Technology, Nanjing, 3.Laboratory for Climate Studies, National Climate Center, China Meteorological Administration, Beijing)

[AAS05-P10] Analysis of specific energy in zonal currents focusing on the analogy between jet stream and open channel flow

*Yoshikazu Kitano[1], Tomohito J. Yamada[2] (1.Central Research Institute of Electric Power Industry, 2.Faculty of Engineering, Hokkaido University)

[AAS05-P11] Analysis of the ozone reduction event over the southern tip of South America in November 2009

*Hideharu Akiyoshi[1], Masanao Kadowaki[2], Haruna Nakamura[3], Takafumi Sugita[1], Toshihiko Hirooka[4], Yayoi Harada[5], Akira Mizuno[6] (1.National Institute for Environmental Studies, 2.Japan Atomic Energy Agency, 3.Fujitsu FIP Corporation, 4.Department of Earth and Planetary Sciences, Kyushu University, 5.Meteorological Research Institute, 6.Institute for Space-Earth Environmental Research, Nagoya University)

[AAS05-P12] **Analysis of relatively low ozone in Arctic spring during the QBO-westerly and solar-minimum years**

*Yousuke Yamashita[1,2], Hideharu Akiyoshi[2], Masaaki Takahashi[2] (1.Japan Agency for Marine-Earth Science and Technology, 2.National Institute for Environmental Studies)

[AAS05-P13] Evaluation of ozone in the upper troposphere and lower stratosphere derived from multi-species satellite data assimilation

*Takashi Sekiya[1], Kazuyuki Miyazaki[2,1], Koji Ogochi[1], Kengo Sudo[3,1], Masayuki Takigawa[1] (1.Japan Agency for Marine-Earth Science and Technology, 2.Jet Propulsion Laboratory/California Institute for Technology, 3.Graduate School of Environmental Studies, Nagoya University)

[AAS05-P14] Characteristics of Initial Perturbation of JMA GEPS during Sudden Stratospheric Warmings

★Invited Papers

*Shunsuke Noguchi[1,2] (1.Japan Agency for Marine-Earth Science and Technology, 2.Meteorological Research institute, Japan Meteorological Agency)

An advanced impact of Arctic stratospheric ozone changes on spring precipitation in China

*Fei Xie[1]

1. Beijing Normal University

The effect of spring Arctic Stratospheric Ozone (ASO) changes on spring precipitation in China is analyzed using observations, reanalysis data, and the Whole Atmosphere Community Climate Model version 4 (WACCM4). We find that February–March mean ASO changes have a significant impact on April–May mean precipitation over the Loess Plateau and the middle–lower reaches of the Yangtze River—two important grain-producing regions with large populations. Changes in the polar vortex link the ASO to precipitation in China. Stratospheric circulation anomalies caused by ASO changes can propagate to the North Pacific. An increase in ASO leads to enhanced westerlies in the high and low latitudes of the North Pacific but weakened westerlies in the mid-latitudes of the North Pacific. The circulation anomalies over the North Pacific, forced by the increase of ASO, can extend westwards to East Asia, leading to an abnormal anticyclone in the East Asian upper and middle troposphere, and an abnormal cyclone in the lower troposphere. This enhances the warm and humid airstream from the Western Pacific to the Chinese mainland and strengthens upwelling over the Loess Plateau and the middle–lower reaches of the Yangtze River. These conditions enhance precipitation in central China during positive ASO anomaly events and reduce precipitation during negative events. The WACCM4 simulations support the results from our statistical analysis of observations and reanalysis data. Our results suggest that ASO variation can serve as a predictor of spring precipitation variation over the Loess Plateau and the middle–lower reaches of the Yangtze River.

Keywords: Arctic Stratospheric Ozone, Spring precipitation

©2019. Japan Geoscience Union. All Right Reserved.

Global Cooling System installed on the beach by means of Artificial Convection and Artificial Rain

*Murakami Hideyo[1]

1. Ii Ecology Development

In recent years the Earth is warming. The sun radiates sunlight energy and warms the Earth. The Earth reflects a part of sunlight energy to space and radiates infrared ray including latent heat energy to space. An amount of sunlight energy received by the earth is almost the same as an amount of energy sent out by the earth. The amount of sunlight energy is almost constant. On the other hand Greenhouse gas such as CO_2 decreases a ratio of a heat enrgy which air sent out to space to a heat enrgy which air radiates. Then global mean temperature is increasing and many severe climate events due to mean temperature increase happen. In the world many people study to decrease CO_2 accumulation in air and not to increase global mean temperature. However a useful system for decreasing CO_2 accumulation cannot be developed.

This paper studies Global Cooling System. Global Cooling System is composed of Artificial Convection Equipment (type II) and a control center. Global Cooling System can cancel mean temperature increase and cools the Earth, even if air has a lot of greenhouse gas and mean temperature increase is 2℃.

Artificial Convection Equipment looks like a large greenhouse, which is composed of 1 roof, 1 wall, 1 air inlet, 1 air outlet and 1 heater. Artificial Convection Equipment is installed on a tropical beach where it is hot and humidity (35℃, 26.2g kg^{-1}), and a sea breeze during daytime. The roof and the wall are made of transparent plastic sheet and there are the heater (black sheet) under the roof. The heater receives sunlight energy under the roof and changes sunlight energy to heat energy, and warms air inputted from the inlet and sends out heated air from the outlet. Heated air is lighter than circumstance air and is lifted up to the troposphere. The lifted air, which includes a lot of vapor, is cooled in the troposphere. Then vapor is cooled and is changed to artificial rain or snow in the troposphere. The artificial rain or snow falls down to the land. As a result Artificial Convection Equipment artificially makes convection between the beach surface and the troposphere, by transporting warmed air from the beach surface to the troposphere upward and bringing down artificial rain or snow with high altitude air downward. The lifted air sends out latent heat and sensing heat energy of circumstance air including vapor on the beach surface to space, and the artificial rain or snow with the high altitude air absorbs sensing heat and dissolution heat from circumstance air on the land, and cools the land surface too. Furthermore in a region where it is hot and small rain, a half amount of artificial rain is absorbed by plants. Plants vaporize it and absorbs latent heat from circumstance air. Then the earth is cooled by plants too.

This paper analyses Global Cooling System by means of Artificial Convection and Artificial Rain, and shows that mean temperature increase can be stop by Global Cooling System. A large scale of experiment is required to reconfirm a characteristics of Global Cooling System.

Keywords: global cooling, artificial convection, latent heat, artificial rain

©2019. Japan Geoscience Union. All Right Reserved.

Stratospheric front-like temperature structure and gravity wave activity during a stratospheric sudden warming event in 2016

*Yukari Sumi[1], Kaoru Sato[1]

1. University of Tokyo

A large-scale front-like temperature structure is observed in the Arctic stratosphere during a stratospheric sudden warming (SSW) event in 2016. As reported by previous studies, it is shown that a stratospheric front with a vertical scale of about 15 km is formed near the polar vortex edge and vertically tilts toward a colder region. Moreover, we found that the front is the strongest a few days prior to the major warming and that a local maximum of temperature appears in the exit region of a jet streak. These characteristics of the front are roughly common among other SSW events. However, it is not clear as to why the front-like structure is strengthened during the SSW event, which still needs more observational analysis. In the present study, the semi-geostrophic system is considered to better understand the frontogenesis in the stratosphere. Q-vector and frontogenesis function are computed by using MERRA-2 reanalysis data. Near the front region, the geostrophic and ageostrophic parts of the frontogenesis function have large negative and small positive values, respectively. Therefore, it is suggested that the weakening of the front due to geostrophic flow is dominant over the strengthening of the front due to ageostrophic flow. The ageostrophic part is further separated into horizontal and vertical components. The vertical component is positive and significantly larger than the horizontal component. This result implies that the frontogenetic effect of the ageostrophic motion mainly comes from the vertical motion, which seems to be different from the tropospheric front: convergence of the horizontal ageostrophic wind is dominant for the tropospheric front because the vertical motion is suppressed near the ground surface. In addition, gravity wave (GW) activity near the front is examined by using dry temperature data from FORMOSAT-3/COSMIC satellite. The vertical wavelength of the GW is estimated from 1D-Stockwell transform (S-transform) for the temperature data. The S-transform spectra have a peak around 4–7 km in the vertical range between 25 and 35 km where the stratospheric front is the strongest.

Keywords: stratosphere, stratospheric sudden warming

©2019. Japan Geoscience Union. All Right Reserved.

The effects of a well-resolved stratosphere on the simulated boreal winter circulation in a climate model

*Yoshio Kawatani[1], Kevin Hamilton[2], Lesley J. Gray[3], Scott M. Osprey[3], Shingo Watanabe[1], Yousuke Yamashita[1]

1. Japan Agency for Marine-Earth Science and Technology, 2. International Pacific Research Center, University of Hawaii, 3. Atmospheric, Oceanic and Planetary Physics, Department of Physics, University of Oxford

The impact of stratospheric representation is investigated using the Model for Interdisciplinary Research On Climate Atmospheric General Circulation Model (MIROC-AGCM) run with different model-lid heights and stratospheric vertical resolutions, but unchanged horizontal resolutions (~1.125°) and subgrid parameterizations. One hundred year integrations of the model were conducted using configurations with 34, 42, 72 and 168 vertical layers and model-lid heights of ~27 km (L34), 47 km (L42), 47 km (L72) and 100 km (L168). Analysis of the results focused on the Northern Hemisphere in winter. Compared with the L42 model, the L34 model produces a poorer simulation of the stratospheric Brewer-Dobson circulation (BDC) in the lower stratosphere, with weaker polar downwelling and accompanying cold pole and westerly jet biases. The westerly bias extends into the troposphere and even to the surface. The tropospheric westerlies and zone of baroclinic wave activity shift northward; surface pressure has negative (positive) biases in the high (mid) latitudes, with concomitant precipitation shifts. The L72/L168 models generate a Quasi-Biennial Oscillation (QBO) while the L34/42 models do not. The L168 model includes the mesosphere, and thus resolves the upper branch of the BDC. The L72 model simulates stronger polar downwelling associated with the BDC than does the L42 model. However, experiments with prescribed nudging of the tropical stratospheric winds suggest differences in the QBO representation cannot account for L72-L42 differences in the climatological polar night jet structure. The results show that the stratospheric vertical resolution and inclusion of the full middle atmosphere significantly affect tropospheric circulations.

Keywords: middle atmosphere

©2019. Japan Geoscience Union. All Right Reserved.

On the relation between three-dimensional wave activity flux and pseudo momentum without using intrinsic phase velocities

*Takenari Kinoshita[1]

1. Japan Agency for Marine-Earth Science and Technology

The middle-atmosphere general circulation is driven by various wave activities. The transformed Eulerian-Mean (TEM) are the useful tools to diagnose interaction between waves and mean state. The three-dimensional (3D) extension of TEM equations has been conducted since 1980s and the recent study uses the 3D wave activity flux for the analysis of special structure of Rossby wave activities during Stratospheric Sudden Warming. It was proved that divergence of wave activity flux corresponds to the time variation of pseudo momentum in the TEM equations (Eliassen-Palm relation). Also, this relation is proved in the 3D-TEM equations. However, the pseudo momentum used in the relation is defined as the wave energy divided by intrinsic phase velocities and is difficult to use in the data analysis. In this study, referring Double Impulse pseudo momentum of Aiki et al. (2015), the pseudo momentum without using intrinsic phase velocities are introduced and the relation between 3D wave activity flux divergence and time variation of pseudo momentum in the middle atmosphere is reported.

Keywords: wave activity flux, pseudo momentum

©2019. Japan Geoscience Union. All Right Reserved.

Hindcasts of the 2016 Disruption of the Stratospheric Quasi-biennial Oscillation

*Shingo Watanabe[1], Kevin Hamilton[2], Scott Osprey[3], Yoshio Kawatani[1], Eriko Nishimoto

1. Japan Agency for Marine-Earth Science and Technology, 2. International Pacific Research Center, University of Hawaii at Manoa, 3. NCAS-Climate, University of Oxford

In early 2016 the quasi-biennial oscillation in tropical stratospheric winds was disrupted by an anomalous easterly jet centered at ~40 hPa, a development that was completely missed by all operational extended range weather forecast systems. This event and its predictability are investigated through ensemble hindcasts using a global model notable for its sophisticated representation of the upper atmosphere. Key to prediction of this event is simulating the slowly evolving mean winds in the winter subtropics that provide a waveguide for Rossby waves propagating from the winter hemisphere. Its association to the strong El Nino condition in 2015 is also investigated by changing sea surface temperatures.

Keywords: quasi-biennial oscillation, Rossby wave, extended range hindcast

©2019. Japan Geoscience Union. All Right Reserved.

Selection bias of quasi-fixed-point observations in the ExUTLS and its impact on the seasonal record

*Yoichi Inai[1], Toshinobu Machida[2], Hidekazu Matsueda[3], Yousuke Sawa[3], Kazuhiro Tsuboi[3], Keiichi Katsumata[2,4], Shinji Morimoto[1], Shuji Aoki[1], Takakiyo Nakazawa[1], Ryo Fujita[5,1]

1. Tohoku Univ., 2. NIES, 3. MRI, 4. Takachiho Chem. Industrial, 5. Imperial College London

Fixed-point observations are essential for long-term monitoring of the atmospheric environment. However, some attention might be paid to the interpretation of seasonal variations appearing in the observational record, particularly for regions with large seasonal variations. In the extra-tropical upper troposphere/lower stratosphere (ExUTLS), the climatological tropopause height changes with season. This leads to a seasonal dependence of whether individual fixed-point observations are included in the stratosphere or the troposphere. In this study, using the reanalysis fields, quasi-fixed-point observations in the ExUTLS are simulated and categorized as being in the troposphere or stratosphere based on their position relative to the dynamic tropopause, to investigate seasonal tendencies of the categorization. The influence of these tendencies on seasonal variations of atmospheric composition in the categorized data is estimated. The seasonal cycles of CH_4, N_2O and SF_6 mixing ratios are found to change with the categorization method. In particular, the minimum values for these tropospheric tracers in observations categorized as stratospheric occur 1–2 months later than in uncategorized observations. This delay in stratospheric record is interpreted as the selection bias, that is, the air mass categorized as the stratospheric atmosphere biased to some specific meteorological situation due to the seasonal variation of ExUTLS meteorological field.

Keywords: Earth atmosphere, Observation

©2019. Japan Geoscience Union. All Right Reserved.

Varying Rossby Wave Trains from the Developing to Decaying Period of the Upper Atmospheric Heat Source over the Tibetan Plateau in Boreal Summer

*Chuandong Zhu[1,2], Rongcai Ren[1]

1. Institute of Atmospheric Physics, Chinese Academy of Sciences, 2. University of Chinese Academy of Sciences

This study demonstrates the two different Rossby wave train (RWT) patterns related to the developing/decaying upper atmospheric heat source over the Tibetan Plateau (TPUHS) in boreal summer. The results show that the summer TPUHS is dominated by quasi-biweekly variability, particularly from late July to mid-August when the subtropical jet steadily stays to the north of the TP. During the developing period of TPUHS events, the intensifying TPUHS corresponds to an anomalous upper-tropospheric high over the TP, which acts as the main source of a RWT that extends northeastward, via North China, the central Pacific and Alaska, to the northeastern Pacific region. This RWT breaks up while the anomalous high is temporarily replaced by an anomalous low due to the further deepened convective heating around the TPUHS peak. However, this anomalous low, though existing for only three to four days due to the counteracting dynamical effects of the persisting upper/lower divergence/convergence over the TP, acts as a new wave source to connect to an anomalous dynamical high over the Baikal region. Whilst the anomalous low is diminishing rapidly, this Baikal high becomes the main source of a new RWT, which develops eastward over the North Pacific region till around eight days after the TPUHS peak. Nevertheless, the anomaly centers along this decaying-TPUHS-related RWT mostly appear much weaker than those along the previous RWT. Therefore, their impacts on circulation and weather differ considerably from the developing to the decaying period of TPUHS events.

Keywords: Tibetan Plateau, upper atmospheric heat source, Rossby wave train, circulation and weather

©2019. Japan Geoscience Union. All Right Reserved.

Equilibrium Climate Responses of the East Asian Summer Monsoon to Various Anthropogenic Aerosol Species

*Qiuyan Wang[2,1], Zhili Wang[1,2], Hua Zhang[3,2]

1. State Key Laboratory of Severe Weather & Key Laboratory of Atmospheric Chemistry of CMA, Chinese Academy of Meteorological Sciences, Beijing, 2. Collaborative Innovation Center on Forecast and Evaluation of Meteorological Disasters, Nanjing University of Information Science and Technology, Nanjing, 3. Laboratory for Climate Studies, National Climate Center, China Meteorological Administration, Beijing

The equilibrium climate responses of the East Asian summer monsoon (EASM) to increases in various types of anthropogenic aerosol emissions, including sulfate, organic carbon (OC), and black carbon (BC), from 1850 to 2000 are studied using an aerosol-climate online model. The results show that various aerosol species have substantially different impacts on the EASM by changing the local sea-land surface thermal difference and atmospheric circulation. The increased sulfate leads to decrease in the surface thermal difference between the land and ocean, the southward shift of the East Asian subtropical jet (EASJ), and significant northerly wind anomalies at 850 hPa over eastern China and the ambient oceans, thus dampening the EASM markedly. Pronounced surface cooling appears and an anomalous anticyclone is formed over the oceans north of 30˚N due to the increase of OC. These cause slight increase in sea-land surface thermal difference and southerly flow anomalies to the west of the anticyclonic center, thereby strengthening the northern East Asian summer monsoon (NEASM). However, the increased OC decreases the sea-land surface thermal contrast over southern China, which weakens the southern East Asian summer monsoon (SEASM). The responses of summer 850 hPa winds and rainfall over the East Asian monsoon region (EAMR) to increase in BC are generally consistent with those to increase in OC. The increased BC leads to the strengthening of the NEASM north of 35˚N and slight weakening of the SEASM south of 35˚N. Also, the simulated responses of the EASM to increase in BC are not changed when BC emission is scaled up by five times its 2000 levels, but the intensities of responses are enhanced. Overall, the increase in sulfate primarily weakens the EASM, while the increases in BC and OC mitigate the weakening of the NEASM to some extent.

Keywords: EASM, various aerosol species, equilibrium climate response

©2019. Japan Geoscience Union. All Right Reserved.

Analysis of specific energy in zonal currents focusing on the analogy between jet stream and open channel flow

*Yoshikazu Kitano[1], Tomohito J. Yamada[2]

1. Central Research Institute of Electric Power Industry, 2. Faculty of Engineering, Hokkaido University

Atmospheric blocking is one of the important causes of meteorological extremes in mid-latitude, such as cold spells, heat waves and long-term heavy rainfalls. Rossby (1950) focused on dynamical analogies between the hydraulic jump in open channel flow and the atmospheric blocking in jet stream, and proposed a theoretical formula to explain the two dynamically possible states in zonal currents which are compatible with supercritical and subcritical flow in an open channel flow. Armi (1989) focused on the specific energy flux in zonal currents and showed that a dimensionless parameter, which is called Froude/Rossby number, is analogous to the Froude number of open channel flow. Kitano and Yamada (2017) extended these theories to realistic conditions in atmosphere and showed a relationship between typical blocking flow and specific energy flux in jet stream. In this study, we analyzed several blocking episodes using specific energy flux and found energetic signals over Japan and its surroundings before Pacific blocking occasions. These signals may contribute to prediction on blocking.

Keywords: atmospheric blocking, jet stream, open channel flow

©2019. Japan Geoscience Union. All Right Reserved.

Analysis of the ozone reduction event over the southern tip of South America in November 2009

*Hideharu Akiyoshi[1], Masanao Kadowaki[2], Haruna Nakamura[3], Takafumi Sugita[1], Toshihiko Hirooka[4], Yayoi Harada[5], Akira Mizuno[6]

1. National Institute for Environmental Studies, 2. Japan Atomic Energy Agency, 3. Fujitsu FIP Corporation, 4. Department of Earth and Planetary Sciences, Kyushu University, 5. Meteorological Research Institute, 6. Institute for Space-Earth Environmental Research, Nagoya University

A reduction of the total ozone over the southern tip of South America lasting 3 weeks occurred in November 2009. Analyses of the ERA-Interim reanalysis data and the total ozone observed by the OMI indicate that the total ozone reduction event was caused by a migration of the polar vortex toward the South American continent at the time of the vortex breakup. The vortex migration is associated with an enhanced wave flux from the troposphere at 120–150˚W and 50–60˚S to the west of the South American continent to the stratosphere over the southern part of the continent, which led to a large negative geopotential height anomaly in the lower stratosphere. In November, a blocking pattern was diagnosed from the 500 hPa geopotential height over the west of the South American continent. These results suggest a relation between the long-lasting reduction of the total ozone over the southern tip of South America and the blocking phenomenon in the troposphere of the Southern Hemisphere through wave propagation from the blocking region in 2009.

The total ozone, the geopotential height at 50 hPa and 500 hPa, the wave activity flux, the polar vortex migration and elongation, and the blocking pattern in the Southern Hemisphere November for 1979–2015 as well as 2009 were investigated. The results show that the relation between the blocking pattern in the troposphere and the large polar vortex migration and elongation in the stratosphere is also evident in November 1987, 1994, 1997, 2001, and 2011. Especially, in November 1994, 1997, and 2011, the blocking pattern and the polar vortex migration occurred near the South American continent.

These results indicate that the migration of the Antarctic polar vortex to the southern tip of South America in November occurred occasionally in the past. They also suggest that diagnosis of blocking pattern in the Southern Hemisphere troposphere may be useful for prediction of the direction of polar vortex migration in the stratosphere, and hence, prediction of high UV radiation risk over the southern tip of South America in early summer.

This research was supported by JST/JICA, SATREPS, the Environment Research and Technology Development Fund.

Keywords: ozone hole, South America, polar vortex, blocking, November 2009, ERA-Interim reanalysis data

©2019. Japan Geoscience Union. All Right Reserved.

Analysis of relatively low ozone in Arctic spring during the QBO-westerly and solar-minimum years

*Yousuke Yamashita[1,2], Hideharu Akiyoshi[2], Masaaki Takahashi[2]

1. Japan Agency for Marine-Earth Science and Technology, 2. National Institute for Environmental Studies

The equatorial quasi-biennial oscillation (QBO) and the 11-year solar cycle are known to cause year-to-year variability of the Northern Hemisphere (NH) polar vortex (e.g. Holton and Tan, 1980; Labitzke, 1987). Labitzke (1987) and several studies following her work have been used the four categories of the QBO and 11-year solar cycle, according to the westerly/easterly phase of the QBO (QBO-W/QBO-E) and the maximum/minimum phase of the 11-year solar cycle (S_{max}/ S_{min}). Camp and Tung (2007) suggested that the NH polar vortex is the most stable and the least perturbed state in late winter during the QBO-W/S_{min} years relative to the other three groups (QBO-W/S_{max}, QBO-E/S_{max}, and QBO-E/S_{min}), in agreement with the work of Labitzke and van Loon (1988). Their findings are in agreement with the smallest magnitude of the Arctic total ozone in QBO-W/S_{min} years among the four categories (Li and Tung 2014), because the ozone depletion is enhanced in the stable and cold polar vortex associated with an increase in chemical destruction through heterogeneous reactions on the Polar Stratospheric Clouds (PSCs). Since the Arctic ozone amount is related to the ozone transport as well as the chemical ozone destruction, the estimation of their influences is still challenging issue for understanding the small amount of the Arctic total ozone in March.

In this study, we analyze the Arctic ozone amount using TOMS/OMI observations, ERA-interim reanalysis data, and the outputs of a chemistry climate model (CCM) with REF-C1SD hindcast simulation, in which the model’s zonal/meridional wind and temperature are nudged toward those of the ERA-interim reanalysis data with a 6-hour interval. The anomaly from the average for all the years of 1979–2011 in the Arctic total ozone amount is calculated for QBO-W/S_{min} group in late winter. We estimate the amounts of ozone transport and chemical ozone destruction and their effects on the derived Arctic ozone anomaly for the QBO-W/S_{min} group with CCM outputs.

Result of the composite mean for QBO-W/S_{min} years shows negative anomaly (relatively small amount) of total ozone in February–March compared to the 1979–2011 average from the CCM output, in agreement with the satellite observation, reanalysis data. To distinguish the effect of chemical ozone destruction from that of ozone transport for the total ozone anomaly in February–March, we analyze the total ozone anomaly of the passive ozone tracer without any chemical change in the CCM. The negative anomalies of the passive ozone tracer have a similar distribution to that of chemically reactive ozone with similar magnitude, suggesting that the negative anomalies of total ozone are mainly caused by ozone transport.

The outputs of CCM are also analyzed for vertical profile of ozone concentration, which indicates negative anomaly of the Arctic ozone in the upper troposphere and the lower stratosphere for the QBO-W/S_{min} condition, the maximum anomaly of ozone partial column is located around 50–70 hPa. The partial column of the passive ozone tracer at these levels also shows negative anomalies, whilst their magnitudes are small, especially at 50 hPa in March. These results suggest the significant influence of ozone transport on the negative ozone anomaly in February–March, whilst the influence of chemistry is partially large at 50 hPa in March.

©2019. Japan Geoscience Union. All Right Reserved.

Keywords: stratospheric ozone, Northern Hemisphere polar vortex, chemistry climate mode

©2019. Japan Geoscience Union. All Right Reserved.

Evaluation of ozone in the upper troposphere and lower stratosphere derived from multi-species satellite data assimilation

*Takashi Sekiya[1], Kazuyuki Miyazaki[2,1], Koji Ogochi[1], Kengo Sudo[3,1], Masayuki Takigawa[1]

1. Japan Agency for Marine-Earth Science and Technology, 2. Jet Propulsion Laboratory/California Institute for Technology, 3. Graduate School of Environmental Studies, Nagoya University

Ozone (O_3) in the upper troposphere and lower stratosphere (UTLS) has a stronger greenhouse effect than in the lower troposphere. However, information on O_3 in the UTLS from observations with the global coverage is still limited. Multi-species satellite data assimilation of stratospheric O_3, and tropospheric O_3 and its precursors is expected to provide better constraints on O_3 in the UTLS, because O_3 in the UTLS is controlled by stratospheric O_3 intrusions, O_3 transport from middle and lower troposphere, and in-situ O_3 chemical production. In this study, we evaluate O_3 in the UTLS derived from the multi-species data assimilation with horizontal resolutions of 2.8, 1.1, and 0.56 degree using ozonesonde observations (not used for data assimilation) in April 2008. Assimilated data were obtained from the OMI, GOME-2, and SCIAMACHY for tropospheric NO_2 column, the TES for O_3 profile, the MOPITT for total CO column, the MLS for O_3 and HNO_3 profiles, and the OMI for total SO_2 column. At 200 hPa, 300 hPa, and 500 hPa, the data assimilation at 0.56-degree resolution reduced root mean square errors (RMSEs) against ozonesonde observations in the northern midlatitudes by 32%, 31%, and 13%, respectively, compared to the model simulation without data assimilation. The overall data assimilation performance for O_3 concentrations is not sensitive to horizontal resolution in the altitudes between 200 hPa and 500 hPa (i.e., the RMSEs were within 7% at all resolutions). Meanwhile, the data assimilation at 0.56-degree resolution improved agreements with ozonesonde observations at 300 hPa by up to 55% compared to 1.1- and 2.8-degree resolutions during a deep stratospheric intrusion episode at Trinidad Head (124˚W, 41˚N) through resolving small-scale transport processes. These results confirm that O_3 analyses derived from multi-species data assimilation are suitable for understanding spatial and temporal variations in O_3 in the UTLS and their controlling processes.

Keywords: Satellite data assimilation, Ozone, Atmospheric chemistry

©2019. Japan Geoscience Union. All Right Reserved.

Characteristics of Initial Perturbation of JMA GEPS during Sudden Stratospheric Warmings

*Shunsuke Noguchi[1,2]

1. Japan Agency for Marine-Earth Science and Technology, 2. Meteorological Research institute, Japan Meteorological Agency

In order to sophisticate the ensemble forecasting and data assimilation system of the whole atmosphere, it is necessary to accumulate the knowledge about the uncertainty of the analysis in the stratosphere and mesosphere, which is poor in comparison with that in the troposphere. Therefore, this study investigates characteristics of initial perturbation of the Japan Meteorological Agency (JMA) Global Ensemble Prediction System (GEPS), which has been replaced in March 2017.

By focusing on two Sudden Stratospheric Warming (SSW) events occurred in 2017-2018 and 2018-2019 winters, several aspects of the new JMA GEPS are revealed as follows: (1) There is large uncertainty above the upper stratosphere (which has not been reflected in the previous system). (2) The analysis ensemble spread increases and penetrates downward from the upper stratosphere during the onset period of both SSW events, though its precursory nature is not so evident as pointed by previous studies (e.g. Enomoto et al. 2010). (3) After SSW events, the analysis ensemble spread in the middle and upper stratosphere shrinks in association with the change of dominant physical processes. However, relatively large spreads, which may have implications for the stratosphere-troposphere coupling, are sometimes found in the lower stratosphere.

The quality of forecasts and analyses above the upper stratosphere would be inevitable from the artificial effect of sponge layers near the model top. Therefore, it is worth comparing or communicating with results of some high-top system to validate the appropriateness of above-mentioned aspects (e.g. (1)) and recognize limitations of current operational settings.

Keywords: Sudden Stratospheric Warming, Ensemble Prediction System

©2019. Japan Geoscience Union. All Right Reserved.

[E] Poster | A (Atmospheric and Hydrospheric Sciences)：A-OS Ocean Sciences & Ocean Environment

Wed. May 29, 2019 10:45 AM - 12:15 PM JST | Wed. May 29, 2019 1:45 AM - 3:15 AM UTC | Poster Hall International Exhibition Hall8, Makuhari Messe_4

[A-OS08] ECS-Kuroshio and Ryukyu Current System -Observation, modeling and theory-

convener:Hirohiko Nakamura(Kagoshima University, Faculy of Fisheries), Xiao-Hua Zhu(Second Institute of Oceanography)

The East China Sea (ECS) is separated from the North Pacific basin by the Ryukyu Islands. On each side of the Ryukyu Islands, there lies two western boundary currents -the Kuroshio on the northwest and the Ryukyu Current on the southeast. These two currents play an important role in the global substance cycle and have a remarkable impact on the climate and adjacent marginal seas. Our knowledge of the Kuroshio and the Ryukyu Current's dynamics, variability, and impact has advanced significantly over the last decade, because of recent international collaborative field programs, improvement in satellite measurements, and advancement in high-resolution numerical models. This session seeks contributions from ECS-Kuroshio and Ryukyu Current studies and will cover a wide range of topics of observation, modeling and theory. The dynamics of the Kuroshio and the Ryukyu Current's variability at all spatio-temporal scales, the influence of the Kuroshio on typhoons and climate, the interactions among the Kuroshio, Ryukyu Current and eddies, internal waves including near-internal waves and their interactions with background currents, and the water mass exchanges through the gaps between the Ryukyu Islands are welcome to be discussed in this session.

[AOS08-P01] Impact of the mesosacle eddies on the western boundary current over the entire western North Pacific

*Kako Shinichiro[1], Hirohiko Nakamura[2] (1.Graduate School of Science and Engineering, Kagoshima University, 2.Faculty of Fisheries, Kagoshima University)

[AOS08-P02] Glider observations of interleaving layers in the Kuroshio

*Sen Jan[1], Shih-Hong Wang[1], Kai-Chieh Yang[1], Yiing Jang Yang[1], Ming-Huei Chang[1] (1.Institute of Oceanography, National Taiwan Univ.)

[AOS08-P03] Bottom Pressure in the East China Sea -Observation and modeling

*Hua Zheng[1], Xiao-Hua Zhu[1], Hirohiko Nakamura[2], Jae-Hun Park[3], Chanhyung Jeon[4], Ruixiang Zhao[1], Ayako Nishina[2], Chuanzheng Zhang[1], Hanna Na[5], Ze-Nan Zhu[1], Hong Sik Min[6] (1.Second Institute of Oceanography, Ministry of Natural Resources, China, 2.Faculty of Fisheries, Kagoshima University, Kagoshima, Japan, 3.Department of Ocean Sciences, Inha University, Incheon, South Kore, 4.Department of Marine Science and Biological Engineering, Inha University, Incheon, Korea, 5.School of Earth and Environmental Sciences, Seoul National University, Seoul, Korea, 6.Ocean Circulation and Climate Research Center, Korea Institute of Ocean Science and Technology, Busan, Korea)

[AOS08-P04] A numerical study on the dynamics of seasonal velocity variation in the East China Sea

*ZHENLONG ZHANG[1], Nakamura Hirohiko[1], Xiao-Hua Zhu[2] (1.Kagoshima University, 2.Ministry of Natural Resources, CHINA.)

[AOS08-P05] Temporal and spatial velocity variations over the Kuroshio Extension, Kuroshio and Ryukyu Current System in 1982-2014

*YUXIANG QIAO[1], Hirohiko Nakamura[2], AYAKO NISHINA[2] (1.Kagoshima University, Graduate School of Fisheries, 2.Kagoshima University, Faculty of Fishries)

[AOS08-P06] Characteristics of water in the southern Okinawa Trough.

*Ayako Nishina[1], Hirohiko Nakamura[1], Jae-Hun Park[2], Xiao-Hua Zhu[3], Hong Sik Min[4], Hanna Na[5] (1.Kagoshima University, 2.Inha University, 3.Second Institute of Oceanography, 4.Korea Institute of Ocean Science and Technology, 5.Seoul National University)

Impact of the mesosacle eddies on the western boundary current over the entire western North Pacific

*Kako Shinichiro[1], Hirohiko Nakamura[2]

1. Graduate School of Science and Engineering, Kagoshima University, 2. Faculty of Fisheries, Kagoshima University

Although many previous studies have suggested that the mesoscale eddies affect the variations of the Kuroshio and Ryukyu current systems, the generated regions and paths to the western boundary have not been well explained yet. We constructed a mesosacle eddy tracking dataset using FORA-WNP30 in conjunction with Okubo-Weiss parameters to investigate the effects of eddies on the western boundary current over the entire North Pacific. We observed that cyclonic eddies with relatively long durations (>120 days) were mainly generated around the southern Kuroshio Extension region, while anti-cyclonic eddies were generated around the subtropical counter current. In addition, we found that the cyclonic eddies propagate westward along the Kuroshio region and reach the western boundary, while the anti-cyclonic eddies propagate westward from their regions of origin and thereafter reach the Kuroshio recirculation region and Ryukyu current. The comparison of the Ryukyu-current at a depth of 600 m and the number of times the meso-scale eddies passed over the Ryukyu current demonstrated that the weakening (strengthening) of the northward current in the northern part of the Ryukyu region was consistent with the number of times the cyclonic (anti-cyclonic) eddies passed over the northern part of the Ryukyu current.

Keywords: mesoscale eddy, Kuroshio, Ryukyu current

©2019. Japan Geoscience Union. All Right Reserved.

Glider observations of interleaving layers in the Kuroshio

*Sen Jan[1], Shih-Hong Wang[1], Kai-Chieh Yang[1], Yiing Jang Yang[1], Ming-Huei Chang[1]

1. Institute of Oceanography, National Taiwan Univ.

Interleaving layers (or thermohaline intrusions) were sometimes observed by repeated ship-based hydrographic surveys with coarse spacing between adjacent stations in the Kuroshio off Taiwan, but have never been examined in a dynamic context. A Seaglider was navigated along a triangle track east of Taiwan to complete two repeated high-resolution hydrographic observations from December 2016 to March 2017. Prominent interleaving layers were observed between dissimilar intermediate water masses across the Kuroshio. During the observations, a diple eddy pair and a relatively large anticyclonic eddy impinged on the offshore flank of the Kuroshio, respectively, which brought certain impacts on the formation and growth of the interleaving. Aside from the complicated physical processes in the upper 200 m, salinity profiles indicate that interleaving layers appeared within 500 and 800 m with vertical and horizontal length scales of O(50 m) and O(10-100 km), respectively. The time scale for the interleaving layers should be much less than 30 days, inferred from the discrepancy in the interleaving features between the two surveys. The instability analysis together with values of the Turner angle calculated from the hydrographic data suggests that the double-diffusive instability is the primary driving mechanism for the observed interleaving layers.

Keywords: Kuroshio, Interleaving, Double-diffusive instability, Glider observation

©2019. Japan Geoscience Union. All Right Reserved.

Bottom Pressure in the East China Sea -Observation and modeling

*Hua Zheng[1], Xiao-Hua Zhu[1], Hirohiko Nakamura[2], Jae-Hun Park[3], Chanhyung Jeon[4], Ruixiang Zhao[1], Ayako Nishina[2], Chuanzheng Zhang[1], Hanna Na[5], Ze-Nan Zhu[1], Hong Sik Min[6]

1. Second Institute of Oceanography, Ministry of Natural Resources, China, 2. Faculty of Fisheries, Kagoshima University, Kagoshima, Japan, 3. Department of Ocean Sciences, Inha University, Incheon, South Kore, 4. Department of Marine Science and Biological Engineering, Inha University, Incheon, Korea, 5. School of Earth and Environmental Sciences, Seoul National University, Seoul, Korea, 6. Ocean Circulation and Climate Research Center, Korea Institute of Ocean Science and Technology, Busan, Korea

A two-year ocean bottom pressure record acquired between June 2015 and June 2017 observed by two pressure-recording inverted echo sounders (PIESs) and five current and pressure-recording inverted echo sounders (CPIESs) deployed along a section southwest of the Kerama Gap showed a significant 21-day variability. This 21-day bottom pressure variability (P_{bot21}) was particularly strong from July 2016 to January 2017, and it showed a squared coherence of 0.72 with wind stress curl around the Yangtze estuary in the East China Sea (ECS) during this period with a nearly 3-day time lag. A barotropic ocean model demonstrated the generation, spread, and dissipation of P_{bot21}. The modeling results showed that the P_{bot21} was driven by wind stress curl on the continental shelf of the ECS, where depths are shallower than 100 m, and spread southeastward to the Ryukyu Island Chain (RIC). The P_{bot21} was generated and remained on the shallow continental shelf, and only little power spread toward the RIC; thus, whether the signal could be observed by the mooring array was related to where it was generated. Significant P_{bot21} was generated southeast of the Yangtze estuary and measured by the mooring array from July 2016 to January 2017. However, P_{bot21} generated northeast of the Yangtze estuary, far from the mooring section, from January 2016 to April 2016 was exhausted before reaching the mooring array due to the long distance. It is suggested that the spatial pattern of 21-day wind stress curl over the ECS strongly influences P_{bot21} near the RIC.

©2019. Japan Geoscience Union. All Right Reserved.

A numerical study on the dynamics of seasonal velocity variation in the East China Sea

*ZHENLONG ZHANG[1], Nakamura Hirohiko[1], Xiao-Hua Zhu[2]

1. Kagoshima University, 2. Ministry of Natural Resources, CHINA.

In our previous study, we investigated the seasonal velocity variations at different depths over the entire Kuroshio path. It showed that the upper layer (< ~500 m depth) velocity variation over the entire Kuroshio path has a coherent seasonal feature, which reaches a maximum in July and a minimum in autumn or winter, over most of the regions along the Kuroshio path. However, the lower layer velocity (> ~500 m depth, in the continental slope area from the east of Luzon Island to the east of the Ryukyu Island chain) shows a reversed seasonal variation with a maximum in winter. Several numerical experiments were carried out to clarify the essential mechanisms. Although it was shown that the local wind stress upon the current region is a key factor for the seasonal velocity variation in the upper layer, the detailed driving mechanism has been still unknown. Thus, we perform further numerical experiments to clarify the concreate mechanism in this study. Using a rectilinear regional model with idealized continental slope, we have successfully reproduced the seasonal velocity variation of the jet (the Kuroshio) by the seasonal wind stress variation over the jet. It turns out that the velocity of the jet increases (decreases) when the wind stress is directed to downstream (upstream) direction of the jet. We will report the concrete process underlying acceleration and deceleration processes of the upper layer velocity related to the local wind stress.

Keywords: Kuroshio, Seasonal variation

©2019. Japan Geoscience Union. All Right Reserved.

Temporal and spatial velocity variations over the Kuroshio Extension, Kuroshio and Ryukyu Current System in 1982-2014

*YUXIANG QIAO[1], Hirohiko Nakamura[2], AYAKO NISHINA[2]

1. Kagoshima University, Graduate School of Fisheries, 2. Kagoshima University, Faculty of Fishries

Four dimensional variational Ocean ReAnalysis for the Western North Pacific (FORA-WNP30) from 1982 to 2014 is used to investigate temporal and spatial velocity variations over the regions consisting of Kuroshio Extension (KE), Kuroshio and Ryukyu Current System (RCS). In order to identify such temporal and spatial features, we made Hovmöller diagrams at several depths, which display temporal variations of along-stream velocity along the current path from Luzon Island to KE region. In this study, we particularly examine long-term (> 1 year) variations for their regional characteristics (Luzon Island to KE region) and their vertical features (sea surface to 1000 m depth). The results revealed that 1) the KE is dominated by decadal signals while the upstream regions include clearer interannual signals in addition to decadal ones, 2) decadal variations in the KE tends to be almost out of phase to those variations in the upstream regions from Luzon Island to Izu-Ridge, and 3) the velocity variations at the sea surface tend to be similar to those variations at 1000 m depth.

Keywords: Kuroshio, Ryukyu Current, Kuroshio Extension, Velocity, Long-term variations

©2019. Japan Geoscience Union. All Right Reserved.

Characteristics of water in the southern Okinawa Trough.

*Ayako Nishina[1], Hirohiko Nakamura[1], Jae-Hun Park[2], Xiao-Hua Zhu[3], Hong Sik Min[4], Hanna Na[5]

1. Kagoshima University, 2. Inha University, 3. Second Institute of Oceanography, 4. Korea Institute of Ocean Science and Technology, 5. Seoul National University

The Okinawa Trough is a basin within the East China Sea, where maximum depth reaches 2300 m. There are two characteristic water masses in the Okinawa Trough. One is the high salinity water in the sub-surface layer shallower than 300 m and the other is the low salinity water in the intermediate layer from 400 m to 700 m. According to the previous studies, the former water is occupied by the South China Sea Tropical Water (SCSTW) and the Kuroshio Tropical Water (KTW), and the latter is dominated by modified water masses of the North Pacific Intermediate Water (NPIW) and the South China Sea Intermediate Water (SCSIW). However, in the previous studies, the southern part of the Okinawa Trough remains to be observed, and it should be confirmed whether the previous results can apply to the southern part.
In this study, water mass properties in the southern part of the Okinawa Trough are investigated in detail. We mainly used CTD data from T/V Kagoshima-maru cruises in Junes from 2013 to 2018. The high salinity waters in the sub-surface layer were classified into three groups: SCSTW, KTW and the tropical waters in the east of Ryukyu Islands chain. The low salinity water in the intermediate layer had a complicated distribution in which the low salinity water from the east of Taiwan and that from the Kerama Gap.

Keywords: Okinawa Trough, water mass

©2019. Japan Geoscience Union. All Right Reserved.

[E] Poster | A (Atmospheric and Hydrospheric Sciences)：A-OS Ocean Sciences & Ocean Environment

Wed. May 29, 2019 5:15 PM - 6:30 PM JST | Wed. May 29, 2019 8:15 AM - 9:30 AM UTC | Poster Hall International Exhibition Hall8, Makuhari Messe_11

[A-OS08] ECS-Kuroshio and Ryukyu Current System -Observation, modeling and theory-

convener:Hirohiko Nakamura(Kagoshima University, Faculy of Fisheries), Xiao-Hua Zhu(Second Institute of Oceanography)

The East China Sea (ECS) is separated from the North Pacific basin by the Ryukyu Islands. On each side of the Ryukyu Islands, there lies two western boundary currents -the Kuroshio on the northwest and the Ryukyu Current on the southeast. These two currents play an important role in the global substance cycle and have a remarkable impact on the climate and adjacent marginal seas. Our knowledge of the Kuroshio and the Ryukyu Current's dynamics, variability, and impact has advanced significantly over the last decade, because of recent international collaborative field programs, improvement in satellite measurements, and advancement in high-resolution numerical models. This session seeks contributions from ECS-Kuroshio and Ryukyu Current studies and will cover a wide range of topics of observation, modeling and theory. The dynamics of the Kuroshio and the Ryukyu Current's variability at all spatio-temporal scales, the influence of the Kuroshio on typhoons and climate, the interactions among the Kuroshio, Ryukyu Current and eddies, internal waves including near-internal waves and their interactions with background currents, and the water mass exchanges through the gaps between the Ryukyu Islands are welcome to be discussed in this session.

[AOS08-P01] Impact of the mesosacle eddies on the western boundary current over the entire western North Pacific

*Kako Shinichiro[1], Hirohiko Nakamura[2] (1.Graduate School of Science and Engineering, Kagoshima University, 2.Faculty of Fisheries, Kagoshima University)

[AOS08-P02] Glider observations of interleaving layers in the Kuroshio

*Sen Jan[1], Shih-Hong Wang[1], Kai-Chieh Yang[1], Yiing Jang Yang[1], Ming-Huei Chang[1] (1.Institute of Oceanography, National Taiwan Univ.)

[AOS08-P03] Bottom Pressure in the East China Sea -Observation and modeling

*Hua Zheng[1], Xiao-Hua Zhu[1], Hirohiko Nakamura[2], Jae-Hun Park[3], Chanhyung Jeon[4], Ruixiang Zhao[1], Ayako Nishina[2], Chuanzheng Zhang[1], Hanna Na[5], Ze-Nan Zhu[1], Hong Sik Min[6] (1.Second Institute of Oceanography, Ministry of Natural Resources, China, 2.Faculty of Fisheries, Kagoshima University, Kagoshima, Japan, 3.Department of Ocean Sciences, Inha University, Incheon, South Kore, 4.Department of Marine Science and Biological Engineering, Inha University, Incheon, Korea, 5.School of Earth and Environmental Sciences, Seoul National University, Seoul, Korea, 6.Ocean Circulation and Climate Research Center, Korea Institute of Ocean Science and Technology, Busan, Korea)

[AOS08-P04] A numerical study on the dynamics of seasonal velocity variation in the East China Sea

*ZHENLONG ZHANG[1], Nakamura Hirohiko[1], Xiao-Hua Zhu[2] (1.Kagoshima University, 2.Ministry of Natural Resources, CHINA.)

[AOS08-P05] Temporal and spatial velocity variations over the Kuroshio Extension, Kuroshio and Ryukyu Current System in 1982-2014

*YUXIANG QIAO[1], Hirohiko Nakamura[2], AYAKO NISHINA[2] (1.Kagoshima University, Graduate School of Fisheries, 2.Kagoshima University, Faculty of Fishries)

[AOS08-P06] Characteristics of water in the southern Okinawa Trough.

*Ayako Nishina[1], Hirohiko Nakamura[1], Jae-Hun Park[2], Xiao-Hua Zhu[3], Hong Sik Min[4], Hanna Na[5] (1.Kagoshima University, 2.Inha University, 3.Second Institute of Oceanography, 4.Korea Institute of Ocean Science and Technology, 5.Seoul National University)

Impact of the mesosacle eddies on the western boundary current over the entire western North Pacific

*Kako Shinichiro[1], Hirohiko Nakamura[2]

1. Graduate School of Science and Engineering, Kagoshima University, 2. Faculty of Fisheries, Kagoshima University

Although many previous studies have suggested that the mesoscale eddies affect the variations of the Kuroshio and Ryukyu current systems, the generated regions and paths to the western boundary have not been well explained yet. We constructed a mesosacle eddy tracking dataset using FORA-WNP30 in conjunction with Okubo-Weiss parameters to investigate the effects of eddies on the western boundary current over the entire North Pacific. We observed that cyclonic eddies with relatively long durations (>120 days) were mainly generated around the southern Kuroshio Extension region, while anti-cyclonic eddies were generated around the subtropical counter current. In addition, we found that the cyclonic eddies propagate westward along the Kuroshio region and reach the western boundary, while the anti-cyclonic eddies propagate westward from their regions of origin and thereafter reach the Kuroshio recirculation region and Ryukyu current. The comparison of the Ryukyu-current at a depth of 600 m and the number of times the meso-scale eddies passed over the Ryukyu current demonstrated that the weakening (strengthening) of the northward current in the northern part of the Ryukyu region was consistent with the number of times the cyclonic (anti-cyclonic) eddies passed over the northern part of the Ryukyu current.

Keywords: mesoscale eddy, Kuroshio, Ryukyu current

©2019. Japan Geoscience Union. All Right Reserved.

Glider observations of interleaving layers in the Kuroshio

*Sen Jan[1], Shih-Hong Wang[1], Kai-Chieh Yang[1], Yiing Jang Yang[1], Ming-Huei Chang[1]

1. Institute of Oceanography, National Taiwan Univ.

Interleaving layers (or thermohaline intrusions) were sometimes observed by repeated ship-based hydrographic surveys with coarse spacing between adjacent stations in the Kuroshio off Taiwan, but have never been examined in a dynamic context. A Seaglider was navigated along a triangle track east of Taiwan to complete two repeated high-resolution hydrographic observations from December 2016 to March 2017. Prominent interleaving layers were observed between dissimilar intermediate water masses across the Kuroshio. During the observations, a diple eddy pair and a relatively large anticyclonic eddy impinged on the offshore flank of the Kuroshio, respectively, which brought certain impacts on the formation and growth of the interleaving. Aside from the complicated physical processes in the upper 200 m, salinity profiles indicate that interleaving layers appeared within 500 and 800 m with vertical and horizontal length scales of O(50 m) and O(10-100 km), respectively. The time scale for the interleaving layers should be much less than 30 days, inferred from the discrepancy in the interleaving features between the two surveys. The instability analysis together with values of the Turner angle calculated from the hydrographic data suggests that the double-diffusive instability is the primary driving mechanism for the observed interleaving layers.

Keywords: Kuroshio, Interleaving, Double-diffusive instability, Glider observation

©2019. Japan Geoscience Union. All Right Reserved.

Bottom Pressure in the East China Sea -Observation and modeling

*Hua Zheng[1], Xiao-Hua Zhu[1], Hirohiko Nakamura[2], Jae-Hun Park[3], Chanhyung Jeon[4], Ruixiang Zhao[1], Ayako Nishina[2], Chuanzheng Zhang[1], Hanna Na[5], Ze-Nan Zhu[1], Hong Sik Min[6]

1. Second Institute of Oceanography, Ministry of Natural Resources, China, 2. Faculty of Fisheries, Kagoshima University, Kagoshima, Japan, 3. Department of Ocean Sciences, Inha University, Incheon, South Kore, 4. Department of Marine Science and Biological Engineering, Inha University, Incheon, Korea, 5. School of Earth and Environmental Sciences, Seoul National University, Seoul, Korea, 6. Ocean Circulation and Climate Research Center, Korea Institute of Ocean Science and Technology, Busan, Korea

A two-year ocean bottom pressure record acquired between June 2015 and June 2017 observed by two pressure-recording inverted echo sounders (PIESs) and five current and pressure-recording inverted echo sounders (CPIESs) deployed along a section southwest of the Kerama Gap showed a significant 21-day variability. This 21-day bottom pressure variability (P_{bot21}) was particularly strong from July 2016 to January 2017, and it showed a squared coherence of 0.72 with wind stress curl around the Yangtze estuary in the East China Sea (ECS) during this period with a nearly 3-day time lag. A barotropic ocean model demonstrated the generation, spread, and dissipation of P_{bot21}. The modeling results showed that the P_{bot21} was driven by wind stress curl on the continental shelf of the ECS, where depths are shallower than 100 m, and spread southeastward to the Ryukyu Island Chain (RIC). The P_{bot21} was generated and remained on the shallow continental shelf, and only little power spread toward the RIC; thus, whether the signal could be observed by the mooring array was related to where it was generated. Significant P_{bot21} was generated southeast of the Yangtze estuary and measured by the mooring array from July 2016 to January 2017. However, P_{bot21} generated northeast of the Yangtze estuary, far from the mooring section, from January 2016 to April 2016 was exhausted before reaching the mooring array due to the long distance. It is suggested that the spatial pattern of 21-day wind stress curl over the ECS strongly influences P_{bot21} near the RIC.

©2019. Japan Geoscience Union. All Right Reserved.

A numerical study on the dynamics of seasonal velocity variation in the East China Sea

*ZHENLONG ZHANG[1], Nakamura Hirohiko[1], Xiao-Hua Zhu[2]

1. Kagoshima University, 2. Ministry of Natural Resources, CHINA.

In our previous study, we investigated the seasonal velocity variations at different depths over the entire Kuroshio path. It showed that the upper layer (< ~500 m depth) velocity variation over the entire Kuroshio path has a coherent seasonal feature, which reaches a maximum in July and a minimum in autumn or winter, over most of the regions along the Kuroshio path. However, the lower layer velocity (> ~500 m depth, in the continental slope area from the east of Luzon Island to the east of the Ryukyu Island chain) shows a reversed seasonal variation with a maximum in winter. Several numerical experiments were carried out to clarify the essential mechanisms. Although it was shown that the local wind stress upon the current region is a key factor for the seasonal velocity variation in the upper layer, the detailed driving mechanism has been still unknown. Thus, we perform further numerical experiments to clarify the concreate mechanism in this study. Using a rectilinear regional model with idealized continental slope, we have successfully reproduced the seasonal velocity variation of the jet (the Kuroshio) by the seasonal wind stress variation over the jet. It turns out that the velocity of the jet increases (decreases) when the wind stress is directed to downstream (upstream) direction of the jet. We will report the concrete process underlying acceleration and deceleration processes of the upper layer velocity related to the local wind stress.

Keywords: Kuroshio, Seasonal variation

©2019. Japan Geoscience Union. All Right Reserved.

Temporal and spatial velocity variations over the Kuroshio Extension, Kuroshio and Ryukyu Current System in 1982-2014

*YUXIANG QIAO[1], Hirohiko Nakamura[2], AYAKO NISHINA[2]

1. Kagoshima University, Graduate School of Fisheries, 2. Kagoshima University, Faculty of Fishries

Four dimensional variational Ocean ReAnalysis for the Western North Pacific (FORA-WNP30) from 1982 to 2014 is used to investigate temporal and spatial velocity variations over the regions consisting of Kuroshio Extension (KE), Kuroshio and Ryukyu Current System (RCS). In order to identify such temporal and spatial features, we made Hovmöller diagrams at several depths, which display temporal variations of along-stream velocity along the current path from Luzon Island to KE region. In this study, we particularly examine long-term (> 1 year) variations for their regional characteristics (Luzon Island to KE region) and their vertical features (sea surface to 1000 m depth). The results revealed that 1) the KE is dominated by decadal signals while the upstream regions include clearer interannual signals in addition to decadal ones, 2) decadal variations in the KE tends to be almost out of phase to those variations in the upstream regions from Luzon Island to Izu-Ridge, and 3) the velocity variations at the sea surface tend to be similar to those variations at 1000 m depth.

Keywords: Kuroshio, Ryukyu Current, Kuroshio Extension, Velocity, Long-term variations

©2019. Japan Geoscience Union. All Right Reserved.

Characteristics of water in the southern Okinawa Trough.

*Ayako Nishina[1], Hirohiko Nakamura[1], Jae-Hun Park[2], Xiao-Hua Zhu[3], Hong Sik Min[4], Hanna Na[5]

1. Kagoshima University, 2. Inha University, 3. Second Institute of Oceanography, 4. Korea Institute of Ocean Science and Technology, 5. Seoul National University

The Okinawa Trough is a basin within the East China Sea, where maximum depth reaches 2300 m. There are two characteristic water masses in the Okinawa Trough. One is the high salinity water in the sub-surface layer shallower than 300 m and the other is the low salinity water in the intermediate layer from 400 m to 700 m. According to the previous studies, the former water is occupied by the South China Sea Tropical Water (SCSTW) and the Kuroshio Tropical Water (KTW), and the latter is dominated by modified water masses of the North Pacific Intermediate Water (NPIW) and the South China Sea Intermediate Water (SCSIW). However, in the previous studies, the southern part of the Okinawa Trough remains to be observed, and it should be confirmed whether the previous results can apply to the southern part.
In this study, water mass properties in the southern part of the Okinawa Trough are investigated in detail. We mainly used CTD data from T/V Kagoshima-maru cruises in Junes from 2013 to 2018. The high salinity waters in the sub-surface layer were classified into three groups: SCSTW, KTW and the tropical waters in the east of Ryukyu Islands chain. The low salinity water in the intermediate layer had a complicated distribution in which the low salinity water from the east of Taiwan and that from the Kerama Gap.

Keywords: Okinawa Trough, water mass

©2019. Japan Geoscience Union. All Right Reserved.

[E] Oral | A (Atmospheric and Hydrospheric Sciences)：A-OS Ocean Sciences & Ocean Environment

Wed. May 29, 2019 1:45 PM - 3:15 PM JST | Wed. May 29, 2019 4:45 AM - 6:15 AM UTC | 105 1F

[A-OS08] ECS-Kuroshio and Ryukyu Current System -Observation, modeling and theory-

convener:Hirohiko Nakamura(Kagoshima University, Faculy of Fisheries), Xiao-Hua Zhu(Second Institute of Oceanography), Chairperson:Hirohiko Nakamura(Kagoshima University), Jae-Hun Park(Inha University)

The East China Sea (ECS) is separated from the North Pacific basin by the Ryukyu Islands. On each side of the Ryukyu Islands, there lies two western boundary currents -the Kuroshio on the northwest and the Ryukyu Current on the southeast. These two currents play an important role in the global substance cycle and have a remarkable impact on the climate and adjacent marginal seas. Our knowledge of the Kuroshio and the Ryukyu Current's dynamics, variability, and impact has advanced significantly over the last decade, because of recent international collaborative field programs, improvement in satellite measurements, and advancement in high-resolution numerical models. This session seeks contributions from ECS-Kuroshio and Ryukyu Current studies and will cover a wide range of topics of observation, modeling and theory. The dynamics of the Kuroshio and the Ryukyu Current's variability at all spatio-temporal scales, the influence of the Kuroshio on typhoons and climate, the interactions among the Kuroshio, Ryukyu Current and eddies, internal waves including near-internal waves and their interactions with background currents, and the water mass exchanges through the gaps between the Ryukyu Islands are welcome to be discussed in this session.

1:45 PM - 1:50 PM JST | 4:45 AM - 4:50 AM UTC

Introduction

1:50 PM - 2:10 PM JST | 4:50 AM - 5:10 AM UTC

[AOS08-01] Downstream Evolution of the Kuroshio Velocity Structure and Transport

★Invited Papers

*Magdalena Andres[1], Sen Jan[2] (1.Woods Hole Oceanographic Institution, 2.National Taiwan University)

2:10 PM - 2:25 PM JST | 5:10 AM - 5:25 AM UTC

[AOS08-02] **Non-seasonal variability of the Kuroshio shelf intrusion and its associated changes in the ocean environment over the East China Sea during 1993-2017**

*Jiwon Kang[1], Hanna Na[1] (1.School of Earth and Environmental Sciences, Seoul National University, Republic of Korea)

2:25 PM - 2:40 PM JST | 5:25 AM - 5:40 AM UTC

[AOS08-03] The temporal and spatial variability of the Kuroshio in the East China Sea and its associated mechanisms

*Yanzhou Wei[1] (1.State Key Laboratory of Satellite Ocean Environment Dynamics, Second Institute of Oceanography, Ministry of Natural Resources, Hangzhou, China)

2:40 PM - 2:55 PM JST | 5:40 AM - 5:55 AM UTC

[AOS08-04] The Joint Kuroshio–Ryukyu Current System Study and a rapid report about mooring observations southeast of Miyakojima

*Xiao-Hua Zhu[1], Hirohiko Nakamura[2], Jae-Hun Park[3], Ruixiang Zhao[1], Ayako Nishina[2], Chuanzheng Zhang[1], Chanhyung Jeon[4], Hanna Na[5], Ze-Nan Zhu[1], Hong Sik Min[6] (1.State Key Laboratory of Satellite Ocean Environment Dynamics, Second Institute of Oceanography, Ministry of Natural Resources, Hangzhou, China, 2.Faculty of Fisheries, Kagoshima University, Kagoshima, Japan, 3.Department of Ocean Sciences, Inha University, Incheon, South Korea, 4.Department of Marine Science and Biological Engineering, Inha University, Incheon, Korea, 5.School of Earth and Environmental Sciences, Seoul National University, Seoul, Korea, 6.Ocean Circulation and Climate Research Center, Korea Institute of Ocean Science and Technology, Busan, Korea)

2:55 PM - 3:10 PM JST | 5:55 AM - 6:10 AM UTC

[AOS08-05] Relationship of the Kuroshio with the current fields in the East China Sea from observations and model results

*Hong Sik Min[1], Chorong Hwang[1], Dong Guk Kim[1], Hirohiko Nakamura[2], Ayako Nishina[2], Xiao-Hua Zhu[3], Jae-Hun Park[4], Chanhyung Jeon[4], Hanna Na[5], Naoki Hirose[6] (1.Korea Institute of Ocean Science & Technology, 2.Kagoshima University, 3.Second Institute of Oceanography, 4.Inha University, 5.Seoul National University, 6.Kyushu University)

3:10 PM - 3:15 PM JST | 6:10 AM - 6:15 AM UTC

Discussion

Downstream Evolution of the Kuroshio Velocity Structure and Transport

*Magdalena Andres[1], Sen Jan[2]

1. Woods Hole Oceanographic Institution, 2. National Taiwan University

The Kuroshio flows along the North Pacific western boundary carrying heat, mass and momentum poleward. Along this route, the Kuroshio’ s strength and vertical structure undergo significant temporal and spatial variability. Recent observational studies have examined the Kuroshio between Luzon and Taiwan, just before the Kuroshio flows into the East China Sea and upstream of the beginning of the Ryukyu Current (a subsurface-intensified current that carries part of the total poleward western boundary current flow). These observations were part of the recent US Origins of the Kuroshio and Mindanao Currents (OKMC) and Taiwan Observations of Kuroshio Transport Variability (OKTV) and Study of the Kuroshio II (SK-II) observational programs. These studies, together with previous observational efforts, build a comprehensive picture of the Kuroshio on its route from its origins near Luzon to southeastern Japan, where the current finally transitions from a western boundary current into the Kuroshio Extension, a vigorously meandering free jet. Through the joint OKMC/OKTV efforts, Kuroshio strength and velocity structure were measured between June 2012 and November 2014 with pressure-sensor equipped inverted echo sounders (PIESs) and upward- looking acoustic Doppler current profilers (ADCPs) deployed across the current northeast of Luzon, Philippines, and east of Taiwan with an 8 month overlap in the two arrays’ deployment periods. The time-mean net (i.e., integrated from the surface to the bottom) absolute transport increases downstream and the observed downstream increase is consistent with the return flow predicted by the simple Sverdrup relation and the mean wind stress curl field over the North Pacific (despite the complicated bathymetry and gaps along the North Pacific western boundary). Northeast of Luzon, the Kuroshio is shallower than 750 dbar, while east of Taiwan areas of positive flow reach to the seafloor (3000 m). A similar deepening of the subtropical western boundary current is observed in the North Atlantic in the region where the Gulf Stream leaves Cape Hatteras. In addition, there is a deep counterflow beneath the poleward-flowing Kuroshio. Time-varying transports and velocities indicate the strong influence at both sections of westward propagating eddies from the ocean interior. Topography associated with the ridges east of Taiwan also influences the mean and time-varying velocity structure there. By comparison, in the North Atlantic there is also a deep counterflow beneath the Gulf Stream at Cape Hatteras, however, this is likely due to different processes than those at play in the North Pacific, due to the presence of the Deep Western Boundary Current there which carries equatorward flow in the Atlantic Meridional Overturning Circulation (AMOC) cold limb flow.

Keywords: Kuroshio, mesoscale eddies, PIES, ADCP

©2019. Japan Geoscience Union. All Right Reserved.

Non-seasonal variability of the Kuroshio shelf intrusion and its associated changes in the ocean environment over the East China Sea during 1993-2017

*Jiwon Kang[1], Hanna Na[1]

1. School of Earth and Environmental Sciences, Seoul National University, Republic of Korea

The Kuroshio in the East China Sea (ECS) exhibits strong variability over the northeast of Taiwan; weakening of the Kuroshio has been understood to be associated with shelf-ward shift of the Kuroshio axis, which induces shelf intrusion of the Kuroshio water. The Kuroshio intrusion plays an important role for understanding the characteristics of water masses over the shelf region that, in turn, influences ocean environment in the marginal seas. In this study, non-seasonal variability of the intrusion, which was reported to be more significant in comparison with its seasonal variability, is examined during 1993-2017.

The Kuroshio intrusion index was defined based on the Empirical Orthogonal Function analysis of satellite-altimetry-derived geostrophic velocity data. The composite analysis of oceanic and atmospheric variables according to the intrusion index reveals that strong Kuroshio intrusion is associated with increase of sea surface temperature and eddy kinetic energy, strengthening of northwesterly wind and upward surface heat flux in the continental shelf region. The strong Kuroshio intrusion would also be related to sub-mesoscale eddy variability inside the ECS, and its relationship is discussed by examining surface drifter data over the region.

Keywords: Kuroshio, shelf intrusion, East China Sea, sub-mesoscale eddy

©2019. Japan Geoscience Union. All Right Reserved.

The temporal and spatial variability of the Kuroshio in the East China Sea and its associated mechanisms

*Yanzhou Wei[1]

1. State Key Laboratory of Satellite Ocean Environment Dynamics, Second Institute of Oceanography, Ministry of Natural Resources, Hangzhou, China

The Kuroshio is a strong western boundary current of the North Pacific subtropical gyre. It transports huge amounts of heat and nutrients poleward, and has a profound effect on the hydrography, fisheries, and climate of countries surrounding the Northwestern Pacific. As such, the temporal and spatial variability of the Kuroshio on multiple scales is of wide interest to the oceanographic and climate communities. In this study, we examine the temporal and spatial variability of the Kuroshio based on long term hydrographic observation and satellite data, and discuss the associated mechanisms.

Keywords: Kuroshio, East China Sea

©2019. Japan Geoscience Union. All Right Reserved.

The Joint Kuroshio–Ryukyu Current System Study and a rapid report about mooring observations southeast of Miyakojima

*Xiao-Hua Zhu[1], Hirohiko Nakamura[2], Jae-Hun Park[3], Ruixiang Zhao[1], Ayako Nishina[2], Chuanzheng Zhang[1], Chanhyung Jeon[4], Hanna Na[5], Ze-Nan Zhu[1], Hong Sik Min[6]

1. State Key Laboratory of Satellite Ocean Environment Dynamics, Second Institute of Oceanography, Ministry of Natural Resources, Hangzhou, China, 2. Faculty of Fisheries, Kagoshima University, Kagoshima, Japan, 3. Department of Ocean Sciences, Inha University, Incheon, South Korea, 4. Department of Marine Science and Biological Engineering, Inha University, Incheon, Korea, 5. School of Earth and Environmental Sciences, Seoul National University, Seoul, Korea, 6. Ocean Circulation and Climate Research Center, Korea Institute of Ocean Science and Technology, Busan, Korea

From June 2015 to June 2017, an international cooperative research project called “Joint Kuroshio-Ryukyu Current System Study” (JKRYCSS) was conducted by scientists from Japan, China, and South Korea. Tall moorings with current meters (CMs) and upward-looking acoustic Doppler current profilers (ADCPs), and current and pressure-recording inverted echo sounders (CPIESs) were deployed on northwestern and southeastern sides of Miyakojima Island to observe the Kuroshio and the Ryukyu Current, simultaneously. These mooring sites lay along the altimeter track used by TOPEX/Poseidon and Jason-1/2/3, which is roughly perpendicular to the isobath of the continental shelf break.

In this talk, we will illustrate the velocity structure and variability of the Ryukyu Current by analyzing the 2-year record from a mooring array southeast of Miyakojima Island. The results showed that the shoreward intensified currents flowed northeastward. The subsurface core of the Ryukyu Current was located near the 1000 m isobath, with a maximum of 19.4 cm/s at 500 m. The observed velocity structure was reproduced well by the HYCOM reanalysis, except that the observed current core was stronger and shallower. The mean estimated volume transport across the observation section was 9.0 Sv with a standard deviation of 8.7 Sv, with a near 100-day variability dominant in the upper layer but absent in the deep layer.

©2019. Japan Geoscience Union. All Right Reserved.

Relationship of the Kuroshio with the current fields in the East China Sea from observations and model results

*Hong Sik Min[1], Chorong Hwang[1], Dong Guk Kim[1], Hirohiko Nakamura[2], Ayako Nishina[2], Xiao-Hua Zhu[3], Jae-Hun Park[4], Chanhyung Jeon[4], Hanna Na[5], Naoki Hirose[6]

1. Korea Institute of Ocean Science & Technology, 2. Kagoshima University, 3. Second Institute of Oceanography, 4. Inha University, 5. Seoul National University, 6. Kyushu University

We investigated relationship between variations of the Kuroshio in the southern East China Sea (ECS) and the current structure across the Korea/Tsushima Strait (KTS) using observational data and numerical simulation results. Variability of the Kuroshio in the southern ECS was obtained from moored current measurements located near the Kuroshio axis for 2 years (June 2015-June 2017), while current pattern across the KTS was obtained from acoustic Doppler current profiler (ADCP) measurements by a ferryboat between Hakata and Pusan. Comparisons between the two time series of observations reveal a significant relationship : when the Kuroshio in the southern ECS was strengthened the current in the western channel of KTS was also strengthened with a shift of the Tsushima Current (TC) to the coast. This correlated feature was also seen in the data-assimilated HYCOM, confirming that the HYCOM can reasonably reproduce the current field in the ECS. Further investigations using 25-year-long HYCOM outputs exhibit that the Kuroshio can vary the TC in the KTS. This presentation will show the connectivity of current fields in the northern ECS to the Kuroshio in the southern ECS.

Keywords: Kuroshio, East China Sea, observation

©2019. Japan Geoscience Union. All Right Reserved.

[E] Oral | A (Atmospheric and Hydrospheric Sciences)：A-OS Ocean Sciences & Ocean Environment

Wed. May 29, 2019 3:30 PM - 5:00 PM JST | Wed. May 29, 2019 6:30 AM - 8:00 AM UTC | 105 1F

[A-OS08] ECS-Kuroshio and Ryukyu Current System -Observation, modeling and theory-

convener:Hirohiko Nakamura(Kagoshima University, Faculy of Fisheries), Xiao-Hua Zhu(Second Institute of Oceanography), Chairperson:Jae-Hun Park(Inha University), Hirohiko Nakamura(Kagoshima University)

The East China Sea (ECS) is separated from the North Pacific basin by the Ryukyu Islands. On each side of the Ryukyu Islands, there lies two western boundary currents -the Kuroshio on the northwest and the Ryukyu Current on the southeast. These two currents play an important role in the global substance cycle and have a remarkable impact on the climate and adjacent marginal seas. Our knowledge of the Kuroshio and the Ryukyu Current's dynamics, variability, and impact has advanced significantly over the last decade, because of recent international collaborative field programs, improvement in satellite measurements, and advancement in high-resolution numerical models. This session seeks contributions from ECS-Kuroshio and Ryukyu Current studies and will cover a wide range of topics of observation, modeling and theory. The dynamics of the Kuroshio and the Ryukyu Current's variability at all spatio-temporal scales, the influence of the Kuroshio on typhoons and climate, the interactions among the Kuroshio, Ryukyu Current and eddies, internal waves including near-internal waves and their interactions with background currents, and the water mass exchanges through the gaps between the Ryukyu Islands are welcome to be discussed in this session.

3:30 PM - 3:35 PM JST | 6:30 AM - 6:35 AM UTC

Introduction

3:35 PM - 3:55 PM JST | 6:35 AM - 6:55 AM UTC

[AOS08-06] Separating Small-Scale Oceanic Internal Waves and Vortical Motions

★Invited Papers

*Ren-Chieh Lien[1] (1.University of Washington, Seattle, WA, USA)

3:55 PM - 4:10 PM JST | 6:55 AM - 7:10 AM UTC

[AOS08-07] Structure and variability of the Kuroshio current in the Tokara Strait

*Zhao-Jun Liu[1], Hirohiko Nakamura[2], Xiao-Hua Zhu[1], Ayako Nishina[2], Xinyu Guo[3], Menghong Dong[1] (1.Second Institute of Oceanography, China, 2.Kagoshima University, Japan, 3.Ehime University, Japan)

4:10 PM - 4:25 PM JST | 7:10 AM - 7:25 AM UTC

[AOS08-08] **Near-inertial waves advected by the Kuroshio from observation and simulation**

*CHANHYUNG JEON[1], Jae-Hun Park[1], Hirohiko Nakamura[2], Ayako Nishina[2], Xiao-Hua Zhu[3], Dong Guk Kim[4], Hong Sik Min[4], Sok Kuh Kang[4], Hanna Na[5], Naoki Hirose[6], Youngseok Choi[1] (1.Inha University, 2.Kagoshima University, 3.Second Institute of Oceanography, 4.Korea Institute of Ocean Science and Technology, 5.Seoul National University, 6.Kyushu University)

4:25 PM - 4:40 PM JST | 7:25 AM - 7:40 AM UTC

[AOS08-09] Turbulent mixing and near-inertial internal waves induced by the Kuroshio over seamounts in the Tokara Strait

*Takeyoshi Nagai[1], Daisuke Hasegawa[2], Eisuke Tsutsumi[3], Hirohiko Nakamura[4], Ayako Nishina[4], Tomoharu Senjyu[3], Takahiro Endoh[3], Takeshi Matsuno[3], Ryuichiro Inoue[5], Amit Tandon[6] (1.Department of Ocean Sciences, Tokyo University of Marine Science and Technology, 2.Tohoku National Fisheries Research Institute, Japan Fisheries Research and Education Agency, 3.Kyushu University, Research Institute for Applied Mechanics, 4.Faculty of Fisheries Kagoshima University, 5.Ocean Circulation Research Group, Japan Agency for Marine-Earth Science and Technology, 6.Mechanical Engineering Department & SMAST, University of Massachusetts Dartmouth)

4:40 PM - 4:55 PM JST | 7:40 AM - 7:55 AM UTC

[AOS08-10] Microstructure and mooring observations of enhanced mixing in the Kerama Gap

*Ryuichiro Inoue[1], Hirohiko Nakamura[2], Takahiro Tanaka[3], Shinzou Fujio[4], Daigo Yanagimoto[4], Ichiro Yasuda[4] (1.Japan Agency for Marine-Earth Science and Technology, 2.Kagoshima University, Faculy of Fisheries, 3.Tohoku National Fisheries Research Institute, Japan Fisheries Research and Education Agency, 4.The University of Tokyo, Atmosphere and Ocean Research Institute)

4:55 PM - 5:00 PM JST | 7:55 AM - 8:00 AM UTC

Discussion

Separating Small-Scale Oceanic Internal Waves and Vortical Motions

*Ren-Chieh Lien[1]

1. University of Washington, Seattle, WA, USA

Internal waves and vortical motions coexist in the ocean, sometimes at same temporal and spatial scales. Observations taken by 20 EM-APEX floats in the upper ocean thermocline of the summer Sargasso Sea capture the temporal and vertical variations of Ertel potential vorticity (PV) in 7–70 m vertical scale, averaged over horizontal scales of O(4–8 km). PV is dominated by its linear components —vertical vorticity and vortex stretching, each with rms value of ~0.15 f. In the internal wave frequency band, they are coherent and in phase, expected for linear internal waves. Packets of strong vertical vorticity and vortex stretching, > 0.2 f, balance each other closely such that the rms PV ~0.03 f. PV is dominant at frequencies less than 1.4 f and peaks at vertical wavenumber $<$~0.1 cpm , our highest resolvable vertical wavenumber. PV frequency spectrum plateaus at subinertial frequencies and has a −1 spectral slope in the internal wave frequencies with a small peak at inertial frequency. The PV at near-inertial frequency is likely attributed to the differential advection of background PV by near inertial waves. Measurement errors might also contribute to PV in the internal wave frequency band. Vertical vorticity and vortex stretching are separated into linear vortical mode and internal wave components following the normal mode decomposition. The theoretical prediction of a negative correlation between vertical vorticity and vortex stretching for the linear vortical mode, i.e., reinforcing PV, is confirmed at subinertial frequencies. The Burger number of the vortical mode is ~0.84, implying HKE/APE of ~0.7. The vortical mode frequency and vertical wavenumber spectra are 1-2 decades less than internal wave components. A joint experiment will be conducted in Tokara Strait in the next 3 years to study Kuroshio interaction with seamounts in Tokara Strait. We will discuss the importance of separating internal lee waves and vortical motions behind the seamount on quantifying turbulence mixing and watermass transformation.

Keywords: Internal Lee Waves, Vortical Motions, Turbulence, Kuroshio, Tokara Strait

©2019. Japan Geoscience Union. All Right Reserved.

Structure and variability of the Kuroshio current in the Tokara Strait

*Zhao-Jun Liu[1], Hirohiko Nakamura[2], Xiao-Hua Zhu[1], Ayako Nishina[2], Xinyu Guo[3], Menghong Dong[1]

1. Second Institute of Oceanography, China, 2. Kagoshima University, Japan, 3. Ehime University, Japan

Transverse-vertical structure and temporal variability of the Kuroshio current across the Tokara Strait during 2003–2012 measured by ferryboat acoustic Doppler current profiler (ADCP) with a 2-km horizontal resolution and a 2-day interval are presented. The Kuroshio passing through the Tokara Strait exhibits a nearly permanent multicore velocity structure. The mean eastward Kuroshio transport is 25.84 Sv (1 Sv ≡10^6 m^3 s^{-1}) and the net baroclinic transport relative to 700 m is 19.57 Sv. The seasonal variation of the Kuroshio transport via the Tokara Strait is a “W”-shaped curve with a maximum in July and a second maximum in December–January. The baroclinic transport shows seasonal variation similar to that of the undecomposed transport, with a maximum in July. However, the barotropic transport displays a reversed seasonal variation—a “V”-shaped distribution—with a maximum in December. In the empirical orthogonal function (EOF) analyses of the cross-sectional velocity, with the exception of the well-known meander (EOF1: 41.1%) and transport (EOF2: 26.3%) modes, the third mode (EOF3: 19.2%) is first observed. The EOF3 mode exhibits a band-like structure, with a smaller horizontal scale than the first two EOF modes; such a band-like structure may be related to the wakes in the lee of the Tokara Islands. Additional analysis based on high-resolution JCOPE-T reanalysis data revealed that (1) many vortexes were generated around the Tokara Strait due to the strong flow-topography interaction; (2) the intensities of the island-induced wakes depend on the Kuroshio path position around the Tokara Strait.

Keywords: Tempo-spatial variations, Kuroshio, Tokara Strait

©2019. Japan Geoscience Union. All Right Reserved.

Near-inertial waves advected by the Kuroshio from observation and simulation

*CHANHYUNG JEON[1], Jae-Hun Park[1], Hirohiko Nakamura[2], Ayako Nishina[2], Xiao-Hua Zhu[3], Dong Guk Kim[4], Hong Sik Min[4], Sok Kuh Kang[4], Hanna Na[5], Naoki Hirose[6], Youngseok Choi[1]

1. Inha University, 2. Kagoshima University, 3. Second Institute of Oceanography, 4. Korea Institute of Ocean Science and Technology, 5. Seoul National University, 6. Kyushu University

Advection of near-inertial waves (NIWs) by background currents has been predicted using numerical simulations, while supporting in-situ observations were rare. A pair of tall current moorings, deployed around 26˚N and 125˚E in Okinawa Trough from June 2015 to June 2016, provides a clear evidence exhibiting NIWs advected by the Kuroshio. Energetic NIWs are observed after two-typhoon passages in early August and late September 2015. Both typhoon passages occurred across the Kuroshio east of Taiwan upstream of the observation sites about 250-km southwest with a difference of about 2-degree in latitude. One site (KCM1), relatively close to the center of the Kuroshio axis, exhibits more energetic NIWs than near the edge of the Kuroshio (KCM2), ~32 km away from KCM1. The frequency of NIWs shifts to the lower band from the local inertial frequency (0.91*f*), inferring propagation from the south. The data-assimilative three-dimensional numerical model forced by 6-hourly atmospheric forcings including tides and oceanic circulation demonstrates local NIW generation is weak at observation sites during and after typhoon passages, while its generation upstream of observation sites is quite energetic. Current patterns and frequency shifts of NIWs between observation and simulation agree well at observation sites. Analyses of simulation provide that negative relative vorticity region works like a waveguide for NIW propagation, and the strong Kuroshio current advects the waves poleward with a speed ~85% of the local current.

Keywords: Near-inertial waves, Advection, Kuroshio, observation, simulation

©2019. Japan Geoscience Union. All Right Reserved.

Turbulent mixing and near-inertial internal waves induced by the Kuroshio over seamounts in the Tokara Strait

*Takeyoshi Nagai[1], Daisuke Hasegawa[2], Eisuke Tsutsumi[3], Hirohiko Nakamura[4], Ayako Nishina[4], Tomoharu Senjyu[3], Takahiro Endoh[3], Takeshi Matsuno[3], Ryuichiro Inoue[5], Amit Tandon[6]

1. Department of Ocean Sciences, Tokyo University of Marine Science and Technology, 2. Tohoku National Fisheries Research Institute, Japan Fisheries Research and Education Agency, 3. Kyushu University, Research Institute for Applied Mechanics, 4. Faculty of Fisheries Kagoshima University, 5. Ocean Circulation Research Group, Japan Agency for Marine-Earth Science and Technology, 6. Mechanical Engineering Department & SMAST, University of Massachusetts Dartmouth

Recent observations in the upstream side of the Tokara Strait during November 2016, where the Kuroshio south of Kyushu flows over a number of seamounts, show banded structures of large amplitude high vertical wavenumber shear roughly along isopycnal, which are suggestive of near-inertial internal waves. The measured vertical section of laterally high resolution (~1 km) tow-yo microstructure measurements show the banded layers of large turbulent kinetic energy dissipation rates clearly associated with the near inertial shear banding. In this study, the results from the similar tow-yo microstructure surveys during November 2017 and June 2018 cruise, which are extended further downstream side of the Tokara Strait in the Kuroshio are analyzed. It is found that the high vertical wavenumber near-inertial shear is amplified near the seamounts in the Kuroshio, and that turbulent kinetic energy dissipation rates are elevated near the seamounts over 100 km along the Kuroshio axis by a factor of 100-1000. This length scale, over 100 km, is much larger than that of the hydraulically controlled isopycnal displacements with large Froude number in close proximity to the seamounts ~5km. In the presentation, mechanisms of the amplified near-inertial shear and elevated turbulence over such a wide length scale are discussed with the results from June 2018 cruise and using numerical simulations with and without tide.

Keywords: Kuroshio, Near-inertial internal waves, Turbulence

©2019. Japan Geoscience Union. All Right Reserved.

©2019. Japan Geoscience Union. All Right Reserved.

Microstructure and mooring observations of enhanced mixing in the Kerama Gap

*Ryuichiro Inoue[1], Hirohiko Nakamura[2], Takahiro Tanaka[3], Shinzou Fujio[4], Daigo Yanagimoto[4], Ichiro Yasuda[4]

1. Japan Agency for Marine-Earth Science and Technology, 2. Kagoshima University, Faculy of Fisheries, 3. Tohoku National Fisheries Research Institute, Japan Fisheries Research and Education Agency, 4. The University of Tokyo, Atmosphere and Ocean Research Institute

Microstructure and mooring observations were conducted around the Kerama Gap, near the midpoint of the Ryukyu Island chain, in December 2016. We observed the enhanced mixing near the topography, with vertical diffusivities of 10^{-2}~10^{-1} m^2 s^{-1} and found that tides are important to drive the enhanced mixing at the sill. To understand tidal processes, we conducted two-dimensional numerical simulations. The numerical simulation indicated that hydraulic jump or lee wave breaking are important for the enhanced mixing behind the sill. It also indicated that there are interferences between M2 internal tides radiated from entrance and exit of the Kerama Gap, which may correspond to observed enhanced vertical shear and mixing at a bottom of the North Pacific Intermediate Water in the Kerama Gap. These results suggest that enhanced mixing around Kerama Gap is important for ventilating deep water as well as renewal of the North Pacific Intermediate Water in the Okinawa Trough.

©2019. Japan Geoscience Union. All Right Reserved.

[E] Oral | A (Atmospheric and Hydrospheric Sciences)：A-OS Ocean Sciences & Ocean Environment

Wed. May 29, 2019 9:00 AM - 10:30 AM JST | Wed. May 29, 2019 12:00 AM - 1:30 AM UTC | 301A 3F

[A-OS11] Continental-Oceanic Mutual Interaction: Planetary scale Material Circulation

convener:Yosuke Alexandre Yamashiki(Earth & Planetary Water Resources Assessment Laboratory Graduate School of Advanced Integrated Studies in Human Survivability Kyoto University), Yukio Masumoto(Graduate School of Science, The University of Tokyo), Swadhin Behera(Climate Variation Predictability and Applicability Research Group, Application Laboratory, JAMSTEC, 3173-25 Showa-machi, Yokohama 236-0001), Takanori Sasaki(Department of Astronomy, Kyoto University), Chairperson:Yukio Masumoto, Behera Swadhin(JAMSTEC)

The main purpose of this session is to promote discussion on mutual interaction between Continental zone and Oceanic zone. The global-scale material circulation induced by River runoff through oceanic general circulation as major topic on Continental-Oceanic Interaction, where the ENSO / IOD influence into continental climate as major topics on Oceanic-Continental Interaction. Numerical simulation and field observation of radionuclide transport from continental zone into ocean and its potential impact is also important topics of this session. The session also extend discussion on planetary hydrology and oceanography focusing on subsurface ocean in Jupiter's moon & Ancient Martian Oceanography & Hydrology by possible application of terrestrial GCM into Ancient Mars.

9:00 AM - 9:15 AM JST | 12:00 AM - 12:15 AM UTC

[AOS11-01] Explorations and current understandings for subsurface ocean of icy bodies

★Invited Papers

*Jun Kimura[1] (1.Osaka University)

9:15 AM - 9:30 AM JST | 12:15 AM - 12:30 AM UTC

[AOS11-02] **Climate predictability for societal applications including AI/ML**

*Swadhin Behera[1], Manali Pal[2], J.V. Ratnam[1], Rajib Maity[2], Takeshi Doi[1], Yushi Morioka[1], Masami Nonaka[1] (1.Application Laboratory, JAMSTEC, 3173-25 Showa-machi, Yokohama 236-0001, 2.Indian Institute of Technology, Kharagpur, India)

9:30 AM - 9:45 AM JST | 12:30 AM - 12:45 AM UTC

[AOS11-03] Re-entry of giant-impact fragments and early evolution of the Earth's ocean

*Takanori Sasaki[1] (1.Department of Astronomy, Kyoto University)

9:45 AM - 10:00 AM JST | 12:45 AM - 1:00 AM UTC

[AOS11-04] Modeling of Extreme Freshwater Discharge and influence from Japanese First-Class Rivers to Coastal zones

*Ryusuke Kuroki, Yosuke Alexandre Yamashiki[1], Sergey Varlamov[2], Yasumasa Miyazawa[2], Racault Fanny Marie[3], Hoshin Vijai Gupta[4] (1.Kyoto University, 2.Application Laboratory, Japan Agency for Marine-Earth Science and Technology, Japan, 3.Plymouth Marine Laboratory, Plymouth, United Kingdom, 4.University of Arizona)

10:00 AM - 10:15 AM JST | 1:00 AM - 1:15 AM UTC

[AOS11-05] Establishment of new curriculum at Biosphere 2

*Kenji Miki[1], Takao Doi[2], Yosuke Yamashiki[3], Masahiro Terada[2] (1.Kyoto University Graduate School of Agriculture, 2.Kyoto University Unit of Synergetic Studies for Space, 3.Graduate School of Advanced Integrated Studies in Human Survivability)

10:15 AM - 10:30 AM JST | 1:15 AM - 1:30 AM UTC

[AOS11-06] Development of the highly precise high-speed photometry technique with the photometer mounted with PIRKA telescope

*Nami Kimura[1] (1.Hokkaido University)

Explorations and current understandings for subsurface ocean of icy bodies

*Jun Kimura[1]

1. Osaka University

Most of solid bodies in the outer solar system, around Jupiter's orbit and beyond, are covered with ice on its surface, which are called as "Icy bodies".
In these icy bodies, e.g., Jovian moon Europa and Saturnian moon Enceladus, existence of the global liquid water ocean under the icy crust, called as "subsurface ocean", has been strongly suggested through the past remote sensing (mainly by geodetic and electromagnetic measurement) and theoretical modelling.
In this talk, I introduce the results of previous observations and theoretical calculations, and summarize the current
understandings focusing on the geophysical knowledge about the subsurface ocean of icy bodies.

©2019. Japan Geoscience Union. All Right Reserved.

Climate predictability for societal applications including AI/ML

*Swadhin Behera[1], Manali Pal[2], J.V. Ratnam[1], Rajib Maity[2], Takeshi Doi[1], Yushi Morioka[1], Masami Nonaka[1]

1. Application Laboratory, JAMSTEC, 3173-25 Showa-machi, Yokohama 236-0001, 2. Indian Institute of Technology, Kharagpur, India

The tropical Indo-Pacific domain is important for global climate. Particularly, the warm pool region rooted in both basins plays an important role in the modulation of ocean and atmosphere variability on several spatio-temporal scales. While both basins share the extended warm pool, each of the two basins has its own modes of ocean and climate variations. Tropical Pacific Ocean is well-known for the El Niñ o/Southern Oscillation (ENSO) phenomenon, the influence of which is seen world-wide during ENSO occurrence years. Recently, another mode of climate variability called the ENSO Modoki is discovered in the tropical Pacific Ocean. The ENSO Modoki is distinct from ENSO in terms of its characteristics and global impacts. Therefore, predictability of ENSO and ENSO Modoki is important for reducing their impacts on the society. Coupled models like SINTEX-F has been predicting the ENSO Modokis quite well. Here an attempt is made to compare those predictabilities using predictions from an AI/ML based statistical approach.

Keywords: ENSO , ENSO Modoki, Prediction

©2019. Japan Geoscience Union. All Right Reserved.

Re-entry of giant-impact fragments and early evolution of the Earth's ocean

*Takanori Sasaki[1]

1. Department of Astronomy, Kyoto University

The late stages of Earth's formation remain a mystery. No building blocks remain in Earth's orbit and no geological evidence is available for the first 700 million years Earth's history. Herein we propose that protoplanetary fragments produced by the giant impacts during terrestrial planet formation may give some important clues to the era. Iron-bearing giant impact fragments provide significant reducing agent that could transform primitive CO2–H2O atmosphere and ocean into more reducing H2-bearing atmosphere. Re-entry of the giant-impact fragments into eary Earth would be important for the origin of Earth’ s life and its early evolution.

Keywords: Earth, ocean, giant impact

©2019. Japan Geoscience Union. All Right Reserved.

Modeling of Extreme Freshwater Discharge and influence from Japanese First-Class Rivers to Coastal zones

*Ryusuke Kuroki, Yosuke Alexandre Yamashiki[1], Sergey Varlamov[2], Yasumasa Miyazawa[2], Racault Fanny Marie[3], Hoshin Vijai Gupta[4]

1. Kyoto University, 2. Application Laboratory, Japan Agency for Marine-Earth Science and Technology, Japan, 3. Plymouth Marine Laboratory, Plymouth, United Kingdom, 4. University of Arizona

We estimated the effects of extreme fresh water discharge from Japanese first-class rivers to coastal zones of the Japanese coast. Our targeted event was a typhoon Etau from 06/09/2015 to 12/09/2015, a week, and we could success to optimize 5 parameters, soil roughness coefficient, river roughness coefficient, effective porosity, saturated hydraulic conductivity, and effective rainfall by using Shuffled Complex Evolution method developed by University of Arizona (SCE-UA method), that is one of the optimization method for hydrologic model during this week. In addition to this, we made a set of hourly simulated river outflow data of almost all of Japanese first-class rivers from these basins to the Pacific Ocean and the Sea of Japan during the period by using our model “Cell Distributed Runoff Model Version 3.1.1 (CDRMV3.1.1)”. After the simulation, we used these calculated discharge data with a coupled hydrological-oceanographic model JCOPE-T for estimation of sea surface salinity distribution (SSS) in Japanese coastal zones. And simulated SSS results were verified by comparison with Chlorophyll-a distribution, observed by satellite re-mote sensing. Therefore we successfully reproduced peak discharge prediction of extreme typhoon events on river mouth and the coastal oceanic circulation.

©2019. Japan Geoscience Union. All Right Reserved.

Establishment of new curriculum at Biosphere 2

*Kenji Miki[1], Takao Doi[2], Yosuke Yamashiki[3], Masahiro Terada[2]

1. Kyoto University Graduate School of Agriculture, 2. Kyoto University Unit of Synergetic Studies for Space, 3. Graduate School of Advanced Integrated Studies in Human Survivability

We are currently planning to start up a new practical training programme at Biosphere 2 under a contract between Kyoto University and Arizona State University.
Biosphere 2 was established in1991 and was designed to produce a closed-complete ecosystem in the institute. Although the ecosystem-establishment was not fully successful, the institute still has been used for various research such as ecology, terraforming, and closed-environental impact to human health.
Our practical training programme will include hands-on training for exoplanet observation, and lectures about water-cycle and atmospheric science.
Although the programme is going to be carried out in August 2019, the pilot programme were put into practice with ten participants including lecturers and students from the states and Japan.
At the conference, we would give a presentation about the detailed programme schedule and expected educational and academic results from this programme.

Keywords: Biosphere 2, ecosystem

©2019. Japan Geoscience Union. All Right Reserved.

Development of the highly precise high-speed photometry technique with the photometer mounted with PIRKA telescope

*Nami Kimura[1]

1. Hokkaido University

There is a few striped pattern on Jupiter when we observe by visible light, and we can see white bands called " belt” and dark band called " zone". The cloud top altitude is high at zone, low at belt by infrared observation.Various models are proposed to figure out, but we cannot elucidate the mechanism of this large scale structure.The Galileo datas tell us that the zonal jets are located on boundaries between the belts and zones, with the westward jets on the poleward edges of belts and the eastward jets on the poleward edges of zones.It is still not clear that the wind occurs by sun light in atmospheric layer or internal heat source makes the global structure including the wind.One of the mechanism making zonal wind is that small eddies combine each other and make eddy flow, but it is not sufficiently to observe the cumulonimbus the source of small eddies. In the case of thunders of the earth, the study of the activity of cumulonimbus such a strong upward current and thunder storms makes progress. Upward current can help hydrologic cycle. There is a relationship of frequency of thunders and the altitude go the cumulonimbus on the earth, and the CMC is known to be proportion to brightness of the thunder, too. I developed a photometer equipped to PIRKA telescope to arrest the time change and the frequency of thunder lightning in the Jupiter.First I estimated the time of the duration and freqency and spatial distribution of lightnings of Jupiter by using parameters of lightnings on the earth and observation data of satellites.Then it is necessary to divide into 10 to observe lightning activity which continue 1ms and to focus on one cumulonimbus and to get high signal-noise ratio. I designed the equipment which can achieve these numerical goal and examined observation methods for example exposure time and field of view.

©2019. Japan Geoscience Union. All Right Reserved.

[E] Oral | A (Atmospheric and Hydrospheric Sciences)：A-OS Ocean Sciences & Ocean Environment

Wed. May 29, 2019 10:45 AM - 12:15 PM JST | Wed. May 29, 2019 1:45 AM - 3:15 AM UTC | 301A 3F

[A-OS11] Continental-Oceanic Mutual Interaction: Planetary scale Material Circulation

convener:Yosuke Alexandre Yamashiki(Earth & Planetary Water Resources Assessment Laboratory Graduate School of Advanced Integrated Studies in Human Survivability Kyoto University), Yukio Masumoto(Graduate School of Science, The University of Tokyo), Swadhin Behera(Climate Variation Predictability and Applicability Research Group, Application Laboratory, JAMSTEC, 3173-25 Showa-machi, Yokohama 236-0001), Takanori Sasaki(Department of Astronomy, Kyoto University), Chairperson:Yosuke Yamashiki(GSAIS Kyoto University), Takanori Sasaki(Department of Astronomy, Kyoto University)

The main purpose of this session is to promote discussion on mutual interaction between Continental zone and Oceanic zone. The global-scale material circulation induced by River runoff through oceanic general circulation as major topic on Continental-Oceanic Interaction, where the ENSO / IOD influence into continental climate as major topics on Oceanic-Continental Interaction. Numerical simulation and field observation of radionuclide transport from continental zone into ocean and its potential impact is also important topics of this session. The session also extend discussion on planetary hydrology and oceanography focusing on subsurface ocean in Jupiter's moon & Ancient Martian Oceanography & Hydrology by possible application of terrestrial GCM into Ancient Mars.

10:45 AM - 11:00 AM JST | 1:45 AM - 2:00 AM UTC

[AOS11-07] The Drivers of early Archean Earth’s Hydrology: Resolving the Faint Young Sun's Paradox

★Invited Papers

*Vladimir Airapetian[1], Guillaume Gronoff[2], Michael Way[3], Meng Jin[4] (1.NASA Goddard Space Flight Center/SEEC and American University, 2.NASA LaRC/SSAI, 3.NASA GISS/SEEC, 4.SETI)

11:00 AM - 11:15 AM JST | 2:00 AM - 2:15 AM UTC

[AOS11-08] Experimental study on elementary hydrological process of rainfall in a forested continental hinterland

*Shigeki Murakami[1] (1.Kyushu Research Cente, Forestry and Forest Products Research Institute)

11:15 AM - 11:30 AM JST | 2:15 AM - 2:30 AM UTC

[AOS11-09] Radiological Assessment of Martian and Terrestrial Surface during Young Sun

*Yosuke Alexandre Yamashiki[1], Hiroyuki Maehara[6], Yuta Notsu[3], Tatsuhiko Sato[2], Airapetian Vladimir[7], Shota Notsu[3], Ryusuke Kuroki[1], keiya murashima[5], Hiroaki Sato[4], Hina Bando[5], Kosuke Namekata[3], Takanori Sasaki[3], Scott Thomas[8], Nogami Daisaku[3], Kazunari Shibata[9] (1.Earth & Planetary Water Resources Assessment Laboratory Graduate School of Advanced Integrated Studies in Human Survivability Kyoto University, 2.Japan Atomic Energy Agency, 3.Graduate School of Science, Kyoto University, 4.School of Engineering, 5.School of Science, 6.National Astronomical Observatory of Japan, 7.NASA / Goddard Space Flight Center, 8.University of Bristol , 9.Kwasan Astronomical Observatory, Kyoto University)

11:30 AM - 11:45 AM JST | 2:30 AM - 2:45 AM UTC

[AOS11-10] Evaluation of scintillator detection materials for application within environmental radiation monitoring

*Peter George Martin[1], D. Connor[1], M. Lowden[1], T. B. Scott[1] (1.School of Physics, University of Bristol, Bristol, UK)

11:45 AM - 12:00 PM JST | 2:45 AM - 3:00 AM UTC

[AOS11-11] The important factors for future human space activity in terms of space medicine

*Masahiro Terada[1], Yosuke Yamashiki[1], Kenji Miki[1], Satoko Tsujihiro[1], Takao Doi[1] (1.Kyoto University, Unit of Synergetic Studies for Space)

12:00 PM - 12:15 PM JST | 3:00 AM - 3:15 AM UTC

[AOS11-12] Storm Surge Response to Freshwater Outflow from Typhoons on the Ibaraki Coast

*Josko Troselj[1], Nobuhito Mori[1] (1.Coastal Engineering Laboratory, Disaster Prevention Research Institute, Kyoto University)

The Drivers of early Archean Earth’ s Hydrology: Resolving the Faint Young Sun's Paradox

*Vladimir Airapetian[1], Guillaume Gronoff[2], Michael Way[3], Meng Jin[4]

1. NASA Goddard Space Flight Center/SEEC and American University, 2. NASA LaRC/SSAI, 3. NASA GISS/SEEC, 4. SETI

Understanding how the early Archean Earth supported standing bodies of liquid surface water under the faint young Sun is one of the greatest challenges of modern science. Can this problem be resolved as a part of the puzzle of understanding of the origin of building blocks of life on early Earth? Here, we present a new concept of how these two pieces of the mystery of life can be reconciled if we reconstruct the eruptive history of space weather from the young Sun at the time when life started on Earth. Our three-dimensional (3D) magnetohydrodynamic model of the young Sun suggests that energetic protons can be accelerated in shock waves driven by frequent and powerful Coronal Mass Ejection events and Corotating Interacting Regions produced by the young Sun's wind. Accelerated protons at energies > 300 MeV penetrated into the nitrogen-rich weakly reducing atmosphere and initiated the reactive chemistry by breaking molecular nitrogen, carbon dioxide, and methane, producing nitrous oxide, the potent greenhouse gas, and hydrogen cyanide, an essential feedstock molecule of life. Our Global Climate Model, ROCKE-3D, suggests that at 4(1000) ppmv of nitrous oxide produced in a 1(0.5) bar atmospheres outputs the mean annualized Earth’ s temperature of +16(5.2)C, and thus may provide a resolution of the FYS paradox and explain the presence of early oceans.

Keywords: Earth, Sun, climate, chemistry

©2019. Japan Geoscience Union. All Right Reserved.

©2019. Japan Geoscience Union. All Right Reserved.

Experimental study on elementary hydrological process of rainfall in a forested continental hinterland

*Shigeki Murakami[1]

1. Kyushu Research Cente, Forestry and Forest Products Research Institute

There is an observational fact that a rainfall amount is constant or increases with increasing the distance from the coast (x) in a forest covered continent up to a few thousands kilometers, e.g. Amazon and Yenisei river basins. However, it contradicts the basic law of hydrology as shown in Fig 1a; rainfall (P) is partitioned into evapotranspiration (ET) and discharge (Q) that means P_0 at $x = x_0$ is larger than P_1 at $x = x_1$ ($x_0 < x_1$), because $P_0 = ET_0 + Q_0$ and $P_1 =< ET_0$. The contradiction is solved by Makarieva and Gorshkov (2007, hereafter refer to MG 2007) in which they proposed Biotic Pump of Atmospheric Moisture (BP) as illustrated in Fig. 1b. The principle of BP is that ET from forests (ET(F)) is greater than that from the ocean (ET(O)) that is the driving force to transport moisture from the ocean to a forested continental hinterland.

Nonetheless, MG (2007) and their series of studies did not explicitly mention the reason of large ET from forests. It is great in forests because evaporation of canopy interception (hereafter refer to interception; typically some 20% of rainfall) at the time of rainfall is larger than that from any other vegetative surfaces, though the amount of transpiration is similar independent of vegetation types under a certain climate condition.

Some studies showed that interception is proportional to the rainfall amount on an hourly basis. For example Hashino et al. (2012) observed evaporation rate of more than 10 mm/hour during rainfall that requires latent heat of five times as large as the solar constant. To explain such huge amount of evaporation during rainfall Murakami (2006) proposed splash droplet evaporation mechanism. I believe it is the only explanation of enormous evaporation because small droplets can evaporate and disappear quickly even under very high humidity based on the theory and experiments of cloud physics. On top of that, latent heat is supplied from clouds upon condensation of water vaper. However, splash droplet evaporation along with BP is still a hypothesis.

To prove the splash droplet evaporation hypothesis stable isotope of water is used. Over 1000 of rainwater samples were collected on an hourly basis both under the forest canopy and at the opening simultaneously (Fig. 2). The isotopic ratios are measured and are being analyzed in combine with the meteorological data. The outline of the methodology is presented at the meeting.

References

Hashino, M., Yao H., Tamura T. 2010 Micro-Droplet Flux in Forest and its Contribution to Interception Loss of Rainfall –Theoretical Study and Field Experiment. Journal of Water Resource and Protection, 2,

©2019. Japan Geoscience Union. All Right Reserved.

872-879. DOI: 10.4236/jwarp.2010.2101

Makarieva, A. M., Gorshkov V. G. 2007 Biotic pump of atmospheric moisture as driver of the hydrological cycle on land. 11, 1013–1033. DOI: 10.5194/hess-11-1013-2007

Murakami, S. 2006 A proposal for a new forest canopy interception mechanism: Splash droplet evaporation. Journal of Hydrology, 319, 72-82. DOI: 10.1016/j.jhydrol.2005.07.002

Keywords: Biotic Pump of Atmospheric Moisture, canopy interception, splash droplet evaporation, stable isotope of water

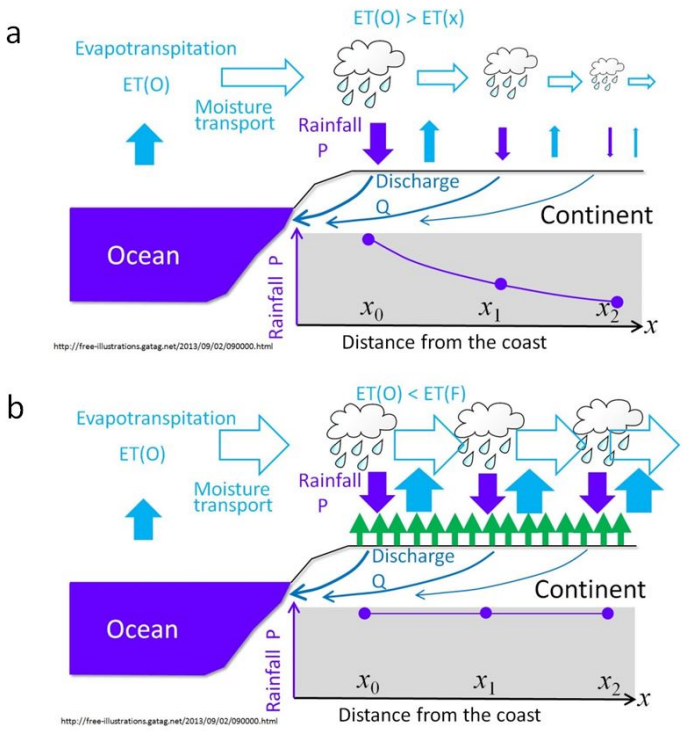

Fig. 1

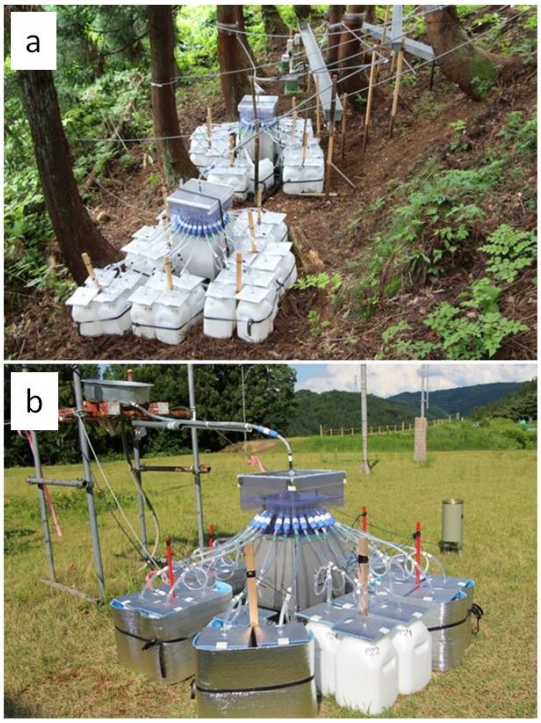

Fig. 2

©2019. Japan Geoscience Union. All Right Reserved.

Radiological Assessment of Martian and Terrestrial Surface during Young Sun

*Yosuke Alexandre Yamashiki[1], Hiroyuki Maehara[6], Yuta Notsu[3], Tatsuhiko Sato[2], Airapetian Vladimir[7], Shota Notsu[3], Ryusuke Kuroki[1], keiya murashima[5], Hiroaki Sato[4], Hina Bando[5], Kosuke Namekata[3], Takanori Sasaki[3], Scott Thomas[8], Nogami Daisaku[3], Kazunari Shibata[9]

1. Earth & Planetary Water Resources Assessment Laboratory Graduate School of Advanced Integrated Studies in Human Survivability Kyoto University, 2. Japan Atomic Energy Agency, 3. Graduate School of Science, Kyoto University, 4. School of Engineering, 5. School of Science, 6. National Astronomical Observatory of Japan, 7. NASA / Goddard Space Flight Center, 8. University of Bristol , 9. Kwasan Astronomical Observatory, Kyoto University

For a terrestrial planetary system, during the initiation period of planetary formation, the activity of a young Sun is extremely important in order to comprehend the atmospheric behavior of the planet. Relatively lower luminosity associated with lower surface temperature of the young Sun brings the planets a cooler surface environment. Terrestrial and Martian surfaces become icy cold in this environment without considering extensive GHG formation. Within such environments, the dose from SEP from a young Sun might play an important role in primordial atmospheric composition.

Here, we propose a reasonable radiological assssessment of the possible exposure intensity in SEP from a young Sun, by evaluating the possible magnitude and frequency of early solar flares by using possible star spot area, derived from their rotational period. We evaluated annual and maximum flare energy in different cases of solar spot areas for 3 %, 5 % ,and 10 % of solar surfaces. The maximum dose at the Martian TOA reaches 5.86 k Gy (265 Sv) when the solar spot area reaches 10 % of the solar surface. Such higher radiation dose may have influenced significantly atmospheric composition of Early Mars and Young Earth.

Keywords: Young Sun, Solar Flare, Radiological Condition

©2019. Japan Geoscience Union. All Right Reserved.

Evaluation of scintillator detection materials for application within environmental radiation monitoring

*Peter George Martin[1], D. Connor[1], M. Lowden[1], T. B. Scott[1]

1. School of Physics, University of Bristol, Bristol, UK

The last five years has seen the unabated growth in the number of airborne platforms performing radiation mapping –each using various iterations of low-altitude unmanned aerial vehicle (UAV). Alongside the associated advancements in the base airborne system transporting the radiation detection payload, from the earliest radiological analyses performed using gas-filled Geiger-Muller tube detectors, modern radiation mapping platforms are now based near-exclusively on solid-state scintillator (and to a lesser-extent semiconductor) detectors. With numerous types of these light-emitting crystalline materials now in existence, this combined desk and computational modelling study sought to evaluate the best-available detector material compatible with the requirements for low-altitude autonomous radiation mapping –of naturally-occurring but also anthropogenically-derived radionuclides.

Aside from ground-based radiation surveying undertaken by humans; environmental mapping of radiation distribution (resulting from both anthropogenic activities as well as from naturally-occurring radioactive material) has been performed historically using manned, fixed-wing aircraft. In contrast to the more limited detector volumes carried during on-ground operations (due to size and weight practicalities), the systems carried during these extensive spatial extent aerial surveys are typically not less than 33 litres in detector volume. For the gamma-ray measurements of naturally-occurring radionuclides, the key emission peaks are associated with the daughter products of the U (^{214}Bi) and Th (^{208}Tl) decay chains, alongside a strong contribution from radiogenic potassium (^{40}K). In contrast to the higher-energy (>1.0 MeV) gamma-ray emissions characteristic of the aforementioned naturally-occurring radionuclides, the primary anthropogenically-derived radionuclide released into the environment in extensive quantities during an emergency release event (such as at both Fukushima and Chernobyl) is radiocesium –specifically ^{137}Cs (half-life: 30.17 years), which emits a single gamma-ray photon at 0.662 MeV.

While the currently and widely-used NaI and CsI (both of which are Tl-doped) are the mainstays of radiation monitoring, during this study, LaBr scintillator detectors were determined to possess not only a greater sensitivity to incident gamma-radiation, but also a far superior spectral (energy) resolution over existing detector materials. Combined with their current competitive cost, an array of three such composition cylindrical detectors were determined to provide the best means of detecting and discriminating the various incident gamma-rays incident onto the detector owing to both naturally-occurring or anthropogenically-derived sources.
In this talk, we will present the results of multiple GEANT4 simulations that will inform the potential future development of the next generation of radiation detection materials and their optimal configurations for deployment.

©2019. Japan Geoscience Union. All Right Reserved.

The important factors for future human space activity in terms of space medicine

*Masahiro Terada[1], Yosuke Yamashiki[1], Kenji Miki[1], Satoko Tsujihiro[1], Takao Doi[1]

1. Kyoto University, Unit of Synergetic Studies for Space

When humans stay in space for long term, our body has various phyisiological effects by the specific space environments. Recently, space agency, such as NASA and JAXA, has the plan to send human to Moon or Mars. Therefore, it is very important to understand how we are effected during space staying. For example, our skeletal muscles on the leg become atrophy and bone volume decrease by spaceflight. And, astronauts must spend time in closed environment during human space mission. So, we need to know the mental or emotional changes during space mission.
Now, we have space camps which is simulated for future space misson. In this time, I will present the phyisiological data of mental factors in simulated space camps.

Keywords: Space medicine, Human space activity, Closed environment

©2019. Japan Geoscience Union. All Right Reserved.

Storm Surge Response to Freshwater Outflow from Typhoons on the Ibaraki Coast

*Josko Troselj[1], Nobuhito Mori[1]

1. Coastal Engineering Laboratory, Disaster Prevention Research Institute, Kyoto University

Introduction and Objective

Collaborative results (Troselj et al., 2017) have permitted for the first time to quantitatively evaluate the influence of extreme freshwater outflow to the coastal ocean due to typhoon passage by combining river and ocean models using hourly time step data and remote-sensing technology. They found that projection of coastal Sea Surface Salinity was improved (up to 10 PSU difference) and became more realistic with included freshwater impact and concluded that extreme events freshwater outflows significantly decrease Sea Surface Salinity distribution in the coastal zone.

With the advance of weather forecasting systems and specific availability of forecasting typhoon trajectory and intensity, the research team aims to be able to apprehend freshwater impacts on the coastal marine environment in advance of typhoon events, and contribute to the comprehensive management and protection of coastal zones.

In our JpGU presentation (2018), we concluded that our findings that the freshwater outflow impact to the storm surge is negligible during the typhoon passage but is important to be considered in evaluating an after-runner storm surge mechanism should be further confirmed in future works by testing the applicability of using the same method with many other typhoon event cases.

A follow up of the previous studies is shown here. As parameters which affect the total sea level are storm surge, tides, waves and freshwater impact, the main objective of the study is to test dependence between storm surge heights and the freshwater impact before and after passing of several typhoons over the Ibaraki Coast, Japan.

Methods

We continued the study from Troselj et al. (2018) with improved downscaling model methodology and extended analyzed period into 7 years (2000-2006). We applied better vertical transformation equation (Vtransform=2, new formulation developed by A. Shchepetkin) and different vertical stretching function (Vstretching=4, where A. Shchepetkin improved double stretching) compared to Troselj et al. (2018). River forcing conditions were applied as observed river temperature and discharge (MLIT, 2017) with constant salinity of 0.5 PSU for Tone, Naka and Kuji rivers.

Discussions

We compared coastal storm surge heights for cases with and without freshwater outflow impact and discussed differences in results, for several typhoons passing over Ibaraki Coast during the analysed period. With new results, our conclusions from JpGU presentation (2018) cannot yet be certainly

©2019. Japan Geoscience Union. All Right Reserved.

confirmed. The mechanism which we found then, presence of so called after-runner storm surge occurring about 4 days after passage of the event, is occurring in some typhoon cases but not every time. Therefore, its occurrence is function of many parameters occurring simultaneously such as typhoon trajectory, intensity and central pressure, actual state of the ocean (tides, waves), river discharge magnitude and temporal distribution and model conditions.

Summary

Using dynamic downscaling for reanalysis of coastal current system in the Ibaraki Coast, our goal was to test dependence between storm surge heights and the freshwater impact before and after typhoon events. We found that the mechanism found in the previous study is not occurring every time on the same way but is rather function of many other dependent parameters.

References

Troselj J, Sayama T, Varlamov SM, Sasaki T, Racault M-F, Takara K, Miyazawa Y, Kuroki R, Yamagata T, Yamashiki Y (2017). Modeling of extreme freshwater outflow from the north-eastern Japanese river basins to western Pacific Ocean, Journal of Hydrology, Vol. 555, pp. 956-970, doi:10.1016/j.jhydrol.2017.10.042.

Troselj, J, Imai, Y, Ninomiya, J, Mori, N (2018). Coastal Current Downscaling Emphasizing Freshwater Impact on Ibaraki Coast, Journal of Japan Society of Civil Engineers, Ser. B2 (Coastal Engineering), vol.74, no.2, pp. 1357-1362.

Keywords: storm surge, freshwater impact, typhoon events, downscaling, coastal current, COAWST

Keywords: storm surge, freshwater impact, typhoon events, downscaling, coastal current, COAWST

©2019. Japan Geoscience Union. All Right Reserved.

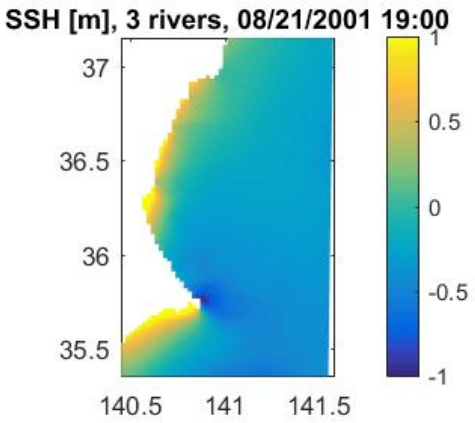

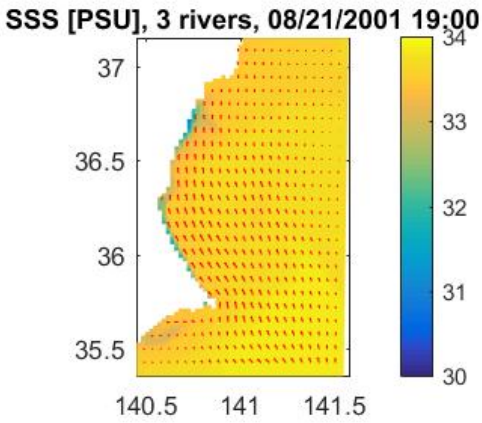

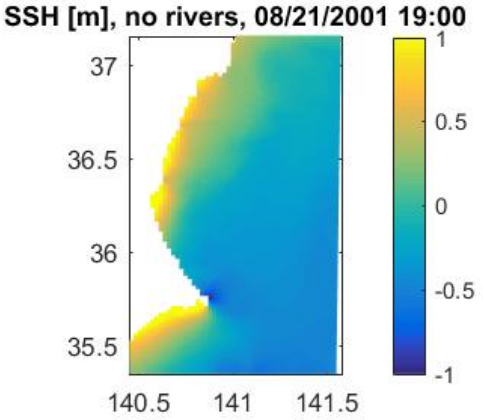

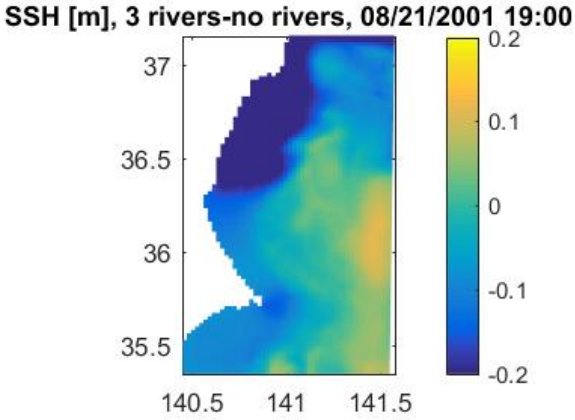

©2019. Japan Geoscience Union. All Right Reserved.

[E] Poster | A (Atmospheric and Hydrospheric Sciences)：A-OS Ocean Sciences & Ocean Environment

Wed. May 29, 2019 3:30 PM - 5:00 PM JST | Wed. May 29, 2019 6:30 AM - 8:00 AM UTC | Poster Hall International Exhibition Hall8, Makuhari Messe_7

[A-OS11] Continental-Oceanic Mutual Interaction: Planetary scale Material Circulation

convener:Yosuke Alexandre Yamashiki(Earth & Planetary Water Resources Assessment Laboratory Graduate School of Advanced Integrated Studies in Human Survivability Kyoto University), Yukio Masumoto(Graduate School of Science, The University of Tokyo), Swadhin Behera(Climate Variation Predictability and Applicability Research Group, Application Laboratory, JAMSTEC, 3173-25 Showa-machi, Yokohama 236-0001), Takanori Sasaki(Department of Astronomy, Kyoto University)

The main purpose of this session is to promote discussion on mutual interaction between Continental zone and Oceanic zone. The global-scale material circulation induced by River runoff through oceanic general circulation as major topic on Continental-Oceanic Interaction, where the ENSO / IOD influence into continental climate as major topics on Oceanic-Continental Interaction. Numerical simulation and field observation of radionuclide transport from continental zone into ocean and its potential impact is also important topics of this session. The session also extend discussion on planetary hydrology and oceanography focusing on subsurface ocean in Jupiter's moon & Ancient Martian Oceanography & Hydrology by possible application of terrestrial GCM into Ancient Mars.

[AOS11-P01] Remote Sensing of Chlorophyll-a and Submerged Aquatic Vegetation for a Freshwater Lake in Japan

*Shweta Yadav[1], Yamashiki Yosuke[1], Junichi Susaki[1], Kanako Ishikawa[2] (1.Kyoto University, 2.Lake Biwa Environmental Research Institute)

[AOS11-P02] Hydrological and Debris-flow simulation of Martian Surface in Hesperian & early Amazonian epoch

*Hiroaki Sato[2], Yosuke Alexandre Yamashiki[1], Ryusuke Kuroki[1], Hideaki Miyamoto[3], Ryodo Hemmi[3] (1.Earth & Planetary Water Resources Assessment Laboratory Graduate School of Advanced Integrated Studies in Human Survivability Kyoto University, 2.Faculty of Engineering, Kyoto University, 3.Graduate School of Engineering, The University of Tokyo)

[AOS11-P03] Global Lakes & reservoirs Repository and their application for terrestrial surface environment

*Yosuke Alexandre Yamashiki[1], Ryusuke Kuroki[1], Botong Gao[1], Hina Bando[2], Fuka Takagi[3], Shweta Yadav[4] (1.Earth & Planetary Water Resources Assessment Laboratory Graduate School of Advanced Integrated Studies in Human Survivability Kyoto University, 2.Faculty of Science, Kyoto University, 3.Faculty of Agriculture, Kyoto University, 4.Educational Unit for Studies on Connectivity of Hills, Humans and Ocean, Kyoto University)

[AOS11-P04] Numerical simulation of Tidal Heating using SPH and its application to inner sea formation

*keiya murashima[1], Yosuke Alexandre Yamashiki[1], Natsuki Hosono[2] (1.Kyoto University, 2.Japan Agency for Marine-Earth Science and Technology)

Remote Sensing of Chlorophyll-a and Submerged Aquatic Vegetation for a Freshwater Lake in Japan

*Shweta Yadav[1], Yamashiki Yosuke[1], Junichi Susaki[1], Kanako Ishikawa[2]

1. Kyoto University, 2. Lake Biwa Environmental Research Institute

Freshwater lakes, particularly shallow lakes often exhibit alternative vegetative states, a clear-water state dominated by submerged aquatic vegetation (SAV) and a turbid-water state dominated by phytoplankton. Phytoplankton and SAV constitute the base of the aquatic food web and are the primary driver of the biogeochemical process in both the freshwater and coastal water bodies. The abundance of phytoplankton biomass can potentially indicate the degree of eutrophication in a specific waterbody. On the other hand, the massive overgrowth of invasive SAV species can also pose a serious threat to the aquatic ecosystem. Conventional methods (eg. Site-specific Boat survey) used to monitor the large water bodies are often time-consuming and expensive. In this study, we used a remote sensing based approach to monitor SAV and phytoplankton of the Lake. A multi-spectral satellite image (Landsat-8 Operational Land Imager) was used to assess the phytoplankton concentration and SAV biomass. A spectral decomposing algorithm was used to estimate and quantify both phytoplankton and SAV. Based on the peak growth period of SAV in the lake, the estimations were limited to a certain period of the year (i.e. mainly August and September). The image was used to classify and map the SAV coverage area using the spectral mixture analysis. The SAV biomass estimation model was used to determine the biomass of the SAV classified pixels in the lake. The satellite-derived phytoplankton and SAV were validated using the in-situ measured data of the lake. The result indicates the time and location-specific variation in the dominance of the phytoplankton and SAV.

Keywords: Phytoplankton, Submerged Aquatic Vegetation, Remote Sensing, Lake Water Quality

©2019. Japan Geoscience Union. All Right Reserved.

Hydrological and Debris-flow simulation of Martian Surface in Hesperian & early Amazonian epoch

*Hiroaki Sato[2], Yosuke Alexandre Yamashiki[1], Ryusuke Kuroki[1], Hideaki Miyamoto[3], Ryodo Hemmi[3]

1. Earth & Planetary Water Resources Assessment Laboratory Graduate School of Advanced Integrated Studies in Human Survivability Kyoto University, 2. Faculty of Engineering, Kyoto University, 3. Graduate School of Engineering, The University of Tokyo

It is considered that the Mars in Noachian ecoch to early Amazonian was much warmer temperature than current condition, with atmosphere and ocean supported by its magnetic activity. Several valley which seems to be developed by ancient hydrological processes are obsered in Martian surface, is being considered to be built long time before. Some fluvial fun was formed during the following Hesperian to early Amazonian epoch, which is considered as much cooler and drier than Noachian epoch. In this study, we applied Hydro-debris 2D model into Martian surface in Hesperian epoch in order to try develping surface vallay formation throughout hydrological processes.

Sediment transport and associated small-scale debris-flow occurrence may be the key for valley formation, where might be the micro-habitable zone in ancient period. At the same time it is still uncertain how much precipitation and erosion should have been required to formulate such topography. Following the last year’ s calculation we attempted to compare several cases of debris flow experiments by changing hypothetical precipitation rate and erosive coefficients in the initially distributed regolith.

Keywords: Hesperian Epoch, Debris flow

©2019. Japan Geoscience Union. All Right Reserved.

Global Lakes & reservoirs Repository and their application for terrestrial surface environment

*Yosuke Alexandre Yamashiki[1], Ryusuke Kuroki[1], Botong Gao[1], Hina Bando[2], Fuka Takagi[3], Shweta Yadav[4]

1. Earth & Planetary Water Resources Assessment Laboratory Graduate School of Advanced Integrated Studies in Human Survivability Kyoto University, 2. Faculty of Science, Kyoto University, 3. Faculty of Agriculture, Kyoto University, 4. Educational Unit for Studies on Connectivity of Hills, Humans and Ocean, Kyoto University

Global Lakes & Reservoirs Repository (GLR) has been developed in order to list global scale freshwater storage focusing on Lakes & Reservoirs. In this presentation we'll introduce their application, combining this with the ecological model for lakes & reservoirs for their surface environmental assessment under different climatic conditions. A two-layer aquatic ecological model (consisted with three types of phytoplanktons & zooplankton) is linked for a number of global lakes for the evaluation of future trends of aquatic ecosystems, mainly focusing on phytoplankton growth. The application of the database, by coupling it with satellite remote sensing for monitoring aquatic environment, together with the three-dimensional lake & reservoir aquatic environment model, are also introduced in the database.

Keywords: GLR, Remote sensing of aquatic environment

©2019. Japan Geoscience Union. All Right Reserved.

Numerical simulation of Tidal Heating using SPH and its application to inner sea formation

*keiya murashima[1], Yosuke Alexandre Yamashiki[1], Natsuki Hosono[2]

1. Kyoto University, 2. Japan Agency for Marine-Earth Science and Technology

There are some traces of liquid in icy moons, such as a plume of vapor of Europa acquired by Hubble Space Telescope and tiger stripes of Enceladus observed by Cassini. Since liquid water is essential for the origin of life, it can be important to understand the development of inner sea and also the temperature distribution inside of such icy moons.

It is considered that the tidal heating caused by tidal acceleration melts the inner icy layer which results in the presence of liquid water beneath its surface. Thus, we aim at simulating the tidal heating of an icy moon by 3-dimensional numerical fluid calculation in Smoothed Particle Hydrodynamics (SPH) method. As the tidal heating model, we apply the viscosity model which was used for numerical calculation of tidal stripping.

It is confirmed that this viscosity model lead to qualitatively correct result about tidal disruption, but the possibility of its application to tidal heating is not validiated. Therefore, as a first step, we tried to compare the result of this simulation with the result which is estimated theoretically. We made a rotation of a differentiated Titan-sized tidally locked object around a Saturn-mass material point with the radius of orbit being 1.1 times larger than its Roche limit. We also considered how to applicate this simulation to the calculation of actual icy moons. We will report the progress.

Keywords: icy moon, tidal heating

©2019. Japan Geoscience Union. All Right Reserved.

[E] Poster | A (Atmospheric and Hydrospheric Sciences)：A-OS Ocean Sciences & Ocean Environment

Wed. May 29, 2019 5:15 PM - 6:30 PM JST | Wed. May 29, 2019 8:15 AM - 9:30 AM UTC | Poster Hall International Exhibition Hall8, Makuhari Messe_12

[A-OS11] Continental-Oceanic Mutual Interaction: Planetary scale Material Circulation

convener:Yosuke Alexandre Yamashiki(Earth & Planetary Water Resources Assessment Laboratory Graduate School of Advanced Integrated Studies in Human Survivability Kyoto University), Yukio Masumoto(Graduate School of Science, The University of Tokyo), Swadhin Behera(Climate Variation Predictability and Applicability Research Group, Application Laboratory, JAMSTEC, 3173-25 Showa-machi, Yokohama 236-0001), Takanori Sasaki(Department of Astronomy, Kyoto University)

The main purpose of this session is to promote discussion on mutual interaction between Continental zone and Oceanic zone. The global-scale material circulation induced by River runoff through oceanic general circulation as major topic on Continental-Oceanic Interaction, where the ENSO / IOD influence into continental climate as major topics on Oceanic-Continental Interaction. Numerical simulation and field observation of radionuclide transport from continental zone into ocean and its potential impact is also important topics of this session. The session also extend discussion on planetary hydrology and oceanography focusing on subsurface ocean in Jupiter's moon & Ancient Martian Oceanography & Hydrology by possible application of terrestrial GCM into Ancient Mars.

[AOS11-P01] Remote Sensing of Chlorophyll-a and Submerged Aquatic Vegetation for a Freshwater Lake in Japan

*Shweta Yadav[1], Yamashiki Yosuke[1], Junichi Susaki[1], Kanako Ishikawa[2] (1.Kyoto University, 2.Lake Biwa Environmental Research Institute)

[AOS11-P02] Hydrological and Debris-flow simulation of Martian Surface in Hesperian & early Amazonian epoch

*Hiroaki Sato[2], Yosuke Alexandre Yamashiki[1], Ryusuke Kuroki[1], Hideaki Miyamoto[3], Ryodo Hemmi[3] (1.Earth & Planetary Water Resources Assessment Laboratory Graduate School of Advanced Integrated Studies in Human Survivability Kyoto University, 2.Faculty of Engineering, Kyoto University, 3.Graduate School of Engineering, The University of Tokyo)

[AOS11-P03] Global Lakes & reservoirs Repository and their application for terrestrial surface environment

*Yosuke Alexandre Yamashiki[1], Ryusuke Kuroki[1], Botong Gao[1], Hina Bando[2], Fuka Takagi[3], Shweta Yadav[4] (1.Earth & Planetary Water Resources Assessment Laboratory Graduate School of Advanced Integrated Studies in Human Survivability Kyoto University, 2.Faculty of Science, Kyoto University, 3.Faculty of Agriculture, Kyoto University, 4.Educational Unit for Studies on Connectivity of Hills, Humans and Ocean, Kyoto University)

[AOS11-P04] Numerical simulation of Tidal Heating using SPH and its application to inner sea formation

*keiya murashima[1], Yosuke Alexandre Yamashiki[1], Natsuki Hosono[2] (1.Kyoto University, 2.Japan Agency for Marine-Earth Science and Technology)

Remote Sensing of Chlorophyll-a and Submerged Aquatic Vegetation for a Freshwater Lake in Japan

*Shweta Yadav[1], Yamashiki Yosuke[1], Junichi Susaki[1], Kanako Ishikawa[2]

1. Kyoto University, 2. Lake Biwa Environmental Research Institute

Freshwater lakes, particularly shallow lakes often exhibit alternative vegetative states, a clear-water state dominated by submerged aquatic vegetation (SAV) and a turbid-water state dominated by phytoplankton. Phytoplankton and SAV constitute the base of the aquatic food web and are the primary driver of the biogeochemical process in both the freshwater and coastal water bodies. The abundance of phytoplankton biomass can potentially indicate the degree of eutrophication in a specific waterbody. On the other hand, the massive overgrowth of invasive SAV species can also pose a serious threat to the aquatic ecosystem. Conventional methods (eg. Site-specific Boat survey) used to monitor the large water bodies are often time-consuming and expensive. In this study, we used a remote sensing based approach to monitor SAV and phytoplankton of the Lake. A multi-spectral satellite image (Landsat-8 Operational Land Imager) was used to assess the phytoplankton concentration and SAV biomass. A spectral decomposing algorithm was used to estimate and quantify both phytoplankton and SAV. Based on the peak growth period of SAV in the lake, the estimations were limited to a certain period of the year (i.e. mainly August and September). The image was used to classify and map the SAV coverage area using the spectral mixture analysis. The SAV biomass estimation model was used to determine the biomass of the SAV classified pixels in the lake. The satellite-derived phytoplankton and SAV were validated using the in-situ measured data of the lake. The result indicates the time and location-specific variation in the dominance of the phytoplankton and SAV.

Keywords: Phytoplankton, Submerged Aquatic Vegetation, Remote Sensing, Lake Water Quality

©2019. Japan Geoscience Union. All Right Reserved.

Hydrological and Debris-flow simulation of Martian Surface in Hesperian & early Amazonian epoch

*Hiroaki Sato[2], Yosuke Alexandre Yamashiki[1], Ryusuke Kuroki[1], Hideaki Miyamoto[3], Ryodo Hemmi[3]

1. Earth & Planetary Water Resources Assessment Laboratory Graduate School of Advanced Integrated Studies in Human Survivability Kyoto University, 2. Faculty of Engineering, Kyoto University, 3. Graduate School of Engineering, The University of Tokyo

It is considered that the Mars in Noachian ecoch to early Amazonian was much warmer temperature than current condition, with atmosphere and ocean supported by its magnetic activity. Several valley which seems to be developed by ancient hydrological processes are obsered in Martian surface, is being considered to be built long time before. Some fluvial fun was formed during the following Hesperian to early Amazonian epoch, which is considered as much cooler and drier than Noachian epoch. In this study, we applied Hydro-debris 2D model into Martian surface in Hesperian epoch in order to try develping surface vallay formation throughout hydrological processes.

Sediment transport and associated small-scale debris-flow occurrence may be the key for valley formation, where might be the micro-habitable zone in ancient period. At the same time it is still uncertain how much precipitation and erosion should have been required to formulate such topography. Following the last year’ s calculation we attempted to compare several cases of debris flow experiments by changing hypothetical precipitation rate and erosive coefficients in the initially distributed regolith.

Keywords: Hesperian Epoch, Debris flow

©2019. Japan Geoscience Union. All Right Reserved.

Global Lakes & reservoirs Repository and their application for terrestrial surface environment

*Yosuke Alexandre Yamashiki[1], Ryusuke Kuroki[1], Botong Gao[1], Hina Bando[2], Fuka Takagi[3], Shweta Yadav[4]

1. Earth & Planetary Water Resources Assessment Laboratory Graduate School of Advanced Integrated Studies in Human Survivability Kyoto University, 2. Faculty of Science, Kyoto University, 3. Faculty of Agriculture, Kyoto University, 4. Educational Unit for Studies on Connectivity of Hills, Humans and Ocean, Kyoto University

Global Lakes & Reservoirs Repository (GLR) has been developed in order to list global scale freshwater storage focusing on Lakes & Reservoirs. In this presentation we'll introduce their application, combining this with the ecological model for lakes & reservoirs for their surface environmental assessment under different climatic conditions. A two-layer aquatic ecological model (consisted with three types of phytoplanktons & zooplankton) is linked for a number of global lakes for the evaluation of future trends of aquatic ecosystems, mainly focusing on phytoplankton growth. The application of the database, by coupling it with satellite remote sensing for monitoring aquatic environment, together with the three-dimensional lake & reservoir aquatic environment model, are also introduced in the database.

Keywords: GLR, Remote sensing of aquatic environment

©2019. Japan Geoscience Union. All Right Reserved.

Numerical simulation of Tidal Heating using SPH and its application to inner sea formation

*keiya murashima[1], Yosuke Alexandre Yamashiki[1], Natsuki Hosono[2]

1. Kyoto University, 2. Japan Agency for Marine-Earth Science and Technology

There are some traces of liquid in icy moons, such as a plume of vapor of Europa acquired by Hubble Space Telescope and tiger stripes of Enceladus observed by Cassini. Since liquid water is essential for the origin of life, it can be important to understand the development of inner sea and also the temperature distribution inside of such icy moons.

It is considered that the tidal heating caused by tidal acceleration melts the inner icy layer which results in the presence of liquid water beneath its surface. Thus, we aim at simulating the tidal heating of an icy moon by 3-dimensional numerical fluid calculation in Smoothed Particle Hydrodynamics (SPH) method. As the tidal heating model, we apply the viscosity model which was used for numerical calculation of tidal stripping.

It is confirmed that this viscosity model lead to qualitatively correct result about tidal disruption, but the possibility of its application to tidal heating is not validiated. Therefore, as a first step, we tried to compare the result of this simulation with the result which is estimated theoretically. We made a rotation of a differentiated Titan-sized tidally locked object around a Saturn-mass material point with the radius of orbit being 1.1 times larger than its Roche limit. We also considered how to applicate this simulation to the calculation of actual icy moons. We will report the progress.

Keywords: icy moon, tidal heating

©2019. Japan Geoscience Union. All Right Reserved.

[J] Poster | A (Atmospheric and Hydrospheric Sciences)：A-OS Ocean Sciences & Ocean Environment

Wed. May 29, 2019 10:45 AM - 12:15 PM JST | Wed. May 29, 2019 1:45 AM - 3:15 AM UTC | Poster Hall International Exhibition Hall8, Makuhari Messe_5

[A-OS14] Coastal physical processes associated with mixing, eddies, internal waves

convener:Eiji Masunaga(Ibaraki University), Taira Nagai(Graduate School of Science, The University of Tokyo), TSUTSUMI EISUKE(Atmosphere and Ocean Research Institute, The University of Tokyo)

Recently developed observational and numerical approaches have revealed details of physical processes in coastal regions, which is a key to understanding global ocean circulations and ecosystems. This session aims to provide discussions of mixing, eddies, nonlinear internal waves in coastal and marginal oceans, estuaries and lakes. Observations, numerical modeling and laboratory experiments associated with these phenomena are encouraged to submit an abstract to this session. In addition, studies that consider linkages between coastal physical processes and large scale open ocean processes, e.g., the Kuroshio, global ocean circulations.

[AOS14-P01] Development of methods and systems for vertical mixing and observations (OMIX-A01-1)

*Ichiro Yasuda[1], Koenjong Lee[1], Shinzo Fujio[1], Daigo Yanagimoto[1], Maki Nagasawa[1], Yusuke Kawaguchi[1], Eitarou Oka[1], Shuo Zhai[1], Shino Kimura[1], Ryuichiro Inoue[2], Daisuke Hasegawa[3], Takahiro Tanaka[3], Masao Ishii[4], Toshiya Nakano[4], Yasutaka Goto[4] (1.Atmosphere and Ocean Research Institute, The University of Tokyo, 2.Japan Agency of Marine-Earth Science and Technology, 3.Fisheries Research Agency, 4.Japan Meteorological Agency)

[AOS14-P02] Observation of enhanced nonlinear interactions after the passage of typhoon in the western South China Sea

*gui ying Chen, chang rong Liang, xiao dong Shang

[AOS14-P03] Investigating vertical mixing in estuarine pycnocline: a case study in the Ariake Sea, Japan

*Takeshi Matsuno[1], Eisuke Tsutsumi[1] (1.Kyushu University)

[AOS14-P04] Possibility of interactions between the coastal and offshore branch of Tsushima Warm Current over the submarine canyon in the Sea of Japan.

*Yosuke Igeta[1], Alexander Yankovsky [2], Mizuki Kuga[1], Naoki Hirose[3], Kenichi Fukudome[4] (1.Japan Sea National Fishseries Research Institute, 2.University of South Carolina, 3.RIAM Kyushu Univ., 4.National Institute of Technology, Toyama College)

Development of methods and systems for vertical mixing and observations (OMIX-A01-1)

*Ichiro Yasuda[1], Koenjong Lee[1], Shinzo Fujio[1], Daigo Yanagimoto[1], Maki Nagasawa[1], Yusuke Kawaguchi[1], Eitarou Oka[1], Shuo Zhai[1], Shino Kimura[1], Ryuichiro Inoue[2], Daisuke Hasegawa[3], Takahiro Tanaka[3], Masao Ishii[4], Toshiya Nakano[4], Yasutaka Goto[4]

1. Atmosphere and Ocean Research Institute, The University of Tokyo, 2. Japan Agency of Marine-Earth Science and Technology, 3. Fisheries Research Agency, 4. Japan Meteorological Agency

In order to know the distribution of vertical mixing and generating mechanisms in the western North Pacific and to elucidate the influence on ocean circulations, this team developed/introduced/made practical following three observational systems that are capable to concurrently observe turbulence with vertical mm-scales and currents with 10m-scale which can be resolved by numerical models, and perform in-situ observations. 1) Developed turbulence estimate method with fast response thermistors attached to CTD platform, and obtained numerous microstructure data down to deep/intermediate depths or bottom by use of Japan Meteorological Agency, JAMSTEC and fisheries-related CTD observational array. 2) Developed autonomous observation system of underwater gliders with turbulence sensors and ADCP. 3) Developed long-term time series observation system with autonomous floats or moorings with turbulence sensors or current sensors. These new observing systems were or being tested in the real oceans. This team conducted cruises of R/V Hakuho-maru KH-16-3, KH-16-7, KH-17-5 and R/V Shinsei-maru KS-15-5, KS-16-10, KS-19-6, and microstructure and mooring observations in the Multanovskiiy 2018 cruise. This poster presentation reports this team activity and some results.

Keywords: Turbulence, Ocean Mixing, Observation system

©2019. Japan Geoscience Union. All Right Reserved.

Observation of enhanced nonlinear interactions after the passage of typhoon in the western South China Sea

*gui ying Chen, chang rong Liang, xiao dong Shang

Typhoon Chanchu passed the subsurface mooring in the western South China Sea (SCS) in June 2004 and the effects of typhoon on the internal wave field and nonlinear interactions were examined. The internal wave field was characterized by diurnal (D_1) and semidiurnal (D_2) tides before typhoon. After the passage of typhoon, the internal wave field was characterized not only by diurnal and semidiurnal tides but also by near-inertial (f) waves, higher harmonic ($fD_2=f+D_2$ and $D_3=D_1+D_2$) frequency internal waves, and enhanced diurnal currents. Analysis on the rotary coefficient and bicoherence suggests that the observed fD_2 waves, D_3 waves, and enhanced diurnal currents were derived from nonlinear interactions of $f+D_2=fD_2$, $D_1+D_2=D_3$, and $f+f=2f$, respectively. Previous researches indicated that nonlinear interactions induced by typhoon mainly occur between near-inertial waves and internal tides ($f+D_1=fD_1$ or $f+D_2=fD_2$). Our observations first indicate that typhoon can also induce the self-interaction of near-inertial waves ($f+f=2f$) and enhance the nonlinear interaction between diurnal tides and semidiurnal tides ($D_1+D_2=D_3$). Critical diurnal latitudes (where $2f\approx D_1$) play an important role in the occurrence of these nonlinear interactions. Typhoon-induced near-inertial waves undergo self-interaction ($f+f=2f$) near the critical diurnal latitudes and transfer energy to diurnal waves. Enhanced diurnal waves further contribute to the nonlinear interaction of $D_1+D_2=D_3$. These nonlinear processes might promote the energy cascade of the typhoon-induced near-inertial waves near the critical diurnal latitudes and play an important role in ocean mixing.

Keywords: typhoon, nonlinear interaction, internal wave, near-inertial wave

©2019. Japan Geoscience Union. All Right Reserved.

Investigating vertical mixing in estuarine pycnocline: a case study in the Ariake Sea, Japan

*Takeshi Matsuno[1], Eisuke Tsutsumi[1]

1. Kyushu University

Turbulent mixing controls coastal environment and primary production through transportation of heat, freshwater, and various materials. Vertical mixing in pycnocline plays a key role in occurrence of major environmental problems in semi-enclosed seas and estuaries, such as bottom hypoxia and red tides, although it is not fully understood. For better understanding and prediction of coastal mixing processes, we investigate pycnocline mixing in a tidally-energetic shallow (~20 m) estuary, the Ariake Sea, Japan, where stratification is maintained almost throughout a year by large amounts of freshwater inputs from major rivers. We collected more than 5,000 microstructure turbulence profiles (~530-hour measurements) in several stations in the central area of the sea during 24-cruises conducted in various seasons over 2002-2012, and examined Turbulent kinetic energy (TKE) dissipation rate in the shear- and buoyancy-frequency space. TKE dissipation rates in pycnocline exhibited a broad variability, $O(10^{-9})$ - $O(10^{-5})$ W kg^{-1} , while most of them fell into a range where the gradient Richardson number is larger than a critical value, i.e., $Ri_g > 1/4$. In stratified seasons, we frequently observed high-vertical wavenumber internal tides in the pycnocline around the microstructure stations from separately-conducted mooring observations using acoustic Doppler current profilers. The large variability in the mixing around pycnocline is therefore likely to be originated from internal wave breaking and shear instability. We found an ordered structure of mean dissipation rate where it correlates positively with vertical shear, which gives a clue to improving a “background” vertical diffusion parameterization in numerical ocean models.

Keywords: turbulent mixing, stratification, vertical shear, parameterization

©2019. Japan Geoscience Union. All Right Reserved.

Possibility of interactions between the coastal and offshore branch of Tsushima Warm Current over the submarine canyon in the Sea of Japan.

*Yosuke Igeta[1], Alexander Yankovsky [2], Mizuki Kuga[1], Naoki Hirose[3], Kenichi Fukudome[4]

1. Japan Sea National Fishseries Research Institute, 2. University of South Carolina, 3. RIAM Kyushu Univ., 4. National Institute of Technology, Toyama College

Tsushima warm current (TWC) is known to flow northeastward over continental shelf off the northern coast of Japan. Coastal branch of TWC (CBTWC) is fundamentally current trapped by the coastline, whereas offshore branch of TWC (OBTWC) are interpreted as current steered by continental slope. The coastal line and continental shelf have alongshore discontinuity around the Toyama Trough (TT) which is a submarine canyon cutting across the continental shelf off the downstream side of the Noto Peninsula (NP) and almost reaching the coastline. The CBTWC is observed to change its path from coastal mode to offshore mode when encountering the TT (Igeta et al., 2017). This process results in transformation from the barotropic coastal current into baroclinic jet detached from the coast over the TT. On the other hand, the details of the OBTWC current path change are not well understood, as well as interaction between the CBTWC and OBTWC.
To clarify these, we analyzed re-analysis current data calculated by DR_C (Hirose et al., 2017) that is high resolution nested ocean model. Current paths of CBTWC around the TT were extracted by using current data from 2005 to 2014. The results showed that complete and incomplete current path transition of the CBTWC from coastal mode to offshore mode in 2013 and 2014, respectively. The OBTWC-like current was explicitly confirmed over continental slope just off the current path of the CBTWC over continental shelf around the northern off the NP in 2013, however such current was not able to be found out in 2014. These results suggest that interaction between the CBTWC and the OBTWC makes current path transition of the CBTWC fast.
To interpret these simply, we demonstrated numerical experiment using 2-layered ocean model with simplified continental shelf, continental slope and submarine canyon. Barotropic current trapped by continental slope, modeling the OBTWC, was applied from the upstream boundary. The OBTWC changed its current path from coast to offshore almost in the same manner as the CBTWC over the TT. The detached current over the submarine canyon was re-arrested by the continental slope on the opposite side of the submarine canyon. The OBTWC continued to take its current path in the offshore region after reaching steady state. Once the OBTWC has reached a steady state, the CBTWC was specified at the upstream boundary. The CBTWC flowed along the coast despite the existence of the OBTWC bridging over the TT. Although the CBTWC and OBTWC merged around the northern coast of the NP, they seemed to behave independently. Time scale of the CBTWC current path transition, however, was shorten in the presence of the OBTWC. This indicates the OBTWC let the current path transition of the CBTWC accelerate through vorticity generated around the upstream boundary of the TT. It is considered that vorticity supplied from the OBTWC accelerate eddy growth by the CBTWC that results in current path transition.

Keywords: Tushima Warm current, current path transition, current-current interaction, topographic eddy, numerucal experiment

©2019. Japan Geoscience Union. All Right Reserved.

[J] Poster | A (Atmospheric and Hydrospheric Sciences)：A-OS Ocean Sciences & Ocean Environment

Wed. May 29, 2019 5:15 PM - 6:30 PM JST | Wed. May 29, 2019 8:15 AM - 9:30 AM UTC | Poster Hall International Exhibition Hall8, Makuhari Messe_13

[A-OS14] Coastal physical processes associated with mixing, eddies, internal waves

convener:Eiji Masunaga(Ibaraki University), Taira Nagai(Graduate School of Science, The University of Tokyo), TSUTSUMI EISUKE(Atmosphere and Ocean Research Institute, The University of Tokyo)

Recently developed observational and numerical approaches have revealed details of physical processes in coastal regions, which is a key to understanding global ocean circulations and ecosystems. This session aims to provide discussions of mixing, eddies, nonlinear internal waves in coastal and marginal oceans, estuaries and lakes. Observations, numerical modeling and laboratory experiments associated with these phenomena are encouraged to submit an abstract to this session. In addition, studies that consider linkages between coastal physical processes and large scale open ocean processes, e.g., the Kuroshio, global ocean circulations.

[AOS14-P01] Development of methods and systems for vertical mixing and observations (OMIX-A01-1)

*Ichiro Yasuda[1], Koenjong Lee[1], Shinzo Fujio[1], Daigo Yanagimoto[1], Maki Nagasawa[1], Yusuke Kawaguchi[1], Eitarou Oka[1], Shuo Zhai[1], Shino Kimura[1], Ryuichiro Inoue[2], Daisuke Hasegawa[3], Takahiro Tanaka[3], Masao Ishii[4], Toshiya Nakano[4], Yasutaka Goto[4] (1.Atmosphere and Ocean Research Institute, The University of Tokyo, 2.Japan Agency of Marine-Earth Science and Technology, 3.Fisheries Research Agency, 4.Japan Meteorological Agency)

[AOS14-P02] Observation of enhanced nonlinear interactions after the passage of typhoon in the western South China Sea

*gui ying Chen, chang rong Liang, xiao dong Shang

[AOS14-P03] Investigating vertical mixing in estuarine pycnocline: a case study in the Ariake Sea, Japan

*Takeshi Matsuno[1], Eisuke Tsutsumi[1] (1.Kyushu University)

[AOS14-P04] Possibility of interactions between the coastal and offshore branch of Tsushima Warm Current over the submarine canyon in the Sea of Japan.

*Yosuke Igeta[1], Alexander Yankovsky [2], Mizuki Kuga[1], Naoki Hirose[3], Kenichi Fukudome[4] (1.Japan Sea National Fishseries Research Institute, 2.University of South Carolina, 3.RIAM Kyushu Univ., 4.National Institute of Technology, Toyama College)

Development of methods and systems for vertical mixing and observations (OMIX-A01-1)

*Ichiro Yasuda[1], Koenjong Lee[1], Shinzo Fujio[1], Daigo Yanagimoto[1], Maki Nagasawa[1], Yusuke Kawaguchi[1], Eitarou Oka[1], Shuo Zhai[1], Shino Kimura[1], Ryuichiro Inoue[2], Daisuke Hasegawa[3], Takahiro Tanaka[3], Masao Ishii[4], Toshiya Nakano[4], Yasutaka Goto[4]

1. Atmosphere and Ocean Research Institute, The University of Tokyo, 2. Japan Agency of Marine-Earth Science and Technology, 3. Fisheries Research Agency, 4. Japan Meteorological Agency

In order to know the distribution of vertical mixing and generating mechanisms in the western North Pacific and to elucidate the influence on ocean circulations, this team developed/introduced/made practical following three observational systems that are capable to concurrently observe turbulence with vertical mm-scales and currents with 10m-scale which can be resolved by numerical models, and perform in-situ observations. 1) Developed turbulence estimate method with fast response thermistors attached to CTD platform, and obtained numerous microstructure data down to deep/intermediate depths or bottom by use of Japan Meteorological Agency, JAMSTEC and fisheries-related CTD observational array. 2) Developed autonomous observation system of underwater gliders with turbulence sensors and ADCP. 3) Developed long-term time series observation system with autonomous floats or moorings with turbulence sensors or current sensors. These new observing systems were or being tested in the real oceans. This team conducted cruises of R/V Hakuho-maru KH-16-3, KH-16-7, KH-17-5 and R/V Shinsei-maru KS-15-5, KS-16-10, KS-19-6, and microstructure and mooring observations in the Multanovskiiy 2018 cruise. This poster presentation reports this team activity and some results.

Keywords: Turbulence, Ocean Mixing, Observation system

©2019. Japan Geoscience Union. All Right Reserved.

Observation of enhanced nonlinear interactions after the passage of typhoon in the western South China Sea

*gui ying Chen, chang rong Liang, xiao dong Shang

Typhoon Chanchu passed the subsurface mooring in the western South China Sea (SCS) in June 2004 and the effects of typhoon on the internal wave field and nonlinear interactions were examined. The internal wave field was characterized by diurnal (D_1) and semidiurnal (D_2) tides before typhoon. After the passage of typhoon, the internal wave field was characterized not only by diurnal and semidiurnal tides but also by near-inertial (f) waves, higher harmonic ($fD_2=f+D_2$ and $D_3=D_1+D_2$) frequency internal waves, and enhanced diurnal currents. Analysis on the rotary coefficient and bicoherence suggests that the observed fD_2 waves, D_3 waves, and enhanced diurnal currents were derived from nonlinear interactions of $f+D_2=fD_2$, $D_1+D_2=D_3$, and $f+f=2f$, respectively. Previous researches indicated that nonlinear interactions induced by typhoon mainly occur between near-inertial waves and internal tides ($f+D_1=fD_1$ or $f+D_2=fD_2$). Our observations first indicate that typhoon can also induce the self-interaction of near-inertial waves ($f+f=2f$) and enhance the nonlinear interaction between diurnal tides and semidiurnal tides ($D_1+D_2=D_3$). Critical diurnal latitudes (where $2f\approx D_1$) play an important role in the occurrence of these nonlinear interactions. Typhoon-induced near-inertial waves undergo self-interaction ($f+f=2f$) near the critical diurnal latitudes and transfer energy to diurnal waves. Enhanced diurnal waves further contribute to the nonlinear interaction of $D_1+D_2=D_3$. These nonlinear processes might promote the energy cascade of the typhoon-induced near-inertial waves near the critical diurnal latitudes and play an important role in ocean mixing.

Keywords: typhoon, nonlinear interaction, internal wave, near-inertial wave

©2019. Japan Geoscience Union. All Right Reserved.

Investigating vertical mixing in estuarine pycnocline: a case study in the Ariake Sea, Japan

*Takeshi Matsuno[1], Eisuke Tsutsumi[1]

1. Kyushu University

Turbulent mixing controls coastal environment and primary production through transportation of heat, freshwater, and various materials. Vertical mixing in pycnocline plays a key role in occurrence of major environmental problems in semi-enclosed seas and estuaries, such as bottom hypoxia and red tides, although it is not fully understood. For better understanding and prediction of coastal mixing processes, we investigate pycnocline mixing in a tidally-energetic shallow (~20 m) estuary, the Ariake Sea, Japan, where stratification is maintained almost throughout a year by large amounts of freshwater inputs from major rivers. We collected more than 5,000 microstructure turbulence profiles (~530-hour measurements) in several stations in the central area of the sea during 24-cruises conducted in various seasons over 2002-2012, and examined Turbulent kinetic energy (TKE) dissipation rate in the shear- and buoyancy-frequency space. TKE dissipation rates in pycnocline exhibited a broad variability, $O(10^{-9})$ - $O(10^{-5})$ W kg^{-1} , while most of them fell into a range where the gradient Richardson number is larger than a critical value, i.e., $Ri_g > 1/4$. In stratified seasons, we frequently observed high-vertical wavenumber internal tides in the pycnocline around the microstructure stations from separately-conducted mooring observations using acoustic Doppler current profilers. The large variability in the mixing around pycnocline is therefore likely to be originated from internal wave breaking and shear instability. We found an ordered structure of mean dissipation rate where it correlates positively with vertical shear, which gives a clue to improving a “background” vertical diffusion parameterization in numerical ocean models.

Keywords: turbulent mixing, stratification, vertical shear, parameterization

©2019. Japan Geoscience Union. All Right Reserved.

Possibility of interactions between the coastal and offshore branch of Tsushima Warm Current over the submarine canyon in the Sea of Japan.

*Yosuke Igeta[1], Alexander Yankovsky [2], Mizuki Kuga[1], Naoki Hirose[3], Kenichi Fukudome[4]

1. Japan Sea National Fishseries Research Institute, 2. University of South Carolina, 3. RIAM Kyushu Univ., 4. National Institute of Technology, Toyama College

Tsushima warm current (TWC) is known to flow northeastward over continental shelf off the northern coast of Japan. Coastal branch of TWC (CBTWC) is fundamentally current trapped by the coastline, whereas offshore branch of TWC (OBTWC) are interpreted as current steered by continental slope. The coastal line and continental shelf have alongshore discontinuity around the Toyama Trough (TT) which is a submarine canyon cutting across the continental shelf off the downstream side of the Noto Peninsula (NP) and almost reaching the coastline. The CBTWC is observed to change its path from coastal mode to offshore mode when encountering the TT (Igeta et al., 2017). This process results in transformation from the barotropic coastal current into baroclinic jet detached from the coast over the TT. On the other hand, the details of the OBTWC current path change are not well understood, as well as interaction between the CBTWC and OBTWC.
To clarify these, we analyzed re-analysis current data calculated by DR_C (Hirose et al., 2017) that is high resolution nested ocean model. Current paths of CBTWC around the TT were extracted by using current data from 2005 to 2014. The results showed that complete and incomplete current path transition of the CBTWC from coastal mode to offshore mode in 2013 and 2014, respectively. The OBTWC-like current was explicitly confirmed over continental slope just off the current path of the CBTWC over continental shelf around the northern off the NP in 2013, however such current was not able to be found out in 2014. These results suggest that interaction between the CBTWC and the OBTWC makes current path transition of the CBTWC fast.
To interpret these simply, we demonstrated numerical experiment using 2-layered ocean model with simplified continental shelf, continental slope and submarine canyon. Barotropic current trapped by continental slope, modeling the OBTWC, was applied from the upstream boundary. The OBTWC changed its current path from coast to offshore almost in the same manner as the CBTWC over the TT. The detached current over the submarine canyon was re-arrested by the continental slope on the opposite side of the submarine canyon. The OBTWC continued to take its current path in the offshore region after reaching steady state. Once the OBTWC has reached a steady state, the CBTWC was specified at the upstream boundary. The CBTWC flowed along the coast despite the existence of the OBTWC bridging over the TT. Although the CBTWC and OBTWC merged around the northern coast of the NP, they seemed to behave independently. Time scale of the CBTWC current path transition, however, was shorten in the presence of the OBTWC. This indicates the OBTWC let the current path transition of the CBTWC accelerate through vorticity generated around the upstream boundary of the TT. It is considered that vorticity supplied from the OBTWC accelerate eddy growth by the CBTWC that results in current path transition.

Keywords: Tushima Warm current, current path transition, current-current interaction, topographic eddy, numerucal experiment

©2019. Japan Geoscience Union. All Right Reserved.

[J] Oral | A (Atmospheric and Hydrospheric Sciences)：A-OS Ocean Sciences & Ocean Environment

Wed. May 29, 2019 1:45 PM - 3:15 PM JST | Wed. May 29, 2019 4:45 AM - 6:15 AM UTC | 301A 3F

[A-OS14] Coastal physical processes associated with mixing, eddies, internal waves

convener:Eiji Masunaga(Ibaraki University), Taira Nagai(Graduate School of Science, The University of Tokyo), TSUTSUMI EISUKE(Atmosphere and Ocean Research Institute, The University of Tokyo), Chairperson:Eiji Masunaga, Eisuke Tsutsumi

Recently developed observational and numerical approaches have revealed details of physical processes in coastal regions, which is a key to understanding global ocean circulations and ecosystems. This session aims to provide discussions of mixing, eddies, nonlinear internal waves in coastal and marginal oceans, estuaries and lakes. Observations, numerical modeling and laboratory experiments associated with these phenomena are encouraged to submit an abstract to this session. In addition, studies that consider linkages between coastal physical processes and large scale open ocean processes, e.g., the Kuroshio, global ocean circulations.

1:45 PM - 2:00 PM JST | 4:45 AM - 5:00 AM UTC

[AOS14-01] The cooling of sea surface temperature in the southern Indonesian Seas due to a combination of the Ekman transport and tidal mixing in narrow straits

*Taira Nagai[1], Toshiyuki Hibiya[1] (1.Graduate School of Science, The University of Tokyo)

2:00 PM - 2:15 PM JST | 5:00 AM - 5:15 AM UTC

[AOS14-02] A reanalysis of regional circulations in the Southern South China Sea using a HYCOM-ROMS downscaling ocean model

*Naru Takaura[1], Yusuke Uchiyama[1], Nizamani Zafarullah[2], Akihiko Nakayama[2] (1.Kobe Univ, 2.Tunku Abdul Rahman University)

2:15 PM - 2:30 PM JST | 5:15 AM - 5:30 AM UTC

[AOS14-03] Nutrient and phytoplankton dynamics in the continental slope region of the East China Sea associated with the Kuroshio frontal eddy

*Naoki Yoshie[1], Anri Kabe[1], Kazuki Ohgi[1], Eisuke Tsutsumi[2], Shigenobu Takeda[3], Joji Ishizaka[4], Xinyu Guo[1] (1.Center for Marine Environmental Studies, Ehime University, 2.Research Institute for Applied Mechanics, Kyushu University, 3.Faculty of Fisheries, Nagasaki University, 4.Institute for Space-Earth Environmental Research, Nagoya University)

2:30 PM - 2:45 PM JST | 5:30 AM - 5:45 AM UTC

[AOS14-04] Dissipation and transport due to internal tides generated by multiple submarine canyons

*Qiang Li[1], Xianzhong Mao[1], Ran Liao[1] (1.Tsinghua University)

2:45 PM - 3:00 PM JST | 5:45 AM - 6:00 AM UTC

[AOS14-05] Measurement of Physical structure in Kasumigaura using high resolution tow-yo instrument

*Daiki Asaoka[1], Eiji Masunaga[1], Shunsuke Komuro[2], Shunichi Matsumoto[2], Masahiko Ono[3], Hiroaki Banba[3] (1.Ibaraki University, 2.Ibaraki Kasumigaura Environmental Science Center, 3.Ministry of Land, Infrastructure, Transport and Tourism)

3:00 PM - 3:15 PM JST | 6:00 AM - 6:15 AM UTC

[AOS14-06] Mixing and baroclinic structure in a stratified shallow lake, Lake Kasumigaura, Japan

*Eiji Masunaga[1], Daiki Asaoka[1], Shunsuke Komuro[2], Shunichi Matsumoto[2], Masahiko Ono[3], Hiroaki Banba[3] (1.Ibaraki University, 2.Ibaraki Kasumigaura Environmental Science Center, 3.Ministry of Land, Infrastructure, Transport and Tourism)

The cooling of sea surface temperature in the southern Indonesian Seas due to a combination of the Ekman transport and tidal mixing in narrow straits

*Taira Nagai[1], Toshiyuki Hibiya[1]

1. Graduate School of Science, The University of Tokyo

The Indonesian archipelago is characterized by the warmest sea surface temperatures (SSTs) in the world and is a key region of the world climate system. Kida and Wijffels (2012) reported that SST cooling around the Nusa Tenggara Islands (NTIs) located at the southern Indonesia plays a crucial role in the seasonal variation of SST over a large area in the Indonesian Seas. Although they suggested that both the monsoonal winds and tidal mixing might significantly impact such SST cooling, their numerical model settings were somewhat idealized.

In this study, to investigate the mechanisms of SST cooling around the NTIs, we carry out a numerical simulation using a regional ocean model where the realistic distribution of vertical diffusivity estimated from a high resolution baroclinic tide model is incorporated. The simulated results show that significant mixing in the narrow tidal straits between the NTIs creates well-mixed waters, which spread out northward (southward) during Austral summer (winter) and finally causes significant SST cooling over a large area of southern Indonesian Seas.

We therefore carry out numerical experiments where either of the monsoonal wind or localized tidal mixing in the narrow straits is switched off. These numerical experiments show that well-mixed waters in the narrow straits are continuously advected by the northward (southward) flow driven by the western (eastern) monsoonal wind during Austral summer (winter) until the Indonesian Throughflow spreads them out over a large area of southern Indonesian Seas, demonstrating the importance of the combined effect of the Ekman transport and tidal mixing.

Keywords: SST in the Indonesian Seas, Tidal mixing in narrow straits, Ekman transport

©2019. Japan Geoscience Union. All Right Reserved.

A reanalysis of regional circulations in the Southern South China Sea using a HYCOM-ROMS downscaling ocean model

*Naru Takaura[1], Yusuke Uchiyama[1], Nizamani Zafarullah[2], Akihiko Nakayama[2]

1. Kobe Univ, 2. Tunku Abdul Rahman University

A high-resolution, high-precision downscaling oceanic circulation model for the Southern China Sea (SCS) was developed based on the Regional Oceanic Modeling System (ROMS) at a lateral resolution of 5 km, initialized and forced by the Hybrid Coordinate Ocean Model (HYCOM) global reanalysis product. A multi-year reanalysis was conducted for the four-year period from 2012 to 2015 with the HYCOM-ROMS system that properly accounts for wind stress and heat budget at surface, freshwater influences from the atmosphere and major rivers, and tidal variability.
The model results were confirmed to agree well with satellite and in situ measurement, and generally consistent with the findings in previous studies. For instance, prevailing strong meridional currents are provoked along the continental shelves between China and the southern Vietnam, which are driven by seasonally varying monsoons dominated in the winter and summer, followed by current separation to the east off the southern Vietnam occurred in summer.
Prospective applications of the system include assessments of oceanic dispersal of wastewater, quantification of marine ecosystem network, analyses of micro plastic transport, its coastal accumulation and maintenance of offshore structure. In the present study, we utilized the model outcome to evaluate external forcing conditions on offshore oil platforms along the coast of the Malay Peninsular and Borneo Island by using extreme value statistics for surface currents and wind. The maximum surface velocity was found to occur off the coast of Borneo Island, which is influenced by the Mindanao Current. It was suggested that water mass exchange between the Pacific and the SCS is extremely significant as it subsequently controls regional circulations in the coastal margins in the SCS.

Keywords: South China Sea, mass transport, HYCOM-ROMS, seasonal circulation

©2019. Japan Geoscience Union. All Right Reserved.

Nutrient and phytoplankton dynamics in the continental slope region of the East China Sea associated with the Kuroshio frontal eddy

*Naoki Yoshie[1], Anri Kabe[1], Kazuki Ohgi[1], Eisuke Tsutsumi[2], Shigenobu Takeda[3], Joji Ishizaka[4], Xinyu Guo[1]

1. Center for Marine Environmental Studies, Ehime University, 2. Research Institute for Applied Mechanics, Kyushu University, 3. Faculty of Fisheries, Nagasaki University, 4. Institute for Space-Earth Environmental Research, Nagoya University

The lower-trophic level ecosystem in the continental slope region of the East China Sea (ECS) during summer generally shows typical subtropical features, i.e., small size pico-phytoplankton such as cyanobacteria dominates in the euphotic layer under the oligotrophic condition due to the stable stratification. It is also known that such stable physical and chemical conditions are often disturbed by the Kuroshio frontal eddy. In this study, we investigated the phytoplankton dynamics associated with the passing of Kuroshio frontal eddies. We conducted comprehensive observations with the high horizontal resolution (7km) around the continental slope region in the ECS in the late-July, 2018. We observed drastic changes in the depth of subsurface chlorophyll maximum (SCM) and nitrate concentrations around the SCM, and micro-phytoplankton such as diatom mainly changed around SCM. We found cyclonic frontal eddies with 15-35 km diameter around the 40-80 m depth near the drastic change of the SCM. These changes were caused by the horizontal advection of nutrient-rich shelf water associated with the passing of the cyclonic frontal eddies.

Keywords: frontal eddy, nutrient, phytoplankton, East China Sea

©2019. Japan Geoscience Union. All Right Reserved.

Dissipation and transport due to internal tides generated by multiple submarine canyons

*Qiang Li[1], Xianzhong Mao[1], Ran Liao[1]

1. Tsinghua University

Rough seafloor is a major source to generate internal waves in the ocean. High-resolution multibeam survey reveals detailed seafloor with complicated features, however, some are not shown in commonly used topography datasets, such as Smith and Sandwell (1997). A group of canyons on the continental shelf of the northern South China Sea were recently discovered during a geographic survey. Interaction between barotropic tides and concave-shape canyons generates internal tides, showing complex interference patterns. A linear model, based on normal-mode decomposition, reveals complex beam generation and interaction inside and between the canyons. Then, a very high resolution and three dimensional numerical model is employed to validate the linear model result and estimate local energy dissipation for internal wave generation by a group of canyons. Instead of complicated turbulence models, constant viscosity coefficients are used. Nonlinear interaction or shear instability during internal tide generation and propagation causes local diapycnal mixing, which is one of the key processes to drive material transport in continental shelf. Transport due to internal tides in the canyon region is also calculated and its relationship with local internal tide generation and propagation is discussed.

Keywords: internal waves, canyons, mixing

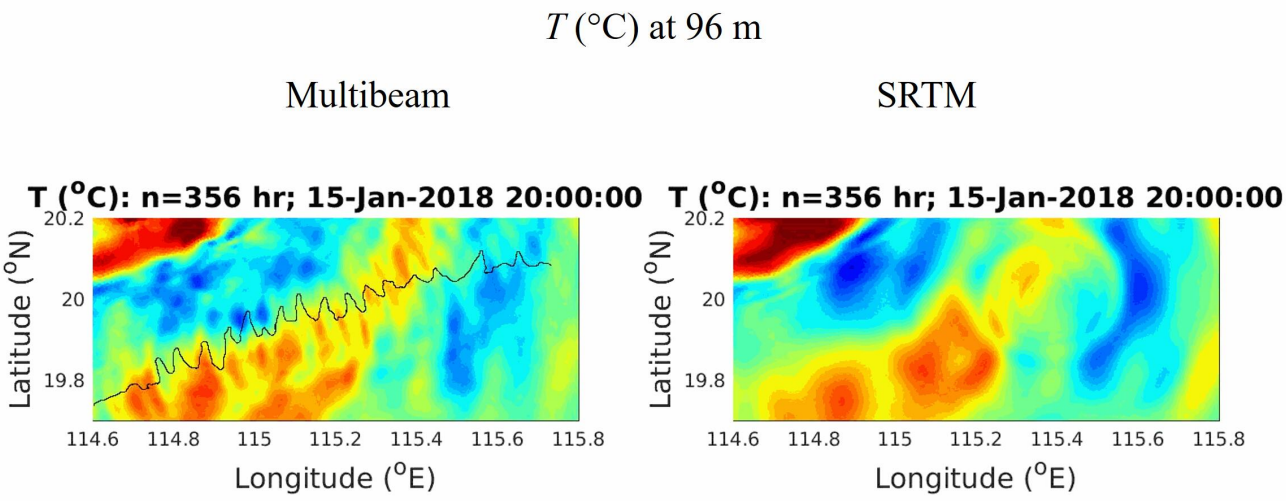

©2019. Japan Geoscience Union. All Right Reserved.

Measurement of Physical structure in Kasumigaura using high resolution tow-yo instrument

*Daiki Asaoka[1], Eiji Masunaga[1], Shunsuke Komuro[2], Shunichi Matsumoto[2], Masahiko Ono[3], Hiroaki Banba[3]

1. Ibaraki University, 2. Ibaraki Kasumigaura Environmental Science Center, 3. Ministry of Land, Infrastructure, Transport and Tourism

This study shows physical processes in Lake Kitaura, Kasumigaura, using field observations by YODA Profiler and Mooring system. Hypoxia and eutrophication have a bad influence on ecosystems in the study area. Understanding physical processes is essential to understand ecosystems in lakes and oceans. Lake Kitaura is a long lake in the north-south direction with 25 km and 4 km in the east-west. The stratified layer is generated due to strong incoming heat flux during the summer season. Mooring observation results show that the thin mixed layer was gradually thickened due to the wind stress and disappeared within several hours. Details of this mixing processes were further investigated by making use of a high-resolution tow-yo instrument, the YODA Profiler. The warm surface water was transported toward on the downwind side due to the wind stress. Small scale K-H instability like motions were observed during this event. According to the data from the YODA Profiler, the Wedderburn number can roughly explain the baroclinic and mixing structures in the east-west direction. However, the Wedderburn number is not able to be used for explaining quantitative vertical displacements of the thermocline, because the complexity of the observed density distribution. The vertical isotherm displacements can be simply explained by wind stress. Time series of the mixed layer depth were calculated to evaluate mixing in the lake. The mixed layer reached the bottom when the daily-averaged wind speed exceeded 8 m/s, resulting in complete vertical mixing. Results from the north-south long transect survey show wavy like baroclinic (or stripe-shaped) temperature distribution with a horizontal scale of several km. In addition, three dimensional numerical simulations were conducted using the SUNTANS. Model results also show a wavy like baroclinic structure in the north-south direction caused by the complicated coastal shape and east-west wind stress. The wavy like baroclinic structure is generated by convergence of warm water into bay-shaped areas.

Keywords: Thermocline, Mixed layer, Wind stress

©2019. Japan Geoscience Union. All Right Reserved.

Mixing and baroclinic structure in a stratified shallow lake, Lake Kasumigaura, Japan

*Eiji Masunaga[1], Daiki Asaoka[1], Shunsuke Komuro[2], Shunichi Matsumoto[2], Masahiko Ono[3], Hiroaki Banba[3]

1. Ibaraki University, 2. Ibaraki Kasumigaura Environmental Science Center, 3. Ministry of Land, Infrastructure, Transport and Tourism

This study presents mixing and baroclinic structure associated with hypoxia in a shallow lake, Lake Kasumigaura, using field observations and numerical simulations. Hypoxia in stratified lakes is one of the pressing issues for maintaining water environment and ecosystems. Mooring observations show that hypoxia events occur when the stratification is enhanced by the surface heat flux. The stratification (N^2) is controlled by the ratio between the surface wind stress and surface heat (buoyanvy) flux. The strength of the stratification/mixing can be simply explained by the Monin-Obukov length scale, L_{MO}. N^2 is linearly related with L_{MO} in a log scale with a correlation coefficient of approximately 0.7. According to the heat budget analysis, the bottom sediment heat flux toward the bottom significantly contribute to the heat content as well as the surface heat flux. The heat flux toward the bottom is roughly an order of 100 W m^{-2} during the summer season, which suppresses mixing near the bottom. The internal wave-like baroclinic structure was observed by high resolution survey using the YODA Profiler. Baroclinic motions are enhanced by the surface wind stress, and they transport the hypoxic water, suspended sediments and phytoplanktons. In addition to field surveys, three-dimensional simulations were conducted with SUNTANS to further investigate physical processes in the lake. Numerical results well agree to observational results and show that baroclinic motions influence in the whole of the lake basin. The wind-induced baroclinic energy is generated in the middle of the lake basin and propagate to the onshore. This study suggests that mixing and baroclinic motions due to buoyancy and wind effects play an important role in the oxygen distribution in Lake Kasumigaura.

Keywords: Mixing, Hypoxia, Internal waves

©2019. Japan Geoscience Union. All Right Reserved.

[J] Oral | A (Atmospheric and Hydrospheric Sciences)：A-OS Ocean Sciences & Ocean Environment

Wed. May 29, 2019 3:30 PM - 5:00 PM JST | Wed. May 29, 2019 6:30 AM - 8:00 AM UTC | 301A 3F

[A-OS14] Coastal physical processes associated with mixing, eddies, internal waves

convener:Eiji Masunaga(Ibaraki University), Taira Nagai(Graduate School of Science, The University of Tokyo), TSUTSUMI EISUKE(Atmosphere and Ocean Research Institute, The University of Tokyo), Chairperson:Eiji Masunaga, Taira Nagai

Recently developed observational and numerical approaches have revealed details of physical processes in coastal regions, which is a key to understanding global ocean circulations and ecosystems. This session aims to provide discussions of mixing, eddies, nonlinear internal waves in coastal and marginal oceans, estuaries and lakes. Observations, numerical modeling and laboratory experiments associated with these phenomena are encouraged to submit an abstract to this session. In addition, studies that consider linkages between coastal physical processes and large scale open ocean processes, e.g., the Kuroshio, global ocean circulations.

3:30 PM - 3:45 PM JST | 6:30 AM - 6:45 AM UTC

[AOS14-07] Turbulent mixing and vertical nitrate flux in the Bungo Channel, Japan

*TSUTSUMI EISUKE[1], Naoki Yoshie[2], Takashi Mano[3], Kanda Taisei[3], Naoki Fujii[4], Xinyu Guo[2] (1.Research Institute for Applied Mechanics, Kyushu University, 2.Center for Marine Environmental Studies, Ehime Univeristy, 3.Graduate School for Science and Engineering, Ehime University, 4.Faculty of Agriculture, Saga Univerisity)

3:45 PM - 4:00 PM JST | 6:45 AM - 7:00 AM UTC

[AOS14-08] Numerical Analysis of Submerged Turbulent Buoyant Jet in River Mouth

*Yen-Chen Mou[1], Gene You[1], Chih-Chieh Young[2] (1.National Taiwan University, 2.National Taiwan Ocean University)

4:00 PM - 4:15 PM JST | 7:00 AM - 7:15 AM UTC

[AOS14-09] Implementing regional downscaling capability in the STEAMER radionuclide dispersion prediction system based on multi-nested ROMS model

*Kamidaira Yuki[1], Hideyuki Kawamura[1], Takuya Kobayashi[1], Yusuke Uchiyama[2] (1.Japan Atomic Energy Agency, 2.Kobe University)

4:15 PM - 4:30 PM JST | 7:15 AM - 7:30 AM UTC

[AOS14-10] Transport processes around the Izu-chain islands investigated with a Lagrangian particle tracking model

*Waku Kimura[1], Eiji Masunaga[1], Taichi Kosako[2], Yusuke Uchiyama[3] (1.Ibaraki University, 2.Port and Airport Research Institute, 3.Kobe University)

4:30 PM - 4:45 PM JST | 7:30 AM - 7:45 AM UTC

[AOS14-11] Fates and dynamical roles of pinch-off mesoscale eddies originated from the Kuroshio Extension Jet

*Yusuke Uchiyama[1], Nobue Okada[1], Changming Dong[2] (1.Graduate School of Engineering, Kobe University, 2.Nanjing University of Information Science & Technology)

4:45 PM - 5:00 PM JST | 7:45 AM - 8:00 AM UTC

Discussion

Turbulent mixing and vertical nitrate flux in the Bungo Channel, Japan

*TSUTSUMI EISUKE[1], Naoki Yoshie[2], Takashi Mano[3], Kanda Taisei[3], Naoki Fujii[4], Xinyu Guo[2]

1. Research Institute for Applied Mechanics, Kyushu University, 2. Center for Marine Environmental Studies, Ehime Univeristy, 3. Graduate School for Science and Engineering, Ehime University, 4. Faculty of Agriculture, Saga Univerisity

Turbulent mixing plays a key role in primary production in coastal seas through supplying nutrients to the euphotic zone from deeper layers and to the ocean from rivers. Understanding of turbulent dynamics in coastal seas is therefore essential for prediction, conservation and management of coastal ecosystems. Here, we studied turbulent mixing and the associated vertical nitrate transport in a tidally-energetic channel between the Kuroshio region and the Seto Inland Sea (Bungo Channel, Japan). Takeoka [1993] hypothesized that strong vertical mixing and the associated secondary circulation in the channel maintains primary production through supplying large amount of nutrients coming from the Kuroshio region. We conducted simultaneous measurements of turbulence and nitrate concentration along a section in the Bungo Channel using a microstructure turbulence profiler (TurboMAP-5, JFE Advantech) and optical nitrate sensor (SUNA-V2, Sea-Bird Scientific) on 27 August, 2017. We found nitrate-rich cold waters in the bottom of the southern part of the section, which coincide with a typical bottom intrusion from the Kuroshio region. Largest vertical eddy diffusivity of O(10^{-2}) m^2 s^{-1} and the associated upward nitrate flux of O(10) mmol m^{-2} day^{-1} were obtained at 20-30 m depth south of deep and narrow strait (Hoyo Strait). Also, subsurface maximum in chlorophyll fluorescence is observed just above the strong turbulence layer, possibly suggesting phytoplankton blooms in response to the high turbulent nitrate flux. The strong vertical turbulent diffusion was associated with density overturns and elevated vertical shear, indicating internal wave breaking. We hypothesis that internal tides generated in the Hoyo Strait is one of the key processes in enhancement of turbulent mixing and nutrient transport in the Bungo Channel.

Keywords: turbulent mixing, vertical nitrate flux, internal tides

©2019. Japan Geoscience Union. All Right Reserved.

Numerical Analysis of Submerged Turbulent Buoyant Jet in River Mouth

*Yen-Chen Mou[1], Gene You[1], Chih-Chieh Young[2]

1. National Taiwan University, 2. National Taiwan Ocean University

The purpose of this study is to investigate the characteristics of submerged turbulent buoyant jet in river mouth by simulating basic fluid mechanisms. The numerical model composes two-dimensional continuity equation, momentum equation, and advective diffusion equation. Since our model is building on basic fluid mechanics formulas, we can test the movement of buoyant jet in the river mouth depends on different parameters, such as environmental and geometrical factors. One of our focuses will be how the phenomena be influenced by inflow hydrograph and sediment concentration, as well as real events and analyze their effect submerged turbulent buoyant jet motion pattern.

Our model will be applied to simulated several characteristic behaviors that are consistent with prior knowledge, including: (1) the inflow concentration is higher at the fixed inflow rate and calculation time, the formed buoyant jet has a large influence range and higher concentration; (2) when the inflow rate is high in a fixed flow concentration and calculation time, the generated buoyant jet has a large influence range and that shape more bulging. Moreover, we will adjust the downstream boundary conditions. When the downstream water level is high, the range and the duration time of the buoyant jet are great. As expected, the concentration of the same location is also higher than other situation that has a lower downstream water level. So far, this model will progress to the extent that it can capture the overall trend of buoyant jet movements, and this simulation is based only on the physical mechanism of the sand-containing fluid itself.

Keywords: Submerged Turbulent Buoyant Jet, River Mouth, Numerical Analysis, Finite-Difference Methods, Buoyancy, Plume

©2019. Japan Geoscience Union. All Right Reserved.

Implementing regional downscaling capability in the STEAMER radionuclide dispersion prediction system based on multi-nested ROMS model

*Kamidaira Yuki[1], Hideyuki Kawamura[1], Takuya Kobayashi[1], Yusuke Uchiyama[2]

1. Japan Atomic Energy Agency, 2. Kobe University

Oceanic regional downscaling capability was implemented into Short-Term Emergency Assessment system of Marine Environmental Radioactivity (STEAMER) developed by Japan Atomic Energy Agency (JAEA) to enable us to predict more realistically the oceanic dispersion of radionuclides at higher spatiotemporal resolutions for broader applications. The system consisted of double-nested Regional Ocean Modeling System (ROMS) with tidal forcing embedded in the Multivariate Ocean Variational Estimation system for the Western North Pacific (MOVE-WNP), assimilative reanalysis/forecast product and an oceanic radionuclide dispersion model SEA-GEARN developed by JAEA. Surface wind stress was provided by the Grid Point Value of the Global Spectral Model (GPV-GSM) atmospheric reanalysis/forecast while surface heat and freshwater fluxes are from the Comprehensive Ocean-Atmosphere Data Set (COADS) monthly climatology. Ten principal tidal constituents from the TPXO 7.0 global tidal reanalysis were additionally imposed on the sea surface height as boundary condition along the perimeter to include barotropic tides and the resultant intrinsic baroclinic tides. The horizontal grid spacing was decreased from ~10 km in the outermost MOVE-WNP, to 3 km in the intermediate ROMS-L1 model, and further down to 1 km in the innermost ROMS-L2 model. The model results showed reasonable agreement with tidal observations. The system was used to comparatively examine downscaling and tidal effects on the dispersion of radionuclides hypothetically released from the Fukushima Daiichi Nuclear Power Plant. The simulated dissolved ^{137}Cs distribution had seasonal variability and was different from that obtained using coarser-resolution models because downscaling enhanced both horizontal and vertical mixing. Temporal ^{137}Cs fluctuations were slightly amplified as a result of the suppression of horizontal mixing and enhancement of vertical mixing by tides. In addition, the submesoscale effects strengthened the three-dimensional ^{137}Cs fluctuations by <10 times, while the tidal effects promoted slightly increased the intensity of three-dimensional ^{137}Cs fluctuations by approximately 3-30%. This indicated that the submesoscale effects substantially surpassed tidal forcing in oceanic mixing in the coastal margin off Fukushima.

Keywords: ROMS, radionuclide dispersion model

©2019. Japan Geoscience Union. All Right Reserved.

Transport processes around the Izu-chain islands investigated with a Lagrangian particle tracking model

*Waku Kimura[1], Eiji Masunaga[1], Taichi Kosako[2], Yusuke Uchiyama[3]

1. Ibaraki University, 2. Port and Airport Research Institute, 3. Kobe University

This study investigated mass transport and dispersion around Izu-chain islands off the Japan mainland using with 3-D Lagrangian particle tracking simulations modeled in a high-resolution reginal ocean modeling system (ROMS). The Kuroshio and eddies, tides largely influence physical processes in the study area. Details of transport processes involving the Kuroshio, eddies and tides have not been understood well. However, these processes are important for understanding oceanic environments and ecosystems in the North Pacific Ocean. Particles were released from three regions: around the Izu-chain islands (north of the Kuroshio), in the Kuroshio, south of the Kuroshio. Model results show that the particle trajectory is different depends on the initial location of particles. Approximately 60% particles released from the Izu-chain islands were transported outside the model domain in 30 days. On the other hands, more than 90% particles released from the Kuroshio and south of the Kuroshio flew out from the domain in 30 days. The vorticity is enhanced by the tidal forcing in the whole study area. The tidal forcing enhances the horizontal diffusion of particles within 2 days scale. By contrast, in the longer time scale longer than 5 days, the dispersion of particles is suppressed by the tidal forcing, because large scale motions are suppressed by tides. The frequency spectrum of the particle velocity shows semi-diurnal peaks and high frequency (low frequency) is enhanced (decreased) by the tidal forcing.

Keywords: Tide, Lagrangian particle tracking model, Kuroshio

©2019. Japan Geoscience Union. All Right Reserved.

Fates and dynamical roles of pinch-off mesoscale eddies originated from the Kuroshio Extension Jet

*Yusuke Uchiyama[1], Nobue Okada[1], Changming Dong[2]

1. Graduate School of Engineering, Kobe University, 2. Nanjing University of Information Science & Technology

Mesoscale eddies are ubiquitous in the world ocean that frequently collide with currents, leading to substantial alteration of the associated dynamics. For instance, the Kuroshio plays a major role in preconditioning the coastal environment around Japan through poleward heat and material transport from the subtropics, while its path is known to meander occasionally by eddy collisions. Pinch-off mesoscale eddies that detach intermittently from the Kuroshio tend to travel westward as Rossby waves and have been found to collide with the Kuroshio again to alter oceanic and coastal environment through alteration of the Kuroshio path.

For realization of such processes, we applied the eddy detection algorithm used in Liu et al. (2012) to ARMOR3D. The ARMOR3D dataset is a 3D global currents and density data set that is reconstructed from a combination of extensive satellite data and in situ observations based on the geostrophic thermal wind relation and statistical methods as described in Guinehut et al. (2012). By conducting several sensitivity tests, we introduced constraints on vorticity magnitude of detected mesoscale eddies and their relative positions to the Kuroshio path to determine pinch-off eddies near the Kuroshio Extension (KE) region. It was found that the constraint on vorticity magnitude of the detected individual eddies greater than $0.15f$, where f is the local Coriolis frequency, throughout eddy lifetime is significant to successfully isolate pinch-off eddies.

With this constraint, we discovered that most of the detected pinch-off eddies are cyclonic on the south side of the KE region, while anticyclonic eddies are predominant on the north side. The former occurred 2.5–3 times as often as the latter, although in the entire North Pacific, cyclonic eddies occurred only 12.1% more frequently than anticyclonic eddies. Hence, it is considered that this cyclone dominance in the pinch-off eddies from the Kuroshio is a unique feature. We also succeeded to determine pinch-off eddies that collide again with the Kuroshio by introducing another constraint, which is the threshold distance between the Kuroshio path and terminal positions of pinch-off eddies traveled westward. In several selected cases with these constraints, comparisons of the surface temperature and salinity before and after the eddy collisions clearly exhibit that the alteration of the Kuroshio path due to eddy collisions is quite influential in modifying the oceanic structures. It was also found that the pinch-off eddies occasionally interact with other mesoscale eddies to modify the upper-ocean structure pronouncedly.

The Kuroshio path in the KE region is known to vary on annual to decadal time scales, where it was rather stable for 1993-1995 and 2002-2005, whereas largely meandered unstably for 1996–2001 and 2006–2009. During the first unstable periods, the number of cyclonic pinch-off eddies were significantly increased in the area between 144 °E and 150 °E for 1996–2001. However, no significant increase was observed during the other unstable period for 2006–2009. More than 70% of the pinch-off eddies that collided with the Kuroshio appeared during the unstable periods, suggesting that the stability of the Kuroshio path in the KE region is a key influencer on vigorous generation of such colliding pinch-off eddies.

©2019. Japan Geoscience Union. All Right Reserved.

Keywords: pinch-off mesoscale eddy, Kuroshio, eddy tracking algorithm, ARMOR3D

©2019. Japan Geoscience Union. All Right Reserved.

[E] Oral | A (Atmospheric and Hydrospheric Sciences)：A-HW Hydrology & Water Environment

Wed. May 29, 2019 3:30 PM - 5:00 PM JST | Wed. May 29, 2019 6:30 AM - 8:00 AM UTC | 201B 2F

[A-HW22] Materials transport and nutrient cycles in watersheds; from headwaters to coastal seas

convener:Masahiro Kobayashi(Forestry and Forest Products Research Institute), Seiko Yoshikawa(Institute for Agro-environmental Sciences, National Agriculture and Food Research Organization), Jun Yasumoto(University of the Ryukyus, Faculty of Agriculuture), Adina Paytan(University of California Santa Cruz), Chairperson:Noboru Okuda(Research Institute for Humanity and Nature)

This session aims to synthetize watershed sciences in order to understand dynamical processes of materials transport and nutrient cycles in watersheds from headwaters to coastal seas. The session will be integrating a variety of research disciplines including limnology, ground water hydrology, coastal oceanography, meteorology, pedology, sedimentology, forestry, agriculture, fishery, ecology, social science and more. This session calls for ideas on new methods for the watershed sciences, such as tracer and molecular technique, hydrological modeling, paleontological approaches, laboratory and field experiments, social-scientific evaluation of ecosystem services and social-ecological systems, and so on, in order to elucidate physical, chemical and biological mechanisms for shedding light on natural phenomena and their changes over time in complex and dynamic watershed systems under human and climate impacts. Through this session, we would like to facilitate interdisciplinary collaboration among participants to create new knowledge on watershed sciences.

3:30 PM - 3:40 PM JST | 6:30 AM - 6:40 AM UTC

Introduction

3:40 PM - 4:00 PM JST | 6:40 AM - 7:00 AM UTC

[AHW22-01] **Coral Skeleton $\delta^{15}N$ as a Tracer of Historic Nutrient Loading to a Coral Reef in Maui, Hawaii**

★Invited Papers

*Adina Paytan[1] (1.University of California Santa Cruz)

4:00 PM - 4:15 PM JST | 7:00 AM - 7:15 AM UTC

[AHW22-02] **The Use of Ammonium and Trace Metals in Identifying Low Redox Environment Zone at Indonesian Coastal Alluvial Groundwater**

*Anna Fadliah Rusydi[1,4], Mitsuyo - Saito[2], Seiichiro - Ioka[3], Shin-ichi - Onodera[1] (1.Graduate School of Integrated Arts and Sciences, Hiroshima University, Japan, 2.Graduate School of Environmental and Life Sciences, Okayama University, Japan, 3.Institute of Regional Innovation, Hirosaki University, Japan, 4.Research Center for Geotechnology, Indonesian Institute of Sciences, Indonesia)

4:15 PM - 4:30 PM JST | 7:15 AM - 7:30 AM UTC

[AHW22-03] Spatial and temporal variation in submarine groundwater discharge (SGD) on a beach scale in a temperate coastal island: a multi-tracer approach

*Mitsuyo Saito[1], Shin-ichi Onodera[2], Yusuke Tomozawa[2], Kazuyoshi Asai[3] (1.Graduate School of Environmental and Life Science, Okayama University, 2.Graduate School of Integrated Arts and Sciences, Hiroshima University, 3.Geo Science Laboratory)

4:30 PM - 4:45 PM JST | 7:30 AM - 7:45 AM UTC

[AHW22-04] **Phosphorus discharge via groundwater into the lake, based on lacustrine groundwater discharge (LGD) and alluvial plain sediment**

*Shin-ichi Onodera[1], Mitsuyo Saito[2], Guangzhe Jin[3], Anna Fadliah Rusydi[1], Yusuke Tomozawa[1], Kunyang Wang[1], Syuhei Ban[4], Noboru Okuda[5] (1.Graduate School of Integrated and Arts Sciences, Hiroshima University, 2. Graduate School of Environmental and Life Science, Okayama University, 3.Guangdong Ocean University, 4.The University of Shiga Prefecture, 5.Research Institute for Humanity and Nature)

4:45 PM - 5:00 PM JST | 7:45 AM - 8:00 AM UTC

[AHW22-05] **Geochemical controls and health implications of water chemistry in Benoue River Basin, North Cameroon: Insights from Major ions**

*Sharon Bih Kimbi[1,2], Wilson Y Fantong[3], Samuel N Ayonghe[2], Robert Kringel[4], Shin-ichi Onodera[1]
(1.Graduate School of Integrate Arts and Sciences, Hiroshima University, 2.Department of Environmental Science, Faculty of science, University of Buea, 3.Institute of Mining and Geological Research (IRGM), 4.Federal Institute for Geoscience and Natural Resources Bundesanstalt fur Geowissenschaften und Rohstoffe (BGR) PRESS NO & SW)

Coral Skeleton $\delta^{15}N$ as a Tracer of Historic Nutrient Loading to a Coral Reef in Maui, Hawaii

*Adina Paytan[1]

1. University of California Santa Cruz

Excess nutrient loading to nearshore environments has been linked to declining water quality and ecosystem health. Macro-algal blooms, eutrophication, and reduction in coral cover have been observed in West Maui, Hawaii, and linked to nutrient inputs from coastal submarine groundwater seeps. Here, we present a forty-year record of nitrogen isotopes ($\delta^{15}N$) of intra-crystalline coral skeletal organic matter in three coral cores collected at this site and evaluate the record in terms of changes in nitrogen sources. Our results show a dramatic increase in coral $\delta^{15}N$ values after 1995, corresponding with the implementation of biological nutrient removal at the nearby Lahaina Wastewater Reclamation Facility (LWRF). High $\delta^{15}N$ values are known to be strongly indicative of denitrification and sewage effluent, corroborating a previously suggested link between local wastewater injection and degradation of the reef environment. This record demonstrates the power of coral skeletal $\delta^{15}N$ as a tool for evaluating nutrient dynamics within coral reef environments.

Keywords: Nitrogen Isotopes, Corals, Submarine Groundwater Discharge

©2019. Japan Geoscience Union. All Right Reserved.

The Use of Ammonium and Trace Metals in Identifying Low Redox Environment Zone at Indonesian Coastal Alluvial Groundwater

*Anna Fadliah Rusydi[1,4], Mitsuyo - Saito[2], Seiichiro - Ioka[3], Shin-ichi - Onodera[1]

1. Graduate School of Integrated Arts and Sciences, Hiroshima University, Japan, 2. Graduate School of Environmental and Life Sciences, Okayama University, Japan, 3. Institute of Regional Innovation, Hirosaki University, Japan, 4. Research Center for Geotechnology, Indonesian Institute of Sciences, Indonesia

Reduction and oxidation (redox) conditions in the aquifer are essential factors; those can determine the behavior of chemicals in the groundwater system. Nowadays, researches concerning the low redox (reduction) environment are growing significantly since some pollutions occur under this condition. The study was taken place in Indramayu, Indonesia. The area is an alluvial plain located on the North Coast of West Java Island. The groundwater in the alluvial area is compelling to study because it has a large aquifer storage capacity but unfortunately vulnerable to contamination. Moreover, the contamination will get severe under reduction environment. The primary objective of this study is to understand groundwater vulnerability by identifying the reduction environmental zone in the study site.

In this research, we used combined chemical parameters: ammonium (NH_4^+-N), dissolve manganese (Mn^{2+}) and ferrous (Fe^{2+}), to trace reduction condition in the groundwater. NH_4^+-N is one form of nitrogen compound that usually arise under reduction condition. Other parameters that arise with the reduction process are Mn^{2+} and Fe^{2+}. Therefore, in this investigation, we assumed the use of NH_4^+-N, combined with the concentrations of Mn^{2+} and Fe^{2+} elements, are able to identify groundwater reduction environment.

Totally, there was ten soil taken from 2 boreholes located at the south and north of the research site and 20 water samples collected from groundwater (18) and river (2). The soil samples were analyzed for NH_4^+-N and C/N ratio parameters. These data were used to explain further about NH_4^+-N presence in groundwater. Additionally, the water samples were analyzed for NH_4^+-N, $Mn^{2+,}$ and Fe^{2+} concentrations. The aquifer materials consist of sandstone, claystone, and sandy claystone. The NH_4^+-N concentrations were ranged from 0.82 until 3.37 mg / L. However; there was no clear relationship between the soil’s depth and compositions with NH_4^+-N concentrations. The soil samples had low C/N ratios, with values of 8.00 to 12.19. This is indicating that N-organic in the soil potentially experiences mineralization, one that produces NH_4^+-N. Furthermore, NH_4^+-N in water samples were detected as the dominant nitrogen form at most sites. Similarly, Mn^{2+} was detected at almost all locations. Moreover, the concentrations of Mn^{2+} were high (> 0.05 mg / L), around 0.07 - 12.8 mg / L, at 16 locations. High concentrations of Fe^{2+} (> 0.3 mg/L), were found in groundwater at 6 locations. The concentrations were ranged from 1.39 to 9.91 mg/L. The presence of NH_4^+-N along with high Mn^{2+} contents indicated that almost all locations experienced reduction condition at a zone of manganese reduction. Moreover, at 6 locations, the reduction process was stronger and lead to becoming ferrous zone. This was shown by NH_4^+-N existence as dominant nitrogen form and high concentrations of Fe^{2+} as well as Mn^{2+}.

Keywords: Ammonium, Manganese, Ferrous, Reduction, Coastal Groundwater, Indramayu

©2019. Japan Geoscience Union. All Right Reserved.

Spatial and temporal variation in submarine groundwater discharge (SGD) on a beach scale in a temperate coastal island: a multi-tracer approach

*Mitsuyo Saito[1], Shin-ichi Onodera[2], Yusuke Tomozawa[2], Kazuyoshi Asai[3]

1. Graduate School of Environmental and Life Science, Okayama University, 2. Graduate School of Integrated Arts and Sciences, Hiroshima University, 3. Geo Science Laboratory

Submarine groundwater discharge (SGD) is defined as subsurface water flow from the seabed to the coastal sea and ocean. Because groundwater often contains higher nutrients than river water, SGD delivers comparatively large quantities of nutrients to coastal ecosystems. However, there are few studies to examine the spatial relation between SGD and coastal ecosystem such as seagrasses and seaweeds. In the present research, we aimed to examine the spatial and temporal variation in SGD on a beach scale in a temperate coastal island.
The study areas are located on Ikuchijima Island in Seto Inland Sea, southern Japan. The regional climate is mild, with an annual mean precipitation of 1,100 mm and temperature of 15.6 ˚C. The whole island is characterized by steep slopes and is widely covered by citrus farms with more than 40% of the island. The previous researches confirmed that SGD can rival or even exceed surface runoff in this island. However, the spatial and temporal variation in SGD on a beach scale was not well examined. We installed piezometers in two beach sites (Gohonmatsu: IKG and Miyabara: IKM) and measured water pressure, water temperature, electric conductivity (EC), and radon (^{222}Rn) concentration in pore water in July and December 2018, and January 2019. In January 2019, SF6 (sulfur hexafluoride) concentration was measured to estimate residence time of pore water. Before the field campaign in July 2018, the study area had an extreme rainfall event. IKG has steeper backland topography than IKM. There is no surface water inflow to IKG, while a small channel inflow to IKM. Main bottom material is sand in both beaches, however, the western part of IKG is covered by coarse gravels. Large spatial variation in hydraulic potential, water temperature, EC and ^{222}Rn concentration in pore water were confirmed in both beaches, with larger variation range in IKG. EC was totally lower and ^{222}Rn was higher in IKG than IKM. These results suggest that higher rate in fresh-SGD in IKG than IKM. In addition, significant low EC and high ^{222}Rn concentration were confirmed in the western part of IKG in July 2018.

Keywords: Submarine groundwater discharge (SGD), Beach scale, Spatial and temporal variation

©2019. Japan Geoscience Union. All Right Reserved.

Phosphorus discharge via groundwater into the lake, based on lacustrine groundwater discharge (LGD) and alluvial plain sediment

*Shin-ichi Onodera[1], Mitsuyo Saito[2], Guangzhe Jin[3], Anna Fadliah Rusydi[1], Yusuke Tomozawa[1], Kunyang Wang[1], Syuhei Ban[4], Noboru Okuda[5]

1. Graduate School of Integrated and Arts Sciences, Hiroshima University, 2. Graduate School of Environmental and Life Science, Okayama University, 3. Guangdong Ocean University, 4. The University of Shiga Prefecture, 5. Research Institute for Humanity and Nature

Groundwater discharge and nutrient flux into a lake has not been confirmed enough in terms of spatial variation including those in deeper zone. Biwa Lake has different characteristics between in northern and southern. In northern, the water depth varies up to 100m, groundwater discharge is also expected not only in beach sides with shallower depth but in deeper zones. We examined to indicate spatial variation of Rn-222 and to compare with the results of seepage observations by Kobayashi (1993).

Radon radioisotope (Rn-222) concentrations were measured by a RAD7 at 500 m interval along the whole shoreline of the northern lake, and surface water samples were coincidently collected. Oxygen stable isotope ratio ($\delta^{18}O$), Chloride anion and nutrients (nitrogen, phosphorus, and silicon) concentrations were measured in the laboratory in order to evaluate inflow of the groundwater into the lake. Those dissolved materials were also measured from the groundwater samples were collected in ca. 20 wells situated along the shore of the lake as well as those in river waters. In the eastern coast (Hikone), artesian groundwater was also collected because of aquiclude at 10m deep under the ground. Lake waters at the surface, middle and bottom layers and interstitial waters in the bottom sediments were collected for measuring Rn-222 concentrations.

At the both sites of Yasu and Takashima, high pressures of groundwater indicated flow of the water to the lake under the ground. Spatial distributions in Rn-222, Cl^- and nutrient concentrations with those in $\delta^{18}O$ along the coasts also indicated discharges of groundwater into the lake. High concentrations of dissolved phosphorus phosphate (> 0.1ppm) were detected from several wells out of 15 ones investigated. Based on the comparative results with the seepage observations, we could confirm good correlation between Rn-222 concentration and seepage observation results.

In addition, Rn-222 concentrations in lake waters were measured in the surface and bottom layers at the 4 stations with different water depths (5m, 10m and 20m) in October 2015 and July 2016. The highest Rn-222 was observed in the bottom layer at 20m-deep site in both periods. The concentration was more than 2-fold of that in the littoral site. It suggests high possibility of deep-LGD from offshore lake floor.

Keywords: Phosphorus, groundwater, alluvial plain, semiment

©2019. Japan Geoscience Union. All Right Reserved.

Geochemical controls and health implications of water chemistry in Benoue River Basin, North Cameroon: Insights from Major ions

*Sharon Bih Kimbi[1,2], Wilson Y Fantong[3], Samuel N Ayonghe[2], Robert Kringel[4], Shin-ichi Onodera[1]

1. Graduate School of Integrate Arts and Sciences, Hiroshima University, 2. Department of Environmental Science, Faculty of science, University of Buea, 3. Institute of Mining and Geological Research (IRGM), 4. Federal Institute for Geoscience and Natural Resources Bundesanstalt fur Geowissenschaften und Rohstoffe (BGR) PRESS NO & SW

Increase population growth in the north region of Cameroon coupled with rapid urbanisation has led to the widespread of informal settlements in urban areas. Multivariate statistics and hydrochemical diagrams were used to investigate the groundwater chemistry, usability and the impact of urbanisation on water resource quality. The purposive random technique was used to sample and collect 86 water samples from 34 boreholes, 37 wells, 14 rivers and 1spring during the month of January, 2017. Major ions were analyzed using an Ion Chromatography. The results revealed that, water pH ranged from slightly acidic to basic meanwhile the water types varied from Ca-Cl in wells, Na-HCO_3 in springs and CaMg-HCO_3 in boreholes and rivers. Water sources did not meet WHO, 2006 quality standard with respect to pH (60.5% <7 & >8.5), EC (58.1%>250 μS/cm) and NO_3^-(60.5%>10mg/l). The Wilcox and USSL diagrams for irrigational uses showed that the water sources are of low to moderate salinity and low alkalinity hazard and thus excellent for use in irrigation. Increase concentrations of NO_3^- and Cl^- from 8.0mg/l to 198.4mg/l and from 2.0mg/l to 59.4mg/l in 1997 and 2017 (20yrs) respectively could be linked to increase population, poor waste disposal and pollution from agricultural fields. While anthropogenic activities are main provenance of NO_3^- and Cl^-, the population is equally affected by fluorosis from lithogenic fluoride and is at risk to nitrate. It is recommended that a monitoring and evaluation system for ground water sources with respect to their quantity and quality be put in place to ensure sustainable management by policy makers.

Keywords: Hydrochemistry, Water resources, Fluorosis, Urbanization, Cameroon

©2019. Japan Geoscience Union. All Right Reserved.

[E] Oral | A (Atmospheric and Hydrospheric Sciences)：A-HW Hydrology & Water Environment

Wed. May 29, 2019 9:00 AM - 10:30 AM JST | Wed. May 29, 2019 12:00 AM - 1:30 AM UTC | 103 1F

[A-HW23] Hydrology & Water Environment

convener:Isao Machida(Geological Survey of Japan), Dai Yamazaki(Institute of Industrial Sciences, The University of Tokyo), Takeshi Hayashi(Faculty of Education and Human Studies, Akita University), Keisuke Fukushi(Institute of Nature & Environmental Technology, Kanazawa University), Chairperson:Takeshi Hayashi(Faculty of Education and Human Studies, Akita University)

We focus on various issues of water cycle and environment and aim to answer questions of hydrological and earth system sciences including 1) surface, subsurface and evapotranspiration processes of water cycle; 2) natural and anthropogenic hydrothermal systems, 3) environments issues and studies on a watershed or global scale, 4) water-related issues with ecological, environmental, and geochemical aspects, and 5) other issues in hydrological sciences. This session welcomes presentations regarding various kinds of approaches and techniques such as field survey, remote sensing, isotope tracers, numerical simulation, and theoretical analysis.

9:00 AM - 9:15 AM JST | 12:00 AM - 12:15 AM UTC

[AHW23-12] Drought Analysis based on Copulas and Poisson Process

*Pei-Yu Wu[1], Gene Jiing-yun You[1] (1.National Taiwan University, Department of Civil Engineering)

9:15 AM - 9:30 AM JST | 12:15 AM - 12:30 AM UTC

[AHW23-13] **Snow melt dynamics in snowfall dominated mountain regions in Shonai**

*Alexander Brandt[1,3], Muhammad Fraz Ismail[2], Larry Maximo Lopez Caceres[1], Wolfgang Bogacki[2] (1.Yamagata University, 2.Hochschule Koblenz, 3.UGAS)

9:30 AM - 9:45 AM JST | 12:30 AM - 12:45 AM UTC

[AHW23-14] Study on transport of particulate organic matter in a small river with forest and paddy filed by using carbon isotopes ($\delta^{13}C$ and $\Delta^{14}C$)

*Seiya Nagao[1], Ryunosuke Tahara[2], Shinya Ochiai[1], Akiko Goto[3], Takashi Hasegawa[3] (1.Institute of Nature and Environmental Technology, Kanazawa University, 2.Graduate School of Natural Science and Technology, Kanazawa University, 3.Institute of Science and Engineering, Kanazawa University)

9:45 AM - 10:00 AM JST | 12:45 AM - 1:00 AM UTC

[AHW23-15] **Sources of Shallow Groundwater Salinity in the Ganges Delta of Bangladesh**

*Masudur Rahman[1,2], Tomochika Tokunaga[1] (1.Department of Environment Systems, Graduate School of Frontier Sciences, The University of Tokyo, 5-1-5, Kashiwa-no-ha, Kashiwa-shi, Chiba 277-8563, Japan, 2.Environmental Science Discipline, Life Science School, Khulna University, Khulna 9208, Bangladesh)

10:00 AM - 10:15 AM JST | 1:00 AM - 1:15 AM UTC

[AHW23-16] **Groundwater chemistry in the Gunii Khooloi basin, Southern Gobi Region of Mongolia using multivariate analysis**

*Batdemberel BAYANZUL[1,2], Isao Machida[3], Kengo Nakamura[2], Noriaki Watanabe[2], Takeshi Komai[2] (1.School of Geology and Mining Engineering, Mongolian University of Science and Technology, 2.Graduate School of Environmental Studies, Tohoku University, 3.Groundwater research group, Advanced Industrial Science and Technology)

10:15 AM - 10:30 AM JST | 1:15 AM - 1:30 AM UTC

[AHW23-17] **Temporal observation of molybdenum concentrations in rivers from Erdenet mining area, Mongolia**

*Solongo Tsetsgee[1], Keisuke Fukushi[1], Altansukh Ochir[2], Takahashi Yoshio[3], Ariuntungalag Yunden[2], Enkhjin Odgerel[2], Noriko Hasebe[1] (1.Kanazawa University, 2.National University of Mongolia, 3.The University of Toyko)

Drought Analysis based on Copulas and Poisson Process

*Pei-Yu Wu[1], Gene Jiing-yun You[1]

1. National Taiwan University, Department of Civil Engineering

Drought is a regular and recurring climatic phenomenon. Because of climate change and the increasing water demand, we have experienced higher drought deficit and severity in recent years. To evaluate the impact of the trend of drought, this study aims to develop an improved framework for streamflow drought analysis and simulation of the future conditions. Based on our proposed framework based on Copulas and Poisson process, this study firstly analyzes historical inflow data to estimate statistical parameters of drought. Secondly, we calculate three defined indices of the drought, drought duration, drought deficit, and interval time between droughts respectively. With statistical test, these three indices are found to be correlated. Following, the marginal distributions of these indices are estimated. Accordingly, this study constructs a stochastic model by three-dimensional Gaussian copulas to simulate the occurrence of drought events. In addition, to more appropriately simulate drought occurrences, a Poisson process is applied in this study to describe the occurrence between drought events. This simulation is based on the stationary assumption in current stage. In the future, we will consider the influence of climate change and simulate drought events under non-stationary condition. The results of this work can be utilized to support the decision or policy making processes in drought management.

Keywords: drought analysis, copulas, poisson process

©2019. Japan Geoscience Union. All Right Reserved.

Snow melt dynamics in snowfall dominated mountain regions in Shonai

*Alexander Brandt[1,3], Muhammad Fraz Ismail[2], Larry Maximo Lopez Caceres[1], Wolfgang Bogacki[2]

1. Yamagata University, 2. Hochschule Koblenz, 3. UGAS

With a total snowfall of 1500 mm, which is the half of the total annual precipitation, Shonai is one of the snowiest regions of the world (*Asaoka et al, 2013*). Snow depth can reach up to 5.2 meters in March before the snow melt finishes in May. The maximum snow depth as 50-year average is 2.7 m in the Yamagata University Research Forest (YURF), southern of the Shonai plains. The relatively warm air in winter (~ 0˚C) leads to several melting and refreezing processes within the snow column, increasing the snow density to 0.5 g/cm³. This huge amount of snow in Yamagata, Akita and Aomori prefecture is the dominating water source for plants in spring and a good thermal insulation for the soil, which is never freezing in YURF. A change of wind direction in winter is the reason for the high amount of snow. Cold air from Siberia is passing the warm Japanese Sea and faces the central mountains of Tohoku (*Asaoka et al., 2013*). These characteristics are very unique in the world leading to snow accumulations higher than in most areas of the world (*Krasting et al., 2013, Masiokas et al., 2006*).

The thick snow pack with high density results in a high Snow Water Equivalent (SWE). Monitoring and modelling of the snow melt period in spring is essential to confirm river discharges, water infiltration into the soil and to calculate the water balance of Japanese mountain forests. A modelling approach was done with the calculation of Degree-Day Factors (DDF) (*Ismail et al., 2015*). Measurements to determine the snow pack differences of forest covered sites and clear-cut sites are conducted this winter and will be intensified in the snow melting period. We expect results comparable to *Jost et al. (2009)* and *Schelker et al. (2013)*.

Automatic and manual measurements of snow density and snow depth were conducted intensively in the last 7 years in YURF. Together with the DDF we already discovered a significant trend of changing melt dynamics after half of the melting season. Results show furthermore, that the snow cover is not losing water, even in the warm periods during the winter. Soil moisture is measured to identify the start of the snow melt period, river flow discharge measurements will be introduced as soon as the snow melt starts. All these measurements together are parameters for the following calculations of snowmelt runoff. Melting dynamic related to temperature, snow cover and season was discovered and will be compared with river discharge measurements.

Literature:

Asaoka, Yoshihiro, Yuji Kominami (2013): Incorporation of satellite-derived snow-cover area in spatial snowmelt modeling for a large area: determination of a gridded degree-day factor

Ismail, Muhammad Fraz, Habib-ur-Rehman, Wolfgang Bogacki, Noor Muhammad (2015): Degree Day Factor models for forecasting the snowmelt runoff for Naran watershed

©2019. Japan Geoscience Union. All Right Reserved.

Jost, Georg, R. Dan Moore, Markus Weiler, David R. Gluns, Younes Alila (2009): Use of distributed snow measurements to test and improve a snowmelt model for predicting the effect of forest clear-cutting

Krasting, John P., Anthony J. Broccoli, Keith W. Dixon, John R. Lanzante (2013): Future Changes in Northern Hemisphere Snowfall

Masiokas, Mariano H., Ricardo Villalba, Brian H. Luckman, Carlos Le Quesne, Juan Carlos Aravena (2006): Snowpack Variations in the Central Andes of Argentina and Chile, 1951–2005: Large-Scale Atmospheric Influences and Implications for Water Resources in the Region

Schelker, J., L. Kuglerová, K. Eklöf, K. Bishop, H. Laudon (2013): Hydrological effects of clear-cutting in a boreal forest –Snowpack dynamics, snowmelt and streamflow responses

Keywords: Snow Water Equivalent, Degree-Day Factor, soil moisture, snowmelt, climate data, snow accumulation

©2019. Japan Geoscience Union. All Right Reserved.

Study on transport of particulate organic matter in a small river with forest and paddy filed by using carbon isotopes ($\delta^{13}C$ and $\Delta^{14}C$)

*Seiya Nagao[1], Ryunosuke Tahara[2], Shinya Ochiai[1], Akiko Goto[3], Takashi Hasegawa[3]

1. Institute of Nature and Environmental Technology, Kanazawa University, 2. Graduate School of Natural Science and Technology, Kanazawa University, 3. Institute of Science and Engineering, Kanazawa University

Radioactive and stable isotopes of carbon (^{14}C and ^{13}C) can serve as powerful tools for identifying sources and estimating turnover times of organic matter in aquatic systems. The present study aims to investigate variations in the characteristics of riverine particulate organic matter running through forests and paddy fields, corresponding to a typical Japanese river system. We selected the Kumaki River located in the central part of the Noto Peninsula in Ishikawa Prefecture, Japan. The river research was conducted at a fixed site of the midstream Kumaki River from April 2016 to March 2018.

Total organic carbon and nitrogen content was measured using the elemental analyzer after the 0.1 M HCl treatment to remove inorganic carbonates. ^{14}C measurements were performed by accelerator mass spectrometry. Final ^{14}C activities are reported in $\Delta^{14}C$. $\delta^{13}C$ values were determined for sub-samples of the CO_2 gas generated during graphite production, using an isotope ratio mass spectrometer.

$\delta^{13}C$ and $\Delta^{14}C$ values of organic matter in the riverine POC of Kumaki River show the range of −27.2‰ to −25.1‰, and −130 to +3 ‰, respectively. There are two negative correlations (correlation factor of 0.78) between the $\delta^{13}C$ and $\Delta^{14}C$ values at winter and the other season except for summer in July and August in 2017. The results indicate that particulate organic matter is mixed with two end-members such as surface forest soil and paddy field soil.

Keywords: Radiocarbon, stable carbon isotope ratio, Particulate organic matter

©2019. Japan Geoscience Union. All Right Reserved.

Sources of Shallow Groundwater Salinity in the Ganges Delta of Bangladesh

*Masudur Rahman[1,2], Tomochika Tokunaga[1]

1. Department of Environment Systems, Graduate School of Frontier Sciences, The University of Tokyo, 5-1-5, Kashiwa-no-ha, Kashiwa-shi, Chiba 277-8563, Japan, 2. Environmental Science Discipline, Life Science School, Khulna University, Khulna 9208, Bangladesh

In Bangladesh, unconsolidated fluvio-deltaic sediments host highly productive aquifer systems that are generally classified as shallow aquifers (depth less than 150 m below ground level, mbgl) and deep aquifers (depth more than 150 mbgl). Elevated groundwater salinity in shallow aquifers underlying the southern deltaic areas, in addition to mass poisoning of arsenic, aggravates freshwater scarcity in the country. However, little is known about the origin of salinity and mechanisms of salinization. Therefore, we analyzed both measured and previously published data on pH (n=585), electrical conductivity (EC, n=737), chloride and bromide (n=120 each), stable isotopes of water (oxygen-18 & deuterium, n=175 each), and radiogenic isotopes (C-14, n=18 & tritium, n=29) to discuss these issues for the upper shallow groundwater (depth around 60 mbgl) in the Ganges delta covering much of the coastal areas of Bangladesh. Stable isotope data from two GNIP (Global Network of Isotopes in Precipitation) stations in the delta were incorporated in this study. A paleo-shoreline, representing the maximum extent of last marine transgression at around 7 ka, was retrieved from a previous study and incorporated as well.
The upper shallow groundwater shows slightly acidic to alkaline in nature (6.1-8.5) over the delta. EC ranges from 210-29,400 microsimens/cm with lower salinity in fluvial area (210-2,000 microsimens/cm) than those in tidal domain (383-29,400 microsimens/cm). Cl^-/Br^- molar ratios are higher in tidal area (160-540,000) than those in fluvial setting (42-2,800). The cross plot between oxygen-18 and deuterium isotopes shows that groundwater data fall on or slightly below the local meteoric water line (Figure 1). Most of the brackish groundwater (n=43, EC>2,000-10,000 microsimens/cm) contains depleted isotope signatures. In EC vs oxygen-18 cross plot, EC mostly increases with almost constant isotopic signatures and this trend does not follow seawater mixing. Tritium concentrations are either low (0.1-2.9 TU, n=6) or below detection limit (<0.3 TU, n=9) in tidal domain, whereas around 57% of data show 0.2-7.2 TU in fluvial area. Radiocarbon (C-14) signatures are also higher in fluvial area (around 50-88 pMC) than those in tidal domain (around 36-86 pMC).
These results indicate that present-day seawater intrusion or connate seawater/estuarine water entrapped within sediments is not a major source of elevated salinity in groundwater. Current seawater intrusion is being occurred probably only in limited areas, i.e., near the coast. Also, it is hypothesized that groundwater salinity was possibly provided through the dissolution of soluble salts in paleosols by paleo-precipitation and concurrent infiltration to aquifers. During the transgression, intertidal environment was dominated in the study area, where evaporites and mud-cracks were likely to be developed during prolonged dry season. Subsequently, the monsoonal precipitation dissolved these evaporite minerals and vertically infiltrated into aquifers through mud-cracks or sediments. The future tasks should concentrate on analyzing whether these processes are occurring currently in the delta as well as reconstruction of paleo-geography for validating the hypothesis.

Keywords: Elevated salinity, Upper shallow groundwater, Electrical conductivity, Isotopes, Intertidal environment, Evaporite minerals

©2019. Japan Geoscience Union. All Right Reserved.

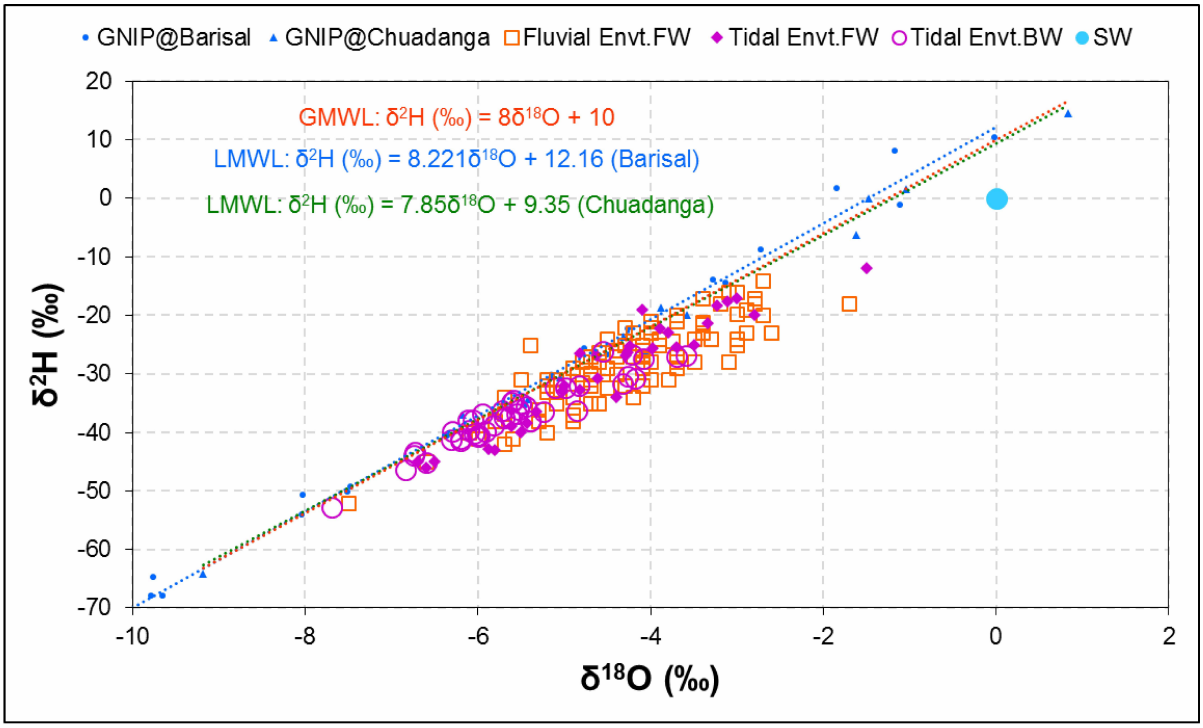

Figure 1: Cross plot between stable oxygen ($\delta^{18}O$) and deuterium ($\delta^{2}H$) isotopes

GNIP: Global Network of Isotopes in Precipitation, Envt.: Environment, FW: Freshwater (≤2000 µS/cm), BW: Brackish water (>2000 µS/cm), SW: Seawater

©2019. Japan Geoscience Union. All Right Reserved.

Groundwater chemistry in the Gunii Khooloi basin, Southern Gobi Region of Mongolia using multivariate analysis

*Batdemberel BAYANZUL[1,2], Isao Machida[3], Kengo Nakamura[2], Noriaki Watanabe[2], Takeshi Komai[2]

1. School of Geology and Mining Engineering, Mongolian University of Science and Technology, 2. Graduate School of Environmental Studies, Tohoku University, 3. Groundwater research group, Advanced Industrial Science and Technology

Water plays a vital role in the southern part of Mongolia where is climatically classified as an arid and semi-arid region, so called Southern Gobi Region of Mongolia (SGR). Groundwater serves as the only source of water supply and is largely utilized by mining companies such as the Tavan Tolgoi and Oyu Tolgoi Mine located in the SGR. The area is expected to face severe water shortages of mining and drinking water, which may be related to changes in groundwater recharge due to climate change. Understanding the geochemical evolution of groundwater and recharge mechanisms in the Gunii Khooloi basin is thus paramount for water resource management in this region. However, chemical compositions of groundwater in the SGR has not been studied so far.

In this study, the hydrogeochemical approaches have been introduced to characterize hydrogeochemical characteristics and its associated recharge processes in the Gunii Khooloi basin. To investigate this hydrogeochemical study, springs, groundwater in shallow wells and deep wells in the study area were sampled twice (in September 2016, and in June 2017). A total of 95 groundwater samples were collected within these two years for major chemical analysis in order to understand the general hydrogeochemical conditions of the Gunii Khooloi basin.

Here, we will present the groundwater chemical properties and relationship between shallow and deep groundwater in the Gunii Khooloi basin clarified by multivariate statistical analysis, such as principal component analysis (PCA) and hierarchical cluster analysis (HCA).

Keywords: Groundwater chemistry, Principal component analysis, Southern Gobi Region of Mongolia

©2019. Japan Geoscience Union. All Right Reserved.

Temporal observation of molybdenum concentrations in rivers from Erdenet mining area, Mongolia

*Solongo Tsetsgee[1], Keisuke Fukushi[1], Altansukh Ochir[2], Takahashi Yoshio[3], Ariuntungalag Yunden[2], Enkhjin Odgerel[2], Noriko Hasebe[1]

1. Kanazawa University, 2. National University of Mongolia, 3. The University of Toyko

Erdenet mine is one of the world’ s largest copper–molybdenum mine. This study is conducted the temporal observation of Mo concentrations in river waters. The waters were collected from three rivers, flowing thought Erdenet city, during 9 months in 2018 March to November.
During the summer Mo concentration was increasing with temperature and pH. On the other hand, When the winter was starting low concentration of Mo with low temperature and pH. The Mo concentration is positively correlated with pH and temperature. The tailing pond sample pH slightly lower than rivers due to it couldn’ t be increase of pH in river water. And also, sediment result showed that Mo concentration is lower than water. Therefore, another possibility of reason could be relating to the white dust and it can be increase pH of water.
A huge tailing pond is located in the north of the Erdenet area. It is recognized that the dried precipitates formed by the neutralization of the acidic mine water in the tailing ponds are dispersed widely in the Erdenet area by wind. The dried precipitates (so called white dust) are mainly composed with lime or carbonates containing high amount of Mo. It can be expected that the white dust may dissolve with rainwater. The increase of Mo concentrations associated with the increase of pH may be caused by the dissolution of the white dust at summer rainy season.

Keywords: Molybdenum , pH, Erdenet mine, River water, Temporal observation

©2019. Japan Geoscience Union. All Right Reserved.

[E] Oral | A (Atmospheric and Hydrospheric Sciences)：A-HW Hydrology & Water Environment

Wed. May 29, 2019 10:45 AM - 12:15 PM JST | Wed. May 29, 2019 1:45 AM - 3:15 AM UTC | 103 1F

[A-HW23] Hydrology & Water Environment

convener:Isao Machida(Geological Survey of Japan), Dai Yamazaki(Institute of Industrial Sciences, The University of Tokyo), Takeshi Hayashi(Faculty of Education and Human Studies, Akita University), Keisuke Fukushi(Institute of Nature & Environmental Technology, Kanazawa University), Chairperson:Keisuke Fukushi

We focus on various issues of water cycle and environment and aim to answer questions of hydrological and earth system sciences including 1) surface, subsurface and evapotranspiration processes of water cycle; 2) natural and anthropogenic hydrothermal systems, 3) environments issues and studies on a watershed or global scale, 4) water-related issues with ecological, environmental, and geochemical aspects, and 5) other issues in hydrological sciences. This session welcomes presentations regarding various kinds of approaches and techniques such as field survey, remote sensing, isotope tracers, numerical simulation, and theoretical analysis.

10:45 AM - 11:05 AM JST | 1:45 AM - 2:05 AM UTC

[AHW23-18] Solid-water interaction of Mn and As near the bottom of Lake Biwa. –Implications for the spatio-temporal change of these elements for past 40 years-

★Invited Papers

*TAKAAKI ITAI[1], SACHIKA NATORI[1] (1.Department of Earth and Planetary Science, The University of Tokyo)

11:05 AM - 11:20 AM JST | 2:05 AM - 2:20 AM UTC

[AHW23-19] **Sources, pathways and treatment of contaminants in surface water: Applicability in developing countries**

*Mst. Shamsun Nahar[1] (1.Earth Consultant Co. Ltd, Toyama, Japan)

11:20 AM - 11:35 AM JST | 2:20 AM - 2:35 AM UTC

[AHW23-20] **Numerical simulations (COMSOL) of γ-Fe_2O_3 nanohybrids for transport (3D) and arsenic removal in homogeneous porous media**

*Ajay Kumar[1], Himanshu Joshi[1], Anil Kumar[1] (1.INDIAN INSTITUTE OF TECHNOLOGY ROORKEE, INDIA)

11:35 AM - 11:50 AM JST | 2:35 AM - 2:50 AM UTC

[AHW23-21] **Transport processes of suspended solids in the Kumaki River inferred from atmospheric radionuclides**

*Shinya Ochiai[1], Ryunosuke Tahara[2], Tetsuya Matsunaka[1], Seiya Nagao[1] (1.Institute of Nature and Environmental Technology, Kanazawa University, 2.Graduate School of Natural Science and Technology, Kanazawa University)

11:50 AM - 12:05 PM JST | 2:50 AM - 3:05 AM UTC

[AHW23-22] Using tritium in Japanese precipitation for tritium-tracer transit time studies across Asia

*Maksym Gusyev[1], Yoshito Kikumori[1], Terumasa Nishihara[2], Takeshi Hayashi[3], Kimpei Ichiyanagi[4], Naofumi Akata[5], Tomoki Oda[6], Uwe Morgenstern[7], Michael Stewart[7] (1.International Centre for Water Hazard and Risk Management (ICHARM), Public Works Research Institute (PWRI), 2.Civil Engineering Research Institute for Cold Region, PWRI, 3.Akita University, 4.Kumamoto University, 5.National Institute for Fusion Science (NIFS), 6.University of Tokyo, 7.GNS Science, New Zealand)

12:05 PM - 12:15 PM JST | 3:05 AM - 3:15 AM UTC

Discussion

Solid-water interaction of Mn and As near the bottom of Lake Biwa. –Implications for the spatio-temporal change of these elements for past 40 years-

*TAKAAKI ITAI[1], SACHIKA NATORI[1]

1. Department of Earth and Planetary Science, The University of Tokyo

Enrichment of Mn and As in the surface of sediment caused by diagenetic process has been reported from various lakes in the world. Lake Biwa is a typical example, in which clear enrichments of Mn (up to 5.7 wt%) and As (up to 900 mg/kg) within thin surface enriched layer (< 2 cm) of sediment were observed. This enrichment is caused by the accumulation of manganese oxide and arsenate both of which show lower mobility than these reducing chemical forms. However, decreasing trend of interannual minimum dissolved oxygen level reported from the lake-bottom can change redox behavior of these elements near the sediment-water interface (Itai et al. 2012, Sohrin et al. 2016, Fukushima et al. 2019). Through the geochemical survey after 2009, some specific scientific questions have been arisen.

(i) The degree of surface enrichment of Mn and As from 7 stations in northern lake were markedly increased in 2009 relative to 1977 (Itai et al., 2012). However, the source of them and process of this change are unclear.

(ii) The temporal increase of As in sediment is particularly significant in southern basin of northern lake (so called “first-basin”). The As accumulated on the surface of sediment is likely by scavenging from water column rather than upward diffusion from buried sediment. Nevertheless, difference between northern and southern basin (so called “second-basin”) is unclear.

(iii) Past study suggest that Mn and As level in sediment can be a unique indicator of palaeo water depth (Takamatsu, 1985). This is plausibly caused by higher enrichment of Mn and As toward deeper part of the lake. We confirmed this trend via measurement of 22 core sediments from northern lake. We hypothesize that this distribution is attributed to the geochemical focusing (Schaller et al., 1997), although scientific evidences are still not enough. Besides, there should be some specific mechanism to keep Mn and As enrichment after buried into deep sediment.

In order to answer these questions, we need comprehensive geochemical survey between water column and sediment with focusing speciation of these metals. In the presentation, we would like to present our dataset of lake water (3 stations, 10 m depth interval, 1 year), sediment core (30-40 cm depth, 22 stations), porewater (30 - 40 cm depth, 7 stations), filtered materials of 1, 3, 5, 7, 9 m from lake bottom (7 stations) characterized by X-ray absorption spectroscopy, micro beam chemical analysis, water chemistry analysis, porous diffusion model, and aqueous speciation calculation. Coupling with available monitoring data after 1950s, we make some constraints for the above questions.

Keywords: manganese, arsenic, speciation, redox environment, temporal change, lake sediment

©2019. Japan Geoscience Union. All Right Reserved.

Sources, pathways and treatment of contaminants in surface water: Applicability in developing countries

*Mst. Shamsun Nahar[1]

1. Earth Consultant Co. Ltd, Toyama, Japan

This report presents the contamination degree, occurrence, distribution characteristics in the surface water and sediments from Dhaka Rivers (Buriganga and Shitalakshya River) and the Bay of Bengal coast of Bangladesh. A model water treatment method is developing using Baburail Canal Water linked with Shitalakshya River, a World Bank supported project, under Narayanganj City Corporation, Bangladesh. By evaluating hypoxic to anoxic low dissolve oxygen (DO) (below the 0.85 mg/L critical level) associated with very high concentrations of biological oxygen demands (BOD) (5-10 mg/L) and toxic metals (Cr, As, Pb, Cd etc.) in surface water, a model treatment process is developing by using micro bubbling system for increasing the DO level, Neem leaves and bamboo powder are for heavy metals removal process and finally TiO_2 (P25)/ Fe^{+++} method is for the degradation and coagulation of organic content in treated water. The model method of this study should be applied to future water treatment focused on the potential to improve water quality in urban and surrounding areas in developing countries.

Keywords: Surface Water, Bay of Bengal, Dissolve Oxygen, Micro Bubbling System

©2019. Japan Geoscience Union. All Right Reserved.

Numerical simulations (COMSOL) of γ-Fe_2O_3 nanohybrids for transport (3D) and arsenic removal in homogeneous porous media

*Ajay Kumar[1], Himanshu Joshi[1], Anil Kumar[1]

1. INDIAN INSTITUTE OF TECHNOLOGY ROORKEE, INDIA

Worldwide, arsenic is a menace among the living communities due to its contamination in groundwater. It leaches moderately into groundwater from earth crust and bedrocks enriched with its ores. The countries like India and Bangladesh are being critically affected due to their densely populated areas. Several nanomaterials have been developed and examined as adsorbents for its removal, which are being utilized in *ex-situ* remediation technique. This technique has the disadvantages in terms of generating highly toxic waste, causes due to its easy mobilization in the living ecosystems. Nowadays, *in-situ* (subterranean) sequestration of arsenic is gaining considerable attention in respect to reduce the chance of its mobilization in living environment.

To this aim, the γ-Fe_2O_3 nanohybrids are developed using a novel approach of synthesis which include the usage of industry waste as one of precursor material. These nanoparticles have been found significantly stable in aqueous solutions representing real world groundwater conditions. The measured zeta (ζ)-potential value of -31.6 mV, indicated their significant colloidal stability. In respect to *in-situ* application, the understanding of transport modeling and retardation of nanomaterials in aquifer systems by simulating through numerical models in complex 3-dimensional scenario are necessary. Therefore, a modeling approach based on modified advection-dispersion-retardation equations has been investigated, considering the coupled influence of head difference and reaction rate of particle transport.

All the experiments were performed in a sand-tank set up (0.6 x 0.3 x 0.50 m) having several injection ports at variable depths. The tank was packed with the porous media (medium size sand) having the grain size (mm), grain density (g cm^{-3}), bulk density (g cm^{-3}) and effective porosity (%) values of 0.5-1.0, 2.33 ± 0.2, 1.55 ±0.09 and 0.34 ±0.1, respectively. The longitudinal and traverse dispersivity of consolidated media were calculated using NaCl as a tracer. The COMSOL Multiphysics model (subsurface module) was investigated for simulation of γ-Fe_2O_3 nanohybrids injection and their transport through porous media. Transport of arsenic and as-synthesized nanomaterial were modelled by considering these as solute and colloid, respectively, under fully saturated homogenous porous media and variable flow rate conditions. After simulation, the colloidal solution of nanoparticles was allowed to inject at the concentration of 1.25 x 10^{-4} mol m^{-3} and flow rate of 1.2 L h^{-1}. The simulation results were matched with the experimental observations which provided estimates of transport parameters. The retardation efficiency utilized to predict the γ-Fe_2O_3 nanohybrids in similar porous media, although the extend of injection pressure, colloid concentration and pumping rate may be underpredicted which require further investigations.

Keywords: Numerical modeling, In-situ arsenic sequestration, Groundwater

©2019. Japan Geoscience Union. All Right Reserved.

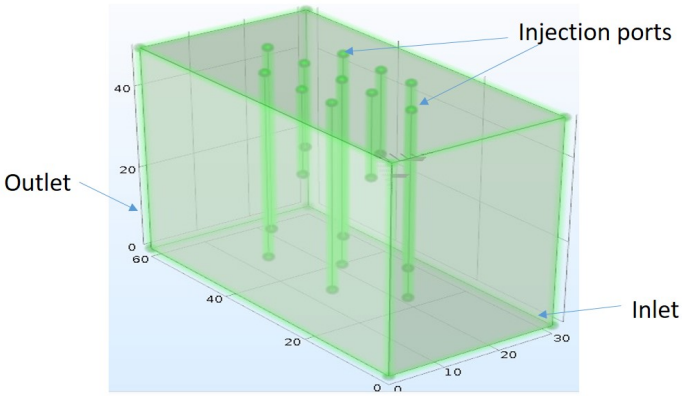

3-Dimesional view of Sand-Tank set up

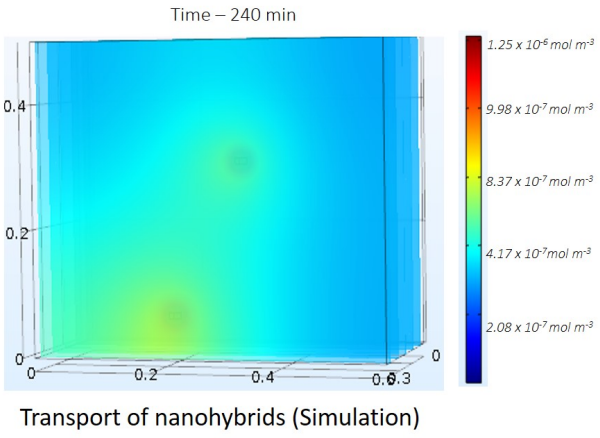

Transport of nanohybrids (Simulation)

©2019. Japan Geoscience Union. All Right Reserved.

Transport processes of suspended solids in the Kumaki River inferred from atmospheric radionuclides

*Shinya Ochiai[1], Ryunosuke Tahara[2], Tetsuya Matsunaka[1], Seiya Nagao[1]

1. Institute of Nature and Environmental Technology, Kanazawa University, 2. Graduate School of Natural Science and Technology, Kanazawa University

The Kumaki River, which drains into the Nanao Bay, is in the central part of the Noto Peninsula. Over recent years, the vegetation in the catchment area of the Kumaki River has changed, and the areas of unmanaged forest and cultivated areas have progressively increased because of plantation activities and decreasing and aging population. These anthropogenic catchment environmental changes may affect the erosion and transport of clastic materials and particulate organic matter to the lower reaches and coastal areas. It is therefore important to clarify the transport processes of these materials to achieve proper management and prediction of environmental changes in river watersheds and coastal areas.
To investigate the transport processes of suspended solids (SS) in the Kumaki River, the atmospheric radionuclides ($^{210}Pb_{ex}$, ^{7}Be, and ^{137}Cs) of SS samples were observed. The SS samples were obtained with a continuous centrifuge of the river water (100 L) collected at the three sampling points (upstream, midstream, and downstream) in Kumaki River every month since April 2016. The concentrations of atmospheric radionuclides in SS samples were measured with a Ge detector. The water discharge was also measured based on cross-sectional profiles of water depth and the flow velocity with a leveling rod and a flow meter at each sampling point.
The $^{7}Be/^{210}Pb_{ex}$ activity ratio of SS sample, which is related to the residence time of these radionuclides in the catchment area, showed clear positive correlation with the water discharge and it was high during winter season with higher precipitation in each sampling point. This result indicates that SS was transported in a shorter time scale during rainfall event and winter season. On the other hand, $^{7}Be/^{210}Pb_{ex}$ ratio exceptionally decreased during heavy rainfall events with the higher water discharge over the threshold value, implying that older stored sediment and subsurface soil were eroded and transported under these conditions. Temporal and spatial changes in ^{137}Cs concentration and $^{137}Cs/^{210}Pb_{ex}$ ratio of SS sample showed different fluctuation in each sampling point, suggesting that changes in discharge amount and source of SS were affected by the subcatchment-scale local hydrological environments and land use conditions.

Keywords: suspended solids, river catchment area, atmospheric radionuclides

©2019. Japan Geoscience Union. All Right Reserved.

Using tritium in Japanese precipitation for tritium-tracer transit time studies across Asia

*Maksym Gusyev[1], Yoshito Kikumori[1], Terumasa Nishihara[2], Takeshi Hayashi[3], Kimpei Ichiyanagi[4], Naofumi Akata[5], Tomoki Oda[6], Uwe Morgenstern[7], Michael Stewart[7]

1. International Centre for Water Hazard and Risk Management (ICHARM), Public Works Research Institute (PWRI), 2. Civil Engineering Research Institute for Cold Region, PWRI, 3. Akita University, 4. Kumamoto University, 5. National Institute for Fusion Science (NIFS), 6. University of Tokyo, 7. GNS Science, New Zealand

In order to improve management of water resources, water circulation times are estimated with the use of tritium-tracer in catchments across Asia. As an environmental tracer generated in the upper atmosphere, tritium in precipitation is influenced by latitude, season and altitude, and understanding of tritium inputs in water cycle components is needed to estimate mean transit times (MTTs). For future studies, we established the latitude scaling factors to the north and south of the Tokyo area, which has the tritium measurements in monthly precipitation from 1961 to present, by investigating the latitude tritium effect at selected coastal stations in Asia (Gusyev et al., 2016; 2019). In Japan, higher spring tritium was confirmed with winter and spring precipitation samples in 2016 and we observed the altitude effect in March-April snowpack in Hokkaido. The importance of latitude and altitude effects is demonstrated with annual tritium in precipitation at Japanese meteorological stations compared to Tokyo tritium, and with estimated MTTs using 2016 tritium winter and summer baseflow samples at headwater catchments of the Tone and Ishikari River basins, Japan.

References:

Gusyev M.A., Morgenstern U., Nishihara T., Hayashi T., Akata N., Ichiyanagi K., Sugimoto A., Hasegawa A., Stewart, M.K. (2019). Evaluating anthropogenic and environmental tritium effects using precipitation and Hokkaido snowpack at selected coastal locations in Asia. Science of the Total Environment 659: 1307-1321, doi: 10.1016/j.scitotenv.2018.12.342

Gusyev M.A., Morgenstern U., Stewart M.K., Yamazaki Y., Kashiwaya K., Nishihara T., Kuribayashi D., Sawano H. and Y. Iwami (2016). Application of tritium in precipitation and baseflow in Japan: a case study of groundwater transit times and storage in Hokkaido watersheds. *Hydrol. Earth Syst. Sci.*, 20, 1-16, doi:10.5194/hess-20-1-2016

Keywords: tritium in precipitation, scaling factors, tritium input, mean transit times

©2019. Japan Geoscience Union. All Right Reserved.

[E] Poster | A (Atmospheric and Hydrospheric Sciences)：A-HW Hydrology & Water Environment

Wed. May 29, 2019 3:30 PM - 5:00 PM JST | Wed. May 29, 2019 6:30 AM - 8:00 AM UTC | Poster Hall International Exhibition Hall8, Makuhari Messe_8

[A-HW23] Hydrology & Water Environment

convener:Isao Machida(Geological Survey of Japan), Dai Yamazaki(Institute of Industrial Sciences, The University of Tokyo), Takeshi Hayashi(Faculty of Education and Human Studies, Akita University), Keisuke Fukushi(Institute of Nature & Environmental Technology, Kanazawa University)

We focus on various issues of water cycle and environment and aim to answer questions of hydrological and earth system sciences including 1) surface, subsurface and evapotranspiration processes of water cycle; 2) natural and anthropogenic hydrothermal systems, 3) environments issues and studies on a watershed or global scale, 4) water-related issues with ecological, environmental, and geochemical aspects, and 5) other issues in hydrological sciences. This session welcomes presentations regarding various kinds of approaches and techniques such as field survey, remote sensing, isotope tracers, numerical simulation, and theoretical analysis.

[AHW23-P01] A multiobjective risk management model for real-time reservoir flood control operation

*Juan Chen[1,2], Ping-An Zhong[2], XinYu Wan[2], Yu Zhang[2] (1.College of Earth Sciences and Engineering, Hohai University, 2.College of Hydrology and Water Resources, Hohai University)

[AHW23-P02] Assessment of the Flow Regime of Roanoke River due to Climatic and Anthropogenic Activities

*Rahul Kumar Singh[1], Dr. Manoj Kumar Jain[1] (1.Indian Institute of Technology, Roorkee, India)

[AHW23-P03] Predictive Analysis of Climate, Water, Health and the Environment Nexus

*Abhishek [1], Deepika [2] (1.Technical University Dresden, GERMANY, 2.BPS Government Medical College for Women, Sonepat, INDIA)

[AHW23-P05] Severe droughts provide huge fuel for widespread wildfires in California in USA

*Linghua Qiu[1], Ji Chen[1], Haiyun Shi[2], Liqun Sun[3], Jun Niu[4] (1.the University of Hong Kong, 2.Southern University of Science and Technology, 3.Shenzhen Institutes of Advanced Technology, Chinese Academy of Sciences, 4.China Agricultural University)

[AHW23-P06] A comprehensive evaluation of MODIS-based water use efficiency with global eddy covariance flux data and a process model

*Shanshan YANG[1,2], Jiahua ZHANG[1], Sha ZHANG[1,2], Jingwen WANG[1,2], Yun BAI[1,2], Fengmei YAO[2], Huadong GUO[1] (1.Institute of Remote Sensing and Digital Earth, Chinese Academy of Sciences, 2.University of Chinese Academy of Sciences, Beijing, China)

[AHW23-P07] Impact of variability and anisotropy in the correlation decay distance for precipitation spatial interpolation in China

*yingxian zhang[1] (1.National Climate Center, China Meteorological Administration)

[AHW23-P08] New Record-Breaking Frequency of Annual Maximum Daily Precipitation of 58 stations in the whole Japan, an increasing of extreme values.

*Chhay Ngorn SEANG[1], Tomohito YAMADA[1] (1.Hokkaido University)

[AHW23-P09] Quantifying stemflow to better express its ecohydrological significance

*Shin'ichi Iida[1], Darryl E. Carlye-Moses[2], Sonja Germer[3], Pilar Llorens[4], Beate Michalzik[5], Kazuki Nanko[1], Alexander Tischer[5], Delphis F. Levia[6] (1.Department of Disaster Prevention, Meteorology and Hydrology, Forestry and Forest Products Research Institute, 2.Department of Geography and Environmental Studies, Thompson Rivers University, Kamloops, British Columbia, Canada, 3.Department of Bioengineering,

Leibniz Institute for Agricultural Engineering and Bioeconomy, Potsdam, Germany, 4.Institute of Environmental Assessment and Water Research (IDAEA-CSIC), Barcelona, Spain, 5.Soil Science, Institute of Geography, Friedrich Schiller University Jena, Jena, Germany, 6.Department of Geography and Department of Plant and Soil Sciences, University of Delaware, Newark, DE, USA)

[AHW23-P10] **Hydraulic analysis of overland flow caused by temporally varying rainfall**

*PING-CHENG HSIEH[1], Ming-Chang Wu[1] (1.National Chung Hsing University)

[AHW23-P11] A comparative Study on Water Environment of Isolated Islands - Focusing on Islands in Nagasaki Prefecture - (3)

*Go Yamaki[1], Koji Kodera[2], Kazuki Asami[1], Yoshihiro IGARI[1], Masaki Horiuchi[1] (1.Grad. Student, Hosei Univ., 2.Dep. of Geography, Hosei Univ.)

[AHW23-P12] **Water environment around Kusatsu-Shirane volcano and consideration of the effect of eruption in January 2018**

*Igari Yoshihiro[1], Koji Kodera[2], Kazuki Asami[1] (1.Grad.Student,Hosei Univ., 2.Dep.of Geography Hosei Univ.)

[AHW23-P13] Re-consideration of discharge rate of spring water in Lake Ezu, Kumamoto

*Kimpei Ichiyanagi[1], Kiyoshi Ide[1], Jun Shimada[1], Tsutomu Ichikawa[2] (1.Kumamoto University, 2.Tokai University)

[AHW23-P14] **Evaluating the efficacy of hydrologically and hydrodynamically driven methods of e-flow assessment for Upper Godavari River Basin, India**

*GAURAV KALIDAS PAKHALE[1], Jyoti Punjahari Nale[2], Ashvin Kumar Gosain[3], Rakesh Khosa[3] (1.PhD Research Scholar, Civil Engineering Department, Indian Institute of Technology, Delhi, 2.Project Advisor, IEWP, GIZ India, New Delhi, India, 3.Professor, Civil Engineering Department, Indian Institute of Technology, Delhi)

[AHW23-P15] Presence of pharmaceutical compounds in freshwater lakes and their impact on phytoplankton

*Nandakumar Kanavillil[1], Cassandra Fligg[1], Sreekumari Kurissery[1] (1.Lakehead University, Canada)

[AHW23-P16] **Novel approximate solutions for solute transport due to injections: considering the scale-dependent dispersion and non-integer flow dimension**

*Ye-Chen Lin[1], Hund-Der Yeh[1] (1.National Chiao Tung Univ.)

[AHW23-P17] Experimemtal study on the residual saturation of Porous Media using Pore Doublets Micromodel

*Chun-Wei Peng[1] (1.Taiwan National Chiao Tung University)

[AHW23-P18] Assessment of Synergy between Biomedical Waste and Shallow Groundwater Pollution

*Deepika [1], Abhishek [2] (1.BPS Government Medical College for Women, Sonepat, INDIA, 2.Technical University Dresden, GERMANY)

[AHW23-P19] Erosion and transport processes of earth surface materials in a reservoir-catchment system inferred from atmospheric radionuclides ^{7}Be and ^{210}Pb

*Mikiya Tsuruoka[1], Shinya Ochiai[2], Atsushi Matsuki[2], Seiya Nagao[2] (1.Graduate School of Natural Science and Technology, Kanazawa University, 2.Institute of Nature and Environmental Technology, Kanazawa University)

[AHW23-P20] Fluctuation of groundwater level in a sloping unconfined aquifer due to time varying recharge

*Ming-Chang Wu[1], Ping-Cheng Hsieh[1] (1.National Chung Hsing University)

[AHW23-P21] **Effect of cutoff wall on recharge water storage volume**

*Pei-hsun Tsai[1], Jung-hsing Tai[1] (1.Chaoyang University of Technology)

[AHW23-P22] **Studying Operation Parameters on Flat-Plate Membrane Bioreactor for Sewage Treatment**

*Jen Hung Chiu[1], Wen Chin Chen[1] (1.Studying Operation Parameters on Flat-Plate Membrane Bioreactor for Sewage Treatment)

[AHW23-P23] **Mine-water quality at a tertiary coalfield in India: Characterisation and treatment using novel polyvinyl alcohol (PVA) gel bioreactor**

*Aparna Dutta[1], Sudipta Sarkar[1] (1.Indian Institute of Technology Roorkee)

A multiobjective risk management model for real-time reservoir flood control operation

*Juan Chen[1,2], Ping-An Zhong[2], XinYu Wan[2], Yu Zhang[2]

1. College of Earth Sciences and Engineering, Hohai University, 2. College of Hydrology and Water Resources, Hohai University

Many uncertainties exit in the real-time reservoir flood control operation and bring risks to flood control decisions. A multiobjective optimization model is developed for the real-time risk management for the flood control operation of a reservoir system considering multiple uncertainties such as inflow forecast errors and outflow errors. The two competing objectives considered are: (1) minimizing the risk of reservoir upstream flooding and (2) minimizing the risk of downstream flooding. The optimization model seeks to find the operation schedules that satisfy the flood control objectives and simultaneously minimize the overall risks. The decision variables are the hourly reservoir releases. The formulated multiobjective optimization problem is nonlinear and non-convex, and is solved with an improved Non-dominated Sorting Genetic Algorithm-II (INSGA-II). We use a filtering algorithm to select representative non-dominated solutions from the Pareto front generated by INSGA-II to assist in real-time decision making. The proposed risk management model is applied to the Foziling reservoir in Huaihe river basin of China. The results show that the proposed method can provide a practical way to optimize the real-time flood control operation for risk management of a reservoir.

Keywords: Flood, Reservoir, Flood control operation, Risk assessment, Multiobjective optimization

©2019. Japan Geoscience Union. All Right Reserved.

Assessment of the Flow Regime of Roanoke River due to Climatic and Anthropogenic Activities

*Rahul Kumar Singh[1], Dr. Manoj Kumar Jain[1]

1. Indian Institute of Technology, Roorkee, India

The natural flow regime of many rivers around the world has been significantly altered due to climatic and anthropogenic modifications such as the construction of dams and reservoirs. The natural flow regime plays an important role in the development of the riverine ecosystem. Therefore, quantification of the extent of the alterations in the natural flow regime would be helpful in the river’ s ecological assessment. The Roanoke River in southeastern United States had one of the biggest and least disturbed forest ecosystems but due to climatic changes and anthropogenic actions such as construction of dam, artificial regulations of the natural flow regime, the overall riverine ecosystem has severely impacted. In this study, SWAT (Soil Water Assessment Tool) has been used to reconstruct the long-term unaltered streamflow for a hypothetical no-dam scenario condition, in order to assess the impact of climate change as well as due to construction of the John H Kerr reservoir on Roanoke River streamflow from 1956-2012. In order to simulate the unaltered streamflow series post construction of John H Kerr reservoir, 32 years (1916-1948) of observed gauge inflow prior to anthropogenic disturbance (due to construction of John H Kerr Reservoir) was used for calibration and validation of the parameters of the SWAT model. Historical land use and land cover backcasting data for the year 1938 has been used in the hydrological model to simulate the flow regime prior to construction of the dam and it was kept same during the whole simulation period. The SWAT model simulated observed gauge data with Nash-Sutcliffe efficiency coefficient (NSE) = 0.70, Percent bias (PBIAS) = 0.00 and the determination coefficient (R^2) = 0.73 during the calibration period (1916 - 1936), and performed equally better during the validation period (1937-1948) with NSE = 0.72, PBIAS = 0.00 and R^2 = 0.74. The indicators of hydrologic alteration (IHA) methodology has been used to assess the natural flow regime (no dam or reservoir moderated flow regime) characteristics under a simulated no-reservoir scenario (scenario1) and compare with the IHA results obtained based on the gauged streamflow downstream of the dam (scenario2). Hence, in case of scenario 1, the post-impact period has been taken as the simulated flow series using SWAT model from 1956-2012 and in case of scenario 2 the post-impact period has been taken as the gauged observed streamflow from 1956-2012 at Roanoke Rapids gauging station downstream of the reservoir. The pre-impact period for both the scenario was kept the same i.e. from 1912 to 1949. The results reveal that in case of the IHA assessment based on scenario 1, significant alterations have been observed in 5 out of 32 indicators compared to 13 out 32 indicators in case of scenario 2. The overall hydrologic alteration in case of scenario 1 was 45.65% and it was 55.17% in the case of scenario 2. The alteration during the scenario 1 could be attributed to the overall natural climatic variability. The results also indicate that flow variability in terms of high and low flows were better in scenario 1 compared to scenario 2 where the high flows were completely absorbed including the low pulse count and duration due to regulation in the flow. However, the reservoir operations enhanced the monthly flows including the multiday minima low flows. Thus, the present method can be treated as an easy-to-implement comprehensive approach for designing natural flow regimes to mimic the pre-impact flow condition in order to restore the ecosystem of modified rivers due to anthropogenic interventions.

Keywords: SWAT, IHA, Streamflow, Hydrologic Alteration, Ecosystem

©2019. Japan Geoscience Union. All Right Reserved.

Predictive Analysis of Climate, Water, Health and the Environment Nexus

*Abhishek -[1], Deepika -[2]

1. Technical University Dresden, GERMANY, 2. BPS Government Medical College for Women, Sonepat, INDIA

Amid the major demographic transition of developing world from a rural, agrarian society to an urban, industrial one, there is a need for predictive analytics of impact of the major biotic and abiotic stressors on the environmental constituents. The current study emphasizes the connections between climate, water, environment, and health and their interdependency followed by an impact assessment focusing on an urban environment. A data-driven hybrid framework for water resources assessment and management based on machine learning techniques was developed, calibrated and validated with the ground data for the sub-region scale of North-East Indian regime (mean spatial coordinates: 28° 38' 41.2800" N and 77° 13' 0.1956" E). The remote sensing data for land cover and land change were coupled with the climate model simulations to formulate the health risk assessment framework. The large ensemble of downscaled scenario based outputs including the effects of anthropogenic factors was used to drive the hybrid model framework.

Multi-dimensional Random Walk Metropolis (RWM) algorithms used to optimize the sample observations converged with an RMSE error of 0.18 with a range of 0.006. Pearson Product Moment Correlation coefficient range of all the ensemble members was 0.886-0.904. The prediction accuracy construed from 95 % model uncertainty bounds was 89-91 % for the constituent parameters. The sensitivity analysis revealed that the climate is the key parameter and is the most sensitive for all other linkage units followed by water availability and health factors. Comparative analysis of the simulated- and experimental results enforced comprehensive clarification of the assumptions made therein. By real-time monitoring and forecasting the vital impacts, this research will serve and benefit local policymakers and in the decision-making process, particularly regarding water resources vulnerability and future availability with significant economic consequences. The upscaling of the model form sub-regional to regional scale is well underway.

Keywords: Climate Change, Urbanization, RWM algorithm, Ensemble model

©2019. Japan Geoscience Union. All Right Reserved.

Severe droughts provide huge fuel for widespread wildfires in California in USA

*Linghua Qiu[1], Ji Chen[1], Haiyun Shi[2], Liqun Sun[3], Jun Niu[4]

1. the University of Hong Kong, 2. Southern University of Science and Technology, 3. Shenzhen Institutes of Advanced Technology, Chinese Academy of Sciences, 4. China Agricultural University

The frequently occurred large wildfires in California caught the public’ s attention in recent years and the ability to identify and prevent such disasters is pressing. The study built the rational relationship between soil moisture and vegetation based on remote sensing, hydrology and wildfire data during 2001-2017 in California. The purpose is to estimate the effects of droughts on wildfires and to detect the valid fuel for wildfires. The study results reported that severe droughts could cause huge fuel for wildfires and made them even much more widespread and longer sustained. The consequences could provide significant information for identification and prevention of future wildfires in California and even other regions in the world.

Keywords: Fuel, Wildfires, Droughts, Soil moisture, Vegetation

©2019. Japan Geoscience Union. All Right Reserved.

A comprehensive evaluation of MODIS-based water use efficiency with global eddy covariance flux data and a process model

*Shanshan YANG[1,2], Jiahua ZHANG[1], Sha ZHANG[1,2], Jingwen WANG[1,2], Yun BAI[1,2], Fengmei YAO[2], Huadong GUO[1]

1. Institute of Remote Sensing and Digital Earth, Chinese Academy of Sciences, 2. University of Chinese Academy of Sciences, Beijing, China

Ecosystem water use efficiency (WUE), defined as the ratio of gross primary productivity (GPP) to evapotranspiration (ET), is an important indicator to investigate the interaction between the terrestrial carbon and water cycles. The spatiotemporal patterns of WUE inferred from MODIS GPP and ET products and its responses to environmental factors have been analyzed, however, the accuracy of MODIS-derived WUE (MODIS WUE) has not been well evaluated. In this study, we evaluated monthly and annual MODIS WUE using global covariance flux data (FLUXNET2015 dataset) during 2000-2014, and conducted global intercomparisons (2001-2011) among annual WUE from MODIS, gridded FLUXNET (MTE) and a process model (BESS). Site scale (53 sites) evaluation results revealed that MODIS gave reliable estimates for GPP and ET, however, the performances of MODIS WUE was poor for monthly WUE (R2=0.14) and even worse for annual WUE (R2=0.08). MODIS WUE was generally underestimated with a bias of -0.21 gC kg-1 H2O (-8.43%) and RMSE of 1.20 gC kg-1 H2O for monthly WUE, and a bias of -0.28 gC kg-1 H2O (-11.31%) and RMSE of 0.98 gC kg-1 H2O for annual WUE. Among all land cover types, MODIS WUE performed relatively better in savannas and woody savannas for monthly WUE and grasslands for annual WUE, but significantly overestimated WUE in open shrublands. Likewise, MODIS WUE was obviously overestimated in hot and cold semiarid and arid climate zones. The global intercomparison results demonstrated that the spatial pattern of MODIS WUE was broadly similar to that of MTE and BESS WUE, except for the tropical and subtropical arid and semiarid areas. In these regions MODIS WUE showed extremely high values with large uncertainty and different linear trends compared with MTE and BESS WUE. These disagreements were mainly caused by the discrepancies in MODIS ET. Therefore, the uncertainty of MODIS WUE in the tropical arid and semiarid areas should be taken with caution when using MODIS WUE to investigate and interpret how WUE varies spatially and its responses to climate change. Furthermore, the accuracy of MODIS GPP and ET datasets should be paid extra attention since the quality of both GPP and ET would directly affect the WUE accuracy.

Keywords: Water use efficiency (WUE), Evaluation, Intercomparison, MODIS, FLUXNET, BESS

©2019. Japan Geoscience Union. All Right Reserved.

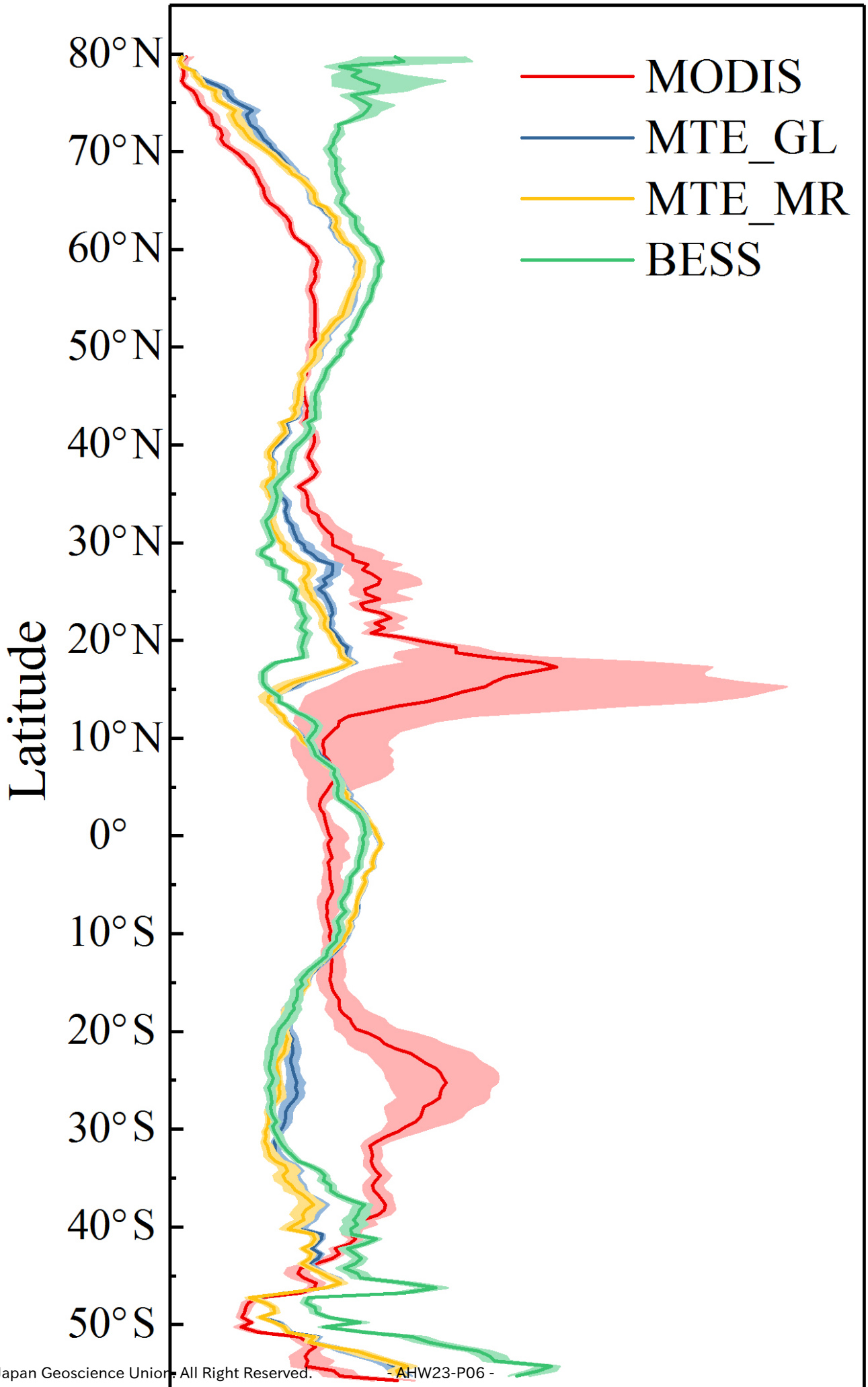

©2019. Japan Geoscience Union. All Right Reserved.

©2019. Japan Geoscience Union. All Right Reserved.

Impact of variability and anisotropy in the correlation decay distance for precipitation spatial interpolation in China

*yingxian zhang[1]

1. National Climate Center, China Meteorological Administration

The correlation decay distance (CDD) plays a key role in the angular-distance weighting (ADW) interpolation technique, being used as the searching radius to select correlated neighbors and to calculate the relative weights. The CDD of daily precipitation in China varies spatially and seasonally, and it presents anisotropic behavior, as a result of topography and the predominant atmospheric circulation. In general, CDD is largest in winter and smallest in summer, except for limited regions such as the Tibetan plateau. From a cross validation analysis, it is found that taking account of spatial and seasonal variations in CDD generally improves the ADW interpolation. Utilization of anisotropic CDDs increases the interpolation skill scores in regions with a dense monitoring network, significant elevation variation (southwestern China) or strongly anisotropic CDDs (Tibetan plateau).

Keywords: daily precipitation, correlation decay distance, ADW interpolation

©2019. Japan Geoscience Union. All Right Reserved.

New Record-Breaking Frequency of Annual Maximum Daily Precipitation of 58 stations in the whole Japan, an increasing of extreme values.

*Chhay Ngorn SEANG[1], Tomohito YAMADA[1]

1. Hokkaido University

The changes in daily temperature extremes in global scale have affected the weather and climate extreme events when there is an increase of greenhouse gas GHG compare to the industrialization in the 19th century (IPCC, 2014). Yamada et al. (2014) illustrate that the water vapor and convective instability follow the Clausius-Clapeyron-like rate of change with 99th percentile hourly precipitation intensity. Lehmann, J. et al. (2015), on another hand, studied globally the characteristic of precipitation change anomaly using a relation of the Clausius-Clapeyron model. By the way, the climate change tends to include another factor, which is more statistical base. The theory of record values in independent and identically distributed (i.i.d) random variable is studied more extensively and is more applicable with an assumption of stationary climate. The Clausius-Clapeyron equation is then also applicable base on the thermodynamic term which illustrates the relation of the temperature, vapor pressure and precipitation formation characteristic which also mentioned in the above previous studies. At the first stage, 58 stations of AMeDAS data with 117-years period across Japan are used for this analysis. The result shows that mean long-term precipitation of these 58 stations is higher than the mean value from theory i.i.d random variable of stationary climate. From this result, it can be implied that the change of precipitation in Japan is influenced by the drift term either of climate change or the heat island. In this case, the Clausius-Clapeyron equation is applied to identify the temperature term of change. This study tries to formulate a theory which more statistical base of climate drifts, non-stationary and non-identically to extreme events in accordance with time series. Clausius-Clapeyron Model and the Linear Drift Model is considered to form an empirical stochastically based on climate trend.

Keywords: Clausius-Clapeyron, New record Breaking, i.i.d

©2019. Japan Geoscience Union. All Right Reserved.

Quantifying stemflow to better express its ecohydrological significance

*Shin'ichi Iida[1], Darryl E. Carlye-Moses[2], Sonja Germer[3], Pilar Llorens[4], Beate Michalzik[5], Kazuki Nanko[1], Alexander Tischer[5], Delphis F. Levia[6]

1. Department of Disaster Prevention, Meteorology and Hydrology, Forestry and Forest Products Research Institute, 2. Department of Geography and Environmental Studies, Thompson Rivers University, Kamloops, British Columbia, Canada, 3. Department of Bioengineering, Leibniz Institute for Agricultural Engineering and Bioeconomy, Potsdam, Germany, 4. Institute of Environmental Assessment and Water Research (IDAEA-CSIC), Barcelona, Spain, 5. Soil Science, Institute of Geography, Friedrich Schiller University Jena, Jena, Germany, 6. Department of Geography and Department of Plant and Soil Sciences, University of Delaware, Newark, DE, USA

Stemflow is the flow of rainwater over the exterior of a tree stem to its base. Due to water balance calculations to obtain interception loss of forest stands, and the sometimes low percentage of stemflow as a function of rainfall, some literature ignores the ecohydrological significance of stemflow. However, stemflow is much more concentrated than throughfall per unit area. In recognition of the extreme amounts of water input to the small area around tree trunks, we advocate for two metrics to better express stemflow in relation to its ecohydrological importance: namely, the stand-scale funneling ratio and the stand-scale infiltration funneling ratio. We calculated these metrics based on measurements carried out in a tropical dry deciduous forest and a subpolar juvenile coniferous stand, and found that these are significantly larger than throughfall on both sites. The data cited from recent papers (n=34) showed that very small stand-scale amount of stemflow (approximately 0.5% on average) were necessary to make the stand-scale funneling ratio to be equal or more than unity. Moreover, the infiltration area of stemflow is generally < 0.2 m^2 due to the high infiltration capacity of top soil of forests, generally resulting in the stand-scale infiltration funneling ratio substantially greater than unity. Thus, stemflow is more effective for soil water recharge than throughfall. We recommend use of these metrics to better express ecohydrological importance of stemflow.

This presentation is based on the published paper as follows:
Carlye-Moses, D.E., Iida, S., Germer, S., Llorens, P., Michalzik, B., Nanko, K., Tischer, A., Levia, D.F. (2018): Expressing stemflow commensurate with its ecohydrological importance. Advances in Water Resources, 121, 472-479. Free open access article to: https://doi.org/10.1016/j.advwatres.2018.08.015

Keywords: Stemflow, Funneling ratio, Forest hydrology

©2019. Japan Geoscience Union. All Right Reserved.

Hydraulic analysis of overland flow caused by temporally varying rainfall

*PING-CHENG HSIEH[1], Ming-Chang Wu[1]

1. National Chung Hsing University

With the development of human civilization and population migration, we use many different types of pervious or impervious materials to cover the original surface. As a result, the surface friction and water permeability are reduced, resulting in increased flow velocity and runoff, and thus increasing the frequency and scale of flood occurrence. Therefore, predicting changes in overland flow caused by rainfall has become an important issue.

This study intends to simulate the overland flow under different rainfall patterns by the theory of diffusion wave model. The diffusion wave equation was used as the governing equation, and an analytical solution of the water depth by the generalized integral transformation method was presented. Since the values of the parameters used in previous research for diffusion wave models vary in an extensive range. In this study, the parameters were adjusted for each location to ensure the rationality of the simulation results according to the law of mass conservation.
The results show that for the non-uniform rainfall, the peak water depth and peak flow due to the post-peak rainfall are the largest, followed by the third quarter peak rainfall; whereas the average flow velocity of the mid-peak rainfall is the largest, followed by the third quarter peak rainfall. The peak water depth, peak flow rate and average flow rate due to the double peak rainfall are the smallest among the six rainfall patterns in this study.

Keywords: overland flow, nonuniform rainfall, diffusion wave

©2019. Japan Geoscience Union. All Right Reserved.

A comparative Study on Water Environment of Isolated Islands - Focusing on Islands in Nagasaki Prefecture - (3)

*Go Yamaki[1], Koji Kodera[2], Kazuki Asami[1], Yoshihiro IGARI[1], Masaki Horiuchi[1]

1. Grad. Student, Hosei Univ., 2. Dep. of Geography, Hosei Univ.

1. Introduction Research on islands in Nagasaki prefecture has hardly been investigated and research has been promoted since 2014 from Goto Island Islands, Tsushima, Iki, Hirado. For this time, we will clarify the water environment in each area from the relationship with land use and climate, and make it a foothold to clarify the material cycle of each island.

2. Target area Iki is rugged with a maximum altitude of 213 m, and there are numerous reservoirs in various parts of the island. In Tsushima, the altitude of the entire island is relatively high, and the mountains occupy about 89%. The Goto Islands Island consists of about 140 large and small islands, with large geological differences on each island. The Hirado Islands have many mountains while the fields are also relatively large. The population penetration rate of wastewater treatment in both areas is as low as 20-40%.

3. Research method Field survey was conducted 2 to 4 times a year from 2014 after organizing and examining existing research. On the site, water temperature, temperature, electric conductivity (EC), pH and RpH, COD were measured, and water was taken to measure the total organic carbon and the main dissolved components.

4. Results and discussion In Iki, the influence of agriculture appears in EC and TOC, but it is interesting that there is almost no effect of nitric acid. On the other hand, although many nitric acid was detected in the Goto Islands, it is thought that factors are due to paddy fields in Iki and upland fields in Goto Islands. Tsushima showed relatively low concentrations of EC and dissolved components, and seasonal changes also appeared. In Hirado Island, especially in the southern part, the geological influence is large in many places, the impact of sea salt is strong in Ikitsuki island and Azuchi Oshima. EC tends to rise in rainwater from October to March, pH tends to decrease. From the above, it is considered that the difference in the quality of the islands is greatly influenced by the difference of geology, topography and agricultural form.

Keywords: Iki island, Tsushima islands, Goto islands, Hirado islands, Water environment

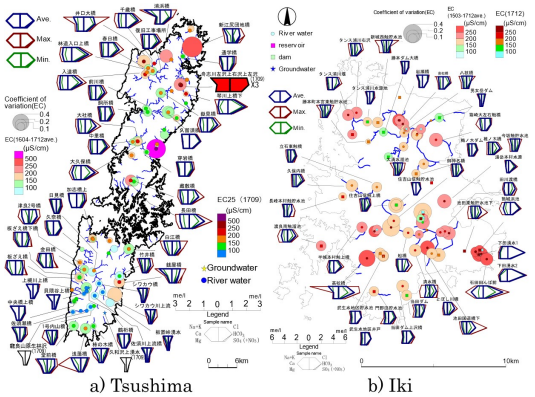

a) Tsushima b) Iki c) Hirado

Fig.1 Water quality

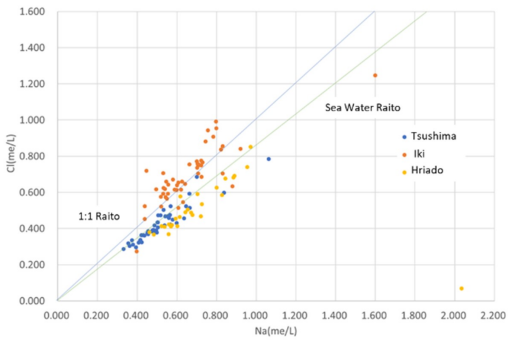

Fig.2 Na / Cl ratio

©2019. Japan Geoscience Union. All Right Reserved.

Water environment around Kusatsu-Shirane volcano and consideration of the effect of eruption in January 2018

*Igari Yoshihiro[1], Koji Kodera[2], Kazuki Asami[1]

1. Grad.Student,Hosei Univ., 2. Dep.of Geography Hosei Univ.

1. Introduction

The eruption (steam explosion) occurred in Mt.Motoshirane (One of Kusatsu-Shirane Volcano) on January 23, 2018. In this area, water quality survey of water environment began in May 2017 before the eruption. In addition to examining the influence on the water quality before and after the eruption, we studied the elution component of volcanic ash and the influence on the water environment. We also attempted to consider water quality forming factors in river water around Kusatsu-Shirane volcano.

2. Research method

We conducted about 21 field surveys from May 2017 to March 2019. The survey site is about 45 sites, centering on rivers flowing in the east and south of the mountain. Temperature, water temperature, pH, RpH, EC, and flow rate were measured locally, and the sampled sample was analyzed for the main dissolved components. In February 2018, we investigated the deposition situation and ash fall volume of volcanic ash and conducted sampling, and carried out dissolution experiment. In addition to rivers, field surveys and sampling of lakes and precipitation, snow cover, hot spring water were conducted.

3. Results and discussion

In Shirasuna River flowing to the east side of the mountain, groundwater and river water influenced by hot spring drainage and volcanic activity flow in from the tributary. There are points where the EC value fluctuates greatly, and it is influenced by the discharge and conduction of the dam which stores the neutralizing water of acidic rivers. In the Gando Swamp where the site of sulfur mine is located in the upstream part, the water quality is around pH:2.0, EC:6000 μS/cm. It is conceivable that the deposited volcanic ash affects the quality of the surrounding river due to snow melting water and precipitation.

Keywords: Mt.Kusatsu-Shirane, Volcano, Water environment, Eruption, Hot spring

©2019. Japan Geoscience Union. All Right Reserved.

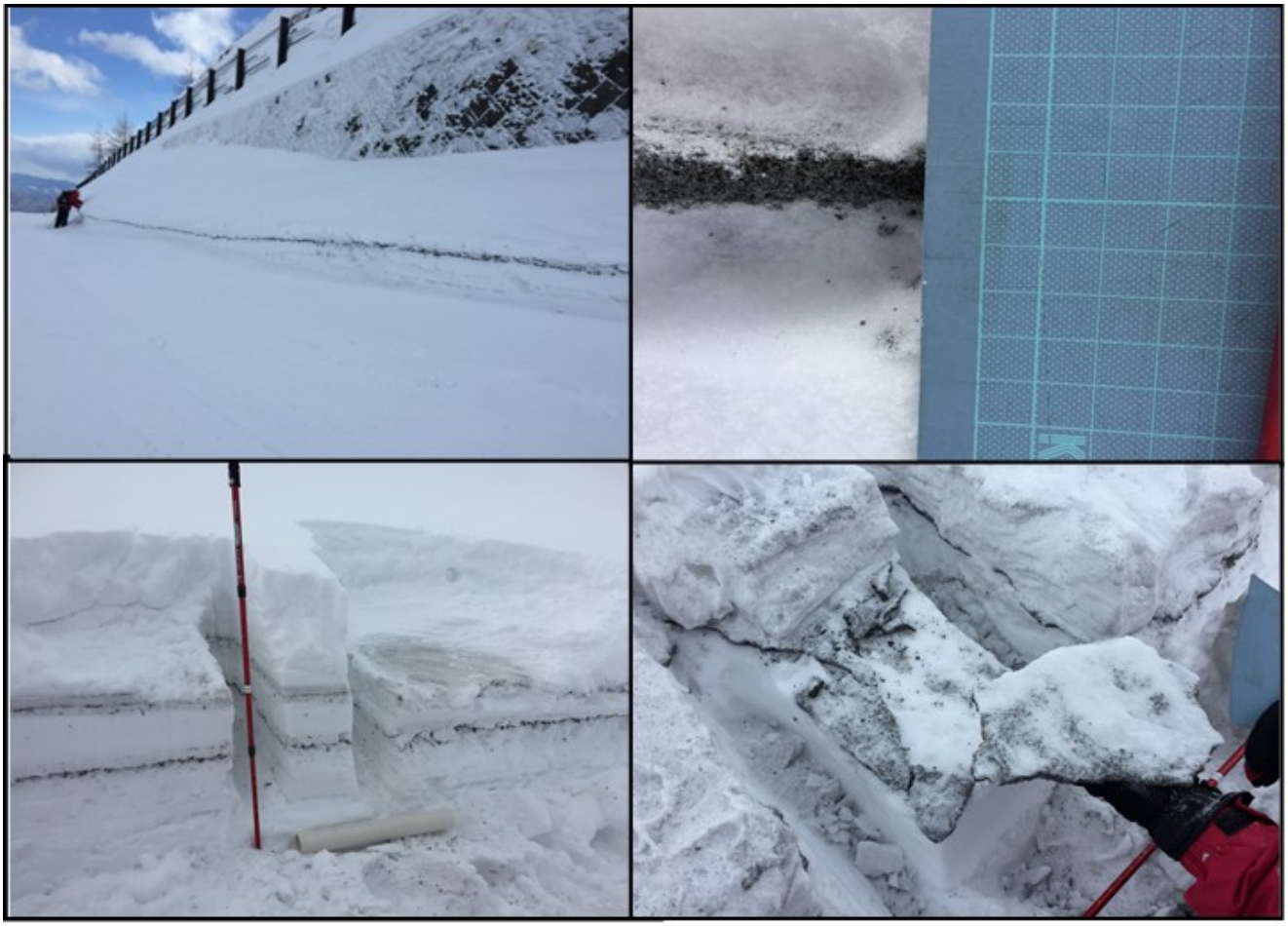

Picture.1 Ash fall in the east foot of Kusatsu-Shirane volcano (February 6, 2018)

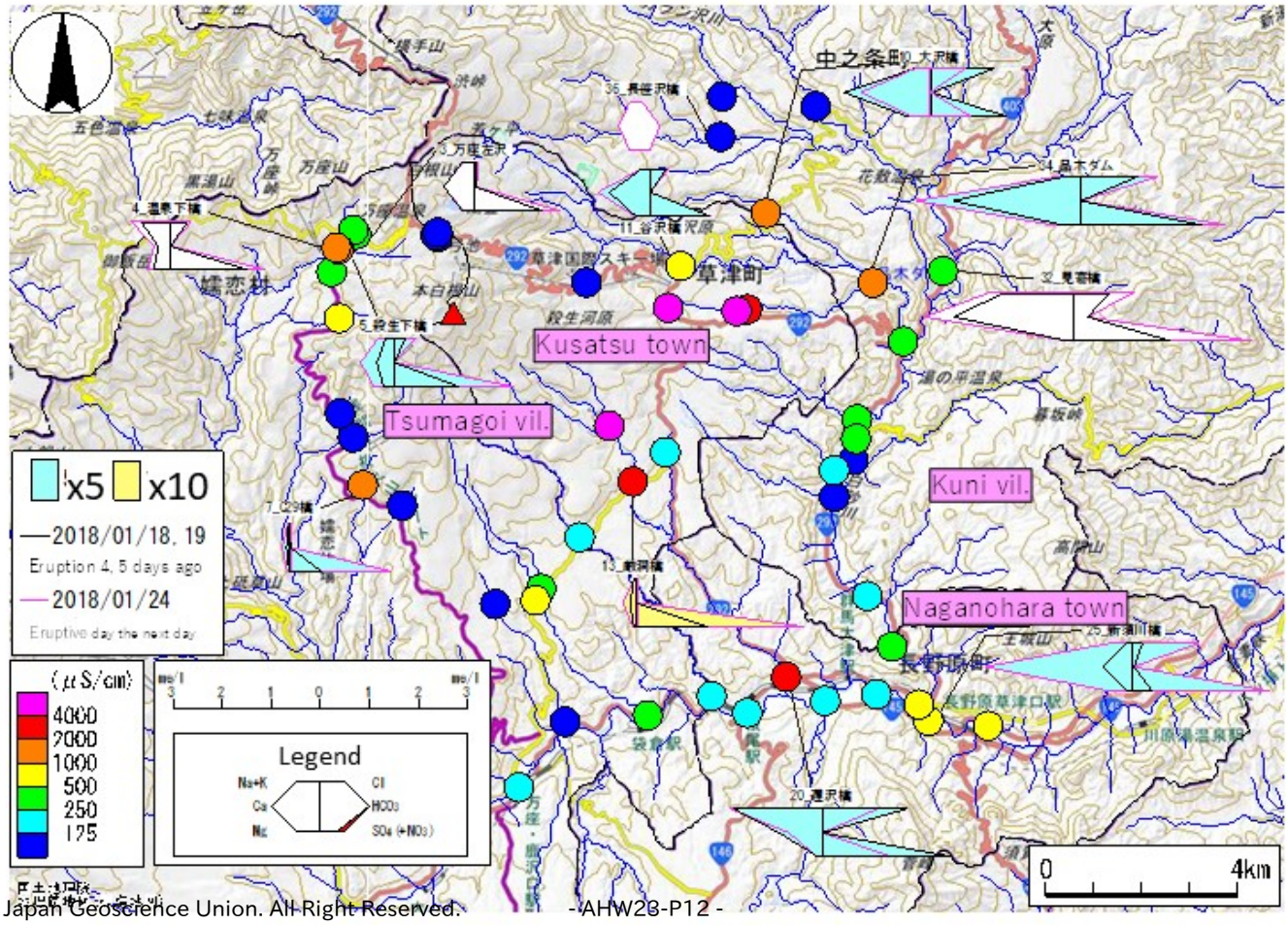

©2019. Japan Geoscience Union. All Right Reserved.

©2019. Japan Geoscience Union. All Right Reserved.

Re-consideration of discharge rate of spring water in Lake Ezu, Kumamoto

*Kimpei Ichiyanagi[1], Kiyoshi Ide[1], Jun Shimada[1], Tsutomu Ichikawa[2]

1. Kumamoto University, 2. Tokai University

In Kumamoto area, 100% of tap water is sourced from abundant groundwater. Recently, there is a great fear of groundwater level decreasing. To estimate discharge rete of spring water in Lake Ezu, the flow rate at 13 sites has been observed every month since December 1991. In previous studies, the total discharge rate of spring water was calculated by flow rates only at the most downstream, the most upper-stream, and incoming streams. In this study, total discharge rate from December 1991 to December 2014 was re-considered as a sum of three zones, that is upper-stream area, Kami-Ezu Lake, and Shimo-Ezu lake. When the discharge rate in each zone became negative, the case 1 where calculation was carried out with minus and the case 2 where it assumed to 0m^3/day were compared. As a result, total discharge rate gradually declined from about 450,000m^3/day in 1992 to about 360,000m^3/day (case 1) and to about 410,000m^3/day (case 2) in 2005. In July 2006, total discharge rate rapidly increased with heavy rainfall. After that, it had fluctuated about 400,000 to 500,000m^3/day in both cases. The discharge rate of Shimo-Ezu Lake sometimes became negative after 2003, and that averaged after July 2006 in case 2 was about 90,000m^3/day more than the case 1. As a result of comparing seasonal variability of discharge rate, monthly mean values of total and Shimo-Ezu Lake are low in April-May and high in October-November. However, monthly mean values of upper-stream area and Kami-Ezu Lake show no significant seasonal fluctuation. Monthly mean values of Shimo-Ezu Lake in August averaged after 2006 was about -14,000m^3/day in case 1 and about 32,000 m^3/day in case 2. Since negative value is not suitable to represent seasonal fluctuation, case 2 is proper to represent the discharge rate of spring water.

Keywords: spring water, Lake Ezu, long-term trend, seasonal variability

©2019. Japan Geoscience Union. All Right Reserved.

Evaluating the efficacy of hydrologically and hydrodynamically driven methods of e-flow assessment for Upper Godavari River Basin, India

*GAURAV KALIDAS PAKHALE[1], Jyoti Punjahari Nale[2], Ashvin Kumar Gosain[3], Rakesh Khosa[3]

1. PhD Research Scholar, Civil Engineering Department, Indian Institute of Technology, Delhi, 2. Project Advisor, IEWP, GIZ India, New Delhi, India, 3. Professor, Civil Engineering Department, Indian Institute of Technology, Delhi

In Peninsular India, pronounced seasonality in the precipitation and tropical semi-arid climate have compelled the tremendous development in the water resources sector. The major proportion of this fertile plateau falls in the rainshadow region of Western Ghats and is rightfully supported through enormous irrigation schemes which include the operation of several large reservoirs. These developments have resulted in alteration of various components of a natural hydrological regime like low as well as high flows. Environmental flows (e-flows), though acknowledged widely for their benefits, have not been attempted vigorously for peninsular river basins due to the prioritised issues related to water scarcity and disputes over water sharing. Also, many of these river streams have historically been known as non-perennial, thus further weakening the case of e-flows. Effectively, many recent e-flow assessments, have been observed to be elementary, quick and based on methods that are less intensive in terms of data and time requirements. In this view, the present study attempts to verify the efficiency of various hydrology and hydrodynamics-based e-flow assessment methods in one of such river basins, Upper Godavari River Basin. For this, hydrological observations of 16 sites with long term record availability (20 years or more) have been used and latest cross section data for these sites have been used for hydrodynamic computations.

Hydrological indices based on concepts like Percentage of Flow (POF) and Range of Variability Approach (RVA) have been estimated using a natural flow regime obtained from SWAT rainfall-runoff modelling. POF approaches like Tennant Method, Tessman Method, Variable Monthly Flow Methods are analysed while RVA approach has been analysed using Indicators of Hydrological Alteration (IHA) platform. These indices have been analysed for their feasibility and acceptability under the natural flow regime to understand the efficacy of these indices in providing optimum e-flow suggestions. Present observed flow regime has been juxtaposed with these indices to assess the present flow health in their comparison.

Hydrodynamic computations have been performed in HEC-RAS using 1-dimensional steady state conditions. Flow discharge versus flow depth, wetted perimeter, etc. relationships obtained for these study sites have been utilised to understand the critical flow levels which ensure the maximum bed inundations preferable for ecological sustainability. Wetted perimeter method of e-flow assessment has been evaluated for its suitability to provide the optimum e-flow suggestions. It has been found that hydrology based simple and quick methods of e-flow assessment fail the basic criteria of feasibility even under natural flow regime while hydrodynamic approach gives site-specific solutions which may not be relatable in longitudinal e-flow implementation.

Keywords: environmental flows, Range of Variability Approach, Wetted perimeter method

©2019. Japan Geoscience Union. All Right Reserved.

Presence of pharmaceutical compounds in freshwater lakes and their impact on phytoplankton

*Nandakumar Kanavillil[1], Cassandra Fligg[1], Sreekumari Kurissery[1]

1. Lakehead University, Canada

Historically, microalgae have been used as bio-indicators of aquatic health and this can be seen in several studies across the world. Often, at the bottom of the food chain microalgae constitute the primary producer of energy of many freshwater ecosystems. Diatoms, a group of microalgae, have been shown to exhibit extreme sensitivity to varying environmental parameters thereby making themselves an excellent candidate for studying the impacts of pollutants such as Pharmaceuticals and Personal Care Products (PPCPs). The contamination by PPCPs is common in our inland water bodies with a potential to get into our drinking water supply. This study explores the presence of PPCPs (Ibuprofen, 17-β Estradiol, and Triclosan) in the nearshore waters of Lake Simcoe, Ontario, Canada and their impacts on microalgal community. The study involved assessment of several environmental and algal parameters in the surrounding freshwater systems of three Waste Water Treatment Plants (WWTPs) that discharge their effluents *via* a creek/water channel to Lake Simcoe. Water samples were also drawn from a control location located away from the WWTPs. The results indicated that 1) PPCPs contamination is prevalent in the water outside of WWTPs (as far as the point of confluence with Lake Simcoe), and 2) The algal parameters varied according to the presence of PPCPs in the surface waters. Thus the study supported the growing concern of pharmaceutical contamination in the freshwater systems and its impacts on primary producers.

Keywords: Water quality, Bioindicators, Freshwater lakes, Pharmaceuticals, Phytoplankton

©2019. Japan Geoscience Union. All Right Reserved.

Novel approximate solutions for solute transport due to injections: considering the scale-dependent dispersion and non-integer flow dimension

*Ye-Chen Lin[1], Hund-Der Yeh[1]

1. National Chiao Tung Univ.

Prior research indicated that the flow dimension in a fractured medium may be of non-integer. In this article, we aim at developing a mathematical model for solute transport problems due to continuous or pulse injection in a non-integer dimensional flow field. The model allows the flow dimension ranging from linear flow to spherical flow. Our model also considers the effect of scale-dependent dispersion. The approximate solutions of the model are derived by applying the arrival times of mean and variance and validated through the comparison with finite-difference solutions of the present model. The results show that the approximate solutions give reasonable predictions when the value of dispersion or flow dimension is not large.

Keywords: solute transport, non-integer flow dimension, approximate solution, scale-dependent dispersion

©2019. Japan Geoscience Union. All Right Reserved.

Experimemtal study on the residual saturation of Porous Media using Pore Doublets Micromodel

*Chun-Wei Peng[1]

1. Taiwan National Chiao Tung University

In this study, we use a micromodel of PDM with different channel diameter ratios to study the fluid entrapment and mobilization. This study focuses on the evolution of the trapping and the amount of residuals saturation in the porous media. We observed the movement of wetting and non-wet liquids during the imbibition and drainage processes.We found that, with the low injection flow rates, the residual amount was strongly related to the contact angle; with the high injection flow rates, viscous force was dominated the trapping process. The results also showed that the liquids were trapped in the small tube for low injection rate, and in the large tube for the high injection rate. Our findings can help to control the residual saturation during water-flooding oil recovery, groundwater remediation, and the storage of carbon dioxide in deep subsurface.

©2019. Japan Geoscience Union. All Right Reserved.

Assessment of Synergy between Biomedical Waste and Shallow Groundwater Pollution

*Deepika -[1], Abhishek -[2]

1. BPS Government Medical College for Women, Sonepat, INDIA, 2. Technical University Dresden, GERMANY

Rapid urbanization and increasing population growth rate followed by the high rates of resource consumption patterns and increased waste generation have had an unintended negative impact on the prevailing environment. In a developing country like India where 50.34 % groundwater resources are not suitable for drinking as per WHO standards (United Nations, 2016), scrutinizing the open dumping of pathogenic biomedical waste becomes of paramount importance. Poor waste management practices pose a huge risk to the health of the public, patients, professionals and contribute to environmental degradation (land, air, and water pollution) if dumped untreated on the open ground. To assess this nexus, a prevalence study of the patients affected with waterborne diseases was conducted in a total of 35 hospitals comprising of government-, government-aided- and private hospitals of Ambala city. With a pronounced steppe climate, Ambala is located in North-Eastern (mean spatial coordinates: 30˚ 22' 41.4480" N and 76˚ 46' 36.1020" E) edge of Haryana, India. The city is drained by non-perennial streams and therefore the inhabitants depend solely on shallow groundwater resources for meeting their domestic water demand.

Data about the sources, quantity produced, treatment facilities, and awareness of biomedical waste, collected by questionnaire method based survey revealed that the mean waste generation was 8.08 kg/day with SD 5.371 kg/day. The biomedical waste consisted of approximately 1.2 % of the total municipal waste generated by the city and the patients affected with waterborne diseases were about 36 % of the total patients recorded. A latin hypercube Pareto distribution coupled with AMALGAM algorithm was employed for the initial sampling states of the proposals from the observed data (no. of patients). Thereafter, posterior estimates were generated using the Markov Chain Monte Carlo (MCMC) methods which showed a close fit with the observed and simulated data with RMSE 0.158. Furthermore, regression analysis with R^2=0.868 construed strong positive linear correlation between two variables viz. the number of patients and biomedical waste generated (and dumped). Recommendations are made for prioritizing the waste segregation and employing the indispensable management processes including waste treatment to avoid the further deterioration of the drinking water quality. The hospital authorities are advised to conduct the periodic seminars for enhancing awareness among the workforce from present 93.3 % to a maximum possible level.

Keywords: Groundwater, Biomedical waste, MCMC methods, Environmental awareness

©2019. Japan Geoscience Union. All Right Reserved.

Erosion and transport processes of earth surface materials in a reservoir-catchment system inferred from atmospheric radionuclides ^{7}Be and ^{210}Pb

*Mikiya Tsuruoka[1], Shinya Ochiai[2], Atsushi Matsuki[2], Seiya Nagao[2]

1. Graduate School of Natural Science and Technology, Kanazawa University, 2. Institute of Nature and Environmental Technology, Kanazawa University

Erosion and transport processes of earth surface materials are related to landform development in river catchment area and material discharge from the land area to the ocean. It is necessary to understand erosion and transport processes of earth surface materials to achieve proper management and prediction of river watershed and coastal area. However, since discharge behavior of earth surface materials in a large-scale river system is complicated by various processes, it is difficult to trace individual processes. On the other hand, earth surface materials eroded from catchment is transported and accumulated in reservoir. Therefore, discharge behavior of earth surface materials from catchment can be observed by monitoring of reservoir sediment. In this study, erosion and transport processes of earth surface materials in catchment were investigated based on atmospheric deposition flux to the catchment and sedimentation flux in the reservoir of ^{7}Be (half-life: 53 days) and ^{210}Pb (half-life: 22.3 years). From July 2016, rain water sample was collected every month with a collecting pan installed on the roof of Noto Atmospheric Observatory in Suzu City. ^{7}Be and ^{210}Pb in rain water were collected on ion exchange resins and measured with a Ge semiconductor detector to obtain atmospheric deposition fluxes. Sediment samples were collected with two sediment traps installed on the bottom of the reservoir (Shin-ike Reservoir) near the Noto Atmospheric Observatory at the same interval with rain sampling. Another trap was also set up in the middle layer (1.5 m above the bottom) since May 2018. Sediment samples were freeze-dried and measured with a Ge semiconductor detector to obtain sedimentation fluxes of ^{7}Be and ^{210}Pb. The atmospheric deposition fluxes of ^{7}Be and ^{210}Pb ranged 1.06-30.7 and 0.334-7.68 Bq/m^{2}/day, respectively. It shows clear seasonal fluctuation with high deposition in winter. The sedimentation fluxes of ^{7}Be in the bottom and middle layers were same level with the deposition flux. This result indicates that the contribution of ^{7}Be from the catchment is small. On the other hand, the sedimentation flux of ^{210}Pb in the middle layer was about 1.7-7.3 times higher than the atmospheric deposition flux of ^{210}Pb. This result suggests that sedimentation flux of ^{210}Pb in the middle layer reflects the contribution of ^{210}Pb from the catchment. The sedimentation flux of ^{210}Pb in the bottom layer was much higher than the atmospheric deposition flux, implying that sedimentation flux in the bottom was largely affected by resuspension in addition to the contribution of ^{210}Pb from the catchment. Residence time of these radionuclides in the reservoir-catchment system was estimated from the ^{7}Be/^{210}Pb$_{ex}$ ratios of rain water and sediment samples. The average residence times of the bottom layer samples and middle layer sample were estimated at 278 days and 141 days, respectively. This difference in the residence time may result from resuspension effect in the reservoir bottom.

Keywords: sediment, reservoir-catchment system, Be-7, Pb-210

©2019. Japan Geoscience Union. All Right Reserved.

Fluctuation of groundwater level in a sloping unconfined aquifer due to time varying recharge

*Ming-Chang Wu[1], Ping-Cheng Hsieh[1]

1. National Chung Hsing University

When a water-permeable slope is recharged by rainfall, the variation of the groundwater level is usually observed by setting up observation wells. However, the point observations are not sufficient to represent the vast domain of an aquifer and are constrained by the high cost of instrumentation and excavated wells. Therefore, the development of mathematical models for groundwater simulations can help us to understand the change of groundwater level more easily.
This study considers the variation of the groundwater level in a sloping aquifer with an impervious bottom. We divided the aquifer into two areas with and without rainfall recharge, and then use the nonlinear Boussinesq equation with a source term derived from the law of mass conservation. Analytical solutions to the nonlinear equation was acquired by the perturbation method for a finite region and a semi-infinite domain. After the transformation of variables, the general integral transformation method was used. The groundwater level varying with time under different factors (such as the dip angle of impervious bed, hydraulic conductivity, storage coefficient and different recharge rates) was discussed.
The present results were compared with the observed data from an observation well, and the difference in between was discussed. It is expected that the research results can better understand the physical mechanism of groundwater level change, and help to manage the groundwater.

Keywords: nonlinear Boussinesq equation, perturbation method, general integral transform method (GITM)

©2019. Japan Geoscience Union. All Right Reserved.

Effect of cutoff wall on recharge water storage volume

*Pei-hsun Tsai[1], Jung-hsing Tai[1]

1. Chaoyang University of Technology

Artificial groundwater recharge is used to increase groundwater in areas with water scarcity. Understanding the hydromechanical features of aquifers during groundwater withdrawal and recharge is necessary for managing groundwater resources effectively. In practice, an artificial pool can be used to collect surface runoff so that it infiltrates the aquifer and recharges groundwater. A cutoff wall can be constructed to seal recharge water and prevent it from flowing from the recharge area. Additional studies are required to understand the effect of the various parameters of cutoff walls on groundwater recharge. This study used the finite difference software FLAC 8.0 to examine the influence of the location and size of gaps of a cutoff wall on recharge water storage volume. Each aquifer was in an unsaturated state before groundwater recharging; therefore, groundwater recharge analyses were simulated by the two-phase flow in unsaturated porous media. The results revealed that when the groundwater layer was sand and the cutoff wall was not extended into the fully impermeable layer, the recharge water completely flowed from the gap between the bottom of the cutoff wall and the fully impermeable layer after stopping groundwater recharge. The recharge water volume related to the size of the gap at the bottom of the cutoff wall. When the cutoff wall was not extended into the groundwater layer, the cutoff wall did not intercept water. The gap at the top of the cutoff wall retained more recharge water compared with the gap at the bottom of the cutoff wall.

Keywords: Groundwater recharge, Cutoff wall, Water storage volume

©2019. Japan Geoscience Union. All Right Reserved.

Studying Operation Parameters on Flat-Plate Membrane Bioreactor for Sewage Treatment

*Jen Hung Chiu[1], Wen Chin Chen[1]

1. Studying Operation Parameters on Flat-Plate Membrane Bioreactor for Sewage Treatment

The flat-plate membrane bioreactor is applied to the domestic sewage treatment, which has a high quality of effluent than the traditional activated sludge process, and decreasing the susceptible of hair entanglement with the hollow fiber membrane. It has become a priority for recent sewage treatment applications.

A flat-plate membrane bioreactor pilot plant with a reaction volume of 4 m^3 was installed in the existing sewage treatment plant. In this research, the parallel treatment of the same influent water quality and hydraulic retention time was carried out to compare the treatment efficiency between the MBR and traditional activated sludge process, and the operational effects of the membrane flux were discussed.

With one year of long-term research, the average removal efficiencies of MBR process, regardless of the COD, SS and E.coli were over 99%, wchih was better than the activated sludge process only 90~95%. Meanwhile, the optimal operation mode of the MBR was obtained in the study. The aeration flow rate in the system was adjusted to 10~13 NL/min per film, the effluent flux was controlled under 50% of the maximum recommended flux of membrane with 9-minute operation and 1 minute stop in a cycle, there is no significant change in operating flux and pressure. These operational mode of MBR can extend the life time of membrane and effectively improve the application of flat-plate MBR to domestic sewage treatment.It is suggested that, in view of water treatment and resource sustainability, the flat plate MBR technology is feasible, and can serve as a green guide to the sewage treatment.

Keywords: Membrane Bioreactor, Flat-Plate Membrane, Sewage

©2019. Japan Geoscience Union. All Right Reserved.

Mine-water quality at a tertiary coalfield in India: Characterisation and treatment using novel polyvinyl alcohol (PVA) gel bioreactor

*Aparna Dutta[1], Sudipta Sarkar[1]

1. Indian Institute of Technology Roorkee

Nearly 78 percent of the total measured (proved) tertiary coal reserves of India is concentrated in the north-eastern state of Assam. The Tertiary coal of North–Eastern Coalfields (NEC) has been found to contain as high as 8% sulphur with varying percentage of pyrite, sulfate, organic and free sulphur. The pyrites are often associated with toxic heavy metals. Acid mine drainage (AMD) is generated when mining activities expose the pyrite and sulfides to atmospheric oxygen, moisture and micro-organisms that catalyse the oxidation process to release large amounts of sulfate into the mine water along with protons and dissolved metals. Microbial dissimilatory sulfate reduction (DSR) in the presence of a suitable organic carbon source can be engineered to treat such water. This study is significant because this region is rich in biodiversity and such mining impacted water may have adverse ecological impact, if discharged without appropriate treatment.The objective of the work is to characterise water samples collected from two open cast mines of Makum coalfield under NEC and evaluate the performance of a novel polyvinyl alcohol (PVA) gel packed bed bioreactor to treat the same. Sample collection, storage and physico-chemical analysis are carried out as per Standard methods of American Public Health Association. The biological treatment process is studied in a cylindrical continuous flow lab scale bioreactor under relevant acidic pH at different feed chemical oxygen demand (COD) to sulfate ratio and hydraulic retention time (HRT). Sludge from a lab scale anaerobic bioreactor treating very high sulfate industrial water is used as inoculum. The sulfate reducing microorganisms are enriched within the bioreactor in fed-batch mode using modified Postgate’ s medium for one month.Oxidation Reduction Potential (ORP), pH, sulfate removal, total inorganic carbon (TIC) and alkalinity produced are measured at the bioreactor outlet to evaluate the process performance. The mine water samples exhibit low pH, high sulfate, conductivity, dissolved solids, hardness, iron and manganese, which indicates the occurrence of AMD. The treatment process reduces the sulfate concentration and increases pH of the treated water. The use of highly porous PVA gel beads as packing material in the bioreactor treating sulfate rich acidic water imparts resilience to operational variation. The study evaluates the novel application of PVA gel beads to bioreactor for treating acidic mine waters from an ecologically important region. The research finding provides an understanding of the process for application to other biological AMD treatment configurations.

Keywords: acid mine drainage (AMD), polyvinyl alcohol (PVA), sulfate, sulfate reducing microorganism (SRM), dissimilatory sulfate reduction(DSR), pyrite

©2019. Japan Geoscience Union. All Right Reserved.

[E] Poster | A (Atmospheric and Hydrospheric Sciences)：A-HW Hydrology & Water Environment

Wed. May 29, 2019 5:15 PM - 6:30 PM JST | Wed. May 29, 2019 8:15 AM - 9:30 AM UTC | Poster Hall International Exhibition Hall8, Makuhari Messe_14

[A-HW23] Hydrology & Water Environment

convener:Isao Machida(Geological Survey of Japan), Dai Yamazaki(Institute of Industrial Sciences, The University of Tokyo), Takeshi Hayashi(Faculty of Education and Human Studies, Akita University), Keisuke Fukushi(Institute of Nature & Environmental Technology, Kanazawa University)

We focus on various issues of water cycle and environment and aim to answer questions of hydrological and earth system sciences including 1) surface, subsurface and evapotranspiration processes of water cycle; 2) natural and anthropogenic hydrothermal systems, 3) environments issues and studies on a watershed or global scale, 4) water-related issues with ecological, environmental, and geochemical aspects, and 5) other issues in hydrological sciences. This session welcomes presentations regarding various kinds of approaches and techniques such as field survey, remote sensing, isotope tracers, numerical simulation, and theoretical analysis.

[AHW23-P01] A multiobjective risk management model for real-time reservoir flood control operation

*Juan Chen[1,2], Ping-An Zhong[2], XinYu Wan[2], Yu Zhang[2] (1.College of Earth Sciences and Engineering, Hohai University, 2.College of Hydrology and Water Resources, Hohai University)

[AHW23-P02] Assessment of the Flow Regime of Roanoke River due to Climatic and Anthropogenic Activities

*Rahul Kumar Singh[1], Dr. Manoj Kumar Jain[1] (1.Indian Institute of Technology, Roorkee, India)

[AHW23-P03] Predictive Analysis of Climate, Water, Health and the Environment Nexus

*Abhishek [1], Deepika [2] (1.Technical University Dresden, GERMANY, 2.BPS Government Medical College for Women, Sonepat, INDIA)

[AHW23-P05] Severe droughts provide huge fuel for widespread wildfires in California in USA

*Linghua Qiu[1], Ji Chen[1], Haiyun Shi[2], Liqun Sun[3], Jun Niu[4] (1.the University of Hong Kong, 2.Southern University of Science and Technology, 3.Shenzhen Institutes of Advanced Technology, Chinese Academy of Sciences, 4.China Agricultural University)

[AHW23-P06] A comprehensive evaluation of MODIS-based water use efficiency with global eddy covariance flux data and a process model

*Shanshan YANG[1,2], Jiahua ZHANG[1], Sha ZHANG[1,2], Jingwen WANG[1,2], Yun BAI[1,2], Fengmei YAO[2], Huadong GUO[1] (1.Institute of Remote Sensing and Digital Earth, Chinese Academy of Sciences, 2.University of Chinese Academy of Sciences, Beijing, China)

[AHW23-P07] Impact of variability and anisotropy in the correlation decay distance for precipitation spatial interpolation in China

*yingxian zhang[1] (1.National Climate Center, China Meteorological Administration)

[AHW23-P08] New Record-Breaking Frequency of Annual Maximum Daily Precipitation of 58 stations in the whole Japan, an increasing of extreme values.

*Chhay Ngorn SEANG[1], Tomohito YAMADA[1] (1.Hokkaido University)

[AHW23-P09] Quantifying stemflow to better express its ecohydrological significance

*Shin'ichi Iida[1], Darryl E. Carlye-Moses[2], Sonja Germer[3], Pilar Llorens[4], Beate Michalzik[5], Kazuki Nanko[1], Alexander Tischer[5], Delphis F. Levia[6] (1.Department of Disaster Prevention, Meteorology and Hydrology, Forestry and Forest Products Research Institute, 2.Department of Geography and Environmental Studies, Thompson Rivers University, Kamloops, British Columbia, Canada, 3.Department of Bioengineering,

Leibniz Institute for Agricultural Engineering and Bioeconomy, Potsdam, Germany, 4.Institute of Environmental Assessment and Water Research (IDAEA-CSIC), Barcelona, Spain, 5.Soil Science, Institute of Geography, Friedrich Schiller University Jena, Jena, Germany, 6.Department of Geography and Department of Plant and Soil Sciences, University of Delaware, Newark, DE, USA)

[AHW23-P10] **Hydraulic analysis of overland flow caused by temporally varying rainfall**

*PING-CHENG HSIEH[1], Ming-Chang Wu[1] (1.National Chung Hsing University)

[AHW23-P11] A comparative Study on Water Environment of Isolated Islands - Focusing on Islands in Nagasaki Prefecture - (3)

*Go Yamaki[1], Koji Kodera[2], Kazuki Asami[1], Yoshihiro IGARI[1], Masaki Horiuchi[1] (1.Grad. Student, Hosei Univ., 2.Dep. of Geography, Hosei Univ.)

[AHW23-P12] **Water environment around Kusatsu-Shirane volcano and consideration of the effect of eruption in January 2018**

*Igari Yoshihiro[1], Koji Kodera[2], Kazuki Asami[1] (1.Grad.Student,Hosei Univ., 2.Dep.of Geography Hosei Univ.)

[AHW23-P13] Re-consideration of discharge rate of spring water in Lake Ezu, Kumamoto

*Kimpei Ichiyanagi[1], Kiyoshi Ide[1], Jun Shimada[1], Tsutomu Ichikawa[2] (1.Kumamoto University, 2.Tokai University)

[AHW23-P14] **Evaluating the efficacy of hydrologically and hydrodynamically driven methods of e-flow assessment for Upper Godavari River Basin, India**

*GAURAV KALIDAS PAKHALE[1], Jyoti Punjahari Nale[2], Ashvin Kumar Gosain[3], Rakesh Khosa[3] (1.PhD Research Scholar, Civil Engineering Department, Indian Institute of Technology, Delhi, 2.Project Advisor, IEWP, GIZ India, New Delhi, India, 3.Professor, Civil Engineering Department, Indian Institute of Technology, Delhi)

[AHW23-P15] Presence of pharmaceutical compounds in freshwater lakes and their impact on phytoplankton

*Nandakumar Kanavillil[1], Cassandra Fligg[1], Sreekumari Kurissery[1] (1.Lakehead University, Canada)

[AHW23-P16] **Novel approximate solutions for solute transport due to injections: considering the scale-dependent dispersion and non-integer flow dimension**

*Ye-Chen Lin[1], Hund-Der Yeh[1] (1.National Chiao Tung Univ.)

[AHW23-P17] Experimemtal study on the residual saturation of Porous Media using Pore Doublets Micromodel

*Chun-Wei Peng[1] (1.Taiwan National Chiao Tung University)

[AHW23-P18] Assessment of Synergy between Biomedical Waste and Shallow Groundwater Pollution

*Deepika [1], Abhishek [2] (1.BPS Government Medical College for Women, Sonepat, INDIA, 2.Technical University Dresden, GERMANY)

[AHW23-P19] Erosion and transport processes of earth surface materials in a reservoir-catchment system inferred from atmospheric radionuclides ^{7}Be and ^{210}Pb

*Mikiya Tsuruoka[1], Shinya Ochiai[2], Atsushi Matsuki[2], Seiya Nagao[2] (1.Graduate School of Natural Science and Technology, Kanazawa University, 2.Institute of Nature and Environmental Technology, Kanazawa University)

[AHW23-P20] Fluctuation of groundwater level in a sloping unconfined aquifer due to time varying recharge

*Ming-Chang Wu[1], Ping-Cheng Hsieh[1] (1.National Chung Hsing University)

[AHW23-P21] **Effect of cutoff wall on recharge water storage volume**

*Pei-hsun Tsai[1], Jung-hsing Tai[1] (1.Chaoyang University of Technology)

[AHW23-P22] **Studying Operation Parameters on Flat-Plate Membrane Bioreactor for Sewage Treatment**

*Jen Hung Chiu[1], Wen Chin Chen[1] (1.Studying Operation Parameters on Flat-Plate Membrane Bioreactor for Sewage Treatment)

[AHW23-P23] **Mine-water quality at a tertiary coalfield in India: Characterisation and treatment using novel polyvinyl alcohol (PVA) gel bioreactor**

*Aparna Dutta[1], Sudipta Sarkar[1] (1.Indian Institute of Technology Roorkee)

A multiobjective risk management model for real-time reservoir flood control operation

*Juan Chen[1,2], Ping-An Zhong[2], XinYu Wan[2], Yu Zhang[2]

1. College of Earth Sciences and Engineering, Hohai University, 2. College of Hydrology and Water Resources, Hohai University

Many uncertainties exit in the real-time reservoir flood control operation and bring risks to flood control decisions. A multiobjective optimization model is developed for the real-time risk management for the flood control operation of a reservoir system considering multiple uncertainties such as inflow forecast errors and outflow errors. The two competing objectives considered are: (1) minimizing the risk of reservoir upstream flooding and (2) minimizing the risk of downstream flooding. The optimization model seeks to find the operation schedules that satisfy the flood control objectives and simultaneously minimize the overall risks. The decision variables are the hourly reservoir releases. The formulated multiobjective optimization problem is nonlinear and non-convex, and is solved with an improved Non-dominated Sorting Genetic Algorithm-II (INSGA-II). We use a filtering algorithm to select representative non-dominated solutions from the Pareto front generated by INSGA-II to assist in real-time decision making. The proposed risk management model is applied to the Foziling reservoir in Huaihe river basin of China. The results show that the proposed method can provide a practical way to optimize the real-time flood control operation for risk management of a reservoir.

Keywords: Flood, Reservoir, Flood control operation, Risk assessment, Multiobjective optimization

©2019. Japan Geoscience Union. All Right Reserved.

Assessment of the Flow Regime of Roanoke River due to Climatic and Anthropogenic Activities

*Rahul Kumar Singh[1], Dr. Manoj Kumar Jain[1]

1. Indian Institute of Technology, Roorkee, India

The natural flow regime of many rivers around the world has been significantly altered due to climatic and anthropogenic modifications such as the construction of dams and reservoirs. The natural flow regime plays an important role in the development of the riverine ecosystem. Therefore, quantification of the extent of the alterations in the natural flow regime would be helpful in the river’ s ecological assessment. The Roanoke River in southeastern United States had one of the biggest and least disturbed forest ecosystems but due to climatic changes and anthropogenic actions such as construction of dam, artificial regulations of the natural flow regime, the overall riverine ecosystem has severely impacted. In this study, SWAT (Soil Water Assessment Tool) has been used to reconstruct the long-term unaltered streamflow for a hypothetical no-dam scenario condition, in order to assess the impact of climate change as well as due to construction of the John H Kerr reservoir on Roanoke River streamflow from 1956-2012. In order to simulate the unaltered streamflow series post construction of John H Kerr reservoir, 32 years (1916-1948) of observed gauge inflow prior to anthropogenic disturbance (due to construction of John H Kerr Reservoir) was used for calibration and validation of the parameters of the SWAT model. Historical land use and land cover backcasting data for the year 1938 has been used in the hydrological model to simulate the flow regime prior to construction of the dam and it was kept same during the whole simulation period. The SWAT model simulated observed gauge data with Nash-Sutcliffe efficiency coefficient (NSE) = 0.70, Percent bias (PBIAS) = 0.00 and the determination coefficient (R^2) = 0.73 during the calibration period (1916 - 1936), and performed equally better during the validation period (1937-1948) with NSE = 0.72, PBIAS = 0.00 and R^2 = 0.74. The indicators of hydrologic alteration (IHA) methodology has been used to assess the natural flow regime (no dam or reservoir moderated flow regime) characteristics under a simulated no-reservoir scenario (scenario1) and compare with the IHA results obtained based on the gauged streamflow downstream of the dam (scenario2). Hence, in case of scenario 1, the post-impact period has been taken as the simulated flow series using SWAT model from 1956-2012 and in case of scenario 2 the post-impact period has been taken as the gauged observed streamflow from 1956-2012 at Roanoke Rapids gauging station downstream of the reservoir. The pre-impact period for both the scenario was kept the same i.e. from 1912 to 1949. The results reveal that in case of the IHA assessment based on scenario 1, significant alterations have been observed in 5 out of 32 indicators compared to 13 out 32 indicators in case of scenario 2. The overall hydrologic alteration in case of scenario 1 was 45.65% and it was 55.17% in the case of scenario 2. The alteration during the scenario 1 could be attributed to the overall natural climatic variability. The results also indicate that flow variability in terms of high and low flows were better in scenario 1 compared to scenario 2 where the high flows were completely absorbed including the low pulse count and duration due to regulation in the flow. However, the reservoir operations enhanced the monthly flows including the multiday minima low flows. Thus, the present method can be treated as an easy-to-implement comprehensive approach for designing natural flow regimes to mimic the pre-impact flow condition in order to restore the ecosystem of modified rivers due to anthropogenic interventions.

Keywords: SWAT, IHA, Streamflow, Hydrologic Alteration, Ecosystem

©2019. Japan Geoscience Union. All Right Reserved.

Predictive Analysis of Climate, Water, Health and the Environment Nexus

*Abhishek -[1], Deepika -[2]

1. Technical University Dresden, GERMANY, 2. BPS Government Medical College for Women, Sonepat, INDIA

Amid the major demographic transition of developing world from a rural, agrarian society to an urban, industrial one, there is a need for predictive analytics of impact of the major biotic and abiotic stressors on the environmental constituents. The current study emphasizes the connections between climate, water, environment, and health and their interdependency followed by an impact assessment focusing on an urban environment. A data-driven hybrid framework for water resources assessment and management based on machine learning techniques was developed, calibrated and validated with the ground data for the sub-region scale of North-East Indian regime (mean spatial coordinates: 28° 38' 41.2800" N and 77° 13' 0.1956" E). The remote sensing data for land cover and land change were coupled with the climate model simulations to formulate the health risk assessment framework. The large ensemble of downscaled scenario based outputs including the effects of anthropogenic factors was used to drive the hybrid model framework.

Multi-dimensional Random Walk Metropolis (RWM) algorithms used to optimize the sample observations converged with an RMSE error of 0.18 with a range of 0.006. Pearson Product Moment Correlation coefficient range of all the ensemble members was 0.886-0.904. The prediction accuracy construed from 95 % model uncertainty bounds was 89-91 % for the constituent parameters. The sensitivity analysis revealed that the climate is the key parameter and is the most sensitive for all other linkage units followed by water availability and health factors. Comparative analysis of the simulated- and experimental results enforced comprehensive clarification of the assumptions made therein. By real-time monitoring and forecasting the vital impacts, this research will serve and benefit local policymakers and in the decision-making process, particularly regarding water resources vulnerability and future availability with significant economic consequences. The upscaling of the model form sub-regional to regional scale is well underway.

Keywords: Climate Change, Urbanization, RWM algorithm, Ensemble model

©2019. Japan Geoscience Union. All Right Reserved.

Severe droughts provide huge fuel for widespread wildfires in California in USA

*Linghua Qiu[1], Ji Chen[1], Haiyun Shi[2], Liqun Sun[3], Jun Niu[4]

1. the University of Hong Kong, 2. Southern University of Science and Technology, 3. Shenzhen Institutes of Advanced Technology, Chinese Academy of Sciences, 4. China Agricultural University

The frequently occurred large wildfires in California caught the public’ s attention in recent years and the ability to identify and prevent such disasters is pressing. The study built the rational relationship between soil moisture and vegetation based on remote sensing, hydrology and wildfire data during 2001-2017 in California. The purpose is to estimate the effects of droughts on wildfires and to detect the valid fuel for wildfires. The study results reported that severe droughts could cause huge fuel for wildfires and made them even much more widespread and longer sustained. The consequences could provide significant information for identification and prevention of future wildfires in California and even other regions in the world.

Keywords: Fuel, Wildfires, Droughts, Soil moisture, Vegetation

©2019. Japan Geoscience Union. All Right Reserved.

A comprehensive evaluation of MODIS-based water use efficiency with global eddy covariance flux data and a process model

*Shanshan YANG[1,2], Jiahua ZHANG[1], Sha ZHANG[1,2], Jingwen WANG[1,2], Yun BAI[1,2], Fengmei YAO[2], Huadong GUO[1]

1. Institute of Remote Sensing and Digital Earth, Chinese Academy of Sciences, 2. University of Chinese Academy of Sciences, Beijing, China

Ecosystem water use efficiency (WUE), defined as the ratio of gross primary productivity (GPP) to evapotranspiration (ET), is an important indicator to investigate the interaction between the terrestrial carbon and water cycles. The spatiotemporal patterns of WUE inferred from MODIS GPP and ET products and its responses to environmental factors have been analyzed, however, the accuracy of MODIS-derived WUE (MODIS WUE) has not been well evaluated. In this study, we evaluated monthly and annual MODIS WUE using global covariance flux data (FLUXNET2015 dataset) during 2000-2014, and conducted global intercomparisons (2001-2011) among annual WUE from MODIS, gridded FLUXNET (MTE) and a process model (BESS). Site scale (53 sites) evaluation results revealed that MODIS gave reliable estimates for GPP and ET, however, the performances of MODIS WUE was poor for monthly WUE (R2=0.14) and even worse for annual WUE (R2=0.08). MODIS WUE was generally underestimated with a bias of -0.21 gC kg-1 H2O (-8.43%) and RMSE of 1.20 gC kg-1 H2O for monthly WUE, and a bias of -0.28 gC kg-1 H2O (-11.31%) and RMSE of 0.98 gC kg-1 H2O for annual WUE. Among all land cover types, MODIS WUE performed relatively better in savannas and woody savannas for monthly WUE and grasslands for annual WUE, but significantly overestimated WUE in open shrublands. Likewise, MODIS WUE was obviously overestimated in hot and cold semiarid and arid climate zones. The global intercomparison results demonstrated that the spatial pattern of MODIS WUE was broadly similar to that of MTE and BESS WUE, except for the tropical and subtropical arid and semiarid areas. In these regions MODIS WUE showed extremely high values with large uncertainty and different linear trends compared with MTE and BESS WUE. These disagreements were mainly caused by the discrepancies in MODIS ET. Therefore, the uncertainty of MODIS WUE in the tropical arid and semiarid areas should be taken with caution when using MODIS WUE to investigate and interpret how WUE varies spatially and its responses to climate change. Furthermore, the accuracy of MODIS GPP and ET datasets should be paid extra attention since the quality of both GPP and ET would directly affect the WUE accuracy.

Keywords: Water use efficiency (WUE), Evaluation, Intercomparison, MODIS, FLUXNET, BESS

©2019. Japan Geoscience Union. All Right Reserved.

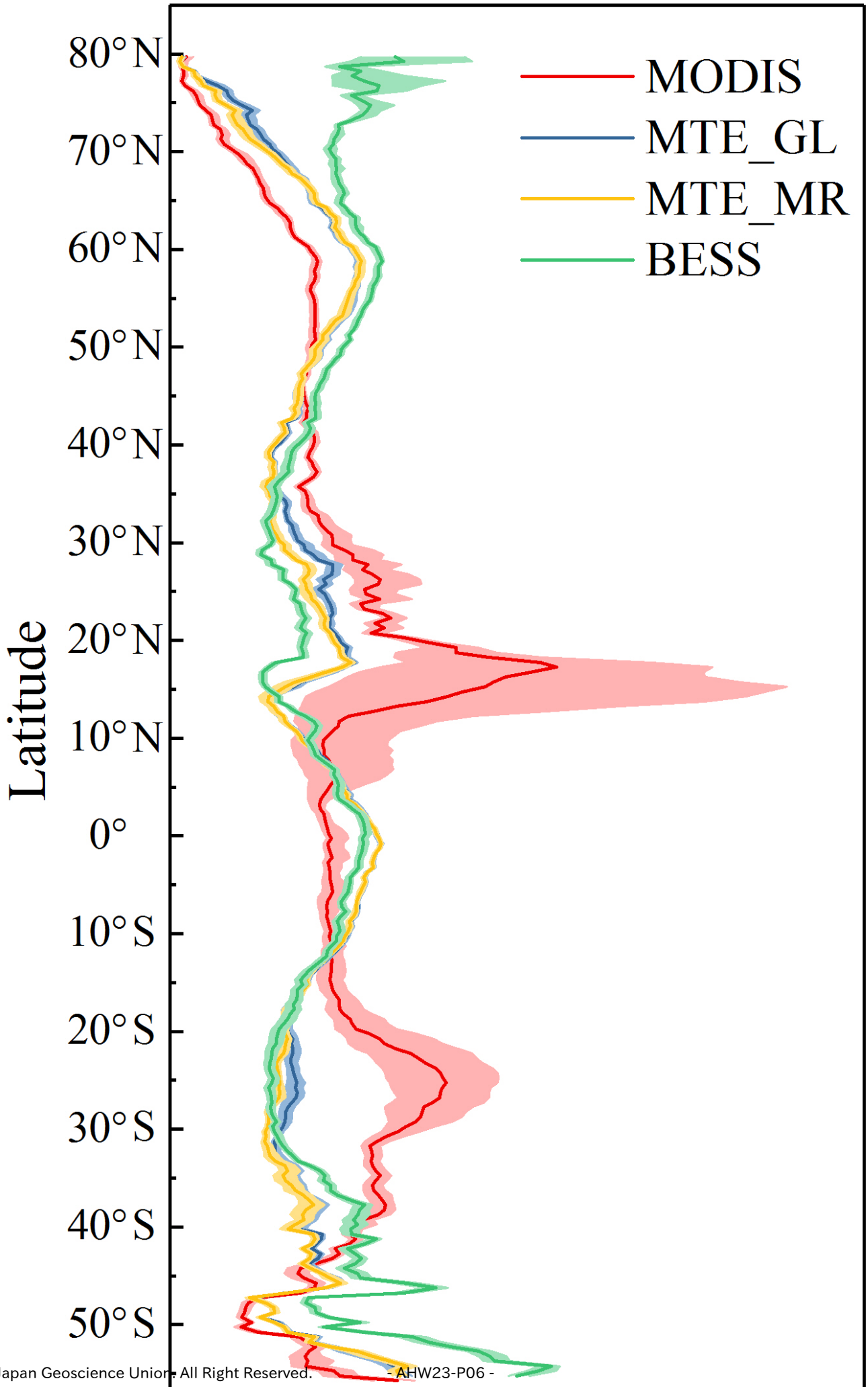

©2019. Japan Geoscience Union. All Right Reserved.

©2019. Japan Geoscience Union. All Right Reserved.

Impact of variability and anisotropy in the correlation decay distance for precipitation spatial interpolation in China

*yingxian zhang[1]

1. National Climate Center, China Meteorological Administration

The correlation decay distance (CDD) plays a key role in the angular-distance weighting (ADW) interpolation technique, being used as the searching radius to select correlated neighbors and to calculate the relative weights. The CDD of daily precipitation in China varies spatially and seasonally, and it presents anisotropic behavior, as a result of topography and the predominant atmospheric circulation. In general, CDD is largest in winter and smallest in summer, except for limited regions such as the Tibetan plateau. From a cross validation analysis, it is found that taking account of spatial and seasonal variations in CDD generally improves the ADW interpolation. Utilization of anisotropic CDDs increases the interpolation skill scores in regions with a dense monitoring network, significant elevation variation (southwestern China) or strongly anisotropic CDDs (Tibetan plateau).

Keywords: daily precipitation, correlation decay distance, ADW interpolation

©2019. Japan Geoscience Union. All Right Reserved.

New Record-Breaking Frequency of Annual Maximum Daily Precipitation of 58 stations in the whole Japan, an increasing of extreme values.

*Chhay Ngorn SEANG[1], Tomohito YAMADA[1]

1. Hokkaido University

The changes in daily temperature extremes in global scale have affected the weather and climate extreme events when there is an increase of greenhouse gas GHG compare to the industrialization in the 19th century (IPCC, 2014). Yamada et al. (2014) illustrate that the water vapor and convective instability follow the Clausius-Clapeyron-like rate of change with 99th percentile hourly precipitation intensity. Lehmann, J. et al. (2015), on another hand, studied globally the characteristic of precipitation change anomaly using a relation of the Clausius-Clapeyron model. By the way, the climate change tends to include another factor, which is more statistical base. The theory of record values in independent and identically distributed (i.i.d) random variable is studied more extensively and is more applicable with an assumption of stationary climate. The Clausius-Clapeyron equation is then also applicable base on the thermodynamic term which illustrates the relation of the temperature, vapor pressure and precipitation formation characteristic which also mentioned in the above previous studies. At the first stage, 58 stations of AMeDAS data with 117-years period across Japan are used for this analysis. The result shows that mean long-term precipitation of these 58 stations is higher than the mean value from theory i.i.d random variable of stationary climate. From this result, it can be implied that the change of precipitation in Japan is influenced by the drift term either of climate change or the heat island. In this case, the Clausius-Clapeyron equation is applied to identify the temperature term of change. This study tries to formulate a theory which more statistical base of climate drifts, non-stationary and non-identically to extreme events in accordance with time series. Clausius-Clapeyron Model and the Linear Drift Model is considered to form an empirical stochastically based on climate trend.

Keywords: Clausius-Clapeyron, New record Breaking, i.i.d

©2019. Japan Geoscience Union. All Right Reserved.

Quantifying stemflow to better express its ecohydrological significance

*Shin'ichi Iida[1], Darryl E. Carlye-Moses[2], Sonja Germer[3], Pilar Llorens[4], Beate Michalzik[5], Kazuki Nanko[1], Alexander Tischer[5], Delphis F. Levia[6]

1. Department of Disaster Prevention, Meteorology and Hydrology, Forestry and Forest Products Research Institute, 2. Department of Geography and Environmental Studies, Thompson Rivers University, Kamloops, British Columbia, Canada, 3. Department of Bioengineering, Leibniz Institute for Agricultural Engineering and Bioeconomy, Potsdam, Germany, 4. Institute of Environmental Assessment and Water Research (IDAEA-CSIC), Barcelona, Spain, 5. Soil Science, Institute of Geography, Friedrich Schiller University Jena, Jena, Germany, 6. Department of Geography and Department of Plant and Soil Sciences, University of Delaware, Newark, DE, USA

Stemflow is the flow of rainwater over the exterior of a tree stem to its base. Due to water balance calculations to obtain interception loss of forest stands, and the sometimes low percentage of stemflow as a function of rainfall, some literature ignores the ecohydrological significance of stemflow. However, stemflow is much more concentrated than throughfall per unit area. In recognition of the extreme amounts of water input to the small area around tree trunks, we advocate for two metrics to better express stemflow in relation to its ecohydrological importance: namely, the stand-scale funneling ratio and the stand-scale infiltration funneling ratio. We calculated these metrics based on measurements carried out in a tropical dry deciduous forest and a subpolar juvenile coniferous stand, and found that these are significantly larger than throughfall on both sites. The data cited from recent papers (n=34) showed that very small stand-scale amount of stemflow (approximately 0.5% on average) were necessary to make the stand-scale funneling ratio to be equal or more than unity. Moreover, the infiltration area of stemflow is generally < 0.2 m^2 due to the high infiltration capacity of top soil of forests, generally resulting in the stand-scale infiltration funneling ratio substantially greater than unity. Thus, stemflow is more effective for soil water recharge than throughfall. We recommend use of these metrics to better express ecohydrological importance of stemflow.

This presentation is based on the published paper as follows:
Carlye-Moses, D.E., Iida, S., Germer, S., Llorens, P., Michalzik, B., Nanko, K., Tischer, A., Levia, D.F. (2018): Expressing stemflow commensurate with its ecohydrological importance. Advances in Water Resources, 121, 472-479. Free open access article to: https://doi.org/10.1016/j.advwatres.2018.08.015

Keywords: Stemflow, Funneling ratio, Forest hydrology

©2019. Japan Geoscience Union. All Right Reserved.

Hydraulic analysis of overland flow caused by temporally varying rainfall

*PING-CHENG HSIEH[1], Ming-Chang Wu[1]

1. National Chung Hsing University

With the development of human civilization and population migration, we use many different types of pervious or impervious materials to cover the original surface. As a result, the surface friction and water permeability are reduced, resulting in increased flow velocity and runoff, and thus increasing the frequency and scale of flood occurrence. Therefore, predicting changes in overland flow caused by rainfall has become an important issue.

This study intends to simulate the overland flow under different rainfall patterns by the theory of diffusion wave model. The diffusion wave equation was used as the governing equation, and an analytical solution of the water depth by the generalized integral transformation method was presented. Since the values of the parameters used in previous research for diffusion wave models vary in an extensive range. In this study, the parameters were adjusted for each location to ensure the rationality of the simulation results according to the law of mass conservation.
The results show that for the non-uniform rainfall, the peak water depth and peak flow due to the post-peak rainfall are the largest, followed by the third quarter peak rainfall; whereas the average flow velocity of the mid-peak rainfall is the largest, followed by the third quarter peak rainfall. The peak water depth, peak flow rate and average flow rate due to the double peak rainfall are the smallest among the six rainfall patterns in this study.

Keywords: overland flow, nonuniform rainfall, diffusion wave

©2019. Japan Geoscience Union. All Right Reserved.

A comparative Study on Water Environment of Isolated Islands - Focusing on Islands in Nagasaki Prefecture - (3)

*Go Yamaki[1], Koji Kodera[2], Kazuki Asami[1], Yoshihiro IGARI[1], Masaki Horiuchi[1]

1. Grad. Student, Hosei Univ., 2. Dep. of Geography, Hosei Univ.

1. Introduction Research on islands in Nagasaki prefecture has hardly been investigated and research has been promoted since 2014 from Goto Island Islands, Tsushima, Iki, Hirado. For this time, we will clarify the water environment in each area from the relationship with land use and climate, and make it a foothold to clarify the material cycle of each island.

2. Target area Iki is rugged with a maximum altitude of 213 m, and there are numerous reservoirs in various parts of the island. In Tsushima, the altitude of the entire island is relatively high, and the mountains occupy about 89%. The Goto Islands Island consists of about 140 large and small islands, with large geological differences on each island. The Hirado Islands have many mountains while the fields are also relatively large. The population penetration rate of wastewater treatment in both areas is as low as 20-40%.

3. Research method Field survey was conducted 2 to 4 times a year from 2014 after organizing and examining existing research. On the site, water temperature, temperature, electric conductivity (EC), pH and RpH, COD were measured, and water was taken to measure the total organic carbon and the main dissolved components.

4. Results and discussion In Iki, the influence of agriculture appears in EC and TOC, but it is interesting that there is almost no effect of nitric acid. On the other hand, although many nitric acid was detected in the Goto Islands, it is thought that factors are due to paddy fields in Iki and upland fields in Goto Islands. Tsushima showed relatively low concentrations of EC and dissolved components, and seasonal changes also appeared. In Hirado Island, especially in the southern part, the geological influence is large in many places, the impact of sea salt is strong in Ikitsuki island and Azuchi Oshima. EC tends to rise in rainwater from October to March, pH tends to decrease. From the above, it is considered that the difference in the quality of the islands is greatly influenced by the difference of geology, topography and agricultural form.

Keywords: Iki island, Tsushima islands, Goto islands, Hirado islands, Water environment

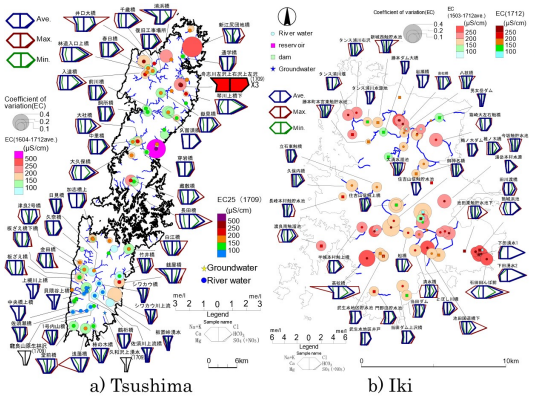

a) Tsushima b) Iki c) Hirado

Fig.1 Water quality

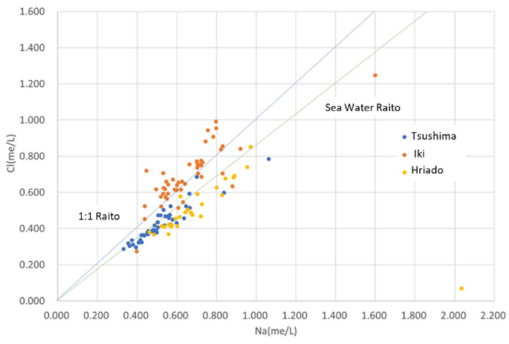

Fig.2 Na / Cl ratio

©2019. Japan Geoscience Union. All Right Reserved.

Water environment around Kusatsu-Shirane volcano and consideration of the effect of eruption in January 2018

*Igari Yoshihiro[1], Koji Kodera[2], Kazuki Asami[1]

1. Grad.Student,Hosei Univ., 2. Dep.of Geography Hosei Univ.

1. Introduction

The eruption (steam explosion) occurred in Mt.Motoshirane (One of Kusatsu-Shirane Volcano) on January 23, 2018. In this area, water quality survey of water environment began in May 2017 before the eruption. In addition to examining the influence on the water quality before and after the eruption, we studied the elution component of volcanic ash and the influence on the water environment. We also attempted to consider water quality forming factors in river water around Kusatsu-Shirane volcano.

2. Research method

We conducted about 21 field surveys from May 2017 to March 2019. The survey site is about 45 sites, centering on rivers flowing in the east and south of the mountain. Temperature, water temperature, pH, RpH, EC, and flow rate were measured locally, and the sampled sample was analyzed for the main dissolved components. In February 2018, we investigated the deposition situation and ash fall volume of volcanic ash and conducted sampling, and carried out dissolution experiment. In addition to rivers, field surveys and sampling of lakes and precipitation, snow cover, hot spring water were conducted.

3. Results and discussion

In Shirasuna River flowing to the east side of the mountain, groundwater and river water influenced by hot spring drainage and volcanic activity flow in from the tributary. There are points where the EC value fluctuates greatly, and it is influenced by the discharge and conduction of the dam which stores the neutralizing water of acidic rivers. In the Gando Swamp where the site of sulfur mine is located in the upstream part, the water quality is around pH:2.0, EC:6000 μS/cm. It is conceivable that the deposited volcanic ash affects the quality of the surrounding river due to snow melting water and precipitation.

Keywords: Mt.Kusatsu-Shirane, Volcano, Water environment, Eruption, Hot spring

©2019. Japan Geoscience Union. All Right Reserved.

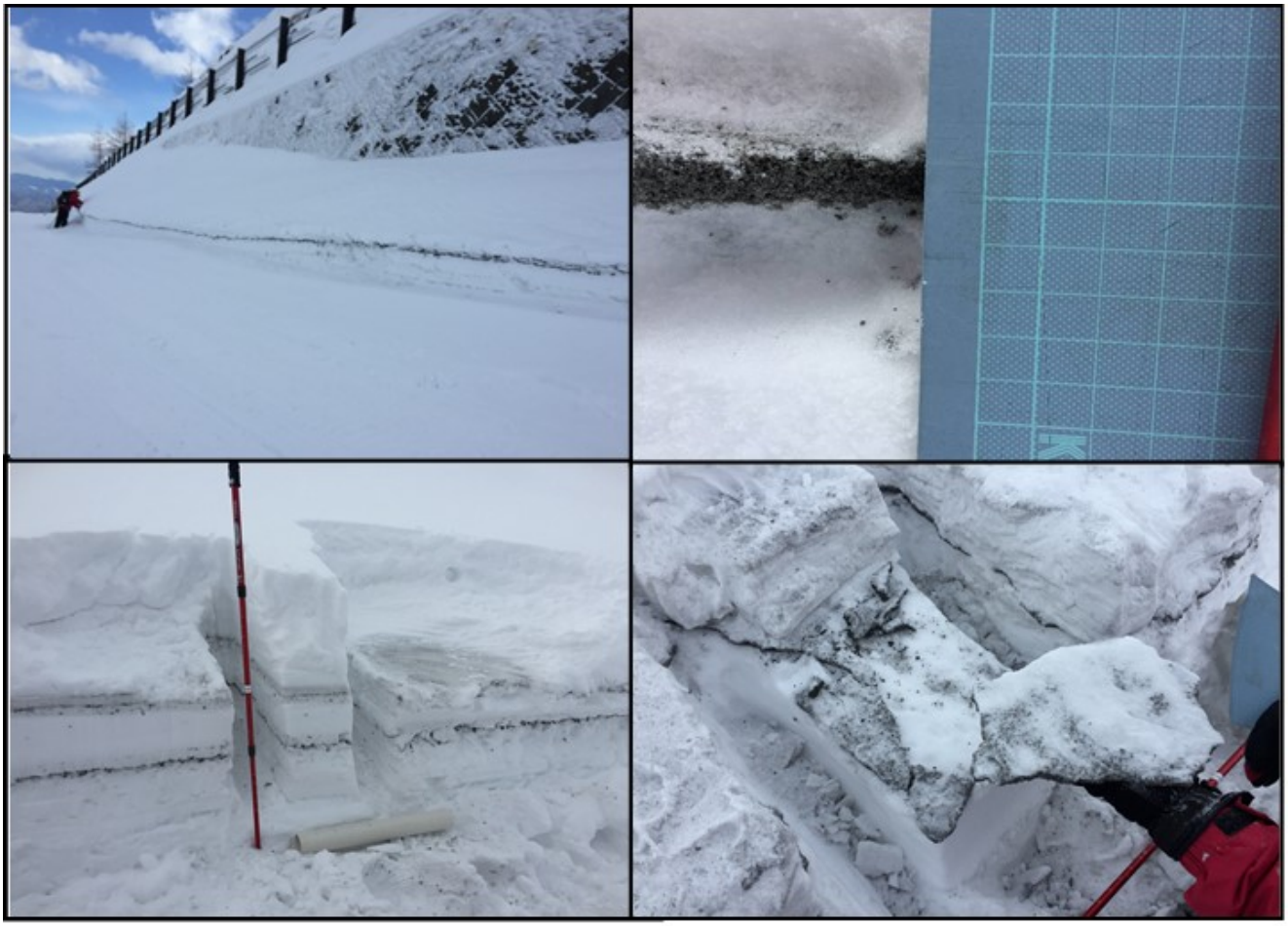

Picture.1 Ash fall in the east foot of Kusatsu-Shirane volcano (February 6, 2018)

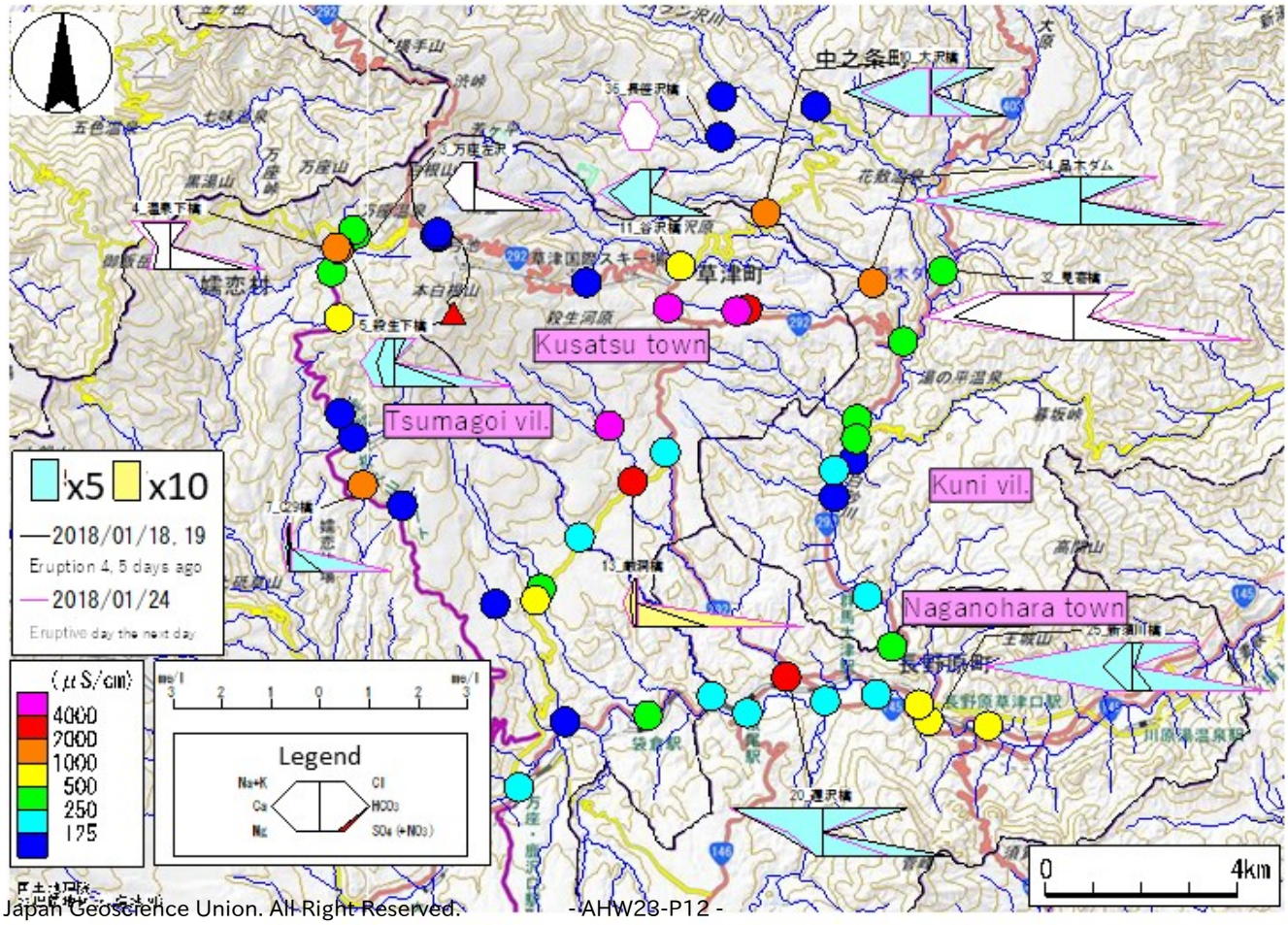

©2019. Japan Geoscience Union. All Right Reserved.

©2019. Japan Geoscience Union. All Right Reserved.

Re-consideration of discharge rate of spring water in Lake Ezu, Kumamoto

*Kimpei Ichiyanagi[1], Kiyoshi Ide[1], Jun Shimada[1], Tsutomu Ichikawa[2]

1. Kumamoto University, 2. Tokai University

In Kumamoto area, 100% of tap water is sourced from abundant groundwater. Recently, there is a great fear of groundwater level decreasing. To estimate discharge rete of spring water in Lake Ezu, the flow rate at 13 sites has been observed every month since December 1991. In previous studies, the total discharge rate of spring water was calculated by flow rates only at the most downstream, the most upper-stream, and incoming streams. In this study, total discharge rate from December 1991 to December 2014 was re-considered as a sum of three zones, that is upper-stream area, Kami-Ezu Lake, and Shimo-Ezu lake. When the discharge rate in each zone became negative, the case 1 where calculation was carried out with minus and the case 2 where it assumed to 0m^3/day were compared. As a result, total discharge rate gradually declined from about 450,000m^3/day in 1992 to about 360,000m^3/day (case 1) and to about 410,000m^3/day (case 2) in 2005. In July 2006, total discharge rate rapidly increased with heavy rainfall. After that, it had fluctuated about 400,000 to 500,000m^3/day in both cases. The discharge rate of Shimo-Ezu Lake sometimes became negative after 2003, and that averaged after July 2006 in case 2 was about 90,000m^3/day more than the case 1. As a result of comparing seasonal variability of discharge rate, monthly mean values of total and Shimo-Ezu Lake are low in April-May and high in October-November. However, monthly mean values of upper-stream area and Kami-Ezu Lake show no significant seasonal fluctuation. Monthly mean values of Shimo-Ezu Lake in August averaged after 2006 was about -14,000m^3/day in case 1 and about 32,000 m^3/day in case 2. Since negative value is not suitable to represent seasonal fluctuation, case 2 is proper to represent the discharge rate of spring water.

Keywords: spring water, Lake Ezu, long-term trend, seasonal variability

©2019. Japan Geoscience Union. All Right Reserved.

Evaluating the efficacy of hydrologically and hydrodynamically driven methods of e-flow assessment for Upper Godavari River Basin, India

*GAURAV KALIDAS PAKHALE[1], Jyoti Punjahari Nale[2], Ashvin Kumar Gosain[3], Rakesh Khosa[3]

1. PhD Research Scholar, Civil Engineering Department, Indian Institute of Technology, Delhi, 2. Project Advisor, IEWP, GIZ India, New Delhi, India, 3. Professor, Civil Engineering Department, Indian Institute of Technology, Delhi

In Peninsular India, pronounced seasonality in the precipitation and tropical semi-arid climate have compelled the tremendous development in the water resources sector. The major proportion of this fertile plateau falls in the rainshadow region of Western Ghats and is rightfully supported through enormous irrigation schemes which include the operation of several large reservoirs. These developments have resulted in alteration of various components of a natural hydrological regime like low as well as high flows. Environmental flows (e-flows), though acknowledged widely for their benefits, have not been attempted vigorously for peninsular river basins due to the prioritised issues related to water scarcity and disputes over water sharing. Also, many of these river streams have historically been known as non-perennial, thus further weakening the case of e-flows. Effectively, many recent e-flow assessments, have been observed to be elementary, quick and based on methods that are less intensive in terms of data and time requirements. In this view, the present study attempts to verify the efficiency of various hydrology and hydrodynamics-based e-flow assessment methods in one of such river basins, Upper Godavari River Basin. For this, hydrological observations of 16 sites with long term record availability (20 years or more) have been used and latest cross section data for these sites have been used for hydrodynamic computations.

Hydrological indices based on concepts like Percentage of Flow (POF) and Range of Variability Approach (RVA) have been estimated using a natural flow regime obtained from SWAT rainfall-runoff modelling. POF approaches like Tennant Method, Tessman Method, Variable Monthly Flow Methods are analysed while RVA approach has been analysed using Indicators of Hydrological Alteration (IHA) platform. These indices have been analysed for their feasibility and acceptability under the natural flow regime to understand the efficacy of these indices in providing optimum e-flow suggestions. Present observed flow regime has been juxtaposed with these indices to assess the present flow health in their comparison.

Hydrodynamic computations have been performed in HEC-RAS using 1-dimensional steady state conditions. Flow discharge versus flow depth, wetted perimeter, etc. relationships obtained for these study sites have been utilised to understand the critical flow levels which ensure the maximum bed inundations preferable for ecological sustainability. Wetted perimeter method of e-flow assessment has been evaluated for its suitability to provide the optimum e-flow suggestions. It has been found that hydrology based simple and quick methods of e-flow assessment fail the basic criteria of feasibility even under natural flow regime while hydrodynamic approach gives site-specific solutions which may not be relatable in longitudinal e-flow implementation.

Keywords: environmental flows, Range of Variability Approach, Wetted perimeter method

©2019. Japan Geoscience Union. All Right Reserved.

Presence of pharmaceutical compounds in freshwater lakes and their impact on phytoplankton

*Nandakumar Kanavillil[1], Cassandra Fligg[1], Sreekumari Kurissery[1]

1. Lakehead University, Canada

Historically, microalgae have been used as bio-indicators of aquatic health and this can be seen in several studies across the world. Often, at the bottom of the food chain microalgae constitute the primary producer of energy of many freshwater ecosystems. Diatoms, a group of microalgae, have been shown to exhibit extreme sensitivity to varying environmental parameters thereby making themselves an excellent candidate for studying the impacts of pollutants such as Pharmaceuticals and Personal Care Products (PPCPs). The contamination by PPCPs is common in our inland water bodies with a potential to get into our drinking water supply. This study explores the presence of PPCPs (Ibuprofen, 17-β Estradiol, and Triclosan) in the nearshore waters of Lake Simcoe, Ontario, Canada and their impacts on microalgal community. The study involved assessment of several environmental and algal parameters in the surrounding freshwater systems of three Waste Water Treatment Plants (WWTPs) that discharge their effluents *via* a creek/water channel to Lake Simcoe. Water samples were also drawn from a control location located away from the WWTPs. The results indicated that 1) PPCPs contamination is prevalent in the water outside of WWTPs (as far as the point of confluence with Lake Simcoe), and 2) The algal parameters varied according to the presence of PPCPs in the surface waters. Thus the study supported the growing concern of pharmaceutical contamination in the freshwater systems and its impacts on primary producers.

Keywords: Water quality, Bioindicators, Freshwater lakes, Pharmaceuticals, Phytoplankton

©2019. Japan Geoscience Union. All Right Reserved.

Novel approximate solutions for solute transport due to injections: considering the scale-dependent dispersion and non-integer flow dimension

*Ye-Chen Lin[1], Hund-Der Yeh[1]

1. National Chiao Tung Univ.

Prior research indicated that the flow dimension in a fractured medium may be of non-integer. In this article, we aim at developing a mathematical model for solute transport problems due to continuous or pulse injection in a non-integer dimensional flow field. The model allows the flow dimension ranging from linear flow to spherical flow. Our model also considers the effect of scale-dependent dispersion. The approximate solutions of the model are derived by applying the arrival times of mean and variance and validated through the comparison with finite-difference solutions of the present model. The results show that the approximate solutions give reasonable predictions when the value of dispersion or flow dimension is not large.

Keywords: solute transport, non-integer flow dimension, approximate solution, scale-dependent dispersion

©2019. Japan Geoscience Union. All Right Reserved.

Experimemtal study on the residual saturation of Porous Media using Pore Doublets Micromodel

*Chun-Wei Peng[1]

1. Taiwan National Chiao Tung University

In this study, we use a micromodel of PDM with different channel diameter ratios to study the fluid entrapment and mobilization. This study focuses on the evolution of the trapping and the amount of residuals saturation in the porous media. We observed the movement of wetting and non-wet liquids during the imbibition and drainage processes.We found that, with the low injection flow rates, the residual amount was strongly related to the contact angle; with the high injection flow rates, viscous force was dominated the trapping process. The results also showed that the liquids were trapped in the small tube for low injection rate, and in the large tube for the high injection rate. Our findings can help to control the residual saturation during water-flooding oil recovery, groundwater remediation, and the storage of carbon dioxide in deep subsurface.

©2019. Japan Geoscience Union. All Right Reserved.

Assessment of Synergy between Biomedical Waste and Shallow Groundwater Pollution

*Deepika -[1], Abhishek -[2]

1. BPS Government Medical College for Women, Sonepat, INDIA, 2. Technical University Dresden, GERMANY

Rapid urbanization and increasing population growth rate followed by the high rates of resource consumption patterns and increased waste generation have had an unintended negative impact on the prevailing environment. In a developing country like India where 50.34 % groundwater resources are not suitable for drinking as per WHO standards (United Nations, 2016), scrutinizing the open dumping of pathogenic biomedical waste becomes of paramount importance. Poor waste management practices pose a huge risk to the health of the public, patients, professionals and contribute to environmental degradation (land, air, and water pollution) if dumped untreated on the open ground. To assess this nexus, a prevalence study of the patients affected with waterborne diseases was conducted in a total of 35 hospitals comprising of government-, government-aided- and private hospitals of Ambala city. With a pronounced steppe climate, Ambala is located in North-Eastern (mean spatial coordinates: 30˚ 22' 41.4480" N and 76˚ 46' 36.1020" E) edge of Haryana, India. The city is drained by non-perennial streams and therefore the inhabitants depend solely on shallow groundwater resources for meeting their domestic water demand.

Data about the sources, quantity produced, treatment facilities, and awareness of biomedical waste, collected by questionnaire method based survey revealed that the mean waste generation was 8.08 kg/day with SD 5.371 kg/day. The biomedical waste consisted of approximately 1.2 % of the total municipal waste generated by the city and the patients affected with waterborne diseases were about 36 % of the total patients recorded. A latin hypercube Pareto distribution coupled with AMALGAM algorithm was employed for the initial sampling states of the proposals from the observed data (no. of patients). Thereafter, posterior estimates were generated using the Markov Chain Monte Carlo (MCMC) methods which showed a close fit with the observed and simulated data with RMSE 0.158. Furthermore, regression analysis with R^2=0.868 construed strong positive linear correlation between two variables viz. the number of patients and biomedical waste generated (and dumped). Recommendations are made for prioritizing the waste segregation and employing the indispensable management processes including waste treatment to avoid the further deterioration of the drinking water quality. The hospital authorities are advised to conduct the periodic seminars for enhancing awareness among the workforce from present 93.3 % to a maximum possible level.

Keywords: Groundwater, Biomedical waste, MCMC methods, Environmental awareness

©2019. Japan Geoscience Union. All Right Reserved.

Erosion and transport processes of earth surface materials in a reservoir-catchment system inferred from atmospheric radionuclides ^{7}Be and ^{210}Pb

*Mikiya Tsuruoka[1], Shinya Ochiai[2], Atsushi Matsuki[2], Seiya Nagao[2]

1. Graduate School of Natural Science and Technology, Kanazawa University, 2. Institute of Nature and Environmental Technology, Kanazawa University

Erosion and transport processes of earth surface materials are related to landform development in river catchment area and material discharge from the land area to the ocean. It is necessary to understand erosion and transport processes of earth surface materials to achieve proper management and prediction of river watershed and coastal area. However, since discharge behavior of earth surface materials in a large-scale river system is complicated by various processes, it is difficult to trace individual processes. On the other hand, earth surface materials eroded from catchment is transported and accumulated in reservoir. Therefore, discharge behavior of earth surface materials from catchment can be observed by monitoring of reservoir sediment. In this study, erosion and transport processes of earth surface materials in catchment were investigated based on atmospheric deposition flux to the catchment and sedimentation flux in the reservoir of ^{7}Be (half-life: 53 days) and ^{210}Pb (half-life: 22.3 years). From July 2016, rain water sample was collected every month with a collecting pan installed on the roof of Noto Atmospheric Observatory in Suzu City. ^{7}Be and ^{210}Pb in rain water were collected on ion exchange resins and measured with a Ge semiconductor detector to obtain atmospheric deposition fluxes. Sediment samples were collected with two sediment traps installed on the bottom of the reservoir (Shin-ike Reservoir) near the Noto Atmospheric Observatory at the same interval with rain sampling. Another trap was also set up in the middle layer (1.5 m above the bottom) since May 2018. Sediment samples were freeze-dried and measured with a Ge semiconductor detector to obtain sedimentation fluxes of ^{7}Be and ^{210}Pb. The atmospheric deposition fluxes of ^{7}Be and ^{210}Pb ranged 1.06-30.7 and 0.334-7.68 Bq/m^{2}/day, respectively. It shows clear seasonal fluctuation with high deposition in winter. The sedimentation fluxes of ^{7}Be in the bottom and middle layers were same level with the deposition flux. This result indicates that the contribution of ^{7}Be from the catchment is small. On the other hand, the sedimentation flux of ^{210}Pb in the middle layer was about 1.7-7.3 times higher than the atmospheric deposition flux of ^{210}Pb. This result suggests that sedimentation flux of ^{210}Pb in the middle layer reflects the contribution of ^{210}Pb from the catchment. The sedimentation flux of ^{210}Pb in the bottom layer was much higher than the atmospheric deposition flux, implying that sedimentation flux in the bottom was largely affected by resuspension in addition to the contribution of ^{210}Pb from the catchment. Residence time of these radionuclides in the reservoir-catchment system was estimated from the ^{7}Be/^{210}Pb$_{ex}$ ratios of rain water and sediment samples. The average residence times of the bottom layer samples and middle layer sample were estimated at 278 days and 141 days, respectively. This difference in the residence time may result from resuspension effect in the reservoir bottom.

Keywords: sediment, reservoir-catchment system, Be-7, Pb-210

©2019. Japan Geoscience Union. All Right Reserved.

Fluctuation of groundwater level in a sloping unconfined aquifer due to time varying recharge

*Ming-Chang Wu[1], Ping-Cheng Hsieh[1]

1. National Chung Hsing University

When a water-permeable slope is recharged by rainfall, the variation of the groundwater level is usually observed by setting up observation wells. However, the point observations are not sufficient to represent the vast domain of an aquifer and are constrained by the high cost of instrumentation and excavated wells. Therefore, the development of mathematical models for groundwater simulations can help us to understand the change of groundwater level more easily.
This study considers the variation of the groundwater level in a sloping aquifer with an impervious bottom. We divided the aquifer into two areas with and without rainfall recharge, and then use the nonlinear Boussinesq equation with a source term derived from the law of mass conservation. Analytical solutions to the nonlinear equation was acquired by the perturbation method for a finite region and a semi-infinite domain. After the transformation of variables, the general integral transformation method was used. The groundwater level varying with time under different factors (such as the dip angle of impervious bed, hydraulic conductivity, storage coefficient and different recharge rates) was discussed.
The present results were compared with the observed data from an observation well, and the difference in between was discussed. It is expected that the research results can better understand the physical mechanism of groundwater level change, and help to manage the groundwater.

Keywords: nonlinear Boussinesq equation, perturbation method, general integral transform method (GITM)

©2019. Japan Geoscience Union. All Right Reserved.

Effect of cutoff wall on recharge water storage volume

*Pei-hsun Tsai[1], Jung-hsing Tai[1]

1. Chaoyang University of Technology

Artificial groundwater recharge is used to increase groundwater in areas with water scarcity. Understanding the hydromechanical features of aquifers during groundwater withdrawal and recharge is necessary for managing groundwater resources effectively. In practice, an artificial pool can be used to collect surface runoff so that it infiltrates the aquifer and recharges groundwater. A cutoff wall can be constructed to seal recharge water and prevent it from flowing from the recharge area. Additional studies are required to understand the effect of the various parameters of cutoff walls on groundwater recharge. This study used the finite difference software FLAC 8.0 to examine the influence of the location and size of gaps of a cutoff wall on recharge water storage volume. Each aquifer was in an unsaturated state before groundwater recharging; therefore, groundwater recharge analyses were simulated by the two-phase flow in unsaturated porous media. The results revealed that when the groundwater layer was sand and the cutoff wall was not extended into the fully impermeable layer, the recharge water completely flowed from the gap between the bottom of the cutoff wall and the fully impermeable layer after stopping groundwater recharge. The recharge water volume related to the size of the gap at the bottom of the cutoff wall. When the cutoff wall was not extended into the groundwater layer, the cutoff wall did not intercept water. The gap at the top of the cutoff wall retained more recharge water compared with the gap at the bottom of the cutoff wall.

Keywords: Groundwater recharge, Cutoff wall, Water storage volume

©2019. Japan Geoscience Union. All Right Reserved.

Studying Operation Parameters on Flat-Plate Membrane Bioreactor for Sewage Treatment

*Jen Hung Chiu[1], Wen Chin Chen[1]

1. Studying Operation Parameters on Flat-Plate Membrane Bioreactor for Sewage Treatment

The flat-plate membrane bioreactor is applied to the domestic sewage treatment, which has a high quality of effluent than the traditional activated sludge process, and decreasing the susceptible of hair entanglement with the hollow fiber membrane. It has become a priority for recent sewage treatment applications.

A flat-plate membrane bioreactor pilot plant with a reaction volume of 4 m^3 was installed in the existing sewage treatment plant. In this research, the parallel treatment of the same influent water quality and hydraulic retention time was carried out to compare the treatment efficiency between the MBR and traditional activated sludge process, and the operational effects of the membrane flux were discussed.

With one year of long-term research, the average removal efficiencies of MBR process, regardless of the COD, SS and E.coli were over 99%, wchih was better than the activated sludge process only 90~95%. Meanwhile, the optimal operation mode of the MBR was obtained in the study. The aeration flow rate in the system was adjusted to 10~13 NL/min per film, the effluent flux was controlled under 50% of the maximum recommended flux of membrane with 9-minute operation and 1 minute stop in a cycle, there is no significant change in operating flux and pressure. These operational mode of MBR can extend the life time of membrane and effectively improve the application of flat-plate MBR to domestic sewage treatment.It is suggested that, in view of water treatment and resource sustainability, the flat plate MBR technology is feasible, and can serve as a green guide to the sewage treatment.

Keywords: Membrane Bioreactor, Flat-Plate Membrane, Sewage

©2019. Japan Geoscience Union. All Right Reserved.

Mine-water quality at a tertiary coalfield in India: Characterisation and treatment using novel polyvinyl alcohol (PVA) gel bioreactor

*Aparna Dutta[1], Sudipta Sarkar[1]

1. Indian Institute of Technology Roorkee

Nearly 78 percent of the total measured (proved) tertiary coal reserves of India is concentrated in the north-eastern state of Assam. The Tertiary coal of North–Eastern Coalfields (NEC) has been found to contain as high as 8% sulphur with varying percentage of pyrite, sulfate, organic and free sulphur. The pyrites are often associated with toxic heavy metals. Acid mine drainage (AMD) is generated when mining activities expose the pyrite and sulfides to atmospheric oxygen, moisture and micro-organisms that catalyse the oxidation process to release large amounts of sulfate into the mine water along with protons and dissolved metals. Microbial dissimilatory sulfate reduction (DSR) in the presence of a suitable organic carbon source can be engineered to treat such water. This study is significant because this region is rich in biodiversity and such mining impacted water may have adverse ecological impact, if discharged without appropriate treatment.The objective of the work is to characterise water samples collected from two open cast mines of Makum coalfield under NEC and evaluate the performance of a novel polyvinyl alcohol (PVA) gel packed bed bioreactor to treat the same. Sample collection, storage and physico-chemical analysis are carried out as per Standard methods of American Public Health Association. The biological treatment process is studied in a cylindrical continuous flow lab scale bioreactor under relevant acidic pH at different feed chemical oxygen demand (COD) to sulfate ratio and hydraulic retention time (HRT). Sludge from a lab scale anaerobic bioreactor treating very high sulfate industrial water is used as inoculum. The sulfate reducing microorganisms are enriched within the bioreactor in fed-batch mode using modified Postgate’ s medium for one month.Oxidation Reduction Potential (ORP), pH, sulfate removal, total inorganic carbon (TIC) and alkalinity produced are measured at the bioreactor outlet to evaluate the process performance. The mine water samples exhibit low pH, high sulfate, conductivity, dissolved solids, hardness, iron and manganese, which indicates the occurrence of AMD. The treatment process reduces the sulfate concentration and increases pH of the treated water. The use of highly porous PVA gel beads as packing material in the bioreactor treating sulfate rich acidic water imparts resilience to operational variation. The study evaluates the novel application of PVA gel beads to bioreactor for treating acidic mine waters from an ecologically important region. The research finding provides an understanding of the process for application to other biological AMD treatment configurations.

Keywords: acid mine drainage (AMD), polyvinyl alcohol (PVA), sulfate, sulfate reducing microorganism (SRM), dissimilatory sulfate reduction(DSR), pyrite

©2019. Japan Geoscience Union. All Right Reserved.

[J] Oral | A (Atmospheric and Hydrospheric Sciences)：A-CC Cryospheric Sciences & Cold District Environment

Wed. May 29, 2019 9:00 AM - 10:30 AM JST | Wed. May 29, 2019 12:00 AM - 1:30 AM UTC | 303 3F

[A-CC27] Glaciology

convener:Takayuki Nuimura(Tokyo Denki University), Ishikawa Mamoru(Hokkaido University), Kzutaka Tateyama(National University Corporation Kitami Institute of Technology), Hiroto Nagai(Waseda Univ., School of Education), Chairperson:Hiroto Nagai(Japan Aerospace Exploration Agency)

The cryosphere is a fundamental component of the earth system. It is a region where snow and ice exist in the form of glacier/ice sheet, snow cover and snowfall, frozen ground, sea ice and fresh water ice, and they play a critical role in the global environment under the interactions with atmosphere, ocean, ecosystem and others. In this session, research results on physical and chemical characteristics of snow and ice, variations and dynamics of cryospheric environment, roles of the cryosphere on the earth and other planets will be discussed broadly, regardless of the research method.

9:00 AM - 9:15 AM JST | 12:00 AM - 12:15 AM UTC

[ACC27-01] The early validation results of the GCOM-C/SGLI cryosphere standard product

★Invited Papers

*Rigen Shimada[1], Masahiro Hori[1], Teruo Aoki[2,3], Tomonori Tanikawa[2], Sumito Matoba[4], Masashi Niwano[2], Knut Stamnes[5], Wei Li[5], Nan Chen[5] (1.Japan Aerospace Exploration Agency, 2.Meteorological Research Institute, 3.Okayama University, 4.Institute of Low Temperature Science, Hokkaido University, 5.Stevens Institute of Technology)

9:15 AM - 9:30 AM JST | 12:15 AM - 12:30 AM UTC

[ACC27-02] Overview of the cryospheric variables derived from GCOM-C/SGLI observations: The first-year results

★Invited Papers

*Masahiro Hori[1], Teruo Aoki[2,4], Knut Stamnes[3], Wei Li[3], Nan Chen[3], Rigen Shimada[1], Tomonori Tanikawa[4], Masashi Niwano[4] (1.Earth Observation Reseacrh Center, Japan Aerospace Exploration Agency, 2.Okayama University, 3.Stevens Institute of Technology, 4.Meteorological Research Institute)

9:30 AM - 9:45 AM JST | 12:30 AM - 12:45 AM UTC

[ACC27-03] Relationships between PASAR-2 backscatter amplitude changes and snow depths

*Hiroto Nagai[1], Satoru Yamaguchi[2], Katsuya Yamashita[2], Mayumi Kashima[3] (1.Waseda University, School of Education, 2. National Research Institute for Earth Science and Disaster Resilience, 3.Esri Japan Corporation)

9:45 AM - 10:00 AM JST | 12:45 AM - 1:00 AM UTC

[ACC27-04] Breaking-off of hanging glaciers at Mt. Langtang-Lirung in Nepal

Honami Watanabe[2], *Chiyuki Narama[1], Yoshitaka Mori[2], Katsuhisa Kawashima[3] (1.Niigata University, Program of Field Research in the Environmental Sciences, 2.Graduate School of Science and Technology, Niigata University, 3.Research Institute for Natural Hazards & Disaster Recovery, Niigata University)

10:00 AM - 10:15 AM JST | 1:00 AM - 1:15 AM UTC

[ACC27-05] Spatial distribution of ice cliff in the Trakarding glacier, Nepal Himalaya

*Yota Sato[1], Koji Fujita[1], Hiroshi Inoue[2], Sojiro Sunako[1], Akiko Sakai[1], Akane Tsushima[1], Evgeny Podolskiy[3,4], Etienne Berthier[5], Rijan Kayastha[6] (1.Graduate School of Environmental Studies, Nagoya University, 2.National Research Institute for Earth Science and Disaster Resilience, 3.Arctic Research Center, Hokkaido University, 4.Global Station for Arctic Research, Global Institution for Collaborative Research and Education, Hokkaido University, 5.Centre National de la Recherche Scientifique, 6.School of Science, Kathmandu University)

10:15 AM - 10:30 AM JST | 1:15 AM - 1:30 AM UTC

[ACC27-06] Quantify the range of projections of future changes in glacier mass caused by differences among observed past climate datasets

*Megumi Watanabe[1], Aki Yanagawa[2], Yukiko Hirabayashi[3], Satoshi Watanabe[4], Shinjiro Kanae[1] (1.Tokyo Institute of Technology, 2.Meisei University, 3.Shibaura Institute of Technology, 4.The University of Tokyo)

The early validation results of the GCOM-C/SGLI cryosphere standard product

*Rigen Shimada[1], Masahiro Hori[1], Teruo Aoki[2,3], Tomonori Tanikawa[2], Sumito Matoba[4], Masashi Niwano[2], Knut Stamnes[5], Wei Li[5], Nan Chen[5]

1. Japan Aerospace Exploration Agency, 2. Meteorological Research Institute, 3. Okayama University, 4. Institute of Low Temperature Science, Hokkaido University, 5. Stevens Institute of Technology

Japan Aerospace Exploration Agency (JAXA) polar-orbit satellite, Global Change Observation Mission for Climate (GCOM-C) has been launched on 23 December 2017. The Second-generation Global Imager (SGLI) which is carried on GCOM-C observes various geophysical variables in the Atmosphere, Ocean, Land and Cryosphere for long-term monitoring of earth environment using multi wavelength, high resolution and multi angles. When focusing on the cryosphere: snow, sea-ice, glacier and ice sheet, their high albedo affect the cooling mechanism of the radiative balance. The GCOM-C/SGLI regularly creates cryosphere standard products including C1: snow, ice and cloud classification product and C2: snow grain size and snow surface temperature product. We validated these products by comparison with other satellite products and in-situ observation data. C1 product was validated by comparing other similar satellite product (e.g. Terra/MODIS) focusing on the snow and ice extent. C2 product was validated by match-up comparison with in-situ data and satellite retrieval results. Snow grain size of shallow layer was measured at the in-situ observation carried out at the East GRIP site on the North-eastern Greenland Ice Sheet in July 2018. Snow and ice surface temperature was derived from automatic weather station (AWS). From these validation results, all standard product was achieved the release threshold and JAXA decided to release the GCOM-C/SGLI product. In the presentation, some examples and case study of the GCOM-C/SGLI observation results will be shown.

Keywords: GCOM-C/SGLI, remote sensing, snow grain size

©2019. Japan Geoscience Union. All Right Reserved.

Overview of the cryospheric variables derived from GCOM-C/SGLI observations: The first-year results

*Masahiro Hori[1], Teruo Aoki[2,4], Knut Stamnes[3], Wei Li[3], Nan Chen[3], Rigen Shimada[1], Tomonori Tanikawa[4], Masashi Niwano[4]

1. Earth Observation Reseacrh Center, Japan Aerospace Exploration Agency, 2. Okayama University, 3. Stevens Institute of Technology, 4. Meteorological Research Institute

The “Global Change Observation Mission-Climate” (GCOM-C) is an Earth observing satellite of Japan Aerospace Exploration Agency (JAXA) for the global observation of the Earth environment. GCOM-C carries a multi-spectral optical radiometer named Second Generation Global Imager (SGLI), which has special features of wide spectral coverage from 380 nm to 12 μm, a high spatial resolution of 250 m, a field of view exceeding 1000 km, two-direction simultaneous observation, and polarization observation. The GCOM-C satellite was successfully launched from the Tanegashima Space Center in Japan on December 23, 2017 and SGLI started the Earth observations on January 1st, 2018. From the SGLI observations snow-related variables such as snow and ice cover extent, snow grain size, and snow surface temperature are being retrieved and the products of those variables have been released to the public from the JAXA’s satellite data providing service “G-Portal” (https://gportal.jaxa.jp/gpr/index/index) since December 20th 2018. These snow physical variables are important for determining spectral albedo and radiation budget at the snow surface. In this presentation, the first-year results of SGLI snow observations are presented as well as the introduction of the SGLI products with the special attention to the thermal infrared observations at 250-m spatial resolution.

Keywords: GCOM-C, SGLI, Snow Cover, Snow Grain Size, Surface Temperature, Remote Sensing

©2019. Japan Geoscience Union. All Right Reserved.

Relationships between PASAR-2 backscatter amplitude changes and snow depths

*Hiroto Nagai[1], Satoru Yamaguchi[2], Katsuya Yamashita[2], Mayumi Kashima[3]

1. Waseda University, School of Education, 2. National Research Institute for Earth Science and Disaster Resilience, 3. Esri Japan Corporation

For local governments heavy snowfall gives a very big economic burden. A large amount of tax will be put into operation of the snow removal vehicle, for example. The snow removal expenses of Niigata prefecture approaches 10 billion yen annually, but the operation plan (route selection and operation count) of the snow removal vehicle is not based on objective awareness of snow depth which can vary year by year.
In order to solve this problem, it is important to grasp the snow depth deep space distribution. The estimation of snow accumulation by the conventional satellite-mounted synthetic aperture radar (SAR) was mostly based on the C-band, and adaptation to the snow layer including liquid moisture have difficulty due to the short wavelength (Bernier et al., 1999; Li et al., 2017; Rignot et al., 2001; Shi et al., 1993; Shi and Dozier, 1995). However, in the L-band SAR, the correlation between the snow depth and the backscattering intensity was confirmed to be wet snow, which was a negative correlation (the snow is deeper the reflected intensity decreases) in the night observation assumed to be dry snow It was shown that positive correlation was obtained by day observation (Nagai et al., 2018a, 2018b).
In this research, we examined the image processing algorithm suitable for snow depth estimation for PALSAR-2 which is the L-band SAR equipped with "Daichi-2". First of all, the night observation data was used to minimize the influence of liquid moisture. Obtain data of the observation as 2015/11/22, 2016/11/20 as the no-snow period and 2018/01/28 as the snowy season, convert the backscattering intensity (dB). A series of moving average filter of 0, 5, 10, 15...55 pixels were carried out for each. Then statistical comparison of the ground measurement value compiled by Niigata University (Iyobe and Kawashima, 2016) and the SAR-derived backscatter amplitude changes was carried out.
As a result, the moving average filter with 10 pixels or more shows a negative correlation of $r < -0.3$, $p < 0.1\%$ in all cases, and the correlation coefficient decreased as the number of pixels of the filter increased. There was no significant difference between the November average image and the single scene image. For the linear approximation between the intensity difference and the measured value, the slope was almost constant with the moving average filter of 10 pixels or more.
By using data at night during the winter season, we can estimate snow depth from SAR with high negative correlation. In order to create a snow depth map with a better correlation coefficient, it is necessary to apply a stronger moving average filter, but since it becomes a coarse and smooth snow depth map according to it, it is necessary to consider a filter according to the application.
In addition to this, statistical analysis is also presented in this presentation on other seasons as the standard as well as for snow melting daytime observations presumed to contain a large amount of snow in the snow, and a snow depth estimation method using SAR deepens in the discussion.

(References)
Bernier, M., Fortin, J.-P., 1998. The potential of times series of C-Band SAR data to monitor dry and shallow snow cover. IEEE Trans. Geosci. Remote Sens. 36, 226–243.
Bernier, M., Fortin, J.P., Gauthier, Y., Gauthier, R., Roy, R., Vincent, P., 1999. Determination of Snow Water Equivalent using RADARSAT SAR data in eastern Canada. Hydrol. Process. 13, 3041–3051.
Li, H., Wang, Z., He, G., Man, W., 2017. Estimating snow depth and snow water equivalence using repeat-pass interferometric SAR in the northern piedmont region of the Tianshan Mountains. J. Sensors

©2019. Japan Geoscience Union. All Right Reserved.

2017.
Rignot, E., Echelmeyer, K., Krabill, W., 2001. Penetration depth of interferometric synthetic-aperture radar signals in snow and ice. Geophys. Res. Lett. 28, 3501–3504.
Shi, J., Dozier, J., 1995. Inferring snow wetness using C-band data from SIR-C’ s polarimetric synthetic aperture radar. IEEE Trans. Geosci. Remote Sens. 33, 905–914.
Shi, J., Dozier, J., Rott, H., 1993. Deriving snow liquid water content using C-band polarimetric SAR. Proc. IGARSS ’ 93 - IEEE Int. Geosci. Remote Sens. Symp. 1038–1041.
Nagai, H., Watanabe, T., Tadono, T., Motohka, T., 2018a. Development of snow-depth map using ALOS-2. JpGU 2018 ACC28-04.
Nagai, H., Watanabe, T., Tadono, T., Motohka, T., 2018b. Feasibility assessment of SAR-derived snow-depth map for Japanese wet snow conditions. AGU2018 NH31D–1196.
Iyobe, T., Kawashima, K., 2016. Development of a quasi-real-time monitoring system for snow depth distribution in Japan. JSSI JSSE Jt. Conf. Nagoya 119.

Keywords: SAR, snowpack, backscatter amplitude

©2019. Japan Geoscience Union. All Right Reserved.

Breaking-off of hanging glaciers at Mt. Langtang-Lirung in Nepal

Honami Watanabe[2], *Chiyuki Narama[1], Yoshitaka Mori[2], Katsuhisa Kawashima[3]

1. Niigata University, Program of Field Research in the Environmental Sciences, 2. Graduate School of Science and Technology, Niigata University, 3. Research Institute for Natural Hazards & Disaster Recovery, Niigata University

On 25 April 2015, an earthquake (M7.8) occurred at Gurkha region located northwest of Kathmandu, the capital of Nepal. On 12 May, an earthquake of M 7.3 occurred at 80 km northeast from Kathmandu. Due to this series of large earthquakes, slope failure events (ice avalanche, snow avalanche, snow-rock avalanche, rock avalanche) occurred frequently in snow mountain area of the Himalaya. In Langtang valley, a huge snow-rock avalanche caused more than 100 victims in Langtang village. We investigated the characteristics of bereaking-off from hunging glaciers around Mt. Langtang-Lirung using satellite data and digital aerial images in 2015 and 2018.

Keywords: hanging glacier, breaking-off, Mt. Langtang-Lirung, Gurkha earthquake

©2019. Japan Geoscience Union. All Right Reserved.

Spatial distribution of ice cliff in the Trakarding glacier, Nepal Himalaya

*Yota Sato[1], Koji Fujita[1], Hiroshi Inoue[2], Sojiro Sunako[1], Akiko Sakai[1], Akane Tsushima[1], Evgeny Podolskiy[3,4], Etienne Berthier[5], Rijan Kayastha[6]

1. Graduate School of Environmental Studies, Nagoya University, 2. National Research Institute for Earth Science and Disaster Resilience, 3. Arctic Research Center, Hokkaido University, 4. Global Station for Arctic Research, Global Institution for Collaborative Research and Education, Hokkaido University, 5. Centre National de la Recherche Scientifique, 6. School of Science, Kathmandu University

Glaciers in High Mountain Asia are valuable indicator of climate change, and its melt water have an important role for the regional water resources (e.g. Immerzeel et al., 2010). We thus need to estimate Himalayan glacier melting amount. However, the lower part of large Himalayan glaciers is generally covered with debris mantle, which makes the melting process complicated. Several previous works pointed out a role of ice cliffs that promote local enhancement of the ice melting (e.g. Brun et al., 2018). In previous studies, digital elevation models (DEMs) based on satellite imageries have been analyzed to estimate glacier mass change. However, it is difficult to extract ice cliffs due to their low resolution. Recently, Structure from Motion (SfM), image analysis technology, has been dramatically developed. This method enables to obtain high resolution glacial terrain data and identify the small features on glacier surface such as ice cliffs.
In this study, we generated high resolution DEMs and orthomosaic images from aerial photographs taken at three different times at the Trakarding glacier, Rolwaling region, Nepal Himalaya in order to evaluate area and aspect of ice cliffs, and analyzed the relation between cliff distribution and glacier surface elevation change. We carried out field observations and conducted aerial photogrammetry by fixed wing UAV in 2017 and helicopter in 2018 at the entire debris-covered area (3.1 km^2). We also analyzed photographs taken in 2007, and then created high resolution (0.2~2.0 m/pix) DEMs and orthomosaic images, from which about 500 ice cliffs were extracted.
DEMs shows that the surface elevation of the Trakarding Glacier declined between 2007 and 2017 by -1.65 m w.e. yr^{-1} while it lifted up between 2017 and 2018 by +1.25 m w.e. yr^{-1}. We find that the surface elevation changes are spatially heterogeneous. The more significant surface lowering happens, the higher cliff density is observed, suggesting that the ice cliff locally enhances glacier melting. In addition, the ice cliff length density was 7.9×10^{-3} m m^{-2} in 2017, which remarks the highest density comparing to a previous study in the Khumbu region (Watson et al., 2017). Further, we find significant correlation between ice cliff length and its slope area, which means that it is possible to estimate the slope area of cliff from the cliff length, which can be obtained from satellite images.

Reference

Immerzeel et al., 2010 : Climate change will affect the Asian water towers. Science., 328, 1382-1385.
Brun et al., 2018 : Ice cliff contribution to the tongue-wide ablation of Changri Nup Glacier, Nepal, central Himalaya. The Cryosphere., 12, 3439-3457.
Watson et al., 2017 : Ice cliff dynamics in the Everest region of the central Himalaya. Geomorphology., 278, 238-251.

©2019. Japan Geoscience Union. All Right Reserved.

Keywords: Glacier, Himalaya, UAV, SfM, Remote Sensing

©2019. Japan Geoscience Union. All Right Reserved.

Quantify the range of projections of future changes in glacier mass caused by differences among observed past climate datasets

*Megumi Watanabe[1], Aki Yanagawa[2], Yukiko Hirabayashi[3], Satoshi Watanabe[4], Shinjiro Kanae[1]

1. Tokyo Institute of Technology, 2. Meisei University, 3. Shibaura Institute of Technology, 4. The University of Tokyo

Observed climate data used as input in glacier models are expected to differ among datasets particularly at high elevations. Differences among datasets have not yet been described as a cause of uncertainty in projections of future changes in glacier mass, although uncertainty caused by varying future climate projections among general circulation models (GCMs) has often been discussed. Differences among climate datasets are expected to propagate as uncertainty in future changes in glacier mass due to bias correction of GCMs and calibration of glacier models. We project ensemble future changes in the mass of glaciers in Asia through the year 2100 using a glacier model. A set of 18 combinations of inputs, including two observed past air temperature datasets, three observed past precipitation datasets, and future air temperature and precipitation projections from three GCMs were used. The uncertainty in projected changes in glacier mass was partitioned into three distinct sources: GCM uncertainty, observed past air temperature uncertainty, and observed past precipitation uncertainty. Our findings indicate that, in addition to the differences in climate projections among GCMs, differences among climate datasets can propagate uncertainty into projected changes in glacier mass. Significant differences in observed precipitation did not cause major uncertainty in projected changes in glacier mass.

Keywords: propagation of uncertainty, glacier model, bias correction, calibration, air temperature, precipitation

©2019. Japan Geoscience Union. All Right Reserved.

[J] Oral | A (Atmospheric and Hydrospheric Sciences)：A-CC Cryospheric Sciences & Cold District Environment

Wed. May 29, 2019 10:45 AM - 12:15 PM JST | Wed. May 29, 2019 1:45 AM - 3:15 AM UTC | 303 3F

[A-CC27] Glaciology

convener:Takayuki Nuimura(Tokyo Denki University), Ishikawa Mamoru(Hokkaido University), Kzutaka Tateyama(National University Corporation Kitami Institute of Technology), Hiroto Nagai(Waseda Univ., School of Education), Chairperson:Takayuki Nuimura(Chiba Institute of Science)

The cryosphere is a fundamental component of the earth system. It is a region where snow and ice exist in the form of glacier/ice sheet, snow cover and snowfall, frozen ground, sea ice and fresh water ice, and they play a critical role in the global environment under the interactions with atmosphere, ocean, ecosystem and others. In this session, research results on physical and chemical characteristics of snow and ice, variations and dynamics of cryospheric environment, roles of the cryosphere on the earth and other planets will be discussed broadly, regardless of the research method.

10:45 AM - 11:00 AM JST | 1:45 AM - 2:00 AM UTC

[ACC27-07] Preliminary analysis result of the Handheld Integrating Sphere Snow Grain Sizer (HISSGraS)

*Teruo Aoki[1,2,3], Masashi Niwano[2], Satoru Yamaguchi[4], Sumito Matoba[5], Tomonori Tanikawa[2], Masahiro Hori[6], Rigen Shimada[6], Akihiro Hachikubo[7] (1.The Graduate School of Natural Science and Technology, Okayama University, 2.Meteorological Research Institute, Japan Meteorological Agency, 3.National Institute of Polar Research, 4.National Research Institute for Earth Science and Disaster Resilience, 5.Institute of Low Temperature Sciences, Hokkaido University, 6.Earth Observation Research Center, Japan Aerospace Exploration Agency, 7.Kitami Institute of Technology)

11:00 AM - 11:15 AM JST | 2:00 AM - 2:15 AM UTC

[ACC27-08] Experimental study on compaction process of highly porous ice: Implications for density change of icy regolith layer on icy bodies

Minami Yabe[1], *Minami Yasui[1], Masahiko Arakawa[1] (1.Department of Planetology, Graduate School of Science, Kobe University)

11:15 AM - 11:30 AM JST | 2:15 AM - 2:30 AM UTC

[ACC27-09] **Effect of snow impurities on the radiation budget and snow melting observed at Sapporo during 10 winter seasons**

*Yoichiro Hirozawa[1], Teruo Aoki[1,2], Masashi Niwano[2], Sumito Matoba[3], Yuji Kodama[4], Tomonori Tanikawa[2] (1.Okayama University, Graduate School of Natural Science and Technology, 2.Meteorological Research Institute, 3.Institute of Low Temperature Science, Hokkaido University, 4.National Institute of Polar Research)

11:30 AM - 12:15 PM JST | 2:30 AM - 3:15 AM UTC

Discussion

Preliminary analysis result of the Handheld Integrating Sphere Snow Grain Sizer (HISSGraS)

*Teruo Aoki[1,2,3], Masashi Niwano[2], Satoru Yamaguchi[4], Sumito Matoba[5], Tomonori Tanikawa[2], Masahiro Hori[6], Rigen Shimada[6], Akihiro Hachikubo[7]

1. The Graduate School of Natural Science and Technology, Okayama University, 2. Meteorological Research Institute, Japan Meteorological Agency, 3. National Institute of Polar Research, 4. National Research Institute for Earth Science and Disaster Resilience, 5. Institute of Low Temperature Sciences, Hokkaido University, 6. Earth Observation Research Center, Japan Aerospace Exploration Agency, 7. Kitami Institute of Technology

Snow grain size is one of the most important factors as a snow physical parameter expressing the snow metamorphism as well as controlling the albedo. As snow grains are generally non-spherical and complicated shapes, the optically-equivalent grain size is not a common glaciological grain size[1)]. Thus, various techniques to measure the specific surface area (SSA) as an optically-equivalent grain size have been developed[2-5)]. It is known from intercomparisons of those techniques so far that one of the most accurate field instruments is IceCube (A2 Photonics Sensor, France)[2)]. The IceCube measures a reflectance of snow sample at the wavelength of 1,310 nm using an integrating sphere and a laser light source. The value of SSA is transformed from the reflectance. A weight of the IceCube is as much as about 20 kg and the snow sampling into a sampling case is needed. These impose not only a workload to the observer but also a certain observation time. We therefore developed a small and light-weight (1/10) instrument, the Handheld Integrating Sphere Snow Grain Sizer (HISSGraS), which operates on the same principle as the IceCube and can measure snow pit face or snow surface directly. This direct measurement enables us to measure the SSA of snow of natural condition in a short time. We measured the SSAs with HISSGraS and IceCube for several snow samples in a cold laboratory and for natural snow pit face in Japan and Greenland. When the SSAs were measured for the same snow samples with both HISSGraS and IceCube, the those SSAs agreed well with each other. When HISSGraS measured snow pit face directly and IceCube measured snow samples collected from the same snow pit, the SSAs by HISSGraS were somewhat larger than those by IceCube. This is because the snow crystals in a sampling case would be compressed at the sampling and the snow grain size could differ from that under natural snow condition.

References

1) Aoki et al. (2007): Remote Sens. Environ., 111, 320–336.
2) Gallet et al. (2009): The Cryosphere, 3, 167-182.
3) Legagneux et al. (2002): J. Geophys. Res., 107(D17), 4335.
4) Hachikubo et al. (2012): Seppyo in Hokkaido, 31, 45–48.
5) Matzl and Schneebeli (2010): Cold Reg. Sci. Tech., 64, 1-8.

Keywords: snow grain size, specific surface area, albedo, snow metamorphism

©2019. Japan Geoscience Union. All Right Reserved.

Experimental study on compaction process of highly porous ice: Implications for density change of icy regolith layer on icy bodies

Minami Yabe[1], *Minami Yasui[1], Masahiko Arakawa[1]

1. Department of Planetology, Graduate School of Science, Kobe University

Ice sheets are found on the polar regions of Earth and Mars. Ice sheets were formed as snow was piled up and compacted into ice. Icy satellites are covered with ice regolith layer which is generated from impact craters by collisions of small bodies. It is supposed that this regolith layer is compacted by self-gravity, but the gravity of small icy satellites is very small and also the surface temperature is quite low, compared with that on the surfaces of Earth and Mars, so the compaction rate of ice regolith layer could be very low, then the deep icy regolith layer might be kept at high porosity on their surfaces. This icy regolith layer could be attributed to the evolution of the surface geology on icy satellites such as topographic relaxation and impact cratering. In this study, we focused on the compaction process of icy regolith layer on icy satellites and conducted compression experiments for highly porous ice under low stresses to examine the relationship between the compaction rate and the porosity.

Snow samples were prepared by filling ice particles with the diameter of ~20 μm into the cylinder mold and by compressing them by a piston into the cylinder with the diameter of 20 mm and the height of 40 mm. The initial porosity was 0.5-0.65. In order to examine the effect of sintering among ice particles on the compression rate, the sintering duration was changed from 0 to 200 hours. We conducted creep tests under constant stresses from 21 to 42 kPa. The displacement of the sample height was measured by a laser or a contact-typed displacement sensors while the diameter change was measured by using images take by a time lapse camera. The temperature was set to be -9and -11 ˚C.

First, we examined the relationship between the strain in a height direction, dh/h, and that in a horizontal direction (diameter change), dr/r, and found to be (dr/r)=-0.11(dh/h). Thus, the compaction rate, $(1/\rho \cdot d\rho/dt)$, was found to be obtained to be -0.78 times the strain rate in a height direction (we call this rate as “compression rate” hereafter), $1/h \cdot dh/h$.

Next, we examined the effect of sintering duration on the compression rate. Under same stress condition, the compression rate was smaller as the sintering duration was longer. However, when the sintering duration passed the critical period, the compression rate was nearly constant even if the sintering duration passed longer. This critical period became shorter as the initial porosity was larger. In this study, to exclude the effect of sintering duration on the compression rate, we examined the effects of porosity, stress, and temperature on the compression rate that was expected for the sample sintering at the period loger than the critical period.

We examined the relationship between the compression rate and the porosity, ϕ, and found that the compression rate could be fitted by the following power equation under a constant stress, irrespective of the initial porosity, $1/h \cdot dh/dt = B\exp(C\phi)$, where B and C are constants. The constant increased exponentially with the increase of the stress, σ, that is, $B \propto \sigma^n$, where n is constant. The constants, C, and n, did not depend on the stress and obtained to be C=24, and n=1.8.

Finally, we evaluated the compaction processes due to self-gravity on the Antarctica and a saturnian icy satellite, Enceladus, by using our obtained empirical equation. We calculated the density and the elevation change of the snow layer on the Antarctica and the icy regolith layer on Enceladus. In this calculation, we assumed that the initial density was homogeneous, 180 kg/m^3, in the whole layer and the stress on the ground surface was 100 kPa. In the case of the Antarctica (a layer thickness of 10 m), the density just above the ground surface increased about three times and the thickness was changed to be a half after 100 years. In the case of Enceladus (a layer thickness of 5 km), the thickness was changed to be

©2019. Japan Geoscience Union. All Right Reserved.

a half after 100 years, as same as the case of the Antarctica, but the density just above the ground surface increased about only twice and the density in the layer on Enceladus was smaller than that on the Antarctica on the whole.

Keywords: highly porous ice, compaction, creep experiment, sintering duration, icy regolith layer

©2019. Japan Geoscience Union. All Right Reserved.

Effect of snow impurities on the radiation budget and snow melting observed at Sapporo during 10 winter seasons

*Yoichiro Hirozawa[1], Teruo Aoki[1,2], Masashi Niwano[2], Sumito Matoba[3], Yuji Kodama[4], Tomonori Tanikawa[2]

1. Okayama University, Graduate School of Natural Science and Technology, 2. Meteorological Research Institute, 3. Institute of Low Temperature Science, Hokkaido University, 4. National Institute of Polar Research

Snow impurities originated from light-absorbing aerosols in the atmosphere have an effect to accelerate the cryospheric warming by reducing the albedo. According to IPCC AR5, black carbon (BC) on snow and ice was assessed to have a global and annual mean radiative forcing (RF) of +0.04 Wm^{-2}. However, the larger effect on the radiation budget and snow melting could be expected in urban area where the snow impurity concentrations are high. In this study, we investigated the effect of snow impurity (BC and mineral dust) concentration on albedo and snow melting from snow and meteorological data observed at Sapporo using physical based snow albedo model (PBSAM) (Aoki et al., 2011). The observation site is the meteorological observation field (43° 04' 56"N, 141° 20' 30"E, 15 m a.s.l) of the Institute of Low Temperature Science of Hokkaido University and the observation period analyzed is 10 winter seasons from 2007 to 2017. The observed broadband albedos were compared with the theoretical values calculated with the PBSAM to which the observed data of snow grain size, impurity concentrations, and downward radiation were input. In addition, we conducted numerical sensitivity experiments on the albedo change due to snow impurities and calculated their RFs. We also estimated a contribution of snow impurities to snow melting from the energy balance analysis.
Comparing the time series of the observed broadband albedos with the theoretically calculated values, the calculated albedo variations due to the change in snow grain size and impurity concentration agreed well with the observations in each year of the analysis period. The determination coefficient (R^2) and the root mean square error (RMSE) for the whole period obtained from the albedo comparison in the shortwave (SW) spectral region were 0.847 and 0.046, respectively, confirming the high accuracy of PBSAM. Next, sensitivity experiments were conducted on the albedo changes in the visible (VIS), near-infrared (NIR), and SW regions depending on the presence and absence of snow impurities. The albedo change and RF due to snow impurities (BC + mineral dust) in the whole period were -0.053 and +6.7 Wm^{-2}, respectively for the SW region. In addition, we estimated total snowmelt amount from the surface energy balance calculation and measured energy flux between the bottom of the snowpack and the underlying ground. The total estimated amount of snow melt for the whole period was 398 mm w. e..The contributions from surface melting and melting at the ground were 76% and 24%, respectively. The melting energy due to snow impurity-induced albedo reduction is equivalent to 28% of total amount of snow melting, which is larger than the melting at the ground and is not negligible. Furthermore, the contributions from BC and dust to this value are 21% and 7%, respectively.

References

Aoki, T., K. Kuchiki, M. Niwano, Y. Kodama, M. Hosaka and T. Tanaka (2011), Physically based snow albedo model for calculating broadband albedos and the solar heating profile in snowpack for general circulation models. *J. Geophys. Res.*, **116**, D11114, doi:10.1029/2010JD015507.

©2019. Japan Geoscience Union. All Right Reserved.

[J] Poster | A (Atmospheric and Hydrospheric Sciences)：A-CC Cryospheric Sciences & Cold District Environment

Wed. May 29, 2019 3:30 PM - 5:00 PM JST | Wed. May 29, 2019 6:30 AM - 8:00 AM UTC | Poster Hall International Exhibition Hall8, Makuhari Messe_9

[A-CC27] Glaciology

convener:Takayuki Nuimura(Tokyo Denki University), Ishikawa Mamoru(Hokkaido University), Kzutaka Tateyama(National University Corporation Kitami Institute of Technology), Hiroto Nagai(Waseda Univ., School of Education)

The cryosphere is a fundamental component of the earth system. It is a region where snow and ice exist in the form of glacier/ice sheet, snow cover and snowfall, frozen ground, sea ice and fresh water ice, and they play a critical role in the global environment under the interactions with atmosphere, ocean, ecosystem and others. In this session, research results on physical and chemical characteristics of snow and ice, variations and dynamics of cryospheric environment, roles of the cryosphere on the earth and other planets will be discussed broadly, regardless of the research method.

[ACC27-P01] Recent surface changes of rock glaciers in Tien Shan Mountains

*Hideyuki Takadama[1], Narama Chiyuki[2], Tsutomu Yamanokuchi[3], Takeo Tadono[4] (1.Graduate school of Science and Technology, Niigata university, 2.Department of Science, Niigata University , 3.RESTEC, 4.JAXA)

[ACC27-P02] **Verification of AMSR-2 sea ice concentration and utilization of ship navigation in the Arctic Ocean**

*Nodoka Ono[1] (1.Earth Observation Research Center, Japan Aerospace Exploration Agency)

[ACC27-P03] **Ice thickness and flow of the perennial snow patch at Karamatsu-sawa in Hida mountain range**

*Kenshiro Arie[1], Chiyuki Narama[2], Kotaro FUKUI[3], Hajime IIDA[3] (1.Graduate School of Science and Technology, Niigata University, 2.Faculty of Science, Niigata University, 3.Tateyama Caldera Sabo Museum)

[ACC27-P04] **Meltwater discharge from Wilkes Basin, East Antarctica at around 4.2 ka revealed from Beryllium-10 analysis of marine sediments**

*Bethany Behrens[1,2], Yosuke Miyairi[1], Adam Sproson[1], Masako Yamane[3], Yusuke Yokoyama[1,2,4,5] (1.Atmosphere and Ocean Research Institute, University of Tokyo, 5-1-5 Kashiwanoha, Kashiwa, Chiba 277-8564, Japan, 2.Graduate Program on Environmental Science, University of Tokyo, Komaba, Meguro, Tokyo 153-0041, Japan, 3.Institute for Space-Earth Environmental Research, Nagoya University, Furocho, Chikusa, Nagoya, Aichi, 464-8601, Japan, 4.Japan Agency for Marine-Earth Science and Technology (JAMSTEC), Natsushimacho, Yokosuka, Kanagawa Prefecture 237-0061, Japan, 5.Department of Earth and Planetary Science, Graduate School of Science, University of Tokyo, Hongo, Bunkyo, Tokyo 113-8654, Japan)

[ACC27-P05] Daily variation of supraglacial lakes in the southern Inylchek Glacier

*Naoki Sakurai[1], Chiyuki Narama[2], Hiroshi Inoue[3], Muhammed Esenamanov[4], Zarylbek Usekov[4] (1.Niigata University, 2. Niigata University Department of Science, 3.National Research Institute for Earth Science and Disaster Prevention, 4.Central Asian Institute for Applied Geosciences)

[ACC27-P06] Historical development of Spillway Lake on Ngozompa Glacier, Nepal

*Mohan Bahadur Chand[1], Teiji Watanabe[2], Yusuki Kobayashi[1] (1.Graduate School of Environmental Science, Hokkaido University, 2.Faculty of Environmental Earth Science, Hokkaido University)

[ACC27-P07] Feature analysis of the spectral of snow, ice, and water in Lake Suwa using MODIS data

*Tomohiro Nakazawa[1], Takashi Nonaka[2], Keishi Iwashita[2] (1.Department of Civil Engineering, College of Industrial Technology, Nihon University , 2.College of Industrial Technology, Nihon University)

Recent surface changes of rock glaciers in Tien Shan Mountains

*Hideyuki Takadama[1], Narama Chiyuki[2], Tsutomu Yamanokuchi[3], Takeo Tadono[4]

1. Graduate school of Science and Technology, Niigata university, 2. Department of Science, Niigata University , 3. RESTEC, 4. JAXA

The rock glacier which composed of ice (permafrost) and debris is one of topographies to confirm periglacial area. It normally moves down at about 0.1-1m/yr by ice creeping, but the velocity of rock glacier in the study area is more faster than any other mountain regions. It has come to understand that the rock glacier is significantly accelerated in the Alps recently, and it is attributed to increasing temperature. But as for the rock glacier in the Tien Shan, it does not have sufficient data to know how fast it moves in the present and past. In this study, we tried to investigate the surface changes of rock glaciers in the Tien Shan Mountains at various time interval using DInSAR analysis. In addition, we observed the surface motion using GNSS measurement, and air and ground surface temperatures.

Keywords: rock glacier, DInSAR, Tien Shan

©2019. Japan Geoscience Union. All Right Reserved.

Verification of AMSR-2 sea ice concentration and utilization of ship navigation in the Arctic Ocean

*Nodoka Ono[1]

1. Earth Observation Research Center, Japan Aerospace Exploration Agency

Mitsui O.S.K. Lines, Ltd. (MOL) plans to transport LNG produced in Yamaru through the Arctic Ocean for 28 years from 2018 using the Northern Sea Route.

JAXA offers sea ice products (sea ice concentration, etc.) from the Advanced Microwave Scanning Radiometer-2 (AMSR-2) carried by the Global Change Observation Mission-Water (GCOM-W) via the ship navigation support service 'VENUS' developed by the National Institute of Polar Research and verifies the availability of AMSR2 products for ship navigation.

In addition, JAXA has installed interval cameras developed by Weathernews Inc. on the LNG ship, which enables the acquisition of sea ice information in the Arctic Ocean for long periods.

Based on these field data, sea ice concentrations are calculated using the image analysis system developed by Tanaka et al. (2015), which are then verified against products from the AMSR-2 and the MODerate resolution Imaging Spectroradiometer (MODIS) carried by Terra/Aqua satellite.

In this study, the result of verification are reported.

Keywords: satellite remote sensing, passive microwave, Northern Sea Route

©2019. Japan Geoscience Union. All Right Reserved.

Ice thickness and flow of the perennial snow patch at Karamatsu-sawa in Hida mountain range

*Kenshiro Arie[1], Chiyuki Narama[2], Kotaro FUKUI[3], Hajime IIDA[3]

1. Graduate School of Science and Technology, Niigata University, 2. Faculty of Science, Niigata University, 3. Tateyama Caldera Sabo Museum

We investigated ice thickness and flow speed of the perennial snow patch at Karamatsu-sawa by GPR observation and GNSS observation. As a result, ice thickness of the perennial snow patch was about 30m and the flow speed was several centimeter.

Keywords: glacier, perennial snow patch, equilibrium line altitude, GPR, GNSS

©2019. Japan Geoscience Union. All Right Reserved.

Meltwater discharge from Wilkes Basin, East Antarctica at around 4.2 ka revealed from Beryllium-10 analysis of marine sediments

*Bethany Behrens[1,2], Yosuke Miyairi[1], Adam Sproson[1], Masako Yamane[3], Yusuke Yokoyama[1,2,4,5]

1. Atmosphere and Ocean Research Institute, University of Tokyo, 5-1-5 Kashiwanoha, Kashiwa, Chiba 277-8564, Japan, 2. Graduate Program on Environmental Science, University of Tokyo, Komaba, Meguro, Tokyo 153-0041, Japan, 3. Institute for Space-Earth Environmental Research, Nagoya University, Furocho, Chikusa, Nagoya, Aichi, 464-8601, Japan, 4. Japan Agency for Marine-Earth Science and Technology (JAMSTEC), Natsushimacho, Yokosuka, Kanagawa Prefecture 237-0061, Japan, 5. Department of Earth and Planetary Science, Graduate School of Science, University of Tokyo, Hongo, Bunkyō, Tokyo 113-8654, Japan

Understanding Antarctic ice sheet dynamics related to global climate change is of scientific and societal interest as the future behavior of the ice sheets under currently changing climate is unknown. We present beryllium-10 analysis of a high-resolution marine sediment core from Adélie Basin near the Wilkes Land ice sheet, which is susceptible to retreat due to the low-lying nature and down-sloping trough of the Wilkes Basin. Combined with a newly constructed age model using compound specific radiocarbon dates, the data reveal three ice sheet meltwater discharge events at ca. ~10 ka, ca. ~6.5 ka and ca. ~4 ka. The earlier events correspond to the disappearance of Northern Hemisphere ice sheets and interglacial level atmospheric CO_2. The timing of the latest meltwater influx complements the 4.2 ka event, a period of abrupt global climatic change and the beginning of the Meghalayan Age.

Keywords: Holocene, East Antarctica, Adelie Basin, 4.2 ka event, Beryllium-10

©2019. Japan Geoscience Union. All Right Reserved.

Daily variation of supraglacial lakes in the southern Inylchek Glacier

*Naoki Sakurai[1], Chiyuki Narama[2], Hiroshi Inoue[3], Muhammed Esenamanov[4], Zarylbek Usekov[4]

1. Niigata University, 2. Niigata University Department of Science, 3. National Research Institute for Earth Science and Disaster Prevention, 4. Central Asian Institute for Applied Geosciences

In the eastern Himalayas and Karakoram, sudden large-scale drainage and flooding can occur from debris-covered glaciers that lack a large proglacial lake.This type of glacial lake outburst flood (GLOF) differs clearly from large proglacial lakes. Thus, these studies indicate that debris-covered glaciers that lack a large proglacial lake can have one or more supraglacial lakes vanish when a sudden, large drainage occurs through englacial/subglacial channels, sometime leading to dangerous flooding.

It has been clarified that seasonal variation of supraglacial lakes exist as variation of supraglacial lakes, but shorter period variation are not disclosed. Therefore, in this research it is to elucidate the daily variation of supraglacial lakes.

Using field survey in 2017 and 2018 plus satellite data from the 2014-2018 period, we analyze the daily variation of supraglacial lakes on the Southern Inylchek Glacier in the central Tien Shan.

Keywords: supragracial lake, drainage, debris-covered glacier , englacial channel

©2019. Japan Geoscience Union. All Right Reserved.

Historical development of Spillway Lake on Ngozompa Glacier, Nepal

*Mohan Bahadur Chand[1], Teiji Watanabe[2], Yusuki Kobayashi[1]

1. Graduate School of Environmental Science, Hokkaido University, 2. Faculty of Environmental Earth Science, Hokkaido University

Continuous loss of glacier mass in the recent period resulted the growth of several moraine-dammed glacial lakes at the terminus of the glaciers in the Himalayan region. It increases the risk of glacier lake outburst floods with the increase in size and volume of lakes. The loss of glacier mass decreases the elevation of the glacier surface and leads to the formation of elevated moraine dam which increase the possibility for developing new glacial lakes. In this study, we document the historical development of the spillway lake on Ngozompa Glacier, Nepal using a combination of Unmanned Aerial Vehicle (UAV) photos, WorldView imageries (0.5 –2 m), and Landsat imageries. We used Landsat imageries from 1989-2018 to prepare the long-term development of the lakes. High-resolution WorldView images and UAV photos were used for accuracy assessment. We also processed the UAV photos to prepare the Digital Elevation Model to understand the possibility of future development of the lakes. We observed the three small supraglacial ponds (0.03 km^2) near the terminus of the glacier in 1989 and they have undergone rapid change in their area till 2018 (0.32 km^2), increased by more than ten times. Several supraglacial ponds are merging together to become a large lake and it will be likely to continue in the future. The further growth of the lake is dependent largely on the subaqueous melting and calving of glacier ice, and on undercutting action of lake water. Subaqueous melting of the glacier ice leads to increase of lake depth and volume of water. However, future development of the lake depends largely on the level of the outlet channel. Presence of glacier ice under the channel may continuously lower its level and drain the water from lake. Geophysical studies are needed to understand the condition of the outlet channel.

Keywords: Glacier, Himalaya, Glacial lake, Glacier lake outburst floods, Nepal, Unmanned Aerial Vehicle (UAV)

©2019. Japan Geoscience Union. All Right Reserved.

Feature analysis of the spectral of snow, ice, and water in Lake Suwa using MODIS data

*Tomohiro Nakazawa[1], Takashi Nonaka[2], Keishi Iwashita[2]

1. Department of Civil Engineering, College of Industrial Technology, Nihon University , 2. College of Industrial Technology, Nihon University

The freezing and breakup dates of the lake are important as an index of climate change. There is not enough record of freezing and breakup dates of the lakes in Japan though various publication reports are available in Europe and United States. Estimating freezing and breakup dates in Japanese lakes contributes to grasp the trend of climate change in Japan. Satellite data is expected to complement the dates of such lakes without in-situ observations.
Therefore, our study team has developed the methodology to classify the lake surface on Lake Suwa using optical satellite data. Currently, we tried to classify the lake surface into snow, ice, and water and estimate the temporal surface changes of the lake using the spectral reflectance data and the surface temperature acquired by MODIS on daily observed Terra satellite. However, we found the difficulty to distinguish thin ice and water by the difference of the surface reflectance.
The purpose of this study was to grasp the feature of reflectance of the Lake Suwa, and we used the surface reflectance data derived by MODIS in winter season mainly in 2014 and 2018. This study acquired the lake surface status referring to the newspaper articles.
From the analysis of the reflectance of each band, it showed that the variation of the reflectance between snow, ice, and water was different depending on the wavelength. The ice showed the relatively high reflectance on band 3 (visible blue) and 4 (visible green), while snow had high reflectance on band 1 (visible red) and 2 (near infrared). The water also showed the high reflectance on band 3 and 4, and classification between ice and water was difficult only by the reflectance data. This study also compared the observations derived by the spectral band values of Landsat-8, and confirmed the validity of the result.

Keywords: MODIS, Lake Suwa, Reflectance, Freezing state

©2019. Japan Geoscience Union. All Right Reserved.

[J] Poster | A (Atmospheric and Hydrospheric Sciences)：A-CC Cryospheric Sciences & Cold District Environment

Wed. May 29, 2019 5:15 PM - 6:30 PM JST | Wed. May 29, 2019 8:15 AM - 9:30 AM UTC | Poster Hall International Exhibition Hall8, Makuhari Messe_15

[A-CC27] Glaciology

convener:Takayuki Nuimura(Tokyo Denki University), Ishikawa Mamoru(Hokkaido University), Kzutaka Tateyama(National University Corporation Kitami Institute of Technology), Hiroto Nagai(Waseda Univ., School of Education)

The cryosphere is a fundamental component of the earth system. It is a region where snow and ice exist in the form of glacier/ice sheet, snow cover and snowfall, frozen ground, sea ice and fresh water ice, and they play a critical role in the global environment under the interactions with atmosphere, ocean, ecosystem and others. In this session, research results on physical and chemical characteristics of snow and ice, variations and dynamics of cryospheric environment, roles of the cryosphere on the earth and other planets will be discussed broadly, regardless of the research method.

[ACC27-P01] Recent surface changes of rock glaciers in Tien Shan Mountains

*Hideyuki Takadama[1], Narama Chiyuki[2], Tsutomu Yamanokuchi[3], Takeo Tadono[4] (1.Graduate school of Science and Technology, Niigata university, 2.Department of Science, Niigata University , 3.RESTEC, 4.JAXA)

[ACC27-P02] **Verification of AMSR-2 sea ice concentration and utilization of ship navigation in the Arctic Ocean**

*Nodoka Ono[1] (1.Earth Observation Research Center, Japan Aerospace Exploration Agency)

[ACC27-P03] **Ice thickness and flow of the perennial snow patch at Karamatsu-sawa in Hida mountain range**

*Kenshiro Arie[1], Chiyuki Narama[2], Kotaro FUKUI[3], Hajime IIDA[3] (1.Graduate School of Science and Technology, Niigata University, 2.Faculty of Science, Niigata University, 3.Tateyama Caldera Sabo Museum)

[ACC27-P04] **Meltwater discharge from Wilkes Basin, East Antarctica at around 4.2 ka revealed from Beryllium-10 analysis of marine sediments**

*Bethany Behrens[1,2], Yosuke Miyairi[1], Adam Sproson[1], Masako Yamane[3], Yusuke Yokoyama[1,2,4,5] (1.Atmosphere and Ocean Research Institute, University of Tokyo, 5-1-5 Kashiwanoha, Kashiwa, Chiba 277-8564, Japan, 2.Graduate Program on Environmental Science, University of Tokyo, Komaba, Meguro, Tokyo 153-0041, Japan, 3.Institute for Space-Earth Environmental Research, Nagoya University, Furocho, Chikusa, Nagoya, Aichi, 464-8601, Japan, 4.Japan Agency for Marine-Earth Science and Technology (JAMSTEC), Natsushimacho, Yokosuka, Kanagawa Prefecture 237-0061, Japan, 5.Department of Earth and Planetary Science, Graduate School of Science, University of Tokyo, Hongo, Bunkyo, Tokyo 113-8654, Japan)

[ACC27-P05] Daily variation of supraglacial lakes in the southern Inylchek Glacier

*Naoki Sakurai[1], Chiyuki Narama[2], Hiroshi Inoue[3], Muhammed Esenamanov[4], Zarylbek Usekov[4] (1.Niigata University, 2. Niigata University Department of Science, 3.National Research Institute for Earth Science and Disaster Prevention, 4.Central Asian Institute for Applied Geosciences)

[ACC27-P06] Historical development of Spillway Lake on Ngozompa Glacier, Nepal

*Mohan Bahadur Chand[1], Teiji Watanabe[2], Yusuki Kobayashi[1] (1.Graduate School of Environmental Science, Hokkaido University, 2.Faculty of Environmental Earth Science, Hokkaido University)

[ACC27-P07] Feature analysis of the spectral of snow, ice, and water in Lake Suwa using MODIS data

*Tomohiro Nakazawa[1], Takashi Nonaka[2], Keishi Iwashita[2] (1.Department of Civil Engineering, College of Industrial Technology, Nihon University , 2.College of Industrial Technology, Nihon University)

Recent surface changes of rock glaciers in Tien Shan Mountains

*Hideyuki Takadama[1], Narama Chiyuki[2], Tsutomu Yamanokuchi[3], Takeo Tadono[4]

1. Graduate school of Science and Technology, Niigata university, 2. Department of Science, Niigata University , 3. RESTEC, 4. JAXA

The rock glacier which composed of ice (permafrost) and debris is one of topographies to confirm periglacial area. It normally moves down at about 0.1-1m/yr by ice creeping, but the velocity of rock glacier in the study area is more faster than any other mountain regions. It has come to understand that the rock glacier is significantly accelerated in the Alps recently, and it is attributed to increasing temperature. But as for the rock glacier in the Tien Shan, it does not have sufficient data to know how fast it moves in the present and past. In this study, we tried to investigate the surface changes of rock glaciers in the Tien Shan Mountains at various time interval using DInSAR analysis. In addition, we observed the surface motion using GNSS measurement, and air and ground surface temperatures.

Keywords: rock glacier, DInSAR, Tien Shan

©2019. Japan Geoscience Union. All Right Reserved.

Verification of AMSR-2 sea ice concentration and utilization of ship navigation in the Arctic Ocean

*Nodoka Ono[1]

1. Earth Observation Research Center, Japan Aerospace Exploration Agency

Mitsui O.S.K. Lines, Ltd. (MOL) plans to transport LNG produced in Yamaru through the Arctic Ocean for 28 years from 2018 using the Northern Sea Route.

JAXA offers sea ice products (sea ice concentration, etc.) from the Advanced Microwave Scanning Radiometer-2 (AMSR-2) carried by the Global Change Observation Mission-Water (GCOM-W) via the ship navigation support service 'VENUS' developed by the National Institute of Polar Research and verifies the availability of AMSR2 products for ship navigation.

In addition, JAXA has installed interval cameras developed by Weathernews Inc. on the LNG ship, which enables the acquisition of sea ice information in the Arctic Ocean for long periods.

Based on these field data, sea ice concentrations are calculated using the image analysis system developed by Tanaka et al. (2015), which are then verified against products from the AMSR-2 and the MODerate resolution Imaging Spectroradiometer (MODIS) carried by Terra/Aqua satellite.

In this study, the result of verification are reported.

Keywords: satellite remote sensing, passive microwave, Northern Sea Route

©2019. Japan Geoscience Union. All Right Reserved.

Ice thickness and flow of the perennial snow patch at Karamatsu-sawa in Hida mountain range

*Kenshiro Arie[1], Chiyuki Narama[2], Kotaro FUKUI[3], Hajime IIDA[3]

1. Graduate School of Science and Technology, Niigata University, 2. Faculty of Science, Niigata University, 3. Tateyama Caldera Sabo Museum

We investigated ice thickness and flow speed of the perennial snow patch at Karamatsu-sawa by GPR observation and GNSS observation. As a result, ice thickness of the perennial snow patch was about 30m and the flow speed was several centimeter.

Keywords: glacier, perennial snow patch, equilibrium line altitude, GPR, GNSS

©2019. Japan Geoscience Union. All Right Reserved.

Meltwater discharge from Wilkes Basin, East Antarctica at around 4.2 ka revealed from Beryllium-10 analysis of marine sediments

*Bethany Behrens[1,2], Yosuke Miyairi[1], Adam Sproson[1], Masako Yamane[3], Yusuke Yokoyama[1,2,4,5]

1. Atmosphere and Ocean Research Institute, University of Tokyo, 5-1-5 Kashiwanoha, Kashiwa, Chiba 277-8564, Japan, 2. Graduate Program on Environmental Science, University of Tokyo, Komaba, Meguro, Tokyo 153-0041, Japan, 3. Institute for Space-Earth Environmental Research, Nagoya University, Furocho, Chikusa, Nagoya, Aichi, 464-8601, Japan, 4. Japan Agency for Marine-Earth Science and Technology (JAMSTEC), Natsushimacho, Yokosuka, Kanagawa Prefecture 237-0061, Japan, 5. Department of Earth and Planetary Science, Graduate School of Science, University of Tokyo, Hongo, Bunkyō, Tokyo 113-8654, Japan

Understanding Antarctic ice sheet dynamics related to global climate change is of scientific and societal interest as the future behavior of the ice sheets under currently changing climate is unknown. We present beryllium-10 analysis of a high-resolution marine sediment core from Adélie Basin near the Wilkes Land ice sheet, which is susceptible to retreat due to the low-lying nature and down-sloping trough of the Wilkes Basin. Combined with a newly constructed age model using compound specific radiocarbon dates, the data reveal three ice sheet meltwater discharge events at ca. ~10 ka, ca. ~6.5 ka and ca. ~4 ka. The earlier events correspond to the disappearance of Northern Hemisphere ice sheets and interglacial level atmospheric CO_2. The timing of the latest meltwater influx complements the 4.2 ka event, a period of abrupt global climatic change and the beginning of the Meghalayan Age.

Keywords: Holocene, East Antarctica, Adelie Basin, 4.2 ka event, Beryllium-10

©2019. Japan Geoscience Union. All Right Reserved.

Daily variation of supraglacial lakes in the southern Inylchek Glacier

*Naoki Sakurai[1], Chiyuki Narama[2], Hiroshi Inoue[3], Muhammed Esenamanov[4], Zarylbek Usekov[4]

1. Niigata University, 2. Niigata University Department of Science, 3. National Research Institute for Earth Science and Disaster Prevention, 4. Central Asian Institute for Applied Geosciences

In the eastern Himalayas and Karakoram, sudden large-scale drainage and flooding can occur from debris-covered glaciers that lack a large proglacial lake.This type of glacial lake outburst flood (GLOF) differs clearly from large proglacial lakes. Thus, these studies indicate that debris-covered glaciers that lack a large proglacial lake can have one or more supraglacial lakes vanish when a sudden, large drainage occurs through englacial/subglacial channels, sometime leading to dangerous flooding.

It has been clarified that seasonal variation of supraglacial lakes exist as variation of supraglacial lakes, but shorter period variation are not disclosed. Therefore, in this research it is to elucidate the daily variation of supraglacial lakes.

Using field survey in 2017 and 2018 plus satellite data from the 2014-2018 period, we analyze the daily variation of supraglacial lakes on the Southern Inylchek Glacier in the central Tien Shan.

Keywords: supragracial lake, drainage, debris-covered glacier , englacial channel

©2019. Japan Geoscience Union. All Right Reserved.

Historical development of Spillway Lake on Ngozompa Glacier, Nepal

*Mohan Bahadur Chand[1], Teiji Watanabe[2], Yusuki Kobayashi[1]

1. Graduate School of Environmental Science, Hokkaido University, 2. Faculty of Environmental Earth Science, Hokkaido University

Continuous loss of glacier mass in the recent period resulted the growth of several moraine-dammed glacial lakes at the terminus of the glaciers in the Himalayan region. It increases the risk of glacier lake outburst floods with the increase in size and volume of lakes. The loss of glacier mass decreases the elevation of the glacier surface and leads to the formation of elevated moraine dam which increase the possibility for developing new glacial lakes. In this study, we document the historical development of the spillway lake on Ngozompa Glacier, Nepal using a combination of Unmanned Aerial Vehicle (UAV) photos, WorldView imageries (0.5 –2 m), and Landsat imageries. We used Landsat imageries from 1989-2018 to prepare the long-term development of the lakes. High-resolution WorldView images and UAV photos were used for accuracy assessment. We also processed the UAV photos to prepare the Digital Elevation Model to understand the possibility of future development of the lakes. We observed the three small supraglacial ponds (0.03 km^2) near the terminus of the glacier in 1989 and they have undergone rapid change in their area till 2018 (0.32 km^2), increased by more than ten times. Several supraglacial ponds are merging together to become a large lake and it will be likely to continue in the future. The further growth of the lake is dependent largely on the subaqueous melting and calving of glacier ice, and on undercutting action of lake water. Subaqueous melting of the glacier ice leads to increase of lake depth and volume of water. However, future development of the lake depends largely on the level of the outlet channel. Presence of glacier ice under the channel may continuously lower its level and drain the water from lake. Geophysical studies are needed to understand the condition of the outlet channel.

Keywords: Glacier, Himalaya, Glacial lake, Glacier lake outburst floods, Nepal, Unmanned Aerial Vehicle (UAV)

©2019. Japan Geoscience Union. All Right Reserved.

Feature analysis of the spectral of snow, ice, and water in Lake Suwa using MODIS data

*Tomohiro Nakazawa[1], Takashi Nonaka[2], Keishi Iwashita[2]

1. Department of Civil Engineering, College of Industrial Technology, Nihon University , 2. College of Industrial Technology, Nihon University

The freezing and breakup dates of the lake are important as an index of climate change. There is not enough record of freezing and breakup dates of the lakes in Japan though various publication reports are available in Europe and United States. Estimating freezing and breakup dates in Japanese lakes contributes to grasp the trend of climate change in Japan. Satellite data is expected to complement the dates of such lakes without in-situ observations.
Therefore, our study team has developed the methodology to classify the lake surface on Lake Suwa using optical satellite data. Currently, we tried to classify the lake surface into snow, ice, and water and estimate the temporal surface changes of the lake using the spectral reflectance data and the surface temperature acquired by MODIS on daily observed Terra satellite. However, we found the difficulty to distinguish thin ice and water by the difference of the surface reflectance.
The purpose of this study was to grasp the feature of reflectance of the Lake Suwa, and we used the surface reflectance data derived by MODIS in winter season mainly in 2014 and 2018. This study acquired the lake surface status referring to the newspaper articles.
From the analysis of the reflectance of each band, it showed that the variation of the reflectance between snow, ice, and water was different depending on the wavelength. The ice showed the relatively high reflectance on band 3 (visible blue) and 4 (visible green), while snow had high reflectance on band 1 (visible red) and 2 (near infrared). The water also showed the high reflectance on band 3 and 4, and classification between ice and water was difficult only by the reflectance data. This study also compared the observations derived by the spectral band values of Landsat-8, and confirmed the validity of the result.

Keywords: MODIS, Lake Suwa, Reflectance, Freezing state

©2019. Japan Geoscience Union. All Right Reserved.

[E] Oral | A (Atmospheric and Hydrospheric Sciences)：A-CG Complex & General

Wed. May 29, 2019 3:30 PM - 5:00 PM JST | Wed. May 29, 2019 6:30 AM - 8:00 AM UTC | 302 3F

[A-CG34] Satellite Earth Environment Observation

convener:Riko Oki(Japan Aerospace Exploration Agency), Yoshiaki HONDA(Center for Environmental Remote Sensing, Chiba University), Yukari Takayabu(Atmosphere and Ocean Research Institute, the University of Tokyo), Tsuneo Matsunaga(Center for Global Environmental Research and Satellite Observation Center, National Institute for Environmental Studies), Chairperson:Misako Kachi(Earth Observation Research Center, Japan Aerospace Exploration Agency)

In recent years, we cannot avoid facing issues on global environmental changes that occur in various spatiotemporal scales. The earth environmental observation data by satellites became the necessary basic data to tackle and solve those issues. Due to the recent advancement in the observation sensor technique and the data processing technique, the satellite observation has been showing rapid progress, and the time is changing from examining the accuracy of the observation sensor data to the advancement of the data application, leading to broaden potential users. In these days application became synergetic, so we comprehensively pick
up this topic in the Atmospheric and Hydrospheric Sciences Session of this Union Meeting that enables to comprise the atmospheric, oceanic and land sciences; by combining the intelligence and the knowledge of the party, we propose a session that aims to prompt further studies towards the issues on earth environmental change, the advancement in the data application and future plans of Earth Observation missions.

3:30 PM - 3:45 PM JST | 6:30 AM - 6:45 AM UTC

[ACG34-01] Current Status and Future Plan of the Global Change Observation Mission - Water (GCOM-W) and Advanced Microwave Scanning Radiometer 2 (AMSR2)

*Misako Kachi[1], Takashi Maeda[1], Nodoka Ono[1], Hideyuki Fujii[1], Marehito Kasahara[1], Naoto Ebuchi[1,2] (1.Earth Observation Research Center, Japan Aerospace Exploration Agency, 2.Institute of Low Temperature Science, Hokkaido University)

3:45 PM - 4:00 PM JST | 6:45 AM - 7:00 AM UTC

[ACG34-02] Testing and Evaluation for JPSS-1 Algorithms using Algorithm Development Library Block 2.1

*Bigyani Das[1,2], Weizhong Chen[1,2], Thomas S King[1,2], Walter Wolf[2] (1.IMSG, 2.STAR/NESDIS/NOAA)

4:00 PM - 4:15 PM JST | 7:00 AM - 7:15 AM UTC

[ACG34-03] Remote Sensing of Atmospheric and Surface Properties using Hyperspectral satellite Sensors

*Xu Liu[1] (1.NASA Langley Research Center)

4:15 PM - 4:30 PM JST | 7:15 AM - 7:30 AM UTC

[ACG34-04] **RADIOMETRIC UNIFORMITY AND STABILITY OF GROUND SITE CHARACTERIZATION FOR INSAT-3D**

*Shailesh Parihar[1], R. Bhatla[1], A. K. Mitra[2] (1.Banaras Hindu University, Varanasi, India, 2.India Meteorological Department, New Delhi, India)

4:30 PM - 4:45 PM JST | 7:30 AM - 7:45 AM UTC

[ACG34-05] Vicarious calibration activities of ASTER Thermal Infrared Radiometer (TIR) for Earth environmental observation

*Satoru Yamamoto[1], Hideyuki Tonooka[2], Soushi Kato[3], Kazuki Ayuzawa[2], Tsuneo Matsunaga[4] (1.Japan Space Systems, 2.Ibaraki University, 3.Remote Sensing Technology Center of Japan, 4.National Institute for Environmental Studies)

4:45 PM - 5:00 PM JST | 7:45 AM - 8:00 AM UTC

[ACG34-06] **Overview of Vegetation Lidar MOLI**

★Invited Papers

*Haruhisa Shimoda[1], Toshiyoshi Kimura[2], Rei Mituhashi [2], Junpei Muruoka [2], Daisuke Sakaizawa[2], Tadashi Imai [2], Kazuhiro Asai[3] (1.Tokai University, 2.JAXA, 3.Tohoku Institute of Technology)

Current Status and Future Plan of the Global Change Observation Mission - Water (GCOM-W) and Advanced Microwave Scanning Radiometer 2 (AMSR2)

*Misako Kachi[1], Takashi Maeda[1], Nodoka Ono[1], Hideyuki Fujii[1], Marehito Kasahara[1], Naoto Ebuchi[1,2]

1. Earth Observation Research Center, Japan Aerospace Exploration Agency, 2. Institute of Low Temperature Science, Hokkaido University

The Global Change Observation Mission (GCOM) –Water (GCOM-W) is one of two medium sized satellites to provide comprehensive information of the Essential Climate Variables (ECV) of atmosphere, ocean, land, cryosphere, and ecosystem. The GCOM-W (Water) or “SHIZUKU” satellite that carries the Advanced Microwave Scanning Radiometer 2 (AMSR2), which was launched on May 2012; and GCOM-C (Climate) or “SHIKISAI” satellite that carries the Second-generation Global Imager (SGLI) and launched in December 2017. Both satellites are currently operating, and their data are distributed through the JAXA G-Portal (https://gportal.jaxa.jp/gpr/).

AMSR2 is multi-frequency, total-power microwave radiometer system with dual polarization channels for all frequency bands, and a successor of JAXA’s Advanced Microwave Scanning Radiometer for EOS (AMSR-E) on the NASA's Aqua satellite. Sensor specification of AMSR2 is almost identical to that of AMSR-E, except larger (2.0 m) antenna, additional 7.3 GHz channels to mitigate Radio Frequency Interference (RFI) and improved internal calibration. Due to its higher spatial resolution, all-weather capability, near-real-time availability and observation stability, AMSR2 data is routinely used in many operational and science applications. To provide consistent dataset between AMSR2 and AMSR-E for long-term water cycle monitoring and climate studies, we applied the latest AMSR2 algorithms and formats to AMSR-E data and have provided products through the G-Portal system. Level 1B and 1R (resampled L1B) products have been released since April 2018, and Level 2 products will be released early summer in 2019. We have also released new AMSR2 research products, Thin Ice Detection (sea ice thinner than 30 cm) and Total Precipitable Water over Land, since January 2019 through the GCOM-W Research Product Data Providing Service (https://suzaku.eorc.jaxa.jp/GCOM_W/research/resdist.html).

The GCOM-W satellite has been in extended mission phase since 2017, and we expect to operate satellite and instrument as long as possible to reduce observation gaps between AMSR2 follow-on mission, which has been in Pre-project Phase (Phase A) since September 2018.

Keywords: satellite remote sensing, water cycle, microwave radiometer

©2019. Japan Geoscience Union. All Right Reserved.

Testing and Evaluation for JPSS-1 Algorithms using Algorithm Development Library Block 2.1

*Bigyani Das[1,2], Weizhong Chen[1,2], Thomas S King[1,2], Walter Wolf[2]

1. IMSG, 2. STAR/NESDIS/NOAA

The Joint Polar Satellite System 1 (JPSS-1) is the next generation polar-orbiting operational environmental satellite which was launched on November 18, 2017. It carries advanced versions of the instruments Advanced Technology Microwave Sounder (ATMS), Cross-track Infrared Sounder (CrIS), Ozone Mapping and Profiler Suite (OMPS) and Visible Infrared Imaging Radiometer Suite (VIIRS) that are on board of Suomi National Polar-Orbiting Partnership (S-NPP) satellite which was launched on October 28, 2011. All the Sensor Data Record (SDR) algorithms for the instruments are processed in the Interactive Data Processing Segment (IDPS) system designed and maintained by Raytheon. The Algorithm Development Library (ADL) Block 2.1 is an updated offline test system developed by Raytheon to mimic the operational system. Current version of the algorithm has gone through many recent code updates as well as Look-up-Table (LUT) updates for improving product quality. The center for Satellite Applications and Research (STAR) Algorithm Scientific Software Integration and System Transition Team (ASSISTT) uses ADL Block 2.1 to test and integrate updates to JPSS-1 algorithms, both code and the Lookup Tables (LUTs). Weekly updates are made to Dark tables for both OMPS Nadir Mapper (NM) and Nadir Profiler (NP) instruments and for both SNPP and JPSS-1 (J01) satellites. These are tested, integrated and submitted as packages with inputs, outputs and guide documents for further verification by the Data Products Engineering and Services (DPES) team and final integration by Raytheon in the operational system IDPS. Updates are also made to bi-weekly Wavelength and Solar tables for OMPS NP for SNPP satellite. They are tested and submitted in the package for operational implementation. We have created scripts to automate the staging and processing of weekly and bi-weekly updated LUTs in ADL Block 2.1. Details of the process of integration and application of the scripts for testing and integration of LUTs for OMPS as well as other instruments will be discussed.

Keywords: JPSS, Algorithm Integration, STAR ASSISTT, Algorithm Development Library

©2019. Japan Geoscience Union. All Right Reserved.

Remote Sensing of Atmospheric and Surface Properties using Hyperspectral satellite Sensors

*Xu Liu[1]

1. NASA Langley Research Center

Hyperspectral remote sensors from satellite platforms provide high information content on clouds, atmospheric temperatures, moisture, and trace gases profiles. They also provide surface information. In order to retrieve these information from hyperspectral remote sensing data, a fast and accurate radiative transfer model and a robust inversion algorithm are needed. We will describe a Principal Component-based Radiative Transfer Model (PCRTM) and an associated non-linear inversion algorithm. The PCRTM model can provide fast and accurate top of atmosphere high spectral resolution radiance or reflectance spectra from far infrared spectral region to UV-VIS spectral region. The forward model has been used to analyse hyperspectral data such as AIRS, CrIS, IASI, and SCIAMACHY. Examples of retrieval results from some of these satellite sensors will be given.

Keywords: remote sensing, atmospheric profiles, radiative transfer

©2019. Japan Geoscience Union. All Right Reserved.

RADIOMETRIC UNIFORMITY AND STABILITY OF GROUND SITE CHARACTERIZATION FOR INSAT-3D

*Shailesh Parihar[1], R. Bhatla[1], A. K. Mitra[2]

1. Banaras Hindu University, Varanasi, India, 2. India Meteorological Department, New Delhi, India

Radiometric phenomena of Earth Observation Satellite sensors vary between ground pre-launch calibration campaign, after launch and over satellite lifetime due to launching vibration, eventual optical element misalignments, generally space harsh environment. One of vicarious calibration methods is the reflectance-based approach that is applied here to radiometric calibration of INSAT-3D visible channel. In-situ vicarious calibration method for radiometric calibration of visible (VIS 550–750 nm) sensor onboard geostationary satellite INSAT-3D has been carried out for characterizing the radiometric uniformity of the site at Bhuj, Gujarat. The measurements of ground reflectance (spectral range of 350–2500 nm), aerosol optical depth (AOD), total column ozone from Spectroradiometer (spectral range of 350–2500 nm), Sunphotometer, Ozonometer respectively and other meteorological variables were obtained from site during the field campaigns and calibration coefficients with bias and relative error for optical sensor of the INSAT-3D satellite is presented. Based on these measurements, simulations of radiance reaching at top of the atmosphere (TOA) were carried out using radiative transfer model 6S (Second Simulation of the Satellite Signal in the Solar Spectrum). The computed TOA radiances when compared with the sensor measured radiances for various dates and sites show an over-estimation of TOA radiance. The analysis suggested that Bhuj site has been preferred for post launch vicarious calibration of optical sensor of INSAT-3D satellite as well as upcoming geostationary INSAT satellite series.

Keywords: INSAT-3D, vicarious calibration, radiative transfer model 6S

©2019. Japan Geoscience Union. All Right Reserved.

Vicarious calibration activities of ASTER Thermal Infrared Radiometer (TIR) for Earth environmental observation

*Satoru Yamamoto[1], Hideyuki Tonooka[2], Soushi Kato[3], Kazuki Ayuzawa[2], Tsuneo Matsunaga[4]

1. Japan Space Systems, 2. Ibaraki University, 3. Remote Sensing Technology Center of Japan, 4. National Institute for Environmental Studies

The Advanced Spaceborne Thermal Emission and Reflection Radiometer (ASTER) instrument on the Terra satellite has been retrieving multiband images with 14 spectral bands from the visible through thermal infrared and stereo images over the Earth's surface since 2000. The data set by ASTER has provided the composition and distribution of materials, temperature/emissivity map, and digital elevation topography models (DEM), contributing to a variety of Earth's science applications, i.e., natural resources, agricultural applications, natural disasters, geology, and urban development as well as monitoring global environmental change. In addition, the data of ASTER is being used for space business involved in space-enabled economic activity and service.

In order to establish the ASTER data for high-accuracy applications, radiometric calibration and atmospheric correction are highly important. Since any optical sensor is expected to degrade in space, we need to monitor the performance of the sensor over time based on onboard and vicarious calibrations. One of vicarious calibration approaches characterizes instrument performance based on comparison with the data measured by field campaigns at homogeneous ground areas such as lake and desert sites. The field campaigns for ASTER took place at various test sites such as Railroad Valley Playa, Lunar Lake, and Alkali Lake in Nevada and water sites such as Lake Kasumigaura in Japan during about two decades.

On 30 August through 1 September 2018, as part of annual vicarious calibrations for ASTER Thermal Infrared Radiometer (TIR), we conducted the field campaigns at Railroad Valley playa and Alkali Lake in Nevada. We also made the vicarious calibration at Lone Mountain playa in Nevada, which is a new test site discovered during this campaign. In this presentation, we will report the activity of the 2018's field campaigns at Nevada, and discuss how important the radiometric calibration after launch is to Earth's science applications including assessment of global environmental change based on satellites.

Keywords: multispectral data, remote-sensing, ASTER, Earth observation satellite, vicarious calibration

©2019. Japan Geoscience Union. All Right Reserved.

Overview of Vegetation Lidar MOLI

*Haruhisa Shimoda[1], Toshiyoshi Kimura[2], Rei Mituhashi [2], Junpei Muruoka [2], Daisuke Sakaizawa[2], Tadashi Imai [2], Kazuhiro Asai[3]

1. Tokai University, 2. JAXA, 3. Tohoku Institute of Technology

Under the PARIS AGREEMENT (Adopted at COP 21 in 2015), each country, including developing countries, is obliged to declare its emissions, but an objective verification method was considered necessary from the perspective of credibility and accuracy. It is said that one of the largest errors today is in the evaluation of CO_2 absorption by forests. Regarding the assessment of forests as a CO_2 absorption source, biomass and the change of biomass observed. We propose the use of airborne and satellite-mounted LIDAR as an effective method of directly measuring tree height. JAXA has begun studying the space vegetation LIDAR mission using the Multi-footprint Observation Lidar and Imager (MOLI) in collaboration with scientists. The main objective of this mission is to globally and precisely measure canopy height from space for improving biomass estimation. MOLI is designed to be mounted on the Exposed Facility (EF) of the Japanese Experiment Module on the International Space Station (ISS). The mission requirements for MOLI were set through discussions with scientists, and are listed as follows:

1. MOLI measures canopy height globally with accuracy of ±2 m (for canopy height less than 20 m) or ± 10% (for canopy height above 20 m) so as to generate map data of canopy heights and biomass, combined with imagery data from other satellites. The measurement data are also used as inputs or for validation in carbon cycle models.

2. Simultaneously, MOLI also measures the vegetation index and vegetation phenology for generating more accurate map data of canopy height and biomass.

3. MOLI measures the average amount of carbon per sub-national-scale area (80 km grid) to an uncertainty level of 20% or less (95% confidence interval).

The system requirements for MOLI are set based on the mission requirements. Regarding the waveform generated by the Geoscience Laser Altimeter System (GLAS) installed in the ICESat. However, waveforms with a lower S/N (less than 10) were excluded from analysis, as it greatly reduced the accuracy of canopy height measurement. Based on this result, the S/N requirement of MOLI was set to 10 or more, and the measurement precision of canopy height reached ±2 m or 10 %.

The tilted ground causes significant errors in measuring the canopy height due to the difference in height of the ground in the footprint. MOLI must be able to detect the inclination of the ground in order to estimate the difference in height of the footprint ground. Thus, MOLI must have a multi-footprint to estimate the tilt of the ground surface by detecting the time lag of each footprint.

Since MOLI needs to acquire data on vegetation phenology and vegetation index at the same time as the LIDAR observation to generate map data, it also has an optical imager with multiple bands. Using the imager, MOLI also measures the canopy height to identify the trees observed by MOLI for ground verification. The imager GSD is 5m. The imager also has green, red and NIR bands for measuring vegetation phenology and vegetation index.

©2019. Japan Geoscience Union. All Right Reserved.

To realize the sampling design, it is necessary to irradiate two laser beams and receive two reflection signals with the array detector. We considered dividing the laser beam into two laser beams by using an optical system. Based on this method, one laser transmitter is attached and the pulse energy is 40 mJ

Keywords: vegetation Lidar, MOLI, biomass

©2019. Japan Geoscience Union. All Right Reserved.

[E] Poster | A (Atmospheric and Hydrospheric Sciences)：A-CG Complex & General

Wed. May 29, 2019 10:45 AM - 12:15 PM JST | Wed. May 29, 2019 1:45 AM - 3:15 AM UTC | Poster Hall International Exhibition Hall8, Makuhari Messe_6

[A-CG35] Projection and detection of global environmental change

convener:Michio Kawamiya(Japan Agency for Marine-Earth Science and Technology), Hiroaki Tatebe(Japan Agency for Marine-Earth Science and Technology), Kaoru Tachiiri(Japan Agency for Marine-Earth Science and Technology)

Anthropogenic forcings on global environment are expected to cause intensification of extreme events, sea level rise, ocean acidification and deoxygenation, as well as large-scale ecosystem changes. The CMIP6 experimental protocol has been established based on which modeling groups across the world are starting to provide environmental projection data toward 6th IPCC assessment report due in 2021. Various new types of studies, such as event attribution and coupling of socio-economic processes and Earth system dynamics, are also emerging in the field of global change projection. In addition, observational studies are becoming increasingly more important for grasping changes in the global environment and evaluating model projections. Interactions and collaborations beyond boundaries of conventional scientific disciplines are desired for dealing with the issue of global changes. This session thus aims to deepen our understanding on global change, from both disciplinary and interdisciplinary viewpoints. This session is co-organized by AIMES - Future Earth project "Analysis, Integration and Modelling of the Earth System" (https://aimesproject.org/).

[ACG35-P01] World Regionalization of Climate Change (1961–2010)

*Shao Sun[1,2], Peijun Shi[2,3,4], Daoyi Gong[2], Tao Zhou[2] (1.National Climate Center, China Meteorological Administration, Beijing 100081, China, 2.State Key Laboratory of Earth Surface Processes and Resource Ecology, Beijing Normal University, Beijing 100875, China, 3.Key Laboratory of Environmental Change and Natural Disaster of Ministry of Education, Beijing Normal University, Beijing 100875, China, 4.Academy of Disaster Reduction and Emergency Management, Ministry of Civil Affairs & Ministry of Education, Beijing 100875, China)

[ACG35-P02] Quantifying and identifying future climate signal, noise, and internal variability at finer temporal scales

*Jongho Kim[1], Manh Van Doi[1] (1.University of Ulsan)

[ACG35-P03] Basic evaluation of MIROC6 and current status of CMIP6 experiments

*Hiroaki Tatebe[1] (1.Japan Agency for Marine-Earth Science and Technology)

[ACG35-P04] Synchronized increase of extreme cold and warm events in China during the recent global warming slowdown

*Xiubao Sun[1,3], Chunzai Wang[1], Guoyu Ren[2,3], Panfeng Zhang[2] (1.State Key Laboratory of Tropical Oceanography (LTO), South China Sea Institute of Oceanology(SCSIO), Chinese Academy of Sciences (CAS), 2.Department of Atmospheric Science, School of Environmental Studies, China University of Geosciences (CUG), 3.Laboratory for Climate Studies, National Climate Center (NCC), China Meteorological Administration (CMA))

[ACG35-P05] Quantification of thermodynamical and dynamical contributions to the anthropogenic influences on tropical cyclone rainfall extremes

*Cheng-Ta Chen[1], Shih-How Lo[1], Chung-Chieh Wang[1], Kazuhisa Tsuboki[2] (1.Department of Earth Sciences, National Taiwan Normal University, 2.Hydrospheric-Atmospheric Research Center, Nagoya University)

[ACG35-P06] Temporal Evolution of the Long-Term Distributional Biases of Climate Models as a Parameter for the Regional Evaluation of the Simulation of Climate Change

*Martin Gomez-Garcia[1], Akiko Matsumura[1], Shiro Hishinuma[1], Daikichi Ogawada[1] (1.Nippon Koei Co. Ltd., Reasearch and Development Center)

[ACG35-P07] A global simulation of bioenergy crop yield

*Zhipin Ai[1], Naota Hanasaki[1] (1.National Institute for Environmental Studies)

[ACG35-P08] Integrated Research Program for Advancing Climate Models - Theme B: national research program in Japan on earth system modeling

*Michio Kawamiya[1], Tomohiro Hajima[1], Kaoru Tachiiri[1], Jun'ichi Tsutsui[2], Tokuta Yokohata[3], Takashi Arakawa[4], Takahiro Inoue[4] (1.Japan Agency for Marine-Earth Science and Technology, 2.Central Research Institute of Electric Power Industry, 3.National Institute for Environmental Studies, 4.Research Organization for Information Science and Technology)

[ACG35-P09] Towards probabilistic climate projections based on the CMIP6 multi-model ensemble

*Junichi Tsutsui[1] (1.Central Research Institute of Electric Power Industry)

[ACG35-P10] Effect on the earth system of realizing 1.5 degree climate target by overshooting after reaching 2 degree level

*Kaoru Tachiiri[1], Herran Diego Silva[2], Xuanming Su[1], Michio Kawamiya[1] (1.Japan Agency for Marine-Earth Science and Technology, 2.Institute for Global Environmental Strategies)

[ACG35-P11] **Historical regional and sectoral contributions to climate change**

*Xuanming Su[1], Kaoru Tachiiri[1], Katsumasa TANAKA[2], Michio Watanabe[1] (1.Japan Agency for Marine-Earth Science and Technology, 2.National Institute for Environmental Studies)

[ACG35-P12] **Future projection of global climate, water, food, bio-energy, and land investigated with MIROC-INTEG: a global bio-geophysical land surface model with human components**

*Tokuta Yokohata[1], Yusuke Satoh[1], Tsuguki Kinoshita[2], Gen Sakurai[3], Yadu Pokhrel[4], Akihiko Ito[1], Etsushi Kato[5], Masashi Okada[1], Naota Hanasaki[1], Tomoko Nitta[6], Seita Emori[1] (1.National Institute for Environmental Studies, 2.Ibaraki University, 3.National Agriculture and Food Research Organization, 4.Michigan State University, 5.The Institute of Applied Energy, 6.University of Tokyo)

[ACG35-P13] **Downscaling a global agricultural land use model to country level for national SSP analysis**

*Wenchao Wu[1], Tomoko Hasegawa[1], Kiyoshi Takahashi[1], Shinichiro Fujimori[2] (1.National Institute for Environmental Studies, 2.Kyoto Univ.)

[ACG35-P14] Extreme Events and Emergent Trends in Marine Ecosystem Stressors under a historical/RCP8.5 Climate Change Pathway

*Keith Bradley Rodgers[1,2], Sarah Schlunegger[3], Richard Slater[3], Burke Hales[4], Axel Timmermann[1,2] (1.IBS Center for Climate Physics, Busan, South Korea, 2.Pusan National University, Busan, South Korea, 3.AOS Program, Princeton University, Princeton NJ, USA, 4.College of Ocean and Atmospheric Sciences, Oregon State Universitym, Corvallis, OR, USA)

World Regionalization of Climate Change (1961–2010)

*Shao Sun[1,2], Peijun Shi[2,3,4], Daoyi Gong[2], Tao Zhou[2]

1. National Climate Center, China Meteorological Administration, Beijing 100081, China, 2. State Key Laboratory of Earth Surface Processes and Resource Ecology, Beijing Normal University, Beijing 100875, China, 3. Key Laboratory of Environmental Change and Natural Disaster of Ministry of Education, Beijing Normal University, Beijing 100875, China, 4. Academy of Disaster Reduction and Emergency Management, Ministry of Civil Affairs & Ministry of Education, Beijing 100875, China

Existing climate regionalization aims to characterize the regional differences in climate based on years of the mean values of climate indices. However, with the accelerating climate change nowadays, existing climate regionalization cannot represent the regional difference of climate change, nor can it reflect the extreme weather and climate disasters and environmental risks incurred from climate changes. This paper utilizes the tendency value and fluctuation value of temperature and precipitation from 1961 to 2010 to identify the climate change quantitatively, and completes world regionalization of climate change (1961–2010) with administrative subdivisions of countries as the basic unit in combination with world's terrain feature. Level-I regionalization divides world's climate change (1961–2010) into twelve tendency zones based on the tendency of temperature and precipitation; level-II regionalization refers to twenty-eight fluctuation regions based on level-I regionalization according to the fluctuation of temperature and precipitation. Climate change regionalization provides a basis for countries and regions in the world to develop plans for adapting to climate change, especially for managing extreme weather and climate disasters and environmental risks.

Keywords: Climate change, Regionalization, Tendency, Fluctuation, World

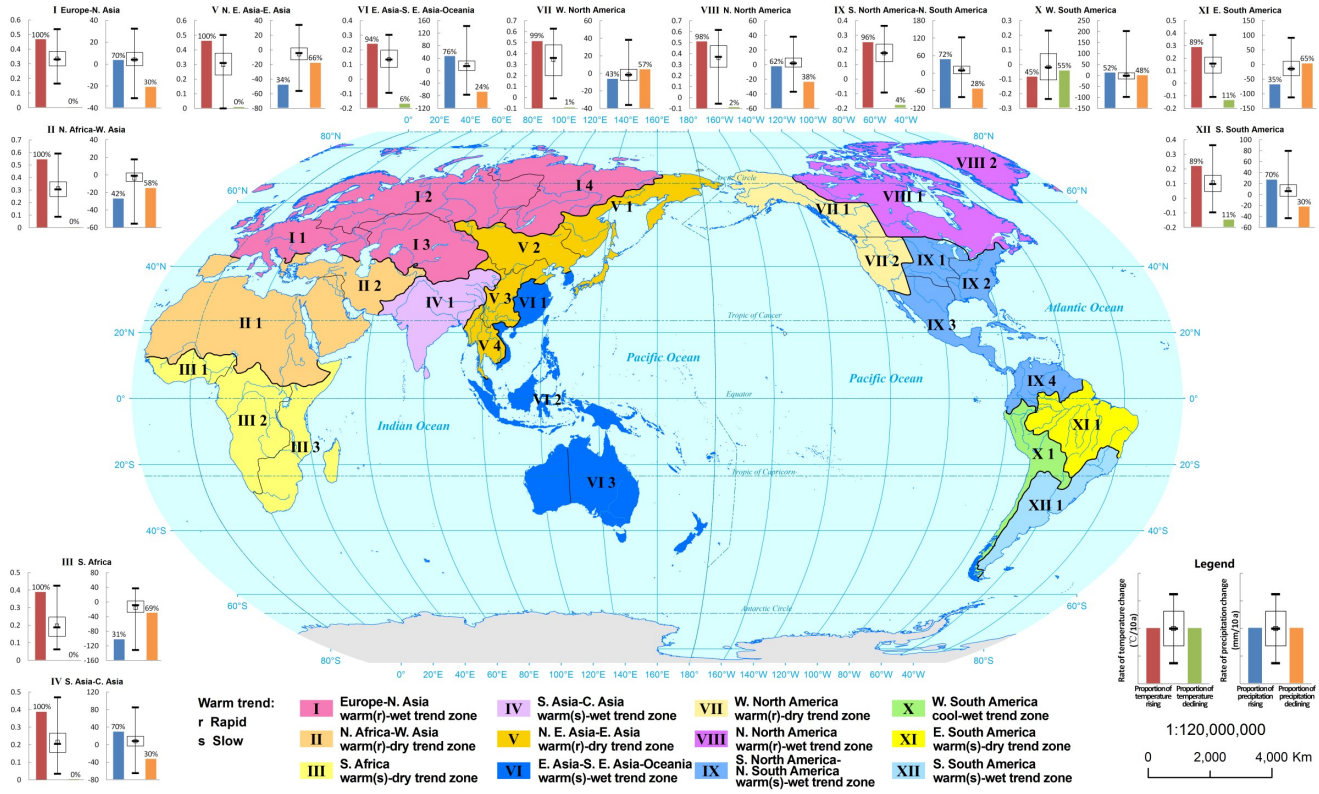

©2019. Japan Geoscience Union. All Right Reserved.

Quantifying and identifying future climate signal, noise, and internal variability at finer temporal scales

*Jongho Kim[1], Manh Van Doi[1]

1. University of Ulsan

Quantifying and identifying climate internal variability (CIV) plays an important role in climate change studies because of its irreducible and unpredictable characteristics. A large number of studies have addressed such an issue; however, the issue was only resolved at coarser resolution on the first order moments of few climate variables. Our recent study has estimated CIV of climate variables for a “current” period at finer spatial and temporal scales; however, whether CIV will change or remain constant in the future under the impact of representative concentration pathways (RCP45 and RCP85) is still questionable. To investigate how CIV will change in the future in both spatial pattern and magnitude, CIV is assessed over 30-year periods in both current and future periods with two scenarios in Korea by analyzing an ensemble of 100 simulations generated by an hourly weather generator. In this study, signal to noise ratio (SNR) used to evaluate the model performance will be applied to simulating ensemble for different periods. CIV is then estimated by two methods: “detrended” and “differenced”; SNR is estimated by “analysis of variance” and “trend analysis” methods. Both SNR and CIV are evaluated with four proposed matrices signifying rainfall volume, extremes and occurrence of rainfall. To consider the change of CIV in the future periods, t-test (test for mean difference) and f-test (test for variance difference) are applied to the ensemble of CIV. In this study, analyzing SNR’s values shows that the four proposed matrices are controlled by non-linear stochastic process and the change tend to increase in the future with increase of CO2 concentration. CIV is proved to change in the future periods under impact of CO2 scenarios. Spatial distribution of CIV’s change over future periods of which locations provides the important and useful information for decision making of water resources planning and proposing mitigation measures of disaster protection.

Acknowledgment:

This research was supported by the Water Management Research Program funded by Ministry of Environment of Korean government (127554), and by the Basic Science Research Program of the National Research Foundation of Korea funded by the Ministry of Education (2016R1D1A1B03931886).

Keywords: climate internal variability, signal to noise ratio, t-test, f-test

©2019. Japan Geoscience Union. All Right Reserved.

Basic evaluation of MIROC6 and current status of CMIP6 experiments

*Hiroaki Tatebe[1]

1. Japan Agency for Marine-Earth Science and Technology

The sixth version of the Model for Interdisciplinary Research on Climate (MIROC), called MIROC6, was cooperatively developed by a Japanese climate modeling community. Overall reproducibility of mean climate and internal climate variability in MIROC6 is better than that in the previous version (MIROC5). The tropical climate systems (e.g., summertime precipitation in the western Pacific and the eastward propagating Madden-Julian Oscillation) and the mid-latitude atmospheric circulations (e.g., the westerlies, the polar night jet, and troposphere-stratosphere interactions) are significantly improved in MIROC6. These improvements can be attributed to the newly implemented parameterization for shallow convective processes and to the directly resolved stratosphere. In the present study, simulated mean climate, internal climate variability in MIROC6 are evaluated and briefly summarized in comparison with MIROC5 and observations. Using MIROC6, designated simulations tackling a wide range of climate science issues, as well as seasonal-to-decadal climate predictions and future climate projections, are currently ongoing with an aim towards contributing to the sixth phase of the Coupled Model Intercomparison Project (CMIP6). Preliminary results of historical climate simulations from the middle of the 19th century, climate projections from the present to the end of the 21th century based on future scenarios of the Shared Socio-economic Pathways, and initialized climate predictions on seasonal-to-decadal timescales will be given in this talk.

Keywords: Climate model, CMIP6, climate projections/predictions

©2019. Japan Geoscience Union. All Right Reserved.

Synchronized increase of extreme cold and warm events in China during the recent global warming slowdown

*Xiubao Sun[1,3], Chunzai Wang[1], Guoyu Ren[2,3], Panfeng Zhang[2]

1. State Key Laboratory of Tropical Oceanography (LTO), South China Sea Institute of Oceanology(SCSIO), Chinese Academy of Sciences (CAS), 2. Department of Atmospheric Science, School of Environmental Studies, China University of Geosciences (CUG), 3. Laboratory for Climate Studies, National Climate Center (NCC), China Meteorological Administration (CMA)

From the end of 1990s to the middle of 2010s, global mean temperature experienced a process of warming slowdown. However, global warm extremes did not show the slowdown phenomenon during the recent global warming slowdown. Based on the observation data of 2362 land surface stations in China, we analyzed the cold and warm extremes changes over mainland China between global warming period (1961-1999) and warming slowdown period (2000-2014). Results indicate that the warming trend in the cold season (MAM and DJF) is significantly higher than that in the warm season (JJA and SON) in the period of global warming (1961-1999), while the warming trend in the warm season is significantly higher than that in the cold season in the period of global warming slowdown. That is, the trend of warm season and the cool season in China have reversed. At the same time, we also found that the synchronous increase occurrence of extreme warm events in summer (JJA) and extreme cold events in winter (DJF) leads to the seasonal trend reverse phenomenon, but there are differences in the spatial variation characteristics between cold and warm extremes. The increase of warm extremes in summer is mainly due to the strong increase of warm events in south China, while the increase of cold events in winter is due to the increase of cold events over China. Further, we also found that the variability of extreme temperature has increased more significantly in the warming slowdown period than that in global warming period. East Asian winter monsoon and summer monsoon both show enhanced characteristics during the global warming slowdown period, which indicates that the increase of sea-land temperature difference in summer and winter results in the synchronous increase of extreme cold and warm events by increasing the climate variability in China.

Keywords: Global warming, Global warming slowdown, Extreme warm events, Extreme cold events, Land-sea temperature difference

©2019. Japan Geoscience Union. All Right Reserved.

Quantification of thermodynamical and dynamical contributions to the anthropogenic influences on tropical cyclone rainfall extremes

*Cheng-Ta Chen[1], Shih-How Lo[1], Chung-Chieh Wang[1], Kazuhisa Tsuboki[2]

1. Department of Earth Sciences, National Taiwan Normal University, 2. Hydrospheric-Atmospheric Research Center, Nagoya University

The rainfall extremes and strong winds associated with tropical cyclones lead to significant damages and lost to where they make landfalling. Upward trend in term of financial lost was indicated for the past few decades from the report of major reinsurance firms. Whether the past anthropogenic warming played a significant role in such extreme event and their changes remained very controversial. On one hand, people argue it’s nearly impossible to attribute an individual extreme event to global warming. On the other hand, the increase of heavy rainfall is consistent with the expected effects of climate change on tropical cyclone. To diagnose possible anthropogenic contributions to the odds of heavy rainfall associated with tropical cyclone, we adapt an existing event attribution framework of modeling a ‘world that was’ and comparing it to a modeled ‘world that might have been’ for that same time but for the absence of historical anthropogenic drivers of climate. One limitation for applying such approach to high-impact weather system is that it will require models capable of capturing the essential processes lead to the studied extremes. Using a cloud system resolving model that can properly simulate the complicated interactions between tropical cyclone, large-scale background, topography, we first perform the ensemble ‘world that was’ simulations forced by the high resolution ECMWF YOTC analysis. We then re-simulate with the adjusted ‘world that might have been conditions’ by removing the regional atmospheric and oceanic forcing due to human influences estimated from the CMIP5 model ensemble mean conditions between all forcing and natural forcing only historical runs. Thus our findings are highly conditional on the driving analysis and adjustments therein, but the setup allows us to elucidate possible contribution of anthropogenic forcing to changes in the likelihood of heavy rainfall associated tropical cyclone. With only less than half of degree anthropogenic warming over the study area, we found that this forcing very likely (9 out of 10 cases) increase the risk of heavy rainfall event (grid rainfall greater than 33 mm per hour) by at least 16%. The role of dynamical processes that leads to precipitation extreme increases beyond the moisture content increase will be further analyzed and discussed.

Keywords: Tropical Cyclone, Extreme rainfall, extreme event attribution

©2019. Japan Geoscience Union. All Right Reserved.

Temporal Evolution of the Long-Term Distributional Biases of Climate Models as a Parameter for the Regional Evaluation of the Simulation of Climate Change

*Martin Gomez-Garcia[1], Akiko Matsumura[1], Shiro Hishinuma[1], Daikichi Ogawada[1]

1. Nippon Koei Co. Ltd., Reasearch and Development Center

Owing to the climate variability of the General Circulation Models (GCM), the discrepancy between their outputs and observational datasets at scales that range from hours to years is practically random. Thus, the associated errors need to be evaluated in terms of the long-term (multidecadal) distributional properties of the atmospheric variables. A recently developed bias-correction method corrects the systematic errors (i.e., biases) in the climate mean state and in three distributional measures of the daily and the interannual variability (namely the frequency of extremes, the skewness, and the scale of the variable at each timescale). The adjustment of these biases is done in such a way that the corrections at one timescale do not affect the probability distribution at another. Therefore, this bias-correction method is able to preserve the GCM-simulated climate trends and extensively reproduce the long-term frequency of the observed extreme weather (e.g. 98th percentile of wet days, maximum seasonal mean of surface temperature).

Generally, the bias-correction of GCMs faces the challenge of including the simulated changes of climate, which supposes alterations in not only the mean but also other aspects like the skewness and the frequency of extremes. The abovementioned bias-correction method includes the effect of the simulated climate change in the correction of the distributional biases. However, considering the coarse resolution of the GCMs and the imperfections in the parameterizations of the subgrid physical processes, the fundamental assumption that the distributional biases are predictable (i.e., stationary) is made.

In this study, we explored the possibility of evaluating the sensibility with which GCMs simulate the response of the earth-system components to external forcing (i.e., climate change) by comparing the temporal evolution of the distributional biases at different timescales over specific regions. For the short period in which the observed data was available, our results revealed that many CMIP5 GCMs are indeed able to simulate with a quasi-stationary bias the changes caused by climate change. Moreover, being able to identify the regions in which certain models do not show the errors with a systematic behavior in either the climate mean state, the daily variability or the interannual variability can be useful for the further development of climate models. We expect that with the data of the GCM outputs of the future phases of the CMIP project, the period in which the observed and the modeled data coincide becomes longer and, thus, our conclusions can be supported by more robust evidence.

Keywords: Bias correction of GCMs at different timescales, Climate trends and climate variability, Evaluation of the ability of GCMs to simulate climate change

©2019. Japan Geoscience Union. All Right Reserved.

A global simulation of bioenergy crop yield

*Zhipin Ai[1], Naota Hanasaki[1]

1. National Institute for Environmental Studies

Large-scale development of bioenergy is considered as an effective pathway to achieve the 2 degrees target of the Paris Agreement. To avoid the competition with food crops, so-called the second-generation bioenergy crops such as miscanthus and switchgrass are regarded as potential dedicated biomass crop. However, the models to estimate the yield of miscanthus and switchgrass at a global scale which enable analyzing the effects of irrigation water application are seldom seen as of today. Here, we firstly updated the crop module in the global hydrological model H08 for miscanthus and switchgrass. Then, we conducted a global simulation and validation of the yield for miscanthus and switchgrass at 0.5 degree. The results indicated that the updated H08 have a good ability in simulating the yield of perennial bioenergy crops, which provides a good foundation for further integrated assessment of the impacts of bioenergy crop production on water sector.

Acknowledgement: This research was supported by the Environment Research and Technology Development Fund (S-14-5) of the Environmental Restoration and Conservation Agency.

Keywords: Bioenergy, Crop yield, H08

©2019. Japan Geoscience Union. All Right Reserved.

Integrated Research Program for Advancing Climate Models - Theme B: national research program in Japan on earth system modeling

*Michio Kawamiya[1], Tomohiro Hajima[1], Kaoru Tachiiri[1], Jun'ichi Tsutsui[2], Tokuta Yokohata[3], Takashi Arakawa[4], Takahiro Inoue[4]

1. Japan Agency for Marine-Earth Science and Technology, 2. Central Research Institute of Electric Power Industry, 3. National Institute for Environmental Studies, 4. Research Organization for Information Science and Technology

The Integrated Research Program for Advancing Climate Models, or TOUGOU (abbreviation taken from its Japanese name), is a national project for projection of global change. Its aim to provide information for adaptation and mitigation, based on scientific evaluation of changes including those in extreme events and carbon cycle. The project was launched in April, 2017. While the entire program deals with a wide range of physical aspects and consequent impacts of climate change, Theme B (TOUGOU-B) focuses on the development of a state-of-the-art Earth system model (ESM) incorporating biogeochemical processes, such as sophisticated carbon and nitrogen cycles, as well as its application to exploring future socio-economic pathways of climate change mitigation. MIROC-ESM, an ESM developed under TOUGOU-B (and the previous SOUSEI-B) has been significantly improved since the 5th phase of coupled model intercomparison project (CMIP5), and has started to be run for CMIP6. During the three years since TOUGOU was launched, results have been obtained that may contribute to 6th Assessment Report (AR6) of Intergovernmental Panel on Climate Change (IPCC) including those on impacts of pyrogenic iron on oceanic ecosystem, assessment of the outcome of labor productivity change due to warming, and effects of high dust amount on surface temperature during the Last Glacial Maximum. Besides, efforts to secure ways to disseminate projection data are ongoing under TOUGOU-B. Specifically, collaboration has been established between climate modeling community in Japan and Data Integration and Analysis System (DIAS), a national IT project for environmental data, have been continuing, in order for Japan to participate in Earth System Grid Federation (ESGF). ESGF is an international cooperative activity to construct a data distributing system for climate related data such as CMIP6 outputs. Some of the details of these results will be explained in the presentation.

Keywords: IPCC, Earth system model , carbon cycle, socio-economic scenario, CMIP6, climate mitigation

©2019. Japan Geoscience Union. All Right Reserved.

Towards probabilistic climate projections based on the CMIP6 multi-model ensemble

*Junichi Tsutsui[1]

1. Central Research Institute of Electric Power Industry

Research on climate change mitigation uses a climate model emulator that represents the average and range over a specific multi-model ensemble of complex climate simulations. The Coupled Model Intercomparison Project (CMIP) has provided such multi-model ensembles, and its latest Phase 6 (CMIP6) results are being revealed. As a first step to applying the CMIP6 results to probabilistic climate projections, we focus on the distribution of key parameters representing atmospheric CO_2-induced forcing and transient temperature responses.

In this study, we develop a procedure to determine the forcing-response parameters of a complex climate model. We simultaneously fit a curve built on an impulse response function to the global mean time series of the model's surface temperature anomaly and top-of-atmosphere energy imbalance from two basic CO_2 -forced experiments, i.e., an abrupt quadrupling and a 1%-per-year increase in atmospheric CO_2 concentration. This scheme serves as an improved alternative to the widely-used regression method of Gregory et al. (2004). Furthermore, it makes a complete set of parameters to emulate the target model from which equilibrium climate sensitivity (ECS) and transient climate response (TCR) are derived. The properties of a multi-model ensemble are quantified through a statistical approach including a principal component analysis for the parameters.

The two CO_2-forced experiments are included in the set of common experiments which is designed to maintain continuity across different CMIP phases. Here, we compare the parameters of individual CMIP6 models with those of the previous-phase CMIP5 models. The parameters of the CMIP5 ensemble have several features. The ratio of TCR to ECS is distributed in the range of approximately 0.5 to 0.7, and for models with large ECS, the ratio tends to decrease. The scaling parameter for the effective radiative forcing of CO_2 varies from model to model and tends to be less than a reference value used in a conventional formula of CO_2 radiative forcing. Although the number of CMIP6 models is currently limited, their parameters show similar distributions within the CMIP5 ranges.

Keywords: climate sensitivity, effective radiative forcing, impulse response model, climate model emulator, ensemble climate experiment

©2019. Japan Geoscience Union. All Right Reserved.

Effect on the earth system of realizing 1.5 degree climate target by overshooting after reaching 2 degree level

*Kaoru Tachiiri[1], Herran Diego Silva[2], Xuanming Su[1], Michio Kawamiya[1]

1. Japan Agency for Marine-Earth Science and Technology, 2. Institute for Global Environmental Strategies

By using an Earth system model (ESM) with emissions and land use scenarios consistent with socio-economic projections from an integrated assessment model, the effect of overshooting to 1.5 degree target (in Celsius from pre-industrial periods) after reaching 2 degree level is investigated in selected indicators of the global environment. Unlike the internationally coordinated model intercomparison project, the scenario is developed for a specific climatic model. The ESM output results in delayed achievements for both of 1.5 and 2 degree targets in terms of global surface mean air temperature, but achieved before or around 2100 as expected when we use global mean surface temperature (for which sea surface temperature and surface air temperature are used for ocean and land, respectively) masked with observation areas. In the overshooting scenario more heat is absorbed by the ocean compared to a case without overshooting, but still we found significant difference between the two scenarios in Arctic sea ice, while in both scenarios corals seem difficult to survive the 21st century (when no thermal adaptation is assumed) . The difference in steric sea level rise between the scenarios is only below 2 cm in 2100. In addition, vegetation productivity in broad regions shows slight (~5%) increase. Emission pathways in the scenarios rely on a large amount of carbon sequestration. In the 2 degree scenario CO2 emissions in 2100 are slightly below zero, while for 1.5 degree scenario they are below -20 GtCO2.. When the Earth system has high climate sensitivity and TCRE, to reach the 1.5 degree target we need to take an overshooting temperature pathway, but in case the overshooting is large, difference in some indicators between 1.5 degree and 2 degree scenarios can be non-significant, which is an important indication in implementing adaptive mitigation in the coming decades.

Keywords: Earth system model, integrated assessment model, 1.5 degree target, 2 degree target, stabilization, overshooting

©2019. Japan Geoscience Union. All Right Reserved.

Historical regional and sectoral contributions to climate change

*Xuanming Su[1], Kaoru Tachiiri[1], Katsumasa TANAKA[2], Michio Watanabe[1]

1. Japan Agency for Marine-Earth Science and Technology, 2. National Institute for Environmental Studies

Regional or sectoral contributions to climate change are important in the formulation of climate change policy. After the industrial revolution, developed countries emit CO_2 and non-CO_2 greenhouse gases (GHGs), and the historical emissions are large; while developing countries contribute relative fewer emissions in historical period but increase significantly in recent years or visible future. To assess the contributions to climate change, using cumulative emissions is a general and direct method. However, such method may ignore the lifetime of GHGs since part of the GHGs sink into the biosphere, ocean, soil or diminish during biogeochemical cycles. In this study, we evaluate the historical regional and sectoral contributions to climate change by using an improved version of Simple Climate Model for OPTimization (SCM4OPT) with a normalized marginal method. Based on the results, we analyze ten major GHG emitting countries and 12 sectors.

First, current emissions with relative long lifetime like CO_2 and N_2O, from developing countries increase significantly, like China, India, Mexico and Brazil, however, their contributions to climate change are still relatively smaller, compared with the developed countries such as USA, Japan, Germany, Canada and UK, of which countries the cumulative emissions are in relatively larger scale and current emissions are already under controlled. We can conclude here that the GHGs with relatively long lifetime need to be controlled stringently to reduce the long-term effects on climate change. For CH_4, which has a relatively shorter lifetime, the contributions to climate change are closely related to emissions within recent decades. These imply that reductions on short lifetime emissions can make immediate alleviation regarding climate change.

Second, energy sector contributes most of the CO_2 emissions, and therefore contribute almost half to the climate change among all the sectors. However, for CH_4 and N_2O, agriculture sector contributes most of the emissions and therefore their contributions to climate change are remarkable. Reduction policiesneed to targetthesesectors. In addition, CO_2 from land transportation and CH_4 from waste treatment increase rapidly in recent years, attention also needs to be paid to these sectors for making climate change policies.

Keywords: region emissions, sector emissions, climate change contribution, simple climate model

©2019. Japan Geoscience Union. All Right Reserved.

Future projection of global climate, water, food, bio-energy, and land investigated with MIROC-INTEG: a global bio-geophysical land surface model with human components

*Tokuta Yokohata[1], Yusuke Satoh[1], Tsuguki Kinoshita[2], Gen Sakurai[3], Yadu Pokhrel[4], Akihiko Ito[1], Etsushi Kato[5], Masashi Okada[1], Naota Hanasaki[1], Tomoko Nitta[6], Seita Emori[1]

1. National Institute for Environmental Studies, 2. Ibaraki University, 3. National Agriculture and Food Research Organization, 4. Michigan State University, 5. The Institute of Applied Energy, 6. University of Tokyo

Future climate changes possibly affect water resources, food production, energy supply, and ecosystem services. It is critical to better understand the interactions between the changes in these complicated factors. While earth system models and integrated assessment models are applicable to explore this topic, parts of their natural and/or human processes tend to be simplified depending on their scope. As such, it still remains a challenge to realistically model the human-natural interface. In this context, the MIROC integrated terrestrial model (MIROC-INTEG) was developed. One of the features of MIROC-INTEG is that the natural ecosystem and human activity models are coupled to a global land surface model MATSIRO (Nitta et al. 2014, Journal of Climate), which is a component of a state-of-the-art global climate model, MIROC (Watanabe et al. 2010, Journal of Climate). As a natural ecosystem model, we use a global vegetation model, VISIT (Ito and Inatomi 2012, Biogeosciences). As human activity models, we use a global land-surface model with anthropogenic water regulation modules, HiGW-MAT (Pokhrel et al, 2012, Journal of Hydrometeorology), and a global crop model, PRYSBI2 (Sakurai et al, 2014, Scientific Reports). In HiGW-MAT, models of human water regulations such as water withdrawal from river, dam operation, and irrigation (Hanasaki et al. 2008, Hydrol. Earth Syst. Sci.) are incorporated to the above-mentioned global land surface model, MATSIRO. In PRYSBI2, the growth and yield of four crops (wheat, maize, soybean, rice) are calculated. In addition to these models, a global land use model (Terrestrial Land-use Model, TeLMO) is newly developed in the present study. TeLMO calculate the grid ratio of cropland (food and bio-energy crops), pasture, forest (managed and un-managed), as well as their transition. Output variables of each sub-model are passed to other sub-models during the time integration.
We will present an analysis of historical and future simulations with a focus on the interactions between water, food, energy, and land. In the historical simulations, we validated the model output such as irrigated water, crop yield, ecosystem productions, and cropland area by comparing to the observed or reanalysis data. In the future simulations, we investigated the role of uncertainties in climate (Representative Concentration Pathways) and socio-economic (Shared Socio-economic Pathways) scenarios. We also investigate the role of uncertainties in model parameters, and found that an uncertainty in the fertilization effect of crop growth model PRYSBI2 strongly affect uncertainty in future projection of crop yield and land use change in TeLMO. We found that future changes in precipitation and/or temperature possibly cause decrease in soil moisture, leading to decreases in crop yield (especially in high emission scenario such as RCP8.5). Decrease in crop yield bring about increase in crop land area, which also causes the increase in irrigation demands. Interaction between water, crop yield, and land use, as well as possible impacts on ecosystem service will be discussed in the presentation.

Keywords: Global Climate Model, Earth System Model, Human activity

©2019. Japan Geoscience Union. All Right Reserved.

Downscaling a global agricultural land use model to country level for national SSP analysis

*Wenchao Wu[1], Tomoko Hasegawa[1], Kiyoshi Takahashi[1], Shinichiro Fujimori[2]

1. National Institute for Environmental Studies, 2. Kyoto Univ.

The Shared Socioeconomic Pathways (SSPs) has been part of latest scenario framework developed by the climate change research society in the recent decade, serving the integrated analysis of future climate impacts, vulnerabilities, adaptation, and mitigation, in which the agriculture, food system and land use are important components. Multiple integrated assessment models (IAMs) have been used for the quantitative projections of future agriculture, food system and land use in the global scale. However, the tool and application of IAMs to the quantification of SSPs on regional or national level is limited. Meanwhile, there are growing needs for the quantification of SSPs on regional or national level for a more detailed understanding of agriculture, food, and land use, and their interactions with other nexus, such as energy, water, and biodiversity. One obstacle for such application is the coarse spatial resolution of global IAMs for land use module. This study aims to apply the Asian-Pacific Integrated Model/Platform for Land-Use and Environmental Model (AIM/PLUM) for the quantification of agriculture, food system, and land use in Japan under its national-specific SSPs narratives. To achieve this, a regional land use model, AIM/PLUM-Japan, was developed, by improving the spatial resolution to 0.05˚ (targeting 1km) from global model of 0.5˚. We combined the statistical production area data and spatial land use data to produce a refined base crop map. Agricultural land use could be downscaled to 0.05˚ resolution and gridded agricultural land use information could be generated using this model. Aside from providing quantitative land use information for Japan’ s SSPs, this study also contributes to the IAMs and SSPs societies by testing the applicability and feasibility of global IAMs, especially land use models, to the regional or national extension. For example, regional (national) SSPs quantifications for other regions could be easily implemented by a similar paradigm using AIM/PLUM.

Keywords: downscaling, land use, national SSP

©2019. Japan Geoscience Union. All Right Reserved.

Extreme Events and Emergent Trends in Marine Ecosystem Stressors under a historical/RCP8.5 Climate Change Pathway

*Keith Bradley Rodgers[1,2], Sarah Schlunegger[3], Richard Slater[3], Burke Hales[4], Axel Timmermann[1,2]

1. IBS Center for Climate Physics, Busan, South Korea, 2. Pusan National University, Busan, South Korea, 3. AOS Program, Princeton University, Princeton NJ, USA, 4. College of Ocean and Atmospheric Sciences, Oregon State Universitym, Corvallis, OR, USA

It is important to identify the degree to which climate change will impact ocean ecosystems over the 21st century. Over the last decade there has been increasing application of Earth System Models (ESMs) to project changes in ecosystem stressors (acidification, warming, and de-oxygenation) with a focus on surface and/or thermocline-integrated conditions. Recent efforts have made combined use of CMIP5 models, large ensemble simulations, and/or scenario sensitivity experiments to estimate uncertainties in future projections. Nevertheless very little to date has been done to evaluate how the frequency of extreme events with ecosystem stressors will respond to future climate perturbations. Here we consider for an ensemble suite of simulations with GFDL's ESM2M changes in the frequency of marine ecosystem extreme events over the 21stcentury. We focus on the contrast between the behavior at the ocean's surface vs. base of the ocean's euphotic zone, as these are both important horizons for ocean ecosystems, and on the contrast between the Time of Emergence of decadal trends vs. frequency changes of extreme events, as these are both important ecological timescales. Particular attention is devoted to acidification at the base of the euphotic zone, as this pertains to the life cycle of pteropods. Preliminary results indicate that in addition to the subpolar Northern Oceans and the Southern Ocean, the Large Marine Ecosystems (LME) regions of the eastern Pacific become increasingly exposed to corrosive waters over the 21stcentury.

Keywords: Climate Change, Ecosystem Stressors, Extreme Events, Large Ensemble

©2019. Japan Geoscience Union. All Right Reserved.

[E] Poster | A (Atmospheric and Hydrospheric Sciences)：A-CG Complex & General

Wed. May 29, 2019 5:15 PM - 6:30 PM JST | Wed. May 29, 2019 8:15 AM - 9:30 AM UTC | Poster Hall International Exhibition Hall8, Makuhari Messe_16

[A-CG35] Projection and detection of global environmental change

convener:Michio Kawamiya(Japan Agency for Marine-Earth Science and Technology), Hiroaki Tatebe(Japan Agency for Marine-Earth Science and Technology), Kaoru Tachiiri(Japan Agency for Marine-Earth Science and Technology)

Anthropogenic forcings on global environment are expected to cause intensification of extreme events, sea level rise, ocean acidification and deoxygenation, as well as large-scale ecosystem changes. The CMIP6 experimental protocol has been established based on which modeling groups across the world are starting to provide environmental projection data toward 6th IPCC assessment report due in 2021. Various new types of studies, such as event attribution and coupling of socio-economic processes and Earth system dynamics, are also emerging in the field of global change projection. In addition, observational studies are becoming increasingly more important for grasping changes in the global environment and evaluating model projections. Interactions and collaborations beyond boundaries of conventional scientific disciplines are desired for dealing with the issue of global changes. This session thus aims to deepen our understanding on global change, from both disciplinary and interdisciplinary viewpoints. This session is co-organized by AIMES - Future Earth project "Analysis, Integration and Modelling of the Earth System" (https://aimesproject.org/).

[ACG35-P01] World Regionalization of Climate Change (1961–2010)

*Shao Sun[1,2], Peijun Shi[2,3,4], Daoyi Gong[2], Tao Zhou[2] (1.National Climate Center, China Meteorological Administration, Beijing 100081, China, 2.State Key Laboratory of Earth Surface Processes and Resource Ecology, Beijing Normal University, Beijing 100875, China, 3.Key Laboratory of Environmental Change and Natural Disaster of Ministry of Education, Beijing Normal University, Beijing 100875, China, 4.Academy of Disaster Reduction and Emergency Management, Ministry of Civil Affairs & Ministry of Education, Beijing 100875, China)

[ACG35-P02] Quantifying and identifying future climate signal, noise, and internal variability at finer temporal scales

*Jongho Kim[1], Manh Van Doi[1] (1.University of Ulsan)

[ACG35-P03] Basic evaluation of MIROC6 and current status of CMIP6 experiments

*Hiroaki Tatebe[1] (1.Japan Agency for Marine-Earth Science and Technology)

[ACG35-P04] Synchronized increase of extreme cold and warm events in China during the recent global warming slowdown

*Xiubao Sun[1,3], Chunzai Wang[1], Guoyu Ren[2,3], Panfeng Zhang[2] (1.State Key Laboratory of Tropical Oceanography (LTO), South China Sea Institute of Oceanology(SCSIO), Chinese Academy of Sciences (CAS), 2.Department of Atmospheric Science, School of Environmental Studies, China University of Geosciences (CUG), 3.Laboratory for Climate Studies, National Climate Center (NCC), China Meteorological Administration (CMA))

[ACG35-P05] Quantification of thermodynamical and dynamical contributions to the anthropogenic influences on tropical cyclone rainfall extremes

*Cheng-Ta Chen[1], Shih-How Lo[1], Chung-Chieh Wang[1], Kazuhisa Tsuboki[2] (1.Department of Earth Sciences, National Taiwan Normal University, 2.Hydrospheric-Atmospheric Research Center, Nagoya University)

[ACG35-P06] Temporal Evolution of the Long-Term Distributional Biases of Climate Models as a Parameter for the Regional Evaluation of the Simulation of Climate Change

*Martin Gomez-Garcia[1], Akiko Matsumura[1], Shiro Hishinuma[1], Daikichi Ogawada[1] (1.Nippon Koei Co. Ltd., Reasearch and Development Center)

[ACG35-P07] A global simulation of bioenergy crop yield

*Zhipin Ai[1], Naota Hanasaki[1] (1.National Institute for Environmental Studies)

[ACG35-P08] Integrated Research Program for Advancing Climate Models - Theme B: national research program in Japan on earth system modeling

*Michio Kawamiya[1], Tomohiro Hajima[1], Kaoru Tachiiri[1], Jun'ichi Tsutsui[2], Tokuta Yokohata[3], Takashi Arakawa[4], Takahiro Inoue[4] (1.Japan Agency for Marine-Earth Science and Technology, 2.Central Research Institute of Electric Power Industry, 3.National Institute for Environmental Studies, 4.Research Organization for Information Science and Technology)

[ACG35-P09] Towards probabilistic climate projections based on the CMIP6 multi-model ensemble

*Junichi Tsutsui[1] (1.Central Research Institute of Electric Power Industry)

[ACG35-P10] Effect on the earth system of realizing 1.5 degree climate target by overshooting after reaching 2 degree level

*Kaoru Tachiiri[1], Herran Diego Silva[2], Xuanming Su[1], Michio Kawamiya[1] (1.Japan Agency for Marine-Earth Science and Technology, 2.Institute for Global Environmental Strategies)

[ACG35-P11] **Historical regional and sectoral contributions to climate change**

*Xuanming Su[1], Kaoru Tachiiri[1], Katsumasa TANAKA[2], Michio Watanabe[1] (1.Japan Agency for Marine-Earth Science and Technology, 2.National Institute for Environmental Studies)

[ACG35-P12] **Future projection of global climate, water, food, bio-energy, and land investigated with MIROC-INTEG: a global bio-geophysical land surface model with human components**

*Tokuta Yokohata[1], Yusuke Satoh[1], Tsuguki Kinoshita[2], Gen Sakurai[3], Yadu Pokhrel[4], Akihiko Ito[1], Etsushi Kato[5], Masashi Okada[1], Naota Hanasaki[1], Tomoko Nitta[6], Seita Emori[1] (1.National Institute for Environmental Studies, 2.Ibaraki University, 3.National Agriculture and Food Research Organization, 4.Michigan State University, 5.The Institute of Applied Energy, 6.University of Tokyo)

[ACG35-P13] **Downscaling a global agricultural land use model to country level for national SSP analysis**

*Wenchao Wu[1], Tomoko Hasegawa[1], Kiyoshi Takahashi[1], Shinichiro Fujimori[2] (1.National Institute for Environmental Studies, 2.Kyoto Univ.)

[ACG35-P14] Extreme Events and Emergent Trends in Marine Ecosystem Stressors under a historical/RCP8.5 Climate Change Pathway

*Keith Bradley Rodgers[1,2], Sarah Schlunegger[3], Richard Slater[3], Burke Hales[4], Axel Timmermann[1,2] (1.IBS Center for Climate Physics, Busan, South Korea, 2.Pusan National University, Busan, South Korea, 3.AOS Program, Princeton University, Princeton NJ, USA, 4.College of Ocean and Atmospheric Sciences, Oregon State Universitym, Corvallis, OR, USA)

World Regionalization of Climate Change (1961–2010)

*Shao Sun[1,2], Peijun Shi[2,3,4], Daoyi Gong[2], Tao Zhou[2]

1. National Climate Center, China Meteorological Administration, Beijing 100081, China, 2. State Key Laboratory of Earth Surface Processes and Resource Ecology, Beijing Normal University, Beijing 100875, China, 3. Key Laboratory of Environmental Change and Natural Disaster of Ministry of Education, Beijing Normal University, Beijing 100875, China, 4. Academy of Disaster Reduction and Emergency Management, Ministry of Civil Affairs & Ministry of Education, Beijing 100875, China

Existing climate regionalization aims to characterize the regional differences in climate based on years of the mean values of climate indices. However, with the accelerating climate change nowadays, existing climate regionalization cannot represent the regional difference of climate change, nor can it reflect the extreme weather and climate disasters and environmental risks incurred from climate changes. This paper utilizes the tendency value and fluctuation value of temperature and precipitation from 1961 to 2010 to identify the climate change quantitatively, and completes world regionalization of climate change (1961–2010) with administrative subdivisions of countries as the basic unit in combination with world's terrain feature. Level-I regionalization divides world's climate change (1961–2010) into twelve tendency zones based on the tendency of temperature and precipitation; level-II regionalization refers to twenty-eight fluctuation regions based on level-I regionalization according to the fluctuation of temperature and precipitation. Climate change regionalization provides a basis for countries and regions in the world to develop plans for adapting to climate change, especially for managing extreme weather and climate disasters and environmental risks.

Keywords: Climate change, Regionalization, Tendency, Fluctuation, World

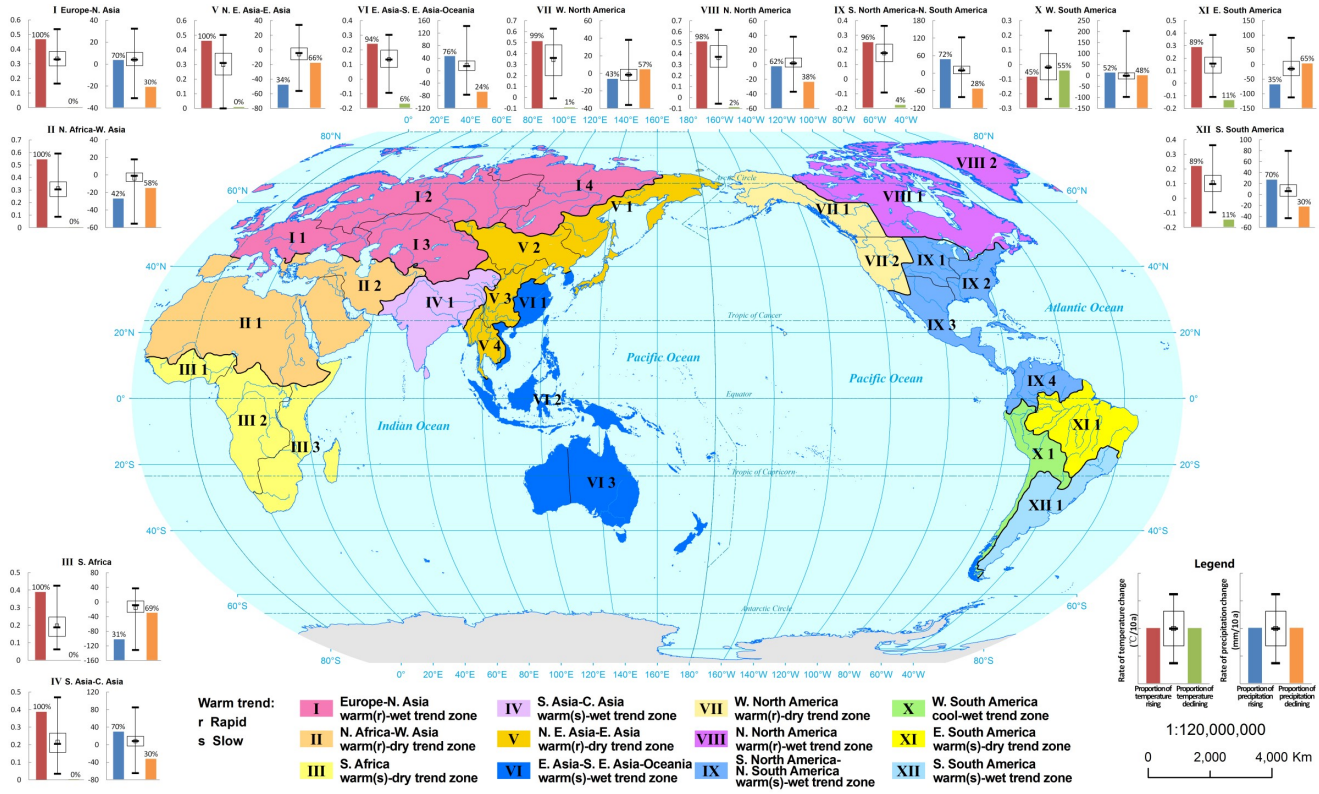

©2019. Japan Geoscience Union. All Right Reserved.

Quantifying and identifying future climate signal, noise, and internal variability at finer temporal scales

*Jongho Kim[1], Manh Van Doi[1]

1. University of Ulsan

Quantifying and identifying climate internal variability (CIV) plays an important role in climate change studies because of its irreducible and unpredictable characteristics. A large number of studies have addressed such an issue; however, the issue was only resolved at coarser resolution on the first order moments of few climate variables. Our recent study has estimated CIV of climate variables for a “current” period at finer spatial and temporal scales; however, whether CIV will change or remain constant in the future under the impact of representative concentration pathways (RCP45 and RCP85) is still questionable. To investigate how CIV will change in the future in both spatial pattern and magnitude, CIV is assessed over 30-year periods in both current and future periods with two scenarios in Korea by analyzing an ensemble of 100 simulations generated by an hourly weather generator. In this study, signal to noise ratio (SNR) used to evaluate the model performance will be applied to simulating ensemble for different periods. CIV is then estimated by two methods: “detrended” and “differenced”; SNR is estimated by “analysis of variance” and “trend analysis” methods. Both SNR and CIV are evaluated with four proposed matrices signifying rainfall volume, extremes and occurrence of rainfall. To consider the change of CIV in the future periods, t-test (test for mean difference) and f-test (test for variance difference) are applied to the ensemble of CIV. In this study, analyzing SNR’s values shows that the four proposed matrices are controlled by non-linear stochastic process and the change tend to increase in the future with increase of CO2 concentration. CIV is proved to change in the future periods under impact of CO2 scenarios. Spatial distribution of CIV’s change over future periods of which locations provides the important and useful information for decision making of water resources planning and proposing mitigation measures of disaster protection.

Acknowledgment:

This research was supported by the Water Management Research Program funded by Ministry of Environment of Korean government (127554), and by the Basic Science Research Program of the National Research Foundation of Korea funded by the Ministry of Education (2016R1D1A1B03931886).

Keywords: climate internal variability, signal to noise ratio, t-test, f-test

©2019. Japan Geoscience Union. All Right Reserved.

Basic evaluation of MIROC6 and current status of CMIP6 experiments

*Hiroaki Tatebe[1]

1. Japan Agency for Marine-Earth Science and Technology

The sixth version of the Model for Interdisciplinary Research on Climate (MIROC), called MIROC6, was cooperatively developed by a Japanese climate modeling community. Overall reproducibility of mean climate and internal climate variability in MIROC6 is better than that in the previous version (MIROC5). The tropical climate systems (e.g., summertime precipitation in the western Pacific and the eastward propagating Madden-Julian Oscillation) and the mid-latitude atmospheric circulations (e.g., the westerlies, the polar night jet, and troposphere-stratosphere interactions) are significantly improved in MIROC6. These improvements can be attributed to the newly implemented parameterization for shallow convective processes and to the directly resolved stratosphere. In the present study, simulated mean climate, internal climate variability in MIROC6 are evaluated and briefly summarized in comparison with MIROC5 and observations. Using MIROC6, designated simulations tackling a wide range of climate science issues, as well as seasonal-to-decadal climate predictions and future climate projections, are currently ongoing with an aim towards contributing to the sixth phase of the Coupled Model Intercomparison Project (CMIP6). Preliminary results of historical climate simulations from the middle of the 19th century, climate projections from the present to the end of the 21th century based on future scenarios of the Shared Socio-economic Pathways, and initialized climate predictions on seasonal-to-decadal timescales will be given in this talk.

Keywords: Climate model, CMIP6, climate projections/predictions

©2019. Japan Geoscience Union. All Right Reserved.

Synchronized increase of extreme cold and warm events in China during the recent global warming slowdown

*Xiubao Sun[1,3], Chunzai Wang[1], Guoyu Ren[2,3], Panfeng Zhang[2]

1. State Key Laboratory of Tropical Oceanography (LTO), South China Sea Institute of Oceanology(SCSIO), Chinese Academy of Sciences (CAS), 2. Department of Atmospheric Science, School of Environmental Studies, China University of Geosciences (CUG), 3. Laboratory for Climate Studies, National Climate Center (NCC), China Meteorological Administration (CMA)

From the end of 1990s to the middle of 2010s, global mean temperature experienced a process of warming slowdown. However, global warm extremes did not show the slowdown phenomenon during the recent global warming slowdown. Based on the observation data of 2362 land surface stations in China, we analyzed the cold and warm extremes changes over mainland China between global warming period (1961-1999) and warming slowdown period (2000-2014). Results indicate that the warming trend in the cold season (MAM and DJF) is significantly higher than that in the warm season (JJA and SON) in the period of global warming (1961-1999), while the warming trend in the warm season is significantly higher than that in the cold season in the period of global warming slowdown. That is, the trend of warm season and the cool season in China have reversed. At the same time, we also found that the synchronous increase occurrence of extreme warm events in summer (JJA) and extreme cold events in winter (DJF) leads to the seasonal trend reverse phenomenon, but there are differences in the spatial variation characteristics between cold and warm extremes. The increase of warm extremes in summer is mainly due to the strong increase of warm events in south China, while the increase of cold events in winter is due to the increase of cold events over China. Further, we also found that the variability of extreme temperature has increased more significantly in the warming slowdown period than that in global warming period. East Asian winter monsoon and summer monsoon both show enhanced characteristics during the global warming slowdown period, which indicates that the increase of sea-land temperature difference in summer and winter results in the synchronous increase of extreme cold and warm events by increasing the climate variability in China.

Keywords: Global warming, Global warming slowdown, Extreme warm events, Extreme cold events, Land-sea temperature difference

©2019. Japan Geoscience Union. All Right Reserved.

Quantification of thermodynamical and dynamical contributions to the anthropogenic influences on tropical cyclone rainfall extremes

*Cheng-Ta Chen[1], Shih-How Lo[1], Chung-Chieh Wang[1], Kazuhisa Tsuboki[2]

1. Department of Earth Sciences, National Taiwan Normal University, 2. Hydrospheric-Atmospheric Research Center, Nagoya University

The rainfall extremes and strong winds associated with tropical cyclones lead to significant damages and lost to where they make landfalling. Upward trend in term of financial lost was indicated for the past few decades from the report of major reinsurance firms. Whether the past anthropogenic warming played a significant role in such extreme event and their changes remained very controversial. On one hand, people argue it’s nearly impossible to attribute an individual extreme event to global warming. On the other hand, the increase of heavy rainfall is consistent with the expected effects of climate change on tropical cyclone. To diagnose possible anthropogenic contributions to the odds of heavy rainfall associated with tropical cyclone, we adapt an existing event attribution framework of modeling a ‘world that was’ and comparing it to a modeled ‘world that might have been’ for that same time but for the absence of historical anthropogenic drivers of climate. One limitation for applying such approach to high-impact weather system is that it will require models capable of capturing the essential processes lead to the studied extremes. Using a cloud system resolving model that can properly simulate the complicated interactions between tropical cyclone, large-scale background, topography, we first perform the ensemble ‘world that was’ simulations forced by the high resolution ECMWF YOTC analysis. We then re-simulate with the adjusted ‘world that might have been conditions’ by removing the regional atmospheric and oceanic forcing due to human influences estimated from the CMIP5 model ensemble mean conditions between all forcing and natural forcing only historical runs. Thus our findings are highly conditional on the driving analysis and adjustments therein, but the setup allows us to elucidate possible contribution of anthropogenic forcing to changes in the likelihood of heavy rainfall associated tropical cyclone. With only less than half of degree anthropogenic warming over the study area, we found that this forcing very likely (9 out of 10 cases) increase the risk of heavy rainfall event (grid rainfall greater than 33 mm per hour) by at least 16%. The role of dynamical processes that leads to precipitation extreme increases beyond the moisture content increase will be further analyzed and discussed.

Keywords: Tropical Cyclone, Extreme rainfall, extreme event attribution

©2019. Japan Geoscience Union. All Right Reserved.

Temporal Evolution of the Long-Term Distributional Biases of Climate Models as a Parameter for the Regional Evaluation of the Simulation of Climate Change

*Martin Gomez-Garcia[1], Akiko Matsumura[1], Shiro Hishinuma[1], Daikichi Ogawada[1]

1. Nippon Koei Co. Ltd., Reasearch and Development Center

Owing to the climate variability of the General Circulation Models (GCM), the discrepancy between their outputs and observational datasets at scales that range from hours to years is practically random. Thus, the associated errors need to be evaluated in terms of the long-term (multidecadal) distributional properties of the atmospheric variables. A recently developed bias-correction method corrects the systematic errors (i.e., biases) in the climate mean state and in three distributional measures of the daily and the interannual variability (namely the frequency of extremes, the skewness, and the scale of the variable at each timescale). The adjustment of these biases is done in such a way that the corrections at one timescale do not affect the probability distribution at another. Therefore, this bias-correction method is able to preserve the GCM-simulated climate trends and extensively reproduce the long-term frequency of the observed extreme weather (e.g. 98th percentile of wet days, maximum seasonal mean of surface temperature).

Generally, the bias-correction of GCMs faces the challenge of including the simulated changes of climate, which supposes alterations in not only the mean but also other aspects like the skewness and the frequency of extremes. The abovementioned bias-correction method includes the effect of the simulated climate change in the correction of the distributional biases. However, considering the coarse resolution of the GCMs and the imperfections in the parameterizations of the subgrid physical processes, the fundamental assumption that the distributional biases are predictable (i.e., stationary) is made.

In this study, we explored the possibility of evaluating the sensibility with which GCMs simulate the response of the earth-system components to external forcing (i.e., climate change) by comparing the temporal evolution of the distributional biases at different timescales over specific regions. For the short period in which the observed data was available, our results revealed that many CMIP5 GCMs are indeed able to simulate with a quasi-stationary bias the changes caused by climate change. Moreover, being able to identify the regions in which certain models do not show the errors with a systematic behavior in either the climate mean state, the daily variability or the interannual variability can be useful for the further development of climate models. We expect that with the data of the GCM outputs of the future phases of the CMIP project, the period in which the observed and the modeled data coincide becomes longer and, thus, our conclusions can be supported by more robust evidence.

Keywords: Bias correction of GCMs at different timescales, Climate trends and climate variability, Evaluation of the ability of GCMs to simulate climate change

©2019. Japan Geoscience Union. All Right Reserved.

A global simulation of bioenergy crop yield

*Zhipin Ai[1], Naota Hanasaki[1]

1. National Institute for Environmental Studies

Large-scale development of bioenergy is considered as an effective pathway to achieve the 2 degrees target of the Paris Agreement. To avoid the competition with food crops, so-called the second-generation bioenergy crops such as miscanthus and switchgrass are regarded as potential dedicated biomass crop. However, the models to estimate the yield of miscanthus and switchgrass at a global scale which enable analyzing the effects of irrigation water application are seldom seen as of today. Here, we firstly updated the crop module in the global hydrological model H08 for miscanthus and switchgrass. Then, we conducted a global simulation and validation of the yield for miscanthus and switchgrass at 0.5 degree. The results indicated that the updated H08 have a good ability in simulating the yield of perennial bioenergy crops, which provides a good foundation for further integrated assessment of the impacts of bioenergy crop production on water sector.

Acknowledgement: This research was supported by the Environment Research and Technology Development Fund (S-14-5) of the Environmental Restoration and Conservation Agency.

Keywords: Bioenergy, Crop yield, H08

©2019. Japan Geoscience Union. All Right Reserved.

Integrated Research Program for Advancing Climate Models - Theme B: national research program in Japan on earth system modeling

*Michio Kawamiya[1], Tomohiro Hajima[1], Kaoru Tachiiri[1], Jun'ichi Tsutsui[2], Tokuta Yokohata[3], Takashi Arakawa[4], Takahiro Inoue[4]

1. Japan Agency for Marine-Earth Science and Technology, 2. Central Research Institute of Electric Power Industry, 3. National Institute for Environmental Studies, 4. Research Organization for Information Science and Technology

The Integrated Research Program for Advancing Climate Models, or TOUGOU (abbreviation taken from its Japanese name), is a national project for projection of global change. Its aim to provide information for adaptation and mitigation, based on scientific evaluation of changes including those in extreme events and carbon cycle. The project was launched in April, 2017. While the entire program deals with a wide range of physical aspects and consequent impacts of climate change, Theme B (TOUGOU-B) focuses on the development of a state-of-the-art Earth system model (ESM) incorporating biogeochemical processes, such as sophisticated carbon and nitrogen cycles, as well as its application to exploring future socio-economic pathways of climate change mitigation. MIROC-ESM, an ESM developed under TOUGOU-B (and the previous SOUSEI-B) has been significantly improved since the 5th phase of coupled model intercomparison project (CMIP5), and has started to be run for CMIP6. During the three years since TOUGOU was launched, results have been obtained that may contribute to 6th Assessment Report (AR6) of Intergovernmental Panel on Climate Change (IPCC) including those on impacts of pyrogenic iron on oceanic ecosystem, assessment of the outcome of labor productivity change due to warming, and effects of high dust amount on surface temperature during the Last Glacial Maximum. Besides, efforts to secure ways to disseminate projection data are ongoing under TOUGOU-B. Specifically, collaboration has been established between climate modeling community in Japan and Data Integration and Analysis System (DIAS), a national IT project for environmental data, have been continuing, in order for Japan to participate in Earth System Grid Federation (ESGF). ESGF is an international cooperative activity to construct a data distributing system for climate related data such as CMIP6 outputs. Some of the details of these results will be explained in the presentation.

Keywords: IPCC, Earth system model , carbon cycle, socio-economic scenario, CMIP6, climate mitigation

©2019. Japan Geoscience Union. All Right Reserved.

Towards probabilistic climate projections based on the CMIP6 multi-model ensemble

*Junichi Tsutsui[1]

1. Central Research Institute of Electric Power Industry

Research on climate change mitigation uses a climate model emulator that represents the average and range over a specific multi-model ensemble of complex climate simulations. The Coupled Model Intercomparison Project (CMIP) has provided such multi-model ensembles, and its latest Phase 6 (CMIP6) results are being revealed. As a first step to applying the CMIP6 results to probabilistic climate projections, we focus on the distribution of key parameters representing atmospheric CO_2-induced forcing and transient temperature responses.

In this study, we develop a procedure to determine the forcing-response parameters of a complex climate model. We simultaneously fit a curve built on an impulse response function to the global mean time series of the model's surface temperature anomaly and top-of-atmosphere energy imbalance from two basic CO_2 -forced experiments, i.e., an abrupt quadrupling and a 1%-per-year increase in atmospheric CO_2 concentration. This scheme serves as an improved alternative to the widely-used regression method of Gregory et al. (2004). Furthermore, it makes a complete set of parameters to emulate the target model from which equilibrium climate sensitivity (ECS) and transient climate response (TCR) are derived. The properties of a multi-model ensemble are quantified through a statistical approach including a principal component analysis for the parameters.

The two CO_2-forced experiments are included in the set of common experiments which is designed to maintain continuity across different CMIP phases. Here, we compare the parameters of individual CMIP6 models with those of the previous-phase CMIP5 models. The parameters of the CMIP5 ensemble have several features. The ratio of TCR to ECS is distributed in the range of approximately 0.5 to 0.7, and for models with large ECS, the ratio tends to decrease. The scaling parameter for the effective radiative forcing of CO_2 varies from model to model and tends to be less than a reference value used in a conventional formula of CO_2 radiative forcing. Although the number of CMIP6 models is currently limited, their parameters show similar distributions within the CMIP5 ranges.

Keywords: climate sensitivity, effective radiative forcing, impulse response model, climate model emulator, ensemble climate experiment

©2019. Japan Geoscience Union. All Right Reserved.

Effect on the earth system of realizing 1.5 degree climate target by overshooting after reaching 2 degree level

*Kaoru Tachiiri[1], Herran Diego Silva[2], Xuanming Su[1], Michio Kawamiya[1]

1. Japan Agency for Marine-Earth Science and Technology, 2. Institute for Global Environmental Strategies

By using an Earth system model (ESM) with emissions and land use scenarios consistent with socio-economic projections from an integrated assessment model, the effect of overshooting to 1.5 degree target (in Celsius from pre-industrial periods) after reaching 2 degree level is investigated in selected indicators of the global environment. Unlike the internationally coordinated model intercomparison project, the scenario is developed for a specific climatic model. The ESM output results in delayed achievements for both of 1.5 and 2 degree targets in terms of global surface mean air temperature, but achieved before or around 2100 as expected when we use global mean surface temperature (for which sea surface temperature and surface air temperature are used for ocean and land, respectively) masked with observation areas. In the overshooting scenario more heat is absorbed by the ocean compared to a case without overshooting, but still we found significant difference between the two scenarios in Arctic sea ice, while in both scenarios corals seem difficult to survive the 21st century (when no thermal adaptation is assumed) . The difference in steric sea level rise between the scenarios is only below 2 cm in 2100. In addition, vegetation productivity in broad regions shows slight (~5%) increase. Emission pathways in the scenarios rely on a large amount of carbon sequestration. In the 2 degree scenario CO2 emissions in 2100 are slightly below zero, while for 1.5 degree scenario they are below -20 GtCO2.. When the Earth system has high climate sensitivity and TCRE, to reach the 1.5 degree target we need to take an overshooting temperature pathway, but in case the overshooting is large, difference in some indicators between 1.5 degree and 2 degree scenarios can be non-significant, which is an important indication in implementing adaptive mitigation in the coming decades.

Keywords: Earth system model, integrated assessment model, 1.5 degree target, 2 degree target, stabilization, overshooting

©2019. Japan Geoscience Union. All Right Reserved.

Historical regional and sectoral contributions to climate change

*Xuanming Su[1], Kaoru Tachiiri[1], Katsumasa TANAKA[2], Michio Watanabe[1]

1. Japan Agency for Marine-Earth Science and Technology, 2. National Institute for Environmental Studies

Regional or sectoral contributions to climate change are important in the formulation of climate change policy. After the industrial revolution, developed countries emit CO_2 and non-CO_2 greenhouse gases (GHGs), and the historical emissions are large; while developing countries contribute relative fewer emissions in historical period but increase significantly in recent years or visible future. To assess the contributions to climate change, using cumulative emissions is a general and direct method. However, such method may ignore the lifetime of GHGs since part of the GHGs sink into the biosphere, ocean, soil or diminish during biogeochemical cycles. In this study, we evaluate the historical regional and sectoral contributions to climate change by using an improved version of Simple Climate Model for OPTimization (SCM4OPT) with a normalized marginal method. Based on the results, we analyze ten major GHG emitting countries and 12 sectors.

First, current emissions with relative long lifetime like CO_2 and N_2O, from developing countries increase significantly, like China, India, Mexico and Brazil, however, their contributions to climate change are still relatively smaller, compared with the developed countries such as USA, Japan, Germany, Canada and UK, of which countries the cumulative emissions are in relatively larger scale and current emissions are already under controlled. We can conclude here that the GHGs with relatively long lifetime need to be controlled stringently to reduce the long-term effects on climate change. For CH_4, which has a relatively shorter lifetime, the contributions to climate change are closely related to emissions within recent decades. These imply that reductions on short lifetime emissions can make immediate alleviation regarding climate change.

Second, energy sector contributes most of the CO_2 emissions, and therefore contribute almost half to the climate change among all the sectors. However, for CH_4 and N_2O, agriculture sector contributes most of the emissions and therefore their contributions to climate change are remarkable. Reduction policiesneed to targetthesesectors. In addition, CO_2 from land transportation and CH_4 from waste treatment increase rapidly in recent years, attention also needs to be paid to these sectors for making climate change policies.

Keywords: region emissions, sector emissions, climate change contribution, simple climate model

©2019. Japan Geoscience Union. All Right Reserved.

Future projection of global climate, water, food, bio-energy, and land investigated with MIROC-INTEG: a global bio-geophysical land surface model with human components

*Tokuta Yokohata[1], Yusuke Satoh[1], Tsuguki Kinoshita[2], Gen Sakurai[3], Yadu Pokhrel[4], Akihiko Ito[1], Etsushi Kato[5], Masashi Okada[1], Naota Hanasaki[1], Tomoko Nitta[6], Seita Emori[1]

1. National Institute for Environmental Studies, 2. Ibaraki University, 3. National Agriculture and Food Research Organization, 4. Michigan State University, 5. The Institute of Applied Energy, 6. University of Tokyo

Future climate changes possibly affect water resources, food production, energy supply, and ecosystem services. It is critical to better understand the interactions between the changes in these complicated factors. While earth system models and integrated assessment models are applicable to explore this topic, parts of their natural and/or human processes tend to be simplified depending on their scope. As such, it still remains a challenge to realistically model the human-natural interface. In this context, the MIROC integrated terrestrial model (MIROC-INTEG) was developed. One of the features of MIROC-INTEG is that the natural ecosystem and human activity models are coupled to a global land surface model MATSIRO (Nitta et al. 2014, Journal of Climate), which is a component of a state-of-the-art global climate model, MIROC (Watanabe et al. 2010, Journal of Climate). As a natural ecosystem model, we use a global vegetation model, VISIT (Ito and Inatomi 2012, Biogeosciences). As human activity models, we use a global land-surface model with anthropogenic water regulation modules, HiGW-MAT (Pokhrel et al, 2012, Journal of Hydrometeorology), and a global crop model, PRYSBI2 (Sakurai et al, 2014, Scientific Reports). In HiGW-MAT, models of human water regulations such as water withdrawal from river, dam operation, and irrigation (Hanasaki et al. 2008, Hydrol. Earth Syst. Sci.) are incorporated to the above-mentioned global land surface model, MATSIRO. In PRYSBI2, the growth and yield of four crops (wheat, maize, soybean, rice) are calculated. In addition to these models, a global land use model (Terrestrial Land-use Model, TeLMO) is newly developed in the present study. TeLMO calculate the grid ratio of cropland (food and bio-energy crops), pasture, forest (managed and un-managed), as well as their transition. Output variables of each sub-model are passed to other sub-models during the time integration.
We will present an analysis of historical and future simulations with a focus on the interactions between water, food, energy, and land. In the historical simulations, we validated the model output such as irrigated water, crop yield, ecosystem productions, and cropland area by comparing to the observed or reanalysis data. In the future simulations, we investigated the role of uncertainties in climate (Representative Concentration Pathways) and socio-economic (Shared Socio-economic Pathways) scenarios. We also investigate the role of uncertainties in model parameters, and found that an uncertainty in the fertilization effect of crop growth model PRYSBI2 strongly affect uncertainty in future projection of crop yield and land use change in TeLMO. We found that future changes in precipitation and/or temperature possibly cause decrease in soil moisture, leading to decreases in crop yield (especially in high emission scenario such as RCP8.5). Decrease in crop yield bring about increase in crop land area, which also causes the increase in irrigation demands. Interaction between water, crop yield, and land use, as well as possible impacts on ecosystem service will be discussed in the presentation.

Keywords: Global Climate Model, Earth System Model, Human activity

©2019. Japan Geoscience Union. All Right Reserved.

Downscaling a global agricultural land use model to country level for national SSP analysis

*Wenchao Wu[1], Tomoko Hasegawa[1], Kiyoshi Takahashi[1], Shinichiro Fujimori[2]

1. National Institute for Environmental Studies, 2. Kyoto Univ.

The Shared Socioeconomic Pathways (SSPs) has been part of latest scenario framework developed by the climate change research society in the recent decade, serving the integrated analysis of future climate impacts, vulnerabilities, adaptation, and mitigation, in which the agriculture, food system and land use are important components. Multiple integrated assessment models (IAMs) have been used for the quantitative projections of future agriculture, food system and land use in the global scale. However, the tool and application of IAMs to the quantification of SSPs on regional or national level is limited. Meanwhile, there are growing needs for the quantification of SSPs on regional or national level for a more detailed understanding of agriculture, food, and land use, and their interactions with other nexus, such as energy, water, and biodiversity. One obstacle for such application is the coarse spatial resolution of global IAMs for land use module. This study aims to apply the Asian-Pacific Integrated Model/Platform for Land-Use and Environmental Model (AIM/PLUM) for the quantification of agriculture, food system, and land use in Japan under its national-specific SSPs narratives. To achieve this, a regional land use model, AIM/PLUM-Japan, was developed, by improving the spatial resolution to 0.05˚ (targeting 1km) from global model of 0.5˚. We combined the statistical production area data and spatial land use data to produce a refined base crop map. Agricultural land use could be downscaled to 0.05˚ resolution and gridded agricultural land use information could be generated using this model. Aside from providing quantitative land use information for Japan’ s SSPs, this study also contributes to the IAMs and SSPs societies by testing the applicability and feasibility of global IAMs, especially land use models, to the regional or national extension. For example, regional (national) SSPs quantifications for other regions could be easily implemented by a similar paradigm using AIM/PLUM.

Keywords: downscaling, land use, national SSP

©2019. Japan Geoscience Union. All Right Reserved.

Extreme Events and Emergent Trends in Marine Ecosystem Stressors under a historical/RCP8.5 Climate Change Pathway

*Keith Bradley Rodgers[1,2], Sarah Schlunegger[3], Richard Slater[3], Burke Hales[4], Axel Timmermann[1,2]

1. IBS Center for Climate Physics, Busan, South Korea, 2. Pusan National University, Busan, South Korea, 3. AOS Program, Princeton University, Princeton NJ, USA, 4. College of Ocean and Atmospheric Sciences, Oregon State Universitym, Corvallis, OR, USA

It is important to identify the degree to which climate change will impact ocean ecosystems over the 21st century. Over the last decade there has been increasing application of Earth System Models (ESMs) to project changes in ecosystem stressors (acidification, warming, and de-oxygenation) with a focus on surface and/or thermocline-integrated conditions. Recent efforts have made combined use of CMIP5 models, large ensemble simulations, and/or scenario sensitivity experiments to estimate uncertainties in future projections. Nevertheless very little to date has been done to evaluate how the frequency of extreme events with ecosystem stressors will respond to future climate perturbations. Here we consider for an ensemble suite of simulations with GFDL's ESM2M changes in the frequency of marine ecosystem extreme events over the 21stcentury. We focus on the contrast between the behavior at the ocean's surface vs. base of the ocean's euphotic zone, as these are both important horizons for ocean ecosystems, and on the contrast between the Time of Emergence of decadal trends vs. frequency changes of extreme events, as these are both important ecological timescales. Particular attention is devoted to acidification at the base of the euphotic zone, as this pertains to the life cycle of pteropods. Preliminary results indicate that in addition to the subpolar Northern Oceans and the Southern Ocean, the Large Marine Ecosystems (LME) regions of the eastern Pacific become increasingly exposed to corrosive waters over the 21stcentury.

Keywords: Climate Change, Ecosystem Stressors, Extreme Events, Large Ensemble

©2019. Japan Geoscience Union. All Right Reserved.

[E] Oral | A (Atmospheric and Hydrospheric Sciences)：A-CG Complex & General

Wed. May 29, 2019 1:45 PM - 3:15 PM JST | Wed. May 29, 2019 4:45 AM - 6:15 AM UTC | 303 3F

[A-CG35] Projection and detection of global environmental change

convener:Michio Kawamiya(Japan Agency for Marine-Earth Science and Technology), Hiroaki Tatebe(Japan Agency for Marine-Earth Science and Technology), Kaoru Tachiiri(Japan Agency for Marine-Earth Science and Technology), Chairperson:Hiroaki Tatebe

Anthropogenic forcings on global environment are expected to cause intensification of extreme events, sea level rise, ocean acidification and deoxygenation, as well as large-scale ecosystem changes. The CMIP6 experimental protocol has been established based on which modeling groups across the world are starting to provide environmental projection data toward 6th IPCC assessment report due in 2021. Various new types of studies, such as event attribution and coupling of socio-economic processes and Earth system dynamics, are also emerging in the field of global change projection. In addition, observational studies are becoming increasingly more important for grasping changes in the global environment and evaluating model projections. Interactions and collaborations beyond boundaries of conventional scientific disciplines are desired for dealing with the issue of global changes. This session thus aims to deepen our understanding on global change, from both disciplinary and interdisciplinary viewpoints. This session is co-organized by AIMES - Future Earth project "Analysis, Integration and Modelling of the Earth System" (https://aimesproject.org/).

1:45 PM - 2:00 PM JST | 4:45 AM - 5:00 AM UTC

[ACG35-01] Sour and anoxic Sea of Japan in the near future

*Chen-Tung Arthur Chen[1], Hon-Kit Lui[1], Masao Ishii[2] (1.National Sun Yat Sen University, 2.Japan Meteorological Agency)

2:00 PM - 2:15 PM JST | 5:00 AM - 5:15 AM UTC

[ACG35-02] Decadal predictions of the variable ocean carbon uptake

★Invited Papers

*Hongmei Li[1], Tatiana Ilyina[1], Wolfgang A. Müller[1,2], Peter Landschützer[1] (1.Max Planck Institute for Meteorology, Bundesstraße 53, 20146 Hamburg, Germany, 2.Deutscher Wetterdienst, Bernhard-Nocht-Straße 76, 20359 Hamburg, Germany)

2:15 PM - 2:30 PM JST | 5:15 AM - 5:30 AM UTC

[ACG35-03] Air-sea CO_2 flux variations in the tropical Pacific simulated with two ESMs embedded an ocean data assimilation system

*Michio Watanabe[1], Hiroaki Tatebe[1], Hiroshi Koyama[1], Tomohiro Hajima[1], Masahiro Watanabe[2], Michio Kawamiya[1] (1.Japan Agency for Marine-Earth Science and Technology, 2.Atmosphere and Ocean Research Institute, the University of Tokyo)

2:30 PM - 2:45 PM JST | 5:30 AM - 5:45 AM UTC

[ACG35-04] A Study of Decadal Ocean Deoxygenation and Heat Uptake from a suite of OMIP Simulations

*Yohei Takano[1], Jerry Tjiputra[2], Jörg Schwinger[2], Matthias Gröger[3], Sarah Berthet[4], Roland Séférian[4], Andrew Yool[5], Julien Palmieri[5], Michio Watanabe[6], Irene Stemmler[1], Tatiana Ilyina[1] (1.Max Planck Institute for Meteorology, 2.Norwegian Research Centre, 3.Swedish Meteorological and Hydrological Institute, 4.Centre National de Recherche Météorologique, Unite mixte de recherche 3589 Météo-France/CNRS, 5. National Oceanography Centre, 6.Japan Agency for Marine-Earth Science and Technology)

2:45 PM - 3:00 PM JST | 5:45 AM - 6:00 AM UTC

[ACG35-05] Role of large-scale environmental variability in changing storm climate

*Nilima Aditya Natoo[1] (1.University of Bremen, Germany)

3:00 PM - 3:15 PM JST | 6:00 AM - 6:15 AM UTC

[ACG35-06] The forced response of the climate system: The case of climatic teleconnections

*Tamas Bodai[1], Matyas Herein[2], Gabor Drotos[3] (1.University of Reading, 2.Eotvos University Budapest, 3.Universitat de les Illes Balears)

Sour and anoxic Sea of Japan in the near future

*Chen-Tung Arthur Chen[1], Hon-Kit Lui[1], Masao Ishii[2]

1. National Sun Yat Sen University, 2. Japan Meteorological Agency

The ocean acidification is frequently related to hypoxia. In the paper "An anoxic Sea of Japan in 2200?" (Chen, Marine Chemistry, 1999) it was suggested that the sea is undergoing rapid de-oxygenation, and that the sea may become anoxic by the year 2200. But, a question mark was used in the title because of large uncertainties. In a recent Nature Climate Change paper (Chen et al., 2017), however, it was further concluded that the deep Sea of Japan has acidified at a faster rate than anywhere else in the world oceans. The conclusion of rapid acidification is in line with the conclusion of de-oxygenation. In addition, adding 20 years of new data confirms that the assessment of 1999 was correct. Likely the Sea of Japan would become sour and anoxic within the next two hundred years, if not sooner, based on nutrients, oxygen and pH data.

Keywords: Sea of Japan, acidification, hypoxia

©2019. Japan Geoscience Union. All Right Reserved.

Decadal predictions of the variable ocean carbon uptake

*Hongmei Li[1], Tatiana Ilyina[1], Wolfgang A. Müller[1,2], Peter Landschützer[1]

1. Max Planck Institute for Meteorology, Bundesstraße 53, 20146 Hamburg, Germany, 2. Deutscher Wetterdienst, Bernhard-Nocht-Straße 76, 20359 Hamburg, Germany

The global ocean, as a major carbon sink, absorbs about 25% of the contemporary anthropogenic CO_2 emissions; hence the carbon uptake by the ocean largely mitigates the CO_2concentration increase in the atmosphere and hence the global warming. Moreover, the strength of the carbon flux into the ocean, varies substantially from annual to decadal time-scale. Therefore, predicting the variable ocean carbon uptake and global carbon cycle is of essential value of tracing the fate of carbon and the corresponding climate and ecosystem changes.

By assimilating atmosphere and ocean physical observations into the decadal prediction system based on the Max Planck Institute Earth System Model (MPI-ESM), we reproduce the ocean carbon uptake variations in consistent with the data-based estimates. The retrospective predictions starting from the assimilation states show a predictive skill of 2 years in the ocean carbon uptake globally. Regionally the predictive skill is up to 5 years in the Southern Ocean and the North Pacific. To understand the mechanisms in maintaining the predictability of the ocean carbon uptake, we separate the ocean surface pCO_2, which is the main driver of the variability in carbon fluxes, into thermal and non-thermal components. The thermal component is affected by the solubility of CO_2via temperature variations, and the non-thermal component is affected by the ocean circulation and biology, i.e., is not first order affected by the temperature. We find that the thermal component contributes mainly to shorter-term (of <3 years) of predictive skill of the ocean carbon uptake, while the non-thermal component is responsible for longer-term (of >3 years) of predictive skill of the ocean carbon uptake.

Decadal prediction study of the global carbon cycle and corresponding ecosystem based on the ESMs is still at its early stage and facing a number of challenges arising from limited ocean biogeochemical observations and lack of proper initialization strategies. An extension of our predictions in the context of multi-model framework is in progress and this will facilitate deeper understanding of the mechanisms and further improvement of the predictive skill in the global carbon cycle.

Keywords: Decadal predictions, Ocean carbon uptake, Climate variability

©2019. Japan Geoscience Union. All Right Reserved.

Air-sea CO_2 flux variations in the tropical Pacific simulated with two ESMs embedded an ocean data assimilation system

*Michio Watanabe[1], Hiroaki Tatebe[1], Hiroshi Koyama[1], Tomohiro Hajima[1], Masahiro Watanabe[2], Michio Kawamiya[1]

1. Japan Agency for Marine-Earth Science and Technology, 2. Atmosphere and Ocean Research Institute, the University of Tokyo

Interannual-to-decadal fluctuations of the global-mean atmospheric CO_2 concentration are observed associated with internal climate variations, and these fluctuations sometimes cancel out and at other times support the centennial increasing trend of the global-mean atmospheric CO_2 concentration due to accumulation of anthropogenic CO_2 emissions. One direct cause of the fluctuations is the oceanic absorption or release of CO_2 through the global air-sea CO_2 flux variations which are mainly dominated by the tropical Pacific. Therefore, deeper understanding of the tropical oceanic processes and properly initializing oceanic states including marine ecosystem are of importance in future predictions of the global CO_2 concentration together with quantification of human-influences. In the present study, we examined the simulated air-sea CO_2 flux variations in the tropical Pacific in two ESMs (MIROC-ES2L and MIROC-ESM) with the same ocean data assimilation system. Although the assimilation procedures are the same, observed anti-correlated relationship between interannual variations of the upward air-sea CO_2 flux and the sea surface temperature (SST) in the tropical Pacific are well captured in MIROC-ES2L, but the relationship is reversed in MIROC-ESM. Tropical climatic-mean state of MIROC-ESM shows significant biases of weaker trade winds as well as more diffuse equatorial thermocline than observations, and simulated amplitude of interannual variations of NINO3-SST is about half as large as observations. When observations are assimilated into the model, these biases lead to non-negligible correction terms on the governing equations of ocean temperature and salinity, which induces an anomalous spurious equatorial upwelling during El-Niño events. The spurious upwelling brings dissolved inorganic carbon rich water in the subsurface layer to the surface mixed layer. Consequently, an anomalous upward air-sea CO_2 flux is occurred during El-Niño, as opposed to observations and MIROC-ES2L. Better modeling physical processes in the tropical climate system is suggested to be essential for better marine ecosystem modeling and reanalysis.

Keywords: Earth system model, data assimilation, air-sea CO2 flux, ENSO

©2019. Japan Geoscience Union. All Right Reserved.

A Study of Decadal Ocean Deoxygenation and Heat Uptake from a suite of OMIP Simulations

*Yohei Takano[1], Jerry Tjiputra[2], Jörg Schwinger[2], Matthias Gröger[3], Sarah Berthet[4], Roland Séférian[4], Andrew Yool[5], Julien Palmieri[5], Michio Watanabe[6], Irene Stemmler[1], Tatiana Ilyina[1]

1. Max Planck Institute for Meteorology, 2. Norwegian Research Centre, 3. Swedish Meteorological and Hydrological Institute, 4. Centre National de Recherche Météorologique, Unite mixte de recherche 3589 Météo-France/CNRS, 5. National Oceanography Centre, 6. Japan Agency for Marine-Earth Science and Technology

Observational studies reveal substantial ocean deoxygenation and increased heat uptake in the past decades. These two properties are known to be tightly connected. The Earth System Models (ESMs) struggle to simulate the observed trends in oxygen inventory (O_2-Inv) and the tight global O_2-heat relationship. One possible reason is the role of decadal climate variability.

The past decadal changes in oxygen inventory and tight global O_2-heat relationship cannot be fully explained by changes in solubility alone, indicating the important role of changes in ocean circulation and biology. Climate variability could modulate O_2-Inv and heat uptake on decadal timescales but the observed climate variability is not necessarily simulated in the ESMs historical simulations due to the fact that the models have their own internal climate variability, which vary in magnitude and phase, in the coupled climate system. Here we address the question how the observed decadal climate variability modulates O_2-Inv and heat uptake using a suite of OMIP simulations.

We will present results from the comparison of state-of-the-art ocean model simulations driven by the atmospheric reanalysis forcing. The main focus is to understand decadal changes in global and regional upper ocean O_2-Inv and OHC based on the results from six different model simulations (NorESM-OC, EC-EARTH3.3.0, CNRM-ESM2-1, UKESM1, MIROC-ES2L, and MPI-OM-HAMOCC), and observations. The model structural differences result in different physical and biogeochemical mean states, which lead to different decadal variability of O_2-Inv and OHC. The regional O_2-heat relationship among the models and observations would be presented to discern the biases in the simulated ocean circulations and biological processes. Our study will provide first indications of the importance of decadal climate variability on determining changes in O_2-Inv and OHC. Hence, it will also provide guidance on accuracy and uncertainty of future deoxygenation and warming projected in the ESMs. We aim on stimulating the discussion on near term strategy of how we analyze upcoming OMIP simulations within the context of climate variability and changes in ocean physics and biogeochemistry based on our multi-model analysis.

Keywords: Multi-model comparison, ocean deoxygenation, ocean heat uptake, decadal variability and trend

©2019. Japan Geoscience Union. All Right Reserved.

Role of large-scale environmental variability in changing storm climate

*Nilima Aditya Natoo[1]

1. University of Bremen, Germany

This paper focusses sequentially on two different aspects: (a) recent changes in observed storms, and (b) its linkages to the changes in large-scale environmental (LSE) variability. The analysis of observed storm show that in spite of an overall reduction in the Southwest Pacific (SWP) storminess over the past four decades, the number of extreme storms corresponding to the mean maximum sustained storm wind speed, has increased. At the same time, a slight reduction in the corresponding mean minimum central pressure is observed. The transition time from category 1 to 3 has also reduced substantially (by ~12 hours). Possible conditions for some of these observed behavioural change in terms of quick intensification and traveling longer distance towards south pole will be discussed.
The second aspect explores the linkages between above changes in storm indices and corresponding variability in LSE variability. The methodology uses multiple linear regression analysis to establish their relationship. This relationship is used to construct scenarios of likely change in future storminess using simulated (RCP8.5 minus historical) differences. The analysis will show how the role of some of the environmental indices when in combination can aid in modulating the Southwest Pacific change in storminess.

Keywords: Southwest Pacific, Storminess, Regression analysis

©2019. Japan Geoscience Union. All Right Reserved.

The forced response of the climate system: The case of climatic teleconnections

*Tamas Bodai[1], Matyas Herein[2], Gabor Drotos[3]

1. University of Reading, 2. Eotvos University Budapest, 3. Universitat de les Illes Balears

We frame the forced response of the climate system in terms of an ensemble that represents the so-called snapshot/pullback attractor, and explore the implications and power of this approach. Teleconnections as cross-correlations can be defined in the ensemble-based framework by evaluating the correlations over ensemble members. As a specific example, we studied the teleconnection between the El Niño–Southern Oscillation (ENSO) and the Indian summer monsoon in ensemble simulations from state-of-the-art climate models, the Max Planck Institute Earth System Model (MPI-ESM) and the Community Earth System Model (CESM). We detect an increase in the strength of the teleconnection in the MPI-ESM under historical forcing between 1890 and 2005, which is in contrast with scientific consensus. In the MPI-ESM no similar increase is present between 2006 and 2099 under the Representative Concentration Pathway 8.5 (RCP8.5), and in a 110-year-long 1-percent pure CO2 scenario; neither is in the CESM between 1960 and 2100 with historical forcing and RCP8.5. This is also a puzzling result inasmuch as the historical forcing is the weakest. Accordingly, we evaluated that the static susceptibility of the strength of the teleconnection with respect to radiative forcing (assuming an instantaneous and linear response) is at least three times larger in the historical MPI-ESM ensemble than in the others.

Keywords: teleconnection, ENSO, Indian monsoon, forced response, trajectory ensemble

©2019. Japan Geoscience Union. All Right Reserved.

[E] Oral | A (Atmospheric and Hydrospheric Sciences)：A-CG Complex & General

Wed. May 29, 2019 3:30 PM - 5:00 PM JST | Wed. May 29, 2019 6:30 AM - 8:00 AM UTC | 303 3F

[A-CG35] Projection and detection of global environmental change

convener:Michio Kawamiya(Japan Agency for Marine-Earth Science and Technology), Hiroaki Tatebe(Japan Agency for Marine-Earth Science and Technology), Kaoru Tachiiri(Japan Agency for Marine-Earth Science and Technology), Chairperson:Kaoru Tachiiri(Japan Agency for Marine-Earth Science and Technology), Michio Kawamiya(JAMSTEC)

Anthropogenic forcings on global environment are expected to cause intensification of extreme events, sea level rise, ocean acidification and deoxygenation, as well as large-scale ecosystem changes. The CMIP6 experimental protocol has been established based on which modeling groups across the world are starting to provide environmental projection data toward 6th IPCC assessment report due in 2021. Various new types of studies, such as event attribution and coupling of socio-economic processes and Earth system dynamics, are also emerging in the field of global change projection. In addition, observational studies are becoming increasingly more important for grasping changes in the global environment and evaluating model projections. Interactions and collaborations beyond boundaries of conventional scientific disciplines are desired for dealing with the issue of global changes. This session thus aims to deepen our understanding on global change, from both disciplinary and interdisciplinary viewpoints. This session is co-organized by AIMES - Future Earth project "Analysis, Integration and Modelling of the Earth System" (https://aimesproject.org/).

3:30 PM - 3:45 PM JST | 6:30 AM - 6:45 AM UTC

[ACG35-07] Guiding Mother Earth: taking stock of progress to a long-term temperature goal

★Invited Papers

*Myles Robert Allen[1] (1.Environmental Change Institute, School of Geography and the Environment and Department of Physics, University of Oxford)

3:45 PM - 4:00 PM JST | 6:45 AM - 7:00 AM UTC

[ACG35-08] Uneven distributions of four hazard indicators of climate change with the Paris Agreement's goals

*Hideo Shiogama[1] (1.Center for Global Environmental Research, National Institute for Environmental Studies)

4:00 PM - 4:15 PM JST | 7:00 AM - 7:15 AM UTC

[ACG35-09] Understanding the centennial-scale human-natural interactions using an integrated terrestrial model MIROC-INTEG under ISIMIP2 project

*Yusuke Satoh[1], Julien Boulange[1], Naota Hanasaki[1], Kumiko Takata[1], Yadu Pokhrel[3], Ted Veldkamp[2,4], Peter Burek[2], Tokuta Yokohata[1] (1.National Institute for Environmental Studies, 2.International Institute for Applied Systems Analysis, 3.Department of Civil and Environmental Engineering, Michigan State University, 4.Institute for Environmental Studies (IVM), VU Amsterdam)

4:15 PM - 4:30 PM JST | 7:15 AM - 7:30 AM UTC

[ACG35-10] Radiative forcing of the physiological CO_2 response

*Victor Brovkin[1], Veronika Gayler[1], Sonia I Seneviratne[2], Pierre Gentine[3] (1.Max Planck Institute for Meteorology, Hamburg, Germany, 2.ETH, Institute for Atmospheric and Climate Science, Zurich, Switzerland, 3.Columbia University, Earth and Environmental Engineering, New York, USA)

4:30 PM - 4:45 PM JST | 7:30 AM - 7:45 AM UTC

[ACG35-11] Progress of MIROC-ES2 simulations in CMIP6 and the analysis of the biogeochemical feedbacks

*Tomohiro Hajima[1], Shingo Watanabe[1], Michio Kawamiya[1], Kaoru Tachiiri[1], Hiroaki Tatebe[1], Akihiko Ito[2], Kumiko TAKATA[2], Michio Watanabe[1], Maki Noguchi[1], Akitomo Yamamoto[1], Akinori Ito[1], Manabu

Abe[1], Rumi Ohgaito[1], Dai Yamazaki[3] (1.Japan Agency for Marine-Earth Science and Technology, 2.National Institute for Environmental Studies, 3.Institute of Industrial Science, the University of Tokyo)

4:45 PM - 5:00 PM JST | 7:45 AM - 8:00 AM UTC

[ACG35-12] The impact of long-term historical warming on the global terrestrial gross primary production

*Irina Melnikova[1], Takahiro Sasai[1] (1.Tohoku University)

Guiding Mother Earth: taking stock of progress to a long-term temperature goal

*Myles Robert Allen[1]

1. Environmental Change Institute, School of Geography and the Environment and Department of Physics, University of Oxford

The IPCC Special Report on 1.5˚C found that human-induced global warming had reached 1˚C ±0.2˚C, increasing at 0.2˚C per decade, leaving only a few decades for emissions to be reduced to net zero to limit warming to 1.5˚C. The Paris Climate Agreement introduced a regime of periodic stocktakes of progress to the long-term temperature goal of limiting warming to well below 2˚C, pursuing efforts to 1.5˚C. While there is general agreement that these stocktakes are to be informed by science, these is less consensus on how this will be done. I will explain how we can robustly estimate the level of human-induced warming to date, and how this information was used to support a revision in the remaining carbon budget for cumulative future CO_2 emissions consistent with limiting warming to 1.5˚C. CO_2 budgets in the IPCC Special Report were contingent on scenarios for non-CO_2 forcing, but the concept of a carbon budget can be generalised if we recognise how other anthropogenic forcing agents affect climate on different timescales, either expressing them as CO_2-forcing-equivalent emissions, or applying the traditional GWP_{100} metric in a new way. Taken together, these insights provide a simple, transparent, scenario-independent and model-independent method of assessing the implications of current and future emissions for progress towards a long-term temperature goal.

Keywords: Climate change, Greenhouse-gases, Stocktake, Attribution, Metrics, Forcing

©2019. Japan Geoscience Union. All Right Reserved.

Uneven distributions of four hazard indicators of climate change with the Paris Agreement's goals

*Hideo Shiogama[1]

1. Center for Global Environmental Research, National Institute for Environmental Studies

Clarifying characteristics of hazards and risks of climate change at 2ºC and 1.5ºC global warming is important for understanding the implications of the Paris Agreement. We perform and analyse large ensembles of 2ºC and 1.5ºC warming simulations. In the 2ºC runs, we find substantial increases in extreme hot days, heavy rainfalls, high streamflow and labor capacity reduction related to heat stress. For example, about half of the world's population will experience a present day 1-in-10 year hot day event every other year at 2ºC warming. The regions with largely increases of these four hazard indicators coincide with countries characterized by small CO_2 emissions, low-income and high vulnerability. Limiting global warming to 1.5ºC, compared to 2ºC, will lower increases in the four hazard indicators especially in those regions.

Keywords: Climate change, Paris Agreement

©2019. Japan Geoscience Union. All Right Reserved.

Understanding the centennial-scale human-natural interactions using an integrated terrestrial model MIROC-INTEG under ISIMIP2 project

*Yusuke Satoh[1], Julien Boulange[1], Naota Hanasaki[1], Kumiko Takata[1], Yadu Pokhrel[3], Ted Veldkamp[2,4], Peter Burek[2], Tokuta Yokohata[1]

1. National Institute for Environmental Studies, 2. International Institute for Applied Systems Analysis, 3. Department of Civil and Environmental Engineering, Michigan State University, 4. Institute for Environmental Studies (IVM), VU Amsterdam

Within the earth system, changing-climate, -human society, and -ecosystems interact mutually. It is crucial to better understand the interconnectedness among such human-natural systems in order to assess the potential impacts of climate and socioeconomic changes on each system and identify sustainable pathways. Although existing earth system models and integrated assessment models are applicable to explore this field, parts of their natural and/or human processes tend to be simplified depending on their scope. Therefore, it still remains a challenge to improve integrated modeling frameworks. For these reasons, a process-based integrated terrestrial model, MIROC INTEGrated terrestrial model (MIROC-INTEG), was developed. The modeling framework is composed of five natural/human subcomponents. At its core is a land surface model (MATSIRO), which is coupled to three human modules; water use (H08), food and biofuel crop production(PRYSBI2) and land use change (TELMO). An ecosystem model (VISIT) calculates the C and N cycles among atmosphere-vegetation-soil. While each sub-model can run independently, MIROC-INTEG dynamically simulates their interactions, embracing the water-food-energy nexus within a system.

The goal of this study is to improve our quantitative understanding on coupled terrestrial systems at the global scale for past and future time-scales. Hence, we have run MIROC-INTEG following the Inter-Sectoral Impact Model Inter-comparison Project phase 2a (ISIMIP2a) and 2b (ISIMIP2b) simulation protocols. Using 3 hourly climate forcing data and considering anthropogenic activities, MIROC-INTEG simulated agro-hydrological condition at a spatial resolution of 0.5˚, globally. As its inputs, ISIMIP2a makes use of three reanalysis-base metrological data for historical periods, and ISIMIP2b employs an ensemble of bias-corrected forcing data set of four general circulation models covering preindustrial, historical, and future time-periods under four representative concentration pathways. Furthermore, ISIMIP provides a unique opportunity for validation of simulation skill in comparison with other models' under consistent protocols.
Within this contribution we present the first results of MIROC-INTEG looking specifically at the centennial-scale human-natural interactions over the period 1851-2099 and its consequences for long-term changes in fundamental hydrological variables. The results are presented at global, regional and large-basin scale and are compared against existing ISIMIP runs of other hydrological and land surface models.

Keywords: Integrated terrestrial model, Human intervention, climate and socio-economic change, multi-forcing, model inter comparison

©2019. Japan Geoscience Union. All Right Reserved.

Radiative forcing of the physiological CO_2 response

*Victor Brovkin[1], Veronika Gayler[1], Sonia I Seneviratne[2], Pierre Gentine[3]

1. Max Planck Institute for Meteorology, Hamburg, Germany, 2. ETH, Institute for Atmospheric and Climate Science, Zurich, Switzerland, 3. Columbia University, Earth and Environmental Engineering, New York, USA

Theory and observations indicate that plant stomatal conductance decreases in response to increase in the atmospheric CO_2. This physiological CO_2 response causes reduction in the evapotranspiration and modification of the global hydrological cycle, affecting the global radiative fluxes and climate sensitivity. While this biogeophysical mechanism is included into all comprehensive Earth System Models, its radiative forcing has not been isolated from the other biospheric feedbacks. To evaluate the scale of its radiative forcing, we performed two sensitivity experiments with the CMIP6 version of the MPI Earth system model (MPI-ESM1.2-LR). In addition to the standard 4xCO_2 simulation, in which both climate and carbon cycle respond to an instantaneous 4-fold increase in CO_2, we performed the 4xCO_2rad simulation in which biogeochemistry and plants were not affected by elevated CO_2. We analyse changes in outgoing radiation and surface temperature using the Gregory et al. (2004) approach for radiative forcing, and compare results with- and without physiological CO_2 response. Rescaling to the doubling of the CO_2 concentration, stomatal conductance response increases equilibrium climate sensitivity of the model by ca. 10%, and its radiative feedback is estimated at 0.14 W/m^2/K. This suggest that the magnitude of this positive biogeophysical feedback is comparable with the magnitude of biogeochemical (climate-carbon) feedback.

Keywords: climate feedbacks, vegetation cover, radiative forcing

©2019. Japan Geoscience Union. All Right Reserved.

Progress of MIROC-ES2 simulations in CMIP6 and the analysis of the biogeochemical feedbacks

*Tomohiro Hajima[1], Shingo Watanabe[1], Michio Kawamiya[1], Kaoru Tachiiri[1], Hiroaki Tatebe[1], Akihiko Ito[2], Kumiko TAKATA[2], Michio Watanabe[1], Maki Noguchi[1], Akitomo Yamamoto[1], Akinori Ito[1], Manabu Abe[1], Rumi Ohgaito[1], Dai Yamazaki[3]

1. Japan Agency for Marine-Earth Science and Technology, 2. National Institute for Environmental Studies, 3. Institute of Industrial Science, the University of Tokyo

In order to reveal how climate-biogeochemical system responds to anthropogenic forcing, a new Earth system model “MIROC-ES2L” has been developed for CMIP6. The physical core of the model is “MIROC5.2”, and the biogeochemical component are updated from that used for CMIP5: the new model has explicit CN interaction in land ecosystem, and ocean component has been improved to include P, Fe, and O in addition to C and N cycles that were already incorporated into that of CMIP5 ver. In the new model, ocean N cycle is opened to other subsystems: N input via biological fixation, deposition and riverine transport are considered, and denitrification process controls N loss from the ocean. This model is used for CMIP6 runs, by participating in endorsed MIPs such as C4MIP, PMIP, OMIP, LUMIP, CDRMIP, ScenarioMIP, VolMIP, etc.
A provisional historical simulation by MIROC-ES2L with CMIP6 official forcing (v6.2.1) clearly showed a global warming trend from 1970’s, which is consistent with observation (HadCRU4). Carbon stored in land ecosystem decreased by responding to the land-use change forcing, and started to increase around 1960 by responding to CO2 increase and increased N input into land (N deposition and fertilizer), in addition to the response to LUC. Ocean continuously store the anthropogenic CO2: the increase during 1850-2005 is about 150PgC, which is almost similar level to the number reported in Global Carbon Budget 2017. In addition to C cycle, the historical simulation showed drastic changes in global N budget, by directly responding to the anthropogenic forcing (LUC and agriculture), and indirectly affected by climate–carbon cycle change. Agriculture increased both land N2O emission (diagnosed) and N leaching, the latter of which impacted on ocean biogeochemistry near river mouths.

Keywords: Earth system model, Biogeochemistry, CMIP6, Carbon cycle, Feedback

©2019. Japan Geoscience Union. All Right Reserved.

The impact of long-term historical warming on the global terrestrial gross primary production

*Irina Melnikova[1], Takahiro Sasai[1]

1. Tohoku University

The recent increase of carbon dioxide in the atmosphere from anthropogenic emissions resulted in the increase of carbon uptake by the global biosphere. The most uncertain contributor to the interannual global uptake variability is land, and the largest and primary land carbon flux is gross primary production (GPP). In this study, we aim to estimate the impact of the long-term (1951–2010) historical warming on the global terrestrial GPP. We use the Biosphere model integrating Eco-physiological And Mechanistic approaches using Satellite data (BEAMS ver.1.3) [*Sasai et al.*, 2016] forced by historical and nonwarming simulation climates of the Database for Policy Decision making for Future climate change (d4PDF) [*Mizuta et al.*, 2017]. This is a pioneer study to apply a diagnostic GPP estimation approach on the large-size ensembles climate data to simulate the long-term global GPP.

First, we evaluated the surface d4PDF climatology in comparison with existing modern datasets, including reanalyses, and discussed the benefits and limitations of the database in the studies of the terrestrial carbon fluxes. Second, we validated the BEAMS GPP forced by d4PDF data against observations and evaluated the BEAMS performance against existing GPP grid-datasets by other approaches (data-driven datasets and process-driven models). Finally, we discussed the impact of the long-term historical warming on the global GPP in terms of decadal trends and density histograms.

We confirmed that d4PDF surface climatology is appropriate for use in the studies of the terrestrial carbon fluxes, and d4PDF historical climate data is comparable to existing modern datasets. BEAMS estimated both the magnitude and decadal trends of the global terrestrial GPP realistically by using the benefits of the diagnostic approach. The global long-term (1951–2010) mean GPP equaled 144.0 ±2.3 GtC $year^{-1}$ for historical and 140.3 ±1.3 GtC $year^{-1}$ for nonwarming climates. The accumulated increase of the historical warming-induced GPP equaled 184.8 ±5.8 GtC for the period of 1951–2010 and accounted for nearly half of all anthropogenic emissions. The GPP increase intensified over time. The density histogram analyses showed that the global GPP distribution in the present (2001–2010) share neither the mean nor spread of GPP in the nonwarming climate.
This study provides the evidence of the impact of long-term historical warming on the global GPP by a novel approach using the benefits of the diagnostic model and large-size ensemble climate data.

Keywords: GPP, climate change, BEAMS, diagnostic approach, large-size ensemble, d4PDF

©2019. Japan Geoscience Union. All Right Reserved.

[J] Oral | A (Atmospheric and Hydrospheric Sciences)：A-CG Complex & General

Wed. May 29, 2019 10:45 AM - 12:15 PM JST | Wed. May 29, 2019 1:45 AM - 3:15 AM UTC | 102 1F

[A-CG42] Biogeochemical linkages between the surface ocean and atmosphere

convener:Yuzo Miyazaki(Institute of Low Temperature Science, Hokkaido University), Jun Nishioka(Hokkaido University, Institute of low temperature sciences), Koji Suzuki(Hokkaido University), Yoko Iwamoto(Graduate School of Biosphere Science, Hiroshima University), Chairperson:Yuzo Miyazaki(Institute of low temperature science, Hokkaido University), Jun Nishioka(Institute of low temperature science, Hokkaido University)

Multi-scale vertical and horizontal ocean mixing processes can strongly influence the distribution of dissolved and suspended substances including macro- and micro-nutrients, and may impact on phytoplankton bloom formation. The changes in nutrient dynamics generally affect the abundance, composition and metabolic activity of marine organisms such as phytoplankton and bacteria during the bloom. Marine phytoplankton can produce volatile organic compounds (VOCs) and marine atmospheric aerosols, which strongly influence on atmospheric chemistry. Primary and secondary organic and inorganic components produced via marine phytoplankton activity can contribute to the Earth's radiative forcing, and in turn marine ecosystems including biogeochemical processes directly or indirectly. Therefore, the biogeochemical cycles have a tight linkage between the ocean and the atmosphere. In order to understand physical, chemical and biological processes relevant to phytoplankton bloom formation in the ocean, dynamics of VOCs and marine aerosols in the atmosphere, and the biogeochemical linkage between the ocean and the atmosphere, we welcome new interdisciplinary presentations and active discussions on physical, chemical, and biological sciences both from ocean and atmospheric fields in this session. Studies linked to the Surface Ocean-Lower Atmosphere Study (SOLAS) project are good examples, but other related studies are also invited.

10:45 AM - 11:00 AM JST | 1:45 AM - 2:00 AM UTC

[ACG42-01] Production of bromoform in sea ice and emission to the atmosphere

*Daiki Nomura[1], Atsushi Ooki[1], Ellen Damm[2], Gerhard Dieckmann[2], Bruno Delille[3], Markus Frey[4], Mats Granskog[5], Klaus Meiners[6,7], Anna Silyakova[8], Takeshi Tamura[9], Jean-Louis Tison[10], Youhei Yamashita[11] (1.Faculty of Fisheries Sciences, Hokkaido University, 2.Alfred Wegener Institute for Polar and Marine Research, Bremerhaven, Germany, 3.Université de Liège, Liège, Belgium., 4.British Antarctic Survey, Cambridge, United Kingdom., 5.Norwegian Polar Institute, Tromsø, Norway., 6.Antarctic Climate andEcosystems Cooperative Research Centre, University of Tasmania, Hobart, Australia., 7.Australian Antarctic Division, Kingston, Australia., 8.Centre for Arctic Gas Hydrate, Environment and Climate, Tromsø, Norway., 9.National Institute of Polar Research, Tokyo, Japan., 10.Université Libre de Bruxelles, Bruxelles, Belgium., 11.Graduate School of Environmental Sceince, Hokkaido University, Sapporo, Japan.)

11:00 AM - 11:15 AM JST | 2:00 AM - 2:15 AM UTC

[ACG42-02] Accumulation processes of trace metals into arctic sea ice: distribution of Fe, Mn and Cd associated with ice structure

*La Kenya Evans[1], Jun Nishioka[1] (1.Institute of Low Temperature Sciences, Hokkaido University)

11:15 AM - 11:30 AM JST | 2:15 AM - 2:30 AM UTC

[ACG42-03] Is halogen chemistry responsible for low ozone levels observed over western Pacific equatorial region? - From observations on R/V Mirai

*Yugo Kanaya[1], Kazuyuki Miyazaki[1], Fumikazu Taketani[1], Takuma Miyakawa[1], Hisahiro Takashima[1,2], Yuichi Komazaki[1], Xiaole PAN[3,1], Saki Kato[2], Kengo Sudo[4,1] (1.Research and Development Center for Global Change, Japan Agency for Marine-Earth Science and Technology, 2.Fukuoka University, 3.Institute of Atmospheric Physics, Chinese Academy of Sciences, China, 4.Nagoya University)

11:30 AM - 11:45 AM JST | 2:30 AM - 2:45 AM UTC

[ACG42-04] Very low $\delta^{15}N$ of atmospheric nitrate found in the earstern equatorial Pacific and its implication to dynamic nitrogen recycle between ocean and lower atmosphere

*Shohei Hattori[1], Kazuki Kamezaki[1], Yoko Iwamoto[2], Sakiko Ishino[1], Mitsuo Uematsu[3], Kazuhiko Miura[4], Naohiro Yoshida[1] (1.Department of Chemical Science and Engineering, School of Materials and Chemical Technology, Tokyo Institute of Technology, 2.Hiroshima University, 3.University of Tokyo, 4.Tokyo University of Science)

11:45 AM - 12:00 PM JST | 2:45 AM - 3:00 AM UTC

[ACG42-05] **Origin of water-soluble organic nitrogen in marine atmospheric aerosols in the subtropical North Pacific**

*Tsukasa Dobashi[1,2], Yuzo Miyazaki[1], Eri Tachibana[1], Yoko Iwamoto[3], Kazutaka Takahashi[4], Sachiko Horii[4], Shu-Kuan Wong[5], Koji Hamasaki[5] (1.Institute of Low Temperature Science, Hokkaido Univ., 2.Graduate School of Env. Sci., Hokkaido Univ., 3.Graduate School of Biosphere Science, Hiroshima Univ., 4.Graduate School of Agricultural and Life Sciences, Univ. of Tokyo, 5.Atmosphere and Ocean Research Institute, Univ. of Tokyo)

12:00 PM - 12:15 PM JST | 3:00 AM - 3:15 AM UTC

[ACG42-06] Impacts of ammonia on gas-particle partition and AWC during the 2016 APHH-Beijing campaign: inducing effects of nitrate ammonium

*baozhu Ge[1], Xiaobin Xu[2], Zhiqiang Ma[3], Xiaole PAN[1], Zhe WANG[1,4], Weili Lin[5], Bin Ouyang[6], Danhui Xu[1], James Lee[7], Mei Zheng[8], Dongsheng Ji[1], Yele Sun[1], Huabin Dong[8], Freya Anne Squires[7], Pingqing Fu[1], Zifa Wang[1] (1.State Key Laboratory of Atmospheric Boundary Layer Physics and Atmospheric Chemistry, Institute of Atmospheric Physics, Chinese Academy of Sciences, Beijing 100029, China, 2.State Key Laboratory of Severe Weather & Key Laboratory for Atmospheric Chemistry of China Meteorological Administration, Chinese Academy of Meteorological Sciences, Beijing 100081, China, 3.Institute of Urban Meteorology, China Meteorological Administration, Beijing, China, 4.Research Institute for Applied Mechanics (RIAM), Kyushu University, Fukuoka, Japan, 5.College of Life and Environmental Sciences, Minzu University of China, Beijing 100081, China, 6.Lancaster Environment Centre, Lancaster University, Lancaster, LA1 4YQ, UK, 7.National Centre for Atmospheric Science Department of Chemistry, University of York, York, YO10 5DD, UK, 8.State Key Joint Laboratory of Environmental Simulation and Pollution Control, College of Environmental Sciences and Engineering, Peking University, Beijing, 100871, China)

Production of bromoform in sea ice and emission to the atmosphere

*Daiki Nomura[1], Atsushi Ooki[1], Ellen Damm[2], Gerhard Dieckmann[2], Bruno Delille[3], Markus Frey[4], Mats Granskog[5], Klaus Meiners[6,7], Anna Silyakova[8], Takeshi Tamura[9], Jean-Louis Tison[10], Youhei Yamashita[11]

1. Faculty of Fisheries Sciences, Hokkaido University, 2. Alfred Wegener Institute for Polar and Marine Research, Bremerhaven, Germany, 3. Université de Liège, Liège, Belgium., 4. British Antarctic Survey, Cambridge, United Kingdom., 5. Norwegian Polar Institute, Tromsø, Norway., 6. Antarctic Climate andEcosystems Cooperative Research Centre, University of Tasmania, Hobart, Australia., 7. Australian Antarctic Division, Kingston, Australia., 8. Centre for Arctic Gas Hydrate, Environment and Climate, Tromsø, Norway., 9. National Institute of Polar Research, Tokyo, Japan., 10. Université Libre de Bruxelles, Bruxelles, Belgium., 11. Graduate School of Environmental Sceince, Hokkaido University, Sapporo, Japan.

Bromoform ($CHBr_3$) is one of the important bromine containing volatile halocarbons that are involved in ozone depletion in the atmosphere. Although the possible source of reactive bromine species from snow and sea ice has been discussed, mechanisms that control $CHBr_3$ production within sea ice and emission to the atmosphere remain unclear. Here, we show evidence of massive $CHBr_3$ production at sea ice surface-snow interfaces and its strong emission to the atmosphere from five field-campaigns to the Arctic Ocean, the Southern Ocean, and the Sea of Okhotsk in the winter and spring, in addition to supporting laboratory experiments. We found that the ice-related strong $CHBr_3$ emission was linked to the production of the $CHBr_3$ at the snow-sea ice interface through the haloform reaction. Our results suggest that sea ice acts as a strong $CHBr_3$ source for the atmosphere, indicating a significant contribution to the atmospheric bromine cycle.

Keywords: sea ice, bromoform, polar ocean

©2019. Japan Geoscience Union. All Right Reserved.

Accumulation processes of trace metals into arctic sea ice: distribution of Fe, Mn and Cd associated with ice structure

*La Kenya Evans[1], Jun Nishioka[1]

1. Institute of Low Temperature Sciences, Hokkaido University

Increased loss of Arctic summer sea ice can influence the cycling of biogeochemical materials (trace metals, nutrients, etc.), affecting seawater’ s biology and chemistry. Sea ice is important for the supply of biogeochemical materials, especially trace metals, to the surface waters of the polar oceans; but its role is not clear. Understanding the accumulation and release mechanisms into Arctic sea ice will clarify the geochemical behaviour of trace metals. This study compared dissolved (D) and labile particulate (LP) Fe, Mn, and Cd to the observed sea ice structure from a single Arctic sea ice core. The structure of sea ice reflects the process of ice formation, which may aid in the determination of accumulation processes. Using photographic analysis for the percentage of pore microstructure and $\delta^{18}O$ analysis, sea ice structure was observed as: snow, granular (frazil), mixed (granular and columnar) and columnar ice. Salinity and nutrients were low, indicating brine drainage and multi-year ice. High trace metal concentrations in snow ice indicated meteoric snow as a source and accumulation during snow ice formation. High concentrations of LPFe in granular ice indicated accumulation via suspension freezing by frazil ice followed by entrainment. Dissolved Mn and Cd accumulated in snow and granular ice through chemical transformation processes. Elevated DMn and DCd in granular ice resulted from the reduction and release from accumulated Fe and Mn oxides. Elevated DMn and DCd in snow ice may have been due to the photochemical reduction of LPFe and LPMn. Low trace metal concentrations in mixed and columnar ice indicated trace metal release due to brine drainage. Our study clearly indicated that the differences observed in trace metals, within sea ice structure, showed that sea ice formation, chemical reduction and brine release were the processes behind trace metal accumulation and release in this Arctic sea ice.

Keywords: Trace Metals, Dissolved , Labile Particulate , Sea Ice Structure

©2019. Japan Geoscience Union. All Right Reserved.

Is halogen chemistry responsible for low ozone levels observed over western Pacific equatorial region? - From observations on R/V Mirai

*Yugo Kanaya[1], Kazuyuki Miyazaki[1], Fumikazu Taketani[1], Takuma Miyakawa[1], Hisahiro Takashima[1,2], Yuichi Komazaki[1], Xiaole PAN[3,1], Saki Kato[2], Kengo Sudo[4,1]

1. Research and Development Center for Global Change, Japan Agency for Marine-Earth Science and Technology, 2. Fukuoka University, 3. Institute of Atmospheric Physics, Chinese Academy of Sciences, China, 4. Nagoya University

Constraints from ozone (O_3) observations over oceans are needed in addition to those from terrestrial regions to fully understand global tropospheric chemistry and its impact on the climate. Here, we provide a large data set of ozone and carbon monoxide (CO) levels observed (for 11666 and 10681 h, respectively) over oceans. The data set is derived from observations made during 24 research cruise legs of R/V *Mirai* during 2012 to 2017, in the Southern, Indian, Pacific, and Arctic Oceans, covering the region from 67˚S to 75˚N. The data are suitable for critical evaluation of the over-ocean distribution of ozone derived from chemical transport models. We first give an overview of the statistics in the data set and highlight key features in terms of geographical distribution and air mass type. We then use the data set to evaluate ozone concentration fields from Tropospheric Chemistry Reanalysis version 2 (TCR-2), produced by assimilating a suite of satellite observations of multiple species into a chemical transport model, namely CHASER. Over the western Pacific equatorial region (125-165˚E, 10˚S to 25˚N), the observed O_3 level frequently decreased to less than 10 ppb in comparison to that obtained with TCR-2, and also those obtained in most of the Atmospheric Chemistry Climate Model Intercomparison Project (ACCMIP) model runs for the decade from 2000. These results imply loss processes that are unaccounted for in the models. We found that the model's positive bias positively correlated with the daytime residence times of air masses over a particular grid, namely 165-180˚E and 15-30˚N; an additional loss rate of 0.25 ppb h^{-1} in the grid best explained the gap. Halogen chemistry, which is commonly omitted from currently used models, might be active in this region and could have contributed to additional losses. Our open data set covering wide ocean regions is complementary to the Tropospheric Ozone Assessment Report data set, which basically comprises ground-based observations, and enables a fully global study of the behavior of O_3.

Keywords: Over-ocean atmospheric composition observations, Missing sink of ozone, Halogens, Western Pacific equatorial region

©2019. Japan Geoscience Union. All Right Reserved.

Very low $\delta^{15}N$ of atmospheric nitrate found in the earstern equatorial Pacific and its implication to dynamic nitrogen recycle between ocean and lower atmosphere

*Shohei Hattori[1], Kazuki Kamezaki[1], Yoko Iwamoto[2], Sakiko Ishino[1], Mitsuo Uematsu[3], Kazuhiko Miura[4], Naohiro Yoshida[1]

1. Department of Chemical Science and Engineering, School of Materials and Chemical Technology, Tokyo Institute of Technology, 2. Hiroshima University, 3. University of Tokyo, 4. Tokyo University of Science

Atmospheric nitrogen sources in the marine boundary layer of the remote ocean have been known to include long-range transport (LRT) of anthropogenic pollutants, and the LRT of anthropogenic atmospheric particulate nitrate ($p\text{-}NO_3^-$) within the free troposphere has been observed in regions influenced by westerlies from the Asian continent over Pacific Ocean. This traditional paradigm that the ocean is considered a passive recipient of anthropogenic N deposition can be applied western north Pacific regions. However, for the equatorial Pacific under the influence of pristine air, the sources of such $p\text{-}NO_3^-$ remain unresolved. To address this, we present $\delta^{15}N$ of $p\text{-}NO_3^-$ collected over the Pacific Ocean between 40˚S and 68˚N on two cruises, carried out by the Research Vessel *Hakuho Maru*, and estimated $\delta^{15}N$ of source NO_x of each sample. We categorized six marine regions within the Pacific Ocean, based on backward trajectory analysis to determine their source regions and various ion concentrations to assess whether anthropogenic or non-anthropogenic sources were dominant.

We found remarkably low $\delta^{15}N(NO_x)$ values for the equatorial Pacific regions compared to those in other regions over Pacific Ocean. These low source $\delta^{15}N(NO_x)$ values cannot be explained using conventional NO_x apportionment. Given that the eastern equatorial Pacific is one of the biologically active ocean regions resulted from upwelling water, here we postulate the alternative biogenic nitrogen source (NH_3 or alkyl nitrate) in this region. In the presentation, we will discuss important feature of self-recycle process of nitrogen between ocean and lower atmosphere in the eastern equatorial Pacific. We will also discuss its implication to nitrogen deposition for this region, which may contribute to new marine biological production and/or nitrous oxide emissions.

Keywords: Nitrate, Stable Isotopes, Pacific Ocean, Equatorial Pacific

©2019. Japan Geoscience Union. All Right Reserved.

Origin of water-soluble organic nitrogen in marine atmospheric aerosols in the subtropical North Pacific

*Tsukasa Dobashi[1,2], Yuzo Miyazaki[1], Eri Tachibana[1], Yoko Iwamoto[3], Kazutaka Takahashi[4], Sachiko Horii[4], Shu-Kuan Wong[5], Koji Hamasaki[5]

1. Institute of Low Temperature Science, Hokkaido Univ., 2. Graduate School of Env. Sci., Hokkaido Univ., 3. Graduate School of Biosphere Science, Hiroshima Univ., 4. Graduate School of Agricultural and Life Sciences, Univ. of Tokyo, 5. Atmosphere and Ocean Research Institute, Univ. of Tokyo

Marine atmospheric aerosol is one of the most important factors that determine the climate change, because it absorbs and reflects the sunlight which affects radiative balance of the atmosphere. In particular, water-soluble organic nitrogen (WSON) in aerosol affect physicochemical properties of aerosol such as water-solubility characteristics, acidity, light-absorption properties of the particles. However, little is known about the origin of WSON in marine atmospheric aerosols. The purpose of this study is to elucidate the origin of WSON by cruise observation in subtropical North Pacific where very limited data are available.

Size-segregated aerosol samples were collected on board the R/V *Hakuho Maru* (KH-17-4) over the subtropical North Pacific, mainly along 23ºN, during August–October in 2017. Water-soluble organic carbon (WSOC) and water-soluble total nitrogen (WSTN) were measured by a total organic carbon analyzer with a TN unit. The concentrations of inorganic nitrogen (IN) were measured by ion chromatograph. The WSON concentration was derived from the difference between WSTN and IN. The stable carbon isotope ratio ($\delta^{13}C$) was measured by elemental analyzer-isotope ratio mass spectrometer (EA-IRMS). Longitudinal distributions of WSON at 23ºN showed that the submicrometer WSON concentration (av. 5.9 ±6.0 ng N m^{-3}) to the east of 160ºW was significantly larger than that to the west (av. 2.2 ±2.0 ng N m^{-3}). Additionally, the mass fraction of WSON to WSTN in the eastern oceanic region reached as large as 40% with an average of 14.1%, suggesting the importance of WSON in this oceanic region. Backward trajectory, the chlorophyll *a* concentration in seawater, and the $\delta^{13}C$ value suggested that the majority of the observed WSON was derived from microbial activity in the sea surface. WSON did not show any significant correlation with a tracer of primary emission (i.e., Na^{+}), indicating that the majority of WSON were not directly emitted as aerosol particles from the ocean surface, but were produced from N-containing gas species released into the atmosphere. Furthermore, a significant correlation between the concentrations of WSON and the nitrogen fixation rate in the sea surface indicates that reactive nitrogen, produced by nitrogen fixing organisms (e.g., cyanobacteria), are emitted from sea surface to the atmosphere, which significantly contributed to the formation of aerosol WSON.

Keywords: Organic nitrogen, Marine atmospheric aerosol, Biogeochemical linkage between atmosphere and ocean, Nitrogen fixation

©2019. Japan Geoscience Union. All Right Reserved.

Impacts of ammonia on gas-particle partition and AWC during the 2016 APHH-Beijing campaign: inducing effects of nitrate ammonium

*baozhu Ge[1], Xiaobin Xu[2], Zhiqiang Ma[3], Xiaole PAN[1], Zhe WANG[1,4], Weili Lin[5], Bin Ouyang[6], Danhui Xu[1], James Lee[7], Mei Zheng[8], Dongsheng Ji[1], Yele Sun[1], Huabin Dong[8], Freya Anne Squires[7], Pingqing Fu[1], Zifa Wang[1]

1. State Key Laboratory of Atmospheric Boundary Layer Physics and Atmospheric Chemistry, Institute of Atmospheric Physics, Chinese Academy of Sciences, Beijing 100029, China, 2. State Key Laboratory of Severe Weather & Key Laboratory for Atmospheric Chemistry of China Meteorological Administration, Chinese Academy of Meteorological Sciences, Beijing 100081, China, 3. Institute of Urban Meteorology, China Meteorological Administration, Beijing, China, 4. Research Institute for Applied Mechanics (RIAM), Kyushu University, Fukuoka, Japan, 5. College of Life and Environmental Sciences, Minzu University of China, Beijing 100081, China, 6. Lancaster Environment Centre, Lancaster University, Lancaster, LA1 4YQ, UK, 7. National Centre for Atmospheric Science Department of Chemistry, University of York, York, YO10 5DD, UK, 8. State Key Joint Laboratory of Environmental Simulation and Pollution Control, College of Environmental Sciences and Engineering, Peking University, Beijing, 100871, China

Atmospheric NH_3 plays a vital role not only in the environmental ecosystem but also in atmosphere chemistry. To fully understand the effects of NH_3 on the formation of haze pollution in Beijing, ambient NH_3 and related species were measured at high resolutions during the wintertime Air Pollution and Human Health-Beijing (APHH-Beijing) campaign in 2016. Simulations were made to gain insights into impacts of NH_3 on the formation of secondary inorganic aerosols (SIAs) and regional fine particle pollution. We found that the total NH_x (gaseous NH_3+particle NH_4^+) was mostly in excess of the SO_4^{2-}-NO_3^--NH_4^+-water equilibrium system during our campaign. This NH_x excess made medium aerosol acidity, with the median pH value being 3.6 and 4.5 for polluted and non-polluted conditions, respectively, and enhanced the formation of particle phase nitrate. During polluted periods, SIAs contributed most to $PM_{2.5}$ and were highly correlated with aerosol water content (AWC), indicating the importance of heterogeneous reactions in haze formation. Our analysis suggests that NH_4NO_3 is the most important factor driving the formation of AWC, with NO_3^- controlling the prior pollution stage and NH_4^+ the most polluted stage. Increased formation of NH_4NO_3 under excess NH_x, especially during the nighttime, may trigger the decreasing of aerosol DRH and hence lead to hygroscopic growth even under lower RH conditions and the wet aerosol particles become better medium for rapid heterogeneous reactions. A further increase of RH promotes the positive feedback "AWC-heterogeneous reactions" and ultimately leads to the formation of severe haze. Both our observational and modelling results suggest that the control of NH_3 may be more effective in reducing $PM_{2.5}$ under current emissions conditions in the North China Plain (NCP).

Keywords: Ammonia, partition, aerosol acidity, APHH-Beijing, PM2.5, NCP

©2019. Japan Geoscience Union. All Right Reserved.

[J] Poster | A (Atmospheric and Hydrospheric Sciences)：A-CG Complex & General

Wed. May 29, 2019 3:30 PM - 5:00 PM JST | Wed. May 29, 2019 6:30 AM - 8:00 AM UTC | Poster Hall International Exhibition Hall8, Makuhari Messe_10

[A-CG42] Biogeochemical linkages between the surface ocean and atmosphere

convener:Yuzo Miyazaki(Institute of Low Temperature Science, Hokkaido University), Jun Nishioka(Hokkaido University, Institute of low temperature sciences), Koji Suzuki(Hokkaido University), Yoko Iwamoto(Graduate School of Biosphere Science, Hiroshima University)

Multi-scale vertical and horizontal ocean mixing processes can strongly influence the distribution of dissolved and suspended substances including macro- and micro-nutrients, and may impact on phytoplankton bloom formation. The changes in nutrient dynamics generally affect the abundance, composition and metabolic activity of marine organisms such as phytoplankton and bacteria during the bloom. Marine phytoplankton can produce volatile organic compounds (VOCs) and marine atmospheric aerosols, which strongly influence on atmospheric chemistry. Primary and secondary organic and inorganic components produced via marine phytoplankton activity can contribute to the Earth's radiative forcing, and in turn marine ecosystems including biogeochemical processes directly or indirectly. Therefore, the biogeochemical cycles have a tight linkage between the ocean and the atmosphere. In order to understand physical, chemical and biological processes relevant to phytoplankton bloom formation in the ocean, dynamics of VOCs and marine aerosols in the atmosphere, and the biogeochemical linkage between the ocean and the atmosphere, we welcome new interdisciplinary presentations and active discussions on physical, chemical, and biological sciences both from ocean and atmospheric fields in this session. Studies linked to the Surface Ocean-Lower Atmosphere Study (SOLAS) project are good examples, but other related studies are also invited.

[ACG42-P01] Mixing States of Aged Black Carbon Collected over the Western North Pacific Ocean

*Momoka Yoshizue[1], Masahiro Momoi[1], Kouji Adachi[2], Masanori Yabuki[3], Tatsuhiro Mori[1], Akiho Suizu[4], Shinichi Kodama[1,4], Kazuhiko Miura[1], Mitsuo Uematsu[4] (1.Tokyo University of Science, 2.Meteorological Research Institute, 3.Kyoto University, 4.The University of Tokyo)

[ACG42-P02] Influence of Deposition of Atmospheric Inorganic Nitrogen Compounds to Marine Ecosystem at Bay of Bengal

*Fumikazu Taketani[1], Maki Noguchi Aita[1], Kazuyo Yamaji[1,2], Takashi Sekiya[1], Kohei Ikeda[3], Taketo Hashioka[1], Makio Honda[1], Kazuhiko Matsumoto[1], Yugo Kanaya[1] (1.Japan Agency for Marine-Earth Science and Technology, 2.Kobe University, 3.National Institute for Environmental Studies)

[ACG42-P03] Carbon isotopic characterization of organic aerosols in tropical marine atmosphere at the Maïdo high-altitude observatory, Reunion Island

Sharmine Akter Simu[1], *Yuzo Miyazaki[1], OCTAVE Science Team (1.Institute of Low Temperature Science, Hokkaido University)

Mixing States of Aged Black Carbon Collected over the Western North Pacific Ocean

*Momoka Yoshizue[1], Masahiro Momoi[1], Kouji Adachi[2], Masanori Yabuki[3], Tatsuhiro Mori[1], Akiho Suizu[4], Shinichi Kodama[1,4], Kazuhiko Miura[1], Mitsuo Uematsu[4]

1. Tokyo University of Science, 2. Meteorological Research Institute, 3. Kyoto University, 4. The University of Tokyo

Atmospheric aerosol particles can play a vital role in the climate change because they influence the radiative forcing on the Earth through absorbing and scattering of solar radiation. Especially, black carbon (BC) is known to a strong absorber of visible spectrum solar radiation in the atmosphere. However, its radiative forcing changes variably depending on its microphysical properties (e.g. mixing state, compositions, and shape). Therefore, it is important to accurately measure their parameters, especially, over the ocean because the observation is limited. In this study, the morphology and chemical compositions of marine aerosol particles including BC over the western north Pacific Ocean were analyzed by the individual particle analyses.

Measurement and samplings of atmospheric aerosol particles were carried out during the R/V Hakuho-Maru cruise (14-30/11/2017). The ambient BC mass concentrations were measured by a particle soot/absorption photometer (PSAP). In this study, we focused on relatively high BC mass concentration events over the western north Pacific Ocean at 26.62˚N, 137.93˚E and at 25.51˚N, 135.77˚E on 19/11/2017. The aerosols collected in both events were analyzed using a transmission electron microscope and an energy dispersive X-ray spectrometer.

In both samples, most BCs were embedded in sulfate particles that have organic coatings. Only a few BCs were attached to sea-salt particles. The backward trajectory analyses suggested that the air masses of both events passed through the land of China and Japan. These results indicate that BCs were emitted in or around the land, and then SO_2 condensed on their surface before organic carbon condensed during transportation. Our result is useful to understand the aging process of BC over the ocean.

Keywords: Marine atmospheric aerosol, Black carbon, Sulfate, Organic carbon, The western north Pacific Ocean, TEM-EDX

©2019. Japan Geoscience Union. All Right Reserved.

Influence of Deposition of Atmospheric Inorganic Nitrogen Compounds to Marine Ecosystem at Bay of Bengal

*Fumikazu Taketani[1], Maki Noguchi Aita[1], Kazuyo Yamaji[1,2], Takashi Sekiya[1], Kohei Ikeda[3], Taketo Hashioka[1], Makio Honda[1], Kazuhiko Matsumoto[1], Yugo Kanaya[1]

1. Japan Agency for Marine-Earth Science and Technology, 2. Kobe University, 3. National Institute for Environmental Studies

To investigate the influence for the deposition of inorganic nitrogen compounds derived from the continent on the marine ecosystem at Bay of Bengal (BOB) in the North East Indian Ocean, we performed numerical simulations with and without atmospheric deposition of inorganic nitrogen compounds, using a 3-D lower trophic-marine ecosystem model (COCO-NEMURO), coupled with an atmospheric regional chemical transport model (WRF-CMAQ). The monthly mean data of wet and dry deposition of inorganic nitrogen compounds consisted of gases (HNO_3 and NH_3) and aerosol particles (NO_3^- and NH_4^+) at BOB region in 2009 –2016 produced by WRF-CMAQ were inputted to the COCO-NEMURO as a new nitrogen nutrient supplying process from the atmosphere. The results indicated that monthly average chlorophyll mass concentration at the surface in BOB was significant increase. This study indicates that the supply of atmospheric inorganic nitrogen compounds from continent to the BOB could lead to a high nutrient impact on the marine ecosystem within the subtropical region.

Keywords: Deposition, Bay of Bengal, Marine Ecosystem, nutrient

©2019. Japan Geoscience Union. All Right Reserved.

Carbon isotopic characterization of organic aerosols in tropical marine atmosphere at the Maïdo high-altitude observatory, Reunion Island

Sharmine Akter Simu[1], *Yuzo Miyazaki[1], OCTAVE Science Team

1. Institute of Low Temperature Science, Hokkaido University

Ocean-derived atmospheric aerosols can affect radiative forcing via formation of cloud droplets and ice nuclei as well as biogeochemical cycle of bioelements. Moreover, oxygenated volatile organic compounds (OVOCs) give significant impact on the atmospheric oxidative capacity and climate, which serve as key precursors of climatically active secondary organic aerosol (SOA) in the marine boundary layer. Atmospheric reactions of OVOCs and aerosols are closely linked to those of halogens, emissions of which are significant in the tropical oceans. However, current atmospheric models significantly underestimate the budget of OVOCs as well as SOA especially over tropical oceans, primarily due to poor knowledge of sources and paucity of observations of these parameters in tropical remote regions.
To improve our knowledge on the role of tropical oceans in the formation of atmospheric organic aerosols, size-segregated aerosol sampling was conducted for the first time at the Maïdo observatory (2,200m a.s.l) in Reunion Island in the Indian Ocean. The aerosol measurements were made during the Oxygenated Compounds in the Tropical Atmosphere–Variability and Exchanges (OCTAVE) project in March-June 2018, with integrated approach combining in situ/off-line measurements, satellite retrievals, and modelling. Stable carbon isotopic compositions together with molecular characterization of organic aerosols showed clear seasonal changes with significant contribution of marine sources to the observed aerosols in March when the microbial activity in sea surface was most active in that oceanic region. The effect of the changes in conditions of marine boundary layer and free troposphere on the observed organic aerosols are also discussed.

Keywords: Marine atmospheric organic aerosol, OVOCs, Tropical marine atmosphere, Halogen chemistry

©2019. Japan Geoscience Union. All Right Reserved.

[J] Poster | A (Atmospheric and Hydrospheric Sciences)：A-CG Complex & General

Wed. May 29, 2019 5:15 PM - 6:30 PM JST | Wed. May 29, 2019 8:15 AM - 9:30 AM UTC | Poster Hall International Exhibition Hall8, Makuhari Messe_17

[A-CG42] Biogeochemical linkages between the surface ocean and atmosphere

convener:Yuzo Miyazaki(Institute of Low Temperature Science, Hokkaido University), Jun Nishioka(Hokkaido University, Institute of low temperature sciences), Koji Suzuki(Hokkaido University), Yoko Iwamoto(Graduate School of Biosphere Science, Hiroshima University)

Multi-scale vertical and horizontal ocean mixing processes can strongly influence the distribution of dissolved and suspended substances including macro- and micro-nutrients, and may impact on phytoplankton bloom formation. The changes in nutrient dynamics generally affect the abundance, composition and metabolic activity of marine organisms such as phytoplankton and bacteria during the bloom. Marine phytoplankton can produce volatile organic compounds (VOCs) and marine atmospheric aerosols, which strongly influence on atmospheric chemistry. Primary and secondary organic and inorganic components produced via marine phytoplankton activity can contribute to the Earth's radiative forcing, and in turn marine ecosystems including biogeochemical processes directly or indirectly. Therefore, the biogeochemical cycles have a tight linkage between the ocean and the atmosphere. In order to understand physical, chemical and biological processes relevant to phytoplankton bloom formation in the ocean, dynamics of VOCs and marine aerosols in the atmosphere, and the biogeochemical linkage between the ocean and the atmosphere, we welcome new interdisciplinary presentations and active discussions on physical, chemical, and biological sciences both from ocean and atmospheric fields in this session. Studies linked to the Surface Ocean-Lower Atmosphere Study (SOLAS) project are good examples, but other related studies are also invited.

[ACG42-P01] Mixing States of Aged Black Carbon Collected over the Western North Pacific Ocean

*Momoka Yoshizue[1], Masahiro Momoi[1], Kouji Adachi[2], Masanori Yabuki[3], Tatsuhiro Mori[1], Akiho Suizu[4], Shinichi Kodama[1,4], Kazuhiko Miura[1], Mitsuo Uematsu[4] (1.Tokyo University of Science, 2.Meteorological Research Institute, 3.Kyoto University, 4.The University of Tokyo)

[ACG42-P02] Influence of Deposition of Atmospheric Inorganic Nitrogen Compounds to Marine Ecosystem at Bay of Bengal

*Fumikazu Taketani[1], Maki Noguchi Aita[1], Kazuyo Yamaji[1,2], Takashi Sekiya[1], Kohei Ikeda[3], Taketo Hashioka[1], Makio Honda[1], Kazuhiko Matsumoto[1], Yugo Kanaya[1] (1.Japan Agency for Marine-Earth Science and Technology, 2.Kobe University, 3.National Institute for Environmental Studies)

[ACG42-P03] Carbon isotopic characterization of organic aerosols in tropical marine atmosphere at the Maïdo high-altitude observatory, Reunion Island

Sharmine Akter Simu[1], *Yuzo Miyazaki[1], OCTAVE Science Team (1.Institute of Low Temperature Science, Hokkaido University)

Mixing States of Aged Black Carbon Collected over the Western North Pacific Ocean

*Momoka Yoshizue[1], Masahiro Momoi[1], Kouji Adachi[2], Masanori Yabuki[3], Tatsuhiro Mori[1], Akiho Suizu[4], Shinichi Kodama[1,4], Kazuhiko Miura[1], Mitsuo Uematsu[4]

1. Tokyo University of Science, 2. Meteorological Research Institute, 3. Kyoto University, 4. The University of Tokyo

Atmospheric aerosol particles can play a vital role in the climate change because they influence the radiative forcing on the Earth through absorbing and scattering of solar radiation. Especially, black carbon (BC) is known to a strong absorber of visible spectrum solar radiation in the atmosphere. However, its radiative forcing changes variably depending on its microphysical properties (e.g. mixing state, compositions, and shape). Therefore, it is important to accurately measure their parameters, especially, over the ocean because the observation is limited. In this study, the morphology and chemical compositions of marine aerosol particles including BC over the western north Pacific Ocean were analyzed by the individual particle analyses.

Measurement and samplings of atmospheric aerosol particles were carried out during the R/V Hakuho-Maru cruise (14-30/11/2017). The ambient BC mass concentrations were measured by a particle soot/absorption photometer (PSAP). In this study, we focused on relatively high BC mass concentration events over the western north Pacific Ocean at 26.62˚N, 137.93˚E and at 25.51˚N, 135.77˚E on 19/11/2017. The aerosols collected in both events were analyzed using a transmission electron microscope and an energy dispersive X-ray spectrometer.

In both samples, most BCs were embedded in sulfate particles that have organic coatings. Only a few BCs were attached to sea-salt particles. The backward trajectory analyses suggested that the air masses of both events passed through the land of China and Japan. These results indicate that BCs were emitted in or around the land, and then SO_2 condensed on their surface before organic carbon condensed during transportation. Our result is useful to understand the aging process of BC over the ocean.

Keywords: Marine atmospheric aerosol, Black carbon, Sulfate, Organic carbon, The western north Pacific Ocean, TEM-EDX

©2019. Japan Geoscience Union. All Right Reserved.

Influence of Deposition of Atmospheric Inorganic Nitrogen Compounds to Marine Ecosystem at Bay of Bengal

*Fumikazu Taketani[1], Maki Noguchi Aita[1], Kazuyo Yamaji[1,2], Takashi Sekiya[1], Kohei Ikeda[3], Taketo Hashioka[1], Makio Honda[1], Kazuhiko Matsumoto[1], Yugo Kanaya[1]

1. Japan Agency for Marine-Earth Science and Technology, 2. Kobe University, 3. National Institute for Environmental Studies

To investigate the influence for the deposition of inorganic nitrogen compounds derived from the continent on the marine ecosystem at Bay of Bengal (BOB) in the North East Indian Ocean, we performed numerical simulations with and without atmospheric deposition of inorganic nitrogen compounds, using a 3-D lower trophic-marine ecosystem model (COCO-NEMURO), coupled with an atmospheric regional chemical transport model (WRF-CMAQ). The monthly mean data of wet and dry deposition of inorganic nitrogen compounds consisted of gases (HNO_3 and NH_3) and aerosol particles (NO_3^- and NH_4^+) at BOB region in 2009 –2016 produced by WRF-CMAQ were inputted to the COCO-NEMURO as a new nitrogen nutrient supplying process from the atmosphere. The results indicated that monthly average chlorophyll mass concentration at the surface in BOB was significant increase. This study indicates that the supply of atmospheric inorganic nitrogen compounds from continent to the BOB could lead to a high nutrient impact on the marine ecosystem within the subtropical region.

Keywords: Deposition, Bay of Bengal, Marine Ecosystem, nutrient

©2019. Japan Geoscience Union. All Right Reserved.

Carbon isotopic characterization of organic aerosols in tropical marine atmosphere at the Maïdo high-altitude observatory, Reunion Island

Sharmine Akter Simu[1], *Yuzo Miyazaki[1], OCTAVE Science Team

1. Institute of Low Temperature Science, Hokkaido University

Ocean-derived atmospheric aerosols can affect radiative forcing via formation of cloud droplets and ice nuclei as well as biogeochemical cycle of bioelements. Moreover, oxygenated volatile organic compounds (OVOCs) give significant impact on the atmospheric oxidative capacity and climate, which serve as key precursors of climatically active secondary organic aerosol (SOA) in the marine boundary layer. Atmospheric reactions of OVOCs and aerosols are closely linked to those of halogens, emissions of which are significant in the tropical oceans. However, current atmospheric models significantly underestimate the budget of OVOCs as well as SOA especially over tropical oceans, primarily due to poor knowledge of sources and paucity of observations of these parameters in tropical remote regions.
To improve our knowledge on the role of tropical oceans in the formation of atmospheric organic aerosols, size-segregated aerosol sampling was conducted for the first time at the Maïdo observatory (2,200m a.s.l) in Reunion Island in the Indian Ocean. The aerosol measurements were made during the Oxygenated Compounds in the Tropical Atmosphere–Variability and Exchanges (OCTAVE) project in March-June 2018, with integrated approach combining in situ/off-line measurements, satellite retrievals, and modelling. Stable carbon isotopic compositions together with molecular characterization of organic aerosols showed clear seasonal changes with significant contribution of marine sources to the observed aerosols in March when the microbial activity in sea surface was most active in that oceanic region. The effect of the changes in conditions of marine boundary layer and free troposphere on the observed organic aerosols are also discussed.

Keywords: Marine atmospheric organic aerosol, OVOCs, Tropical marine atmosphere, Halogen chemistry

©2019. Japan Geoscience Union. All Right Reserved.

[E] Oral | H (Human Geosciences)：H-GM Geomorphology

Wed. May 29, 2019 1:45 PM - 3:15 PM JST | Wed. May 29, 2019 4:45 AM - 6:15 AM UTC | 101 1F

[H-GM03] Geomorphology

convener:Tsuyoshi Hattanji(Faculty of Life and Environmental Sciences, University of Tsukuba), Masayuki Seto(Fukushima Future Center for Regional Revitalization, Fukushima University), Chairperson:Thomas Parkner, Tsuyoshi Hattanji

The main subject of this session is interdisciplinary discussion on the whole range of themes relating to geomorphology, especially geomorphic processes, landform development and its relation to environmental changes, geomorphological hazards and their mitigation, relationships among geomorphic processes, other natural phenomena and human activities, and various techniques of geomorphological measurements and landform classification. All presentations and discussion of this session are made in English.

1:45 PM - 2:00 PM JST | 4:45 AM - 5:00 AM UTC

[HGM03-01] Surface structure as a control for gully complex development in the Mackey`s block, North Island, New Zealand

*Thomas Parkner[1] (1.University of Tsukuba, Graduate School of Life and Environmental Sciences)

2:00 PM - 2:15 PM JST | 5:00 AM - 5:15 AM UTC

[HGM03-02] Model Linking Landslides and River Evolution of Incisional Channel Created by River Erosion

*Chia-Ting Kao[1], Gene Jiing-yun You[1] (1.National Taiwan University)

2:15 PM - 2:30 PM JST | 5:15 AM - 5:30 AM UTC

[HGM03-03] **A semi-automated method for extracting channels and channel profiles from LiDAR-derived digital elevation models**

*Pinliang Dong[1] (1.University of North Texas)

2:30 PM - 2:45 PM JST | 5:30 AM - 5:45 AM UTC

[HGM03-04] Laboratory experiments on the landform development

*Shunji Ouchi[1] (1.Faculty of Science and Engineering, Chuo University)

2:45 PM - 3:00 PM JST | 5:45 AM - 6:00 AM UTC

[HGM03-05] Characteristics of lake sediment from southern part of Mongolia and comparison to meteorological data

*Uyangaa Udaanjargal[1], Noriko Hasebe[1], Keisuke Fukushi[1], Tanaka Yukiya[2], Davaadorj Davaasuren[4], Makoto Sambo[1], Baasansuren Gankhurel[1], Nagayoshi Katsuta[3], Shinya Ochiai[1], Tuvshin Gerelmaa[4] (1.Kanazawa University, 2.Kyunghee University, 3.Gifu University, 4.National University of Mongolia)

3:00 PM - 3:15 PM JST | 6:00 AM - 6:15 AM UTC

[HGM03-06] **Evaluation of geomorphological changes on Kujukuri beach based on UAV SfM**

*Mergen Kungaa[1], Toshihiko Sugai[1], Natsuki Sasaki[1], Taiga Kimori[1], Taro Funatsu (1.Tokyo University, Graduate School of Frontier Sciences, Department of Natural Environmental Studies)

Surface structure as a control for gully complex development in the Mackey`s block, North Island, New Zealand

*Thomas Parkner[1]

1. University of Tsukuba, Graduate School of Life and Environmental Sciences

Gully erosion occurs on many steep, erosion-prone slopes. While most research focusses on gully formation by water erosion, gullies can also enlarge by mass movement processes. In New Zealand, such process combinations are named gully complexes. While concepts on gully complex development are available, material variability - other than lithology –is not included. In this study, development of gullies and gully complexes is analyzed by focusing on properties of the initial surface into with gullies and gully complexes erode to relate gully orientation and erosion intensity to surface structure.

The study area consists of 12 headwater catchments in the Mackey`s Block, North Island, New Zealand. Bedrock consists of Cretaceous-aged, highly crushed and sheared mudstones and sandstones. Deforestation by European settlers at the beginning of the 20th century for pastoral farming was followed by reforestation for wood production from the 1980s. Sequential aerial photographs from 1939 to 2005 were interpreted to map mass movements and the development of gullies. Digital elevation models were extracted from aerial photography from 1957 to 2002 using ERDAS to relate surface structure to gully orientation and erosion intensity.

Mapping results indicate that prior to a severe gully erosion phase, which started shortly before the first aerial photography in 1939, the surface structure is charaterized by (revegetated) small gullies, deep-seated landsliding with double ridges, and shallow flows. Deep (few meters to 15m) gullies complexes incised at the toe of mass movement bodies and eroded upslope. Such gullies developed oversteepened sidewalls, which in turn initiate extensive mass movements at the gully walls. Erosion intensity increased suddenly, where gullies destabilized mass movement deposits. Above the deep gully complexes, shallow (about 1 -2m deep), hundreds of meter long gully arms extended along boundaries of mass movements. These results indicate that next to morphometric parameters (slope, catchment size), material type, vegetation change, and moisture conditions, the development of gully complexes is also controlled by surface structure.

Keywords: gully, mass movement

©2019. Japan Geoscience Union. All Right Reserved.

Model Linking Landslides and River Evolution of Incisional Channel Created by River Erosion

*Chia-Ting Kao[1], Gene Jiing-yun You[1]

1. National Taiwan University

Landslides produce enormous volumes of sediment in mountainous watersheds. However, quantifying landslide-derived sediment transported downstream remains a challenge. This study makes effort in determine the amount of landslide-derived sediment that eroded by the water and the ratio of sediment yield of this problem. We try to use a coupled two-dimensional model to investigate the evolution of landslide aggregation influenced by the channel flow.In this study, the shallow water equations consider the two-dimensional distribution flow velocity to estimate the shear stress. In addition, the Exner equation is applied to calculate the sediment transport the landslide aggregation evolution. By assuming constant inflow, the Exner equation can be derived as a diffusion equation. Besides, both of the two equations under a horizontal 2D straight, non-erodible banks, and no secondary flow channel can be derived as our governing equation which has the nonlinear terms, and the analytical method may not work to solve the two equations under the 2D condition. As a result, this study adopts the finite volume method to proceed this work. This proposed model will be able to have a better presentation in estimating the landslide-derived sediment in channel, and these sequences are expected to be useful indicators in the watershed management according to the predicted the upstream of watershed sediment yield .

Keywords: Landslide aggregation, River erosion, Finite volume method, Exner equation, Shallow water equations, Numerical modeling

©2019. Japan Geoscience Union. All Right Reserved.

A semi-automated method for extracting channels and channel profiles from LiDAR-derived digital elevation models

*Pinliang Dong[1]

1. University of North Texas

Stream channels are an integral part of hydrology, alluvial geomorphology and tectonic geomorphology, and have long been studied qualitatively and quantitatively. With the advent of digital elevation models (DEMs) and geographic information systems (GIS), several methods have been proposed to extract channels from raster DEMs. This presentation introduces a semi-automated method for extracting stream channels from high resolution DEMs. The methodology flowchart includes the following major steps: (1) channel detection, (2) mathematical morphological operation, (3) vectorization, (4) profile generation, and (5) accuracy assessment. The method is implemented as an ArcGIS Python add-in toolbar. The application of the toolbar is demonstrated using a LiDAR-derived DEM in a study area along the San Andreas Fault in California, USA.

Keywords: Stream channel, Digital elevation model, Geographic information system, Light detection and ranging (LiDAR), Python

©2019. Japan Geoscience Union. All Right Reserved.

Laboratory experiments on the landform development

*Shunji Ouchi[1]

1. Faculty of Science and Engineering, Chuo University

Geomorphic experiments with uplift and rainfall erosion are expected to provide some important knowledge to interpret the development of landform, which has left only scarce and hard-to-find evidence. This type of experiments had not been conducted so often, probably because no one had a good idea to scale down the processes of landform development. In recent years, however, laboratory experiments on the development of landform were increasingly conducted for the purpose to verify numerical/analytical models, which have been promoted by the development of computer technology and the spread of DEM, while the fundamental problems of huge scale difference have not been solved yet. Some of these recent experiments demonstrated a certain mechanism or a law governing the experimental landform development, such as the self-organized criticality or the competition between diffusive hill slope transport and advective transport in channels, which was suggested by numerical analyses. This indicates the applicability of numerical models to the experimental landform, but not to the real landform yet, although the authors believed it. Real landforms we see today have developed in the geographical space through the historical time, and inevitably have infinite varieties. We can find landscapes similar to the experimentally formed landscapes somewhere in the world, but this does not mean that mechanisms or laws dominated in the experiment also work on the real landform. The experimental landform develops within a certain setting, which is restricted by the facilities and arranged for the purpose. We still have a lot to do before taking the experiments as a bridge between numerical models and natural landscapes. I have been conducting a series of geomorphic experiments with changing experimental settings (40 runs by now), and I here try to make clear the significance of experiments in the study of geomorphology on the basis of these experiments.
A mixture of fine sand and kaolinite (10:1 by weight) compacted in a square prism-shaped stainless container (ca. 60×60×40cm) is pushed up by the uplift-generating device put under the bottom plate of container. Mist-type rainfall is generated by a pump through spray nozzles. The results of experiments suggested the existence of two thresholds of uplift rate, which is the most important independent controlling factor. Below the lower threshold, fluvial erosion offsets the surface rising by slow uplift, and gentle landforms reflecting the mound erodibility and rainfall intensity appear (Characteristic relief phase). Above the upper threshold, uplift overwhelms and a massive mountain grows until it hits the limit of experimental facilities (Mountain building phase). When the uplift rate is between the lower and upper thresholds, average surface height stops increasing and changes around a certain height depending on the uplift rate, after valley systems develop and slopes grow enough to cause landslides (Steady state phase). This steady state phase is the most common condition through the series of experiments. Rainfall intensity is expected to affect the amount of surface flow; and therefore, the rate of erosion. Low rainfall generates less surface flow, and this reduces erosion and make the surface grow higher. Permeability of the sand mound is considered to have a similar effect concerning the surface flow. However, more permeable material, associated with lower sear strength, promotes slope failures even in the earlier stage. The surface, therefore, becomes lower even with less rainfall. These factors, which relate each other themselves, apparently have complex effects on the development of experimental landform. The relationships among these controlling factors can be compared to those concerning real landform. Revealing these relationships and their effects on the experimental landform is probably the key to make geomorphic experiments meaningful in the study of geomorphology.

©2019. Japan Geoscience Union. All Right Reserved.

Keywords: geomorphic experiment, uplift, rainfall intensity, fluvial erosion, landslide, permeability

©2019. Japan Geoscience Union. All Right Reserved.

Characteristics of lake sediment from southern part of Mongolia and comparison to meteorological data

*Uyangaa Udaanjargal[1], Noriko Hasebe[1], Keisuke Fukushi[1], Tanaka Yukiya[2], Davaadorj Davaasuren[4], Makoto Sambo[1], Baasansuren Gankhurel[1], Nagayoshi Katsuta[3], Shinya Ochiai[1], Tuvshin Gerelmaa[4]

1. Kanazawa University, 2. Kyunghee University, 3. Gifu University, 4. National University of Mongolia

Mongolia is located in center of the Central Asia and it provides an important key archive for the research of climate characteristics inside continents. Lake sediments are an excellent archive to study long-term fluctuations of environmental conditions (Gunten et al. 2009). Lake is the subject to a variety of extrinsic and intrinsic forcing variables that regulate the subsequent history of the lake, such as climate, watershed bedrock composition, tectonic and volcanic activity, vegetation, aquatic biota, and human activities (Gierlowski-Kordesch, 2004). To understand how climate system works in Mongolia and how we can extract information from the lake sediments, sediment cores of about 30 cm long from Boontsagaan, Orog and Olgoy lakes are analyzed and compared to the meteorological data (air temperature, precipitation and wind) of Galuut and Baatsagaan stations, Bayanhongor Province. The sedimentary features include whole and mineral grain size, grain density, water, organic matter, carbonate, and amorphous silica contents. Sedimentary ages were estimated by excess 210Pb measurement. According to the comparison between sediment characteristics and climate condition, temperature is correlated to whole grain size in three of lakes.

Further comparison reveals that calcium carbonate concentration, amorphous silica concentration, and mineral grain size correlate to temperature in Boontsagaan and Olgoy lakes. In Orog lake, wetter years with high wind and much rainfall result in fine grain size, while the high amount of $CaCO_3$and organic flux is found during the low precipitation. Some of the major fluctuations may indicate indirect consequence of climate change, for instance, some events such as the earthquake or a permafrost degradation.

Keywords: lakes , sediment characteristics, climate condition

©2019. Japan Geoscience Union. All Right Reserved.

Evaluation of geomorphological changes on Kujukuri beach based on UAV SfM

*Mergen Kungaa[1], Toshihiko Sugai[1], Natsuki Sasaki[1], Taiga Kimori[1], Taro Funatsu

1. Tokyo University, Graduate School of Frontier Sciences, Department of Natural Environmental Studies

Nowadays, structure from motion (SfM) photogrammetry became a powerful tool in the hands of coastal researchers. During 2018-2019 we conducted 4 aerial survey by UAV on the 4 km long stretch on Kujukuri beach between Nabakigawa and Horikawa rivers, Chiba Prefecture. These 2 rivers separate research area from rest of 60-km long Kujukuri beach, forming separate morpho- and lithodynamical unit. The results of the research were high-resolution digital elevation models (DEM) and orthomosaics for February 2018, June 2018, September 2018 and February 2019. Based on DEM and orhomosaics we were able evaluate geomorphological changes throughout the year. From February 2018 to September 2018 we recorded active accumulation along the entire length of the beach. But accumulation intensity varied in different zones of beach as if foreshore, backshore or dunes. Also, the accumulation processes did not occur evenly for 7 months, but mostly intensified in the summer. From September 2018 to February 2019 erosional processes prevailed having different intensity at various sites. Thus, we were able to record in high resolution the process of transition from the winter profile of the beach to the summer profile and back.

Keywords: Coastal geomorphology, UAV SfM, Kujukuri beach

©2019. Japan Geoscience Union. All Right Reserved.

[E] Poster | H (Human Geosciences)：H-GM Geomorphology

Wed. May 29, 2019 3:30 PM - 5:00 PM JST | Wed. May 29, 2019 6:30 AM - 8:00 AM UTC | Poster Hall International Exhibition Hall8, Makuhari Messe_11

[H-GM03] Geomorphology

convener:Tsuyoshi Hattanji(Faculty of Life and Environmental Sciences, University of Tsukuba), Masayuki Seto(Fukushima Future Center for Regional Revitalization, Fukushima University)

The main subject of this session is interdisciplinary discussion on the whole range of themes relating to geomorphology, especially geomorphic processes, landform development and its relation to environmental changes, geomorphological hazards and their mitigation, relationships among geomorphic processes, other natural phenomena and human activities, and various techniques of geomorphological measurements and landform classification. All presentations and discussion of this session are made in English.

[HGM03-P01] Honeycomb Weathering (Tafoni) of Sandstone and Environmental Factors in Yonaguni Island, Okinawa Prefecture, Japan

*Takayuki Ogata[1] (1.Disaster Prevention Research Center for Island Regions, University of the Ryukyus)

[HGM03-P02] Colluvial deposits in first-order streams and channel head migration by shallow landslides: Case study in granitic basins, Asaminami, Hiroshima, Japan

*Tsuyoshi Hattanji[1], Ryuya Kodama[2], Takahisa Furuichi[3], Shoji Doshida[4], Yasushi Tanaka[5] (1.Faculty of Life and Environmental Sciences, University of Tsukuba, 2.former College of Geoscience, University of Tsukuba, 3.Hokkaido University, 4.National Research Institute of Fire and Disaster, 5.Komazawa University)

[HGM03-P03] Rock restrictions on topographical features of rivers: model experiment

*Yuta Takase[1], Noritaka Endo[1] (1.Kanazawa University)

[HGM03-P04] Stream power incision model and the stage of topographic equilibrium, using physical experiments

*Imamura Akihiro[1], Noritaka Endo[1] (1.Kanazawa University)

[HGM03-P05] Downstream variation in gravel size of the Tenjin River system

*Kazuaki Hori[1], Kazuya Yonehara[1] (1.Department of Geography, Graduate School of Environmental Studies, Nagoya University)

[HGM03-P06] Talus slope development in the time of deglaciation: a case study of the Rev Valley, SW Spitsbergen

*Krzysztof Senderak[1], Marta Kondracka[1], Bogdan Gądek[1] (1.Faculty of Earth Sciences, University of Silesia)

[HGM03-P07] Distribution of Large Benthic Foraminifers in one of Majuro's Conservation Areas – Drenmeo Island

*Benedict Yamamura[1], Kazuhiko Fujita[2], Melba White[3], Kyotak Ishiguro[3], Hironobu Kan[1] (1.Kyushu University, Integrated Sciences for Global Society - Research Center for Coastal Seafloor , 2.Department of Physics and Earth Sciences, University of the Ryukyus, 3.Marshall Islands Marine Resources Authority)

[HGM03-P08] Luminescence chronology of fluvial and marine records from subsurface sediment cores: An insight into the geomorphic evolution of Kaveri delta, India

*kartika goswami[1], Anbarasu Kumaresan[2], Sivakumar Krishnan[2], Senthil K. Sadasivam[2], Manoj Kumar Jaiswal[1] (1.Department of Earth Sciences, Indian Institute of Science Education and Reserach Kolkata, 2.National College Tiruchirappalli, India)

Honeycomb Weathering (Tafoni) of Sandstone and Environmental Factors in Yonaguni Island, Okinawa Prefecture, Japan

*Takayuki Ogata[1]

1. Disaster Prevention Research Center for Island Regions, University of the Ryukyus

Sandstone surfaces of Yonaguni Island (westernmost of the Ryukyu Arc) often show a honeycomb structure (tafoni) derived from physical disintegration in relation to salt weathering. Miocene sandstone (Yaeyama Group) is extensively exposed on the island surface, and forms sea cliffs along rocky coasts. The honeycomb structure is especially observed along the coasts where wave splashes produce wetting and drying processes assisted by strong wind and active evaporation. The geometry and density of tafoni seem to be controlled by vertical height from the sea level and horizontal distance of the coast line. Field observations at the rocky coasts of Yonaguni Island suggest that larger holes are developed along the north-faced coasts than the south-faced coasts, which depends mainly on the northeastern monsoon during the winter period.

Keywords: weathering, sandstone, rocky coast, tafoni, monsoon, Yaeyama group

©2019. Japan Geoscience Union. All Right Reserved.

Colluvial deposits in first-order streams and channel head migration by shallow landslides: Case study in granitic basins, Asaminami, Hiroshima, Japan

*Tsuyoshi Hattanji[1], Ryuya Kodama[2], Takahisa Furuichi[3], Shoji Doshida[4], Yasushi Tanaka[5]

1. Faculty of Life and Environmental Sciences, University of Tsukuba, 2. former College of Geoscience, University of Tsukuba, 3. Hokkaido University, 4. National Research Institute of Fire and Disaster, 5. Komazawa University

Relationship between dates of colluvial deposits and channel-head migration was examined in granitic mountains where a debris-flow disaster occurred in 2014. Topographic analysis using 1-m grid DEMs before and after the disaster indicates that post-event channel heads were located upslope from pre-event channel heads due to landslide or erosion by debris flow. Post-event channel heads with shallow landslides had strong inverse correlations between local slope and drainage area. Charcoal samples were collected in colluvial deposits of two post-event channel heads (A and B) where the channel heads migrated more than 50 m upslope with shallow landslides. The radiocarbon dates of the samples were 1162–1194 y BP for channel head A and 786 y BP for channel head B. Another sample was collected in colluvial deposits of a post-event channel head (C) with shallow landslide but no migration. The radiocarbon date of the sample at the channel head C was 670 y BP. These radiocarbon data explain contrasting intervals of landslide events in hollows. The channel head A with older radiocarbon dates has the longer interval of landslide events and therefore the valley head has been buried in longer distance (more than 50 m) along the channel since the last landslide event to 2014.

Keywords: High-resolution DEM, Micro-topography, Radiocarbon dating, Valley head

©2019. Japan Geoscience Union. All Right Reserved.

Rock restrictions on topographical features of rivers: model experiment

*Yuta Takase[1], Noritaka Endo[1]

1. Kanazawa University

Landforms of mountainous areas is developed by both downcutting and lateral erosion of rivers. For example, ingrown meanders develop when the lateral erosion is predominant, while entrenched meanders form when the downcutting is dominant. It is a generally accepted understanding that the relative superiority or inferiority between the downcutting and lateral erosion is determined by the uplift rate of the land, rock strength difference, riverbed gradient, deflection of flow in a channel, but the systematic discussion remains insufficient. In this study, we conducted flume experiments to investigate the relationship between bedrock strength and sinuosity, and the relationship between time series pattern of uplift and meandering development. We prepared a single channel that cut a uniform substrate in a two-dimensional flume. The substrates were made of the mixture of fine sand and clay, and we examined two types of substrate, hard and soft ones, which can be formed by changing the ratio of sand and clay (the mixure including more clay is harder). Uplift of the experimental land was realized by lowering a weir set at the downstream end of the channel, i.e. the base-level lowering.

Knickpoints were observed more frequently in the case of hard substrate, which is consistent with previous study (Grimaud, 2016). Sinuosity of the channel tended to be higher for the hard substrate than the soft substrate, which is seemingly opposite the conventional understanding, but can be attributed to sustainability of the channel shape due to erosion resistance of the hard substrate. In all the experiments, the sinuosity tended to be higher after the uplift ceased rather than during the period of uplift.

Keywords: labo, sinuosity, bedrock strength, knickpoint, uplift

©2019. Japan Geoscience Union. All Right Reserved.

Stream power incision model and the stage of topographic equilibrium, using physical experiments

*Imamura Akihiro[1], Noritaka Endo[1]

1. Kanazawa University

Bedrock rivers develop their landforms very slowly, compared with alluvial river, thus bedrock rivers and their surrounding topographies are expected to record long-term environmental changes such as tectonics and climate. The stream power incision model (SPIM) is an empirical model that expresses the erosion rate due to rivers by the product of two power functions of the contributing area and river bed slope. Using this equation with an uplift term, the differential equation of the temporal change in the altitude of riverbed is constituted. When applying the model to a natural drainage basin, the equilibrium state between erosion and uplift is often assumed, partially because the uplift rate is usually unknown. Under the assumption of equilibrium state, SPIM is reduced to the relationship in which the riverbed slope is a power function of the contributing area, known as Flint’s law, which is the basis of “slope-area analysis” to determine the concavity (equivalent to the ratio of two power exponents in SPIM). Usually the two power exponents in SPIM are presumed to be constant if lithology, climate, and other factors are the same. This postulation, however, is difficult to verify for natural landforms, because of heterogeneity of various kind of property within a single drainage basin and difficulty in evaluation of the incision rate.

This study investigates the relation between the incision rate and topographic properties in river basins, through the observation of small-sized physical experiments under well-controlled conditions. A flume used was 90×180 cm, and the substrate to be dissected composed of the uniform mixture of sand and clay was installed. Rainfall was simulated by supplying mist from 10 nozzles. Uplift was realized by lowering a weir that was installed at the downstream end of the flume and determined the base level. The landform was measured by photogrammetry using several hundred photos taken during intermission from rainfall for photographing.

We compared the results of (1) this and (2) the previous studies (Imamura and Endo, 2018) realizing different kinds of uplift: (1) sudden base level lowering from a stable state of basin, to observe the response processes of the landforms until the basin became stable again (about 5 hours); (2) Sudden change in the uplift rate, to observe the change from a stable state under constant uplift of 4.5 mm/h to a new stable state under faster uplift rate of 6.0 mm/h (about 6 hours).

The results of Experiment (1) showed that the incision rate decreased with time (presumably asymptotic to zero), while Experiment (2) always displayed a certain finite value of the incision rate. The power exponents in SPIM, m (for the contributing area) and n (for the slope) did not seem to be constant in both experiments. The ratio m/n also changed, but seemed to converge to a certain value in each experiment.

We evaluated the correlation of the incision rate with the fitted function for each measurement time. In Experiment (1), although the denudation rate decreased with time, the first half of the run time showed good correlations but the latter half showed the worse. By contrast, Experiment (2) exhibited increasing correlations in the latter half of the run. These results suggests that SPIM holds for dynamic equilibrium (tectonic steady state (Montgomery, 2001)) or the early stage of static quasi-equilibrium (erosional stead state (Montgomery, 2001)), but fails for mature or later stages in which a landform proceeds to a

©2019. Japan Geoscience Union. All Right Reserved.

peneplane.

Imamura and Endo, 2018. Incision rate, riverbed slope and contributing area of an experimental drainage basin. JPGU 2018 Abstract.

Montgomery, 2001, Slope distributions, threshold hillslopes, and steady-state topography. American Journal of Science, 301, 432–454.

Keywords: stream power model, laboratory experiment, bedrock river

©2019. Japan Geoscience Union. All Right Reserved.

Downstream variation in gravel size of the Tenjin River system

*Kazuaki Hori[1], Kazuya Yonehara[1]

1. Department of Geography, Graduate School of Environmental Studies, Nagoya University

Many researchers have studied downstream variation in river-bed material size and its controlling factors, because they are important to understand the evolution of fluvial landforms and drainage basin. Many of these studies have focused only on rivers flowing through mountains or alluvial plains. Thus, it is desirable to examine a much broader range, i.e. from head to mouth of a river. We investigated the downstream variation of gravel size and channel gradient in the Tenjin River system (Tenjin, Ogamo, and Mitoku rivers) located in the central part of Tottori prefecture, Japan. The Tenjin River is approximately 34 km in length and major tributaries, the Ogamo and Mitoku rivers, join the Tenjin River at approximately 7 km and 12 km upstream from the mouth, respectively. Mean gravel size tends to decrease toward the downstream between 5 and 23 km upstream from the Tenjin River mouth where exposed gravel bars are easily found. Channel gradient is usually less than 0.03 and its variation is relatively small in this range. On the other hand, exposed gravel bars are uncommon between 23 and 34 km upstream from the mouth. The channel gradient become larger (> 0.06) and shows large variation. Large boulders (> 500 mm) are distributed in the channel. The number of boulders, especially > 1000 mm, seems to be inversely proportional to the distance from the valley wall. Buffers along the rivers regulate the supply of boulders from the valley wall in the upper reaches and reduce the connectivity of sediment supply from the tributaries in the middle and lower reaches. Barriers typified by weirs reduce the connectivity in the longitudinal direction throughout the basin.

Keywords: sediment connectivity, grain size, channel gradient

©2019. Japan Geoscience Union. All Right Reserved.

Talus slope development in the time of deglaciation: a case study of the Rev Valley, SW Spitsbergen

*Krzysztof Senderak[1], Marta Kondracka[1], Bogdan Gądek[1]

1. Faculty of Earth Sciences, University of Silesia

Every high-mountain area is characterized by the occurrence of talus slopes. A process of development this kind of forms depends on among other things climatic conditions. Currently in Spitsbergen, we observe the deglaciation process caused climate changes. This causes that the evolution’ s tempo of all environments linked with glaciers is very high. It also concerns the talus slopes, which, in the last time, are more often used as key element to paleo-environmental reconstructions for last thousands. In this paper, we present the geophysical surveys of talus slopes conducted in the Rev Valley (SW Spitsbergen). The valley was shaped by glacier, which left behind among other things glacial lake and buried glacial ice in mixed slope-moraine material. Nowadays, the talus slopes in this valley develop under the typical conditions of periglacial environment. In the studies of 15 talus slopes we used the ground-penetrating radar (GPR) and electrical resistivity tomography method (ERT). The studies allowed to recognize the internal structure of talus slopes and to determine a character of their elements, such as thickness of slopes, permafrost table and a depth of active layer, present of buried glacial ice, sediementological structures caused by various deposition of material on the slope surface, and finally a shape of bedrock. A comparison obtained results indicates on relevant regularity in the development of internal structure of talus slopes. These are for example visible differences in the terms of present of permafrost, which is located from a depth 2-3 m in the oldest slopes to a depth 4-5 m in the youngest. On the other hands, the studies discovers the deviations from the typical evolution models. The buried glacial ice has not been survived in a younger forms, whereas it is present in these older slopes. Based on the results we created the proposition of model of talus slope evolution developing in a periglacial period. In this time the development of slopes characterize a very high variability, not much lower than in previous paraglacial period. This work was financed from the funds of the National Science Centre in Poland received by Krzysztof Senderak in the Preludium 12 project: Determination of the evolution of slopes of southern Spitsbergen on the background of climate changes (2016/23/N/ST10/00162).

Keywords: talus slope evolution, permafrost, deglaciation, electrical resistivity tomography (ERT), ground-penetrating radar (GPR)

©2019. Japan Geoscience Union. All Right Reserved.

Distribution of Large Benthic Foraminifers in one of Majuro's Conservation Areas –Drenmeo Island

*Benedict Yamamura[1], Kazuhiko Fujita[2], Melba White[3], Kyotak Ishiguro[3], Hironobu Kan[1]

1. Kyushu University, Integrated Sciences for Global Society - Research Center for Coastal Seafloor , 2. Department of Physics and Earth Sciences, University of the Ryukyus, 3. Marshall Islands Marine Resources Authority

Climate change is having a huge impact on the island formation. In this study, we examined the composition and distribution of large benthic foraminifers (LBF) from 12 chosen sample sites (see map) within and outside of Drenmeo islet, one of the designated conservation areas in Majuro atoll. Samples were collected from the area to further investigate the sand built-up between the conservation area and the adjacent islet. The preliminary findings showed that the area is predominantly composed of two island-building LBF, namely *Calcarina sp.* and *Amphistegina sp.* The final results from this study will help stakeholders to amend the management plan to include the adjacent islet under the current management plan.

Keywords: Drenmeo island, conservation area, large benthic foraminifers, management plan

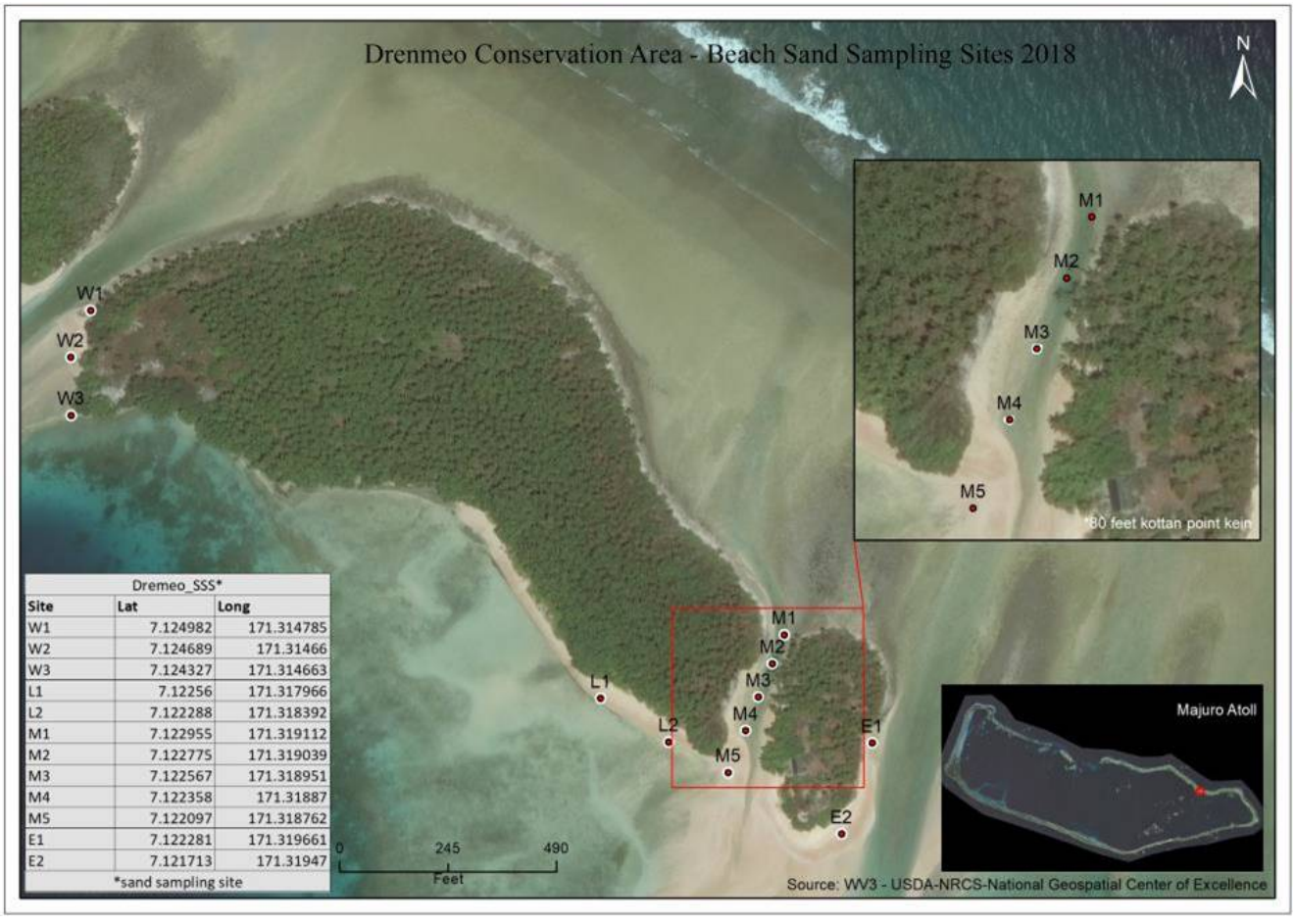

©2019. Japan Geoscience Union. All Right Reserved.

Luminescence chronology of fluvial and marine records from subsurface sediment cores: An insight into the geomorphic evolution of Kaveri delta, India

*kartika goswami[1], Anbarasu Kumaresan[2], Sivakumar Krishnan[2], Senthil K. Sadasivam[2], Manoj Kumar Jaiswal[1]

1. Department of Earth Sciences, Indian Institute of Science Education and Reserach Kolkata, 2. National College Tiruchirappalli, India

Long-term evolution of river deltas is a result of forcings (tectonics, climate, sea level, avulsion, compaction etc). We present the results of luminescence dating of sediments from four sediment cores (VKI, TNR, SY and KKI) of 25 m depth each, retrieved from the Kaveri delta in south India. The coring sites are ~2.5 km, ~11 km, ~17 km and ~20 km away from the present coastline respectively. The cores were analysed for OSL dating, 14C dating, lithology and microfossils and represent various stages of fluvial and marine activity in the region over the last ~150 ka. The chronology of the core closet to the coast (VKI) reflects eight major phases of increased sea level during the late quaternary period (142-140 ka, 104-100 ka, ~121 ka, 87-81 ka, 60-57 ka, 9-6 ka, ~5 ka and ~3 ka) partly coinciding with the global climate cycles MIS 6, MIS 5, MIS 3, MIS 1 respectively. During ~121 ka and 9-6 ka, marine transgression reached the core location to leave marine signatures in the forms of foraminifera. VKI core replicates the quaternary sea level curve, showing strong control of the sea in coastal deposition.

The oldest age of VKI is ~140 ka. The three cores situated further inland give oldest/bottom most ages of~120 ka. This indicates the coastal land has uplifted in the recent years with deeper sediments being encountered at relative shallower depth. The uplift is expected to occur around post 50 ka, creating a basin fill situation for riverine sediments to accumulate and restricting the delta to prograde. This is observed from the sedimentation pattern and robust chronology of the other three inland cores. Analysis of DEM also supported the occurrence of uplift. Thus, the present work examines the geomorphic evolution of Kaveri delta, an archive of fluvial, shoreline and tectonic activities.

Keywords: OSL Dating, Kaveri Delta , GIS, Foraminifera

©2019. Japan Geoscience Union. All Right Reserved.

[E] Poster | H (Human Geosciences)：H-GM Geomorphology

Wed. May 29, 2019 5:15 PM - 6:30 PM JST | Wed. May 29, 2019 8:15 AM - 9:30 AM UTC | Poster Hall International Exhibition Hall8, Makuhari Messe_18

[H-GM03] Geomorphology

convener:Tsuyoshi Hattanji(Faculty of Life and Environmental Sciences, University of Tsukuba), Masayuki Seto(Fukushima Future Center for Regional Revitalization, Fukushima University)

The main subject of this session is interdisciplinary discussion on the whole range of themes relating to geomorphology, especially geomorphic processes, landform development and its relation to environmental changes, geomorphological hazards and their mitigation, relationships among geomorphic processes, other natural phenomena and human activities, and various techniques of geomorphological measurements and landform classification. All presentations and discussion of this session are made in English.

[HGM03-P01] Honeycomb Weathering (Tafoni) of Sandstone and Environmental Factors in Yonaguni Island, Okinawa Prefecture, Japan

*Takayuki Ogata[1] (1.Disaster Prevention Research Center for Island Regions, University of the Ryukyus)

[HGM03-P02] Colluvial deposits in first-order streams and channel head migration by shallow landslides: Case study in granitic basins, Asaminami, Hiroshima, Japan

*Tsuyoshi Hattanji[1], Ryuya Kodama[2], Takahisa Furuichi[3], Shoji Doshida[4], Yasushi Tanaka[5] (1.Faculty of Life and Environmental Sciences, University of Tsukuba, 2.former College of Geoscience, University of Tsukuba, 3.Hokkaido University, 4.National Research Institute of Fire and Disaster, 5.Komazawa University)

[HGM03-P03] Rock restrictions on topographical features of rivers: model experiment

*Yuta Takase[1], Noritaka Endo[1] (1.Kanazawa University)

[HGM03-P04] Stream power incision model and the stage of topographic equilibrium, using physical experiments

*Imamura Akihiro[1], Noritaka Endo[1] (1.Kanazawa University)

[HGM03-P05] Downstream variation in gravel size of the Tenjin River system

*Kazuaki Hori[1], Kazuya Yonehara[1] (1.Department of Geography, Graduate School of Environmental Studies, Nagoya University)

[HGM03-P06] Talus slope development in the time of deglaciation: a case study of the Rev Valley, SW Spitsbergen

*Krzysztof Senderak[1], Marta Kondracka[1], Bogdan Gądek[1] (1.Faculty of Earth Sciences, University of Silesia)

[HGM03-P07] Distribution of Large Benthic Foraminifers in one of Majuro's Conservation Areas – Drenmeo Island

*Benedict Yamamura[1], Kazuhiko Fujita[2], Melba White[3], Kyotak Ishiguro[3], Hironobu Kan[1] (1.Kyushu University, Integrated Sciences for Global Society - Research Center for Coastal Seafloor , 2.Department of Physics and Earth Sciences, University of the Ryukyus, 3.Marshall Islands Marine Resources Authority)

[HGM03-P08] Luminescence chronology of fluvial and marine records from subsurface sediment cores: An insight into the geomorphic evolution of Kaveri delta, India

*kartika goswami[1], Anbarasu Kumaresan[2], Sivakumar Krishnan[2], Senthil K. Sadasivam[2], Manoj Kumar Jaiswal[1] (1.Department of Earth Sciences, Indian Institute of Science Education and Reserach Kolkata, 2.National College Tiruchirappalli, India)

Honeycomb Weathering (Tafoni) of Sandstone and Environmental Factors in Yonaguni Island, Okinawa Prefecture, Japan

*Takayuki Ogata[1]

1. Disaster Prevention Research Center for Island Regions, University of the Ryukyus

Sandstone surfaces of Yonaguni Island (westernmost of the Ryukyu Arc) often show a honeycomb structure (tafoni) derived from physical disintegration in relation to salt weathering. Miocene sandstone (Yaeyama Group) is extensively exposed on the island surface, and forms sea cliffs along rocky coasts. The honeycomb structure is especially observed along the coasts where wave splashes produce wetting and drying processes assisted by strong wind and active evaporation. The geometry and density of tafoni seem to be controlled by vertical height from the sea level and horizontal distance of the coast line. Field observations at the rocky coasts of Yonaguni Island suggest that larger holes are developed along the north-faced coasts than the south-faced coasts, which depends mainly on the northeastern monsoon during the winter period.

Keywords: weathering, sandstone, rocky coast, tafoni, monsoon, Yaeyama group

©2019. Japan Geoscience Union. All Right Reserved.

Colluvial deposits in first-order streams and channel head migration by shallow landslides: Case study in granitic basins, Asaminami, Hiroshima, Japan

*Tsuyoshi Hattanji[1], Ryuya Kodama[2], Takahisa Furuichi[3], Shoji Doshida[4], Yasushi Tanaka[5]

1. Faculty of Life and Environmental Sciences, University of Tsukuba, 2. former College of Geoscience, University of Tsukuba, 3. Hokkaido University, 4. National Research Institute of Fire and Disaster, 5. Komazawa University

Relationship between dates of colluvial deposits and channel-head migration was examined in granitic mountains where a debris-flow disaster occurred in 2014. Topographic analysis using 1-m grid DEMs before and after the disaster indicates that post-event channel heads were located upslope from pre-event channel heads due to landslide or erosion by debris flow. Post-event channel heads with shallow landslides had strong inverse correlations between local slope and drainage area. Charcoal samples were collected in colluvial deposits of two post-event channel heads (A and B) where the channel heads migrated more than 50 m upslope with shallow landslides. The radiocarbon dates of the samples were 1162–1194 y BP for channel head A and 786 y BP for channel head B. Another sample was collected in colluvial deposits of a post-event channel head (C) with shallow landslide but no migration. The radiocarbon date of the sample at the channel head C was 670 y BP. These radiocarbon data explain contrasting intervals of landslide events in hollows. The channel head A with older radiocarbon dates has the longer interval of landslide events and therefore the valley head has been buried in longer distance (more than 50 m) along the channel since the last landslide event to 2014.

Keywords: High-resolution DEM, Micro-topography, Radiocarbon dating, Valley head

©2019. Japan Geoscience Union. All Right Reserved.

Rock restrictions on topographical features of rivers: model experiment

*Yuta Takase[1], Noritaka Endo[1]

1. Kanazawa University

Landforms of mountainous areas is developed by both downcutting and lateral erosion of rivers. For example, ingrown meanders develop when the lateral erosion is predominant, while entrenched meanders form when the downcutting is dominant. It is a generally accepted understanding that the relative superiority or inferiority between the downcutting and lateral erosion is determined by the uplift rate of the land, rock strength difference, riverbed gradient, deflection of flow in a channel, but the systematic discussion remains insufficient. In this study, we conducted flume experiments to investigate the relationship between bedrock strength and sinuosity, and the relationship between time series pattern of uplift and meandering development. We prepared a single channel that cut a uniform substrate in a two-dimensional flume. The substrates were made of the mixture of fine sand and clay, and we examined two types of substrate, hard and soft ones, which can be formed by changing the ratio of sand and clay (the mixure including more clay is harder). Uplift of the experimental land was realized by lowering a weir set at the downstream end of the channel, i.e. the base-level lowering.

Knickpoints were observed more frequently in the case of hard substrate, which is consistent with previous study (Grimaud, 2016). Sinuosity of the channel tended to be higher for the hard substrate than the soft substrate, which is seemingly opposite the conventional understanding, but can be attributed to sustainability of the channel shape due to erosion resistance of the hard substrate. In all the experiments, the sinuosity tended to be higher after the uplift ceased rather than during the period of uplift.

Keywords: labo, sinuosity, bedrock strength, knickpoint, uplift

©2019. Japan Geoscience Union. All Right Reserved.

Stream power incision model and the stage of topographic equilibrium, using physical experiments

*Imamura Akihiro[1], Noritaka Endo[1]

1. Kanazawa University

Bedrock rivers develop their landforms very slowly, compared with alluvial river, thus bedrock rivers and their surrounding topographies are expected to record long-term environmental changes such as tectonics and climate. The stream power incision model (SPIM) is an empirical model that expresses the erosion rate due to rivers by the product of two power functions of the contributing area and river bed slope. Using this equation with an uplift term, the differential equation of the temporal change in the altitude of riverbed is constituted. When applying the model to a natural drainage basin, the equilibrium state between erosion and uplift is often assumed, partially because the uplift rate is usually unknown. Under the assumption of equilibrium state, SPIM is reduced to the relationship in which the riverbed slope is a power function of the contributing area, known as Flint’s law, which is the basis of “slope-area analysis” to determine the concavity (equivalent to the ratio of two power exponents in SPIM). Usually the two power exponents in SPIM are presumed to be constant if lithology, climate, and other factors are the same. This postulation, however, is difficult to verify for natural landforms, because of heterogeneity of various kind of property within a single drainage basin and difficulty in evaluation of the incision rate.

This study investigates the relation between the incision rate and topographic properties in river basins, through the observation of small-sized physical experiments under well-controlled conditions. A flume used was 90×180 cm, and the substrate to be dissected composed of the uniform mixture of sand and clay was installed. Rainfall was simulated by supplying mist from 10 nozzles. Uplift was realized by lowering a weir that was installed at the downstream end of the flume and determined the base level. The landform was measured by photogrammetry using several hundred photos taken during intermission from rainfall for photographing.

We compared the results of (1) this and (2) the previous studies (Imamura and Endo, 2018) realizing different kinds of uplift: (1) sudden base level lowering from a stable state of basin, to observe the response processes of the landforms until the basin became stable again (about 5 hours); (2) Sudden change in the uplift rate, to observe the change from a stable state under constant uplift of 4.5 mm/h to a new stable state under faster uplift rate of 6.0 mm/h (about 6 hours).

The results of Experiment (1) showed that the incision rate decreased with time (presumably asymptotic to zero), while Experiment (2) always displayed a certain finite value of the incision rate. The power exponents in SPIM, m (for the contributing area) and n (for the slope) did not seem to be constant in both experiments. The ratio m/n also changed, but seemed to converge to a certain value in each experiment.

We evaluated the correlation of the incision rate with the fitted function for each measurement time. In Experiment (1), although the denudation rate decreased with time, the first half of the run time showed good correlations but the latter half showed the worse. By contrast, Experiment (2) exhibited increasing correlations in the latter half of the run. These results suggests that SPIM holds for dynamic equilibrium (tectonic steady state (Montgomery, 2001)) or the early stage of static quasi-equilibrium (erosional stead state (Montgomery, 2001)), but fails for mature or later stages in which a landform proceeds to a

©2019. Japan Geoscience Union. All Right Reserved.

peneplane.

Imamura and Endo, 2018. Incision rate, riverbed slope and contributing area of an experimental drainage basin. JPGU 2018 Abstract.

Montgomery, 2001, Slope distributions, threshold hillslopes, and steady-state topography. American Journal of Science, 301, 432–454.

Keywords: stream power model, laboratory experiment, bedrock river

©2019. Japan Geoscience Union. All Right Reserved.

Downstream variation in gravel size of the Tenjin River system

*Kazuaki Hori[1], Kazuya Yonehara[1]

1. Department of Geography, Graduate School of Environmental Studies, Nagoya University

Many researchers have studied downstream variation in river-bed material size and its controlling factors, because they are important to understand the evolution of fluvial landforms and drainage basin. Many of these studies have focused only on rivers flowing through mountains or alluvial plains. Thus, it is desirable to examine a much broader range, i.e. from head to mouth of a river. We investigated the downstream variation of gravel size and channel gradient in the Tenjin River system (Tenjin, Ogamo, and Mitoku rivers) located in the central part of Tottori prefecture, Japan. The Tenjin River is approximately 34 km in length and major tributaries, the Ogamo and Mitoku rivers, join the Tenjin River at approximately 7 km and 12 km upstream from the mouth, respectively. Mean gravel size tends to decrease toward the downstream between 5 and 23 km upstream from the Tenjin River mouth where exposed gravel bars are easily found. Channel gradient is usually less than 0.03 and its variation is relatively small in this range. On the other hand, exposed gravel bars are uncommon between 23 and 34 km upstream from the mouth. The channel gradient become larger (> 0.06) and shows large variation. Large boulders (> 500 mm) are distributed in the channel. The number of boulders, especially > 1000 mm, seems to be inversely proportional to the distance from the valley wall. Buffers along the rivers regulate the supply of boulders from the valley wall in the upper reaches and reduce the connectivity of sediment supply from the tributaries in the middle and lower reaches. Barriers typified by weirs reduce the connectivity in the longitudinal direction throughout the basin.

Keywords: sediment connectivity, grain size, channel gradient

©2019. Japan Geoscience Union. All Right Reserved.

Talus slope development in the time of deglaciation: a case study of the Rev Valley, SW Spitsbergen

*Krzysztof Senderak[1], Marta Kondracka[1], Bogdan Gądek[1]

1. Faculty of Earth Sciences, University of Silesia

Every high-mountain area is characterized by the occurrence of talus slopes. A process of development this kind of forms depends on among other things climatic conditions. Currently in Spitsbergen, we observe the deglaciation process caused climate changes. This causes that the evolution’ s tempo of all environments linked with glaciers is very high. It also concerns the talus slopes, which, in the last time, are more often used as key element to paleo-environmental reconstructions for last thousands. In this paper, we present the geophysical surveys of talus slopes conducted in the Rev Valley (SW Spitsbergen). The valley was shaped by glacier, which left behind among other things glacial lake and buried glacial ice in mixed slope-moraine material. Nowadays, the talus slopes in this valley develop under the typical conditions of periglacial environment. In the studies of 15 talus slopes we used the ground-penetrating radar (GPR) and electrical resistivity tomography method (ERT). The studies allowed to recognize the internal structure of talus slopes and to determine a character of their elements, such as thickness of slopes, permafrost table and a depth of active layer, present of buried glacial ice, sediementological structures caused by various deposition of material on the slope surface, and finally a shape of bedrock. A comparison obtained results indicates on relevant regularity in the development of internal structure of talus slopes. These are for example visible differences in the terms of present of permafrost, which is located from a depth 2-3 m in the oldest slopes to a depth 4-5 m in the youngest. On the other hands, the studies discovers the deviations from the typical evolution models. The buried glacial ice has not been survived in a younger forms, whereas it is present in these older slopes. Based on the results we created the proposition of model of talus slope evolution developing in a periglacial period. In this time the development of slopes characterize a very high variability, not much lower than in previous paraglacial period. This work was financed from the funds of the National Science Centre in Poland received by Krzysztof Senderak in the Preludium 12 project: Determination of the evolution of slopes of southern Spitsbergen on the background of climate changes (2016/23/N/ST10/00162).

Keywords: talus slope evolution, permafrost, deglaciation, electrical resistivity tomography (ERT), ground-penetrating radar (GPR)

©2019. Japan Geoscience Union. All Right Reserved.

Distribution of Large Benthic Foraminifers in one of Majuro's Conservation Areas –Drenmeo Island

*Benedict Yamamura[1], Kazuhiko Fujita[2], Melba White[3], Kyotak Ishiguro[3], Hironobu Kan[1]

1. Kyushu University, Integrated Sciences for Global Society - Research Center for Coastal Seafloor , 2. Department of Physics and Earth Sciences, University of the Ryukyus, 3. Marshall Islands Marine Resources Authority

Climate change is having a huge impact on the island formation. In this study, we examined the composition and distribution of large benthic foraminifers (LBF) from 12 chosen sample sites (see map) within and outside of Drenmeo islet, one of the designated conservation areas in Majuro atoll. Samples were collected from the area to further investigate the sand built-up between the conservation area and the adjacent islet. The preliminary findings showed that the area is predominantly composed of two island-building LBF, namely *Calcarina sp.* and *Amphistegina sp.* The final results from this study will help stakeholders to amend the management plan to include the adjacent islet under the current management plan.

Keywords: Drenmeo island, conservation area, large benthic foraminifers, management plan

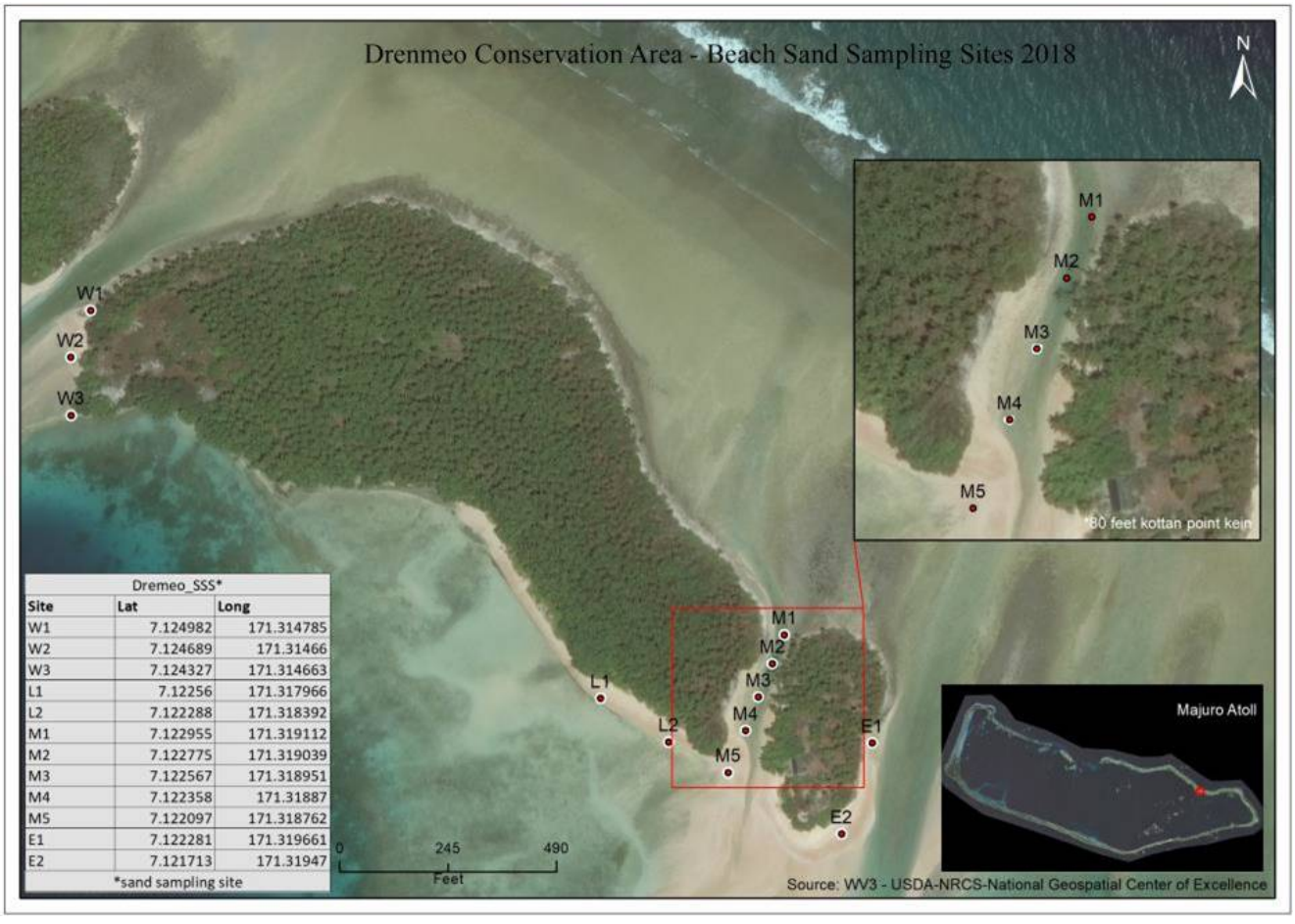

©2019. Japan Geoscience Union. All Right Reserved.

Luminescence chronology of fluvial and marine records from subsurface sediment cores: An insight into the geomorphic evolution of Kaveri delta, India

*kartika goswami[1], Anbarasu Kumaresan[2], Sivakumar Krishnan[2], Senthil K. Sadasivam[2], Manoj Kumar Jaiswal[1]

1. Department of Earth Sciences, Indian Institute of Science Education and Reserach Kolkata, 2. National College Tiruchirappalli, India

Long-term evolution of river deltas is a result of forcings (tectonics, climate, sea level, avulsion, compaction etc). We present the results of luminescence dating of sediments from four sediment cores (VKI, TNR, SY and KKI) of 25 m depth each, retrieved from the Kaveri delta in south India. The coring sites are ~2.5 km, ~11 km, ~17 km and ~20 km away from the present coastline respectively. The cores were analysed for OSL dating, 14C dating, lithology and microfossils and represent various stages of fluvial and marine activity in the region over the last ~150 ka. The chronology of the core closet to the coast (VKI) reflects eight major phases of increased sea level during the late quaternary period (142-140 ka, 104-100 ka, ~121 ka, 87-81 ka, 60-57 ka, 9-6 ka, ~5 ka and ~3 ka) partly coinciding with the global climate cycles MIS 6, MIS 5, MIS 3, MIS 1 respectively. During ~121 ka and 9-6 ka, marine transgression reached the core location to leave marine signatures in the forms of foraminifera. VKI core replicates the quaternary sea level curve, showing strong control of the sea in coastal deposition.

The oldest age of VKI is ~140 ka. The three cores situated further inland give oldest/bottom most ages of~120 ka. This indicates the coastal land has uplifted in the recent years with deeper sediments being encountered at relative shallower depth. The uplift is expected to occur around post 50 ka, creating a basin fill situation for riverine sediments to accumulate and restricting the delta to prograde. This is observed from the sedimentation pattern and robust chronology of the other three inland cores. Analysis of DEM also supported the occurrence of uplift. Thus, the present work examines the geomorphic evolution of Kaveri delta, an archive of fluvial, shoreline and tectonic activities.

Keywords: OSL Dating, Kaveri Delta , GIS, Foraminifera

©2019. Japan Geoscience Union. All Right Reserved.

[J] Oral | H (Human Geosciences)：H-GM Geomorphology

Wed. May 29, 2019 9:00 AM - 10:30 AM JST | Wed. May 29, 2019 12:00 AM - 1:30 AM UTC | 101 1F

[H-GM04] Geomorphology

convener:Tsuyoshi Hattanji(Faculty of Life and Environmental Sciences, University of Tsukuba), Masayuki Seto(Fukushima Future Center for Regional Revitalization, Fukushima University), Chairperson:Tsuyoshi Hattanji

The main subject of this session is the whole range of themes relating to geomorphology, especially geomorphic processes, landform development and its relation to environmental changes, geomorphological hazards and their mitigation and reports of recent events of disaster occurred in Japan, various kind of hazard maps, relationships among geomorphic processes, other natural phenomena and human activities, and various techniques of geomorphological measurements and automatic landform classification. Japanese can be used in this session.

9:00 AM - 9:15 AM JST | 12:00 AM - 12:15 AM UTC

[HGM04-01] Salt weathering in humidity-change environments: a laboratory experiment

*Masato Sato[1], Tsuyoshi Hattanji[2] (1.Graduate School of Life and environmental Sciences, University of Tsukuba, 2.Faculty of Life and Environmental Sciences, University of Tsukuba)

9:15 AM - 9:30 AM JST | 12:15 AM - 12:30 AM UTC

[HGM04-02] Verification a new control device of blown sand transport rate by wind tunnel experiments

*Yoshinori Kodama[1], Riko Saikusa[2] (1.Faculty of Agriculture, 2.Faculty of Regional Sciences)

9:30 AM - 9:45 AM JST | 12:30 AM - 12:45 AM UTC

[HGM04-03] Bedrock landslides, river blockage, and barrier-lake outburst as general geomorphic processes in high-relief mountainous landscape: an example from the Marshyangdi River, central Nepal

*Yuki Matsushi[1], Hiroshi YAGI[2], Hiroyuki Matsuzaki[3] (1.Disaster Prevention Research Institute, Kyoto University, 2.Department of Education, Art and Science, Yamagata University, 3.icro Analysis Laboratory, Tandem Accelerator, The University of Tokyo)

9:45 AM - 10:00 AM JST | 12:45 AM - 1:00 AM UTC

[HGM04-04] Influence of lithology on production and transport of soils on hillslopes underlain by granite and hornfels

*Takuma Watakabe[1], Yuki Matsushi[2], Hiroyuki Matsuzaki[3] (1.Graduate School of Science, Kyoto University, 2.Disaster Prevention Research Institute, Kyoto University, 3.The University Museum, The University of Tokyo)

10:00 AM - 10:15 AM JST | 1:00 AM - 1:15 AM UTC

[HGM04-05] Characterization of the vertical unsaturated flow for an integrated prediction of the storm runoff response and landslide initiation on a hillslope

*Makoto Tani[1], Yuki Matsushi[2], Takahiro Sayama[2], Nagahiro Kojima[3] (1.University of Human Environments, 2.Disaster Prevention Research Institute, Kyoto University, 3.Lake Biwa Environmental Research Institute)

10:15 AM - 10:30 AM JST | 1:15 AM - 1:30 AM UTC

Discussion

Salt weathering in humidity-change environments: a laboratory experiment

*Masato Sato[1], Tsuyoshi Hattanji[2]

1. Graduate School of Life and environmental Sciences, University of Tsukuba, 2. Faculty of Life and Environmental Sciences, University of Tsukuba

A laboratory weathering experiment simulating under changing humidity conditions were carried out using five types of rocks (porous tuff, porous sandstone, dense sandstone, and two porous mudstones) with three types of salts (sodium chloride, sodium sulfate, or magnesium sulfate). The rock specimens were subjected to humidity oscillations in a climatic cabinet where air humidity ranged from 20%RH to 98%RH during 6-hour periods 20˚C. Prior to the weathering experiment, the specimens were oven-dried, and the water supply was restricted only from air humidity during the experiment.
Humidity oscillation induced cycles of repeated of salt deliquescence-recrystallization and hydration-dehydration. Salts on rock surface deliquesced and hydrated in a high-humidity period, while they crystallized in a low-humidity period. The degrees of damage were correlated with moisture amounts absorbed to the rock specimens in the high-humidity period.
Sodium chloride which deliquesces at humidity of more than 80%RH caused the most intensive weathering. Porous sandstone with sodium chloride was completely broken down after 100 cycles of humidity changes. Dense sandstone and porous tuff showed flaking or swelling on their surfaces. Equotip surface hardness of dense sandstone with sodium chloride decreased with increasing number of humidity cycles. Sodium chloride can easily induce salt weathering by salt deliquesce and recrystallize in environment where air humidity fluctuates in a short time interval, such as the surfaces of rock cliff in coastal spray zones.
Magnesium sulfate induced a weight loss in porous sandstone, through flaking from the surface of porous tuff, and through swelling and cracking on the surface of dense sandstone. Sodium sulfate was not effective in the humidity-change experiment, although salt efflorescence was extensively produced. Slow hydration rate of sodium sulfate can cause the ineffectiveness of sodium sulfate. In addition, volumetric expansion with hydration of sodium sulfate may result in pore clogging, and hinder infiltration of moisture into the rock specimens. The restricted activity of sodium sulfate suggests that sodium sulfate rarely induces salt weathering by daily humidity fluctuation. Magnesium sulfate might influence rock decay more than sodium sulfate when air humidity fluctuates in a short period.

Keywords: salt weathering, humidity, sodium chloride, sodium sulfate, magnesium sulfate, surface hardness

©2019. Japan Geoscience Union. All Right Reserved.

Verification a new control device of blown sand transport rate by wind tunnel experiments

*Yoshinori Kodama[1], Riko Saikusa[2]

1. Faculty of Agriculture, 2. Faculty of Regional Sciences

A new water-pool device for reducing blown sand transport rate was proposed from a view point of saltating particle motion. Wind duct experiments were conducted to check sediment trap efficiencies of a proposed device. In our experimental conditions, maximum wind velocity: 12.9 m/s, it worked well: reducing blown sand transport rate less than 6 % within 4.55 m distance. We estimated that the least length of the device is 11.3 m at 18.0 m/s wind condition, which is almost maximum in Tottori Sand Dunes.

Keywords: a water-pool method for reducing blown sand transport rate, wind tunnel experiment, saltation particle, Tottori Sand Dunes

©2019. Japan Geoscience Union. All Right Reserved.

Bedrock landslides, river blockage, and barrier-lake outburst as general geomorphic processes in high-relief mountainous landscape: an example from the Marshyangdi River, central Nepal

*Yuki Matsushi[1], Hiroshi YAGI[2], Hiroyuki Matsuzaki[3]

1. Disaster Prevention Research Institute, Kyoto University, 2. Department of Education, Art and Science, Yamagata University, 3. icro Analysis Laboratory, Tandem Accelerator, The University of Tokyo

This study demonstrates generality of large-scale bedrock landslides, river blockage by the slid mass, and debris flow by the barrier-lake outburst in landscape evolution of high-relief mountainous watersheds. We focused on the Marshyangdi River, south-eastern range of the Annapurna massif, central Nepal, to conduct ground-based surveys and geo-spatial analyses. Geology along the river consists mainly of Paleozoic and Mesozoic sedimentary rocks, gneiss, phyllite, schist, and shale from the upper to lower reach. Deeply-incised gorge develops in the area of massive gneiss, while fill terraces occupy the wide area of valley floor downstream from the Main Central Thrust. The lower- to mid-level terraces exhibit characteristic morphology with hummocky mounds with gneiss boulders settled on the surface, indicating their origin that may be relevant to large scale debris flow events by deep-seated bedrock landslide and subsequent barrier lake breach. Exposure ages of the boulders ranges from 2 to 4 ka, indicating repeated occurrence of such events under the Holocene climate. On the upstream area, several sets of lacustrine deposits remain along the main channel. The sequence and distribution indicate that the paleo landslide-dammed lakes expanded few-kilometers in length and few hundreds meters in depth before breaching. The debris flow ran through the river for tens of kilometers, spreading out over the downstream valley. Results of evidence mapping and topographic analysis indicate that these kind of large-scale sequential phenomena play a general function in landscape evolution of a high-relief steep mountainous watershed in tectonically-active settings. Disaster mitigation for such possible event requires enhancement of preparedness through prediction and risk assessment for conceivable hillslope and/or fluvial processes.

Keywords: Mountain geography, Disaster mitigation, Landslide-dammed lake, Debris flow, Climate change

©2019. Japan Geoscience Union. All Right Reserved.

Influence of lithology on production and transport of soils on hillslopes underlain by granite and hornfels

*Takuma Watakabe[1], Yuki Matsushi[2], Hiroyuki Matsuzaki[3]

1. Graduate School of Science, Kyoto University, 2. Disaster Prevention Research Institute, Kyoto University, 3. The University Museum, The University of Tokyo

We measured rates of soil production and transport using cosmogenic ^{10}Be and measured characteristics of soil properties in hillslopes underlain by granite and hornfels in Shirakawa watershed, eastern Kyoto City. Rates of soil production and transport of the granite hillslope were faster than those of the hornfels hillslope. Soil on the granite hillslope was incohesive sand with large saturated hydraulic conductivity and low water retention ability. In contrast, soil on the hornfels hillslope was cohesive sand with low saturated hydraulic conductivity and high water retention ability. Characteristics of the granite soil promote wet–dry weathering effect in the shallow subsurface materials of the granite hillslope. Thus, physical, mechanical, and hydrological properties of soils on each bedrock control the rates of soil production and transport.

Keywords: Soil production rate, Soil transport coefficient, Cosmogenic nuclides, Geotechnical properties

©2019. Japan Geoscience Union. All Right Reserved.

Characterization of the vertical unsaturated flow for an integrated prediction of the storm runoff response and landslide initiation on a hillslope

*Makoto Tani[1], Yuki Matsushi[2], Takahiro Sayama[2], Nagahiro Kojima[3]

1. University of Human Environments, 2. Disaster Prevention Research Institute, Kyoto University, 3. Lake Biwa Environmental Research Institute

Studies on hillslope hydrology have demonstrated storm runoff responses are generated mainly through subsurface flow instead of overland flow, and studies on erosion control have empirically revealed landslides usually occur at the time of intense rainfall after a large cumulative rainfall. based on these findings, we have to explain with consistency that the flow generation mechanism for large magnitude storms on hillslope can produce both hydrograph responses below a threshold condition of rainfall and a landslide initiation above the threshold. Recent observational studies have shown vertical unsaturated flow within a hillslope soil layer may dominantly control the responses of ephemeral groundwater table to storm rainfall through the pressure-head propagation and that the responses are rather transmitted to the stream runoff with little modification. The present study discusses the reason why the vertical unsaturated flow can produce the runoff responses during large magnitude storms and provides a perspective on an integrative prediction of the storm runoff response and landslide initiation

Keywords: Integrated prediction of storm runoff and landslide initiation , Hillslope hydrology, Vertical unsaturated flow, Soil-layer evolution

©2019. Japan Geoscience Union. All Right Reserved.

[J] Oral | H (Human Geosciences)：H-GM Geomorphology

Wed. May 29, 2019 10:45 AM - 12:15 PM JST | Wed. May 29, 2019 1:45 AM - 3:15 AM UTC | 101 1F

[H-GM04] Geomorphology

convener:Tsuyoshi Hattanji(Faculty of Life and Environmental Sciences, University of Tsukuba), Masayuki Seto(Fukushima Future Center for Regional Revitalization, Fukushima University), Chairperson:Masayuki Seto, Hiroshi Shimazu

The main subject of this session is the whole range of themes relating to geomorphology, especially geomorphic processes, landform development and its relation to environmental changes, geomorphological hazards and their mitigation and reports of recent events of disaster occurred in Japan, various kind of hazard maps, relationships among geomorphic processes, other natural phenomena and human activities, and various techniques of geomorphological measurements and automatic landform classification. Japanese can be used in this session.

10:45 AM - 11:00 AM JST | 1:45 AM - 2:00 AM UTC

[HGM04-06] The landform and flood characteristics of the Iron Gate on the ancient road from Samarkand to Bamian, south Uzbekistan

*Hiroshi Shimazu[1] (1.Department of Geography, Faculty of Geo-Environmental Science, Rissho University)

11:00 AM - 11:15 AM JST | 2:00 AM - 2:15 AM UTC

[HGM04-07] OSL dating of sediment core in Olgoi lake, Mongolia

*Yudai Igarashi[1], Noriko Hasebe[1], Nagayoshi Katsuta[2], Hitoshi Hasegawa[3], Davaadorj Davaasuren[4], Yukiya Tanaka[5], Uyangaa Udaanjargal[1], Keisuke Fukushi[1], Ichinnorov Niiden[6] (1.Kanazawa University, 2.Gihu University, 3.Kochi University, 4.National University of Mongolia, 5.Kyunghee University, 6.Mongolian Academy of Science)

11:15 AM - 11:30 AM JST | 2:15 AM - 2:30 AM UTC

[HGM04-08] Paleo Lake level change in southern part of Mongolia

*Noriko Hasebe[1], Makoto Sambo[2], Uyangaa Udaanjargal[2,3], Shuukaaz Ganbat[3], Keisuke Fukushi[1], Yukiya Tanaka[4], Davaadorj Davaasuren[3] (1.Institute of Nature and Environmental Technology, Kanazawa University, 2.Department of Earth Sciences, Kanazawa University, 3.National University of Mongolia, 4.Kyunghee University)

11:30 AM - 11:45 AM JST | 2:30 AM - 2:45 AM UTC

[HGM04-09] Numerical modeling of wave propagation on the coral reef based on high resolution 3D topography

*Kenta Minamidate[1], Kazuhisa Goto[2], Masashi Watanabe[3,4], Volker Roeber[5,6], Ken Toguchi[7], Masami Sannoh[8], Yosuke Nakashima[9], Hironobu Kan[10] (1.Graduate School of Science, Tohoku University, 2.International Research Institute of Disaster Science (IRIDeS), Tohoku University, 3.Graduate School of Engineering, Tohoku University, 4.Graduate School of Science and Engineering, Chuo University, 5.Hawaii University, 6.Université de Pau et des Pays de l'Adour, 7.Ryukyu University, 8.Mikuniya Corporation, 9.NIT, Ariake College, 10.Graduate School of Integrated Sciences for Global Society, Kyushu University)

11:45 AM - 12:00 PM JST | 2:45 AM - 3:00 AM UTC

[HGM04-10] Coastal Seafloor Geomorphology: launching of a new field and perspectives

*Hironobu Kan[1], Nobuyuki Hori[2], Tatsuro Nakai[3], Yusuke Yokoyama[4], Kazuhiko Fujita[5], Hitoshi Hasegawa[3], Yosuke Nakashima[6], Kensaku Urata[1], Atsushi Suzuki[7], Masayuki Nagao[7], Kazuhisa Goto[8] (1.Graduate School of Integrated Sciences for Global Society, Kyushu University, 2.Emeritus Professor, Department of Geography, Tokyo Metropolitan University, 3.Department of Geography and Environmental Studies, Kokushikan University, 4.AORI, University of Tokyo, 5.Department of Physics and Earth Sciences, Faculty of Science, University of the Ryukyus, 6.National Institute of Technology, Ariake College, 7.Research Institute of Geology and Geoinformation, AIST, 8.IRIDeS, Tohoku University)

12:00 PM - 12:15 PM JST | 3:00 AM - 3:15 AM UTC

Discussion

The landform and flood characteristics of the Iron Gate on the ancient road from Samarkand to Bamian, south Uzbekistan

*Hiroshi Shimazu[1]

1. Department of Geography, Faculty of Geo-Environmental Science, Rissho University

“The Iron Gate” is located on the ancient road from Samarkand, which has been one of the largest cities in the central Asia from ancient times, via Termes, where is the crossing point of the Amudarya, to Bamian, which has been one of the important cities as Buddhism. The Iron Gate is a narrow gorge located several kilometers east of the main mountain ridge of the Hissar Mountains. Its length is 2 kilometers and its width of the narrowest part is 10 meters. Both valley side slopes are very steep and their relative height is about 200 meters. Genjo, who is one of the most famous Buddhism priest of 7th century walked through the gorge on the way to India.

Debris flow deposits, whose maximum diameter in b-axis is over 50cm, and sorted and clear laminated flood sediments, which are more rounded and smaller sandy gravels are distributed in the canyon. The relative height between these surface top and valley bottom is several meters. Present valley floor is buried valley bottom, whose surface is flat or covered with lobate large gravel deposits. Although there is poor vegetation on the both valley side slopes and surface of the sediments, only sporadic shrubs are on the valley bottom and both side of the eroded cliff of the sediments Heavy flood event frequent occurred in this region and debris flow and sediment flow buried the Iron Gate canyon section. After the event the buried valley bottom was dissected by water flow. Sediment transport events repeated more than once in a year and heavy flood event repeated once in several years. Samarkand and Termes have precipitation between October and April. The temperature in cold season of the city is below zero and this region has some snow. Snow melt is accelerated by rain in March and April and flood events are caused in this region.

The reason why this important road was constructed in the area of such higher risk of flood is that this place was the important checkpoint of this road. The forts of this region, located the ridge of hill, were favorable to watch passers pass through the canyon road, where sometimes closed by flood.

Keywords: Iron Gate, gorge, flooding, fluvial sediments, Surkhandarya, Uzbekistan

©2019. Japan Geoscience Union. All Right Reserved.

OSL dating of sediment core in Olgoi lake, Mongolia

*Yudai Igarashi[1], Noriko Hasebe[1], Nagayoshi Katsuta[2], Hitoshi Hasegawa[3], Davaadorj Davaasuren[4], Yukiya Tanaka[5], Uyangaa Udaanjargal[1], Keisuke Fukushi[1], Ichinnorov Niiden[6]

1. Kanazawa University, 2. Gihu University, 3. Kochi University, 4. National University of Mongolia, 5. Kyunghee University, 6. Mongolian Academy of Science

In the southern part of Mongolia, there are many lakes in the basin between mountain ranges, which is called “Valley of the Lakes”. These lakes experienced lake level fluctuations during the Quaternary period. This lake level variation is considered important information to understand climate change. The influx from the Khangai Mountains is a major source of water for the Valley of the Gobi lakes, a large southern basin. Olgoi lake is the research target of this study and locates closer to the summit of the Khangai mountain range than other lakes of Valley of the Gobi lakes, so it is highly likely that it reflects influx sensitively. A sediment core was collected from Olgoi lake to investigate the environmental change of the region. In this study, OSL dating of quartz was carried out to date core samples from Olgoi lake. This Core sample showed the age value of 0.7 to 10 ka covering the Holocene. In addition, it is suggested that the sedimentation of gravels, which is the most characteristic feature of the lower part of the Olgoi lake core sample, was related to the Holocene rapid temperature change events. There is a large gap in age values in this core sample at 7.5-9.0m. There is a high possibility that it reflects past sedimentary environment and even the climate, but I could not reach the final argument by the ages obtained in this research. To understand the complex transition of sedimentary environment of Olgoi lake, high resolution analyses of sediment characteristics and precise age control would be necessary.

Keywords: Mongolia, Lake sediment, OSL dating

©2019. Japan Geoscience Union. All Right Reserved.

Paleo Lake level change in southern part of Mongolia

*Noriko Hasebe[1], Makoto Sambo[2], Uyangaa Udaanjargal[2,3], Shuukaaz Ganbat[3], Keisuke Fukushi[1], Yukiya Tanaka[4], Davaadorj Davaasuren[3]

1. Institute of Nature and Environmental Technology, Kanazawa University, 2. Department of Earth Sciences, Kanazawa University, 3. National University of Mongolia, 4. Kyunghee University

Lake Boontsagaan, Orog and Olgoy are located in the Valley of the Lakes, Gobi-Altai transition zone, which stretches from central to western Mongolia. This area suffers desertification probably due to the ongoing global worming and dried up lake sediments are worried as a source of contaminated sand storm. The flat surface in Valley of Lakes is covered with Quaternary lake sediments. Paleoshorelines are identified near the lakes. This study observed the sedimentary structures of the outcrops on the paleoshoreline and samples were collected to estimate the time when lake level was high by Quartz OSL dating method. The outcrop near the Ology, Boontsagaan, and Orog lakes are higher than the present lake level by 8 m, 15 m and 3 m, respectively.
The history of lake level change is proposed based on the age, altitude of the localities, and sedimentary structure of the outcrops. Data from Boontsagaan lake, for which coarse grains were analysed, scatter, therefore the youngest age component is extracted by plotting the data on the radial plot (Galbraith, 1988, Vermeesch, 2009). Ages from Boontsagaan Lake are around ~4-9 ka, while ages from Olgoy and Orog lakes are around ~1-2 ka. Because Boontsagaan Lake is larger and deeper than other lakes, its lake level change would be less active. Besides, relative height of the locality to the current lake level is higher then other two lakes. Therefore, the lake level was very high before ~5 ka, and relatively high at ~1-2 ka. The obtained results are consistent with previously reported data from the nearby sites (Lehmkuhl et al., 2018).

Keywords: Lake level change, OSL dating, Mongolia, Holocene

©2019. Japan Geoscience Union. All Right Reserved.

Numerical modeling of wave propagation on the coral reef based on high resolution 3D topography

*Kenta Minamidate[1], Kazuhisa Goto[2], Masashi Watanabe[3,4], Volker Roeber[5,6], Ken Toguchi[7], Masami Sannoh[8], Yosuke Nakashima[9], Hironobu Kan[10]

1. Graduate School of Science, Tohoku University, 2. International Research Institute of Disaster Science (IRIDeS), Tohoku University, 3. Graduate School of Engineering, Tohoku University, 4. Graduate School of Science and Engineering, Chuo University, 5. Hawaii University, 6. Université de Pau et des Pays de l'Adour, 7. Ryukyu University, 8. Mikuniya Corporation, 9. NIT, Ariake College, 10. Graduate School of Integrated Sciences for Global Society, Kyushu University

Coral reefs commonly act as natural barrier against swell wave impact. Conventionally, reefs efficiently attenuate storm waves. However, recent studies have indicated that during energetic typhoon swells, generation of infragravity waves can lead to hazardous conditions where the reef does not act like a protecting barrier anymore. In order to know the wave behavior near and over the reef, high-resolution 3D topographic data is required for the numerical calculation. However, most of the previous studies result from one- or two-dimensional numerical calculations based on low-resolution topographic data. This is mainly due to the challenging environment for conducting bathymetry/topography surveys in the vicinity of the reef. Hence, it was difficult to discuss the wave processes under the influence of the microtopography. In this study, we developed high resolution and complete set of the 3D topographic data (girid size: 1 m) from land to about 95 m water depth at the east coast of Kudaka Island, Okinawa Prefecture (an area of approximately 3 ×5 km) by UAV topographic and multibeam bathymetric surveys. Based on the terrain data with 5 m mesh size, we conducted two-dimensional wave-by-wave calculations with the Boussinesq-type wave model, BOSZ. The results show that the deformation and propagation mechanisms of the waves near the reef are highly controlled by microtopography features such as the differences in slope angles and the presence of spurs and grooves.

Keywords: Wave, Storm wave, Coral reef, Multi-beam survey, UAV, Numerical simulation

©2019. Japan Geoscience Union. All Right Reserved.

Coastal Seafloor Geomorphology: launching of a new field and perspectives

*Hironobu Kan[1], Nobuyuki Hori[2], Tatsuro Nakai[3], Yusuke Yokoyama[4], Kazuhiko Fujita[5], Hitoshi Hasegawa[3], Yosuke Nakashima[6], Kensaku Urata[1], Atsushi Suzuki[7], Masayuki Nagao[7], Kazuhisa Goto[8]

1. Graduate School of Integrated Sciences for Global Society, Kyushu University, 2. Emeritus Professor, Department of Geography, Tokyo Metropolitan University, 3. Department of Geography and Environmental Studies, Kokushikan University, 4. AORI, University of Tokyo, 5. Department of Physics and Earth Sciences, Faculty of Science, University of the Ryukyus, 6. National Institute of Technology, Ariake College, 7. Research Institute of Geology and Geoinformation, AIST, 8. IRIDeS, Tohoku University

The coastal seafloor at depths shallower than ~130 m was subjected to alternating subaerial erosion and sedimentation during Quaternary sea-level change. However, the coastal seafloor is rarely discussed in conventional geomorphology. Recently, the development of exploration technology such as multibeam echo sounder survey enables us to observe the accurate and detailed coastal seafloor geomorphology. In this presentation, we discuss the novelty and possibilities of coastal seafloor geomorphology based on case studies from around the world and research materials of our group.

Keywords: multibeam bathymetry, echo sounder, sea level change, shelf

©2019. Japan Geoscience Union. All Right Reserved.

[J] Poster | H (Human Geosciences)：H-GM Geomorphology

Wed. May 29, 2019 3:30 PM - 5:00 PM JST | Wed. May 29, 2019 6:30 AM - 8:00 AM UTC | Poster Hall International Exhibition Hall8, Makuhari Messe_12

[H-GM04] Geomorphology

convener:Tsuyoshi Hattanji(Faculty of Life and Environmental Sciences, University of Tsukuba), Masayuki Seto(Fukushima Future Center for Regional Revitalization, Fukushima University)

The main subject of this session is the whole range of themes relating to geomorphology, especially geomorphic processes, landform development and its relation to environmental changes, geomorphological hazards and their mitigation and reports of recent events of disaster occurred in Japan, various kind of hazard maps, relationships among geomorphic processes, other natural phenomena and human activities, and various techniques of geomorphological measurements and automatic landform classification. Japanese can be used in this session.

[HGM04-P01] Automatic landform classification using Self-Organizing Map (SOM) by geomorphological features calculated from DEM

*Ito Yoshiki[1], Yoshiya Oda[1], Toshifumi Matsuoka[2] (1.Tokyo Metropolitan University, 2.Fukada Geological Institute)

[HGM04-P02] **Functionalization of the Average Erosion of Drainage Basin Using DEM**

*Rei Yamanaka[1], Tatsuto Aoki[1] (1.Kanazawa University)

[HGM04-P03] The Movement of Sediment and Development of Gullies Inside of Landslide area

*Yasuhiro Horikawa[1], Tatsuto Aoki[2] (1.Tsukuba University, 2.Kanazawa University)

[HGM04-P04] Detailed topographic survey of valley head in hill by terrestrial laser scanning

*KIYOSHI SAIJO[1], Takahisa Furuichi[2], Asaka Konno[3] (1.Miyagi University of Education, 2.Graduate School of Agriculture, Hokkaido University, 3.Tokoha University)

[HGM04-P05] Preliminary application of electrical resistivity tomography to estimate subsurface structure of unchanneled valley: A case at granitic hillslope near Mt. Tsukuba, Japan

*Naoyuki Yoshihara[1], Tsuyoshi Hattanji[2] (1.Graduate School of Life and Environmental Sciences, University of Tsukuba, 2.Faculty of Life and Environmental Sciences, University of Tsukuba)

[HGM04-P06] Estimating distribution of soil thickness in doline from electrical resistivity tomography:A case study in the Akiyoshi-dai Karst Plateau, Japan

*Naoya Hiramoto[1], Tsuyoshi Hattanji[2] (1.Graduate School of Life and Environmental Sciences, University of Tsukuba, 2.Faculty of Life and Environmental Sciences, University of Tsukuba)

[HGM04-P07] Occurrence and origin of potholes developed on the eastern slope of Miharayama in Hachijojima, Izu Islands, Tokyo Prefecture, Japan

*Takashi Ishibashi[1], Tomoaki Mastumi[2], Ren Higuchi[2], Yuki Yamatmoto[2], Keigo Shimada[2], Hirotomo Morimoto[2], Tsutomu Shimada[3], Kenji Asakura[4] (1.Masutomi Museum of Geocience, 2.Ritsumeikan University Explorers Club, 3.Pothole Survey Team, 4.Kyoto University Graduate School of Science)

[HGM04-P08] Temporal and spatial changes of sediment supply processes from tributaries since the last glacial period in the upper valleys of the Tama and Ara rivers, central Japan

*Takayuki Takahashi[1], Toshihiko Sugai[1] (1.Graduate School of Frontier Sciences, The University of Tokyo)

[HGM04-P09] Landform evolution and active tectonics in the eastern part of Oiso Hills inferred by characteristics of gravels composing Kissawa Formation, Japan

*Masahiro Muraki[1], Toshihiko Sugai[1] (1.Graduate School of Frontier Science, The University of Tokyo)

[HGM04-P10] Sediment movement and collapse of bank protections by a series of large flood events at the Sendai River, Tottori, southwest Japan

*Yoshinori Kodama[1], Kento Takemoto[2] (1.Faculty of Agriculture, 2.Hyogo Prefecture)

[HGM04-P11] Channel incision history with knickpoint retreat in the Kushira River after the deposition of Ata pyroclastic flow, Osumi Peninsula, Kyushu, Japan

*Shintaro Takanami[1] (1.Meiji University)

[HGM04-P12] **Implications of the distribution of marine terraces and submerged terraces in Japanese Island**

*Tetsuya Komatsu[1], Hiura Yuki[1], Takayuki Takahashi[2], Taro Funatsu[2], Masahiro Muraki[2], Taiga Kimori[2], Toshihiko Sugai[2] (1.Japan Atomic Energy Agency, 2.Graduate School of Frontier Sciences, The University of Tokyo)

[HGM04-P13] Marine erosional landforms along the southern coast of Yonaguni Island, Ryukyus

*Hayate Kimura[1], Kensaku Urata[2], HASEGAWA Hitoshi[3], Toshihiko Ichihara[4], Atsushi Suzuki[5], Nobuyuki Hori[6], Hironobu Kan[2] (1.Graduate school of integrated sciences for global society, 2.Graduate School of Integrated Sciences for Global Society, Kyushu University, 3.Kokushikan University, 4.Sedimentary Environments Research, 5.Geological Survey of Japan National Institute of Advanced Industrial Science and Technology (AIST), 6.Department of Geography, Nara University)

[HGM04-P14] Seafloor topography of Amami Sumiyo Bay -Visualization of Seafloor derived from multibeam bathymetric survey-

*Miho Tanaka[1], Ken Toguchi[2], Nobuyuki Hori[3], Hayate Kimura[4], Yukihiko Imai[5], Yosuke Nakashima[6], Yayoi Najima[7], Hironobu Kan[8] (1.Graduate School of Integrated Sciences for Global Society, 2.University of the Ryukyus, 3.Tokyo Metropolitan University, 4.School of Engineering, Kyushu University, 5.Faculty of science, Okayama University, 6.National Institute of Technology, Ariake College, 7.The Graduate University for Advanced Studies, 8.Kyushu University)

Automatic landform classification using Self-Organizing Map (SOM) by geomorphological features calculated from DEM

*Ito Yoshiki[1], Yoshiya Oda[1], Toshifumi Matsuoka[2]

1. Tokyo Metropolitan University, 2. Fukada Geological Institute

The landform classification map based on the various geomorphological features which calculated from DEM data is adopted in many scenes of the modern society. As is well known, Iwahashi and Pike (2007) had proposed a classification method of terrain by using slope gradient, local convexity, and surface texture. In this research, we tried to automate landform classification by using Self-Organizing Map (SOM) which is an unsupervised neural network. It is aimed at grasping the influence on the classification result depending on the combination of the geomorphological features used. The target area in this preliminary study is the same area as Iwahashi and Pike (2007); the southern part of Yatsugatake located at the prefecture boundary between Yamanashi prefecture and Nagano prefectures (about 22.5 km east-west, about 20.0 km north and south).

The SOM was carried out by the following procedure. Calculate the amount of slope gradient, surface texture, local convexity, direction of dip, the ridge valley degree, surface curvature, and the hill figure from DEM data. ② These geomorphological features were combined and adopted as input data to SOM. Totally seven patterns of geomorphological features were selected. ③ For these data, learning by SOM was conducted, and seven landform classification maps were obtained. Also, in order to visualize the features of classification by SOM, a histogram of each feature was also calculated. (4) The classification results were compared based on the landform classification maps and histograms, and the influence of the classification result by combination of the geomorphological features used was examined. We also compared SOM results with the classification results by Iwahashi and Pike (2007) method. In concludingly, it was found that in the automatic landform classification by SOM using multiple geomorphological features, the relatively uniformly distributed topographical feature quantities greatly affect classification compared to biased terrain feature. We also found that the topographic features with histograms with symmetric distribution and narrow histograms do not have a significant effect on topographic classification results by SOM. We would like to consider an application of supervised neural network and to obtain a landform

Keywords: digital elevation model(DEM), Self-Organizing Maps(SOM), landform classifications

©2019. Japan Geoscience Union. All Right Reserved.

Functionalization of the Average Erosion of Drainage Basin Using DEM

*Rei Yamanaka[1], Tatsuto Aoki[1]

1. Kanazawa University

1.First.

Geomorphic development model of tectonically active and intensive denuded regions in japan has been discussed.
Yoshikawa (1985) showed the need to discuss as a geomorphic development model considering the changing terrain in the wet variation zone in Japan.
Ohmori (1978), using a 50mDEM, to determine the dispersion of altitude. Moreover, he will evaluate the stages in the geomorphic development of the mountains.
In this study, 10 m DEM available nationwide was used.
The average amount of erosion per basin was obtained by ArcGIS and compared with the data of the dispersion of altitude of Ohmori (1978).

2.Target area

Soya Hill, Taihei Mountain, Abukuma Plateau, Shirakami Mountains, Mikawa Plateau, Hakusan Mountains, Kanto Mountains, Akaishan Mountains, Hida Mountain Range with different stages in geomorphic development is Target areas. Selected from the mountains that are analyzed by Ohmori (1978).

3.Analysis method

This is a procedure with ArcGIS, calculation of average erosion amount per watershed.
First, I made summit level map with grid sizes 3 to 301. The summit level map can be regarded as a virtual ground surface before erosion. For this reason, I set "summit level map - DEM" as the depth of erosion.

4.Functionalization of average erosion amount

We made a function of the relationship between grid size and erosion amount. At that time, graph fitting to the linear function, power function, exponential function, logarithmic function, approximate curve and its error were obtained. As a result, the most fitted function was logarithmic function "y = alog (1 + bx)", and the error was the smallest. a is considered to represent the depth of the valley and b is the width of the valley.

5.Evaluation of average erosion amount by mountain area

A scatter diagram based on the coefficients was prepared from the average erosion amount by mountainous area which was functionalized. According to Ohmori (1978), Mikawa Plateau is topography development more advanced than Shirakami mountain range. However, it was found that the Shirakami mountain area is deep in the valley, and the Shirakami mountain area was found to have a steep valley.

6.Evaluation

Functionalization of the average erosion amount has made it possible to identify eroded parts within the same mountainous region. Also, together with ohmori's topography development classification, you can also grasp the place of erosion from now. Furthermore, it is possible to consider the expansion of the mountainous area, it is possible to estimate the developmental stage, to narrow down the scale to the contrary, also to consider in the catchment area unit, so it is thought that it is possible to evaluate the future topography change.

©2019. Japan Geoscience Union. All Right Reserved.

Keywords: Geomorphic development, Digital elevation model(DEM), Average erosion, Altitudinal dispersion, Geographic Information System(GIS)

©2019. Japan Geoscience Union. All Right Reserved.

The Movement of Sediment and Development of Gullies Inside of Landslide area

*Yasuhiro Horikawa[1], Tatsuto Aoki[2]

1. Tsukuba University, 2. Kanazawa University

There are many researches focusing on gully network. Distinguishing these researches into some groups, two major approaches are found. One is inductive approach. This approach of study makes the theory based on the specific observation of current terrains. From this approach, some famous theories, such as Horton’s Law, are led and discussions based on natural condition are realized. However this type of survey has a limitation in researching the formation of gully network in short time scale. Other one is deductive approach. This approach researches the formation of gully network by doing slope experiments. This kind of research invokes some theories led by inductive approach. By doing experiments, the formation of gull network in short time scale is discussed. But because the experiments have to equalize conditions of soil, rainfall, slope angle, etc. The result based on natural conditions cannot be observed. For these reasons the researches connecting two approaches are required.
To meet this condition, researching formation of gully network in short time scale, analyze based on the real terrain is ideal. One of the study areas meeting the condition is a landslide area. This study researched newly formed landslide area located in Kanazawa city, Japan. This landslide had few gullies when the observation was begun. Research was done for five months, from July 2018 to November 2018.In this research, by using an Unmanned Ariel Vehicle (UAV), observation of gully network was done. From the images taken by the UAV, Digital Surface Models (DSMs) are made. Comparing these DSMs, in drainage systems expansion of gully network was measured. At the same time, to understand the movement of sediment was measured by using pins and bricks. Also the profile of each gully was taken.

In five months, gully network extended to the top of the landslide. Analyzing the gully network, the tendency of network matched Horton’s 1stlaw. But the gully network’s tendency did not match Horton’s 2ndlaw. On the landslide surface and inside of gullies, erosion and sedimentation occurred. This can be said to the small gravels to big ones. The erosion and sedimentation occurs intermittently not continuity. Gullies became deeper by downward erosion, and they became wider by lateral erosion. However sedimentation inside of gullies was also observed. By sedimentation, small scale of channel changes happened. Small scale of sedimentation is ignored or omitted in experiments of gully network. But in reality, small-scale sedimentation can play an important role in forming gully network. Small sedimentation can interrupt the formation of gully network. Adding to this, landslide’ original terrains controlled the gully formation. For these reasons, to gully network in landslide area it can be said that the gullies adopted Horton’s 1st law but by the small sedimentation and the terrain of landslide, gully network did not adopt Horton’s 2ndlaw. From the result of the observation, slope experiment and the real terrain have both common points and different points. This survey is primitive research of gully network in real terrain. To make the data for sure, more researches are required.

Keywords: Gully Erosion, Landslide, Mass Movement

©2019. Japan Geoscience Union. All Right Reserved.

Detailed topographic survey of valley head in hill by terrestrial laser scanning

*KIYOSHI SAIJO[1], Takahisa Furuichi[2], Asaka Konno[3]

1. Miyagi University of Education, 2. Graduate School of Agriculture, Hokkaido University, 3. Tokoha University

Detailed contour map 0.5 m of a valley head in the Ohmatsuzawa Hills in Miyagi Prefecture, northeast Japan was produced based on the topographic survey by terrestrial laser scanning. As the results, we could make more accurate geomorphic map, and recognize some micro landforms which suggest tiny slope processes and artificial landforms related to human activity such as charcoal burning.

Keywords: hill, head hollow, microtopography, terrestrial laser scanning

©2019. Japan Geoscience Union. All Right Reserved.

Preliminary application of electrical resistivity tomography to estimate subsurface structure of unchanneled valley: A case at granitic hillslope near Mt. Tsukuba, Japan

*Naoyuki Yoshihara[1], Tsuyoshi Hattanji[2]

1. Graduate School of Life and Environmental Sciences, University of Tsukuba, 2. Faculty of Life and Environmental Sciences, University of Tsukuba

Subsurface structure, for example, depth of soil-bedrock interface, is one of the important factors for shallow landslide. Estimating spatially continuous subsurface structure requires an enormous amount of work and time, and more efficient survey method improves our understanding as well as the work time. Electrical resistivity tomography (ERT), which has conventionally been used for groundwater survey, is potentially useful for visualization of shallow subsurface structure. Therefore, we conducted ERT, cone penetration test and some soil tests at an unchanneled valley underlain by weathered granite near Mt. Tsukuba, Japan, and discussed the applicability of ERT imaging for estimation of shallow subsurface structure.
Little antecedent precipitation was observed before the ERT survey. Distribution of resistivity obtained from ERT with 0.5-m electrode spacing visualized the depth of loose soil (N_c = 3) as a band of a specific resistivity range (4000–10000 Ωm). However, the depth of soil-bedrock boundary (N_c = 30) did not correspond to any specific resistivity range. The resistivity distribution and the result of some soil tests indicate that surface layer was dry at the survey, and the deeper layer was wet because of bedrock groundwater. Thus, we presumed that surface electrical conductivity of the slope materials affected the resistivity value in the shallower layer, and that liquid electrical conductivity affected the resistivity value in the deeper layer that contain bedrock groundwater.

Keywords: Shallow landslide, Unchanneled valley, Granite, Electrical resistivity tomography, Subsurface structure

©2019. Japan Geoscience Union. All Right Reserved.

Estimating distribution of soil thickness in doline from electrical resistivity tomography: A case study in the Akiyoshi-dai Karst Plateau, Japan

*Naoya Hiramoto[1], Tsuyoshi Hattanji[2]

1. Graduate School of Life and Environmental Sciences, University of Tsukuba, 2. Faculty of Life and Environmental Sciences, University of Tsukuba

Distribution of soil thickness in doline was estimated based on 2-D electrical resistivity tomography in ten dolines on Akiyoshi-dai Karst Plateau in Yamaguchi Prefecture, western Japan. Relationship between topographic parameters and soil thickness was examined based on topographic analysis using GIS software. The 2-D electrical resistivity tomography revealed a clear transition zone of resistivity in subsurface doline. The resistivity ranging from 280 Ω·m to 400 Ω·m represents transition layer of soil and bedrock. The layers above (< 280 Ω·m) and below (> 400 Ω·m) the transition layer were identified as soil and bedrock, respectively. Electrical resistivity survey for each doline revealed that (1) soil at the upper slope of doline (max. 6.5 m) was thinner than that at the lower slope (max. 9 m), and (2) soil at doline bottom (max. 11 m) was thicker than that of slope (max. 9 m). For doline bottom, mean soil thickness increased with increasing catchment area, and catchment area is one of the main factors determining soil thickness on doline bottom.

Keywords: Karst landform, GIS, Bottom diameter, Slope, Catchment area

©2019. Japan Geoscience Union. All Right Reserved.

Occurrence and origin of potholes developed on the eastern slope of Miharayama in Hachijojima, Izu Islands, Tokyo Prefecture, Japan

*Takashi Ishibashi[1], Tomoaki Mastumi[2], Ren Higuchi[2], Yuki Yamatmoto[2], Keigo Shimada[2], Hirotomo Morimoto[2], Tsutomu Shimada[3], Kenji Asakura[4]

1. Masutomi Museum of Geocience, 2. Ritsumeikan University Explorers Club, 3. Pothole Survey Team, 4. Kyoto University Graduate School of Science

Introduction

In Hachijojima (Hachijo Town, Tokyo), a lot of potholes are seen along swamps on the eastern slope of Miharayama. The finding of the potholes was in recent years, and they were designed as cultural property by Hachijo Town in 2016. But the distribution and its origin had not been elucidated enough, the potholes had surveyed in many aspects of geography four times over from 2014 to 2016. We will report the knowledge obtained from the survey and discuss the origin of the potholes. The study area is the special area of Fuji Hakone Izu National Park. The sampling of study specimens approved by the permission of the Minister of the Environment specified by Natural Park Act (No.1509143).

Definition of pothole

"Cyclopedia of Earth Science" (The Association for the Geological Collaboration in Japan, 1996) defines pothole as ‘a round shape structural failure developed on the surface of riverbed by erosion’, but the definition of pothole is not strict in general. So, in the case of Hachijojima potholes, we measured the size of pothole as follows. 1. The depth of pothole is the vertical distance from the surface of bedrock to the bottom of pothole. 2. The width of pothole is average of the major axis and the minor axis, which are the horizonal distance at the attitude of the surface of pothole. We accept the hole whose depth and width are bigger than 10 cm and 30 cm, respectively. Furthermore, the holes developed on the soil made by water current are excluded.

Potholes developed on the eastern slope of Miharayam

Potholes occur in Sueyoshi district, eastern Miharayama. On the eastern slope of Miharayama, some small valleys are lined in the WNW-ESE direction. Potholes are formed on the waterway of the valleys continuously. Over 700 potholes are found in 9 valleys. Among them, the “main” valley is the biggest one. In addition, schematic occurrence of potholes is recognized in the main valley. So, we will report the survey of the main valley chiefly. The types of the potholes are divided into two types. 1. Pothole type : a typical pothole removed by pebbles deeply. 2. Spoon type : a pothole whose depth is small as compared with its width. In the main valley, we found 19 pothole type potholes and 122 spoon type potholes. Some potholes had captured pebbles. The waterways are commonly step-wise. The steps of the waterway are several meters away from each other. Waterfalls are common on the step. The bedrock of the potholes is basaltic lava, which has 1-2 cm euhedral anorthite crystals. Under the microscope, the lava shows intersertal texture, and plagioclase, clinopyroxene and orthopyroxene (up to 1 mm) were recognized. Intergranular basaltic xenoliths usually occur in the lava. They seem to be crusts of volcanic vent when the lavas erupted. Potholes exist only in the area the basaltic lavas occur. The lavas must be a part of the main volcanic body of Miharayama, whose age is estimated to be 26-30 ka (Suga, 1998).

©2019. Japan Geoscience Union. All Right Reserved.

Origin of potholes
It is necessary to form potholes that water flow and pebbles which remove the bedrock exist. Over and under the basaltic lavas, scoriaceous beds are recognized. Waterfalls are formed usually on the scoriaceous beds because they are weak and water-permeable layer although the basaltic lavas are impermeable layer. Basaltic rocks over the waterfall turn to pebbles when the waterfall goes back. The occurrence of pebbles is a factor of formation of potholes as described above. In addition, sands which are formed by boll mill crushing accelerate erosion of the bedrocks. They must be a factor of spoon type pothole.

Reference : Suga(1998): *The Quaternary research*, **37**, 59-75. ; The Association for the Geological Collaboration in Japan (1996): 1228.

Keywords: pothole, Hachijojima, Izu Islands, volcano, basaltic lava

©2019. Japan Geoscience Union. All Right Reserved.

Temporal and spatial changes of sediment supply processes from tributaries since the last glacial period in the upper valleys of the Tama and Ara rivers, central Japan

*Takayuki Takahashi[1], Toshihiko Sugai[1]

1. Graduate School of Frontier Sciences, The University of Tokyo

To understand the sediment routing systems in the long-term, it is important to reveal the temporal and spatial changes of sediment supply processes from tributaries to the trunk river in upper reaches. Although Shimazu (1990; 1991) discuss the relationship between the longitudinal changes of the gravel size on the trunk riverbed and the tributary slope based on the slope 8% (the slope which debris flow deposition occurs), few studies discuss the temporal changes of the sediment supply processes of tributaries. Fill terrace formed in the last glacial period are developed in the upper reaches of the rivers in the Hokkaido, northeastern and central Japan. In the upper valley of the Tama and Ara rivers, most fill terraces are toe-cut terraces formed by tributaries (e.g. Takahashi and Sugai, 2018). The slope of their tread (Sg) indicates the tributary slope in the last glacial period. This study compares Sg and the present tributary slope (Sp) and discusses the temporal and spatial changes of the tributary slope and the sediment supply process from tributaries based on the slope 8%.

Sg is greater than Sp at the same tributary. This indicates that the tributary channels have been steepened because of the incision of the trunk river in the postglacial. Based on 8%, the tributaries can be classified as the three types (Type-A, B and C). Type-A tributaries (Sg and Sp > 8%) have been able to supply the sediment the debris flow to trunk river since the last glacial period. Type-B tributaries (Sg is less than 8%, Sp > 8%) supply the sediment by debris flow in the post glacial and by traction in the postglacial. Type-C tributaries (Sg and Sp are less than 8%) have supplied the sediment the traction to trunk river since the last glacial period. Based on the tributary Types above, the upper valleys of the Tama and Ara rivers were classified as three segment types (Seg. A, B and C). Seg. A is the segment that Type-A tributaries frequently join and appears in the upper part of the Tama and Ara river valleys. Seg. B is the segment that Type-B tributaries frequently join and appears in the lower part of the Tama River valley, and the upper part of the Chichibu Basin and the gorge of the Ara River valley. Seg. C is the segment that Type-C tributaries frequently join and appears in the lower part of the Chichibu Basin and gorge of the Ara River valley.

Seg. A appears the upper part of Tama and Ara river valleys, the sorting of the trunk river was dominated in their downstream in the last glacial period. The reason why Seg. C appears in the lower part of the Chichibu Basin is that the tributaries from the hills composed of the Neogene sedimentary rocks join. In contrast steep tributaries join in the gorge mainly because metamorphic rocks partly appear along the gorge of the Ara River and because the valley width are narrow by rock control. Sp and Sg are positively correlated with the relief ratio (Rr) of the tributary catchment. Sp, Sg and Rr decrease toward downstream (the east) in the Tama River valley. In the Ara River valley, these values decrease downstream from the headwaters to the Chichibu Basin, and increase in the gorge. The tendency for Sp, Sg and Rr to decrease downstream reflects the lowering of mountain ridges toward the east. It is suggested that the changes of tributary slope and the sediment supply process from tributaries are affected by the distribution of lithology and mountain relief along with the elevation changes of the trunk riverbed.

Keywords: fluvial terrace, debris flow, mountain river, sediment routing system

©2019. Japan Geoscience Union. All Right Reserved.

©2019. Japan Geoscience Union. All Right Reserved.

Landform evolution and active tectonics in the eastern part of Oiso Hills inferred by characteristics of gravels composing Kissawa Formation, Japan

*Masahiro Muraki[1], Toshihiko Sugai[1]

1. Graduate School of Frontier Science, The University of Tokyo

Introduction

Oiso Hills are uplift blocks bounded by active faults and uplifted rapidly in the late Quaternary period (Fig. 1: Active Fault Research Group, 1991). In the eastern part of Oiso Hills, however, the relationships between the landform development and active tectonics have not been clarified. The aim of this study is to clarify the landform evolution and the active tectonics in the eastern part of Oiso Hills based on the paleo-geography inferred from the depositional environments of gravel layers of the Pleistocene Kissawa Formation (KF: Machida and Moriyama, 1968), marine deposits of the last interglacial period (125 ka). The study area is divided into Mt. Koma area and Hinataoka area. Furthermore, Mt. Koma area can be subdivided into four blocks of OSA, OSB, OSC and OSD bounded with the active faults defined by Active Fault Research Group (1991) (Fig. 2).

Methods

In order to compare the present fluvial and beach gravels with gravels of KF, we established a frame of 1 m ×1 m at each gravel sampling site along the Kaname River, the Sagami bay beach, and at the outcrop of gravel layers of KF to collect 100 gravels from the largest size. The size, lithology, roundness and degree of weathering of the gravels were measured. Also, the matrix was analyzed with a sieve. And besides, chemical composition of tephras intervening or covering KF was analyzed.
Terrace surfaces were identified by aerial photo interpretation and field observation.

Results

The average middle diameter of the Kaname River gravels decreased downstream from 7 to 3 cm, and the average roundness increased from 0.3 to 0.6. Average flatness was 0.3 ~ 0.4. As the lithologic composition of sampled gravels, pyroclastic rocks occupied the majority upstream, and the ratio of sandstone, mudstone, and conglomerate increased to downstream. The average middle diameter of the Sagami Bay beach gravels was about 3 cm, roundness was about 0.7 and flatness was about 0.6. As the lithologic composition of sampled gravels, pyroclastic rocks, sandstone and mudstone occupied the majority. The average middle diameter of the sampled gravels of KF was about 2 cm, roundness was 0.6 ~ 0.7 and flatness was 0.3 ~ 0.4. As the lithologic composition of the gravels, pyroclastic rocks, sandstone and chart occupied the majority.
Kissawa Terrace (KT) I, II and Nanakuni-touge Terrace (230 ~ 250 ka) were identified in the study area. KT I (Shonan daira surface) develop in OSB and KT II in OSA, OSC and OSD. Eastern Takatori Terrace (ETT) formed around 30 ka by tributaries was also identified along the Fudou River.

Discussion

The flatness of the Kaname River bed gravel did not increase to downstream, while the roundness increased associated with the decrease of the particle size. Lithologic composition of the lowest reach of the Kaname River bed gravels was similar with that of the Sagami River, suggesting that the Sagami River flowed to the west side of the Sagami plain in the late Holocene, depositing gravel of the Sagami River

©2019. Japan Geoscience Union. All Right Reserved.

system at around the lowest reach of the present Kaname River. Sagami Bay beach gravels were characterized by well-rounded flat shape influenced by coastal current. Kaname River gravels and Sagami Bay beach gravels were distinguished from roundness 0.6, lower was the former and higher was the latter. Spatial variation of characteristics of the KF gravels implies that KT I is older than the last interglacial period and OSB may be a hilly island during the last interglacial period while the Kaname River flowed into the present Fudou River and formed KT II. This interpretation suggests that the Hinataoka and Komukai fault activities triggered the change of the river course in the last glacial period. After that ETT was probably formed by tributaries flowed into the present Fudou River.

Reference
Active Fault Research Group (1991) University of Tokyo Press, 437 p. Machida H. and Moriyama A. (1968) Geographical Review of Japan, 41, 241-257. Machida H. and Moriyama A. (2003) University of Tokyo Press, 336 p. Smith, V. C. et al., (2013) Quaternary Science Reviews 67, 121-137.

Keywords: Kissawa formation, depositional environment, landform evolution, active tectonics, Oiso hills

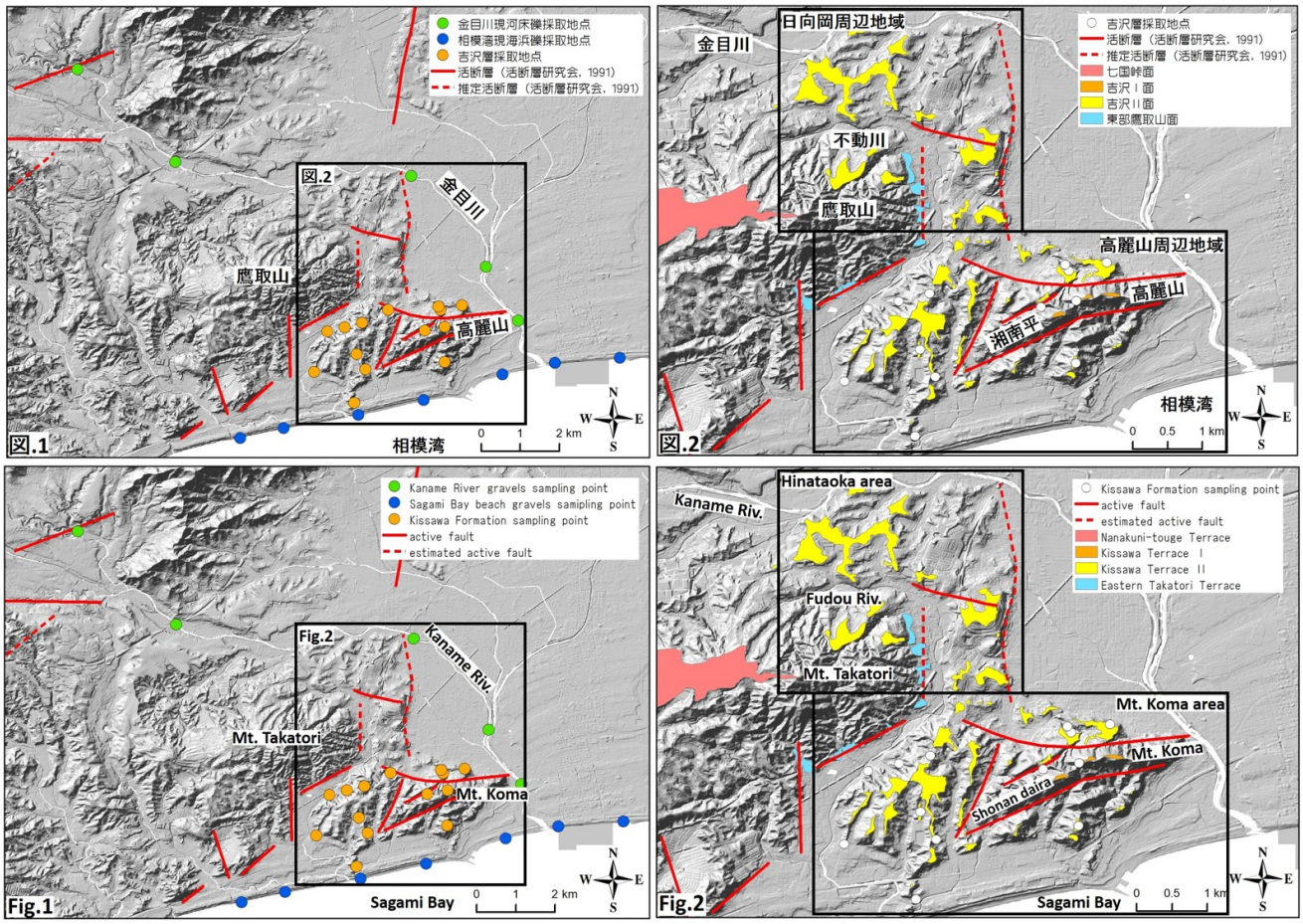

©2019. Japan Geoscience Union. All Right Reserved.

Sediment movement and collapse of bank protections by a series of large flood events at the Sendai River, Tottori, southwest Japan

*Yoshinori Kodama[1], Kento Takemoto[2]

1. Faculty of Agriculture, 2. Hyogo Prefecture

In recent two years, large flood events more than 15 year-occurrence interval happened in a row at the Sendai River (Ad=1,190 km^2, L=52 km), southwest Japan. We surveyed recording artificial bank damages and sediment movements to build bars. We also analyzed satellite images for pre-events, middle, post events. The results show that the Sendai River could be divided into three sections, except uppermost 6.6 km reach: i) 6.6-11.8 km: river bed sediments were washed away to be bedrock exposure, ii) 11.8-31.0 km: alternate bars with small wavelength (less than 1000 m) were formed and iii) 31.0-48.4 km: alternate or multiple bars with larger wavelength (less than 4000 m) were formed, some of them were covered by vegetation. Many sites of artificial bank protection collapse were observed in bedrock exposure reach, where basement of artificial bank protection lost support by removing sediments. The other many sites of bank collapse were in adjacent points of small wavelength (less than 800 m) and high in relief (c.a. 2m) alternate bars, where convergent flood flow occurred scouring of river bed material.

Keywords: Large flood events, collapse of bank protection, bedrock exposure, alternate bar, satellite image, 2018 torrential rain in western Japan

©2019. Japan Geoscience Union. All Right Reserved.

Channel incision history with knickpoint retreat in the Kushira River after the deposition of Ata pyroclastic flow, Osumi Peninsula, Kyushu, Japan

*Shintaro Takanami[1]

1. Meiji University

The Ata welded ignimbrite (110 ka B.P.) lies concealed in the Osumi pumice fall deposits and the Ito pyroclastic flow deposits (non-welded, 30 ka B. P.), having been exposed along the Kushira River valley in the northern margin of Kasanohara ignimbrite plateau, southern Kyushu of Japan (Aramaki and Ui 1966). The Kushira River has a number of knickpoints along its course. Riverbed of Kushira River is composed of the Ata ignimbrite in the upstream reach after the Tanida waterfall. The preceding research by Yokoyama (2000) revealed rapid erosion processes on the Ito non-welded ignimbrite plateau. By contrast, almost no studies reported on the processes of the Ata ignimbrite exposed along Kushira River. Here, to gain a better understanding of this topic, the present study estimated the recession rates of knickpoints in various duration (i.e., from 110 ka to 30 ka, from 30 ka to present and during 110 kyrs), by restoring and comparing the three longitudinal profiles based on field observation and existing borehole data.

In this study, the bottom elevation of Osumi pumice fall deposits in the Kushira River valley was identified as the maximum elevation of riverbed just before the deposition of Osumi pumice. And the elevation of riverbed immediately after the Ata pyroclastic flow was also provided by the distributional top of the Ata ignimbrite. At 11 outcrops, unconfined compressive strength of the Ata ignimbrite was evaluated by KS-type Schmidt rock hammer.

Restored longitudinal profile of 110 ka indicates that the Kushira River had a marked knickpoint at the edge of Ata ignimbrite plateau that was 16 km away from present river mouth. The recession rate of this knickpoint is estimated to 5.4 cm/yr considering that it has retreated to the present position of Tanida waterfall. Estimated unconfined compressive strength of the Ata ignimbrite is gradually decreasing toward its upper part, and showing the exceptionally highest value at the “lower-positioned” Tanida waterfall ($421\times10^6 N/m^2$). Taking this into consideration, another knickpoint located now observed at 26 km from the present river mouth is also candidate for the original knickpoint at 110 ka and had retreated from the edge of Ata ignimbrite plateau to such above position (26 km inland). In this latter case, the recession rate of the knickpoint in the past 110,000 years is calculated as 8.6 cm/yr. The maximum elevation of estimated riverbed at 30 ka indicates that the Kushira River had a steeper gradient than any other timing (probably except for LGM) and incised deeper into the Ata ignimbrite plateau along the downstream side. At that time, the former Tanida waterfall was likely situated in the downstream side of 19 km from the present river mouth. Therefore, its recession rates were estimated more than 2.6 cm/yr during the period from 110 ka to 30 ka, and less than 10 cm/yr in the last 30,000 years. Based on these, this study concludes that continuous bedrock incision might have been occurred with knickpoint retreat since the formation of Ata welded ignimbrite until the deposition of Osumi pumice fall. And it is highly probable that this incision in the Kushira River valley was definitely controlled by the sea level lowering during the period of LGM.

This work was financially supported by the School of Arts and Letters, Meiji University.

©2019. Japan Geoscience Union. All Right Reserved.

References

Aramaki, S. and Ui, T. 1966. Ata pyroclastic flows and the Ata caldera in Southern Kyushu, Japan. *The Journal of the Geological Society of Japan* 72: 337-349.
Yokoyama, S. 2000. Rapid Formation of Kasanohara Ignimbrite Plateau, South Kyushu, Japan. *Transactions, Japanese Geomorphological Union* 21: 277-290.

Keywords: Ata welded ignimbrite, knickpoint, Kasanohara, Kushira River, sea-level change

©2019. Japan Geoscience Union. All Right Reserved.

Implications of the distribution of marine terraces and submerged terraces in Japanese Island

*Tetsuya Komatsu[1], Hiura Yuki[1], Takayuki Takahashi[2], Taro Funatsu[2], Masahiro Muraki[2], Taiga Kimori[2], Toshihiko Sugai[2]

1. Japan Atomic Energy Agency, 2. Graduate School of Frontier Sciences, The University of Tokyo

One of the primary issues of the geological disposal technology is to advance the techniques associated with investigation/assessment for long-term uplift and erosion in terrestrial-marine transitional zone in Japan. To examine this issue, it is inevitable to understand the geomorphic features indicating uplift and erosion in the continental shelf, which widely emerged during glacial periods. Submerged terraces defined as step-like and lobate seabed features can be identified along the continental shelfs. These landforms morphologically mimic marine terraces in terrestrial areas. This study compared the distribution of submerged terraces and MIS 5e terraces in Japan. As a result, the trends of the depth change of submerged terraces in some areas appear to be consistent with the trends of the elevation change of MIS 5e terraces. Furthermore, some cases show the depth of submerged terraces changes abruptly at the seaward extension of terrestrial active fault. These results imply submerged terraces in Japan can be an indicator of regional tectonics in the seafloor.

This study was carried out under a contract with METI (Ministry of Economy, Trade and Industry) as part of its R&D supporting program for developing geological disposal technology.

Keywords: seafloor landform, submerged terrace, marine terrace, geological disposal

©2019. Japan Geoscience Union. All Right Reserved.

Marine erosional landforms along the southern coast of Yonaguni Island, Ryukyus

*Hayate Kimura[1], Kensaku Urata[2], HASEGAWA Hitoshi[3], Toshihiko Ichihara[4], Atsushi Suzuki[5], Nobuyuki Hori[6], Hironobu Kan[2]

1. Graduate school of integrated sciences for global society, 2. Graduate School of Integrated Sciences for Global Society, Kyushu University, 3. Kokushikan University, 4. Sedimentary Environments Research, 5. Geological Survey of Japan National Institute of Advanced Industrial Science and Technology (AIST), 6. Department of Geography, Nara University

Yonaguni Island is located at the westernmost of Japan, where marine erosional landform is widely seen. However, high sea cliffs refuse the investigator’ s approach. We created three-dimensional models by taking photographs from drone. The coastal area of Yonaguni Island is composed of the Middle Miocene sedimentary rocks of the Yaeyama Group and Pleistocene limestone of the Ryukyu Group. We observed characteristic erosional landforms which varies depending on geology along the southern coast of Yonaguni Island.
We surveyed 6 areas where locate the east and south coasts in Yonaguni Island. Photogrammetric surveys were carried out using DJI Phantom 4 Pro. We installed a GCP at accessible places. PhotoScan Professional was used as SfM-MVS software to create terrain models.
Coastal landforms are largely different depending on geological structure. In the limestone coast, collapsed areas of several hundred meters wide are formed. These collapses seem to originate from the unconsolidated layer of unconformity below the limestone or the detrital layer in the limestone. In the coast of sedimentary rocks, coastal landform varies with sedimentary facies. Shore platform is formed at the base of cliff which composed of layers of sandstone and shale. On the other hand, large boulders are distributed at the base of cliff composed of massive sandstone without layers.

Keywords: SfM-MVS, Photogrammetry, Sea cliff, Shore platform, Yaeyama Group, Ryukyu Limestone

©2019. Japan Geoscience Union. All Right Reserved.

Seafloor topography of Amami Sumiyo Bay -Visualization of Seafloor derived from multibeam bathymetric survey-

*Miho Tanaka[1], Ken Toguchi[2], Nobuyuki Hori[3], Hayate Kimura[4], Yukihiko Imai[5], Yosuke Nakashima[6], Yayoi Najima[7], Hironobu Kan[8]

1. Graduate School of Integrated Sciences for Global Society, 2. University of the Ryukyus, 3. Tokyo Metropolitan University, 4. School of Engineering, Kyushu University, 5. Faculty of science, Okayama University, 6. National Institute of Technology, Ariake College, 7. The Graduate University for Advanced Studies, 8. Kyushu University

The shallow water area is a very important area to reveal the sea level change during the last glacial period. In this study, we conducted multibeam bathymetric survey at Amami Sumiyo Bay and created a seafloor topographic map with high accuracy of 1 m grid.
Sumiyo Bay is located on the eastern coast of Amami Island. The Kawauchi River and the Sumiyo River are flowing into that bay. Multibeam bathymetric survey was conducted from August 20th to September 2nd, 2018 by using R2SONIC 2022 Broadband Multibeam Echosounder. Also, we measured the reflection intensity to discriminate sediment by using the side scan sonar function (TruePix / Snippets) installed in that device.
As a result of this survey, the topography distribution of the seafloor was revealed. Terrace scarp can be confirmed near the water depth of 100m in the central part of Sumiyo Bay, and it is thought that it was formed by erosion at the low sea level of the glacial period.
In this study, I integrated 10m DEM data of terrestrial area provided by Geographical Survey Institute to the highly accurate seafloor topographic map created by us and consider about geomorphology.

Keywords: multibeam bathymetry, seafloor topography, last glacial stage, sea level, Digital Elevation Model (DEM)

©2019. Japan Geoscience Union. All Right Reserved.

[J] Poster | H (Human Geosciences)：H-GM Geomorphology

Wed. May 29, 2019 5:15 PM - 6:30 PM JST | Wed. May 29, 2019 8:15 AM - 9:30 AM UTC | Poster Hall International Exhibition Hall8, Makuhari Messe_19

[H-GM04] Geomorphology

convener:Tsuyoshi Hattanji(Faculty of Life and Environmental Sciences, University of Tsukuba), Masayuki Seto(Fukushima Future Center for Regional Revitalization, Fukushima University)

The main subject of this session is the whole range of themes relating to geomorphology, especially geomorphic processes, landform development and its relation to environmental changes, geomorphological hazards and their mitigation and reports of recent events of disaster occurred in Japan, various kind of hazard maps, relationships among geomorphic processes, other natural phenomena and human activities, and various techniques of geomorphological measurements and automatic landform classification. Japanese can be used in this session.

[HGM04-P01] Automatic landform classification using Self-Organizing Map (SOM) by geomorphological features calculated from DEM

*Ito Yoshiki[1], Yoshiya Oda[1], Toshifumi Matsuoka[2] (1.Tokyo Metropolitan University, 2.Fukada Geological Institute)

[HGM04-P02] **Functionalization of the Average Erosion of Drainage Basin Using DEM**

*Rei Yamanaka[1], Tatsuto Aoki[1] (1.Kanazawa University)

[HGM04-P03] The Movement of Sediment and Development of Gullies Inside of Landslide area

*Yasuhiro Horikawa[1], Tatsuto Aoki[2] (1.Tsukuba University, 2.Kanazawa University)

[HGM04-P04] Detailed topographic survey of valley head in hill by terrestrial laser scanning

*KIYOSHI SAIJO[1], Takahisa Furuichi[2], Asaka Konno[3] (1.Miyagi University of Education, 2.Graduate School of Agriculture, Hokkaido University, 3.Tokoha University)

[HGM04-P05] Preliminary application of electrical resistivity tomography to estimate subsurface structure of unchanneled valley: A case at granitic hillslope near Mt. Tsukuba, Japan

*Naoyuki Yoshihara[1], Tsuyoshi Hattanji[2] (1.Graduate School of Life and Environmental Sciences, University of Tsukuba, 2.Faculty of Life and Environmental Sciences, University of Tsukuba)

[HGM04-P06] Estimating distribution of soil thickness in doline from electrical resistivity tomography:A case study in the Akiyoshi-dai Karst Plateau, Japan

*Naoya Hiramoto[1], Tsuyoshi Hattanji[2] (1.Graduate School of Life and Environmental Sciences, University of Tsukuba, 2.Faculty of Life and Environmental Sciences, University of Tsukuba)

[HGM04-P07] Occurrence and origin of potholes developed on the eastern slope of Miharayama in Hachijojima, Izu Islands, Tokyo Prefecture, Japan

*Takashi Ishibashi[1], Tomoaki Mastumi[2], Ren Higuchi[2], Yuki Yamatmoto[2], Keigo Shimada[2], Hirotomo Morimoto[2], Tsutomu Shimada[3], Kenji Asakura[4] (1.Masutomi Museum of Geocience, 2.Ritsumeikan University Explorers Club, 3.Pothole Survey Team, 4.Kyoto University Graduate School of Science)

[HGM04-P08] Temporal and spatial changes of sediment supply processes from tributaries since the last glacial period in the upper valleys of the Tama and Ara rivers, central Japan

*Takayuki Takahashi[1], Toshihiko Sugai[1] (1.Graduate School of Frontier Sciences, The University of Tokyo)

[HGM04-P09] Landform evolution and active tectonics in the eastern part of Oiso Hills inferred by characteristics of gravels composing Kissawa Formation, Japan

*Masahiro Muraki[1], Toshihiko Sugai[1] (1.Graduate School of Frontier Science, The University of Tokyo)

[HGM04-P10] Sediment movement and collapse of bank protections by a series of large flood events at the Sendai River, Tottori, southwest Japan

*Yoshinori Kodama[1], Kento Takemoto[2] (1.Faculty of Agriculture, 2.Hyogo Prefecture)

[HGM04-P11] Channel incision history with knickpoint retreat in the Kushira River after the deposition of Ata pyroclastic flow, Osumi Peninsula, Kyushu, Japan

*Shintaro Takanami[1] (1.Meiji University)

[HGM04-P12] **Implications of the distribution of marine terraces and submerged terraces in Japanese Island**

*Tetsuya Komatsu[1], Hiura Yuki[1], Takayuki Takahashi[2], Taro Funatsu[2], Masahiro Muraki[2], Taiga Kimori[2], Toshihiko Sugai[2] (1.Japan Atomic Energy Agency, 2.Graduate School of Frontier Sciences, The University of Tokyo)

[HGM04-P13] Marine erosional landforms along the southern coast of Yonaguni Island, Ryukyus

*Hayate Kimura[1], Kensaku Urata[2], HASEGAWA Hitoshi[3], Toshihiko Ichihara[4], Atsushi Suzuki[5], Nobuyuki Hori[6], Hironobu Kan[2] (1.Graduate school of integrated sciences for global society, 2.Graduate School of Integrated Sciences for Global Society, Kyushu University, 3.Kokushikan University, 4.Sedimentary Environments Research, 5.Geological Survey of Japan National Institute of Advanced Industrial Science and Technology (AIST), 6.Department of Geography, Nara University)

[HGM04-P14] Seafloor topography of Amami Sumiyo Bay -Visualization of Seafloor derived from multibeam bathymetric survey-

*Miho Tanaka[1], Ken Toguchi[2], Nobuyuki Hori[3], Hayate Kimura[4], Yukihiko Imai[5], Yosuke Nakashima[6], Yayoi Najima[7], Hironobu Kan[8] (1.Graduate School of Integrated Sciences for Global Society, 2.University of the Ryukyus, 3.Tokyo Metropolitan University, 4.School of Engineering, Kyushu University, 5.Faculty of science, Okayama University, 6.National Institute of Technology, Ariake College, 7.The Graduate University for Advanced Studies, 8.Kyushu University)

Automatic landform classification using Self-Organizing Map (SOM) by geomorphological features calculated from DEM

*Ito Yoshiki[1], Yoshiya Oda[1], Toshifumi Matsuoka[2]

1. Tokyo Metropolitan University, 2. Fukada Geological Institute

The landform classification map based on the various geomorphological features which calculated from DEM data is adopted in many scenes of the modern society. As is well known, Iwahashi and Pike (2007) had proposed a classification method of terrain by using slope gradient, local convexity, and surface texture. In this research, we tried to automate landform classification by using Self-Organizing Map (SOM) which is an unsupervised neural network. It is aimed at grasping the influence on the classification result depending on the combination of the geomorphological features used. The target area in this preliminary study is the same area as Iwahashi and Pike (2007); the southern part of Yatsugatake located at the prefecture boundary between Yamanashi prefecture and Nagano prefectures (about 22.5 km east-west, about 20.0 km north and south).

The SOM was carried out by the following procedure. Calculate the amount of slope gradient, surface texture, local convexity, direction of dip, the ridge valley degree, surface curvature, and the hill figure from DEM data. ② These geomorphological features were combined and adopted as input data to SOM. Totally seven patterns of geomorphological features were selected. ③ For these data, learning by SOM was conducted, and seven landform classification maps were obtained. Also, in order to visualize the features of classification by SOM, a histogram of each feature was also calculated. (4) The classification results were compared based on the landform classification maps and histograms, and the influence of the classification result by combination of the geomorphological features used was examined. We also compared SOM results with the classification results by Iwahashi and Pike (2007) method. In concludingly, it was found that in the automatic landform classification by SOM using multiple geomorphological features, the relatively uniformly distributed topographical feature quantities greatly affect classification compared to biased terrain feature. We also found that the topographic features with histograms with symmetric distribution and narrow histograms do not have a significant effect on topographic classification results by SOM. We would like to consider an application of supervised neural network and to obtain a landform

Keywords: digital elevation model(DEM), Self-Organizing Maps(SOM), landform classifications

©2019. Japan Geoscience Union. All Right Reserved.

Functionalization of the Average Erosion of Drainage Basin Using DEM

*Rei Yamanaka[1], Tatsuto Aoki[1]

1. Kanazawa University

1.First.

Geomorphic development model of tectonically active and intensive denuded regions in japan has been discussed.
Yoshikawa (1985) showed the need to discuss as a geomorphic development model considering the changing terrain in the wet variation zone in Japan.
Ohmori (1978), using a 50mDEM, to determine the dispersion of altitude. Moreover, he will evaluate the stages in the geomorphic development of the mountains.
In this study, 10 m DEM available nationwide was used.
The average amount of erosion per basin was obtained by ArcGIS and compared with the data of the dispersion of altitude of Ohmori (1978).

2.Target area

Soya Hill, Taihei Mountain, Abukuma Plateau, Shirakami Mountains, Mikawa Plateau, Hakusan Mountains, Kanto Mountains, Akaishan Mountains, Hida Mountain Range with different stages in geomorphic development is Target areas. Selected from the mountains that are analyzed by Ohmori (1978).

3.Analysis method

This is a procedure with ArcGIS, calculation of average erosion amount per watershed.
First, I made summit level map with grid sizes 3 to 301. The summit level map can be regarded as a virtual ground surface before erosion. For this reason, I set "summit level map - DEM" as the depth of erosion.

4.Functionalization of average erosion amount

We made a function of the relationship between grid size and erosion amount. At that time, graph fitting to the linear function, power function, exponential function, logarithmic function, approximate curve and its error were obtained. As a result, the most fitted function was logarithmic function "y = alog (1 + bx)", and the error was the smallest. a is considered to represent the depth of the valley and b is the width of the valley.

5.Evaluation of average erosion amount by mountain area

A scatter diagram based on the coefficients was prepared from the average erosion amount by mountainous area which was functionalized. According to Ohmori (1978), Mikawa Plateau is topography development more advanced than Shirakami mountain range. However, it was found that the Shirakami mountain area is deep in the valley, and the Shirakami mountain area was found to have a steep valley.

6.Evaluation

Functionalization of the average erosion amount has made it possible to identify eroded parts within the same mountainous region. Also, together with ohmori's topography development classification, you can also grasp the place of erosion from now. Furthermore, it is possible to consider the expansion of the mountainous area, it is possible to estimate the developmental stage, to narrow down the scale to the contrary, also to consider in the catchment area unit, so it is thought that it is possible to evaluate the future topography change.

©2019. Japan Geoscience Union. All Right Reserved.

Keywords: Geomorphic development, Digital elevation model(DEM), Average erosion, Altitudinal dispersion, Geographic Information System(GIS)

©2019. Japan Geoscience Union. All Right Reserved.

The Movement of Sediment and Development of Gullies Inside of Landslide area

*Yasuhiro Horikawa[1], Tatsuto Aoki[2]

1. Tsukuba University, 2. Kanazawa University

There are many researches focusing on gully network. Distinguishing these researches into some groups, two major approaches are found. One is inductive approach. This approach of study makes the theory based on the specific observation of current terrains. From this approach, some famous theories, such as Horton’s Law, are led and discussions based on natural condition are realized. However this type of survey has a limitation in researching the formation of gully network in short time scale. Other one is deductive approach. This approach researches the formation of gully network by doing slope experiments. This kind of research invokes some theories led by inductive approach. By doing experiments, the formation of gull network in short time scale is discussed. But because the experiments have to equalize conditions of soil, rainfall, slope angle, etc. The result based on natural conditions cannot be observed. For these reasons the researches connecting two approaches are required.
To meet this condition, researching formation of gully network in short time scale, analyze based on the real terrain is ideal. One of the study areas meeting the condition is a landslide area. This study researched newly formed landslide area located in Kanazawa city, Japan. This landslide had few gullies when the observation was begun. Research was done for five months, from July 2018 to November 2018.In this research, by using an Unmanned Ariel Vehicle (UAV), observation of gully network was done. From the images taken by the UAV, Digital Surface Models (DSMs) are made. Comparing these DSMs, in drainage systems expansion of gully network was measured. At the same time, to understand the movement of sediment was measured by using pins and bricks. Also the profile of each gully was taken.

In five months, gully network extended to the top of the landslide. Analyzing the gully network, the tendency of network matched Horton’s 1stlaw. But the gully network’s tendency did not match Horton’s 2ndlaw. On the landslide surface and inside of gullies, erosion and sedimentation occurred. This can be said to the small gravels to big ones. The erosion and sedimentation occurs intermittently not continuity. Gullies became deeper by downward erosion, and they became wider by lateral erosion. However sedimentation inside of gullies was also observed. By sedimentation, small scale of channel changes happened. Small scale of sedimentation is ignored or omitted in experiments of gully network. But in reality, small-scale sedimentation can play an important role in forming gully network. Small sedimentation can interrupt the formation of gully network. Adding to this, landslide’ original terrains controlled the gully formation. For these reasons, to gully network in landslide area it can be said that the gullies adopted Horton’s 1st law but by the small sedimentation and the terrain of landslide, gully network did not adopt Horton’s 2ndlaw. From the result of the observation, slope experiment and the real terrain have both common points and different points. This survey is primitive research of gully network in real terrain. To make the data for sure, more researches are required.

Keywords: Gully Erosion, Landslide, Mass Movement

©2019. Japan Geoscience Union. All Right Reserved.

Detailed topographic survey of valley head in hill by terrestrial laser scanning

*KIYOSHI SAIJO[1], Takahisa Furuichi[2], Asaka Konno[3]

1. Miyagi University of Education, 2. Graduate School of Agriculture, Hokkaido University, 3. Tokoha University

Detailed contour map 0.5 m of a valley head in the Ohmatsuzawa Hills in Miyagi Prefecture, northeast Japan was produced based on the topographic survey by terrestrial laser scanning. As the results, we could make more accurate geomorphic map, and recognize some micro landforms which suggest tiny slope processes and artificial landforms related to human activity such as charcoal burning.

Keywords: hill, head hollow, microtopography, terrestrial laser scanning

©2019. Japan Geoscience Union. All Right Reserved.

Preliminary application of electrical resistivity tomography to estimate subsurface structure of unchanneled valley: A case at granitic hillslope near Mt. Tsukuba, Japan

*Naoyuki Yoshihara[1], Tsuyoshi Hattanji[2]

1. Graduate School of Life and Environmental Sciences, University of Tsukuba, 2. Faculty of Life and Environmental Sciences, University of Tsukuba

Subsurface structure, for example, depth of soil-bedrock interface, is one of the important factors for shallow landslide. Estimating spatially continuous subsurface structure requires an enormous amount of work and time, and more efficient survey method improves our understanding as well as the work time. Electrical resistivity tomography (ERT), which has conventionally been used for groundwater survey, is potentially useful for visualization of shallow subsurface structure. Therefore, we conducted ERT, cone penetration test and some soil tests at an unchanneled valley underlain by weathered granite near Mt. Tsukuba, Japan, and discussed the applicability of ERT imaging for estimation of shallow subsurface structure.
Little antecedent precipitation was observed before the ERT survey. Distribution of resistivity obtained from ERT with 0.5-m electrode spacing visualized the depth of loose soil (N_c = 3) as a band of a specific resistivity range (4000–10000 Ωm). However, the depth of soil-bedrock boundary (N_c = 30) did not correspond to any specific resistivity range. The resistivity distribution and the result of some soil tests indicate that surface layer was dry at the survey, and the deeper layer was wet because of bedrock groundwater. Thus, we presumed that surface electrical conductivity of the slope materials affected the resistivity value in the shallower layer, and that liquid electrical conductivity affected the resistivity value in the deeper layer that contain bedrock groundwater.

Keywords: Shallow landslide, Unchanneled valley, Granite, Electrical resistivity tomography, Subsurface structure

©2019. Japan Geoscience Union. All Right Reserved.

Estimating distribution of soil thickness in doline from electrical resistivity tomography: A case study in the Akiyoshi-dai Karst Plateau, Japan

*Naoya Hiramoto[1], Tsuyoshi Hattanji[2]

1. Graduate School of Life and Environmental Sciences, University of Tsukuba, 2. Faculty of Life and Environmental Sciences, University of Tsukuba

Distribution of soil thickness in doline was estimated based on 2-D electrical resistivity tomography in ten dolines on Akiyoshi-dai Karst Plateau in Yamaguchi Prefecture, western Japan. Relationship between topographic parameters and soil thickness was examined based on topographic analysis using GIS software. The 2-D electrical resistivity tomography revealed a clear transition zone of resistivity in subsurface doline. The resistivity ranging from 280 Ω·m to 400 Ω·m represents transition layer of soil and bedrock. The layers above (< 280 Ω·m) and below (> 400 Ω·m) the transition layer were identified as soil and bedrock, respectively. Electrical resistivity survey for each doline revealed that (1) soil at the upper slope of doline (max. 6.5 m) was thinner than that at the lower slope (max. 9 m), and (2) soil at doline bottom (max. 11 m) was thicker than that of slope (max. 9 m). For doline bottom, mean soil thickness increased with increasing catchment area, and catchment area is one of the main factors determining soil thickness on doline bottom.

Keywords: Karst landform, GIS, Bottom diameter, Slope, Catchment area

©2019. Japan Geoscience Union. All Right Reserved.

Occurrence and origin of potholes developed on the eastern slope of Miharayama in Hachijojima, Izu Islands, Tokyo Prefecture, Japan

*Takashi Ishibashi[1], Tomoaki Mastumi[2], Ren Higuchi[2], Yuki Yamatmoto[2], Keigo Shimada[2], Hirotomo Morimoto[2], Tsutomu Shimada[3], Kenji Asakura[4]

1. Masutomi Museum of Geocience, 2. Ritsumeikan University Explorers Club, 3. Pothole Survey Team, 4. Kyoto University Graduate School of Science

Introduction

In Hachijojima (Hachijo Town, Tokyo), a lot of potholes are seen along swamps on the eastern slope of Miharayama. The finding of the potholes was in recent years, and they were designed as cultural property by Hachijo Town in 2016. But the distribution and its origin had not been elucidated enough, the potholes had surveyed in many aspects of geography four times over from 2014 to 2016. We will report the knowledge obtained from the survey and discuss the origin of the potholes. The study area is the special area of Fuji Hakone Izu National Park. The sampling of study specimens approved by the permission of the Minister of the Environment specified by Natural Park Act (No.1509143).

Definition of pothole

"Cyclopedia of Earth Science" (The Association for the Geological Collaboration in Japan, 1996) defines pothole as ‘a round shape structural failure developed on the surface of riverbed by erosion’, but the definition of pothole is not strict in general. So, in the case of Hachijojima potholes, we measured the size of pothole as follows. 1. The depth of pothole is the vertical distance from the surface of bedrock to the bottom of pothole. 2. The width of pothole is average of the major axis and the minor axis, which are the horizonal distance at the attitude of the surface of pothole. We accept the hole whose depth and width are bigger than 10 cm and 30 cm, respectively. Furthermore, the holes developed on the soil made by water current are excluded.

Potholes developed on the eastern slope of Miharayam

Potholes occur in Sueyoshi district, eastern Miharayama. On the eastern slope of Miharayama, some small valleys are lined in the WNW-ESE direction. Potholes are formed on the waterway of the valleys continuously. Over 700 potholes are found in 9 valleys. Among them, the “main” valley is the biggest one. In addition, schematic occurrence of potholes is recognized in the main valley. So, we will report the survey of the main valley chiefly. The types of the potholes are divided into two types. 1. Pothole type : a typical pothole removed by pebbles deeply. 2. Spoon type : a pothole whose depth is small as compared with its width. In the main valley, we found 19 pothole type potholes and 122 spoon type potholes. Some potholes had captured pebbles. The waterways are commonly step-wise. The steps of the waterway are several meters away from each other. Waterfalls are common on the step. The bedrock of the potholes is basaltic lava, which has 1-2 cm euhedral anorthite crystals. Under the microscope, the lava shows intersertal texture, and plagioclase, clinopyroxene and orthopyroxene (up to 1 mm) were recognized. Intergranular basaltic xenoliths usually occur in the lava. They seem to be crusts of volcanic vent when the lavas erupted. Potholes exist only in the area the basaltic lavas occur. The lavas must be a part of the main volcanic body of Miharayama, whose age is estimated to be 26-30 ka (Suga, 1998).

©2019. Japan Geoscience Union. All Right Reserved.

Origin of potholes
It is necessary to form potholes that water flow and pebbles which remove the bedrock exist. Over and under the basaltic lavas, scoriaceous beds are recognized. Waterfalls are formed usually on the scoriaceous beds because they are weak and water-permeable layer although the basaltic lavas are impermeable layer. Basaltic rocks over the waterfall turn to pebbles when the waterfall goes back. The occurrence of pebbles is a factor of formation of potholes as described above. In addition, sands which are formed by boll mill crushing accelerate erosion of the bedrocks. They must be a factor of spoon type pothole.

Reference : Suga(1998): *The Quaternary research*, **37**, 59-75. ; The Association for the Geological Collaboration in Japan (1996): 1228.

Keywords: pothole, Hachijojima, Izu Islands, volcano, basaltic lava

©2019. Japan Geoscience Union. All Right Reserved.

Temporal and spatial changes of sediment supply processes from tributaries since the last glacial period in the upper valleys of the Tama and Ara rivers, central Japan

*Takayuki Takahashi[1], Toshihiko Sugai[1]

1. Graduate School of Frontier Sciences, The University of Tokyo

To understand the sediment routing systems in the long-term, it is important to reveal the temporal and spatial changes of sediment supply processes from tributaries to the trunk river in upper reaches. Although Shimazu (1990; 1991) discuss the relationship between the longitudinal changes of the gravel size on the trunk riverbed and the tributary slope based on the slope 8% (the slope which debris flow deposition occurs), few studies discuss the temporal changes of the sediment supply processes of tributaries. Fill terrace formed in the last glacial period are developed in the upper reaches of the rivers in the Hokkaido, northeastern and central Japan. In the upper valley of the Tama and Ara rivers, most fill terraces are toe-cut terraces formed by tributaries (e.g. Takahashi and Sugai, 2018). The slope of their tread (Sg) indicates the tributary slope in the last glacial period. This study compares Sg and the present tributary slope (Sp) and discusses the temporal and spatial changes of the tributary slope and the sediment supply process from tributaries based on the slope 8%.

Sg is greater than Sp at the same tributary. This indicates that the tributary channels have been steepened because of the incision of the trunk river in the postglacial. Based on 8%, the tributaries can be classified as the three types (Type-A, B and C). Type-A tributaries (Sg and Sp > 8%) have been able to supply the sediment the debris flow to trunk river since the last glacial period. Type-B tributaries (Sg is less than 8%, Sp > 8%) supply the sediment by debris flow in the post glacial and by traction in the postglacial. Type-C tributaries (Sg and Sp are less than 8%) have supplied the sediment the traction to trunk river since the last glacial period. Based on the tributary Types above, the upper valleys of the Tama and Ara rivers were classified as three segment types (Seg. A, B and C). Seg. A is the segment that Type-A tributaries frequently join and appears in the upper part of the Tama and Ara river valleys. Seg. B is the segment that Type-B tributaries frequently join and appears in the lower part of the Tama River valley, and the upper part of the Chichibu Basin and the gorge of the Ara River valley. Seg. C is the segment that Type-C tributaries frequently join and appears in the lower part of the Chichibu Basin and gorge of the Ara River valley.

Seg. A appears the upper part of Tama and Ara river valleys, the sorting of the trunk river was dominated in their downstream in the last glacial period. The reason why Seg. C appears in the lower part of the Chichibu Basin is that the tributaries from the hills composed of the Neogene sedimentary rocks join. In contrast steep tributaries join in the gorge mainly because metamorphic rocks partly appear along the gorge of the Ara River and because the valley width are narrow by rock control. Sp and Sg are positively correlated with the relief ratio (Rr) of the tributary catchment. Sp, Sg and Rr decrease toward downstream (the east) in the Tama River valley. In the Ara River valley, these values decrease downstream from the headwaters to the Chichibu Basin, and increase in the gorge. The tendency for Sp, Sg and Rr to decrease downstream reflects the lowering of mountain ridges toward the east. It is suggested that the changes of tributary slope and the sediment supply process from tributaries are affected by the distribution of lithology and mountain relief along with the elevation changes of the trunk riverbed.

Keywords: fluvial terrace, debris flow, mountain river, sediment routing system

©2019. Japan Geoscience Union. All Right Reserved.

©2019. Japan Geoscience Union. All Right Reserved.

Landform evolution and active tectonics in the eastern part of Oiso Hills inferred by characteristics of gravels composing Kissawa Formation, Japan

*Masahiro Muraki[1], Toshihiko Sugai[1]

1. Graduate School of Frontier Science, The University of Tokyo

Introduction

Oiso Hills are uplift blocks bounded by active faults and uplifted rapidly in the late Quaternary period (Fig. 1: Active Fault Research Group, 1991). In the eastern part of Oiso Hills, however, the relationships between the landform development and active tectonics have not been clarified. The aim of this study is to clarify the landform evolution and the active tectonics in the eastern part of Oiso Hills based on the paleo-geography inferred from the depositional environments of gravel layers of the Pleistocene Kissawa Formation (KF: Machida and Moriyama, 1968), marine deposits of the last interglacial period (125 ka). The study area is divided into Mt. Koma area and Hinataoka area. Furthermore, Mt. Koma area can be subdivided into four blocks of OSA, OSB, OSC and OSD bounded with the active faults defined by Active Fault Research Group (1991) (Fig. 2).

Methods

In order to compare the present fluvial and beach gravels with gravels of KF, we established a frame of 1 m ×1 m at each gravel sampling site along the Kaname River, the Sagami bay beach, and at the outcrop of gravel layers of KF to collect 100 gravels from the largest size. The size, lithology, roundness and degree of weathering of the gravels were measured. Also, the matrix was analyzed with a sieve. And besides, chemical composition of tephras intervening or covering KF was analyzed.
Terrace surfaces were identified by aerial photo interpretation and field observation.

Results

The average middle diameter of the Kaname River gravels decreased downstream from 7 to 3 cm, and the average roundness increased from 0.3 to 0.6. Average flatness was 0.3 ~ 0.4. As the lithologic composition of sampled gravels, pyroclastic rocks occupied the majority upstream, and the ratio of sandstone, mudstone, and conglomerate increased to downstream. The average middle diameter of the Sagami Bay beach gravels was about 3 cm, roundness was about 0.7 and flatness was about 0.6. As the lithologic composition of sampled gravels, pyroclastic rocks, sandstone and mudstone occupied the majority. The average middle diameter of the sampled gravels of KF was about 2 cm, roundness was 0.6 ~ 0.7 and flatness was 0.3 ~ 0.4. As the lithologic composition of the gravels, pyroclastic rocks, sandstone and chart occupied the majority.
Kissawa Terrace (KT) I, II and Nanakuni-touge Terrace (230 ~ 250 ka) were identified in the study area. KT I (Shonan daira surface) develop in OSB and KT II in OSA, OSC and OSD. Eastern Takatori Terrace (ETT) formed around 30 ka by tributaries was also identified along the Fudou River.

Discussion

The flatness of the Kaname River bed gravel did not increase to downstream, while the roundness increased associated with the decrease of the particle size. Lithologic composition of the lowest reach of the Kaname River bed gravels was similar with that of the Sagami River, suggesting that the Sagami River flowed to the west side of the Sagami plain in the late Holocene, depositing gravel of the Sagami River

©2019. Japan Geoscience Union. All Right Reserved.

system at around the lowest reach of the present Kaname River. Sagami Bay beach gravels were characterized by well-rounded flat shape influenced by coastal current. Kaname River gravels and Sagami Bay beach gravels were distinguished from roundness 0.6, lower was the former and higher was the latter. Spatial variation of characteristics of the KF gravels implies that KT I is older than the last interglacial period and OSB may be a hilly island during the last interglacial period while the Kaname River flowed into the present Fudou River and formed KT II. This interpretation suggests that the Hinataoka and Komukai fault activities triggered the change of the river course in the last glacial period. After that ETT was probably formed by tributaries flowed into the present Fudou River.

Reference
Active Fault Research Group (1991) University of Tokyo Press, 437 p. Machida H. and Moriyama A. (1968) Geographical Review of Japan, 41, 241-257. Machida H. and Moriyama A. (2003) University of Tokyo Press, 336 p. Smith, V. C. et al., (2013) Quaternary Science Reviews 67, 121-137.

Keywords: Kissawa formation, depositional environment, landform evolution, active tectonics, Oiso hills

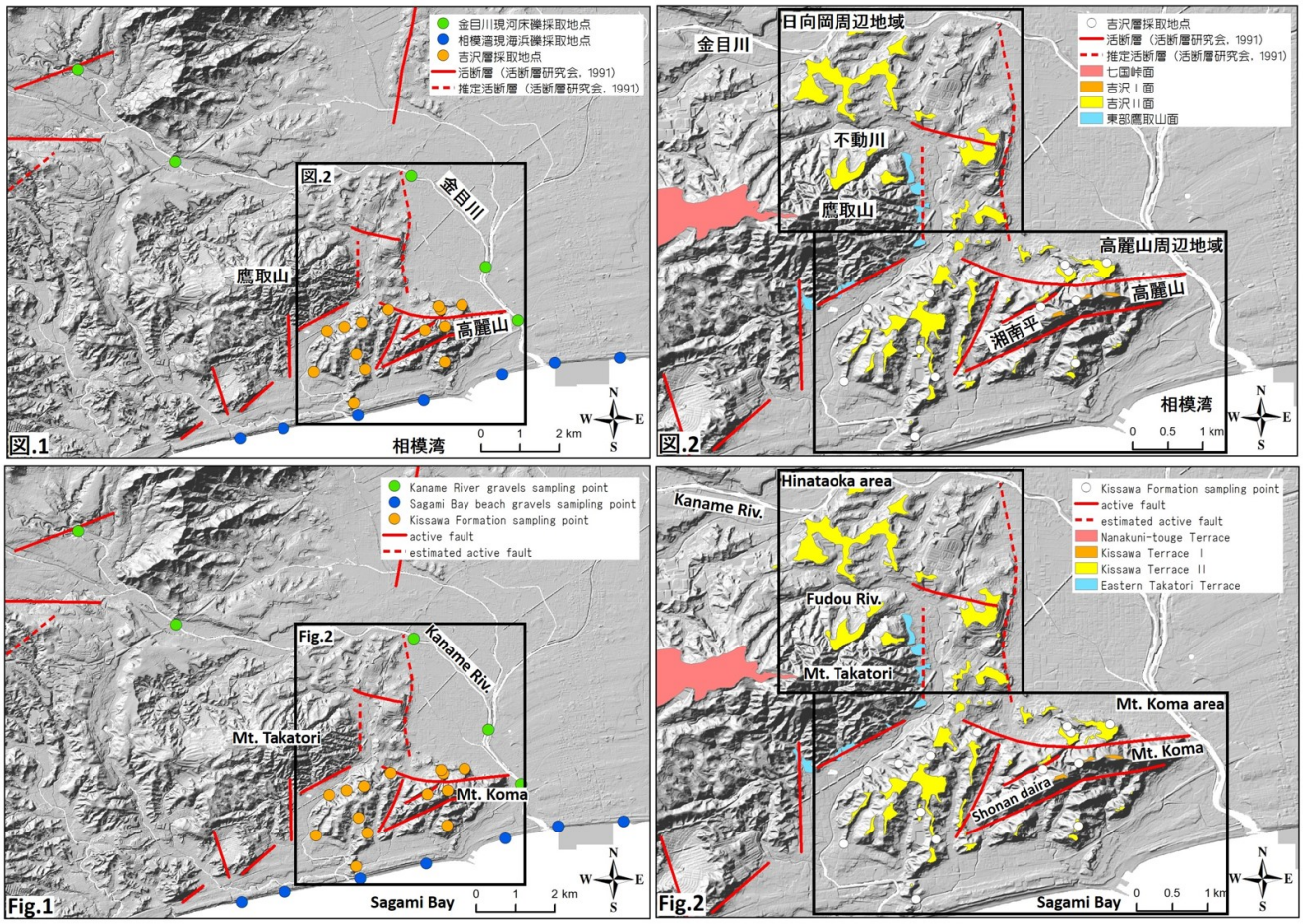

©2019. Japan Geoscience Union. All Right Reserved.

Sediment movement and collapse of bank protections by a series of large flood events at the Sendai River, Tottori, southwest Japan

*Yoshinori Kodama[1], Kento Takemoto[2]

1. Faculty of Agriculture, 2. Hyogo Prefecture

In recent two years, large flood events more than 15 year-occurrence interval happened in a row at the Sendai River (Ad=1,190 km^2, L=52 km), southwest Japan. We surveyed recording artificial bank damages and sediment movements to build bars. We also analyzed satellite images for pre-events, middle, post events. The results show that the Sendai River could be divided into three sections, except uppermost 6.6 km reach: i) 6.6-11.8 km: river bed sediments were washed away to be bedrock exposure, ii) 11.8-31.0 km: alternate bars with small wavelength (less than 1000 m) were formed and iii) 31.0-48.4 km: alternate or multiple bars with larger wavelength (less than 4000 m) were formed, some of them were covered by vegetation. Many sites of artificial bank protection collapse were observed in bedrock exposure reach, where basement of artificial bank protection lost support by removing sediments. The other many sites of bank collapse were in adjacent points of small wavelength (less than 800 m) and high in relief (c.a. 2m) alternate bars, where convergent flood flow occurred scouring of river bed material.

Keywords: Large flood events, collapse of bank protection, bedrock exposure, alternate bar, satellite image, 2018 torrential rain in western Japan

©2019. Japan Geoscience Union. All Right Reserved.

Channel incision history with knickpoint retreat in the Kushira River after the deposition of Ata pyroclastic flow, Osumi Peninsula, Kyushu, Japan

*Shintaro Takanami[1]

1. Meiji University

The Ata welded ignimbrite (110 ka B.P.) lies concealed in the Osumi pumice fall deposits and the Ito pyroclastic flow deposits (non-welded, 30 ka B. P.), having been exposed along the Kushira River valley in the northern margin of Kasanohara ignimbrite plateau, southern Kyushu of Japan (Aramaki and Ui 1966). The Kushira River has a number of knickpoints along its course. Riverbed of Kushira River is composed of the Ata ignimbrite in the upstream reach after the Tanida waterfall. The preceding research by Yokoyama (2000) revealed rapid erosion processes on the Ito non-welded ignimbrite plateau. By contrast, almost no studies reported on the processes of the Ata ignimbrite exposed along Kushira River. Here, to gain a better understanding of this topic, the present study estimated the recession rates of knickpoints in various duration (i.e., from 110 ka to 30 ka, from 30 ka to present and during 110 kyrs), by restoring and comparing the three longitudinal profiles based on field observation and existing borehole data.

In this study, the bottom elevation of Osumi pumice fall deposits in the Kushira River valley was identified as the maximum elevation of riverbed just before the deposition of Osumi pumice. And the elevation of riverbed immediately after the Ata pyroclastic flow was also provided by the distributional top of the Ata ignimbrite. At 11 outcrops, unconfined compressive strength of the Ata ignimbrite was evaluated by KS-type Schmidt rock hammer.

Restored longitudinal profile of 110 ka indicates that the Kushira River had a marked knickpoint at the edge of Ata ignimbrite plateau that was 16 km away from present river mouth. The recession rate of this knickpoint is estimated to 5.4 cm/yr considering that it has retreated to the present position of Tanida waterfall. Estimated unconfined compressive strength of the Ata ignimbrite is gradually decreasing toward its upper part, and showing the exceptionally highest value at the “lower-positioned” Tanida waterfall ($421\times10^6 N/m^2$). Taking this into consideration, another knickpoint located now observed at 26 km from the present river mouth is also candidate for the original knickpoint at 110 ka and had retreated from the edge of Ata ignimbrite plateau to such above position (26 km inland). In this latter case, the recession rate of the knickpoint in the past 110,000 years is calculated as 8.6 cm/yr. The maximum elevation of estimated riverbed at 30 ka indicates that the Kushira River had a steeper gradient than any other timing (probably except for LGM) and incised deeper into the Ata ignimbrite plateau along the downstream side. At that time, the former Tanida waterfall was likely situated in the downstream side of 19 km from the present river mouth. Therefore, its recession rates were estimated more than 2.6 cm/yr during the period from 110 ka to 30 ka, and less than 10 cm/yr in the last 30,000 years. Based on these, this study concludes that continuous bedrock incision might have been occurred with knickpoint retreat since the formation of Ata welded ignimbrite until the deposition of Osumi pumice fall. And it is highly probable that this incision in the Kushira River valley was definitely controlled by the sea level lowering during the period of LGM.

This work was financially supported by the School of Arts and Letters, Meiji University.

©2019. Japan Geoscience Union. All Right Reserved.

References

Aramaki, S. and Ui, T. 1966. Ata pyroclastic flows and the Ata caldera in Southern Kyushu, Japan. *The Journal of the Geological Society of Japan* 72: 337-349.
Yokoyama, S. 2000. Rapid Formation of Kasanohara Ignimbrite Plateau, South Kyushu, Japan. *Transactions, Japanese Geomorphological Union* 21: 277-290.

Keywords: Ata welded ignimbrite, knickpoint, Kasanohara, Kushira River, sea-level change

©2019. Japan Geoscience Union. All Right Reserved.

Implications of the distribution of marine terraces and submerged terraces in Japanese Island

*Tetsuya Komatsu[1], Hiura Yuki[1], Takayuki Takahashi[2], Taro Funatsu[2], Masahiro Muraki[2], Taiga Kimori[2], Toshihiko Sugai[2]

1. Japan Atomic Energy Agency, 2. Graduate School of Frontier Sciences, The University of Tokyo

One of the primary issues of the geological disposal technology is to advance the techniques associated with investigation/assessment for long-term uplift and erosion in terrestrial-marine transitional zone in Japan. To examine this issue, it is inevitable to understand the geomorphic features indicating uplift and erosion in the continental shelf, which widely emerged during glacial periods. Submerged terraces defined as step-like and lobate seabed features can be identified along the continental shelfs. These landforms morphologically mimic marine terraces in terrestrial areas. This study compared the distribution of submerged terraces and MIS 5e terraces in Japan. As a result, the trends of the depth change of submerged terraces in some areas appear to be consistent with the trends of the elevation change of MIS 5e terraces. Furthermore, some cases show the depth of submerged terraces changes abruptly at the seaward extension of terrestrial active fault. These results imply submerged terraces in Japan can be an indicator of regional tectonics in the seafloor.

This study was carried out under a contract with METI (Ministry of Economy, Trade and Industry) as part of its R&D supporting program for developing geological disposal technology.

Keywords: seafloor landform, submerged terrace, marine terrace, geological disposal

©2019. Japan Geoscience Union. All Right Reserved.

Marine erosional landforms along the southern coast of Yonaguni Island, Ryukyus

*Hayate Kimura[1], Kensaku Urata[2], HASEGAWA Hitoshi[3], Toshihiko Ichihara[4], Atsushi Suzuki[5], Nobuyuki Hori[6], Hironobu Kan[2]

1. Graduate school of integrated sciences for global society, 2. Graduate School of Integrated Sciences for Global Society, Kyushu University, 3. Kokushikan University, 4. Sedimentary Environments Research, 5. Geological Survey of Japan National Institute of Advanced Industrial Science and Technology (AIST), 6. Department of Geography, Nara University

Yonaguni Island is located at the westernmost of Japan, where marine erosional landform is widely seen. However, high sea cliffs refuse the investigator’ s approach. We created three-dimensional models by taking photographs from drone. The coastal area of Yonaguni Island is composed of the Middle Miocene sedimentary rocks of the Yaeyama Group and Pleistocene limestone of the Ryukyu Group. We observed characteristic erosional landforms which varies depending on geology along the southern coast of Yonaguni Island.
We surveyed 6 areas where locate the east and south coasts in Yonaguni Island. Photogrammetric surveys were carried out using DJI Phantom 4 Pro. We installed a GCP at accessible places. PhotoScan Professional was used as SfM-MVS software to create terrain models.
Coastal landforms are largely different depending on geological structure. In the limestone coast, collapsed areas of several hundred meters wide are formed. These collapses seem to originate from the unconsolidated layer of unconformity below the limestone or the detrital layer in the limestone. In the coast of sedimentary rocks, coastal landform varies with sedimentary facies. Shore platform is formed at the base of cliff which composed of layers of sandstone and shale. On the other hand, large boulders are distributed at the base of cliff composed of massive sandstone without layers.

Keywords: SfM-MVS, Photogrammetry, Sea cliff, Shore platform, Yaeyama Group, Ryukyu Limestone

©2019. Japan Geoscience Union. All Right Reserved.

Seafloor topography of Amami Sumiyo Bay -Visualization of Seafloor derived from multibeam bathymetric survey-

*Miho Tanaka[1], Ken Toguchi[2], Nobuyuki Hori[3], Hayate Kimura[4], Yukihiko Imai[5], Yosuke Nakashima[6], Yayoi Najima[7], Hironobu Kan[8]

1. Graduate School of Integrated Sciences for Global Society, 2. University of the Ryukyus, 3. Tokyo Metropolitan University, 4. School of Engineering, Kyushu University, 5. Faculty of science, Okayama University, 6. National Institute of Technology, Ariake College, 7. The Graduate University for Advanced Studies, 8. Kyushu University

The shallow water area is a very important area to reveal the sea level change during the last glacial period. In this study, we conducted multibeam bathymetric survey at Amami Sumiyo Bay and created a seafloor topographic map with high accuracy of 1 m grid.
Sumiyo Bay is located on the eastern coast of Amami Island. The Kawauchi River and the Sumiyo River are flowing into that bay. Multibeam bathymetric survey was conducted from August 20th to September 2nd, 2018 by using R2SONIC 2022 Broadband Multibeam Echosounder. Also, we measured the reflection intensity to discriminate sediment by using the side scan sonar function (TruePix / Snippets) installed in that device.
As a result of this survey, the topography distribution of the seafloor was revealed. Terrace scarp can be confirmed near the water depth of 100m in the central part of Sumiyo Bay, and it is thought that it was formed by erosion at the low sea level of the glacial period.
In this study, I integrated 10m DEM data of terrestrial area provided by Geographical Survey Institute to the highly accurate seafloor topographic map created by us and consider about geomorphology.

Keywords: multibeam bathymetry, seafloor topography, last glacial stage, sea level, Digital Elevation Model (DEM)

©2019. Japan Geoscience Union. All Right Reserved.

[J] Oral | H (Human Geosciences)：H-SC Social Earth Sciences & Civil/Urban System Sciences

Wed. May 29, 2019 9:00 AM - 10:30 AM JST | Wed. May 29, 2019 12:00 AM - 1:30 AM UTC | 301B 3F

[H-SC07] CCUS (Carbon Dioxide Capture, Utilization, and Storage) for Climate Mitigation

convener:Masao Sorai(Institute for Geo-Resources and Environment, National Institute of Advanced Industrial Science and Technology), Ziqiu Xue(Research Institute of Innovative Tech for the Earth), Masaatsu Aichi(Graduate School of Frontier Sciences, University of Tokyo), Chairperson:Masao Sorai(National Institute of Advanced Industrial Science and Technology)

The prevention of the global warming, which is the urgent challenge facing the world, requires the full-out efforts of science and technology. This session focuses on the CCUS (Carbon Dioxide Capture, Utilization, and Storage) as one of the useful countermeasures for the CO2 emission reduction. It not only targets various scientific phenomenon caused by the capture and storage of CO2, CO2 utilization, and CO2-EOR/EGR, but also discusses the latest R&D developments of each method for the environmental impact assessment, safety assessment, the measuring, monitoring and verification (MMV), and public acceptance. The main theme is the recognition of key issues toward the practical use of CCUS, in addition to the deepening of our knowledge about the CO2 behavior on the underground.

9:00 AM - 9:15 AM JST | 12:00 AM - 12:15 AM UTC

[HSC07-01] Numerical simulation of variational pore pressure response to ocean tidal loading during CO2 injection

*Toshifumi Akaki[1], Hajime Yamamoto[1] (1.Taisei Corporation)

9:15 AM - 9:30 AM JST | 12:15 AM - 12:30 AM UTC

[HSC07-02] Relationship between rock deformation and permeability evolution during fracturing in rocks for CCUS technology

*Takashi Fujii[1], Xinglin Lei[1], Masao Sorai[1] (1.National Institute of Advanced Industrial Science and Technology)

9:30 AM - 9:45 AM JST | 12:30 AM - 12:45 AM UTC

[HSC07-03] Comparison of Optical Fiber Sensing Technique and Strain Gauge in a Measurement of Rock Deformation Caused by Chemical Osmosis

*Shogo Hirota[1], Tomochika Tokunaga[1], Ziqiu Xue[2], Hyuck Park[2] (1.Department of Environmental Systems, Graduate School of Frontier Science, the University of Tokyo, 2.Research Institute of Innovative Technology for the Earth)

9:45 AM - 10:00 AM JST | 12:45 AM - 1:00 AM UTC

[HSC07-04] Experiment of precipitation of salt for dry-out condition caused by CO_2 storage in saline aquifer

*Hayato Morigaki[1,2], Masaatsu Aichi[1] (1.University of Tokyo, 2.Toshiba Energy Systems & Solution Corporation)

10:00 AM - 10:15 AM JST | 1:00 AM - 1:15 AM UTC

[HSC07-05] Thermodynamic Approach to Wettability of CO_2/Brine/Mineral System by Augmented Young Laplace Equation

*Masashige Shiga[1,2], Masao Sorai[1], Masaatsu Aichi[2], Hiromi Honda[2] (1.AIST, 2.The University of Tokyo)

10:15 AM - 10:30 AM JST | 1:15 AM - 1:30 AM UTC

[HSC07-06] A proposal of CO2 underground storage using hydrate

*Takaomi Tobase[1] (1.Electric Power Development Co., Ltd.)

Numerical simulation of variational pore pressure response to ocean tidal loading during CO2 injection

*Toshifumi Akaki[1], Hajime Yamamoto[1]

1. Taisei Corporation

As a promising measure against global warming, CCS (Carbon dioxide capture and storage) has been extensively studied over recent decades and some large-scale projects are currently in operation worldwide. Carbon dioxide is captured from flue gases emitted from large sources such as coal-fired power plant, and injected and kept stored in a deep geologic formation for long-term. In the geologic CO2 storage, reliable and cost-effective monitoring techniques of the injected CO2 need to be established. It is well known that the pore-pressure of groundwater is affected by the earth and ocean tides. Recently, at a geologic CO2 storage project, it has been reported that the pore-pressure fluctuation at a monitoring well is explained by diurnal earth tides, and the amplitude of the pressure fluctuation significantly attenuated when the carbon dioxide arrived at the well due to the changes in compressibility of pore fluid around the well (i.e. the compressibility of CO2 is much smaller than that of water). This suggests a potential low-cost CO2 monitoring technique through monitoring and analyzing tidal responses of pore pressure during geologic CO2 storage. The tidal response of pressure is understood as a hydro-geomechanical coupled phenomena in deformable porous media containing water and CO2. Previous studies indicated that the changes in amplitude of pore-pressure before and after CO2 arrival at a monitoring well can be simply explained by poroelasticity theory. However, numerical simulations are required to further quantitatively investigate the tidal effects on pressure fluctuation at monitoring wells during CO2 injection. For example, the pressure response is possibly affected by many geometrical and geological settings in three-dimensional space, such as distance between the monitoring wells and CO2 plume, geometry of CO2 plume, and pressure dissipation induced by fluid flow. In this study, we developed a numerical simulator in the framework of poromechanics to simulate three-dimensional deformations and stress changes of geological formations under two-phase flow conditions of water-CO2, which was enhanced to be adoptive to cyclic loading by diurnal and semi-diurnal tide. Using this simulator, we investigate variation of responses of pore water pressure to the ocean tide loading during CO2 injection. Amplitude of the response at injection well decrease during CO2 injection, and somewhat recovered due to upward movement of CO2 plume after injection. The final amplitude in this simulation is smaller than initial amplitude under water saturated condition due to an effect of CO2 plume staying top of the reservoir.

Keywords: Ocean tide, Carbon dioxide geologic storage, Numerical simulation

©2019. Japan Geoscience Union. All Right Reserved.

Relationship between rock deformation and permeability evolution during fracturing in rocks for CCUS technology

*Takashi Fujii[1], Xinglin Lei[1], Masao Sorai[1]

1. National Institute of Advanced Industrial Science and Technology

An understanding of relationship between fluid flow transport and geo-mechanical response within geological reservoirs is of a fundamental concept for a suitable utilization of deep underground repositories (e.g., Carbon Capture and Storage (CCS), Carbon Capture Utilization and Storage (CCUS), shale gas exploration). Particularly, fracture permeability within caprocks plays an important role in producing hydrocarbon during the trapping of buoyant gas fluids in reservoirs for CCUS projects. Wide variations of permeability value depending on rock deformation (including fracturing process) for several types of rocks has been determined using the coupled fluid flow transport (TOUGH2) and geo-mechanical response (FLAC3D) simulator (e.g., Rutqvist et al., 2002) so far. However, the evolution of permeability during fracturing in such rocks is very complex, and there now are being reported few constitute law for the linked deformation and fracture permeability. Furthermore, few laboratory studies have experimentally been conducted so as to replicate this process by simultaneously fracturing specimens and measuring permeability at in situ fracturing stress states (Carey et al., 2015; Fujii et al., 2015; Frash et al., 2016).
The purpose of this study is to investigate experimentally permeability change during fracturing in (i) caprocks (shale, mudstone, slate) and (ii) reservoir rock (sandstone, tuff), the conditions of which assumes that CO_2 is injected into geological media. We attempt to fit a model to obtained experimental data (i.e., permeability: K, volumetric strain: e_v) in order to develop suitable constitute law for the optimize use of coupled geo-mechanics and fluid flow simulator.
Our results demonstrate that there could mainly be classified into the two patterns of relationship between e_v and K of all materials tested. Particularly, it is apparent that the permeability behavior throughout fracturing and slipping processes are quite different between rock groups of (i) and (ii). Caprocks have a sharp-jumped increase of permeability during fracturing in the rock matrix, but reservoir rocks have significantly smaller permeability change, compared to the caprocks in post-failure regime. Furthermore, model fitting results suggest that the relationship between e_v and K of all materials tested could be explained fully by modification of conventional model (e.g., Cappa et al., 2009)
In light of findings of our study, it can be concluded that the propsed constitute law might be contributed to the simplification and optimization of the coupled fluid flow and geomechanical simulator.

Keywords: rock deformation, fracture permeability, Constitute law

©2019. Japan Geoscience Union. All Right Reserved.

Comparison of Optical Fiber Sensing Technique and Strain Gauge in a Measurement of Rock Deformation Caused by Chemical Osmosis

*Shogo Hirota[1], Tomochika Tokunaga[1], Ziqiu Xue[2], Hyuck Park[2]

1. Department of Environmental Systems, Graduate School of Frontier Science, the University of Tokyo, 2. Research Institute of Innovative Technology for the Earth

Mass transport and water flow in subsurface are generally considered to be much smaller than those on surface environment. Stability of subsurface environment is useful to isolate specific substances (e.g. CO_2 or high-level radioactive wastes) from human societies for a long time. For these purposes, argillaceous formations perform as effective seal layer because of its low permeability and smaller diffusion coefficient.

It is known that some argillaceous rocks show semipermeable membrane behavior, i.e., the process called chemical osmosis. Chemical osmosis causes water flow across semipermeable membrane driven by the gradient of osmotic pressure between two solutions (Marine and Fritz, 1981). Previous research showed that the pressure change caused by chemical osmosis can reach to about 20 MPa (Neuzil, 2000). Osmosis-induced pore pressure change can cause deformation of porous medium (Greenberg et al., 1973: Noy et al., 2004), however, the detailed discussion on the osmosis-induced deformation behavior of argillaceous rocks is still premature because of the difficulty for measuring multiple strain in the sample.

Generally, normal strain gauges by measuring the changes of the electrical resistance are used for laboratory-scale rock deformation experiments. Experiments for measuring deformation caused by chemical osmosis take a long time and drifts caused by water intrusion and/or delayed heat dissipation is considered to be the issue for the accurate measurements. Distributed optical fiber sensing (DOFS) is a technique for possibly avoiding the measurement drift. In DOFS measurement, the backscattering light is used to measure strains along the fiber, and DOFS can use entire optical fiber as a sensor, thus, strain behavior at multiple points along the optical fiber can be obtained.

The purpose of this study is to investigate the applicability of both strain gauges and DOFS to the laboratory-scale chemical osmosis experiments through the comparison of both results, and to discuss the strain behavior of argillaceous rocks by chemical osmosis. In this experiment, core samples with the height of about 30mm and diameter of about 50mm made from mudstones collected from the Wakkanai Formation in Hokkaido prefecture and the Oganocho Formation in the Chichibu Basin, Saitama prefecture, were used. Strain gauges were attached to the sample, and axial and circumstantial strains near the both edges were measured. Optical fiber was attached helically to the sample, and the strains along the direction of the fiber were measured. The lateral and top surfaces of the specimen were sealed by silicon rubber to prevent water flow through these surfaces. In the experiment, the bottom surface of the sample was contacted to NaCl solution with 10g/L higher concentration than that of pore water, and osmotic flow was induced by the concentration gradient. The strains of the specimen caused by osmotic flow were measured by both DOFS and strain gauges. Temperature was kept almost constant throughout 240 hours by putting the apparatus into a box made with heat insulating material and the experimental room was controlled by air conditioner.

In the initial phase of the experiments, the strain behaviors measured by both strain gauges and DOFS showed a good agreement. Initial strain behavior characteristic to the poroelastic effect was found only in the measurement by strain gauges because of the much shorter sampling interval compared with that in

©2019. Japan Geoscience Union. All Right Reserved.

DOFS. On the other hand, after 20 hours, strains measured by the strain gauges near the bottom of the sample, i.e., high-concentration side, started to increase while those measured by DOFS not. It is considered to be caused by the unstable behavior of strain gauges.

Keywords: Chemical osmosis, optical fiber sensing technique, argillaceous formation, poroelasticity

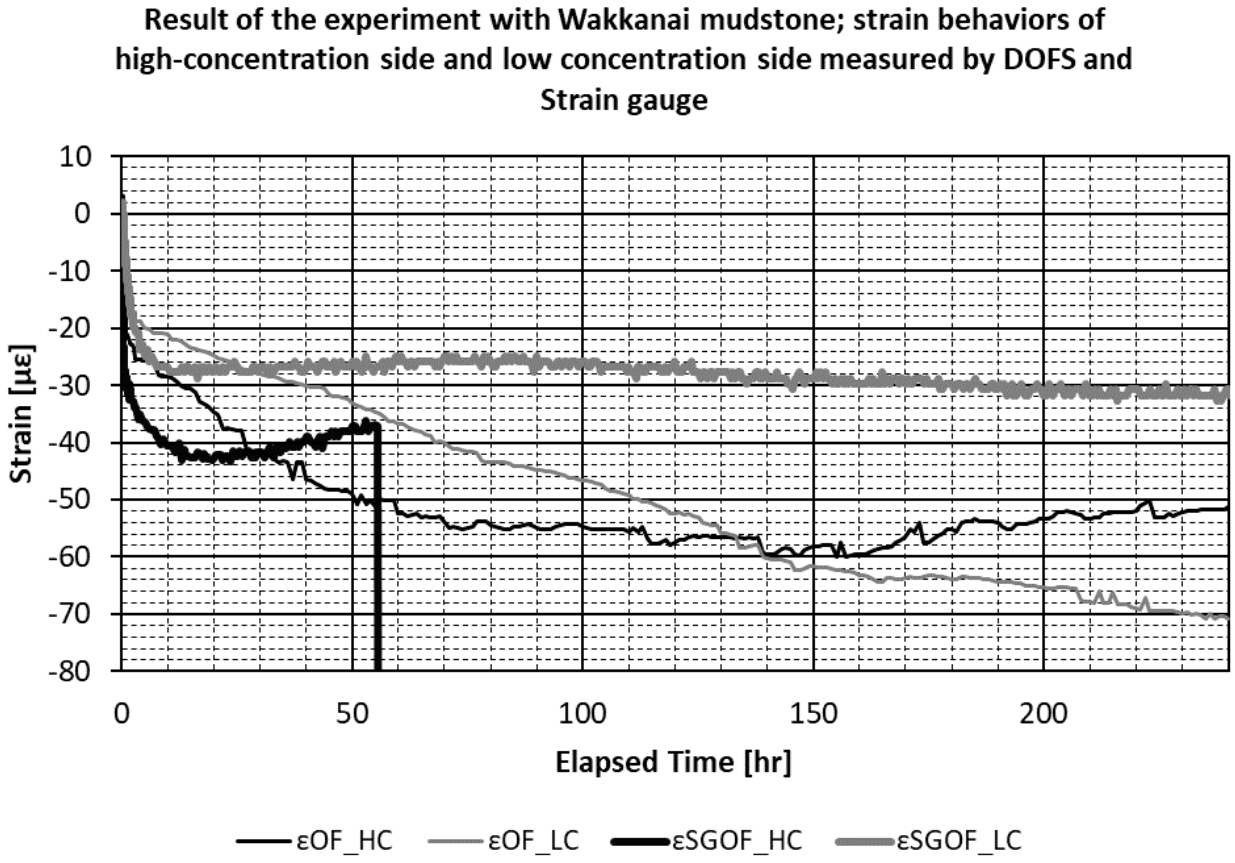

©2019. Japan Geoscience Union. All Right Reserved.

Experiment of precipitation of salt for dry-out condition caused by CO_2 storage in saline aquifer

*Hayato Morigaki[1,2], Masaatsu Aichi[1]

1. University of Tokyo, 2. Toshiba Energy Systems & Solution Corporation

Since CO_2 is transported in dry condition to prevent corrosion of the press-in pipe, CO_2 injected into the saline aquifer may evaporate water and dry the formation. In this case, there is concern that the porosity and permeability of the reservoir will decrease due to salt precipitation and clogging. On the other hand, the influence of cap rock on the sealing ability has not been considered sufficiently.
In this study, in order to observe the state of salt precipitation while controlling the degree of drying, the experiment was carried out with humidity control to generate a suction of about 100 MPa using a thermo-hygrostat. In the experiment, the core sample with the side sealed and the brine reservoir attached at the bottom was placed in the humidity control space, and the water evaporation from the top of the core sample was measured and the precipitation of salt was observed. In addition, in the comparison between before and after this experiment, we also tried to evaluate the influence of semipermeable membrane performance of mudstone on the presence or absence of precipitation and change in salt concentration of brine in the reservoir. The salt concentration of the reservoir, which was assumed to be the saline aquifer, was set at 0.6 mol / L as seawater, and when experiments were conducted assuming that the brine saturated rock was exposed to dryness, it was confirmed that the flux of moisture did not change remarkably before and after salt precipitation on the muddy sandstone of the Otadai Formation, the mudstone of the Otadai Formation and the mudstone of Wakkanai Formation. Also, the salt transport inhibition due to the semipermeable membrane effect was not noticeable. This suggests it is not necessarily expected that the precipitation of salt by drying improves CO_2 shielding performance of cap rock.

Keywords: saline aquifer, salt precipitation, reflection coefficient

©2019. Japan Geoscience Union. All Right Reserved.

Thermodynamic Approach to Wettability of CO_2/Brine/Mineral System by Augmented Young Laplace Equation

*Masashige Shiga[1,2], Masao Sorai[1], Masaatsu Aichi[2], Hiromi Honda[2]

1. AIST, 2. The University of Tokyo

CO_2 Geo-Sequestration (CGS)has been regarded as one of the most significant technologies to reduce the amount of CO_2 emissions into the atmosphere.

Sealing performance of the caprock in the geological formation is largely influenced by wettability which is evaluated by the contact angle of the CO_2/Brine/Mineral system.

A lot of researchers have measured the angles in various conditions (e.g. pressure, temperature, salinity, or types of minerals) by various methods.

However, the value and the trend of the contact angle have not been confirmed yet.

This is mainly because there are a lot of inconsistencies in the experimental data due to the difficulties of controlling the surface roughness or impurities.

In order to tackle this problem,we calculated the contact angle and studied the key factor to affect its value by using augmented Young Laplace equation in which a thickness of the film on the mineral substrate is considered as a thermodynamic variable.

Parameters of the interfacial properties were calculated by PhreeqC, which is a simulator performing a wide variety of aqueous geochemical calculations.

Keywords: CO2 Geo-Sequestration, Wettability, Contact Angle

©2019. Japan Geoscience Union. All Right Reserved.

A proposal of CO2 underground storage using hydrate

*Takaomi Tobase[1]

1. Electric Power Development Co., Ltd.

There is a fact that methane exists naturally and stably in the form of hydrate (solid).
As natural analog with methane hydrate, form CO2 hydrate using gas hydrate mechanism based on temperature and pressure, propose that could also be applied to underground storage of CO2. The concepts of the CO2 hydrate storage are as follows.
(1) Injection liquid or supercritical CO2 in the storage layer.
(2) Injected CO2 moves above by a density difference, when temperature and pressure condition reached the domain that formed hydrate, make clogging in a pore (come to have seal function).
(3) CO2 becomes able to storage under layer of CO2 hydrate having seal function. (not need the cap rock as geological structure)
As a result of investigating the temperature in the surrounding sea area of Japan, we confirm that temperature and pressure condition to form CO2 hydrate in the underground of sea bottom. It is thought that very likely to be the CO2 hydrate storage.
Aquifer storage (including CO2-EOR) to have the cap rock as a method of the CO2 storage is popular. But if CO2 hydrate storage is realized, we can hope that contribute to right lot expansion of the CO2 storage.

Keywords: carbon storage, gas hydrate, seal function

©2019. Japan Geoscience Union. All Right Reserved.

[J] Oral | H (Human Geosciences)：H-SC Social Earth Sciences & Civil/Urban System Sciences

Wed. May 29, 2019 10:45 AM - 12:15 PM JST | Wed. May 29, 2019 1:45 AM - 3:15 AM UTC | 301B 3F

[H-SC07] CCUS (Carbon Dioxide Capture, Utilization, and Storage) for Climate Mitigation

convener:Masao Sorai(Institute for Geo-Resources and Environment, National Institute of Advanced Industrial Science and Technology), Ziqiu Xue(Research Institute of Innovative Tech for the Earth), Masaatsu Aichi(Graduate School of Frontier Sciences, University of Tokyo), Chairperson:Ziqiu Xue(Research Institute of Innovative Technology for the Earth)

The prevention of the global warming, which is the urgent challenge facing the world, requires the full-out efforts of science and technology. This session focuses on the CCUS (Carbon Dioxide Capture, Utilization, and Storage) as one of the useful countermeasures for the CO2 emission reduction. It not only targets various scientific phenomenon caused by the capture and storage of CO2, CO2 utilization, and CO2-EOR/EGR, but also discusses the latest R&D developments of each method for the environmental impact assessment, safety assessment, the measuring, monitoring and verification (MMV), and public acceptance. The main theme is the recognition of key issues toward the practical use of CCUS, in addition to the deepening of our knowledge about the CO2 behavior on the underground.

10:45 AM - 11:00 AM JST | 1:45 AM - 2:00 AM UTC

[HSC07-07] CO_2 behavior simulation using large scale geological model

*Yuuki Shigeoka[1], Haruki Nishiyama[1], Hiroshi Kinoto[1], Takaomi Tobase[2], Takahiro Nakajima[3], Ziqiu Xue[3] (1.JP Business Survice Corporation, 2.Electric Power Development Co., Ltd., 3.Research Institute of Innovative Technology for the Earth)

11:00 AM - 11:15 AM JST | 2:00 AM - 2:15 AM UTC

[HSC07-08] **Monitoring hydromechanical responses in aquifer by distributed fiber-optic strain sensing: From lab to field**

*Yi Zhang[1,2], Ziqiu Xue[1,2], Tsutomu Hashimoto[1,2], Hyuck Park[1,2] (1.Geological Carbon dioxide Storage Technology Research Association, 2.Research Institute of Innovative Tech for the Earth)

11:15 AM - 11:30 AM JST | 2:15 AM - 2:30 AM UTC

[HSC07-09] **Field Testing of Hybrid Brillouin-Rayleigh Distributed Sensing System for Subsurface Water Injection Monitoring**

*Yankun Sun[1,2], Ziqiu Xue[1,2], Tsutomu Hashimoto[1,2], Xinglin Lei[3], Yi Zhang[1,2] (1.Geological Carbon Dioxide Storage Technology Research Association, 2.Research Institute of Innovative Technology for the Earth, 3.National Institute of Advanced Industrial Science and Technology)

11:30 AM - 11:45 AM JST | 2:30 AM - 2:45 AM UTC

[HSC07-10] Gravity monitoring using superconducting gravimeters near the seashore at the Tomakomai CCS demonstration site

*Hiroki Goto[1,2], Mituhiko Sugihara[1,2], Hiroshi Ikeda[3], Yuji Nishi[1,2], Tsuneo Ishido[1,2], Masao Sorai[1,2] (1.Geological Carbon Dioxide Storage Technology Research Association, 2.National Institute of Advanced Industrial Science and Technology, 3.University of Tsukuba)

11:45 AM - 12:00 PM JST | 2:45 AM - 3:00 AM UTC

[HSC07-11] Pilot test for microbubble CO_2 injection to reservoir in oil field - Test planning and preparation -

*Kazunori Nakagawa[1], Ryo Ueda[1], Masanori Nakano[1], Ziqiu Xue[2] (1.Japan Petroleum Exploration Co., Ltd., 2.Research Institute of Innovative Technology for the Earth)

12:00 PM - 12:15 PM JST | 3:00 AM - 3:15 AM UTC

[HSC07-12] Mechanisms inducing anomalously high pCO_2 without CO_2 leakage in coastal environment

*Yuji Watanabe[1,2], Keisuke Uchimoto[1,2], Makoto Nishimura[1,2], Saeko Mito[1,2], Ziqiu Xue[1,2] (1.Geological CO2 Storage Technology Research Association, 2.RITE)

CO_2 behavior simulation using large scale geological model

*Yuuki Shigeoka[1], Haruki Nishiyama[1], Hiroshi Kinoto[1], Takaomi Tobase[2], Takahiro Nakajima[3], Ziqiu Xue[3]

1. JP Business Survice Corporation, 2. Electric Power Development Co., Ltd., 3. Research Institute of Innovative Technology for the Earth

Carbon Capture and Storage (CCS) is expected as a mitigation measure of climate change and global warming causing by the rise in atmospheric carbon dioxide (CO_2) concentration. CCS is a technology that can reduce the amount of CO_2 emissions from large point sources, such as electricity power plant, by separating and recovering CO_2 from atmosphere-releasing gas and storing it in the basement. Main items of reservoir evaluation are (1) evaluation of injection performance and (2) evaluation of storage capacity. In this research, the above two evaluation items were investigated by numerical analysis. Analysis module, TOUGH2-ECO2N which deals with multicomponent and multiphase fluid was used.

(1) Evaluation of injection performance
The influence of basic physical parameter (permeability and porosity) on the CO_2 injection performance of the reservoir layer was investigated. As a result, it has been found that permeability affects whole pressure level of the reservoir layer and porosity affects the slope of pressure rise. Furthermore, their influence on the long-term distribution range of pressure and CO_2 plume has been revealed clearly.

(2) Evaluation of storage capacity
The basic physical parameter of analysis model for the evaluation of the storage capacity was determined with history matching based on the monitoring and the prediction simulation of the pressure, which was conducted in the CCS project in Canada Quest. In order to reveal the factors affecting the storage capacity evaluation were carried out, case studies such as changing placement of injection wells, etc. It is expected that the findings from this study can contribute to the evaluation of the storage capacity, such as predicting pressure rise in the reservoir layer and distribution of CO_2 plume, and the helpful for enabling "reservoir management", such as arrangement of injection wells, number of wells, injection rate and time, and installation of a pressure relief well.

Keywords: Carbon dioxide Capture and Storage, TOUGH2, Large scale Reservoir Simulation

©2019. Japan Geoscience Union. All Right Reserved.

Monitoring hydromechanical responses in aquifer by distributed fiber-optic strain sensing: From lab to field

*Yi Zhang[1,2], Ziqiu Xue[1,2], Tsutomu Hashimoto[1,2], Hyuck Park[1,2]

1. Geological Carbon dioxide Storage Technology Research Association, 2. Research Institute of Innovative Tech for the Earth

Pore fluids control deformation of porous media by the fluid-to-solid hydromechanical (HM) coupling in which a change in fluid pressure can modify the effective stress and deform the porous medium (Wang, 2000). The HM coupling mechanism provides a possibility that to understand aquifer characteristics and fluid activities during fluid extraction and/or injection operations, e.g., in geological CO_2 storage (GCS), by monitoring rock strain changes. We successfully measured such HM deformations using a high-resolution distributed fiber optic strain sensing (DFOSS) tool in both laboratory and field scale studies. From the DFOSS-obtained HM information, we are able to track the pressure impact zone, understand the permeability structure of the aquifer formation and identify the preferential flow layers. Moreover, we can track the fluid migration front during CO_2 displacing water and the mechanical response of CO_2 breaking through to a low-permeability layer or caprock. The application of DFOSS would be beneficial to guide the aquifer pressure management for safe GCS with prior or simultaneous water extraction (Buscheck et al., 2012).

Keywords: Distributed fiber-optic strain sensing, Aquifer test, Hydromechanical deformation, CO2 storage

©2019. Japan Geoscience Union. All Right Reserved.

Field Testing of Hybrid Brillouin-Rayleigh Distributed Sensing System for Subsurface Water Injection Monitoring

*Yankun Sun[1,2], Ziqiu Xue[1,2], Tsutomu Hashimoto[1,2], Xinglin Lei[3], Yi Zhang[1,2]

1. Geological Carbon Dioxide Storage Technology Research Association, 2. Research Institute of Innovative Technology for the Earth, 3. National Institute of Advanced Industrial Science and Technology

Massive fluid injections into underground formations inevitably alter stress state and even induce damaging earthquakes, so robust high-resolution monitoring technologies are urgent to track geomechanical behaviors of injected fluids. Here we present one of the first case studies demonstrating the use of distributed fiber optic sensing (DFOS) technique based on hybrid Brillouin-Rayleigh backscattering for well-based monitoring of geomechanical deformations induced by field water injection. Injection tests were conducted with different injection scenarios between injection well (230 m, IW #2) and 5.5 m away from fibered monitoring well (300 m, MW #1) deployed cable behind casing in Mobara, Japan. Geomechanical responses were real- time recorded using DFOS approach; the resulting strain profiles were used to capture fluid evolution behaviors; thus evidencing that induced strains significantly depend on injection rate, injection pressure and lithological heterogeneity using this approach. Concurrent borehole logging was utilized to detect injection-induced variation of near- wellbore formations, which results agreed reasonably well with DFOS readings. This field application of hybrid DFOS technology conclusively enables speedy improvement of finely monitoring subsurface geoscience engineering activities, such as CO_2 storage.

Based on this methodology, some conclusions in this study can be drawn below:
1. An advanced DFOS system based hybrid Brillouin-Rayleigh backscattering is successfully applied to real-time monitor water injection tests between two adjacent wells. Two different injection formations ① and ② are investigated.
2. Field testing demonstrates that induced geomechanical deformation (i.e., strain) is mainly dependent on injection volume rather than injection temperature, which has no significant effect on the strain changes.
3. Geomechanical deformations harmoniously emerge and eliminate with injection schemes, although the effect of packers on the strain profile results in slight emergency of strain leaps. The impacted zones expand along vertical direction beyond corresponding injection sections.
4. Formation heterogeneity results in lateral transport of injected water and its pressure propagation in the pore space. Compared with *V*sh -GR and BH, the lower *V*sh related to formation is easier for strain accumulation. In addition, although the impact acting on clay-rich formations is relatively small, the existence of shale just weakens the induced deformation intensity rather than completely stops the strain expansion.
5. According to open-hole resistively logs of IW and MW, simplified simulation result further confirms strong small-scale formation heterogeneity and discontinuities of shale-sand distribution in the injection formations.
6. Testing results also reveal that there are two main reasons accounting for vertical expansion of impacted zones during water injections. First reason is formation heterogeneity, which is quantified by open-hole resistivity logging and GR data, largely affecting fluid behaviors, including migration, evolution and diffusion in subsurface. Second reason is that due to poroelastic deformation, different injection scenarios can generate different injection pressure, which will ultimately lead to different geomechanical deformation responses and first-arrival pressure front patterns of injected water propagating to the

©2019. Japan Geoscience Union. All Right Reserved.

fibered well.

References
Xue, Z., Hashimoto, T., 2017. Geomechanical Monitoring of Caprock and Wellbore Integrity Using Fiber Optic Cable: Strain Measurement from the Fluid Injection and Extraction Field Tests. *Energy Procedia* 114, 3305–3311.
Sun, Y., Li, Q., Fan, C., 2017. Laboratory core flooding experiments in reservoir sandstone under different sequestration pressures using multichannel fiber Bragg grating sensor arrays. *International Journal of Greenhouse Gas Control.* 60, 186–198.
Sun, Y., Xue, Z., Hashimoto, T., 2018. Fiber optic distributed sensing technology for real-time monitoring water jet tests: Implications for wellbore integrity diagnostics. *Journal of Natural Gas Science and Engineering.* 58, 241–250.
Sun, Y., Xue, Z., Hashimoto T., Zhang, Y., 2019. Hybrid Brillouin-Rayleigh Sensing System for Cross-well Monitoring Fluid Injection Tests—A Geomechanical Responses Perspective. *Water Resource Research.* (Under review).

Keywords: Distributed fiber optic sensing, Fluid injection and storage, Hybrid Brillouin-Rayleigh backscattering, Real-time monitoring, Strain responses, Geomechanical deformation

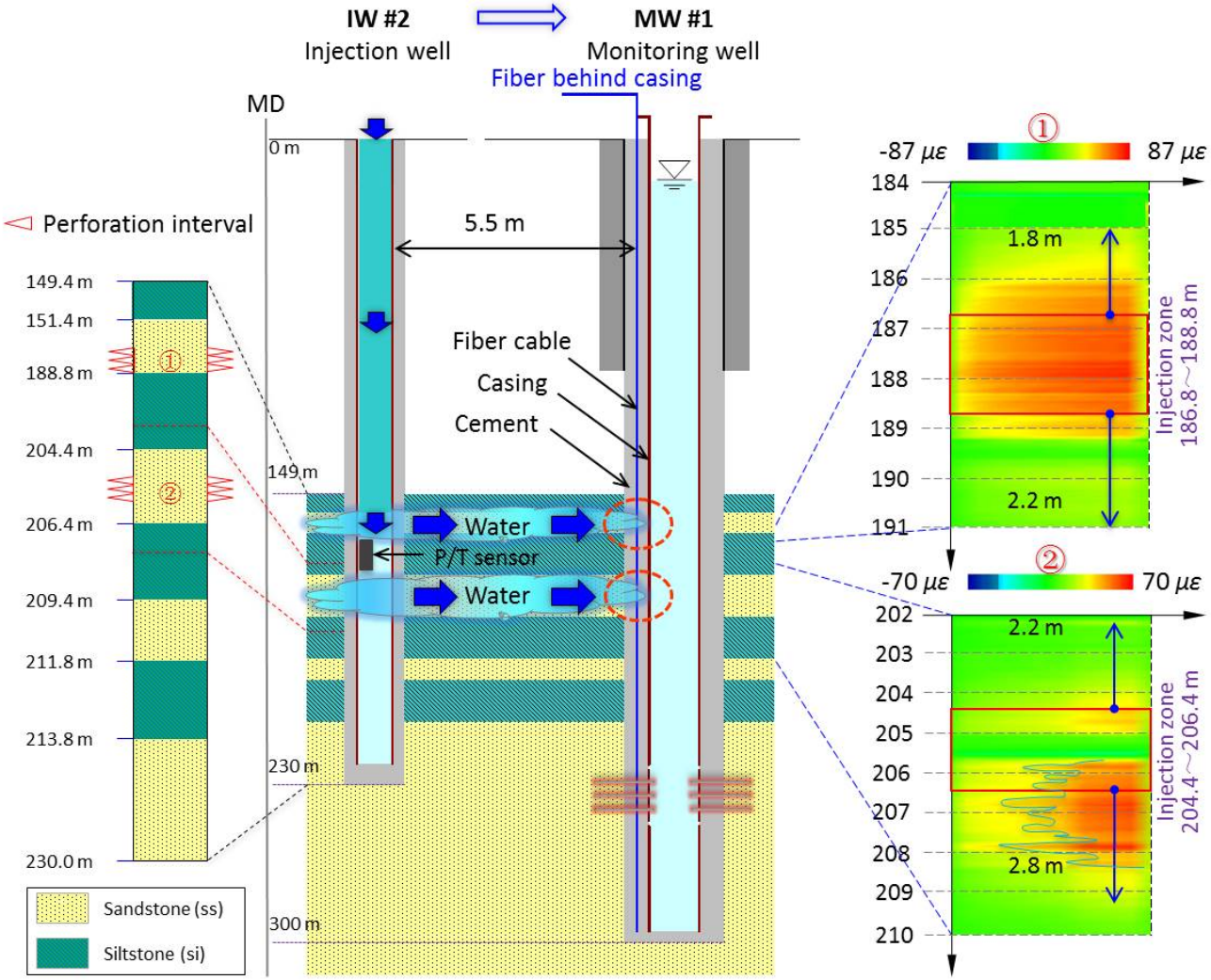

A schematic for fiber optic sensors deployment (left) and the mapped strain by the fiber optic cable (right).

©2019. Japan Geoscience Union. All Right Reserved.

Gravity monitoring using superconducting gravimeters near the seashore at the Tomakomai CCS demonstration site

*Hiroki Goto[1,2], Mituhiko Sugihara[1,2], Hiroshi Ikeda[3], Yuji Nishi[1,2], Tsuneo Ishido[1,2], Masao Sorai[1,2]

1. Geological Carbon Dioxide Storage Technology Research Association, 2. National Institute of Advanced Industrial Science and Technology, 3. University of Tsukuba

Monitoring the distribution and migration of CO_2 injected into geological formations is needed for management of geological storage of CO_2. Superconducting gravimeters (SG’s) potentially enable monitoring of offshore CO_2 storage at ground-based stations because of its high precision. We conducted continuous gravity observations using SG’s near the seashore at the Tomakomai CCS (carbon dioxide capture and storage) demonstration site, Japan to study variation in the observed gravity near the seashore. The gravity data after correcting for tides, polar motion, and barometric pressure changes was strongly affected by shallow groundwater level changes but it was corrected by expressing their effects as a summation of linear functions of groundwater level changes. The standard deviation of the gravity residuals was reduced to less than 1 μGal after correcting for the groundwater effects. The small variation in the observed gravity residuals suggests that the ground-based gravity monitoring using SG's can be useful in long-term monitoring of offshore CO_2 storage.

Keywords: offshore CO2 geological storage, superconducting gravimeter, groundwater

©2019. Japan Geoscience Union. All Right Reserved.

Pilot test for microbubble CO_2 injection to reservoir in oil field - Test planning and preparation -

*Kazunori Nakagawa[1], Ryo Ueda[1], Masanori Nakano[1], Ziqiu Xue[2]

1. Japan Petroleum Exploration Co., Ltd., 2. Research Institute of Innovative Technology for the Earth

In this study we have studied to evaluate the effect of microbubble CO_2 injection to CO_2 storage by core flooding test in laboratory and develop the tools for microbubble CO_2 injection in reservoir and we reached at the step which we plan to conduct the field pilot test in 2019.

We provide an introduction to the planning and preparation to the field pilot test for microbubble injection technology.
Summary of the pilot test
We plan to conduct this test at a part of oil field in Japan. This oil reservoir is consisted of the alternate layers of sand and mud and has high hetrogeneity which the advantage in the microbubble injection technology is expected. Huff' n Puff method will be applied in this test and pressure and flow rate at CO_2 injection and reproduction (flow back) from reservoir after CO_2 injection are measured as field test data. Two CO_2 injection tests, microbubble and normal injection are planned to estimate the effect of microbubble injection technology and behavior. Injected CO_2 volume is 100t at each test, microbubble and normal injection. Moreover, we construct the flow simulation model and estimate the microbubble CO_2 injection before and after field test.
preparation
We produced the tools for microbubble CO_2 injection in well based on prototype tools developed in this study and constructed facility which consisted of CO2 storage tank, CO2 injection pump and warming apparatus in test field.

Acknowledgements

This presentation is based on results obtained from a project commissioned by the New Energy and Industrial Technology Development Organization (NEDO) and the New Energy the Ministry of Economy, Trade and Industry (METI) and attributed to basic study for micro bubble CO_2 injection technology by Tokyo-gas Co., Ltd. and RITE. We deeply appreciate them.

Keywords: Geological CO2 Storage, microbubble, field test

©2019. Japan Geoscience Union. All Right Reserved.

Mechanisms inducing anomalously high pCO_2 without CO_2 leakage in coastal environment

*Yuji Watanabe[1,2], Keisuke Uchimoto[1,2], Makoto Nishimura[1,2], Saeko Mito[1,2], Ziqiu Xue[1,2]

1. Geological CO2 Storage Technology Research Association, 2. RITE

When CO_2 is stored in sub-seabed geological formations in Japan, marine monitoring is mandatory to detect CO_2 leakage as soon as possible should it occur. In the Tomakomai CCS Demonstration Project, a threshold line based on a negative correlation between partial pressure of CO_2 (pCO_2) and dissolved Oxygen saturation in seawater is used to detect an anomalously high value of pCO_2, which is suspected to be a sign of CO_2 leakage. Although CO_2 leakage has never occurred in Tomakomai, pCO_2 values obtained in the monitoring have frequently exceeded the threshold line; that is, many false-positives have been produced. It is important to consider what can be causes of the false-positives. To discuss the causes, we analyzed data observed in the marine monitoring of the Tomakomai project, and meteorological data at Tomakomai. It is implied that weather conditions, such as wind speeds and precipitation, were related with false-positives. Also, we found that total alkalinity was remarkably low at a monitoring survey where many false-positives were observed. The low values of total alkalinity make pCO_2 values higher than usual, and consequently they might produce many false-positives. Based on the results, we are going to present how to avoid or reduce false-positives.

Keywords: Sub-seabed CO2 storage, Marine monitoring, CO2 leakage, pCO2, Total alkalinity

©2019. Japan Geoscience Union. All Right Reserved.

[J] Poster | H (Human Geosciences)：H-SC Social Earth Sciences & Civil/Urban System Sciences

Wed. May 29, 2019 3:30 PM - 5:00 PM JST | Wed. May 29, 2019 6:30 AM - 8:00 AM UTC | Poster Hall International Exhibition Hall8, Makuhari Messe_13

[H-SC07] CCUS (Carbon Dioxide Capture, Utilization, and Storage) for Climate Mitigation

convener:Masao Sorai(Institute for Geo-Resources and Environment, National Institute of Advanced Industrial Science and Technology), Ziqiu Xue(Research Institute of Innovative Tech for the Earth), Masaatsu Aichi(Graduate School of Frontier Sciences, University of Tokyo)

The prevention of the global warming, which is the urgent challenge facing the world, requires the full-out efforts of science and technology. This session focuses on the CCUS (Carbon Dioxide Capture, Utilization, and Storage) as one of the useful countermeasures for the CO2 emission reduction. It not only targets various scientific phenomenon caused by the capture and storage of CO2, CO2 utilization, and CO2-EOR/EGR, but also discusses the latest R&D developments of each method for the environmental impact assessment, safety assessment, the measuring, monitoring and verification (MMV), and public acceptance. The main theme is the recognition of key issues toward the practical use of CCUS, in addition to the deepening of our knowledge about the CO2 behavior on the underground.

[HSC07-P01] Evaluation of seismic event location accuracy of Tomakomai CO2 injection site: a numerical simulation case study

*Luchen Wang[1], Takahiro Nakajima[1], Ziqiu Xue[1] (1.RITE, Research Institute of Innovative Technology for the Earth)

[HSC07-P02] Technical Challenges of Machine Learning Approach for Porosity Estimation in Nagaoka CCS site

*Takayuki Miyoshi[1], Takahiro Nakajima[1], Ziqiu Xue[1] (1.Research Institute of Innovative Technology for the Earth)

[HSC07-P03] Utilization of wave attenuation in time-lapse sonic logging data to evaluate the effect of super-critical CO_2 in the reservoir

*Takahiro Nakajima[2,1], Luchen Wang[2,1], Ziqiu Xue[2,1] (1.Research Institute of Innovative Technology for the Earth, 2.Geological Carbon Dioxide Storage Technology Research Association)

[HSC07-P04] Geological sequestration in saline carbonate formations: CO_2-brine-rock interaction

*Shachi Shachi[1], Brijesh Kumar Yadav[1], Mohammad Azizur Rahman[2], Mayur Pal[3] (1.Indian Institute of Technology Roorkee, 2.Texas A&M University Qatar, 3.North Oil Company, Qatar)

[HSC07-P05] Changes in sealing performance of artificial caprocks caused by carbonate reactions

*Masao Sorai[1] (1.Geological Survey of Japan, National Institute of Advanced Industrial Science and Technology)

[HSC07-P06] CO_2 migration characteristics of microbubble and conventional sequestration in Berea sandstone revealed by X-ray CT imaging

*Hongyu Zhai[1,2], Yi Zhang[1,2], Hyuck Park[1,2], Ziqiu Xue[1,2] (1.Geological Carbon dioxide Storage Technology Research Association,9-2, Kizugawadai, Kizugawa Shi, Kyoto, 6190292 Japan, 2.Research Institute of Innovative Technology for the Earth (RITE),9-2, Kizugawadai, Kizugawa Shi, Kyoto, 6190292 Japan)

[HSC07-P07] Strain detection by optical fiber for CO_2 injected core specimen

*Hyuck Park[1], Yankun Sun[1], Ziqiu Xue[1] (1.Research Institute of Innovative Technology for the Earth)

[HSC07-P08] Bed deformation measured by distributed optical fiber and its sedimentological interpretation: alternated sandstone and mudstone aquifer, Boso Peninsula, Japan

*Takuma Ito[1,2], Tsutomu Hashimoto[1,2], Ziqiu Xue[1,2] (1.Research Institute of Innovative Technology for the Earth, 2.Geological Carbon Dioxide Storage Technology Research Association)

[HSC07-P09] How many data are necessary to make a suitable threshold for anomalous pCO_2 owing to CO_2 leakage?

*Keisuke Uchimoto[1,2], Yuji Watanabe[1,2], Makoto Nishimura[1,2], Ziqiu Xue[1,2] (1.Geological Carbon dioxide Storage Technology Research Association , 2.Research Institute of Innovative Technology for the Earth)

Evaluation of seismic event location accuracy of Tomakomai CO2 injection site: a numerical simulation case study

*Luchen Wang[1], Takahiro Nakajima[1], Ziqiu Xue[1]

1. RITE, Research Institute of Innovative Technology for the Earth

For CO2 injection monitoring in many CCS project, the most basic monitoring information is the seismic events. The seismic event location is the first step to understanding the causal process of a natural or induced fracture. In the case of CO2 geological storage, the location of an event is of special importance. The events in the reservoir may affect the storage capability. The events in the cap-rock may indicate the CO2 leakage. However, the location of the seismic event is probably to contain bias, especially for the limited seismic observation system. Therefore, the operator should understand that there is uncertainty in the location estimation of a detected event. In this study, we use the Tomakomai (Ocean Bottom Cable) OBC and borehole system (OB1 well) to study the seismic location accuracy in Tomakomai site. We believe that it can help to evaluate the event location effect with different azimuths and different depths. Moreover, this study may also be applied to the optimization of the seismic observation system.

At Tomakomai site, the permanent OBC is arranged as a line (length 3.6 km, containing 55 available sensors), deployed 2 m under the seabed. It is located above the CO2 reservoir and the center point is 3 km from the coast. The OB1 contains 4 sensors in the well with depths ranging from 2 km to 2.2 km. All sensors of OBC and OB1 contain a three-component geophone. Therefore, we can use only detected P phase signal for seismic location. We assume that the velocity model is layered and homogeneous, so that a simple model can be built based on the logging result. The ray-tracing method is employed in the seismic simulation and location process.

We compared the modelling event location accuracy for different azimuths and different depths. All events were distributed around Tomakomai site. The results showed that as the epicenter distance increases, the location errors increases. For the events which the epicenter is far away from the area enclosed by OBC and OB1, the locating effect is significantly worse. In addition, as the event depth increases, the location error also increases. The location error of shallow (0-1 km) events can be maintained within 1 m, while the location error of deep (8 km) events can reach the scale of several hundred meters. Ignoring the effects of the simulation method, it is obviously affected by the geometric distribution of the observation system.

Secondly, we also compared different observation system optimization strategies. The result indicated that, based on the Tomakomai seismic monitoring system, if the number of sensor is fixed, the longer OBC line can provide a better location result. Based on these analyses, future seismic monitoring system designs can be optimized for specific purposes (number of sensors, expected depth of monitoring, etc.).

Keywords: event location, Seismic monitoring, 3D ray tracing, Tomakomai site

©2019. Japan Geoscience Union. All Right Reserved.

Technical Challenges of Machine Learning Approach for Porosity Estimation in Nagaoka CCS site

*Takayuki Miyoshi[1], Takahiro Nakajima[1], Ziqiu Xue[1]

1. Research Institute of Innovative Technology for the Earth

In CCS, the distribution of hydraulic parameters such as porosity and permeability is one of the key parameters for evaluation of CO_2 storage capacity and CO_2 saturations. These parameters are measured as 1D profiles through well-logging. CCS projects, in general, have only a few wells available in the area of target. The 3D seismic data which covers the three dimensional space does not represent the hydraulic features directly. A technique to integrate these different types of data is required to estimate appropriate geological models.
Machine learning (ML) is a technique for predicting a target property from unknown input data by learning the relationship between known input data and prediction target. In this research, we apply ML approaches to Nagaoka CCS site data for predicting porosity distribution from seismic attributes created from the 3D seismic data. Determination of hyper-parameters of the ML model is often site-specific in predicting geological models. We present the technical challenges when using multiple attributes as input data.

Keywords: CCS, Machine Learning, Geological model

©2019. Japan Geoscience Union. All Right Reserved.

Utilization of wave attenuation in time-lapse sonic logging data to evaluate the effect of super-critical CO_2 in the reservoir

*Takahiro Nakajima[2,1], Luchen Wang[2,1], Ziqiu Xue[2,1]

1. Research Institute of Innovative Technology for the Earth, 2. Geological Carbon Dioxide Storage Technology Research Association

This paper discusses seismic wave attenuation by injected CO_2 in the formation. Seismic methods have been broadly used for the monitoring of injected CO_2 at many CCS sites. Concerning the velocity change by the existence of CO_2, the relationship between P-wave velocity and CO_2 saturation in rock samples and formation have been studied well. Some laboratory experiments studied amplitude of P-wave as well as the velocity change by the invasion of CO_2, and the change in amplitude was larger than that of time delay (e.g. Muller et al., 2010). Meanwhile investigations on amplitude attenuation were rather limited. In this paper, we investigated P-wave data in the results of time-lapse sonic logging at the Nagaoka site.
At the Nagaoka site, time-lapse well loggings have been conducted during the injection period and post injection period at observation wells, which are 40 m and 60 m apart from the injection well. The sonic logging was conducted 45 times during 12 years using Halliburton’ s LFDL (Low Frequency Dipole-Sonic Logging Tool). Since it is not ascertain that the monopole transmitter has emitted the same energy at every logging, we chose a reference point in the cap rock 10 m above the target zone. At this depth, the formation was highly cemented with very small slowness, so the position was easily recognized in wave data and its wave field would not change during the CO_2 injection. We took the amplitude of the first P-wave arrival as the reference. We also assume that the emitted energy from the transmitter would not change at the reservoir within 15 m interval from the reference point.
Firstly, we compared the wave data at the depth where the largest change observed by CO_2 injected. We can see that the first arrival of P-wave at the nearest observation logging was shifted from 1.64 to 1.8 micro-sec at 14-th run. Amplitude of the peak was also gradually decreased after the CO_2 breakthrough, and the amplitude at 21-st run was clearly small. Next we calculated spectrum around the first P-wave arrivals, and found that high frequency components decreased much than the lower frequency components. This frequency shift looked like to be recovered during the imbibition process. These could be an evidence of wave-induced flow of two phase liquid.
From these analyses, amplitude attenuation can be observed in the sonic logging at geological storage site. The combination of seismic wave amplitude and time-delay could be applied for more reliable evaluation of CO_2 saturation as Azuma et al. (2014) pointed out. The amplitude change might be effective in the early detection of CO_2 leakage along the well, if results as the laboratory experiments were obtained in the field. An effective measurement for this purpose could be realized with the use of DAS-VSP.

Keywords: Geological CO2 storage, Sonic logging wave data, P-wave velocity, P-wave amplitude, Nagaoka site

©2019. Japan Geoscience Union. All Right Reserved.

Geological sequestration in saline carbonate formations: CO_2 -brine-rock interaction

*Shachi Shachi[1], Brijesh Kumar Yadav[1], Mohammad Azizur Rahman[2], Mayur Pal[3]

1. Indian Institute of Technology Roorkee, 2. Texas A&M University Qatar, 3. North Oil Company, Qatar

To reduce unequivocal global warming due to continuous emission of greenhouse gas CO_2 into atmosphere, geo-sequestration is one such emerging technology. For geologic sequestration, CO_2 is injected into suitable deep subsurface formations at supercritical temperature and pressure conditions. Saline carbonate formations are one such promising sink due to its wide spread availability and enormous storage potential. In this study, a series of experiments have been performed on carbonate cores for finding out the effect of injected supercritical CO_2 in subsurface formations. The laboratory study reported here investigated the cyclic injection of $scCO_2$ and brine on two types (Edward White and Edward Yellow) of core samples under reservoir conditions. Further, the pre and post flooded carbonate core samples are analysed for mineralogical changes of CO_2-brine-rock interaction using image analysis techniques such as FeSEM and EDX. The cyclic injection provides the differential pressure (DP) profile of the two samples with time, and is found to have increased with successive injection cycles. The FeSEM images showed that there was some dissolution and precipitation of minerals after the CO_2 flooding emphasizing on solubility trapping and EDX provides the quantitative information about mineral compositions. The results are also compared for both porosity and permeability changes which are found to have decreased post $scCO_2$ flooding. The results of this study provide vital information about mineralogical changes and thus will enhance the knowledge of implementing full scale CO_2 sequestration in subsurface carbonate formations.

Keywords: Global warming, geo-sequestration, image analysis, mineralogical changes

©2019. Japan Geoscience Union. All Right Reserved.

Changes in sealing performance of artificial caprocks caused by carbonate reactions

*Masao Sorai[1]

1. Geological Survey of Japan, National Institute of Advanced Industrial Science and Technology

Geological CO_2 storage assumes that a caprock retains injected CO_2 stably within a reservoir. However, there is little knowledge whether the caprock geochemically-reacted over a long time keep equal sealing performance. This study aims to quantify the change of the rock's sealing performance caused by geochemical reactions.

To understand the rock reaction and the resultant changes in pore structure, it is reasonable to perform experiments under the system with clear reaction process and of controlled pore structures. I used sintered compacts comprising of differently packed uniform silica beads, whose particle size were respectively 0.5, 1 and 10 μm. Here, attention was focused on reactions of carbonate minerals because carbonates have the highest reactivity of usual aquifer minerals. Therefore, products were immersed into the calcium acetate solution and heated up to 700˚C, which resulted in the precipitation of carbonates within their pore space. In the current experiment, samples were reacted in a supercritical CO_2-water system at 10 MPa and 40ºC, which corresponds to the condition of 1000 m depth. The reaction was performed separately setting the reaction time to 1, 2, and 4 weeks. Each sample after reactions was made available for the measurement of permeability *k*.

It is generally expected that the dissolution of carbonates in rock's pore space causes an increase in *k*, whereas that the precipitation of carbonates results in a decrease in *k*. Applying this presumption to experimental results, the *k* change caused by carbonate reactions was considered. On high density samples, carbonates dissolve from the sample surface by the CO_2-dissolved water, but once the surrounding water reaches a concentration saturated to carbonates, no more dissolution occurs. In addition, even if the water does not reach a saturating concentration, most of leaching components have no way out. Therefore, they are concentrated and re-precipitated in the central part of a sample. This scenario expects that the permeability is initially increased and then maintained constant or decreased to a prior level. In contrast, low density samples dissolve more carbonates because of the penetration of CO_2 -dissolved water deep into a sample and of active material transport between surface and interior. This results in an increase in *k*. Hereafter, we should quantify the leakage risk through a caprock based on both penetration rate within a rock and the carbonates content.

Keywords: Geological CO2 storage, Sealing performance, Geochemical reactions, Caprock, Carbonate minerals

©2019. Japan Geoscience Union. All Right Reserved.

CO_2 migration characteristics of microbubble and conventional sequestration in Berea sandstone revealed by X-ray CT imaging

*Hongyu Zhai[1,2], Yi Zhang[1,2], Hyuck Park[1,2], Ziqiu Xue[1,2]

1. Geological Carbon dioxide Storage Technology Research Association,9-2, Kizugawadai, Kizugawa Shi, Kyoto, 6190292 Japan, 2. Research Institute of Innovative Technology for the Earth (RITE),9-2, Kizugawadai, Kizugawa Shi, Kyoto, 6190292 Japan

CO_2 geological sequestration is an effective technique to mitigate the increase of global CO_2 emission and warming effect. To improve CO_2 storage capacity in porous sediments, we applied a new technology, of which a particular filter is utilized to generate supercritical CO_2 (SC) microbubble, for the SC injection. A Berea sandstone sample was used for the tests: the microbubble injection (MBI) and conventional injection (CI). By X-ray CT imaging, we find that the MBI can enhance the SC migration and sweep efficiency, and finally result in a higher SC saturation. To quantify the difference in SC saturation variation for MBI and CI, we classify the porous space (as imaged volume) into three subsets (low-porosity: $\Phi_L \leqq$ 19%; medium-porosity: 19%$<\Phi_M \leqq$22%; and high-porosity: 22%$<\Phi_H$). We identify that there are different SC migration patterns (P1: rapid and high-massed SC flow occupied large-sized porosity sites with an apparent migration trace; P2: slow and low-massed SC flow diffused into small-sized porosity sites; and P3: a mixed migration pattern of P1 and P2) dominated by the porosity distribution and sediment layers. The main differences in the flow characteristics of MBI and CI for the three groups of porosity sites are outlined as follows.

(1)-Φ_H: At the beginning, the MBI formed a step-increased SC saturation gradient in the Φ_H sites along the axial direction. Subsequently, several times of SC saturation accumulation occurred before the injected SC reached 0.15 PV. In contrast, in the CI, there was a continuous SC flow migrated in the high-porosity sites from the inlet side to the outlet side before the injected SC reached 0.1 PV. After the SC flow transported to the left part (with a distance >150 mm from inlet side), the SC sweep efficiency became weakened. When the injected SC was greater than 0.08 PV, the increase of SC saturation propagated simultaneously from the central position towards inlet and outlet sides.

(2)-Φ_M: In the Φ_M sites, before the injected SC smaller than 0.9 PV, the P1 model controlled the flow migration for MBI. Then the P3 model dominated the SC flow migration. In the CI, similar SC flow transport features also occurred, however, with a lower SC sweep efficiency, and the P3 model commenced until the injected SC approximated 0.15 PV.

(3)-Φ_L: In the Φ_L sites, both the MBI and CI produced only the P1-type SC transport pattern. But the MBI had an earlier trigger time and higher SC saturation than CI.

These analyses demonstrate that the SC flow in the MBI can permeate into more porous space and build a higher CO_2 saturation than CI. The MBI has the potential to provide a more efficient and lower cost choice for the CO_2 geological storage.

Keywords: CO2 migration, Microbubble sequestration, Conventional sequestration, X-ray CT imaging

©2019. Japan Geoscience Union. All Right Reserved.

Strain detection by optical fiber for CO_2 injected core specimen

*Hyuck Park[1], Yankun Sun[1], Ziqiu Xue[1]

1. Research Institute of Innovative Technology for the Earth

In order to detect strain of rock specimen during CO_2 injection using optical fiber, a laboratory experiment was carried out using porous sandstone. Spiral direction strain of core specimen was detected by optical fiber. We compared the strain profiles in the case of one-phase flow (water only) and the case of two-phase flow (CO_2 in water saturated specimen). CT image analysis was also used to determine the internal state of the specimen. Sarukawa sandstone (diameter: 34.83mm, length: 179.50mm) was used in this study. Porosity of the specimen determined by X-ray CT imaging is 23.38%. This specimen is homogeneous overall, but there are some gravels in some places. The permeability is about 7 mDarcy. The experiment was conducted under the pressure and temperature conditions that simulate underground environments; pore pressure: 10MPa, temperature: 40 degrees Celsius. The confining pressure selected in this study is 12MPa. The specimen was first saturated with KI aqueous solution (11.5 wt%). The permeability was confirmed using the KI aqueous solution. The upstream pump was prepared at 10.5 MPa for differential pressure of 0.5MPa. The CO_2 flooding was carried out until the total fluid injection reaches about 7.6PV (pore volume). Optical fiber measurement and X-ray CT imaging were performed in all experimental steps. In the case of one-phase flow (water only), as soon as the water injection started, the strain profile was completed. And the strain profile was almost constant until the test ended. In the case of two-phase flow (CO_2 flooding in water saturated specimen), there was a small strain increase up to CO_2 breakthrough and there was a sudden strain increase after the breakthrough. In this study, it was possible to measure the spiral direction strain of 180mm long core specimen. At the same time, we could visualize the process of CO_2 flooding by X-ray CT image analysis. It has become possible to measure distortion of a long distance under the ground with a single optical fiber. It reveals that the optical fiber sensing is a potential tool for future CO_2 storage industries.

Keywords: Optical fiber, CO2 flooding, strain detection, strain profile, X-ray CT

©2019. Japan Geoscience Union. All Right Reserved.

Bed deformation measured by distributed optical fiber and its sedimentological interpretation: alternated sandstone and mudstone aquifer, Boso Peninsula, Japan

*Takuma Ito[1,2], Tsutomu Hashimoto[1,2], Ziqiu Xue[1,2]

1. Research Institute of Innovative Technology for the Earth, 2. Geological Carbon Dioxide Storage Technology Research Association

We have been developing a technology to monitor real-time bed deformation by utilizing the distributed fiber optic sensing. Pumping test results illustrated that uneven bed deformation in an aquifer during pumping groundwater. This uneven bed deformation may be related to geological heterogeneity. For investigating geological heterogeneity, sediment cores were taken from the target aquifer, however detailed sedimentological features are less studied. Purposes of this study are to clarify sedimentary environment and grain size features on the basis of core analysis, and to compare core analysis results with bed deformation signature during the pumping test.

Sediment cores were taken from a Middle Pleistocene alternated sandstone and mudstone aquifer on Boso Peninsula, Japan. Facies analysis indicates that 3 types of sand layers were recognized in the cores: type 1 is single normally graded bed, type 2 is inversely-to-normally graded bed, and type3 is deformed beds in association with rip-up clasts. These features indicate that these sand layers are event deposits. This interpretation supports the view from the previous study that sandstone beds in the target aquifer are interpreted as event deposits in front of a shelf-margin delta. Grain-size analysis of the cores indicates that three depositional cycles were recognized at the depth between 164 and 230 m. Depositional cycles are the origin of the geological heterogeneity in the aquifer, which appears to be related to transgressive-regressive cycles.

Pumping test results showed four intervals with no bed deformation at the depth between 164 and 230 m. These intervals with no bed deformation appear to be related to the geological feature of the aquifer. Comparison between strain measured by optical fiber and depositional cycles identified by detailed core analysis indicates that depths with compressive strain correspond to that composing of coarse-grained sand beds. This pumping test result suggests that compressive strain, which can be used as an indicator of the groundwater pathway in the aquifer, largely depends on the lithology and grain size features. The field experimental results demonstrated that the bed deformation monitoring using distributed fiber optic sensing is useful for as indirect evaluation of the hydraulic properties of aquifer, which is closely linked to geological heterogeneity.

Keywords: Alternated sandstone and mudstone, Optic fiber sensing, Monitoring of bed deformation

©2019. Japan Geoscience Union. All Right Reserved.

How many data are necessary to make a suitable threshold for anomalous pCO_2 owing to CO_2 leakage?

*Keisuke Uchimoto[1,2], Yuji Watanabe[1,2], Makoto Nishimura[1,2], Ziqiu Xue[1,2]

1. Geological Carbon dioxide Storage Technology Research Association , 2. Research Institute of Innovative Technology for the Earth

In Japan, the offshore storage of CO_2 is regulated by Act on Prevention of Marine Pollution and Maritime Disaster, which requires monitoring to be able to detect CO_2 leakage should it occur. If CO_2 stored in deep geological formations leaks into the sea, carbonate variables in seawater such as pH, dissolved inorganic carbon, and partial pressure of CO_2 (pCO_2) would change. Hence, to find anomalous values of the carbonate variables can be a method of the marine monitoring. It is, however, difficult to judge whether an observed carbonate value is anomalous, because the natural variability of carbonate variables is relatively great. Actually, many data were judged as anomalous at Tomakomai CCS Demonstration Project, where pCO_2 have been monitored, although CO_2 leakage has never occurred. Although false-positives (natural variability misjudged as anomalous) themselves are unavoidable, there are also avoidable false-positives, some of which are caused by an unsuitable threshold based on insufficient baseline data. In this study, we studied how many data are necessary to make a suitable threshold. For this purpose, we analyzed quarterly data observed in a semi-enclosed bay, Osaka Bay, from 2002 to 2010. Using N ($1 \leqq N \leqq 9$) years' data out of them, we calculated a threshold line based on a correlation between pCO_2 and dissolved oxygen saturation, applied all the 9 years' data to the threshold line, and counted the number of data exceeding the threshold line, i.e. false-positives. We suggest that at least around 5 years' data are necessary to make a reasonable threshold line based on quarterly data.

Keywords: offshore CO2 storage, leakage, marine monitoring, CCS

©2019. Japan Geoscience Union. All Right Reserved.

[J] Poster | H (Human Geosciences)：H-SC Social Earth Sciences & Civil/Urban System Sciences

Wed. May 29, 2019 5:15 PM - 6:30 PM JST | Wed. May 29, 2019 8:15 AM - 9:30 AM UTC | Poster Hall International Exhibition Hall8, Makuhari Messe_20

[H-SC07] CCUS (Carbon Dioxide Capture, Utilization, and Storage) for Climate Mitigation

convener:Masao Sorai(Institute for Geo-Resources and Environment, National Institute of Advanced Industrial Science and Technology), Ziqiu Xue(Research Institute of Innovative Tech for the Earth), Masaatsu Aichi(Graduate School of Frontier Sciences, University of Tokyo)

The prevention of the global warming, which is the urgent challenge facing the world, requires the full-out efforts of science and technology. This session focuses on the CCUS (Carbon Dioxide Capture, Utilization, and Storage) as one of the useful countermeasures for the CO2 emission reduction. It not only targets various scientific phenomenon caused by the capture and storage of CO2, CO2 utilization, and CO2-EOR/EGR, but also discusses the latest R&D developments of each method for the environmental impact assessment, safety assessment, the measuring, monitoring and verification (MMV), and public acceptance. The main theme is the recognition of key issues toward the practical use of CCUS, in addition to the deepening of our knowledge about the CO2 behavior on the underground.

[HSC07-P01] Evaluation of seismic event location accuracy of Tomakomai CO2 injection site: a numerical simulation case study

*Luchen Wang[1], Takahiro Nakajima[1], Ziqiu Xue[1] (1.RITE, Research Institute of Innovative Technology for the Earth)

[HSC07-P02] Technical Challenges of Machine Learning Approach for Porosity Estimation in Nagaoka CCS site

*Takayuki Miyoshi[1], Takahiro Nakajima[1], Ziqiu Xue[1] (1.Research Institute of Innovative Technology for the Earth)

[HSC07-P03] Utilization of wave attenuation in time-lapse sonic logging data to evaluate the effect of super-critical CO_2 in the reservoir

*Takahiro Nakajima[2,1], Luchen Wang[2,1], Ziqiu Xue[2,1] (1.Research Institute of Innovative Technology for the Earth, 2.Geological Carbon Dioxide Storage Technology Research Association)

[HSC07-P04] Geological sequestration in saline carbonate formations: CO_2-brine-rock interaction

*Shachi Shachi[1], Brijesh Kumar Yadav[1], Mohammad Azizur Rahman[2], Mayur Pal[3] (1.Indian Institute of Technology Roorkee, 2.Texas A&M University Qatar, 3.North Oil Company, Qatar)

[HSC07-P05] Changes in sealing performance of artificial caprocks caused by carbonate reactions

*Masao Sorai[1] (1.Geological Survey of Japan, National Institute of Advanced Industrial Science and Technology)

[HSC07-P06] CO_2 migration characteristics of microbubble and conventional sequestration in Berea sandstone revealed by X-ray CT imaging

*Hongyu Zhai[1,2], Yi Zhang[1,2], Hyuck Park[1,2], Ziqiu Xue[1,2] (1.Geological Carbon dioxide Storage Technology Research Association,9-2, Kizugawadai, Kizugawa Shi, Kyoto, 6190292 Japan, 2.Research Institute of Innovative Technology for the Earth (RITE),9-2, Kizugawadai, Kizugawa Shi, Kyoto, 6190292 Japan)

[HSC07-P07] Strain detection by optical fiber for CO_2 injected core specimen

*Hyuck Park[1], Yankun Sun[1], Ziqiu Xue[1] (1.Research Institute of Innovative Technology for the Earth)

[HSC07-P08] Bed deformation measured by distributed optical fiber and its sedimentological interpretation: alternated sandstone and mudstone aquifer, Boso Peninsula, Japan

*Takuma Ito[1,2], Tsutomu Hashimoto[1,2], Ziqiu Xue[1,2] (1.Research Institute of Innovative Technology for the Earth, 2.Geological Carbon Dioxide Storage Technology Research Association)

[HSC07-P09] How many data are necessary to make a suitable threshold for anomalous pCO_2 owing to CO_2 leakage?

*Keisuke Uchimoto[1,2], Yuji Watanabe[1,2], Makoto Nishimura[1,2], Ziqiu Xue[1,2] (1.Geological Carbon dioxide Storage Technology Research Association , 2.Research Institute of Innovative Technology for the Earth)

Evaluation of seismic event location accuracy of Tomakomai CO2 injection site: a numerical simulation case study

*Luchen Wang[1], Takahiro Nakajima[1], Ziqiu Xue[1]

1. RITE, Research Institute of Innovative Technology for the Earth

For CO2 injection monitoring in many CCS project, the most basic monitoring information is the seismic events. The seismic event location is the first step to understanding the causal process of a natural or induced fracture. In the case of CO2 geological storage, the location of an event is of special importance. The events in the reservoir may affect the storage capability. The events in the cap-rock may indicate the CO2 leakage. However, the location of the seismic event is probably to contain bias, especially for the limited seismic observation system. Therefore, the operator should understand that there is uncertainty in the location estimation of a detected event. In this study, we use the Tomakomai (Ocean Bottom Cable) OBC and borehole system (OB1 well) to study the seismic location accuracy in Tomakomai site. We believe that it can help to evaluate the event location effect with different azimuths and different depths. Moreover, this study may also be applied to the optimization of the seismic observation system.

At Tomakomai site, the permanent OBC is arranged as a line (length 3.6 km, containing 55 available sensors), deployed 2 m under the seabed. It is located above the CO2 reservoir and the center point is 3 km from the coast. The OB1 contains 4 sensors in the well with depths ranging from 2 km to 2.2 km. All sensors of OBC and OB1 contain a three-component geophone. Therefore, we can use only detected P phase signal for seismic location. We assume that the velocity model is layered and homogeneous, so that a simple model can be built based on the logging result. The ray-tracing method is employed in the seismic simulation and location process.

We compared the modelling event location accuracy for different azimuths and different depths. All events were distributed around Tomakomai site. The results showed that as the epicenter distance increases, the location errors increases. For the events which the epicenter is far away from the area enclosed by OBC and OB1, the locating effect is significantly worse. In addition, as the event depth increases, the location error also increases. The location error of shallow (0-1 km) events can be maintained within 1 m, while the location error of deep (8 km) events can reach the scale of several hundred meters. Ignoring the effects of the simulation method, it is obviously affected by the geometric distribution of the observation system.

Secondly, we also compared different observation system optimization strategies. The result indicated that, based on the Tomakomai seismic monitoring system, if the number of sensor is fixed, the longer OBC line can provide a better location result. Based on these analyses, future seismic monitoring system designs can be optimized for specific purposes (number of sensors, expected depth of monitoring, etc.).

Keywords: event location, Seismic monitoring, 3D ray tracing, Tomakomai site

©2019. Japan Geoscience Union. All Right Reserved.

Technical Challenges of Machine Learning Approach for Porosity Estimation in Nagaoka CCS site

*Takayuki Miyoshi[1], Takahiro Nakajima[1], Ziqiu Xue[1]

1. Research Institute of Innovative Technology for the Earth

In CCS, the distribution of hydraulic parameters such as porosity and permeability is one of the key parameters for evaluation of CO_2 storage capacity and CO_2 saturations. These parameters are measured as 1D profiles through well-logging. CCS projects, in general, have only a few wells available in the area of target. The 3D seismic data which covers the three dimensional space does not represent the hydraulic features directly. A technique to integrate these different types of data is required to estimate appropriate geological models.
Machine learning (ML) is a technique for predicting a target property from unknown input data by learning the relationship between known input data and prediction target. In this research, we apply ML approaches to Nagaoka CCS site data for predicting porosity distribution from seismic attributes created from the 3D seismic data. Determination of hyper-parameters of the ML model is often site-specific in predicting geological models. We present the technical challenges when using multiple attributes as input data.

Keywords: CCS, Machine Learning, Geological model

©2019. Japan Geoscience Union. All Right Reserved.

Utilization of wave attenuation in time-lapse sonic logging data to evaluate the effect of super-critical CO_2 in the reservoir

*Takahiro Nakajima[2,1], Luchen Wang[2,1], Ziqiu Xue[2,1]

1. Research Institute of Innovative Technology for the Earth, 2. Geological Carbon Dioxide Storage Technology Research Association

This paper discusses seismic wave attenuation by injected CO_2 in the formation. Seismic methods have been broadly used for the monitoring of injected CO_2 at many CCS sites. Concerning the velocity change by the existence of CO_2, the relationship between P-wave velocity and CO_2 saturation in rock samples and formation have been studied well. Some laboratory experiments studied amplitude of P-wave as well as the velocity change by the invasion of CO_2, and the change in amplitude was larger than that of time delay (e.g. Muller et al., 2010). Meanwhile investigations on amplitude attenuation were rather limited. In this paper, we investigated P-wave data in the results of time-lapse sonic logging at the Nagaoka site.
At the Nagaoka site, time-lapse well loggings have been conducted during the injection period and post injection period at observation wells, which are 40 m and 60 m apart from the injection well. The sonic logging was conducted 45 times during 12 years using Halliburton’ s LFDL (Low Frequency Dipole-Sonic Logging Tool). Since it is not ascertain that the monopole transmitter has emitted the same energy at every logging, we chose a reference point in the cap rock 10 m above the target zone. At this depth, the formation was highly cemented with very small slowness, so the position was easily recognized in wave data and its wave field would not change during the CO_2 injection. We took the amplitude of the first P-wave arrival as the reference. We also assume that the emitted energy from the transmitter would not change at the reservoir within 15 m interval from the reference point.
Firstly, we compared the wave data at the depth where the largest change observed by CO_2 injected. We can see that the first arrival of P-wave at the nearest observation logging was shifted from 1.64 to 1.8 micro-sec at 14-th run. Amplitude of the peak was also gradually decreased after the CO_2 breakthrough, and the amplitude at 21-st run was clearly small. Next we calculated spectrum around the first P-wave arrivals, and found that high frequency components decreased much than the lower frequency components. This frequency shift looked like to be recovered during the imbibition process. These could be an evidence of wave-induced flow of two phase liquid.
From these analyses, amplitude attenuation can be observed in the sonic logging at geological storage site. The combination of seismic wave amplitude and time-delay could be applied for more reliable evaluation of CO_2 saturation as Azuma et al. (2014) pointed out. The amplitude change might be effective in the early detection of CO_2 leakage along the well, if results as the laboratory experiments were obtained in the field. An effective measurement for this purpose could be realized with the use of DAS-VSP.

Keywords: Geological CO2 storage, Sonic logging wave data, P-wave velocity, P-wave amplitude, Nagaoka site

©2019. Japan Geoscience Union. All Right Reserved.

Geological sequestration in saline carbonate formations: CO_2 -brine-rock interaction

*Shachi Shachi[1], Brijesh Kumar Yadav[1], Mohammad Azizur Rahman[2], Mayur Pal[3]

1. Indian Institute of Technology Roorkee, 2. Texas A&M University Qatar, 3. North Oil Company, Qatar

To reduce unequivocal global warming due to continuous emission of greenhouse gas CO_2 into atmosphere, geo-sequestration is one such emerging technology. For geologic sequestration, CO_2 is injected into suitable deep subsurface formations at supercritical temperature and pressure conditions. Saline carbonate formations are one such promising sink due to its wide spread availability and enormous storage potential. In this study, a series of experiments have been performed on carbonate cores for finding out the effect of injected supercritical CO_2 in subsurface formations. The laboratory study reported here investigated the cyclic injection of $scCO_2$ and brine on two types (Edward White and Edward Yellow) of core samples under reservoir conditions. Further, the pre and post flooded carbonate core samples are analysed for mineralogical changes of CO_2-brine-rock interaction using image analysis techniques such as FeSEM and EDX. The cyclic injection provides the differential pressure (DP) profile of the two samples with time, and is found to have increased with successive injection cycles. The FeSEM images showed that there was some dissolution and precipitation of minerals after the CO_2 flooding emphasizing on solubility trapping and EDX provides the quantitative information about mineral compositions. The results are also compared for both porosity and permeability changes which are found to have decreased post $scCO_2$ flooding. The results of this study provide vital information about mineralogical changes and thus will enhance the knowledge of implementing full scale CO_2 sequestration in subsurface carbonate formations.

Keywords: Global warming, geo-sequestration, image analysis, mineralogical changes

©2019. Japan Geoscience Union. All Right Reserved.

Changes in sealing performance of artificial caprocks caused by carbonate reactions

*Masao Sorai[1]

1. Geological Survey of Japan, National Institute of Advanced Industrial Science and Technology

Geological CO_2 storage assumes that a caprock retains injected CO_2 stably within a reservoir. However, there is little knowledge whether the caprock geochemically-reacted over a long time keep equal sealing performance. This study aims to quantify the change of the rock's sealing performance caused by geochemical reactions.

To understand the rock reaction and the resultant changes in pore structure, it is reasonable to perform experiments under the system with clear reaction process and of controlled pore structures. I used sintered compacts comprising of differently packed uniform silica beads, whose particle size were respectively 0.5, 1 and 10 μm. Here, attention was focused on reactions of carbonate minerals because carbonates have the highest reactivity of usual aquifer minerals. Therefore, products were immersed into the calcium acetate solution and heated up to 700˚C, which resulted in the precipitation of carbonates within their pore space. In the current experiment, samples were reacted in a supercritical CO_2-water system at 10 MPa and 40ºC, which corresponds to the condition of 1000 m depth. The reaction was performed separately setting the reaction time to 1, 2, and 4 weeks. Each sample after reactions was made available for the measurement of permeability *k*.

It is generally expected that the dissolution of carbonates in rock's pore space causes an increase in *k*, whereas that the precipitation of carbonates results in a decrease in *k*. Applying this presumption to experimental results, the *k* change caused by carbonate reactions was considered. On high density samples, carbonates dissolve from the sample surface by the CO_2-dissolved water, but once the surrounding water reaches a concentration saturated to carbonates, no more dissolution occurs. In addition, even if the water does not reach a saturating concentration, most of leaching components have no way out. Therefore, they are concentrated and re-precipitated in the central part of a sample. This scenario expects that the permeability is initially increased and then maintained constant or decreased to a prior level. In contrast, low density samples dissolve more carbonates because of the penetration of CO_2 -dissolved water deep into a sample and of active material transport between surface and interior. This results in an increase in *k*. Hereafter, we should quantify the leakage risk through a caprock based on both penetration rate within a rock and the carbonates content.

Keywords: Geological CO2 storage, Sealing performance, Geochemical reactions, Caprock, Carbonate minerals

©2019. Japan Geoscience Union. All Right Reserved.

CO_2 migration characteristics of microbubble and conventional sequestration in Berea sandstone revealed by X-ray CT imaging

*Hongyu Zhai[1,2], Yi Zhang[1,2], Hyuck Park[1,2], Ziqiu Xue[1,2]

1. Geological Carbon dioxide Storage Technology Research Association,9-2, Kizugawadai, Kizugawa Shi, Kyoto, 6190292 Japan, 2. Research Institute of Innovative Technology for the Earth (RITE),9-2, Kizugawadai, Kizugawa Shi, Kyoto, 6190292 Japan

CO_2 geological sequestration is an effective technique to mitigate the increase of global CO_2 emission and warming effect. To improve CO_2 storage capacity in porous sediments, we applied a new technology, of which a particular filter is utilized to generate supercritical CO_2 (SC) microbubble, for the SC injection. A Berea sandstone sample was used for the tests: the microbubble injection (MBI) and conventional injection (CI). By X-ray CT imaging, we find that the MBI can enhance the SC migration and sweep efficiency, and finally result in a higher SC saturation. To quantify the difference in SC saturation variation for MBI and CI, we classify the porous space (as imaged volume) into three subsets (low-porosity: $\Phi_L \leqq$ 19%; medium-porosity: 19%$<\Phi_M \leqq$22%; and high-porosity: 22%$<\Phi_H$). We identify that there are different SC migration patterns (P1: rapid and high-massed SC flow occupied large-sized porosity sites with an apparent migration trace; P2: slow and low-massed SC flow diffused into small-sized porosity sites; and P3: a mixed migration pattern of P1 and P2) dominated by the porosity distribution and sediment layers. The main differences in the flow characteristics of MBI and CI for the three groups of porosity sites are outlined as follows.

(1)-Φ_H: At the beginning, the MBI formed a step-increased SC saturation gradient in the Φ_H sites along the axial direction. Subsequently, several times of SC saturation accumulation occurred before the injected SC reached 0.15 PV. In contrast, in the CI, there was a continuous SC flow migrated in the high-porosity sites from the inlet side to the outlet side before the injected SC reached 0.1 PV. After the SC flow transported to the left part (with a distance >150 mm from inlet side), the SC sweep efficiency became weakened. When the injected SC was greater than 0.08 PV, the increase of SC saturation propagated simultaneously from the central position towards inlet and outlet sides.

(2)-Φ_M: In the Φ_M sites, before the injected SC smaller than 0.9 PV, the P1 model controlled the flow migration for MBI. Then the P3 model dominated the SC flow migration. In the CI, similar SC flow transport features also occurred, however, with a lower SC sweep efficiency, and the P3 model commenced until the injected SC approximated 0.15 PV.

(3)-Φ_L: In the Φ_L sites, both the MBI and CI produced only the P1-type SC transport pattern. But the MBI had an earlier trigger time and higher SC saturation than CI.

These analyses demonstrate that the SC flow in the MBI can permeate into more porous space and build a higher CO_2 saturation than CI. The MBI has the potential to provide a more efficient and lower cost choice for the CO_2 geological storage.

Keywords: CO2 migration, Microbubble sequestration, Conventional sequestration, X-ray CT imaging

©2019. Japan Geoscience Union. All Right Reserved.

Strain detection by optical fiber for CO_2 injected core specimen

*Hyuck Park[1], Yankun Sun[1], Ziqiu Xue[1]

1. Research Institute of Innovative Technology for the Earth

In order to detect strain of rock specimen during CO_2 injection using optical fiber, a laboratory experiment was carried out using porous sandstone. Spiral direction strain of core specimen was detected by optical fiber. We compared the strain profiles in the case of one-phase flow (water only) and the case of two-phase flow (CO_2 in water saturated specimen). CT image analysis was also used to determine the internal state of the specimen. Sarukawa sandstone (diameter: 34.83mm, length: 179.50mm) was used in this study. Porosity of the specimen determined by X-ray CT imaging is 23.38%. This specimen is homogeneous overall, but there are some gravels in some places. The permeability is about 7 mDarcy. The experiment was conducted under the pressure and temperature conditions that simulate underground environments; pore pressure: 10MPa, temperature: 40 degrees Celsius. The confining pressure selected in this study is 12MPa. The specimen was first saturated with KI aqueous solution (11.5 wt%). The permeability was confirmed using the KI aqueous solution. The upstream pump was prepared at 10.5 MPa for differential pressure of 0.5MPa. The CO_2 flooding was carried out until the total fluid injection reaches about 7.6PV (pore volume). Optical fiber measurement and X-ray CT imaging were performed in all experimental steps. In the case of one-phase flow (water only), as soon as the water injection started, the strain profile was completed. And the strain profile was almost constant until the test ended. In the case of two-phase flow (CO_2 flooding in water saturated specimen), there was a small strain increase up to CO_2 breakthrough and there was a sudden strain increase after the breakthrough. In this study, it was possible to measure the spiral direction strain of 180mm long core specimen. At the same time, we could visualize the process of CO_2 flooding by X-ray CT image analysis. It has become possible to measure distortion of a long distance under the ground with a single optical fiber. It reveals that the optical fiber sensing is a potential tool for future CO_2 storage industries.

Keywords: Optical fiber, CO2 flooding, strain detection, strain profile, X-ray CT

©2019. Japan Geoscience Union. All Right Reserved.

Bed deformation measured by distributed optical fiber and its sedimentological interpretation: alternated sandstone and mudstone aquifer, Boso Peninsula, Japan

*Takuma Ito[1,2], Tsutomu Hashimoto[1,2], Ziqiu Xue[1,2]

1. Research Institute of Innovative Technology for the Earth, 2. Geological Carbon Dioxide Storage Technology Research Association

We have been developing a technology to monitor real-time bed deformation by utilizing the distributed fiber optic sensing. Pumping test results illustrated that uneven bed deformation in an aquifer during pumping groundwater. This uneven bed deformation may be related to geological heterogeneity. For investigating geological heterogeneity, sediment cores were taken from the target aquifer, however detailed sedimentological features are less studied. Purposes of this study are to clarify sedimentary environment and grain size features on the basis of core analysis, and to compare core analysis results with bed deformation signature during the pumping test.

Sediment cores were taken from a Middle Pleistocene alternated sandstone and mudstone aquifer on Boso Peninsula, Japan. Facies analysis indicates that 3 types of sand layers were recognized in the cores: type 1 is single normally graded bed, type 2 is inversely-to-normally graded bed, and type3 is deformed beds in association with rip-up clasts. These features indicate that these sand layers are event deposits. This interpretation supports the view from the previous study that sandstone beds in the target aquifer are interpreted as event deposits in front of a shelf-margin delta. Grain-size analysis of the cores indicates that three depositional cycles were recognized at the depth between 164 and 230 m. Depositional cycles are the origin of the geological heterogeneity in the aquifer, which appears to be related to transgressive-regressive cycles.

Pumping test results showed four intervals with no bed deformation at the depth between 164 and 230 m. These intervals with no bed deformation appear to be related to the geological feature of the aquifer. Comparison between strain measured by optical fiber and depositional cycles identified by detailed core analysis indicates that depths with compressive strain correspond to that composing of coarse-grained sand beds. This pumping test result suggests that compressive strain, which can be used as an indicator of the groundwater pathway in the aquifer, largely depends on the lithology and grain size features. The field experimental results demonstrated that the bed deformation monitoring using distributed fiber optic sensing is useful for as indirect evaluation of the hydraulic properties of aquifer, which is closely linked to geological heterogeneity.

Keywords: Alternated sandstone and mudstone, Optic fiber sensing, Monitoring of bed deformation

©2019. Japan Geoscience Union. All Right Reserved.

How many data are necessary to make a suitable threshold for anomalous pCO_2 owing to CO_2 leakage?

*Keisuke Uchimoto[1,2], Yuji Watanabe[1,2], Makoto Nishimura[1,2], Ziqiu Xue[1,2]

1. Geological Carbon dioxide Storage Technology Research Association , 2. Research Institute of Innovative Technology for the Earth

In Japan, the offshore storage of CO_2 is regulated by Act on Prevention of Marine Pollution and Maritime Disaster, which requires monitoring to be able to detect CO_2 leakage should it occur. If CO_2 stored in deep geological formations leaks into the sea, carbonate variables in seawater such as pH, dissolved inorganic carbon, and partial pressure of CO_2 (pCO_2) would change. Hence, to find anomalous values of the carbonate variables can be a method of the marine monitoring. It is, however, difficult to judge whether an observed carbonate value is anomalous, because the natural variability of carbonate variables is relatively great. Actually, many data were judged as anomalous at Tomakomai CCS Demonstration Project, where pCO_2 have been monitored, although CO_2 leakage has never occurred. Although false-positives (natural variability misjudged as anomalous) themselves are unavoidable, there are also avoidable false-positives, some of which are caused by an unsuitable threshold based on insufficient baseline data. In this study, we studied how many data are necessary to make a suitable threshold. For this purpose, we analyzed quarterly data observed in a semi-enclosed bay, Osaka Bay, from 2002 to 2010. Using N ($1 \leqq N \leqq 9$) years' data out of them, we calculated a threshold line based on a correlation between pCO_2 and dissolved oxygen saturation, applied all the 9 years' data to the threshold line, and counted the number of data exceeding the threshold line, i.e. false-positives. We suggest that at least around 5 years' data are necessary to make a reasonable threshold line based on quarterly data.

Keywords: offshore CO2 storage, leakage, marine monitoring, CCS

©2019. Japan Geoscience Union. All Right Reserved.

[E] Oral | H (Human Geosciences)：H-DS Disaster geosciences

Wed. May 29, 2019 9:00 AM - 10:30 AM JST | Wed. May 29, 2019 12:00 AM - 1:30 AM UTC | 304 3F

[H-DS10] Natural hazards impacts on human society, economics and technological systems

convener:ELENA PETROVA(Lomonosov Moscow State University, Faculty of Geography), Hajime Matsushima(Research Faculty of Agriculture, Hokkaido University), Chairperson:Elena Petrova, Hajime Matsushima

The last decade set a record for the number and scale of natural disasters and demonstrates high vulnerability of human society and technosphere to their impacts. The most serious consequences have the so-called natural-technological disasters in which natural hazards trigger accidents at technology and infrastructure such as nuclear power and chemical plants, oil refineries and pipelines, power supply systems, buildings, and roads. A distinctive feature of natural-technological events, such as of the 2011 Tohoku earthquake, is their multi-hazard and synergistic nature, which creates cascading impacts, resulting in simultaneous occurrences of myriad catastrophes. The main goal of this multidisciplinary session is to summarize case studies of relationships between natural hazards and technological disasters, their social and economic consequences; and to encourage a discussion about tools and methods to prevent disasters and to minimize their consequences, disaster reconstruction, and tourism for reconstruction, Eco-DRR, and green infrastructure.

9:00 AM - 9:15 AM JST | 12:00 AM - 12:15 AM UTC

[HDS10-01] People's lives utilizing coastal dunes ecosystem service

★Invited Papers

*Kaneko Korehisa[1] (1.Hokuso Creature Association)

9:15 AM - 9:30 AM JST | 12:15 AM - 12:30 AM UTC

[HDS10-02] Survey on the Impact of Sea wall on the Vegetation of Coastal sand dune

*XIANGMEI ZHONG[1], Hajime Matsushima[2], Akira Suzuki[3], Yoshihiko Hirabuki[4], Kouji Kimura[5] (1.Graduate school of Agriculture, Hokkaido University, 2.Research Faculty of Agriculture, Hokkaido University, 3.Kita-no-satohama Hana-no-kanehashi Network, 4.Faculty of Liberal Arts, Tohoku Gakuin University, 5.Snow Brand Seed Co., Ltd.)

9:30 AM - 9:45 AM JST | 12:30 AM - 12:45 AM UTC

[HDS10-03] Greening on the seawall: challenge to conversion from gray to green infrastructure.

★Invited Papers

*Hajime Matsushima[1], Akira Suzuki[2], Kouji Kimura[4], Xiangmei Zhong[5], Yoshihiko Hirabuki[3] (1.Research Faculty of Agriculture, Hokkaido University, 2.Kita-no-satohama Hana-no-kakehashi Network, 3.Faculty of Liberal Arts, Tohoku Gakuin University, 4.Snow Brand Seed Co., Ltd., 5.Graduate school of Agriculture, Hokkaido University)

9:45 AM - 10:00 AM JST | 12:45 AM - 1:00 AM UTC

[HDS10-04] Distribution Characteristics of Informal Green Space and Its Extension of perspective into Green Infrastructure

*minseo kim[1], Katsunori Furuya[1] (1.Chiba University Graduate School of Horticulture)

10:00 AM - 10:15 AM JST | 1:00 AM - 1:15 AM UTC

[HDS10-05] DISASTER ANALYSIS OF LIGHTNING STRIKE DENSITY BASED ON LANDFORM FOR REDUCING VICTIMS IN WONOSOBO, INDONESIA

*Astry Zulky Permatasari[1], Gagad Nur Ridho[1], Yan Abdi Rahmanu[1], Emilya Nurjani[1] (1.Gadjah Mada University)

10:15 AM - 10:30 AM JST | 1:15 AM - 1:30 AM UTC

[HDS10-06] Development of Cost Competitive Unmanned Aerial Vehicle for Search and Rescue

*Aditya Keshav Natoo

People's lives utilizing coastal dunes ecosystem service

*Kaneko Korehisa[1]

1. Hokuso Creature Association

1. Introduction

The coastal sand system is a buffer zone between the sea and the land, and originally, it has a function to mitigate the natural disasters such as tsunamis and the formation of biodiversity. People form a settlement "town" in the coastal sand dunes for a long time. However, because natural coastal sand dunes have been destroyed due to the progress of development, opportunities to receive the benefits of nature have decreased since the period of high economic growth.
In this research, I evaluate the functions and ecosystem services from people's living in the coastal sand dunes before large-scale coastal development, we will also discuss about the regeneration of the coastal sand dunes in regard to social changes.

2. Method

The study sites are coastal cities in the coastal areas of Chiba Prefecture. In coastal area of Tokyo Bay side, large scale development has been conducted since the 1960’ s. Therefore, I judged it to be an effective place for evaluating coastal sand dunes before development. We investigated the environment of study sites, including the soil and groundwater. There were supported as necessities and luxury items in the area.

3. Results

In distance ratio of coastal type in Chiba Prefecture in 1993, natural coast was 23.5%, the artificial coast was 70.0%. The coastal cities of study site existed brewing industry such as soy sauce, miso, sake brewery. It was an industry that utilized ecosystem services such as the freshwater layer of the coastal dunes and the sea creatures. As a result investigated the location environment of the main coastal cities (soil, groundwater level, water quality), the coastal cities were often located on the geographical features consisting of sand, sandbanks and natural levees. The surface geology consisted of sand-rich sediments, including sand 1(i.e., exceedingly soft), the depth of the groundwater was 3-10 m. I believe that the coastal cities benefited from the proximity of the coast.

4. Themes for the future

The future prediction in Japanese society are ①progress of population decline, declining birthrate and aging population, ②economic decline, financial tightening, ③infrastructure (roads, railroads etc.) aging and the maintenance problem, the social situation change drastically. Moreover, in the coastal industrial area, the number of companies that suspended or stopped production facilities and the expansion of idle land have increased due to the shift of major manufacturing to overseas due to the shrinking domestic

©2019. Japan Geoscience Union. All Right Reserved.

demand over the medium to long term and intensified global competition. As a future task, it is important to work on the regeneration (green infrastructure) of the natural coast sand dune utilizing idle land while cooperating with the government, enterprises, local residents, and academics.

Keywords: Ecosystem Service, Coastal Sand System, Industry, Regeneration

©2019. Japan Geoscience Union. All Right Reserved.

Survey on the Impact of Sea wall on the Vegetation of Coastal sand dune

*XIANGMEI ZHONG[1], Hajime Matsushima[2], Akira Suzuki[3], Yoshihiko Hirabuki[4], Kouji Kimura[5]

1. Graduate school of Agriculture, Hokkaido University, 2. Research Faculty of Agriculture, Hokkaido University, 3. Kita-no-satohama Hana-no-kanehashi Network, 4. Faculty of Liberal Arts, Tohoku Gakuin University, 5. Snow Brand Seed Co., Ltd.

[Introduction]

In recent years, many extreme events have come out due to climate change such as heavy rain, typhoon, etc. Large amounts of expenses are required for disaster-management measures. However, with the declining of population, the government budget is gradually lessening. On the other hand, people’s interests about disasters risk reduction are increasing. Before the disaster in 2011, at Yuriage district in Miyagi prefecture, coastal sand dune, pine forest and backward wetlands can be seen from the shoreline to the landward. In 2011, it is clear that the tsunami disturbed the organisms that support the coastal ecosystem and the environment which is the foundation of its habitat on a large scale. Since the coastal sand dune ecosystem here was disturbed, it has been restored naturally over time and then as a tsunami protection measure, a large seawall was built. Later, on the land side of the Sea wall was reclaimed by the mountain soil. However, the impact of them on the coastal dune ecosystem is unclear. This study clarifies the ecological impact on coastal sand dune vegetation of the Sea wall and mountain soil. And if there is a negative effect, how can we reduce that effect? This study records it as a reference for future solutions.

Three sites at the Yuriage district were selected as survey targets(figure 1.). From the north to the south: the Yuriage area 1(Y1), the Yuriage area 2(Y2), and the Yuriage area 3(Y3). In Y1, the Sea wall was built about 2 years ago and the coastal ecology recovered in nature. In August 2017, plants (*Ixeris repens*) were planted on both sides of the Sea wall in Y2. In Y3, the Sea wall was built about 5 years ago, and the coastal ecology recovered naturally. Additionally, the land sides of the three survey areas were reclaimed with mountain soil.

[Methods]

A belt was set up from the coastal forest to the shoreline. Then, the terrain was recorded with Unmanned aerial vehicle(UAV). Vegetation surveys were conducted at 5m intervals and Plant species / Coverage(%) / Grass height(cm) were investigated. Furthermore, samples of sand were collected at intervals of 10m, and the particle diameter composition(mm) as well as Electrical Conductivity(mS / m)(EC) of each sample were measured. After that, the average plant volume(mm^3) was calculated. Based on the above data, the current status of the plants on both sides of the Sea wall and the physical environment were analyzed.

[Results&Discussion]

About the result of vegetation, there are three plant species on both sides of the Sea wall: *Imperata cylindrica, Digitaria ciliaris* and *Artemisia capillaris*. On the land side, *Artemisia capillaris,* and *Setaria viridis* are the dominant species. On the sea side, *Carex kobomugi, Glehnia littoralis, Calystegia soldanella* and *Ixeris repens* are the dominant species. It is obvious that the plant species on land side and sea side are different because of the separation by the sea wall. It can be seen that the distribution of plants on the

©2019. Japan Geoscience Union. All Right Reserved.

land side is significantly affected by the mountain soils, resulting in an increase in the number of inland plants, such as *Setaria viridis* and *Trifolium repens.* From the EC value, it is evident that the trend from the shoreline to the sea wall is gradually decreasing, and the trend from the sea wall to the inland is increasing. The phenomenon that the EC value increases inland can be considered as the impact of artificial coverage of mountain soil. About the result of particle diameter composition, it is obvious that the medium sand has a decreasing trend from the shoreline to the inland side. Closer to the shoreline, the proportion of the very fine sand is increasing. The closer to the inland, the greater the proportion of the very coarse sand and the coarse sand.

In general, the composition of particle diameter on both sides of the sea and land of the sea wall is of difference, and this phenomenon may be caused by the barrier effect of the sea wall. This phenomenon may become larger as time goes by.

Keywords: coastal plants, ecotone, green infrastructure, the sea wall

figure 1. Survey area

©2019. Japan Geoscience Union. All Right Reserved.

Greening on the seawall: challenge to conversion from gray to green infrastructure.

*Hajime Matsushima[1], Akira Suzuki[2], Kouji Kimura[4], Xiangmei Zhong[5], Yoshihiko Hirabuki[3]

1. Research Faculty of Agriculture, Hokkaido University, 2. Kita-no-satohama Hana-no-kakehashi Network, 3. Faculty of Liberal Arts, Tohoku Gakuin University, 4. Snow Brand Seed Co., Ltd., 5. Graduate school of Agriculture, Hokkaido University

After the Tsunami disaster in March 11th, 2011 at east Japan area, especially on the pacific side of Tohoku region, our government built huge seawalls along the coastline about 400 km long to protect inland area from Tsunami disaster. We aimed to regenerate the ecotone of coastal ecosystem using the dune plants by greening the seawall. We were planting the seven species of dune plants on the seawall in 2017. On this presentation we report the survival rate for a year of planted dune plants on the seawall.
As a result, most dune plants were survived around 80% or more on the seaside seawall. But the survival rates were decreased around 70% on the landside seawall because of dried out by soil loss. Comparison between natural recovered seaside seawall and planted seaside seawall, the dominant species *Ischaemum anthephoroides* were similar. But *Ixeris repens* were less survived on the planted seaside seawall, in spite of one of the dominant species on the natural recovered seaside seawall. On the other hand, species of landside seawall were completely different with natural recovered landside seawall. This results shows that the greening on the seawall, especially on the landside seawall, were important for regeneration of coastal dune ecotone.

Keywords: Green infrastructure, Ecotone, Coastal dune system, Dune plants, Seawall

©2019. Japan Geoscience Union. All Right Reserved.

Fig. 1 Planting of dune plants on the seawall with citizens

©2019. Japan Geoscience Union. All Right Reserved.

Distribution Characteristics of Informal Green Space and Its Extension of perspective into Green Infrastructure

*minseo kim[1], Katsunori Furuya[1]

1. Chiba University Graduate School of Horticulture

1. introduction

The issues of Green Infrastructure (GI) and urban natural disasters are being addressed around the world, not only in North America and Europe, where the discussion first began, but throughout Asia. GI is a planned network strategically between natural and semi-natural areas, along with environmental factors designed for overall ecosystem services. A well-connected network provides positive benefits for quality of life and biodiversity and can receive ecosystem services such as reduction of disaster risk, water purification, air quality, recreational space, and climate change mitigation and adaptation. GI is a widely applicable element that can effectively respond to the various damage caused by climate change. Examples include efficient use of water resources, water restoration, protection of plant species susceptible to disasters, implementation of water conservation measures, reduction of heat island phenomena. In the case of the U.S. and Europe, a network of natural or semi-natural spaces with multidisciplinary functions is defined with the aim of restoring the functions of the ecosystem, and the policy is to utilize the combined spatial plan of domestic or countries. However, in recent years, the decline of cities has increased and limitations have been considered to create new urban green space as GI. Accordingly, the interest in informal green space such as vacant lots, street verges, water verges, and brownfields is increasing as an open space that is abandoned or overlooked in interstices in a city. In particular, interest is growing in strategies to enhance the urban environment and the vitality of residents by converting the value of vacant properties in urban areas to GI. Therefore, this study aims to examine the potential of informal green space as GI, and to suggests a connection with natural disaster prevention.

2. method

Since informal green spaces do not have an officially documented database, fieldwork on the site should be involved to derive the implications of this study. Therefore, in this study, Ichikawa City was analyzed as a study site, and informal green space and urban structures were analyzed using the spatial information collected from the field and the official open data sources. The sampling strategy used in this study was to set a square sample site of 50 meters at the intersection of a grid 500m and collect site information in focusing on the sample site. The total number of sample sites set up is 229 and the total area is about 1% of the entire city area.

3. results

Informal green space was found on 106 sample sites out of 229 sample sites in this study area. The total area of collected informal green space is 26,458 m^2 and consists of 229 patches. The total area of the informal green space found accounts for about 4.62% of the entire sample sites area, with an average area of about 115 m^2. Informal green space was distributed 123 patches and 67.6 m^2 mean size in residential areas, 15 patches and 48 m^2 mean size in commercial area, 16 patches and 230 m^2 mean size in industrial area, and 75 patches and 183 m^2 mean size in the urbanization control area. In the residential and commercial area, where are population density, informal green spaces are frequently distributed with a small scale. On the other hand, the informal green space of the urbanization control area with low population density and high elderly density is relatively large scale compared to residential and commercial area.

©2019. Japan Geoscience Union. All Right Reserved.

4. discussion and conclusion

Informal green space is a secondary green space created by human activities. Therefore, the distribution characteristics of informal green space differ according to the land use patterns that are related to human activities. Given the accessibility according to the distribution characteristics of informal green space and the linkage with the surrounding natural environment, a supplementary system of urban green infrastructure can be proposed.

Keywords: vacant land, urban green space, green infrastructure policy , Asia

©2019. Japan Geoscience Union. All Right Reserved.

DISASTER ANALYSIS OF LIGHTNING STRIKE DENSITY BASED ON LANDFORM FOR REDUCING VICTIMS IN WONOSOBO, INDONESIA

*Astry Zulky Permatasari[1], Gagad Nur Ridho[1], Yan Abdi Rahmanu[1], Emilya Nurjani[1]

1. Gadjah Mada University

Wonosobo regency is a region with diverse configuration landforms. The morphological and material aspects of the landform different responses to the lightning strike density. The incident of lightning strikes in Wonosobo Regency has negative impacts on people, buildings, and environment. Therefore, a lightning strike density analysis is important to minimize the negative impact of lightning strikes. This study aims to determine the condition of landform, analyze the relationship of lightning strike density and the landform, to know the risk of a lightning strike and give a recommendation of mitigation to reduce the negative impacts caused lightning strike. The research was conducted in Wonosobo Regency, Central Java Province. The data used are lightning strike type Cloud to Ground (CG) on 2015 - 2017 obtained from BMKG Yogyakarta station. Data is processed using ArcGIS 10.3 software with Kernel Density modeling and analyzed quantitatively-qualitative. Lightning strike density in Wonosobo shows a lower pattern from the southeast to the northwest. Wonosobo's landforms are volcanic and structural. Structural landform in Wonosobo Regency is anticlinal mountains with a strong or moderate incision that has the highest lightning strike density. The condition of the lithology of Wonosobo Regency dominated by Breccia, Lava and Tuff rocks that effect on the number of lightning strikes, because it has a low resistivity value (conductor). Kepil District and Wonosobo District are areas that have the highest risk of lightning strikes. Some mitigation activities that can be applied to reduce the risk of losses and death are installing a lightning rod, unplug the cable of electronic device inside the house during a lightning strike and immediately ending the outdoor activities when Cumulonimbus clouds begin to appear, and protect yourself by going into permanent buildings.

Keywords: Landform, Cloud to Ground, Wonosobo Regency, Risk, Lightning Strikes

©2019. Japan Geoscience Union. All Right Reserved.

LIGHTNING STRIKE DENSITY MAP IN WONOSOBO DISTRICT 2017

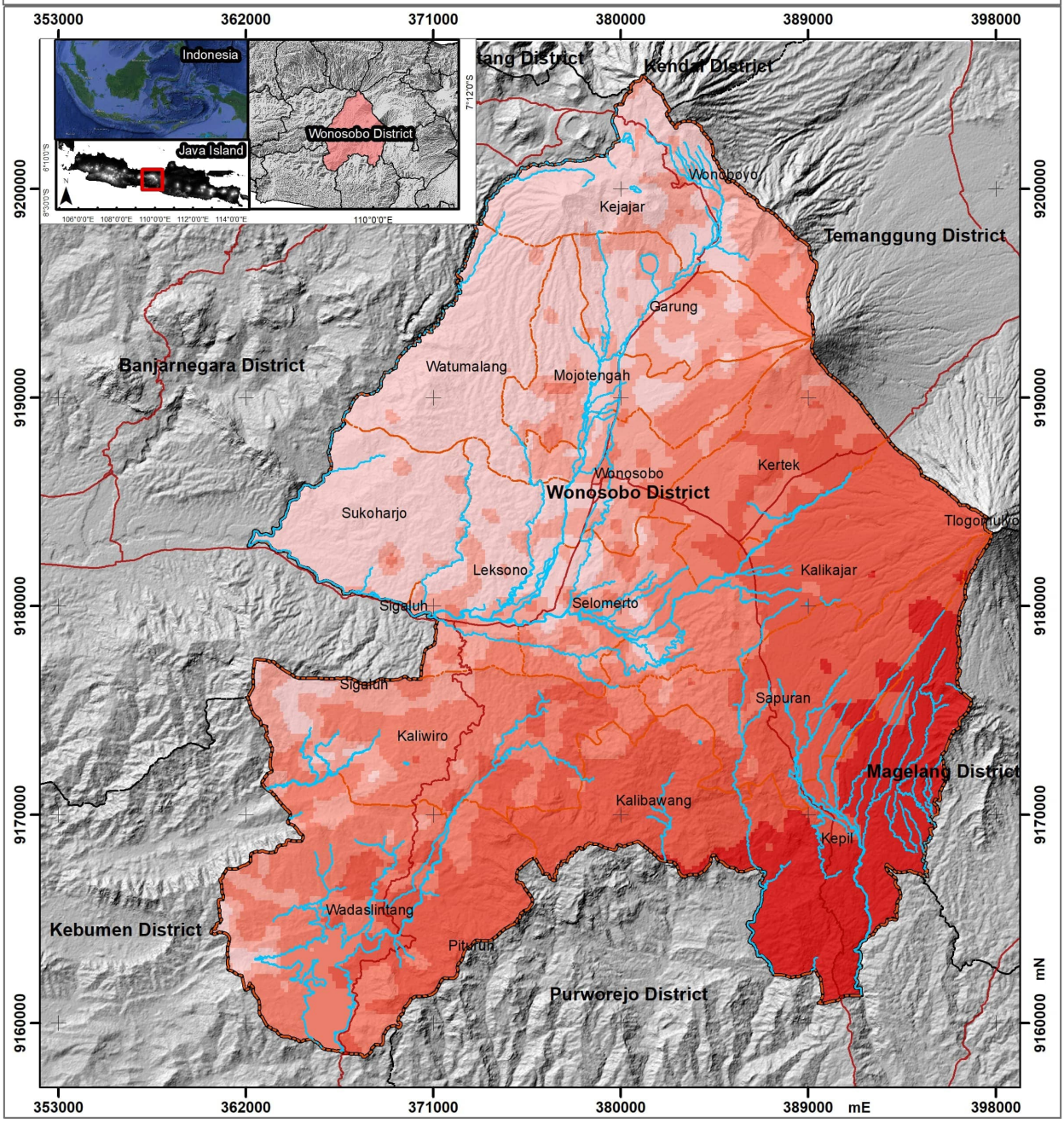

Legend

- Road
- River
- Subdistrict Border
- District Border

N

0 2 4 Km

Scale 1: 250.000

Density Class (in hectar)

Very Low	< 4.020
Low	4.021 - 5.303
Medium	5.306 - 8.330
High	8.331 - 15.435
Very High	15.436 - 32.138

Projection System : Transvers Mercator
Coordinate System : UTM
Datum : WGS 1984 Zone 49S
Source : 1.Lightning Strike Data's in Wonosobo District 2017 (Yogyakarta BMKG Station)
Made By : PKM-PE UGM Sambaran Petir's Team 2018

Faculty of Geography
Gadjah Mada University
Yogyakarta
2018

©2019. Japan Geoscience Union. All Right Reserved.

Development of Cost Competitive Unmanned Aerial Vehicle for Search and Rescue

*Aditya Keshav Natoo

UAV Technology is progressing at a rapid pace around the world. Some organizations have tried to develop Enterprise class UAVs which aim to cater to large section of users.
A dedicated cost competitive UAV to be used during and after disaster and for search and rescue missions is currently not available.

An effort is made to develop quad/hexa copter based UAVs with thermal and/or regular video cameras alongwith a servo controlled arm for transporting objects during search and rescue mission.

The thermal camera can transmit video images to the UAV operator to check for presence of victims during floods, earthquakes, forest fires, landslides, avalanches, tsunamis and cyclones.
During the search and rescue operations, items like inflatable lifejackets, harness, food and water supply etc can be dropped to the victims as well as rescue teams.

Keywords: Cost Competitive, Unmanned Aerial Vehicle, Search and Rescue

©2019. Japan Geoscience Union. All Right Reserved.

[E] Poster | H (Human Geosciences)：H-DS Disaster geosciences

Wed. May 29, 2019 10:45 AM - 12:15 PM JST | Wed. May 29, 2019 1:45 AM - 3:15 AM UTC | Poster Hall International Exhibition Hall8, Makuhari Messe_7

[H-DS10] Natural hazards impacts on human society, economics and technological systems

convener:ELENA PETROVA(Lomonosov Moscow State University, Faculty of Geography), Hajime Matsushima(Research Faculty of Agriculture, Hokkaido University)

The last decade set a record for the number and scale of natural disasters and demonstrates high vulnerability of human society and technosphere to their impacts. The most serious consequences have the so-called natural-technological disasters in which natural hazards trigger accidents at technology and infrastructure such as nuclear power and chemical plants, oil refineries and pipelines, power supply systems, buildings, and roads. A distinctive feature of natural-technological events, such as of the 2011 Tohoku earthquake, is their multi-hazard and synergistic nature, which creates cascading impacts, resulting in simultaneous occurrences of myriad catastrophes. The main goal of this multidisciplinary session is to summarize case studies of relationships between natural hazards and technological disasters, their social and economic consequences; and to encourage a discussion about tools and methods to prevent disasters and to minimize their consequences, disaster reconstruction, and tourism for reconstruction, Eco-DRR, and green infrastructure.

[HDS10-P01] The 2018 Activity of Kamchatka Volcanoes and Danger to Aviation

*Olga Girina[1], Dmitry Melnikov[1], Alexander Manevich[1], Anton Nuzhdaev[1], Elena Petrova[2] (1.Institute of Volcanology and Seismology, Far East Division, Russian Academy of Sciences, 2.M.V. Lomonosov Moscow State University)

[HDS10-P02] Planning Methodology on the Effective Use of Green Infrastructure for Disaster Risk Reduction

★Invited Papers

*Keita Aragane[1], Satoshi Funakubo[1] (1.National Institute for Land Infrastructure Management)

[HDS10-P03] EMERGENCY CALL PATTERN IN PETROZAVODSK

*Boris Zalmanovich Belashev[1], Natalia Vladimirovna Krutskikh[1], Anna Aleksandrovna Gerasimova[1] (1.Karelian research center of Russian academy of science)

[HDS10-P04] IDENTIFYING “REGIMES” IN THE TIME SEQUENCES OF PROCESSES

*Boris Zalmanovich Belashev[1] (1.Karelian research center of Russian academy of science)

[HDS10-P05] Investigation of status and demand on public service of earthquake disaster mitigation in China

*Lina Dong[1], Weiping Lian[1], Weitao Chen[1] (1.Development Research Center, China Earthquake Administration)

[HDS10-P06] Analysis of Eco-DRR and Ecological Services using InVEST at the Disaster Areas of Kumamoto Earthquake

*Minghui Tang[1], Naoko Fujita[1] (1.Kyushu University)

[HDS10-P07] Transformation as praxis: Exploring socially just and transdisciplinary pathways to sustainability in marginal environments (TAPESTRY)

*Nobuhito Ohte[1], Lyla Mehta[2], Synne Movik[3], Devanathan Parthasarathy[4] (1.Department of Social Informatics, Graduate School of Informatics, Kyoto University, 2.Institute of Development Studies at the University of Sussex, 3.Department of Urban and Regional Planning, Norwegian University of Life Sciences, 4.Department of Humanities and Social Sciences, Indian Institute of Technology)

[HDS10-P08] Study for the Establishment of the Design for Disaster prevention through the survey of Recognition of tsunami disaster prevention from the viewpoint of green infrastructure in the coastal area of Kyushu-Pacific region.

*Shanshan Xu[1], Naoko Fujita[1], Minghui Tang[1] (1.Kyushu University)

[HDS10-P09] Design for Green Infrastructure: Analysis of Landscape change in the Kumamoto earthquake area

★Invited Papers

*Naoko Fujita[1] (1.Kyushu University)

The 2018 Activity of Kamchatka Volcanoes and Danger to Aviation

*Olga Girina[1], Dmitry Melnikov[1], Alexander Manevich[1], Anton Nuzhdaev[1], Elena Petrova[2]

1. Institute of Volcanology and Seismology, Far East Division, Russian Academy of Sciences, 2. M.V. Lomonosov Moscow State University

Strong explosive eruptions of volcanoes are the most dangerous for aircraft because they can produce in a few hours or days to the atmosphere and the stratosphere till several cubic kilometers of volcanic ash and aerosols. Ash plumes and the clouds, depending on the power of the eruption, the strength and wind speed, can travel thousands of kilometers from the volcano for several days, remaining hazardous to aircraft, as the melting temperature of small particles of ash below the operating temperature of jet engines.

There are 30 active volcanoes in the Kamchatka, and several of them are continuously active. Scientists of KVERT monitor Kamchatkan volcanoes since 1993. In 2018, three of these volcanoes (Sheveluch, Klyuchevskoy, Karymsky) had strong and moderate explosive eruptions.
The eruptive activity of Sheveluch volcano began since 1980 (growth of the lava dome) and is continuing at present. In 2018, strong explosions sent ash up to 10-11 km a.s.l. on 09 January, 26 and 30 December; and up to 6-7 km a.s.l. –on 09 November, and 12, 14, 26-27 and 29 December; ash plumes extended more 2000 km to the different directions of the volcano. Satellite data by KVERT showed a thermal anomaly over the volcano all year. Activity of the volcano was dangerous to international and local aviation.

The moderate explosive events (ash up to 5-6 km a.s.l.) of Klyuchevskoy volcano were observing from 01 till 18 January, on 08 May, and 06 and 15 June. Strong explosions sent ash up to 10.5 km a.s.l. on 14 May. Ash plumes extended more 350 km to the eastern and south-western directions from the volcano. Satellite data by KVERT showed a thermal anomaly over the volcano all year. Activity of the volcano was dangerous to international and local aviation.

The thermal anomaly over Karymsky volcano was recorded on satellite images from time to time, most brightly it manifested in January, May, June-August, September and December. According to visual and satellite data, at this time explosions rose ash up to 6.5 km a.s.l., ash plumes drifted for about 860 km to the different directions from the volcano. The most intense eruptive activity of the volcano was observed on 10, 14-20 and 26-31 July, besides, isolated strong explosive events were observed on 07 and 25 August, on 10-11, 22-23 and 30 September, and 01 December. The size of the ash clouds varied from 5-6 to 240 km. Activity of the volcano was dangerous to local aviation.
This work was supported by the Russian Science Foundation, project No. 16-17-00042.

Keywords: volcano, eruption, Kamchatka, danger to Aviation

©2019. Japan Geoscience Union. All Right Reserved.

Planning Methodology on the Effective Use of Green Infrastructure for Disaster Risk Reduction

*Keita Aragane[1], Satoshi Funakubo[1]

1. National Institute for Land Infrastructure Management

Green Infrastructure (GI) is a concept based on infrastructure development and land utilization that take advantage of natural environments' various functions for creating sustainable and attractive national land or regions. In Japan, since 2015, the concept of GI has been include in National Spatial Strategy, National Land Use Plan, and Priority Plan for Infrastructure Development, etc. Also, lessons learned from the Great East Japan Earthquake raised awareness of the need for more-comprehensive disaster risk reduction strategies in preparing for disasters that surpass worst-case scenarios. Additionally, there is concern over anticipated the Nankai Trough Earthquakes that might cause greater damage in near future, and increasingly frequent urban flooding owing to climate change. Thus, initiative for disaster risks reduction by utilizing GI's multiple functions in addition to approaches focusing on artificial infrastructure has become increasingly important.

This study aims to discuss planning methodology regarding the effective use of GI for disaster risk reduction in urban area by examining the “Green Master Plan (GMP)” through 72 case studies. In Japan, 680 municipal governments have developed GMPs as their basic policy for green space planning, management, and greening. These municipal governments in Japan are recommended to emphasize the viewpoint of disaster risk reduction in their GMPs, and to implement disaster risk reduction systematically through effective use of green spaces such as parks, roadside trees, waterways, private domestic gardens, agricultural land, and woodlands. Result from the case studies revealed that almost all GMPs designated green spaces such as parks as evacuation sites for mega-earthquakes or large-scale fires. Several GMPs were also found to present countermeasures that make effective use of GI for tsunami-related disasters and urban flooding.

Through these findings and through discussions with scholars at a workshop, we published “Technical Note on Green Infrastructure Planning for Urban Resilience” in June 2018. In this technical note, we explain six key points for developing GMPs that enhance the role of GI in disaster risk reduction: (1) combining various measures for disaster risk reduction by utilizing GI from a comprehensive perspective, (2) examining the role and combination of GI and other artificial infrastructure in urban disaster risk reduction, (3) building cooperative relationships with various stakeholders and citizens, (4) taking advantage of multiple functions of GI not only during disasters but also in normal times, (5) establishing a mechanism for maintaining and using GI from a long-term perspective, and (6) considering regional conditions and social situations.

Keywords: Green Infrastructure, Dsaster Risk Reduction, Green Master Plan

©2019. Japan Geoscience Union. All Right Reserved.

EMERGENCY CALL PATTERN IN PETROZAVODSK

*Boris Zalmanovich Belashev[1], Natalia Vladimirovna Krutskikh[1], Anna Aleksandrovna Gerasimova[1]

1. Karelian research center of Russian academy of science

The aim of the study is to analyze the emergency call distribution for Petrozavodsk, Russia, to obtain quantitative disease estimates and to assess the effect of environmental factors on them.

The study was based on medical statistical data and geophysical and geochemical monitoring. Environmental factors, such as magnetic storms and air and urban soil pollution, were assessed. The impersonified catalogue of emergency calls of Petrozavodsk Ambulance from 2015.1.1 to 2017.12.19, database of geomagnetic field variations at Petrozavodsk Geophysical Observatory, data on Kp index monitoring at the Laboratory of Tesis X-ray Astronomy at Lebedev Physical Institute, and the results of geochemical soil sampling in Petrozavodsk were used. Emergency call and geomagnetic activity distributions were constructed and processed in MATLAB computer mathematics system and Qgis software package. Analytical results were demonstrated on cardiovascular diseases.

The number of emergency call for patients with cardiac diseases in 2015-2017 is at about the same level. Seasonal factors affect the time distribution trends of calls for patients with essential hypertension, stenocardia and ischemic cardiac disease and do not affect the distribution trends of myocardial infarction and cerebral crisis. Time distribution spectra display a 25.6 day cycle similar to a geomagnetic activity period, two- and one-week cycles and cycles with periods of about 6, 4 and 3 days. Emergency calls for patients with myocardial infarction reflect the gender and age of the patients. The number of calls on weekends is typically low. On week-days, the number of calls at rush hours is maximum. The number of calls on days close to magnetic storms is not necessarily great. An elevated number of calls on these days for patients with stenocardia and myocardial infarction is observed.

The spatial distribution of the number of emergency calls were obtained using the Ambulance Geoinformation System. The system constructs the spatial distributions of the number of emergency team calls with known diagnoses for the streets and blocks of the city and is used to compare call frequency with district factors. With its help the link of distribution of quantity of calls of ambulance with diagnoses of cardiovascular diseases, bronchial asthma, vegeto-vascular dystonia, new growths, other diseases on districts of the city with the soils contamination indicated by the environmental hazard index –a total of the weighted average concentration values of As, Pb, Zn, Cd, Co, Cu, V, W is studied. No significant correlations between these values have been revealed.

3, 6-daily cycles in the analyzed ranges can be connected to thyroid gland hormone activity and a 4-day cycle to glucocorticoid hormone activity. Circadian rhythms are either thought to be general or to be due to the unwillingness of people to be sent to hospital or call for a doctor on weekends. In case of myocardial infarction, when help is needed urgently, the latter factor does not work, and a one-week cycle in the spectrum, showing the time dependence of the number of calls, is displayed.

This fact and the weekend effect can be understood, based on the properties of hydrocortisone. Stress from production activity stimulates the supply of the hormone into the blood, which rushes to the heart and muscles. When the heart fails to cope with the rush of blood, a cardiac disease becomes more acute.

©2019. Japan Geoscience Union. All Right Reserved.

As the hydrocortisone level in the blood on weekends and holidays declines, the number of emergency calls for patients with cardiovascular diseases decreases.

Peaks in the daily emergency call dynamics distribution on week-days are interpreted to be due to air pollution with car gases at rush hours (9-10 a.m., 1-2 and 6-7 p.m.) and an approximately one-hour delay caused by progress in disease and the need to apply for a doctor.
The emergency call distributions analyzed are highly informative, showing the complete dynamic disease pattern of the urban population.

Keywords: diseases, emergency call, patient, diagnose, magnetic storms, contamination

©2019. Japan Geoscience Union. All Right Reserved.

IDENTIFYING “REGIMES” IN THE TIME SEQUENCES OF PROCESSES

*Boris Zalmanovich Belashev[1]

1. Karelian research center of Russian academy of science

A process is represented as a sequence of “regimes” when describing climatic variations and complex systems, detecting the malfunctioning of instruments and illegal interference in computer and hardware networks. For natural, technological and social processes such representation is comfortable to detect precursors of disastrous events.
The shifts of “regimes” in the sequences are commonly detected by checking statistical hypotheses by Student’s test and tests of non-parametric statistics when comparing the characteristics of the sequence at one or another site. Algorithms often use a priori information, work in unstable fashion over short intervals and at sequences boundaries, find it hard to recognize the shifts and trends of “regimes”.
Widespread R-algorithm [1] analyze data consecutively in a sliding window, operate with a small number of parameters and filter off “red” noise. The boundary regimes it detect may reflect distortions characteristic of the beginning and end of measurements.
The goal of the present study is to develop B-algorithm which automatically recognizes stable “regimes” in time data sequences.
The main stages of the algorithm are clusterization, comparison and optimization. Clusterization preliminary divides a normalized time sequence into “regimes”. While comparing the characteristics of the “regimes”, the division obtained is re-estimated. The final model of division is formed during optimization, which minimizes the variance of deviations from the trends of the “regimes” by varying the internal boundaries of the sites.
The algorithm, developed as a software in the MATLAB computer mathematics system, fulfils procedures automatically, decreases the amount of a priori data, increases operation speed and brings solutions closer to optima.
The operation of B- and R-algorithms is exemplified by the PDO (Pacific Decade Oscillation) sequence of mean January temperatures [2].
In both algorithms the number of “regimes” and their approximate positions coincide. The delay of part of R-“regimes” emphasize the sensitivity of B-algorithm to new “regimes”. Discrepancies are connected with the last “regime” identified by R- and B-algorithms on 2 and 15 members of sequence, respectively.
B- algorithm can operate with constant, linear and complex trends.
B- and R-algorithms, applied to the time sequences of river runoff, solar and seismic activity and the sequences of the annual rings of trees, have provided new information on the stages of processes.
The simplified schematic “regime” representation of a process reveals trends commonly obscured by the abundance of details. B- algorithm identifies stable “regimes” and recognizes the shifts and trends of “regimes”. The use of MATLAB functions increases the potential of the algorithm, admits the fulfilment of procedures by various methods, brings solutions closer to optimum solutions and ensures high operation speed. The ability of the algorithm to automatically process data makes it suitable for working with extensive data in various earth sciences.
References:
1.Rodionov, S. (2006) Use of prewhitening in climate region shift detection. Geophysical Research Letters 33, L12707.
2.Pacific Decadal Oscillation Index Data.
https://www.rdocumentation.org/packages/rpdo/versions/0.2.5.

©2019. Japan Geoscience Union. All Right Reserved.

Keywords: time sequence, shift regime, algorithm, clusterization, comparision, optimization

©2019. Japan Geoscience Union. All Right Reserved.

Investigation of status and demand on public service of earthquake disaster mitigation in China

*Lina Dong[1], Weiping Lian[1], Weitao Chen[1]

1. Development Research Center, China Earthquake Administration

In order to make a comprehensive and systematic evaluation of the status and demands of public service of earthquake disaster mitigation, we launched an investigation with National Bureau of Statistics on the current situation of public service of earthquake disaster mitigation and the demands for it in 2018. The investigation was conducted in 31 provinces of China mainland using the Computer Assisted Telephone Interview(CATI) method and received 20078 valid samples in total.

The results indicate that 52.2% of the population have received the scientific knowledge education for earthquake disaster mitigation in Different levels. It shows that the public still possesses a high expectation of earthquake prediction and farmers have a low level of scientific knowledge of earthquake disaster mitigation. And TV, network, and the new media app such as wechat and weibo become the most important information channels for the public to obtain the earthquake related information. Furthermore, the degree of satisfaction evaluation of public service of earthquake disaster mitigation is marked on 81.22 points (the full mark is 100 points). And the most expectative services for the public are reconstruction, earthquake warning, and house earthquake resilience test. The results of the investigation have provided a scientific evidence for the government to provide better services of earthquake disaster mitigation and to make scientific knowledge popularization in a more scientific way.

Keywords: scientific knowledge popularization of earthquake disaster mitigation, public service, satisfaction evaluation

©2019. Japan Geoscience Union. All Right Reserved.

Analysis of Eco-DRR and Ecological Services using InVEST at the Disaster Areas of Kumamoto Earthquake

*Minghui Tang[1], Naoko Fujita[1]

1. Kyushu University

When compared with other countries in a global point of view, Japan is a country with high number of natural calamities, significant causalities, economic loss and damages by earthquakes, typhoons, and eruption. The damage is especially big when a hazard comes right after another one.

Complex disaster refers to the occurrence of multiple disasters instead of one. Such as, in 2016, Kumamoto prefecture was hit by earthquakes with magnitude as large as 7 and within another 2 months, by heavy rain and the damage was tremendous.

There is a huge number of researches on the eco-application of proceeding in various countries and it is vitally important to verify their validity. Here, InVEST refers to the ArcGIS tool for the integrated review for ecological services and its compensation.

This research focuses on the analysis of the changes of the land cover as reflected in satellite pictures of the whole Kumamoto prefecture taken after the complex disaster, the earthquake in April 2016 and heavy rain in June 2016. Also, it’ s a review on the ecological services with the use of InVEST. A special focus is paid on the review of the soil retention and the quality changes of the eco-habitant as reflection of the disaster damage reduction measures.

In addition, there is an analysis on the change of land coverage on area-unit level with Mashiki-machi, the epicenter, as the target. Furthermore, projection was plotted for the ecological services implemented as the reconstruction plan.

Keywords: Kumamoto Earthquake, Eco-DRR, Ecological services, Complex Disasters, local governments/local communities, InVEST

©2019. Japan Geoscience Union. All Right Reserved.

Transformation as praxis: Exploring socially just and transdisciplinary pathways to sustainability in marginal environments (TAPESTRY)

*Nobuhito Ohte[1], Lyla Mehta[2], Synne Movik[3], Devanathan Parthasarathy[4]

1. Department of Social Informatics, Graduate School of Informatics, Kyoto University, 2. Institute of Development Studies at the University of Sussex, 3. Department of Urban and Regional Planning, Norwegian University of Life Sciences, 4. Department of Humanities and Social Sciences, Indian Institute of Technology

Climate change related uncertainties are the main threats to the sustainability of societies and their environments. To tackle these challenges, systemic transformations are required. Our project focuses on three cases of transformation in marginal environments in India and Bangladesh, and is concerned with: How transformation happens through bottom up processes in these sites; and how they can be scaled up and facilitate wider societal changes. Both require transdisciplinary co-production and the praxis of transformation which presupposes change in social arrangements and reconstruction by individuals. Our project addresses issues concerning governance, wellbeing, identity and quality of life in relation to transformations to sustainability in a lower middle income country (India) and a least developed country (Bangladesh). Our results should help inform processes that ultimately improve the quality of life in marginal environments, and build action and capacity among all partners.

Keywords: Transformation, Sustainability, Marginal environment, Transdisciplinary study, India, Bangladesh

©2019. Japan Geoscience Union. All Right Reserved.

Study for the Establishment of the Design for Disaster prevention through the survey of Recognition of tsunami disaster prevention from the viewpoint of green infrastructure in the coastal area of Kyushu-Pacific region.

*Shanshan Xu[1], Naoko Fujita[1], Minghui Tang[1]

1. Kyushu University

Considering the possibility of Nankai Trough large-scale earthquake predicted to occur in the nearest future, the issue of the tsunami in the coastal area of Kyushu-Pacific region is becoming extremely important. Efforts to utilize the various functions of the ecosystem internationally for the society creation are expanding in recent years, and even in the situation of toughening of the land in Japan, the initiative to incorporate Green Infrastructure (GI) which utilizes the disaster prevention and reduction functions of the natural ecosystem are being observed. Also, during the process of self-help/mutual assistance action and disaster reconstruction at the time of disaster, attention is paid as regional ties are affected, which are being considered as Social capital (SC).

The purpose of this study is to clarify the actual situation of tsunami disaster prevention of Nankai Trough earthquake based on the viewpoint of GI. We conducted a questionnaire survey on tsunami disaster prevention and GI at local governments and local communities. After analyzing the questionnaire, we analyzed the needs of the self-governing president's disaster prevention measures, the problems of the area, and the deviation of the improved situation of municipalities' disaster prevention measures. A correlation analysis was conducted to grasp the relationship between the consciousness concerning GI utilization, the strength of regional linkage SC and the recognition of evacuation.

1. Misalignment between demand and maintenance situation desired by the region

Policy regarding the issue of disaster helpers was extracted as a gap between needs and maintenance situation. Regarding the needs of the soft pattern in disaster prevention, a lot of measures were taken by disaster support supporters, however as it comes from the municipality questionnaire results, the measures related to the introduction of the barrier-free system and evacuation action supporters were introduced only partially. Further improvement is necessary for welfare evacuation sites, measures against supporters requiring evacuation actions, barrier-free formation.

2. SC regarded from the viewpoint of the relationship between intentions to utilize GI and recognition on disaster.

©2019. Japan Geoscience Union. All Right Reserved.

Especially, the correlation coefficient was 0.701 between No.7 and No.6. This shows that those who responded that disaster can happen among residents can respond that regional ties are stronger. For items with a high correlation coefficient between No.3 and No.8, the correlation became 0.437. This means the respondents who answered that evacuation is possible for all area inhabitants including elderly people in case of disaster (flooding, earthquakes, and tsunami) are able to use local well water and spring water in the event of a disaster.

Between No.2 and No.4, the correlation coefficient became 3.380. This is because those who respond that they think they can fully utilize the resources of the area (resources such as firewood, foods that can be harvested in mountains) even in the event of disasters will escape by utilizing the nearby natural landforms such as plateaus and mountains for tsunami evacuation. Between No.2 and No.8, the correlation coefficient became 0.351. This is because it shows those who responded that they thought that they could escape by utilizing nearby plateau and mountains such as mountains during the tsunami evacuation, even if disasters (flood, earthquake, tsunami) occurred, everyone including the elderly in the area evacuated. Between No.2 and No.6, the correlation coefficient became 0.343. This indicates that those who responded that they believe that they can escape by utilizing nearby plateaus and mountains when evacuating the tsunami think that the connection of the community people is strong. Between No.3 and No.6, the correlation coefficient became 0.287. This indicates that those who responded as they thought they could use local well water and spring water at the time of a disaster replied that they think that the regional connection is stronger.

Based on the above, we clarified the SC from the viewpoint of the gap between the request and the maintenance situation the region desires and the relationship between the intention to utilize GI and the perception of disaster. The fact that utilization of natural resources such as well water and spring water and understanding that natural topography can be utilized for evacuation leads to a positive feeling making people believe it is possible for everyone to evacuate even if the tsunami comes, can be suggested from this study.

Keywords: the Design for Disaster prevention, tsunami disaster, green infrastructure, the coastal area of Kyushu-Pacific region, Nankai Trough large-scale earthquake

©2019. Japan Geoscience Union. All Right Reserved.

Design for Green Infrastructure: Analysis of Landscape change in the Kumamoto earthquake area

*Naoko Fujita[1]

1. Kyushu University

The concept of “Green Infrastructure” and “Eco-DRR” is developed in Europe and North America lately, and it started to spread around in Japan after the Tohoku earthquake and tsunami in 2011. Landscape ecology is parallel with this conceptually, as well as in terms of spatial scale. Its successful focused researches and social implementation are becoming pervasive.

The new concept is to solve various problems by local resources and pearls of wisdom, it connects local communities to the world while it’s mainly led by front liners and researchers in engineering and ecological fields that little attention is paid to the aspects of arts and designs. It’s still not well-penetrated despite the validity and functions of the concept are well verified. Thus, it’s vitally important to work on the insufficient.

The purpose of this research is to analyze the reconstruction plan prepared by the affected municipalities of the Kumamoto earthquake and compare the landscape change read from the plan and the actual landscape change actually occurred and make clear how the cities and nature have changed during the reconstruction process.

In this research, we firstly gathered and analyzed the earthquake reconstruction plans created by each local government for all 45 municipalities in Kumamoto prefecture. In this analysis, while studying each municipal original plan, we primarily focused on the background, features, and landscape references of the plan formulation. During this analysis, we grasped the relations between the reconstruction plan and the landscape change, and also clarified what exactly each local government emphasizes independently. As the next step, basing on the field survey, we analyzed the actual state of the landscape changes described in the plan. As a method, we took the photographs at places where the plans adopted by each municipality in Kumamoto prefecture were scheduled or executed, and after recording the current situation and the surrounding landscape, we made a comparison with the photographs taken at the same place in the past. By doing this, we revealed what kind of changes have occurred between the past and the present due to the disaster, and how they affected the surrounding landscape.

Among the 45 municipalities in downtown Kumamoto Prefecture, we found that earthquake reconstruction plan was formulated in 16 municipalities, and 5 municipalities planned to formulate. There were references that "consideration of the landscape when promoting housing improvement and infrastructure development" and "to consider the landscape from the tourism viewpoint". Also, there were plans to utilize the process of reconstruction itself as a resource for tourist attraction. Furthermore, as a result of analyzing the individual plans described in the reconstruction plan, the reference to landscape,

©2019. Japan Geoscience Union. All Right Reserved.

reference to the prediction of landscape change, reference to landscape protection exists in all 16 cities, towns, and villages. Totally 117 relevant plans have been found. Although many of them were intended to cope with the damage at the time of the disaster, there were several plans originally adopted by the local governments to make necessary improvements of the problems they had from the past by conducting disaster recovery.

The field survey was conducted for 16 municipalities in total in Kumamoto Prefecture. One year has passed since the earthquake disaster, and recovery works progressed in a wide range in Kumamoto Prefecture. In the recovery sites in various places, a secondary change of the landscape, which caused the recovery activity aimed at improving the convenience of life and safety, has already been taking place. Moreover, recovery works progressed also in Kumamoto castle which is also cultural asset and tourist attraction, as well as the station and the government office which are the center of town. As a result, we could confirm the change of landscape.

In this research, through the analysis of the reconstruction plan created by the municipalities affected by the Kumamoto earthquake and the field survey, from the viewpoint of Green Infrastructure, we could make clear the process of the landscape change occurred during the process of recovery/reconstruction of the living base, the tourist resources, the natural environment in the affected areas and its influence respectively. Although few local governments have formulated landscape-friendly reconstruction plans, to gain medium- and long-term benefits, we should make landscape-friendly reconstructions from the original planning stage. This is because it is the factor determining the richness of living base, tourism resources, and natural environment.

Keywords: Green Infrastructure, the Kumamoto earthquake , Design

©2019. Japan Geoscience Union. All Right Reserved.

[E] Poster | H (Human Geosciences)：H-DS Disaster geosciences

Wed. May 29, 2019 5:15 PM - 6:30 PM JST | Wed. May 29, 2019 8:15 AM - 9:30 AM UTC | Poster Hall International Exhibition Hall8, Makuhari Messe_21

[H-DS10] Natural hazards impacts on human society, economics and technological systems

convener:ELENA PETROVA(Lomonosov Moscow State University, Faculty of Geography), Hajime Matsushima(Research Faculty of Agriculture, Hokkaido University)

The last decade set a record for the number and scale of natural disasters and demonstrates high vulnerability of human society and technosphere to their impacts. The most serious consequences have the so-called natural-technological disasters in which natural hazards trigger accidents at technology and infrastructure such as nuclear power and chemical plants, oil refineries and pipelines, power supply systems, buildings, and roads. A distinctive feature of natural-technological events, such as of the 2011 Tohoku earthquake, is their multi-hazard and synergistic nature, which creates cascading impacts, resulting in simultaneous occurrences of myriad catastrophes. The main goal of this multidisciplinary session is to summarize case studies of relationships between natural hazards and technological disasters, their social and economic consequences; and to encourage a discussion about tools and methods to prevent disasters and to minimize their consequences, disaster reconstruction, and tourism for reconstruction, Eco-DRR, and green infrastructure.

[HDS10-P01] The 2018 Activity of Kamchatka Volcanoes and Danger to Aviation

*Olga Girina[1], Dmitry Melnikov[1], Alexander Manevich[1], Anton Nuzhdaev[1], Elena Petrova[2] (1.Institute of Volcanology and Seismology, Far East Division, Russian Academy of Sciences, 2.M.V. Lomonosov Moscow State University)

[HDS10-P02] Planning Methodology on the Effective Use of Green Infrastructure for Disaster Risk Reduction

★Invited Papers

*Keita Aragane[1], Satoshi Funakubo[1] (1.National Institute for Land Infrastructure Management)

[HDS10-P03] EMERGENCY CALL PATTERN IN PETROZAVODSK

*Boris Zalmanovich Belashev[1], Natalia Vladimirovna Krutskikh[1], Anna Aleksandrovna Gerasimova[1] (1.Karelian research center of Russian academy of science)

[HDS10-P04] IDENTIFYING “REGIMES” IN THE TIME SEQUENCES OF PROCESSES

*Boris Zalmanovich Belashev[1] (1.Karelian research center of Russian academy of science)

[HDS10-P05] Investigation of status and demand on public service of earthquake disaster mitigation in China

*Lina Dong[1], Weiping Lian[1], Weitao Chen[1] (1.Development Research Center, China Earthquake Administration)

[HDS10-P06] Analysis of Eco-DRR and Ecological Services using InVEST at the Disaster Areas of Kumamoto Earthquake

*Minghui Tang[1], Naoko Fujita[1] (1.Kyushu University)

[HDS10-P07] Transformation as praxis: Exploring socially just and transdisciplinary pathways to sustainability in marginal environments (TAPESTRY)

*Nobuhito Ohte[1], Lyla Mehta[2], Synne Movik[3], Devanathan Parthasarathy[4] (1.Department of Social Informatics, Graduate School of Informatics, Kyoto University, 2.Institute of Development Studies at the University of Sussex, 3.Department of Urban and Regional Planning, Norwegian University of Life Sciences, 4.Department of Humanities and Social Sciences, Indian Institute of Technology)

[HDS10-P08] Study for the Establishment of the Design for Disaster prevention through the survey of Recognition of tsunami disaster prevention from the viewpoint of green infrastructure in the coastal area of Kyushu-Pacific region.

*Shanshan Xu[1], Naoko Fujita[1], Minghui Tang[1] (1.Kyushu University)

[HDS10-P09] Design for Green Infrastructure: Analysis of Landscape change in the Kumamoto earthquake area

★Invited Papers

*Naoko Fujita[1] (1.Kyushu University)

The 2018 Activity of Kamchatka Volcanoes and Danger to Aviation

*Olga Girina[1], Dmitry Melnikov[1], Alexander Manevich[1], Anton Nuzhdaev[1], Elena Petrova[2]

1. Institute of Volcanology and Seismology, Far East Division, Russian Academy of Sciences, 2. M.V. Lomonosov Moscow State University

Strong explosive eruptions of volcanoes are the most dangerous for aircraft because they can produce in a few hours or days to the atmosphere and the stratosphere till several cubic kilometers of volcanic ash and aerosols. Ash plumes and the clouds, depending on the power of the eruption, the strength and wind speed, can travel thousands of kilometers from the volcano for several days, remaining hazardous to aircraft, as the melting temperature of small particles of ash below the operating temperature of jet engines.

There are 30 active volcanoes in the Kamchatka, and several of them are continuously active. Scientists of KVERT monitor Kamchatkan volcanoes since 1993. In 2018, three of these volcanoes (Sheveluch, Klyuchevskoy, Karymsky) had strong and moderate explosive eruptions.
The eruptive activity of Sheveluch volcano began since 1980 (growth of the lava dome) and is continuing at present. In 2018, strong explosions sent ash up to 10-11 km a.s.l. on 09 January, 26 and 30 December; and up to 6-7 km a.s.l. –on 09 November, and 12, 14, 26-27 and 29 December; ash plumes extended more 2000 km to the different directions of the volcano. Satellite data by KVERT showed a thermal anomaly over the volcano all year. Activity of the volcano was dangerous to international and local aviation.

The moderate explosive events (ash up to 5-6 km a.s.l.) of Klyuchevskoy volcano were observing from 01 till 18 January, on 08 May, and 06 and 15 June. Strong explosions sent ash up to 10.5 km a.s.l. on 14 May. Ash plumes extended more 350 km to the eastern and south-western directions from the volcano. Satellite data by KVERT showed a thermal anomaly over the volcano all year. Activity of the volcano was dangerous to international and local aviation.

The thermal anomaly over Karymsky volcano was recorded on satellite images from time to time, most brightly it manifested in January, May, June-August, September and December. According to visual and satellite data, at this time explosions rose ash up to 6.5 km a.s.l., ash plumes drifted for about 860 km to the different directions from the volcano. The most intense eruptive activity of the volcano was observed on 10, 14-20 and 26-31 July, besides, isolated strong explosive events were observed on 07 and 25 August, on 10-11, 22-23 and 30 September, and 01 December. The size of the ash clouds varied from 5-6 to 240 km. Activity of the volcano was dangerous to local aviation.
This work was supported by the Russian Science Foundation, project No. 16-17-00042.

Keywords: volcano, eruption, Kamchatka, danger to Aviation

©2019. Japan Geoscience Union. All Right Reserved.

Planning Methodology on the Effective Use of Green Infrastructure for Disaster Risk Reduction

*Keita Aragane[1], Satoshi Funakubo[1]

1. National Institute for Land Infrastructure Management

Green Infrastructure (GI) is a concept based on infrastructure development and land utilization that take advantage of natural environments' various functions for creating sustainable and attractive national land or regions. In Japan, since 2015, the concept of GI has been include in National Spatial Strategy, National Land Use Plan, and Priority Plan for Infrastructure Development, etc. Also, lessons learned from the Great East Japan Earthquake raised awareness of the need for more-comprehensive disaster risk reduction strategies in preparing for disasters that surpass worst-case scenarios. Additionally, there is concern over anticipated the Nankai Trough Earthquakes that might cause greater damage in near future, and increasingly frequent urban flooding owing to climate change. Thus, initiative for disaster risks reduction by utilizing GI's multiple functions in addition to approaches focusing on artificial infrastructure has become increasingly important.

This study aims to discuss planning methodology regarding the effective use of GI for disaster risk reduction in urban area by examining the “Green Master Plan (GMP)” through 72 case studies. In Japan, 680 municipal governments have developed GMPs as their basic policy for green space planning, management, and greening. These municipal governments in Japan are recommended to emphasize the viewpoint of disaster risk reduction in their GMPs, and to implement disaster risk reduction systematically through effective use of green spaces such as parks, roadside trees, waterways, private domestic gardens, agricultural land, and woodlands. Result from the case studies revealed that almost all GMPs designated green spaces such as parks as evacuation sites for mega-earthquakes or large-scale fires. Several GMPs were also found to present countermeasures that make effective use of GI for tsunami-related disasters and urban flooding.

Through these findings and through discussions with scholars at a workshop, we published “Technical Note on Green Infrastructure Planning for Urban Resilience” in June 2018. In this technical note, we explain six key points for developing GMPs that enhance the role of GI in disaster risk reduction: (1) combining various measures for disaster risk reduction by utilizing GI from a comprehensive perspective, (2) examining the role and combination of GI and other artificial infrastructure in urban disaster risk reduction, (3) building cooperative relationships with various stakeholders and citizens, (4) taking advantage of multiple functions of GI not only during disasters but also in normal times, (5) establishing a mechanism for maintaining and using GI from a long-term perspective, and (6) considering regional conditions and social situations.

Keywords: Green Infrastructure, Dsaster Risk Reduction, Green Master Plan

©2019. Japan Geoscience Union. All Right Reserved.

EMERGENCY CALL PATTERN IN PETROZAVODSK

*Boris Zalmanovich Belashev[1], Natalia Vladimirovna Krutskikh[1], Anna Aleksandrovna Gerasimova[1]

1. Karelian research center of Russian academy of science

The aim of the study is to analyze the emergency call distribution for Petrozavodsk, Russia, to obtain quantitative disease estimates and to assess the effect of environmental factors on them.

The study was based on medical statistical data and geophysical and geochemical monitoring. Environmental factors, such as magnetic storms and air and urban soil pollution, were assessed. The impersonified catalogue of emergency calls of Petrozavodsk Ambulance from 2015.1.1 to 2017.12.19, database of geomagnetic field variations at Petrozavodsk Geophysical Observatory, data on Kp index monitoring at the Laboratory of Tesis X-ray Astronomy at Lebedev Physical Institute, and the results of geochemical soil sampling in Petrozavodsk were used. Emergency call and geomagnetic activity distributions were constructed and processed in MATLAB computer mathematics system and Qgis software package. Analytical results were demonstrated on cardiovascular diseases.

The number of emergency call for patients with cardiac diseases in 2015-2017 is at about the same level. Seasonal factors affect the time distribution trends of calls for patients with essential hypertension, stenocardia and ischemic cardiac disease and do not affect the distribution trends of myocardial infarction and cerebral crisis. Time distribution spectra display a 25.6 day cycle similar to a geomagnetic activity period, two- and one-week cycles and cycles with periods of about 6, 4 and 3 days. Emergency calls for patients with myocardial infarction reflect the gender and age of the patients. The number of calls on weekends is typically low. On week-days, the number of calls at rush hours is maximum. The number of calls on days close to magnetic storms is not necessarily great. An elevated number of calls on these days for patients with stenocardia and myocardial infarction is observed.

The spatial distribution of the number of emergency calls were obtained using the Ambulance Geoinformation System. The system constructs the spatial distributions of the number of emergency team calls with known diagnoses for the streets and blocks of the city and is used to compare call frequency with district factors. With its help the link of distribution of quantity of calls of ambulance with diagnoses of cardiovascular diseases, bronchial asthma, vegeto-vascular dystonia, new growths, other diseases on districts of the city with the soils contamination indicated by the environmental hazard index –a total of the weighted average concentration values of As, Pb, Zn, Cd, Co, Cu, V, W is studied. No significant correlations between these values have been revealed.

3, 6-daily cycles in the analyzed ranges can be connected to thyroid gland hormone activity and a 4-day cycle to glucocorticoid hormone activity. Circadian rhythms are either thought to be general or to be due to the unwillingness of people to be sent to hospital or call for a doctor on weekends. In case of myocardial infarction, when help is needed urgently, the latter factor does not work, and a one-week cycle in the spectrum, showing the time dependence of the number of calls, is displayed.

This fact and the weekend effect can be understood, based on the properties of hydrocortisone. Stress from production activity stimulates the supply of the hormone into the blood, which rushes to the heart and muscles. When the heart fails to cope with the rush of blood, a cardiac disease becomes more acute.

©2019. Japan Geoscience Union. All Right Reserved.

As the hydrocortisone level in the blood on weekends and holidays declines, the number of emergency calls for patients with cardiovascular diseases decreases.

Peaks in the daily emergency call dynamics distribution on week-days are interpreted to be due to air pollution with car gases at rush hours (9-10 a.m., 1-2 and 6-7 p.m.) and an approximately one-hour delay caused by progress in disease and the need to apply for a doctor.
The emergency call distributions analyzed are highly informative, showing the complete dynamic disease pattern of the urban population.

Keywords: diseases, emergency call, patient, diagnose, magnetic storms, contamination

©2019. Japan Geoscience Union. All Right Reserved.

IDENTIFYING “REGIMES” IN THE TIME SEQUENCES OF PROCESSES

*Boris Zalmanovich Belashev[1]

1. Karelian research center of Russian academy of science

A process is represented as a sequence of “regimes” when describing climatic variations and complex systems, detecting the malfunctioning of instruments and illegal interference in computer and hardware networks. For natural, technological and social processes such representation is comfortable to detect precursors of disastrous events.
The shifts of “regimes” in the sequences are commonly detected by checking statistical hypotheses by Student’s test and tests of non-parametric statistics when comparing the characteristics of the sequence at one or another site. Algorithms often use a priori information, work in unstable fashion over short intervals and at sequences boundaries, find it hard to recognize the shifts and trends of “regimes”.
Widespread R-algorithm [1] analyze data consecutively in a sliding window, operate with a small number of parameters and filter off “red” noise. The boundary regimes it detect may reflect distortions characteristic of the beginning and end of measurements.
The goal of the present study is to develop B-algorithm which automatically recognizes stable “regimes” in time data sequences.
The main stages of the algorithm are clusterization, comparison and optimization. Clusterization preliminary divides a normalized time sequence into “regimes”. While comparing the characteristics of the “regimes”, the division obtained is re-estimated. The final model of division is formed during optimization, which minimizes the variance of deviations from the trends of the “regimes” by varying the internal boundaries of the sites.
The algorithm, developed as a software in the MATLAB computer mathematics system, fulfils procedures automatically, decreases the amount of a priori data, increases operation speed and brings solutions closer to optima.
The operation of B- and R-algorithms is exemplified by the PDO (Pacific Decade Oscillation) sequence of mean January temperatures [2].
In both algorithms the number of “regimes” and their approximate positions coincide. The delay of part of R-“regimes” emphasize the sensitivity of B-algorithm to new “regimes”. Discrepancies are connected with the last “regime” identified by R- and B-algorithms on 2 and 15 members of sequence, respectively.
B- algorithm can operate with constant, linear and complex trends.
B- and R-algorithms, applied to the time sequences of river runoff, solar and seismic activity and the sequences of the annual rings of trees, have provided new information on the stages of processes.
The simplified schematic “regime” representation of a process reveals trends commonly obscured by the abundance of details. B- algorithm identifies stable “regimes” and recognizes the shifts and trends of “regimes”. The use of MATLAB functions increases the potential of the algorithm, admits the fulfilment of procedures by various methods, brings solutions closer to optimum solutions and ensures high operation speed. The ability of the algorithm to automatically process data makes it suitable for working with extensive data in various earth sciences.
References:
1.Rodionov, S. (2006) Use of prewhitening in climate region shift detection. Geophysical Research Letters 33, L12707.
2.Pacific Decadal Oscillation Index Data.
https://www.rdocumentation.org/packages/rpdo/versions/0.2.5.

©2019. Japan Geoscience Union. All Right Reserved.

Keywords: time sequence, shift regime, algorithm, clusterization, comparision, optimization

©2019. Japan Geoscience Union. All Right Reserved.

Investigation of status and demand on public service of earthquake disaster mitigation in China

*Lina Dong[1], Weiping Lian[1], Weitao Chen[1]

1. Development Research Center, China Earthquake Administration

In order to make a comprehensive and systematic evaluation of the status and demands of public service of earthquake disaster mitigation, we launched an investigation with National Bureau of Statistics on the current situation of public service of earthquake disaster mitigation and the demands for it in 2018. The investigation was conducted in 31 provinces of China mainland using the Computer Assisted Telephone Interview(CATI) method and received 20078 valid samples in total.

The results indicate that 52.2% of the population have received the scientific knowledge education for earthquake disaster mitigation in Different levels. It shows that the public still possesses a high expectation of earthquake prediction and farmers have a low level of scientific knowledge of earthquake disaster mitigation. And TV, network, and the new media app such as wechat and weibo become the most important information channels for the public to obtain the earthquake related information. Furthermore, the degree of satisfaction evaluation of public service of earthquake disaster mitigation is marked on 81.22 points (the full mark is 100 points). And the most expectative services for the public are reconstruction, earthquake warning, and house earthquake resilience test. The results of the investigation have provided a scientific evidence for the government to provide better services of earthquake disaster mitigation and to make scientific knowledge popularization in a more scientific way.

Keywords: scientific knowledge popularization of earthquake disaster mitigation, public service, satisfaction evaluation

©2019. Japan Geoscience Union. All Right Reserved.

Analysis of Eco-DRR and Ecological Services using InVEST at the Disaster Areas of Kumamoto Earthquake

*Minghui Tang[1], Naoko Fujita[1]

1. Kyushu University

When compared with other countries in a global point of view, Japan is a country with high number of natural calamities, significant causalities, economic loss and damages by earthquakes, typhoons, and eruption. The damage is especially big when a hazard comes right after another one.

Complex disaster refers to the occurrence of multiple disasters instead of one. Such as, in 2016, Kumamoto prefecture was hit by earthquakes with magnitude as large as 7 and within another 2 months, by heavy rain and the damage was tremendous.

There is a huge number of researches on the eco-application of proceeding in various countries and it is vitally important to verify their validity. Here, InVEST refers to the ArcGIS tool for the integrated review for ecological services and its compensation.

This research focuses on the analysis of the changes of the land cover as reflected in satellite pictures of the whole Kumamoto prefecture taken after the complex disaster, the earthquake in April 2016 and heavy rain in June 2016. Also, it’ s a review on the ecological services with the use of InVEST. A special focus is paid on the review of the soil retention and the quality changes of the eco-habitant as reflection of the disaster damage reduction measures.

In addition, there is an analysis on the change of land coverage on area-unit level with Mashiki-machi, the epicenter, as the target. Furthermore, projection was plotted for the ecological services implemented as the reconstruction plan.

Keywords: Kumamoto Earthquake, Eco-DRR, Ecological services, Complex Disasters, local governments/local communities, InVEST

©2019. Japan Geoscience Union. All Right Reserved.

Transformation as praxis: Exploring socially just and transdisciplinary pathways to sustainability in marginal environments (TAPESTRY)

*Nobuhito Ohte[1], Lyla Mehta[2], Synne Movik[3], Devanathan Parthasarathy[4]

1. Department of Social Informatics, Graduate School of Informatics, Kyoto University, 2. Institute of Development Studies at the University of Sussex, 3. Department of Urban and Regional Planning, Norwegian University of Life Sciences, 4. Department of Humanities and Social Sciences, Indian Institute of Technology

Climate change related uncertainties are the main threats to the sustainability of societies and their environments. To tackle these challenges, systemic transformations are required. Our project focuses on three cases of transformation in marginal environments in India and Bangladesh, and is concerned with: How transformation happens through bottom up processes in these sites; and how they can be scaled up and facilitate wider societal changes. Both require transdisciplinary co-production and the praxis of transformation which presupposes change in social arrangements and reconstruction by individuals. Our project addresses issues concerning governance, wellbeing, identity and quality of life in relation to transformations to sustainability in a lower middle income country (India) and a least developed country (Bangladesh). Our results should help inform processes that ultimately improve the quality of life in marginal environments, and build action and capacity among all partners.

Keywords: Transformation, Sustainability, Marginal environment, Transdisciplinary study, India, Bangladesh

©2019. Japan Geoscience Union. All Right Reserved.

Study for the Establishment of the Design for Disaster prevention through the survey of Recognition of tsunami disaster prevention from the viewpoint of green infrastructure in the coastal area of Kyushu-Pacific region.

*Shanshan Xu[1], Naoko Fujita[1], Minghui Tang[1]

1. Kyushu University

Considering the possibility of Nankai Trough large-scale earthquake predicted to occur in the nearest future, the issue of the tsunami in the coastal area of Kyushu-Pacific region is becoming extremely important. Efforts to utilize the various functions of the ecosystem internationally for the society creation are expanding in recent years, and even in the situation of toughening of the land in Japan, the initiative to incorporate Green Infrastructure (GI) which utilizes the disaster prevention and reduction functions of the natural ecosystem are being observed. Also, during the process of self-help/mutual assistance action and disaster reconstruction at the time of disaster, attention is paid as regional ties are affected, which are being considered as Social capital (SC).

The purpose of this study is to clarify the actual situation of tsunami disaster prevention of Nankai Trough earthquake based on the viewpoint of GI. We conducted a questionnaire survey on tsunami disaster prevention and GI at local governments and local communities. After analyzing the questionnaire, we analyzed the needs of the self-governing president's disaster prevention measures, the problems of the area, and the deviation of the improved situation of municipalities' disaster prevention measures. A correlation analysis was conducted to grasp the relationship between the consciousness concerning GI utilization, the strength of regional linkage SC and the recognition of evacuation.

1. Misalignment between demand and maintenance situation desired by the region

Policy regarding the issue of disaster helpers was extracted as a gap between needs and maintenance situation. Regarding the needs of the soft pattern in disaster prevention, a lot of measures were taken by disaster support supporters, however as it comes from the municipality questionnaire results, the measures related to the introduction of the barrier-free system and evacuation action supporters were introduced only partially. Further improvement is necessary for welfare evacuation sites, measures against supporters requiring evacuation actions, barrier-free formation.

2. SC regarded from the viewpoint of the relationship between intentions to utilize GI and recognition on disaster.

©2019. Japan Geoscience Union. All Right Reserved.

Especially, the correlation coefficient was 0.701 between No.7 and No.6. This shows that those who responded that disaster can happen among residents can respond that regional ties are stronger. For items with a high correlation coefficient between No.3 and No.8, the correlation became 0.437. This means the respondents who answered that evacuation is possible for all area inhabitants including elderly people in case of disaster (flooding, earthquakes, and tsunami) are able to use local well water and spring water in the event of a disaster.

Between No.2 and No.4, the correlation coefficient became 3.380. This is because those who respond that they think they can fully utilize the resources of the area (resources such as firewood, foods that can be harvested in mountains) even in the event of disasters will escape by utilizing the nearby natural landforms such as plateaus and mountains for tsunami evacuation. Between No.2 and No.8, the correlation coefficient became 0.351. This is because it shows those who responded that they thought that they could escape by utilizing nearby plateau and mountains such as mountains during the tsunami evacuation, even if disasters (flood, earthquake, tsunami) occurred, everyone including the elderly in the area evacuated. Between No.2 and No.6, the correlation coefficient became 0.343. This indicates that those who responded that they believe that they can escape by utilizing nearby plateaus and mountains when evacuating the tsunami think that the connection of the community people is strong. Between No.3 and No.6, the correlation coefficient became 0.287. This indicates that those who responded as they thought they could use local well water and spring water at the time of a disaster replied that they think that the regional connection is stronger.

Based on the above, we clarified the SC from the viewpoint of the gap between the request and the maintenance situation the region desires and the relationship between the intention to utilize GI and the perception of disaster. The fact that utilization of natural resources such as well water and spring water and understanding that natural topography can be utilized for evacuation leads to a positive feeling making people believe it is possible for everyone to evacuate even if the tsunami comes, can be suggested from this study.

Keywords: the Design for Disaster prevention, tsunami disaster, green infrastructure, the coastal area of Kyushu-Pacific region, Nankai Trough large-scale earthquake

©2019. Japan Geoscience Union. All Right Reserved.

Design for Green Infrastructure: Analysis of Landscape change in the Kumamoto earthquake area

*Naoko Fujita[1]

1. Kyushu University

The concept of “Green Infrastructure” and “Eco-DRR” is developed in Europe and North America lately, and it started to spread around in Japan after the Tohoku earthquake and tsunami in 2011. Landscape ecology is parallel with this conceptually, as well as in terms of spatial scale. Its successful focused researches and social implementation are becoming pervasive.

The new concept is to solve various problems by local resources and pearls of wisdom, it connects local communities to the world while it’s mainly led by front liners and researchers in engineering and ecological fields that little attention is paid to the aspects of arts and designs. It’s still not well-penetrated despite the validity and functions of the concept are well verified. Thus, it’s vitally important to work on the insufficient.

The purpose of this research is to analyze the reconstruction plan prepared by the affected municipalities of the Kumamoto earthquake and compare the landscape change read from the plan and the actual landscape change actually occurred and make clear how the cities and nature have changed during the reconstruction process.

In this research, we firstly gathered and analyzed the earthquake reconstruction plans created by each local government for all 45 municipalities in Kumamoto prefecture. In this analysis, while studying each municipal original plan, we primarily focused on the background, features, and landscape references of the plan formulation. During this analysis, we grasped the relations between the reconstruction plan and the landscape change, and also clarified what exactly each local government emphasizes independently. As the next step, basing on the field survey, we analyzed the actual state of the landscape changes described in the plan. As a method, we took the photographs at places where the plans adopted by each municipality in Kumamoto prefecture were scheduled or executed, and after recording the current situation and the surrounding landscape, we made a comparison with the photographs taken at the same place in the past. By doing this, we revealed what kind of changes have occurred between the past and the present due to the disaster, and how they affected the surrounding landscape.

Among the 45 municipalities in downtown Kumamoto Prefecture, we found that earthquake reconstruction plan was formulated in 16 municipalities, and 5 municipalities planned to formulate. There were references that "consideration of the landscape when promoting housing improvement and infrastructure development" and "to consider the landscape from the tourism viewpoint". Also, there were plans to utilize the process of reconstruction itself as a resource for tourist attraction. Furthermore, as a result of analyzing the individual plans described in the reconstruction plan, the reference to landscape,

©2019. Japan Geoscience Union. All Right Reserved.

reference to the prediction of landscape change, reference to landscape protection exists in all 16 cities, towns, and villages. Totally 117 relevant plans have been found. Although many of them were intended to cope with the damage at the time of the disaster, there were several plans originally adopted by the local governments to make necessary improvements of the problems they had from the past by conducting disaster recovery.

The field survey was conducted for 16 municipalities in total in Kumamoto Prefecture. One year has passed since the earthquake disaster, and recovery works progressed in a wide range in Kumamoto Prefecture. In the recovery sites in various places, a secondary change of the landscape, which caused the recovery activity aimed at improving the convenience of life and safety, has already been taking place. Moreover, recovery works progressed also in Kumamoto castle which is also cultural asset and tourist attraction, as well as the station and the government office which are the center of town. As a result, we could confirm the change of landscape.

In this research, through the analysis of the reconstruction plan created by the municipalities affected by the Kumamoto earthquake and the field survey, from the viewpoint of Green Infrastructure, we could make clear the process of the landscape change occurred during the process of recovery/reconstruction of the living base, the tourist resources, the natural environment in the affected areas and its influence respectively. Although few local governments have formulated landscape-friendly reconstruction plans, to gain medium- and long-term benefits, we should make landscape-friendly reconstructions from the original planning stage. This is because it is the factor determining the richness of living base, tourism resources, and natural environment.

Keywords: Green Infrastructure, the Kumamoto earthquake , Design

©2019. Japan Geoscience Union. All Right Reserved.

[E] Oral | H (Human Geosciences)：H-DS Disaster geosciences

Wed. May 29, 2019 1:45 PM - 3:15 PM JST | Wed. May 29, 2019 4:45 AM - 6:15 AM UTC | 301B 3F

[H-DS10] Natural hazards impacts on human society, economics and technological systems

convener:ELENA PETROVA(Lomonosov Moscow State University, Faculty of Geography), Hajime Matsushima(Research Faculty of Agriculture, Hokkaido University), Chairperson:Hajime Matsushima, Elena Petrova

The last decade set a record for the number and scale of natural disasters and demonstrates high vulnerability of human society and technosphere to their impacts. The most serious consequences have the so-called natural-technological disasters in which natural hazards trigger accidents at technology and infrastructure such as nuclear power and chemical plants, oil refineries and pipelines, power supply systems, buildings, and roads. A distinctive feature of natural-technological events, such as of the 2011 Tohoku earthquake, is their multi-hazard and synergistic nature, which creates cascading impacts, resulting in simultaneous occurrences of myriad catastrophes. The main goal of this multidisciplinary session is to summarize case studies of relationships between natural hazards and technological disasters, their social and economic consequences; and to encourage a discussion about tools and methods to prevent disasters and to minimize their consequences, disaster reconstruction, and tourism for reconstruction, Eco-DRR, and green infrastructure.

1:45 PM - 2:00 PM JST | 4:45 AM - 5:00 AM UTC

[HDS10-07] **Seasonal variations of atmospheric hazard impacts on infrastructure**

★Invited Papers

*ELENA PETROVA[1] (1.Lomonosov Moscow State University, Faculty of Geography)

2:00 PM - 2:15 PM JST | 5:00 AM - 5:15 AM UTC

[HDS10-08] Assessment of water supply function and measures for chemical release accidents triggered by major earthquakes

*Lisa Ito[1], Toyohiko Nakakubo[2], Naoya Kojima[1], Akihiro Tokai[1] (1.Graduate School of Engineering, Osaka University, 2.Faculty of Core Research, Ochanomizu University)

2:15 PM - 2:30 PM JST | 5:15 AM - 5:30 AM UTC

[HDS10-09] Development of disaster risk management plan of a thermal power plant: Spearheading the paradigm shift from disaster management to disaster risk management of NATECH in India

*Repaul Kanji[1], Madan Mohan Rout[2], Ankur Srivastava[3] (1.Gujarat Institute of Disaster Management, Gandhinagar, Gujarat, India, 2.Institute of Seismological Research, Gandhinagar, India, 3.Indian Institute of Technology Delhi, India)

2:30 PM - 2:45 PM JST | 5:30 AM - 5:45 AM UTC

[HDS10-10] **Applying Transfer Learning to Improve Machine Learning Impact Model at Extremes**

*Peter Lawrence Watson[1], Manos Anagnostou[1], David Wanik[1] (1.University of Connecticut)

2:45 PM - 3:00 PM JST | 5:45 AM - 6:00 AM UTC

[HDS10-11] rescEU, the European Union Civil Protection System UCPM and the future role of Geosciences in natural disaster reduction

*Andreas Nikolaus Kueppers[1] (1.GFZ - Deutsches Geoforschungszentrum - Helmholtz Zentrum Potsdam)

3:00 PM - 3:15 PM JST | 6:00 AM - 6:15 AM UTC

[HDS10-12] The Probability of Satellite Anomalies by a Disastrous Solar Flare

*Daikichi SEKI[1,2,3] (1.Graduate School of Advanced Integrated Studies in Human Survivability, Kyoto University, 2.Centre for the Study of Existential Risk, University of Cambridge, 3.Astronomical

Observatory, Kyoto University)

Seasonal variations of atmospheric hazard impacts on infrastructure

*ELENA PETROVA[1]

1. Lomonosov Moscow State University, Faculty of Geography

Infrastructure facilities consist of power, heat and water supply systems, communication lines, transport infrastructure including roads and bridges, railways, airports, oil and gas pipelines, etc. Above-ground and ground infrastructure facilities are most affected by impacts of various natural hazards, especially those of atmospheric origin. More than 90% of all natural-technological accidents in infrastructure facilities of Russia are triggered by atmospheric hazards such as strong winds, heavy snowfalls and rainfalls, snowdrifts, torrents, thunderstorms and lightning, hailstorms, hard frost, icing, etc. Natural factors cause about 70 percent of “blackouts”, more than 10 percent of accidents at heat and water supply systems as well as water accidents; about four percent of air crashes, automobile and railway accidents, and about two percent of pipeline ruptures. Various atmospheric hazards can also cause long delays in automobile, railway and air transportation of passengers and goods. The majorities of these events are triggered by windstorms and hurricanes (37 percent), snowfalls and snowstorms (27 percent), rainfalls (16 percent), hard frost and icing (12 percent), thunderstorms and lightning (nearly 4 percent). All of these weather conditions are subject to seasonal variations. During the cold season, there are much more weather events influencing the growth in the number of accidents than in the warm season. The author created a database of natural-technological accidents occurring in Russia, including those in infrastructure facilities. More than 18.5 thousands events are registered in the database between 1991 and 2018. The collected information allows analyzing the main causes and triggers of accidents, their distribution within area of Russia, temporal variations, and revealing “weak spots” to cope with. The risk of natural-technological accidents in infrastructure facilities was assessed for Russian federal regions. The Far Eastern, South and North-Western parts of Russia are at the most risk of atmospheric hazard impacts. The risk of natural-technological accidents is highest in Sakhalin region, Krasnodarsky and Primorsky territories.

Keywords: infrastructure facilities , atmospheric hazards , risk assessment, seasonal variations

©2019. Japan Geoscience Union. All Right Reserved.

Assessment of water supply function and measures for chemical release accidents triggered by major earthquakes

*Lisa Ito[1], Toyohiko Nakakubo[2], Naoya Kojima[1], Akihiro Tokai[1]

1. Graduate School of Engineering, Osaka University, 2. Faculty of Core Research, Ochanomizu University

In recent years, natural disasters called Natech (Natural hazard triggered technological accident) has become a big issue around Europe. Also, in Japan, Natech becomes social issues by the recent major earthquake such as the Great East Japan Earthquake, in which highly concentrated toxic chemical substances was released due to tsunami or fire. Such an accident causes risks related to serious environmental contamination. However, chemical behaviors in the environments and degrees of the impact on the infrastructure after the accident have not been clarified especially under the unstable situation. In this research, we aimed i) to clarify the influence of toxic chemicals released into the environment due to the major earthquake and ii) to evaluate the efficiency of the countermeasure option, focusing on unintended releases of chemicals from manufacturing or on-site storage facilities to water. As the research area, we selected Yodo River in Osaka, which is an essential water source that supports the infrastructure of Kansai area. On the other hand, there are growing concerns for the risks caused by seismic motion and liquefaction as there are many chemical factories with drainage pouring into Yodo River.

We selected 38 chemical substances with high risk such as acrylonitrile in addition to toluene and xylene that are used in large quantities. These chemicals are also included in Pollutant Release and Transfer Register (PRTR) which make it possible to grasp more actual discharge status. Among PRTR, these 38 substances have especially high toxicity for human (LD_{50} ≦300 mg/kg) (UN, 2015), and have difficulty to remove even in the water treatment process because of its high solubility in water (≧10,000 mg/L) and hydrophilic properties (octanol/water partition coefficients (Log Kow)≦ 1.5) (Ito et al., 2014). The prediction occurrence of chemical release accident caused by the earthquake was calculated as the expected value (Y) based on the statistical data in the world (Santella et al., 2011). Probability (P_n) of occurrence of the accident in Yodo basin area caused by Hanaore fault was calculated by the Poisson distribution. Subsequently, we calculated the maximum expected concentration of chemical substances at the water-intake points in the river after the accident using the hydrology-exposure analysis model (AIST-SHANEL ver. 3)(AIST, 2015). The accident date on the model was set for winter season since the streamflow is relatively low throughout the year from a factory which has the largest storage of target chemicals. Emergency shut-off valve was adopted as a countermeasure in this scenario. As judgement criteria for suspension of water supply, we evaluated subacute toxicity as a criterion ($JC_i^{subacute}$).

As a result of the model calculation, the concentration of acrylonitrile in the purified water was calculated to be 2.19×10^{-1} mg/L for a maximum. In this case, water supply system would stop, since it exceeds $JC_i^{subacute}$ ($=6.25\times10^{-2}$ mg/L) based on the no observable adverse effect level (NOAEL) (Ministry of the Environment, 2003) obtained from rats. Furthermore, as it exceeds the predicted no effect concentration (PNEC) of aquatic organisms, 7.6×10^{-3} mg/L (Ministry of the Environment, 2003), intake of the water would also stop. On the other hand, if the Emergency shut-off valve works properly, the outflow rate is 2% or less of the storage tank, calculating from the length of pipe and tube diameter outside the valve (Osaka, 2013). In that condition, the concentration of acrylonitrile in the river is less than $JC_i^{subacute}$ and PNEC, which suggested that outage of water supply function can be avoided. According to these analyses, we found that an emergency shut-off valve is a useful option as a countermeasure for an earthquake. Furthermore, it would be possible to implement more quick and proper responses applying the method of this study, even in the case that the released chemicals are not included in the criteria for tap water.

©2019. Japan Geoscience Union. All Right Reserved.

Keywords: Chemical accidents, Water supply function, Major earthquake, Modeling, Natech

©2019. Japan Geoscience Union. All Right Reserved.

Development of disaster risk management plan of a thermal power plant: Spearheading the paradigm shift from disaster management to disaster risk management of NATECH in India

*Repaul Kanji[1], Madan Mohan Rout[2], Ankur Srivastava[3]

1. Gujarat Institute of Disaster Management, Gandhinagar, Gujarat, India, 2. Institute of Seismological Research, Gandhinagar, India, 3. Indian Institute of Technology Delhi, India

With global phenomenon like climate change looming large on the horizon, occurrences of extreme events are expected to rise eventually. Rapid urbanisation and the powerful want of globalisation does little to control the exposure of our ‘assets’ to such events, thereby increasing the disaster risks. The quantum of risk rises exponentially if the exposed asset is a critical infrastructure like a nuclear power plant or a thermal power plant which might lead to ‘natural hazard triggered technological disasters’ like that of Fukushima. The damage and loss in such cases is borne not only by the infrastructure in question but also by the community in its immediate surrounding. Management of disasters, which has long been the usual trend, has a very little effectiveness in such tragic scenarios, thus rather than managing disasters, one should manage the disaster risks. Even the Sendai Framework for Disaster Risk Reduction (SFDRR) talks about reduction of the acceptable risks and management of the residual risks. However, for all this to be implemented, one needs to understand and anticipate risks, which is way more than the current practice of risk identification.

The researchers, when provided with the opportunity to develop a disaster management plan for a thermal power plant in India, took cognisance of the priorities of SFDRR embarked on a strategy of disaster risk management and disaster risk reduction rather than mere disaster management. This study elaborates on the strategy adopted during the development of the plan. The first step was to conduct field survey and collect primary geo-technical and meteorological data. Content analysis of hazard maps were done to identify the possible hazards which can affect the critical infrastructure. Earthquake, cyclone and technological hazards were identified as the main probable hazards. The methodology developed by Cornell (1968) for Probabilistic Seismic Hazard Assessment (PSHA) was applied for the estimation of seismic hazard for 10% and 2% probability of exceedence in 50 years. In this method, seismogenic zones were delineated and then seismicity parameters were estimated using the decluttered earthquake catalog and finally the ground motion was estimated using different ground motion prediction equations (GMPE). In addition to this, probable intensities of earthquakes were evaluated according to the seismic zonation and the corresponding grade of damage was estimated, taking into account the typology of building construction. To elucidate assessment of cyclonic winds and rainfall over the critical infrastructure an experiment was designed in which 9 major cyclonic systems occurring in the region in last ten years were considered. These cyclonic events were numerically simulated around the geographical location of the infrastructure. Weather Research Forecasting (WRF) model was used to carry out the simulations. As a result, the maximum windspeed and the maximum rainfall was obtained. In addition to these natural hazards, content analysis was done to enumerate all the possible technological hazards and Maximum Credible Accident Analysis (MCAA) was performed. These steps were integral in assessing the hazards and the outputs of these simulations were fed as inputs of the Quick Risk Estimation (QRE) tool developed by UNISDR. Based on the outputs of the QRE tool, the disaster risk management plan was developed.

This particular study tries to identify and assess the hazards, vulnerabilities and capacities and estimates

©2019. Japan Geoscience Union. All Right Reserved.

the risks which is then used to develop risk management plans. Offcourse, management of extreme events through institutionalisation of Incident Response System (IRS) is a part of the plan but it forms only a part of it. Thus, in a way, this plan marks the first step taken towards disaster risk management of critical infrastructures in India; a step towards the management of risks of technological disasters due to natural hazards.

Keywords: Disaster risk management, Disaster risk reduction, Weather Research Forecasting, Ground Motion Prediction Equation, Quick Risk Estimation Tool

©2019. Japan Geoscience Union. All Right Reserved.

Applying Transfer Learning to Improve Machine Learning Impact Model at Extremes

*Peter Lawrence Watson[1], Manos Anagnostou[1], David Wanik[1]

1. University of Connecticut

Machine learning can be useful for modeling the impacts of natural hazards on infrastructural systems. By relying on empirical observations, these methods lack the prohibitive complexity of large-scale physical models, but can also operate in high-dimensional spaces: where a large number factors contribute to the observed damages to the system. However, modeling extreme events can be challenging with machine learning. Unlike parametric models, the dynamic range of these models is constrained to the training data, and the training data from extreme events is as rare as the events themselves. However, transfer learning, where a model trained on data from one system is retrained for another system, may enable the use of additional training data to improve the prediction of extreme events. This would allow for more examples of extreme events from more places to be included in the training data, and should improve the performance of machine learning based impact models at the extremes. In this study, we apply transfer learning methods to the University of Connecticut's Outage Prediction Model (OPM), a machine-learning based electrical power outage model. The OPM has a large domain that spans three states in the US: Connecticut, Massachusetts, and New Hampshire, and there is much more training data available for Connecticut than the other states. We investigate the effects of applying this additional data on the accuracy and dynamic range of models for the other states using transfer learning methods, in an effort to better predict the impacts of the most extreme weather events.

Keywords: Machine Learning, Impact Model, Transfer Learning, Extreme Events, Power Outage, Infrastructure

©2019. Japan Geoscience Union. All Right Reserved.

rescEU, the European Union Civil Protection System UCPM and the future role of Geosciences in natural disaster reduction

*Andreas Nikolaus Kueppers[1]

1. GFZ - Deutsches Geoforschungszentrum - Helmholtz Zentrum Potsdam

On February 12, 2019, the European Parliament in Strassbourg adopted the decision* for a substantial enhancement of the Union Civil Protection Mechanism which includes the 28 EU Member States plus a major number of affiliated nations. The actual legislational move had been directly instigated by the very serious impact of large wildfires in Europe with many fatalities in Portugal, Greece, Spain, Sweden, among others. It became clear in a dramatic way that sufficient technical resources for fire fighting, in particular aircraft, were neither available on a national nor an international base. The new and financially strengthened Mechanism embraces a large number of disaster types where geology based disasters like earthquakes, tsunami, volcanic eruptions including volcanic ash clouds and gravitational movements are among the most prominent. Expressis verbis, the decision calls for substantial foresight for the early discovery of future disasters which even may be not known to us today. While this without doubt means a great chance for broad geosciences to actively contribute from the start, the integration of more nations into the system and a possible globalisation constitute next stage challenges.

*Official text is expected to be published by the European Commission in due time.

Keywords: Earthquake, Tsunami, Volcanic Eruption, Landslide, European Civil Protection Mechanism, Globalisation

©2019. Japan Geoscience Union. All Right Reserved.

The Probability of Satellite Anomalies by a Disastrous Solar Flare

*Daikichi SEKI[1,2,3]

1. Graduate School of Advanced Integrated Studies in Human Survivability, Kyoto University, 2. Centre for the Study of Existential Risk, University of Cambridge, 3. Astronomical Observatory, Kyoto University

The Sun has a potential risk of various socioeconomic impacts on our human society. It often produces various eruptive phenomena such as a solar flare and a coronal mass ejection, which sometimes bring adverse effect to us like satellite anomalies, radiation exposure, and huge blackouts. For example, in 2003 October 28, X17-class flares (roughly once-in-10-year level severity) occurred and more than 60 % of NASA scientific satellites were affected.

Similar to other terrestrial disasters like an earthquake, the solar eruptive phenomena also follow the power-law distribution between frequency and severity, and low-frequency-high-impact solar disaster could also happen. Recently, it was revealed that a “super-flare”, a flare whose energy is 100 times larger than X10-class flare, can occur once in 1000 years from statistical and theoretical points of view [Maehara et al. 2012, Shibayama et al. 2013, Shibata et al. 2013].

However, though there are many assessment studies of “moderate” solar eruptive phenomena, the assessment of “disastrous” solar eruptive phenomena like a super-flare has been little conducted. For this reason, this research aims to evaluate the frequency (or probability) and the possible socioeconomic damage of a super-flare, especially focusing on satellite anomalies.

Using various data sets about satellites, their anomalies, flares, and plasma environment around the Earth*, 154 X-class flare events with 9 relating parameters (peak flux of X-ray (0.1–0.8 nm), integral fluxes of electron (> 2 MeV) and of proton (> 1, 5, 10, 30, 50, 60, 100 MeV)) were selected. To avoid multi-collinearity, Ridge regression model was used to compute the regression to the satellite anomaly rate (1/satellite/event). Also 10-fold cross validation was performed. After obtaining the model, the possible plasma parameters in case of X1000-class flare assumed by Takahashi et al. 2016 were input into the model.

As a result, we obtained the model with its coefficient of determination of 0.607 and its Pearson correlation coefficients of 0.691±0.212 (for 100 times randomly chosen dataset). Assuming that electron and proton follow the same scaling law, with applying scaling law by Takahashi et al. 2016, 0.573 satellite anomaly rate (57.3% per satellite per event) was obtained. It should be noted that the scaling law provided by Takahashi et al. 2016 is upper limit, so in the actual case, rate should be lower. The validity of assumption, the comparison between this research and others (Pilipenko et al. 2006; Iucci et al. 2005; Odenwald et al, 2006, 2007), and the possible socioeconomic loss will be also discussed.

* NOAA NGDC Spacecraft Anomaly Data, Satellite Catalogue (https://www.celestrak.com/satcat/search.php), NOAA GOES flare report (https://www.ngdc.noaa.gov/stp/space-weather/solar-data/solar-features/solar-flares/x-rays/goes/xrs/) , and OMNI 2 database

©2019. Japan Geoscience Union. All Right Reserved.

Keywords: Space weather disaster, satellite anomaly, super-flare

©2019. Japan Geoscience Union. All Right Reserved.

[E] Oral | H (Human Geosciences)：H-DS Disaster geosciences

Wed. May 29, 2019 3:30 PM - 5:00 PM JST | Wed. May 29, 2019 6:30 AM - 8:00 AM UTC | 301B 3F

[H-DS10] Natural hazards impacts on human society, economics and technological systems

convener:ELENA PETROVA(Lomonosov Moscow State University, Faculty of Geography), Hajime Matsushima(Research Faculty of Agriculture, Hokkaido University), Chairperson:Elena Petrova, Hajime Matsushima

The last decade set a record for the number and scale of natural disasters and demonstrates high vulnerability of human society and technosphere to their impacts. The most serious consequences have the so-called natural-technological disasters in which natural hazards trigger accidents at technology and infrastructure such as nuclear power and chemical plants, oil refineries and pipelines, power supply systems, buildings, and roads. A distinctive feature of natural-technological events, such as of the 2011 Tohoku earthquake, is their multi-hazard and synergistic nature, which creates cascading impacts, resulting in simultaneous occurrences of myriad catastrophes. The main goal of this multidisciplinary session is to summarize case studies of relationships between natural hazards and technological disasters, their social and economic consequences; and to encourage a discussion about tools and methods to prevent disasters and to minimize their consequences, disaster reconstruction, and tourism for reconstruction, Eco-DRR, and green infrastructure.

3:30 PM - 3:50 PM JST | 6:30 AM - 6:50 AM UTC

[HDS10-13] Management and Maintenance for Disaster prevention park in Tokyo Metropolitan Government

★Invited Papers

*Masayshi Kikuchi[1] (1.Tokyo Metropolitan Park Association)

3:50 PM - 4:05 PM JST | 6:50 AM - 7:05 AM UTC

[HDS10-14] Rebuilding Tourism after the Great East Japan Earthquake and Examining Post-Disaster Tourism in Kamaishi City

*Satoshi Sasaki[1], Kiyotatsu Yamamoto[2], Kaoruko Sasaki[3] (1.Iwate University, 2.The University of Tokyo, 3.Hokkaido University)

4:05 PM - 4:20 PM JST | 7:05 AM - 7:20 AM UTC

[HDS10-15] Population Change in Ishinomaki City, Miyagi Prefecture, with a Focus on the Area around the Earthquake Ruins

*Ryo Nishisaka[1], Katsunori Furuya[1] (1.Chiba University)

4:20 PM - 4:35 PM JST | 7:20 AM - 7:35 AM UTC

[HDS10-16] The Way of Seeing the Atomic Bomb Dome and the Relationship with Viewers' Attributes

*yasuhara arisa[1], Kiyotatsu Yamamoto[1], Akio Shimomura[1] (1.Graduate School of Agricultural and Life Sciences, The University of Tokyo)

4:35 PM - 4:50 PM JST | 7:35 AM - 7:50 AM UTC

[HDS10-17] Flood Disaster Risk Analysis at Ratnapura in Sri Lanka

*Tsuchida Ryo[1], Kaoru Takara[1] (1.Graduate School of Advanced Integrated Studies in Human Survivability, Kyoto University)

4:50 PM - 5:00 PM JST | 7:50 AM - 8:00 AM UTC

Discussion

Management and Maintenance for Disaster prevention park in Tokyo Metropolitan Government

*Masayshi Kikuchi[1]

1. Tokyo Metropolitan Park Association

Tokyo has experienced great damage by many earthquakes since ancient times, has a history that has repeatedly been destroyed and reconstructed. Every time Tokyo suffered an earthquake disaster, the park has been required to have new functions. Every time Tokyo suffered an earthquake disaster, the park has been required to have new functions. The first is a role as evacuation site and the second is a role as Base for Large-scald and Life-saving Operations. Currently, there are 82 parks in metropolitan parks, but the 21 major parks are not only functions as evacuation places but also Base for Large-scald and Life-saving Operations when disasters such as large earthquakes occur in the capital Tokyo Function. We name them as disaster prevention parks and manage them. First, the function as an evacuation site is a function that all parks have and is to secure places where many citizens can escape as safe places in the event of a disaster. To that end, there are three distinctive park facilities. One is a "solar-type park light" so that you can check the location from anywhere even at the time of a power outage. The second type is "manhole type disaster prevention toilet" directly connected to the drain pipe so that many evacuees can use it even if they temporarily stay in the park. The third one is a normal bench in peacetime, but in the event of a disaster it is a "kamado bench" that can be used as a "kettle" that can be boiled. Next, the function as Base for Large-scald and Life-saving Operations is a function that serves as a helicopter departure station or a large emergency vehicle collecting base as an activity base of relief units, medical troops, etc. in the afflicted area. Therefore, although a park having a large-scale square is designated as a large-scale rescue and relief activity base, the characteristic maintenance is to expand and strengthen the school path so that large vehicles can pass, securing helicopter take-off and landing spots, etc. is there. What you need to fully demonstrate these functions is day-to-day disaster prevention drills. In the park, including citizens, police, fire fighting companies, companies, etc., training is conducted several times a year "Manhole type disaster prevention toilet" and "Kamado bench", and helicopter takeoff and landing training etc. are also carried out.

Keywords: disaster prevention park, evacuation site , Base for Large-scald and Life-saving Operations

©2019. Japan Geoscience Union. All Right Reserved.

Rebuilding Tourism after the Great East Japan Earthquake and Examining Post-Disaster Tourism in Kamaishi City

*Satoshi Sasaki[1], Kiyotatsu Yamamoto[2], Kaoruko Sasaki[3]

1. Iwate University, 2. The University of Tokyo, 3. Hokkaido University

1. Introduction

Natural hazards can have a devastating effect on tourism. In the case of the Great East Japan Earthquake (GEJE) of 2011, the tsunami caused damage to not only human lives but also to critical infrastructures in coastal areas in the Tohoku region. Tourist attractions and facilities were also damaged by the tsunami, and people who lived in the metropolitan and Kinki regions understood that they should avoid traveling to the Tohoku region (Yamamoto, 2013). Thus, a decrease in the number of visitors to the tsunami-hit area was reported in the Tohoku region immediately following the disaster (Igarashi et al., 2017). Fortunately, after suffering a drop in the number of tourists, the disaster area is experiencing a trend in recovery these days. “Disaster tourism”—defined as the practice of visiting natural or man-made environmental disaster sites (Amujo et al., 2012)—has succeeded in bringing visitors to the disaster area. However, eight years have already passed since the disaster, and the time lapse should be taken into account for promoting post-disaster tourism (Sasaki et al., 2018). From this viewpoint, the purposes of this study were established as follows: 1) to clarify the current situation of tourism after the GEJE of 2011 and 2) to examine post-disaster tourism in the Tohoku region.

2. Methods

The case study area for this study was Kamaishi City, which is located in Iwate Prefecture in northeast Japan; it was hit by the tsunami in 2011 and more than 1,000 lives were lost to the disaster. Thanks to disaster prevention efforts, however, almost all of the nearly 3,000 elementary and junior high school students miraculously survived (i.e., the “Miracle of Kamaishi”). Accordingly, many people have been infused with hope. To grasp the awareness and behaviors of visitors to the city, two post-recall questionnaires were distributed to Japanese people over age 17 from July to September in 2018. One was disseminated to visitors who participated in the guided tours conducted by storytellers with the Kamaishi Volunteer Guide Association. The other was given to tourists at the JR Kamaishi Station, Kamaishi Sennin-toge roadside rest area, and Hashino Iron Mining and Smelting Site (listed as a UNESCO World Heritage Site). The survey focused on the following aspects: (1) visitor attributes (e.g., age, gender), (2) characteristics of visits (e.g., number of visits, group size, objectives of trips, places visited), (3) familiarity with guided tours (e.g., expectations, sources of information), (4) changes in awareness after a visit, (5) appreciation for disaster lore, and (6) the satisfaction and intention to revisit.

3. Results and Conclusion

In total, 478 people (guided: N = 155, non-guided: N = 323) participated in the survey, representing a response rate of 22%. As a result, the largest proportion of respondents included people over age 59 (47%); further, the total number was almost equally divided between the two genders (male: 51%, female: 47%). The most frequent group size of visitors was two or three people (43%); moreover, approximately 50% of visitors used private cars. The most common trip type was the day trip (46%), and the majority of visitors were not there for the first time (32%). The most commonly mentioned trip objectives were engaging in tourism (46%), visiting the disaster area (29%), and eating delicious food (25%). Additionally, the degree to which visitors intended to join a tour guided by a storyteller was high (77%), with the most common contents of interest being stories recounted from the time of the disaster (77%) and lessons from

©2019. Japan Geoscience Union. All Right Reserved.

the disaster (68%). A few people acknowledged enjoying the storytelling tour locally (12%) and on the Web (6%). On the whole, the GEJE experience was regarded as worth handing down to future generations and sharing with the world (very valuable: 82%, somewhat valuable: 11%). Compared to non-guided visitors, guided visitors had a greater sense of being present during the disaster ($P < .01$, T-test) and were encouraged to change their attitudes toward disasters ($P < .01$, based on a single regression analysis). In conclusion, Kamaishi City still functions as a disaster tourism site but it is thought that efforts to increase the city’ s appeal in the future are necessary.

Keywords: tourism, Great East Japan Earthquake, storyteller, questionnaire

©2019. Japan Geoscience Union. All Right Reserved.

Population Change in Ishinomaki City, Miyagi Prefecture, with a Focus on the Area around the Earthquake Ruins

*Ryo Nishisaka[1], Katsunori Furuya[1]

1. Chiba University

1. Introduction

Eight years have passed since the Great East Japan Earthquake of 2011. There is a movement to preserve buildings and structures affected by the earthquake and resulting tsunami as earthquake ruins and to utilize them for storytelling and disaster prevention. In the Tohoku region, where the birthrate is declining and the population is aging, sustainable management of the earthquake ruins will be an issue.

So far, the bereaved families and storytellers (called the kataribe) who live around the earthquake ruins of Ishinomaki are known to have been working on the management of flowers from visitors, cleaning up the earthquake ruins, and improving the flowerbeds. At the same time, residents around the earthquake ruins might be affected by the increase in the number of visitors when the earthquake ruins are opened to the public, so consideration of them is necessary. Therefore, this paper aims to clarify the population change around the former Kadonowaki Elementary School and the former Okawa Elementary School, which are the two earthquake ruins in Ishinomaki.

2. Methods

We investigated mesh population data of 500-meter mesh areas from “Population Census,” published by the Statistics Bureau, Ministry of Internal Affairs and Communications, Japan, and analyzed the population change of Ishinomaki between 2010, before the earthquake, and 2015, after the earthquake, using Geographic Information Systems (GIS). We extracted the two earthquake ruins and created buffers of 2,000 meters. We considered the population change within 2,000 meters of the two earthquake ruins as well as the situation regarding Ishinomaki’s recovery.

3. Results

As a general overview of the population change in the whole city of Ishinomaki, we can confirm a large population decline in coastal areas that were reached by the tsunami, such as Kadonowaki-*cho*. In addition, large-scale temporary housing was constructed and a population migration to the inland area was confirmed.

Although the overall population decline was significant within 2,000 meters of the former Kadonowaki Elementary School, a population increase was confirmed in a small area near the temporary housing in Hiyorigaoka.

Even within 2,000 meters of the former Okawa Elementary School, the population was decreasing as a

©2019. Japan Geoscience Union. All Right Reserved.

whole, but we could confirm an area where the population increased slightly. There were no large temporary housing structures around the former Okawa Elementary School, and the population did not accumulate.

4. Discussion

In Ishinomaki, after the Great East Japan Earthquake, the population of the coastal area drastically decreased, and population increase in the inland area was confirmed. Both the former Kadonowaki Elementary School and the former Okawa Elementary School had a drastic decrease in population within 2,000 meters. However, the existence of areas where the population was increasing even within 2,000 meters was confirmed. It seems that the presence of temporary housing greatly influenced the change in population.

The population changes around both earthquake ruins were large, so it is thought that there were many cases in which bereaved families and residents involved in the elementary schools had relocated. Particularly concerning the former Okawa Elementary School, there is a possibility that there was a large-scale relocation to the southwestern part of the city, where population increase advanced. In Ishinomaki, the situation with tenancy in temporary housing continues to change even after 2015, and now temporary housing is being demolished and residents are moving into public housing. In the future, it is necessary to track the population changes and consider how to support the activities in the earthquake ruins by residents who cannot easily get there.

Keywords: Earthquake Ruins, Ishinomaki, GIS, Population Change

©2019. Japan Geoscience Union. All Right Reserved.

Fig. Population change in Ishinomaki <2010-2015>

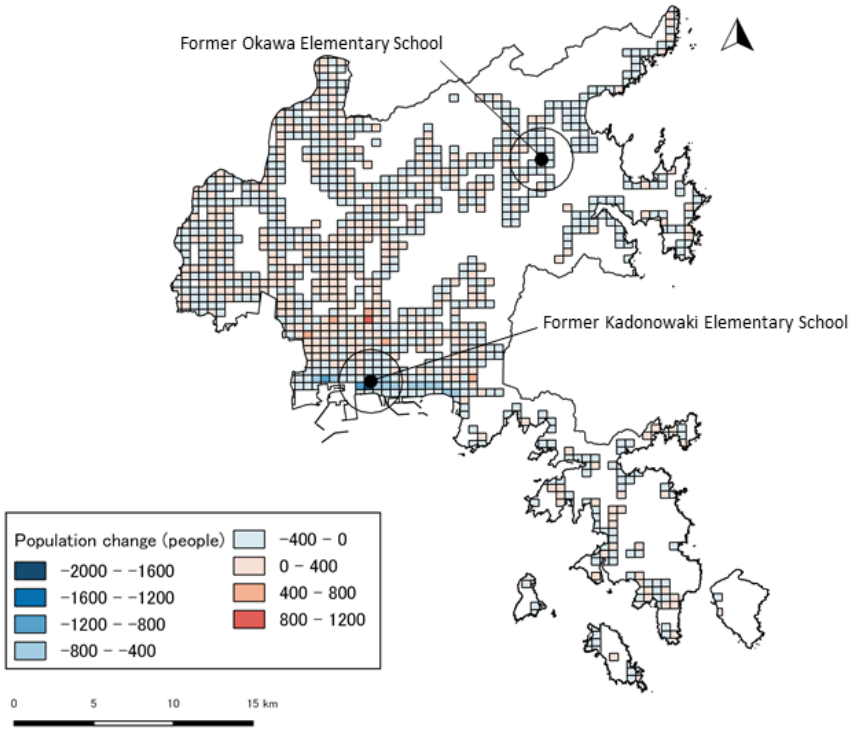

©2019. Japan Geoscience Union. All Right Reserved.

The Way of Seeing the Atomic Bomb Dome and the Relationship with Viewers' Attributes

*yasuhara arisa[1], Kiyotatsu Yamamoto[1], Akio Shimomura[1]

1. Graduate School of Agricultural and Life Sciences, The University of Tokyo

1. Introduction

The Atomic Bomb Dome (ABD) is one of the major atomic bombing sites in Hiroshima. In 1996, it was registered as an UNESCO World Heritage Site under the name "Hiroshima Peace Memorial," and its lasting preservation was secured. However, like other world heritage sites, its maintenance and management were not easy. Hiroshima City, taking charge of the management, established "Preservation and maintenance policies of peace memorial museums (2006)," in which the role of the ABD was specified as "The witness of history who suffered heavy damage by an atomic bomb" and "The symbol of hope for nuclear weapon extinction and lasting peace." This policy considered the mindset of the people who wished for peace, tried to preserve the history, and achieve World heritage-registration. This description meant regarding the ABD as the memory of Hiroshima. In other words, it was aimed to include not only the Dome's visual image (the visual aspect) but also the history of Hiroshima and people who had an emotional connection with the town (the semantic aspect), and to preserve both. To embody the idea in a preservation plan, it is necessary to clarify the history of Hiroshima as the background of the ABD and the mindset of people. This study analyzes the "way of seeing" to reveal "how" and "by whom" the ABD has been seen until today, and to understand the memory of Hiroshima.
In light of the above issues and viewpoints, the objectives of this study are 1) to classify the way of seeing the dome and 2) to address the meaning of the relationship between the landscape types and viewers' attributes.

2. Methods

Photographs were collected to understand how ABD is seen by a variety of viewers. Approximately 561 photographs in which the ABD appeared were found in 52 books at the Hiroshima City Central Library. These were selected as materials for analysis, excluding those wherein who took the photograph and when it was taken could not be identified. Time, locations, and photographers were identified, and the constituent elements of each scene were counted to understand the characteristics of the photographs. The attributes of photographing through identification are as follows: (1) time: year of photographing; (2) locations: 6 areas of photographing; and (3) photographers: 4 categories extracted by combining "people who visited Hiroshima," "people who were born or lived in Hiroshima," "photographers," and "amateur photographers." After this process, the sceneries were divided into typical patterns by using quantification method of the third type and cluster analysis. Finally, the relationship between the landscape types and the photographers' attributes was analyzed.

3. Results and Conclusion

The ways of seeing were classified into 6 types, which were related to photographers' attributes. These were: I) landscape hit by atomic bomb, II) landscape with low buildings, III) landscape viewed through the Hiroshima Peace Memorial Monument, IV) landscape of the ABD, V) landscape with plants, and VI) landscape with high buildings. Moreover, it was revealed that landscape I) was photographed more by "people who visited Hiroshima." Likewise, II), III), and IV) were related to "photographers who were born or lived in Hiroshima," "people who were born or lived in Hiroshima," and "photographers who visited Hiroshima," respectively. Additionally, the elements included in the photographs, the main period

©2019. Japan Geoscience Union. All Right Reserved.

of photographing, and the viewpoint of photographing differ according to the landscape types. In conclusion, it was suggested that the meaning of Hiroshima’ s memory as understood by the photographers was diverse and it was necessary to provide the visitors to ABD with various landscape experiences related to the ways of seeing the ABD.

Keywords: Atomic Bomb Dome, way of seeing, landscape, photograph, world heritage

©2019. Japan Geoscience Union. All Right Reserved.

Flood Disaster Risk Analysis at Ratnapura in Sri Lanka

*Tsuchida Ryo[1], Kaoru Takara[1]

1. Graduate School of Advanced Integrated Studies in Human Survivability, Kyoto University

This paper describes disaster risk at a flood-prone area in southwest Sri Lanka where a severe flood disaster took place in May 2017. First, the author conducted frequency analysis at Ratunapura by using a 125-year annual maximum rainfall series to evaluate the probability of the 2017 event. Second, land use change was also detected by Landsat-8 images before and after the flood. Visiting Ratunapura a couple of times, the author interviewed people and the local government to understand the situation of the flood disaster and how they coped with the flood by utilizing a framework based on disaster ethnography. Results obtained from the interview survey showed that the residents, who acted on their own experience and knowledge, could not respond to disasters when enormous floods occurred, and the flood disaster brought them bad influences in many ways. In addition, external organizations including governments, UN agencies and Non Profits Organizations for disaster relief could not provide adequate supports to reflect the needs of residents worth covering vulnerabilities. Moreover, this survey found that the government’s assessment of the house and livelihood damage was delayed. Also, distribution of allowance and supplementary from the government was delayed. The research results in this paper would be useful for flood disaster risk reduction and for understanding recovery proesses in Sri Lanka.

Keywords: Flood Disaster, Frequent Analysis, Land Use Change, Recovery and Rehabilitation, Sri Lanka

©2019. Japan Geoscience Union. All Right Reserved.

[J] Oral | H (Human Geosciences)：H-DS Disaster geosciences

Wed. May 29, 2019 9:00 AM - 10:30 AM JST | Wed. May 29, 2019 12:00 AM - 1:30 AM UTC | Convention Hall B 2F

[H-DS13] Tsunami and Tsunami Forecast

convener:Naotaka YAMAMOTO CHIKASADA(National Research Institute for Earth Science and Disaster Resilience), Hiroaki Tsushima(Japan Meteorological Agency), Tatsuya Kubota(National Research Institute for Earth Science and Disaster Resilience), Chairperson:Masaaki Minami(気象研究所), Naotaka Chikasada(National Res. Inst. for Earth Science and Disaster Resilience)

This session discusses issues related to improving real-time and long-term prediction accuracy of tsunami from earthquakes, landslides, and volcanoes, which include such as a better understanding of tsunami dynamics, new real-time tsunami observing systems deployed in the open ocean and coastal waters, methodologies of more rapid and accurate prediction during tsunami emergencies, more extensive and accurate inundation maps, and long-term tsunami potential forecast.

9:00 AM - 9:15 AM JST | 12:00 AM - 12:15 AM UTC

[HDS13-07] Functions of Real-time Tsunami Inundation Forecast System Using S-net Pressure Data

*Wataru Suzuki[1], Naotaka YAMAMOTO CHIKASADA[1], Takayuki Miyoshi[1], Shin Aoi[1] (1.National Research Institute for Earth Science and Disaster Resilience)

9:15 AM - 9:30 AM JST | 12:15 AM - 12:30 AM UTC

[HDS13-08] Improvement of Real-time Tsunami Forecast System for Outer-rise Earthquake

*Naotaka YAMAMOTO CHIKASADA[1], Toshitaka Baba[2] (1.NIED, 2.Tokushima University)

9:30 AM - 9:45 AM JST | 12:30 AM - 12:45 AM UTC

[HDS13-09] Maximum tsunami height prediction using Ocean-Bottom Pressure Values based on Gaussian Process Regression

*Kotaro Takahashi[1], Kenjiro Kashiwabara[1], Yasuhiko Igarashi[1,2], Toshitaka Baba[3], Takane Hori[4], Masato Okada[1] (1.Graduate School of Frontier Sciences, The University of Tokyo, 2.Japan Science and Technology Agency PRESTO, 3.Institute of Technology and Science, The University of Tokushima, 4.Research and Development Center for Earthquake and Tsunami, Japan Agency for Marine-Earth Science and Technology)

9:45 AM - 10:00 AM JST | 12:45 AM - 1:00 AM UTC

[HDS13-10] Improvement for Finite-Difference Formula of Non-Linear Longwave Equations to Express Tsunami Decay

*Masaaki MINAMI[1] (1.Meteorological Research Institute)

10:00 AM - 10:15 AM JST | 1:00 AM - 1:15 AM UTC

[HDS13-11] Real time tsunami inundation forecast method developed for Central America Region

*Yuichiro Tanioka[1], Ulbert Gleb Grillo[2], Greyving Jose Argrello[2], Amilcar Cabrera[2] (1.Hokkaido University, Institute of Seismology and Volcanology, 2.Nicaraguan Institute of Territorial Studies, Nicaragua)

10:15 AM - 10:30 AM JST | 1:15 AM - 1:30 AM UTC

[HDS13-12] Near-fault observations of an offshore earthquake by DONET: Comparison of ocean bottom pressure gauges and strong-motion accelerometers

*Ayumu Mizutani[1], Kiyoshi Yomogida[1] (1.Natural History Science, Graduate School of Science, Hokkaido University, Earth and Planetary Dynamics)

Functions of Real-time Tsunami Inundation Forecast System Using S-net Pressure Data

*Wataru Suzuki[1], Naotaka YAMAMOTO CHIKASADA[1], Takayuki Miyoshi[1], Shin Aoi[1]

1. National Research Institute for Earth Science and Disaster Resilience

We have developed real-time tsunami inundation forecast system using S-net ocean bottom pressure data (Aoi et al., 2019, JDR). The forecast methodology of the system is mainly based on the multi-index method (Yamamoto et al., 2016, EPS) coupled with tsunami scenario bank (Chikasada et al., 2019, Technical Note NIED). In addition, the system has many functions to perform appropriate forecast considering a nature of the observed S-net pressure data, additional seismological data, regression targeted for specific region and alerting for tsunami without search for tsunami scenario bank. In this presentation, we introduce the developed forecast system focusing on these various functions.

The system has a redundancy and robustness in processing the observed S-net data by receiving the data from dual receiver with quality check. The pressure data are corrected for offset, band-pass filtered to extract the tsunami components. It was found that high waves due to typhoon or storm cause noises even in the ocean bottom pressure data and scenarios are selected by multi-index method. Therefore, the system does not make forecast information if no stations have larger amplitude than criterion value.

Forecast information, i.e., coastal tsunami heights and inundation depth distribution, is produced from the selected scenarios from the multi-index method by taking the maximum and average value of the selected scenarios. The scenario with the largest variance reduction between the observed and scenario data can be forecast information too. Standard deviation can be used to present the scattering of the forecast. As additional information, the system imposes the consistency with the hypocenter information on the selected scenarios by the multi-index method. This works well for the tsunamis generated at the edge or outside of S-net region. Moreover, most possible tsunami scenario for specific region can be derived from the selected scenarios in comparison with the forecast tsunami inundation depth at representative points based on neural network regression. The system also has functions to alert the tsunami by detecting the large pressure changes as well as using the tsunami warnings issued by the Japan Meteorological Agency. Detailed information based on the tsunami simulation based on 10-m mesh topography model is output for Kujukuri-Sotobo region of Chiba prefecture and rough and limited information is output from Ibaraki prefecture to Pacific coast of Hokkaido.

Acknowledgements: This work is partly supported by Council for Science, Technology and Innovation (CSTI), Cross-ministerial Strategic Innovation Promotion Program (SIP), “Enhancement of societal resiliency against natural disasters” (Funding agency: JST).

Keywords: Tsunami, Inundation, Real-time forecast, S-net

©2019. Japan Geoscience Union. All Right Reserved.

Improvement of Real-time Tsunami Forecast System for Outer-rise Earthquake

*Naotaka YAMAMOTO CHIKASADA[1], Toshitaka Baba[2]

1. NIED, 2. Tokushima University

The outer-rise earthquakes often induce the behavior of the unusual tsunamis. For example, it induces an abnormally larger tsunami than expected from its seismic ground motion, called tsunami earthquake and/or contains short wavelength components produced by sea floor displacements caused by shallow depth fault slip. Additionally, the depressed wave usually arrives preceding the first elevated wave for the normal fault earthquake tsunamis. National Research Institute for Earth Science and Disaster Resilience (NIED) has developed real-time tsunami inundation forecasting method using real-time ocean bottom pressure data taken by the dense offshore observation network such as the Seafloor observation network for earthquakes and tsunamis (S-net) that has been constructed along the Japan Trench (Chikasada et al., 2019, Technical Report of NIED; Yamamoto et al., 2016, EPS). They calculated synthetic tsunami waveforms at the observation locations by solving nonlinear long-wave equations using a staggered leapfrog finite-difference scheme. A run-up boundary condition was applied to the coastal regions and an open boundary condition was applied to the rims of calculation region. But they did not consider about dispersive wave (Baba et al., 2017, Ocean Modeling) neither the attenuation effect of ocean bottom pressure changes (Chikasada et al., 2018, AGU).
Therefore, we reconsidered the effects of the dispersion term and the attenuation for a few thousands tsunami scenarios stored in the Tsunami Scenario Bank (TSB). As a result, we confirmed that these two effects possibly cause underestimation in real-time tsunami forecast. Therefore, we need to update waveforms calculated and registered for outer-rise earthquake into the TSB with a dispersion term. However, it is quite time-consuming task to solve non-linear long-wave equations with Boussinesq terms. In order to reduce calculation time, the linear long-wave equations with Boussinesq terms could be used to generate offshore synthetic waveforms. We considered the attenuation effect as well.
This work was partially supported by JSPS KAKENHI Grant Number JP15H05718 and JP18K04674.

Keywords: Tsunami, Outer-rise earthquake, Ocean bottom pressure observation

©2019. Japan Geoscience Union. All Right Reserved.

Maximum tsunami height prediction using Ocean-Bottom Pressure Values based on Gaussian Process Regression

*Kotaro Takahashi[1], Kenjiro Kashiwabara[1], Yasuhiko Igarashi[1,2], Toshitaka Baba[3], Takane Hori[4], Masato Okada[1]

1. Graduate School of Frontier Sciences, The University of Tokyo, 2. Japan Science and Technology Agency PRESTO, 3. Institute of Technology and Science, The University of Tokushima, 4. Research and Development Center for Earthquake and Tsunami, Japan Agency for Marine-Earth Science and Technology

Tsunami early warning systems using water pressure gauges operate around the world to cope with human damage caused by tsunami waves. The systems use a correlation between observed pressure gauges value around coast and tsunami height at prediction points near shore, based on prior insights such that tsunami height highly depends on the topography (bathymetry) during its propagation.

In predicting the tsunami height, it is important both to avoid underestimation for minimizing the damage and to increase accuracy for minimizing the evacuation cost. Takahashi et al. [2018] proposed a method making use of a database of the tsunami height and the observed pressure-gauge-values. While it is good at avoiding underestimation, it puts the prediction accuracy second; its prediction is likely to be highly overestimated. To improve the accuracy, Igarashi et al. [2016] proposed a method based on Gaussian Process regression, but it does not avoid underestimation. In this work, we extend the method by Igarashi et al. [2016], and proposed a prediction method with less underestimation and higher accuracy. We used pressure gauges data from the Dense Ocean-floor Network System for Earthquakes and Tsunamis (DONET) in the Nankai trough to investigate the prediction accuracy and the possibility of underestimation by our proposed method. Compared to the method by Takahashi et al. [2018], our method dropped the average prediction error from 4.44m to 1.61m, at the cost of an increase in the average underestimation rate of only 3.5%. Likewise, compared to the method by Igarashi et al. [2016],

our method dropped the average underestimation rate from 43.2% to 4.38%, at the cost of an increase in the average prediction error of only 0.84m. These facts prove the effectiveness of our method, which is good at making predictions with both little underestimation and high accuracy.

Keywords: Gaussian Process, Machine Learning, Disaster prevention, tsunami height prediction

©2019. Japan Geoscience Union. All Right Reserved.

Improvement for Finite-Difference Formula of Non-Linear Longwave Equations to Express Tsunami Decay

*Masaaki MINAMI[1]

1. Meteorological Research Institute

In the current, we can not correctly express the decay process of the tsunami by numerical calculation. In the meantime, social demands for accurately expressing the tsunami decay are strengthening, for judging the timing of cancellation of the tsunami warning and information on the outlook of the tsunami. Therefore, at the Meteorological Research Institute, we are conducting research to improve the accuracy of the subsequent wave and decay process of the far-field tsunami and modeling of the decay process using observation waveforms (Hayashi et al., 2010, JSCE papers B2 (coastal engineering) etc.). We are conducting large-scale and highly accurate tsunami calculations using supercomputer using nonlinear longwave equations, which is a conventional tsunami numerical calculation method. (Minami et al., 2018, Japan Seismological Society Autumn Meeting etc.) Nevertheless, the decay process of the tsunami was not correctly expressed like the results of various calculations so far.

In this paper, we focused on bottom friction of tsunamis, which is an important factor in decay, and improved the differential formula of nonlinear longwave equations. First, in the friction term in the equation, the position difference of the total water depth (D) for calculating the friction term has been calculated as the arithmetic mean of the two adjacent meshes (central difference). If you use arithmetic averaging, there is a possibility that non-negligible errors may occur compared to when solving continuously. This is because D changes in the friction term on the order of -1/3. Therefore, the positional difference was improved to the one using the average value theorem (fig1). Furthermore, with regard to the time difference, assuming that dt is dt/n within one calculation step dt seconds and assuming that the calculation is repeated n times, it is possible to take the limit at $n \rightarrow \infty$, and the difference expression can be transformed as shown in fig 2.

Using these improved difference formula and appropriate coefficients, we calculated in the case of the 2010 Chile earthquake tsunami (Mw 8.8), and as a result its deay is larger than the conventional formula. In the example of fig3, the total energy amount of the later part, which became larger than the observation amount, decreased by about 4% and approached the observation amount. As a calculation condition of the tsunami, all areas including the entire Pacific Ocean (E100° to W90°) are assumed to be 30 seconds mesh (GEBCO 30 sec-grid), and in the area surrounding Hokkaido, Honshu, Shikoku and Kyushu, nesting is performed with a 10 second mesh, and we calculated for a long time (72 hours) in order to see the decay process. For the calculation we use JAGURS (Baba et al., 2015) , considering the elastic loading of the crust and the density effect of seawater, and using the result of the fault parameter (Fujii & Satake, 2013).

By using this formula, the decay of the tsunami becomes larger than the conventional formula by about 5%, and it is 10% or more in large case when the total depth D is small (generally less than 1 m) such as run-up and exposure. Also, by improving the time difference, it is possible to take longer time steps and it is possible to shorten the calculation time.

Although the decay process of the tsunami was not correctly expressed by the previous numerical calculation, it became possible to express the decay process more correctly by this method. In the future,

©2019. Japan Geoscience Union. All Right Reserved.

we will continue to study this method and apply this method to various cases to improve the accuracy of the tsunami decay process.

Keywords: Far-field tsunami, Numerical simulation, Supercomputer

$$gn^2\left(\frac{D_{i,j}^k+D_{i+1,j}^k}{2}\right)^{-7/3}\frac{M_{i+1/2,j}^{k+1/2}+M_{i+1/2,j}^{k-1/2}}{2}\sqrt{(M_{i+1/2,j}^{k-1/2})^2+(N_{i+1/2,j}^{k-1/2})^2}$$

$$\downarrow$$

$$gn^2\frac{3}{2}\frac{(D_{i+1,j}^k)^{\frac{2}{3}}-(D_{i,j}^k)^{\frac{2}{3}}}{D_{i+1,j}^k-D_{i,j}^k}\left(\frac{D_{i,j}^k+D_{i+1,j}^k}{2}\right)^{-2}\frac{M_{i+1/2,j}^{k+1/2}+M_{i+1/2,j}^{k-1/2}}{2}\sqrt{(M_{i+1/2,j}^{k-1/2})^2+(N_{i+1/2,j}^{k-1/2})^2}$$

fig1. Bottom Friction Term Using Mean Value Theorem

Conventional difference formula is

$$\mathrm{M_new(i,j)}=(\mathrm{M'\ (i,j)}-\frac{1}{2}\mathrm{fric}*\mathrm{M_old(i,j)})\ /\ (1+\frac{1}{2}\mathrm{fric})$$

$$\mathrm{M'\ (i,j)=M_old(i,j)-(gravity\ term)-(advection\ term)}$$

$$\mathrm{fric=\ dt\cdot g\cdot n\hat{}2\cdot D\hat{}-7/3\cdot \bar{M}}$$

solving n times

$$\begin{cases}\mathrm{M_{1/n}(i,j)=M'(i,j)}-\frac{1}{n}*\mathrm{fric}*\mathrm{M_old(i,j)}\\ \mathrm{M_{2/n}(i,j)=M_{1/n}(i,j)}-\frac{1}{n}*\mathrm{fric}*\mathrm{M_{1/n}(i,j)}\\ \vdots\\ \mathrm{M_{n/n}(i,j)=M_{n-1/n}(i,j)}-\frac{1}{n}*\mathrm{fric}*\mathrm{M_{n-1/n}(i,j)}\end{cases}$$

$$\mathrm{M_new(i,j)}=(\mathrm{M'(i,j)}-\tfrac{1}{n}*\mathrm{fric}*\mathrm{M_old(i,j)})\cdot(1-\tfrac{\mathrm{fric}}{n})^{n-1}$$

$$n\to\infty,\ (1\text{-}a/n)\hat{}n=\exp(-a)$$

$$\mathrm{M_new(i,j)}=\mathrm{M'(i,j)}\cdot\exp(-\mathrm{fric})$$

fig2. Bottom Friction Term Using Limit of a function

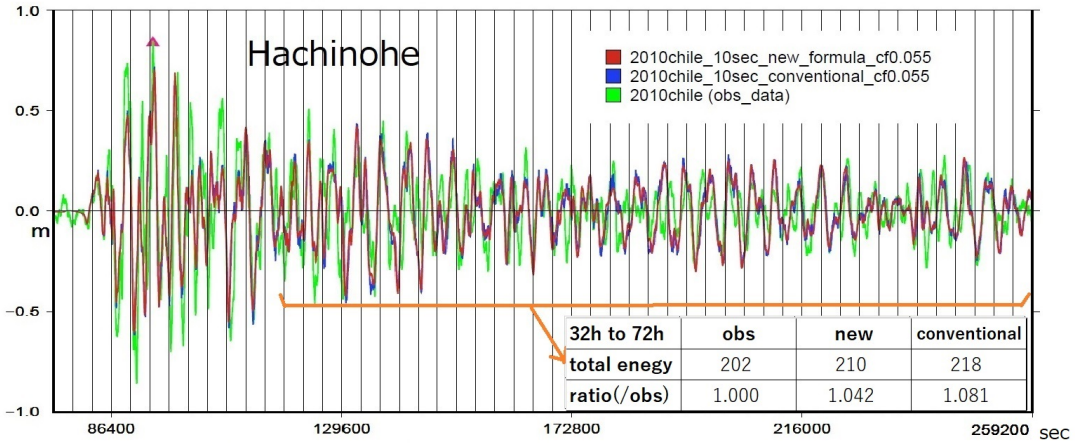

fig3. Time Series of Comparisons between New and Conventional Formula

©2019. Japan Geoscience Union. All Right Reserved.

Real time tsunami inundation forecast method developed for Central America Region

*Yuichiro Tanioka[1], Ulbert Gleb Grillo[2], Greyving Jose Argrello[2], Amilcar Cabrera[2]

1. Hokkaido University, Institute of Seismology and Volcanology, 2. Nicaraguan Institute of Territorial Studies, Nicaragua

In 1992, the Nicaragua tsunami earthquake generated a large tsunami which caused a significant disaster along the coast. In Central America, it has been an issue to develop a tsunami warning system which can manage a tsunami earthquake such as the 1992 Nicaragua earthquake. Recently, the Intergovernmental Oceanographic Commission of UNESCO (IOC/USESCO) decided to make the Central America Tsunami Advisory Center (CATAC) in Nicaragua. Therefore, Japan International Cooperation Agency (JICA) with Japan Meteorological Agency (JMA) run a technical program to support the establishment of CATAC. In this paper, we develop a tsunami inundation forecast method for CATAC which can manage a tsunami earthquake.

First, we previously developed the method to appropriately estimate the source model (Tanioka et al., 2017). The technique was tested for four large earthquakes, the 1992 Nicaragua tsunami earthquake (Mw7.7), the 2001 El Salvador earthquake (Mw7.7), the 2004 El Astillero earthquake (Mw7.0), and the 2012 El Salvador-Nicaragua earthquake (Mw7.3), which occurred off Central America. At first, fault parameters were estimated from the W-phase inversion. Then the fault length and width were determined from scaling relationships. To estimate a slip amount, we constructed a depth dependent rigidity curve, similar to that suggested by Bilek and Lay (1999). The curve with a central depth estimated by the W-phase inversion was used to calculate the slip amount of the fault model. Using that slip amount, the tsunami numerical simulation with inundations was carried out. The result indicated that the observed tsunami heights, run-up heights, and inundation areas for the 1992 Nicaragua tsunami earthquake were well explained by the computed one. The other tsunamis from the other large earthquakes were also reasonably well explained by the computed ones.

In this paper, we applied the near-field tsunami forecast method (NearTIF) using a data base (Gusman et al., 2014) by computing a tsunami from the appropriate fault model which estimated in the above. First, we built a data-base which contained tsunami waveforms at several reference points for each region and inundation results at 6 regions, Gulf of Fonseca, Corinto, Puerto Sandino, El Transito, Masachapa,El Astillero, along the Pacific coast of the Central America. We put source models of Mw7.0, 7.2, 7.4, 7.6, 7.8, 8.0, 8.2 along the subduction interface. Totally, 135 source models are in the data base. The best tsunami inundation distribution for the forecast will be chosen by comparing the tsunami waveforms at the reference points computed in a real time with the tsunami waveforms at those points in the data base. Nest, the method is applied for the 1992 Nicaragua tsunami earthquake case. The source model for the 1992 Nicaragua earthquake was previously estimated from the W-phase inversion with the scaling relationship. The slip amount is estimated using the depth dependent rigidity curve. The tsunami forecast result shows that the observed tsunami heights, run-up heights, and inundation areas are reasonably well explained by the tsunami forecasted inundation map. The method developed in this paper should be useful for the tsunami early warning system at CATAC.

Keywords: Real time tsunami inundation forecast, Nicaragua, CATAC

©2019. Japan Geoscience Union. All Right Reserved.

©2019. Japan Geoscience Union. All Right Reserved.

Near-fault observations of an offshore earthquake by DONET: Comparison of ocean bottom pressure gauges and strong-motion accelerometers

*Ayumu Mizutani[1], Kiyoshi Yomogida[1]

1. Natural History Science, Graduate School of Science, Hokkaido University, Earth and Planetary Dynamics

New ocean-bottom networks for earthquakes and tsunami such as S-net and DONET have been recently deployed in the offshore Japan. One important feature of these networks is that seismometers and ocean bottom pressure (OBP) gauges are installed at the same sites. Tsunamis are designed to be recorded in terms of water pressure changes. During an earthquake, the water pressure near its fault area changes not only by tsunamis (i.e., sea surface heights) but also by water depth change of instruments themselves, vertical accelerations of a seafloor itself (i.e., reaction force from water column), and the seismic waves radiated (including ocean acoustic waves) (e.g. Saito and Tsushima, 2016).

In this study, we analyzed the OBP and strong-motion accelerogram records provided by DONET1 that associated with the 2016 Off-Mie earthquake (Mw 6). First, we compared the pressure records in the forms of acceleration, velocity and displacement recorded in strong-motion accelerograms. Velocity and displacement records were calculated by integrations of accelerometer seismograms. Because a simple integration leads to unreasonable results, we conducted the baseline correction by the method based on Iwan et al. (1985). Second, we estimated tsunami heights at stations near the fault in near real-time basis, using the records of OBPs and accelerograms combined.

We obtained the following results by these comparisons: (1) the pressure change proportional to ocean-bottom velocity especially for each first motion, (2) in contrast, at around 0.1Hz, the pressure proportional to ocean-bottom acceleration at some stations, and (3) during the coseismic period, the effect of displacement not contributing to the pressure change at the same site. (1) and (2) are consistent with the numerical simulations by Saito (2017).

Next, we removed the effect of accelerations using 0.05-0.1Hz band-pass filter from the OBP records that were processed by 0.1Hz low-pass filtering, enabling us to extract tsunami and displacement signals at 10s intervals. The resulted waveforms are matched well with 0.01Hz low-pass filtered OBP records, suggesting that this method would be useful for tsunami early warning with near-fault combined records of OBP and accelerograms.

Keywords: DONET, tsunami

©2019. Japan Geoscience Union. All Right Reserved.

[J] Oral | H (Human Geosciences)：H-DS Disaster geosciences

Wed. May 29, 2019 10:45 AM - 12:15 PM JST | Wed. May 29, 2019 1:45 AM - 3:15 AM UTC | Convention Hall B 2F

[H-DS13] Tsunami and Tsunami Forecast

convener:Naotaka YAMAMOTO CHIKASADA(National Research Institute for Earth Science and Disaster Resilience), Hiroaki Tsushima(Japan Meteorological Agency), Tatsuya Kubota(National Research Institute for Earth Science and Disaster Resilience), Chairperson:Kentaro Imai, Toshitaka Baba(Graduate School of Science and Technology, Tokushima University)

This session discusses issues related to improving real-time and long-term prediction accuracy of tsunami from earthquakes, landslides, and volcanoes, which include such as a better understanding of tsunami dynamics, new real-time tsunami observing systems deployed in the open ocean and coastal waters, methodologies of more rapid and accurate prediction during tsunami emergencies, more extensive and accurate inundation maps, and long-term tsunami potential forecast.

10:45 AM - 11:00 AM JST | 1:45 AM - 2:00 AM UTC

[HDS13-13] **Investigation of variation in multiple tsunami inundation modelling**

*Yoshinori Shigihara[1], Kentaro Imai[2], Hiroyuki Iwase[3], Koji Kawasaki[4], Makoto Nemoto[5], Toshitaka Baba[6], Naotaka YAMAMOTO CHIKASADA[7], Yu Chida[8], Taro Arikawa[9] (1.Department of Civil and Environmental Engineering, National Dedense Academy, 2.Japan Agency for Marine-Earth Science and Technology, 3.Ecoh Corporation, 4.Hydro Technology Institute, Co., Ltd., 5.OYO Corporation, 6.Graduate School of Science and Technology, Tokushima University, 7.National Research Institute for Earth Science and Disaster Resilience, 8.Port and Airport Research Institute, 9.Civil and Environmental Engineering, Faculty of Science and Engineering, Chuo University)

11:00 AM - 11:15 AM JST | 2:00 AM - 2:15 AM UTC

[HDS13-14] **Numerical Modeling of Tsunami Inundation in Urban Area using Sub-Grid Scale Drag Force Model**

*Nobuki Fukui[1], Nobuhito Mori[2] (1.Graduate School of Engineering, Kyoto University, 2.Disaster Prevention Research Institute, Kyoto University)

11:15 AM - 11:30 AM JST | 2:15 AM - 2:30 AM UTC

[HDS13-15] Numerical experiment of tsunami deposits related to fault parameters by sediment transport model

*Ako YAMAMOTO[1], Tomoyuki Takahashi[2], Kenji Harada[3] (1.Forest of Research and Management Organization Forestry and Forest Products Research Institute, 2.Kansai University, 3.Shizuoka University)

11:30 AM - 11:45 AM JST | 2:30 AM - 2:45 AM UTC

[HDS13-16] Evaluation of potential impact of tsunami-induced sediment transport in Kochi Prefecture during the Nankai Trough megathrust earthquake and tsunami

*Kei Yamashita[1], Daisuke Sugawara[2], Shuji Seto[1], Taro Arikawa[3], Tomoyuki Takahashi[4], Fumihiko Imamura[1] (1.International Research Institute of Disaster Science, Tohoku University, 2.Museum of Natural and Environmental History, Shizuoka, 3.Faculty of Science and Engineering , Chuo University, 4.Faculty of Societal Safety Sciences, Kansai University)

11:45 AM - 12:00 PM JST | 2:45 AM - 3:00 AM UTC

[HDS13-17] Tsunami damage of the Keicho Earthquake of February 3rd, 1605 on the coasts of Tokai, Shikoku, and Kyushu Districts

*Yoshinobu Tsuji[1], Kentaro Imai[2], Yuuichi Ebina[3], Hiroyuki Iwase[4], Ryoko Oobayashi[2] (1.Shimanto City, 2.JAMSTEC, 3.IRIDeS, 4.Ecoh co. LTD)

12:00 PM - 12:15 PM JST | 3:00 AM - 3:15 AM UTC

[HDS13-18] Re-examination of tsunami heights distribution during the 1854 Ansei Tokai Earthquake

*Kentaro Imai[1], ebina yuichi[2], Yoshinobu Tsuji[3], Hiroyuki Iwase[4], Takane Hori[1], Narumi Takahashi[1,5], Takashi Furumura[6] (1.Japan Agency for Marine-Earth Science and Technology, 2.International Research Institute of Disaster Science, 3.Shimanto City, 4.ECOH CORPORATION, 5.National Research Institute for Earth Science and Disaster Resilience, 6.Earthquake Research Institute The University of Tokyo)

Investigation of variation in multiple tsunami inundation modelling

*Yoshinori Shigihara[1], Kentaro Imai[2], Hiroyuki Iwase[3], Koji Kawasaki[4], Makoto Nemoto[5], Toshitaka Baba[6], Naotaka YAMAMOTO CHIKASADA[7], Yu Chida[8], Taro Arikawa[9]

1. Department of Civil and Environmental Engineering, National Dedense Academy, 2. Japan Agency for Marine-Earth Science and Technology, 3. Ecoh Corporation, 4. Hydro Technology Institute, Co., Ltd., 5. OYO Corporation, 6. Graduate School of Science and Technology, Tokushima University, 7. National Research Institute for Earth Science and Disaster Resilience, 8. Port and Airport Research Institute, 9. Civil and Environmental Engineering, Faculty of Science and Engineering, Chuo University

Many researchers have developed numerical models based on the nonlinear shallow water equations to estimate the propagation and inundation of tsunamis. Several models have been distributed as the software packages including source code, thus tsunami inundation simulation can be performed easily with bathymetric and topographic data available free. However, the tsunami modelling researchers also empirically understand that no tsunami simulation results agree perfectly with that of other research institutes even if the same numerical model is used. The maximum inundation depth, flow velocity and inundated area are different to a certain extent. To clarify the variation in tsunami simulation is very important to establish the standard method that confirm the reliability of tsunami inundation models and it will be useful for the tsunami countermeasure/mitigation planning.

The present study aims to evaluate magnitude of the variation in tsunami inundation simulation quantitatively. We conducted tsunami simulations under the same input data: the initial source model of tsunami, bathymetry, topography and land-use model provided by Cabinet Office, Government of Japan are adopted. A total of eight research institutes participated this project using four kinds of numerical models that are widely employed for the tsunami hazard/risk assessment. Comparison of the time history of water surface elevation and flow velocity at the specific points indicated that a significant difference was confirmed among the model results to the maximum value of physical quantities. The spatial distribution maps of the maximum inundation depth also showed that large variation occurs around the front of tsunami run-up. In order to explain the variation in tsunami inundation model quantitatively, the total flooded volume and the total momentum flux were newly defined. By statistical procedures using these variables, we were able to show the mean value, confidence interval and coefficient of variation of the tsunami inundation models.

Keywords: tsunami, numerical model, variation

©2019. Japan Geoscience Union. All Right Reserved.

Numerical Modeling of Tsunami Inundation in Urban Area using Sub-Grid Scale Drag Force Model

*Nobuki Fukui[1], Nobuhito Mori[2]

1. Graduate School of Engineering, Kyoto University, 2. Disaster Prevention Research Institute, Kyoto University

Numerical simulation of tsunami inundation using high-resolution topography (resolution is less than 1m) needs to consider the effect of structures on wave run-up. However, numerical simulation with medium resolution (resolution over 50m to 100m) is still important for practical use due to computational cost. This study developed Drag Force Model (DFM) and individual Drag Force Model (iDFM) as an urban roughness parameterization to obtain acceptable accuracy in medium resolution tsunami inundation model based on physical modeling. The model treats the effect of structures as grid-averaged drag force and projected area in x and y-direction in Cartesian coordinate and characteristic structure height are used as parameters representing the sub-grid scale structure. Furthermore, iDFM considers the number of structures and structure height in the area of interests individually. The edge detection technology for image processing tool is used to count the number of structures. Moreover, various mesh size 10cm to 40cm (25m to 100m in real scale) are used to check mesh size dependency. The validation DFM and iDFM is conducted using numerical simulation and physical modeling of tsunami inundation targeting available tsunami inundation experiments.

Keywords: tsunami, bottom roughness, drag force

©2019. Japan Geoscience Union. All Right Reserved.

Numerical experiment of tsunami deposits related to fault parameters by sediment transport model

*Ako YAMAMOTO[1], Tomoyuki Takahashi[2], Kenji Harada[3]

1. Forest of Research and Management Organization Forestry and Forest Products Research Institute, 2. Kansai University, 3. Shizuoka University

Large tsunamis cause extensive damage to coastal areas. Underestimation of the tsunami risk can increase the extent of damage and delay reconstruction. To improve tsunami estimation requires review of many records of tsunami cycles and sources (i.e., geologic faults). Sand deposits from tsunamis provide many paleo tsunami records; however, the relationship between tsunami sand deposits and the magnitude of tsunamis is not understood. Takahashi et al. (1999) proposed a sediment transport model for tsunamis. This model was adapted using data from the 1960 Chilean tsunami in Kesennuma Bay, although the amount of sand transportation was underestimated due to the local topography. Takahashi et al. (2011) improved the model based on a hydraulic experiment using three types of sand grains, although verification using other grain sizes and mixed sand compositions has not been conducted. Furthermore, numerical analysis focusing on tsunami sand deposits in inundation areas has fewer verification examples. Yamamoto et al. (2017, 2018) carried out a hydraulic experiment to validate the sediment transport model. This experiment used three types of sand grains, which had sizes different from those used by Takahashi et al. (2011). The model of Takahashi et al. (2011) was confirmed to be very accurate for medium sand. However, the relationship between the tsunami sand deposits and fault parameters has not been verified.

To clarify the relation between tsunami sand deposits and fault parameters, we carried out numerical experiments of sediment transport in a simple topography. The numerical experiments consisted of two steps. The first step investigated the influence of fault conditions on the tsunami waveform. The fault condition was changed according to fault width, length, slip, and position. The waveform observed in this experiment was used as the boundary condition for the second step of the experiment. The second step investigated the effect of the tsunami waveform on the sand deposits in the land area. The topography conditions were changed by changing the slope of the sea area and land area. Furthermore, we investigated the effect of setting a structure in the land area on the sand deposits. Numerical experiments confirmed the points at which the nature of sediment deposits changes according to fault and topography conditions.

Keywords: Tsunami deposit, Numerical experiment, Fault parameter

©2019. Japan Geoscience Union. All Right Reserved.

Evaluation of potential impact of tsunami-induced sediment transport in Kochi Prefecture during the Nankai Trough megathrust earthquake and tsunami

*Kei Yamashita[1], Daisuke Sugawara[2], Shuji Seto[1], Taro Arikawa[3], Tomoyuki Takahashi[4], Fumihiko Imamura[1]

1. International Research Institute of Disaster Science, Tohoku University, 2. Museum of Natural and Environmental History, Shizuoka, 3. Faculty of Science and Engineering , Chuo University, 4. Faculty of Societal Safety Sciences, Kansai University

Introduction

Strong flows due to giant tsunamis may cause large-scale sediment erosion, deposition and resulting morphological changes in coastal areas, in which sometimes alter the nature and size of tsunami hazards (e.g., Sugawara, 2017). The tsunamis flow loaded with a large amount of sediments possesses an increased hydrodynamic force, which causes not only loss of lives and properties but also incidental injuries to human healths, such as “Tsunami lung”. Flush-out of coastal sediments into deeper sea often cause irreversible changes in sandy beaches, on which post-tsunami natural coastal processes may form an altered beach morphology. Sediment deposition on lands and shallow waters hampers not only emergent rescue and support, but also post-disaster recovery and reconstruction. Environmental pollutions due to chemical elements in sludge deposits are additional consequences of the tsunami-induced sediment transport.

In 2012, the Cabinet Office of Japan updated the tsunami risk assessment of the Nankai Trough earthquake and tsunami. However, influences of the sediment transport have not been included quantitatively in the tsunami scenarios. In this study, numerical simulations of tsunami sediment transport caused by the Nankai Trough earthquake have been performed to investigate the potential impacts of sediment erosion, deposition and morphological change in Tosa Bay, Kochi Prefecture, where severest damages are presumed by the Case 4 of the assessment of the Nankai Trough earthquake.

Numerical Calculation Methods

The tsunami sediment transport model (STM) proposed by Takahashi et al. (1999) was used. The STM takes into account exchange of bed- and suspended loads, in which parameters of the transport formula depend on the grain size of the sediment. Computational region covers a wide area of Tosa Bay including Kure Bay in Takaoka-gun to Hane Cape in Muroto City. To assess the uncertainties due to the grain size, three types of median size d_{50} were assumed, i.e., d_{50} = 0.127, 0.267 and 0.394 mm.

Results and Discussion

The numerical simulations demonstrated that in the mouths of class A (Niyodo and Mononobe) and B

©2019. Japan Geoscience Union. All Right Reserved.

(Shinjo, Aki, Ioki and Nahari) rivers, strong flows caused severe erosion greater than 10 m in depth, regardless of the choice of the grain size. A large amount of the sediments were flushed out to the offshore zone deeper than the wave base. In addition, extensive sediment deposition occurred on the lands neighborhood of the class A rivers. For example, deposit thickness near Niyodo River was as large as 1 m. Note that thickness of known paleotsunami deposits in this area is much smaller than the simulations. Further comparison of the field data and modeling results is needed to examine the assumptions of the size of the Nankai Trough earthquake. Based on the findings from the 2011 Tohoku tsunami, averaged deposit thickness is estimated at 4-5 cm. Choice of the grain size caused variations of the averaged deposit thickness ranging from 4.2 to 11.3 cm.

Sediment erosion and deposition were significant around harbors and bays along the coast. Bottom sediments of the mouth and inner part of Susaki Bay were eroded and that the sediments were deposited over a wide area of Susaki City. However, the simulated thickness of the deposit on Ikenouchi area including Tadasu-ike was quite thin compared to the paleotsunami deposits (Okamura and Matsuoka, 2012). Coastal defenses and changes in the land use might have affected to the difference between the deposits. In the mouth of Usa and Urado Bays, the simulations showed that part of the sediments were transported to the land near the source meanwhile most sediments were deposited on the seaward the bay mouth and the head of the bay.

The simulated morphological changes became larger with decreasing grain size. Increase in the maximum inundation heights was 2 and 1 m for d_{50} = 0.127 and 0.394 mm, respectively. In some of the investigated areas (i.e., Geisei-mura), effect of the morphological change to the inundation height was totally different. These results imply importance of sediment transport modeling for regional tsunami hazard assessments.

Conclusions

In Kochi Prefecture, tsunami-induced sediment transport may cause not only large-scale morphological changes of the coasts but also increase in tsunami hazards. Note that the influences of the sediment transport depend significantly on uncertainties in bed materials. Acquisition of detailed sedimentary data will benefit improved assessment of impacts from tsunamis. Further discussions are needed regarding countermeasures to tsunami hazards considering the regional characteristics of tsunami-induced sediment transport.

Keywords: tsunami-induced sediment transport, Nankai Trough earthquake and tsunami, Kochi Prefecture, Numerical simulation

©2019. Japan Geoscience Union. All Right Reserved.

Tsunami damage of the Keicho Earthquake of February 3rd, 1605 on the coasts of Tokai, Shikoku, and Kyushu Districts

*Yoshinobu Tsuji[1], Kentaro Imai[2], Yuuichi Ebina[3], Hiroyuki Iwase[4], Ryoko Oobayashi[2]

1. Shimanto City, 2. JAMSTEC, 3. IRIDeS, 4. Ecoh co. LTD

We conducted field survey of the tsunami damaged coast of the Keicho 9 earthquake of February 3rd, 1605 on the coasts of Tokai, Shikoku And Kyushu and tsunami inundation or run-up heights were measured newly at 17 points by using GPS. Tsunami height distribution along Boso Peninsula had been clarified by Tsuji et al(2018). At Nishina, Nishiizu Town, Shizuoka prefecture, sea water went upstream along Nishina River about 1.4 km from the river mouth and run up height was estimated at 8.9 meters above mean sea level. At Hashimoto in Arai Town, Kosai City, Shizuoka prefecture, 80 houses out of 100 houses were swept away, and tsunami height was 8.2 meters. At Shirasuka, a post town of Tokaido houses were swept away and severel people, horses, and cows were killed, and tsunami height was 9.4 meters. At Horikiri village, Tahara city, near the to of Atsumi Peninsula, Aichi preffecture, all fishing ships were wrecked but no house and human damage took place, and height was estimeted at 3 meters. At Sakihama, Muroto city, Kochi prefecture, sea water rose up to the entrance step stone of the main building of Dainichiji temple, and tsunami height was 14.4 meters. Coastal villages near cape Muroto, about 400 people were killed due to the tsunami. At Saga, Kuroshio Town, documents given by Lord Motochika Chosokabe was lost in Sakamoto's house, where tsunami height was estimated at 6.2 meters. At Misaki, in Tosashimizu city, 153 peoples were killed due to the tsunami, and tsunami height was estimated at 8.1 meters. Tsunami height distribution is illustrated in the figure.
This research was supported by MEXT (“Research project for compound disaster mitigation on the great earthquakes and tsunamis around the Nankai Trough region”).

Keywords: the tsunami of the 1605 Keicho earthquake, historical earthquake, historical tsunami

©2019. Japan Geoscience Union. All Right Reserved.

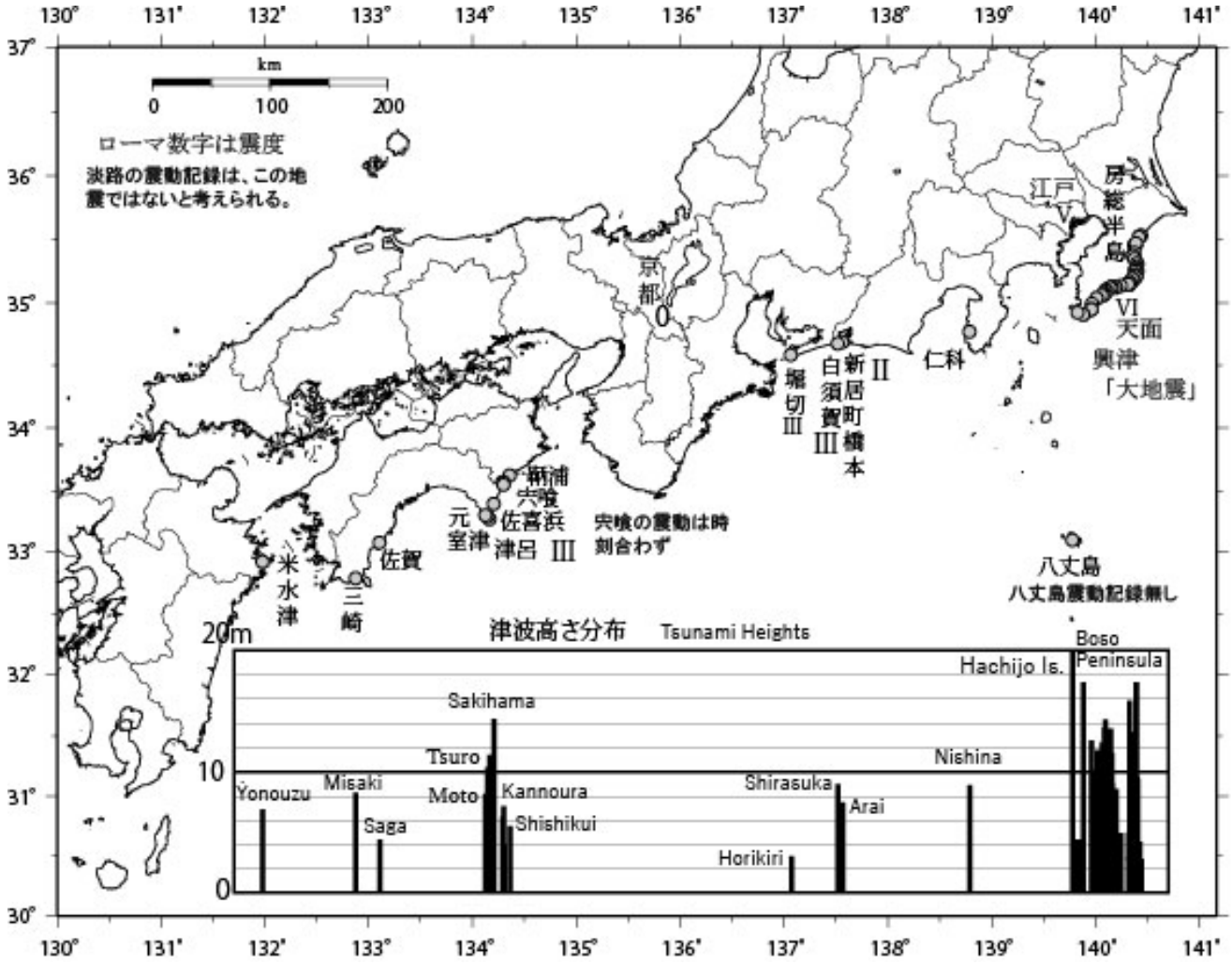

©2019. Japan Geoscience Union. All Right Reserved.

Re-examination of tsunami heights distribution during the 1854 Ansei Tokai Earthquake

*Kentaro Imai[1], ebina yuichi[2], Yoshinobu Tsuji[3], Hiroyuki Iwase[4], Takane Hori[1], Narumi Takahashi[1,5], Takashi Furumura[6]

1. Japan Agency for Marine-Earth Science and Technology, 2. International Research Institute of Disaster Science, 3. Shimanto City, 4. ECOH CORPORATION, 5. National Research Institute for Earth Science and Disaster Resilience, 6. Earthquake Research Institute The University of Tokyo

The great Nankai Trough earthquake has been accepted for the recurrence on the characteristic earthquake based on the plate tectonic interpretation. On the other hand, Seno (2012) pointed out the possibility that overlapping regions are few and complementary in the seismic zone of the Ansei Tokai Earthquake and the Showa Tonankai Earthquake. It is necessary to similar reinterpretation of the tsunami source. In this research, we reexamined the historical documents related to the Ansei Tokai earthquake Tsunami, along the coast of the Izu Peninsula from the coast of the Kii Peninsula, close to the source area of the Ansei Tokai earthquake. Furthermore, field survey for tsunami trace height based on historical documents conducted to clarify the characteristics of the tsunami height distributions.

We extracted historical materials on the 1854 Ansei Tokai Earthquake published in the Japan Earthquake reference material as “Zotei Dai Nippon Jishin shiryo”, “Shinshu Nihon Jishin Shiryo” and so on. 801 documents stored in these collections were selected and checked for newly found documents that have not been used in previous research. We conducted a field survey on tsunami trace height information obtained through historical document. We reviewed carefully these selected historical documents, and evaluation for tsunami trace height on the field was carried out by GNSS and laser range finder measurement. For the comprehensive tsunami trace height distribution, the data evaluated by previous research [Hatori (1977); Tsuji et al. (1991); Namegaya & Tsuji (2005); Tsuji et al. (2013); Tsuji & Saito (2014); Imai et al. (2017)] were partially used.
There are two peaks of the tsunami height during the tsunami trace height distributions on the Ansei Tokai earthquake tsunami, the one as the tsunami trace height was reached 22 m at Kuzaki the east of the Shima Peninsula. the other one as the tsunami trace height was exceeding 15 m at Iruma the south east of Izu Peninsula. This information are extremely important clues to re-examine for the tsunami source of the Ansei Tokai earthquake. We examine the tsunami source that explains such tsunami trace height distribution in this presentation.

Acknowledgments: This research was supported by MEXT (“Research project for compound disaster mitigation on the great earthquakes and tsunamis around the Nankai Trough region”).

Keywords: The great Nankai Trough earthquak, the 1854 Ansei Tokai Earthquake, tsunami trace heights distribution

©2019. Japan Geoscience Union. All Right Reserved.

[J] Oral | H (Human Geosciences)：H-RE Resource and Engineering Geology

Wed. May 29, 2019 10:45 AM - 12:15 PM JST | Wed. May 29, 2019 1:45 AM - 3:15 AM UTC | 106 1F

[H-RE16] Resource Geology

convener:Tsubasa Otake(Division of Sustainable Resources Engineering, Faculty of Engineering, Hokkaido University), Daisuke Araoka(Geological Survey of Japan, National Institute of Advanced Industrial Science and Technology), Ryohei Takahashi(Graduate School of International Resource Sciences, Akita University), Tatsuo Nozaki(Research and Development Center for Submarine Resources, Japan Agency for Marine-Earth Science and Technology), Chairperson:Tsubasa Otake(Faculty of Engineering, Hokkaido University), Daisuke Araoka

Ore deposits containing valuable elements and minerals at high concentrations in supracrustal rocks are formed by the Earth's dynamics including magmatism, hydrothermal activity, metamorphism, and weathering. The formation of ore deposits is also closely associated with global environmental changes and biological evolution in the Earth's history. Involvement of difference academic fields in earth sciences including geology, petrology, geochemistry, mineralogy, and microbiology is required to understand the genesis of ore deposits. The field of resource geology is essential not only for efficient exploration and development of ore deposits but also for better understanding and assessment of hazardous elements that may be caused by the resource development. This session widely covers various topics of field investigation and observation, laboratory experiments, theoretical calculation, development of analytical methods and others related to the supracrustal migration and concentration of elements.

10:45 AM - 11:15 AM JST | 1:45 AM - 2:15 AM UTC

[HRE16-01] The role of water in the concentration of Cr

★Invited Papers

*Shoji Arai[1] (1.Department of Earth Sciences, Faculty of Science, Kanazawa University)

11:15 AM - 11:30 AM JST | 2:15 AM - 2:30 AM UTC

[HRE16-02] Mineralogical Features of Silver-Bearing Minerals in Chimney Ore from Myojinsho Caldera, Myojin Knoll and Bayonnaise Knoll Seafloor Hydrothermal Area, Izu-Bonin Arc

Shinji Kawaguchi[1], *Kotaro Yonezu[1], Thomas Tindell[1], Jun-ichiro Ishibashi[2], Tatsuo Nozaki[3], Yoko Ohtomo[4], Koichiro Watanabe[1] (1.Deaprtment of Earth Resources Engineering, Faculty of Engineering, Kyushu University, 2.Department of Earth and Planetary Sciences, Faculty of Sciences, Kyushu University, 3.Research and Development Center for Submarine Resources, Japan Agency for Marine-Earth Science and Technology, 4.Faculty of Engineering, Hokkaido University)

11:30 AM - 11:45 AM JST | 2:30 AM - 2:45 AM UTC

[HRE16-03] Organic matters and acid-sulfate alteration in Itomuka Mine, Hokkaido, Japan: implications for the transportation and deposition mechanisms of mercury

*Takuya Echigo[1], Mitsuyoshi Kimata[2], Masahiro Shimizu[2] (1.Graduate School of International Resource Sciences, Akita University, 2.Graduate School of Life and Environmental Sciences, University of Tsukuba)

11:45 AM - 12:00 PM JST | 2:45 AM - 3:00 AM UTC

[HRE16-04] **Significances of 12 Ma manganese ores in the Hokuroku district, Akita: unique Mn accumulation and interaction with organic matter during submarine hydrothermal activities**

*Yuya Tsukamoto[1], Takeshi Kakegawa[1] (1.Tohoku Univ.)

12:00 PM - 12:15 PM JST | 3:00 AM - 3:15 AM UTC

[HRE16-05] Microbial communities around ca. 2.7 Ga submarine hydrothermal fields at the Potterdoal deposit in Abitibi Greenstone Belt, Canada

*Takeru Osato[1], Akizumi Ishida[1], Takeshi Kakegawa[1] (1.Tohoku University)

The role of water in the concentration of Cr

*Shoji Arai[1]

1. Department of Earth Sciences, Faculty of Science, Kanazawa University

The role of water in the formation of chromitites, which have been designated as a typical orthomagmatic ores, has been long controversial. Johan et al. (1983, 2017), for example, concluded that chromites are precipitated from water-rich fluids at relatively low temperatures (< 1000 ºC) to form podiform chromitites in the mantle. Those arguments are mainly based on two observations; (1) podiform chromitites and surrounding peridotites have been preferentially hydrated, which may mean the initial water enrichment, and (2) chromite grains contain fluid and hydrous mineral inclusions of apparently primary origin. I criticize the related interpretations based on those observations. The selective hydration in and around chromitite pods is due to the Mg-rich character of olivines, which has been obtained during a subsolidus cooling stage (Arai, 1978), and does not definitely show the involvement of water-rich fluid in chromitite formation. The origin of the chromite-hosted hydrous mineral inclusions has not been left unclear. Many authors a priori interpreted the inclusions as being representative of the trapped melts or fluids that precipitated the host chromites. This is, however, highly questionable. The inclusions are most probably formed during a stage of peridotite-melt reaction within a complicated igneous stage of podiform chromitite generation in the mantle. Hydrothermal fluids can transport Cr and precipitate chromite, but may not form most of the podifrom chromitites.

Keywords: Chromium, Chromitite, Water

©2019. Japan Geoscience Union. All Right Reserved.

Mineralogical Features of Silver-Bearing Minerals in Chimney Ore from Myojinsho Caldera, Myojin Knoll and Bayonnaise Knoll Seafloor Hydrothermal Area, Izu-Bonin Arc

Shinji Kawaguchi[1], *Kotaro Yonezu[1], Thomas Tindell[1], Jun-ichiro Ishibashi[2], Tatsuo Nozaki[3], Yoko Ohtomo[4], Koichiro Watanabe[1]

1. Deaprtment of Earth Resources Engineering, Faculty of Engineering, Kyushu University, 2. Department of Earth and Planetary Sciences, Faculty of Sciences, Kyushu University, 3. Research and Development Center for Submarine Resources, Japan Agency for Marine-Earth Science and Technology, 4. Faculty of Engineering, Hokkaido University

Submarine hydrothermal deposits in western Pacific is characterized as volcanic massive sulfide deposits mainly consisting of Cu-Pb-Zn (± Au ±Ag). Recent explorations have resulted in discoveries of submarine mineral resources in the exclusive economic zones around Japan. The previous study reported chimney ores collected from Izu-Bonin arc are of high grade (Au; 24.1 ppm, Ag; 1275 ppm, Cu: 1.14%, Pb: 5.57%, Zn: 35.03%), (Tanahashi et al, 2004). According to this study, chimney ores were characterized by porous constituents and concentric ring structures, white colored barite layer and sulfide mineral layer mainly composed of sphalerite and galena are recognized from the outer surface to the center part. This concentric ring structures may be attributed to order of precipitations during formation of the chimney ores, however only few studies have discussed mineralization of the chimney along the growth axis (e.g., Watanabe & Hayashi, 2014). Purpose of our research is to clarify mineralogical features of silver minerals in chimney ore by identifying the precipitation conditions of hydrothermal fluids in the Izu-Bonin arc. We studied chimney ores collected during the NT13-09 scientific cruise and NT14-06 scientific cruise.The chimney ores collected from Izu-Bonin arc have quite similar mineralogical features. They have a tubular structure and can be divided into three groups along growth axis from outside to inside of chimney; G1: composed of barite; G2: mainly composed of barite and the principal sulfide minerals of submarine hydrothermal ore deposit (sphalerite, pyrite, chalcopyrite and galena); and G3: composed of main sulfides. According to EPMA analysis, barite is observed in G1 and G2 in addition to pore filling barite in G3. These barite formations are considered to mixing of the hydrothermal fluid with ambient seawater and formation temperature estimated for the initial barite mineralization recognized in G1 and G2 as 190-215℃, and for the second barite mineralization in G3 is as 150-195℃, suggesting temperature decrease of the hydrothermal fluid during the formation of chimney ores (Iizasa, et al. 1997). Based on these results, we propose following formation stages. First, G1 are formed by mixing of the hydrothermal fluid with seawater. Subsequently, porous G2 is formed by a change in the mixing ratio of seawater and hydrothermal fluid. Finally, the hydrothermal contribution becomes greater, so that exclusively sulfide mineral can be precipitated in G3. In addition, as shown in barite observed in G3, after the hydrothermal activity stopped, the second barite is precipitated in the void of the porous chimney ore by mixing ambient seawater and hydrothermal fluid. We noticed that the silver-bearing minerals can be observed in G2 and G3 as tetrahedrite-tennantite series minerals (Ave (wt.%): Ag; 2.9, Cu: 11.1, Zn: 7.0, Pb: 46.6, Sb: 4.0, As: 3.0 and S: 10.9) of 1-20 μm. Silver bearing minerals are associated with sphalerite and galena. According to Ag vs. Sb/(Sb+As) diagram, relatively silver-rich hydrothermal fluids contributed to form the chimney ore in Izu-Bonin arc as compared to that of typical with Kuroko type deposits. Especially from the chimney ore of the Bayonaissea knoll, 1-10 μm of tetrahedrite-tennantite series containing a high content of silver (Ave (wt.%): Ag: 52.9, Cu: 9.6, Zn: 1.6, Pb: 37.5 and S: 13.8) are observed at the rims of galena in the boundary between G1 and G2. Silver mineralization may be explained as follows. Firstly, silver present in galena formed during the principal sulfide mineralization moves by equilibrium equation,

©2019. Japan Geoscience Union. All Right Reserved.

$2Pb^{2+} = Ag^{+} + Sb^{3+}$ (Karup-Moller, 1971 and Foord, 1989) towards the right side by decreasing in temperature. As a result, tetrahedrite-tennantite series minerals are precipitated at G2 and G3. After hydrothermal active vent stopped, further temperature drop was introduced and furutobeite is formed from tetrahedrite-tennantite series minerals.

Keywords: Submarine hydrothermal ore deposit, Chimney ore, Izu-Bonin arc

©2019. Japan Geoscience Union. All Right Reserved.

Organic matters and acid-sulfate alteration in Itomuka Mine, Hokkaido, Japan: implications for the transportation and deposition mechanisms of mercury

*Takuya Echigo[1], Mitsuyoshi Kimata[2], Masahiro Shimizu[2]

1. Graduate School of International Resource Sciences, Akita University, 2. Graduate School of Life and Environmental Sciences, University of Tsukuba

We investigated the ore and hydrothermal alteration minerals and solid organic matters from Itomuka mercury mine which is located in the eastern part of central Hokkaido to examine the transportation and deposition mechanisms of mercury. In addition to the ore minerals, native mercury and cinnabar, powder X-ray diffraction (XRD) analysis showed that the mercury ore consist of quartz, marcasite, alunite, kaolinite and minor amounts of pyrite and smectite. This mineral assemblage suggests that mercury deposition occurred with the advanced argillic alteration under low temperature and low pH condition. Two types of solid organic matter were recognized in quartz vein by yellow-green fluorescence under the ultraviolet radiation: (1) film-shaped organic matter occurring on the surface of quartz vein and (2) globule-shaped organic matter filling pores of quartz vein. Both of these organic matters occur with mercury minerals, cinnabar, native mercury and calomel (Hg_2Cl_2). These organic matters were analyzed with SEM-EDS, micro-X-ray diffraction and micro-FTIR. SEM-EDS analysis showed that film-shaped organic matter is closely associated with mercury and silica minerals though globule-shaped organic matter is not associated with such minerals. Micro-FTIR spectra of both organic matters are similar and suggested that these contain aromatic rings, carboxyl group (-COOH) and adamantine ($C_{16}H_{10}$). Micro-XRD showed that film-shaped organic matter consists quartz, opal- and adamantine crystals and globule-shaped organic matter consists of quartz and amorphous organic matter, respectively. The occurrence of these organic matters suggests that hydrothermal fluid which transported mercury was highly reduced. Because the solubility of Hg in acidic fluid is low, neutral to alkaline fluid seems to have leached mercury from the basement sedimentary rocks of Hidaka formation. The mercury-bearing fluid ascended along the faults in Itomuka formation and oxidized at near the surface. Reduced sulfur (HS^-) in the fluid oxidized into sulfate (SO_4^{2-}) and reduced pH, which resulted in mercury deposition and advanced argillic alteration. Probably, rapid oxidation of ore-forming fluid promoted the precipitation of marcasite, a metastable phase of iron sulfide. The dominance of native mercury over cinnabar indicates that mercury was transported by biphase (liquid+vapor) hydrothermal fluid.

Keywords: Mercury, Organic matter, Advanced argillic alteration

©2019. Japan Geoscience Union. All Right Reserved.

Significances of 12 Ma manganese ores in the Hokuroku district, Akita: unique Mn accumulation and interaction with organic matter during submarine hydrothermal activities

*Yuya Tsukamoto[1], Takeshi Kakegawa[1]

1. Tohoku Univ.

Various Mn ores are found in the Hokuroku district in Akita through the course of the present study. Stratified and veined Mn ores, which lengths are up to 10 cm, are formed during volcanic recession periods (less than 1 Ma) with associated with carbonaceous sediments and local hydrothermal systems. Such short-term precipitation of “pure” Mn ores is unusual, compared to normal Fe-Mn nodules or crusts. In order to understand detailed mechanisms, in particular, role of organic matter, of Mn ore formations, we performed standard mineralogical characterization, magnetic field analyses and oxygen isotope analyses on Mn ores. The first type of Mn ores appear on mudstone and veins in hydrothermally altered hyaloclastite of rhyolite lavas. Detailed geological and geochemical studies revealed that local submarine hydrothermal processes mobilized Mn and Fe in host rocks, Fe-oxides were precipitated first and then discharged Mn were precipitated as oxides (rhodonite and todorokite) on mudstone. $\delta^{18}O_{SMOW}$ value of Mn oxide is + 7.7‰ showing the precipitation temperature less than 112 C. Mn carbonate (rhodochlosite and kutnohorite) also appears in the same region. $\delta^{13}C_{PDB}$values of Mn carbonate were -21‰ (PDB), suggesting interaction with organic matters during intrusive activities of later rhyolite. The second type of Mn ores appear as veins in rhyolitic tuff or stratified lenticular forms with mud/tuffs. Ca. 30 μm colloform structures consisted of organic matter and Mn oxides can be observed. Major Mn mineral in these second type is todorokite. $\delta^{18}O_{SMOW}$value of second types of Mn ores is + 8.5‰ indicating low temperature precipitation of Mn oxides less than 101 C. Magnetic field was detected on Mn oxides in colloform structure by magnetic field microscopy (MFM). Such magnetic fields indicate high cation vacancies and abundance of Mn^{4+}, which are common in biogenic Mn oxides. Formational processes of both Mn ores provide new insight of the unique formational process of Mn ores, especially geological separation from $Fe^{2+}$and interaction with organic matter, in hydrothermal systems at the subseafloor on felsic volcanic setting. Further, this study indicates that low temperature (<100 C) hydrothermal activities can form the Mn ores with high precipitation rates.

Keywords: Manganese, Hokuroku district, Hydrothermal system

©2019. Japan Geoscience Union. All Right Reserved.

Microbial communities around ca. 2.7 Ga submarine hydrothermal fields at the Potterdoal deposit in Abitibi Greenstone Belt, Canada

*Takeru Osato[1], Akizumi Ishida[1], Takeshi Kakegawa[1]

1. Tohoku University

The Archean submarine hydrothermal environment is often considered as a cradle of early life. Large uncertainties still exist as to which microorganisms were active around Archean submarine hydrothermal systems and if hydrothermal communities could be the primary producers for the global biosphere. To approach this problem, we studied ca. 2.7 Ga volcanogenic massive sulfides (VMSs) and associated sedimentary rocks at the Potterdoal deposit in Abitibi Greenstone Belt, Canada. Purposes of the present study are (1) to evaluate which type of microorganisms were active in 2.7 Ga submarine hydrothermal environments, and (2) to find new biosignature in nanoscale analysis of organic matter (OM).
VMS ores were mainly composed of chalcopyrite, sphalerite, pyrrhotite and pyrite, mostly showing layered and sorting textures. They often contained brecciated shale or actinolite or chlorite. Chert and sandstone appeared in the distal area from the VMSs. Most examined VMSs did not have OM, but some samples had up to 0.5 wt.% of carbon concentration. Those OM were found together with actinolite or chlorite or shale fragments trapped in VMSs. Carbon concentration in sedimentary rocks were moderate in general, ranging from 0.0 to 0.9 wt.%C. The thermal alteration temperature was estimated as below 300 ˚C based on the full widths of half maximum of the D1 band in the Raman spectra of kerogen, indicating that less altered features. Overall carbon isotope compositions of kerogen were ranging from -44.6 to -23.6 ‰ (PDB). These values suggest that the presence of contrast microbial ecosystems at this region, utilizing either hydrothermal CH_4 or atmospheric CO_2. Transmitted electron microscope analysis revealed that examined kerogen were mainly composed of immature OM with minor graphene layers. Novel nanostructures of Mo-sulfides stacked with graphene or Fe-sulfides were newly found in immature kerogen structures.These nano-sulfides associated with kerogen may suggest incorporation of biological sulfides in OM during the early diagenesis, possibly giving new evidence of sulfur metabolisms for the early life.

©2019. Japan Geoscience Union. All Right Reserved.

[J] Oral | H (Human Geosciences)：H-RE Resource and Engineering Geology

Wed. May 29, 2019 1:45 PM - 3:15 PM JST | Wed. May 29, 2019 4:45 AM - 6:15 AM UTC | 106 1F

[H-RE16] Resource Geology

convener:Tsubasa Otake(Division of Sustainable Resources Engineering, Faculty of Engineering, Hokkaido University), Daisuke Araoka(Geological Survey of Japan, National Institute of Advanced Industrial Science and Technology), Ryohei Takahashi(Graduate School of International Resource Sciences, Akita University), Tatsuo Nozaki(Research and Development Center for Submarine Resources, Japan Agency for Marine-Earth Science and Technology), Chairperson:Tatsuo Nozaki(JAMSTEC), Ryohei Takahashi(Faculty of International Resource Sciences, Akita University)

Ore deposits containing valuable elements and minerals at high concentrations in supracrustal rocks are formed by the Earth's dynamics including magmatism, hydrothermal activity, metamorphism, and weathering. The formation of ore deposits is also closely associated with global environmental changes and biological evolution in the Earth's history. Involvement of difference academic fields in earth sciences including geology, petrology, geochemistry, mineralogy, and microbiology is required to understand the genesis of ore deposits. The field of resource geology is essential not only for efficient exploration and development of ore deposits but also for better understanding and assessment of hazardous elements that may be caused by the resource development. This session widely covers various topics of field investigation and observation, laboratory experiments, theoretical calculation, development of analytical methods and others related to the supracrustal migration and concentration of elements.

1:45 PM - 2:15 PM JST | 4:45 AM - 5:15 AM UTC

[HRE16-06] Development of nano-fabrication and high-resolution electron microscopy techniques: their possible applications to resource geology

★Invited Papers

*Naotaka Tomioka[1], Satoko Motai[1], Yu Kodama[2], Motoo Ito[1] (1.Kochi Institute for Core Sample Research, Japan Agency for Marine-Earth Science and Technology, 2.Marine Works Japan)

2:15 PM - 2:30 PM JST | 5:15 AM - 5:30 AM UTC

[HRE16-07] Microscopic study on rare earth elements in ion-adsorption type ore of China

*Hiroki Mukai[1], Yoshiaki Kon[1], Kenzo Sanematsu[1], Yoshio Takahashi[2], Motoo Ito[3] (1.National Institute of Advanced Industrial Science and Technology, 2.Graduate School of Science, the University of Tokyo, 3.Kochi Institute for Core Sample Research JAMSTEC)

2:30 PM - 2:45 PM JST | 5:30 AM - 5:45 AM UTC

[HRE16-08] Geochemical features of “invisible gold” in pyrites from the Akeshi and Kasuga deposits, Kagoshima, Japan

*Mizuki Ishida[1], Rurik Romeo[2,3], Mathieu Leisen[2,3], Junji Torimoto[4], Tatsuo Nozaki[4,5,6,7], Kazutaka Yasukawa[1,6], Koichiro Fujinaga[6,1], Kentaro Nakamura[1], Martin Reich[2,3], Yasuhiro Kato[1,6,5] (1.Department of Systems Innovation, School of Engineering, The University of Tokyo, 2.Department of Geology and Andean Geothermal Center of Excellence (CEGA), FCFM, 3.Millennium Nucleus for Metal Tracing Along Subduction, FCFM, Universidad de Chile, FCFM, 4.Japan Agency for Marine-Earth Science and Technology (JAMSTEC), 5.Frontier Research Center for Energy and Resources, School of Engineering, The University of Tokyo, 6.Ocean Resources Research Center for Next Generation, Chiba Institute of Technology, 7.Department of Planetology, Graduate School of Science, Kobe University)

2:45 PM - 3:00 PM JST | 5:45 AM - 6:00 AM UTC

[HRE16-09] Hydrothermal Mineral Assemblage of the Southwest Prospect, in the Vicinity Sto. Tomas II (Philex) Porphyry Cu-Au Deposit, Baguio District, Philippines

*Avriel Venis Literal Cirineo[1], Akira Imai[2], Ryohei Takahashi[1], Noel C. Oliveros[3], Redempta P. Baluda[3], Victor B. Maglambayan[3], Roy Ronald C. Luis[3], Maria Lourdes M. Faustino[3] (1.Graduate School of International Resource Sciences, Akita University, 2.Faculty of Engineering, Kyushu University, 3.Philex Mining Corporation)

3:00 PM - 3:15 PM JST | 6:00 AM - 6:15 AM UTC

[HRE16-10] Characteristics and genesis of weathering REE deposits

★Invited Papers

*Kenzo Sanematsu[1] (1.Mineral Resource Research Group, Institute for Geo-Resources and Environment, Geological Survey of Japan, National Institute of Advanced Industrial Science and Technology)

Development of nano-fabrication and high-resolution electron microscopy techniques: their possible applications to resource geology

*Naotaka Tomioka[1], Satoko Motai[1], Yu Kodama[2], Motoo Ito[1]

1. Kochi Institute for Core Sample Research, Japan Agency for Marine-Earth Science and Technology, 2. Marine Works Japan

In order to explore accessible and profitable natural resources, scientific elucidation of their origin and evolution are an essential issue. The natural resources often have fine-grained textures and minute mineral/fluid inclusions in the host minerals. Therefore, microanalysis is required to clarify their mineralogical and geochemical characteristics in detail. Focused-ion beam (FIB) microfabrication and transmission electron microscopy (TEM) are potentially effective techniques for this purpose. FIB allows to precisely extract portions of interest in sub-micron scale from various types of samples. Using TEM, microtextural, chemical, and crystallographic information can be obtained in nano-scale spatial resolution from ultrathin-film (100–200 nm) samples. With taking these technical advantages, state-of-the-art FIB and TEM at JAMSTEC KOCHI have been applied to a variety of geosciences including clay mineralogy [1], biomineralization [2], mantle rheology [3], and meteoritics [4].

One of uniqueness of the FIB/TEM laboratory at KOCHI is a combined FIB-FESEM instrument equipped with an energy dispersive spectrometer (EDS) and a cryo-holder system [5]. We are currently developing a FIB-fabrication scheme of fluid inclusions in minerals such as olivine and halite, so that those fluids are exposed in frozen state for their in-situ chemical analysis including X-ray elemental mapping using EDS [6]. 3D tomography by micro X-ray CT is effective to visualize distribution of fluid inclusions especially in nontransparent minerals prior to nanofabrication and analysis by the FIB-FESEM system.

The nanoscale occurrence of fluid (as voids) and mineral inclusions can be further characterized by high-resolution TEM. This technique would be useful for mineralogical analysis of fine-grained resource materials such as deep-sea mud containing abundant rare-earth elements [7] and manganese deposits. As a typical example, we have mineralogically characterized several-micron-sized Mn-rich microparticles recently discovered in seafloor sediments, and found vernadite-like mineral therein based on their electron diffraction patterns and elemental mappings [8]. We are further developing the linkage fabrication/analysis scheme to extend toward more comprehensive sample analysis including trace elemental and isotopic analyses using NanoSIMS [9]. These microanalysis techniques would play a key role for our better understanding of environments for the formation of resource materials.

References: [1] Ijiri et al. (2018) *Front. Earth. Sci.*,doi.org/10.3389/feart.2018.00036. [2] Shiraishi et al. (2017) *Sci. Rep.*, 7, 11805. [3] Yamamoto et al. (2017) *Phys. Chem. Minerals.*, 44, 247. [4] Tomioka & Okuchi (2017)*Sci. Rep.*, 17351. [5] Kodama et al. (2019) (submitted) [6] Kodama et al. (2019) *JpGU* [7] Takaya et al. (2018) *Sci. Rep.*, 8, 5763. [8] Uramoto et al. (2019)*Nature Comm.*(in press)[9] Ito et al. (2017) *LPSC*, XLVIII, #1776.

Keywords: microanalysis, Transmission electron microscopy, Focused ion beam

©2019. Japan Geoscience Union. All Right Reserved.

Microscopic study on rare earth elements in ion-adsorption type ore of China

*Hiroki Mukai[1], Yoshiaki Kon[1], Kenzo Sanematsu[1], Yoshio Takahashi[2], Motoo Ito[3]

1. National Institute of Advanced Industrial Science and Technology, 2. Graduate School of Science, the University of Tokyo, 3. Kochi Institute for Core Sample Research JAMSTEC

At present, China constitutes more than 80 % of the rare earth elements (REE) production in the world. Among REE ores, ion-adsorption type ones existing mainly in southern China are a major supply source of heavy REE (HREE) which are especially valuable. The ion-adsorption type ore is formed under weathering of the underlying parent granite rocks. This ore typically contains more than 50 % of ion-exchangeable REE that can be extractable with electrolyte solution such as ammonium sulfate $(NH_4)_2SO_4$ solution. It has been estimated that permanent negative charge on clay minerals, such as kaolinite, leads to surface adsorption of REE in the ore. However, the direct observations or analyses for the individual minerals have been rarely conducted due to the relatively low concentrations of REE (<2000 ppm). In the present study, we analyzed weathered granite collected from an ion-adsorption ore in Dingnan County, Jiangxi Province, China on a submicroscopic scale by using various experimental apparatuses.
XRD measurements indicated that the weathered granite is mainly composed of quartz, K-feldspar and kaolinite. The results of SEM-EDS and LA-ICP-MS measurements showed that “kaolinitic particle” is abundant with REE compared to the other minerals. These results suggest that the kaolinitic particles are major reservoir of REE in the ore. The elemental mapping for a kaolinitic particle by LA-ICP-MS showed that each element is distributed heterogeneously in the particle. The SEM-EDS analyses also suggested that the kaolinitic particle is composed of several minerals. For further micro-analyses, cross sections were processed from the kaolinitic particles by FIB. XAFS study on the cross sections suggested that REE are basically hydrated in the particle. STEM-EDS analyses revealed that the kaolinitic particle contains illite and hematite in addition to kaolinite. Considering general weathering process, it can be assumed that K-feldspar was altered into illite and further into kaolinite during chemical weathering. Elemental mapping with high spatial resolution by NanoSIMS clarified that REE are distributed in kaolinite and illite.

Keywords: Ion-adsorption type rare earth ore, LA-ICP-MS, FIB-TEM, XAFS, NanoSIMS

©2019. Japan Geoscience Union. All Right Reserved.

Geochemical features of “invisible gold” in pyrites from the Akeshi and Kasuga deposits, Kagoshima, Japan

*Mizuki Ishida[1], Rurik Romeo[2,3], Mathieu Leisen[2,3], Junji Torimoto[4], Tatsuo Nozaki[4,5,6,7], Kazutaka Yasukawa[1,6], Koichiro Fujinaga[6,1], Kentaro Nakamura[1], Martin Reich[2,3], Yasuhiro Kato[1,6,5]

1. Department of Systems Innovation, School of Engineering, The University of Tokyo, 2. Department of Geology and Andean Geothermal Center of Excellence (CEGA), FCFM, 3. Millennium Nucleus for Metal Tracing Along Subduction, FCFM, Universidad de Chile, FCFM, 4. Japan Agency for Marine-Earth Science and Technology (JAMSTEC), 5. Frontier Research Center for Energy and Resources, School of Engineering, The University of Tokyo, 6. Ocean Resources Research Center for Next Generation, Chiba Institute of Technology, 7. Department of Planetology, Graduate School of Science, Kobe University

The occurrence of gold in ore is one of the most important information in gold deposit research. This information allows us to optimize beneficiation and smelting processes, as well as providing valuable insights into the mineralization mechanism, which can improve exploration strategies (e.g., [1]).

In hydrothermal gold deposits, gold is not always visible as native gold, electrum, caraverite (AuTe2) or other gold minerals. In many cases, it also exists as submicrometer-size inclusions and solid solution in other minerals, which is so-called “*invisible gold*” [2]. Pyrite is the most ubiquitous and well-known host mineral for this invisible gold, and its trace element geochemistry has been increasingly recognized as a useful tool to understand the mineralization processes (e.g., [3]).

In this study, we report the geochemical features of invisible gold in pyrites collected from the Akeshi and Kasuga deposits. These deposits, located in the southern part of the Kagoshima Prefecture, Japan, are currently under operation, and are classified as high-sulfidation gold deposits. In both Akeshi and Kasuga, gold minerals are only reported from high-grade ores, and other hosts of gold in lower-grade ores remain still uncertain [4]. Pyrite is the most common sulfide mineral in these deposits. Here, we report the results of EPMA (Electron Probe Micro Analyzer) and LA-ICP-MS (Laser Ablation Inductively Coupled Plasma Mass Spectrometry) trace element analyses of pyrite, in order to determine their mineralization processes.

[1] Morishita et al. (2018) *Ore Geology Reviews*, **95**, 79-93.

[2] Cook and Chryssoulis (1990) *Canadian Mineralogist*, **28**, 1-16.

[3] Román et al. (2019) *Geochimica et Cosmochimica Acta*, **246**, 60-85.

[4] Nakamura et al. (1994) *Resource Geology*, **44**(3), 155-171.

Keywords: Pyrite, Trace elements, Invisible gold, High-sulfidation deposit, Nansatsu-type

©2019. Japan Geoscience Union. All Right Reserved.

Hydrothermal Mineral Assemblage of the Southwest Prospect, in the Vicinity Sto. Tomas II (Philex) Porphyry Cu-Au Deposit, Baguio District, Philippines

*Avriel Venis Literal Cirineo[1], Akira Imai[2], Ryohei Takahashi[1], Noel C. Oliveros[3], Redempta P. Baluda[3], Victor B. Maglambayan[3], Roy Ronald C. Luis[3], Maria Lourdes M. Faustino[3]

1. Graduate School of International Resource Sciences, Akita University, 2. Faculty of Engineering, Kyushu University, 3. Philex Mining Corporation

Overprinting relationship between intrusive rocks, diatreme-breccias and mineralized porphyry-type veinlets are documented in the Southwest prospect was recently discovered along the contact of the basement Pugo metavolcanics and conglomerates of the Zigzag formation, overlain by dacitic tuff termed as the Keratophyre (KTP). The prospect is located at the southwestern periphery of the Sto. Tomas II orebody, a 60-year old porphyry Cu-Au mine being operated by Philex Mining Corporation (PMC).
At least four intrusive rocks were recognized. In chronological order, they are the: (1) coarse-grained biotite quartz diorite (ODP –Old Diorite Porphyry), (2) fine-grained quartz diorite porphyry (EMD -Early Mineralization Diorite), (3) medium-grained porphyritic hornblende quartz diorite (LD –Late Diorite) and (4) hornblende andesite porphyry (DP –Diorite Porphyry). Meanwhile, at least five breccia facies were identified: (1) Phreatomagmatic Breccia facies 1 or PMBx1, (2) Phreatomagmatic facies 2a or PMBx2a, (3) Phreatomagmatic Breccia facies 2b or PMBx2b, (4) Early Mineralization Diorite Breccia or EMDBx and (5) Diorite Porphyry Breccia or DPBx. The PMBx facies are polymictic breccias with chaotic mixture of clasts set in a matrix composed of rock flour of earlier formed rocks and juvenile tuffaceous matrix. They are sub-vertical pipes that flare upwards and may represent diatreme breccias (Sillitoe, 1985, Baker et al., 1986, Lawless and White, 1990). On the other hand, EMDBx and DPBx are intrusion breccias that were formed during the emplacement of their intrusive equivalents (Sillitoe, 1985). Porphyry-type veinlets are observed overprinting ODP, EMD and PMBx1, while at the same time, quartz vein fragments are included in the latter. These veinlets are also commonly found along the contacts between LD and the PMBx1. PMBx2a and PMBx2b crosscut all the earlier intrusions and breccias. Spatial and temporal associations suggest syn-mineralization timing of the EMD, PMBx1 during porphyry-type quartz veining, while LD and some of the porphyry-type veinlets associated with the LD suggest a late-mineralization timing.
Intense potassic alteration is characterized by secondary biotite-quartz-magnetite-anhydrite-chalcopyrite-bornite. It is exhibited by EMD and andesitic clasts of Pugo Metavolcanics occurring as clasts in the diatreme breccias. It is also well-developed in the EMD at the deeper central portion of the prospect, in the matrix of the adjacent EMDBx and PMBx1. Secondary biotite is present as fine disseminations in the groundmass and as polygrain aggregates completely altering former ferromagnesian minerals, such as hornblende. It is often accompanied with quartz, anhydrite, magnetite and copper iron sulfides. Occasional K-feldspar, chlorite, illite and epidote are present in the assemblage. Associated sheeted quartz and granular quartz veinlets indicated a wide range of liquid-vapor homogenization temperature (T_h(L-V)) from 436˚C to 578˚C and 461˚C to >720˚C, respectively, and salinities from 41 to 43 wt% $NaCl_{equivalent}$ and 37 to 43 wt% $NaCl_{equiv.}$ This alteration is overprinted by illite-chlorite-carbonate-magnetite±K-feldspar alteration with abundant chalcopyrite and bornite. It pervasively overprinted the quartz stockwork zone hosted in the PMBx1 adjacent to the EMD at the central deeper portion of the prospect. Associated banded quartz veinlets indicated Th(L-V) >720˚C and salinities ranging from 55 to 70 wt% $NaCl_{equiv.}$ The shallower portions dominated by the later breccias were altered by chlorite-illite-pyrite±chalcopryite with associated quartz-gypsum cement. Lastly, propylitic

©2019. Japan Geoscience Union. All Right Reserved.

alteration is exhibited by LD. It is characterized by chlorite-epidote-calcite±illite. Associated crystalline quartz-chlorite veinlets indicated lower Th(L-V) 246˚C and lower salinity of 40 wt% $NaCl_{equivalent.}$
K-Ar ages determined on the secondary biotite of the EMD sample that exhibited intense hydrothermal biotitization typical at the potassic core in Southwest and on the hornblende grains of LD that showed no hydrothermal alteration are both 3.5Ma. This indicates that the hydrothermal biotitization prevalent in the potassic alteration in EMD and the emplacement of the LD could have happened in a single magmatic-hydrothermal event. This may also indicate that the timing between the potassic alteration and intrusion are close in Southwest, and also constrained an older age than the mineralization at the Sto. Tomas II orebody (Imai, 2001, Waters et al., 2011).

Keywords: Baguio district, Southwest prospect, Sto. Tomas II orebody, potassic alteration, overprinting porphyry-type veinlets, diatreme breccias

©2019. Japan Geoscience Union. All Right Reserved.

Characteristics and genesis of weathering REE deposits

*Kenzo Sanematsu[1]

1. Mineral Resource Research Group, Institute for Geo-Resources and Environment, Geological Survey of Japan, National Institute of Advanced Industrial Science and Technology

The world rare earth deposits can be classified into carbonatite, alkaline-rocks related, placer and ion-adsorption types. Rare earth elements (REE) which are present as trace elements in the mantle and crusts can be geologically condensed by either or both of the formation of alkaline magma and weathering. This talk reviews on the characteristics and genesis of weathering REE deposits consisting of weathered carbonatites, placer and ion-adsorption type deposits.

Weathered carbonatite deposits are characterized by high REE grades. Carbonatites are high in REE (>1%, approximately) and these elements are condensed by dissolution of carbonate minerals during chemical weathering. The dominant REE minerals are primary and secondary phosphate minerals including monazite. The ores are rich in LREE (light REE) and Th and poor in HREE (heavy REE), reflecting compositions of the unweathered carbonatites. REE minerals are generally fine-grained compared to unweathered carbonatites and this may influence the recovery of REE during mineral processing.

Placer deposits are formed by weathering and erosion of igneous and metamorphic rocks and deposition of heavy minerals in alluvium and beach sands. Placer ore minerals are mainly Ti minerals (ilmenite and rutile), zircon and cassiterite. REE-bearing placer deposits contain monazite and lesser amount of xenotime. Although the bulk REE grade is low, the ore consisting of sand and gravels can be mined and heavy minerals are processed easily. This deposit type was the leading world REE producer in the world until 1965. Since monazite is the dominant REE mineral, placer deposits are rich in LREE and Th and poor in HREE. Zircon is the common HREE-bearing mineral in placer deposits, however they are not economically extractable.

Contrasting to the two types of residual deposits mentioned above, ion-adsorption type deposits are characterized by REE adsorbed electrostatically on the surface of clays (not in the crystal structure of minerals) and they are extractable by ion exchange from the REE ores. The ores, called ion-adsorption ores, are formed mainly from granite by chemical weathering. Although these deposits are generally low in REE, they can be rich HREE. Parent granites contain weatherable REE bearing minerals such as fluorocarbonates (e.g., bastnaesite, synchysite) and REE-bearing silicates (e.g., allanite, titanite) and LREE/HREE ratios of these minerals constrain those of ion-adsorption ores. In contrast, parent granite rich in phosphate minerals (e.g., monazite and apatite) tends to form weathered granites with low ion-exchangeable REE because most REE are incorporated in phosphate minerals which resistant to chemical weathering. Kaolinite, halloysite, illite and vermiculite appear to have ion-exchangeable REE. Since the ores and extracted solutions are generally low in Th, ion-adsorption type deposits are poor in Th compared with the other REE deposits.

Keywords: rare earths, weathering, deposits, resources, adsorption

©2019. Japan Geoscience Union. All Right Reserved.

[J] Poster | H (Human Geosciences)：H-RE Resource and Engineering Geology

Wed. May 29, 2019 3:30 PM - 5:00 PM JST | Wed. May 29, 2019 6:30 AM - 8:00 AM UTC | Poster Hall International Exhibition Hall8, Makuhari Messe_14

[H-RE16] Resource Geology

convener:Tsubasa Otake(Division of Sustainable Resources Engineering, Faculty of Engineering, Hokkaido University), Daisuke Araoka(Geological Survey of Japan, National Institute of Advanced Industrial Science and Technology), Ryohei Takahashi(Graduate School of International Resource Sciences, Akita University), Tatsuo Nozaki(Research and Development Center for Submarine Resources, Japan Agency for Marine-Earth Science and Technology)

Ore deposits containing valuable elements and minerals at high concentrations in supracrustal rocks are formed by the Earth's dynamics including magmatism, hydrothermal activity, metamorphism, and weathering. The formation of ore deposits is also closely associated with global environmental changes and biological evolution in the Earth's history. Involvement of difference academic fields in earth sciences including geology, petrology, geochemistry, mineralogy, and microbiology is required to understand the genesis of ore deposits. The field of resource geology is essential not only for efficient exploration and development of ore deposits but also for better understanding and assessment of hazardous elements that may be caused by the resource development. This session widely covers various topics of field investigation and observation, laboratory experiments, theoretical calculation, development of analytical methods and others related to the supracrustal migration and concentration of elements.

[HRE16-P01] Mineral Chemistry and Petrogenesis of the Mazua Ultramafic Massif, Northern Mozambique: Constraints on the Associated Fe-Ti Oxides Deposit

*David Augusto Bene Unganai[1], Akira Imai[2], Ryohei Takahashi[1], Daud Liace Jamal[3], Takashi Hoshide[1] (1.Akita University, 2.Kyushu University, 3.Eduardo Mondlane University)

[HRE16-P02] Ni-Cu-PGM Mineralisation in the Bastard Reef and Merensky Reef of the Flatreef section, Turfspruit Farm, Northern Limb, Bushveld Igneous Complex, South Africa.

*MOKHIRI MALESELA MAKHAFOLA[1], Tsubasa Otake[1], Tsutomu Sato[1], Danie Grobler[2] (1.Hokkaido University, 2.Ivanplats Pty. Ltd)

[HRE16-P03] Characteristics of Porphyry Copper-Gold Mineralization in the Grasberg Mine, Papua, Indonesia

*Kanehiko Kawasaki[1], Kotaro Yonezu[2], Reza Al Furqan[3], Benny Bensaman[4], Mega Fatimah Rosana[4] (1.Kyushu University Facurity of Engineering, 2.Deaprtment of Earth Resources Engineering, Faculty of Engineering, Kyushu University, 3.PT Freeport Indonesia, 4.Department of Geology, Padjadjaran University)

[HRE16-P04] Formation of Ni-bearing minerals during chemical weathering of ultramafic rocks in Myanmar

*Ayaka Murofushi[1], Akane Ito[1], Tsubasa Otake[2], Kenzo Sanematsu[3], Kyaw Zay Ya[1,4], Tsutomu Sato[2] (1.Graduate school of Engineering, Hokkaido University, 2.Facility of Engineering, Hokkaido University, 3.Geological Survey of Japan, National Institute of Advanced Industrial Science and Technology, 4.Department of Geological Survey and Mineral Exploration)

[HRE16-P05] Geological Characteristics and Mineralogy of the Makorungo and Nalia Gold Prospects, Northeastern Mozambique

*Manuel Augusto Manuel Nopeia[1], Ryohei Takahashi[1], Akira Imai[2], Daud Liace Jamal[3] (1.Akita University, 2.Kyushu University, 3.Eduardo Mondlane University)

[HRE16-P06] Geochemical features of the Hishikari epithermal gold deposit based on simultaneous multi-element analysis

*Sota Nishida[1], Mizuki Ishida[1], Kazutaka Yasukawa[1,2], Kentaro Nakamura[1], Koichiro Fujinaga[2,1], Yasuhiro Kato[3,1,2] (1.Department of Systems Innovation, School of Engineering, The University of Tokyo, 2.Ocean Resources Research Center for Next Generation, Chiba Institute of Technology, 3.Frontier Research Center for Energy and Resources, School of Engineering, The University of Tokyo)

[HRE16-P07] Transformation of ore minerals and their geochemical signatures in submarine hydrothermal ore deposits in Izena Hole, Okinawa Trough

*IKESHIMA TAKURO[1], Tsubasa Otake[1], Tsutomu Sato[1], Akane Ito[1], Shuji Ono[1], Jun-ichiro Ishibashi[2], Tatsuo Nozaki[3], Hidenori Kumagai[3], Lena Maeda[3] (1.Hokkaido University, 2.Kyushu University, 3.Japan Agency for Marine-Earth Science and Technology (JAMSTEC))

[HRE16-P08] Geochemical behavior of heavy metals during wastewater treatment in Chingola Stream of the Zambia Copperbelt

*Cryton Phiri[1], Daiki Shimazui[2], Tsutomu Sato[2], Tsubasa Otake[2] (1.University of Zambia, 2.Hokkaido University)

Mineral Chemistry and Petrogenesis of the Mazua Ultramafic Massif, Northern Mozambique: Constraints on the Associated Fe-Ti Oxides Deposit

*David Augusto Bene Unganai[1], Akira Imai[2], Ryohei Takahashi[1], Daud Liace Jamal[3], Takashi Hoshide[1]

1. Akita University, 2. Kyushu University, 3. Eduardo Mondlane University

Economic magmatic Fe-Ti-V deposits are commonly hosted by mafic-ultramafic intrusions and massif-type anorthosites. The Mazua Ultramafic Massif (MUM), located in northeast Mozambique, is one of the most promising intrusions that host Fe-Ti oxides ore deposit in the country. The orebody is a 10-km long ilmenite-rich hornblende pyroxenite, which is in sharp contact with a banded biotite gneiss. The ore commonly occurs as layers/lenses, massive and dissemination in host rocks. The average grade of the ore is 27 wt.% TiO_2, 35 wt.% Fe_2O_{3tot} and ~2 ppm V (Norconsult Consortium, 2007). However, detailed studies regarding the petrogenesis of the intrusion and its related Fe-Ti oxides ores are still scarce. Thus, we carried out microprobe and petrographic analyses to elucidate these issues.

The hornblende pyroxenite consists of ilmenite, diopside, and magnesiohornblende as main phases. Petrography reveals that the Fe-Ti oxides and pyroxenes are syngenetic. The composition of diopside ($Wo_{43.5–48.5}En_{36.0–41.4}Fs_{11.1–20.5}$) and occurrence of magnesiohornblende suggest tholeiitic, non-alkaline and hydrous (>3.0 wt.% H_2O) parental ultrabasic melt. In addition, the absence of olivine and orthopyroxene supported by wide range of #Mg in diopside (63.8–78.7) and magnesiohornblende (68.9–85.4) confirms the idea that the magma which formed MUM was differentiated.

Texture and variable mineral composition suggest that Fe-Ti oxides underwent extensive subsolidus re-equilibration during cooling, supported by the following evidences: (1) The Fe-Ti oxides show different types of micro-intergrowths such as (a) lamellae of ilmenite with clothing textures hosted in magnetite, (b) fine pattern exsolution lamellae (trellis) and blebs of aluminous spinel in magnetite, (c) reaction rims of aluminous spinel distributed along the boundary between magnetite and ilmenite and (d) re-equilibration textures involving Fe-Ti oxides and silicate phases. (2) The very low MgO content of primary ilmenite (<2 wt.%) is interpreted as a result of postcumulus oxide-silicate re-equilibration involving clinopyroxene and amphibole. (3) Determination of equilibrium conditions using geothermobarometer by Spencer & Lindsley (1981) indicates that Mazua Fe-Ti oxides last equilibrated at subsolidus temperatures (<600 ˚C) and high oxygen fugacity ($\log fO_2 > -20.0$ bars). The reconstruction of the primary composition of Fe-Ti oxides, by reintegration of exsolved with the host phases, leads to primary titanomagnetite with an ulvospinel component of ~20 mol%.

©2019. Japan Geoscience Union. All Right Reserved.

Ni-Cu-PGM Mineralisation in the Bastard Reef and Merensky Reef of the Flatreef section, Turfspruit Farm, Northern Limb, Bushveld Igneous Complex, South Africa.

*MOKHIRI MALESELA MAKHAFOLA[1], Tsubasa Otake[1], Tsutomu Sato[1], Danie Grobler[2]

1. Hokkaido University, 2. Ivanplats Pty. Ltd

The Bushveld Igneous Complex of South Africa is the largest layered igneous complex in the world and it is the current leading producer of platinum group metals globally. The Northern Limb is the northern extension of the complex currently mined (open pit) for a Ni-Cu-PGM rich deposit hosted in a lithologically variable igneous sequence dipping at about 45 degrees and has been intensively affected by contamination and alteration termed the Platreef (Kinnaird et al, 2005). Westwards of the Platreef lies the Flatreef section, which is a recently discovered sub-horizontal down-dip extension of the Platreef. It hosts the Ni-Cu-PGM rich deposit in two successive high-grade reefs termed the Bastard Reef and the Merensky Reef that are amenable for underground mining methods (Grobler et al, 2018). The Flatreef has not been studied in detail and this study reports on the petrographical and semi-quantitative investigations done on the mineralized reefs.
Logging and petrographical investigations revealed the Bastard Reef to comprise a fine to medium-grained equigranular feldspathic orthopyroxenite. Several metres below the Bastard Reef lies the Merensky Reef, which has been subdivided into 3 different units (M2, M1U and M1L) mainly based on mineralogical and textural variations. The M2 is the uppermost layer comprising medium to coarse-grained equigranular orthopyroxenite, denoted by cumulus orthopyroxene and is bound irregularly by a chromite seam at its top contact. The M2 orthopyroxenite is underlain by the M1U denoted by a cumulate textured pegmatoidal orthopyroxenite and is commonly bound by a chromite stringer at its top contact and a less consistent one at its base. The M1L, which is laterally less continuous, comprises a poikilitic textured harzburgite and/or varied-textured olivine-bearing orthopyroxenite. SEM analysis revealed sulphide mineral assemblages in the reefs usually comprising pyrrhotite, pentlandite and chalcopyrite as fine to medium-grained disseminations, blebs and net-textured sulphides. PGM mineralisation comprise a wide range of PGMs, mostly Platinum and Palladium dominated, grouped into bismithotellurides (-Bi-Te), antimonides, arsenides, Fe and Sn alloys, sulphides, as well as laurite (RuS_2) and Ir-Ru-Rh-Pt-Pd sulfoarsenides alongside chromite seams. Semi-quantitative analysis illustrates the Flatreef section to be an undisturbed magmatic sequence that is much less affected by assimilation and contamination. It retains much of its magmatic characteristics and provides a great opportunity to furthermore study magmatic processes that resulted in the formation of such an enigmatic deposit.

References

Grobler, D.F., Brits, J.A.N., Maier, W.D. and Crossingham, A. (2018) Litho- and Chemostratigraphy of the Flatreef PGE deposit, northern Bushveld Complex. Mineralium Deposita, 126, 1-26.

Kinnaird, J.A., Hutchinson, D., Schurman, L., Nex, P. and de Lange, R. (2005) Petrology and Mineralisation of the Southern Platreef: Northern Limb of the Bushveld Complex, South Africa. Mineralium Deposita, 40, 576-597.

Keywords: Ni-Cu-PGM, Bushveld Igneous Complex, Flatreef Section, Northern Limb

©2019. Japan Geoscience Union. All Right Reserved.

©2019. Japan Geoscience Union. All Right Reserved.

Characteristics of Porphyry Copper-Gold Mineralization in the Grasberg Mine, Papua, Indonesia

*Kanehiko Kawasaki[1], Kotaro Yonezu[2], Reza Al Furqan[3], Benny Bensaman[4], Mega Fatimah Rosana[4]

1. Kyushu University Facurity of Engineering, 2. Deaprtment of Earth Resources Engineering, Faculty of Engineering, Kyushu University, 3. PT Freeport Indonesia, 4. Department of Geology, Padjadjaran University

The Grasberg-Ertsberg district is located in the west of the remote highlands of the Sudirman Mountain in the province of Papua, Indonesia. The district is well-known copper-gold mine area as “Grasberg mine” in the world. In this district, Pliocene intrusive rocks host copper and gold mineralization. These intrusive rocks are named “Grasberg Igneous Complex” (GIC), which is composed of Kali Intrusion (KI), Main Grasberg Intrusion (MGI) and Dalam Intrusion (DI). The purpose of this study is to clarify characteristics of ore forming fluid and copper-gold mineralization, especially in the western part of MGI hosted porphyry mineralization in the Grasberg district.
In this study, all samples used is collected from a drill core, AM-30-08H-05. It penetrates KI and DI through MGI. Petrography revealed that Cu bearing mineralization style can be divided into three types: Cu(-Fe) sulfides vein type in quartz vein, Cu(-Fe) sulfides veinlet type and disseminated Cu(-Fe) sulfides type. Chalcopyrite is major ore mineral in vein type and veinlet type. In these types, bornite is often distributed in or by the chalcopyrite, therefore it could be explained by exsolution from intermediate solid solution and bornite solid solution. In disseminated Cu(-Fe) sulfides, chalcopyrite and bornite is major and primary Cu bearing minerals. They are often co-existing, therefore they also seemed to be exsoluted from intermediate solid solution and bornite solution. However, the other Cu bearing minerals (chalcocite, covellite, digenite) sometimes form foliated texture with chalcopyrite and bornite, clearly indicating that those Cu bearing minerals are formed by replacement from bornite. In addition, rim of bornite is sometimes replaced by chalcocite, covellite and digenite, suggesting interaction with ground water after primary mineralization. Native gold is precipitated in chalcopyrite vein in quartz vein and in disseminated chalcopyrite. In chalcopyrite vein, native gold is precipitated with bornite and merenskyite, which is determined by SEM-EDX as $Pd_{1.0}Te_{2.0}$. Merenskyite is newly identified in the western part of GIC, while it has already reported in northern and southern part of GIC. Merenskyite is a common in ultramafic rocks related to PGE mineralization (e.g., merensky reef in Bushveld Igneous Complex). Precipitation of merenskyite in this area suggests the presence and contribution of primitive mafic magma. The fact merenskyite can be observed widely in MGI, the contribution may cover the whole MGI.
Since clear cross-cutting relationship among quartz veins is not observed in this research, SEM-Cathodoluminescence observation is conducted for identifying quartz crystal growth pattern in quartz vein, hosting chalcopyrite vein. Luminescence contrast anomaly can be recognized in quartz vein, suggesting that there are two different occurrence of quartz veins which are early quartz vein and later quartz vein. Only late quartz vein is associated with chalcopyrite vein. Fluid inclusion microthermometry in early quartz vein was conducted. Homogenization temperature of fluid inclusion in early quartz is over 600 degree Celsius with high salinity (61.32 wt%). These results are harmonious with previous research, suggesting weak or none of Cu and Au mineralization is associated with early quartz vein, however late quartz vein introduced intensive copper-gold mineralization.

Keywords: Grasberg Mine, Porphyry Copper Deposit, Mineralization

©2019. Japan Geoscience Union. All Right Reserved.

Formation of Ni-bearing minerals during chemical weathering of ultramafic rocks in Myanmar

*Ayaka Murofushi[1], Akane Ito[1], Tsubasa Otake[2], Kenzo Sanematsu[3], Kyaw Zay Ya[1,4], Tsutomu Sato[2]

1. Graduate school of Engineering, Hokkaido University, 2. Facility of Engineering, Hokkaido University, 3. Geological Survey of Japan, National Institute of Advanced Industrial Science and Technology, 4. Department of Geological Survey and Mineral Exploration

Ni laterite deposit, an important resource for Ni, is formed by chemical weathering of ultramafic rocks under tropical climate conditions. Whereas many studies have aimed to understand the formation processes of Ni laterites in Indonesia and Philippines, few studies have investigated those in Myanmar, which also has a high potential of Ni laterite resources. The highest grade of Ni in a weathering profile is usually found in a saprolite zone, a weakly weathered section underlain by intensively-weathered laterite zone. Mobilization of Ni from the bedrock as well as laterite zone together with Fe has been proposed to be an important process for Ni enrichment in saprolite zone (e.g., Golightly, 2010). However, formation of various Ni-bearing minerals in saprolite zone (Tauler et al., 2017) may also govern the Ni enrichment though the common Ni-bearing mineral in saprolite zone is secondary-formed serpentine (Ser-II). It is important to understand the formation processes of Ni laterite deposits for efficient exploration and mine development. Therefore, in this study, we are focused on the formation of secondary minerals at different weathering degrees and its relationship to Ni enrichment during chemical weathering of ultramafic rocks in Myanmar by investigating 6 different weathering profiles in the Western and Central Ophiolite Belts.

The results of the bulk chemical analysis by XRF show that Ni is concentrated in saprolite zones up to 1.6 wt% as chemical weathering progresses as indicated by thickness of profiles and depletion of major elements (e.g., Mg). Ni is associated more closely with 0.2-2 μm fraction (e.g., clay minerals) of the samples as Ni concentration in this fraction was determined by acid digestion and ICP-AES. The results of mineralogical analysis by XRD and petrographic microscope show that minerals formed in saprolite zones varies depending on the degree of weathering regardless that all the bedrocks are serpentinite. Whereas smectite dominates in the saprolite zone of the least weathered profile, both smectite and Ser-II were present in the saprolite zone of the most weathered profile. This suggests that smectite is formed at the initial stage of chemical weathering of the ultramafic rocks in Myanmar. However, the results of SEM-EDS analysis show that Mn-oxide (e.g., asbolane) is the main mineral concentrating Ni in the least weathered profile whereas secondary silicate minerals (e.g., Ser-II, smectite, unidentified Fe-Ni silicates) are the main minerals in the most weathered profile. Therefore, Ni is preferentially associated with Mn-oxide possibly because of a strong electrostatic interaction. However, as weathering progresses and Mn-oxide dissolved away, Ni is enriched into secondary silicate minerals (e.g., Ser-II, smectite). No preferential incorporation of Ni was observed between Ser-II and smectite. Further progress in chemical weathering may result in the transformation of other silicate minerals into Ser-II, which would be then the main Ni-bearing mineral in Ni laterite deposit in Myanmar.

©2019. Japan Geoscience Union. All Right Reserved.

Geological Characteristics and Mineralogy of the Makorungo and Nalia Gold Prospects, Northeastern Mozambique

*Manuel Augusto Manuel Nopeia[1], Ryohei Takahashi[1], Akira Imai[2], Daud Liace Jamal[3]

1. Akita University, 2. Kyushu University, 3. Eduardo Mondlane University

The northeastern Mozambique is composed of medium-high grade metamorphic complexes of the Mozambique Belt, intruded by Neoproterozoic-Paleozoic granitoids (Norconsult, 2007). Mozambique Belt (MB) is a part of the East African Orogeny and has been associated with a large variety of mineralization, including base metals, gemstones, and gold (Lächelt, 2004). The lack of studies on gold deposits associated with metamorphic terrains in Mozambique weakens the discovery and further exploration of gold. This study focuses on the Makorungo and Nalia gold prospects, northeastern Mozambique, where artisanal and small-scale mining of placer and primary gold is conducted mainly by local people. These prospects belong to Xixano complex, interpreted as a Pan-African nappe, which is composed of supercrustal rocks, enveloping mafic and ganulitic rocks (Viola et al, 2008). This study aims to reveal the geological and mineralogical characteristics of the gold prospects to better understand the ore-forming process. Field observation and laboratory analysis, including petrography of host rocks and ores, and whole-rock and ore chemistry were applied. Quartz veins parallel and at low angle to amphibolite foliation host the gold mineralization in the Nalia and Makorungo prospects. The amphibolites in the Nalia prospect are strongly foliated and composed mainly of hornblende, plagioclase, quartz and clinopyroxene with minor titanite. Secondary minerals include hornblende replacing clinopyroxenes, and biotite replacing hornblende. Whole-rock geochemistry of the amphibolites indicates high silica and total alkali ($K_2O + Na_2O$) contents, 50 to 64 wt. % and 3.3 to 5.2 wt. %, respectively. On the other hand, the amphibolite rocks in the Makorungo prospect are less foliated and mainly comprises amphiboles, plagioclase, and biotite, with minor quartz. Secondary biotite replaces amphiboles. Based on the extinction angles, the plagioclase in the Makorungo prospect is more Na-rich, while the plagioclase from the Nalia prospect is more Ca-rich. The TiO_2 vs. MnO diagram shows that the amphibolites in both prospects are ortho-amphibolites. Total alkali and silica diagram (TAS diagram) indicates protolith of basaltic composition. The mineralized veins in the Nalia prospect show deformation textures including triple-point texture, undulose extinction and variability in cathodoluminescence brightness within individual quartz grain. Evidence of post-deformation is less common in the Makorungo prospect. The ore mineralogy in the Nalia and Makorungo prospects is very similar, despite the absence of sphalerite in the former. Pyrite, pyrrhotite, galena, magnetite and chalcopyrite commonly occur with minor tellurides and electrum (the Makorungo prospect) or native gold (the Nalia prospect). Bismuth, Te, Pb, and W bearing minerals commonly occur as sulfides and tellurides in both prospects. Sphalerite in the Makorungo prospect is characterized by high Fe and Cd contents, ranging 9.2-11.8 wt. %, and 2.9-3.4 wt. %, respectively. Pressure formation estimated from FeS contents in sphalerite coexisting with pyrite and pyrrhotite (sphalerite geobarometry) is within 1.6 and 2.1 Kb, which corresponds to a depth from 5.9 to7.4 Km. The coeval existence of pyrrhotite and sphalerite in the Makorungo prospect suggests a low sulfidation state, along the pyrite-pyrrhotite equilibrium.

©2019. Japan Geoscience Union. All Right Reserved.

Geochemical features of the Hishikari epithermal gold deposit based on simultaneous multi-element analysis

*Sota Nishida[1], Mizuki Ishida[1], Kazutaka Yasukawa[1,2], Kentaro Nakamura[1], Koichiro Fujinaga[2,1], Yasuhiro Kato[3,1,2]

1. Department of Systems Innovation, School of Engineering, The University of Tokyo, 2. Ocean Resources Research Center for Next Generation, Chiba Institute of Technology, 3. Frontier Research Center for Energy and Resources, School of Engineering, The University of Tokyo

The Hishikari gold deposit, located in the northern part of Kagoshima prefecture, Japan, is known as one of the highest-grade gold deposits in the world. The origin of this low-sulfidation vein-type deposit has been extensively investigated since its discovery in the early 1980s. For example, Ishihara et al. (1986) suggested a magmatic source for gold (Au) and sulfur (S) based on sulfur isotope compositions of pyrites [1]. More recently, Morishita et al. (2018) demonstrated a positive correlation between Au and arsenic (As) in pyrites of the Hishikari veins and discussed their genetic relationship [2].

Understanding the mineralization process of the Hishikari deposit can provide key insights into an exploration strategy for new and high-grade gold deposits. To this end, identifying elements that show behaviors closely associated with Au can be one of the effective approaches. In this study, therefore, major and trace element geochemistry of the Hishikari ore samples have been investigated in order to obtain a new constraint on the Au mineralization processes. We determined multi-elemental composition (including Au) of the host rocks and vein samples by inductively coupled plasma mass spectrometry (ICP-MS).

Previous studies suggested that adularia content is closely related to the Au content of the ore [3]. In the present study, however, we found no correlation between Au and adularia contents in the vein samples. The results of X-ray diffraction (XRD) analysis indicated that the samples with high Au mostly consist of quartz. The Au mineralization thus seems to have occurred concurrently with the quartz mineralization that followed the adularia mineralization.

Among the 49 elements measured in this study, silver (Ag) content was positively correlated with Au content, which is consistent with the fact that electrum is the main host of Au in the Hishikari deposit. Arsenic (As) content had no correlation with Au, although it is well known for a coupling behavior with Au. Most notably, bismuth (Bi) content had clear correlation with Ag ($r = 0.88$) and Au ($r = 0.91$) contents, whereas it had no clear correlation with cobalt (Co), copper (Cu), iron (Fe), zinc (Zn), lead (Pb), or As contents. Bi is known to be enriched in high-sulfidation gold deposits where the common host of Bi is sulfide minerals (e.g. [4]), and closely associated with Au in these deposits. However, elemental behavior of Bi in low-sulfidation gold deposits has so far been poorly understood. Our results imply that Bi in the Hishikari deposit is likely to be involved not in sulfide but in electrum. This in turn suggests that Bi could be an important tracer for Au mineralization in low-sulfidation deposits such as the Hishikari deposit.

[1] S. Ishihara, Y. Sakamaki, A. Sasaki et al. (1986) *Mining Geology*, **36**(200), 495-509.

[2] Y. Morishita, N. Shimada and K. Shimada (2018) *Ore Geology Reviews*, **95**, 79-93.

©2019. Japan Geoscience Union. All Right Reserved.

[3] K. Ibaraki, R. Suzuki and E. Fukuda (1991) *Mining Geology*, **41**(2), 63-75.

[4] B. Zheng, Y. Zhu, F. An et al. (2015) *Ore Geology Reviews*, **69**, 17-32.

Keywords: gold, Hishikari deposit, bulk chemical analysis, ICP-MS, trace element composition

©2019. Japan Geoscience Union. All Right Reserved.

Transformation of ore minerals and their geochemical signatures in submarine hydrothermal ore deposits in Izena Hole, Okinawa Trough

*IKESHIMA TAKURO[1], Tsubasa Otake[1], Tsutomu Sato[1], Akane Ito[1], Shuji Ono[1], Jun-ichiro Ishibashi[2], Tatsuo Nozaki[3], Hidenori Kumagai[3], Lena Maeda[3]

1. Hokkaido University, 2. Kyushu University, 3. Japan Agency for Marine-Earth Science and Technology (JAMSTEC)

It is important for exploration and development of submarine hydrothermal ore deposits to understand zoning of ore bodies and their mineral assemblages, particularly with depth from the seafloor. Transformation of ore minerals via dissolution and re-precipitation may cause such a zoning corresponding to the evolution of a hydrothermal system because geochemical conditions may then vary with the depth from the seafloor. In this study, we aimed (1) to clarify the mineral assemblage changes with increasing depth of a mound sulfide deposit by microscopic observations and SEM-EDS analyses, (2) to understand geochemical evolution of hydrothermal fluids based on Fe contents in sphalerite determined by EPMA, and (3) to understand the formation processes of Fe sulfides by analyzing Fe isotopic composition of the bulk samples with MC-ICP-MS. The samples used for the analyses were obtained from Site C9027, which drilled up to 72.5 meter below seafloor (mbsf) through a mound sulfide deposit in Hakurei site, Izena Hole, middle Okinawa Trough during the CK16-05 cruise operated from November to December, 2016 under the SIP program.
Results of microscopic observations show that sphalerite and galena are comparatively dominant with minor occurrence of pyrrhotite and anglesite in the samples at shallow depths. In contrast, samples from middle and deep depths are more abundant on pyrite and chalcopyrite, and pyrite, respectively. The texture that pyrrhotite was dissolved and replaced by pyrite or marcasite was observed in the samples in the depth of 0.05 –44.0 mbsf. The Fe content in sphalerite tends to decrease with increasing depth, and also change within single sphalerite grain. These results suggest that hydrothermal fluid geochemistry such as fugacity of S_2 and O_2, and temperature changes for the depth and time. The δ^{56}Fe values (δ^{56}Fe (‰) = 1000 * [(^{56}Fe/^{54}Fe) sample / (^{56}Fe/^{54}Fe)$_{IRMM-014}$ -1]) of the bulk samples range from -0.62 to +0.11‰, which tends to increase toward the deeper part. This indicates that Fe sulfides at shallow depths was formed by non-equilibrium precipitation with a rapid cooling, which caused a kinetic isotope effect. In contrast, those at deeper depths were likely formed near the equilibrium conditions.

Keywords: Submarine hydrothermal ore deposits, Izena Hole, SIP, Replacement, Fe isotope, D/V Chikyu

©2019. Japan Geoscience Union. All Right Reserved.

Geochemical behavior of heavy metals during wastewater treatment in Chingola Stream of the Zambia Copperbelt

*Cryton Phiri[1], Daiki Shimazui[2], Tsutomu Sato[2], Tsubasa Otake[2]

1. University of Zambia, 2. Hokkaido University

The study focuses on an area at a copper mine in Chingola town of the Zambian Copperbelt where wastewater containing heavy metals (Cu-Co-Mn) at variable pH (3.5-6.5) mixes with a nearby municipal wastewater in Chingola Stream. The metal concentration of discharge is below the regulation limit because lime treatment has been conducted in the stream. However, remaining volume of ponds for sludge produced by lime treatment was limited. The objective of the study was therefore to understand the geochemical behavior of the metals for the optimization of wastewater treatment. Representative water and soil samples were obtained along the affected stream and analyzed for their target heavy metal content and geochemical distribution using ICP-AES/MS and sequential extraction (SQE) methods. Analyses of sediment mineralogy were made by XRD, optical microscopy, FE-SEM/EDS and TEM/EDS. Water chemistry results revealed relatively low metal concentrations of Cu-Co-Mn ranging from below detection limit (bdl) to 60mg/l. SQE analyses show high total target metal concentrations ranging from (1-12000mg/kg) in sediments, which obviously supports the possible adsorption and precipitation processes to be taking place. Low concentrations are as a result of the increasing pH and possible metal adsorption and precipitation on sediment. The target metal contents were highest in exchangeable fraction Cu (100-2500mg/kg), Co (1-50mg/kg), Mn (bdl-2g/kg), and in carbonate fraction Cu (2-500mg/kg), Co (0.5-20mg/kg), Mn (bdl-1.2g/kg) and in amorphous Fe mineral fraction Cu (2-1000mg/kg), Co (1-100mg/kg) and Mn (0.5-2.5g/kg) respectively. The other remaining fractions had very low metal concentrations. FE-SEM/EDS and TEM/EDS techniques showed some metal adsorption phases on biotite and kaolinite confirming the earlier results of SQE. The amorphous Fe mineral determined using SQE reveal an average of between 3.5-12 g/kg. From the surface complexation modeling between amorphous Fe mineral and the metals shows that the range of pH condition, 6.5-7.5 is strongly recommended for better sorbed fraction of Cu-Co-Mn on amorphous Fe mineral. From the above results, it was found that the geochemical partitioning of metals to the most labile exchangeable fraction which easily releases metals to the environment depending on the prevailing conditions (i.e pH) can as well be treated by ion exchange, surface complexation by amorphous Fe mineral and carbonation. The advantages of this treatment method is that heavy metal can easily be recovered from sludge through the application of relatively weak acid and at the same time reducing the sludge volumes through utilization of the sediments as sand for engineering purposes.

Keywords: Heavy metals, Geochemical behavior, Treatment

©2019. Japan Geoscience Union. All Right Reserved.

[J] Poster | H (Human Geosciences)：H-RE Resource and Engineering Geology

Wed. May 29, 2019 5:15 PM - 6:30 PM JST | Wed. May 29, 2019 8:15 AM - 9:30 AM UTC | Poster Hall International Exhibition Hall8, Makuhari Messe_22

[H-RE16] Resource Geology

convener:Tsubasa Otake(Division of Sustainable Resources Engineering, Faculty of Engineering, Hokkaido University), Daisuke Araoka(Geological Survey of Japan, National Institute of Advanced Industrial Science and Technology), Ryohei Takahashi(Graduate School of International Resource Sciences, Akita University), Tatsuo Nozaki(Research and Development Center for Submarine Resources, Japan Agency for Marine-Earth Science and Technology)

Ore deposits containing valuable elements and minerals at high concentrations in supracrustal rocks are formed by the Earth's dynamics including magmatism, hydrothermal activity, metamorphism, and weathering. The formation of ore deposits is also closely associated with global environmental changes and biological evolution in the Earth's history. Involvement of difference academic fields in earth sciences including geology, petrology, geochemistry, mineralogy, and microbiology is required to understand the genesis of ore deposits. The field of resource geology is essential not only for efficient exploration and development of ore deposits but also for better understanding and assessment of hazardous elements that may be caused by the resource development. This session widely covers various topics of field investigation and observation, laboratory experiments, theoretical calculation, development of analytical methods and others related to the supracrustal migration and concentration of elements.

[HRE16-P01] Mineral Chemistry and Petrogenesis of the Mazua Ultramafic Massif, Northern Mozambique: Constraints on the Associated Fe-Ti Oxides Deposit

*David Augusto Bene Unganai[1], Akira Imai[2], Ryohei Takahashi[1], Daud Liace Jamal[3], Takashi Hoshide[1] (1.Akita University, 2.Kyushu University, 3.Eduardo Mondlane University)

[HRE16-P02] **Ni-Cu-PGM Mineralisation in the Bastard Reef and Merensky Reef of the Flatreef section, Turfspruit Farm, Northern Limb, Bushveld Igneous Complex, South Africa.**

*MOKHIRI MALESELA MAKHAFOLA[1], Tsubasa Otake[1], Tsutomu Sato[1], Danie Grobler[2] (1.Hokkaido University, 2.Ivanplats Pty. Ltd)

[HRE16-P03] Characteristics of Porphyry Copper-Gold Mineralization in the Grasberg Mine, Papua, Indonesia

*Kanehiko Kawasaki[1], Kotaro Yonezu[2], Reza Al Furqan[3], Benny Bensaman[4], Mega Fatimah Rosana[4] (1.Kyushu University Facurity of Engineering, 2.Deaprtment of Earth Resources Engineering, Faculty of Engineering, Kyushu University, 3.PT Freeport Indonesia, 4.Department of Geology, Padjadjaran University)

[HRE16-P04] Formation of Ni-bearing minerals during chemical weathering of ultramafic rocks in Myanmar

*Ayaka Murofushi[1], Akane Ito[1], Tsubasa Otake[2], Kenzo Sanematsu[3], Kyaw Zay Ya[1,4], Tsutomu Sato[2] (1.Graduate school of Engineering, Hokkaido University, 2.Facility of Engineering, Hokkaido University, 3.Geological Survey of Japan, National Institute of Advanced Industrial Science and Technology, 4.Department of Geological Survey and Mineral Exploration)

[HRE16-P05] Geological Characteristics and Mineralogy of the Makorungo and Nalia Gold Prospects, Northeastern Mozambique

*Manuel Augusto Manuel Nopeia[1], Ryohei Takahashi[1], Akira Imai[2], Daud Liace Jamal[3] (1.Akita University, 2.Kyushu University, 3.Eduardo Mondlane University)

[HRE16-P06] Geochemical features of the Hishikari epithermal gold deposit based on simultaneous multi-element analysis

*Sota Nishida[1], Mizuki Ishida[1], Kazutaka Yasukawa[1,2], Kentaro Nakamura[1], Koichiro Fujinaga[2,1], Yasuhiro Kato[3,1,2] (1.Department of Systems Innovation, School of Engineering, The University of Tokyo, 2.Ocean Resources Research Center for Next Generation, Chiba Institute of Technology, 3.Frontier Research Center for Energy and Resources, School of Engineering, The University of Tokyo)

[HRE16-P07] Transformation of ore minerals and their geochemical signatures in submarine hydrothermal ore deposits in Izena Hole, Okinawa Trough

*IKESHIMA TAKURO[1], Tsubasa Otake[1], Tsutomu Sato[1], Akane Ito[1], Shuji Ono[1], Jun-ichiro Ishibashi[2], Tatsuo Nozaki[3], Hidenori Kumagai[3], Lena Maeda[3] (1.Hokkaido University, 2.Kyushu University, 3.Japan Agency for Marine-Earth Science and Technology (JAMSTEC))

[HRE16-P08] Geochemical behavior of heavy metals during wastewater treatment in Chingola Stream of the Zambia Copperbelt

*Cryton Phiri[1], Daiki Shimazui[2], Tsutomu Sato[2], Tsubasa Otake[2] (1.University of Zambia, 2.Hokkaido University)

Mineral Chemistry and Petrogenesis of the Mazua Ultramafic Massif, Northern Mozambique: Constraints on the Associated Fe-Ti Oxides Deposit

*David Augusto Bene Unganai[1], Akira Imai[2], Ryohei Takahashi[1], Daud Liace Jamal[3], Takashi Hoshide[1]

1. Akita University, 2. Kyushu University, 3. Eduardo Mondlane University

Economic magmatic Fe-Ti-V deposits are commonly hosted by mafic-ultramafic intrusions and massif-type anorthosites. The Mazua Ultramafic Massif (MUM), located in northeast Mozambique, is one of the most promising intrusions that host Fe-Ti oxides ore deposit in the country. The orebody is a 10-km long ilmenite-rich hornblende pyroxenite, which is in sharp contact with a banded biotite gneiss. The ore commonly occurs as layers/lenses, massive and dissemination in host rocks. The average grade of the ore is 27 wt.% TiO_2, 35 wt.% Fe_2O_{3tot} and ~2 ppm V (Norconsult Consortium, 2007). However, detailed studies regarding the petrogenesis of the intrusion and its related Fe-Ti oxides ores are still scarce. Thus, we carried out microprobe and petrographic analyses to elucidate these issues.

The hornblende pyroxenite consists of ilmenite, diopside, and magnesiohornblende as main phases. Petrography reveals that the Fe-Ti oxides and pyroxenes are syngenetic. The composition of diopside ($Wo_{43.5–48.5}En_{36.0–41.4}Fs_{11.1–20.5}$) and occurrence of magnesiohornblende suggest tholeiitic, non-alkaline and hydrous (>3.0 wt.% H_2O) parental ultrabasic melt. In addition, the absence of olivine and orthopyroxene supported by wide range of #Mg in diopside (63.8–78.7) and magnesiohornblende (68.9–85.4) confirms the idea that the magma which formed MUM was differentiated.

Texture and variable mineral composition suggest that Fe-Ti oxides underwent extensive subsolidus re-equilibration during cooling, supported by the following evidences: (1) The Fe-Ti oxides show different types of micro-intergrowths such as (a) lamellae of ilmenite with clothing textures hosted in magnetite, (b) fine pattern exsolution lamellae (trellis) and blebs of aluminous spinel in magnetite, (c) reaction rims of aluminous spinel distributed along the boundary between magnetite and ilmenite and (d) re-equilibration textures involving Fe-Ti oxides and silicate phases. (2) The very low MgO content of primary ilmenite (<2 wt.%) is interpreted as a result of postcumulus oxide-silicate re-equilibration involving clinopyroxene and amphibole. (3) Determination of equilibrium conditions using geothermobarometer by Spencer & Lindsley (1981) indicates that Mazua Fe-Ti oxides last equilibrated at subsolidus temperatures (<600 ˚C) and high oxygen fugacity ($\log fO_2 > -20.0$ bars). The reconstruction of the primary composition of Fe-Ti oxides, by reintegration of exsolved with the host phases, leads to primary titanomagnetite with an ulvospinel component of ~20 mol%.

©2019. Japan Geoscience Union. All Right Reserved.

Ni-Cu-PGM Mineralisation in the Bastard Reef and Merensky Reef of the Flatreef section, Turfspruit Farm, Northern Limb, Bushveld Igneous Complex, South Africa.

*MOKHIRI MALESELA MAKHAFOLA[1], Tsubasa Otake[1], Tsutomu Sato[1], Danie Grobler[2]

1. Hokkaido University, 2. Ivanplats Pty. Ltd

The Bushveld Igneous Complex of South Africa is the largest layered igneous complex in the world and it is the current leading producer of platinum group metals globally. The Northern Limb is the northern extension of the complex currently mined (open pit) for a Ni-Cu-PGM rich deposit hosted in a lithologically variable igneous sequence dipping at about 45 degrees and has been intensively affected by contamination and alteration termed the Platreef (Kinnaird et al, 2005). Westwards of the Platreef lies the Flatreef section, which is a recently discovered sub-horizontal down-dip extension of the Platreef. It hosts the Ni-Cu-PGM rich deposit in two successive high-grade reefs termed the Bastard Reef and the Merensky Reef that are amenable for underground mining methods (Grobler et al, 2018). The Flatreef has not been studied in detail and this study reports on the petrographical and semi-quantitative investigations done on the mineralized reefs.
Logging and petrographical investigations revealed the Bastard Reef to comprise a fine to medium-grained equigranular feldspathic orthopyroxenite. Several metres below the Bastard Reef lies the Merensky Reef, which has been subdivided into 3 different units (M2, M1U and M1L) mainly based on mineralogical and textural variations. The M2 is the uppermost layer comprising medium to coarse-grained equigranular orthopyroxenite, denoted by cumulus orthopyroxene and is bound irregularly by a chromite seam at its top contact. The M2 orthopyroxenite is underlain by the M1U denoted by a cumulate textured pegmatoidal orthopyroxenite and is commonly bound by a chromite stringer at its top contact and a less consistent one at its base. The M1L, which is laterally less continuous, comprises a poikilitic textured harzburgite and/or varied-textured olivine-bearing orthopyroxenite. SEM analysis revealed sulphide mineral assemblages in the reefs usually comprising pyrrhotite, pentlandite and chalcopyrite as fine to medium-grained disseminations, blebs and net-textured sulphides. PGM mineralisation comprise a wide range of PGMs, mostly Platinum and Palladium dominated, grouped into bismithotellurides (-Bi-Te), antimonides, arsenides, Fe and Sn alloys, sulphides, as well as laurite (RuS_2) and Ir-Ru-Rh-Pt-Pd sulfoarsenides alongside chromite seams. Semi-quantitative analysis illustrates the Flatreef section to be an undisturbed magmatic sequence that is much less affected by assimilation and contamination. It retains much of its magmatic characteristics and provides a great opportunity to furthermore study magmatic processes that resulted in the formation of such an enigmatic deposit.

References

Grobler, D.F., Brits, J.A.N., Maier, W.D. and Crossingham, A. (2018) Litho- and Chemostratigraphy of the Flatreef PGE deposit, northern Bushveld Complex. Mineralium Deposita, 126, 1-26.

Kinnaird, J.A., Hutchinson, D., Schurman, L., Nex, P. and de Lange, R. (2005) Petrology and Mineralisation of the Southern Platreef: Northern Limb of the Bushveld Complex, South Africa. Mineralium Deposita, 40, 576-597.

Keywords: Ni-Cu-PGM, Bushveld Igneous Complex, Flatreef Section, Northern Limb

©2019. Japan Geoscience Union. All Right Reserved.

©2019. Japan Geoscience Union. All Right Reserved.

Characteristics of Porphyry Copper-Gold Mineralization in the Grasberg Mine, Papua, Indonesia

*Kanehiko Kawasaki[1], Kotaro Yonezu[2], Reza Al Furqan[3], Benny Bensaman[4], Mega Fatimah Rosana[4]

1. Kyushu University Facurity of Engineering, 2. Deaprtment of Earth Resources Engineering, Faculty of Engineering, Kyushu University, 3. PT Freeport Indonesia, 4. Department of Geology, Padjadjaran University

The Grasberg-Ertsberg district is located in the west of the remote highlands of the Sudirman Mountain in the province of Papua, Indonesia. The district is well-known copper-gold mine area as “Grasberg mine” in the world. In this district, Pliocene intrusive rocks host copper and gold mineralization. These intrusive rocks are named “Grasberg Igneous Complex” (GIC), which is composed of Kali Intrusion (KI), Main Grasberg Intrusion (MGI) and Dalam Intrusion (DI). The purpose of this study is to clarify characteristics of ore forming fluid and copper-gold mineralization, especially in the western part of MGI hosted porphyry mineralization in the Grasberg district.
In this study, all samples used is collected from a drill core, AM-30-08H-05. It penetrates KI and DI through MGI. Petrography revealed that Cu bearing mineralization style can be divided into three types: Cu(-Fe) sulfides vein type in quartz vein, Cu(-Fe) sulfides veinlet type and disseminated Cu(-Fe) sulfides type. Chalcopyrite is major ore mineral in vein type and veinlet type. In these types, bornite is often distributed in or by the chalcopyrite, therefore it could be explained by exsolution from intermediate solid solution and bornite solid solution. In disseminated Cu(-Fe) sulfides, chalcopyrite and bornite is major and primary Cu bearing minerals. They are often co-existing, therefore they also seemed to be exsoluted from intermediate solid solution and bornite solution. However, the other Cu bearing minerals (chalcocite, covellite, digenite) sometimes form foliated texture with chalcopyrite and bornite, clearly indicating that those Cu bearing minerals are formed by replacement from bornite. In addition, rim of bornite is sometimes replaced by chalcocite, covellite and digenite, suggesting interaction with ground water after primary mineralization. Native gold is precipitated in chalcopyrite vein in quartz vein and in disseminated chalcopyrite. In chalcopyrite vein, native gold is precipitated with bornite and merenskyite, which is determined by SEM-EDX as $Pd_{1.0}Te_{2.0}$. Merenskyite is newly identified in the western part of GIC, while it has already reported in northern and southern part of GIC. Merenskyite is a common in ultramafic rocks related to PGE mineralization (e.g., merensky reef in Bushveld Igneous Complex). Precipitation of merenskyite in this area suggests the presence and contribution of primitive mafic magma. The fact merenskyite can be observed widely in MGI, the contribution may cover the whole MGI.
Since clear cross-cutting relationship among quartz veins is not observed in this research, SEM-Cathodoluminescence observation is conducted for identifying quartz crystal growth pattern in quartz vein, hosting chalcopyrite vein. Luminescence contrast anomaly can be recognized in quartz vein, suggesting that there are two different occurrence of quartz veins which are early quartz vein and later quartz vein. Only late quartz vein is associated with chalcopyrite vein. Fluid inclusion microthermometry in early quartz vein was conducted. Homogenization temperature of fluid inclusion in early quartz is over 600 degree Celsius with high salinity (61.32 wt%). These results are harmonious with previous research, suggesting weak or none of Cu and Au mineralization is associated with early quartz vein, however late quartz vein introduced intensive copper-gold mineralization.

Keywords: Grasberg Mine, Porphyry Copper Deposit, Mineralization

©2019. Japan Geoscience Union. All Right Reserved.

Formation of Ni-bearing minerals during chemical weathering of ultramafic rocks in Myanmar

*Ayaka Murofushi[1], Akane Ito[1], Tsubasa Otake[2], Kenzo Sanematsu[3], Kyaw Zay Ya[1,4], Tsutomu Sato[2]

1. Graduate school of Engineering, Hokkaido University, 2. Facility of Engineering, Hokkaido University, 3. Geological Survey of Japan, National Institute of Advanced Industrial Science and Technology, 4. Department of Geological Survey and Mineral Exploration

Ni laterite deposit, an important resource for Ni, is formed by chemical weathering of ultramafic rocks under tropical climate conditions. Whereas many studies have aimed to understand the formation processes of Ni laterites in Indonesia and Philippines, few studies have investigated those in Myanmar, which also has a high potential of Ni laterite resources. The highest grade of Ni in a weathering profile is usually found in a saprolite zone, a weakly weathered section underlain by intensively-weathered laterite zone. Mobilization of Ni from the bedrock as well as laterite zone together with Fe has been proposed to be an important process for Ni enrichment in saprolite zone (e.g., Golightly, 2010). However, formation of various Ni-bearing minerals in saprolite zone (Tauler et al., 2017) may also govern the Ni enrichment though the common Ni-bearing mineral in saprolite zone is secondary-formed serpentine (Ser-II). It is important to understand the formation processes of Ni laterite deposits for efficient exploration and mine development. Therefore, in this study, we are focused on the formation of secondary minerals at different weathering degrees and its relationship to Ni enrichment during chemical weathering of ultramafic rocks in Myanmar by investigating 6 different weathering profiles in the Western and Central Ophiolite Belts.

The results of the bulk chemical analysis by XRF show that Ni is concentrated in saprolite zones up to 1.6 wt% as chemical weathering progresses as indicated by thickness of profiles and depletion of major elements (e.g., Mg). Ni is associated more closely with 0.2-2 μm fraction (e.g., clay minerals) of the samples as Ni concentration in this fraction was determined by acid digestion and ICP-AES. The results of mineralogical analysis by XRD and petrographic microscope show that minerals formed in saprolite zones varies depending on the degree of weathering regardless that all the bedrocks are serpentinite. Whereas smectite dominates in the saprolite zone of the least weathered profile, both smectite and Ser-II were present in the saprolite zone of the most weathered profile. This suggests that smectite is formed at the initial stage of chemical weathering of the ultramafic rocks in Myanmar. However, the results of SEM-EDS analysis show that Mn-oxide (e.g., asbolane) is the main mineral concentrating Ni in the least weathered profile whereas secondary silicate minerals (e.g., Ser-II, smectite, unidentified Fe-Ni silicates) are the main minerals in the most weathered profile. Therefore, Ni is preferentially associated with Mn-oxide possibly because of a strong electrostatic interaction. However, as weathering progresses and Mn-oxide dissolved away, Ni is enriched into secondary silicate minerals (e.g., Ser-II, smectite). No preferential incorporation of Ni was observed between Ser-II and smectite. Further progress in chemical weathering may result in the transformation of other silicate minerals into Ser-II, which would be then the main Ni-bearing mineral in Ni laterite deposit in Myanmar.

©2019. Japan Geoscience Union. All Right Reserved.

Geological Characteristics and Mineralogy of the Makorungo and Nalia Gold Prospects, Northeastern Mozambique

*Manuel Augusto Manuel Nopeia[1], Ryohei Takahashi[1], Akira Imai[2], Daud Liace Jamal[3]

1. Akita University, 2. Kyushu University, 3. Eduardo Mondlane University

The northeastern Mozambique is composed of medium-high grade metamorphic complexes of the Mozambique Belt, intruded by Neoproterozoic-Paleozoic granitoids (Norconsult, 2007). Mozambique Belt (MB) is a part of the East African Orogeny and has been associated with a large variety of mineralization, including base metals, gemstones, and gold (Lächelt, 2004). The lack of studies on gold deposits associated with metamorphic terrains in Mozambique weakens the discovery and further exploration of gold. This study focuses on the Makorungo and Nalia gold prospects, northeastern Mozambique, where artisanal and small-scale mining of placer and primary gold is conducted mainly by local people. These prospects belong to Xixano complex, interpreted as a Pan-African nappe, which is composed of supercrustal rocks, enveloping mafic and ganulitic rocks (Viola et al, 2008). This study aims to reveal the geological and mineralogical characteristics of the gold prospects to better understand the ore-forming process. Field observation and laboratory analysis, including petrography of host rocks and ores, and whole-rock and ore chemistry were applied. Quartz veins parallel and at low angle to amphibolite foliation host the gold mineralization in the Nalia and Makorungo prospects. The amphibolites in the Nalia prospect are strongly foliated and composed mainly of hornblende, plagioclase, quartz and clinopyroxene with minor titanite. Secondary minerals include hornblende replacing clinopyroxenes, and biotite replacing hornblende. Whole-rock geochemistry of the amphibolites indicates high silica and total alkali ($K_2O + Na_2O$) contents, 50 to 64 wt. % and 3.3 to 5.2 wt. %, respectively. On the other hand, the amphibolite rocks in the Makorungo prospect are less foliated and mainly comprises amphiboles, plagioclase, and biotite, with minor quartz. Secondary biotite replaces amphiboles. Based on the extinction angles, the plagioclase in the Makorungo prospect is more Na-rich, while the plagioclase from the Nalia prospect is more Ca-rich. The TiO_2 vs. MnO diagram shows that the amphibolites in both prospects are ortho-amphibolites. Total alkali and silica diagram (TAS diagram) indicates protolith of basaltic composition. The mineralized veins in the Nalia prospect show deformation textures including triple-point texture, undulose extinction and variability in cathodoluminescence brightness within individual quartz grain. Evidence of post-deformation is less common in the Makorungo prospect. The ore mineralogy in the Nalia and Makorungo prospects is very similar, despite the absence of sphalerite in the former. Pyrite, pyrrhotite, galena, magnetite and chalcopyrite commonly occur with minor tellurides and electrum (the Makorungo prospect) or native gold (the Nalia prospect). Bismuth, Te, Pb, and W bearing minerals commonly occur as sulfides and tellurides in both prospects. Sphalerite in the Makorungo prospect is characterized by high Fe and Cd contents, ranging 9.2-11.8 wt. %, and 2.9-3.4 wt. %, respectively. Pressure formation estimated from FeS contents in sphalerite coexisting with pyrite and pyrrhotite (sphalerite geobarometry) is within 1.6 and 2.1 Kb, which corresponds to a depth from 5.9 to7.4 Km. The coeval existence of pyrrhotite and sphalerite in the Makorungo prospect suggests a low sulfidation state, along the pyrite-pyrrhotite equilibrium.

©2019. Japan Geoscience Union. All Right Reserved.

Geochemical features of the Hishikari epithermal gold deposit based on simultaneous multi-element analysis

*Sota Nishida[1], Mizuki Ishida[1], Kazutaka Yasukawa[1,2], Kentaro Nakamura[1], Koichiro Fujinaga[2,1], Yasuhiro Kato[3,1,2]

1. Department of Systems Innovation, School of Engineering, The University of Tokyo, 2. Ocean Resources Research Center for Next Generation, Chiba Institute of Technology, 3. Frontier Research Center for Energy and Resources, School of Engineering, The University of Tokyo

The Hishikari gold deposit, located in the northern part of Kagoshima prefecture, Japan, is known as one of the highest-grade gold deposits in the world. The origin of this low-sulfidation vein-type deposit has been extensively investigated since its discovery in the early 1980s. For example, Ishihara et al. (1986) suggested a magmatic source for gold (Au) and sulfur (S) based on sulfur isotope compositions of pyrites [1]. More recently, Morishita et al. (2018) demonstrated a positive correlation between Au and arsenic (As) in pyrites of the Hishikari veins and discussed their genetic relationship [2].

Understanding the mineralization process of the Hishikari deposit can provide key insights into an exploration strategy for new and high-grade gold deposits. To this end, identifying elements that show behaviors closely associated with Au can be one of the effective approaches. In this study, therefore, major and trace element geochemistry of the Hishikari ore samples have been investigated in order to obtain a new constraint on the Au mineralization processes. We determined multi-elemental composition (including Au) of the host rocks and vein samples by inductively coupled plasma mass spectrometry (ICP-MS).

Previous studies suggested that adularia content is closely related to the Au content of the ore [3]. In the present study, however, we found no correlation between Au and adularia contents in the vein samples. The results of X-ray diffraction (XRD) analysis indicated that the samples with high Au mostly consist of quartz. The Au mineralization thus seems to have occurred concurrently with the quartz mineralization that followed the adularia mineralization.

Among the 49 elements measured in this study, silver (Ag) content was positively correlated with Au content, which is consistent with the fact that electrum is the main host of Au in the Hishikari deposit. Arsenic (As) content had no correlation with Au, although it is well known for a coupling behavior with Au. Most notably, bismuth (Bi) content had clear correlation with Ag ($r = 0.88$) and Au ($r = 0.91$) contents, whereas it had no clear correlation with cobalt (Co), copper (Cu), iron (Fe), zinc (Zn), lead (Pb), or As contents. Bi is known to be enriched in high-sulfidation gold deposits where the common host of Bi is sulfide minerals (e.g. [4]), and closely associated with Au in these deposits. However, elemental behavior of Bi in low-sulfidation gold deposits has so far been poorly understood. Our results imply that Bi in the Hishikari deposit is likely to be involved not in sulfide but in electrum. This in turn suggests that Bi could be an important tracer for Au mineralization in low-sulfidation deposits such as the Hishikari deposit.

[1] S. Ishihara, Y. Sakamaki, A. Sasaki et al. (1986) *Mining Geology*, **36**(200), 495-509.

[2] Y. Morishita, N. Shimada and K. Shimada (2018) *Ore Geology Reviews*, **95**, 79-93.

©2019. Japan Geoscience Union. All Right Reserved.

[3] K. Ibaraki, R. Suzuki and E. Fukuda (1991) *Mining Geology*, **41**(2), 63-75.

[4] B. Zheng, Y. Zhu, F. An et al. (2015) *Ore Geology Reviews*, **69**, 17-32.

Keywords: gold, Hishikari deposit, bulk chemical analysis, ICP-MS, trace element composition

©2019. Japan Geoscience Union. All Right Reserved.

Transformation of ore minerals and their geochemical signatures in submarine hydrothermal ore deposits in Izena Hole, Okinawa Trough

*IKESHIMA TAKURO[1], Tsubasa Otake[1], Tsutomu Sato[1], Akane Ito[1], Shuji Ono[1], Jun-ichiro Ishibashi[2], Tatsuo Nozaki[3], Hidenori Kumagai[3], Lena Maeda[3]

1. Hokkaido University, 2. Kyushu University, 3. Japan Agency for Marine-Earth Science and Technology (JAMSTEC)

It is important for exploration and development of submarine hydrothermal ore deposits to understand zoning of ore bodies and their mineral assemblages, particularly with depth from the seafloor. Transformation of ore minerals via dissolution and re-precipitation may cause such a zoning corresponding to the evolution of a hydrothermal system because geochemical conditions may then vary with the depth from the seafloor. In this study, we aimed (1) to clarify the mineral assemblage changes with increasing depth of a mound sulfide deposit by microscopic observations and SEM-EDS analyses, (2) to understand geochemical evolution of hydrothermal fluids based on Fe contents in sphalerite determined by EPMA, and (3) to understand the formation processes of Fe sulfides by analyzing Fe isotopic composition of the bulk samples with MC-ICP-MS. The samples used for the analyses were obtained from Site C9027, which drilled up to 72.5 meter below seafloor (mbsf) through a mound sulfide deposit in Hakurei site, Izena Hole, middle Okinawa Trough during the CK16-05 cruise operated from November to December, 2016 under the SIP program.
Results of microscopic observations show that sphalerite and galena are comparatively dominant with minor occurrence of pyrrhotite and anglesite in the samples at shallow depths. In contrast, samples from middle and deep depths are more abundant on pyrite and chalcopyrite, and pyrite, respectively. The texture that pyrrhotite was dissolved and replaced by pyrite or marcasite was observed in the samples in the depth of 0.05 –44.0 mbsf. The Fe content in sphalerite tends to decrease with increasing depth, and also change within single sphalerite grain. These results suggest that hydrothermal fluid geochemistry such as fugacity of S_2 and O_2, and temperature changes for the depth and time. The δ^{56}Fe values (δ^{56}Fe (‰) = 1000 * [(^{56}Fe/^{54}Fe) sample / (^{56}Fe/^{54}Fe)$_{IRMM-014}$ -1]) of the bulk samples range from -0.62 to +0.11‰, which tends to increase toward the deeper part. This indicates that Fe sulfides at shallow depths was formed by non-equilibrium precipitation with a rapid cooling, which caused a kinetic isotope effect. In contrast, those at deeper depths were likely formed near the equilibrium conditions.

Keywords: Submarine hydrothermal ore deposits, Izena Hole, SIP, Replacement, Fe isotope, D/V Chikyu

©2019. Japan Geoscience Union. All Right Reserved.

Geochemical behavior of heavy metals during wastewater treatment in Chingola Stream of the Zambia Copperbelt

*Cryton Phiri[1], Daiki Shimazui[2], Tsutomu Sato[2], Tsubasa Otake[2]

1. University of Zambia, 2. Hokkaido University

The study focuses on an area at a copper mine in Chingola town of the Zambian Copperbelt where wastewater containing heavy metals (Cu-Co-Mn) at variable pH (3.5-6.5) mixes with a nearby municipal wastewater in Chingola Stream. The metal concentration of discharge is below the regulation limit because lime treatment has been conducted in the stream. However, remaining volume of ponds for sludge produced by lime treatment was limited. The objective of the study was therefore to understand the geochemical behavior of the metals for the optimization of wastewater treatment. Representative water and soil samples were obtained along the affected stream and analyzed for their target heavy metal content and geochemical distribution using ICP-AES/MS and sequential extraction (SQE) methods. Analyses of sediment mineralogy were made by XRD, optical microscopy, FE-SEM/EDS and TEM/EDS. Water chemistry results revealed relatively low metal concentrations of Cu-Co-Mn ranging from below detection limit (bdl) to 60mg/l. SQE analyses show high total target metal concentrations ranging from (1-12000mg/kg) in sediments, which obviously supports the possible adsorption and precipitation processes to be taking place. Low concentrations are as a result of the increasing pH and possible metal adsorption and precipitation on sediment. The target metal contents were highest in exchangeable fraction Cu (100-2500mg/kg), Co (1-50mg/kg), Mn (bdl-2g/kg), and in carbonate fraction Cu (2-500mg/kg), Co (0.5-20mg/kg), Mn (bdl-1.2g/kg) and in amorphous Fe mineral fraction Cu (2-1000mg/kg), Co (1-100mg/kg) and Mn (0.5-2.5g/kg) respectively. The other remaining fractions had very low metal concentrations. FE-SEM/EDS and TEM/EDS techniques showed some metal adsorption phases on biotite and kaolinite confirming the earlier results of SQE. The amorphous Fe mineral determined using SQE reveal an average of between 3.5-12 g/kg. From the surface complexation modeling between amorphous Fe mineral and the metals shows that the range of pH condition, 6.5-7.5 is strongly recommended for better sorbed fraction of Cu-Co-Mn on amorphous Fe mineral. From the above results, it was found that the geochemical partitioning of metals to the most labile exchangeable fraction which easily releases metals to the environment depending on the prevailing conditions (i.e pH) can as well be treated by ion exchange, surface complexation by amorphous Fe mineral and carbonation. The advantages of this treatment method is that heavy metal can easily be recovered from sludge through the application of relatively weak acid and at the same time reducing the sludge volumes through utilization of the sediments as sand for engineering purposes.

Keywords: Heavy metals, Geochemical behavior, Treatment

©2019. Japan Geoscience Union. All Right Reserved.

[E] Poster | H (Human Geosciences)：H-TT Technology & Techniques

Wed. May 29, 2019 1:45 PM - 3:15 PM JST | Wed. May 29, 2019 4:45 AM - 6:15 AM UTC | Poster Hall International Exhibition Hall8, Makuhari Messe_2

[H-TT21] Non-destructive techniques applied to stone cultural heritage

convener:Chiaki T. Oguchi(Institute for Environmental Science and Technology, Graduate School of Science and Engineering, Saitama University), Celine Elise Thomachot-Schneider(Groupe d'etude des environnements naturels, anthropiques et archeologiques - Universite de Reims-Champagne-Ardenne (France)), Wonsuh Song(Waseda University), Miguel Gomez-Heras(Universidad Autonoma de Madrid)

Non-destructive and non-invasive techniques applying to cultural heritage made of stones, soils and earthen materials have been significantly developed over past years, and thus, the interest in such techniques has greatly increased. Here, we focus the session on new devices, new protocols and new data treatments that allow better understanding of weathering mechanisms, decay states and response to treatments.
A few topics would be listed as follows: 1) The development of new techniques and devices in cultural heritage and new protocols using non-destructive techniques; 2) The application of these techniques and protocols on indoor and outdoor case studies and laboratory studies; 3) The assessment of weathering mechanisms, weathering kinetics, decay state, and response to treatments; and 4) The modeling and simulation of decay processes.

[HTT21-P01] Comparison and Analysis of GNSS-RTK Combined with 3D LiDAR Technology on Monument Maintenance Project

*Lih-Shinn Hwang[1], Chien-Hua Chiu[1], Chien-Wen Wang[1], Hsiao-Hung Chen[1] (1.National Defense Univ.)

[HTT21-P02] Non-destructive field measurement for investigation of deteriorated parts of an artificial cave

Kaisei Sakane[1], *Chiaki T. Oguchi[1], Yasuhiko TAMURA[2] (1.Institute for Environmental Science and Technology, Graduate School of Science and Engineering, Saitama University, 2.The Exective Committee for the Preservation of Taya Cavern)

[HTT21-P03] Ultra-portable thermal cameras for moisture detection

*Miguel Gomez-Heras[1], Laura Lopez-Gonzalez[2], Maria Teresa Gil-Muñoz[3] (1.Universidad Autonoma de Madrid, 2.Artfabrik, 3.Universidad Complutense de Madrid)

[HTT21-P04] A laboratory experiment on stone decay by combination of salt and ice crystallization

*Masato Sato[1], Tsuyoshi Hattanji[2] (1.Graduate School of Life and environmental Sciences, 2.Faculty of Life and EnvironmentalSciences, University of Tsukuba)

[HTT21-P05] Study of the micro-climatic monitoring on the Saint-Remi Basilica (Rheims, France)

*Emilie Huby[1], Celine Elise Thomachot-Schneider[1], Patricia Vazquez[1], Gilles Fronteau[1] (1.Universite de Reims-Champagne-Ardenne)

Comparison and Analysis of GNSS-RTK Combined with 3D LiDAR Technology on Monument Maintenance Project

*Lih-Shinn Hwang[1], Chien-Hua Chiu[1], Chien-Wen Wang[1], Hsiao-Hung Chen[1]

1. National Defense Univ.

The Precision is the first face problem in the restoration and preservation of Monument Maintenance Project. It may be that the initial coordinates of the position cannot be effectively determined by each object of historical antiquities or buildings, which seriously affects the proportional position when the combination is later reconstructed; or because the relative relationship with the natural environment is neglected, the restoration project is time consuming and even there may be errors that cannot be recovered.
Therefore, external reference control points play an important role in the 3D laser scanning operation of historical antiquities or buildings. Especially for long-term monitoring, it almost determines the accuracy of the following article scanning.
However, due to the unexpected situation on the spot, there are often control points lost, and there is a need for a rebuild-point project, which affects the 3D scanning operation of the later cultural relics. Rebuild-point project requires not only consistent precision, but also convenience and speed. This team takes the ancient house of Li-Tengfang, a national monument, as an example. When this term is studying on the restoration and preservation of Monument Maintenance Project, it is, and proposes newly method of rebuild-point project by comparison. A new method based on the viewpoint of engineering measurement is proposed to improve the lack of traditional operations.
The experimental results show that the GNSS-RTK rapidly-precise-positioning technology can replace the traditional static-measurement to practice rebuild-point project, and the 3D LiDAR ground control measurement which accuracy is enough can also be used as a reference for the other control points. Under the premise of high efficiency and constant accuracy, our team not only successfully introduced the concept of engineering measurement into the restoration and preservation of Monument Maintenance Project, but also completed the all 3D laser scanning operation on Li-Tengfang ancient house. All research processes can be provided to relevant units for reference.

Keywords: Monument Maintenance Project, Rebuild-point project, GNSS-RTK rapidly-precise-positioning positioning, 3D LiDAR Ground control measurement

©2019. Japan Geoscience Union. All Right Reserved.

Non-destructive field measurement for investigation of deteriorated parts of an artificial cave

Kaisei Sakane[1], *Chiaki T. Oguchi[1], Yasuhiko TAMURA[2]

1. Institute for Environmental Science and Technology, Graduate School of Science and Engineering, Saitama University, 2. The Exective Committee for the Preservation of Taya Cavern

Non-destructive measurements are useful methods for evaluating weathering degree without any damage on geoarchaeological sites. The present study aims to extract the deteriorated parts by using Silver Schmidt hammer and ultrasonic measurement on the Taya cave in Yokohama city. It is a manmade cave excavated from Kamakura to late Edo periods. Many sculptures and reliefs were carved on the surface of the cave wall made of soft rock. The cave has a complex three-layer structure with a total length of 570 m. Firstly, distribution maps showing cracks and exfoliation parts were created. Then, the points showing low rebound values and slow ultrasonic rates were plotted on the same map. After these on-site measurements, many dangerous parts were turned out within the worship route.

Keywords: Taya Cave, Silver Schmidt Test, Ultrasonic Rate

©2019. Japan Geoscience Union. All Right Reserved.

Ultra-portable thermal cameras for moisture detection

*Miguel Gomez-Heras[1], Laura Lopez-Gonzalez[2], Maria Teresa Gil-Muñoz[3]

1. Universidad Autonoma de Madrid, 2. Artfabrik, 3. Universidad Complutense de Madrid

Thermal imaging technology has grown and costs have decreased exponentially from 1987, when the first portable commercially available radiometric system appeared. Several firms produce nowadays ultra-portable thermal cameras that can be fitted in smartphones and tablets, giving resolutions of thermal images up to 320x240 p at a low cost. This facilitates the use of this tool for practitioners as a part of assessment of the state of conservation of heritage buildings and control and monitoring of conservation measurements. Moisture detection is a particular case in which thermal imaging is useful. This communication presents a case study of ultra-portable thermal camera usage for moisture detection and monitoring in two north-facing chapels in the ambulatory of the 14th to 16th Century Cathedral of Palencia (Spain). [Supported by Top Heritage (P2018/NMT-4372) programe from the Regional Government of Madrid (Spain)]

Keywords: Infrared Termography, Non-Destructive Testing, Moisture

©2019. Japan Geoscience Union. All Right Reserved.

A laboratory experiment on stone decay by combination of salt and ice crystallization

*Masato Sato[1], Tsuyoshi Hattanji[2]

1. Graduate School of Life and environmental Sciences, 2. Faculty of Life and EnvironmentalSciences, University of Tsukuba

A laboratory weathering experiment simulating combination of salt and ice crystallization was carried out using four types of rocks (porous tuff, dense tuff, dense sandstone, and porous andesite) with three types of salts (sodium chloride, sodium sulfate, or magnesium sulfate). The rock specimens were subjected to freeze-thaw cycles in a climatic cabinet where air temperature ranged from -30℃ to 10℃ within 24 hours. Prior to the freeze-thaw experiment, the specimens were immersed in saturated salt solutions at 10˚C or distilled water for 72 hours, and covered with foil for preventing the specimens from drying.
The specimens immersed in saturated salt solutions showed greater weight losses, reductions in Equotip rebound value and longitudinal wave velocity and surface expansion than those immersed in distilled water. Saturated solution of magnesium sulfate induced the greatest damage on rock specimens, although magnesium sulfate has been regarded as an inactive salt in the previous freeze-thaw experiments in which rock specimen were partly immersed in salt solution with dilute or mild concentration. Sodium sulfate induced rock damages comparable with sodium chloride. Sodium and magnesium sulfate crystallized from saturated solution and induced rock expansion prior to freezing. These salt crystals may fill micro-pores in rock and facilitates rock expansion and breakdown due to freezing.

Keywords: alt weathering, frost weathering, freeze-thaw, surface hardness, longitudinal wave velocity, surface expansion

©2019. Japan Geoscience Union. All Right Reserved.

Study of the micro-climatic monitoring on the Saint-Remi Basilica (Rheims, France)

*Emilie Huby[1], Celine Elise Thomachot-Schneider[1], Patricia Vazquez[1], Gilles Fronteau[1]

1. Universite de Reims-Champagne-Ardenne

Historical buildings are subjected to weathering through different factors such as temperature and humidity variations, that have a direct influence on different weathering processes. Insolation produces thermal expansion differences within the stone creating stresses at grain boundaries that can lead to disaggregation. If water is involved, a low temperature can cause the freezing of water inducing ice expansion and cryosuction. These repetitive stresses can damage the stone through fatigue failure. The measurement of environmental parameters on site is essential in order to study the weathering of the stone in its particular environment and anticipate risk areas.
To identify the micro-climatic conditions on a monument, an in situ monitoring was achieved on the Saint-Remi Basilica of Rheims, listed as a UNESCO World Heritage site. A sensor network was set up on the two towers of the monument in December 2017: fourteen temperature-humidity i-Buttons facing different directions, at different heights and recording with a time step of 1 hour, or a time step of 2 minutes for short measurement campaigns.
The data obtained by the sensor network highlighted the microclimates on the building. The height of the measured points had no significant impact on the results, whereas the orientation of the façade had an influence on the surface temperature. This was directly related to the longer solar exposure of the stone throughout the day and allowed to identify micro-climates. The façades exposed to the sun (South, East in the morning, West in the afternoon) present higher temperatures and lower relative humidity compared to the shadowed areas (North, East in the afternoon, West in the morning, other shadowed zones). The relative humidity measured was linked to the temperature: a temperature increase induces a humidity decrease. A mean difference of temperature between South and North of 2,7˚C with a maximum of 18˚C and a mean difference of relative humidity of 4,3% with a maximum of 48% were observed.
Climatic cycles on different time ranges were identified: an annual cycle alternating between winter and summer, a daily cycle due to sun exposure and short cycles identified during short term monitoring. These short abrupt variations of temperature (1-2˚C) on façades lasted between 5 and 40 minutes and were due to cloud cover and/or wind-speed. Four typical days inducing strains were identified: sunny days with a temperature increase superior to 10˚C, rainy days inducing wet/dry cycles, frost days presenting frost/thaw cycles and stormy days where a sudden rain on heated stones caused abrupt temperature and humidity variations. A year can thus be fragmented in those 4 categorized days. This repartition of typical days over a year depended on the micro-climatic variations previously identified: the shadowed zones experienced less sunny days and more rainy days.
This study of climatic monitoring will help anticipate the stone weathering on the Saint-Remi Basilica. The monitoring will continue for the next two years in order to obtain reproducible data and will be coupled with an infrared thermography monitoring. The strains corresponding to the four identified types of day are reproduced through accelerated ageing experiments using the parameters recorded on site. From the repartition of these typical days in one year, this will allow to estimate the behavior of a stone during a year on a sun-exposed façade and on a shadowed zone of the Basilica. The final goal is to be able to anticipate the stone weathering on the monument and identify risk areas.

Keywords: weathering processes, micro-climate, Saint-Remi Basilica, in situ monitoring

©2019. Japan Geoscience Union. All Right Reserved.

©2019. Japan Geoscience Union. All Right Reserved.

[E] Poster | H (Human Geosciences)：H-TT Technology & Techniques

Wed. May 29, 2019 5:15 PM - 6:30 PM JST | Wed. May 29, 2019 8:15 AM - 9:30 AM UTC | Poster Hall International Exhibition Hall8, Makuhari Messe_23

[H-TT21] Non-destructive techniques applied to stone cultural heritage

convener:Chiaki T. Oguchi(Institute for Environmental Science and Technology, Graduate School of Science and Engineering, Saitama University), Celine Elise Thomachot-Schneider(Groupe d'etude des environnements naturels, anthropiques et archeologiques - Universite de Reims-Champagne-Ardenne (France)), Wonsuh Song(Waseda University), Miguel Gomez-Heras(Universidad Autonoma de Madrid)

Non-destructive and non-invasive techniques applying to cultural heritage made of stones, soils and earthen materials have been significantly developed over past years, and thus, the interest in such techniques has greatly increased. Here, we focus the session on new devices, new protocols and new data treatments that allow better understanding of weathering mechanisms, decay states and response to treatments.
A few topics would be listed as follows: 1) The development of new techniques and devices in cultural heritage and new protocols using non-destructive techniques; 2) The application of these techniques and protocols on indoor and outdoor case studies and laboratory studies; 3) The assessment of weathering mechanisms, weathering kinetics, decay state, and response to treatments; and 4) The modeling and simulation of decay processes.

[HTT21-P01] Comparison and Analysis of GNSS-RTK Combined with 3D LiDAR Technology on Monument Maintenance Project

*Lih-Shinn Hwang[1], Chien-Hua Chiu[1], Chien-Wen Wang[1], Hsiao-Hung Chen[1] (1.National Defense Univ.)

[HTT21-P02] Non-destructive field measurement for investigation of deteriorated parts of an artificial cave

Kaisei Sakane[1], *Chiaki T. Oguchi[1], Yasuhiko TAMURA[2] (1.Institute for Environmental Science and Technology, Graduate School of Science and Engineering, Saitama University, 2.The Exective Committee for the Preservation of Taya Cavern)

[HTT21-P03] Ultra-portable thermal cameras for moisture detection

*Miguel Gomez-Heras[1], Laura Lopez-Gonzalez[2], Maria Teresa Gil-Muñoz[3] (1.Universidad Autonoma de Madrid, 2.Artfabrik, 3.Universidad Complutense de Madrid)

[HTT21-P04] A laboratory experiment on stone decay by combination of salt and ice crystallization

*Masato Sato[1], Tsuyoshi Hattanji[2] (1.Graduate School of Life and environmental Sciences, 2.Faculty of Life and EnvironmentalSciences, University of Tsukuba)

[HTT21-P05] Study of the micro-climatic monitoring on the Saint-Remi Basilica (Rheims, France)

*Emilie Huby[1], Celine Elise Thomachot-Schneider[1], Patricia Vazquez[1], Gilles Fronteau[1] (1.Universite de Reims-Champagne-Ardenne)

Comparison and Analysis of GNSS-RTK Combined with 3D LiDAR Technology on Monument Maintenance Project

*Lih-Shinn Hwang[1], Chien-Hua Chiu[1], Chien-Wen Wang[1], Hsiao-Hung Chen[1]

1. National Defense Univ.

The Precision is the first face problem in the restoration and preservation of Monument Maintenance Project. It may be that the initial coordinates of the position cannot be effectively determined by each object of historical antiquities or buildings, which seriously affects the proportional position when the combination is later reconstructed; or because the relative relationship with the natural environment is neglected, the restoration project is time consuming and even there may be errors that cannot be recovered.
Therefore, external reference control points play an important role in the 3D laser scanning operation of historical antiquities or buildings. Especially for long-term monitoring, it almost determines the accuracy of the following article scanning.
However, due to the unexpected situation on the spot, there are often control points lost, and there is a need for a rebuild-point project, which affects the 3D scanning operation of the later cultural relics. Rebuild-point project requires not only consistent precision, but also convenience and speed. This team takes the ancient house of Li-Tengfang, a national monument, as an example. When this term is studying on the restoration and preservation of Monument Maintenance Project, it is, and proposes newly method of rebuild-point project by comparison. A new method based on the viewpoint of engineering measurement is proposed to improve the lack of traditional operations.
The experimental results show that the GNSS-RTK rapidly-precise-positioning technology can replace the traditional static-measurement to practice rebuild-point project, and the 3D LiDAR ground control measurement which accuracy is enough can also be used as a reference for the other control points. Under the premise of high efficiency and constant accuracy, our team not only successfully introduced the concept of engineering measurement into the restoration and preservation of Monument Maintenance Project, but also completed the all 3D laser scanning operation on Li-Tengfang ancient house. All research processes can be provided to relevant units for reference.

Keywords: Monument Maintenance Project, Rebuild-point project, GNSS-RTK rapidly-precise-positioning positioning, 3D LiDAR Ground control measurement

©2019. Japan Geoscience Union. All Right Reserved.

Non-destructive field measurement for investigation of deteriorated parts of an artificial cave

Kaisei Sakane[1], *Chiaki T. Oguchi[1], Yasuhiko TAMURA[2]

1. Institute for Environmental Science and Technology, Graduate School of Science and Engineering, Saitama University, 2. The Exective Committee for the Preservation of Taya Cavern

Non-destructive measurements are useful methods for evaluating weathering degree without any damage on geoarchaeological sites. The present study aims to extract the deteriorated parts by using Silver Schmidt hammer and ultrasonic measurement on the Taya cave in Yokohama city. It is a manmade cave excavated from Kamakura to late Edo periods. Many sculptures and reliefs were carved on the surface of the cave wall made of soft rock. The cave has a complex three-layer structure with a total length of 570 m. Firstly, distribution maps showing cracks and exfoliation parts were created. Then, the points showing low rebound values and slow ultrasonic rates were plotted on the same map. After these on-site measurements, many dangerous parts were turned out within the worship route.

Keywords: Taya Cave, Silver Schmidt Test, Ultrasonic Rate

©2019. Japan Geoscience Union. All Right Reserved.

Ultra-portable thermal cameras for moisture detection

*Miguel Gomez-Heras[1], Laura Lopez-Gonzalez[2], Maria Teresa Gil-Muñoz[3]

1. Universidad Autonoma de Madrid, 2. Artfabrik, 3. Universidad Complutense de Madrid

Thermal imaging technology has grown and costs have decreased exponentially from 1987, when the first portable commercially available radiometric system appeared. Several firms produce nowadays ultra-portable thermal cameras that can be fitted in smartphones and tablets, giving resolutions of thermal images up to 320x240 p at a low cost. This facilitates the use of this tool for practitioners as a part of assessment of the state of conservation of heritage buildings and control and monitoring of conservation measurements. Moisture detection is a particular case in which thermal imaging is useful. This communication presents a case study of ultra-portable thermal camera usage for moisture detection and monitoring in two north-facing chapels in the ambulatory of the 14th to 16th Century Cathedral of Palencia (Spain). [Supported by Top Heritage (P2018/NMT-4372) programe from the Regional Government of Madrid (Spain)]

Keywords: Infrared Termography, Non-Destructive Testing, Moisture

©2019. Japan Geoscience Union. All Right Reserved.

A laboratory experiment on stone decay by combination of salt and ice crystallization

*Masato Sato[1], Tsuyoshi Hattanji[2]

1. Graduate School of Life and environmental Sciences, 2. Faculty of Life and EnvironmentalSciences, University of Tsukuba

A laboratory weathering experiment simulating combination of salt and ice crystallization was carried out using four types of rocks (porous tuff, dense tuff, dense sandstone, and porous andesite) with three types of salts (sodium chloride, sodium sulfate, or magnesium sulfate). The rock specimens were subjected to freeze-thaw cycles in a climatic cabinet where air temperature ranged from -30℃ to 10℃ within 24 hours. Prior to the freeze-thaw experiment, the specimens were immersed in saturated salt solutions at 10˚C or distilled water for 72 hours, and covered with foil for preventing the specimens from drying.
The specimens immersed in saturated salt solutions showed greater weight losses, reductions in Equotip rebound value and longitudinal wave velocity and surface expansion than those immersed in distilled water. Saturated solution of magnesium sulfate induced the greatest damage on rock specimens, although magnesium sulfate has been regarded as an inactive salt in the previous freeze-thaw experiments in which rock specimen were partly immersed in salt solution with dilute or mild concentration. Sodium sulfate induced rock damages comparable with sodium chloride. Sodium and magnesium sulfate crystallized from saturated solution and induced rock expansion prior to freezing. These salt crystals may fill micro-pores in rock and facilitates rock expansion and breakdown due to freezing.

Keywords: alt weathering, frost weathering, freeze-thaw, surface hardness, longitudinal wave velocity, surface expansion

©2019. Japan Geoscience Union. All Right Reserved.

Study of the micro-climatic monitoring on the Saint-Remi Basilica (Rheims, France)

*Emilie Huby[1], Celine Elise Thomachot-Schneider[1], Patricia Vazquez[1], Gilles Fronteau[1]

1. Universite de Reims-Champagne-Ardenne

Historical buildings are subjected to weathering through different factors such as temperature and humidity variations, that have a direct influence on different weathering processes. Insolation produces thermal expansion differences within the stone creating stresses at grain boundaries that can lead to disaggregation. If water is involved, a low temperature can cause the freezing of water inducing ice expansion and cryosuction. These repetitive stresses can damage the stone through fatigue failure. The measurement of environmental parameters on site is essential in order to study the weathering of the stone in its particular environment and anticipate risk areas.
To identify the micro-climatic conditions on a monument, an in situ monitoring was achieved on the Saint-Remi Basilica of Rheims, listed as a UNESCO World Heritage site. A sensor network was set up on the two towers of the monument in December 2017: fourteen temperature-humidity i-Buttons facing different directions, at different heights and recording with a time step of 1 hour, or a time step of 2 minutes for short measurement campaigns.
The data obtained by the sensor network highlighted the microclimates on the building. The height of the measured points had no significant impact on the results, whereas the orientation of the façade had an influence on the surface temperature. This was directly related to the longer solar exposure of the stone throughout the day and allowed to identify micro-climates. The façades exposed to the sun (South, East in the morning, West in the afternoon) present higher temperatures and lower relative humidity compared to the shadowed areas (North, East in the afternoon, West in the morning, other shadowed zones). The relative humidity measured was linked to the temperature: a temperature increase induces a humidity decrease. A mean difference of temperature between South and North of 2,7˚C with a maximum of 18˚C and a mean difference of relative humidity of 4,3% with a maximum of 48% were observed.
Climatic cycles on different time ranges were identified: an annual cycle alternating between winter and summer, a daily cycle due to sun exposure and short cycles identified during short term monitoring. These short abrupt variations of temperature (1-2˚C) on façades lasted between 5 and 40 minutes and were due to cloud cover and/or wind-speed. Four typical days inducing strains were identified: sunny days with a temperature increase superior to 10˚C, rainy days inducing wet/dry cycles, frost days presenting frost/thaw cycles and stormy days where a sudden rain on heated stones caused abrupt temperature and humidity variations. A year can thus be fragmented in those 4 categorized days. This repartition of typical days over a year depended on the micro-climatic variations previously identified: the shadowed zones experienced less sunny days and more rainy days.
This study of climatic monitoring will help anticipate the stone weathering on the Saint-Remi Basilica. The monitoring will continue for the next two years in order to obtain reproducible data and will be coupled with an infrared thermography monitoring. The strains corresponding to the four identified types of day are reproduced through accelerated ageing experiments using the parameters recorded on site. From the repartition of these typical days in one year, this will allow to estimate the behavior of a stone during a year on a sun-exposed façade and on a shadowed zone of the Basilica. The final goal is to be able to anticipate the stone weathering on the monument and identify risk areas.

Keywords: weathering processes, micro-climate, Saint-Remi Basilica, in situ monitoring

©2019. Japan Geoscience Union. All Right Reserved.

©2019. Japan Geoscience Union. All Right Reserved.

[E] Oral | H (Human Geosciences)：H-TT Technology & Techniques

Wed. May 29, 2019 3:30 PM - 5:00 PM JST | Wed. May 29, 2019 6:30 AM - 8:00 AM UTC | 101 1F

[H-TT21] Non-destructive techniques applied to stone cultural heritage

convener:Chiaki T. Oguchi(Institute for Environmental Science and Technology, Graduate School of Science and Engineering, Saitama University), Celine Elise Thomachot-Schneider(Groupe d'etude des environnements naturels, anthropiques et archeologiques - Universite de Reims-Champagne-Ardenne (France)), Wonsuh Song(Waseda University), Miguel Gomez-Heras(Universidad Autonoma de Madrid), Chairperson:Wonsuh Song, Chiaki Oguchi

Non-destructive and non-invasive techniques applying to cultural heritage made of stones, soils and earthen materials have been significantly developed over past years, and thus, the interest in such techniques has greatly increased. Here, we focus the session on new devices, new protocols and new data treatments that allow better understanding of weathering mechanisms, decay states and response to treatments.
A few topics would be listed as follows: 1) The development of new techniques and devices in cultural heritage and new protocols using non-destructive techniques; 2) The application of these techniques and protocols on indoor and outdoor case studies and laboratory studies; 3) The assessment of weathering mechanisms, weathering kinetics, decay state, and response to treatments; and 4) The modeling and simulation of decay processes.

3:30 PM - 3:45 PM JST | 6:30 AM - 6:45 AM UTC

[HTT21-01] Study on creation of 3D model by SfM photogrammetry: An example of Taya Cave

Kisara Shimizu[1], *Chiaki T. Oguchi[1], Yasuhiko TAMURA[2], Yuichi S. Hayakawa[3], Takuro Ogura[4], OGATA KEISUKE[5] (1.Institute for Environmental Science and Technology, Graduate School of Science and Engineering, Saitama University, 2.The Exective Committee for the Preservation of Taya Cavern, 3.Faculty of Environmental Earth Science, Hokkaido University, 4.Graduate School of Frontier Sciences, The University of Tokyo, 5.Tsurumi University)

3:45 PM - 4:00 PM JST | 6:45 AM - 7:00 AM UTC

[HTT21-02] TLS measurement data and 3D printing of an artificial cave for geotechnical and educational applications

*Yuichi S. Hayakawa[1,2], Takuro Ogura[4,5], Yasuhiko Tamura[2], Chiaki T. Oguchi[3], Kisara Shimizu[3] (1.Faculty of Environmental Earth Science, Hokkaido University, 2.Center for Spatial Information Science, The University of Tokyo, 3.Saitama University, 4.Graduate School of Frontier Science, The University of Tokyo, 5.Graduate School of Environmental Science, Hokkaido University)

4:00 PM - 4:15 PM JST | 7:00 AM - 7:15 AM UTC

[HTT21-03] Conservation restoration of the world heritage of Okinawa Prefecture, Sonohyan-utaki Ishimon - Situation after 30 years since filling with mortar and applying silicone resin.

*Wonsuh Song[1], Tadateru Nishiura[2], Chiaki T. Oguchi[3] (1.Waseda University, 2.Kokushika Univeristy, 3.Saitama University)

4:15 PM - 4:30 PM JST | 7:15 AM - 7:30 AM UTC

[HTT21-04] Application of portable XRF analysis for provenance of seabed worked stone in coastal are of Kochi Prefecture

★Invited Papers

*Wataru Tanikawa[1], Go-Ichiro Uramoto[2], Masafumi MURAYAMA[2], Yohei Hamada[1], Yuhji Yamamoto[2], Osamu Tadai[3] (1.Japan Agency for Marine-Earth Science and Technology, Kochi Instutute for Core Sample Research, 2.Kochi University, Center for Advanced Marine Core Research, 3.Marine Works Japan LTD.)

4:30 PM - 4:45 PM JST | 7:30 AM - 7:45 AM UTC

[HTT21-05] pXRF analyses on Assyrain sculptures

★Invited Papers

*Ryo Anma[1], Ki-Cheol Shin[2], Chikako Watanabe[3], Akihiro Tuji[4] (1.Graduate School of Technology, Industrial and Social Sciences, Tokushima University, 2.Research Institute for Humanity and Nature,

3.Faculty of International Studies, Osaka Gakuin University, 4.National Museum of Nature and Science)

4:45 PM - 5:00 PM JST | 7:45 AM - 8:00 AM UTC

[HTT21-06] Discussion

*Chiaki T. Oguchi[1] (1.Institute for Environmental Science and Technology, Graduate School of Science and Engineering, Saitama University)

Study on creation of 3D model by SfM photogrammetry: An example of Taya Cave

Kisara Shimizu[1], *Chiaki T. Oguchi[1], Yasuhiko TAMURA[2], Yuichi S. Hayakawa[3], Takuro Ogura[4], OGATA KEISUKE[5]

1. Institute for Environmental Science and Technology, Graduate School of Science and Engineering, Saitama University, 2. The Exective Committee for the Preservation of Taya Cavern, 3. Faculty of Environmental Earth Science, Hokkaido University, 4. Graduate School of Frontier Sciences, The University of Tokyo, 5. Tsurumi University

SfM (Structure-from-Motion) photogrammetry is one of the methods for creating 3D models of objects by extracting feature points in the images. Taya Cave, the investigation site of the present study, is a historical site of Yokohama City. It has about 200 base-reliefs on the surface of the cave tunnel walls, however, they are suffering from weathering and difficult to preserve from it in the future. The cave was excavated in Kamakura Era originally, and has a total length of 570 m with a three-layer structure. The present study tried to make a 3D model of this complicated, dark and narrow cave by SfM photogrammetry. The accuracy of the created 3D model were evaluated by comparing the values of distances between from the 3D model and from 2016 actual survey data.

Keywords: SfM, Taya Cave

©2019. Japan Geoscience Union. All Right Reserved.

TLS measurement data and 3D printing of an artificial cave for geotechnical and educational applications

*Yuichi S. Hayakawa[1,2], Takuro Ogura[4,5], Yasuhiko Tamura[2], Chiaki T. Oguchi[3], Kisara Shimizu[3]

1. Faculty of Environmental Earth Science, Hokkaido University, 2. Center for Spatial Information Science, The University of Tokyo, 3. Saitama University, 4. Graduate School of Frontier Science, The University of Tokyo, 5. Graduate School of Environmental Science, Hokkaido University

Conservation of an underground cultural heritage is often a controversial issue due partly to its invisibility and insufficient awareness in the local society. Also, the safety assessment is necessary to promote sustainable protection of an underground cultural heritage. The developments in high-definition topographic measurements enable to acquire detailed three-dimensional morphological data of a cave, which can be further utilized for the visualization and structural analyses. Regarding the measurements and visualization, we present a case study at the Taya Cave, a registered cultural heritage in Yokohama City, Kanagawa Prefecture in central Japan. The terrestrial laser scanning was performed from multiple scan positions throughout the cave, and the point clouds were registered using the feature-based iterated closest point algorithm. The registered point clouds were then converted into a mesh model, to which face error corrections and a solid filling were applied. After these processes, the mesh model can be printed out in three dimensions. The 3D print model of the cave is used for the class teaching in an elementary school in the local area, and such the visualization of the cave successfully enhanced the recognition by students regarding the underground cultural heritage. The 3D data can also be utilized for the structural assessment of the cave. Effective and sustainable protection of the cave will further be possible by integrating such geotechnical assessments and outreach activities in the local society.

Keywords: terrestrial laser scanning, point cloud, 3D printing, outreach, underground cultural heritage

©2019. Japan Geoscience Union. All Right Reserved.

Conservation restoration of the world heritage of Okinawa Prefecture, Sonohyan-utaki Ishimon - Situation after 30 years since filling with mortar and applying silicone resin.

*Wonsuh Song[1], Tadateru Nishiura[2], Chiaki T. Oguchi[3]

1. Waseda University, 2. Kokushika Univeristy, 3. Saitama University

Sonohyan-utaki Ishimon in the Shuri Castle Park has been registered as a World Heritage Site in 2000 as a place of "Gusuku and related heritage group of the Ryukyu Kingdom". The stone gate (Ishimon) and the forest behind it are called Sonohyan-utaki and used as a place of worship for praying for safety when the King of the Ryukyu Kingdom goes out. It was built with Ryukyu Limestone in 1519, was designated as the old national treasure in 1933 but was destroyed in the battle against Okinawa, was restored in 1957, and repaired in 1986. It became the national designated building in 1972. At the time of demolition repair, an old roof stone was used, but cleaning and water repellent silicone resin impregnation and surface filling were done at this time. Currently, as can be seen in Figure 1, the color of the entire stone gate becomes darker, the difference in color between the filling part of the roof and the original stone is becoming noticeable. The purpose of this study is to be used for the repair treatment in the future.
In order to understand the color of the surface of the repaired roof and the overall color of the stone gate, quantitative measurements were made using a spectroscopic colorimeter (Konica Minolta, CM-700d) at 51 locations on the surface of the stone gate. The proportion of blackened parts was determined from the front of the stone gate using Photoshop. To measure the surface temperature of the stone gate, we grasped the temperature distribution of the surface using the FLIR thermal camera.
We installed a button type temperature and humidity measuring instrument in the upper left side of the stone gate with the permission of Naha City to grasp the change of temperature and humidity in the year-round. As a result of the measurement by the spectrophotometer, the color of limestone was bright, and it was almost the same color as the repair material in the roof part. However, the discoloration rate and the situation were different after 30 years. The repair material was gray, and it was found that the original stone was darker. The average annual temperature observed under the roof of the stone gate was 24 ˚c, and the average humidity was 81.5%, and the characteristics of the hot and humid subtropical climate were observed. The average temperature in winter was 22.1 ˚c, and the humidity was 80% and the lowest temperature was 8.5 ˚c. Therefore, it seems that the growth of vegetation is very fast and it may affect the color of rock surface.

Keywords: Stone cultural heritage, Restoration, Okinawa , Limestone, Colorimeter

©2019. Japan Geoscience Union. All Right Reserved.

Fig. 1. After completing conservation restoration work of Sonohyan-utaki Ishimon (left) and situation of thirty years later (right).

©2019. Japan Geoscience Union. All Right Reserved.

Application of portable XRF analysis for provenance of seabed worked stone in coastal are of Kochi Prefecture

*Wataru Tanikawa[1], Go-Ichiro Uramoto[2], Masafumi MURAYAMA[2], Yohei Hamada[1], Yuhji Yamamoto[2], Osamu Tadai[3]

1. Japan Agency for Marine-Earth Science and Technology, Kochi Instutute for Core Sample Research, 2. Kochi University, Center for Advanced Marine Core Research, 3. Marine Works Japan LTD.

Many stone pillars around 1m long, which look like artifacts, lie on the seafloor in off Tsumajiro, Kochi Prefecture, Japan. Tsumajiro area has been repeatedly damaged by tsunami from Nankai earthquakes, and extreme rainfalls by typhoon events. Therefore, we suggest that a tsunami or river floods might have transported the pillars offshore, or coseismic land subsidence might have caused them to become submerged. To assess the origin of the submerged stone pillars in the Tsumajiro area (Tsumajiro pillars), we analyzed mineralogy, geochemistry and physical property of Tsumajiro pillars, of rocks from natural expores and quarries in Tsumajiro and neighboring areas, and of building stones in use in the Tsumajiro area. We analyzed concentrations of major and trace elements in samples using a portable X-ray fluorescence (pXRF) spectrometer, and estimated mineral composition of samples using powdered XRD analysis. Porosity and grain density were also measured on all samples.

In the XRF spectral data, we clearly recognized peaks for 12 elements (Mg, Si, S, K, Ca, Ti, Mn, Fe, Rb, Sr, Zr, and Pd) in all samples. Therefore, we selected these 12 elements for PCA. In the PCA results for all samples, we could clearly divide those into sandstone group and shale group from the first principle component, where components of Mg, Fe, and Ti strongly influenced. In PCA results for sandstone only, we could see the characteristics of each samples much more clearly. Submerged pillars showed similar characteristics, where a component of Zr was strongly contributed, with Tatsukushi formation in Misaki group (natural exposures and quarries) and foundation stones for main building at Tsumajiro area. Porosity, grain density, and mineral composition were also similar between Tsumajiro pillars, Tatsukushi formation, and a foundation stone.
Our results suggest that the submerged stone pillars were made from Tatsukushi sandstone and had been utilized as building stones for structures such as steps and foundations in Tsumajiro village.

Keywords: Principle Component Analysis (PCA), Provenance, pXRF, sedimentary rock, Nankai earthquake

©2019. Japan Geoscience Union. All Right Reserved.

pXRF analyses on Assyrain sculptures

*Ryo Anma[1], Ki-Cheol Shin[2], Chikako Watanabe[3], Akihiro Tuji[4]

1. Graduate School of Technology, Industrial and Social Sciences, Tokushima University, 2. Research Institute for Humanity and Nature, 3. Faculty of International Studies, Osaka Gakuin University, 4. National Museum of Nature and Science

To evaluate a possibility of reconstruction and understanding the provenance of stone materials used in the ancient cities of Western Asia, some of which have been destroyed and/or dismantled, and are moved to different places of the world, we characterized the bulk geochemical composition of gypsum-carbonate rocks, on which the Assyrians carved sculptures to decollate their palaces, using an Olympus VANTA portable X-ray fluorescence spectroscopy (pXRF). To establish the methodology, we started with the Assyrian sculptures with known provenance: i.e. the collections of the British Museum, the Ashmolean Museum, Magdalen College (Oxford), the Okayama Orient Museum and the MIHO museum.
The pXRF analysis was performed using a Rh target at 40 kV and 100 μA. Beam time was 20 seconds for Beam 1 and 15 and 30 seconds, in later sessions, for Beam 2. The accuracy and precision of the analyses were assessed by analyzing several powdered reference samples of igneous rocks (JB-2 basalt, JA-1, JA-2 andesites, JR-2 rhyolite JG1, JG2 granites and JGb-1 gabbro) and sedimentary rocks (JLk-1 lake sediment, JSd-1 and JSd-2 river sediments, JLs-1 limestone and JDo-1 dolomite) distributed by the Geological Survey of Japan, and gypsum samples (alabaster, selenite and satin spar) distributed by Nichika Inc. We performed the measurement three-times for each spot to assess repeatability of the measurement and/or inhomogeneity of the samples.
Our results showed that ~ 99% of the measured Assyrian sculptures were made of gypsum-anhydrate rocks. Although their distribution fields largely overlap, the gypsum sculptures from Nineveh tend to have more impurities when compared with those from Nimrud and Khorsabad. Visually, the stone materials used in the sculptures in Nimrud often have homogeneously distributed large gypsum crystals, whereas those from Nineveh are rather inhomogeneous and finer in grain size, and often exhibit developed bedding planes. Together with the textural changes, we provisionally conclude that degraded stone materials became used over time.
The Til-Tuba sculpture from Room 33 of the Southwest Palace of Nineveh has higher Ca and lower S contents compared with others. Visually, it contains numerous foraminifera shells of *Alveolinidae Sp*. The different chemical composition could be attributed to the amount of the included foraminifera shells. Stones from Room 36 of Nineveh Southwest Palace have slightly higher Al and Fe contents than others. Although, few such examples have somewhat different compositions, the exact provenance would not be able to identify from a single chemical data. More information obtained through destructive analyses would be necessary for the reconstruction and understanding the provenance of stone materials, such as textural and mineralogical information through thin-section observation, crystallographic information through XRD analysis and analyses of micro-fossils.
Nevertheless, our observation from a material science point of view can provide evidence to what Sennacherib (705-681 BCE) described in his text. The king states that he used “Na_4.^{d}Še.tir” stone from Nipur (Judi Dagh in SE Turkey) that looks like cucumber seeds to construct the statues of Aladlammû and *Apsātu*. Based on this, Mitchel and Middleton (2002) speculated that this same stone was used for the reliefs in Room 33 of the Southwest Palace, Nineveh. If their speculation is correct, evaporites of the middle to late Miocene Fars formation should have comprised the quarry.

Keywords: pXRF, Assyrian sculpture

©2019. Japan Geoscience Union. All Right Reserved.

©2019. Japan Geoscience Union. All Right Reserved.

Discussion

*Chiaki T. Oguchi[1]

1. Institute for Environmental Science and Technology, Graduate School of Science and Engineering, Saitama University

Discussion on non-destructive techniques for geoheritage.

Keywords: non-destructive techniques

©2019. Japan Geoscience Union. All Right Reserved.

[E] Poster | H (Human Geosciences)：H-CG Complex & General

Wed. May 29, 2019 3:30 PM - 5:00 PM JST | Wed. May 29, 2019 6:30 AM - 8:00 AM UTC | Poster Hall International Exhibition Hall8, Makuhari Messe_15

[H-CG25] International Comparison of Landscape Appreciation

convener:Anastasia Petrova(Institute of Oriental Studies of the Russian Academy of Sciences), yoji aoki(Open University of Japan)

Evaluation of landscape has been developed in a variety of fields, such as geography, landscape architecture, nature protection, and some others. Landscape appreciation is a complex and sophisticated psychological phenomenon. There is no consensus among researchers on what the phenomenon of "landscape" truly is, how people physiologically and mentally experience it, which human attributes affect the perception of it, and why it is apprehended the way it is. The concept of landscape appreciation has yet to be clearly defined and there is a lack of agreement on evaluation methods, the factors that determine landscape preferences, the steps in appreciation, and so forth. This session aims to discuss the research findings of landscape evaluation in various fields, including geography, geomorphology, landscape planning, architecture, engineering, social sciences, environmental psychology, meteorology, phenology, and so on.

[HCG25-P01] The Globally Important Agricultural Heritage of Aso from the perspective of landscape and its supporting systems

*REIKO MACHIDA[1] (1.TOKYO UNIVERSITY OF AGRICULTURE)

[HCG25-P02] Hazardous natural phenomena and weather conditions appreciation in Russian landscape painting

*ELENA PETROVA[1] (1.Lomonosov Moscow State University, Faculty of Geography)

[HCG25-P03] Trends of evaluation items to landscape appreciation until 2017 in the English journals

*yoji aoki[1], keisuke mukagai[2], Anastasia Petrova[3] (1.Open University of Japan, 2.Nagano University, 3.Institute of Oriental Studies, Russian Academy of Sciences)

The Globally Important Agricultural Heritage of Aso from the perspective of landscape and its supporting systems

*REIKO MACHIDA[1]

1. TOKYO UNIVERSITY OF AGRICULTURE

Globally Important Agricultural Heritage Systems (GIAHS) is a partnership initiative of the Food and Agriculture Organization of the United Nations which began in 2002 with the aim to identify, support and safeguard remarkable land use systems and landscapes that are rich in globally significant biological diversity evolving from the co-adaptation of a community with its environment and its needs and aspirations for sustainable development. There are 19 countries and 45 areas around the world, and among them 9 areas in Japan that are listed as GIAHS at present.The Aso area located in Northern Kyusyu features the world's largest caldera, which is 25 km wide from north to south and 18 km from east to west and grassland landscapes. The vast grasslands of the Aso area have been managed throughout history by local agricultural activities such as controlled burning, mowing and pasturage since the Heian period. The historical land use in Aso has been a balanced combination of rice fields at the caldera floor, forestry and fungiculture at the foot of the caldera, and grazing pasture at the top of caldera, which is carried out in harmony with the environment. The management of the Aso grasslands for sustainable agriculture have been recognized and certified as Globally Important Agricultural Heritage Systems (GIAHS) in 2013.In terms of landscape, the values of Aso as Globally Important Agricultural Heritage System are the dynamic grassland landscapes of the large caldera, the historical paddies and rice terraces, which vary in size from small to large as a result of the local human activities. There are beautiful rural landscapes on various scales.However, the productivity oriented rural development and the division of land has been having a negative impact on the landscape value of the GIAHS. There are cases of rice paddies and buildings that contribute to the landscape value being lost. From such cases, it is evident that the landscape structures that should be protected since they are GIHS are not recognized widely enough.This study investigated the landscape value and landscape structure as GIAHS and its value supports landscape policy. As a result, it became clear that the landscape structure of Minamiaso village consist of the traditional combination of grasslands and paddy fields retains significant wildlife habitat and picturesque agricultural landscapes. It has become clear that development activities do not influence to landscape in large-scale, however development activities as land readjustment project influenced to landscape in small and medium-scale. "Landscape planning" "Landscape agricultural development plan" can support the landscape structure in small and medium -scale. It is important to plan the land use for the landscape value of GIAHS.

Keywords: Globally Important Agricultural Heritage Systems (GIAHS), Landscape, Landscape Planning

©2019. Japan Geoscience Union. All Right Reserved.

Hazardous natural phenomena and weather conditions appreciation in Russian landscape painting

*ELENA PETROVA[1]

1. Lomonosov Moscow State University, Faculty of Geography

The fixation of various natural phenomena by landscape artists of different historical periods in different regions and countries has not only purely aesthetic interest, but also particular interest to science. During the period of Romanticism that has spread in the European and Russian art in the 19th century, Russian art turned to real living nature. Landscapes of the native country began to play a dominant role in the formation of landscape image. Romanticism aroused interest not only in the picturesque and exotic landscapes, but also in the majestic forces of nature. Volcanic eruptions, earthquakes, storms, thunderstorms, floods, and other natural hazards were new motifs for artists of that time. Romantic artists were inclined to exaggerate the power and destructive forces of natural phenomena they portrayed, elevating any event of this kind to the rank of a natural disaster. Often, they portrayed the rather ordinary storm, thunderstorm, flood as a universal natural catastrophe, comparable, perhaps, only to the biblical flood. What to say about really extraordinary events. Most vividly, the theme of the turbulent, dramatic landscape was developed in the works by Aivazovsky who quite realistically showed the sea element in various stages of its manifestation - from complete calm to the strongest storm. Being in Italy, Russian artists could not disregard such an extraordinary event as the violent eruption of the volcano Vesuvius, which occurred in 1822; many have captured it in their landscape images.

Thanks to the rapid development of scientific knowledge and discoveries in the field of geosciences, including meteorology, artists were encouraged to observe various atmospheric phenomena and weather conditions. Gradually, the sky ceased to be depicted simply as a smooth blue background, as was customary in the tradition of classicism; carefully traced clouds of various types, shapes and shades began to appear in pictures. In addition, various evaporations, fogs, haze, etc. became objects of the landscape image. Romantic artists were little interested in depicting winter and snow, despite the fact that the cold season with a steady snow cover continues in Russia for almost half a year from November to early April. The painting “Russian Winter” (1827) by Nikifore Krylov became perhaps the first winter landscape image in Russian painting. Krylov depicted a somewhat naive, but quite real, winter landscape on the bank of the Tosna River in the vicinity of St. Petersburg, which he painted from life. He was able to reliably convey the atmosphere of the Russian winter: a valley covered with snow, a frozen river, a dark strip of forest in the distance and the peasants with their daily affairs on the road down to the river in the foreground. The first bright and joyful snow-covered landscape image was created, apparently, by Alexey Savrasov in his famous painting “The Rooks Have Come Back” (1871). The spring snow melting and sparkling in the sun became later the favorite motif of the Russian painting. Comparative analysis of landscape pictures can be an important tool, in addition to scientific methods, in studying the nature and dynamics of various hazardous natural processes and phenomena, including hydrological and meteorological ones in conditions of changing climate.

Keywords: hazardous natural phenomena , weather conditions , landscape painting, landscape images

©2019. Japan Geoscience Union. All Right Reserved.

Trends of evaluation items to landscape appreciation until 2017 in the English journals

*yoji aoki[1], keisuke mukagai[2], Anastasia Petrova[3]

1. Open University of Japan, 2. Nagano University, 3. Institute of Oriental Studies, Russian Academy of Sciences

Introduction
We have considered trends of landscape appreciation since JpGU2013-2018. According to the definition of landscape phenomena proposed by Prof. O. Shinohara (Fig. 1), we reported the trends of studies in each part of the phenomena.

Aoki, Y. (1999) described the first landscape evaluation using psychometrical methods to be pioneered by Peterson, G.L. (1967). Before this development, they tried to find the landscape appreciation using various descriptors. They were mostly belonging to the literature or the paintings. As for the literature, the first description of mountain was found in Francesco Petrarca in 1336 of France (Kondo, T. 2002). But his description has no reliable evidence to ensure the landscape. In the field of art, Albrecht Altdorfer drew the first natural landscape in the beginning of 15th century of Germany (Cavaliere, B. 1989). But we could not measure the physical data from his picture. The literature and the art found the beauty of natural landscape by these examples. They recorded the aesthetic beauty in landscape (Thiel, P. 1968).

Jay Appleton (1980) explained the scientific reason of the landscape phenomena with physical data, e.g. geomorphysical data and meteorological data. He explained the landscape phenomena of two pictures, Constable's Weymouth Bay and Constable's sunset study of Hampstead Heath. His approach must be the scientific based explanation to find psychological phenomena of landscape using the geology and meteorology. But the psychological phenomena could deviate by the person observed and the results must be happened statistically. So the process of the landscape phenomena should be explained by stochastic process of psychology. Then scientists developed psychological approach to it.

Here, we summarize the appreciation item (the third component of the landscape phenomena).

1. The developments to establish the psychological scale of appraisal

In the trial of psychometrical method, Ekman & Kuennapas (1962) tested the difference of Nominal scale and Interval scale, and the development of SD method promoted to use many adjectives in the visual complexities (Berlyne & Peckham 1966). Hart & Graham (1967) considered “How to rate & rank landscape”.

In the development of the psychological scale, Heise (1969) tested the scale -3 to 3, and Zube, Anderson & Pitt (1973) used the numerical scale 3 to 14.

2. The psychological evaluation item of preference

Kaplan, Kaplan, & Wendt (1972) proposed to use preference for the landscape appreciation. Compared to the results obtained by SD method, “preference” is easy to understand among different cultural back ground and was popularized in many countries.

©2019. Japan Geoscience Union. All Right Reserved.

3. The developments and the use of SD method

As for the SD method proposed by Osgood & Suci (1955), it employed many pairs of adjectives to evaluate landscape and provided detailed impressions of landscape. The largest number of 240 adjectives was tested by Craik (1975). The results were too complicated and scientists would like to summarize the results. SBE (Terry & Boster 1976), AVQ (Arriaza etc. 2004) and others were statistical aggregation examples of this trial and the example of meaningful aggregation was “Coherence, Complexity, Legibility and Mystery” proposed by Kaplan (1987). These indicators were tested with the relation to the preference and other appreciations by many scientists (Stamps III 2004, and so on.).

4. Method of monetary term evaluation

Monetary term is another evaluation of landscapes and sometimes used in the physical planning (Fukahori & Kubota 2003).

5. Items based on the human behavior of landscape evaluation

The origin of the landscape appreciation was explained from the animal behavior of predation (Appleton 1975). This theory had discussed for a long time. And this behavior might propose a base appreciation of landscape (Aoki & Kitamura 2001). Consideration on the human activities, the reason of visit (Andereck et al. 1989) and the visitability (Abdulkarim & Nasar 2014) were examined and the photographing (Oku & Fukamachi 2006, Sugimoto 2013) were reported.

6. Other appraisals

There are many appreciation descriptors and even now the scientists are finding new descriptors (Collier & Scott 2008). Until now, we could find examples of this trial in absorption (Berlyne 1958), quietness (Womble & Studebaker 1981), beauty (Hull IV, Buhyoff & Daniel 1984), size (Coeterier 1994), fear and stress (Nasar & Jones 1997), positive and negative (Ryan 1998), aggression and violence (Kuo 2001), satisfaction (Kaplan & Austin 2004), overcrowding (Manning & Freimund 2004), openness (Dramstad et al. 2006), ugly (Ruell, Halleux & Teller 2013), and other descriptions.

Keywords: landscape appreciation, appreciation items, until 2017

©2019. Japan Geoscience Union. All Right Reserved.

Table Historical review of landscape appreciation items

Interesting subject	Name of authors	Year
Development of the SD method	Osgood, C.E. and Suci, G.J.	1955
absorption	Berlyne, D.E.,	1958
descriptive appreciation as aesthetic beauty	Thiel, P.,	1961
difference of Nominal scale and Interval scale	Ekman, G. and Kuennapas, T.	1962
SD method	Wright, B. and Rainwater, L.	1962
description	Halprin, L.,	1965
absorption	Berlyne, D.E. and Peckham, S.	1966
description	Noe, S. and Abernathy, B.L.	1966
landscape type	Hart W. J. and William W. Graham,	1967
absorption	Wohlwill, J.F.	1968
numerical scale from -3 to +3	Heise, D.R.,	1969
aesthetic and emotional	Shafer, E.L. and Mietz, J.	1969
objectivity	Craik, K.H.	1972
preference	Kaplan, S., Kaplan, R. and Wendt, J.S.	1972
scaling	Acking, C.A and Sorte, G.J.	1973
numerical scale from 3 to 14	Zube, E.H., Anderson, T. and Pitt, D.	1973
prospect-refuge theory	Appleton, J.	1975
SD method with 240 pairs of adjectives	Craik, K.H.	1975
SBE method; normalization of the results	Daniel, T.C. and Boster, R.S.	1976
monetary	McConnell, K.E.,	1977
SD method	Pedersen, D.M.	1978
SD method	Shuttleworth, S.	1980
preference	Nasar, J.L.,	1981
meaning	Russell, J.A. and Ward, L.M.	1981
quiet	Womble, P. and Studebaker, S.	1981
quiet	Hammitt, W.E.,	1982
preference	Mudrak, L.Y.,	1983
preference	Nasar, J.L.,	1983
SD method	Ruiz, J.P. and Gonzalez-Bernaldez, F.	1983
scenic beauty	Hull IV, R.B., Buhyoff, G.J. and Daniel, T.C.	1984
needs and fears	Talbot, J.F. and Kaplan, R.	1984
preference	Herzog, T.R.	1985
SD method	Abello, R.P., Bernaldez, F.G. and Galiano, E.F.	1986
preference	Talbot, J.F. and Kaplan, R.	1986
survey paper: Coherence, Complexity, Legibility, Mystery	Kaplan, S.	1987
SD method	Kobayashi, M., Higashiyama, J. and Kawasaki, K.	1987
preference	Talbot, J.F., Bardwell, L.V. and Kaplan, R.	1987
monetary	Anderson, L.M. and Cordell, H.K.	1988
preference	Herzog, T. and Smith, G.A.	1988
motivation to visit	Andereck, K. et al.	1989
evaluation by monetary term	Daniel, T.C., et al.	1989
SD method	Kaplan, R., Kaplan, S. and Brown, T.	1989
SD method	Ruiz, M. and Ruiz, J.P.	1989
preference	Gimblett, H.R.	1990
monetary	Green, C.H., et al.	1990
motivation to visit	Uysal, M., McDonald, C.D. and Reid, L.J.	1990
quiet	Ulrich, R.S. et al.	1991
preference	Chokor, B.A	1992
preference	Herzog, T.	1992
refuge provides shelter	Hudson, B.J.	1992
effect to land price	Orland, B., Vinning, J. and Ebreo, A.	1992
familiarity	Purcell, A.T.	1992
description: literature works	Ikeda, T. and Konno, A.	1993
size of space	Coeterier, J.F.,	1994
identity	Hull IV, R.B., Lam, M. and Vigo, G.	1994
preference	Stamps III, A.E.	1994
preference	Strumse, E.	1994
preference	Sullivan III, W.C.,	1994
prospect-refuge theory reviewed	Appleton, J.,	1995
motivation to visit	Cha, S., McCleary, K.W. and Uysal, M.	1995
preference	Mealey, L.	1995
preference on tree form	Sommer, R. and Summit, J.	1995
preference	Herzog, T.R. and Gale, T.A.	1996
scenic preference in Finland	Karjalainen, E.	1996
scaling	Tahvanainen, L., Tyrvainen, L. and Nousiainen, I.	1996
Notation for a Participatory Envirotecture	Thiel, P.,	1996
fear and stress	Nasar, J.L. and Jones, K.M.	1997
landscape preferences of USA, Ireland, Senegal	Newell, P.B.	1997
quiet	Caffyn, A. and Prosser, B.	1998
preference	Herzog, T.R.,	1998
consistency of evaluation by rank order and graphical scale	Karjalainen, E. and Komulainen, M.	1998
preference	Kuo, F.E., Bacaicoa, M. and Sullivan, W.C.	1998
preference and naturalness using Scrub-forest, wide-close view, nature-altered	Purcell, A.T. and Lamb, R.J.	1998
positive and negative scenery of river frontland	Ryan, R.L.	1998
monetary	Tyrvainen, L. and Vaananen, H.	1998
preference	Brown, T.J., Kaplan R. and Quaderer, G.	1999
tranquility and preference	Herzog, T.R. and Barnes, G.J.	1999
preference	Summit, J. and Sommer, R.	1999
landscape preference in Australia	Herzog, T.R. et al	2000
landscape preference in Israel	Misgav, A.	2000
Phylogenic and Ontogenic evolution of landscape appreciation	Aoki, Y. and Kitamura, S.	2001
correlation between preference and likeliness	Hagerhall, C.M.	2001
motivation of ecological behavior	Hartig, T.	2001
aggression and violence	Kuo, F.E.,	2001
preference and danger	Herzog, T.R. and Kutzli, G.E.	2002
landscape preference in Norway	Kaltenborn, B.P. and Bjerke, T.	2002
positive and negative scenery of rural living	Ryan, R.L.,	2002
comparison of VOC and SBE	Franco, D. et al.	2003
cost and amenity level of road scenery	Fukahori, K. and Kubota, Y.	2003
preference	Herzog, T.R. and Leverich, O.L.	2003
AVQ index for visual quality	Arriaza, M. et al.	2004
preference	Herzog, T.R. and Kropscott, L.S.	2004
satisfaction of nature	Kaplan, R. and Austin, M.E.	2004
over crowding by photo montage method	Manning, R.E. and Freimund, W.A	2004
SBE difference 1976-1996	Palmer, J.F.	2004
preference did not correlate to mystery, complexity, legibility, coherence	Stamps, III, A.E.	2004
preference and danger by visibility	Herzog, T.R., & Kirk, K.M.	2005
preference by pair comparison	Rodiek, S.D. and Fried, J.T.	2005
proper openness, student and locals	Dramstad, W.E., et al.	2006
essential features for scenic beauty	Ergin, A., Williams, A.T. and Micallef, A.	2006
landscape preferred in Turkey	Kaplan, A., Taskin, T. and Onenc, A.,	2006
photographing by activity	Oku, H., & Fukamachi, K.	2006
disturbance, naturalness, visual scale, place identity in the photographs	Tveit, M., Ode, A. and Fry, G.	2006
mystery did not affect preference	Herzog, T.R. and Bryce, A.G.,	2007
words interested in the interview	Collier, M.J. and Scott, M.J.	2008
preference of transportation system; vegetation, distance, side fascia affected	Bernasconi, C. et al.	2009
beautiful high mountain, Sherpa appreciate flora, ugly garbage site no vegetation at Everest	Beza, B.B.	2010
species-rich of middle ground affect like of alpine landscape	Lindemann-Matthies, P. et al.	2010
naturalness, unity affect preference of Spruce forest landscape in Turkey	Eroglu, E. and Acar, C.	2011
surprise and Mystery affect preference, Turkey find Mystery at curved street	Nasar, J.L. and Cubukcu, E.	2011
ugly impression of brown fields and montage support improvement in Belgium	Ruelle, C., Halleux, J.-M. & Teller, J.	2013
Visitability	Abdulkarim, D. and Nasar, J. L.	2014
oppressiveness	Asgarzadeh, M. et al.	2014
threat	Chiang, Y-C., Nasal, J. and Ko, C-C.	2014
variance affected by evaluation value	Kalivoda, O. et al.	2014
forest and park affected stress relief	Tyrvainen, L., Ojala, A., Korpela, K. Lanki, T., Tsunetsugu, Y., Kagawa, T.	2014
proper understorey affect preference	van der Wal, R., Miller, D., Irvine, J., Fiorini, S., Amar, A., Yearley, S. Gill, R. & Dandy, N.	2014
openness	Weitkamp, G., Lammeren, R. and Bregt, A.	2014
risk of bushfire	Gill, N. et al.	2015
water use affect landscaping preference	Hayden, L., et al	2015
panorama tree cover density affect to preference	Jiang, B., et al.	2015
green roof affect restorativeness	Lee, K.E., Williams,K.J.H., Sargent, L.D., Williams, N.S.G., Johnson, K.A	2015
aesthetic, morphological condition and ecological integrity	McCormick, A, Fisher, K. and Brierley, G.	2015
water, reed, litter, dead wood affected preference	Eder, R., & Arnberger, A.	2016
tree coverage affect stress recovery	Jiang, B., Li, D., Larsen, L. & Sullivan, W.C.	2016
visual realism and sound affect preference	Lindquist, M., Lange, E. & Kang J.	2016
change of motivation	Shalev, I.	2016
cultural values in visual object	Sowinska-Swierkosz, B.N., Chmielewski, T.J.	2016
visual green reduces noise annoyance	Van Renterghem, T. & Botteldooren, D.	2016
public litter and fishing litter affect preference	Wyles, K.J., Pahl, S. Thomas, K. & Thompson, R.	2016
disorder affect fear of crime	Biasi, Alaina De	2017
nature contact reduce depression, anxiety, stress in outside experience	Brooks, A.M. et al.	2017
biodiversity affected preference	Cracknell, D. et. al.	2017
dead wood affected preference	Gundersen, V., Stange, E.E., Kaltenborn, B.P. Vistad	2017
EAB infestation affect crime, theft, breaking entering, property crime	Kondo, M.C., Han, S., Donovan, G.H., MacDonald, J.M.	2017
preference increase 4bit designed complexinformation entropy values	Kuper, R.	2017
wind generator affect to EEG (electroencephalographic)	Murcia, G. et al.	2017
natural scenery affect change of heart rate by CT scan	Zijlstra, E. et. Al.	2017
attributes affected to landscape aesthetic value of CVM	Dupras, J. et al.	2018
point elements affect preference	Haefner, K. et al.	2018
dense vegetation preferred in city	Harris, V. et al.	2018
motivation of park visit	Hecke, Linde, et al.	2018
firing affect emotional wellbeing	Knez, I. et al.	2018
mature oak with anemone preferred	Nielsen, A.B., Gundersen, V.S. & Jensen, F.S.	2018
traditional landscape preferred by residents in central Alps	Pecher, C., et al.	2018
photo points located by GIS	Sugimoto, K.	2018
setting and arrangement affect restrativeness	Tabrizian, P., et al.	2018
forest preference of 4 seasons	Bravo-Vargas, V. et al.	2019

behavioral consideration
developments in scaling
monetary approaches
use of preference
developments in SD method
other appreciation

©2019. Japan Geoscience Union. All Right Reserved.

[E] Poster | H (Human Geosciences)：H-CG Complex & General

Wed. May 29, 2019 5:15 PM - 6:30 PM JST | Wed. May 29, 2019 8:15 AM - 9:30 AM UTC | Poster Hall International Exhibition Hall8, Makuhari Messe_24

[H-CG25] International Comparison of Landscape Appreciation

convener:Anastasia Petrova(Institute of Oriental Studies of the Russian Academy of Sciences), yoji aoki(Open University of Japan)

Evaluation of landscape has been developed in a variety of fields, such as geography, landscape architecture, nature protection, and some others. Landscape appreciation is a complex and sophisticated psychological phenomenon. There is no consensus among researchers on what the phenomenon of "landscape" truly is, how people physiologically and mentally experience it, which human attributes affect the perception of it, and why it is apprehended the way it is. The concept of landscape appreciation has yet to be clearly defined and there is a lack of agreement on evaluation methods, the factors that determine landscape preferences, the steps in appreciation, and so forth. This session aims to discuss the research findings of landscape evaluation in various fields, including geography, geomorphology, landscape planning, architecture, engineering, social sciences, environmental psychology, meteorology, phenology, and so on.

[HCG25-P01] The Globally Important Agricultural Heritage of Aso from the perspective of landscape and its supporting systems

*REIKO MACHIDA[1] (1.TOKYO UNIVERSITY OF AGRICULTURE)

[HCG25-P02] Hazardous natural phenomena and weather conditions appreciation in Russian landscape painting

*ELENA PETROVA[1] (1.Lomonosov Moscow State University, Faculty of Geography)

[HCG25-P03] Trends of evaluation items to landscape appreciation until 2017 in the English journals

*yoji aoki[1], keisuke mukagai[2], Anastasia Petrova[3] (1.Open University of Japan, 2.Nagano University, 3.Institute of Oriental Studies, Russian Academy of Sciences)

The Globally Important Agricultural Heritage of Aso from the perspective of landscape and its supporting systems

*REIKO MACHIDA[1]

1. TOKYO UNIVERSITY OF AGRICULTURE

Globally Important Agricultural Heritage Systems (GIAHS) is a partnership initiative of the Food and Agriculture Organization of the United Nations which began in 2002 with the aim to identify, support and safeguard remarkable land use systems and landscapes that are rich in globally significant biological diversity evolving from the co-adaptation of a community with its environment and its needs and aspirations for sustainable development. There are 19 countries and 45 areas around the world, and among them 9 areas in Japan that are listed as GIAHS at present.The Aso area located in Northern Kyusyu features the world's largest caldera, which is 25 km wide from north to south and 18 km from east to west and grassland landscapes. The vast grasslands of the Aso area have been managed throughout history by local agricultural activities such as controlled burning, mowing and pasturage since the Heian period. The historical land use in Aso has been a balanced combination of rice fields at the caldera floor, forestry and fungiculture at the foot of the caldera, and grazing pasture at the top of caldera, which is carried out in harmony with the environment. The management of the Aso grasslands for sustainable agriculture have been recognized and certified as Globally Important Agricultural Heritage Systems (GIAHS) in 2013.In terms of landscape, the values of Aso as Globally Important Agricultural Heritage System are the dynamic grassland landscapes of the large caldera, the historical paddies and rice terraces, which vary in size from small to large as a result of the local human activities. There are beautiful rural landscapes on various scales.However, the productivity oriented rural development and the division of land has been having a negative impact on the landscape value of the GIAHS. There are cases of rice paddies and buildings that contribute to the landscape value being lost. From such cases, it is evident that the landscape structures that should be protected since they are GIHS are not recognized widely enough.This study investigated the landscape value and landscape structure as GIAHS and its value supports landscape policy. As a result, it became clear that the landscape structure of Minamiaso village consist of the traditional combination of grasslands and paddy fields retains significant wildlife habitat and picturesque agricultural landscapes. It has become clear that development activities do not influence to landscape in large-scale, however development activities as land readjustment project influenced to landscape in small and medium-scale. "Landscape planning" "Landscape agricultural development plan" can support the landscape structure in small and medium -scale. It is important to plan the land use for the landscape value of GIAHS.

Keywords: Globally Important Agricultural Heritage Systems (GIAHS), Landscape, Landscape Planning

©2019. Japan Geoscience Union. All Right Reserved.

Hazardous natural phenomena and weather conditions appreciation in Russian landscape painting

*ELENA PETROVA[1]

1. Lomonosov Moscow State University, Faculty of Geography

The fixation of various natural phenomena by landscape artists of different historical periods in different regions and countries has not only purely aesthetic interest, but also particular interest to science. During the period of Romanticism that has spread in the European and Russian art in the 19th century, Russian art turned to real living nature. Landscapes of the native country began to play a dominant role in the formation of landscape image. Romanticism aroused interest not only in the picturesque and exotic landscapes, but also in the majestic forces of nature. Volcanic eruptions, earthquakes, storms, thunderstorms, floods, and other natural hazards were new motifs for artists of that time. Romantic artists were inclined to exaggerate the power and destructive forces of natural phenomena they portrayed, elevating any event of this kind to the rank of a natural disaster. Often, they portrayed the rather ordinary storm, thunderstorm, flood as a universal natural catastrophe, comparable, perhaps, only to the biblical flood. What to say about really extraordinary events. Most vividly, the theme of the turbulent, dramatic landscape was developed in the works by Aivazovsky who quite realistically showed the sea element in various stages of its manifestation - from complete calm to the strongest storm. Being in Italy, Russian artists could not disregard such an extraordinary event as the violent eruption of the volcano Vesuvius, which occurred in 1822; many have captured it in their landscape images.

Thanks to the rapid development of scientific knowledge and discoveries in the field of geosciences, including meteorology, artists were encouraged to observe various atmospheric phenomena and weather conditions. Gradually, the sky ceased to be depicted simply as a smooth blue background, as was customary in the tradition of classicism; carefully traced clouds of various types, shapes and shades began to appear in pictures. In addition, various evaporations, fogs, haze, etc. became objects of the landscape image. Romantic artists were little interested in depicting winter and snow, despite the fact that the cold season with a steady snow cover continues in Russia for almost half a year from November to early April. The painting “Russian Winter” (1827) by Nikifore Krylov became perhaps the first winter landscape image in Russian painting. Krylov depicted a somewhat naive, but quite real, winter landscape on the bank of the Tosna River in the vicinity of St. Petersburg, which he painted from life. He was able to reliably convey the atmosphere of the Russian winter: a valley covered with snow, a frozen river, a dark strip of forest in the distance and the peasants with their daily affairs on the road down to the river in the foreground. The first bright and joyful snow-covered landscape image was created, apparently, by Alexey Savrasov in his famous painting “The Rooks Have Come Back” (1871). The spring snow melting and sparkling in the sun became later the favorite motif of the Russian painting. Comparative analysis of landscape pictures can be an important tool, in addition to scientific methods, in studying the nature and dynamics of various hazardous natural processes and phenomena, including hydrological and meteorological ones in conditions of changing climate.

Keywords: hazardous natural phenomena , weather conditions , landscape painting, landscape images

©2019. Japan Geoscience Union. All Right Reserved.

Trends of evaluation items to landscape appreciation until 2017 in the English journals

*yoji aoki[1], keisuke mukagai[2], Anastasia Petrova[3]

1. Open University of Japan, 2. Nagano University, 3. Institute of Oriental Studies, Russian Academy of Sciences

Introduction
We have considered trends of landscape appreciation since JpGU2013-2018. According to the definition of landscape phenomena proposed by Prof. O. Shinohara (Fig. 1), we reported the trends of studies in each part of the phenomena.

Aoki, Y. (1999) described the first landscape evaluation using psychometrical methods to be pioneered by Peterson, G.L. (1967). Before this development, they tried to find the landscape appreciation using various descriptors. They were mostly belonging to the literature or the paintings. As for the literature, the first description of mountain was found in Francesco Petrarca in 1336 of France (Kondo, T. 2002). But his description has no reliable evidence to ensure the landscape. In the field of art, Albrecht Altdorfer drew the first natural landscape in the beginning of 15th century of Germany (Cavaliere, B. 1989). But we could not measure the physical data from his picture. The literature and the art found the beauty of natural landscape by these examples. They recorded the aesthetic beauty in landscape (Thiel, P. 1968).

Jay Appleton (1980) explained the scientific reason of the landscape phenomena with physical data, e.g. geomorphysical data and meteorological data. He explained the landscape phenomena of two pictures, Constable's Weymouth Bay and Constable's sunset study of Hampstead Heath. His approach must be the scientific based explanation to find psychological phenomena of landscape using the geology and meteorology. But the psychological phenomena could deviate by the person observed and the results must be happened statistically. So the process of the landscape phenomena should be explained by stochastic process of psychology. Then scientists developed psychological approach to it.

Here, we summarize the appreciation item (the third component of the landscape phenomena).

1. The developments to establish the psychological scale of appraisal

In the trial of psychometrical method, Ekman & Kuennapas (1962) tested the difference of Nominal scale and Interval scale, and the development of SD method promoted to use many adjectives in the visual complexities (Berlyne & Peckham 1966). Hart & Graham (1967) considered “How to rate & rank landscape”.

In the development of the psychological scale, Heise (1969) tested the scale -3 to 3, and Zube, Anderson & Pitt (1973) used the numerical scale 3 to 14.

2. The psychological evaluation item of preference

Kaplan, Kaplan, & Wendt (1972) proposed to use preference for the landscape appreciation. Compared to the results obtained by SD method, “preference” is easy to understand among different cultural back ground and was popularized in many countries.

©2019. Japan Geoscience Union. All Right Reserved.

3. The developments and the use of SD method

As for the SD method proposed by Osgood & Suci (1955), it employed many pairs of adjectives to evaluate landscape and provided detailed impressions of landscape. The largest number of 240 adjectives was tested by Craik (1975). The results were too complicated and scientists would like to summarize the results. SBE (Terry & Boster 1976), AVQ (Arriaza etc. 2004) and others were statistical aggregation examples of this trial and the example of meaningful aggregation was “Coherence, Complexity, Legibility and Mystery” proposed by Kaplan (1987). These indicators were tested with the relation to the preference and other appreciations by many scientists (Stamps III 2004, and so on.).

4. Method of monetary term evaluation

Monetary term is another evaluation of landscapes and sometimes used in the physical planning (Fukahori & Kubota 2003).

5. Items based on the human behavior of landscape evaluation

The origin of the landscape appreciation was explained from the animal behavior of predation (Appleton 1975). This theory had discussed for a long time. And this behavior might propose a base appreciation of landscape (Aoki & Kitamura 2001). Consideration on the human activities, the reason of visit (Andereck et al. 1989) and the visitability (Abdulkarim & Nasar 2014) were examined and the photographing (Oku & Fukamachi 2006, Sugimoto 2013) were reported.

6. Other appraisals

There are many appreciation descriptors and even now the scientists are finding new descriptors (Collier & Scott 2008). Until now, we could find examples of this trial in absorption (Berlyne 1958), quietness (Womble & Studebaker 1981), beauty (Hull IV, Buhyoff & Daniel 1984), size (Coeterier 1994), fear and stress (Nasar & Jones 1997), positive and negative (Ryan 1998), aggression and violence (Kuo 2001), satisfaction (Kaplan & Austin 2004), overcrowding (Manning & Freimund 2004), openness (Dramstad et al. 2006), ugly (Ruell, Halleux & Teller 2013), and other descriptions.

Keywords: landscape appreciation, appreciation items, until 2017

©2019. Japan Geoscience Union. All Right Reserved.

Table Historical review of landscape appreciation items

Interesting subject	Name of authors	Year
Development of the SD method	Osgood, C.E. and Suci, G.J.	1955
absorption	Berlyne, D.E.,	1958
descriptive appreciation as aesthetic beauty	Thiel, P.,	1961
difference of Nominal scale and Interval scale	Ekman, G. and Kuennapas, T.	1962
SD method	Wright, B. and Rainwater, L.	1962
description	Halprin, L.,	1965
absorption	Berlyne, D.E. and Peckham, S.	1966
description	Noe, S. and Abernathy, B.L.	1966
landscape type	Hart W. J. and William W. Graham,	1967
absorption	Wohlwill, J.F.	1968
numerical scale from -3 to +3	Heise, D.R.,	1969
aesthetic and emotional	Shafer, E.L. and Mietz, J.	1969
objectivity	Craik, K.H.	1972
preference	Kaplan, S., Kaplan, R. and Wendt, J.S.	1972
scaling	Acking, C.A and Sorte, G.J.	1973
numerical scale from 3 to 14	Zube, E.H., Anderson, T. and Pitt, D.	1973
prospect-refuge theory	Appleton, J.	1975
SD method with 240 pairs of adjectives	Craik, K.H.	1975
SBE method; normalization of the results	Daniel, T.C. and Boster, R.S.	1976
monetary	McConnell, K.E.,	1977
SD method	Pedersen, D.M.	1978
SD method	Shuttleworth, S.	1980
preference	Nasar, J.L.,	1981
meaning	Russell, J.A. and Ward, L.M.	1981
quiet	Womble, P. and Studebaker, S.	1981
quiet	Hammitt, W.E.,	1982
preference	Mudrak, L.Y.,	1983
preference	Nasar, J.L.,	1983
SD method	Ruiz, J.P. and Gonzalez-Bernaldez, F.	1983
scenic beauty	Hull IV, R.B., Buhyoff, G.J. and Daniel, T.C.	1984
needs and fears	Talbot, J.F. and Kaplan, R.	1984
preference	Herzog, T.R.	1985
SD method	Abello, R.P., Bernaldez, F.G. and Galiano, E.F.	1986
preference	Talbot, J.F. and Kaplan, R.	1986
survey paper: Coherence, Complexity, Legibility, Mystery	Kaplan, S.	1987
SD method	Kobayashi, M., Higashiyama, J. and Kawasaki, K.	1987
preference	Talbot, J.F., Bardwell, L.V. and Kaplan, R.	1987
monetary	Anderson, L.M. and Cordell, H.K.	1988
preference	Herzog, T. and Smith, G.A.	1988
motivation to visit	Andereck, K. et al.	1989
evaluation by monetary term	Daniel, T.C., et al.	1989
SD method	Kaplan, R., Kaplan, S. and Brown, T.	1989
SD method	Ruiz, M. and Ruiz, J.P.	1989
preference	Gimblett, H.R.	1990
monetary	Green, C.H., et al.	1990
motivation to visit	Uysal, M., McDonald, C.D. and Reid, L.J.	1990
quiet	Ulrich, R.S. et al.	1991
preference	Chokor, B.A	1992
preference	Herzog, T.	1992
refuge provides shelter	Hudson, B.J.	1992
effect to land price	Orland, B., Vinning, J. and Ebreo, A.	1992
familiarity	Purcell, A.T.	1992
description: literature works	Ikeda, T. and Konno, A.	1993
size of space	Coeterier, J.F.,	1994
identity	Hull IV, R.B., Lam, M. and Vigo, G.	1994
preference	Stamps III, A.E.	1994
preference	Strumse, E.	1994
preference	Sullivan III, W.C.,	1994
prospect-refuge theory reviewed	Appleton, J.,	1995
motivation to visit	Cha, S., McCleary, K.W. and Uysal, M.	1995
preference	Mealey, L.	1995
preference on tree form	Sommer, R. and Summit, J.	1995
preference	Herzog, T.R. and Gale, T.A.	1996
scenic preference in Finland	Karjalainen, E.	1996
scaling	Tahvanainen, L., Tyrvainen, L. and Nousiainen, I.	1996
Notation for a Participatory Envirotecture	Thiel, P.,	1996
fear and stress	Nasar, J.L. and Jones, K.M.	1997
landscape preferences of USA, Ireland, Senegal	Newell, P.B.	1997
quiet	Caffyn, A. and Prosser, B.	1998
preference	Herzog, T.R.,	1998
consistency of evaluation by rank order and graphical scale	Karjalainen, E. and Komulainen, M.	1998
preference	Kuo, F.E., Bacaicoa, M. and Sullivan, W.C.	1998
preference and naturalness using Scrub-forest, wide-close view, nature-altered	Purcell, A.T. and Lamb, R.J.	1998
positive and negative scenery of river frontland	Ryan, R.L.	1998
monetary	Tyrvainen, L. and Vaananen, H.	1998
preference	Brown, T.J., Kaplan R. and Quaderer, G.	1999
tranquility and preference	Herzog, T.R. and Barnes, G.J.	1999
preference	Summit, J. and Sommer, R.	1999
landscape preference in Australia	Herzog, T.R. et al	2000
landscape preference in Israel	Misgav, A.	2000
Phylogenic and Ontogenic evolution of landscape appreciation	Aoki, Y. and Kitamura, S.	2001
correlation between preference and likeliness	Hagerhall, C.M.	2001
motivation of ecological behavior	Hartig, T.	2001
aggression and violence	Kuo, F.E.,	2001
preference and danger	Herzog, T.R. and Kutzli, G.E.	2002
landscape preference in Norway	Kaltenborn, B.P. and Bjerke, T.	2002
positive and negative scenery of rural living	Ryan, R.L.,	2002
comparison of VOC and SBE	Franco, D. et al.	2003
cost and amenity level of road scenery	Fukahori, K. and Kubota, Y.	2003
preference	Herzog, T.R. and Leverich, O.L.	2003
AVQ index for visual quality	Arriaza, M. et al.	2004
preference	Herzog, T.R. and Kropscott, L.S.	2004
satisfaction of nature	Kaplan, R. and Austin, M.E.	2004
over crowding by photo montage method	Manning, R.E. and Freimund, W.A	2004
SBE difference 1976-1996	Palmer, J.F.	2004
preference did not correlate to mystery, complexity, legibility, coherence	Stamps, III, A.E.	2004
preference and danger by visibility	Herzog, T.R., & Kirk, K.M.	2005
preference by pair comparison	Rodiek, S.D. and Fried, J.T.	2005
proper openness, student and locals	Dramstad, W.E., et al.	2006
essential features for scenic beauty	Ergin, A., Williams, A.T. and Micallef, A.	2006
landscape preferred in Turkey	Kaplan, A., Taskin, T. and Onenc, A.,	2006
photographing by activity	Oku, H., & Fukamachi, K.	2006
disturbance, naturalness, visual scale, place identity in the photographs	Tveit, M., Ode, A. and Fry, G.	2006
mystery did not affect preference	Herzog, T.R. and Bryce, A.G.,	2007
words interested in the interview	Collier, M.J. and Scott, M.J.	2008
preference of transportation system; vegetation, distance, side fascia affected	Bernasconi, C. et al.	2009
beautiful high mountain, Sherpa appreciate flora, ugly garbage site no vegetation at Everest	Beza, B.B.	2010
species-rich of middle ground affect like of alpine landscape	Lindemann-Matthies, P. et al.	2010
naturalness, unity affect preference of Spruce forest landscape in Turkey	Eroglu, E. and Acar, C.	2011
surprise and Mystery affect preference, Turkey find Mystery at curved street	Nasar, J.L. and Cubukcu, E.	2011
ugly impression of brown fields and montage support improvement in Belgium	Ruelle, C., Halleux, J.-M. & Teller, J.	2013
Visitability	Abdulkarim, D. and Nasar, J. L.	2014
oppressiveness	Asgarzadeh, M. et al.	2014
threat	Chiang, Y-C., Nasal, J. and Ko, C-C.	2014
variance affected by evaluation value	Kalivoda, O. et al.	2014
forest and park affected stress relief	Tyrvainen, L., Ojala, A., Korpela, K. Lanki, T., Tsunetsugu, Y., Kagawa, T.	2014
proper understorey affect preference	van der Wal, R., Miller, D., Irvine, J., Fiorini, S., Amar, A., Yearley, S. Gill, R. & Dandy, N.	2014
openness	Weitkamp, G., Lammeren, R. and Bregt, A.	2014
risk of bushfire	Gill, N. et al.	2015
water use affect landscaping preference	Hayden, L., et al	2015
panorama tree cover density affect to preference	Jiang, B., et al.	2015
green roof affect restorativeness	Lee, K.E., Williams,K.J.H., Sargent, L.D., Williams, N.S.G., Johnson, K.A	2015
aesthetic, morphological condition and ecological integrity	McCormick, A, Fisher, K. and Brierley, G.	2015
water, reed, litter, dead wood affected preference	Eder, R., & Arnberger, A.	2016
tree coverage affect stress recovery	Jiang, B., Li, D., Larsen, L. & Sullivan, W.C.	2016
visual realism and sound affect preference	Lindquist, M., Lange, E. & Kang J.	2016
change of motivation	Shalev, I.	2016
cultural values in visual object	Sowinska-Swierkosz, B.N., Chmielewski, T.J.	2016
visual green reduces noise annoyance	Van Renterghem, T. & Botteldooren, D.	2016
public litter and fishing litter affect preference	Wyles, K.J., Pahl, S. Thomas, K. & Thompson, R.	2016
disorder affect fear of crime	Biasi, Alaina De	2017
nature contact reduce depression, anxiety, stress in outside experience	Brooks, A.M. et al.	2017
biodiversity affected preference	Cracknell, D. et. al.	2017
dead wood affected preference	Gundersen, V., Stange, E.E., Kaltenborn, B.P. Vistad	2017
EAB infestation affect crime, theft, breaking entering, property crime	Kondo, M.C., Han, S., Donovan, G.H., MacDonald, J.M.	2017
preference increase 4bit designed complexinformation entropy values	Kuper, R.	2017
wind generator affect to EEG (electroencephalographic)	Murcia, G. et al.	2017
natural scenery affect change of heart rate by CT scan	Zijlstra, E. et. Al.	2017
attributes affected to landscape aesthetic value of CVM	Dupras, J. et al.	2018
point elements affect preference	Haefner, K. et al.	2018
dense vegetation preferred in city	Harris, V. et al.	2018
motivation of park visit	Hecke, Linde, et al.	2018
firing affect emotional wellbeing	Knez, I. et al.	2018
mature oak with anemone preferred	Nielsen, A.B., Gundersen, V.S. & Jensen, F.S.	2018
traditional landscape preferred by residents in central Alps	Pecher, C., et al.	2018
photo points located by GIS	Sugimoto, K.	2018
setting and arrangement affect restrativeness	Tabrizian, P., et al.	2018
forest preference of 4 seasons	Bravo-Vargas, V. et al.	2019

behavioral consideration
developments in scaling
monetary approaches
use of preference
developments in SD method
other appreciation

©2019. Japan Geoscience Union. All Right Reserved.

[J] Poster | S (Solid Earth Sciences)：S-SS Seismology

Wed. May 29, 2019 1:45 PM - 3:15 PM JST | Wed. May 29, 2019 4:45 AM - 6:15 AM UTC | Poster Hall International Exhibition Hall8, Makuhari Messe_3

[S-SS09] Earthquake prediction and forecast

convener:Masayuki Obayashi(Japan Agency for Marine-Earth Science and Technology), Toshitaka Baba(Graduate School of Science and Technology, Tokushima University)

This session provides the opportunity for contributions that fall within the scientific spectrum of earthquake prediction and forecasting. We welcome theoretical, observational or numerical papers that are either on long- or short-term predictions, and either based on deterministic or probabilistic approaches.

[SSS09-P01] A method to ditect seismic precursors

*Kozo Takahashi

[SSS09-P02] Difference of foreshock characteristics between real data and synthetic ETAS catalogs: through the application of an empirical earthquake forecast model based on foreshocks

*Fuyuki Hirose[1], Koji Tamaribuchi[1], Kenji Maeda[2] (1.Seismology and Tsunami Research Department, Meteorological Research Institute, 2.Seismology and Volcanology Department, Japan Meteorological Agency)

[SSS09-P03] The increase in missing waveform images of the F-net broadband seismograph network preceding the 2011 Tohoku earthquake (2)

*Yoshiki SUE[1] (1.none)

[SSS09-P04] On the *b*-value of the OBS seismic observation around the Suruga Bay Senoumi

*Taiyo Sotani[1], Hisatoshi Baba[4], Takahito Nishimiya[2], Nakao Nagisa[1], Toshiyasu Nagao[3] (1.Toukai Univrsity, 2.Meteorological Research Institute, Japan Meteorological Agency, 3.Institute of Oceanic Research and development, Tokai University, 4.Department of Marine and Earth Science, Tokai University)

[SSS09-P05] Trial Result of Long-term Occurrence Probabilities with The Moderate Repeating Earthquakes Using The Lognormal Distribution Model with Bayesian Approach

*Masayuki Tanaka[1] (1.Meteorological Research Institute)

[SSS09-P06] **Structural heterogeneity under the 2018 Mw6.6 Eastern Iburi earthquake in Hokkaido, Japan and its implications for rupture initiations**

*ZHI WANG[1] (1.Key Laboratory of Marginal Sea Geology at South China Sea Institute of Oceanology of CAS of China)

A method to ditect seismic precursors

*Kozo Takahashi

A method to detect seismic precursors precursory seismic electric fields
earthquake prediction Introduction
Many precursors have been observed before a big earthquake. Most of them are regarded as the result of microcracks in the source region. Therefore, if we can detect the microcracks, it will become possible to predict directly or indirectly the earthquakes. Detection of microcracks
By arranging four electrodes around the earthquake region, we measure the electric potential and resistance (though this method is difficult at seabed), then we can detect the microcrack. But this method is nearly impossible, as we can't know the precise location of the earthquake region.
If Gravitational Waves (GWs)are
emitting from the source region, it becomes possible to detect the region and to predict the earthquakes. But the following shows this is perfectly impossible.
Receiving GW
First the intensity of GW is shown which was detected.
The intensity of GW150914, which emitted when the two Black Holes (BHs) combined, is calculated as follows:
Symbols and approximate values of constants are as follows:
???Fraise to the power ˜
Light velocity:????3?˜(10??5) km/sec
One light-year??9.46?˜(10??12) km
Solar Mass:?Q?˜(10??30) kg
The values of GW150914 when it combined: The distance to the BHs:
??=13 hundred million light-years
The mass of the smaller BH:
M=29 Solar mass
The collision between BHs means that the each BH enters partner's Event Horizon. So the collision means the combine. Then the kinetic energy turns into wave energy of GW.
The relative speed between BHs can't be beyond the light speed, so the speed of each BH is less than about c/2.
The GW is generated by the rapid change of the gravitational field, so the wave is also generated by the change of the momentum. As the GW is a kind of wave, so GW is inversely proportional to the square of the distance r to the observing point. Therefore the GW150914 observed on the earth is proportional to the value expressed by the following formula:
GWbh?? 29 ?˜2?˜(10??30)?˜1.5?˜(10??5)??{(13?˜9.46?˜(10??12)?p??2
?@?? 5.75 ?˜10??8) (kg?^sec?Ekm)
The GW which might be generated accompanied by a earthquake is calculated as follows:
The energy E of a earthquake, magnitude M is expressed as follows:
?@?@log E??4.8 + 1.5 M When M=7,
log E ?? 4.8 + 10.5 ?? 15.3
E ?? 10??15.3 J??2?˜10??15 J
??2?˜10??9 kg (km?^sec)??2
The mass which moves by the earthquake is calculated from
?@ E??0.5?˜m ?˜v??2

©2019. Japan Geoscience Union. All Right Reserved.

When the speed of the earthquake wave on the surface v=5.45 km/sec is substituted, the momentum is
??v ??2 E?^??
?? 4?˜10??9?^5.45 kg?E?q?^sec
??0.734?˜10??9 kg?E?q?^sec
In the case of GW150914, only the speed of more than about c/2 contributed to generate the GW, so it is thought that only when the speed is more than about c/2, the GW is generated.
In general, the speed is distributed as normal distribution. The part of the earthquake wave speed more than c/2 becomes neglectfully small, when it is calculated from the mean value and standard deviation of earthquake wave speed. So, it will be concluded that any earthquake never generates GW.
Now let try in any case we can observe the GW
Let calculate GW when a meteorite falls on the earth with the speed of c/2. By the way, the moon never falls on the earth, because the tidal force breaks the moon into pieces, and the falling pieces burn out in the atmosphere. And the radar can't detect the object which approach with the speed of more than c/2, because the object with the speed more than c/2 arrives before it is detected.
The observed GW, when the Meteorite of the mass of the moon falls at the distance of r, is proportional to
GWme??m v?^????2 ?@kg?^km?Esec
where
mass of the moon: m??7.343?˜10??22?s
r??10000 km
GWme??1.10 ?˜10??21?@ kg?^?q?Esec
Now,
GWme?^GWbh??1.10?˜10??21?^5.75?˜10??8
??1.91?˜10??11
This value means that the meteor of the mass of 1?^1.91?˜10??11 of the moon causes the GW.
The maximum Meteor we know is about ten thousand tons, so if more than one hundred thousand tons meteor falls on the earth, all the life on the earth disappears. Ending Remark
It will be clear that predicting all earthquakes is impossible because even the precursors are difficult to predict. Even the locating the place of the microcrack, which is origin of precursors, is nearly impossible.
Reference
Kozo Takahashi: Mechanism of generating electromagnetic fields just before great earthquakes, Japan Geoscience Union Meeting 2011, S-SS024-13 Introduction

Keywords: Earthquake Prediction, precursory seismic electric fields, eruption predicion, precursory eruptional magma, gravitational wave

©2019. Japan Geoscience Union. All Right Reserved.

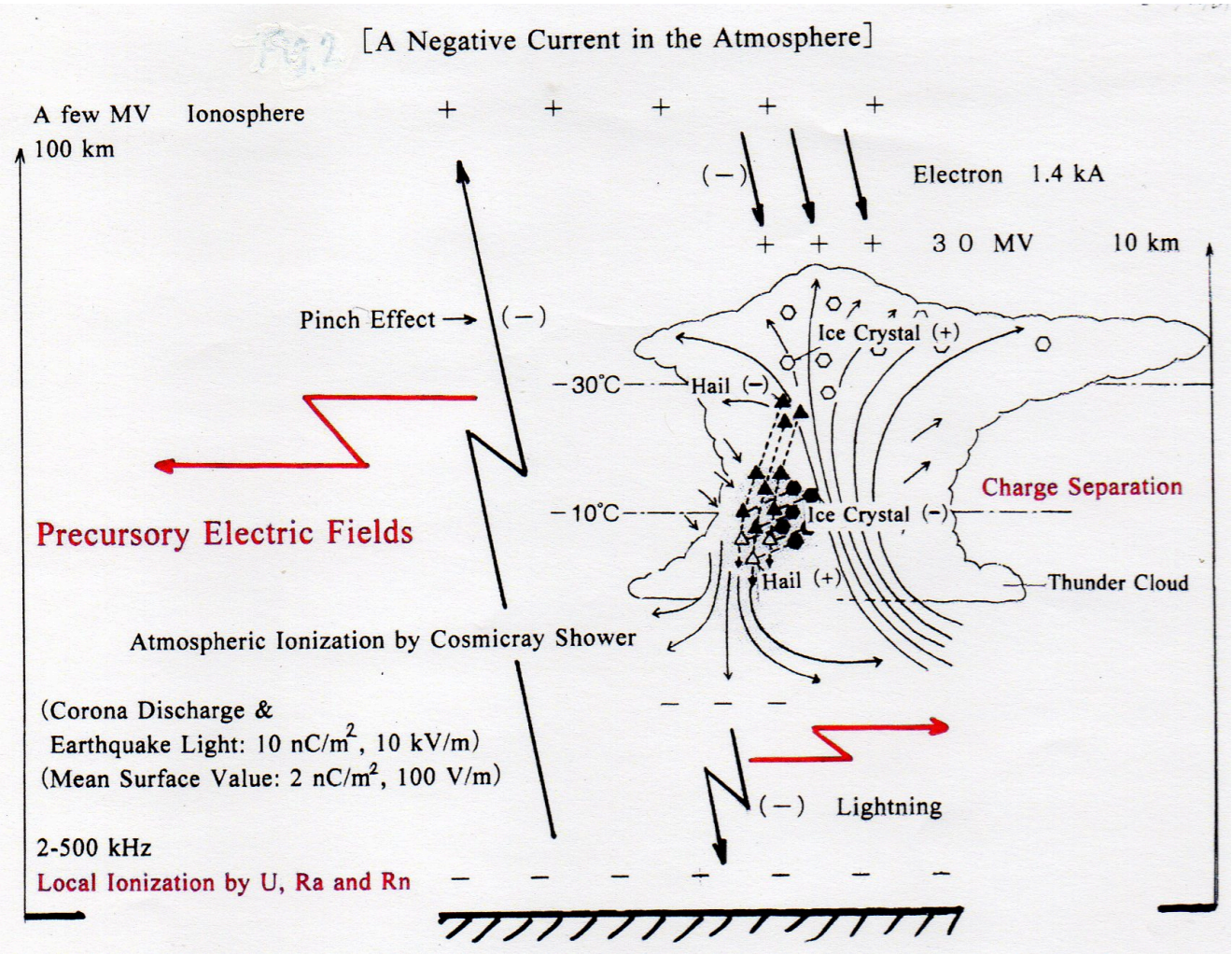

©2019. Japan Geoscience Union. All Right Reserved.

Difference of foreshock characteristics between real data and synthetic ETAS catalogs: through the application of an empirical earthquake forecast model based on foreshocks

*Fuyuki Hirose[1], Koji Tamaribuchi[1], Kenji Maeda[2]

1. Seismology and Tsunami Research Department, Meteorological Research Institute, 2. Seismology and Volcanology Department, Japan Meteorological Agency

It is pointed out that there is no effective earthquake forecast model than ETAS model [Ogata, 1988, JASA] because earthquakes are probabilistic phenomena driven by seismically cascading process represented by a superposition of background activity and epidemic-type aftershock sequence [e.g., Felzer et al., 2004, BSSA; 2015, NatureGeo]. On the other hand, it is also pointed out that the information of foreshock characteristics could be an effective clue of earthquake forecast because foreshocks are a part of the nucleation process, including precursory slips, which ETAS model cannot represent [e.g., Lippiello et al., 2012, SciRep; Bouchon et al., 2013, NatureGeo].
To investigate reproducibility of real data by ETAS model, we made synthetic earthquake catalogs (hereafter ETAS catalogs) based on ETAS parameters obtained from real data, and then we applied the earthquake forecast model that was formulated using real foreshock data [e.g., Maeda & Hirose, 2017, Yochiren98] to ETAS catalogs, and investigated the efficiency of the forecast. The forecast model optimized for Izu Islands is as follows: when 3 events (foreshocks) of M >= 3.0 occur in area of latitude 0.2˚ ×longitude 0.2˚ during 3 days, a mainshock of M >= 5.0 will occur within 5 days just after the event. This model with specific parameters is the most efficient one among those with other parameters by the measurement of likelihood.
Our investigation resulted in that real data yielded higher scores than ETAS catalogs. In other words, it is hard for ETAS model to reproduce foreshock characteristics, which might be related to precursory slips, well, indicating the earthquake forecast model based on foreshock characteristics is more efficient rather than ETAS model. However, our investigation might be biased because our forecast model based on foreshocks was optimized for real data. To perform reliable testing, it may also be necessary to investigate using our forecast model parameters optimized for ETAS catalogs.

Keywords: Earthquake forecast model, Foreshocks, ETAS model, Izu Islands

©2019. Japan Geoscience Union. All Right Reserved.

The increase in missing waveform images of the F-net broadband seismograph network preceding the 2011 Tohoku earthquake (2)

*Yoshiki SUE[1]

1. none

1. Introduction
For the themed earthquake, it is reported that number of the stations with missing waveform images (i.e. data) in the broadband seismic network F-net increased over several months before and after the main shock.
There was the first increase from December 22, 2010 to January 18, 2011, and reached the number of 4. Then there was the 2nd increase from February 16, 2011 to March 2, 2011. Especially from February 19 to March 2, it again became 4 stations (Sapporo (Code: HSS), Yamagata (IYG, Iwate pref.), Kesennuma (KSN) and Shiramine (SRN)). ... The period of 2nd increase overlapped seismically active period of February 13 to March 2 when M5 earthquakes occurred continuously in the epicentral region. (Sue, 2013)

2. Further investigations
We conducted further investigations for the period from the middle of February 2011 to the beginning of March 2011 and obtained the following results.
<Slow slip>
·Slow slip occurred near the epicenter before occurrence of the main shock. Slow slip began on January 29, 2011, expanded the active area around February 19, existed till the time just before occurrence of the Off Sanriku earthquake M7.3 on March 9. The slow slip induced the earthquake, which is thought the foreshock. (Uchida, Kato, Ito, Ota, 2014)
<Missing data of F-net>
·The second deterioration started from February 16, 2011, and from February 19 to March 2, it became the worst condition with 4 data-missing stations (Sapporo (HSS), Iwate Yamagata (IYG), Kesennuma (KSN), and Shiramine (SRN)).
·Sapporo (HSS) and Iwate Yamagata (IYG) were the stations with missing data before starting of deterioration.
·Kesennuma station (KSN) joined this group from February 16 to March 2.
·Shiramine station (SRN) joined this group from February 19 to April 25. Shiramine station is located in Hakusan city, Ishikawa prefecture where is far from off-Sanriku area, but on February 27, there was an earthquake swarm including a M5.5 Earthquake in Hida area near the station.
·The increase of data-missing stations ended on March 2, then number decreased. On March 8, the day before occurrence of the foreshock with a magnitude of 7.3, two stations; Iwate Yamagata (IYG) and Shiramine (SRN) remained.

3. Summary
Increase of missing data for the F-net stations from mid February to early March coincides the slow slip which occurred from January 29 through March 9 as well as the earthquake activities in off-Sanriku region from mid-February to late February in terms of time and location. On February 19, slow slip expanded the area, and on the same day, it reached the largest number of missing stations of F-net. It is thought that F-net responded to some kind of vibration generated near the future epicentral region.

©2019. Japan Geoscience Union. All Right Reserved.

Acknowledgement
The author thanks NIED for using the data of the F-net.

References

Sue, Y., 2013, The increase in missing waveform images of the F-net broadband seismograph network preceding the 2011 Tohoku earthquake, JpGU.
Uchida, N., Kato, A., Ito, Y., and Ota, Y., 2014, Special issue −3 years passed since the Tohoku earthquake, the slow slip existed prior to the earthquake, Naifuru, Vol97.

Keywords: 2011 Tohoku earthquake, F-net, slow slip

©2019. Japan Geoscience Union. All Right Reserved.

On the *b*-value of the OBS seismic observation around the Suruga Bay Senoumi

*Taiyo Sotani[1], Hisatoshi Baba[4], Takahito Nishimiya[2], Nakao Nagisa[1], Toshiyasu Nagao[3]

1. Toukai Univrsity, 2. Meteorological Research Institute, Japan Meteorological Agency, 3. Institute of Oceanic Research and development, Tokai University, 4. Department of Marine and Earth Science, Tokai University

Suruga Bay is a steep bay with Suruga trough and is presumed to be the focal region of the Tokai earthquake. At the plate boundary from the Suruga Through to the Nankai Trough, massive earthquakes of M 8.0 classes have repeatedly occurred in the past. In Suruga Bay, in August 2009, "Shizuoka Offshore Earthquake (M6.5)" and August 2011 "Suruga Bay Earthquake (M6.2)" as an opportunity, from November 2011, we set up the pup-up ocean bottom seismograph (OBS) at the sea area around Senoumi in central Suruga Bay and started seismic observation.

We will make the presentation about the following.
The *b*-value every 3 months using the hypocenters located by OBS observation from October 2012 to August 2018 The comparison of the *b*-value calculated every 3 months and the data of Japan Meteorological Agency (JMA) from October 2012 to August 2018. The *b*-values in the vicinity of the Senoumi located a lot of hypocenters.

Keywords: Tokai Earthquake, b-value

©2019. Japan Geoscience Union. All Right Reserved.

Trial Result of Long-term Occurrence Probabilities with The Moderate Repeating Earthquakes Using The Lognormal Distribution Model with Bayesian Approach

*Masayuki Tanaka[1]

1. Meteorological Research Institute

We are investigating the moderate repeating earthquakes. And we are verifying the long-term probability forecast using the log-normal distribution model with Bayesian approach (LN-Bayes) by Okada et al. (2007). This model is that probability distribution of recurrence interval is given in the inverse gamma prior distribution. The parameters of inverse gamma use shape, ϕ=2.5 and scale, ζ=0.23. This model can be calculated from one sample. We calculated the probability of occurrence during one year from February 2016 (2016.2). Then in February 2017 (2017.2) and February 2018 (2018.2) we did the same calculation. We confirm the outcome of the forecast using evaluation index. Then compares with the result of another model.
We use three models for comparison.
(1) LN-SST: Lognormal distribution model base on the small sample theory.
(2) BPT: BPT distribution model. The coefficient of variation α use 0.24. This value is based on the Headquarters for Earthquake Research Promotion (2010).
(3) Exp: Exponential distribution model. The parameter plugged is the sample mean.

The "Mean log-likelihood (*MLL*)" and "Brier Score (*BS*)" mentioned below are used to score the forecast results.
MLL: Average of $Ev \log_e (P) + (1-Ev) \log_e (1-P)$
BS: Average of $(P - Ev)^2$
Here *P* means forecast probability for event and *Ev* means presence (*Ev*=1) or absence (*Ev*=0) of the event. The *MLL* has a negative value. The closer to 0, the better. The *MLL* is -0.693 when the probability is 0.5, and it is very bad if the value is smaller than that. The *BS* has a positive value. The closer to 0, the better. The *BS* is 0.25 when the probability is 0.5, and it is very bad if the value is larger than that.

In Figure 1 shows the forecast results of the MLL for the four models. With the 2016.2 trial, The LN-SST model is better than other models. With the 2017.2 and 2018.2 trials, result of the LN-Bayes model is better than the other models one. Three predictions are independent, and combining of results for three times, the result of the LN-Bayes model is superior to the other models. But results of the LN-Bayes, the LN-SST and the Exp models are gradually getting worse. The results of the LN-SST model change more than the other two models. In February 2018 results, result of the LN-SST model is inferior to result of the Exp model. The cause is unknown. The BPT model is a very bad results in all three times.

Keywords: Repeating earthquakes, Forecast results, Mean log-likelihood

©2019. Japan Geoscience Union. All Right Reserved.

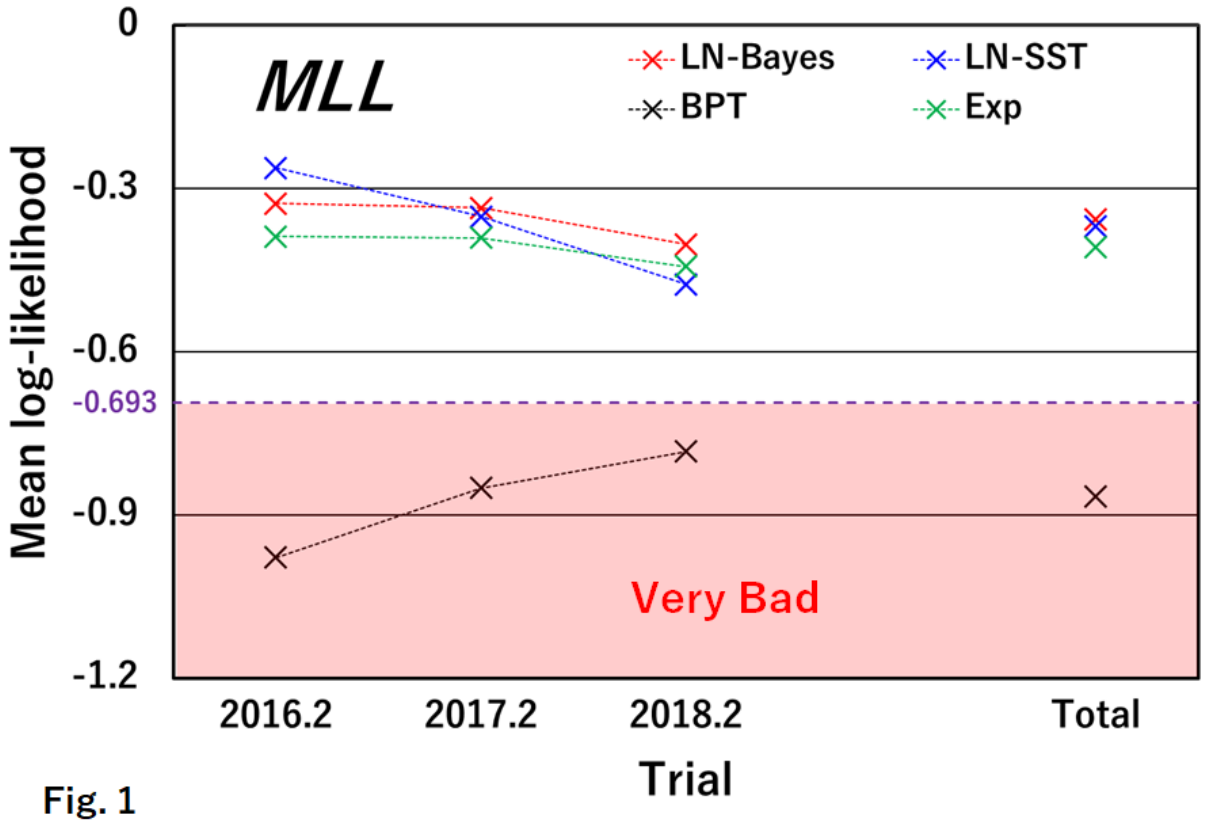

Fig. 1

©2019. Japan Geoscience Union. All Right Reserved.

Structural heterogeneity under the 2018 Mw6.6 Eastern Iburi earthquake in Hokkaido, Japan and its implications for rupture initiations

*ZHI WANG[1]

1. Key Laboratory of Marginal Sea Geology at South China Sea Institute of Oceanology of CAS of China

On September 6, 2018, an Mw6.6 (moment magnitude) crustal earthquake occurred at Eastern Iburi on the island of Hokkaido, Japan (hereafter referred to as the Iburi Earthquake), where the northeastern Japan arc obliquely collides with the Kuril arc. It is the first time an earthquake has ever reached a maximum intensity of 7 (on scale of JMA: Japan Meteorological Agency) in Hokkaido. The 2018 Iburi earthquake caused serious damage across Hokkaido Prefecture and adjacent regions, including the death of 44 people, as many as 680 injuries, and a large number of landslides around the town of Atsuma. The focal mechanism solution of the earthquake showed that initiation occurred on either a moderately dipping reverse fault striking northwest (NW), or on a shallow-to-moderately dipping fault striking southeast (SE).

The hypocenter area is characterized by the mutual interactions of three plates: the Pacific plate, the North American (Okhotsk) plate, and the Eurasian plate. This reverse-faulting earthquake occurred close to the Hidaka main thrust belt, whose tectonics are driven by the convergence of the above three plates. The plate boundary between the Eurasian and Okhotsk plates is located near the eastern coastline of the Japan Sea. Under the Iburi earthquake, the Pacific slab is subducting towards the west (W) -NW beneath the Eurasian and North American plates from the northeastern (NE) Japan and Kuril Trenches. In the Hokkaido subduction zone, there have been 18 earthquakes (M_J > 6.5: JMA magnitude) recorded since 1926; however, the majority are interplate thrust earthquakes associated with the Pacific slab subduction, and only five of these occurred at shallow depths under Hokkaido according to JMA focal depths.
The hypocenter determined by JMA indicated a focal depth of ~37 km. Given the focal mechanism solutions and depth, the main-shock was likely an intraplate event within the North American (upper) plate (or Okhotsk microplate), rather than on the interface between the subducting Pacific and North America plates. This was because the iso-depth of the upper boundary for the Pacific slab was about ~100 km beneath the epicenter. Although numerous seismic tomographic studies in the crust and uppermost mantle have been conducted in Hokkaido, the structure in the 2018 Iburi source area remains poorly resolved. It is worth noting that the seismic velocity and Poisson ratio images, together with geology and geothermal data, in the source area could provide some important information for a better understanding of earthquake generation. To investigate the rupture initiation of the earthquake, we conduct a high resolution seismic tomography study to determine the seismic velocity and Poisson ratio structures under the entire Hokkaido arc. Our results indicated that the main-shock was likely located at a blind-thrust fault close to the boundary between the negative and positive seismic anomalies. A strong low velocity and high Poisson ratio body that extended to a depth of ~120 km was clearly imaged northwest of the hypocenter under the back-arc side of the mantle wedge, indicating fluids were released from the subducting Pacific slab dehydration. Fluids released from the great depth of the back-arc mantle wedge would intrude into the positive anomaly from the more saturated negative side in the lower crust, leading to high pore-fluid pressure accumulation in that region. The descending brittle crustal material sandwiched by two negative zones in the hypocenter was sufficiently large, resulting in strain concentration, decrease of rock effective stress in the hypocenter, and contributing to brittle deformation.

©2019. Japan Geoscience Union. All Right Reserved.

Keywords: 2018 Mw6.6 Eastern Iburi earthquake, Fluid pore-pressure concentration, Role of fluids in triggering of earthquake

©2019. Japan Geoscience Union. All Right Reserved.

[J] Poster | S (Solid Earth Sciences)：S-SS Seismology

Wed. May 29, 2019 5:15 PM - 6:30 PM JST | Wed. May 29, 2019 8:15 AM - 9:30 AM UTC | Poster Hall International Exhibition Hall8, Makuhari Messe_25

[S-SS09] Earthquake prediction and forecast

convener:Masayuki Obayashi(Japan Agency for Marine-Earth Science and Technology), Toshitaka Baba(Graduate School of Science and Technology, Tokushima University)

This session provides the opportunity for contributions that fall within the scientific spectrum of earthquake prediction and forecasting. We welcome theoretical, observational or numerical papers that are either on long- or short-term predictions, and either based on deterministic or probabilistic approaches.

[SSS09-P01] A method to ditect seismic precursors

*Kozo Takahashi

[SSS09-P02] Difference of foreshock characteristics between real data and synthetic ETAS catalogs: through the application of an empirical earthquake forecast model based on foreshocks

*Fuyuki Hirose[1], Koji Tamaribuchi[1], Kenji Maeda[2] (1.Seismology and Tsunami Research Department, Meteorological Research Institute, 2.Seismology and Volcanology Department, Japan Meteorological Agency)

[SSS09-P03] The increase in missing waveform images of the F-net broadband seismograph network preceding the 2011 Tohoku earthquake (2)

*Yoshiki SUE[1] (1.none)

[SSS09-P04] On the *b*-value of the OBS seismic observation around the Suruga Bay Senoumi

*Taiyo Sotani[1], Hisatoshi Baba[4], Takahito Nishimiya[2], Nakao Nagisa[1], Toshiyasu Nagao[3] (1.Toukai Univrsity, 2.Meteorological Research Institute, Japan Meteorological Agency, 3.Institute of Oceanic Research and development, Tokai University, 4.Department of Marine and Earth Science, Tokai University)

[SSS09-P05] Trial Result of Long-term Occurrence Probabilities with The Moderate Repeating Earthquakes Using The Lognormal Distribution Model with Bayesian Approach

*Masayuki Tanaka[1] (1.Meteorological Research Institute)

[SSS09-P06] **Structural heterogeneity under the 2018 Mw6.6 Eastern Iburi earthquake in Hokkaido, Japan and its implications for rupture initiations**

*ZHI WANG[1] (1.Key Laboratory of Marginal Sea Geology at South China Sea Institute of Oceanology of CAS of China)

A method to ditect seismic precursors

*Kozo Takahashi

A method to detect seismic precursors precursory seismic electric fields
earthquake prediction Introduction
Many precursors have been observed before a big earthquake. Most of them are regarded as the result of microcracks in the source region. Therefore, if we can detect the microcracks, it will become possible to predict directly or indirectly the earthquakes. Detection of microcracks
By arranging four electrodes around the earthquake region, we measure the electric potential and resistance (though this method is difficult at seabed), then we can detect the microcrack. But this method is nearly impossible, as we can't know the precise location of the earthquake region.
If Gravitational Waves (GWs)are
emitting from the source region, it becomes possible to detect the region and to predict the earthquakes. But the following shows this is perfectly impossible.
Receiving GW
First the intensity of GW is shown which was detected.
The intensity of GW150914, which emitted when the two Black Holes (BHs) combined, is calculated as follows:
Symbols and approximate values of constants are as follows:
???Fraise to the power ˜
Light velocity:????3?˜(10??5) km/sec
One light-year??9.46?˜(10??12) km
Solar Mass:?Q?˜(10??30) kg
The values of GW150914 when it combined: The distance to the BHs:
??=13 hundred million light-years
The mass of the smaller BH:
M=29 Solar mass
The collision between BHs means that the each BH enters partner's Event Horizon. So the collision means the combine. Then the kinetic energy turns into wave energy of GW.
The relative speed between BHs can't be beyond the light speed, so the speed of each BH is less than about c/2.
The GW is generated by the rapid change of the gravitational field, so the wave is also generated by the change of the momentum. As the GW is a kind of wave, so GW is inversely proportional to the square of the distance r to the observing point. Therefore the GW150914 observed on the earth is proportional to the value expressed by the following formula:
GWbh?? 29 ?˜2?˜(10??30)?˜1.5?˜(10??5)??{(13?˜9.46?˜(10??12)?p??2
?@?? 5.75 ?˜10??8) (kg?^sec?Ekm)
The GW which might be generated accompanied by a earthquake is calculated as follows:
The energy E of a earthquake, magnitude M is expressed as follows:
?@?@log E??4.8 + 1.5 M When M=7,
log E ?? 4.8 + 10.5 ?? 15.3
E ?? 10??15.3 J??2?˜10??15 J
??2?˜10??9 kg (km?^sec)??2
The mass which moves by the earthquake is calculated from
?@ E??0.5?˜m ?˜v??2

©2019. Japan Geoscience Union. All Right Reserved.

When the speed of the earthquake wave on the surface v=5.45 km/sec is substituted, the momentum is
??v ??2 E?^??
?? 4?˜10??9?^5.45 kg?E?q?^sec
??0.734?˜10??9 kg?E?q?^sec
In the case of GW150914, only the speed of more than about c/2 contributed to generate the GW, so it is thought that only when the speed is more than about c/2, the GW is generated.
In general, the speed is distributed as normal distribution. The part of the earthquake wave speed more than c/2 becomes neglectfully small, when it is calculated from the mean value and standard deviation of earthquake wave speed. So, it will be concluded that any earthquake never generates GW.
Now let try in any case we can observe the GW
Let calculate GW when a meteorite falls on the earth with the speed of c/2. By the way, the moon never falls on the earth, because the tidal force breaks the moon into pieces, and the falling pieces burn out in the atmosphere. And the radar can't detect the object which approach with the speed of more than c/2, because the object with the speed more than c/2 arrives before it is detected.
The observed GW, when the Meteorite of the mass of the moon falls at the distance of r, is proportional to
GWme??m v?^????2 ?@kg?^km?Esec
where
mass of the moon: m??7.343?˜10??22?s
r??10000 km
GWme??1.10 ?˜10??21?@ kg?^?q?Esec
Now,
GWme?^GWbh??1.10?˜10??21?^5.75?˜10??8
??1.91?˜10??11
This value means that the meteor of the mass of 1?^1.91?˜10??11 of the moon causes the GW.
The maximum Meteor we know is about ten thousand tons, so if more than one hundred thousand tons meteor falls on the earth, all the life on the earth disappears. Ending Remark
It will be clear that predicting all earthquakes is impossible because even the precursors are difficult to predict. Even the locating the place of the microcrack, which is origin of precursors, is nearly impossible.
Reference
Kozo Takahashi: Mechanism of generating electromagnetic fields just before great earthquakes, Japan Geoscience Union Meeting 2011, S-SS024-13 Introduction

Keywords: Earthquake Prediction, precursory seismic electric fields, eruption predicion, precursory eruptional magma, gravitational wave

©2019. Japan Geoscience Union. All Right Reserved.

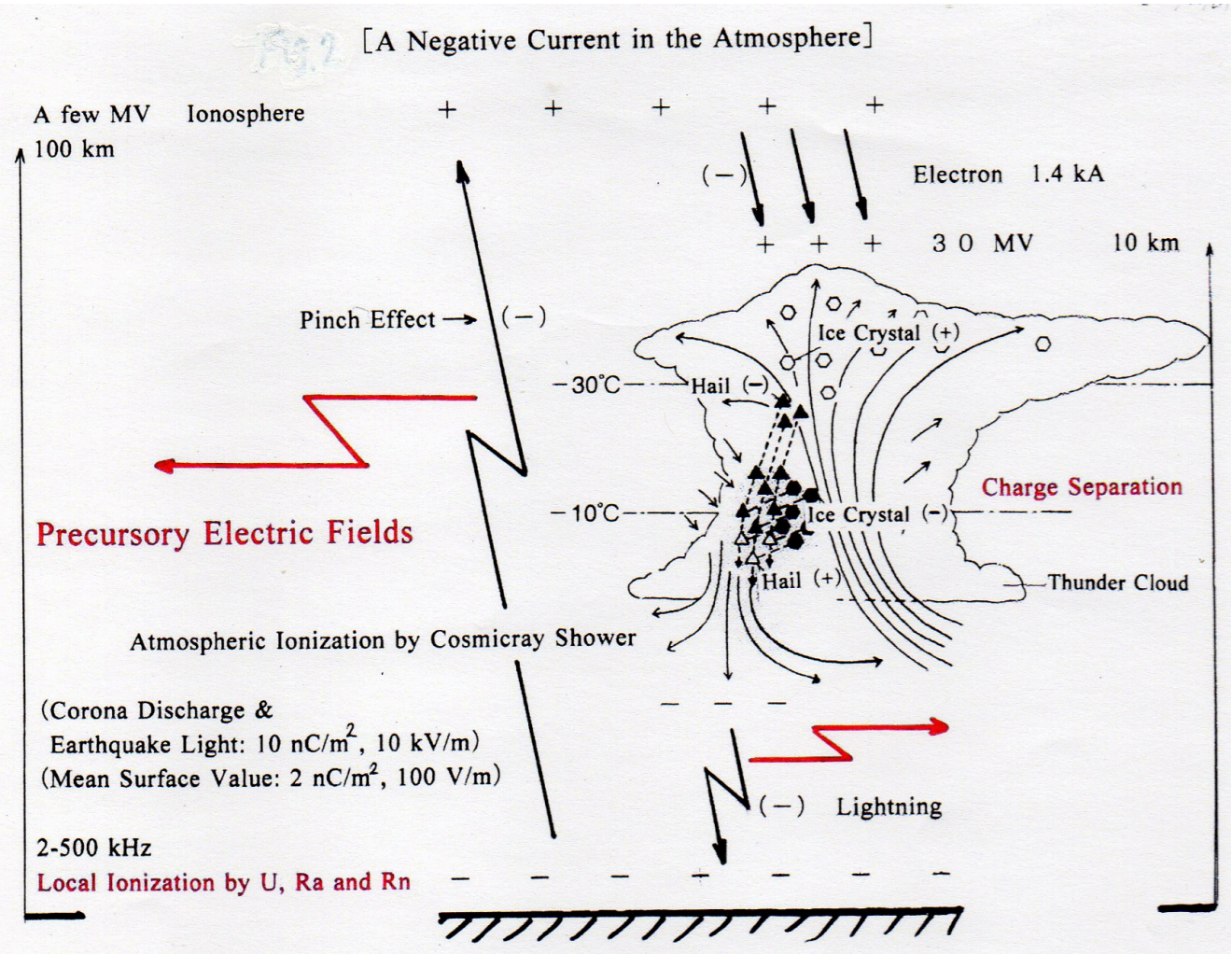

©2019. Japan Geoscience Union. All Right Reserved.

Difference of foreshock characteristics between real data and synthetic ETAS catalogs: through the application of an empirical earthquake forecast model based on foreshocks

*Fuyuki Hirose[1], Koji Tamaribuchi[1], Kenji Maeda[2]

1. Seismology and Tsunami Research Department, Meteorological Research Institute, 2. Seismology and Volcanology Department, Japan Meteorological Agency

It is pointed out that there is no effective earthquake forecast model than ETAS model [Ogata, 1988, JASA] because earthquakes are probabilistic phenomena driven by seismically cascading process represented by a superposition of background activity and epidemic-type aftershock sequence [e.g., Felzer et al., 2004, BSSA; 2015, NatureGeo]. On the other hand, it is also pointed out that the information of foreshock characteristics could be an effective clue of earthquake forecast because foreshocks are a part of the nucleation process, including precursory slips, which ETAS model cannot represent [e.g., Lippiello et al., 2012, SciRep; Bouchon et al., 2013, NatureGeo].
To investigate reproducibility of real data by ETAS model, we made synthetic earthquake catalogs (hereafter ETAS catalogs) based on ETAS parameters obtained from real data, and then we applied the earthquake forecast model that was formulated using real foreshock data [e.g., Maeda & Hirose, 2017, Yochiren98] to ETAS catalogs, and investigated the efficiency of the forecast. The forecast model optimized for Izu Islands is as follows: when 3 events (foreshocks) of M >= 3.0 occur in area of latitude 0.2˚ ×longitude 0.2˚ during 3 days, a mainshock of M >= 5.0 will occur within 5 days just after the event. This model with specific parameters is the most efficient one among those with other parameters by the measurement of likelihood.
Our investigation resulted in that real data yielded higher scores than ETAS catalogs. In other words, it is hard for ETAS model to reproduce foreshock characteristics, which might be related to precursory slips, well, indicating the earthquake forecast model based on foreshock characteristics is more efficient rather than ETAS model. However, our investigation might be biased because our forecast model based on foreshocks was optimized for real data. To perform reliable testing, it may also be necessary to investigate using our forecast model parameters optimized for ETAS catalogs.

Keywords: Earthquake forecast model, Foreshocks, ETAS model, Izu Islands

©2019. Japan Geoscience Union. All Right Reserved.

The increase in missing waveform images of the F-net broadband seismograph network preceding the 2011 Tohoku earthquake (2)

*Yoshiki SUE[1]

1. none

1. Introduction
For the themed earthquake, it is reported that number of the stations with missing waveform images (i.e. data) in the broadband seismic network F-net increased over several months before and after the main shock.
There was the first increase from December 22, 2010 to January 18, 2011, and reached the number of 4. Then there was the 2nd increase from February 16, 2011 to March 2, 2011. Especially from February 19 to March 2, it again became 4 stations (Sapporo (Code: HSS), Yamagata (IYG, Iwate pref.), Kesennuma (KSN) and Shiramine (SRN)). ... The period of 2nd increase overlapped seismically active period of February 13 to March 2 when M5 earthquakes occurred continuously in the epicentral region. (Sue, 2013)

2. Further investigations
We conducted further investigations for the period from the middle of February 2011 to the beginning of March 2011 and obtained the following results.
<Slow slip>
·Slow slip occurred near the epicenter before occurrence of the main shock. Slow slip began on January 29, 2011, expanded the active area around February 19, existed till the time just before occurrence of the Off Sanriku earthquake M7.3 on March 9. The slow slip induced the earthquake, which is thought the foreshock. (Uchida, Kato, Ito, Ota, 2014)
<Missing data of F-net>
·The second deterioration started from February 16, 2011, and from February 19 to March 2, it became the worst condition with 4 data-missing stations (Sapporo (HSS), Iwate Yamagata (IYG), Kesennuma (KSN), and Shiramine (SRN)).
·Sapporo (HSS) and Iwate Yamagata (IYG) were the stations with missing data before starting of deterioration.
·Kesennuma station (KSN) joined this group from February 16 to March 2.
·Shiramine station (SRN) joined this group from February 19 to April 25. Shiramine station is located in Hakusan city, Ishikawa prefecture where is far from off-Sanriku area, but on February 27, there was an earthquake swarm including a M5.5 Earthquake in Hida area near the station.
·The increase of data-missing stations ended on March 2, then number decreased. On March 8, the day before occurrence of the foreshock with a magnitude of 7.3, two stations; Iwate Yamagata (IYG) and Shiramine (SRN) remained.

3. Summary
Increase of missing data for the F-net stations from mid February to early March coincides the slow slip which occurred from January 29 through March 9 as well as the earthquake activities in off-Sanriku region from mid-February to late February in terms of time and location. On February 19, slow slip expanded the area, and on the same day, it reached the largest number of missing stations of F-net. It is thought that F-net responded to some kind of vibration generated near the future epicentral region.

©2019. Japan Geoscience Union. All Right Reserved.

Acknowledgement
The author thanks NIED for using the data of the F-net.

References

Sue, Y., 2013, The increase in missing waveform images of the F-net broadband seismograph network preceding the 2011 Tohoku earthquake, JpGU.
Uchida, N., Kato, A., Ito, Y., and Ota, Y., 2014, Special issue −3 years passed since the Tohoku earthquake, the slow slip existed prior to the earthquake, Naifuru, Vol97.

Keywords: 2011 Tohoku earthquake, F-net, slow slip

©2019. Japan Geoscience Union. All Right Reserved.

On the *b*-value of the OBS seismic observation around the Suruga Bay Senoumi

*Taiyo Sotani[1], Hisatoshi Baba[4], Takahito Nishimiya[2], Nakao Nagisa[1], Toshiyasu Nagao[3]

1. Toukai Univrsity, 2. Meteorological Research Institute, Japan Meteorological Agency, 3. Institute of Oceanic Research and development, Tokai University, 4. Department of Marine and Earth Science, Tokai University

Suruga Bay is a steep bay with Suruga trough and is presumed to be the focal region of the Tokai earthquake. At the plate boundary from the Suruga Through to the Nankai Trough, massive earthquakes of M 8.0 classes have repeatedly occurred in the past. In Suruga Bay, in August 2009, "Shizuoka Offshore Earthquake (M6.5)" and August 2011 "Suruga Bay Earthquake (M6.2)" as an opportunity, from November 2011, we set up the pup-up ocean bottom seismograph (OBS) at the sea area around Senoumi in central Suruga Bay and started seismic observation.

We will make the presentation about the following.
The *b*-value every 3 months using the hypocenters located by OBS observation from October 2012 to August 2018 The comparison of the *b*-value calculated every 3 months and the data of Japan Meteorological Agency (JMA) from October 2012 to August 2018. The *b*-values in the vicinity of the Senoumi located a lot of hypocenters.

Keywords: Tokai Earthquake, b-value

©2019. Japan Geoscience Union. All Right Reserved.

Trial Result of Long-term Occurrence Probabilities with The Moderate Repeating Earthquakes Using The Lognormal Distribution Model with Bayesian Approach

*Masayuki Tanaka[1]

1. Meteorological Research Institute

We are investigating the moderate repeating earthquakes. And we are verifying the long-term probability forecast using the log-normal distribution model with Bayesian approach (LN-Bayes) by Okada et al. (2007). This model is that probability distribution of recurrence interval is given in the inverse gamma prior distribution. The parameters of inverse gamma use shape, ϕ=2.5 and scale, ζ=0.23. This model can be calculated from one sample. We calculated the probability of occurrence during one year from February 2016 (2016.2). Then in February 2017 (2017.2) and February 2018 (2018.2) we did the same calculation. We confirm the outcome of the forecast using evaluation index. Then compares with the result of another model.
We use three models for comparison.
(1) LN-SST: Lognormal distribution model base on the small sample theory.
(2) BPT: BPT distribution model. The coefficient of variation α use 0.24. This value is based on the Headquarters for Earthquake Research Promotion (2010).
(3) Exp: Exponential distribution model. The parameter plugged is the sample mean.

The "Mean log-likelihood (*MLL*)" and "Brier Score (*BS*)" mentioned below are used to score the forecast results.
MLL: Average of $Ev \log_e (P) + (1-Ev) \log_e (1-P)$
BS: Average of $(P - Ev)^2$
Here *P* means forecast probability for event and *Ev* means presence (*Ev*=1) or absence (*Ev*=0) of the event. The *MLL* has a negative value. The closer to 0, the better. The *MLL* is -0.693 when the probability is 0.5, and it is very bad if the value is smaller than that. The *BS* has a positive value. The closer to 0, the better. The *BS* is 0.25 when the probability is 0.5, and it is very bad if the value is larger than that.

In Figure 1 shows the forecast results of the MLL for the four models. With the 2016.2 trial, The LN-SST model is better than other models. With the 2017.2 and 2018.2 trials, result of the LN-Bayes model is better than the other models one. Three predictions are independent, and combining of results for three times, the result of the LN-Bayes model is superior to the other models. But results of the LN-Bayes, the LN-SST and the Exp models are gradually getting worse. The results of the LN-SST model change more than the other two models. In February 2018 results, result of the LN-SST model is inferior to result of the Exp model. The cause is unknown. The BPT model is a very bad results in all three times.

Keywords: Repeating earthquakes, Forecast results, Mean log-likelihood

©2019. Japan Geoscience Union. All Right Reserved.

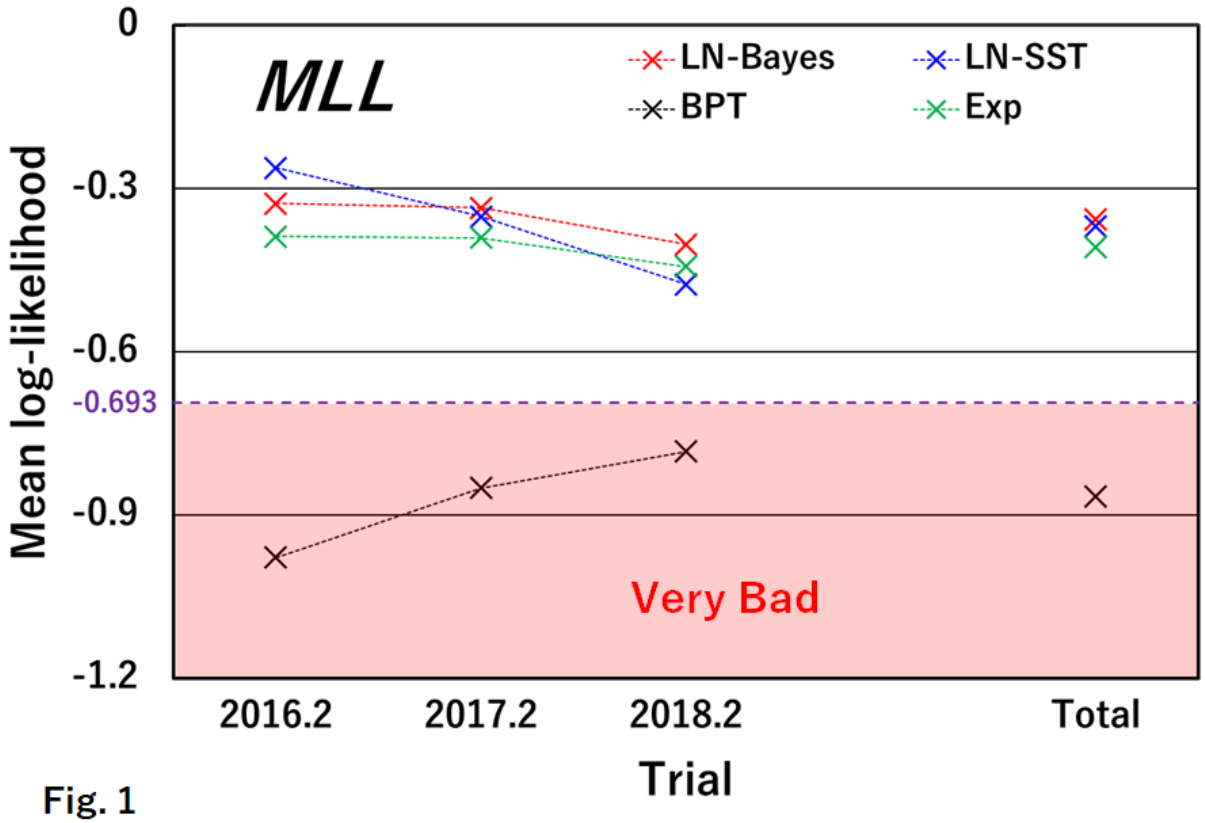

Fig. 1

©2019. Japan Geoscience Union. All Right Reserved.

Structural heterogeneity under the 2018 Mw6.6 Eastern Iburi earthquake in Hokkaido, Japan and its implications for rupture initiations

*ZHI WANG[1]

1. Key Laboratory of Marginal Sea Geology at South China Sea Institute of Oceanology of CAS of China

On September 6, 2018, an Mw6.6 (moment magnitude) crustal earthquake occurred at Eastern Iburi on the island of Hokkaido, Japan (hereafter referred to as the Iburi Earthquake), where the northeastern Japan arc obliquely collides with the Kuril arc. It is the first time an earthquake has ever reached a maximum intensity of 7 (on scale of JMA: Japan Meteorological Agency) in Hokkaido. The 2018 Iburi earthquake caused serious damage across Hokkaido Prefecture and adjacent regions, including the death of 44 people, as many as 680 injuries, and a large number of landslides around the town of Atsuma. The focal mechanism solution of the earthquake showed that initiation occurred on either a moderately dipping reverse fault striking northwest (NW), or on a shallow-to-moderately dipping fault striking southeast (SE).

The hypocenter area is characterized by the mutual interactions of three plates: the Pacific plate, the North American (Okhotsk) plate, and the Eurasian plate. This reverse-faulting earthquake occurred close to the Hidaka main thrust belt, whose tectonics are driven by the convergence of the above three plates. The plate boundary between the Eurasian and Okhotsk plates is located near the eastern coastline of the Japan Sea. Under the Iburi earthquake, the Pacific slab is subducting towards the west (W) -NW beneath the Eurasian and North American plates from the northeastern (NE) Japan and Kuril Trenches. In the Hokkaido subduction zone, there have been 18 earthquakes (M_J > 6.5: JMA magnitude) recorded since 1926; however, the majority are interplate thrust earthquakes associated with the Pacific slab subduction, and only five of these occurred at shallow depths under Hokkaido according to JMA focal depths.
The hypocenter determined by JMA indicated a focal depth of ~37 km. Given the focal mechanism solutions and depth, the main-shock was likely an intraplate event within the North American (upper) plate (or Okhotsk microplate), rather than on the interface between the subducting Pacific and North America plates. This was because the iso-depth of the upper boundary for the Pacific slab was about ~100 km beneath the epicenter. Although numerous seismic tomographic studies in the crust and uppermost mantle have been conducted in Hokkaido, the structure in the 2018 Iburi source area remains poorly resolved. It is worth noting that the seismic velocity and Poisson ratio images, together with geology and geothermal data, in the source area could provide some important information for a better understanding of earthquake generation. To investigate the rupture initiation of the earthquake, we conduct a high resolution seismic tomography study to determine the seismic velocity and Poisson ratio structures under the entire Hokkaido arc. Our results indicated that the main-shock was likely located at a blind-thrust fault close to the boundary between the negative and positive seismic anomalies. A strong low velocity and high Poisson ratio body that extended to a depth of ~120 km was clearly imaged northwest of the hypocenter under the back-arc side of the mantle wedge, indicating fluids were released from the subducting Pacific slab dehydration. Fluids released from the great depth of the back-arc mantle wedge would intrude into the positive anomaly from the more saturated negative side in the lower crust, leading to high pore-fluid pressure accumulation in that region. The descending brittle crustal material sandwiched by two negative zones in the hypocenter was sufficiently large, resulting in strain concentration, decrease of rock effective stress in the hypocenter, and contributing to brittle deformation.

©2019. Japan Geoscience Union. All Right Reserved.

Keywords: 2018 Mw6.6 Eastern Iburi earthquake, Fluid pore-pressure concentration, Role of fluids in triggering of earthquake

©2019. Japan Geoscience Union. All Right Reserved.

[J] Oral | S (Solid Earth Sciences)：S-SS Seismology

Wed. May 29, 2019 3:30 PM - 5:00 PM JST | Wed. May 29, 2019 6:30 AM - 8:00 AM UTC | A05 TOKYO BAY MAKUHARI HALL

[S-SS09] Earthquake prediction and forecast

convener:Masayuki Obayashi(Japan Agency for Marine-Earth Science and Technology), Toshitaka Baba(Graduate School of Science and Technology, Tokushima University), Chairperson:Sumio Yoshikawa(気象研究所), Mamoru Kato(Graduate School of Human and Environmental Studies Kyoto University)

This session provides the opportunity for contributions that fall within the scientific spectrum of earthquake prediction and forecasting. We welcome theoretical, observational or numerical papers that are either on long- or short-term predictions, and either based on deterministic or probabilistic approaches.

3:30 PM - 3:45 PM JST | 6:30 AM - 6:45 AM UTC

[SSS09-01] **Objective evaluationof precursory seismic quiescence and activation phenomenon in wide area**

*Sumio Yoshikawa[1] (1.Meteorological Research Institute)

3:45 PM - 4:00 PM JST | 6:45 AM - 7:00 AM UTC

[SSS09-02] Long-term Probability of a Great Earthquake along the Kurile Trench, Hokkaido Japan (2)

*Masajiro Imoto[1], Morilkawa Nobuyuki[1], Fujiwara Hiroyuki[1] (1.National Research Institute for Earth Science and Disaster Resilience)

4:00 PM - 4:15 PM JST | 7:00 AM - 7:15 AM UTC

[SSS09-03] Parallel and Focused Increase Trends in Time Series (M-T Diagram) of Earthquake Occurrences

*Satoshi Hashimoto[1] (1.none)

4:15 PM - 4:30 PM JST | 7:15 AM - 7:30 AM UTC

[SSS09-04] Revisiting a simple method for short-term earthquake probabilities derived from past Seismicity

*Mamoru Kato[1] (1.Graduate School of Human and Environmental Studies Kyoto University)

4:30 PM - 4:45 PM JST | 7:30 AM - 7:45 AM UTC

[SSS09-05] Recent anomalous groundwater temperature and water level changes at the frontier land zone of Nanki region for impending great earthquakes at the Nankai trough

*Tameshige Tsukuda[1] (1.none)

4:45 PM - 5:00 PM JST | 7:45 AM - 8:00 AM UTC

[SSS09-06] What happen on the East Japan Megaquake; answer to sufferers

*Nobuaki Niitsuma[1] (1.Institute of Geosciences,Shizuoka University)

Objective evaluationof precursory seismic quiescence and activation phenomenon in wide area

*Sumio Yoshikawa[1]

1. Meteorological Research Institute

The 1995 Kobe earthquake of M7.3 is an earthquake known to have observed abnormal changes in seismic activity accompanied by various changes such as crustal deformation, groundwater and electromagnetism before the main shock. Especially Mogi (1995) pointed out the seismicity gap and the quiescent phenomenon of the seismic activity with a long-term and wide-area perspective. Yoshida (1995) pointed out the wide range of the preceding phenomena of seismic activity and showed that the area wider than the epicenter area is involved in the earthquake occurrence process. Therefore, if any prediction method is supposed, it is a problem how much accuracy it is possible to know based on such a preceding phenomenon in wide area.

eMAP is a tool to evaluate the appearance probability of seismic activity by Poisson's probability (Yoshikawa et al., 2017). In this method a region is set for each individual epicenter and the degree of abnormality is displayed in all regions. In order to consider the above problem, we examined the possibility of diagnosis of wide area seismic activity by this method.

By analysis of the quiescence and activation phenomenon in wide area during the Kobe earthquake, mainly in the Kinki, Chugoku and Shikoku districts, the following features were found. At that time, in the JMA seismic catalog before the unification, the magnitude threshold is considered to be around M 2.0 since 1988. The spatial distribution of the seismic activity has changed in a relatively short time scale and a stable pattern is not seen until 5 to 6 years before the main shock, but about 2 years before, a quiet phenomenon is confirmed in the area with the range of 50 km in the eastern part of Hyogo Prefecture. About a year before to the main shock, we can see activation in the epicenter area and a wide area surrounding it. This seems to be due to the small foreshock activity occurred along various active faults and geological lineaments. Based on this seismic sequence, it is possible to suppose a forecasting tactics as follows. First of all, by grasping the location and extent of the quiescence phenomenon, we assume the location and the scale of the main shock (Yoshikawa, 2015), and then estimate the urgency of earthquake occurrence by detecting the simultaneity of temporal changes.

Keywords: Kobe eq, Seismic quiescence and activation

©2019. Japan Geoscience Union. All Right Reserved.

Long-term Probability of a Great Earthquake along the Kurile Trench, Hokkaido Japan (2)

*Masajiro Imoto[1], Morilkawa Nobuyuki[1], Fujiwara Hiroyuki[1]

1. National Research Institute for Earth Science and Disaster Resilience

Great earthquakes (M8 and larger) repeatedly occur along the Kurile Trench off Hokkaido. A much larger one in the 17-th century (17-th type earthquake) is indicated by studies of tsunami deposits, which is considered as representing the simultaneous of Tokachi-oki and Nemuro-oki earthquakes. The Earthquake Research Committee, the Government of Japan has reported the long-term probability of the 17-th type earthquake. We discuss the uncertainty of the long-term probability of the 17-th type earthquake, applying the method by Parsons (2008) to compare the likelihood of both the Brownian Passage Time distribution and the Poisson distribution for recurrent earthquakes. We adopted the seven probable ranges of origin times observed at Mochirippu-toh, and the five ranges at Kiritappu Marsh (Table 7 in the ERC report). Considering two probable ranges of 68% and 95% listed, two different functions of a origin time are adopted as weights; a modified Gaussian function and a step-function. The latter function is fixed so as to reserve the 68% and 95% probabilities in their ranges.
The likelihood ratios of the BPT model to the Poisson one are 0.70-0.79 for the Mochirippu-toh and 1.9-2.0 for the Kiritappu Marsh. The mean of the 17-th type earthquake probability in the next 30 years over the model parameters is about 11% for the Mochirippu-toh and around 21% for the Kiritappu Marsh. Only slight differences of both likelihood ratios and the thirty year probabilities among the three weight functions are observed.

Keywords: Great Earthquake, Kurile Trench, Probability

©2019. Japan Geoscience Union. All Right Reserved.

Parallel and Focused Increase Trends in Time Series (M-T Diagram) of Earthquake Occurrences

*Satoshi Hashimoto[1]

1. none

Usually time sequence of earthquakes is not used as continuous variations because of special property of its occurrences. A few cases such as aftershocks and repeated earthquakes are attributed to continuous series. However, in a time series downloaded from HP of earthquake catalog continuous increase variations are seen clearly in almost all M-T diagrams, here M and T mean magnitude and occurrence time of earthquakes, respectively.

For example, since 2000 a time series of earthquake is shown under the conditions that M > 5.5, D (depth) < 50km, and main 4 islands of Japan with sea areas. In this series clear increase trend consisted from 13 earthquakes (M > 6) can be recognized on a time period from 2002 to 2005. Note that 3 points deviated largely from the straight line are excluded. Surprisingly the straight line connects roughly to the M9 of 2011/3/11 Tohoku-oki Earthquake. If we focus our attention to the increase trend, several lines with similar slope can be seen in other time durations since 2000. These lines are parallel with each other and interrupted at some value of M.

One more important character is seen in the M-T diagram since 2000. Before 2011/3/11 extrapolated more lines gather to the value M9 of Tohoku-oki Earthquake in detailed observations. These are called focused lines. Focused lines are coexisted with the parallel series. Both series are exhibited in whole time span of about 100 years of the catalog. The excluded points described above are probably included by other parallel or focused lines. In short, almost all earthquakes are included in many increase trends of earthquake time sequences.

Little work has be done to the regularity shown above. If several focused time series are found for a few and several years at present, extrapolation of the series will cross in near future. Just the crossing point is the predicted point.

In order to obtain further information about two kinds of the time series, several blocks of Japanese islands are analyzed together with sea areas. From the results two kinds of the time series can be seen in the all blocks. In a small region, increase trend of M~7 does not appear, but in a case of M~6, focused trends are also seen. This fact means that possibility of the prediction is successfully performed to M~6.

Appearance of two kinds of time series is not understood at present. Statistical rule of earthquake occurrences called G-R (Gutenberg-Richter) law is well known. This is one of the power laws, in which number of very large earthquakes are very small, and number of small earthquakes are order of magnitude greater than that of large earthquakes. Comparison of this law with the present results can give us important suggestion. This law does not include the factor of time. Present results shows linear increase trends are very simple but real time series are very complex. Time plays main role in the time series. G-R law is obtained from just after many earthquake occurrences. Present results do not show the individual earthquakes, but show continuous processes in earthquake preparation time span.

At the first stage of this study, present trends are presumably attributed to the constant rate of strain

©2019. Japan Geoscience Union. All Right Reserved.

energy accumulation. However, this idea does not interpret the both parallel and focused trend in the time series. Namely mechanism that long time of several years are spent for accumulating the energy is not adequate in the present results. Perhaps critical state of the crust on the earth did exist hundreds of millions of years ago. At present the state can occur the earthquake both at all time and all places, crust give rise to the earthquake occurrences depending on the time durations. Trial of the prediction is now under planning, but origin of the mechanism is an important problem to be solved.

Keywords: M-T diagram, Earthhquake Time Series, Palallel Time Series, Focused Time Series

©2019. Japan Geoscience Union. All Right Reserved.

Revisiting a simple method for short-term earthquake probabilities derived from past Seismicity

*Mamoru Kato[1]

1. Graduate School of Human and Environmental Studies Kyoto University

We revisit the method of Kato (2016, doi:10.4294/zisin.68.163) to estimate the probability that random earthquake predictions would hit using the seismicity data after 2011. When the seismicity rate is high, a random earthquake prediction without scientific evidence often becomes successful. Accidental, occasional hits will not guarantee that such methods of earthquake prediction are worthy of trust, and we should have a measure to judge whether the method is reliable. Kato (2016) proposed a method to roughly compute the probability that a random earthquake prediction accidentally hits. In this method, assuming that the rate of background seismicity is nearly constant in any period. This presentation is a follow-up to this study, and we reevaluate the method of Kato using the other seismicity data in Japan. We also revisit two probabilities of Utsu (1977) and argue how to make apparently successful earthquake predictions

Keywords: Earthquake prediction, seismicity

©2019. Japan Geoscience Union. All Right Reserved.

Recent anomalous groundwater temperature and water level changes at the frontier land zone of Nanki region for impending great earthquakes at the Nankai trough

*Tameshige Tsukuda[1]

1. none

Earthquakes are generated by the anisotropic principal stress regime in the rock medium. In the preparing process of a large earthquake, the medium would be deformed generating regions of contraction and dilatation around the nucleus of the shearing stresses. According to a hydraulic model, pore fluid flow is driven upward to the ground surface through crack systems serving as flowing pipes by high pressure pumps at a deep spot. The change in the quantity of the upwelling hot water from deep underground causes a change of groundwater temperature(Tsukuda et al., 2005).
We have 16 groundwater observation stations for temperature, and 3 stations for water level in the Tokai and Nanki regions, central and southwest Japan, respectively, where are close to the source regions of the great Nakai-trough earthquakes. This paper reports the seismological meaning of the data from Nanki region.
At stations HA and WA in Shionomisaki, Nanki region, Wakayama Prefecture, the long-term trend of the water level is rising, corresponding to the ground subsidence found by levelling and GNSS data (Kobayashi, 2013). The trend of temperature is similarly rising, suggesting contraction of the rock medium under Shionomisaki, the southernmost end of Honshu. At KZ(Kozagawa)about 15km northeast of HA or WA in the Nanki region, the temperature is monotonously falling since the observation started in 2002. However, the decreasing temperature changed to severely increase in the middle of 2015, and changed to decrease again in 2017.
As mentioned above, the deformations of the rock medium are accelerated under the regions close to the source regions of the great erthquakes at the Nankai trough. For prediction studies for the impending great erthquakes, we should start to conduct detailed and multidisciplinary observations.

Keywords: dilatation, contraction , groundwater temperature, water level, precursor, earthquake prediction

©2019. Japan Geoscience Union. All Right Reserved.

What happen on the East Japan Megaquake; answer to sufferers

*Nobuaki Niitsuma[1]

1. Institute of Geosciences,Shizuoka University

Significant change on stress field was appeared on Northeast Japan. The difference on stress field can be identified by Euler rotation of principal stress axes (Niitsuma, JpGU2015, s-ss27), and the stress fields rotated toward trench side in southeastern part of Northeast Japan but not in northwestern, comparing to stress field of Megaquake. The foci of Megaquake was located on the boundary of the rotation, which indicate the rotation was caused by Megaquake.

Hida area in the central Japan sits on the southwest extinction of the rotation boundary. Hida area had earthquakes from 6 February 2011, 10 days before foreshocks of Megaquake. The activity was complementary with the foreshocks, and the polarities of the stress field (Niitsuma, JpGU2017, sss05-P01) were normal, except the last of 6th March with reversed polarity, comparing with stress field of Megaquake. The maximum foreshock happened 3 days and mainshock of Megaquake 4 days later the polarity reversal, which means Hida area was a part of the constitution to block subduction of Pacific Plate along Japan Trench. The southwestern extinction of Hida area consistent of continental crust, connecting to Korean Peninsula, and the strain for Megaquake had been accumulated in the longest continental crust in Japan and Pacific Plate.

The activity of earthquakes can be converted to Plate relative motion, using area of earthquake fault S from the magnitude M based on log S =1.2M −9.9 (Matsuda,1975). The total area of earthquake faults in North East Japan from 1923/9/2 (just after Kanto Earthquake) to 2011/3/10 (just before East Japan Megaquake) is stepwise increasing on Benioff Chart and reaches to area of M9.0 as same for East Japan Megaquake. The area of relative Plate motion along the Japan Trench for the time interval is 9% less than the earthquake faults, which means the strain for East Japan Megaquake could not be accumulated after Kanto Earthquake, but before.

The area of earthquake faults in North East Japan reached to area for M9.0 before Kanto Earthquake 1923 from 1793, for which area of relative Plate motion was 1.34 of M9.0 and could accumulate strain of 0.34 for M9.0. The Plate motion is not enough for the strain of M9.0 which should be accumulated before 1793.

Because records on historical earthquakes in Northeast Japan are poor comparing with Southwest Japan, the ratio 1.65 on areas of historical earthquake faults in Northeast to Southwest Japan from 1793 to 1923 for calculation on corrected area of earthquake faults in Northeast Japan before 1793.

The corrected area of earthquake faults in Northeast Japan is 0.73 of M9.0 from 1611 to 1793, whose area of Plate motion is 2.06 in which 1.33 could be accumulated enough for the Megaquake. The history of strain accumulation indicates that the Megaquake strain could be kept after filled up with spending for usual earthquake.

Before Megaquake, the focal distribution around non seismic Megaquake foci indicates that rupture was reaching to Megaquake foci. The difference in magnitude of CMT to initial moment in CMT solutions for Hida-side were small than 0.4, which means the main moments were smaller than one forth of estimated

©2019. Japan Geoscience Union. All Right Reserved.

moment from initial moment. Such magnitude differences were identified on the foreshock of Kumamoto Earthquake in April 2016.

Keywords: East Japan Megaquake, Area of earthquake fault, Area of relative plate Motion, Benioff Chart, Difference in Magnitude of Earthquake, Hida

©2019. Japan Geoscience Union. All Right Reserved.

[J] Oral | S (Solid Earth Sciences)：S-SS Seismology

Wed. May 29, 2019 9:00 AM - 10:30 AM JST | Wed. May 29, 2019 12:00 AM - 1:30 AM UTC | A05 TOKYO BAY MAKUHARI HALL

[S-SS14] Fault Rheology and Earthquake Physics

convener:Keishi Okazaki(Japan Agency for Marine-Earth Science and Technology), Hideki Mukoyoshi(Department of Geoscience Interdisciplinary Graduate School of Science and Engineering, Shimane University), Hiroyuki Noda(Kyoto University, Disaster Prevention Research Institute), Keisuke Yoshida(Tohoku University), Chairperson:Hideki Mukoyoshi, Shunya Kaneki(Osaka University)

The goal of this session is to integrate theoretical, experimental, observational, and numerical perspectives from various fields such as seismology, geodesy, geology, mineralogy, and so on, to define what is known about earthquake source processes and the physical and chemical elementary processes of faulting. This session welcomes studies that address such issues as pre-, co-, and post-seismic processes, the rheology of seismogenic faults and fault rocks, laboratory experiments on elementary processes, numerical models based on frictional laws, and estimates of the stress field in the seismogenic zones. We also welcome studies on fault-zone drilling projects and in situ stress measurements.

9:00 AM - 9:15 AM JST | 12:00 AM - 12:15 AM UTC

[SSS14-07] Effect of slickenside on the crustal strength

*Jun-ichi Ando[1], Takayoshi Nagaoka[1], Naotaka Tomioka[2], Hiroyuki Kagi[3], Kaushik Das[1] (1.Department of Earth and Planetary Systems Science, Hiroshima University, 2.Kochi Institute for core sample research, Japan Agency for Marine-Earth Science and Technology, 3.Geochemical Research Center, Graduate School of Science, University of Tokyo)

9:15 AM - 9:30 AM JST | 12:15 AM - 12:30 AM UTC

[SSS14-08] Dehydroxylation kinetics of clay minerals and its application to friction heating along an imbricate thrust in an accretionary prism

★Invited Papers

*Hirokazu Masumoto[1], Jun Kameda[1] (1.Faculty of Science, Hokkaido University)

9:30 AM - 9:45 AM JST | 12:30 AM - 12:45 AM UTC

[SSS14-09] Origin of frictional melt in the Jurassic accretionary complex of the Mino Belt on the basis of trace element and isotope analysis

*Chizuru Ozawa[1], Tsuyoshi Ishikawa[2], Kohtaro Ujiie[1] (1.University of Tsukuba, 2.JAMSTEC)

9:45 AM - 10:00 AM JST | 12:45 AM - 1:00 AM UTC

[SSS14-10] Geochemical constraint on the origin of albite-bearing black fault rocks in the Kodiak accretionary complex

*Tsuyoshi Ishikawa[1], Asuka Yamaguchi[2] (1.Kochi Institute for Core Sample Research, Japan Agency for Marine-Earth Science and Technology, 2.AORI, The University of Tokyo)

10:00 AM - 10:15 AM JST | 1:00 AM - 1:15 AM UTC

[SSS14-11] Importance of initial maturity and reaction kinetics on maturation of carbonaceous material and its implications for thermal maturity as a proxy for temperature in estimation of coseismic slip parameters

*Shunya Kaneki[1], Ichiba Tatsuya[1], Shuhei Yamashita[1], Tetsuro Hirono[1] (1.Graduate School of Science, Osaka University)

10:15 AM - 10:30 AM JST | 1:15 AM - 1:30 AM UTC

[SSS14-12] Experimental investigation of cumulative effect on thermal maturation of carbonaceous material as a proxy for earthquake slip

*Tetsuro Hirono[1], Yuhtaro Shimamura[1], Shunya Kaneki[2] (1.Department of Earth and Space Science, Graduate School of Science, Osaka University, 2.Disaster Prevention Research Institute, Kyoto University)

Effect of slickenside on the crustal strength

*Jun-ichi Ando[1], Takayoshi Nagaoka[1], Naotaka Tomioka[2], Hiroyuki Kagi[3], Kaushik Das[1]

1. Department of Earth and Planetary Systems Science, Hiroshima University, 2. Kochi Institute for core sample research, Japan Agency for Marine-Earth Science and Technology, 3. Geochemical Research Center, Graduate School of Science, University of Tokyo

Slickenside is a glossy and smoothly surface developed on the fault slip plane. Although the slickenside is a common and well-known microstructure, its microstructural characterization and effect on the fault behaviour have not fully studied so far. To understand these points, we characterized the microstructures of natural samples and conducted the frictional experiments. The recovery samples from the experiments were also characterized.

Samples and experiment: The natural samples we characterized were slickensides found on the following rocks collected from several localities. 4-Cherts, 3-Limestones, 1-Amphibolite, 1-Serpentinite, 1-Chromitite, 1-Sandstone, 2-Mudstones, 1-Coaly mudstone and 1-Tuff breccia. The frictional experiments were conducted using limestone and gabbro blocks, and calcite powder with 45 to 75 μm in grain size, with a biaxial friction apparatus. The experimental conditions were 3 - 80 MPa of normal stress, 0.1 m/s and 30 μm/s of slip velocity. The characterization methods of samples were optical microscopy, SEM, TEM, AFM and XANES measurements.
Results and conclusion: The present characterization of natural samples demonstrates that the slickenside is composed of nano-size grains, whose aspect ratio (h/d) of height (h) and diameter (d) is constant at about 0.02 –0.05 for each sample. These nano-size grains can be identified as same minerals, not amorphous, composed of the parent rocks with some minor exceptions. This fact indicates that the nano-size grains were created during fault slip only by grinding of parent rocks without any reaction including the heating-induced reaction. Therefore, our first conclusion is that the slickenside is a product of aseismic faulting. The slickensides were created by all frictional experiments. The characteristics of these slickensides are same as those of natural samples described above. The interesting results are that the aspect ratio (h/d) of nano-size grains is constant for each experiment and tends to decrease with increasing normal stress from ca. 0.23 to ca. 0.07. The h/d values of nano-size grains composed of natural samples are much smaller than those of the recovered samples, which suggests that the studied natural slickensides were created by faulting at the higher normal stress conditions than at least 80 MPa, and preserved during exhumation from original depth to earth’ s surface. This consideration indicates that the fault having slickenside exists at depth corresponding to at least 80 MPa normal stress, ca. 3 km and more. The experimental results using limestone block having pre-existing mirror polished slip plane show that the static and dynamic friction coefficients are very low, ca. 0.3 and 0.2, respectively. In general, it is believed that the frictional sliding on pre-existing fault governs the crustal strength. Therefore, our second conclusion is that the slip behaviour of fault having slickenside might governs the crustal strength. However, the experiments using gabbro block did not show the low static and dynamic friction coefficients. Hence the further detail experiments using simulated slickenside are needed to understand the crustal strength.

Keywords: Slickenside, Nano-size grain, Shear experiment, Fault strength

©2019. Japan Geoscience Union. All Right Reserved.

Dehydroxylation kinetics of clay minerals and its application to friction heating along an imbricate thrust in an accretionary prism

*Hirokazu Masumoto[1], Jun Kameda[1]

1. Faculty of Science, Hokkaido University

Dehydroxylation of clay minerals within fault gouges is significant for assessing transient thermogenesis due to high-velocity, frictional slip along fault zones. The clay minerals kaolinite and chlorite are common in fault zones hosted in sedimentary rocks at subduction margins. To better understand the dehydroxylation processes of these clay minerals, high-temperature X-ray diffraction (XRD) analyses were carried out by using a 1:1 mixture of kaolinite and chlorite standard samples. We evaluated the kinetic parameters of each dehydroxylation reaction by thermogravimetric analysis Thermal models of frictional heating employing this calibration show that the frictional heating can explain the reported clay mineralogy in a fossil imbricate thrust from a shallow part in an ancient accretionary prism (Shirako Fault, Japan). This result supports the previous assertion, and the observed temperature anomaly appears to demonstrate the frictional heating caused by coseismic slip on this fault.

©2019. Japan Geoscience Union. All Right Reserved.

Origin of frictional melt in the Jurassic accretionary complex of the Mino Belt on the basis of trace element and isotope analysis

*Chizuru Ozawa[1], Tsuyoshi Ishikawa[2], Kohtaro Ujiie[1]

1. University of Tsukuba, 2. JAMSTEC

Pseudotachylytes (solidified frictional melts) in exhumed accretionary complexes have great significance for understanding the dynamics of earthquake faulting in subduction zones. However, they are rarely preserved in a recognizable form mainly due to subsequent hydrothermal alteration. Recently, a pseudotachylyte was found in the Jurassic accretionary complex of the Mino Belt, central Japan. The pseudotachylyte is ~2 mm-thick and separates gray chert above from cataclasite below. Although the pseudotachylyte has been hydrothermally altered, its microstructures are characterized by presence of fault and injection veins, intensely cracked gray chert fragments incorporated from wall rocks, and locally embayed and rounded wall rocks, suggesting thermal cracking and thermal erosion associated with increased heating. Here, we analyzed major and trace elements and Sr and Pb isotopes of the milligram-level samples taken by micro-milling technique along the structures of the pseudotachylyte, cataclasite and gray chert, as well as the black chert and black carbonaceous mudstone near the pseudotachylyte. The pseudochylyte exhibits remarkably high trace element concentrations compared to those of gray chert. The trace element composition of the pseudotachylyte requires the involvement of black carbonaceous mudstone as well as gray chert, suggesting that the frictional melt originated from the mixture of gray chert and black carbonaceous mudstone. Based on major and trace element chemistry, the mixing ratio is estimated to be ~50–60% of gray chert and ~40–50% of black carbonaceous mudstone, and the ratio is consistent with the Sr and Pb isotope compositions. Despite the hydrothermally alteration, the chemistry of the pseudotachylyte well preserves melt-derived characteristics, thus provides useful information for understanding the frictional melting on faults and its source materials.

Keywords: pseudotachylyte, frictional melting, trace element analysis

©2019. Japan Geoscience Union. All Right Reserved.

Geochemical constraint on the origin of albite-bearing black fault rocks in the Kodiak accretionary complex

*Tsuyoshi Ishikawa[1], Asuka Yamaguchi[2]

1. Kochi Institute for Core Sample Research, Japan Agency for Marine-Earth Science and Technology, 2. AORI, The University of Tokyo

The Pasagshak Point thrust in the Kodiak accretionary complex is considered to represent the paleo-plate-boundary décollement at seismogenic depths. The fault rocks in this thrust consist of cataclasites and ultrafine-grained black fault rocks (BFRs), and the latter makes up the principal shear zones (Rowe et al., 2005; Meneghini et al., 2010). The BFRs contain crystalline microlayers characterized by the presence of fine-grained albitic plagioclase (Meneghini et al., 2010). Previously Yamaguchi et al. (2014) showed that the trace element characteristics of BFRs are consistent with the occurrence of fluid-rock interactions at >350 deg. C. Here we present further trace element and isotope analyses on the same samples, and re-examine the data in detail. Plagioclase abundances (albite + anorthite) calculated from major element compositions are distinctly higher in BFRs than in host rocks and cataclasites. Distinctly high Sr concentrations and low 87Sr/86Sr ratios observed in BFRs are well correlated with the plagioclase abundances. This indicates that the petrogenesis of BFRs requires additions of Na and Sr derived from external sources, possibly migrating saline fluids. The 87Sr/86Sr ratio estimated for end-component fluid is as low as 0.705, strongly suggesting the involvement of fluids from basaltic source. Li isotope ratios of BFRs are also consistent with equilibration with basalt-derived fluids. Thus, it is likely that saline fluids largely derived from basaltic oceanic crust of the lower plate migrated through the plate boundary décollement, and frictional heating combined with comminution induced high-temperature fluid-rock interactions at >350 deg. C to produce the unique geochemical characteristics observed for BFRs.
Refs: Meneghini et al. (2010) GSA Bull., 122, 1280-1297; Rowe et al. (2005) Geology, 33, 937-940; Yamaguchi et al. (2014) Earth Planet Space, 66:58.

Keywords: fault rocks, geochemistry, fluid-rock interactions, plate-boundary faults, accretionary complex

©2019. Japan Geoscience Union. All Right Reserved.

Importance of initial maturity and reaction kinetics on maturation of carbonaceous material and its implications for thermal maturity as a proxy for temperature in estimation of coseismic slip parameters

*Shunya Kaneki[1], Ichiba Tatsuya[1], Shuhei Yamashita[1], Tetsuro Hirono[1]

1. Graduate School of Science, Osaka University

Most of total seismic energy during earthquake slip is considered to convert into frictional heat, which activates many physicochemical reactions in faults. Various thermal indicators for detecting frictional heat recorded in fault rocks have been suggested, such as formation of pseudotachylyte and thermal transformation of fault-forming minerals. Among these reactions, thermal maturation of carbonaceous materials (CM) has been received a considerable attention, because CM changes its maturity in response to ambient temperature even with short-term heating duration.

On the basis of these backgrounds, CM maturity has been applied to estimate maximum temperature and coseismic slip parameters experienced by various faults during earthquakes (e.g., Hirono et al., 2015; Kaneki et a., 2016). These studies, however, may contain several concerns when evaluating amount of frictional heat from CM maturity: (1) mechanochemical effect, (2) kinetic effect of heating rate, (3) effect of initial maturity, and (4) cumulative effect of repeated earthquakes. Recently, Kaneki et al. (2018) and Kaneki and Hirono (2018) experimentally investigated the impacts of (1) and (2), and suggested that kinetic effects of both shear-induced mechanochemistry and heating rate can strongly dominate maturation process of CM, indicating that such kinetic effects should be considered to establish CM as a more rigorous fault geo-thermometer. However, the impacts of (3) and (4) on CM maturation process still remain unknown, leading to uncertainties in estimation of maximum temperatures from CM maturity.

In this study, we aim to understand the impact of (3) on CM maturation process and its implication for CM-based fault geo-thermometer. We adopted four grades of CM for our starting materials (lignite, bituminous coal, anthracite, and graphite), and performed low-velocity friction experiments with slip rate of 1 mm $s^{-1}$and normal stresses of 1 and 3 MPa under dry condition, to reproduce coseismic shear damage on CM samples without frictional heating. We then conducted heating experiments on both intact and sheared CM samples with targeted temperatures of 100, 200, 300, ..., 1300 ˚C (100 ˚C interval) and heating rates of approximately 1 and several hundreds of ˚C s^{-1}. We finally carried out infrared and Raman spectroscopies to evaluate maturity of both intact CM samples and products after friction and heating experiments. The results show that mechanochemical effect can enhance maturation process of lignite by ~100 ˚C whereas no significant difference between maturities of intact and sheared CM samples are present in bituminous coal, anthracite, and graphite. All CM samples, except for graphite that showed no significant change in maturity with heating, show higher reaction temperature by ~500 ˚C in heating experiments with higher heating rate. These results indicate that kinetic effects of both mechanochemistry and heating rate affect CM maturation process and the effects depends on initial maturity of CM. Thus, by taking consideration into initial maturity and kinetic effects, thermal maturation of CM could be an universal proxy for temperature in estimation of coseismic slip parameters.

Keywords: Earthquake, Carbonaceous material, Frictional heat, Initial maturity, Chemical kinetics

©2019. Japan Geoscience Union. All Right Reserved.

Experimental investigation of cumulative effect on thermal maturation of carbonaceous material as a proxy for earthquake slip

*Tetsuro Hirono[1], Yuhtaro Shimamura[1], Shunya Kaneki[2]

1. Department of Earth and Space Science, Graduate School of Science, Osaka University, 2. Disaster Prevention Research Institute, Kyoto University

Estimation of the maximum temperature recorded in fault rocks gives us important information about earthquake enegetics and fault slip behavior, because the frictional heat is directly related to dynamic parameters and to fault-weakening mechanisms. The thermal maturity of carbonaceous material (CM) has received considerable attention as a new temperature proxy because the organochemical characteristics of CM change irreversibly with increasing temperature. Various approaches by using infrared and Raman spectroscopies, elemental composition analyzer, biomarker method, and vitrinite reflectance measurement have been performed. However, for more accurate estimation of frictional heat, not only shear-enhanced mechanochemical effects but also chemical kinetics should be considered. In particular, cumulative effect by repeated earthquake events, related to the kinetics of the maturation, has not well understood. Here we demonstrated repeated heating events on bituminous coal and anthracite by using a tube furnace. We heated the samples 1, 10, and 100 times under conditions of 100, 300, 500, 700, 900, 1100, and 1300 degree C and 40-s heating duration, and conducted infrared and Raman spectroscopic analyses on the samples after heating. The disappearance of aliphatic C-H at 500 degree C were observed on all samples, and the intensity ratio of D and G bands on the Raman spectra of all samples increased beyond 700 degree C. Thus, we could conclude no significant cumulative effect on the thermal maturation of CM under rapid heating, indicating that the detected temperature on a fault corresponds to the largest earthquake slip event.

Keywords: fault, carbonaceous material, frictional heat

©2019. Japan Geoscience Union. All Right Reserved.

[J] Oral | S (Solid Earth Sciences)：S-SS Seismology

Wed. May 29, 2019 10:45 AM - 12:15 PM JST | Wed. May 29, 2019 1:45 AM - 3:15 AM UTC | A05 TOKYO BAY MAKUHARI HALL

[S-SS14] Fault Rheology and Earthquake Physics

convener:Keishi Okazaki(Japan Agency for Marine-Earth Science and Technology), Hideki Mukoyoshi(Department of Geoscience Interdisciplinary Graduate School of Science and Engineering, Shimane University), Hiroyuki Noda(Kyoto University, Disaster Prevention Research Institute), Keisuke Yoshida(Tohoku University), Chairperson:Hiroyuki Noda(DPRI, Kyoto University), Keishi Okazaki(JAMSTEC)

The goal of this session is to integrate theoretical, experimental, observational, and numerical perspectives from various fields such as seismology, geodesy, geology, mineralogy, and so on, to define what is known about earthquake source processes and the physical and chemical elementary processes of faulting. This session welcomes studies that address such issues as pre-, co-, and post-seismic processes, the rheology of seismogenic faults and fault rocks, laboratory experiments on elementary processes, numerical models based on frictional laws, and estimates of the stress field in the seismogenic zones. We also welcome studies on fault-zone drilling projects and in situ stress measurements.

10:45 AM - 11:00 AM JST | 1:45 AM - 2:00 AM UTC

[SSS14-13] **Fault rheology at the depth limits of the seismogenic zone**

★Invited Papers

*Berend Antonie Verberne[1] (1.Geological Survey of Japan, National Institute of Industrial Science and Technology)

11:00 AM - 11:15 AM JST | 2:00 AM - 2:15 AM UTC

[SSS14-14] Fault models revisited based on friction to flow law

*Toshihiko Shimamoto[1] (1.State Key Laboratory of Earthquake Dynamics, Institute of Geology, China Earthquake Administration)

11:15 AM - 11:30 AM JST | 2:15 AM - 2:30 AM UTC

[SSS14-15] Timing of Earthquakes on Intraplate Active Faults Subjected to Stress Perturbation by Megathrust Earthquakes: Insights from Earthquake Sequence Simulation

*Hiroyuki Noda[1] (1.Kyoto University, Disaster Prevention Research Institute)

11:30 AM - 11:45 AM JST | 2:30 AM - 2:45 AM UTC

[SSS14-16] Physics of earthquake triggering: effect of stress perturbation to slip acceleration

★Invited Papers

*Takahiro Hatano[1] (1.Earthquake Research Institute, University of Tokyo)

11:45 AM - 12:00 PM JST | 2:45 AM - 3:00 AM UTC

[SSS14-17] Foreshock activities controlled by slip rate on a 4-meter-long laboratory fault

*Futoshi Yamashita[1], Eiichi Fukuyama[1], Shiqing Xu[1] (1.National Research Institute for Earth Science and Disaster Resilience)

12:00 PM - 12:15 PM JST | 3:00 AM - 3:15 AM UTC

[SSS14-18] Supersonic propagation of slow slip rupture during rock friction experiments

*Eiichi Fukuyama[1], Futoshi Yamashita[1], Shiqing Xu[1] (1.National Research Institute for Earth Science and Disaster Resilience)

Fault rheology at the depth limits of the seismogenic zone

*Berend Antonie Verberne[1]

1. Geological Survey of Japan, National Institute of Industrial Science and Technology

The limits of the seismogenic zone demarcate changes in fault behaviour with increasing depth in Earth's crust, from aseismic, velocity (*v*-)strengthening to seismogenic, *v*-weakening, and vice versa. Significantly, the *v*-dependence of fault strength is a material property of the sliding medium present in the core of fault, or the fault gouge. I conducted shear tests using simulated fault gouge composed of calcite ($CaCO_3$) at an effective normal stress of 50 MPa, at temperatures of 20 to 600ºC, employing sliding velocities (*v*) of 0.03 to 300 μm/s –sufficient to span the brittle-plastic transition in this material. Mechanical results showed (unstable) *v*-weakening behaviour from ~80-100ºC to ~550ºC, but stable *v*-strengthening for <80-100ºC and >550ºC. All gouges sheared at temperatures <=550˚C showed localization into nanocrystalline principal slip zones, while samples sheared at >550˚C were characterized by distributed deformation. Using the post-test micro- and nanostructures observed in calcite gouge as a basis, plus a previously established microphysical model, I argue that transitions in fault stability are caused by changes in the (nano)granular flow processes accommodating shear. Specifically, the rate of intergranular compaction by Arrhenius-type processes such as diffusion or crystal plasticity, is key to thermally-activated transitions in the velocity dependence of gouge-filled faults. At the low-temperature transition from *v*-strengthening to *v*-weakening, at shallow crustal levels representing the upper-limit of the seismogenic zone, diffusion creep (e.g. pressure solution) may be dramatically accelerated due to the nanogranular nature of the fault rock that forms. At higher temperatures, towards the base of the seismogenic zone, a transition occurs from nanogranular flow in localized faults to distributed, fully creep-controlled flow in ductile shear zones.

Keywords: earthquake, seismogenic zone, rheology, nanograins, localization, brittle-ductile

©2019. Japan Geoscience Union. All Right Reserved.

Fault models revisited based on friction to flow law

*Toshihiko Shimamoto[1]

1. State Key Laboratory of Earthquake Dynamics, Institute of Geology, China Earthquake Administration

Friction to flow law (Shimamoto and Noda, 2014, JGR) can describe a transition from friction to flow using only friction and flow parameters, and shear zone width *w*. Friction and flow laws are described in terms of velocity and displacement, and shear strain rate and shear strain, respectively, and *w* is needed to relate velocity and shear strain rate to merge the two laws. The friction to flow law is a mixing law connecting friction and flow laws smoothly, and no other parameters are required probably because no new deformation mechanisms operate in the intermediate regime. In JpGU last year, Shimamoto and Noda argued (i) that the velocity dependency of shear resistance is by far the most heterogeneous in the intermediate regime between friction and flow, and (ii) that frictional patches can be surrounded by viscous matrix in the middle part of lithosphere because temperature for the onset of flow depends on rock types. This presentation will discuss (1) how fault models change in view of the friction to flow law, (2) how to construct realistic mechanical models of faults and plate boundaries that are usable in modelling earthquake generation, and (3) how to reproduce friction to flow transition for important rocks in laboratory.

Shimamoto and Noda (cited above) already discussed a revised fault model using results from earthquake modelling based on friction to flow law. A new problem addressed here is a question which of power law (dislocation creep) and grain-size sensitive flow law (diffusion creep or superplasticity) should be used as a flow law to describe fault properties. The latter law has often be favoured because the cores of deep shear zones are often composed of very fine-grained ultramylonites, grain size being on the order of microns or even smaller. Both flow laws are determined for calcite and plagioclase (Heard and Raleigh, 1972, GSA Bull.; Schmit et al., 1977, Tectonophysics; Rybacki and Dresen, 2000, JGR). Thus, strength profiles were constructed with the friction to flow law, assuming $w = 0.1 \sim 10$ m and velocity = 10 mm/yr. Results clearly show that diffusion creep occurs at lower stresses for both minerals (although this is not the case in laboratory experiments). Power-law creep is expected in the middle and lower parts of lithospheres, whereas diffusion creep is expected to be dominant in fault and plate-boundary zones. Thus, frictional patches can be surrounded by linear or nearly linear viscous flow matrix at some depths, and this can be quite important in analysing low-frequency earthquakes and slow slips.

Traditional fault models, started from Sibson (1977, J. Geol. Soc. London), have proposed how materials controlling friction and flow properties, types of fault rocks reflecting deformation mechanisms, and fault geometry such as fault and shear zone widths changes with increasing depth. Such models are bases for constructing realistic mechanical models for faults and plate boundaries. However, the models alone are not usable in modelling earthquakes and plate-boundary behaviours. Friction to flow law captures essential changes in fault properties with depth in a very simplified manner. Both transient and steady-state properties are included and the law can be used in earthquake modelling. However, the law for single material can never describe complex and variable properties of faults and plate boundaries. I want to discuss what has to be done to connect fault and earthquake studies, as much as possible in my presentation. Here I point out the importance of three problems; (I) to check if the friction to flow laws holds for important rocks or not in laboratory experiments, (II) to determine flow laws for important rocks constituting fault and plate-boundary zones, and (III) to determine transient flow properties in flow laws (see Noda and Shimamoto, 2010, GRL). I will give apparatus capabilities required for (I). Unfortunately,

©2019. Japan Geoscience Union. All Right Reserved.

there are only small amount data on (II) and (III).

Keywords: Friction to flow law, fault rheology, earthquake mechanisms

©2019. Japan Geoscience Union. All Right Reserved.

Timing of Earthquakes on Intraplate Active Faults Subjected to Stress Perturbation by Megathrust Earthquakes: Insights from Earthquake Sequence Simulation

*Hiroyuki Noda[1]

1. Kyoto University, Disaster Prevention Research Institute

Estimation of likelyhood of occurrence of intraplate large earthquakes is crutially important because of expected large amplitude of ground motion in nearby cities and short distance between source and human society which makes earthquake early warning difficult. Currently issued National Seismic Hazard Maps for Japan [2018, the Headquarter for Earthquake Research Promotion] adopts assumptions of Poisson process or Brownian passage time distribution depending on available information for each active fault. They yield rather wide distribution of temporal probability density for a timescale of the reccurence interval or the estimation error of history of events. The timelscale is typicaly much longer than recurrence intervals of megathrust earthquakes T_{cyc} which causes semi-periodic stress perturbation to intraplate faults. In the present study, effects of the semi-periodic stress perturbation to an intraplate active fault having a ductile shear zone beneath the seismogenic part [e.g., Shimamoto and Noda, 2014] are investigated by means of dynamic earthquake sequence simulation using a spectral boundary integral method [e.g., Lapusta et al., 2000].

Utsu [1974] pointed out that historical earthquakes in Southwest Japan are concentrated in -50 and +10 years from Nankai trough megathrust earthquakes. Such active periods of intraplate earthquakes may be due to semi-periodic stress perturbation by the megathrust earthquakes [e.g., Hori and Oike, 1996; Shikakura et al., 2014]. An important question is how its duration is scaled for different tectonic settings. T_{cyc} of megathrust earthquakes in Japan trench subduction zone is 500-800 years [e.g., Sawai et al., 2015] and much longer than in Nanka trough. Parameter studies on T_{cyc} and amplitude of the stress perturbation have been conducted to elucidate what controls the timing of intraplate earthquakes.

A 2D numerical simulation of a strike-slip fault [e.g., Lapusta et al., 2000] with ductile shear zone was considered as a model for an intraplate fault, accounting for a friction-to-flow fault constitutive law [Shimamoto and Noda, 2014] composed of the aging law and a quartzite flow law [Hirth et al., 2001], and effective normal stress distribution with maximum value of 50 MPa. The model was drived by far-field shear stress which was perturbed as a sawtooth wave function of variable amplitude about 1 MPa and T_{cyc} from 100 to 1000 years. If the perturbation was perfectly periodic, the system synchronized with the perturbation and the intraplate earthquakes ocurr at a specific phase in the cycle of megathrust earthquakes. If the interval was randomized by Gaussian distribution of 10% standard deviation, then the timing of the intraplate earthquakes distributed more widely, and concentrate in the latter half of the cycle, consistently with the notion of the active period. The shape of the distribution can be explained by a seismicity model based on ΔCFF [e.g., Shikakura et al., 2014], not by a rate-and-state spring-slider model [Dieterich, 1994; Ader et al., 2014]. The result of the parameter study suggests that not only the history of the activity of the fault, but also stress change on it due to recurring megathrust earthquakes or other events may be useful in constrainig the likelihood of intraplate earthquakes.

Keywords: Intraplate earthquakes, Earthquake sequense simulation, Brittle-plastic transition

©2019. Japan Geoscience Union. All Right Reserved.

©2019. Japan Geoscience Union. All Right Reserved.

Physics of earthquake triggering: effect of stress perturbation to slip acceleration

*Takahiro Hatano[1]

1. Earthquake Research Institute, University of Tokyo

Recent observation studies have revealed that the occurrence of tremors is sensitive to faint stress changes such as ocean tides. This might not be surprising in light of the low stress drop caused by tremors. Interestingly, however, ordinary earthquakes too may be sensitive to weak stress perturbations, although it is not so common as for tremors. Dynamic triggering should be the most prominent illustration of such sensitivity, but the occurrence of ordinary earthquakes could be also correlated to ocean tides, snowfalls, and rainfalls.

To understand such sensitivities to stress perturbation in a unified point of view, here we analyze the rupture nucleation process on a fault subject to weak periodic stress modulation. Assuming the rate- and state-dependent friction law with one state variable, we calculate the threshold amplitude above which the rupture initiation exhibits correlation with the perturbation phase. It is found that the crack-like nucleation is more sensitive to the perturbations than the patch-like nucleation. The estimated threshold amplitude for the crack-like nucleation is significantly lower than the tidal stress change. Time-to-failure for the both nucleation types in the presence of perturbation is estimated, and it is not significantly affected by the stress perturbation. We also discuss the optimum frequency at which the correlation is enhanced.

Keywords: earthquake triggering

©2019. Japan Geoscience Union. All Right Reserved.

Foreshock activities controlled by slip rate on a 4-meter-long laboratory fault

*Futoshi Yamashita[1], Eiichi Fukuyama[1], Shiqing Xu[1]

1. National Research Institute for Earth Science and Disaster Resilience

We report foreshock activities associated with evolving local slow slip events preceding the main rupture on a laboratory fault. To investigate the preparation process of laboratory earthquake with enough spatial resolution, we used a large-scale friction apparatus newly developed and installed at National Research Institute for Earth Science and Disaster Resilience (NIED) as shown in Figure 1. We used two rectangular metagabbro blocks as experimental specimens, whose nominal contacting area was 4.0 m long and 0.1 m wide. Height of each specimen was 0.2 m. Normal load was applied by eight flat jacks on the top surface of the upper specimen, and the associated pressures were kept at around 6 MPa during the experiments. After applying normal load, we applied shear load to the side surface of the lower specimen by manually pumping up a hydraulic jack, which was fixed at the western end of the apparatus. To monitor local phenomena on the fault, we installed 16 AE sensors, 40 triaxial rosette strain gauges, and 10 eddy current displacement sensors along the fault. We conducted experiments with relatively high shear loading rate (67-185 kPa/s) and low shear loading rate (2-7 kPa/s). In each experiment, displacement data showed that both the eastern and western edges of the fault kept slipping during the shear loading, though the slip rate was very low (< ~20 μm/s). It is consistent with FEM calculation that fault should start to slip at both edges in this configuration. This steady slip was significant during the experiments with low loading rate, in both quantity and area. However, such steady slip did not immediately trigger seismic events. Most of seismic events occurred just before the main rupture, and therefore should better be termed foreshocks. To understand what controls the occurrence of foreshocks, we first investigated the amount of stable slow slip accumulated after the previous main rupture. We found that foreshocks were not activated at around both fault edges even after the accumulated slip attained around 10 μm there (Figure 2a). On the other hand, foreshocks occurred around the central locked area with only a small amount of slip. We next compared the spatiotemporal distribution of foreshocks with that of slip rate. Displacement and strain data indicated that precursory slow slip began at the central locked area and then propagated outward over the fault area preceding the main rupture. We found that this slow slip had caused high slip rate (several hundreds of μm/s), which coincided with the occurrence of foreshocks (Figure 2b). These observations suggest that the key factor controlling the occurrence of foreshocks in this experiment is not the amount of accumulated slip but that of slip rate. The mechanism may be associated with the unstable fault slip triggered by fast loading in the laboratory (McLaskey and Yamashita, 2017, JGR; Xu et al., 2018, Tectonophysics), and the seismicity episodically activated in nature such as emergence of repeating earthquakes due to increased loading rate by afterslip of the 2011 *M*9.0 Tohoku-oki earthquake (Hatakeyama et al., 2017, JGR).

Keywords: Rock friction experiment, Slow slip, Foreshock, Slip rate

©2019. Japan Geoscience Union. All Right Reserved.

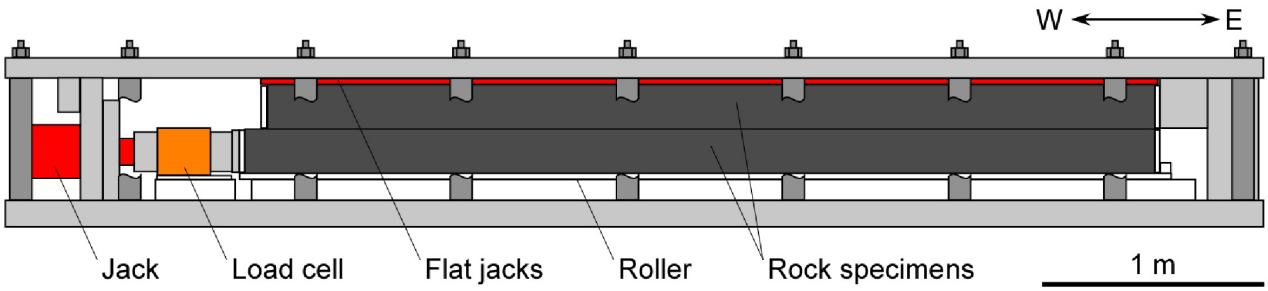

Figure 1

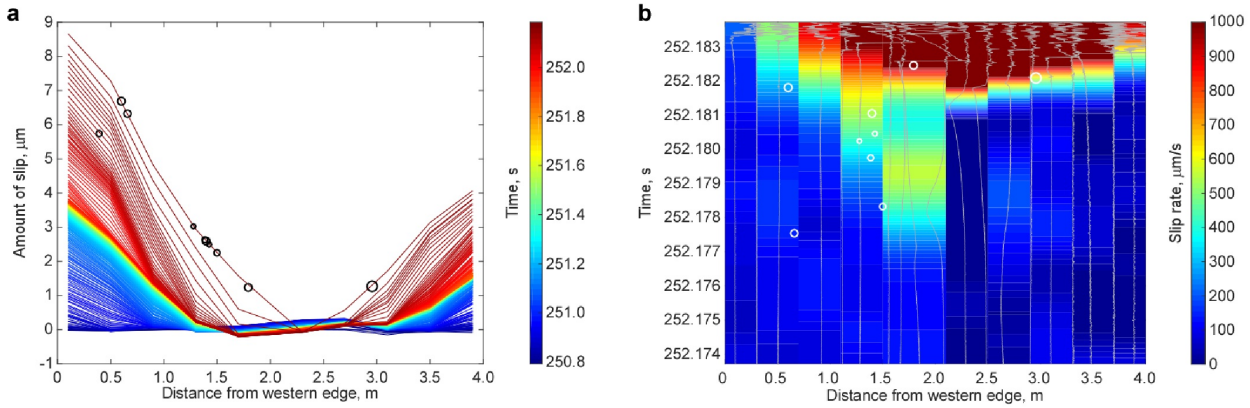

Figure 2

©2019. Japan Geoscience Union. All Right Reserved.

Supersonic propagation of slow slip rupture during rock friction experiments

*Eiichi Fukuyama[1], Futoshi Yamashita[1], Shiqing Xu[1]

1. National Research Institute for Earth Science and Disaster Resilience

Rupture propagation speed on the fault has been considered to be slower than elastic wave velocities of the material. Exceptions were when extremely high energy is imposed, much higher than the fracture energy needed for the rupture to advance. The rupture propagating faster than the elastic velocities is called supersonic rupture. We observed such supersonic rupture propagation of slow slip events during large scale rock on rock friction experiments on a 1.5×0.1 m^2 fault using Indian metagabbro rock specimens. Such slow slip events were accompanied by low frequency vibrations whose onsets were synchronized with those of slow slip events; they also propagated faster than the elastic wave velocities of the rock. Since typical precursory slow slip and coseismic slip events have been observed on the same fault in a sequence of the friction experiment, the slow slip events with supersonic rupture might share the same friction environment as that for the typical preslip-mainshock type events. We interpret this phenomenon as an occurrence of non-linear deformation of a very thin layer on the fault surface. For linear deformation case, the limitation of propagation velocity comes from the elastic property of rock specimens, but non-linear deformation can propagate independently of the material elastic constants but the propagation velocity tend to be proportional to the strain rate. In addition, because there are several similarities between the present observation and the slow slip events observed in the subduction zone worldwide, it may provide a clue to understand these phenomena.

Keywords: supersonic rupture proapgation, rock friction experiment, slow slip event

©2019. Japan Geoscience Union. All Right Reserved.

[J] Oral | S (Solid Earth Sciences)：S-SS Seismology

Wed. May 29, 2019 1:45 PM - 3:15 PM JST | Wed. May 29, 2019 4:45 AM - 6:15 AM UTC | A05 TOKYO BAY MAKUHARI HALL

[S-SS14] Fault Rheology and Earthquake Physics

convener:Keishi Okazaki(Japan Agency for Marine-Earth Science and Technology), Hideki Mukoyoshi(Department of Geoscience Interdisciplinary Graduate School of Science and Engineering, Shimane University), Hiroyuki Noda(Kyoto University, Disaster Prevention Research Institute), Keisuke Yoshida(Tohoku University), Chairperson:Hiroyuki Noda(DPRI, Kyoto University), Keisuke Yoshida(東北大学大学院理学研究科 地球物理学専攻)

The goal of this session is to integrate theoretical, experimental, observational, and numerical perspectives from various fields such as seismology, geodesy, geology, mineralogy, and so on, to define what is known about earthquake source processes and the physical and chemical elementary processes of faulting. This session welcomes studies that address such issues as pre-, co-, and post-seismic processes, the rheology of seismogenic faults and fault rocks, laboratory experiments on elementary processes, numerical models based on frictional laws, and estimates of the stress field in the seismogenic zones. We also welcome studies on fault-zone drilling projects and in situ stress measurements.

1:45 PM - 2:00 PM JST | 4:45 AM - 5:00 AM UTC

[SSS14-19] The role of fault damage zone in the supershear rupture of the 2018 Mw 7.5 Palu earthquake

*Lingsen Meng[1], Han Bao[1], Jean-Paul Ampuero[2], Eric Fielding[3], Cunren Liang[4], Christopher Milliner [3], Tian Feng[1], Hui Huang[1] (1.University of California Los Angeles, 2.Université Côte d'Azur and IRD, 3.Jet Propulsion Laboratory , 4.California Institute of Technology)

2:00 PM - 2:15 PM JST | 5:00 AM - 5:15 AM UTC

[SSS14-20] The role of curvature in earthquake mechanics

*Pierre Romanet[1], Daisuke Sato[2], Ryosuke Ando[1] (1.Earth and Planetary Science Department, University of Tokyo, 2.Disaster Prevention Research Institute, Kyoto University)

2:15 PM - 2:30 PM JST | 5:15 AM - 5:30 AM UTC

[SSS14-21] **Heterogeneous source modelling by the fully dynamic simulations of earthquake cycles on a strike-slip fault and scaling relations.**

*Percy Galvez[1,5], Anatoly Petukhin[2], Paul Somerville[3], Ken Miyakoshi[2], Kojiro Irikura[4] (1.KAUST University, Saudi Arabia, 2.Geo-Research Institute, Osaka Japan, 3.AECOM, Los Angeles, USA., 4.Aichi Institute of Technology, Japan, 5.ETH Zurich, Switzerland)

2:30 PM - 2:45 PM JST | 5:30 AM - 5:45 AM UTC

[SSS14-22] **Strain energy released by an earthquake: Contributions of random slip fluctuations**

*Tatsuhiko Saito[1], Akemi Noda[1] (1.National Research Institute for Earth Science and Disaster Resilience)

2:45 PM - 3:00 PM JST | 5:45 AM - 6:00 AM UTC

[SSS14-23] The change in the elastic strain energy due to the 1992 Landers earthquake and triggering mechanisms of aftershock activity

*Toshiko Terakawa[1], Mitsuhiro Matsu'ura[2], Akemi Noda[3] (1.Graduate School of Environmental Studies, Nagoya University, 2.Institute of Statistical Mathematics, 3.National Research Institute for Earth Science and Disaster Resilience)

3:00 PM - 3:15 PM JST | 6:00 AM - 6:15 AM UTC

[SSS14-24] Toward understanding generation mechanism of crustal earthquakes based on accumulation/release of elastic strain energy

★Invited Papers

*Akemi Noda[1] (1.National Research Institute for Earth Science and Disaster Resilience)

The role of fault damage zone in the supershear rupture of the 2018 Mw 7.5 Palu earthquake

*Lingsen Meng[1], Han Bao[1], Jean-Paul Ampuero[2], Eric Fielding[3], Cunren Liang[4], Christopher Milliner [3], Tian Feng[1], Hui Huang[1]

1. University of California Los Angeles, 2. Université Côte d'Azur and IRD, 3. Jet Propulsion Laboratory , 4. California Institute of Technology

The powerful M 7.2 earthquake that shock the Sulawesi island of Indonesia on September 28, 2018, was a seismic standout for many reasons, not the least of which is that it triggers tsunami and landslides and causes major life and economic loss in the city of Palu. In this study, integrated geophysical observations of the 2018 Mw 7.5 Palu, Indonesia earthquake, provide robust evidence of an early and persistent supershear rupture speed. Slowness-enhanced back-projection (SEBP) of teleseismic data provides a sharp image of the rupture process, consistently across multiple arrays. The inferred rupture path agrees with the surface rupture trace inferred from the net surface displacement field derived by sub-pixel InSAR image correlation. The SEBP results indicate a sustained rupture velocity of 4.1 km/s from the rupture initiation to the end, despite large fault bends. The persistent supershear speed is further validated by evidence of far-field Rayleigh Mach waves in regional seismograms. Supershear earthquakes with rupture velocity exceeding shear-wave speeds, previously observed in laboratory experiments and large strike-slip events, often have an initial sub-shear stage before they transition to supershear. The rupture speed of the 2018 Palu earthquake is supershear from very early on. The short or absent supershear transition distance can be caused by high initial shear stress or short critical slip-weakening distance, and promoted by fault roughness near the hypocenter. Steady rupture propagation at a supershear speed considered to be unstable, lower than the Eshelby speed, could result from the presence of a damaged fault zone.

Keywords: Palu Earthquake, Supershear, Fault Damage Zone

©2019. Japan Geoscience Union. All Right Reserved.

The role of curvature in earthquake mechanics

*Pierre Romanet[1], Daisuke Sato[2], Ryosuke Ando[1]

1. Earth and Planetary Science Department, University of Tokyo, 2. Disaster Prevention Research Institute, Kyoto University

In recent years, many studies have tried to catch the influence of geometry in earthquake mechanics. In this paper, we suggest a new interpretation of the effect of geometry on the stress on a fault, as a direct effect of local curvature and torsion of line field of slip along the surface of the fault. Within this framework, it is possible to unify the understanding of bends, kinks and roughness, as an effect of local parameters along the fault. Starting from the representation theorem, that links the displacement in a medium to the slip distribution on his boundary, and assuming homogeneous infinite medium, we first derive a new regularized boundary element method. Using this equation, we were able to separate the influence of geometry, express by curvature and torsion of the fault surface geometry and the slip direction, from the effect of the gradient of slip. This allows us to shed a new light on the mechanical effects of geometrical complexities on fault surface. We used that new discovery to solve a paradox between smooth and abrupt kink [Tada and Fukuyama 1996] as well as re-interpret the effect of roughness on the fault: It can be shown that the effect of drag stress [Fang and Dunham 2013] along the fault it actually exactly equal to the effect of curvature along the fault.

Keywords: Fault mechanics, Curvature, Fault geometry

©2019. Japan Geoscience Union. All Right Reserved.

Heterogeneous source modelling by the fully dynamic simulations of earthquake cycles on a strike-slip fault and scaling relations.

*Percy Galvez[1,5], Anatoly Petukhin[2], Paul Somerville[3], Ken Miyakoshi[2], Kojiro Irikura[4]

1. KAUST University, Saudi Arabia, 2. Geo-Research Institute, Osaka Japan, 3. AECOM, Los Angeles, USA., 4. Aichi Institute of Technology, Japan, 5. ETH Zurich, Switzerland

Numerical modeling is a necessary tool for the assessment of variability strong ground motions in potential devastating large earthquakes. In a simulation-based seismic hazard analysis, it is critical to be able to generate a large number of physically self-consistent source models whose rupture process captures the main physics of earthquake rupture and is consistent with the spatio-temporal heterogeneity of past earthquakes. An inherent difficulty in such efforts is that, from a mechanical point of view, stress and strength heterogeneities cannot be prescribed arbitrarily as was done in earlier work. Their interdependence must be consistent with a mechanical model of deformation and stress evolution over the longer time scale of the earthquake cycle.

In this work, a set of spontaneous source models have been generated in a wide magnitude range (*Mw* 5.5-7.5) by using multicycle simulations under the rate-and-state friction law with the goal of studying the characteristics of source scaling relations and strong ground motions. To get realistic irregular seismic sequence, several realizations of 2D correlated heterogeneous random distributions of characteristic weakening distance "*Dc*" in rate and state friction are tested. A mesh grid size of 125 meters has been used to resolve properly the nucleation and cohesive zone of the seismic events. The fault is 128 km in length and 30km in width, the seismogenic width is 18km. The quasi-dynamic solver QDYN (Luo, et al., 2017) has been used to nucleate the seismic events and SPECFEM3D (Galvez et al, 2014; 2016) to resolve the rupture process. Other important parameters are the normal stress, which controls the stress drop and rupture velocity during an earthquake, and the maximum value of *Dc* distribution, that controls rupture velocity but not stress drop. Following these ideas, we perform dynamic rupture modeling to take into account the free surface effects and perform a parametrization study; parameters of our final friction model are shown in Fig.1.

In order to validate source models we compare the source scaling relations vs. seismic moment *Mo* for the modeled rupture area *S*(*Mo*), average slip of the ruptures *Dave*(*Mo*) and the slip asperity area *Sa*(*Mo*), with similar scaling relations from the source inversions. Fig. 2 shows result for *S*(*Mo*). The seismogenic zone width plays a fundamental role in the *S* vs *Mo* scaling. In fact, Luo et al. (2017) reported that events which break the whole seismogenic width and reach the free surface are exposed to an attraction effect from the free surface. This attraction effect may explain the transition regime from Stage 1 (self-similar rupture, $Mw < 6.5$) to Stage 2 ($6.5 < Mw < 7.4$). Ground motions have been also computed from our models. Their peak ground velocities (*PGV*) agree well with the GMPE values.

Acknowledgements. This study is based on the 2018 research project 'Examination for uncertainty of strong ground motion prediction for inland crustal earthquakes' by the Secretariat of Nuclear Regulation Authority (NRA), Japan. The Super Computer Shaheen II at KAUST University has been used to run the models presented in this study.

Keywords: earthquake rupture dynamics, earthquake cycles, rate-and-state friction, source scaling

©2019. Japan Geoscience Union. All Right Reserved.

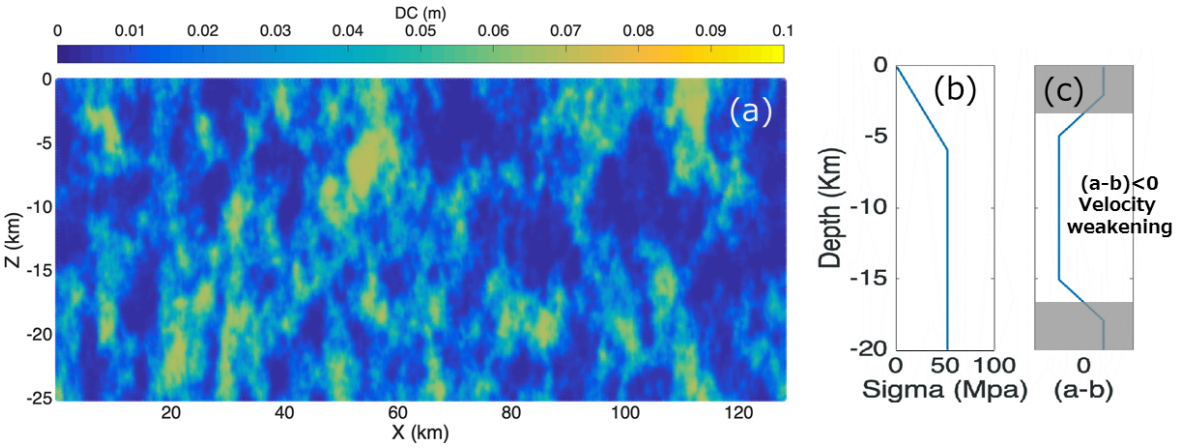

Fig 1. Friction settings: (a) heterogeneous *Dc*, (b) normal stress, and (c) *a-b* friction parameters.

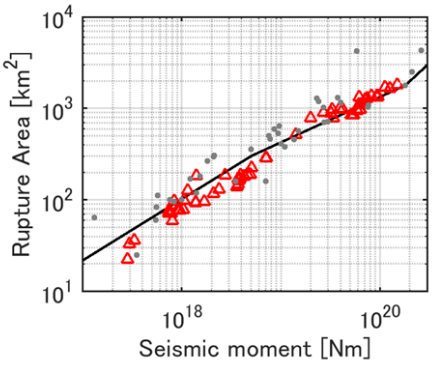

Fig 2. Comparison of *S*-values of modeled events vs. *Mo* (triangles) and observed (dots).
Line is 3-stage scaling assumed for strong-motion simulations.

©2019. Japan Geoscience Union. All Right Reserved.

Strain energy released by an earthquake: Contributions of random slip fluctuations

*Tatsuhiko Saito[1], Akemi Noda[1]

1. National Research Institute for Earth Science and Disaster Resilience

Strain energy in the lithosphere is the source of earthquake generation. For example, the shear strain energy change caused by the interplate coupling along the Nankai Trough, Japan affects the seismicity in the inland area (Saito et al. 2018 JGR). The aftershocks of the 2016 Kumamoto earthquakes were activated by the shear strain energy brought by the mainshocks (Noda et al. 2018 ACES; Tanaka et al. 2018 JpGU). The strain energy change caused by an earthquake is one of the most fundamental quantity for earthquake mechanics. When the stress change occurs uniformly on the earthquake fault (constant stress drop), a simple theoretical equation gives the relation between the seismic moment, initial stress, stress drop, and the strain energy liberated by the earthquake (e.g., Aki and Richards 2002). This relation leads that the strain energy released by an earthquake is proportional to the seismic moment. However, for actual earthquakes, the stress change on the fault is considerably heterogeneous.

The present study theoretically investigates the relation between the strain energy released by an earthquake and the seismic moment when the stress change is not uniform on the fault plane due to heterogeneous slip distribution. We assume that the initial stress is homogeneous in space and suppose that the heterogeneous slip distribution is given by the sum of the reference slip distribution causing the constant stress drop and the randomly fluctuating slip distribution. We adopt a stochastic approach using an ensemble of the slip fluctuations characterized by the power spectral density functions such as Gaussian and von Karman type function. The derived theoretical relation gives a scaling law of the strain energy with the power spectral density function of the slip fluctuation. This deduces the following results. (1) When an earthquake contains randomly fluctuating slip distribution, the liberated strain energy is smaller than that of the constant stress-drop earthquake. (2) This indicates that a representative value of stress drop becomes large due to the randomly fluctuating slip distribution in the view point of the energy partition. This study refers to this stress drop as effective stress drop. This was also reported by some studies such as Noda et al (2003 GJI) and Hirano and Yagi (2017 GJI). This study derived a theoretical equation of the effective stress drop with the power spectral density function of the random slip fluctuation. (3) When the stress change is not constant on the fault, the strain energy is not proportional to the seismic moment unless the correlation distance of the slip fluctuation is proportional to cube root of the seismic moment. (4) The energy balance gives a value of the initial stress that is required for the earthquake generation. In order to generate an earthquake, the initial stress needs to be larger than the sum of the half of the effective stress drop and the apparent stress (the apparent stress is given by rigidity, radiation energy, and seismic moment (Wyss and Brune 1968,1971)).

Keywords: strain energy, random slip fluctuations, stress

©2019. Japan Geoscience Union. All Right Reserved.

The change in the elastic strain energy due to the 1992 Landers earthquake and triggering mechanisms of aftershock activity

*Toshiko Terakawa[1], Mitsuhiro Matsu'ura[2], Akemi Noda[3]

1. Graduate School of Environmental Studies, Nagoya University, 2. Institute of Statistical Mathematics, 3. National Research Institute for Earth Science and Disaster Resilience

Earthquakes are physical processes to release elastic strain energy stored in the Earth’s crust by shear faulting. This quantity is essentially important for understanding earthquake generation. However, we have little knowledge on the quantity, because it is difficult to measure stress in-situ. Recently, Terakawa and Hauksson (2018) developed a method to model and estimate the 3-D absolute stress field from earthquake focal mechanism data, using the reference pore pressure as a single parameter (the reference pore pressure). In this study, we directly investigated changes in elastic strain energy, based on 3-D abosolute stress fields modeled by Terakawa and Hauksson (2018). Then, we tried to propose a new criterion to understand aftershock activity following large earthquakes instead of the change in Coulomb Failure Function (CFF), based on elastic strain energy.

First, we investigated partitioning of changes in shear and volumetric strain energies due to the 1992 Landers earthquake (M_W 7.3). Changes in volumetric strain energy did not depend on the reference pore pressure, or the level of deviatoric stress field. On the other hand, those in shear strain energy was closely related to the parameter. More shear strain energy were released when the background deviatoric stress magnitudes were higher. The elastic strain energy released by the mainshock is consumed as radiated, fracture and thermal energies. The amount of change (decrease) in the elastic stain energy must be at leaset larger than radiatied energy, which can be estimated (e.g., Kostrov, 1974; Ide, 2002). Therefore, the change in shear strain energy plays a crucial role to constrain the the most plausible reference pore pressure and eventually the level of the (absolute) deviatoric stress field.

When a stress field is compressed due to the mainshock, frictional strength as well as volumetric strain energy in the region will increase after the mainshock. This means that an increase in elastic strain energy do not necessarily mean activation of seismicity. The shear and volumetric strain energy are closely related to the average shear and normal stresses acting on faults randomly and isotropically distributed in the crust (e.g., Saito et al., 2018; Matsu’ura et al., under review). Increases in shear and volumetric strain energies have positive and negative effects on triggering aftershocks following the mainshock. In order to understand aftershock activity, we need to correctly consider both effects of the two kinds of strain energies into account. As the elastic strain energy is scalar quantity, we do not have to set any receiver faults, unlike using the change in CFF. In the source region of the Big Bear earthquake (M_W 6.5), which is the largest aftershock following the Landers mainshock, the shear strain energy increased, but the volumetric strain energy decreased. Both changes would have promoted this event. In the region just south of the hypocenter of the mainshock, the total effect from the two kinds of strain energies suggest that seismicity would have become inactive, contrary to the actual activation. Focal mechanism solutions of some of these events were normal faulting with NW-SE tension. We can understand that these events would have reactivated by decrease in fault strength under the stress field characterized by strike-slip faulting with NE-SW compression and NW-SE tension. This suggest that many aftershocks in the region may have been triggered by overpressurized fluids.

©2019. Japan Geoscience Union. All Right Reserved.

Keywords: absolute stress fields, elastic strain energy, pore fluid pressures

©2019. Japan Geoscience Union. All Right Reserved.

Toward understanding generation mechanism of crustal earthquakes based on accumulation/release of elastic strain energy

*Akemi Noda[1]

1. National Research Institute for Earth Science and Disaster Resilience

Although the physical process of interplate earthquakes has been modeled from the viewpoint of accumulation and release of shear stress on plate boundaries, it is difficult to apply the framework directly to cycles of crustal (inland) earthquakes. It is necessary to assume a fault plane to obtain shear stress in a stress field, but the faults in the crust are not a continuous and unique plane of weakness like plate boundaries. Furthermore, there are many unknown faults covered by sedimentary layers.

The shear strain energy is a scalar quantity appropriate for evaluating the potential of earthquake occurrence in the case that the fault plane cannot be specified. The scalar quantity corresponds to the average value of the shear stress acting on randomly distributed cracks in the crust (Saito et al., 2018). In other words, an increase and decrease in the shear strain energy correspond to the accumulation and release of crustal stress, respectively. In addition, since the work done for shear faulting is related to the release of elastic strain energy in the surrounding region (Aki & Richards, 1980; Matsu'ura et al., 2019), the strain energy can be thought of as an essential physical quantity for earthquake generation. Evaluating the accumulate and release of the shear strain energy in the crust, therefore, would help to understand the generation mechanism of crustal earthquakes.

To evaluate the shear strain energy changes, we must have not only stress changes but also background stress fields. However, it is difficult to know the absolute value of the background stress. Under the assumption that the absolute level of the background stress is much greater than the stress changes, Saito et al. (2018) derived an expression of shear strain energy changes normalized by the differential stress of the background stress using the spatial pattern of background stress orientation and the stress changes. Then, they calculated the normalized shear strain energy changes in the inland seismogenic layer caused by interplate coupling along the Nankai Trough, and found the correlation between the shear strain energy changes and seismicity in the southwestern Japan.

In order to apply this framework to tectonic zones in the crust, Noda et al. (2018 AGU) developed a method to evaluate the shear strain energy changes using elastic/inelastic strain analysis method (Noda & Matsu'ura, 2010). Firstly, we inverted the 3-D moment tensor density distribution in the crust as the source of crustal deformation from GNSS displacement data. The 3-D elastic/inelastic strain distribution in the crust was obtained from the estimated moment tensor density distribution. The stress changes were calculated by multiplying the elastic strain distribution by assumed elastic constants. Secondly, given a background stress field, the 3-D shear strain energy changes in the crust was evaluated from the calculated stress changes.
This method was applied to coseismic and preseismic GNSS data associated with the 2016 Kumamoto earthquake. For the background stress, we used the 3-D tectonic stress field estimated by CMT data inversion (Terakawa & Matsu'ura, 2010). The coseismic shear strain energy changes were estimated from the coseismic GNSS displacement data and showed its correlation with the spatial pattern of aftershock activity. Next, we evaluated preseismic changes in shear strain energy from GNSS displacement rate data (2005~2011), and found an increase (accumulation) in a part of the Futagawa fault, which is one of the main faults coseismically slipped during the earthquake, and a large decrease (release) in the

©2019. Japan Geoscience Union. All Right Reserved.

northeastern end of the fault, where the coseismic slip terminated. The shear strain energy change was caused by a large inelastic deformation (brittle fracture/plastic deformation) in the shallow crust along the Aso-Kuju volcanoes.

Keywords: elastic strain energy, crustal earthquake, elastic/inelastic strain, background stress field, 2016 Kumamoto earthquake

©2019. Japan Geoscience Union. All Right Reserved.

[J] Poster | S (Solid Earth Sciences)：S-SS Seismology

Wed. May 29, 2019 3:30 PM - 5:00 PM JST | Wed. May 29, 2019 6:30 AM - 8:00 AM UTC | Poster Hall International Exhibition Hall8, Makuhari Messe_16

[S-SS14] Fault Rheology and Earthquake Physics

convener:Keishi Okazaki(Japan Agency for Marine-Earth Science and Technology), Hideki Mukoyoshi(Department of Geoscience Interdisciplinary Graduate School of Science and Engineering, Shimane University), Hiroyuki Noda(Kyoto University, Disaster Prevention Research Institute), Keisuke Yoshida(Tohoku University)

The goal of this session is to integrate theoretical, experimental, observational, and numerical perspectives from various fields such as seismology, geodesy, geology, mineralogy, and so on, to define what is known about earthquake source processes and the physical and chemical elementary processes of faulting. This session welcomes studies that address such issues as pre-, co-, and post-seismic processes, the rheology of seismogenic faults and fault rocks, laboratory experiments on elementary processes, numerical models based on frictional laws, and estimates of the stress field in the seismogenic zones. We also welcome studies on fault-zone drilling projects and in situ stress measurements.

[SSS14-P01] Measurement of shear-wave polarization anisotropy in crack-bearing Aji granite during shear experiment

*Jinki Tanaka[1], Ikuo Katayama[1] (1.Hiroshima University)

[SSS14-P02] Effects of talc content on frictional properties of quartz gouge

Risako Shirahige[1], Inori Tatara[1], *Ken-ichi Hirauchi[1], Takato Takemura[2] (1.Department of Geosciences, Faculty of Science, Shizuoka University, 2.Department of Earth and Environmental Sciences, College of Humanities and Sciences, Nihon University)

[SSS14-P03] Mechanism controlling the frictional strength of quartz rocks at intermediate slip rates

*Kyuichi Kanagawa[1], Asuka Sugita[2], Miki Takahashi[3], Michiyo Sawai[1] (1.School of Science, Chiba University, 2.Faculty of Science, Chiba University, 3.Research Institute of Earthquake and Volcano Geology, Geological Survey of Japan)

[SSS14-P04] **Evolution of hydraulic and frictional properties of incoming hemipelagic sediments during diagenetic reactions**

*Keishi Okazaki[1], Ikuo Katayama[2], Asuka Yamaguchi[3] (1.Japan Agency for Marine-Earth Science and Technology, 2.Dept. of Earth & Planetary Systems Science, Hiroshima University, 3.AORI, the University of Tokyo)

[SSS14-P05] Contrasting silica precipitation via flash vaporization and fluid flow and possible effects on fault properties

*Takamasa Niibe[1], Atsushi Okamoto[1], Takashi Amagai[2], Noriyoshi Tsuchiya[1] (1.Graduate School of Environmental Studies, Tohoku University, 2.Japan Oil, Gas and Metals National Corporation)

[SSS14-P06] Temporal variations of reflected and transmitted wave during a slide-hold-slide experiment on a biaxial friction testing machine

*Miyuu Uemura[1], Yoshihiro Ito[2], Ikuo Katayama[3] (1.Kyoto University, 2.Disaster Prevention Research Institute, Kyoto University, 3.Department of Earth and Planetary Systems Science, Hiroshima University)

[SSS14-P07] Monitoring stress-induced changes of laboratory fault by ultrasonic coda wavesMonitoring stress-induced changes of laboratory fault by ultrasonic coda waves

*Fan XIE[1], Yaqiong REN[1] (1.Institute of Geophysics, China Earthquake Administration)

[SSS14-P08] Longer duration of meta-instability stage of laboratory earthquakes on a 1.5m granite fault

*yaqiong Ren[1] (1.Institute of Geophysics, China Earthquake Administration)

[SSS14-P09] Estimation of the frictional heat and the amount of wall rock incorporation by thermal fracturing during an earthquake: An example from the pseudotachylyte in Jurassic accretionary complex

*Ayaka Nagate[1], Kohtaro Ujiie[1] (1.University of Tsukuba)

[SSS14-P10] Porosity variation of fault rocks accompanied the Median Tectonic Line in Shikoku, southwestern Japan

*Michiharu Ikeda[1], Takeshi Tsuji[2], Tomohiro Tsuji[1], Kozo Onishi[3], Naoki Nishizaka[3] (1.Shikoku Research Institute Incorporated, 2.Kyushu University, 3.Shikoku Electric Power Company, Incorporated)

[SSS14-P11] Characteristics of inactive section of the Median Tectonic Line from drillcore samples in Shikoku, southwestern Japan

*Hideto Uchida[1], Michiharu Ikeda[1], Takeshi Tsuji[2], Kozo Onishi[3], Naoki Nishizaka[3] (1.Department of Civil Engineering, Shikoku Research Institute incorporated, 2.Department of Earth Resources Engineering, Kyusyu University, 3.Shikoku Electronic Power)

[SSS14-P12] Surface and internal textures of clasts in incohesive fault rocks and their significance

*Tetsuhiro Togo[1], Toshihiko Shimamoto[2], Michiyo Sawai[3] (1.THE EARTH, 2.Institute of Geology, China Earthquake Administration, 3.Chiba Univ.)

[SSS14-P13] **Fault Displacement Assessment of Surface-rupturing Earthquakes for Nuclear Installations and the use of Physics-based Rupture Models**

*Luis Angel Dalguer[1], Yoshimitsu Fukushima[2] (1.3Q-Lab GmbH, 2.International Atomic Energy Agency)

[SSS14-P14] Dynamic rupture simulation for seismic hazard assessment: Application to the Futagawa and Hinagu fault zones (Part 2)

*Yuko Kase[1] (1.Geological Survey of Japan, AIST)

[SSS14-P15] Quantification of gaps between slip-length scaling law of earthquakes and stick-slip experiments.

*Shinichi Oba[1], Yuta Mitsui[2] (1.Graduate School of Science and Tecnology, Shizuoka University, 2.Faculty of Science, Shizuoka University)

[SSS14-P16] Effect of Wear Process on Earthquake Recurrence

*Jeen-Hwa Wang[1] (1.Academia Sinica)

[SSS14-P17] On the Mechanical Relation between Individual Interaction and Collective Behavior of Multiple Fault Sets Subjected to Quasi-Static Loading

*Koji Uenishi[1,2], Yuki Fukuda[2], Nobuki Kame[3] (1.Department of Advanced Energy, The University of Tokyo, 2.Department of Aeronautics and Astronautics, The University of Tokyo, 3.Earthquake Research Institute, The University of Tokyo)

[SSS14-P18] Inelastic deformation in a region of the transient and forced extensional horizontal crustal strain

*Takao Eguchi, Yasuyuki Iwase[1] (1.National Defense Academy, Japan)

[SSS14-P19] Representation Theorem and Green's Function (3) - - Strain, Stress, and Density Perturbation Fields due to a Point Source Using 2nd Derivative of Green's Function in an Unbounded Homogeneous Isotropic Elastic Medium - -

*Masaya Kimura[1], Nobuki Kame[1] (1.Earthquake Research Institute,The University of Tokyo)

[SSS14-P20] Development of a method of visualization of abrupt changes in slip-rate and rupture velocity toward better understanding of high-frequency radiation on a fault.

*Takahiro ayukai[1], Yuji Yagi[2], Ryo Okuwaki[3], Keita Kayano[3], Kousuke Shimizu[3] (1.School of Life and Environmental Sciences, University of Tsukuba, 2.Graduate School of Life and Environmental Sciences, University of Tsukuba, Tsukuba, 3.Graduate School of Life and Environmental Sciences, University of Tsukuba)

[SSS14-P21] Issues in earthquake-source-inversion analysis, evaluated through singular value decomposition

*Keita Kayano[1], Yuji Yagi[1], Ryo Okuwaki[1], Kousuke Shimizu[1] (1.Tsukuba University)

[SSS14-P22] **Source process of recent M6-class inland earthquakes in Japan**

*Ritsuya Shibata[1], Naofumi Aso[1], Junichi Nakajima[1], Satoshi Ide[2] (1.Department of Earth and Planetary Sciences, Tokyo Institute of Technology, 2.Department of Earth and Planetary Science, University of Tokyo)

[SSS14-P23] Expected slip direction on assumed fault planes of large earthquakes inferred from stress field after the 2016 Kumamoto earthquake sequence, in central Kyushu, Japan

*Ayaho Mitsuoka[1], Satoshi Matsumoto[2], Azusa Shito[2], Hiroshi Shimizu[2], Group for urgent joint seismic observation of the 2016 Kumamoto earthquake (1.Department of Earth and Planetary Sciences, Graduate School of Science, Kyushu University, 2.Institute of Seismology and Volcanology, Faculty of Sciences, Kyushu University)

[SSS14-P24] Spaciotemporal change of source parameters of repeaters due to the 2011 Tohoku-Oki earthquake

*Kazuya Tateiwa[1], Tomomi Okada[1], Toshio Kono[1], Naoki Uchida[1] (1.Research Center for Prediction of Earthquakes and Volcanic Eruptions, Graduate School of Science, Tohoku University)

[SSS14-P25] Slip distributions and relation of slip-rate and shear stress for the Boso slow slip events

*Takuma Kobayashi[1], Toshinori Sato[2] (1.Graduate School of Science and Engineering, Chiba University, 2.Graduate School of Science, Chiba University)

[SSS14-P26] Repeating inland earthquakes in northern Ibaraki Prefecture activated after the 2011 Tohoku-Oki earthquake

Ryo Takahashi[1], *Keisuke Yoshida[1], Akira Hasegawa[1], Toru Matsuzawa[1] (1.Tohoku University)

Measurement of shear-wave polarization anisotropy in crack-bearing Aji granite during shear experiment

*Jinki Tanaka[1], Ikuo Katayama[1]

1. Hiroshima University

The stress drop at the time of the earthquake not only releases the stress applied to the fault plane but also causes the rotation of the principal stress axis applied to the fault plane. In fact, the change in the direction of the principal stress axis after the earthquake is reported by the mechanism solution of aftershocks and the seismic wave anisotropy(e.g. Tadokoro and Ando 2002; Boness and Zoback 2006). It is thought that this is because the closing (opening) direction of the cracks around the fault plane correspond to the stress axis. Therefore, in this study, the elastic wave velocity was monitored during the shear experiment of the rock and the relation between the shear stress and the principal stress axis and elastic wave velocity was measured in the laboratory. Since the shear-wave polarization anisotropy has a characteristic which is sensitive to the direction of the crack, measurement of different vibration components of S wave is performed in addition to measurement of P wave velocity.

For the experiment, we investigated the change in elastic wave velocity according to shear deformation using a High-T biaxial frictional testing machine in Hiroshima University. For the experimental samples, Aji granite which generated thermal cracks inside by heating to 600 degrees Celsius was used. In the shear experiment, it was carried out by loading the central rock block at a constant speed while keeping the vertical stress constant. The shear sliding velocity was about 0.9 μm/s and the normal stress was 5 MPa. For measurement of elastic waves, probes with a resonance frequency of 1 MHz (manufactured by Olympus Corporation) were used, and S wave and P wave were measured by pulse transmission method. The propagation direction of elastic wave is parallel to the shear plane and perpendicular to the shear sliding direction, and for the S wave, we measured two components, wave (SH) oscillating in the plane orthogonal to the shear plane and wave (SV) oscillating parallel to the shear plane.

From the experimental results, with the increase of the shear stress, it was found that the velocity of SH wave rises earlier and the SV wave rises late. In addition, there was a phenomenon in which the initial motion of the SV wave jumped suddenly as the shear stress increased. This means that when the shear stress is low and the maximum principal stress axis in the sample is close to the direction of the normal stress, the shear direction cracks are frequently closed and the SH wave velocity increases, and the shear stress increases, when the inclination of the maximum principal stress axis becomes steeper with respect to the normal stress, it is considered that the direction of the crack which closes is correspondingly inclined. In this way, since the SH wave and SV wave behave differently due to the increase of the shear stress and the corresponding change of the principal stress axis angle, by utilizing this property, a good index for monitoring the stress state around the fault.

Keywords: Earthquake prediction, Shear-wave polarization anisotropy

©2019. Japan Geoscience Union. All Right Reserved.

Effects of talc content on frictional properties of quartz gouge

Risako Shirahige[1], Inori Tatara[1], *Ken-ichi Hirauchi[1], Takato Takemura[2]

1. Department of Geosciences, Faculty of Science, Shizuoka University, 2. Department of Earth and Environmental Sciences, College of Humanities and Sciences, Nihon University

Phyllosilicates have low coefficients of friction and an effect of weakening fault strength. To understand effects of talc content on frictional strength and sliding stability, we conducted frictional sliding experiments on dry gouge mixtures of quartz and talc at room humidity, room temperature, a normal stress of 10 MPa and sliding velocities of 0.66–2 μm/s, using a single direct-shear apparatus. The coefficient of friction for the mixture ranged from 0.18 to 0.69 and fell between pure quartz and talc values. The overall trend was a decrease in the coefficient of friction with increasing talc content. The velocity dependence of friction, ($a-b$), ranged from −0.0018 to 0.0039 and increased with increasing talc content. The ($a-b$) values are highest in the mixture with a talc content of 80 wt.%. For the mixture with talc contents below 10 wt.%, the ($a-b$) values become negative, with the occurrence of slow to fast stick-slip behavior.

Keywords: friction, stick slip, fault weakening, phyllosilicate

©2019. Japan Geoscience Union. All Right Reserved.

Mechanism controlling the frictional strength of quartz rocks at intermediate slip rates

*Kyuichi Kanagawa[1], Asuka Sugita[2], Miki Takahashi[3], Michiyo Sawai[1]

1. School of Science, Chiba University, 2. Faculty of Science, Chiba University, 3. Research Institute of Earthquake and Volcano Geology, Geological Survey of Japan

Frictional strength of quartz rocks is known to be extraordinary low at subseismic slip rates ranging from 1 mm/s to 10 cm/s, which has been ascribed to the hydration of comminuted amorphous silica, i.e., silica gel. In order to testify this hypothesis, we conducted rotary-shear friction experiments on intact agate or silica gel gouge at a normal stress of 1.5 MPa and slip rates (V) ranging from 1 mm/s to 10 cm/s. We also measured temperature (T) adjacent to the slip surface or the gouge layer during the experiments.

Steady-state friction coefficient of agate μ_{ss} was ≈0.6 at V = 1 mm/s, ≈0.5 at V = 7 mm/s, and ≦0.1 at V = 10 cm/s. T was ≈25˚C at V = 1 mm/s, ≈30˚C at V = 7 mm/s, and up to 85˚C at V = 10 cm/s, but the actual temperature along the slip surface must have been much higher. μ_{ss} of silica gel gouge was ≈0.7 at V = 1 mm/s, 0.4–0.5 at V = 7 mm/s, and ≦0.2 at V = 10 cm/s. T was 25–28˚C at V = 1 mm/s, 30–37˚C at V = 7 mm/s, and 80–100˚C at V = 10 cm/s, but again, the actual temperature in the gouge layer must have been much higher.

Thus our results show that agate or silica gel exhibits weakening with increasing T, and that the presence of silica gel does not reduce the frictional strength when T is not high enough. Shear strength of quartz rocks is high so that significant amount of frictional heat would be produced at asperity contacts even at V ≈1 cm/s, which must be responsible for weakening of quartz rocks at intermediate slip rates.

Keywords: agate, silica gel, frictional strength, intermediate slip rates

©2019. Japan Geoscience Union. All Right Reserved.

Evolution of hydraulic and frictional properties of incoming hemipelagic sediments during diagenetic reactions

*Keishi Okazaki[1], Ikuo Katayama[2], Asuka Yamaguchi[3]

1. Japan Agency for Marine-Earth Science and Technology, 2. Dept. of Earth & Planetary Systems Science, Hiroshima University, 3. AORI, the University of Tokyo

Deployments of seismic and geodetic observation networks had revealed the activity of slow earthquakes along the subduction plate boundaries, which are characterized as intermediate fault slip rate between earthquake (~1m/s) and stable sliding along the plate boundary (~1 nm/s). Diagenesis of subducting sediments has stimulated interest in their relationship to regular and slow seismicity in the subduction zone. We report experimental results on the effect of diagenetic reactions to hydraulic and frictional properties of incoming hemipelagic sediments. Hemipelagic sediments taken from KS-15-3 Shinseimaru cruise are used as the starting sample. Friction experiments and permeability measurements were carried out with a confining pressure of 150 MPa and a pore pressure of 58 MPa and temperatures ranging RT–230 degC. When the sample is sheared immediately after reaching the experimental condition, all experimental data at the temperature below 150 degC showed a velocity-strengthening behavior. On the other hand, at the temperature of 230 degC, the frictional behavior is no longer stable, but stick-slip behavior was observed during the experiments. We also measured a time-dependent permeability evolution of hemipelagic sediments to assess how diagenetic reactions consolidate the sediments. Permeability decreased about an order magnitude due to the mechanical compaction from the effective pressure of 3 MPa to 92 MPa, and decrease additional an order magnitude of permeability is observed during the hot-pressing of the sample at the pressure and the temperature of 92 MPa and 100 degC, respectively. Those experimental observations suggest that thermally activated compactions, possibly pressure solution creep, could contribute key role for understanding the physical property of subducting sediments.

Keywords: subduction zone, frictional property

©2019. Japan Geoscience Union. All Right Reserved.

Contrasting silica precipitation via flash vaporization and fluid flow and possible effects on fault properties

*Takamasa Niibe[1], Atsushi Okamoto[1], Takashi Amagai[2], Noriyoshi Tsuchiya[1]

1. Graduate School of Environmental Studies, Tohoku University, 2. Japan Oil, Gas and Metals National Corporation

It is thought that precipitation of silica plays crucial roles on mechanical and hydrological properties of faults. The solubility of silica minerals varies significantly depending on temperature and water density (e.g., Manning, 1994). Okamoto *et al.* (2010) conducted the hydrothermal flow-through experiments at vapor-like supercritical condition (430 ℃, 31 MPa) and showed that silica precipitation predominantly occurred via quartz overgrowth and quartz nucleation (Okamoto *et al.*, 2010). In contrast, precipitation of silica is thought to be induced by decompression of fluids. Weatherley and Henley (2013) suggested that silica particles precipitate by flash vaporization at fault jog; however, the process of silica precipitation under such extreme condition has not been verified experimentally. The purpose of this study is to understand the mechanism of silica precipitation by hydrothermal experiments. In particular we focus on the difference in the mode of occurrences of silica precipitates between flashing and fluid flow system.
We conducted two types of experiments: (1) flash + batch experiments, and (2) flow-through experiments. Both experiments were carried out with using high-silica solutions (Si = 250-300 mg/kgH_2O, Na, Al, K = 4-6 mg/kgH_2O), that was prepared by dissolution of granite sand at 370 ℃ and 40 MPa. In the flashing experiments, after the input solution was enclosed into the autoclaves, elevated pressure and temperature, and flashed by opening the valve. Alumina filter (average pore size of 60 μm) was placed on the flow pathway to catch the silica particles. The flash P-T conditions were 261 ℃, 353 ℃, 400 ℃, and 450 ℃ at pressure of 35-38 MPa. In all conditions, silica precipitates did not include quartz, but spherical particles of amorphous silica with size of 0.1-10 μm were produced. Such amorphous silica was probably formed by nucleation and aggregation during the evaporation of water droplet. Then, we investigated the transformation of the flashing products (removed from the alumina filter and enclosed in Au tube) by the batch experiments at 261 ℃ and 351 ℃ at vapor saturated pressure, and at 400 ℃ and 450 ℃ under supercritical conditions. There was no change of silica after the batch experiments at 261℃ and 351℃ conditions within 5 days. In contrast, small quartz crystals (size of less than 10 μm) were produced in 5 days at 400 ℃ and in 3 days at 450 ℃. Albite was partly produced as the results of interaction with alumina-filter.
The silica precipitation was also investigated by the flow-through experiments at 390-430 ℃ and 25 MPa (supercritical condition) with constant flow-rate of 0.5 or 1 mL/min by using the granite-dissolved solution similar to the flash experiments. The silica was precipitated in alumina tube filled with alumina ball (diameter with 1 and 2mm). We found the silica precipitates clogged the pores within few days. Based on the XRD and SEM observation, the products of the flow-through experiments were mixture of amorphous silica and quartz. Some quartz crystals grew up to 100 micrometers and amorphous silica were precipitated on the alumina balls and the alumina pipe.
In both cases, amorphous silica was easily produced in response to the drop of water density at high temperatures. Such amorphous silica can move and clog effectively the pores. Also, our experiments revealed that such amorphous silica was changed to quartz, which depends on the temperature and fluid states (flow or batch). Such variation of silica by precipitation and transformation potentially would provide a significant influence on the fault strength.

Weatherley D. K. and Henley R. W. (2013), *Nature Geoscience*, **6(4)**, 294.
Okamoto A., Saishu H., Hirano N. and Tsuchiya N. (2010), *Geochemica et Cosmochimica Acta*, **74**,

©2019. Japan Geoscience Union. All Right Reserved.

3692-3706.
Manning C. E. (1994), *Geochemica et Cosmochimica Acta*, **58**, 4831-4839.

Keywords: Water-Rock Interaction, Silica, Flash Vaporization

©2019. Japan Geoscience Union. All Right Reserved.

Temporal variations of reflected and transmitted wave during a slide-hold-slide experiment on a biaxial friction testing machine

*Miyuu Uemura[1], Yoshihiro Ito[2], Ikuo Katayama[3]

1. Kyoto University, 2. Disaster Prevention Research Institute, Kyoto University, 3. Department of Earth and Planetary Systems Science, Hiroshima University

Slow slip events (SSEs), which is one of the slow earthquakes differing from regular earthquakes, have been detected at both shallower and deeper portions of the seismogenic zones, such as Japan and New Zealand. We carried slide-hold-slide experiments with gouge layer under a slip velocity of an SSE using a biaxial friction testing machine under the condition with the temperature and the humidity of room. We measured temporal changes of acoustic impedance in the gouge layer with reflected and transmitted wave during slides and holds. As a result, we detected variations in travel time, amplitude, and cross-correlation coefficient on first arrival of reflected and transmitted wave.

The features of observed waveforms were classified clearly by a slide-hold-slide conditions into two categories: sliding and holing. We chose two materials as gouge powder, which were clay mineral (Ca-montmorillonite) and quartz. Regardless of the kinds of the gouge powder, the amplitude both of reflected and transmitted waves showed opposite temporal variation during the slide-hold-slide sequences; the amplitude of transmitted wave decreased during slides and increased during holds, respectively. This suggests that the amplitudes of reflected and transmitted waves indicate a change of an elastic-wave speed in the gouge layer.

The travel times of transmitted waves increased during slides and decrease during holds. According to Birch (1961), a propagation speed of elastic waves normally decreases as the density of media decreases, or as the porosity increases. Increasing travel times of transmitted waves in our experiments may indicate the change of the density, or porosity in the gouge layer. Although the travel times of reflected waves decreased during slides and increased during holds in the case of clay mineral, the travel time on quartz powder did not change through our experiment.

The temporal change on correlation of observed transmitted wave also shows significant changes from a slide to a hold. The change of travel time, the amplitude, and the cross-correlation coefficient of transmitted waves were more sensitive to a slide-hold-slide condition, such as slip rate on the gouge later than those of reflected wave. Those result suggests that a transmitted wave is more suitable for monitoring SSE although a reflected wave is also useful for monitoring, and that a beginning and an end of an SSE can be detected by reflected and transmitted waves.

Keywords: slow slip event, biaxial friction experiment, gouge

©2019. Japan Geoscience Union. All Right Reserved.

Monitoring stress-induced changes of laboratory fault by ultrasonic coda wavesMonitoring stress-induced changes of laboratory fault by ultrasonic coda waves

*Fan XIE[1], Yaqiong REN[1]

1. Institute of Geophysics, China Earthquake Administration

It is increasing important to understand evolution in fault zone and find clear precursors to the earthquake. Nevertheless, the evolving behavior of crustal faults remains changeling due to its inaccessible and weakness.

Duo to their highly sensitivity, the seismic coda waves have been long used at kilometer scale to investigate stress changes by tracking seismic relative velocity changes during earthquake. However, detecting such changes and imaging their spatial distribution with satisfied resolution are still an ongoing project, for which laboratory developments may be useful.

This work aims to explore the applicability of coda waves to monitor spatiotemporal changes of laboratory fault.

Laboratory-scale experiments are performed by meter-scale biaxial loading apparatus in which coda waves at ultrasonic frequencies (100 kHz to 400 kHz) are transmitted and received by 16 broadband piezoelectric transducers using the state-of-the-art ultrasound research platform (Verasonics Vantage 64 Low Frequency Edition) across a 1.5-meter long granite simulated fault.

Before stick-slip events occurred by increasing shear stress at loading rate of 1 um/s , the normal stress was kept 500KPa constant for 60 minutes. The ultrasonic coda waves were recorded throughout the entire process of stress accumulation along the fault.

Coda wave interferometry (CWI) and Coda wave decorrelation (CWD) are performed to detect relative velocity changes and microstructural changes along the fault by measuring phase shifts and loss of coherence of received coda waves respectively.

We observe a ~0.4e-3 velocity increase and ~0.5% coherence loss within logarithm of stationary contact time during 1-hour normal stress holding time. A significant 1.4e-3 increase in relative velocity changes and 8% coherence loss during shear stress increasing test followed by 0.5e4 decease in relative velocity changes and 2% decrease in coherence loss respectively caused by ~200kPa stress drop of the emerging stick-slip event. We also observe that the such changes are localized at upper center of the fault by comparing the changes extracted at different transducers along the fault.

The results suggest that ultrasonic coda waves are a promising means to monitor weak but localized stress-induced changes of laboratory fault by detecting and characterization velocity and micro-structural changes. Considering such advantages, further works to temporal critical observations, such as nucleation process of laboratory earthquake, are conceivable from a practical and instrumental point of view.

©2019. Japan Geoscience Union. All Right Reserved.

Keywords: laboratory earthquake , stick slip , coda waves, stress-induced changes

©2019. Japan Geoscience Union. All Right Reserved.

Longer duration of meta-instability stage of laboratory earthquakes on a 1.5m granite fault

*yaqiong Ren[1]

1. Institute of Geophysics, China Earthquake Administration

Laboratory earthquakes are a series of stick slip events occurred on an old or newly formed fracture in laboratory. It is widely used to study the properties and mechanisms of earthquake nucleation, dynamic rupture and post-seismic process since its similarities with nature earthquakes. Meta-instability stage is the later stage of the nucleation process. It holds that when the stress release accelerates and synergizes, the deformation enters an irreversible stage to instability. Thus studying its evolutionary characteristics is more conducive to identifying the arrival of earthquakes in advance.

We perform a series stick slip experiments on a 1.5m granite fault. Using a meter-scale rock as experimental sample can indirectly improve the spatial resolution of observation. More importantly, the scale effect of earthquake preparation process can be studied by comparing the results of centimeter-scale and meter-scale samples, which is helpful to the field application of experimental results.

The experiment was carried out on a large horizontal two-direction servo-control press at the Institute of Geophysics, China Earthquake Administration. The maximum loading capacity of the press in two directions is 100 tons and 200 tons respectively. The local variations of stress and displacement along the fault as well as the variation of the whole sample were recorded during the experiment. The stiffness of the meter-scale sample and press system is 0.003 MPa/um, which is one order of magnitude smaller than that of the centimeter-scale sample and press system in the Institute of Geology, China Earthquake Administration. This enables us to obtain stick-slip events with small stress drop, large displacement and audible energy release at lower confining pressure.

For a single stick-slip event, the beginning of meta-instability stage and quasi-dynamic stage (the later stage of meta-instability stage) can be identified based on the relative displacement and strain observations along the fault. The meta-instability begins in the middle of the fault and extends toward both ends as the instability approaches. During the meta-instability stage, the variation rate of different parts of the fault varies greatly, and tends to synergize with the approach of instability.

The duration of meta-instability is longer under lower loading rate, and the change of normal stress has little effect on the duration of meta-instability under lower normal stress. The duration of meta-instability increases with the increase of fault scale, showing obvious scale effect. The results suggest that meta-instability on natural faults in the field may last for several years, and could be monitored. The non-uniformity of faults with the increase of fault scale may be an important mechanism for the scale effect of the duration of meta-instability.

Keywords: stick slip, earthquake nucleation, meta-instability stage, scale effect, meter-scale rock

©2019. Japan Geoscience Union. All Right Reserved.

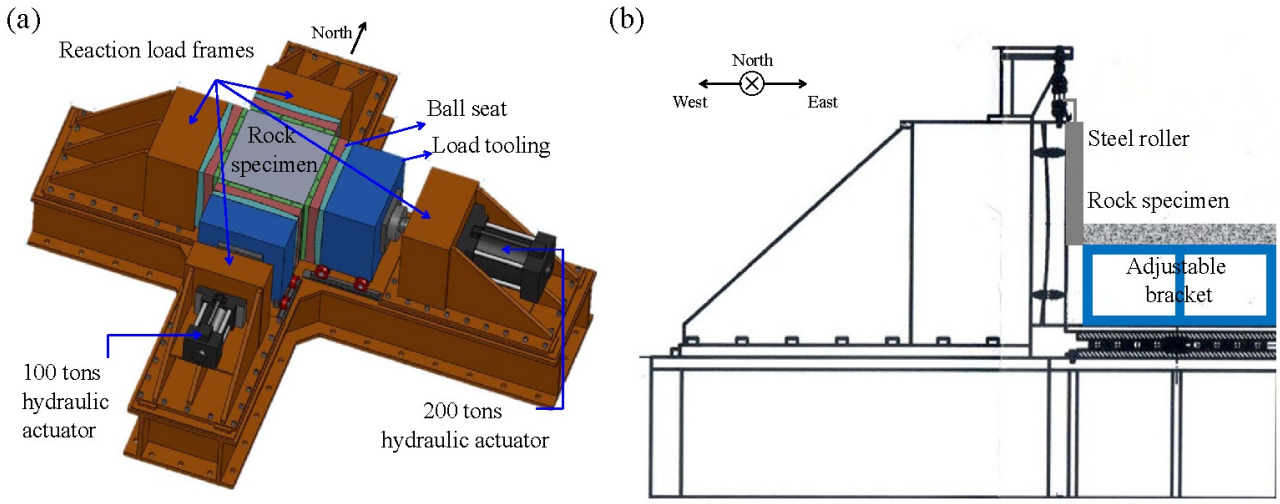

©2019. Japan Geoscience Union. All Right Reserved.

Estimation of the frictional heat and the amount of wall rock incorporation by thermal fracturing during an earthquake: An example from the pseudotachylyte in Jurassic accretionary complex

*Ayaka Nagate[1], Kohtaro Ujiie[1]

1. University of Tsukuba

Estimation of frictional heat is crucial to evaluate dynamic shear strength and fault behavior during an earthquake. Pseudotachylyte produced by solidification of frictional melt is an unequivocal geological evidence of seismic slip on faults. Here, we estimated frictional heat and amount of wall rock incorporation into coseismic slipping zone during an earthquake, based on microstructural observation and numerical analysis of the pseudotachylyte in the Jurassic accretionary complex. The pseudotachylyte-bearing thrust develops as an out-of-sequence thrust in the coherent chert-clastic sequence, which bounds middle Triassic chert above from early Jurassic siliceous mudstone below. The pseudotachylyte is ~2 mm-thick and sharply separates fractured grey chert above from cataclasite below. The pelagic black carbonaceous mudstone layer is distributed at the stratigraphic equivalent interval of the pseudotachylyte.

The microstructures of the pseudotachylyte are characterized by fault and injection veins, fragments of grey chert and quartz in the dark matrix of illite composition, and irregularly and embayed pseudotachylyte boundaries. The gray chert adjacent to the pseudotachylyte and fragments in the pseudotachylyte consisted of grey chert are intensely cracked, showing jigsaw puzzle-like structure. These microstructural features suggest that thermal erosion, thermal fracturing, and preferential melting of illite occurred during earthquake faulting. Frictional heat, which was estimated from temperature rise, volume fraction of fragments, and pseudotachylyte thickness, is ~7.1 MJ m^{-2}.

The comparison of volume fraction of fragments in the matrix between the pseudotachylyte and the black carbonaceous mudstone layer suggests that half amount of fragments in the pseudotachylyte were derived from wall rocks. The numerical modeling considering temperature rise, heating duration, and thermal properties of gray chert indicates that the temperatures of wall rocks a few millimeters away from the pseudotachylyte boundaries exceed the temperature of a-b transition in quartz (~573 ˚C) during earthquake faulting. This distance is consistent with spatial distribution of crack density, which shows exponentially decrease away from the pseudotachylyte boundaries. Thus, intensely cracked wall rocks are considered to represent thermal expansion of quartz grains in gray chert, which could contribute to unstable fault slip associated with decrease in stiffness of surrounding rocks.

Keywords: Frictional heat, Pseudotachylyte, Jurassic accretionary complex

©2019. Japan Geoscience Union. All Right Reserved.

Porosity variation of fault rocks accompanied the Median Tectonic Line in Shikoku, southwestern Japan

*Michiharu Ikeda[1], Takeshi Tsuji[2], Tomohiro Tsuji[1], Kozo Onishi[3], Naoki Nishizaka[3]

1. Shikoku Research Institute Incorporated, 2. Kyushu University, 3. Shikoku Electric Power Company, Incorporated

Petrophysical properties of fault rocks are important information to understand evolution processes of fault rocks. Among their properties, hydraulic properties of fault rocks are closely related to fault dynamics and potential of reservoirs of fluid or gas. In this research, we focused on distribution of porosities through fault rocks of the Median Tectonic Line in Shikoku.

The Median Tecotnic Line (MTL) is the longest geological terrane boundary fault. The northern and southern parts from the MTL are Ryoke Belt composed of low P/T metamorphic rocks, granitic rocks and sedimentary rocks and Sanbagawa metamorphic rocks consisted of high P/T metamorphic rocks, respectively. We drilled a bore hole to obtain a geological core sample penetrating the MTL. The total core length is 250 m-long. The fault plane of the MTL is within 37.45 m-depth. The hanging wall and foot wall zones are Izumi Group in Ryoke Belt and Sanbagawa metamorphic rocks, respectively.

The fault rocks in Izumi Group are composed of three zones, fault breccia zone (ca.4– ca.12.5 m-depth), transition zone (ca.12.5–ca.31.6 m-depth) and fault gouge zone (ca.31.6–ca.37.2 m-depth), based on geological observation. On the other hand, the fault rocks of the Sanbagawa metamorphic rocks are cataclasite just below the MTL fault plane (37.45–ca.47 m-depth) and intact rocks in the deeper parts of the core (ca.47–250.0 m-depth).

We measured 49 samples (24 samples in Izumi Group and 20 samples in Sanbagawa metramorphic rocks) from the core. In addition to them, 5 samples from outcrops of Izumi Group were measured to get porosities of intact rocks of Izumi Group, because all parts of Izumi Group in the core are damaged.

The porosities of the hanging wall (Izumi Group) range between 4.54% and 20.35%, whereas those of the foot wall (Sanbagawa metamorphic rocks) are lower (2.06%–11.4%) than those of the hanging wall. Additionally, the porosities of the outcrop samples of Izumi Group show quite low (0.97%–1.75%), corresponding to those of intact rocks of Izumi Group, whereas those of the intact rocks of Sanbagwa metamorphic rocks are estimated to be ca.2%–ca.3%. These porosities are measured for samples in the deep zone (ca.75–ca.200 m-depth) of the core, which are quite far from the fault plane. The porosities of the three zones of fault rocks in the hanging wall are 5.19%–15.27% for the fault breccia zone, 4.54–15.30% for the transition zone and 11.02–20.35% for the gouge zone. It should be noted that the porosities are corrected on the basis of CT values. As the fault rocks of Izumi Group are composed of matrix and clasts, we measured the porosities of both matrix and clasts (or blocks) for each sample. Then, we calculated the correction porosities based on the ratio of matrix and clasts of CT values.
The porosities in the hanging wall (Izumi Group) widely vary depending on characteristics of fault damage, however those gradually increase toward the fault plane. In addition, the porosities are quite higher than those of intact rocks. On the other hand, the high porosity zone in the foot wall (Sanbagawa metamorphic rocks) is limited in a narrow zone (37.45–ca.50 m-depth). These facts suggest that the hanging wall (Izumi Group) are strongly damaged compared to the foot wall (Sanbagawa metamorphic rocks). This is an intriguing characteristics for understanding petrophysical properties of fault rocks.

©2019. Japan Geoscience Union. All Right Reserved.

Keywords: Median Tectonic Line, porosity, fault rocks

©2019. Japan Geoscience Union. All Right Reserved.

Characteristics of inactive section of the Median Tectonic Line from drillcore samples in Shikoku, southwestern Japan

*Hideto Uchida[1], Michiharu Ikeda[1], Takeshi Tsuji[2], Kozo Onishi[3], Naoki Nishizaka[3]

1. Department of Civil Engineering, Shikoku Research Institute incorporated, 2. Department of Earth Resources Engineering, Kyusyu University, 3. Shikoku Electronic Power

The Median Tectonic Line (MTL) is a geological boundary fault that divides southwestern Japan into Inner and Outer zones. The MTL is generally considered to be a long-lived fault system from the middle Cretaceous, although the details of the movement history are complex. On the other hand, it has been revealed from geomorphological and paleo-seismological surveys that the MTL from Shikoku to western Kii Peninsula has caused right-lateral slip during Quaternary. Therefore, the part of the MTL is active, and called as the Median Tectonic Line active fault system (MTLAFS) (e.g., Ikeda et al.,2017). To estimate present seismic condition (or environment) of the MTLAFS, we should understand details of its paleo-activities. However, outcrops widely exposed for geological survey about paleo-activities inactive MTL are limited. In this study, we obtained a geological core sample (125 m-long) penetrating the MTL and conducted downhole logging in Saijyo city, Ehime prefecture.
We focused on three points as follows. Firstly, we observed and described the core samples in detail. Secondly, we obtained structural data from the geological core and a borehole image data in order to predict paleo-stress conditions. Finally, we estimated physical properties around a fracture zone of the MTL based on the geological and geophysical data.

[Description of fault rocks]
The fault plane of the MTL is at about 109.45 m-depth in the borehole. The hanging wall and footwall of the fault system are Izumi Group (mainly alternating beds of mud and sand) and Sanbagawa metamorphic rocks (mainly pelitic schist), respectively. Orientation of the fault plane of the MTL is NE-SW strike with moderate-angle northwest dipping in our study area, and its fault zone is approximately 4m-width. The fault zone is composed of fault gouge, fault breccia and cataclasite. The altered dikes that is Ishizuchi volcanic rocks erupted in c.a. 15 Ma distribute in the fault zone. The MTL in this region reactivated after 15 Ma, because the altered dikes are fragmentated in the fault zone.

[Structural analysis]
Orientations of bedding planes of Izumi Group and schistosity planes of Sanbagawa metamorphic rocks are generally N–S strike with low-angle east dipping and ENE–WSW strike with low-angle north dipping. The dikes intrude into the fault zone in orientation of NE–SW strike with moderate-angle northwest dipping. Orientations of fractures concentrate in N–S strike with east dipping and E–W strike with north dipping based on the borehole camera data.
Moreover, we conducted paleo-stress analysis based on fault orientations and slickenlines and slickensteps on the fault surfaces. We adopted Hough transform inverse method (Sato, 2006) to estimate paleo-stress conditions of the MTL. As the result, a stress condition around the MTL is dominantly normal-faulting stress-regime, however strike-slip and reverse-faulting stress-regimes are also recognized.

[Physical properties]
There is a remarkable trend of the elastic wave velocity data around the fracture zone. P-wave velocity *Vp* in fracture zone (95–109.5 m-depth) drastically decreases as compared with host rock in the upper zone due to intensive crack and lower elastic moduli. On the other hand, S-wave velocity *Vs* does not change in

©2019. Japan Geoscience Union. All Right Reserved.

the fracture zone such as the trend of *Vp*.

The paleo-stress condition data are useful information for inactiveness of the MTL. And the physical properties are also crucial to understand the physical conditions what the MTL in this region have experienced. Therefore, the information derived in this study could contribute to understand fault evolution processes and activities of the MTL.

Keywords: Median Tectonic Line, fault rocks, paleostress field, physical property

©2019. Japan Geoscience Union. All Right Reserved.

Surface and internal textures of clasts in incohesive fault rocks and their significance

*Tetsuhiro Togo[1], Toshihiko Shimamoto[2], Michiyo Sawai[3]

1. THE EARTH, 2. Institute of Geology, China Earthquake Administration, 3. Chiba Univ.

Fault rocks are classified based on the fraction of clasts (visible under naked eyes) and fine-grained matrix (e.g., Sibson, J. Geol. Soc. London). Studies on clasts are important at least for the following three purposes. First, clasts must have formed by fracturing of host rocks and/or old cohesive fault rocks during their formation and past movements, and hence clasts may provide us with old fault rocks and may yield information on deeper parts of fault zones. Second, clasts must have undergone series of physical and chemical intrafault processes and might give clues to recover some of those processes. Third, comparison of surface and internal textures of clasts with those of borehole cuttings may lead to identifying fault zones from the cuttings. Recovering all cores in drilling is very costly and the textural studies on fault-zone clasts may have many practical applications.

Kanaori and his coworkers conducted very detailed SEM (scanning electron microscope) observations on quartz or quartz-rich clasts in fault gouge, collected from more than ten mostly-active faults (e.g., Kanaori et al., 1980, Eng. Geol.). They demonstrated that characteristic surface textures, completely different from those of fresh fracture surfaces, developed on clasts primarily due to dissolution of surface materials. They pointed out that those textures were similar to the surface textures of quartz grains in sediments that had been reported in many publications (note that fault-zone clasts and clastic sediments were exposed to underground water in geological time scale). They classified the surface textures of quartz clasts into 8 types and 4 groups, and proposed a sequence of changes in surface textures with time. The primary target of the work by Kanaori and others was to make rough estimate of timing of fault motion from the surface textures. However, this was not easy and their pioneering work did not progress further.

Present work was motivated from the third purpose listed above. We have not followed the classifications of Kanaori et al, but rather we have intended to study surface and cross-sectional textures of clasts, using all clasts from all parts of fault zones, with broad perspectives. We have studied so far Nojima fault and Arima-Takatsuki Tectonic Line in Japan, and Yangsan fault and Yeongdeok fault in southeast Korea (all granitic fault zones). We have recognized surface textures similar to the orange peel-like and fish scale-like textures of Kanaori and others, but we have not yet confirmed all textures that they have classified. A broken clast from clayey fault gouge in Yeongdeok fault zone exhibits quite interesting internal texture with a broken mineral (probably feldspar) in the center, mantled by thick fine-grained and still-porous fault rock that is rich in phyllosilicates. The texture clearly demonstrates that the surface textures of this clast did not form simply by dissolution of surface material, and there is a possibility that reactions between the clast and matrix formed the fault rock surrounding the clast. If this is the case, such textures may record some physical and chemical processes in fault zones (useful for the second purpose listed above), and we plan to do more detailed work on such textures. Pulverized rock is reported in a wide granitic fault zone along the Arima-Takatsuki Tectonic Line (Mitchell et al., 2011, EPSL). Distinction between clasts and matrix is not always clear in this fault rock and we could observe many fractures in minerals under a SEM. Interestingly, many of those fractures exhibit dissolution textures similar to those of fault-zone clasts and clastic sediments, and old existing fractures in rocks can be distinguished from fresh new fractures from surface textures. All of those textures will be useful in identifying faults from borehole cuttings.

©2019. Japan Geoscience Union. All Right Reserved.

Keywords: fault gouge, fault breccia, drill cuttings

©2019. Japan Geoscience Union. All Right Reserved.

Fault Displacement Assessment of Surface-rupturing Earthquakes for Nuclear Installations and the use of Physics-based Rupture Models

*Luis Angel Dalguer[1], Yoshimitsu Fukushima[2]

1. 3Q-Lab GmbH, 2. International Atomic Energy Agency

Surface-rupturing faulting is usually expected from large earthquakes, but this phenomenon has been also observed sometimes in moderate earthquakes. The coseismic fault displacement (defined as the surface rupture offset or slip on the free-surface) associated to earthquakes can seriously compromise the safety of critical infra-structures located near faults, such as bridges, dams, railroads, pipelines, nuclear installations (NI) and nuclear waste repositories. The draft IAEA specific safety requirements (Site Evaluation for Nuclear Installations No.SSR-1, DS484) requires that the capability for surface faulting shall be assessed for the site of a NI. But current practices of fault displacement hazard assessments (FDHA) are in general very challenging and quite limited because recorded fault displacement data to develop empirical models are very sparse, as such, at present very few empirical models with large uncertainty are available for this purpose. IAEA has already recognised this issue and currently is making the effort to implement the physics-based rupture modelling in practice for FDHA. In general for seismic hazard assessments (SHA), the empirical and physics-based rupture models complement each other and all available efforts are encouraged for the nuclear safety. These efforts have been discussed through different international working group activities, being the most outstanding two international workshops on **Best** Practices in **P**hysics-based Fault Rupture Models for **S**eismic **H**azard **A**ssessment of **N**uclear **I**nstallations (BestPSHANI) in 2015 and 2018. Here we discuss the feasibility of the use of Physics-based rupture models for FDHA and presenting couple of examples of fault displacement prediction of past earthquakes.

Keywords: Fault displacement, Fault displacement hazard assessment, Dynamic rupture modeling, Earthquake physics

©2019. Japan Geoscience Union. All Right Reserved.

Dynamic rupture simulation for seismic hazard assessment: Application to the Futagawa and Hinagu fault zones (Part 2)

*Yuko Kase[1]

1. Geological Survey of Japan, AIST

For probabilistic seismic hazard assessment, evaluations of rupture area to estimate a magnitude for a scenario earthquake and frequency are needed. We propose to provide the basic information for the evaluations using dynamic rupture simulations. Kase et al. (2017) applied the dynamic rupture model for seismic hazard assessment to the Futagawa and Hinagu fault zones. They simulated dynamic rupture models based on information observed before the 2016 Kumamoto earthquake, and showed that the rupture processes initiated at the northeastern end of the Takano-Shirahata segment were consistent with the rupture process of the 2016 Kumamoto earthquake. In this study, we investigate the effect of variations in initial crack locations and the other source parameters on simulation results.
A fault geometry and tectonic stress fields are assumed in the same way as Kase et al. (2017). The Futagawa segment of the Futagawa fault zone and the Takano-Shirahata and Hinagu segments of the Hinagu fault zone are modeled as a continuous vertical right-lateral strike-slip fault plane about 75 km long with surface rupture, based on HERP (2013). Azimuths of the minimum principal stress and stress ratios are assumed, considering the stress inversion result of Matsumoto et al. (2015). We also assume that the principal stresses are proportional to depth, and that the intermediate principal stress is vertical and overburden load.
Two initial crack locations, the southwestern ends of the Futagawa and Takano-Shirahata segment, are assumed. We calculate dynamic rupture processes, using a finite-difference method (Kase and Day, 2006), to search the azimuth of the minimum principal stress and depth coefficient of stress drop consistent with observed right-lateral dislocation on each segment.
Among ruptures initiating at the southwestern end of the Futagawa segment, the ruptures propagating only on the Futagawa segment have right-lateral slips consistent with the observation. Among ruptures initiating at the southwestern end of the Takano-Shirahata segment, on the other hand, the ruptures propagating on the Takano-Shirahata and Futagawa segments have right-lateral slips consistent with the observation. These results agree with the cases initiating at the northeastern ends of both segments (Kase et al., 2017). Thus, the initial crack location does not affect the rupture propagation to the adjacent segments in the ruptures initiating on the Futagawa and Takano-Shirahata segments. In the ruptures initiating on the Hinagu segment, a rupture initiating at the southwestern end is easier to propagate to the Takano-Shirahata segment than that initiating at the northeastern end (AIST, 2018). The difference is caused by rupture directivity. The lengths of the Futagawa and Takano-Shirahata segments are less than 20 km, while the Hinagu segment is 40 km long. Thus, the difference of rupture propagation between the initial crack locations clearly appears in the Hinagu segment.
We also investigate the effect of variations in a critical displacement and a ratio of strength excess and stress drop on simulation results.

Acknowledgment: This research was funded by the project commissioning disaster prevention for nuclear facilities (consideration of uncertainty factors in probabilistic seismic hazard analysis) in FY2018 by Regulatory Standard and Research Department, Secretariat of Nuclear Regulation Authority.

Keywords: dynamic rupture model, seismic hazard assessment, Futagawa and Hinagu fault zone

©2019. Japan Geoscience Union. All Right Reserved.

©2019. Japan Geoscience Union. All Right Reserved.

Quantification of gaps between slip-length scaling law of earthquakes and stick-slip experiments.

*Shinichi Oba[1], Yuta Mitsui[2]

1. Graduate School of Science and Tecnology, Shizuoka University, 2. Faculty of Science, Shizuoka University

Scaling relations of natural earthquake (over km scales) have been well studied, but their extension to smaller scales is difficult because of limited observation resolution. This study focuses on experimental stick-slip data and compares them with a slip-length scaling law of natural earthquakes. There seem gaps between the extension of the earthquake scaling and the stick-slip experiments. Here we perform correlation and multivariate analyses to investigate effects of apparatus type, mass and stiffness on the gaps. We find that a characteristic time composed of the mass and the stiffness shows a strong correlation with the gaps against the natural scaling in case of direct shear apparatus.

Keywords: stick-slip, earthquake slip-length scaling

©2019. Japan Geoscience Union. All Right Reserved.

Effect of Wear Process on Earthquake Recurrence

*Jeen-Hwa Wang[1]

1. Academia Sinica

Earthquake recurrence is studied from the temporal variation in slip through numerical simulations based on the normalized form of equation of motion of a one-body spring-slider model with thermal-pressurized slip-weakening friction and viscosity. The wear process, whose effect is included in the friction law, is also taken into account in this study. The main parameters are the normalized characteristic displacement, U_c, of the friction law and the normalized damping coefficient (to represent viscosity), η. Define T_R, D, and t_D to be the recurrence time of events, the final slip of an event, and the duration time of an event, respectively. Simulation results show that T_R increases when U_c decreases or η increases; D and t_D decrease with increasing η; and t_D increases with U_c. The time- and slip-predictable model can describe the temporal variation in cumulative slip. When the wear process is considered, the thickness of slip zone, h which depends on the cumulated slip, $S(t)=\Sigma D(t)$, i.e., $h(t)=CS(t)$ (C=a dimensionless increasing rate of h with S) is an important parameter influencing T_R and D. U_c is a function of h and thus depends on cumulated slip, ΣU, with an increasing rate of C. In the computational time period, the wear process influences the recurrence of events and such an effect increases with C when C>0.0001. When viscosity is present, the effect due to wear process becomes stronger. Both T_R and D decrease when the fault becomes more mature, thus suggesting that it is more difficult to produce large earthquakes along a fault when it becomes more mature. Neither the time-predictable model nor the slip-predictable one can describe the temporal variation in cumulative slip of earthquakes under the wear process with large C.

Keywords: Earthquake, Recurrence, Slip, Friction, Viscosity, Wear

©2019. Japan Geoscience Union. All Right Reserved.

On the Mechanical Relation between Individual Interaction and Collective Behavior of Multiple Fault Sets Subjected to Quasi-Static Loading

*Koji Uenishi[1,2], Yuki Fukuda[2], Nobuki Kame[3]

1. Department of Advanced Energy, The University of Tokyo, 2. Department of Aeronautics and Astronautics, The University of Tokyo, 3. Earthquake Research Institute, The University of Tokyo

In order to deepen our essential understanding of the connection between the local and the global or collective mechanical behavior of sets of geological faults in the solid earth, we have been performing laboratory rupture experiments using two-dimensional rectangular, linear elastic solid specimens with preset parallel cracks that model multiple fault planes under quasi-static tensile (mode-I) or tensile with in-plane shearing (mixed mode) loading conditions (Uenishi et al., SSJ Fall Meeting, 2017, 2018). Our special attention has been paid to the identification of when and how ruptures develop on each individual fault plane and interact with one another, and how the interaction influences the global nature of the solid. For that purpose, we have observed the local evolution of the isochromatic fringe patterns, i.e. the contours of the maximum in-plane shear stress, around the modeled fault planes in the photoelastic polycarbonate specimens with a high-speed digital video camera. At the same time, we have measured the global stress-strain relation utilizing a tensile testing machine that externally exerts a prescribed constant displacement rate to the specimen, and have compared its time history with the local observations of the isochromatic fringe patterns. Although the externally applied displacement or strain rate has been still in a relatively low, quasi-static range, the comparison may imply the effect of the local rupture development on the global properties of the solid specimen, and we have found that local rupture may not always propagate unidirectionally in the prepared specimens and ruptures may run into each other even on a single fault plane under very simple external loading conditions. We are now trying to investigate the mechanical characteristics of multiple fault sets that are subjected to more dynamic, impact loads and identify difference in the local-global relation, if any, between the dynamically-controlled and quasi-statically governed ruptures.

Keywords: fault rupture, fault stability, strain rate

©2019. Japan Geoscience Union. All Right Reserved.

Inelastic deformation in a region of the transient and forced extensional horizontal crustal strain

*Takao Eguchi, Yasuyuki Iwase[1]

1. National Defense Academy, Japan

Just after the focal rebound displacement by the 2011 Off-Tohoku Earthquake *(M~9)*, forced horizontal extension was confirmed in the Japanese archipelago. For example, from Miyagi to Yamagata prefectures on the overriding lithosphere, it was approximately stretching in the E-W direction.
We here investigate the "*transient inelastic deformation process*" in the adjacent island-arc environment immediately after such horizontally forced arc-extension.
For simplicity, let us assume that the main origin of inelastic island-arc deformation is not due to biaxial extension but due to transient elongation in a specific direction.
Since the island-arc is not necessarily an isotropic homogeneous elastic body, the mode of inelastic deformation depends on geometrical characteristics such as zonal contrast in elastic constants at pre-existing material block boundaries and/or at active faults within the island-arc.
We discuss the stress-strain relationship in the island-arc as an inelastic deformable body in the environment after the above-mentioned unidirectional elongation.
The response to the stress change in the subsequent environment becomes a nonlinear phenomenon that is transiently time-space dependent at least, and it will be different from the case of the linear elastic body.
In particular, even a small subsequent stress change will result in greater strain than in the case of linear elastics.
In this study, incorporating rheology such as thixotropy, we present some hypothetic models on the inelastic deformation of the island-arc system with the geometric distributed blocks, etc.

Keywords: inelastic deformation, island-arc system just after a greater interplate earthquake, block deformation, thixotropy

©2019. Japan Geoscience Union. All Right Reserved.

Representation Theorem and Green's Function (3) -- Strain, Stress, and Density Perturbation Fields due to a Point Source Using 2nd Derivative of Green's Function in an Unbounded Homogeneous Isotropic Elastic Medium --

*Masaya Kimura[1], Nobuki Kame[1]

1. Earthquake Research Institute,The University of Tokyo

Here we derive the second spatial derivative of Green's fuction in an unbounded homogeneous isotropic elastic medium. Following this formula, we obtain the expressions for strain, stress, and density perturbation fields due to a point source described by a moment tensor or a single force. These fomulae are useful for theoretical modeling of the prompt detection of earthquake occurrences by means of piezoelectricity, piezomagneticity, and transient gravity perturbations. We propose two applications of the formulae: (1) volumetric moment tensor mass redistribution and (2) dynamically induced quadratic earthquake mass redistribution. Regarding the latter application, we show the relationship between the moment magnitude M_w of an earthquake and dynamically induced quadratic earthquake mass redistribution (Table 1).

Table 1. The relationship between M_w of an earthquake and dynamically induced quadratic earthquake mass redistribution.

Reference: M. Kimura and N. Kame, 2018, Representation Theorem and Green's Function (3) -- Strain, Stress, and Density Perturbation Fields due to a Point Source Using 2nd Derivative of Green's Function in an Unbounded Homogeneous Isotropic Elastic Medium --, Zisin 2, 71, 153-160, doi:10.4294/zisin.2017-20

Keywords: Green's Function

©2019. Japan Geoscience Union. All Right Reserved.

M_w	$\delta m^{DQM}(M_w) = 10^{1.5M_w+1}[\mathrm{kg}]$
1.0	$10^{2.5} \sim 3 \times 10^2$
2.0	$10^{4.0} \sim 1 \times 10^4$
3.0	$10^{5.5} \sim 3 \times 10^5$
4.0	$10^{7.0} \sim 1 \times 10^7$
5.0	$10^{8.5} \sim 3 \times 10^8$
6.0	$10^{10.0} \sim 1 \times 10^{10}$
7.0	$10^{11.5} \sim 3 \times 10^{11}$
8.0	$10^{13.0} \sim 1 \times 10^{13}$
9.0	$10^{14.5} \sim 3 \times 10^{14}$

©2019. Japan Geoscience Union. All Right Reserved.

Development of a method of visualization of abrupt changes in slip-rate and rupture velocity toward better understanding of high-frequency radiation on a fault.

*Takahiro ayukai[1], Yuji Yagi[2], Ryo Okuwaki[3], Keita Kayano[3], Kousuke Shimizu[3]

1. School of Life and Environmental Sciences, University of Tsukuba, 2. Graduate School of Life and Environmental Sciences, University of Tsukuba, Tsukuba, 3. Graduate School of Life and Environmental Sciences, University of Tsukuba

High-frequency waves are thought to be generated by abrupt changes of slip-rate or rupture velocity on a fault during an earthquake rupture based on theoretical studies (e.g. Spudich and Frazer, 1984, BSSA). Finite-fault inversion of seismic waveforms is a tool to estimate spatiotemporal distribution of slip-rate function. Slip-rate function is composed of some basis functions at each subfault which an assumed fault is divided into in a reticular pattern. Back Projection (BP) (Ishii et al., 2005, Nature) and Hybrid BP (HBP) (Yagi et al., 2012, EPSL) methods are techniques for tracking high-frequency radiation sources and have been used to discuss the detailed source process by comparison with slip distribution resolved by waveform inversion. However, the physical meaning of the BP/HBP images is ambiguous, and the quantitative evaluation of the high-frequency radiation has been difficult solely by the BP/HBP methods. In order to reveal what rupture behavior generates high-frequency radiation, we proposed a method to image acceleration and deceleration of slip and rupture from spatiotemporal distribution of slip-rate function resolved by waveform inversion. We derived a representative slip-rate as a maximum value of slip-rate function and a representative rupture time at each sub-fault, and then calculated spatial gradients of the slip-rates and the rupture time to derive acceleration and deceleration of slip and rupture front, respectively. We used the slip-rate function which was obtained by the waveform inversion introducing uncertainty of Green’ s function (Yagi and Fukahata, 2011, GJI), where the high-frequency components of observed waveform were well reproduced compared to the conventional scheme because the waveform inversion can get a slip-rate functions which have a number of basis functions. We applied the developed method to the slip-rate functions of the M_W 7.9 2015 Gorkha, Nepal and the M_W 8.8 2010 Maule, Chile, earthquakes, which were presented in Yagi & Okuwaki (2015, GRL) and Pulido et al. (2011, EPS), respectively. For both the two earthquakes, the results showed that the rapid acceleration of slip was found at the edge of the large slip area facing to the hypocenter, while rapid deceleration of slip was found at the edge across the large slip area. The results also showed that the rapid deceleration of rupture was observed just before the rupture front penetrates into and escaped out of the large slip area. The estimated areas of rapid acceleration and deceleration are consistent with the spatial distribution of intense high-frequency radiation sources tracked by HBP methods (Yagi & Okuwaki, 2015, GRL; Okuwaki et al., 2014, Sci. Rep.). Our developed method well distinguished the behavior of slip evolution related to the generation of high-frequency waves, that is, spatiotemplrally separated slip and rupture front acceleration/deceleration, which has not been evaluated by the BP/HBP methods alone.

Keywords: High frequency, Waveform inversion, Slip rate, Rupture velocity, 2015 Gorkha, Nepal, earthquake, 2010 Maule, Chile, earthquake

©2019. Japan Geoscience Union. All Right Reserved.

Issues in earthquake-source-inversion analysis, evaluated through singular value decomposition

*Keita Kayano[1], Yuji Yagi[1], Ryo Okuwaki[1], Kousuke Shimizu[1]

1. Tsukuba University

Toward solving an inverse problem in Geophysics (e.g., earthquake-source inversion), prior information is used for stabilizing the solution, and an optimal weight between the observed data and prior information is objectively determined by minimizing Akaike's Bayesian Information Criterion (ABIC; Akaike, 1980). However, individual role of observed data and prior information on the resultant solution has not been evaluated in ABIC-based inversion, which makes it difficult to evaluate how much the prior information and its strength are valid in the solution, even though its weight is determined statistically by minimizing ABIC.

Here we resolved each characteristic of the observed data and the prior information that constrains the resultant image by applying singular value decomposition to a kernel of an inverted-source model of the Mw 7.0, 2016 Kumamoto, Japan, earthquake. The source model is represented as five-basis moment tensors (Kikuchi & Kanamori, 1991) distributed at 0.3-sec time and 2-km space intervals in the model space, which can simultaneously model slip evolution and fault geometry (Shimizu et al., 2019, under review). We used models with different weight: one with the weight minimizing ABIC, and the others with the weight artificially weakened and strengthened compared to the ABIC minimum. As prior information, we tested two types of condition: smoothing and L2-norm minimization.

Under the condition of smoothing, the model showed north side uplifting and reverse faulting at the weight stronger and weaker than the one minimizing ABIC, respectively, which is not consistent with the aftershock distribution and field observations (e.g., Yoshida et al., 2016; Shirahama et al., 2016). We found that the specific moment-tensor components, where the amplitudes of Green's function are larger, determining the characteristic of the singular vectors. It is suggested that if the weight of the prior information is stronger and weaker than the one minimizing ABIC, observed-data kernel (corresponding to Green's function) and smoothing-information kernel heavily controls the model characteristics, respectively. Under the condition of the L2 norm, the model showed north side uplifting, which is not evidenced by the aftershock distribution and the field surveys, even though we used ABIC for determining the "optimal" weight of the prior information. We found that the specific moment-tensor components, where the amplitudes of Green's function are larger, determining the characteristic of the singular vectors as is the case under the condition of smoothing. However, regardless of the weight of prior information, Green's function heavily controls the model characteristics.

Our study highlights that, under the condition of smoothing, the ABIC-based inversion works successfully for suppressing bias that violates the final solution generated by kernels of observed data and prior information. We also clarify that the L2-norm-minimization condition does not work properly for constraining source process of the 2016 Kumamoto earthquake.

Keywords: singular value decomposition, prior information, smoothing, L2 norm minimization, Green’s function, Akaike's Bayesian Information Criterion

©2019. Japan Geoscience Union. All Right Reserved.

Source process of recent M6-class inland earthquakes in Japan

*Ritsuya Shibata[1], Naofumi Aso[1], Junichi Nakajima[1], Satoshi Ide[2]

1. Department of Earth and Planetary Sciences, Tokyo Institute of Technology, 2. Department of Earth and Planetary Science, University of Tokyo

In recent years, inland earthquakes frequently occur in Japan including the 2016 Kumamoto earthquake (Mw7.0). Among them, M6-class events are the best targets to study the mechanics of two-dimensional rupture propagation, since smaller events are more difficult to study finite slip distribution while rupture area of larger events tend to be restricted in depth. For this purpose, we investigate the source process of the 2016 Central Tottori earthquake (Mw6.2) and the 2018 Hokkaido Eastern Iburi earthquake (Mw6.6), which are characterized by strike-slip and reverse-fault types, respectively, by applying slip inversion to strong-motion seismograms.

We use KiK-net stations deployed and maintained by NIED (National Research Institute for Earth Science and Disaster Resilience) within 50 km from the epicenter for both earthquakes. Fault geometry is assumed to be same as Kubo et al. (2017) for the 2016 Central Tottori earthquake, while we assume the fault geometry of the 2018 Hokkaido Eastern Iburi earthquake from the aftershock distribution. Fault discretization, source duration, source time discretization, and band-pass filters are optimized manually for each event.

Regarding 2016 Central Tottori earthquake, there has been discrepancies between previous studies. While Kubo et al. (2017) reported the slip of 0.3–0.6 m widely distributed over 5×8 km^2, Ross et al. (2018) estimated concentrated slip of >4 m in 3×3 km^2. Recently, Meneses-Gutierrez et al. (2019) obtained the slip of 1–2 m over 5×5 km^2 by analyzing GNSS (Global Navigation Satellite System) data. Our results mainly agree with Kubo et al. (2017), but larger slip is distributed more heterogeneously in our model because we do not apply smoothing. The concentration of slip near the hypocenter as reported by Ross et al. (2018) is also confirmed especially when we use finer model resolution. Therefore, the discrepancy reported in the previous studies may be due to the resolvability of slip with strong directivity in ordinary finite fault inversion, which usually requires sparse discretization and/or a smoothing constraint.

As a result of slip distribution of the 2018 Hokkaido Eastern Iburi earthquake, we obtained the slip in between right-lateral strike-slip type and reverse-fault types at the beginning, which is consistent with the mechanism determined by JMA (Japan Meteorological Agency) using first-motion polarities, while total slip is predominated by the reverse-fault component, which is consistent with the CMT (centroid moment tensor) solution determined by NIED using surface wave amplitudes. The final slip is separated in the shallow part and the deep part, similar to the distribution of aftershocks.

In both earthquakes, the rupture tends to expand in the direction parallel to the slip regardless of the rake direction. The prevailing mode II rupture over mode III rupture is consistent with the expectation from rupture mechanics (e.g., Day, 1982; Madariaga et al., 1998).

Keywords: 2016 Central Tottori earthquake, 2018 Hokkaido Eastern Iburi earthquake, inland earthquake

©2019. Japan Geoscience Union. All Right Reserved.

Expected slip direction on assumed fault planes of large earthquakes inferred from stress field after the 2016 Kumamoto earthquake sequence, in central Kyushu, Japan

*Ayaho Mitsuoka[1], Satoshi Matsumoto[2], Azusa Shito[2], Hiroshi Shimizu[2], Group for urgent joint seismic observation of the 2016 Kumamoto earthquake

1. Department of Earth and Planetary Sciences, Graduate School of Science, Kyushu University, 2. Institute of Seismology and Volcanology, Faculty of Sciences, Kyushu University

In order to understand generation of earthquake, knowing the force acting on a fault plane is the great interest problem for us. We should find with which direction and magnitude a fault plane slips. Shear and normal stresses on a fault plane can be estimated from the stress field around a fault. Maximum shear stress direction on a fault plane constrains the slip direction of an earthquake on the fault based on Wallace-Bott hypothesis. In this study, we estimated the maximum shear stress directions on some fault planes from the stress field at hypocentral area of the 2016 Kumamoto earthquake sequence.
The 2016 Kumamoto earthquake sequence occurred at Hinagu and Futagawa fault zones in Kumamoto prefecture, central Kyushu Island, Japan. The area was high seismicity area before the sequence. The largest foreshock with Mj 6.5 (Mj: magnitude by Japan Metrological Agency) on April 14, 2016 was located in Hingau fault zone. The mainshock (Mj 7.3) occurred on April 16, 2016. Many earthquakes occurred around these faults after the mainshock and continue until now. Some fault planes are determined from the aftershock hypocenter distribution.
Maximum shear stress direction on a fault is a projection of a traction vector that is calculated from the fault geometry and the stress field. In other word, we can consider slip direction on a fault from stress tensor and fault geometry. In the hypocentral area of the 2016 Kumamoto Earthquake sequence, evaluation of strong ground motion is important to mitigate damage of further coming earthquake. Slip direction is one of the key for the evaluation. Here, we showed expected slip direction on fault plane proposed by Iwata et al. [2019] from their geometry and the stress field estimated by Mitsuoka et al. [2019] using the seismic moment tensors.Most of the expected slip direction on the assumed faults reveal either simple strike slip or normal fault types. However the maximum shear stress directions on some faults change to have large upward component at shallow depth. The result suggests complicated slip could occur on the candidate faults in a case of large earthquake faulting.

Keywords: stress field, shear stress, 2016 Kumamoto earthquake

©2019. Japan Geoscience Union. All Right Reserved.

Spaciotemporal change of source parameters of repeaters due to the 2011 Tohoku-Oki earthquake

*Kazuya Tateiwa[1], Tomomi Okada[1], Toshio Kono[1], Naoki Uchida[1]

1. Research Center for Prediction of Earthquakes and Volcanic Eruptions, Graduate School of Science, Tohoku University

A number of small to moderate repeating earthquakes occur at the upper boundary of subducting Pacific plate in NE Japan. Understanding the source characteristics of repeating earthquakes and their spaciotemporal changes give us insight about the loading rate and its variation due to the plate motion and physical mechanisms of earthquakes, which can be common with major earthquakes because they would have the same occurrence structure as the small repeaters. In this study, we investigated the spatiotemporal change of source parameters of repeating earthquakes occurred on the Pacific interplate before and after the 2011 Tohoku-Oki earthquake. We analyzed seismic waveforms from about 3,000 repeating earthquake groups and about 7,000 repeating earthquakes in total. In this study, we show the results obtained by analysis of repeaters located off-Kamaishi and near Iwaizumi, Iwate, NE Japan.
In off-Kamaishi, repeaters are observed in a very constant recurrence cycle (~5.5 yr) and magnitude (~4.9) before the Tohoku-Oki earthquake, however, the recurrence interval was extremely shortened and the size of the earthquake was substantially enlarged immediately after the Tohoku-Oki earthquake. The recurrence interval and magnitude are becoming close to those of before the Tohoku-Oki earthquake with time. Although stress drop calculated with spectral ratio method is about 14 MPa before the Tohoku-Oki earthquake, it is estimated that stress drop after the Tohoku-Oki earthquake became smaller than before to have roughly a constant value (~2 MPa). The radius of ruptured fault estimated from corner frequency become about 5 times larger just after the Tohoku-Oki earthquake and later it became about 1 km. The radius of rupture fault of post-Tohoku events is becoming close to that of pre-Tohoku event with time. These results agree with Uchida et al. (2015) that estimated the rupture area of off-Kamaishi sequence by slip inversion. We consider that these changes of source parameters before and after the Tohoku-Oki earthquake are caused by its afterslip.
On the other hand, the repeating earthquake sequences in Iwaizumi does not have obvious changes in magnitude and stress drop before and after the Tohoku-Oki earthquake. If this region was less affected by afterslip than off-Kamaishi, small aftership might make the difference from the results of off-Kamaishi. We found the directivity estimated from corner frequency is observed only for repeaters of M<4, which indicates these small repeating earthquakes are composed of complex rupture. As it was suggested that repeaters of Iwaizumi sometimes rupture multiple patches in previous study (Arao et al., 2007), such complexities in rupture and the interaction between small ruptures would affect the recurrence of repeaters.

©2019. Japan Geoscience Union. All Right Reserved.

Slip distributions and relation of slip-rate and shear stress for the Boso slow slip events

*Takuma Kobayashi[1], Toshinori Sato[2]

1. Graduate School of Science and Engineering, Chiba University, 2. Graduate School of Science, Chiba University

Slow slip events (SSEs), which radiate no seismic waves, were detected 6 times off the Boso Peninsula since the GNSS observation in Japan started in 1996. This presentation shows slip distributions and stress changes of 6 SSEs, and discusses frictional properties on the plate boundary where the SSEs occur.

We used the daily F3 coordinate values of GNSS stations from the Geospatial Information Authority of Japan. The GNSS data were fitted with a time series model that takes account of the linear trend and seasonal variations in the data, and then the fitted data were smoothed. We made every 3 days transient movements from the smoothed data. From the 3 days data, we estimated slip distributions using ABIC inversion method. We calculated stress changes from the slip distributions using Coulomb 3.3.

The results show that the amount and location of the slip distributions differ each events. Maximum amount of slips is about 7 cm for 1996 and 2014 events, and 14-20 cm for the other events (2002, 2007, 2011, 2018). 1996 and 2014 events slipped at a location during the event. The other events, on the other hand, moved southward during the event. Shear stress changes were about 0.1-0.3 MPa at main slip areas. From graphs of logarithm of slip rate and the stress change, we can see starting phase, stable phase, and stopping phase for the SSEs. Slopes of the stable phase increase with depth.

The slopes of the stable phase represent (a-b)* σn, where σn is normal stress, from an equation of steady state friction for rate and state dependent friction low. Since the SSEs are quasi stable slip, the shear stress changes estimated from slip distributions may equal to frictional stress changes. Using also results of quasi stable slip simulation, we can estimate (a-b) and effective normal stresses from the slope of the stable phase for the SSEs. Assuming (a-b)=-0.003, the effective normal stresses are estimated about 2-20 MPa. These values are much smaller than lithostatic stresses at the depth. This indicates a possibility of very high pore pressure on the plate boundary.

Acknowledgements: We used the daily F3 coordinate values by GSI, and Coulomb 3.3 program by USGS.

Keywords: slow slip, slip rate, stress change, effective normal stress, rate and state dependent friction low

©2019. Japan Geoscience Union. All Right Reserved.

Repeating inland earthquakes in northern Ibaraki Prefecture activated after the 2011 Tohoku-Oki earthquake

Ryo Takahashi[1], *Keisuke Yoshida[1], Akira Hasegawa[1], Toru Matsuzawa[1]

1. Tohoku University

The 2016 M6.3 earthquake in northern Ibaraki Prefecture is estimated to have reruptured the same portion of the fault already ruptured in 2011 by an M6.1 earthquake (Fukushima et al., 2018) in 2011. Since repeated slips with such a short interval are rare in inland area far from the plate boundary, it provides a unique opportunity to investigate the earthquake cycle. In this presentation, we introduce our ongoing study about the generation processes of the 2011 and 2016 M6 earthquakes in northern Ibaraki Prefecture.

We start by relocating hypocenters using precise differential arrival time obtained by the waveform cross-correlation. The target is 13,410 earthquakes with M>2 listed in the JMA unified catalog for the period from Apr. 2003 to Oct. 31, 2018 in the M6.3 and M6.1 earthquake sequences near the Ibaraki-Fukushima border. We applied the double-difference hypocenter relocation method (Waldhauser & Ellsworth, 2002) to the differential arrival times of P- and S-wave based on a similar procedure to that by Yoshida & Hasegawa (2018).

Although the distribution of relocated hypocenters shows some complicated features, there is one dominant planar structure with west-dipping in northern Ibaraki prefecture. Comparison with the focal mechanisms supports that this planar structure corresponds to the fault plane of the 2011 and the 2016 M6 earthquakes. A planar structure of hypocenter did not newly appear after the 2016 earthquake; their aftershocks are concentrated on the existing planar structure. This supports that the 2011 and 2016 M6 earthquakes ruptured the same fault as pointed out by Fukushima et al. (2018).

The existence of repeating M6 earthquakes suggests that there are other smaller-magnitude repeating earthquake sequences along the plane. Based on the precise hypocenter locations and the waveform similarity, we detected many small repeating earthquakes (M>2) along the plane, which surround the large coseismic slip area of the M6 earthquakes. These small repeating earthquakes are estimated to be caused by the afterslip of the 2011 and 2016 M6 earthquakes. According to the empirical relationship between seismic moment and slip amount (Nadeau & Johnson, 1998), the slip amount is roughly estimated to be a few tens centimeter, which is comparable to the slip amounts of the two mainshocks. Moreover, the slip amount after the 2011 earthquake is larger than that after the 2016 earthquake, which is consistent with Fukushima et al. (2018). These suggest the importance of the effects of afterslip for the aftershock occurrence and the earthquake cycle.

Keywords: repeating earthquake, afterslip, the 2011 Tohoku-Oki earthquake

©2019. Japan Geoscience Union. All Right Reserved.

[J] Poster | S (Solid Earth Sciences)：S-SS Seismology

Wed. May 29, 2019 5:15 PM - 6:30 PM JST | Wed. May 29, 2019 8:15 AM - 9:30 AM UTC | Poster Hall International Exhibition Hall8, Makuhari Messe_26

[S-SS14] Fault Rheology and Earthquake Physics

convener:Keishi Okazaki(Japan Agency for Marine-Earth Science and Technology), Hideki Mukoyoshi(Department of Geoscience Interdisciplinary Graduate School of Science and Engineering, Shimane University), Hiroyuki Noda(Kyoto University, Disaster Prevention Research Institute), Keisuke Yoshida(Tohoku University)

The goal of this session is to integrate theoretical, experimental, observational, and numerical perspectives from various fields such as seismology, geodesy, geology, mineralogy, and so on, to define what is known about earthquake source processes and the physical and chemical elementary processes of faulting. This session welcomes studies that address such issues as pre-, co-, and post-seismic processes, the rheology of seismogenic faults and fault rocks, laboratory experiments on elementary processes, numerical models based on frictional laws, and estimates of the stress field in the seismogenic zones. We also welcome studies on fault-zone drilling projects and in situ stress measurements.

[SSS14-P01] Measurement of shear-wave polarization anisotropy in crack-bearing Aji granite during shear experiment

*Jinki Tanaka[1], Ikuo Katayama[1] (1.Hiroshima University)

[SSS14-P02] Effects of talc content on frictional properties of quartz gouge

Risako Shirahige[1], Inori Tatara[1], *Ken-ichi Hirauchi[1], Takato Takemura[2] (1.Department of Geosciences, Faculty of Science, Shizuoka University, 2.Department of Earth and Environmental Sciences, College of Humanities and Sciences, Nihon University)

[SSS14-P03] Mechanism controlling the frictional strength of quartz rocks at intermediate slip rates

*Kyuichi Kanagawa[1], Asuka Sugita[2], Miki Takahashi[3], Michiyo Sawai[1] (1.School of Science, Chiba University, 2.Faculty of Science, Chiba University, 3.Research Institute of Earthquake and Volcano Geology, Geological Survey of Japan)

[SSS14-P04] **Evolution of hydraulic and frictional properties of incoming hemipelagic sediments during diagenetic reactions**

*Keishi Okazaki[1], Ikuo Katayama[2], Asuka Yamaguchi[3] (1.Japan Agency for Marine-Earth Science and Technology, 2.Dept. of Earth & Planetary Systems Science, Hiroshima University, 3.AORI, the University of Tokyo)

[SSS14-P05] Contrasting silica precipitation via flash vaporization and fluid flow and possible effects on fault properties

*Takamasa Niibe[1], Atsushi Okamoto[1], Takashi Amagai[2], Noriyoshi Tsuchiya[1] (1.Graduate School of Environmental Studies, Tohoku University, 2.Japan Oil, Gas and Metals National Corporation)

[SSS14-P06] Temporal variations of reflected and transmitted wave during a slide-hold-slide experiment on a biaxial friction testing machine

*Miyuu Uemura[1], Yoshihiro Ito[2], Ikuo Katayama[3] (1.Kyoto University, 2.Disaster Prevention Research Institute, Kyoto University, 3.Department of Earth and Planetary Systems Science, Hiroshima University)

[SSS14-P07] Monitoring stress-induced changes of laboratory fault by ultrasonic coda wavesMonitoring stress-induced changes of laboratory fault by ultrasonic coda waves

*Fan XIE[1], Yaqiong REN[1] (1.Institute of Geophysics, China Earthquake Administration)

[SSS14-P08] Longer duration of meta-instability stage of laboratory earthquakes on a 1.5m granite fault

*yaqiong Ren[1] (1.Institute of Geophysics, China Earthquake Administration)

[SSS14-P09] Estimation of the frictional heat and the amount of wall rock incorporation by thermal fracturing during an earthquake: An example from the pseudotachylyte in Jurassic accretionary complex

*Ayaka Nagate[1], Kohtaro Ujiie[1] (1.University of Tsukuba)

[SSS14-P10] Porosity variation of fault rocks accompanied the Median Tectonic Line in Shikoku, southwestern Japan

*Michiharu Ikeda[1], Takeshi Tsuji[2], Tomohiro Tsuji[1], Kozo Onishi[3], Naoki Nishizaka[3] (1.Shikoku Research Institute Incorporated, 2.Kyushu University, 3.Shikoku Electric Power Company, Incorporated)

[SSS14-P11] Characteristics of inactive section of the Median Tectonic Line from drillcore samples in Shikoku, southwestern Japan

*Hideto Uchida[1], Michiharu Ikeda[1], Takeshi Tsuji[2], Kozo Onishi[3], Naoki Nishizaka[3] (1.Department of Civil Engineering, Shikoku Research Institute incorporated, 2.Department of Earth Resources Engineering, Kyusyu University, 3.Shikoku Electronic Power)

[SSS14-P12] Surface and internal textures of clasts in incohesive fault rocks and their significance

*Tetsuhiro Togo[1], Toshihiko Shimamoto[2], Michiyo Sawai[3] (1.THE EARTH, 2.Institute of Geology, China Earthquake Administration, 3.Chiba Univ.)

[SSS14-P13] **Fault Displacement Assessment of Surface-rupturing Earthquakes for Nuclear Installations and the use of Physics-based Rupture Models**

*Luis Angel Dalguer[1], Yoshimitsu Fukushima[2] (1.3Q-Lab GmbH, 2.International Atomic Energy Agency)

[SSS14-P14] Dynamic rupture simulation for seismic hazard assessment: Application to the Futagawa and Hinagu fault zones (Part 2)

*Yuko Kase[1] (1.Geological Survey of Japan, AIST)

[SSS14-P15] Quantification of gaps between slip-length scaling law of earthquakes and stick-slip experiments.

*Shinichi Oba[1], Yuta Mitsui[2] (1.Graduate School of Science and Tecnology, Shizuoka University, 2.Faculty of Science, Shizuoka University)

[SSS14-P16] Effect of Wear Process on Earthquake Recurrence

*Jeen-Hwa Wang[1] (1.Academia Sinica)

[SSS14-P17] On the Mechanical Relation between Individual Interaction and Collective Behavior of Multiple Fault Sets Subjected to Quasi-Static Loading

*Koji Uenishi[1,2], Yuki Fukuda[2], Nobuki Kame[3] (1.Department of Advanced Energy, The University of Tokyo, 2.Department of Aeronautics and Astronautics, The University of Tokyo, 3.Earthquake Research Institute, The University of Tokyo)

[SSS14-P18] Inelastic deformation in a region of the transient and forced extensional horizontal crustal strain

*Takao Eguchi, Yasuyuki Iwase[1] (1.National Defense Academy, Japan)

[SSS14-P19] Representation Theorem and Green's Function (3) - - Strain, Stress, and Density Perturbation Fields due to a Point Source Using 2nd Derivative of Green's Function in an Unbounded Homogeneous Isotropic Elastic Medium - -

*Masaya Kimura[1], Nobuki Kame[1] (1.Earthquake Research Institute,The University of Tokyo)

[SSS14-P20] Development of a method of visualization of abrupt changes in slip-rate and rupture velocity toward better understanding of high-frequency radiation on a fault.

*Takahiro ayukai[1], Yuji Yagi[2], Ryo Okuwaki[3], Keita Kayano[3], Kousuke Shimizu[3] (1.School of Life and Environmental Sciences, University of Tsukuba, 2.Graduate School of Life and Environmental Sciences, University of Tsukuba, Tsukuba, 3.Graduate School of Life and Environmental Sciences, University of Tsukuba)

[SSS14-P21] Issues in earthquake-source-inversion analysis, evaluated through singular value decomposition

*Keita Kayano[1], Yuji Yagi[1], Ryo Okuwaki[1], Kousuke Shimizu[1] (1.Tsukuba University)

[SSS14-P22] **Source process of recent M6-class inland earthquakes in Japan**

*Ritsuya Shibata[1], Naofumi Aso[1], Junichi Nakajima[1], Satoshi Ide[2] (1.Department of Earth and Planetary Sciences, Tokyo Institute of Technology, 2.Department of Earth and Planetary Science, University of Tokyo)

[SSS14-P23] Expected slip direction on assumed fault planes of large earthquakes inferred from stress field after the 2016 Kumamoto earthquake sequence, in central Kyushu, Japan

*Ayaho Mitsuoka[1], Satoshi Matsumoto[2], Azusa Shito[2], Hiroshi Shimizu[2], Group for urgent joint seismic observation of the 2016 Kumamoto earthquake (1.Department of Earth and Planetary Sciences, Graduate School of Science, Kyushu University, 2.Institute of Seismology and Volcanology, Faculty of Sciences, Kyushu University)

[SSS14-P24] Spaciotemporal change of source parameters of repeaters due to the 2011 Tohoku-Oki earthquake

*Kazuya Tateiwa[1], Tomomi Okada[1], Toshio Kono[1], Naoki Uchida[1] (1.Research Center for Prediction of Earthquakes and Volcanic Eruptions, Graduate School of Science, Tohoku University)

[SSS14-P25] Slip distributions and relation of slip-rate and shear stress for the Boso slow slip events

*Takuma Kobayashi[1], Toshinori Sato[2] (1.Graduate School of Science and Engineering, Chiba University, 2.Graduate School of Science, Chiba University)

[SSS14-P26] Repeating inland earthquakes in northern Ibaraki Prefecture activated after the 2011 Tohoku-Oki earthquake

Ryo Takahashi[1], *Keisuke Yoshida[1], Akira Hasegawa[1], Toru Matsuzawa[1] (1.Tohoku University)

Measurement of shear-wave polarization anisotropy in crack-bearing Aji granite during shear experiment

*Jinki Tanaka[1], Ikuo Katayama[1]

1. Hiroshima University

The stress drop at the time of the earthquake not only releases the stress applied to the fault plane but also causes the rotation of the principal stress axis applied to the fault plane. In fact, the change in the direction of the principal stress axis after the earthquake is reported by the mechanism solution of aftershocks and the seismic wave anisotropy(e.g. Tadokoro and Ando 2002; Boness and Zoback 2006). It is thought that this is because the closing (opening) direction of the cracks around the fault plane correspond to the stress axis. Therefore, in this study, the elastic wave velocity was monitored during the shear experiment of the rock and the relation between the shear stress and the principal stress axis and elastic wave velocity was measured in the laboratory. Since the shear-wave polarization anisotropy has a characteristic which is sensitive to the direction of the crack, measurement of different vibration components of S wave is performed in addition to measurement of P wave velocity.

For the experiment, we investigated the change in elastic wave velocity according to shear deformation using a High-T biaxial frictional testing machine in Hiroshima University. For the experimental samples, Aji granite which generated thermal cracks inside by heating to 600 degrees Celsius was used. In the shear experiment, it was carried out by loading the central rock block at a constant speed while keeping the vertical stress constant. The shear sliding velocity was about 0.9 μm/s and the normal stress was 5 MPa. For measurement of elastic waves, probes with a resonance frequency of 1 MHz (manufactured by Olympus Corporation) were used, and S wave and P wave were measured by pulse transmission method. The propagation direction of elastic wave is parallel to the shear plane and perpendicular to the shear sliding direction, and for the S wave, we measured two components, wave (SH) oscillating in the plane orthogonal to the shear plane and wave (SV) oscillating parallel to the shear plane.

From the experimental results, with the increase of the shear stress, it was found that the velocity of SH wave rises earlier and the SV wave rises late. In addition, there was a phenomenon in which the initial motion of the SV wave jumped suddenly as the shear stress increased. This means that when the shear stress is low and the maximum principal stress axis in the sample is close to the direction of the normal stress, the shear direction cracks are frequently closed and the SH wave velocity increases, and the shear stress increases, when the inclination of the maximum principal stress axis becomes steeper with respect to the normal stress, it is considered that the direction of the crack which closes is correspondingly inclined. In this way, since the SH wave and SV wave behave differently due to the increase of the shear stress and the corresponding change of the principal stress axis angle, by utilizing this property, a good index for monitoring the stress state around the fault.

Keywords: Earthquake prediction, Shear-wave polarization anisotropy

©2019. Japan Geoscience Union. All Right Reserved.

Effects of talc content on frictional properties of quartz gouge

Risako Shirahige[1], Inori Tatara[1], *Ken-ichi Hirauchi[1], Takato Takemura[2]

1. Department of Geosciences, Faculty of Science, Shizuoka University, 2. Department of Earth and Environmental Sciences, College of Humanities and Sciences, Nihon University

Phyllosilicates have low coefficients of friction and an effect of weakening fault strength. To understand effects of talc content on frictional strength and sliding stability, we conducted frictional sliding experiments on dry gouge mixtures of quartz and talc at room humidity, room temperature, a normal stress of 10 MPa and sliding velocities of 0.66–2 μm/s, using a single direct-shear apparatus. The coefficient of friction for the mixture ranged from 0.18 to 0.69 and fell between pure quartz and talc values. The overall trend was a decrease in the coefficient of friction with increasing talc content. The velocity dependence of friction, ($a-b$), ranged from −0.0018 to 0.0039 and increased with increasing talc content. The ($a-b$) values are highest in the mixture with a talc content of 80 wt.%. For the mixture with talc contents below 10 wt.%, the ($a-b$) values become negative, with the occurrence of slow to fast stick-slip behavior.

Keywords: friction, stick slip, fault weakening, phyllosilicate

©2019. Japan Geoscience Union. All Right Reserved.

Mechanism controlling the frictional strength of quartz rocks at intermediate slip rates

*Kyuichi Kanagawa[1], Asuka Sugita[2], Miki Takahashi[3], Michiyo Sawai[1]

1. School of Science, Chiba University, 2. Faculty of Science, Chiba University, 3. Research Institute of Earthquake and Volcano Geology, Geological Survey of Japan

Frictional strength of quartz rocks is known to be extraordinary low at subseismic slip rates ranging from 1 mm/s to 10 cm/s, which has been ascribed to the hydration of comminuted amorphous silica, i.e., silica gel. In order to testify this hypothesis, we conducted rotary-shear friction experiments on intact agate or silica gel gouge at a normal stress of 1.5 MPa and slip rates (V) ranging from 1 mm/s to 10 cm/s. We also measured temperature (T) adjacent to the slip surface or the gouge layer during the experiments.

Steady-state friction coefficient of agate μ_{ss} was ≈0.6 at V = 1 mm/s, ≈0.5 at V = 7 mm/s, and ≦0.1 at V = 10 cm/s. T was ≈25˚C at V = 1 mm/s, ≈30˚C at V = 7 mm/s, and up to 85˚C at V = 10 cm/s, but the actual temperature along the slip surface must have been much higher. μ_{ss} of silica gel gouge was ≈0.7 at V = 1 mm/s, 0.4–0.5 at V = 7 mm/s, and ≦0.2 at V = 10 cm/s. T was 25–28˚C at V = 1 mm/s, 30–37˚C at V = 7 mm/s, and 80–100˚C at V = 10 cm/s, but again, the actual temperature in the gouge layer must have been much higher.

Thus our results show that agate or silica gel exhibits weakening with increasing T, and that the presence of silica gel does not reduce the frictional strength when T is not high enough. Shear strength of quartz rocks is high so that significant amount of frictional heat would be produced at asperity contacts even at V ≈1 cm/s, which must be responsible for weakening of quartz rocks at intermediate slip rates.

Keywords: agate, silica gel, frictional strength, intermediate slip rates

©2019. Japan Geoscience Union. All Right Reserved.

Evolution of hydraulic and frictional properties of incoming hemipelagic sediments during diagenetic reactions

*Keishi Okazaki[1], Ikuo Katayama[2], Asuka Yamaguchi[3]

1. Japan Agency for Marine-Earth Science and Technology, 2. Dept. of Earth & Planetary Systems Science, Hiroshima University, 3. AORI, the University of Tokyo

Deployments of seismic and geodetic observation networks had revealed the activity of slow earthquakes along the subduction plate boundaries, which are characterized as intermediate fault slip rate between earthquake (~1m/s) and stable sliding along the plate boundary (~1 nm/s). Diagenesis of subducting sediments has stimulated interest in their relationship to regular and slow seismicity in the subduction zone. We report experimental results on the effect of diagenetic reactions to hydraulic and frictional properties of incoming hemipelagic sediments. Hemipelagic sediments taken from KS-15-3 Shinseimaru cruise are used as the starting sample. Friction experiments and permeability measurements were carried out with a confining pressure of 150 MPa and a pore pressure of 58 MPa and temperatures ranging RT–230 degC. When the sample is sheared immediately after reaching the experimental condition, all experimental data at the temperature below 150 degC showed a velocity-strengthening behavior. On the other hand, at the temperature of 230 degC, the frictional behavior is no longer stable, but stick-slip behavior was observed during the experiments. We also measured a time-dependent permeability evolution of hemipelagic sediments to assess how diagenetic reactions consolidate the sediments. Permeability decreased about an order magnitude due to the mechanical compaction from the effective pressure of 3 MPa to 92 MPa, and decrease additional an order magnitude of permeability is observed during the hot-pressing of the sample at the pressure and the temperature of 92 MPa and 100 degC, respectively. Those experimental observations suggest that thermally activated compactions, possibly pressure solution creep, could contribute key role for understanding the physical property of subducting sediments.

Keywords: subduction zone, frictional property

©2019. Japan Geoscience Union. All Right Reserved.

Contrasting silica precipitation via flash vaporization and fluid flow and possible effects on fault properties

*Takamasa Niibe[1], Atsushi Okamoto[1], Takashi Amagai[2], Noriyoshi Tsuchiya[1]

1. Graduate School of Environmental Studies, Tohoku University, 2. Japan Oil, Gas and Metals National Corporation

It is thought that precipitation of silica plays crucial roles on mechanical and hydrological properties of faults. The solubility of silica minerals varies significantly depending on temperature and water density (e.g., Manning, 1994). Okamoto *et al.* (2010) conducted the hydrothermal flow-through experiments at vapor-like supercritical condition (430 ℃, 31 MPa) and showed that silica precipitation predominantly occurred via quartz overgrowth and quartz nucleation (Okamoto *et al.*, 2010). In contrast, precipitation of silica is thought to be induced by decompression of fluids. Weatherley and Henley (2013) suggested that silica particles precipitate by flash vaporization at fault jog; however, the process of silica precipitation under such extreme condition has not been verified experimentally. The purpose of this study is to understand the mechanism of silica precipitation by hydrothermal experiments. In particular we focus on the difference in the mode of occurrences of silica precipitates between flashing and fluid flow system.
We conducted two types of experiments: (1) flash + batch experiments, and (2) flow-through experiments. Both experiments were carried out with using high-silica solutions (Si = 250-300 mg/kgH_2O, Na, Al, K = 4-6 mg/kgH_2O), that was prepared by dissolution of granite sand at 370 ℃ and 40 MPa. In the flashing experiments, after the input solution was enclosed into the autoclaves, elevated pressure and temperature, and flashed by opening the valve. Alumina filter (average pore size of 60 μm) was placed on the flow pathway to catch the silica particles. The flash P-T conditions were 261 ℃, 353 ℃, 400 ℃, and 450 ℃ at pressure of 35-38 MPa. In all conditions, silica precipitates did not include quartz, but spherical particles of amorphous silica with size of 0.1-10 μm were produced. Such amorphous silica was probably formed by nucleation and aggregation during the evaporation of water droplet. Then, we investigated the transformation of the flashing products (removed from the alumina filter and enclosed in Au tube) by the batch experiments at 261 ℃ and 351 ℃ at vapor saturated pressure, and at 400 ℃ and 450 ℃ under supercritical conditions. There was no change of silica after the batch experiments at 261℃ and 351℃ conditions within 5 days. In contrast, small quartz crystals (size of less than 10 μm) were produced in 5 days at 400 ℃ and in 3 days at 450 ℃. Albite was partly produced as the results of interaction with alumina-filter.
The silica precipitation was also investigated by the flow-through experiments at 390-430 ℃ and 25 MPa (supercritical condition) with constant flow-rate of 0.5 or 1 mL/min by using the granite-dissolved solution similar to the flash experiments. The silica was precipitated in alumina tube filled with alumina ball (diameter with 1 and 2mm). We found the silica precipitates clogged the pores within few days. Based on the XRD and SEM observation, the products of the flow-through experiments were mixture of amorphous silica and quartz. Some quartz crystals grew up to 100 micrometers and amorphous silica were precipitated on the alumina balls and the alumina pipe.
In both cases, amorphous silica was easily produced in response to the drop of water density at high temperatures. Such amorphous silica can move and clog effectively the pores. Also, our experiments revealed that such amorphous silica was changed to quartz, which depends on the temperature and fluid states (flow or batch). Such variation of silica by precipitation and transformation potentially would provide a significant influence on the fault strength.

Weatherley D. K. and Henley R. W. (2013), *Nature Geoscience*, **6(4)**, 294.
Okamoto A., Saishu H., Hirano N. and Tsuchiya N. (2010), *Geochemica et Cosmochimica Acta*, **74**,

©2019. Japan Geoscience Union. All Right Reserved.

3692-3706.
Manning C. E. (1994), *Geochemica et Cosmochimica Acta*, **58**, 4831-4839.

Keywords: Water-Rock Interaction, Silica, Flash Vaporization

©2019. Japan Geoscience Union. All Right Reserved.

Temporal variations of reflected and transmitted wave during a slide-hold-slide experiment on a biaxial friction testing machine

*Miyuu Uemura[1], Yoshihiro Ito[2], Ikuo Katayama[3]

1. Kyoto University, 2. Disaster Prevention Research Institute, Kyoto University, 3. Department of Earth and Planetary Systems Science, Hiroshima University

Slow slip events (SSEs), which is one of the slow earthquakes differing from regular earthquakes, have been detected at both shallower and deeper portions of the seismogenic zones, such as Japan and New Zealand. We carried slide-hold-slide experiments with gouge layer under a slip velocity of an SSE using a biaxial friction testing machine under the condition with the temperature and the humidity of room. We measured temporal changes of acoustic impedance in the gouge layer with reflected and transmitted wave during slides and holds. As a result, we detected variations in travel time, amplitude, and cross-correlation coefficient on first arrival of reflected and transmitted wave.

The features of observed waveforms were classified clearly by a slide-hold-slide conditions into two categories: sliding and holing. We chose two materials as gouge powder, which were clay mineral (Ca-montmorillonite) and quartz. Regardless of the kinds of the gouge powder, the amplitude both of reflected and transmitted waves showed opposite temporal variation during the slide-hold-slide sequences; the amplitude of transmitted wave decreased during slides and increased during holds, respectively. This suggests that the amplitudes of reflected and transmitted waves indicate a change of an elastic-wave speed in the gouge layer.

The travel times of transmitted waves increased during slides and decrease during holds. According to Birch (1961), a propagation speed of elastic waves normally decreases as the density of media decreases, or as the porosity increases. Increasing travel times of transmitted waves in our experiments may indicate the change of the density, or porosity in the gouge layer. Although the travel times of reflected waves decreased during slides and increased during holds in the case of clay mineral, the travel time on quartz powder did not change through our experiment.

The temporal change on correlation of observed transmitted wave also shows significant changes from a slide to a hold. The change of travel time, the amplitude, and the cross-correlation coefficient of transmitted waves were more sensitive to a slide-hold-slide condition, such as slip rate on the gouge later than those of reflected wave. Those result suggests that a transmitted wave is more suitable for monitoring SSE although a reflected wave is also useful for monitoring, and that a beginning and an end of an SSE can be detected by reflected and transmitted waves.

Keywords: slow slip event, biaxial friction experiment, gouge

©2019. Japan Geoscience Union. All Right Reserved.

Monitoring stress-induced changes of laboratory fault by ultrasonic coda wavesMonitoring stress-induced changes of laboratory fault by ultrasonic coda waves

*Fan XIE[1], Yaqiong REN[1]

1. Institute of Geophysics, China Earthquake Administration

It is increasing important to understand evolution in fault zone and find clear precursors to the earthquake. Nevertheless, the evolving behavior of crustal faults remains changeling due to its inaccessible and weakness.

Duo to their highly sensitivity, the seismic coda waves have been long used at kilometer scale to investigate stress changes by tracking seismic relative velocity changes during earthquake. However, detecting such changes and imaging their spatial distribution with satisfied resolution are still an ongoing project, for which laboratory developments may be useful.

This work aims to explore the applicability of coda waves to monitor spatiotemporal changes of laboratory fault.

Laboratory-scale experiments are performed by meter-scale biaxial loading apparatus in which coda waves at ultrasonic frequencies (100 kHz to 400 kHz) are transmitted and received by 16 broadband piezoelectric transducers using the state-of-the-art ultrasound research platform (Verasonics Vantage 64 Low Frequency Edition) across a 1.5-meter long granite simulated fault.

Before stick-slip events occurred by increasing shear stress at loading rate of 1 um/s , the normal stress was kept 500KPa constant for 60 minutes. The ultrasonic coda waves were recorded throughout the entire process of stress accumulation along the fault.

Coda wave interferometry (CWI) and Coda wave decorrelation (CWD) are performed to detect relative velocity changes and microstructural changes along the fault by measuring phase shifts and loss of coherence of received coda waves respectively.

We observe a ~0.4e-3 velocity increase and ~0.5% coherence loss within logarithm of stationary contact time during 1-hour normal stress holding time. A significant 1.4e-3 increase in relative velocity changes and 8% coherence loss during shear stress increasing test followed by 0.5e4 decease in relative velocity changes and 2% decrease in coherence loss respectively caused by ~200kPa stress drop of the emerging stick-slip event. We also observe that the such changes are localized at upper center of the fault by comparing the changes extracted at different transducers along the fault.

The results suggest that ultrasonic coda waves are a promising means to monitor weak but localized stress-induced changes of laboratory fault by detecting and characterization velocity and micro-structural changes. Considering such advantages, further works to temporal critical observations, such as nucleation process of laboratory earthquake, are conceivable from a practical and instrumental point of view.

©2019. Japan Geoscience Union. All Right Reserved.

Keywords: laboratory earthquake , stick slip , coda waves, stress-induced changes

©2019. Japan Geoscience Union. All Right Reserved.

Longer duration of meta-instability stage of laboratory earthquakes on a 1.5m granite fault

*yaqiong Ren[1]

1. Institute of Geophysics, China Earthquake Administration

Laboratory earthquakes are a series of stick slip events occurred on an old or newly formed fracture in laboratory. It is widely used to study the properties and mechanisms of earthquake nucleation, dynamic rupture and post-seismic process since its similarities with nature earthquakes. Meta-instability stage is the later stage of the nucleation process. It holds that when the stress release accelerates and synergizes, the deformation enters an irreversible stage to instability. Thus studying its evolutionary characteristics is more conducive to identifying the arrival of earthquakes in advance.

We perform a series stick slip experiments on a 1.5m granite fault. Using a meter-scale rock as experimental sample can indirectly improve the spatial resolution of observation. More importantly, the scale effect of earthquake preparation process can be studied by comparing the results of centimeter-scale and meter-scale samples, which is helpful to the field application of experimental results.

The experiment was carried out on a large horizontal two-direction servo-control press at the Institute of Geophysics, China Earthquake Administration. The maximum loading capacity of the press in two directions is 100 tons and 200 tons respectively. The local variations of stress and displacement along the fault as well as the variation of the whole sample were recorded during the experiment. The stiffness of the meter-scale sample and press system is 0.003 MPa/um, which is one order of magnitude smaller than that of the centimeter-scale sample and press system in the Institute of Geology, China Earthquake Administration. This enables us to obtain stick-slip events with small stress drop, large displacement and audible energy release at lower confining pressure.

For a single stick-slip event, the beginning of meta-instability stage and quasi-dynamic stage (the later stage of meta-instability stage) can be identified based on the relative displacement and strain observations along the fault. The meta-instability begins in the middle of the fault and extends toward both ends as the instability approaches. During the meta-instability stage, the variation rate of different parts of the fault varies greatly, and tends to synergize with the approach of instability.

The duration of meta-instability is longer under lower loading rate, and the change of normal stress has little effect on the duration of meta-instability under lower normal stress. The duration of meta-instability increases with the increase of fault scale, showing obvious scale effect. The results suggest that meta-instability on natural faults in the field may last for several years, and could be monitored. The non-uniformity of faults with the increase of fault scale may be an important mechanism for the scale effect of the duration of meta-instability.

Keywords: stick slip, earthquake nucleation, meta-instability stage, scale effect, meter-scale rock

©2019. Japan Geoscience Union. All Right Reserved.

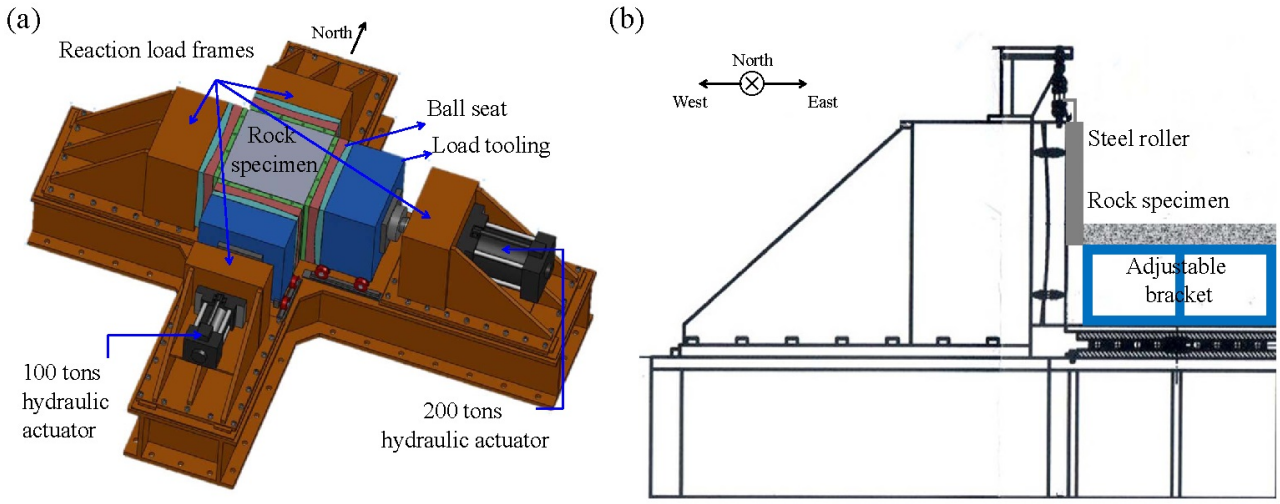

©2019. Japan Geoscience Union. All Right Reserved.

Estimation of the frictional heat and the amount of wall rock incorporation by thermal fracturing during an earthquake: An example from the pseudotachylyte in Jurassic accretionary complex

*Ayaka Nagate[1], Kohtaro Ujiie[1]

1. University of Tsukuba

Estimation of frictional heat is crucial to evaluate dynamic shear strength and fault behavior during an earthquake. Pseudotachylyte produced by solidification of frictional melt is an unequivocal geological evidence of seismic slip on faults. Here, we estimated frictional heat and amount of wall rock incorporation into coseismic slipping zone during an earthquake, based on microstructural observation and numerical analysis of the pseudotachylyte in the Jurassic accretionary complex. The pseudotachylyte-bearing thrust develops as an out-of-sequence thrust in the coherent chert-clastic sequence, which bounds middle Triassic chert above from early Jurassic siliceous mudstone below. The pseudotachylyte is ~2 mm-thick and sharply separates fractured grey chert above from cataclasite below. The pelagic black carbonaceous mudstone layer is distributed at the stratigraphic equivalent interval of the pseudotachylyte.

The microstructures of the pseudotachylyte are characterized by fault and injection veins, fragments of grey chert and quartz in the dark matrix of illite composition, and irregularly and embayed pseudotachylyte boundaries. The gray chert adjacent to the pseudotachylyte and fragments in the pseudotachylyte consisted of grey chert are intensely cracked, showing jigsaw puzzle-like structure. These microstructural features suggest that thermal erosion, thermal fracturing, and preferential melting of illite occurred during earthquake faulting. Frictional heat, which was estimated from temperature rise, volume fraction of fragments, and pseudotachylyte thickness, is ~7.1 MJ m^{-2}.

The comparison of volume fraction of fragments in the matrix between the pseudotachylyte and the black carbonaceous mudstone layer suggests that half amount of fragments in the pseudotachylyte were derived from wall rocks. The numerical modeling considering temperature rise, heating duration, and thermal properties of gray chert indicates that the temperatures of wall rocks a few millimeters away from the pseudotachylyte boundaries exceed the temperature of a-b transition in quartz (~573 ˚C) during earthquake faulting. This distance is consistent with spatial distribution of crack density, which shows exponentially decrease away from the pseudotachylyte boundaries. Thus, intensely cracked wall rocks are considered to represent thermal expansion of quartz grains in gray chert, which could contribute to unstable fault slip associated with decrease in stiffness of surrounding rocks.

Keywords: Frictional heat, Pseudotachylyte, Jurassic accretionary complex

©2019. Japan Geoscience Union. All Right Reserved.

Porosity variation of fault rocks accompanied the Median Tectonic Line in Shikoku, southwestern Japan

*Michiharu Ikeda[1], Takeshi Tsuji[2], Tomohiro Tsuji[1], Kozo Onishi[3], Naoki Nishizaka[3]

1. Shikoku Research Institute Incorporated, 2. Kyushu University, 3. Shikoku Electric Power Company, Incorporated

Petrophysical properties of fault rocks are important information to understand evolution processes of fault rocks. Among their properties, hydraulic properties of fault rocks are closely related to fault dynamics and potential of reservoirs of fluid or gas. In this research, we focused on distribution of porosities through fault rocks of the Median Tectonic Line in Shikoku.

The Median Tecotnic Line (MTL) is the longest geological terrane boundary fault. The northern and southern parts from the MTL are Ryoke Belt composed of low P/T metamorphic rocks, granitic rocks and sedimentary rocks and Sanbagawa metamorphic rocks consisted of high P/T metamorphic rocks, respectively. We drilled a bore hole to obtain a geological core sample penetrating the MTL. The total core length is 250 m-long. The fault plane of the MTL is within 37.45 m-depth. The hanging wall and foot wall zones are Izumi Group in Ryoke Belt and Sanbagawa metamorphic rocks, respectively.

The fault rocks in Izumi Group are composed of three zones, fault breccia zone (ca.4– ca.12.5 m-depth), transition zone (ca.12.5–ca.31.6 m-depth) and fault gouge zone (ca.31.6–ca.37.2 m-depth), based on geological observation. On the other hand, the fault rocks of the Sanbagawa metamorphic rocks are cataclasite just below the MTL fault plane (37.45–ca.47 m-depth) and intact rocks in the deeper parts of the core (ca.47–250.0 m-depth).

We measured 49 samples (24 samples in Izumi Group and 20 samples in Sanbagawa metramorphic rocks) from the core. In addition to them, 5 samples from outcrops of Izumi Group were measured to get porosities of intact rocks of Izumi Group, because all parts of Izumi Group in the core are damaged.

The porosities of the hanging wall (Izumi Group) range between 4.54% and 20.35%, whereas those of the foot wall (Sanbagawa metamorphic rocks) are lower (2.06%–11.4%) than those of the hanging wall. Additionally, the porosities of the outcrop samples of Izumi Group show quite low (0.97%–1.75%), corresponding to those of intact rocks of Izumi Group, whereas those of the intact rocks of Sanbagwa metamorphic rocks are estimated to be ca.2%–ca.3%. These porosities are measured for samples in the deep zone (ca.75–ca.200 m-depth) of the core, which are quite far from the fault plane. The porosities of the three zones of fault rocks in the hanging wall are 5.19%–15.27% for the fault breccia zone, 4.54–15.30% for the transition zone and 11.02–20.35% for the gouge zone. It should be noted that the porosities are corrected on the basis of CT values. As the fault rocks of Izumi Group are composed of matrix and clasts, we measured the porosities of both matrix and clasts (or blocks) for each sample. Then, we calculated the correction porosities based on the ratio of matrix and clasts of CT values.
The porosities in the hanging wall (Izumi Group) widely vary depending on characteristics of fault damage, however those gradually increase toward the fault plane. In addition, the porosities are quite higher than those of intact rocks. On the other hand, the high porosity zone in the foot wall (Sanbagawa metamorphic rocks) is limited in a narrow zone (37.45–ca.50 m-depth). These facts suggest that the hanging wall (Izumi Group) are strongly damaged compared to the foot wall (Sanbagawa metamorphic rocks). This is an intriguing characteristics for understanding petrophysical properties of fault rocks.

©2019. Japan Geoscience Union. All Right Reserved.

Keywords: Median Tectonic Line, porosity, fault rocks

©2019. Japan Geoscience Union. All Right Reserved.

Characteristics of inactive section of the Median Tectonic Line from drillcore samples in Shikoku, southwestern Japan

*Hideto Uchida[1], Michiharu Ikeda[1], Takeshi Tsuji[2], Kozo Onishi[3], Naoki Nishizaka[3]

1. Department of Civil Engineering, Shikoku Research Institute incorporated, 2. Department of Earth Resources Engineering, Kyusyu University, 3. Shikoku Electronic Power

The Median Tectonic Line (MTL) is a geological boundary fault that divides southwestern Japan into Inner and Outer zones. The MTL is generally considered to be a long-lived fault system from the middle Cretaceous, although the details of the movement history are complex. On the other hand, it has been revealed from geomorphological and paleo-seismological surveys that the MTL from Shikoku to western Kii Peninsula has caused right-lateral slip during Quaternary. Therefore, the part of the MTL is active, and called as the Median Tectonic Line active fault system (MTLAFS) (e.g., Ikeda et al.,2017). To estimate present seismic condition (or environment) of the MTLAFS, we should understand details of its paleo-activities. However, outcrops widely exposed for geological survey about paleo-activities inactive MTL are limited. In this study, we obtained a geological core sample (125 m-long) penetrating the MTL and conducted downhole logging in Saijyo city, Ehime prefecture.
We focused on three points as follows. Firstly, we observed and described the core samples in detail. Secondly, we obtained structural data from the geological core and a borehole image data in order to predict paleo-stress conditions. Finally, we estimated physical properties around a fracture zone of the MTL based on the geological and geophysical data.

[Description of fault rocks]
The fault plane of the MTL is at about 109.45 m-depth in the borehole. The hanging wall and footwall of the fault system are Izumi Group (mainly alternating beds of mud and sand) and Sanbagawa metamorphic rocks (mainly pelitic schist), respectively. Orientation of the fault plane of the MTL is NE-SW strike with moderate-angle northwest dipping in our study area, and its fault zone is approximately 4m-width. The fault zone is composed of fault gouge, fault breccia and cataclasite. The altered dikes that is Ishizuchi volcanic rocks erupted in c.a. 15 Ma distribute in the fault zone. The MTL in this region reactivated after 15 Ma, because the altered dikes are fragmentated in the fault zone.

[Structural analysis]
Orientations of bedding planes of Izumi Group and schistosity planes of Sanbagawa metamorphic rocks are generally N–S strike with low-angle east dipping and ENE–WSW strike with low-angle north dipping. The dikes intrude into the fault zone in orientation of NE–SW strike with moderate-angle northwest dipping. Orientations of fractures concentrate in N–S strike with east dipping and E–W strike with north dipping based on the borehole camera data.
Moreover, we conducted paleo-stress analysis based on fault orientations and slickenlines and slickensteps on the fault surfaces. We adopted Hough transform inverse method (Sato, 2006) to estimate paleo-stress conditions of the MTL. As the result, a stress condition around the MTL is dominantly normal-faulting stress-regime, however strike-slip and reverse-faulting stress-regimes are also recognized.

[Physical properties]
There is a remarkable trend of the elastic wave velocity data around the fracture zone. P-wave velocity *Vp* in fracture zone (95–109.5 m-depth) drastically decreases as compared with host rock in the upper zone due to intensive crack and lower elastic moduli. On the other hand, S-wave velocity *Vs* does not change in

©2019. Japan Geoscience Union. All Right Reserved.

the fracture zone such as the trend of *Vp*.

The paleo-stress condition data are useful information for inactiveness of the MTL. And the physical properties are also crucial to understand the physical conditions what the MTL in this region have experienced. Therefore, the information derived in this study could contribute to understand fault evolution processes and activities of the MTL.

Keywords: Median Tectonic Line, fault rocks, paleostress field, physical property

©2019. Japan Geoscience Union. All Right Reserved.

Surface and internal textures of clasts in incohesive fault rocks and their significance

*Tetsuhiro Togo[1], Toshihiko Shimamoto[2], Michiyo Sawai[3]

1. THE EARTH, 2. Institute of Geology, China Earthquake Administration, 3. Chiba Univ.

Fault rocks are classified based on the fraction of clasts (visible under naked eyes) and fine-grained matrix (e.g., Sibson, J. Geol. Soc. London). Studies on clasts are important at least for the following three purposes. First, clasts must have formed by fracturing of host rocks and/or old cohesive fault rocks during their formation and past movements, and hence clasts may provide us with old fault rocks and may yield information on deeper parts of fault zones. Second, clasts must have undergone series of physical and chemical intrafault processes and might give clues to recover some of those processes. Third, comparison of surface and internal textures of clasts with those of borehole cuttings may lead to identifying fault zones from the cuttings. Recovering all cores in drilling is very costly and the textural studies on fault-zone clasts may have many practical applications.

Kanaori and his coworkers conducted very detailed SEM (scanning electron microscope) observations on quartz or quartz-rich clasts in fault gouge, collected from more than ten mostly-active faults (e.g., Kanaori et al., 1980, Eng. Geol.). They demonstrated that characteristic surface textures, completely different from those of fresh fracture surfaces, developed on clasts primarily due to dissolution of surface materials. They pointed out that those textures were similar to the surface textures of quartz grains in sediments that had been reported in many publications (note that fault-zone clasts and clastic sediments were exposed to underground water in geological time scale). They classified the surface textures of quartz clasts into 8 types and 4 groups, and proposed a sequence of changes in surface textures with time. The primary target of the work by Kanaori and others was to make rough estimate of timing of fault motion from the surface textures. However, this was not easy and their pioneering work did not progress further.

Present work was motivated from the third purpose listed above. We have not followed the classifications of Kanaori et al, but rather we have intended to study surface and cross-sectional textures of clasts, using all clasts from all parts of fault zones, with broad perspectives. We have studied so far Nojima fault and Arima-Takatsuki Tectonic Line in Japan, and Yangsan fault and Yeongdeok fault in southeast Korea (all granitic fault zones). We have recognized surface textures similar to the orange peel-like and fish scale-like textures of Kanaori and others, but we have not yet confirmed all textures that they have classified. A broken clast from clayey fault gouge in Yeongdeok fault zone exhibits quite interesting internal texture with a broken mineral (probably feldspar) in the center, mantled by thick fine-grained and still-porous fault rock that is rich in phyllosilicates. The texture clearly demonstrates that the surface textures of this clast did not form simply by dissolution of surface material, and there is a possibility that reactions between the clast and matrix formed the fault rock surrounding the clast. If this is the case, such textures may record some physical and chemical processes in fault zones (useful for the second purpose listed above), and we plan to do more detailed work on such textures. Pulverized rock is reported in a wide granitic fault zone along the Arima-Takatsuki Tectonic Line (Mitchell et al., 2011, EPSL). Distinction between clasts and matrix is not always clear in this fault rock and we could observe many fractures in minerals under a SEM. Interestingly, many of those fractures exhibit dissolution textures similar to those of fault-zone clasts and clastic sediments, and old existing fractures in rocks can be distinguished from fresh new fractures from surface textures. All of those textures will be useful in identifying faults from borehole cuttings.

©2019. Japan Geoscience Union. All Right Reserved.

Keywords: fault gouge, fault breccia, drill cuttings

©2019. Japan Geoscience Union. All Right Reserved.

Fault Displacement Assessment of Surface-rupturing Earthquakes for Nuclear Installations and the use of Physics-based Rupture Models

*Luis Angel Dalguer[1], Yoshimitsu Fukushima[2]

1. 3Q-Lab GmbH, 2. International Atomic Energy Agency

Surface-rupturing faulting is usually expected from large earthquakes, but this phenomenon has been also observed sometimes in moderate earthquakes. The coseismic fault displacement (defined as the surface rupture offset or slip on the free-surface) associated to earthquakes can seriously compromise the safety of critical infra-structures located near faults, such as bridges, dams, railroads, pipelines, nuclear installations (NI) and nuclear waste repositories. The draft IAEA specific safety requirements (Site Evaluation for Nuclear Installations No.SSR-1, DS484) requires that the capability for surface faulting shall be assessed for the site of a NI. But current practices of fault displacement hazard assessments (FDHA) are in general very challenging and quite limited because recorded fault displacement data to develop empirical models are very sparse, as such, at present very few empirical models with large uncertainty are available for this purpose. IAEA has already recognised this issue and currently is making the effort to implement the physics-based rupture modelling in practice for FDHA. In general for seismic hazard assessments (SHA), the empirical and physics-based rupture models complement each other and all available efforts are encouraged for the nuclear safety. These efforts have been discussed through different international working group activities, being the most outstanding two international workshops on **Best** Practices in **P**hysics-based Fault Rupture Models for **S**eismic **H**azard **A**ssessment of **N**uclear **I**nstallations (BestPSHANI) in 2015 and 2018. Here we discuss the feasibility of the use of Physics-based rupture models for FDHA and presenting couple of examples of fault displacement prediction of past earthquakes.

Keywords: Fault displacement, Fault displacement hazard assessment, Dynamic rupture modeling, Earthquake physics

©2019. Japan Geoscience Union. All Right Reserved.

Dynamic rupture simulation for seismic hazard assessment: Application to the Futagawa and Hinagu fault zones (Part 2)

*Yuko Kase[1]

1. Geological Survey of Japan, AIST

For probabilistic seismic hazard assessment, evaluations of rupture area to estimate a magnitude for a scenario earthquake and frequency are needed. We propose to provide the basic information for the evaluations using dynamic rupture simulations. Kase et al. (2017) applied the dynamic rupture model for seismic hazard assessment to the Futagawa and Hinagu fault zones. They simulated dynamic rupture models based on information observed before the 2016 Kumamoto earthquake, and showed that the rupture processes initiated at the northeastern end of the Takano-Shirahata segment were consistent with the rupture process of the 2016 Kumamoto earthquake. In this study, we investigate the effect of variations in initial crack locations and the other source parameters on simulation results.
A fault geometry and tectonic stress fields are assumed in the same way as Kase et al. (2017). The Futagawa segment of the Futagawa fault zone and the Takano-Shirahata and Hinagu segments of the Hinagu fault zone are modeled as a continuous vertical right-lateral strike-slip fault plane about 75 km long with surface rupture, based on HERP (2013). Azimuths of the minimum principal stress and stress ratios are assumed, considering the stress inversion result of Matsumoto et al. (2015). We also assume that the principal stresses are proportional to depth, and that the intermediate principal stress is vertical and overburden load.
Two initial crack locations, the southwestern ends of the Futagawa and Takano-Shirahata segment, are assumed. We calculate dynamic rupture processes, using a finite-difference method (Kase and Day, 2006), to search the azimuth of the minimum principal stress and depth coefficient of stress drop consistent with observed right-lateral dislocation on each segment.
Among ruptures initiating at the southwestern end of the Futagawa segment, the ruptures propagating only on the Futagawa segment have right-lateral slips consistent with the observation. Among ruptures initiating at the southwestern end of the Takano-Shirahata segment, on the other hand, the ruptures propagating on the Takano-Shirahata and Futagawa segments have right-lateral slips consistent with the observation. These results agree with the cases initiating at the northeastern ends of both segments (Kase et al., 2017). Thus, the initial crack location does not affect the rupture propagation to the adjacent segments in the ruptures initiating on the Futagawa and Takano-Shirahata segments. In the ruptures initiating on the Hinagu segment, a rupture initiating at the southwestern end is easier to propagate to the Takano-Shirahata segment than that initiating at the northeastern end (AIST, 2018). The difference is caused by rupture directivity. The lengths of the Futagawa and Takano-Shirahata segments are less than 20 km, while the Hinagu segment is 40 km long. Thus, the difference of rupture propagation between the initial crack locations clearly appears in the Hinagu segment.
We also investigate the effect of variations in a critical displacement and a ratio of strength excess and stress drop on simulation results.

Acknowledgment: This research was funded by the project commissioning disaster prevention for nuclear facilities (consideration of uncertainty factors in probabilistic seismic hazard analysis) in FY2018 by Regulatory Standard and Research Department, Secretariat of Nuclear Regulation Authority.

Keywords: dynamic rupture model, seismic hazard assessment, Futagawa and Hinagu fault zone

©2019. Japan Geoscience Union. All Right Reserved.

©2019. Japan Geoscience Union. All Right Reserved.

Quantification of gaps between slip-length scaling law of earthquakes and stick-slip experiments.

*Shinichi Oba[1], Yuta Mitsui[2]

1. Graduate School of Science and Tecnology, Shizuoka University, 2. Faculty of Science, Shizuoka University

Scaling relations of natural earthquake (over km scales) have been well studied, but their extension to smaller scales is difficult because of limited observation resolution. This study focuses on experimental stick-slip data and compares them with a slip-length scaling law of natural earthquakes. There seem gaps between the extension of the earthquake scaling and the stick-slip experiments. Here we perform correlation and multivariate analyses to investigate effects of apparatus type, mass and stiffness on the gaps. We find that a characteristic time composed of the mass and the stiffness shows a strong correlation with the gaps against the natural scaling in case of direct shear apparatus.

Keywords: stick-slip, earthquake slip-length scaling

©2019. Japan Geoscience Union. All Right Reserved.

Effect of Wear Process on Earthquake Recurrence

*Jeen-Hwa Wang[1]

1. Academia Sinica

Earthquake recurrence is studied from the temporal variation in slip through numerical simulations based on the normalized form of equation of motion of a one-body spring-slider model with thermal-pressurized slip-weakening friction and viscosity. The wear process, whose effect is included in the friction law, is also taken into account in this study. The main parameters are the normalized characteristic displacement, U_c, of the friction law and the normalized damping coefficient (to represent viscosity), η. Define T_R, D, and t_D to be the recurrence time of events, the final slip of an event, and the duration time of an event, respectively. Simulation results show that T_R increases when U_c decreases or η increases; D and t_D decrease with increasing η; and t_D increases with U_c. The time- and slip-predictable model can describe the temporal variation in cumulative slip. When the wear process is considered, the thickness of slip zone, h which depends on the cumulated slip, $S(t)=\Sigma D(t)$, i.e., $h(t)=CS(t)$ (C=a dimensionless increasing rate of h with S) is an important parameter influencing T_R and D. U_c is a function of h and thus depends on cumulated slip, ΣU, with an increasing rate of C. In the computational time period, the wear process influences the recurrence of events and such an effect increases with C when C>0.0001. When viscosity is present, the effect due to wear process becomes stronger. Both T_R and D decrease when the fault becomes more mature, thus suggesting that it is more difficult to produce large earthquakes along a fault when it becomes more mature. Neither the time-predictable model nor the slip-predictable one can describe the temporal variation in cumulative slip of earthquakes under the wear process with large C.

Keywords: Earthquake, Recurrence, Slip, Friction, Viscosity, Wear

©2019. Japan Geoscience Union. All Right Reserved.

On the Mechanical Relation between Individual Interaction and Collective Behavior of Multiple Fault Sets Subjected to Quasi-Static Loading

*Koji Uenishi[1,2], Yuki Fukuda[2], Nobuki Kame[3]

1. Department of Advanced Energy, The University of Tokyo, 2. Department of Aeronautics and Astronautics, The University of Tokyo, 3. Earthquake Research Institute, The University of Tokyo

In order to deepen our essential understanding of the connection between the local and the global or collective mechanical behavior of sets of geological faults in the solid earth, we have been performing laboratory rupture experiments using two-dimensional rectangular, linear elastic solid specimens with preset parallel cracks that model multiple fault planes under quasi-static tensile (mode-I) or tensile with in-plane shearing (mixed mode) loading conditions (Uenishi et al., SSJ Fall Meeting, 2017, 2018). Our special attention has been paid to the identification of when and how ruptures develop on each individual fault plane and interact with one another, and how the interaction influences the global nature of the solid. For that purpose, we have observed the local evolution of the isochromatic fringe patterns, i.e. the contours of the maximum in-plane shear stress, around the modeled fault planes in the photoelastic polycarbonate specimens with a high-speed digital video camera. At the same time, we have measured the global stress-strain relation utilizing a tensile testing machine that externally exerts a prescribed constant displacement rate to the specimen, and have compared its time history with the local observations of the isochromatic fringe patterns. Although the externally applied displacement or strain rate has been still in a relatively low, quasi-static range, the comparison may imply the effect of the local rupture development on the global properties of the solid specimen, and we have found that local rupture may not always propagate unidirectionally in the prepared specimens and ruptures may run into each other even on a single fault plane under very simple external loading conditions. We are now trying to investigate the mechanical characteristics of multiple fault sets that are subjected to more dynamic, impact loads and identify difference in the local-global relation, if any, between the dynamically-controlled and quasi-statically governed ruptures.

Keywords: fault rupture, fault stability, strain rate

©2019. Japan Geoscience Union. All Right Reserved.

Inelastic deformation in a region of the transient and forced extensional horizontal crustal strain

*Takao Eguchi, Yasuyuki Iwase[1]

1. National Defense Academy, Japan

Just after the focal rebound displacement by the 2011 Off-Tohoku Earthquake *(M~9)*, forced horizontal extension was confirmed in the Japanese archipelago. For example, from Miyagi to Yamagata prefectures on the overriding lithosphere, it was approximately stretching in the E-W direction.
We here investigate the "*transient inelastic deformation process*" in the adjacent island-arc environment immediately after such horizontally forced arc-extension.
For simplicity, let us assume that the main origin of inelastic island-arc deformation is not due to biaxial extension but due to transient elongation in a specific direction.
Since the island-arc is not necessarily an isotropic homogeneous elastic body, the mode of inelastic deformation depends on geometrical characteristics such as zonal contrast in elastic constants at pre-existing material block boundaries and/or at active faults within the island-arc.
We discuss the stress-strain relationship in the island-arc as an inelastic deformable body in the environment after the above-mentioned unidirectional elongation.
The response to the stress change in the subsequent environment becomes a nonlinear phenomenon that is transiently time-space dependent at least, and it will be different from the case of the linear elastic body.
In particular, even a small subsequent stress change will result in greater strain than in the case of linear elastics.
In this study, incorporating rheology such as thixotropy, we present some hypothetic models on the inelastic deformation of the island-arc system with the geometric distributed blocks, etc.

Keywords: inelastic deformation, island-arc system just after a greater interplate earthquake, block deformation, thixotropy

©2019. Japan Geoscience Union. All Right Reserved.

Representation Theorem and Green's Function (3) -- Strain, Stress, and Density Perturbation Fields due to a Point Source Using 2nd Derivative of Green's Function in an Unbounded Homogeneous Isotropic Elastic Medium --

*Masaya Kimura[1], Nobuki Kame[1]

1. Earthquake Research Institute,The University of Tokyo

Here we derive the second spatial derivative of Green's fuction in an unbounded homogeneous isotropic elastic medium. Following this formula, we obtain the expressions for strain, stress, and density perturbation fields due to a point source described by a moment tensor or a single force. These fomulae are useful for theoretical modeling of the prompt detection of earthquake occurrences by means of piezoelectricity, piezomagneticity, and transient gravity perturbations. We propose two applications of the formulae: (1) volumetric moment tensor mass redistribution and (2) dynamically induced quadratic earthquake mass redistribution. Regarding the latter application, we show the relationship between the moment magnitude M_w of an earthquake and dynamically induced quadratic earthquake mass redistribution (Table 1).

Table 1. The relationship between M_w of an earthquake and dynamically induced quadratic earthquake mass redistribution.

Reference: M. Kimura and N. Kame, 2018, Representation Theorem and Green's Function (3) -- Strain, Stress, and Density Perturbation Fields due to a Point Source Using 2nd Derivative of Green's Function in an Unbounded Homogeneous Isotropic Elastic Medium --, Zisin 2, 71, 153-160, doi:10.4294/zisin.2017-20

Keywords: Green's Function

©2019. Japan Geoscience Union. All Right Reserved.

M_w	$\delta m^{DQM}(M_w) = 10^{1.5M_w+1}[\mathrm{kg}]$
1.0	$10^{2.5} \sim 3 \times 10^2$
2.0	$10^{4.0} \sim 1 \times 10^4$
3.0	$10^{5.5} \sim 3 \times 10^5$
4.0	$10^{7.0} \sim 1 \times 10^7$
5.0	$10^{8.5} \sim 3 \times 10^8$
6.0	$10^{10.0} \sim 1 \times 10^{10}$
7.0	$10^{11.5} \sim 3 \times 10^{11}$
8.0	$10^{13.0} \sim 1 \times 10^{13}$
9.0	$10^{14.5} \sim 3 \times 10^{14}$

©2019. Japan Geoscience Union. All Right Reserved.

Development of a method of visualization of abrupt changes in slip-rate and rupture velocity toward better understanding of high-frequency radiation on a fault.

*Takahiro ayukai[1], Yuji Yagi[2], Ryo Okuwaki[3], Keita Kayano[3], Kousuke Shimizu[3]

1. School of Life and Environmental Sciences, University of Tsukuba, 2. Graduate School of Life and Environmental Sciences, University of Tsukuba, Tsukuba, 3. Graduate School of Life and Environmental Sciences, University of Tsukuba

High-frequency waves are thought to be generated by abrupt changes of slip-rate or rupture velocity on a fault during an earthquake rupture based on theoretical studies (e.g. Spudich and Frazer, 1984, BSSA). Finite-fault inversion of seismic waveforms is a tool to estimate spatiotemporal distribution of slip-rate function. Slip-rate function is composed of some basis functions at each subfault which an assumed fault is divided into in a reticular pattern. Back Projection (BP) (Ishii et al., 2005, Nature) and Hybrid BP (HBP) (Yagi et al., 2012, EPSL) methods are techniques for tracking high-frequency radiation sources and have been used to discuss the detailed source process by comparison with slip distribution resolved by waveform inversion. However, the physical meaning of the BP/HBP images is ambiguous, and the quantitative evaluation of the high-frequency radiation has been difficult solely by the BP/HBP methods. In order to reveal what rupture behavior generates high-frequency radiation, we proposed a method to image acceleration and deceleration of slip and rupture from spatiotemporal distribution of slip-rate function resolved by waveform inversion. We derived a representative slip-rate as a maximum value of slip-rate function and a representative rupture time at each sub-fault, and then calculated spatial gradients of the slip-rates and the rupture time to derive acceleration and deceleration of slip and rupture front, respectively. We used the slip-rate function which was obtained by the waveform inversion introducing uncertainty of Green’ s function (Yagi and Fukahata, 2011, GJI), where the high-frequency components of observed waveform were well reproduced compared to the conventional scheme because the waveform inversion can get a slip-rate functions which have a number of basis functions. We applied the developed method to the slip-rate functions of the M_W 7.9 2015 Gorkha, Nepal and the M_W 8.8 2010 Maule, Chile, earthquakes, which were presented in Yagi & Okuwaki (2015, GRL) and Pulido et al. (2011, EPS), respectively. For both the two earthquakes, the results showed that the rapid acceleration of slip was found at the edge of the large slip area facing to the hypocenter, while rapid deceleration of slip was found at the edge across the large slip area. The results also showed that the rapid deceleration of rupture was observed just before the rupture front penetrates into and escaped out of the large slip area. The estimated areas of rapid acceleration and deceleration are consistent with the spatial distribution of intense high-frequency radiation sources tracked by HBP methods (Yagi & Okuwaki, 2015, GRL; Okuwaki et al., 2014, Sci. Rep.). Our developed method well distinguished the behavior of slip evolution related to the generation of high-frequency waves, that is, spatiotemplrally separated slip and rupture front acceleration/deceleration, which has not been evaluated by the BP/HBP methods alone.

Keywords: High frequency, Waveform inversion, Slip rate, Rupture velocity, 2015 Gorkha, Nepal, earthquake, 2010 Maule, Chile, earthquake

©2019. Japan Geoscience Union. All Right Reserved.

Issues in earthquake-source-inversion analysis, evaluated through singular value decomposition

*Keita Kayano[1], Yuji Yagi[1], Ryo Okuwaki[1], Kousuke Shimizu[1]

1. Tsukuba University

Toward solving an inverse problem in Geophysics (e.g., earthquake-source inversion), prior information is used for stabilizing the solution, and an optimal weight between the observed data and prior information is objectively determined by minimizing Akaike's Bayesian Information Criterion (ABIC; Akaike, 1980). However, individual role of observed data and prior information on the resultant solution has not been evaluated in ABIC-based inversion, which makes it difficult to evaluate how much the prior information and its strength are valid in the solution, even though its weight is determined statistically by minimizing ABIC.

Here we resolved each characteristic of the observed data and the prior information that constrains the resultant image by applying singular value decomposition to a kernel of an inverted-source model of the Mw 7.0, 2016 Kumamoto, Japan, earthquake. The source model is represented as five-basis moment tensors (Kikuchi & Kanamori, 1991) distributed at 0.3-sec time and 2-km space intervals in the model space, which can simultaneously model slip evolution and fault geometry (Shimizu et al., 2019, under review). We used models with different weight: one with the weight minimizing ABIC, and the others with the weight artificially weakened and strengthened compared to the ABIC minimum. As prior information, we tested two types of condition: smoothing and L2-norm minimization.

Under the condition of smoothing, the model showed north side uplifting and reverse faulting at the weight stronger and weaker than the one minimizing ABIC, respectively, which is not consistent with the aftershock distribution and field observations (e.g., Yoshida et al., 2016; Shirahama et al., 2016). We found that the specific moment-tensor components, where the amplitudes of Green's function are larger, determining the characteristic of the singular vectors. It is suggested that if the weight of the prior information is stronger and weaker than the one minimizing ABIC, observed-data kernel (corresponding to Green's function) and smoothing-information kernel heavily controls the model characteristics, respectively. Under the condition of the L2 norm, the model showed north side uplifting, which is not evidenced by the aftershock distribution and the field surveys, even though we used ABIC for determining the "optimal" weight of the prior information. We found that the specific moment-tensor components, where the amplitudes of Green's function are larger, determining the characteristic of the singular vectors as is the case under the condition of smoothing. However, regardless of the weight of prior information, Green's function heavily controls the model characteristics.

Our study highlights that, under the condition of smoothing, the ABIC-based inversion works successfully for suppressing bias that violates the final solution generated by kernels of observed data and prior information. We also clarify that the L2-norm-minimization condition does not work properly for constraining source process of the 2016 Kumamoto earthquake.

Keywords: singular value decomposition, prior information, smoothing, L2 norm minimization, Green’s function, Akaike's Bayesian Information Criterion

©2019. Japan Geoscience Union. All Right Reserved.

Source process of recent M6-class inland earthquakes in Japan

*Ritsuya Shibata[1], Naofumi Aso[1], Junichi Nakajima[1], Satoshi Ide[2]

1. Department of Earth and Planetary Sciences, Tokyo Institute of Technology, 2. Department of Earth and Planetary Science, University of Tokyo

In recent years, inland earthquakes frequently occur in Japan including the 2016 Kumamoto earthquake (Mw7.0). Among them, M6-class events are the best targets to study the mechanics of two-dimensional rupture propagation, since smaller events are more difficult to study finite slip distribution while rupture area of larger events tend to be restricted in depth. For this purpose, we investigate the source process of the 2016 Central Tottori earthquake (Mw6.2) and the 2018 Hokkaido Eastern Iburi earthquake (Mw6.6), which are characterized by strike-slip and reverse-fault types, respectively, by applying slip inversion to strong-motion seismograms.

We use KiK-net stations deployed and maintained by NIED (National Research Institute for Earth Science and Disaster Resilience) within 50 km from the epicenter for both earthquakes. Fault geometry is assumed to be same as Kubo et al. (2017) for the 2016 Central Tottori earthquake, while we assume the fault geometry of the 2018 Hokkaido Eastern Iburi earthquake from the aftershock distribution. Fault discretization, source duration, source time discretization, and band-pass filters are optimized manually for each event.

Regarding 2016 Central Tottori earthquake, there has been discrepancies between previous studies. While Kubo et al. (2017) reported the slip of 0.3–0.6 m widely distributed over 5×8 km^2, Ross et al. (2018) estimated concentrated slip of >4 m in 3×3 km^2. Recently, Meneses-Gutierrez et al. (2019) obtained the slip of 1–2 m over 5×5 km^2 by analyzing GNSS (Global Navigation Satellite System) data. Our results mainly agree with Kubo et al. (2017), but larger slip is distributed more heterogeneously in our model because we do not apply smoothing. The concentration of slip near the hypocenter as reported by Ross et al. (2018) is also confirmed especially when we use finer model resolution. Therefore, the discrepancy reported in the previous studies may be due to the resolvability of slip with strong directivity in ordinary finite fault inversion, which usually requires sparse discretization and/or a smoothing constraint.

As a result of slip distribution of the 2018 Hokkaido Eastern Iburi earthquake, we obtained the slip in between right-lateral strike-slip type and reverse-fault types at the beginning, which is consistent with the mechanism determined by JMA (Japan Meteorological Agency) using first-motion polarities, while total slip is predominated by the reverse-fault component, which is consistent with the CMT (centroid moment tensor) solution determined by NIED using surface wave amplitudes. The final slip is separated in the shallow part and the deep part, similar to the distribution of aftershocks.

In both earthquakes, the rupture tends to expand in the direction parallel to the slip regardless of the rake direction. The prevailing mode II rupture over mode III rupture is consistent with the expectation from rupture mechanics (e.g., Day, 1982; Madariaga et al., 1998).

Keywords: 2016 Central Tottori earthquake, 2018 Hokkaido Eastern Iburi earthquake, inland earthquake

©2019. Japan Geoscience Union. All Right Reserved.

Expected slip direction on assumed fault planes of large earthquakes inferred from stress field after the 2016 Kumamoto earthquake sequence, in central Kyushu, Japan

*Ayaho Mitsuoka[1], Satoshi Matsumoto[2], Azusa Shito[2], Hiroshi Shimizu[2], Group for urgent joint seismic observation of the 2016 Kumamoto earthquake

1. Department of Earth and Planetary Sciences, Graduate School of Science, Kyushu University, 2. Institute of Seismology and Volcanology, Faculty of Sciences, Kyushu University

In order to understand generation of earthquake, knowing the force acting on a fault plane is the great interest problem for us. We should find with which direction and magnitude a fault plane slips. Shear and normal stresses on a fault plane can be estimated from the stress field around a fault. Maximum shear stress direction on a fault plane constrains the slip direction of an earthquake on the fault based on Wallace-Bott hypothesis. In this study, we estimated the maximum shear stress directions on some fault planes from the stress field at hypocentral area of the 2016 Kumamoto earthquake sequence.
The 2016 Kumamoto earthquake sequence occurred at Hinagu and Futagawa fault zones in Kumamoto prefecture, central Kyushu Island, Japan. The area was high seismicity area before the sequence. The largest foreshock with Mj 6.5 (Mj: magnitude by Japan Metrological Agency) on April 14, 2016 was located in Hingau fault zone. The mainshock (Mj 7.3) occurred on April 16, 2016. Many earthquakes occurred around these faults after the mainshock and continue until now. Some fault planes are determined from the aftershock hypocenter distribution.
Maximum shear stress direction on a fault is a projection of a traction vector that is calculated from the fault geometry and the stress field. In other word, we can consider slip direction on a fault from stress tensor and fault geometry. In the hypocentral area of the 2016 Kumamoto Earthquake sequence, evaluation of strong ground motion is important to mitigate damage of further coming earthquake. Slip direction is one of the key for the evaluation. Here, we showed expected slip direction on fault plane proposed by Iwata et al. [2019] from their geometry and the stress field estimated by Mitsuoka et al. [2019] using the seismic moment tensors.Most of the expected slip direction on the assumed faults reveal either simple strike slip or normal fault types. However the maximum shear stress directions on some faults change to have large upward component at shallow depth. The result suggests complicated slip could occur on the candidate faults in a case of large earthquake faulting.

Keywords: stress field, shear stress, 2016 Kumamoto earthquake

©2019. Japan Geoscience Union. All Right Reserved.

Spaciotemporal change of source parameters of repeaters due to the 2011 Tohoku-Oki earthquake

*Kazuya Tateiwa[1], Tomomi Okada[1], Toshio Kono[1], Naoki Uchida[1]

1. Research Center for Prediction of Earthquakes and Volcanic Eruptions, Graduate School of Science, Tohoku University

A number of small to moderate repeating earthquakes occur at the upper boundary of subducting Pacific plate in NE Japan. Understanding the source characteristics of repeating earthquakes and their spaciotemporal changes give us insight about the loading rate and its variation due to the plate motion and physical mechanisms of earthquakes, which can be common with major earthquakes because they would have the same occurrence structure as the small repeaters. In this study, we investigated the spatiotemporal change of source parameters of repeating earthquakes occurred on the Pacific interplate before and after the 2011 Tohoku-Oki earthquake. We analyzed seismic waveforms from about 3,000 repeating earthquake groups and about 7,000 repeating earthquakes in total. In this study, we show the results obtained by analysis of repeaters located off-Kamaishi and near Iwaizumi, Iwate, NE Japan.
In off-Kamaishi, repeaters are observed in a very constant recurrence cycle (~5.5 yr) and magnitude (~4.9) before the Tohoku-Oki earthquake, however, the recurrence interval was extremely shortened and the size of the earthquake was substantially enlarged immediately after the Tohoku-Oki earthquake. The recurrence interval and magnitude are becoming close to those of before the Tohoku-Oki earthquake with time. Although stress drop calculated with spectral ratio method is about 14 MPa before the Tohoku-Oki earthquake, it is estimated that stress drop after the Tohoku-Oki earthquake became smaller than before to have roughly a constant value (~2 MPa). The radius of ruptured fault estimated from corner frequency become about 5 times larger just after the Tohoku-Oki earthquake and later it became about 1 km. The radius of rupture fault of post-Tohoku events is becoming close to that of pre-Tohoku event with time. These results agree with Uchida et al. (2015) that estimated the rupture area of off-Kamaishi sequence by slip inversion. We consider that these changes of source parameters before and after the Tohoku-Oki earthquake are caused by its afterslip.
On the other hand, the repeating earthquake sequences in Iwaizumi does not have obvious changes in magnitude and stress drop before and after the Tohoku-Oki earthquake. If this region was less affected by afterslip than off-Kamaishi, small aftership might make the difference from the results of off-Kamaishi. We found the directivity estimated from corner frequency is observed only for repeaters of M<4, which indicates these small repeating earthquakes are composed of complex rupture. As it was suggested that repeaters of Iwaizumi sometimes rupture multiple patches in previous study (Arao et al., 2007), such complexities in rupture and the interaction between small ruptures would affect the recurrence of repeaters.

©2019. Japan Geoscience Union. All Right Reserved.

Slip distributions and relation of slip-rate and shear stress for the Boso slow slip events

*Takuma Kobayashi[1], Toshinori Sato[2]

1. Graduate School of Science and Engineering, Chiba University, 2. Graduate School of Science, Chiba University

Slow slip events (SSEs), which radiate no seismic waves, were detected 6 times off the Boso Peninsula since the GNSS observation in Japan started in 1996. This presentation shows slip distributions and stress changes of 6 SSEs, and discusses frictional properties on the plate boundary where the SSEs occur.

We used the daily F3 coordinate values of GNSS stations from the Geospatial Information Authority of Japan. The GNSS data were fitted with a time series model that takes account of the linear trend and seasonal variations in the data, and then the fitted data were smoothed. We made every 3 days transient movements from the smoothed data. From the 3 days data, we estimated slip distributions using ABIC inversion method. We calculated stress changes from the slip distributions using Coulomb 3.3.

The results show that the amount and location of the slip distributions differ each events. Maximum amount of slips is about 7 cm for 1996 and 2014 events, and 14-20 cm for the other events (2002, 2007, 2011, 2018). 1996 and 2014 events slipped at a location during the event. The other events, on the other hand, moved southward during the event. Shear stress changes were about 0.1-0.3 MPa at main slip areas. From graphs of logarithm of slip rate and the stress change, we can see starting phase, stable phase, and stopping phase for the SSEs. Slopes of the stable phase increase with depth.

The slopes of the stable phase represent (a-b)* σn, where σn is normal stress, from an equation of steady state friction for rate and state dependent friction low. Since the SSEs are quasi stable slip, the shear stress changes estimated from slip distributions may equal to frictional stress changes. Using also results of quasi stable slip simulation, we can estimate (a-b) and effective normal stresses from the slope of the stable phase for the SSEs. Assuming (a-b)=-0.003, the effective normal stresses are estimated about 2-20 MPa. These values are much smaller than lithostatic stresses at the depth. This indicates a possibility of very high pore pressure on the plate boundary.

Acknowledgements: We used the daily F3 coordinate values by GSI, and Coulomb 3.3 program by USGS.

Keywords: slow slip, slip rate, stress change, effective normal stress, rate and state dependent friction low

©2019. Japan Geoscience Union. All Right Reserved.

Repeating inland earthquakes in northern Ibaraki Prefecture activated after the 2011 Tohoku-Oki earthquake

Ryo Takahashi[1], *Keisuke Yoshida[1], Akira Hasegawa[1], Toru Matsuzawa[1]

1. Tohoku University

The 2016 M6.3 earthquake in northern Ibaraki Prefecture is estimated to have reruptured the same portion of the fault already ruptured in 2011 by an M6.1 earthquake (Fukushima et al., 2018) in 2011. Since repeated slips with such a short interval are rare in inland area far from the plate boundary, it provides a unique opportunity to investigate the earthquake cycle. In this presentation, we introduce our ongoing study about the generation processes of the 2011 and 2016 M6 earthquakes in northern Ibaraki Prefecture.

We start by relocating hypocenters using precise differential arrival time obtained by the waveform cross-correlation. The target is 13,410 earthquakes with M>2 listed in the JMA unified catalog for the period from Apr. 2003 to Oct. 31, 2018 in the M6.3 and M6.1 earthquake sequences near the Ibaraki-Fukushima border. We applied the double-difference hypocenter relocation method (Waldhauser & Ellsworth, 2002) to the differential arrival times of P- and S-wave based on a similar procedure to that by Yoshida & Hasegawa (2018).

Although the distribution of relocated hypocenters shows some complicated features, there is one dominant planar structure with west-dipping in northern Ibaraki prefecture. Comparison with the focal mechanisms supports that this planar structure corresponds to the fault plane of the 2011 and the 2016 M6 earthquakes. A planar structure of hypocenter did not newly appear after the 2016 earthquake; their aftershocks are concentrated on the existing planar structure. This supports that the 2011 and 2016 M6 earthquakes ruptured the same fault as pointed out by Fukushima et al. (2018).

The existence of repeating M6 earthquakes suggests that there are other smaller-magnitude repeating earthquake sequences along the plane. Based on the precise hypocenter locations and the waveform similarity, we detected many small repeating earthquakes (M>2) along the plane, which surround the large coseismic slip area of the M6 earthquakes. These small repeating earthquakes are estimated to be caused by the afterslip of the 2011 and 2016 M6 earthquakes. According to the empirical relationship between seismic moment and slip amount (Nadeau & Johnson, 1998), the slip amount is roughly estimated to be a few tens centimeter, which is comparable to the slip amounts of the two mainshocks. Moreover, the slip amount after the 2011 earthquake is larger than that after the 2016 earthquake, which is consistent with Fukushima et al. (2018). These suggest the importance of the effects of afterslip for the aftershock occurrence and the earthquake cycle.

Keywords: repeating earthquake, afterslip, the 2011 Tohoku-Oki earthquake

©2019. Japan Geoscience Union. All Right Reserved.

[J] Oral | S (Solid Earth Sciences)：S-SS Seismology

Wed. May 29, 2019 9:00 AM - 10:30 AM JST | Wed. May 29, 2019 12:00 AM - 1:30 AM UTC | A02 TOKYO BAY MAKUHARI HALL

[S-SS15] Active faults and paleoseismology

convener:Mamoru Koarai(Earth Science course, College of Science, Ibaraki University), Takashi OGAMI(National Institute of Advanced Industrial Science and Technology), Ryosuke Doke(Hot Springs Research Institute of Kanagawa Prefecture), Hisao Kondo(Geological Survey of Japan, National Institute of Advanced Industrial Science and Technology), Chairperson:Takashi Azuma(AIST), Mamoru KOARAI(Ibaraki University)

Geologic and historic information on seismic cycles and on the magnitude and source faults of past earthquakes is essential information to understand future large earthquakes. The study of past faulting and seismicity is an important issue for an interdisciplinary community of seismologists, geologists, geomorphologists, archaeologists, and historians.

9:00 AM - 9:15 AM JST | 12:00 AM - 12:15 AM UTC

Introduction

9:15 AM - 9:30 AM JST | 12:15 AM - 12:30 AM UTC

[SSS15-05] Paleoseismological survey on the Shibetsu fault zone in the eastern part of Hokkaido, Japan

*Takashi Azuma[1], Daisuke Hirouchi[2], Koji Okumura[3], Kaoru Taniguchi[4], Masashi Omata[4], Yorihide Kohriya[4] (1.National Institute of Advanced Industrial Science and Technology, 2.Shinshu University, 3.Hiroshima University, 4.Pasco CORPORATION)

9:30 AM - 9:45 AM JST | 12:30 AM - 12:45 AM UTC

[SSS15-06] Deformation of marine terrace surfaces associated with active Rokkasho fault in southern Shimokita peninsula, northern Japan

*Mitsuhisa Watanabe[1] (1.Faculty of Sociology, Toyo University)

9:45 AM - 10:00 AM JST | 12:45 AM - 1:00 AM UTC

[SSS15-07] **Vertical crustal movement during the past 600 years in the Kikai Island, deduced from the height distribution and ages of coral microatolls**

*Masanobu Shishikura[1], Hideaki Maemoku[2], Tomoo Echigo[3], Yuichi Namegaya[1], Tatsuya Ishiyama[4], Ryo Kinjo[2], Naoto Inoue[3] (1.Institute of Earthquake and Volcano Geology, National Institute of Advanced Industrial Science and Technology, 2.Hosei University, 3.Geo-Reserch Institute, 4.Earthquake Research Institute, University of Tokyo)

10:00 AM - 10:15 AM JST | 1:00 AM - 1:15 AM UTC

[SSS15-08] Variation of coseismic fault displacements on multiple seismic cycles at a site: An example from the Kamishiro fault, Itoigawa-Shizuoka Tectonic Line active fault system, central Japan

*Naoya Takahashi[1], Shinji Toda[2] (1.Graduate school of Science, Department of Earth Science, Tohoku University, 2.International Research Institute of Disaster Science, Tohoku University)

10:15 AM - 10:30 AM JST | 1:15 AM - 1:30 AM UTC

[SSS15-09] High-resolution shear-wave seismic reflection surveys across the Kamishiro fault, Itoigawa-Shizuoka Tectonic Line active fault system, central Japan

*Naoki IKEGUCHI[1], Nobuhisa Matsuta[2], Kyoko Kagohara[3], Shinsuke Okada[4], Daisuke Hirouchi[5], Tatsuya Ishiyama[1], Katsuya Noda[6], Hiroshi Sato[1] (1.Earthquake Resarch Institute University of Tokyo, 2.Graduate School of Education, Okayama University, 3.Faculty of Education, Yamaguchi University, 4.Graduate school of Science, Tohoku University, 5.Faculty of Education, Shinshu University, 6.GEOSYS Inc.)

Paleoseismological survey on the Shibetsu fault zone in the eastern part of Hokkaido, Japan

*Takashi Azuma[1], Daisuke Hirouchi[2], Koji Okumura[3], Kaoru Taniguchi[4], Masashi Omata[4], Yorihide Kohriya[4]

1. National Institute of Advanced Industrial Science and Technology, 2. Shinshu University, 3. Hiroshima University, 4. Pasco CORPORATION

We conducted a paleoseimological survey on the Shibetsu fault zone in the eastern part of Hokkaido in 2018.
This fault zone has a length more than 52 km but no data was obtained about slip-rate and history of fault activeity in previous study (Hokkaido, 2004 and 2005). On a detailed topographic map with an air-borne LiDAR data, we found a new fault scarp with height of 2-5 m on fan produced the lastglacial age at Kotanuka site, and excurvated a trench (25 m in length, 8 m in width, 4 m in depth) and 4 drilling surveys (5 m in depth). We observed a high-angle fault cutting a tephra layer (Ma-l: ca.12,000 yrBP) and black soil with 40 cm on the trench wall. Based on drilling survey, the fan gravel layers, which covered with sandy sediment containing humic silt with 14C ages of 22,140-21,690 cal.BC and 20,587-20,343 cal.BC, is offset ca.3 m in vertical. We discuss the fault event and slip-rate of this fault with careful, because there are deformation of strata not only faulting but also periglacial process in the trench walls.

Keywords: active fault, paleoseismology, trenching survey, tephrochronology, the Shibetsu fault zone, Hokkaido

©2019. Japan Geoscience Union. All Right Reserved.

Deformation of marine terrace surfaces associated with active Rokkasho fault in southern Shimokita peninsula, northern Japan

*Mitsuhisa Watanabe[1]

1. Faculty of Sociology, Toyo University

The marine terrace surfaces formed in MIS 5e and MIS 5c have successively deformed, resulting in a 1 km wide flexural scarp tilting to the east. These surfaces dipping to the same direction converged upon in the scarp. The flexure is consistent with the prevailing Neogene structure. Some bedding reverse faults are observed, which indicates that the structure is an active one. The marine terrace surfaces and the Tertiary system have been folded convincingly owing to the activity of west-dipping blind active thrust (the active Rokkasho fault), merging into the extensive submarine fault along shelf edge in the north.

Keywords: marine terrace, flexural scarp, bedding reverse fault, active fault

©2019. Japan Geoscience Union. All Right Reserved.

Vertical crustal movement during the past 600 years in the Kikai Island, deduced from the height distribution and ages of coral microatolls

*Masanobu Shishikura[1], Hideaki Maemoku[2], Tomoo Echigo[3], Yuichi Namegaya[1], Tatsuya Ishiyama[4], Ryo Kinjo[2], Naoto Inoue[3]

1. Institute of Earthquake and Volcano Geology, National Institute of Advanced Industrial Science and Technology, 2. Hosei University, 3. Geo-Reserch Institute, 4. Earthquake Research Institute, University of Tokyo

The Kikai Island is known as a tectonically active region due to the MIS 5e coral terrace reaching over 200 m in altitude. Holocene marine terraces divided into four levels suggest that 1-2 m of uplift has intermittently occurred every 1500-2000 years (Sugihara et al., 2003). However, recently simulation results propose that the main factor of terrace formation is a combination of steady uplift and erosive action triggered by relatively small coseismic uplift (Shikakura, 2014). According to the geodetic observation, GNSS data shows uplifting at about 2 mm/year, but it is contradictory that the leveling survey results (comparison between Sep. 1997 and Apr. 2014) indicate subsiding at approximately 1 mm/year (Ito et al., 2015).

As described above, there are various views and observation results on the crustal vertical movement pattern of the Kikai Island. Therefore, we focused on coral microatoll which is a natural tide gauge and reconstructed the long-term crustal vertical deformation based on its distribution and age.

Since the microatoll formed by *Polites sp.*, grows on the basis of the low tide level, and records sea level change annually, it is good paleoshoreline indicator to reconstruct past crustal vertical deformation. We found a total of 25 living microatolls at three areas in the northern part, eastern part and southern part of the Kikai Island and one emerged microatoll. We obtained detailed cross-sections of five living micro-atolls and sliced samples of emerged microatoll to take a CT-scan image, and also obtained some samples for 14C age which were calibrated of marine reservoir effect based on data of Hirabayashi et al. (2017).

In the northern area (Onozu), the height of the top surface of all living microatolls was almost flat at -1.01 - 1.07 m (TP), and the maximum was 78.8 cm in radius. Emerged microatoll found in this area is 270 cm in radius. Its shape of the top surface is almost flat but the altitude is decreasing gently from the center (-0.80 m TP) to the edge (-0.87 m TP) and is 20 cm higher than the living microatolls. From the CT scan image, 237 lines of annual band can be counted in the range of 260 cm showing clearly growing in the horizontal direction. Therefore, the mean horizontal growth rate is estimated to 1.1 cm/year. It is consistent with 14C age data which shows AD 1305-1425 in the center and AD 1489-1650 in the margin. Based on the growth rate obtained from analysis of emerged microatoll, the age of growth of the living microatoll in this region can be estimated to about 72 years ago.

The largest one of the living microatolls confirmed in the eastern area (Kadon) has a radius of 145.6 cm and can be estimated to about 132 years ago, which is no contradiction to the 14C age of the center (AD 1680-1880). The shape of the top surface is roughly horizontal throughout the growth period, but the altitude is slightly uneven between -1.06 m (TP) and -1.20 m (TP).

©2019. Japan Geoscience Union. All Right Reserved.

Based on the above results, the relative sea level change of the Kikai Island slowly decreased by 7 + α cm within 300 years from the 14th to the 17th century, and rapidly fall by 20 - α cm at the 17th century or in the period until the 19th century. Also, since at least 137 years ago, the sea level is almost stable while fluctuating about 10 cm at the maximum. Although it is difficult to distinguish the crustal deformation and the eustatic sea level change, if it is regarded that all of the change was the tectonic influence, it can be denied the steady uplift at a constant rate for the past 600 years. The rapid sea level fall during the 17th century or until the 19th century may have been an intermittent coseismic uplift.

Keywords: Kikai Island, earthquake, crustal movement, sea level change, coral microatoll

©2019. Japan Geoscience Union. All Right Reserved.

Variation of coseismic fault displacements on multiple seismic cycles at a site: An example from the Kamishiro fault, Itoigawa-Shizuoka Tectonic Line active fault system, central Japan

*Naoya Takahashi[1], Shinji Toda[2]

1. Graduate school of Science, Department of Earth Science, Tohoku University, 2. International Research Institute of Disaster Science, Tohoku University

Predicting coseismic fault slip at a site on an active fault is crucial from the view point of fault displacement hazard assessment. The characteristic earthquake model, where an amount of coseismic slip at a point on a fault is roughly consistent through seismic cycles (Schwartz & Coppersmith, 1984), has been widely accepted and applied for hazard assessment. However, recent paleoseismic studies, high-resolution topographic data and quantitative more precise dating techniques have revealed that many faults do not repeat persistently their characteristic displacements (e.g., Zielke, 2018).To further discuss this issue, however, more case studies in particular on a dip-slip fault are required.
We estimated co-seismic slips of paleo-earthquakes at Oide site (36.7˚N, 137.87˚E) on the Kamishiro fault and evaluated variability in co-seismic slips through seismic cycles. The Kamishiro fault is a reverse fault which is located at the northernmost part of the Itoigawa-Shizuoka Tectonic Line active fault system in Japan. Advantages of this fault are that the co-seismic slip distribution of the most recent event, the 2014 Nagano-ken-hokubu earthquake (Mw 6.2), is precisely measured by field observation and differential LiDAR analysis, and that there is a flight of displaced terraces that record slips of recent earthquakes. Several paleoseismic studies share the evidence for the penultimate and the antepenultimate events that occurred in AD 1714 and ~1.2 ka (AD 841 or AD 762) respectively, whereas the event ages older than 1.2 ka are not well constrained. Here we mapped five displaced terraces (T1-T5, from the older) at Oide using aerial photographs taken by the US Armed Forces in the 1940s. Then, we estimated cumulative net slip of T1, T2 and T5 terraces using a tool developed by Wolfe et al. (2018) which incorporates topographic and fault properties with uncertainties and enables us to objectively estimate a plausible cumulative net slip. We made 30 topographic profiles for each terrace, and sought the mean and standard deviation of the cumulative net slip. We also constrained terrace ages based on radio carbon dating. As a result, we estimated coseismic slips of the penultimate and the antepenultimate events, 1.5±0.2 m and 2.7±0.4 m, respectively. Next, we performed a Monte Carlo simulation to estimate slips of events before the antepenultimate earthquake and then explore a possible range of CV (Coefficient of Variation) for co-seismic slips. CV is a ratio of a data set’ s standard deviation to mean and used to assess variability. Low CV indicates co-seismic slips are nearly the among seismic cycles, and high CV (close to 1) means slips are variable. Because previous paleoseismic studies found one to three earthquakes occurred between T1 formation (5-2.7 ka) and 1.2 ka, we iteratively computed one to three co-seismic slips before 1.2 ka so that the simulated slip sequences can reproduce the cumulative terrace offsets. This approach enabled us to calculate CV that ranged from 0.3 to 0.5 (1 σ), which indicates that a recent sequence of co-seismic slips at Oide does not follow the characteristic earthquake model but varies in a narrow range.

Keywords: Active fault, Paleoseismology, Co-seismic slip, Monte Carlo simulation

©2019. Japan Geoscience Union. All Right Reserved.

High-resolution shear-wave seismic reflection surveys across the Kamishiro fault, Itoigawa-Shizuoka Tectonic Line active fault system, central Japan

*Naoki IKEGUCHI[1], Nobuhisa Matsuta[2], Kyoko Kagohara[3], Shinsuke Okada[4], Daisuke Hirouchi[5], Tatsuya Ishiyama[1], Katsuya Noda[6], Hiroshi Sato[1]

1. Earthquake Resarch Institute University of Tokyo, 2. Graduate School of Education, Okayama University, 3. Faculty of Education, Yamaguchi University, 4. Graduate school of Science, Tohoku University, 5. Faculty of Education, Shinshu University, 6. GEOSYS Inc.

Coseismic net fault slip based on very shallow fault trajectories offers insights to understand properties of source faults for assessing seismic risk from crustal earthquakes in the overriding plate. To illuminate very shallow fault geometries, we carried out new shear-wave very shallow seismic reflection profiling across coseismic surface ruptures emerged along the Kamishiro fault, a northernmost segment of the Itoigawa-Shizuoka tectonic line (ISTL) active fault system, during the 2014 Nagano-ken-hokubu earthquake (Mw = 6.2) (c.f., Hirouchi et al., 2015; Ishimura et al., 2015; Katsube et al., 2017; Okada et al., 2015).

We collected seismic data along six seismic lines (Shiojima, North-Oide, South-Oide, Wing-21, Iimori, Horinouchi, respectively) in 2017 and 2018 by using Electrodynamic Vibrator System (ELVIS; GEOSYM) as an SH seismic source, a land streamer composed of 96 channels, and recording system GEODE (GeoMetrics). Acquisition parameters are: sweep length, 10 sec: sweep frequency, 20-120 Hz: source intervals, 1 m (2 m only in the Wing 21 seismic line); receiver intervals: 0.5 m; sampling rate: 1 msec.

By correlation of processed depth sections based on standard CMP stacking with surface geology and drill-hole data, the seismic sections up to a depth of approximately 100 m resolve thrust geometries extending from the 2014 coseismic surface ruptures that are mostly consistent with previous results in field mapping (e.g., Togo and Hasegawa, 2015; Lin et al., 2015; Okada et al., 2015), ground-penetrating radar (Kimura and Taniguchi, 2015; Nakano and Une, 2015). Our new seismic sections also successfully illuminate previously unrecognized blind thrust faults deforming Quaternary sediments which were not activated during the 2015 event. Our results show that shear-wave seismic reflection surveys using Electrodynamic Vibrator System and a land streamer are very effective to obtain detailed subsurface images of not only active faults but also unrecognized blind thrust structures.

Keywords: seismic reflection survey, Kamishiro fault, active fault, coseismic surface rupture, Itoigawa-Shizuoka Tectonic Line, subsurface structure

©2019. Japan Geoscience Union. All Right Reserved.

[J] Oral | S (Solid Earth Sciences)：S-SS Seismology

Wed. May 29, 2019 10:45 AM - 12:15 PM JST | Wed. May 29, 2019 1:45 AM - 3:15 AM UTC | A02 TOKYO BAY MAKUHARI HALL

[S-SS15] Active faults and paleoseismology

convener:Mamoru Koarai(Earth Science course, College of Science, Ibaraki University), Takashi OGAMI(National Institute of Advanced Industrial Science and Technology), Ryosuke Doke(Hot Springs Research Institute of Kanagawa Prefecture), Hisao Kondo(Geological Survey of Japan, National Institute of Advanced Industrial Science and Technology), Chairperson:HISAO KONDO(Geological Survey of Japan, National Institute of Advanced Industrial Science and Technology), Nobuhiko Sugito(Hosei University)

Geologic and historic information on seismic cycles and on the magnitude and source faults of past earthquakes is essential information to understand future large earthquakes. The study of past faulting and seismicity is an important issue for an interdisciplinary community of seismologists, geologists, geomorphologists, archaeologists, and historians.

10:45 AM - 11:00 AM JST | 1:45 AM - 2:00 AM UTC

[SSS15-10] Paleoseismic investigations on the un-ruptured section during the 2014 earthquake along the Kamishiro fault, ISTL active fault zone, Central Japan

*Hisao Kondo[1], Hideki Kurosawa[2], Yoko Hirakura[2], Keita Takada[3], Kohei Abe[2], Miwako Ito[2], Atsuo Igarashi[3], Tetsuya Ikeda[3], Atsushi Miwa[2] (1.Geological Survey of Japan, National Institute of Advanced Industrial Science and Technology, 2.OYO Cooperation, 3.Fukken Co., Ltd)

11:00 AM - 11:15 AM JST | 2:00 AM - 2:15 AM UTC

[SSS15-11] P-wave seismic reflection profiling across the northern central ISTL active fault system, central Japan

*Haruo Kimura[1], Hisao Kondo[2], Yasuhiko Akinaga[3], Shigeru Okamoto[3], Masaki Suehiro[3] (1.Central Research Institute of Electric Power Industry, 2.Geological Survey of Japan, AIST, 3.Hanshin Consultants Co., Ltd.)

11:15 AM - 11:30 AM JST | 2:15 AM - 2:30 AM UTC

[SSS15-12] History of interplate earthquakes along the Sagami Trough from uplifted coasts in the Boso Peninsula

*Junki Komori[1], Masanobu Shishikura[2], Ryosuke Ando[1] (1.The University of Tokyo, 2.The National Institute of Advanced Industrial Science and Technology)

11:30 AM - 11:45 AM JST | 2:30 AM - 2:45 AM UTC

[SSS15-13] Inferring location and activity of the Iriyamase fault, the Fujikawa-kako fault zone, based on boring core sample analyses and physical fault model

*Namiki Ryo[1], Ryosuke Ando[1], Masanobu Shishikura[2] (1.The University of Toyko, 2.National Institute of Advanced Industrial Science and Technology)

11:45 AM - 12:00 PM JST | 2:45 AM - 3:00 AM UTC

[SSS15-14] **Coastal submergence events identified by fossil diatoms and plant macrofossils at Ukishima-ga-hara adjacent to the Suruga Trough (eastern Nankai Trough), central Japan**

*Yuki Sawai[1], Arata Momohara[2], DAN MATSUMOTO[1], Yumi Shimada[1,3] (1.Geological Survey of Japan, AIST, 2.Chiba University, 3.University of Tsukuba)

12:00 PM - 12:15 PM JST | 3:00 AM - 3:15 AM UTC

Discussion

Paleoseismic investigations on the un-ruptured section during the 2014 earthquake along the Kamishiro fault, ISTL active fault zone, Central Japan

*Hisao Kondo[1], Hideki Kurosawa[2], Yoko Hirakura[2], Keita Takada[3], Kohei Abe[2], Miwako Ito[2], Atsuo Igarashi[3], Tetsuya Ikeda[3], Atsushi Miwa[2]

1. Geological Survey of Japan, National Institute of Advanced Industrial Science and Technology, 2. OYO Cooperation, 3. Fukken Co., Ltd

We perfomed paleoseismological invetigations on the un-ruptured fault section along the Kamishiro fault, ISTL active fault zone, central Japan. The un-ruptured section extends for about 15 km, consisting of the southernmost section of the Kamishiro fault. The northern most section have activated during the 2014 Nagano-ken Hokubu earthquake, Mj 6.7. Near Lake Nakatsuna, the Kamishiro fault forms tentonic geomorphic features such as fault scarp on the lucustrin terrace and fluvial terrace, monoclinal scarp on the lowland. Beside the eastern side of Lake Nakatsuna, we obtained two bore holes in order to estimate vertical slip rate based on lucustrin terrace deposite at hanging-wall side and fine sediments at foot-wall side. We estimated about 1.0 mm/yr of vertical slip rate as the minimum value. The fault exposure at the depth of -29 m in the borehole core at the foot-wall side implies that thrust front is located at the west of the borehole site. It indicates that the slip rate at present is the minimum estimatation. 350 meter south of this site, we obtained several Geoslicer across the fault scarp. The scarp hight is about 2 m. Based on geomorphic and geologica section, we identified two paleoseismic events after the depositon of alluvial fun deposite. At this moment, we estimated that the most recent event occurred after 664 A.D. More carbon dating samples will allow us to constrain teh timing of paleoseismic events. Near the sourthern most termination of the Kamishiro fault, south of Lake Kizaki, we re-investigated timing and slip per event during 5-6 paleoseismic events. Here, 2-3 events has been identified based on the shallow geologic section up to 6 m deep revealed by Geoslicer technique. We added four borehole cores to identify thrust structures and older events. At present, fine sediments and carbon dating results yeild 1.0 mm/yr of vertical slip rate after 1.2 ka. More dating results will provide high-resolution chronology of past events and slip per events, that will help us to discuss the occurrence of past multi-segment earthquakes.

Keywords: active fault, paleoseismology, ISTL active fault zone

©2019. Japan Geoscience Union. All Right Reserved.

P-wave seismic reflection profiling across the northern central ISTL active fault system, central Japan

*Haruo Kimura[1], Hisao Kondo[2], Yasuhiko Akinaga[3], Shigeru Okamoto[3], Masaki Suehiro[3]

1. Central Research Institute of Electric Power Industry, 2. Geological Survey of Japan, AIST, 3. Hanshin Consultants Co., Ltd.

We carried out P-wave seismic reflection profiling to reveal the subsurface structure across the northern central Itoigawa–Shizuoka tectonic line active fault system. Obtained migrated depth-converted section has shown a steeply (about 75 degree) eastward dipping fault.

Keywords: Itoigawa–Shizuoka tectonic line active fault system, East Matsumoto Basin fault, active fault, seismic reflection profiling, subsurface structure

©2019. Japan Geoscience Union. All Right Reserved.

History of interplate earthquakes along the Sagami Trough from uplifted coasts in the Boso Peninsula

*Junki Komori[1], Masanobu Shishikura[2], Ryosuke Ando[1]

1. The University of Tokyo, 2. The National Institute of Advanced Industrial Science and Technology

We surveyed tectonically uplifted coast, Heisa-ura, in the southernmost part of the Boso Peninsula, central Japan, for the estimation of the recurrence history of subduction earthquakes. The megathrust earthquakes along the Sagami Trough, located to the south of Tokyo, are known to repeatedly occur as represented by the 1703 M8.2 Genroku Kanto Earthquake. The interval time of these earthquakes is previously believed to be longer than 2,000 years from the investigations of the marine terraces in the Boso Peninsula (e.g. Nakata+, 1980). However, the recent dating survey indicated that their interval time might be 500–800 years at the shortest (Komori+, 2017) and required more detailed investigation. The Heisa-ura coast, we surveyed in this study, has not been investigated well before because no significant landform such as marine terraces are developed there. This region is, however, considered to suffer the fastest averaged uplift rate in the surrounding area from the recent study of the marine terrace distribution. Thus the buried sedimentary structure in Heisa-ura possibly records the emergence history of this coast. Here we show the result of the detailed geological survey using Geoslicer done in Heisa-ura for the first time. We obtained 8 sedimentary structure ~2 m deep along a survey line perpendicular to the coast. This investigation revealed that shoreface deposit contains shell fragments is placed deeper than 0.5–1.0 m beneath the surface. Additionally, the sedimentary structure is different between the survey points above and below the estimated elevation of the paleo-shoreline angle. These results indicate that the sedimentary structure beneath the Heisa-ura coast might records the chronicle of crustal deformations which has not been explored. This survey would give us several important factors for the discussion of the mechanisms of the subduction earthquakes along the Sagami Trough and the future hazard assessment of them.

Keywords: Sagami Trough, interplate earthquakes, marine terrace

©2019. Japan Geoscience Union. All Right Reserved.

Inferring location and activity of the Iriyamase fault, the Fujikawa-kako fault zone, based on boring core sample analyses and physical fault model

*Namiki Ryo[1], Ryosuke Ando[1], Masanobu Shishikura[2]

1. The University of Toyko, 2. National Institute of Advanced Industrial Science and Technology

The Fujikawa-kako (estuary) fault zone, located in the northern end of the Suruga-Nankai-trough, is claimed to be possible to be activated with the Nankai megathrust earthquakes, resulting in fatal damage in this region. However, it is difficult to accurately estimate the activity of the Iriyamase fault, which is considered as one of the most active faults in this fault zone, because no clear tectonic landform is found on the alluvial fan developed in the Fujikawa estuary area. Recently, three boring cores drilled in the Fujikawa estuary area are preliminarily analyzed by Shisikura et al. (2018). The KNB core is taken at the west side of the Fuji river as well as the hanging wall side of the Iriyamase fault, whose location is estimated by AIST (2016); The SKB core is at the west side of the Fuji river and the footwall side; the FGB core is at the east side of the river and the footwall side.

Based on the result of these analyses, it is estimated that the average displacement rate of Iriyamase fault is about 1~3 m / ky, which is smaller than the previous estimates (Yamazaki, 1992). Moreover, it is also pointed out that the both hanging wall and footwall sides of Iriyamase fault has been subsiding in the long term because Late Holocene terrestrial sediments are buried at the depth beneath the present sea level even in the KNB core located at the hanging side. According to the depth of layers deposited in the peak of the postglacial transgression, this subsiding rate is estimated to be at the 3m/ky.

In this presentation, we show the result of radiocarbon dating and a diatom analysis in these three cores based on more detail analyses of the core samples. Furthermore, we construct physical models based on these results to consider the underlying tectonic conditions.

The diatom analysis of the SKB core shows that diatoms are rarely found at depths shallower than 56 m, and the shallower strata are found to be terrestrial sediments. This result agrees with the long-term subsidence suggested by Shisikura et al. (2018). Moreover, the average displacement rate of Iriyamase fault is estimated about 2 m / ky by comparing the results of the diatom analyses of two cores (KNB and SKB). In order to understand the tectonic origin of the long-term subsidence in the Fujikawa estuary area, we construct the two physics-based models, called the Fuji volcano model and the fault model. In the Fuji volcano model, we calculated the amount of the subsidence caused by the isostasy effects due to the development of the Fuji volcano; the amount of subsidence is calculated to be about 0.7m by the volume increase of Fuji volcano in the past 17 thousand years, 41.37 km^3 (Miyazi, 2007). Thus, this result is far smaller than the amount of the long-term subsidence based on the boring core analysis. In the fault model, we calculate the average displacement rate of the Iriyamase fault, assuming faults as the finite rectangles in the semi-infinite elastic medium based on Okada (1992). We assume two faults to explain both the subsidence at the KNB core and the vertical offset between KNB and SKB; fault A is located between KNB and SKB and Fault B is located in the western side of KNB. The result shows that the average displacement rate of fault B is required to be much larger than that of fault A, because subsidence due to fault B in its footwall side must overcome the uplift due to fault A in the hanging side of fault A.

©2019. Japan Geoscience Union. All Right Reserved.

Keywords: Fujikawa-kako fault zone, Suruga trough, Tōkai earthquake, Active fault, Boring survey

©2019. Japan Geoscience Union. All Right Reserved.

Coastal submergence events identified by fossil diatoms and plant macrofossils at Ukishima-ga-hara adjacent to the Suruga Trough (eastern Nankai Trough), central Japan

*Yuki Sawai[1], Arata Momohara[2], DAN MATSUMOTO[1], Yumi Shimada[1,3]

1. Geological Survey of Japan, AIST, 2. Chiba University, 3. University of Tsukuba

We identified eight episodic submergence events based on paleontological analyses on peaty sediment samples at Ukishima-ga-hara lowland in Shizuoka Prefecture, central Japan. Lithostratigraphy of sediment samples from Ukushima-ga-hara has no clear changes in facies, but changes in compositions of diatom assemblages and plant macrofossils suggest episodic submergence events. For example, at about 2.3 m and 3.1 m below the ground surface, while aerophilic diatoms (such as *Diadesmis contenta*) dominate underlying peaty layer, freshwater and brackish planktonic taxa (*Aulacoseira* and *Thalassiosira*) abound in overlying layer. Radiocarbon ages of plant macrofossils taken from samples just above and below the event horizons were used to constrain event ages. As the results of applying Bayesian estimation, the youngest one may be correlated with either 1707 or 1498 earthquake. The second one was with either 1361 or 1498 earthquake. The third one covers ages of 1096 and 887 earthquakes. These submergence events may be generated with coastal deformation associated with subduction zone earthquake along Suruga Trough and/or active fault earthquake at Fujikawa-kako-fault zone.

Keywords: submergence event, diatom, plant macrofossil, radiocarbon dating, Fujikawa-kako fault zone

©2019. Japan Geoscience Union. All Right Reserved.

[J] Oral | S (Solid Earth Sciences)：S-SS Seismology

Wed. May 29, 2019 1:45 PM - 3:15 PM JST | Wed. May 29, 2019 4:45 AM - 6:15 AM UTC | A02 TOKYO BAY MAKUHARI HALL

[S-SS15] Active faults and paleoseismology

convener:Mamoru Koarai(Earth Science course, College of Science, Ibaraki University), Takashi OGAMI(National Institute of Advanced Industrial Science and Technology), Ryosuke Doke(Hot Springs Research Institute of Kanagawa Prefecture), Hisao Kondo(Geological Survey of Japan, National Institute of Advanced Industrial Science and Technology), Chairperson:Takashi Ogami(AIST), Koji Okumura(Hiroshima University)

Geologic and historic information on seismic cycles and on the magnitude and source faults of past earthquakes is essential information to understand future large earthquakes. The study of past faulting and seismicity is an important issue for an interdisciplinary community of seismologists, geologists, geomorphologists, archaeologists, and historians.

1:45 PM - 2:00 PM JST | 4:45 AM - 5:00 AM UTC

[SSS15-15] Shallow structures and tectonic geomorphology of active blind thrusts imaged by new hi-resolution seismic reflection profiling, Hokkaido, Northern Japan

*Tatsuya Ishiyama[1], Naoko Kato[1], Hiroshi Sato[1], Taro Koike[2], Katsuya Noda[2] (1.Earthquake Research Institute, University of Tokyo, 2.Geosys, Inc.)

2:00 PM - 2:15 PM JST | 5:00 AM - 5:15 AM UTC

[SSS15-16] Paleo-seismological survey on the Idenokuchi fault, Nishihara village, Kumamoto prefecture

*Daisuke Ishimura[1], Hiroyuki Tsutsumi[2], Naoya Takahashi[3], Ryuhei Oda[1], Jun Matsukaze[1], Heitaro Kaneda[4], Motoya Kobayashi[4], Yasuhiro Kumahara[5], Makoto Kobayashi[6], Toshihiko Ichihara[7] (1.Department of Geography, Tokyo Metropolitan University, 2.Department of Environmental Systems Science, Faculty of Science and Engineering, Doshisha University, 3.Department of EarthScience, Tohoku University, 4.Graduate School of Science, Chiba University, 5.Graduate School of Education, Hiroshima University, 6.Research Center for Volcanic Hazards and Their Mitigation, Tokyo Metropolitan University, 7.Sedimentary Environments Research)

2:15 PM - 2:30 PM JST | 5:15 AM - 5:30 AM UTC

[SSS15-17] Paleoseismic investigations of the Hinagu fault zone, Kumamoto, Japan: Preliminary result of trenching survey at Yatsushiro city

*Yukari Miyashita[1], Takashi Azuma[1], Yusuke Komine[2], Masao Kametaka[2], Midori Kishiyama[2] (1.Institute of Earthquake and Volcano Geology, Geological Survey of Japan, National Institute of Advanced Industrial Science and Technology, 2.Dia Consultants Co. Ltd.)

2:30 PM - 2:45 PM JST | 5:30 AM - 5:45 AM UTC

[SSS15-18] Seismic trenching on offshore part of the Hinagu Fault Zone, Kyushu, Japan −3D structure and paleo-seismicity of offshore dextral strike-slip fault

*Takashi OGAMI[1], Shintaro Abe[2], Kenjiro Mukaiyama[3], Shigeyuki Suda[4] (1.Geological Survey of Japan, AIST, 2.ADEP, 3.Kawasaki Geological Engineering Co. Ltd., 4.JGI Inc.)

2:45 PM - 3:00 PM JST | 5:45 AM - 6:00 AM UTC

[SSS15-19] Conductivity Structure models of large and small slip regions at the 2016 Kumamoto earthquake sequence

*Satoru Yamaguchi[1], Yuto Yamanaka[2], Akira Mimura[1], Kazuki Fkue[1], Daigo Furukawa[1], Tada-nori Goto[3], Hisatoshi Koji[3], Sota Kawaguchi[3], Koki Aizawa[4], Shinichi Takakura[5] (1.Department of Geosciences, Graduate School of Science, Osaka City University, 2.Faculty of Science, Osaka City University, 3.Department of Urban Management, Graduate School of Engineering, Kyoto University, 4.Institute of

Seismology and Volcanology, Kyushu University, 5. Geological Survey of Japan, National Institute of Advanced Industrial Science and Technology)

3:00 PM - 3:15 PM JST | 6:00 AM - 6:15 AM UTC

[SSS15-20] The Timing and Extent of the Last Surface Rupture Event on the Himalayan Frontal Thrust in Central Nepal around Butwal

*Koji Okumura[1], Soma Nath Sapkota[2], Prakash Pokhrel[2], Hisao Kondo[4], Takuya Furuhashi[3] (1.Graduate School of Letters, Hiroshima University, 2.Department of Mines and Geology, 3.Taiheiyo Cement Corporation, 4.Geological Survey of Japan, AIST)

Shallow structures and tectonic geomorphology of active blind thrusts imaged by new hi-resolution seismic reflection profiling, Hokkaido, Northern Japan

*Tatsuya Ishiyama[1], Naoko Kato[1], Hiroshi Sato[1], Taro Koike[2], Katsuya Noda[2]

1. Earthquake Research Institute, University of Tokyo, 2. Geosys, Inc.

Active structures of central Hokkaido are characterized by north-striking active thrusts along the western flanks of the Hidaka Mountains and eastern flanks of the Kabato Mountains. Whereas structural styles and positions of active thrusts along the Umaoi and Kurisawa Hills are clearly related to frontal Hidaka fold-and-thrust belt, structural relations between east-facing folded fluvial terraces along the eastern flanks of the Kabato Mountains and pre-Neogene basement-cored folds remain poorly understood. In addition, geomorphic expression of active faults/folds along the northern Yubari Mountains is quite insufficiently recognized in contrast to both their northern southern extension. To define these unsolved questions, we collected new seismic reflection data from the eastern flank of the Kabato Mountains, through alluvial plain of the Ishikari River to the western flank of the northern Yubari Mountains, by use of both ca. 14.5 km long array of seismic recorders at 20 m intervals and a vibroseis truck as seismic sources at 10 m intervals. Our processed seismic profile based on standard CMP stacking and its preliminary interpretation suggest the eastern flank of the Kabato Mountains is underlain by a tight, east-vergent, asymmetric anticline that deforms Paleogene to Pliocene sediments. Synclinal and anticlinal axial surfaces newly identified on folded, middle to late Pleistocene fluvial terraces on the eastern flank of the Kabato Mountains are apparently consistent with those recognized in the seismic section. This may suggest recent growth of the fault-related anticline and activities of underling west-dipping blind thrusts imaged in this experiment. In contrast to the east-vergent asymmetric anticline beneath the eastern flank of the Kabato Mountains, structural styles beneath the western flank of the northern Yubari Mountains in the eastern half of the section include more gentle westerly dipping Pliocene-Pleistocene (?) sedimentary units with steeper dip panels, possibly suggesting an east-dipping blind thrust fault. Previously unrecognized, very subtle, west facing scarps on alluvial plain and late Pleistocene fluvial terraces are consistent with these underlying thrusts and may indicate their recent fault activities.

Keywords: Active fault, Ishikari Lowland, Seismic reflection profile, Blind thrust, Hokkaido

©2019. Japan Geoscience Union. All Right Reserved.

Paleo-seismological survey on the Idenokuchi fault, Nishihara village, Kumamoto prefecture

*Daisuke Ishimura[1], Hiroyuki Tsutsumi[2], Naoya Takahashi[3], Ryuhei Oda[1], Jun Matsukaze[1], Heitaro Kaneda[4], Motoya Kobayashi[4], Yasuhiro Kumahara[5], Makoto Kobayashi[6], Toshihiko Ichihara[7]

1. Department of Geography, Tokyo Metropolitan University, 2. Department of Environmental Systems Science, Faculty of Science and Engineering, Doshisha University, 3. Department of EarthScience, Tohoku University, 4. Graduate School of Science, Chiba University, 5. Graduate School of Education, Hiroshima University, 6. Research Center for Volcanic Hazards and Their Mitigation, Tokyo Metropolitan University, 7. Sedimentary Environments Research

In the 2016 Kumamoto earthquake, surface ruptures appeared not only on the Futagawa fault, source fault of this event but also on the other active faults. Especially, on the Idenokuchi fault located about 2 km south of and subparallel to the Futagawa fault, normal fault scarps (10 km length and Max. 2 m vertical offset) appeared (Toda et al., 2016). Toda et al. (2016) presented that the slip-partition occurred using the Futagawa (strike-slip fault) and Idenokuchi (normal fault) faults, indicating the structural relationship between both faults. Additionally, in considering the 2016 event, there is one question whether the activity of Idenokuchi fault coincides that of the Futagawa fault or not. Recent paleoseismological survey (Kumahara et al., 2017; Iwasa et al., 2018; Shirahama et al., 2018; Toda et al., 2018; Tsutsumi et al., 2018; Ueta et al., 2018) revealed that 3 or 4 events including the 2016 event were estimated since Kikai-Akahoya (K-Ah) tephra (7.3 ka; Machida and Arai, 2003) fall. Thus, if the Idenokuchi fault ruptures together with the Futagawa fault, we would find multi-events on the Idenokuchi fault during the last seven thousand years.

We excavated a 14-m-long, 6-m-wide, 3-m-deep trench on the antithetic fault of the Idenokuchi fault, where we found 30-60 cm vertical offset associated with the 2016 event. In the laboratory, we conducted tephra analysis and radiocarbon dating. Now, we are measuring radiocarbon dates, and thus will estimate depositional and event ages in our presentation.

On the trench walls, we recognized clear, but complex normal and reverse faults. A main normal fault with a high dip angle bounded basement rocks and soil just below the 2016 surface rupture. On the hanging wall side, we found many antithetic normal faults and reverse faults. In the soil sediments, we identified K-Ah tephra (thickness of 40 cm) based on volcanic glass morphology and refractive index. Soil sequence on the hanging wall side is shown from the surface: surface soil, brown soil, black soil (paleosol1), brown soil, K-Ah, black soil (paleosol2) and yellowish soil.
At present, we identified at least four events including the 2016 event since paleosol2. Especially, after K-Ah deposition, we confidently three events including the 2016 event, corresponding with the frequency of the Futagawa fault activity (Kumahara et al., 2017; Toda et al., 2018; Tsutsumi et al., 2018; Ueta et al., 2018). This preliminary result suggests that the Idenokuchi fault ruptured with the Futagawa fault. Additionally, we also identified a few probable events and will discuss this with radiocarbon dates in the presentation.

Keywords: 2016 Kumamoto earthquake, Idenokuchi fault, Paleo-seismological survey, K-Ah tephra, Normal fault

©2019. Japan Geoscience Union. All Right Reserved.

©2019. Japan Geoscience Union. All Right Reserved.

Paleoseismic investigations of the Hinagu fault zone, Kumamoto, Japan: Preliminary result of trenching survey at Yatsushiro city

*Yukari Miyashita[1], Takashi Azuma[1], Yusuke Komine[2], Masao Kametaka[2], Midori Kishiyama[2]

1. Institute of Earthquake and Volcano Geology, Geological Survey of Japan, National Institute of Advanced Industrial Science and Technology, 2. Dia Consultants Co. Ltd.

We conducted paleoseismic investigations such as drilling and trenching surveys across the Hinagu segment of the Hinagu fault zone, Kumamoto, Japan. The result based on the careful trench wall observation and preliminary radiocarbon dating of sediments show that paleoearthquake cycle of the Hinagu segment is shorter than previous evaluation of the fault.

Keywords: Hinagu fault zone, 2016 Kumamoto Earthquake, paleoseismology, trenching survey

©2019. Japan Geoscience Union. All Right Reserved.

Seismic trenching on offshore part of the Hinagu Fault Zone, Kyushu, Japan −3D structure and paleo-seismicity of offshore dextral strike-slip fault

*Takashi OGAMI[1], Shintaro Abe[2], Kenjiro Mukaiyama[3], Shigeyuki Suda[4]

1. Geological Survey of Japan, AIST, 2. ADEP, 3. Kawasaki Geological Engineering Co. Ltd., 4. JGI Inc.

As a part of "Comprehensive research project for the major active faults related to the 2016 Kumamoto earthquake" of MEXT, we conducted offshore-fault surveys at the offshore part of the Hinagu-Fault-Zone, Kyushu, Japan. We have obtained ultra-high-resolution 3D-seismic data and two offshore drilling cores, and integrated them to clarify detailed geological structure and paleo-seismicity of the fault zone since the Last glacial maximum (LGM).

We chose coastal area of the Yatsushiro Sea, off the Tsunagi town, Kumamoto Prefecture, as study area. The sedimentary body of the postglacial period is formed thicker than 10 m at the area. Inside a rectangle area of 1 km by 2 km, we obtained ultra-high-resolution 3D-seismic data using the boomer source. Two drilling cores are obtained at both sides of the target fault.

3D geological structure and shape of the fault are figured out based on the 3D-seismic data. We distinguished extensional duplex structure at right-stepover section along the fault, which strongly suggest dextral strike-slip faulting. The structural depression associated with the extensional duplex would emphasize vertical faulting, which would provide clues to clarify the paleo-seismic events based on sedimentary analysis.

Two drilling cores penetrates the sedimentary body of the postglacial period, and are classified into Facies B, A4, A3, A2 and A1, in ascending order. Our interpretion of them are followings. Facies B: Sediment before LGM. Facies A4: Terrestrial sediment after LGM. Facies A3: Muddy bay sediment of transgressive stage. Facies A2: Sandy sediment overlapping ravinement surface. Facies A1: Sandy and muddy bay sediment of highstand. Based on 3D-seismic data, we classified strata of facies A4, A3, A2 and A1 into 7 seismic units (U7-U1, in ascending order) . The seismic units of U7-U3 are composed of facies A4 and A3. The seismic unit of U2 and U1 correspond with facies A2 and A1, respectively. The basement of seismic unit of U7 corresponds to the boundary of facies B/A4, and is interpreted as an erosional surface during lowstand of LGM around 18 ka.
Thickness of the seismic unit of U7, U5, U3, U2 and U1 changes abruptly at the fault, which should have result of 5 faulting events of E5-E1, in ascending order. Based on age-depth curve at drilling site on the downthrown side of the fault, faulting events of E5-E3 could be estimated as followings. E5: 18 ka-12.01 cal kBP, E4: 9.96-9.50 cal kBP, E3: 8.86-8.62 cal kBP. E2 should occurred during formation of seismic unit U2, which corresponds to the sediment of facies A2 (8.31-1.65 cal kBP). E1 displaces top of seismic unit U2, and we don’ t recognize displacement inside U1 and sea floor. Therefore, E1 should have occurred just before U1 deposition. Facies A1 corresponds to U1 and its deposition started after 1.59 cal kBP. Therefore, E1 should have occurred just before 1.59 cal kBP.
This study successfully demonstrated "3D-seismic trenching", which comprises ultra-high-resolution 3D seismic survey and offshore drilling surveys, can figure out detailed geological structure and paleo-seismicity of strike-slip fault.

©2019. Japan Geoscience Union. All Right Reserved.

Keywords: offshore active fault survey, Holocene, paleo-seismicity, offshore drilling survey, 3D-seismic survey

©2019. Japan Geoscience Union. All Right Reserved.

Conductivity Structure models of large and small slip regions at the 2016 Kumamoto earthquake sequence

*Satoru Yamaguchi[1], Yuto Yamanaka[2], Akira Mimura[1], Kazuki Fkue[1], Daigo Furukawa[1], Tada-nori Goto[3], Hisatoshi Koji[3], Sota Kawaguchi[3], Koki Aizawa[4], Shinichi Takakura[5]

1. Department of Geosciences, Graduate School of Science, Osaka City University, 2. Faculty of Science, Osaka City University, 3. Department of Urban Management, Graduate School of Engineering, Kyoto University, 4. Institute of Seismology and Volcanology, Kyushu University, 5. Geological Survey of Japan, National Institute of Advanced Industrial Science and Technology

The 2016 Kumamoto earthquake sequence in Japan started with M_{JMA} 6.5 foreshock and the M_{JMA} 7.3 mainshock occurred 28 hours after the foreshock. The events occurred mainly within the Hinagu and Futagawa fault zone, which are known to be active faults.
Asano and Iwata (2016), Kubo *et al.* (2016), and Kobayashi *et al.* (2017) analyzed the detailed source rupture process of the foreshock, mainshock, and another notable event and proposed the source rupture models. It is important and interesting to reveal conductivity structure of the fault and compare it the source rupture models above mentioned because resistivity structure is one of the crucial elements to reveal subsurface structure of the fault.
We made magnetotelluric (MT) surveys using an audio- frequency MT (AMT) method, which is suitable for revealing shallow part (0 -2 km in depth) with high spatial resolution, along two lines (MSK and NSH lines) of ~2 km across the Futagawa Fault. The MKS line crosses the large slipped region and along the line, we made measurements at 11 stations. The NSH line crosses the small slipped region and along the line, we made measurements at 14 stations. We obtained two-dimensional resistivity models between depths 0 - ~1.0 km along the two lines, we call them MSK model and NSH model, respectively.
We recognize two common conducive regions in both models. One is highly and near vertical conductor below the surface fault traces of the Futagawa Fault. The conductor is located just beneath the surface fault trace in the MSK model and is shifted south in the NSH model. Another is deep and wider conductor which includes deep part of the conductor mentioned above. This conductor of the MSK model is wider and shallower than that of the NSH model. These features are consistent with that of source rupture models, further we can say that our conductivity models figured out more detailed subsurface structure of the Futagawa Fault.

Keywords: 2016 Kumamoto earthquake sequence, Futagawa fault, magnetotellurics, resistivity, active fault

©2019. Japan Geoscience Union. All Right Reserved.

The Timing and Extent of the Last Surface Rupture Event on the Himalayan Frontal Thrust in Central Nepal around Butwal

*Koji Okumura[1], Soma Nath Sapkota[2], Prakash Pokhrel[2], Hisao Kondo[4], Takuya Furuhashi[3]

1. Graduate School of Letters, Hiroshima University, 2. Department of Mines and Geology, 3. Taiheiyo Cement Corporation, 4. Geological Survey of Japan, AIST

The 2015 Gorkha earthquake ruptured only the deeper northern part of the thrust during the Mw 7.8 earthquake, but did not rupture the surface and shallow portion of the Himalayan Frontal Thrust (HFT) in south. Since then, the evaluation of the potential of the future surface rupture event on the HFT in central Nepal in south of 2015 rupture became an important task for paleoseismology. Mishra et al. (2016), Bollinger et al. (2016), and Wesnousky et al. (2017) proposed respective 1100 CE, 1344 CE and/or 1408 CE, and 1221 CE to 1262 CE (possibly 1255 CE) for the timing of the last surface-rupture event. Each report eliminates the timing of earthquake proposed by the other authors. Therefore, it is necessary to think over the possibility of multiple events in short (less than 100 km) segments or of misleading radiocarbon dates. Also, the existence and the east termination of 1505 CE Indian central seismic gap event (Malik et al., 2017) are not certain yet. In order to solve the rupture history and rupture extents in central and western Nepal, we excavated two trenches across the HFT around the city of Butwal. One is at 12 km west of Butwal at Sorauli (27.70˚N 83.36˚E) and another is at 60 km ESE of Butwal at Susto (27.48˚ N 83.86˚E). Around the Sorauli trench site there is no clear continuous scarp along the Siwalik hill front, but ~100 m wide zone of alluvial surface adjacent to the foot of the hills tilt toward south and juxtaposed to flat alluvial surface. The boundary between the tilted surface and the flat plain is continuous and looks like the active front of a flexure scarp. The trench across a small scarp on the tilted surface did not expose any fault, but a fine sand layer was tilted towards the boundary. An Baesian model of radiocarbon dates indicates the timing of tilting is between 1328 CE and 1435 CE. This period coincides with the 1344 CE earthquake (Bollinger et al., 2016). The Susto trench in the east of Butwal was dug into the foot of ~20 m high fault/flexure scarp below an uplifted terrace surface. In this trench also, 13˚ south-dipping fine sand layers appeared but the fault was below the water table and not exposed. The timing of the tilt in Susuto trench as well as results from investigation in further west in the boundary area between 1344 CE and 1505 CE event will be reported.

Keywords: Himalayan frontal thrust, paleoseismology, trenching study

©2019. Japan Geoscience Union. All Right Reserved.

[J] Oral | S (Solid Earth Sciences)：S-SS Seismology

Wed. May 29, 2019 3:30 PM - 5:00 PM JST | Wed. May 29, 2019 6:30 AM - 8:00 AM UTC | A02 TOKYO BAY MAKUHARI HALL

[S-SS15] Active faults and paleoseismology

convener:Mamoru Koarai(Earth Science course, College of Science, Ibaraki University), Takashi OGAMI(National Institute of Advanced Industrial Science and Technology), Ryosuke Doke(Hot Springs Research Institute of Kanagawa Prefecture), Hisao Kondo(Geological Survey of Japan, National Institute of Advanced Industrial Science and Technology), Chairperson:Ryosuke Doke(Hot Springs Research Institute of Kanagawa Prefecture), Mamoru KOARAI(Ibaraki University)

Geologic and historic information on seismic cycles and on the magnitude and source faults of past earthquakes is essential information to understand future large earthquakes. The study of past faulting and seismicity is an important issue for an interdisciplinary community of seismologists, geologists, geomorphologists, archaeologists, and historians.

3:30 PM - 4:00 PM JST | 6:30 AM - 7:00 AM UTC

[SSS15-21] Linear surface ruptures detected by SAR - - *the Kumamoto earthquake, the Northern Osaka earthquake and the Hokkaido Eastern Iburi earthquake*

★Invited Papers

*Satoshi Fujiwara[1], Hiroshi Une[1], Takayuki Nakano[1], Hiroshi Yarai[1], Tomokazu Kobayashi[1], Yu Morishita[1] (1.GSI of Japan)

4:00 PM - 4:15 PM JST | 7:00 AM - 7:15 AM UTC

[SSS15-22] Acquisition of micro-landforms in the forest using small UAV-LiDAR: An example from surface rupture of the 2008 Iwate-Miyagi Nairiku, Japan, earthquake

*Asaka Konno[1], Taro Suzuki[2], Shinji Toda[1] (1.International Research Institute of Disaster Science, Tohoku University, 2.Waseda University)

4:15 PM - 4:30 PM JST | 7:15 AM - 7:30 AM UTC

[SSS15-23] **Bayesian Inference and Forecast on Renewal Processes for Recurrent Earthquakes with Uncertain Occurrence Times**

*Shunichi Nomura[1], Yosihiko Ogata[1] (1.The Institute of Statistical Mathematics)

4:30 PM - 4:45 PM JST | 7:30 AM - 7:45 AM UTC

[SSS15-24] **Slip rate of the Chaman fault: estimates based on ^{10}Be exposure dating for offset geomorphic surfaces in Afghanistan**

*Zakeria Shnizai[1], Yuki Matsushi[2], Hiroyuki Tsutsumi[1] (1.Doshisha University, 2.Kyoto University)

4:45 PM - 5:00 PM JST | 7:45 AM - 8:00 AM UTC

Discussion

Linear surface ruptures detected by SAR -- *the Kumamoto earthquake, the Northern Osaka earthquake and the Hokkaido Eastern Iburi earthquake*

*Satoshi Fujiwara[1], Hiroshi Une[1], Takayuki Nakano[1], Hiroshi Yarai[1], Tomokazu Kobayashi[1], Yu Morishita[1]

1. GSI of Japan

1. Introduction

The radar interferogram of ALOS-2 for the 2016 Kumamoto earthquake (M7.3) generally shows elastic deformation caused by the main earthquakes but many other linear discontinuities showing displacement are also found (Fujiwara et al., 2016).

We also found similar linear surface ruptures of the Northern Osaka earthquake on June 18, 2018 (M6.1) and the 2018 Hokkaido Eastern Iburi earthquake (M6.7).

In this presentation, we will show the characteristics of these linear surface ruptures.

2.General characteristics of the linear surface ruptures

The linear surface ruptures are those that Sangawa *et al.* (1985) presented about active faults in the southern part of Suruga Bay West Coast, and did not cause a large earthquake independently and the faults moved as a result of other large earthquakes.

The followings are the common features of the linear surface ruptures:

(1) The standard length of them is several kilometers, with linear or gentle curvilinear shape. The displacement is on the order of a few centimeters to several tens of centimeters.
(2) They are far from the seismogenic fault, and it is unlikely that they are the main seismic fault itself or the branch faults.
(3) There is no evidence that they generated large earthquake ground motions at the time of the main earthquake.
(4) They were likely moved passively, and it is considered to be the resultant faults, not the cause of the main big earthquake.
(5) Since there is a correlation between the topography and the displacement, some of them are recognized as "active faults" from their topographical features. Therefore, there is a possibility that similar fault movements have been accumulating from the past.
(6) The direction of strike and the displacement pattern of them are consistent with the surrounding stress field.

3. Characteristics for each earthquake

3-1) 2016 Kumamoto Earthquake
(1) About 230 linear surface ruptures have been confirmed.

©2019. Japan Geoscience Union. All Right Reserved.

(2) The form of displacement accounts for most of the normal fault.
(3) The interval, depth and displacement of them are almost constant and uniform for each area, and they form several groups of the linear surface faults.
(4) There are fault groups of similar shape from Beppu Bay to Unzen in the central part of Kyushu, Japan. This implies a possibility that there is a common form of them in central Kyushu.
(5) ΔCFF based on the fault model of the Futagawa fault zone and the Hinagu fault zone for the Kumamoto earthquake can not explain the cause of the displacement of them.

3-2) Northern Osaka earthquake on June 18, 2018
(1) The linear surface rupture was recognized at a place coincident with one of the faults of the Arima–Takatsuki fault zone (Makami fault). Makami fault has been confirmed that it moved at the time of the 1596 Keicho–Fushimi earthquake (M 7.5).
(2) Although the right–lateral fault component is dominant, the rupture does not reach the surface of the ground, but the displacement of the deviation component spreads by a width of about several hundred meters.
(3) On the linear surface rupture, vertical displacement of the south side down is found.
(4) According to the long-term observation before the earthquake, a wide belt around the linear surface rupture has continuously sunk.
(5) The general crustal deformation due to the main shock is small, and it is about several cm at the maximum.

3-3) 2018 Hokkaido Eastern Iburi earthquake
(1) The displacement shows east–west shortening, and there are almost no vertical components. Then, they can be described as reverse fault motion with very low dip angle.
(2) The trace on the ground surface is not a straight line but a somewhat complicated curve that follows the terrain.
(3) The traces of them have not been recognized as active faults.
(4) In the seismic exploration (Yokokura et al., 2014), deviations in the basement are recognized just under them and they may be a hidden fault.

Keywords: Kumamoto earthquake, Northern Osaka earthquake, Hokkaido Eastern Iburi earthquake, Crustal deformation, Active fault, ALOS-2

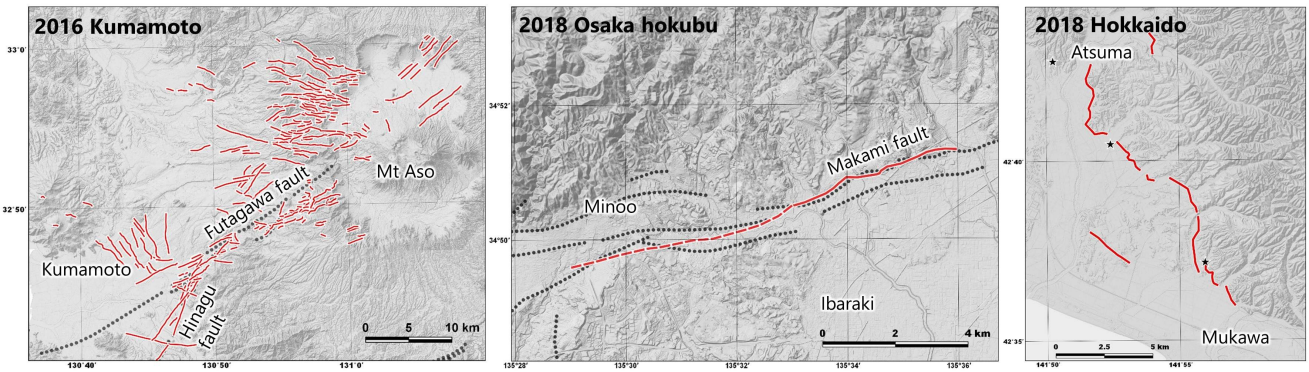

Figure Comparison of linear surface ruptures for three earthquakes.
The red lines demote linear surface ruptures. The black dotted lines demote known active faults by HERP.
The stars denote estimated fault positions by seismic reflection survey (Yokokura et al., 2014)

©2019. Japan Geoscience Union. All Right Reserved.

Acquisition of micro-landforms in the forest using small UAV-LiDAR: An example from surface rupture of the 2008 Iwate-Miyagi Nairiku, Japan, earthquake

*Asaka Konno[1], Taro Suzuki[2], Shinji Toda[1]

1. International Research Institute of Disaster Science, Tohoku University, 2. Waseda University

For active fault research, photogrammetry (e.g., Photoscan) with UAV (Unmanned Aerial Vehicle) has been introduced to map surface ruptures for the recent earthquakes. However, this method has mainly two drawbacks: it is necessary to set reference points (GCP: Ground Control Point), and it cannot be applied to ground in the dense forest. A small LiDAR equipment attached to the UAV laser is expected to overcome these issues. Although this approach is considered to be effective for detailed mapping of earthquake surface ruptures, none of the papers has been published such an application in the forest. Here we investigate the effectiveness of UAV laser surveying under the forest comparing to the topographical data acquired by terrestrial laser survey (Maruyama et al., 2008; Yoshimi et al., 2010) for the surface rupture that appeared at the 2008 Iwate Miyagi Nairiku earthquake.

Our study field is along the ~0.7-km-long surface rupture located in the north-east of the Aratozawa Dam. The heights of the free faces was several tens of cm to 2 m. We conducted the UAV flights at an altitude of 50-70 m on November 15, 2018. The area is densely covered with cedar plantations and broad-leaved trees, and thus surface rupture is almost invisible from aerial photographs. For the UAV aviation laser surveying, DJI Matrice 600 Pro owned by Waseda University was used. Six GNSS receivers mounted on the UAV allows us to precisely calculate the UAV location only with the errors of the attitude (0.1 °) and the position (1 cm). Based on the precise position information of the UAV, we attached the LiDAR equipment Velodyne's VLP-32C to the UAV to acquire detailed topographical data in the forest. We filtered the point cloud data using Landforms of ISP's software, and then extracted only the ground surface removing the points reflected from vegetation. The swath of ~0.16 km^2 along the surface rupture, measured in about 15 minutes of flight, enable us to provide about 69-million-point cloud data. Among them, the ground point data of ~200,000 points were only screened (~0.3%). Even though it is much fewer than the 8 million points obtained by terrestrial laser surveying of Mariuyama et al. (2008), the points are more homogeneously distributed and data loss is small. Since the terrestrial laser irradiates the beam to the horizontal direction from the installed machine, the data could not be acquired from a blind spot behind trees. In terms of data precision, we confirmed the DEM model from UAV LiDAR is comparable with the terrestrial LiDAR DEM with centimeter-order accuracy. An absolute advantage of the UAV LiDAR is overwhelmingly short operation that allows us to perform not only urgent post-earthquake survey but also repeating measurements to follow degradation process of fault scarps.

Acknowledgements. This research was supported by ImPACT program of Japan Science and Technology Agency.

References.

Maruyama, T., Toda, S., Yoshimi, M., Omata, M., Kohriya, Y., & Nihei, T. (2008). Ground-based LiDAR Mapping of Surface Rupture Associated with the 2008 Iwate-Miyagi Nairiku, Japan, Earthquake (Mw 6.9). In Eos Trans. AGU, Vol. 89, p. Meet. Suppl., Abstract T53D-1998.

©2019. Japan Geoscience Union. All Right Reserved.

Yoshimi, M., Maruyama, T., & Toda, S. (2010). Surface deformation extracted from trees ' tilt around surface ruptures of the 2008 Iwate-Miyagi inland earthquake, Japan, using ground-based LiDAR point clouds. In Eos Trans. AGU, Vol. 91, p. West. Pac. Geophys. Meet. Suppl., Abstract T33A-07.

Keywords: UAV LiDAR, Terrestrial LiDAR, Micro-landforms, Surface rupturing, 2008 Iwate-Miyagi Nairiku, Japan, earthquake

©2019. Japan Geoscience Union. All Right Reserved.

Bayesian Inference and Forecast on Renewal Processes for Recurrent Earthquakes with Uncertain Occurrence Times

*Shunichi Nomura[1], Yosihiko Ogata[1]

1. The Institute of Statistical Mathematics

We discuss parameter inference and forecast in renewal processes for recurrent earthquakes suffering from uncertainties in their occurrence times. Exact likelihood and hazard evaluation in point process theory involves multiple integral with respect to uncertain occurrence dates and are often difficult to calculate even numerically. Alternatively, Monte Carlo simulation of the uncertain occurrence histories can be used for the evaluation by calculating the integrated functions for respective simulated histories and simply averaging them. We apply a renewal model with the Brownian Passage Time (BPT) distribution to Japanese paleoseismic catalog in which at least 2 latest events are specified for each fault segment. It is shown that the Monte Carlo method yields almost the same results as numerical integration. In parameter inference, we assume a common coefficient of variation (COV) parameter for recurrence intervals of Japanese paleoearthquakes due to scarcity of their histories. From datasets in 73 inland paleoseismic sites in Japan, we obtain a Bayes estimate of the common COV at 0.50, which is significantly larger than the COV estimate at 0.24 currently applied in the long-term forecast held by the Headquarters for Earthquake Research Promotion (HERP) of Japan. The difference in COV’ s estimates makes critical influences on long-term probability forecast in several fault segments. We also show numeric experiments of parameter inference and forecast for virtual active fault and compare Bayesian inference and forecast to plug-in methods with maximum likelihood estimates.

Keywords: Bayesian forecast, Coefficient of variation, Renewal process

©2019. Japan Geoscience Union. All Right Reserved.

Slip rate of the Chaman fault: estimates based on ^{10}Be exposure dating for offset geomorphic surfaces in Afghanistan

*Zakeria Shnizai[1], Yuki Matsushi[2], Hiroyuki Tsutsumi[1]

1. Doshisha University, 2. Kyoto University

Afghanistan is located in a tectonically active part of the world near the collision boundary between the Eurasian and Indian plates. The Chaman fault traverses the eastern part of the country and is a major left-lateral strike-slip fault that accommodates much of the differential movement between the Indian and Eurasian plates. The fault starts from Makaran coast and extends to northeast through the Chaman City, Pakistan. Then it extends to north-northeast into Afghanistan and runs in west of Kabul and finally merges with the Pamir faults system. It is ~1000 km long and strikes from N10˚E to N35˚E. High slip-rates of the fault are known by previous works in the Pakistan side. In Afghanistan no research has been done, therefore we prepared a detailed fault map based on visual images interpretation and previous literatures. The fault offset older and younger alluvial fans and stream deposits of late Pleistocene and Holocene age. Along the fault, relative ages of geomorphic surfaces are known but their absolute ages are unknown. In the absence of absolute ages for faulted deposits, it is not possible to determine the fault slip-rate. Therefore we have conducted cosmogenic dating as was done in Pakistan side to provide age controls for fluvial deposits in the study area. Terrestrial Cosmogenic Nuclide (TCN) uses the interactions between cosmic rays and nuclides in transported boulders, and therefore is an excellent method to directly date alluvial deposits. TCN is particularly useful in Afghanistan due to lack of terrestrial organic materials for radiocarbon dating. Our study focuses on three different areas located at Wardak Province. One of the sites is Ghat Bandakul south of Kabul where the distal part of alluvial fan deposited at the mouth of a stream channel is offset left-laterally. The fan slopes 3-5˚ westward for ~1 km from the foot of the Syah-Tapa Mountain. The deposits are composed of clay, sandstone and granitic clasts originating from bedrocks. Analysis of ALOS images and field work indicate that younger and older terrace risers are displaced left-laterally along the fault for 165 m and 235 m respectively. We collected 6 samples from the top 1-3 cm of each desired sandstone boulders that were >1m in diameter and well-embedded in surface to ensure their long-term stability. The sandstone has large amounts of quartz mineral, which yields ^{10}Be TCN nuclide ideal for dating deposits over Quaternary timescale. Samples were processed at the laboratories of DPRI, Kyoto University and MALT, University of Tokyo.
Based on ~165 m displaced alluvial fan with a ^{10}Be exposure age of ~46 kyr, we obtained the first geomorphologically determined slip-rate of 3.5 mm/yr along the Chaman fault. This slip-rate is considerably smaller than the geologically and geomorphologically defined slip-rates of 19–24 mm/yr and 33 mm/yr along the fault in the border region of Afghanistan and Pakistan. Along the southern section at Ghazni and Zabul Provinces, we mapped east-dipping thrust faults as well as the multiple fault splays indicating a complex interplay between left-lateral faulting and northwest compression, which may cause slower slip-rate at the northern end of the fault. We plan to date two other alluvial surfaces in the southern part of the study area to determine exact slip-rate of the fault in Afghanistan.

Keywords: Chaman fault, 10Be exposure dating, offset geomorphic surface , Afghansitan

©2019. Japan Geoscience Union. All Right Reserved.

[J] Oral | S (Solid Earth Sciences)：S-SS Seismology

Wed. May 29, 2019 1:45 PM - 3:15 PM JST | Wed. May 29, 2019 4:45 AM - 6:15 AM UTC | A08 TOKYO BAY MAKUHARI HALL

[S-SS17] Seismic evidence of volcanic roots

convener:Naofumi Aso(Tokyo Institute of Technology), Yohei Yukutake(Hot Springs Research Institute of Kanagawa Prefecture), Chairperson:Naofumi Aso, Yohei Yukutake

Magma transport system beneath volcanoes is a key to understand long-term geodynamics and the evolution of the Earth. Especially, deep long-period earthquakes around the Moho beneath active volcanoes are supposed to relate to the magma transport system, although their activities and mechanisms are not understood well. Revealing the role of deep long-period earthquakes in the magma transport system is a key to understand deep volcanic roots around the lower crust, including deep magma chambers. It is therefore essential to estimate complete seismicity with a high-resolution hypocenter distribution and focal mechanisms of deep long-period earthquakes, based on innovative techniques including template matching, relocation methods using waveform cross-correlations, and waveform inversions. Also, high-resolution seismic imaging using advanced tomography techniques, including tomography using ambient noise interferometry, with a dense seismic network is essential to visualize the magma transport system. We welcome studies to understand volcanic roots from a variety of seismological approaches including but not limited to the methods mentioned above.

1:45 PM - 2:00 PM JST | 4:45 AM - 5:00 AM UTC

[SSS17-01] Spectral characteristics of deep low frequency earthquakes at Mount Fuji

★Invited Papers

*Motoo Ukawa[1] (1.Nihon University)

2:00 PM - 2:15 PM JST | 5:00 AM - 5:15 AM UTC

[SSS17-02] Deep low-frequency earthquakes corresponding to the 2011 and 2018 eruptions in Kirishima volcano

*Ryo Kurihara[1], Kazushige Obara[1], Akiko Takeo[1], Yusaku Tanaka[1] (1.Earthquake Research Institute, The University of Tokyo)

2:15 PM - 2:30 PM JST | 5:15 AM - 5:30 AM UTC

[SSS17-03] Origin of long-duration of deep low-frequency earthquakes and activity of shallow low-frequency earthquakes beneath northeastern Japan

*Masahiro Kosuga[1], Taichi Haruyama[1], Yuki Matsuno[2], Iori Narita[2], Takuto Maeda[1] (1.Graduate School of Science and Technology, Hirosaki University, 2.Faculty of Science and Technology, Hirosaki University)

2:30 PM - 2:45 PM JST | 5:30 AM - 5:45 AM UTC

[SSS17-04] Deep low-frequency earthquakes, tomography and magmatic system beneath active volcanoes

★Invited Papers

*Dapeng Zhao[1] (1.Department of Geophysics, Tohoku University)

2:45 PM - 3:00 PM JST | 5:45 AM - 6:00 AM UTC

[SSS17-05] Seismic imaging of deep structure beneath active volcanoes

*Junichi Nakajima[1] (1.Department of Earth and Planetary Sciences, Tokyo Institute of Technology)

3:00 PM - 3:15 PM JST | 6:00 AM - 6:15 AM UTC

[SSS17-06] Deep low-frequency volcanic earthquakes and their implication for deep crustal processes in the magmatic arc

*Haruhisa Nakamichi[1] (1.Sakurajima Volcano Research Center, Disaster Prevention Research Institute, Kyoto University)

Spectral characteristics of deep low frequency earthquakes at Mount Fuji

*Motoo Ukawa[1]

1. Nihon University

Source processes of deep low frequency (DLF) earthquakes beneath volcanoes have poorly understood, mainly because of the small magnitudes of the earthquakes. In this study, we investigate spectral characteristics of the DLF earthquakes beneath Mount Fuji, focusing 11 events with long durations of 5 to 20 minutes including relatively large maximum earthquakes of M0.9 to M1.8. Spectral characteristics of earthquakes, as well as the amplitudes of seismic waves, provide us constraints for their source models. In the present spectral analysis, wavelet analysis with Morlet analyzing wavelet is applied to the DLF events. The results show following characteristics of the DLF earthquakes. The predominant frequencies of the 11 events range relatively narrow frequency band of 1 to 2 Hz. High frequency components of mainly 5-10 Hz are superposed onto the main low frequency waves in the events with large amplitudes. One event shows gradual change of the predominant frequency from 1.5 Hz to 1.0 Hz during 5 minutes. Source models of DLF earthquakes should explain the above spectral characteristics.

Keywords: Deep low frequency earthquakes, Spectra, Mount Fuji

©2019. Japan Geoscience Union. All Right Reserved.

Deep low-frequency earthquakes corresponding to the 2011 and 2018 eruptions in Kirishima volcano

*Ryo Kurihara[1], Kazushige Obara[1], Akiko Takeo[1], Yusaku Tanaka[1]

1. Earthquake Research Institute, The University of Tokyo

Deep low-frequency earthquakes (LFEs), or sometimes called as deep long-period earthquakes (DLPs), are earthquakes whose dominant frequencies are lower than those of regular earthquakes of the same magnitudes. Deep LFEs occur beneath Kirishima volcano in southwest Japan at the depths of about 10-15 km and 20-25 km according to the catalog of Japan meteorology agency (JMA), while deep LFEs at most volcanoes in Japan occur at the depth of about 30 km.The LFEs near volcanoes can be a key to reveal physical processes of volcanic activities including eruptions because deep LFE activities are supposed to correlate with eruptions. For example, White (1996) showed that the deep long-period earthquakes (DLPs), so-called LFEs, occurred before the 1991 eruption of Pinatubo volcano, Philippine. Shapiro et al. (2017) showed the relationship between DLPs and long period earthquake near the surface beneath the Klyuchevskoy volcano group at Kamchatka, Russia. However, the relationships are still unknown in many volcanoes in Japan. Takahashi and Miyamura (2009) analyzed deep LFEs all over Japan using the catalog of JMA and concluded that they could not find deep LFEs corresponding with the surface volcanic activity such as eruptions. In fact, LFEs were constantly observed in Kirishima volcano in the JMA catalog. In this study, in order to reveal the relationships between activities of volcano such as eruptions and activities of deep LFEs, we first investigated spatial distribution of LFEs by relocation of the hypocenters of LFEs occurred from April 2004 to December 2015 in the JMA catalog using Network correlation coefficient method (Ohta and Ide, 2011). We then obtained time-series change of LFEs by comprehensive detection of deep LFEs based on matched filter technique (Gibbons and Ringdal, 2006; Shelly et al., 2007) from April 2004 to March 2018.

In results of relocation, hypocenters of the deep LFEs are concentrated in small clusters at the depth of 13 km and 22 km, especially many LFEs are located at the depth of about 22 km. On the other hand, result of the matched filter technique shows that deep LFEs at the depth of 23-25 km are activated for about two years including 2011 subplinian eruptions of Shinmoe-dake in Kirishima volcano group. The period of activation corresponds to the period of crustal deformation due to the volume change of the magma reservoir located beneath Ebino plateau at the depth of about 8 km (Nakao et al., 2013). From both results, we find that deep LFEs activated in the two years are located at the depth of 23-25 km, deeper than the locations of deep LFEs which constantly occurred from 2004 to 2018. Waveforms of deep LFEs activated around the 2011 eruptions have different characteristics such as lower frequencies and weak P wave onsets. The locations of activated deep LFEs migrated from shallow part to deep part of the small cluster at the depth of about 23-25 km during the two years of activation. In addition, there are some characteristic deep LFEs which were intensively observed in the periods of phreatic eruptions from March 2010 to July 2010 and phreatomagmatic eruptions from June 2011 to September 2011.Activation of deep LFEs was also observed in the period of eruptions in 2018, however, the depth and waveforms of the deep LFEs are same as those of deep LFEs which constantly occur at the depth of 20-23 km.
These results suggest that the deep LFEs occurring at the depths of 20-25 km are triggered by fluid flow. The difference of deep LFEs in 2011 and 2018 suggest that the fluid paths of the 2011 eruptions and 2018 eruptions are different. Activation of deep LFEs was not observed at the depth of 13 km in the periods of both eruptions, therefore, this deep LFEs may correspond to Ohachi volcano which did not erupt in the periods.

©2019. Japan Geoscience Union. All Right Reserved.

Keywords: Deep low-frequency earthquake, Kirishima volcano

©2019. Japan Geoscience Union. All Right Reserved.

Origin of long-duration of deep low-frequency earthquakes and activity of shallow low-frequency earthquakes beneath northeastern Japan

*Masahiro Kosuga[1], Taichi Haruyama[1], Yuki Matsuno[2], Iori Narita[2], Takuto Maeda[1]

1. Graduate School of Science and Technology, Hirosaki University, 2. Faculty of Science and Technology, Hirosaki University

We investigated the origin of long duration of deep low-frequency (DLF) earthquakes and the activity of shallow low-frequency (SLF) earthquakes beneath northeastern Japan. Source mechanism of DLF events has attracted attention because the events are anomalous with very low predominant frequencies and with a very deep hypocentral location, suggesting a possible link to a magma transport system. Previous studies have shown that the source mechanisms are variable, double couple, CLVD, and single force, among the events. However, the other aspect of the characteristics of DLF events, long duration of the seismic signal, has not been well studied. We firstly searched for typical DLF events with low frequency and long duration. ThenWe we evaluatedthe frequency content by employing frequency index (FI) defined by the logarithm of the amplitude ratio of spectra between high- low-frequency ranges. We specify specified the range as 2–4 Hz and 10–20 Hz for low- and high-frequency ranges, respectively. These ranges correspond to the predominant frequencies of DLF and shallow ordinary earthquakes. We specified determined the location of typical DLF eventsbased on the FI and durationmeasurements. For the case of Hijiori in Yamagata prefecture, long-lasting (> 10 s) monochromatic vibration is was in phase among the stations, which suggests that the source effect is the origin of extended coda is a source origin rather than some path effects. Spectrogram of this event shows no hint of overtones expected from a resonance mechanism. We next numericallysimulated seismograms from several source models by the OpenSWPC code for seismic wave propagation in 2D/3D media. Simulation indicates that the resonance of seismic waves in a low-velocity body could produce monochromatic vibration, but under an exceptional condition of the size and physical properties of the resonant body, and restricted location of the initial source that trigger the resonance. We are conducting the following simulation for a moving source through multiple channels of the fluid transport system.

Event detection using FI is effective for SLF earthquakes that have no low-frequency flag in the JMA earthquake catalog. We searched for the SLF events in the Hakkoda area in Aomori prefecture and the Hakodate area in southern Hokkaido. SLF events in Hakkoda exhibit a cylindrical distribution beneath the Odake volcano in a depth range from the surface to about 5 km, clearly separated from the distribution of VT earthquakes around the volcano. Since the activity of SLF events are restricted in time when the expansion of volcanic body was suggested by GNSS observation, the SLF activity probably related to a magmatic activity of the volcano. In Hakodate area, the SLF earthquakes are located apart from the active volcano, Esan, and with focal depths shallower than 10 km. We confirmed the depth of several SLF earthquakes by adding travel time data from our two temporary seismic stations just above the SLF sources. Thus, the SLF events in this area are collocated with ordinary high-frequency events. Investigation of the generation mechanism of SLF earthquakes in the brittle regime is also important to comparably understand the mechanism of DLF earthquakes in the ductile regime.

Keywords: low-frequency earthquakes, Frequency Index, duration

©2019. Japan Geoscience Union. All Right Reserved.

©2019. Japan Geoscience Union. All Right Reserved.

Deep low-frequency earthquakes, tomography and magmatic system beneath active volcanoes

*Dapeng Zhao[1]

1. Department of Geophysics, Tohoku University

We made a systematic study of deep low-frequency earthquakes, high-resolution tomography and magmatic system beneath active volcanoes on the Japan Islands. Low-frequency earthquakes (LFEs) in the lower crust and uppermost mantle are widely observed, and they occur not only along the subducting Philippine Sea (PHS) slab interface but also beneath active arc volcanoes. The volcanic LFEs are still not well understood because of their limited quantities and less reliable hypocenter locations. We used seismic tomography to determine detailed three-dimensional (3-D) P and S-wave velocity (Vp and Vs) models of the crust and upper mantle beneath the Japan Islands, and used the obtained 3-D Vp and Vs models to relocate the volcanic LFEs precisely (Niu et al., 2008; Yu et al., 2018). Our results show that the volcanic LFEs can be classified into two types: pipe-like and swarm-like LFEs, and both of them are located in or around zones of low-velocity (low-V) and high-Poisson's ratio (high-σ) in the crust and uppermost mantle beneath the active volcanoes. The pipe-like LFEs may be related to fluid migration from the lower crust or the uppermost mantle, whereas the swarm-like LFEs may be related to local magmatic activities or small magma chambers. The number of LFEs sometimes increases sharply before or after a nearby large crustal earthquake that may cause cracks and fluid migration. The spatiotemporal distribution of the LFEs may indicate the track of migrating fluids. As compared with the tectonic LFEs along the PHS slab interface, the volcanic LFEs are more sensitive to fluid migration and local magmatic activities. High pore pressures play an important role in triggering both types of LFEs.

We also investigated the 3-D seismic structure of source areas of the 6 October 2000 Western Tottori earthquake (M 7.3) and the 21 October 2016 Central Tottori earthquake (M 6.6) that occurred near the Daisen volcano in SW Japan (Zhao et al., 2018a). The two large events took place in a high-velocity (high-V) zone in the upper crust, whereas low-V and high-σ anomalies are revealed in the lower crust and upper mantle. LFEs (M 0.0–2.1) occurred in or around the low-V and high-σ zones, which reflect upward migration of magmatic fluids from the upper mantle to the crust under the Daisen volcano. The nucleation of the Tottori earthquakes may be affected by the ascending fluids. The flat subducting PHS slab has a younger lithosphere age and so a higher temperature beneath the Daisen and Tottori area, facilitating the PHS slab melting. It is also possible that a PHS slab window has formed along the extinct Shikoku Basin spreading ridge beneath SW Japan, and mantle materials below the PHS slab may ascend to the shallow area through the slab window. These results suggest that the Daisen adakite magma was affected by the PHS slab melting and upwelling flow in the upper mantle above the subducting Pacific slab.

Detailed 3-D Vp, Vs and σ images of the crust and upper mantle beneath Kyushu are determined, with a focus on the source area of the 2016 Kumamoto earthquake (M 7.3) that occurred in the Beppu-Shimabara graben (BSG) where four active volcanoes and many active faults exist (Zhao et al., 2018b). The 2016 Kumamoto earthquake took place in a high-V and low-σ zone in the upper crust, which is surrounded and underlain by low-V and high-σ anomalies in the upper mantle. This result suggests that, in and around the source zone of the 2016 Kumamoto earthquake, strong structural heterogeneities relating to active volcanoes and magmatic fluids exist, which may affect the seismogenesis. Along the BSG, low-V and high-σ anomalies do not exist everywhere in the upper mantle but mainly beneath the active volcanoes, suggesting that hot mantle upwelling is not the only cause of the

©2019. Japan Geoscience Union. All Right Reserved.

graben. The BSG was most likely formed by joint effects of northward extension of the Okinawa Trough, westward extension of the Median Tectonic Line, and hot upwelling flow in the mantle wedge beneath the active volcanoes.

References

Niu, X., D. Zhao, J. Li (2018). Precise relocation of low-frequency earthquakes in Northeast Japan: New insight into arc magma and fluids. *Geophys. J. Int.* 212, 1183-1200.
Yu, Z., D. Zhao, X. Niu, J. Li (2018). Spatiotemporal distribution of low-frequency earthquakes in Southwest Japan: Evidence for fluid migration and magmatic activity. *J. Asian Earth Sci.* 151, 148-172.
Zhao, D., X. Liu, Y. Hua (2018a). Tottori earthquakes and Daisen volcano: Effects of fluids, slab melting and hot mantle upwelling. *Earth Planet. Sci. Lett.* 485, 121-129.
Zhao, D., K. Yamashita, G. Toyokuni (2018b). Tomography of the 2016 Kumamoto earthquake area and the Beppu-Shimabara graben. *Scientific Reports* 8, 15488.

Keywords: deep low-frequency earthquakes, seismic tomography, active volcano

©2019. Japan Geoscience Union. All Right Reserved.

Seismic imaging of deep structure beneath active volcanoes

*Junichi Nakajima[1]

1. Department of Earth and Planetary Sciences, Tokyo Institute of Technology

Seismological observations clearly show that flux melting in the mantle wedge is a deep source of magmatism in subduction zones and generated melts are transported to the continental crust through a mantle upwelling flow. However, physical processes of magmatism beneath deep crust are poorly understood. Here I review seismological structures (seismic velocity and attenuation, S-wave reflectors, and low-frequency earthquakes) beneath active volcanoes in Japan, focusing on deep magma chambers and possible pathways of magmatic fluids to the upper crustal levels.

Keywords: S-wave reflector, seismic tomography, low-frequency earthquakes

©2019. Japan Geoscience Union. All Right Reserved.

Deep low-frequency volcanic earthquakes and their implication for deep crustal processes in the magmatic arc

*Haruhisa Nakamichi[1]

1. Sakurajima Volcano Research Center, Disaster Prevention Research Institute, Kyoto University

Under temperatures and pressures of the lower crust and the upper mantle, rocks typically deform in a ductile manner, and it is unlikely that a sufficient deviatoric stress accumulates to generate brittle failure. However, earthquakes do occur in the upper mantle and in the lower crust beneath active volcanoes, and they are known as volcanic deep low-frequency earthquakes (VDLFs). They release energy mostly in the low-frequency range (<5 Hz), and are characterized by emergent arrivals and long-duration codas. VDLF activity observed at depths of 10-50 km in Japan, the Philippines, Alaska, and the Western US (Power et al., 2004; Ukawa, 2005; Nichols et al. 20011) has generally been attributed to magma transport in the mid-to-lower crustal and uppermost mantle regions. However, because VDLF seismicity is infrequent, with relatively weak and emergent signals, the relationship between deep magma transport and seismic radiation remains poorly understood. Dense seismic observation systems in boreholes, such as the high-sensitivity seismograph network “Hi-net” in Japan (Obara et al. 2005), are effective at detecting not only non-VDLFs (Obara, 2002) but also VDLFs. Since 1997, the Japan Meteorological Agency has routinely detected and located DLFs using the Hi-net dataset, and have identified DLFs in and around most quaternary volcanoes in Japan (Takahashi and Miyamura, 2009). Several studies have attempted to estimate source mechanisms of VDLFs in Japan. The first attempt, carried out by Ukawa and Ohtake (1987), provided a single force as the source mechanism of a VDLF beneath Izu-Ohshima by using the particle motion directions of *S*-waves. More recently, strike-slip type and non-double-couple source mechanisms were obtained using waveform inversions for VDLFs in Northeast Japan (Nishidomi and Takeo 1996; Okada and Hasegawa, 2000). Nakamichi et al. (2003; 2004) estimated the source mechanisms of Mts. Iwate and Fuji through the moment tensor inversion of spectral ratios of body waves, using data from a dense seismic network. The authors explained the source mechanisms as the motion of a tensile crack coupled either with a shear crack or with a chamber. No significant common features have been found in these estimated source mechanisms of VDLFs in Japan. The depths of VDLFs correspond to the depth interval where CO_2-rich fluids are expected to be liberated from ascending basaltic magmas, suggesting that such fluids play an important role in facilitating earthquake instabilities in the presence of tectonic stresses. The striking temporal correlation between VDLF activity and CO_2 gas emissions has been pointed out by Mammoth Mountain (Hill, 1996) and Izu-Ohshima (Watanabe, 2013). However, a temporal correlation between the VDLF activity and surficial geological and shallow geophysical activity is currently debated. The intrusion of basaltic magma before the eruption of Mt. Pinatubo in 1991 was correlated with VDLFs (White, 1996), and temporal correlations are clear for the 1998-1999 unrest of Mt. Iwate, where VDLF seismicity started 5 days before the initiation of the volcano tectonic (VT) seismicity (Nakamichi et al., 2003). We are currently investigating this correlation for the volcanic activity of Sakurajima, which is located in the southern part of the Aira caldera. There is a correlation between VT and VDLF seismicity in the Aira caldera since 2000. For example, both VT and VDLF increased in number between 2017 and 2018. On the other hand, no clear correlation between the VDLF seismicity and the eruption activity of Sakurajima volcano has been identified thus far.

Keywords: Deep low-frequency volcanic earthquake, Non-double-couple source mechanism, Volcanic activity

©2019. Japan Geoscience Union. All Right Reserved.

©2019. Japan Geoscience Union. All Right Reserved.

[J] Poster | S (Solid Earth Sciences)：S-SS Seismology

Wed. May 29, 2019 3:30 PM - 5:00 PM JST | Wed. May 29, 2019 6:30 AM - 8:00 AM UTC | Poster Hall International Exhibition Hall8, Makuhari Messe_17

[S-SS17] Seismic evidence of volcanic roots

convener:Naofumi Aso(Tokyo Institute of Technology), Yohei Yukutake(Hot Springs Research Institute of Kanagawa Prefecture)

Magma transport system beneath volcanoes is a key to understand long-term geodynamics and the evolution of the Earth. Especially, deep long-period earthquakes around the Moho beneath active volcanoes are supposed to relate to the magma transport system, although their activities and mechanisms are not understood well. Revealing the role of deep long-period earthquakes in the magma transport system is a key to understand deep volcanic roots around the lower crust, including deep magma chambers. It is therefore essential to estimate complete seismicity with a high-resolution hypocenter distribution and focal mechanisms of deep long-period earthquakes, based on innovative techniques including template matching, relocation methods using waveform cross-correlations, and waveform inversions. Also, high-resolution seismic imaging using advanced tomography techniques, including tomography using ambient noise interferometry, with a dense seismic network is essential to visualize the magma transport system. We welcome studies to understand volcanic roots from a variety of seismological approaches including but not limited to the methods mentioned above.

[SSS17-P01] S-wave reflectors beneath the earthquake swarm in the Yonezawa-Kitakata area, NE Japan

*Manami Suzuki [1], Akiko Hasemi[1], Tomomi Okada[1], Toru Matsuzawa[1], Norihito Umino[1], Takashi Nakayama[1], Noriko Tsumura[2], Tadashi Yamashina[3], Group for the aftershock observations of the 2011 off the Pacific of Tohoku Earthquake (1.Research Center for Prediction of Earthquakes and Volcanic Eruptions, Graduate School of Science, Tohoku University, 2.Graduate School of Science, Chiba University, 3.Faculty of Science and Technology, Kochi University)

[SSS17-P02] Imaging of the magma pathway beneath Kirishima volcanoes by seismic interferometry

*Yutaka Nagaoka[1], Kiwamu Nishida[2], Yosuke Aoki[2], Minoru Takeo[2], Takahiro Ohkura[3], Shin Yoshikawa[3] (1.Volcanology Research Department, Meteorological Research Institute, 2.Earthquake Research Institute, The University of Tokyo, 3.Aso Volcanological Laboratory, Institute for Geothermal Sciences, Graduate School of Science, Kyoto University)

[SSS17-P03] Finite element three-dimensional seismic waveform calculations of volcanic deep low frequency earthquake including true topographic effects of Hakone volcano

*Lina Yamaya[1], Kimihiro Mochizuki[1], Tsuyoshi Ichimura[1], Kohei Fujita[1], Takeshi Akuhara[1], Takane Hori[2], Ryou Honda[3], Yohei Yukutake[3] (1.Earthquake Research Institute, Univ. of Tokyo, 2.JAMSTEC, 3.Hot Springs Research Institute of Kanagawa)

[SSS17-P04] Magma transport system beneath Hakone volcano inferred from deep low frequency earthquakes

*Yohei Yukutake[1], Yuki Abe[1] (1.Hot Springs Research Institute of Kanagawa Prefecture)

[SSS17-P05] Hypocenter and waveform characteristics of deep low-frequency earthquakes beneath Zao volcano

*Takuma Ikegaya[1], Mare Yamamoto[1] (1.Graduate School of Science, Tohoku University)

[SSS17-P06] Mechanisms transition of LFEs beneath Zao volcano due to the stress change induced by the 2011 Tohoku earthquake

*Genki Oikawa[1], Naofumi Aso[1], Junichi Nakajima[1], Toru Matsuzawa[2] (1.Tokyo Institute of Technology, 2.Tohoku University)

[SSS17-P07] Magma/gas intrusion process of Shinmoedake Eruption in 2017 suggested by volcanic tremors location with ASL method

Shoya Imamura[1], *Makoto OKUBO[2] (1.Faculty of Science, Kochi University, 2.Natural Science Cluster, Kochi University)

[SSS17-P08] Source depth estimation of a magmatic inflation in 2008-2010 at Mt. Fuji, Japan, based on sparsity-promoting L1 inversion of GNSS data

*Yuta Mitsui[1], Takahiro Kato[2] (1.Department of Geosciences, Shizuoka University, 2.formerly at Department of Geosciences, Shizuoka University)

S-wave reflectors beneath the earthquake swarm in the Yonezawa-Kitakata area, NE Japan

*Manami Suzuki [1], Akiko Hasemi[1], Tomomi Okada[1], Toru Matsuzawa[1], Norihito Umino[1], Takashi Nakayama[1], Noriko Tsumura[2], Tadashi Yamashina[3], Group for the aftershock observations of the 2011 off the Pacific of Tohoku Earthquake -

1. Research Center for Prediction of Earthquakes and Volcanic Eruptions, Graduate School of Science, Tohoku University, 2. Graduate School of Science, Chiba University, 3. Faculty of Science and Technology, Kochi University

Research on reflected S wave around volcanic regions and inland earthquake faults has been conducted throughout Japan. Mizoue et al. (1982) showed the spatial distribution of S wave reflection points in Nikko-Ashio area, and the amplitude ratio of SxP wave and SxS wave was explained by layered partially melt. In the Tohoku region, reflected S wave is from reflector contains fluid which was released during the cooling process of the melt suggested by Umino et al. (2002) and Hori et al. (2004). It is pointed out that the dehydrated fluid is involved in the mechanism of the occurrence of an inland earthquake [e.g., Hasegawa et al., 2005], and it is important to understand the behavior of the fluid in the crust in the Tohoku region in more details.

In the Yonezawa - Kitakata area, NE Japan, which is the target area of this research, it is thought that a swarm earthquake occurred 7 days after the 2011 Tohoku Region Pacific Offshore Earthquake, and the cause is the decrease in strength due to increase in fluid pressure [eg, Okada et al., 2015]. The focal region is located in and around the Otoge caldera [Yamamoto et al., 1994] which formed in the Miocene, and the possibility of existence of the fluid dehydrated from the melt as described above is sufficient. Since S wave reflected waves in Yonezawa - Kitakata area have already been discovered by Hasemi et al. (2016), this study aims to obtain the spatial distribution of the S wave reflector. In this area, temporary stations are deployed densely by Group of the aftershock observations of 2011 off the Pacific coast of Tohoku Earthquake. In this research, seismic waveform data at these temporal stations and the permanent stations by Hi-net is used. In order to accurately obtain the spatial distribution of the S wave reflector, we use the hypocenters determined by the Double Difference method using the temporary observation data.

First of all, I carefully read the travel time of the S wave reflected wave visually. For ten observation stations/clusters pairs which were able to confirm the S wave reflected wave remarkably, the travel time of the seismic waveform was converted to the depth as in Inamori et al. (1992). As a result, 16 reflectors in the northeast clusters, 14 in the center, and 3 in the southwest were read.

Next, using the read travel time, the mirror observation stations were calculated by grid search [e.g., Horiuchi et al., 1988]. We assume that the reflector is a single plane, and the wave ray path is a straight line with a uniform velocity structure of 3.4 km/s. We will find the reflector with minimum of the least squared square root between observed and calculated traveling times. From the equation of the reflector obtained by the above process, the strike/dip and the position of the reflection point with respect to each epicenter were obtained.

As a result, the reflectors are located from the lower part of the source region to the depth of 10 - 20 km below it. The strike seems to be drawing a circle or an arc, and the dips are smaller beneath the source region. Comparing this reflector distribution with the seamless geological map [AIST], for the reflectors just beneath the Otoge caldera their strikes seems to be along the edge of the caldera, and for the

©2019. Japan Geoscience Union. All Right Reserved.

reflector in the western part, their strikes follows the western marginal fault zone of Aizu Basin and the boundaries of geological structure. Comparing this with the seismic velocity structure, the reflectors are located at the periphery of the low velocity zone, being consistent with the results obtained by Umino et al. (2002) and Hori et al. (2004). By this reason, fluids promoting swarm earthquakes in the Yonezawa - Kitakata area may be migrated from the melt below the epicenter area and may have passed boundary of the existing geological structure.

Keywords: reflected wave, crustal fluid

©2019. Japan Geoscience Union. All Right Reserved.

Imaging of the magma pathway beneath Kirishima volcanoes by seismic interferometry

*Yutaka Nagaoka[1], Kiwamu Nishida[2], Yosuke Aoki[2], Minoru Takeo[2], Takahiro Ohkura[3], Shin Yoshikawa[3]

1. Volcanology Research Department, Meteorological Research Institute, 2. Earthquake Research Institute, The University of Tokyo, 3. Aso Volcanological Laboratory, Institute for Geothermal Sciences, Graduate School of Science, Kyoto University

Shinmoe-dake, one of Kirishima volcanoes, experienced magmatic eruptions in 2011. The analysis of ground deformation shows that the pressure source locates 5 km to the northwest of the Shinmoe-dake summit at a depth of 8 km, which implies the existence of a magma reservoir. We are trying to resolve a better image by a seismological technique toward ensuring its existence and deriving precise crustal structure and reveal a magma pathway.

The technique we employed is seismic wave interferometry, which extracts the seismic wave propagation between two seismic stations by taking cross correlations of random wavefields, such as the ambient seismic noise or the seismic coda wave. The cross correlations of random wavefields recorded at two stations can be represented as if the source is at one station and the recorder is at the other. This technique is suitable for exploring local structure since the extracted wave is sensitive to the internal structure between the two stations.

We inferred the crustal phase velocity anomaly using three-component records of the ambient seismic noise recorded by a seismic array between April 2011 and December 2013. Rayleigh and Love waves are extracted by taking cross correlations (Rayleigh waves from cross correlation functions of pairs of vertical components, and Love waves from transverse components). We derived reference dispersion curves of Rayleigh and Love waves, respectively, using all possible pairs of stations, then measured phase velocity anomalies of all possible pairs with respect to the reference in multiple frequency bands (0.1-0.2 Hz, 0.2-0.4 Hz, 0.3-0.6 Hz, and 0.4-0.8 Hz). Finally, three-dimensional V_{SV} and V_{SH} structures were obtained from a collection of local one-dimensional velocity profiles derived by inverting phase velocities of Rayleigh and Love waves, respectively, at each grid point.

Kirishima volcanoes exhibit a low V_{SV} body that is embedded beneath the deformation source and extends horizontally by about 15 km at around 10 km below sea level beneath the volcanoes. We interpret it as a crustal magma reservoir. V_{SH} did not detect low velocity bodies, implying the radial anisotropy generated by a sill complex in the magma reservoir. The ground deformation source of the eruptions in 2011 locates at uppermost and northwesternmost of the low velocity body, indicating that the low velocity body is a magma reservoir of the volcanoes. Moreover, low frequency earthquakes occur beneath the southeasternmost of the low velocity body. We can, therefore, present a model of a magma pathway that magma rising up from the deeper region right beneath the volcanoes is once stored at a magma reservoir and further ascend toward the surface from the uppermost and northwesternmost of the magma reservoir.

Our study presents the effectiveness of the estimation of S wave velocity structure using phase velocities of Rayleigh and Love waves in deciphering the magma pathway beneath the active volcanoes and the importance of further investigation of magma plumbing systems beneath various types of volcanoes.

©2019. Japan Geoscience Union. All Right Reserved.

Keywords: Kirishima, seismic interferometry, ambient seismic noise, radial anisotropy

©2019. Japan Geoscience Union. All Right Reserved.

Finite element three-dimensional seismic waveform calculations of volcanic deep low frequency earthquake including true topographic effects of Hakone volcano

*Lina Yamaya[1], Kimihiro Mochizuki[1], Tsuyoshi Ichimura[1], Kohei Fujita[1], Takeshi Akuhara[1], Takane Hori[2], Ryou Honda[3], Yohei Yukutake[3]

1. Earthquake Research Institute, Univ. of Tokyo, 2. JAMSTEC, 3. Hot Springs Research Institute of Kanagawa

Volcanic deep low frequency (DLF) earthquakes play an important role on revealing magma volcanic system because they are thought to reflect movements of volcanic fluid. Nakamichi et al. (2003) showed that the DLF earthquakes occurring beneath Iwate volcano have compensated linear vector dipole components, which suggests the relation with volcanic fluid.

Hakone volcano also has DLF earthquakes whose depths are from 10 to 30 km. Yukutake et al. (2018) showed that the number of DLF earthquakes increased just before crustal movement or increase of volcanic tremors in 2006, 2013, 2015, but mechanisms of the DLF earthquakes are still unrevealed. JMA reported that DLF earthquakes occur not just beneath Owakudani (the main crater of Hakone volcano) but around 10 km north from Owakudani, which is needed to be studied in detail. One of the difficulties to infer the source mechanisms and centroids is that the volcanic structure is complex not only due to its velocity structure but also due to its geometry. Calculation of three-dimensional seismic wave propagation are still challenging due to its computational cost, but it has become less difficult due to the recent development of efficient calculation techniques of computational science.

In this study, we used a technique of finite element three-dimensional waveform computation (Ichimura et al., 2017) to calculate the synthetic waveforms of the DLF earthquakes in Hakone volcano with respect to two different structure representations; direct inclusion of topography and flat surface with squashed topography in to the subsurface (Aagaard et al. 2008), and compared the resulted synthetic waveforms. We assumed the modified seismic velocity model reported in Yukutake et al. (2014). We used K computer and calculated the synthetics up to 1.5 Hz. As a result, although the arrival times of direct waves are similar, shapes of subsequent arrival phases are different. The amplitudes of subsequent arrival waves calculated including the true topography are larger than those calculated for the flat surface model with squashed topography. Observed data have such large amplitudes in subsequent arrival phases. Therefore, it is needed to calculate the synthetics including true topography for comparisons between data and synthetics. We further investigate generation mechanisms of such DLF earthquakes by synthetic modeling of the observed waveforms.

Keywords: Deep low frequency earthquake, Finite element three-dimensional seismic waveform calculation, K computer

©2019. Japan Geoscience Union. All Right Reserved.

Magma transport system beneath Hakone volcano inferred from deep low frequency earthquakes

*Yohei Yukutake[1], Yuki Abe[1]

1. Hot Springs Research Institute of Kanagawa Prefecture

It has been recognized that the occurrence of deep low-frequency earthquakes (DLFEs) beneath a volcano is related to a behavior of magmatic fluid (e.g. Nakamichi et al., 2003). On the other hand, the linkage between the DLFE and shallow volcanic activities such as a swarm activity and crustal deformation has not been well understood. In the present study, we compared the temporal sequence of the DLFEs occurred around the depth of 25 km beneath Hakone volcano, central Japan, with the swarm activity and the inflation of pressure source occurred in the area shallower than the depth of 10 km.

During recent two decades, we observed the remarkable swarm activities at Hakone volcano in 2001, 2006, 2009, 2013 and 2015. In each swarm activity, crustal deformation associated with an inflation of pressure source was estimated at the depth of 7km beneath the central cone of caldera, by using the GNSS data (Harada et al., 2018). Tthe tomography analysis (Yukutake et al., 2015; Yukutake et al., 2018) reveals that the crystalizing magma body locates around the depth of 10km and the hydrothermal fluid dehydrated from the magma exists above it.

The DLFEs were detected by using the Matched Filter method. We used continuous seismic waveforms at 12 permanent stations around Hakone volcano in the period from January, 2000 to January, 2017. The template waveforms of 94 DLFs were prepared on the basis of the JMA catalog. We also estimated the temporal sequence of b-value by using the DLFE catalog. The temporal change was calculated by using the method in Wiemer and Wyss (2000), using the moving time-windows containing a constant event number of 300 events.

As a result, we could detect the numerous DLFEs corresponding to 46 times in comparison with the number detected by JMA. It is clearly evident that the DLFEs activated prior the swarm activity in 2006, 2009, 2013 and 2015, and synchronized with the onset time of crustal expansion caused by the inflation of pressure source. We estimated the increment of b-values by accompanied with the activation of DLFEs. An increase of b-values during the swarm activity in several volcanic regions can be explained by assuming the increment of pore pressure or the change of thermal gradient associated with the intrusion of magma/hydrothermal fluid (Jacobs and McNutt, 2010; Nanjo et al., 2018). It is likely that the activation of DLFEs accompanied by the increase of b-values reflects the inclusion of magma at the depth. The inflation of pressure source at the depth of 7 km may suggest the increase of a volatile component at the shallow magma/hydrothermal fluid from the deep intruded magma at the source region of DLFEs or the increment of temperature due to the migration of hot material. The increase of strain rate due to the inflation can promote the migration of highly pressurized to the shallow brittle zone (Fournier, 1999), triggering the earthquake swarms. On the other hand, the remarkable activation of DLFE was observed in the later stage of swarm activity in 2001, rather than precursory activity for the earthquake swarms. This result may imply that the activation of volcanic phenomena such as the shallow swarm activity and crustal deformation is not necessary initiated by the deep magma intrusion.

Acknowledgments
We used the waveform record obtained by the permanent stations of National Research Institute for Earth

©2019. Japan Geoscience Union. All Right Reserved.

Science and Disaster Resilience and GNSS data of Geospatial Information Authority of Japan. We used zmap program code (Wiemer, 2001) to estimate b-value.

Keywords: Deep low frequency earthquake, earthquake swarm, Hakone volcano

©2019. Japan Geoscience Union. All Right Reserved.

Hypocenter and waveform characteristics of deep low-frequency earthquakes beneath Zao volcano

*Takuma Ikegaya[1], Mare Yamamoto[1]

1. Graduate School of Science, Tohoku University

The 2011 Tohoku Earthquake (Mw 9.0) caused large crustal deformation in and around the Tohoku region, and strongly affected volcanic fluids in the crust. As an example suggesting such influence, the change in activities of deep low-frequency earthquakes (DLFs) occurring in the lower crust. The analysis of DLFs is thus considered to be one of the important keys to infer the activity of deep magma and to assess the potential risks of mid- to long-term volcanic activity after a huge earthquake. In this presentation, we report the results of our analysis of the DLFs beneath Zao volcano where activation of volcanic activities has been observed after the 2011 Tohoku Earthquake.

Zao volcano is located on the border between Yamagata and Miyagi prefectures. After the 2011 Tohoku Earthquake, the number of DLFs beneath Zao volcano started increasing, and increase in shallow seismicity have been observed since 2013. To investigate such seismic activities, the JMA unified hypocenter catalog (JMA catalog) is often used. However, the completeness of the catalog is not guaranteed in small DLFs. To improve the completeness of event detection, Ikegaya and Yamamoto (2018, JpGU) applied Matched Filter method (MF method) to the continuous waveform data recorded in 2015 and detected DLFs having high correlation to the template DLFs listed in JMA catalog. They successfully increased the number of small DLFs and revealed the spatial distribution of hypocenters showing two clusters above and below 28 km. However, due to the assumption that the hypocenters of the detected events are the same as those of the templates yielding maximum correlation value, it is difficult to discuss the details of the hypocenter clustering. In this study, aiming to understand the detailed spatio-temporal characteristics of DLF activity, we apply MF method to the waveform data for the last seven years, and determine relative hypocenters of the detected events.

In the analysis, we used the continuous three-components waveform data recorded at four permanent stations operated by Tohoku Univ., NIED, and JMA. 146 DLFs listed in JMA catalog between Jan. 2012 and Sept. 2016 were selected as templates for the MF analysis. We used a frequency band of 1-8 Hz and set the detection threshold to 0.2. The time windows exceeding the threshold were visually checked to eliminate false detections. For each detected DLFs, using cross spectrum and correlation functions, we estimated the differential travel times between the detected DLF and the template having maximum correlation, and determined the relative hypocenter using the master event method.

As a result, we detected 1361 DLFs between Jan. 2012 to May 2018, which is about 10 times the number of templates, and determined 1357 hypocenters which spread over wider depth range compared to those estimated with the assumption that the hypocenters of the detected events are the same as those of the templates having maximum correlation. We also checked the individual waveforms of the detected DLFs to understand the spatial clustering of DLFs, and revealed that DLFs can be classified into the following two types in a large sense: the first type (354 events) shows high-frequency (3-4 Hz) component in the initial part (1-2 s) of the waveform, and low-frequency (1-2 Hz) component in the remaining part of the waveform; the second type (1007 events) shows low-frequency (1-2 Hz) component over the entire waveform. The depth distribution of the former type has a peak around 33 km and widely spreads (20-38 km) whereas that of the latter type is confined within a narrow range (20-26 km). These results suggest

©2019. Japan Geoscience Union. All Right Reserved.

that source processes of DLFs differ between two types. On the other hand, there is no clear difference in the Gutenberg-Richter law *b* values of both types.

Our further analysis including estimation of the source mechanisms of the detected DLFs may contribute to the understanding of the distribution and activities of deep volcanic fluid.

Keywords: Zao volcano, deep low-frequency earthquakes, Matched Filter method

©2019. Japan Geoscience Union. All Right Reserved.

Mechanisms transition of LFEs beneath Zao volcano due to the stress change induced by the 2011 Tohoku earthquake

*Genki Oikawa[1], Naofumi Aso[1], Junichi Nakajima[1], Toru Matsuzawa[2]

1. Tokyo Institute of Technology, 2. Tohoku University

Deep low-frequency earthquakes (LFEs) with dominant frequencies of 2–8 Hz occur at depths of 20–40 km, which is deeper than the depth of regular crustal earthquakes. Many previous studies indicated that focal mechanisms of LFEs have non-double-couple components such as CLVD (compensated linear vector dipole) and volumetric deformation. Therefore, LFEs are thought to be related to the magma or crustal fluid, but their physical mechanisms are still unknown. The focal mechanisms of LFEs are key information for understanding the physics underlying LFEs. Seismicity of LFEs in Zao has increased about two years after the Tohoku earthquake, so we are also interested in the potential variations of focal mechanisms in association with the seismicity change.
We analyze the mechanisms of 48 LFEs beneath Zao volcano by using the amplitude ratios of S-wave to P-wave.The site effect at each station is corrected using the radiation from regular earthquakes with known mechanisms. We assume four focal models (double-couple, CLVD, tensile-crack, and single-force) and determine an optimal model based on AIC (Akaike information criteria), to minimize the residuals between observed and theoretical S/P ratios with a penalty for the number of parameters.
We successfully determined focal mechanisms of 29 events. While the majorities are double couples (18 events; 62%), there are notable numbers of non-double-couple LFEs. The obtained mechanisms are classified into five groups, three types of double-couple (DC-A, DC-B, DC-C), a CLVD type (CLVD-D) and a single-force type (SF-E). Whereas the DC-A LFEs are observed only before the increase of LFE seismicity, most of the other types are generated after the increase of seismicity. The DC-A is consistent with the local stress field, and the symmetry axis of CLVD-D is sub-parallel to the P-axis of DC-A, so the CLVD-D is interpreted to be a shear-tensile-crack under the similar stress field. Considering that the transition of focal mechanisms was two years later than the Tohoku earthquake, we suggest that the lateral compressional stress field became less dominant near the source of LFEs two years after the Tohoku Earthquake, probably associated with afterslip and viscoelastic relaxation, and the change in local stress field altered the occurrence of LFEs.

Keywords: Low-frequency earthquake, The 2011 Tohoku earthquake, Focal Mechanisms

©2019. Japan Geoscience Union. All Right Reserved.

Magma/gas intrusion process of Shinmoedake Eruption in 2017 suggested by volcanic tremors location with ASL method

Shoya Imamura[1], *Makoto OKUBO[2]

1. Faculty of Science, Kochi University, 2. Natural Science Cluster, Kochi University

Kirishima volcanoes, which located on border Miyazaki and Kagoshima prefecture in Kyushu, is still active after the large scale eruption in 2011. In this study, by using volcanic tremor/events distribution, we would like to discuss magma/gas intrusion process around magma chamber.

Recentlly, source location of volcanic tremors is usually determined by ASL (Amplitude Source Location) method (*c.f.* Nakamichi *et.al.*, 2017). ASL method is based on the idea that seismic (S) waves at higher frequency range (> 5 Hz) will propagate isotropically, an its amplitude will be simply attenuate with distance. If we can use dense seismic observation records around volcano, we can calculate the volcanic tremor location in automatically every time window. Thus, using with ASL we can easily discuss volcanic tremor/events distribution and its time variation.

According to Kirishima volcanoes activities reported by JMA (Oct, 2017), numbers of volcanic earthquakes/tremors located at southwestward of the Shinmoedake have been rapidly increased from Oct. 2017, and erupsed on 11th until 16th. Therefore, In this study we analyzed three stages, **(1)** stable condition on 9th, **(2)** earthquake/tremor activation on 10th, and **(3)** continuous eruption on 16th.

In this study, we choiced and used 10 stations, which were operated by JMA, NIED and ERI, established around Shinmoedake. For analysis, we assumed V_S = 2.2 km/s, Q_f = 175 @10Hz for volcanic events, and Q_f = 300 for volcanic tremors beneath Shinmoedake and used 5 - 10 Hz band-passed envelope amplitude for ASL. Thus, we obtained three stages time-spatial volcanic tremor/events distribution.

According to Volcanic tremor/events distribution, these were located at southward of magma source at ~ 4 km depth estimated with GPS observations (Nakao et al., 2013); stage (1). After 18 o'clock, volcanic tremor/events were activated with numbers and magnitudes around magma source, and these location were move to shallower until -1 km; stage (2). Small magnitude and shallower tremors occurred continuously at Oct. 10th.
On 16th, tremor activity became in quiet, and just only located around southward of magma source; stage (3).

These results imply that magma/gas intrusion was occurred at stage (2), might have been occurred after magma vaporization in chamber. And we can considered that at stage(2), magma vent was already constructed, magma/gas was continuously supplyed from chamber at stage (3).

Acknowledgments:
In this study, we used seismic observation records obtained by JMA, NIED, ERI(University of Tokyo). A tool of ASL method was provided by Dr. Nakamichi, Kyoto university. We are very thanks to these cooperation.

Keywords: ASL, Kirishima volcanoes, Volcanic tremors/events

©2019. Japan Geoscience Union. All Right Reserved.

Source depth estimation of a magmatic inflation in 2008-2010 at Mt. Fuji, Japan, based on sparsity-promoting L1 inversion of GNSS data

*Yuta Mitsui[1], Takahiro Kato[2]

1. Department of Geosciences, Shizuoka University, 2. formerly at Department of Geosciences, Shizuoka University

Mt. Fuji has not erupted since the Plinian eruption in 1707, but its volcanic activity such as low-frequency earthquakes has not finished. Here, using GNSS (Global Navigation Satellite System) time-series data, we investigate an inflation event of Mt. Fuji in 2008-2010. Referring to recent studies of igneous processes, we focus on “vertically-extensive” magma systems and estimate depth distribution of geodetic inflation sources. A sparsity-promoting L1 regularization algorithm for inversion analysis allows us to estimate concentrated distribution of the sources with sufficient performance of data fitting. Our result shows that the inflation sources were mainly distributed in a depth range from 20 km to 15 km, and the total volume change was on the order of 0.01 cubic kilometers. The magma clot might move upward, and not move back downward as far as we observed. Our sparsity-promoting method is useful to constrain magma movement from limited observation data.

Keywords: Mt. Fuji, GNSS, L1 regularization

©2019. Japan Geoscience Union. All Right Reserved.

[J] Poster | S (Solid Earth Sciences)：S-SS Seismology

Wed. May 29, 2019 5:15 PM - 6:30 PM JST | Wed. May 29, 2019 8:15 AM - 9:30 AM UTC | Poster Hall International Exhibition Hall8, Makuhari Messe_27

[S-SS17] Seismic evidence of volcanic roots

convener:Naofumi Aso(Tokyo Institute of Technology), Yohei Yukutake(Hot Springs Research Institute of Kanagawa Prefecture)

Magma transport system beneath volcanoes is a key to understand long-term geodynamics and the evolution of the Earth. Especially, deep long-period earthquakes around the Moho beneath active volcanoes are supposed to relate to the magma transport system, although their activities and mechanisms are not understood well. Revealing the role of deep long-period earthquakes in the magma transport system is a key to understand deep volcanic roots around the lower crust, including deep magma chambers. It is therefore essential to estimate complete seismicity with a high-resolution hypocenter distribution and focal mechanisms of deep long-period earthquakes, based on innovative techniques including template matching, relocation methods using waveform cross-correlations, and waveform inversions. Also, high-resolution seismic imaging using advanced tomography techniques, including tomography using ambient noise interferometry, with a dense seismic network is essential to visualize the magma transport system. We welcome studies to understand volcanic roots from a variety of seismological approaches including but not limited to the methods mentioned above.

[SSS17-P01] S-wave reflectors beneath the earthquake swarm in the Yonezawa-Kitakata area, NE Japan

*Manami Suzuki [1], Akiko Hasemi[1], Tomomi Okada[1], Toru Matsuzawa[1], Norihito Umino[1], Takashi Nakayama[1], Noriko Tsumura[2], Tadashi Yamashina[3], Group for the aftershock observations of the 2011 off the Pacific of Tohoku Earthquake (1.Research Center for Prediction of Earthquakes and Volcanic Eruptions, Graduate School of Science, Tohoku University, 2.Graduate School of Science, Chiba University, 3.Faculty of Science and Technology, Kochi University)

[SSS17-P02] Imaging of the magma pathway beneath Kirishima volcanoes by seismic interferometry

*Yutaka Nagaoka[1], Kiwamu Nishida[2], Yosuke Aoki[2], Minoru Takeo[2], Takahiro Ohkura[3], Shin Yoshikawa[3] (1.Volcanology Research Department, Meteorological Research Institute, 2.Earthquake Research Institute, The University of Tokyo, 3.Aso Volcanological Laboratory, Institute for Geothermal Sciences, Graduate School of Science, Kyoto University)

[SSS17-P03] Finite element three-dimensional seismic waveform calculations of volcanic deep low frequency earthquake including true topographic effects of Hakone volcano

*Lina Yamaya[1], Kimihiro Mochizuki[1], Tsuyoshi Ichimura[1], Kohei Fujita[1], Takeshi Akuhara[1], Takane Hori[2], Ryou Honda[3], Yohei Yukutake[3] (1.Earthquake Research Institute, Univ. of Tokyo, 2.JAMSTEC, 3.Hot Springs Research Institute of Kanagawa)

[SSS17-P04] Magma transport system beneath Hakone volcano inferred from deep low frequency earthquakes

*Yohei Yukutake[1], Yuki Abe[1] (1.Hot Springs Research Institute of Kanagawa Prefecture)

[SSS17-P05] Hypocenter and waveform characteristics of deep low-frequency earthquakes beneath Zao volcano

*Takuma Ikegaya[1], Mare Yamamoto[1] (1.Graduate School of Science, Tohoku University)

[SSS17-P06] Mechanisms transition of LFEs beneath Zao volcano due to the stress change induced by the 2011 Tohoku earthquake

*Genki Oikawa[1], Naofumi Aso[1], Junichi Nakajima[1], Toru Matsuzawa[2] (1.Tokyo Institute of Technology, 2.Tohoku University)

[SSS17-P07] Magma/gas intrusion process of Shinmoedake Eruption in 2017 suggested by volcanic tremors location with ASL method

Shoya Imamura[1], *Makoto OKUBO[2] (1.Faculty of Science, Kochi University, 2.Natural Science Cluster, Kochi University)

[SSS17-P08] Source depth estimation of a magmatic inflation in 2008-2010 at Mt. Fuji, Japan, based on sparsity-promoting L1 inversion of GNSS data

*Yuta Mitsui[1], Takahiro Kato[2] (1.Department of Geosciences, Shizuoka University, 2.formerly at Department of Geosciences, Shizuoka University)

S-wave reflectors beneath the earthquake swarm in the Yonezawa-Kitakata area, NE Japan

*Manami Suzuki [1], Akiko Hasemi[1], Tomomi Okada[1], Toru Matsuzawa[1], Norihito Umino[1], Takashi Nakayama[1], Noriko Tsumura[2], Tadashi Yamashina[3], Group for the aftershock observations of the 2011 off the Pacific of Tohoku Earthquake -

1. Research Center for Prediction of Earthquakes and Volcanic Eruptions, Graduate School of Science, Tohoku University, 2. Graduate School of Science, Chiba University, 3. Faculty of Science and Technology, Kochi University

Research on reflected S wave around volcanic regions and inland earthquake faults has been conducted throughout Japan. Mizoue et al. (1982) showed the spatial distribution of S wave reflection points in Nikko-Ashio area, and the amplitude ratio of SxP wave and SxS wave was explained by layered partially melt. In the Tohoku region, reflected S wave is from reflector contains fluid which was released during the cooling process of the melt suggested by Umino et al. (2002) and Hori et al. (2004). It is pointed out that the dehydrated fluid is involved in the mechanism of the occurrence of an inland earthquake [e.g., Hasegawa et al., 2005], and it is important to understand the behavior of the fluid in the crust in the Tohoku region in more details.

In the Yonezawa - Kitakata area, NE Japan, which is the target area of this research, it is thought that a swarm earthquake occurred 7 days after the 2011 Tohoku Region Pacific Offshore Earthquake, and the cause is the decrease in strength due to increase in fluid pressure [eg, Okada et al., 2015]. The focal region is located in and around the Otoge caldera [Yamamoto et al., 1994] which formed in the Miocene, and the possibility of existence of the fluid dehydrated from the melt as described above is sufficient. Since S wave reflected waves in Yonezawa - Kitakata area have already been discovered by Hasemi et al. (2016), this study aims to obtain the spatial distribution of the S wave reflector. In this area, temporary stations are deployed densely by Group of the aftershock observations of 2011 off the Pacific coast of Tohoku Earthquake. In this research, seismic waveform data at these temporal stations and the permanent stations by Hi-net is used. In order to accurately obtain the spatial distribution of the S wave reflector, we use the hypocenters determined by the Double Difference method using the temporary observation data.

First of all, I carefully read the travel time of the S wave reflected wave visually. For ten observation stations/clusters pairs which were able to confirm the S wave reflected wave remarkably, the travel time of the seismic waveform was converted to the depth as in Inamori et al. (1992). As a result, 16 reflectors in the northeast clusters, 14 in the center, and 3 in the southwest were read.

Next, using the read travel time, the mirror observation stations were calculated by grid search [e.g., Horiuchi et al., 1988]. We assume that the reflector is a single plane, and the wave ray path is a straight line with a uniform velocity structure of 3.4 km/s. We will find the reflector with minimum of the least squared square root between observed and calculated traveling times. From the equation of the reflector obtained by the above process, the strike/dip and the position of the reflection point with respect to each epicenter were obtained.

As a result, the reflectors are located from the lower part of the source region to the depth of 10 - 20 km below it. The strike seems to be drawing a circle or an arc, and the dips are smaller beneath the source region. Comparing this reflector distribution with the seamless geological map [AIST], for the reflectors just beneath the Otoge caldera their strikes seems to be along the edge of the caldera, and for the

©2019. Japan Geoscience Union. All Right Reserved.

reflector in the western part, their strikes follows the western marginal fault zone of Aizu Basin and the boundaries of geological structure. Comparing this with the seismic velocity structure, the reflectors are located at the periphery of the low velocity zone, being consistent with the results obtained by Umino et al. (2002) and Hori et al. (2004). By this reason, fluids promoting swarm earthquakes in the Yonezawa - Kitakata area may be migrated from the melt below the epicenter area and may have passed boundary of the existing geological structure.

Keywords: reflected wave, crustal fluid

©2019. Japan Geoscience Union. All Right Reserved.

Imaging of the magma pathway beneath Kirishima volcanoes by seismic interferometry

*Yutaka Nagaoka[1], Kiwamu Nishida[2], Yosuke Aoki[2], Minoru Takeo[2], Takahiro Ohkura[3], Shin Yoshikawa[3]

1. Volcanology Research Department, Meteorological Research Institute, 2. Earthquake Research Institute, The University of Tokyo, 3. Aso Volcanological Laboratory, Institute for Geothermal Sciences, Graduate School of Science, Kyoto University

Shinmoe-dake, one of Kirishima volcanoes, experienced magmatic eruptions in 2011. The analysis of ground deformation shows that the pressure source locates 5 km to the northwest of the Shinmoe-dake summit at a depth of 8 km, which implies the existence of a magma reservoir. We are trying to resolve a better image by a seismological technique toward ensuring its existence and deriving precise crustal structure and reveal a magma pathway.

The technique we employed is seismic wave interferometry, which extracts the seismic wave propagation between two seismic stations by taking cross correlations of random wavefields, such as the ambient seismic noise or the seismic coda wave. The cross correlations of random wavefields recorded at two stations can be represented as if the source is at one station and the recorder is at the other. This technique is suitable for exploring local structure since the extracted wave is sensitive to the internal structure between the two stations.

We inferred the crustal phase velocity anomaly using three-component records of the ambient seismic noise recorded by a seismic array between April 2011 and December 2013. Rayleigh and Love waves are extracted by taking cross correlations (Rayleigh waves from cross correlation functions of pairs of vertical components, and Love waves from transverse components). We derived reference dispersion curves of Rayleigh and Love waves, respectively, using all possible pairs of stations, then measured phase velocity anomalies of all possible pairs with respect to the reference in multiple frequency bands (0.1-0.2 Hz, 0.2-0.4 Hz, 0.3-0.6 Hz, and 0.4-0.8 Hz). Finally, three-dimensional V_{SV} and V_{SH} structures were obtained from a collection of local one-dimensional velocity profiles derived by inverting phase velocities of Rayleigh and Love waves, respectively, at each grid point.

Kirishima volcanoes exhibit a low V_{SV} body that is embedded beneath the deformation source and extends horizontally by about 15 km at around 10 km below sea level beneath the volcanoes. We interpret it as a crustal magma reservoir. V_{SH} did not detect low velocity bodies, implying the radial anisotropy generated by a sill complex in the magma reservoir. The ground deformation source of the eruptions in 2011 locates at uppermost and northwesternmost of the low velocity body, indicating that the low velocity body is a magma reservoir of the volcanoes. Moreover, low frequency earthquakes occur beneath the southeasternmost of the low velocity body. We can, therefore, present a model of a magma pathway that magma rising up from the deeper region right beneath the volcanoes is once stored at a magma reservoir and further ascend toward the surface from the uppermost and northwesternmost of the magma reservoir.

Our study presents the effectiveness of the estimation of S wave velocity structure using phase velocities of Rayleigh and Love waves in deciphering the magma pathway beneath the active volcanoes and the importance of further investigation of magma plumbing systems beneath various types of volcanoes.

©2019. Japan Geoscience Union. All Right Reserved.

Keywords: Kirishima, seismic interferometry, ambient seismic noise, radial anisotropy

©2019. Japan Geoscience Union. All Right Reserved.

Finite element three-dimensional seismic waveform calculations of volcanic deep low frequency earthquake including true topographic effects of Hakone volcano

*Lina Yamaya[1], Kimihiro Mochizuki[1], Tsuyoshi Ichimura[1], Kohei Fujita[1], Takeshi Akuhara[1], Takane Hori[2], Ryou Honda[3], Yohei Yukutake[3]

1. Earthquake Research Institute, Univ. of Tokyo, 2. JAMSTEC, 3. Hot Springs Research Institute of Kanagawa

Volcanic deep low frequency (DLF) earthquakes play an important role on revealing magma volcanic system because they are thought to reflect movements of volcanic fluid. Nakamichi et al. (2003) showed that the DLF earthquakes occurring beneath Iwate volcano have compensated linear vector dipole components, which suggests the relation with volcanic fluid.

Hakone volcano also has DLF earthquakes whose depths are from 10 to 30 km. Yukutake et al. (2018) showed that the number of DLF earthquakes increased just before crustal movement or increase of volcanic tremors in 2006, 2013, 2015, but mechanisms of the DLF earthquakes are still unrevealed. JMA reported that DLF earthquakes occur not just beneath Owakudani (the main crater of Hakone volcano) but around 10 km north from Owakudani, which is needed to be studied in detail. One of the difficulties to infer the source mechanisms and centroids is that the volcanic structure is complex not only due to its velocity structure but also due to its geometry. Calculation of three-dimensional seismic wave propagation are still challenging due to its computational cost, but it has become less difficult due to the recent development of efficient calculation techniques of computational science.

In this study, we used a technique of finite element three-dimensional waveform computation (Ichimura et al., 2017) to calculate the synthetic waveforms of the DLF earthquakes in Hakone volcano with respect to two different structure representations; direct inclusion of topography and flat surface with squashed topography in to the subsurface (Aagaard et al. 2008), and compared the resulted synthetic waveforms. We assumed the modified seismic velocity model reported in Yukutake et al. (2014). We used K computer and calculated the synthetics up to 1.5 Hz. As a result, although the arrival times of direct waves are similar, shapes of subsequent arrival phases are different. The amplitudes of subsequent arrival waves calculated including the true topography are larger than those calculated for the flat surface model with squashed topography. Observed data have such large amplitudes in subsequent arrival phases. Therefore, it is needed to calculate the synthetics including true topography for comparisons between data and synthetics. We further investigate generation mechanisms of such DLF earthquakes by synthetic modeling of the observed waveforms.

Keywords: Deep low frequency earthquake, Finite element three-dimensional seismic waveform calculation, K computer

©2019. Japan Geoscience Union. All Right Reserved.

Magma transport system beneath Hakone volcano inferred from deep low frequency earthquakes

*Yohei Yukutake[1], Yuki Abe[1]

1. Hot Springs Research Institute of Kanagawa Prefecture

It has been recognized that the occurrence of deep low-frequency earthquakes (DLFEs) beneath a volcano is related to a behavior of magmatic fluid (e.g. Nakamichi et al., 2003). On the other hand, the linkage between the DLFE and shallow volcanic activities such as a swarm activity and crustal deformation has not been well understood. In the present study, we compared the temporal sequence of the DLFEs occurred around the depth of 25 km beneath Hakone volcano, central Japan, with the swarm activity and the inflation of pressure source occurred in the area shallower than the depth of 10 km.

During recent two decades, we observed the remarkable swarm activities at Hakone volcano in 2001, 2006, 2009, 2013 and 2015. In each swarm activity, crustal deformation associated with an inflation of pressure source was estimated at the depth of 7km beneath the central cone of caldera, by using the GNSS data (Harada et al., 2018). Tthe tomography analysis (Yukutake et al., 2015; Yukutake et al., 2018) reveals that the crystalizing magma body locates around the depth of 10km and the hydrothermal fluid dehydrated from the magma exists above it.

The DLFEs were detected by using the Matched Filter method. We used continuous seismic waveforms at 12 permanent stations around Hakone volcano in the period from January, 2000 to January, 2017. The template waveforms of 94 DLFs were prepared on the basis of the JMA catalog. We also estimated the temporal sequence of b-value by using the DLFE catalog. The temporal change was calculated by using the method in Wiemer and Wyss (2000), using the moving time-windows containing a constant event number of 300 events.

As a result, we could detect the numerous DLFEs corresponding to 46 times in comparison with the number detected by JMA. It is clearly evident that the DLFEs activated prior the swarm activity in 2006, 2009, 2013 and 2015, and synchronized with the onset time of crustal expansion caused by the inflation of pressure source. We estimated the increment of b-values by accompanied with the activation of DLFEs. An increase of b-values during the swarm activity in several volcanic regions can be explained by assuming the increment of pore pressure or the change of thermal gradient associated with the intrusion of magma/hydrothermal fluid (Jacobs and McNutt, 2010; Nanjo et al., 2018). It is likely that the activation of DLFEs accompanied by the increase of b-values reflects the inclusion of magma at the depth. The inflation of pressure source at the depth of 7 km may suggest the increase of a volatile component at the shallow magma/hydrothermal fluid from the deep intruded magma at the source region of DLFEs or the increment of temperature due to the migration of hot material. The increase of strain rate due to the inflation can promote the migration of highly pressurized to the shallow brittle zone (Fournier, 1999), triggering the earthquake swarms. On the other hand, the remarkable activation of DLFE was observed in the later stage of swarm activity in 2001, rather than precursory activity for the earthquake swarms. This result may imply that the activation of volcanic phenomena such as the shallow swarm activity and crustal deformation is not necessary initiated by the deep magma intrusion.

Acknowledgments
We used the waveform record obtained by the permanent stations of National Research Institute for Earth

©2019. Japan Geoscience Union. All Right Reserved.

Science and Disaster Resilience and GNSS data of Geospatial Information Authority of Japan. We used zmap program code (Wiemer, 2001) to estimate b-value.

Keywords: Deep low frequency earthquake, earthquake swarm, Hakone volcano

©2019. Japan Geoscience Union. All Right Reserved.

Hypocenter and waveform characteristics of deep low-frequency earthquakes beneath Zao volcano

*Takuma Ikegaya[1], Mare Yamamoto[1]

1. Graduate School of Science, Tohoku University

The 2011 Tohoku Earthquake (Mw 9.0) caused large crustal deformation in and around the Tohoku region, and strongly affected volcanic fluids in the crust. As an example suggesting such influence, the change in activities of deep low-frequency earthquakes (DLFs) occurring in the lower crust. The analysis of DLFs is thus considered to be one of the important keys to infer the activity of deep magma and to assess the potential risks of mid- to long-term volcanic activity after a huge earthquake. In this presentation, we report the results of our analysis of the DLFs beneath Zao volcano where activation of volcanic activities has been observed after the 2011 Tohoku Earthquake.

Zao volcano is located on the border between Yamagata and Miyagi prefectures. After the 2011 Tohoku Earthquake, the number of DLFs beneath Zao volcano started increasing, and increase in shallow seismicity have been observed since 2013. To investigate such seismic activities, the JMA unified hypocenter catalog (JMA catalog) is often used. However, the completeness of the catalog is not guaranteed in small DLFs. To improve the completeness of event detection, Ikegaya and Yamamoto (2018, JpGU) applied Matched Filter method (MF method) to the continuous waveform data recorded in 2015 and detected DLFs having high correlation to the template DLFs listed in JMA catalog. They successfully increased the number of small DLFs and revealed the spatial distribution of hypocenters showing two clusters above and below 28 km. However, due to the assumption that the hypocenters of the detected events are the same as those of the templates yielding maximum correlation value, it is difficult to discuss the details of the hypocenter clustering. In this study, aiming to understand the detailed spatio-temporal characteristics of DLF activity, we apply MF method to the waveform data for the last seven years, and determine relative hypocenters of the detected events.

In the analysis, we used the continuous three-components waveform data recorded at four permanent stations operated by Tohoku Univ., NIED, and JMA. 146 DLFs listed in JMA catalog between Jan. 2012 and Sept. 2016 were selected as templates for the MF analysis. We used a frequency band of 1-8 Hz and set the detection threshold to 0.2. The time windows exceeding the threshold were visually checked to eliminate false detections. For each detected DLFs, using cross spectrum and correlation functions, we estimated the differential travel times between the detected DLF and the template having maximum correlation, and determined the relative hypocenter using the master event method.

As a result, we detected 1361 DLFs between Jan. 2012 to May 2018, which is about 10 times the number of templates, and determined 1357 hypocenters which spread over wider depth range compared to those estimated with the assumption that the hypocenters of the detected events are the same as those of the templates having maximum correlation. We also checked the individual waveforms of the detected DLFs to understand the spatial clustering of DLFs, and revealed that DLFs can be classified into the following two types in a large sense: the first type (354 events) shows high-frequency (3-4 Hz) component in the initial part (1-2 s) of the waveform, and low-frequency (1-2 Hz) component in the remaining part of the waveform; the second type (1007 events) shows low-frequency (1-2 Hz) component over the entire waveform. The depth distribution of the former type has a peak around 33 km and widely spreads (20-38 km) whereas that of the latter type is confined within a narrow range (20-26 km). These results suggest

©2019. Japan Geoscience Union. All Right Reserved.

that source processes of DLFs differ between two types. On the other hand, there is no clear difference in the Gutenberg-Richter law *b* values of both types.

Our further analysis including estimation of the source mechanisms of the detected DLFs may contribute to the understanding of the distribution and activities of deep volcanic fluid.

Keywords: Zao volcano, deep low-frequency earthquakes, Matched Filter method

©2019. Japan Geoscience Union. All Right Reserved.

Mechanisms transition of LFEs beneath Zao volcano due to the stress change induced by the 2011 Tohoku earthquake

*Genki Oikawa[1], Naofumi Aso[1], Junichi Nakajima[1], Toru Matsuzawa[2]

1. Tokyo Institute of Technology, 2. Tohoku University

Deep low-frequency earthquakes (LFEs) with dominant frequencies of 2–8 Hz occur at depths of 20–40 km, which is deeper than the depth of regular crustal earthquakes. Many previous studies indicated that focal mechanisms of LFEs have non-double-couple components such as CLVD (compensated linear vector dipole) and volumetric deformation. Therefore, LFEs are thought to be related to the magma or crustal fluid, but their physical mechanisms are still unknown. The focal mechanisms of LFEs are key information for understanding the physics underlying LFEs. Seismicity of LFEs in Zao has increased about two years after the Tohoku earthquake, so we are also interested in the potential variations of focal mechanisms in association with the seismicity change.
We analyze the mechanisms of 48 LFEs beneath Zao volcano by using the amplitude ratios of S-wave to P-wave.The site effect at each station is corrected using the radiation from regular earthquakes with known mechanisms. We assume four focal models (double-couple, CLVD, tensile-crack, and single-force) and determine an optimal model based on AIC (Akaike information criteria), to minimize the residuals between observed and theoretical S/P ratios with a penalty for the number of parameters.
We successfully determined focal mechanisms of 29 events. While the majorities are double couples (18 events; 62%), there are notable numbers of non-double-couple LFEs. The obtained mechanisms are classified into five groups, three types of double-couple (DC-A, DC-B, DC-C), a CLVD type (CLVD-D) and a single-force type (SF-E). Whereas the DC-A LFEs are observed only before the increase of LFE seismicity, most of the other types are generated after the increase of seismicity. The DC-A is consistent with the local stress field, and the symmetry axis of CLVD-D is sub-parallel to the P-axis of DC-A, so the CLVD-D is interpreted to be a shear-tensile-crack under the similar stress field. Considering that the transition of focal mechanisms was two years later than the Tohoku earthquake, we suggest that the lateral compressional stress field became less dominant near the source of LFEs two years after the Tohoku Earthquake, probably associated with afterslip and viscoelastic relaxation, and the change in local stress field altered the occurrence of LFEs.

Keywords: Low-frequency earthquake, The 2011 Tohoku earthquake, Focal Mechanisms

©2019. Japan Geoscience Union. All Right Reserved.

Magma/gas intrusion process of Shinmoedake Eruption in 2017 suggested by volcanic tremors location with ASL method

Shoya Imamura[1], *Makoto OKUBO[2]

1. Faculty of Science, Kochi University, 2. Natural Science Cluster, Kochi University

Kirishima volcanoes, which located on border Miyazaki and Kagoshima prefecture in Kyushu, is still active after the large scale eruption in 2011. In this study, by using volcanic tremor/events distribution, we would like to discuss magma/gas intrusion process around magma chamber.

Recentlly, source location of volcanic tremors is usually determined by ASL (Amplitude Source Location) method (*c.f.* Nakamichi *et.al.*, 2017). ASL method is based on the idea that seismic (S) waves at higher frequency range (> 5 Hz) will propagate isotropically, an its amplitude will be simply attenuate with distance. If we can use dense seismic observation records around volcano, we can calculate the volcanic tremor location in automatically every time window. Thus, using with ASL we can easily discuss volcanic tremor/events distribution and its time variation.

According to Kirishima volcanoes activities reported by JMA (Oct, 2017), numbers of volcanic earthquakes/tremors located at southwestward of the Shinmoedake have been rapidly increased from Oct. 2017, and erupsed on 11th until 16th. Therefore, In this study we analyzed three stages, **(1)** stable condition on 9th, **(2)** earthquake/tremor activation on 10th, and **(3)** continuous eruption on 16th.

In this study, we choiced and used 10 stations, which were operated by JMA, NIED and ERI, established around Shinmoedake. For analysis, we assumed V_S = 2.2 km/s, Q_f = 175 @10Hz for volcanic events, and Q_f = 300 for volcanic tremors beneath Shinmoedake and used 5 - 10 Hz band-passed envelope amplitude for ASL. Thus, we obtained three stages time-spatial volcanic tremor/events distribution.

According to Volcanic tremor/events distribution, these were located at southward of magma source at ~ 4 km depth estimated with GPS observations (Nakao et al., 2013); stage (1). After 18 o'clock, volcanic tremor/events were activated with numbers and magnitudes around magma source, and these location were move to shallower until -1 km; stage (2). Small magnitude and shallower tremors occurred continuously at Oct. 10th.
On 16th, tremor activity became in quiet, and just only located around southward of magma source; stage (3).

These results imply that magma/gas intrusion was occurred at stage (2), might have been occurred after magma vaporization in chamber. And we can considered that at stage(2), magma vent was already constructed, magma/gas was continuously supplyed from chamber at stage (3).

Acknowledgments:
In this study, we used seismic observation records obtained by JMA, NIED, ERI(University of Tokyo). A tool of ASL method was provided by Dr. Nakamichi, Kyoto university. We are very thanks to these cooperation.

Keywords: ASL, Kirishima volcanoes, Volcanic tremors/events

©2019. Japan Geoscience Union. All Right Reserved.

Source depth estimation of a magmatic inflation in 2008-2010 at Mt. Fuji, Japan, based on sparsity-promoting L1 inversion of GNSS data

*Yuta Mitsui[1], Takahiro Kato[2]

1. Department of Geosciences, Shizuoka University, 2. formerly at Department of Geosciences, Shizuoka University

Mt. Fuji has not erupted since the Plinian eruption in 1707, but its volcanic activity such as low-frequency earthquakes has not finished. Here, using GNSS (Global Navigation Satellite System) time-series data, we investigate an inflation event of Mt. Fuji in 2008-2010. Referring to recent studies of igneous processes, we focus on “vertically-extensive” magma systems and estimate depth distribution of geodetic inflation sources. A sparsity-promoting L1 regularization algorithm for inversion analysis allows us to estimate concentrated distribution of the sources with sufficient performance of data fitting. Our result shows that the inflation sources were mainly distributed in a depth range from 20 km to 15 km, and the total volume change was on the order of 0.01 cubic kilometers. The magma clot might move upward, and not move back downward as far as we observed. Our sparsity-promoting method is useful to constrain magma movement from limited observation data.

Keywords: Mt. Fuji, GNSS, L1 regularization

©2019. Japan Geoscience Union. All Right Reserved.

[E] Poster | S (Solid Earth Sciences)：S-IT Science of the Earth's Interior & Techtonophysics

Wed. May 29, 2019 10:45 AM - 12:15 PM JST | Wed. May 29, 2019 1:45 AM - 3:15 AM UTC | Poster Hall International Exhibition Hall8, Makuhari Messe_8

[S-IT26] New perspectives on the geodynamics of East Asia

convener:Timothy B Byrne(University of Connecticut), Asuka Yamaguchi(Atomosphere and Ocean Research Institute, The University of Tokyo), Jonny Wu(University of Houston), Kyoko Okino(Atmosphere and Ocean Research Institute, The University of Tokyo)

The Pacific, Indo-Australia and Eurasian plates converge around the Philippine Sea plates in south and East Asia, resulting in one of the most tectonically active regions on earth. The area is also geologically and tectonically complex with numerous active tectonic environments, ranging from subduction to collision, and a long history of plate boundary interactions. The last decade has yielded a wide range of new observations, including detailed geologic data and high resolution crustal to mantle imaging. Here we seek oral and poster presentations that bear on the geologic history and geophysical character of modern and ancient plates in East Asia and their interactions since the Mesozoic. We also invite geodynamic models that integrate these diverse datasets into a more holistic view of this dynamic environment.

[SIT26-P01] Geochemical characteristics of effusive rocks (greenstones) in the Hidaka Belt, Hokkaido, Japan

*Toru Yamasaki[1], Futoshi Nanayama[1] (1.Geol. Survey of Japan (AIST))

[SIT26-P02] Large gas reservoir in continental back-arc basin, revealed by automatic seismic velocity analysis in the Okinawa Trough

*Kota Mukumoto[1], Takeshi Tsuji[1], Andri Hendriyana[1] (1.Kyushu University)

[SIT26-P03] Characterize coseismic deformation of Mw 7.5 Palu earthquake in a triple junction in Sulawesi, Indonesia

*MIN-CHIEN TSAI[1], Ying-Hui Yang[2], Chun-Ying Chiu[3], Jyr-Ching Hu[3] (1.Seismological center, Central Weather Bureau, Taipei, Taiwan, R.O.C., 2.School of Civil Engineering and Architecture, Southwest Petroleum University, Chengdu, China, 3.Department of Geosciences, National Taiwan University, Taipei, Taiwan, R.O.C.)

Geochemical characteristics of effusive rocks (greenstones) in the Hidaka Belt, Hokkaido, Japan

*Toru Yamasaki[1], Futoshi Nanayama[1]

1. Geol. Survey of Japan (AIST)

Igneous rocks in a subduction complex typically occur as greenstones, and petrological and geochemical investigations of such greenstones can provide important insights into the oceanic magmatism, origin of the accretionary complex, and growth of the continental margin. The Hidaka Belt in Central Hokkaido, Japan consists of an early Paleogene subduction complex, referred to as the Hidaka Supergroup (HSG), dominated by clastic rocks. Locally, the terrigenous sediments of the HSG were intruded by the contemporary, normal-type mid-ocean ridge basalts (“*in situ*N-MORBs”) that were formed at an oceanic ridge near the Eurasian continent (Miyashita and Katsushima, 1986: GSJ). The southern area of the HSG has been referred to as the Nakanogawa Group (NKG), which gradually leads to the high-temperature Hidaka metamorphic belt (HMB) in the western part. The lower sequence of the HMB consists mainly of high-grade metabasites, which are assumed to be equivalent to the N-MORBs in the HSG, based on their geochemical features. Recently, Yamasaki and Nanayama (2018a: Lithos) reported about the unique Daimaruyama greenstones from the NKG, formed by an immature intra-oceanic arc-type volcanism. In addition, highly-alkaline basalts, presumably formed at the seamount, exist as exotic blocks in the NKG and are named as Tachiiwa blocks (Owada et al., 1992: JMPEG). In fact, the N-MORBs in the HSG and the Tachiiwa alkaline rocks are characterized by the whole-rock major and minor element geochemistry, but the trace element geochemistry, including the rare earth elements (REEs), has not been reported yet for these rocks. Therefore, we collected 18 samples of greenstones from the entire Hidaka Belt and examined their whole-rock major and trace element geochemistry.

Including those in our previous reports (Yamasaki and Nanayama, 2018a, b: JpGU Abs.), there are three distinct types of greenstones in the Hidaka Belt. The first type are the MORB-type greenstones which show relatively flat chondrite-normalized (CN) REE patterns and N-MORB-normalized (NMN) multi-element patterns with Ti/V = 26–53 and Zr/Nb = 21–117. Although Miyashita and Kiminami (1999: MemGSJ) showed the flat NMN minor element (Nb, P, Zr, Ti, and Y) patterns of basalts from the northern HSG, trace element patterns of the MORB-type rocks in this study show rather light REE (LREE)-rich NMN multi-element patterns. The second type are the ocean island basalt (OIB)-type greenstones. The NMN multi-element and CN REE patterns for this type of greenstones show a gentle slope up to the left, with Ti/V>62 and Zr/Nb<15. The third type are the Daimaruyama greenstones. This type of greenstones show similar NMN multi-element patterns and CN REE patterns to those in the OIB-type, but with a clear relative depletion of Nb, Ta, and Ti. In addition, their Ti-V relations are similar to those in the MORB-type greenstones.

MORB-type greenstones are distributed from the northernmost part of the HSG to the southern Rakko River area in the NKG. OIB-type greenstones occur in the Tachiiwa block and the Rakko River area. Daimaruyama greenstones occur only in the Daimaruyama megablock in the NKG. Since the Tachiiwa and Daimaruyama blocks are presumably derived from the neighboring Tokoro Belt, the absence of the OIB-type and Daimaruyama greenstones in the northern HSG implies a difference in provenance between the HSG and NKG. The MORB-type greenstones do not show the typical N-MORB-type (LREE-depleted) trace element patterns, whereas the metabasite in the HMB shows the typical N-MORB-type geochemical features. In addition, the distribution of the MORB-type greenstones is separated from the metabasites of

©2019. Japan Geoscience Union. All Right Reserved.

the HMB in the southern Hidaka Belt. These lines of evidence suggest that the protolith of the HMB is not an equivalent of the “*in-situ*MORB” in the HSG, and is probably an accreted fragment of the older oceanic plate.

Keywords: Hidaka Belt, greenstones, trace elements

©2019. Japan Geoscience Union. All Right Reserved.

Large gas reservoir in continental back-arc basin, revealed by automatic seismic velocity analysis in the Okinawa Trough

*Kota Mukumoto[1], Takeshi Tsuji[1], Andri Hendriyana[1]

1. Kyushu University

P-wave velocity acquired from seismic reflection data allows us to quantify submarine geological structures. In the Iheya North Knoll of the Okinawa Trough, intense hydrothermal activity occurs due to continental rifting. The hydrothermal system in the Iheya North Knoll has been explored by geophysical surveys, geochemical measurements and drilling campaign. Based on these surveys, gas reservoir could be considered to exist around the Iheya North Knoll. However, gas reservoir around the Iheya North Knoll has not been identified in previous studies. Here we show P-wave velocity structure derived from automatic velocity analysis of multi-channel seismic reflection data. P-wave velocity is sensitive to free gas in sediments. Therefore, P-wave velocity is key information to quantify gas distribution in sediments. Automatic velocity analysis estimated P-wave velocity structure with remarkable high spatial and temporal resolution. The P-wave velocity structure revealed gas reservoirs around the Iheya North Knoll. Although many gas components can be generated by magmatic activity, hydrothermal alteration of organic-rich sediments and biogenic processes, CH_4 and CO_2 could be major gas components which is derived by hydrothermal system in marine sediment. Therefore, main gas components could be CH_4 or CO_2. The strong amplitude reflector above the gas reservoir could be the interface between CH_4 hydrate and gas, because the depth of strong amplitude reflector is well consistent with pressure-temperature conditions of the phase transition. If the main gas component is CH_4, the gas reservoir could be important as resource. Whereas, if the gas reservoir includes CO_2, the gas distribution could be important to consider carbon flux between earth and ocean. Furthermore, widely distributed gas reservoir may influence on the chemical components of hydrothermal fluids in the Iheya North Knoll.

Keywords: Seismic reflection data, Okinawa Trough, Gas reservoir

©2019. Japan Geoscience Union. All Right Reserved.

Characterize coseismic deformation of Mw 7.5 Palu earthquake in a triple junction in Sulawesi, Indonesia

*MIN-CHIEN TSAI[1], Ying-Hui Yang[2], Chun-Ying Chiu[3], Jyr-Ching Hu[3]

1. Seismological center, Central Weather Bureau, Taipei, Taiwan, R.O.C., 2. School of Civil Engineering and Architecture, Southwest Petroleum University, Chengdu, China, 3. Department of Geosciences, National Taiwan University, Taipei, Taiwan, R.O.C.

We first use SAR satellite data to map the coseismic deformation for the 2018 Mw=7.5 strike-slip earthquake of 28 September 2018 in Palu, Sulawesi, Indonesia. The seismogenic fault is a left-lateral a strike-slip event along the Palu-Koro fault at shallow depth that occurred within the interior of the Molucca Sea microplate, which is part of the Sunda plate. We use D-InSAR technique with ALOS-2 descending orbit radar images to characterize coseismic and deformation pattern induced by Palu earthquake.We also plan to use with sub-pixel correlation form Sentinel-2 and Planet imagery to map the surface rupture area and the coseismic offsets in order to provide the near-field deformation data located in decorrelation zone from the D-InSAR result. Thus we can inverse the distribution of slip on the fault patches. In addition, we also calculate the Coulomb stress transfer for assessing the stress increasing and shadow on the major fault systems, such as the active Poso Fault Zone and Mamuju –Lariang Active Fault Zone. In particular, we will assess the seismic potential by Coulomb stress transfer in Minahasa Active Subduction Zone together with two events with Mw 7.9 and Mw 7.0 happened on 1996/01/01 and 1996/07/22. We try to assess the seismogenic potential in terms of interseismic slip rate, slip rate deficit and coupling ratio for the Palu-Koro fault system in a triple junction of the Sulawesi island.

Keywords: InSAR , pixel offset , Palu earthquake, Triple junction

©2019. Japan Geoscience Union. All Right Reserved.

[E] Poster | S (Solid Earth Sciences)：S-IT Science of the Earth's Interior & Techtonophysics

Wed. May 29, 2019 5:15 PM - 6:30 PM JST | Wed. May 29, 2019 8:15 AM - 9:30 AM UTC | Poster Hall International Exhibition Hall8, Makuhari Messe_28

[S-IT26] New perspectives on the geodynamics of East Asia

convener:Timothy B Byrne(University of Connecticut), Asuka Yamaguchi(Atomosphere and Ocean Research Institute, The University of Tokyo), Jonny Wu(University of Houston), Kyoko Okino(Atmosphere and Ocean Research Institute, The University of Tokyo)

The Pacific, Indo-Australia and Eurasian plates converge around the Philippine Sea plates in south and East Asia, resulting in one of the most tectonically active regions on earth. The area is also geologically and tectonically complex with numerous active tectonic environments, ranging from subduction to collision, and a long history of plate boundary interactions. The last decade has yielded a wide range of new observations, including detailed geologic data and high resolution crustal to mantle imaging. Here we seek oral and poster presentations that bear on the geologic history and geophysical character of modern and ancient plates in East Asia and their interactions since the Mesozoic. We also invite geodynamic models that integrate these diverse datasets into a more holistic view of this dynamic environment.

[SIT26-P01] Geochemical characteristics of effusive rocks (greenstones) in the Hidaka Belt, Hokkaido, Japan

*Toru Yamasaki[1], Futoshi Nanayama[1] (1.Geol. Survey of Japan (AIST))

[SIT26-P02] Large gas reservoir in continental back-arc basin, revealed by automatic seismic velocity analysis in the Okinawa Trough

*Kota Mukumoto[1], Takeshi Tsuji[1], Andri Hendriyana[1] (1.Kyushu University)

[SIT26-P03] Characterize coseismic deformation of Mw 7.5 Palu earthquake in a triple junction in Sulawesi, Indonesia

*MIN-CHIEN TSAI[1], Ying-Hui Yang[2], Chun-Ying Chiu[3], Jyr-Ching Hu[3] (1.Seismological center, Central Weather Bureau, Taipei, Taiwan, R.O.C., 2.School of Civil Engineering and Architecture, Southwest Petroleum University, Chengdu, China, 3.Department of Geosciences, National Taiwan University, Taipei, Taiwan, R.O.C.)

Geochemical characteristics of effusive rocks (greenstones) in the Hidaka Belt, Hokkaido, Japan

*Toru Yamasaki[1], Futoshi Nanayama[1]

1. Geol. Survey of Japan (AIST)

Igneous rocks in a subduction complex typically occur as greenstones, and petrological and geochemical investigations of such greenstones can provide important insights into the oceanic magmatism, origin of the accretionary complex, and growth of the continental margin. The Hidaka Belt in Central Hokkaido, Japan consists of an early Paleogene subduction complex, referred to as the Hidaka Supergroup (HSG), dominated by clastic rocks. Locally, the terrigenous sediments of the HSG were intruded by the contemporary, normal-type mid-ocean ridge basalts (“*in situ*N-MORBs”) that were formed at an oceanic ridge near the Eurasian continent (Miyashita and Katsushima, 1986: GSJ). The southern area of the HSG has been referred to as the Nakanogawa Group (NKG), which gradually leads to the high-temperature Hidaka metamorphic belt (HMB) in the western part. The lower sequence of the HMB consists mainly of high-grade metabasites, which are assumed to be equivalent to the N-MORBs in the HSG, based on their geochemical features. Recently, Yamasaki and Nanayama (2018a: Lithos) reported about the unique Daimaruyama greenstones from the NKG, formed by an immature intra-oceanic arc-type volcanism. In addition, highly-alkaline basalts, presumably formed at the seamount, exist as exotic blocks in the NKG and are named as Tachiiwa blocks (Owada et al., 1992: JMPEG). In fact, the N-MORBs in the HSG and the Tachiiwa alkaline rocks are characterized by the whole-rock major and minor element geochemistry, but the trace element geochemistry, including the rare earth elements (REEs), has not been reported yet for these rocks. Therefore, we collected 18 samples of greenstones from the entire Hidaka Belt and examined their whole-rock major and trace element geochemistry.

Including those in our previous reports (Yamasaki and Nanayama, 2018a, b: JpGU Abs.), there are three distinct types of greenstones in the Hidaka Belt. The first type are the MORB-type greenstones which show relatively flat chondrite-normalized (CN) REE patterns and N-MORB-normalized (NMN) multi-element patterns with Ti/V = 26–53 and Zr/Nb = 21–117. Although Miyashita and Kiminami (1999: MemGSJ) showed the flat NMN minor element (Nb, P, Zr, Ti, and Y) patterns of basalts from the northern HSG, trace element patterns of the MORB-type rocks in this study show rather light REE (LREE)-rich NMN multi-element patterns. The second type are the ocean island basalt (OIB)-type greenstones. The NMN multi-element and CN REE patterns for this type of greenstones show a gentle slope up to the left, with Ti/V>62 and Zr/Nb<15. The third type are the Daimaruyama greenstones. This type of greenstones show similar NMN multi-element patterns and CN REE patterns to those in the OIB-type, but with a clear relative depletion of Nb, Ta, and Ti. In addition, their Ti-V relations are similar to those in the MORB-type greenstones.

MORB-type greenstones are distributed from the northernmost part of the HSG to the southern Rakko River area in the NKG. OIB-type greenstones occur in the Tachiiwa block and the Rakko River area. Daimaruyama greenstones occur only in the Daimaruyama megablock in the NKG. Since the Tachiiwa and Daimaruyama blocks are presumably derived from the neighboring Tokoro Belt, the absence of the OIB-type and Daimaruyama greenstones in the northern HSG implies a difference in provenance between the HSG and NKG. The MORB-type greenstones do not show the typical N-MORB-type (LREE-depleted) trace element patterns, whereas the metabasite in the HMB shows the typical N-MORB-type geochemical features. In addition, the distribution of the MORB-type greenstones is separated from the metabasites of

©2019. Japan Geoscience Union. All Right Reserved.

the HMB in the southern Hidaka Belt. These lines of evidence suggest that the protolith of the HMB is not an equivalent of the “*in-situ*MORB” in the HSG, and is probably an accreted fragment of the older oceanic plate.

Keywords: Hidaka Belt, greenstones, trace elements

©2019. Japan Geoscience Union. All Right Reserved.

Large gas reservoir in continental back-arc basin, revealed by automatic seismic velocity analysis in the Okinawa Trough

*Kota Mukumoto[1], Takeshi Tsuji[1], Andri Hendriyana[1]

1. Kyushu University

P-wave velocity acquired from seismic reflection data allows us to quantify submarine geological structures. In the Iheya North Knoll of the Okinawa Trough, intense hydrothermal activity occurs due to continental rifting. The hydrothermal system in the Iheya North Knoll has been explored by geophysical surveys, geochemical measurements and drilling campaign. Based on these surveys, gas reservoir could be considered to exist around the Iheya North Knoll. However, gas reservoir around the Iheya North Knoll has not been identified in previous studies. Here we show P-wave velocity structure derived from automatic velocity analysis of multi-channel seismic reflection data. P-wave velocity is sensitive to free gas in sediments. Therefore, P-wave velocity is key information to quantify gas distribution in sediments. Automatic velocity analysis estimated P-wave velocity structure with remarkable high spatial and temporal resolution. The P-wave velocity structure revealed gas reservoirs around the Iheya North Knoll. Although many gas components can be generated by magmatic activity, hydrothermal alteration of organic-rich sediments and biogenic processes, CH_4 and CO_2 could be major gas components which is derived by hydrothermal system in marine sediment. Therefore, main gas components could be CH_4 or CO_2. The strong amplitude reflector above the gas reservoir could be the interface between CH_4 hydrate and gas, because the depth of strong amplitude reflector is well consistent with pressure-temperature conditions of the phase transition. If the main gas component is CH_4, the gas reservoir could be important as resource. Whereas, if the gas reservoir includes CO_2, the gas distribution could be important to consider carbon flux between earth and ocean. Furthermore, widely distributed gas reservoir may influence on the chemical components of hydrothermal fluids in the Iheya North Knoll.

Keywords: Seismic reflection data, Okinawa Trough, Gas reservoir

©2019. Japan Geoscience Union. All Right Reserved.

Characterize coseismic deformation of Mw 7.5 Palu earthquake in a triple junction in Sulawesi, Indonesia

*MIN-CHIEN TSAI[1], Ying-Hui Yang[2], Chun-Ying Chiu[3], Jyr-Ching Hu[3]

1. Seismological center, Central Weather Bureau, Taipei, Taiwan, R.O.C., 2. School of Civil Engineering and Architecture, Southwest Petroleum University, Chengdu, China, 3. Department of Geosciences, National Taiwan University, Taipei, Taiwan, R.O.C.

We first use SAR satellite data to map the coseismic deformation for the 2018 Mw=7.5 strike-slip earthquake of 28 September 2018 in Palu, Sulawesi, Indonesia. The seismogenic fault is a left-lateral a strike-slip event along the Palu-Koro fault at shallow depth that occurred within the interior of the Molucca Sea microplate, which is part of the Sunda plate. We use D-InSAR technique with ALOS-2 descending orbit radar images to characterize coseismic and deformation pattern induced by Palu earthquake.We also plan to use with sub-pixel correlation form Sentinel-2 and Planet imagery to map the surface rupture area and the coseismic offsets in order to provide the near-field deformation data located in decorrelation zone from the D-InSAR result. Thus we can inverse the distribution of slip on the fault patches. In addition, we also calculate the Coulomb stress transfer for assessing the stress increasing and shadow on the major fault systems, such as the active Poso Fault Zone and Mamuju –Lariang Active Fault Zone. In particular, we will assess the seismic potential by Coulomb stress transfer in Minahasa Active Subduction Zone together with two events with Mw 7.9 and Mw 7.0 happened on 1996/01/01 and 1996/07/22. We try to assess the seismogenic potential in terms of interseismic slip rate, slip rate deficit and coupling ratio for the Palu-Koro fault system in a triple junction of the Sulawesi island.

Keywords: InSAR , pixel offset , Palu earthquake, Triple junction

©2019. Japan Geoscience Union. All Right Reserved.

[E] Oral | S (Solid Earth Sciences)：S-IT Science of the Earth's Interior & Techtonophysics

Wed. May 29, 2019 1:45 PM - 3:15 PM JST | Wed. May 29, 2019 4:45 AM - 6:15 AM UTC | A09 TOKYO BAY MAKUHARI HALL

[S-IT26] New perspectives on the geodynamics of East Asia

convener:Timothy B Byrne(University of Connecticut), Asuka Yamaguchi(Atomosphere and Ocean Research Institute, The University of Tokyo), Jonny Wu(University of Houston), Kyoko Okino(Atmosphere and Ocean Research Institute, The University of Tokyo), Chairperson:Jonny Wu, Okino Kyoko

The Pacific, Indo-Australia and Eurasian plates converge around the Philippine Sea plates in south and East Asia, resulting in one of the most tectonically active regions on earth. The area is also geologically and tectonically complex with numerous active tectonic environments, ranging from subduction to collision, and a long history of plate boundary interactions. The last decade has yielded a wide range of new observations, including detailed geologic data and high resolution crustal to mantle imaging. Here we seek oral and poster presentations that bear on the geologic history and geophysical character of modern and ancient plates in East Asia and their interactions since the Mesozoic. We also invite geodynamic models that integrate these diverse datasets into a more holistic view of this dynamic environment.

1:45 PM - 2:00 PM JST | 4:45 AM - 5:00 AM UTC

[SIT26-01] How to solve controversies in Cenozoic tectonics in western Pacific margin

*Gaku Kimura[1] (1.Tokyo University of Marine Science and Technology)

2:00 PM - 2:15 PM JST | 5:00 AM - 5:15 AM UTC

[SIT26-02] Plio-Pleistocene plate interactions associated the Philippine Sea Plate

*Timothy B Byrne[1], Gaku Kimura[3], Jonny Wu[2] (1.University of Connecticut, 2.University of Houston, 3.Tokyo University of Science and Technology)

2:15 PM - 2:30 PM JST | 5:15 AM - 5:30 AM UTC

[SIT26-03] A regional mylonite zone between the Mesozoic metamorphic basement and the subducted Miocene covered schists in eastern Range of Taiwan: A possible Plio-Pleistocene transform fault between Eurasia and the Philippine Sea plate

*Gong-Ruei Ho[1], Jian-Cheng Lee[1], Timothy B Byrne[2], En-Chao Yeh[3] (1.Institute of Earth Sciences, Academia Sinica, 2.Department of Geography, University of Connecticut, 3.Department of Earth Sciences, National Taiwan Normal University)

2:30 PM - 2:45 PM JST | 5:30 AM - 5:45 AM UTC

[SIT26-04] **Coeval exhumation or subduction channel extrusion of the high pressure Yuli belt? Insights from the Shoufeng fault in eastern Taiwan**

*Jian-Cheng Lee[1,5], Gong-Ruei Ho[1,5], Timothy B Byrne[2], Yuan Hsi Lee[3,5], En-Chao Yeh[4,5] (1.Academia Sinica, 2.Univerity of Connecticut, 3.National Chung Cheng University, 4.National Taiwan Normal University, 5.The Yuli Exhumation Study team (YES Team))

2:45 PM - 3:00 PM JST | 5:45 AM - 6:00 AM UTC

[SIT26-05] Metamorphic temperature variation across the Yuli belt: a clue about exhumation of high-pressure rocks?

*Chin-Ho Tsai[1], Chih-Ying Yeh[1], Yui Kouketsu[2], Masaki Enami[3] (1.Department of Natural Resources & Environmental Studies, National Dong Hwa Univ., 2.Department of Earth & Planetary Sciences, Nagoya Univ., 3.Institute for Space-Earth Environmental Research, Nagoya Univ.)

3:00 PM - 3:15 PM JST | 6:00 AM - 6:15 AM UTC

[SIT26-06] **Thermal state, slab metamorphism and interface seismicity in Mariana based on 3-D modeling**

*Yingfeng Ji[1,2,3], Shoichi Yoshioka[3,4] (1.Center of Excellence in Tibetan Plateau Earth Science, Chinese Academy of Sciences, 2.Key laboratory of continental collision and plateau uplift, Institute of Tibetan Plateau, Chinese Academy of Sciences, 3.Research Center for Urban Safety and Security, Kobe University, 4.Graduate School of Science, Kobe University)

How to solve controversies in Cenozoic tectonics in western Pacific margin

*Gaku Kimura[1]

1. Tokyo University of Marine Science and Technology

Tectonics and their geodynamic backgrounds are difficult theme and keep controversial. Cenozoic tectonics in the western Pacific margin are of them. 1) Oceanic ridge subduction, 2) Back-arc spreading, 3) interaction between the Philippine Sea Plate and SW Japan, 4) collision and bending of the Japanese islands, 5) onset of present tectonic and dynamic frameworks, and 6) dynamic background of the earthquakes and volcanic eruption are key events but controversial.

To solve these controversies, a classic geological philosophy of “uniformitarianism” is significant. It means “the present is the key to the past”.

1. To solve the controversy of the Izanagi-Pacific Ridge subduction in early Cenozoic, a comparative study with modern examples of the ridge subduction at the Chile triple junction, Woodlrack Basin and Middle America trench with a new data set and simlation is a key.
2. To solve the back arc spreading controversy of Kuril and Japan Basins and Okinawa Trough, the promotion of International collaboration to acquire a new data set is necessary together with a comparative study among the modern backarc spreading. A classic controversy of double door opening vs pull-apart spreading will be progressed by comparison with progressed modern examples. A large scale perspective beyond the back-arc basins themselves is also necessary for geodynamic solution for the back-arc spreading.
3. To solve the controversy of the interaction between the Philippine Sea Plate and SW Japan; switch from the Pacific plate to Philippine Sea Plate at ~15Ma vs ~12Ma- 6Ma, detailed tomographic study with new perspectives and data sets from on-and geology and geophysics is necessary with simulation.
4. To solve the controversy of the collision and bending of the Japanese islands, not only the geological data set but more comprehensive data set of geophysics and geochemistry with simulation are necessary. Differentiation between the hypothesis and fact promotes a constructive controversy. In geology, data reliability and re-productablity is the most significance part of science.
5. To solve the controversy of onset of present tectonic and dynamic frameworks is the most essential part of “uniformitarianism”. The definition of “present” depends on the scientific field even in geoscience, Seismological “present” is a moment to minutes, days and month scale, That of geodesy is ~10s to 100 years. Geomorphology combined with geology is 100s to 10^4 scale. That of most geology is beyond 10^4 scale. Establishment of seamless “uniformitarianism” with seamless space perspective is a key to understand this controversy.
6. To solve dynamic background of the earthquakes and volcanic eruption, I like to emphasize the viewpoint of evolving effect of hysteresis. A final trigger of earthquakes and volcanic eruption is no doubt of physical consequence resulted from long and short term hysteresis.

Keywords: western Pacific, ridge subduction, back-arc spreading, collision, subduction, Japanese islands

©2019. Japan Geoscience Union. All Right Reserved.

Plio-Pleistocene plate interactions associated the Philippine Sea Plate

*Timothy B Byrne[1], Gaku Kimura[3], Jonny Wu[2]

1. University of Connecticut, 2. University of Houston, 3. Tokyo University of Science and Technology

Geologists have long recognized the possible significance of a change in motion of the Philippine Sea Plate (PSP) in the middle to late Cenozoic (Huchon, 1983; Seno and Maruyama, 1984), although the detailed timing and kinematics have remained elusive. The most recent reconstructions suggest a ~50° counterclockwise rotation of the plate motion vector relative to Eurasia possibly as recently as 2 Ma (Wu et al., 2015), which would have significant implications for the tectonics of east-central Asia. In southern Japan, for example, CCW rotation of the plate motion vector predicts a change from generally orthogonal plate convergence to the present NW-directed and oblique motion. In Taiwan, in contrast, plate convergence obliquity would decrease significantly. To better understand and possibly better constrain the geometry, kinematics and timing of this change in motion, we review the geologic histories of different geologic units and terranes along the boundary of the PSP, including: the Okinawa Trough, Kyushu and Shikoku Islands, Kumano Basin, Boso and Miura Peninsulas, the southern Marianas, the Philippines and Taiwan. Several areas in southern Japan also appear to provide critical constraints on the kinematics and timing of a possible change in motion. For example, geological and geophysical studies of the accretionary prism in SW Japan show a transition from shortening perpendicular to the plate boundary to extension perpendicular to the boundary <1.0 Ma (Gulick et al., 2010, and Sacks et al., 2013). Although these authors suggest that this change reflects changes in subduction zone dynamics, we propose that the change to extension relates to the decrease in the rate of convergence across the prism as the plate motion changed from nearly orthogonal to more oblique at ~1.0 Ma. Hayman et al. (2012) also documented a CCW rotation in the shortening direction deep in the Nankai accretionary prism just south of Shikoku Island, although the timing of this rotation was only constrained to be younger than ~5 Ma (the age of the youngest deformed sediments). In the eastern Nankai, Yamaji et al. (2003) interpreted a similar suite of faults to be related to a similar change in plate motion at ~1 Ma. Further landward, studies of the Median Tectonic Line on Shikoku Island document a change from thrusting to right-lateral strike-slip faulting at about ~0.8 Ma (Mizuno, 1999; Sato et al., 2015). This change in kinematics and timing is consistent with previous ideas on the age of formation of the Nankai forearc sliver (~0.8 Ma) based primarily on geologic and geomorphic data from Shikoku Island (Ohmori, 1978; Saito, 1999; Okamura, 1990). Finally, in Taiwan, Hsu et al. (2016) have proposed an acceleration in rock uplift at ~0.8 Ma based on low-temperature thermochronology data that may reflect an acceleration in plate convergence related to changing plate motions. Taken together, these observations suggest that a significant change in the plate motion vector (i.e., CCW rotation) occurred relatively recently and probably < 1 Ma.

Keywords: plate tectonics, philippine sea plate

©2019. Japan Geoscience Union. All Right Reserved.

A regional mylonite zone between the Mesozoic metamorphic basement and the subducted Miocene covered schists in eastern Range of Taiwan: A possible Plio-Pleistocene transform fault between Eurasia and the Philippine Sea plate

*Gong-Ruei Ho[1], Jian-Cheng Lee[1], Timothy B Byrne[2], En-Chao Yeh[3]

1. Institute of Earth Sciences, Academia Sinica, 2. Department of Geography, University of Connecticut, 3. Department of Earth Sciences, National Taiwan Normal University

As one of the youngest orogenic belts, Taiwan offers insights into mountain building processes operating from the Earth’ s surface. In the eastern Central Range of the Taiwan mountain belt, the Tananao metamorphic belt, comprising the Tailuko Belt, high temperature/low pressure Mesozoic basement, was attached by the Yuli belt, a Miocene pelitic quartz-mica schist with high-pressure exotic mafic to ultra-mafic blocks (Yen, 1960; Tsai et al., 2013). Observations of meso- and microscopic structures show predominant asymmetric folds with top-to-east S2/S3 on the eastern Yuli belt and isoclinal folds with west dipping S2 on the western Tailuko belt. In the boundary between these two geological rock units, we observed a mylonite zone distributed about 2 kilometers wide, which has been called the Shoufeng Fault, which indicated sinistral sense of shear and shallow stretching lineation within the mylonite zone. The structural style of other area is relatively irregular and disordered (Stanley et al., 1981; Lu and Wang Lee, 1986; Pulver et al., 2002; Ho, 2007; Liao, 2011; Ji, 2011). This pattern was found from north to south in a distance of 100 km along the Yuli belt along the Mugua, Shoufeng, Wanliqiao, and Chinshui Rivers to the Southern Cross island highway and the Dawushan map (Usami, 1940). The above observations pointed out an apparently down-dip folding coupled with a dominant orogen-parallel lineation pattern around the Shoufeng mylonite zone between the Miocene Yuli belt and the Mesozoic Tananao complex. It provides structural constraints on the deformation associated with ductile metamorphism of the high-pressure Yuli belt terrane while attached against the much older continental crust of the Tananao complex as well as during the subsequent rapid exhumation processes.

Keywords: Tananao metamorphic belt, mylonite zone, left-lateral strike slip motion

©2019. Japan Geoscience Union. All Right Reserved.

Coeval exhumation or subduction channel extrusion of the high pressure Yuli belt? Insights from the Shoufeng fault in eastern Taiwan

*Jian-Cheng Lee[1,5], Gong-Ruei Ho[1,5], Timothy B Byrne[2], Yuan Hsi Lee[3,5], En-Chao Yeh[4,5]

1. Academia Sinica, 2. Univerity of Connecticut, 3. National Chung Cheng University, 4. National Taiwan Normal University, 5. The Yuli Exhumation Study team (YES Team)

Based on field investigations, microscopic observations, and available geophysical, geochemical and geochronological data, this study intends to better understand the structural characteristics of the Eurasian continental margin (e.g., the eastern Central Range in Taiwan) during subduction and exhumation while the Philippine Sea plate has been approaching in the vicinity of Taiwan since the Miocene time. The eastern Central Range is composed of two major geological units: 1) the Tailuko belt, the Mesozoic metamorphic subduction complex, retro-metamorphosed in green schist facies and exhumed since late Miocene, and 2) the Yuli belt, continental margin rocks that contain high-pressure minerals (omphacite, glaucophane, garnet) with Miocene-Pliocene ages suggesting rapid exhumation from mantle depths of 40-50 km.

We conducted detailed field surveys around the Shoufeng fault which represents the boundary between the Tailuko belt and the Yuli belt. We found a mylonite zone of several kilometers wide in the boundary of these two belts. Based on the meso- and microscopic scale observations we define the boundary as ultra-mylonite, mylonite, and proto-mylonite zones. Within the ultra-mylonite and mylonite zones, rocks from two belts are intercalated each other in varied widths. The main dominant schistosity/cleavage in the mylonite zones (Sm/S3) remains the same orientation of striking in NE/NNE and dipping to the west. Also, the main composition layers, which we tentatively called S2 for the sake of field investigations, were more intensively deformed (i.e., crenulated, folded, etc.) from outside toward the core of the mylonite zones. As a result, the Sm/S3 becomes less persistent outside of the mylonite zones in the Yuli belt.
The mylonite zones exhibit left-lateral Sm/S3-related shearing without significant down-dip component. We also observed a general S2/S3-related top-to-west sense of shear across the two belts. As a consequence, we tend to interpret that the Yuli belt and the Tailuko belt have been mylonitically sheared (Sm/S3) in a left-lateral movement at the depth and that they exhumed coevally up to the surface level. The schistosity of the main composition layers S2 probably occurred before the mylonization during the transition from subduction to exhumation. The shallow dipping and less dominant S3 outside the mylonite zone might imply a upward and unroofing process during the rapid exhumation of the eastern Central Range of Taiwan.

Keywords: Mylonite, Exhumation, Shoufeng fault, Yuli belt, Taiwan

©2019. Japan Geoscience Union. All Right Reserved.

Metamorphic temperature variation across the Yuli belt: a clue about exhumation of high-pressure rocks?

*Chin-Ho Tsai[1], Chih-Ying Yeh[1], Yui Kouketsu[2], Masaki Enami[3]

1. Department of Natural Resources & Environmental Studies, National Dong Hwa Univ., 2. Department of Earth & Planetary Sciences, Nagoya Univ., 3. Institute for Space-Earth Environmental Research, Nagoya Univ.

We applied Raman spectra of carbonaceous material (RSCM) geothermometer to estimate peak metamorphic temperatures of pelitic and psammitic schists across the Yuli belt, eastern Taiwan. The analyzed samples mainly consist of phengitic mica, quartz, chlorite, and albite, with accessory graphitic carbonaceous material, titanite, zircon, and tourmaline. In samples from the Juisui Schist and Chinshuichi Plantation units (both containing high-pressure allochthonous blocks), garnet, ilmenite, and paragonite may occur and albite tends to be porphyroblastic. Serpentinite and metabasite pods occur in these units, whereas the neighboring metasedimentary units lack such rocks and porphyroblastic phases. The yielded metamorphic temperatures reveal a systematic variation in spatial distribution across the Yuli belt. In the Wanjung and Juisui areas, peak temperatures of the four schist units are in the range of 430-510˚C, 410-470˚C, 560-620˚C and 420-450˚C, from west (structurally upper) to east (lower), respectively. In the Chinshuichi area, temperatures of the two units are in the range of 540-560˚C (structurally lower) and 400-450˚C (higher), whereas the temperatures of the low-grade Slate unit (Chulai Formation) bordering the Yuli belt in the east are 330-340˚C. The high-pressure Juisui Schist and Chinshuichi Plantation are apparently warmer than their neighboring units in each area, although boundaries of the units are poorly exposed or characterized. The spatial distribution of metamorphic temperatures requires a structural explanation. Possible interpretations include doming, extension, or extrusion, and the inferred structures and processes may shed new lights on the exhumation of high-pressure metamorphic rocks in the Yuli belt.

Keywords: metasedimentary rocks, thermobarometry, carbonaceous material, exhumation, high-pressure metamorphism

©2019. Japan Geoscience Union. All Right Reserved.

Thermal state, slab metamorphism and interface seismicity in Mariana based on 3-D modeling

*Yingfeng Ji[1,2,3], Shoichi Yoshioka[3,4]

1. Center of Excellence in Tibetan Plateau Earth Science, Chinese Academy of Sciences, 2. Key laboratory of continental collision and plateau uplift, Institute of Tibetan Plateau, Chinese Academy of Sciences, 3. Research Center for Urban Safety and Security, Kobe University, 4. Graduate School of Science, Kobe University

The Marina arc system represents a typical mode of intra-oceanic convergent boundary characterizing circum-Pacific subduction zones, together with the Izu-Bonin, Kuril and Tonga-Kermadec margins well known for the tectonically formed deep trenches. Active back-arc extension driven by hydrothermal mantle upwell comprises one of the significant features of Mariana caused by steep subduction. Previous studies document that the narrow subduction constrains the seismicity in Mariana to be less than M7. However, the subduction thermal regime remains still unclear in detail. Based on the 3-D thermal model constructed for Mariana, we found that the highly curved Mariana arc presenting such a particular tectonic setting caused by trench retreat produces a cold thermal structure beneath the central and northern Mariana influenced by an oblique subduction. The deep earthquakes (>100 km) are therefore frequently detected compared with the southern Mariana. The subducted Pacific plate entraining the oceanic crust components is calculated to obtain their pressure-temperature conditions for different petrological faces undergoing multiple phase transition including the paths from amphibolite to eclogite or harzburgite at a high temperature of >500 degrees in Celsius which is conjectured to facilitate the deep earthquakes at Mariana. The dewatered oceanic plate is expected to releases ample fluids for the backarc volcanism and hydrous circulation at Mariana mantle wedge. The 3-D temperature structure of Mariana obtained in this study sheds lights on regional earthquake genesis and slab metamorphism in such an intro-oceanic subduction system featured by deep events.

Keywords: Thermal state, slab metamorphism , interface seismicity, Mariana, 3-D modeling

©2019. Japan Geoscience Union. All Right Reserved.

[E] Oral | S (Solid Earth Sciences)：S-IT Science of the Earth's Interior & Techtonophysics

Wed. May 29, 2019 3:30 PM - 5:00 PM JST | Wed. May 29, 2019 6:30 AM - 8:00 AM UTC | A09 TOKYO BAY MAKUHARI HALL

[S-IT26] New perspectives on the geodynamics of East Asia

convener:Timothy B Byrne(University of Connecticut), Asuka Yamaguchi(Atomosphere and Ocean Research Institute, The University of Tokyo), Jonny Wu(University of Houston), Kyoko Okino(Atmosphere and Ocean Research Institute, The University of Tokyo), Chairperson:Asuka Yamaguchi(Atomosphere and Ocean Research Institute, The University of Tokyo), Tim Byrne

The Pacific, Indo-Australia and Eurasian plates converge around the Philippine Sea plates in south and East Asia, resulting in one of the most tectonically active regions on earth. The area is also geologically and tectonically complex with numerous active tectonic environments, ranging from subduction to collision, and a long history of plate boundary interactions. The last decade has yielded a wide range of new observations, including detailed geologic data and high resolution crustal to mantle imaging. Here we seek oral and poster presentations that bear on the geologic history and geophysical character of modern and ancient plates in East Asia and their interactions since the Mesozoic. We also invite geodynamic models that integrate these diverse datasets into a more holistic view of this dynamic environment.

3:30 PM - 3:45 PM JST | 6:30 AM - 6:45 AM UTC

[SIT26-07] **A tomography-led plate reconstruction of NE Asia during the late Cretaceous**

*Jonny Wu[1], Yi-An Lin[1], Nicolas Flament[2], Tsung-Jui Wu[1], Yiduo Liu[1] (1.University of Houston, 2.University of Wollongong)

3:45 PM - 4:00 PM JST | 6:45 AM - 7:00 AM UTC

[SIT26-08] Geodynamic models of late Mesozoic intraoceanic subduction offshore NE Asia caused by growing Izanagi plate

*Lorenzo Colli[1], Jonny Wu[1], Yi-An Lin[1] (1.University of Houston)

4:00 PM - 4:15 PM JST | 7:00 AM - 7:15 AM UTC

[SIT26-09] **Early Cretaceous to Paleocene magmatism in the Sikhote-Alin area and their implications for Paleo-Pacific plate subduction and continental evolution**

*Tsung-Jui Wu[1], Jonny Wu[1], Igor Alexandrov[2], Thomas Lapen[1] (1.Department of Earth and Atmospheric sciences, University of Houston, Houston, U.S., 2.Far East Geological Institute, Russian Academy of Sciences, Vladivostok, Russia)

4:15 PM - 4:30 PM JST | 7:15 AM - 7:30 AM UTC

[SIT26-10] Processes of subduction initiation revealed by P-T paths of amphibolite and blueschist tectonic blocks in serpentinite mélange: An example from the Kamuikotan high-P/T metamorphic rocks in Hokkaido, northern Japan

*Toru Takeshita[1], Ayumi S. Okamoto, Wonji Shin[1], Mizuho Ando[1] (1.Department of Natural History Sciences, Graduate School of Science, Hokkaido University)

4:30 PM - 4:50 PM JST | 7:30 AM - 7:50 AM UTC

[SIT26-11] Metamorphism in the Sanbagawa belt of SW Japan as a record of subduction processes

★Invited Papers

*Simon Richard Wallis[1] (1.University of Tokyo)

4:50 PM - 5:00 PM JST | 7:50 AM - 8:00 AM UTC

[SIT26-12] Subduction and exhumation of the high pressure metamorphic rocks: What we know and what we need to know.

*Timothy B Byrne[1] (1.University of Connecticut)

A tomography-led plate reconstruction of NE Asia during the late Cretaceous

*Jonny Wu[1], Yi-An Lin[1], Nicolas Flament[2], Tsung-Jui Wu[1], Yiduo Liu[1]

1. University of Houston, 2. University of Wollongong

Contrasted plate tectonic reconstructions have been proposed for the northeast Asian margin during the late Cretaceous, including: an Andean-type subduction margin, the existence of marginal seas, the subduction of a spreading ridge, the subduction of remnant arcs, or continental block collision and continental subduction. Here we investigate which scenarios are consistent with tomography models by mapping and unsubducting the vanished western Pacific slabs along the Kurile-Kamchatka, Japan, and Izu-Bonin-Marianas trenches from global tomography models. We show that a mapped 4,000 km-long slab gap within the East Asian lower mantle is the tomographic signature of the subducted Izanagi-Pacific spreading ridge based on a comparison to global mantle flow models. We reconstruct the size of the lost Izanagi conjugate from the geometry of the unsubducted western Pacific slabs, the age of Pacific oceanic crust, and published synthetic seafloor isochrons.

Our tomography-based plate reconstruction implies that: (1) the Izanagi ocean basin crust (i.e. formed by Pacific MORB) first reached and subducted along Sikhote-Alin and northern Japan around ~100 Ma; (2) subduction of the Izanagi plate along northeast Asia during the late Cretaceous ~75 Ma was limited to north of southernmost Korea and Bohai Bay, China, and west of westernmost Alaska; and, (3) the Izanagi-Pacific ridge intersected with the northeast Asian margin at a low angle in the early Cenozoic. We discuss our plate model against proposed northeast Asian margin plate tectonics during the Cretaceous.

Keywords: NW Pacific Ocean, Izanagi plate, NE Asia

©2019. Japan Geoscience Union. All Right Reserved.

Geodynamic models of late Mesozoic intraoceanic subduction offshore NE Asia caused by growing Izanagi plate

*Lorenzo Colli[1], Jonny Wu[1], Yi-An Lin[1]

1. University of Houston

The existence of the Izanagi plate is well established both from magnetic lineations and fracture zones in the western Pacific and from tomographic imaging of the deep mantle underneath East Asia. But its spatial extent, position and motion through time remain poorly known.

A common scenario envisages the Izanagi as a large and long-lived plate extending from central Panthalassa to the eastern margin of Eurasia. In this scenario the Izanagi plate is conjugate to the Farallon and Phoenix plates before the inception of the Pacific plate and it subducts continuously beneath East Asia during the Mesozoic (e.g. Müller et al., 2016).

A conservative choice for the spatial and temporal extent of the Izanagi plate, limiting it to what can be extrapolated using the conjugate Pacific plate, leads to a very different scenario: in this case the Izanagi plate is born together with the Pacific plate around 190 Ma and grows triangular in shape. It overrides preexisting oceanic lithosphere causing extended intraoceanic subduction in western Panthalassa characterized by fast trench retreat towards the Eurasian margin. The tip of the Izanagi plate reaches the Eurasian continental margin near Japan and Sikhote-Alin around 100 Ma.

Here we assimilate these two scenarios in geodynamic models of global mantle convection in the form of time-dependent velocity boundary condition at the Earth’ s surface. Their implications for the evolution of mantle structure in East Asia during Mesozoic time up to present-day are presented and discussed.

Keywords: Izanagi plate, intraoceanic subduction, Panthalassa, East Asia, Mesozoic, Numerical model

©2019. Japan Geoscience Union. All Right Reserved.

Early Cretaceous to Paleocene magmatism in the Sikhote-Alin area and their implications for Paleo-Pacific plate subduction and continental evolution

*Tsung-Jui Wu[1], Jonny Wu[1], Igor Alexandrov[2], Thomas Lapen[1]

1. Department of Earth and Atmospheric sciences, University of Houston, Houston, U.S., 2. Far East Geological Institute, Russian Academy of Sciences, Vladivostok, Russia

The Sikhote-Alin area in southern Russian Far East is one of the few places in the East Asian margin that has extensively exposed Mesozoic geological units. In particular, Cretaceous to Cenozoic igneous rocks are abundant and formed in response to periodic subduction of Paleo-Pacific plates. Previous geochemical studies of igneous rocks, mainly from southern Sikhote-Alin, resulted in significant insights into the continental evolution of East Aisan margin and subduction history of Paleo-Pacific plates (Kruk et al., 2014; Jahn et al., 2015; Grebennikov et al., 2016). In this study, we present new zircon U-Pb chronology and geochemical data from ~50 samples in across the entire Sikhote-Alin area. We combine our new results with published data to discuss the history of arc magmatic evolution in the region.

In general, the data show a cycle of arc magmatism that started from the early Cretaceous to Paleocene in Sikhote-Alin. Zircon U-Pb geochronology of igneous rocks indicate a major population of granitoids that had ages of 135-57 Ma; a small population of volcaniclastic rocks were dated at 55-53 Ma. Three magmatic episodes with distinct geochemical characteristics were recognized: 135-120 Ma, 110-100 Ma and 100-57 Ma. The 135-120 Ma granitoids are dominated by S-type granites; zircons with inherited cores were frequently observed in this episode. The 110-100 Ma episode has mostly I-type granites, whereas the 100-57 Ma magmatism had I-type granites that show greater degrees at fractional crystallization than the other groups. Some magmatic rocks with 67-57 Ma and ~100 Ma were A2 type granites, suggesting that two periods of intraplate magmatism could had occurred within this subduction setting. The La/Yb ratio and Nd isotopic ratios of the granitoids remained relatively similar during the Cretaceous and even showed a La/Yb ratio decrease in the late Cretaceous, implying that the Andean subduction margin crustal thickening model (Haschke et al., 2002) may not applicable to the Sikhote-Alin area.

Keywords: continental arc, paleo-pacific plate subduction, Northeast Aisa, Sikhote-Alin, continental evolution

©2019. Japan Geoscience Union. All Right Reserved.

Processes of subduction initiation revealed by P-T paths of amphibolite and blueschist tectonic blocks in serpentinite mélange: An example from the Kamuikotan high-P/T metamorphic rocks in Hokkaido, northern Japan

*Toru Takeshita[1], Ayumi S. Okamoto, Wonji Shin[1], Mizuho Ando[1]

1. Department of Natural History Sciences, Graduate School of Science, Hokkaido University

It has been recently noted that serpentinite mélange which contains tectonic blocks of high-*P/T* type metamorphic rocks such as blueschist and eclogite and their counterclockwise P-T paths could indicate the subduction initiation (e.g. Willner et al., 2004; Escuder-Viruete et al., 2011; Agard et al., 2016; Bhowmik and Ao, 2016; Hunziker et al., 2017). We investigated tectonics in amphibolite and blueschist tectonic blocks in mélange, which are distributed at the highest structural level of the high-*P/T* type Kamuikotan metamorphic rocks in Hokkaido, northern Japan. We reconstructed their individual pressure-temperature (*P-T*) paths based on petrography, mineral chemistry and phase equilibria modeling. As a result, tectonic blocks in this study area are divided into six rock types: garnet-epidote amphibolite, epidote amphibolite, amphibolite, plagioclase-poor amphibolite, blueschist and quartz-rich blueschist. From the reconstruction of *P-T* paths, it is found that most of the tectonic blocks experienced blueschist facies metamorphism probably at the maximum depth, while the initial paths vary from a counterclockwise *P-T* path shown by different kinds of amphibolite to a prograde *P-T* path shown by blueschist and quartz-rich blueschist. We have concluded that these *P-T* paths, on the whole, could have reflected the cooling history of subduction channel from the beginning to steady state of subduction. The geothermal gradient could have been changed from ~25 ˚C/km to ~10 ˚C/km within *c.* 25 myr estimated by previously reported radiometric ages. These tectonic blocks could have started to subduct at a different timing to show the different *P-T* paths, and juxtaposed against each other at a certain depth in the subduction channel. Since these tectonic blocks show little deformation structures formed during exhumation stage, they might have behaved as a rigid body in serpentinite (i.e. mélange matrix) after they were incorporated in it during subduction stage.

Keywords: Kamuikotan high-P/T type metamorrphic rocks, amphibolite and blueschist tectonic blocks in serpentinite mélange, counterclockwise P-T paths, subduction initiation

©2019. Japan Geoscience Union. All Right Reserved.

Metamorphism in the Sanbagawa belt of SW Japan as a record of subduction processes

*Simon Richard Wallis[1]

1. University of Tokyo

The Sanbagawa belt of SW Japan records Cretaceous suduction processes off the eastern Asian margin. The Sanbagawa belt can be traced for around 800 km throughout SW Japan, but the main exposure is found in Shikoku. The main constituent rock types are pelitic, quartz and mafic schists which were derived from the subducted oceanic slab. These are associated with widespread blocks and lenses of serpentinite and related rocks types derived from the mantle wedge.

A long running dispute about the age of peak metamorphism has recently been resolved. Evidence for an early stage of subduction associated at around 115 Ma is locally preserved with anticlockwise P-T paths. This is followed at around 90 Ma by the main been long disputed with estimates of the peak

Keywords: Tectonics, Sanbagawa belt, subduction

©2019. Japan Geoscience Union. All Right Reserved.

Subduction and exhumation of the high pressure metamorphic rocks: What we know and what we need to know.

*Timothy B Byrne[1]

1. University of Connecticut

Although great strides have been made in understanding the subduction and, to a lesser extent the exhumation, of high pressure rocks, the links between these two processes is much less clear. As a result, many of the regional-scale models of these processes are poorly constrained and weakly supported by data. In this discussion session, we would like to better understand the data and observations that provide evidence for exhumation of high pressure rocks and, in areas were data gaps remain, what data are necessary to advance our understanding.

©2019. Japan Geoscience Union. All Right Reserved.

[J] Oral | S (Solid Earth Sciences)：S-MP Mineralogy & Petrology

Wed. May 29, 2019 9:00 AM - 10:30 AM JST | Wed. May 29, 2019 12:00 AM - 1:30 AM UTC | A08 TOKYO BAY MAKUHARI HALL

[S-MP32] Deformed rocks, Metamorphic rocks and Tectonics

convener:Yumiko Harigane(Geological Survey of Japan, National Institute of Advanced Industrial Science and Technology (AIST)), Yoshihiro Nakamura(Geological Survey of Japan, National Institute of Advanced Industrial Science and Technology), Chairperson:Yoshihiro Nakamura(産総研), Yumiko Harigane(産総研)

We invite all researchers who aim to understand the dynamics of the earth's crust and mantle at the plate boundaries, to discuss the latest results from various viewpoints. The scope will include contributions through petrology and structural geology as well as various techniques including rheology and transformation of heat and mass.

9:00 AM - 9:15 AM JST | 12:00 AM - 12:15 AM UTC

[SMP32-01] Argon release mechanism of deformed phengite

*Tetsumaru Itaya[1] (1.Engineering Geology Center, Hiruzen Institute for Geology and Chronology)

9:15 AM - 9:30 AM JST | 12:15 AM - 12:30 AM UTC

[SMP32-02] Detrital zircons from a traverse along the Asemi River (Sanbagawa Metamorphic Belt, Shikoku, Japan): U-Pb geochronology and Hf isotopic composition

*Ulrich Knittel[1], Shigeyuki Suzuki[2], Monika Walia[3], Juan-Hsi Lee[4], Hao-Yang Lee[5] (1.RWTH Aachen University, 2.Okayama University, 3.Nat. Taiwan University , 4.Chung Cheng University, 5.Academia Sinica)

9:30 AM - 9:45 AM JST | 12:30 AM - 12:45 AM UTC

[SMP32-03] Tectonic process of the Sanbagawa eclogite: zircon U–Pb and REE composition analyses

*Shogo Aoki[1], Kazumasa Aoki[2], Tatsuki Tsujimori[3], Yuta Tsuchiya[1], Daichi Kato[2] (1.Department of Biosphere-Geosphere Science, Okayama University of Science, 2.Department of Applied Science, Okayama University of Science, 3.Center for Northeast Asian Studies, Tohoku University)

9:45 AM - 10:00 AM JST | 12:45 AM - 1:00 AM UTC

[SMP32-04] Petrological implications of a new occurrence of retrogressed eclogite from the Sanbagawa belt of southwest Japan

*Tomoki Taguchi[1], Shunsuke Endo[2], Yohei Igami[1,3], Akira Miyake[1] (1.Graduate School of Science, Kyoto University, 2.Interdisciplinary Faculty of Science and Engineering, Shimane University, 3.Institute of Materials and Systems for Sustainability, Nagoya University)

10:00 AM - 10:15 AM JST | 1:00 AM - 1:15 AM UTC

[SMP32-05] *P-T* estimations of Kashio mylonite in Oshika, Nagano, Japan: Constraints on the amalgamation of Ryoke and Sambagawa belts

*Yoshihiro Nakamura[1], Yutaka Takahasi[1], Tohru Danhara[2], Hideki Iwano[2], Takehumi Hirata[3] (1.Geological Survey of Japan, National Institute of Advanced Industrial Science and Technology, 2.Kyoto Fission-Track Co., Ltd., 3.Geochemical Research Center, The University of Tokyo)

10:15 AM - 10:30 AM JST | 1:15 AM - 1:30 AM UTC

[SMP32-06] **Static phenomena retained by garnet during exhumation of metamorphic rocks**

*Masaki Enami[1], Yui Kouketsu[2] (1.Institute for Space–Earth Environmental Research, Nagoya University, 2. Nagoya University)

Argon release mechanism of deformed phengite

*Tetsumaru Itaya[1]

1. Engineering Geology Center, Hiruzen Institute for Geology and Chronology

The author has proposed the argon release from phengites in HP-UHP metamorphic rocks by their ductile deformation in the exhumation and cooling of the metamorphic sequences to explain the relationships between K-Ar phengite ages and the metamorphic grade since Itaya and Takasugi (1988). This argon release hypothesis has not been accepted for 20 years until Nuong et al. (2008) described the age (K-Ar phengite)-temperature-structure relations in the Ishigaki high-pressure schist belt, southern Ryukyu Arc, Japan. Its main reason would be that the argon release mechanism is vague. Recently, the author made its mechanism clear in the literature that is in submission to journal. This paper will focus on the argon release mechanism of deformed phengites.

Cosca et al. (2011) described the effect of deformation on radiogenic argon retentivity from high pressure experiments (10kb and 600 ˚C over a period of 29 hours, giving ca. 10% shortening) performed on rock samples of peraluminous granite containing euhedral muscovite and biotite. Intragrain in-situ $^{40}Ar/^{39}Ar$ analyses for deformed muscovite provided 309 to 264 Ma, consistent with 0-16 % argon loss relative to the undeformed muscovite (311 Ma). They interpreted that the reduction in the effective diffusion length scale in naturally deformed rocks occurs most probably through productions of mesoscopic and submicroscopic defects such as stacking faults. The extreme size reduction of phengite observed at domains close to the rigid garnet in pelitic schists of the Sanbagawa belt are identical to the reduction in the effective diffusion length scale described by Cosca et al. (2011), likely enhancing the argon release. The Sanbagawa pelitic schists suffered extremely long deformation (longer than 31 million years) during the exhumation and had the extremely slow exhumation rate (slower than 0.7 mm/y). In this case, the phengite could grow up with “Ostwald ripening phenomenon” consuming the extremely fine-grained phengite close to the rigid garnet. The size reduction and “Ostwald ripening” growth would continue to become final stage of static phengite crystal size (0.02-0.06 mm in width and 0.4-1.0 mm in length) observed in matrix. During these processes phengite could experience chemical change depending on local bulk chemistry under the P/T conditions changing from moment to moment during the exhumation, making heterogeneous chemistry. On the other hand, Lago di Cignana UHP unit in western Alps suffered relatively quick deformation (shorter than 5 million years) during the exhumation and had the extremely fast exhumation rate (15 - 26 mm/y). In this case, the phengite crystals could record heterogeneously deformed domains in a crystal as well as among the grains, resulting in heterogeneous argon release. In fact, the laser step heating $^{40}Ar/^{39}Ar$ analyses of single phengite crystal in the UHP schists of Lago di Cignana provided significantly irregular age spectrum in comparison with the phengite from the Sanbagawa schists of which the age spectra show the perfect plateau for both the phengite separates and a phengite crystal.

A muscovite in metagranitoid from Grand Paradiso Massif in western Alps yielded heterogeneous age values, giving 54 to 218 Ma (Beltrando et al., 2013). The dated points by the crystal edge are significantly younger than the ages in the part far from the edge. These features suggest that the submicrosopic defects occurring preferentially near the crystal edges are affected by the rubbing with other phases, enhancing preferentially the argon release.

Keywords: deformation of phengite, duration of deformation, in-situ Ar-Ar ages, exhumation rate, argon release mechanism, effective diffusion length scale

©2019. Japan Geoscience Union. All Right Reserved.

©2019. Japan Geoscience Union. All Right Reserved.

Detrital zircons from a traverse along the Asemi River (Sanbagawa Metamorphic Belt, Shikoku, Japan): U-Pb geochronology and Hf isotopic composition

*Ulrich Knittel[1], Shigeyuki Suzuki[2], Monika Walia[3], Juan-Hsi Lee[4], Hao-Yang Lee[5]

1. RWTH Aachen University, 2. Okayama University, 3. Nat. Taiwan University , 4. Chung Cheng University, 5. Academia Sinica

Sanbagawa Belt is a classic high-P/low-T metamorphic belt that is exposed over a distance of about 1000 km on Kyushu, Shikoku and Honshu Islands in Japan. The age of this belt has been the focus of many studies in recent years since the discovery of young detrital zircon grains (80 - 95 Ma), younger than the presumed age of peak metamorphism.

Samples for this study come from a traverse along the Asemi River in central Shikoku. Dating of single zircon grains using the LA–ICP–MS U–Pb dating method shows that zircons from all sites investigated are younger than 90 Ma and thus the protoliths are younger than the previously accepted age of metamorphism for this part of the Sanbagawa Belt at ca. 116 Ma. Our sampling sites include the site sampled by Minamishin et al. (1979) which is the reference for metamorphism at ca. 116 Ma in this part of the belt. We therefore conclude that the linear arrays found by Minamishin et al. are mixing lines rather than isochrones. Another sample was taken within the area recently delineated as having experienced eclogite facies metamorphism prior to overprinting in the epidote-amphibolite facies(Taguchi et al., 2018). This implies that the eclogite facies metamorphim took place after 90 Ma, the maximum deposition age of the protolith.

Within the detrital zircon populations contained in the Sanbagawa meta-sediments several age groups are recognized that are also known from SE China. However, compared to those from mainland China, zircons from the Sanbagawa meta-sediments are usually characterized by higher eHf(T) values suggesting higher input of material derived from the depleted mantle. For example, eHf(T) values of zircons of the age group 82-116 Ma range from -2.4 to +9.6 and those of the 127–146 Ma group have altogether positive eHf(T) values of +11.5 to +19.0 indicating depleted mantle sources. We envisage these zircons to have been derived from the ocean side of a magmatic arc. All grains in the range 215-250 Ma are characterized by negative eHf(T) ranging from -2.3 to -15.2, suggesting re-melting of already existing crust.

Keywords: Sanbagawa Belt, detrital zircon, U-Pb dating, Hf-isotopes

©2019. Japan Geoscience Union. All Right Reserved.

Tectonic process of the Sanbagawa eclogite: zircon U–Pb and REE composition analyses

*Shogo Aoki[1], Kazumasa Aoki[2], Tatsuki Tsujimori[3], Yuta Tsuchiya[1], Daichi Kato[2]

1. Department of Biosphere-Geosphere Science, Okayama University of Science, 2. Department of Applied Science, Okayama University of Science, 3. Center for Northeast Asian Studies, Tohoku University

High-pressure and low-temperature (HP) metamorphic rocks in the Pacific-type orogeny are relicts of deeply-subducted accretionary prisms along the past subduction zones. The geochronological data of the HP rocks provide us with the time-scale information involved in material cycle from surface to deep mantle.
The Sanbagawa metamorphic belt in SW Japan is one of well-studied HP metamorphic belts in the world. However, the timing of the prograde metamorphism, especially of the eclogite-facies metamorphism has been controversial (e.g. Okamoto et al., 2004; Wallis et al., 2009).In order to solve this issue, we applied in-situ zircon U–Pb age and rare earth element (REE) composition analyses to the Sanbagawa eclogite in central Shikoku.
Igneous core and metamorphic rim domains of the separated zircons can be recognized, based on their cathodoluminescence images and Th/U ratios. The U–Pb datings of those domains clearly show existence of two different metamorphic units in the Sanbagawa metamorphic belt; i.e., one is ca. 120-100 Ma older metamorphic unit and the other is ca. 90 Ma younger one. Chondrite-normalized REE patterns obtained from the metamorphic rims in both units show no Eu anomaly and HREE depletion. These characteristics suggest that each unit suffered the eclogite-facies metamorphism at ca. 120-100 Ma and ca. 90 Ma, respectively.
Our new data combined with the mode of occurrence of the Sanbagawa eclogite in Shikoku are suggestive of the following tectonic scenario:
1. The highest-grade part of the older unit was subducted to the depth over 15 kbar at ca. 120 Ma, and stagnated there until ca. 90Ma.
2. The highest-grade part of the younger unit underwent the eclogite-facies metamorphism at ca. 90 Ma, and was juxtaposed with the eclogite of the older unit at the depth.
3. Both units were exhumed at the same time after the juxtaposition.

Keywords: Sanbagawa metamorphic belt, zircon U–Pb dating, rare earth element

©2019. Japan Geoscience Union. All Right Reserved.

Petrological implications of a new occurrence of retrogressed eclogite from the Sanbagawa belt of southwest Japan

*Tomoki Taguchi[1], Shunsuke Endo[2], Yohei Igami[1,3], Akira Miyake[1]

1. Graduate School of Science, Kyoto University, 2. Interdisciplinary Faculty of Science and Engineering, Shimane University, 3. Institute of Materials and Systems for Sustainability, Nagoya University

The Sanbagawa belt is one of the most famous subduction-related high-pressure (HP) metamorphic belts in the world, and the metamorphic facies series of the belt reaches the eclogite facies. Sanbagawa eclogites are found within coarse-grained mafic-ultramafic masses (Iratsu type) and their surrounding fine-grained mafic, pelitic, and siliceous schists (Seba type) in central and eastern Shikoku, southwest, Japan (Aoya & Endo, 2017 JGSJ). However, the regional extent of the eclogite facies region (eclogite unit) has not yet been established because most were overprinted by lower-pressure assemblages during the exhumation stage. In order to document the eclogite facies metamorphic features of the belt, we recently conducted comprehensive petrological studies of the pelitic schists in the Asemi-gawa region of central Shikoku (Taguchi & Enami, 2014a, 2014b JMPS; Taguchi et al., 2019 JMG). Our previous studies have revealed that a new eclogite unit exists in a limited high-grade area of this region and is composed primarily of pelitic schists. A number of petrological studies have been conducted on the mafic lithology of this region (e.g. Otsuki & Banno, 1990 JMG; Aoki et al. 2009 Lithos; Uno et al., 2015 CMP). However, none of these works recognize the presence of a definitive eclogitic indicator (omphacite, jadeite) within the mafic lithologies, which contrasts with the other eclogite units of Shikoku. This hinders the reliable reconstruction of the extent of the eclogite facies metamorphism in the Sanbagawa belt. Based on an integrated petrological and mineralogical approach, this study reports that mafic schist with garnet + omphacite + quartz paragenesis was first discovered in the Asemi-gawa region. The mafic schist occurs as thin layers within pelitic schist of the albite–biotite zone. This rock includes abundant garnet porphyroblasts up to 5 mm in diameter and shows prograde-type compositional zoning with no textural or compositional break. Omphacite in the mafic schist only occurs as inclusions in garnet, and albite is the major Na phase in the matrix, suggesting that the mafic schist represents highly retrogressed eclogite. The omphacite in the sample displays a strong Raman peak at 678 cm^{-1}, and concomitant Raman peaks are all consistent with those of the reference omphacite Raman spectrum. Transmission electron microscopy (TEM) observations showed that the selected area electron diffraction pattern of the omphacite is compatible with the common $P2/n$ omphacite structure. The combination of Raman geothermobarometries and conventional thermodynamic calculations gives peak (pressure–temperature) P–T conditions of 1.7–2.0 GPa and 440–540 ˚C for the mafic schist. The peak P–T values are comparable to those of the schistose eclogitic rocks (Seba type) in other Sanbagawa eclogite units of Shikoku. These findings suggest that most of the schistose eclogites and associated metasedimentary rocks along the Sanbagawa subduction zone probably share similar simple P–T histories.

Keywords: eclogite, FIB–TEM, omphacite, Raman spectroscopy, Sanbagawa belt

©2019. Japan Geoscience Union. All Right Reserved.

P-T estimations of Kashio mylonite in Oshika, Nagano, Japan: Constraints on the amalgamation of Ryoke and Sambagawa belts

*Yoshihiro Nakamura[1], Yutaka Takahasi[1], Tohru Danhara[2], Hideki Iwano[2], Takehumi Hirata[3]

1. Geological Survey of Japan, National Institute of Advanced Industrial Science and Technology, 2. Kyoto Fission-Track Co., Ltd., 3. Geochemical Research Center, The University of Tokyo

Sambagawa (*LTHP*-type) and Ryoke (*HTLP*-type) metamorphic belts are classically termed as a “paired metamorphic belt” and closely related to the island arc magmatism and regional metamorphism in subduction zone (e.g., Brown, 2010). Although almost all Ryoke metamorphic belt in SW Japan are not directly in contact with Sambagawa metamorphic belt, Oshika area in Nagano prefecture, Japan, is one of the few examples of the geological field where can be directly observed the amalgamation of Ryoke and Sambagawa belts along the Median Tectonic Line (MTL). Hence, it is the best place for discussing the relationship between metamorphism and deformation related to the tectonic evolution of MTL. Our detailed investigations of both metamorphic rocks lead to be constraints on the exhumation tectonics of *HPLT*-type metamorphic rocks and tectonic evolution from ductile to brittle deformations in subduction zone.

In this area, it is well known that the medium-*T* mylonite (so called “Kashio mylonite”) is widely exposed along the MTL (Takagi, 1986). We newly found that the low-*T* mylonites, as indicated by the Z-maximum *c*-axis lattice preferred orientations (LPOs) of recrystallized quartz, were also distributed. Both Ryoke and Sambagawa metamorphic rocks were deformed by low-*T* mylonitization within ~500m of the MTL. The mineral stretching with a gentle plunge to the NNE or SSW, suggesting the sinistral shearing, are well developed on the mylonite foliation. In the low-*T* mylonite zone, garnet porphyroclasts showed a significant chemical zoning of the grossular (X_{Grs}) from core to rim. The mylonite foliation was composed of white mica (Si in apfu = 3.38-3.49) and chlorite (X_{Mg} = 0.39-0.41). Based on the chemical analyses of recrystallized minerals, we attempted to apply the geothermometry and barometry. The *P-T* conditions of the low-*T* mylonites were estimated at 420~450 ˚C /0.5-0.6 GPa. A part of the Ryoke pelitic gneiss origin mylonites was estimated at ~540 ˚C /0.9 GPa. These *P-T* conditions of the mylonites are consistent of peak *P-T* conditions during Sambagawa metamorphism (e.g., Enami et al., 1994), suggesting the amalgamation of Ryoke and Sambagawa metamorphic belt during mylonitization.

In addition, U-Pb ages of zircons in the Kashio mylonite of Ryoke metamorphic belt were analysed by LA-ICPMS. The prominent age spectra of the mylonite showed 69.0 +/- 0.6 Ma (*n*=10), suggesting the solidification age of host Ryoke granite. Our data on protolith demonstrate a younger age than previously reported ages during mylonitization (>83 Ma, Kubota and Takeshita, 2008; or 95~85 Ma, Takagi, 1997). This suggests that the host Ryoke granite and Sambagawa metamorphic rocks were deformed by low-*T* mylonitization during 58-69 Ma. After the mylonitization and amalgamation of both metamorphic rocks, the exhumation of Ryoke and Sambagawa belts might be occurred owing to the change in plate motion at around 55 Ma (Seton et al. 2015).

[Reference] M. Brown, Gondwana Research, 18 (2010) 46-59. H. Takagi, J. Struct. Gel. 8 (1986) 3-14. M. Enami, S.R. Wallis, Y. Banno, 116 (1994), 182-198. Y. Kubota, T. Takeshita, Island Arc, 17, (2008) 129-151. H. Takagi, Chikyu, 19 (1997) 111-116. K. Shibata, H. Takagi, J. Geol. Soc. Jpn., 94 (1988) 35-50.

©2019. Japan Geoscience Union. All Right Reserved.

M. Seton, N. Flament, J. Whittaker, R.D. Muller, M. Gurnis, D.J. Bower, Geol. Rea. Let. 42 (2015) 1732-1740.

Keywords: Mylonite, EBSD, Ryoke metamorphic belt, Sambagawa metamorphic belt

©2019. Japan Geoscience Union. All Right Reserved.

Static phenomena retained by garnet during exhumation of metamorphic rocks

*Masaki Enami[1], Yui Kouketsu[2]

1. Institute for Space–Earth Environmental Research, Nagoya University, 2. Nagoya University

Electron back scatter diffraction (EBSD) method was employed for the analysis of crystallographic orientations of garnet grains to discuss tectonic behavior of various types of metamorphic rocks during exhumation. Selected metamorphic rocks were coesite-eclogite from the Sulu belt, China, granulite in the Mogok belt, Myanmar, and epidote-amphibolite and quartz schist of eclogite and non-eclogite units, respectively, in the Sanbagawa belt, Japan. The garnet grains are grouped into segmentation and honeycomb types. The segments forming an aggregate, which formed by hydration reaction during the exhumation stage, share similar crystallographic orientations, with misorientations of less than 3—4°. This suggests that the segmentation textures were not formed by deformational crush and the grains recorded a static environment during exhumation. The Sulu and Mogok garnet grains segmented under granulite-upper amphibolite facies conditions have been continually exhumed to the earth's surface without incurring specific deformation and/or rotation. The garnet grains in the epidote-amphibolite from the Sanbagawa eclogite unit were once fragmented by hydration reactions during exhumation and have subsequently become unified by hydration reactions during prograde epidote-amphibolite facies metamorphism. This fact indicates that the Sanbagawa garnet grains in the eclogite unit have recorded static conditions during the hydration and dehydration stages. Honeycomb garnet in a quartz schist from the Sanbagawa non-eclogite unit, which formed during prograde stage under the lower epidote-amphibolite facies, also shows no evidence suggesting deformation processes. This sample might not have undergone significant deformation during exhumation from depths of 25—30 km (0.8—0.9 GPa) to the earth's surface. Such undeformed phenomena recorded in these metamorphic garnet grains during exhumation might have been promoted by episodic exhumation, buoyancy-driven and static exhumation of the metamorphic belt, or local concentration of tectonic stress and heterogeneities of deformation impacts caused by the contrast of lithologic competency and tectonic discontinuity development.

Keywords: EBSD, exhumation, garnet, metamorphic rock

©2019. Japan Geoscience Union. All Right Reserved.

[J] Oral | S (Solid Earth Sciences)：S-MP Mineralogy & Petrology

Wed. May 29, 2019 10:45 AM - 12:15 PM JST | Wed. May 29, 2019 1:45 AM - 3:15 AM UTC | A08 TOKYO BAY MAKUHARI HALL

[S-MP32] Deformed rocks, Metamorphic rocks and Tectonics

convener:Yumiko Harigane(Geological Survey of Japan, National Institute of Advanced Industrial Science and Technology (AIST)), Yoshihiro Nakamura(Geological Survey of Japan, National Institute of Advanced Industrial Science and Technology), Chairperson:Tomoki Taguchi(京都大学　大学院理学研究科), Kenta Yoshida(JAMSTEC)

We invite all researchers who aim to understand the dynamics of the earth's crust and mantle at the plate boundaries, to discuss the latest results from various viewpoints. The scope will include contributions through petrology and structural geology as well as various techniques including rheology and transformation of heat and mass.

10:45 AM - 11:00 AM JST | 1:45 AM - 2:00 AM UTC

[SMP32-07] Garnet zoning suggesting the correlation between the Higo and Abukuma metamorphic rocks

*Tadao Nishiyama[1], Yuto Wakida[1] (1.Department of Earth and Environmental Sciences, School of Science, Graduate School of Science and Technology, Kumamoto University)

11:00 AM - 11:15 AM JST | 2:00 AM - 2:15 AM UTC

[SMP32-08] $FeAlO_3$ phase at ultrahigh-temperature metamorphic conditions: Evidences from the sillimanite—Fe_2O_3 and sillimanite—Fe_3O_4 systems at 9 kbar and 1050 °C

*Toshisuke Kawasaki[1], Tatsuro Adachi[2], Hiroaki Ohfuji[1], Yasuhito Osanai[2] (1.Ehime University, 2.Kyushu University)

11:15 AM - 11:30 AM JST | 2:15 AM - 2:30 AM UTC

[SMP32-09] **Halogens in nanogranitoids entrapped during granulite facies to ultrahigh-temperature metamorphism in the lower crust**

*Fumiko Higashino[1], Tetsuo Kawakami[2] (1. Graduate School of Environmental Studies, Tohoku University, 2.Graduate School of Science, Kyoto University)

11:30 AM - 11:45 AM JST | 2:30 AM - 2:45 AM UTC

[SMP32-10] Significance of high-Ti biotite and anatectic conditions of paragneiss in the Oki-Dogo Island, Japan

Hiroshi Yoshida[1], *Shunsuke Endo[1], Mai Fujiwara[1], Atsushi Kamei[1] (1.Department of Earth Science, Interdisciplinary Faculty of Science and Engineering, Shimane University)

11:45 AM - 12:00 PM JST | 2:45 AM - 3:00 AM UTC

[SMP32-11] Eclogite-to-granulite transition in the Ufipa Complex (Tanzania): the time-lag between collision and the granulitization

*Morita Isamu[1], Tatsuki Tsujimori[1], Nelson Boniface[2], Shogo Aoki[3], Kazumasa Aoki[3] (1.Tohoku University, 2.University of Dar es Salaam, 3.Okayama University of Science)

12:00 PM - 12:15 PM JST | 3:00 AM - 3:15 AM UTC

[SMP32-12] **Switching of metamorphic growth kinetics due to volume fraction of metamorphic fluid**

*Kazuhiro Miyazaki[1] (1.Orogenic Processes Research Group, Institute of Geology and Geoinformation, Geological Survey of Japan/National Institute of Advanced Industrial Science and Technology)

Garnet zoning suggesting the correlation between the Higo and Abukuma metamorphic rocks

*Tadao Nishiyama[1], Yuto Wakida[1]

1. Department of Earth and Environmental Sciences, School of Science, Graduate School of Science and Technology, Kumamoto University

The Higo and Abukuma metamorphic rocks are both Cretaceous low P/T metamorphic rocks, located in central Kyushu (the former) and in northeast Japan (the latter), respectively. The correlation between the two metamorphic rocks has been discussed in terms of SHRIMP U-Pb ages of plutonism, metamorphism and sedimentation (Sakashima et al., 2003), although they are separated by more than 1,000 km. This paper presents new evidence for this hypothesis by reporting garnet zoning in the Higo metamorphic rock (HMR) which is very similar to that in the Abukuma metamorphic rock (AMR).

Pelitic and psammitic gneisses in the garnet-cordierite zone in the HMR contains commonly garnet crystals, which are subhedral to euhedral grains of several millimeters in size. We examined chemical zoning of these garnets from 41 samples of pelitic gneiss in the Kousadake area, Kousa and Tomochi Towns, Kumamoto Prefecture. Typical mineral assemblage of the pelitic gneiss is garnet + biotite + K-spar + plagioclase + quartz ± cordierite ± sillimanite. Ilmenite, titanite, and rutile (less common) occur as inclusions in garnet. Garnet zoning can be classified into three types: flat, simple and complex types. The flat type shows no concentration gradient of any component from the core to the rim. The composition ranges from Prp9Alm68Sps3Grs20 to Prp20Alm73Sps3Grs4, depending on the bulk composition of the sample. The simple type shows a gradual change in composition from the core richer in Sps and Grs components (Prp15Alm51Sps26Grs8) to the rim richer in Alm component (Prp15Alm61Sps19Grs3). The complex type has several variations in the zoning, however, all the variations show discontinuous or rapid changes in composition. The complex A type consists of the plateau-like core richer in Sps and Grs components (Prp2Alm36Sps33Grs29) and the rim richer in Alm and Prp components (Prp23Alm67Sps7Grs3). The complex B type shows a core-mantle-rim structure. The core is nearly constant composition with Prp6Alm61Sps14Grs19, followed by a rapid increment of Grs component up to 28 mol % associated with counterpart decrement of Alm and Sps components in the mantle (Prp6Alm58Sps8Grs28). In the rim, Grs and Sps components gradually decrease with counterpart increment of Prp and Alm components to Prp12Alm73Sps5Grs10. The Grs contents in the core of the complex A type and also in the mantle of the complex B type are much higher than those of the simple and flat types, indicating higher pressure condition for the formation. Garnets with these three types of zoning occur randomly in the garnet-cordierite zone of the studied area, suggesting the different nucleation timing of these garnets rather than diffusive homogenization of zoning in higher grade rocks (Yoshimura,1995).

The complex A and B types of zoning are quite similar to those of sector-zoned garnets from the AMR reported by Hiroi et al. (1998), who suggested the followings. These zonings may indicate three stages of garnet growth at different pressures: the earliest stage characterized by relatively low T (~650 C) and medium P (~0.6 GPa), the second stage with much higher pressure up to 1.2 GPa, and the third stage with higher T (~800 C) and lower P (~0.5 GPa). Thus, the HMR may have experienced the P-T path similar to that of the AMR. This similarity of the P-T path together with the consistency of the age of plutonism, metamorphism and sedimentation (Sakashima et a., 2003) strongly suggests that the HMR and AMR may have formed the same geological terrane. The tectonics leading to the large-sale displacement between

©2019. Japan Geoscience Union. All Right Reserved.

the HMR and AMR can be either a nappe tectonics or strike-slip tectonics, although this study cannot provide any information on the tectonics.

References: Hiroi, Y. et al., (1998) JMG, 16, 67-81; Sakashima, T. et al., (2003) Jour. Asian Earth Sci., 21, 1019-1039. Yoshimura,Y.(1995) Mem. Fac. Sci. Kumamoto Univ., 14, 1, 1-18.

Keywords: garnet, zoning, Higo metamorphic rock, Abukuma metamorphic rock

©2019. Japan Geoscience Union. All Right Reserved.

$FeAlO_3$ phase at ultrahigh-temperature metamorphic conditions: Evidences from the sillimanite—Fe_2O_3 and sillimanite—Fe_3O_4 systems at 9 kbar and 1050 ℃

*Toshisuke Kawasaki[1], Tatsuro Adachi[2], Hiroaki Ohfuji[1], Yasuhito Osanai[2]

1. Ehime University, 2. Kyushu University

Two high pressure experiments at 9 kbar and 1050 ℃ under moisture condition reveal $FeAlO_3$ phase is stable under ultrahigh-temperature metamorphic conditions. $FeAlO_3$ and corundum newly crystallised accompanying SiO_2-rich melt and vapour among sillimanite crystals from the mixture of Rundvågshetta sillimanite and reagent-grade Fe_2O_3 (weight ratio of 95:5) within Pt capsule. We found no hematite in the charge. In contrast, we found $FeAlO_3$ phase, SiO_2-rich melt and vapour among sillimanite from the mixture of Rundvågshetta sillimanite and reagent-grade Fe_3O_4 at (weight ratio of 86:14) within AuPd capsule. We found a domain composed by $FeAlO_3$, corundum, magnetite—hercynite spinel and ulvöspinel at the bottom part of the charge. The domain was contact with melt among sillimanite. The present results suggest the possibility that $FeAlO_3$ phase would be an index mineral of ultrahigh-temperature metamorphism for the partially melted Fe—Al-rich granulites under hydrous and oxidised environments.

Keywords: FeAlO3 phase, sillimanite, corundum, spinel, ultrahigh-temperature granulies

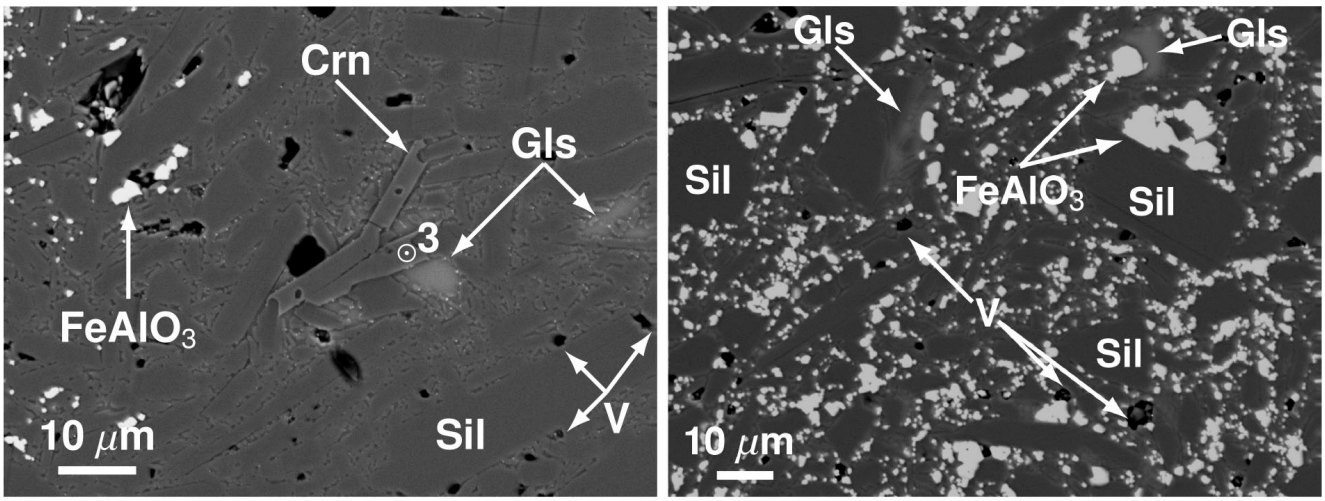

Fig. 1. Backscattered electron image (BSEI) of run products recrystallised from the mixture of Rundvågshetta sillimanite and Fe_2O_3 in the Pt capsule (left: run no. 171018A) and the mixture of Rundvågshetta sillimanite and Fe_3O_4 in the AuPd capsule (right: run no. 171018D) at 9 kbar 1050 ℃ under moisture condition. Left: euhedral corundum with fine vapour hole, $FeAlO_3$ phase, glass and vapour (dark holes) fill among sillimanite crystals. Number 3 is the analysed point by Raman spectroscopy. Right: euhedral 5–10 μm size $FeAlO_3$ phase and fine (<1 μm) $FeAlO_3$ phase are scattered among sillimanite crystals accompanying melt and vapour (dark hole). Crn, corundum. $FeAlO_3$, $FeAlO_3$ phase. Gls, glass. Sil, sillimanite. V, vapour.

©2019. Japan Geoscience Union. All Right Reserved.

Halogens in nanogranitoids entrapped during granulite facies to ultrahigh-temperature metamorphism in the lower crust

*Fumiko Higashino[1], Tetsuo Kawakami[2]

1. Graduate School of Environmental Studies, Tohoku University, 2. Graduate School of Science, Kyoto University

Granulite facies to ultrahigh-temperature (UHT) metamorphic terranes in the deep crust are considered as a potential source region of granitoid melts that eventually form plutons (e.g., Sawyer et al., 2011; Brown et al., 2011). Melt inclusions such as “nanogranitoids” and “felsite inclusions” recently found from such granulite facies and UHT metamorphic terranes are the explicit evidence of partial melting (Cesare et al., 2009; 2015; Hiroi et al., 2014). Such inclusions enable us to estimate the melt composition formed by partial melting (Cesare et al., 2015) and to estimate the timing of partial melting when combined with pressure-temperature-time (*P-T-t*) paths (Kawakami et al., 2013; 2016).
In determining the melt compositions using nanogranitoids, re-melting and re-homogenization of nanogranitoid inclusions using piston cylinder is often performed, and nanogranitoids with decrepitation texture are avoided from such experiments (Cesare et al., 2015). However, nanogranitoids that has decrepitation texture are common in high-*T* pelitic gneisses (e.g., Hiroi et al., 2014; Cesare et al., 2015; Kawakami et al., 2016) and if development of such texture is related to the *P-T* path of the host rock as in the case of fluid inclusions (Vityk and Bodnar, 1995), neglecting the decrepitated nanogranitoids might mean neglecting of specific metamorphic history. Therefore, efforts in determining chemical compositions of melt inclusions of decrepitated nanogranitoid inclusions is also valuable. Among various chemical aspects, information on major halogens (F and Cl) in lower crustal nanogranitoids is extremely poor (e.g., Cesare et al., 2015; Acosta-Vigil et al., 2016; Ferrero et al., 2018). This study aims to provide some new data on the halogen contents in nanogranitoids to better understand the partial melting in the granulite facies active lower crust using fully crystallized nanogranitoids.
Nanogranitoid inclusions are found as inclusions in garnet from granulite facies mafic and pelitic gneisses from Balchenfjella (Sør Rondane Mountains, East Antarctica). Mineral assemblages of the large-sized (>100 μm) nanogranitoid inclusions are Bt + Pl + Qtz in mafic gneiss, and Bt + Pl + Qtz + And + Sil in pelitic gneiss. Mesoperthite in the nanogranitoid inclusion and in the matrix of the pelitic gneiss gave temperature of >900 ºC based on ternary feldspar thermometry. These observation evidences that Balchenfjella experienced UHT metamorphism and the nanogranitoid inclusions represent the UHT melt. The re-integrated composition of nanogranitoids range from granodioritic in the mafic gneiss to granitic in the pelitic gneiss, and mostly peraluminous. The peraluminous melt compositions might be a result of post-entrapment interaction between the melt and host garnet. F/Cl ratio of biotite in the nanogranitoids can be an indicator of F/Cl of the nanogranitoid melts, and low F/Cl ratio observed in this study contrasts with high values observed in peraluminous silicic melts from intrusive and extrusive igneous rocks. This suggests that F/Cl ratio in shallower level silicic igneous rocks is mainly controlled by the magmatic processes in the shallow crust, and chemical characteristics of source rocks or F/Cl ratio of the original melts in the source region is of secondary importance.

Keywords: nanogranitoids, partial melting, chlorine, fluorine

©2019. Japan Geoscience Union. All Right Reserved.

Significance of high-Ti biotite and anatectic conditions of paragneiss in the Oki-Dogo Island, Japan

Hiroshi Yoshida[1], *Shunsuke Endo[1], Mai Fujiwara[1], Atsushi Kamei[1]

1. Department of Earth Science, Interdisciplinary Faculty of Science and Engineering, Shimane University

The Oki Gneiss exposed on the eastern side of the Oki-Dogo Island in SW Japan consists mainly of paragneiss and subordinate orthogneiss. These lithologies were originated from Paleoproterozoic (~1800 Ma) clastic rocks and granitoids, and subjected to low-P/T type metamorphism associated with anatexis at around 240 Ma (Tsutsumi et al., 2006; Cho et al., 2012). The Oki Gneiss must be a key to understand the correlation with Precambrian basements in the Korean Peninsula and Permo-Triassic tectonic framework of East Asia. In the present study, we conducted field survey in the entire areas of the Oki Gneiss and examined the spatial extent and P–T conditions of high-grade metamorphism and anatexis. Although structures of the Oki Gneiss were affected by intensive Cenozoic volcanic activities, the main foliation (gneissosity) largely strikes E–W and dips to the south or north. Migmatitic gneiss shows complex ptigmatic folding, but outcrops showing polyphase deformation are uncommon and the main foliation probably represents a single deformation phase. Migmatitic pelitic gneiss consists of biotite- and sillimanite-rich melanosome and plagioclase- and quartz-rich leucosome parallel to the main foliation, and is commonly cut by discordant leucogranite dikes. The peak mineral assemblage of aluminous pelitic gneiss is garnet + biotite + sillimanite + cordierite + plagioclase + quartz + spinel (hercynite-gahnite) + ilmenite + rutile + graphite or its partial assemblages. Spinel only occurs in southern areas. Occasionally, euhedral andalusite enclosing sillimanite occurs in the leucosome, and they might be cotectic minerals crystallized during cooling. Garnet grains are chemically homogeneous except for the reverse-zoned (i.e., increase in Mn and decrease in Mg) grain margins. However, some garnet in northern localities faintly preserves growth zoning characterized by high Mn, Ca and Y contents at the core of garnet grains. To estimate peak-T conditions, we used Ti-in-biotite and Zr-in-rutile geothermometers for biotite and rutile in equilibrium with quartz and zircon. High-Ti biotite (up to 5.9 wt% TiO_2) is found as inclusions in garnet and tiny rounded grains completely enclosed within single crystals of matrix quartz or plagioclase. These high-Ti biotite grains imply high-T metamorphism (up to 760˚C), but high-Ti biotite in garnet shows significantly higher Mg#, suggesting Fe-Mg exchange with the host garnet during cooling. Coarse-grained platy biotite aligned in the gneissosity shows low Ti and is associated with low-Zr rutile and sillimanite, suggesting re-equilibration (~550–650˚C) and pervasive ductile deformation during an early retrograde stage. High-Zr rutile (1200–1700 ppm Zr) only occurs as inclusions in garnet with no any associated cracks, and implies high-T conditions of ~750–780˚C. Presuming high-Ti biotite in quartz/plagioclase and homogenous core of garnet are in equilibrium at the thermal peak, combination of conventional geothermobarometers gives peak P–T conditions of ~0.42–0.60 GPa and 760–780˚C for samples from widely-spaced localities. Samples from southern localities tend to show lower P conditions. Calculated phase equilibria verify the coexistence of cordierite, garnet and spinel during anatexis at the estimated peak conditions for the southern samples. The ubiquitous occurrence of high-Ti biotite implies the Oki Gneiss entirely underwent high-grade metamorphism (transitional upper amphibolite to granulite facies). Taken together, the Oki Gneiss represents a Paleoproterozoic basement that was overprinted by a 240 Ma thermal event associated with ductile flow, low-P/T metamorphism and anatexis at mid-crustal levels (~15–20 km).

Keywords: Oki Gneiss, biotite, metamorphism

©2019. Japan Geoscience Union. All Right Reserved.

©2019. Japan Geoscience Union. All Right Reserved.

Eclogite-to-granulite transition in the Ufipa Complex (Tanzania): the time-lag between collision and the granulitization

*Morita Isamu[1], Tatsuki Tsujimori[1], Nelson Boniface[2], Shogo Aoki[3], Kazumasa Aoki[3]

1. Tohoku University, 2. University of Dar es Salaam, 3. Okayama University of Science

Eclogite-to-granulite transition found in the collisional tectonic regime can provide not only regional tectonic history but also basic principles underlying crustal thickening attributed to the continent-continent collision at convergent plate boundary. In order to understand the dynamics and timescale of collision-induced crustal thickening, we conducted petrological and geochronological research for partially granulitized eclogite and associated metamorphic rocks of the Ufipa Complex (Tanzania).

The Ufipa Complex is a newly confirmed Neoproterozoic metamorphic complex that is equivalent to the Mozambique Belt formed during 'Pan-African orogeny'. Granulitized eclogite is a coarse-grained kyanite-bearing retrograde eclogite with the major mineral assemblage of garnet + omphacite + kyanite + rutile; kyanite contains both omphacite and clinozoisite. Kyanite-free eclogite is medium-grained less-retrograded, bimineralic eclogite. Garnet–omphacite–kyanite–quartz geothermobarometry yielded a P = ~1.9–2.1 GPa and T = ~920–960°C for eclogite stage and P = ~1.3–1.6 GPa and T = ~900–940℃ for high-pressure granulite stage.

LA-ICPQMS zircon U–Pb geochronology for the eclogites revealed that time-lag Δt between collision at ~588 Ma and granulite-facies recrystallization at ~559 Ma was ~30 m.y. Zircon growth during eclogite-facies was confirmed by both mineral inclusions and trace-element abundances. In-situ zircon dating using petrographic thin-sections also confirmed the timing of granulitization. The inferred Δt of ~30 m.y. is consistent with other continental collision zones even in Cenozoic orogens in the literatures.

Keywords: Eclogite, Granulitization, Zircon U-Pb age, In-situ dating, Neoproterozoic, East Africa

©2019. Japan Geoscience Union. All Right Reserved.

Switching of metamorphic growth kinetics due to volume fraction of metamorphic fluid

*Kazuhiro Miyazaki[1]

1. Orogenic Processes Research Group, Institute of Geology and Geoinformation, Geological Survey of Japan/National Institute of Advanced Industrial Science and Technology

In general, it is predicted that the growth kinetics should switch from interface-controlled to diffusion-controlled kinetics with increasing grain size. Rate constant and diffusion coefficient are required for estimate the critical grain size for the switching. It is assumed that the effective diffusivity is a product among diffusivity of solute in water, volume fraction of metamorphic fluid and tortuosity. Using rate constant of silicate in aqueous fluid and diffusion coefficient of solutes in aqueous fluids, the switching will occur around 1 mm in diameter at 500 degree C and 1 G Pa with 0.02 volume % of metamorphic fluid. The switching will occur around 1 cm with 0.2 volume % of metamorphic fluid, and will occur around 10 cm with 2 % volume of metamorphic fluid, respectively. Accompanying the switching with diffusional instability, growth kinetics can be predicted by degree of supersaturation. Recently, degree of supersaturation or reaction affinity, which is a function of degree of supersaturation, were reported from different metamorphic belts (e.g. Miyazaki, 2015; Spear and Pattison, 2017). Typical value for reaction affinity of the nucleation of a porphyroblast, such as garnet, is 300 J/mol oxygen (Spear and Pattison, 2017). Using this value, diffusional instability will occur above 1 μm. Therefore, garnet should grow unstable and result in highly irregular morphology after the switching. However, such garnet is rare in general regional metamorphic belt. In other word, existence of euhedral to subhedral garnet larger than cm-scale implies interface-controlled growth under sufficient metamorphic fluid condition at deep crustal depths. Unlike in the case of garnet porphyroblast, matrix mineral, such as phengite, probably grew by interface-controlled dissolution-precipitation with non-hydrostatic condition, because supersaturation of the dissolution-precipitation is perhaps much lower than that of net-transfer reaction and size of phengite is usually less than 1 mm.

Keywords: Metamorphism, Metamorphic reaction, Garnet

©2019. Japan Geoscience Union. All Right Reserved.

[J] Poster | S (Solid Earth Sciences)：S-MP Mineralogy & Petrology

Wed. May 29, 2019 1:45 PM - 3:15 PM JST | Wed. May 29, 2019 4:45 AM - 6:15 AM UTC | Poster Hall International Exhibition Hall8, Makuhari Messe_4

[S-MP32] Deformed rocks, Metamorphic rocks and Tectonics

convener:Yumiko Harigane(Geological Survey of Japan, National Institute of Advanced Industrial Science and Technology (AIST)), Yoshihiro Nakamura(Geological Survey of Japan, National Institute of Advanced Industrial Science and Technology)

We invite all researchers who aim to understand the dynamics of the earth's crust and mantle at the plate boundaries, to discuss the latest results from various viewpoints. The scope will include contributions through petrology and structural geology as well as various techniques including rheology and transformation of heat and mass.

[SMP32-P01] Pressure-temperature estimates of the Lützow-Holm Complex utilizing distributions of trace elements and inclusions in garnet porphyroblasts in pelitic gneisses

*Kota Suzuki[1], Tetsuo Kawakami[1], Yohei Igami[2] (1.Department of Geology and Mineralogy, Graduate School of Science, Kyoto University, 2.Institute of Materials and Systems for Sustainability, Nagoya University)

[SMP32-P02] Microstructures and pressure-temperature condition in pelitic gneisses from the Lützow-Holm Complex at Akarui Point, East Antarctica

*Hayato Yodoya[1], Takeshi Ikeda[2] (1.Department of Earth and Planetary Sciences, Graduate School of Scinece, Kyushu University, 2.Department of Earth and Planetary Sciences, Faculty of School of Scinece, Kyushu University)

[SMP32-P03] Long-lived (>90 Myr) granulite-facies metamorphism in the Trivandrum Block, southern India.

*Hikaru Kadowaki[1], Toshiaki Tsunogae[2], Santosh M.[3], Shaji E.[4], Yusuke Takamura[5], Yukiyasu Tsutsumi[6] (1.College of Geoscience, Graduate School of Life and Environmental Sciences, University of Tsukuba, 2.Faculty of Life and Environmental Sciences, University of Tsukuba, 3.School of Earth Sciences and Resources, China University of Geosciences Beijing, 4.Department of Geology, University of Kerala, 5. Doctoral Program in Earth Evolution Sciences, Graduate School of Life and Environmental Sciences, University of Tsukuba, 6.Department of Geology and Paleontology, National Museum of Nature and Science)

[SMP32-P04] Dislocation microstructures in garnet: Thermal effect during deeper crustal seismic slip in orogen-boundary shear zone

*Kaushik Das[1], Naotaka Tomioka[2], Proloy Ganguly[3], Jun-ichi Ando[1], Gautam Ghosh[3], Sankar Bose[3] (1.Hiroshima University, 2.Kochi Institute for Core Sample Research, JAMSTEC, 3.Presidency University, India)

[SMP32-P05] U-Pb zircon ages of migmatitic rocks from the Ryoke belt in the Mikawa and eastern Sanuki areas

*Keiichi Kazuratachi[1], Tetsuo Kawakami[1], Etienne Skrzypek[1], Shuhei Sakata[2], Takafumi Hirata[3] (1.Kyoto University, 2.Gakushuin University, 3.The University of Tokyo)

[SMP32-P06] Structural geology of Hidaka metamorphic belt in the Mt.Nozuka area, Hokkaido, Japan -Growth and formation process of the Cenozoic continental crust by island arc/arc join and its mechanism-

*Moeko Kanno[1], Tsuyoshi Toyoshima[2] (1.Graduate school of Science and Technology, Niigata University , 2.Department of Geology,Faculty of Science,Niigata University)

[SMP32-P07] THE PRESSURE-TEMPERATURE PATH AND MINERAL ASSEMBLAGE OF THE KHONICHIIN OVOO AREA, SOUTHEASTERN MONGOLIA.

*Undarmaa Batsaikhan[1], Noriyoshi Tsuchiya[1], Masaoki Uno[1], Yukio Isozaki[2], Uyanga Bold[2], OTGONBAYAR DANDAR[1], Hikaru Sawada[2] (1.Graduate School of Environmental Studies, Tohoku University, 2.Graduate School of Arts and Sciences the University of Tokyo)

[SMP32-P08] **Pressure-temperature conditions of contact metamorphism in Nokita area, Itoshima Peninsula, northwest Kyushu**

*Takeshi Ikeda[1], Kento Ota[2] (1.Department of Earth and Planetary Sciences,Faculty of Scinece, Kyushu University, 2.Department of Earth and Planetary Sciences,Graduate School of Scinece, Kyushu University)

[SMP32-P09] Evidence of Partial Melting of Migmatitic Felsic Gneiss from Nagasaki Metamorphic Complex in Amakusa-Shimoshima, western Kyushu, Japan

*Yuki Mori[1], Takeshi Ikeda[2], Kazuhiro Miyazaki[3] (1.Department of Earth and Planetary Sciences, Graduate School of Sciences, Kyushu University, 2.Department of Earth and Planetary Sciences, Faculty of Sciences, Kyushu University, 3.Research Institute of Geology and Geoinformation, Geological Survey of Japan, National Institute of Advanced Industrial Science and Technology)

[SMP32-P10] **Microstructural Analysis of Quartz grains in Monomineralic and Polyphase domains: A case study from Main Central Thrust (MCT) Zone Mylonites, western Himalaya, India**

*Shivaji Saha[1], Toru Takeshita[1], Subhajit Ghosh[2], Hari Bahadur Srivastava[3] (1.Department of Natural History Sciences, Hokkaido University, 2.Earthquake Research Institute, The University of Tokyo, 3.Department of Geology, Banaras Hindu University)

[SMP32-P11] **Tectono-thermal evolution of the Main Central Thrust (MCT) zone rocks of the Himalayan Crystalline Complex (*HCC*), Darjeeling-Sikkim Himalaya**

*Subhajit Ghosh[1,2], Santanu Bose[2,3], Nibir Mandal[4], Arijit Laik[2] (1.Earthquake Research Institute, The University of Tokyo, 1-1-1 Yayoi, Bunkyo-Ku, Tokyo 113-0032, 2.Department of Geology, University of Calcutta, 35, Ballygunge Circular Road, Kolkata 700019, India, 3.Department of Geology, Presidency University, 86/1 College Street, Kolkata 700073, India, 4.Department of Geological Sciences, Jadavpur University, Kolkata 700032, India)

[SMP32-P12] Thermal structure and deformation history of the low-grade Sanbagawa belt in the central of Kii Peninsula and tectonic implications

*Ken Yamaoka[1,2], Simon Wallis[1], Hiroshi Mori[2] (1.University of Tokyo, 2.Shinshu University)

[SMP32-P13] Antigorite Raman spectrum: a case study in Shiraga region of the central Shikoku, Sanbagawa metamorphic belt, SW Japan

*Kota Ando[1], Yui Kouketsu[1], Katsuyoshi Michibayashi[1] (1.Nagoya University)

[SMP32-P14] A fluid inclusion study from the late Paleozoic retrograde eclogite from the Yunotani Valley of the Omi area, Hida-Gaien Belt, Japan

*Yuzuki Shinji[1], Tatsuki Tsujimori[1], Tatsuhiko Kawamoto[2] (1.Tohoku University, 2.Shizuoka University)

[SMP32-P15] Development of reaction-induced stress and permeability in MgO-H_2O system

*Hisamu Kasahara[1], Masaoki Uno[1], Atsushi Okamoto[1], Noriyoshi Tsuchiya[1] (1.Graduate School of Environmental Studies, Tohoku University)

[SMP32-P16] Crystal orientation analysis of olivine in ultra-mylonite using TKD method: progress in spatial resolution from EBSD

*Yohei Igami[1], Katsuyoshi Michibayashi[2], Kakihata Yuki[2], Yui Kouketsu[2] (1.Institute of Materials and Systems for Sustainability, Nagoya University, 2.Graduate School of Environmental Studies, Nagoya University)

[SMP32-P17] Elucidation of effective diffusion coefficient along grain boundaries by hydrothermal experiment using low porosity rocks

*Naoki Sugisawa[1], Masaoki Uno[1], Noriyoshi Tsuchiya[1] (1.Graduate school of environmental studies Tohoku university)

[SMP32-P18] **Seismic slipping events recorded in a fault gouge zone: evidence from the Nojima Fault drill holes, SW Japan**

*Aiming Lin[1], Takafumi Nishiwaki[1] (1.Department of Geophysics, Graduate School of Science, Kyoto University)

[SMP32-P19] Evolution of fluid chemistry during basalt-water and basalt-seawater interactions revealed by hydrothermal flow-through experiments

*Yusuke Netsu[1], Atsushi Okamoto[1], Nobuo Hirano[1], Masaoki Uno[1], Noriyoshi Tsuchiya[1] (1.Tohoku University, Graduate School of Environment Studies)

[SMP32-P20] **3D microstructural analyses of fault rocks using CT and μCT scanning techniques**

*Bingcheng Liu[1], Aiming Lin[1], Takafumi Nishiwaki[1] (1.Kyoto University)

[SMP32-P21] **Dissolution kinetics of forsterite olivine at >200 °C: implication for the kinetics of serpentinization.**

*Ryosuke Oyanagi[1], Tatsu Kuwatani[1], Katsuhiko Suzuki[1] (1.Japan Agency for Marine-Earth Science and Technology)

Pressure-temperature estimates of the Lützow-Holm Complex utilizing distributions of trace elements and inclusions in garnet porphyroblasts in pelitic gneisses

*Kota Suzuki[1], Tetsuo Kawakami[1], Yohei Igami[2]

1. Department of Geology and Mineralogy, Graduate School of Science, Kyoto University, 2. Institute of Materials and Systems for Sustainability, Nagoya University

The Lützow-Holm Complex (LHC) in East Antarctica is a late Neoproterozoic to early Cambrian orogenic belt, formed during the amalgamation of Gondwana and composed of various bulk compositions of high-grade metamorphic rocks. Based on matrix mineral assemblages of mafic to intermediate mafic rocks, the LHC has been divided into three metamorphic facies zones; upper-amphibolite facies zone, transitional zone and granulite facies zone [1]. Because of the continuous distribution of upper-amphibolite facies to granulite facies metamorphic rocks, the LHC has been considered as a good exposure of the cross section of lower crust during continental collision events.
However, recent studies have found that high-*T* conditions above 850 °C are common even in the transitional zone and such temperatures are attained under kyanite stability field [3, 6, 7]. The aim of this study is to re-examine the peak metamorphic *P-T* conditions and *P-T* paths of selected regions in the LHC (Rundvågshetta, Skallen, Skarvsnes and Akarui Point) utilizing distributions of trace elements and inclusions such as Al_2SiO_5 minerals and rutile in garnet porphyroblasts in high-grade pelitic gneisses.
The Zr content of rutile coexisting with zircon+quartz strongly depends on the temperature condition and has been calibrated as Zr-in-rutile geothermometers that is more robust than the traditional Fe-Mg exchange type geothermometers during high-*T* metamorphism. In this study, experimentally calibrated Zr-in-rutile geothermometer [8] was applied to rutile grains in garnet and matrix.
The polymorphs of Al_2SiO_5 minerals are known as valuable indicators of the *P-T* conditions. In the course of this study, sillimanite with a characteristic Raman peak around 420 cm^{-1} which is not listed as a sillimanite peak in the Lyon database (http://www.geologie-lyon.fr/Raman/) were found as inclusion minerals in garnet and as matrix minerals from all of the four studied regions. In order to examine whether such a peak is related to the phase transition from kyanite or mullite to sillimanite, we observed them in detail by TEM. However, no evidence for such transition was found. Therefore, sillimanite with 420 cm^{-1} peak is dealt as normal sillimanite in this study.
Chemical zoning of garnet in high-*T* metamorphic rocks in terms of major elements (Fe, Mg, Ca and Mn) are commonly obscured by the diffusion under high-*T* conditions. On the other hand, chemical zoning of garnet in terms of trace elements, especially P, is less affected by the later diffusion, and commonly preserves sharp growth zoning [e.g., 2, 4]. Utilizing the sharp P zoning as a contemporaneous surface during garnet growth to define core and rim of garnet, and utilizing relic inclusions in garnet such as Al_2SiO_5 minerals and rutile to constrain the *P-T* conditions of each metamorphic stage [e.g., 5], we estimated metamorphic *P-T* conditions recorded in pelitic gneisses from the four regions in the LHC. Although Akarui Point is located in the “transitional zone” and three other regions are in the “granulite facies zone”, all of the inferred *P-T* paths of high-grade pelitic gneisses from Skallen, Skarvsnes and Akarui Point indicate nearly isothermal decompression starting from kyanite stability field at temperature around 850 °C. From Rundvågshetta, although pressure condition could not be well constrained, extremely high peak metamorphic temperature (> 900 °C) was inferred.
Since the peak metamorphic grades inferred from inclusion minerals in garnet porphyroblasts from Skallen, Skarvsnes and Akarui Point are almost the same, the traditional metamorphic zone mapping

©2019. Japan Geoscience Union. All Right Reserved.

based on matrix mineral assemblages does not represent the highest metamorphic conditions attained, and needs re-evaluation utilizing petrochronological approach.

References

[1]Hiroi et al, 1991 [2]Hiroi et al, 1997 [3]Iwamura et al, 2013 [4]Kawakami and Motoyoshi, 2004 [5]Kawakami and Hokada, 2010 [6]Kawakami et al, 2016 [7]Nakamura et al, 2013 [8]Tomkins et al, 2007

Keywords: chemical zoning, Phosphorus, kyanite, sillimanite, Zr-in-rutile geothermometer, partial melting

©2019. Japan Geoscience Union. All Right Reserved.

Microstructures and pressure-temperature condition in pelitic gneisses from the Lützow-Holm Complex at Akarui Point, East Antarctica

*Hayato Yodoya[1], Takeshi Ikeda[2]

1. Department of Earth and Planetary Sciences, Graduate School of Scinece, Kyushu University, 2. Department of Earth and Planetary Sciences, Faculty of School of Scinece, Kyushu University

Metamorphic rocks have been considered to preserve the mineral assemblage and composition at the peak condition in each pressure (*P*) –temperature (*T*) path. If this assumption is valid, the metamorphic rocks in the same outcrop are expected to show the same *P-T* condition. However, different *P-T* conditions have been estimated based on different geothermobarometers for rocks even from the same outcrop. Systematic difference among the methods could be responsible for these differences. However, this study revealed that use of the same pair of geothermobarometers provides significantly different P-T conditions for two pelitic gneisses from the same outcrop of the Lützow-Holm Complex, at Akarui Point, East Antarctica. An alternative interpretation is proposed to account for this difference.

The mineral assemblages of the studied gneisses are garnet, biotite, plagioclase, K-feldspar, quartz with and without sillimanite. Garnet grains in the Sil-bg. sample show round shape and contain large amount of fine quartz inclusions, whereas those in the Sil-free sample represent irregular shape and sporadically include coarse-grained plagioclase.

Garnet in both samples have chemically heterogeneity such that X_{Ca} (=Ca/Fe+Mg+Ca+Mn) and Mg/Fe decrease from the core to the rim. Furthermore, garnet in contact with biotite represents lower Mg/Fe than that in contact with other minerals. Garnet in the Sil-bg. sample is low in X_{Ca} and Mg/Fe as compared with garnet in the Sil-free sample. Phosphorus in garnet of the Sil-bg. sample represents euhedral shape of chemical contour in contrast to the garnet in the Sil-free sample where phosphorus shows no zoning. Biotite in the Sil-bg. sample shows Al-rich and low Mg/Fe as compared with that in the Sil-free sample. No systematic difference in Ti content in biotite is recognized. The Sil-free sample contains plagioclase with higher anorthite content than the Sil-bg. sample.

In the AFM approximation, garnet and biotite coexisting with sillimanite are expected to show higher Mg/Fe than those free from sillimanite. However, the present observations disagree with the prediction. Garnet contains significant amount of Ca, requiring addition of CaO to the chemical system. A calculated garnet composition diagram with respect to Ca-Mg-Fe shows that garnet coexisting with sillimanite represents a univariant line lower Ca and Mg/Fe than that free from sillimanite, and the present data are consistent with it. This suggests that two samples were not necessarily equilibrated at different *P-T* condition.

Geothermobarometry, in contrast, indicates significant difference in *P-T* condition. That is, garnet-biotite geothermometer (Ferry and Spear., 1978) and garnet-biotite-plagioclase-quartz geobarometer (Hoisch., 1990) show 685-718 ℃ at 6.4-6.6 kbar for the Sil-free sample and 828-855 ℃ at 7.2-7.8 kbar for the Sil-bg. sample.

It is puzzling feature that different samples from the same outcrop provide different *P-T* estimations using

©2019. Japan Geoscience Union. All Right Reserved.

the same geothermobarometers. The Sil-bg. sample records higher temperature than the Sil-free sample, as described before. Preservation of euhedral chemical contour of phosphorus in the Sil-bg. sample would indicate that the garnet grew maintaining surface equilibrium, at high temperatures. In contrast, absence of such euhedral contour and highly-rough surface of garnet in the Sil-free sample suggest relatively high growth rate, at low temperatures.

The *P-T* path of Akarui Point contains pressure decrease during temperature decrease (Iwamura et al., 2013). Considering this *P-T* path, it is expected that the garnet of Sil-free sample didn't exist at high temperatures and formed at low pressures and temperatures. The difference in estimated *P-T* conditions in the same outcrop can be attributed to not only the difference in the method but also the difference in the timing of the formation of minerals.

Keywords: pressure-temperature condition, phase relation, Lützow-Holm Complex

©2019. Japan Geoscience Union. All Right Reserved.

Long-lived (>90 Myr) granulite-facies metamorphism in the Trivandrum Block, southern India.

*Hikaru Kadowaki[1], Toshiaki Tsunogae[2], Santosh M.[3], Shaji E.[4], Yusuke Takamura[5], Yukiyasu Tsutsumi[6]

1. College of Geoscience, Graduate School of Life and Environmental Sciences, University of Tsukuba, 2. Faculty of Life and Environmental Sciences, University of Tsukuba, 3. School of Earth Sciences and Resources, China University of Geosciences Beijing, 4. Department of Geology, University of Kerala, 5. Doctoral Program in Earth Evolution Sciences, Graduate School of Life and Environmental Sciences, University of Tsukuba, 6. Department of Geology and Paleontology, National Museum of Nature and Science

The Southern Granulite Terrane in India is composed of various Archean to Neoproterozoic continental blocks, magmatic arcs, and supracrustal units amalgamated through complex subduction-accretion-collision event and high-grade metamorphism during the Latest Neoproterozoic to Cambrian Gondwana amalgamation. The Trivandrum Block corresponds to a unit in the southern part of the terrane with abundant metasediments and orthogneisses. The pressure-temperature (*P-T*) evolution of the high-grade metamorphism and its time scale are important for unraveling metamorphic processes during the collisional event. The *P-T* evolution recorded in various lithologies in the Trivandrum Block has been argued in numerous previous studies, and it is a subject of ongoing debate. The peak metamorphic ages reported in previous studies from the Trivandrum Block also show a wide range of ca. 600-510 Ma. It is therefore still not known whether the Trivandrum Block underwent single metamorphism with *P-T* variations within the block, or it experienced two discrete metamorphic events at 800-900 ˚C and >950 ˚C. In this study, we present new petrological, geothermobarometric, and geochronological data from khondalites, charnockites, bleached charnockites in the western part of the Trivandrum Block and discuss pressure-temperature-time (*P–T–t*) evolution of the block for unraveling the duration and heat source of high-grade metamorphism.

Phase equilibria modeling of the khondalite from Elavinmoodu quarry located in the western part of the Trivandrum Block indicates peak *P-T* condition of 920-1030 ˚C and 6.0-7.6 kbar, suggesting UHT metamorphism. Prograde and retrograde *P-T* conditions of ~750 ˚C/~7 kbar and ~750 ˚C/~4 kbar, respectively, were also obtained, based on which a clockwise *P-T* path with geotherm-parallel slow cooling is inferred. Consistent *P-T* conditions are obtained from khondalite exposed at Kakkod quarry where incipient charnockite patches within khondalite and foliation-parallel bleached layers within massive charnockite are preserved. Phase equilibria modeling of the incipient charnockite and the bleached rock indicate metamorphic *P-T* conditions of 820-950 ˚C/ 5-10 kbar and 800-1000 ˚C/~6 kbar, respectively. These data suggest that the bleaching of charnockite occurred during high-grade (or UHT) metamorphism, possibly because of fluid flow around the peak metamorphism.

Zircon and monazite U-Pb geochronology for a khondalite sample from Elavinmoodu quarry suggests that prograde, peak, and retrograde metamorphisms took place at around 582±17 Ma, 555.1±8.1 Ma, and 527.3±8.0 to 501.9±8.5 Ma, respectively. Later infiltration of hydrous fluid and hydration of garnet to form biotite occurred at around 489±12 Ma. Our results suggest that high-grade metamorphism continued at least 90 Myr, from 582 Ma to 489 Ma, suggesting a long-lived thermal event possibly related to the input of radiogenic heat from the crust and/or magmatic heat from syn- to post-tectonic intrusions.

The results of this study suggest single metamorphic event along a clockwise *P-T* path. The duration of

©2019. Japan Geoscience Union. All Right Reserved.

high-grade metamorphism (>90 Myr) is nearly consistent with that of metasediments from the Wanni Complex (>50 Myr; Hirayama et al., 2018), but it is shorter than that of long-lived high-grade metamorphism of the Highland Complex (~180 Myr; He et al., 2018). Although previous studies suggested that the supracrustal units of the Trivandrum Block could be a continuation of the Highland Complex (e.g., Dharmapriya et al., 2016; Takamura et al., 2018), the high-grade metamorphism of the Highland Complex might have started earlier than that of the Trivandrum Block possibly due to complex and multi-stage collisional processes related to the amalgamation of Gondwana Supercontinent.

Keywords: Trivandrum Block, P–T–t evolution, Ultrahigh-temperature metamorphism, Phase equilibria modeling, U–Pb geochronology

©2019. Japan Geoscience Union. All Right Reserved.

Dislocation microstructures in garnet: Thermal effect during deeper crustal seismic slip in orogen-boundary shear zone

*Kaushik Das[1], Naotaka Tomioka[2], Proloy Ganguly[3], Jun-ichi Ando[1], Gautam Ghosh[3], Sankar Bose[3]

1. Hiroshima University, 2. Kochi Institute for Core Sample Research, JAMSTEC, 3. Presidency University, India

A considerable amount of information regarding the growth and evolution of old continents are preserved at the boundaries between the orogenic belts and pre-existing cratonic blocks. These are the areas of intense and repeated deformation, metamorphism and activities of crustal fluids. Apart from the precise estimation of the pressure-temperature-fluid evolution through time, one of the major existing challenges is to understand the deformation mechanisms operated in the deep to shallow crustal depths for such geologically complex areas. The Phulbani domain in the north-western part of the Eastern Ghats Granulite Belt, India (EGB) provides a good opportunity as it is juxtaposed in its north and west by the Archean Singbhum Craton and Bastar Craton, respectively. Recent petrological and geochronological works of our group on the metapelitic granulite-charnockite-granitic gneiss of this domain reveal the pressure-temperature-fluid evolution with time. Though this domain is differentiated from the Visakhapatnam domain situated further south-southwest, the overall evolutionary history is observed to be very similar in style and time of occurrence. The Si-poor aluminous granulites preserve exotic reaction textures implying prograde heating-dominated path culminating at UHT condition (~1000 ˚C at 8 Kbar) followed by a retrograde cooling-decompression path, both in presence of CO_2-rich fluids. The age of metamorphism and associated magmatism ranges between ca. 1000 Ma and 900 Ma, similar to that of the Visakhapatnam domain.
The Phulbani domain, however, is bound on its north by a pronounced east-west shear zone, known as the Ranipathar shear zone. This deep crustal shearing affected the pelitic granulite and granitic gneiss. The mylonitic garnet-bearing granite gneiss preserves east-west foliation-parallel ultramylonite layers. Moreover, broadly east-west and north-south oriented black veins occur in these rocks. Thick (cm-scale) to thin (mm-scale) veins have mesoscopic characters of a pseudotachylite, e.g. injection veins. The microscopic observations on the foliation-parallel veins reveal that the vesicular groundmass of the veins is composed of micron-scale quartz-feldspar-biotite with clasts of garnet, at places. These veins, in certain cases, contain mm-scale clasts of the host granite mylonite gneiss.

Keywords: Garnet dislocation microstructures, Cataclastic flow, Seismic slip, Orogen-boundary shear zone

©2019. Japan Geoscience Union. All Right Reserved.

U-Pb zircon ages of migmatitic rocks from the Ryoke belt in the Mikawa and eastern Sanuki areas

*Keiichi Kazuratachi[1], Tetsuo Kawakami[1], Etienne Skrzypek[1], Shuhei Sakata[2], Takafumi Hirata[3]

1. Kyoto University, 2. Gakushuin University, 3. The University of Tokyo

Petrochronological studies of the migmatitic part of the high-temperature, low-pressure type Ryoke metamorphic belt enables us to understand the duration of partial melting of the mid-crustal depths during the Cretaceous ignimbrite flare-up event (Takatsuka et al., 2018a). In order to link multiple metamorphic zircon growths in migmatitic rocks with metamorphic stages of the Ryoke metamorphism, we performed LA-ICP-MS U-Pb zircon dating for samples from the Mikawa and eastern Sanuki areas (Ryoke belt, SW Japan).

In the Mikawa area, U-Pb ages of zircon from ~20 cm thick leucosome subparallel to the migmatitic banding of the psammitic metatexite has been already reported (Takatsuka et al., 2018a). The U-Pb dates of metamorphic rims in this part continuously spread on concordia from ~103 Ma to ~83 Ma. These metamorphic rims were separated into two stages of rim growth by discontinuous zoning in CL images, supported by their chronological and chemical difference: Inner rims were interpreted as the zircon growth during prograde metamorphism (97.0±4.4 Ma) and outer rim as the zircon crystallization from the partial melt during early retrograde metamorphism (88.5±2.5 Ma) (Takatsuka et al., 2018a). However, since the sample used in Takatsuka et al. (2018a) was a notably thick leucosome sample different from the surrounding metatexite leucosomes, whether zircon in the typical metatexite migmatites from the same area give the similar characteristics or not has been not clear.

In this study, we performed LA-ICP-MS U-Pb zircon dating for 4 migmatitic rock samples from the high-grade part of the Mikawa area. Migmatite samples mainly consist of Qtz+Pl+Kfs+Bt±Crd+Sil±Grt. Zircon grains commonly have metamorphic rims in which sillimanite and muscovite inclusions are found. We obtained continuous spread of U-Pb dates on concordia from ~98 Ma to ~81 Ma. Based on presence/absence of sillimanite inclusions, Th/U ratio, and U concentration of zircon rims in addition to the U-Pb dates, three metamorphic stages were recognized; (1) 91.4±0.8 Ma (weighted average age, MSWD=1.4, Th/U<0.08, n=29) possibly representing the zircon rim growth in the presence of partial melts during regional metamorphism, (2) 87.1±1.7 Ma (weighted average age, MSWD=2.1, Th/U=~0.002-0.01, n=3) representing the formation of U-rich zircon through fluid-rock interaction at early retrograde metamorphism, (3) ~81 Ma (80.9±2.9 Ma and 81.5±7.3 Ma; Th/U<0.03) overgrowth on metamorphic rim (1). The zircon rim (3) might represent the growth or recrystallization during contact metamorphism caused by the intrusion of 81-75 Ma granitoids (Takatsuka et al., 2018b), as sampling point of the migmatite was 1.7 km distant from the 81-75 Ma granitoids and the obtained U-Pb zircon dates are close to the granitoids.

We also determined U-Pb ages of metamorphic zircon in 2 samples from the eastern Sanuki area (Kutsukake et al., 1979) where ages of metamorphic zircon have not been reported so far. One sample is a pelitic gneiss from a metamorphic rock body of about 800 m in size surrounded by granitoids, and mainly consists of Qtz+Pl+Kfs+Bt+Grt. Zircon grains in this sample have metamorphic rims (Th/U=~0.02-0.18). The weighted average U-Pb age of the metamorphic zircon rims is 93.4±0.7 Ma (MSWD=0.85, n=27). Another sample is a pelitic gneiss from a metamorphic rock body of 4 km wide, surrounded by gneissose granitoids. The gneissose structure of pelitic gneiss is concordant with surrounding granitoids. This sample mainly consists of Qtz+Pl+Kfs+Bt+Sil. Metamorphic rims (Th/U=~0.05-0.08) of zircon include sillimanite, and the weighted average U-Pb age is 95.4±2.4 Ma (MSWD=0.47, n=6). As these ages are consistent with U-Pb zircon ages of surrounding ~93 Ma gneissose granitoids (Iida et al., 2015), it is likely

©2019. Japan Geoscience Union. All Right Reserved.

that the rims grew during contact metamorphism by the granitoids under sillimanite-stable condition.

Keywords: U-Pb zircon dating, migmatite, high-temperature metamorphism

©2019. Japan Geoscience Union. All Right Reserved.

Structural geology of Hidaka metamorphic belt in the Mt.Nozuka area, Hokkaido, Japan -Growth and formation process of the Cenozoic continental crust by island arc/arc join and its mechanism-

*Moeko Kanno[1], Tsuyoshi Toyoshima[2]

1. Graduate school of Science and Technology, Niigata University , 2. Department of Geology,Faculty of Science,Niigata University

The Hidaka Metamorphic Belt (HMB) in Hokkaido, northern Japan, consists of metamorphic and plutonic rocks, and is regarded as a crustal section of Tertiary immature parts of the Kurile island arc exposed along with collision to the NE Japan arc in the Miocene (Komatsu et al., 1982 etc.) . Metamorphic grade increases from very low-grade sediments in the east to granulite facies in the west. It was considered to be a single and coherent crustal section, however, Shimura et al. (2015) proposed that HMB is a composite of two crusts of 19 Ma and 37 Ma. This hypothesis should be tested by detailed filed relationships of rocks of different ages. This paper presents deformation phase of metamorphic rock and plutonic rock and zircon U-Pb ages along the Niobetsu River route of the Nozuka dake area, southern HMB, and discusses on the mode of crustal evolution there.

In the study area, HMB consists mainly of S-Type tonalite (Grt Tonalite, Grt-Bt Tonalite), I-Type tonalite (Hbl-Bt tonalite), Diorite, Amphibolite, Gneiss.
Most of the rocks aligned with NW—SE trends except for a diorite intrusion with N—S margins. The diorite is accompanied with migmatite along its margins. Blocks of metamorphic rocks are included in I-Type tonalite and Diorite. Imbricated hornblende crystals in marginal parts of the diorite imply a normal fault-sense magmatic flow. Heterogeneous amphibolite on the southern margin of the diorite are severely folded and deformed with S-C fabric suggesting partial melting.
Mylonitization is observed in S-type tonalite near the Hidaka Main Thrust (HMT), the western margin of HMB. The mylonites show right lateral shear structures with or without normal-slip component. The mylonitization can be classified into 3 stages: 1st Mylonitization by shear deformation of nomal dip-slip, 2nd Mylonitization by shear deformation of normal dip-slip ~ dextral shear, 3rd Mylonitization by shear deformation of dextral shear ~ reverse dip-slip.

We obtained zircon U-Pb ages from S-type tonalites, I-type tonalite, and Diorite.
S-type: about 45Ma, I-type: About 33Ma, Diorite: about 19Ma.

Heterogeneous amphibolite is considered as the boundary deformation zone between 19 Ma plutonic and metamorphic rocks and the older plutonic and metamorphic rocks, because Heterogeneous amphibolite is severely folded and deformed with partial melting. Diorite is penetration in a tensile field is expected. Because the asymmetric flow structure inside the diorite shows normal fault sense.

Zircon U - Pb ages suggest three magmatic stages (about 33 Ma, about 19 Ma and older then 33Ma) in HMB of this area. Igneous rocks include migmatite and metamorphic rocks . So, it is suggested that the magmatism activities of 3 stages are accompanied by metamorphism. Therefore, it is considered that the Hidaka metamorphic belt was formed by three stage metamorphisms.

©2019. Japan Geoscience Union. All Right Reserved.

Keywords: Structural geology, Hidaka Metamorphic belt, Tectonics

©2019. Japan Geoscience Union. All Right Reserved.

THE PRESSURE-TEMPERATURE PATH AND MINERAL ASSEMBLAGE OF THE KHONICHIIN OVOO AREA, SOUTHEASTERN MONGOLIA.

*Undarmaa Batsaikhan[1], Noriyoshi Tsuchiya[1], Masaoki Uno[1], Yukio Isozaki[2], Uyanga Bold[2], OTGONBAYAR DANDAR[1], Hikaru Sawada[2]

1. Graduate School of Environmental Studies, Tohoku University, 2. Graduate School of Arts and Sciences the University of Tokyo

The Khonichiin ovoo area is located in the southeastern part of Mongolia of the Central Asian Orogenic belt, which is largest amalgamation history of during Phanerozoic time. The Khonichiin ovoo area mainly consists of the Khutaguul, the Norovzeeg metamorphic complexes that underwent high grade facies metamorphism, with rare igneous rocks. The Khutaguul metamorphic complex is composed of garnet-biotite, amphibolite-biotite, two mica gneiss, amphibolite schist, quartzite, marble, granite-gneiss, granulite and migmatites. The Norovzeeg metamorphic complex is composed of metasedimentary and metavolcanic rocks. P-T condition and mineral assemblage data/information for these metamorphic complexes are extremely limited. This is because international and local researchers had focused on investigations on Paleozoic igneous, volcanic and sedimentary rocks, which are somehow related to the porphyry copper deposits (Tsagaan suvarga Cu-Mo, Kharmagtai Cu-Au) in the south of Mongolia in the last two-decade years.
We will show new age dating and P-T conditions of the Khutaguul and the Norovzeeg metamorphic rocks.

Keywords: P-T path, Petrology, Southeastern Mongolia

©2019. Japan Geoscience Union. All Right Reserved.

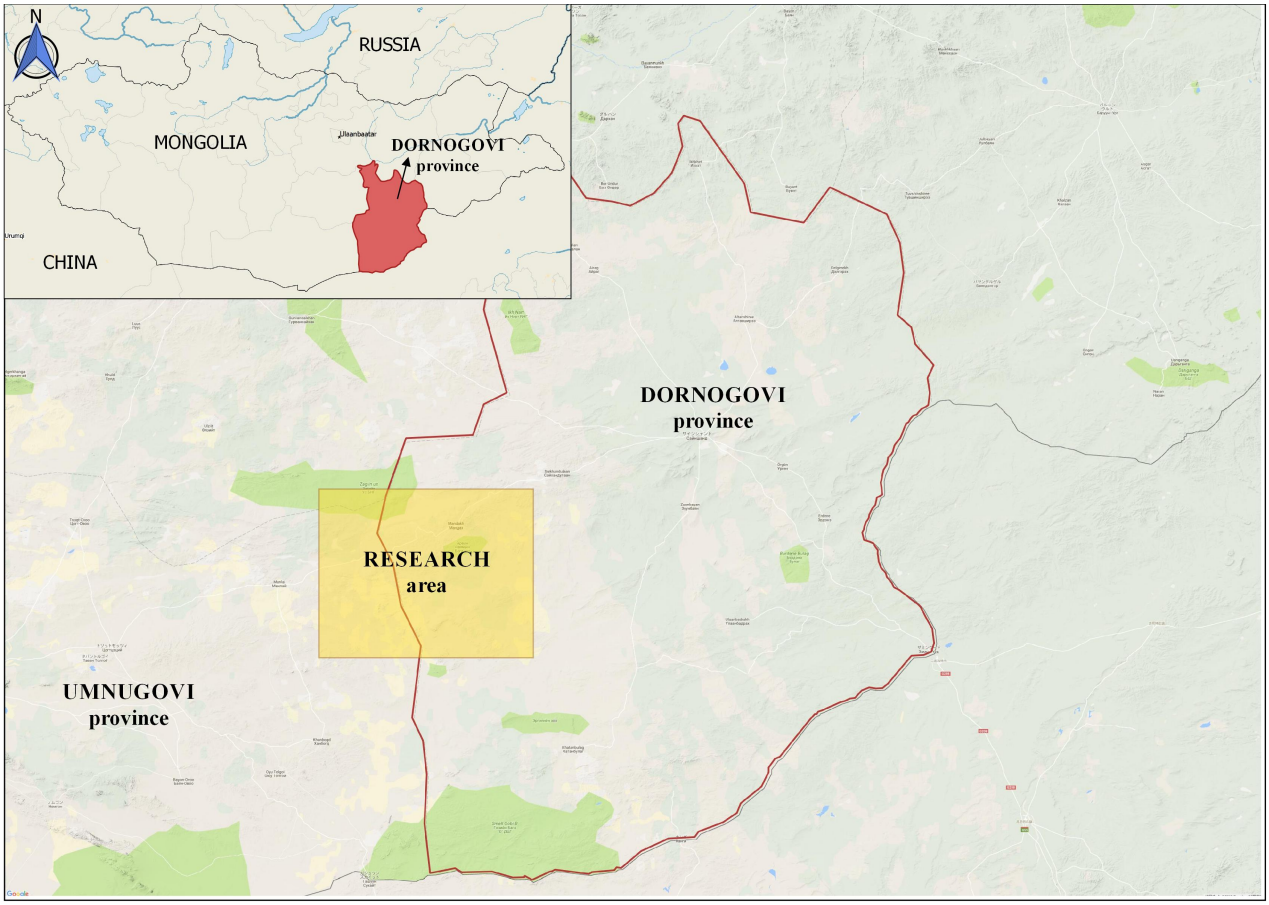

©2019. Japan Geoscience Union. All Right Reserved.

Pressure-temperature conditions of contact metamorphism in Nokita area, Itoshima Peninsula, northwest Kyushu

*Takeshi Ikeda[1], Kento Ota[2]

1. Department of Earth and Planetary Sciences,Faculty of Scinece, Kyushu University, 2. Department of Earth and Planetary Sciences,Graduate School of Scinece, Kyushu University

Gneissose granitic rocks are common in high-grade areas of high-temperature low-pressure metamorphic complex. Similarity in age and concordant relation to the surrounding rocks imply that they supplied heat to cause the high-temperature low-pressure metamorphism. Parallelism of internal structures of granitic and metamorphic rocks also suggests that both rocks underwent simultaneous deformation during and after the intrusion of the granitic rocks. The post-metamorphic deformation would rearrange the thermal structure formed at the heat supply.

The Renge metamorphic complex in the Nokita area of Itoshima Peninsula, northwest Kyushu, was intruded by the Kitazaki and Itoshima granodiorites on the north and south at Cretaceous, respectively. The complex was recrystallized by thses intrusions and underwent significant deformation that belongs to flattening after the peak of contact metamorphism (Yamasaki & Ikeda, 2018). This study estimates the pressure-temperature condition preserved in pelitic rocks to evaluate the post-metamorphic deformation.

The pelitic schists in the study area are composed of leucocratic and melanocratic layers depending on the modal amount of biotite. The common constituent minerals are quartz, plagioclase, biotite. Garnet, muscovite, and K-feldspar locally occur. In addition, chlorite is present as veins and schistosity-forming mineral, which is interpreted as retrograde products.

Four pelitic schists were employed to estimate the metamorphic conditions. Garnet shows euhedral shape and so-called normal zoning where Mg increases and Fe and Mn decreases towards the rim. The composition of rim ranges such that Xalm=0.72-0.80, Xprp=0.09-0.12, Xsps=0.06-0.16, and Xgrs=0.04-0.06. On the other hand, that of core varies Xalm=0.50-0.66, Xprp=0.03-0.05, Xsps=0.24-0.40, and Xgrs=0.04-0.10. The Mg/Fe of rim and core ranges 0.13-0.15 and 0.06-0.08, respectively. Biotite also shows significant variation in composition, i.e., Ti of 0.15 - 0.46 based on 22 oxygen, and Mg/Fe of 0.44 - 0.76. The Ti content of biotite near chlorite is low as compared with that far from chlorite. Plagioclase is chemically homogeneous in one sample. The anorthite content shows southward increase from 0.23 to 0.42.

We chose the composition equilibrated at peak of the metamorphism such as the highest Mg/Fe in the rim of garnet, highest Ti in biotite and highest anorthite content in plagioclase. Geothermobarometry using garnet-biotite geothermometer (Ferry & Spear 1978) and a garnet-biotite-plagioclase-quartz geobarometer (Hoisch 1990) provide the metamorphic conditions of 590 °C, 1.4 kbar, 650 °C, 3.5 kbar, 770 °C, 4.2 kbar, and 650 °C, 2.8 kbar from south to north ,which corresponds to 5.3-16 km depth. The pressure and temperature vary by 2.8 kbar and 180 °C, respectively, within ca. 300 m distance. The lithostatic pressure relevant to 300 m thickness cannot explain the pressure difference of 2.8 kbar. The present result also supports the significant thinning deformation after the contact metamorphism.

Keywords: Contact metamorphism, Post-metamorphic deformation, Geothermobarometry

©2019. Japan Geoscience Union. All Right Reserved.

©2019. Japan Geoscience Union. All Right Reserved.

Evidence of Partial Melting of Migmatitic Felsic Gneiss from Nagasaki Metamorphic Complex in Amakusa-Shimoshima, western Kyushu, Japan

*Yuki Mori[1], Takeshi Ikeda[2], Kazuhiro Miyazaki[3]

1. Department of Earth and Planetary Sciences, Graduate School of Sciences, Kyushu University, 2. Department of Earth and Planetary Sciences, Faculty of Sciences, Kyushu University, 3. Research Institute of Geology and Geoinformation, Geological Survey of Japan, National Institute of Advanced Industrial Science and Technology

The Nagasaki Metamorphic Complex in Amakusa-Shimoshima is divided into the lower and upper units. The former and the latter are composed mainly of pelitic schists and gneisses with mafic and felsic composition, respectively. The upper unit is considered to have located at lower crust that was shortened due to ductile flow toward trench side (Miyazaki et al., 2013). The unit belongs to the high-pressure granulite facies and represents migmatitic mode of occurrence, which implies potential presence of melt that enhanced the ductile deformation. This study reports microstructural features indicative of partial melting in a felsic migmatitic gneiss.

The migmatitic felsic gneiss dealt with this study represents U-Pb zircon age of 125.8±1.8 Ma (Mori et al., 2018 JpGU). It is composed mainly of garnet, quartz, muscovite, zoisite and aggregate of fine-grained zoisite + albite + muscovite that is former plagioclase. Minor amounts of graphite, zircon, apatite, rutile, chlorite, and iron sulfide also occur. Tiny grains of hornblende are included in the rim of garnet. The matrix zoisite commonly includes epidote in the core. The epidote contains significant amounts of rare earth elements (REE) and is composed of Y-poor core and Y-rich rim. The garnet grains are roughly divided into two types of coarse- and fine-grained. The X_{Mg} [=Mg/(Mg+Fe)] of the coarse-grained garnet increases from the core to the rim and decreases at the extreme periphery, while that of the fine-grained garnet monotonically decreases from the core to the rim. The coarse-grained garnet represents Y-rich and P-poor core and Y-poor and P-rich rim whereas Y-poor and P-rich domain is dominant in the fine-grained garnet. A polyphase inclusion composed of chlorite + muscovite + quartz + $CaCO_3$ is found from the rim of coarse-grained garnet. The inclusion shows polygonal shape and has cuspate offshoots filled with chlorite or muscovite. Apatite is included in the core of the coarse-grained garnet but is not found from the rim. The fine-grained garnet and the rim of the coarse-grained garnet include Y-rich REE-epidote.

We applied Zr-in-rutile geothermometer (Ferry & Watson, 2007), garnet-hornblende geothermometers (Graham & Powell, 1984; Powell, 1985; Ravna, 2000), and hornblende-plagioclase geothermometer (Holland & Blundy, 1994). These results are consistent among them within their errors and represent 720 −770 ˚C as the peak condition. The pressure at the peak condition was estimated utilizing garnet-hornblende-plagioclase-quartz geobarometer of Kohn & Spear (1990), and we obtained the pressure of 9.1 −10.2 kbar.

The estimated condition lies above the melting reaction of zoisite + muscovite + quartz + water = kyanite + melt (cf. Schliestedt & Johannes, 1984). The polygonal shape of the polyphase inclusion in the rim of coarse-grained garnet could represent negative crystal of garnet. Combining the constituent minerals of the inclusion, it is likely that the polyphase inclusion was originally melt inclusion.

The concentration of yttrium and phosphorus in the rim of coarse-grained garnet is similar to that in fine-grained garnet. Based on the presence of melt inclusion in the rim of coarse-grained garnet, we

©2019. Japan Geoscience Union. All Right Reserved.

consider that fine-grained garnet nucleated during the partial melting with the formation of the rim of coarse-grained garnet. The Y-rich REE-epidote is in the matrix and included in the fine-grained garnet and the rim of the coarse-grained garnet, so we consider that Y-poor garnet and Y-rich REE-epidote coexisted with the melt. The lack of apatite inclusion in P-rich domain of both garnets may indicate that the phosphorus in P-rich domain in garnet was supplied by breakdown of apatite during the melting.

Keywords: partial melting, melt inclusion, garnet, REE-epidote, apatite

©2019. Japan Geoscience Union. All Right Reserved.

Microstructural Analysis of Quartz grains in Monomineralic and Polyphase domains: A case study from Main Central Thrust (MCT) Zone Mylonites, western Himalaya, India

*Shivaji Saha[1], Toru Takeshita[1], Subhajit Ghosh[2], Hari Bahadur Srivastava[3]

1. Department of Natural History Sciences, Hokkaido University, 2. Earthquake Research Institute, The University of Tokyo, 3. Department of Geology, Banaras Hindu University

Ongoing collision in the Himalayan orogeny causes crustal deformation owing to the thrust activity. Hence, the movement along the Main Central Thrust (MCT) enhances ductile deformation of the crust widely distributed across the orogenic belt. Therefore, detailed microstructural analysis is necessary to define the shear zone by the degree of strain intensification across the MCT. A study area along Madhmaheswar Ganga valley, Rudraprayag district, Uttarakhand, India, has been chosen. Purpose of this study is to perceive the heterogeneity of the deformational behavior of quartz grains in terms of thickness of quartz layers and other associated phases along with the understanding of fabric development with respect to the MCT. In this research, the lower Greater Himalayan Sequence (L-GHS) of *c.* 1.5 km thickness on the hangingwall side and upper Lesser Himalayan Sequence (U-LHS or Munsiari formation) of *c.* 4 km thickness on the footwall side of the MCT, has been studied.

Microstructural observations are essentially focused on the quartzo-feldspathic gneiss of the Munsiari formation and L-GHS. At lower Munsiari formation, Quartz microstructures are characterized by subgrain rotation recrystallization (SGR). Polygonal quartz grains with triple point junction indicate SGR followed by static grain growth. At upper Munsiari formation, lobate boundaries of quartz grains with sweeping extinction and deformation lamellae indicate high temperature grain boundary migration (GBM) overprinted by late stage low temperature deformation. Quartz grains in the lower GHS rocks are coarser than that of the Munsiari rocks and highly amoeboid in shape. High temperature deformation is evidenced by the presence of elongated sub-grains within these irregular grains.

To carry out further microstructural studies, 14 samples were selected for EBSD analysis. Quartz *c*-axis fabric from ~500-829 μm thick quartz-rich monomineralic layer shows a series of type-*II* crossed girdle fabrics with *Y*-maximum. Here, the quartz *c*-axes are aligned parallel to intermediate finite strain axis *Y*, revealing the intracrystalline deformation by active prism {10 -10} *a* slip system. In contrast, c-axis orientations obtained from thin monomineralic quartz layers (thickness ~72-163 μm) records girdles ranging from small circle girdles to type-*I* crossed girdle fabric with r-maxima. In this case, the rhombohedral plane of quartz is aligned parallel to the foliation plane (*XY*), which indicate basal (0001) *a* slip and rhomb {10 -11} *a* slip system activity. Thus, there is an effect of thickness of monophase layers on fabric development and, perhaps the role of other phases has a strong impact on the fabric development for thin monomineralic layers.

On the other hand, polyphase domains are characterized by the quartz grains totally surrounded by other phases. The size of recrystallized quartz grains within polyphase domain increases from ~64.4 μm in Munsiari to ~109 μm in L-GHS. C-axes orientations are random for the Munsiari samples. Whereas, C-axis fabric with point maxima is observed for the L-GHS samples. However, those fabric patterns are strengthened with increasing modal abundance of quartz.

©2019. Japan Geoscience Union. All Right Reserved.

The strength of the quartz *c*-axis fabric is quantified as a function of eigenvectors (λ_1 = maximum; λ_2 = intermediate; λ_3 = minimum) from *c*-axes orientation distribution. Following, Vollmer (1990), three end member fabric types are determined from these eigenvectors; those are point (*P*), girdle (*G*) and random (*R*). Then, by introducing cylindricity index (*B*) of Vollmer (1990), the variation in fabric strength of quartz LPO is shown as a function of strain localization throughout the Munsiari formation. Progressive increase in fabric intensity for both thin and thick monomineralic quartz layers indicate an increase in strain towards the MCT.

Keywords: Main Central Thrust Zone, Quart c-axis fabric, Strain intensification

©2019. Japan Geoscience Union. All Right Reserved.

Tectono-thermal evolution of the Main Central Thrust (MCT) zone rocks of the Himalayan Crystalline Complex (*HCC*), Darjeeling-Sikkim Himalaya

*Subhajit Ghosh[1,2], Santanu Bose[2,3], Nibir Mandal[4], Arijit Laik[2]

1. Earthquake Research Institute, The University of Tokyo, 1-1-1 Yayoi, Bunkyo-Ku, Tokyo 113-0032, 2. Department of Geology, University of Calcutta, 35, Ballygunge Circular Road, Kolkata 700019, India, 3. Department of Geology, Presidency University, 86/1 College Street, Kolkata 700073, India, 4. Department of Geological Sciences, Jadavpur University, Kolkata 700032, India

The rheology of the Himalayan Crystalline Complex (*HCC*) laying above the Main Central Thrust (MCT), is the key boundary condition for all the tectonic models that deals with extrusion of lower crustal material. Therefore, it is important to understand the intricate relationship between the processes of crustal thickening, Barrovian metamorphism and strain localization in the high-grade rocks of the *HCC* that controls the rheology of a deforming wedge. Initially deformation was distributed and a series of repeated folding leads to crustal thickening and pro-grade metamorphism. The similarity between the peak metamorphic and peak deformation temperature, as documented by frozen high-temperature microstructures is indicative of this phase. The '*locked in*' deformation microstructures and syn-kinematic growth of metamorphic index minerals reveal that the MCT related shearing begins at or near the peak metamorphic condition (16-12 Ma), where grain size reduction by dislocation-controlled creep was the most effective mechanism for strain localization. The observed deformation microstructures and the available P-T data shows that the peak deformation and metamorphic condition progressively increases (~500 to >700˚C) towards the mountain interior. It is further evident that the now-exposed *HCC* begun to extrude under dominantly ductile mid-crustal condition at a temperature >700˚C, where the hotter mid-crustal rocks can flow in a viscous manner by melt enhanced depth-dependent ductile flow. Hence, initially the MCT represents a rheological and metamorphic boundary that separates material which can or cannot flow. Then with subsequent exhumation, cooling and strengthening of the *HCC* produced diffuse ductile shear zones along the same rheological boundary, where deformation was distributed for 4-6 km width (~ MCT zone). The base of the high strain zone is marked by base of the compressed reverse paleo-isograds that coincides with the SGR-GMB transition for quartz, leading to steep P-T gradient locally constrained within the MCT zone before it flattened in the migmatite gneisses. At further lowering of temperature (shallower depth), the MCT localized into narrow shear zone under dominantly brittle condition, transporting the entire *HCC* thrust sheets to the foreland.

Keywords: Himalaya, India-Asia collision, Superposed folding, Strain localization , Main Central Thrust Zone

©2019. Japan Geoscience Union. All Right Reserved.

Thermal structure and deformation history of the low-grade Sanbagawa belt in the central of Kii Peninsula and tectonic implications

*Ken Yamaoka[1,2], Simon Wallis[1], Hiroshi Mori[2]

1. University of Tokyo, 2. Shinshu University

The Sanbagawa belt in SW Japan is one of the best-documented regions of relatively warm subduction-type metamorphism and information from such regions are important to clarify our understanding of convergent plate margins. Much of the present knowledge is based on petrological studies in the higher grade parts of this belt. However, most of the Sanbagawa belt belongs to the lowest grade domain, the chlorite zone. The lack of reliable methods to determine the thermal structure in this low-grade zone has meant that information from the majority of the belt has been underrepresented. Development of the Raman carbonaceous material thermometer (RCMT) has opened up possibilities of determining the temperature structure of low-grade metamorphic domains such as the chlorite zone of the Sanbagawa metamorphism. Application of RCMT to pelitic rocks of the central Kii peninsula shows a progressive decrease in T from ~390 ˚C close to the northern boundary marked by the Median Tectonic Line (MTL) to ~270 ˚C ~7 km to the south and roughly constant thereafter. The thermal structure is not significantly affected by fault boundaries between different geological units. Meso and microstructural observations combined with strain analysis based on deformed shapes of detrital grains in metamudstone indicate a similar deformation history throughout the area and no correlation between strain and temperature gradients. These features can be used to asses possible models for the observed temperature rise. On this basis, we suggest the rise in T was not due to return flow of high T material in a subduction channel. We also conclude that the rise in T takes place over too narrow a distance to be explained as part of the expected thermal warping in a warm subduction zone. We find no evidence for heating related to the rise of magma or hot fluids. Shear heating along the MTL does provide a plausible explanation for the observed thermal structure compatible with all observations. One-dimensional thermal modeling shows that to account for the observed thermal structure requires slip rates of several mm/yr and relatively high coefficients of friction (μ=??). A similar result was reported from an area to the east but with a much more limited domain of elevated temperatures, probably due to late-stage thinning related to normal faulting. Our results imply that long-lived major crustal faults such as the MTL are at least locally associated with high stresses and are relatively strong. Evidence for the faults being weak at shallow depth implies there is a rapid decrease in strength over the upper few km of the MTL fault zone.

Keywords: Sanbagawa belt, Raman carbonaceous material thermometry, shear heating

©2019. Japan Geoscience Union. All Right Reserved.

Antigorite Raman spectrum: a case study in Shiraga region of the central Shikoku, Sanbagawa metamorphic belt, SW Japan

*Kota Ando[1], Yui Kouketsu[1], Katsuyoshi Michibayashi[1]

1. Nagoya University

Serpentinites are important rocks and are associtated with water circulating in the earth's interior. However, it is difficult to estimate their metamorphic conditions because serpentine minerals are stable at wide P-T condition. In this study, we compared Raman spectrum of antigorite in different metamorphic grade samples and determined whether Raman spectrum could constrain metamorphic conditions of serpentinites. Serpentinites in this study have been sampled from Shiraga region of the central Shikoku, the Sanbagawa metamorphic belt, SW Japan. All samples experienced the metamorphic conditions in which olivine were formed by the dehydration reaction of antigorite with brucite. Some samples show retrograde antigorite formed during exhumation. Raman spectrum were measured from various sizes and textures of antigorite grains. Comparing full width at half maximum (FWHM) of Raman spectrum, we found that the prograde-antigorite had different features from retrograde-antigorite. As a consequence, FWHM of Antigorite Raman spectrum could be used to constrain the timing of antigorite formation.

Keywords: antigorite, Serpentinite, Raman spectrum, Sanbagawa metamorphic belt

©2019. Japan Geoscience Union. All Right Reserved.

A fluid inclusion study from the late Paleozoic retrograde eclogite from the Yunotani Valley of the Omi area, Hida-Gaien Belt, Japan

*Yuzuki Shinji[1], Tatsuki Tsujimori[1], Tatsuhiko Kawamoto[2]

1. Tohoku University, 2. Shizuoka University

Primary fluid inclusions trapped in subduction metamorphic rocks can provide direct information concerning composition and origin of slab-derived fluids. In order to investigate fluid signatures at the mantle wedge beneath forearc regions, we conducted microthermometry for primary fluid inclusions in both prograde eclogite-stage omphacite and retrograde blueschist-stage quartz, in the late Paleozoic retrograde eclogite from the Yunotani Valley of the Omi area, Hida-Gaien Belt, Japan. Note that the investigated blueschist-stage quartz forms a microvein along cracks of omphacite. The investigated eclogite occurs as mafic layers or lenses which are intercalated in metasedimentary rocks with the mineral assemblage paragonite + phengite + garnet ±glaucophane + quartz + rutile. Recent study confirmed that the retrograde blueschist-stage reached the pumpellyite stability field of P = ~0.62–0.70 GPa and T = ~280–320°C (Shinji and Tsujimori 2019 doi:10.2465/jmps.180716).

The primary fluid-inclusions in both omphacite and quartz are aqueous two-phase inclusions of liquid and vapor. Their molecular species in a liquid and gas phase were identified using micro-Raman spectroscopy. The fluid inclusions of the eclogite-stage omphacite are characterized by relatively high salinity of ~8.0–8.2 wt% NaCl equivalent and the brine freezing temperatures at ~-70°C suggests presence of divalent ions such as Ca^{2+} and/or Mg^{2+}. In contrast, fluid inclusion in blueschist-stage quartz shows relatively low value of ~2.4 wt% NaCl equivalent. The liquid phase of the fluid inclusion transforms completely into solid phases at ~-38°C, suggesting existence of the limited monovalent ions such as Na^{+} or/and K^{+} in the fluids.

Our preliminary data demonstrates that the pervasive fluids entrapped at prograde eclogite-stage and retrograde blueschist-stage had different chemical compositions. This suggests different fluid sources at eclogite and blueschist depth. Our observation is consistent with the different fluid compositions recorded in zoned lawsonite in Guatemalan eclogite (Hara et al. 2018 doi: 10.1016/j.lithos.2018.09.001). In our study, the existence of higher salinity fluids in the eclogite-facies conditions can suggest more effective transportation of the lithophile elements into the mantle wedge at deeper forearc regions.

Keywords: Slab-derived fluid, Mantle wedge beneath forearc region, Fluid inclusion, Microthermometry, Retrograde eclogite, Retrograde blueschist-stage pumpellyite

©2019. Japan Geoscience Union. All Right Reserved.

Development of reaction-induced stress and permeability in MgO-H_2O system

*Hisamu Kasahara[1], Masaoki Uno[1], Atsushi Okamoto[1], Noriyoshi Tsuchiya[1]

1. Graduate School of Environmental Studies, Tohoku University

Fractures are dominant flow path of fluid transport in the crust, and fluid flow through the fractures is important for the progress of fluid-rock interaction and material transport in the crust. The fractures enhance permeability in rocks, which has significant effects on the efficiency oil mining, geothermal development and Carbon dioxide Capture and Storage (CCS). Thus, the research on the fracture formations and associated permeability developments are increasingly important for geoscience and engineering.

Especially during fluid-rock interactions in the crust, hydration reactions increase solid-volume and generate stress. Recently such reaction-induced stress has been investigated as a new fracture generation process. For example, the fractures associated with reaction-induced stress are observed in serpentinized olivine (Jamtveit and Austrheim, 2010). In addition, the stress exceeding rock strength is reported from thermodynamic prediction (Kelemen and Hirth, 2012) and experimental measurements (e.g., Lambart et al., 2018). However, the existence of non-fractured rocks despite the volumetric expansion reaction (Centerrea et al., 2015) and the discrepancies between the experimental and theoretical values of reaction-induced stress have not yet been clarified. To understand the causes of these phenomena, it is important to constrain the controlling factors and the generation processes of reaction-induced stress. Therefore, we conducted direct measurements of reaction-induced stress and permeability development during hydration reactions, to clarify the relation between the reaction, stress generation, fracturing and permeability developments.

In our previous study, we measured the reaction-induced stress in MgO–H_2O system, and observed stress generation of approximately 40 MPa, exceeding common tensile strength of rocks. It is indicated that temperature dependence exists in stress generation behavior: the higher the temperature, the higher stress are generated and the stronger stress relaxation are observed after a peak stress. We also showed that this behavior can be explained by competition between reaction and deformation strain rate. This result was consistent to a certain extent with the result of $CaSO_4 \cdot 1/2H_2O$–H_2O system reported by Skarbek et al. (2018).

In this report, we aimed to clarify the influence of reaction and deformation rate on stress generation and the permeability development during volumetric expansion reaction. We conducted two experiments, the stress measurement experiments and the permeability experiments. In the former, experiments were conducted using pellets (ϕ=45–55%) of MgO powder as a starting material under conditions of approximately 80 to 120 ˚C and fluid pressure of approximately 0.100 MPa. The developments of reaction-induced stress were measured as a function of temperature. In the same experimental systems, the reaction and deformation rate were determined by measuring the strain and the reaction rate. In the latter, the experiment was conducted using the sintered MgO as a starting material under the conditions of approximately 100 to 300 ˚C, a fluid pressure of 0 to 10 MPa, and a confining pressure of 0 to 50 MPa. The permeability developments were measured under conditions of various temperatures, confining pressures and fluid pressures. From the results, we consider the relation between stress, fracturing and permeability and discuss the modes of rock fracturing and fluid transfer enhancement during hydration

©2019. Japan Geoscience Union. All Right Reserved.

reactions in the crust.

Keywords: Reaction-induced stress

©2019. Japan Geoscience Union. All Right Reserved.

Crystal orientation analysis of olivine in ultra-mylonite using TKD method: progress in spatial resolution from EBSD

*Yohei Igami[1], Katsuyoshi Michibayashi[2], Kakihata Yuki[2], Yui Kouketsu[2]

1. Institute of Materials and Systems for Sustainability, Nagoya University, 2. Graduate School of Environmental Studies, Nagoya University

Mantle, which is the dominant component consisting of the earth making up 80 %, is the key to understanding material cycle and/or formation history of the earth. The uppermost part of the mantle is composed of peridotite which is aggregate mostly of olivine [$(Mg,Fe)_2SiO_4$] grains. Olivine has orthorhombic crystal system and its mechanical property is anisotropic. Thus the olivine polycrystalline in peridotite shows various crystal-preferred orientation (CPO) patterns formed by share deformation processes (Karato et al., 2008). Therefore, the CPO pattern can be an indicator of deformation environment and is also used as a key parameter to estimate seismic anisotropy. Thus, the CPO is very important for tectonic geology.

To evaluate CPO of olivine, Scanning Electron Microscope equipped with Electron BackScatter Diffraction detector (SEM-EBSD) is widely used. The SEM-EBSD is a method to analyze crystal orientation using the Kikuchi diffraction pattern formed by the interaction between scattered electrons and lattice planes of sample surface. Recently, improvements of high-speed detectors and userfriendly computer programs have enabled automatic, rapid and easy EBSD mapping. Using the method, olivine CPO patterns in peridotite of various localities have been studied. However, effect of fine grains (<1 μm in diameter) might have been overlooked in such studies, because it is difficult to obtain clear EBSD pattern from sub-micrometric mineral grains.

On the other hand, it was reported that the Kikuchi pattern can be obtained also by transmitted electrons through thin film (~100 nm) using SEM (Keller and Geiss, 2011). This method, which is called transmission EBSD (t-EBSD) or transmission Kikuchi diffraction (TKD), can restrict area in which electrons are scattered and improve spatial resolution even by the conventional SEM-EBSD system. In this study, therefore, we tried CPO analysis for ultra-mylonite using the TKD, to investigate usefulness of this method for tectonic geology.

The analyzed sample is an ultra-mylonite from Marion Transform fault by PROTEA5 cruise. The sample contains amphibole and olivine as porphyroclasts and fine-grained matrix, with a small amount of orthopyroxene and spinel (Kakihata et al., 2018, AGU). We obtained EBSD map from petrographic-thin section of this sample, and then an ultra-thin section for TKD was made using a focused ion beam apparatus(FIB, HITACHI FB2100). Finally, TKD map of the ultra-thin section was obtained. For both of the EBSD and TKD analyses, the same SEM-EBSD system (HITACH, S-3400N + OXFORD Instruments, NordlysNano) was used.

As the result, we successfully obtained TKD map dataset, in which patterns are indexed even at the region over boundaries between sub-micrometric olivine grains. This TKD map which was obtained by W-filament gun SEM is clearer than the FESEM-EBSD map we obtained from the same sample. The TKD map dataset was able to be processed by the same software with EBSD (following configuration parameters suggested by Miyake et al., 2016, JAMS). The processed TKD map of olivine displays CPO of *b* -axis perpendicular to shear plane. In addition, spatial distribution of sub-grain boundaries and irregular shaped grains is well displayed. TKD requires much less time and labor than TEM analyses in such orientation analysis throughout the ultra-thin section, although TEM is of course much better in spatial resolution or detailed crystallographic/chemical analyses. The TKD should be useful as a pre-analysis before the detailed TEM analyses for polycristalline samples such as ultra-mylonite. Application of the

©2019. Japan Geoscience Union. All Right Reserved.

TKD method may reveal various effects of fine grains in tectonic geology.

Keywords: EBSD, TKD, crystal preferred orientation, ultra-mylonite, peridotite

©2019. Japan Geoscience Union. All Right Reserved.

Elucidation of effective diffusion coefficient along grain boundaries by hydrothermal experiment using low porosity rocks

*Naoki Sugisawa[1], Masaoki Uno[1], Noriyoshi Tsuchiya[1]

1. Graduate school of environmental studies Tohoku university

Elucidation of the time scale of the fluid activity recorded in the rock is important for understanding the actual condition of fluid activity in the crust. In recent years, it has become possible to estimate time-scale of fluid activity in the crust from isotopes and element concentration profile of natural metamorphic rocks. (e.g.John et al.,2012) To estimate the time-scale, the effective diffusion coefficient (Deff) is important as an indicator of diffusion via grain boundary fluid. It is known that the effective diffusion coefficient depends on the porosity (Φ) of rock and time due to grain boundary diffusion. (e.g.Boving and Grathwohl, 2001) The effective diffusion coefficient is conventionally substituted by the product of self-diffusion coefficient (D_{self}) and porosity ($D_{self}\Phi^{x}$). However, the effective diffusion coefficient varies depending on the power factor (x) of the porosity, and the estimated timescales depend significantly on the power factor (x). Therefore, we clarified the relationship between porosity vs effective diffusion coefficient and confining pressure vs effective diffusion coefficient using hydrothermal experiment under crustal condition with various low porosity granite. In this paper, we mention the following two experiments as the first step : (1) Fluorapatite (F-Ap) substitution reaction (2) Determination of effective diffusion coefficient using low porosity hydroxyapatite sintered body (OH-Ap).

In this study, natural F-Ap from Mexico and OH-Ap (Wako Pure Chemical corporation) were used as starting materials. In experiment (1), first, natural F-Ap was cut in the c-axis direction. And it was put in the gold tube with 0.0006-6 M HCl or 0.01-1 M NaOH two types solution. After that gold tube was putted in the batch type hydrothermal equipment and conducted hydrothermal experiment under 400 ℃, 50 MPa for168 hour. In experiment (2), OH-Ap powder was pressed under 200 MPa for 30 minutes and then the porosity was varied by sintering at deference temperature from 1500 ℃ to 1200 ℃. After cooling, the porosity was measured by the wet method. NaF solution saturated at room temperature and OH-Ap sintered body was added to the same apparatus as above and a hydrothermal experiment was conducted at 300 ℃ and 20 MPa for 168 hours. After the experiment (1) and (2), the samples were evaluated by quantitative analysis and mapping analysis with EPMA in both cases. Before the experiment, phase diagram of apatite under experimental temperature and pressure was prepared using SUPCRT92, GEMS to expect these reactions.

As a result of the hydrothermal experiment, in the experiment (1), it is suggested that the OH in F-Ap is substituted with Cl under HCl solution and the NaOH substitutes OH for F. In experiment (2), F diffusion zoning was generated along the clacks in the sintered OH-Ap, and an effective diffusion coefficient was calculated using diffusion equation. There was no apparent porosity dependency of the effective diffusion coefficient at porosities 1.68-5.83%. The effective diffusion coefficient obtained in this experiment was equivalent to the self-diffusion coefficient of fluorine multiplied by the porosity 2.26 power. ($D_{eff} = D_{self}\Phi^{x}$) (e.g. Oelkers and Helgeson, 1988) However, the porosity measured by the wet method needs to be investigated because it contains the cracks generated in making the sintered body. (e.g. mercury porosimeter)

Based on the above experimental results, it is discussed that the influence of temperature, pressure, solution condition, on substitution of monovalent halogen and hydroxyl group between apatite and fluid and relationship between porosity and effective diffusion coefficients.

©2019. Japan Geoscience Union. All Right Reserved.

References
John et al. Nature Geosience, Vol.5, July 2012, Pages 489-492 Boving and Grathwohl Journal of Contaminant Hydrology, Vol.53, 8 May 2001, Pages 85-100 Oelkers and Helgeson, Geochemica et Cosmochimica Acta, Vol.52, October 1988, 63-85

Keywords: effective diffusion coefficient, porosity, Crustal fluid

©2019. Japan Geoscience Union. All Right Reserved.

Seismic slipping events recorded in a fault gouge zone: evidence from the Nojima Fault drill holes, SW Japan

*Aiming Lin[1], Takafumi Nishiwaki[1]

1. Department of Geophysics, Graduate School of Science, Kyoto University

It is well known that large intra-continental earthquakes occur repeatedly along mature active faults and that the seismic slip may be recorded by cataclastic rocks, including fault gouge zones, that form at shallow depths in the upper crust (e.g., Lin, 2008). A fault gouge zone, bounded by a principal fault plane, is considered to represent the seismic slip zone that accommodates most of the accumulated fault displacement in the seismogenic regime. Therefore, studies of fault gouge zones along mature active faults would provide important information for reconstructing the long-term seismic faulting behavior of such faults, as well as providing new insights into the individual seismic slipping processes of active faults and their paleoseismic histories.

In the present study, we focused on the structural features of the fault gouge zone observed in drill cores acquired from nine holes that were drilled through the Nojima Fault (NF) at different depths from ~260 to 900 m at the Ogura site (Lin and Nishiwaki, 2019). Drilling investigations and structural analyses of drill cores reveal that a ~60 m wide fault damage zone containing a 10–30 cm thick fault gouge zone developed along the Nojima Fault (NF), on which the 1995 M_w 6.9 Kobe (Japan) earthquake occurred. The fault gouge zone was observed at depths of ~260 to 900 m in nine drill holes that intersected the NF. Our findings show that i) the fault gouge zone observed at different depths in the nine drill cores is the principal fault slip zone of the NF, ii) the fault gouge zone can be divided into 11–20 thin layers of different color, and iii) the individually colored layers contain different color breccias of fault gouge that are offset and/or cut by cracks and crack-filled calcite and quartz veinlets. Our results reveal that the fault gouge zone probably records more than 11–20 paleoseismic faulting events along the NF during the late Pleistocene-Holocene.

References:

1) Lin, A., 2008. Fossil Earthquakes: The Formation and Preservation of Pseudotachylytes. Springer, Berlin, 348p (ISBN 978-3-540-74235-7).
2) Lin, A., Nishiwaki, T., 2019. Repeated seismic slipping events recorded in a fault gouge zone: evidence from the Nojima Fault drill holes, SW Japan. Geophys. Res. Lett., doi: 10.1029/2019GL081927.

Keywords: Fault gouge zone, Nojima Fault, Seismic slipping event

©2019. Japan Geoscience Union. All Right Reserved.

Evolution of fluid chemistry during basalt-water and basalt-seawater interactions revealed by hydrothermal flow-through experiments

*Yusuke Netsu[1], Atsushi Okamoto[1], Nobuo Hirano[1], Masaoki Uno[1], Noriyoshi Tsuchiya[1]

1. Tohoku University, Graduate School of Environment Studies

Recently, several deep drilling projects for exploiting the supercritical geothermal reservoirs in the world. For example, in 2017, the Island Deep Drilling Project (IDDP-2) reached 427 ˚C and 34 MPa, which exceeds the critical point of seawater. The drillcores revealed that the intense water-rock interaction under greenschist to amphibolite facies metamorphism. Although such deep drilling provides us direct information of active metamorphic processes. however, it is still unclear whether conventional petrological analyses could apply to reaction processes in open systems at high temperature hydrothermal alteration at seafloor. There have been few experiment studies on the water-rock interaction under supercritical conditions with some exceptions (Yardley et al. 2014).

In this study, we conducted hydrothermal flow-through experiments on the basalt-H_2O, basalt-NaCl.aq, basalt-seawater systems under the sub or supercritical conditions. The temperature and pressure were set to be 400 ˚C and 37 - 39 MPa, and the input solutions was flowed at constant flow rate (0.1 ml/min) for 1 –6 days. We placed a powder of MORB (Island, 250-500 μm), which is composed of plagioclase (Pl), olivine (Ol) phenocrysts and clinopyroxnene (Cpx), Pl groundmass, with lessor amount of volcanic glass, in a Ti inner tube (L=275 mm, I.D.= 4.35 mm). During the run, the solution was continuously pumped into the reaction vessel, and the output solution was collected every few hours. The concentration of Si, Al, Ti, Fe, Mg, Ca, Na, and K in the output solution was analyzed by ICP-AES.

In the basalt-H_2O experiment, the products varied with distance from the inlet. At the inlet and middle of tube, Ca-rich Pl (An# 0.98) formed around primary Pl grain with producing abundant pores, whereas chlorite was dominantly formed around Ol and Pl at the middle to outlet of inner tube. The solution chemistry evolves with time: Si concentration was initially high and then decreases toward the steady state. pH, Na and Al increases with decreasing Si, whereas the Ca, Mg and Fe concentrations were low. These features indicate the dissolution of volcanic glass at the initial stage, and then the solution chemistry was controlled by preferential leaching of albite component of plagioclase.

In the basalt-saline water (2.5 wt% of NaCl) experiment, we observed pH rises accompanying the decrease Si concentration, indicating the leaching of Si and dissolution of Pl similar to the basalt- H_2O experiment. One of the large differences between the two experiments was the extremely high Na concentration of saline water, resulting in the leaching of Ca (Ca concentration of the output solution was 40 to 80 times that of H_2O experiment), or breakdown of Ca-bearing minerals. In the basalt reaction with artificial seawater, which contains a lot of Mg^{2+}, SO_4^{2-}, CO_3^{2-} ions, revealed that the significant amount of precipitation of sulfate minerals occurred in the pre-heating parts of the vessel (before pass through the fluid reached the basalt sand), and that chlorite was formed throughout the reaction tube, which clogged the reaction vessel in a day. In contrast to the H_2O and saline water experiments, pH decreased to 3. In spite that we conducted the experiments with the same rock sample (basalt sand) and the same P-T conditions, the products and solubitions after the water-rock interaction were quite different in response to the input solutions, probably because the open system, in which new fluids are continuously supplied, is never rock-buffered. We will analyse the complicated reaction systems which control te evolution of solutions and minerals, based on the analyses of speciation of aqueous species, saturation of minerals

©2019. Japan Geoscience Union. All Right Reserved.

and variation of replacement textures of minerals.

Reference
Yardley, B. W., Harlov, D. E., & Heinrich, W. (2010). Rates of retrograde metamorphism and their implications for crustal rheology. Geofluids, 10(1-2), 234-240.

Keywords: Fluid-rock interaction, Flow through experiment, Supercritical condition, Basalt-seawater system, Garnet synthesis

©2019. Japan Geoscience Union. All Right Reserved.

3D microstructural analyses of fault rocks using CT and μCT scanning techniques

*Bingcheng Liu[1], Aiming Lin[1], Takafumi Nishiwaki[1]

1. Kyoto University

Meso- and microstructures of fault rocks including fault gouge developed in the active fault shear zone can reflect the deformation processes of fault motion and faulting mechanisms (Lin, 2008). Therefore, the study on structural features of fault rocks may provide new insights for understanding the nature of active faults. However, it is difficult to understand the spatial variation of microstructures of fault core zone based on traditional methods using two dimensional images under naked-eye and microscopic observations. Accordingly, it is necessary to develop an analytical method for three dimension (3D) analysis for understanding the spatial variation and internal structures of fault core zone. Computed tomography (CT) apparatus with micro-CT (μCT) accessories is a powerful tool which allows non-destructive 3D X-ray imaging and analyzing the spatial and internal structures within non-transparent objects, mainly determined by variations in density, chemical composition (effective atomic number) as well as thickness (Cnudde, 2005).

In this study, the CT and μCT imaging techniques are exploited to observe the 3D internal structures of a series of representative fault rocks: 1) pseudotachylytes of different origins (melting and crushing), and 2) cataclasitic rocks including fault gouge, fault breccia and cataclasite, by utilizing two types of scanning apparatuses (Bruker microCT, 2014): 1) μCT flat panel (FP), and 2) μCT charge coupled device (CCD). The samples of pseudotachylyte are from Fuyun, NW China (Lin, 1994), Ohsumi, Japan (Fabbri et al., 2000), and Musgrave Mt, Australia (Lin et al., 2005), respectively. The samples of fault gouge were acquired from two typical active fault zones in Japan: The Nojima Fault and Arima-Takatsuki Tectonic Line, SW Japan (Lin and Nishiwaki, 2019). The FP analysis shows that 1) the flow structures within the melting-origin pseudotachylytes are denoted by parallel colored glassy matrix layers with numerous rounded quartz clasts and quartz-filled amygdules which are oriented along the flow layers, and 2) chilled margins are characterized by fine-grained microlites orientated parallel to the margins. The 3D scanning images show that the layering structures developed within the fault gouge and fault breccia zones which are marked by sharp colored boundaries, oriented clasts and fine-grained matrixes. Our results demonstrate that 1) the CCD imaging makes it possible to observe sub-micron and even nano-scale 3D microsturctures fault rocks without destruction, and 2) μCT imaging can be further combined with traditional methods (such as optical microscope and SEM observation) to determine the spatial variations for both the meso- and microstructures and chemical compositions of fault rocks.

References:

1). Lin, A., 2008. Fossil Earthquakes: The Formation and Preservation of Pseudotachylytes. Springer, Berlin, 348p (ISBN 978-3-540-74235-7).

2). Veerle Cnudde, 2005. Exploring the potential of X-ray tomography as a new non-destructive research tool in conservation studies of natural building stones. Diss. Ghent University.

©2019. Japan Geoscience Union. All Right Reserved.

3). Bruker microCT. SkyScan 2211 User Manual, 2014.

4). Lin, A., 1994. Jour. Struct. Geol., 16, 71-83.

5). Fabbri, O., Lin, A., Totsushige, H., 2000. Jour. Struct. Geol., 22, 1015-1026.

6). Lin et al., 2005. Tectonophysics, 402, 21-35.

7). Lin, A., Nishiwaki,T., 2019. Geophy. Res. Lett., 46, DOI: 10.1029/2019GL081927.

Keywords: computed tomography, fault rocks, microstructure

©2019. Japan Geoscience Union. All Right Reserved.

Dissolution kinetics of forsterite olivine at >200 ˚C: implication for the kinetics of serpentinization.

*Ryosuke Oyanagi[1], Tatsu Kuwatani[1], Katsuhiko Suzuki[1]

1. Japan Agency for Marine-Earth Science and Technology

Serpentinization (hydration of mantle peridotite) gives significant changes to both chemical and physical properties of the oceanic lithosphere. Several studies suggested that the rate of serpentinization is maximized at 250-300˚C, and the rate-limiting process of serpentinization is the dissolution of primary mineral (e.g., Malvoisin et al., 2012). Therefore, the dissolution rate of olivine at 250-300˚C is consequently a critical parameter to understand the progress of serpentinization in the oceanic lithosphere. However, the olivine dissolution rates at > 150˚C have never been measured (Rimstidt et al. 2012), and the olivine dissolution rate extrapolatory calculated at 300˚C was inconsistent with the olivine serpentinization kinetics (Malvoisin et al., 2012). Towards the improved understanding of serpentinization kinetics, measuring dissolution rates of olivine as a function of solution composition and the temperature is required.

In this study, the dissolution rate of natural olivine ($(Mg_{0.91}, Fe_{0.09})_2SiO_4$) was measured at 200-400 ˚C and 50 MPa using a flow-through reactor (Suzuki et al., 2015). A 0.5 mol/kg NaCl solution was introduced at a constant rate of 2.0 mL/min during experiments. A preliminary experiment revealed that steady-state dissolution rate of olivine at 200 ˚C and far-from-equilibrium conditions was ca. -4.8 [mol/m^2/s] in log units. The obtained dissolution rate was consistent with the extrapolated dissolution rate (log_{10}(Rate) = ca. -4.72 [mol/m^2/s]), which was extrapolated from their pH-temperature dependence at 25-150 ˚C (Rimstidt et al., 2012). Based on dependences of temperature, salinity, and ΔG on dissolution rate, the timescales on hydrothermal alteration of peridotite will be discussed.

References

Malvoisin B, Brunet F, Carlut J, et al (2012) Serpentinization of oceanic peridotites: 2. Kinetics and processes of San Carlos olivine hydrothermal alteration. J Geophys Res Solid Earth 117:1–13. doi: 10.1029/2011JB008842

Rimstidt JD, Brantley SL, Olsen AA (2012) Systematic review of forsterite dissolution rate data. Geochim Cosmochim Acta 99:159–178. doi: 10.1016/j.gca.2012.09.019

Suzuki K, Kato S, Shibuya T, et al (2015) Development of Hydrothermal and Frictional Experimental Systems to Simulate Sub-seafloor Water–Rock–Microbe Interactions. In: Subseafloor Biosphere Linked to Hydrothermal Systems. Springer Japan, Tokyo, pp 71–85

Keywords: Serpentine, Reaction rate, Olivine, Dissolution rate

©2019. Japan Geoscience Union. All Right Reserved.

[J] Poster | S (Solid Earth Sciences)：S-MP Mineralogy & Petrology

Wed. May 29, 2019 5:15 PM - 6:30 PM JST | Wed. May 29, 2019 8:15 AM - 9:30 AM UTC | Poster Hall International Exhibition Hall8, Makuhari Messe_29

[S-MP32] Deformed rocks, Metamorphic rocks and Tectonics

convener:Yumiko Harigane(Geological Survey of Japan, National Institute of Advanced Industrial Science and Technology (AIST)), Yoshihiro Nakamura(Geological Survey of Japan, National Institute of Advanced Industrial Science and Technology)

We invite all researchers who aim to understand the dynamics of the earth's crust and mantle at the plate boundaries, to discuss the latest results from various viewpoints. The scope will include contributions through petrology and structural geology as well as various techniques including rheology and transformation of heat and mass.

[SMP32-P01] Pressure-temperature estimates of the Lützow-Holm Complex utilizing distributions of trace elements and inclusions in garnet porphyroblasts in pelitic gneisses

*Kota Suzuki[1], Tetsuo Kawakami[1], Yohei Igami[2] (1.Department of Geology and Mineralogy, Graduate School of Science, Kyoto University, 2.Institute of Materials and Systems for Sustainability, Nagoya University)

[SMP32-P02] Microstructures and pressure-temperature condition in pelitic gneisses from the Lützow-Holm Complex at Akarui Point, East Antarctica

*Hayato Yodoya[1], Takeshi Ikeda[2] (1.Department of Earth and Planetary Sciences, Graduate School of Scinece, Kyushu University, 2.Department of Earth and Planetary Sciences, Faculty of School of Scinece, Kyushu University)

[SMP32-P03] Long-lived (>90 Myr) granulite-facies metamorphism in the Trivandrum Block, southern India.

*Hikaru Kadowaki[1], Toshiaki Tsunogae[2], Santosh M.[3], Shaji E.[4], Yusuke Takamura[5], Yukiyasu Tsutsumi[6] (1.College of Geoscience, Graduate School of Life and Environmental Sciences, University of Tsukuba, 2.Faculty of Life and Environmental Sciences, University of Tsukuba, 3.School of Earth Sciences and Resources, China University of Geosciences Beijing, 4.Department of Geology, University of Kerala, 5. Doctoral Program in Earth Evolution Sciences, Graduate School of Life and Environmental Sciences, University of Tsukuba, 6.Department of Geology and Paleontology, National Museum of Nature and Science)

[SMP32-P04] Dislocation microstructures in garnet: Thermal effect during deeper crustal seismic slip in orogen-boundary shear zone

*Kaushik Das[1], Naotaka Tomioka[2], Proloy Ganguly[3], Jun-ichi Ando[1], Gautam Ghosh[3], Sankar Bose[3] (1.Hiroshima University, 2.Kochi Institute for Core Sample Research, JAMSTEC, 3.Presidency University, India)

[SMP32-P05] U-Pb zircon ages of migmatitic rocks from the Ryoke belt in the Mikawa and eastern Sanuki areas

*Keiichi Kazuratachi[1], Tetsuo Kawakami[1], Etienne Skrzypek[1], Shuhei Sakata[2], Takafumi Hirata[3] (1.Kyoto University, 2.Gakushuin University, 3.The University of Tokyo)

[SMP32-P06] Structural geology of Hidaka metamorphic belt in the Mt.Nozuka area, Hokkaido, Japan -Growth and formation process of the Cenozoic continental crust by island arc/arc join and its mechanism-

*Moeko Kanno[1], Tsuyoshi Toyoshima[2] (1.Graduate school of Science and Technology, Niigata University , 2.Department of Geology,Faculty of Science,Niigata University)

[SMP32-P07] THE PRESSURE-TEMPERATURE PATH AND MINERAL ASSEMBLAGE OF THE KHONICHIIN OVOO AREA, SOUTHEASTERN MONGOLIA.

*Undarmaa Batsaikhan[1], Noriyoshi Tsuchiya[1], Masaoki Uno[1], Yukio Isozaki[2], Uyanga Bold[2], OTGONBAYAR DANDAR[1], Hikaru Sawada[2] (1.Graduate School of Environmental Studies, Tohoku University, 2.Graduate School of Arts and Sciences the University of Tokyo)

[SMP32-P08] **Pressure-temperature conditions of contact metamorphism in Nokita area, Itoshima Peninsula, northwest Kyushu**

*Takeshi Ikeda[1], Kento Ota[2] (1.Department of Earth and Planetary Sciences,Faculty of Scinece, Kyushu University, 2.Department of Earth and Planetary Sciences,Graduate School of Scinece, Kyushu University)

[SMP32-P09] Evidence of Partial Melting of Migmatitic Felsic Gneiss from Nagasaki Metamorphic Complex in Amakusa-Shimoshima, western Kyushu, Japan

*Yuki Mori[1], Takeshi Ikeda[2], Kazuhiro Miyazaki[3] (1.Department of Earth and Planetary Sciences, Graduate School of Sciences, Kyushu University, 2.Department of Earth and Planetary Sciences, Faculty of Sciences, Kyushu University, 3.Research Institute of Geology and Geoinformation, Geological Survey of Japan, National Institute of Advanced Industrial Science and Technology)

[SMP32-P10] **Microstructural Analysis of Quartz grains in Monomineralic and Polyphase domains: A case study from Main Central Thrust (MCT) Zone Mylonites, western Himalaya, India**

*Shivaji Saha[1], Toru Takeshita[1], Subhajit Ghosh[2], Hari Bahadur Srivastava[3] (1.Department of Natural History Sciences, Hokkaido University, 2.Earthquake Research Institute, The University of Tokyo, 3.Department of Geology, Banaras Hindu University)

[SMP32-P11] **Tectono-thermal evolution of the Main Central Thrust (MCT) zone rocks of the Himalayan Crystalline Complex (*HCC*), Darjeeling-Sikkim Himalaya**

*Subhajit Ghosh[1,2], Santanu Bose[2,3], Nibir Mandal[4], Arijit Laik[2] (1.Earthquake Research Institute, The University of Tokyo, 1-1-1 Yayoi, Bunkyo-Ku, Tokyo 113-0032, 2.Department of Geology, University of Calcutta, 35, Ballygunge Circular Road, Kolkata 700019, India, 3.Department of Geology, Presidency University, 86/1 College Street, Kolkata 700073, India, 4.Department of Geological Sciences, Jadavpur University, Kolkata 700032, India)

[SMP32-P12] Thermal structure and deformation history of the low-grade Sanbagawa belt in the central of Kii Peninsula and tectonic implications

*Ken Yamaoka[1,2], Simon Wallis[1], Hiroshi Mori[2] (1.University of Tokyo, 2.Shinshu University)

[SMP32-P13] Antigorite Raman spectrum: a case study in Shiraga region of the central Shikoku, Sanbagawa metamorphic belt, SW Japan

*Kota Ando[1], Yui Kouketsu[1], Katsuyoshi Michibayashi[1] (1.Nagoya University)

[SMP32-P14] A fluid inclusion study from the late Paleozoic retrograde eclogite from the Yunotani Valley of the Omi area, Hida-Gaien Belt, Japan

*Yuzuki Shinji[1], Tatsuki Tsujimori[1], Tatsuhiko Kawamoto[2] (1.Tohoku University, 2.Shizuoka University)

[SMP32-P15] Development of reaction-induced stress and permeability in MgO-H_2O system

*Hisamu Kasahara[1], Masaoki Uno[1], Atsushi Okamoto[1], Noriyoshi Tsuchiya[1] (1.Graduate School of Environmental Studies, Tohoku University)

[SMP32-P16] Crystal orientation analysis of olivine in ultra-mylonite using TKD method: progress in spatial resolution from EBSD

*Yohei Igami[1], Katsuyoshi Michibayashi[2], Kakihata Yuki[2], Yui Kouketsu[2] (1.Institute of Materials and Systems for Sustainability, Nagoya University, 2.Graduate School of Environmental Studies, Nagoya University)

[SMP32-P17] Elucidation of effective diffusion coefficient along grain boundaries by hydrothermal experiment using low porosity rocks

*Naoki Sugisawa[1], Masaoki Uno[1], Noriyoshi Tsuchiya[1] (1.Graduate school of environmental studies Tohoku university)

[SMP32-P18] **Seismic slipping events recorded in a fault gouge zone: evidence from the Nojima Fault drill holes, SW Japan**

*Aiming Lin[1], Takafumi Nishiwaki[1] (1.Department of Geophysics, Graduate School of Science, Kyoto University)

[SMP32-P19] Evolution of fluid chemistry during basalt-water and basalt-seawater interactions revealed by hydrothermal flow-through experiments

*Yusuke Netsu[1], Atsushi Okamoto[1], Nobuo Hirano[1], Masaoki Uno[1], Noriyoshi Tsuchiya[1] (1.Tohoku University, Graduate School of Environment Studies)

[SMP32-P20] **3D microstructural analyses of fault rocks using CT and μCT scanning techniques**

*Bingcheng Liu[1], Aiming Lin[1], Takafumi Nishiwaki[1] (1.Kyoto University)

[SMP32-P21] **Dissolution kinetics of forsterite olivine at >200 °C: implication for the kinetics of serpentinization.**

*Ryosuke Oyanagi[1], Tatsu Kuwatani[1], Katsuhiko Suzuki[1] (1.Japan Agency for Marine-Earth Science and Technology)

Pressure-temperature estimates of the Lützow-Holm Complex utilizing distributions of trace elements and inclusions in garnet porphyroblasts in pelitic gneisses

*Kota Suzuki[1], Tetsuo Kawakami[1], Yohei Igami[2]

1. Department of Geology and Mineralogy, Graduate School of Science, Kyoto University, 2. Institute of Materials and Systems for Sustainability, Nagoya University

The Lützow-Holm Complex (LHC) in East Antarctica is a late Neoproterozoic to early Cambrian orogenic belt, formed during the amalgamation of Gondwana and composed of various bulk compositions of high-grade metamorphic rocks. Based on matrix mineral assemblages of mafic to intermediate mafic rocks, the LHC has been divided into three metamorphic facies zones; upper-amphibolite facies zone, transitional zone and granulite facies zone [1]. Because of the continuous distribution of upper-amphibolite facies to granulite facies metamorphic rocks, the LHC has been considered as a good exposure of the cross section of lower crust during continental collision events.
However, recent studies have found that high-*T* conditions above 850 °C are common even in the transitional zone and such temperatures are attained under kyanite stability field [3, 6, 7]. The aim of this study is to re-examine the peak metamorphic *P-T* conditions and *P-T* paths of selected regions in the LHC (Rundvågshetta, Skallen, Skarvsnes and Akarui Point) utilizing distributions of trace elements and inclusions such as Al_2SiO_5 minerals and rutile in garnet porphyroblasts in high-grade pelitic gneisses.
The Zr content of rutile coexisting with zircon+quartz strongly depends on the temperature condition and has been calibrated as Zr-in-rutile geothermometers that is more robust than the traditional Fe-Mg exchange type geothermometers during high-*T* metamorphism. In this study, experimentally calibrated Zr-in-rutile geothermometer [8] was applied to rutile grains in garnet and matrix.
The polymorphs of Al_2SiO_5 minerals are known as valuable indicators of the *P-T* conditions. In the course of this study, sillimanite with a characteristic Raman peak around 420 cm^{-1} which is not listed as a sillimanite peak in the Lyon database (http://www.geologie-lyon.fr/Raman/) were found as inclusion minerals in garnet and as matrix minerals from all of the four studied regions. In order to examine whether such a peak is related to the phase transition from kyanite or mullite to sillimanite, we observed them in detail by TEM. However, no evidence for such transition was found. Therefore, sillimanite with 420 cm^{-1} peak is dealt as normal sillimanite in this study.
Chemical zoning of garnet in high-*T* metamorphic rocks in terms of major elements (Fe, Mg, Ca and Mn) are commonly obscured by the diffusion under high-*T* conditions. On the other hand, chemical zoning of garnet in terms of trace elements, especially P, is less affected by the later diffusion, and commonly preserves sharp growth zoning [e.g., 2, 4]. Utilizing the sharp P zoning as a contemporaneous surface during garnet growth to define core and rim of garnet, and utilizing relic inclusions in garnet such as Al_2SiO_5 minerals and rutile to constrain the *P-T* conditions of each metamorphic stage [e.g., 5], we estimated metamorphic *P-T* conditions recorded in pelitic gneisses from the four regions in the LHC. Although Akarui Point is located in the “transitional zone” and three other regions are in the “granulite facies zone”, all of the inferred *P-T* paths of high-grade pelitic gneisses from Skallen, Skarvsnes and Akarui Point indicate nearly isothermal decompression starting from kyanite stability field at temperature around 850 °C. From Rundvågshetta, although pressure condition could not be well constrained, extremely high peak metamorphic temperature (> 900 °C) was inferred.
Since the peak metamorphic grades inferred from inclusion minerals in garnet porphyroblasts from Skallen, Skarvsnes and Akarui Point are almost the same, the traditional metamorphic zone mapping

©2019. Japan Geoscience Union. All Right Reserved.

based on matrix mineral assemblages does not represent the highest metamorphic conditions attained, and needs re-evaluation utilizing petrochronological approach.

References

[1]Hiroi et al, 1991 [2]Hiroi et al, 1997 [3]Iwamura et al, 2013 [4]Kawakami and Motoyoshi, 2004 [5]Kawakami and Hokada, 2010 [6]Kawakami et al, 2016 [7]Nakamura et al, 2013 [8]Tomkins et al, 2007

Keywords: chemical zoning, Phosphorus, kyanite, sillimanite, Zr-in-rutile geothermometer, partial melting

©2019. Japan Geoscience Union. All Right Reserved.

Microstructures and pressure-temperature condition in pelitic gneisses from the Lützow-Holm Complex at Akarui Point, East Antarctica

*Hayato Yodoya[1], Takeshi Ikeda[2]

1. Department of Earth and Planetary Sciences, Graduate School of Scinece, Kyushu University, 2. Department of Earth and Planetary Sciences, Faculty of School of Scinece, Kyushu University

Metamorphic rocks have been considered to preserve the mineral assemblage and composition at the peak condition in each pressure (*P*) –temperature (*T*) path. If this assumption is valid, the metamorphic rocks in the same outcrop are expected to show the same *P-T* condition. However, different *P-T* conditions have been estimated based on different geothermobarometers for rocks even from the same outcrop. Systematic difference among the methods could be responsible for these differences. However, this study revealed that use of the same pair of geothermobarometers provides significantly different P-T conditions for two pelitic gneisses from the same outcrop of the Lützow-Holm Complex, at Akarui Point, East Antarctica. An alternative interpretation is proposed to account for this difference.

The mineral assemblages of the studied gneisses are garnet, biotite, plagioclase, K-feldspar, quartz with and without sillimanite. Garnet grains in the Sil-bg. sample show round shape and contain large amount of fine quartz inclusions, whereas those in the Sil-free sample represent irregular shape and sporadically include coarse-grained plagioclase.

Garnet in both samples have chemically heterogeneity such that X_{Ca} (=Ca/Fe+Mg+Ca+Mn) and Mg/Fe decrease from the core to the rim. Furthermore, garnet in contact with biotite represents lower Mg/Fe than that in contact with other minerals. Garnet in the Sil-bg. sample is low in X_{Ca} and Mg/Fe as compared with garnet in the Sil-free sample. Phosphorus in garnet of the Sil-bg. sample represents euhedral shape of chemical contour in contrast to the garnet in the Sil-free sample where phosphorus shows no zoning. Biotite in the Sil-bg. sample shows Al-rich and low Mg/Fe as compared with that in the Sil-free sample. No systematic difference in Ti content in biotite is recognized. The Sil-free sample contains plagioclase with higher anorthite content than the Sil-bg. sample.

In the AFM approximation, garnet and biotite coexisting with sillimanite are expected to show higher Mg/Fe than those free from sillimanite. However, the present observations disagree with the prediction. Garnet contains significant amount of Ca, requiring addition of CaO to the chemical system. A calculated garnet composition diagram with respect to Ca-Mg-Fe shows that garnet coexisting with sillimanite represents a univariant line lower Ca and Mg/Fe than that free from sillimanite, and the present data are consistent with it. This suggests that two samples were not necessarily equilibrated at different *P-T* condition.

Geothermobarometry, in contrast, indicates significant difference in *P-T* condition. That is, garnet-biotite geothermometer (Ferry and Spear., 1978) and garnet-biotite-plagioclase-quartz geobarometer (Hoisch., 1990) show 685-718 ℃ at 6.4-6.6 kbar for the Sil-free sample and 828-855 ℃ at 7.2-7.8 kbar for the Sil-bg. sample.

It is puzzling feature that different samples from the same outcrop provide different *P-T* estimations using

©2019. Japan Geoscience Union. All Right Reserved.

the same geothermobarometers. The Sil-bg. sample records higher temperature than the Sil-free sample, as described before. Preservation of euhedral chemical contour of phosphorus in the Sil-bg. sample would indicate that the garnet grew maintaining surface equilibrium, at high temperatures. In contrast, absence of such euhedral contour and highly-rough surface of garnet in the Sil-free sample suggest relatively high growth rate, at low temperatures.

The *P-T* path of Akarui Point contains pressure decrease during temperature decrease (Iwamura et al., 2013). Considering this *P-T* path, it is expected that the garnet of Sil-free sample didn't exist at high temperatures and formed at low pressures and temperatures. The difference in estimated *P-T* conditions in the same outcrop can be attributed to not only the difference in the method but also the difference in the timing of the formation of minerals.

Keywords: pressure-temperature condition, phase relation, Lützow-Holm Complex

©2019. Japan Geoscience Union. All Right Reserved.

Long-lived (>90 Myr) granulite-facies metamorphism in the Trivandrum Block, southern India.

*Hikaru Kadowaki[1], Toshiaki Tsunogae[2], Santosh M.[3], Shaji E.[4], Yusuke Takamura[5], Yukiyasu Tsutsumi[6]

1. College of Geoscience, Graduate School of Life and Environmental Sciences, University of Tsukuba, 2. Faculty of Life and Environmental Sciences, University of Tsukuba, 3. School of Earth Sciences and Resources, China University of Geosciences Beijing, 4. Department of Geology, University of Kerala, 5. Doctoral Program in Earth Evolution Sciences, Graduate School of Life and Environmental Sciences, University of Tsukuba, 6. Department of Geology and Paleontology, National Museum of Nature and Science

The Southern Granulite Terrane in India is composed of various Archean to Neoproterozoic continental blocks, magmatic arcs, and supracrustal units amalgamated through complex subduction-accretion-collision event and high-grade metamorphism during the Latest Neoproterozoic to Cambrian Gondwana amalgamation. The Trivandrum Block corresponds to a unit in the southern part of the terrane with abundant metasediments and orthogneisses. The pressure-temperature (*P-T*) evolution of the high-grade metamorphism and its time scale are important for unraveling metamorphic processes during the collisional event. The *P-T* evolution recorded in various lithologies in the Trivandrum Block has been argued in numerous previous studies, and it is a subject of ongoing debate. The peak metamorphic ages reported in previous studies from the Trivandrum Block also show a wide range of ca. 600-510 Ma. It is therefore still not known whether the Trivandrum Block underwent single metamorphism with *P-T* variations within the block, or it experienced two discrete metamorphic events at 800-900 ˚C and >950 ˚C. In this study, we present new petrological, geothermobarometric, and geochronological data from khondalites, charnockites, bleached charnockites in the western part of the Trivandrum Block and discuss pressure-temperature-time (*P–T–t*) evolution of the block for unraveling the duration and heat source of high-grade metamorphism.

Phase equilibria modeling of the khondalite from Elavinmoodu quarry located in the western part of the Trivandrum Block indicates peak *P-T* condition of 920-1030 ˚C and 6.0-7.6 kbar, suggesting UHT metamorphism. Prograde and retrograde *P-T* conditions of ~750 ˚C/~7 kbar and ~750 ˚C/~4 kbar, respectively, were also obtained, based on which a clockwise *P-T* path with geotherm-parallel slow cooling is inferred. Consistent *P-T* conditions are obtained from khondalite exposed at Kakkod quarry where incipient charnockite patches within khondalite and foliation-parallel bleached layers within massive charnockite are preserved. Phase equilibria modeling of the incipient charnockite and the bleached rock indicate metamorphic *P-T* conditions of 820-950 ˚C/ 5-10 kbar and 800-1000 ˚C/~6 kbar, respectively. These data suggest that the bleaching of charnockite occurred during high-grade (or UHT) metamorphism, possibly because of fluid flow around the peak metamorphism.

Zircon and monazite U-Pb geochronology for a khondalite sample from Elavinmoodu quarry suggests that prograde, peak, and retrograde metamorphisms took place at around 582±17 Ma, 555.1±8.1 Ma, and 527.3±8.0 to 501.9±8.5 Ma, respectively. Later infiltration of hydrous fluid and hydration of garnet to form biotite occurred at around 489±12 Ma. Our results suggest that high-grade metamorphism continued at least 90 Myr, from 582 Ma to 489 Ma, suggesting a long-lived thermal event possibly related to the input of radiogenic heat from the crust and/or magmatic heat from syn- to post-tectonic intrusions.

The results of this study suggest single metamorphic event along a clockwise *P-T* path. The duration of

©2019. Japan Geoscience Union. All Right Reserved.

high-grade metamorphism (>90 Myr) is nearly consistent with that of metasediments from the Wanni Complex (>50 Myr; Hirayama et al., 2018), but it is shorter than that of long-lived high-grade metamorphism of the Highland Complex (~180 Myr; He et al., 2018). Although previous studies suggested that the supracrustal units of the Trivandrum Block could be a continuation of the Highland Complex (e.g., Dharmapriya et al., 2016; Takamura et al., 2018), the high-grade metamorphism of the Highland Complex might have started earlier than that of the Trivandrum Block possibly due to complex and multi-stage collisional processes related to the amalgamation of Gondwana Supercontinent.

Keywords: Trivandrum Block, P–T–t evolution, Ultrahigh-temperature metamorphism, Phase equilibria modeling, U–Pb geochronology

©2019. Japan Geoscience Union. All Right Reserved.

Dislocation microstructures in garnet: Thermal effect during deeper crustal seismic slip in orogen-boundary shear zone

*Kaushik Das[1], Naotaka Tomioka[2], Proloy Ganguly[3], Jun-ichi Ando[1], Gautam Ghosh[3], Sankar Bose[3]

1. Hiroshima University, 2. Kochi Institute for Core Sample Research, JAMSTEC, 3. Presidency University, India

A considerable amount of information regarding the growth and evolution of old continents are preserved at the boundaries between the orogenic belts and pre-existing cratonic blocks. These are the areas of intense and repeated deformation, metamorphism and activities of crustal fluids. Apart from the precise estimation of the pressure-temperature-fluid evolution through time, one of the major existing challenges is to understand the deformation mechanisms operated in the deep to shallow crustal depths for such geologically complex areas. The Phulbani domain in the north-western part of the Eastern Ghats Granulite Belt, India (EGB) provides a good opportunity as it is juxtaposed in its north and west by the Archean Singbhum Craton and Bastar Craton, respectively. Recent petrological and geochronological works of our group on the metapelitic granulite-charnockite-granitic gneiss of this domain reveal the pressure-temperature-fluid evolution with time. Though this domain is differentiated from the Visakhapatnam domain situated further south-southwest, the overall evolutionary history is observed to be very similar in style and time of occurrence. The Si-poor aluminous granulites preserve exotic reaction textures implying prograde heating-dominated path culminating at UHT condition (~1000 ˚C at 8 Kbar) followed by a retrograde cooling-decompression path, both in presence of CO_2-rich fluids. The age of metamorphism and associated magmatism ranges between ca. 1000 Ma and 900 Ma, similar to that of the Visakhapatnam domain.
The Phulbani domain, however, is bound on its north by a pronounced east-west shear zone, known as the Ranipathar shear zone. This deep crustal shearing affected the pelitic granulite and granitic gneiss. The mylonitic garnet-bearing granite gneiss preserves east-west foliation-parallel ultramylonite layers. Moreover, broadly east-west and north-south oriented black veins occur in these rocks. Thick (cm-scale) to thin (mm-scale) veins have mesoscopic characters of a pseudotachylite, e.g. injection veins. The microscopic observations on the foliation-parallel veins reveal that the vesicular groundmass of the veins is composed of micron-scale quartz-feldspar-biotite with clasts of garnet, at places. These veins, in certain cases, contain mm-scale clasts of the host granite mylonite gneiss.

Keywords: Garnet dislocation microstructures, Cataclastic flow, Seismic slip, Orogen-boundary shear zone

©2019. Japan Geoscience Union. All Right Reserved.

U-Pb zircon ages of migmatitic rocks from the Ryoke belt in the Mikawa and eastern Sanuki areas

*Keiichi Kazuratachi[1], Tetsuo Kawakami[1], Etienne Skrzypek[1], Shuhei Sakata[2], Takafumi Hirata[3]

1. Kyoto University, 2. Gakushuin University, 3. The University of Tokyo

Petrochronological studies of the migmatitic part of the high-temperature, low-pressure type Ryoke metamorphic belt enables us to understand the duration of partial melting of the mid-crustal depths during the Cretaceous ignimbrite flare-up event (Takatsuka et al., 2018a). In order to link multiple metamorphic zircon growths in migmatitic rocks with metamorphic stages of the Ryoke metamorphism, we performed LA-ICP-MS U-Pb zircon dating for samples from the Mikawa and eastern Sanuki areas (Ryoke belt, SW Japan).

In the Mikawa area, U-Pb ages of zircon from ~20 cm thick leucosome subparallel to the migmatitic banding of the psammitic metatexite has been already reported (Takatsuka et al., 2018a). The U-Pb dates of metamorphic rims in this part continuously spread on concordia from ~103 Ma to ~83 Ma. These metamorphic rims were separated into two stages of rim growth by discontinuous zoning in CL images, supported by their chronological and chemical difference: Inner rims were interpreted as the zircon growth during prograde metamorphism (97.0±4.4 Ma) and outer rim as the zircon crystallization from the partial melt during early retrograde metamorphism (88.5±2.5 Ma) (Takatsuka et al., 2018a). However, since the sample used in Takatsuka et al. (2018a) was a notably thick leucosome sample different from the surrounding metatexite leucosomes, whether zircon in the typical metatexite migmatites from the same area give the similar characteristics or not has been not clear.

In this study, we performed LA-ICP-MS U-Pb zircon dating for 4 migmatitic rock samples from the high-grade part of the Mikawa area. Migmatite samples mainly consist of Qtz+Pl+Kfs+Bt±Crd+Sil±Grt. Zircon grains commonly have metamorphic rims in which sillimanite and muscovite inclusions are found. We obtained continuous spread of U-Pb dates on concordia from ~98 Ma to ~81 Ma. Based on presence/absence of sillimanite inclusions, Th/U ratio, and U concentration of zircon rims in addition to the U-Pb dates, three metamorphic stages were recognized; (1) 91.4±0.8 Ma (weighted average age, MSWD=1.4, Th/U<0.08, n=29) possibly representing the zircon rim growth in the presence of partial melts during regional metamorphism, (2) 87.1±1.7 Ma (weighted average age, MSWD=2.1, Th/U=~0.002-0.01, n=3) representing the formation of U-rich zircon through fluid-rock interaction at early retrograde metamorphism, (3) ~81 Ma (80.9±2.9 Ma and 81.5±7.3 Ma; Th/U<0.03) overgrowth on metamorphic rim (1). The zircon rim (3) might represent the growth or recrystallization during contact metamorphism caused by the intrusion of 81-75 Ma granitoids (Takatsuka et al., 2018b), as sampling point of the migmatite was 1.7 km distant from the 81-75 Ma granitoids and the obtained U-Pb zircon dates are close to the granitoids.

We also determined U-Pb ages of metamorphic zircon in 2 samples from the eastern Sanuki area (Kutsukake et al., 1979) where ages of metamorphic zircon have not been reported so far. One sample is a pelitic gneiss from a metamorphic rock body of about 800 m in size surrounded by granitoids, and mainly consists of Qtz+Pl+Kfs+Bt+Grt. Zircon grains in this sample have metamorphic rims (Th/U=~0.02-0.18). The weighted average U-Pb age of the metamorphic zircon rims is 93.4±0.7 Ma (MSWD=0.85, n=27). Another sample is a pelitic gneiss from a metamorphic rock body of 4 km wide, surrounded by gneissose granitoids. The gneissose structure of pelitic gneiss is concordant with surrounding granitoids. This sample mainly consists of Qtz+Pl+Kfs+Bt+Sil. Metamorphic rims (Th/U=~0.05-0.08) of zircon include sillimanite, and the weighted average U-Pb age is 95.4±2.4 Ma (MSWD=0.47, n=6). As these ages are consistent with U-Pb zircon ages of surrounding ~93 Ma gneissose granitoids (Iida et al., 2015), it is likely

©2019. Japan Geoscience Union. All Right Reserved.

that the rims grew during contact metamorphism by the granitoids under sillimanite-stable condition.

Keywords: U-Pb zircon dating, migmatite, high-temperature metamorphism

©2019. Japan Geoscience Union. All Right Reserved.

Structural geology of Hidaka metamorphic belt in the Mt.Nozuka area, Hokkaido, Japan -Growth and formation process of the Cenozoic continental crust by island arc/arc join and its mechanism-

*Moeko Kanno[1], Tsuyoshi Toyoshima[2]

1. Graduate school of Science and Technology, Niigata University , 2. Department of Geology,Faculty of Science,Niigata University

The Hidaka Metamorphic Belt (HMB) in Hokkaido, northern Japan, consists of metamorphic and plutonic rocks, and is regarded as a crustal section of Tertiary immature parts of the Kurile island arc exposed along with collision to the NE Japan arc in the Miocene (Komatsu et al., 1982 etc.) . Metamorphic grade increases from very low-grade sediments in the east to granulite facies in the west. It was considered to be a single and coherent crustal section, however, Shimura et al. (2015) proposed that HMB is a composite of two crusts of 19 Ma and 37 Ma. This hypothesis should be tested by detailed filed relationships of rocks of different ages. This paper presents deformation phase of metamorphic rock and plutonic rock and zircon U-Pb ages along the Niobetsu River route of the Nozuka dake area, southern HMB, and discusses on the mode of crustal evolution there.

In the study area, HMB consists mainly of S-Type tonalite (Grt Tonalite, Grt-Bt Tonalite), I-Type tonalite (Hbl-Bt tonalite), Diorite, Amphibolite, Gneiss.
Most of the rocks aligned with NW—SE trends except for a diorite intrusion with N—S margins. The diorite is accompanied with migmatite along its margins. Blocks of metamorphic rocks are included in I-Type tonalite and Diorite. Imbricated hornblende crystals in marginal parts of the diorite imply a normal fault-sense magmatic flow. Heterogeneous amphibolite on the southern margin of the diorite are severely folded and deformed with S-C fabric suggesting partial melting.
Mylonitization is observed in S-type tonalite near the Hidaka Main Thrust (HMT), the western margin of HMB. The mylonites show right lateral shear structures with or without normal-slip component. The mylonitization can be classified into 3 stages: 1st Mylonitization by shear deformation of nomal dip-slip, 2nd Mylonitization by shear deformation of normal dip-slip ~ dextral shear, 3rd Mylonitization by shear deformation of dextral shear ~ reverse dip-slip.

We obtained zircon U-Pb ages from S-type tonalites, I-type tonalite, and Diorite.
S-type: about 45Ma, I-type: About 33Ma, Diorite: about 19Ma.

Heterogeneous amphibolite is considered as the boundary deformation zone between 19 Ma plutonic and metamorphic rocks and the older plutonic and metamorphic rocks, because Heterogeneous amphibolite is severely folded and deformed with partial melting. Diorite is penetration in a tensile field is expected. Because the asymmetric flow structure inside the diorite shows normal fault sense.

Zircon U - Pb ages suggest three magmatic stages (about 33 Ma, about 19 Ma and older then 33Ma) in HMB of this area. Igneous rocks include migmatite and metamorphic rocks . So, it is suggested that the magmatism activities of 3 stages are accompanied by metamorphism. Therefore, it is considered that the Hidaka metamorphic belt was formed by three stage metamorphisms.

©2019. Japan Geoscience Union. All Right Reserved.

Keywords: Structural geology, Hidaka Metamorphic belt, Tectonics

©2019. Japan Geoscience Union. All Right Reserved.

THE PRESSURE-TEMPERATURE PATH AND MINERAL ASSEMBLAGE OF THE KHONICHIIN OVOO AREA, SOUTHEASTERN MONGOLIA.

*Undarmaa Batsaikhan[1], Noriyoshi Tsuchiya[1], Masaoki Uno[1], Yukio Isozaki[2], Uyanga Bold[2], OTGONBAYAR DANDAR[1], Hikaru Sawada[2]

1. Graduate School of Environmental Studies, Tohoku University, 2. Graduate School of Arts and Sciences the University of Tokyo

The Khonichiin ovoo area is located in the southeastern part of Mongolia of the Central Asian Orogenic belt, which is largest amalgamation history of during Phanerozoic time. The Khonichiin ovoo area mainly consists of the Khutaguul, the Norovzeeg metamorphic complexes that underwent high grade facies metamorphism, with rare igneous rocks. The Khutaguul metamorphic complex is composed of garnet-biotite, amphibolite-biotite, two mica gneiss, amphibolite schist, quartzite, marble, granite-gneiss, granulite and migmatites. The Norovzeeg metamorphic complex is composed of metasedimentary and metavolcanic rocks. P-T condition and mineral assemblage data/information for these metamorphic complexes are extremely limited. This is because international and local researchers had focused on investigations on Paleozoic igneous, volcanic and sedimentary rocks, which are somehow related to the porphyry copper deposits (Tsagaan suvarga Cu-Mo, Kharmagtai Cu-Au) in the south of Mongolia in the last two-decade years.
We will show new age dating and P-T conditions of the Khutaguul and the Norovzeeg metamorphic rocks.

Keywords: P-T path, Petrology, Southeastern Mongolia

©2019. Japan Geoscience Union. All Right Reserved.

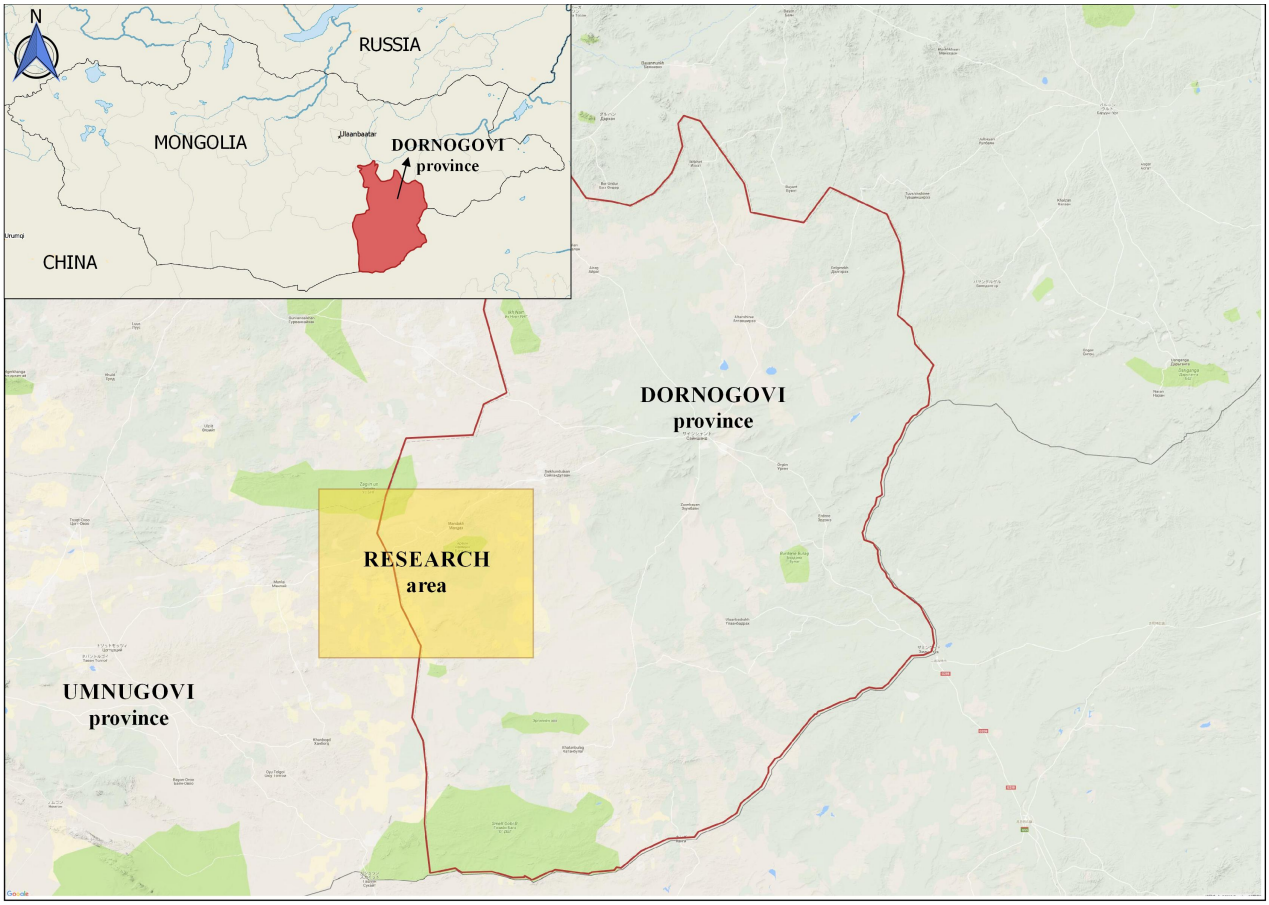

©2019. Japan Geoscience Union. All Right Reserved.

Pressure-temperature conditions of contact metamorphism in Nokita area, Itoshima Peninsula, northwest Kyushu

*Takeshi Ikeda[1], Kento Ota[2]

1. Department of Earth and Planetary Sciences,Faculty of Scinece, Kyushu University, 2. Department of Earth and Planetary Sciences,Graduate School of Scinece, Kyushu University

Gneissose granitic rocks are common in high-grade areas of high-temperature low-pressure metamorphic complex. Similarity in age and concordant relation to the surrounding rocks imply that they supplied heat to cause the high-temperature low-pressure metamorphism. Parallelism of internal structures of granitic and metamorphic rocks also suggests that both rocks underwent simultaneous deformation during and after the intrusion of the granitic rocks. The post-metamorphic deformation would rearrange the thermal structure formed at the heat supply.

The Renge metamorphic complex in the Nokita area of Itoshima Peninsula, northwest Kyushu, was intruded by the Kitazaki and Itoshima granodiorites on the north and south at Cretaceous, respectively. The complex was recrystallized by thses intrusions and underwent significant deformation that belongs to flattening after the peak of contact metamorphism (Yamasaki & Ikeda, 2018). This study estimates the pressure-temperature condition preserved in pelitic rocks to evaluate the post-metamorphic deformation.

The pelitic schists in the study area are composed of leucocratic and melanocratic layers depending on the modal amount of biotite. The common constituent minerals are quartz, plagioclase, biotite. Garnet, muscovite, and K-feldspar locally occur. In addition, chlorite is present as veins and schistosity-forming mineral, which is interpreted as retrograde products.

Four pelitic schists were employed to estimate the metamorphic conditions. Garnet shows euhedral shape and so-called normal zoning where Mg increases and Fe and Mn decreases towards the rim. The composition of rim ranges such that Xalm=0.72-0.80, Xprp=0.09-0.12, Xsps=0.06-0.16, and Xgrs=0.04-0.06. On the other hand, that of core varies Xalm=0.50-0.66, Xprp=0.03-0.05, Xsps=0.24-0.40, and Xgrs=0.04-0.10. The Mg/Fe of rim and core ranges 0.13-0.15 and 0.06-0.08, respectively. Biotite also shows significant variation in composition, i.e., Ti of 0.15 - 0.46 based on 22 oxygen, and Mg/Fe of 0.44 - 0.76. The Ti content of biotite near chlorite is low as compared with that far from chlorite. Plagioclase is chemically homogeneous in one sample. The anorthite content shows southward increase from 0.23 to 0.42.

We chose the composition equilibrated at peak of the metamorphism such as the highest Mg/Fe in the rim of garnet, highest Ti in biotite and highest anorthite content in plagioclase. Geothermobarometry using garnet-biotite geothermometer (Ferry & Spear 1978) and a garnet-biotite-plagioclase-quartz geobarometer (Hoisch 1990) provide the metamorphic conditions of 590 °C, 1.4 kbar, 650 °C, 3.5 kbar, 770 °C, 4.2 kbar, and 650 °C, 2.8 kbar from south to north ,which corresponds to 5.3-16 km depth. The pressure and temperature vary by 2.8 kbar and 180 °C, respectively, within ca. 300 m distance. The lithostatic pressure relevant to 300 m thickness cannot explain the pressure difference of 2.8 kbar. The present result also supports the significant thinning deformation after the contact metamorphism.

Keywords: Contact metamorphism, Post-metamorphic deformation, Geothermobarometry

©2019. Japan Geoscience Union. All Right Reserved.

©2019. Japan Geoscience Union. All Right Reserved.

Evidence of Partial Melting of Migmatitic Felsic Gneiss from Nagasaki Metamorphic Complex in Amakusa-Shimoshima, western Kyushu, Japan

*Yuki Mori[1], Takeshi Ikeda[2], Kazuhiro Miyazaki[3]

1. Department of Earth and Planetary Sciences, Graduate School of Sciences, Kyushu University, 2. Department of Earth and Planetary Sciences, Faculty of Sciences, Kyushu University, 3. Research Institute of Geology and Geoinformation, Geological Survey of Japan, National Institute of Advanced Industrial Science and Technology

The Nagasaki Metamorphic Complex in Amakusa-Shimoshima is divided into the lower and upper units. The former and the latter are composed mainly of pelitic schists and gneisses with mafic and felsic composition, respectively. The upper unit is considered to have located at lower crust that was shortened due to ductile flow toward trench side (Miyazaki et al., 2013). The unit belongs to the high-pressure granulite facies and represents migmatitic mode of occurrence, which implies potential presence of melt that enhanced the ductile deformation. This study reports microstructural features indicative of partial melting in a felsic migmatitic gneiss.

The migmatitic felsic gneiss dealt with this study represents U-Pb zircon age of 125.8±1.8 Ma (Mori et al., 2018 JpGU). It is composed mainly of garnet, quartz, muscovite, zoisite and aggregate of fine-grained zoisite + albite + muscovite that is former plagioclase. Minor amounts of graphite, zircon, apatite, rutile, chlorite, and iron sulfide also occur. Tiny grains of hornblende are included in the rim of garnet. The matrix zoisite commonly includes epidote in the core. The epidote contains significant amounts of rare earth elements (REE) and is composed of Y-poor core and Y-rich rim. The garnet grains are roughly divided into two types of coarse- and fine-grained. The X_{Mg} [=Mg/(Mg+Fe)] of the coarse-grained garnet increases from the core to the rim and decreases at the extreme periphery, while that of the fine-grained garnet monotonically decreases from the core to the rim. The coarse-grained garnet represents Y-rich and P-poor core and Y-poor and P-rich rim whereas Y-poor and P-rich domain is dominant in the fine-grained garnet. A polyphase inclusion composed of chlorite + muscovite + quartz + $CaCO_3$ is found from the rim of coarse-grained garnet. The inclusion shows polygonal shape and has cuspate offshoots filled with chlorite or muscovite. Apatite is included in the core of the coarse-grained garnet but is not found from the rim. The fine-grained garnet and the rim of the coarse-grained garnet include Y-rich REE-epidote.

We applied Zr-in-rutile geothermometer (Ferry & Watson, 2007), garnet-hornblende geothermometers (Graham & Powell, 1984; Powell, 1985; Ravna, 2000), and hornblende-plagioclase geothermometer (Holland & Blundy, 1994). These results are consistent among them within their errors and represent 720 −770 ˚C as the peak condition. The pressure at the peak condition was estimated utilizing garnet-hornblende-plagioclase-quartz geobarometer of Kohn & Spear (1990), and we obtained the pressure of 9.1 −10.2 kbar.

The estimated condition lies above the melting reaction of zoisite + muscovite + quartz + water = kyanite + melt (cf. Schliestedt & Johannes, 1984). The polygonal shape of the polyphase inclusion in the rim of coarse-grained garnet could represent negative crystal of garnet. Combining the constituent minerals of the inclusion, it is likely that the polyphase inclusion was originally melt inclusion.

The concentration of yttrium and phosphorus in the rim of coarse-grained garnet is similar to that in fine-grained garnet. Based on the presence of melt inclusion in the rim of coarse-grained garnet, we

©2019. Japan Geoscience Union. All Right Reserved.

consider that fine-grained garnet nucleated during the partial melting with the formation of the rim of coarse-grained garnet. The Y-rich REE-epidote is in the matrix and included in the fine-grained garnet and the rim of the coarse-grained garnet, so we consider that Y-poor garnet and Y-rich REE-epidote coexisted with the melt. The lack of apatite inclusion in P-rich domain of both garnets may indicate that the phosphorus in P-rich domain in garnet was supplied by breakdown of apatite during the melting.

Keywords: partial melting, melt inclusion, garnet, REE-epidote, apatite

©2019. Japan Geoscience Union. All Right Reserved.

Microstructural Analysis of Quartz grains in Monomineralic and Polyphase domains: A case study from Main Central Thrust (MCT) Zone Mylonites, western Himalaya, India

*Shivaji Saha[1], Toru Takeshita[1], Subhajit Ghosh[2], Hari Bahadur Srivastava[3]

1. Department of Natural History Sciences, Hokkaido University, 2. Earthquake Research Institute, The University of Tokyo, 3. Department of Geology, Banaras Hindu University

Ongoing collision in the Himalayan orogeny causes crustal deformation owing to the thrust activity. Hence, the movement along the Main Central Thrust (MCT) enhances ductile deformation of the crust widely distributed across the orogenic belt. Therefore, detailed microstructural analysis is necessary to define the shear zone by the degree of strain intensification across the MCT. A study area along Madhmaheswar Ganga valley, Rudraprayag district, Uttarakhand, India, has been chosen. Purpose of this study is to perceive the heterogeneity of the deformational behavior of quartz grains in terms of thickness of quartz layers and other associated phases along with the understanding of fabric development with respect to the MCT. In this research, the lower Greater Himalayan Sequence (L-GHS) of *c.* 1.5 km thickness on the hangingwall side and upper Lesser Himalayan Sequence (U-LHS or Munsiari formation) of *c.* 4 km thickness on the footwall side of the MCT, has been studied.

Microstructural observations are essentially focused on the quartzo-feldspathic gneiss of the Munsiari formation and L-GHS. At lower Munsiari formation, Quartz microstructures are characterized by subgrain rotation recrystallization (SGR). Polygonal quartz grains with triple point junction indicate SGR followed by static grain growth. At upper Munsiari formation, lobate boundaries of quartz grains with sweeping extinction and deformation lamellae indicate high temperature grain boundary migration (GBM) overprinted by late stage low temperature deformation. Quartz grains in the lower GHS rocks are coarser than that of the Munsiari rocks and highly amoeboid in shape. High temperature deformation is evidenced by the presence of elongated sub-grains within these irregular grains.

To carry out further microstructural studies, 14 samples were selected for EBSD analysis. Quartz *c*-axis fabric from ~500-829 μm thick quartz-rich monomineralic layer shows a series of type-*II* crossed girdle fabrics with *Y*-maximum. Here, the quartz *c*-axes are aligned parallel to intermediate finite strain axis *Y*, revealing the intracrystalline deformation by active prism {10 -10} *a* slip system. In contrast, c-axis orientations obtained from thin monomineralic quartz layers (thickness ~72-163 μm) records girdles ranging from small circle girdles to type-*I* crossed girdle fabric with r-maxima. In this case, the rhombohedral plane of quartz is aligned parallel to the foliation plane (*XY*), which indicate basal (0001) *a* slip and rhomb {10 -11} *a* slip system activity. Thus, there is an effect of thickness of monophase layers on fabric development and, perhaps the role of other phases has a strong impact on the fabric development for thin monomineralic layers.

On the other hand, polyphase domains are characterized by the quartz grains totally surrounded by other phases. The size of recrystallized quartz grains within polyphase domain increases from ~64.4 μm in Munsiari to ~109 μm in L-GHS. C-axes orientations are random for the Munsiari samples. Whereas, C-axis fabric with point maxima is observed for the L-GHS samples. However, those fabric patterns are strengthened with increasing modal abundance of quartz.

©2019. Japan Geoscience Union. All Right Reserved.

The strength of the quartz *c*-axis fabric is quantified as a function of eigenvectors (λ_1 = maximum; λ_2 = intermediate; λ_3 = minimum) from *c*-axes orientation distribution. Following, Vollmer (1990), three end member fabric types are determined from these eigenvectors; those are point (*P*), girdle (*G*) and random (*R*). Then, by introducing cylindricity index (*B*) of Vollmer (1990), the variation in fabric strength of quartz LPO is shown as a function of strain localization throughout the Munsiari formation. Progressive increase in fabric intensity for both thin and thick monomineralic quartz layers indicate an increase in strain towards the MCT.

Keywords: Main Central Thrust Zone, Quart c-axis fabric, Strain intensification

©2019. Japan Geoscience Union. All Right Reserved.

Tectono-thermal evolution of the Main Central Thrust (MCT) zone rocks of the Himalayan Crystalline Complex (*HCC*), Darjeeling-Sikkim Himalaya

*Subhajit Ghosh[1,2], Santanu Bose[2,3], Nibir Mandal[4], Arijit Laik[2]

1. Earthquake Research Institute, The University of Tokyo, 1-1-1 Yayoi, Bunkyo-Ku, Tokyo 113-0032, 2. Department of Geology, University of Calcutta, 35, Ballygunge Circular Road, Kolkata 700019, India, 3. Department of Geology, Presidency University, 86/1 College Street, Kolkata 700073, India, 4. Department of Geological Sciences, Jadavpur University, Kolkata 700032, India

The rheology of the Himalayan Crystalline Complex (*HCC*) laying above the Main Central Thrust (MCT), is the key boundary condition for all the tectonic models that deals with extrusion of lower crustal material. Therefore, it is important to understand the intricate relationship between the processes of crustal thickening, Barrovian metamorphism and strain localization in the high-grade rocks of the *HCC* that controls the rheology of a deforming wedge. Initially deformation was distributed and a series of repeated folding leads to crustal thickening and pro-grade metamorphism. The similarity between the peak metamorphic and peak deformation temperature, as documented by frozen high-temperature microstructures is indicative of this phase. The '*locked in*' deformation microstructures and syn-kinematic growth of metamorphic index minerals reveal that the MCT related shearing begins at or near the peak metamorphic condition (16-12 Ma), where grain size reduction by dislocation-controlled creep was the most effective mechanism for strain localization. The observed deformation microstructures and the available P-T data shows that the peak deformation and metamorphic condition progressively increases (~500 to >700˚C) towards the mountain interior. It is further evident that the now-exposed *HCC* begun to extrude under dominantly ductile mid-crustal condition at a temperature >700˚C, where the hotter mid-crustal rocks can flow in a viscous manner by melt enhanced depth-dependent ductile flow. Hence, initially the MCT represents a rheological and metamorphic boundary that separates material which can or cannot flow. Then with subsequent exhumation, cooling and strengthening of the *HCC* produced diffuse ductile shear zones along the same rheological boundary, where deformation was distributed for 4-6 km width (~ MCT zone). The base of the high strain zone is marked by base of the compressed reverse paleo-isograds that coincides with the SGR-GMB transition for quartz, leading to steep P-T gradient locally constrained within the MCT zone before it flattened in the migmatite gneisses. At further lowering of temperature (shallower depth), the MCT localized into narrow shear zone under dominantly brittle condition, transporting the entire *HCC* thrust sheets to the foreland.

Keywords: Himalaya, India-Asia collision, Superposed folding, Strain localization , Main Central Thrust Zone

©2019. Japan Geoscience Union. All Right Reserved.

Thermal structure and deformation history of the low-grade Sanbagawa belt in the central of Kii Peninsula and tectonic implications

*Ken Yamaoka[1,2], Simon Wallis[1], Hiroshi Mori[2]

1. University of Tokyo, 2. Shinshu University

The Sanbagawa belt in SW Japan is one of the best-documented regions of relatively warm subduction-type metamorphism and information from such regions are important to clarify our understanding of convergent plate margins. Much of the present knowledge is based on petrological studies in the higher grade parts of this belt. However, most of the Sanbagawa belt belongs to the lowest grade domain, the chlorite zone. The lack of reliable methods to determine the thermal structure in this low-grade zone has meant that information from the majority of the belt has been underrepresented. Development of the Raman carbonaceous material thermometer (RCMT) has opened up possibilities of determining the temperature structure of low-grade metamorphic domains such as the chlorite zone of the Sanbagawa metamorphism. Application of RCMT to pelitic rocks of the central Kii peninsula shows a progressive decrease in T from ~390 ˚C close to the northern boundary marked by the Median Tectonic Line (MTL) to ~270 ˚C ~7 km to the south and roughly constant thereafter. The thermal structure is not significantly affected by fault boundaries between different geological units. Meso and microstructural observations combined with strain analysis based on deformed shapes of detrital grains in metamudstone indicate a similar deformation history throughout the area and no correlation between strain and temperature gradients. These features can be used to asses possible models for the observed temperature rise. On this basis, we suggest the rise in T was not due to return flow of high T material in a subduction channel. We also conclude that the rise in T takes place over too narrow a distance to be explained as part of the expected thermal warping in a warm subduction zone. We find no evidence for heating related to the rise of magma or hot fluids. Shear heating along the MTL does provide a plausible explanation for the observed thermal structure compatible with all observations. One-dimensional thermal modeling shows that to account for the observed thermal structure requires slip rates of several mm/yr and relatively high coefficients of friction (μ=??). A similar result was reported from an area to the east but with a much more limited domain of elevated temperatures, probably due to late-stage thinning related to normal faulting. Our results imply that long-lived major crustal faults such as the MTL are at least locally associated with high stresses and are relatively strong. Evidence for the faults being weak at shallow depth implies there is a rapid decrease in strength over the upper few km of the MTL fault zone.

Keywords: Sanbagawa belt, Raman carbonaceous material thermometry, shear heating

©2019. Japan Geoscience Union. All Right Reserved.

Antigorite Raman spectrum: a case study in Shiraga region of the central Shikoku, Sanbagawa metamorphic belt, SW Japan

*Kota Ando[1], Yui Kouketsu[1], Katsuyoshi Michibayashi[1]

1. Nagoya University

Serpentinites are important rocks and are associtated with water circulating in the earth's interior. However, it is difficult to estimate their metamorphic conditions because serpentine minerals are stable at wide P-T condition. In this study, we compared Raman spectrum of antigorite in different metamorphic grade samples and determined whether Raman spectrum could constrain metamorphic conditions of serpentinites. Serpentinites in this study have been sampled from Shiraga region of the central Shikoku, the Sanbagawa metamorphic belt, SW Japan. All samples experienced the metamorphic conditions in which olivine were formed by the dehydration reaction of antigorite with brucite. Some samples show retrograde antigorite formed during exhumation. Raman spectrum were measured from various sizes and textures of antigorite grains. Comparing full width at half maximum (FWHM) of Raman spectrum, we found that the prograde-antigorite had different features from retrograde-antigorite. As a consequence, FWHM of Antigorite Raman spectrum could be used to constrain the timing of antigorite formation.

Keywords: antigorite, Serpentinite, Raman spectrum, Sanbagawa metamorphic belt

©2019. Japan Geoscience Union. All Right Reserved.

A fluid inclusion study from the late Paleozoic retrograde eclogite from the Yunotani Valley of the Omi area, Hida-Gaien Belt, Japan

*Yuzuki Shinji[1], Tatsuki Tsujimori[1], Tatsuhiko Kawamoto[2]

1. Tohoku University, 2. Shizuoka University

Primary fluid inclusions trapped in subduction metamorphic rocks can provide direct information concerning composition and origin of slab-derived fluids. In order to investigate fluid signatures at the mantle wedge beneath forearc regions, we conducted microthermometry for primary fluid inclusions in both prograde eclogite-stage omphacite and retrograde blueschist-stage quartz, in the late Paleozoic retrograde eclogite from the Yunotani Valley of the Omi area, Hida-Gaien Belt, Japan. Note that the investigated blueschist-stage quartz forms a microvein along cracks of omphacite. The investigated eclogite occurs as mafic layers or lenses which are intercalated in metasedimentary rocks with the mineral assemblage paragonite + phengite + garnet ±glaucophane + quartz + rutile. Recent study confirmed that the retrograde blueschist-stage reached the pumpellyite stability field of P = ~0.62–0.70 GPa and T = ~280–320°C (Shinji and Tsujimori 2019 doi:10.2465/jmps.180716).

The primary fluid-inclusions in both omphacite and quartz are aqueous two-phase inclusions of liquid and vapor. Their molecular species in a liquid and gas phase were identified using micro-Raman spectroscopy. The fluid inclusions of the eclogite-stage omphacite are characterized by relatively high salinity of ~8.0–8.2 wt% NaCl equivalent and the brine freezing temperatures at ~-70°C suggests presence of divalent ions such as Ca^{2+} and/or Mg^{2+}. In contrast, fluid inclusion in blueschist-stage quartz shows relatively low value of ~2.4 wt% NaCl equivalent. The liquid phase of the fluid inclusion transforms completely into solid phases at ~-38°C, suggesting existence of the limited monovalent ions such as Na^{+} or/and K^{+} in the fluids.

Our preliminary data demonstrates that the pervasive fluids entrapped at prograde eclogite-stage and retrograde blueschist-stage had different chemical compositions. This suggests different fluid sources at eclogite and blueschist depth. Our observation is consistent with the different fluid compositions recorded in zoned lawsonite in Guatemalan eclogite (Hara et al. 2018 doi: 10.1016/j.lithos.2018.09.001). In our study, the existence of higher salinity fluids in the eclogite-facies conditions can suggest more effective transportation of the lithophile elements into the mantle wedge at deeper forearc regions.

Keywords: Slab-derived fluid, Mantle wedge beneath forearc region, Fluid inclusion, Microthermometry, Retrograde eclogite, Retrograde blueschist-stage pumpellyite

©2019. Japan Geoscience Union. All Right Reserved.

Development of reaction-induced stress and permeability in MgO-H_2O system

*Hisamu Kasahara[1], Masaoki Uno[1], Atsushi Okamoto[1], Noriyoshi Tsuchiya[1]

1. Graduate School of Environmental Studies, Tohoku University

Fractures are dominant flow path of fluid transport in the crust, and fluid flow through the fractures is important for the progress of fluid-rock interaction and material transport in the crust. The fractures enhance permeability in rocks, which has significant effects on the efficiency oil mining, geothermal development and Carbon dioxide Capture and Storage (CCS). Thus, the research on the fracture formations and associated permeability developments are increasingly important for geoscience and engineering.

Especially during fluid-rock interactions in the crust, hydration reactions increase solid-volume and generate stress. Recently such reaction-induced stress has been investigated as a new fracture generation process. For example, the fractures associated with reaction-induced stress are observed in serpentinized olivine (Jamtveit and Austrheim, 2010). In addition, the stress exceeding rock strength is reported from thermodynamic prediction (Kelemen and Hirth, 2012) and experimental measurements (e.g., Lambart et al., 2018). However, the existence of non-fractured rocks despite the volumetric expansion reaction (Centerrea et al., 2015) and the discrepancies between the experimental and theoretical values of reaction-induced stress have not yet been clarified. To understand the causes of these phenomena, it is important to constrain the controlling factors and the generation processes of reaction-induced stress. Therefore, we conducted direct measurements of reaction-induced stress and permeability development during hydration reactions, to clarify the relation between the reaction, stress generation, fracturing and permeability developments.

In our previous study, we measured the reaction-induced stress in MgO–H_2O system, and observed stress generation of approximately 40 MPa, exceeding common tensile strength of rocks. It is indicated that temperature dependence exists in stress generation behavior: the higher the temperature, the higher stress are generated and the stronger stress relaxation are observed after a peak stress. We also showed that this behavior can be explained by competition between reaction and deformation strain rate. This result was consistent to a certain extent with the result of $CaSO_4 \cdot 1/2H_2O$–H_2O system reported by Skarbek et al. (2018).

In this report, we aimed to clarify the influence of reaction and deformation rate on stress generation and the permeability development during volumetric expansion reaction. We conducted two experiments, the stress measurement experiments and the permeability experiments. In the former, experiments were conducted using pellets (ϕ=45–55%) of MgO powder as a starting material under conditions of approximately 80 to 120 ˚C and fluid pressure of approximately 0.100 MPa. The developments of reaction-induced stress were measured as a function of temperature. In the same experimental systems, the reaction and deformation rate were determined by measuring the strain and the reaction rate. In the latter, the experiment was conducted using the sintered MgO as a starting material under the conditions of approximately 100 to 300 ˚C, a fluid pressure of 0 to 10 MPa, and a confining pressure of 0 to 50 MPa. The permeability developments were measured under conditions of various temperatures, confining pressures and fluid pressures. From the results, we consider the relation between stress, fracturing and permeability and discuss the modes of rock fracturing and fluid transfer enhancement during hydration

©2019. Japan Geoscience Union. All Right Reserved.

reactions in the crust.

Keywords: Reaction-induced stress

©2019. Japan Geoscience Union. All Right Reserved.

Crystal orientation analysis of olivine in ultra-mylonite using TKD method: progress in spatial resolution from EBSD

*Yohei Igami[1], Katsuyoshi Michibayashi[2], Kakihata Yuki[2], Yui Kouketsu[2]

1. Institute of Materials and Systems for Sustainability, Nagoya University, 2. Graduate School of Environmental Studies, Nagoya University

Mantle, which is the dominant component consisting of the earth making up 80 %, is the key to understanding material cycle and/or formation history of the earth. The uppermost part of the mantle is composed of peridotite which is aggregate mostly of olivine [$(Mg,Fe)_2SiO_4$] grains. Olivine has orthorhombic crystal system and its mechanical property is anisotropic. Thus the olivine polycrystalline in peridotite shows various crystal-preferred orientation (CPO) patterns formed by share deformation processes (Karato et al., 2008). Therefore, the CPO pattern can be an indicator of deformation environment and is also used as a key parameter to estimate seismic anisotropy. Thus, the CPO is very important for tectonic geology.

To evaluate CPO of olivine, Scanning Electron Microscope equipped with Electron BackScatter Diffraction detector (SEM-EBSD) is widely used. The SEM-EBSD is a method to analyze crystal orientation using the Kikuchi diffraction pattern formed by the interaction between scattered electrons and lattice planes of sample surface. Recently, improvements of high-speed detectors and userfriendly computer programs have enabled automatic, rapid and easy EBSD mapping. Using the method, olivine CPO patterns in peridotite of various localities have been studied. However, effect of fine grains (<1 μm in diameter) might have been overlooked in such studies, because it is difficult to obtain clear EBSD pattern from sub-micrometric mineral grains.

On the other hand, it was reported that the Kikuchi pattern can be obtained also by transmitted electrons through thin film (~100 nm) using SEM (Keller and Geiss, 2011). This method, which is called transmission EBSD (t-EBSD) or transmission Kikuchi diffraction (TKD), can restrict area in which electrons are scattered and improve spatial resolution even by the conventional SEM-EBSD system. In this study, therefore, we tried CPO analysis for ultra-mylonite using the TKD, to investigate usefulness of this method for tectonic geology.

The analyzed sample is an ultra-mylonite from Marion Transform fault by PROTEA5 cruise. The sample contains amphibole and olivine as porphyroclasts and fine-grained matrix, with a small amount of orthopyroxene and spinel (Kakihata et al., 2018, AGU). We obtained EBSD map from petrographic-thin section of this sample, and then an ultra-thin section for TKD was made using a focused ion beam apparatus(FIB, HITACHI FB2100). Finally, TKD map of the ultra-thin section was obtained. For both of the EBSD and TKD analyses, the same SEM-EBSD system (HITACH, S-3400N + OXFORD Instruments, NordlysNano) was used.

As the result, we successfully obtained TKD map dataset, in which patterns are indexed even at the region over boundaries between sub-micrometric olivine grains. This TKD map which was obtained by W-filament gun SEM is clearer than the FESEM-EBSD map we obtained from the same sample. The TKD map dataset was able to be processed by the same software with EBSD (following configuration parameters suggested by Miyake et al., 2016, JAMS). The processed TKD map of olivine displays CPO of *b* -axis perpendicular to shear plane. In addition, spatial distribution of sub-grain boundaries and irregular shaped grains is well displayed. TKD requires much less time and labor than TEM analyses in such orientation analysis throughout the ultra-thin section, although TEM is of course much better in spatial resolution or detailed crystallographic/chemical analyses. The TKD should be useful as a pre-analysis before the detailed TEM analyses for polycristalline samples such as ultra-mylonite. Application of the

©2019. Japan Geoscience Union. All Right Reserved.

TKD method may reveal various effects of fine grains in tectonic geology.

Keywords: EBSD, TKD, crystal preferred orientation, ultra-mylonite, peridotite

©2019. Japan Geoscience Union. All Right Reserved.

Elucidation of effective diffusion coefficient along grain boundaries by hydrothermal experiment using low porosity rocks

*Naoki Sugisawa[1], Masaoki Uno[1], Noriyoshi Tsuchiya[1]

1. Graduate school of environmental studies Tohoku university

Elucidation of the time scale of the fluid activity recorded in the rock is important for understanding the actual condition of fluid activity in the crust. In recent years, it has become possible to estimate time-scale of fluid activity in the crust from isotopes and element concentration profile of natural metamorphic rocks. (e.g.John et al.,2012) To estimate the time-scale, the effective diffusion coefficient (Deff) is important as an indicator of diffusion via grain boundary fluid. It is known that the effective diffusion coefficient depends on the porosity (Φ) of rock and time due to grain boundary diffusion. (e.g.Boving and Grathwohl, 2001) The effective diffusion coefficient is conventionally substituted by the product of self-diffusion coefficient (D_{self}) and porosity ($D_{self}\Phi^{x}$). However, the effective diffusion coefficient varies depending on the power factor (x) of the porosity, and the estimated timescales depend significantly on the power factor (x). Therefore, we clarified the relationship between porosity vs effective diffusion coefficient and confining pressure vs effective diffusion coefficient using hydrothermal experiment under crustal condition with various low porosity granite. In this paper, we mention the following two experiments as the first step : (1) Fluorapatite (F-Ap) substitution reaction (2) Determination of effective diffusion coefficient using low porosity hydroxyapatite sintered body (OH-Ap).

In this study, natural F-Ap from Mexico and OH-Ap (Wako Pure Chemical corporation) were used as starting materials. In experiment (1), first, natural F-Ap was cut in the c-axis direction. And it was put in the gold tube with 0.0006-6 M HCl or 0.01-1 M NaOH two types solution. After that gold tube was putted in the batch type hydrothermal equipment and conducted hydrothermal experiment under 400 ℃, 50 MPa for168 hour. In experiment (2), OH-Ap powder was pressed under 200 MPa for 30 minutes and then the porosity was varied by sintering at deference temperature from 1500 ℃ to 1200 ℃. After cooling, the porosity was measured by the wet method. NaF solution saturated at room temperature and OH-Ap sintered body was added to the same apparatus as above and a hydrothermal experiment was conducted at 300 ℃ and 20 MPa for 168 hours. After the experiment (1) and (2), the samples were evaluated by quantitative analysis and mapping analysis with EPMA in both cases. Before the experiment, phase diagram of apatite under experimental temperature and pressure was prepared using SUPCRT92, GEMS to expect these reactions.

As a result of the hydrothermal experiment, in the experiment (1), it is suggested that the OH in F-Ap is substituted with Cl under HCl solution and the NaOH substitutes OH for F. In experiment (2), F diffusion zoning was generated along the clacks in the sintered OH-Ap, and an effective diffusion coefficient was calculated using diffusion equation. There was no apparent porosity dependency of the effective diffusion coefficient at porosities 1.68-5.83%. The effective diffusion coefficient obtained in this experiment was equivalent to the self-diffusion coefficient of fluorine multiplied by the porosity 2.26 power. ($D_{eff} = D_{self}\Phi^{x}$) (e.g. Oelkers and Helgeson, 1988) However, the porosity measured by the wet method needs to be investigated because it contains the cracks generated in making the sintered body. (e.g. mercury porosimeter)

Based on the above experimental results, it is discussed that the influence of temperature, pressure, solution condition, on substitution of monovalent halogen and hydroxyl group between apatite and fluid and relationship between porosity and effective diffusion coefficients.

©2019. Japan Geoscience Union. All Right Reserved.

References
John et al. Nature Geosience, Vol.5, July 2012, Pages 489-492 Boving and Grathwohl Journal of Contaminant Hydrology, Vol.53, 8 May 2001, Pages 85-100 Oelkers and Helgeson, Geochemica et Cosmochimica Acta, Vol.52, October 1988, 63-85

Keywords: effective diffusion coefficient, porosity, Crustal fluid

©2019. Japan Geoscience Union. All Right Reserved.

Seismic slipping events recorded in a fault gouge zone: evidence from the Nojima Fault drill holes, SW Japan

*Aiming Lin[1], Takafumi Nishiwaki[1]

1. Department of Geophysics, Graduate School of Science, Kyoto University

It is well known that large intra-continental earthquakes occur repeatedly along mature active faults and that the seismic slip may be recorded by cataclastic rocks, including fault gouge zones, that form at shallow depths in the upper crust (e.g., Lin, 2008). A fault gouge zone, bounded by a principal fault plane, is considered to represent the seismic slip zone that accommodates most of the accumulated fault displacement in the seismogenic regime. Therefore, studies of fault gouge zones along mature active faults would provide important information for reconstructing the long-term seismic faulting behavior of such faults, as well as providing new insights into the individual seismic slipping processes of active faults and their paleoseismic histories.

In the present study, we focused on the structural features of the fault gouge zone observed in drill cores acquired from nine holes that were drilled through the Nojima Fault (NF) at different depths from ~260 to 900 m at the Ogura site (Lin and Nishiwaki, 2019). Drilling investigations and structural analyses of drill cores reveal that a ~60 m wide fault damage zone containing a 10–30 cm thick fault gouge zone developed along the Nojima Fault (NF), on which the 1995 M_w 6.9 Kobe (Japan) earthquake occurred. The fault gouge zone was observed at depths of ~260 to 900 m in nine drill holes that intersected the NF. Our findings show that i) the fault gouge zone observed at different depths in the nine drill cores is the principal fault slip zone of the NF, ii) the fault gouge zone can be divided into 11–20 thin layers of different color, and iii) the individually colored layers contain different color breccias of fault gouge that are offset and/or cut by cracks and crack-filled calcite and quartz veinlets. Our results reveal that the fault gouge zone probably records more than 11–20 paleoseismic faulting events along the NF during the late Pleistocene-Holocene.

References:

1) Lin, A., 2008. Fossil Earthquakes: The Formation and Preservation of Pseudotachylytes. Springer, Berlin, 348p (ISBN 978-3-540-74235-7).
2) Lin, A., Nishiwaki, T., 2019. Repeated seismic slipping events recorded in a fault gouge zone: evidence from the Nojima Fault drill holes, SW Japan. Geophys. Res. Lett., doi: 10.1029/2019GL081927.

Keywords: Fault gouge zone, Nojima Fault, Seismic slipping event

©2019. Japan Geoscience Union. All Right Reserved.

Evolution of fluid chemistry during basalt-water and basalt-seawater interactions revealed by hydrothermal flow-through experiments

*Yusuke Netsu[1], Atsushi Okamoto[1], Nobuo Hirano[1], Masaoki Uno[1], Noriyoshi Tsuchiya[1]

1. Tohoku University, Graduate School of Environment Studies

Recently, several deep drilling projects for exploiting the supercritical geothermal reservoirs in the world. For example, in 2017, the Island Deep Drilling Project (IDDP-2) reached 427 ˚C and 34 MPa, which exceeds the critical point of seawater. The drillcores revealed that the intense water-rock interaction under greenschist to amphibolite facies metamorphism. Although such deep drilling provides us direct information of active metamorphic processes. however, it is still unclear whether conventional petrological analyses could apply to reaction processes in open systems at high temperature hydrothermal alteration at seafloor. There have been few experiment studies on the water-rock interaction under supercritical conditions with some exceptions (Yardley et al. 2014).

In this study, we conducted hydrothermal flow-through experiments on the basalt-H_2O, basalt-NaCl.aq, basalt-seawater systems under the sub or supercritical conditions. The temperature and pressure were set to be 400 ˚C and 37 - 39 MPa, and the input solutions was flowed at constant flow rate (0.1 ml/min) for 1 –6 days. We placed a powder of MORB (Island, 250-500 μm), which is composed of plagioclase (Pl), olivine (Ol) phenocrysts and clinopyroxnene (Cpx), Pl groundmass, with lessor amount of volcanic glass, in a Ti inner tube (L=275 mm, I.D.= 4.35 mm). During the run, the solution was continuously pumped into the reaction vessel, and the output solution was collected every few hours. The concentration of Si, Al, Ti, Fe, Mg, Ca, Na, and K in the output solution was analyzed by ICP-AES.

In the basalt-H_2O experiment, the products varied with distance from the inlet. At the inlet and middle of tube, Ca-rich Pl (An# 0.98) formed around primary Pl grain with producing abundant pores, whereas chlorite was dominantly formed around Ol and Pl at the middle to outlet of inner tube. The solution chemistry evolves with time: Si concentration was initially high and then decreases toward the steady state. pH, Na and Al increases with decreasing Si, whereas the Ca, Mg and Fe concentrations were low. These features indicate the dissolution of volcanic glass at the initial stage, and then the solution chemistry was controlled by preferential leaching of albite component of plagioclase.

In the basalt-saline water (2.5 wt% of NaCl) experiment, we observed pH rises accompanying the decrease Si concentration, indicating the leaching of Si and dissolution of Pl similar to the basalt- H_2O experiment. One of the large differences between the two experiments was the extremely high Na concentration of saline water, resulting in the leaching of Ca (Ca concentration of the output solution was 40 to 80 times that of H_2O experiment), or breakdown of Ca-bearing minerals. In the basalt reaction with artificial seawater, which contains a lot of Mg^{2+}, SO_4^{2-}, CO_3^{2-} ions, revealed that the significant amount of precipitation of sulfate minerals occurred in the pre-heating parts of the vessel (before pass through the fluid reached the basalt sand), and that chlorite was formed throughout the reaction tube, which clogged the reaction vessel in a day. In contrast to the H_2O and saline water experiments, pH decreased to 3. In spite that we conducted the experiments with the same rock sample (basalt sand) and the same P-T conditions, the products and solubitions after the water-rock interaction were quite different in response to the input solutions, probably because the open system, in which new fluids are continuously supplied, is never rock-buffered. We will analyse the complicated reaction systems which control te evolution of solutions and minerals, based on the analyses of speciation of aqueous species, saturation of minerals

©2019. Japan Geoscience Union. All Right Reserved.

and variation of replacement textures of minerals.

Reference
Yardley, B. W., Harlov, D. E., & Heinrich, W. (2010). Rates of retrograde metamorphism and their implications for crustal rheology. Geofluids, 10(1-2), 234-240.

Keywords: Fluid-rock interaction, Flow through experiment, Supercritical condition, Basalt-seawater system, Garnet synthesis

©2019. Japan Geoscience Union. All Right Reserved.

3D microstructural analyses of fault rocks using CT and μCT scanning techniques

*Bingcheng Liu[1], Aiming Lin[1], Takafumi Nishiwaki[1]

1. Kyoto University

Meso- and microstructures of fault rocks including fault gouge developed in the active fault shear zone can reflect the deformation processes of fault motion and faulting mechanisms (Lin, 2008). Therefore, the study on structural features of fault rocks may provide new insights for understanding the nature of active faults. However, it is difficult to understand the spatial variation of microstructures of fault core zone based on traditional methods using two dimensional images under naked-eye and microscopic observations. Accordingly, it is necessary to develop an analytical method for three dimension (3D) analysis for understanding the spatial variation and internal structures of fault core zone. Computed tomography (CT) apparatus with micro-CT (μCT) accessories is a powerful tool which allows non-destructive 3D X-ray imaging and analyzing the spatial and internal structures within non-transparent objects, mainly determined by variations in density, chemical composition (effective atomic number) as well as thickness (Cnudde, 2005).

In this study, the CT and μCT imaging techniques are exploited to observe the 3D internal structures of a series of representative fault rocks: 1) pseudotachylytes of different origins (melting and crushing), and 2) cataclasitic rocks including fault gouge, fault breccia and cataclasite, by utilizing two types of scanning apparatuses (Bruker microCT, 2014): 1) μCT flat panel (FP), and 2) μCT charge coupled device (CCD). The samples of pseudotachylyte are from Fuyun, NW China (Lin, 1994), Ohsumi, Japan (Fabbri et al., 2000), and Musgrave Mt, Australia (Lin et al., 2005), respectively. The samples of fault gouge were acquired from two typical active fault zones in Japan: The Nojima Fault and Arima-Takatsuki Tectonic Line, SW Japan (Lin and Nishiwaki, 2019). The FP analysis shows that 1) the flow structures within the melting-origin pseudotachylytes are denoted by parallel colored glassy matrix layers with numerous rounded quartz clasts and quartz-filled amygdules which are oriented along the flow layers, and 2) chilled margins are characterized by fine-grained microlites orientated parallel to the margins. The 3D scanning images show that the layering structures developed within the fault gouge and fault breccia zones which are marked by sharp colored boundaries, oriented clasts and fine-grained matrixes. Our results demonstrate that 1) the CCD imaging makes it possible to observe sub-micron and even nano-scale 3D microsturctures fault rocks without destruction, and 2) μCT imaging can be further combined with traditional methods (such as optical microscope and SEM observation) to determine the spatial variations for both the meso- and microstructures and chemical compositions of fault rocks.

References:

1). Lin, A., 2008. Fossil Earthquakes: The Formation and Preservation of Pseudotachylytes. Springer, Berlin, 348p (ISBN 978-3-540-74235-7).

2). Veerle Cnudde, 2005. Exploring the potential of X-ray tomography as a new non-destructive research tool in conservation studies of natural building stones. Diss. Ghent University.

©2019. Japan Geoscience Union. All Right Reserved.

3). Bruker microCT. SkyScan 2211 User Manual, 2014.

4). Lin, A., 1994. Jour. Struct. Geol., 16, 71-83.

5). Fabbri, O., Lin, A., Totsushige, H., 2000. Jour. Struct. Geol., 22, 1015-1026.

6). Lin et al., 2005. Tectonophysics, 402, 21-35.

7). Lin, A., Nishiwaki,T., 2019. Geophy. Res. Lett., 46, DOI: 10.1029/2019GL081927.

Keywords: computed tomography, fault rocks, microstructure

©2019. Japan Geoscience Union. All Right Reserved.

Dissolution kinetics of forsterite olivine at >200 ˚C: implication for the kinetics of serpentinization.

*Ryosuke Oyanagi[1], Tatsu Kuwatani[1], Katsuhiko Suzuki[1]

1. Japan Agency for Marine-Earth Science and Technology

Serpentinization (hydration of mantle peridotite) gives significant changes to both chemical and physical properties of the oceanic lithosphere. Several studies suggested that the rate of serpentinization is maximized at 250-300˚C, and the rate-limiting process of serpentinization is the dissolution of primary mineral (e.g., Malvoisin et al., 2012). Therefore, the dissolution rate of olivine at 250-300˚C is consequently a critical parameter to understand the progress of serpentinization in the oceanic lithosphere. However, the olivine dissolution rates at > 150˚C have never been measured (Rimstidt et al. 2012), and the olivine dissolution rate extrapolatory calculated at 300˚C was inconsistent with the olivine serpentinization kinetics (Malvoisin et al., 2012). Towards the improved understanding of serpentinization kinetics, measuring dissolution rates of olivine as a function of solution composition and the temperature is required.

In this study, the dissolution rate of natural olivine ($(Mg_{0.91}, Fe_{0.09})_2SiO_4$) was measured at 200-400 ˚C and 50 MPa using a flow-through reactor (Suzuki et al., 2015). A 0.5 mol/kg NaCl solution was introduced at a constant rate of 2.0 mL/min during experiments. A preliminary experiment revealed that steady-state dissolution rate of olivine at 200 ˚C and far-from-equilibrium conditions was ca. -4.8 [mol/m^2/s] in log units. The obtained dissolution rate was consistent with the extrapolated dissolution rate (log_{10}(Rate) = ca. -4.72 [mol/m^2/s]), which was extrapolated from their pH-temperature dependence at 25-150 ˚C (Rimstidt et al., 2012). Based on dependences of temperature, salinity, and ΔG on dissolution rate, the timescales on hydrothermal alteration of peridotite will be discussed.

References

Malvoisin B, Brunet F, Carlut J, et al (2012) Serpentinization of oceanic peridotites: 2. Kinetics and processes of San Carlos olivine hydrothermal alteration. J Geophys Res Solid Earth 117:1–13. doi: 10.1029/2011JB008842

Rimstidt JD, Brantley SL, Olsen AA (2012) Systematic review of forsterite dissolution rate data. Geochim Cosmochim Acta 99:159–178. doi: 10.1016/j.gca.2012.09.019

Suzuki K, Kato S, Shibuya T, et al (2015) Development of Hydrothermal and Frictional Experimental Systems to Simulate Sub-seafloor Water–Rock–Microbe Interactions. In: Subseafloor Biosphere Linked to Hydrothermal Systems. Springer Japan, Tokyo, pp 71–85

Keywords: Serpentine, Reaction rate, Olivine, Dissolution rate

©2019. Japan Geoscience Union. All Right Reserved.

[J] Oral | S (Solid Earth Sciences)：S-MP Mineralogy & Petrology

Wed. May 29, 2019 3:30 PM - 5:00 PM JST | Wed. May 29, 2019 6:30 AM - 8:00 AM UTC | A08 TOKYO BAY MAKUHARI HALL

[S-MP32] Deformed rocks, Metamorphic rocks and Tectonics

convener:Yumiko Harigane(Geological Survey of Japan, National Institute of Advanced Industrial Science and Technology (AIST)), Yoshihiro Nakamura(Geological Survey of Japan, National Institute of Advanced Industrial Science and Technology), Chairperson:Shunsuke Endo(島根大学 総合理工学部 地球科学科), Ryosuke Oyanagi(国立研究開発法人 海洋研究開発機構 地球内部物質循環研究分野)

We invite all researchers who aim to understand the dynamics of the earth's crust and mantle at the plate boundaries, to discuss the latest results from various viewpoints. The scope will include contributions through petrology and structural geology as well as various techniques including rheology and transformation of heat and mass.

3:30 PM - 3:45 PM JST | 6:30 AM - 6:45 AM UTC

[SMP32-13] Early Paleozoic subduction-zone metamorphism in Japan: A geochronological reappraisal of Kitomyo Schists

*Shota Matsunaga [1], Tatsuki Tsujimori[1], Atsushi MIYASHITA[2], Shogo Aoki[3], Kazumasa Aoki[3] (1.Tohoku University, 2.Seikei University, 3. Okayama University of Science)

3:45 PM - 4:00 PM JST | 6:45 AM - 7:00 AM UTC

[SMP32-14] Dating a 'princess': U–Pb age determination of 'nunakawaite' (strontio-orthojoaquinite)

*Tatsuki Tsujimori[1], Tomomi Hara[1], Yuzuki Shinji[1], Tomohiro Ishizaka[1], Hiroshi Miyajima[2], Jun-Ichi Kimura[3], Shogo Aoki[4], Kazumasa Aoki[4] (1.Tohoku University, 2.Fossa Magna Museum, 3.JAMSTEC, 4.Okayama University of Science)

4:00 PM - 4:15 PM JST | 7:00 AM - 7:15 AM UTC

[SMP32-15] Modeling of the progressive evolution of subducting slab composition by sparse modeling

*Kenta Yoshida[1], Tatsu Kuwatani[1,2], Kenta Ueki[1], Ryosuke Oyanagi[1], Shotaro Akaho[3] (1.Japan Agency for Marine-earth Science and Technology (JAMSTEC), 2.PRESTO, Japan Science and Technology Agency, 3.National Institute of Advanced Industrial Science and Technology (AIST))

4:15 PM - 4:30 PM JST | 7:15 AM - 7:30 AM UTC

[SMP32-16] Bayesian statistical evaluation method for detrital zircon geochronology: Applications

*Tan Furukawa[1], Tatsuki Tsujimori[2], Shogo Aoki[3], Kazumasa Aoki[4] (1.Tohoku University, Department of Earth Science, 2.Tohoku University, 3.Faculty of Biosphere-Geosphere Science, Okayama University of Science, 4.Department of Applied Science Okayama University of Science)

4:30 PM - 4:45 PM JST | 7:30 AM - 7:45 AM UTC

[SMP32-17] 3D structural analysis using X-ray Computed Tomography technique: a case study for fault rocks from the Nojima Fault, southwest Japan

*Takafumi Nishiwaki[1], Aiming Lin[1], Bingcheng Liu[1] (1.Kyoto University)

4:45 PM - 5:00 PM JST | 7:45 AM - 8:00 AM UTC

[SMP32-18] High- and low-stress subduction zones recognized in the rock record

*Kazuhiko Ishii[1], Simon Richard Wallis[2] (1.Department of Physical Science, Graduate School of Sciences, Osaka Prefecture University, 2.Department of Earth and Planetary Science, Faculty of Science, The University of Tokyo)

Early Paleozoic subduction-zone metamorphism in Japan: A geochronological reappraisal of Kitomyo Schists

*Shota Matsunaga [1], Tatsuki Tsujimori[1], Atsushi MIYASHITA[2], Shogo Aoki[3], Kazumasa Aoki[3]

1. Tohoku University, 2. Seikei University, 3. Okayama University of Science

Early Paleozoic subduction-related high-pressure metamorphic rocks have been reported from the Kitomyo Schists of the Kurosegawa Belt (Maruyama and Ueda 1975 [doi: 10.2465/ganko1941.70.47]) and the Fuko Pass Metacumulates (FPMC) of the Oeyama Belt (Tsujimori and Liou 2004 [doi: 10.1111/j.1525-1314.2004.00515.x]). In order better to understand the earliest subduction zone record of the ‘proto-Japan’, we revisited the Kitomyo Schists petrologically and gecohronologically. The metasedimentary sample is a well-deformed, quartzo-feldspathic mica schist, with the mineral assemblage of garnet + clinozoisite + phengite (Si p.f.u. = 3.3–3.5) + quartz + albite. Euhedral grains show distinct prograde chemical zoning in spessartine decrease toward the rims. The lack of biotite, oligoclase and paragonite indicate that the schist underwent a HP intermediate type metamorphism. The metabasaltic rock is a well-deformed, amphibolite. Although the amphibolite was overprinted severely at a greenschist-facies condition, relict barroisitic amphibole [B]Na (Na in the B-site) = ~0.69 and rutile, indicating HP metamorphism. LA-ICPQMS and HR-SIMS zircon geochronology yielded 445.5 ±3 Ma for the timing of HP intermediate type metamorphism of the Kitomyo Schists. Metamorphic zircon in metasedimentary sample is characterized by lower U (117–132 μg/g) and lower Th (34–143 μg/g) than detrital magmatic zircons. Our reapproval suggests that the Kitomyo Schists formed in an Early Paleozoic subduction zone with geothermal gradient in the order of ~15°C/km. Such a relatively high geothermal gradient in the subduction zone has produced the HP intermediate type metamorphism. The earliest subduction record in the ‘proto-Japan’ was not ‘cool’ enough to produce blueschist.

Keywords: metamorphic zircon, zircon geochronology

©2019. Japan Geoscience Union. All Right Reserved.

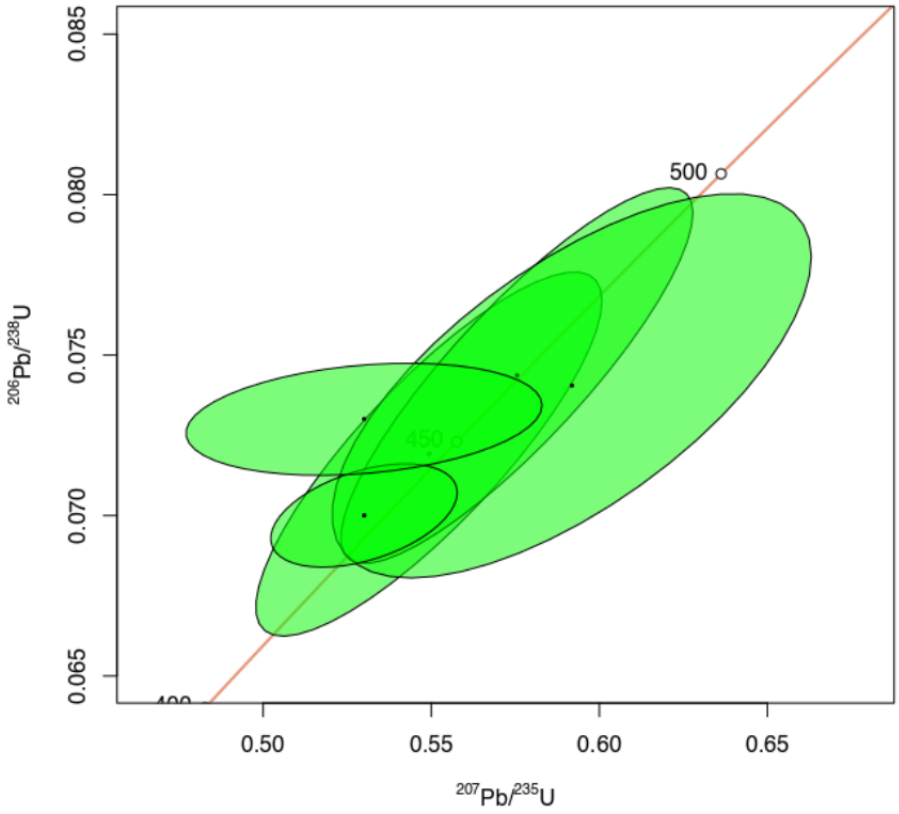

LA-ICPQMS and HR-SIMS U-Pb analysis of metamorphic zircons. Data are plotted on Concordia diagram

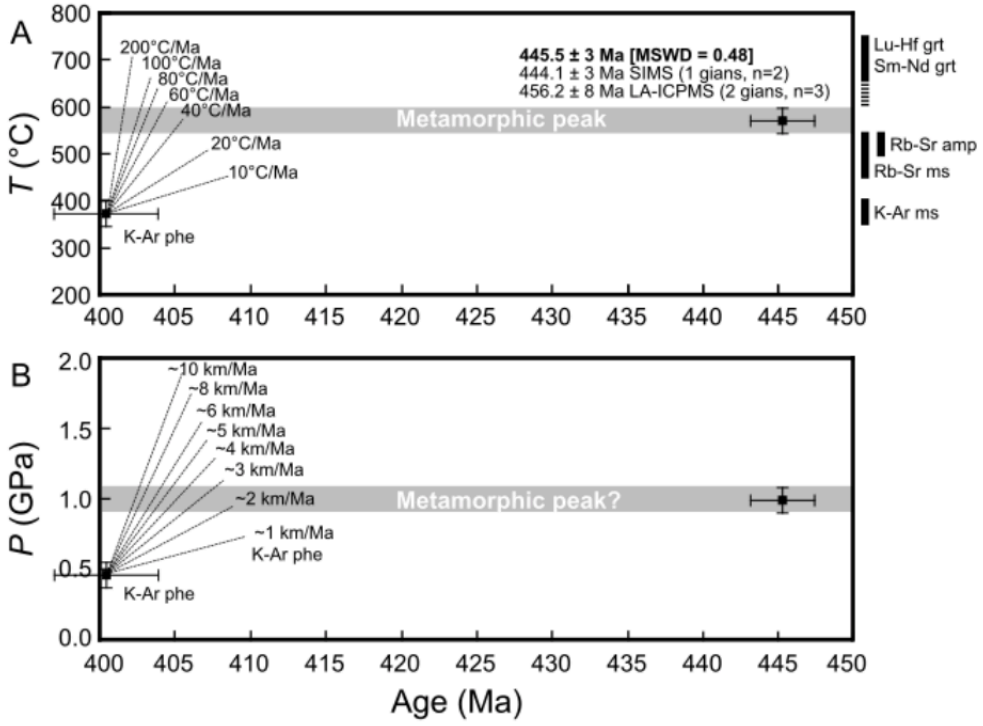

P-T condition of metamorphism

©2019. Japan Geoscience Union. All Right Reserved.

©2019. Japan Geoscience Union. All Right Reserved.

Dating a 'princess': U–Pb age determination of 'nunakawaite' (strontio-orthojoaquinite)

*Tatsuki Tsujimori[1], Tomomi Hara[1], Yuzuki Shinji[1], Tomohiro Ishizaka[1], Hiroshi Miyajima[2], Jun-Ichi Kimura[3], Shogo Aoki[4], Kazumasa Aoki[4]

1. Tohoku University, 2. Fossa Magna Museum, 3. JAMSTEC, 4. Okayama University of Science

'Nunakawaite' (strontiojoaquinite) is an orthorhombic variety of strontiojoaquinite [$Sr_2Ba_2(Na,Fe)_2Ti_2[Si_4O_{12}]_2O_2(O,OH)_2 \cdot H_2O$]; it is a rare joaquinite group mineral that is only found in a riebeckite-bearing albitite in the serpentinite-matrix mélange of the Itoigawa–Omi area. The mineral was originally named after 'Princess Nunakawa' (*nunakawa hime*) in the Japanese Shinto mythology '*Kojiki*'.

'Nunakawaite' is characterized by remarkably high Ba, Zr, Nb, Zn, LREEs, MREEs, and enriched in U (35.8–721 $\mu g \cdot g^{-1}$), Pb (2.2–31 $\mu g \cdot g^{-1}$), and Th (7.42–2365 $\mu g \cdot g^{-1}$). LA-ICPMS analyses show highly variable U/Pb ($^{238}U/^{206}Pb$ = 9.245–68.98) and Pb ($^{207}Pb/^{206}Pb$ = 0.0758–0.756) isotope ratios, and the scattered trend define an isochron line with a lower intercept at 89.19 ±1.07 Ma. The 'nunakawaite' U–Pb age confirms that the 'nunakawaite'-hosted riebeckite-bearing albitite formed at late Cretaceous. This implies that the serpentinite-matrix mélange unit with early Paleozoic jadeitites and late Paleozoic blueschist, eclogite and amphibolite was reactivated by a significantly younger tectonic event.

In-situ Sr-Pb isotope analyses show two different isotope trends between Sr-rich accessory minerals in riebeckite-bearing albitite ('nunakawaite' and ohmilite) and those in jadeitite (itoigawaite, stronalsite, vesvianite, Sr-rich epidote). The Sr-Pb isotopes also support the idea that the riebeckite-bearing albitite formed by a fluid-induced metasomatic event different from the jadeitite-forming metasomatism at early Paleozoic. The formation of riebeckite-bearing albitite at ~90 Ma is coeval with late Cretaceous granitic intrusion of the Omi area (youngest zircon U–Pb: 90.8 ±1.1 Ma: Nagamori et al. 2018). The granitic intrusion might have acted an important role in the formation of 'nunakawaite'. In other words, reactivation of metasomatic mineralization in the Paleozoic serpentinite mélange is recorded in the Cretaceous riebeckite-bearing albitite.

Keywords: 'nunakawaite' (strontio-orthojoaquinite), U–Pb dating, metasomatism, serpentinite mélange, Itoigawa–Omi area

©2019. Japan Geoscience Union. All Right Reserved.

Modeling of the progressive evolution of subducting slab composition by sparse modeling

*Kenta Yoshida[1], Tatsu Kuwatani[1,2], Kenta Ueki[1], Ryosuke Oyanagi[1], Shotaro Akaho[3]

1. Japan Agency for Marine-earth Science and Technology (JAMSTEC), 2. PRESTO, Japan Science and Technology Agency, 3. National Institute of Advanced Industrial Science and Technology (AIST)

The progressive evolution of subducting rocks under intermediate high-*P/T* type metamorphism is modelled by using thermodynamic calculation combined with mass-transfer calculation. On the basis of non-negative matrix factorization analysis, Yoshida et al. (2018 J. Metamorph. Geol.) pointed out the evolutional change of the composition of metapelites collected from the Sanbagawa metamorphic belt. The evolutional change can be approximated as the increase of stoichiometric garnet, which may have resulted from the fixation of garnet and the effusion of other components by high-temperature aqueous fluids. To model this progressive compositional evolution more quantitatively, we performed mass-transfer calculation to determine a specific reference frame of the evolutionally-changing whole-rock compositions. Generally, mass-transfer calculation defines one or multiple immobile elements on the basis of petrographic observation, common knowledge of mobility of elements, deviation of the concentration among the dataset used, and so on (e.g., Baumgartner and Olsen, 1995; Ague 2011). The Data-driven Isocon analysis, newly proposed method applying a sparse modeling approach, is designed to determine reference frame of mass-transfer being mostly free from the arbitrariness to choose immobile element(s), and also applicable for the case where no elements can be assumed as a completely immobile element (Kuwatani et al., 2019 in this meeting M-GI33). This new method defines a reference frame of a series of dataset on the basis of the data structure, finding a least-mobile (not necessary to be “immobile”) element. To figure out the mass gain/loss behavior of the subducting metapelites, applying the Data-driven Isocon analysis is suitable because (1) the dataset show weak but mostly monotonous compositional trend (Yoshida et al., 2018); (2) it is difficult to assume a specific immobile element on the basis of the petrographic observation provided previously. We performed the Data-driven Isocon analysis to the major component dataset of the metapelites collected from the Sanbagawa metamorphic belt of the central Shikoku (Goto et al., 1996). The Isocon analysis indicated a total of 6% of mass loss during the progressive metamorphism, which is characterized by the decrease of Na and Si and the increase of divalent cations assuming Al as the least-mobile element. This result indicated that the evolutional change of the Sanbagawa metapelites is characterized not only by mass loss possibly because of the high-temperature fluid, but also some addition of mafic components. Among the high metamorphic grade zone (> garnet zone) of the relevant area, common existence of the ultramafic blocks are observed, suggesting the previous contact with the wedge mantle (Aoya et al., 2013). The addition of the mafic components may have originated from the material transfer from the ultramafic bodies. On the basis of actual mass loss obtained from the Isocon analysis and the thermodynamic modelling, the water production rate can be calculated (e.g., Dragovic et al., 2018). From the chlorite zone (approximately 350 degC, 0.5 GPa) to the oligoclase-biotite zone (approximately 610 degC, 1.0 GPa), water production rate of 64 kg/m3/Myr, being consistent with the previously indicated values (6-90 kg/m3/Myr: Peacock, 1989; 5-20 kg/m3/Myr: Lyubetskaya and Ague, 2009), was obtained.

Keywords: Sanbagawa metamorphic belt, subduction zone, sparse modeling, deep fluid

©2019. Japan Geoscience Union. All Right Reserved.

Bayesian statistical evaluation method for detrital zircon geochronology: Applications

*Tan Furukawa[1], Tatsuki Tsujimori[2], Shogo Aoki[3], Kazumasa Aoki[4]

1. Tohoku University, Department of Earth Science, 2. Tohoku University, 3. Faculty of Biosphere-Geosphere Science, Okayama University of Science, 4. Department of Applied Science Okayama University of Science

Detrital zircon geochoronology is an essential method for determining the provenance and maximum depositional age of sedimentary and metamorphic strata. The age distribution is conventionally evaluated by using histograms. However the lack of the statistical verification of the histograms can cause misunderstanding of data. In order to overcome the raised statistical issues, we established new statistical evaluation method to evaluate distribution for detrital zircon ages, based on Bayesian Statistics (Furukawa and Tsujimori, 2019 JpGU, session M-GI33). As the application of our new statistical evaluation method, LA-ICPMS U-Pb dating for detrital zircon separates from the Carboniferous lawsonite-bearing metagreywacke of the Osayama serpentinite mélange (OSM) and the Cretaceous arkose sandstone of the Akaiwa Formation (AFS), Tetori Group was conducted.

The OSM of the Renge Belt tectonically overlies the pre-Triassic geotectonic units of the Chugoku Mountains (e.g., Tsujimori 1997 Min. Mag.; Tsujimori and Itaya 1999 IAR). The geological and lithological features are similar to those of late Paleozoic blueschist-bearing serpentinite mélange units of the Kurosegawa Belt in Shikoku, Kyushu and Kii Peninsula. Our new data shows that the OSM zircons show at least bimodal age distributions at ~500 Ma and ~1,100 Ma with 95% certainty; the group of the oldest concordant ages reaches 3,300 Ma and the youngest concordant age was 412 Ma.Comparison with existing data in the literatures (e.g. metasediments in the Kii Peninsula: Yoshimoto et al. 2013 JMPS), our Bayesian-based statistical evaluation shows a strong similarity.

We also applied our new evaluation method to the Tetori Group sandstones. The youngest grain yields 187 Ma, and the oldest concordant age was 2,940 Ma. Our evaluation found statistical 'discrepancy' with more than 90% certainty between our AFS data and the existing data of the Itsuki Formation (Kawagoe et al., 2012 Mem. FPDM), which stratigraphically occupy higher portion of the AFS and unconformably overlies the AFS. Throughout the two applications, we introduce how our new statistical evaluation works and its advantages in geological sciences.

Keywords: Bayesian statistics, detrital zircon geochoronology

©2019. Japan Geoscience Union. All Right Reserved.

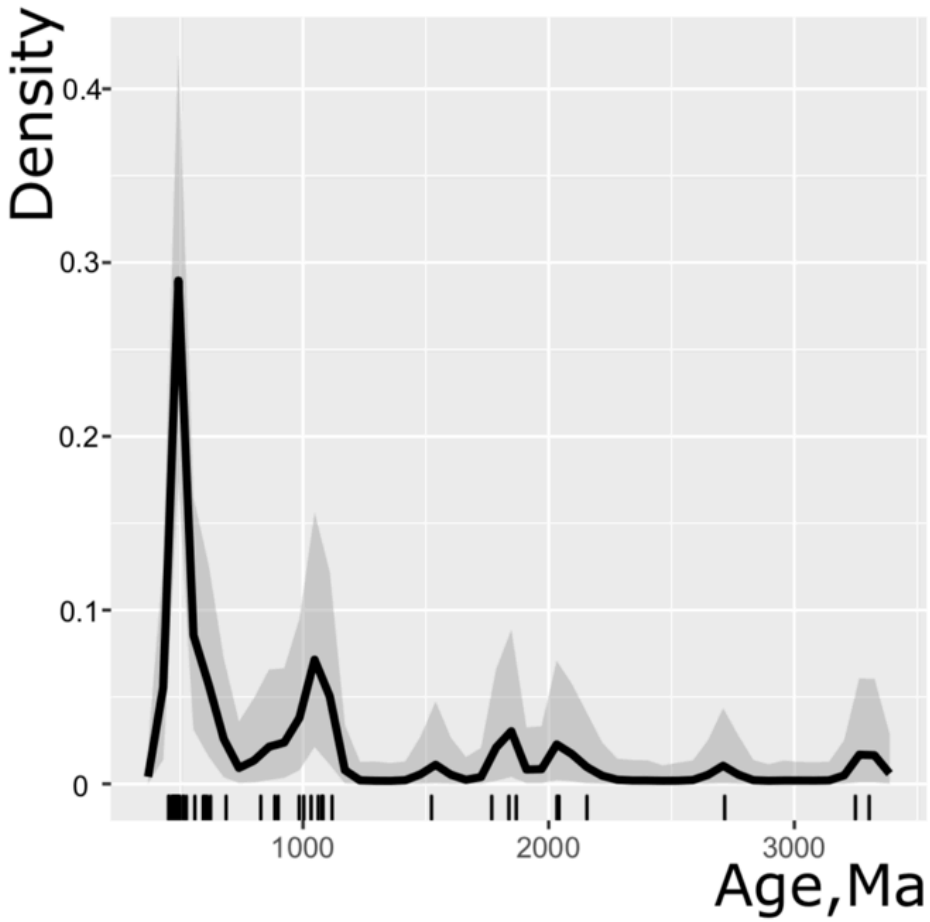

The distribution of OSM detrital zircons and its 95% credible interval

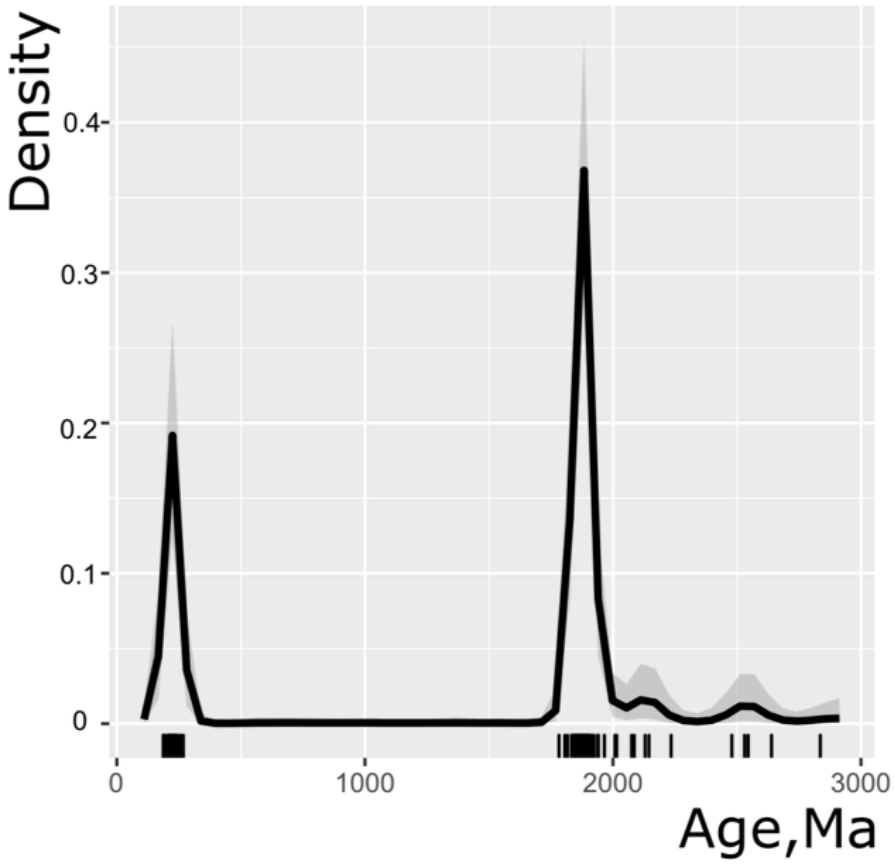

©2019. Japan Geoscience Union. All Right Reserved.

©2019. Japan Geoscience Union. All Right Reserved.

3D structural analysis using X-ray Computed Tomography technique: a case study for fault rocks from the Nojima Fault, southwest Japan

*Takafumi Nishiwaki[1], Aiming Lin[1], Bingcheng Liu[1]

1. Kyoto University

Fault rock structures in active fault shear zone can contain important information of seismic slip mechanism (e.g. Lin et al, 2013; Lin and Nishiwaki, 2019). The micro- to macro-structural characteristics of fault rocks formed pass entirely throughout faulting periods, resulting in a broad suite of deformation processes being recorded by deformation structures and textures in spatial within the fault zone (Lin, 2008). Therefore, to understand the spatial variation of meso- and microstructures of fault shear zones, it is important to analyze the three dimensional (3D) images of fault rocks.
In this study, we conducted the 3D structural analysis using X-ray computed tomography (XCT) technique for the cataclastic rock samples including fault gouge obtained from the scientific drilling project "Drilling into Fault Damage Zone (DFDZ)" penetrated throughout the Nojima Fault (NF) Zone that triggered the 1995 M_w 6.9 Kobe earthquake. XCT technique is a non-destructive imaging analysis using CT-value, a function of density and chemical composition. Drilling investigations and 3D structural analyses of drill cores reveal that a ~60 m wide fault damage zone containing a 10–30 cm thick fault gouge zone developed along NF (Nishiwaki et al., 2018; Lin and Nishiwaki, 2019). The fault gouge zone consists of many different color gouge layers 1-2 mm to ~10 cm thick in both sides of the fault plane. In the gouge layer, there is foliations oriented parallel or sub-parallel to the boundaries of each gouge layer. XCT analysis shows the 3D structural features as followings: 1) the main fault plane shows a sharp boundary between two fault gouge layers and cut or offset all other fault gouge layers and fragments, 2) foliations developed within individual fault gouge layers defining the composite planer structures on the X-Z section which show a right-lateral shear sense as that inferred from the topographical and geological evidence, and 3) fine-grained materials were injected into the cataclastic rocks and formed veinlet network structures with complicated spatial variation. These results indicate that the XCT imaging technique is a powerful tool to study 3D deformational structures and textures of fault rocks combining with conventional structural analysis.
References:
1) Aiming Lin, 2008. Fossil Earthquakes: The Formation and Preservation of Pseudotachylytes. Springer, Berlin, 348p (ISBN 978-3-540-74235-7).
2) Lin, A., Yamashita, K., Tanaka, M., 2013. J. Struct. Geol., 48, 3-13. http://dx.doi.org/10.1016/j.jsg.2013.01.005.
3) Lin, A., Nishiwaki, T., 2019. Geophys. Res. Lett., doi: 10.1029/2019GL081927. https://doi.org/10.1029/ 2019GL081927.
4) Nishiwaki, T., Lin, A., Lin, W., 2018. Geophys. Res. Lett., 45, 12814-12820, https://doi.org/10.1029/2018GL079317.

Keywords: Nojima fault, fault rock, structural analysis, CT scan

©2019. Japan Geoscience Union. All Right Reserved.

High- and low-stress subduction zones recognized in the rock record

*Kazuhiko Ishii[1], Simon Richard Wallis[2]

1. Department of Physical Science, Graduate School of Sciences, Osaka Prefecture University, 2. Department of Earth and Planetary Science, Faculty of Science, The University of Tokyo

Knowledge of the frictional strength along subduction plate boundaries is an essential part of understanding the conditions necessary for plate tectonics, the processes leading to great earthquakes occur along subduction megathrusts and the thermal structure of subduction zones. The frictional strength of faults increases with depth until ductile deformation becomes dominant and is usually expressed as the ratio of shear to normal stress known as the coefficient of friction, mu or the apparent coefficient, mu', when the effects of fluid pressure are taken into account. Lamb (2006) uses force balance for forearc domains to infer mu' = 0.03-0.09 along subduction boundaries. Gao and Wang (2014) infer mu' = 0.02-0.13 based on the comparison between heat flow data and numerical modeling, while England (2018) estimates relatively uniform values mu' = 0.05-0.07 from analytical modeling of heat flow data. In addition, a global 3D thermo-mechanical model presented by Osei Tutu et al. (2018) suggests the average mu' along plate boundaries is required to be <= 0.05 to match the observed present-day plate motion and net rotation.

The published estimates of mu' for subduction boundaries are significantly lower than Byerlee's Law (mu' ~ 0.4, assuming hydrostatic fluid pressure) and closer to values published for seismic slip rates with mu' ~ 0.1 (Di Toro et al., 2011). However, estimates for different subduction zones or obtained by different methods show variations over an order of magnitude. It is desirable to obtain direct estimates of shear stresses from ancient subduction zones both as an independent test of the suggested values and because if high- and low-stress subduction zones can be identified in the ancient record then observations of the associated geology can help identify those characteristics that are responsible for differences in shear strength along subduction zone boundaries.

Thermal modelling shows that high- and low-stress subduction zones can potentially be recognized in the ancient record based on the shape of the prograde P-T path in the forearc region. For all but very young and very slowly subducting slabs, high-stress subduction can be distinguished by curved P–T paths with higher P/T gradients at greater depths. Low-stress subduction over the same domain results in straight paths.

The Cretaceous Sanbagawa belt of SW Japan records metamorphism developed as a result of rapid (20-24 cm/yr) subduction of the Izanagi plate with a slab age of around 60 Ma. The prograde P-T paths show the characteristics predicted for high-stress subduction. Comparisons with thermal modelling suggest an apparent coefficient of friction, mu', of > 0.11, and the corresponding peak shear stresses are ~60 MPa.

Prograde P–T paths and geochronological information from high grade blocks of the Franciscan Complex, USA, indicate rapid cooling during the initial 10-20 Myr subduction with low mu' <= 0.02.

P–T paths in subduction-type metamorphic belts have the potential to be used as paleo stress indicators. Examining differences between high- and low-stress subduction-type metamorphic belts can help determine what controls the strength of different subduction boundaries and assess the potential for

©2019. Japan Geoscience Union. All Right Reserved.

great earthquakes in modern settings.

Keywords: High pressure metamorphic rocks, Stress along subduction boundaries, Sanbagawa belt, Franciscan complex

©2019. Japan Geoscience Union. All Right Reserved.

[J] Oral | S (Solid Earth Sciences)：S-MP Mineralogy & Petrology

Wed. May 29, 2019 9:00 AM - 10:30 AM JST | Wed. May 29, 2019 12:00 AM - 1:30 AM UTC | A07 TOKYO BAY MAKUHARI HALL

[S-MP33] Physics and Chemistry of Minerals

convener:Seiji Kamada(Frontier Research Institute for Interdisciplinary Sciences, Tohoku University), Masahiro KAYAMA(Department of Earth and Planetary Material Sciences, Faculty of Science, Tohoku University), Chairperson:Seiji Kamada(FRIS, Tohoku Univ.)

In this session, we will discuss the physics and chemistry of the Earth and planetary materials (including amorphous and melts) based on the results obtained from various experimental methods such as X-ray diffraction, FT-IR, Raman spectroscopy, electron microscopic observations, and computer simulations.

9:00 AM - 9:15 AM JST | 12:00 AM - 12:15 AM UTC

[SMP33-01] High-temperature Raman spectroscopic study of CO_2-containing melanophlogite

*Masami Kanzaki[1] (1.Institute for Planetary Matereials, Okayama University)

9:15 AM - 9:30 AM JST | 12:15 AM - 12:30 AM UTC

[SMP33-02] Synthesis of barium carbonate with calcite structure and rotational disorder of carbonate ions

*Hiroyuki Kagi[1], Ayaka Saito[1], Kazuki Komatsu[1], Jun Kawano[2] (1.Geochemical Research Center, Graduate School of Science, University of Tokyo, 2.Fuculty of Science, Hokkaido University)

9:30 AM - 9:45 AM JST | 12:30 AM - 12:45 AM UTC

[SMP33-03] In-situ Raman spectroscopy of ε-FeOOH under high pressures

*Osamu Ikeda[1], Tatsuya Sakamaki[1], Akio Suzuki[1] (1.Department of Earth Science, Graduate School of Science, Tohoku University)

9:45 AM - 10:00 AM JST | 12:45 AM - 1:00 AM UTC

[SMP33-04] **Strong hydrogen-bond generation in dense hydrous magnesium silicate phase E observed by single-crystal neutron diffraction**

*Narangoo Purevjav[1], Takuo Okuchi[1], Christina Hoffmann[2] (1.Institute for Planetary Materials, Okayama University, 2.Neutron Scattering Division, Neutron Sciences Directorate, Oak Ridge National Laboratory)

10:00 AM - 10:15 AM JST | 1:00 AM - 1:15 AM UTC

[SMP33-05] **Water partitioning between upper mantle minerals and melts**

*Dmitry Bondar[1], Hongzhan Fei[1], Tony Withers[1], Tomoo Katsura[1] (1.Bayerisches Geoinstitut, University of Bayreuth, 95440 Bayreuth, Germany)

10:15 AM - 10:30 AM JST | 1:15 AM - 1:30 AM UTC

[SMP33-06] Drop-solution enthalpy measurement of $MgSiO_3$ majorite

*Hiroshi Kojitani[1], Masamichi Noda[2], Toru Inoue[2,3], Masaki Akaogi[1] (1.Department of Chemistry, Faculty of Science, Gakushuin University, 2.GRC, Ehime University, 3.Dept. of Earth and Planetary systems Science, Hiroshima University)

High-temperature Raman spectroscopic study of CO_2-containing melanophlogite

*Masami Kanzaki[1]

1. Institute for Planetary Matereials, Okayama University

Introduction: Melanophlogite is one of natural silica minerals with a clathrate structure. The structure has two kinds of cages which can host small guest molecules such as CH_4, CO_2, N_2 and H_2S. These are M^{12} and M^{14} cages correspond to pentagondodecahedral [5^{12}] and tetrakaidecahedral [$5^{12}6^2$] units made of 5- and 6-membered SiO_4 rings, respectively. Previous crystal structural studies suggested that CO_2 is mostly locating in larger M^{14} cage. A few years ago, we found a very intense and broad peak below 100 cm^{-1} in CO_2-containing melanophlogite. To clarify the origin of this peak in relation with CO_2 guest molecule, heat treatment experiments and in-situ high-temperature Raman spectroscopy measurements were conducted up to 1100 ^{o}C.
Experimental: Micro-Raman spectra were obtained using a home-built Raman system made of single-monochromator, CCD detector and Ondax SureBlock filters for low frequency measurement. The heat treatment was conducted using a muffle furnace, and the in-situ study was conducted with a wire-heater cell. Natural shperical single crystals from Fortunillo, Italy were crushed and small fragments were used for the experiments.
Results and discussion (origin of low-freq. peak): For the heat treatment experiments, nearly CO_2-free melanophlogite was obtained at 950 ^{o}C for 6 h, judging from intensities of CO_2 vibrational peaks (Fermi diad). Simultaneously, the low-frequency peak nearly disappeared. For shorter time durations or lower treatment temperatures, CO_2 vibrational peaks and low-frequency peak were still visible. We found that CO_2 vibrational peaks of the heat treated samples were split.
For the in-situ study, integrated total intensity of CO_2 vibrational peaks started to drop at around 450 ^{o}C, and simultaneously the low-frequency peak intensity decreased. These peaks completely disappeared at 1100 ^{o}C, while melanophlogite itself remained intact. Thus, it was concluded that the low-frequency peak is originated from CO_2 molecules, not from melanophlogite structure. Librational and translational modes of CO_2 molecules in the cages of melanophlogite would be responsible for the low-frequency peak. Thus, degassing behavior can be studied by monitoring both the low frequency band and the vibrational peaks.
(vibrational peak splitting): At about 450 ^{o}C, we noted that the vibrational CO_2 peak started to split (or more precisely, new peak appeared at slightly higher frequency and grew with temperature while the original peak became weaker). This splitting is partly quenchable, as demonstrated in the heat treated sample mentioned above. Vibrational peak splitting has been reported for CH_4 and H_2S in melanophlogites, and has interpreted as occupancy of those molecules in both M^{14} and M^{12} cages. Thus, peak splitting observed in our study can be interpreted similarly. No splitting of CO_2 has been reported before, except one report at very low temperature. From those observations, we speculated that at above 450 ^{o}C, CO_2 molecule is able to migrate from original M^{14} cage to next M^{14} or M^{12} cages. Because M^{14} cages make an infinite chain by sharing 6-membered rings, migration of CO_2 from M^{14} to M^{14} cages through the 6-membered ring will contribute to long-range diffusion (i.e., degassing). On the other hand, migration of CO_2 from M^{14} to next M^{12} through 5-membered ring will contribute to disordered distribution of CO_2 in M^{12} and M^{14} cages, which caused vibrational peak splittings. Thus, high-temperature Raman spectroscopic study could provide us more insight of diffusion behavior of CO_2 and possibly other gas molecules in melanophlogite structure.

©2019. Japan Geoscience Union. All Right Reserved.

Keywords: CO2-containing melanophlogite, In-situ high-temperature Raman spectroscopy, Low-frequency Raman spectroscopy, clathrasil, degassing process

©2019. Japan Geoscience Union. All Right Reserved.

Synthesis of barium carbonate with calcite structure and rotational disorder of carbonate ions

*Hiroyuki Kagi[1], Ayaka Saito[1], Kazuki Komatsu[1], Jun Kawano[2]

1. Geochemical Research Center, Graduate School of Science, University of Tokyo, 2. Fuculty of Science, Hokkaido University

Structures of divalent metal carbonate is constrained by the ionic radii of cations. Cations larger than Ca^{2+} take the aragonite structure and cations smaller than Ca^{2+} take the aragonite structure. Barium carbonate (witherite) takes the aragonite structure and Ba2+ is incompatible to calcite. We have reported that large incompatible cations can be introduced to calcite through amorphous calcium carbonate (ACC). In this study, we synthesized $Ba_{0.7}Ca0.3CO_3$ with the calcite structure by heating treatment on ACC containing Ba^{2+}. The obtained crystal can be interpreted as Ca-containing barium carbonate with the calcite structure, which cannot be found in nature or synthesized from a direct precipitation from the supersaturated solutions.

X-ray diffraction (XRD) patterns of Ba-doped calcite measured at 300 K shows the extinction of 113 reflection with increasing Ba concentration (see Figure 1). The extinction of the 113 reflection was reported on pure calcite at temperatures higher than 1240 K (Ishizawa et al., 2013). The change was attributed to the rotational disorder of CO_3^{2-} ions. In contrast, we have observed the extinction of 113 reflection on the Ba-doped calcite at 300 K.

To investigate the behavior of CO_3^{2-} ions at an atomistic level, molecular dynamics (MD) simulation of Ba-doped calcite was conductedusing the MD program, MXDTRICL (Kawamura 1997). Intensity ratio of reflections 113 to 104 (I_{113}/I_{104}) was measured from XRD patterns obtained from experimental study and MD simulation. $I_{113}/I_{104}$from experiment dropped to 0 at Ba/(Ba + Ca) = 26.8 ±1.6 mol% while that of MD-simulated Ba-doped calcite gradually weakened and did not fall to zero. MD simulations of 25.5% and 50.9% Ba-doped calcite at high temperature were also conducted. In 25.5% Ba-doped calcite, I_{113}/I_{104} remarkably dropped at around 1050 K with the structure of rotationally disordered CO_3^{2-} ions. The transition temperature to the rotational disorder was at around 850 K for 50.9% Ba-doped calcite. These simulated temperatures are much lower than the transition temperature (1250 K) obtained from MD simulation on pure calcite (Kawano et al., 2009). The simulated results showed that the transition temperature to the rotational disordered phase dramatically decreased with increasing Ba/(Ba + Ca) in calcite.

Keywords: barium carbonate, molecular dynamics simulation, rotational disorder, calcium carbonate (calcite)

©2019. Japan Geoscience Union. All Right Reserved.

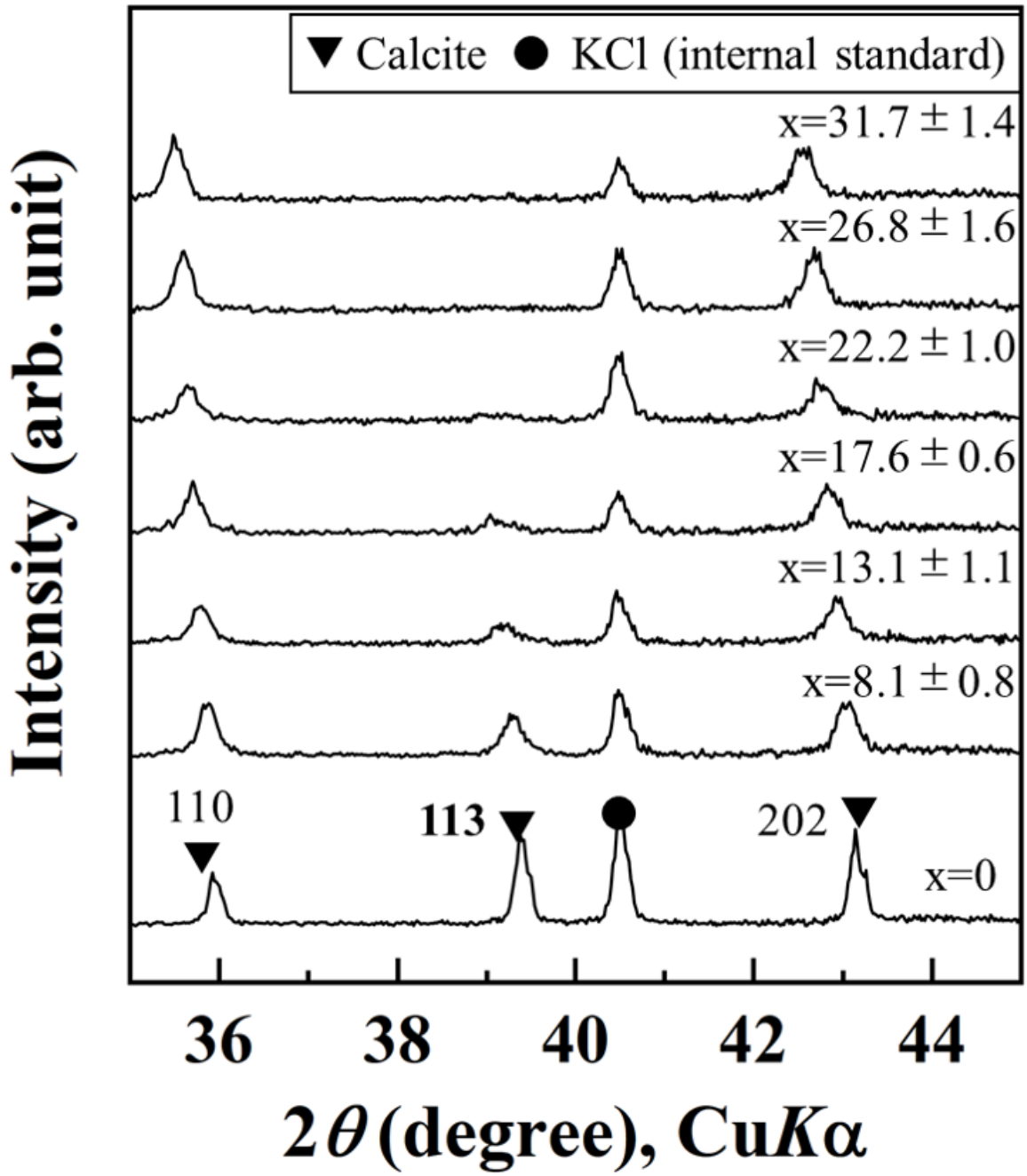

Figure 1. Broadening and disappearance of reflection 113 observed from powder X-ray patterns of Ba-doped calcite samples. x stands for Ba/(Ba+Ca) mol% in Ba-doped calcite.

©2019. Japan Geoscience Union. All Right Reserved.

In-situ Raman spectroscopy of ε-FeOOH under high pressures

*Osamu Ikeda[1], Tatsuya Sakamaki[1], Akio Suzuki[1]

1. Department of Earth Science, Graduate School of Science, Tohoku University

ε-FeOOH is one of crucial high-pressure hydrous phases in the Earth's mantle, and is isostructural to δ-AlOOH. A first principles calculation (Gleason et al., 2013) has indicated pressure-induced hydrogen bond symmetrization at 43 GPa, and spin transition of iron at 65 GPa. These transitions cause changes in physical properties, and knowledge of the transition changes can help us to understand the behaviors of hydrous phases under high pressure.

We present a first study of Raman spectroscopy of ε-FeOOH at high pressure and room temperature. The measured sample was polycrystalline ε-FeOOH, which was synthesized in advance from a powder of reagent grade 99 % α-FeOOH at the pressure-temperature condition of 8 GPa and 480 ℃ for 2 hour. Micro-Raman spectrometer NRS-4100TOR (JASCO Corporation), which has a laser with the wavelength 532 nm and power 50 mW installed in Tohoku University, was used to obtain Raman spectra. Symmetric diamond anvil cell with 300 μm culet size was used to generate high pressure. The sample was loaded in the sample chamber of tungsten gasket with NaCl pressure medium. The pressure in the chamber was calculated by means of the ruby luminescence pressure scale (Dewaele et al., 2004).

Along compression, the frequencies of most of peak tops have positive pressure dependences but some peaks (298, 386, 698, and 1099 cm^{-1} at 15 GPa) changed the dependences to negative around 14 GPa. Above 15 GPa some peaks (197, 298, and 443 cm^{-1} at 15 GPa) disappeared and the others (364, 386, 549, 646, 698, and 1099 cm^{-1} at 15 GPa) jumped by frequency 10–30 cm^{-1}. This change around 15 GPa may correspond to the replacement of vibrational modes in Raman spectra of δ-AlOOH at the pressure of 5.6 GPa (Mashino et al., 2016), which indicates a hydrogen-bond related space-group transition from $P2_1nm$ to *Pnnm* (Tsuchiya et al., 2008).

Reference:
Dewaele, A., Loubeyre, P., and Mezouar, M. (2004). Equations of state of six metals above 94 GPa. Phys. Rev. B *70*, 094112.
Gleason, A.E., Quiroga, C.E., Suzuki, A., Pentcheva, R., and Mao, W.L. (2013). Symmetrization driven spin transition in ε-FeOOH at high pressure. Earth Planet. Sci. Lett. *379*, 49–55.
Mashino, I., Murakami, M., and Ohtani, E. (2016). Sound velocities of δ-AlOOH up to core-mantle boundary pressures with implications for the seismic anomalies in the deep mantle. J. Geophys. Res. Solid Earth *121*, 595–609.
Tsuchiya, J., Tsuchiya, T., and Wentzcovitch, R.M. (2008). Vibrational properties of δ-AlOOH under pressure. Am. Mineral. *93*, 477–482.

Keywords: ε-FeOOH, high pressure, Raman spectroscopy, H-bond symmetrization

©2019. Japan Geoscience Union. All Right Reserved.

Strong hydrogen-bond generation in dense hydrous magnesium silicate phase E observed by single-crystal neutron diffraction

*Narangoo Purevjav[1], Takuo Okuchi[1], Christina Hoffmann[2]

1. Institute for Planetary Materials, Okayama University, 2. Neutron Scattering Division, Neutron Sciences Directorate, Oak Ridge National Laboratory

Dense hydrous magnesium silicates (DHMS) are considered as the most major water transporters in cold subducting slabs, which are descending into the deep mantle. Phase E [$Mg_2SiH_4O_6$ –ideal] is one of the most important DHMS phases which is stable at conditions between 13 –17 GPa and 800 –1200 ˚C [1]. Besides its stability at such high temperatures, it stores up to 18 wt.% of water within its crystal structure, which is one of the largest among DHMS phases. Thus phase E is one of the most important carriers and transporter of water in the subducting slabs. The crystal structure of phase E was first investigated by single crystal x-ray diffraction except for its hydrogen position [2]. Its structure has brucite-like layers of MgO6 octahedra which are crosslinked by SiO4 tetrahedra [2]. The hydrogen atoms were expected to be located between these MgO6 octahedra layers like those in brucite, $Mg(OH)_2$. The previous expectation on the structure of phase E was recently confirmed by our powder neutron diffraction study [3]. In contrast, present single-crystal neutron diffraction is conducted to investigate hydrogen bonding geometry in phase E structure, including the Debye-Waller factor of the hydrogen, for which we utilize much higher spatial resolution of the single crystal method. The method has been well confirmed to be very sensitive for investigating such properties of the hydrogen atoms within a series of hydrous minerals [4, 5].
We expect that such information is helpful to understand the reason of stability of phase E at the high-temperature condition. A deuterated phase E single crystal was measured by neutron time-of-flight single-crystal Laue diffraction at Spallation Neutron Source, Oak Ridge National Laboratory. From preliminary structure refinement results, we found that the covalent bond O-D was inclined and displaced from the three-fold axis. Such O-D inclination should occur due to interlayer strong hydrogen-bond generation in the phase E structure. The details of the results will be given in the presentation.

References: [1] Kanzaki, M. *Trans Am Geophys Union* (1991) **70**:508. [2] Kudoh, Y., Finger, L. W., Hazen, R. M., Prewitt, C. T., Kanzaki, M. and Veblen, D. R., *Phys. Chem. Minerals* (1993) **19**:357. [3] Tomioka, N., Okuchi, T., Purevjav, N., Abe, J. and Harjo, S., *Phys. Chem. Mineral.* (2016) **43**:267. [4] Purevjav, N., Okuchi, T., Tomioka, N., Wang, X. and Hoffmann, C. *Sci. Rep.* (2016) **6**:34988. [5] Purevjav, N., Okuchi, T., Wang, X., Hoffmann, C. and Tomioka, N. *Acta Cryst.* (2018) B**74**:115.

Keywords: hydrogen-bond, dense hydrous magnesium silicate, neutron diffraction

©2019. Japan Geoscience Union. All Right Reserved.

Water partitioning between upper mantle minerals and melts

*Dmitry Bondar[1], Hongzhan Fei[1], Tony Withers[1], Tomoo Katsura[1]

1. Bayerisches Geoinstitut, University of Bayreuth, 95440 Bayreuth, Germany

Water in the Earth's upper mantle is predominantly stored in nominally anhydrous minerals (NAMs) such as olivine, orthopyroxene, clinopyroxene and garnet. Since incorporated water has a strong influence on mantle properties, namely melting temperature, rheology, electrical conductivity and seismic velocity, it is important to know the distribution of water among phases. Knowledge of how water partitions between upper mantle minerals and melts is essential for estimation of water content in incipient melts at different depths, water transport by these melts, and total amount of water in the upper mantle.
There are quite a few studies providing data on water partitioning between NAMs and melts. The most challenging part of these studies is to quench melt coexisting with mineral phases to form glass at elevated pressures (>2 GPa), which is necessary to measure water partitioning with high accuracy. It also becomes more difficult to quench melt with higher Mg/Si ratio into glass, which is necessary in order to crystallize olivine from the melt. Previous studies produced mantle minerals coexisting with quenched melt up to only 5 GPa, namely olivine up to 3 GPa, orthopyroxene up to 4 GPa, clinopyroxene and garnet up to 5 GPa. As a result, there is no systematic pressure, temperature and water content dependence of water partitioning from the data scattered over the narrow pressure range. Many authors also reported that glasses in some run products were not transparent, which implies micro-crystals may have crystallized in those studies.
The difficulty of quenching melt into glass lies in the insufficient cooling rate. The cooling rates of regular piston-cylinder and multi-anvil experiments used for these purposes are 120˚/sec and 500˚/sec, respectively. Quenching glass at elevated pressures and at various compositions is important not only for measuring water partitioning, but also for a number of other tasks, such as melt structure studies and partitioning of other components and elements.
The purposes of the present study are (1) to develop a multi-anvil technique allowing much faster cooling rate than conventional ones and (2) to measure water partitioning between upper mantle minerals and melts for a pressure range from 1 to 13 GPa, which covers the whole upper mantle. Our design for a fast-cooling multi-anvil technique has already been shown to produce a very high quenching rate (5200˚ /sec) in comparison with those of regular piston cylinder and multi-anvil apparatus (120˚C/sec and 500˚ C/sec, respectively) (Fig. 1a). Using this technique, completely transparent glass coexisting with garnet was successfully quenched at 6 GPa (Fig.1b,c). We plan to improve the fast quenching technique to allow quenching melts under even wider conditions.
Fig 1. (a) Comparison of cooling rate among different assemblies. 1/2 and 18/8 are piston-cylinder and multi-anvil assemblies, respectively. Cooling rate was calculated for the temperature range between target temperature and 600˚C; (b) Glass coexisting with garnet at 6 GPa; (c) BSE image of the area in the red box from picture b.

Keywords: Water partitioning, Water distribution, Upper mantle, Nominally anhydrous minerals , Quenched melts, Basaltic glass

©2019. Japan Geoscience Union. All Right Reserved.

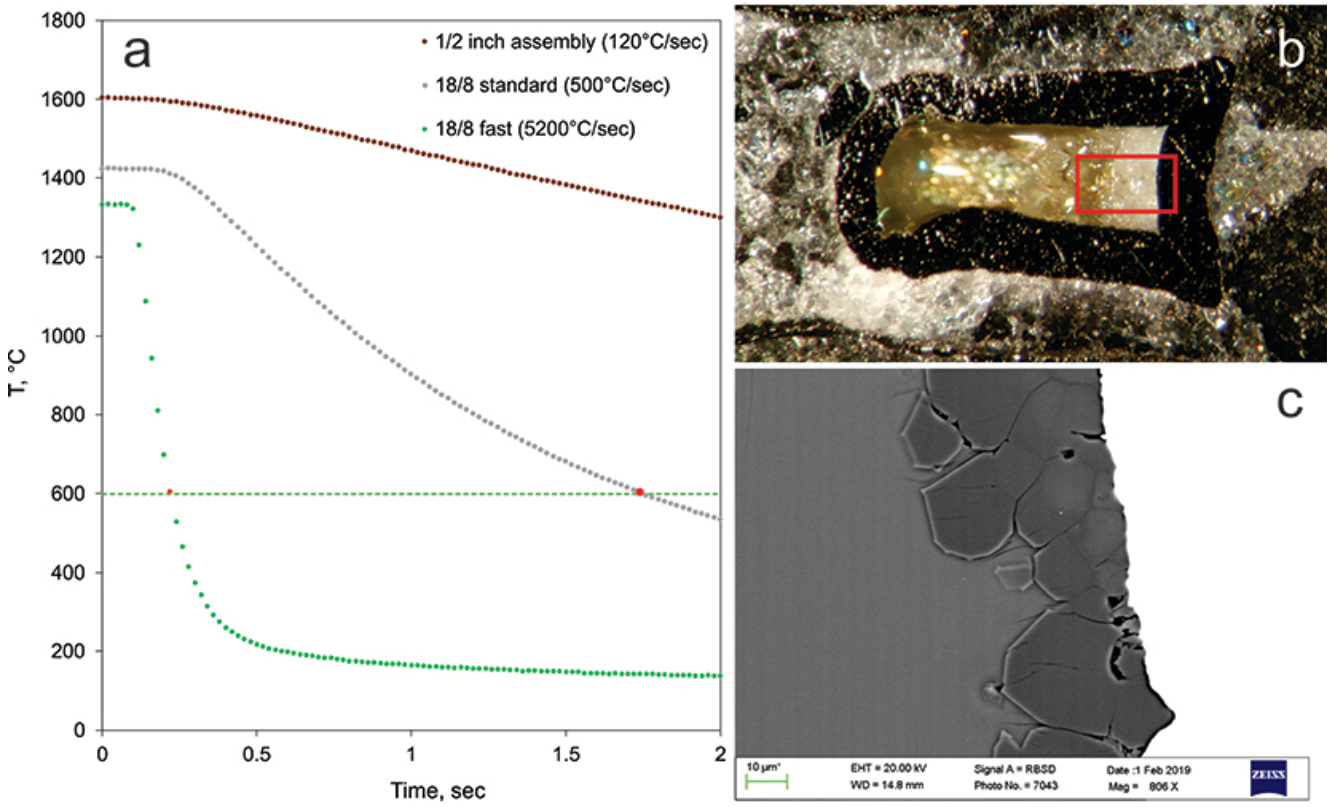

©2019. Japan Geoscience Union. All Right Reserved.

Drop-solution enthalpy measurement of $MgSiO_3$ majorite

*Hiroshi Kojitani[1], Masamichi Noda[2], Toru Inoue[2,3], Masaki Akaogi[1]

1. Department of Chemistry, Faculty of Science, Gakushuin University, 2. GRC, Ehime University, 3. Dept. of Earth and Planetary systems Science, Hiroshima University

Silicate garnet is one of the major Earth's mantle constituent minerals. With increasing depth, pyroxene components dissolve into the silicate garnet. $MgSiO_3$ majorite (Mj) is an important endmember to express such the pyroxene component dissolving in the silicate garnet solid solution. Recently, we experimentally determined isobaric heat capacity and entropy of $MgSiO_3$ Mj. The stability field of $MgSiO_3$ Mj in the $MgSiO_3$ system thermodynamically calculated using these new thermodynamic data of $MgSiO_3$ Mj together with its enthalpy data measured by Yusa et al. (1993) and Saikia (2008) is not consistent with that determined by previous high-pressure phase relation experiments. In this study, the standard enthalpy of $MgSiO_3$ Mj was determined by drop-solution enthalpy measurement and the obtained enthalpy value was applied to examine the phase stability field of $MgSiO_3$ Mj by thermodynamic calculation.

$MgSiO_3$ Mj samples for the drop-solution calorimetry was the same as those used in the heat capacity measurement, which were synthesized at 19 GPa and 2173 K using a high-pressure apparatus at Ehime University, GRC. The sintered polycrystalline samples were crushed into powder. The drop-solution calorimetry was performed using a Calvet-type high-temperature calorimeter (SETARAM, HT-1000). The powdered sample with weight of about 4 mg was compressed into a pellet and it was dropped into the lead borate solvent ($2PbO{\cdot}B_2O_3$) placed in the calorimeter which was kept at 978 K. The summation of heat content from room temperature to 978 K and solution enthalpy at 978 K, namely drop-solution enthalpy ($\Delta H_{d\text{-}s}$), was measured. To hasten the solution of the samples, the solvent was stirred by bubbling with Ar gas.

$\Delta H_{d\text{-}s}$ ($MgSiO_3$ Mj) was determined to be 69.57±0.77 kJ/mol from the average of five data. This value is the middle between 80.0±2.5 kJ/mol (Yusa et al., 1993) and 59.5±3.2 kJ/mol (Saikia, 2008). From the difference between $\Delta H_{d\text{-}s}$ (MgO) (33.74±0.99 kJ/mol, Kojitani et al. 2012) + $\Delta H_{d\text{-}s}$ (SiO_2 quartz) (40.05± 0.36 kJ/mol, Akaogi et al. 1995) and our $\Delta H_{d\text{-}s}$ ($MgSiO_3$ Mj), the formation enthalpy from the oxides was obtained as 4.2±1.3 kJ/mol. The thermodynamic calculation of the *P-T* phase diagram by adopting the present enthalpy value suggests that the stability field of $MgSiO_3$ Mj would expand to lower temperature region than that determined by previous high-pressure high-temperature experiments and thermodynamic calculations.

Keywords: garnet, majorite, enthalpy, thermodynamic stability, thermodynamic calculation

©2019. Japan Geoscience Union. All Right Reserved.

[J] Oral | S (Solid Earth Sciences)：S-MP Mineralogy & Petrology

Wed. May 29, 2019 10:45 AM - 12:15 PM JST | Wed. May 29, 2019 1:45 AM - 3:15 AM UTC | A07 TOKYO BAY MAKUHARI HALL

[S-MP33] Physics and Chemistry of Minerals

convener:Seiji Kamada(Frontier Research Institute for Interdisciplinary Sciences, Tohoku University), Masahiro KAYAMA(Department of Earth and Planetary Material Sciences, Faculty of Science, Tohoku University), Chairperson:Masahiro Kayama(東北大学)

In this session, we will discuss the physics and chemistry of the Earth and planetary materials (including amorphous and melts) based on the results obtained from various experimental methods such as X-ray diffraction, FT-IR, Raman spectroscopy, electron microscopic observations, and computer simulations.

10:45 AM - 11:00 AM JST | 1:45 AM - 2:00 AM UTC

[SMP33-07] High-pressure phase transitions of minerals in the system MgO-TiO_2

*Masaki Akaogi[1], Tetsuya Fujimura[1], Shunto Arai[1], Masaki Okano[1], Hiroshi Kojitani[1] (1.Department of Chemistry, Faculty of Science, Gakushuin University)

11:00 AM - 11:15 AM JST | 2:00 AM - 2:15 AM UTC

[SMP33-08] Phase change process of iron sulfide nanoparticle from amorphous to crystalline with grain growth

*Yoshinari Sano[1], Atsushi Kyono[2], Yasuhiro Yoneda[3], Gen-ichiro Yamamoto[1] (1.Graduate School of Life and Environmental Sciences, University of Tsukuba, 2.Faculty of Life and Environmental Sciences, University of Tsukuba, 3.Japan Atomic Energy Agency)

11:15 AM - 11:30 AM JST | 2:15 AM - 2:30 AM UTC

[SMP33-09] Texture formation in quenching of Fe-S-O micro melt spherules

*Hiroshi Isobe[1] (1.Department of Earth and Environmental Sciences, Faculty of Advanced Science and Technology, Kumamoto University)

11:30 AM - 11:45 AM JST | 2:30 AM - 2:45 AM UTC

[SMP33-10] Development of a software for electron diffraction simulation based on dynamical theory and its application to mineralogy

*Yusuke Seto[1], Masahiro Ohtuka[3], Akira Miyake[2] (1.Graduate School of Science, Kobe University, 2.Graduate School of Science, Kyoto University, 3.Graduate School of Technology, Nagoya University)

11:45 AM - 12:15 PM JST | 2:45 AM - 3:15 AM UTC

[SMP33-11] Site occupation analysis for cation in minerals by analytical electron microscopy: application of TEM-ALCHEMI for earth and planetary science

★Invited Papers

*Yohei Igami[1], Shunsuke Muto[1], Masahiro Ohtsuka[3], Akira Miyake[2], Takahiro Kuribayashi[4], Shoichi Toh[5] (1.Institute of Materials and Systems for Sustainability, Nagoya University, 2.Graduate School of Science, Kyoto University, 3.Graduate School of Engineering, Nagoya University, 4.Graduate School of Science, Tohoku University, 5.Faculty of Science, Fukuoka University)

High-pressure phase transitions of minerals in the system MgO-TiO_2

*Masaki Akaogi[1], Tetsuya Fujimura[1], Shunto Arai[1], Masaki Okano[1], Hiroshi Kojitani[1]

1. Department of Chemistry, Faculty of Science, Gakushuin University

Mg_2TiO_4, $MgTiO_3$ and $MgTi_2O_5$ form spinel(Sp)-, ilmenite(Ilm)-, and pseudobrookite(Pbr)-type solid solutions, respectively, with other endmembers such as Fe_2TiO_4, $FeTiO_3$ and $FeTi_2O_5$. These phases occur as minor minerals in various igneous and metamorphic rocks. Previous studies on stability relations of Mg_2TiO_4, $MgTiO_3$ and $MgTi_2O_5$ at high pressure were limited below about 3 GPa, except for that the transitions in $MgTiO_3$ were examined up to about 18 GPa. In this study, we have examined the phase transitions of these magnesium titanates up to 28 GPa and 1800 ˚C.

We have determined the high-pressure phase relations in Mg_2TiO_4, $MgTiO_3$ and $MgTi_2O_5$ at 4-28 GPa and 1000-1800 ˚C using multianvil apparatus with the quench method. $MgTiO_3$ ilm transformed to the $LiNbO_3$ (Ln)-type high-pressure phase at 16-20 GPa and 1200-1600 ˚C. The Ln phase was interpreted as the retrograde transformation product from perovskite(Pv)-type $MgTiO_3$ stable at high pressure and high temperature (Linton et al., 1999). Above 21-25 GPa, the recovered phases were MgO and a-PbO_2-type TiO_2, the latter of which was interpreted to be converted from baddeleyite(Bd)-type TiO_2. The transition boundary from Pv to MgO + TiO_2(Bd) has a positive Clapeyron slope. Mg_2TiO_4 Sp dissociates to MgO + $MgTiO_3$ Ilm at about 1 GPa, and at higher pressure they changes to MgO + $MgTiO_3$ Pv and subsequently to 2MgO + TiO_2(Bd). $MgTi_2O_5$ Pbr decomposes at 1-2 GPa to $MgTiO_3$ Ilm + TiO_2 rutile(Ru), the latter of which transforms to a-PbO_2-type TiO_2. At higher pressure, the assemblage changes to $MgTiO_3$ Pv + a-PbO_2-type TiO_2, and subsequently to MgO + 2TiO_2(Bd). These results show that the mixtures of MgO and TiO_2 (Bd) are stable above 20-25 GPa in the three magnesium titanates. We also performed Rietveld structure refinement of Ln-type $MgTiO_3$ using synchrotron powder X-ray diffraction data, and confirmed that Ti^{4+} and Mg^{2+} ions are slightly deviated from the centrosymmetric positions in the octahedra which gives polarity of the $MgTiO_3$ Ln-phase.

The high-pressure transition behaviors of Mg_2TiO_4, $MgTiO_3$ and $MgTi_2O_5$ are similar to those of Fe_2TiO_4, $FeTiO_3$ and $FeTi_2O_5$, respectively, up to moderate pressures, where the phases transform to the assemblages involving $MTiO_3$ Ilm and Pv (M = Mg, Fe). However, the transition behaviors are different at higher pressures: Fe_2TiO_4 transforms to $CaTi_2O_4$(CT)-type phase, and $FeTiO_3$ dissociates to Fe_2TiO_4 CT + a dense orthorhombic $FeTi_2O_5$ phase (Akaogi et al., 2017).

Keywords: high pressure, titanate mineral, phase transition

©2019. Japan Geoscience Union. All Right Reserved.

Phase change process of iron sulfide nanoparticle from amorphous to crystalline with grain growth

*Yoshinari Sano[1], Atsushi Kyono[2], Yasuhiro Yoneda[3], Gen-ichiro Yamamoto[1]

1. Graduate School of Life and Environmental Sciences, University of Tsukuba, 2. Faculty of Life and Environmental Sciences, University of Tsukuba, 3. Japan Atomic Energy Agency

1. Introduction

In anaerobic marine sediments, sulfate-reducing bacteria (SRB) acquires metabolic energy by reducing sulfate ions (SO_4^{2-}) to sulfide ions (S^{2-}). Sulfide ions are, furthermore, oxidized from sulfur (S^0) to sulfate ions by the metabolic activity of sulfur bacteria (SB). These series of reaction are called geochemical sulfur cycle and considered as one of the most important elemental cycle. In the reaction, a part of the sulfide ions is readily reacted with ferrous ions (Fe^{2+}) to produce iron sulfide nanoparticle (FeS), and which grows to more stable mackinawite (FeS). In the previous study, it was reported that the crystal growth from iron sulfide nanoparticle to mackinawite occurred in hydrothermal aging experiment at 120°C (Csákberé nyi-Malasics et al., 2012). Despite its importance as a precursor of mackinawite, phase change process of the iron sulfide nanoparticle from amorphous to crystalline has not been elucidated yet. In this study, synchrotron X-ray total scattering measurement and atomic Pair Distribution Function (PDF) analysis were performed to clarify the crystal structure change of iron sulfide nanoparticle with grain growth.

2. Experimental method

At first, iron sulfide nanoparticle suspension was synthesized by the mixing 10 mL of 0.2 M $(NH_4)_2Fe(SO_4)_2 \cdot 6H_2O$ solution with 10 mL of 0.4 M $Na_2S \cdot 9H_2O$ solution in N_2 gas atmosphere. The synthesized suspensions were heated in a Teflon container at 120°C for 2, 4, 6, 8 and 12 hours, respectively. After the end of heating experiments, the solid phases were dried by blowing N_2 gas and stored in vacuum. Synchrotron X-ray total scattering measurements were performed at beamline BL14B1 in SPring-8. The incident beam was monochromatized to a wavelength of 0.20606 Å. X-ray total scattering data at 20 K and 300 K were collected in the Q range between 0 and 25 $Å^{-1}$. Atomic Pair Distribution Function (PDF) analysis was applied to X-ray total scattering data.

3. Results and discussion

The PDF pattern of iron sulfide nanoparticle synthesized in the study almost disappeared at about 2 nm. Those of samples heated for 2, 4, 6, 8, 12 h are, on the other hand, were continuously observed up to 4 nm. This result showed that the particle size of iron sulfide nanoparticle was grown to 4 nm by the heating at 120°C. The Fe-S and Fe-Fe distances obtained by the PDF analysis are 2.25 and 2.65 Å, respectively, which suggests that the local atomic structure around Fe, ie FeS_4 tetrahedra, in iron sulfide nanoparticle almost remains unchanged by particle growth. Compared with the structure model of mackinawite, the iron sulfide nanoparticle would consist of disordered arrangement of FeS_4 tetrahedra. This is consistent with the structure model of iron sulfide nanoparticle proposed by the previous study (Wolthers et al., 2003; Ohfuji and Rickard, 2006; Jeong et al., 2008). In the presentation, we will discuss structure change associated with medium-range atomic order and propose phase change process from amorphous to crystalline by particle growth.

Keywords: atomic Pair Distribution Function , iron sulfide nanoparticle, mackinawite

©2019. Japan Geoscience Union. All Right Reserved.

Texture formation in quenching of Fe-S-O micro melt spherules

*Hiroshi Isobe[1]

1. Department of Earth and Environmental Sciences, Faculty of Advanced Science and Technology, Kumamoto University

Microtexture of minerals records physical, chemical and kinetic conditions at crystal growth. Local processes at crystal growth and migration of elements have important role in the rapid crystal growth. Especially, Fe and S-bearing systems are oxidation and evaporation sensitive. And fine particles can be quenched very quickly from high temperature, quench crystals show characteristic textures of crystals. In this study, quick heating and cooling experiments of powdered iron sulfide particles were carried out with a fine particles free falling apparatus with controlled gas flow (Isobe and Gondo, 2013). Oxygen fugacity was controlled to FMQ -0.5, +0.9 or +2.4 log unit. Particles can be heated to the maximum temperatures of approximately 1600˚C within two seconds, are kept approximately one second and quenched within a second.

Run products particles were completely melted and show rounded shape with smooth surface or characteristic texture. Spherical products were initially well homogenized from inhomogeneous starting materials by complete melting. Then, spherules are oxidized and show growth of secondary crystals with rapid cooling.

FeS dendritic crystals occur in sulfur-rich spherules with low fO2 condition. In the higher fO2 experiments, rapid growth of magnetite in Fe-O melt produces iron metal phase from an excess iron in melt phase relative to magnetite.

Compositions of iron sulfide melt in fine spherules are initially close to FeS and are losing S with oxidation following Fe-S-O phase relations depending on oxygen fugacity even in a few seconds. Crystallization of FeS crystals can reduce sulfur content in melt, then evaporation of sulfur can be suppressed. Evaporation of sulfur may be promoted by oxidation of iron sulfide melt to occur magnetite as liquidus phase.

Keywords: iron sulfide, magnetite, quench crystals, spherules, dendrite

©2019. Japan Geoscience Union. All Right Reserved.

Development of a software for electron diffraction simulation based on dynamical theory and its application to mineralogy

*Yusuke Seto[1], Masahiro Ohtuka[3], Akira Miyake[2]

1. Graduate School of Science, Kobe University, 2. Graduate School of Science, Kyoto University, 3. Graduate School of Technology, Nagoya University

Electron diffraction technique is widely used for the phase identification and crystal structure determination of Earth and planetary materials. Electrons are scattered by the positive potential inside the electron cloud, resulting that the interaction of electrons with matter is much stronger (10^6-10^7) than that of X-rays. This has the advantage that the diffracted electron beams have a high intensity and the patterns can directly be observed on the viewing screen of the electron microscope. The strong interaction, however, easily causes multiple scattering, and thereby the intensities of the reflections are much influenced by the dynamical effects. This makes structure determinations from electron diffraction more difficult and less reliable than that from XRD data. In order to treat the dynamical effects, a lot of computer resources of Fourier transform and/or eigenvalue problem are required, and consequently, such a dynamical analysis was limited to simple structured materials. However, that situation has been changing. In recent years, many-core CPUs can make a lot of computation possible. Moreover, with the rapid spread of field emission transmission electron microscopes (TEM) and sensitive detectors (CCD or CMOS), the quantitative analyses of electron intensities become available even from nanometer-sized minerals.

In the present study, the authors developed a GUI-based software, ReciPro, that simulates electron diffraction patterns using one of the dynamical theories, called the Bethe method (or Bloch wave eigenvalue method), in which the three dimensional eigenvalues of the electron wave function in a crystalline specimen are solved with the appropriate boundary conditions on the entrance and exit face of the crystal. By this method, the diffraction patterns (SAED and CBED) can be obtained with a good accuracy and speed regardless of the specimen thickness. Moreover, ReciPro provides following features: i) Loading any crystal structure including AMCSD (American Mineralogist Crystal Structure Database) database or COD (Crystallography Open Database). ii) Changing a specimen orientation and TEM conditions freely by a mouse operation. iii) Displaying Digital Micrograph file, the de facto standard of TEM image file format developed by Gatan inc., can be read and displayed. iv) Fitting diffraction spots by two dimensional pseudo-Voigt functions. v) Quantitative comparison of simulated and experimental diffraction patterns, and many more features. In the presentation, the authors will report examples of reproducibility of simulated diffraction patterns (SAED and CBED) for several minerals, and future prospects of this approach.

Keywords: electron diffraction, dynamical theory, transmission electron microscopy

©2019. Japan Geoscience Union. All Right Reserved.

Site occupation analysis for cation in minerals by analytical electron microscopy: application of TEM-ALCHEMI for earth and planetary science

*Yohei Igami[1], Shunsuke Muto[1], Masahiro Ohtsuka[3], Akira Miyake[2], Takahiro Kuribayashi[4], Shoichi Toh[5]

1. Institute of Materials and Systems for Sustainability, Nagoya University, 2. Graduate School of Science, Kyoto University, 3. Graduate School of Engineering, Nagoya University, 4. Graduate School of Science, Tohoku University, 5. Faculty of Science, Fukuoka University

Cation site occupation in natural minerals is very important for earth and planetary science, because it should reflect thermal histories such as peak temperatures and cooling rates. However, natural minerals generally have various complex micro-textures. Therefore, determination of cation site occupation from micrometric regions has been required.
Spence and Taftø [1] developed the ALCHEMI (Atom Location by CHanneling-Enhanced MIcroanalysis) method in which transmission electron microscope with energy dispersive X-ray spectrometer (TEM-EDS) is used to determine the crystallographic sites of impurity elements from micrometric regions in crystals on the basis of channeling-enhanced X-ray emissions. Subsequent improvements in the ALCHEMI have led to more statistical method called HARECXS (High Angular Resolution Electron Channeling X-ray Spectroscopy) or St-ALCHEMI (statistical ALCHEMI). This method is widely applicable including minerals with low symmetric structures (reviewed by [2]). Recently, we successfully determined the order parameter of Al and Si in the tetrahedral sites in sillimanite (Al_2SiO_5) at the areas free from precipitates of mullite ($3Al_2O_3$ $2SiO_2$) and glasses [3]. In this study, we carried out the ALCHEMI/HARECXS method for major rock forming minerals to extend its applicability in earth and planetary science.
Sample minerals are olivine ($[Mg, Fe]_2SiO_4$), diopside ($Ca[Mg, Fe]Si_2O_6$) and sillimanite. The samples were prepared by a focused ion beam system (FIB, FEI Quanta 200 3DS or Helios NanoLab G3 CX), and examined by using TEM-EDS (JEOL JEM-2100F, JED-2300T). X-ray signals generated under illumination of 200 keV electrons were collected as a function of electron beam direction. The homogeneous areas free from dislocations or inclusions were selected as regions of interest.
The one-dimensional tilting ALCHEMI datasets under the condition exciting the particular systematic reflection row (HARECXS profiles) were successfully obtained from regions ~1 μm in diameter by automated control of beam tilting and X-ray detection following Muto and Ohtsuka [2]. For determination of cation site occupation, we performed theoretical calculations of HARECXS profiles using ICSC code [4] and evaluated sample thicknesses by convergent-beam electron diffraction. The experimentally obtained HARECXS profiles were fitted by linear combinations of calculated profiles, and the site occupations of constituent cations were quantitatively determined. Obtained results were almost consistent with the results determined by single crystal X-ray diffraction experiments. Moreover, the cation distributions in annealed samples showed continuous disordering with increasing temperature. This study suggests that the ALCHEMI/HARECXS method is one of the most promising candidates for accurate analysis of minerals in particular the samples having heterogeneous textures.

[1] J. H. Spence and J. Taftø, J. Microscopy 130 (1983) 147-154.
[2] S. Muto and M. Ohtsuka, Prog. Cryst. Growth Ch. 63 (2017) 40-61.
[3] Y. Igami, T. Kuribayashi and A. Miyake, Am. Mineral. 130 (2018) 944-951.
[4] M. P. Oxley and L. J. Allen, J. Appl. Cryst. 36 (2003) 940-943.

©2019. Japan Geoscience Union. All Right Reserved.

Keywords: Analytical electron microscopy, ALCHEMI, HARECXS, Site occupancy, Cation ordering

©2019. Japan Geoscience Union. All Right Reserved.

[J] Oral | S (Solid Earth Sciences)：S-MP Mineralogy & Petrology

Wed. May 29, 2019 1:45 PM - 3:15 PM JST | Wed. May 29, 2019 4:45 AM - 6:15 AM UTC | A07 TOKYO BAY MAKUHARI HALL

[S-MP33] Physics and Chemistry of Minerals

convener:Seiji Kamada(Frontier Research Institute for Interdisciplinary Sciences, Tohoku University), Masahiro KAYAMA(Department of Earth and Planetary Material Sciences, Faculty of Science, Tohoku University), Chairperson:Fumiya Noritake(Materials Science, Faculty of Engineering, Graduate Faculty of Interdisciplinary Research, UNIVERSITY OF YAMANASHI), Seiji Kamada(FRIS, Tohoku Univ.)

In this session, we will discuss the physics and chemistry of the Earth and planetary materials (including amorphous and melts) based on the results obtained from various experimental methods such as X-ray diffraction, FT-IR, Raman spectroscopy, electron microscopic observations, and computer simulations.

1:45 PM - 2:15 PM JST | 4:45 AM - 5:15 AM UTC

[SMP33-12] Molecular Dynamics Study of Soret Effect in Silicate Liquids

★Invited Papers

*Fumiya Noritake[1] (1.Graduate Faculty of interdisciplinary Research, University of Yamanashi)

2:15 PM - 2:30 PM JST | 5:15 AM - 5:30 AM UTC

[SMP33-13] Seebeck coefficient of olivine: Implausible Mercury's thermoelectric dynamo

*Hitoshi Gomi[1], Takashi Yoshino[1], Akira Yoneda[1] (1.Okayama University)

2:30 PM - 2:45 PM JST | 5:30 AM - 5:45 AM UTC

[SMP33-14] Density measurement of liquid gallium using externally heated diamond anvil cell

*Ryo Tsuruoka[1], Hidenori Terasaki[1], Seiji Kamada[2], Iori Yamada[1], Fumiya Maeda[3], Tadashi Kondo[1], Satoru Urakawa[4], Naohisa Hirao[5], Akihiko Machida[6] (1.Department of Earth and Space Science, Graduate School of Science Osaka University, 2.Frontier Research Institute for Interdisciplinary Sciences, Tohoku University, 3.Department of Earth and Planetary Materials Science, Graduate School of Science, Tohoku University, 4.Department of Earth Science, Okayama University, 5.Japan Synchrotron Radiation Research Institute, 6.National Institutes for Quantum and Radiological Science and Technology)

2:45 PM - 3:00 PM JST | 5:45 AM - 6:00 AM UTC

[SMP33-15] Density measurements of crystalline Fe and amorphous materials at high pressure

*Seiji Kamada[1,2], Hidenori Terasaki[3], Yusaku Takubo[3], Ryo Tsuruoka[3], Fumiya Maeda[2], Rui Yamada[1], Saori Kawaguchi[4], Naohisa Hirao[4], Akihiko Machida[5] (1.Frontier Research Institute for Interdisciplinary Sciences, Tohoku University, 2.Department of Earth Science, Graduate School of Science, Tohoku University, 3.Department of Earth and Space Science, Graduate School of Science, Osaka University, 4.JASRI, 5.QST)

3:00 PM - 3:15 PM JST | 6:00 AM - 6:15 AM UTC

[SMP33-16] DAC-GHz ultrasonic P wave velocity measurement on KCl and natural olivine

*Akira Yoneda[1], Shinichiro Kobayashi[2], Seiji Kamada[3] (1.Institute for planetary materials, Okayama University, 2.Department of Earth Science, Graduate school of Science, Tohoku Univ., 3.Frontier Research Institute for Interdisciplinary Sciences, Tohoku Univ.)

Molecular Dynamics Study of Soret Effect in Silicate Liquids

*Fumiya Noritake[1]

1. Graduate Faculty of interdisciplinary Research, University of Yamanashi

There are various transportation phenomena driven a potential gradient. The Soret effect is diffusion driven by a temperature gradient (Soret, 1879; Ludwig, 1856). The inverse effect is known as Dufour effect. The Soret effect is sometime used in explanation of fractionation phenomena in geology (Lesher, 1986; Dominguez et al., 2011). Recently Kishi et al. (2018) reports a distribution anomaly of composition in calcium aluminosilicate glass made by migration of high-temperature metal sphere induced by laser irradiation (Hidai et al., 2016). The rate of fractionation by temperature gradient is determined by both thermal diffusivity (D_T) and mass diffusivities (D) because the total net flux must be zero in a steady state. Consequently, understanding the Soret coefficient (D_T/D, or $\partial \log \rho / \partial T$) is difficult because the coefficient might be affected by not only atomic mass and inter-atomic interaction that affect activation energy but also geometric/structural factor.
I applied the molecular dynamics (MD) simulations for pseudo binary and aluminosilicate liquids to investigate the mechanism of fractionation by temperature gradient. The MD simulation appropriate method for this study because it gives trajectories of each atoms in the simulation cells and potentials of each atom at any point in simulation time. MD simulations of sodium/calcium-silicate/aluminosilicate liquids were performed using MXDORTO code (Sakuma & Kawamura, 2009). The simulation conditions are as follows: The inter-atomic potential model was taken from Feuston & Garofalini (1988). Systems of approximately 30000 particles in rod-shaped (approximately 5 x 5 x 17 nm) simulation cell in periodic boundary condition were firstly annealed for 2 ns at 2000 K from randomly generated structure. Then we started the simulations in temperature gradient. The temperatures in sliced region (approximately 0.35 nm thickness) perpendicular to the longest axis at the end and the center of simulation cell were maintained 2000 and 3500 K using the scaling procedure. After several tens nano-second simulations, we confirmed the changes in distribution of composition. The concentration of SiO_2 in the high-temperature center part slightly increases as simulation proceeds. In contrast the concentration of CaO and Na_2O in that part slightly decreases. Soret coefficients for each cation has linear relation with the half width of potential energy distribution in binary silicates. The existence of Al_2O_3 content impedes fractionation in sodium-aluminosilicate whereas it enhances in calcium-aluminosilicate. This behavior might be caused by the charge compensation of 4-fold aluminum cation.

Keywords: Silicate Liquids, Molecular Dynamics Simulation, Soret Effect

©2019. Japan Geoscience Union. All Right Reserved.

Seebeck coefficient of olivine: Implausible Mercury's thermoelectric dynamo

*Hitoshi Gomi[1], Takashi Yoshino[1], Akira Yoneda[1]

1. Okayama University

The Mercury's magnetic fields are known to be weaker than that predicted by conventional dynamo models. In order to explain the Mercury's weak magnetic field, several models are proposed (Stanley and Glatzmaier, 2010). One of them is the thermoelectric dynamo, which drive the dynamo via the thermoelectric force (Stevenson, 1987). The field strength is proportional to the relative Seebeck coefficient between the core and the mantle. Because the Seebeck coefficient of insulators is more than one order larger than that of metals, the Seebeck coefficient of Mercury's mantle is the central parameter. Therefore, we investigated the Seebeck coefficient of mantle minerals from the first-principles calculations. The structure relaxation and band structure calculations were conducted by using the Quantum ESPRESSO package. The bandgap energy was calibrated by means of the quasiparticles self-consistent GW (QSGW) approximation adopted in the ecalj package. The Seebeck coefficient was calculated via the Boltzmann equation implemented in the BoltzTraP package. The results indicate that the Seebeck coefficient of forsterite with a small amount of dopant exhibit comparable to that previously thought (|S| ~ 1000 mV/K). This value may constrain the upper limit. The Mercury's mantle may contain ~3wt% FeO (Robinson and Taylor, 2001). The Fe substitution and O vacancy act as donor, which is predicted to reduce the Seebeck coefficient, significantly. The field strength also depends on the electrical conductivity of the mangle. Recent high pressure experiments suggest that the electrical conductivity of the Earth's mantle is ~ 10^{-2} Sm. Considering the both of the Seebeck coefficient and the electrical conductivity of mantle material, the field strength is calculated to be ~ 0.1 nT, which is significantly weaker than the observed value of 300 nT. Therefore, we conclude that the thermoelectric dynamo cannot generate the Mercury's magnetic fields.

Keywords: Seebeck coefficient, Mercury, thermoelectric dynamo

©2019. Japan Geoscience Union. All Right Reserved.

Density measurement of liquid gallium using externally heated diamond anvil cell

*Ryo Tsuruoka[1], Hidenori Terasaki[1], Seiji Kamada[2], Iori Yamada[1], Fumiya Maeda[3], Tadashi Kondo[1], Satoru Urakawa[4], Naohisa Hirao[5], Akihiko Machida[6]

1. Department of Earth and Space Science, Graduate School of Science Osaka University, 2. Frontier Research Institute for Interdisciplinary Sciences, Tohoku University, 3. Department of Earth and Planetary Materials Science, Graduate School of Science, Tohoku University, 4. Department of Earth Science, Okayama University, 5. Japan Synchrotron Radiation Research Institute, 6. National Institutes for Quantum and Radiological Science and Technology

Density of a liquid metal at high pressure and high temperature is fundamental information to determine its equation of state (EOS). Gallium (Ga) which has a low melting temperature at ambient pressure has been reported to have complex liquid structures. The densities of Ga at high pressures have been reported based on the measurement of volume changes (Lyapin et al. 2008), that of liquid structures (Yu et al. 2012), and that of sound velocity (Ayrinhac et al. 2015). However, these densities were not consistent each other. In this study, we measured densities of liquid Ga at high pressure using an X-ray absorption method with an externally heated diamond anvil cell (EHDAC).

Ga sample and reference materials (KBr, RbBr) were loaded into each hole drilled on a pre-indented Re gasket. The reference materials were used for estimation of sample thickness and for determination of experimental pressures (Takubo et al. 2018). The Re gasket was coated with Al_2O_3 to avoid a reaction between the Ga sample and the gasket. High pressure was generated using a symmetric DAC with a lever-arm frame. The culet size of the diamond anvils used was 600 μm. High temperature was generated using external heaters composed of Pt-Rh wires with a ZrO_2 insulator. X-ray absorption measurements were conducted with monochromatic X-ray of 30 keV at BL10XU and BL22XU beamlines in SPring-8. Intensities of incident and transmitted X-rays were detected using a photo-diode or ion chambers. Experimental pressures were determined based on EOSs of KBr and RbBr using their volumes from XRD patterns collected using a flat panel detector.

The densities of liquid Ga were measured up to 9.4 GPa and 500 K. The densities of liquid Ga obtained at 4–9 GPa range 6.53(7)–7.25(14) g/cm^3. The measured density at 4 GPa is consistent with the density calculated from sound velocity data reported by Ayrinhac et al. (2015).

Keywords: gallium, diamond anvil cell, X-ray absorption method

©2019. Japan Geoscience Union. All Right Reserved.

Density measurements of crystalline Fe and amorphous materials at high pressure

*Seiji Kamada[1,2], Hidenori Terasaki[3], Yusaku Takubo[3], Ryo Tsuruoka[3], Fumiya Maeda[2], Rui Yamada[1], Saori Kawaguchi[4], Naohisa Hirao[4], Akihiko Machida[5]

1. Frontier Research Institute for Interdisciplinary Sciences, Tohoku University, 2. Department of Earth Science, Graduate School of Science, Tohoku University, 3. Department of Earth and Space Science, Graduate School of Science, Osaka University, 4. JASRI, 5. QST

Terrestrial planets, such as Earth, Venus, Mars, and Mercury, have metallic liquid and/or solid cores. The cores consistent of mainly Fe and Ni with small amounts of light elements. Chemical compositions of solid state cores have been estimated by density measurements of crystalline core materials in a number of previous studies. On the other hand, there are a few previous studies on density measurements of liquid samples because of technical difficulties. Although Morard et al. (2008, 2013) obtained densities of liquid Fe with light elements by structure analyses from XRD patterns, accuracy of the densities was under debate because they used XRD patterns with narrow reciprocal lattice spaces. In this study, we have measured densities of crystalline Fe and amorphous materials using an X-ray absorption method in order to avoid problems of small diffraction angles due to a diamond anvil cell (DAC).
High pressure measurements were performed using a DAC with a gasket having 3 sample chambers. Fe or amorphous samples were loaded in a sample chamber for density measurements. Powders of KCl, KBr, or RbBr as references for thickness were also loaded in the other sample chambers. After XRD patterns were taken from all samples and references, absorption profiles were also measured. Experimental pressures were determined using pressure averages between KCl and KBr, or KBr and RbBr. Densities based on the X-ray absorption method were obtained using the Lambert Beer law with mass absorption coefficients from NIST data base. Densities of crystalline Fe were obtained up to 20 GPa and density differences between XRD and the absorption method were less than 2%. This technique was applied to densities of amorphous materials as well. We will report the densities based on the X-ray absorption method.

Keywords: X-ray absorption method, diamond anvil cell

©2019. Japan Geoscience Union. All Right Reserved.

DAC-GHz ultrasonic P wave velocity measurement on KCl and natural olivine

*Akira Yoneda[1], Shinichiro Kobayashi[2], Seiji Kamada[3]

1. Institute for planetary materials, Okayama University, 2. Department of Earth Science, Graduate school of Science, Tohoku Univ., 3. Frontier Research Institute for Interdisciplinary Sciences, Tohoku Univ.

GHz ultrasonic velocity measurements has been developed up to 14 GPa in diamond anvil cell (DAC). In order for GHz ultrasonic measurement, both P and S wave buffer rods were manufactured through sputtering ZnO piezoelectric film on single crystal rods, such as sapphire, rutile, and YAG. Several technical breakthroughs were achieved before observing stable signals from the specimen squeezed in DAC: (1) Wiping by aqueous ammonia on the contact surfaces enhances transmissibility of GHz wave from buffer rod to diamond. (2) Cleaning by lathery detergent and water jet is effective to remove sticky staff on rear surface of diamond. (3) Steel ball supporter provides easier adjustment of contact between buffer rod and diamond. Consequently, we succeeded to demonstrate performance of DAC-GHz system through KCl and natural olivine samples.

Keywords: elasticity, DAC, GHz ultrasonics

©2019. Japan Geoscience Union. All Right Reserved.

[J] Poster | S (Solid Earth Sciences)：S-MP Mineralogy & Petrology

Wed. May 29, 2019 3:30 PM - 5:00 PM JST | Wed. May 29, 2019 6:30 AM - 8:00 AM UTC | Poster Hall International Exhibition Hall8, Makuhari Messe_18

[S-MP33] Physics and Chemistry of Minerals

convener:Seiji Kamada(Frontier Research Institute for Interdisciplinary Sciences, Tohoku University), Masahiro KAYAMA(Department of Earth and Planetary Material Sciences, Faculty of Science, Tohoku University)

In this session, we will discuss the physics and chemistry of the Earth and planetary materials (including amorphous and melts) based on the results obtained from various experimental methods such as X-ray diffraction, FT-IR, Raman spectroscopy, electron microscopic observations, and computer simulations.

[SMP33-P01] Raman spectroscopy of seifertite

*Masahiro KAYAMA[1], Eiji Ohtani[1], Masaaki Miyahara[2], Shohei Kaneko[1], Toshimori Sekine[3], Shin Ozawa[1], Naohisa Hirao[4] (1.Tohoku University, 2.Hiroshima University, 3.HPSTAR, 4.Japan Synchrotron Radiation Research Institute)

[SMP33-P02] Microtexture and crystallization process of impact diamonds

*Hiroaki Ohfuji[1], Motosuke Nakaya[1] (1.Geodynamics Research Center, Ehime University)

[SMP33-P03] Metamorphic temperature analysis of H chondrites: Using revised Lindsley's pyroxene thermometer

*Ryo Uehara[1], Yoshihiro Kuwahara[1], Kazuhiko Shimada[1], Yoshihiro Nakamuta[1], Seiichiro Uehara[1], Tatsuro Adachi[1] (1.Kyushu university)

[SMP33-P04] The occurrence combinations of Zeolites at Chichijima, Ogasawara Islands

Michiharu Ito[1], *Yuki Inoue[1], Mana Yasui[2], Atsushi Yamazaki[2], Hiroshi Hagiya[1] (1. Tokyo City University, 2.Waseda research institute for science and engineering)

[SMP33-P05] Title: Single-crystal X-ray diffraction study of mirabilite ($Na_2SO_4 \cdot 10H_2O$) from 213 to 303 K

*Ryutaro Ikeda[1] (1.University of tsukuba)

[SMP33-P06] Elastic constants of single-crystal topaz studied via sphere-resonance method

*Kako Aradachi[1], Tohru Watanabe[1], Morihisa Hamada[2] (1.University of Toyama, 2.JAMSTEC)

[SMP33-P07] Verification of damage by polishing of sheet-like minerals

*Yui Kouketsu[1], Kota Ando[1], Katsuyoshi Michibayashi[1] (1.Department of Earth & Planetary Sciences, Graduate School of Environmental Studies, Nagoya University)

[SMP33-P08] Description of Zebra Rock and the pattern formation model

*Kaoru Yoshimura[1], Atsushi Toramaru[2], Mie Ichihara[3], Takaaki Noguchi[4], Toru Matsumoto[5] (1.Department of Earth and Planetary Science, Graduate School of Science, Kyushu University, 2.Department of Earth and Planetary Sciences, Faculty of Sciences, Kyushu University, 3.Earthquake Research Institute, University of Tokyu, 4.Department of Arts and Science, Kyushu University, 5.Japan Aerospace Exploration Agency/ Institute of Space and Astronautical Science)

[SMP33-P09] Thermal conductivity anomaly of (Mg,Fe)CO_3 solid solution across the spin transition

*Keng-Hsien Chao[1], Wen-Pin Hsieh[1,2] (1.Institute of Earth Sciences, Academia Sinica, Taiwan, 2.Department of Geosciences, National Taiwan University, Taiwan)

[SMP33-P10] **Melting experiments in the $MgSiO_3$ – SiO_2 system under high pressures**

*Takuya Moriguti[1], Akira Yoneda[1], Eiji Ito[1] (1.Institute for Planetary Materials, Okayama University)

[SMP33-P11] Melting relations of the Fe-Ni-S-C system and the formation of superdeep diamonds

*Yu Itami[1], Satoru Urakawa[1] (1.Okayama University)

[SMP33-P12] Effect of ammonia on the stability of methane hydrate under high-pressure and high-temperature

*Hirokazu Kadobayashi[1], Hisako Hirai[2], Hiroaki Ohfuji[1], Hideaki Kawamura[1], Michika Ohtake[3], Yoshitaka Yamamoto[3] (1.Geodynamics Research Center, Ehime University, 2.Department of Environment System, Faculty of Geo-environmental Science, Rissho University, 3.National Institute of Advanced Industrial Science and Technology)

[SMP33-P13] Study on magnetite-maghemite-hematite transformation

*Ibuki Kinebuchi[1], Atsushi Kyono[1], Yoshinari Sano[1] (1.University of Tsukuba)

[SMP33-P14] The Effects of Temperature and Pressure on Hydromagnesite

*Gen-ichiro Yamamoto[1], Atsushi Kyono[1], Jun Abe[2], Takanori Hattori[3], Yoshitaka Matsushita[4], Yasuhiro Yoneda[3] (1.University of Tsukuba, 2.CROSS, 3.JAEA, 4.NIMS)

[SMP33-P15] Synthesis and crystal structure of Mg-bearing Fe_9O_{11}: New insight in the complexity of Fe-Mg oxides at conditions of the deep upper mantle

*Takayuki Ishii[1], Uenver-Thiele Laura[2], Alan B Woodland[2], Edith Alig[3], Tiziana Boffa Ballaran[1] (1.Bavarian Research Institute, University of Bayreuth, 2.Institut für Geowissenschaften, Goethe-Universität Frankfurt, 3.Institut für Anorganische und Analytische Chemie, Goethe-Universität Frankfurt)

[SMP33-P16] **Changes in specific surface area and morphology of kaolin group minerals with pressure treatment**

*Soyeon Kwon[1], Yongjae Lee[1] (1.YONSEI University)

Raman spectroscopy of seifertite

*Masahiro KAYAMA[1], Eiji Ohtani[1], Masaaki Miyahara[2], Shohei Kaneko[1], Toshimori Sekine[3], Shin Ozawa[1], Naohisa Hirao[4]

1. Tohoku University, 2. Hiroshima University, 3. HPSTAR, 4. Japan Synchrotron Radiation Research Institute

Seifertite is one of the SiO_2 polymorphs and is a high pressure phase with an α-PbO_2 structure. It is known to lie in lunar and martian meteorites and constrains shock pressure and duration of an impact event that these meteorites have experienced on the host bodies. Seifertite is thermodynamically stable at more than ~100 GPa, which is not realistic for an impact event on the Moon and Mars. However, it can be transformed as a metastable phase from cristobalite at least ~11 GPa and 0.01 s, and can consequently be quenched down to an ambient condition. As a result of this process, seifertite remains present in some of the lunar and martian meteorites. The estimated shock pressure and duration provide valuable information on the size of the crater and impactor that collided don the host bodies. Although Raman spectroscopy has been previously measured for seifertite in meteorites, it was not successful to obtain the seifertite signature because of a potential vitrification or transition into other SiO_2 phase by heating due to the laser irradiation. Therefore, only synchrotron-XRD and TEM analyses allow us to determine the structure, where silica grains are excavated with a focused ion beam (FIB) system from meteorite. Here, Raman spectral signatures of seifertite has been obtained from synthetic and meteoritic silica grains, implying its identification with high-spatial resolution as nondestructive analysis.

Seifertite in silica grains of synthetic samples and lunar (NWA 4734) and martian meteorites (Zagami, NWA 2975) were identifications by a synchrotron XRD analysis at Spring-8 BL-10 and were employed for Raman spectroscopy. Seifertite were synthetized from synthetic cristobalite powders using multi-anvil press at 16 GPa, 673 K and 0.5 hour. Raman spectroscopy were performed for synthetic and meteoritic silica grains using Nd: YAG 532 nm at 20 mW for 3 minutes exposure time.
Raman spectra of synthetic seifertite have pronounced peaks at 380, 515, 564, 739 and 796 cm^{-1} and weak peaks at 401, 496, 539, 547, 606 and 749 cm^{-1}. Similar Raman signature was obtained from seifertite in lunar and martian meteorites. These Raman shifts and relative intensities are well corresponding to the values calculated within the density-functional perturbation theory for seifertite. Based on the calculation, thee Raman peaks at 380, 515, 564, and 796 cm^{-1} are assigned to Ag, those at 401, 496, and 539 cm^{-1} to B1g, 606 and 749 cm^{-1} to B2g, and 547 and 739 cm^{-1} to B3g modes. After laser beam irradiation for 30 minutes, the distinct Raman signature can be detected from synthetic and meteoritic seifertite. Therefore, Raman spectroscopy enables determination of the structure and identification of SiO2 polymorphs with high-spatial resolution and without destruction.

Keywords: Seifertite, Raman spectroscopy, Meteorite

©2019. Japan Geoscience Union. All Right Reserved.

Microtexture and crystallization process of impact diamonds

*Hiroaki Ohfuji[1], Motosuke Nakaya[1]

1. Geodynamics Research Center, Ehime University

Impact diamonds from the Popigai crater located in the central Siberia, Russia show unique nano-polycrystalline texture composed of diamond and a small amount of lonsdaleite of ~50 nm (Ohfuji et al., 2015), which is well comparable to the nano-polycrystalline diamond synthesized by direct conversion of graphite under high pressure and high temperature (Irifune et al., 2003). However, subsequent studies noted that they show a variety of microtexture such as lamellar or layer textures and granular textures. In the present study, we investigated the mineralogical and crystallographic characteristics of the various microtextures shown by the Popigai diamonds by TEM.

The microtextures found in Popigai diamonds are divided into two types, 1) lamellar type and 2) granular type. The former is further classified into two types, 1a) less-mosaiced lamellar and 1b) mosaiced lamellar. The latter can also be divided further into 2a) granular texture composed of fine crystals of <50 nm and 2b) granular texture composed of larger (~100 nm) crystals. Careful textural observations and electron diffraction analysis revealed that the microtextures of Popigai diamonds vary from layered texture to granular texture (1a →1b →2a →2b) as the phase transitions from graphite to lonsdaleite to diamond proceed. The phase transition mechanism also changes from martensitic process involving a lattice relationship (Graphite (001) // Lonsdaleite (100) // Diamond (111)) to diffusion process where the nucleation of new grains and the their growth are promoted.

The most important factor controlling the degree of the phase transitions and the resulting microtexture is probably the shock temperature, which is supposed to have decreased gradually from the center to rim in the crater.

Keywords: Impact diamonds, Pipogai crater, High temperature and high pressure

©2019. Japan Geoscience Union. All Right Reserved.

Metamorphic temperature analysis of H chondrites: Using revised Lindsley's pyroxene thermometer

*Ryo Uehara[1], Yoshihiro Kuwahara[1], Kazuhiko Shimada[1], Yoshihiro Nakamuta[1], Seiichiro Uehara[1], Tatsuro Adachi[1]

1. Kyushu university

1. Introduction
The thermal evolution models of asteroids have been proposed and discussed by many researchers to provide insight into the internal structure and thermal history of those (e.g., Wood,1979; Miyamoto et al., 1981; Yomogida and Matsui, 1984; McSween et al., 2002). As important parameters for the thermal evolution models, the highest peak temperatures, ages, and cooling rates of meteorite parent bodies are mentioned (McSween et al., 2002). The peak temperature inside the parent body has been estimated using various thermometers (Olsen and Bunch, 1984; Nakamuta and Motomura, 1999; Kessel et al., 2002; Slater-Reynolds and McSween, 2005). Pyroxene thermometer by Lindsley (1983) has been widely used because it allows us to derive temperatures from both orthopyroxene (Opx) and clinopyroxene (Cpx) in a meteorite. However, the temperatures determined from clinopyroxenes, especially for type 6 chondrites, are systematically 50˚C to 150˚C higher than those from orthopyroxenes (Nakamuta et al., 2017). The Lindsley’s pyroxene thermometer is made empirically for terrestrial rocks and therefore the kosmochlor component is not considered in the calculation. So, Nakamuta et al. (2017) proposed the revised Lindsley’s pyroxene thermometer in which the kosmochlor pyroxene component is added to evaluate the effect of the component on the thermometry. They also showed that the difference in temperature between clinopyroxene and orthopyroxene in LL chondrites using the revised thermometer was less than 20˚C.
In this study, we have attempted to estimate the metamorphic temperatures of H chondrites (type 4 to 7) using the Lindsley’s pyroxene thermometer revised by Nakamuta et al (2017). Here we report the results of the estimation.
2. Samples and method
The chondrite samples used were four types of H chondrite with different metamorphic degrees; Edmondson(b) (H4), Faucett (H5), Faith (H5), Plainview (H5), Mulga(north) (H6), Great Bend (H6) and NWA7875 (H7). Polished thin sections of the seven H chondrites were prepared and observed using transmitted and reflecting light microscopes. Then, chemical compositions of pyroxenes, olivines, and plagioclases in the seven H chondrites were analyzed by an EPMA, JEOL JXA-8530F. Beased on these results, the classification of each meteorite sample was reconfirmed, and metamorphism temperatures estimated using the revised Lindsley pyroxene thermometer.
3. Results and discussion
From results of the texture observation and chemical analysis of the chondrite sample, we reconfirmed that there is no mistake in classification of each meteorites (H4, H5, H6, H7). The temperatures for Edmondson(b) (H4), Faucett (H5), Faith (H5), Plainview (H5), Mulga(north) (H6), Great Bend (H6) and NWA7875 (H7) are 779-1236˚C (Opx-Cpx), 814-875˚C, 832-843˚C, 844-838˚C, 807-797˚C, 811-818˚C and 1183-1247˚C, respectively, using the revised Lindsley pyroxene thermometer. Most of H5 and H6 meteorite samples showed that the difference in temperature between Opx and Cpx was less than 20˚C. This result, this suggests that the revised Lindsley pyroxene thermometer by Nakamuta et al. (2017) is also effective for H chondrite. The metamorphic temperatures of the H5 type chondrite (Faucett, Faith and Plainview) and the H6 type chondrite (Mulga(north), Great Bend) are approximately 840˚C and 810˚C, respectively, while the H4 type Edmondson(b) chondrite is less than 780˚C judging from the temperature

©2019. Japan Geoscience Union. All Right Reserved.

estimated from Opx. Regarding the H7 type NWA7875 chondrite which showed the highest metamorphic temperature and lamella structure in some Cpx crystals, the H7 material that existed already in H5 and/or H6 conditions may have experienced impact metamorphism, redrawing the previous metamorphic temperature and the H5 and/or H6 conditions.
Comparing these estimated temperature data with the results of the model simulation reported by Monnereau et al. (2013), it is estimated that the H chondrite meteorite parent body had an onion shell type internal thermal structure formed when the accumulation period was short (<0.2 Myr).

Keywords: H chondrite, Lindsley pyroxene thermometer, Kosmoclor, Peak temperature, Onion-shell model

©2019. Japan Geoscience Union. All Right Reserved.

The occurrence combinations of Zeolites at Chichijima, Ogasawara Islands

Michiharu Ito[1], *Yuki Inoue[1], Mana Yasui[2], Atsushi Yamazaki[2], Hiroshi Hagiya[1]

1. Tokyo City University, 2. Waseda research institute for science and engineering

The Ogasawara Islands are located in the Pacific Ocean about 1000 km south of Tokyo, Japan. These Islands are situated in the outer of the Izu-Bonin-Mariana Arc. The Ogasawara Islands are composed by paleogene submarine volcanic formation, and is well known by andesitic volcanic rock called boninite. Boninite is a feldspar-free and glass-rich olivine-bronzite andesite with higher MgO, SiO_2, H_2O and Cr contents. Zeolites, co-exist with calcite, quartz/chalcedony and celadonite, fill the vesicles of volcanic gas, radial and columnar cooling joint of pillow lava, and also occur in interpillow sediment with large aggregate of crystals.

In this study, various habits of zeolites at Chichijima, Ogasawara Islands are obtained, also more than two-step growth of zeolites in amygdale were confirmed. Between these two-step growth, cation ratio have changed at the border of two faces.

These cation's contents are similar to neighboring rock. It is considered that there is another hydrothermal activity after the first-step growth.

Keywords: Zeolite, boninite, hydrothermal activity, occurrence combinations

©2019. Japan Geoscience Union. All Right Reserved.

Title: Single-crystal X-ray diffraction study of mirabilite ($Na_2SO_4 \cdot 10H_2O$) from 213 to 303 K

*Ryutaro Ikeda[1]

1. University of tsukuba

Introduction

Renewable energy is of increasing importance in modern society due to its low environmental impact, ubiquity and sustainability. Since some renewable energy resources (e.g. sunlight, wind and tides) have variable outputs, storage technologies have great potential for affording the supply from these resources. In recent years, much attention has been paid to phase change materials (PCMs) due to its high energy storage capacity. PCMs are substances with a heat of fusion which can store and releasing large amounts of energy. Mirabilite ($Na_2SO_4 \cdot 10H_2O$) is known as one of the PCMs. With increasing temperature, mirabilite transforms to thenardite (Na_2SO_4) at a dehydration temperature of 306 K. On the contrary, thenardite is rehydrated back to mirabilite at 283 K. The reversible reaction involves large exothermic and endothermic heats. To date, however, there is little information on temperature dependence of crystal structure in mirabilite. The structure of mirabilite contains ribbons consisting of edge-sharing $Na(H_2O)_6$ octahedra along the *c*-axis. These ribbons alternate with chains of the SO_4 tetrahedra and the two H_2O molecules. Levy and Lisensky (1978) identified disorder over two orientations of the SO_4 tetrahedra by single-crystal neutron diffraction measurement at room temperature. The characteristic two orientations, related by a rotation of about 30° about the S×××O5 vector, generate pairs of partially occupied sulfate oxygen sites (O4’/O4’’, O6’/O6’’, and O7’/O7’’). Levy and Lisensky (1978) found that the primed sites are about 25% occupied, and the double-primed sites are about 75% occupied. Recently, Brand et al. (2008) performed powder neutron diffraction measurements on mirabilite ($Na_2SO_4 \cdot 10D_2O$) in the temperature range from 10 to 300 K. They reported that the unit cell of mirabilite is isotopically expanded up to 300 K. The authors however couldn’t observe the two orientations for the SO_4 tetrahedra in the structure, which was previously identified by Levy and Lisensky (1978). In the study, we performed temperature-dependent single-crystal X-ray diffraction measurement of mirabilite in the temperature range between 213 and 303 K. Here, we report the crystal structure change of mirabilite associated with the characteristic exothermic and endothermic heats.

Methods

Single crystals of mirabilite were obtained by slow cooling of a saturated solution of Na_2SO_4. After the synthesis, a single crystal was stored in a 0.7 mm Lindemann glass capillary to avoid dehydration. Temperature dependent single-crystal X-ray diffraction study on mirabilite was performed using a single-crystal diffractometer (APEXII ULTRA, Bruker AXS Inc., Germany) equipped with a liquid nitrogen cryostat, a CCD detector, multilayer optics, and graphite monochromated Mo$K\alpha$ radiation (λ = 0.71073 Å) generated by a rotating anode. The measurements were conducted at temperature ranges between 213 and 303 K with 10 K step in both heating and cooling processes.

Results and Discussion

The *a* and *c* lattice parameters and unit cell volume were monotonously changed with temperature, whereas the *b* lattice parameter remained almost unchanged. The result is entirely consistent with the

©2019. Japan Geoscience Union. All Right Reserved.

previous report that thermal expansivities of the *a*- and *c*-axes are of similar magnitude, while the *b*-axis shows a much smaller thermal expansion (Brand et al. 2008). The disorder over two orientations of the SO_4 tetrahedra was observed in the present study. At room temperature, the primed and double-primed sites are about 25% and 75% occupied, respectively, which is completely consistent with the result by single-crystal neutron diffraction study (Levy and Lisensky 1978). A clear temperature dependence of the disorder over two orientations was, however, unobserved in the study. It is noteworthy that the SO_4 tetrahedral volume coordinated by primed oxygen atoms showed a pronounced temperature dependence. In the vicinity of dehydration temperature of mirabilite, it approached to that of thenardite (Na_2SO_4), which would be a trigger initiating the dehydration of mirabilite.

Keywords: sodium sulfate, Single crystal XRD, mirabilite, Phase change

©2019. Japan Geoscience Union. All Right Reserved.

Elastic constants of single-crystal topaz studied via sphere-resonance method

*Kako Aradachi[1], Tohru Watanabe[1], Morihisa Hamada[2]

1. University of Toyama, 2. JAMSTEC

Transport of ocean floor sediments by plate motions might play an important role in the circulation of materials within the Earth. Imaging subducted sediments through seismological observations requires a thorough understanding of elastic properties of sediment origin hydrous minerals. Topaz is a hydrous mineral, which can be formed from subducted sediment at high pressures. We have studied elastic constants of single-crystal topaz by the sphere-resonance method.

A sphere sample (D=2.665(1) mm) was made from a topaz single-crystal (Al1.97SiO4(F1.17,OH0.82)) collected from Ouro preto, Mines Gerais, Brazil by the two-pipe method. Lattice parameters are a=4.663, b=8.835, c=8.386 A (orthorhombic). Resonant frequencies were measured at frequencies from 1.6 MHz to 3.5 MHz with different specimen-holding forces. Extrapolating to the specimen-holding force of zero, we obtained frequencies of "free" oscillation. Elastic constants were determined by comparing measured and calculated resonant frequencies. The xyz algorithm (Visscher et al., 1991) was employed to calculate resonant frequencies of the sphere sample. At an ambient temperature, C11=281.2(5), C22=350.3(7), C33=288.4(5), C44=108.8(2), C55=130.9(2), C66=131.4(2), C12=121.3(2), C13=81.6(2), C23=82.1(2) (GPa).

Keywords: Topaz, Elastic constants, Water

©2019. Japan Geoscience Union. All Right Reserved.

Verification of damage by polishing of sheet-like minerals

*Yui Kouketsu[1], Kota Ando[1], Katsuyoshi Michibayashi[1]

1. Department of Earth & Planetary Sciences, Graduate School of Environmental Studies, Nagoya University

Sheet-like minerals such as mica, serpentine, clay minerals and graphite are affected by shearing due to polishing. In addition, a damage due to electron beam irradiation during observation by the electron microscope also occurs. In this study, the damage due to polishing and irradiation of the electron beam for sheet-like minerals of graphite and serpentine minerals was evaluated by Raman spectroscopic analysis. First, we evaluated the crystallinity change of graphite in each polishing stage. As a result, a decrease in crystallinity was observed in all stages from rough polishing to fine grain polishing by diamond paste. The chemical polishing with colloidal silica also lowered the crystallinity of graphite. In order to reduce the shearing effect to graphite, we tested a low load polishing using the polisher ISPP-1000 (Ikegami Seiki Co., Ltd.) which is controlling the load by a weight. However, it was revealed that even a load of only 25g was damaged to graphite. Next we examined the polishing effect of serpentine minerals. Raman spectroscopic analysis was performed after polishing, however no spectral change at each polishing stage like graphite was detected. On the other hand, the antigorite Raman spectra after SEM-EBSD analysis showed a decrease in intensity at the depth of about 3 micrometre from the surface, suggesting that the crystal structure was damaged by electron beam irradiation. We also tried a low load polishing for serpentine minerals, and we detected an electron backscatter pattern of lizardite for the first time. In the case of pure lizardite sample, a clear Kikuchi band was confirmed. On the other hand, almost no pattern was detected for serpentine minerals (antigorite, lizardite, chrysotile) in the serpentinite samples, because of the contrast of hardness with surrounding hard minerals such as olivine. For analysis of sheet-like minerals contained in rock samples including minerals of various hardness, further improvement of the polishing method or other methods such as ion milling is needed.

Keywords: graphite, antigorite, lizardite, low load polish, Raman spectroscopy, EBSD

©2019. Japan Geoscience Union. All Right Reserved.

Description of Zebra Rock and the pattern formation model

*Kaoru Yoshimura[1], Atsushi Toramaru[2], Mie Ichihara[3], Takaaki Noguchi[4], Toru Matsumoto[5]

1. Department of Earth and Planetary Science, Graduate School of Science, Kyushu University, 2. Department of Earth and Planetary Sciences, Faculty of Sciences, Kyushu University, 3. Earthquake Research Institute, University of Tokyu, 4. Department of Arts and Science, Kyushu University, 5. Japan Aerospace Exploration Agency/ Institute of Space and Astronautical Science

Zebra Rock is a sedimentary rock characterized by a pattern consisting of red and whitein color, which is characteristically seen in Australia. Loughnan and Roberts (1990) conclude that the origin of the pattern is due to the diffusion process in a sediment on the basis of their study of the mineral assemblage.However, the mechanism of the specific reaction is not explained, lacking the detailed description. Our aim is to describe Zebra Rock in more detail and to develop a pattern formation model including the reaction of mineral formation.
Six samples taken from the vicinity of Lake Argyle in the East Kimberley region of Western Australia are used. We refer to the characteristic banding pattern consisting of red bands and white bands as Red and White, respectively.
We examined the mineral compositions with XRD (Mac science CuKα radiation) and SEM-EDS (FE-SEM 15 kev, OXFORD Aztec) and the occurrence of minerals with SEM (FE-SEM 15 kev) and TEM (JEM-3200FSk) for each White and Red. By using BSD images, we examined the fraction of minerals, and the characteristics of the spatial correlations between minerals and void for White and Red. As a result, we found that there are two distinctive differences in the mineral abundance and occurrence of iron oxide between White and Red. Red contains more iron oxide than White as shown by previous study. In the occurrence of iron oxide is different. The iron oxide in White takes a shape of planer sheet of polycrystal (<100 μm) which consists of hematite grains (~100 nm), whereas the iron oxides in Red are aligned in interstitial spaces between kaolinite and quartz crystals, as aggregates (<100 μm) which consists of granular hematite grains (~ μm). In addition, from the spatial distribution analysis it is found that the iron oxides concentrate near voids both in White and Red.
Integrating these results,on the basis of the idea that the formation of iron oxide plays an essential role in the formation of zebra pattern,we develop a pattern formation model using a reaction diffusion system. In our model, the pattern is defined as the variation of concentration of ferric irons. We assume the formation process ofhematite in an aqueous solution is simplified as “ferrous ion →goethite (monomers) →goethite (precipitates) →hematite”. We propose an autocatalytic reaction in which ferrous ion are adsorbed in goethite, and thereby the reaction is accelerated. As a result of the linear stability analysis for this simplest model, it is found that the equilibrium point is stable and no pattern forms. Thus, we will develop more complex reaction models to produce the zebra pattern.

Keywords: Zebra Rock, pattern formation, reaction diffusion system

©2019. Japan Geoscience Union. All Right Reserved.

Thermal conductivity anomaly of $(Mg,Fe)CO_3$ solid solution across the spin transition

*Keng-Hsien Chao[1], Wen-Pin Hsieh[1,2]

1. Institute of Earth Sciences, Academia Sinica, Taiwan, 2. Department of Geosciences, National Taiwan University, Taiwan

Deep carbon cycle is a process carrying carbon into Earth's interior by subduction of slabs and returning to Earth's surface by volcanic activities. Given the abundance of iron in Earth's interior, it is believed that $(Mg,Fe)CO_3$ solid solution is an important candidate of carbon-hosting mineral in the mantle. Prior studies have shown that the iron in the $(Mg,Fe)CO_3$ solid solution undergoes a pressure-induced spin transition at 40-55 GPa and the iron content has a minor effect on the onset pressure of spin transition. Across the spin transition, the physical properties of $(Mg,Fe)CO_3$ solid solution, e.g. sound velocity and unit cell volume, typically change accordingly. Lattice thermal conductivity of mantle minerals is key to control the heat flux and temperature profile of the mantle. However, the thermal conductivity of $(Mg,Fe)CO_3$ solid solution under relevant mantle pressure-temperature conditions remains largely unknown. Here we used Raman spectroscopy to characterize the extent of spin transition of natural $(Fe_{0.18}Mn_{0.01}Mg_{0.80}Ca_{0.01})CO_3$ ferromagnesite and time-domain thermoreflectance to measure its thermal conductivity from ambient conditions to 65 GPa. Our preliminary study shows that the thermal conductivity of $(Fe_{0.18}Mn_{0.01}Mg_{0.80}Ca_{0.01})CO_3$ ferromagnesite is 20 W m^{-1} K^{-1} at 40 GPa and drastically increases to 80 W m^{-1} K^{-1} at the beginning of spin transition, and then suddenly drops to 20 W m^{-1} K^{-1} during the middle period of spin transition, similar to its iron-rich counterpart, $(Fe_{0.78}Mg_{0.22})CO_3$ siderite, investigated in our previous work. Our results suggest that if the $(Mg,Fe)CO_3$ carbonates can be transported by the subduction slabs to 1400-1800 km depth with iron contents of 18 to 78 %, their thermal conductivity anomalies across the spin transition may induce anomalies in local thermo-chemical profiles in subduction zones, which in turn alter the distribution fields of subducting minerals.

Keywords: Spin transition, Thermal conductivity, Ferromagnesite, Siderite

©2019. Japan Geoscience Union. All Right Reserved.

Melting experiments in the $MgSiO_3$ –SiO_2 system under high pressures

*Takuya Moriguti[1], Akira Yoneda[1], Eiji Ito[1]

1. Institute for Planetary Materials, Okayama University

Melting of silicates played important roles in chemical differentiation in a deep magma ocean in the early Earth. Therefore, melting relations of the MgO–SiO_2 system have been extensively studied since a pioneer work by Bowen and Anderson (1914). Furthermore, chemical differentiation in the deep magma ocean has been simulated extensively based on results of high pressure melting experiments (e.g. Kato and Kumazawa, 1985; Ito and Katsura, 1992). However, almost all of these works have been carried out on the compositions ranging from MgO to $MgSiO_3$, assuming that the bulk mantle composition is peridotitic or close to that derived from CI chondrite. Recently, enstatite chondrite (E-chondrite) has been attracted as the bulk earth source material (Javoy et al., 2010) because the isotope systematics of the Earth and Moon are nearly identical to those of E-chondrite over O, N, Mo, Re, Os, and Cr. In E-chondrite, the silicate composition is characterized by SiO_2/(SiO_2+MgO) = ˜0.6, which is substantially higher than that of the peridotitic mantle (˜0.4).

In this context, understanding of the melting relations over compositions between $MgSiO_3$ and SiO_2 is indispensable to clarify the mantle fractionation. That also relates to investigations of chemical compositions of the crust at early stage of the Earth. Nevertheless, there have been very limited works on the pressure effect on melting in the $MgSiO_3$–SiO_2 system. Available information regarding phase relations in the system has been so far limited to 5 GPa (Dalton and Presnall, 1997). In this study, we are determining the melting relations in the $MgSiO_3$–SiO_2 system at pressures 5 to 20 GPa. Here we present the results obtained at 10 GPa.

References

Bowen and Anderson (1914) The binary system MgO-SiO_2. Am. J. Sci. 4th ser. 37, 487-500.

Dalton and Presnall (1997) No liquid immiscibility in the system $MgSiO_3$-SiO_2 at 5.0 GPa. Geochim. Cosmochim. Acta 61, 2367-2373.

Ito and Katsura (1992) Melting of ferromagnesian silicates under the lower mantle conditions. Am. Geophys. Union Monogr. 67, 315-322.

Javoy et al. (2010) The chemical composition of the Earth: Enstatite chondrite models. Earth Planet. Sci. Lett. 293, 259-268.

Kato and Kumazawa (1985) Garnet phase of $MgSiO_3$ filling the pyroxene-ilmenite gap at very high temperature. Nature 316, 803-805.

.

©2019. Japan Geoscience Union. All Right Reserved.

Keywords: enstatite chondrite, melting relation, magma ocean, mantle differentiation, high pressure

©2019. Japan Geoscience Union. All Right Reserved.

Melting relations of the Fe-Ni-S-C system and the formation of superdeep diamonds

*Yu Itami[1], Satoru Urakawa[1]

1. Okayama University

Superdeep diamonds derived from the mantle transition zone or the lower mantle have been found in recent years , while most diamonds are thought to form in the upper mantle between 150 and 200 km depth. Smith et al. (2016) discovered solidified Fe-Ni-S-C melt in the inclusions of CLIPPIR diamond, which is one of the superdeep diamonds, and concluded that these diamonds have formed from the metallic liquid in the slabs subducted into the mantle transition zone. In this research, we have performed high-pressure and high-temperature quench experiments of the Fe-Ni-S-C system to investigate diamond formation in the mantle transition zone.

High-pressure and high-temperature experiments were carried out at a pressure of 15 GPa and temperatures of 900-1400 K using a Kawai-type apparatus. Diamonds can coexist with Fe-Ni-S-C melt above 1400 K at 15 GPa. Although the maximum carbon solubility in the liquid coexisting with diamond decreases to 1.5 wt.% with increasing sulfur content up to 12 wt.%, the maximum carbon solubility increases with increasing sulfur content above 12 wt.%. Taking into consideration of the carbon content in the mantle, diamonds can be crystallized from the liquid alloy by supersaturation at 15 GPa when sulfur content in the liquid ranges from 5 to 15 wt.%.

Since the temperature of the mantle transition zone at 450 km depth (15 GPa) is higher than 1400 K, diamonds can form from the Fe-Ni-S-C melt. On the other hand, the diamond cannot form within the top of subducting slab, due to its lower temperature. Thus it is considered that CLIPPIR diamonds have formed in the ancient hotter slab. Meanwhile, in the case that the mantle transition zone has a basaltic composition, it is feasible that the eclogitic diamonds such as CLIPPIR diamonds have been crystallized from liquid alloy in the mantle transition zone.

Keywords: diamond, mantle transition zone, the Fe-Ni-S-C system, liquid alloy, subducting slab

©2019. Japan Geoscience Union. All Right Reserved.

Effect of ammonia on the stability of methane hydrate under high-pressure and high-temperature

*Hirokazu Kadobayashi[1], Hisako Hirai[2], Hiroaki Ohfuji[1], Hideaki Kawamura[1], Michika Ohtake[3], Yoshitaka Yamamoto[3]

1. Geodynamics Research Center, Ehime University, 2. Department of Environment System, Faculty of Geo-environmental Science, Rissho University, 3. National Institute of Advanced Industrial Science and Technology

Methane hydrate may be present in significant amounts in the interior of Titan and other icy moons and is thought to be a candidate for a source of their atmospheric methane [e.g., Loveday *et al.* (2001); Choukroun *et al.* (2010)]. The icy mantles of these moons mainly consist of water, methane and ammonia, but the stability of methane hydrate coexisting with these components under high-pressure and high-temperature have been still unknown. In this study, we report a high-pressure and high-temperature investigation of the effect of ammonia on the stability of methane hydrate using X-ray diffraction and Raman spectroscopy combined with externally heated diamond anvil cell under 0.2-20 GPa and 298-413 K. X-ray diffraction studies revealed that methane hydrate in water-methane-ammonia system transforms from sI cage structure into sH cage structure at approximately 0.8 GPa at room temperature, and further transforms into a filled-ice Ih structure at approximately 1.8 GPa without decomposition into water ice and solid methane. These transition pressures at room temperature were same as those reported for pure methane hydrate [Hirai *et al.* (2001); Loveday *et al.* (2001); Shimizu *et al.* (2002)]. At higher temperature, the melting temperatures for the sI and sH cage structures below 1.8 GPa determined by in situ Raman spectroscopy were good agreement with those of pure methane hydrate reported by previous studies [Dyadin *et al.* (1997); Bezacier *et al.* (2014)]. On the other hand, the decomposition temperatures of filled-ice Ih above 1.8 GPa were about 10-20 K lower than those of water-methane system reported by Kadobayashi *et al.* (2018). Our results suggest that ammonia has a potential to vary the stability of filled-ice Ih of methane hydrate in the interiors of icy moons. Finally, we briefly discuss the implications of our new results for the fate of methane hydrate in concerned with a source of atmospheric methane in Titan.

Keywords: icy satellite, Titan, methane hydrate, diamond anvil cell, high-pressure experiment

©2019. Japan Geoscience Union. All Right Reserved.

Study on magnetite-maghemite-hematite transformation

*Ibuki Kinebuchi[1], Atsushi Kyono[1], Yoshinari Sano[1]

1. University of Tsukuba

Magnetite (Fe_3O_4) widely distributed in the Earth's crust changes into hematite (α-Fe_2O_3) by the oxidization of Fe^{2+} to Fe^{3+}. In the oxidization process, maghemite (γ-Fe_2O_3) with the same spinel structure as magnetite emerges as an intermediate phase. Maghemite differs from magnetite by the presence of cationic vacancies within the octahedral site. It is important to understand the oxidization mechanism of magnetite, however, the local structure change during the oxidization has been still nuclear. In the study, therefore, the phase transition mechanism from magnetite to hematite through maghemite was investigated by using, thermal analysis (TG・DTA), powder X-ray diffraction (XRD) measurement, and high-temperature ex-situ and in-situ X-ray absorption fine structure (XAFS) measurement. The TG・DTA curves of magnetite showed continuous oxidization up to 400 °C.
High-temperature ex-situ EXAFS spectrum of magnetite heated up to 250 °C exhibited weaker peaks concerning Fe_{oct}-O, Fe_{oct}-Fe_{oct}, and Fe_{tet}-Fe_{oct} than those of magnetite. In addition, the averaged Fe-O bond distance appears to become shorter. The results suggest that magnetite is continuously transformed to maghemite in the temperature range from room temperature to 400 °C. The high-temperature ex-situ EXAFS spectrum of magnetite heated up to 500 °C finally displayed characteristic peaks corresponding to hematite, suggesting that the phase transition from magnetite to hematite was completed.
High-temperature in-situ XANES spectrum indicated that the average oxidation number of Fe gradually increased for 135 min from the start of heating at 500 °C, and then became almost constant. The radial structure function obtained from the high-temperature in-situ EXAFS revealed that the peaks of Fe-O, Fe_{oct}-Fe_{oct} and Fe_{tet}-Fe_{oct} become weakened continuously until 70 min from the start of heating. After 80 min peaks corresponding to hematite began to increase. It can be concluded from these results that the phase transition from magnetite to hematite through maghemite starts from the diffusion of the Fe^{2+} in the octahedral sites, resulting in the formations of cationic vacancies and amorphous phase concentrating Fe^{2+}. Subsequently, the reconstruction of the octahedral coordination of Fe and additional oxidization of the amorphous phase lead to the crystallization into hematite.

Keywords: magnetite, maghemite, hematite, thermal analysis, X-ray diffraction, X-ray absorpition fine structure

©2019. Japan Geoscience Union. All Right Reserved.

The Effects of Temperature and Pressure on Hydromagnesite

*Gen-ichiro Yamamoto[1], Atsushi Kyono[1], Jun Abe[2], Takanori Hattori[3], Yoshitaka Matsushita[4], Yasuhiro Yoneda[3]

1. University of Tsukuba, 2. CROSS, 3. JAEA, 4. NIMS

In recent years, the global warming is the most important environment problem. Therefore, attempts of CO_2 geological storage have been made to reduce carbon dioxide in the atmosphere all over the world (Xue and Nakano 2008). Among some CO_2 geological storage methods, the CO_2 mineral trapping can store the carbon dioxide safety for a long time. In the case of geological storage, magnesium carbonate hydrates are important minerals since they precipitate easily from water saturated with carbon dioxide. The major magnesium carbonate hydrates formed from aqueous solution are nesquehonite $MgCO_3 \cdot 3H_2O$ and hydromagnesite $Mg_5(CO_3)_4(OH)_2 \cdot 4H_2O$. The stability of these minerals are critically important factors to assess environmental safety and phase stability over geological time scale, but they have not been fully investigated yet, especially of hydromagnesite. Here, we investigated the effects of pressure and temperature on hydromagnesite by using thermal analysis, high-temperature X-ray diffraction, X-ray total scattering, high-pressure X-ray diffraction, and high-pressure and high-temperature neutron diffraction techniques.

With temperature, hydromagnesite was decomposed into periclase MgO through the poor crystalline phase, accompanied with dehydration, dihydroxylation, and decarbonation of hydromagnesite. The *a* and *c* lattice parameters were monotonously increased as increasing temperature whereas *b* lattice parameter almost remained unchanged. At just before the dehydration reaction, the unit cell was contracted due to the dehydration. With pressure, hydromagnesite structure was maintained up to 8.7 GPa. Decomposition into magnesite $MgCO_3$ or periclase was unobserved up to at least 21.0 GPa. With compression, the unit cell was isotopically contracted. The fit to the Birch-Murnaghan equation of state gives $K_0 = 32(2)$ and $V_0 = 658(4)$ with $K' = 4.0$ (fixed). Under high-pressure and high-temperature conditions, hydromagnesite broke down into magnesite and brucite $Mg(OH)_2$ at 200 $^{\circ}C$ and 1.2 GPa. The unit cell was isotopically expanded up to just before the breakdown. The breakdown of hydromagnesite could be caused by the dissolution by dehydration water, and subsequently magnesite and brucite were hydrothermally grown from the solution at the condition. The results obtained from this study would provide insight the CO_2 geological storage.

Keywords: Hydromagnesite, magnesite, phase change, high-pressure, high-temperature, CO2 geological storage

©2019. Japan Geoscience Union. All Right Reserved.

Synthesis and crystal structure of Mg-bearing Fe_9O_{11}: New insight in the complexity of Fe-Mg oxides at conditions of the deep upper mantle

*Takayuki Ishii[1], Uenver-Thiele Laura[2], Alan B Woodland[2], Edith Alig[3], Tiziana Boffa Ballaran[1]

1. Bavarian Research Institute, University of Bayreuth, 2. Institut für Geowissenschaften, Goethe-Universität Frankfurt, 3. Institut für Anorganische und Analytische Chemie, Goethe-Universität Frankfurt

The Fe-O system is fundamental for understanding redox processes operating in the Earth's interior. Recent experimental studies have revealed several new mixed-valence Fe-oxides to be stable at high pressures and temperatures, such as the orthorhombic-structured phases $Fe^{2+}_2Fe^{3+}_2O_5$ and $Fe^{2+}_3Fe^{3+}_2O_6$. and the monoclinic-structured $Fe^{2+}_3Fe^{3+}_4O_9$. It has been also demonstrated that Fe_4O_5 and Fe_7O_9 form solid solutions with the Mg-endmembers such as $Mg_2Fe_2O_5$ and $Mg_3Fe_4O_9$, suggesting possible existence of complicated Mg-Fe oxides in the deep mantle. We synthesized a new Mg-Fe oxide with a composition of $Mg_{0.9}Fe_{8.1}O_{11}$. We report the synthesis and crystal structure analyzed by the Rietveld method.

A novel Mg-bearing iron oxide $Mg_{0.87(1)}Fe^{2+}_{4.13(1)}Fe^{3+}_4O_{11}$ was synthesized at 12 GPa and 1300 ˚C using a large volume press. Rietveld structural analysis was conducted with a laboratory X-ray diffraction pattern obtained at ambient conditions.
The crystal structure, which has one oxygen trigonal prism site and four octahedral sites for the cations, was found to be isostructural with $Ca_2Fe_7O_{11}$. The unit-cell lattice parameters are a = 9.8441(5) Å, b = 2.8920(1) Å, c = 14.1760(6) Å, β = 99.956(4)˚, V = 397.50(3) Å, and Z = 2 (monoclinic, $C2/m$). Mg and Fe cations are disordered on the trigonal prism site and on two of the four octahedral sites, and the remaining Fe is accommodated at the other two octahedral sites. The present structure is closely related to the other recently discovered Fe oxide structures, e.g. Fe_4O_5 and Fe_5O_6, by distortion derived either from incorporation (Fe_4O_5) or removal (Fe_5O_6) of an edge-shared FeO_6 single octahedral chain in their structures. The present synthesis at deep upper mantle conditions and the structural relationships observed between various novel Mg-Fe oxides indicate that a series of different phases become stable above 10 GPa and that their relative stabilities (Fe^{2+}/Fe^{3+}) must be controlled by oxygen fugacity.

Keywords: iron oxide, mantle, oxygen fugacity, multi-anvil apparatus, Rietveld analysis

©2019. Japan Geoscience Union. All Right Reserved.

Changes in specific surface area and morphology of kaolin group minerals with pressure treatment

*Soyeon Kwon[1], Yongjae Lee[1]

1. YONSEI University

Pressure can tailor the properties of a material by changing its atomistic arrangements and/or crystal morphology. We have investigated the changes in the adsorption properties of kaolin group minerals as a function of pressure treatment in gigapascal range. External pressure has been applied using a Large Volume Press (LVP) to kaolinite ($Al_2Si_2O_5(OH)_4$) and halloysite ($H_4Al_2O_9Si_2{\cdot}2H_2O$), which represent natural 2D layered and 1D nanowire structures, respectively. Powdered samples have been compressed up to 3 GPa in 1 GPa steps at room temperature and recovered by up to ~0.35g from each pressure step. The BET (Brunauer, Emmett, Teller) measurement was conducted using N_2 gas to measure the specific surface area, pore size distribution, and pore volume of the pressure-treated samples. Before pressure-treatment, the specific surface area of kaolinite has been measured to be 10.702(m^2g^{-1}), which increases to 12.090(m^2g^{-1}) after 1 GPa, 17.101(m^2g^{-1}) after 2 GPa, and 17.864(m^2g^{-1}) after 3 GPa treatments. These lead to a gradual increase in the total volume of adsorbed pores from 0.01216 (cm^3g^{-1}) at ambient, to 0.01368(cm^3g^{-1}) after 1 GPa, 0.074337(cm^3g^{-1}) after 2 GPa, and 0.09546(cm^3g^{-1}) after 3 GPa treatments. Unlike Kaolinite, the specific surface area of halloysite decreases from 47.476($m2g^{-1}$) from ambient to 44.348(m^2g^{-1}) after 1 GPa, 41.579(m^2g^{-1}) after 2 GPa, and 42.796(m^2g^{-1}) after 3 GPa treatment, which results in overall decrease in the total volume of the pore from 0.1914(cm^3g^{-1}) at ambient to 0.1863(cm^3g^{-1}) after 1 GPa, 0.1572(cm^3g^{-1}) after 2 GPa, and 0.1187(cm^3g^{-1}) after 3 GPa treatments.
We discuss the contrasting effects of pressure-treatment on the two morphologically-distinct kaolin group minerals based on SEM (Scanning Electron Microscope) images and analyses of selected diffraction peaks measured on each recovered material. We observe that the layers in kaolinite separate into smaller units upon increasing pressure treatment, whereas the tubes in halloysite become flattened, which led to the contrasting changes in surface area and pore volume. Further study is in progress to compare these results to when water is used as a pore-penetrating pressure-transmitting medium.

Keywords: kaolinite, halloysite, high pressure treatment, specific surface area, morphology

©2019. Japan Geoscience Union. All Right Reserved.

Changes in specific surface area and morphology of kaolin group minerals with pressure treatment

Soyeon Kwon, Yongjae Lee*

Department of Earth System Sciences, Yonsei University

yongjaelee@yonsei.ac.kr

ABSTRACT

Pressure can tailor the properties of a material by changing its atomistic arrangements and/or crystal morphology. We have investigated the changes in the adsorption properties of kaolin group minerals as a function of pressure treatment in gigapascal range. External pressure has been applied using a Large Volume Press (LVP) to kaolinite ($Al_2Si_2O_5(OH)_4$) and halloysite ($H_4Al_2O_9Si_2 \cdot 2H_2O$), which represent natural 2D layered and 1D nanowire structures, respectively. Powdered samples have been compressed up to 3 GPa in 1 GPa steps at room temperature and recovered by up to ~0.35g from each pressure step. The BET (Brunauer, Emmett, Teller) measurement was conducted using N_2 gas to measure the specific surface area, pore size distribution, and pore volume of the pressure-treated samples. Before pressure-treatment, the specific surface area of kaolinite has been measured to be 10.702(m^2g^{-1}), which increases to 12.090(m^2g^{-1}) after 1 GPa, 17.101(m^2g^{-1}) after 2 GPa, and 17.864(m^2g^{-1}) after 3 GPa treatments. These lead to a gradual increase in the total volume of adsorbed pores from 0.01216 (cm^3g^{-1}) at ambient, to 0.01368(cm^3g^{-1}) after 1 GPa, 0.074337(cm^3g^{-1}) after 2 GPa, and 0.09546(cm^3g^{-1}) after 3 GPa treatments. Unlike Kaolinite, the specific surface area of halloysite decreases from 47.476(m2g^{-1}) from ambient to 44.348(m^2g^{-1}) after 1 GPa, 41.579(m^2g^{-1}) after 2 GPa, and 42.796(m^2g^{-1}) after 3 GPa treatment, which results in overall decrease in the total volume of the pore from 0.1914(cm^3g^{-1}) at ambient to 0.1863(cm^3g^{-1}) after 1 GPa, 0.1572(cm^3g^{-1}) after 2 GPa, and 0.1187(cm^3g^{-1}) after 3 GPa treatments.

We discuss the contrasting effects of pressure-treatment on the two morphologically-distinct kaolin group minerals based on SEM (Scanning Electron Microscope) images and analyses of selected diffraction peaks measured on each recovered material. We observe that the layers in kaolinite separate into smaller units upon increasing pressure treatment, whereas the tubes in halloysite become flattened, which led to the contrasting changes in surface area and pore volume. Further study is in progress to compare these results to when water is used as a pore-penetrating pressure-transmitting medium.

©2019. Japan Geoscience Union. All Right Reserved.

[J] Poster | S (Solid Earth Sciences)：S-MP Mineralogy & Petrology

Wed. May 29, 2019 5:15 PM - 6:30 PM JST | Wed. May 29, 2019 8:15 AM - 9:30 AM UTC | Poster Hall International Exhibition Hall8, Makuhari Messe_30

[S-MP33] Physics and Chemistry of Minerals

convener:Seiji Kamada(Frontier Research Institute for Interdisciplinary Sciences, Tohoku University), Masahiro KAYAMA(Department of Earth and Planetary Material Sciences, Faculty of Science, Tohoku University)

In this session, we will discuss the physics and chemistry of the Earth and planetary materials (including amorphous and melts) based on the results obtained from various experimental methods such as X-ray diffraction, FT-IR, Raman spectroscopy, electron microscopic observations, and computer simulations.

[SMP33-P01] Raman spectroscopy of seifertite

*Masahiro KAYAMA[1], Eiji Ohtani[1], Masaaki Miyahara[2], Shohei Kaneko[1], Toshimori Sekine[3], Shin Ozawa[1], Naohisa Hirao[4] (1.Tohoku University, 2.Hiroshima University, 3.HPSTAR, 4.Japan Synchrotron Radiation Research Institute)

[SMP33-P02] Microtexture and crystallization process of impact diamonds

*Hiroaki Ohfuji[1], Motosuke Nakaya[1] (1.Geodynamics Research Center, Ehime University)

[SMP33-P03] Metamorphic temperature analysis of H chondrites: Using revised Lindsley's pyroxene thermometer

*Ryo Uehara[1], Yoshihiro Kuwahara[1], Kazuhiko Shimada[1], Yoshihiro Nakamuta[1], Seiichiro Uehara[1], Tatsuro Adachi[1] (1.Kyushu university)

[SMP33-P04] The occurrence combinations of Zeolites at Chichijima, Ogasawara Islands

Michiharu Ito[1], *Yuki Inoue[1], Mana Yasui[2], Atsushi Yamazaki[2], Hiroshi Hagiya[1] (1. Tokyo City University, 2.Waseda research institute for science and engineering)

[SMP33-P05] Title: Single-crystal X-ray diffraction study of mirabilite ($Na_2SO_4 \cdot 10H_2O$) from 213 to 303 K

*Ryutaro Ikeda[1] (1.University of tsukuba)

[SMP33-P06] Elastic constants of single-crystal topaz studied via sphere-resonance method

*Kako Aradachi[1], Tohru Watanabe[1], Morihisa Hamada[2] (1.University of Toyama, 2.JAMSTEC)

[SMP33-P07] Verification of damage by polishing of sheet-like minerals

*Yui Kouketsu[1], Kota Ando[1], Katsuyoshi Michibayashi[1] (1.Department of Earth & Planetary Sciences, Graduate School of Environmental Studies, Nagoya University)

[SMP33-P08] Description of Zebra Rock and the pattern formation model

*Kaoru Yoshimura[1], Atsushi Toramaru[2], Mie Ichihara[3], Takaaki Noguchi[4], Toru Matsumoto[5] (1.Department of Earth and Planetary Science, Graduate School of Science, Kyushu University, 2.Department of Earth and Planetary Sciences, Faculty of Sciences, Kyushu University, 3.Earthquake Research Institute, University of Tokyu, 4.Department of Arts and Science, Kyushu University, 5.Japan Aerospace Exploration Agency/ Institute of Space and Astronautical Science)

[SMP33-P09] Thermal conductivity anomaly of (Mg,Fe)CO_3 solid solution across the spin transition

*Keng-Hsien Chao[1], Wen-Pin Hsieh[1,2] (1.Institute of Earth Sciences, Academia Sinica, Taiwan, 2.Department of Geosciences, National Taiwan University, Taiwan)

[SMP33-P10] **Melting experiments in the $MgSiO_3$ – SiO_2 system under high pressures**

*Takuya Moriguti[1], Akira Yoneda[1], Eiji Ito[1] (1.Institute for Planetary Materials, Okayama University)

[SMP33-P11] Melting relations of the Fe-Ni-S-C system and the formation of superdeep diamonds

*Yu Itami[1], Satoru Urakawa[1] (1.Okayama University)

[SMP33-P12] Effect of ammonia on the stability of methane hydrate under high-pressure and high-temperature

*Hirokazu Kadobayashi[1], Hisako Hirai[2], Hiroaki Ohfuji[1], Hideaki Kawamura[1], Michika Ohtake[3], Yoshitaka Yamamoto[3] (1.Geodynamics Research Center, Ehime University, 2.Department of Environment System, Faculty of Geo-environmental Science, Rissho University, 3.National Institute of Advanced Industrial Science and Technology)

[SMP33-P13] Study on magnetite-maghemite-hematite transformation

*Ibuki Kinebuchi[1], Atsushi Kyono[1], Yoshinari Sano[1] (1.University of Tsukuba)

[SMP33-P14] The Effects of Temperature and Pressure on Hydromagnesite

*Gen-ichiro Yamamoto[1], Atsushi Kyono[1], Jun Abe[2], Takanori Hattori[3], Yoshitaka Matsushita[4], Yasuhiro Yoneda[3] (1.University of Tsukuba, 2.CROSS, 3.JAEA, 4.NIMS)

[SMP33-P15] Synthesis and crystal structure of Mg-bearing Fe_9O_{11}: New insight in the complexity of Fe-Mg oxides at conditions of the deep upper mantle

*Takayuki Ishii[1], Uenver-Thiele Laura[2], Alan B Woodland[2], Edith Alig[3], Tiziana Boffa Ballaran[1] (1.Bavarian Research Institute, University of Bayreuth, 2.Institut für Geowissenschaften, Goethe-Universität Frankfurt, 3.Institut für Anorganische und Analytische Chemie, Goethe-Universität Frankfurt)

[SMP33-P16] **Changes in specific surface area and morphology of kaolin group minerals with pressure treatment**

*Soyeon Kwon[1], Yongjae Lee[1] (1.YONSEI University)

Raman spectroscopy of seifertite

*Masahiro KAYAMA[1], Eiji Ohtani[1], Masaaki Miyahara[2], Shohei Kaneko[1], Toshimori Sekine[3], Shin Ozawa[1], Naohisa Hirao[4]

1. Tohoku University, 2. Hiroshima University, 3. HPSTAR, 4. Japan Synchrotron Radiation Research Institute

Seifertite is one of the SiO_2 polymorphs and is a high pressure phase with an α-PbO_2 structure. It is known to lie in lunar and martian meteorites and constrains shock pressure and duration of an impact event that these meteorites have experienced on the host bodies. Seifertite is thermodynamically stable at more than ~100 GPa, which is not realistic for an impact event on the Moon and Mars. However, it can be transformed as a metastable phase from cristobalite at least ~11 GPa and 0.01 s, and can consequently be quenched down to an ambient condition. As a result of this process, seifertite remains present in some of the lunar and martian meteorites. The estimated shock pressure and duration provide valuable information on the size of the crater and impactor that collided don the host bodies. Although Raman spectroscopy has been previously measured for seifertite in meteorites, it was not successful to obtain the seifertite signature because of a potential vitrification or transition into other SiO_2 phase by heating due to the laser irradiation. Therefore, only synchrotron-XRD and TEM analyses allow us to determine the structure, where silica grains are excavated with a focused ion beam (FIB) system from meteorite. Here, Raman spectral signatures of seifertite has been obtained from synthetic and meteoritic silica grains, implying its identification with high-spatial resolution as nondestructive analysis.

Seifertite in silica grains of synthetic samples and lunar (NWA 4734) and martian meteorites (Zagami, NWA 2975) were identifications by a synchrotron XRD analysis at Spring-8 BL-10 and were employed for Raman spectroscopy. Seifertite were synthetized from synthetic cristobalite powders using multi-anvil press at 16 GPa, 673 K and 0.5 hour. Raman spectroscopy were performed for synthetic and meteoritic silica grains using Nd: YAG 532 nm at 20 mW for 3 minutes exposure time.
Raman spectra of synthetic seifertite have pronounced peaks at 380, 515, 564, 739 and 796 cm^{-1} and weak peaks at 401, 496, 539, 547, 606 and 749 cm^{-1}. Similar Raman signature was obtained from seifertite in lunar and martian meteorites. These Raman shifts and relative intensities are well corresponding to the values calculated within the density-functional perturbation theory for seifertite. Based on the calculation, thee Raman peaks at 380, 515, 564, and 796 cm^{-1} are assigned to Ag, those at 401, 496, and 539 cm^{-1} to B1g, 606 and 749 cm^{-1} to B2g, and 547 and 739 cm^{-1} to B3g modes. After laser beam irradiation for 30 minutes, the distinct Raman signature can be detected from synthetic and meteoritic seifertite. Therefore, Raman spectroscopy enables determination of the structure and identification of SiO2 polymorphs with high-spatial resolution and without destruction.

Keywords: Seifertite, Raman spectroscopy, Meteorite

©2019. Japan Geoscience Union. All Right Reserved.

Microtexture and crystallization process of impact diamonds

*Hiroaki Ohfuji[1], Motosuke Nakaya[1]

1. Geodynamics Research Center, Ehime University

Impact diamonds from the Popigai crater located in the central Siberia, Russia show unique nano-polycrystalline texture composed of diamond and a small amount of lonsdaleite of ~50 nm (Ohfuji et al., 2015), which is well comparable to the nano-polycrystalline diamond synthesized by direct conversion of graphite under high pressure and high temperature (Irifune et al., 2003). However, subsequent studies noted that they show a variety of microtexture such as lamellar or layer textures and granular textures. In the present study, we investigated the mineralogical and crystallographic characteristics of the various microtextures shown by the Popigai diamonds by TEM.

The microtextures found in Popigai diamonds are divided into two types, 1) lamellar type and 2) granular type. The former is further classified into two types, 1a) less-mosaiced lamellar and 1b) mosaiced lamellar. The latter can also be divided further into 2a) granular texture composed of fine crystals of <50 nm and 2b) granular texture composed of larger (~100 nm) crystals. Careful textural observations and electron diffraction analysis revealed that the microtextures of Popigai diamonds vary from layered texture to granular texture (1a →1b →2a →2b) as the phase transitions from graphite to lonsdaleite to diamond proceed. The phase transition mechanism also changes from martensitic process involving a lattice relationship (Graphite (001) // Lonsdaleite (100) // Diamond (111)) to diffusion process where the nucleation of new grains and the their growth are promoted.

The most important factor controlling the degree of the phase transitions and the resulting microtexture is probably the shock temperature, which is supposed to have decreased gradually from the center to rim in the crater.

Keywords: Impact diamonds, Pipogai crater, High temperature and high pressure

©2019. Japan Geoscience Union. All Right Reserved.

Metamorphic temperature analysis of H chondrites: Using revised Lindsley's pyroxene thermometer

*Ryo Uehara[1], Yoshihiro Kuwahara[1], Kazuhiko Shimada[1], Yoshihiro Nakamuta[1], Seiichiro Uehara[1], Tatsuro Adachi[1]

1. Kyushu university

1. Introduction
The thermal evolution models of asteroids have been proposed and discussed by many researchers to provide insight into the internal structure and thermal history of those (e.g., Wood,1979; Miyamoto et al., 1981; Yomogida and Matsui, 1984; McSween et al., 2002). As important parameters for the thermal evolution models, the highest peak temperatures, ages, and cooling rates of meteorite parent bodies are mentioned (McSween et al., 2002). The peak temperature inside the parent body has been estimated using various thermometers (Olsen and Bunch, 1984; Nakamuta and Motomura, 1999; Kessel et al., 2002; Slater-Reynolds and McSween, 2005). Pyroxene thermometer by Lindsley (1983) has been widely used because it allows us to derive temperatures from both orthopyroxene (Opx) and clinopyroxene (Cpx) in a meteorite. However, the temperatures determined from clinopyroxenes, especially for type 6 chondrites, are systematically 50˚C to 150˚C higher than those from orthopyroxenes (Nakamuta et al., 2017). The Lindsley’s pyroxene thermometer is made empirically for terrestrial rocks and therefore the kosmochlor component is not considered in the calculation. So, Nakamuta et al. (2017) proposed the revised Lindsley’s pyroxene thermometer in which the kosmochlor pyroxene component is added to evaluate the effect of the component on the thermometry. They also showed that the difference in temperature between clinopyroxene and orthopyroxene in LL chondrites using the revised thermometer was less than 20˚C.
In this study, we have attempted to estimate the metamorphic temperatures of H chondrites (type 4 to 7) using the Lindsley’s pyroxene thermometer revised by Nakamuta et al (2017). Here we report the results of the estimation.
2. Samples and method
The chondrite samples used were four types of H chondrite with different metamorphic degrees; Edmondson(b) (H4), Faucett (H5), Faith (H5), Plainview (H5), Mulga(north) (H6), Great Bend (H6) and NWA7875 (H7). Polished thin sections of the seven H chondrites were prepared and observed using transmitted and reflecting light microscopes. Then, chemical compositions of pyroxenes, olivines, and plagioclases in the seven H chondrites were analyzed by an EPMA, JEOL JXA-8530F. Beased on these results, the classification of each meteorite sample was reconfirmed, and metamorphism temperatures estimated using the revised Lindsley pyroxene thermometer.
3. Results and discussion
From results of the texture observation and chemical analysis of the chondrite sample, we reconfirmed that there is no mistake in classification of each meteorites (H4, H5, H6, H7). The temperatures for Edmondson(b) (H4), Faucett (H5), Faith (H5), Plainview (H5), Mulga(north) (H6), Great Bend (H6) and NWA7875 (H7) are 779-1236˚C (Opx-Cpx), 814-875˚C, 832-843˚C, 844-838˚C, 807-797˚C, 811-818˚C and 1183-1247˚C, respectively, using the revised Lindsley pyroxene thermometer. Most of H5 and H6 meteorite samples showed that the difference in temperature between Opx and Cpx was less than 20˚C. This result, this suggests that the revised Lindsley pyroxene thermometer by Nakamuta et al. (2017) is also effective for H chondrite. The metamorphic temperatures of the H5 type chondrite (Faucett, Faith and Plainview) and the H6 type chondrite (Mulga(north), Great Bend) are approximately 840˚C and 810˚C, respectively, while the H4 type Edmondson(b) chondrite is less than 780˚C judging from the temperature

©2019. Japan Geoscience Union. All Right Reserved.

estimated from Opx. Regarding the H7 type NWA7875 chondrite which showed the highest metamorphic temperature and lamella structure in some Cpx crystals, the H7 material that existed already in H5 and/or H6 conditions may have experienced impact metamorphism, redrawing the previous metamorphic temperature and the H5 and/or H6 conditions.
Comparing these estimated temperature data with the results of the model simulation reported by Monnereau et al. (2013), it is estimated that the H chondrite meteorite parent body had an onion shell type internal thermal structure formed when the accumulation period was short (<0.2 Myr).

Keywords: H chondrite, Lindsley pyroxene thermometer, Kosmoclor, Peak temperature, Onion-shell model

©2019. Japan Geoscience Union. All Right Reserved.

The occurrence combinations of Zeolites at Chichijima, Ogasawara Islands

Michiharu Ito[1], *Yuki Inoue[1], Mana Yasui[2], Atsushi Yamazaki[2], Hiroshi Hagiya[1]

1. Tokyo City University, 2. Waseda research institute for science and engineering

The Ogasawara Islands are located in the Pacific Ocean about 1000 km south of Tokyo, Japan. These Islands are situated in the outer of the Izu-Bonin-Mariana Arc. The Ogasawara Islands are composed by paleogene submarine volcanic formation, and is well known by andesitic volcanic rock called boninite. Boninite is a feldspar-free and glass-rich olivine-bronzite andesite with higher MgO, SiO_2, H_2O and Cr contents. Zeolites, co-exist with calcite, quartz/chalcedony and celadonite, fill the vesicles of volcanic gas, radial and columnar cooling joint of pillow lava, and also occur in interpillow sediment with large aggregate of crystals.

In this study, various habits of zeolites at Chichijima, Ogasawara Islands are obtained, also more than two-step growth of zeolites in amygdale were confirmed. Between these two-step growth, cation ratio have changed at the border of two faces.

These cation's contents are similar to neighboring rock. It is considered that there is another hydrothermal activity after the first-step growth.

Keywords: Zeolite, boninite, hydrothermal activity, occurrence combinations

©2019. Japan Geoscience Union. All Right Reserved.

Title: Single-crystal X-ray diffraction study of mirabilite ($Na_2SO_4 \cdot 10H_2O$) from 213 to 303 K

*Ryutaro Ikeda[1]

1. University of tsukuba

Introduction

Renewable energy is of increasing importance in modern society due to its low environmental impact, ubiquity and sustainability. Since some renewable energy resources (e.g. sunlight, wind and tides) have variable outputs, storage technologies have great potential for affording the supply from these resources. In recent years, much attention has been paid to phase change materials (PCMs) due to its high energy storage capacity. PCMs are substances with a heat of fusion which can store and releasing large amounts of energy. Mirabilite ($Na_2SO_4 \cdot 10H_2O$) is known as one of the PCMs. With increasing temperature, mirabilite transforms to thenardite (Na_2SO_4) at a dehydration temperature of 306 K. On the contrary, thenardite is rehydrated back to mirabilite at 283 K. The reversible reaction involves large exothermic and endothermic heats. To date, however, there is little information on temperature dependence of crystal structure in mirabilite. The structure of mirabilite contains ribbons consisting of edge-sharing $Na(H_2O)_6$ octahedra along the *c*-axis. These ribbons alternate with chains of the SO_4 tetrahedra and the two H_2O molecules. Levy and Lisensky (1978) identified disorder over two orientations of the SO_4 tetrahedra by single-crystal neutron diffraction measurement at room temperature. The characteristic two orientations, related by a rotation of about 30° about the S×××O5 vector, generate pairs of partially occupied sulfate oxygen sites (O4’/O4’’, O6’/O6’’, and O7’/O7’’). Levy and Lisensky (1978) found that the primed sites are about 25% occupied, and the double-primed sites are about 75% occupied. Recently, Brand et al. (2008) performed powder neutron diffraction measurements on mirabilite ($Na_2SO_4 \cdot 10D_2O$) in the temperature range from 10 to 300 K. They reported that the unit cell of mirabilite is isotopically expanded up to 300 K. The authors however couldn’t observe the two orientations for the SO_4 tetrahedra in the structure, which was previously identified by Levy and Lisensky (1978). In the study, we performed temperature-dependent single-crystal X-ray diffraction measurement of mirabilite in the temperature range between 213 and 303 K. Here, we report the crystal structure change of mirabilite associated with the characteristic exothermic and endothermic heats.

Methods

Single crystals of mirabilite were obtained by slow cooling of a saturated solution of Na_2SO_4. After the synthesis, a single crystal was stored in a 0.7 mm Lindemann glass capillary to avoid dehydration. Temperature dependent single-crystal X-ray diffraction study on mirabilite was performed using a single-crystal diffractometer (APEXII ULTRA, Bruker AXS Inc., Germany) equipped with a liquid nitrogen cryostat, a CCD detector, multilayer optics, and graphite monochromated Mo$K\alpha$ radiation (λ = 0.71073 Å) generated by a rotating anode. The measurements were conducted at temperature ranges between 213 and 303 K with 10 K step in both heating and cooling processes.

Results and Discussion

The *a* and *c* lattice parameters and unit cell volume were monotonously changed with temperature, whereas the *b* lattice parameter remained almost unchanged. The result is entirely consistent with the

©2019. Japan Geoscience Union. All Right Reserved.

previous report that thermal expansivities of the *a*- and *c*-axes are of similar magnitude, while the *b*-axis shows a much smaller thermal expansion (Brand et al. 2008). The disorder over two orientations of the SO_4 tetrahedra was observed in the present study. At room temperature, the primed and double-primed sites are about 25% and 75% occupied, respectively, which is completely consistent with the result by single-crystal neutron diffraction study (Levy and Lisensky 1978). A clear temperature dependence of the disorder over two orientations was, however, unobserved in the study. It is noteworthy that the SO_4 tetrahedral volume coordinated by primed oxygen atoms showed a pronounced temperature dependence. In the vicinity of dehydration temperature of mirabilite, it approached to that of thenardite (Na_2SO_4), which would be a trigger initiating the dehydration of mirabilite.

Keywords: sodium sulfate, Single crystal XRD, mirabilite, Phase change

©2019. Japan Geoscience Union. All Right Reserved.

Elastic constants of single-crystal topaz studied via sphere-resonance method

*Kako Aradachi[1], Tohru Watanabe[1], Morihisa Hamada[2]

1. University of Toyama, 2. JAMSTEC

Transport of ocean floor sediments by plate motions might play an important role in the circulation of materials within the Earth. Imaging subducted sediments through seismological observations requires a thorough understanding of elastic properties of sediment origin hydrous minerals. Topaz is a hydrous mineral, which can be formed from subducted sediment at high pressures. We have studied elastic constants of single-crystal topaz by the sphere-resonance method.

A sphere sample (D=2.665(1) mm) was made from a topaz single-crystal (Al1.97SiO4(F1.17,OH0.82)) collected from Ouro preto, Mines Gerais, Brazil by the two-pipe method. Lattice parameters are a=4.663, b=8.835, c=8.386 A (orthorhombic). Resonant frequencies were measured at frequencies from 1.6 MHz to 3.5 MHz with different specimen-holding forces. Extrapolating to the specimen-holding force of zero, we obtained frequencies of "free" oscillation. Elastic constants were determined by comparing measured and calculated resonant frequencies. The xyz algorithm (Visscher et al., 1991) was employed to calculate resonant frequencies of the sphere sample. At an ambient temperature, C11=281.2(5), C22=350.3(7), C33=288.4(5), C44=108.8(2), C55=130.9(2), C66=131.4(2), C12=121.3(2), C13=81.6(2), C23=82.1(2) (GPa).

Keywords: Topaz, Elastic constants, Water

©2019. Japan Geoscience Union. All Right Reserved.

Verification of damage by polishing of sheet-like minerals

*Yui Kouketsu[1], Kota Ando[1], Katsuyoshi Michibayashi[1]

1. Department of Earth & Planetary Sciences, Graduate School of Environmental Studies, Nagoya University

Sheet-like minerals such as mica, serpentine, clay minerals and graphite are affected by shearing due to polishing. In addition, a damage due to electron beam irradiation during observation by the electron microscope also occurs. In this study, the damage due to polishing and irradiation of the electron beam for sheet-like minerals of graphite and serpentine minerals was evaluated by Raman spectroscopic analysis. First, we evaluated the crystallinity change of graphite in each polishing stage. As a result, a decrease in crystallinity was observed in all stages from rough polishing to fine grain polishing by diamond paste. The chemical polishing with colloidal silica also lowered the crystallinity of graphite. In order to reduce the shearing effect to graphite, we tested a low load polishing using the polisher ISPP-1000 (Ikegami Seiki Co., Ltd.) which is controlling the load by a weight. However, it was revealed that even a load of only 25g was damaged to graphite. Next we examined the polishing effect of serpentine minerals. Raman spectroscopic analysis was performed after polishing, however no spectral change at each polishing stage like graphite was detected. On the other hand, the antigorite Raman spectra after SEM-EBSD analysis showed a decrease in intensity at the depth of about 3 micrometre from the surface, suggesting that the crystal structure was damaged by electron beam irradiation. We also tried a low load polishing for serpentine minerals, and we detected an electron backscatter pattern of lizardite for the first time. In the case of pure lizardite sample, a clear Kikuchi band was confirmed. On the other hand, almost no pattern was detected for serpentine minerals (antigorite, lizardite, chrysotile) in the serpentinite samples, because of the contrast of hardness with surrounding hard minerals such as olivine. For analysis of sheet-like minerals contained in rock samples including minerals of various hardness, further improvement of the polishing method or other methods such as ion milling is needed.

Keywords: graphite, antigorite, lizardite, low load polish, Raman spectroscopy, EBSD

©2019. Japan Geoscience Union. All Right Reserved.

Description of Zebra Rock and the pattern formation model

*Kaoru Yoshimura[1], Atsushi Toramaru[2], Mie Ichihara[3], Takaaki Noguchi[4], Toru Matsumoto[5]

1. Department of Earth and Planetary Science, Graduate School of Science, Kyushu University, 2. Department of Earth and Planetary Sciences, Faculty of Sciences, Kyushu University, 3. Earthquake Research Institute, University of Tokyu, 4. Department of Arts and Science, Kyushu University, 5. Japan Aerospace Exploration Agency/ Institute of Space and Astronautical Science

Zebra Rock is a sedimentary rock characterized by a pattern consisting of red and whitein color, which is characteristically seen in Australia. Loughnan and Roberts (1990) conclude that the origin of the pattern is due to the diffusion process in a sediment on the basis of their study of the mineral assemblage.However, the mechanism of the specific reaction is not explained, lacking the detailed description. Our aim is to describe Zebra Rock in more detail and to develop a pattern formation model including the reaction of mineral formation.
Six samples taken from the vicinity of Lake Argyle in the East Kimberley region of Western Australia are used. We refer to the characteristic banding pattern consisting of red bands and white bands as Red and White, respectively.
We examined the mineral compositions with XRD (Mac science CuKα radiation) and SEM-EDS (FE-SEM 15 kev, OXFORD Aztec) and the occurrence of minerals with SEM (FE-SEM 15 kev) and TEM (JEM-3200FSk) for each White and Red. By using BSD images, we examined the fraction of minerals, and the characteristics of the spatial correlations between minerals and void for White and Red. As a result, we found that there are two distinctive differences in the mineral abundance and occurrence of iron oxide between White and Red. Red contains more iron oxide than White as shown by previous study. In the occurrence of iron oxide is different. The iron oxide in White takes a shape of planer sheet of polycrystal (<100 μm) which consists of hematite grains (~100 nm), whereas the iron oxides in Red are aligned in interstitial spaces between kaolinite and quartz crystals, as aggregates (<100 μm) which consists of granular hematite grains (~ μm). In addition, from the spatial distribution analysis it is found that the iron oxides concentrate near voids both in White and Red.
Integrating these results,on the basis of the idea that the formation of iron oxide plays an essential role in the formation of zebra pattern,we develop a pattern formation model using a reaction diffusion system. In our model, the pattern is defined as the variation of concentration of ferric irons. We assume the formation process ofhematite in an aqueous solution is simplified as “ferrous ion →goethite (monomers) →goethite (precipitates) →hematite”. We propose an autocatalytic reaction in which ferrous ion are adsorbed in goethite, and thereby the reaction is accelerated. As a result of the linear stability analysis for this simplest model, it is found that the equilibrium point is stable and no pattern forms. Thus, we will develop more complex reaction models to produce the zebra pattern.

Keywords: Zebra Rock, pattern formation, reaction diffusion system

©2019. Japan Geoscience Union. All Right Reserved.

Thermal conductivity anomaly of $(Mg,Fe)CO_3$ solid solution across the spin transition

*Keng-Hsien Chao[1], Wen-Pin Hsieh[1,2]

1. Institute of Earth Sciences, Academia Sinica, Taiwan, 2. Department of Geosciences, National Taiwan University, Taiwan

Deep carbon cycle is a process carrying carbon into Earth's interior by subduction of slabs and returning to Earth's surface by volcanic activities. Given the abundance of iron in Earth's interior, it is believed that $(Mg,Fe)CO_3$ solid solution is an important candidate of carbon-hosting mineral in the mantle. Prior studies have shown that the iron in the $(Mg,Fe)CO_3$ solid solution undergoes a pressure-induced spin transition at 40-55 GPa and the iron content has a minor effect on the onset pressure of spin transition. Across the spin transition, the physical properties of $(Mg,Fe)CO_3$ solid solution, e.g. sound velocity and unit cell volume, typically change accordingly. Lattice thermal conductivity of mantle minerals is key to control the heat flux and temperature profile of the mantle. However, the thermal conductivity of $(Mg,Fe)CO_3$ solid solution under relevant mantle pressure-temperature conditions remains largely unknown. Here we used Raman spectroscopy to characterize the extent of spin transition of natural $(Fe_{0.18}Mn_{0.01}Mg_{0.80}Ca_{0.01})CO_3$ ferromagnesite and time-domain thermoreflectance to measure its thermal conductivity from ambient conditions to 65 GPa. Our preliminary study shows that the thermal conductivity of $(Fe_{0.18}Mn_{0.01}Mg_{0.80}Ca_{0.01})CO_3$ ferromagnesite is 20 W m^{-1} K^{-1} at 40 GPa and drastically increases to 80 W m^{-1} K^{-1} at the beginning of spin transition, and then suddenly drops to 20 W m^{-1} K^{-1} during the middle period of spin transition, similar to its iron-rich counterpart, $(Fe_{0.78}Mg_{0.22})CO_3$ siderite, investigated in our previous work. Our results suggest that if the $(Mg,Fe)CO_3$ carbonates can be transported by the subduction slabs to 1400-1800 km depth with iron contents of 18 to 78 %, their thermal conductivity anomalies across the spin transition may induce anomalies in local thermo-chemical profiles in subduction zones, which in turn alter the distribution fields of subducting minerals.

Keywords: Spin transition, Thermal conductivity, Ferromagnesite, Siderite

©2019. Japan Geoscience Union. All Right Reserved.

Melting experiments in the $MgSiO_3$ –SiO_2 system under high pressures

*Takuya Moriguti[1], Akira Yoneda[1], Eiji Ito[1]

1. Institute for Planetary Materials, Okayama University

Melting of silicates played important roles in chemical differentiation in a deep magma ocean in the early Earth. Therefore, melting relations of the MgO–SiO_2 system have been extensively studied since a pioneer work by Bowen and Anderson (1914). Furthermore, chemical differentiation in the deep magma ocean has been simulated extensively based on results of high pressure melting experiments (e.g. Kato and Kumazawa, 1985; Ito and Katsura, 1992). However, almost all of these works have been carried out on the compositions ranging from MgO to $MgSiO_3$, assuming that the bulk mantle composition is peridotitic or close to that derived from CI chondrite. Recently, enstatite chondrite (E-chondrite) has been attracted as the bulk earth source material (Javoy et al., 2010) because the isotope systematics of the Earth and Moon are nearly identical to those of E-chondrite over O, N, Mo, Re, Os, and Cr. In E-chondrite, the silicate composition is characterized by SiO_2/(SiO_2+MgO) = ˜0.6, which is substantially higher than that of the peridotitic mantle (˜0.4).

In this context, understanding of the melting relations over compositions between $MgSiO_3$ and SiO_2 is indispensable to clarify the mantle fractionation. That also relates to investigations of chemical compositions of the crust at early stage of the Earth. Nevertheless, there have been very limited works on the pressure effect on melting in the $MgSiO_3$–SiO_2 system. Available information regarding phase relations in the system has been so far limited to 5 GPa (Dalton and Presnall, 1997). In this study, we are determining the melting relations in the $MgSiO_3$–SiO_2 system at pressures 5 to 20 GPa. Here we present the results obtained at 10 GPa.

References

Bowen and Anderson (1914) The binary system MgO-SiO_2. Am. J. Sci. 4th ser. 37, 487-500.

Dalton and Presnall (1997) No liquid immiscibility in the system $MgSiO_3$-SiO_2 at 5.0 GPa. Geochim. Cosmochim. Acta 61, 2367-2373.

Ito and Katsura (1992) Melting of ferromagnesian silicates under the lower mantle conditions. Am. Geophys. Union Monogr. 67, 315-322.

Javoy et al. (2010) The chemical composition of the Earth: Enstatite chondrite models. Earth Planet. Sci. Lett. 293, 259-268.

Kato and Kumazawa (1985) Garnet phase of $MgSiO_3$ filling the pyroxene-ilmenite gap at very high temperature. Nature 316, 803-805.

.

©2019. Japan Geoscience Union. All Right Reserved.

Keywords: enstatite chondrite, melting relation, magma ocean, mantle differentiation, high pressure

©2019. Japan Geoscience Union. All Right Reserved.

Melting relations of the Fe-Ni-S-C system and the formation of superdeep diamonds

*Yu Itami[1], Satoru Urakawa[1]

1. Okayama University

Superdeep diamonds derived from the mantle transition zone or the lower mantle have been found in recent years , while most diamonds are thought to form in the upper mantle between 150 and 200 km depth. Smith et al. (2016) discovered solidified Fe-Ni-S-C melt in the inclusions of CLIPPIR diamond, which is one of the superdeep diamonds, and concluded that these diamonds have formed from the metallic liquid in the slabs subducted into the mantle transition zone. In this research, we have performed high-pressure and high-temperature quench experiments of the Fe-Ni-S-C system to investigate diamond formation in the mantle transition zone.

High-pressure and high-temperature experiments were carried out at a pressure of 15 GPa and temperatures of 900-1400 K using a Kawai-type apparatus. Diamonds can coexist with Fe-Ni-S-C melt above 1400 K at 15 GPa. Although the maximum carbon solubility in the liquid coexisting with diamond decreases to 1.5 wt.% with increasing sulfur content up to 12 wt.%, the maximum carbon solubility increases with increasing sulfur content above 12 wt.%. Taking into consideration of the carbon content in the mantle, diamonds can be crystallized from the liquid alloy by supersaturation at 15 GPa when sulfur content in the liquid ranges from 5 to 15 wt.%.

Since the temperature of the mantle transition zone at 450 km depth (15 GPa) is higher than 1400 K, diamonds can form from the Fe-Ni-S-C melt. On the other hand, the diamond cannot form within the top of subducting slab, due to its lower temperature. Thus it is considered that CLIPPIR diamonds have formed in the ancient hotter slab. Meanwhile, in the case that the mantle transition zone has a basaltic composition, it is feasible that the eclogitic diamonds such as CLIPPIR diamonds have been crystallized from liquid alloy in the mantle transition zone.

Keywords: diamond, mantle transition zone, the Fe-Ni-S-C system, liquid alloy, subducting slab

©2019. Japan Geoscience Union. All Right Reserved.

Effect of ammonia on the stability of methane hydrate under high-pressure and high-temperature

*Hirokazu Kadobayashi[1], Hisako Hirai[2], Hiroaki Ohfuji[1], Hideaki Kawamura[1], Michika Ohtake[3], Yoshitaka Yamamoto[3]

1. Geodynamics Research Center, Ehime University, 2. Department of Environment System, Faculty of Geo-environmental Science, Rissho University, 3. National Institute of Advanced Industrial Science and Technology

Methane hydrate may be present in significant amounts in the interior of Titan and other icy moons and is thought to be a candidate for a source of their atmospheric methane [e.g., Loveday *et al.* (2001); Choukroun *et al.* (2010)]. The icy mantles of these moons mainly consist of water, methane and ammonia, but the stability of methane hydrate coexisting with these components under high-pressure and high-temperature have been still unknown. In this study, we report a high-pressure and high-temperature investigation of the effect of ammonia on the stability of methane hydrate using X-ray diffraction and Raman spectroscopy combined with externally heated diamond anvil cell under 0.2-20 GPa and 298-413 K. X-ray diffraction studies revealed that methane hydrate in water-methane-ammonia system transforms from sI cage structure into sH cage structure at approximately 0.8 GPa at room temperature, and further transforms into a filled-ice Ih structure at approximately 1.8 GPa without decomposition into water ice and solid methane. These transition pressures at room temperature were same as those reported for pure methane hydrate [Hirai *et al.* (2001); Loveday *et al.* (2001); Shimizu *et al.* (2002)]. At higher temperature, the melting temperatures for the sI and sH cage structures below 1.8 GPa determined by in situ Raman spectroscopy were good agreement with those of pure methane hydrate reported by previous studies [Dyadin *et al.* (1997); Bezacier *et al.* (2014)]. On the other hand, the decomposition temperatures of filled-ice Ih above 1.8 GPa were about 10-20 K lower than those of water-methane system reported by Kadobayashi *et al.* (2018). Our results suggest that ammonia has a potential to vary the stability of filled-ice Ih of methane hydrate in the interiors of icy moons. Finally, we briefly discuss the implications of our new results for the fate of methane hydrate in concerned with a source of atmospheric methane in Titan.

Keywords: icy satellite, Titan, methane hydrate, diamond anvil cell, high-pressure experiment

©2019. Japan Geoscience Union. All Right Reserved.

Study on magnetite-maghemite-hematite transformation

*Ibuki Kinebuchi[1], Atsushi Kyono[1], Yoshinari Sano[1]

1. University of Tsukuba

Magnetite (Fe_3O_4) widely distributed in the Earth's crust changes into hematite (α-Fe_2O_3) by the oxidization of Fe^{2+} to Fe^{3+}. In the oxidization process, maghemite (γ-Fe_2O_3) with the same spinel structure as magnetite emerges as an intermediate phase. Maghemite differs from magnetite by the presence of cationic vacancies within the octahedral site. It is important to understand the oxidization mechanism of magnetite, however, the local structure change during the oxidization has been still nuclear. In the study, therefore, the phase transition mechanism from magnetite to hematite through maghemite was investigated by using, thermal analysis (TG・DTA), powder X-ray diffraction (XRD) measurement, and high-temperature ex-situ and in-situ X-ray absorption fine structure (XAFS) measurement. The TG・DTA curves of magnetite showed continuous oxidization up to 400 °C.
High-temperature ex-situ EXAFS spectrum of magnetite heated up to 250 °C exhibited weaker peaks concerning Fe_{oct}-O, Fe_{oct}-Fe_{oct}, and Fe_{tet}-Fe_{oct} than those of magnetite. In addition, the averaged Fe-O bond distance appears to become shorter. The results suggest that magnetite is continuously transformed to maghemite in the temperature range from room temperature to 400 °C. The high-temperature ex-situ EXAFS spectrum of magnetite heated up to 500 °C finally displayed characteristic peaks corresponding to hematite, suggesting that the phase transition from magnetite to hematite was completed.
High-temperature in-situ XANES spectrum indicated that the average oxidation number of Fe gradually increased for 135 min from the start of heating at 500 °C, and then became almost constant. The radial structure function obtained from the high-temperature in-situ EXAFS revealed that the peaks of Fe-O, Fe_{oct}-Fe_{oct} and Fe_{tet}-Fe_{oct} become weakened continuously until 70 min from the start of heating. After 80 min peaks corresponding to hematite began to increase. It can be concluded from these results that the phase transition from magnetite to hematite through maghemite starts from the diffusion of the Fe^{2+} in the octahedral sites, resulting in the formations of cationic vacancies and amorphous phase concentrating Fe^{2+}. Subsequently, the reconstruction of the octahedral coordination of Fe and additional oxidization of the amorphous phase lead to the crystallization into hematite.

Keywords: magnetite, maghemite, hematite, thermal analysis, X-ray diffraction, X-ray absorpition fine structure

©2019. Japan Geoscience Union. All Right Reserved.

The Effects of Temperature and Pressure on Hydromagnesite

*Gen-ichiro Yamamoto[1], Atsushi Kyono[1], Jun Abe[2], Takanori Hattori[3], Yoshitaka Matsushita[4], Yasuhiro Yoneda[3]

1. University of Tsukuba, 2. CROSS, 3. JAEA, 4. NIMS

In recent years, the global warming is the most important environment problem. Therefore, attempts of CO_2 geological storage have been made to reduce carbon dioxide in the atmosphere all over the world (Xue and Nakano 2008). Among some CO_2 geological storage methods, the CO_2 mineral trapping can store the carbon dioxide safety for a long time. In the case of geological storage, magnesium carbonate hydrates are important minerals since they precipitate easily from water saturated with carbon dioxide. The major magnesium carbonate hydrates formed from aqueous solution are nesquehonite $MgCO_3 \cdot 3H_2O$ and hydromagnesite $Mg_5(CO_3)_4(OH)_2 \cdot 4H_2O$. The stability of these minerals are critically important factors to assess environmental safety and phase stability over geological time scale, but they have not been fully investigated yet, especially of hydromagnesite. Here, we investigated the effects of pressure and temperature on hydromagnesite by using thermal analysis, high-temperature X-ray diffraction, X-ray total scattering, high-pressure X-ray diffraction, and high-pressure and high-temperature neutron diffraction techniques.

With temperature, hydromagnesite was decomposed into periclase MgO through the poor crystalline phase, accompanied with dehydration, dihydroxylation, and decarbonation of hydromagnesite. The *a* and *c* lattice parameters were monotonously increased as increasing temperature whereas *b* lattice parameter almost remained unchanged. At just before the dehydration reaction, the unit cell was contracted due to the dehydration. With pressure, hydromagnesite structure was maintained up to 8.7 GPa. Decomposition into magnesite $MgCO_3$ or periclase was unobserved up to at least 21.0 GPa. With compression, the unit cell was isotopically contracted. The fit to the Birch-Murnaghan equation of state gives $K_0 = 32(2)$ and $V_0 = 658(4)$ with $K' = 4.0$ (fixed). Under high-pressure and high-temperature conditions, hydromagnesite broke down into magnesite and brucite $Mg(OH)_2$ at 200 $^{\circ}C$ and 1.2 GPa. The unit cell was isotopically expanded up to just before the breakdown. The breakdown of hydromagnesite could be caused by the dissolution by dehydration water, and subsequently magnesite and brucite were hydrothermally grown from the solution at the condition. The results obtained from this study would provide insight the CO_2 geological storage.

Keywords: Hydromagnesite, magnesite, phase change, high-pressure, high-temperature, CO2 geological storage

©2019. Japan Geoscience Union. All Right Reserved.

Synthesis and crystal structure of Mg-bearing Fe_9O_{11}: New insight in the complexity of Fe-Mg oxides at conditions of the deep upper mantle

*Takayuki Ishii[1], Uenver-Thiele Laura[2], Alan B Woodland[2], Edith Alig[3], Tiziana Boffa Ballaran[1]

1. Bavarian Research Institute, University of Bayreuth, 2. Institut für Geowissenschaften, Goethe-Universität Frankfurt, 3. Institut für Anorganische und Analytische Chemie, Goethe-Universität Frankfurt

The Fe-O system is fundamental for understanding redox processes operating in the Earth's interior. Recent experimental studies have revealed several new mixed-valence Fe-oxides to be stable at high pressures and temperatures, such as the orthorhombic-structured phases $Fe^{2+}_2Fe^{3+}_2O_5$ and $Fe^{2+}_3Fe^{3+}_2O_6$. and the monoclinic-structured $Fe^{2+}_3Fe^{3+}_4O_9$. It has been also demonstrated that Fe_4O_5 and Fe_7O_9 form solid solutions with the Mg-endmembers such as $Mg_2Fe_2O_5$ and $Mg_3Fe_4O_9$, suggesting possible existence of complicated Mg-Fe oxides in the deep mantle. We synthesized a new Mg-Fe oxide with a composition of $Mg_{0.9}Fe_{8.1}O_{11}$. We report the synthesis and crystal structure analyzed by the Rietveld method.

A novel Mg-bearing iron oxide $Mg_{0.87(1)}Fe^{2+}_{4.13(1)}Fe^{3+}_4O_{11}$ was synthesized at 12 GPa and 1300 ˚C using a large volume press. Rietveld structural analysis was conducted with a laboratory X-ray diffraction pattern obtained at ambient conditions.
The crystal structure, which has one oxygen trigonal prism site and four octahedral sites for the cations, was found to be isostructural with $Ca_2Fe_7O_{11}$. The unit-cell lattice parameters are a = 9.8441(5) Å, b = 2.8920(1) Å, c = 14.1760(6) Å, β = 99.956(4)˚, V = 397.50(3) Å, and Z = 2 (monoclinic, $C2/m$). Mg and Fe cations are disordered on the trigonal prism site and on two of the four octahedral sites, and the remaining Fe is accommodated at the other two octahedral sites. The present structure is closely related to the other recently discovered Fe oxide structures, e.g. Fe_4O_5 and Fe_5O_6, by distortion derived either from incorporation (Fe_4O_5) or removal (Fe_5O_6) of an edge-shared FeO_6 single octahedral chain in their structures. The present synthesis at deep upper mantle conditions and the structural relationships observed between various novel Mg-Fe oxides indicate that a series of different phases become stable above 10 GPa and that their relative stabilities (Fe^{2+}/Fe^{3+}) must be controlled by oxygen fugacity.

Keywords: iron oxide, mantle, oxygen fugacity, multi-anvil apparatus, Rietveld analysis

©2019. Japan Geoscience Union. All Right Reserved.

Changes in specific surface area and morphology of kaolin group minerals with pressure treatment

*Soyeon Kwon[1], Yongjae Lee[1]

1. YONSEI University

Pressure can tailor the properties of a material by changing its atomistic arrangements and/or crystal morphology. We have investigated the changes in the adsorption properties of kaolin group minerals as a function of pressure treatment in gigapascal range. External pressure has been applied using a Large Volume Press (LVP) to kaolinite ($Al_2Si_2O_5(OH)_4$) and halloysite ($H_4Al_2O_9Si_2{\cdot}2H_2O$), which represent natural 2D layered and 1D nanowire structures, respectively. Powdered samples have been compressed up to 3 GPa in 1 GPa steps at room temperature and recovered by up to ~0.35g from each pressure step. The BET (Brunauer, Emmett, Teller) measurement was conducted using N_2 gas to measure the specific surface area, pore size distribution, and pore volume of the pressure-treated samples. Before pressure-treatment, the specific surface area of kaolinite has been measured to be 10.702(m^2g^{-1}), which increases to 12.090(m^2g^{-1}) after 1 GPa, 17.101(m^2g^{-1}) after 2 GPa, and 17.864(m^2g^{-1}) after 3 GPa treatments. These lead to a gradual increase in the total volume of adsorbed pores from 0.01216 (cm^3g^{-1}) at ambient, to 0.01368(cm^3g^{-1}) after 1 GPa, 0.074337(cm^3g^{-1}) after 2 GPa, and 0.09546(cm^3g^{-1}) after 3 GPa treatments. Unlike Kaolinite, the specific surface area of halloysite decreases from 47.476($m2g^{-1}$) from ambient to 44.348(m^2g^{-1}) after 1 GPa, 41.579(m^2g^{-1}) after 2 GPa, and 42.796(m^2g^{-1}) after 3 GPa treatment, which results in overall decrease in the total volume of the pore from 0.1914(cm^3g^{-1}) at ambient to 0.1863(cm^3g^{-1}) after 1 GPa, 0.1572(cm^3g^{-1}) after 2 GPa, and 0.1187(cm^3g^{-1}) after 3 GPa treatments.
We discuss the contrasting effects of pressure-treatment on the two morphologically-distinct kaolin group minerals based on SEM (Scanning Electron Microscope) images and analyses of selected diffraction peaks measured on each recovered material. We observe that the layers in kaolinite separate into smaller units upon increasing pressure treatment, whereas the tubes in halloysite become flattened, which led to the contrasting changes in surface area and pore volume. Further study is in progress to compare these results to when water is used as a pore-penetrating pressure-transmitting medium.

Keywords: kaolinite, halloysite, high pressure treatment, specific surface area, morphology

©2019. Japan Geoscience Union. All Right Reserved.

Changes in specific surface area and morphology of kaolin group minerals with pressure treatment

Soyeon Kwon, Yongjae Lee*

Department of Earth System Sciences, Yonsei University

yongjaelee@yonsei.ac.kr

ABSTRACT

Pressure can tailor the properties of a material by changing its atomistic arrangements and/or crystal morphology. We have investigated the changes in the adsorption properties of kaolin group minerals as a function of pressure treatment in gigapascal range. External pressure has been applied using a Large Volume Press (LVP) to kaolinite ($Al_2Si_2O_5(OH)_4$) and halloysite ($H_4Al_2O_9Si_2 \cdot 2H_2O$), which represent natural 2D layered and 1D nanowire structures, respectively. Powdered samples have been compressed up to 3 GPa in 1 GPa steps at room temperature and recovered by up to ~0.35g from each pressure step. The BET (Brunauer, Emmett, Teller) measurement was conducted using N_2 gas to measure the specific surface area, pore size distribution, and pore volume of the pressure-treated samples. Before pressure-treatment, the specific surface area of kaolinite has been measured to be 10.702(m^2g^{-1}), which increases to 12.090(m^2g^{-1}) after 1 GPa, 17.101(m^2g^{-1}) after 2 GPa, and 17.864(m^2g^{-1}) after 3 GPa treatments. These lead to a gradual increase in the total volume of adsorbed pores from 0.01216 (cm^3g^{-1}) at ambient, to 0.01368(cm^3g^{-1}) after 1 GPa, 0.074337(cm^3g^{-1}) after 2 GPa, and 0.09546(cm^3g^{-1}) after 3 GPa treatments. Unlike Kaolinite, the specific surface area of halloysite decreases from 47.476(m2g^{-1}) from ambient to 44.348(m^2g^{-1}) after 1 GPa, 41.579(m^2g^{-1}) after 2 GPa, and 42.796(m^2g^{-1}) after 3 GPa treatment, which results in overall decrease in the total volume of the pore from 0.1914(cm^3g^{-1}) at ambient to 0.1863(cm^3g^{-1}) after 1 GPa, 0.1572(cm^3g^{-1}) after 2 GPa, and 0.1187(cm^3g^{-1}) after 3 GPa treatments.

We discuss the contrasting effects of pressure-treatment on the two morphologically-distinct kaolin group minerals based on SEM (Scanning Electron Microscope) images and analyses of selected diffraction peaks measured on each recovered material. We observe that the layers in kaolinite separate into smaller units upon increasing pressure treatment, whereas the tubes in halloysite become flattened, which led to the contrasting changes in surface area and pore volume. Further study is in progress to compare these results to when water is used as a pore-penetrating pressure-transmitting medium.

©2019. Japan Geoscience Union. All Right Reserved.

[E] Poster | S (Solid Earth Sciences)：S-GC Geochemistry

Wed. May 29, 2019 10:45 AM - 12:15 PM JST | Wed. May 29, 2019 1:45 AM - 3:15 AM UTC | Poster Hall International Exhibition Hall8, Makuhari Messe_9

[S-GC40] Volatile Cycles in the Deep Earth - from Subduction Zone to Hot Spot

convener:Hirochika Sumino(Department of Basic Science, Graduate School of Arts and Sciences, The University of Tokyo), Takeshi Hanyu(Japan Agency for Marine-Earth Science and Technology, Department of Solid Earth Geochemistry), Yuji Sano(Division of Ocean and Earth Systems, Atmosphere and Ocean Research Institute, University of Tokyo), Gray E Bebout(Lehigh University)

Volatiles play an important role in the geodynamics and chemical differentiation in the mantle and crust by drastically changing mineral stability and rheological behavior. Fractionation-processes such as partial melting, hydration, and dehydration are all controlled by volatiles in the rocks. A significant portion of the volatiles in the Earth has been thought to be present in the atmosphere and oceans as a consequence of extensive degassing during accretion and subsequent mantle degassing. On the other hand, it has been recently recognized that substantial amounts of volatiles are recycled back into the mantle at subduction zones, where intensive devolatilization of descended materials during arc magma generation was once thought to act as an effective "subduction barrier". However, fundamental questions still remain, such as: how are volatiles species distributed throughout the early and present Earth? What are the mechanisms for, and rate at which, volatiles are fluxed between the atmosphere, crust, and mantle? And what role have volatiles played in driving the evolution of the Earth? The possible role of the core in storing primordial volatiles is also poorly constrained. We therefore welcome contributions from experimental, observational, and modeling studies that help shed light on the deep cycles of volatiles, such as hydrogen, carbon, nitrogen, noble gases, halogens and sulfur. We particularly encourage studies linking the behavior of multiple volatile elements and their isotopic compositions. Studies investigating the linkage between volatile and solid geochemical tracers, the phase equilibria of volatile-bearing mantle assemblages, and the effect of volatiles on the physical properties of the mantle are also welcome.

[SGC40-P01] Continental growth models demystified

*Jun Korenaga[1] (1.Department of Geology and Geophysics, Yale University)

[SGC40-P02] Mass-independent sulfur isotope signature from the 2.7 Ga Belingwe komatiite: Recycling of crustal material in Archean

*Yusuke Kubota[1], Yuichiro Ueno[1,2,3], Kenji Shimizu[3], Fumihiro Matsuura[2], Akira Ishikawa[1,3] (1.Department of Earth and Planetary Sciences, Tokyo Institute of Technology, 2.Earth-Life Science Institute, Tokyo Institute of Technology, 3.Japan Agency for Marine-Earth Science and Technology (JAMSTEC))

[SGC40-P03] Determination of halogens in some standard materials using the neutron irradiation noble gas mass spectrometric technique

*Hirochika Sumino[1], Masahiro Kobayashi[2], Takehiko Saito[3], Keisuke Nagao[3] (1.Department of Basic Science, Graduate School of Arts and Sciences, The University of Tokyo, 2.Tokyo Metropolitan Industrial Technology Research Institute, 3.Geochemical Research Center, Graduate School of Science, University of Tokyo)

[SGC40-P04] FTIR spectroscopy and noble gas mass spectrometry for a single olivine grain

*Sota Niki[1], Hirochika Sumino[2], Masahiro Kobayashi[3], Hiroyuki Kagi[1], Takafumi Hirata[1], Chris J. Ballentine[4] (1.Geochemical Research Center, Grad. School of Science, Univ. of Tokyo, 2.Dept. of Basic Science, Grad. School of Arts and Sciences, Univ. of Tokyo, 3.Tokyo Metropolitan Industrial Technology Research Institute, 4.Dept. of Earth Sciences, Univ. of Oxford)

[SGC40-P05] New halogen incorporation mechanism in serpentine group minerals: Crystal chemical consideration

*Masami Kanzaki[1] (1.Institute for Planetary Matereials, Okayama University)

[SGC40-P06] Mineralogical and geochemical characteristics of cuttings from Taketomi hot spring

*Noriyuki Shingaki[1], Tomohiro Toki[1], Syogo Oshima[2], Masaaki chinen[3], Arito Sakaguchi[4], Naoto Takahata[5], Yuji Sano[5], Shirai Kotaro[5], Kentaro Tanaka[5] (1.University of the Ryukyus , 2.West Japan Engineering Consultants, Inc., 3.MicroRange, 4.Faculty of Science, Yamaguchi University, 5.Atmosphere and Ocean Research Institute, The University of Tokyo)

[SGC40-P07] Variation of helium isotope compositions at Lake Mashu

*Takanori Kagoshima[1], Yuji Sano[1], Atsushi Tanaka[2] (1.Atmosphere and Ocean Research Institute, University of Tokyo, 2.National Institute for Environmental Studies)

[SGC40-P08] Helium isotopes in Tachibana Bay and Shimabara Bay, Nagasaki

*Ma. Teresa Escobar[1], Yama Tomonaga[2], Hajime Obata[1], Shigenobu Takeda[3], Naoto Takahata[1], Yuji Sano[1] (1.Atmosphere and Ocean Research Institute, University of Tokyo, Kashiwanoha, Kashiwa, Chiba, Japan, 2.Eawag,, Swiss Federal Institute of Aquatic Science and Technology, Department of Water Resources and Drinking Water, Überlandstrasse 133 CH-8600 ,Dübendorf, Switzerland, 3.Graduate School of Fisheries and Environmental Sciences, Nagasaki University, Nagasaki, Japan)

Continental growth models demystified

*Jun Korenaga[1]

1. Department of Geology and Geophysics, Yale University

So far proposed models of continental growth exhibit bewildering diversity, but this diversity is rather superficial. By understanding how different growth models are built and what they are meant to constrain, we can gain deeper insight into the evolution of continental crust as well as the dynamics of the early Earth. There are three kinds of growth models: crust-based, mantle-based, and others. Crust-based models provide only the lower bound on net crustal growth, and mantle-based models aim at constraining net crustal growth itself. Other models are also about net crustal growth, but they are subject to greater uncertainty. In the presence of crustal recycling, crust-based models are expected to be different from mantle-based models, and more important, the difference between these two kinds of models provides important constraints on the operation of plate tectonics in the early Earth. Some popular misconceptions in the recent literature are also discussed.

Keywords: Continental crust, Plate tectonics, Chemical differentiation

©2019. Japan Geoscience Union. All Right Reserved.

Mass-independent sulfur isotope signature from the 2.7 Ga Belingwe komatiite: Recycling of crustal material in Archean

*Yusuke Kubota[1], Yuichiro Ueno[1,2,3], Kenji Shimizu[3], Fumihiro Matsuura[2], Akira Ishikawa[1,3]

1. Department of Earth and Planetary Sciences, Tokyo Institute of Technology, 2. Earth-Life Science Institute, Tokyo Institute of Technology, 3. Japan Agency for Marine-Earth Science and Technology (JAMSTEC)

Recycling of the Earth's crustal material has long been discussed mainly through the radiogenic isotopes of modern Ocean Island Basalts (OIB). Recent finding of Sulfur Mass Independent Fractionation (S-MIF) from HIMU and EM I basalts supports recycling of crustal material in mantle (Cabral et al., 2013; Delavault et al., 2016). Since photochemical reactions under reducing Archean atmosphere are thought to be a plausible process of large S-MIF generation (Farquhar et al., 2001; Farquhar and Wings, 2003), these discoveries demonstrated that the S-MIF is a useful signature for tracing Archean crustal material. However, it has been difficult to estimate when the subduction started in the history of the Earth. Here, we report multiple sulfur isotope analysis of the 2.7 Ga Belingwe komatiites and related rocks, which has potential to elucidate earlier subduction or recycling of crustal material before 2.7 Ga. The Belingwe komatiite are one of the best-preserved Archean komatiites in the world. The results show clear S-MIF signature in several komatiites and basalts. Sulfide minerals in the S-MIF bearing samples occur as pyrrhotite and chalcopyrite scattered within groundmass around the quenched olivine and pyroxene crystals, indicating that the sulfides crystalized at the time of eruption. The original nature of the sulfide is also supported by the correlation between sulfur contents and magnesium number. Based on Nd, Sr, and Pb isotope composition measured in the previous study (Shimizu et al., 2005), the S-MIF bearing komatiites and basalts are likely to be derived from depleted mantle source, whereas more enriched samples do not show S-MIF. Therefore, the S-MIF component is not likely derived from assimilated crust at the time of the komatiite volcanism, but originally incorporated in the depleted source mantle. Consequently, our results suggest that subduction of S-MIF bearing surface material into the mantle had been operated at least prior to 2.7 Ga.

Keywords: Sulfur mass independent fractionation, Mantle geochemistry, Komatiite, Archean

©2019. Japan Geoscience Union. All Right Reserved.

Determination of halogens in some standard materials using the neutron irradiation noble gas mass spectrometric technique

*Hirochika Sumino[1], Masahiro Kobayashi[2], Takehiko Saito[3], Keisuke Nagao[3]

1. Department of Basic Science, Graduate School of Arts and Sciences, The University of Tokyo, 2. Tokyo Metropolitan Industrial Technology Research Institute, 3. Geochemical Research Center, Graduate School of Science, University of Tokyo

Halogens are among the most powerful tracers of volatile cycling in subduction zones, because of (i) the large contrast in concentrations between the surface and interior of the Earth [1], (ii) their high affinities to gas- and fluid-phases relative to mineral [2], (iii) distinct elemental and/or isotopic compositions in each reservoir in the Earth [3-7]. However, few analytical techniques can determine trace amounts of halogens, particularly bromine and iodine in mantle-derived samples. Consequently, there have been relatively few previous studies of halogens in mantle-derived samples.

The neutron irradiation noble gas mass spectrometric technique (NI-NGMS) is capable of measuring very low concentrations of halogens (<1 ppb) in very small samples (<1 mg). The NI-NGMS is an extension of the Ar-Ar and I-Xe dating methods [8-10]. Halogens (chlorine, bromine, and iodine) and other elements (potassium, calcium, barium, and uranium) are converted to corresponding isotopes of argon, krypton, and xenon by neutron irradiation in a nuclear reactor. The noble gas isotopes in neutron-irradiated samples are analyzed by noble gas mass spectrometry. Irradiation conditions such as neutron fluence are monitored using standard materials of the Ar-Ar and I-Xe dating methods. Relatively high cross-sections of halogens for neutron capture and high sensitivity of noble gas mass spectrometry enable determination of trace amounts of halogens using NI-NGMS.

We report new halogen concentrations determined for scapolite standards and geological reference materials distributed by Geological Survey of Japan and US Geological Survey using NI-NGMS. Consistent results with those regarded as reference values were obtained from scapolite standards, which indicate that the scapolite standards are reliable in halogen analysis. On the other hand, the halogen concentrations obtained from geological reference materials are systematically lower than the reference values for samples with low concentrations of halogens. The higher concentrations reported for the geological reference materials probably result from contamination on the sample surface during preparation of these reference materials. We also propose a fluorine determination method using NI-NGMS based on neon systematics, although reliable determination of fluorine has been thought to be impossible.

[1] Pyle & Mather, *Chem. Geol.* 2009. [2] Bureau *et al.*, *GCA* 2016. [3] Sumino *et al.*, *EPSL* 2010. [4] Chavrit *et al.*, *GCA* 2016. [5] Kobayashi *et al.*, *EPSL* 2017. [6] Kendrick *et al.*, *Nature Geosci.* 2017. [7] Kobayashi *et al.*, *G-cubed* 2019. [8] Turner, *JGR* 1965. [9] Kendrick, *Chem. Geol.* 2012. [10] Ruzié-Hamilton *et al.*, *Chem. Geol.* 2016.

Keywords: Halogen, Noble gas, Nuetron irradiation, Noble gas mass spectrometry

©2019. Japan Geoscience Union. All Right Reserved.

FTIR spectroscopy and noble gas mass spectrometry for a single olivine grain

*Sota Niki[1], Hirochika Sumino[2], Masahiro Kobayashi[3], Hiroyuki Kagi[1], Takafumi Hirata[1], Chris J. Ballentine[4]

1. Geochemical Research Center, Grad. School of Science, Univ. of Tokyo, 2. Dept. of Basic Science, Grad. School of Arts and Sciences, Univ. of Tokyo, 3. Tokyo Metropolitan Industrial Technology Research Institute, 4. Dept. of Earth Sciences, Univ. of Oxford

Volatiles have been degassed from the mantle and recycled back into the mantle at subduction zones. Water is the main component of volatiles and plays a key role in dynamics of the subduction zones because even a small water content in rocks has an influence on the physical and chemical properties of the rocks (e.g. friction coefficient, melting point, etc.) which are closely related to phenomena studied in earth sciences including volcanic or seismic activities. It is still unclear to what extent of water have been subducted into the mantle and released to the Earth’ s surface. To elucidate the volatile recycling, noble gases are powerful tracers because they have unique compositions in geochemical reservoirs. Previous researches have mainly reported results of bulk analysis of mantle peridotites. On the contrary, in this study, FTIR measurements and noble gas analysis of a single olivine grain were conducted to determine the noble gas concentrations in fluid inclusions.

The olivine samples used for this study were separated from mantle xenoliths collected from an intraplate setting (Hualalai in Hawaii) and two subduction zones (the Avacha volcano in the Kamchatka arc and the Pinatubo volcano in the Luzon arc). The Hualalai olivine was expected to show mantle-derived noble gas compositions (Kobayashi et al., G-cubed 2019) and was used for checking the accuracy of noble gas analysis. The Avacha and Pinatubo olivines contained H_2O-rich fluid inclusions and the noble gas concentrations in the inclusions had been estimated from salinities, and halogen and noble gas compositions (Kobayashi et al., EPSL 2017). The Avacha and Pinatubo olivines were used to confirm the accuracy of the analytical method used in this study for determining the noble gas concentrations in the inclusions.

FTIR measurements were conducted to determine the H_2O concentration in the Avacha and Pinatubo olivines. The mantle xenoliths were crushed into 0.5 to 2 mm and olivine grains were separated. The olivine grains were embedded in resin (Ortho Bright) and polished to a thickness of several hundred micrometers. The weight of samples was 0.7 to 16 mg. The H_2O concentration was calculated from the absorbance at 3404 cm^{-1}. After the FTIR measurements, resin was removed from each grain by heating at 50ºC and dissolving in acetone.

Noble gas analysis was conducted using multicollector noble gas mass spectrometers (Helix SFT and Argus, Thermo Fisher Scientific). After the sample loading into a laser heating cell, the cell was baked out with pumping to desorb atmospheric noble gases to achieve low blank levels required for single-grain analysis. Consequently, noble gases were extracted by laser heating (Fusion Diode Stepped Heating System, Teledyne CETAC) at about 1000 ºC for 5 minutes. The gases released from samples were purified by removing active gases using a getter, and then, absorbed on two cryo-traps (one was for helium and neon and the other was for argon, krypton, and xenon). Each noble gas was desorbed from the trap at a certain temperature and introduced into the mass spectrometers. Helium was measured with Helix SFT and other noble gases were measured with Argus. The abundances and isotopic ratios of noble gases in a

©2019. Japan Geoscience Union. All Right Reserved.

single olivine grain were obtained. The accuracy of the isotopic ratios was checked by the Hualalai samples.

The noble gas concentrations in the inclusions obtained will be compared with the previous bulk analysis to discuss the accuracy of the method in this study. This method of determining the noble gas concentrations in fluid inclusions from single-grain analysis has a potential to clarify the heterogeneity of the mantle volatiles in terms of a single-grain mineral and the flux quantification during the volatile recycling.

Keywords: noble gas, FTIR spectroscopy, mantle

©2019. Japan Geoscience Union. All Right Reserved.

New halogen incorporation mechanism in serpentine group minerals: Crystal chemical consideration

*Masami Kanzaki[1]

1. Institute for Planetary Matereials, Okayama University

Introduction: Recent geochemical studies revealed that serpentinites contain a significant amount of halogens. However, how halogen ions are incorporated into serpentinites is not well understood. Commonly assumed mechanism is "OH^- substitution" in serpentine group minerals (chrysotile, lizardite and antigorite). Although this mechanism will be fine for F, but may not be adequate for larger halogens (Cl, Br, I). Here, I propose new halogen incorporation mechanism in lizardite and antigorite from crystal chemical point of view.

Calculation methods: In order to assess present new incorporation model, first-principles calculation was conducted. Quantum-Espresso package was used to optimize the halogen incooporated model structures. In the present study, lizardite and antigorite (*m*=17 polysome) are considered. For our proposed mechanism, charge balance should be observed; so $Mg^{2+} = X^- + Al^{3+}$ substitution (X^- = halogen) is assumed to introduce halogen to a vacant site. For lizardite, enthalpy difference between two models (OH^- substitution and our model) was calculated for following equation: $Mg_2AlSi_2O_8XH_2 + H_2O = Mg_2AlSi_2O_9XH_4$. Former corresponds to the OH substituted model (with Al introduced), and latter corresponds to our new model. Although this comparison is crude (as free H_2O is included in the equation), it could provide systematic trend with kinds of halogen atoms. Since antigorite has a very large unit cell and many vacant sites, only $Mg^{2+} = Cl^- + Al^{3+}$ substitute in five vacant sites are considered so far.

Results and Discussion: From close inspection of crystal structures of lizardite and antigorite, vacant sites ideal for halogens are identified. The vacant sites are surrounded by four protons (of OH^-) forming elongated tetrahedon (i.e., XH_4^{3+}) if halogen is located. Such vacant sites provide local structure similar to halogen ions in aqueous solution.

In order to further assess present incorporation mechanism, first-principles calculations of lizardite and antigorite containing halogens in those sites were conducted. The structural optimizations confirmed that halogens could be well accommodated into the tetrahedral vacant sites in lizardite. The calculated enthalpy difference between OH substitution and present models in lizardite revealed that larger halogens prefer our model over the OH substitution model. There is sinlge vacant site in lizardite, but antigorite (*m*=17) has 17 crystallographically different vacant sites. Most sites have local structures more or less similar to that of lizardite (locating in 6-membered SiO_4 ring). But there is another kind of vacant site which is locating in 8-membered SiO_4 ring. This local structure is surrounded by six protons, but it can be regareded as two tetrahedral proton sites with edge sharing. Substitution of Cl^- to this site (one of tetrahedral sites) showed lower enthalpy compared to those of other lizardite-like sites, and can accept more larger ions. Therefore, Cl^- (and other larger halogens) will prefet this site in antigorite (*m*=17). Not all antogorite polysomes have this site.

Present study suggests that our new proposed incorporation mechanism is promising, and it should be further studied experimentally. Present new incorporation mechanism would be important to understand elemental partition behavior of halogens in subduction zones.

Keywords: halogen site, serpentine, crystal chemistry, incorporation mechanism, elemental partition

©2019. Japan Geoscience Union. All Right Reserved.

Mineralogical and geochemical characteristics of cuttings from Taketomi hot spring

*Noriyuki Shingaki[1], Tomohiro Toki[1], Syogo Oshima[2], Masaaki chinen[3], Arito Sakaguchi[4], Naoto Takahata[5], Yuji Sano[5], Shirai Kotaro[5], Kentaro Tanaka[5]

1. University of the Ryukyus , 2. West Japan Engineering Consultants, Inc., 3. MicroRange, 4. Faculty of Science, Yamaguchi University, 5. Atmosphere and Ocean Research Institute, The University of Tokyo

It is important to grasp carbon cycle on the earth’ s surface for thinking about global environmental change. A hot spring with a maximum temperature of 64℃ is venting with gas containing 70% of methane from several spots on the seafloor at depth of 22 m at 1 km northeast off Taketomi Island. Based on methane and helium isotope ratios in the venting gas, the influence of magmatic gas has been pointed out. In spite of Taketomi Island located on the trench side from island arc, magmatic gas is venting. It suggests the forearc where magma cannot generate, might form new supply path of carbon from the Earth’ s interior. The mass balance from new supply path of carbon may change estimation of carbon cycle on earth’ s surface. Therefore, the purpose of this study is to elucidate venting mechanism and quantitative grasp of magmatic gas from forearc, and the history of hot spring activities will be investigated to predict future activities.

In 2017, the hot spring was drilled up to depth of 940 m in Taketomi Island. The cuttings with muddy water were sampled every 10 m. The thin sections were prepared from cuttings to be observed using polarization microscope, and the chemical compositions of grains were analyzed by SEM-EDX. The ground samples were analyzed for mineral and chemical compositions by XRD and EDX. The clay minerals gathered by levitation were measured for half-value width of illite using XRD. He and CO_2 contained in samples that were crashed in vacuum were measured for isotope ratios by mass spectrometer. Calcite and dolomite collected from the cuttings were measured for the carbon and oxygen isotope ratios by mass spectrometer. The vitrinite in the cuttings was separated by a heavy liquid, and the reflectance was measured by a reflecting microscope.

In the microscopy, the stratum was roughly divided two formations; cryptocrystalline quartz layer and sand stone layer. Carbonaceous materials were observed in most of the stratum. Dolomite was limitedly observed in the vicinity of 800 m. In the XRD analysis, Quartz was detected at all depth. Calcite was detected at shallower depth than 30 m, and dolomite was detected only around 800 m. As a result of the EDX analysis, silicon was the most dominant in all layers, and especially, it was contained around 0-100 m, 300 m and around 900 m over 80%. There was a layer that contained much calcium. Around 0-30 m, 400-500 m and around 800 m, calcite was contained 15 % or more. The half-value width of illite was large, 0.8 $\Delta^\circ 2\theta$, in only 10 m surface, and as low as 0.2 to 0.4 $\Delta^\circ 2\theta$ below 50 m. Vitrinite reflectance was around 5% in the whole layer, close to measurement limit. The helium content was 10^{-14}-10^{-11} mol per 1g of cuttings, and tended to increase with increasing depth. The highest content was detected at 800 m depth. The helium isotope ratio($^3He/^4He$)have value of 0.4-3.6 times that of atmosphere, and tended to increase with increasing depth. Particularly, it was higher at 100 m, 300-400 m and 700-800 m. The CO_2 content per gram of cuttings, was in the range of 10^{-8}-10^{-6} mol in most layers, but it showed

©2019. Japan Geoscience Union. All Right Reserved.

higher values at 400 m and 800 m depth. the water tended to decrease with increasing depth, and showed especially high values at 400 m and 900 m. The carbon isotope ratio ($\delta^{13}C$) of calcite was -4.7‰ VPDB, and the oxygen isotope ratio ($\delta^{18}O$) is -16.3‰VPDB. The $\delta^{13}C$ value of dolomite was -1‰VPDB, and the $\delta^{18}O$ value was -10.9‰VPDB. The $\delta^{13}C$ value of CO_2 from cuttings at 800 m was -7.3‰VPDB, which contained sufficiently amount of carbon to measure carbon isotope ratio.

Keywords: Taketomi Island, Hot spring, cuttings, vitrinite reflectance, carbon cycle, helium isotope

©2019. Japan Geoscience Union. All Right Reserved.

Variation of helium isotope compositions at Lake Mashu

*Takanori Kagoshima[1], Yuji Sano[1], Atsushi Tanaka[2]

1. Atmosphere and Ocean Research Institute, University of Tokyo, 2. National Institute for Environmental Studies

Helium-3 is one of the most sensitive geochemical tracers which reflects addition of mantle components to gas and fluids in volcanic hydrothermal systems, and $^{3}He/^{4}He$ ratios may be useful to assess temporal change of hydrothermal activity at volcanic lakes. Lake Mashu is a caldera lake which formed around 7000 years ago in Hokkaido. Igarashi et al. (1992) measured He and Ne isotopes in water of Lake Mashu, and concluded that the depth profile of isotopic compositions reflect injection of mantle-derived He due to hot spring activity at the lake bottom. After that, there is no subsequent study reporting He isotope data. The lack of observational data may be due to difficulty of water sampling at caldera lakes. Igarashi et al. (1992) collected water samples into copper tubes. However, this method requires heavy and large sampling tools, and people who can transfer water and seal the tubes properly. In May and September 2017, we investigated Lake Mashu in order to check volcanic activity and practical sampling methods for caldera lakes. We collected water using a Niskin bottle at several depths (surface to 210 m) around the deepest point (211 m). Collected water was immediately transferred into lead-glass containers with vacuum valves at both ends. In Atmosphere and Ocean Research Institute, dissolved gases were extracted by the head space method, and introduced into a purification vacuum line. In the line, He and Ne were purified for isotope analyses. $^{3}He/^{4}He$ and $^{4}He/^{20}Ne$ ratios were measured using Helix-SFT and QMS, respectively. The highest $^{3}He/^{4}He$ ratios were observed at 205-210 m depth, indicating that injection of fluids with the high $^{3}He/^{4}He$ ratio at the bottom. The linear correlation between $^{4}He/^{20}Ne$ and $^{3}He/^{20}Ne$ ratios in water samples indicated mixing of two components: injected fluids and the atmosphere. The estimated $^{3}He/^{4}He$ ratio of the fluid end member was indistinguishable from the value reported by Igarashi et al. (1992), implying a possibility that there was no significant change in volcanic activity at Lake Mashu in the past 30 years.

Keywords: Helium isotope, Volcanic lake, Lake Mashu

©2019. Japan Geoscience Union. All Right Reserved.

Helium isotopes in Tachibana Bay and Shimabara Bay, Nagasaki

*Ma. Teresa Escobar[1], Yama Tomonaga[2], Hajime Obata[1], Shigenobu Takeda[3], Naoto Takahata[1], Yuji Sano[1]

1. Atmosphere and Ocean Research Institute, University of Tokyo, Kashiwanoha, Kashiwa, Chiba, Japan, 2. Eawag,, Swiss Federal Institute of Aquatic Science and Technology, Department of Water Resources and Drinking Water, Ü berlandstrasse 133 CH-8600 ,Dübendorf, Switzerland, 3. Graduate School of Fisheries and Environmental Sciences, Nagasaki University, Nagasaki, Japan

Noble gases are powerful tracers to study physical transport processes in aquatic system. Moreover, helium isotopes have been shown to be very useful to infer the origin of fluids. Shimabara Peninsula is located on western side of the Beppu-Shimabara graben in Kyushu, SW Japan. In the region, there are some hot springs and groundwaters which indicate magmatic helium with high 3He/4He ratio. Although some researchers report helium isotopic ratio on land, there is no data in the sea.

The surrounding bays around Shimabara Peninsula in Nagasaki were recently studied for the existence of hydrothermal springs and vents. Physico-chemical properties characteristic of hydrothermal activity were detected on the seafloor. For this study, we use helium isotopes to detect the occurrence of hydrothermal springs on the seafloor in both Tachibana Bay and Shimabara Bay. Samples were collected using a CTD-CMS system and analyzed using a Noble Gas Mass Spectrometer. Our data supplements the discovery of hydrothermal venting along known faults on the seafloor. We present the results of noble gas measurements conducted on water samples and discuss the relationship between our observations and the tectonic setup of the surrounding region.

Keywords: Helium Isotopes, Hydrothermal vents, Tachibana Bay

©2019. Japan Geoscience Union. All Right Reserved.

[E] Poster | S (Solid Earth Sciences)：S-GC Geochemistry

Wed. May 29, 2019 5:15 PM - 6:30 PM JST | Wed. May 29, 2019 8:15 AM - 9:30 AM UTC | Poster Hall International Exhibition Hall8, Makuhari Messe_31

[S-GC40] Volatile Cycles in the Deep Earth - from Subduction Zone to Hot Spot

convener:Hirochika Sumino(Department of Basic Science, Graduate School of Arts and Sciences, The University of Tokyo), Takeshi Hanyu(Japan Agency for Marine-Earth Science and Technology, Department of Solid Earth Geochemistry), Yuji Sano(Division of Ocean and Earth Systems, Atmosphere and Ocean Research Institute, University of Tokyo), Gray E Bebout(Lehigh University)

Volatiles play an important role in the geodynamics and chemical differentiation in the mantle and crust by drastically changing mineral stability and rheological behavior. Fractionation-processes such as partial melting, hydration, and dehydration are all controlled by volatiles in the rocks. A significant portion of the volatiles in the Earth has been thought to be present in the atmosphere and oceans as a consequence of extensive degassing during accretion and subsequent mantle degassing. On the other hand, it has been recently recognized that substantial amounts of volatiles are recycled back into the mantle at subduction zones, where intensive devolatilization of descended materials during arc magma generation was once thought to act as an effective "subduction barrier". However, fundamental questions still remain, such as: how are volatiles species distributed throughout the early and present Earth? What are the mechanisms for, and rate at which, volatiles are fluxed between the atmosphere, crust, and mantle? And what role have volatiles played in driving the evolution of the Earth? The possible role of the core in storing primordial volatiles is also poorly constrained. We therefore welcome contributions from experimental, observational, and modeling studies that help shed light on the deep cycles of volatiles, such as hydrogen, carbon, nitrogen, noble gases, halogens and sulfur. We particularly encourage studies linking the behavior of multiple volatile elements and their isotopic compositions. Studies investigating the linkage between volatile and solid geochemical tracers, the phase equilibria of volatile-bearing mantle assemblages, and the effect of volatiles on the physical properties of the mantle are also welcome.

[SGC40-P01] Continental growth models demystified

*Jun Korenaga[1] (1.Department of Geology and Geophysics, Yale University)

[SGC40-P02] Mass-independent sulfur isotope signature from the 2.7 Ga Belingwe komatiite: Recycling of crustal material in Archean

*Yusuke Kubota[1], Yuichiro Ueno[1,2,3], Kenji Shimizu[3], Fumihiro Matsuura[2], Akira Ishikawa[1,3] (1.Department of Earth and Planetary Sciences, Tokyo Institute of Technology, 2.Earth-Life Science Institute, Tokyo Institute of Technology, 3.Japan Agency for Marine-Earth Science and Technology (JAMSTEC))

[SGC40-P03] Determination of halogens in some standard materials using the neutron irradiation noble gas mass spectrometric technique

*Hirochika Sumino[1], Masahiro Kobayashi[2], Takehiko Saito[3], Keisuke Nagao[3] (1.Department of Basic Science, Graduate School of Arts and Sciences, The University of Tokyo, 2.Tokyo Metropolitan Industrial Technology Research Institute, 3.Geochemical Research Center, Graduate School of Science, University of Tokyo)

[SGC40-P04] FTIR spectroscopy and noble gas mass spectrometry for a single olivine grain

*Sota Niki[1], Hirochika Sumino[2], Masahiro Kobayashi[3], Hiroyuki Kagi[1], Takafumi Hirata[1], Chris J. Ballentine[4] (1.Geochemical Research Center, Grad. School of Science, Univ. of Tokyo, 2.Dept. of Basic Science, Grad. School of Arts and Sciences, Univ. of Tokyo, 3.Tokyo Metropolitan Industrial Technology Research Institute, 4.Dept. of Earth Sciences, Univ. of Oxford)

[SGC40-P05] New halogen incorporation mechanism in serpentine group minerals: Crystal chemical consideration

*Masami Kanzaki[1] (1.Institute for Planetary Matereials, Okayama University)

[SGC40-P06] Mineralogical and geochemical characteristics of cuttings from Taketomi hot spring

*Noriyuki Shingaki[1], Tomohiro Toki[1], Syogo Oshima[2], Masaaki chinen[3], Arito Sakaguchi[4], Naoto Takahata[5], Yuji Sano[5], Shirai Kotaro[5], Kentaro Tanaka[5] (1.University of the Ryukyus , 2.West Japan Engineering Consultants, Inc., 3.MicroRange, 4.Faculty of Science, Yamaguchi University, 5.Atmosphere and Ocean Research Institute, The University of Tokyo)

[SGC40-P07] Variation of helium isotope compositions at Lake Mashu

*Takanori Kagoshima[1], Yuji Sano[1], Atsushi Tanaka[2] (1.Atmosphere and Ocean Research Institute, University of Tokyo, 2.National Institute for Environmental Studies)

[SGC40-P08] Helium isotopes in Tachibana Bay and Shimabara Bay, Nagasaki

*Ma. Teresa Escobar[1], Yama Tomonaga[2], Hajime Obata[1], Shigenobu Takeda[3], Naoto Takahata[1], Yuji Sano[1] (1.Atmosphere and Ocean Research Institute, University of Tokyo, Kashiwanoha, Kashiwa, Chiba, Japan, 2.Eawag,, Swiss Federal Institute of Aquatic Science and Technology, Department of Water Resources and Drinking Water, Überlandstrasse 133 CH-8600 ,Dübendorf, Switzerland, 3.Graduate School of Fisheries and Environmental Sciences, Nagasaki University, Nagasaki, Japan)

Continental growth models demystified

*Jun Korenaga[1]

1. Department of Geology and Geophysics, Yale University

So far proposed models of continental growth exhibit bewildering diversity, but this diversity is rather superficial. By understanding how different growth models are built and what they are meant to constrain, we can gain deeper insight into the evolution of continental crust as well as the dynamics of the early Earth. There are three kinds of growth models: crust-based, mantle-based, and others. Crust-based models provide only the lower bound on net crustal growth, and mantle-based models aim at constraining net crustal growth itself. Other models are also about net crustal growth, but they are subject to greater uncertainty. In the presence of crustal recycling, crust-based models are expected to be different from mantle-based models, and more important, the difference between these two kinds of models provides important constraints on the operation of plate tectonics in the early Earth. Some popular misconceptions in the recent literature are also discussed.

Keywords: Continental crust, Plate tectonics, Chemical differentiation

©2019. Japan Geoscience Union. All Right Reserved.

Mass-independent sulfur isotope signature from the 2.7 Ga Belingwe komatiite: Recycling of crustal material in Archean

*Yusuke Kubota[1], Yuichiro Ueno[1,2,3], Kenji Shimizu[3], Fumihiro Matsuura[2], Akira Ishikawa[1,3]

1. Department of Earth and Planetary Sciences, Tokyo Institute of Technology, 2. Earth-Life Science Institute, Tokyo Institute of Technology, 3. Japan Agency for Marine-Earth Science and Technology (JAMSTEC)

Recycling of the Earth's crustal material has long been discussed mainly through the radiogenic isotopes of modern Ocean Island Basalts (OIB). Recent finding of Sulfur Mass Independent Fractionation (S-MIF) from HIMU and EM I basalts supports recycling of crustal material in mantle (Cabral et al., 2013; Delavault et al., 2016). Since photochemical reactions under reducing Archean atmosphere are thought to be a plausible process of large S-MIF generation (Farquhar et al., 2001; Farquhar and Wings, 2003), these discoveries demonstrated that the S-MIF is a useful signature for tracing Archean crustal material. However, it has been difficult to estimate when the subduction started in the history of the Earth. Here, we report multiple sulfur isotope analysis of the 2.7 Ga Belingwe komatiites and related rocks, which has potential to elucidate earlier subduction or recycling of crustal material before 2.7 Ga. The Belingwe komatiite are one of the best-preserved Archean komatiites in the world. The results show clear S-MIF signature in several komatiites and basalts. Sulfide minerals in the S-MIF bearing samples occur as pyrrhotite and chalcopyrite scattered within groundmass around the quenched olivine and pyroxene crystals, indicating that the sulfides crystalized at the time of eruption. The original nature of the sulfide is also supported by the correlation between sulfur contents and magnesium number. Based on Nd, Sr, and Pb isotope composition measured in the previous study (Shimizu et al., 2005), the S-MIF bearing komatiites and basalts are likely to be derived from depleted mantle source, whereas more enriched samples do not show S-MIF. Therefore, the S-MIF component is not likely derived from assimilated crust at the time of the komatiite volcanism, but originally incorporated in the depleted source mantle. Consequently, our results suggest that subduction of S-MIF bearing surface material into the mantle had been operated at least prior to 2.7 Ga.

Keywords: Sulfur mass independent fractionation, Mantle geochemistry, Komatiite, Archean

©2019. Japan Geoscience Union. All Right Reserved.

Determination of halogens in some standard materials using the neutron irradiation noble gas mass spectrometric technique

*Hirochika Sumino[1], Masahiro Kobayashi[2], Takehiko Saito[3], Keisuke Nagao[3]

1. Department of Basic Science, Graduate School of Arts and Sciences, The University of Tokyo, 2. Tokyo Metropolitan Industrial Technology Research Institute, 3. Geochemical Research Center, Graduate School of Science, University of Tokyo

Halogens are among the most powerful tracers of volatile cycling in subduction zones, because of (i) the large contrast in concentrations between the surface and interior of the Earth [1], (ii) their high affinities to gas- and fluid-phases relative to mineral [2], (iii) distinct elemental and/or isotopic compositions in each reservoir in the Earth [3-7]. However, few analytical techniques can determine trace amounts of halogens, particularly bromine and iodine in mantle-derived samples. Consequently, there have been relatively few previous studies of halogens in mantle-derived samples.

The neutron irradiation noble gas mass spectrometric technique (NI-NGMS) is capable of measuring very low concentrations of halogens (<1 ppb) in very small samples (<1 mg). The NI-NGMS is an extension of the Ar-Ar and I-Xe dating methods [8-10]. Halogens (chlorine, bromine, and iodine) and other elements (potassium, calcium, barium, and uranium) are converted to corresponding isotopes of argon, krypton, and xenon by neutron irradiation in a nuclear reactor. The noble gas isotopes in neutron-irradiated samples are analyzed by noble gas mass spectrometry. Irradiation conditions such as neutron fluence are monitored using standard materials of the Ar-Ar and I-Xe dating methods. Relatively high cross-sections of halogens for neutron capture and high sensitivity of noble gas mass spectrometry enable determination of trace amounts of halogens using NI-NGMS.

We report new halogen concentrations determined for scapolite standards and geological reference materials distributed by Geological Survey of Japan and US Geological Survey using NI-NGMS. Consistent results with those regarded as reference values were obtained from scapolite standards, which indicate that the scapolite standards are reliable in halogen analysis. On the other hand, the halogen concentrations obtained from geological reference materials are systematically lower than the reference values for samples with low concentrations of halogens. The higher concentrations reported for the geological reference materials probably result from contamination on the sample surface during preparation of these reference materials. We also propose a fluorine determination method using NI-NGMS based on neon systematics, although reliable determination of fluorine has been thought to be impossible.

[1] Pyle & Mather, *Chem. Geol.* 2009. [2] Bureau *et al.*, *GCA* 2016. [3] Sumino *et al.*, *EPSL* 2010. [4] Chavrit *et al.*, *GCA* 2016. [5] Kobayashi *et al.*, *EPSL* 2017. [6] Kendrick *et al.*, *Nature Geosci.* 2017. [7] Kobayashi *et al.*, *G-cubed* 2019. [8] Turner, *JGR* 1965. [9] Kendrick, *Chem. Geol.* 2012. [10] Ruzié-Hamilton *et al.*, *Chem. Geol.* 2016.

Keywords: Halogen, Noble gas, Nuetron irradiation, Noble gas mass spectrometry

©2019. Japan Geoscience Union. All Right Reserved.

FTIR spectroscopy and noble gas mass spectrometry for a single olivine grain

*Sota Niki[1], Hirochika Sumino[2], Masahiro Kobayashi[3], Hiroyuki Kagi[1], Takafumi Hirata[1], Chris J. Ballentine[4]

1. Geochemical Research Center, Grad. School of Science, Univ. of Tokyo, 2. Dept. of Basic Science, Grad. School of Arts and Sciences, Univ. of Tokyo, 3. Tokyo Metropolitan Industrial Technology Research Institute, 4. Dept. of Earth Sciences, Univ. of Oxford

Volatiles have been degassed from the mantle and recycled back into the mantle at subduction zones. Water is the main component of volatiles and plays a key role in dynamics of the subduction zones because even a small water content in rocks has an influence on the physical and chemical properties of the rocks (e.g. friction coefficient, melting point, etc.) which are closely related to phenomena studied in earth sciences including volcanic or seismic activities. It is still unclear to what extent of water have been subducted into the mantle and released to the Earth’ s surface. To elucidate the volatile recycling, noble gases are powerful tracers because they have unique compositions in geochemical reservoirs. Previous researches have mainly reported results of bulk analysis of mantle peridotites. On the contrary, in this study, FTIR measurements and noble gas analysis of a single olivine grain were conducted to determine the noble gas concentrations in fluid inclusions.

The olivine samples used for this study were separated from mantle xenoliths collected from an intraplate setting (Hualalai in Hawaii) and two subduction zones (the Avacha volcano in the Kamchatka arc and the Pinatubo volcano in the Luzon arc). The Hualalai olivine was expected to show mantle-derived noble gas compositions (Kobayashi et al., G-cubed 2019) and was used for checking the accuracy of noble gas analysis. The Avacha and Pinatubo olivines contained H_2O-rich fluid inclusions and the noble gas concentrations in the inclusions had been estimated from salinities, and halogen and noble gas compositions (Kobayashi et al., EPSL 2017). The Avacha and Pinatubo olivines were used to confirm the accuracy of the analytical method used in this study for determining the noble gas concentrations in the inclusions.

FTIR measurements were conducted to determine the H_2O concentration in the Avacha and Pinatubo olivines. The mantle xenoliths were crushed into 0.5 to 2 mm and olivine grains were separated. The olivine grains were embedded in resin (Ortho Bright) and polished to a thickness of several hundred micrometers. The weight of samples was 0.7 to 16 mg. The H_2O concentration was calculated from the absorbance at 3404 cm^{-1}. After the FTIR measurements, resin was removed from each grain by heating at 50ºC and dissolving in acetone.

Noble gas analysis was conducted using multicollector noble gas mass spectrometers (Helix SFT and Argus, Thermo Fisher Scientific). After the sample loading into a laser heating cell, the cell was baked out with pumping to desorb atmospheric noble gases to achieve low blank levels required for single-grain analysis. Consequently, noble gases were extracted by laser heating (Fusion Diode Stepped Heating System, Teledyne CETAC) at about 1000 ºC for 5 minutes. The gases released from samples were purified by removing active gases using a getter, and then, absorbed on two cryo-traps (one was for helium and neon and the other was for argon, krypton, and xenon). Each noble gas was desorbed from the trap at a certain temperature and introduced into the mass spectrometers. Helium was measured with Helix SFT and other noble gases were measured with Argus. The abundances and isotopic ratios of noble gases in a

©2019. Japan Geoscience Union. All Right Reserved.

single olivine grain were obtained. The accuracy of the isotopic ratios was checked by the Hualalai samples.

The noble gas concentrations in the inclusions obtained will be compared with the previous bulk analysis to discuss the accuracy of the method in this study. This method of determining the noble gas concentrations in fluid inclusions from single-grain analysis has a potential to clarify the heterogeneity of the mantle volatiles in terms of a single-grain mineral and the flux quantification during the volatile recycling.

Keywords: noble gas, FTIR spectroscopy, mantle

©2019. Japan Geoscience Union. All Right Reserved.

New halogen incorporation mechanism in serpentine group minerals: Crystal chemical consideration

*Masami Kanzaki[1]

1. Institute for Planetary Matereials, Okayama University

Introduction: Recent geochemical studies revealed that serpentinites contain a significant amount of halogens. However, how halogen ions are incorporated into serpentinites is not well understood. Commonly assumed mechanism is "OH^- substitution" in serpentine group minerals (chrysotile, lizardite and antigorite). Although this mechanism will be fine for F, but may not be adequate for larger halogens (Cl, Br, I). Here, I propose new halogen incorporation mechanism in lizardite and antigorite from crystal chemical point of view.

Calculation methods: In order to assess present new incorporation model, first-principles calculation was conducted. Quantum-Espresso package was used to optimize the halogen incooporated model structures. In the present study, lizardite and antigorite (*m*=17 polysome) are considered. For our proposed mechanism, charge balance should be observed; so $Mg^{2+} = X^- + Al^{3+}$ substitution (X^- = halogen) is assumed to introduce halogen to a vacant site. For lizardite, enthalpy difference between two models (OH^- substitution and our model) was calculated for following equation: $Mg_2AlSi_2O_8XH_2 + H_2O = Mg_2AlSi_2O_9XH_4$. Former corresponds to the OH substituted model (with Al introduced), and latter corresponds to our new model. Although this comparison is crude (as free H_2O is included in the equation), it could provide systematic trend with kinds of halogen atoms. Since antigorite has a very large unit cell and many vacant sites, only $Mg^{2+} = Cl^- + Al^{3+}$ substitute in five vacant sites are considered so far.

Results and Discussion: From close inspection of crystal structures of lizardite and antigorite, vacant sites ideal for halogens are identified. The vacant sites are surrounded by four protons (of OH^-) forming elongated tetrahedon (i.e., XH_4^{3+}) if halogen is located. Such vacant sites provide local structure similar to halogen ions in aqueous solution.

In order to further assess present incorporation mechanism, first-principles calculations of lizardite and antigorite containing halogens in those sites were conducted. The structural optimizations confirmed that halogens could be well accommodated into the tetrahedral vacant sites in lizardite. The calculated enthalpy difference between OH substitution and present models in lizardite revealed that larger halogens prefer our model over the OH substitution model. There is sinlge vacant site in lizardite, but antigorite (*m*=17) has 17 crystallographically different vacant sites. Most sites have local structures more or less similar to that of lizardite (locating in 6-membered SiO_4 ring). But there is another kind of vacant site which is locating in 8-membered SiO_4 ring. This local structure is surrounded by six protons, but it can be regareded as two tetrahedral proton sites with edge sharing. Substitution of Cl^- to this site (one of tetrahedral sites) showed lower enthalpy compared to those of other lizardite-like sites, and can accept more larger ions. Therefore, Cl^- (and other larger halogens) will prefet this site in antigorite (*m*=17). Not all antogorite polysomes have this site.

Present study suggests that our new proposed incorporation mechanism is promising, and it should be further studied experimentally. Present new incorporation mechanism would be important to understand elemental partition behavior of halogens in subduction zones.

Keywords: halogen site, serpentine, crystal chemistry, incorporation mechanism, elemental partition

©2019. Japan Geoscience Union. All Right Reserved.

Mineralogical and geochemical characteristics of cuttings from Taketomi hot spring

*Noriyuki Shingaki[1], Tomohiro Toki[1], Syogo Oshima[2], Masaaki chinen[3], Arito Sakaguchi[4], Naoto Takahata[5], Yuji Sano[5], Shirai Kotaro[5], Kentaro Tanaka[5]

1. University of the Ryukyus , 2. West Japan Engineering Consultants, Inc., 3. MicroRange, 4. Faculty of Science, Yamaguchi University, 5. Atmosphere and Ocean Research Institute, The University of Tokyo

It is important to grasp carbon cycle on the earth’ s surface for thinking about global environmental change. A hot spring with a maximum temperature of 64℃ is venting with gas containing 70% of methane from several spots on the seafloor at depth of 22 m at 1 km northeast off Taketomi Island. Based on methane and helium isotope ratios in the venting gas, the influence of magmatic gas has been pointed out. In spite of Taketomi Island located on the trench side from island arc, magmatic gas is venting. It suggests the forearc where magma cannot generate, might form new supply path of carbon from the Earth’ s interior. The mass balance from new supply path of carbon may change estimation of carbon cycle on earth’ s surface. Therefore, the purpose of this study is to elucidate venting mechanism and quantitative grasp of magmatic gas from forearc, and the history of hot spring activities will be investigated to predict future activities.

In 2017, the hot spring was drilled up to depth of 940 m in Taketomi Island. The cuttings with muddy water were sampled every 10 m. The thin sections were prepared from cuttings to be observed using polarization microscope, and the chemical compositions of grains were analyzed by SEM-EDX. The ground samples were analyzed for mineral and chemical compositions by XRD and EDX. The clay minerals gathered by levitation were measured for half-value width of illite using XRD. He and CO_2 contained in samples that were crashed in vacuum were measured for isotope ratios by mass spectrometer. Calcite and dolomite collected from the cuttings were measured for the carbon and oxygen isotope ratios by mass spectrometer. The vitrinite in the cuttings was separated by a heavy liquid, and the reflectance was measured by a reflecting microscope.

In the microscopy, the stratum was roughly divided two formations; cryptocrystalline quartz layer and sand stone layer. Carbonaceous materials were observed in most of the stratum. Dolomite was limitedly observed in the vicinity of 800 m. In the XRD analysis, Quartz was detected at all depth. Calcite was detected at shallower depth than 30 m, and dolomite was detected only around 800 m. As a result of the EDX analysis, silicon was the most dominant in all layers, and especially, it was contained around 0-100 m, 300 m and around 900 m over 80%. There was a layer that contained much calcium. Around 0-30 m, 400-500 m and around 800 m, calcite was contained 15 % or more. The half-value width of illite was large, 0.8 $\Delta^\circ 2\theta$, in only 10 m surface, and as low as 0.2 to 0.4 $\Delta^\circ 2\theta$ below 50 m. Vitrinite reflectance was around 5% in the whole layer, close to measurement limit. The helium content was 10^{-14}-10^{-11} mol per 1g of cuttings, and tended to increase with increasing depth. The highest content was detected at 800 m depth. The helium isotope ratio($^3He/^4He$)have value of 0.4-3.6 times that of atmosphere, and tended to increase with increasing depth. Particularly, it was higher at 100 m, 300-400 m and 700-800 m. The CO_2 content per gram of cuttings, was in the range of 10^{-8}-10^{-6} mol in most layers, but it showed

©2019. Japan Geoscience Union. All Right Reserved.

higher values at 400 m and 800 m depth. the water tended to decrease with increasing depth, and showed especially high values at 400 m and 900 m. The carbon isotope ratio ($\delta^{13}C$) of calcite was -4.7‰ VPDB, and the oxygen isotope ratio ($\delta^{18}O$) is -16.3‰VPDB. The $\delta^{13}C$ value of dolomite was -1‰VPDB, and the $\delta^{18}O$ value was -10.9‰VPDB. The $\delta^{13}C$ value of CO_2 from cuttings at 800 m was -7.3‰VPDB, which contained sufficiently amount of carbon to measure carbon isotope ratio.

Keywords: Taketomi Island, Hot spring, cuttings, vitrinite reflectance, carbon cycle, helium isotope

©2019. Japan Geoscience Union. All Right Reserved.

Variation of helium isotope compositions at Lake Mashu

*Takanori Kagoshima[1], Yuji Sano[1], Atsushi Tanaka[2]

1. Atmosphere and Ocean Research Institute, University of Tokyo, 2. National Institute for Environmental Studies

Helium-3 is one of the most sensitive geochemical tracers which reflects addition of mantle components to gas and fluids in volcanic hydrothermal systems, and $^{3}He/^{4}He$ ratios may be useful to assess temporal change of hydrothermal activity at volcanic lakes. Lake Mashu is a caldera lake which formed around 7000 years ago in Hokkaido. Igarashi et al. (1992) measured He and Ne isotopes in water of Lake Mashu, and concluded that the depth profile of isotopic compositions reflect injection of mantle-derived He due to hot spring activity at the lake bottom. After that, there is no subsequent study reporting He isotope data. The lack of observational data may be due to difficulty of water sampling at caldera lakes. Igarashi et al. (1992) collected water samples into copper tubes. However, this method requires heavy and large sampling tools, and people who can transfer water and seal the tubes properly. In May and September 2017, we investigated Lake Mashu in order to check volcanic activity and practical sampling methods for caldera lakes. We collected water using a Niskin bottle at several depths (surface to 210 m) around the deepest point (211 m). Collected water was immediately transferred into lead-glass containers with vacuum valves at both ends. In Atmosphere and Ocean Research Institute, dissolved gases were extracted by the head space method, and introduced into a purification vacuum line. In the line, He and Ne were purified for isotope analyses. $^{3}He/^{4}He$ and $^{4}He/^{20}Ne$ ratios were measured using Helix-SFT and QMS, respectively. The highest $^{3}He/^{4}He$ ratios were observed at 205-210 m depth, indicating that injection of fluids with the high $^{3}He/^{4}He$ ratio at the bottom. The linear correlation between $^{4}He/^{20}Ne$ and $^{3}He/^{20}Ne$ ratios in water samples indicated mixing of two components: injected fluids and the atmosphere. The estimated $^{3}He/^{4}He$ ratio of the fluid end member was indistinguishable from the value reported by Igarashi et al. (1992), implying a possibility that there was no significant change in volcanic activity at Lake Mashu in the past 30 years.

Keywords: Helium isotope, Volcanic lake, Lake Mashu

©2019. Japan Geoscience Union. All Right Reserved.

Helium isotopes in Tachibana Bay and Shimabara Bay, Nagasaki

*Ma. Teresa Escobar[1], Yama Tomonaga[2], Hajime Obata[1], Shigenobu Takeda[3], Naoto Takahata[1], Yuji Sano[1]

1. Atmosphere and Ocean Research Institute, University of Tokyo, Kashiwanoha, Kashiwa, Chiba, Japan, 2. Eawag,, Swiss Federal Institute of Aquatic Science and Technology, Department of Water Resources and Drinking Water, Ü berlandstrasse 133 CH-8600 ,Dübendorf, Switzerland, 3. Graduate School of Fisheries and Environmental Sciences, Nagasaki University, Nagasaki, Japan

Noble gases are powerful tracers to study physical transport processes in aquatic system. Moreover, helium isotopes have been shown to be very useful to infer the origin of fluids. Shimabara Peninsula is located on western side of the Beppu-Shimabara graben in Kyushu, SW Japan. In the region, there are some hot springs and groundwaters which indicate magmatic helium with high 3He/4He ratio. Although some researchers report helium isotopic ratio on land, there is no data in the sea.

The surrounding bays around Shimabara Peninsula in Nagasaki were recently studied for the existence of hydrothermal springs and vents. Physico-chemical properties characteristic of hydrothermal activity were detected on the seafloor. For this study, we use helium isotopes to detect the occurrence of hydrothermal springs on the seafloor in both Tachibana Bay and Shimabara Bay. Samples were collected using a CTD-CMS system and analyzed using a Noble Gas Mass Spectrometer. Our data supplements the discovery of hydrothermal venting along known faults on the seafloor. We present the results of noble gas measurements conducted on water samples and discuss the relationship between our observations and the tectonic setup of the surrounding region.

Keywords: Helium Isotopes, Hydrothermal vents, Tachibana Bay

©2019. Japan Geoscience Union. All Right Reserved.

[E] Oral | S (Solid Earth Sciences)：S-GC Geochemistry

Wed. May 29, 2019 1:45 PM - 3:15 PM JST | Wed. May 29, 2019 4:45 AM - 6:15 AM UTC | A10 TOKYO BAY MAKUHARI HALL

[S-GC40] Volatile Cycles in the Deep Earth - from Subduction Zone to Hot Spot

convener:Hirochika Sumino(Department of Basic Science, Graduate School of Arts and Sciences, The University of Tokyo), Takeshi Hanyu(Japan Agency for Marine-Earth Science and Technology, Department of Solid Earth Geochemistry), Yuji Sano(Division of Ocean and Earth Systems, Atmosphere and Ocean Research Institute, University of Tokyo), Gray E Bebout(Lehigh University), Chairperson:Takeshi Hanyu, Gray Bebout(Lehigh University), Yuji Sano, Hirochika Sumino

Volatiles play an important role in the geodynamics and chemical differentiation in the mantle and crust by drastically changing mineral stability and rheological behavior. Fractionation-processes such as partial melting, hydration, and dehydration are all controlled by volatiles in the rocks. A significant portion of the volatiles in the Earth has been thought to be present in the atmosphere and oceans as a consequence of extensive degassing during accretion and subsequent mantle degassing. On the other hand, it has been recently recognized that substantial amounts of volatiles are recycled back into the mantle at subduction zones, where intensive devolatilization of descended materials during arc magma generation was once thought to act as an effective "subduction barrier". However, fundamental questions still remain, such as: how are volatiles species distributed throughout the early and present Earth? What are the mechanisms for, and rate at which, volatiles are fluxed between the atmosphere, crust, and mantle? And what role have volatiles played in driving the evolution of the Earth? The possible role of the core in storing primordial volatiles is also poorly constrained. We therefore welcome contributions from experimental, observational, and modeling studies that help shed light on the deep cycles of volatiles, such as hydrogen, carbon, nitrogen, noble gases, halogens and sulfur. We particularly encourage studies linking the behavior of multiple volatile elements and their isotopic compositions. Studies investigating the linkage between volatile and solid geochemical tracers, the phase equilibria of volatile-bearing mantle assemblages, and the effect of volatiles on the physical properties of the mantle are also welcome.

1:45 PM - 2:15 PM JST | 4:45 AM - 5:15 AM UTC

[SGC40-01] Continental growth, crustal recycling, and global water cycle

★Invited Papers

*Jun Korenaga[1] (1.Department of Geology and Geophysics, Yale University)

2:15 PM - 2:30 PM JST | 5:15 AM - 5:30 AM UTC

[SGC40-02] Role of volatiles in magma genesis of ascending mantle plume

*Eiichi Takahashi[1], Jintuan Wang[1], Li Li[1] (1.Guangzhou Institute of Geochemistry, Chinese Academy of Science)

2:30 PM - 2:45 PM JST | 5:30 AM - 5:45 AM UTC

[SGC40-03] DH partitioning experiment among high-pressure polymorph of olivine

*Asami Sano-Furukawa[1], Shoichi Itoh[2], Toru Inoue[3], Masamichi Noda[3] (1.J-PARC center, Japan Atomic Energy Agency, 2.Kyoto University, 3.Hiroshima University)

2:45 PM - 3:00 PM JST | 5:45 AM - 6:00 AM UTC

[SGC40-04] Formation of Fe-rich volatile-bearing phases in the deep lower mantle and the implications for deep Earth volatile cycles

*Li Zhang[1], Hongsheng Yuan[1], Eiji Ohtani[2], Lianjie Man[1], Duck Young Kim[1], Dmitry Popov[3], Yue Meng[3], Eran Greenberg[4], Vitali Prakapenka[4] (1.Center for High Pressure Science and Technology Advanced Research (HPSTAR), 2.Department of Earth Science, Graduate School of Science, Tohoku University, 3.HPCAT, X-ray Science Division, Argonne National Laboratory, 4.GeoSoilEnviroCARS, University of Chicago)

3:00 PM - 3:15 PM JST | 6:00 AM - 6:15 AM UTC

[SGC40-05] Estimation of the origin of Pitcairn Island OIB by Independent Component Analysis

*Takahiro Ozawa[1], Hikaru Iwamori[1,2,3], Takeshi Hanyu[2], Morihisa Hamada[2], Kenji Shimizu[4], Ushikubo Takayuki[4], Jun-Ichi Kimura[2], Q. Chang[2], Hitomi Nakamura[5], Motoo Ito[4] (1.Tokyo Institute of Tokyo, 2.Geochemical Evolution Research Program, Japan Agency for Marine-Earth Science and Technology, 3.Earthquake Research Institute, The University Tokyo, 4.Kochi Core Center, Japan Agency for Marine-Earth Science and Technology, 5.Geological Survey of Japan, National Institute of Advanced Industrial Science and Technology)

Continental growth, crustal recycling, and global water cycle

*Jun Korenaga[1]

1. Department of Geology and Geophysics, Yale University

The evolution of continental crust provides first-order control on Earth’ s surface environment, but relevant studies on this important issue have long been in a confused state since 1990s. There are mainly two reasons for this situation. First, the volume of the global database of detrital zircons has been continuously growing in the last three decades, and as a result, the most of new crustal growth models have been built solely on such a zircon database. Zircons that have survived to the present day, however, do not constrain the amount of crust that has been lost to the mantle by subduction, so there is no way to reconstruct net crustal growth from zircon data. Second, this situation further deteriorated by two influential papers, Belousova et al. (2010) and Dhuime et al. (2012), with the former introducing an illogical method of using zircon age data to construct a growth model, and the latter claiming falsely that this method can actually reconstruct net crustal growth. The situation has recently been rescued by the development of a sensible method of utilizing zircon age data as well as a new geochemical box modeling of Nd isotope data. These new studies point to the possibility of rapid crustal growth and efficient crustal recycling in early Earth, and such crustal evolution is consistent with the operation of plate tectonics throughout Earth history. In particular, the secular evolution of crustal recycling, when considered jointly with the constancy of continental freeboard, indicates a novel connection between global water cycle and the stability of continental crust, which can naturally explain both the Hadean/Archean and Archean/Proterozoic transitions.

Keywords: Plate tectonics, Continental crust, Origin of geologic eons

©2019. Japan Geoscience Union. All Right Reserved.

Role of volatiles in magma genesis of ascending mantle plume

*Eiichi Takahashi[1], Jintuan Wang[1], Li Li[1]

1. Guangzhou Institute of Geochemistry, Chinese Academy of Science

It is now widely accepted that recycled former oceanic crust component (eclogite) plays a great role in magma genesis of OIBs and flood basalts (Hauri, 1996; Takahashi et al, 1998; Sobolev et al, 2005). In this study we investigated the effect of H_2O and K_2O in magma genesis of heterogeneous mantle plume that contains large amount of recycled eclogite component. K_2O was studied as a group of volatile component, because it is incompatible to most mantle minerals at P<7 GPa (Tsuruta and Takahashi, 1998) and it drops the solidus of both peridotite and eclogite dramatically (Wang and Takahashi, 1999, 2000).

High-pressure melting experiments were carried out using a piston-cylinder and a 2500 ton cubic-type multi-anvil that have been moved from Tokyo Institute of Technology to Guangzhou Institute of Geochemistry in 2017. In order to understand the melting reaction between recycled eclogite and surrounding peridotite, we investigated melting of layered eclogite/peridotite starting materials both under dry and wet conditions. Spinel lherzolite KLB-1 (Takahashi 1986) was employed as peridotite component in this study. Two basalt components were used as recycled crust component: 1) Columbia River basalt (CRB72-180, Takahashi et al., 1998) which is relatively enriched in K, Ti and LREE (K_2O=1wt%, TiO_2=3.2wt%), N-type MORB (NAM-7, Yasuda et al., 1994). The 2.9GPa experiments (corresponding to about 80km depth which is the top most horizon of the Hawaiian plume head) were carried out with Boyd-England type piston-cylinder apparatus at (1460~1540˚C for dry experiments; 1400~1500˚C for hydrous experiments), The 5GPa and 8 GPa experiments (corresponding to about 150km and 200km depth on the plume axis) were conducted cubic-type multi-anvil apparatus (1550~1650˚C for dry experiments; 1350~1550˚C for hydrous experiments).

Melts formed by reactive melting of dry eclogite and peridotite changes dramatically in the temperature range across the solidus of peridotite KLB-1 from basalt (below dry solidus) to picrite (20-40˚C above dry solidus). Basaltic melts are not saturated with olivine both at 2.9 and 5 GPa and therefore they are separated by peridotite matrix by Opx film. Chemical reaction between the basalt melt and the peridotite matrix proceeds only slowly by solid-diffusion across the Opx film. In hydrous experiments, solidus of peridotite decreases significantly, Opx film was not formed, therefore, the reaction between hydrous melt and the partially molten peridotite matrix proceeds significantly even at temperatures much below peridotite dry solidus.

Melt composition produced by reactive melting of dry basalt and peridotite are similar to basaltic andesite (below peridotite solidus), Hawaiian tholeiite (slightly below peridotite solidus) to picrite (above peridotite dry solidus). On the other hand, melt compositions formed by reactive melting between hydrous basalt and peridotite show a great diversity depending on the amount of H_2O and K_2O. At H_2O-rich conditions (3 to 5 wt.% in bulk), melting took place both in peridotite and eclogite layers and composition of partial melts are similar to silica-deficient basanite and nephelinite at temperatures 1300-1400˚C both at 3 and 5 GPa. At low H_2O conditions (1 wt.% in bulk) partial melts formed in the MORB layer at 1300˚C are similar to silica-rich dacite both at 3 and 5 GPa. On the other hand, partial melts formed in the CRB72-180 layer with 1 wt.% H_2O at 3 and 5 GPa are similar to K-rich alkali acidic magma (phonolite, tracyte, hawaiite).

©2019. Japan Geoscience Union. All Right Reserved.

Post shield stage phonolite and hawaiite magmas in Hawaii were considered to be fractionation product of alkali basalts under crustal magma chambers (e.g., Frey et al, 1990). However, our experimental results demonstrated an alternative scenario that phonolite and hawaiite magma were derived from partial melting of alkali basaltic blocks at deeper part (150-200km) of the plume. On the other hand, basanite and nephelinite which appears in rejuvenated stage in Oahu and Kawai may represent partial melts of peridotite portion of the plume beneath Pacific plate. Volatiles control the solidus and the depth of melting as well as enhancing chemical interaction between the peridotite and entrained eclogite component in the ascending plume. In this presentation, we discuss the role of volatile and K_2O in magma genesis in ascending plume based on our melting experiments and field occurrence of diverse magma types both geographically and in growth history of given shield volcanoes in Hawaii.

Keywords: magma genesis, effect of volatile, mantle plume, Hawaii hot spot

©2019. Japan Geoscience Union. All Right Reserved.

DH partitioning experiment among high-pressure polymorph of olivine

*Asami Sano-Furukawa[1], Shoichi Itoh[2], Toru Inoue[3], Masamichi Noda[3]

1. J-PARC center, Japan Atomic Energy Agency, 2. Kyoto University, 3. Hiroshima University

Mantle is known to have homogeneous hydrogen isotope composition with δD = -80 ~ -60 ‰based on the analysis of MORB and OIB [1, 2]. The reason of the depletion of deuterium compared to the present ocean has been explained by the existence of isolated primordial reservoir in the mantle [1], evolution by the subduction of deuterium-poor hydrous mineral through the geological timescale [3], and addition of cometary water after the formation of ocean [4]. Hydrogen isotope partitioning factor among minerals is a key in these discussions, but little is known under high pressure and high temperature of mantle conditions. In this study we focused on DH partitioning between olivine and wadsleyite, which is a main constituent of upper mantle and mantle transition zone (MTZ). High pressure experiments suggest that wadsleyite and its high pressure polymorph of ringwoodite can contain significant amount of water up to 3.3 wt.% thus MTZ has an ability to keep water up to several times of ocean [5]. Finding of Ringwoodite with 1.4 wt.% H_2O in a diamond inclusion also reveals hydrated MTZ at least locally [6].

The partitioning experiment was conducted using Kawai-type multianvil press at GRC, Ehime University. Powder of $Mg(OH)_2$ and $Mg(OD)_2$ was mixed with synthetic olivine so that the starting composition is equivalent to $Mg_{1.8}Fe_{0.2}SiO_4$ + 1.0 wt.% HDO. The sample was sealed in the Au75Pd25 capsule and kept at 1300 ˚C and around 13 GPa, which is the condition of olivine and wadsleyite coexist. The recovered sample was polished and analyzed by micro-focused X-ray diffractometer, Raman spectroscopy and EPMA. Hydrogen isotope composition was determined using SIMS at Kyoto University.

To test for equilibrium, partitioning experiments are made with changing duration times from 1 h to 72 h. The fractionation factor decreases with increasing of duration time. After keeping for 30 h, $1000\ln\alpha_{\text{Olivine-Wadsleyite}}$ seems to reach almost equilibrium around -60 ‰. Assuming that the δD of olivine of upper mantle to -80, the δD of wadsleyite at MTZ become -20 to 0, which is more comparable to the composition of the ocean. The present result shows that the depletion of deuterium of upper mantle can be explained as a result of DH fractionation between upper mantle and MTZ.

[1] Kyser and O’ Neil, 1984, *Geochim Cosmochim. Acta.* [2] Clog et al., 2013, *Earth Planet. Sci. Lett.* [3] Kurokawa et al., 2018, *Earth Planet. Sci. Lett.* [4] Kokubu et al., 1961, *Geochim. Cosmochim. Acta* [5] Smyth et al., 1987, *Am. Mineral.* [6] Pearson et al., 2014, *Nature.*

Keywords: mantle transition zone, olivine, wadsleyite, hydrogen isotope

©2019. Japan Geoscience Union. All Right Reserved.

Formation of Fe-rich volatile-bearing phases in the deep lower mantle and the implications for deep Earth volatile cycles

*Li Zhang[1], Hongsheng Yuan[1], Eiji Ohtani[2], Lianjie Man[1], Duck Young Kim[1], Dmitry Popov[3], Yue Meng[3], Eran Greenberg[4], Vitali Prakapenka[4]

1. Center for High Pressure Science and Technology Advanced Research (HPSTAR), 2. Department of Earth Science, Graduate School of Science, Tohoku University, 3. HPCAT, X-ray Science Division, Argonne National Laboratory, 4. GeoSoilEnviroCARS, University of Chicago

Inclusions in deep diamonds provide a window to the actual deep mantle processes. The observation of hydrous ringwoodite with ~1 wt.% H_2O as a diamond inclusion indicates the transition zone is, at least locally, very wet [1]. Furthermore, the recent discovery of Ice-VII and halite inclusions at pressures as high as 24 GPa in diamonds provides direct evidence for the existence of saline fluid at least down to the shallow lower mantle [2]. To understand the interaction of water and Cl with the Fe-bearing lower mantle, we performed experiments to simulate the behavior of volatile-bearing systems in laser-heated diamond anvil cells (DACs) under high pressure-temperature (*P-T*) conditions corresponding to the deep lower mantle. The phase assemblages were determined by a combination of *in-situ* synchrotron-based X-ray diffraction (XRD) and *ex situ* transmission electron microscope (TEM) analysis. In the system MgO-Al_2O_3-Fe_2O_3-SiO_2-H_2O containing ~7 wt.% water, the hydrous Fe-bearing δ-phase coexists with both bridgmanite (Bdg) and post-perovskite (pPv) in a broad *P-T* range of 104-126 GPa and 1900-2500 K, whereas the pyrite-type (py) FeOOH phase was observed coexisting with the pPv phase. *In situ* XRD data further revealed that saline fluid reacts with Fe-bearing pPv to form a previously unknown cubic phase of $FeCl_2$ that adopts the identical space group of *Pa3* with the py-phase FeOOH. The TEM chemical analysis revealed that the composition of the pPv phase contains 3.5 wt.% Na_2O and 16.5 wt.% FeO after the reaction with the oversaturated saline fluid. Formation of the very dense Fe-rich volatile-bearing phases in the lowermost mantle provides clues for the deep storage of water and Cl and may contribute to the chemical heterogeneities in this region.

[1] D. G. Pearson *et al.*, Nature **507** (2014).
[2] O. Tschauner *et al.*, Science **359** (2018).

Keywords: deep lower mantle, volatile cycle, post-perovskite, synchrotron X-ray diffraction

©2019. Japan Geoscience Union. All Right Reserved.

Estimation of the origin of Pitcairn Island OIB by Independent Component Analysis

*Takahiro Ozawa[1], Hikaru Iwamori[1,2,3], Takeshi Hanyu[2], Morihisa Hamada[2], Kenji Shimizu[4], Ushikubo Takayuki[4], Jun-Ichi Kimura[2], Q. Chang[2], Hitomi Nakamura[5], Motoo Ito[4]

1. Tokyo Institute of Tokyo, 2. Geochemical Evolution Research Program, Japan Agency for Marine-Earth Science and Technology, 3. Earthquake Research Institute, The University Tokyo, 4. Kochi Core Center, Japan Agency for Marine-Earth Science and Technology, 5. Geological Survey of Japan, National Institute of Advanced Industrial Science and Technology

Ocean island basalts (OIB) are thought to bring information concerning geochemistry and material cycling of the deep mantle. For this reason, OIB have been studied extensively, among which Pitcairn Island in the South Pacific is regarded as a unique and important location as a hotspot volcano. Previous studies reported that the lavas in Pitcairn involve multiple components from DM (depleted mantle) to EM1 (enriched mantle) (Woodhead & McCulloch, 1989), of which EM1 component has been argued to originate from recycling oceanic plate, delaminated lower crust, continental marine sediment and others (Eisele et al., 2002; Garapic et al., 2015). The mechanism to produce the specific isotopic composition of EM1 is still under extensive debate.

We analyzed concentrations of major elements, volatile elements (CO_2, H_2O, F, S, and Cl), and trace elements, as well as lead isotopic ratios, by using SIMS, EPMA and LA - ICP - MS for melt inclusions contained in olivine from basalt and pyroclastic rock in Pitcairn Island. Melt inclusions are thought to retain the volatile elements without losing them upon eruption, which is suitable for discussing the origin of the EM1 component. In this study, four lavas (PC-2, PC-16, PC-38, and PC-40) and a pyroclastic rock collected from the Tedside formation of Pitcairn Island were analyzed. The whole-rock composition of these lavas show EM1 signatures. Melt inclusions in olivine are crystallized, but those of pyroclastic rock are all glassy and homogeneous as they are. The crystalized melt inclusion samples from the four lavas were homogenized at the individual liquidus temperatures (1150 degrees and 1175 degrees). A small amount of H2O loss was found for 10 min heating for homogenization, by comparing the analyses of both melt inclusion with/without reheating of the pyroclastic rock samples. On the other hand, virtually no effect was seen for F and Cl.

Multivariate statistical analysis is useful to extract the geochemical features from these data set. McKenzie et al. (2004) identified the coherence between the trace element concentrations and the isotopic ratios, and argued that such coherence must indicate multiple sources of different origin. Instead of Principal Component Analysis (PCA) as used by McKenzie et al. (2004), we utilize Independent Component Analysis (ICA) to extract geochemically independent features. At the same time, we also performed k-means cluster analysis on the whitened data set (Iwamori et al., 2017) to clarify the multiple sources hidden in the lavas from a small area within the Pitcairn Island. In this paper, we will present the results of the geochemical analyses and statistical analyses to identify and discuss the nature of the sources involved in the Pitcairn volcanism.

©2019. Japan Geoscience Union. All Right Reserved.

[E] Oral | S (Solid Earth Sciences)：S-GC Geochemistry

Wed. May 29, 2019 3:30 PM - 5:00 PM JST | Wed. May 29, 2019 6:30 AM - 8:00 AM UTC | A10 TOKYO BAY MAKUHARI HALL

[S-GC40] Volatile Cycles in the Deep Earth - from Subduction Zone to Hot Spot

convener:Hirochika Sumino(Department of Basic Science, Graduate School of Arts and Sciences, The University of Tokyo), Takeshi Hanyu(Japan Agency for Marine-Earth Science and Technology, Department of Solid Earth Geochemistry), Yuji Sano(Division of Ocean and Earth Systems, Atmosphere and Ocean Research Institute, University of Tokyo), Gray E Bebout(Lehigh University), Chairperson:Takeshi Hanyu, Gray Bebout(Lehigh University), Yuji Sano, Hirochika Sumino

Volatiles play an important role in the geodynamics and chemical differentiation in the mantle and crust by drastically changing mineral stability and rheological behavior. Fractionation-processes such as partial melting, hydration, and dehydration are all controlled by volatiles in the rocks. A significant portion of the volatiles in the Earth has been thought to be present in the atmosphere and oceans as a consequence of extensive degassing during accretion and subsequent mantle degassing. On the other hand, it has been recently recognized that substantial amounts of volatiles are recycled back into the mantle at subduction zones, where intensive devolatilization of descended materials during arc magma generation was once thought to act as an effective "subduction barrier". However, fundamental questions still remain, such as: how are volatiles species distributed throughout the early and present Earth? What are the mechanisms for, and rate at which, volatiles are fluxed between the atmosphere, crust, and mantle? And what role have volatiles played in driving the evolution of the Earth? The possible role of the core in storing primordial volatiles is also poorly constrained. We therefore welcome contributions from experimental, observational, and modeling studies that help shed light on the deep cycles of volatiles, such as hydrogen, carbon, nitrogen, noble gases, halogens and sulfur. We particularly encourage studies linking the behavior of multiple volatile elements and their isotopic compositions. Studies investigating the linkage between volatile and solid geochemical tracers, the phase equilibria of volatile-bearing mantle assemblages, and the effect of volatiles on the physical properties of the mantle are also welcome.

3:30 PM - 4:00 PM JST | 6:30 AM - 7:00 AM UTC

[SGC40-06] Tracing recycled volatiles in MORB with halogens

★Invited Papers

*Ray Burgess[1], Lorraine Ruzie-Hamilton[1], Patricia Clay[1], Bastian Joachim[2], Christopher Ballentine[3] (1.School of Earth and Environmental Sciences, University of Manchester, Manchester, M13 9PL UK, 2.Institute for Mineralogy and Petrography, University of Innsbruck, Innrain, 52A-6020, Innsbruck, Austria, 3.Department of Earth Sciences, University of Oxford, South Parks Road, Oxford, OX1 3AN UK)

4:00 PM - 4:15 PM JST | 7:00 AM - 7:15 AM UTC

[SGC40-07] Volatile composition in ocean island basalts

*Takeshi Hanyu[1] (1.Japan Agency for Marine-Earth Science and Technology, Department of Solid Earth Geochemistry)

4:15 PM - 4:30 PM JST | 7:15 AM - 7:30 AM UTC

[SGC40-08] Halogen heterogeneity in the subcontinental lithospheric mantle

*Hirochika Sumino[1], Masahiro Kobayashi[2], Ray Burgess[3], Chris J Ballentine[4] (1.Department of Basic Science, Graduate School of Arts and Sciences, University of Tokyo, 2.Tokyo Metropolitan Industrial Technology Research Institute, 3.School of Earth and Environmental Sciences, University of Manchester, 4.Department of Earth Sciences, University of Oxford)

4:30 PM - 4:45 PM JST | 7:30 AM - 7:45 AM UTC

[SGC40-09] Efficiency of Deep Carbon Subduction: Input, Metamorphic Records, and Bearing on Estimated Sources of Arc Volcanic Gases

*Gray E Bebout[1,2], Gabe S Epstein[2], Brian M House[3] (1.Institute for Planetary Materials, Okayama University, 2.Lehigh University, 3.University of California, San Diego)

4:45 PM - 5:00 PM JST | 7:45 AM - 8:00 AM UTC

[SGC40-10] Helium isotope variations in subduction-type volcanic hydrothermal systems

*Yuji Sano[1], Takanori Kagoshima[1], Naoto Takahata[1], Tetsuji Onoue[2], Tomo Shibata[3], Tobias P Fischer[4]
(1.Division of Ocean and Earth Systems, Atmosphere and Ocean Research Institute, University of Tokyo, 2.Department of Earth and Environmental Sciences, Kumamoto University, 3.Institute for Geothermal Sciences, Kyoto University, 4.Department of Earth and Planetary Sciences, University of New Mexico)

Tracing recycled volatiles in MORB with halogens

*Ray Burgess[1], Lorraine Ruzie-Hamilton[1], Patricia Clay[1], Bastian Joachim[2], Christopher Ballentine[3]

1. School of Earth and Environmental Sciences, University of Manchester, Manchester, M13 9PL UK, 2. Institute for Mineralogy and Petrography, University of Innsbruck, Innrain, 52A-6020, Innsbruck, Austria, 3. Department of Earth Sciences, University of Oxford, South Parks Road, Oxford, OX1 3AN UK

Interactions between the Earth’ s mantle and the surface have controlled the evolution of the crust, the oceans, and the atmosphere. The mantle is by many orders of magnitude the largest silicate reservoir for volatiles, and volcanic release of these species has played a major role throughout Earth history in global chemical cycles. Understanding the distribution and geochemical evolution of volatiles in the terrestrial mantle is therefore central to understanding the unique planetary history of Earth. The input and output of volatiles at plate boundaries provides major controls on the cycles of many important elements and exerts long-term controls on habitibale conditions at the surface.

Noble gases have provided key insight into the processes controlling the mantle system. Primordial heavy noble gases in the MORB-source mantle are accompanied by atmosphere noble gases with an elemental composition consistent with subduction of an ocean/pore-fluid signature into the mantle (1). Pore fluid subduction represents an important opportunity to use halogens, in particualr iodine which is highly enriched in marine pore fluids, in conjunction with noble gases as sensitive tracers of water and volatile enrichment processes in the mantle.

To assess the control of subduction zones on the mantle halogen budget we have investigated basaltic glass samples from the Manus Back-Arc Basin as some of the volatiles may survive forearc to subarc devolatilization to depths beyond arcs/back-arcs and contribute to the long term volatile budget of the mantle. We also investigated two sets of samples: one from the Central Indian Ridge (2) containing D(epleted)-MORB, N(ormal)-MORB and E(nriched)-MORB and one from the Siqueiros Transform Fault (STF) known for sampling the depleted upper mantle (3). In contrast to axial MORB, lavas from STF are tapping smaller mantle melt without mixing in large magmatic chambers. These melts provide better estimates of the volatile contents of the potential mantle sources.

Based on new halogen determinations, we show that the volatile budget in the mantle sampled by the mid oceanic ridge basalts is a mixture between the depleted upper mantle and a fluid-modified mantle enriched during its residency in subduction zone. This enables us to revisit the global halogen budget and assess how subduction of halogens has affected the habitability of our planet.

1. Holland & Ballentine, Nature 441, 186-191, 2006.

2. Nauret et al. Earth Planet. Sci Lett. 245, 137-152, 2006.

3. Saal et al., Nature 419, 451-455, 2002.

Keywords: Halogens, Recycling, Mantle, Volatiles

©2019. Japan Geoscience Union. All Right Reserved.

©2019. Japan Geoscience Union. All Right Reserved.

Volatile composition in ocean island basalts

*Takeshi Hanyu[1]

1. Japan Agency for Marine-Earth Science and Technology, Department of Solid Earth Geochemistry

Volatile reservoirs and transport mechanisms in the mantle are one of fundamental questions in mantle geochemistry. The atmosphere and hydrosphere are major volatile reservoirs in the Earth. Portions of volatiles in the surface layers can be incorporated into oceanic crust and sediment by fluidal reaction and organic and inorganic sedimentation, and then they are delivered to the mantle via slab subduction. However, the efficiency of volatile transport against subduction barrier is poorly constrained. Studies of volatiles in ocean island basalts (OIBs) should document the origin and distribution of volatiles in the deep mantle. This presentation provides an overview of previous studies of volatiles on OIBs using submarine quenched glasses and olivine-hosted melt inclusions.

Whether the mantle source of OIBs is enriched in H_2O is measured by taking H_2O/Ce ratio, where Ce is a lithophile element that has similar incompatibility to H_2O during partial melting. While many OIBs exhibit H_2O/Ce that overlap with the MORB range, OIBs with robust EM1, EM2, and HIMU signatures have significantly lower H_2O/Ce. The fact that H_2O/Ce decreases proportionately with increasing $^{87}Sr/^{86}Sr$ for Pitcairn, Kerguelen (EM1), and Society (EM2), and with decreasing $^{207}Pb/^{206}Pb$ for Tuvalu (HIMU) documents that the mantle components with robust EM1, EM2, and HIMU signatures are commonly depleted in H_2O relative to Ce [1-3]. If their precursor was any type of subducted material, fluid or hydrous melt extraction from the subducted slab reasonably explains the low H_2O/Ce. However, an alternative explanation is a contribution from pyroxenite components in the magma sources, where Ce is more efficiently partitioned into pyroxene than H [4].

Enrichment in F (i.e., F/Nd) in the EM1 and EM2 OIBs from Pitcairn and Samoa is equivocal [2,5]. In contrast, melt inclusions from Mangaia HIMU basalts have high F/Nd (~30) as a group relative to the average MORB value (~21) [1,6], which is best explained by the efficient transfer of F to the mantle by F-bearing minerals such as amphibole, serpentinite, mica, and clinohumite in subducted slabs [7]. Detecting Cl enrichment is not always straightforward because shallow-level magma assimilation with seawater, brines, and altered oceanic crust easily alter the Cl composition [8]. Submarine glasses from Pitcairn and Society exhibit decreasing Cl/K with increasing $^{87}Sr/^{86}Sr$ [2]. Such covariation precludes assimilation as the principal cause of Cl/K variation, and therefore low Cl/K is the source feature of EM1 and EM2. Chlorine loss from subducted components due to fluid release or hydrous melt extraction accounts for low Cl/K. In contrast, HIMU OIBs show increase of Cl/K and Cl/Nb along with decreasing $^{207}Pb/^{206}Pb$ (more robust HIMU signature from ancient altered oceanic crust) as observed in olivine-hosted melt inclusions in Raivavae basalts from Austral Islands [9]. Because such correlation is not ascribed to shallow-level assimilation, this fact requires a mechanism to return Cl from the hydrosphere to the HIMU mantle source via altered oceanic crust against subduction dehydration. Although Cl-hosting minerals beyond the sub-arc depth have not been thus far identified, the lattice defects in major minerals or mineral grain boundaries may be a carrier of small amounts of Cl in subducted oceanic crust. Subduction of altered oceanic crust would transfer Cl from seawater to the deep mantle, forming Cl-rich HIMU mantle reservoir in the deep mantle.

©2019. Japan Geoscience Union. All Right Reserved.

[1] Jackson et al., Geochem. Geophys. Geosyst. 16, 3210-3234 (2015).

[2] Kendrick et al., Chem. Geol. 370, 69-81 (2014).

[3] Wallace, J. Petrol. 43, 1311-1326 (2002).

[4] Bizimis & Peslier, Chem. Geol. 397, 61-75 (2015).

[5] Kendrick et al., Earth Planet. Sci. Lett. 410, 197-209 (2015).

[6] Cabral et al., Geochem. Geophys. Geosyst. 15, 4445-4467 (2014).

[7] Grützner et al., Geology 45, 443-446 (2017).

[8] Stroncik & Haase, Geology 32, 945-948 (2004).

[9] Hanyu et al., Nat. Commun. 10, 60 (2019).

Keywords: volatile, recycle, mantle

©2019. Japan Geoscience Union. All Right Reserved.

Halogen heterogeneity in the subcontinental lithospheric mantle

*Hirochika Sumino[1], Masahiro Kobayashi[2], Ray Burgess[3], Chris J Ballentine[4]

1. Department of Basic Science, Graduate School of Arts and Sciences, University of Tokyo, 2. Tokyo Metropolitan Industrial Technology Research Institute, 3. School of Earth and Environmental Sciences, University of Manchester, 4. Department of Earth Sciences, University of Oxford

Volatile recycling back to the Earth’ s mantle at subduction zones has a significant, yet poorly constrained impact to the volatile budget in the mantle. Halogen and noble gas systematics are powerful tracers of volatile recycling. The presence of noble gases and halogens with seawater and sedimentary pore-fluid signatures in exhumed mantle wedge peridotites from the Sanbagawa-metamorphic belt, southwest Japan [1], and in forearc serpentinites [2] along with seawater-like heavy noble gases (Ar, Kr, and Xe) in the convecting mantle [3] strongly suggest the subduction of sedimentary-pore-fluid-like noble gases and halogens. In order to better constrain how such subduction fluids may modify the halogen composition of subcontinental lithospheric mantle, we have analyzed halogens in mantle-derived xenoliths from volcanic front and back-arc regions of subduction zones, and intraplate continental settings.

In addition to a MORB-like halogen component observed in most of the samples, three other distinct components were identified: (A) a marine-pore-fluid-like component with high Br/Cl and I/Cl ratios similar to mantle wedge peridotites [1], (B) a Cl-enriched component relative to MORB, similar to bulk altered oceanic crust [4]; and (C) a component enriched in Br and moderately in I compared to MORB, which resembles to fluid components in altered oceanic crust and diamonds [4,5].

The component (A) is typically observed in the volcanic front samples containing abundant H_2O-rich fluid inclusions. This suggests that marine pore fluids in deep-sea sediments are carried by serpentine and supplied to the mantle wedge, preserving their original halogen and noble gas compositions. However, the measured Cl/H_2O and $^{36}Ar/H_2O$ in the peridotites are higher than those in sedimentary pore fluids and serpentine in oceanic plates [2]. The halogen/noble gas/H_2O systematics are interpreted within a model where water is incorporated into serpentine in a closed system formed along fracture zones developed at the outer rise, where oceanic plates bend prior to entering subduction zones, preserving Cl/H_2O and $^{36}Ar/H_2O$ values of sedimentary pore fluids. Dehydration-hydration process within the oceanic lithospheric mantle maintains the closed system until the final stage of serpentine dehydration. The sedimentary pore fluid-like halogen and noble gas signatures in fluids released at the final stage of serpentine dehydration are preserved due to highly channelized flow [6].

The samples involving the component (B) have higher Cl concentration and trace elements ratios, whereas the samples involving the component (C) have relatively low Cl concentration and low ratios of highly incompatible elements relative to heavy rare earth elements. Considering that these two components are observed in some back-arc samples having radiogenic/nucleogenic noble gases [7], they could be remnants of metasomatic agents derived from subducted altered oceanic crust, or could result from secondary processes of volatile loss during partial melting and secondary phase formation during interaction with melts [8].

The common primary MORB-like halogen ratios in mantle xenoliths from different parts of the globe indicate that the mantle itself must have a relatively uniform composition over a wide scale. The mantle has maintained its halogen composition over billion year timescales without being affected by I-rich

©2019. Japan Geoscience Union. All Right Reserved.

halogens being transported into the mantle. Mass balance calculations suggest that, in order to maintain the I/Cl ratio of the convecting mantle over 2 Gyr, the I/Cl ratio of the subducted halogens must be no more than several times higher than the present-day mantle value [8].

[1] Sumino *et al. EPSL* 2010. [2] Kendrick *et al. EPSL* 2013. [3] Holland & Ballentine *Nature* 2006. [4] Chavrit *et al.*, *GCA* 2016. [5] Burgess *et al.*, *GCA* 2009. [6] Kobayashi *et al. EPSL* 2017. [7] Jalowizki *et al.*, *EPSL* 2016. [8] Kobayashi *et al.*, *G-cubed* 2019.

Keywords: halogen , subcontinental mantle, noble gas, subduction, volatile recycling

©2019. Japan Geoscience Union. All Right Reserved.

Efficiency of Deep Carbon Subduction: Input, Metamorphic Records, and Bearing on Estimated Sources of Arc Volcanic Gases

*Gray E Bebout[1,2], Gabe S Epstein[2], Brian M House[3]

1. Institute for Planetary Materials, Okayama University, 2. Lehigh University, 3. University of California, San Diego

Circum-Pacific and Italian Alps high- and ultrahigh-pressure metasedimentary rocks record the subduction of organic (reduced) and carbonate (oxidized) C through forearcs (10-70 km) to depths approaching those beneath volcanic fronts. Still uncertain are the efficiency of delivery of such sections to subarc depths, as related to varying degrees of accretion and underplating, the mobilization of C during prograde metamorphism and fluid-rock interactions, and the fractions of C recycled in arcs, stored in forearc reservoirs (e.g., the mantle wedge), or added to the deeper mantle.

Franciscan Complex (FC) blueschist-facies rocks, and lower-grade units (lawsonite-albite and lawsonite-blueschist) of the carbonate-poor Catalina Schist (CS), preserve reduced C (RC) concentrations and $\delta^{13}C$, and C:N, similar to those of sediment protoliths, as does the lowest-grade unit of the Schistes Lustres (SL) exposed in the Alps (regardless of carbonate content). In CS units that experienced warmer prograde *P-T* paths (epidote-blueschist grade and higher), RC is shifted in $\delta^{13}C_{VPDB}$ from -25 per mil to as high as -19 per mil, seemingly related to minor loss of C as CH_4 during prograde devolatilization. The higher-grade units of the SL extend, to depths of ~70km, the extremely low-*P/T* trajectory represented by the FC and low-grade CS. Across this range of grade, RC shows little evidence of loss but considerable increase in $\delta^{13}C$ toward mantle values (-5 to -6 per mil) related to isotopic exchange with coexisting carbonate. In SL metashales, RC preserves protolith $\delta^{13}C$ of -24 to -21 per mil independent of grade and degrees of devolatilization. Reduced C occurs as amorphous carbonaceous matter at low grades, and its transformation to graphite at higher grades presumably enhances isotopic exchange with carbonate. This work implies that much of the RC reservoir is retained to depths beneath volcanic fronts and could be available for transfer into the sub-arc mantle wedge, likely via partial melting (K. Kraft, Lehigh Univ. M.S. thesis, 2018).

The blueschist to eclogite facies SL contains carbonate-rich flysch formed prior to and during Eocene subduction of the Piemonte-Liguria Ocean and underplated at 40-70 km depths. We analyzed $\delta^{13}C$ and $\delta^{18}O$ of carbonate in this unit, over a regional scale, and made field and petrographic observations bearing on mechanisms of C mobilization. A study of decarbonation history by Cook-Kollars et al. (2014) for the same suite demonstrated that, depending on extents of open-system infiltration by H_2O-rich fluid, large fractions of initially subducted carbonate could be retained in such rocks to at least 70 km depths. Assessing the magnitude of removal of carbonate via dissolution, at the whole-unit scale, has proven difficult. Isotopic exchange between the reduced and oxidized C reservoirs, and any fractionation during sub-arc mobilization and delivery into the mantle wedge, would have implications for the approach of Sano and Marty (1995) used to estimate proportions of gas from mantle and disparate sediment sources.

Study of along-margin C input flux at the Sunda margin (House et al., 2016; Fall AGU) emphasizes the role of sediment composition, source, and degree of accretion on the nature and size of the deeply subducted C reservoir. Ongoing NSF-funded work on the Hikurangi margin, New Zealand (collaborative with Bruce Christenson-GNS-NZ, Hirochika Sumino-Univ. Tokyo, and Ikuko Wada-Univ. Minnesota), is aimed at resolving C inputs vs. outputs in arc volcanoes and associated hydrothermal systems, in part considering the makeup of the incoming sediment section (based on drilling by IODP Exp. 375), extents of accretion,

©2019. Japan Geoscience Union. All Right Reserved.

along-margin thermal structure, and calculated extents of devolatilization. Studies of the Schistes Lustrés and other HP and UHP suites provide insight regarding the structural and geochemical evolution of sediments similar in composition to those subducting at modern margins (e.g., Sunda).

Keywords: carbon, subduction, arc volcanism, metamorphism

©2019. Japan Geoscience Union. All Right Reserved.

Helium isotope variations in subduction-type volcanic hydrothermal systems

*Yuji Sano[1], Takanori Kagoshima[1], Naoto Takahata[1], Tetsuji Onoue[2], Tomo Shibata[3], Tobias P Fischer[4]

1. Division of Ocean and Earth Systems, Atmosphere and Ocean Research Institute, University of Tokyo, 2. Department of Earth and Environmental Sciences, Kumamoto University, 3. Institute for Geothermal Sciences, Kyoto University, 4. Department of Earth and Planetary Sciences, University of New Mexico

Large variations of $^{3}He/^{4}He$ ratios of gas and fluid samples were observed in subduction-type modern hydrothermal systems (0.3Ra −8Ra where Ra is the atmospheric ratio of $1.38x10^{-6}$) compared with those of mid-ocean ridge basalt (MORB) glasses (7.5Ra −9.5Ra). These variations are principally attributable to binary mixing of two components: mantle He (8Ra) and crustal helium (0.1Ra). Major source of the latter component could be due to radiogenic helium in the subsurface crustal material. Thus, shallow assimilation would result in helium isotope variations around an isolated volcano. Early case study on the Ontake volcanic hydrothermal system showed that high-Ra was located in hot spring close to the central cone and decreased with distance from the volcano. Subsequent studies around Mt Nevado del Ruiz and Mt Kusatsu-Shirane confirmed the negative correlation between the $^{3}He/^{4}He$ ratio and the distance. There may be three necessary conditions to produce such a tendency. First, the volcano is independent strato-type and there is no other volcano close to the subject. Second, the magma chamber is located just beneath the volcano so that the conduit is not inclined significantly. Third, the hydrothermal system is well developed and the emission of mantle helium is stable for a long time. In order to apply these hypothetical conditions to a caldera volcano, we have carried out helium isotope survey around Aso volcano in Southwest Japan. Mt Aso is the largest active volcano in Japan with a caldera 25 km north-south and 18 km east-west. Post caldera activity is currently observed in central cone at Mt Nakadake. We have collected hot spring gas and fluid samples within the Aso caldera together with the outside and measured $^{3}He/^{4}He$ and $^{4}He/^{20}Ne$ ratios by a noble gas mass spectrometer. The helium isotopes, after correction of air contribution, decrease with the distance from the central cone in the region. The tendency is consistent with those of strato-volcanoes reported in literatures.

Keywords: helium, isotopes

©2019. Japan Geoscience Union. All Right Reserved.

[J] Poster | S (Solid Earth Sciences)：S-GC Geochemistry

Wed. May 29, 2019 3:30 PM - 5:00 PM JST | Wed. May 29, 2019 6:30 AM - 8:00 AM UTC | Poster Hall International Exhibition Hall8, Makuhari Messe_19

[S-GC41] Solid Earth Geochemistry, Cosmochemistry

convener:Gen Shimoda(Geological Survey of Japan, AIST), Katsuhiko Suzuki(Research and Development Center for Submarine Resources, Japan Agency for Marine-Earth Science and Technology), Katsuyuki Yamashita(Graduate School of Natural Science and Technology, Okayama University), Akira Ishikawa(Department of Earth and Planetary Sciences, Tokyo Institute of Technology)

"Solid Earth Geochemistry, Cosmochemistry" session aims at evaluating processes during the 4.6 billion years of the solar system and the Earth. Any approaches to this issue is welcomed, including, geochemistry, geophysics, geology, mineralogy and petrology.

[SGC41-P01] Experimental and Simulation Study on the Migration Rule of Arsenic in the Soil of Surface Karst Zone in Southwest China

*bin zeng[1] (1.China University of Geosciences)

[SGC41-P02] H_2 production and CO_2 storage during peridotite serpentinization under CO_2-rich hydrothermal conditions: Influence of pyroxene

*Jiajie Wang[1], Noriaki Watanabe[1], Atsushi Okamoto[1], Kengo Nakamura[1], Takeshi Komai[1] (1.Tohoku Univ.)

[SGC41-P03] **Age determination of spherical carbonate concretions by Sr isotope stratigraphy**

*Yoshihiro Asahara[1], Hidekazu Yoshida[2], Koshi Yamamoto[1], Nagayoshi Katsuta[3], Masayo Minami[4], Richard Metcalfe[5] (1.Graduate School of Environmental Studies, Nagoya University, 2.Material Research Section, Nagoya University, University Museum, 3.Faculty of Education, Gifu University, 4.Institute for Space-Earth Environmental Research, Nagoya University, 5.Quintessa UK)

[SGC41-P04] Origin of mantle xenoliths from Kaula Island, Hawaii:Constrains from Os isotope and highly siderophile element compositions

*Ryo Fujita[1], Akira Ishikawa[1], Tetsuya Yokoyama[1], Michael O Garcia[2] (1.Tokyo Institute of Technology, 2.University of Hawaii)

[SGC41-P05] Petrological and Geochemical features of Miocene adakitic volcanic rocks in eastern part of Hokuriku region, SW Japan

*Watanabe Syun[1], Toshiro Takahashi[1] (1.Niigata university)

[SGC41-P06] Trace element and isotopic characteristics of high Nb basalts from Kyushu arc and back arc

*Bidisha Dey[1], Tomoyuki Shibata[1] (1.Department of Earth and Planetary Systems Science, Hiroshima University)

[SGC41-P07] Evaluation of digestion methods for Molybdenum concentration analysis for geological materials

Yu Mutsushika[1], *Akira Ishikawa[1], Tetsuya Yokoyama[1] (1.Department of Earth and Planetary Sciences, Tokyo Institute of Technology)

[SGC41-P08] *fs*LA-ICPMS analysis of XRF glass beads

*Q. Chang[1], T. Sato[2], J.-I. Kimura[1] (1.Dept. Solid Earth Geochem., JAMSTEC, 2.R&D Center for Ocean Drilling Sci., JAMSTEC)

Experimental and Simulation Study on the Migration Rule of Arsenic in the Soil of Surface Karst Zone in Southwest China

*bin zeng[1]

1. China University of Geosciences

Karst Underground River is an important water source in southwest China. In addition to entering and polluting the groundwater directly through the sinkholes, arsenic pollutants produced from the industrial production process will also adsorb, remain, and concentrate in the dissolution cracks and gaps in the surface karst zone, and remigrate under certain conditions to become a "secondary pollution source". Taking an arsenic pollution event in Guangxi province as an example, the dynamic adsorption and desorption experiments of arsenic were carried out by using narrow slot physical model device, and the migration rule of arsenic contamination in the soil of surface karst zone was studied, combined with geochemical simulation. The experimental results show that the adsorption of arsenic in the surface karst zone is mainly physical adsorption (diffusion process), and the desorption rate is slow compared with the adsorption process, while the acid solution can promote the desorption process of arsenic compared with deionized water. The results of geochemical simulation show that goethite contributes most to arsenic adsorption in soil minerals, while acid solution weakens the ability of arsenic adsorption by corroding goethite and other minerals. It is concluded that in the karst area of southwest China, once the surface karst zone system is integrated with arsenic pollutants, the desorption process is slow, and it is easy to form the retention and enrichment of arsenic pollutants; while the accelerated desorption and migration process of arsenic under acid rain will increase the pollution risk of groundwater system.

Keywords: surface karst zone, arsenic pollution, physical model experiment, geochemical simulation

©2019. Japan Geoscience Union. All Right Reserved.

H_2 production and CO_2 storage during peridotite serpentinization under CO_2-rich hydrothermal conditions: Influence of pyroxene

*Jiajie Wang[1], Noriaki Watanabe[1], Atsushi Okamoto[1], Kengo Nakamura[1], Takeshi Komai[1]

1. Tohoku Univ.

Serpentinization of peridotite (mainly includes olivine and pyroxene) usually produces molecular H_2, which may potentially contribute to today’s always-increasing energy demands. On the other hand, peridotite also appears to be a good candidate for CO_2 sequestration by mineralization. Based on this, our previous research has successfully combined the strategies of H_2 production and CO_2 mineralization by olivine alteration in CO_2-rich hydrothermal system. However, olivine may not necessarily act as a peridotite equivalent during alteration, and the pyroxene influence is still poorly understood.
In this study, we examined the reactions in H_2O-olivine/pyroxene-CO_2 systems by performing hydrothermal experiments in 0.5 mol/L $NaHCO_3$ solutions under conditions of 300 °C and 10 MPa. The results show that H_2 was produced when olivine and/or pyroxene reacted in $NaHCO_3$ solution, and the presence of pyroxene in starting material suppressed H_2 production from per kg of mineral. Pyroxene was converted solely to serpentine, rather than brucite and magnesite even in CO_2-contained solutions, which indicates CO_2 mineralization was only realized in olivine-contained systems. In addition, the pyroxene serpentinization process is quicker than olivine. In the experiment with olivine/pyroxene weight ratio of 3/2, all of the pyroxene was altered after 72 h reaction, whereas half of the olivine particles have remained. Based on experimental results, we propose that the presence of pyroxene in starting material will suppress the H_2 production and CO_2 storage during peridotite alteration; however, the inhibition effect will be decreased along the reaction time.

Keywords: Pyroxene, Olivine, Hydrothermal, H2 production, CO2 storage

©2019. Japan Geoscience Union. All Right Reserved.

Age determination of spherical carbonate concretions by Sr isotope stratigraphy

*Yoshihiro Asahara[1], Hidekazu Yoshida[2], Koshi Yamamoto[1], Nagayoshi Katsuta[3], Masayo Minami[4], Richard Metcalfe[5]

1. Graduate School of Environmental Studies, Nagoya University, 2. Material Research Section, Nagoya University, University Museum, 3. Faculty of Education, Gifu University, 4. Institute for Space-Earth Environmental Research, Nagoya University, 5. Quintessa UK

Isolated spherical carbonate ($CaCO_3$) concretions are frequently observed in marine clayey sediments but do not always contain index fossils. Although carbonate concretions with fossil inside can be used to estimate sedimentation ages, concretions without fossils inside have never previously been used for age determination. In this study, we used $^{87}Sr/^{86}Sr$ ratios to determine the ages of these spherical concretions.

The studied concretions formed in the Yatsuo Group of Miocene age in central Japan. Some formed post-mortem around tusk-shells (*Fissidentalium*spp.), while other concretions have no shell fossils inside. The concretions formed under highly constrained conditions by reactions between the decay products of organic matter and Ca^{2+} from the marine water (Yoshida et al., 2015; 2018). And the sedimentary structure around the concretions and geochemical analyses reveal that Sr was incorporated into the $CaCO_3$ concretions during their rapid formation.

The $^{87}Sr/^{86}Sr$ ratios of calcite in the tusk-shell concretions lie within 0.70865~0.70867 and vary little. The values are similar to those of tusk-shell aragonite, 0.70865~0.70868. In addition, the isolated carbonate concretions without shell fossils have $^{87}Sr/^{86}Sr$ ratios of 0.70865~0.70868, which are also well consistent with the tusk-shell aragonite values. Based on the Sr isotope stratigraphy (McArthur et al., 2001) and the measured $^{87}Sr/^{86}Sr$ values, the age of the tusk-shell concretions lies within a narrow range of 17.08 (+0.27, −0.28) Ma. The age determined from the $^{87}Sr/^{86}Sr$ of the tusk-shells themselves (16.86 +/− 0.34 Ma) is almost the same. The age determined from the $^{87}Sr/^{86}Sr$ of concretions without fossils, 16.95 (+0.36, −0.37) Ma, is almost the same as that of the tusk-shell concretions. Strontium isotopic stratigraphy using $^{87}Sr/^{86}Sr$ ratios of all concretions with tusk-shell and without fossils indicates an age of 17.02 +/− 0.27 Ma, with higher accuracy than the ages estimated using microfossils from the Yatsuo Group. The results imply that the $^{87}Sr/^{86}Sr$ ratio of isolated spherical carbonate concretions can be applied generally to estimate the ages of all kinds of spherical concretions in marine sediments (Yoshida et al., 2019).

Keywords: carbonate concretion, fossil, Sr isotope, age determination, marine sediment

©2019. Japan Geoscience Union. All Right Reserved.

Origin of mantle xenoliths from Kaula Island, Hawaii:Constrains from Os isotope and highly siderophile element compositions

*Ryo Fujita[1], Akira Ishikawa[1], Tetsuya Yokoyama[1], Michael O Garcia[2]

1. Tokyo Institute of Technology, 2. University of Hawaii

The Emperor Seamount-Hawaiian island chain is thought to originate from melting of a heterogeneous mantle plume, although the nature and extent of heterogeneity remain unclear. It has been suggested that some Hawaiian mantle xenoliths with highly unradiogenic Os isotope ratios (down to 187Os/188Os=0.1138) represent the depleted part of ascending Hawaiian plume, and that the depleted materials are more commonly distributed in mantle plumes than has been inferred from the compositions of erupted lavas. To better understand the lithological and geochemical variations of Hawaiian xenoliths and to evaluate the robustness of the above model, we conducted petrological and geochemical studies on 11 peridotite xenoliths (9 lherzolites, 1 dunite, and 1 wehlrite) collected from the island of Kaula, Hawaii. Here we present the results on the whole-rock Re-Os isotope systematics and highly siderophile element compositions in the xenoliths, together with the major element compositions of constituent minerals (olivine, clinopyroxene, orthopyroxene and spinel). The rock texture and mineral compositions indicate that the Kaula peridotites are samples from normal oceanic mantle and residues of variable degrees of melting. However, they have highly unradiogenic Os isotope ratios (down to 187Os/188Os=0.1187) yielding minimum rhenium-depletion ages of up to ~1.3 Ga, which are similar to those of O’ahu peridotites. Such unradiogenic Os isotopic compositions are not found in Hawaiian lavas and in depleted mantles (e.g., mid-oceanic ridge basalts). Importantly, as is observed in the O’ahu peridotites, the 187Os/188Os ratios of Kaula peridotites correlate with the degree of depletion, suggesting that they are related to an ancient melting event. Therefore, the Kaula peridotites are possibly the fragments of a Hawaiian mantle plume that consists of ancient depleted and recycled mantle lithosphere.

Keywords: Os isotope, hawaii, mantle xenolith

©2019. Japan Geoscience Union. All Right Reserved.

Petrological and Geochemical features of Miocene adakitic volcanic rocks in eastern part of Hokuriku region, SW Japan

*Watanabe Syun[1], Toshiro Takahashi[1]

1. Niigata university

Miocene volcanic rocks are widely distribution from the eastern part of Toyama prefecture to the northern part of Fukui prefecture in Hokuriku region, Central Japan. These volcanic rocks are broadly classified in to mafic volcanic rocks and felsic volcanic rocks, and in this study the petrological and geochemical features of mafic volcanic rocks are considered. Mafic volcanic rocks of the Hokuriku region consists of various types that have characteristic petrologic and geochemical features; tholeiitic volcanic rocks, calc-alkaline volcanic rocks, high-magnesia andesite and adakitic andesite (Takahashi and Shuto, 1999; Ishiwatari and Ohama, 1997).

The present study area is in the eastern part of the Miocene volcanic rocks. Volcanic rocks of this study area can be classified into four groups; Group-1 basalts, bulk rock chemical composition of group-1 indicate low SiO_2 (<53 wt %) composition and Nd and Ta depletion. Group-2 tholeiitic andesites, bulk rock chemical composition of group-2 indicate increasing FeO*/MgO ratio with increasing SiO_2. Group-3 calc-alkaline andesites, bulk rock chemical composition of group-3 indicate stable FeO*/MgO ratio with increasing SiO_2. Group-4 Hornblende-bearing andesites, Bulk rock chemical composition of group-4 indicate low FeO*/MgO ratio, high Sr, MgO, Cr, Ni concentration and low LILE and HFSE concentration. All types of volcanic rocks are distributed in Iwaine formation except in Fukuhira formation, only group-1 and group-2 are distributed.

The volcanic rocks of this study area can be classified two types by their isotopic features. First type have nearly bulk earth isotopic composition (SrI=0.7040-0.7060, NdI=0.5125-0.5129) whereas the second type have very enriched isotopic composition (SrI=0.7085-0.7100, NdI=0.5119-0.5125). In terms of rock types Groups-1 to 3 shows both the isotopic composition, whereas only group-4 rocks have only bulk earth isotopic composition.

Here, we focus on petrological and geochemical features, because these features of group-4 is different from other groups. Group-4 have hornblende, plagioclase, clinopyroxene and olthopyroxene phenocrysts. Pyroxene phenocrysts have a wide range of composition (Mg#= Cpx 70-86; Opx 69-85).

It is difficult to explain the petrological features of group-4 by crystallization differentiation of magma that formed group-1 to 3 rocks types. This study uses trace element composition of clinopyroxene phenocryst for magma genesis of group-4. The results indicate that the group-4 magma is a product of magma mixing of high Mg# magma that have adakitic signatures (Defant and Drummond, 1991) and low Mg# magma that have enriched isotopic signature. In general, adakitic volcanic rocks are formed by partial melting of subducted oceanic crust, and so adakitic magma usually have depleted isotopic composition like a subducted oceanic crust (MORB; Castillo, 2012). However, adakitic rocks in this study area has more depleted isotopic signatures. Previous study indicated a model that involves the addition of sediment on subducted basaltic crust melt during slab melting (Sato et al., 2013). However, this model cannot explain the observed isotopic compositions. Therefore, this study proposes a model that involved an enriched component of magma mixing that resulted in the observed isotopic features.

©2019. Japan Geoscience Union. All Right Reserved.

In general, adakitic magma genesis needs heat source for slab melting. Previous studies suggest that heat source is hot asthenospheric upwelling preceding Japan sea opening (Takahashi and Shuto, 1999). Petrological features of group-4, for example, high MgO, Cr, Ni concentration are similar to bajaite (Rogers et al., 1985). Previous studies suggest that magma genesis of bajaitic magma result from ridge subducting (Tsuchiya et al., 1995). But this study area doesn’ t show evidence of ridge subducting. It is necessary to discuss from more various view point.

Keywords: Hokuriku region, adakite, island-arc magmatism

©2019. Japan Geoscience Union. All Right Reserved.

Trace element and isotopic characteristics of high Nb basalts from Kyushu arc and back arc

*Bidisha Dey[1], Tomoyuki Shibata[1]

1. Department of Earth and Planetary Systems Science, Hiroshima University

Basalts and basaltic andesites from south-west Japan arc and Back arc region show signature of HFSE enrichment similar to high Nb basalts (HNB) and Nb enriched basalts (NEB) (i.e. Philippines, Castillo et al., 2007; Central America, Hastie et al., 2011).

We use previously published data from Kyushu basalts and basaltic andesites from both arc and back arc setting to compare the geochemical characteristics of these rocks. We observe that the rocks of our interest in this area, show a much higher Nb/Zr and Nb/Hf ratio than that of typical MORB values (0.032, Sun and McDonough, 1989) or of NE Japan arc (similar to MORB, Shibata and Nakamura, 1997). The samples from Kita-Matsuura area as reported by Sakuyama et al (2009, 2014) and Fukuejima- Goto island volcanoes (Uto et al., 2004; Hoang et al., 2013; Kuritani et al., 2017) also show significantly high Nb content, up to 50 ppm and 60 ppm respectively. This type of signature is more common to OIB type mantle than to MORB type mantle (Sun and McDonough, 1989); however, isotopic plots using Sr, Nd and Pb isotopic data in 2D and 3D space show that these rocks are not likely to be related to the enriched mantle (EM1, EM2) or the HIMU components and more likely to be related to MORB type mantle and a mixture with Philippine sea plate (PHS) sediments or slab melt as suggested by Shibata et al. (2014). Samples from Fukuejima islands show the same trend as arc rocks in Pb-Pb isotopic space despite not likely to be affected by PHS plate sediment or slab melt. This suggests that the mantle geochemistry beneath Kyushu is the product of mixing between MORB type mantle and slab or sediment like Pb isotope enriched component, which may have also contributed to the HFSE enrichment. The nature of this component is subject to further investigation.

Keywords: Kyushu basalts, High Nb basalts

©2019. Japan Geoscience Union. All Right Reserved.

Evaluation of digestion methods for Molybdenum concentration analysis for geological materials

Yu Mutsushika[1], *Akira Ishikawa[1], Tetsuya Yokoyama[1]

1. Department of Earth and Planetary Sciences, Tokyo Institute of Technology

Molybdenum, one of redox-sensitive trace elements showing slightly chalcophile and moderately siderophile character, is recognized as a useful element for tracing chemical evolution of the Earth ranging from core-mantle differentiation to low temperatures surface processes. Despite this, determination of Mo concentration is frequently abandoned for the studies of rock samples dominated by silicate materials because formation of insoluble molybdenum oxides in hydrochloric (HCl) or nitric (HNO_3) acid solutions precludes accurate measurements of Mo concentration with ICP-MS in typical multi-element determination methods for other lithophile trace elements such as Rb, Sr, and rare earth elements (REE). Makishima and Nakamura (1999) and Lu et al. (2007) proposed that isotope-dilution ICP-MS (ID-ICP-MS) employing dissolution with hydrofluoric (HF) acid is a well-suited method for the simultaneous determination of Mo and other elements such as W, Sb and high-field strength elements (HFSE). However, most of these elements are hosted in acid resistant minerals such zircon and Cr-spinel in rock samples, high-temperature/pressure HF digestions with longer duration are sometimes required in order to achieve complete recovery of these elements. Here we develop a rapid and universal method for the determination of Mo in geological samples using ID-ICP-MS combined with fused-glass bead digestion (sample + lithium tetraborate). The fused-glass beads were properly dissolved into a diluted HF with spike solution. The optimized procedure and analytical capability using ICP-QMS with HF-resistant setting will be presented by showing results of replicate analyses for reference materials such as volcanic rocks (JB-1, JB-1a, JB-2, JB-3, JA-1, JA-1a, JA-2, JA-3, JR-1, JR-2, JR-3, BIR-1a, BCR-2, BHVO-2 and W-2a), plutonic rocks (JGb-1, JGb-2, WMG-1, JG-1, JG-1a, JG-2, JG-3 andJSy-1), ultramafic rocks (JP-1, JH-1, OKUM, GP-13 and UB-N), sedimentary rocks (SCo-1, SDo-1, Jdo-1, JLs-1, JCp-1, NIST694, JCh-1, JSd-1, JSd-2, JSd-3, JSl-1, JSl-2 and JLk-1) and ore-materials (JF-1, JF-2, JZn-1, JMn-1 and SARM32).

Keywords: Molybdenum, ICP-MS, isotope dilution

©2019. Japan Geoscience Union. All Right Reserved.

*fs*LA-ICPMS analysis of XRF glass beads

*Q. Chang[1], T. Sato[2], J.-I. Kimura[1]

1. Dept. Solid Earth Geochem., JAMSTEC, 2. R&D Center for Ocean Drilling Sci., JAMSTEC

Analysis of naturally heterogeneous rock samples by ICP-MS requires laborious sample preparation including acid/alkali digestion. Crystalline plutonic rocks or sediments remains as challenging analysis by ICP-MS because of the difficulty in complete digestion of acid resistant minerals which contain significant fraction of high field strength elements (HFSE) or rare earth elements (REE). We tested femto-second laser ablation (fsLA) ICP-MS analysis of glass beads prepared for X-ray fluorescence spectrometry (XRF). This method maintains benefits of no sample digestion by wet chemistry, high sensitivity, high sample throughput and low costs. A comprehensive examination of measurement parameters was made on wave length and repetition rate of the laser beam. Choice of internal standard and external calibration method were also examined. Using high-diluted glass beads (1:10 sample to lithium tetraborate ratio) and optimized in-house developed fsLA system coupled to a quadruple-type ICP-MS (iCAP Qs, ThermoFisher Sci.), the parameters and methods were validated by determining 48 elements including ten major (Si, Ti, Al, Fe, Mn, Mg, Ca, Na, K, P), refractory lithophile (Sr, Ba, REE and HFSE) and volatile (Ga, Rb, Cs, Tl, Pb) elements in well-established geological reference materials (GSJ JB-1, JG-1a, JG-2 and JR-1) and synthetic reference glasses (NIST SRM 612, USGS GSD-1G). Laboratory bias (or trueness by ISO 5725-1) for most elements was better than 10% when compared to the reference or consensus values. Poorly determined or failed elements were P, Sc, V, Ni, Sn, Sb, and W, whose data deviated from the reference values >20%. Volatile elements such as Rb, Cs and Ga showed no substantial loss; however, Tl and Pb exhibited always lower values suggesting their loss during fusion in the glass bead preparation. Repeatability and intermediate precision (ISO 5725-1) of all measured elements were better than 5–7% RSD except Cu, Sn, Sb, Cs and Tl which showed 10–40% RSD due to extremely low abundances or strong spectral interferences. The low limits of detection by this method were comparable to those obtained by solution ICP-MS for most elements of geochemical interests. Our results demonstrate that the fsLA-ICPMS using XRF glass bead can be used for rapid bulk-rock analyses of trace, minor and major elements.

Keywords: femto-second LA-ICP-MS, bulk analysis, XRF glass bead, geological reference materials

©2019. Japan Geoscience Union. All Right Reserved.

[J] Poster | S (Solid Earth Sciences)：S-GC Geochemistry

Wed. May 29, 2019 5:15 PM - 6:30 PM JST | Wed. May 29, 2019 8:15 AM - 9:30 AM UTC | Poster Hall International Exhibition Hall8, Makuhari Messe_32

[S-GC41] Solid Earth Geochemistry, Cosmochemistry

convener:Gen Shimoda(Geological Survey of Japan, AIST), Katsuhiko Suzuki(Research and Development Center for Submarine Resources, Japan Agency for Marine-Earth Science and Technology), Katsuyuki Yamashita(Graduate School of Natural Science and Technology, Okayama University), Akira Ishikawa(Department of Earth and Planetary Sciences, Tokyo Institute of Technology)

"Solid Earth Geochemistry, Cosmochemistry" session aims at evaluating processes during the 4.6 billion years of the solar system and the Earth. Any approaches to this issue is welcomed, including, geochemistry, geophysics, geology, mineralogy and petrology.

[SGC41-P01] Experimental and Simulation Study on the Migration Rule of Arsenic in the Soil of Surface Karst Zone in Southwest China

*bin zeng[1] (1.China University of Geosciences)

[SGC41-P02] H_2 production and CO_2 storage during peridotite serpentinization under CO_2-rich hydrothermal conditions: Influence of pyroxene

*Jiajie Wang[1], Noriaki Watanabe[1], Atsushi Okamoto[1], Kengo Nakamura[1], Takeshi Komai[1] (1.Tohoku Univ.)

[SGC41-P03] **Age determination of spherical carbonate concretions by Sr isotope stratigraphy**

*Yoshihiro Asahara[1], Hidekazu Yoshida[2], Koshi Yamamoto[1], Nagayoshi Katsuta[3], Masayo Minami[4], Richard Metcalfe[5] (1.Graduate School of Environmental Studies, Nagoya University, 2.Material Research Section, Nagoya University, University Museum, 3.Faculty of Education, Gifu University, 4.Institute for Space-Earth Environmental Research, Nagoya University, 5.Quintessa UK)

[SGC41-P04] Origin of mantle xenoliths from Kaula Island, Hawaii:Constrains from Os isotope and highly siderophile element compositions

*Ryo Fujita[1], Akira Ishikawa[1], Tetsuya Yokoyama[1], Michael O Garcia[2] (1.Tokyo Institute of Technology, 2.University of Hawaii)

[SGC41-P05] Petrological and Geochemical features of Miocene adakitic volcanic rocks in eastern part of Hokuriku region, SW Japan

*Watanabe Syun[1], Toshiro Takahashi[1] (1.Niigata university)

[SGC41-P06] Trace element and isotopic characteristics of high Nb basalts from Kyushu arc and back arc

*Bidisha Dey[1], Tomoyuki Shibata[1] (1.Department of Earth and Planetary Systems Science, Hiroshima University)

[SGC41-P07] Evaluation of digestion methods for Molybdenum concentration analysis for geological materials

Yu Mutsushika[1], *Akira Ishikawa[1], Tetsuya Yokoyama[1] (1.Department of Earth and Planetary Sciences, Tokyo Institute of Technology)

[SGC41-P08] *fs*LA-ICPMS analysis of XRF glass beads

*Q. Chang[1], T. Sato[2], J.-I. Kimura[1] (1.Dept. Solid Earth Geochem., JAMSTEC, 2.R&D Center for Ocean Drilling Sci., JAMSTEC)

Experimental and Simulation Study on the Migration Rule of Arsenic in the Soil of Surface Karst Zone in Southwest China

*bin zeng[1]

1. China University of Geosciences

Karst Underground River is an important water source in southwest China. In addition to entering and polluting the groundwater directly through the sinkholes, arsenic pollutants produced from the industrial production process will also adsorb, remain, and concentrate in the dissolution cracks and gaps in the surface karst zone, and remigrate under certain conditions to become a "secondary pollution source". Taking an arsenic pollution event in Guangxi province as an example, the dynamic adsorption and desorption experiments of arsenic were carried out by using narrow slot physical model device, and the migration rule of arsenic contamination in the soil of surface karst zone was studied, combined with geochemical simulation. The experimental results show that the adsorption of arsenic in the surface karst zone is mainly physical adsorption (diffusion process), and the desorption rate is slow compared with the adsorption process, while the acid solution can promote the desorption process of arsenic compared with deionized water. The results of geochemical simulation show that goethite contributes most to arsenic adsorption in soil minerals, while acid solution weakens the ability of arsenic adsorption by corroding goethite and other minerals. It is concluded that in the karst area of southwest China, once the surface karst zone system is integrated with arsenic pollutants, the desorption process is slow, and it is easy to form the retention and enrichment of arsenic pollutants; while the accelerated desorption and migration process of arsenic under acid rain will increase the pollution risk of groundwater system.

Keywords: surface karst zone, arsenic pollution, physical model experiment, geochemical simulation

©2019. Japan Geoscience Union. All Right Reserved.

H_2 production and CO_2 storage during peridotite serpentinization under CO_2-rich hydrothermal conditions: Influence of pyroxene

*Jiajie Wang[1], Noriaki Watanabe[1], Atsushi Okamoto[1], Kengo Nakamura[1], Takeshi Komai[1]

1. Tohoku Univ.

Serpentinization of peridotite (mainly includes olivine and pyroxene) usually produces molecular H_2, which may potentially contribute to today’s always-increasing energy demands. On the other hand, peridotite also appears to be a good candidate for CO_2 sequestration by mineralization. Based on this, our previous research has successfully combined the strategies of H_2 production and CO_2 mineralization by olivine alteration in CO_2-rich hydrothermal system. However, olivine may not necessarily act as a peridotite equivalent during alteration, and the pyroxene influence is still poorly understood.
In this study, we examined the reactions in H_2O-olivine/pyroxene-CO_2 systems by performing hydrothermal experiments in 0.5 mol/L $NaHCO_3$ solutions under conditions of 300 °C and 10 MPa. The results show that H_2 was produced when olivine and/or pyroxene reacted in $NaHCO_3$ solution, and the presence of pyroxene in starting material suppressed H_2 production from per kg of mineral. Pyroxene was converted solely to serpentine, rather than brucite and magnesite even in CO_2-contained solutions, which indicates CO_2 mineralization was only realized in olivine-contained systems. In addition, the pyroxene serpentinization process is quicker than olivine. In the experiment with olivine/pyroxene weight ratio of 3/2, all of the pyroxene was altered after 72 h reaction, whereas half of the olivine particles have remained. Based on experimental results, we propose that the presence of pyroxene in starting material will suppress the H_2 production and CO_2 storage during peridotite alteration; however, the inhibition effect will be decreased along the reaction time.

Keywords: Pyroxene, Olivine, Hydrothermal, H2 production, CO2 storage

©2019. Japan Geoscience Union. All Right Reserved.

Age determination of spherical carbonate concretions by Sr isotope stratigraphy

*Yoshihiro Asahara[1], Hidekazu Yoshida[2], Koshi Yamamoto[1], Nagayoshi Katsuta[3], Masayo Minami[4], Richard Metcalfe[5]

1. Graduate School of Environmental Studies, Nagoya University, 2. Material Research Section, Nagoya University, University Museum, 3. Faculty of Education, Gifu University, 4. Institute for Space-Earth Environmental Research, Nagoya University, 5. Quintessa UK

Isolated spherical carbonate ($CaCO_3$) concretions are frequently observed in marine clayey sediments but do not always contain index fossils. Although carbonate concretions with fossil inside can be used to estimate sedimentation ages, concretions without fossils inside have never previously been used for age determination. In this study, we used $^{87}Sr/^{86}Sr$ ratios to determine the ages of these spherical concretions.

The studied concretions formed in the Yatsuo Group of Miocene age in central Japan. Some formed post-mortem around tusk-shells (*Fissidentalium*spp.), while other concretions have no shell fossils inside. The concretions formed under highly constrained conditions by reactions between the decay products of organic matter and Ca^{2+} from the marine water (Yoshida et al., 2015; 2018). And the sedimentary structure around the concretions and geochemical analyses reveal that Sr was incorporated into the $CaCO_3$ concretions during their rapid formation.

The $^{87}Sr/^{86}Sr$ ratios of calcite in the tusk-shell concretions lie within 0.70865~0.70867 and vary little. The values are similar to those of tusk-shell aragonite, 0.70865~0.70868. In addition, the isolated carbonate concretions without shell fossils have $^{87}Sr/^{86}Sr$ ratios of 0.70865~0.70868, which are also well consistent with the tusk-shell aragonite values. Based on the Sr isotope stratigraphy (McArthur et al., 2001) and the measured $^{87}Sr/^{86}Sr$ values, the age of the tusk-shell concretions lies within a narrow range of 17.08 (+0.27, −0.28) Ma. The age determined from the $^{87}Sr/^{86}Sr$ of the tusk-shells themselves (16.86 +/− 0.34 Ma) is almost the same. The age determined from the $^{87}Sr/^{86}Sr$ of concretions without fossils, 16.95 (+0.36, −0.37) Ma, is almost the same as that of the tusk-shell concretions. Strontium isotopic stratigraphy using $^{87}Sr/^{86}Sr$ ratios of all concretions with tusk-shell and without fossils indicates an age of 17.02 +/− 0.27 Ma, with higher accuracy than the ages estimated using microfossils from the Yatsuo Group. The results imply that the $^{87}Sr/^{86}Sr$ ratio of isolated spherical carbonate concretions can be applied generally to estimate the ages of all kinds of spherical concretions in marine sediments (Yoshida et al., 2019).

Keywords: carbonate concretion, fossil, Sr isotope, age determination, marine sediment

©2019. Japan Geoscience Union. All Right Reserved.

Origin of mantle xenoliths from Kaula Island, Hawaii:Constrains from Os isotope and highly siderophile element compositions

*Ryo Fujita[1], Akira Ishikawa[1], Tetsuya Yokoyama[1], Michael O Garcia[2]

1. Tokyo Institute of Technology, 2. University of Hawaii

The Emperor Seamount-Hawaiian island chain is thought to originate from melting of a heterogeneous mantle plume, although the nature and extent of heterogeneity remain unclear. It has been suggested that some Hawaiian mantle xenoliths with highly unradiogenic Os isotope ratios (down to 187Os/188Os=0.1138) represent the depleted part of ascending Hawaiian plume, and that the depleted materials are more commonly distributed in mantle plumes than has been inferred from the compositions of erupted lavas. To better understand the lithological and geochemical variations of Hawaiian xenoliths and to evaluate the robustness of the above model, we conducted petrological and geochemical studies on 11 peridotite xenoliths (9 lherzolites, 1 dunite, and 1 wehlrite) collected from the island of Kaula, Hawaii. Here we present the results on the whole-rock Re-Os isotope systematics and highly siderophile element compositions in the xenoliths, together with the major element compositions of constituent minerals (olivine, clinopyroxene, orthopyroxene and spinel). The rock texture and mineral compositions indicate that the Kaula peridotites are samples from normal oceanic mantle and residues of variable degrees of melting. However, they have highly unradiogenic Os isotope ratios (down to 187Os/188Os=0.1187) yielding minimum rhenium-depletion ages of up to ~1.3 Ga, which are similar to those of O’ahu peridotites. Such unradiogenic Os isotopic compositions are not found in Hawaiian lavas and in depleted mantles (e.g., mid-oceanic ridge basalts). Importantly, as is observed in the O’ahu peridotites, the 187Os/188Os ratios of Kaula peridotites correlate with the degree of depletion, suggesting that they are related to an ancient melting event. Therefore, the Kaula peridotites are possibly the fragments of a Hawaiian mantle plume that consists of ancient depleted and recycled mantle lithosphere.

Keywords: Os isotope, hawaii, mantle xenolith

©2019. Japan Geoscience Union. All Right Reserved.

Petrological and Geochemical features of Miocene adakitic volcanic rocks in eastern part of Hokuriku region, SW Japan

*Watanabe Syun[1], Toshiro Takahashi[1]

1. Niigata university

Miocene volcanic rocks are widely distribution from the eastern part of Toyama prefecture to the northern part of Fukui prefecture in Hokuriku region, Central Japan. These volcanic rocks are broadly classified in to mafic volcanic rocks and felsic volcanic rocks, and in this study the petrological and geochemical features of mafic volcanic rocks are considered. Mafic volcanic rocks of the Hokuriku region consists of various types that have characteristic petrologic and geochemical features; tholeiitic volcanic rocks, calc-alkaline volcanic rocks, high-magnesia andesite and adakitic andesite (Takahashi and Shuto, 1999; Ishiwatari and Ohama, 1997).

The present study area is in the eastern part of the Miocene volcanic rocks. Volcanic rocks of this study area can be classified into four groups; Group-1 basalts, bulk rock chemical composition of group-1 indicate low SiO_2 (<53 wt %) composition and Nd and Ta depletion. Group-2 tholeiitic andesites, bulk rock chemical composition of group-2 indicate increasing FeO*/MgO ratio with increasing SiO_2. Group-3 calc-alkaline andesites, bulk rock chemical composition of group-3 indicate stable FeO*/MgO ratio with increasing SiO_2. Group-4 Hornblende-bearing andesites, Bulk rock chemical composition of group-4 indicate low FeO*/MgO ratio, high Sr, MgO, Cr, Ni concentration and low LILE and HFSE concentration. All types of volcanic rocks are distributed in Iwaine formation except in Fukuhira formation, only group-1 and group-2 are distributed.

The volcanic rocks of this study area can be classified two types by their isotopic features. First type have nearly bulk earth isotopic composition (SrI=0.7040-0.7060, NdI=0.5125-0.5129) whereas the second type have very enriched isotopic composition (SrI=0.7085-0.7100, NdI=0.5119-0.5125). In terms of rock types Groups-1 to 3 shows both the isotopic composition, whereas only group-4 rocks have only bulk earth isotopic composition.

Here, we focus on petrological and geochemical features, because these features of group-4 is different from other groups. Group-4 have hornblende, plagioclase, clinopyroxene and olthopyroxene phenocrysts. Pyroxene phenocrysts have a wide range of composition (Mg#= Cpx 70-86; Opx 69-85).

It is difficult to explain the petrological features of group-4 by crystallization differentiation of magma that formed group-1 to 3 rocks types. This study uses trace element composition of clinopyroxene phenocryst for magma genesis of group-4. The results indicate that the group-4 magma is a product of magma mixing of high Mg# magma that have adakitic signatures (Defant and Drummond, 1991) and low Mg# magma that have enriched isotopic signature. In general, adakitic volcanic rocks are formed by partial melting of subducted oceanic crust, and so adakitic magma usually have depleted isotopic composition like a subducted oceanic crust (MORB; Castillo, 2012). However, adakitic rocks in this study area has more depleted isotopic signatures. Previous study indicated a model that involves the addition of sediment on subducted basaltic crust melt during slab melting (Sato et al., 2013). However, this model cannot explain the observed isotopic compositions. Therefore, this study proposes a model that involved an enriched component of magma mixing that resulted in the observed isotopic features.

©2019. Japan Geoscience Union. All Right Reserved.

In general, adakitic magma genesis needs heat source for slab melting. Previous studies suggest that heat source is hot asthenospheric upwelling preceding Japan sea opening (Takahashi and Shuto, 1999). Petrological features of group-4, for example, high MgO, Cr, Ni concentration are similar to bajaite (Rogers et al., 1985). Previous studies suggest that magma genesis of bajaitic magma result from ridge subducting (Tsuchiya et al., 1995). But this study area doesn’ t show evidence of ridge subducting. It is necessary to discuss from more various view point.

Keywords: Hokuriku region, adakite, island-arc magmatism

©2019. Japan Geoscience Union. All Right Reserved.

Trace element and isotopic characteristics of high Nb basalts from Kyushu arc and back arc

*Bidisha Dey[1], Tomoyuki Shibata[1]

1. Department of Earth and Planetary Systems Science, Hiroshima University

Basalts and basaltic andesites from south-west Japan arc and Back arc region show signature of HFSE enrichment similar to high Nb basalts (HNB) and Nb enriched basalts (NEB) (i.e. Philippines, Castillo et al., 2007; Central America, Hastie et al., 2011).

We use previously published data from Kyushu basalts and basaltic andesites from both arc and back arc setting to compare the geochemical characteristics of these rocks. We observe that the rocks of our interest in this area, show a much higher Nb/Zr and Nb/Hf ratio than that of typical MORB values (0.032, Sun and McDonough, 1989) or of NE Japan arc (similar to MORB, Shibata and Nakamura, 1997). The samples from Kita-Matsuura area as reported by Sakuyama et al (2009, 2014) and Fukuejima- Goto island volcanoes (Uto et al., 2004; Hoang et al., 2013; Kuritani et al., 2017) also show significantly high Nb content, up to 50 ppm and 60 ppm respectively. This type of signature is more common to OIB type mantle than to MORB type mantle (Sun and McDonough, 1989); however, isotopic plots using Sr, Nd and Pb isotopic data in 2D and 3D space show that these rocks are not likely to be related to the enriched mantle (EM1, EM2) or the HIMU components and more likely to be related to MORB type mantle and a mixture with Philippine sea plate (PHS) sediments or slab melt as suggested by Shibata et al. (2014). Samples from Fukuejima islands show the same trend as arc rocks in Pb-Pb isotopic space despite not likely to be affected by PHS plate sediment or slab melt. This suggests that the mantle geochemistry beneath Kyushu is the product of mixing between MORB type mantle and slab or sediment like Pb isotope enriched component, which may have also contributed to the HFSE enrichment. The nature of this component is subject to further investigation.

Keywords: Kyushu basalts, High Nb basalts

©2019. Japan Geoscience Union. All Right Reserved.

Evaluation of digestion methods for Molybdenum concentration analysis for geological materials

Yu Mutsushika[1], *Akira Ishikawa[1], Tetsuya Yokoyama[1]

1. Department of Earth and Planetary Sciences, Tokyo Institute of Technology

Molybdenum, one of redox-sensitive trace elements showing slightly chalcophile and moderately siderophile character, is recognized as a useful element for tracing chemical evolution of the Earth ranging from core-mantle differentiation to low temperatures surface processes. Despite this, determination of Mo concentration is frequently abandoned for the studies of rock samples dominated by silicate materials because formation of insoluble molybdenum oxides in hydrochloric (HCl) or nitric (HNO_3) acid solutions precludes accurate measurements of Mo concentration with ICP-MS in typical multi-element determination methods for other lithophile trace elements such as Rb, Sr, and rare earth elements (REE). Makishima and Nakamura (1999) and Lu et al. (2007) proposed that isotope-dilution ICP-MS (ID-ICP-MS) employing dissolution with hydrofluoric (HF) acid is a well-suited method for the simultaneous determination of Mo and other elements such as W, Sb and high-field strength elements (HFSE). However, most of these elements are hosted in acid resistant minerals such zircon and Cr-spinel in rock samples, high-temperature/pressure HF digestions with longer duration are sometimes required in order to achieve complete recovery of these elements. Here we develop a rapid and universal method for the determination of Mo in geological samples using ID-ICP-MS combined with fused-glass bead digestion (sample + lithium tetraborate). The fused-glass beads were properly dissolved into a diluted HF with spike solution. The optimized procedure and analytical capability using ICP-QMS with HF-resistant setting will be presented by showing results of replicate analyses for reference materials such as volcanic rocks (JB-1, JB-1a, JB-2, JB-3, JA-1, JA-1a, JA-2, JA-3, JR-1, JR-2, JR-3, BIR-1a, BCR-2, BHVO-2 and W-2a), plutonic rocks (JGb-1, JGb-2, WMG-1, JG-1, JG-1a, JG-2, JG-3 andJSy-1), ultramafic rocks (JP-1, JH-1, OKUM, GP-13 and UB-N), sedimentary rocks (SCo-1, SDo-1, Jdo-1, JLs-1, JCp-1, NIST694, JCh-1, JSd-1, JSd-2, JSd-3, JSl-1, JSl-2 and JLk-1) and ore-materials (JF-1, JF-2, JZn-1, JMn-1 and SARM32).

Keywords: Molybdenum, ICP-MS, isotope dilution

©2019. Japan Geoscience Union. All Right Reserved.

*fs*LA-ICPMS analysis of XRF glass beads

*Q. Chang[1], T. Sato[2], J.-I. Kimura[1]

1. Dept. Solid Earth Geochem., JAMSTEC, 2. R&D Center for Ocean Drilling Sci., JAMSTEC

Analysis of naturally heterogeneous rock samples by ICP-MS requires laborious sample preparation including acid/alkali digestion. Crystalline plutonic rocks or sediments remains as challenging analysis by ICP-MS because of the difficulty in complete digestion of acid resistant minerals which contain significant fraction of high field strength elements (HFSE) or rare earth elements (REE). We tested femto-second laser ablation (fsLA) ICP-MS analysis of glass beads prepared for X-ray fluorescence spectrometry (XRF). This method maintains benefits of no sample digestion by wet chemistry, high sensitivity, high sample throughput and low costs. A comprehensive examination of measurement parameters was made on wave length and repetition rate of the laser beam. Choice of internal standard and external calibration method were also examined. Using high-diluted glass beads (1:10 sample to lithium tetraborate ratio) and optimized in-house developed fsLA system coupled to a quadruple-type ICP-MS (iCAP Qs, ThermoFisher Sci.), the parameters and methods were validated by determining 48 elements including ten major (Si, Ti, Al, Fe, Mn, Mg, Ca, Na, K, P), refractory lithophile (Sr, Ba, REE and HFSE) and volatile (Ga, Rb, Cs, Tl, Pb) elements in well-established geological reference materials (GSJ JB-1, JG-1a, JG-2 and JR-1) and synthetic reference glasses (NIST SRM 612, USGS GSD-1G). Laboratory bias (or trueness by ISO 5725-1) for most elements was better than 10% when compared to the reference or consensus values. Poorly determined or failed elements were P, Sc, V, Ni, Sn, Sb, and W, whose data deviated from the reference values >20%. Volatile elements such as Rb, Cs and Ga showed no substantial loss; however, Tl and Pb exhibited always lower values suggesting their loss during fusion in the glass bead preparation. Repeatability and intermediate precision (ISO 5725-1) of all measured elements were better than 5–7% RSD except Cu, Sn, Sb, Cs and Tl which showed 10–40% RSD due to extremely low abundances or strong spectral interferences. The low limits of detection by this method were comparable to those obtained by solution ICP-MS for most elements of geochemical interests. Our results demonstrate that the fsLA-ICPMS using XRF glass bead can be used for rapid bulk-rock analyses of trace, minor and major elements.

Keywords: femto-second LA-ICP-MS, bulk analysis, XRF glass bead, geological reference materials

©2019. Japan Geoscience Union. All Right Reserved.

[J] Oral | S (Solid Earth Sciences)：S-VC Volcanology

Wed. May 29, 2019 10:45 AM - 12:15 PM JST | Wed. May 29, 2019 1:45 AM - 3:15 AM UTC | IC 2F

[S-VC38] Active Volcanism

convener:Yuta Maeda(Nagoya University), Takahiro Miwa(National research institute for earth science and disaster prevention), Takeshi Nishimura(Department of Geophysics, Graduate School of Science, Tohoku University), Chairperson:Nobukazu Seama, Tetsuo Matsuno

This session discusses various aspects of active volcanisms including, but not limited to, recent and historical eruptions, various phenomena associated with the volcanic activities, underground structures of the volcanoes, and developments of new instruments based on geophysical, geochemical, geological, and multidiscipline approaches. We also welcome studies on understanding and predicting the transitions of the eruptive activities from observational, theoretical, and experimental approaches.

10:45 AM - 11:00 AM JST | 1:45 AM - 2:00 AM UTC

[SVC38-30] Summary of Kikai submarine caldera researches conducted by KOBEC (Kobe Ocean-Bottom Exploration Center)

*Nobukazu Seama[1,2], Tetsuo Matsuno[2,1], Koji Kiyosugi[3,2], Satoshi Shimizu[2], Reina Nakaoka[2], Keiko Suzuki-Kamata[2,1], Yasutomo Seto[1], Mamoru Sano[2], Yuiko Morita[4], Hikaru Iwamaru[2], Haruhisa Morozumi[2], Misaki Horiuchi[1], Kimihiro Nishimura[1], Hiroshi Ichihara[5], Kazuki Hayashi[1], Toki Hirose[1], Katsuya Kaneko[1,2], Hiroto Yamaguchi[4], Yuki Okizono[4], Hiroko Sugioka[1,2], Kazuo Nakahigashi[6,2], Yojiro Yamamoto[7], Tatsuya KODA[2], Shuichi Kodaira[7,2], Yoshiyuki Tatsumi[2,1], Scientific party of T/S Fukae-maru Kikai caldera research cruises (1.Department of Planetology, Graduate School of Science, Kobe University, 2.Kobe Ocean Bottom Exploration Center, Kobe University, 3.Organization of Advanced Science and Technology, Kobe University, 4.Department of Planetology, Faculty of Science, Kobe University, 5.Graduate school of environmental studies, Nagoya University, 6.Tokyo University of Marine Science and Technology, 7.Japan Agency for Marine-Earth Science and Technology)

11:00 AM - 11:15 AM JST | 2:00 AM - 2:15 AM UTC

[SVC38-31] Distribution of submarine pyroclastic-flow deposits of Akahoya eruption, Kikai caldera

*Satoshi Shimizu[1,2], Nobukazu Seama[3,1], Reina NAKAOKA[1], Tetsuo Matsuno[1,3], Koji Kiyosugi[5], Hikaru Iwamaru[1,2], Mamoru Sano[1,2], Kimihiro Nishimura[3], Keiko Suzuki-Kamata[1,3], Katsuya Kaneko[3], hiroto yamaguchi[4], Misaki Horiuchi[3], Toki Hirose[3], Kazuki Hayashi[3], Yoshiyuki Tatsumi[1,3] (1.Ocean Bottom Exploraiton Center, Kobe University, 2.Nippon Marine Enterprises, Ltd., 3.Department of Planetology, Graduate School of Science, Kobe University, 4.Department of Planetology, Faculty of Science, Kobe University, 5.Organization of Advanced Science and Technology, Kobe University)

11:15 AM - 11:30 AM JST | 2:15 AM - 2:30 AM UTC

[SVC38-32] Identification of submarine volcanic ash around the Kikai caldera with the Koya pyroclastic flow deposit inferred from glass composition

*Reina NAKAOKA[1], Keiko Suzuki-Kamata[1,2], Satoshi Shimizu[1], Yoshiyuki Tatsumi[1,2], Katsuya Kaneko[2,1], Koji Kiyosugi[3,1], Nobukazu Seama[2,1], Tetsuo Matsuno[1,2], Kimihiro Nishimura[2], Kazuki Hayashi[2] (1.Kobe Ocean-Bottom Exploration Center, Kobe University, 2.Department of Planetology, Graduate School ofScience, Kobe University, 3.Organization of Advanced Science and Technology, Kobe University)

11:30 AM - 11:45 AM JST | 2:30 AM - 2:45 AM UTC

[SVC38-33] Preliminary report of the sea floor survey by a remotely operated vehicle (ROV) at the Kikai caldera, SW Japan

*Koji Kiyosugi[1], Keiko Suzuki-Kamata[2], Haruhisa Morozumi[2,4], Yoshiyuki Tatsumi[2], Katsuya Kaneko[3], Reina NAKAOKA[2], Mamoru Sano[2], Satoshi Shimizu[2], Hikaru Iwamaru[2], Nobukazu Seama[3], Tetsuo Matsuno[2], Kimihiro Nishimura[3], Kazuki Hayashi[3], Misaki Horiuchi[3] (1.Organization for Advanced and Integrated Research, Kobe University, 2.Kobe Ocean-Bottom Exploration Center, Kobe University,

3.Department of Planetology, Graduate School of Science, Kobe University, 4.Japan Oil, Gas and Metals National Corporation)

11:45 AM - 12:00 PM JST | 2:45 AM - 3:00 AM UTC

[SVC38-34] Seismic activity beneath Kikai Caldera by using Ocean Bottom Observation

*Yasutomo Seto[1], Hiroko Sugioka[2], Yojiro Yamamoto[3], Tsutomu Takahashi[4] (1.Department of Planetology, Graduate School of Science, Kobe University, 2.Department of Planetology, Kobe University, 3.Japan Agency for Marine-Earth Science and Technology, 4.Research and Developement Center for Earthquake and Tsunami, Japan Agency for Marine-Earth Science and Technology)

12:00 PM - 12:15 PM JST | 3:00 AM - 3:15 AM UTC

[SVC38-35] An investigation of three-dimensional electrical resistivity structure under Kikai Caldera

*Tetsuo Matsuno[1,2], Toki Hirose[2], Yuuki Okizono[3], Nobukazu Seama[2,1], Hiroshi Ichihara[4], Hiroko Sugioka[2,1], Yoshiyuki Tatsumi[1,2] (1.Kobe Ocean Bottom Exploration Center, Kobe University, 2.Department of Planetology, Graduate School of Science, Kobe University, 3.Department of Planetology, Faculty of Science, Kobe University, 4.Graduate school of environmental studies, Nagoya University)

Summary of Kikai submarine caldera researches conducted by KOBEC (Kobe Ocean-Bottom Exploration Center)

*Nobukazu Seama[1,2], Tetsuo Matsuno[2,1], Koji Kiyosugi[3,2], Satoshi Shimizu[2], Reina Nakaoka[2], Keiko Suzuki-Kamata[2,1], Yasutomo Seto[1], Mamoru Sano[2], Yuiko Morita[4], Hikaru Iwamaru[2], Haruhisa Morozumi[2], Misaki Horiuchi[1], Kimihiro Nishimura[1], Hiroshi Ichihara[5], Kazuki Hayashi[1], Toki Hirose[1], Katsuya Kaneko[1,2], Hiroto Yamaguchi[4], Yuki Okizono[4], Hiroko Sugioka[1,2], Kazuo Nakahigashi[6,2], Yojiro Yamamoto[7], Tatsuya KODA[2], Shuichi Kodaira[7,2], Yoshiyuki Tatsumi[2,1], Scientific party of T/S Fukae-maru Kikai caldera research cruises -

1. Department of Planetology, Graduate School of Science, Kobe University, 2. Kobe Ocean Bottom Exploration Center, Kobe University, 3. Organization of Advanced Science and Technology, Kobe University, 4. Department of Planetology, Faculty of Science, Kobe University, 5. Graduate school of environmental studies, Nagoya University, 6. Tokyo University of Marine Science and Technology, 7. Japan Agency for Marine-Earth Science and Technology

Kikai submarine caldera to the south of the Kyushu Island, SW Japan, had at least three eruptions at 140, 95 and 7.3 ka, and its collapse occurred at 7.3 ka during the latest supereruption (>500 $km^3$of magma) in the Japanese Archipelago. We have conducted series of research cruises using the T/S Fukae-maru in this caldera to understand the melt supply system for the supereruption through tracing past supereruptions, identifying current volcanic activities, and imaging current structure.

The surveys to trace past supereruptions include multi-channel seismic reflection (MCS) surveys, visual observation and sediments sampling using remotely operated vehicle (ROV; SHINDAI-2K), and land observation. The MCS surveys provide high resolution marine seismic reflection images, which are classified into seven seismic units characterized by distinctive seismic facies. We interpreted that the upper most seismic unit should be a candidate layer for Koya ignimbrite due to 7.3 ka Akahoya eruption, because the deposit from the Kagoshima mainland with regressive surface erosion on progradational HST (highstand system tract) locates beneath this seismic unit and the deposit probably corresponds to the last glacial period (18 ka) (Shimizu et al., this meeting). This interpretation is supported by the chemical composition of glass shard samples on the sea floor near the caldera wall, which were obtained by ROV divings. The chemical composition of the glass shards indicates characteristic bimodal SiO_2 contents, which consistent with unique characteristic for the Akahoya eruption (Nakaoka et al., this meeting). This seismic unit distributes around the caldera and its whole volume will be calculated to estimate reliable magma volume during the Akahoya eruption. Further, visual observation of the ocean bottom by ROV (Kiyosugi et al., this meeting) and land observation (Suzuki-Kamata et al., this meeting) suggest eruption styles of submarine volcanoes and ignimbrite deposition modes.

Current volcanic activities and structures are obtained using geophysical approaches. High volcanic activities are identified by five months of seismicity data using five ocean bottom seismometers (OBSs): 1100 volcanic tremor events with its fundamental frequency of 2 Hz, high frequency seismic events with obvious P and S arrival, and monochromatic variation events are detected beneath and/or around the caldera (Seto et al., this meeting). Imaging current structures are provided by multi-beam echosounder mapping with backscatter imaging, gravity analysis, and marine electromagnetic experiment. All these structures outside of the caldera wallshows asymmetric features between the trench side and the back-arc side. The backscatter images show rough morphological features in the back-arc side, suggesting recent local eruptions, in contrast with smooth morphology in the trench side. The gravity analysis indicates that thinner upper crust in the back-arc side than that in the trench side (Morita, 2019). The

©2019. Japan Geoscience Union. All Right Reserved.

electromagnetic field variation data obtained by 10 ocean-bottom electro-magnetometers (OBEMs) observation allowed us to image a 3-D electrical resistivity structure, which also shows asymmetric feature at <5-10 km depths (Matsuno et al., this meeting). These asymmetric features between the trench side and the back-arc side suggest that Kikai submarine caldera formation is basically controlled by the subducting slab.

Keywords: Kikai Caldera, Supereruption, Akahoya eruption

©2019. Japan Geoscience Union. All Right Reserved.

Distribution of submarine pyroclastic-flow deposits of Akahoya eruption, Kikai caldera

*Satoshi Shimizu[1,2], Nobukazu Seama[3,1], Reina NAKAOKA[1], Tetsuo Matsuno[1,3], Koji Kiyosugi[5], Hikaru Iwamaru[1,2], Mamoru Sano[1,2], Kimihiro Nishimura[3], Keiko Suzuki-Kamata[1,3], Katsuya Kaneko[3], hiroto yamaguchi[4], Misaki Horiuchi[3], Toki Hirose[3], Kazuki Hayashi[3], Yoshiyuki Tatsumi[1,3]

1. Ocean Bottom Exploraiton Center, Kobe University, 2. Nippon Marine Enterprises, Ltd., 3. Department of Planetology, Graduate School of Science, Kobe University, 4. Department of Planetology, Faculty of Science, Kobe University, 5. Organization of Advanced Science and Technology, Kobe University

Kikai caldera, most of which is submerged in the seawater of the south of the Kyusyu Island, southwest Japan, is the Quaternary active caldera volcano. Latest eruption accompanied by caldera collapse taken place in 7.3 ka is the biggest Holocene eruption in Japan Archipelago. The ash-fall known as Akahoya was spread to entire southwest Japan and the pyroclastic flow thought as a low-aspect ratio ignimbrite is distributed in subaerial parts of the surrounding islands 40-80 km away from the source. Such submarine caldera must supplied the products not only in air, but largely in the water which has not been identified yet.

In order to understand the distribution of the pyroclastic-flow deposits beneath the sea around Kikai caldera, we conducted high resolution marine seismic studies from 2016 to 2018 by T/V Fukae-maru. We identified the uppermost unit widely recognized around Kikai caldera as the pyroclastic-flow deposit associated with 7.3-ka Akahoya eruption from the seismic sequence stratigraphic analysis and glass composition of sediments. The uppermost unit, characterized by subparallel to hummocky configurations of high amplitude reflections, covers the slope fan and progradational deposits of shelf edge developed between the Kyusyu Island and Kikai caldera. These secondary deposits under the uppermost unit are interpreted to deposit around the last glacial by reason of the erosion structure seen on the top-lap surface of regressive clinoform at 120 m below current sea level. Since uppermost unit is deposited after the last glacial (18 ka) and shows consistent seismic facies around Kikai caldera, the unit is inferred as products of 7.3-ka eruption. This is supported by analysis of glass composition of the sediments sampled at the seafloors interpreted as the above seismic unit, which shows the bimodal geochemical characteristic of high SiO_2 glass shards and lesser amount of low SiO_2 glass shards by which Koya pyroclastic-flow deposits are characterized (Nakaoka et al., this meeting).

This uppermost seismic unit interpreted as pyroclastic-flow deposit represents Akahoya eruption is distributed with a thickness of ~50 m around Kikai caldera. It maintains a certain amount of thickness until it reaches the shelf edge of the Kyusyu and surrounding islands. At least 40 km radius circle around the caldera, this unit is recognizable in most of the area of the seismic profiles. This result shows that a large amount of volcanic materials are ejected not only in air rather in the water at 7.3-ka Akahoya eruption.

Keywords: Caldera, Pyroclastic flow deposits, Sesimic survey, Sequence stratigraphy

©2019. Japan Geoscience Union. All Right Reserved.

Identification of submarine volcanic ash around the Kikai caldera with the Koya pyroclastic flow deposit inferred from glass composition

*Reina NAKAOKA[1], Keiko Suzuki-Kamata[1,2], Satoshi Shimizu[1], Yoshiyuki Tatsumi[1,2], Katsuya Kaneko[2,1], Koji Kiyosugi[3,1], Nobukazu Seama[2,1], Tetsuo Matsuno[1,2], Kimihiro Nishimura[2], Kazuki Hayashi[2]

1. Kobe Ocean-Bottom Exploration Center, Kobe University, 2. Department of Planetology, Graduate School ofScience, Kobe University, 3. Organization of Advanced Science and Technology, Kobe University

Koya pyroclastic flow deposit (PFD) is large scale ignimbrite generated during formation of the Kikai caldera in Kikai-Akahoya eruption at 7.3 ka. Kikai caldera is located ~50 km south of the Satsuma Peninsula and largely presents at the bottom of sea. Koya PFD is thickly distributed on land of Takeshima and Satsuma-Iwojima which represent subaerial part of the northern rim of the Kikai caldera. It is also thinly distributed over distal area, adjacent islands and mainland of south Kyusyu which is 40-60 km away from the source across the sea. This pyroclastic flow deposit has been suggested to exhibit rather low aspect ratio ignimbrite (Ui, 1973). However, on-land survey revealed that the maximum pumice size tends to decrease with increasing the distance across the sea. This may lead to a hypothesis that a significant amount of pyroclastics was lost during traveling over the sea and deposited on the sea floor (Yamane and Suzuki-Kamata, 2017). Our multi-channel seismic (MCS) reflection experiments around the Kikai caldera further suggested several seismic units (Shimizu et al., 2018). We have concluded that the uppermost unit should be a candidate layer for Koya PFD. This layer is recognized extensive distribution around the proximal islands (~30 m thick) and continuous to the Kagoshima bay (~10 m thick). As mentioned above, the Koya PFD is expected to be thickly distributed on the sea floor around the Kikai caldera. However, identification of submarine deposit with the subaerial Koya PFD is not sufficiently. In this study, we measured chemical composition of glass shards on the sea floor obtained by remotely operated vehicle (ROV) and compared with the subaerial Koya PFD.

The ROV conducted four dives to sea floor where MCS data indicate that uppermost unit is distributed near sea floor around the caldera wall and one dive in the south of the Satsuma Peninsula and collected volcanic ash on the sea floor using nozzle. The chemical composition of glass shards (<200 micrometers) from both subaerial and submarine were measured by Electron Probe Micro Analyzer (EPMA).
The glass shards on the sea floor around the caldera wall show bimodal geochemical characteristic which contain a high proportion of high SiO_2 glass shards (SiO_2=72-78 wt.%) and lesser amount of low SiO_2 glass shards (SiO_2=64-68 wt.%). The low SiO_2 glass was reported by Fujihara and Suzuki-Kamata (2013) and confirmed that it is unique characteristic for the Kikai-Akahoya eruption by glass and whole rock composition of other volcanics of the Kikai caldera. This indicate that the sea floor around the Kikai caldera covered by volcanic ash derived from the Koya PFD. Samples from the sea floor in the south of the Satsuma Peninsula were also confirmed that they contain small amount of glass shard corresponding the Koya PFD. These results correspond to the MCS data showing that candidate layer for the Koya PFD is thickly and widely distributed at uppermost part around the Kikai caldera. The vertical variation for contents of low SiO_2 glass on Takeshima Island, which is proximal area of the Koya PHD with a thickness of ~20 m, shows that the content of low SiO_2 glass lacks at the basal level and increases upward and reaches >10% at early stage (~10% level of the total thickness). While, the contents of low SiO_2 glass at distal areas across the sea tend to increase upward to <5%, which are lesser than value of proximal area. The contents of low SiO_2 glass of the sea floor samples around the caldera rim are >10%. Ash size grains are considered to be less under the influence of segregation by difference of density (Nakaoka and

©2019. Japan Geoscience Union. All Right Reserved.

Suzuki-Kamata, 2018). Thus, the Koya pyroclastic flow reached distal area across the sea between the start of eruption and the beginning of containment of low SiO_2 glass and was waning to not reach distal area and deposit on sea floor after the content of low SiO_2 glass increases to >10%.

Keywords: Kikai caldera, Koya pyroclastic flow

©2019. Japan Geoscience Union. All Right Reserved.

Preliminary report of the sea floor survey by a remotely operated vehicle (ROV) at the Kikai caldera, SW Japan

*Koji Kiyosugi[1], Keiko Suzuki-Kamata[2], Haruhisa Morozumi[2,4], Yoshiyuki Tatsumi[2], Katsuya Kaneko[3], Reina NAKAOKA[2], Mamoru Sano[2], Satoshi Shimizu[2], Hikaru Iwamaru[2], Nobukazu Seama[3], Tetsuo Matsuno[2], Kimihiro Nishimura[3], Kazuki Hayashi[3], Misaki Horiuchi[3]

1. Organization for Advanced and Integrated Research, Kobe University, 2. Kobe Ocean-Bottom Exploration Center, Kobe University, 3. Department of Planetology, Graduate School of Science, Kobe University, 4. Japan Oil, Gas and Metals National Corporation

Submarine volcanoes are one of the frontiers in volcanology: many volcanoes are located under the sea and most of them are not well studied. Since 2016, the Kobe Ocean-Bottom Exploration Center (KOBEC) at Kobe University has investigated a submarine volcano (the Kikai caldera) to understand the structure of the caldera and the style of the caldera forming eruption. The Kikai caldera is located about 45 km off southern Kyushu Island, Japan. Except two islands on the northern part of the caldera rim, most of the caldera structure is under the sea. The caldera has double caldera structure: the outer caldera has width of 19 km and length of 24 km and the inner caldera has width of 15 km and length of 17 km. The formation of, at least, the inner caldera must be related with one of the largest eruption of this volcano occurred about 7300 years ago. In the inner caldera, a giant rhyolite lava dome (~32 km^3) was created after the caldera collapse (Tatsumi et al., 2018).

A remotely operated vehicle (ROV) is a tethered underwater robot connected with a support surface vessel by a cable for power supply and signal transmission. To observe and sample sea floor material, we introduced a ROV (SHINDAI-2K) in 2016. In this presentation, we show preliminary results of 9 dives of the ROV at 8 sites in the following 3 areas in the Kikai caldera.

Outer caldera: We investigated two sites at the northeastern rim of the outer caldera. At one of the sites, we found a massive angular outcrop of dense rock in the caldera wall. This result and andesitic gravel sampled at this site confirmed the presence of igneous rock expected by our prior multi-channel seismic reflection survey. Another site had a sandy seafloor. We sampled the sediments with the ROV and identified volcanic glass fragments ejected by the caldera forming eruption.

Inner caldera: We had two dives around the inner caldera. At the northeast caldera wall of the inner caldera, basement rock appeared as a massive and angular upright outcrop of dense mudstone which had several centimeters wide horizontal banded structure. On the other hand, at the southeastern site in the inner caldera, the sea floor was covered by sandy or muddy sediments. Volcanic glass fragments ejected by the caldera forming eruption were also identified from the sediments. Furthermore, some isolated vesiculated lava blocks were observed at this site. Those blocks had fractured surface, suggesting chilling of hot ejecta due to lava/water interaction.

Lava dome: We had four dives at the lava dome. The outline of the results was already reported by Tatsumi et al (2018). The most surface of the lava dome was covered by meter-scale vesiculated lava blocks (pillow lobes; Tatsumi et al., 2018). These blocks also had water-chilled structures. Relatively dense angular chilled blocks were observed at the east flank of the lava dome where gully-like features had been determined with our prior bathymetry analysis. Furthermore, a small amount of gas emission was observed at the northern flank of the lava dome where water column was expected in our prior

©2019. Japan Geoscience Union. All Right Reserved.

side-scan sonar acoustic images.

Visual observation and sediments sampling using ROV provides valuable information to understand the history and eruption style of submarine volcanoes. Our preliminary observations suggests that (1) the amount and size of vesiculated lava blocks decrease with distance from the lava dome, showing that they were provided from the dome, (2) basement rock of the volcano is exposed at the sea floor in, at least, some areas of the Kikai caldera, (3) as well as old volcanic edifices in the two islands, old submarine volcanic edifices were cut by the caldera collapse and some of them are exposed in the outer caldera wall. These results and further ROV survey will provide new insight into the eruption history of submarine volcanoes.

Keywords: Submarine volcanoes, Caldera volcanoes, Kikai caldera, ROV

©2019. Japan Geoscience Union. All Right Reserved.

Seismic activity beneath Kikai Caldera by using Ocean Bottom Observation

*Yasutomo Seto[1], Hiroko Sugioka[2], Yojiro Yamamoto[3], Tsutomu Takahashi[4]

1. Department of Planetology, Graduate School of Science, Kobe University, 2. Department of Planetology, Kobe University, 3. Japan Agency for Marine-Earth Science and Technology, 4. Research and Developement Center for Earthquake and Tsunami, Japan Agency for Marine-Earth Science and Technology

Kikai submarine caldera located in the southern part of Kagoshima prefecture is located on the volcanic front of the southwestern Japan arc. It was recently revealed that a giant lava dome with a volume of 32km ^{3} is created after super eruption at 7.3 K.a. (Tatsumi et al., 2018). Seismic observation with the T/S Fukae-maru of Kobe University is conducted by five short-period ocean bottom seismographs (OBSs) which were in the deepest part of the caldera from October 19, 2016 to March 14, 2017. As the result, about 1100 volcanic tremors like as swarm with a fundamental frequency of around 2Hz were detected during the period and it was occurred very frequently beneath the caldera. In addition to these low frequency tremors, about 32 high frequency earthquakes with dominant frequency of over 5Hz and many monochromatic tremors were detected, but at the onshore station of Satsuma Iwo-jima no signals corresponding to these volcanic earthquakes have been detected.

In general, volcanoes are strongly inhomogeneous regions compared with ordinary crusts. The seismic waves propagate to stations under the influence of scattering and diffraction due to random inhomogeneities along the seismic ray paths. Actually, the monochromatic tremor observed in the Kikai caldera is detected only at the stations near the place where the hydrothermal activities were observed by the high-performance camera of the remotely operated vehicle (ROV) and multi-beam echosounder mapping, suggesting strong three-dimensional inhomogeneity in the volcanic body. An amplitude envelope method is powerful tool for analyzing seismic waves propagating through such a three-dimensional inhomogeneous medium. In this study, a method based on Takahashi et al. (2007) focusing on peak delay time from direct S-wave onset to the maximum amplitude arrival of its envelope was applied to about 1100 low frequency tremors and about 32 high frequency earthquakes.

For high frequency earthquakes and some low frequency tremors, we picked up the onset times arrival of P- and S-waves recorded clearly to determine the hypocenters. The hypocenters were vertically divided into two parts at a depth of around 10 km, most of which occurred at the shallower parts were laterally expanded within the lava dome. In addition, we measured the peak delay times for S-wave seismograms filtered at four frequency bands of 2-4, 4-8, 8-16 and 16-32 Hz and calculated root mean square envelope for the sum of two components in those bands to investigate a frequency. In this presentation, we will discuss characteristics of the obtained peak delay times.

©2019. Japan Geoscience Union. All Right Reserved.

An investigation of three-dimensional electrical resistivity structure under Kikai Caldera

*Tetsuo Matsuno[1,2], Toki Hirose[2], Yuuki Okizono[3], Nobukazu Seama[2,1], Hiroshi Ichihara[4], Hiroko Sugioka[2,1], Yoshiyuki Tatsumi[1,2]

1. Kobe Ocean Bottom Exploration Center, Kobe University, 2. Department of Planetology, Graduate School of Science, Kobe University, 3. Department of Planetology, Faculty of Science, Kobe University, 4. Graduate school of environmental studies, Nagoya University

We have conducted an electromagnetic experiment to reveal a 3-D electrical resistivity (or conductivity) structure under Kikai Caldera, SW Japan. The electrical resistivity is highly sensitive to thermal structure and the presence of partial melt or magma and fluid in the crust and in the upper mantle. Imaging an electrical resistivity structure provides key constraints on the distribution of magma reservoirs in the crust and in the upper mantle and volcanic structures and activities of this submarine caldera. Our electromagnetic experiment is one part of an integrated marine investigation of Kikai Caldera since October 2016 with T/S Fukae-maru, Kobe University. By semiannual research cruises to the Kikai Caldera region, we have repeatedly deployed and recovered ocean-bottom electro-magnetometers (OBEMs) by changing their locations to obtain a data set that is useful for imaging a 3-D electrical resistivity structure. We set 13 observational sites so far, and we have 10-sites data available for analysis. The 10 sites cover an area of 13 km ×16 km within the submarine double caldera with site-distances of ~5-10 km. The OBEMs measured time variations of electromagnetic fields at sampling rates of 8 Hz and 60 s with instrumental tilts and temperature at seafloor. Data suggested instrumental vibrations during observations, likely because of strong ocean current near the Kuroshio Current or between islands, and unstable positions of OBEMs on very rugged seafloor of lavas in this volcanic area. We carefully checked the time-series data and selected available data terms. We finally obtained magnetotelluric (MT) response functions at the 10 sites at a period range from 21 s to 8192 s, using the BIRRP program [Chave and Thomson, 2004]. For imaging a 3-D electrical resistivity structure, we carried out a 3-D inversion of the MT response functions using an inversion program of Usui et al. [2018]. Undulating seafloor in the study area, which can severely distort the MT responses, was incorporated into a 3-D inversion model with tetrahedron meshes. A preliminary 3-D inversion model (RMS misfit = ~1.7) shows a shallow conductive area of 3-10 Ω-m at <5-10 km depths, which is thin to the west and is thick to the east, and an underlying deep resistive area of 30-300 Ω-m at 10-30 km depths.

©2019. Japan Geoscience Union. All Right Reserved.

[J] Oral | S (Solid Earth Sciences)：S-VC Volcanology

Wed. May 29, 2019 1:45 PM - 3:15 PM JST | Wed. May 29, 2019 4:45 AM - 6:15 AM UTC | IC 2F

[S-VC38] Active Volcanism

convener:Yuta Maeda(Nagoya University), Takahiro Miwa(National research institute for earth science and disaster prevention), Takeshi Nishimura(Department of Geophysics, Graduate School of Science, Tohoku University), Chairperson:Takeshi Ohba, Akihiko Terada

This session discusses various aspects of active volcanisms including, but not limited to, recent and historical eruptions, various phenomena associated with the volcanic activities, underground structures of the volcanoes, and developments of new instruments based on geophysical, geochemical, geological, and multidiscipline approaches. We also welcome studies on understanding and predicting the transitions of the eruptive activities from observational, theoretical, and experimental approaches.

1:45 PM - 2:00 PM JST | 4:45 AM - 5:00 AM UTC

[SVC38-36] Time variation in the chemical and isotopic composition of fumarolic gases at Hakone volcano Japan

*Takeshi Ohba[1], Muga Yaguchi[2], Kana NISHINO[1], Nozomi Numanami[1], Yasushi DAITA[3], Urumu Tsunogai[4], Masanori Ito[4], Chiho Sukigara[4] (1.Department of chemistry, School of Science, Tokia University, 2.Meteorological Research Institute, JMA, 3.Kanagawa Environmental Research Center, 4.Nagoya University Graduate School of Environmental Studies)

2:00 PM - 2:15 PM JST | 5:00 AM - 5:15 AM UTC

[SVC38-37] Chemical and isotopic composition of volcanic gases at Mt Kirishima Iwoyama, Japan

*Takeshi Ohba[1], Muga Yaguchi[2], Kotaro Toyama[3], Hirochika Sumino[3], Urumu Tsunogai[4], Masanori Ito[4], Ryo Shingubara[4] (1.Department of chemistry, School of Science, Tokia University, 2.Meteorological Research Institute, 3.The University of Tokyo Graduate School of Arts and Sciences Department of Basic Science, 4.Nagoya University Graduate School of Environmental Studies)

2:15 PM - 2:30 PM JST | 5:15 AM - 5:30 AM UTC

[SVC38-38] Temporal and spatial variations of helium isotope ratios in volcanic gases in Kirishima volcanic group, Japan

*Kotaro Toyama[1], Hirochika Sumino[1], Kaori Kawana[1], Takeshi Ohba[2], Muga Yaguchi[3], Yoshihide Akiyama[1], Koki Aizawa[4], Kaori Tsukamoto[4] (1.Department of Basic Science, Graduate School of Arts and Sciences, The University of Tokyo, 2.Department of chemistry, School of Science, Tokia University, 3.Meteorological Research Institute, 4.Institute of Seismology and Volcanology, Faculty of Science, Kyushu University)

2:30 PM - 2:45 PM JST | 5:30 AM - 5:45 AM UTC

[SVC38-39] Emission regions of gaseous elemental mercury around Yugama crater lake at Kusatsu-Shirane volcano, Japan

*Akihiko Terada[1], Noriaki Mizutani[1] (1.Volcanic Fluid Research Center, Faculty of Science, Tokyo Institute of Technology)

2:45 PM - 3:00 PM JST | 5:45 AM - 6:00 AM UTC

[SVC38-40] Magnetotelluric images of Kusatsu-Shirane volcano, revisited by 3-D modeling with tetrahedral elements considered topography effect

*Kuo Hsuan Tseng[1], Yasuo Ogawa[1], Nurhassan .[2], Sabri Bulent Tank[3], Akihiko Terada[1], Wataru Kanda[1], Masato Fukai[1] (1.Tokyo Institute of Technology, 2.Bandung Institute of Technology, Indonesia, 3.Bogazici University, Turkey)

3:00 PM - 3:15 PM JST | 6:00 AM - 6:15 AM UTC

[SVC38-41] Magma conduit and associated hydrothermal systems of Aso volcano as revealed by broadband magnetotelluric data

*Nobuo Matsushima[1], Mitsuru Utsugi[2], Shinichi Takakura[1], Tadashi Yamasaki[1], Maki Hata[3], Takeshi Hashimoto[4], Makoto Uyeshima[3] (1.Geological Survey of Japan,AIST, 2.Kyoto University, 3.The University of Tokyo, 4.Hokkaido University)

Time variation in the chemical and isotopic composition of fumarolic gases at Hakone volcano Japan

*Takeshi Ohba[1], Muga Yaguchi[2], Kana NISHINO[1], Nozomi Numanami[1], Yasushi DAITA[3], Urumu Tsunogai[4], Masanori Ito[4], Chiho Sukigara[4]

1. Department of chemistry, School of Science, Tokia University, 2. Meteorological Research Institute, JMA, 3. Kanagawa Environmental Research Center, 4. Nagoya University Graduate School of Environmental Studies

A geochemical observation method that analyzes substances released from magma and hydrothermal systems such as volcanic gas, hot spring water, volcanic ash, etc. is a potentially effective means for predicting steam eruption and elucidating the structure of hydrothermal system. In Hakone volcano, an earthquake swarm began in late April 2015, and a small steam explosion occurred at the end of June. Prior to the earthquake swarm, the stable isotopic ratio of H2O in the volcanic gas declined and fluctuations in the CO2/H20 ratio synchronized with the increase and decrease in the number of earthquakes were observed. Analyzing the volcanic ash released at the end of June 2015 and using the constituent mineral species and the Cl/S ratio of the component adhered on ash surface, it was presumed that the source depth of the volcanic ash was shallower than about 350-500m. Hakone volcano repeats earthquake swarm and the associated volcanic gas anomalies every few years, and it is expected that means to predict the transition of earthquake swarm can be established by ongoing volcanic gas geochemical observation.

We collected and analyzed monthly fumarolic gases T and S, respectively, that are releasing naturally in Owakudani and Kamiyuba, which are geothermal zones developed in the central volcanic cone of Hakone volcano, and obtained the following results. The CO2/H2S ratio of T reached its maximum value around October 2017, and then showed a tendency to gradually decrease toward to January 2019. At T, a similar tendency was also observed for He/CH4 ratio. The CO2/H2S ratio of S remained nearly constant from February 2018 to February 2019, but decreased once in November 2018. The He/CH4 ratio of S showed a declining trend in 2018 like T, but the rate of decline was slower than T. CO2 and He are derived from magma that degas, H2S and CH4 are derived from hydrothermal system. Therefore the declining trend of CO2/H2S ratio and He/CH4 ratio observed in 2018 indicates that the flux of magmatic gas to shallow hydrothermal system was decreasing. The cause of the decreasing trend may be due to the development of the sealing zone surrounding the magma. The declining trend of the CO2/H2S ratio and the He/CH4 ratio in 2018 looks to disappear in 2019. The CO2/H2S ratio of T and S rose slightly from January 2019 to February. Corresponding to the rise, a minor swarm earthquake was observed on Hakone volcano on January 24, 2019 (based on Hot Springs Research Institute of Kanagawa prefecture HP). The N2/He ratio of T and S remained low from 2018 to 2019, but T was exceptionally high in January 2019. N2 is a component derived from the atmosphere, and an increase in N2 in T indicates that the fluid pressure in the shallow part hydrothermal system decreased and a part of atmospheric contamination occurred. The apparent equilibrium temperature (AETD) can be calculated by combining the hydrogen isotope ratios of H2O and H2 contained in T and S. A decline phenomenon preceding the earthquake swarm were observed in 2014 and 2017. From early 2018 to the October, AETD is declining especially for S. The decrease may be a preceding sign of earthquake swarm.

©2019. Japan Geoscience Union. All Right Reserved.

Chemical and isotopic composition of volcanic gases at Mt Kirishima Iwoyama, Japan

*Takeshi Ohba[1], Muga Yaguchi[2], Kotaro Toyama[3], Hirochika Sumino[3], Urumu Tsunogai[4], Masanori Ito[4], Ryo Shingubara[4]

1. Department of chemistry, School of Science, Tokia University, 2. Meteorological Research Institute, 3. The University of Tokyo Graduate School of Arts and Sciences Department of Basic Science, 4. Nagoya University Graduate School of Environmental Studies

INTRODUCTION

At Mt Kirishima Iwoyama, several fumarolic gases appeared in the vicinity of the summit in December 2015, and the discharge of fumarolic gas was enhanced in May 2017. In addition, a small steam eruption occurred in April 2018. Volcanic gas contains components degassed from magma and is useful for evaluating volcanic activity. In this study, from December 2015 to January 2019, fumarolic gases were repeatedly collected and analyzed at Mt Kirishima Iwoyama. We consider the relationship between the variation of the chemical composition and stable isotope ratio of these samples and the recent volcanic activity.

SAMPLING OF FUMAROLIC GAS

Fumarolic gases a, b, c were collected near the summit of Mt. Kirishima Iwoyama. The location of fumarole-a is the place where fumarolic gas first appeared in Dec. 2015. The fumarole-b is located about 40 m south of fumarole-a. The fumarole-c is about 200 m away from the fumarole-a in the south-southwest direction. The outlet temperature of the fumaroles was all close to the boiling point of water and the discharge pressure of fumarolic gases was low.

RESULTS AND DISCUSSIONS

The SO2/H2S ratio of fumarolic gas-a fell sharply from May to October 2018, but again rose in January 2019. The ratio at fumarolic gas-b also rose from October 2018 to January 2019. The Oxygen isotope ratios of H2O rose at three fumarolic gases from October 2018 to January 2019. At all three fumarolic gases, the CO2/H2O and the H2S/H2O ratio fell from October 2018 to January 2019.

In general, CO2 is a component originating in magma, H2S is a component originating in hydrothermal system, and the CO2/H2S ratio rises as the flux of magmatic gas to a shallow hydrothermal system increases. In Mt Kusatsu Shirane and Mt Hakone, the H2S/H2O ratio of the fumaroles is stable in time, and the CO2/H2S ratio could be a good indicator of the magmatic gas flow rate for the shallow hydrothermal system. The H2S/H2O ratio of Mt Kirishima Iwoyama is variable, and the situation is different from Mt Kusatsu Shirane and Mt Hakone. For example, from January to March 2018, the H2S/H2O ratio of fumarolic gas-a changed little, but fumaroles b and c greatly decreased. From March to May 2018 the H2S/H2O ratio dropped greatly in fumarolic gas-a, but in fumarolic gas-c it increased in reverse. Thus, the change in H2S/H2O ratio was not coordinated between fumaroles, and the cause of H2S/H2O ratio change is estimtated to be local. For this reason, it is not appropriate to use the CO2/H2S ratio of fumarolic as an indicator of the flux of magmatic CO2 to the shallow hydrothermal system at Mt Kirishima Iwoyama. The reason why the H2S/H2O ratio of fumarolic gases greatly fluctuates may be

©2019. Japan Geoscience Union. All Right Reserved.

attributed to the insufficient development of shallow hydrothermal system.

The SO2/H2S ratio of fumarolic gas gas was low in January 2018, but it rapidly rose in March 2018 just before the steam eruption. In addition, the increase in SO2/H2S ratio occurred simultaneously in three fumarolic gases. At this time, the apparent equilibrium temperature (AETD) calculated by combining the hydrogen isotopic ratios of H2O and H2 sharply increased to values close to the magmatic temperature at the fumaroles-a and b. A similar increases in SO2/H2S ratio and AETD also occurred in May 2017, when the discharge of fumarolic gas was enhanced. The H2O oxygen isotopic ratios of the three fumaroles have been similarly fluctuated. The oxygen isotopic ratio reached the maximum value in fumaroles a and b in March 2018 just before the eruption in April. Considering the SO2/H2S ratio and the high oxygen isotope ratio in May 2017, it is highly likely that so-called the attempted eruption occurred.

©2019. Japan Geoscience Union. All Right Reserved.

Temporal and spatial variations of helium isotope ratios in volcanic gases in Kirishima volcanic group, Japan

*Kotaro Toyama[1], Hirochika Sumino[1], Kaori Kawana[1], Takeshi Ohba[2], Muga Yaguchi[3], Yoshihide Akiyama[1], Koki Aizawa[4], Kaori Tsukamoto[4]

1. Department of Basic Science, Graduate School of Arts and Sciences, The University of Tokyo, 2. Department of chemistry, School of Science, Tokia University, 3. Meteorological Research Institute, 4. Institute of Seismology and Volcanology, Faculty of Science, Kyushu University

In Kirishima volcanic group in Kyushu, Southwest Japan, Shinmoe-dake is an active volcano and erupted in 2008, 2011, 2017 and 2018, and Iwo-yama also erupted in 2018. For the volcanic disaster preservation, forecasting the timing of the volcanic eruption is required. It is known that the temporal variations in chemical and isotopic compositions of volcanic gases are useful to evaluate the present state of volcanic activity [1]. Especially, helium isotope ratio ($^3He/^4He$) exhibits unique values corresponding to the origin (e.g., 7-8 Ra in the mantle and about 0.02 Ra in the crust, where 1 Ra denotes atmospheric $^3He/^4He$ ratio of 1.4×10^{-6} [2]). Some studies have reported pre-eruptive $^3He/^4He$ anomalies, suggesting the increase of the magmatic helium supply into the hydrothermal system preceding eruption [1, 3, 4].

We report spatial and temporal variations of $^3He/^4He$ ratios of fumaroles and hot spring gases collected from 10 sites in Kirishima volcanic group during 2016 to 2018. The measured $^3He/^4He$ ratios were corrected for atmospheric contamination based on $^4He/^{20}Ne$ ratios. The air-corrected $^3He/^4He$ ratios (6.8 to 7.7 Ra) of the central craters in the active volcanos (i.e., Iwo-yama and Shinmoe-dake) are higher than those (4.3 to 5.3 Ra) of the other sites. These $^3He/^4He$ ratios decrease with the increase of the distance from the magma reservoir, location of which is estimated as pressure source of crustal deformation associated with the 2011 Shinmoe-dake eruption, to each sampling site. This trend reflects that the contribution of radiogenic ^4He in old groundwater increases with migration distance of the gas from the magma to the site [5].

The $^3He/^4He$ ratios of fumaroles in Iwo-yama slightly increase before Shinmoe-dake eruptions, and decrease after the eruption. This variation cannot be accounted for by the contribution of the radiogenic ^4He relative to total helium in the fumaroles before and after the eruptions, because it is estimated that the amount of radiogenic ^4He which volcanic gas can acquire during its migration from magma to the surface is negligible. Alternatively, the variation results from the change in mixing ratio of gases derived from two reservoirs having high and low $^3He/^4He$ ratios. Assuming that the magma chamber has high $^3He/^4He$ ratio, the increase of $^3He/^4He$ ratios of the fumaroles before the eruption would be resulted from increase of the supply of the gas from the chamber to the Iwo-yama fumaroles. Once an eruption occurs at Shinmoe-dake, magmatic gas is effectively released through the volcanic vent, resulting in decrease of its supply to the Iwo-yama fumaroles. Thus, the temporal variation of $^3He/^4He$ ratios in volcanic gases may reflect the pressure variation of the magma chamber.

References: [1]Paonita et al. (2016) Geol.; [2] Ozima and Podosek (2002) Noble Gas Geochemistry.; [3] Padrón et al. (2013) Geol.; [4] Sano et al. (2015) Sci. Rep.; [5] Sano et al. (1994) Appl. Geochem.

Keywords: Kirishima volcanic group, Helium isotope ratios, Volcanic gas, Temporal and spatial variations, Volcanic eruption

©2019. Japan Geoscience Union. All Right Reserved.

©2019. Japan Geoscience Union. All Right Reserved.

Emission regions of gaseous elemental mercury around Yugama crater lake at Kusatsu-Shirane volcano, Japan

*Akihiko Terada[1], Noriaki Mizutani[1]

1. Volcanic Fluid Research Center, Faculty of Science, Tokyo Institute of Technology

Kusatsu-Shirane volcano is one of the most active volcanoes in terms of release of a large amount of heat as volcanic gas and thermal hot waters. In addition to a hot crater lake, locally referred to as Yugama, the Shirane pyroclastic cone exhibits thermal features such as steaming grounds and fumaroles. Because many visitors visit around the Shirane pyroclastic cone for sightseeing, risk evaluations of phreatic eruptions are valuable. Gaseous mercury emissions from ground surface at active volcanoes suggest thermal activities such as shallow hydrothermal system. Mercury contained in geothermal hot water separated from hydrothermal reservoirs as a gas phase and is transported to the surface along relatively high permeable zones. Thus, a spacial distribution of gaseous mercury emission rates from ground surface is one of a clue used to detect fracture zones. Such fracture zones may correspond to areas where explosion vents are formed in future. Furthermore, changes in flux of gaseous mercury may reflect temperature changes in a hydrothermal reservoir although mercury flux from ground surface is affected by environmental factors including air temperature, soil moisture content and organic carbon. Recently, portable apparatuses enabling to measure concentrations of gaseous elementary mercury (GEM) have been developed. To detect fracture zones around the Shirane pyroclastic cone, we applied the portable GEM analyzer which is low power consumption and light weight. On the basis of a simple numerical model which we have developed, we calculated GEM flux from GEM density measured around the soil. As a result, two GEM emission zones, A and B were found at the southern flank of the Shirane pyroclastic cone. The zone A corresponds to a locality of fissure vents formed by phreatic eruptions occurred at the beginning of 20 century. No volcanic vents are observed at ground surface at the zone B while its direction is parallel to an orientation of past fissure vents at the bottom of Yugama crater lake. We believe the zone B is fracture zone which was buried by thick ejecta emitted by following eruptions.

This work is supported by Japan Society for the Promotion of Science under the Grants-in-Aid for Scientific Research of 18H01290.

Keywords: Gaseous elemental mercury, Kusatsu-Shirane volcano, Hydrothermal system, Phreatic eruption

©2019. Japan Geoscience Union. All Right Reserved.

Magnetotelluric images of Kusatsu-Shirane volcano, revisited by 3-D modeling with tetrahedral elements considered topography effect

*Kuo Hsuan Tseng[1], Yasuo Ogawa[1], Nurhassan .[2], Sabri Bulent Tank[3], Akihiko Terada[1], Wataru Kanda[1], Masato Fukai[1]

1. Tokyo Institute of Technology, 2. Bandung Institute of Technology, Indonesia, 3. Bogazici University, Turkey

Mount Kusatsu-Shirane, Japan, is an active volcano with temporary phreatic eruptions. The distribution of subsurface conductor was previously inferred with 2-D inversion of magnetotelluric data which considered the topography effect. We combine the magnetotelluric data from 94 stations which were investigated in 2001-2002 and 8 stations which were investigated in 2017-2018 for inverse modeling. The stations were located on the volcano, mostly around Yugama crater. We selected the data by 15 frequencies for the 3-D inverse modeling. The model was calculated by FEMTIC (Usui, 2015; Usui et al., 2017), considering the topographic effect.

The final model presents two major electric conductive structures. A 0.5-3 ohm-m conductive structure with 500-1000 meters thickness is located at 300 meters depth, beneath Yugama crater and extend to the east slope of Kusatsu-Shirane volcano until Sesshogahara fumarole field. Another conductor at the west of Yugama crater has 600-1000 meters thickness at 1500-2000 meters depth.

Comparing the final model with microseismic data, most of the hypocenters are under a low conductive (<2 ohm-m) structure beneath Yugama crater. This conductive structure infers a hydrothermal deposit of volcano, which cut-off the seismicity as a cap rock. At the north of Mizugama crater, a high resistivity structure at the edge of conductor infers the path of fumarole. The deep conductor between Kusatsu-Shirane volcano and Manza geothermal field infers the geothermal source of Kusatsu-Shirane volcano system.

Keywords: data inversion, geothermal field, clay, fumerole

©2019. Japan Geoscience Union. All Right Reserved.

Magma conduit and associated hydrothermal systems of Aso volcano as revealed by broadband magnetotelluric data

*Nobuo Matsushima[1], Mitsuru Utsugi[2], Shinichi Takakura[1], Tadashi Yamasaki[1], Maki Hata[3], Takeshi Hashimoto[4], Makoto Uyeshima[3]

1. Geological Survey of Japan,AIST, 2. Kyoto University, 3. The University of Tokyo, 4. Hokkaido University

Aso volcano is one of the most active volcanoes in Japan. The caldera forming eruptions occurred from 210 ka to 90 ka, emitting the volcanic product of 600 m^3 in total. The caldera has a dimension of 25 ×18 km^2. After the caldera forming eruptions, post-caldera cones more than 17 were formed at the center of the caldera. Resent eruptions occurred repeatedly at Naka-dake cone. The count of the eruption events from Naka-dake crater was 73 times from 1901 to 2015. These volcanic activities suggest the stable magma supply from deep seated magma source to the surface. To investigate the magma plumbing system, the resistivity structure under Aso volcano was analyzed using the broadband magnetotelluric (MT) data. The four components of MT impedance and two components of tipper vector were used to obtain the resistivity structure by three-dimension inversion (Siripunvaraporn and Egbert, 2009). Overall structure was obtained using 55 measurement sites in and around of Aso caldera (Hata et al., 2016). We observed additional 9 sites near Naka-dake crater and revised the previous model to examine mainly the shallow structure near the active crater. The resistivity structure represents the low resistivity (< a few Ω•m) body which extends from near surface to a depth of 15 km (bsl) with a columnar shape, dipping northward and roughly directs to the epicenter of deep low-frequency earthquakes. The top of the low resistivity body is just located below the Naka-dake crater at sea level, which corresponds to the upper bound of magma depth estimated by melt inclusion analysis (Saito et al., 2018). From these results, we conclude that the low resistivity body indicates the upper part of the magma plumbing system of Aso volcano from deep seated magma source to the present active crater.

Keywords: Aso volcano, resistivity structure, magma plumbing system

©2019. Japan Geoscience Union. All Right Reserved.

[E] Oral | S (Solid Earth Sciences)：S-CG Complex & General

Wed. May 29, 2019 9:00 AM - 10:30 AM JST | Wed. May 29, 2019 12:00 AM - 1:30 AM UTC | IC 2F

[S-CG48] Science of slow earthquakes: Toward unified understandings of whole earthquake process

convener:Satoshi Ide(Department of Earth an Planetary Science, University of Tokyo), Hitoshi Hirose(Research Center for Urban Safety and Security, Kobe University), Kohtaro Ujiie(Graduate School of Life and Environmental Sciences, University of Tsukuba), Takahiro Hatano(Earthquake Research Institute, University of Tokyo), Chairperson:Hitoshi Hirose, Yoshiyuki Tanaka

Accumulating observational studies on various types of slow deformation events, such as tectonic tremors, very low frequency events, and slow slip events, portrays some universal characteristics in generally complex behavior, including interaction among events and influence by various outer loadings. Some of these phenomena seem to have causal relation with the occurrence of very large earthquakes. A unified understanding of these slow and fast earthquake processes requires an approach integrating geophysics, seismology, geodesy, geology, and non-equilibrium statistical physics. We welcome presentations based on, but not limited to, geophysical observation, data analysis, analytical theory, numerical simulation, field study, and laboratory experiments.

9:00 AM - 9:30 AM JST | 12:00 AM - 12:30 AM UTC

[SCG48-01] Variability of the space-time evolution of slow slip events off the Boso Peninsula, central Japan, from 1996 to 2018

★Invited Papers

*Jun'ichi Fukuda[1] (1.Earthquake Research Institute, University of Tokyo)

9:30 AM - 9:45 AM JST | 12:30 AM - 12:45 AM UTC

[SCG48-02] Cumulative slip distribution of short-term slow slip events in the western Shikoku area, southwest Japan based on tilt change measurements

*Hitoshi Hirose[1,2], Wakako Tamura[2], Takeshi Kimura[3] (1.Research Center for Urban Safety and Security, Kobe University, 2.Graduate School of Science, Kobe University, 3.National Research Institute for Earth Science and Disaster Resilience)

9:45 AM - 10:00 AM JST | 12:45 AM - 1:00 AM UTC

[SCG48-03] Shallow undersea SSEs off the western Japan monitored by the GNSS-A

*Yusuke Yokota[1], Tadashi Ishikawa[2] (1.Institute of Industrial Science, The University of Tokyo, 2.Hydrographic and Oceanographic department, Japan Coast Guard)

10:00 AM - 10:15 AM JST | 1:00 AM - 1:15 AM UTC

[SCG48-04] Co- and Post-seismic deformation due to the 2016 moderate earthquake sequence at the Chaman fault

*Fumiko Matsumoto[1], Masato Furuya[1] (1.Hokkaido University)

10:15 AM - 10:30 AM JST | 1:15 AM - 1:30 AM UTC

[SCG48-05] An attempt to quantify transient fluid flow during slow slip event using GNSS and gravity data-1st report

*Yusuke Umemiya[1], Yoshiyuki Tanaka[1] (1.The University of Tokyo)

Variability of the space-time evolution of slow slip events off the Boso Peninsula, central Japan, from 1996 to 2018

*Jun'ichi Fukuda[1]

1. Earthquake Research Institute, University of Tokyo

Continuous geodetic measurements over the past two decades have identified numerous recurrent slow slip events (SSEs) in subduction zones and other tectonic settings. Many previous studies revealed static source characteristics of SSEs, including the magnitudes, durations, recurrence intervals, and spatial slip distributions. However, our current knowledge of the time-dependent evolution of SSEs and their variability is much more limited.

In this study, we focus on a series of SSEs that occurred off the Boso Peninsula, central Japan. Since the installation of a dense GNSS network in Japan in the early 1990s, six Mw 6.6-6.7 SSEs, accompanied by swarms of regular earthquakes, have been identified on the subducting Philippine Sea Plate interface offshore of the Boso Peninsula in 1996, 2002, 2007, 2011, 2013-2014, and 2018. We invert GNSS time series to estimate the space-time evolution of the six SSEs using a modified version of the Network Inversion Filter (NIF) [Fukuda et al., 2008]. Our analyses reveal the similarities and differences in the time-dependent evolution of the six SSEs. We find that the nucleation style and space-time evolution of slip vary among the SSEs. The 2002, 2007, and 2011 SSEs nucleated more rapidly, with slip accelerations significantly higher than those of the 1996 and 2013-2014 SSEs. Furthermore, the 2002, 2007, and 2011 SSEs exhibited more rapid temporal variations in their slip and slip rates, and showed larger seismic moments and higher maximum slip rates than the 1996 and 2013-2014 SSEs. The along-strike expansion/propagation of slip is identified for the SSEs, revealing that the expansion/propagation patterns vary from event to event. Our results also show that the swarm seismicity accompanying the SSEs is highly correlated in space and time with slip rate, and seismicity only occurred after the slip rate exceeded ~4 m/yr, suggesting that the evolution of seismicity is controlled by the instantaneous stressing rate determined by slip rate.

Finally, we show that the space-time evolution of slow slip obtained here can potentially be used to study mechanisms governing the SSEs. We model the spatiotemporal evolution of shear stress on the plate interface due to slow slip obtained in the NIF analysis using the rate-and-state friction law. The rate-and-state friction parameters and initial state variable are adjusted to reproduce the stress histories. Results show that the rate-and-state friction law well reproduces the spatiotemporal evolution of stress on the plate interface during the SSEs. The critical fault size calculated from the estimated friction parameters is similar to the size of the SSE region, suggesting that the evolution of slow slip is governed by frictional properties near the stability boundary between stable and unstable slip.

Keywords: slow slip event, GNSS, crustal deformation

©2019. Japan Geoscience Union. All Right Reserved.

Cumulative slip distribution of short-term slow slip events in the western Shikoku area, southwest Japan based on tilt change measurements

*Hitoshi Hirose[1,2], Wakako Tamura[2], Takeshi Kimura[3]

1. Research Center for Urban Safety and Security, Kobe University, 2. Graduate School of Science, Kobe University, 3. National Research Institute for Earth Science and Disaster Resilience

In the western Shikoku area, southwest Japan, so-called short-term slow slip events (SSE) accompanying tremor activities repeatedly occur with an average recurrence interval of about six months (e.g., Obara et al., 2004; Sekine et al., 2010). This activity has been detected by high-sensitivity accelerometers (tiltmeters) equipped at NIED Hi-net stations (Obara et al., 2005). Using the observed tilt records, Sekine et al. (2010) estimated a history of released seismic moment by short-term SSEs and reported that about 65\% of the accumulated moment by the relative plate convergence is released as short-term SSEs in the western Shikoku area. Because this estimation is based on a fault model such that slip is uniform on a plane rectangular fault and a location of the fault, especially a depth of the fault, is an unknown (nonlinear) parameter in their inversion, it is possible that an estimated seismic moment of an SSE could be biased.

In this study, we apply an inversion method that can express a spatial fault slip distribution assuming the slip is on the plate interface to the same tilt change data set that were detected in Sekine et al. (2010). They measured a tilt change caused by a short-term SSE as a difference between two averages of tilt values in one-day-long time interval (this can vary on a case-by-case basis) just before and after the SSE episode. We estimated each slip distribution of 18 short-term SSEs in western Shikoku between January 2001 and March 2008 although a reliable slip distribution is not estimated in a couple of episodes because of the limited number of available stations.

A cumulative slip distribution of the 18 SSEs shows that (1) slip area is localized within a narrow zone with its width of about 30-40~km in dip direction and about 70~km in strike direction of the subducting plate; (2) accumulated moment by the plate subduction is considered as fully released by SSEs at an area with larger cumulative slip; (3) the width of the slip zone is wider in the western part and narrower in the eastern part. The last characteristics is in agreement with the tremor epicenter distribution in this area (e.g., Obara et al., 2010). This suggests that there is a segment boundary that separates the western and eastern part of the SSE area in the western Shikoku region, and these segments likely have different frictional property and/or different pore fluid distribution.

Acknowledgments: This work was supported by JSPS KAKENHI Grant Number JP16H06474.

Keywords: subduction zone, slow earthquakes, tilt changes, earthquake cycle

©2019. Japan Geoscience Union. All Right Reserved.

Shallow undersea SSEs off the western Japan monitored by the GNSS-A

*Yusuke Yokota[1], Tadashi Ishikawa[2]

1. Institute of Industrial Science, The University of Tokyo, 2. Hydrographic and Oceanographic department, Japan Coast Guard

In the last two decades, many kinds of SEQs including non-seismic SSE have been detected using the onshore high-precision seismometer and GNSS networks. Along the Nankai Trough having dense seismic and geodetic monitoring network, their relationships were discussed and compared in detail [e.g., Hirose et al., 2010, Science; Obara and Kato, 2016, Science]. Observation of deep and shallow SEQ analogies and differences has multidisciplinary value for the physical properties of the plate boundary, submarine geology and earthquake disaster research. However, comparison between deep underground SEQs and shallow undersea SEQs cannot easily be performed due to the undersea observation technical constraint.

In these several years that the technology has been upgraded, shallow SEQs (tremor, LFE, VLF and short-term SSE) have been detected along the pan-Pacific subduction zones in high-precision onshore seismometers, seafloor seismometers, ocean bottom pressure gauges and submarine borehole strainmeters [e.g., Wallace et al., 2016, Science; Araki et al., 2017, Science]. However, there was no geodetic monitoring technology for detecting undersea longer sequence of SSE than week-scale. Longer-term SSE than week-scale cannot be monitored except for the GNSS-A technique.

Recently, we improved the GNSS-A technology and upgraded observation frequency and precision [Yokota et al., 2017, Rep. Hydro. Ocean. Res; Yokota et al., 2018, MGR]. With the present observation capability, yearly time change of the amount of undersea crustal deformation was newly unclosed. Then, the GNSS-A monitoring uncloses the occurrence situation of undersea SSE which could not be observed by the onshore geodetic network.

We detected SSE signals in the GNSS-A data using c-AIC detection process based on the method of Nishimura et al. [2013, JGR]. Then, SSE rectangle models were estimated by the grid search process using the GNSS-A signals and the onshore GEONET data. The detected models are located off the Kii channel and the Bungo channel at shallow side around the Nankai Trough historical seismogenic zone and strong coupling regions estimated by Yokota et al. [2016, Nature] and Nishimura et al. [2018, Geosphere]. We detected about M_w 6.0 and 6.5 events off the Kii channel and a migration of about M_w 6.1 ~ 6.2 events off the Bungo channel.

Shallow VLF events [NIED and Asano et al., 2008, EPS] were also activated simultaneously with these undersea SSEs. Off the Kii channel, VLF activity in 2009 was a little closer to the western side than 2018. Off the Bungo channel, VLF activity after 2015 was synchronized with the undersea SSEs. These suggest the temporal synchronization and the spatial relationship between SSE and VLF in these regions.

Keywords: SSE, GNSS-A, Nankai Trough

©2019. Japan Geoscience Union. All Right Reserved.

Co- and Post-seismic deformation due to the 2016 moderate earthquake sequence at the Chaman fault

*Fumiko Matsumoto[1], Masato Furuya[1]

1. Hokkaido University

Chaman fault system, located in Pakistan and Afghanistan, forms a transform boundary between Indian and Eurasian plates. Previous geological survey found the relative velocity of the Indian plate to the Eurasian at ~36mm/yr. Chaman fault is the major sinistral strike-slip fault which has ~900km long in the system. However, no large earthquakes (M>7) have been documented on the Chaman fault. Low seismicity results from either a long recurrence interval or aseismic creeping. Recent studies indicate a heterogeneous distribution of locked and creeping segments along the fault. In previous work, Furuya and Satyabala(2008) revealed a long lasted afterslip following a moderate earthquake (M5) in 2005 on the Chaman fault. We examine other earthquakes on the Chaman fault and their behavior comparing with the results in Furuya and Satyabala(2008). We find two moderate events occurred on May 13 and July 10 in 2016, first events larger than M5 on the Chaman fault after the M5 earthquake in 2005. The first event on May 13 was the largest M5-class earthquake since the 2005 M5 event examined by Furuya and Satyabala (2008). According to USGS catalogue, this May 13 event has three earthquakes observed within a few kilometers every minute in a row. We use ascending Sentinel-1 SAR data from March 31, 2016 to January 13, 2017. We generate InSAR images that suggest that the co- and post-seismic deformation of left-lateral strike-slip. Especially the second July 10 event almost implies the same behavior with the results in Furuya and Satyabala(2008). We must pick up real deformation except atmospheric trend, so we stack five InSAR images using different master date for each events before estimation of fault source model.

Keywords: InSAR, Slow slip, Crustal deformation

©2019. Japan Geoscience Union. All Right Reserved.

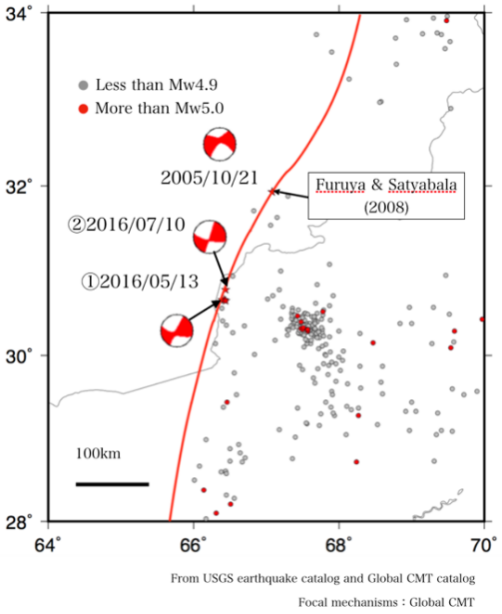

Figure1. Location map of Chaman fault and earthquakes after 2005/10/21. Gray dots show events less than Mw4.9 while red dots show more than Mw5.0. We pick up two events from more than Mw5.0 along the fault.

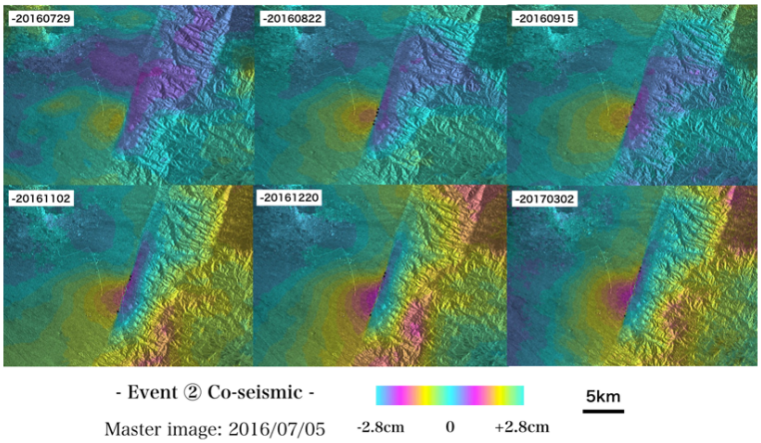

Figure2. Co-seismic deformation regarding the second event on 2016/07/10. There are six interferograms using same master image on 2016/07/05. These patterns are consistent with left lateral deformation. The phase and extent of deformation area gradually become larger.

©2019. Japan Geoscience Union. All Right Reserved.

An attempt to quantify transient fluid flow during slow slip event using GNSS and gravity data-1st report

*Yusuke Umemiya[1], Yoshiyuki Tanaka[1]

1. The University of Tokyo

Slow slip events (SSEs) cause crustal deformation. The observed deformations are usually explained with a fault model based on elasticity dislocation theory and fault slip distributions on plate interfaces have been inferred. On the other hand, a recent study analyzing the temporal gravity change which was obtained in the Tokai area indicates that long-term SSEs could cause transient fluid flow within the fault fracture zone. According to their study, fault slip cannot explain the observed negative gravity anomalies because the density redistribution which is expected from a dislocation theory is too small. However, their fluid-flow model neglects the deformation outside the fault fracture zone for simplicity. Therefore, how large surface deformation occurs due to such fluid flow (if it exists) has not yet been estimated. In this study, we propose a model which can consider the crustal deformation outside the fault fracture zone, which is induced by fluid flow. Instead of poroelasticity theories, we combine Mogi model with an ordinary dislocation model. Our model does not include a physical mechanism to drive the fluid flow itself. However, the kinematic approach allows us to quantify the fluid volume which is injected within the fault fracture zone during the SSEs in a very simple manner, using crustal deformation and gravity anomaly data. A preliminary result indicates that the injected fluid volume is approximately 0.01% if assuming that the thickness of the fault fracture zone is 200 m and the length and the width of the area where the fluid flow occurs are of the fault model of the SSE. For this volume change, our model can explain the crustal deformation and the gravity anomaly simultaneously.

Keywords: slow slip, fluid flow, GNSS, Gravity

©2019. Japan Geoscience Union. All Right Reserved.

[E] Poster | S (Solid Earth Sciences)：S-CG Complex & General

Wed. May 29, 2019 10:45 AM - 12:15 PM JST | Wed. May 29, 2019 1:45 AM - 3:15 AM UTC | Poster Hall International Exhibition Hall8, Makuhari Messe_10

[S-CG48] Science of slow earthquakes: Toward unified understandings of whole earthquake process

convener:Satoshi Ide(Department of Earth an Planetary Science, University of Tokyo), Hitoshi Hirose(Research Center for Urban Safety and Security, Kobe University), Kohtaro Ujiie(Graduate School of Life and Environmental Sciences, University of Tsukuba), Takahiro Hatano(Earthquake Research Institute, University of Tokyo)

Accumulating observational studies on various types of slow deformation events, such as tectonic tremors, very low frequency events, and slow slip events, portrays some universal characteristics in generally complex behavior, including interaction among events and influence by various outer loadings. Some of these phenomena seem to have causal relation with the occurrence of very large earthquakes. A unified understanding of these slow and fast earthquake processes requires an approach integrating geophysics, seismology, geodesy, geology, and non-equilibrium statistical physics. We welcome presentations based on, but not limited to, geophysical observation, data analysis, analytical theory, numerical simulation, field study, and laboratory experiments.

[SCG48-P01] Off the Kii Peninsula Shallow Low Frequency Earthquake in 2004 revealed by Ocean Bottom Seismometer

*Koji Tamaribuchi[1], Akio Kobayashi[1], Takahito Nishimiya[1], Satoshi Annoura[2] (1.Meteorological Research Institute, 2.Japan Meteorological Agency)

[SCG48-P02] The development of pressure vessel on gouges for rock deformation at seismic rates under water-saturated conditions

*Wei-Ting Lin[1], Li-Wei Kuo[1], Wen-Jie Wu[1], Jia-Jyun Dong[1], Yi-Hung Huang[2] (1.National Central University, 2.MATSUKI HYDRAULIC INDUSTRIAL CO. LTD)

[SCG48-P03] Spatial variations of shallow very low-frequency earthquake activity along the Nankai Trough based on CMT inversion using the 3D heterogeneous model

*Shunsuke Takemura[1], Takanori Matsuzawa[1], Akemi Noda[1], Takashi Tonegawa[2], Youichi Asano[1], Takeshi Kimura[1], Katsuhiko Shiomi[1] (1.National Research Institute for Earth Science and Disaster Resilience, 2.Japan Agency for Marine-Earth Science and Technology)

[SCG48-P04] Evaluation of Magnitude and Characteristics of Seismicity of Low Frequency Earthquakes in Parkfield

*Miki Aso[1,3], Naofumi Aso[2], Satoshi Ide[1] (1.Department of Earth and Planetary Science, The University of Tokyo, 2.Tokyo Institute of Technology, School of Science, 3.OYO RMS Corporation)

[SCG48-P05] Tectonic tremor catalog in the Tohoku-Hokkaido-Oki region using S-net

*Satoshi Ide[1], Tomoaki Nishikawa[2], Takanori Matsuzawa[3], Kazuaki Ohta[2], Naoki Uchida[4], Takuya NISHIMURA[2] (1.Department of Earth an Planetary Science, University of Tokyo, 2.Disaster Prevention Research Institute, Kyoto University, 3.National Research Institute for Earth Science and Disaster Resilience, 4.Graduate School of Science and International Research Institute of Disaster Science, Tohoku University)

[SCG48-P06] Spontaneous Slow Slip and Runaway Slip in Laboratory

*Miki Takahashi[1] (1.Institute of Earthquake and Volcano Geology, Geological Survey of Japan, AIST)

[SCG48-P07] Hydration and amorphization of quartz rocks during high-velocity frictional sliding: An examination of fault gouge from friction experiments of synthetic quartz

*Yuko Onoe[1], Hirotaka Iida[2], Akito Tsutsumi[1], Aki Takigawa[1] (1.Graduate School of Science, Kyoto University, 2.Geothermal Engineering Co., Ltd.)

[SCG48-P08] Constraining S Wave Velocity of the Source Region of Shallow Very Low-Frequency Earthquakes

*Takeshi Akuhara[1], Takashi Tonegawa[2] (1.Earthquake Research Institute, The University of Tokyo, 2.Research and Development center for Earthquake and Tsunami, Japan Agency for Marine-Earth Science and Technology)

[SCG48-P09] **Quantitative relationship between aseismic slip propagation speed and frictional properties**

*Keisuke Ariyoshi[1], Jean-Paul Ampuero[2,3], Roland Burgmann[4], Toru Matsuzawa[5], Akira Hasegawa[5], Ryota Hino[5], Takane Hori[1] (1.Japan Agency for Marine-Earth Science and Technology, 2.Université Côte d'Azur, 3.California Institute of Technology, 4.University of California, Berkeley, 5.Graduate School of Science, Tohoku University)

[SCG48-P10] Comprehensive detection of very low frequency earthquakes off the Pacific coasts of Hokkaido and Tohoku, northeastern Japan

*Satoru Baba[1], Akiko Takeo[1], Kazushige Obara[1], Takanori Matsuzawa[2], Takuto Maeda[3] (1.Earthquake Research Institute, University of Tokyo, 2.National Research Institute for Earth Science and Disaster Resilience, 3.Graduate School of Science and Technology, Hirosaki University)

[SCG48-P11] **Spatio-temporal evolution of long- and short-term slow slip events in the Tokai region, central Japan estimated from a very dense GNSS network, during 1997-2017**

*Hiromu Sakaue[1], Takuya NISHIMURA[2], Jun'ichi Fukuda[3], Teruyuki Kato[4] (1.Graduate School of Science, Kyoto University, 2.Disaster Prevention Research Institute Kyoto University, 3.Earthquake Research Institute,The University of Tokyo, 4.Hot Springs Research Institute of Kanagawa Prefecture)

[SCG48-P12] Broadband excitation of acoustic emission in granular stick-slip : experiments and spectral analyses

*Hidekazu Fukumizu[1], Ikuro Sumita[2] (1.Earth and Environmental Science Course, Division of Natural System, Graduate school of Natural Science and Technology, Kanazawa University, 2.School of Geosciences and Civil Engineering, Kanazawa University)

[SCG48-P13] Episodic tremor and slip silently invades strongly locked megathrust in the Nankai Trough

*Masayuki Kano[1], Aitaro Kato[2], Kazushige Obara[2] (1.Graduate school of science, Tohoku University, 2.Earthquake Research Institute, The University of Tokyo)

[SCG48-P14] Spatial distribution of the electrical resistivity beneath western part of Shikoku Island where long-term SSE events have repeatedly occurred

*Makoto Uyeshima[1], Maki Hata[1], Hiroshi Ichihara[2], Ryokei Yoshimura[3], Koki Aizawa[4] (1.Earthquake Research Institute, The University of Tokyo, 2.Graduate School of Environmental Studies, Nagoya University, 3.Disaster Prevention Research Institute, Kyoto University, 4.Institute of Seismology and Volcanology, Faculty of Sciences, Kyushu University)

[SCG48-P15] Variations of scaling relationships for shallow tremor observed along the Nankai trough

*Masaru Nakano[1], Suguru Yabe[1] (1.Japan Agency for Marine-Earth Science and Technology)

[SCG48-P16] Low-frequency earthquakes triggered by teleseismic surface waves by Ryukyu subduction zone.

Ayumi Kinjo[1], *Mamoru Nakamura[1] (1.Faculty of Science, University of the Ryukyus)

[SCG48-P17] Detection of small surface displacement accompanying deep low-frequency tremor in Shikoku region, southwest Japan

*Yutaro Okada[1], Takao Tabei[2] (1.Faculty of Science, Kochi University, 2.Faculty of Science and Technology, Kochi University)

[SCG48-P18] Long-term temporal change in crustal resistivity beneath western Shikoku

*Futoshi Yamashita[1], Yoshimori Honkura[1] (1.National Research Institute for Earth Science and Disaster Resilience)

[SCG48-P19] Slow decay of postseismic deformation compared with aftershocks following the 2011 Tohoku-oki Earthquake

*Yuta Mitsui[1], Shunsuke Morikami[2] (1.Department of Geosciences, Shizuoka University, 2.Formerly at Graduate School of Science and Technology, Shizuoka University)

[SCG48-P20] Serpentinite dehydration in subduction shear zones formed at source depths of slow earthquakes

*Yasushi Mori[1], Miki Shigeno[1], Kohtaro Ujiie[2], Kazuya Noro[2], Tadao Nishiyama[3] (1.Kitakyushu Museum of Natural History and Human History, 2.University of Tsukuba, 3.Kumamoto University)

[SCG48-P21] Earthquake swarms following very low-frequency earthquakes in the central Ryukyu Trench

*Mamoru Nakamura[1] (1.Faculty of Science, University of the Ryukyus)

[SCG48-P22] Seismic imaging in the central Nankai trough, off Shionomisaki to Kii channel

*Yasuyuki Nakamura[1], Shuichi Kodaira[1], Tetsuo No[1], Yuka Kaiho[1], Gou Fujie[1], Seiichi Miura[1], Kazuya Shiraishi[1] (1.Japan Agency for Marine Earth Science and Technology)

[SCG48-P23] Attempt to Detect Intra-plate SSEs Based on F3 Solution of GEONET

*Yusaku Tanaka[1] (1.Earthquake Research Institute)

[SCG48-P24] A new hydrothermal, low to high speed rotary-shearing apparatus: Reproduction of slow/megathrust earthquakes in laboratory

*Takehiro Hirose[1], Wataru Tanikawa[1], Yohei Hamada[1], Keishi Okazaki[1] (1.Kochi Institute for Core Sample Research, Japan Agency for Marine-Earth Science and Technology)

[SCG48-P25] Very low-frequency earthquakes in western Shikoku remotely triggered by the 2016 Mw5.9 off-Kii Peninsula earthquake

*Masatoshi Miyazawa[1] (1.Disaster Prevention Research Institute, Kyoto University)

[SCG48-P26] **Underground structure around source region of slow earthquakes in western Shikoku obtained by receiver function analysis**

Akira Hikita[1], Aitaro Kato[1], *Kazushige Obara[1], Akiko Takeo[1], Takeshi Akuhara[1] (1.Earthquake Research Institute, The University of Tokyo)

[SCG48-P27] Hypocenter determination of deep low frequency tremors beneath the Kii Peninsula by backprojection of seismic array data

*Kodai Sagae[1], Hisashi Nakahara[1], Takeshi Nishimura[1], Kazutoshi Imanishi[2] (1.Graduate School of Science,Tohoku University, 2.National Institute of Advanced Industrial Science and Technology (AIST))

[SCG48-P28] Triggered tremors and stress perturbations due to surface waves

*Ryohei Ikeda[1], Naoki Suda[1] (1.Hiroshima University)

[SCG48-P29] Numerical modeling of long- and shallow slow slip events including shallow region in Hyuganada and western Nankai, Japan

*Takanori Matsuzawa[1], Bunichiro Shibazaki[2] (1.National Research Institute for Earth Science and Disaster Resilience, 2.Building Research Institute)

[SCG48-P30] Further evidence for the influence of a subducting-ridge on the spatial strain accumulation and release pattern in the shallow eastern Nankai Trough, based on VLFE distribution

*Akiko Toh[1], Chen Wan-Jou [2], Doug Dreger[3], Wu-Cheng Chi[2], Satoshi Ide[1] (1.University of Tokyo, 2.Institute of Earth Sciences, Academia Sinica, 3.UC Berkeley)

[SCG48-P31] Evidence for semi-brittle flow in mantle-wedge serpentinites under high pore fluid pressure and their implications for deep low frequency earthquakes

Kengo Kataoka[1], Yurina Nagata[1], *Ken-ichi Hirauchi[1], Ryosuke Oyanagi[2], Atsushi Okamoto[3], Katsuyoshi Michibayashi[4] (1.Department of Geosciences, Faculty of Science, Shizuoka University, 2.Japan Agency for Marine-Earth Science and Technology, 3.Graduate School of Environmental studies, Tohoku University, 4.Department of Earth and Planetary Sciences, Nagoya University)

[SCG48-P32] Spatial distribution of slow slip events off the Boso peninsula from 1996 to 2018 under sparsity constraints

*Ryoko Nakata[1], Hideitsu Hino[2], Tatsu Kuwatani[3,4], Takahiro Akiyama[5], Shoichi Yoshioka[6], Masato Okada[7], Takane Hori[1] (1.Japan Agency for Marine-Earth Science and Technology, 2.The Institute of Statistical Mathematics, 3.Department of Solid Earth Geochemistry, Japan Agency for Marine-Earth Science and Technology, 4.PRESTO, Japan Science and Technology Agency, 5.Graduate School of Science, Kobe University, 6.Research Center for Urban Safety and Security, Kobe University, 7.Graduate School of Frontier Sciences, The University of Tokyo)

[SCG48-P33] Marine electromagnetic observations around a slow earthquake region in the western Nankai trough

*Hiroshi Ichihara[1], Tada-nori Goto[2], Tetsuo Matsuno[3], Noriko Tada[4], Shinya Sato[2] (1.Earthquake and Volcano Research Center, Nagoya University, 2.Graduate School of Engineering, Kyoto University, 3.Ocean Bottom Exploration Center, Kobe University, 4.JAMSTEC)

[SCG48-P34] Dynamics of precipitating injection fronts inside of structured medium

*Yutaka Sumino[1], Shunsuke Tanaka[1], Miyuki Kunihiro[1] (1.Tokyo University of Science)

[SCG48-P35] Permeability changes of simulated low permeable fault rocks induced by intermediate velocity friction test

*Wataru Tanikawa[1] (1.Japan Agency for Marine-Earth Science and Technology, Kochi Instutute for Core Sample Research)

[SCG48-P36] Modified relation between the coupling and tremor rates around the Shikoku region

*Tadafumi Ochi[1] (1.Institute of Earthquake and Volcano Geology, Geological Survey of Japan, The National Institute of Advanced Industrial Science and Technology)

[SCG48-P37] Spatiotemporal distribution of regular and very low-frequency earthquakes in the northern part of the Ryukyu subduction zone

*Youichi Asano[1], Kazuhiko Goto[2], Hiroshi Yakiwara[3], Shuichiro Hirano[3] (1.National Research Institute for Earth Science and Disaster Resilience, 2.Association for the development of earthquake prediction,

3.Nansei-toko Observatory for Earthquakes and Volcanoes, Kagoshima University)

[SCG48-P38] Possible tectonic tremor activities near the VLFE epicenters in the Sanriku-Oki region in 2011

*Hidenobu Takahashi[1], Ryota Hino[1], Yusaku Ohta[1], Naoki Uchida[1], Syuichi Suzuki[1], Masanao Shinohara[2], Takanori Matsuzawa[3] (1.Graduate school of Science Tohoku University , 2.Earthquake Research Institute, University of Tokyo, 3.National Research Institute for Earth Science and Disaster Resilience)

[SCG48-P39] Heterogeneous structure around a region of slow earthquake activity off Ibaraki prefecture along the Japan Trench

*Kimihiro Mochizuki[1], Tomoaki Yamada[1], Masanao Shinohara[1], Ryota Hino[2], Ryosuke Azuma[2], Yoshihiro Ito[3], Yoshio Murai[4], Kenji Uehira[5], Toshinori Sato[6] (1.ERI, Univ. of Tokyo, 2.Graduate School of Science, Tohoku Univ., 3.DPRI, Kyoto Univ., 4.Faculty of Science, Hokkaido Univ., 5.NIED, 6.Graduate School of Science, Chiba Univ.)

[SCG48-P40] Shallow low-frequency tremor triggered by nearby moderate earthquakes off Sanriku

*Sachiko Tanaka[1], Takanori Matsuzawa[1], Youichi Asano[1] (1.National Research Institute for Earth Science and Disaster Resilience)

[SCG48-P41] Slow slip events in the Bungo Channel over 15 years as inferred from GNSS data (1996-2011)

Takatoshi Yokoi[1], *SHINICHI MIYAZAKI[1], Hiromu Sakaue[1], Jun'ichi Fukuda[2] (1.Graduate School of Science, Kyoto University, 2.Earthquake Research Institute, The University of Tokyo)

[SCG48-P42] Investigations of sensor orientation and a possibility of detecting crustal deformation based on accelerometer records of S-net

*Ryota Takagi[1], Naoki Uchida[1], Takashi NAKAYAMA[1], Ryosuke Azuma[1], Akira Ishigami[1], Tomomi Okada[1], Yusaku Ohta[1], Ryota Hino[1] (1.Research Center for Prediction of Earthquakes and Volcanic Eruptions, Graduate School of Science, Tohoku University)

[SCG48-P43] Spatiotemporal variation of released seismic energy from shallow low-frequency tremor in Hyuga-nada, revealed by ocean bottom seismological observation

*Yusuke Yamashita[1], Saki Watanabe[2], Tomoaki Yamada[3], Masanao Shinohara[3], Takeshi Matsushima[2] (1.Disaster Prevention Research Institute, Kyoto University, 2.Institute of Seismology and Volcanology, Kyushu University, 3.Earthquake Research Institute, The University of Tokyo)

[SCG48-P44] Unified description of fast and slow earthquakes using velocity strengthening patches

*So Ozawa[1], Takahiro Hatano[1] (1.Earthquake Research Institute, the University of Tokyo)

[SCG48-P45] The b-value of the earthquake swarm activities accompanied by the Boso slow slip events

*Yuki Noda[1], Hitoshi Hirose[2,1] (1.Department of Planetology, Faculty of Science, Kobe University , 2.Research Center for Urban Safety and Security, Kobe University)

[SCG48-P46] **Three-dimensional thermal modeling associated with subduction of the Philippine Sea plate at the Ryukyu Trench, and its relation to the occurrence of interplate seismic events**

*Nobuaki Suenaga[1], Shoichi Yoshioka[2,1], Yinfeng Ji[3] (1.Graduate School of Science, Kobe University, Japan, 2.Research Center for Urban Safety and Security, Kobe University, Japan, 3.Chinese Academy of Science, Beijin, China)

Off the Kii Peninsula Shallow Low Frequency Earthquake in 2004 revealed by Ocean Bottom Seismometer

*Koji Tamaribuchi[1], Akio Kobayashi[1], Takahito Nishimiya[1], Satoshi Annoura[2]

1. Meteorological Research Institute, 2. Japan Meteorological Agency

The 2004 off the Kii Peninsula earthquakes (Mj7.1, 7.4) occurred near the Nankai trough axis, southeast off the Kii Peninsula, Japan, on September 5, 2004. After the earthquakes, the Meteorological Research Institute conducted OBS observation to examine the aftershock distribution accurately. Although the analysis was limited to hypocenter relocation of "ordinary aftershocks", no analysis was done for slow events. In this study, it is shown that many low-frequency earthquakes (LFEs) occurred in "ordinary aftershocks" from the detailed inspection of our observation. During the observation period, the frequency of LFE gradually decreased. Since P- and S-arrival times are unclear, it is difficult to determine the distribution of the hypocenter accurately. However, by using the Amplitude Source Location (ASL; Battaglia and Aki, 2003), the LFEs are located between a splay fault and trench axis. The 2004 OBS stations are located east of the DONET, and many LFEs are detected in the 2004 OBS network. In addition, there are many very-low-frequency events (VLFEs) in the F-net waveforms with very-low-frequency band-pass filter (0.02 - 0.05 Hz) during the observation period. We found that the identified LFEs were associated with VLFEs since their amplitudes seemed to be correlated. This means that the LFEs and VLFEs show the same phenomenon. Our observations might contribute to reveal the relationship between ordinary aftershocks, slow-events, and megathrust events such as Nankai trough earthquake.

Keywords: LFE, OBS, 2004 off the Kii Peninsula earthquakes

©2019. Japan Geoscience Union. All Right Reserved.

The development of pressure vessel on gouges for rock deformation at seismic rates under water-saturated conditions

*Wei-Ting Lin[1], Li-Wei Kuo[1], Wen-Jie Wu[1], Jia-Jyun Dong[1], Yi-Hung Huang[2]

1. National Central University, 2. MATSUKI HYDRAULIC INDUSTRIAL CO. LTD

To understand earthquake mechanism and fault behavior during earthquake ruptures, experimentalists commonly conduct rock deformation tests with rotary shear apparatus (e.g., low-to high-velocity rock friction experiment, LHVR) which allow deformed at seismic rates. In general, the materials utilized for rotary shear apparatus are both cohesive rocks (e.g., gabbro and carbonate) and incohesive rocks (natural fault gouges and synthetic rock powders), while the latter are deformed at seismic rates and, commonly at low normal stresses (0.5 to 2 MPa confining with a plastic Teflon ring). However, using Teflon rings has issues of gouge extrusion and chemical contamination, in particular, at high normal stresses (>3MPa) and water-saturated condition, and the obtained mechanical data and associated experimental products seem to be questionable. Here we develop a metal pressure vessel for LHVR to deform gouges at seismic rates and, importantly, expand the normal stress capability (up to 15 MPa) and under water-saturated condition. Our results show the resistance from the pressure vessel itself (metal-to-metal contact) is extremely low (friction coefficient ≈0.02), and the result of kaolinite is similar to the previously published data. In particular, both gouge-extrusion and water-leaking was not observed deformed at a normal stress of 15 MPa and equivalent velocity 1 m/s. The designed pressure vessel could fill the gap of experimental conditions among the current used pressure vessels and complete the understanding of fault ruptures.

Keywords: pressure vessel, water-saturated condition, fault gouge, rotary shear experiment

©2019. Japan Geoscience Union. All Right Reserved.

Spatial variations of shallow very low-frequency earthquake activity along the Nankai Trough based on CMT inversion using the 3D heterogeneous model

*Shunsuke Takemura[1], Takanori Matsuzawa[1], Akemi Noda[1], Takashi Tonegawa[2], Youichi Asano[1], Takeshi Kimura[1], Katsuhiko Shiomi[1]

1. National Research Institute for Earth Science and Disaster Resilience, 2. Japan Agency for Marine-Earth Science and Technology

To reveal structural properties around the Philippine Sea plate boundary, we investigated spatial variation of shallow very low-frequency earthquake (SVLFE) activity along the Nankai Trough. By using F-net velocity seismograms for periods of 20-50s, we conducted centroid moment tensor (CMT) inversion of SVLFEs detected by array analysis of Asano et al. (2008 EPS). Our CMT method is basically same as in Takemura et al. (2018 GRL). Source grids were assumed on the boundary of the Philippine Sea plate at horizontal intervals of 0.1°. Green's functions from source grids to F-net stations were evaluated by finite-difference method simulations of seismic wave propagation within the 3D heterogeneous structure model of Takemura et al. (2019 PAGEOPH).

We applied our CMT method to SVLFEs occurred from June 2003 to May 2018. Almost of CMT solutions are low-angle thrust faulting mechanism occurred around the accretionary prism toe. We evaluated spatial variations of SVLFE activity along the Nankai trough by calculating cumulative moment at each source grid. The areas with large cumulative moments appeared near the trench axis of off the Cape Muroto, the Kii Channel and the southeastern Kii Peninsula. We found spatial correlations between cumulative moment, slip-deficit rate (Noda et al. 2018 JGR) and *S*-wave velocities (Tonegawa et al. 2017 Nature Comm.) around the Philippine Sea plate boundary. Such spatial correlations suggest that SVLFEs are effectively activated by mechanically weakening due to pore fluid at surrounding area of strongly locked zone of the Philippine Sea plate.

Acknowledgement
NIED F-net broadband velocity seismograms were used. The catalogs of slow earthquakes were downloaded from the website of slow earthquake database (Kano et al., 2018 SRL). Finite-different method simulations were conducted on the Earth Simulator at the JAMSTEC.

Keywords: Nankai Trough, Shallow very low-frequency earthquake, CMT inversion, Pore fluid pressure, Slip deficit rate

©2019. Japan Geoscience Union. All Right Reserved.

Evaluation of Magnitude and Characteristics of Seismicity of Low Frequency Earthquakes in Parkfield

*Miki Aso[1,3], Naofumi Aso[2], Satoshi Ide[1]

1. Department of Earth and Planetary Science, The University of Tokyo, 2. Tokyo Institute of Technology, School of Science, 3. OYO RMS Corporation

Over a million tectonic low frequency earthquakes (LFEs) have been found in Parkfield along the San Andreas Fault, as 88 families by Shelly and Hardebeck [2010]. Thanks to enormous event detection, interesting characteristics focusing on their event amplitudes have been reported such as the spatial variation along the fault, the exponential frequency distribution for each family, and the relationship with recurrence time [Shelly and Hardebeck, 2010; Shelly, 2010]. However, the relative size of families has not been quantified accurately, because we have to consider various factors such as radiation pattern depending on focal mechanisms, attenuation during wave propagation, and site amplification effects. For quantitative comparison of scale among differently located events, here we estimate the absolute magnitude of each event considered those effects.

We estimate the seismic moment Mo [Nm] and moment magnitude Mw of all LFE events in the catalog of Shelly [2017]. We first stack seismograms of over one million events in the catalog to improve the signal-to-noise (S/N) ratio. Then, we evaluate the absolute amplitude of the original seismograms using the stacked waveforms. Specifically, we evaluate seismic moment Mo by assuming focal mechanisms of each family, attenuation quality factor, site effect estimated by Aso et al. [2019, submitted to JpGU meeting, “Variations of Focal Mechanisms of Low Frequency Earthquake in Parkfield”], and the source time function estimated by Thomas et al. [2016]. Note that we consider the frequency-limited seismic moment Mo, though it is not exactly the same as the original definition of seismic moment measured at a lower frequency than the minimum frequency contained in one phenomenon.

As previously reported by reported by Shelly and Hardebeck [2010], LFEs in the southern part has larger magnitude. We also find that shallower events are smaller than deeper events.

Similarly, most of the frequency distribution for each family shows an exponential distribution which is also reported for LFEs in Cascadia [Sweet et al., 2014] and New Zealand [Chamberlain et al., 2014].

By comparing size and recurrence interval, the events during LFE burst (seconds interval) tend to be larger than the first event of burst, which occurs after hours-to-days quiescence. A similar tendency is found in tremor burst occurring with a longer time scale (~1-week-long) than that of LFEs (~1-minute-long) [Yabe and Ide, 2014]. These might suggest some temporal change in fault rheology and/or some characteristic spatiotemporal behavior such as Brownian slow earthquake processes [Ide, 2008].

Keywords: San Andreas Fault, Parkfield, seismicity, waveform stacking, low frequency earthquake, amplitude evaluation

©2019. Japan Geoscience Union. All Right Reserved.

Tectonic tremor catalog in the Tohoku-Hokkaido-Oki region using S-net

*Satoshi Ide[1], Tomoaki Nishikawa[2], Takanori Matsuzawa[3], Kazuaki Ohta[2], Naoki Uchida[4], Takuya NISHIMURA[2]

1. Department of Earth an Planetary Science, University of Tokyo, 2. Disaster Prevention Research Institute, Kyoto University, 3. National Research Institute for Earth Science and Disaster Resilience, 4. Graduate School of Science and International Research Institute of Disaster Science, Tohoku University

Recently, various slow earthquakes have discovered in the subduction zone off Tohoku and Hokkaido regions along the Japan Trench. In this presentation, we report the detection of tectonic tremors using the Seafloor Observation Network for Earthquakes and Tsunamis along the Japan Trench (S-net), operated by The National Research Institute for Earth Science and Disaster Resilience (NIED).

We used continuous seismograms from August 2016 to August 2018 recorded by short-period sensors at 150 S-net stations. The original data were converted to envelope waveforms and analyzed using the envelope correlation method coded by Ide (2010), for each 300 s time windows with 150 s overlap. Since the results included many ordinary earthquakes with short durations, we regarded the events with durations longer than 20 s as tremors. This number is twice longer than that used for deep tremors in western Japan, reflecting the long-lasting waves in ocean bottom observation.

We found that the detection completeness is not high due to the high seismic activity in the Japan Trench, especially after the occurrence of large earthquakes, with numerous aftershocks falsely detected. We therefore divided the study area into 18 overlapping sub-regions that cover the locations of tremor activity to solve this problem. We detected tremors in each sub-region and merged the results into one catalogue by removing one of any two events within 10 s and 1 degree of each other, depending on their root-mean-square errors. Some tremor-like signals were found near the triple junction off the Boso Peninsula at approximately 34.8˚N. However, visual inspection revealed these events to be ordinary earthquakes, which we excluded from our tremor catalogue. The resultant tremor catalogue will be available in Slow Earthquake Database (Kano et al., 2018).

Keywords: tectonic tremor, slow earthquake, ocean bottom seismometer, S-net, Japan trench

©2019. Japan Geoscience Union. All Right Reserved.

Spontaneous Slow Slip and Runaway Slip in Laboratory

*Miki Takahashi[1]

1. Institute of Earthquake and Volcano Geology, Geological Survey of Japan, AIST

Earthquake nucleation and propagation involves the acceleration of slip on a fault from a background, quasi-static, low-velocity state towards meter-per-second values. From shear experiments using brine-saturated simulated gouge composed of 80:20 wt.% mixtures of halite and muscovite (following e.g. Niemeijer & Spiers, 2007, JGR), Takahashi et al., [2017, G-cubed] recently reported a switch in the dominant deformation process, from distributed viscous flow (pressure solution creep) to localized brittle deformation, at a critical velocity V_c (~20 μm/sec). The direct effect which is normally observed upon perturbations in sliding rate disappears for $V > V_c$, suggesting that runaway fault-slip may be achieved when the sliding velocity exceeds V_c.
At relatively low shear stress, flow mechanisms, such as pressure solution creep and dislocation creep, will be fast enough to effectively suppress slip acceleration. However, with increasing the shear stress, there may be a velocity range in which flow mechanisms still works but not as effective. Hypothesizing that, under constant shear stress boundary conditions, this may lead to spontaneous acceleration followed by deceleration, analogous to a slow slip event. Moreover, imposing the constant shear stress with equal or larger value of the maximum strength of the simulated gouge, I also hypothesize that slip acceleration may proceed as $V > V_c$, inducing a dynamic weakening.
To address these hypotheses, I conducted torque-controlled rotary shear experiments, using brine-saturated, 80:20 wt % mixtures of halite (grain size < 75 μm) and muscovite (grain size < 33 μm) powders. Approximately 1.65 g of the gouge mixture was sandwiched between two teethed steel piston rings, forming an initially 1 mm thick layer. The piston rings had an inner diameter of 38 mm, and an outer diameter of 50 mm. I used a high-velocity rotary shear apparatus designed by T. Shimamoto [e.g., Togo and Shimamoto, 2012], and now installed at the Geological Survey of Japan (GSJ). The apparatus was modified to enable torque control with an accuracy of ±0.002 in the friction coefficient (μ), at a normal stress of 5 MPa. Rotation displacement is measured using a potentiometer installed close to the piston ring at the rotating side.
A preliminary result shows the velocity evolution after stepwise changes in the shear stress. At low shear stresses, corresponding to the pressure solution creep-controlled regime, transient increasing velocity towards a steady-state values suggests stable sliding. At $\mu \approx 0.6$, the simulated gouge shows spontaneous acceleration to $V \approx 1$ μm/sec, followed by deceleration. Lastly, under a constant shear stress condition equivalent to $\mu = 0.67$, spontaneous slip acceleration occurred followed by dynamic weakening at $V \approx V_c = 20$ μm/sec. More experiments and microstructural observations will help to elucidate the relationship between the critical velocity and the switch among dominant deformation mechanisms.

Keywords: shear stress control test, spontaneous acceleration/deceleration, dynamic weakening

©2019. Japan Geoscience Union. All Right Reserved.

Hydration and amorphization of quartz rocks during high-velocity frictional sliding: An examination of fault gouge from friction experiments of synthetic quartz

*Yuko Onoe[1], Hirotaka Iida[2], Akito Tsutsumi[1], Aki Takigawa[1]

1. Graduate School of Science, Kyoto University, 2. Geothermal Engineering Co., Ltd.

Various types of rocks and fault gouges display weakening of frictional strength at high-velocities, and in many cases, it is caused by high-temperature faulting processes such as frictional melting and thermal decomposition of fault materials. On the other hand, siliceous rocks display weakening of frictional strength at relatively slow slip velocity of ~1 mm/s. This weakening is a specific phenomenon because frictional heat is not sufficient to induce the high-temperature transformation reactions in this slip velocity range [Di Toro et al., 2004]. Goldsby and Tullis [2002] proposed gel lubrication model to explain the weakening of siliceous rocks; in which model frictional weakening likely results from production and shearing of hydrated amorphous silica layer along a fault in quartz rocks. But the relationship between the frictional weakening and hydration and amorphization of fault gouge is not clear yet.

This study aims to elucidate the mechanism of the frictional weakening observed for siliceous rocks. We conducted a series of friction experiments on synthetic quartz samples using a rotary-shear, intermediate-to high-velocity friction testing machine. Experiments were carried out under a constant normal stress condition of 1.5 MPa and at slip velocities of 5 μm/s, 10 μm/s, 105 μm/s, 1 mm/s, 10 mm/s and 105 mm/s. In this study effect of drying the sample on the frictional behavior were examined by introducing dry air to the chamber of the sample. After the friction tests, the gouge material on the slip surfaces were collected and analyzed by FTIR.

The frictional behavior of the synthetic quartz differs between room humidity and dry conditions; velocity weakening was observed for both conditions, however, velocity weakening starts at lower slip velocities for the dry experiments. Under DRY conditions, the frictional weakening occurs at slip velocity around 10 μm/s. From the results of the FTIR analysis, hydration of the gouge is confirmed for all the samples tested in this study. The FTIR result also indicates that the faster the slip velocity, the more the crystal structure of the gouge is destructed.
It is showed that under both DRY and Room Humidity conditions, at least the gouge generated on the friction surface of the sample which showed slip weakening is hydrated, consistent with the weakening model of Goldsby and Tullis [2002].

©2019. Japan Geoscience Union. All Right Reserved.

Constraining S Wave Velocity of the Source Region of Shallow Very Low-Frequency Earthquakes

*Takeshi Akuhara[1], Takashi Tonegawa[2]

1. Earthquake Research Institute, The University of Tokyo, 2. Research and Development center for Earthquake and Tsunami, Japan Agency for Marine-Earth Science and Technology

Shallow very low-frequency earthquakes (VLFEs), which are believed to occur in the vicinity of megathrusts, have been often associated with elevated pore fluid pressure. Lines of evidence for this idea include a small amount of stress drop, high tidal sensitivity, and reduced P wave velocity inferred from active source seismic surveys. Revealing the physical properties of the source region of shallow VLFEs will lead to a better understanding of their generation mechanisms. However, the challenge lies in the difficulty of acquiring S wave velocity in fine resolution.

Recent achievements by the authors may help overcome this issue. Akuhara et al. (2019) developed a robust technique to estimate Green's functions of receiver side structures from offshore seismograms, which are typically ill-conditioned due to water reverberations. Tonegawa et al. (2017) inverted Rayleigh wave admittance (i.e., a ratio of ground displacement to hydraulic pressure) for shallow S wave velocity structures beneath DONET seafloor observatories at the Nankai Trough subduction zone. Their velocity models show low-velocity zones that characterize the source regions of shallow VLFEs. However, a smoothing constraint imposed on the models renders their interpretation somewhat difficult.

This study presents preliminary results from transdimensional inversion of receiver-side Green's function estimated by the method of Akuhara et al. (2019), where we adopt a prior constraint by the velocity models of Tonegawa et al. (2017). Complementary to the Rayleigh admittance, the Green's function approach is sensitive to velocity contrasts and thus will offer an improved resolution.

Keywords: shallow very low frequency earthquake, seismic velocity structure, ocean bottom seismometer, bayesian analysis

©2019. Japan Geoscience Union. All Right Reserved.

Quantitative relationship between aseismic slip propagation speed and frictional properties

*Keisuke Ariyoshi[1], Jean-Paul Ampuero[2,3], Roland Burgmann[4], Toru Matsuzawa[5], Akira Hasegawa[5], Ryota Hino[5], Takane Hori[1]

1. Japan Agency for Marine-Earth Science and Technology, 2. Université Côte d'Azur, 3. California Institute of Technology, 4. University of California, Berkeley, 5. Graduate School of Science, Tohoku University

Recent observations show evidence of propagation of postseismic slip, whose propagation speed may contain information about the mechanical properties of faults. Here, we develop a new analytical relationship between the propagation speed of aseismic slip transients and fault frictional properties, modeled by a rate- and state-dependent friction law. The relationship explains the propagation speed of afterslip in 3-D numerical simulations to first order. Based on this relationship, we identify systematic dependencies of afterslip propagation speed on effective normal stress σ and frictional properties (the coefficients a and a-b which quantify the instantaneous and the steady-state velocity-dependence of friction, respectively, and the characteristic slip distance d_c of fault state evolution). Lower values of the parameter $A=a\sigma$ cause faster propagation in areas where the passage of the postseismic slip front induces large shear stress changes $\Delta\tau$ compared to A, which are typically located near the mainshock rupture. In areas where $\Delta\tau/A$ is small, typically more distant from the mainshock, afterslip propagation speed is more sensitive to (a-b) σ. The propagation speed is proportional to initial slip velocity and inversely proportional to d_c. The relationship developed here should be useful to constrain the frictional properties of faults based on observed propagation speeds, independently of rock laboratory experiments, which can then be used in predictive numerical simulations of aseismic slip phenomena.

Keywords: rate- and state-dependent friction, effective normal stress, stress perturbation

©2019. Japan Geoscience Union. All Right Reserved.

Comprehensive detection of very low frequency earthquakes off the Pacific coasts of Hokkaido and Tohoku, northeastern Japan

*Satoru Baba[1], Akiko Takeo[1], Kazushige Obara[1], Takanori Matsuzawa[2], Takuto Maeda[3]

1. Earthquake Research Institute, University of Tokyo, 2. National Research Institute for Earth Science and Disaster Resilience, 3. Graduate School of Science and Technology, Hirosaki University

Very low frequency earthquakes (VLFEs), classified as one type of slow earthquakes, occur near seismogenic zones. VLFEs off the Pacific coasts of Hokkaido and Tohoku in northeastern Japan occur around subducting plate interfaces near trenches. Asano et al. (2008) found VLFEs in the off-Tokachi region, the southern part of the Pacific coast of Hokkaido along the Kuril Trench, by array signal processing using high-sensitivity accelerometers of Hi-net operated by National Research Institute for Earth Science and Disaster Resilience (NIED). In recent years, VLFEs off the Pacific coast of Tohoku were found by visually checking broadband seismograms of F-net operated by NIED and other events were detected by the matched-filter technique using waveforms of detected events as templates (Matsuzawa et al., 2015). However, the number of detected VLFEs may have been limited because of the small number of the VLFE templates in previous studies. Baba et al. (2018, SSJ) set four virtual epicenters off the Pacific coasts of Hokkaido and Tohoku and detected VLFEs by the matched-filter technique using numerically simulated waveforms as templates. We extended virtual epicentral gridsto make more comprehensive detection of VLFEs.

We used continuous seismograms of F-net seismometers from January 2003 to July 2018 after applying a band-pass filter of 0.02–0.05 Hz. We set 123 virtual epicentral grids off the Pacific coasts of Hokkaido and Tohoku, and computed the synthetic waveform from the source at each virtual epicenter by the finite difference method with a three-dimensional velocity structure model, namely, Japan Integrated Velocity Structure Model (Koketsu et al., 2012). The fault mechanisms were assumed to be consistent with the geometry of the plate boundary and a plate motion model, NUVEL-1A. We then calculated station- and component-averaged cross-correlation coefficients (averaged CC) between synthetic waveforms and the data of F-net seismograms every 1 s, and selected the events which have averaged CC above nine times of the median absolute deviation of the distribution. This method is, however, sensitive to regular earthquakes and teleseismic events as well. We then excluded the signal of regular earthquakes by discarding events with the amplitudes of more than 160 nm/s at 1-2 Hz in vertical components at the nearest stations. Moreover, to remove teleseismic events, we used the USGS earthquake catalog and discarded events with high amplitudes and low averaged cross-correlation coefficients.

VLFE activities in the off-Tokachi and off-Aomori regions show synchronized episodic bursts in the interval of several months. VLFEs in the off-Tokachi region was rapidly increased by the afterslip of the 2003 Tokachi-Oki earthquake. Those in the off-Iwate and off-Ibaraki regions, located out of the coseismic slip area of the 2011 off the Pacific coast of Tohoku Earthquake (hereinafter, the Tohoku earthquake), were also rapidly increased by the afterslip of the Tohoku earthquake. VLFE activity in the off-Miyagi region is characterized by episodic bursts in the interval of several months to one year before the Tohoku earthquake, but it became low since then. VLFE activity in the off-Fukushima region show dramatic increase after an Mw 6.9 earthquake at off-Fukushima on July 19, 2008. In the off-Miyagi and off-Fukushima regions, located within or at the edge of the coseismic slip area of the Tohoku earthquake, VLFE activity has been low since the Tohoku earthquake probably because the earthquake released the

©2019. Japan Geoscience Union. All Right Reserved.

stress almost completely. These results suggest that VLFEs are sensitive to the stress perturbation and can be a slip meter that reflect spatiotemporal change of the interplate slip, as has been indicated by previous studies. Consequently, one possible cause of these episodic VLFE bursts in the off-Tokachi, off-Aomori and off-Miyagi regions may be the intermittent release of small portion of stress accumulated by interplate locking between plates in the interval of several months to one year. The interval of episodic bursts is shorter than a periodicity of slow slips ranging from 1 to 6 years off the Pacific coasts of Tohoku indicated by Uchida et al. (2016).

©2019. Japan Geoscience Union. All Right Reserved.

Spatio-temporal evolution of long- and short-term slow slip events in the Tokai region, central Japan estimated from a very dense GNSS network, during 1997-2017

*Hiromu Sakaue[1], Takuya NISHIMURA[2], Jun'ichi Fukuda[3], Teruyuki Kato[4]

1. Graduate School of Science, Kyoto University, 2. Disaster Prevention Research Institute Kyoto University, 3. Earthquake Research Institute,The University of Tokyo, 4. Hot Springs Research Institute of Kanagawa Prefecture

The long-term slow slip events (SSEs) have been reported on the subducting Philippine Sea Plate in the Tokai region, central Japan during 2001-2005 and 2013-2016. Many short-term slow slip events have been also observed there since 1996. We analyzed GNSS data from 1997 to 2017 to estimate spatiotemporal distribution of interplate slip associated with these SSEs in this study. The GIPSY-OASIS II software (version 6.1) was used to estimate daily coordinates of GNSS stations operated by GSI and JUNCO (the Japanese University Consortium for GPS Research). It is well known that GNSS time series have many systematic signals and noises that do not result from SSEs. They include, for example, seasonal variations, co- and post-seismic deformation of the 2004 southeast off Kii Peninsula earthquakes (M_w 7.3/7.4), the 2008 Ibaraki-ken-oki earthquake (M_w6.9), the 2008 Fukushima-ken-oki earthquake (M_w7.0) and the 2011 Tohoku-oki earthquake (M_w9.0), and crustal deformation of volcanic activity on the northern Izu Islands in 2000. After removing them, we applied a modified Network Inversion Filter (NIF) [Fukuda et al., 2008] to estimate daily slip and slip rate on the subduction plate interface.
Our results suggest that not only long-term SSEs (M_w~7.1 and M_w~6.7) in 2000-2005 and 2013-2016, but also short-term SSEs (M_w<6.1). The maximum estimated daily slip rates for short-term SSEs are an order of magnitude larger than those of the long-term SSE, and peak slip for short-term SSEs migrates along strike with LFTs synchronously. It suggests that LFTs are loaded directly by SSEs, and that slip rate regulates LFT genesis. We will present the change of back slip rate between inter short-term SSEs and characteristics of short-term SSEs (e.g. slip rates and recurrence interval) depending on the occurrence of long-term SSE.

Keywords: slow slip event, Tokai region, GNSS

©2019. Japan Geoscience Union. All Right Reserved.

Broadband excitation of acoustic emission in granular stick-slip : experiments and spectral analyses

*Hidekazu Fukumizu[1], Ikuro Sumita[2]

1. Earth and Environmental Science Course, Division of Natural System, Graduate school of Natural Science and Technology, Kanazawa University, 2. School of Geosciences and Civil Engineering, Kanazawa University

Slow slip and tremor are observed to occur simultaneously (e.g., Rogers and Dragert, Science, 2003). Such observation can be modelled using granular stick-slip experiments which show that the timing of the slips and acoustic emission (AE) are well correlated (e.g., Johnson et al., GRL, 2013, Jiang et al. GRL, 2017). AE waveforms are complex (e.g., Michlmayr & Or, Gran. Matt., 2014), and we do not fully understand the details of the temporal change of AE during the slip. Here we report the results of granular stick-slip experiments which focus on how their spectra depend on the shear rate, particle size and container size.

We shear glass beads contained in a stainless steel beaker using a rotating viscometer to which a vane spindle is attached (Higashi and Sumita, JGR, 2009), and measure the shear stress and AE at 200kHz. We use broadband accelerometers and microphones to measure AE. Four accelerometers are attached at the outer rim of the beaker, and each are separated by an angle of 90 degrees.

We integrate the acceleration to obtain AE velocity –time series data and analyze their characteristics in broad band. We find that although AE has a broad spectrum, the spectra show that there are two characteristic frequency (f) components ; a high-f (of the order of 100 Hz) and a low-f (of the order of 10Hz) components. The velocity waveforms recorded at antipodal positions, show that the high-f components are in phase, whereas the low-f components are of the opposite phase. This indicates that the mechanism which excite these components differ : the high-f component may correspond to AE excited by particle rearrangement, whereas the low-f component may correspond to the translational motion of the container. Indeed we find that the frequency of the low-f component depends on the container size.

We also conducted experiments using a rheometer in a parallel-plate setup and confirmed that these two different components exist. When the particle size becomes larger, the amplitude of the shear stress and the AE velocity increases. Furthermore we find that the mean frequency of the normalized power spectra rose to a higher frequency, thus correlating with the stress increase.

Our experiments indicate that AE is excited in broadband, and that their frequency components can be used to infer the interparticle stress. Such excitation appear to be analogous to tremors and very low frequency earthquakes that are also excited simultaneously.

Keywords: granular matter, stick-slip, acoustic emission, earthquake, tremor

©2019. Japan Geoscience Union. All Right Reserved.

Episodic tremor and slip silently invades strongly locked megathrust in the Nankai Trough

*Masayuki Kano[1], Aitaro Kato[2], Kazushige Obara[2]

1. Graduate school of science, Tohoku University, 2. Earthquake Research Institute, The University of Tokyo

Recent seismic and geodetic observations in subduction zones have revealed that slow earthquakes have preceded some large earthquakes (e.g., Kato et al., 2012; Mavrommatis et al., 2014; Ruiz et al., 2014). Characterization of slow earthquakes and their relation to large earthquakes provides important clues to constrain a wide spectrum of slip rates on tectonic faults. In this study, we report new evidence of a slow slip transient at the downdip edge of the strongly locked seismogenic zone in the western Nankai Trough in southwest Japan based on GNSS time series. This slow slip transient was remotely excited during an episodic tremor and slip at the downdip extension of the locked zone. Through this remote triggering, the frequent occurrence of the deep episodic tremor and slip invades the strongly locked megathrust zone and may intermittently increase the probability of large earthquakes in the Nankai Trough.

Acknowledgments

We used GNSS data provided by the Geospatial Information Authority of Japan. This study was supported by the JSPS KAKENHI Grant Number JP15K17743 in Grant-in-Aid for Young Scientists (B), JP18K03796 in Grant-in-Aid for Scientific Research (C), JP16H06473 and JP16H06474 in Scientific Research on Innovative Areas “Science of Slow Earthquakes.”

Keywords: Slow slip events, Slow earthquakes, Western Shikoku, GNSS

©2019. Japan Geoscience Union. All Right Reserved.

Spatial distribution of the electrical resistivity beneath western part of Shikoku Island where long-term SSE events have repeatedly occurred

*Makoto Uyeshima[1], Maki Hata[1], Hiroshi Ichihara[2], Ryokei Yoshimura[3], Koki Aizawa[4]

1. Earthquake Research Institute, The University of Tokyo, 2. Graduate School of Environmental Studies, Nagoya University, 3. Disaster Prevention Research Institute, Kyoto University, 4. Institute of Seismology and Volcanology, Faculty of Sciences, Kyushu University

In the Bungo channel area at the western margin of the Nankai megathrust rupture zones, the long-term slow slip events (SSE) repeatedly occurred about every 6 or 7 years. Since the last large-scale SSE event occurred in 2010, we will have a next large event soon. In order to obtain the electrical resistivity structure in the vicinity of the SSE area and examine its temporal change, we have started the Network-MT survey in the western part of the Shikoku Island facing the Bungo channel since April, 2016. Just before beginning of the observation, a tiny-scale SSE event occurred in the Bungo-channel (Ozawa, 2017, Hirose et al., 2018). We selected 17 areas in the western part of the Shikoku Island and installed 3 or 4 electrodes in the respective areas. The electrical potential differences with typical electrode spacing of several km are measured by using metallic telephone line network. We also measure the geomagnetic field at two stations in the target region. With the aid of the BIRRP code (Chave and Thomson, 2004), we could estimate the frequency-domain Network-MT response functions of good quality between the voltage difference and the magnetic field. The Network-MT response functions were directly inverted to estimate the 3-D resistivity structure in this area with the aid of the DASOCC Network-MT 3-D inversion code (Siripunvaraporn, Uyeshima & Egbert, 2004).

Conductive portions are commonly detected in the mid-crust of the target region. Their roots are just on the upper surface of the subducting Philippine Sea slab. This may suggest dehydration there. Among the spatial distribution of resistivity, that of seismic P-wave attenuation (Kita and Matsubara, 2016), and that of SSE slips (e.g. Ozawa et al., 2013, Yoshioka et al., 2015, Hirose et al., 2018), some mutually related features are detected. Low Qp (high attenuation) areas tend to correspond to highly conductive areas. The low Qp and highly conductive area are detected just above the subducting slab and outside of the SSE area. Inside the SSE area, while Qp takes generally high values, a patchy conductive area is detected in overall resistive background structure.

This study is supported by JSPS KAKENHI Grand Number JP16H06475 in Scientific Research on Innovative Areas "Science of Slow Earthquakes". It is also partly supported by the Ministry of Education, Culture, Sports, Science and Technology (MEXT) of Japan, under its Earthquake and Volcano Hazards Observation and Research Program. We acknowledge staffs of the Nippon Telegraph and Telephone WEST Corporation for their cordial support in the survey. We also thank H. Abe, A. Takeuchi and Y. Suwa for their help in preparing and installing instruments.

Keywords: slow slip event beneath the Bungo Channel, 3-D resistivity structure, Network-MT observation

©2019. Japan Geoscience Union. All Right Reserved.

Variations of scaling relationships for shallow tremor observed along the Nankai trough

*Masaru Nakano[1], Suguru Yabe[1]

1. Japan Agency for Marine-Earth Science and Technology

Scaling relationships of seismic phenomena is one of keys to understand the source processes. Size distributions of slow earthquakes as low-frequency earthquakes (LFEs), non-volcanic tremor (NVT), very-low-frequency earthquakes (VLFE), and slow-slip events (SSEs) have been studied in many locations. Some studies showed that the size distribution follow an exponential law (e.g. Watanabe et al., 2007; Hiramatsu et al., 2008; Chestler and Creager, 2017), while others showed that power law distributions better explain the observations (e.g. Kao et al., 2010; Bostock et al., 2015; Nakamura and Sunagawa, 2015).

Most of previous studies are for slow earthquakes that occur in regions deeper than the source region of megathrust earthquakes, and only a limited number of studies have been carried out for shallow slow earthquakes beneath accretionary prism as observed along the Nankai trough. Although observed characteristics of shallow and deep ones are very similar, physical conditions as temperature and pressure much differs in these region.

In our previous studies (Nakano et al., 2018SSJ, AGU), we obtained the result that shallow tremor follows a power law distribution with b values of about 1. In this study, we further analyzed tremor activities beneath the Muroto fore-arc basin. using data from DONET2. We estimated the seismic energy of tremor signals using the same method as our previous studies, during intensive activities starting in September 2015, April 2016, February 2017, and February 2018. The source region of each activity is different from each other, spanning between off Shiono-Misaki and off Cape Muroto.

The size distribution of each activity mostly follow power-law distributions, but the b value varies from 0.7 and 1.7. We note that the activity in 2016 is also well fitted by an exponential law, probably due to narrow range of observed event size distribution. Similar result has been obtained in the 2018 activity in Kumano. The size distribution deviate from a power law for largest events as observed in Kumano activities. This deviation at larger events would be due to limited system size, expected from the theoretical stochastic model of tremor by Ide and Yabe (2018). The upper limit of event size, and accordingly the system size, varies from activity to activity.

We also investigated the relation between the seismic energy and duration of tremor events. The relation also follows a power law, with slopes of 2.0 to 2.6 in Kumano, and 1.5 to 3.3 in Muroto. These values are again consistent with the expectation value of 2 from the model of Ide and Yabe (2018).

These investigations represent that the scaling relationships of shallow tremor are mostly consistent with the 2D PCA model by Ide and Yabe (2018). Further studies would be necessary to reproduce the observed variations of the scaling parameters.

Acknowledgments: We used DONET data and JMA and USGS earthquake catalogs in the analysis. This research was supported by JSPS KAKENHI Grant Number 16H06477 in Scientific Research on Innovative Areas “Science of Slow Earthquakes”

Keywords: DONET, Nankai trough, earthquake size distributions

©2019. Japan Geoscience Union. All Right Reserved.

Low-frequency earthquakes triggered by teleseismic surface waves by Ryukyu subduction zone.

Ayumi Kinjo[1], *Mamoru Nakamura[1]

1. Faculty of Science, University of the Ryukyus

We investigated low-frequency earthquakes (LFEs) in the Ryukyu Trench region that were triggered by surface waves from teleseismic earthquakes. Although these LFEs in the southwestern Ryukyu arc have previously been explored by Chao et al. (2016), their hypocenter distribution is not known in detail.

We selected 50 earthquakes from January 2004 to December 2016, which had magnitudes greater than 7.5 and epicentral distances between 9–150˚. We used the waveforms of 6 broadband seismometers in the Ryukyu arc from F-net (NIED) to analyze the surface waves. We also used the waveforms of 20 short-period seismometers in the Ryukyu arc from the Japan Meteorological Agency to detect trace LFEs in Ryukyu Island and determine their hypocenters.

The LFEs in the Yaeyama and Okinawa regions were observed. In the former region, during the passage of the surface waves, spindle-shaped LFE waveforms were first observed at Hateruma (south of Yaeyama Islands), and later at other stations in the Yaeyama region. Similarly, for the latter region, during the passage of the surface waves, spindle-shaped LFE waveforms were first observed at ZMM or Tamagusuku (south of Okinawa Island), and later at other stations in the Okinawa region. These observations suggest that the sources of the triggered LFEs were near or south of Hateruma and Tamagusuku.

We subsequently determined the hypocenters of the triggered LFEs. We computed the LFE travel-time difference between two stations using cross-correlations of the waveforms (Obara, 2002). The travel-time difference of waveforms of the LFEs corresponded to travel-time difference of the S-phase because S-waves were dominant in the LFEs, and P-waves were weak. The hypocenters were determined using the grid search method (Chao et al., 2013). In the Yaeyama region, the LFE hypocenters were mainly distributed near Hateruma Island. In the Okinawa region, they were distributed south of Okinawa Island. These positions are similar to the positions of the LFE hypocenters that accompany very low frequency earthquakes (LFE-VLFEs). This suggests that faulting in a cluster of LFE-VLFEs would be active with dynamic stress change.

In the Okinawa and Yaeyama regions, LFEs are triggered when the peak ground velocity of the surface wave is greater than 0.1 cm/s. This threshold value is similar to that for LFEs in Taiwan (Chao et al., 2013), suggesting that the weak friction coefficient at the plate interface of the Ryukyu Trench is similar to that in Taiwan.

Keywords: low frequency earthquake, surface wave, Ryukyu Trench

©2019. Japan Geoscience Union. All Right Reserved.

Detection of small surface displacement accompanying deep low-frequency tremor in Shikoku region, southwest Japan

*Yutaro Okada[1], Takao Tabei[2]

1. Faculty of Science, Kochi University, 2. Faculty of Science and Technology, Kochi University

In many subduction zones in the world, several types of slow earthquakes occur with different depths on the plate interface and some of them are accompanied by surface displacement. In this study, we focus on small surface displacements coincident with non-volcanic deep low-frequency tremor in Shikoku region in the Nankai subduction zone, southwest Japan.

We use daily coordinates time series from 107 GEONET stations located in Shikoku and tremor catalog compiled by NIED (Maeda and Obara, 2009; Obara et al., 2010) in the period from Jan. 1 2004 to Dec. 31 2008. Since GNSS coordinates changes due to the Bungo Channel long-term slow slip events are well reproduced by S-shaped logistic function, we use the same function to extract small displacement coincident with tremor activity. At first, we convert horizonal components into N50°W direction after removing annual and semiannual variations and common-mode errors. Next, we fit the logistic function to a data segment with variable time window of 5, 7, and 9 days and estimate an amplitude of the function. The fitting is checked by a correlation coefficient between the observation and calculation. We apply this fitting for entire data period at all stations sliding data segment. Finally, we extract displacement when the amplitude of the fitted logistic function exceeds a certain criterion (1.8 mm in this study) and the correlation coefficient is large enough. If the extracted displacement is coincident with tremor activity within 30 m from the GNSS station, we adopt it as the tremor-related displacement. As a result, 225 events are adopted.

Spatial pattern of the tremor-related displacement seems to be related with the location and mechanism of the tremor event though closer inspection is needed. However, we extract much more small displacements by fitting a logistic function, of which the source is unknown. The logistic function is effective to reproduce transient displacement of the surface but we need to reconsider noise reduction of GNSS time series, time constant of logistic function, time window of the fitting, and so on.

Keywords: GNSS, southwest Japan, Deep low frequency tremor

©2019. Japan Geoscience Union. All Right Reserved.

Long-term temporal change in crustal resistivity beneath western Shikoku

*Futoshi Yamashita[1], Yoshimori Honkura[1]

1. National Research Institute for Earth Science and Disaster Resilience

In southwest Japan, various slow earthquakes such as deep low-frequency tremor and short/long-term slow slip events occur at the subducting plate interface (e.g. Obara and Kato, 2016, Scinence). In western Shikoku, Magneto-telluric (MT) survey was carried out along the dip direction of subducting Philippine Sea plate. The survey revealed an existence of low-resistivity structure in the lower crust in this region (Yamashita and Obara, 2009, AGU). In order to investigate a relationship between this characteristic structure and the activity of slow earthquakes, NIED has been carrying out continuous MT observations in western Shikoku since 2008. Here we show the observational records over 10 years and then discuss a relationship between observed temporal change in crustal resistivity and activity of the long-term slow slip event (L-SSE). Two observational sites KBN and IKT are available as of 2019. Qualities of data recorded at these sites are relatively fine. However, in order to improve the quality for discussing subtle change in MT parameters, we apply a data processing method same as Honkura *et al.* (2013, Nature comm.); we use only data whose coherency between electric and magnetic field is higher than a threshold. The lowest frequency of processed data is 0.00028 Hz. The processed MT parameters, apparent resistivity and phase, do not show any long-term temporal changes at KBN site even after temporal stops of observation over some months. On the other hand, apparent resistivity at IKT site, which is around 10 km southwest away from KBN site, shows temporal reduction at a frequency lower than 0.0022 Hz between 2010 and the middle of 2012. It is known that L-SSE occurred beneath the Bungo Channel in 2010 (e.g. Yoshioka *et al.*, 2015, GJI), which could induce resistivity change in the lower crust and then it might be detected by our MT observation.

Keywords: Crustal resistivity, Long-term slow slip event, Magneto-telluric method

©2019. Japan Geoscience Union. All Right Reserved.

Slow decay of postseismic deformation compared with aftershocks following the 2011 Tohoku-oki Earthquake

*Yuta Mitsui[1], Shunsuke Morikami[2]

1. Department of Geosciences, Shizuoka University, 2. Formerly at Graduate School of Science and Technology, Shizuoka University

In the literature, decays of postseismic deformation rates of large earthquakes were almost comparable to aftershock decays for subduction earthquakes (e.g. Hsu et al. (2006), Lange et al. (2014)). They are characterized by the modified Omori law with p~1, which means "afterslip-triggerred aftershocks". In this study, we focus on the 2011 Tohoku-oki megathrust earthquake using GNSS and seismicity data. On the basis of high-rate analysis of RINEX data and the F3 solution provided by the Geographical Survey Institute (GSI), we clarify the characteristics of postseismic deformation and aftershocks up to five orders of magnitude of time scale. We find that the p value for the postseismic deformation (p_m) is ~0.7, by contrast, that for the aftershocks (p_n) is ~1. Because a rate-and-state-friction model (Helmstetter and Shaw (2009)) predicted $p_m>=p_n$, another or an additional physical mechanism is necessary to explain the data of $p_m<p_n$. One important mechanism is viscoelastic relaxation of asthenosphere, thus we try fitting the postseismic deformation data by combination of afterslip and viscoelastic relaxation (a model of Suito (2017)). The fitting is not poor but fails to reproduce the Omori-like decay. More complex combination models may improve the fitting, but would not make simple Omori-like power-law decays. We need more sophisticated physical model to represent the decay characteristics of postseismic deformation.

Keywords: aftershocks, postseismic deformation, afterslip, viscoelastic relaxation, the 2011 Tohoku Earthquake

©2019. Japan Geoscience Union. All Right Reserved.

Serpentinite dehydration in subduction shear zones formed at source depths of slow earthquakes

*Yasushi Mori[1], Miki Shigeno[1], Kohtaro Ujiie[2], Kazuya Noro[2], Tadao Nishiyama[3]

1. Kitakyushu Museum of Natural History and Human History, 2. University of Tsukuba, 3. Kumamoto University

Long-term slow slip events (L-SSEs) and episodic tremor and slip (ETS) occur along the subduction plate boundary at depths of 30–45 km (Obara, 2002; Shelly et al., 2006). These deep slow earthquakes are probably induced by high pore-fluid pressure. Based on geological study, we propose that the high pore-fluid pressure can be produced by metasomatic dehydration of serpentinite in subduction shear zones at source depths of deep slow earthquakes.

The Nishisonogi metamorphic rocks in Kyushu, Japan, are part of a Late Cretaceous subduction complex metamorphosed at $P \approx 1$ GPa and $T \approx 470$ ˚C. The P-T conditions are close to those of source depths of deep slow earthquakes. Serpentinite mélanges intercalated with the metamorphic rocks contain blocks of metabasite, metapelite and albitite. The mélange matrix consists of chlorite-actinolite schist (CAS), talc schist and schistose serpentinite. Intense shear deformation is concentrated in the CAS, and the serpentinite mélanges have the characteristics of anastomosing shear zones.

Bulk chemical composition of the rocks suggests that the CAS is the metasomatized mixture of serpentinite and metabasite. In addition, chemical mass balance indicates considerable dehydration during the CAS formation, along with a slight increase of solid volume. These findings suggest that the CAS formation involves the build-up of pore-fluid pressure. The high pore-fluid pressure results in the concentration of shear deformation into the weakened CAS.

Dehydration of serpentinite probably plays a key role in deep slow earthquakes (Poulet et al., 2014; Okazaki and Katayama, 2015). Thermal dehydration of serpentinite occurs at ~600 ˚C along the subduction plate boundary (Auzende et al., 2006), which is much higher temperature than that of source depths of deep slow earthquakes. In contrast, metasomatic dehydration of serpentinite described here could occur at source depths of deep slow earthquakes.

Auzende, A-L., et al., 2006, EJM, 18, 21–33. Obara, K., 2002, Science, 296, 1679–1681. Okazaki, K., Katayama, I, 2015, GRL, 42, 1099–1104. Poulet, T., et al., 2014, JGR, 119, 4606–4625. Shelly, D.R., et al., 2006, Nature, 442, 188–191.

Keywords: serpentinite mélange, shear zone, dehydration, pore fluid pressure, Nishisonogi metamorphic rocks, deep slow earthquakes

©2019. Japan Geoscience Union. All Right Reserved.

Earthquake swarms following very low-frequency earthquakes in the central Ryukyu Trench

*Mamoru Nakamura[1]

1. Faculty of Science, University of the Ryukyus

Earthquake swarms occur frequently from Amami Island to Okinawa Island, near the axis of the central Ryukyu Trench. These earthquake swarms recur every few years and typically followed swarms of very-low frequency earthquakes (VLFE) that occur in a similar area. I have investigated the relationship between the VLFEs and the subsequent earthquake swarms in the central Ryukyu Trench, using the earthquake catalog provided by the Japan Meteorological Agency (JMA). For the VLFEs, I used the catalog by Nakamura and Sunagawa (2015) and the extended catalog to December 2018.

Results show that the VLFE swarms occurred approximately one month before the subsequent earthquake swarms began near the trench axis in this region. Previous noteworthy earthquake swarms occurred on August 2005 (with a maximum magnitude of 4.7), April 2009 (with a maximum magnitude of 5.1), May 2016 (with a maximum magnitude of 5.6), and September 2018 (with a maximum magnitude of 6.2).

Prior to the earthquake swarm that occurred in August 2005, a VLFE swarm started near Okinawa Island three months before and its activity moved intermittently from Okinawa Island to Amami Island. In the case of the earthquake swarm that occurred in April 2009, a VLFE swarm started near Amami Island and the subsequent swarm occurred two weeks after the start of the VLFE swarm. The location of the VLFE swarm moved intermittently closer to Okinawa Island. In the case of the earthquake swarm that occurred on May 2016, the VLFE swarm started near Amami Island and its active cluster moved intermittently towards Okinawa Island. The subsequent earthquake swarm started near the trench axis, approximately twenty days after the occurrence of the VLFE swarm. In the case of the earthquake swarm that occurred in September 2018, the VLFE swarm started near Okinoerabu Island (the midpoint between Amami Island and Okinawa Island) and the activity moved intermittently to Okinawa Island. The earthquake swarm occurred approximately twenty-five days after the start of the VLFE swarm. The location of the cluster of the 2018 earthquake swarm was slightly landward from the trench axis.

The faulting associated with these earthquake swarms was of normal type, corresponding to intra-slab earthquakes in the subducting Philippine Sea plate. I calculated the Coulomb Failure Stress (delta-CFS) assuming that a small slow slip event (SSE) occurred on the plate interface. Our results show that the positive delta-CFS that accelerated the normal faulting could not have occurred in the subducted slab near the trench axis until the slip of the SSE had reached close to the trench axis. This suggests that the SSE propagated from Amami Island to Okinawa Island accompanying the activation of the VLFE swarm, the slip of the SSE then propagated close to the trench axis, and the normal-faulting earthquake swarm in the slab was induced by the positive delta-CFS caused by the SSE.

Keywords: Very low frequency earthquake, Ryukyu Trench, Earthquake swarm

©2019. Japan Geoscience Union. All Right Reserved.

Seismic imaging in the central Nankai trough, off Shionomisaki to Kii channel

*Yasuyuki Nakamura[1], Shuichi Kodaira[1], Tetsuo No[1], Yuka Kaiho[1], Gou Fujie[1], Seiichi Miura[1], Kazuya Shiraishi[1]

1. Japan Agency for Marine Earth Science and Technology

Shallow very low frequency events (sVLFE) have been reported in the Nankai Trough subduction zone recently. In the central part of the Nankai trough, sVLFE were observed off Kii channel and Shinomisaki, but not reported in the area between them, off western Kii peninsula. We conducted a seismic survey with R/V *Kaimei* in November and December 2018 in Nankai subduction zone off Kii channel to Shonomisaki to investigate the structural features and its possible relationship to the sVLFE. R/V *Kaimei* fired 10600 $inch^3$ air gun array at every 50 m and a streamer cable (4.3 km at shortest, 5.7 km at longest) recorded the seismic signals. We acquired 23 seismic profiles with the length of ~ 75 km in dip direction at 4 km line separation and four profiles of ~ 90 km in strike direction at the shallowest part of the subduction zone. In addition, seven dip profiles with the length of 35 km were acquired off Kii channel to cover the lowermost part of the landward slope densely. The streamer cable was towed at a depth of 25 m to relatively enhance the lower frequency signals for better imaging of the deeper structure. Preliminary processed seismic profiles exhibited the structural variation in the survey area. Deformation of the hanging wall sediments and decollement were well imaged especially ~ 20 –30 km from the trough axis. Top of subducting Philippine Sea plate can be observed through ~ 40 –50 km from the trough axis in some of the obtained profiles. A pair of apparently low angle deep strong reflections were imaged at ~ 7 –8 s two-way time around 40 - 50 km from the trough axis off the western Kii peninsula, which was located slightly east and landward of the area with sVLFE. The shallowest part of the subduction zone in the area where the recent sVLFE activity was not reported, a slope basin with younger sediments deposited over the body of the accretionary prism is imaged, and the deformation was not observed in the slope basin. This suggests the thrust faults within the accretionary prism have not been active recently in this area. We will further process acquired data to obtain clearer seismic images and discuss the structural features and its connection to the observed seismological events in the Nankai Trough.

Keywords: Nankai Trough, seismic imaging

©2019. Japan Geoscience Union. All Right Reserved.

Attempt to Detect Intra-plate SSEs Based on F3 Solution of GEONET

*Yusaku Tanaka[1]

1. Earthquake Research Institute

Slow earthquakes have been detected all over the world and providing new insights into earthquakes. However, most of slow slip events (SSEs) were detected only on plate boundaries and intra-plate SSE was detected only once in Hokkaido. Thus, I attempt to detect intra-plate SSEs all over Japan using F3 solution of GEONET by GSI. I analyze the F3 data with six steps, i.e., (1) removing outliers by setting a term of mean + two times standard deviation for 1/4+1/4 year before-and-after each datum except for the datum itself and considering it is an outlier when it is out of the term, (2) removing disconnections estimated from the offsets and linear trends of 60+60 days before-and-after each datum with the least square method, (3) searching statistically significant temporal changes of the trends by using AIC, (4) cheking visually the time series in which the temporal changes are detected, (5) estimating the displacements from the trend chagnes, and (6) verifying the deformations by numerical calculation by setting rectangular faults.

As of 18th Feb 2019, my study has proceeded to the step (4). In the JpGU meeting, I will report the results of this analysis.

Keywords: crustal deformation, slow slip event, geonet

©2019. Japan Geoscience Union. All Right Reserved.

A new hydrothermal, low to high speed rotary-shearing apparatus: Reproduction of slow/megathrust earthquakes in laboratory

*Takehiro Hirose[1], Wataru Tanikawa[1], Yohei Hamada[1], Keishi Okazaki[1]

1. Kochi Institute for Core Sample Research, Japan Agency for Marine-Earth Science and Technology

Earthquakes involve a wide range of slip rates, from slow/aseismic to fast/seismic slip along faults. Thus, frictional properties of faults over wide slip rates (nm/s to m/s), in particular under hydrothermal conditions similar to those expected in seismogenic zones are essential for a unified understanding of all earthquake events. A new hydrothermal, low to high speed rotary-shearing apparatus has been installed at Kochi/JAMSTEC, in order to study the fault constitutive properties at slow to fast slip rates and the physicochemical mechanisms underlying mechanical responses. The apparatus is currently capable of applying slip rates from 100 nm/s to 2 m/s, normal stress up to 55 MPa, fluid pressure up to 120 MPa and temperature up to 450oC with infinite displacement. We have been improving the apparatus to work as we intended. In pilot tests, we used metamorphic rocks (pelitic and green schists) as starting materials that are potentially distributed at and below seismogenic zones along hot and young subduction zones. We will present our preliminary results with the basic design of the apparatus.

Keywords: friction, hydrothermal, slow to fast slip

©2019. Japan Geoscience Union. All Right Reserved.

Very low-frequency earthquakes in western Shikoku remotely triggered by the 2016 Mw5.9 off-Kii Peninsula earthquake

*Masatoshi Miyazawa[1]

1. Disaster Prevention Research Institute, Kyoto University

Slow tectonic events are known to be sensitive to external stress perturbations due to passing seismic waves and earth tides. High-amplitude surface waves from large earthquakes have transiently triggered low-frequency earthquakes (LFEs) and slow slip events (SSEs) in subduction zones. However, dynamic triggering of very low-frequency (VLF) earthquakes during the arrival of seismic waves from a large, distant earthquake has not been observed. Because both the VLF earthquake and the surface wave have similar characteristic periods, remote triggering is not easily detected by using existing methods. We developed a particle filter/smoother for time series analysis combined with Markov chain Monte-Carlo methods, to detect seismic signals and estimate the maximum likelihood source parameters of VLF events that might have been remotely triggered. We apply this method to seismic data from the Mw5.9 earthquake, which occurred on 1 April 2016 (UTC), off Kii Peninsula. We found that six VLF events with magnitudes about 4, likely occurred in the seismogenic regions of ambient LFEs, and were likely triggered by the arrivals of high-amplitude surface waves. The triggering stress changes are from 0.4 to 1.5 kPa, which are similar to the values for LFEs triggering reported previously. Since there were no triggered LFEs in western Shikoku following the 2016 earthquake, these VLF earthquakes are more sensitive to stress changes caused by surface waves from large earthquakes.

Keywords: Very low-frequency earthquake, Remote triggering

©2019. Japan Geoscience Union. All Right Reserved.

Underground structure around source region of slow earthquakes in western Shikoku obtained by receiver function analysis

Akira Hikita[1], Aitaro Kato[1], *Kazushige Obara[1], Akiko Takeo[1], Takeshi Akuhara[1]

1. Earthquake Research Institute, The University of Tokyo

Various types of slow earthquakes have been observed at subduction zones surrounding the Pacific Ocean. It has been suggested that elevated pore fluid pressure plays an essential role in the generation of slow earthquakes because low velocity or high Vp/Vs zones have been also reported along the plate boundaries where they occur. In Tokai region of the Nankai subduction zone, Kato et al. (2010) revealed that long-term slow slip event (SSE) occurs at the boundary between the continental lower crust and the subducting Philippine Sea plate and episodic tremor and slip (ETS) occurs between the mantle wedge and the subducting plate. Kato et al (2010) also revealed that oceanic crust indicates higher Vp/Vs in the long-term SSE region than in the ETS region. In contrast, Toya et al. (2017) reported that the oceanic crust indicates higher Vp/Vs in the ETS region than in the long-term SSE region in western Shikoku of the same subduction zone. In this study, we revealed configurations of continental Moho discontinuity and subducting oceanic crust and investigated relationship between slow earthquakes and the surrounding seismic velocity structure by receiver function analysis using a dense seismic array in western Shikoku.

As a result, continuous continental Moho and oceanic crust are clearly imaged along both north-south and east-west oriented seismic lines. The plate boundary in the south part, where the distinct continental Moho is not imaged, has steeper slope than the north part along the north-south line. ETS occurs between the mantle wedge and the subducting plate, and long-term SSE occurs along a contact between the continental crust and the oceanic crust.
We show that the oceanic crust indicates much higher Vp/Vs than the hanging wall by using also the reverberation phases. This high Vp/Vs means the elevated fluid pore pressure within oceanic crust due to dehydration. Vp/Vs in the oceanic crust is higher in the deep part of the long-term SSE region than in the ETS region like as the case of Tokai. It is assumed that fluid would accumulate within the oceanic crust owing to low permeability of the continental crust in the long-term SSE region. In contrast, serpentinization of the mantle wedge just above the ETS region could reduce fluid pressure in the oceanic crust. Furthermore, Vp/Vs in the oceanic crust becomes lower in the deeper part beyond the ETS depths, suggesting that eclogization is completed at the depths.

Keywords: Receiver function, episodic tremor and slip, long-term slow slip event, low seismic velocity layer

©2019. Japan Geoscience Union. All Right Reserved.

Hypocenter determination of deep low frequency tremors beneath the Kii Peninsula by backprojection of seismic array data

*Kodai Sagae[1], Hisashi Nakahara[1], Takeshi Nishimura[1], Kazutoshi Imanishi[2]

1. Graduate School of Science,Tohoku University, 2. National Institute of Advanced Industrial Science and Technology (AIST)

A seismic array analysis enables us to detect weak signals if they are coherent. In Cascadia, a high accuracy hypocenter determination of tremors has been carried out by using dense seismic arrays (e.g.,Ghosh et al.,2012). In Southwest Japan, previous studies (e.g.,Ueno et al.,2010) applied the **MU**ltiple **SI**gnal **C**lassification (MUSIC) method (Schmidt,1986) to data of surface seismic arrays at Western Shikoku and carried out the hypocenter determination. However, a quantitative threshold for event detection was not considered. Sagae et al.,(2018 SSJ) introduced an event detection threshold based on the coherence of waveforms among stations, and improved tremor detection by using a surface seismic array installed by AIST at the Kii Peninsula. We applied the MUSIC method to this data in times when tremor events were detected and estimated slownesses and arrival azimuths of tremor signals. Their temporal variations suggested tremor migration. However, we did not carry out hypocenter determination. In this study, we determine hypocenters of tremors by backprojection using the estimated slownesses and arrival azimuths.
The surface seismic array installed by AIST at the Kii Peninsula was composed of 39 three component velocity sensors with a natural frequency of 2.0 Hz and a sampling frequency of 200 Hz. This array had an aperture of about 1.5 km and the sensors were arranged in a cross shape with interval spacings of 50~100 m. We analyze data for 1 year (between July 7,2013 and July 7,2014), because the number of sensors is stable in this period.
We focus on a frequency of 3Hz, which is within the tremor's dominant frequency band of 2-10 Hz. Data processing is described as follows. (1) We calculate averaged coherence of waveforms for all station's pairs. (2) We detect tremor events by setting a detection threshold based on the averaged coherence. (3) We estimate slownesses and arrival azimuths by applying the MUSIC method to the data when tremors are detected. (4) We project them back to the plate boundary (Hirose et al.,2008) and determine source locations by using S wave velocity model JMA2001 (Ueno et al.,2002).
We detected 5 periods of high tremor activities during the 1 year period. We compared the hypocenter distributions determined by our method and those of AIST tremor catalogue which were determined from an envelope cross correlation method. Temporal variation of tremors in this study were almost consistent with the AIST catalogue. We were also able to detect about 2.5 times as many events as the AIST catalogue. It is easier to identify temporal variation of tremors in more detail because our study improved temporal resolution up to 10 sec.
We projected temporal variations of tremor distributions into along-strike and along-dip directions. The results show tremors tend to migrate along the strike in time scales of several days with migration velocities of 6.0~9.3 km/day. Along-dip migrations of tremors with a short timescale of several hours are also detected. When we focused on the initial part of tremor activities, tremors tend to start in deeper parts and gradually migrate to shallow parts. These migration velocities were estimated to be about 1.0 km/hr (24 km/day) in the up-dip direction.
In this study, we were able to improve tremor detection by setting the event detection threshold based on the coherence of seismograms for stations pairs in a surface seismic array. Thanks to this, we were able to locate 2.5 times more tremors than the conventional method. We made it easier to keep track of tremor migrations by improving the temporal resolution of hypocenter determination to 10 sec.
We used the plate boundary model (Hirose et al.,2008). We downloaded the AIST catalogue from Slow

©2019. Japan Geoscience Union. All Right Reserved.

Earthquake Database (Kano et al.,2018).

Keywords: Deep low frequency tremor, Seismic array analysis, Backprojection, MUSIC method, Kii Peninsula, Hypocenter determination

©2019. Japan Geoscience Union. All Right Reserved.

Triggered tremors and stress perturbations due to surface waves

*Ryohei Ikeda[1], Naoki Suda[1]

1. Hiroshima University

Surface waves radiated from distant large earthquakes sometimes trigger a series of deep non-volcanic tremors with intervals of 20-30 seconds, which are the same as dominant periods of surface waves [e.g. Miyazawa & Brodsky 2008]. Understanding the triggering mechanism is important because it provides us clues to the slip process occurring along the transition zone of subducting plate interface. Dynamic stress perturbations due to surface waves that triggered tremors were estimated on the order of 1 to 10 kPa [e.g. Chao & Obara 2016]. To study the relationship between triggered tremors and stress perturbations due to surface waves, we computed theoretical dynamic stresses due to surface waves from large earthquakes by using observed and theoretical surface waves.

We focused on the triggered tremors in the western Shikoku region of the Nankai subduction zone. Most of them occurred in two clusters where tectonic tremors actively occur. We computed theoretical dynamic stress perturbations due to surface waves from 106 earthquakes between 2004 and 2016 with moment magnitudes of 7.0 or grater. The receiver points at which the stress components were computed are at the plate boundary below the N.TSAF and N.KWBH stations, which are the nearest stations of the triggered tremors in F-net and Hi-net, respectively. PREM [Dziewonski & Anderson 1981] and Global CMT catalog [Dziewonski et al. 1981; Ekstrom et al. 2012] were used for the Earth model and the seismic sources for computing theoretical surface waves. Source time functions were approximated with triangular functions whose half durations are equal to the centroid time lags.

The stress change at the plate boundary by the surface wave was estimated based on the method of Spudich et al. (1995). This method consists of two stages: (1) Estimate the stress at the surface from the observed ground velocity and (2) Estimate the stress at the plate boundary from the stress at the surface estimated in (1). In these estimations, we used theoretical proportional relations between the ground velocity and the surface stress and those between the surface and the deep stresses in the frequency domain, which were obtained from the theoretical surface waves. We used the N.TSAF and N.KWBH records as the observed ground velocity. The records from the latter were corrected using the method of Maeda et al. (2011).

The stress components in the source coordinates were transformed to the stress normal to the plate interface and the stress along the possible slip direction of tremor source. The normal and slip directions were obtained from the model plate interface [Baba et al. 2002; Nakajima & Hasegawa 2007; Hirose et al. 2008] and plate convergence vectors [Miyazaki & Heki 2001]. We computed waveforms of the Coulomb failure function (ΔCFF) using a frictional coefficient of 0.2 at periods between 20 and 50 seconds.

©2019. Japan Geoscience Union. All Right Reserved.

Results from the N.TSAF records show that the maximum ΔCFF for the events that triggered tremors are greater than 0.5 kPa. The magnitudes of triggering earthquakes are greater than 7.5. ΔCFFs were generally overestimated when we used the corrected N.KWBH records because the correction did not well work, in particular, for the earthquakes with magnitudes less than 7.5. The important point is that not all of the events that provided the stress perturbations greater than 0.5 kPa triggered tremors. This shows that the stress perturbation due to surface waves cannot be the unique triggering condition: other conditions, for example, stress perturbations due to possible background slow slip events and/or high pore fluid pressure are required.

©2019. Japan Geoscience Union. All Right Reserved.

Numerical modeling of long- and shallow slow slip events including shallow region in Hyuganada and western Nankai, Japan

*Takanori Matsuzawa[1], Bunichiro Shibazaki[2]

1. National Research Institute for Earth Science and Disaster Resilience, 2. Building Research Institute

Recent studies reported deep long-term slow slip events (SSEs) in the Hyuganada and western Nankai region (e.g., Kobayashi, 2014; Takagi et al., 2016; Ozawa. 2017). Shallow SSEs are also recently reported with low-frequency tremor and very low-frequency earthquakes (e.g., Araki et al., 2017; Nakano et al., 2018). In our previous study, we have numerically reproduced recurring deep long- and short-term SSEs in the Shikoku region (Matsuzawa et al., 2013), considering the actual distribution of slow earthquakes and configuration of the subducting Philippine Sea plate. We aim to reproduce deep long- and short-term SSEs and shallow SSEs in a single numerical model applying a similar approach in Matsuzawa et al. (2013).

We adopt a rate- and state-dependent friction law (RS-law) with cutoff velocities. We assume that (a-b) value in the RS-law is negative within the deep short-term SSE region, and positive outside that region. The deep short-term SSE region is modeled based on the actual distribution of deep low frequency tremor. Deep long-term SSE region is assumed based on the geodetic observation (Hirose et al., 2011). To focus on the Hyuganada and western Nankai region, we assume stable sliding region with positive (a-b) in the south of the Kyushu-Palau ridge. We also assume low cutoff velocity at the depth shallower than 9 km to reproduce shallow SSEs. Low effective normal stress is assumed at the depth of SSEs. Temporal evolution of slip velocity is numerically simulated, introducing elastic response and realistic configuration of the plate interface.

In terms of deep long-term SSEs in Hyuganada, a simple extension of the long-term SSE region in the Bungo Channel cannot reproduce the segments of observed SSEs. Narrowed long-term SSE region in the dip direction between Bungo and southern Hyuganada can reproduce three observed segments of SSEs, i.e., Bungo, northern Hyuganada, and southern Hyuganada. In addition, recurring shallow SSEs along trench in Hyuganada and off Ashizuri are reproduced in our result. Megathrust earthquakes are divided into two regions; off Shikoku and Hyuganada in our result. The segments of these large earthquakes may be attributed to the long-term SSE region in the Bungo Channel. Our model comprehensively reproduces various SSEs and megathrust earthquakes, including newly found long-term SSEs.

Keywords: Slow Earthquake, Slow Slip Event, Hyuganada

©2019. Japan Geoscience Union. All Right Reserved.

Further evidence for the influence of a subducting-ridge on the spatial strain accumulation and release pattern in the shallow eastern Nankai Trough, based on VLFE distribution

*Akiko Toh[1], Chen Wan-Jou [2], Doug Dreger[3], Wu-Cheng Chi[2], Satoshi Ide[1]

1. University of Tokyo, 2. Institute of Earth Sciences, Academia Sinica, 3. UC Berkeley

We investigated the distribution and focal mechanisms of very low frequency earthquakes (VLFEs) located in the shallow part of the eastern Nankai trough. While they are mainly explained as low angle thrust faulting along the plate boundary (Sugioka et al., 2012; Nakano et al, 2016), along the strike variation in their distribution has also been observed, likely caused by a subducting-ridge (Toh et al., 2018). Such variations could be closely related to the strain release pattern, or the tsunamigenic potential, of this region, thus warrant a further comprehensive study.

We used 3 component records of broadband ocean bottom seismometers equipped in Dense Oceanfloor Network system for Earthquakes and Tsunamis 1 (DONET1). Records of VLFE activities that occurred immediately beneath the network in 2015, 2016 and 2017 for 1-2 weeks each year, are used. Through visual inspections, we detected 335 VLFEs whose signals are observed at least 6 stations on vertical component filtered between 16-32s.

Instead of estimating the source parameters for one after another for all the events, we searched for densely located event groups inferred by similarities of the maximum amplitude variations measured per event, and, so far, worked only on the grouped events. The purpose of this event selection process is to get an overview of the distribution using the simple quantity (i.e. max. amplitude variation) that can be evaluated for every VLFE, and to avoid a bias that may be caused by eliminating events that are merely difficult to process (i.e. do not fit synthetic waveforms) mostly due to complicated long source time functions that characterize VLFEs. The grouping is conducted by a hieratical density-based clustering method HDBSCAN (Campello et al., 2003), and 197 events were grouped into 26 groups that consists of 2 to 35 events.

We determined the centroid origin time, location and 5-component of moment tensor of VLFEs that maximize the normalized variance reduction (VR) between the observed and synthetic velocity waveforms. The waveforms are bandpass filtered either between 16-32s or 20-50s, depending on signal duration and S/N per event. The time and location are grid-searched at intervals of 0.01 degree in horizontal, 1 km in depth between 5 and 10km bsl., and 1 s in time. At each grid, the moment tensor is estimated using the code TDMT_INV (Dreger, 2003) that conducts full-waveform linearized inversion in time domain. Green’s functions are calculated using the code by Herrmann (2013) based on wavenumber integration. We used a 1D structural model based on a 2D model obtained by an active source survey (Nakanishi et al., 2008). Although the 1D structure is assumed, the large variations in station elevation (1.9-4.3 km bsl) are considered in Green’s function calculations.

We obtained 50 events with good VR (>65%). Among the 26 groups, 6 groups ended up with no events of high VR, mostly due to being located outside of the network. Almost all the VLFEs are reasonably explained by low angle thrust faulting. From the obtained distribution, the strong influence of the subduction-ridge located on the northwestern side of DONET1 is inferred. On the southwestern side

©2019. Japan Geoscience Union. All Right Reserved.

where there is no ridge-subduction, VLFEs are distributed beneath outer-ridge toward the trench axis. The estimated depths for the ones located beneath the outer-ridge are deep (7–10km with median at 8km), which are consistent with the depth of the plate boundary of this area. In contrast, on the northeastern side, VLFEs are mostly distributed landward of outer-ridge and their estimated depth are shallow (5–8km with the median at 7km) as previously suggested (To et al., 2015). The shallow depths can be explained by the uplifted plate boundary in this area due to the subducting-ridge. Furthermore, they are located to landward of the peak of the subducting-ridge, which can be reasonably explained by the change in shear stresses and pore pressures caused by the subducting-ridge.

Keywords: Nankai trough, Very low frequency earthquake (VLFE), Accretionary prism, HDBSCAN, Broadband ocean bottom seismometer

©2019. Japan Geoscience Union. All Right Reserved.

Evidence for semi-brittle flow in mantle-wedge serpentinites under high pore fluid pressure and their implications for deep low frequency earthquakes

Kengo Kataoka[1], Yurina Nagata[1], *Ken-ichi Hirauchi[1], Ryosuke Oyanagi[2], Atsushi Okamoto[3], Katsuyoshi Michibayashi[4]

1. Department of Geosciences, Faculty of Science, Shizuoka University, 2. Japan Agency for Marine-Earth Science and Technology, 3. Graduate School of Environmental studies, Tohoku University, 4. Department of Earth and Planetary Sciences, Nagoya University

In southwest Japan, deep low frequency earthquakes occur at the base of the shallow serpentinized mantle wedge. In order to understand deformation styles of the mantle wedge serpentinite, we conducted structural and petrological analysis of a paleo-mantle wedge body that has experienced serpentinization at pressure–temperature conditions corresponding to source areas of low-frequency earthquakes, in the Sanbagawa belt, central Shikoku. The serpentinite body has a block-in-matrix structure that result from pervasive fragmentation. At outcrop and thin section scales, the distribution of blocks follows a power law distribution with exponent $2.32 < D < 2.37$ (2-D). The block has experienced complete serpentinization, characterized by randomly-oriented antigorite aggregates. The matrix also consists of antigorite, which was formed due to dissolution–precipitation process of the block in the presence of H_2O. Antigorite aggregates in the matrix along localized shear planes is characterized by a strong crystallographic preferred orientation with a dominant [010](001) slip system, suggesting dislocation glide on (001) planes. We suggest that deep slow earthquakes occur by semi-plastic deformation of the serpentinized mantle wedge, under low effective normal stresses.

Keywords: slow earthquakes, low frequency earthquake, mantle wedge, serpentinite

©2019. Japan Geoscience Union. All Right Reserved.

Spatial distribution of slow slip events off the Boso peninsula from 1996 to 2018 under sparsity constraints

*Ryoko Nakata[1], Hideitsu Hino[2], Tatsu Kuwatani[3,4], Takahiro Akiyama[5], Shoichi Yoshioka[6], Masato Okada[7], Takane Hori[1]

1. Japan Agency for Marine-Earth Science and Technology, 2. The Institute of Statistical Mathematics, 3. Department of Solid Earth Geochemistry, Japan Agency for Marine-Earth Science and Technology, 4. PRESTO, Japan Science and Technology Agency, 5. Graduate School of Science, Kobe University, 6. Research Center for Urban Safety and Security, Kobe University, 7. Graduate School of Frontier Sciences, The University of Tokyo

We estimated spatial distribution of the six slow slip events (SSEs) off the Boso peninsula, central Japan, from 1996 to 2018. We have applied an inversion method called fused regularization, a type of sparsity constraint, suitable for detecting discontinuous changes in the model parameters, for evaluation function [Nakata et al., 2017]. In this study, to shorten calculation time, we used a type of approximation method by Obuchi and Kabashima [2016] to search hyperparameters, not LOO-CV (leave-one-out cross validation).

From our tentative results, the maximum slips for the 2002, 2011 and 2018 SSEs were large, and the 1996, 2007 and 2013 SSEs were small. The slip distributions of the 2011 and 2018 SSEs seem to be distributed southward than 2002. It is confirmed by numerical experiments that the difference in slip distribution is not due to GNSS station distribution.

Furthermore, we are conducting numerical simulation of earthquake generation cycles, which modelling SSEs off the Boso peninsula and M~8 earthquakes along the Sagami Trough. We will discuss slip distributions of SSEs and locked area during an interseismic period.

©2019. Japan Geoscience Union. All Right Reserved.

Marine electromagnetic observations around a slow earthquake region in the western Nankai trough

*Hiroshi Ichihara[1], Tada-nori Goto[2], Tetsuo Matsuno[3], Noriko Tada[4], Shinya Sato[2]

1. Earthquake and Volcano Research Center, Nagoya University, 2. Graduate School of Engineering, Kyoto University, 3. Ocean Bottom Exploration Center, Kobe University, 4. JAMSTEC

Slow earthquakes have been believed to relate to fraction of pore fluid around plate boundary. Thus, imaging of electrical resistivity (conductivity) distribution is essential to understand slow earthquakes. However, many of SSE areas are distributed beneath the ocean, we need marine electromagnetic (EM) observations. In this presentation, we report preliminary results of marine EM observations in the western part of Nankai Trough (off Miyazaki prefecture and off western Kochi prefecture, Japan) where SSEs, VLF events and regular earthquakes (e.g. 1968 off-Hyuga earthquake, M7.5) are known. We deployed eight ocean bottom electro-magnetometers (OBEMs) and recovered seven of them between 2017 and 2018. In addition to EM fields, two OBEMs measure absolute pressure to detect short period crustal deformations caused by SSE. We estimated high quality magnetotelluric responses based on Chave and Thomson (2004). However, the responses show strong three-dimensionality of resistivity distribution and strong coast effect (e.g. Key and Constable, 2011). They indicate that we need to apply three-dimensional imaging techniques for seafloor magnetotelluric data.

Keywords: Slow earthquake, magnetotelluric, OBEM, Nankai trough, off Miyazaki

©2019. Japan Geoscience Union. All Right Reserved.

Dynamics of precipitating injection fronts inside of structured medium

*Yutaka Sumino[1], Shunsuke Tanaka[1], Miyuki Kunihiro[1]

1. Tokyo University of Science

Recent study on a slow earthquake elucidates that the migration of water within a mantle wedge may play relevant roles[1]. The flow inside of confined geometry, such as within a soil, is often described by the Darcy’s law, where flow velocity is described by the gradient of fluid pressure. Interestingly, however, the water within a mantle wedge contains large amount of solid contents, and hence, a precipitation can be formed within the water[2]. For this reason, the dynamics of fluid flow under the effect of precipitation reaction should be explored.

Based on the above motivation, we explored the 2-dimensional confined chemical garden[3] as an analogue experiment for the fluid flow within a mantle wedge[4]. The system consists of two fluids with a quasi-two dimensional thin cell, so called a Hele-Shaw cell. The cell was filled with a fluid, and the other fluid is injected from the center of the cell. The flow in a Hele-Shaw cell can be described by the Darcy’s law. Furthermore, the mixing of these fluids leads to the precipitation. Thus, the flow observed in 2-dimensional confined chemical garden system is analogous to the one of water in a mantle wedge with precipitation formation.

Our previous study[4] showed that a filamentous pattern appears when the injection speed is high enough, whereas the symmetrical circular front was formed for lower injection speed. This results indicates that the propagation radius of injection front can be drastically different depending on the injection speed. In addition, the number of moving filaments saturate whose value is proportional to the injection speed. Such tendency can be understood with our boundary model adopting the effect Laplace pressure and the conservation of precipitation at the boundary. The model further predicts existence of optimal curvature for the moving front with which the required pressure for the motion is minimum. The curvature, and the speed of the optimal boundary motion is independent of the injection speed. These experimental and theoretical study thus worked well in the 2-dimensional Hele-Shaw cell. However, actual condition in a mantle wedge should have quenched structure, which is absent in a Hele-Shaw cell.

In order to fill the gap between actual condition in a mantle wedge and our analogue experiments, we modified our Hele-Shaw cell to have periodic pillar structure. As a control parameter, we changed the pillar to pillar distance, w, as shown in attached figure. The filament pattern showed meandering motion without pillar structures ($w = \infty$). We found that the filament pattern showed straight motion especially when w agreed with the typical filament width. Our modified mathematical model adopting nonlinear response of permeability with precipitation density numerically reproduced such experimental results. This results indicates that the propagation distance of injected fluid can be modified by the locally quenched disorder within a mantle wedge.

In this paper, we show detailed setup for experiments, as well as mathematical model.

[1] A. Tanaka et al. Earth, Planets and Space 70, 25 (2018).
[2] K. Ujiie, et al., *Geophys. Res. Lett.* **45**, 5371–5379 (2018).

©2019. Japan Geoscience Union. All Right Reserved.

[3] F. Haudin et al., *Proc. Natl. Acad. Sci. U.S.A.* **111**, 17363–17367 (2014).
[4] S. Wagatsuma, et, al., *Phys. Rev. E* **95**,052220 (2017).

Keywords: injection, fluid, precipitation

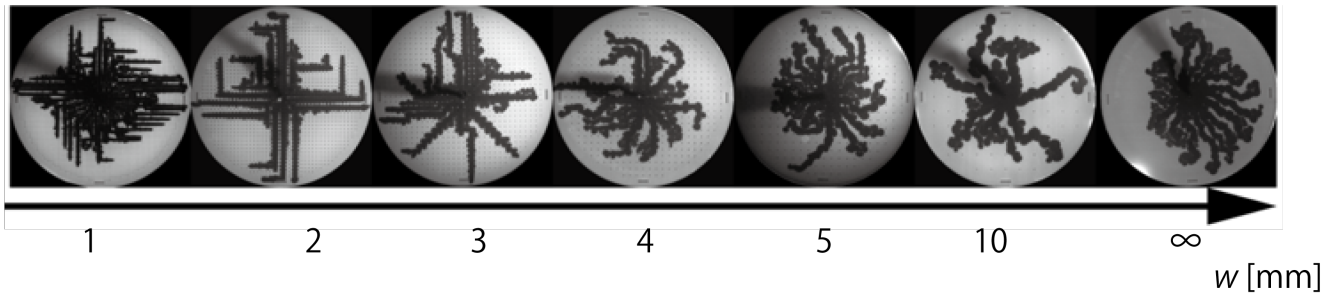

©2019. Japan Geoscience Union. All Right Reserved.

Permeability changes of simulated low permeable fault rocks induced by intermediate velocity friction test

*Wataru Tanikawa[1]

1. Japan Agency for Marine-Earth Science and Technology, Kochi Instutute for Core Sample Research

Earthquake events often associate with fluctuations of flow rate, pore pressure and pore fluid chemistry at a subsurface of earthquake rupture zones. The co-seismic hydrological changes are explained by changes in fluid permeability of fault zones during earthquakes, and the permeability change plays an important role for dynamic fault processes as well. Therefore, we newly designed a system to estimate water permeability changes during and after low to high velocity shear deformation using a rotary shear apparatus and simulated fault rocks.

A pair of hollow cylindrical samples made by low permeable Belfast dolerite and Aji granite were used as test specimens. To calculate permeability, a radial flow from the inner wall to the outer wall of the specimen was induced by applying a differential pore pressure (0.01 to 0.2 MPa) between inner and outer walls. We performed friction tests at normal stress of 2 MPa, rotation speed from 0.0003 to 0.6 m/s, and slip displacement of 1 m.

The results showed that permeability increased during sliding at every slip velocity condition, and higher velocity friction caused more abrupt increase in permeability. After the end of sliding, permeability gradually decreased with time and then became nearly constant value. Reduction rate of permeability 5 min after slip increased with slip rate. Fiction coefficient was decreased with sliding velocity. Frictional heating is a key to explain slip velocity dependence of permeability (flow rate). Temperature rise caused by frictional heating will reduce fluid viscosity, therefore, apparent permeability reduction after sliding can be explained by an increase in fluid viscosity by cooling. Pore pressure build-up by frictional heating can increase aperture, therefore, this process can explain permeability enhancement during sliding and velocity dependences on permeability increase and friction coefficient.

Keywords: permeability, friction coefficient, frictional heating

©2019. Japan Geoscience Union. All Right Reserved.

Modified relation between the coupling and tremor rates around the Shikoku region

*Tadafumi Ochi[1]

1. Institute of Earthquake and Volcano Geology, Geological Survey of Japan, The National Institute of Advanced Industrial Science and Technology

In Ochi and Takeda (2018, EPS), I examined the relation between the interplate coupling velocity and the number of deep low-frequency tremors in the same place around the Shikoku region, southwest Japan. I found that there were some spot-like points where the coupling and the tremor count were well correlated, and that the regression line required the coupling rate to be the plate convergence rate in this region under conditions of zero tremor count rate. One of the problems to be resolved is the interpretation of the first matter 'spot-like points' mentioned above. According to the pairs of time series of the coupling rate and tremor count rate, some pairs show a time delay, and the others show a small fluctuation in the tremor count rate that seems to be independent of the coupling rate. It is interesting that whether the an ill-correlation just comes from an oversimple model of the linear regression I used in the previous study, or really reflects some physical background. In order to answer this question, I construct the model which allows the fluctuation in the tremor count rate that is independent from the coupling rate and observe the fitness of the model. At this time, some trial models that allow the shorter period fluctuation in the tremor count rate than in the coupling rate and temporal change in the period achieve clear correlations. In the presentation, I will show the results of the various trials.

Keywords: Interplate coupling, Low-frequency tremor

©2019. Japan Geoscience Union. All Right Reserved.

Spatiotemporal distribution of regular and very low-frequency earthquakes in the northern part of the Ryukyu subduction zone

*Youichi Asano[1], Kazuhiko Goto[2], Hiroshi Yakiwara[3], Shuichiro Hirano[3]

1. National Research Institute for Earth Science and Disaster Resilience, 2. Association for the development of earthquake prediction, 3. Nansei-toko Observatory for Earthquakes and Volcanoes, Kagoshima University

We have investigated detailed spatiotemporal distribution of regular and very low-frequency (VLF) earthquakes including an Mw 6.3 interplate event near Tanegashima along the Ryukyu trench on Jun. 08, 2019. This earthquake was followed four Mw4-5 class regular and many VLF earthquakes by the end of Jan., 2019. At first we estimated centroid moment tensors of these regular and several VLF earthquakes, respectively, from broadband seismograms recorded at the NIED F-net and temporally observation stations. In the next step, the known VLF earthquakes were selected to be template events for searching unknown VLF earthquakes from continuous seismograms. If there are several candidates of VLF earth quake, we select the most coherent event with a maximum cross-correlation coefficient averaged over all stations in every 180 seconds. Finally we estimated locations of the selected events from phase shift of the wavelets between the template and these selected events. Obtained result shows that activity of VLF earthquakes after the Mw 6.3 earthquake was started in the adjacent area east of this Mw 6.3 earthquake; however, the following Mw4-5 regular earthquakes occurred south of this area in the period of Jan. 25-30, 2019. In this period, the front of the VLF activity migrated toward east from these Mw4-5 events. Such a spatiotemporal distribution of regular and VLF earthquakes suggests that the after slip of the Mw 6.3 and/or an SSE caused these regular and VLF earthquakes.

Acknowledgment

This study is partly supported by JSPS KAKENHI Grant Number JP16H06473.

Keywords: very low-frequency earthquake, Ryukyu subduction zone

©2019. Japan Geoscience Union. All Right Reserved.

Possible tectonic tremor activities near the VLFE epicenters in the Sanriku-Oki region in 2011

*Hidenobu Takahashi[1], Ryota Hino[1], Yusaku Ohta[1], Naoki Uchida[1], Syuichi Suzuki[1], Masanao Shinohara[2], Takanori Matsuzawa[3]

1. Graduate school of Science Tohoku University , 2. Earthquake Research Institute, University of Tokyo, 3. National Research Institute for Earth Science and Disaster Resilience

Recently various kind of slow earthquakes have been discovered along the Japan Trench subduction zone. Prior to the occurrence of the 2011 Tohoku-oki earthquake, occurrence of slow slip events associated with migration of small earthquake epicenters and tectonic tremors was reported near the hypocenter of the Tohoku-Oki earthquake (e.g. Kato et al., 2012; Ito et al., 2015; Katakami et al., 2018). As a different type of a slow-earthquake family, Very Low Frequency Earthquakes (VLFEs) have been detected in more broad areas (Matsuzawa et al., 2015). Takahashi et al. (in prep.) detected the seismic signals from the VLFEs by short-period ocean bottom seismograms (OBS) deployed in the vicinity of the VLFE epicenters in the Sanriku-Oki region, just after the Tohoku-Oki earthquake. They further identified a number of VLFE-like events, not recognized by the onshore data. Here, we report on possible tectonic tremor activities in the same area based on the OBS data after the 2011 Tohoku-oki earthquake.
We detected four sequences of continuous rises of amplitudes on the OBS records. Each of the sequence has a duration of ~ half a day. The sequences were composed of numerous wave trains with good correlations in their growths and decays in observed amplitudes among the stations, but no distinct P- or S-wave onsets were identified for individual wave trains. Interestingly, the spatial variation of the wave trains amplitudes is similar to those of the previously identified VLFEs. These observations suggest that the sequences were composed of small seismic events closely located each other and to the known VLFEs. It is also notable that some of the VLFE-like events discovered by the OBS data were contained in the sequences. We regard the discovered sequence as a kind of tectonic tremor activity and will inspect their characteristics, such as frequency content and its variability, to clarify their nature and discuss their relevance to slow slip events along the shallow subduction interface, which might promote the activities.

Keywords: tectonic tremor, Sanriku−oki

©2019. Japan Geoscience Union. All Right Reserved.

Heterogeneous structure around a region of slow earthquake activity off Ibaraki prefecture along the Japan Trench

*Kimihiro Mochizuki[1], Tomoaki Yamada[1], Masanao Shinohara[1], Ryota Hino[2], Ryosuke Azuma[2], Yoshihiro Ito[3], Yoshio Murai[4], Kenji Uehira[5], Toshinori Sato[6]

1. ERI, Univ. of Tokyo, 2. Graduate School of Science, Tohoku Univ., 3. DPRI, Kyoto Univ., 4. Faculty of Science, Hokkaido Univ., 5. NIED, 6. Graduate School of Science, Chiba Univ.

Large earthquakes of magnitude (M) ~7 have repeatedly occurred in the Ibaraki-oki region, about 100 km offshore of the Ibaraki prefecture along the Japan Trench, at a constant interval of ~20 years. Mochizuki et al. (2008) conducted a marine seismic survey and revealed that there exists a subducted seamount in the region. They also conducted an offshore seismic observation using ocean bottom seismometers (OBSs) to show that the seismicity in the region can be seen off of the subducted seamount, but not along the plate interface over it. They found that the location of the subducted seamount did not agree with the focal region of the repeating M7 earthquakes. From these results, they argued that the plate interface over the subducted seamount does not constitute an asperity of the repeating M7 earthquakes. Wang and Bilek (2011) introduced an idea that the seamount subduction causes formation of a fracture network within the overriding plate, and such a fracture network would prevent accumulation of large strain energy along the plate interface over the subducted seamount to generate large earthquakes. In addition to the repeating M7 earthquakes, recent studies (e.g. Matsuzawa et al., 2015; Nishikawa and Ide, 2018) have reported activity of slow earthquakes in the region. Relationship between activity of various types of earthquakes and structural features around the plate interface is one of the key topics to better understand controlling factors over earthquake types to be generated.

Recent studies in the Hikurangi subduction margin off the North Island of New Zealand show spatial relationship between variety of fault slips and topographic features of the plate interface. Wallace et al. (2016) successfully observed a large slow slip event just beneath an offshore array of ocean bottom pressure gauges, and precisely determined its slip distribution. They revealed that its slip propagation appeared to have circumvented subducted seamounts that have been imaged by magnetic anomalies as well as seismic reflection sections. Todd et al. (2018), for the first time, detected offshore tremor activity in the Hikurangi margin. The activity appears to have started just after the cessation of the slow slip, and its spatial distribution is only limited within regions of subducted seamounts. These results show that distributions of slow slip and tremor activity do not appear coincident, and thus the physical properties of the plate interface may be different. Further seismic surveys are supposed to provide vital information on structural variations that control physical characteristics of the plate interface.

In February, 2011, we acquired wide-angle reflection and refraction seismic data using 21 OBSs along a 150 km transect in the Ibaraki-oki region during the KH11-2 R/V Hakuho-maru cruise. We also included data from an OBS array that had already been deployed for a long-term seismic observation above the subduction front of the subducted seamount. Thus, we could construct a dense OBS profile above the subducted seamount with a receiver interval of ~3 km to achieve a high spatial resolution, whereas the largest interval is 10 km near both ends of the profile. First arrivals from the airgun sources can be traced up to ~95 km on most of the OBSs. The OBS record sections show significant heterogeneity that may include very rough structural features of the subducting oceanic crust along strike. Such heterogeneity may control seismic activity in the region.

©2019. Japan Geoscience Union. All Right Reserved.

Keywords: Ibaraki-oki, Active source seismic survey, Heterogeneous structure

©2019. Japan Geoscience Union. All Right Reserved.

Shallow low-frequency tremor triggered by nearby moderate earthquakes off Sanriku

*Sachiko Tanaka[1], Takanori Matsuzawa[1], Youichi Asano[1]

1. National Research Institute for Earth Science and Disaster Resilience

In the region off Sanriku, we have observed shallow low-frequency tremor, which occurs between the 12 km and 20 km depth contours of the plate interface, applying an envelope correlation method (Obara, 2002) to the records from the Seafloor observation network for earthquakes and tsunamis along the Japan Trench (S-net) (Tanaka et al., 2018). Several episodes of tremor, each of which lasted for half a day to six days, were detected in 2017, with intervals of one to three months. In the present study, we found tremor triggered by nearby moderate earthquakes. On July 24, 2017, an Mw 5.6 earthquake, showing reverse faulting consistent with the slip on the plate interface, occurred at the downdip end of the tremor zone off Sanriku, which was the largest event within 100 km of that tremor zone in the year. Immediately after the Mw 5.6 earthquake, coherent tremor signals were identified at surrounding stations. These signals continued for 20 hours, and the locations of their sources spanned 40 km along strike and 50 km along dip. Similar triggered tremor was observed following an Mw 5.1 earthquake on July 22, two days before the Mw 5.6 earthquake. This tremor activity was smaller and shorter than that triggered by the Mw 5.6 earthquake; tremor was localized to an area of 20 km by 15 km, and lasted for twelve hours. After a quiescence of nearly one day, the Mw 5.6 earthquake occurred at an adjacent area and triggered tremor was detected again. Triggering of tremor by moderate interplate earthquakes in or very close to the tremor zone we observed may imply small-scale (~ a few kilometers) heterogeneities in frictional properties on the plate interface in the area.

Keywords: shallow low-frequency tremor, triggered tremor, Japan Trench

©2019. Japan Geoscience Union. All Right Reserved.

Slow slip events in the Bungo Channel over 15 years as inferred from GNSS data (1996-2011)

Takatoshi Yokoi[1], *SHINICHI MIYAZAKI[1], Hiromu Sakaue[1], Jun'ichi Fukuda[2]

1. Graduate School of Science, Kyoto University, 2. Earthquake Research Institute, The University of Tokyo

We estimated space-time evolution of inter-plate slip and slip velocity associated with slow slip events (SSE) in the Bungo Channel over 15 years between January 1, 1996 and February 28, 2011, from GNSS data.

We use GNSS time series at 80 stations around the Bungo Channel out of GEONET stations. Time series were obtained with GIPSY-OASIS II software by Nishimura (personal communication). We removed data during SSE and estimated secular velocities, annual and semi-annual seasonal variations, and offsets associated with earthquakes, SSEs and instrumental events. Then we remove contributions of those components from time series with SSE to prepare time series for the inversion. We constructed plate interface based on iso-depth data by Baba et al. (2002) and Hirose et al. (2008), and setup the model region that is 200km long east to west and 280km long north to south. The model region was subdivided into 719 small triangular patches. We employed the inversion method based on the Monte Carlo Mixture Kalman Filter (Fukuda et al. 2008) and estimated slip and slip velocities on the fault continuously over 15 years.

First, Long-term slow slip events (L-SSE hereafter) that lasted for several months were inferred in 1997, 2003 and 2010 as obtained by, such as, Ozawa et al. (2012, 2017) and Yoshioka et al. (2015). In addition to basic characteristics described in these previous studies, short-term slow slip events (S-SSE hereafter) were inferred just before or just after the main slip event. This result suggests that stress perturbations by SSEs trigger other SSEs. Therefore the inferred cumulative moment in this study was smaller than previous studies because we successfully excluded contributions from S-SSEs. Second, S-SSEs have repeatedly occurred with the interval of about three or four months over 15 years. Those S-SSE were located at depths of about 30-40km and associated with low frequency tremors.

In this presentation, we focus space-time evolutions of L-SSE in 2010 and S-SSE in 2005.

Keywords: Slow slip in the Bungo Channel, crustal deformation, Monte Carlo Mixture Kalman Filter

©2019. Japan Geoscience Union. All Right Reserved.

Investigations of sensor orientation and a possibility of detecting crustal deformation based on accelerometer records of S-net

*Ryota Takagi[1], Naoki Uchida[1], Takashi NAKAYAMA[1], Ryosuke Azuma[1], Akira Ishigami[1], Tomomi Okada[1], Yusaku Ohta[1], Ryota Hino[1]

1. Research Center for Prediction of Earthquakes and Volcanic Eruptions, Graduate School of Science, Tohoku University

Seafloor Observation Network for Earthquakes and Tsunamis along the Japan Trench (S-net) of National Research Institute for Earth Science and Disaster Resilience (NIED) will greatly improve our knowledge of subsurface structure beneath offshore region along Japan trench and understanding of regular and slow earthquakes on the subducting plate boundary. We estimated the orientations of S-net sensors that are fundamental information for further data analysis and investigated the possibility of detecting crustal deformation based on accelerometer records.

We determined three parameters of sensor orientations: tilt angle of the long axis of a cable, rotation angle around the long axis, azimuth of the long axis. We estimated the tilt and rotation angles by assuming the DC components of accelerometers record the gravitational acceleration. The tilt and rotation angles slightly vary within the range of 0.01-0.1 degree during the period from 2016 to 2018 except for coseismic steps of rotation angles larger than 1 degree due to the M6.4 off Sanriku earthquake (August 20, 2016) and M7.4 off Fukushima earthquake (November 20, 2016). The long-axis azimuths are estimated by particle motions of long-period Rayleigh waves. We used the accelerometer records in 30-100 s of 7-14 teleseismic earthquakes with Mw 7.0-8.2. The azimuths are constrained in the range of 5-10 degrees. After correcting waveforms based on the estimated sensor orientation, we found coherent waveforms within the whole S-net stations and separation of Rayleigh and Love waves in radial and transverse components.

The capability of the DC components of accelerometers implies a possibility to detect crustal deformation from accelerometer records. We made time series of tilt and rotation angle with the sampling rate of one hour. During the period without offsets partly due to earthquakes, the root-mean-square (RMS) amplitudes of tilt and rotation angles are about 2 micro radians at most stations. The buried stations shallower than 1500 m show smaller variations and RMS amplitudes are about 0.2 micro radians. Some buried stations show tidal response with amplitude of about 1 micro radians. Since the maximum tilt change of land stations by a slow slip event (SSE) near the Boso Peninsula is about 1 micro radians, it might be possible to detect crustal deformation due to similar SSEs based on the accelerometer records.

Acknowledgement: We used continuous records of S-net managed by NIED. We thank NIED for providing the data.

Keywords: S-net, Sensor orientation, Crustal deformation, Slow slip, Tilt observation

©2019. Japan Geoscience Union. All Right Reserved.

Spatiotemporal variation of released seismic energy from shallow low-frequency tremor in Hyuga-nada, revealed by ocean bottom seismological observation

*Yusuke Yamashita[1], Saki Watanabe[2], Tomoaki Yamada[3], Masanao Shinohara[3], Takeshi Matsushima[2]

1. Disaster Prevention Research Institute, Kyoto University, 2. Institute of Seismology and Volcanology, Kyushu University, 3. Earthquake Research Institute, The University of Tokyo

In this study, we estimate the released seismic energy by shallow low-frequency tremors (shallow tremors) and clarify spatiotemporal variation of shallow tremor activity in Hyuga-nada, east off Kyushu. We used the data obtained from the temporal ocean bottom seismological observation for 3 months in 2013 [Yamashita *et al*., 2015] and long-term ocean bottom seismological observation from 2014 to 2017. The source location and released seismic energy of each shallow tremor was simultaneously estimated by Hybrid Envelope Cross-correlation Method [Maeda and Obara, 2009]. Observation data were obtained by the long-term continuous ocean bottom seismic observation in Hyuga-nada from 2013 to 2017. Site amplification factors were estimated by the coda normalization method [e.g., Sato and Fehler, 1998].

Spatial distribution of released seismic energy rate (energy rate) shows a heterogeneity although the average value of that is generally 10^4 J/s. The regions where the energy rate is relatively small are roughly coincident with the subducting or passed areas of the Kyushu-Palau Ridge. This result suggests that the structure and/or shape of the subducting plate such as seamounts or ridges may have an effect on the frictional property of the shallow plate interface. The 2013 activity was similar characteristics of shallow tremor location in space and time as the previous study, including two migrations episode. In addition, the characteristics of the released seismic energy were revealed as follows: (1) the energy rate was large at the both initiation point and the front of the migration, (2) the total released energy amount of the first migration was larger than that of the second migration, (3) both migrations were stopped at the region of small amount of released energy. Migration episode occurred while the 2015 activity and similar characteristics were documented.

Migration speed of shallow tremor is a few times faster, and energy rate of that is one or two orders of magnitude greater than the deep tremor. Applying the model of Ando *et al*. [2010, 2012] and Yabe and Ide [2014] to the result in this study, the average fault strength of shallow tremor is stronger than that of deep tremor, which leads up to a faster fault slip both brittle and ductile area. As a result, migration speed may become to be faster than deep tremor.

Acknowledgements: This study is supported by the research project for compound disaster mitigation on the great earthquakes and tsunami around the Nankai trough region, the MEXT of Japan, and JSPS KAKENHI Grant Number JP16H06471, JP16H06472. We thank Dr. Takuto Maeda for valuable discussions and comments. The observation data in 2013 obtained by T/S Nagasaki-maru. We used the JMA unified earthquake catalog and the seismic data obtained by Kagoshima University.

Keywords: Shallow low frequency tremor, Shallow slow earthquake, Ocean bottom seismological observation

©2019. Japan Geoscience Union. All Right Reserved.

©2019. Japan Geoscience Union. All Right Reserved.

Unified description of fast and slow earthquakes using velocity strengthening patches

*So Ozawa[1], Takahiro Hatano[1]

1. Earthquake Research Institute, the University of Tokyo

In a prevalent view, seismicity in subduction zones is governed by the distribution of the frictional properties of the plate interface. Regions with velocity-weakening (VW) friction generate earthquakes, whereas velocity-strengthening (VS) regions creep aseismically. Although most models consider isolated VW regions (patches) from the idea of asperities (e.g. Dublanchet et al., 2013), isolated VS patches also would exist given the frictional properties on faults are inferred to be complex and hierarchical. Therefore, the role of VS patches is to be studied.

Here we perform 3-D numerical simulation of the seismic cycle of faults governed by the rate and state friction law with the aging law. We distribute randomly circular VS patches on a VW background. We mainly focus on the effect of the ratio of VS and VW areas.

In our preliminary simulation, we identified two important effects. First, the VS patches act as the “stability barriers” during dynamic rupture propagation, which makes the rupture process more complicated than a single propagating crack. Rupture decelerates by encountering a stability barrier, followed by reacceleration due to overcoming the barrier. Such a process gives rise to multiple rupture fronts in the slipping area.

Second, dynamic rupture is inhibited by increasing the number of VS patches, and the fault slips aseismically with strong fluctuation in slip velocity. This is because there are no enough VW regions to accelerate the slip to dynamic rupture. Although a similar mechanism for slow earthquakes is proposed by Skarbek et al. (2012) and Yabe & Ide (2017), our 3-D modeling enables detailed studies on the spatiotemporal evolution of slip. In the presentation, we further discuss our results in the context of the dynamic scaling of rupture growth and the phenomenological law of slow earthquakes.

Keywords: Slow earthquake, Rate and state friction

©2019. Japan Geoscience Union. All Right Reserved.

The b-value of the earthquake swarm activities accompanied by the Boso slow slip events

*Yuki Noda[1], Hitoshi Hirose[2,1]

1. Department of Planetology, Faculty of Science, Kobe University , 2. Research Center for Urban Safety and Security, Kobe University

Slow slip events (SSEs) which are accompanying earthquake swarms repeatedly occur at intervals of about 2 to 7 years off Boso Peninsula (e.g., Sagiya, 2004; Hirose et al., 2012, 2014; Fukuda, 2018). These SSEs and swarms are thought to occur on the upper boundary of the subducting Philippine Sea plate.

As a statistical property of earthquakes, Gutenberg-Righter’ s law is well-known, that is, the relationship between the magnitude and the logarithm of occurrence frequency of earthquakes is expressed well with a straight line a-bM (Gutenberg and Richter, 1944). Although the b-value (slope of the line) often takes values around 1, there are many reports about the temporal changes of the b-value. For example, a decade-scale b-value decrease prior to the 2011 Tohoku Earthquake is reported (Nanjo et al., 2012). Although the relationship between the temporal change of b-value and aseismic slip is suggested, but the lack of near field geodetic observations prevents the direct evidence for the relationship. Here we examine the b-value of the earthquake swarms accompanied by the Boso SSEs, of which the aseismic slip is revealed by geodetic observations.

In this study, we estimate the b-value of the earthquake swarms in 2002, 2007, 2011 and 2014. We use the JMA unified earthquake catalog. As a preliminary analysis, we investigated the earthquakes with focal depths of 5 km to 40 km occurring at 35.05˚ to 35.56˚N in latitude and 140.15˚ to 140.73˚E in longitude. Eventually, “event period” estimated in the previous studies of the crustal deformation by geodetic observation does not necessarily agree with the period of the swarms occurring at the same time. Therefore, in this research, “event period” was redefined from seismic activity and used. In other words, we extracted swarms including a SSE period from crustal deformation studies and the time when the seismicity rate (the number of earthquakes per unit time) is significantly higher than the other time is defined as “event period”. In addition, the period other than the event period is defined as “inter-swarm period”.

We find that the b-values in the event periods tend to be lower than that during inter-swarm period. In more detail, different trends that seem to correspond to the difference in slip zone and location of earthquake activity of each SSE (Hirose et al. 2014) are seen in the b-values for the event periods. A seismic activity near the southern coast of the Boso Peninsula was hardly observed in the 2007 event period, whereas an active seismic activity was seen there in the 2011 event period. In order to clarify the dependence of the b-value on the difference in the location of the earthquakes, we divided the survey area into two areas, that is, the northern area (area A) and the southern area (area B). The seismic activity is observed in all event periods in the area A, whereas an active seismic activity is observed only in the event periods of 2002 and 2011 in the area B. Then a b- value is estimated in each period in the same way. As a result, for the earthquakes occurred in the northern region (area A), there is a tendency that the b-value in each of the event periods is lower by about 0.2-0.4 than that during inter-swarm. On the other hand, such a tendency is not observed in the southern area (area B). Such differences in the northern and southern regions may suggest that the effects of stress changes caused by SSEs vary from region to region.

©2019. Japan Geoscience Union. All Right Reserved.

Keywords: Gutenberg-Richter's law

©2019. Japan Geoscience Union. All Right Reserved.

Three-dimensional thermal modeling associated with subduction of the Philippine Sea plate at the Ryukyu Trench, and its relation to the occurrence of interplate seismic events

*Nobuaki Suenaga[1], Shoichi Yoshioka[2,1], Yinfeng Ji[3]

1. Graduate School of Science, Kobe University, Japan, 2. Research Center for Urban Safety and Security, Kobe University, Japan, 3. Chinese Academy of Science, Beijin, China

Interplate seismic events such as short-term slow slip evens (S-SSEs) (Nakamura, 2017), low-frequency earthquakes (LFEs) (Ando et al., 2012), and shallow very low-frequency earthquakes (VLFEs) (Nakamura et al., 2015) have been identified at the Ryukyu Trench, southwestern Japan. As the specific characteristics of these distributions, depths where S-SSEs and LFEs occur at the plate interface beneath the Okinawa island, whose depth is ranging from 15 km to 25 km, is about 10-20 km shallower than that beneath the Yaeyama islands, whose depth is ranging from 35 km to 50 km.

In this study, we constructed three-dimensional parallelepiped thermal convection model associated with subduction of the Philippine Sea (PHS) plate beneath the Amurian (AM) plate at the Ryukyu subduction zone. We considered subduction history of the PHS plate in the model region, referring to the plate rotation model (Mathews et al., 2016). We performed the numerical simulation as the time-dependent problem in the last 15 Myr to elucidate relationships among calculated thermal structures, dehydrations from the subducting plate, and the interplate seismic events. We used observed heat flow data to constrain thermal structures.

As a result at 0 Ma, we found that interplate temperature where S-SSEs and LFEs occur beneath the Yaeyama islands is lower than that beneath the Okinawa island when compared with the same depth along the direction of the trench axis. This is mainly because the convergence rate (PHS-AM) becomes gradually fast toward the southwest. Therefore, interplate temperatures where S-SSEs and LFEs occur were estimated ranging from 500℃ to 700℃ both beneath the Okinawa island and the Yaeyama islands.

We also calculated water content distribution within the PHS plate, using the calculated thermal structures and the phase diagram of MORB in an oceanic crust (Omori et al., 2008) and ultramafic rock in a slab mantle (Hacker et al., 2003). As for dehydration of MORB, we found that epidote eclogite transforms into amphibole eclogite in the neighboring area where S-SSEs and LFEs occur beneath the Okinawa island, and amphibole eclogite transforms into eclogite beneath the Yaeyama islands. The former and the latter dehydrate a total amount of 1.4 wt% and 0.7 wt% associated with their phase transformations, respectively.

Keywords: three dimensional thermal modeling

©2019. Japan Geoscience Union. All Right Reserved.

[E] Poster | S (Solid Earth Sciences)：S-CG Complex & General

Wed. May 29, 2019 5:15 PM - 6:30 PM JST | Wed. May 29, 2019 8:15 AM - 9:30 AM UTC | Poster Hall International Exhibition Hall8, Makuhari Messe_33

[S-CG48] Science of slow earthquakes: Toward unified understandings of whole earthquake process

convener:Satoshi Ide(Department of Earth an Planetary Science, University of Tokyo), Hitoshi Hirose(Research Center for Urban Safety and Security, Kobe University), Kohtaro Ujiie(Graduate School of Life and Environmental Sciences, University of Tsukuba), Takahiro Hatano(Earthquake Research Institute, University of Tokyo)

Accumulating observational studies on various types of slow deformation events, such as tectonic tremors, very low frequency events, and slow slip events, portrays some universal characteristics in generally complex behavior, including interaction among events and influence by various outer loadings. Some of these phenomena seem to have causal relation with the occurrence of very large earthquakes. A unified understanding of these slow and fast earthquake processes requires an approach integrating geophysics, seismology, geodesy, geology, and non-equilibrium statistical physics. We welcome presentations based on, but not limited to, geophysical observation, data analysis, analytical theory, numerical simulation, field study, and laboratory experiments.

[SCG48-P01] Off the Kii Peninsula Shallow Low Frequency Earthquake in 2004 revealed by Ocean Bottom Seismometer

*Koji Tamaribuchi[1], Akio Kobayashi[1], Takahito Nishimiya[1], Satoshi Annoura[2] (1.Meteorological Research Institute, 2.Japan Meteorological Agency)

[SCG48-P02] The development of pressure vessel on gouges for rock deformation at seismic rates under water-saturated conditions

*Wei-Ting Lin[1], Li-Wei Kuo[1], Wen-Jie Wu[1], Jia-Jyun Dong[1], Yi-Hung Huang[2] (1.National Central University, 2.MATSUKI HYDRAULIC INDUSTRIAL CO. LTD)

[SCG48-P03] Spatial variations of shallow very low-frequency earthquake activity along the Nankai Trough based on CMT inversion using the 3D heterogeneous model

*Shunsuke Takemura[1], Takanori Matsuzawa[1], Akemi Noda[1], Takashi Tonegawa[2], Youichi Asano[1], Takeshi Kimura[1], Katsuhiko Shiomi[1] (1.National Research Institute for Earth Science and Disaster Resilience, 2.Japan Agency for Marine-Earth Science and Technology)

[SCG48-P04] Evaluation of Magnitude and Characteristics of Seismicity of Low Frequency Earthquakes in Parkfield

*Miki Aso[1,3], Naofumi Aso[2], Satoshi Ide[1] (1.Department of Earth and Planetary Science, The University of Tokyo, 2.Tokyo Institute of Technology, School of Science, 3.OYO RMS Corporation)

[SCG48-P05] Tectonic tremor catalog in the Tohoku-Hokkaido-Oki region using S-net

*Satoshi Ide[1], Tomoaki Nishikawa[2], Takanori Matsuzawa[3], Kazuaki Ohta[2], Naoki Uchida[4], Takuya NISHIMURA[2] (1.Department of Earth an Planetary Science, University of Tokyo, 2.Disaster Prevention Research Institute, Kyoto University, 3.National Research Institute for Earth Science and Disaster Resilience, 4.Graduate School of Science and International Research Institute of Disaster Science, Tohoku University)

[SCG48-P06] Spontaneous Slow Slip and Runaway Slip in Laboratory

*Miki Takahashi[1] (1.Institute of Earthquake and Volcano Geology, Geological Survey of Japan, AIST)

[SCG48-P07] Hydration and amorphization of quartz rocks during high-velocity frictional sliding: An examination of fault gouge from friction experiments of synthetic quartz

*Yuko Onoe[1], Hirotaka Iida[2], Akito Tsutsumi[1], Aki Takigawa[1] (1.Graduate School of Science, Kyoto University, 2.Geothermal Engineering Co., Ltd.)

[SCG48-P08] Constraining S Wave Velocity of the Source Region of Shallow Very Low-Frequency Earthquakes

*Takeshi Akuhara[1], Takashi Tonegawa[2] (1.Earthquake Research Institute, The University of Tokyo, 2.Research and Development center for Earthquake and Tsunami, Japan Agency for Marine-Earth Science and Technology)

[SCG48-P09] **Quantitative relationship between aseismic slip propagation speed and frictional properties**

*Keisuke Ariyoshi[1], Jean-Paul Ampuero[2,3], Roland Burgmann[4], Toru Matsuzawa[5], Akira Hasegawa[5], Ryota Hino[5], Takane Hori[1] (1.Japan Agency for Marine-Earth Science and Technology, 2.Université Côte d'Azur, 3.California Institute of Technology, 4.University of California, Berkeley, 5.Graduate School of Science, Tohoku University)

[SCG48-P10] Comprehensive detection of very low frequency earthquakes off the Pacific coasts of Hokkaido and Tohoku, northeastern Japan

*Satoru Baba[1], Akiko Takeo[1], Kazushige Obara[1], Takanori Matsuzawa[2], Takuto Maeda[3] (1.Earthquake Research Institute, University of Tokyo, 2.National Research Institute for Earth Science and Disaster Resilience, 3.Graduate School of Science and Technology, Hirosaki University)

[SCG48-P11] **Spatio-temporal evolution of long- and short-term slow slip events in the Tokai region, central Japan estimated from a very dense GNSS network, during 1997-2017**

*Hiromu Sakaue[1], Takuya NISHIMURA[2], Jun'ichi Fukuda[3], Teruyuki Kato[4] (1.Graduate School of Science, Kyoto University, 2.Disaster Prevention Research Institute Kyoto University, 3.Earthquake Research Institute,The University of Tokyo, 4.Hot Springs Research Institute of Kanagawa Prefecture)

[SCG48-P12] Broadband excitation of acoustic emission in granular stick-slip : experiments and spectral analyses

*Hidekazu Fukumizu[1], Ikuro Sumita[2] (1.Earth and Environmental Science Course, Division of Natural System, Graduate school of Natural Science and Technology, Kanazawa University, 2.School of Geosciences and Civil Engineering, Kanazawa University)

[SCG48-P13] Episodic tremor and slip silently invades strongly locked megathrust in the Nankai Trough

*Masayuki Kano[1], Aitaro Kato[2], Kazushige Obara[2] (1.Graduate school of science, Tohoku University, 2.Earthquake Research Institute, The University of Tokyo)

[SCG48-P14] Spatial distribution of the electrical resistivity beneath western part of Shikoku Island where long-term SSE events have repeatedly occurred

*Makoto Uyeshima[1], Maki Hata[1], Hiroshi Ichihara[2], Ryokei Yoshimura[3], Koki Aizawa[4] (1.Earthquake Research Institute, The University of Tokyo, 2.Graduate School of Environmental Studies, Nagoya University, 3.Disaster Prevention Research Institute, Kyoto University, 4.Institute of Seismology and Volcanology, Faculty of Sciences, Kyushu University)

[SCG48-P15] Variations of scaling relationships for shallow tremor observed along the Nankai trough

*Masaru Nakano[1], Suguru Yabe[1] (1.Japan Agency for Marine-Earth Science and Technology)

[SCG48-P16] Low-frequency earthquakes triggered by teleseismic surface waves by Ryukyu subduction zone.

Ayumi Kinjo[1], *Mamoru Nakamura[1] (1.Faculty of Science, University of the Ryukyus)

[SCG48-P17] Detection of small surface displacement accompanying deep low-frequency tremor in Shikoku region, southwest Japan

*Yutaro Okada[1], Takao Tabei[2] (1.Faculty of Science, Kochi University, 2.Faculty of Science and Technology, Kochi University)

[SCG48-P18] Long-term temporal change in crustal resistivity beneath western Shikoku

*Futoshi Yamashita[1], Yoshimori Honkura[1] (1.National Research Institute for Earth Science and Disaster Resilience)

[SCG48-P19] Slow decay of postseismic deformation compared with aftershocks following the 2011 Tohoku-oki Earthquake

*Yuta Mitsui[1], Shunsuke Morikami[2] (1.Department of Geosciences, Shizuoka University, 2.Formerly at Graduate School of Science and Technology, Shizuoka University)

[SCG48-P20] Serpentinite dehydration in subduction shear zones formed at source depths of slow earthquakes

*Yasushi Mori[1], Miki Shigeno[1], Kohtaro Ujiie[2], Kazuya Noro[2], Tadao Nishiyama[3] (1.Kitakyushu Museum of Natural History and Human History, 2.University of Tsukuba, 3.Kumamoto University)

[SCG48-P21] Earthquake swarms following very low-frequency earthquakes in the central Ryukyu Trench

*Mamoru Nakamura[1] (1.Faculty of Science, University of the Ryukyus)

[SCG48-P22] Seismic imaging in the central Nankai trough, off Shionomisaki to Kii channel

*Yasuyuki Nakamura[1], Shuichi Kodaira[1], Tetsuo No[1], Yuka Kaiho[1], Gou Fujie[1], Seiichi Miura[1], Kazuya Shiraishi[1] (1.Japan Agency for Marine Earth Science and Technology)

[SCG48-P23] Attempt to Detect Intra-plate SSEs Based on F3 Solution of GEONET

*Yusaku Tanaka[1] (1.Earthquake Research Institute)

[SCG48-P24] A new hydrothermal, low to high speed rotary-shearing apparatus: Reproduction of slow/megathrust earthquakes in laboratory

*Takehiro Hirose[1], Wataru Tanikawa[1], Yohei Hamada[1], Keishi Okazaki[1] (1.Kochi Institute for Core Sample Research, Japan Agency for Marine-Earth Science and Technology)

[SCG48-P25] Very low-frequency earthquakes in western Shikoku remotely triggered by the 2016 Mw5.9 off-Kii Peninsula earthquake

*Masatoshi Miyazawa[1] (1.Disaster Prevention Research Institute, Kyoto University)

[SCG48-P26] **Underground structure around source region of slow earthquakes in western Shikoku obtained by receiver function analysis**

Akira Hikita[1], Aitaro Kato[1], *Kazushige Obara[1], Akiko Takeo[1], Takeshi Akuhara[1] (1.Earthquake Research Institute, The University of Tokyo)

[SCG48-P27] Hypocenter determination of deep low frequency tremors beneath the Kii Peninsula by backprojection of seismic array data

*Kodai Sagae[1], Hisashi Nakahara[1], Takeshi Nishimura[1], Kazutoshi Imanishi[2] (1.Graduate School of Science,Tohoku University, 2.National Institute of Advanced Industrial Science and Technology (AIST))

[SCG48-P28] Triggered tremors and stress perturbations due to surface waves

*Ryohei Ikeda[1], Naoki Suda[1] (1.Hiroshima University)

[SCG48-P29] Numerical modeling of long- and shallow slow slip events including shallow region in Hyuganada and western Nankai, Japan

*Takanori Matsuzawa[1], Bunichiro Shibazaki[2] (1.National Research Institute for Earth Science and Disaster Resilience, 2.Building Research Institute)

[SCG48-P30] Further evidence for the influence of a subducting-ridge on the spatial strain accumulation and release pattern in the shallow eastern Nankai Trough, based on VLFE distribution

*Akiko Toh[1], Chen Wan-Jou [2], Doug Dreger[3], Wu-Cheng Chi[2], Satoshi Ide[1] (1.University of Tokyo, 2.Institute of Earth Sciences, Academia Sinica, 3.UC Berkeley)

[SCG48-P31] Evidence for semi-brittle flow in mantle-wedge serpentinites under high pore fluid pressure and their implications for deep low frequency earthquakes

Kengo Kataoka[1], Yurina Nagata[1], *Ken-ichi Hirauchi[1], Ryosuke Oyanagi[2], Atsushi Okamoto[3], Katsuyoshi Michibayashi[4] (1.Department of Geosciences, Faculty of Science, Shizuoka University, 2.Japan Agency for Marine-Earth Science and Technology, 3.Graduate School of Environmental studies, Tohoku University, 4.Department of Earth and Planetary Sciences, Nagoya University)

[SCG48-P32] Spatial distribution of slow slip events off the Boso peninsula from 1996 to 2018 under sparsity constraints

*Ryoko Nakata[1], Hideitsu Hino[2], Tatsu Kuwatani[3,4], Takahiro Akiyama[5], Shoichi Yoshioka[6], Masato Okada[7], Takane Hori[1] (1.Japan Agency for Marine-Earth Science and Technology, 2.The Institute of Statistical Mathematics, 3.Department of Solid Earth Geochemistry, Japan Agency for Marine-Earth Science and Technology, 4.PRESTO, Japan Science and Technology Agency, 5.Graduate School of Science, Kobe University, 6.Research Center for Urban Safety and Security, Kobe University, 7.Graduate School of Frontier Sciences, The University of Tokyo)

[SCG48-P33] Marine electromagnetic observations around a slow earthquake region in the western Nankai trough

*Hiroshi Ichihara[1], Tada-nori Goto[2], Tetsuo Matsuno[3], Noriko Tada[4], Shinya Sato[2] (1.Earthquake and Volcano Research Center, Nagoya University, 2.Graduate School of Engineering, Kyoto University, 3.Ocean Bottom Exploration Center, Kobe University, 4.JAMSTEC)

[SCG48-P34] Dynamics of precipitating injection fronts inside of structured medium

*Yutaka Sumino[1], Shunsuke Tanaka[1], Miyuki Kunihiro[1] (1.Tokyo University of Science)

[SCG48-P35] Permeability changes of simulated low permeable fault rocks induced by intermediate velocity friction test

*Wataru Tanikawa[1] (1.Japan Agency for Marine-Earth Science and Technology, Kochi Instutute for Core Sample Research)

[SCG48-P36] Modified relation between the coupling and tremor rates around the Shikoku region

*Tadafumi Ochi[1] (1.Institute of Earthquake and Volcano Geology, Geological Survey of Japan, The National Institute of Advanced Industrial Science and Technology)

[SCG48-P37] Spatiotemporal distribution of regular and very low-frequency earthquakes in the northern part of the Ryukyu subduction zone

*Youichi Asano[1], Kazuhiko Goto[2], Hiroshi Yakiwara[3], Shuichiro Hirano[3] (1.National Research Institute for Earth Science and Disaster Resilience, 2.Association for the development of earthquake prediction,

3.Nansei-toko Observatory for Earthquakes and Volcanoes, Kagoshima University)

[SCG48-P38] Possible tectonic tremor activities near the VLFE epicenters in the Sanriku-Oki region in 2011

*Hidenobu Takahashi[1], Ryota Hino[1], Yusaku Ohta[1], Naoki Uchida[1], Syuichi Suzuki[1], Masanao Shinohara[2], Takanori Matsuzawa[3] (1.Graduate school of Science Tohoku University , 2.Earthquake Research Institute, University of Tokyo, 3.National Research Institute for Earth Science and Disaster Resilience)

[SCG48-P39] Heterogeneous structure around a region of slow earthquake activity off Ibaraki prefecture along the Japan Trench

*Kimihiro Mochizuki[1], Tomoaki Yamada[1], Masanao Shinohara[1], Ryota Hino[2], Ryosuke Azuma[2], Yoshihiro Ito[3], Yoshio Murai[4], Kenji Uehira[5], Toshinori Sato[6] (1.ERI, Univ. of Tokyo, 2.Graduate School of Science, Tohoku Univ., 3.DPRI, Kyoto Univ., 4.Faculty of Science, Hokkaido Univ., 5.NIED, 6.Graduate School of Science, Chiba Univ.)

[SCG48-P40] Shallow low-frequency tremor triggered by nearby moderate earthquakes off Sanriku

*Sachiko Tanaka[1], Takanori Matsuzawa[1], Youichi Asano[1] (1.National Research Institute for Earth Science and Disaster Resilience)

[SCG48-P41] Slow slip events in the Bungo Channel over 15 years as inferred from GNSS data (1996-2011)

Takatoshi Yokoi[1], *SHINICHI MIYAZAKI[1], Hiromu Sakaue[1], Jun'ichi Fukuda[2] (1.Graduate School of Science, Kyoto University, 2.Earthquake Research Institute, The University of Tokyo)

[SCG48-P42] Investigations of sensor orientation and a possibility of detecting crustal deformation based on accelerometer records of S-net

*Ryota Takagi[1], Naoki Uchida[1], Takashi NAKAYAMA[1], Ryosuke Azuma[1], Akira Ishigami[1], Tomomi Okada[1], Yusaku Ohta[1], Ryota Hino[1] (1.Research Center for Prediction of Earthquakes and Volcanic Eruptions, Graduate School of Science, Tohoku University)

[SCG48-P43] Spatiotemporal variation of released seismic energy from shallow low-frequency tremor in Hyuga-nada, revealed by ocean bottom seismological observation

*Yusuke Yamashita[1], Saki Watanabe[2], Tomoaki Yamada[3], Masanao Shinohara[3], Takeshi Matsushima[2] (1.Disaster Prevention Research Institute, Kyoto University, 2.Institute of Seismology and Volcanology, Kyushu University, 3.Earthquake Research Institute, The University of Tokyo)

[SCG48-P44] Unified description of fast and slow earthquakes using velocity strengthening patches

*So Ozawa[1], Takahiro Hatano[1] (1.Earthquake Research Institute, the University of Tokyo)

[SCG48-P45] The b-value of the earthquake swarm activities accompanied by the Boso slow slip events

*Yuki Noda[1], Hitoshi Hirose[2,1] (1.Department of Planetology, Faculty of Science, Kobe University , 2.Research Center for Urban Safety and Security, Kobe University)

[SCG48-P46] **Three-dimensional thermal modeling associated with subduction of the Philippine Sea plate at the Ryukyu Trench, and its relation to the occurrence of interplate seismic events**

*Nobuaki Suenaga[1], Shoichi Yoshioka[2,1], Yinfeng Ji[3] (1.Graduate School of Science, Kobe University, Japan, 2.Research Center for Urban Safety and Security, Kobe University, Japan, 3.Chinese Academy of Science, Beijin, China)

Off the Kii Peninsula Shallow Low Frequency Earthquake in 2004 revealed by Ocean Bottom Seismometer

*Koji Tamaribuchi[1], Akio Kobayashi[1], Takahito Nishimiya[1], Satoshi Annoura[2]

1. Meteorological Research Institute, 2. Japan Meteorological Agency

The 2004 off the Kii Peninsula earthquakes (Mj7.1, 7.4) occurred near the Nankai trough axis, southeast off the Kii Peninsula, Japan, on September 5, 2004. After the earthquakes, the Meteorological Research Institute conducted OBS observation to examine the aftershock distribution accurately. Although the analysis was limited to hypocenter relocation of "ordinary aftershocks", no analysis was done for slow events. In this study, it is shown that many low-frequency earthquakes (LFEs) occurred in "ordinary aftershocks" from the detailed inspection of our observation. During the observation period, the frequency of LFE gradually decreased. Since P- and S-arrival times are unclear, it is difficult to determine the distribution of the hypocenter accurately. However, by using the Amplitude Source Location (ASL; Battaglia and Aki, 2003), the LFEs are located between a splay fault and trench axis. The 2004 OBS stations are located east of the DONET, and many LFEs are detected in the 2004 OBS network. In addition, there are many very-low-frequency events (VLFEs) in the F-net waveforms with very-low-frequency band-pass filter (0.02 - 0.05 Hz) during the observation period. We found that the identified LFEs were associated with VLFEs since their amplitudes seemed to be correlated. This means that the LFEs and VLFEs show the same phenomenon. Our observations might contribute to reveal the relationship between ordinary aftershocks, slow-events, and megathrust events such as Nankai trough earthquake.

Keywords: LFE, OBS, 2004 off the Kii Peninsula earthquakes

©2019. Japan Geoscience Union. All Right Reserved.

The development of pressure vessel on gouges for rock deformation at seismic rates under water-saturated conditions

*Wei-Ting Lin[1], Li-Wei Kuo[1], Wen-Jie Wu[1], Jia-Jyun Dong[1], Yi-Hung Huang[2]

1. National Central University, 2. MATSUKI HYDRAULIC INDUSTRIAL CO. LTD

To understand earthquake mechanism and fault behavior during earthquake ruptures, experimentalists commonly conduct rock deformation tests with rotary shear apparatus (e.g., low-to high-velocity rock friction experiment, LHVR) which allow deformed at seismic rates. In general, the materials utilized for rotary shear apparatus are both cohesive rocks (e.g., gabbro and carbonate) and incohesive rocks (natural fault gouges and synthetic rock powders), while the latter are deformed at seismic rates and, commonly at low normal stresses (0.5 to 2 MPa confining with a plastic Teflon ring). However, using Teflon rings has issues of gouge extrusion and chemical contamination, in particular, at high normal stresses (>3MPa) and water-saturated condition, and the obtained mechanical data and associated experimental products seem to be questionable. Here we develop a metal pressure vessel for LHVR to deform gouges at seismic rates and, importantly, expand the normal stress capability (up to 15 MPa) and under water-saturated condition. Our results show the resistance from the pressure vessel itself (metal-to-metal contact) is extremely low (friction coefficient ≈0.02), and the result of kaolinite is similar to the previously published data. In particular, both gouge-extrusion and water-leaking was not observed deformed at a normal stress of 15 MPa and equivalent velocity 1 m/s. The designed pressure vessel could fill the gap of experimental conditions among the current used pressure vessels and complete the understanding of fault ruptures.

Keywords: pressure vessel, water-saturated condition, fault gouge, rotary shear experiment

©2019. Japan Geoscience Union. All Right Reserved.

Spatial variations of shallow very low-frequency earthquake activity along the Nankai Trough based on CMT inversion using the 3D heterogeneous model

*Shunsuke Takemura[1], Takanori Matsuzawa[1], Akemi Noda[1], Takashi Tonegawa[2], Youichi Asano[1], Takeshi Kimura[1], Katsuhiko Shiomi[1]

1. National Research Institute for Earth Science and Disaster Resilience, 2. Japan Agency for Marine-Earth Science and Technology

To reveal structural properties around the Philippine Sea plate boundary, we investigated spatial variation of shallow very low-frequency earthquake (SVLFE) activity along the Nankai Trough. By using F-net velocity seismograms for periods of 20-50s, we conducted centroid moment tensor (CMT) inversion of SVLFEs detected by array analysis of Asano et al. (2008 EPS). Our CMT method is basically same as in Takemura et al. (2018 GRL). Source grids were assumed on the boundary of the Philippine Sea plate at horizontal intervals of 0.1°. Green's functions from source grids to F-net stations were evaluated by finite-difference method simulations of seismic wave propagation within the 3D heterogeneous structure model of Takemura et al. (2019 PAGEOPH).

We applied our CMT method to SVLFEs occurred from June 2003 to May 2018. Almost of CMT solutions are low-angle thrust faulting mechanism occurred around the accretionary prism toe. We evaluated spatial variations of SVLFE activity along the Nankai trough by calculating cumulative moment at each source grid. The areas with large cumulative moments appeared near the trench axis of off the Cape Muroto, the Kii Channel and the southeastern Kii Peninsula. We found spatial correlations between cumulative moment, slip-deficit rate (Noda et al. 2018 JGR) and *S*-wave velocities (Tonegawa et al. 2017 Nature Comm.) around the Philippine Sea plate boundary. Such spatial correlations suggest that SVLFEs are effectively activated by mechanically weakening due to pore fluid at surrounding area of strongly locked zone of the Philippine Sea plate.

Acknowledgement
NIED F-net broadband velocity seismograms were used. The catalogs of slow earthquakes were downloaded from the website of slow earthquake database (Kano et al., 2018 SRL). Finite-different method simulations were conducted on the Earth Simulator at the JAMSTEC.

Keywords: Nankai Trough, Shallow very low-frequency earthquake, CMT inversion, Pore fluid pressure, Slip deficit rate

©2019. Japan Geoscience Union. All Right Reserved.

Evaluation of Magnitude and Characteristics of Seismicity of Low Frequency Earthquakes in Parkfield

*Miki Aso[1,3], Naofumi Aso[2], Satoshi Ide[1]

1. Department of Earth and Planetary Science, The University of Tokyo, 2. Tokyo Institute of Technology, School of Science, 3. OYO RMS Corporation

Over a million tectonic low frequency earthquakes (LFEs) have been found in Parkfield along the San Andreas Fault, as 88 families by Shelly and Hardebeck [2010]. Thanks to enormous event detection, interesting characteristics focusing on their event amplitudes have been reported such as the spatial variation along the fault, the exponential frequency distribution for each family, and the relationship with recurrence time [Shelly and Hardebeck, 2010; Shelly, 2010]. However, the relative size of families has not been quantified accurately, because we have to consider various factors such as radiation pattern depending on focal mechanisms, attenuation during wave propagation, and site amplification effects. For quantitative comparison of scale among differently located events, here we estimate the absolute magnitude of each event considered those effects.

We estimate the seismic moment Mo [Nm] and moment magnitude Mw of all LFE events in the catalog of Shelly [2017]. We first stack seismograms of over one million events in the catalog to improve the signal-to-noise (S/N) ratio. Then, we evaluate the absolute amplitude of the original seismograms using the stacked waveforms. Specifically, we evaluate seismic moment Mo by assuming focal mechanisms of each family, attenuation quality factor, site effect estimated by Aso et al. [2019, submitted to JpGU meeting, “Variations of Focal Mechanisms of Low Frequency Earthquake in Parkfield”], and the source time function estimated by Thomas et al. [2016]. Note that we consider the frequency-limited seismic moment Mo, though it is not exactly the same as the original definition of seismic moment measured at a lower frequency than the minimum frequency contained in one phenomenon.

As previously reported by reported by Shelly and Hardebeck [2010], LFEs in the southern part has larger magnitude. We also find that shallower events are smaller than deeper events.

Similarly, most of the frequency distribution for each family shows an exponential distribution which is also reported for LFEs in Cascadia [Sweet et al., 2014] and New Zealand [Chamberlain et al., 2014].

By comparing size and recurrence interval, the events during LFE burst (seconds interval) tend to be larger than the first event of burst, which occurs after hours-to-days quiescence. A similar tendency is found in tremor burst occurring with a longer time scale (~1-week-long) than that of LFEs (~1-minute-long) [Yabe and Ide, 2014]. These might suggest some temporal change in fault rheology and/or some characteristic spatiotemporal behavior such as Brownian slow earthquake processes [Ide, 2008].

Keywords: San Andreas Fault, Parkfield, seismicity, waveform stacking, low frequency earthquake, amplitude evaluation

©2019. Japan Geoscience Union. All Right Reserved.

Tectonic tremor catalog in the Tohoku-Hokkaido-Oki region using S-net

*Satoshi Ide[1], Tomoaki Nishikawa[2], Takanori Matsuzawa[3], Kazuaki Ohta[2], Naoki Uchida[4], Takuya NISHIMURA[2]

1. Department of Earth an Planetary Science, University of Tokyo, 2. Disaster Prevention Research Institute, Kyoto University, 3. National Research Institute for Earth Science and Disaster Resilience, 4. Graduate School of Science and International Research Institute of Disaster Science, Tohoku University

Recently, various slow earthquakes have discovered in the subduction zone off Tohoku and Hokkaido regions along the Japan Trench. In this presentation, we report the detection of tectonic tremors using the Seafloor Observation Network for Earthquakes and Tsunamis along the Japan Trench (S-net), operated by The National Research Institute for Earth Science and Disaster Resilience (NIED).

We used continuous seismograms from August 2016 to August 2018 recorded by short-period sensors at 150 S-net stations. The original data were converted to envelope waveforms and analyzed using the envelope correlation method coded by Ide (2010), for each 300 s time windows with 150 s overlap. Since the results included many ordinary earthquakes with short durations, we regarded the events with durations longer than 20 s as tremors. This number is twice longer than that used for deep tremors in western Japan, reflecting the long-lasting waves in ocean bottom observation.

We found that the detection completeness is not high due to the high seismic activity in the Japan Trench, especially after the occurrence of large earthquakes, with numerous aftershocks falsely detected. We therefore divided the study area into 18 overlapping sub-regions that cover the locations of tremor activity to solve this problem. We detected tremors in each sub-region and merged the results into one catalogue by removing one of any two events within 10 s and 1 degree of each other, depending on their root-mean-square errors. Some tremor-like signals were found near the triple junction off the Boso Peninsula at approximately 34.8˚N. However, visual inspection revealed these events to be ordinary earthquakes, which we excluded from our tremor catalogue. The resultant tremor catalogue will be available in Slow Earthquake Database (Kano et al., 2018).

Keywords: tectonic tremor, slow earthquake, ocean bottom seismometer, S-net, Japan trench

©2019. Japan Geoscience Union. All Right Reserved.

Spontaneous Slow Slip and Runaway Slip in Laboratory

*Miki Takahashi[1]

1. Institute of Earthquake and Volcano Geology, Geological Survey of Japan, AIST

Earthquake nucleation and propagation involves the acceleration of slip on a fault from a background, quasi-static, low-velocity state towards meter-per-second values. From shear experiments using brine-saturated simulated gouge composed of 80:20 wt.% mixtures of halite and muscovite (following e.g. Niemeijer & Spiers, 2007, JGR), Takahashi et al., [2017, G-cubed] recently reported a switch in the dominant deformation process, from distributed viscous flow (pressure solution creep) to localized brittle deformation, at a critical velocity V_c (~20 μm/sec). The direct effect which is normally observed upon perturbations in sliding rate disappears for $V > V_c$, suggesting that runaway fault-slip may be achieved when the sliding velocity exceeds V_c.
At relatively low shear stress, flow mechanisms, such as pressure solution creep and dislocation creep, will be fast enough to effectively suppress slip acceleration. However, with increasing the shear stress, there may be a velocity range in which flow mechanisms still works but not as effective. Hypothesizing that, under constant shear stress boundary conditions, this may lead to spontaneous acceleration followed by deceleration, analogous to a slow slip event. Moreover, imposing the constant shear stress with equal or larger value of the maximum strength of the simulated gouge, I also hypothesize that slip acceleration may proceed as $V > V_c$, inducing a dynamic weakening.
To address these hypotheses, I conducted torque-controlled rotary shear experiments, using brine-saturated, 80:20 wt % mixtures of halite (grain size < 75 μm) and muscovite (grain size < 33 μm) powders. Approximately 1.65 g of the gouge mixture was sandwiched between two teethed steel piston rings, forming an initially 1 mm thick layer. The piston rings had an inner diameter of 38 mm, and an outer diameter of 50 mm. I used a high-velocity rotary shear apparatus designed by T. Shimamoto [e.g., Togo and Shimamoto, 2012], and now installed at the Geological Survey of Japan (GSJ). The apparatus was modified to enable torque control with an accuracy of ±0.002 in the friction coefficient (μ), at a normal stress of 5 MPa. Rotation displacement is measured using a potentiometer installed close to the piston ring at the rotating side.
A preliminary result shows the velocity evolution after stepwise changes in the shear stress. At low shear stresses, corresponding to the pressure solution creep-controlled regime, transient increasing velocity towards a steady-state values suggests stable sliding. At $\mu \approx 0.6$, the simulated gouge shows spontaneous acceleration to $V \approx 1$ μm/sec, followed by deceleration. Lastly, under a constant shear stress condition equivalent to $\mu = 0.67$, spontaneous slip acceleration occurred followed by dynamic weakening at $V \approx V_c = 20$ μm/sec. More experiments and microstructural observations will help to elucidate the relationship between the critical velocity and the switch among dominant deformation mechanisms.

Keywords: shear stress control test, spontaneous acceleration/deceleration, dynamic weakening

©2019. Japan Geoscience Union. All Right Reserved.

Hydration and amorphization of quartz rocks during high-velocity frictional sliding: An examination of fault gouge from friction experiments of synthetic quartz

*Yuko Onoe[1], Hirotaka Iida[2], Akito Tsutsumi[1], Aki Takigawa[1]

1. Graduate School of Science, Kyoto University, 2. Geothermal Engineering Co., Ltd.

Various types of rocks and fault gouges display weakening of frictional strength at high-velocities, and in many cases, it is caused by high-temperature faulting processes such as frictional melting and thermal decomposition of fault materials. On the other hand, siliceous rocks display weakening of frictional strength at relatively slow slip velocity of ~1 mm/s. This weakening is a specific phenomenon because frictional heat is not sufficient to induce the high-temperature transformation reactions in this slip velocity range [Di Toro et al., 2004]. Goldsby and Tullis [2002] proposed gel lubrication model to explain the weakening of siliceous rocks; in which model frictional weakening likely results from production and shearing of hydrated amorphous silica layer along a fault in quartz rocks. But the relationship between the frictional weakening and hydration and amorphization of fault gouge is not clear yet.

This study aims to elucidate the mechanism of the frictional weakening observed for siliceous rocks. We conducted a series of friction experiments on synthetic quartz samples using a rotary-shear, intermediate-to high-velocity friction testing machine. Experiments were carried out under a constant normal stress condition of 1.5 MPa and at slip velocities of 5 μm/s, 10 μm/s, 105 μm/s, 1 mm/s, 10 mm/s and 105 mm/s. In this study effect of drying the sample on the frictional behavior were examined by introducing dry air to the chamber of the sample. After the friction tests, the gouge material on the slip surfaces were collected and analyzed by FTIR.

The frictional behavior of the synthetic quartz differs between room humidity and dry conditions; velocity weakening was observed for both conditions, however, velocity weakening starts at lower slip velocities for the dry experiments. Under DRY conditions, the frictional weakening occurs at slip velocity around 10 μm/s. From the results of the FTIR analysis, hydration of the gouge is confirmed for all the samples tested in this study. The FTIR result also indicates that the faster the slip velocity, the more the crystal structure of the gouge is destructed.
It is showed that under both DRY and Room Humidity conditions, at least the gouge generated on the friction surface of the sample which showed slip weakening is hydrated, consistent with the weakening model of Goldsby and Tullis [2002].

©2019. Japan Geoscience Union. All Right Reserved.

Constraining S Wave Velocity of the Source Region of Shallow Very Low-Frequency Earthquakes

*Takeshi Akuhara[1], Takashi Tonegawa[2]

1. Earthquake Research Institute, The University of Tokyo, 2. Research and Development center for Earthquake and Tsunami, Japan Agency for Marine-Earth Science and Technology

Shallow very low-frequency earthquakes (VLFEs), which are believed to occur in the vicinity of megathrusts, have been often associated with elevated pore fluid pressure. Lines of evidence for this idea include a small amount of stress drop, high tidal sensitivity, and reduced P wave velocity inferred from active source seismic surveys. Revealing the physical properties of the source region of shallow VLFEs will lead to a better understanding of their generation mechanisms. However, the challenge lies in the difficulty of acquiring S wave velocity in fine resolution.

Recent achievements by the authors may help overcome this issue. Akuhara et al. (2019) developed a robust technique to estimate Green's functions of receiver side structures from offshore seismograms, which are typically ill-conditioned due to water reverberations. Tonegawa et al. (2017) inverted Rayleigh wave admittance (i.e., a ratio of ground displacement to hydraulic pressure) for shallow S wave velocity structures beneath DONET seafloor observatories at the Nankai Trough subduction zone. Their velocity models show low-velocity zones that characterize the source regions of shallow VLFEs. However, a smoothing constraint imposed on the models renders their interpretation somewhat difficult.

This study presents preliminary results from transdimensional inversion of receiver-side Green's function estimated by the method of Akuhara et al. (2019), where we adopt a prior constraint by the velocity models of Tonegawa et al. (2017). Complementary to the Rayleigh admittance, the Green's function approach is sensitive to velocity contrasts and thus will offer an improved resolution.

Keywords: shallow very low frequency earthquake, seismic velocity structure, ocean bottom seismometer, bayesian analysis

©2019. Japan Geoscience Union. All Right Reserved.

Quantitative relationship between aseismic slip propagation speed and frictional properties

*Keisuke Ariyoshi[1], Jean-Paul Ampuero[2,3], Roland Burgmann[4], Toru Matsuzawa[5], Akira Hasegawa[5], Ryota Hino[5], Takane Hori[1]

1. Japan Agency for Marine-Earth Science and Technology, 2. Université Côte d'Azur, 3. California Institute of Technology, 4. University of California, Berkeley, 5. Graduate School of Science, Tohoku University

Recent observations show evidence of propagation of postseismic slip, whose propagation speed may contain information about the mechanical properties of faults. Here, we develop a new analytical relationship between the propagation speed of aseismic slip transients and fault frictional properties, modeled by a rate- and state-dependent friction law. The relationship explains the propagation speed of afterslip in 3-D numerical simulations to first order. Based on this relationship, we identify systematic dependencies of afterslip propagation speed on effective normal stress σ and frictional properties (the coefficients a and a-b which quantify the instantaneous and the steady-state velocity-dependence of friction, respectively, and the characteristic slip distance d_c of fault state evolution). Lower values of the parameter $A=a\sigma$ cause faster propagation in areas where the passage of the postseismic slip front induces large shear stress changes $\Delta\tau$ compared to A, which are typically located near the mainshock rupture. In areas where $\Delta\tau/A$ is small, typically more distant from the mainshock, afterslip propagation speed is more sensitive to (a-b) σ. The propagation speed is proportional to initial slip velocity and inversely proportional to d_c. The relationship developed here should be useful to constrain the frictional properties of faults based on observed propagation speeds, independently of rock laboratory experiments, which can then be used in predictive numerical simulations of aseismic slip phenomena.

Keywords: rate- and state-dependent friction, effective normal stress, stress perturbation

©2019. Japan Geoscience Union. All Right Reserved.

Comprehensive detection of very low frequency earthquakes off the Pacific coasts of Hokkaido and Tohoku, northeastern Japan

*Satoru Baba[1], Akiko Takeo[1], Kazushige Obara[1], Takanori Matsuzawa[2], Takuto Maeda[3]

1. Earthquake Research Institute, University of Tokyo, 2. National Research Institute for Earth Science and Disaster Resilience, 3. Graduate School of Science and Technology, Hirosaki University

Very low frequency earthquakes (VLFEs), classified as one type of slow earthquakes, occur near seismogenic zones. VLFEs off the Pacific coasts of Hokkaido and Tohoku in northeastern Japan occur around subducting plate interfaces near trenches. Asano et al. (2008) found VLFEs in the off-Tokachi region, the southern part of the Pacific coast of Hokkaido along the Kuril Trench, by array signal processing using high-sensitivity accelerometers of Hi-net operated by National Research Institute for Earth Science and Disaster Resilience (NIED). In recent years, VLFEs off the Pacific coast of Tohoku were found by visually checking broadband seismograms of F-net operated by NIED and other events were detected by the matched-filter technique using waveforms of detected events as templates (Matsuzawa et al., 2015). However, the number of detected VLFEs may have been limited because of the small number of the VLFE templates in previous studies. Baba et al. (2018, SSJ) set four virtual epicenters off the Pacific coasts of Hokkaido and Tohoku and detected VLFEs by the matched-filter technique using numerically simulated waveforms as templates. We extended virtual epicentral gridsto make more comprehensive detection of VLFEs.

We used continuous seismograms of F-net seismometers from January 2003 to July 2018 after applying a band-pass filter of 0.02–0.05 Hz. We set 123 virtual epicentral grids off the Pacific coasts of Hokkaido and Tohoku, and computed the synthetic waveform from the source at each virtual epicenter by the finite difference method with a three-dimensional velocity structure model, namely, Japan Integrated Velocity Structure Model (Koketsu et al., 2012). The fault mechanisms were assumed to be consistent with the geometry of the plate boundary and a plate motion model, NUVEL-1A. We then calculated station- and component-averaged cross-correlation coefficients (averaged CC) between synthetic waveforms and the data of F-net seismograms every 1 s, and selected the events which have averaged CC above nine times of the median absolute deviation of the distribution. This method is, however, sensitive to regular earthquakes and teleseismic events as well. We then excluded the signal of regular earthquakes by discarding events with the amplitudes of more than 160 nm/s at 1-2 Hz in vertical components at the nearest stations. Moreover, to remove teleseismic events, we used the USGS earthquake catalog and discarded events with high amplitudes and low averaged cross-correlation coefficients.

VLFE activities in the off-Tokachi and off-Aomori regions show synchronized episodic bursts in the interval of several months. VLFEs in the off-Tokachi region was rapidly increased by the afterslip of the 2003 Tokachi-Oki earthquake. Those in the off-Iwate and off-Ibaraki regions, located out of the coseismic slip area of the 2011 off the Pacific coast of Tohoku Earthquake (hereinafter, the Tohoku earthquake), were also rapidly increased by the afterslip of the Tohoku earthquake. VLFE activity in the off-Miyagi region is characterized by episodic bursts in the interval of several months to one year before the Tohoku earthquake, but it became low since then. VLFE activity in the off-Fukushima region show dramatic increase after an Mw 6.9 earthquake at off-Fukushima on July 19, 2008. In the off-Miyagi and off-Fukushima regions, located within or at the edge of the coseismic slip area of the Tohoku earthquake, VLFE activity has been low since the Tohoku earthquake probably because the earthquake released the

©2019. Japan Geoscience Union. All Right Reserved.

stress almost completely. These results suggest that VLFEs are sensitive to the stress perturbation and can be a slip meter that reflect spatiotemporal change of the interplate slip, as has been indicated by previous studies. Consequently, one possible cause of these episodic VLFE bursts in the off-Tokachi, off-Aomori and off-Miyagi regions may be the intermittent release of small portion of stress accumulated by interplate locking between plates in the interval of several months to one year. The interval of episodic bursts is shorter than a periodicity of slow slips ranging from 1 to 6 years off the Pacific coasts of Tohoku indicated by Uchida et al. (2016).

©2019. Japan Geoscience Union. All Right Reserved.

Spatio-temporal evolution of long- and short-term slow slip events in the Tokai region, central Japan estimated from a very dense GNSS network, during 1997-2017

*Hiromu Sakaue[1], Takuya NISHIMURA[2], Jun'ichi Fukuda[3], Teruyuki Kato[4]

1. Graduate School of Science, Kyoto University, 2. Disaster Prevention Research Institute Kyoto University, 3. Earthquake Research Institute,The University of Tokyo, 4. Hot Springs Research Institute of Kanagawa Prefecture

The long-term slow slip events (SSEs) have been reported on the subducting Philippine Sea Plate in the Tokai region, central Japan during 2001-2005 and 2013-2016. Many short-term slow slip events have been also observed there since 1996. We analyzed GNSS data from 1997 to 2017 to estimate spatiotemporal distribution of interplate slip associated with these SSEs in this study. The GIPSY-OASIS II software (version 6.1) was used to estimate daily coordinates of GNSS stations operated by GSI and JUNCO (the Japanese University Consortium for GPS Research). It is well known that GNSS time series have many systematic signals and noises that do not result from SSEs. They include, for example, seasonal variations, co- and post-seismic deformation of the 2004 southeast off Kii Peninsula earthquakes (M_w 7.3/7.4), the 2008 Ibaraki-ken-oki earthquake (M_w6.9), the 2008 Fukushima-ken-oki earthquake (M_w7.0) and the 2011 Tohoku-oki earthquake (M_w9.0), and crustal deformation of volcanic activity on the northern Izu Islands in 2000. After removing them, we applied a modified Network Inversion Filter (NIF) [Fukuda et al., 2008] to estimate daily slip and slip rate on the subduction plate interface.
Our results suggest that not only long-term SSEs (M_w~7.1 and M_w~6.7) in 2000-2005 and 2013-2016, but also short-term SSEs (M_w<6.1). The maximum estimated daily slip rates for short-term SSEs are an order of magnitude larger than those of the long-term SSE, and peak slip for short-term SSEs migrates along strike with LFTs synchronously. It suggests that LFTs are loaded directly by SSEs, and that slip rate regulates LFT genesis. We will present the change of back slip rate between inter short-term SSEs and characteristics of short-term SSEs (e.g. slip rates and recurrence interval) depending on the occurrence of long-term SSE.

Keywords: slow slip event, Tokai region, GNSS

©2019. Japan Geoscience Union. All Right Reserved.

Broadband excitation of acoustic emission in granular stick-slip : experiments and spectral analyses

*Hidekazu Fukumizu[1], Ikuro Sumita[2]

1. Earth and Environmental Science Course, Division of Natural System, Graduate school of Natural Science and Technology, Kanazawa University, 2. School of Geosciences and Civil Engineering, Kanazawa University

Slow slip and tremor are observed to occur simultaneously (e.g., Rogers and Dragert, Science, 2003). Such observation can be modelled using granular stick-slip experiments which show that the timing of the slips and acoustic emission (AE) are well correlated (e.g., Johnson et al., GRL, 2013, Jiang et al. GRL, 2017). AE waveforms are complex (e.g., Michlmayr & Or, Gran. Matt., 2014), and we do not fully understand the details of the temporal change of AE during the slip. Here we report the results of granular stick-slip experiments which focus on how their spectra depend on the shear rate, particle size and container size.

We shear glass beads contained in a stainless steel beaker using a rotating viscometer to which a vane spindle is attached (Higashi and Sumita, JGR, 2009), and measure the shear stress and AE at 200kHz. We use broadband accelerometers and microphones to measure AE. Four accelerometers are attached at the outer rim of the beaker, and each are separated by an angle of 90 degrees.

We integrate the acceleration to obtain AE velocity –time series data and analyze their characteristics in broad band. We find that although AE has a broad spectrum, the spectra show that there are two characteristic frequency (f) components ; a high-f (of the order of 100 Hz) and a low-f (of the order of 10Hz) components. The velocity waveforms recorded at antipodal positions, show that the high-f components are in phase, whereas the low-f components are of the opposite phase. This indicates that the mechanism which excite these components differ : the high-f component may correspond to AE excited by particle rearrangement, whereas the low-f component may correspond to the translational motion of the container. Indeed we find that the frequency of the low-f component depends on the container size.

We also conducted experiments using a rheometer in a parallel-plate setup and confirmed that these two different components exist. When the particle size becomes larger, the amplitude of the shear stress and the AE velocity increases. Furthermore we find that the mean frequency of the normalized power spectra rose to a higher frequency, thus correlating with the stress increase.

Our experiments indicate that AE is excited in broadband, and that their frequency components can be used to infer the interparticle stress. Such excitation appear to be analogous to tremors and very low frequency earthquakes that are also excited simultaneously.

Keywords: granular matter, stick-slip, acoustic emission, earthquake, tremor

©2019. Japan Geoscience Union. All Right Reserved.

Episodic tremor and slip silently invades strongly locked megathrust in the Nankai Trough

*Masayuki Kano[1], Aitaro Kato[2], Kazushige Obara[2]

1. Graduate school of science, Tohoku University, 2. Earthquake Research Institute, The University of Tokyo

Recent seismic and geodetic observations in subduction zones have revealed that slow earthquakes have preceded some large earthquakes (e.g., Kato et al., 2012; Mavrommatis et al., 2014; Ruiz et al., 2014). Characterization of slow earthquakes and their relation to large earthquakes provides important clues to constrain a wide spectrum of slip rates on tectonic faults. In this study, we report new evidence of a slow slip transient at the downdip edge of the strongly locked seismogenic zone in the western Nankai Trough in southwest Japan based on GNSS time series. This slow slip transient was remotely excited during an episodic tremor and slip at the downdip extension of the locked zone. Through this remote triggering, the frequent occurrence of the deep episodic tremor and slip invades the strongly locked megathrust zone and may intermittently increase the probability of large earthquakes in the Nankai Trough.

Acknowledgments

We used GNSS data provided by the Geospatial Information Authority of Japan. This study was supported by the JSPS KAKENHI Grant Number JP15K17743 in Grant-in-Aid for Young Scientists (B), JP18K03796 in Grant-in-Aid for Scientific Research (C), JP16H06473 and JP16H06474 in Scientific Research on Innovative Areas “Science of Slow Earthquakes.”

Keywords: Slow slip events, Slow earthquakes, Western Shikoku, GNSS

©2019. Japan Geoscience Union. All Right Reserved.

Spatial distribution of the electrical resistivity beneath western part of Shikoku Island where long-term SSE events have repeatedly occurred

*Makoto Uyeshima[1], Maki Hata[1], Hiroshi Ichihara[2], Ryokei Yoshimura[3], Koki Aizawa[4]

1. Earthquake Research Institute, The University of Tokyo, 2. Graduate School of Environmental Studies, Nagoya University, 3. Disaster Prevention Research Institute, Kyoto University, 4. Institute of Seismology and Volcanology, Faculty of Sciences, Kyushu University

In the Bungo channel area at the western margin of the Nankai megathrust rupture zones, the long-term slow slip events (SSE) repeatedly occurred about every 6 or 7 years. Since the last large-scale SSE event occurred in 2010, we will have a next large event soon. In order to obtain the electrical resistivity structure in the vicinity of the SSE area and examine its temporal change, we have started the Network-MT survey in the western part of the Shikoku Island facing the Bungo channel since April, 2016. Just before beginning of the observation, a tiny-scale SSE event occurred in the Bungo-channel (Ozawa, 2017, Hirose et al., 2018). We selected 17 areas in the western part of the Shikoku Island and installed 3 or 4 electrodes in the respective areas. The electrical potential differences with typical electrode spacing of several km are measured by using metallic telephone line network. We also measure the geomagnetic field at two stations in the target region. With the aid of the BIRRP code (Chave and Thomson, 2004), we could estimate the frequency-domain Network-MT response functions of good quality between the voltage difference and the magnetic field. The Network-MT response functions were directly inverted to estimate the 3-D resistivity structure in this area with the aid of the DASOCC Network-MT 3-D inversion code (Siripunvaraporn, Uyeshima & Egbert, 2004).

Conductive portions are commonly detected in the mid-crust of the target region. Their roots are just on the upper surface of the subducting Philippine Sea slab. This may suggest dehydration there. Among the spatial distribution of resistivity, that of seismic P-wave attenuation (Kita and Matsubara, 2016), and that of SSE slips (e.g. Ozawa et al., 2013, Yoshioka et al., 2015, Hirose et al., 2018), some mutually related features are detected. Low Qp (high attenuation) areas tend to correspond to highly conductive areas. The low Qp and highly conductive area are detected just above the subducting slab and outside of the SSE area. Inside the SSE area, while Qp takes generally high values, a patchy conductive area is detected in overall resistive background structure.

This study is supported by JSPS KAKENHI Grand Number JP16H06475 in Scientific Research on Innovative Areas "Science of Slow Earthquakes". It is also partly supported by the Ministry of Education, Culture, Sports, Science and Technology (MEXT) of Japan, under its Earthquake and Volcano Hazards Observation and Research Program. We acknowledge staffs of the Nippon Telegraph and Telephone WEST Corporation for their cordial support in the survey. We also thank H. Abe, A. Takeuchi and Y. Suwa for their help in preparing and installing instruments.

Keywords: slow slip event beneath the Bungo Channel, 3-D resistivity structure, Network-MT observation

©2019. Japan Geoscience Union. All Right Reserved.

Variations of scaling relationships for shallow tremor observed along the Nankai trough

*Masaru Nakano[1], Suguru Yabe[1]

1. Japan Agency for Marine-Earth Science and Technology

Scaling relationships of seismic phenomena is one of keys to understand the source processes. Size distributions of slow earthquakes as low-frequency earthquakes (LFEs), non-volcanic tremor (NVT), very-low-frequency earthquakes (VLFE), and slow-slip events (SSEs) have been studied in many locations. Some studies showed that the size distribution follow an exponential law (e.g. Watanabe et al., 2007; Hiramatsu et al., 2008; Chestler and Creager, 2017), while others showed that power law distributions better explain the observations (e.g. Kao et al., 2010; Bostock et al., 2015; Nakamura and Sunagawa, 2015).

Most of previous studies are for slow earthquakes that occur in regions deeper than the source region of megathrust earthquakes, and only a limited number of studies have been carried out for shallow slow earthquakes beneath accretionary prism as observed along the Nankai trough. Although observed characteristics of shallow and deep ones are very similar, physical conditions as temperature and pressure much differs in these region.

In our previous studies (Nakano et al., 2018SSJ, AGU), we obtained the result that shallow tremor follows a power law distribution with b values of about 1. In this study, we further analyzed tremor activities beneath the Muroto fore-arc basin. using data from DONET2. We estimated the seismic energy of tremor signals using the same method as our previous studies, during intensive activities starting in September 2015, April 2016, February 2017, and February 2018. The source region of each activity is different from each other, spanning between off Shiono-Misaki and off Cape Muroto.

The size distribution of each activity mostly follow power-law distributions, but the b value varies from 0.7 and 1.7. We note that the activity in 2016 is also well fitted by an exponential law, probably due to narrow range of observed event size distribution. Similar result has been obtained in the 2018 activity in Kumano. The size distribution deviate from a power law for largest events as observed in Kumano activities. This deviation at larger events would be due to limited system size, expected from the theoretical stochastic model of tremor by Ide and Yabe (2018). The upper limit of event size, and accordingly the system size, varies from activity to activity.

We also investigated the relation between the seismic energy and duration of tremor events. The relation also follows a power law, with slopes of 2.0 to 2.6 in Kumano, and 1.5 to 3.3 in Muroto. These values are again consistent with the expectation value of 2 from the model of Ide and Yabe (2018).

These investigations represent that the scaling relationships of shallow tremor are mostly consistent with the 2D PCA model by Ide and Yabe (2018). Further studies would be necessary to reproduce the observed variations of the scaling parameters.

Acknowledgments: We used DONET data and JMA and USGS earthquake catalogs in the analysis. This research was supported by JSPS KAKENHI Grant Number 16H06477 in Scientific Research on Innovative Areas “Science of Slow Earthquakes”

Keywords: DONET, Nankai trough, earthquake size distributions

©2019. Japan Geoscience Union. All Right Reserved.

Low-frequency earthquakes triggered by teleseismic surface waves by Ryukyu subduction zone.

Ayumi Kinjo[1], *Mamoru Nakamura[1]

1. Faculty of Science, University of the Ryukyus

We investigated low-frequency earthquakes (LFEs) in the Ryukyu Trench region that were triggered by surface waves from teleseismic earthquakes. Although these LFEs in the southwestern Ryukyu arc have previously been explored by Chao et al. (2016), their hypocenter distribution is not known in detail.

We selected 50 earthquakes from January 2004 to December 2016, which had magnitudes greater than 7.5 and epicentral distances between 9–150˚. We used the waveforms of 6 broadband seismometers in the Ryukyu arc from F-net (NIED) to analyze the surface waves. We also used the waveforms of 20 short-period seismometers in the Ryukyu arc from the Japan Meteorological Agency to detect trace LFEs in Ryukyu Island and determine their hypocenters.

The LFEs in the Yaeyama and Okinawa regions were observed. In the former region, during the passage of the surface waves, spindle-shaped LFE waveforms were first observed at Hateruma (south of Yaeyama Islands), and later at other stations in the Yaeyama region. Similarly, for the latter region, during the passage of the surface waves, spindle-shaped LFE waveforms were first observed at ZMM or Tamagusuku (south of Okinawa Island), and later at other stations in the Okinawa region. These observations suggest that the sources of the triggered LFEs were near or south of Hateruma and Tamagusuku.

We subsequently determined the hypocenters of the triggered LFEs. We computed the LFE travel-time difference between two stations using cross-correlations of the waveforms (Obara, 2002). The travel-time difference of waveforms of the LFEs corresponded to travel-time difference of the S-phase because S-waves were dominant in the LFEs, and P-waves were weak. The hypocenters were determined using the grid search method (Chao et al., 2013). In the Yaeyama region, the LFE hypocenters were mainly distributed near Hateruma Island. In the Okinawa region, they were distributed south of Okinawa Island. These positions are similar to the positions of the LFE hypocenters that accompany very low frequency earthquakes (LFE-VLFEs). This suggests that faulting in a cluster of LFE-VLFEs would be active with dynamic stress change.

In the Okinawa and Yaeyama regions, LFEs are triggered when the peak ground velocity of the surface wave is greater than 0.1 cm/s. This threshold value is similar to that for LFEs in Taiwan (Chao et al., 2013), suggesting that the weak friction coefficient at the plate interface of the Ryukyu Trench is similar to that in Taiwan.

Keywords: low frequency earthquake, surface wave, Ryukyu Trench

©2019. Japan Geoscience Union. All Right Reserved.

Detection of small surface displacement accompanying deep low-frequency tremor in Shikoku region, southwest Japan

*Yutaro Okada[1], Takao Tabei[2]

1. Faculty of Science, Kochi University, 2. Faculty of Science and Technology, Kochi University

In many subduction zones in the world, several types of slow earthquakes occur with different depths on the plate interface and some of them are accompanied by surface displacement. In this study, we focus on small surface displacements coincident with non-volcanic deep low-frequency tremor in Shikoku region in the Nankai subduction zone, southwest Japan.

We use daily coordinates time series from 107 GEONET stations located in Shikoku and tremor catalog compiled by NIED (Maeda and Obara, 2009; Obara et al., 2010) in the period from Jan. 1 2004 to Dec. 31 2008. Since GNSS coordinates changes due to the Bungo Channel long-term slow slip events are well reproduced by S-shaped logistic function, we use the same function to extract small displacement coincident with tremor activity. At first, we convert horizonal components into N50°W direction after removing annual and semiannual variations and common-mode errors. Next, we fit the logistic function to a data segment with variable time window of 5, 7, and 9 days and estimate an amplitude of the function. The fitting is checked by a correlation coefficient between the observation and calculation. We apply this fitting for entire data period at all stations sliding data segment. Finally, we extract displacement when the amplitude of the fitted logistic function exceeds a certain criterion (1.8 mm in this study) and the correlation coefficient is large enough. If the extracted displacement is coincident with tremor activity within 30 m from the GNSS station, we adopt it as the tremor-related displacement. As a result, 225 events are adopted.

Spatial pattern of the tremor-related displacement seems to be related with the location and mechanism of the tremor event though closer inspection is needed. However, we extract much more small displacements by fitting a logistic function, of which the source is unknown. The logistic function is effective to reproduce transient displacement of the surface but we need to reconsider noise reduction of GNSS time series, time constant of logistic function, time window of the fitting, and so on.

Keywords: GNSS, southwest Japan, Deep low frequency tremor

©2019. Japan Geoscience Union. All Right Reserved.

Long-term temporal change in crustal resistivity beneath western Shikoku

*Futoshi Yamashita[1], Yoshimori Honkura[1]

1. National Research Institute for Earth Science and Disaster Resilience

In southwest Japan, various slow earthquakes such as deep low-frequency tremor and short/long-term slow slip events occur at the subducting plate interface (e.g. Obara and Kato, 2016, Scinence). In western Shikoku, Magneto-telluric (MT) survey was carried out along the dip direction of subducting Philippine Sea plate. The survey revealed an existence of low-resistivity structure in the lower crust in this region (Yamashita and Obara, 2009, AGU). In order to investigate a relationship between this characteristic structure and the activity of slow earthquakes, NIED has been carrying out continuous MT observations in western Shikoku since 2008. Here we show the observational records over 10 years and then discuss a relationship between observed temporal change in crustal resistivity and activity of the long-term slow slip event (L-SSE). Two observational sites KBN and IKT are available as of 2019. Qualities of data recorded at these sites are relatively fine. However, in order to improve the quality for discussing subtle change in MT parameters, we apply a data processing method same as Honkura *et al.* (2013, Nature comm.); we use only data whose coherency between electric and magnetic field is higher than a threshold. The lowest frequency of processed data is 0.00028 Hz. The processed MT parameters, apparent resistivity and phase, do not show any long-term temporal changes at KBN site even after temporal stops of observation over some months. On the other hand, apparent resistivity at IKT site, which is around 10 km southwest away from KBN site, shows temporal reduction at a frequency lower than 0.0022 Hz between 2010 and the middle of 2012. It is known that L-SSE occurred beneath the Bungo Channel in 2010 (e.g. Yoshioka *et al.*, 2015, GJI), which could induce resistivity change in the lower crust and then it might be detected by our MT observation.

Keywords: Crustal resistivity, Long-term slow slip event, Magneto-telluric method

©2019. Japan Geoscience Union. All Right Reserved.

Slow decay of postseismic deformation compared with aftershocks following the 2011 Tohoku-oki Earthquake

*Yuta Mitsui[1], Shunsuke Morikami[2]

1. Department of Geosciences, Shizuoka University, 2. Formerly at Graduate School of Science and Technology, Shizuoka University

In the literature, decays of postseismic deformation rates of large earthquakes were almost comparable to aftershock decays for subduction earthquakes (e.g. Hsu et al. (2006), Lange et al. (2014)). They are characterized by the modified Omori law with p~1, which means "afterslip-triggerred aftershocks". In this study, we focus on the 2011 Tohoku-oki megathrust earthquake using GNSS and seismicity data. On the basis of high-rate analysis of RINEX data and the F3 solution provided by the Geographical Survey Institute (GSI), we clarify the characteristics of postseismic deformation and aftershocks up to five orders of magnitude of time scale. We find that the p value for the postseismic deformation (p_m) is ~0.7, by contrast, that for the aftershocks (p_n) is ~1. Because a rate-and-state-friction model (Helmstetter and Shaw (2009)) predicted $p_m>=p_n$, another or an additional physical mechanism is necessary to explain the data of $p_m<p_n$. One important mechanism is viscoelastic relaxation of asthenosphere, thus we try fitting the postseismic deformation data by combination of afterslip and viscoelastic relaxation (a model of Suito (2017)). The fitting is not poor but fails to reproduce the Omori-like decay. More complex combination models may improve the fitting, but would not make simple Omori-like power-law decays. We need more sophisticated physical model to represent the decay characteristics of postseismic deformation.

Keywords: aftershocks, postseismic deformation, afterslip, viscoelastic relaxation, the 2011 Tohoku Earthquake

©2019. Japan Geoscience Union. All Right Reserved.

Serpentinite dehydration in subduction shear zones formed at source depths of slow earthquakes

*Yasushi Mori[1], Miki Shigeno[1], Kohtaro Ujiie[2], Kazuya Noro[2], Tadao Nishiyama[3]

1. Kitakyushu Museum of Natural History and Human History, 2. University of Tsukuba, 3. Kumamoto University

Long-term slow slip events (L-SSEs) and episodic tremor and slip (ETS) occur along the subduction plate boundary at depths of 30–45 km (Obara, 2002; Shelly et al., 2006). These deep slow earthquakes are probably induced by high pore-fluid pressure. Based on geological study, we propose that the high pore-fluid pressure can be produced by metasomatic dehydration of serpentinite in subduction shear zones at source depths of deep slow earthquakes.

The Nishisonogi metamorphic rocks in Kyushu, Japan, are part of a Late Cretaceous subduction complex metamorphosed at $P \approx 1$ GPa and $T \approx 470$ ˚C. The P-T conditions are close to those of source depths of deep slow earthquakes. Serpentinite mélanges intercalated with the metamorphic rocks contain blocks of metabasite, metapelite and albitite. The mélange matrix consists of chlorite-actinolite schist (CAS), talc schist and schistose serpentinite. Intense shear deformation is concentrated in the CAS, and the serpentinite mélanges have the characteristics of anastomosing shear zones.

Bulk chemical composition of the rocks suggests that the CAS is the metasomatized mixture of serpentinite and metabasite. In addition, chemical mass balance indicates considerable dehydration during the CAS formation, along with a slight increase of solid volume. These findings suggest that the CAS formation involves the build-up of pore-fluid pressure. The high pore-fluid pressure results in the concentration of shear deformation into the weakened CAS.

Dehydration of serpentinite probably plays a key role in deep slow earthquakes (Poulet et al., 2014; Okazaki and Katayama, 2015). Thermal dehydration of serpentinite occurs at ~600 ˚C along the subduction plate boundary (Auzende et al., 2006), which is much higher temperature than that of source depths of deep slow earthquakes. In contrast, metasomatic dehydration of serpentinite described here could occur at source depths of deep slow earthquakes.

Auzende, A-L., et al., 2006, EJM, 18, 21–33. Obara, K., 2002, Science, 296, 1679–1681. Okazaki, K., Katayama, I, 2015, GRL, 42, 1099–1104. Poulet, T., et al., 2014, JGR, 119, 4606–4625. Shelly, D.R., et al., 2006, Nature, 442, 188–191.

Keywords: serpentinite mélange, shear zone, dehydration, pore fluid pressure, Nishisonogi metamorphic rocks, deep slow earthquakes

©2019. Japan Geoscience Union. All Right Reserved.

Earthquake swarms following very low-frequency earthquakes in the central Ryukyu Trench

*Mamoru Nakamura[1]

1. Faculty of Science, University of the Ryukyus

Earthquake swarms occur frequently from Amami Island to Okinawa Island, near the axis of the central Ryukyu Trench. These earthquake swarms recur every few years and typically followed swarms of very-low frequency earthquakes (VLFE) that occur in a similar area. I have investigated the relationship between the VLFEs and the subsequent earthquake swarms in the central Ryukyu Trench, using the earthquake catalog provided by the Japan Meteorological Agency (JMA). For the VLFEs, I used the catalog by Nakamura and Sunagawa (2015) and the extended catalog to December 2018.

Results show that the VLFE swarms occurred approximately one month before the subsequent earthquake swarms began near the trench axis in this region. Previous noteworthy earthquake swarms occurred on August 2005 (with a maximum magnitude of 4.7), April 2009 (with a maximum magnitude of 5.1), May 2016 (with a maximum magnitude of 5.6), and September 2018 (with a maximum magnitude of 6.2).

Prior to the earthquake swarm that occurred in August 2005, a VLFE swarm started near Okinawa Island three months before and its activity moved intermittently from Okinawa Island to Amami Island. In the case of the earthquake swarm that occurred in April 2009, a VLFE swarm started near Amami Island and the subsequent swarm occurred two weeks after the start of the VLFE swarm. The location of the VLFE swarm moved intermittently closer to Okinawa Island. In the case of the earthquake swarm that occurred on May 2016, the VLFE swarm started near Amami Island and its active cluster moved intermittently towards Okinawa Island. The subsequent earthquake swarm started near the trench axis, approximately twenty days after the occurrence of the VLFE swarm. In the case of the earthquake swarm that occurred in September 2018, the VLFE swarm started near Okinoerabu Island (the midpoint between Amami Island and Okinawa Island) and the activity moved intermittently to Okinawa Island. The earthquake swarm occurred approximately twenty-five days after the start of the VLFE swarm. The location of the cluster of the 2018 earthquake swarm was slightly landward from the trench axis.

The faulting associated with these earthquake swarms was of normal type, corresponding to intra-slab earthquakes in the subducting Philippine Sea plate. I calculated the Coulomb Failure Stress (delta-CFS) assuming that a small slow slip event (SSE) occurred on the plate interface. Our results show that the positive delta-CFS that accelerated the normal faulting could not have occurred in the subducted slab near the trench axis until the slip of the SSE had reached close to the trench axis. This suggests that the SSE propagated from Amami Island to Okinawa Island accompanying the activation of the VLFE swarm, the slip of the SSE then propagated close to the trench axis, and the normal-faulting earthquake swarm in the slab was induced by the positive delta-CFS caused by the SSE.

Keywords: Very low frequency earthquake, Ryukyu Trench, Earthquake swarm

©2019. Japan Geoscience Union. All Right Reserved.

Seismic imaging in the central Nankai trough, off Shionomisaki to Kii channel

*Yasuyuki Nakamura[1], Shuichi Kodaira[1], Tetsuo No[1], Yuka Kaiho[1], Gou Fujie[1], Seiichi Miura[1], Kazuya Shiraishi[1]

1. Japan Agency for Marine Earth Science and Technology

Shallow very low frequency events (sVLFE) have been reported in the Nankai Trough subduction zone recently. In the central part of the Nankai trough, sVLFE were observed off Kii channel and Shinomisaki, but not reported in the area between them, off western Kii peninsula. We conducted a seismic survey with R/V *Kaimei* in November and December 2018 in Nankai subduction zone off Kii channel to Shonomisaki to investigate the structural features and its possible relationship to the sVLFE. R/V *Kaimei* fired 10600 $inch^3$ air gun array at every 50 m and a streamer cable (4.3 km at shortest, 5.7 km at longest) recorded the seismic signals. We acquired 23 seismic profiles with the length of ~ 75 km in dip direction at 4 km line separation and four profiles of ~ 90 km in strike direction at the shallowest part of the subduction zone. In addition, seven dip profiles with the length of 35 km were acquired off Kii channel to cover the lowermost part of the landward slope densely. The streamer cable was towed at a depth of 25 m to relatively enhance the lower frequency signals for better imaging of the deeper structure. Preliminary processed seismic profiles exhibited the structural variation in the survey area. Deformation of the hanging wall sediments and decollement were well imaged especially ~ 20 –30 km from the trough axis. Top of subducting Philippine Sea plate can be observed through ~ 40 –50 km from the trough axis in some of the obtained profiles. A pair of apparently low angle deep strong reflections were imaged at ~ 7 –8 s two-way time around 40 - 50 km from the trough axis off the western Kii peninsula, which was located slightly east and landward of the area with sVLFE. The shallowest part of the subduction zone in the area where the recent sVLFE activity was not reported, a slope basin with younger sediments deposited over the body of the accretionary prism is imaged, and the deformation was not observed in the slope basin. This suggests the thrust faults within the accretionary prism have not been active recently in this area. We will further process acquired data to obtain clearer seismic images and discuss the structural features and its connection to the observed seismological events in the Nankai Trough.

Keywords: Nankai Trough, seismic imaging

©2019. Japan Geoscience Union. All Right Reserved.

Attempt to Detect Intra-plate SSEs Based on F3 Solution of GEONET

*Yusaku Tanaka[1]

1. Earthquake Research Institute

Slow earthquakes have been detected all over the world and providing new insights into earthquakes. However, most of slow slip events (SSEs) were detected only on plate boundaries and intra-plate SSE was detected only once in Hokkaido. Thus, I attempt to detect intra-plate SSEs all over Japan using F3 solution of GEONET by GSI. I analyze the F3 data with six steps, i.e., (1) removing outliers by setting a term of mean + two times standard deviation for 1/4+1/4 year before-and-after each datum except for the datum itself and considering it is an outlier when it is out of the term, (2) removing disconnections estimated from the offsets and linear trends of 60+60 days before-and-after each datum with the least square method, (3) searching statistically significant temporal changes of the trends by using AIC, (4) cheking visually the time series in which the temporal changes are detected, (5) estimating the displacements from the trend chagnes, and (6) verifying the deformations by numerical calculation by setting rectangular faults.

As of 18th Feb 2019, my study has proceeded to the step (4). In the JpGU meeting, I will report the results of this analysis.

Keywords: crustal deformation, slow slip event, geonet

©2019. Japan Geoscience Union. All Right Reserved.

A new hydrothermal, low to high speed rotary-shearing apparatus: Reproduction of slow/megathrust earthquakes in laboratory

*Takehiro Hirose[1], Wataru Tanikawa[1], Yohei Hamada[1], Keishi Okazaki[1]

1. Kochi Institute for Core Sample Research, Japan Agency for Marine-Earth Science and Technology

Earthquakes involve a wide range of slip rates, from slow/aseismic to fast/seismic slip along faults. Thus, frictional properties of faults over wide slip rates (nm/s to m/s), in particular under hydrothermal conditions similar to those expected in seismogenic zones are essential for a unified understanding of all earthquake events. A new hydrothermal, low to high speed rotary-shearing apparatus has been installed at Kochi/JAMSTEC, in order to study the fault constitutive properties at slow to fast slip rates and the physicochemical mechanisms underlying mechanical responses. The apparatus is currently capable of applying slip rates from 100 nm/s to 2 m/s, normal stress up to 55 MPa, fluid pressure up to 120 MPa and temperature up to 450oC with infinite displacement. We have been improving the apparatus to work as we intended. In pilot tests, we used metamorphic rocks (pelitic and green schists) as starting materials that are potentially distributed at and below seismogenic zones along hot and young subduction zones. We will present our preliminary results with the basic design of the apparatus.

Keywords: friction, hydrothermal, slow to fast slip

©2019. Japan Geoscience Union. All Right Reserved.

Very low-frequency earthquakes in western Shikoku remotely triggered by the 2016 Mw5.9 off-Kii Peninsula earthquake

*Masatoshi Miyazawa[1]

1. Disaster Prevention Research Institute, Kyoto University

Slow tectonic events are known to be sensitive to external stress perturbations due to passing seismic waves and earth tides. High-amplitude surface waves from large earthquakes have transiently triggered low-frequency earthquakes (LFEs) and slow slip events (SSEs) in subduction zones. However, dynamic triggering of very low-frequency (VLF) earthquakes during the arrival of seismic waves from a large, distant earthquake has not been observed. Because both the VLF earthquake and the surface wave have similar characteristic periods, remote triggering is not easily detected by using existing methods. We developed a particle filter/smoother for time series analysis combined with Markov chain Monte-Carlo methods, to detect seismic signals and estimate the maximum likelihood source parameters of VLF events that might have been remotely triggered. We apply this method to seismic data from the Mw5.9 earthquake, which occurred on 1 April 2016 (UTC), off Kii Peninsula. We found that six VLF events with magnitudes about 4, likely occurred in the seismogenic regions of ambient LFEs, and were likely triggered by the arrivals of high-amplitude surface waves. The triggering stress changes are from 0.4 to 1.5 kPa, which are similar to the values for LFEs triggering reported previously. Since there were no triggered LFEs in western Shikoku following the 2016 earthquake, these VLF earthquakes are more sensitive to stress changes caused by surface waves from large earthquakes.

Keywords: Very low-frequency earthquake, Remote triggering

©2019. Japan Geoscience Union. All Right Reserved.

Underground structure around source region of slow earthquakes in western Shikoku obtained by receiver function analysis

Akira Hikita[1], Aitaro Kato[1], *Kazushige Obara[1], Akiko Takeo[1], Takeshi Akuhara[1]

1. Earthquake Research Institute, The University of Tokyo

Various types of slow earthquakes have been observed at subduction zones surrounding the Pacific Ocean. It has been suggested that elevated pore fluid pressure plays an essential role in the generation of slow earthquakes because low velocity or high Vp/Vs zones have been also reported along the plate boundaries where they occur. In Tokai region of the Nankai subduction zone, Kato et al. (2010) revealed that long-term slow slip event (SSE) occurs at the boundary between the continental lower crust and the subducting Philippine Sea plate and episodic tremor and slip (ETS) occurs between the mantle wedge and the subducting plate. Kato et al (2010) also revealed that oceanic crust indicates higher Vp/Vs in the long-term SSE region than in the ETS region. In contrast, Toya et al. (2017) reported that the oceanic crust indicates higher Vp/Vs in the ETS region than in the long-term SSE region in western Shikoku of the same subduction zone. In this study, we revealed configurations of continental Moho discontinuity and subducting oceanic crust and investigated relationship between slow earthquakes and the surrounding seismic velocity structure by receiver function analysis using a dense seismic array in western Shikoku.

As a result, continuous continental Moho and oceanic crust are clearly imaged along both north-south and east-west oriented seismic lines. The plate boundary in the south part, where the distinct continental Moho is not imaged, has steeper slope than the north part along the north-south line. ETS occurs between the mantle wedge and the subducting plate, and long-term SSE occurs along a contact between the continental crust and the oceanic crust.
We show that the oceanic crust indicates much higher Vp/Vs than the hanging wall by using also the reverberation phases. This high Vp/Vs means the elevated fluid pore pressure within oceanic crust due to dehydration. Vp/Vs in the oceanic crust is higher in the deep part of the long-term SSE region than in the ETS region like as the case of Tokai. It is assumed that fluid would accumulate within the oceanic crust owing to low permeability of the continental crust in the long-term SSE region. In contrast, serpentinization of the mantle wedge just above the ETS region could reduce fluid pressure in the oceanic crust. Furthermore, Vp/Vs in the oceanic crust becomes lower in the deeper part beyond the ETS depths, suggesting that eclogization is completed at the depths.

Keywords: Receiver function, episodic tremor and slip, long-term slow slip event, low seismic velocity layer

©2019. Japan Geoscience Union. All Right Reserved.

Hypocenter determination of deep low frequency tremors beneath the Kii Peninsula by backprojection of seismic array data

*Kodai Sagae[1], Hisashi Nakahara[1], Takeshi Nishimura[1], Kazutoshi Imanishi[2]

1. Graduate School of Science,Tohoku University, 2. National Institute of Advanced Industrial Science and Technology (AIST)

A seismic array analysis enables us to detect weak signals if they are coherent. In Cascadia, a high accuracy hypocenter determination of tremors has been carried out by using dense seismic arrays (e.g.,Ghosh et al.,2012). In Southwest Japan, previous studies (e.g.,Ueno et al.,2010) applied the **MU**ltiple **SI**gnal **C**lassification (MUSIC) method (Schmidt,1986) to data of surface seismic arrays at Western Shikoku and carried out the hypocenter determination. However, a quantitative threshold for event detection was not considered. Sagae et al.,(2018 SSJ) introduced an event detection threshold based on the coherence of waveforms among stations, and improved tremor detection by using a surface seismic array installed by AIST at the Kii Peninsula. We applied the MUSIC method to this data in times when tremor events were detected and estimated slownesses and arrival azimuths of tremor signals. Their temporal variations suggested tremor migration. However, we did not carry out hypocenter determination. In this study, we determine hypocenters of tremors by backprojection using the estimated slownesses and arrival azimuths.
The surface seismic array installed by AIST at the Kii Peninsula was composed of 39 three component velocity sensors with a natural frequency of 2.0 Hz and a sampling frequency of 200 Hz. This array had an aperture of about 1.5 km and the sensors were arranged in a cross shape with interval spacings of 50~100 m. We analyze data for 1 year (between July 7,2013 and July 7,2014), because the number of sensors is stable in this period.
We focus on a frequency of 3Hz, which is within the tremor's dominant frequency band of 2-10 Hz. Data processing is described as follows. (1) We calculate averaged coherence of waveforms for all station's pairs. (2) We detect tremor events by setting a detection threshold based on the averaged coherence. (3) We estimate slownesses and arrival azimuths by applying the MUSIC method to the data when tremors are detected. (4) We project them back to the plate boundary (Hirose et al.,2008) and determine source locations by using S wave velocity model JMA2001 (Ueno et al.,2002).
We detected 5 periods of high tremor activities during the 1 year period. We compared the hypocenter distributions determined by our method and those of AIST tremor catalogue which were determined from an envelope cross correlation method. Temporal variation of tremors in this study were almost consistent with the AIST catalogue. We were also able to detect about 2.5 times as many events as the AIST catalogue. It is easier to identify temporal variation of tremors in more detail because our study improved temporal resolution up to 10 sec.
We projected temporal variations of tremor distributions into along-strike and along-dip directions. The results show tremors tend to migrate along the strike in time scales of several days with migration velocities of 6.0~9.3 km/day. Along-dip migrations of tremors with a short timescale of several hours are also detected. When we focused on the initial part of tremor activities, tremors tend to start in deeper parts and gradually migrate to shallow parts. These migration velocities were estimated to be about 1.0 km/hr (24 km/day) in the up-dip direction.
In this study, we were able to improve tremor detection by setting the event detection threshold based on the coherence of seismograms for stations pairs in a surface seismic array. Thanks to this, we were able to locate 2.5 times more tremors than the conventional method. We made it easier to keep track of tremor migrations by improving the temporal resolution of hypocenter determination to 10 sec.
We used the plate boundary model (Hirose et al.,2008). We downloaded the AIST catalogue from Slow

©2019. Japan Geoscience Union. All Right Reserved.

Earthquake Database (Kano et al.,2018).

Keywords: Deep low frequency tremor, Seismic array analysis, Backprojection, MUSIC method, Kii Peninsula, Hypocenter determination

©2019. Japan Geoscience Union. All Right Reserved.

Triggered tremors and stress perturbations due to surface waves

*Ryohei Ikeda[1], Naoki Suda[1]

1. Hiroshima University

Surface waves radiated from distant large earthquakes sometimes trigger a series of deep non-volcanic tremors with intervals of 20-30 seconds, which are the same as dominant periods of surface waves [e.g. Miyazawa & Brodsky 2008]. Understanding the triggering mechanism is important because it provides us clues to the slip process occurring along the transition zone of subducting plate interface. Dynamic stress perturbations due to surface waves that triggered tremors were estimated on the order of 1 to 10 kPa [e.g. Chao & Obara 2016]. To study the relationship between triggered tremors and stress perturbations due to surface waves, we computed theoretical dynamic stresses due to surface waves from large earthquakes by using observed and theoretical surface waves.

We focused on the triggered tremors in the western Shikoku region of the Nankai subduction zone. Most of them occurred in two clusters where tectonic tremors actively occur. We computed theoretical dynamic stress perturbations due to surface waves from 106 earthquakes between 2004 and 2016 with moment magnitudes of 7.0 or grater. The receiver points at which the stress components were computed are at the plate boundary below the N.TSAF and N.KWBH stations, which are the nearest stations of the triggered tremors in F-net and Hi-net, respectively. PREM [Dziewonski & Anderson 1981] and Global CMT catalog [Dziewonski et al. 1981; Ekstrom et al. 2012] were used for the Earth model and the seismic sources for computing theoretical surface waves. Source time functions were approximated with triangular functions whose half durations are equal to the centroid time lags.

The stress change at the plate boundary by the surface wave was estimated based on the method of Spudich et al. (1995). This method consists of two stages: (1) Estimate the stress at the surface from the observed ground velocity and (2) Estimate the stress at the plate boundary from the stress at the surface estimated in (1). In these estimations, we used theoretical proportional relations between the ground velocity and the surface stress and those between the surface and the deep stresses in the frequency domain, which were obtained from the theoretical surface waves. We used the N.TSAF and N.KWBH records as the observed ground velocity. The records from the latter were corrected using the method of Maeda et al. (2011).

The stress components in the source coordinates were transformed to the stress normal to the plate interface and the stress along the possible slip direction of tremor source. The normal and slip directions were obtained from the model plate interface [Baba et al. 2002; Nakajima & Hasegawa 2007; Hirose et al. 2008] and plate convergence vectors [Miyazaki & Heki 2001]. We computed waveforms of the Coulomb failure function (ΔCFF) using a frictional coefficient of 0.2 at periods between 20 and 50 seconds.

©2019. Japan Geoscience Union. All Right Reserved.

Results from the N.TSAF records show that the maximum ΔCFF for the events that triggered tremors are greater than 0.5 kPa. The magnitudes of triggering earthquakes are greater than 7.5. ΔCFFs were generally overestimated when we used the corrected N.KWBH records because the correction did not well work, in particular, for the earthquakes with magnitudes less than 7.5. The important point is that not all of the events that provided the stress perturbations greater than 0.5 kPa triggered tremors. This shows that the stress perturbation due to surface waves cannot be the unique triggering condition: other conditions, for example, stress perturbations due to possible background slow slip events and/or high pore fluid pressure are required.

©2019. Japan Geoscience Union. All Right Reserved.

Numerical modeling of long- and shallow slow slip events including shallow region in Hyuganada and western Nankai, Japan

*Takanori Matsuzawa[1], Bunichiro Shibazaki[2]

1. National Research Institute for Earth Science and Disaster Resilience, 2. Building Research Institute

Recent studies reported deep long-term slow slip events (SSEs) in the Hyuganada and western Nankai region (e.g., Kobayashi, 2014; Takagi et al., 2016; Ozawa. 2017). Shallow SSEs are also recently reported with low-frequency tremor and very low-frequency earthquakes (e.g., Araki et al., 2017; Nakano et al., 2018). In our previous study, we have numerically reproduced recurring deep long- and short-term SSEs in the Shikoku region (Matsuzawa et al., 2013), considering the actual distribution of slow earthquakes and configuration of the subducting Philippine Sea plate. We aim to reproduce deep long- and short-term SSEs and shallow SSEs in a single numerical model applying a similar approach in Matsuzawa et al. (2013).

We adopt a rate- and state-dependent friction law (RS-law) with cutoff velocities. We assume that (a-b) value in the RS-law is negative within the deep short-term SSE region, and positive outside that region. The deep short-term SSE region is modeled based on the actual distribution of deep low frequency tremor. Deep long-term SSE region is assumed based on the geodetic observation (Hirose et al., 2011). To focus on the Hyuganada and western Nankai region, we assume stable sliding region with positive (a-b) in the south of the Kyushu-Palau ridge. We also assume low cutoff velocity at the depth shallower than 9 km to reproduce shallow SSEs. Low effective normal stress is assumed at the depth of SSEs. Temporal evolution of slip velocity is numerically simulated, introducing elastic response and realistic configuration of the plate interface.

In terms of deep long-term SSEs in Hyuganada, a simple extension of the long-term SSE region in the Bungo Channel cannot reproduce the segments of observed SSEs. Narrowed long-term SSE region in the dip direction between Bungo and southern Hyuganada can reproduce three observed segments of SSEs, i.e., Bungo, northern Hyuganada, and southern Hyuganada. In addition, recurring shallow SSEs along trench in Hyuganada and off Ashizuri are reproduced in our result. Megathrust earthquakes are divided into two regions; off Shikoku and Hyuganada in our result. The segments of these large earthquakes may be attributed to the long-term SSE region in the Bungo Channel. Our model comprehensively reproduces various SSEs and megathrust earthquakes, including newly found long-term SSEs.

Keywords: Slow Earthquake, Slow Slip Event, Hyuganada

©2019. Japan Geoscience Union. All Right Reserved.

Further evidence for the influence of a subducting-ridge on the spatial strain accumulation and release pattern in the shallow eastern Nankai Trough, based on VLFE distribution

*Akiko Toh[1], Chen Wan-Jou [2], Doug Dreger[3], Wu-Cheng Chi[2], Satoshi Ide[1]

1. University of Tokyo, 2. Institute of Earth Sciences, Academia Sinica, 3. UC Berkeley

We investigated the distribution and focal mechanisms of very low frequency earthquakes (VLFEs) located in the shallow part of the eastern Nankai trough. While they are mainly explained as low angle thrust faulting along the plate boundary (Sugioka et al., 2012; Nakano et al, 2016), along the strike variation in their distribution has also been observed, likely caused by a subducting-ridge (Toh et al., 2018). Such variations could be closely related to the strain release pattern, or the tsunamigenic potential, of this region, thus warrant a further comprehensive study.

We used 3 component records of broadband ocean bottom seismometers equipped in Dense Oceanfloor Network system for Earthquakes and Tsunamis 1 (DONET1). Records of VLFE activities that occurred immediately beneath the network in 2015, 2016 and 2017 for 1-2 weeks each year, are used. Through visual inspections, we detected 335 VLFEs whose signals are observed at least 6 stations on vertical component filtered between 16-32s.

Instead of estimating the source parameters for one after another for all the events, we searched for densely located event groups inferred by similarities of the maximum amplitude variations measured per event, and, so far, worked only on the grouped events. The purpose of this event selection process is to get an overview of the distribution using the simple quantity (i.e. max. amplitude variation) that can be evaluated for every VLFE, and to avoid a bias that may be caused by eliminating events that are merely difficult to process (i.e. do not fit synthetic waveforms) mostly due to complicated long source time functions that characterize VLFEs. The grouping is conducted by a hieratical density-based clustering method HDBSCAN (Campello et al., 2003), and 197 events were grouped into 26 groups that consists of 2 to 35 events.

We determined the centroid origin time, location and 5-component of moment tensor of VLFEs that maximize the normalized variance reduction (VR) between the observed and synthetic velocity waveforms. The waveforms are bandpass filtered either between 16-32s or 20-50s, depending on signal duration and S/N per event. The time and location are grid-searched at intervals of 0.01 degree in horizontal, 1 km in depth between 5 and 10km bsl., and 1 s in time. At each grid, the moment tensor is estimated using the code TDMT_INV (Dreger, 2003) that conducts full-waveform linearized inversion in time domain. Green’s functions are calculated using the code by Herrmann (2013) based on wavenumber integration. We used a 1D structural model based on a 2D model obtained by an active source survey (Nakanishi et al., 2008). Although the 1D structure is assumed, the large variations in station elevation (1.9-4.3 km bsl) are considered in Green’s function calculations.

We obtained 50 events with good VR (>65%). Among the 26 groups, 6 groups ended up with no events of high VR, mostly due to being located outside of the network. Almost all the VLFEs are reasonably explained by low angle thrust faulting. From the obtained distribution, the strong influence of the subduction-ridge located on the northwestern side of DONET1 is inferred. On the southwestern side

©2019. Japan Geoscience Union. All Right Reserved.

where there is no ridge-subduction, VLFEs are distributed beneath outer-ridge toward the trench axis. The estimated depths for the ones located beneath the outer-ridge are deep (7–10km with median at 8km), which are consistent with the depth of the plate boundary of this area. In contrast, on the northeastern side, VLFEs are mostly distributed landward of outer-ridge and their estimated depth are shallow (5–8km with the median at 7km) as previously suggested (To et al., 2015). The shallow depths can be explained by the uplifted plate boundary in this area due to the subducting-ridge. Furthermore, they are located to landward of the peak of the subducting-ridge, which can be reasonably explained by the change in shear stresses and pore pressures caused by the subducting-ridge.

Keywords: Nankai trough, Very low frequency earthquake (VLFE), Accretionary prism, HDBSCAN, Broadband ocean bottom seismometer

©2019. Japan Geoscience Union. All Right Reserved.

Evidence for semi-brittle flow in mantle-wedge serpentinites under high pore fluid pressure and their implications for deep low frequency earthquakes

Kengo Kataoka[1], Yurina Nagata[1], *Ken-ichi Hirauchi[1], Ryosuke Oyanagi[2], Atsushi Okamoto[3], Katsuyoshi Michibayashi[4]

1. Department of Geosciences, Faculty of Science, Shizuoka University, 2. Japan Agency for Marine-Earth Science and Technology, 3. Graduate School of Environmental studies, Tohoku University, 4. Department of Earth and Planetary Sciences, Nagoya University

In southwest Japan, deep low frequency earthquakes occur at the base of the shallow serpentinized mantle wedge. In order to understand deformation styles of the mantle wedge serpentinite, we conducted structural and petrological analysis of a paleo-mantle wedge body that has experienced serpentinization at pressure–temperature conditions corresponding to source areas of low-frequency earthquakes, in the Sanbagawa belt, central Shikoku. The serpentinite body has a block-in-matrix structure that result from pervasive fragmentation. At outcrop and thin section scales, the distribution of blocks follows a power law distribution with exponent $2.32 < D < 2.37$ (2-D). The block has experienced complete serpentinization, characterized by randomly-oriented antigorite aggregates. The matrix also consists of antigorite, which was formed due to dissolution–precipitation process of the block in the presence of H_2O. Antigorite aggregates in the matrix along localized shear planes is characterized by a strong crystallographic preferred orientation with a dominant [010](001) slip system, suggesting dislocation glide on (001) planes. We suggest that deep slow earthquakes occur by semi-plastic deformation of the serpentinized mantle wedge, under low effective normal stresses.

Keywords: slow earthquakes, low frequency earthquake, mantle wedge, serpentinite

©2019. Japan Geoscience Union. All Right Reserved.

Spatial distribution of slow slip events off the Boso peninsula from 1996 to 2018 under sparsity constraints

*Ryoko Nakata[1], Hideitsu Hino[2], Tatsu Kuwatani[3,4], Takahiro Akiyama[5], Shoichi Yoshioka[6], Masato Okada[7], Takane Hori[1]

1. Japan Agency for Marine-Earth Science and Technology, 2. The Institute of Statistical Mathematics, 3. Department of Solid Earth Geochemistry, Japan Agency for Marine-Earth Science and Technology, 4. PRESTO, Japan Science and Technology Agency, 5. Graduate School of Science, Kobe University, 6. Research Center for Urban Safety and Security, Kobe University, 7. Graduate School of Frontier Sciences, The University of Tokyo

We estimated spatial distribution of the six slow slip events (SSEs) off the Boso peninsula, central Japan, from 1996 to 2018. We have applied an inversion method called fused regularization, a type of sparsity constraint, suitable for detecting discontinuous changes in the model parameters, for evaluation function [Nakata et al., 2017]. In this study, to shorten calculation time, we used a type of approximation method by Obuchi and Kabashima [2016] to search hyperparameters, not LOO-CV (leave-one-out cross validation).

From our tentative results, the maximum slips for the 2002, 2011 and 2018 SSEs were large, and the 1996, 2007 and 2013 SSEs were small. The slip distributions of the 2011 and 2018 SSEs seem to be distributed southward than 2002. It is confirmed by numerical experiments that the difference in slip distribution is not due to GNSS station distribution.

Furthermore, we are conducting numerical simulation of earthquake generation cycles, which modelling SSEs off the Boso peninsula and M~8 earthquakes along the Sagami Trough. We will discuss slip distributions of SSEs and locked area during an interseismic period.

©2019. Japan Geoscience Union. All Right Reserved.

Marine electromagnetic observations around a slow earthquake region in the western Nankai trough

*Hiroshi Ichihara[1], Tada-nori Goto[2], Tetsuo Matsuno[3], Noriko Tada[4], Shinya Sato[2]

1. Earthquake and Volcano Research Center, Nagoya University, 2. Graduate School of Engineering, Kyoto University, 3. Ocean Bottom Exploration Center, Kobe University, 4. JAMSTEC

Slow earthquakes have been believed to relate to fraction of pore fluid around plate boundary. Thus, imaging of electrical resistivity (conductivity) distribution is essential to understand slow earthquakes. However, many of SSE areas are distributed beneath the ocean, we need marine electromagnetic (EM) observations. In this presentation, we report preliminary results of marine EM observations in the western part of Nankai Trough (off Miyazaki prefecture and off western Kochi prefecture, Japan) where SSEs, VLF events and regular earthquakes (e.g. 1968 off-Hyuga earthquake, M7.5) are known. We deployed eight ocean bottom electro-magnetometers (OBEMs) and recovered seven of them between 2017 and 2018. In addition to EM fields, two OBEMs measure absolute pressure to detect short period crustal deformations caused by SSE. We estimated high quality magnetotelluric responses based on Chave and Thomson (2004). However, the responses show strong three-dimensionality of resistivity distribution and strong coast effect (e.g. Key and Constable, 2011). They indicate that we need to apply three-dimensional imaging techniques for seafloor magnetotelluric data.

Keywords: Slow earthquake, magnetotelluric, OBEM, Nankai trough, off Miyazaki

©2019. Japan Geoscience Union. All Right Reserved.

Dynamics of precipitating injection fronts inside of structured medium

*Yutaka Sumino[1], Shunsuke Tanaka[1], Miyuki Kunihiro[1]

1. Tokyo University of Science

Recent study on a slow earthquake elucidates that the migration of water within a mantle wedge may play relevant roles[1]. The flow inside of confined geometry, such as within a soil, is often described by the Darcy’s law, where flow velocity is described by the gradient of fluid pressure. Interestingly, however, the water within a mantle wedge contains large amount of solid contents, and hence, a precipitation can be formed within the water[2]. For this reason, the dynamics of fluid flow under the effect of precipitation reaction should be explored.

Based on the above motivation, we explored the 2-dimensional confined chemical garden[3] as an analogue experiment for the fluid flow within a mantle wedge[4]. The system consists of two fluids with a quasi-two dimensional thin cell, so called a Hele-Shaw cell. The cell was filled with a fluid, and the other fluid is injected from the center of the cell. The flow in a Hele-Shaw cell can be described by the Darcy’s law. Furthermore, the mixing of these fluids leads to the precipitation. Thus, the flow observed in 2-dimensional confined chemical garden system is analogous to the one of water in a mantle wedge with precipitation formation.

Our previous study[4] showed that a filamentous pattern appears when the injection speed is high enough, whereas the symmetrical circular front was formed for lower injection speed. This results indicates that the propagation radius of injection front can be drastically different depending on the injection speed. In addition, the number of moving filaments saturate whose value is proportional to the injection speed. Such tendency can be understood with our boundary model adopting the effect Laplace pressure and the conservation of precipitation at the boundary. The model further predicts existence of optimal curvature for the moving front with which the required pressure for the motion is minimum. The curvature, and the speed of the optimal boundary motion is independent of the injection speed. These experimental and theoretical study thus worked well in the 2-dimensional Hele-Shaw cell. However, actual condition in a mantle wedge should have quenched structure, which is absent in a Hele-Shaw cell.

In order to fill the gap between actual condition in a mantle wedge and our analogue experiments, we modified our Hele-Shaw cell to have periodic pillar structure. As a control parameter, we changed the pillar to pillar distance, w, as shown in attached figure. The filament pattern showed meandering motion without pillar structures ($w = \infty$). We found that the filament pattern showed straight motion especially when w agreed with the typical filament width. Our modified mathematical model adopting nonlinear response of permeability with precipitation density numerically reproduced such experimental results. This results indicates that the propagation distance of injected fluid can be modified by the locally quenched disorder within a mantle wedge.

In this paper, we show detailed setup for experiments, as well as mathematical model.

[1] A. Tanaka et al. Earth, Planets and Space 70, 25 (2018).
[2] K. Ujiie, et al., *Geophys. Res. Lett.* **45**, 5371–5379 (2018).

©2019. Japan Geoscience Union. All Right Reserved.

[3] F. Haudin et al., *Proc. Natl. Acad. Sci. U.S.A.* **111**, 17363–17367 (2014).
[4] S. Wagatsuma, et, al., *Phys. Rev. E* **95**,052220 (2017).

Keywords: injection, fluid, precipitation

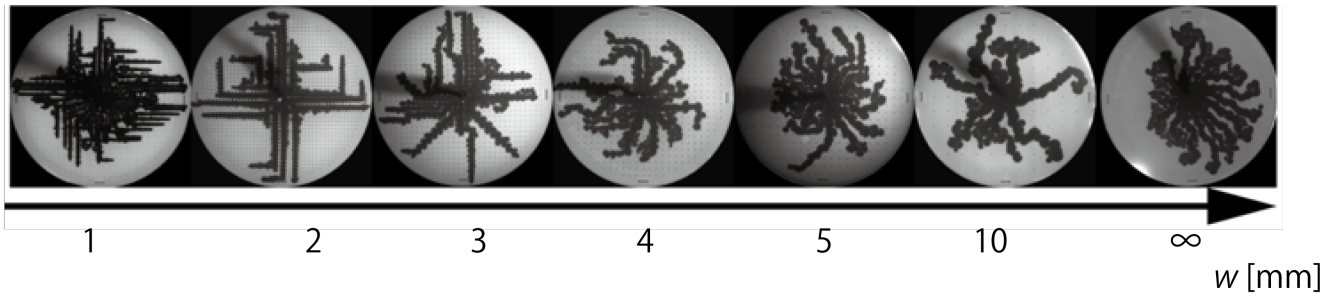

©2019. Japan Geoscience Union. All Right Reserved.

Permeability changes of simulated low permeable fault rocks induced by intermediate velocity friction test

*Wataru Tanikawa[1]

1. Japan Agency for Marine-Earth Science and Technology, Kochi Instutute for Core Sample Research

Earthquake events often associate with fluctuations of flow rate, pore pressure and pore fluid chemistry at a subsurface of earthquake rupture zones. The co-seismic hydrological changes are explained by changes in fluid permeability of fault zones during earthquakes, and the permeability change plays an important role for dynamic fault processes as well. Therefore, we newly designed a system to estimate water permeability changes during and after low to high velocity shear deformation using a rotary shear apparatus and simulated fault rocks.

A pair of hollow cylindrical samples made by low permeable Belfast dolerite and Aji granite were used as test specimens. To calculate permeability, a radial flow from the inner wall to the outer wall of the specimen was induced by applying a differential pore pressure (0.01 to 0.2 MPa) between inner and outer walls. We performed friction tests at normal stress of 2 MPa, rotation speed from 0.0003 to 0.6 m/s, and slip displacement of 1 m.

The results showed that permeability increased during sliding at every slip velocity condition, and higher velocity friction caused more abrupt increase in permeability. After the end of sliding, permeability gradually decreased with time and then became nearly constant value. Reduction rate of permeability 5 min after slip increased with slip rate. Fiction coefficient was decreased with sliding velocity. Frictional heating is a key to explain slip velocity dependence of permeability (flow rate). Temperature rise caused by frictional heating will reduce fluid viscosity, therefore, apparent permeability reduction after sliding can be explained by an increase in fluid viscosity by cooling. Pore pressure build-up by frictional heating can increase aperture, therefore, this process can explain permeability enhancement during sliding and velocity dependences on permeability increase and friction coefficient.

Keywords: permeability, friction coefficient, frictional heating

©2019. Japan Geoscience Union. All Right Reserved.

Modified relation between the coupling and tremor rates around the Shikoku region

*Tadafumi Ochi[1]

1. Institute of Earthquake and Volcano Geology, Geological Survey of Japan, The National Institute of Advanced Industrial Science and Technology

In Ochi and Takeda (2018, EPS), I examined the relation between the interplate coupling velocity and the number of deep low-frequency tremors in the same place around the Shikoku region, southwest Japan. I found that there were some spot-like points where the coupling and the tremor count were well correlated, and that the regression line required the coupling rate to be the plate convergence rate in this region under conditions of zero tremor count rate. One of the problems to be resolved is the interpretation of the first matter 'spot-like points' mentioned above. According to the pairs of time series of the coupling rate and tremor count rate, some pairs show a time delay, and the others show a small fluctuation in the tremor count rate that seems to be independent of the coupling rate. It is interesting that whether the an ill-correlation just comes from an oversimple model of the linear regression I used in the previous study, or really reflects some physical background. In order to answer this question, I construct the model which allows the fluctuation in the tremor count rate that is independent from the coupling rate and observe the fitness of the model. At this time, some trial models that allow the shorter period fluctuation in the tremor count rate than in the coupling rate and temporal change in the period achieve clear correlations. In the presentation, I will show the results of the various trials.

Keywords: Interplate coupling, Low-frequency tremor

©2019. Japan Geoscience Union. All Right Reserved.

Spatiotemporal distribution of regular and very low-frequency earthquakes in the northern part of the Ryukyu subduction zone

*Youichi Asano[1], Kazuhiko Goto[2], Hiroshi Yakiwara[3], Shuichiro Hirano[3]

1. National Research Institute for Earth Science and Disaster Resilience, 2. Association for the development of earthquake prediction, 3. Nansei-toko Observatory for Earthquakes and Volcanoes, Kagoshima University

We have investigated detailed spatiotemporal distribution of regular and very low-frequency (VLF) earthquakes including an Mw 6.3 interplate event near Tanegashima along the Ryukyu trench on Jun. 08, 2019. This earthquake was followed four Mw4-5 class regular and many VLF earthquakes by the end of Jan., 2019. At first we estimated centroid moment tensors of these regular and several VLF earthquakes, respectively, from broadband seismograms recorded at the NIED F-net and temporally observation stations. In the next step, the known VLF earthquakes were selected to be template events for searching unknown VLF earthquakes from continuous seismograms. If there are several candidates of VLF earth quake, we select the most coherent event with a maximum cross-correlation coefficient averaged over all stations in every 180 seconds. Finally we estimated locations of the selected events from phase shift of the wavelets between the template and these selected events. Obtained result shows that activity of VLF earthquakes after the Mw 6.3 earthquake was started in the adjacent area east of this Mw 6.3 earthquake; however, the following Mw4-5 regular earthquakes occurred south of this area in the period of Jan. 25-30, 2019. In this period, the front of the VLF activity migrated toward east from these Mw4-5 events. Such a spatiotemporal distribution of regular and VLF earthquakes suggests that the after slip of the Mw 6.3 and/or an SSE caused these regular and VLF earthquakes.

Acknowledgment

This study is partly supported by JSPS KAKENHI Grant Number JP16H06473.

Keywords: very low-frequency earthquake, Ryukyu subduction zone

©2019. Japan Geoscience Union. All Right Reserved.

Possible tectonic tremor activities near the VLFE epicenters in the Sanriku-Oki region in 2011

*Hidenobu Takahashi[1], Ryota Hino[1], Yusaku Ohta[1], Naoki Uchida[1], Syuichi Suzuki[1], Masanao Shinohara[2], Takanori Matsuzawa[3]

1. Graduate school of Science Tohoku University , 2. Earthquake Research Institute, University of Tokyo, 3. National Research Institute for Earth Science and Disaster Resilience

Recently various kind of slow earthquakes have been discovered along the Japan Trench subduction zone. Prior to the occurrence of the 2011 Tohoku-oki earthquake, occurrence of slow slip events associated with migration of small earthquake epicenters and tectonic tremors was reported near the hypocenter of the Tohoku-Oki earthquake (e.g. Kato et al., 2012; Ito et al., 2015; Katakami et al., 2018). As a different type of a slow-earthquake family, Very Low Frequency Earthquakes (VLFEs) have been detected in more broad areas (Matsuzawa et al., 2015). Takahashi et al. (in prep.) detected the seismic signals from the VLFEs by short-period ocean bottom seismograms (OBS) deployed in the vicinity of the VLFE epicenters in the Sanriku-Oki region, just after the Tohoku-Oki earthquake. They further identified a number of VLFE-like events, not recognized by the onshore data. Here, we report on possible tectonic tremor activities in the same area based on the OBS data after the 2011 Tohoku-oki earthquake.
We detected four sequences of continuous rises of amplitudes on the OBS records. Each of the sequence has a duration of ~ half a day. The sequences were composed of numerous wave trains with good correlations in their growths and decays in observed amplitudes among the stations, but no distinct P- or S-wave onsets were identified for individual wave trains. Interestingly, the spatial variation of the wave trains amplitudes is similar to those of the previously identified VLFEs. These observations suggest that the sequences were composed of small seismic events closely located each other and to the known VLFEs. It is also notable that some of the VLFE-like events discovered by the OBS data were contained in the sequences. We regard the discovered sequence as a kind of tectonic tremor activity and will inspect their characteristics, such as frequency content and its variability, to clarify their nature and discuss their relevance to slow slip events along the shallow subduction interface, which might promote the activities.

Keywords: tectonic tremor, Sanriku−oki

©2019. Japan Geoscience Union. All Right Reserved.

Heterogeneous structure around a region of slow earthquake activity off Ibaraki prefecture along the Japan Trench

*Kimihiro Mochizuki[1], Tomoaki Yamada[1], Masanao Shinohara[1], Ryota Hino[2], Ryosuke Azuma[2], Yoshihiro Ito[3], Yoshio Murai[4], Kenji Uehira[5], Toshinori Sato[6]

1. ERI, Univ. of Tokyo, 2. Graduate School of Science, Tohoku Univ., 3. DPRI, Kyoto Univ., 4. Faculty of Science, Hokkaido Univ., 5. NIED, 6. Graduate School of Science, Chiba Univ.

Large earthquakes of magnitude (M) ~7 have repeatedly occurred in the Ibaraki-oki region, about 100 km offshore of the Ibaraki prefecture along the Japan Trench, at a constant interval of ~20 years. Mochizuki et al. (2008) conducted a marine seismic survey and revealed that there exists a subducted seamount in the region. They also conducted an offshore seismic observation using ocean bottom seismometers (OBSs) to show that the seismicity in the region can be seen off of the subducted seamount, but not along the plate interface over it. They found that the location of the subducted seamount did not agree with the focal region of the repeating M7 earthquakes. From these results, they argued that the plate interface over the subducted seamount does not constitute an asperity of the repeating M7 earthquakes. Wang and Bilek (2011) introduced an idea that the seamount subduction causes formation of a fracture network within the overriding plate, and such a fracture network would prevent accumulation of large strain energy along the plate interface over the subducted seamount to generate large earthquakes. In addition to the repeating M7 earthquakes, recent studies (e.g. Matsuzawa et al., 2015; Nishikawa and Ide, 2018) have reported activity of slow earthquakes in the region. Relationship between activity of various types of earthquakes and structural features around the plate interface is one of the key topics to better understand controlling factors over earthquake types to be generated.

Recent studies in the Hikurangi subduction margin off the North Island of New Zealand show spatial relationship between variety of fault slips and topographic features of the plate interface. Wallace et al. (2016) successfully observed a large slow slip event just beneath an offshore array of ocean bottom pressure gauges, and precisely determined its slip distribution. They revealed that its slip propagation appeared to have circumvented subducted seamounts that have been imaged by magnetic anomalies as well as seismic reflection sections. Todd et al. (2018), for the first time, detected offshore tremor activity in the Hikurangi margin. The activity appears to have started just after the cessation of the slow slip, and its spatial distribution is only limited within regions of subducted seamounts. These results show that distributions of slow slip and tremor activity do not appear coincident, and thus the physical properties of the plate interface may be different. Further seismic surveys are supposed to provide vital information on structural variations that control physical characteristics of the plate interface.

In February, 2011, we acquired wide-angle reflection and refraction seismic data using 21 OBSs along a 150 km transect in the Ibaraki-oki region during the KH11-2 R/V Hakuho-maru cruise. We also included data from an OBS array that had already been deployed for a long-term seismic observation above the subduction front of the subducted seamount. Thus, we could construct a dense OBS profile above the subducted seamount with a receiver interval of ~3 km to achieve a high spatial resolution, whereas the largest interval is 10 km near both ends of the profile. First arrivals from the airgun sources can be traced up to ~95 km on most of the OBSs. The OBS record sections show significant heterogeneity that may include very rough structural features of the subducting oceanic crust along strike. Such heterogeneity may control seismic activity in the region.

©2019. Japan Geoscience Union. All Right Reserved.

Keywords: Ibaraki-oki, Active source seismic survey, Heterogeneous structure

©2019. Japan Geoscience Union. All Right Reserved.

Shallow low-frequency tremor triggered by nearby moderate earthquakes off Sanriku

*Sachiko Tanaka[1], Takanori Matsuzawa[1], Youichi Asano[1]

1. National Research Institute for Earth Science and Disaster Resilience

In the region off Sanriku, we have observed shallow low-frequency tremor, which occurs between the 12 km and 20 km depth contours of the plate interface, applying an envelope correlation method (Obara, 2002) to the records from the Seafloor observation network for earthquakes and tsunamis along the Japan Trench (S-net) (Tanaka et al., 2018). Several episodes of tremor, each of which lasted for half a day to six days, were detected in 2017, with intervals of one to three months. In the present study, we found tremor triggered by nearby moderate earthquakes. On July 24, 2017, an Mw 5.6 earthquake, showing reverse faulting consistent with the slip on the plate interface, occurred at the downdip end of the tremor zone off Sanriku, which was the largest event within 100 km of that tremor zone in the year. Immediately after the Mw 5.6 earthquake, coherent tremor signals were identified at surrounding stations. These signals continued for 20 hours, and the locations of their sources spanned 40 km along strike and 50 km along dip. Similar triggered tremor was observed following an Mw 5.1 earthquake on July 22, two days before the Mw 5.6 earthquake. This tremor activity was smaller and shorter than that triggered by the Mw 5.6 earthquake; tremor was localized to an area of 20 km by 15 km, and lasted for twelve hours. After a quiescence of nearly one day, the Mw 5.6 earthquake occurred at an adjacent area and triggered tremor was detected again. Triggering of tremor by moderate interplate earthquakes in or very close to the tremor zone we observed may imply small-scale (~ a few kilometers) heterogeneities in frictional properties on the plate interface in the area.

Keywords: shallow low-frequency tremor, triggered tremor, Japan Trench

©2019. Japan Geoscience Union. All Right Reserved.

Slow slip events in the Bungo Channel over 15 years as inferred from GNSS data (1996-2011)

Takatoshi Yokoi[1], *SHINICHI MIYAZAKI[1], Hiromu Sakaue[1], Jun'ichi Fukuda[2]

1. Graduate School of Science, Kyoto University, 2. Earthquake Research Institute, The University of Tokyo

We estimated space-time evolution of inter-plate slip and slip velocity associated with slow slip events (SSE) in the Bungo Channel over 15 years between January 1, 1996 and February 28, 2011, from GNSS data.

We use GNSS time series at 80 stations around the Bungo Channel out of GEONET stations. Time series were obtained with GIPSY-OASIS II software by Nishimura (personal communication). We removed data during SSE and estimated secular velocities, annual and semi-annual seasonal variations, and offsets associated with earthquakes, SSEs and instrumental events. Then we remove contributions of those components from time series with SSE to prepare time series for the inversion. We constructed plate interface based on iso-depth data by Baba et al. (2002) and Hirose et al. (2008), and setup the model region that is 200km long east to west and 280km long north to south. The model region was subdivided into 719 small triangular patches. We employed the inversion method based on the Monte Carlo Mixture Kalman Filter (Fukuda et al. 2008) and estimated slip and slip velocities on the fault continuously over 15 years.

First, Long-term slow slip events (L-SSE hereafter) that lasted for several months were inferred in 1997, 2003 and 2010 as obtained by, such as, Ozawa et al. (2012, 2017) and Yoshioka et al. (2015). In addition to basic characteristics described in these previous studies, short-term slow slip events (S-SSE hereafter) were inferred just before or just after the main slip event. This result suggests that stress perturbations by SSEs trigger other SSEs. Therefore the inferred cumulative moment in this study was smaller than previous studies because we successfully excluded contributions from S-SSEs. Second, S-SSEs have repeatedly occurred with the interval of about three or four months over 15 years. Those S-SSE were located at depths of about 30-40km and associated with low frequency tremors.

In this presentation, we focus space-time evolutions of L-SSE in 2010 and S-SSE in 2005.

Keywords: Slow slip in the Bungo Channel, crustal deformation, Monte Carlo Mixture Kalman Filter

©2019. Japan Geoscience Union. All Right Reserved.

Investigations of sensor orientation and a possibility of detecting crustal deformation based on accelerometer records of S-net

*Ryota Takagi[1], Naoki Uchida[1], Takashi NAKAYAMA[1], Ryosuke Azuma[1], Akira Ishigami[1], Tomomi Okada[1], Yusaku Ohta[1], Ryota Hino[1]

1. Research Center for Prediction of Earthquakes and Volcanic Eruptions, Graduate School of Science, Tohoku University

Seafloor Observation Network for Earthquakes and Tsunamis along the Japan Trench (S-net) of National Research Institute for Earth Science and Disaster Resilience (NIED) will greatly improve our knowledge of subsurface structure beneath offshore region along Japan trench and understanding of regular and slow earthquakes on the subducting plate boundary. We estimated the orientations of S-net sensors that are fundamental information for further data analysis and investigated the possibility of detecting crustal deformation based on accelerometer records.

We determined three parameters of sensor orientations: tilt angle of the long axis of a cable, rotation angle around the long axis, azimuth of the long axis. We estimated the tilt and rotation angles by assuming the DC components of accelerometers record the gravitational acceleration. The tilt and rotation angles slightly vary within the range of 0.01-0.1 degree during the period from 2016 to 2018 except for coseismic steps of rotation angles larger than 1 degree due to the M6.4 off Sanriku earthquake (August 20, 2016) and M7.4 off Fukushima earthquake (November 20, 2016). The long-axis azimuths are estimated by particle motions of long-period Rayleigh waves. We used the accelerometer records in 30-100 s of 7-14 teleseismic earthquakes with Mw 7.0-8.2. The azimuths are constrained in the range of 5-10 degrees. After correcting waveforms based on the estimated sensor orientation, we found coherent waveforms within the whole S-net stations and separation of Rayleigh and Love waves in radial and transverse components.

The capability of the DC components of accelerometers implies a possibility to detect crustal deformation from accelerometer records. We made time series of tilt and rotation angle with the sampling rate of one hour. During the period without offsets partly due to earthquakes, the root-mean-square (RMS) amplitudes of tilt and rotation angles are about 2 micro radians at most stations. The buried stations shallower than 1500 m show smaller variations and RMS amplitudes are about 0.2 micro radians. Some buried stations show tidal response with amplitude of about 1 micro radians. Since the maximum tilt change of land stations by a slow slip event (SSE) near the Boso Peninsula is about 1 micro radians, it might be possible to detect crustal deformation due to similar SSEs based on the accelerometer records.

Acknowledgement: We used continuous records of S-net managed by NIED. We thank NIED for providing the data.

Keywords: S-net, Sensor orientation, Crustal deformation, Slow slip, Tilt observation

©2019. Japan Geoscience Union. All Right Reserved.

Spatiotemporal variation of released seismic energy from shallow low-frequency tremor in Hyuga-nada, revealed by ocean bottom seismological observation

*Yusuke Yamashita[1], Saki Watanabe[2], Tomoaki Yamada[3], Masanao Shinohara[3], Takeshi Matsushima[2]

1. Disaster Prevention Research Institute, Kyoto University, 2. Institute of Seismology and Volcanology, Kyushu University, 3. Earthquake Research Institute, The University of Tokyo

In this study, we estimate the released seismic energy by shallow low-frequency tremors (shallow tremors) and clarify spatiotemporal variation of shallow tremor activity in Hyuga-nada, east off Kyushu. We used the data obtained from the temporal ocean bottom seismological observation for 3 months in 2013 [Yamashita *et al*., 2015] and long-term ocean bottom seismological observation from 2014 to 2017. The source location and released seismic energy of each shallow tremor was simultaneously estimated by Hybrid Envelope Cross-correlation Method [Maeda and Obara, 2009]. Observation data were obtained by the long-term continuous ocean bottom seismic observation in Hyuga-nada from 2013 to 2017. Site amplification factors were estimated by the coda normalization method [e.g., Sato and Fehler, 1998].

Spatial distribution of released seismic energy rate (energy rate) shows a heterogeneity although the average value of that is generally 10^4 J/s. The regions where the energy rate is relatively small are roughly coincident with the subducting or passed areas of the Kyushu-Palau Ridge. This result suggests that the structure and/or shape of the subducting plate such as seamounts or ridges may have an effect on the frictional property of the shallow plate interface. The 2013 activity was similar characteristics of shallow tremor location in space and time as the previous study, including two migrations episode. In addition, the characteristics of the released seismic energy were revealed as follows: (1) the energy rate was large at the both initiation point and the front of the migration, (2) the total released energy amount of the first migration was larger than that of the second migration, (3) both migrations were stopped at the region of small amount of released energy. Migration episode occurred while the 2015 activity and similar characteristics were documented.

Migration speed of shallow tremor is a few times faster, and energy rate of that is one or two orders of magnitude greater than the deep tremor. Applying the model of Ando *et al*. [2010, 2012] and Yabe and Ide [2014] to the result in this study, the average fault strength of shallow tremor is stronger than that of deep tremor, which leads up to a faster fault slip both brittle and ductile area. As a result, migration speed may become to be faster than deep tremor.

Acknowledgements: This study is supported by the research project for compound disaster mitigation on the great earthquakes and tsunami around the Nankai trough region, the MEXT of Japan, and JSPS KAKENHI Grant Number JP16H06471, JP16H06472. We thank Dr. Takuto Maeda for valuable discussions and comments. The observation data in 2013 obtained by T/S Nagasaki-maru. We used the JMA unified earthquake catalog and the seismic data obtained by Kagoshima University.

Keywords: Shallow low frequency tremor, Shallow slow earthquake, Ocean bottom seismological observation

©2019. Japan Geoscience Union. All Right Reserved.

©2019. Japan Geoscience Union. All Right Reserved.

Unified description of fast and slow earthquakes using velocity strengthening patches

*So Ozawa[1], Takahiro Hatano[1]

1. Earthquake Research Institute, the University of Tokyo

In a prevalent view, seismicity in subduction zones is governed by the distribution of the frictional properties of the plate interface. Regions with velocity-weakening (VW) friction generate earthquakes, whereas velocity-strengthening (VS) regions creep aseismically. Although most models consider isolated VW regions (patches) from the idea of asperities (e.g. Dublanchet et al., 2013), isolated VS patches also would exist given the frictional properties on faults are inferred to be complex and hierarchical. Therefore, the role of VS patches is to be studied.

Here we perform 3-D numerical simulation of the seismic cycle of faults governed by the rate and state friction law with the aging law. We distribute randomly circular VS patches on a VW background. We mainly focus on the effect of the ratio of VS and VW areas.

In our preliminary simulation, we identified two important effects. First, the VS patches act as the “stability barriers” during dynamic rupture propagation, which makes the rupture process more complicated than a single propagating crack. Rupture decelerates by encountering a stability barrier, followed by reacceleration due to overcoming the barrier. Such a process gives rise to multiple rupture fronts in the slipping area.

Second, dynamic rupture is inhibited by increasing the number of VS patches, and the fault slips aseismically with strong fluctuation in slip velocity. This is because there are no enough VW regions to accelerate the slip to dynamic rupture. Although a similar mechanism for slow earthquakes is proposed by Skarbek et al. (2012) and Yabe & Ide (2017), our 3-D modeling enables detailed studies on the spatiotemporal evolution of slip. In the presentation, we further discuss our results in the context of the dynamic scaling of rupture growth and the phenomenological law of slow earthquakes.

Keywords: Slow earthquake, Rate and state friction

©2019. Japan Geoscience Union. All Right Reserved.

The b-value of the earthquake swarm activities accompanied by the Boso slow slip events

*Yuki Noda[1], Hitoshi Hirose[2,1]

1. Department of Planetology, Faculty of Science, Kobe University , 2. Research Center for Urban Safety and Security, Kobe University

Slow slip events (SSEs) which are accompanying earthquake swarms repeatedly occur at intervals of about 2 to 7 years off Boso Peninsula (e.g., Sagiya, 2004; Hirose et al., 2012, 2014; Fukuda, 2018). These SSEs and swarms are thought to occur on the upper boundary of the subducting Philippine Sea plate.

As a statistical property of earthquakes, Gutenberg-Righter’ s law is well-known, that is, the relationship between the magnitude and the logarithm of occurrence frequency of earthquakes is expressed well with a straight line a-bM (Gutenberg and Richter, 1944). Although the b-value (slope of the line) often takes values around 1, there are many reports about the temporal changes of the b-value. For example, a decade-scale b-value decrease prior to the 2011 Tohoku Earthquake is reported (Nanjo et al., 2012). Although the relationship between the temporal change of b-value and aseismic slip is suggested, but the lack of near field geodetic observations prevents the direct evidence for the relationship. Here we examine the b-value of the earthquake swarms accompanied by the Boso SSEs, of which the aseismic slip is revealed by geodetic observations.

In this study, we estimate the b-value of the earthquake swarms in 2002, 2007, 2011 and 2014. We use the JMA unified earthquake catalog. As a preliminary analysis, we investigated the earthquakes with focal depths of 5 km to 40 km occurring at 35.05˚ to 35.56˚N in latitude and 140.15˚ to 140.73˚E in longitude. Eventually, “event period” estimated in the previous studies of the crustal deformation by geodetic observation does not necessarily agree with the period of the swarms occurring at the same time. Therefore, in this research, “event period” was redefined from seismic activity and used. In other words, we extracted swarms including a SSE period from crustal deformation studies and the time when the seismicity rate (the number of earthquakes per unit time) is significantly higher than the other time is defined as “event period”. In addition, the period other than the event period is defined as “inter-swarm period”.

We find that the b-values in the event periods tend to be lower than that during inter-swarm period. In more detail, different trends that seem to correspond to the difference in slip zone and location of earthquake activity of each SSE (Hirose et al. 2014) are seen in the b-values for the event periods. A seismic activity near the southern coast of the Boso Peninsula was hardly observed in the 2007 event period, whereas an active seismic activity was seen there in the 2011 event period. In order to clarify the dependence of the b-value on the difference in the location of the earthquakes, we divided the survey area into two areas, that is, the northern area (area A) and the southern area (area B). The seismic activity is observed in all event periods in the area A, whereas an active seismic activity is observed only in the event periods of 2002 and 2011 in the area B. Then a b- value is estimated in each period in the same way. As a result, for the earthquakes occurred in the northern region (area A), there is a tendency that the b-value in each of the event periods is lower by about 0.2-0.4 than that during inter-swarm. On the other hand, such a tendency is not observed in the southern area (area B). Such differences in the northern and southern regions may suggest that the effects of stress changes caused by SSEs vary from region to region.

©2019. Japan Geoscience Union. All Right Reserved.

Keywords: Gutenberg-Richter's law

©2019. Japan Geoscience Union. All Right Reserved.

Three-dimensional thermal modeling associated with subduction of the Philippine Sea plate at the Ryukyu Trench, and its relation to the occurrence of interplate seismic events

*Nobuaki Suenaga[1], Shoichi Yoshioka[2,1], Yinfeng Ji[3]

1. Graduate School of Science, Kobe University, Japan, 2. Research Center for Urban Safety and Security, Kobe University, Japan, 3. Chinese Academy of Science, Beijin, China

Interplate seismic events such as short-term slow slip evens (S-SSEs) (Nakamura, 2017), low-frequency earthquakes (LFEs) (Ando et al., 2012), and shallow very low-frequency earthquakes (VLFEs) (Nakamura et al., 2015) have been identified at the Ryukyu Trench, southwestern Japan. As the specific characteristics of these distributions, depths where S-SSEs and LFEs occur at the plate interface beneath the Okinawa island, whose depth is ranging from 15 km to 25 km, is about 10-20 km shallower than that beneath the Yaeyama islands, whose depth is ranging from 35 km to 50 km.

In this study, we constructed three-dimensional parallelepiped thermal convection model associated with subduction of the Philippine Sea (PHS) plate beneath the Amurian (AM) plate at the Ryukyu subduction zone. We considered subduction history of the PHS plate in the model region, referring to the plate rotation model (Mathews et al., 2016). We performed the numerical simulation as the time-dependent problem in the last 15 Myr to elucidate relationships among calculated thermal structures, dehydrations from the subducting plate, and the interplate seismic events. We used observed heat flow data to constrain thermal structures.

As a result at 0 Ma, we found that interplate temperature where S-SSEs and LFEs occur beneath the Yaeyama islands is lower than that beneath the Okinawa island when compared with the same depth along the direction of the trench axis. This is mainly because the convergence rate (PHS-AM) becomes gradually fast toward the southwest. Therefore, interplate temperatures where S-SSEs and LFEs occur were estimated ranging from 500℃ to 700℃ both beneath the Okinawa island and the Yaeyama islands.

We also calculated water content distribution within the PHS plate, using the calculated thermal structures and the phase diagram of MORB in an oceanic crust (Omori et al., 2008) and ultramafic rock in a slab mantle (Hacker et al., 2003). As for dehydration of MORB, we found that epidote eclogite transforms into amphibole eclogite in the neighboring area where S-SSEs and LFEs occur beneath the Okinawa island, and amphibole eclogite transforms into eclogite beneath the Yaeyama islands. The former and the latter dehydrate a total amount of 1.4 wt% and 0.7 wt% associated with their phase transformations, respectively.

Keywords: three dimensional thermal modeling

©2019. Japan Geoscience Union. All Right Reserved.

[E] Oral | S (Solid Earth Sciences)：S-CG Complex & General

Wed. May 29, 2019 1:45 PM - 3:15 PM JST | Wed. May 29, 2019 4:45 AM - 6:15 AM UTC | Convention Hall A 2F

[S-CG48] Science of slow earthquakes: Toward unified understandings of whole earthquake process

convener:Satoshi Ide(Department of Earth an Planetary Science, University of Tokyo), Hitoshi Hirose(Research Center for Urban Safety and Security, Kobe University), Kohtaro Ujiie(Graduate School of Life and Environmental Sciences, University of Tsukuba), Takahiro Hatano(Earthquake Research Institute, University of Tokyo), Chairperson:Kazushige Obara(Earthquake Research Institute, University of Tokyo), Aitaro Kato(Earthquake Research Institute, University of Tokyo)

Accumulating observational studies on various types of slow deformation events, such as tectonic tremors, very low frequency events, and slow slip events, portrays some universal characteristics in generally complex behavior, including interaction among events and influence by various outer loadings. Some of these phenomena seem to have causal relation with the occurrence of very large earthquakes. A unified understanding of these slow and fast earthquake processes requires an approach integrating geophysics, seismology, geodesy, geology, and non-equilibrium statistical physics. We welcome presentations based on, but not limited to, geophysical observation, data analysis, analytical theory, numerical simulation, field study, and laboratory experiments.

1:45 PM - 2:00 PM JST | 4:45 AM - 5:00 AM UTC

[SCG48-06] Interplay between long-term SSE and ETS facilitated by different underground environment

*Kazushige Obara[1] (1.Earthquake Research Institute, The University of Tokyo)

2:00 PM - 2:15 PM JST | 5:00 AM - 5:15 AM UTC

[SCG48-07] **Determination of sVLFE epicenters around the subducted Kyushu-Palau Ridge from coda interferometry**

*Takashi Tonegawa[1], Yusuke Yamashita[2], Aki Ito[1], Masanao Shinohara[3], Daisuke Suetsugu[1], Tsutomu Takahashi[1], Yasushi Ishihara[1], Shuichi Kodaira[1], Yoshiyuki Kaneda[4] (1.JAMSTEC, 2.DPRI, Kyoto University, 3.ERI, The University of Tokyo, 4.Kagawa University)

2:15 PM - 2:30 PM JST | 5:15 AM - 5:30 AM UTC

[SCG48-08] Detection of slow earthquakes in the microseism frequency band (0.05–1.0 Hz) by large-scale waveform stacking

*Koki Masuda[1], Satoshi Ide[1], Kazuaki Ohta[2] (1.Department of Earth an Planetary Science, University of Tokyo, 2.Disaster Prevention Research Institute, Kyoto University)

2:30 PM - 2:45 PM JST | 5:30 AM - 5:45 AM UTC

[SCG48-09] Source characteristics of low-frequency earthquakes in Nankai subduction zone inferred from analysis of large event dataset

*Natalia Poiata[1], Mariano Supino[1,2], Gaetano Festa[2], Jean-Pierre Vilotte[1], Kazushige Obara[3] (1.Institut de Physique du Globe de Paris, 2.Università degli Studi di Napoli “ Federico II ”, Napoli, Italy, 3.Earthquake Research Institute, University of Tokyo, Japan)

2:45 PM - 3:00 PM JST | 5:45 AM - 6:00 AM UTC

[SCG48-10] **High-frequency radiation prior to semi-volcanic low-frequency earthquake in Eastern Shimane, SW Japan, illuminated by “0.1 manten” Hyper Dense Seismic Observation**

*Aitaro Kato[1], Shin'ichi Sakai[1], Satoshi Matsumoto[2], Yoshihisa Iio[3] (1.Earthquake Research Institute, the University of Tokyo, 2.Kyushu University, 3.Kyoto University)

3:00 PM - 3:15 PM JST | 6:00 AM - 6:15 AM UTC

[SCG48-11] Variation of Focal Mechanisms of Low Frequency Earthquakes in Parkfield

*Miki Aso[1,3], Naofumi Aso[2], Satoshi Ide[1] (1.Department of Earth and Planetary Science, The University of Tokyo, 2.Tokyo Institute of Technology, School of Science , 3.OYO RMS Corporation)

Interplay between long-term SSE and ETS facilitated by different underground environment

*Kazushige Obara[1]

1. Earthquake Research Institute, The University of Tokyo

Slow earthquakes consist of fault slip phenomena with various characteristic times. Geodetically detected slow earthquakes are mainly classified into two types; short-term and long-term slow slip events (SSEs) with duration from days to weeks and from months to years, respectively. In southwest Japan, at the deeper part from the seismogenic zone along the subducting plate interface, long-term and short-term SSEs are adjacently distributed and they indicate interaction. Because the short-term SSE usually occurs as an Episodic Tremor and Slip (ETS) associated with low-frequency tremor and very-low-frequency earthquake, the interaction is usually observed clearly in ETS tremor seismicity.
In Bungo channel, the long-term SSE is well known to occur at interval of 6-7 years. After the deployment of dense high-sensitivity seismograph network, major long-term SSEs in 2003 and 2010 were accompanied by activation of tremor seismicity. The activated tremor region is limited within a narrow width of 10 km from the updip edge of ETS zone and the tremor activity of the rest downdip part is constant irrespective to the occurrence of the long-term SSE.
In this region, two small long-term SSEs were detected by GNSS in 2014 and 2016; however, the interaction to ETS tremor were different from cases in 2003 and 2010. In 2014, activated tremor was smaller than that in 2010 according to the difference in the magnitude of SSE. On the other hand, there was no tremor activity associated with 2016 SSE. This is because the slip region of SSE was located southward apart from the tremor zone. By the way, a long-term SSE from the end of 2018 continues associated with activation of tremor lasting for several months. This SSE might be expected as a major SSE since 2010.
The main difference between long-term and short-term SSEs is slip rate. The difference in the slip rate may affect to the tremor rate. During the long-term SSE in 2003 and 2010, the temporal change in cumulative number of tremor increased smoothly similar to the GNSS displacement. However, the gradual increase of tremor number was actually composed of superposition of small bursts corresponding to the faster speed slip compared to the long-term SSE. This suggests that the ETS region has a characteristic slip and frictional property different from the long-term SSE region.
A recent receiver function study conducted along a linear seismic array installed at the west of Shikoku besides from Bungo channel has revealed a low velocity oceanic crust and a continental Moho discontinuity just above ETS activity. This indicates that the ETS occur at the boundary between the subducting oceanic plate and the overlying mantle wedge, whereas that long-term SSE occurs at the boundary between oceanic plate and the continental lower crust. The difference of slow earthquake behavior controlled by the structure in the hanging wall is very similar to the Tokai region (Kato et al., 2010). Therefore, the different environment at the plate interface facilitates these SSEs with different characteristic times.

Keywords: slow earthquake, low frequency tremor, slow slip event, subduction zone

©2019. Japan Geoscience Union. All Right Reserved.

Determination of sVLFE epicenters around the subducted Kyushu-Palau Ridge from coda interferometry

*Takashi Tonegawa[1], Yusuke Yamashita[2], Aki Ito[1], Masanao Shinohara[3], Daisuke Suetsugu[1], Tsutomu Takahashi[1], Yasushi Ishihara[1], Shuichi Kodaira[1], Yoshiyuki Kaneda[4]

1. JAMSTEC, 2. DPRI, Kyoto University, 3. ERI, The University of Tokyo, 4. Kagawa University

Shallow very low frequency earthquakes (sVLFEs) occur at the shallow portion of the plate boundary. The Rayleigh waves at a frequency of 0.03–0.2 Hz radiated from their sources are observed in land and seafloor seismic records. Although sVLFE locations have been estimated from land records, there is a possibility to determine them more precisely if seafloor records near the epicenters are available. In the Hyuga-nada region and off Nansei Islands, ocean bottom seismometer (OBS) arrays were deployed 4 times during 4 years, each of which contained 5–13 OBSs and could observe at least one episode of sVLFE activity. In this study, we estimated the group velocity of the Rayleigh wave in the OBS arrays from coda interferometry, and applied it to the envelope correlation method (ECM) using seafloor seismic records for determining sVLFE epicenters.

As a result, the locations of sVLFE during 2014 and 2016 were determined at the northern edge of the Kyushu-Palau Ridge (KPR) (Yamamoto et al. 2013), while those on 2017 and 2018 were estimated to be the southern edge of the KPR. In particular, the sVLFEs on 2015 firstly occurred at the northern edge of the KPR, but occurred near the trough afterwards. Also, comparing the area of slow slip event (SSE) in the Hyuga-nada region (Ozawa 2017), sVLFE region at the northern part of KPR directly connects to the SSE region, indicating that slow earthquakes potentially occur from deep to shallow plate interface around the KPR.

Acknowledgement
This study was supported by “Research Project for Compound Disaster Mitigation on the Great Earthquakes and Tsunamis around the Nankai Trough Region” of the Ministry of Education, Culture, Sports, Science and Technology (MEXT) of Japan. We thank Shinzaburo Ozawa and Yojiro Yamamoto for providing us SSE and KPR data.

Keywords: shallow very low frequency earthquake, Hyuga-nada region, Kyushu-Palau Ridge

©2019. Japan Geoscience Union. All Right Reserved.

Detection of slow earthquakes in the microseism frequency band (0.05–1.0 Hz) by large-scale waveform stacking

*Koki Masuda[1], Satoshi Ide[1], Kazuaki Ohta[2]

1. Department of Earth an Planetary Science, University of Tokyo, 2. Disaster Prevention Research Institute, Kyoto University

Slow earthquakes have been intensively studied because of the proximity of their source area to that of megathrust earthquakes and their high sensitivity to regional stress change. They have been classified according to their characteristic time scale into tremors and low frequency earthquake (LFE; >1 Hz), very low frequency earthquake (VLFE; 20-100 sec), and slow slip event (SSE; > 1 day). Microseism noise is dominant in the frequency band between LFE and VLFE, which we call the microseism frequency band, and it is difficult to detect signals of slow earthquakes in this band. As a rare exception, signals in this band accompanied with LFEs and VLFEs were detected on the shallow subduction interface by near-field ocean bottom broadband seismometers with fortuitously low microseism noise (Kaneko et al., 2018). The characteristics of signals in this band are totally unknown for deep slow earthquakes.

In this study, we first report the observation of slow earthquake signals in the microseism frequency band in the western Shikoku region of the Nankai subduction zone, Japan, by stacking a lot of seismograms relative to the timing of high-frequency signals. First, we made synthetic template waveforms and conducted a matched filter analysis using these template waveforms (Ohta & Ide, 2017). Utilizing GPU, we detected about 700,000 events in continuous records at 9 Hi-net stations, operated by National Research Institute for Earth Science and Disaster Resilience, from 2005 to 2015. Their temporal distribution suggests that LFEs are episodic phenomena and their spatial distribution indicates the sources are concentrated in several patches, as reported by previous researches (e.g., Ohta & Ide, 2017). Then we stacked seismograms at the timing of these detected events, after band-pass filtering in different frequency bands (4-8 Hz, 2-4 Hz, 1-2 Hz, 0.5-1 Hz, 0.25-0.5 Hz, and 0.125-0.25 Hz). In-phase waveforms are confirmed in all frequency bands, despite low sensitivity of Hi-net seismometers in lower frequencies than 1 Hz. This result suggests that slow earthquakes radiate broadband signals without characteristic frequencies from 0.125 to 8 Hz.

Keywords: slow earthquakes, LFE, microseism, matched filter, Nankai subduction zone

©2019. Japan Geoscience Union. All Right Reserved.

Source characteristics of low-frequency earthquakes in Nankai subduction zone inferred from analysis of large event dataset

*Natalia Poiata[1], Mariano Supino[1,2], Gaetano Festa[2], Jean-Pierre Vilotte[1], Kazushige Obara[3]

1. Institut de Physique du Globe de Paris, 2. Università degli Studi di Napoli “Federico II”, Napoli, Italy, 3. Earthquake Research Institute, University of Tokyo, Japan

Application of advanced detection and location methods to the analysis of low-frequency earthquakes (LFE) allows building large event catalogues rich in information that can provide a better understanding of their source characteristics. Up to now, LFE characterization in terms of size, stress drop and rupture propagation still remains uncertain, the main difficulty owing to the low signal-to noise ratio of corresponding records.

We present a catalog of LFE in western part of Nankai subduction zone derived by applying a full waveform-based detection and location scheme of Poiata et. al. (2016) to the continuous records form Hi-net seismic stations covering a 3-year period from 2013-2016. The applied method is based on the frequency-selective coherence of signals’ statistical features recorded across the stations of seismic network, not requiring a prior assumption about the event source (i.e., template event). The derived catalog (~ 40000 events) allows to look into the details of LFE space-time activity (i.e., clustering and migration patterns) during the energetic tectonic tremor sequences as well as inter-sequence periods as well as characterize source properties of these events.

We derive source parameters of LFEs extracted from this 3-year catalog by applying the probabilistic approach of Supino et al. (2019) based on the conjunction of states of information between data and model and estimating the joint probability density function of the parameters. The events S-wave displacement amplitude spectrum is described by a circular source model, characterized by a plateau at low frequencies and a coherent decay at high frequencies; the frequency of transition between these two regimes is the corner frequency. Processing of this large LFE data set is performed using accurate quality criteria, allowing to automatically reject noisy data and unconstrained solutions.

The resulted moment magnitudes, estimated from low-frequency plateau, range between Mw 0.9 and 2.2, while corner frequencies vary between 0.8 and 12 Hz, being lower than expected for ordinary earthquakes, as already observed for LFEs. We found that LFE sources exhibit a power-law scaling between corner frequency and seismic moment, with an exponent of -3.5, very similar to the scaling observed for classical earthquakes.

Keywords: low-frequency earthquakes, source characteriziation, continuous data analysis, event detection and location

©2019. Japan Geoscience Union. All Right Reserved.

High-frequency radiation prior to semi-volcanic low-frequency earthquake in Eastern Shimane, SW Japan, illuminated by “0.1 manten” Hyper Dense Seismic Observation

*Aitaro Kato[1], Shin'ichi Sakai[1], Satoshi Matsumoto[2], Yoshihisa Iio[3]

1. Earthquake Research Institute, the University of Tokyo, 2. Kyushu University, 3. Kyoto University

Semi-volcanic deep low-frequency earthquake (LFE) that occurs distant from active volcanoes has been investigated by previous several studies [Ohmi and Obara, 2002; Aso et al., 2013]. In eastern Shimane of SW Japan, there is a spot hosting frequent semi-volcanic LFE activity for over 20 years. Above this source area, we installed a thousand of seismic stations from March 2017 to March 2018, which covers an entire aftershock zone of the 2000 Western-Tottori earthquake (Mw 6.7). The spatial interval of each seismic station ranges from 1 to 2 km.

We found out clear arrivals of high-frequency waveforms prior to arrivals of low-frequency signals by a hundred of the dense seismic stations. The differential arrival times between the high- and low-frequency waveforms are approximately 1.5 s. The high-frequency radiation has the strongest amplitude at 28 Hz and 16 Hz and is characterized by stronger P-wave amplitude than faint S-wave. In contrast, the low-frequency component is predominant from 1 to 6 Hz and shows variation of the ratio of P-wave to S-wave with epicentral distance. This observation clarifies that different excitation mechanisms are needed to explain bimodal radiations at the high- and low-frequency bands.

We relocated the high- and low-radiation sources by both visually picked arrival times and Source Scanning Algorithm. Then, each radiation source is located within a cloud of LEFs determined by the JMA. The depth of the high- and low-frequency sources are imaged around the depth of 30 km, namely around Moho discontinuity. But, the high-frequency radiation is slightly deeper than that of the low-frequency with a few km horizontal offset. The origin time of the high-frequency radiation is by 1.5 ~ 2 seconds earlier than that of the low-frequency. This slight spatial gap indicates that the two sources appear to be not collocated, while the spatial separation between the two sources is not so large in terms of the hypocenter accuracy. The present study first shows that the high- and low-frequency radiation sources are close to each other around Moho discontinuity.

Combined with these observations, we interpret that the early high-frequency radiation is derived from brittle breakage of low-permeability seal may arise from hydrothermal cementation. Infiltration of high-pressurized fluids into the bottom of lower crust may trigger slow shear slip or resonance of crustal fluids along a pre-existing fracture.

©2019. Japan Geoscience Union. All Right Reserved.

Variation of Focal Mechanisms of Low Frequency Earthquakes in Parkfield

*Miki Aso[1,3], Naofumi Aso[2], Satoshi Ide[1]

1. Department of Earth and Planetary Science, The University of Tokyo, 2. Tokyo Institute of Technology, School of Science , 3. OYO RMS Corporation

Tectonic low frequency earthquakes (LFEs) occur at plate boundaries around the world, and considered as local slow deformation. LFEs in subduction zones are found to have low-angle thrust fault mechanisms in southwest Japan [Ide et al., 2007], Mexico [Frank et al., 2013], and Cascadia [Royer and Bostock, 2014]. LFEs along Alpine fault, a transform fault in New Zealand, are known to have right-lateral strike slip mechanism [Baratin et al., 2018]. However, the focal mechanisms of LFEs at Parkfield along the San Andreas Fault zone have not been revealed yet, regardless of the frequent activities. The San Andreas Fault is one of the most matured active faults in the world, especially at Parkfield, and large damaging earthquakes also repeatedly occurred in history. Therefore, many seismologists and geologists have been challenging to reveal the cause of earthquakes and LFEs.
In this study, we estimate the focal mechanisms of 88 LFE families in the catalog of Shelly [2017]. We first stack seismograms of over one million events in the catalog to improve the signal-to-noise (S/N) ratio. P-wave polarities of the stacked waveforms suggest the existence of variations in focal mechanisms of the LFE families.
Then, we evaluate the absolute amplitudes of original seismograms using the stacked waveforms. The SH wave amplitudes are inverted to the focal mechanisms for each LFE family. Specifically, the contributions from source radiation, path attenuation, and site amplification are represented by independent terms based on the assumption of simple ray theory, and estimated by solving a two-step inversion problem. The source terms are utilized to determine focal mechanisms. While most of the focal mechanisms are strike-slip consistent with the San Andreas Fault motion, those for families near the central Parkfield and the family off the surface trace contain large dip-slip (Figure 1 and 2). These variations are consistent with tidal sensitivities of LFEs in Parkfield [Thomas et al., 2012]. Our study reveals regional dip-slip focal mechanisms at first glance to be strike-slip along matured San Andreas Fault.

Keywords: San Andreas Fault, Parkfield, focal mechanism inversion, waveform stacking, low frequency earthquake, amplitude evaluation

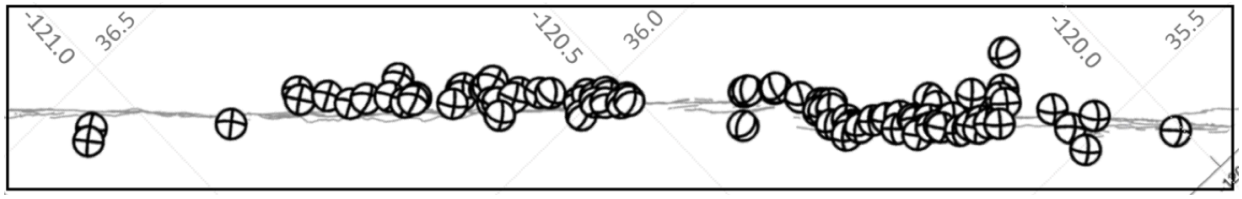

Figure 1. The focal mechanisms of LFE families

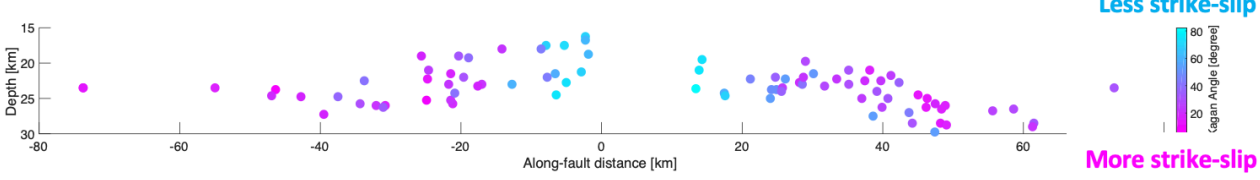

Figure 2. The difference from strike-slip focal mechanism of ordinary earthquake

©2019. Japan Geoscience Union. All Right Reserved.

[E] Oral | S (Solid Earth Sciences)：S-CG Complex & General

Wed. May 29, 2019 3:30 PM - 5:00 PM JST | Wed. May 29, 2019 6:30 AM - 8:00 AM UTC | Convention Hall A 2F

[S-CG48] Science of slow earthquakes: Toward unified understandings of whole earthquake process

convener:Satoshi Ide(Department of Earth an Planetary Science, University of Tokyo), Hitoshi Hirose(Research Center for Urban Safety and Security, Kobe University), Kohtaro Ujiie(Graduate School of Life and Environmental Sciences, University of Tsukuba), Takahiro Hatano(Earthquake Research Institute, University of Tokyo), Chairperson:Satoshi Ide(Graduate School of Science, University of Tokyo), Kazuaki Ohta

Accumulating observational studies on various types of slow deformation events, such as tectonic tremors, very low frequency events, and slow slip events, portrays some universal characteristics in generally complex behavior, including interaction among events and influence by various outer loadings. Some of these phenomena seem to have causal relation with the occurrence of very large earthquakes. A unified understanding of these slow and fast earthquake processes requires an approach integrating geophysics, seismology, geodesy, geology, and non-equilibrium statistical physics. We welcome presentations based on, but not limited to, geophysical observation, data analysis, analytical theory, numerical simulation, field study, and laboratory experiments.

3:30 PM - 4:00 PM JST | 6:30 AM - 7:00 AM UTC

[SCG48-12] Mapping seismic data to slow slip using machine learning

★Invited Papers

*Bertrand Rouet-Leduc[1], Claudia Hulbert[2], Ian McBrearty[1], Paul Johnson[1] (1.Los Alamos National Laboratory, USA, 2.Ecole Normale Superieure, France)

4:00 PM - 4:15 PM JST | 7:00 AM - 7:15 AM UTC

[SCG48-13] Revealing the slow earthquake activity in the Japan Trench and its relation to the 2011 Tohoku-Oki earthquake

*Tomoaki Nishikawa[1], Takanori Matsuzawa[2], Kazuaki Ohta[1], Naoki Uchida[3], Takuya NISHIMURA[1], Satoshi Ide[4] (1.Disaster Prevention Research Institute, Kyoto University, 2.National Research Institute for Earth Science and Disaster Resilience, 3.Graduate School of Science, Tohoku University, 4.Graduate School of Science, The University of Tokyo)

4:15 PM - 4:30 PM JST | 7:15 AM - 7:30 AM UTC

[SCG48-14] Tremor and slow slip associated with afterslip of the 2011 Tohoku earthquake

*Kazuaki Ohta[1], Yoshihiro Ito[1], Ryota Hino[2], Shukei Ohyanagi[1], Takanori Matsuzawa[3], Masanao Shinohara[4], Hajime Shiobara[4] (1.Disaster Prevention Research Institute, Kyoto University, 2.Graduate School of Science, Tohoku University, 3.National Research Institute for Earth Science and Disaster Resilience, 4.Earthquake Research Institute, the University of Tokyo)

4:30 PM - 4:45 PM JST | 7:30 AM - 7:45 AM UTC

[SCG48-15] High definition imaging of the Japan Trench by OBS Array of Arrays: Does shallow tectonic tremor occur in the plate interface?

*Shukei Ohyanagi[1], Kazuaki Ohta[2], Yoshihiro Ito[2], Ryota Hino[3], Yusaku Ohta[3], Ryosuke Azuma[3], Masanao Shinohara[4], Kimihiro Mochizuki[4], Toshinori Sato[5], Yoshio Murai[6] (1.Kyoto University, Graduate School of Science, 2.Kyoto University, Disaster Prevention Research Institute, 3.Tohoku University, 4.Tokyo University, Earthquake Research Institute, 5.Chiba University, 6.Hokkaido University)

4:45 PM - 5:00 PM JST | 7:45 AM - 8:00 AM UTC

[SCG48-16] The activity of small repeating earthquakes after the 2011 Tohoku-oki earthquake: an examination based on the S-net and land networks

*Naoki Uchida[1], Ryota Takagi[1], Satoshi Hirahara[1], Takashi NAKAYAMA[1], Toru Matsuzawa[1], Sachiko Tanaka[2], Youichi Asano[2] (1.Research Center for Prediction of Earthquakes and Volcanic Eruptions Graduate School of Science, Tohoku University, 2.National Research Institute for Earth Science and Disaster Resilience)

Mapping seismic data to slow slip using machine learning

*Bertrand Rouet-Leduc[1], Claudia Hulbert[2], Ian McBrearty[1], Paul Johnson[1]

1. Los Alamos National Laboratory, USA, 2. Ecole Normale Superieure, France

We show that the Cascadia subduction zone is apparently continuously broadcasting a low-amplitude, tremor-like signal that precisely informs of the fault displacement rate throughout the slow slip cycle. Using a method based on machine learning previously developed in the laboratory, we analysed large amounts of raw seismic data from Vancouver Island to separate this signal from the background seismic noise. We posit that this provides indirect real-time access to fault physics on the down-dip portion of the megathrust, and thus may prove useful in determining if and how a slow slip may couple to or evolve into a major earthquake.

In a parallel approach, we show that tremor can be accurately detected on a single seismic station by a deep convolutional neural network. Seismic tremor is posited to provide information on the physical state of the slowly slipping portion of the megathrust, and a single station tremor detector gives a direct access to the tremor signal and its physical characteristics. A deep learning model trained to detect tremor in Cascadia recognizes catalogued tremor in other subduction zones, arguing for the universality of tremor and slow slip characteristics. The detection rate of a deep learning model trained to recognize tremor in Cascadia and applied on waveforms from Northern Chile shows strong correlation with surface displacement rate, arguing for episodic tremor and slip detection where slow earthquakes and associated tremor had not been seen so far, presumably taking place too deep to have been detected using conventional multi-station methods.

Keywords: Tremor, Slow earthquake, Machine learning, Deep learning

©2019. Japan Geoscience Union. All Right Reserved.

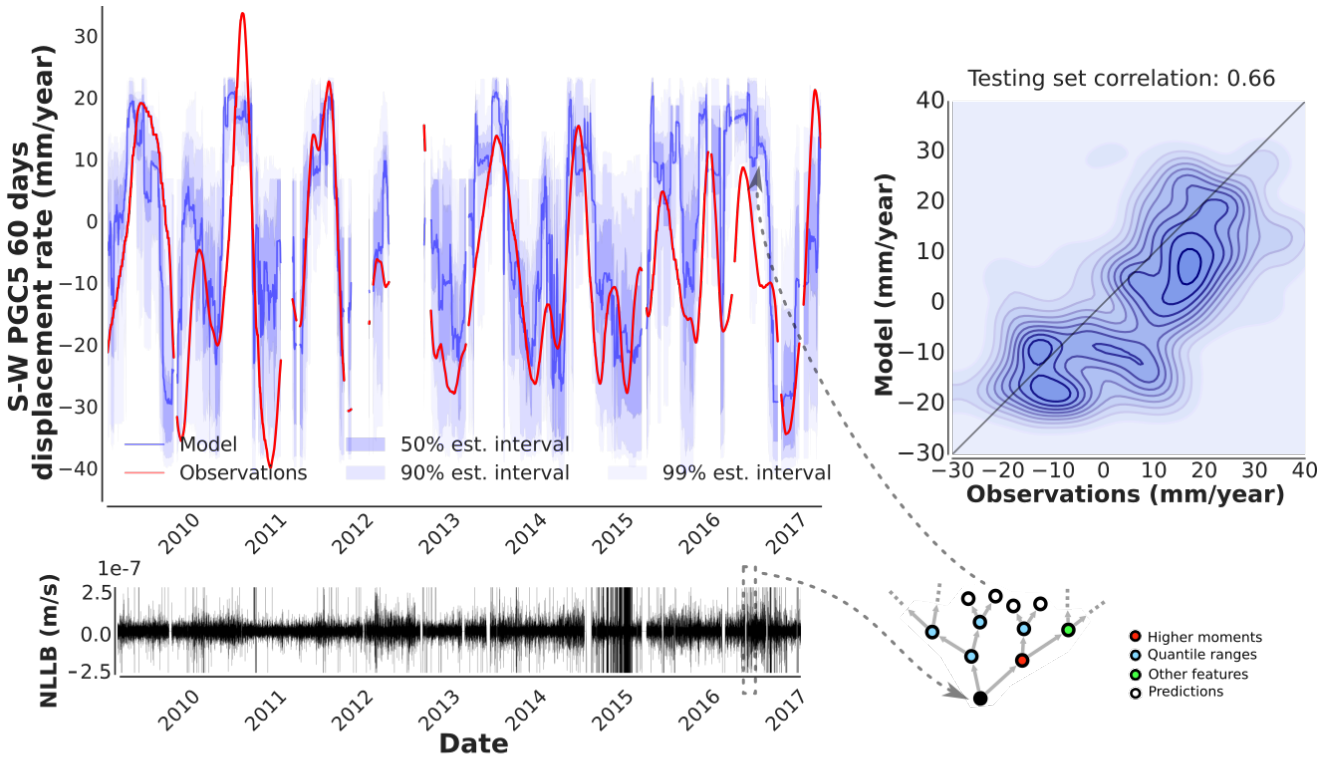

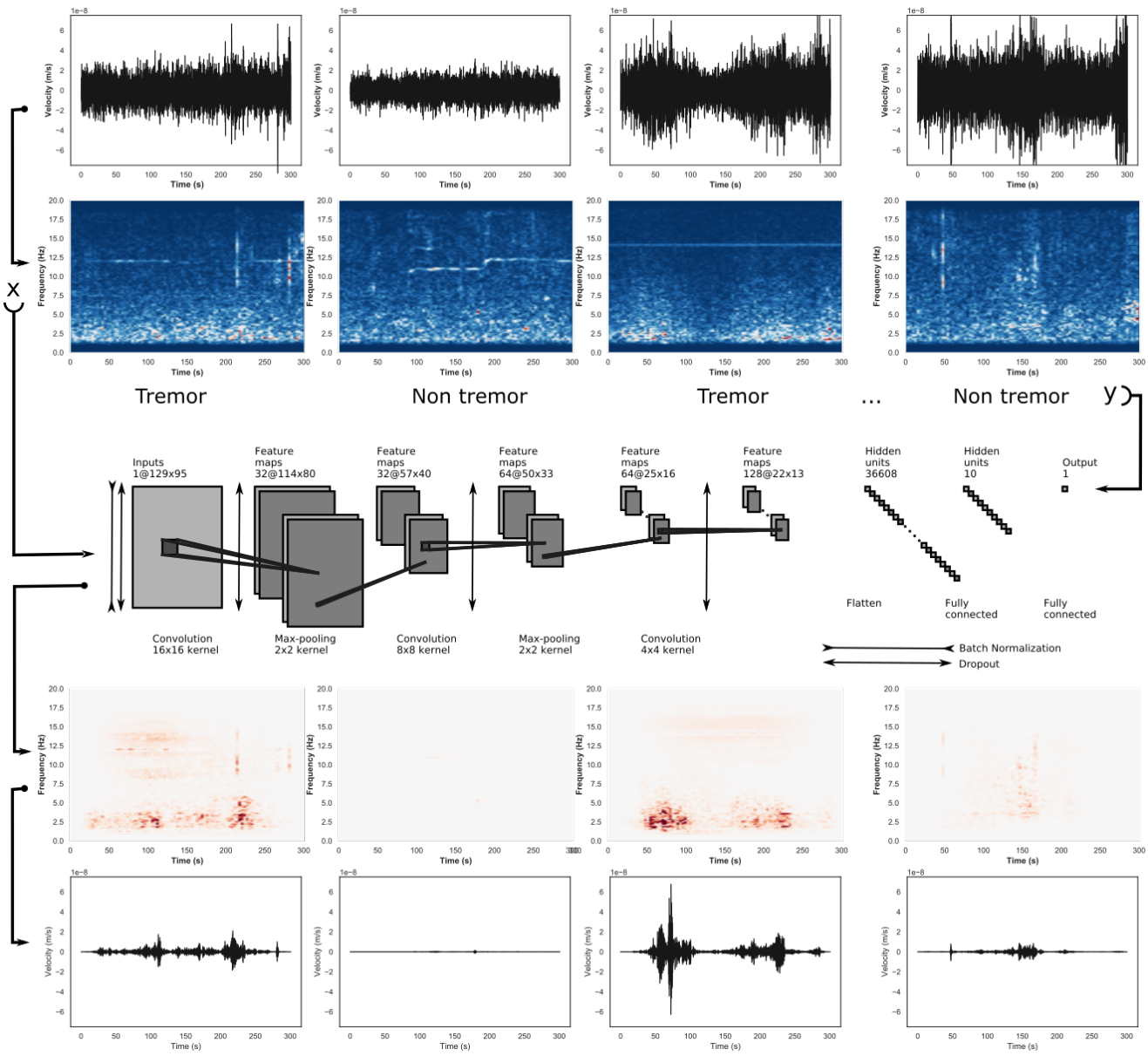

©2019. Japan Geoscience Union. All Right Reserved.

©2019. Japan Geoscience Union. All Right Reserved.

Revealing the slow earthquake activity in the Japan Trench and its relation to the 2011 Tohoku-Oki earthquake

*Tomoaki Nishikawa[1], Takanori Matsuzawa[2], Kazuaki Ohta[1], Naoki Uchida[3], Takuya NISHIMURA[1], Satoshi Ide[4]

1. Disaster Prevention Research Institute, Kyoto University, 2. National Research Institute for Earth Science and Disaster Resilience, 3. Graduate School of Science, Tohoku University, 4. Graduate School of Science, The University of Tokyo

Subduction zone megathrust earthquakes result from the interplay between fast dynamic rupture and slow deformation processes, which are directly observed as various slow earthquakes, including tectonic tremors, very low-frequency earthquake (VLFs) and slow slip events (SSEs), and indirectly suggested by a temporal change in the frequency of repeating earthquakes and the occurrence of episodic earthquake swarms. Some megathrust earthquakes have been preceded by slow earthquakes and terminated near the areas where slow earthquakes were frequently observed. While capturing the entire spectrum of slow earthquake activity is crucial for estimating the occurrence time and rupture extent of future megathrust earthquakes in a given subduction zone, such an observation is generally difficult, and slow earthquake activity is poorly understood in most subduction zones, including the Japan Trench, which hosted the 2011 M_w9.0 Tohoku-Oki earthquake. Here we reveal the slow earthquake activity in the Japan Trench in detail using tectonic tremors, which we detected in the seismograms of a new ocean-bottom seismograph network, VLFs, SSEs, repeating earthquakes, and earthquake swarms. We show that the slow earthquake distribution is complementary to the rupture area of the Tohoku-Oki earthquake and correlates with the structural heterogeneity along the Japan Trench. Concentrated slow earthquake activities were observed in the afterslip area of the Tohoku-Oki earthquake, which is located to the south of the fore-arc geological segment boundary. Our results suggest that the megathrust in the Japan Trench is divided into three segments that are characterised by different frictional properties, and that the rupture of the Tohoku-Oki earthquake, which nucleated in the central segment, was terminated by the two adjacent segments.

Keywords: Slow earthquake, Megathrust earthquake, Subduction zone, The 2011 Tohoku-Oki earthquake

©2019. Japan Geoscience Union. All Right Reserved.

The Japan Trench

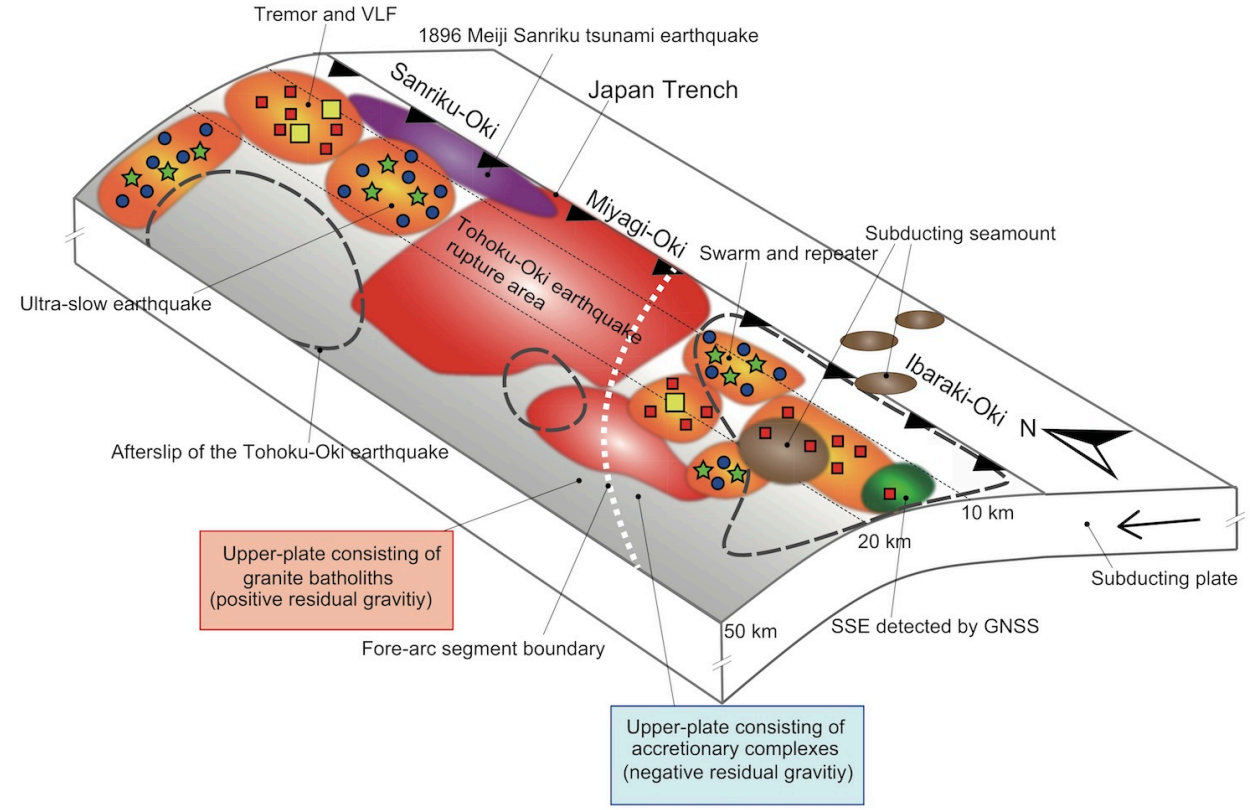

The Nankai Trough

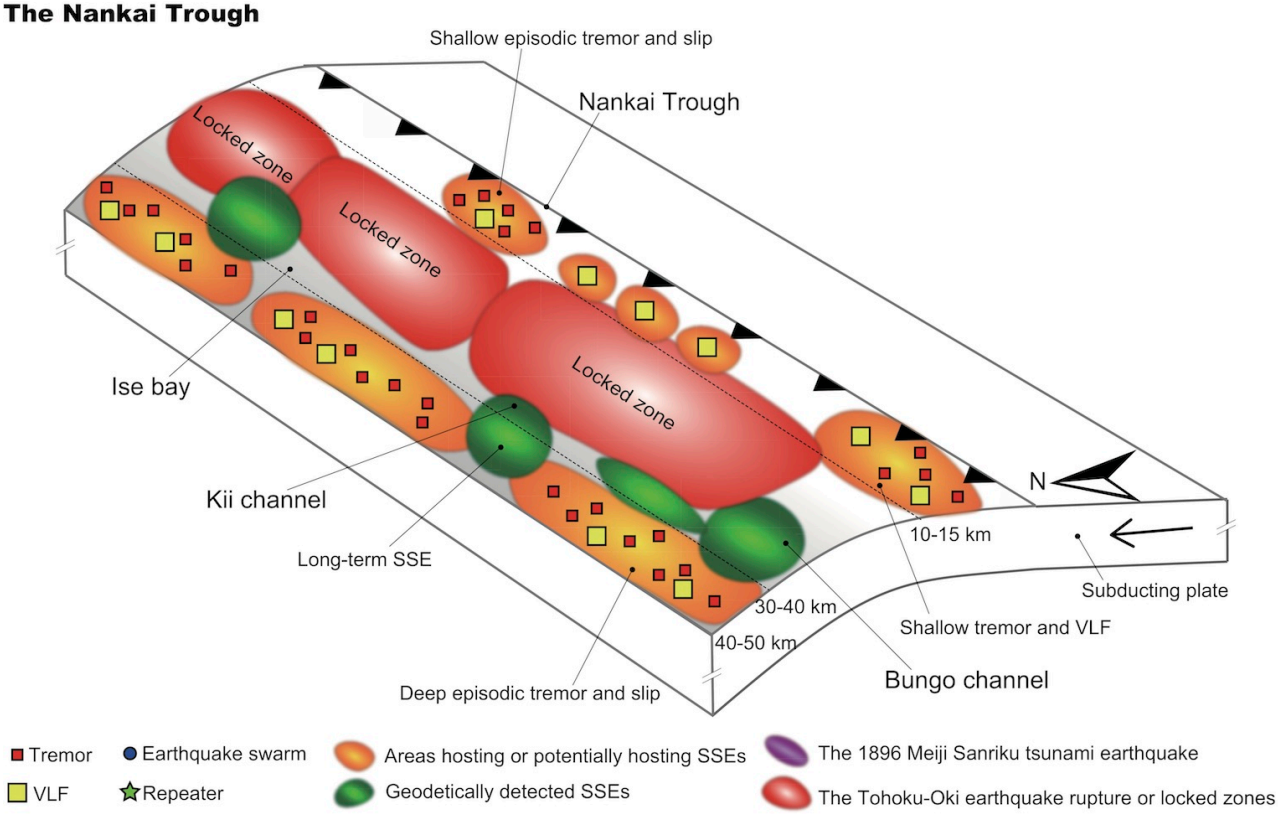

©2019. Japan Geoscience Union. All Right Reserved.

Tremor and slow slip associated with afterslip of the 2011 Tohoku earthquake

*Kazuaki Ohta[1], Yoshihiro Ito[1], Ryota Hino[2], Shukei Ohyanagi[1], Takanori Matsuzawa[3], Masanao Shinohara[4], Hajime Shiobara[4]

1. Disaster Prevention Research Institute, Kyoto University, 2. Graduate School of Science, Tohoku University, 3. National Research Institute for Earth Science and Disaster Resilience, 4. Earthquake Research Institute, the University of Tokyo

Characterizing shallow interplate slip is essential for modeling the potential generation of megathrust earthquakes and tsunamis. Large postseismic crustal deformation caused by the 2011 Tohoku-Oki earthquake suggests the occurrence of shallow afterslip, but it is unclear what kind of slip is dominant at the shallow plate interface. Here we report episodic tremor activity south of the primary rupture area based on ocean bottom seismometer observations.
We deployed 24 OBSs at 6 sites close to the trench axis in the Fukushima-Oki region. Three of these sites were small arrays, each consisting of 1 broad-band OBS and 6 short-period (1 Hz) OBSs. The 3 other sites each had 1 short-period OBS. Continuous observations were made from October 2016 to September 2017. For OBS records, we applied the envelope correlation method to detect and locate tremor activity. We also estimate the focal mechanisms of the detected tremor events using S-wave polarization particle motion.
We identified ~ 2000 tremor events in five burst episodes. The duration of each burst ranges from 6 to 18 days, with recurrence intervals of ~60 days. The tremor region largely coincides with the region of very low frequency earthquakes and lies between geodetically observed coseismic and afterslip region of the Tohoku earthquake. Tremor shows clear migration behavior with the speed of ~ 5 km/day and shear mechanisms consistent with plate subduction direction.
The characteristics of the tremor –episodicity, migration and shear mechanisms –strongly suggest that it is accompanied by slow slip events (SSEs). We further approximated the slip amount of SSEs based on the ground displacement of the tremor seismograms. The estimated slip of 1.5 cm/year corresponding to a seismic moment of ~7.4×10^{17} Nm is slightly smaller than but comparable to that of typical short-term SSEs, however, much smaller than that of afterslip. Thus, both SSEs and afterslip exist in the shallow part of the Japan trench. We propose that the tremor and SSE region illuminate the boundary between coseismic slip and stable aseismic slip that could limit the rupture extent of future megathrust earthquakes. Besides, the observed tremor and slow slip activities may also suggest that the interplate stress state has been recovered to the level of that before the Tohoku earthquake.

Keywords: tremor, slow slip, afterslip, Japan trench, Tohoku earthquake

©2019. Japan Geoscience Union. All Right Reserved.

High definition imaging of the Japan Trench by OBS Array of Arrays: Does shallow tectonic tremor occur in the plate interface?

*Shukei Ohyanagi[1], Kazuaki Ohta[2], Yoshihiro Ito[2], Ryota Hino[3], Yusaku Ohta[3], Ryosuke Azuma[3], Masanao Shinohara[4], Kimihiro Mochizuki[4], Toshinori Sato[5], Yoshio Murai[6]

1. Kyoto University, Graduate School of Science, 2. Kyoto University, Disaster Prevention Research Institute, 3. Tohoku University, 4. Tokyo University, Earthquake Research Institute, 5. Chiba University, 6. Hokkaido University

The Japan Trench is the host to various scale and slip behavior of seismic activities, such as the M9 Tohoku-Oki megathrust earthquake, slow slip events, low frequency tremors and very-low frequency earthquakes (VLFEs). Since these events occur under the seafloor, observation capability of the onshore seismic network is limited due to far distance from their source regions. During 2016 and 2017, we have performed the dense OBS Array of Arrays observation in the offshore Fukushima prefecture near the trench axis to achieve high resolution imaging of the shallow portion of the Japan Trench.
Our network consists of three OBS arrays. Each array consists of one broad band OBS, and six 1Hz short period OBSs. These seven OBSs form a triangular array of 300m to 500m of interstation distance, which results in the array diameter of ~1km. High resolution imaging of complicated seismic phenomena (such as tectonic tremor) is enabled by installing the arrays in the vicinity of the target region.
Based on visual inspection of the observed data, we have identified two episodes of low frequency tremors, triggered dynamically by M7.8 event in offshore Solomon Islands on December 2016, and M7.7 event in offshore Kamchatka Peninsula on July 2017. In both cases, the tremors were accompanied by arrival of Rayleigh waves. The episode of December 2016 lasted 7 minutes, and ceased after passage of Rayleigh wave. On the other hand, the episode of July 2017 continues even after passage of Rayleigh wave, and lasted for more than 12 minutes.
To reveal the origin of these tremors, we apply a beamforming technique to estimate back azimuth and slowness of incoming wave observed by the arrays. Observed tremors are beamformed in horizontal components of OBSs after their absolute orientations are determined using particle-motion of T-phase. From the resulting beam, we have estimated epicenters of the tremors every 60 seconds using only azimuthal information at each array. In this presentation, we are going to discuss about depth of the tremor sources from observed slowness. The tremor activities probably indicate the potential for the occurrence of shallow slow slip events near the Japan Trench, in which VLFEs and after slip were activated after the 2011 Tohoku-Oki earthquake.

Acknowledgements: This study is supported by JSPS KAKENHI (26000002).

Keywords: Low frequency tremor, Ocean Bottom Seismometer, Array analysis, Dynamic triggering, Japan Trench, Slow earthquake

©2019. Japan Geoscience Union. All Right Reserved.

The activity of small repeating earthquakes after the 2011 Tohoku-oki earthquake: an examination based on the S-net and land networks

*Naoki Uchida[1], Ryota Takagi[1], Satoshi Hirahara[1], Takashi NAKAYAMA[1], Toru Matsuzawa[1], Sachiko Tanaka[2], Youichi Asano[2]

1. Research Center for Prediction of Earthquakes and Volcanic Eruptions Graduate School of Science, Tohoku University, 2. National Research Institute for Earth Science and Disaster Resilience

We examined the activity of repeating earthquakes around the 2011 Tohoku-oki earthquake, Japan based on Seafloor Observation Network for Earthquakes and Tsunamis along the Japan Trench (S-net) and permanent land stations. We used earthquakes located by Japan Meteorological Agency to find repeating earthquakes based on the waveform similarity observed at the same station. The waveform coherences for 40 second window including P and S phases are evaluated and if they are larger than 0.8 we select them as repeating earthquakes. We performed long- and short-term analyses respectively to understand long-term activity change of repeating earthquakes and to compare land-based and offshore (S-net) data analyses. For the long-term analysis, we used earthquakes larger than M2.5 for the period from 1993 to 2018 obtained by the land stations. For the short-term analysis, we analyzed land and S-net stations separately for M2.0 or larger earthquakes for the period from August 2016 to October 2018.

The long-term analysis shows that the coseismic slip area of the 2011 Tohoku-oki earthquake continued to be quiet in the activity of the repeating earthquakes suggesting that the area have not reloaded enough after the earthquake. In the shallow area (depth <= 30km), the activity of repeating earthquakes decay with fluctuations to the north of the coseismic slip but decayed monotonically to the south of the coseismic slip area. In the deep area (depth >= 30km), the repeating earthquake activity also decayed but the activity was still high in 2018 especially in the down-dip part of the coseismic slip area. These results show different behavior of postseismic slip of the Tohoku-oki earthquake.

The short-term analysis that use the same set of earthquakes to detect repeating earthquakes (August 2016 to October 2018, M>=2) by the S-net and the land stations show similar number of detected repeating earthquakes (520 and 684 for S-net and land stations respectively). This is probably because the waveforms of earthquakes that are located by land stations (JMA’s catalogue) have good signal-to-noise ratio for the land stations. Since the completeness of magnitudes of the JMA’s catalogue in far off land area is larger than M2.0, the event detection by S-net will contribute to the detection of more repeating earthquakes in the offshore area. In addition to this, the land-station based long-term analysis has more repeating earthquakes (894 M>=2.5) for the 2.2-year period of the S-net data analysis, suggesting the increase of observation period will contribute for the detection of repeating earthquakes whose intervals are larger than the short analysis period .

Acknowledgement:

We used velocity seismometer data obtained by S-net and seismological network of Hokkaido and Tohoku University.

Keywords: repeating earthquakes, S-net, slow slip

©2019. Japan Geoscience Union. All Right Reserved.

[J] Oral | S (Solid Earth Sciences)：S-CG Complex & General

Wed. May 29, 2019 9:00 AM - 10:30 AM JST | Wed. May 29, 2019 12:00 AM - 1:30 AM UTC | A09 TOKYO BAY MAKUHARI HALL

[S-CG57] Structure and evolution of Japanese islands - Formation of island arc systems and earthquake cycles

convener:Hiroshi Sato(Earthquake Prediction Research Center, Earthquake Research Institute, The University of Tokyo), Masanao Shinohara(Earthquake Research Institute, University of Tokyo), Masahiro Ishikawa(Graduate School of Environment and Information Sciences Yokohama National University), Makoto MATSUBARA(National Research Institute for Earth Science and Disaster Resilience), Chairperson:Masanao Shinohara(Earthquake Research Institute, The University of Tokyo), Tatsuya Ishiyama(Earthquake Research Institute, University of Tokyo)

Subduction processes such as accretion, back-arc-spreading, and arc-arc collisions have shaped the Japanese island arc. Recent advances in seismic imaging, both passive and controlled source, have produced new images of the crust-mantle structure under Japan and surrounding regions. Through the influence of pre-existing faults and rheological structures, these crust and mantle structures are exerting strong control on active tectonic processes like seismic activity and crustal deformation in the overriding plate. We seek contributions that document and/or model the deformation of the Japanese islands over a variety of time scales from the earthquake cycle to the tectonic evolution of the Japanese island arc, and from a range of research fields including seismology, geology, geochemistry, tectonic geomorphology, and geodynamics. Multidisciplinary studies are encouraged. We also welcome contributions in numerical or analogue geodynamical modeling that explore deformation processes.

9:00 AM - 9:15 AM JST | 12:00 AM - 12:15 AM UTC

[SCG57-01] Recent Earthquake Activity in Northern Hokkaido, Japan

Cancelled

*Tetsuo Takanami[1,2] (1.Carnegie Institution for Science, 2.Hokkaido Research Center of Geology)

9:15 AM - 9:30 AM JST | 12:15 AM - 12:30 AM UTC

[SCG57-02] Seismic constraints on the crustal structure off the southwestern coast of Hokkaido, Japan Sea

*Tetsuo No[1], Takeshi Sato[1], Shuichi Kodaira[1], Hiroshi Sato[2], Tatsuya Ishiyama[2] (1.JAMSTEC, 2.ERI, University of Tokyo)

9:30 AM - 9:45 AM JST | 12:30 AM - 12:45 AM UTC

[SCG57-03] Deep seismic reflection profiling across the Oshima Peninsula, SW Hokkaido, Japan

*Hiroshi Sato[1], Tatsuya Ishiyama[1], Naoko Kato[1], Hidehiko Shimizu[2], Takeshi Sato[3], Shinji Kawasaki[2], Tetsuo No[3], Shuichi Kodaira[3], Seiichi Miura[3] (1.Earthquake Research Institute, The University of Tokyo, 2.JGI Inc, 3.Japan Agency for Marine-Earth Acience and Technology)

9:45 AM - 10:00 AM JST | 12:45 AM - 1:00 AM UTC

[SCG57-04] Crustal deformation and stress accumulation on source faults around Hokkaido, Japan, due to coupling at the Kuril trench

*Akinori Hashima[1], Hiroshi Sato[1], Tatsuya Ishiyama[1], Andrew M. Freed[2] (1.Earthquake Research Institute, The University of Tokyo, 2.Purdue University)

10:00 AM - 10:15 AM JST | 1:00 AM - 1:15 AM UTC

[SCG57-05] Structural Heterogeneity in and around the Source Region of the 2018 Hokkaido Eastern Iburi Earthquake, Central Hokkaido, Japan

*Takaya Iwasaki[1], Noriko Tsumura[2], Tanio Ito[3], Kazunori Arita[4], Makoto Matsubara[5], Hiroshi Sato[1], Eiji Kurashimo[1], Naoshi Hirata[1], Susumu Abe[6], Katsuya Noda[7], Akira Fujiwara[8], Shinsuke Kikuchi[9], Kazuko Suzuki[10] (1.Eathquake Research Institute, the University of Tokyo, 2.Graduate School of Science, Chiba

University, 3.Association for the Development of Earthquake Prediction, 4.Hokkaido Research Center of Geology, 5.National Research Institute for Earth Science and Disaster Resilience, 6.JAPEX, 7.GEOSYS Inc., 8.JOGMEC, 9.JGI Inc., 10.Schlumberger Ltd.)

10:15 AM - 10:30 AM JST | 1:15 AM - 1:30 AM UTC

[SCG57-06] Electrical resistivity distribution around the middle axis of Hokkaido Island: constraint for tectonics of ultra-mafic rocks

*Hiroshi Ichihara[1], Toru Mogi[1], Yusuke Yamaya[2] (1.Earthquake and Volcano Research Center, Nagoya University, 2.AIST)

Recent Earthquake Activity in Northern Hokkaido, Japan

*Tetsuo Takanami[1,2]

1. Carnegie Institution for Science, 2. Hokkaido Research Center of Geology

In order to understand the future earthquake potential damage in northern Hokkaido, we examined the current seismic activity from the perspective of plate tectonics. An earthquake swarm, with largest earthquake of M_{JMA} 4.3, starting on July 15, 2012 in the town of Nakagawa in northern Hokkaido, Japan, where residents felt the earthquakes of seismic intensity IV three times in 3 days (The Seismological Bulletin of Japan, JMA, 2012). At the same time, a slow earthquake was also detected nearby during the swarm (M. Ohzono et al., 2015; S. Ikeda, 2016). It is inferred from the results that the source area is associated with almost horizontal E-W compressional tectonics. Den and Hotta (1973) first proposed the paleo-tectonic movement of the Okhotsk plate in the Mesozoic to Paleogene time along western Hokkaido and the island of Sakhalin to the north. Nakagawa is located at the western margin of the Okhotsk paleo-plate. The present tectonic movement of the island of Hokkaido is controlled by the triple interaction among the Pacific, the North American and the Eurasian plates. The current activity of an earthquake swarm and slow earthquake near Nakagawa suggests that the tectonic movement on the remnant boundary zone has not completely vanished. Further, according to the geodetic imaging by Loveless and Meade (2010), the slip rates across the corresponding area were estimated as 13.0±2.1 mm/y ~ 8.4±2.1 mm/y of E-W closing or shortening. In order to shed light on the current earthquake behavior in the western boundary of the Okhotsk paleo-plate, we study seismic activity in northern Hokkaido centered on Nakagawa using earthquakes of magnitude 2 or more in the JMA unified catalog from January 1, 1996 to October 30, 2018. The map of epicenters indicates that almost all are inland earthquakes within a western coastal zone extending 40km east-west and 200km north-south with very few earthquakes located in the east side of the Sea of Okhotsk. Here we focus on the earthquake activity in the northern half of the zone (44.2˚N - 45.5˚N; 141.5˚E - 142.5˚E). The topical earthquake swarm and slow earthquake near Nakagawa occurred when the general earthquake activity was at its highest. We apply the Gutenberg-Richter frequency-magnitude formula (G-R law) to our earthquakes set and obtain a b-value of 0.87 that is somewhat small but almost normal. This current seismic activity is also useful in considering future potential damages in northern Hokkaido. The largest earthquake magnitude from the G-R relation is estimated to be about $M_{JMA}5$ consistent with the fact that few moderate to larger earthquakes with magnitude (M_{JMA}) greater than 5 have occurred in the research region. Our results are limited by the number of earthquakes in the region since the installation of the high density network in late 1990. In 2007, the Headquarters for Earthquake Research Promotion, an office of Japanese government estimated the magnitude of the biggest earthquake of $M_{JMA =}$ 7.6 if the Sarobetsu fault zone in northern Hokkaido fails over its entire zone. Since we have a catalog for a certain time interval (2.7 years) the straight line projection to higher magnitudes gives an estimate of the probability of having a larger earthquake. Projecting the line to say M_{max} =7.6 expected gives a value of 0.0055, implying that we could expect one M_{max} =7.6 in 183 years. We are aware that such a long term projection based on a relatively short data interval is subject to significant error. As earthquake data are added in the future, this aspect should be reexamined.

Keywords: Earthquake activity in northern Hokkaido, Earthquake zone in the western margin of Okhotsk sea plate, Earthquake swarm, Slow earthquake, Gutenberg-Richter law, b-value

©2019. Japan Geoscience Union. All Right Reserved.

Seismic constraints on the crustal structure off the southwestern coast of Hokkaido, Japan Sea

*Tetsuo No[1], Takeshi Sato[1], Shuichi Kodaira[1], Hiroshi Sato[2], Tatsuya Ishiyama[2]

1. JAMSTEC, 2. ERI, University of Tokyo

Offshore crustal structure studies have been conducted around Japan, with a primary focus on the Pacific side such as the Nankai Trough and Japan Trench via multichannel seismic reflection (MCS) and ocean bottom seismograph (OBS) surveying since the 1990s (e.g. Kodaira, 2009); moreover, seismic surveys have been conducted in the Japan Sea since the 2000s (e.g. Sato et al., 2018a). In 2018, we conducted a MCS and OBS survey off the southwestern coast of Hokkaido, which was one of the unsurveyed areas in the Japan Sea. Our survey area included the source region of the 1993 Hokkaido Nansei-Oki Earthquake, which is the largest earthquake among the shallow earthquakes that occurred in the Japan Sea since the Meiji period. Therefore, as our survey lines were oriented traverse the source region of the 1993 Hokkaido Nansei-Oki earthquake to the east and west, our data provided very important information for studying the relation between this earthquake source fault and its surrounding crustal structure. Furthermore, we targeted the Japan Basin, which is located to the west of the Hokkaido Nansei-Oki Earthquake source region. The Japan Basin is the widest basin in the Japan Sea, with previous studies estimating that it possesses a standard oceanic crustal structure and thickness (e.g. No et al., 2014; Sato et al., 2018b). Our survey area provides another key piece of information for comparison with a previous geomagnetic study because it overlaps with an area that has been defined by a striped pattern of geomagnetic anomalies (e.g. Kinoshita et al., 1995).

We conducted the seismic survey using the JAMSTEC R/V *KAIREI*. The survey area extends from the Okushiri Basin and Shiribeshi Trough to the Okushiri Ridge, the Japan Basin, and comprises nine MCS lines and one seismic refraction line using OBSs. Furthermore, the seismic refraction survey line was extended onshore to link with a land seismic survey in Oshima Peninsula, which was simultaneously conducted by the Earthquake Research Institute, University of Tokyo.

According to the provisional data processing results, clear shortening structures are imaged in the MCS data that cover the Okushiri Basin, Shiribeshi Trough, and the source region of the Hokkaido Nansei-Oki earthquake. However, a sedimentary layer with a thickness of approximately 2 km is observed in the Japan Basin, and clear reflectors, dense normal faults are observed throughout this sedimentary layer. Furthermore, a strong reflector is identified at approximately 7 km under the sedimentary layer, which we presumed to be the Moho. We image clear reflectors in the crust and uppermost mantle. Furthermore, the Moho reflector is poorly defined in the eastern margin of the Japan Basin, with a shortened structure and clear east-dipping crustal reflector imaged in this region.

The results of data analysis of seismic survey using OBSs indicate that the Japan Basin is a relatively homogeneous structure that possesses a standard oceanic crustal structure. However, the P-wave velocity structure indicates a thicker crust to the east of the region where the MCS data confirmed a shortened structure. Additionally, it is suggested that the crust thickens rapidly across the Okushiri Ridge.

Keywords: Japan Sea, 1993 Hokkaido Nansei-Oki Earthquake, Japan Basin, Okushiri Ridge, Seismic survey

©2019. Japan Geoscience Union. All Right Reserved.

Deep seismic reflection profiling across the Oshima Peninsula, SW Hokkaido, Japan

*Hiroshi Sato[1], Tatsuya Ishiyama[1], Naoko Kato[1], Hidehiko Shimizu[2], Takeshi Sato[3], Shinji Kawasaki[2], Tetsuo No[3], Shuichi Kodaira[3], Seiichi Miura[3]

1. Earthquake Research Institute, The University of Tokyo, 2. JGI Inc, 3. Japan Agency for Marine-Earth Acience and Technology

An onshore-offshore seismic data set was collected across the Oshima peninsula, SW Hokkaido to the Japan basin, off SW-Hokkaido to determine the geometry of seismogenic source faults and basic structure of backarc of NE Honshu arc (Sato, T. et al., 2019 JpGU; No et al., 2019, JpGU). Here, we present the result of deep seismic reflection profiling across the Oshima peninsula, high-reslolution seismic reflection survey across the western boundary fault of Hakodate plain and P-wave velocity structure obtained from onshore-offshore integrated seismic processing.

The deep seismic data set was collected across the Oshima peninsula in May, 2018. Vertical land seismometers (GSR) were deployed with a spacing 50 to 200 m along the 54-km-long seismic line using fixed 1119 channel. The seismic source was four to five vibroseis trucks with standard 150 m shot spacing. As high energy shot, 50 stationary sweep were carried out every 5 km along the seismic line. Sweep frequency was 6 to 60 Hz and sweep length was 16 to 20 sec. The obtained seismic data were processed according to a standard common-midpoint (CMP) stacking and a post stack time migration. We used refraction tomography to determine the P-wave velocity structure, that revealed down to 8 km in depth beneath the western part of the seismic line. Obtained P-wave velocity profile demonstrates the geometry of the top surface of pre-Tertiary rocks. The Kamiiso massif and Esashi range marked by high Vp (> 5 km/s) and 2 km of sediment cover are distributed in the Tate and Hakodate Basins. With a pattern of seismic reflection, main geologic structure is interpreted a series of westward dipping Miocene normal faults. The NS-trending Kamiiso massif is an uplifted zone bounded by a high-angle reverse fault, which formed as a normal fault. The high-resolution seismic reflection profiling was performed across the western boundary fault of the Hakodate plain. Seismic source was a viborseis truck and the seismic signal was recorded fixed 845 channel offline recorders (GSR). Shot and receiver intervals are 10 m. The 8-km-long seismic section portrays the geometry of active fault down to 2 km in depth. The fault dips 45 degrees westward in more than one km depth. Judging from the stratigraphy, it is interpreted as a reactivation of normal fault as reverse fault. On the contrary, the shallower part of active fault forms thin-skinned type of deformation associated with wedge-thrust, fault-related fold and flat-ramp structure. The obtained shallow structure is very concordant with the feature of tectonic geomorphology and frontal part of active thrust is presented as a blind thrust. The air-gun shots along the offshore of Oshima peninsula were recorded by fixed recorders on land and integrated P-wave velocity was obtained covering 310 km seismic line. The basic feature is very similar to the velocity model proposed by Sato, T. et al. (2019) JpGU. The velocity structure portrays the detailed structure produced by Miocene backarc extension and formation of the Sea of Japan crust. In spite of the later shortening deformation, basic structure has extensional tectonic features. There no evidence of the subduction of the Sea of Japan crust beneath the Hokkaido continental crust.

Keywords: Deep seismic reflection profiling, Seismic source fault, SW Hokkaido

©2019. Japan Geoscience Union. All Right Reserved.

Crustal deformation and stress accumulation on source faults around Hokkaido, Japan, due to coupling at the Kuril trench

*Akinori Hashima[1], Hiroshi Sato[1], Tatsuya Ishiyama[1], Andrew M. Freed[2]

1. Earthquake Research Institute, The University of Tokyo, 2. Purdue University

2018 Mw6.7 Hokkaido-Iburi earthquake, Japan, brought about disastrous landslides near epicenter, and a power blackout on the whole Hokkaido island. In order to assess activity of such an intra-plate earthquake, we need to know not only the geometry of local source faults but also stress on them. The geometry model for the source faults over Japan was already published by the Headquarters for Earthquake Research Promotion of the Japanese government. We are now revising the model and adding new source faults in the offshore areas. Stress in the plate interior is essentially formed due to the interplate interaction at plate boundaries. The Kuril trench near Hokkaido has hosted a massive megathrust rupture. GPS observation shows widespread locking region southeast off Hokkaido. Similarities to the preseismic state around the 2011 Mw9.0 Tohoku-oki earthquakes along the Japan trench are pointed out such as decades of subsidence along the southeast Hokkaido and decrease in seismicity in recent years in this region. In order to quantitatively estimate the effect of these plate boundary process, we construct a finite element model (FEM) to estimate regional deformation and stress accumulation rate on source fault around Hokkaido due to the locking along the Kuril trench.

Our model contains the region of 3700 km x 4600 km including the Kuril–Japan trench. The bottom of the model is taken at the depth of 700 km to consider the whole upper mantle. The geometries of the Pacific and Philippine sea slabs under the Northeast Japan –Izu Bonin arcs, and the Southwest Japan –Ryukyu arcs, respectively, are incorporated following the previous studies. The model region is divided into 1000,000 tetrahedral elements. The size of the elements is set 5 km around the slip region and gradually larger close to the boundaries. Fault slip can be modeled by giving constraint equation of displacement discontinuity. Slip region is taken on the upper surface of the Pacific plate shallower than the depth of 80 km. We simply set the Pacific and Philippine sea slabs as the 70-km thick elastic plates over viscoelastic asthenosphere. The continental side is assumed to be elastic-viscoelastic stratified structure. Elastic thickness is tested for the case of 30 and 50 km. Since the interseismic deformation includes the effect of the concurrent viscous relaxation in the asthenosphere, we used response after complete relaxation.

In order to understand the basic feature of crustal deformation around Hokkaido, we compute response to locking of two offshore regions inferred from the past earthquake occurrence: Tokachi and Nemuro. Crustal deformation in Hokkaido obtained from GPS observation shows ~5 cm/yr northwestward movements on the Southeast coast, which decay toward the North and West, except the effect of the 2003 Mw8.0 Tokachi-oki and 2011 Mw9.0 Tohoku-oki earthquakes. This basic feature can be realized in the case of elastic thickness of 50 km and locking rate of 4 cm/yr in Tokachi and 8 cm/yr in Nemuro, respectively. These locking rates form compressive stress fields over the Hokkaido region. The compressive axes are NW-SE in the eastern Hokkaido and E-W in the western Hokkaido. The calculated stress field in the western Hokkaido is consistent with the occurrence of the 2018 Hokkaido-Iburi earthquake. In this study, we also apply the calculated stress field to source fault model around Hokkaido and calculate Coulomb stress to examine the earthquake activities.

Keywords: Kuril trench, Crustal deformation, Finite element method, Viscoelasticity, Coulomb stress

©2019. Japan Geoscience Union. All Right Reserved.

©2019. Japan Geoscience Union. All Right Reserved.

Structural Heterogeneity in and around the Source Region of the 2018 Hokkaido Eastern Iburi Earthquake, Central Hokkaido, Japan

*Takaya Iwasaki[1], Noriko Tsumura[2], Tanio Ito[3], Kazunori Arita[4], Makoto Matsubara[5], Hiroshi Sato[1], Eiji Kurashimo[1], Naoshi Hirata[1], Susumu Abe[6], Katsuya Noda[7], Akira Fujiwara[8], Shinsuke Kikuchi[9], Kazuko Suzuki[10]

1. Eathquake Research Institute, the University of Tokyo, 2. Graduate School of Science, Chiba University, 3. Association for the Development of Earthquake Prediction, 4. Hokkaido Research Center of Geology, 5. National Research Institute for Earth Science and Disaster Resilience, 6. JAPEX, 7. GEOSYS Inc., 8. JOGMEC, 9. JGI Inc., 10. Schlumberger Ltd.

Central Hokkaido, Japan, has complicated tectonic history of subduction, accretion and collision processes from Late Jurassic to the present. Since Paleogene or Early Miocene, compressional stress regime has been dominated by the dextral oblique collision between the Eurasia and North America (Okhotsk) Plates and the subsequent westward movement of the Kuril Arc due to the oblique subduction of the Pacific Plate. The latter event was responsible for the formation of the Hidaka Collision Zone (HCZ) and the foreland fold-and-thrust belt with a very thick (>10 km) sedimentary package. The 2018 Hokkaido Eastern Iburi Earthquake (M=6.7) took place at a very deep depth of 37 km under this foreland fold-and thrust belt. To understand the mechanism on the occurrence of such a deep earthquake from the surrounding structural heterogeneity, we reanalyzed controlled source seismic data from the 1998-2000 Hokkaido Transect Project by applying advanced processing techniques including CRS/MDRS stacking methods and integrated refraction/wide-angle reflection analyses.

The seismic reflection processing imaged for the first time the NE Japan Arc underthrust eastward beneath the thick sedimentary package. The refraction/wide-angle reflection data were re-interpreted by tomography and ray-tracing methods. The latter analysis with aid of the new structural information from the reflection processing indicate that the crust is very thin (15-23 km) and the Moho depth is 22-30 km. The Pn velocity is a normal value of around 8 km/s. These structural features are well consistent with those in the offshore area of NE Japan, which belongs to the same geological unit. Based on the structural information mentioned above, the aftershock distribution was carefully investigated. Aftershocks relocated by the 3D structure model (Matsubara, 2017) with appropriate station corrections are distributed in a depth range of 7-45 km showing a steep geometry facing to the east. We cannot find any evidence that the aftershock distribution is related with shallow west-verging active faults developed in the fold-and-thrust belt. We think that the high-angle fault of this earthquake was formed by a certain tectonic event before the collision, maybe in Late Oligocene to Middle Miocene. The relocated aftershocks are separated into the upper (7-20 km) and lower (22-45 km) groups. The seismicity gap between them corresponds to the lower crust of our velocity model, probably representing its ductile property. According to our results, more than 80 % of relocated events occurred within the uppermost mantle of our structure model. Possible explanation for this high seismic activity is the cold crust delaminated from the Kuril Arc side, whose existence was is confirmed by a series of seismic reflection profiling in the southern part of the HCZ (Arita et al., 1998; Tsumura et al., 1999; Ito, 2000, 2002) and seismic tomography by Matsubara et al. (2017). This delaminated crustal body prevents the thermal circulation and upward migration of dehydrated fluid to cool the forearc mantle and generate more favorable environment for the brittle failure.

©2019. Japan Geoscience Union. All Right Reserved.

Keywords: Hokkaido Island, Hokkaido Eastern Iburi Earthquake, Crust and upper mantle structure, Controlled-source seismic expeditions, Seismic tomography, Fold-and-thrust belt

©2019. Japan Geoscience Union. All Right Reserved.

Electrical resistivity distribution around the middle axis of Hokkaido Island: constraint for tectonics of ultra-mafic rocks

*Hiroshi Ichihara[1], Toru Mogi[1], Yusuke Yamaya[2]

1. Earthquake and Volcano Research Center, Nagoya University, 2. AIST

Middle axis of Hokkaido Island is located on a tectonic boundaries between NE Japan arc and Kurile arc. In the south part of the boundary, collision due to migration of fore-arc aliver is known (Hidaka Collision zone). Huge serpentine rock bodies are exposed in the high P/T metamorphic belt (kamui-kotan belt) located on the NE Japan arc side near the boundary. In addition, a fresh peridotite rock body (Horoman periodotite) is also distributed in the south part around the boundary. However, tectonic process to bring the surface has not been understood although it is the key to understand the tectonics. In this study, we discuss the crustal structure beneath the arc-arc boundary especially for ultra-mafic rock area based on electrical resistivity distribution obtained in following three areas: (1) middle part of Hidaka collision zone where serpentine is exposed, (2) north part of Kamui-kotan belt where serpentine is exposed but the collision is not occurred, and (3) south part of Hidaka collision zone where the Horoman peridotite is distributed. In the area (1) and (2), very low resistivity (1-10 ohm-m) anomalies area found in the depth around 10-40 km beneath the surface serpentine body but they are not significant beneath out of the serpentine area. We interpreted them as high fraction of aqueous fluid area related to serpentine forming and bring them to the surface. In the area (3), we found thin sheet-like high resistivity body near the surface embedded to low resistivity body (Ichihara et al., G3). The surface high resistivity correspond to the peridotite because unaltered igneous rocks are basically resistive. The underlying conductive area possibly reflect cretaceous sedimentary rock based on integrated interpretation of geomagnetic anomaly, gravity anomaly and the resistivity distribution. If these interpretations in the area (3) are true, the Horoman peridotite covers over the sedimentary rock, implying the unknown tectonics processes occurred on the south part of Hidaka collision zone.

Keywords: Hidaka collision zone, serpentine, peridotite, magnetotelluric, kamui-kotan belt, 2018 eastern Iburi earthquake

©2019. Japan Geoscience Union. All Right Reserved.

[J] Oral | S (Solid Earth Sciences)：S-CG Complex & General

Wed. May 29, 2019 10:45 AM - 12:15 PM JST | Wed. May 29, 2019 1:45 AM - 3:15 AM UTC | A09 TOKYO BAY MAKUHARI HALL

[S-CG57] Structure and evolution of Japanese islands - Formation of island arc systems and earthquake cycles

convener:Hiroshi Sato(Earthquake Prediction Research Center, Earthquake Research Institute, The University of Tokyo), Masanao Shinohara(Earthquake Research Institute, University of Tokyo), Masahiro Ishikawa(Graduate School of Environment and Information Sciences Yokohama National University), Makoto MATSUBARA(National Research Institute for Earth Science and Disaster Resilience), Chairperson:Hiroshi Sato(Earthquake Research Institute, Tokyo University), Masahiro Ishikawa(Yokohama National University)

Subduction processes such as accretion, back-arc-spreading, and arc-arc collisions have shaped the Japanese island arc. Recent advances in seismic imaging, both passive and controlled source, have produced new images of the crust-mantle structure under Japan and surrounding regions. Through the influence of pre-existing faults and rheological structures, these crust and mantle structures are exerting strong control on active tectonic processes like seismic activity and crustal deformation in the overriding plate. We seek contributions that document and/or model the deformation of the Japanese islands over a variety of time scales from the earthquake cycle to the tectonic evolution of the Japanese island arc, and from a range of research fields including seismology, geology, geochemistry, tectonic geomorphology, and geodynamics. Multidisciplinary studies are encouraged. We also welcome contributions in numerical or analogue geodynamical modeling that explore deformation processes.

10:45 AM - 11:00 AM JST | 1:45 AM - 2:00 AM UTC

[SCG57-07] Three-dimensional seismic velocity structure beneath and around Japanese Islands including beneath the Pacific Ocean using NIED S-net data

*Makoto MATSUBARA[1], Hiroshi Sato[2], Kenji Uehira[1], Masashi Mochizuki[4], Toshihiko Kanazawa[5], Narumi Takahashi[1], Kensuke Suzuki[3], Shinichiro Kamiya[1] (1.National Research Institute for Earth Science and Disaster Resilience, 2.Earthquake Research Institute, the University of Tokyo, 3.Japan Agency for Marine-Earth Science and Technology, 4.Ministry of Education, Culture, Sports, Science and Technology, Japan , 5.Association for the Development of Earthquake Prediction)

11:00 AM - 11:15 AM JST | 2:00 AM - 2:15 AM UTC

[SCG57-08] Spatio-temporal extent of Cretaceous fore-arc basin in Japan

*Yukio Isozaki[1], Ryo Hasegawa[1], Yukiyasu Tsutsumi[1] (1.Department of Earth Science and Astronomy, Multi-disciplinary Sciences - General Systems Studies, Graduate School of Arts and Sciences, The University of Tokyo)

11:15 AM - 11:30 AM JST | 2:15 AM - 2:30 AM UTC

[SCG57-09] Geotectonic identities of dismembered ancient fore-arc clastics: U-Pb dating of detrital zircons in Cretaceous-Paleogene shallow marine/fluvial sandstones sporadically found in Kanto, central Japan

*Ryo Hasegawa[1], Yukio Isozaki[1], Yukiyasu Tsutsumi[2] (1.Department of Earth Science and Astronomy, The University of Tokyo, 2.Department of Geology and Paleontology, National Museum of Nature and Science)

11:30 AM - 11:45 AM JST | 2:30 AM - 2:45 AM UTC

[SCG57-10] Laboratory Measurements of Vp, Vs and Vp/Vs for polycrystalline labradorite up to 800°C and 1GPa

*Satoko Honda[1], Masahiro Ishikawa[1] (1.Graduate School of Environment and Information Sciences, Yokohama National University)

11:45 AM - 12:00 PM JST | 2:45 AM - 3:00 AM UTC

[SCG57-11] Shallow to deeper structures of the Median Tectonic Line active fault system in Shikoku illuminated by new hi-resolution seismic reflection profiling, southwest Japan

*Tatsuya Ishiyama[1], Naoko Kato[1], Shin Koshiya[2], Hiroshi Sato[1], Makoto MATSUBARA[3], Tomoko Elizabeth Yano[3], Taro Koike[4], Katsuya Noda[4] (1.Earthquake Research Institute, University of Tokyo, 2.Department of Civil and Environmental Engineering, Faculty of Science and Engineering, Iwate University, 3.National Research Institute for Earth Science and Disaster Resilience, 4.Geosys, Inc.)

12:00 PM - 12:15 PM JST | 3:00 AM - 3:15 AM UTC

[SCG57-12] **Cenozoic evolution of the Tsushima Strait and the Fukue Basin, southern Sea of Japan: an interplay of tectonics, palaeo-environment, and volcanism**

*Johan S. Claringbould[1], Hiroshi Sato[1], Tatsuya Ishiyama[1], Anne Van Horne[1,2], Shinji Kawasaki[3], Susume Abe[4] (1.Earthquake Research Institute, The University of Tokyo, 2.Department of Geology and Geophysics, University of Wyoming, 3.JGI, Inc., 4.JAPEX)

Three-dimensional seismic velocity structure beneath and around Japanese Islands including beneath the Pacific Ocean using NIED S-net data

*Makoto MATSUBARA[1], Hiroshi Sato[2], Kenji Uehira[1], Masashi Mochizuki[4], Toshihiko Kanazawa[5], Narumi Takahashi[1], Kensuke Suzuki[3], Shinichiro Kamiya[1]

1. National Research Institute for Earth Science and Disaster Resilience, 2. Earthquake Research Institute, the University of Tokyo, 3. Japan Agency for Marine-Earth Science and Technology, 4. Ministry of Education, Culture, Sports, Science and Technology, Japan , 5. Association for the Development of Earthquake Prediction

1. Introduction
We investigate the 3D seismic velocity structure beneath and around Japanese Islands including beneath the Sea of Japan and Pacific Ocean with seismic tomographic method. National Research Institute for Earth Science and Disaster Resilience (NIED) constructed the High-sensitivity seismograph network (Hi-net) after the 1995 Kobe earthquake, the Seafloor observation network for earthquake and tsunamis along the Japan Trench (S-net) after the 2011 Tohoku-oki earthquake on March 11, and the Dense Oceanfloor Network System for Earthquakes and Tsunamis (DONET) constructed by Japan Agency for Marine-earth Science and Technology (JAMSTEC) was transfered to NIED on April 1, 2016. We used arrival time data detected by these networks operated by NIED as well as other organizations and apply the seismic tomography for these data.

2. Data and method
The target region, 20–48˚N and 120–148˚E, covers the Japanese Islands. In addition to the arrival time data used by Matsubara et al. (2017), we used P- and S-wave arrival times for 32952 earthquakes recorded at approximately 1500 stations including the NIED S-net and DONET from April 2016 to June 2018. We also added the arrival time data detected at the stations operated by universities near the coast of the Sea of Japan from 2000 to 2004. Totally 6356481 P arrival data and 3534482 S arrival data from 112631 events are available. The inversion reduces the RMS of the P-wave traveltime residual from 0.245 s to 0.189 s and that of the S-wave data from 0.287 s to 0.236 s after 11 iterations.

3. Result and discussion
We clarified the seismic velocity structure beneath the Sea of Japan at depths of 10-20 km from off Hokkaido to Wakasa Bay. Vp beneath the Okushiri and Sado Islands is low at a depth of 10 km however, Vp beneath the Sea of Japan is high at depths of 10-35 km. Vp along the coast of Sea of Japan in western Japan is moderate. The lithospheric velocity structure in this region is strongly affected by the mid-Tertiary break up and formation of the Sea of Japan. Through the reactivation of the younger compression, tsunamigenic source faults has been developed. The information of the lithospheric structure provides the essential information to the structure of faults.
Due to the contribution of S-net, the velocity structure of the overlying plate beneath Pacific Ocean has been improved. One important feature is the probable Mesozoic rift structure trending NS from the coast of Tohoku to the west of Hidaka collision zone. Recent the 2018 Hokkaido Eastern Iburi Earthquake (M6.7) may related to the reactivation of the rift related structure in the upper mantle to the lower crust, where marked by high-Vp.

©2019. Japan Geoscience Union. All Right Reserved.

Keywords: seismic tomography, NIED S-net, rift

©2019. Japan Geoscience Union. All Right Reserved.

Spatio-temporal extent of Cretaceous fore-arc basin in Japan

*Yukio Isozaki[1], Ryo Hasegawa[1], Yukiyasu Tsutsumi[1]

1. Department of Earth Science and Astronomy, Multi-disciplinary Sciences - General Systems Studies, Graduate School of Arts and Sciences, The University of Tokyo

Recent analyses on detrital zircon ages in sandstones calrified various new aspects on characteristics and secular changes in provenance for the fore-arc domain of Cretaceous Japan. The shallow marine to fluvial Cretaceous strata are disrtibuted in multiple zones running almost parallel to the coeval arc-trench system in SW Japan, which is represented by the paired granitoid (Ryoke) and blueschist (Sanbagawa) belts. For example, the Upper Cretaceous Izumi Group in Shikoku and Kii peninsula has been regarded as a typical fore-arc sedimentary package deposited between the coeval grnaitoid and blueschist belts. Much emphasis was given to its origin in a pull-apart setting along an imaginary large strike-slip movement of the Median Textonic Line. Nonetheless, the lastest zircon analyses documented that its spatio-temporal dimentsion was much greater than previously believed, e.g., more than 1000 km along-arc, and nearly 100 km wide across-arc in sapce, and extended up into the Paleocene in age. The Izumi Group likely represnt a remnant of much large sedimentary basin, and its current restircted occurrence, ca. ca. 300 km along arc and ca. 20 km across-arc, was made by large-scale removal of fore-arc crust, probably relevant to the back-arc rifting to open the Japan Sea. The missing fore-arc crust can be properly reconstructed by checking ancient provenance through zircon dating in Kyushu and southern Tohoku district.

Keywords: fore-arc basin, detrital zircon, U-Pb dating

©2019. Japan Geoscience Union. All Right Reserved.

Geotectonic identities of dismembered ancient fore-arc clastics: U-Pb dating of detrital zircons in Cretaceous-Paleogene shallow marine/fluvial sandstones sporadically found in Kanto, central Japan

*Ryo Hasegawa[1], Yukio Isozaki[1], Yukiyasu Tsutsumi[2]

1. Department of Earth Science and Astronomy, The University of Tokyo, 2. Department of Geology and Paleontology, National Museum of Nature and Science

For reconstructing the fore-arc basin of Cretaceous arc-trench system in Japan, provenance analysis for sandstones has been carried out by U-Pb dating of detrital zircons, particularly for the “Cretaceous-Paleogene” sandstone-bearing units sporadically occurred in 5 distinct areas in the Kanto Mountains and northern Kanto/southern Tohoku region, i.e. the Shoya Formation in Saku, the Kanohara conglomerate in Shimonita, the Yorii Formation in Yorii (Kanto Mountains), the Nakaminato Group (northern Kanto), and the Futaba Group (southern Tohoku), of which geotectonic identities are ambiguous. The U-Pb dating of detrital zircons from these units constrained the depositional ages of 10 sandstone samples to the Late Cretaceous and early Paleocene, and also their provenance. These results confirmed that 1) the Shoya Fm and the lower-middle Nakaminato Gr are of the Maastrichtian age, which are correlated with the Izumi Group on the Late Cretaceous Ryoke ganitoids in SW Japan, 2) the Kanohara conglomerate, Yorii Fm, and Oarai Fm are of the Danian (early Paleogene) age, which were deposited on the Ryoke belt as well as the Izumi Gr., 3) the Futaba Gr is of the Coniasian age, which is correlated not with the Izumi Gr. but with the coeval units in western Kyushu, i.e., basal Himenoura Group, Kumamoto Gr, and upper Mifune Gr, which were deposited unconformably on a slightly older (Early Cretaceous) granitoids in the same fore-arc domain. These new age data provide new clues in reconstructing paleogegraphy of Cretaceous arc-trench system in Japan, before the Miocene opening of the Japan Sea. The expected discontinutity between pre-Miocene SW and NE Japan crusts in central Japan is currently buried beneath thick Quaternary sediments of the Kanto plain; nonetheless, the present data suggests two candidates, i.e., the seismologically detected major break of the pre-Cenozoic basement along the River Tone and the conventional Tanagura tectonic line to the north.

Keywords: fore-arc basin, detrital zircon, U-Pb age, Cretaceous, Paleocene, Kanto

©2019. Japan Geoscience Union. All Right Reserved.

Laboratory Measurements of Vp, Vs and Vp/Vs for polycrystalline labradorite up to 800˚C and 1GPa

*Satoko Honda[1], Masahiro Ishikawa[1]

1. Graduate School of Environment and Information Sciences, Yokohama National University

In order to estimate the elastic properties of crustal rock-forming minerals at mid-to-lower crustal P-T conditions, we performed simultaneous measurements of compressional-wave (Vp) and shear-wave (Vs) velocities of the labradorite. In this presentation, we report temperature-pressure dependence of the elastic wave velocity for labradorite, intermediate member of plagioclase feldspars, at crustal P-T condition.

The fine-grained pollycrystalline labradorite was fabricated from the nano-sized powders of crushed natural labradorite crystal ($An_{61}Ab_{37}Or_2$, $An_{65}Ab_{34}Or_1$), and was used for the measurements. After milling and forming mineral powders, sintering was carried out at a temperature of 1180–1210˚C with controlled time. Ultrasonic measurements on these samples were conducted up to 1.0 GPa in a temperature range of 25-800˚C with a piston cylinder high pressure apparatus.

The Vp increase rapidly with pressure increase up to 0.40 GPa at room temperature, while it is moderately increasing between 0.40 and 1.00 GPa. At 1.00GPa up to 800 ˚C, the elastic wave velocities decrease with increasing temperature blow 600 ˚C, δVp/δT and δVs/δT of the labradorite sample (An65Ab34Or1) is -1.6×10^{-4} km/s/˚C, -1.0×10^{-4}km/s/˚C . In contrast, above 600 ˚C , the elastic wave velocities show an increasing trend in the range of 600–800 ˚C . At cooling stage, Vp and Vs show an decreasing trend with decreasing temperature above 400˚C.
Previous studies report that elastic wave velocities of polycrystalline anorthite show an increasing trend in the range of 240–640 ˚C (Matsukage et al 2015) and that a polycrystalline plagioclase ($An_{51\pm1}$) at 1.0 GPa show marked increase in Vp and Vs between 700 and 800 ˚C (Kono et al 2008). They suggest that these discontinuous velocity changes in temperature dependence of Vp and Vs would be associated with phase transformation in plagioclase. However, it is unclear whether our measurements results between 650 and 800˚C is phase transformation, because the phase transformation was not determined on our sample using X-ray diffraction analisys. In addition, the temperature conditions of the discontinuous in Vp and Vs at high temperature is not consistent with the phase boundary previously reported. Phase transformation, therefore, would have been only temporary during the experiment.

Keywords: elastic wave velocity, polycrystalline labradorite, sintering

©2019. Japan Geoscience Union. All Right Reserved.

Shallow to deeper structures of the Median Tectonic Line active fault system in Shikoku illuminated by new hi-resolution seismic reflection profiling, southwest Japan

*Tatsuya Ishiyama[1], Naoko Kato[1], Shin Koshiya[2], Hiroshi Sato[1], Makoto MATSUBARA[3], Tomoko Elizabeth Yano[3], Taro Koike[4], Katsuya Noda[4]

1. Earthquake Research Institute, University of Tokyo, 2. Department of Civil and Environmental Engineering, Faculty of Science and Engineering, Iwate University, 3. National Research Institute for Earth Science and Disaster Resilience, 4. Geosys, Inc.

Median Tectonic Line (MTL) active fault system is one of the most pronounced, trench-parallel active dextral slip faults in SWJapan, extending for approx. 300 km (Okada, 1992). With ubiquitous proximity to the north dipping terrane boundary MTL between Samgawa metamorphic rocks (Sm) and Ryoke granitic rocks to the north, their structural links with active strands of the MTL have been widely discussed. Seismic experiments in Kinki (Wakayama) clearly illuminate that near-surface steeply dipping fault plane appears merge into underlying more shallowly dipping reflectors correlated with top Sm (Sato et al., 2015). In Shikoku, however, previous seismic sections have not fully resolved such structural linkages of the major fault strands of the MTL, whereas pioneering deep seismic experiments successfully imaged northerly dipping MTL (Ito et al., 1995). To define structural characters of the shallow to deeper subsurface geometry, we collected new seismic reflection profiles across MTL active fault system in Shikoku island. Our new, processed seismic profile across the Okamura Fault, Komatsu Fault (Goto and Nakata, 1998), and the MTL and its preliminary interpretation suggest northerly dipping Sambagawa metamorphic rocks beneath the northern flank of the Ishizuchi Mountains and Niihama plain to the north. As is the case with previous seismic results, downward extensions of the MTL apparently dips northward, in contrast to near-surface steep fault planes identified in outcrop and trench exposures. In addition, northerly dipping clouds of microseismicity also suggest its deeper extension. Similarly, in our new seismic profile in Wakimachi, Tokushima, Chichio fault (Okada and Tsutsumi, 1997), active dextral slip fault that dips vertically at ground surface, is apparently underlain by very strong and continuous north dipping reflectors from the top of Sm. This observation also suggests that the Chichio fault may merge into, rather than cut across these Sm reflectors. We will mainly discuss on (1) detailed structural characters identified in the new seismic data, (2) their structural linkages with near-surface structures of the active strands, and (3) implications for overall shallow to deeper geometry of the MTL based on both new and previous seismic data, regional seismicity based on JUICE catalogue (Yano et al., 2017), and crustal structures estimated from seismic tomography (Matsubara et al., 2017).

Keywords: Active fault , Median Tectonic Line active fault system, Seismic reflection profile, Seismicity, Shikoku

©2019. Japan Geoscience Union. All Right Reserved.

Cenozoic evolution of the Tsushima Strait and the Fukue Basin, southern Sea of Japan: an interplay of tectonics, palaeo-environment, and volcanism

*Johan S. Claringbould[1], Hiroshi Sato[1], Tatsuya Ishiyama[1], Anne Van Horne[1,2], Shinji Kawasaki[3], Susume Abe[4]

1. Earthquake Research Institute, The University of Tokyo, 2. Department of Geology and Geophysics, University of Wyoming, 3. JGI, Inc., 4. JAPEX

The Japanese island arc is tectonically active with earthquake and tsunami hazard along both the Pacific and Sea of Japan coasts. Following the tsunami disaster from the 2001 Off-Tohoku (M9) earthquake, the Japanese government initiated an extensive evaluation of tsunami hazard around Japan. Since records of prior tsunamis along the southern Japan Sea margin are rare, we here investigate the geologic evolution of the SW Japan back-arc basin to identify and analyse potential tsunami source-faults.

Located between SW Japan and the Korean Peninsula, and connecting the Japan Sea and East China Sea, the Tsushima Strait and the Fukue Basin represent a structurally complex region that formed over the last ~25 Ma as a result of several tectonic phases: (i) back-arc rifting and rotation, (ii) post-rift compression, (iii) weak thrusting, and (iv) subsidence and strike-slip deformation. Syn-depositional volcanism and changes in regional palaeo-environment are known from previous studies surrounding this connecting region, but how these factors fit together in the regional tectonic framework is not well understood. In addition to analysing recent seismic reflection data and detailed gravity data, we here re-evaluate extensive seismic reflection profiles and well data of ten boreholes offshore the SW Japan arc. We observe large basement blocks and igneous bodies, and inverted and cross-cut half grabens filled with syn-kinematic deposits. Clear stratal terminations suggest multiple transitions in regional stress regime. The gravity data allow us to link the syn-depositional igneous bodies to previously-dated volcanism onshore. Additionally, planktonic and calcareous nanno-fossils from the well data provide control on absolute timing of different kinematic stages, while benthic foraminifers and pollen show changes in palaeo-water depth, coeval with local, relative palaeo-climate reversals, respectively.

From ~25 Ma pollen data show warming of the local climate in southern Japan Sea side of the Tsushima Strait, while on the East China Sea side in the Fukue Basin relative cooling is observed. This is related to initial rifting, opening up back-arc basin allowing relative warm water to flow through the Tsushima Strait into the Japan Sea warming the local climate, and relative cold water flowing back cooling the local environment in the Fukue Basin on the opposite side of the Tsushima Strait. Subsequently, negative flower structures and large half-grabens filled with over 5400 m of synrift sediments developed between ~18-16 Ma, containing benthic foraminifera suggesting a deepening marine environment. This is linked to the rapid, clock-wise rotation of SW Japan, which pivot point migrates along a dextral oblique normal fault west of Tsushima. At ~15 Ma rift structures are abruptly inverted or cross-cut by thrust faults and wedge thrusts, with microfossils and pollen on the Japan Sea side suggesting shallowing of the palaeo-waterdepth and cooling of the local climate, respectively. Contrary, in the Fukue Basin, the local climate shows relative warming. We suggest that during this compressional tectonic event a topographic sill developed in the Tsushima Strait that cut off water flow between the cooler Japan Sea and the subtropic East China Sea. From ~6 Ma, the local climate on the Japan Sea side warms again contemporarily with deepening of the marine palaeo-environment and deposition of sub-horizontal

©2019. Japan Geoscience Union. All Right Reserved.

Pliocene sediments, implying a weakening of the compressional stress and renewed water flow through the Tsushima Strait. These observations along with previously published data of the surrounding areas enable us to better understand the connection between the Cenozoic structural development of the SW Japan arc, and the related the palaeo-environment changes and volcanism. As a result, we are better able to identify potential tsunami-source faults along the southern Japan Sea margin based on our understanding of the structural evolution.

Keywords: Structural evolution, Tsushima Strait, Fukue Basin, Palaeo-environment, Back-arc rift basin, Inversion

©2019. Japan Geoscience Union. All Right Reserved.

[J] Poster | S (Solid Earth Sciences)：S-CG Complex & General

Wed. May 29, 2019 3:30 PM - 5:00 PM JST | Wed. May 29, 2019 6:30 AM - 8:00 AM UTC | Poster Hall International Exhibition Hall8, Makuhari Messe_20

[S-CG57] Structure and evolution of Japanese islands - Formation of island arc systems and earthquake cycles

convener:Hiroshi Sato(Earthquake Prediction Research Center, Earthquake Research Institute, The University of Tokyo), Masanao Shinohara(Earthquake Research Institute, University of Tokyo), Masahiro Ishikawa(Graduate School of Environment and Information Sciences Yokohama National University), Makoto MATSUBARA(National Research Institute for Earth Science and Disaster Resilience)

Subduction processes such as accretion, back-arc-spreading, and arc-arc collisions have shaped the Japanese island arc. Recent advances in seismic imaging, both passive and controlled source, have produced new images of the crust-mantle structure under Japan and surrounding regions. Through the influence of pre-existing faults and rheological structures, these crust and mantle structures are exerting strong control on active tectonic processes like seismic activity and crustal deformation in the overriding plate. We seek contributions that document and/or model the deformation of the Japanese islands over a variety of time scales from the earthquake cycle to the tectonic evolution of the Japanese island arc, and from a range of research fields including seismology, geology, geochemistry, tectonic geomorphology, and geodynamics. Multidisciplinary studies are encouraged. We also welcome contributions in numerical or analogue geodynamical modeling that explore deformation processes.

[SCG57-P01] Crustal structure from the Japan Sea back-arc basin to the margin off SW Hokkaido deduced from the seismic survey

*Takeshi Sato[1], Tetsuo No[1], Shuichi Kodaira[1], Seiichi Miura[1], Tatsuya Ishiyama[2], Hiroshi Sato[2] (1.Research and Development Center for Earthquake and Tsunami, Japan Agency for Marine-Earth Science and Technology, 2.ERI, Univ. of Tokyo)

[SCG57-P02] Three-dimensional plate geometry model from the Nankai to the Ryukyu subduction zone

*Ayako Nakanishi[1], Tsutomu Takahashi[1], Yojiro Yamamoto[1], Mikiya Yamashita[1], Minako KATSUYAMA[1], Seiichi Miura[1], Narumi Takahashi[3,1], Hiromi Kamata[1], Shuichi Kodaira[1], Yoshiyuki Kaneda[2,1] (1.Japan Agency for Marine-Earth Science and Technology, 2.Kagawa University, 3.National Research Institute for Earth Science and Disaster Resilience)

[SCG57-P03] Trace elements and Sr-Nd-Hf-Pb isotopic composition of Miocene Tomari volcanic rocks, Shimokita Peninsula, Aomori, NE Japan

*Masataka Aizawa[1], Mitsuru Inaba[2], Satoshi Okamura[3,4], Ryuichi Shinjo[5] (1.Graduate School of Engineering and Sience, University of Ryukyus, 2.GeoPuck Association, 3.Hokkaido Education University, 4.Hokkaido Soil Research Co-op., 5.Faculty of Science, University of Ryukyus)

[SCG57-P04] Acceleration of oceanic plate following megathrust earthquakes

*Mohammad Yuzariyadi[1], Kosuke Heki[1] (1.Hokkaido University)

[SCG57-P05] 3D velocity model in the region of Nankai Trough

*Minako KATSUYAMA[1], Ayako Nakanishi[1], Rei Arai[1], Shigeyoshi Tanaka[1], Narumi Takahashi[2], Hiromi Kamata[1], Yoshiyuki Kaneda[3] (1.Japan Agency for Marine-Earth Science and Technology, 2.National Research Institute for Earth Science and Disaster Resilience, 3.Kagawa University)

[SCG57-P06] Depth of seismogenic layer at the 2018 North Osaka and the 2018 Hokkaido Eastern Iburi earthquake sites

*Tomoko Elizabeth Yano[1], Makoto MATSUBARA[1] (1.National Research Institute of Earth Science and Disaster Prevention)

[SCG57-P07] Seismic reflection profiling across the Median Tectonic Line (MTL) active fault system in Ehime and Tokushima Prefectures

*Naoko Kato[1], Tatsuya Ishiyama[1], Hiroshi Sato[1], Shin Koshiya[2], Taro Koike[3], Katsuya Noda[3]
(1.Earthquake Research Institute,University of Tokyo, 2.Faculty of science and engineering, Iwate University, 3.Geosys, Inc.)

Crustal structure from the Japan Sea back-arc basin to the margin off SW Hokkaido deduced from the seismic survey

*Takeshi Sato[1], Tetsuo No[1], Shuichi Kodaira[1], Seiichi Miura[1], Tatsuya Ishiyama[2], Hiroshi Sato[2]

1. Research and Development Center for Earthquake and Tsunami, Japan Agency for Marine-Earth Science and Technology, 2. ERI, Univ. of Tokyo

The Japan Sea is a back-arc basin in the northwestern Pacific. Along the eastern and southern margins, destructive earthquakes occurred (e.g., the 1983 Nihon-kai-Chubu Earthquake, and the 1993 Hokkaido-Nansei-Oki Earthquake). Moreover, along the eastern margin, fault-fold belts developed as a result of deformation caused by extension associated with the opening of the Japan Sea and by the later compression (e.g., Okamura et al., 1995; Sato, 1994). Results of seismic surveys from the Japan Basin to the eastern margin of this sea indicated that structures related back-arc opening might play a role in the location of large earthquakes and the distribution of the deformation zone including active faults and folds along the margin of the Japan Sea (e.g., No et al., 2014). This result demonstrates that the elucidation of the back-arc opening process is important for understanding not only back-arc extension along the Asian continental margin, but also the mechanism of large earthquakes and the distribution of subsequent deformation in the Japan Sea back-arc basin. In the SW Hokkaido, the 1993 Hokkaido-Nansei-Oki Earthquake (Mj 7.8) occurred and the dip and distribution of active faults show a complication pattern. However, we have little information of detailed opening, deformation processes and mechanism of large earthquakes in this area due to the inadequate detailed crustal structure obtained by sufficiently dense OBS spacing in seismic surveys.

To obtain the crustal structure, we conducted the active-source seismic survey using ocean bottom seismographs (OBSs) and multi-channel streamer (MCS) in the margin of the Japan Sea off southwestern Hokkaido ranging from the Japan Basin to the coastal area on land in 2018. This survey was used at 57 OBSs, a tuned air-gun array having 7,800 cu. inch and MCS system. This survey line has about 243 km length and is a part of an integrated ocean-land seismic survey line.

In record sections of several OBSs, not only the first arrived phases but also later phases reflected from interfaces in the crust and uppermost mantle are visible. Also, the MCS profile clearly images the sedimentary layer and the undulations of the basement. The crustal structure in the Japan Basin resembles the typical oceanic crust (e.g., White et al., 1992). In the transition between the Japan Basin and the southern Okushiri Ridge, the crustal structure drastically changes. The area from the southern Okushiri Ridge to the Okushiri Basin has the upper crust with a P-wave velocity of 5.4-6.2 km/s corresponding to the continental upper crust. Moreover, the P-wave velocity distribution has a variation in this area.

©2019. Japan Geoscience Union. All Right Reserved.

Three-dimensional plate geometry model from the Nankai to the Ryukyu subduction zone

*Ayako Nakanishi[1], Tsutomu Takahashi[1], Yojiro Yamamoto[1], Mikiya Yamashita[1], Minako KATSUYAMA[1], Seiichi Miura[1], Narumi Takahashi[3,1], Hiromi Kamata[1], Shuichi Kodaira[1], Yoshiyuki Kaneda[2,1]

1. Japan Agency for Marine-Earth Science and Technology, 2. Kagawa University, 3. National Research Institute for Earth Science and Disaster Resilience

Considering the large slip distribution of the 2004 Sumatra earthquake, possible coseismic rupture area of megathrust earthquakes from the Tokai to Ryukyu cannot be denied. Characteristics of occurrence of great earthquakes is also different between these neighboring subduction zones. Historically, megathrust earthquakes have been generated repeatedly along the Nankai Trough at intervals of approximately 100-200yrs (e.g. Ando, 1975).Along the Ryukyu Trench, although great earthquakes have occurred only twice over the last 300 years: the 1771 Yaeyama earthquakes and the 1911 earthquake off Kikai, recent studies of tsunami deposits indicated that the Ryukyu Islands have been periodically hit by large tsunamis with an interval of several hundred years [e.g. Ando et al., 2017]. Moreover, the coupling condition of the plate interface along the Ryukyu Trench is different from that of the Nankai Trough based on the seismic survey and observations [Arai et al. 2016]. They reported that the Ryukyu Trench is dominated by slow earthquakes at any depths and lacks a typical locked zone such as the Nankai Trough.
To understand relation between the structure around the subducting Philippine Sea plate and seismicity including slow earthquake phenomena, it is necessary to know the geometry and property of the plate boundary from the Nankai to the Ryukyu subduction zone. Three-dimensional plate geometry model will be also important for a precise estimate of the maximum range of the coseismic rupture zone of the Nankai megathrust earthquake. The model is also very useful to construct a new three-dimensional seismic velocity model of the Nankai Trough for depth conversion of interpreted active faults in time section of seismic reflection data [Katsuyama et al., 2019 JPGU].
Based on the result (three-dimensional plate geometry model of the Nankai Trough) from marine active and passive source seismic data [Nakanishi et al., 2018], three-dimensional plate geometry model from Nankai to Ryukyu subduction zone is tried to be constructed using the result of seismic studies around the Ryukyu Trench [Iwasaki et al, 1990; Kodaira et al., 1996; Arai et al., 2016, 2017; Nishizawa et al, 2017; Yamamoto et al., 2018].The model of Nakanishi et al. [2018] is also updated by using the result of deep seismic tomography off the Kii peninsula [Yamamoto et al., 2014, 2017].
In this presentation, a preliminary version of the combined three-dimensional model will be shown.
This study is part of 'Research project for compound disaster mitigation on the great earthquakes and tsunamis around the Nankai trough region' and the project 'Comprehensive evaluation of faults information on offshore Japan' funded by Ministry of Education, Culture, Sports, Science and Technology, Japan.

Keywords: subducting plate, Nankai Trough, Ryukyu Trench

©2019. Japan Geoscience Union. All Right Reserved.

Trace elements and Sr-Nd-Hf-Pb isotopic composition of Miocene Tomari volcanic rocks, Shimokita Peninsula, Aomori, NE Japan

*Masataka Aizawa[1], Mitsuru Inaba[2], Satoshi Okamura[3,4], Ryuichi Shinjo[5]

1. Graduate School of Engineering and Sience, University of Ryukyus, 2. GeoPuck Association, 3. Hokkaido Education University, 4. Hokkaido Soil Research Co-op., 5. Faculty of Science, University of Ryukyus

Introduction

Tomari volcanic rocks, located in Shimokita Peninsula, Aomori Prefecture, NE Japan, formed volcanic front at Miocene period. They include primitive tholeiitic basalts (Takimoto, 1986), therefore volcanic activity in this area strongly suggest relation to opening Japan Sea back-arc basin caused by upwelling asthenosphere. Volcanic activities divided into 4 stages and their K-Ar dating have been reported 13-15 Ma (Watanabe *et al.*, 1993). This study use boring core sample dug from Shimokita Peninsula (SN-010 core; drilling stop depth is 1484 m). Tomari Formation appear deeper than 308.82 m in this core and it has been reported 13.1-14.5 Ma at 385 m (micro fossils), 16.0 Ma, 24.2 Ma (zircon U-Pb dating) at 467 m and 818 m, respectively (Nuclear Regulatory Agency, 2016).

Lithofacies and occurrence of Tomari volcanic rocks

We collected samples from the 1st and 2nd stage of surface Tomari Formation and 8 depth from SN-010 core. Core samples are volcanic breccia, lava and lapilli tuff. And the 1st stage surface volcanic rocks include reddish rounded gravel and pillow lava fragments into deposition layer with lamination. The 2nd stage surface volcanic rocks mainly erupted as pillow lava and hyaloclastite.

Geochemical characteristics

Shallow core samples (SCS; shallower than 862.26 m) and middle core samples (MCS; 999.00-1003.20 m) show middle-K series and deep core samples (DCS; deeper than 1197.86 m) show low-K series. Incompatible elements (especially LILE) concentrations of SCS and MCS are higher than DCS. Surface 1st and 2nd stage samples are plotted middle-K series. Incompatible elements features are similar as SCS and MCS. Multi-elements diagrams normalized by N-MORB show high LILE, negative Nb-Ta and positive Pb anomalies, they mean these rocks were produced at subduction zone. Sr-Nd isotopic composition of MCS-DCS show more depleted and SCS have more enriched composition. Pb isotopes are plotted into volcanic rocks field of Quaternary volcanic front of NE Japan without difference each strata. Primitive tholeiitic basalts are produced in 2nd stage and they show most enriched isotopic composition (Hanyu *et al.*, 2006). Primitive basalts and SCS-MCS have higher Ba/Nb than DCS.

The relationship to opening Japan Sea event

SN-010 core dating suggest that volcanic activity formed Tomari Formation already started late Oligocene-early Miocene. Whole-rock chemical composition of 563.48 m samples is similar to surface 1st stage volcanic rocks, therefore upper level of core sample may be comparable with surface 1st stage volcanic rocks (Aizawa *et al.*, 2018).

Enriched isotopic composition of primitive basalts cannot be explained by assimilation of lower crust due to their high MgO, Cr, Ni composition. In addition, SCS-MCS and primitive basalts have higher Ba/Nb and MCS-DCS show depleted isotopic composition. Thus, it is considered that partial melting of DMM produced volcanic rocks of MCS-DCS, and MCS (high Ba/Nb) were strongly affected slab derived components. Then, volcanic rocks of SCS and surface samples were originated magma from sub-arc

©2019. Japan Geoscience Union. All Right Reserved.

enriched lithospheric mantle (EM II-like isotopic composition).

Petrography of DCS and MCS suggest volcanic activity on land environment because there are reddish volcanic gravels at 1482.00 m and 1335.87 m, and 999.00 m lapilli tuff matrix color is red. Although SCS have no evidence for judging stationary environment of volcaniclastic rocks, the 1st stage outcrop include rounded reddish volcanic gravels into lamination, and the 2nd stage volcanic rocks are mainly erupted as pillow lava and hyaloclastite. These occurrences suggest the development of lifting at late Oligocene-early Miocene period and stationary environment change from on land to underwater. The change of geochemical features, from depleted to enriched composition, may mean to change partial melting position in sub-arc mantle due to the hot asthenosphere upwelling under this area.

Keywords: Miocene, Volcanic front, Japan Sea, Back-arc basin, Tomari volcanic rocks

©2019. Japan Geoscience Union. All Right Reserved.

Acceleration of oceanic plate following megathrust earthquakes

*Mohammad Yuzariyadi[1], Kosuke Heki[1]

1. Hokkaido University

Accelerated subduction of tectonic plates following megathrust earthquakes was proposed by D. Anderson (1975, Science). Heki and Mitsui (2013 EPSL) found postseismic enhancements of inter-plate coupling in the adjacent segments of the 2003 Tokachi-Oki and the 2011 Tohoku-Oki earthquakes. They hypothesized that these earthquakes caused accelerated subduction of the Pacific plate slab in addition to already-known postseismic processes such as afterslip and viscous relaxation. Melnick et al. (2017 GRL) found a similar enhancement of coupling to the north of the 2010 Maule earthquake rupture zone, and Loveless (2017 GRL) considered this a common phenomenon after megathrust earthquakes and named it as the super-interseismic phase. Accelerated subduction occurs during a period after the earthquakes, but its duration and amount depend on the magnitude. Here we investigate how long and how much is the acceleration over the time period covering several years after the earthquakes. So far, we have been using data from GNSS stations on arcs near the segments adjacent to megathrust ruptures. In the present study, we use data from GNSS stations on the subducting oceanic plates and on a subducted continental plate.

We present GNSS velocity data from oceanic islands showing post-megathrust accelerations. They include the Marcus Island (1098), Japan, that showed significant acceleration following the Mw 9 2011-3-11 Tohoku-Oki Earthquake. The Cocos Island (COCO), Australia, seems to have been accelerated after the Mw 8.4 2007-9-12 Bengkulu earthquake, Southern Sumatra. The JRGN in the west coast tip of Chile was accelerated after the Mw 8.2 2014-4-1 Iquique Earthquake. We also found there was a certain velocity change in Christmas Island (XMIS), Australia, after the Mw 7.7 2006-7-17 South Java earthquake. All stations are located on the oceanic plate except JRGN that is located on the continental plate.

Marcus Island (1098) GNSS station showed a significant velocity change after the 2011 Tohoku-Oki Earthquake. The maximum transient acceleration occurred in the period 2-3 years following the earthquake with a maximum velocity change of 9.4 mm/yr. After 3.0 years, The acceleration has been decaying, and the original velocity resumed by now. Cocos Island (COCO) GNSS station shows that the maximum transient acceleration occurred between 0.75-1.5 years after the 2007 Bengkulu earthquake with a maximum change of 4.9 mm/yr. After 1.5 years, the acceleration has decayed and has been showing the velocity similar to the value before the earthquake since 4.5 years after the earthquake. Chile (JRGN) GNSS station shows that the transient acceleration reached the maximum in ~1 year after the 2014 Iquique earthquake with a maximum change of 4.7 mm/yr. The accelerated velocity decayed to the original value in 2.5 years after that. The acceleration of the Christmas Island (XMIS) GNSS station was 2.7 mm/yr and occurred in ~1.0 year after the 2006 South Java earthquake. The acceleration seems to have decayed in 2.5 years after the earthquake.

In general, we found that the transient acceleration of oceanic plate occurs shortly after a megathrust earthquake and continue over a certain period. Then it decays, and finally the velocity before earthquake recovers in a few years.

Keywords: megathrust earthquake, plate acceleration, Subduction

©2019. Japan Geoscience Union. All Right Reserved.

©2019. Japan Geoscience Union. All Right Reserved.

3D velocity model in the region of Nankai Trough

*Minako KATSUYAMA[1], Ayako Nakanishi[1], Rei Arai[1], Shigeyoshi Tanaka[1], Narumi Takahashi[2], Hiromi Kamata[1], Yoshiyuki Kaneda[3]

1. Japan Agency for Marine-Earth Science and Technology, 2. National Research Institute for Earth Science and Disaster Resilience, 3. Kagawa University

This is a part of the project “Comprehensive evaluation of faults information on offshore Japan”, by the Ministry of Education, Culture, Sports, Science and Technology (MEXT). The project consists of three themes, 1) Collecting seismic survey data and building a database of offshore faults, 2) Interpreting distribution of active faults using seismic data collected, and conducting the seismic re-processing by leading-edge seismic technology for the seismic data obtained in previous decades, 3) Building the fault models for a simulation of strong motion and tsunami disaster, based on the interpreted faults. Our purpose of this study is make a 3D velocity model in the Nankai Trough to provide with the support we needs to interpret faults.

The Nankai Trough, where the Philippine sea plate is subducting beneath the Eurasian plate. Some seamounts and ridges are subducted here.

3D velocity model was constructed by seismic data and ocean bottom seismometer(OBS) refraction survey data which were obtained by a various agencies and private companies. Horizons such as acoustic basment and unconformity were interpreted using reflection seismic sections. Conrad discontinuity and Mohorovicic discontinuity were interpreted on refraction surveys and consulted previous study. Layer structure and velocity model were created on these horizons.

We obtain a result that understands geological structure in Nankai Trough. So in this session, we will take a discussion concerning structural characteristic based on the 3D velocity model.

Keywords: 3D velocity model , Nankai Trough, subduction zone

©2019. Japan Geoscience Union. All Right Reserved.

Depth of seismogenic layer at the 2018 North Osaka and the 2018 Hokkaido Eastern Iburi earthquake sites

*Tomoko Elizabeth Yano[1], Makoto MATSUBARA[1]

1. National Research Institute of Earth Science and Disaster Prevention

Background:
Understanding crustal seismogenic layer on faults is important because it enable us to know the maximum size of possible crustal earthquake on the corresponding fault. Depth of the crustal sesmogenic layer also gives us the depth of brittle zone because it relates to the rheology of the crust. The cutoff depths where total of 95 % of events occurred within the depth column of each grid, referred to as D95, can be calculated from the past microseismicity. We aimed to verify the index, D95, if it indicates as the deeper limit of the seismogenic layer. Using the microeismicity before mainshocks, we investigated if we could foresee the deeper limit of seimogenic layer before the 2018 North Osaka (2018 Osaka) and the 2018 Hokkaido Eastern Iburi (2018 Iburi)earthquakes occurred.

Data and Method:
D95 is calculated from the seismicity before each mainshock. We used JUICE catalog (2001-2012) of the event catalog for miscriseismicity in this study. We calculated D95 from events of M1.5 or greater listed in the JUICE catalog for every grid point of 0.02 degree interval. We only consider when the total number of events within the range of 0.1 degree from the grid point contains 50 events and more.

We also look at the temperature data to see if the estimated depths of 250 degrees (in Celsius), 300 degrees, and 450 degrees correspond to the actual earthquake depth. Using the datasets contain the temperature profile of the depth down to about 300 m and the depth down to about 1000 m from the surface of the earth, we computed the depth at which the crustal temperature reaches 250, 300, 450 degrees (hereafter referred to as D250deg, D300deg, D450deg, respectively).

Result:
For the 2018 Osaka earthquake site, the relocated hypocenter of the mainshock was 13.7 km in depth. Relocated aftershocks are mainly distributed between 8 and 14 km in depth. D95 along the aftershocks was calculated to be between 13 km to 14 km. The range of D250deg to D450deg was between10 km and 24 km. D300deg was about 13 km.

For the 2018 Iburi earthquake site, the relocated hypocenter of the mainshock was 35.9 km in depth. Relocated aftershocks are mainly distributed between 25 to 50 km. D95 was estimated to be around 25 km. The range of D250deg and D400deg is between 10 km and 34 km.

Conclusion/Discussion:
D95 as a seismogenic depth of the 2018 Osaka earthquake site was consistent with the mainshock and aftershock distribution. Conversely, D95 of the 2018 Iburi earthquake was not consistent with an actual event: D95 was about 10 km shallower than the mainshock and about 30 km shallower than the deeper aftershocks. The seismicity on the Ishikari Lowland Eastern edge fault zone (Ishikari Teichi Touen Danso Tai), west from the mainshock site, was used to compute D95 in this study. Therefore, discrepancy in D95 of Iburi earthquake site is due to D95 indicates the seismogenic depth of Ishikari Lowland Eastern edge fault zone but not the fault responsible of the 2018 Ishikari Earthquake.

©2019. Japan Geoscience Union. All Right Reserved.

Keywords: seismogenic depth, North Osaka, Hokkaido Eastern Iburi, Earthquake, heat flow

©2019. Japan Geoscience Union. All Right Reserved.

Seismic reflection profiling across the Median Tectonic Line (MTL) active fault system in Ehime and Tokushima Prefectures

*Naoko Kato[1], Tatsuya Ishiyama[1], Hiroshi Sato[1], Shin Koshiya[2], Taro Koike[3], Katsuya Noda[3]

1. Earthquake Research Institute,University of Tokyo, 2. Faculty of science and engineering, Iwate University, 3. Geosys, Inc.

The Median Tectonic Line (MTL) is the most significant inland fault in SW Japan, which extends more than 1000 km and divides SW Japan into the inner and outer zone. The western part of the MTL shows late Quaternary right-lateral strike-slip movements at several mm/y (eg. Tsutsumi and Okada, 1996). According to the seismic reflection profile, northward gently dipping character of the Median Tectonic Line has already been suggested in the eastern Shikoku (Ito et al., 1996) and eastern Kyushu (Yusa et al., 1992). For the deeper extension of MTL, north-dipping geometry was obtained by low-fold seismic reflection images in Shikoku island (Kawamura et al., 2003; Sato et al., 2005). For the MTL active fault system, the geometry of its deeper extension is poorly understood in Shikoku island. To reveal deeper geometry of fault surface, shallow to deep seismic reflection profiling was performed in Ehime and Tokushima Prefectures. This research was performed as a research program funded by the Ministry of Education, Culture, Sports, Science and Technology, Japan.
Three seismic lines were deployed perpendicular to the MTL and major geologic boundaries. The length of seismic lines is 11 km (Saijo area, Ehime), 4.8 km (Wakimachi area, Tokushima) and 6.4 km (Awa area, Tokushima). To obtain a high-resolution seismic image of the shallow part of MTL, a 10-m spacing receiver array was formed using offline recorders. The seismic source was vibroseis trucks. The sweep signals (5-100 Hz for high resolution reflection profiling, 5-40 Hz for refraction profiling) were recorded 10 Hz vertical geophones. The seismic data were processed using conventional CMP-reflection methods. The high-energy shot gathers at Saijo seismic line clearly demonstrate the reflectors at 1.5, 2-3, 4 sec. (Two-way travel time). The reflectors from 2-3 s (TWT) are interpreted as northward dipping Sambagawa Metamorphic belt. The seismic sections portray the seismic image down to 2 km in Wakimachi and Awa area. The reflectors are interpreted as northward dipping Sambagawa Metamorphic belt. These structural characters found in the seismic section may show that the deeper extension of MTL shows northward dipping in Shikoku.

©2019. Japan Geoscience Union. All Right Reserved.

[J] Poster | S (Solid Earth Sciences)：S-CG Complex & General

Wed. May 29, 2019 5:15 PM - 6:30 PM JST | Wed. May 29, 2019 8:15 AM - 9:30 AM UTC | Poster Hall International Exhibition Hall8, Makuhari Messe_34

[S-CG57] Structure and evolution of Japanese islands - Formation of island arc systems and earthquake cycles

convener:Hiroshi Sato(Earthquake Prediction Research Center, Earthquake Research Institute, The University of Tokyo), Masanao Shinohara(Earthquake Research Institute, University of Tokyo), Masahiro Ishikawa(Graduate School of Environment and Information Sciences Yokohama National University), Makoto MATSUBARA(National Research Institute for Earth Science and Disaster Resilience)

Subduction processes such as accretion, back-arc-spreading, and arc-arc collisions have shaped the Japanese island arc. Recent advances in seismic imaging, both passive and controlled source, have produced new images of the crust-mantle structure under Japan and surrounding regions. Through the influence of pre-existing faults and rheological structures, these crust and mantle structures are exerting strong control on active tectonic processes like seismic activity and crustal deformation in the overriding plate. We seek contributions that document and/or model the deformation of the Japanese islands over a variety of time scales from the earthquake cycle to the tectonic evolution of the Japanese island arc, and from a range of research fields including seismology, geology, geochemistry, tectonic geomorphology, and geodynamics. Multidisciplinary studies are encouraged. We also welcome contributions in numerical or analogue geodynamical modeling that explore deformation processes.

[SCG57-P01] Crustal structure from the Japan Sea back-arc basin to the margin off SW Hokkaido deduced from the seismic survey

*Takeshi Sato[1], Tetsuo No[1], Shuichi Kodaira[1], Seiichi Miura[1], Tatsuya Ishiyama[2], Hiroshi Sato[2] (1.Research and Development Center for Earthquake and Tsunami, Japan Agency for Marine-Earth Science and Technology, 2.ERI, Univ. of Tokyo)

[SCG57-P02] Three-dimensional plate geometry model from the Nankai to the Ryukyu subduction zone

*Ayako Nakanishi[1], Tsutomu Takahashi[1], Yojiro Yamamoto[1], Mikiya Yamashita[1], Minako KATSUYAMA[1], Seiichi Miura[1], Narumi Takahashi[3,1], Hiromi Kamata[1], Shuichi Kodaira[1], Yoshiyuki Kaneda[2,1] (1.Japan Agency for Marine-Earth Science and Technology, 2.Kagawa University, 3.National Research Institute for Earth Science and Disaster Resilience)

[SCG57-P03] Trace elements and Sr-Nd-Hf-Pb isotopic composition of Miocene Tomari volcanic rocks, Shimokita Peninsula, Aomori, NE Japan

*Masataka Aizawa[1], Mitsuru Inaba[2], Satoshi Okamura[3,4], Ryuichi Shinjo[5] (1.Graduate School of Engineering and Sience, University of Ryukyus, 2.GeoPuck Association, 3.Hokkaido Education University, 4.Hokkaido Soil Research Co-op., 5.Faculty of Science, University of Ryukyus)

[SCG57-P04] Acceleration of oceanic plate following megathrust earthquakes

*Mohammad Yuzariyadi[1], Kosuke Heki[1] (1.Hokkaido University)

[SCG57-P05] 3D velocity model in the region of Nankai Trough

*Minako KATSUYAMA[1], Ayako Nakanishi[1], Rei Arai[1], Shigeyoshi Tanaka[1], Narumi Takahashi[2], Hiromi Kamata[1], Yoshiyuki Kaneda[3] (1.Japan Agency for Marine-Earth Science and Technology, 2.National Research Institute for Earth Science and Disaster Resilience, 3.Kagawa University)

[SCG57-P06] Depth of seismogenic layer at the 2018 North Osaka and the 2018 Hokkaido Eastern Iburi earthquake sites

*Tomoko Elizabeth Yano[1], Makoto MATSUBARA[1] (1.National Research Institute of Earth Science and Disaster Prevention)

[SCG57-P07] Seismic reflection profiling across the Median Tectonic Line (MTL) active fault system in Ehime and Tokushima Prefectures

*Naoko Kato[1], Tatsuya Ishiyama[1], Hiroshi Sato[1], Shin Koshiya[2], Taro Koike[3], Katsuya Noda[3]
(1.Earthquake Research Institute,University of Tokyo, 2.Faculty of science and engineering, Iwate University, 3.Geosys, Inc.)

Crustal structure from the Japan Sea back-arc basin to the margin off SW Hokkaido deduced from the seismic survey

*Takeshi Sato[1], Tetsuo No[1], Shuichi Kodaira[1], Seiichi Miura[1], Tatsuya Ishiyama[2], Hiroshi Sato[2]

1. Research and Development Center for Earthquake and Tsunami, Japan Agency for Marine-Earth Science and Technology, 2. ERI, Univ. of Tokyo

The Japan Sea is a back-arc basin in the northwestern Pacific. Along the eastern and southern margins, destructive earthquakes occurred (e.g., the 1983 Nihon-kai-Chubu Earthquake, and the 1993 Hokkaido-Nansei-Oki Earthquake). Moreover, along the eastern margin, fault-fold belts developed as a result of deformation caused by extension associated with the opening of the Japan Sea and by the later compression (e.g., Okamura et al., 1995; Sato, 1994). Results of seismic surveys from the Japan Basin to the eastern margin of this sea indicated that structures related back-arc opening might play a role in the location of large earthquakes and the distribution of the deformation zone including active faults and folds along the margin of the Japan Sea (e.g., No et al., 2014). This result demonstrates that the elucidation of the back-arc opening process is important for understanding not only back-arc extension along the Asian continental margin, but also the mechanism of large earthquakes and the distribution of subsequent deformation in the Japan Sea back-arc basin. In the SW Hokkaido, the 1993 Hokkaido-Nansei-Oki Earthquake (Mj 7.8) occurred and the dip and distribution of active faults show a complication pattern. However, we have little information of detailed opening, deformation processes and mechanism of large earthquakes in this area due to the inadequate detailed crustal structure obtained by sufficiently dense OBS spacing in seismic surveys.

To obtain the crustal structure, we conducted the active-source seismic survey using ocean bottom seismographs (OBSs) and multi-channel streamer (MCS) in the margin of the Japan Sea off southwestern Hokkaido ranging from the Japan Basin to the coastal area on land in 2018. This survey was used at 57 OBSs, a tuned air-gun array having 7,800 cu. inch and MCS system. This survey line has about 243 km length and is a part of an integrated ocean-land seismic survey line.

In record sections of several OBSs, not only the first arrived phases but also later phases reflected from interfaces in the crust and uppermost mantle are visible. Also, the MCS profile clearly images the sedimentary layer and the undulations of the basement. The crustal structure in the Japan Basin resembles the typical oceanic crust (e.g., White et al., 1992). In the transition between the Japan Basin and the southern Okushiri Ridge, the crustal structure drastically changes. The area from the southern Okushiri Ridge to the Okushiri Basin has the upper crust with a P-wave velocity of 5.4-6.2 km/s corresponding to the continental upper crust. Moreover, the P-wave velocity distribution has a variation in this area.

©2019. Japan Geoscience Union. All Right Reserved.

Three-dimensional plate geometry model from the Nankai to the Ryukyu subduction zone

*Ayako Nakanishi[1], Tsutomu Takahashi[1], Yojiro Yamamoto[1], Mikiya Yamashita[1], Minako KATSUYAMA[1], Seiichi Miura[1], Narumi Takahashi[3,1], Hiromi Kamata[1], Shuichi Kodaira[1], Yoshiyuki Kaneda[2,1]

1. Japan Agency for Marine-Earth Science and Technology, 2. Kagawa University, 3. National Research Institute for Earth Science and Disaster Resilience

Considering the large slip distribution of the 2004 Sumatra earthquake, possible coseismic rupture area of megathrust earthquakes from the Tokai to Ryukyu cannot be denied. Characteristics of occurrence of great earthquakes is also different between these neighboring subduction zones. Historically, megathrust earthquakes have been generated repeatedly along the Nankai Trough at intervals of approximately 100-200yrs (e.g. Ando, 1975).Along the Ryukyu Trench, although great earthquakes have occurred only twice over the last 300 years: the 1771 Yaeyama earthquakes and the 1911 earthquake off Kikai, recent studies of tsunami deposits indicated that the Ryukyu Islands have been periodically hit by large tsunamis with an interval of several hundred years [e.g. Ando et al., 2017]. Moreover, the coupling condition of the plate interface along the Ryukyu Trench is different from that of the Nankai Trough based on the seismic survey and observations [Arai et al. 2016]. They reported that the Ryukyu Trench is dominated by slow earthquakes at any depths and lacks a typical locked zone such as the Nankai Trough.
To understand relation between the structure around the subducting Philippine Sea plate and seismicity including slow earthquake phenomena, it is necessary to know the geometry and property of the plate boundary from the Nankai to the Ryukyu subduction zone. Three-dimensional plate geometry model will be also important for a precise estimate of the maximum range of the coseismic rupture zone of the Nankai megathrust earthquake. The model is also very useful to construct a new three-dimensional seismic velocity model of the Nankai Trough for depth conversion of interpreted active faults in time section of seismic reflection data [Katsuyama et al., 2019 JPGU].
Based on the result (three-dimensional plate geometry model of the Nankai Trough) from marine active and passive source seismic data [Nakanishi et al., 2018], three-dimensional plate geometry model from Nankai to Ryukyu subduction zone is tried to be constructed using the result of seismic studies around the Ryukyu Trench [Iwasaki et al, 1990; Kodaira et al., 1996; Arai et al., 2016, 2017; Nishizawa et al, 2017; Yamamoto et al., 2018].The model of Nakanishi et al. [2018] is also updated by using the result of deep seismic tomography off the Kii peninsula [Yamamoto et al., 2014, 2017].
In this presentation, a preliminary version of the combined three-dimensional model will be shown.
This study is part of 'Research project for compound disaster mitigation on the great earthquakes and tsunamis around the Nankai trough region' and the project 'Comprehensive evaluation of faults information on offshore Japan' funded by Ministry of Education, Culture, Sports, Science and Technology, Japan.

Keywords: subducting plate, Nankai Trough, Ryukyu Trench

©2019. Japan Geoscience Union. All Right Reserved.

Trace elements and Sr-Nd-Hf-Pb isotopic composition of Miocene Tomari volcanic rocks, Shimokita Peninsula, Aomori, NE Japan

*Masataka Aizawa[1], Mitsuru Inaba[2], Satoshi Okamura[3,4], Ryuichi Shinjo[5]

1. Graduate School of Engineering and Sience, University of Ryukyus, 2. GeoPuck Association, 3. Hokkaido Education University, 4. Hokkaido Soil Research Co-op., 5. Faculty of Science, University of Ryukyus

Introduction

Tomari volcanic rocks, located in Shimokita Peninsula, Aomori Prefecture, NE Japan, formed volcanic front at Miocene period. They include primitive tholeiitic basalts (Takimoto, 1986), therefore volcanic activity in this area strongly suggest relation to opening Japan Sea back-arc basin caused by upwelling asthenosphere. Volcanic activities divided into 4 stages and their K-Ar dating have been reported 13-15 Ma (Watanabe *et al.*, 1993). This study use boring core sample dug from Shimokita Peninsula (SN-010 core; drilling stop depth is 1484 m). Tomari Formation appear deeper than 308.82 m in this core and it has been reported 13.1-14.5 Ma at 385 m (micro fossils), 16.0 Ma, 24.2 Ma (zircon U-Pb dating) at 467 m and 818 m, respectively (Nuclear Regulatory Agency, 2016).

Lithofacies and occurrence of Tomari volcanic rocks

We collected samples from the 1st and 2nd stage of surface Tomari Formation and 8 depth from SN-010 core. Core samples are volcanic breccia, lava and lapilli tuff. And the 1st stage surface volcanic rocks include reddish rounded gravel and pillow lava fragments into deposition layer with lamination. The 2nd stage surface volcanic rocks mainly erupted as pillow lava and hyaloclastite.

Geochemical characteristics

Shallow core samples (SCS; shallower than 862.26 m) and middle core samples (MCS; 999.00-1003.20 m) show middle-K series and deep core samples (DCS; deeper than 1197.86 m) show low-K series. Incompatible elements (especially LILE) concentrations of SCS and MCS are higher than DCS. Surface 1st and 2nd stage samples are plotted middle-K series. Incompatible elements features are similar as SCS and MCS. Multi-elements diagrams normalized by N-MORB show high LILE, negative Nb-Ta and positive Pb anomalies, they mean these rocks were produced at subduction zone. Sr-Nd isotopic composition of MCS-DCS show more depleted and SCS have more enriched composition. Pb isotopes are plotted into volcanic rocks field of Quaternary volcanic front of NE Japan without difference each strata. Primitive tholeiitic basalts are produced in 2nd stage and they show most enriched isotopic composition (Hanyu *et al.*, 2006). Primitive basalts and SCS-MCS have higher Ba/Nb than DCS.

The relationship to opening Japan Sea event

SN-010 core dating suggest that volcanic activity formed Tomari Formation already started late Oligocene-early Miocene. Whole-rock chemical composition of 563.48 m samples is similar to surface 1st stage volcanic rocks, therefore upper level of core sample may be comparable with surface 1st stage volcanic rocks (Aizawa *et al.*, 2018).

Enriched isotopic composition of primitive basalts cannot be explained by assimilation of lower crust due to their high MgO, Cr, Ni composition. In addition, SCS-MCS and primitive basalts have higher Ba/Nb and MCS-DCS show depleted isotopic composition. Thus, it is considered that partial melting of DMM produced volcanic rocks of MCS-DCS, and MCS (high Ba/Nb) were strongly affected slab derived components. Then, volcanic rocks of SCS and surface samples were originated magma from sub-arc

©2019. Japan Geoscience Union. All Right Reserved.

enriched lithospheric mantle (EM II-like isotopic composition).

Petrography of DCS and MCS suggest volcanic activity on land environment because there are reddish volcanic gravels at 1482.00 m and 1335.87 m, and 999.00 m lapilli tuff matrix color is red. Although SCS have no evidence for judging stationary environment of volcaniclastic rocks, the 1st stage outcrop include rounded reddish volcanic gravels into lamination, and the 2nd stage volcanic rocks are mainly erupted as pillow lava and hyaloclastite. These occurrences suggest the development of lifting at late Oligocene-early Miocene period and stationary environment change from on land to underwater. The change of geochemical features, from depleted to enriched composition, may mean to change partial melting position in sub-arc mantle due to the hot asthenosphere upwelling under this area.

Keywords: Miocene, Volcanic front, Japan Sea, Back-arc basin, Tomari volcanic rocks

©2019. Japan Geoscience Union. All Right Reserved.

Acceleration of oceanic plate following megathrust earthquakes

*Mohammad Yuzariyadi[1], Kosuke Heki[1]

1. Hokkaido University

Accelerated subduction of tectonic plates following megathrust earthquakes was proposed by D. Anderson (1975, Science). Heki and Mitsui (2013 EPSL) found postseismic enhancements of inter-plate coupling in the adjacent segments of the 2003 Tokachi-Oki and the 2011 Tohoku-Oki earthquakes. They hypothesized that these earthquakes caused accelerated subduction of the Pacific plate slab in addition to already-known postseismic processes such as afterslip and viscous relaxation. Melnick et al. (2017 GRL) found a similar enhancement of coupling to the north of the 2010 Maule earthquake rupture zone, and Loveless (2017 GRL) considered this a common phenomenon after megathrust earthquakes and named it as the super-interseismic phase. Accelerated subduction occurs during a period after the earthquakes, but its duration and amount depend on the magnitude. Here we investigate how long and how much is the acceleration over the time period covering several years after the earthquakes. So far, we have been using data from GNSS stations on arcs near the segments adjacent to megathrust ruptures. In the present study, we use data from GNSS stations on the subducting oceanic plates and on a subducted continental plate.

We present GNSS velocity data from oceanic islands showing post-megathrust accelerations. They include the Marcus Island (1098), Japan, that showed significant acceleration following the Mw 9 2011-3-11 Tohoku-Oki Earthquake. The Cocos Island (COCO), Australia, seems to have been accelerated after the Mw 8.4 2007-9-12 Bengkulu earthquake, Southern Sumatra. The JRGN in the west coast tip of Chile was accelerated after the Mw 8.2 2014-4-1 Iquique Earthquake. We also found there was a certain velocity change in Christmas Island (XMIS), Australia, after the Mw 7.7 2006-7-17 South Java earthquake. All stations are located on the oceanic plate except JRGN that is located on the continental plate.

Marcus Island (1098) GNSS station showed a significant velocity change after the 2011 Tohoku-Oki Earthquake. The maximum transient acceleration occurred in the period 2-3 years following the earthquake with a maximum velocity change of 9.4 mm/yr. After 3.0 years, The acceleration has been decaying, and the original velocity resumed by now. Cocos Island (COCO) GNSS station shows that the maximum transient acceleration occurred between 0.75-1.5 years after the 2007 Bengkulu earthquake with a maximum change of 4.9 mm/yr. After 1.5 years, the acceleration has decayed and has been showing the velocity similar to the value before the earthquake since 4.5 years after the earthquake. Chile (JRGN) GNSS station shows that the transient acceleration reached the maximum in ~1 year after the 2014 Iquique earthquake with a maximum change of 4.7 mm/yr. The accelerated velocity decayed to the original value in 2.5 years after that. The acceleration of the Christmas Island (XMIS) GNSS station was 2.7 mm/yr and occurred in ~1.0 year after the 2006 South Java earthquake. The acceleration seems to have decayed in 2.5 years after the earthquake.

In general, we found that the transient acceleration of oceanic plate occurs shortly after a megathrust earthquake and continue over a certain period. Then it decays, and finally the velocity before earthquake recovers in a few years.

Keywords: megathrust earthquake, plate acceleration, Subduction

©2019. Japan Geoscience Union. All Right Reserved.

©2019. Japan Geoscience Union. All Right Reserved.

3D velocity model in the region of Nankai Trough

*Minako KATSUYAMA[1], Ayako Nakanishi[1], Rei Arai[1], Shigeyoshi Tanaka[1], Narumi Takahashi[2], Hiromi Kamata[1], Yoshiyuki Kaneda[3]

1. Japan Agency for Marine-Earth Science and Technology, 2. National Research Institute for Earth Science and Disaster Resilience, 3. Kagawa University

This is a part of the project “Comprehensive evaluation of faults information on offshore Japan”, by the Ministry of Education, Culture, Sports, Science and Technology (MEXT). The project consists of three themes, 1) Collecting seismic survey data and building a database of offshore faults, 2) Interpreting distribution of active faults using seismic data collected, and conducting the seismic re-processing by leading-edge seismic technology for the seismic data obtained in previous decades, 3) Building the fault models for a simulation of strong motion and tsunami disaster, based on the interpreted faults. Our purpose of this study is make a 3D velocity model in the Nankai Trough to provide with the support we needs to interpret faults.

The Nankai Trough, where the Philippine sea plate is subducting beneath the Eurasian plate. Some seamounts and ridges are subducted here.

3D velocity model was constructed by seismic data and ocean bottom seismometer(OBS) refraction survey data which were obtained by a various agencies and private companies. Horizons such as acoustic basment and unconformity were interpreted using reflection seismic sections. Conrad discontinuity and Mohorovicic discontinuity were interpreted on refraction surveys and consulted previous study. Layer structure and velocity model were created on these horizons.

We obtain a result that understands geological structure in Nankai Trough. So in this session, we will take a discussion concerning structural characteristic based on the 3D velocity model.

Keywords: 3D velocity model , Nankai Trough, subduction zone

©2019. Japan Geoscience Union. All Right Reserved.

Depth of seismogenic layer at the 2018 North Osaka and the 2018 Hokkaido Eastern Iburi earthquake sites

*Tomoko Elizabeth Yano[1], Makoto MATSUBARA[1]

1. National Research Institute of Earth Science and Disaster Prevention

Background:
Understanding crustal seismogenic layer on faults is important because it enable us to know the maximum size of possible crustal earthquake on the corresponding fault. Depth of the crustal sesmogenic layer also gives us the depth of brittle zone because it relates to the rheology of the crust. The cutoff depths where total of 95 % of events occurred within the depth column of each grid, referred to as D95, can be calculated from the past microseismicity. We aimed to verify the index, D95, if it indicates as the deeper limit of the seismogenic layer. Using the microeismicity before mainshocks, we investigated if we could foresee the deeper limit of seimogenic layer before the 2018 North Osaka (2018 Osaka) and the 2018 Hokkaido Eastern Iburi (2018 Iburi)earthquakes occurred.

Data and Method:
D95 is calculated from the seismicity before each mainshock. We used JUICE catalog (2001-2012) of the event catalog for miscriseismicity in this study. We calculated D95 from events of M1.5 or greater listed in the JUICE catalog for every grid point of 0.02 degree interval. We only consider when the total number of events within the range of 0.1 degree from the grid point contains 50 events and more.

We also look at the temperature data to see if the estimated depths of 250 degrees (in Celsius), 300 degrees, and 450 degrees correspond to the actual earthquake depth. Using the datasets contain the temperature profile of the depth down to about 300 m and the depth down to about 1000 m from the surface of the earth, we computed the depth at which the crustal temperature reaches 250, 300, 450 degrees (hereafter referred to as D250deg, D300deg, D450deg, respectively).

Result:
For the 2018 Osaka earthquake site, the relocated hypocenter of the mainshock was 13.7 km in depth. Relocated aftershocks are mainly distributed between 8 and 14 km in depth. D95 along the aftershocks was calculated to be between 13 km to 14 km. The range of D250deg to D450deg was between10 km and 24 km. D300deg was about 13 km.

For the 2018 Iburi earthquake site, the relocated hypocenter of the mainshock was 35.9 km in depth. Relocated aftershocks are mainly distributed between 25 to 50 km. D95 was estimated to be around 25 km. The range of D250deg and D400deg is between 10 km and 34 km.

Conclusion/Discussion:
D95 as a seismogenic depth of the 2018 Osaka earthquake site was consistent with the mainshock and aftershock distribution. Conversely, D95 of the 2018 Iburi earthquake was not consistent with an actual event: D95 was about 10 km shallower than the mainshock and about 30 km shallower than the deeper aftershocks. The seismicity on the Ishikari Lowland Eastern edge fault zone (Ishikari Teichi Touen Danso Tai), west from the mainshock site, was used to compute D95 in this study. Therefore, discrepancy in D95 of Iburi earthquake site is due to D95 indicates the seismogenic depth of Ishikari Lowland Eastern edge fault zone but not the fault responsible of the 2018 Ishikari Earthquake.

©2019. Japan Geoscience Union. All Right Reserved.

Keywords: seismogenic depth, North Osaka, Hokkaido Eastern Iburi, Earthquake, heat flow

©2019. Japan Geoscience Union. All Right Reserved.

Seismic reflection profiling across the Median Tectonic Line (MTL) active fault system in Ehime and Tokushima Prefectures

*Naoko Kato[1], Tatsuya Ishiyama[1], Hiroshi Sato[1], Shin Koshiya[2], Taro Koike[3], Katsuya Noda[3]

1. Earthquake Research Institute,University of Tokyo, 2. Faculty of science and engineering, Iwate University, 3. Geosys, Inc.

The Median Tectonic Line (MTL) is the most significant inland fault in SW Japan, which extends more than 1000 km and divides SW Japan into the inner and outer zone. The western part of the MTL shows late Quaternary right-lateral strike-slip movements at several mm/y (eg. Tsutsumi and Okada, 1996). According to the seismic reflection profile, northward gently dipping character of the Median Tectonic Line has already been suggested in the eastern Shikoku (Ito et al., 1996) and eastern Kyushu (Yusa et al., 1992). For the deeper extension of MTL, north-dipping geometry was obtained by low-fold seismic reflection images in Shikoku island (Kawamura et al., 2003; Sato et al., 2005). For the MTL active fault system, the geometry of its deeper extension is poorly understood in Shikoku island. To reveal deeper geometry of fault surface, shallow to deep seismic reflection profiling was performed in Ehime and Tokushima Prefectures. This research was performed as a research program funded by the Ministry of Education, Culture, Sports, Science and Technology, Japan.
Three seismic lines were deployed perpendicular to the MTL and major geologic boundaries. The length of seismic lines is 11 km (Saijo area, Ehime), 4.8 km (Wakimachi area, Tokushima) and 6.4 km (Awa area, Tokushima). To obtain a high-resolution seismic image of the shallow part of MTL, a 10-m spacing receiver array was formed using offline recorders. The seismic source was vibroseis trucks. The sweep signals (5-100 Hz for high resolution reflection profiling, 5-40 Hz for refraction profiling) were recorded 10 Hz vertical geophones. The seismic data were processed using conventional CMP-reflection methods. The high-energy shot gathers at Saijo seismic line clearly demonstrate the reflectors at 1.5, 2-3, 4 sec. (Two-way travel time). The reflectors from 2-3 s (TWT) are interpreted as northward dipping Sambagawa Metamorphic belt. The seismic sections portray the seismic image down to 2 km in Wakimachi and Awa area. The reflectors are interpreted as northward dipping Sambagawa Metamorphic belt. These structural characters found in the seismic section may show that the deeper extension of MTL shows northward dipping in Shikoku.

©2019. Japan Geoscience Union. All Right Reserved.

[J] Oral | B (Biogeosciences)：B-CG Complex & General

Wed. May 29, 2019 9:00 AM - 10:30 AM JST | Wed. May 29, 2019 12:00 AM - 1:30 AM UTC | 201A 2F

[B-CG07] Decoding the history of Earth: From Hadean to the present

convener:Tsuyoshi Komiya(Department of Earth Science & Astronomy Graduate School of Arts and Sciences The University of Tokyo), Yasuhiro Kato(Department of Systems Innovation, Graduate School of Engineering, University of Tokyo), Katsuhiko Suzuki(Research and Development Center for Submarine Resources, Japan Agency for Marine-Earth Science and Technology), Chairperson:Tomohiko Sato(Earth-Life Science Institute, Tokyo Institute of Technology)

The latest results of Earth's evolution and geological processes through 4.6 billion year
s from Hadean to Modern, based on various approaches including fieldworks, chemical
analyses, experiments and computer simulation, will be presented. In this session, we ai
m to discuss and understand causal relationships and interplay among the evolution of
Earth's deep interior, changes in the surface environments, and development and evolut
ion of life. Wide-ranging topics are accepted.

9:00 AM - 9:15 AM JST | 12:00 AM - 12:15 AM UTC

[BCG07-01] Iron-oxidizing bacteria and stromatolites in the Ediacaran hydrothermal carbonate

*Akihiro Kano[1], Aya Miyazaki[1], Jumpei Yoshioka[1], Ibtissam Chraiki[2], Abdelhafed Barzouk[2], Nasrrddine Youbi[2,3], Hassan Admou[2], Moulay Ahmed Boumehdi[2,3], Lhou Maacha[4], Hsaine Baoutoul[4], Ismail Bouskri[4] (1.Graduate School of Science, The University of Tokyo, 2.Department of Geology, Faculty of Sciences-Semlalia, Cadi Ayyad University, 3.Instituto Dom Luiz, Faculdade de Ciências, Universidade de Lisboa, 4.Managem-ONA Group)

9:15 AM - 9:30 AM JST | 12:15 AM - 12:30 AM UTC

[BCG07-02] Carbonate carbon isotope stratigraphy of the Paleoproterozoic Francevillian Group in Gabon

★Invited Papers

*Tomohiko Sato[1], Yusuke Sawaki[2], Hisashi Asanuma[2], Hisahiro Ueda[1], Shigenori Maruyama[1] (1.Tokyo Institute of Technology, 2.The University of Tokyo)

9:30 AM - 9:45 AM JST | 12:30 AM - 12:45 AM UTC

[BCG07-03] The redox condition of late Paleoproterozoic shallow marine environment: The Cape Smith Belt, Canada

*Kento Motomura[1], Shoichi Kiyokawa[1], Minoru Ikehara[2], Takashi Sano[4], Kentaro Tanaka[3], Tsubasa Miki[3], Yuji Sano[3] (1.Kyushu University, 2.Kochi University, 3.University of Tokyo, 4.National Museum of Nature and Science)

9:45 AM - 10:00 AM JST | 12:45 AM - 1:00 AM UTC

[BCG07-04] Paleovegetation changes reconstructed by terrestrial plant biomarker analyses in the sediments deposited across the Cenomanian/Turonian boundary in the Tomamae area, Hokkaido, Japan

*Masashi A. Ikeda[1], Ken Sawada[2], Takuto Ando[3], Hideto Nakamura[4], Reishi Takashima[5], Hiroshi Nishi[5] (1.Graduate School of Science, Hokkaido University, 2.Department of Earth and Planetary Sciences, Faculty of Science, Hokkaido University, 3.Arctic Research Center, Hokkaido University, 4.Faculty of Science, Osaka City University, 5.The Center for Academic Resources and Archives, The Tohoku University Museum, Tohoku University)

10:00 AM - 10:15 AM JST | 1:00 AM - 1:15 AM UTC

[BCG07-05] A general overview of the research progress on REY-rich mud

*Yasuhiro Kato[1,2], Kentaro Nakamura[1], Koichiro Fujinaga[2,1], Kazutaka Yasukawa[1,2], Yutaro Takaya[3,1,2], Junichiro Ohta[2,1], Erika Tanaka[1], Kazuhide Mimura[1], Koichi Iijima[4,1], Shiki Machida[2,1], Tatsuo

Nozaki[4,1,2,5], Jun-Ichi Kimura[4], Hikaru Iwamori[1,4,6] (1.The University of Tokyo, 2.ORCeNG, Chiba Institute of Technology, 3.Waseda University, 4.JAMSTEC, 5.Kobe University, 6.Tokyo Institute of Technology)

10:15 AM - 10:30 AM JST | 1:15 AM - 1:30 AM UTC

[BCG07-06] A cold and alkaline Hadean ocean caused by impact ejecta weathering

*Shintaro Kadoya[1], David C Catling[1] (1.University of Washington)

Iron-oxidizing bacteria and stromatolites in the Ediacaran hydrothermal carbonate

*Akihiro Kano[1], Aya Miyazaki[1], Jumpei Yoshioka[1], Ibtissam Chraiki[2], Abdelhafed Barzouk[2], Nasrrddine Youbi[2,3], Hassan Admou[2], Moulay Ahmed Boumehdi[2,3], Lhou Maacha[4], Hsaine Baoutoul[4], Ismail Bouskri[4]

1. Graduate School of Science, The University of Tokyo, 2. Department of Geology, Faculty of Sciences-Semlalia, Cadi Ayyad University, 3. Instituto Dom Luiz, Faculdade de Ciências, Universidade de Lisboa, 4. Managem-ONA Group

Association of drastic climate change and biological evolution during Neoproterozoic is one of the most enigmatic features of the Earth history. The If the Earth’ s surface has been hardly covered with thick ice-cover during the 58-myr-long Sturtian glaciation, the evolution of organisms was mostly reset. However, there is glowing evidence of protozoan fossils immediately after the Sturtian and Marinoan glaciations. This requires the argument that liquid environments as refugia for protozoans must have occurred in tropical zones or around volcanos.
Moroccan Anti-Atlas exposes several Proterozoic inliers surrounded with Ediacaran, Paleeozoic and Mesozoic strata. Accumulated age data of zircon U-Pb indicate that active tectonics had been sustained here during Cryogenian and Ediacaran. Paleogeographic interpretation based on paleomagnetism reconstructed a high latitude of Anti-Atlas. Neoproterozoic sedimentary sequence here is dominated by volcanics and siliciclastics, and carbonate is developed as lentic bodies on granodiorite rock.
This study focuses on two carbonate bodies near Bleida and Ouarzazate in Anti-Atlas. The Blida section exposes a 25-m-thick sequence of bedded and fine-grained dolostone of red color. This overlies 586Ma volcanic rock, and apparently underlies possible diamictite with a fault contact. Dolostone of the lower part of the section contains relics of iron-oxidizing bacteria. Carbon isotope of the dolostone is low as -6‰, but the stratigraphic position negates the correlation to the Shuram negative excursion of late Ediacaran. The low d13C value likely inherited endogenic carbon, and this interpretation is supported by low d18O indicating high water temperature (around 40-50ºC). While, the 30-m-thick carbonate sequence near Ouarzazate consists of red-colored limestone alternated with volcanoclastic sandstone and siltstone. It rests on 580Ma volcanics. The carbonate sequence exhibit stromatolites at least four stratigraphic levels. The higher d13C value (around -1.5‰) was likely reflected from CO2 degassing or gas exchange with the atmosphere. These stromatolites show regular lamination of ~1 mm interval and appears color changes reflected from a redox gradient within a biofilm.
These carbonate sequences in Anti-Atlas are not directly associated with the Snowball glaciations. However, active volcanism that had sustained latest Neoproterozoic might had provided liquid water environments, as biologic refugia during the Marinoan Snowball Earth.
N.B.Funding was provided by the Academy Hassan II of Science and Technology of Morocco AcadHIIST/SDU/2016-02 (grant to Abderrazzak El Albani and Nasrrddine Youbi and others)and Managem-ONA Group.

Keywords: Neoproterozoic, carbonate rock, Microbe, stromatolite

©2019. Japan Geoscience Union. All Right Reserved.

Carbonate carbon isotope stratigraphy of the Paleoproterozoic Francevillian Group in Gabon

*Tomohiko Sato[1], Yusuke Sawaki[2], Hisashi Asanuma[2], Hisahiro Ueda[1], Shigenori Maruyama[1]

1. Tokyo Institute of Technology, 2. The University of Tokyo

The large fluctuations of δ13C_carb in the Paleoproterozoic are important in terms of the speculation on the atmospheric oxygen level and the global stratigraphic correlations. The interval characterized by the generally high values of δ13C_carb up to +10 ‰is called Lomagundi-Jatuli Event (LJE; ca. 2.2-2.0 Ga) and interpreted as reflecting high rates of oxygen production (e.g. Karhu & Holland, 1996; Martin et al., 2011). The drop of δ13C_carb and δ13C_org at the end of LJE are reported from Shunga in Fennoscandia, and the negative shift of δ13C_org is correlated with that of Franceville in Gabon (Kump et al., 2011); however, the δ13C_carb data in Gabon is still missing because of the scarcity of the carbonate rocks. The Paleoproterozoic Francevillian Group in Gabon consists of FA (fluvial sandstones), FB (black shales/carbonates), FC (cherts), FD (black shales), and FE (sandstones) in ascending order. The lithostratigraphic correlation between the Franceville, Lastoursville, and Okondja basins suggests that the FA-FB-FC units are in different depositional settings and the FD-FE units are in common facies, which indicates the final opening of the intracratonic basins. In order to explore the global correlation of δ13C_carb, the analyses in the FD-FE units are required. In this study, we conducted two drillings in the Lastoursville and Okondja basins to obtain the fresh core-samples of FD. The lithological observations clarified that numbers of carbonate layers are intercalated in black shales in the FD unit in the both areas. We analyzed δ13C_carb of these carbonate layers, and filled in the stratigraphic blanks in the FD unit. In this presentation, we will discuss the propriety of the δ13C_carb stratigraphic correlations.

Keywords: Paleoproterozoic, carbon isotope, Gabon

©2019. Japan Geoscience Union. All Right Reserved.

The redox condition of late Paleoproterozoic shallow marine environment: The Cape Smith Belt, Canada

*Kento Motomura[1], Shoichi Kiyokawa[1], Minoru Ikehara[2], Takashi Sano[4], Kentaro Tanaka[3], Tsubasa Miki[3], Yuji Sano[3]

1. Kyushu University, 2. Kochi University, 3. University of Tokyo, 4. National Museum of Nature and Science

The oceanic redox condition strongly affects the chemical compositions of seawater, especially, redox-sensitive elements such as Fe and Mo. Although it is suggested that bio availability of these bio-essential elements have restricted the biological development through Precambrian ocean, the redox conditions and the trigger of its transition at late Paleoproterozoic era are poorly constrained.

In this study, we reconstructed 50 m lithostratigraphy and chemostratigraphy including major and trace element compositions and C-N-S isotopes ($\delta^{13}C_{org}$, $\delta^{15}N$, $\delta^{34}S$) in order to clarify the sedimentary environment and the trigger of its change.

A part of the drilled hole from the Northern Povungnituk Group, Cape Smith belt of Canada is used for geochemical analyses. The sequence consists of the alteration of sandstone and black shale deposited at northern margin of the Superior province at ~1.9 Ga. Two lithological units, lower and upper units, are identified based on sedimentary sequence. The lower unit is characterized by the transition from coarse sandstone dominant to black shale dominant sequence, while, the upper is fine sandstone dominant sequence.

Vanadium concentrations normalized by total organic carbon (TOC) shows clear evidence for the transition of the redox condition. Although V/TOC at the bottom of the sequence (<~50 ppm/%) is lower than that of black shale from the Bravo Lake Formation of Buffin island in which a previous work cleared the black shale deposited under euxinic condition (H_2S-rich), the value increased and reaches the mean of the black shale (~105ppm/%) from the Formation at lower coarse sandstone dominant portion. These increase of V/TOC suggests ocean redox conditions changed from anoxic (weak-reducing) to euxinic (strongly-reducing). This inference is consistent with redox-sensitive element behavior confirmed from the correlation between the V concentration and TOC.

$\delta^{15}N$ of the sequences (~+7 –+9 ‰) are comparable with that of the modern ocean and that indicates nitrification, denitrification and NH_3assimilation keep $\delta^{15}N$ of dissolved N species high. $\delta^{13}C_{org}$and $\delta^{34}S$ change at the same interval ($\delta^{13}C_{org}$: -30.6 –-33.2 ‰, $\delta^{34}S$: +11.9 –-4.1 ‰) and that suggests some trigger which affects $\delta^{13}C_{org}$and $\delta^{34}S$ caused development of strongly-reducing condition. $\delta^{13}C_{org}$and $\delta^{34}S$ transition are likely to represent input of isotopically light $HCO_3^-$and SO_4^{2-}. The activity of large igneous provinces and oxidative weathering of black shale which relates regression suggested by the change of lithofacies are plausible for these isotope change.

Keywords: Late Paleoproterozoic, Redox condition

©2019. Japan Geoscience Union. All Right Reserved.

Paleovegetation changes reconstructed by terrestrial plant biomarker analyses in the sediments deposited across the Cenomanian/Turonian boundary in the Tomamae area, Hokkaido, Japan

*Masashi A. Ikeda[1], Ken Sawada[2], Takuto Ando[3], Hideto Nakamura[4], Reishi Takashima[5], Hiroshi Nishi[5]

1. Graduate School of Science, Hokkaido University, 2. Department of Earth and Planetary Sciences, Faculty of Science, Hokkaido University, 3. Arctic Research Center, Hokkaido University, 4. Faculty of Science, Osaka City University, 5. The Center for Academic Resources and Archives, The Tohoku University Museum, Tohoku University

The Cretaceous is known as the extreme greenhouse period attributed to the elevated atmospheric CO_2 concentration triggered by the superplume activity. In particular, the Oceanic Anoxic Events (OAEs) caused by the occurrences of the Large Igneous Plateaus (LIPs) in several times during the mid-Cretaceous. Global environmental disturbance events have been extensively investigated in the ocean, but there have been few reports for terrestrial environmental variation during the OAE periods (e.g. Kuypers et al., 2002). In the present study, we analyzed biomarkers of terrestrial plants including lichen and fungi in the sediments deposited across the Cenomanian/Turonian boundary (CTB) from the northern Hokkaido, Japan to reconstruct paleovegetation changes and to evaluate paleoecology of individual plants during environmental disturbance event.

We analyzed sedimentary rocks across the CTB in the Saku Formation,Yezo Group, were collected from the Omagari-zawa sections of the Tomamae area, northern Hokkaido, Japan. The sediments used correspond to the OAE2 intervals (1st build-up, Trough, 2nd build-up and Plateau phases), determined by $\delta^{13}C$ stratigraphy (Omatsu et al., 2014). For the biomarker analysis, the extractions of freeze-dried sediments were fractionated using silica-gel column and analyzed by GC-MS.

By sterane and hopane ratios, we confirmed the high contribution of terrigenous matter input and low maturity of organic matter (vitrinite reflectance ca. 0.4% level; lignite to subbituminous coal rank) in the Omagari-zawa section. These results agree with those reported by Ando et al. (2017). Higher Plant Parameter (HPP) as the vegetation index of higher plants increased in the 1st build-up and 2nd build-up stages, and declined in the Trough and Plateau stages. We interpret that the coniferous vegetation has expanded under arid condition. Moreover, we analyzed the proportion of 1-methyl dibenzofuran in total methyl dibenzofurans as a lichen indicator (1- MDBF ratio), and perylene/ pyrene ratio as a fungal assemblage index. Variations in lichen and fungi vegetation tend to decrease from the 1st build-up to the 2nd build-up stage, which are resemble to those of coniferous vegetation. Thus, it is considered that the vegetation overall declined against the mid-Cretaceous environmental disturbance, especially affected by arid/humid fluctuation.

Keywords: Paleovegetation, lichen, biomarker, Yezo Group, C/T boundary, Cretaceous

©2019. Japan Geoscience Union. All Right Reserved.

A general overview of the research progress on REY-rich mud

*Yasuhiro Kato[1,2], Kentaro Nakamura[1], Koichiro Fujinaga[2,1], Kazutaka Yasukawa[1,2], Yutaro Takaya[3,1,2], Junichiro Ohta[2,1], Erika Tanaka[1], Kazuhide Mimura[1], Koichi Iijima[4,1], Shiki Machida[2,1], Tatsuo Nozaki[4,1,2,5], Jun-Ichi Kimura[4], Hikaru Iwamori[1,4,6]

1. The University of Tokyo, 2. ORCeNG, Chiba Institute of Technology, 3. Waseda University, 4. JAMSTEC, 5. Kobe University, 6. Tokyo Institute of Technology

Deep-sea mud enriched in rare-earth elements and yttrium (REY), termed as REY-rich mud, has been expected as a novel mineral resource for the industrially critical elements [1]. Targeting the Japanese exclusive economic zone around Minamitorishima Island, where highly promising REY-rich mud (total REY content > 5,000 ppm) lies at very shallow depth (2 to 4 m) below the seafloor [2], we have conducted a variety of researches on the mud from both scientific and engineering perspectives.

In the presentation, we report a general overview of the research progress on REY-rich mud, and discuss the importance of the mud from viewpoints of the Japan’s resource security and a new strategy for economic growth.

[1] Kato, Y. et al. (2011) Nature Geoscience 4, 535-539, [2] Iijima, K. et al. (2016) Geochemical Journal 50, 557-573.

Keywords: seafloor mineral resources, rare-earth elements, REY-rich mud, Minamitorishima Island, Pacific Ocean, deep-sea sediment

©2019. Japan Geoscience Union. All Right Reserved.

A cold and alkaline Hadean ocean caused by impact ejecta weathering

*Shintaro Kadoya[1], David C Catling[1]

1. University of Washington

Life probably arose in the Hadean (either on land or in the sea) and then would have spread through the early ocean. Hence, determining constraints on the early marine environment is essential for understanding conditions for the spread of early life, in addition to the history of the Earth itself. In this study, we modelled the evolution of the surface environment of the Earth, including the surface temperature, pCO_2, and oceanic pH.

As revealed by previous works (e.g., Krissansen-Totton et al., 2018, PNAS), Earth's long-term surface environment is controlled by the carbonate-silicate geochemical cycle. This negative feedback has moderated the surface temperature, resulting in the continuous existence of surface liquid water, even when the solar luminosity was smaller in the past than today. To compensate for the faint Sun, the feedback sets a high pCO_2 in the past, which would result in a more acidic ocean. The same mechanism can be applied for modelling the Hadean eon. However, we have to add another factor: impact ejecta weathering. As indicated by impact craters on the Moon, the Earth would also undergo intense meteorite impacts during the Hadean. Since the impact ejecta are easily weathered, they provided an additional sink of CO_2. Hence, previous works (e.g., Sleep & Zahnle et al., 2001, JGR) suggested that the surface temperature and pCO_2 would actually be low, i.e., a cold Hadean Earth –an idea that has been controversial.

In this study, we calculated the evolution of the surface environment by varying parameters in a geologic carbon cycle model within their ranges of uncertainty. Since the ejecta weathering is a source of carbonate alkalinity (i.e., a sink of CO_2), the pCO_2 and surface temperature of cases with ejecta weathering (hereafter, standard cases) are lower than those of cases without ejecta weathering (hereafter, control cases), as shown in Figure 1a and 1b. The surface temperatures of some standard cases are even lower than 273.15 K (Figure 1a). The coldness does not always mean that the Earth was in a snowball state during the early Hadean; instead, it just indicates a high likelihood of a cold climate. The low pCO_2 of standard cases also results in high ocean pH (Figure 1c). In addition, because the high pH results in a high precipitation rate of carbonate, the carbonate alkalinity of standard cases tends to be lower than that of control cases.

For the standard case, such a relatively cold surface and alkaline ocean are confined to the early Hadean, in which the impact flux (i.e., ejecta production rate) is high. However, the impact craters on the Moon also indicate the possibility of an enhanced impact flux around 4 Ga (i.e., the late heavy bombardment; LHB). The estimated impact flux for the LHB is also high enough to result in a cold surface and alkaline ocean. Hence, we should consider the possibility that life existed in a cold and alkaline early ocean.
Fig. 1. Results with control (without ejecta weathering) and standard cases (with ejecta weathering) for the geologic carbon cycle model for (a) atmospheric partial pressure of CO_2, pCO_2, (b) global mean surface temperature, and (c) ocean pH.

Keywords: Hadean, Climate evolution, Carbonate-silicate geochemical cycle

©2019. Japan Geoscience Union. All Right Reserved.

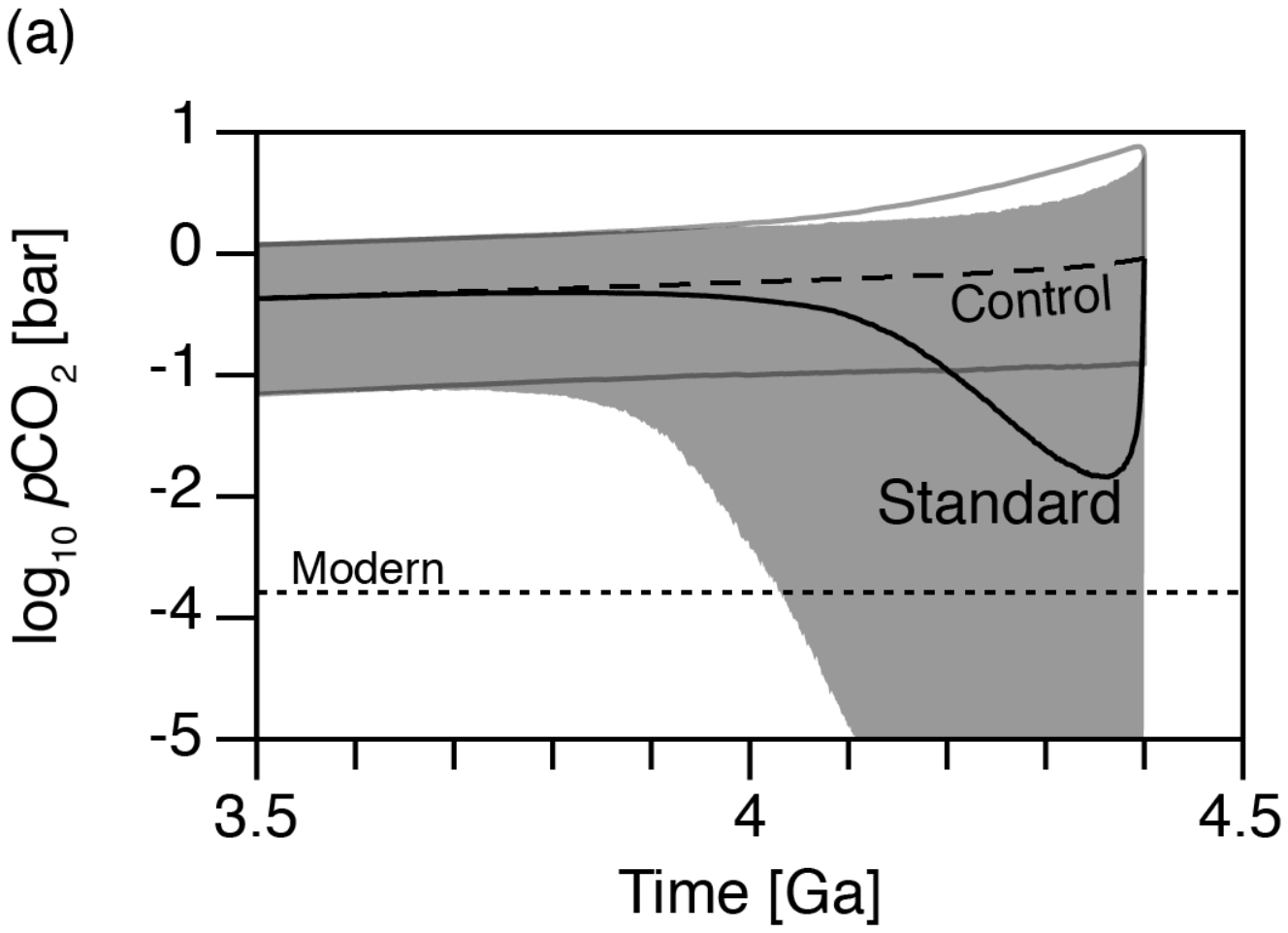

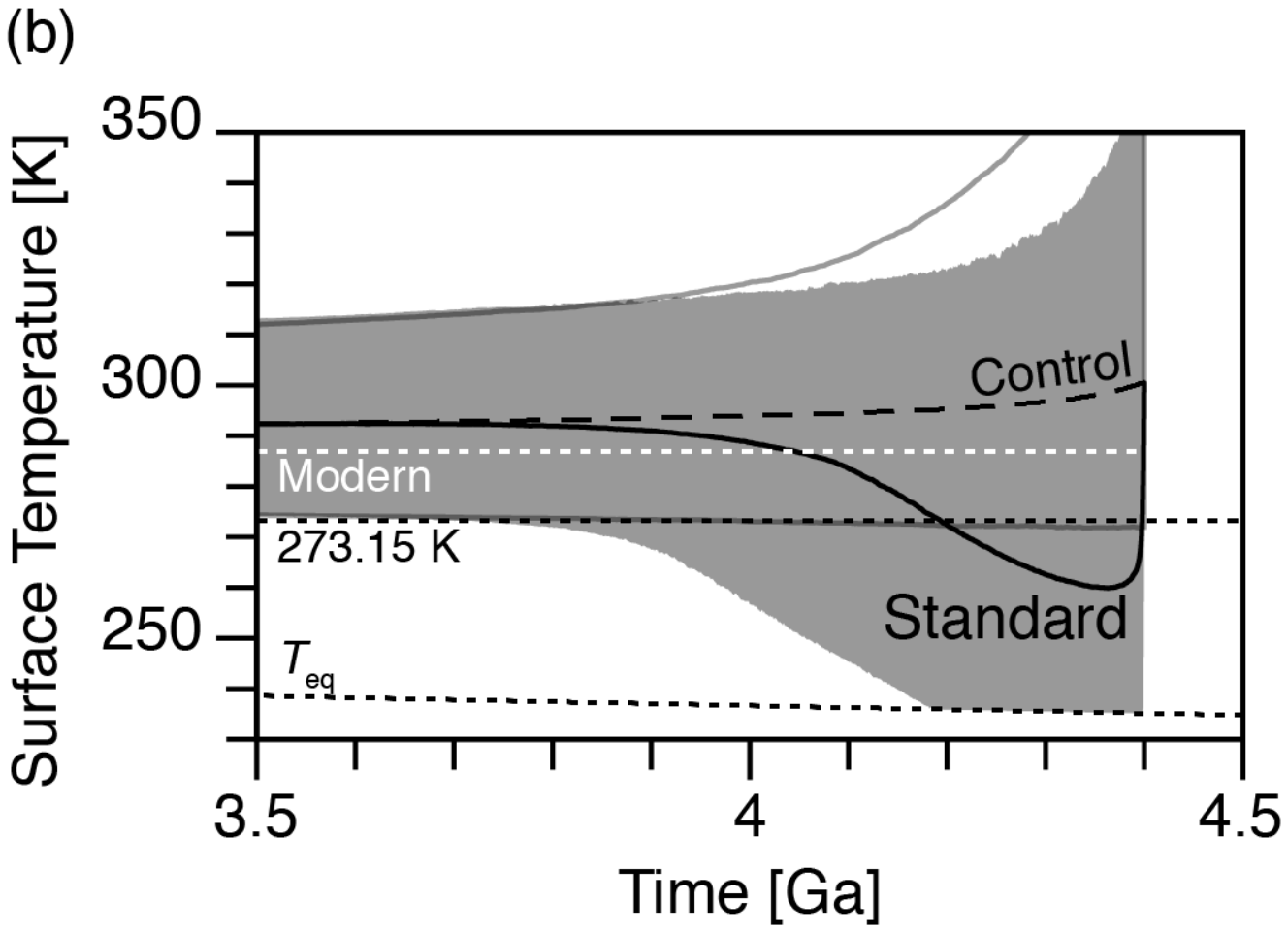

©2019. Japan Geoscience Union. All Right Reserved.

©2019. Japan Geoscience Union. All Right Reserved.

[J] Oral | B (Biogeosciences)：B-CG Complex & General

Wed. May 29, 2019 10:45 AM - 12:15 PM JST | Wed. May 29, 2019 1:45 AM - 3:15 AM UTC | 201A 2F

[B-CG07] Decoding the history of Earth: From Hadean to the present

convener:Tsuyoshi Komiya(Department of Earth Science & Astronomy Graduate School of Arts and Sciences The University of Tokyo), Yasuhiro Kato(Department of Systems Innovation, Graduate School of Engineering, University of Tokyo), Katsuhiko Suzuki(Research and Development Center for Submarine Resources, Japan Agency for Marine-Earth Science and Technology), Chairperson:Satoshi Yoshida(Department of Earth Science & Astronomy, Graduate School of Arts and Sciences, The University of Tokyo)

The latest results of Earth's evolution and geological processes through 4.6 billion year
s from Hadean to Modern, based on various approaches including fieldworks, chemical
analyses, experiments and computer simulation, will be presented. In this session, we ai
m to discuss and understand causal relationships and interplay among the evolution of
Earth's deep interior, changes in the surface environments, and development and evolut
ion of life. Wide-ranging topics are accepted.

10:45 AM - 11:00 AM JST | 1:45 AM - 2:00 AM UTC

[BCG07-07] **Impact-induced magmatism on early Earth**

*Hiroshi Ohmoto[1], Uschi M. Graham[2], Yuya Tsukamoto[3], Yumiko Watanabe[3], Takeshi Kakegawa[3], Hiroshi Hamasaki[4], Andrew Chorney[5], Katherine Crispin[1], Zi-Kui Liu[1] (1.The Pennsylvania State University, 2.Univ. of Kentucky, 3.Tohoku Univ., 4.Tokyo Gas, 5.Temple Univ.)

11:00 AM - 11:15 AM JST | 2:00 AM - 2:15 AM UTC

[BCG07-08] An evaluation of impact dating for shocked zircons with planar features (PFs) in the Vredefort dome by LA-ICP-MS multi-spot analysis

*Shinji Yamamoto[1], Taiga Kato[1] (1.Graduate School of Environment and Information Sciences, Yohohama National University)

11:15 AM - 11:30 AM JST | 2:15 AM - 2:30 AM UTC

[BCG07-09] **Application of acid-washing to trace element and tungsten isotope analyses of Eoarchean rocks from the Isua Supracrustal Belt**

★Invited Papers

*Hatsuki Enomoto[1], Tsuyoshi Iizuka[1], Yoshitaka Homma[1] (1.Department of Earth and Planetary Science, Graduate School of Science, The University of Tokyo)

11:30 AM - 11:45 AM JST | 2:30 AM - 2:45 AM UTC

[BCG07-10] Limited primary production in the early Archean oceans and its biogeochemical consequenses

★Invited Papers

*Kazumi Ozaki[1] (1.Toho University)

11:45 AM - 12:00 PM JST | 2:45 AM - 3:00 AM UTC

[BCG07-11] Behaviors of carbon cycle system and inevitability of the hot climate in the Archean Earth

★Invited Papers

*Yasuto Watanabe[1], Eiichi Tajika[1], Kazumi Ozaki[2], Peng Hong[3] (1.The University of Tokyo, 2.Toho University, 3.Chiba Institute of Technology)

12:00 PM - 12:15 PM JST | 3:00 AM - 3:15 AM UTC

[BCG07-12] Occurrence and chemical composition of metamorphic carbonate rocks in the Isua supracrustal belt, West Greenland: Implications for the origin of carbonate rocks and compositions of the Eoarchean seawater.

*Yoshida Satoshi[1], Kazutaka Yasukawa[2], Yasuhiro Kato[2], Yusuke Sawaki[3], Tsuyoshi Komiya[3]
(1.Department of Earth & Planetary Science, Graduate School of Science, The University of Tokyo, 2.Department of Systems Innovation, Graduate School of Engineering, University of Tokyo, 3.Department of Earth Science & Astronomy Graduate School of Arts and Sciences, The University of Tokyo)

Impact-induced magmatism on early Earth

*Hiroshi Ohmoto[1], Uschi M. Graham[2], Yuya Tsukamoto[3], Yumiko Watanabe[3], Takeshi Kakegawa[3], Hiroshi Hamasaki[4], Andrew Chorney[5], Katherine Crispin[1], Zi-Kui Liu[1]

1. The Pennsylvania State University, 2. Univ. of Kentucky, 3. Tohoku Univ., 4. Tokyo Gas, 5. Temple Univ.

At the JpGU Meeting 2017, we reported the discovery of numerous fragments (<~3 mm in size) of stony meteorites and impact spherules of basalt in the lowest (i.e., the earliest) ~70 m section of the submarine Apex Basalt that overlies the ~110 m-thick Marble Bar Chert Member (MBCM; ca. 3.46 Ga in age) in the ABDP #1 drill core, which was recovered in 2003 at Marble Bar, Pilbara, Western Australia. We suggested that the asteroid body that produced the meteorite fragments was >10 km in diameter, impacted at ~40 km E of Marble Bar, terminated the deposition of the MBCM, and created a crater (“The Apex Impact Crater”) more than ~100 km in diameter. To test this hypothesis, in the summer of 2018 we conducted a geological survey of the proposed “Apex Impact Crater” utilizing a drone equipped with a high-resolution (4K) camera.

Our survey has revealed the presence of “impact tsunami deposits” at the boundary of the MBCM and the Apex Basalt. They are ~1-40 m thick, extending at least 20 km along the strike in the Marble Bar area. They contain numerous fragments (<5 mm size) of stony meteorites, together with various-sized (<1 mm to ~10 m), generally angular-shaped, fragments and blocks of the MBCM. We have also discovered ~15-40 m thick “impact tsunami deposits” underlying the Apex Basalt at ~80 km SE of Marble Bar. Numerous fractures (mostly perpendicular to the bedding planes, and many extending to 100s of meter into the underlying Duffer Formation), the dislocations and rotations of the MBCM in ~cm to ~100 m scales, as well as the “impact tsunami deposits”, were most likely created by an asteroid impact. Our survey has provided evidence that the ~3km-thick Apex Basalt represents the crater-filing komatiite/basalt lavas that were generated by the sudden decompression-melting of the mantle peridotites, triggered by a giant impact, and that the Mt. Edgar Batholiths (~3.46-3.43 Ga in ages), which intruded in the crater, probably represent the rebound of the older continental crust and the products of partial melting of the mantle peridotite and oceanic crust.

Our investigations suggest that the greenstone-granite complexes (“granite dome complexes”) that characterize the geology of the East Pilbara district may represent 8 or more craters created by impacts of asteroid bodies 10-30 km in diameter during the Archean. Consequently, the magmatism and tectonics of early Earth may have been dictated by gigantic asteroid impacts, rather than by the plume- and/or plate tectonics.

Keywords: Asteroid impact crater, Impact tsunami deposits, Early Earth

©2019. Japan Geoscience Union. All Right Reserved.

An evaluation of impact dating for shocked zircons with planar features (PFs) in the Vredefort dome by LA-ICP-MS multi-spot analysis

*Shinji Yamamoto[1], Taiga Kato[1]

1. Graduate School of Environment and Information Sciences, Yohohama National University

Shock-metamorphosed zircons, as an indicator mineral of meteorite impact, have often been utilized for impact dating (e.g. Kamo et al., 2009). Mechanical and thermal effect by impact are thought to lead Pb-loss of shocked zircon, resulting in partly and fully age resetting. The 2.02 Ga Vredefort dome, largest and oldest impact crater, crop out highly-shock metamorphosed basement rocks which include shocked zircons with various shock features such as planar features and granular textures. Previous studies demonstrate that shocked zircons with planar features in the Vredefort show various metamorphic ages from 731 to 3104 Ma, and these ages are interpreted to be correspond to age resetting of regional metamorphism and impact metamorphism. Recent analysis using EBSD, SL and SRIMP for shocked zircon by Moser et al. (2011) reveal that shocked zircons with curvi-planar features have a potential for impact dating in the Vredefort (2.02 Ga), and EBSD misorientation map suggest that deformation of zircon by impact event enhances the age resetting. However, impact dating using shocked zircons with planar features has not been established. Erickson et al. (2013) reported SHRIMP U-Pb ages of detrital shocked zircon with PFs recovered from downriver of the Vredefort dome, and conclude that predominant impact age were identified and that most of shocked zircons record regional metamorphic events. Here we report impact resseting ages from detrital shocked zircons with PFs at the Vaal River sand, cutting along the Vredefort Dome, and identified zircon deformation texture revealed by EBSD misorientation maps. Such deformation in shocked zircon supposed to be formed by impact, and their deformation texture (PFs and EBSD map) may help to identify the ancient impact record.

Keywords: meteorite impact, impact dating, shocked zircon, Vredefort

©2019. Japan Geoscience Union. All Right Reserved.

Application of acid-washing to trace element and tungsten isotope analyses of Eoarchean rocks from the Isua Supracrustal Belt

*Hatsuki Enomoto[1], Tsuyoshi Iizuka[1], Yoshitaka Homma[1]

1. Department of Earth and Planetary Science, Graduate School of Science, The University of Tokyo

The short-lived ^{182}Hf–^{182}W decay system has been widely used to understand early Earth chemical evolution. Recently, ^{182}W anomalies have been found from many Archean terranes (e.g., Willbold et al., 2011; Touboul et al., 2012). These W isotope variations should be produced by the chemical fractionation of Hf/W on the Earth while ^{182}Hf was extant, or contribution of extraterrestrial materials having different W isotope compositions after core formation. While the W isotopic anomalies potentially provide valuable insights into processes on the early Earth, the exact cause of the isotopic anomalies is not yet clearly understood. As the possible causes, early silicate differentiation, early metal-silicate equilibrium at various conditions, and late veneer have been proposed, but these hypotheses respectively are inconsistent with the lack of correlations with Nd, Os isotopic data, and highly siderophile elements abundances (e.g., Rizo et al., 2016b; Puchtel et al., 2018; Touboul et al., 2012). Alternatively, the apparent lack of the correlations may be attributed to secondary disturbance in the W isotope compositions of the Archean rocks, given that W is highly fluid-mobile during metasomatism (e.g., Bali et al., 2012).

In this study, we applied an acid-washing method to Eoarchean metamorphosed rocks from the Isua Supracrustal Belt, with the aims to evaluate the possible effect of metasomatism on the W isotope systems, and to obtain their original W isotope compositions. We measured trace element compositions and W isotope ratios of acid-washes and residues of the metamorphosed basalts using ICP–MS.

The acid-washes show enrichments in light REE, whereas the residues exhibit enrichments in heavy REE. This suggests that acid-washing selectively removed a secondary component gained during metasomatism, given that light REE are relatively fluid-mobile as compared to heavy REE. Negative ^{182}W anomalies were found in the washes showing light REE enrichments. By contrast, non-resolvable ^{182}W anomaly was obtained for the residues displaying heavy REE enrichments. These findings suggest that the Isua metamorphosed basalts have a W isotope heterogeneity even in a single rock sample. Moreover, our results imply that the W isotope compositions of Isua supracrustal rocks could have been modified secondarily as a result of metasomatism. This can account for the lack of correlation between W isotopic data and other geochemical or isotopic data.

Keywords: Hf–W, Isua, acid-washing, early Earth

©2019. Japan Geoscience Union. All Right Reserved.

Limited primary production in the early Archean oceans and its biogeochemical consequenses

*Kazumi Ozaki[1]

1. Toho University

The activity level of the biosphere is a critical factor controlling the chemical composition of the atmosphere. The modern Earth's biosphere is powered by the oxygenic photosynthesis, which utilizes ubiquitous water as their electron donor, with the result that Earth's surface environment is extremely well oxygenated. Before the advent of the oxygenic photosynthesis, in contrast, primary production would have been limited by the geophysical input rate of critical electron donors (e.g., H_2 and Fe^{2+}) from the Earth's interior to the exogenic system. Here, we revisit previous modelling of the global biogeochemical cycles of H, C, and Fe in order to more precisely reconstruct global net primary production (NPP) during an interval of early Archean time before the advent of oxygenic photosynthesis. The biogeochemical model includes a series of metabolic reactions in the primitive anoxic biosphere (e.g., anoxygenic photosynthesis, methanogens, and fermenters) and takes redox (H) balance in the ocean-atmosphere system into account. I explore the effect of a variety of combination of key parameters (e.g., atmospheric CO_2 levels, geophysical input flux of Fe^{2+}, and volcanic outgassing flux of H_2) with a stochastic approach in order to search the possible solutions which allow for creating a warm climate state (>288 K) during the Archean. The results suggest that NPP by anaerobic metabolisms has been a few percent of the modern value. The H-based producers, photoferrotrophs, and CO-consuming acetogens contribute ~80%, ~18%, and ~2% of total NPP, respectively. The estimated extremely low NPP implies the geological fluxes of H_2 and Fe^{2+} as a limiting factor for biological productivity. The results also show that the atmospheric CO_2 levels are needed to be >~70 PAL (present atmospheric level) for maintaining warm climate state and that atmospheric CH_4 levels would have been >100 ppm despite the limited activity of the biosphere.

Keywords: Archean, Biogeochemical cycles, Methane

©2019. Japan Geoscience Union. All Right Reserved.

Behaviors of carbon cycle system and inevitability of the hot climate in the Archean Earth

*Yasuto Watanabe[1], Eiichi Tajika[1], Kazumi Ozaki[2], Peng Hong[3]

1. The University of Tokyo, 2. Toho University, 3. Chiba Institute of Technology

Although the luminosity of the Sun in the Archean (from 4.0 Ga to 2.5 Ga) was dimmer than that of today, geological records of $d^{30}Si$ and $d^{18}O$ from marine cherts suggests that the terrestrial surface environment may have been warm or even hot (328-358 K). Recently, along with these geological records, thermostability of reconstructed ancestral enzymes of cyanobacteria, which reflects the temperature of marine photic zone, also supports the hot surface environment.

To achieve such hot environment under the dimmer Sun, greenhouse effect of carbon dioxide and methane is considered to be necessary. Previous study using a coupled model of atmospheric photochemistry and ocean microbial ecosystem showed that the warm climate can be achieved by non-linearly amplified flux of methane to the atmosphere from the marine ecosystem only when H_2-using photosynthetic bacteria and Fe-using photosynthetic bacteria coexisted in the Archean marine ecosystem. This means that the photochemical processes and the marine microbial processes would have been important in realizing the hot environment under low pO_2 condition in the Archean. However, few studies investigated how these processes affected the global carbon cycle in the Archean.

Here we developed a coupled atmosphere photochemistry-marine microbial ecosystem-global carbon cycle model and assessed how the hot climate suggested from the geologic records can be achieved in the Archean. We found that, there are high pCO_2 (hot climate) stable solutions and low pCO_2 (warm climate) unstable solutions against the range of CO_2 degassing rate similar to that of today. In the low pCO_2 solutions (<~100 PAL), CO_2 is removed from the atmosphere-ocean system as the haze particle, hence such a condition is unstable in the Archean carbon cycle system. This finding strongly supports the results of the hot terrestrial environment in the Archean as suggested from many previous studies. The hot climate may be an inevitable result in the Archean carbon cycle system.

Keywords: Archean, Early Earth, Carbon Cycle

©2019. Japan Geoscience Union. All Right Reserved.

Occurrence and chemical composition of metamorphic carbonate rocks in the Isua supracrustal belt, West Greenland: Implications for the origin of carbonate rocks and compositions of the Eoarchean seawater.

*Yoshida Satoshi[1], Kazutaka Yasukawa[2], Yasuhiro Kato[2], Yusuke Sawaki[3], Tsuyoshi Komiya[3]

1. Department of Earth & Planetary Science, Graduate School of Science, The University of Tokyo, 2. Department of Systems Innovation, Graduate School of Engineering, University of Tokyo, 3. Department of Earth Science & Astronomy Graduate School of Arts and Sciences, The University of Tokyo

The Earth is a unique planet where liquid water and life exist through the geologic time. Therefore, reconstruction of the surface environment of the early Earth is an important issue to consider early life. However, we know little about the early Earth, because the first 500 million years record of the Earth was almost lost.

In recent decades, many studies has been done on the reconstruction of surface environment of the early Earth and early life (c.f. Schidlowski et al., 1979; Ueno et al., 2002; Tashiro et al. 2017). Especially, research on the origin of metamorphic rocks derived from banded iron formation (BIF), carbonate rock and chert in the 3.81 Ga Isua supracrustal belt (ISB), southern West Greenland has been actively carried out in order to reconstruct the surface environment of the early Earth (c.f. Rose et al., 1999; Bolhar et al., 2004; Friend et al., 2008; Nutman et al., 2010).

Recent geochemical studies suggested that the meta-carbonate rock in the ISB originated from a chemical sedimentary rock based on their Post-Archean Average Shale (PAAS)-normalized rare earth element (REE) patterns (Friend et al., 2008; Nutman et al., 2010). They argued that the meta-carbonate rocks have positive La ($[La/La^*]_{PAAS}$; $La^* = 2\,Ce - 2\,Pr$), Eu ($[Eu/Eu^*]_{PAAS}$; $Eu^* = 0.5\,Sm + 0.5\,Gd$) and Y (Y/Ho) anomaly. In the ISB, the carbonate rocks occur with one of three types following rocks: meta-chert, meta-conglomerate and meta-basalt. However, the relationship between the occurrence and the chemical compositons of meta-carbonate rocks is still ambiguous.

We estimated origin of the meta-carbonate rocks with different occurrence, and reconstructed chemical composition of the Eoarchean seawater from geochemistry of the meta-carbonate rocks in the northern part of the ISB. The meta-carbonate layers accompanying the meta-chert are several centimeters thick, and interlayered with meta-chert layer. The meta-carbonate rocks accompanying the meta-conglomerate rock occur as matrix of meta-conglomerate or layer formed centimeter thick. Previous workers considered that those meta-carbonate rocks originated from shallow water sediments (e.g. Dimorth, 1982; Nutman et al., 1984), whereas others interpreted that they formed through metasomatic alteration (e.g. Appel et al., 1998); thus the origin of the meta-carbonate rock are still controversial. The meta-carbonate rocks accompanying meta-basalt occur as veins in the meta-basalt and their thickness are centimeter to tens of centimeters. Those differences in the occurrence are related to their origin.

We analyzed major and trace element (e.g. REE and Zr) contents of the whole rocks of the carbonate rocks with X-ray Fluorescence (XRF) for major elements and High-Resolution Inductively Coupled Plasma Mass Spectrometry (HR-ICP-MS) for trace elements at the University of Tokyo, respectively. Some carbonate rocks have high SiO_2, TiO_2, Al_2O_3, and Zr contents, possibly due to involvement of detrital and

©2019. Japan Geoscience Union. All Right Reserved.

volcanic materials with/without silicification. We selected the carbonate rocks with low SiO_2, TiO_2, Al_2O_3, and Zr contents in order to remove influence of the silicification and contamination of the detrital materials.

The PAAS-normalized REE patterns of meta-carbonate rocks interlayered with the meta-chert show LREE-depleted patterns with positive La (La/La*: 1.18-1.40), Eu (Eu/Eu*: 1.80-5.50) and Y (Y/Ho: 34.9-45.3) anomaly and without Ce anomaly. The meta-carbonate rocks accompanying with meta-conglomerate rocks show LREE-depleted patterns with positive Eu (Eu/Eu*: 1.43-1.91) anomaly, and lack La, Ce and Y anomaly. The meta-carbonate rocks accompanying with the meta-basalt possess LREE-depleted pattern with Eu (Eu/Eu*: 1.35-1.91) anomaly, and lack La, Ce and Y anomaly.

The positive La and Y anomaly indicates that the meta-carbonate rocks were originate from chemical sediments precipitated from seawater (e.g. Webb and Kamber, 1999; Bolhar et al., 2004), and the lack of the Ce anomaly indicates that the Eoarchean seawater was anoxic as many previous works suggested. In addition, the positive Eu anomaly suggests that the meta-carbonate rocks was precipitated from seawater, influenced by hydrothermal activity.
We classified the meta-carbonate rocks in the ISB into two groups based on the occurrence and REE patterns: chemical sedimentary rock and metasomatized rock. The former includes the meta-carbonate rocks interlayered with meta-chert, whereas the latter comprises those accompanied with meta-conglomerate and meta-basalt.

Keywords: Isua supracrustal belt, Carbonate rock, Eoarchean, Rare earth element, Transition metal element

©2019. Japan Geoscience Union. All Right Reserved.

[J] Poster | B (Biogeosciences)：B-CG Complex & General

Wed. May 29, 2019 3:30 PM - 5:00 PM JST | Wed. May 29, 2019 6:30 AM - 8:00 AM UTC | Poster Hall International Exhibition Hall8, Makuhari Messe_21

[B-CG07] Decoding the history of Earth: From Hadean to the present

convener:Tsuyoshi Komiya(Department of Earth Science & Astronomy Graduate School of Arts and Sciences The University of Tokyo), Yasuhiro Kato(Department of Systems Innovation, Graduate School of Engineering, University of Tokyo), Katsuhiko Suzuki(Research and Development Center for Submarine Resources, Japan Agency for Marine-Earth Science and Technology)

The latest results of Earth's evolution and geological processes through 4.6 billion year
s from Hadean to Modern, based on various approaches including fieldworks, chemical
analyses, experiments and computer simulation, will be presented. In this session, we ai
m to discuss and understand causal relationships and interplay among the evolution of
Earth's deep interior, changes in the surface environments, and development and evolut
ion of life. Wide-ranging topics are accepted.

[BCG07-P01] Geology of the Eoarchean Nuvvuagittuq supracrustal belt, northeastern Canada: Reappraisal of Protoliths and ages of the sedimentary rocks

*Tsuyoshi Komiya[1], Shinji Yamamoto[2], Hiroki Uehara[1], Yoshida Satoshi[1], Aoi Murakami[1], Yuki Ishihara[1] (1.Department of Earth Science & Astronomy Graduate School of Arts and Sciences The University of Tokyo, 2.Graduate School of Environment and Information Sciences, Yohohama National University)

[BCG07-P02] Behavior of phosphorus during hydrothermal alteration of basalt under CO_2-rich condition

*Aoi Murakami[1], Yusuke Sawaki[2], Hisahiro Ueda[3], Yuji Orihashi[4], Shiki Machida[5], Tsuyoshi Komiya[2] (1.Department of Earth and Planetary Science, Graduate School of Science, The University of Tokyo, 2.The University of Tokyo, 3.Tokyo Institute of Technology, 4.Hirosaki University, 5.Chiba Institute of Technology)

[BCG07-P03] Origin of chromitites in the Akulleq terrane, southern West Greenland

*Kanta Takahashi[1], Tomoaki Morishita[1], Juan Miguel Ramirez Guotana[1], Kenichiro Tani[2], Yumiko Harigane[3], Ikuya Nishio[1], Kristoffer Szilas[4], Akihiro Tamura[1] (1.Kanazawa University, 2.Department of Geology and Paleontology, National Museum of Nature and Science, 3.Geological Survey of Japan, National Institute of Advanced Industrial Science and Technology (AIST), 4.University of Copenhagen)

[BCG07-P04] Metamorphic P–T condition of the Inyoni shear zone rocks in the Barberton Greenstone Belt, South Africa and its significance

*Daichi Kato[1], Kazumasa Aoki[1], Yuta Tsuchiya[2], Shogo Aoki[2], Tsuyoshi Komiya[3] (1.Department of Applied Science,Okayama University of Science, 2.Department of Biosphere-Geosphere Science,Okayama University of Science, 3.Department of Earth Science and Astronomy,University of Tokyo)

[BCG07-P05] Discovery of possible traces of asteroid impact within the fossil-bearing carbonaceous chert from the 3.4 Ga Strelley Pool Formation, Pilbara Craton of Western Australia - a preliminary study

*Kenichirio Sugitani[1], Ryoko Senda[3], Tsuyoshi Iizuka[2], Simon Wallis[2] (1.Nagoya University, 2.The University of Tokyo, 3.Kyushu University)

[BCG07-P06] High-resolution stable isotopes and chemical analyses on laminations of the early Proterozoic stromatolite

Yuta Miyanishi[1], Kazuki Takamura[1], *Nagayoshi Katsuta[1], Maki Morimoto[1], ATSUSHI YASUDA[2], Shin-ichi Kawakami[3] (1.Faculty of Education, Gifu University, 2.Earthquake Research Institute, University of Tokyo, 3.Faculty of Education, Gifu Shotoku Gakuen University)

[BCG07-P07] Biogeochemical dynamics in during the Great Oxidation Event constrained by a biogeochemical cycle model

*Yuna Miura[1], Kazumi Ozaki[1] (1.Toho University)

[BCG07-P08] Composition of seawater before the Sturtian Snowball Earth estimated by the occurrence of late Tonian evaporitic magnesite

*Aya Miyazaki[1], Akihiro Kano[1], Fumito Shiraishi[2] (1.Department of Earth and Planetary Science, The University of Tokyo, 2.Department of Earth and Planetary Systen Sciences, Hiroshima University)

[BCG07-P09] Geochemical characteristics of black shales in the Japanese accretionary complex across the Permian-Triassic boundary extracted by independent component analysis

*Moei Yano[1], Kazutaka Yasukawa[1,3], Koichiro Fujinaga[3,2], Kentaro Nakamura[1], Yasuhiro Kato[2,1,3] (1.Department of Systems Innvation, School of Engineering, The University of Tokyo, 2.Frontier Research Center for Energy and Resources, School of Engineering, The University of Tokyo, 3.Ocean Resources Research Center for Next Generation, Chiba Institute of Technology)

[BCG07-P10] The Distribution of the Ejecta Deposit derived from Australasian Tektite Event: Implication for the Location of the Impact

*Toshihiro Tada[1], Ryuji Tada[1,2], Paul Carling[3], Wickanet Songtham[4], Le Xuan Thuyen[5], Yu Chang, Eiichi Tajika[1] (1.Department of Earth and Planetary Science, 2.Yunnan University, 3.Geography and Environment, University of Southampton, 4.Northeastern Research institute of Petrified Wood and Mineral Resources, Nakhon Ratchasima Rajabhat University, 5.Ho Chi Minh City University of Science)

[BCG07-P11] Tectonic-sedimentation reconstruction of Neoproterozoic metavolcanic sequences; the El-Dabbah area, Central Eastern Desert, Egypt

*Shoichi Kiyokawa[1], TAISHI SUZUKI[1], Maher Dawoud[3], El-Hasan Mohamed[3], Kenji Horie[2], Mami Takehara[2] (1.Department of Earth and Planetary Sciences Faculty of sciences, Kyuushu University, 2.National Institute of Polar Research, 3.Department of Geology, Faculty of Science, Menoufiya University,)

Geology of the Eoarchean Nuvvuagittuq supracrustal belt, northeastern Canada: Reappraisal of Protoliths and ages of the sedimentary rocks

*Tsuyoshi Komiya[1], Shinji Yamamoto[2], Hiroki Uehara[1], Yoshida Satoshi[1], Aoi Murakami[1], Yuki Ishihara[1]

1. Department of Earth Science & Astronomy Graduate School of Arts and Sciences The University of Tokyo, 2. Graduate School of Environment and Information Sciences, Yohohama National University

The Nuvvuagittuq supracrustal belt in the northeastern Canada is one of the oldest supracrustal rocks in the world, thus the geological, petrological and geochemical study allows us to constrain the evolution of surface environment and sold earth in the early earth. The belt consists of ultramafic rocks, coarse-graind and fine-grained greenstone, banded iron formation (BIF), siliceous rock, carbonate rock, and conglomerate. The ultramafic rocks and coarse-grained greenstone are considered as ultramafic and grabbroic intrusions, respectively. The fine-grained greensone is classified into three types based on the petrography: cummingtonite-bearing amphibolite (faux-amphibolite), hornblende-bearing amphibolite (green-amphibolite) and actinolite-bearing greenschist. The greenschist occurs only in the southwestern area. The faux- and green-amphibolite are ubiquitously present over the belt. Moreover, O'Neil et al. (2011) classified the amphibolite into three types based on their TiO_2 contents and REE patterns. The BIF mainly occurs in three areas, and has different occurrence and petrography. The BIF in the northwestern area is accompanied with the ultramafic rocks, and comprises interlayering of magnetite and amphibole/serpentine/talc. The BIF in the southwestern area occurs together with fine-grained greenstone, and mainly contains hematite and quartz (jaspillite). Dodd et al. (2017) found possible biogenic fabric, formed by iron-oxiding bacteria in the jaspillite. The BIF in the southeastern part is interlayered with the faux-amphibolite, and occurs above the siliceous rock. It mainly comporises magnetite and quartz.

The belt is intruded by some precursors of orthogneiss, whose igneous ages of *ca.* 3.8 Ga and constrain the minimum age of the belt. O'Neil et al. (2008, 2012) proposed that the igneous age of the fine-grained amphibolite is *ca.* 4.38 Ga based on a putative $^{147}Sm/^{144}Nd$-$^{142}Nd/^{144}Nd$ isochron age. On the other hand, Cates et al. (2013) proposed that a felsic layer within the faux-amphibolite originates from a clastic felsic sedimentary rock, and the maximum age of the belt is *ca.* 3.78 Ga based on ages of the zircons. David et al. (2009) interpreted a felsic layer as a volcanosedimentary rock, and proposed that the supracrustal rock was formd at 3817 Ma based on the ages of zircons.

We made a quite detailed geological map using a drone, which enables easily to trace even tens centimeter layers and intrusions. Many tens centimeter thick intrusions with an intermediate composition are present in the faux-amphibolite, whereas no intrusions are apparently found in the green-amphibolite. The distribution of the two types of amphibolite corresponds to that of three geochemical types of greenstone proposed by O'Neil et al. (2011), suggesting that the geochemical signature is due to secondary alteration. In addition, the apparent isochron on the $^{147}Sm/^{144}Nd$-$^{142}Nd/^{144}Nd$ diagram possibly originates from mixing between the mafic/ultramafic component and secondary intermediate component. O'Neil et al. (2008) proposed that the Nd isochron age of gabbroic dikes is 4.3 Ga. But, the gabboric dikes are younger than 3.8 Ga, and the isochron is putative because our map clearly shows that some thin gabbroic dikes are intruded into ambient orthogneiss, whose age is *ca.* 3.8 Ga. We found many conglomerate layers over the belt, but the layers finally change felsic intrusions. The occurrence means that they are putative conglomerate. In addition, the carbonate rocks occur along the felsic intrusions,

©2019. Japan Geoscience Union. All Right Reserved.

suggesting they also have metasomatic origin. The petrograhy and occurrence of the BIF in the northwestern area indicate that the BIF was formed from metamorphism of the ultramafic rock. The siliceous rock is intruded by many felsic intrusions and quartz veins, but the detailed map can differentiate between the siliceous layers and intrusions, and shows that the siliceous layers originate from siliceous sediment.

Keywords: Hadean, Early Earth, Early life, Surface environment

©2019. Japan Geoscience Union. All Right Reserved.

Behavior of phosphorus during hydrothermal alteration of basalt under CO_2-rich condition

*Aoi Murakami[1], Yusuke Sawaki[2], Hisahiro Ueda[3], Yuji Orihashi[4], Shiki Machida[5], Tsuyoshi Komiya[2]

1. Department of Earth and Planetary Science, Graduate School of Science, The University of Tokyo, 2. The University of Tokyo, 3. Tokyo Institute of Technology, 4. Hirosaki University, 5. Chiba Institute of Technology

It is well known that a unique environment is created around seafloor hydrothermal systems by element exchange between circulating seawater and surrounding rocks: enrichment in transition elements and sulfide, emission of quite hot water, and even even electric current flow. In addition, a number of hyperthermophilic microorganisms inhabit around hydrothermal vents. 16S rRNA-based phylogenetic tree suggests that the hyperthermophilic organisms are closest to the earliest lineage; thus the hydrothermal environment is one of the candidates for habitat and evolution of early life.

Phosphorus is one of essential elements for life. In order to maintain an early ecosystem around the hydrothermal vent, phosphorus should have been supplied from the hydrothermal vent through high-temperature water-rock reaction. In the modern basalt-hosted hydrothermal systems, phosphorus is removed due to its adsorption to iron oxide precipitated from hydrothermal fluid and/or formation of metamorphic apatite in the hydrothermally metamorphosed basalt. On the other hand, it is well known that middle Archean basaltic rocks, which constituted upper part of oceanic crust, suffered from severe carbonation during hydrothermal alteration due to quite high atmospheric CO_2 content on the early Earth. Under the CO_2-rich condition, calcium was removed from the seawater/hydrothermal fluid due to extensive carbonate formation. Because the carbonate formation inhibits the formation of apatite, the phosphorus might be released from hydrothermally altered rocks. Actually, the hydrothermally altered basaltic rocks in the Archean are more depleted in phosphorus than hydrothermally altered modern mid-ocean ridge basalt.

In order to quantify phosphorus content of fluid supplied from the basalt-hosted hydrothermal system on the early Earth, we conducted hydrothermal experiments involving hypothetical seawater and basalt under both CO_2-free and CO_2-rich conditions at 200 ˚C, 100 bars. The basalt used in this study was collected from the Indian Ocean Marie Celeste Fracture Zone. The initial solution was prepared by mixture of standard reagents by reference to modern seawater, except for Ca and P. The calcium and phosphorus contents in the solution were regulated to 30 mmol/kg and 0.60 ppm, respectively. The latter is ten times higher than the modern equivalent. For the CO_2-rich experiment, $NaHCO_3$ and HCl were added to the hypothetic seawater to substantialize 400 mmol/kg of ΣCO_2 at the beginning of the experiment.

The CO_2 concentration decreased from 400 mmol/kg to 250 mmol/kg as water-rock reaction advanced, indicating precipitation of carbonate minerals. The SEM-EDS observation demonstrated that the run

©2019. Japan Geoscience Union. All Right Reserved.

products contain calcite, dolomite, and magnesite. Phosphorus content of the fluid decreased to *ca.* 0.10 ppm under the CO_2-rich condition and *ca.* 0.04 ppm under the CO_2-free condition, respectively. The pH value of the produced fluid for the CO_2-rich experiment, measured at room temperature, was 6.6, by *ca.* 2 unit higher than that of the CO_2-free experiment. Calcium concentration decreased from 30 mmol/kg to 25 mmol/kg under the CO_2-free condition. On the other hand, calcium concentration of the formed fluid under the CO_2-rich condition decreased to 18 mmol/kg at 96 hours, and then increased to 25 mmol/kg. The formation of high alkaline and Ca-poor fluid under the CO_2-rich condition suggests that the fluid was oversaturated with carbonate, whereas undersaturated with apatite. Because the produced fluid under the CO_2-rich condition contained more phosphorus than the modern seawater, the basalt-hosted hydrothermal system may have served as a source of phosphorus under the CO_2-rich condition, probably on the early earth.

©2019. Japan Geoscience Union. All Right Reserved.

Origin of chromitites in the Akulleq terrane, southern West Greenland

*Kanta Takahashi[1], Tomoaki Morishita[1], Juan Miguel Ramirez Guotana[1], Kenichiro Tani[2], Yumiko Harigane[3], Ikuya Nishio[1], Kristoffer Szilas[4], Akihiro Tamura[1]

1. Kanazawa University, 2. Department of Geology and Paleontology, National Museum of Nature and Science, 3. Geological Survey of Japan, National Institute of Advanced Industrial Science and Technology (AIST), 4. University of Copenhagen

The studies dealing with the Hadean-Archaean geologic samples are recently expanding. Research on Hadean-Archaean terranes is an important part in reconstructing the geologic past of the Earth which is thought to have differences from the present conditions. Southern West Greenland preserves a wide exposure of ancient geologic materials and structures. This study focuses on chromitites and peridotites from the Ujaragssuit nunāt area in southern West Greenland. The Ujaragssuit nunāt area is about 20 km south from the 3.8 Ga Isua Supracrustal Belt (Moorbath et al., 1977). In Ujaragssuit nunāt, ultramafic rocks occur as lenses of several meters to several hundred meters hosted in silicic gneiss (Chadwick and Crewe, 1986). It is important to understand the origin and processes related to the formation of the peridotites and chromitites in Ujaragssuit nunāt as a contribution to the Archaean magmatic processes and tectonics of the early Earth.

Chromitites are rocks with significant amount of chromites (>20 vol.%) (Arai and Miura, 2016). The unaltered composition of spinel is regarded as a useful petrological indicator (Irvine, 1967). However, chromite composition could be modified as a result of chemical re-equilibration, metamorphism, hydrothermal alteration. The impacts of these processes are evaluated in this study. In Ujaragssuit nunāt, chromitites, dunites and amphibole harzburgites are widely exposed. In some areas, the chromitites occur as layers with thickness ranging from several centimeters to a meter. Massive chromitites (2 m thick) are also exposed. The lithologies present in the area were also described in detail in previous works such as of Rollinson et al. (2002).

Chromites are subhedral and account for about 50-70% of the Ujaragssuit nunāt chromitites. Interstitial grains are mainly phlogopite and minor chlorite and talc. The dunite host consists mainly of olivine (~80%) and accessory spinel and phlogopite. Some spinel grains in the host dunite exhibit zonation as evidenced by darker cores and lighter rims under reflected light microscope and scanning electron microscope observations. The zonation observed is associated with compositional variation from core to rim (Fe enrichment towards the rim). The amphibole harzburgites are mainly composed of amphibole, orthopyroxene, spinel, phlogopite. Orthopyroxenes occur both around olivine and in some parts as inclusions inside olivine grains. Talc replacement of orthopyroxenes is also common. Spinel are surrounded by phlogopite and edenitic amphibole.

Spinel in the host peridotites has a higher Fe^{3+}content. The spinel Fe^{3+} content is higher in samples with higher phlogopite and spinel ratio. This suggests that phlogopite was formed by the reaction of spinel (+olivine) with an alkaline element-rich fluid. Spinel serves as a source of the Al_2O_3 in the phlogopite formation. It is considered that the chemical composition change of spinel is caused by the formation of phlogopite. Furthermore, phlogopite in the sample containing amphiboles has lower K/(K+Na) ratio than samples without amphibole. Amphiboles are also found around the spinel. The K/(K+Na) ratio in the fluid decreases as the alkaline element-rich fluid forms phlogopite and amphibole was formed by the reaction between this differentiated fluid and spinel (+olivine). The abundance of orthopyroxene is higher in the

©2019. Japan Geoscience Union. All Right Reserved.

sample containing amphiboles. The Cr_2O_3- and Al_2O_3- poor characteristic of the orthopyroxenes suggests a secondary origin. The differentiated fluid is also abundant in silica component and reacts with olivine to react to form the secondary orthopyroxenes. Although the possibility of crystal differentiation cannot be completely ruled out, it is thought that these peridotites were originally dunites and chromitites and the chemical composition was modified by alkali alteration.

Keywords: southern West Greenland, chromitite, metasomatism

©2019. Japan Geoscience Union. All Right Reserved.

Metamorphic P–T condition of the Inyoni shear zone rocks in the Barberton Greenstone Belt, South Africa and its significance

*Daichi Kato[1], Kazumasa Aoki[1], Yuta Tsuchiya[2], Shogo Aoki[2], Tsuyoshi Komiya[3]

1. Department of Applied Science,Okayama University of Science, 2. Department of Biosphere-Geosphere Science,Okayama University of Science, 3. Department of Earth Science and Astronomy,University of Tokyo

The metamorphic P–T conditions and processes of the mid-Archean Barberton Greenstone Belt (BGB), South Africa were examined from metamorphosed banded iron formation (BIF) and garnet amphibolite in the Inyoni shear zone (ISZ). Their metamorphic P–T conditions were estimated from thermodynamic calculations combined with several geothermobarometries such as garnet–clinopyroxene geothermometry, Raman geobarometry and Zr-in-sphene geothermometry. Moreover, in order to constrain the protolith age and origin of our studied sample, we conducted zircon U-Pb and trace elements analyses by using Laser Ablation Inductively Coupled Plasma Mass Spectrometry (LA-ICP-MS).The following results were obtained: the P–T conditions of the meta-BIF changed from ca. 600–680 ˚C and 10–12.7 kbar through ca. 510–540 ˚C and 8–11 kbar to less than 500 ˚C and 4 kbar. On the other hand, the P–T conditions of the garnet amphibolite changed from ca. 9.5–10.5 kbar and 620–660˚C to less than 5 kbar and 500 ˚C. Integration of these new results with previous studies for the BGB suggest that the geothermal gradients of the prograde and retrograde metamorphisms were ca. 15–20 ˚C/km and 20–30 ˚C/km, respectively. Igneous zircon separated from the Garnet amphibolite sample yield ^{207}Pb-^{206}Pb age of ca. 3.4-3.2 Ga. This new data together with previous geochronological data indicate that the protoliths of ISZ rocks began to subduct at ca. 3.37-3.24 Ga. The prograde P-T path was kinked at P = 8.0 kbar and T = 560 ℃ by difference in geothermal gradient between crust and upper mantle. The change of geothermal gradient in the ISZ rocks between prograde and retrograde conditions might have relation to the collision of ca. 3.4 Ga Stoluzburg domain. The last P-T trajectory characterized by isothermal decompression might be caused by the intrusion of the ca. 3.23-3.21 Ga TTG Badplaas pluton attendant on plate subduction.

Keywords: Archean, Barberton greenstone belt, Plate tectonics

©2019. Japan Geoscience Union. All Right Reserved.

Discovery of possible traces of asteroid impact within the fossil-bearing carbonaceous chert from the 3.4 Ga Strelley Pool Formation, Pilbara Craton of Western Australia - a preliminary study

*Kenichirio Sugitani[1], Ryoko Senda[3], Tsuyoshi Iizuka[2], Simon Wallis[2]

1. Nagoya University, 2. The University of Tokyo, 3. Kyushu University

Large asteroid impacts are thought to be a common feature of the Archean in particular as a result of the Late Heavy Bombardment (LHB). One line of supporting evidence is the presence of “impact layers” containing silicate spherules that were formed by condensation of rocks vaporized by bombardment events. Two Early Archean impact layers with ages of 3.47 and 3.46 Ga have been identified from the Pilbara greenstone belt, Western Australia (Glikson et al., 2016; Lowe and Byerly, 1986). In contrast 5 separate impact layers with ages of 3.47 to 3.24 Ga have been identified in the Barberton greenstone belt, South Africa (e.g., Lowe et al., 2014; Byerly et al., 2002). Such extraterrestrial impacts likely influenced the Earth’s early environment, including crustal deformation, terrain amalgamation, evaporation of significant volumes of ocean water, and even triggering the development of a modern-like plate tectonic regime (Lowe et al, 2014). It is also reasonable to assume that the early life was influenced significantly by these impacts (Lowe et al., 2003). The early evolution of life might have been accelerated as a consequence of adaptation to such environmental agitations (Kozawa et al., 2018; Oehler et al., 2017). Thus, a close association of traces of life, such as microfossils with cellular preservation, and of impact events recorded in Archean sedimentary successions is of special interest.

In this study we describe the new discovery of traces of asteroid impacts in the ca. 3.4 Ga Strelley Pool Formation (SPF) in the Panorama greenstone belt of the Pilbara Craton, Western Australia. Spherules of possible impact origin were identified in carbonaceous black chert 15 cm thick from which morphologically diverse microfossils have been described (e.g., Sugitani et al., 2013) (Fig. 1). Evidence for an asteroid impact includes the presence of a thin sedimentary layer rich in silicate spherules (Fig. 2) associated with enrichment of platinum-group elements (PGE) (Fig. 3a). However, our detailed analyses revealed that PGE-enrichment is more conspicuous in the lower horizon and are associated with $^{178}Os/^{188}Os$ initial values close to 0.1. In contrast, spherule-rich layers have significantly higher $^{178}Os/^{188}Os$ values ~1.0 (Fig. 3b). One exception is a sample from the upper portion, which has an unusually low value. It is also noteworthy that the spherule-rich layer is enriched in Al and Ti (Fig. 3c). There is a clear higher contribution by clastic materials to this layer, and this feature may explain the apparent contradiction between the PGE-enrichment and Os isotopic values described above. In either case, the layer contains abundant volcanic fragments and clasts in which spherules tend to occur. This occurrence suggests that the spherules were likely reworked from the original site of deposition. A layer composed of carbonaceous grains including rip-up clasts that is found just below the spherule-rich layer (Fig. 1) indicates a steep high-energy depositional environment. This layer contrasts with the fine parallel lamination of carbonaceous chert layers seen at the other horizons, which indicates a quiet depositional environment. We infer that the original impact layer is present below the examined carbonaceous black chert layer and that a high-energy environment related to volcanic activity caused reworking of the spherule-rich deposits, which were transported to the present site of deposition. If this is the case, the high PGE concentrations and the significantly low $^{187}Os/^{188}Os$ initial ratios of the lower cherty samples could be explained as representing the aftermath of an impact event associated with precipitation of vaporized PGE from the atmosphere to the sediment.

©2019. Japan Geoscience Union. All Right Reserved.

References

Byerly et al. (2002) Science 297, 1325-1327; Glikson et al. (2016) Precam. Res. 279: 103-122; Kozawa et al. (2018) *Geobiology* DOI: 10.1111/gbi12319; Lowe et al. (2014) Geology 42: 747-750; Lowe et al. (2003) Astrobiology 3: 7-48; Lowe and Byerly (1986) Geology 14, 83-86; Oehler et al. (2017) Precambrian Research 296, 112-119; Sugitani et al. (2015) Geobiology 13, 507-521.

Keywords: Archean, microfossils, asteroid impact, platinum group elements, osmium isotope

Fig. 1

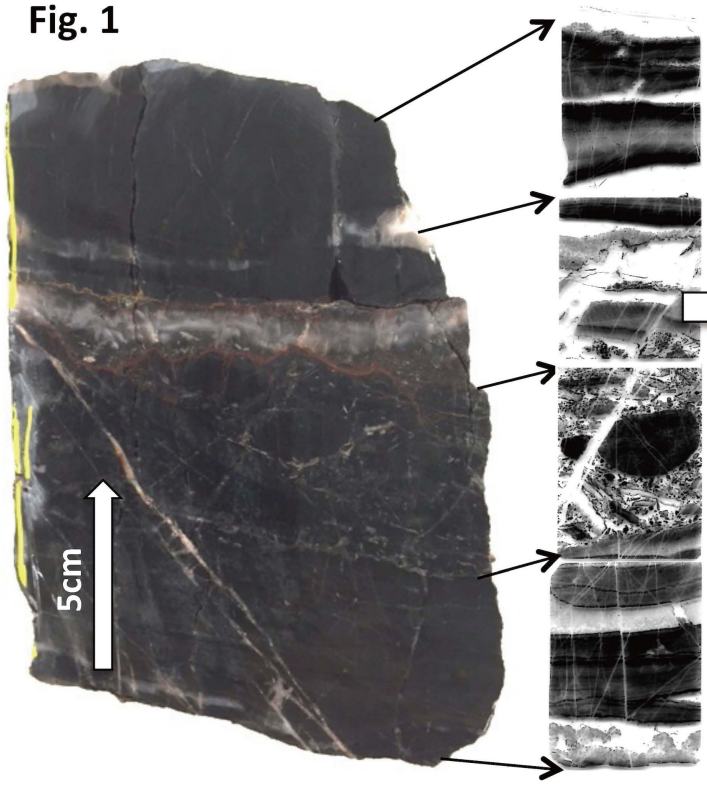

Fig. 2

Fig. 3

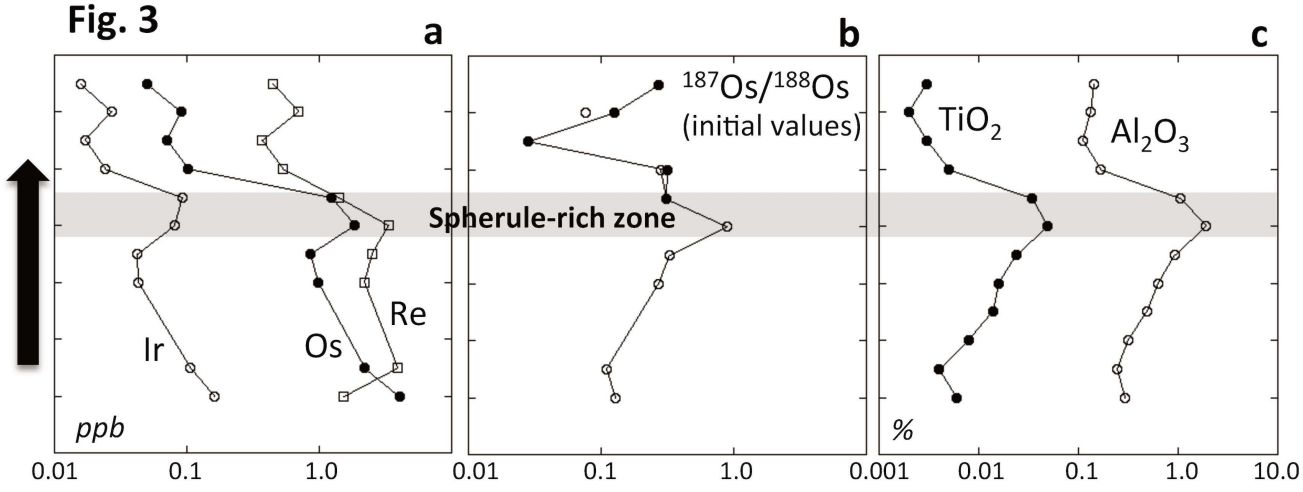

©2019. Japan Geoscience Union. All Right Reserved.

High-resolution stable isotopes and chemical analyses on laminations of the early Proterozoic stromatolite

Yuta Miyanishi[1], Kazuki Takamura[1], *Nagayoshi Katsuta[1], Maki Morimoto[1], ATSUSHI YASUDA[2], Shin-ichi Kawakami[3]

1. Faculty of Education, Gifu University, 2. Earthquake Research Institute, University of Tokyo, 3. Faculty of Education, Gifu Shotoku Gakuen University

In this presentation, we report results of high-resolution analyses on $\delta^{13}C$-$\delta^{18}O$ and chemical compositions of lamination in early Proterozoic stromatolite and then consider the mechanism of the laminae formations and the causes of their fluctuation patterns.

Keywords: Stromatolite, Laminated structure, Stable isotope, Chemical composition

©2019. Japan Geoscience Union. All Right Reserved.

Biogeochemical dynamics in during the Great Oxidation Event constrained by a biogeochemical cycle model

*Yuna Miura[1], Kazumi Ozaki[1]

1. Toho University

The accumulated geological and geochemical data indicate that Earth's ocean-atmosphere system has seen a fundamental increase in oxygen abundances from anoxic conditions (pO_2 <10^{-5} present atmospheric level (PAL)) to oxic conditions (pO_2 >10^{-2} PAL) during the Paleoproterozoic. This marked transition, known as the 'Great Oxidation Event (GOE)', may be accompanied by a transient time of relatively high oxygen levels in the atmosphere and ocean (called an 'oxygen overshoot'). However, the ultimate cause and biogeochemical consequences of the GOE remain unclear.
Harada et al. (2015) hypothesized the snowball Earth glaciation at 2.2 Ga as an ultimate cause of the GOE with a prolonged (~10^8 year) oxygen overshoot. Sedimentary record of iron and manganese oxides above the glacial deposit in the Transvaal Supergroup, South Africa, implies an oxygenation of Earth's surface environments just after the glaciation. The red beds and sulfate evaporites (gypsum, $CaSO_4$) also suggest a sustained oxygenation of the Earth surface environment. They constructed a biogeochemical cycle model of carbon, phosphorous and oxygen, and conducted sensitivity experiments to assess the biogeochemical dynamics after the snowball Earth glaciation. By assuming an atmospheric CO_2 level of 0.7 atm required to end the snowball Earth glaciation, they found that an extremely warm climate accelerates chemical weathering on land and phosphorus riverine input. This marked increase in phosphorus input results in a dramatic increase in biospheric oxygen production, with an oxygen overshoot lasting for ~10^8 years. However, it remains unclear whether their calculations are consistent with available geological constraints (e.g., sulfate evaporite depositions and sulfur isotope data), because they ignore the geochemical cycle of sulfur. A recent geochemical study suggests that concentration of sulfate ($[SO_4^{2-}]$) in the ocean may have been unusually high (>10 mM) during the gypsum formation. If correct, this provides a strong constraint on the biogeochemical conditions.
In this study we constructed a sulfur cycle model with a goal of finding the feasible conditions for the geochemical constraint ($[SO_4^{2-}]$ >10 mM). The model consists of three reservoirs—oceanic sulfate, crustal gypsum, and crustal pyrite. Sulfur enters the ocean through weathering of gypsum and pyrite. We assumed that the oxidative weathering of pyrite is a function of atmospheric O_2 levels and that the gypsum weathering is proportional to the global weathering rate. Sulfur is removed from the ocean via deposition of gypsum and pyrite. We assumed that sulfate burial in the ocean is proportional to seawater sulfate levels. Pyrite burial is assumed to be governed by microbial sulfate reduction dependent on marine sulfate content, biological production (i.e., the availability of organic matter), and oceanic O_2 levels. In this study, we performed a series of sensitivity experiment with a Harada et al.'s model, and obtained biogeochemical dynamics (e.g., atmospheric O_2 levels and weathering rates) were used as a forcing for our sulfur cycle model, enabling us to simulate the evolution of oceanic SO_4^{2-} levels after the glaciation. Our sensitivity experiments of a Harada et al.'s model demonstrate that the biogeochemical dynamics after the glaciation depend mainly on the initial value of atmospheric CO_2 levels: >0.2 bar and >0.25 bar of CO_2 are required for the GOE and the occurrence of an oxygen overshoot, respectively. Our sulfur cycle model, however, demonstrates that 0.25 bar of CO_2 is not sufficient to explain the unusually high levels of $[SO_4^{2-}]$ >10 mM during the overshoot. The systematic sensitivity experiments reveal that at least ~0.75 bar of CO_2 will be required. This result provides an additional support for the hypothesis that the severe glaciation was an ultimate cause of the GOE in the Paleoproterozoic.

©2019. Japan Geoscience Union. All Right Reserved.

Keywords: Great Oxidation Event, biogeochemical cycle, sulfur cycle

©2019. Japan Geoscience Union. All Right Reserved.

Composition of seawater before the Sturtian Snowball Earth estimated by the occurrence of late Tonian evaporitic magnesite

*Aya Miyazaki[1], Akihiro Kano[1], Fumito Shiraishi[2]

1. Department of Earth and Planetary Science, The University of Tokyo, 2. Department of Earth and Planetary Systen Sciences, Hiroshima University

Neoproterozoic is an important period for biological evolution when the spread of algae, protozoan, and multicellular animal were radiated. Understanding of climate changes and fossil records after Ediacaran has been largely improved. But environmental background behind how the Earth’ s surface reached the Snowball Earth state has not been understood.
In Flinders Ranges, South Australia, thick shallow marine sequence preserves excellent geological records especially before and after Sturtian glaciation. This study targets Skillogalee Dolomite exposed at Leigh Creek, Northern Flinders Ranges (LC section) which was deposited around 788±7Ma(Late Tonian) before the Sturtian glaciation (Hood and Wallace 2018). The lithology of LC section contains a small amount of siliciclastics, but mainly consists of shallow water carbonate that exhibits various structures including intraformational conglomerate, stromatolite and tepee structure. However, the most remarkable feature is a large quantity of magnesite. Magnesite alternates with dolostone and occurs as layers of ~1m in thickness or crusts of intraformational conglomerate. The Tepee structure indicates an evaporative environment, and higher d13C and d18O of magnesite indicates that the magnesite deposited after the dolomite. These rocks lack gypsum pseudomorphs.
Evaportive mineral assemblage of the Skillogalee Dolomite can be recognized only in Proterozoic. While the Phanerozoic evaporate sequence starts from Ca carbonate-dolomite, follows to gypsum and halite, but does not include magnesite (Hardie and Eugster 1980). In order to explain this specific mineral assemblage, we made model calculations about the order of precipitated minerals, which expected by continuous evaporation of seawater. Then, we found the Skillogalee mineral sequence was achieved only from seawater of Mg/Ca > 10 and Mg > Alkalinity > Ca. We used sulfate concentration of the modern seawater, but it does no influence to the result. Alkalinity over 10 times higher than the modern level likely reflects from high partial pressure of carbon dioxide or low Ca concentration in seawater. Possible causes of high Mg/Ca ratio were inactive seawater circulation at low mid-ocean ridge, active carbonate sedimentation, or Ca depletion due to extensive evaporite formation including gypsum around 800 Ma. If pH of seawater has been controlled by the solubility equilibrium of CaCO3, the drastic decrease in Ca concentration would encouraged pH rise of sea water and lead to decline of atmospheric carbon dioxide.

Evans 2006, Nature 444, 51-55.
Hardie and Eugster 1980, Science 208, 498-500.
Hood and Wallace 2018. Global and Planetary Change 160, 28-45.

Keywords: Neoproterozoic, evaporite, seawater chemistry

©2019. Japan Geoscience Union. All Right Reserved.

Geochemical characteristics of black shales in the Japanese accretionary complex across the Permian-Triassic boundary extracted by independent component analysis

*Moei Yano[1], Kazutaka Yasukawa[1,3], Koichiro Fujinaga[3,2], Kentaro Nakamura[1], Yasuhiro Kato[2,1,3]

1. Department of Systems Innvation, School of Engineering, The University of Tokyo, 2. Frontier Research Center for Energy and Resources, School of Engineering, The University of Tokyo, 3. Ocean Resources Research Center for Next Generation, Chiba Institute of Technology

The Permian-Triassic boundary (PTB) is characterized by an oxygen-depleted condition in the superocean Panthalassa. However, the degree of the oxygen depletion in deep-sea environments remains an open question.Deep-sea sediments that deposited from the latest Permian to early Triassic constitute black shale within the accretionary complexes of Japan, showing a distinct enrichment of redox sensitive trace metals (e.g., V, Mo, U) that precipitate under reducing conditions.In contrast to the Panthalassa at the PTB, the modern ocean is generally oxygenated from the surface to the bottom due to a sufficiently strong global ocean circulation. However, oxygen-depleted water masses can develop in some specific areas such as restricted basins and coastal upwelling areas, and blackish sediments in these areas show laminated facies and/or high total organic carbon contents reflecting oxygen-depleted conditions.Comparing the black shales at the PTB with the other sediments that deposited in oxygen-depleted conditions can characterize the Panthalassa across the PTB in a context of a broad spectrum of oceanic environmental changes throughout the Earth’ s history. To this end, clarifying geochemical features of multiple elements, especially of redox sensitive trace metals, is quite a useful approach to extract the information of the oceanic environments involving variations in redox conditions. Here we applied independent component analysis to the multi-elemental data set composed of major- and trace-element contents of the samples from the PTB sections within the accretionary complexes of Japan, and black mud and shale of other geological times obtained by scientific drillings in the modern oceans. We will discuss the geochemical characteristics of the PTB black shales and the other blackish sediments, and oceanic environmental conditions across the PTB.

Keywords: Permian-Triassic boundary, black shale, redox sensitive trace metals, independent component analysis, accretionary complex

©2019. Japan Geoscience Union. All Right Reserved.

The Distribution of the Ejecta Deposit derived from Australasian Tektite Event: Implication for the Location of the Impact

*Toshihiro Tada[1], Ryuji Tada[1,2], Paul Carling[3], Wickanet Songtham[4], Le Xuan Thuyen[5], Yu Chang, Eiichi Tajika[1]

1. Department of Earth and Planetary Science, 2. Yunnan University, 3. Geography and Environment, University of Southampton, 4. Northeastern Research institute of Petrified Wood and Mineral Resources, Nakhon Ratchasima Rajabhat University, 5. Ho Chi Minh City University of Science

Tektites are glass spherules formed by large extra-terrestrial impacts and so far reported from 4 strewn fields on the Earth (e.g, McCall, 2001). Australasian tektites—distributed widely from Southeast Asia to Antarctica—are considered to be formed by an impact event at ca. 0.79 Ma in Southeast Asia. This impact event is the youngest among large (diameter of a projectile larger than 1 km) impact events. Because of its young age, it is expected that evidence of the impact (impact crater and ejecta deposits) and the record of environmental perturbation by the impact are well preserved. Therefore, this impact event would serve as an important case study to understand the environmental effects of large impact events on the Earth.

Based on the wide distribution of the tektite—larger than 10% of the Earth’ s surface —the magnitude of the impact has been estimated as large enough to make 30–120 km sized impact crater (e.g., Prasad et al., 2007). The biggest mystery, however, is that no crater has been found and precise location and magnitude of the impact are not well understood.

The location of the impact has been estimated mainly based on the distribution of the tektites. The layered tektites, which are considered to be proximal to the source crater because of their large sizes (larger than 10 cm) and internal inhomogeneity, are distributed in the limited area in Thailand, Laos and Vietnam (Shnetzler, 1992). The number of microtektites per unit area in marine sediment cores decrease with the distance from Indochina peninsula (e.g., Prasad et al., 2007). Such distribution of tektites suggests that the location of the impact is somewhere in the eastern part of Indochina peninsula.

For more precisely constraining the location of the impact, the distribution of the ejecta deposit is important. The ejecta deposit, which is formed by deposition of materials ejected from the source crater, increases its thickness toward the location of the impact. It is also known that the abundance and size of shock-metamorphosed minerals in ejecta deposit increase towards the location of the impact (e.g., Morgan et al., 2006). The ejecta deposit of this impact event, however, has not been reported on the Indochina Peninsula.

In order to identify the ejecta deposit and clarify its distribution in the Indochina Peninsula, we have conducted field surveys in northeastern Thailand, central Vietnam, and southern Laos. We discovered shocked quartz grains—one of the most diagnostic evidence of impact—from the Quaternary sediment unconformably covering the basement rock, and identify the ejecta deposit at Huai Om section located near the border between northeastern Thailand and southern Laos. The ejecta deposit at Huai Om section can be divided into three units: silt–sand layers containing lip-up clasts of the basement rock (Unit 1, approximately 1 m in thickness), a tektite-bearing gravel layer (Unit 2, 20 cm–1 m in thickness), and a massive sand layer (Unit 3, approximately 3 m in thickness), in ascending order.

The tektite bearing gravel layer and the massive sand layer (corresponding to Units 2 and 3 at Huai Om

©2019. Japan Geoscience Union. All Right Reserved.

section) are distributed widely in the eastern part of Indochina Peninsula. Especially, the thickness of the tektite bearing gravel layer (Unit 2) increases toward the area around the southern part of the border between Thailand and Laos. We have measured abundance and size of shocked quartz grains at three sites in northeastern Thailand including Huai Om section. Although the size of shocked quartz grains is similar (approximately 200 μm) among these sites, its abundance varies between 5 and 10% and increases toward the area around the southern part of the border between Thailand and Laos. The distribution of the tektite-bearing gravel layer and abundance of shocked quartz grains indicate that the location of the impact is close to this area.
We are measuring the abundance and size of shocked quartz grains at additional sites in Thailand, Vietnam and Laos. In this presentation, we will report the distribution of the thickness of the ejecta deposit, abundance and size of shocked quartz in the eastern part of Indochina Peninsula to further constrain the location of the impact.

Keywords: Tektite, Shocked quartz, Ejecta, Australasian Tektite

©2019. Japan Geoscience Union. All Right Reserved.

Tectonic-sedimentation reconstruction of Neoproterozoic metavolcanic sequences; the El-Dabbah area, Central Eastern Desert, Egypt

*Shoichi Kiyokawa[1], TAISHI SUZUKI[1], Maher Dawoud[3], El-Hasan Mohamed[3], Kenji Horie[2], Mami Takehara[2]

1. Department of Earth and Planetary Sciences Faculty of sciences, Kyuushu University, 2. National Institute of Polar Research, 3. Department of Geology, Faculty of Science, Menoufiya University,

In the Eastern Desert of Egypt, Neoproterozoic island arc sequence with Banded Iron Formations (BIFs) are reported within volcano-sedimentary sequence whose geological structure and stratigraphy are not well understood. In this study, the geological structure was established to reconstruct the stratigraphy in El Dabbah in the Central Eastern Desert.

It preserves a sequence of relatively undeformed lower greenschist-facies rocks, overlain by subaerial sedimentary strata deposited in strike-slip basins (the Atsham Formation and the Hammamat Group). Reconstructed a stratigraphic–tectonic history of this metavolcanic sequence is understand the Neoproterozoic iron formation stratigraphy and characteristics, which related snowball earth event or not. New geochronological data are used to date the crystallization of granite at *ca.*638.1±2.9 Ma and a rhyodacite at 659.6±3.0 Ma. Four generations of structural deformation have been identified in this area: accretional phase (D_1: 700–680 Ma); strike-slip deformation with transtension, normal faulting, and strong left-lateral shear after the Atsham Formation deposition (D_2: 650–640 Ma); and subaerial sedimentation of the Hammamat Group coincident with the activity of a strike-slip fault and formation of a pull-apart basin (D_3: 638–600 Ma) and followed by extensional deformation. Hear we show stratigraphic and structural interpretation in low grade metamorphosed sequence at the El-Dabbah area, in Central Eastern Desert in Arabian-Nubian Shield.

Keywords: Neoproterozoic, Island arc, strike-slip basin, banded iron formation

©2019. Japan Geoscience Union. All Right Reserved.

[J] Poster | B (Biogeosciences)：B-CG Complex & General

Wed. May 29, 2019 5:15 PM - 6:30 PM JST | Wed. May 29, 2019 8:15 AM - 9:30 AM UTC | Poster Hall International Exhibition Hall8, Makuhari Messe_35

[B-CG07] Decoding the history of Earth: From Hadean to the present

convener:Tsuyoshi Komiya(Department of Earth Science & Astronomy Graduate School of Arts and Sciences The University of Tokyo), Yasuhiro Kato(Department of Systems Innovation, Graduate School of Engineering, University of Tokyo), Katsuhiko Suzuki(Research and Development Center for Submarine Resources, Japan Agency for Marine-Earth Science and Technology)

The latest results of Earth's evolution and geological processes through 4.6 billion year
s from Hadean to Modern, based on various approaches including fieldworks, chemical
analyses, experiments and computer simulation, will be presented. In this session, we ai
m to discuss and understand causal relationships and interplay among the evolution of
Earth's deep interior, changes in the surface environments, and development and evolut
ion of life. Wide-ranging topics are accepted.

[BCG07-P01] Geology of the Eoarchean Nuvvuagittuq supracrustal belt, northeastern Canada: Reappraisal of Protoliths and ages of the sedimentary rocks

*Tsuyoshi Komiya[1], Shinji Yamamoto[2], Hiroki Uehara[1], Yoshida Satoshi[1], Aoi Murakami[1], Yuki Ishihara[1] (1.Department of Earth Science & Astronomy Graduate School of Arts and Sciences The University of Tokyo, 2.Graduate School of Environment and Information Sciences, Yohohama National University)

[BCG07-P02] Behavior of phosphorus during hydrothermal alteration of basalt under CO_2-rich condition

*Aoi Murakami[1], Yusuke Sawaki[2], Hisahiro Ueda[3], Yuji Orihashi[4], Shiki Machida[5], Tsuyoshi Komiya[2] (1.Department of Earth and Planetary Science, Graduate School of Science, The University of Tokyo, 2.The University of Tokyo, 3.Tokyo Institute of Technology, 4.Hirosaki University, 5.Chiba Institute of Technology)

[BCG07-P03] Origin of chromitites in the Akulleq terrane, southern West Greenland

*Kanta Takahashi[1], Tomoaki Morishita[1], Juan Miguel Ramirez Guotana[1], Kenichiro Tani[2], Yumiko Harigane[3], Ikuya Nishio[1], Kristoffer Szilas[4], Akihiro Tamura[1] (1.Kanazawa University, 2.Department of Geology and Paleontology, National Museum of Nature and Science, 3.Geological Survey of Japan, National Institute of Advanced Industrial Science and Technology (AIST), 4.University of Copenhagen)

[BCG07-P04] Metamorphic P–T condition of the Inyoni shear zone rocks in the Barberton Greenstone Belt, South Africa and its significance

*Daichi Kato[1], Kazumasa Aoki[1], Yuta Tsuchiya[2], Shogo Aoki[2], Tsuyoshi Komiya[3] (1.Department of Applied Science,Okayama University of Science, 2.Department of Biosphere-Geosphere Science,Okayama University of Science, 3.Department of Earth Science and Astronomy,University of Tokyo)

[BCG07-P05] Discovery of possible traces of asteroid impact within the fossil-bearing carbonaceous chert from the 3.4 Ga Strelley Pool Formation, Pilbara Craton of Western Australia - a preliminary study

*Kenichirio Sugitani[1], Ryoko Senda[3], Tsuyoshi Iizuka[2], Simon Wallis[2] (1.Nagoya University, 2.The University of Tokyo, 3.Kyushu University)

[BCG07-P06] High-resolution stable isotopes and chemical analyses on laminations of the early Proterozoic stromatolite

Yuta Miyanishi[1], Kazuki Takamura[1], *Nagayoshi Katsuta[1], Maki Morimoto[1], ATSUSHI YASUDA[2], Shin-ichi Kawakami[3] (1.Faculty of Education, Gifu University, 2.Earthquake Research Institute, University of Tokyo, 3.Faculty of Education, Gifu Shotoku Gakuen University)

[BCG07-P07] Biogeochemical dynamics in during the Great Oxidation Event constrained by a biogeochemical cycle model

*Yuna Miura[1], Kazumi Ozaki[1] (1.Toho University)

[BCG07-P08] Composition of seawater before the Sturtian Snowball Earth estimated by the occurrence of late Tonian evaporitic magnesite

*Aya Miyazaki[1], Akihiro Kano[1], Fumito Shiraishi[2] (1.Department of Earth and Planetary Science, The University of Tokyo, 2.Department of Earth and Planetary Systen Sciences, Hiroshima University)

[BCG07-P09] Geochemical characteristics of black shales in the Japanese accretionary complex across the Permian-Triassic boundary extracted by independent component analysis

*Moei Yano[1], Kazutaka Yasukawa[1,3], Koichiro Fujinaga[3,2], Kentaro Nakamura[1], Yasuhiro Kato[2,1,3] (1.Department of Systems Innvation, School of Engineering, The University of Tokyo, 2.Frontier Research Center for Energy and Resources, School of Engineering, The University of Tokyo, 3.Ocean Resources Research Center for Next Generation, Chiba Institute of Technology)

[BCG07-P10] The Distribution of the Ejecta Deposit derived from Australasian Tektite Event: Implication for the Location of the Impact

*Toshihiro Tada[1], Ryuji Tada[1,2], Paul Carling[3], Wickanet Songtham[4], Le Xuan Thuyen[5], Yu Chang, Eiichi Tajika[1] (1.Department of Earth and Planetary Science, 2.Yunnan University, 3.Geography and Environment, University of Southampton, 4.Northeastern Research institute of Petrified Wood and Mineral Resources, Nakhon Ratchasima Rajabhat University, 5.Ho Chi Minh City University of Science)

[BCG07-P11] Tectonic-sedimentation reconstruction of Neoproterozoic metavolcanic sequences; the El-Dabbah area, Central Eastern Desert, Egypt

*Shoichi Kiyokawa[1], TAISHI SUZUKI[1], Maher Dawoud[3], El-Hasan Mohamed[3], Kenji Horie[2], Mami Takehara[2] (1.Department of Earth and Planetary Sciences Faculty of sciences, Kyuushu University, 2.National Institute of Polar Research, 3.Department of Geology, Faculty of Science, Menoufiya University,)

Geology of the Eoarchean Nuvvuagittuq supracrustal belt, northeastern Canada: Reappraisal of Protoliths and ages of the sedimentary rocks

*Tsuyoshi Komiya[1], Shinji Yamamoto[2], Hiroki Uehara[1], Yoshida Satoshi[1], Aoi Murakami[1], Yuki Ishihara[1]

1. Department of Earth Science & Astronomy Graduate School of Arts and Sciences The University of Tokyo, 2. Graduate School of Environment and Information Sciences, Yohohama National University

The Nuvvuagittuq supracrustal belt in the northeastern Canada is one of the oldest supracrustal rocks in the world, thus the geological, petrological and geochemical study allows us to constrain the evolution of surface environment and sold earth in the early earth. The belt consists of ultramafic rocks, coarse-graind and fine-grained greenstone, banded iron formation (BIF), siliceous rock, carbonate rock, and conglomerate. The ultramafic rocks and coarse-grained greenstone are considered as ultramafic and grabbroic intrusions, respectively. The fine-grained greensone is classified into three types based on the petrography: cummingtonite-bearing amphibolite (faux-amphibolite), hornblende-bearing amphibolite (green-amphibolite) and actinolite-bearing greenschist. The greenschist occurs only in the southwestern area. The faux- and green-amphibolite are ubiquitously present over the belt. Moreover, O'Neil et al. (2011) classified the amphibolite into three types based on their TiO_2 contents and REE patterns. The BIF mainly occurs in three areas, and has different occurrence and petrography. The BIF in the northwestern area is accompanied with the ultramafic rocks, and comprises interlayering of magnetite and amphibole/serpentine/talc. The BIF in the southwestern area occurs together with fine-grained greenstone, and mainly contains hematite and quartz (jaspillite). Dodd et al. (2017) found possible biogenic fabric, formed by iron-oxiding bacteria in the jaspillite. The BIF in the southeastern part is interlayered with the faux-amphibolite, and occurs above the siliceous rock. It mainly comporises magnetite and quartz.

The belt is intruded by some precursors of orthogneiss, whose igneous ages of *ca.* 3.8 Ga and constrain the minimum age of the belt. O'Neil et al. (2008, 2012) proposed that the igneous age of the fine-grained amphibolite is *ca.* 4.38 Ga based on a putative $^{147}Sm/^{144}Nd$-$^{142}Nd/^{144}Nd$ isochron age. On the other hand, Cates et al. (2013) proposed that a felsic layer within the faux-amphibolite originates from a clastic felsic sedimentary rock, and the maximum age of the belt is *ca.* 3.78 Ga based on ages of the zircons. David et al. (2009) interpreted a felsic layer as a volcanosedimentary rock, and proposed that the supracrustal rock was formd at 3817 Ma based on the ages of zircons.

We made a quite detailed geological map using a drone, which enables easily to trace even tens centimeter layers and intrusions. Many tens centimeter thick intrusions with an intermediate composition are present in the faux-amphibolite, whereas no intrusions are apparently found in the green-amphibolite. The distribution of the two types of amphibolite corresponds to that of three geochemical types of greenstone proposed by O'Neil et al. (2011), suggesting that the geochemical signature is due to secondary alteration. In addition, the apparent isochron on the $^{147}Sm/^{144}Nd$-$^{142}Nd/^{144}Nd$ diagram possibly originates from mixing between the mafic/ultramafic component and secondary intermediate component. O'Neil et al. (2008) proposed that the Nd isochron age of gabbroic dikes is 4.3 Ga. But, the gabboric dikes are younger than 3.8 Ga, and the isochron is putative because our map clearly shows that some thin gabbroic dikes are intruded into ambient orthogneiss, whose age is *ca.* 3.8 Ga. We found many conglomerate layers over the belt, but the layers finally change felsic intrusions. The occurrence means that they are putative conglomerate. In addition, the carbonate rocks occur along the felsic intrusions,

©2019. Japan Geoscience Union. All Right Reserved.

suggesting they also have metasomatic origin. The petrograhy and occurrence of the BIF in the northwestern area indicate that the BIF was formed from metamorphism of the ultramafic rock. The siliceous rock is intruded by many felsic intrusions and quartz veins, but the detailed map can differentiate between the siliceous layers and intrusions, and shows that the siliceous layers originate from siliceous sediment.

Keywords: Hadean, Early Earth, Early life, Surface environment

©2019. Japan Geoscience Union. All Right Reserved.

Behavior of phosphorus during hydrothermal alteration of basalt under CO_2-rich condition

*Aoi Murakami[1], Yusuke Sawaki[2], Hisahiro Ueda[3], Yuji Orihashi[4], Shiki Machida[5], Tsuyoshi Komiya[2]

1. Department of Earth and Planetary Science, Graduate School of Science, The University of Tokyo, 2. The University of Tokyo, 3. Tokyo Institute of Technology, 4. Hirosaki University, 5. Chiba Institute of Technology

It is well known that a unique environment is created around seafloor hydrothermal systems by element exchange between circulating seawater and surrounding rocks: enrichment in transition elements and sulfide, emission of quite hot water, and even even electric current flow. In addition, a number of hyperthermophilic microorganisms inhabit around hydrothermal vents. 16S rRNA-based phylogenetic tree suggests that the hyperthermophilic organisms are closest to the earliest lineage; thus the hydrothermal environment is one of the candidates for habitat and evolution of early life.

Phosphorus is one of essential elements for life. In order to maintain an early ecosystem around the hydrothermal vent, phosphorus should have been supplied from the hydrothermal vent through high-temperature water-rock reaction. In the modern basalt-hosted hydrothermal systems, phosphorus is removed due to its adsorption to iron oxide precipitated from hydrothermal fluid and/or formation of metamorphic apatite in the hydrothermally metamorphosed basalt. On the other hand, it is well known that middle Archean basaltic rocks, which constituted upper part of oceanic crust, suffered from severe carbonation during hydrothermal alteration due to quite high atmospheric CO_2 content on the early Earth. Under the CO_2-rich condition, calcium was removed from the seawater/hydrothermal fluid due to extensive carbonate formation. Because the carbonate formation inhibits the formation of apatite, the phosphorus might be released from hydrothermally altered rocks. Actually, the hydrothermally altered basaltic rocks in the Archean are more depleted in phosphorus than hydrothermally altered modern mid-ocean ridge basalt.

In order to quantify phosphorus content of fluid supplied from the basalt-hosted hydrothermal system on the early Earth, we conducted hydrothermal experiments involving hypothetical seawater and basalt under both CO_2-free and CO_2-rich conditions at 200 ˚C, 100 bars. The basalt used in this study was collected from the Indian Ocean Marie Celeste Fracture Zone. The initial solution was prepared by mixture of standard reagents by reference to modern seawater, except for Ca and P. The calcium and phosphorus contents in the solution were regulated to 30 mmol/kg and 0.60 ppm, respectively. The latter is ten times higher than the modern equivalent. For the CO_2-rich experiment, $NaHCO_3$ and HCl were added to the hypothetic seawater to substantialize 400 mmol/kg of ΣCO_2 at the beginning of the experiment.

The CO_2 concentration decreased from 400 mmol/kg to 250 mmol/kg as water-rock reaction advanced, indicating precipitation of carbonate minerals. The SEM-EDS observation demonstrated that the run

©2019. Japan Geoscience Union. All Right Reserved.

products contain calcite, dolomite, and magnesite. Phosphorus content of the fluid decreased to *ca.* 0.10 ppm under the CO_2-rich condition and *ca.* 0.04 ppm under the CO_2-free condition, respectively. The pH value of the produced fluid for the CO_2-rich experiment, measured at room temperature, was 6.6, by *ca.* 2 unit higher than that of the CO_2-free experiment. Calcium concentration decreased from 30 mmol/kg to 25 mmol/kg under the CO_2-free condition. On the other hand, calcium concentration of the formed fluid under the CO_2-rich condition decreased to 18 mmol/kg at 96 hours, and then increased to 25 mmol/kg. The formation of high alkaline and Ca-poor fluid under the CO_2-rich condition suggests that the fluid was oversaturated with carbonate, whereas undersaturated with apatite. Because the produced fluid under the CO_2-rich condition contained more phosphorus than the modern seawater, the basalt-hosted hydrothermal system may have served as a source of phosphorus under the CO_2-rich condition, probably on the early earth.

©2019. Japan Geoscience Union. All Right Reserved.

Origin of chromitites in the Akulleq terrane, southern West Greenland

*Kanta Takahashi[1], Tomoaki Morishita[1], Juan Miguel Ramirez Guotana[1], Kenichiro Tani[2], Yumiko Harigane[3], Ikuya Nishio[1], Kristoffer Szilas[4], Akihiro Tamura[1]

1. Kanazawa University, 2. Department of Geology and Paleontology, National Museum of Nature and Science, 3. Geological Survey of Japan, National Institute of Advanced Industrial Science and Technology (AIST), 4. University of Copenhagen

The studies dealing with the Hadean-Archaean geologic samples are recently expanding. Research on Hadean-Archaean terranes is an important part in reconstructing the geologic past of the Earth which is thought to have differences from the present conditions. Southern West Greenland preserves a wide exposure of ancient geologic materials and structures. This study focuses on chromitites and peridotites from the Ujaragssuit nunāt area in southern West Greenland. The Ujaragssuit nunāt area is about 20 km south from the 3.8 Ga Isua Supracrustal Belt (Moorbath et al., 1977). In Ujaragssuit nunāt, ultramafic rocks occur as lenses of several meters to several hundred meters hosted in silicic gneiss (Chadwick and Crewe, 1986). It is important to understand the origin and processes related to the formation of the peridotites and chromitites in Ujaragssuit nunāt as a contribution to the Archaean magmatic processes and tectonics of the early Earth.

Chromitites are rocks with significant amount of chromites (>20 vol.%) (Arai and Miura, 2016). The unaltered composition of spinel is regarded as a useful petrological indicator (Irvine, 1967). However, chromite composition could be modified as a result of chemical re-equilibration, metamorphism, hydrothermal alteration. The impacts of these processes are evaluated in this study. In Ujaragssuit nunāt, chromitites, dunites and amphibole harzburgites are widely exposed. In some areas, the chromitites occur as layers with thickness ranging from several centimeters to a meter. Massive chromitites (2 m thick) are also exposed. The lithologies present in the area were also described in detail in previous works such as of Rollinson et al. (2002).

Chromites are subhedral and account for about 50-70% of the Ujaragssuit nunāt chromitites. Interstitial grains are mainly phlogopite and minor chlorite and talc. The dunite host consists mainly of olivine (~80%) and accessory spinel and phlogopite. Some spinel grains in the host dunite exhibit zonation as evidenced by darker cores and lighter rims under reflected light microscope and scanning electron microscope observations. The zonation observed is associated with compositional variation from core to rim (Fe enrichment towards the rim). The amphibole harzburgites are mainly composed of amphibole, orthopyroxene, spinel, phlogopite. Orthopyroxenes occur both around olivine and in some parts as inclusions inside olivine grains. Talc replacement of orthopyroxenes is also common. Spinel are surrounded by phlogopite and edenitic amphibole.

Spinel in the host peridotites has a higher Fe^{3+}content. The spinel Fe^{3+} content is higher in samples with higher phlogopite and spinel ratio. This suggests that phlogopite was formed by the reaction of spinel (+olivine) with an alkaline element-rich fluid. Spinel serves as a source of the Al_2O_3 in the phlogopite formation. It is considered that the chemical composition change of spinel is caused by the formation of phlogopite. Furthermore, phlogopite in the sample containing amphiboles has lower K/(K+Na) ratio than samples without amphibole. Amphiboles are also found around the spinel. The K/(K+Na) ratio in the fluid decreases as the alkaline element-rich fluid forms phlogopite and amphibole was formed by the reaction between this differentiated fluid and spinel (+olivine). The abundance of orthopyroxene is higher in the

©2019. Japan Geoscience Union. All Right Reserved.

sample containing amphiboles. The Cr_2O_3- and Al_2O_3- poor characteristic of the orthopyroxenes suggests a secondary origin. The differentiated fluid is also abundant in silica component and reacts with olivine to react to form the secondary orthopyroxenes. Although the possibility of crystal differentiation cannot be completely ruled out, it is thought that these peridotites were originally dunites and chromitites and the chemical composition was modified by alkali alteration.

Keywords: southern West Greenland, chromitite, metasomatism

©2019. Japan Geoscience Union. All Right Reserved.

Metamorphic P–T condition of the Inyoni shear zone rocks in the Barberton Greenstone Belt, South Africa and its significance

*Daichi Kato[1], Kazumasa Aoki[1], Yuta Tsuchiya[2], Shogo Aoki[2], Tsuyoshi Komiya[3]

1. Department of Applied Science,Okayama University of Science, 2. Department of Biosphere-Geosphere Science,Okayama University of Science, 3. Department of Earth Science and Astronomy,University of Tokyo

The metamorphic P–T conditions and processes of the mid-Archean Barberton Greenstone Belt (BGB), South Africa were examined from metamorphosed banded iron formation (BIF) and garnet amphibolite in the Inyoni shear zone (ISZ). Their metamorphic P–T conditions were estimated from thermodynamic calculations combined with several geothermobarometries such as garnet–clinopyroxene geothermometry, Raman geobarometry and Zr-in-sphene geothermometry. Moreover, in order to constrain the protolith age and origin of our studied sample, we conducted zircon U-Pb and trace elements analyses by using Laser Ablation Inductively Coupled Plasma Mass Spectrometry (LA-ICP-MS).The following results were obtained: the P–T conditions of the meta-BIF changed from ca. 600–680 ˚C and 10–12.7 kbar through ca. 510–540 ˚C and 8–11 kbar to less than 500 ˚C and 4 kbar. On the other hand, the P–T conditions of the garnet amphibolite changed from ca. 9.5–10.5 kbar and 620–660˚C to less than 5 kbar and 500 ˚C. Integration of these new results with previous studies for the BGB suggest that the geothermal gradients of the prograde and retrograde metamorphisms were ca. 15–20 ˚C/km and 20–30 ˚C/km, respectively. Igneous zircon separated from the Garnet amphibolite sample yield ^{207}Pb-^{206}Pb age of ca. 3.4-3.2 Ga. This new data together with previous geochronological data indicate that the protoliths of ISZ rocks began to subduct at ca. 3.37-3.24 Ga. The prograde P-T path was kinked at P = 8.0 kbar and T = 560 ℃ by difference in geothermal gradient between crust and upper mantle. The change of geothermal gradient in the ISZ rocks between prograde and retrograde conditions might have relation to the collision of ca. 3.4 Ga Stoluzburg domain. The last P-T trajectory characterized by isothermal decompression might be caused by the intrusion of the ca. 3.23-3.21 Ga TTG Badplaas pluton attendant on plate subduction.

Keywords: Archean, Barberton greenstone belt, Plate tectonics

©2019. Japan Geoscience Union. All Right Reserved.

Discovery of possible traces of asteroid impact within the fossil-bearing carbonaceous chert from the 3.4 Ga Strelley Pool Formation, Pilbara Craton of Western Australia - a preliminary study

*Kenichirio Sugitani[1], Ryoko Senda[3], Tsuyoshi Iizuka[2], Simon Wallis[2]

1. Nagoya University, 2. The University of Tokyo, 3. Kyushu University

Large asteroid impacts are thought to be a common feature of the Archean in particular as a result of the Late Heavy Bombardment (LHB). One line of supporting evidence is the presence of “impact layers” containing silicate spherules that were formed by condensation of rocks vaporized by bombardment events. Two Early Archean impact layers with ages of 3.47 and 3.46 Ga have been identified from the Pilbara greenstone belt, Western Australia (Glikson et al., 2016; Lowe and Byerly, 1986). In contrast 5 separate impact layers with ages of 3.47 to 3.24 Ga have been identified in the Barberton greenstone belt, South Africa (e.g., Lowe et al., 2014; Byerly et al., 2002). Such extraterrestrial impacts likely influenced the Earth’s early environment, including crustal deformation, terrain amalgamation, evaporation of significant volumes of ocean water, and even triggering the development of a modern-like plate tectonic regime (Lowe et al, 2014). It is also reasonable to assume that the early life was influenced significantly by these impacts (Lowe et al., 2003). The early evolution of life might have been accelerated as a consequence of adaptation to such environmental agitations (Kozawa et al., 2018; Oehler et al., 2017). Thus, a close association of traces of life, such as microfossils with cellular preservation, and of impact events recorded in Archean sedimentary successions is of special interest.

In this study we describe the new discovery of traces of asteroid impacts in the ca. 3.4 Ga Strelley Pool Formation (SPF) in the Panorama greenstone belt of the Pilbara Craton, Western Australia. Spherules of possible impact origin were identified in carbonaceous black chert 15 cm thick from which morphologically diverse microfossils have been described (e.g., Sugitani et al., 2013) (Fig. 1). Evidence for an asteroid impact includes the presence of a thin sedimentary layer rich in silicate spherules (Fig. 2) associated with enrichment of platinum-group elements (PGE) (Fig. 3a). However, our detailed analyses revealed that PGE-enrichment is more conspicuous in the lower horizon and are associated with $^{178}Os/^{188}Os$ initial values close to 0.1. In contrast, spherule-rich layers have significantly higher $^{178}Os/^{188}Os$ values ~1.0 (Fig. 3b). One exception is a sample from the upper portion, which has an unusually low value. It is also noteworthy that the spherule-rich layer is enriched in Al and Ti (Fig. 3c). There is a clear higher contribution by clastic materials to this layer, and this feature may explain the apparent contradiction between the PGE-enrichment and Os isotopic values described above. In either case, the layer contains abundant volcanic fragments and clasts in which spherules tend to occur. This occurrence suggests that the spherules were likely reworked from the original site of deposition. A layer composed of carbonaceous grains including rip-up clasts that is found just below the spherule-rich layer (Fig. 1) indicates a steep high-energy depositional environment. This layer contrasts with the fine parallel lamination of carbonaceous chert layers seen at the other horizons, which indicates a quiet depositional environment. We infer that the original impact layer is present below the examined carbonaceous black chert layer and that a high-energy environment related to volcanic activity caused reworking of the spherule-rich deposits, which were transported to the present site of deposition. If this is the case, the high PGE concentrations and the significantly low $^{187}Os/^{188}Os$ initial ratios of the lower cherty samples could be explained as representing the aftermath of an impact event associated with precipitation of vaporized PGE from the atmosphere to the sediment.

©2019. Japan Geoscience Union. All Right Reserved.

References

Byerly et al. (2002) Science 297, 1325-1327; Glikson et al. (2016) Precam. Res. 279: 103-122; Kozawa et al. (2018) *Geobiology* DOI: 10.1111/gbi12319; Lowe et al. (2014) Geology 42: 747-750; Lowe et al. (2003) Astrobiology 3: 7-48; Lowe and Byerly (1986) Geology 14, 83-86; Oehler et al. (2017) Precambrian Research 296, 112-119; Sugitani et al. (2015) Geobiology 13, 507-521.

Keywords: Archean, microfossils, asteroid impact, platinum group elements, osmium isotope

Fig. 1

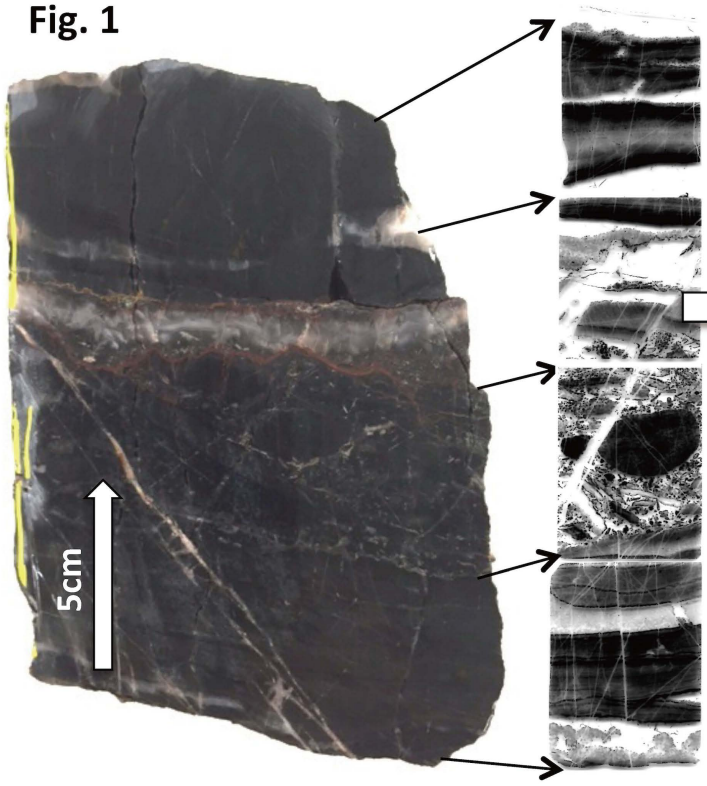

Fig. 2

Fig. 3

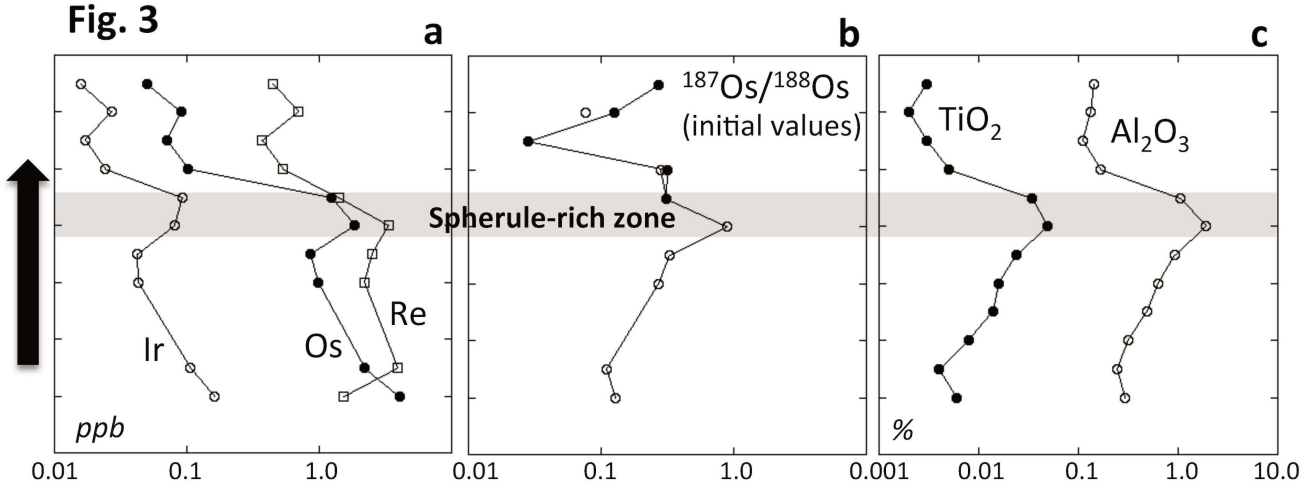

©2019. Japan Geoscience Union. All Right Reserved.

High-resolution stable isotopes and chemical analyses on laminations of the early Proterozoic stromatolite

Yuta Miyanishi[1], Kazuki Takamura[1], *Nagayoshi Katsuta[1], Maki Morimoto[1], ATSUSHI YASUDA[2], Shin-ichi Kawakami[3]

1. Faculty of Education, Gifu University, 2. Earthquake Research Institute, University of Tokyo, 3. Faculty of Education, Gifu Shotoku Gakuen University

In this presentation, we report results of high-resolution analyses on $\delta^{13}C$-$\delta^{18}O$ and chemical compositions of lamination in early Proterozoic stromatolite and then consider the mechanism of the laminae formations and the causes of their fluctuation patterns.

Keywords: Stromatolite, Laminated structure, Stable isotope, Chemical composition

©2019. Japan Geoscience Union. All Right Reserved.

Biogeochemical dynamics in during the Great Oxidation Event constrained by a biogeochemical cycle model

*Yuna Miura[1], Kazumi Ozaki[1]

1. Toho University

The accumulated geological and geochemical data indicate that Earth's ocean-atmosphere system has seen a fundamental increase in oxygen abundances from anoxic conditions (pO_2 <10^{-5} present atmospheric level (PAL)) to oxic conditions (pO_2 >10^{-2} PAL) during the Paleoproterozoic. This marked transition, known as the 'Great Oxidation Event (GOE)', may be accompanied by a transient time of relatively high oxygen levels in the atmosphere and ocean (called an 'oxygen overshoot'). However, the ultimate cause and biogeochemical consequences of the GOE remain unclear.
Harada et al. (2015) hypothesized the snowball Earth glaciation at 2.2 Ga as an ultimate cause of the GOE with a prolonged (~10^8 year) oxygen overshoot. Sedimentary record of iron and manganese oxides above the glacial deposit in the Transvaal Supergroup, South Africa, implies an oxygenation of Earth's surface environments just after the glaciation. The red beds and sulfate evaporites (gypsum, $CaSO_4$) also suggest a sustained oxygenation of the Earth surface environment. They constructed a biogeochemical cycle model of carbon, phosphorous and oxygen, and conducted sensitivity experiments to assess the biogeochemical dynamics after the snowball Earth glaciation. By assuming an atmospheric CO_2 level of 0.7 atm required to end the snowball Earth glaciation, they found that an extremely warm climate accelerates chemical weathering on land and phosphorus riverine input. This marked increase in phosphorus input results in a dramatic increase in biospheric oxygen production, with an oxygen overshoot lasting for ~10^8 years. However, it remains unclear whether their calculations are consistent with available geological constraints (e.g., sulfate evaporite depositions and sulfur isotope data), because they ignore the geochemical cycle of sulfur. A recent geochemical study suggests that concentration of sulfate ($[SO_4^{2-}]$) in the ocean may have been unusually high (>10 mM) during the gypsum formation. If correct, this provides a strong constraint on the biogeochemical conditions.
In this study we constructed a sulfur cycle model with a goal of finding the feasible conditions for the geochemical constraint ($[SO_4^{2-}]$ >10 mM). The model consists of three reservoirs—oceanic sulfate, crustal gypsum, and crustal pyrite. Sulfur enters the ocean through weathering of gypsum and pyrite. We assumed that the oxidative weathering of pyrite is a function of atmospheric O_2 levels and that the gypsum weathering is proportional to the global weathering rate. Sulfur is removed from the ocean via deposition of gypsum and pyrite. We assumed that sulfate burial in the ocean is proportional to seawater sulfate levels. Pyrite burial is assumed to be governed by microbial sulfate reduction dependent on marine sulfate content, biological production (i.e., the availability of organic matter), and oceanic O_2 levels. In this study, we performed a series of sensitivity experiment with a Harada et al.'s model, and obtained biogeochemical dynamics (e.g., atmospheric O_2 levels and weathering rates) were used as a forcing for our sulfur cycle model, enabling us to simulate the evolution of oceanic SO_4^{2-} levels after the glaciation. Our sensitivity experiments of a Harada et al.'s model demonstrate that the biogeochemical dynamics after the glaciation depend mainly on the initial value of atmospheric CO_2 levels: >0.2 bar and >0.25 bar of CO_2 are required for the GOE and the occurrence of an oxygen overshoot, respectively. Our sulfur cycle model, however, demonstrates that 0.25 bar of CO_2 is not sufficient to explain the unusually high levels of $[SO_4^{2-}]$ >10 mM during the overshoot. The systematic sensitivity experiments reveal that at least ~0.75 bar of CO_2 will be required. This result provides an additional support for the hypothesis that the severe glaciation was an ultimate cause of the GOE in the Paleoproterozoic.

©2019. Japan Geoscience Union. All Right Reserved.

Keywords: Great Oxidation Event, biogeochemical cycle, sulfur cycle

©2019. Japan Geoscience Union. All Right Reserved.

Composition of seawater before the Sturtian Snowball Earth estimated by the occurrence of late Tonian evaporitic magnesite

*Aya Miyazaki[1], Akihiro Kano[1], Fumito Shiraishi[2]

1. Department of Earth and Planetary Science, The University of Tokyo, 2. Department of Earth and Planetary Systen Sciences, Hiroshima University

Neoproterozoic is an important period for biological evolution when the spread of algae, protozoan, and multicellular animal were radiated. Understanding of climate changes and fossil records after Ediacaran has been largely improved. But environmental background behind how the Earth’ s surface reached the Snowball Earth state has not been understood.
In Flinders Ranges, South Australia, thick shallow marine sequence preserves excellent geological records especially before and after Sturtian glaciation. This study targets Skillogalee Dolomite exposed at Leigh Creek, Northern Flinders Ranges (LC section) which was deposited around 788±7Ma(Late Tonian) before the Sturtian glaciation (Hood and Wallace 2018). The lithology of LC section contains a small amount of siliciclastics, but mainly consists of shallow water carbonate that exhibits various structures including intraformational conglomerate, stromatolite and tepee structure. However, the most remarkable feature is a large quantity of magnesite. Magnesite alternates with dolostone and occurs as layers of ~1m in thickness or crusts of intraformational conglomerate. The Tepee structure indicates an evaporative environment, and higher d13C and d18O of magnesite indicates that the magnesite deposited after the dolomite. These rocks lack gypsum pseudomorphs.
Evaportive mineral assemblage of the Skillogalee Dolomite can be recognized only in Proterozoic. While the Phanerozoic evaporate sequence starts from Ca carbonate-dolomite, follows to gypsum and halite, but does not include magnesite (Hardie and Eugster 1980). In order to explain this specific mineral assemblage, we made model calculations about the order of precipitated minerals, which expected by continuous evaporation of seawater. Then, we found the Skillogalee mineral sequence was achieved only from seawater of Mg/Ca > 10 and Mg > Alkalinity > Ca. We used sulfate concentration of the modern seawater, but it does no influence to the result. Alkalinity over 10 times higher than the modern level likely reflects from high partial pressure of carbon dioxide or low Ca concentration in seawater. Possible causes of high Mg/Ca ratio were inactive seawater circulation at low mid-ocean ridge, active carbonate sedimentation, or Ca depletion due to extensive evaporite formation including gypsum around 800 Ma. If pH of seawater has been controlled by the solubility equilibrium of CaCO3, the drastic decrease in Ca concentration would encouraged pH rise of sea water and lead to decline of atmospheric carbon dioxide.

Evans 2006, Nature 444, 51-55.
Hardie and Eugster 1980, Science 208, 498-500.
Hood and Wallace 2018. Global and Planetary Change 160, 28-45.

Keywords: Neoproterozoic, evaporite, seawater chemistry

©2019. Japan Geoscience Union. All Right Reserved.

Geochemical characteristics of black shales in the Japanese accretionary complex across the Permian-Triassic boundary extracted by independent component analysis

*Moei Yano[1], Kazutaka Yasukawa[1,3], Koichiro Fujinaga[3,2], Kentaro Nakamura[1], Yasuhiro Kato[2,1,3]

1. Department of Systems Innvation, School of Engineering, The University of Tokyo, 2. Frontier Research Center for Energy and Resources, School of Engineering, The University of Tokyo, 3. Ocean Resources Research Center for Next Generation, Chiba Institute of Technology

The Permian-Triassic boundary (PTB) is characterized by an oxygen-depleted condition in the superocean Panthalassa. However, the degree of the oxygen depletion in deep-sea environments remains an open question.Deep-sea sediments that deposited from the latest Permian to early Triassic constitute black shale within the accretionary complexes of Japan, showing a distinct enrichment of redox sensitive trace metals (e.g., V, Mo, U) that precipitate under reducing conditions.In contrast to the Panthalassa at the PTB, the modern ocean is generally oxygenated from the surface to the bottom due to a sufficiently strong global ocean circulation. However, oxygen-depleted water masses can develop in some specific areas such as restricted basins and coastal upwelling areas, and blackish sediments in these areas show laminated facies and/or high total organic carbon contents reflecting oxygen-depleted conditions.Comparing the black shales at the PTB with the other sediments that deposited in oxygen-depleted conditions can characterize the Panthalassa across the PTB in a context of a broad spectrum of oceanic environmental changes throughout the Earth’ s history. To this end, clarifying geochemical features of multiple elements, especially of redox sensitive trace metals, is quite a useful approach to extract the information of the oceanic environments involving variations in redox conditions. Here we applied independent component analysis to the multi-elemental data set composed of major- and trace-element contents of the samples from the PTB sections within the accretionary complexes of Japan, and black mud and shale of other geological times obtained by scientific drillings in the modern oceans. We will discuss the geochemical characteristics of the PTB black shales and the other blackish sediments, and oceanic environmental conditions across the PTB.

Keywords: Permian-Triassic boundary, black shale, redox sensitive trace metals, independent component analysis, accretionary complex

©2019. Japan Geoscience Union. All Right Reserved.

The Distribution of the Ejecta Deposit derived from Australasian Tektite Event: Implication for the Location of the Impact

*Toshihiro Tada[1], Ryuji Tada[1,2], Paul Carling[3], Wickanet Songtham[4], Le Xuan Thuyen[5], Yu Chang, Eiichi Tajika[1]

1. Department of Earth and Planetary Science, 2. Yunnan University, 3. Geography and Environment, University of Southampton, 4. Northeastern Research institute of Petrified Wood and Mineral Resources, Nakhon Ratchasima Rajabhat University, 5. Ho Chi Minh City University of Science

Tektites are glass spherules formed by large extra-terrestrial impacts and so far reported from 4 strewn fields on the Earth (e.g, McCall, 2001). Australasian tektites—distributed widely from Southeast Asia to Antarctica—are considered to be formed by an impact event at ca. 0.79 Ma in Southeast Asia. This impact event is the youngest among large (diameter of a projectile larger than 1 km) impact events. Because of its young age, it is expected that evidence of the impact (impact crater and ejecta deposits) and the record of environmental perturbation by the impact are well preserved. Therefore, this impact event would serve as an important case study to understand the environmental effects of large impact events on the Earth.

Based on the wide distribution of the tektite—larger than 10% of the Earth’ s surface —the magnitude of the impact has been estimated as large enough to make 30–120 km sized impact crater (e.g., Prasad et al., 2007). The biggest mystery, however, is that no crater has been found and precise location and magnitude of the impact are not well understood.

The location of the impact has been estimated mainly based on the distribution of the tektites. The layered tektites, which are considered to be proximal to the source crater because of their large sizes (larger than 10 cm) and internal inhomogeneity, are distributed in the limited area in Thailand, Laos and Vietnam (Shnetzler, 1992). The number of microtektites per unit area in marine sediment cores decrease with the distance from Indochina peninsula (e.g., Prasad et al., 2007). Such distribution of tektites suggests that the location of the impact is somewhere in the eastern part of Indochina peninsula.

For more precisely constraining the location of the impact, the distribution of the ejecta deposit is important. The ejecta deposit, which is formed by deposition of materials ejected from the source crater, increases its thickness toward the location of the impact. It is also known that the abundance and size of shock-metamorphosed minerals in ejecta deposit increase towards the location of the impact (e.g., Morgan et al., 2006). The ejecta deposit of this impact event, however, has not been reported on the Indochina Peninsula.

In order to identify the ejecta deposit and clarify its distribution in the Indochina Peninsula, we have conducted field surveys in northeastern Thailand, central Vietnam, and southern Laos. We discovered shocked quartz grains—one of the most diagnostic evidence of impact—from the Quaternary sediment unconformably covering the basement rock, and identify the ejecta deposit at Huai Om section located near the border between northeastern Thailand and southern Laos. The ejecta deposit at Huai Om section can be divided into three units: silt–sand layers containing lip-up clasts of the basement rock (Unit 1, approximately 1 m in thickness), a tektite-bearing gravel layer (Unit 2, 20 cm–1 m in thickness), and a massive sand layer (Unit 3, approximately 3 m in thickness), in ascending order.

The tektite bearing gravel layer and the massive sand layer (corresponding to Units 2 and 3 at Huai Om

©2019. Japan Geoscience Union. All Right Reserved.

section) are distributed widely in the eastern part of Indochina Peninsula. Especially, the thickness of the tektite bearing gravel layer (Unit 2) increases toward the area around the southern part of the border between Thailand and Laos. We have measured abundance and size of shocked quartz grains at three sites in northeastern Thailand including Huai Om section. Although the size of shocked quartz grains is similar (approximately 200 μm) among these sites, its abundance varies between 5 and 10% and increases toward the area around the southern part of the border between Thailand and Laos. The distribution of the tektite-bearing gravel layer and abundance of shocked quartz grains indicate that the location of the impact is close to this area.
We are measuring the abundance and size of shocked quartz grains at additional sites in Thailand, Vietnam and Laos. In this presentation, we will report the distribution of the thickness of the ejecta deposit, abundance and size of shocked quartz in the eastern part of Indochina Peninsula to further constrain the location of the impact.

Keywords: Tektite, Shocked quartz, Ejecta, Australasian Tektite

©2019. Japan Geoscience Union. All Right Reserved.

Tectonic-sedimentation reconstruction of Neoproterozoic metavolcanic sequences; the El-Dabbah area, Central Eastern Desert, Egypt

*Shoichi Kiyokawa[1], TAISHI SUZUKI[1], Maher Dawoud[3], El-Hasan Mohamed[3], Kenji Horie[2], Mami Takehara[2]

1. Department of Earth and Planetary Sciences Faculty of sciences, Kyuushu University, 2. National Institute of Polar Research, 3. Department of Geology, Faculty of Science, Menoufiya University,

In the Eastern Desert of Egypt, Neoproterozoic island arc sequence with Banded Iron Formations (BIFs) are reported within volcano-sedimentary sequence whose geological structure and stratigraphy are not well understood. In this study, the geological structure was established to reconstruct the stratigraphy in El Dabbah in the Central Eastern Desert.

It preserves a sequence of relatively undeformed lower greenschist-facies rocks, overlain by subaerial sedimentary strata deposited in strike-slip basins (the Atsham Formation and the Hammamat Group). Reconstructed a stratigraphic–tectonic history of this metavolcanic sequence is understand the Neoproterozoic iron formation stratigraphy and characteristics, which related snowball earth event or not. New geochronological data are used to date the crystallization of granite at *ca.*638.1±2.9 Ma and a rhyodacite at 659.6±3.0 Ma. Four generations of structural deformation have been identified in this area: accretional phase (D_1: 700–680 Ma); strike-slip deformation with transtension, normal faulting, and strong left-lateral shear after the Atsham Formation deposition (D_2: 650–640 Ma); and subaerial sedimentation of the Hammamat Group coincident with the activity of a strike-slip fault and formation of a pull-apart basin (D_3: 638–600 Ma) and followed by extensional deformation. Hear we show stratigraphic and structural interpretation in low grade metamorphosed sequence at the El-Dabbah area, in Central Eastern Desert in Arabian-Nubian Shield.

Keywords: Neoproterozoic, Island arc, strike-slip basin, banded iron formation

©2019. Japan Geoscience Union. All Right Reserved.

[E] Oral | M (Multidisciplinary and Interdisciplinary)：M-IS Intersection

Wed. May 29, 2019 3:30 PM - 5:00 PM JST | Wed. May 29, 2019 6:30 AM - 8:00 AM UTC | 201A 2F

[M-IS07] Astrobiology

convener:Hikaru Yabuta(Hiroshima University, Department of Earth and Planetary Systems Science), Seiji Sugita(Department of Earth and Planetary Science, Graduate School of Science Sciece, The University of Tokyo), Misato Fukagawa(National Astronomical Observatory of Japan), Fujishima Kosuke(Tokyo Institute of Technology, Earth-Life Science Institute), Chairperson:Misato Fukagawa(名古屋大学大学院 理学研究科), Kosuke Fujishima(ELSI 地球生命研究所)

Twenty years have passed since when the field of Astrobiology, which aims to unveil the origins, evolution, and habitability of life by integrating multidisciplinary fields, was established. Individual themes related to Astrobiology, such as chemical evolution in the early Solar System, formation of planetary system, prebiotic chemistry in the early Earth, evolution of life in the Earth's history, extremophile, and habitable planetary environments, has been studied by the knowledge and methods from the multiple fields, which has enabled us to explain "Where we came from" in some ways. However, despite an overwhelming number of investigations and discussions through gathering of the scientists from different fields, there has remained the long-standing unsolved question: How did abiotic materials gain biological function in the Earth and elsewhere in universe? There is still a large gap between prebiotic organic chemistry and biochemistry toward Origins of Life and planetary habitability. Therefore, the JpGU Astrobiology session focuses on pathfinding of "integration of astronomy, geoscience, and biochemistry", which will face an increasing need for the future Astrobiology. In order to enhance our understanding of "What is life", we propose to discuss the biochemical events linked with planetary systems, which is beyond the knowledge in a test tube, by an integration of exoplanets and molecular biology, etc. Through this approach, we will lead the discussions and developments of life-detection strategies for the future exploration of life in universe.

3:30 PM - 3:35 PM JST | 6:30 AM - 6:35 AM UTC

Introduction

3:35 PM - 3:50 PM JST | 6:35 AM - 6:50 AM UTC

[MIS07-01] METEOROID AND DEBRIS IMPACT FLUX IN LOW EARTH ORBIT WITNESSED BY THE TANPOPO CAPTURE PANELS ONBOARD THE ISS IN 2015-2017

*Hajime Yano[1], K. Yamamoto[2], E. Minakami[2], M. Eitel[1,3], S. Sasaki[4], J. Imani[5], K. Okudaira[6], M. Higashide[7], E. Imai[8], Y. Kawaguchi[9], Yoko Kebukawa[10], H. Mita[11], M. Nishi[12], T. Noguchi[13], Makoto Tabata[14], A. Tsuchiyama[12], Hikaru Yabuta[15], K. Arai[8], H. Hashimoto[1], Kensei Kobayashi[10], A. Yamagishi[16] (1.Institute of Space and Astronautical Science, Japan Aerospace Exploration Agency, 2.Hosei University, 3.University of Stuttgart, 4.Tokyo University of Technology, 5.Yuki Seimitsu, Co. Ltd., 6.University of Aizu, 7.JAXA/Aerospace Research and Development Directorate, 8.Nagaoka University of Technology, 9.Chiba Institute of Technology, 10.Yokohama National University, 11.Fukuoka Institute of Technology, 12.Kyoto University, 13.Kyushu University, 14.Chiba University, 15.Hiroshima University, 16.Tokyo University of Pharmacy and Life Science)

3:50 PM - 4:10 PM JST | 6:50 AM - 7:10 AM UTC

[MIS07-02] Growth and transport of dust, ice, and organics in the inner part of protoplanetary disks

★Invited Papers

*Satoshi Okuzumi[1] (1.Department of Earth and Planetary Sciences, Tokyo Institute of Technology)

4:10 PM - 4:25 PM JST | 7:10 AM - 7:25 AM UTC

[MIS07-03] Model Prediction of Complex Organic Molecules in Protoplanetary Disks

*Hideko Nomura[1], Catherine Walsh[2], Tom J. Millar[3] (1.Department of Earth and Planetary Sciences, Tokyo Institute of Technology, 2.School of Physics and Astronomy, University of Leeds, 3.School of Mathematics and Physics, Queen’s University Belfast)

4:25 PM - 4:40 PM JST | 7:25 AM - 7:40 AM UTC

[MIS07-04] Abiotic synthesis of organic matters in environments simulating asteroids and the catalytic effect of minerals on amino acid formation

*Walaa Elmasry[1], Yoko Kebukawa[1], Kensei Kobayashi[1] (1.Yokohama National University)

4:40 PM - 4:55 PM JST | 7:40 AM - 7:55 AM UTC

[MIS07-05] Peptide Formation from amino acid precursors under simulated submarine hydrothermal environments

*Kensei Kobayashi[1], Keisuke Naito[1], Koki Naito[1], Soushi Kuramoto[1], Ei-ichi Imai[2], MITA Hajime[3], Yoko Kebukawa[1] (1.Yokohama National University, 2.Nagaoka University of Technology, 3.Fukuoka Institute of Technology)

4:55 PM - 5:00 PM JST | 7:55 AM - 8:00 AM UTC

Discussion

METEOROID AND DEBRIS IMPACT FLUX IN LOW EARTH ORBIT WITNESSED BY THE TANPOPO CAPTURE PANELS ONBOARD THE ISS IN 2015-2017

*Hajime Yano[1], K. Yamamoto[2], E. Minakami[2], M. Eitel[1,3], S. Sasaki[4], J. Imani[5], K. Okudaira[6], M. Higashide[7], E. Imai[8], Y. Kawaguchi[9], Yoko Kebukawa[10], H. Mita[11], M. Nishi[12], T. Noguchi[13], Makoto Tabata[14], A. Tsuchiyama[12], Hikaru Yabuta[15], K. Arai[8], H. Hashimoto[1], Kensei Kobayashi[10], A. Yamagishi[16]

1. Institute of Space and Astronautical Science, Japan Aerospace Exploration Agency, 2. Hosei University, 3. University of Stuttgart, 4. Tokyo University of Technology, 5. Yuki Seimitsu, Co. Ltd., 6. University of Aizu, 7. JAXA/Aerospace Research and Development Directorate, 8. Nagaoka University of Technology, 9. Chiba Institute of Technology, 10. Yokohama National University, 11. Fukuoka Institute of Technology, 12. Kyoto University, 13. Kyushu University, 14. Chiba University, 15. Hiroshima University, 16. Tokyo University of Pharmacy and Life Science

Twenty-three pairs of silica aerogels and aluminum covers consisted of the Tanpopo capture panels were optically investigated and over 200 hypervelocity impacts signatures were identified and documented for further detailed analyses.
Among them, a low Ca-pyroxene micrometeoroid was captured intact inside the 10mg/cc density silica aerogel. In particular, we compared these data from both space and ram pointing faces of the Tanpopo panels exposed on the International Space Station for deducing meteoroid impact flux by taking into account of effects of local shielding and secondary ejecta impacts. This direct measurement showed that the micrometeoroid impact flux in low Earth orbit in 2015-7 are generally consistent with the previous post-retrieval measurements of LDEF, EuReCa, and SFU in 1980’s to 1990’s.

©2019. Japan Geoscience Union. All Right Reserved.

Growth and transport of dust, ice, and organics in the inner part of protoplanetary disks

*Satoshi Okuzumi[1]

1. Department of Earth and Planetary Sciences, Tokyo Institute of Technology

Dust grains in protoplanetary disks are the fundamental building blocks of planets. Although recent radio interferometric observations have provided us with detailed images of gas and dust in the outer part of protoplanetary disks, it is still poorly understood how solids evolve in the warmer inner regions of the disks. Understanding the physics of gas and dust evolution in the inner part of disks is thus essential to address the question of how Earth-like planets form.

In this talk, I will discuss two topics on the growth and transport of solids (silicates, ices, and organics) in inner protoplanetary disks. The first topic is related to the water content of planets in the habitable zones. Models of protoplanetary disks suggest that the snow line in the dusty disks migrates with time. In the particular case of the solar nebula, the snow line could have moved to the current orbit of Venus in a late stage of its evolution. This raises the question of why the Earth today is so "dry" with the bulk water content of much less than 1 wt%. I will present simulations of ice pebble accretion by terrestrial planetary embryos, showing that Mars-sized rocky embryos would have grown into Neptune-sized waterworlds unless either the solar nebula was compact or a gas giant's core formed early and blocked the inward flux of the ice pebbles. I will also present the results of our latest MHD simulations of protoplanetary disks that imply that the snow line can migrate much faster than expected from the classical accretion model. These results indicate that Earth-like, modestly "water-poor" planets with both oceans and continents do not necessarily form easily in habitable zones.

The second topic is related to the role of organics in the formation of rocky planetesimals. It is widely accepted that silicate grains are poorly sticky and their growth into planetesimal-sized bodies is severely hindered by collisional fragmentation. Here I propose a scenario in which the seeds of rocky planetesimals form through direct coagulation of silicates coated by an organic mantle, like those found in interplanetary dust particles. Our adhesion model for core-mantle particles show that organic-mantled grains are much stickier than bare silicate grains, in particular in warm environments, thanks to the low elasticity of organic matter. I present simulations of the collisional evolution of organic-mantled grains in the inner part of protoplanetary disks, demonstrating that aggregates of organic-mantled grains are able to overcome the fragmentation barrier and directly form km-sized bodies. These organic-rich planetesimals may further evolve into carbon-poor rocky planetesimals by accreting carbon-poor chondrules.

Keywords: protoplanetary disks, planet formation

©2019. Japan Geoscience Union. All Right Reserved.

Model Prediction of Complex Organic Molecules in Protoplanetary Disks

*Hideko Nomura[1], Catherine Walsh[2], Tom J. Millar[3]

1. Department of Earth and Planetary Sciences, Tokyo Institute of Technology, 2. School of Physics and Astronomy, University of Leeds, 3. School of Mathematics and Physics, Queen’ s University Belfast

Protoplanetary disks are the natal place of planets. Understanding chemical components of gas, dust and ice in the disks is essential to investigate the origins of materials in our Solar system and other planetary systems. We investigate the synthesis of complex organic molecules (COMs) in protoplanetary disks using a large gas-grain chemical network including COMs together with a 2D steady-state physical model of a disk irradiated by UV and X-rays from the central star. COMs are efficiently formed on cold and warm grains in the disk midplane via hydrogen adding as well as radical-radical reactions on grain surface. Radiation processing on ice forms reactive radicals and helps build further complexity. Part of the icy molecules are photodesorbed into gas and their transition lines become observable. Actually, ALMA observations have detected CH3CN and CH3OH from protoplanetary disks. The line emitting region of these molecules are the outer relatively cold disk, which suggests that the molecules are non-thermally desorbed from grains following the formation on dust garains. Based on our model calculations, we perform ray-tracing calculations to predict line spectra of complex organic molecules observable with SPICA. Also, we discuss possible connection of COMs in protoplanetary disks to those in the Solar system objects, such as comets.

Keywords: protoplanetary disks, astrochemistry, radiative transfer

©2019. Japan Geoscience Union. All Right Reserved.

Abiotic synthesis of organic matters in environments simulating asteroids and the catalytic effect of minerals on amino acid formation

*Walaa Elmasry[1], Yoko Kebukawa[1], Kensei Kobayashi[1]

1. Yokohama National University

Solar system materials, such as comets, meteorites, and interplanetary dust particles are known to contain extraterrestrial molecules, which might have a heritage from interstellar, nebular, and/or parent body processing. Delivery of these molecules including amino acids to the early Earth may have been important for the origin of life as they are the building blocks of proteins and enzymes. It is suggested that chondritic organic matter was produced through condensation of interstellar formaldehyde, which is an abundant component of the interstellar medium (ISM) organic inventory and, presumably, the solar nebula followed by condensation and carbonization probably during hydrothermal alteration on chondritic asteroids (Cody et al 2011). According to Kebukawa et al. (2013, 2015), the presence of ammonia significantly enhances the formation of organic solids similar to chondritic insoluble organic matter (IOM) from formaldehyde via the formose reaction at 150˚C and could produce amino acids. Carbonaceous chondrites contain abundant clay minerals. Clays may act as absorbents and catalysts for the polymerization of organic interstellar precursor molecules in the early solar system (Pearson et.al 2002).

In this research, we are studying amino acid formation from formaldehyde and ammonia at 150˚C and reveal the expected effect of minerals, namely, montmorillonite clay, olivine and serpentine to simulate the processes of amino acid productions in water-bearing planetesimals.

We synthesized organic compounds using a mixture of water, formaldehyde and ammonia (H_2O, H_2 CO, NH_3) in a ratio of 100:7:1 (mol) with adding minerals (6 mg/ 0.6 mL solution) by simulating primordial materials in comets and asteroids. Aqueous solutions were heated at 150˚C for 24 hours. The resulted products were divided into two parts, the first analyzed using a FT/IR and the other part was acid hydrolyzed, desalted, and subjected to amino acid analysis using a HPLC.

FT/IR spectra indicated that the differences in the spectral intensities are due to synthesis of more organic compounds. In HPLC analysis, various amino acids including glycine and alanine were detected. Presence of non-protein amino acids (β-Ala, γ-ABA) is considered as evidence against terrestrial contamination. Our preliminary results showed that the obtained amount of amino acids was elevated with the presence of minerals. These results suggested that the associated minerals act as catalysts to produce amino acid precursors during aqueous activities in the planetesimals.

References:

1. Cody, G. D. et al. PNAS 108, 19171–19176 (2011).

2. Kebukawa, Y., David Kilcoyne, A. L. & Cody, G. D. The Astrophysical Journal 771, 19 (2013).

3. Kebukawa, Y. & Cody, G. D. Icarus 248, 412–423 (2015).

©2019. Japan Geoscience Union. All Right Reserved.

4. Pearson, V. K. Meteoritics & Planetary Science 37, 1829–1833 (2002).

Keywords: Meteorite, Formaldehyde, Olivine, Serpentine

©2019. Japan Geoscience Union. All Right Reserved.

Peptide Formation from amino acid precursors under simulated submarine hydrothermal environments

*Kensei Kobayashi[1], Keisuke Naito[1], Koki Naito[1], Soushi Kuramoto[1], Ei-ichi Imai[2], MITA Hajime[3], Yoko Kebukawa[1]

1. Yokohama National University, 2. Nagaoka University of Technology, 3. Fukuoka Institute of Technology

Submarine hydrothermal systems have been recognized as one of most promising sites for chemical evolution toward the generation of the first life on the Earth [1]. In order to examine possible reactions in such environments, laboratory simulations by utilizing autoclaves and/or flow reactors have been conducted. Imai et al. reported that peptides were formed when glycine was subjected to heat-quench cycles in a flow reactor simulation submarine hydrothermal systems [2]. Amino acids have been detected in carbonaceous chondrites, and also in the products of experiments simulating interstellar environments. It should be noted that amino acid precursors rather than free amino acids were formed under extraterrestrial environments. Such exogenous amino acid precursors could have been delivered to the primitive Earth and processed in submarine hydrothermal systems. We studied possible reactions of amino acid precursors in simulated submarine hydrothermal environments.

Experimental: We chose the following compounds or materials for hydrothermal experiments: (i) Free glycine (Gly); (ii) aminoacetonitrile (AAN), a Strecker-type precursor; (iii) hydantoin (Hyd), a glycine precursor found in carbonaceous chondrites; (iv) CAW; complex organic molecules formed by proton irradiation of a mixture of CO, NH_3 and H_2O [3]. CAW gave various amino acids after acid hydrolysis, where glycine was predominant. The CAW stock solution used in this study yielded *ca.*10 mM glycine after acid hydrolysis.

In order to simulate submarine hydrothermal reactions, we used a flow reactor, composed of a HPLC pump, an infrared gold image furnace, a cold bath and a backpressure regulator [4]. Injected aqueous samples could be heated up to 400˚C in the furnace, and then quenched in the ice bath (0 ˚C). Carrier used was purified water (neutral) or 1 mM HCl (acidic). In the present study, 0.25 mL of each sample was processed in the furnace at room temperature (reference) or 200-400˚C for 2 min, and then quenched. Amino acids in the effluent were determined by cation exchange HPLC (Shimadzu LC-20 amino acid analyzer with a fluorescence detector) before or after acid-hydrolysis. Peptides were determined by ion-pair HPLC (Shimadzu LC-20 HPLC system with a UV detector).

Results and Discussion: Stability of each material at 300˚C was examined by using 4 mM of Gly, AAN or Hyd, or 10-times diluted CAW. Hyd, AAN and CAW gave some glycine in unhydrolized products. Recovery was calculated by glycine amount after hydrolysis against the reference. Hyd and CAW were more stable than Gly and AAN.

Peptide formation experiments were performed by using 40 mM each of Gly, AAN or Hyd, or the CAW stock solution. Diketopiperazine (DKP; a cyclic dimer of Gly) and diglycine (Gly_2) were detected in the unhydrolized samples after Gly or Hyd was heat-processed. Hyd gave much more Gly_2 and DKP than Gly. The Best yield of Gly_2 was 1.3 %, which was observed when Hyd was processed at 200 or 250˚C under neutral conditions. CAW gave so many peaks in ion-pair chromatograms, so that we could not identify peptides there.

©2019. Japan Geoscience Union. All Right Reserved.

In order to examine possible catalytic abilities of CAW, 10-times diluted CAW was added to 40 mM Gly or 40 mM Hyd and then heat-processed. Yields of Gly_2 were increased when CAW was added to Gly or Hyd and heated at 200˚C under acidic conditions.

It was shown that amino acid precursors such as Hyd and CAW was more stable than free amino acids, and that amino acid precursors like Hyd could yield more peptides than free amino acids. It was also found that CAW (complex amino acid precursors) could facilitate peptide formation. It is known that CAW has amide bonds in its structure, which could be a reason why CAW could work as a condensing agent.

In summary, amino acid precursors were more plausible starting materials than free amino acids in prebiotic reactions in primordial terrestrial environments. Kurihara et al. [5] showed that organic aggregates could be formed from water-soluble organics in hydrothermal environments. It is of interest to examine whether CAW could give such aggregates after processed in the flow reactor.

This work was partly supported by JSPS KAKENHI Grant Number JP17H02991.

References

[1] H. Yanagawa and K. Kobayashi, Orig. Life Evol. Biosph., 22, 147-159 (1995).
[2] E. Imai et al., Science, 283, 831-833 (1999).
[3] Y. Takano et al., Appl. Phys. Lett., 84, 1410-1412 (2004).
[4] Md. N. Islam et al., Bull. Chem. Soc. Jpn., 76, 1172-1178 (2003).
[5] Y. Kurihara et al., Chem. Lett., 41, 441-443 (2012).

Keywords: Submarine hydrothermal systems, Chemical Evolution, Amino acid precursors, Peptides, Flash and quench

©2019. Japan Geoscience Union. All Right Reserved.

[J] Oral | M (Multidisciplinary and Interdisciplinary)：M-IS Intersection

Wed. May 29, 2019 10:45 AM - 12:15 PM JST | Wed. May 29, 2019 1:45 AM - 3:15 AM UTC | 304 3F

[M-IS19] Paleoclimatology and paleoceanography

convener:Yusuke Okazaki(Department of Earth and Planetary Sciences, Graduate School of Science, Kyushu University), Akira Oka(Atmosphere and Ocean Research Institute, The University of Tokyo), Michinobu Kuwae(Center for Marine Environmental Studies), Hitoshi Hasegawa(Faculty of Science and Technology, Kochi University), Chairperson:Yusuke Okazaki

Past environmental changes and events at multi-decadal to tectonic timescale toward an understanding of Earth climate system by an integration of terrestrial and marine proxy studies and numerical modeling will be discussed. At JpGU2019, a series of presentations on present and future climate and environmental changes from paleo-perspective will be held. We welcome a variety of paleo-environmental studies from a wide range of background. We hope that this session will provide an opportunity to promote communication between participants from multidisciplinary field.

10:45 AM - 11:00 AM JST | 1:45 AM - 2:00 AM UTC

[MIS19-01] Development of Longitudinal dunes under the Pangean atmospheric circulation

*Hiroki Shozaki[1], Hitoshi Hasegawa[2] (1.Faculty of Science, Kochi University, 2.Faculty of Science and Technology, Kochi University)

11:00 AM - 11:15 AM JST | 2:00 AM - 2:15 AM UTC

[MIS19-02] Response of primary producers in the ocean anoxic events during the Cretaceous

*Haga Mayuko[1], Eiichi Tajika[1], Kazumi Ozaki[2] (1.The University of Tokyo, 2.Toho University)

11:15 AM - 11:30 AM JST | 2:15 AM - 2:30 AM UTC

[MIS19-03] The linkage between desertification and tectonism inferred from the provenance change of the terrestrial sediments in the Tarim basin

*Aki Sakuma[1], Ryuji Tada[1], Tomohiro Yoshida[1], Hitoshi Hasegawa[2], Naomi Sugiura[1], Akinori Karasuda[1], Ke WANG[1], Hongbo Zheng[3] (1.Department of Earth and Planetary Science, School of Science, the University of Tokyo, 2.Faculty of Science and Technology, Kochi University, 3.School of Resource Environment and Earth Science, Yunnan University)

11:30 AM - 11:45 AM JST | 2:30 AM - 2:45 AM UTC

[MIS19-04] Paleoceanographic reconstruction in the northwestern Pacific during MIS 19 using ultra-high temporal resolution oxygen isotope profiles and planktonic foraminiferal assemblage

*Yuki Haneda[1], Nanako Yokokawa[1], Makoto Okada[1], Hiroki Hayashi[2], Yoshimi Kubota[3], Yusuke Suganuma[4] (1.College of Science, Ibaraki University, 2.Interdisciplinary Factulty of Science and Engineering, Shimane University, 3.National Museum of Nature and Science, 4.National Institute of Polar Research)

11:45 AM - 12:00 PM JST | 2:45 AM - 3:00 AM UTC

[MIS19-05] Paleoclimate reconstruction using fossil pollen analyses from a sedimentary sequence around the Matuyama-Brunhes polarity transition in the Chiba composite section

*Makoto Okada[1], Hitomi Takizawa[1], Yuki Haneda[2], Yusuke Suganuma[3,4], Quentin Simon[5] (1.Department of Earth Sciences, College of Science, Ibaraki University, 2.Graduate school of Science and Technology, Ibaraki University, 3.National Institute of Polar Research, 4.Graduate University for Advanced Studies, 5.Aix-Marseille University)

12:00 PM - 12:15 PM JST | 3:00 AM - 3:15 AM UTC

[MIS19-06] Reconstruction of vertical thermal structure in the western Pacific warm pool over the last 1 Myr

*Fumito Mizuno[1], Takuya Sagawa[2], Keisuke Mukaida[3], Yoshimi Kubota[4], Toshitsugu Yamazaki[5], Junichiro Kuroda[5] (1.Graduate School of Natural Science and Technology. Kanazawa University, 2.Institute of Science & Engineering. Kanazawa University, 3.Collage of Science & Engineering. Kanazawa University, 4.National Museum of Nature & Science, 5.Atmosphere and Ocean Research Institute. The University of Tokyo)

Development of Longitudinal dunes under the Pangean atmospheric circulation

*Hiroki Shozaki[1], Hitoshi Hasegawa[2]

1. Faculty of Science, Kochi University, 2. Faculty of Science and Technology, Kochi University

From the Permian into the Early Jurassic, the supercontinent Pangea dominated our planets. Because of its largest landmass in the Earth’ s history, atmospheric circulation at this period is thought to be significantly different from today. Modelling experiments have suggested cross-equatorial Hadley circulation and its seasonal overturning. However, there are large discrepancy between model-generated surface wind pattern and geological evidence of paleo-wind pattern recorded by eolian sandstones in the central-western U.S.A. Previous study suggested that its discrepancy can be caused by the wrong interpretation of how winds shaped the dune in Pangea. Here, we re-examined Lower Jurassic eolian sandstone records in U.S.A. and reconstructed paleo-wind pattern with focusing on its dune morphology and orientation. Based on the recently revised paleomagnetic reconstructions, sand dune sea was widespread at about 24˚–33˚N. Spatial pattern of paleo-wind directions suggests influence of multi-directed paleo-winds, with dominant westerly winds in northern area and northeasterly winds in southern area. The reconstructed paleo-wind pattern appears to be consistent with the modelling results of paleo-location of subtropical high-pressure belt in the boreal winter of the Early Jurassic. In addition, spatial pattern of eolian slipface orientations suggest that dunes are mainly consists of longitudinal dunes with NNW–SSE orientation in Pangean time, which are markedly different from orientation direction of longitudinal dunes in present desert. We proposed that the development of NNW-SSE oriented longitudinal dunes could be formed by orbitally-induced latitudinal shifts of subtropical high-pressure belt in Pangea supercontinent. Modeling experiments also generated large modulation of strength and location of subtropical high-pressure belt in response to orbital-scale insolation changes. Reconstructed surface wind pattern and different directions of longitudinal dune orientation recorded in Jurassic eolian sandstone records therefore represent a distinct pattern of Pangean atmospheric circulation.

Keywords: Eolian dunes, Navajo sandstone, Pangean supercontinent, Paleowind systems, Atmospheric circulation

©2019. Japan Geoscience Union. All Right Reserved.

Response of primary producers in the ocean anoxic events during the Cretaceous

*Haga Mayuko[1], Eiichi Tajika[1], Kazumi Ozaki[2]

1. The University of Tokyo, 2. Toho University

In the Cretaceous, it is known that the “Ocean Anoxic Events (OAEs)” occurred repeatedly. In the OAEs, marine biogeochemical cycles, biological activity, and process of sedimentation may have been different from those under the oxic condition like today. In fact, biomarkers of cyanobacteria and green sulfur bacteria have been found from the sediments during the OAEs. It is therefore suggested that the redox condition and the primary procedures were quite different at the time of the OAEs. If we regard OAE as a disturbance to the marine biogeochemical cycle system, it is important to understand the response of photosynthetic ecosystem that plays a key role in controlling the ocean redox condition during OAEs.

In the Cretaceous, the climate was warmer and the sea level were higher than today because seafloor spreading rate were very high, hence the shallow water area expanded due to the transgression. Under such conditions, the ocean tends to be oligotrophic and oxic because vast shelf area is locus for the deposition of organic matters and traps large amounts of phosphate and nitrogen (Ozaki et al, 2013). We, however, do not know the marine biogeochemical cycles of nutrients and the behaviors of primary procedures under such a condition in the Cretaceous. We therefore developed a marine biogeochemical cycle model coupled with a marine ecosystem model and investigated the condition of OAEs ,marine biogeochemical cycles of nutrients and the behaviors of primary producers in the Cretaceous.

We found that algae is the dominant primary procedure under the “normal” Cretaceous condition, but once the global surface temperature rises owing to, such as activities of large igneous provinces (LIPs), concentration of phosphate in the ocean increases owing to enhanced chemical weathering of land surface. This leads to increase in the marine primary production which, in turn, promotes anoxic conditions in the ocean because dissolved oxygen is consumed by organic matter decomposition, initiating OAE. In the anoxic ocean, nitrogen is limited because nitrate is consumed by organic matter decomposition and thiodenitrification, inhibiting photosynthetic activity of algae. Cyanobacteria becomes dominant primary procedure because some of them can fix nitrogen. In the upwelling regions, green sulfur bacteria becomes dominant because hydrogen sulfide produced by sulfate reducing bacteria upwells to the euphotic zone.

Keywords: ocean anoxic events, Cretaceous, biomarkers, marine biogeochemical cycle modeling, green sulfur bacteria, cyanobacteria

©2019. Japan Geoscience Union. All Right Reserved.

The linkage between desertification and tectonism inferred from the provenance change of the terrestrial sediments in the Tarim basin

*Aki Sakuma[1], Ryuji Tada[1], Tomohiro Yoshida[1], Hitoshi Hasegawa[2], Naomi Sugiura[1], Akinori Karasuda[1], Ke WANG[1], Hongbo Zheng[3]

1. Department of Earth and Planetary Science, School of Science, the University of Tokyo, 2. Faculty of Science and Technology, Kochi University, 3. School of Resource Environment and Earth Science, Yunnan University

The Tarim basin, which locates to the northwest from the Tibetan Plateau, is the area where the most significant aridification was expected as a result of the uplift of the Himalaya and the Tibetan plateau due to the collision between the Indian subcontinent and the Eurasia continent during Cenozoic (e.g. Kitoh, 2005). However, the geological evidence supporting the relationship between the aridification of the Tarim basin and the tectonism in its surrounding areas is not obtained sufficiently. The reason why the difficulty in examining the relationship between the timing of tectonism and aridification arises is that the timing of the onset of aeolian dune deposition in the Tarim basin, which is the good evidence of the aridification, depends on age models and, thus, there is uncertainty in the timing of the desertification. To solve this problem, it is effective to compare the timing of both tectonic and climatic events on the same section.

In this study, the provenance change of the upper Eocene to the middle Miocene fluvial sandstone deposited in the Aertashi section in the southwestern edge of the Tarim basin was examined using the Electron Spin Resonance (ESR) signal intensity and Crystallinity Index (CI) analyses of quartz in the 64-500 μm fraction and the thin section observation. The timing of the tectonic movement in the Pamir estimated from the provenance change is compared with the timing of the desertification implied by the lithology to examine the relationship between the tectonism and the desertification.

The result of the ESR signal intensity and the CI analyses indicates that the provenance changes of the fluvial sandstone in the Aertashi section are divided into six stages and the boundary between stages are ca. 35Ma, ca. 33Ma, ca. 26Ma, ca. 21Ma, and ca. 17Ma, respectively. Thin section observation shows that the composition of the fluvial sandstone changes significantly at ca. 17Ma with higher content of lithic fragments with wide variety of the types, and the relatively high content of biotite and mafic minerals after ca. 17Ma.
The significant provenance changes at ca. 33Ma, ca. 26Ma, and ca. 17Ma showen by the ESR signal and the CI data imply that the tectonic movement in the Pamir possibly occurred around these times. Since the onset of desertification in the Tarim basin is estimated around 35Ma based on the lithology, the uplift of the Pamir does not seem to have been the cause of the initial aridification in the Tarim basin.

Keywords: Tarim Basin, provenance change, desertification

©2019. Japan Geoscience Union. All Right Reserved.

Paleoceanographic reconstruction in the northwestern Pacific during MIS 19 using ultra-high temporal resolution oxygen isotope profiles and planktonic foraminiferal assemblage

*Yuki Haneda[1], Nanako Yokokawa[1], Makoto Okada[1], Hiroki Hayashi[2], Yoshimi Kubota[3], Yusuke Suganuma[4]

1. College of Science, Ibaraki University, 2. Interdisciplinary Factulty of Science and Engineering, Shimane University, 3. National Museum of Nature and Science, 4. National Institute of Polar Research

The orbital configuration during Marine Isotope Stage (MIS) 19 are characterized by a weak eccentricity-precession forcing and an obliquity maximum associated with a precession minimum as well as MIS 1, although the both absolute values of obliquity are different. Thus, MIS 19c, one of the sub-stages during MIS 19, is assumed as the best analogue for the present interglacial suggesting the timing of the next glacial inception in the future when the anthropogenic influences are excluded.

The Chiba composite section (CbCS) at east-central Japanese island faces the northwestern Pacific containing the Kuroshio Extension Front (KEF) which is north limit of the Kuroshio Current transporting amount of heat and water from the Equatorial to mid-latitude. Modern observation, climate model, and geologic records reveal that variations of the oceanic fronts in the northwestern Pacific (surface temperature and latitudinal position) and atmospheric circulation in the North Pacific interact. However, response of the KEF to external and internal forcings under the modern orbital configuration remain unclear.

Here, we reconstruct detailed paleoceanographic variations in the northwestern Pacific during MIS 19 using stable oxygen isotope ($\delta^{18}O$) and planktonic foraminiferal assemblage records form the CbCS. Spectral and wavelet analyses were conducted in order to assess periodicity of our new $\delta^{18}O$ records. Vertical water temperature structure and their gradient (ΔT), and relative abundance variation of warm-water species exhibit latitudinal displacements of the KEF on multi-millennial scale across the MIS 20–19 transition and during late MIS 19 (MIS 19b to 19a). Results of the spectral and wavelet analyses for the $\delta^{18}O$ records show periodicities of 2,300–6,000 year during late MIS 19. Similarities of timing and periodicity between paleoceanographic records from the CbCS and North Atlantic indicate that disruption of the Atlantic meridional overturning circulation due to freshwater discharge into the North Atlantic caused the southward displacements of the KEF via atmospheric dynamic. A power of the 9,700 year-periodicity in surface planktonic $\delta^{18}O$ and ΔT is stronger during MIS 19c, which probably originates from tropics caused by equatorial insolation at equinoxes with the orbital perihelion. This result indicates the seasonality of the insolation at low-latitudes paced the sea surface condition at the CbCS throughout MIS 19 and this low-latitude influence became larger especially when the North Atlantic forcing by freshwater discharges and AMOC variability was low. Our result suggests that millennial-scale stability and variation of oceanographic condition along the KEF under this orbital configuration depend on North Atlantic climate variability.

Keywords: China composite section, MIS 19, Oxygen isotope, Planktonic foraminifer, northwestern Pacific, Kuroshio Extension Front

©2019. Japan Geoscience Union. All Right Reserved.

Paleoclimate reconstruction using fossil pollen analyses from a sedimentary sequence around the Matuyama-Brunhes polarity transition in the Chiba composite section

*Makoto Okada[1], Hitomi Takizawa[1], Yuki Haneda[2], Yusuke Suganuma[3,4], Quentin Simon[5]

1. Department of Earth Sciences, College of Science, Ibaraki University, 2. Graduate school of Science and Technology, Ibaraki University, 3. National Institute of Polar Research, 4. Graduate University for Advanced Studies, 5. Aix-Marseille University

To examine the “Svensmark effect”, linking climate cooling and geomagnetic field strength decrease, during the time of geomagnetic reversal, we have conducted a pollen analysis in the Chiba Composite Section including the Matuyama-Brunhes polarity reversal boundary, and correlated the quantitative paleoclimatic variation deduced by the modern analog method with the paleomagnetic and ^{10}Be records. The samples used in this study are from 33 horizons in a stratigraphic interval between 4-31 m above the Byk-E tephra bed where the sample density of pollen fossil data used in the previous study (Suganuma et al., 2018) is low. Samples were subjected to KOH-acetolysis treatment (Moore et al., 1991) and hydrofluoric acid treatment as pretreatment to extract pollen fossils. As a result of microscopic examination with an optical microscope, we identified 27 genera in total of 3 families, 24 genera of woody pollen, 2 genus pollen grasses and 2 spores. The abundant pollen fossils are Pinus, and some other genera distributed in the subarctic to cool temperate zones such as Picea, Tsuga, Fagus, etc.
Applying the modern analog method (Nakagawa et al., 2002) to the pollen assemblage data, the reconstructed paleoclimatic parameters show lower overall temperatures than the current study area. Comparing various climatic parameters from the modern analog method with the oxygen isotope records, insolation, ^{10}Be showing the penetration of galactic cosmic ray into the atmosphere and relative paleointensity, the reconstructed climatic parameters showed a variation consistent with paleoceanographic temperatures deduced from oxygen isotopes of planktonic foraminifera. Moreover, we do not recognize any trend of decreasing in air temperature corresponding to geomagnetic field strength collapse at the M-B boundary as reported by Kitaba et al. (2017).

Keywords: Chiba Composite Section, fossil pollen analysis, Matuyama-Brunhes reversal

©2019. Japan Geoscience Union. All Right Reserved.

Reconstruction of vertical thermal structure in the western Pacific warm pool over the last 1 Myr

*Fumito Mizuno[1], Takuya Sagawa[2], Keisuke Mukaida[3], Yoshimi Kubota[4], Toshitsugu Yamazaki[5], Junichiro Kuroda[5]

1. Graduate School of Natural Science and Technology. Kanazawa University, 2. Institute of Science & Engineering. Kanazawa University, 3. Collage of Science & Engineering. Kanazawa University, 4. National Museum of Nature & Science, 5. Atmosphere and Ocean Research Institute. The University of Tokyo

The zonal atmospheric circulation in the tropical Pacific, the Walker circulation, is closely related to the zonal gradients of sea surface temperature (SST) and thermocline through the ocean-atmosphere interaction. Variability of such an interaction in a couple of years timescale is known as El Niño Southern Oscillation (ENSO), which has a great influence on climate not only in the tropics but also in wide areas on the globe. Proxy SST records revealed that the zonal SST gradient has changed in various timescales, and it is interpreted that the ENSO-like ocean-atmosphere interaction also worked on the longer timescale. However, there is no definitive evidence that the change in the zonal SST gradient was accompanied by change of the Walker circulation. Here we reconstruct thermocline temperature variability, which is sensitive to the strength of the Walker circulation. By comparing the variations of zonal and vertical temperature gradients, we examined whether the ENSO-like ocean-atmosphere interaction was functioning on the tens of thousands to hundreds of thousands of years timescale. The sample used in this study is a piston core MR14-02 PC4 collected on the Ontong-Java Plateau located in the western Pacific warm pool (WPWP). Surface and thermocline temperatures were reconstructed by Mg/Ca analyses of planktonic foraminifera, *Globigerinoides ruber* and *Pulleniatina obliquiloculata*, respectively, for the last million years. We compared the vertical temperature gradient (difference between surface and thermocline temperature: ΔT_{WPWP}) and the zonal temperature gradient (difference between *G. ruber* SST in this study and alkenone SST in the East Equatorial Pacific ODP Site 846 : ΔSST_{W-E}). As a result, the relationship between ΔT_{WPWP} and ΔSST_{W-E} in the past was not similar to that of the modern ENSO variability. This result suggests that the change of temperature structure in longer timescale was caused by a mechanism different from today. Also, ΔT_{WPWP} and ΔSST_{W-E} showed a longer time scale change than the glacial-interglacial cycles, and the cycle is approximately 400 kyr. This implies that the thermocline variability in the equatorial Pacific might be related to the Milankovitch cycle. The results of this study suggest that it is necessary to discuss vertical and meridional thermal structures in addition to the zonal SST gradient in order to understand the dynamics of past ocean-atmosphere interaction.

Keywords: Western Pacific warm pool, Planktonic foraminifera, Reconstruction of old water temperature

©2019. Japan Geoscience Union. All Right Reserved.

[J] Oral | M (Multidisciplinary and Interdisciplinary)：M-IS Intersection

Wed. May 29, 2019 1:45 PM - 3:15 PM JST | Wed. May 29, 2019 4:45 AM - 6:15 AM UTC | 304 3F

[M-IS19] Paleoclimatology and paleoceanography

convener:Yusuke Okazaki(Department of Earth and Planetary Sciences, Graduate School of Science, Kyushu University), Akira Oka(Atmosphere and Ocean Research Institute, The University of Tokyo), Michinobu Kuwae(Center for Marine Environmental Studies), Hitoshi Hasegawa(Faculty of Science and Technology, Kochi University), Chairperson:Michinobu Kuwae(愛媛大学沿岸環境科学研究センター)

Past environmental changes and events at multi-decadal to tectonic timescale toward an understanding of Earth climate system by an integration of terrestrial and marine proxy studies and numerical modeling will be discussed. At JpGU2019, a series of presentations on present and future climate and environmental changes from paleo-perspective will be held. We welcome a variety of paleo-environmental studies from a wide range of background. We hope that this session will provide an opportunity to promote communication between participants from multidisciplinary field.

1:45 PM - 2:00 PM JST | 4:45 AM - 5:00 AM UTC

[MIS19-07] Future perspective on the response of marine calcifiers to “evil twins” of climate change due to increased PCO2

*Hodaka Kawahata[1] (1.Atmosphere Ocean Research Institute, the University of Tokyo)

2:00 PM - 2:22 PM JST | 5:00 AM - 5:22 AM UTC

[MIS19-08] Reconstruction of seawater pH and atmospheric CO_2 concentration based on boron isotopic composition of biogenic calcium carbonate

★Invited Papers

*Kaoru Kubota[1] (1.Kochi Institute for Core Sample Research, JAMSTEC)

2:22 PM - 2:37 PM JST | 5:22 AM - 5:37 AM UTC

[MIS19-09] A 70 years changes of the Java Sea surface condition based on geochemical analyses of a coral core

*Ai Genda[1], Atsushi Suzuki[2], Toyoho Ishimura[3], Minoru Ikehara[4], Mayuri Inoue[1] (1.Graduate School of National Science and Technology, Okayama University, 2.Geological Survey of Japan Natinal Institute of Advanced Industrial Science and Technology, 3.National Institute of Technology, Ibaraki College, 4.Center for Advanced Marine Core Research, Kochi University)

2:37 PM - 2:52 PM JST | 5:37 AM - 5:52 AM UTC

[MIS19-10] Reconstruction of paleoenvironments in the western Pacific for the last 220 years

Mutsumi Chihara[1], Ayaka Fukushima[2], Minoru Ikehara[3], Hodaka Kawahata[2], Atsushi Suzuki[4], *Mayuri Inoue[1] (1.Department of Earth Sciences, Okayama University, 2.Atmosphere and Ocean Research Institute, the University of Tokyo, 3.Center for Advanced Marine Core Research, Kochi University, 4.Geological Survey of Japan, AIST)

2:52 PM - 3:15 PM JST | 5:52 AM - 6:15 AM UTC

[MIS19-11] Ocean deoxygenation from the Last Glacial Maximum to the future global warming: inshight from model simulations

★Invited Papers

*Akitomo Yamamoto[1], Ayako Abe-Ouchi[2,1], Rumi Ohgaito[1], Akinori Ito[1], Masahito Shigemitsu[1], Yasuhiro Yamanaka[3], Akira Oka[2] (1.Japan Agency for Marine-Earth Science and TechnologyAtmosphere and Ocean Research Institute, 2.Atmosphere and Ocean Research Institute, The University of Tokyo, 3. Faculty of Environmental Earth Science, Hokkaido University)

Future perspective on the response of marine calcifiers to “evil twins” of climate change due to increased PCO2

*Hodaka Kawahata[1]

1. Atmosphere Ocean Research Institute, the University of Tokyo

This talk is developed from our comprehensive review paper of PEPS: Kawahata, H., Fujita, K., Iguchi, A, Inoue, M., Iwasaki, S., Kuroyanagi, A., Maeda, A., Manaka, T., Moriya, K., Takagi, H., Toyofuku, T., Yoshimura, T., Suzuki, A. (2019) Perspective on the response of marine calcifiers to global warming and ocean acidification –Behavior of corals and foraminifera in a high CO2 world “hot house”. Progress in Earth and Planetary Science 6: 5 (p.1-37).

Our planet will experience global warming and ocean acidification due to increased partial pressure of CO2 in the atmosphere. They are often referred to as the “evil twins” of climate change, potentially inducing severe threats in the near future.

Generally, majority of marine calcifying organisms show decreases in calcification rates in response to acidified seawater by increased pCO2. However, the response often differs depending on situations, species, and life-cycle stage. Calcification of Calcarina gaudichaudii, generally increased with increased pCO2. As one possible cause of these different sensitivities, Calcarina hosts diatoms as its symbiotic algae. High-CO2 seawater is favorable to diatom growth.

X-ray micro-computed tomography will provide valuable information regarding biomineralization including calcification of planktic and benthic foraminifera in response to ocean acidification as well as regarding carbonate dissolution.

Based upon the analysis of the biogeochemical cycle (today, at P/E boundary and in Cretaceous), “high speed” and “high level” pCO2 are the primary and secondary factors, respectively, leading to acidification in the Earth surface’s system. Over the long-term, it is well known that alkalinity has fluctuated largely in the Earth’s surface environment. Therefore, it is important to quantitatively reconstruct alkalinity, which is another key factor determining the saturation state of carbonate minerals.

Keywords: global warming, ocean acidification , calcifiers, carbonate, alkalinity

©2019. Japan Geoscience Union. All Right Reserved.

Reconstruction of seawater pH and atmospheric CO_2 concentration based on boron isotopic composition of biogenic calcium carbonate

*Kaoru Kubota[1]

1. Kochi Institute for Core Sample Research, JAMSTEC

A lot variety of environmental information is recorded in marine biogenic calcium carbonate that is represented by reef building coral skeletons and foraminifera shells. Among these, **boron isotope ($\delta^{11}B$)** proxy is of great importance in the realm of paleoclimatology and paleoceanography, since it can record seawater pH and CO_2 concentration of the overlying atmosphere. Along with the growing interest to recent environmental problems such as global warming and ocean acidification due to anthropogenic CO_2 emission, past carbon cycle research has been actively conducted, and boron isotope proxy is priceless tool to study it. In 1980s, applicability of this proxy was foreseen, but high precision boron isotope measurement with small sample requirement was difficult at that time. As boron exist abundantly around us (the most representative one is borosilicate grass), analytical technique has evolved as the boron-free clean environment improved. Thermal ionization mass spectrometry (**TIMS**) was first developed, and nowadays multi-collector inductively coupled plasma mass spectrometry (**MC-ICPMS**), secondary ionization mass spectrometry (SIMS), and laser-ablation inductively coupled plasma mass spectrometry (LA-ICPMS) (and others) is now available. Measurable minimum sample amount, achievable analytical precision, and spatial resolution of the analysis are largely different among methods, and efforts to measure boron isotope composition more precisely with smaller amount of samples has continued at research institutes around the world. In **Kochi Institute for Core Sample Research, Japan Agency for Marine-Earth Science and Technology**, boron isotope measurements by using TIMS and MC-ICPMS are available: the former realizes the most precise measurement in the world, and the latter realizes analytical precision and required sample amount that is comparable with major overseas laboratory. In this presentation, I will explain theoretical background why boron isotope of marine biogenic calcium carbonate becomes seawater pH proxy and characteristics of two different mass spectrometry, and then overview already-done research and ongoing research topics. Recent development of visualization technology of pH of calcifying fluid of reef building coral and foraminifera has enabled deeper understandings of boron incorporation systematics. On the one hand, boron isotopes of reef building coral is most-likely a direct indicator of pH of calcifying fluid; on the other hand, those of foraminifera is likely influenced by microenvironment pH gradient surrounding foraminifera. Whatever the mechanism is, a clear relationship between boron isotopes and seawater pH is observed in various samples such as cultured, recently live-collected, and fossil samples, thus many studies use this proxy in paleoclimatology and paleoceanography by understanding empirical relationship collectly ("calibration").

Keywords: boron isotope, coral, foraminifera, carbon cycle, calcification, carbon dioxide

©2019. Japan Geoscience Union. All Right Reserved.

A 70 years changes of the Java Sea surface condition based on geochemical analyses of a coral core

*Ai Genda[1], Atsushi Suzuki[2], Toyoho Ishimura[3], Minoru Ikehara[4], Mayuri Inoue[1]

1. Graduate School of National Science and Technology, Okayama University, 2. Geological Survey of Japan Natinal Institute of Advanced Industrial Science and Technology, 3. National Institute of Technology, Ibaraki College, 4. Center for Advanced Marine Core Research, Kochi University

At Indonesian Archipelago, observed and instrumental records have not been well recorded because of complex terrain. In this study, we have reconstructed sea surface condition of the Java Sea for past 70 years based on $\delta^{13}C$, Sr/Ca and U/Ca ratios in the coral skeleton.
A coral core (*Porites* sp.) was collected from the the Seribu Islands located at the Java Sea, Indonesia. Measurements of Sr/Ca, U/Ca ratios and $\delta^{13}C$ were performed by inductively coupled plasma (ICP)-optical emission spectrometer, ICP-mass spectrometer and stable isotope ratio mass spectrometer with about 2-month time resolution.
Although it has been reported that both coral Sr/Ca and U/Ca ratios can be used as paleothermometer [Beck et al., 1992; Min et al., 1995], coral U/Ca ratios also depends on seawater pH [Inoue et al., 2011] and carbonate ion concentration ($[CO_3^{2-}]$) [Anagnostou et al., 2011]. Furthermore, since coral $\delta^{13}C$ reflects DIC of ambient seawater, we will discuss about marine environments such as water temperature and seawater pH at the Java Sea for 70 years.

©2019. Japan Geoscience Union. All Right Reserved.

Reconstruction of paleoenvironments in the western Pacific for the last 220 years

Mutsumi Chihara[1], Ayaka Fukushima[2], Minoru Ikehara[3], Hodaka Kawahata[2], Atsushi Suzuki[4], *Mayuri Inoue[1]

1. Department of Earth Sciences, Okayama University, 2. Atmosphere and Ocean Research Institute, the University of Tokyo, 3. Center for Advanced Marine Core Research, Kochi University, 4. Geological Survey of Japan, AIST

In the tropics, *Porites* corals are recognized as the excellent archives of past climate and environmental and oceanic conditions because coral skeletal geochemistry, such as oxygen and carbon isotopes and Sr/Ca ratios, provides quantitative information on sea surface temperature (SST) and salinity. However, continuous long records more than 200 years based on coral records have been limited.

Here, we present a 224-year SST record with high time resolution (~2 month) derived from Sr/Ca ratios and stable isotopes ($\delta^{18}O$ and $\delta^{13}C$) from Philippines (13°N, 124°E), which located on the northern edge of the western pacific warm pool (WPWP).

Coral Sr/Ca was measured by an inductively coupled plasma optical/atomic emission spectrometer (ICP-OES/AES) with a precision was better than 0.6 % which is equivalent to 0.5 ℃. Analyses of $\delta^{18}O$ and $\delta^{13}C$ were measured by isotope ratio mass spectrometer (IR-MS). Precision was better than 0.05 ‰for $\delta^{13}C$ and 0.10 ‰for $\delta^{18}O$. In this study, spectral analysis was performed by using the kSpectra. Reconstructed SST varies from 25 to 32 ℃ and shows that there were multiple cold events during the last 224 years in the western tropical Pacific. A decreasing trend in $\delta^{13}C$ for the last 50 years was found which may reflect accelerated increase in the amount of anthropogenic CO_2 (Suess effect).The result of $\delta^{18}O$ analyses implies western pacific climate was cooler and drier in the early 19th century which is almost consistent with other coral records. In contrast, warmer and wetter conditions persist since 1950s.The spectral analysis of the annual SST and $\delta^{18}O$ anomaly for 224 years shows significant peaks at 3-8 years. These frequencies are considered to be related to the ENSO variability.

Keywords: the western Pacific, coral skeleton, paleoclimate

©2019. Japan Geoscience Union. All Right Reserved.

Ocean deoxygenation from the Last Glacial Maximum to the future global warming: inshight from model simulations

*Akitomo Yamamoto[1], Ayako Abe-Ouchi[2,1], Rumi Ohgaito[1], Akinori Ito[1], Masahito Shigemitsu[1], Yasuhiro Yamanaka[3], Akira Oka[2]

1. Japan Agency for Marine-Earth Science and TechnologyAtmosphere and Ocean Research Institute, 2. Atmosphere and Ocean Research Institute, The University of Tokyo, 3. Faculty of Environmental Earth Science, Hokkaido University

Global warming is expected to decrease ocean oxygen concentration by less solubility of surface ocean, reduced ventilation and enhanced stratification. The associated expansion of the oxygen minimum zone would have adverse impact on marine organisms and ocean biogeochemical cycles. Earth system models show a consistent deoxygenation trend over the twenty-first century; however, longer-term changes in ocean oxygen are still unclear due to the uncertain response of deep ocean circulation.

During the Last glacial maximum, recent proxy data show that, despite greater oxygen solubility due to sea surface cooling, the oxygen concentrations throughout the deep ocean were generally lower. These records provide the response of oxygen content to climate forcing that are comparable in magnitude to the expected future changes. Therefore, the understanding of glacial deoxygenation will help us to better understand and predict future oxygen changes. In addition, glacial deep-water deoxygenation is crucial to understand glacial-interglacial CO_2 change, since glacial deoxygenation reflects increased accumulation of respired carbon in the glacial deep ocean. However, the mechanisms of deep-water deoxygenation and contribution form the biological pump to glacial CO_2 drawdown are poorly understood due to the difficulties in reproducing glacial deoxygenation.

In this study, we report the importance of glaciogenic dust for the glacial deep-water deoxygenation from our numerical simulation which successfully reproduces the magnitude and large-scale pattern of the observed oxygen changes from the present to Last Glacial Maximum. Sensitivity experiments reveal that physical changes (e.g., more sluggish ocean circulation) contribute to only half of all glacial deep deoxygenation, whereas the other half is driven by enhanced efficiency of the biological pump. We found that iron input from the glaciogenic dust with higher iron solubility is the most significant factor for enhancement of the biological pump and global deep-water deoxygenation. The model-proxy agreement of oxygen change supports the simulated contribution of the enhanced biological pump to the decrease of more than 30 ppm of glacial CO_2.

On the other hand, our model underestimates deoxygenation in the deep Southern Ocean due to enhanced ventilation in the Southern Ocean. Our results suggest that the stratified Southern Ocean is required for reproducing glacial deoxygenation in the Southern Ocean. However, present climate models cannot reproduce the stratified Southern Ocean. A possible reason is that climate models are too coarse to capture the process of dense water formation on the Antarctic shelf and tend to underestimate the strength of stratified Southern Ocean. Similar to glacial oxygen changes, our global warming simulation show that changes in ocean circulation in the Southern Ocean are crucial for long-term projecting future oxygen changes associated with global warming. Therefore, the understanding of glacial oxygen changes will help us to better understand and predict future oxygen changes.

©2019. Japan Geoscience Union. All Right Reserved.

Keywords: Dissolved oxygen, Glacial-interglacial cycle, Global warming, Ocean carbon cycle, Ocean biogeochemical model

©2019. Japan Geoscience Union. All Right Reserved.

[J] Oral | M (Multidisciplinary and Interdisciplinary)：M-IS Intersection

Wed. May 29, 2019 3:30 PM - 5:00 PM JST | Wed. May 29, 2019 6:30 AM - 8:00 AM UTC | 304 3F

[M-IS19] Paleoclimatology and paleoceanography

convener:Yusuke Okazaki(Department of Earth and Planetary Sciences, Graduate School of Science, Kyushu University), Akira Oka(Atmosphere and Ocean Research Institute, The University of Tokyo), Michinobu Kuwae(Center for Marine Environmental Studies), Hitoshi Hasegawa(Faculty of Science and Technology, Kochi University), Chairperson:Akira Oka

Past environmental changes and events at multi-decadal to tectonic timescale toward an understanding of Earth climate system by an integration of terrestrial and marine proxy studies and numerical modeling will be discussed. At JpGU2019, a series of presentations on present and future climate and environmental changes from paleo-perspective will be held. We welcome a variety of paleo-environmental studies from a wide range of background. We hope that this session will provide an opportunity to promote communication between participants from multidisciplinary field.

3:30 PM - 3:52 PM JST | 6:30 AM - 6:52 AM UTC

[MIS19-12] Extraction of high-quality ^{14}C data from terrestrial sediments containing pollen fossils

★Invited Papers

*Takayuki Omori[1], Keitaro Yamada[2], Ikuko Kitaba[2], Takeshi Nakagawa[2] (1.The University Museum, The University of Tokyo, 2.Research Centre for Palaeoclimatology, Ritsumeikan University)

3:52 PM - 4:07 PM JST | 6:52 AM - 7:07 AM UTC

[MIS19-13] Oxygen isotope fluctuations of pollen fossils from Lake Suigetsu, Japan

*Keitaro Yamada[1], Takayuki Omori[2], Ikuko Kitaba[1], Takeshi Nakagawa[1] (1.Research Organization of Science and Technology, Ritsumeikan University, 2.The University museum, The University of Tokyo)

4:07 PM - 4:22 PM JST | 7:07 AM - 7:22 AM UTC

[MIS19-14] Reconstruction of lake-level changes during the last glaciation based on fossil diatom record in Lake Biwa

*Takashi Suzuki[1], Yoshio Inouchi[2], Keisuke Otsuka[1], Kaoru Kawakami[3] (1.Graduate School of Human Science, Waseda University, 2.Faculty of Human Sciences, Waseda University, 3.Graduate School of Environmental Science, Hokkaido University)

4:22 PM - 4:45 PM JST | 7:22 AM - 7:45 AM UTC

[MIS19-15] An estimation of microplatcis sedimentation flux in a coastal sea

★Invited Papers

*Hirofumi Hinata[1], Michinobu Kuwae[1], Issei Masumoto[1], Hayato Kawamata[1] (1.Ehime University)

4:45 PM - 5:00 PM JST | 7:45 AM - 8:00 AM UTC

[MIS19-16] Beppu Bay sediments: Potential palaeoenvironmental archives for a candidate auxiliary stratotype for Anthropocene-Holocene boundary

*Michinobu Kuwae[1], Yoshiaki Suzuki[2] (1.Center for Marine Environmental Studies, Ehime Univ., 2.Department of Eearth Scieces, Fuculty of Education and Integrated Arts and Sciences, Waseda Univ.)

Extraction of high-quality ^{14}C data from terrestrial sediments containing pollen fossils

*Takayuki Omori[1], Keitaro Yamada[2], Ikuko Kitaba[2], Takeshi Nakagawa[2]

1. The University Museum, The University of Tokyo, 2. Research Centre for Palaeoclimatology, Ritsumeikan University

Fossil pollen grains, which are commonly found in various types of sediments, have great potential for radiocarbon chronological research. If measurable amounts of fossil pollen grains can be extracted readily from sediment matrices, then ^{14}C age determination could be performed at any depositional depth, regardless of with or without plant macrofossils, and the quality of the deposition age model can be considerably increased. Thus far, several lake sediments have been tested for pollen ^{14}C. However, technical issues such as complex preparation procedures, collection rate, and purity of concentrated sample persisted and pollen ^{14}C analysis has not been applied routinely. A novel pollen concentration method is developed herein using a next-generation cell sorter to quickly prepare pure concentrates of fossil pollen grains suitable for ^{14}C dating, with a relatively simple preparation procedure.
Cell sorter was originally developed for biomedical researches to instantaneously identify and separate cells of specific fluorescence and shape. Some of the latest model machines can perform machine tuning and sample preparation semi-automatically, and it is designed to solve most issues via the exchange of replacement parts. In the proposed method of pollen purification, pollen-enriched suspension is introduced into cell sorter, which can separate more than a million grains of fossil pollen in half a day. The pollen ^{14}C analysis was conducted using a SG06 sediment core from Lake Suigetsu, which has one of the most reliable age models that we can use as reference. Pollen fossil samples equivalent to 50–100 μgC were extracted from ca. 25-30 g of wet sediment and were measured using a compact AMS system (NEC 0.5 MV 1.5SDH-1) of LRD.UMUT. The ^{14}C data of the pure pollen samples agreed well with the Suigetsu's ^{14}C dataset on terrestrial plant leaf fossils. This result shows that accurate ^{14}C data can be obtained from any depth of the core, even at depths at which plant remains are not present. Using the proposed method, the Suigetsu's ^{14}C data can be enhanced for data density and evenness of the data intervals, both of which would directly contribute to the accuracy of the age model. We also believe that the proposed method can be applied to various sediment types from both marine and terrestrial realms, and will assist high-precision chronological study as well as quantification of marine reservoir age.

Keywords: Radiocarbon dating, Pollen fossil, Cell sorter, Suigetsu

©2019. Japan Geoscience Union. All Right Reserved.

Oxygen isotope fluctuations of pollen fossils from Lake Suigetsu, Japan

*Keitaro Yamada[1], Takayuki Omori[2], Ikuko Kitaba[1], Takeshi Nakagawa[1]

1. Research Organization of Science and Technology, Ritsumeikan University, 2. The University museum, The University of Tokyo

Interactions of atmospheric, marine, terrestrial, and cryospheric realms are important factors in considering mechanisms of climate change (Lowe et al., 2008). Pollen analysis widely used methods to reconstruct past climate changes. However, comparing pollen data with other geochemical proxies, especially stable isotope signals, is not straightforward due to the non-linearity included in the conventional pollen composition signals. On the other hand, pollen grains are composed of sporopollenin and potentially provide isotopic signals which can be more directly compared with key palaeoclimatic records from across the world (Loader and Hemming, 2004). In this study, we first established a method to extract fossil pollen grains from sediment matrix by “cell sorter”. Then we applied that new method to the varved sediments obtained from Lake Suigetsu, Japan (in particular, transition from the Lateglacial to the early Holocene) in order to test if the isotopic signals of pollen grains are keeping meaningful palaeoclimatic information or not.

Lake Suigetsu (35˚35'N, 135˚53'E, 0 m a.s.l.), Fukui prefecture, is one of the Mikata Five lakes, which measures 3 km east-west by 3 km north-south, with the maximum water depth of ca. 34 m. Lake Suigetsu preserves annually laminated sediments over the last ca.70 kyr with a significant number of event layers that allows precise correlation among parallel cores. Two long cores (SG93, SG06) have previously been recovered from the centre of the lake. An exceptionally precise age model has been established for the cores through a combination of over 800 radiocarbon (^{14}C) dates and high precision varve count (Staff et al., 2011; Marshall et al., 2012; Schlolaut et al., 2012; Bronk Ramsey et al., 2012). In this study, we used well-dated SG06 cores and extracted pollen fossils using cell sorter.

Cell sorter is able to characterise particles using optical parameters (mainly fluorescence), and separate specific particles using electrostatic deflection. Pollen fossils can be isolated by cell sorter without fluorescent dyes using cell sorter because sporopollenin constituting pollen grains is naturally auto-fluorescent (Tennant et al., 2013). After chemical and physical pre-treatments, pollen-enriched suspension was introduced into the cell sorter and extracted half a million pollen fossils from each sample. After drying and weighing, δ^{18}O value of the high-purity pollen pellets were determined using High Temperature Conversion Elemental Analyzer (TC/EA, Thermo Scientific) in the University of Tokyo.

The oscillation of the δ^{18}O value of the extracted pollen pellets roughly mirrored that of the NGRIP, showing typical climatic transitions that characterise the Late glacial period. Our results strongly imply that the stable isotope signal of fossil pollen grains is keeping record of past climate changes.

Keywords: Palaeoclimate, Stable isotope, Pollen, Cell sorter, Suigetsu

©2019. Japan Geoscience Union. All Right Reserved.

Reconstruction of lake-level changes during the last glaciation based on fossil diatom record in Lake Biwa

*Takashi Suzuki[1], Yoshio Inouchi[2], Keisuke Otsuka[1], Kaoru Kawakami[3]

1. Graduate School of Human Science, Waseda University, 2. Faculty of Human Sciences, Waseda University, 3. Graduate School of Environmental Science, Hokkaido University

This is a report of a research for reconstruction of lake-level change history of Lake Biwa based on the transfer function of diatom assemblage into water depth. We have analyzed diatom assemblages, sand content, and C/N ratio in drilling core sample from the lake bottom of 23.45 m in depth and surface sediment samples from the lake bottom from 5 m to 30 m in depth off estuary of Echi River, Lake Biwa. The relative abundance of planktonic species in diatom assemblage from surface sediments can be changed into water depth. The transfer function applied to fossil diatom record in drilling core sample into lake-level change history during the last 50 ka.
We compared the record with Sanbao & Hulu cave stalagmites $\delta^{18}O$ records in China and NGRIP $\delta^{18}O$ record in Greenland from 50 ka to 10 ka. The result shows that the lake-level change history in Lake Biwa reflects East Asian winter monsoon intensity. Lake-level rose under relatively cold conditions or abrupt cooling like Heinrich Events and lake-level fell under relatively warm conditions. The lake-level response to climate conditions suggests that snowfall in winter depending on East Asian winter monsoon intensity mainly contributed to water balance of Lake Biwa during the last glacial period.

Keywords: Lake Biwa, Planktonic diatom, Transfer Function, Lake-level change, East Asian winter monsoon

©2019. Japan Geoscience Union. All Right Reserved.

An estimation of microplatcis sedimentation flux in a coastal sea

*Hirofumi Hinata[1], Michinobu Kuwae[1], Issei Masumoto[1], Hayato Kawamata[1]

1. Ehime University

Plastics production has been increasing each year. It is estimated that 4.8-12.7 million tons of plastics flowed out into the ocean in 2010. The plastics weathers due to UV degradation and fragmented into small pieces. Generally, the plastic particles of the 0.3-5mm in size are called microplastics. They are likely to be incorporated into the ecosystem and there is concern about bad influence on ecosystem. Recent studies have found that microplastics sink to the sea bottom. However, the sedimentation flux has not been clarified yet. In this study, the sedimentation flux of microplastics was estimated. We collected and analyzed the sediment cores from the bottom of Beppu Bay. Beppu Bay is suitable for the core sampling, because sediments have not been vertically disturbed.Five cores were taken using Gravity Corer. Four sediment cores were for microplastic analysis, and one for dating sediment layers. The sedimentary age was determined using the Pb-210 method. Microplastics extracted from the four core samples were analyzed by FT-IR to determine the polymer type. A total of 142 pieces of microplastic were detected. The most common polymer type among plastics was polyethylenewhich accounted for 55% of the total in number. The average sedimentary flux from 1998 to 2017 was calculated as 217 [pieces/m^2·y)].

Keywords: microplastics, sedimentation flux

©2019. Japan Geoscience Union. All Right Reserved.

Beppu Bay sediments: Potential palaeoenvironmental archives for a candidate auxiliary stratotype for Anthropocene-Holocene boundary

*Michinobu Kuwae[1], Yoshiaki Suzuki[2]

1. Center for Marine Environmental Studies, Ehime Univ., 2. Department of Eearth Scieces, Fuculty of Education and Integrated Arts and Sciences, Waseda Univ.

A markedly increasing influence of human activity on the Earth system since 1950s has gained attention as one of the notable turning points of Earth's history, which is noteworthy to propose the 'Anthropocene' as a potential new unit of the International Chronostratigraphic Chart which serves as the basis of the Geological Time Scale. Now is ongoing the definition and selection of the Global Boundary Stratotype Section and Point (GSSP) mainly by the Anthropocene Working Group (AWG), a working group of the Subcommission on Quaternary Stratigraphy (SQS) of the International Commission on Stratigraphy (ICS). There are several candidates of a suitable stratotype for hosting an Anthropocene GSSP, including ice core, tree-ring, and coral that record an increasing fallout signal of ^{14}C and ^{239}Pu as well as a rapid decrease in $\delta^{13}C$ during 1950s. However, since (1) radionuclide fallout did not have major biological or other widespread physical repercussions, (2) ice might disappear itself due to global warming, and (3) ^{14}C signal won't detect in 100, 000 years or more, other stable auxiliary stratotypes and markers may be needed for the establishment of GSSP.

GSSPs previously ratified have often been established in marine sediments; anoxic marine sediments emerges as one of the candidates for Anthropocene auxiliary stratotypes (Waters et al., 2018). In anoxic marine sediments, there are the potential Anthropocene boundary markers, including microplastics, diatom and foraminifer assemblages, metals, organic contaminations, and spheroidal carbonaceous particles, which can be used to correlate globally. Several marine anoxic basins have been addressed for a candidate of auxiliary stratotype, such as Santa Barbara Basin, etc., but, an existence of a Japanese marine anoxic basin has not been well-known. Here we introduce laminated sediments in the anoxic Beppu Bay basin for a potential auxiliary stratotype of Anthropocene and discuss its recent progress of stratigraphy and advantage to propose the candidate, and future tasks to acquire a comprehensive dataset for establishment of the boundary.

Keywords: Anthropocene, Beppu Bay sediments, auxiliary stratotype

©2019. Japan Geoscience Union. All Right Reserved.

[J] Poster | M (Multidisciplinary and Interdisciplinary)：M-IS Intersection

Wed. May 29, 2019 1:45 PM - 3:15 PM JST | Wed. May 29, 2019 4:45 AM - 6:15 AM UTC | Poster Hall International Exhibition Hall8, Makuhari Messe_5

[M-IS22] Electromagnetic phenomena associated with seismic and volcanic activities

convener:Tetsuya Kodama(Research Unit I, Research and Development Directorate, Japan Space Exploration Agency), Toshiyasu Nagao(Institute of Oceanic Research and development, Tokai University)

This session deals with reviews and contributions on the recent studies of electromagnetic (EM) phenomena associated with earthquakes and volcanic eruptions. One of the main targets of the session is to clarify the mechanism of seismo-EM emission and Lithosphere-Atmosphere-Ionosphere (LAI) coupling. Recently, some scientists claim that seismic activities are the critical phenomena. These kinds of approach are also welcome.

[MIS22-P01] Ionospheric TEC changes immediately before large earthquakes: Derivation of the standard curve and discussion on the physical mechanisms

*Yuki Takasaka [1], Kosuke Heki[1] (1.Department of Earth and Planetary Science, Faculty of Science, Hokkaido University)

[MIS22-P02] Examination of ionospheric disturbances at different altitudes associated with Tohoku earthquake using HF Doppler sounding

*Natsuki Ono[1], Hiroyuki Nakata[1], Hiroyo Ohya[1], Toshiaki Takano[1], Ichiro Tomizawa[2], Keisuke Hosokawa[2], Takuya Tsugawa[3], Michi Nishioka[3] (1.Department of Electrical and Electronic Engineering, Graduate School of Science and Engineering, Chiba University, 2.The University of Electro-Communications, 3.NICT)

[MIS22-P03] Electromagnetic observation addressed to the short-term earthquake prediction research in VLF band

*Toshiyasu Nagao[1], Jun Izutsu[2], Masashi Kamogawa[3], Yoshiaki Orihara[1], Shigeki Sugiura[4], Hitoshi Kondo[4] (1.Institute of Oceanic Research and development, Tokai University, 2.Intl. Digital Earth Applied Sci. Res. Ctr, Chubu Inst. for Advanced Studies, Chubu Univ., 3.Department of Physics, Tokyo Gakugei University, 4.Genesis Research Institute, Inc.)

[MIS22-P04] ELF electric field intensity at the time of VLF precursor in the DEMETER data

*Masashi Kamogawa[1], Tetsuya Kodama[2], Toshiyasu Nagao[3] (1.Department of Physics, Tokyo Gakugei University, 2.Japan Space Exploration Agency, 3.Tokai University)

Ionospheric TEC changes immediately before large earthquakes: Derivation of the standard curve and discussion on the physical mechanisms

*Yuki Takasaka [1], Kosuke Heki[1]

1. Department of Earth and Planetary Science, Faculty of Science, Hokkaido University

Shortly after the 2011 Tohoku-Oki Earthquake, Heki (2011) found that the ionospheric total electron content (TEC) started to change ~40 minutes before earthquake. Number of earthquakes showing similar immediate precursory TEC changes increased (e.g. He & Heki, 2017), but physical process behind the phenomenon has not been fully understood. Existence of such precursors suggest that the final size of an earthquake is largely prescribed when the fault rupture starts, which would be of sound seismological importance.

Why does the ionospheric TEC increase immediately before large earthquakes? We hypothesize that a certain process weakens the fault by sweeping the fault from one end to the other. It causes micro-scale cracks and dislocations, which cut peroxy bonds within rocks mobilizing positive holes. Electron movements let positive holes diffuse out of the rock and accumulate on the surface. They would make vertical electric fields (**E**) which may reach the ionosphere if the fault is large enough. High conductivity in ionosphere along geomagnetic fields (**B**) prohibits **E** along **B**. Thus, ionospheric electrons come down along **B** to cancel external **E**. This process would increase electron density at the bottom end of the geomagnetic field line and decrease electron density in higher regions. This hypothesis is supported by the 3-dimensional structure of the electron density anomalies just before the 2015 Illapel earthquake by He & Heki (2018).
In this study, we compare vertical TEC changes before and after the 18 earthquakes with Mw 7.3-9.2 that showed significant immediate preseismic TEC anomalies and explore scaling laws of various quantities. Then we derive the ‘standard curve’ of preseismic TEC changes by stacking the time series of individual cases after normalizing their horizontal and vertical axes. Comparing individual cases with the standard curve and highlighting their differences would help us characterize between-earthquake differences and get insight into their physical mechanisms. The current model suggests that the coseismic release of crustal stress would stop further generation of positive changes from faults and halt the TEC anomaly buildup. The derived standard curve suggested that the TEC does not show further increase after the earthquake occurrence time and remain almost constant until acoustic disturbances arrive. Also, the shapes of the pre-earthquake anomaly buildup curves may have regionality, reflecting e.g. the ocean-land proportion around the epicenter. Higher conductivity of the sea water will let electric charges diffuse rapidly and make the TEC anomaly reaches plateau earlier after its start. Comparison of the TEC change curves of individual earthquakes with the standard curve, however, showed that they are highly coincident in most cases with little significant differences in how the TEC anomaly builds up.

Keywords: Total Electron Content (TEC), TEC changes immediately before large earthquakes

©2019. Japan Geoscience Union. All Right Reserved.

Examination of ionospheric disturbances at different altitudes associated with Tohoku earthquake using HF Doppler sounding

*Natsuki Ono[1], Hiroyuki Nakata[1], Hiroyo Ohya[1], Toshiaki Takano[1], Ichiro Tomizawa[2], Keisuke Hosokawa[2], Takuya Tsugawa[3], Michi Nishioka[3]

1. Department of Electrical and Electronic Engineering, Graduate School of Science and Engineering, Chiba University, 2. The University of Electro-Communications, 3. NICT

It is reported that ionospheric disturbances occur after giant earthquakes. One of the reasons for these disturbances are the infrasound wave excited by ground motions.
The infrasound wave propagates upward and produces perturbations of electron density in the ionosphere. Such perturbations are detected by a network of ground-based GPS receivers as TEC perturbations. Using these TEC perturbations, horizontally propagation of the ionospheric disturbances from the epicenter is examined. However, characteristics of vertical propagation of infrasound have been rarely reported. In this study, the coseismic ionospheric disturbances in the different altitudes are examined using HF Doppler (HFD) and GPS-TEC. The HF Doppler sounding system is enable to observe the vertical speed of the ionosphere in the midpoint between the transmitter and the receiver at the different altitudes.We observed fluctuations induced by Tohoku earthquake.The ionospheric disturbances determined by HFD and TEC data were observed about 9 and 10 minutes after the surface wave arrived below the observation point, respectively. Because it takes about 20 minutes for the acoustic wave to arrive directly from the tsunami to HFD observation point, the initial disturbances observed by HFD and TEC were excited by the ground motion. The frequencies of the disturbance. Obtained by the seismograph and HFD data (5.006, 6.055 MHz) were about 3 - 20 mHz, and those in the HFD data (8.006, 9.595 MHz) are 3 - 5 mHz.HFD data (8.006, 9.595 MHz) the frequencies of the disturbances obtained by, 3 - 5 mHz, were the same as those of TEC disturbances associated with earthquakes. In the lower frequency components with 7 - 20 mHz, the acoustic wave excited by the seismic wave tend to attenuate at a high altitudes. Therefore, it is considered that the variation attenuated with the data in HFD data (8.006, 9.595 MHz).

Keywords: ionosphere, earthquake, HF Doppler, TEC

©2019. Japan Geoscience Union. All Right Reserved.

Electromagnetic observation addressed to the short-term earthquake prediction research in VLF band

*Toshiyasu Nagao[1], Jun Izutsu[2], Masashi Kamogawa[3], Yoshiaki Orihara[1], Shigeki Sugiura[4], Hitoshi Kondo[4]

1. Institute of Oceanic Research and development, Tokai University, 2. Intl. Digital Earth Applied Sci. Res. Ctr, Chubu Inst. for Advanced Studies, Chubu Univ., 3. Department of Physics, Tokyo Gakugei University, 4. Genesis Research Institute, Inc.

There have been many reports electromagnetic (EM) waves preceding earthquakes have existed since the 1980s. The late Professor Toshi Asada and his colleagues focused on the VLF band and developed devices and made observations at the Tokai University in the 1990s. As a result, in the apparent arrival direction analysis, the electromagnetic waves, which comes from the epicenter direction were observed. However, after that, the observation was interrupted due to the death of Professor Asada. It seemed promising results, therefore we resumed research from FY 2014. The feature of the present apparatus is that not only the apparent arrival direction analysis but also the wave source determination can be performed using the time difference of arrival (TDOA) of EM waves. Because the apparent arrival direction method can only apply when the observed EM wave has a linear polarization. In the wave source determination using TDOA, the arrival time of the EM wave was determined by using the autoregressive model and AIC. We observed EM waves coming from the epicentral region, two days before the earthquake, which occurred in the southern part of Nagano Prefecture on June 25, 2017 (M5.6). This earthquake was the largest one occurred in the vicinity of our observation network at this moment. In the presentation, we would like to present a detailed waveform analysis and future research plan.

Acknowledgments

This study was partly supported by the Ministry of Education, Culture, Sports, Science and Technology (MEXT) of Japan, under its Earthquake and Volcano Hazards Observation and Research Program, research fund of the core-project of Institute of Oceanic Research and Development (IORD), Tokai University and Genesis Research Institute, Inc.

Keywords: short-term prediction, earthquake prediction, VLF band

©2019. Japan Geoscience Union. All Right Reserved.

ELF electric field intensity at the time of VLF precursor in the DEMETER data

*Masashi Kamogawa[1], Tetsuya Kodama[2], Toshiyasu Nagao[3]

1. Department of Physics, Tokyo Gakugei University, 2. Japan Space Exploration Agency, 3. Tokai University

A decrease of electric field at the 1.7 kHz, i.e., VLF electromagnetic waves, within 4 hours before neighboring earthquake (EQ) with the magnitude of more than 4.8 was statistically shown through the data set of in-situ DEMETER satellite measurement according to French groups (Nemec et al., GRL, 2008). In this study, we investigate the ELF intensity comparing with the pre-seismic VLF intensity decrease data.

Keywords: Earthquake, Ionosphere, DEMETER satellite

©2019. Japan Geoscience Union. All Right Reserved.

[J] Poster | M (Multidisciplinary and Interdisciplinary)：M-IS Intersection

Wed. May 29, 2019 5:15 PM - 6:30 PM JST | Wed. May 29, 2019 8:15 AM - 9:30 AM UTC | Poster Hall International Exhibition Hall8, Makuhari Messe_36

[M-IS22] Electromagnetic phenomena associated with seismic and volcanic activities

convener:Tetsuya Kodama(Research Unit I, Research and Development Directorate, Japan Space Exploration Agency), Toshiyasu Nagao(Institute of Oceanic Research and development, Tokai University)

This session deals with reviews and contributions on the recent studies of electromagnetic (EM) phenomena associated with earthquakes and volcanic eruptions. One of the main targets of the session is to clarify the mechanism of seismo-EM emission and Lithosphere-Atmosphere-Ionosphere (LAI) coupling. Recently, some scientists claim that seismic activities are the critical phenomena. These kinds of approach are also welcome.

[MIS22-P01] Ionospheric TEC changes immediately before large earthquakes: Derivation of the standard curve and discussion on the physical mechanisms

*Yuki Takasaka [1], Kosuke Heki[1] (1.Department of Earth and Planetary Science, Faculty of Science, Hokkaido University)

[MIS22-P02] Examination of ionospheric disturbances at different altitudes associated with Tohoku earthquake using HF Doppler sounding

*Natsuki Ono[1], Hiroyuki Nakata[1], Hiroyo Ohya[1], Toshiaki Takano[1], Ichiro Tomizawa[2], Keisuke Hosokawa[2], Takuya Tsugawa[3], Michi Nishioka[3] (1.Department of Electrical and Electronic Engineering, Graduate School of Science and Engineering, Chiba University, 2.The University of Electro-Communications, 3.NICT)

[MIS22-P03] Electromagnetic observation addressed to the short-term earthquake prediction research in VLF band

*Toshiyasu Nagao[1], Jun Izutsu[2], Masashi Kamogawa[3], Yoshiaki Orihara[1], Shigeki Sugiura[4], Hitoshi Kondo[4] (1.Institute of Oceanic Research and development, Tokai University, 2.Intl. Digital Earth Applied Sci. Res. Ctr, Chubu Inst. for Advanced Studies, Chubu Univ., 3.Department of Physics, Tokyo Gakugei University, 4.Genesis Research Institute, Inc.)

[MIS22-P04] ELF electric field intensity at the time of VLF precursor in the DEMETER data

*Masashi Kamogawa[1], Tetsuya Kodama[2], Toshiyasu Nagao[3] (1.Department of Physics, Tokyo Gakugei University, 2.Japan Space Exploration Agency, 3.Tokai University)

Ionospheric TEC changes immediately before large earthquakes: Derivation of the standard curve and discussion on the physical mechanisms

*Yuki Takasaka [1], Kosuke Heki[1]

1. Department of Earth and Planetary Science, Faculty of Science, Hokkaido University

Shortly after the 2011 Tohoku-Oki Earthquake, Heki (2011) found that the ionospheric total electron content (TEC) started to change ~40 minutes before earthquake. Number of earthquakes showing similar immediate precursory TEC changes increased (e.g. He & Heki, 2017), but physical process behind the phenomenon has not been fully understood. Existence of such precursors suggest that the final size of an earthquake is largely prescribed when the fault rupture starts, which would be of sound seismological importance.

Why does the ionospheric TEC increase immediately before large earthquakes? We hypothesize that a certain process weakens the fault by sweeping the fault from one end to the other. It causes micro-scale cracks and dislocations, which cut peroxy bonds within rocks mobilizing positive holes. Electron movements let positive holes diffuse out of the rock and accumulate on the surface. They would make vertical electric fields (**E**) which may reach the ionosphere if the fault is large enough. High conductivity in ionosphere along geomagnetic fields (**B**) prohibits **E** along **B**. Thus, ionospheric electrons come down along **B** to cancel external **E**. This process would increase electron density at the bottom end of the geomagnetic field line and decrease electron density in higher regions. This hypothesis is supported by the 3-dimensional structure of the electron density anomalies just before the 2015 Illapel earthquake by He & Heki (2018).
In this study, we compare vertical TEC changes before and after the 18 earthquakes with Mw 7.3-9.2 that showed significant immediate preseismic TEC anomalies and explore scaling laws of various quantities. Then we derive the ‘standard curve’ of preseismic TEC changes by stacking the time series of individual cases after normalizing their horizontal and vertical axes. Comparing individual cases with the standard curve and highlighting their differences would help us characterize between-earthquake differences and get insight into their physical mechanisms. The current model suggests that the coseismic release of crustal stress would stop further generation of positive changes from faults and halt the TEC anomaly buildup. The derived standard curve suggested that the TEC does not show further increase after the earthquake occurrence time and remain almost constant until acoustic disturbances arrive. Also, the shapes of the pre-earthquake anomaly buildup curves may have regionality, reflecting e.g. the ocean-land proportion around the epicenter. Higher conductivity of the sea water will let electric charges diffuse rapidly and make the TEC anomaly reaches plateau earlier after its start. Comparison of the TEC change curves of individual earthquakes with the standard curve, however, showed that they are highly coincident in most cases with little significant differences in how the TEC anomaly builds up.

Keywords: Total Electron Content (TEC), TEC changes immediately before large earthquakes

©2019. Japan Geoscience Union. All Right Reserved.

Examination of ionospheric disturbances at different altitudes associated with Tohoku earthquake using HF Doppler sounding

*Natsuki Ono[1], Hiroyuki Nakata[1], Hiroyo Ohya[1], Toshiaki Takano[1], Ichiro Tomizawa[2], Keisuke Hosokawa[2], Takuya Tsugawa[3], Michi Nishioka[3]

1. Department of Electrical and Electronic Engineering, Graduate School of Science and Engineering, Chiba University, 2. The University of Electro-Communications, 3. NICT

It is reported that ionospheric disturbances occur after giant earthquakes. One of the reasons for these disturbances are the infrasound wave excited by ground motions.
The infrasound wave propagates upward and produces perturbations of electron density in the ionosphere. Such perturbations are detected by a network of ground-based GPS receivers as TEC perturbations. Using these TEC perturbations, horizontally propagation of the ionospheric disturbances from the epicenter is examined. However, characteristics of vertical propagation of infrasound have been rarely reported. In this study, the coseismic ionospheric disturbances in the different altitudes are examined using HF Doppler (HFD) and GPS-TEC. The HF Doppler sounding system is enable to observe the vertical speed of the ionosphere in the midpoint between the transmitter and the receiver at the different altitudes.We observed fluctuations induced by Tohoku earthquake.The ionospheric disturbances determined by HFD and TEC data were observed about 9 and 10 minutes after the surface wave arrived below the observation point, respectively. Because it takes about 20 minutes for the acoustic wave to arrive directly from the tsunami to HFD observation point, the initial disturbances observed by HFD and TEC were excited by the ground motion. The frequencies of the disturbance. Obtained by the seismograph and HFD data (5.006, 6.055 MHz) were about 3 - 20 mHz, and those in the HFD data (8.006, 9.595 MHz) are 3 - 5 mHz.HFD data (8.006, 9.595 MHz) the frequencies of the disturbances obtained by, 3 - 5 mHz, were the same as those of TEC disturbances associated with earthquakes. In the lower frequency components with 7 - 20 mHz, the acoustic wave excited by the seismic wave tend to attenuate at a high altitudes. Therefore, it is considered that the variation attenuated with the data in HFD data (8.006, 9.595 MHz).

Keywords: ionosphere, earthquake, HF Doppler, TEC

©2019. Japan Geoscience Union. All Right Reserved.

Electromagnetic observation addressed to the short-term earthquake prediction research in VLF band

*Toshiyasu Nagao[1], Jun Izutsu[2], Masashi Kamogawa[3], Yoshiaki Orihara[1], Shigeki Sugiura[4], Hitoshi Kondo[4]

1. Institute of Oceanic Research and development, Tokai University, 2. Intl. Digital Earth Applied Sci. Res. Ctr, Chubu Inst. for Advanced Studies, Chubu Univ., 3. Department of Physics, Tokyo Gakugei University, 4. Genesis Research Institute, Inc.

There have been many reports electromagnetic (EM) waves preceding earthquakes have existed since the 1980s. The late Professor Toshi Asada and his colleagues focused on the VLF band and developed devices and made observations at the Tokai University in the 1990s. As a result, in the apparent arrival direction analysis, the electromagnetic waves, which comes from the epicenter direction were observed. However, after that, the observation was interrupted due to the death of Professor Asada. It seemed promising results, therefore we resumed research from FY 2014. The feature of the present apparatus is that not only the apparent arrival direction analysis but also the wave source determination can be performed using the time difference of arrival (TDOA) of EM waves. Because the apparent arrival direction method can only apply when the observed EM wave has a linear polarization. In the wave source determination using TDOA, the arrival time of the EM wave was determined by using the autoregressive model and AIC. We observed EM waves coming from the epicentral region, two days before the earthquake, which occurred in the southern part of Nagano Prefecture on June 25, 2017 (M5.6). This earthquake was the largest one occurred in the vicinity of our observation network at this moment. In the presentation, we would like to present a detailed waveform analysis and future research plan.

Acknowledgments

This study was partly supported by the Ministry of Education, Culture, Sports, Science and Technology (MEXT) of Japan, under its Earthquake and Volcano Hazards Observation and Research Program, research fund of the core-project of Institute of Oceanic Research and Development (IORD), Tokai University and Genesis Research Institute, Inc.

Keywords: short-term prediction, earthquake prediction, VLF band

©2019. Japan Geoscience Union. All Right Reserved.

ELF electric field intensity at the time of VLF precursor in the DEMETER data

*Masashi Kamogawa[1], Tetsuya Kodama[2], Toshiyasu Nagao[3]

1. Department of Physics, Tokyo Gakugei University, 2. Japan Space Exploration Agency, 3. Tokai University

A decrease of electric field at the 1.7 kHz, i.e., VLF electromagnetic waves, within 4 hours before neighboring earthquake (EQ) with the magnitude of more than 4.8 was statistically shown through the data set of in-situ DEMETER satellite measurement according to French groups (Nemec et al., GRL, 2008). In this study, we investigate the ELF intensity comparing with the pre-seismic VLF intensity decrease data.

Keywords: Earthquake, Ionosphere, DEMETER satellite

©2019. Japan Geoscience Union. All Right Reserved.

[J] Oral | M (Multidisciplinary and Interdisciplinary)：M-IS Intersection

Wed. May 29, 2019 3:30 PM - 5:00 PM JST | Wed. May 29, 2019 6:30 AM - 8:00 AM UTC | A07 TOKYO BAY MAKUHARI HALL

[M-IS22] Electromagnetic phenomena associated with seismic and volcanic activities

convener:Tetsuya Kodama(Research Unit I, Research and Development Directorate, Japan Space Exploration Agency), Toshiyasu Nagao(Institute of Oceanic Research and development, Tokai University), Chairperson:Tetsuya Kodama, Toshiyasu Nagao

This session deals with reviews and contributions on the recent studies of electromagnetic (EM) phenomena associated with earthquakes and volcanic eruptions. One of the main targets of the session is to clarify the mechanism of seismo-EM emission and Lithosphere-Atmosphere-Ionosphere (LAI) coupling. Recently, some scientists claim that seismic activities are the critical phenomena. These kinds of approach are also welcome.

3:30 PM - 3:45 PM JST | 6:30 AM - 6:45 AM UTC

[MIS22-01] Stress-induced charges in gabbro at high temperature

*Chihiro Yamanaka[1], Daiki Maezono[1] (1.Graduate School of Science, Osaka University)

3:45 PM - 4:00 PM JST | 6:45 AM - 7:00 AM UTC

[MIS22-02] Evaluation of ULF seismo-magnetic precursor phenomena at Kakioka, Japan over 1983 – 2018 by using SEA and Molchan's error diagram

*Katsumi Hattori[1], Kei Takahashi[2], Peng Han[3] (1.Department of Earth Sciences, Graduate School of Science, Chiba University, 2.Department of Earth Sciences, Faculty of Science, Chiba University, 3.Southern University of Science and Technology, China)

4:00 PM - 4:15 PM JST | 7:00 AM - 7:15 AM UTC

[MIS22-03] On the tsunami and electromagnetic pulses appeared abound 10min. after the 2011 Tohoku earthquake

*Yuji Enomoto[1], Tsuneaki Yamabe[1], Shigeki Sugiura[2], Hitoshi Kondo[2] (1.Shinshu Univeristy, Ueda Campus Fii, 2.Genesis Reserach Institute, Inc.)

4:15 PM - 4:30 PM JST | 7:15 AM - 7:30 AM UTC

[MIS22-04] Reinvestigation of correlation between groundwater anomalies and earthquakes carried out by an amateur network in Japan

*Yoshiaki Orihara[1], Masashi Kamogawa[2], Toshiyasu Nagao[1] (1.Institute of Oceanic Research and Development, Tokai University, 2.Dpt. of Phys., Tokyo Gakugei Univ.)

4:30 PM - 4:45 PM JST | 7:30 AM - 7:45 AM UTC

[MIS22-05] Participation Report of S-Booster 2018

*Tetsuya Kodama[1] (1.Research Unit I, Research and Development Directorate, Japan Space Exploration Agency)

4:45 PM - 5:00 PM JST | 7:45 AM - 8:00 AM UTC

[MIS22-06] The future direction of EMSEV, IUGG International Working Group

*Toshiyasu Nagao[1] (1.Institute of Oceanic Research and development, Tokai University)

Stress-induced charges in gabbro at high temperature

*Chihiro Yamanaka[1], Daiki Maezono[1]

1. Graduate School of Science, Osaka University

Preseismic ionospheric disturbance just before large earthquakes was found at the 2011 off the Pacific coast of Tohoku Earthquake (Heki,2011). Similar phenomena up to 18 cases (Heki's TEC anomaly) were found in earthquakes of M 7-9 since 1994. It should be noted all the earthquakes larger than M 8.5 during that duration were 5 times and Heki's TEC anomaly was observed for all of them.
Assuming the phenomena were drived by surface electromagnetic field due to stress induced charges distributed thinly around focal or nucleation zone, we have been studying stress-induced charges from silicate rocks. A dried gabbro sample (10×10×3 cm) was heated up to 350℃, then stress-induced current under uniaxial stress of 10 MPa was observed with the variation of temperature.
Experimental results showed that stress-induced charges increased from room temperature to 200℃ but then decreased at higher temperature. We would like to discuss the mechanism of Heki's TEC anomaly based on the experimental results and computer simulation.

[1] K. Heki (2011), Geophys. Res. Lett. 38, L17312.
[2] L. He and K. Heki (2017), J. Geophys. Res. Space Phys., 122, 8659-8678.
[3] K. Heki and Y. Enomoto (2015), J. Geophys. Res. Space Phys., 120, 7006-7020.
[4] L. He and K. Heki (2017), J. Geophys. Res. Space Phys., 123, 4015-4025.

Keywords: Ionosphere disturbance, Heki’ s TEC anomaly, stress induced charges

©2019. Japan Geoscience Union. All Right Reserved.

Evaluation of ULF seismo-magnetic precursor phenomena at Kakioka, Japan over 1983 –2018 by using SEA and Molchan’ s error diagram

*Katsumi Hattori[1], Kei Takahashi[2], Peng Han[3]

1. Department of Earth Sciences, Graduate School of Science, Chiba University, 2. Department of Earth Sciences, Faculty of Science, Chiba University, 3. Southern University of Science and Technology, China

To clarify and verify the ultralow frequency (ULF) seismo-magnetic phenomena, we have performed statistical studies on the geomagnetic data observed at the Kakioka (KAK) station, Japan, during 1983-2017. We investigated the energy of ULF geomagnetic signals of the frequency around 0.01 Hz using wavelet transform analysis. To minimize the influences of artificial noises and global magnetic perturbations, we used only the geomagnetic data observed at midnight time (LT 2:30 AM to 4:00 AM).We define the geomagnetic anomalies when the Z components of geomagnetic data exceeds median +1.5 IQR, where IQR is the interquartile range. Considering that ionospheric disturbances may also lead to enhancements in the Z component, we exclude the anomaly when the energy of H component exceeds median +3.0 IQR. Statistical analysis of superposed epoch analysis have indicated that ULF magnetic anomalies are more likely to appear before sizable isolated earthquake events rather than after them, especially 6-10 days before the events. Finally, we have evaluated the precursory information of ULF geomagnetic signals for local sizable earthquakes using Molchan’ s error diagram. The results show that the ULF seismo-magnetic phenomena at Kakioka clearly contain precursory information and have a possibility of improving forecasting of large earthquakes. The details will be given in the presentation.

Keywords: Earthquake Precursor Phenomena, Statistical Significance, Molchan's Error Diagram Analysis

©2019. Japan Geoscience Union. All Right Reserved.

On the tsunami and electromagnetic pulses appeared abound 10min. after the 2011 Tohoku earthquake

*Yuji Enomoto[1], Tsuneaki Yamabe[1], Shigeki Sugiura[2], Hitoshi Kondo[2]

1. Shinshu Univeristy, Ueda Campus Fii, 2. Genesis Reserach Institute, Inc.

Tsunami and electromagnetic pulses have appeared about 10 min. after the 2011 Tohoku-Oki earthquake(Heki, GRL, 2011; Utada et al. EPS Lett., 2011; Tsunagawa et al. EPS Lett., 2011). The disturbance to the ionosphere is thought to have been influenced by the atmospheric gravity wave caused by the tsunami. But this model could not explain the variation of geomagnetism, observed at Esahi site. In order to explain geomagnetic variation, we present a model that positively charged mists flied up with the atmospheric gravity wave along with the atmospheric electric field as the tsunami pulse was generated.

Keywords: Seismo-electromagneic phenomena, Tsunami, Geomagnetic change

©2019. Japan Geoscience Union. All Right Reserved.

Reinvestigation of correlation between groundwater anomalies and earthquakes carried out by an amateur network in Japan

*Yoshiaki Orihara[1], Masashi Kamogawa[2], Toshiyasu Nagao[1]

1. Institute of Oceanic Research and Development, Tokai University, 2. Dpt. of Phys., Tokyo Gakugei Univ.

An amateur volunteer group for an earthquake prediction, “the catfish club”, had monitored groundwater levels and the temperature of thermal water to detect earthquake precursor signals since 1976. More than 200 participants in Kanagawa, Tokyo, Shizuoka, and some prefectures monitored them. Their sampled data are sent to the office of the catfish club, and the summarized reports were published every month. Oki and Hiraga (1988) reported the probably predicted events such as the 1978 Izu-Ohshima kinkai earthquake (M 7.0) and the 1978 Miyagiken-Oki earthquake (M 7.4). In this study, we statistically evaluate the anomaly appearance rate, the earthquake occurrence rate, and the probability gain using the data from 1977 to 1987.

Acknowledgment: This study was supported by the Earthquake Research Institute The University of Tokyo Joint Usage/Research Program.

Keywords: the catfish club, earthquake prediction, groundwater, statistical evaluation

©2019. Japan Geoscience Union. All Right Reserved.

Participation Report of S-Booster 2018

*Tetsuya Kodama[1]

1. Research Unit I, Research and Development Directorate, Japan Space Exploration Agency

"Tsunami Early Warning Service by Geostationary Positioning Satellite" and "Prediction of Earthquake Occurrence by Microsatellite Constellation and Global Ground Station Network" which were applied for S-Booster 2018 sponsored by the Cabinet Office, both of which were left in the final selection. The background and results will be reported.

Keywords: S-Booster, tsunami, earthquake prediction, QZS-3, microsatellite

©2019. Japan Geoscience Union. All Right Reserved.

The future direction of EMSEV, IUGG International Working Group

*Toshiyasu Nagao[1]

1. Institute of Oceanic Research and development, Tokai University

EMSEV (Electromagnetic Studies of Earthquakes and Volcanoes) was established in 2001 as a mother foundation of IAGA, IAVCEI, and IASPEI under IUGG (International Union of Geodesy and Geophysics). At that time, many studies of electromagnetic precursory phenomena were reported in earthquake prediction research but never seemed to be recognized by the traditional seismology community. For this reason, the grassroots movement had been expanded for the necessity of promoting international research.

Therefore we urged the establishment of an organization to study earthquake prediction and volcanic eruption prediction based on the electromagnetics in IUGG. It was officially launched in 2001 and the first meeting was made during the IUGG Sapporo in 2003.

Professor emeritus of the University of Tokyo, Seiya Uyeda served as the first chair of EMSEV, then Dr. Jacques Zlotnicki of the French National Science Research Center took the chair till 2018. EMSEV meeting was held, which organizes every two years, in Potenza in Italy in 2018. During the meeting, Professor Toshiyasu Nagao was proposed to serve as the next chair. This proposal was approved through the discussion of the mailing list.

In the future EMSEV, we must show the statistical correlation between the ionospheric anomaly and the earthquake first, then we have to prove why the earthquake precursors phenomena appear in the ionosphere based on the lithosphere - atmosphere - ionosphere coupling hypothesis. In particular, from satellite observations, France launched the DEMETER satellite in 2004, showing the statistical significance of VLF band anomalies just before the earthquake. Inspired by this result, China launched the CSES (Chinese Seismo-Electromagnetic Satellite) in 2018.

We decided that the next meeting of EMSEV will be held in Taiwan in the fall of 2020.

Keywords: IUGG, EMSEV, Earthquake prediction

©2019. Japan Geoscience Union. All Right Reserved.

[E] Poster | M (Multidisciplinary and Interdisciplinary)：M-GI General Geosciences, Information Geosciences & Simulations

Wed. May 29, 2019 10:45 AM - 12:15 PM JST | Wed. May 29, 2019 1:45 AM - 3:15 AM UTC | Poster Hall International Exhibition Hall8, Makuhari Messe_11

[M-GI30] Data assimilation: A fundamental approach in geosciences

convener:Shin ya Nakano(The Institute of Statistical Mathematics), Yosuke Fujii(Meteorological Research Institute, Japan Meteorological Agency), SHINICHI MIYAZAKI(Graduate School of Science, Kyoto University), Takemasa Miyoshi(RIKEN)

Data assimilation is an inversion approach to estimate the evolution of a system by utilizing a constraint given by a dynamical simulation model. Data assimilation is now widely used not only in meteorology and oceanography but also other fields of geosciences such as hydrology, solid earth science, and space science. This session aims at providing an opportunity for discussion on data assimilation studies among researchers of various field of geosciences. We encourage contributions addressing novel methods and theoretical developments of data assimilation. Contributions dealing with useful applications of data assimilation are also welcome.

[MGI30-P01] Superposition of atmospheric states using information redundancy for Numerical Weather Prediction

*Toshiyuki Ishibashi[1] (1.Meteorological Research Institute/Japan Meteorological Agency)

[MGI30-P02] **Numerical Weather Prediction Experiments using a Coupled Atmosphere-Ocean Data Assimilation System in JMA/MRI** (3)

*Toshiyuki Ishibashi[1], Takeshi Iriguchi[1], Yosuke Fujii[1], Tamaki Yasuda[1], Yuhei Takaya[1], Naoki Saito[1], Toshikazu Onogi[1] (1.Meteorological Research Institute/Japan Meteorological Agency)

[MGI30-P03] **Accurate estimation of posterior error covariance in a 4D-Var inverse analysis**

*Yosuke Niwa[1,2], Yosuke Fujii[2,3] (1.National Institute for Environmental Studies, 2.Meteorological Research Institute, Japan Meteorological Agency, 3.The Institute of Statistical Mathematics)

[MGI30-P04] Assimilation CO_2 concentration data in the Kanto region using AIST-MM model and for the estimation of CO_2 emissions

*Yutaka Arai[1], Ryoichi Imasu[1], Hiroaki Kondo[2], Yosuke Niwa[3] (1.Atmosphere and Ocean Research Institute, The University of Tokyo, 2.National Institute of Advanced Industrial Science and Technology, 3.National Institute for Environmental Studies, Independent Administrative Institutions)

[MGI30-P05] **Application of data assimilation method on parameter estimation of flow and nutrient behavior in watershed model**

*Yosuke Horie[1] (1.Nippon Koei Co., Ltd.)

[MGI30-P06] Bayesian inference of grain growth prediction via multi-phase-field models

*Shin-ichi Ito[1], Hiromichi Nagao[1], Takashi Kurokawa[1], Tadashi Kasuya[1], Junya Inoue[1] (1.The University of Tokyo)

[MGI30-P07] GNSS data assimilation for the Bungo channel Long-term SSEs using Ensemble Kalman Filter (EnKF)

*Megumi Fujita[1], Takuya NISHIMURA[2], Kazuro Hirahara[3], SHINICHI MIYAZAKI[1] (1.Graduate School of Science , Kyoto University, 2.Disaster Prevention Research Institute, Kyoto University, 3.Institute of Education, Research and Regional Cooperation for crisis Management Shikoku, Kagawa University)

[MGI30-P08] A data assimilation library with Python for parallel computing

*Shin ya Nakano[1], Yuya Ariyoshi[2], Tomoyuki Higuchi[1] (1.The Institute of Statistical Mathematics, 2.Faculty of Engineering, Nippon Bunri University)

Superposition of atmospheric states using information redundancy for Numerical Weather Prediction

*Toshiyuki Ishibashi[1]

1. Meteorological Research Institute/Japan Meteorological Agency

Atmospheric state analysis is a difficult scientific problem due to our limited ability in computation and observation, and analysed atmospheric states are fluctuating around the true state. The purpose of this paper is to analyse atmospheric state as a superposition of possible atmospheric states using information redundancy, and evaluate its accuracy in the context of numerical weather prediction (NWP). This atmospheric state analysis approach has two novel aspects. First, it uses only real atmospheric information, and no-artificial perturbations unlike existing ensemble based methods. Second, it does not require specific error structures of our knowledge of the atmosphere. We performed this method on a global numerical weather prediction system of Japan Meteorological Agency. The experimental results show the method can clearly reduce forecast root means square errors about 3-5% in average within 2 day forecast compared to existing methods (CNTL). Furthermore, forecast RMSEs of ensemble means of ensemble forecasts using only a few members generated by this method are significantly smaller than CNTL from the forecast initial time.

©2019. Japan Geoscience Union. All Right Reserved.

Numerical Weather Prediction Experiments using a Coupled Atmosphere-Ocean Data Assimilation System in JMA/MRI (3)

*Toshiyuki Ishibashi[1], Takeshi Iriguchi[1], Yosuke Fujii[1], Tamaki Yasuda[1], Yuhei Takaya[1], Naoki Saito[1], Toshikazu Onogi[1]

1. Meteorological Research Institute/Japan Meteorological Agency

An atmosphere-ocean coupled data assimilation system (CDAS) has been developed at the JMA/MRI to investigate feasibility of a CDAS as a future DAS for seamless numerical prediction including both numerical weather prediction (NWP) and numerical seasonal climate prediction (NCP), and for reanalysis of the atmosphere-ocean. Our CDAS (**MRI-CDA1**) has two features. 1) It composed of the JMA operational systems, the global atmospheric DAS (MRI-NAPEX) based on 4D-Var, the global ocean DAS (MOVE-G2) based on 3D-Var, and the atmosphere- ocean coupled global forecast model (CGCM: JMA/MRI-CGCM2). 2) Coupling strategy is “weak coupling” with two different data assimilation window lengths for the atmosphere and ocean. Here, “weak coupling” denotes the approximation that ignores correlations of atmosphere and ocean background forecast errors. Following the previous reports in JpGU2018 and JpGU-AGU joint meeting 2017 (Ishibashi et al. 2018; 2017), we will report basic property of MRI-CDA1 in NWP.

©2019. Japan Geoscience Union. All Right Reserved.

Accurate estimation of posterior error covariance in a 4D-Var inverse analysis

*Yosuke Niwa[1,2], Yosuke Fujii[2,3]

1. National Institute for Environmental Studies, 2. Meteorological Research Institute, Japan Meteorological Agency, 3. The Institute of Statistical Mathematics

The four-dimensional variational method (4D-Var) is one prominent data assimilation/inversion method. However, it is a non-trivial task for a conventional 4D-Var to estimate a posterior error variance-covariance matrix. This study developed a method to estimate a posterior error variance-covariance matrix especially focusing on its off-diagonal elements, i.e., covariance. Off-diagonal elements are usually difficult to be estimated but provide error correlations that are beneficial for interpreting optimized parameter variations. The method was developed within a 4D-Var framework using a quasi-Newton method with the Broyden–Fletcher–Goldfarb–Shanno (BFGS) formula. This study newly introduces numerical techniques that ensure conjugacy among the set of increment vector pairs in the BFGS formula. Through application to an inverse problem of atmospheric CO_2, the developed method was evaluated with three diagnostic measures and compared against existing methods. The evaluation revealed that the developed method could provide accurate estimates of the posterior variance-covariance matrix, in terms not only of the diagonal but also of the off-diagonal elements. Although far more expensive than optimal state estimation, the computational efficiency was found reasonable for practical use, especially in conjunction with an ensemble approach.

Keywords: inversion, data assimilation, posterior error covariance

©2019. Japan Geoscience Union. All Right Reserved.

Assimilation CO_2 concentration data in the Kanto region using AIST-MM model and for the estimation of CO_2 emissions

*Yutaka Arai[1], Ryoichi Imasu[1], Hiroaki Kondo[2], Yosuke Niwa[3]

1. Atmosphere and Ocean Research Institute, The University of Tokyo, 2. National Institute of Advanced Industrial Science and Technology, 3. National Institute for Environmental Studies, Independent Administrative Institutions

Atmospheric carbon dioxide (CO_2) known as greenhouse gas is the most important gas for global warming. For the reason, there have been many researches about CO_2 such as model calculations, satellite observations and direct observations recently. As computer spec get higher, the CO_2 model has been more improved and 3D distributions of CO_2 has been calculated in more detail. In Japan, the satellite observation has been high resolution by satellite, Greenhouse Observing SATellite-2 (GOSAT-2). But in urban area, CO_2 distributions are complicated because of complexed CO_2 emission source and sink around the area. Especially, in the Kanto district mega city, Tokyo is located, CO_2 emissions from power plants and human activities are very huge. Furthermore, around the city there are forests and mountains which strongly affect to CO_2 concentrations in the atmosphere through their respiration and photosynthesis. In case to calculate such the district with high spatial resolutions, the models are required to be able to represent the temporal and spatial variations of the respiration and photosynthesis of the plants precisely. It has been also pointed out that representativeness of the vertical transport of CO_2 in the models is a key subject. About satellite observations, it is not always possible to observe CO2 distributions because of to be influenced by the weather and the frequencies of them are limited, and what ca be observed are not 3 dimensional but 2 dimensional namely vertical column densities of CO_2. On the other hand, the accuracy of the in-situ observations, is best, but there are very limited observation points. These are obstacles to grasping the detailed behavior of CO_2 concentration.

In this study, a regional transport model, AIST-MM has been used to investigate the behavior of CO_2 concentrations in Kanto district (Kondo et al., 2001). Firstly, AIST-MM computes CO_2 concentrations in the outer area (630 km×550 km), and then calculates CO_2 concentrations in the inner area (216 km×216 km) using the results from the former.
Firstly, the model was improved to be able to calculate the CO_2 seasonal variations through a year in order to estimate CO_2 emission source which contained large error. It was found that AIST-MM had uncertainty in the part of plant activities especially respiration in summer. As the calculation of plant respiration strongly depends on the temperature, when the temperature becomes high, the respiration of plants unrealistically increases. So the plant respiration parameter was tuned.
In order to compensate for the CO_2 influx from outside of the calculation region, the result of a global model, NICAM-TM (GL5) were used as the boundary conditions when calculating outer region. This modification led to improve the calculation of the vertical transport.
Furthermore, constant sea surface temperature was replaced with the satellite observation data derived from AVHRR-AMSR. In order to improve the simulating performance, we adjusted many detailed emission information by distinguishing between holidays and weekdays.
Secondly, Local Ensemble Transform Kalman Filter (LETKF) which is one of data assimilation methods is adapted to the adjusted AIST-MM and try to calculate CO_2 concentrations using in-situ observations, satellite observations, and ground remote sensing observations. In the near future, the CO_2 emissions will be estimated using Kalman smoother method.

©2019. Japan Geoscience Union. All Right Reserved.

Keywords: regional CO2 transport model, plant respiration, data assimilation, Local Ensemble Transform Kalman Filter, Kanto region

©2019. Japan Geoscience Union. All Right Reserved.

Application of data assimilation method on parameter estimation of flow and nutrient behavior in watershed model

*Yosuke Horie[1]

1. Nippon Koei Co., Ltd.

In schemes for nutrient reduction from watershed such as Japanese total volume control framework on nutrient or master plan for sewerage system propagation, hydrologic and nutrient behavior in watershed is critical to make an effective plan to fulfill environmental standard of water body. However, there are many uncertainties in constructing a watershed model as follows. First, observation frequency of concentration of water quality, which is a target of such scheme on nutrient reduction, is not enough because they can be obtained in public water quality observation system only about once a month. Second, pollutant load unit, which is used for quantifying pollutant load from watershed, can be fluctuated from place to place. Third, there are many parameters of watershed models which should be calibrated. To resolve these problems, this study applied EnKF, one of data assimilation method, to SWAT (Soil and Water Assessment Tools) model, which can simulate hydrologic and nutrient cycle in watershed, and conducted parameter estimation to achieve more robust result from watershed model under the uncertainties above.

Keywords: Data assimilation, watershed model, water quality simulation, SWAT

©2019. Japan Geoscience Union. All Right Reserved.

Bayesian inference of grain growth prediction via multi-phase-field models

*Shin-ichi Ito[1], Hiromichi Nagao[1], Takashi Kurokawa[1], Tadashi Kasuya[1], Junya Inoue[1]

1. The University of Tokyo

We propose a Bayesian inference methodology to evaluate unobservable parameters involved in multi-phase-field models with the aim of accurately predicting the observed grain growth, such as in metals and rocks. This approach integrates models and a set of observational image data of grain structures. Since the set of image data is not a time series, directly applying conventional inference techniques that require time series as the input data is difficult. The key idea in our methodology to overcome this difficulty is to construct a time series with an appropriate statistic that characterizes static image data of grain structures. Our methodology implements the empirical Bayes method. It can estimate not only a probability density function of the parameters but also an initial phase-field, which is generally unobservable in real experiments. After validating the proposed method through numerical tests using synthetic data, we apply it to real experimental images of grain structures in a steel alloy. The proposed method properly estimates unobservable parameters together with their uncertainties, and successfully selects the initial phase-field that best explains the experimental data from among candidate initial phase-fields.

Keywords: Grain growth, Bayesian inference, Data assimilation, Phase-field model

©2019. Japan Geoscience Union. All Right Reserved.

GNSS data assimilation for the Bungo channel Long-term SSEs using Ensemble Kalman Filter (EnKF)

*Megumi Fujita[1], Takuya NISHIMURA[2], Kazuro Hirahara[3], SHINICHI MIYAZAKI[1]

1. Graduate School of Science , Kyoto University, 2. Disaster Prevention Research Institute, Kyoto University, 3. Institute of Education, Research and Regional Cooperation for crisis Management Shikoku, Kagawa University

Long-term Slow Slip Events (L-SSEs) in the Bungo channel, southwest Japan occur in the down-dip side of the seismogenic zones on the megathrust plate interface. Although L-SSEs release accumulated strain in the L-SSE zones, they can increase strain in the up-dip seismogenic locked zones. Therefore, better understanding of the temporal evolution of L-SSEs is very important for earthquake hazard assessment. Hirahara, and Nishikiori (JpGU, 2018) developed a method for estimating slip evolution and frictional properties on L-SSE area in the Bungo channel, by applying a data assimilation method EnKF (Ensemble Kalman Filter), which has been developed in meteorology and oceanology, to the synthetic GNSS data. Although they used the surface velocity data as GNSS data, the actual data which we can observe at GNSS station is the surface displacement data, not surface velocity data. In order to apply EnKF to the actual GNSS observational data, we conducted two numerical experiments, as follows.

i)We used the surface velocity data converted from the synthetic surface displacement data as observational data.

ii) We used the surface displacement data, not the surface velocity data as observational data.

We used the same model settings in above two numerical experiments as Hirahara and Nishikiori (2018) did. Firstly, we set a plane fault in homogeneous isotropic elastic body, whose angle of dip is 15 degrees. The frictional force on the plane fault follows a Rate and State Friction (RSF) law with an aging law [Dieterich,1979; Ruina,1983]. We set a velocity weakening (A-B<0) circular patch, whose radius R is 35 km, in the velocity strengthen (A-B>0) fault plane. We reproduced the observed L-SSEs in the Bungo Channel, using the frictional parameters in such a way that R is smaller than the critical nucleation size R_c [Rubin and Ampuero (2005), Chen and Lapusta (2009)]. Secondly, we considered the effect the seismogenic locked zones in the up-dip side of the L-SSEs zone. We set a locked zone at the up-dip of the L-SSE fault, whose back-slip rate is 6.0 cm/yr.

As the common analysis settings, we selected several pairs of frictional parameters in a wide range of parameter space which reproduce L-SSEs for the initial ensemble members of frictional parameters. We made the daily synthetic GNSS surface displacement data for 93 GEONET stations around the Bungo channel by calculating the surface displacements using true synthetic frictional parameters and adding random Gaussian noise. We set the assimilation interval to 10 days.

In experiment i), we calculated 31 day moving averages of the synthetic GNSS displacement data, and we obtained the surface velocities at GNSS stations from the derivatives of a 150-day cubic spline function fitting the moving averaged surface displacements. Then we applied EnKF to the obtained surface velocities and we successfully estimated slip evolution and frictional parameters. This result suggests this method for converting the surface displacement data into the surface velocity data at GNSS stations might be applicable.

©2019. Japan Geoscience Union. All Right Reserved.

In experiment ii), we applied EnKF to the synthetic GNSS displacement data directly. When we conducted experiment ii), we changed some analysis settings for stabilizing the assimilation. Firstly, when the slip velocity at the center of fault plane is low, we added larger random noise to the innovations artificially. Secondly, when the slip velocity at the center of fault plane is high, we reduced the assimilation interval to 1 day and introduced additive inflation to prevent the prediction errors from being too small. As a result, we also successfully estimated slip evolution and frictional parameters using the surface displacements, although the experiment sometime fails depending on the start timing of the analysis. Therefore, this method has not been fully stabilized yet, and we need to improve it for robust estimation.

Finally, we applied EnKF to the real GNSS data before the 2011 Tohoku-oki earthquake in the same settings as experiment i) and ii) respectively. We corrected offsets of major earthquakes and antenna changes in the GNSS data. However, both experiments stopped during the assimilation due to negative slip velocities. It manifests an importance of correction of GNSS data including removing annual and semiannual components for a stable assimilation of real GNSS data. Furthermore, we need to consider the realistic model settings including the geometry of the subducting Philippine Sea plate interface and distribution of both L-SSE and locked zones.

Acknowledgement: We used GNSS of GEONET provided by the Geospatial Information Authority of Japan (GSI).

Keywords: GNSS, Ensemble Kalman Filter (EnKF), Long-term SSEs, the Bungo channel

©2019. Japan Geoscience Union. All Right Reserved.

A data assimilation library with Python for parallel computing

*Shin ya Nakano[1], Yuya Ariyoshi[2], Tomoyuki Higuchi[1]

1. The Institute of Statistical Mathematics, 2. Faculty of Engineering, Nippon Bunri University

Parallel computing is essential to reduce the computational time in the ensemble-based data assimilation. However, it requires skills in parallel programming. It is sometimes a hard task to attain high computational efficiency with ensemble-based data assimilation. In particular, the particle filter (PF) algorithm, which is applicable to nonlinear and/or non-Gaussian problems, contains a procedure difficult to parallelize.
It is thus challenging to achieve high computational efficiency with the PF even for experienced users.

We have developed a Python library named P-cubed (Python Parallelized Particle Filter Library), that enables us to use parallel-ready PF algorithms with high parallel efficiency. Now we are also planning to attach a module of other data assimilation algorithms such as the ensemble Kalman filter to this library. In this presentation, we introduce the parallelized PF algorithms which are already available in P-cubed and explain the design and characteristics of the library. Future prospects of this library will also be discussed.

Keywords: data assimilation, particle filter, parallel computing, Python

©2019. Japan Geoscience Union. All Right Reserved.

[E] Poster | M (Multidisciplinary and Interdisciplinary)：M-GI General Geosciences, Information Geosciences & Simulations

Wed. May 29, 2019 5:15 PM - 6:30 PM JST | Wed. May 29, 2019 8:15 AM - 9:30 AM UTC | Poster Hall International Exhibition Hall8, Makuhari Messe_37

[M-GI30] Data assimilation: A fundamental approach in geosciences

convener:Shin ya Nakano(The Institute of Statistical Mathematics), Yosuke Fujii(Meteorological Research Institute, Japan Meteorological Agency), SHINICHI MIYAZAKI(Graduate School of Science, Kyoto University), Takemasa Miyoshi(RIKEN)

Data assimilation is an inversion approach to estimate the evolution of a system by utilizing a constraint given by a dynamical simulation model. Data assimilation is now widely used not only in meteorology and oceanography but also other fields of geosciences such as hydrology, solid earth science, and space science. This session aims at providing an opportunity for discussion on data assimilation studies among researchers of various field of geosciences. We encourage contributions addressing novel methods and theoretical developments of data assimilation. Contributions dealing with useful applications of data assimilation are also welcome.

[MGI30-P01] Superposition of atmospheric states using information redundancy for Numerical Weather Prediction

*Toshiyuki Ishibashi[1] (1.Meteorological Research Institute/Japan Meteorological Agency)

[MGI30-P02] **Numerical Weather Prediction Experiments using a Coupled Atmosphere-Ocean Data Assimilation System in JMA/MRI** (3)

*Toshiyuki Ishibashi[1], Takeshi Iriguchi[1], Yosuke Fujii[1], Tamaki Yasuda[1], Yuhei Takaya[1], Naoki Saito[1], Toshikazu Onogi[1] (1.Meteorological Research Institute/Japan Meteorological Agency)

[MGI30-P03] **Accurate estimation of posterior error covariance in a 4D-Var inverse analysis**

*Yosuke Niwa[1,2], Yosuke Fujii[2,3] (1.National Institute for Environmental Studies, 2.Meteorological Research Institute, Japan Meteorological Agency, 3.The Institute of Statistical Mathematics)

[MGI30-P04] Assimilation CO_2 concentration data in the Kanto region using AIST-MM model and for the estimation of CO_2 emissions

*Yutaka Arai[1], Ryoichi Imasu[1], Hiroaki Kondo[2], Yosuke Niwa[3] (1.Atmosphere and Ocean Research Institute, The University of Tokyo, 2.National Institute of Advanced Industrial Science and Technology, 3.National Institute for Environmental Studies, Independent Administrative Institutions)

[MGI30-P05] **Application of data assimilation method on parameter estimation of flow and nutrient behavior in watershed model**

*Yosuke Horie[1] (1.Nippon Koei Co., Ltd.)

[MGI30-P06] Bayesian inference of grain growth prediction via multi-phase-field models

*Shin-ichi Ito[1], Hiromichi Nagao[1], Takashi Kurokawa[1], Tadashi Kasuya[1], Junya Inoue[1] (1.The University of Tokyo)

[MGI30-P07] GNSS data assimilation for the Bungo channel Long-term SSEs using Ensemble Kalman Filter (EnKF)

*Megumi Fujita[1], Takuya NISHIMURA[2], Kazuro Hirahara[3], SHINICHI MIYAZAKI[1] (1.Graduate School of Science , Kyoto University, 2.Disaster Prevention Research Institute, Kyoto University, 3.Institute of Education, Research and Regional Cooperation for crisis Management Shikoku, Kagawa University)

[MGI30-P08] A data assimilation library with Python for parallel computing

*Shin ya Nakano[1], Yuya Ariyoshi[2], Tomoyuki Higuchi[1] (1.The Institute of Statistical Mathematics, 2.Faculty of Engineering, Nippon Bunri University)

Superposition of atmospheric states using information redundancy for Numerical Weather Prediction

*Toshiyuki Ishibashi[1]

1. Meteorological Research Institute/Japan Meteorological Agency

Atmospheric state analysis is a difficult scientific problem due to our limited ability in computation and observation, and analysed atmospheric states are fluctuating around the true state. The purpose of this paper is to analyse atmospheric state as a superposition of possible atmospheric states using information redundancy, and evaluate its accuracy in the context of numerical weather prediction (NWP). This atmospheric state analysis approach has two novel aspects. First, it uses only real atmospheric information, and no-artificial perturbations unlike existing ensemble based methods. Second, it does not require specific error structures of our knowledge of the atmosphere. We performed this method on a global numerical weather prediction system of Japan Meteorological Agency. The experimental results show the method can clearly reduce forecast root means square errors about 3-5% in average within 2 day forecast compared to existing methods (CNTL). Furthermore, forecast RMSEs of ensemble means of ensemble forecasts using only a few members generated by this method are significantly smaller than CNTL from the forecast initial time.

©2019. Japan Geoscience Union. All Right Reserved.

Numerical Weather Prediction Experiments using a Coupled Atmosphere-Ocean Data Assimilation System in JMA/MRI (3)

*Toshiyuki Ishibashi[1], Takeshi Iriguchi[1], Yosuke Fujii[1], Tamaki Yasuda[1], Yuhei Takaya[1], Naoki Saito[1], Toshikazu Onogi[1]

1. Meteorological Research Institute/Japan Meteorological Agency

An atmosphere-ocean coupled data assimilation system (CDAS) has been developed at the JMA/MRI to investigate feasibility of a CDAS as a future DAS for seamless numerical prediction including both numerical weather prediction (NWP) and numerical seasonal climate prediction (NCP), and for reanalysis of the atmosphere-ocean. Our CDAS (**MRI-CDA1**) has two features. 1) It composed of the JMA operational systems, the global atmospheric DAS (MRI-NAPEX) based on 4D-Var, the global ocean DAS (MOVE-G2) based on 3D-Var, and the atmosphere- ocean coupled global forecast model (CGCM: JMA/MRI-CGCM2). 2) Coupling strategy is “weak coupling” with two different data assimilation window lengths for the atmosphere and ocean. Here, “weak coupling” denotes the approximation that ignores correlations of atmosphere and ocean background forecast errors. Following the previous reports in JpGU2018 and JpGU-AGU joint meeting 2017 (Ishibashi et al. 2018; 2017), we will report basic property of MRI-CDA1 in NWP.

©2019. Japan Geoscience Union. All Right Reserved.

Accurate estimation of posterior error covariance in a 4D-Var inverse analysis

*Yosuke Niwa[1,2], Yosuke Fujii[2,3]

1. National Institute for Environmental Studies, 2. Meteorological Research Institute, Japan Meteorological Agency, 3. The Institute of Statistical Mathematics

The four-dimensional variational method (4D-Var) is one prominent data assimilation/inversion method. However, it is a non-trivial task for a conventional 4D-Var to estimate a posterior error variance-covariance matrix. This study developed a method to estimate a posterior error variance-covariance matrix especially focusing on its off-diagonal elements, i.e., covariance. Off-diagonal elements are usually difficult to be estimated but provide error correlations that are beneficial for interpreting optimized parameter variations. The method was developed within a 4D-Var framework using a quasi-Newton method with the Broyden–Fletcher–Goldfarb–Shanno (BFGS) formula. This study newly introduces numerical techniques that ensure conjugacy among the set of increment vector pairs in the BFGS formula. Through application to an inverse problem of atmospheric CO_2, the developed method was evaluated with three diagnostic measures and compared against existing methods. The evaluation revealed that the developed method could provide accurate estimates of the posterior variance-covariance matrix, in terms not only of the diagonal but also of the off-diagonal elements. Although far more expensive than optimal state estimation, the computational efficiency was found reasonable for practical use, especially in conjunction with an ensemble approach.

Keywords: inversion, data assimilation, posterior error covariance

©2019. Japan Geoscience Union. All Right Reserved.

Assimilation CO_2 concentration data in the Kanto region using AIST-MM model and for the estimation of CO_2 emissions

*Yutaka Arai[1], Ryoichi Imasu[1], Hiroaki Kondo[2], Yosuke Niwa[3]

1. Atmosphere and Ocean Research Institute, The University of Tokyo, 2. National Institute of Advanced Industrial Science and Technology, 3. National Institute for Environmental Studies, Independent Administrative Institutions

Atmospheric carbon dioxide (CO_2) known as greenhouse gas is the most important gas for global warming. For the reason, there have been many researches about CO_2 such as model calculations, satellite observations and direct observations recently. As computer spec get higher, the CO_2 model has been more improved and 3D distributions of CO_2 has been calculated in more detail. In Japan, the satellite observation has been high resolution by satellite, Greenhouse Observing SATellite-2 (GOSAT-2). But in urban area, CO_2 distributions are complicated because of complexed CO_2 emission source and sink around the area. Especially, in the Kanto district mega city, Tokyo is located, CO_2 emissions from power plants and human activities are very huge. Furthermore, around the city there are forests and mountains which strongly affect to CO_2 concentrations in the atmosphere through their respiration and photosynthesis. In case to calculate such the district with high spatial resolutions, the models are required to be able to represent the temporal and spatial variations of the respiration and photosynthesis of the plants precisely. It has been also pointed out that representativeness of the vertical transport of CO_2 in the models is a key subject. About satellite observations, it is not always possible to observe CO2 distributions because of to be influenced by the weather and the frequencies of them are limited, and what ca be observed are not 3 dimensional but 2 dimensional namely vertical column densities of CO_2. On the other hand, the accuracy of the in-situ observations, is best, but there are very limited observation points. These are obstacles to grasping the detailed behavior of CO_2 concentration.

In this study, a regional transport model, AIST-MM has been used to investigate the behavior of CO_2 concentrations in Kanto district (Kondo et al., 2001). Firstly, AIST-MM computes CO_2 concentrations in the outer area (630 km×550 km), and then calculates CO_2 concentrations in the inner area (216 km×216 km) using the results from the former.
Firstly, the model was improved to be able to calculate the CO_2 seasonal variations through a year in order to estimate CO_2 emission source which contained large error. It was found that AIST-MM had uncertainty in the part of plant activities especially respiration in summer. As the calculation of plant respiration strongly depends on the temperature, when the temperature becomes high, the respiration of plants unrealistically increases. So the plant respiration parameter was tuned.
In order to compensate for the CO_2 influx from outside of the calculation region, the result of a global model, NICAM-TM (GL5) were used as the boundary conditions when calculating outer region. This modification led to improve the calculation of the vertical transport.
Furthermore, constant sea surface temperature was replaced with the satellite observation data derived from AVHRR-AMSR. In order to improve the simulating performance, we adjusted many detailed emission information by distinguishing between holidays and weekdays.
Secondly, Local Ensemble Transform Kalman Filter (LETKF) which is one of data assimilation methods is adapted to the adjusted AIST-MM and try to calculate CO_2 concentrations using in-situ observations, satellite observations, and ground remote sensing observations. In the near future, the CO_2 emissions will be estimated using Kalman smoother method.

©2019. Japan Geoscience Union. All Right Reserved.

Keywords: regional CO2 transport model, plant respiration, data assimilation, Local Ensemble Transform Kalman Filter, Kanto region

©2019. Japan Geoscience Union. All Right Reserved.

Application of data assimilation method on parameter estimation of flow and nutrient behavior in watershed model

*Yosuke Horie[1]

1. Nippon Koei Co., Ltd.

In schemes for nutrient reduction from watershed such as Japanese total volume control framework on nutrient or master plan for sewerage system propagation, hydrologic and nutrient behavior in watershed is critical to make an effective plan to fulfill environmental standard of water body. However, there are many uncertainties in constructing a watershed model as follows. First, observation frequency of concentration of water quality, which is a target of such scheme on nutrient reduction, is not enough because they can be obtained in public water quality observation system only about once a month. Second, pollutant load unit, which is used for quantifying pollutant load from watershed, can be fluctuated from place to place. Third, there are many parameters of watershed models which should be calibrated. To resolve these problems, this study applied EnKF, one of data assimilation method, to SWAT (Soil and Water Assessment Tools) model, which can simulate hydrologic and nutrient cycle in watershed, and conducted parameter estimation to achieve more robust result from watershed model under the uncertainties above.

Keywords: Data assimilation, watershed model, water quality simulation, SWAT

©2019. Japan Geoscience Union. All Right Reserved.

Bayesian inference of grain growth prediction via multi-phase-field models

*Shin-ichi Ito[1], Hiromichi Nagao[1], Takashi Kurokawa[1], Tadashi Kasuya[1], Junya Inoue[1]

1. The University of Tokyo

We propose a Bayesian inference methodology to evaluate unobservable parameters involved in multi-phase-field models with the aim of accurately predicting the observed grain growth, such as in metals and rocks. This approach integrates models and a set of observational image data of grain structures. Since the set of image data is not a time series, directly applying conventional inference techniques that require time series as the input data is difficult. The key idea in our methodology to overcome this difficulty is to construct a time series with an appropriate statistic that characterizes static image data of grain structures. Our methodology implements the empirical Bayes method. It can estimate not only a probability density function of the parameters but also an initial phase-field, which is generally unobservable in real experiments. After validating the proposed method through numerical tests using synthetic data, we apply it to real experimental images of grain structures in a steel alloy. The proposed method properly estimates unobservable parameters together with their uncertainties, and successfully selects the initial phase-field that best explains the experimental data from among candidate initial phase-fields.

Keywords: Grain growth, Bayesian inference, Data assimilation, Phase-field model

©2019. Japan Geoscience Union. All Right Reserved.

GNSS data assimilation for the Bungo channel Long-term SSEs using Ensemble Kalman Filter (EnKF)

*Megumi Fujita[1], Takuya NISHIMURA[2], Kazuro Hirahara[3], SHINICHI MIYAZAKI[1]

1. Graduate School of Science , Kyoto University, 2. Disaster Prevention Research Institute, Kyoto University, 3. Institute of Education, Research and Regional Cooperation for crisis Management Shikoku, Kagawa University

Long-term Slow Slip Events (L-SSEs) in the Bungo channel, southwest Japan occur in the down-dip side of the seismogenic zones on the megathrust plate interface. Although L-SSEs release accumulated strain in the L-SSE zones, they can increase strain in the up-dip seismogenic locked zones. Therefore, better understanding of the temporal evolution of L-SSEs is very important for earthquake hazard assessment. Hirahara, and Nishikiori (JpGU, 2018) developed a method for estimating slip evolution and frictional properties on L-SSE area in the Bungo channel, by applying a data assimilation method EnKF (Ensemble Kalman Filter), which has been developed in meteorology and oceanology, to the synthetic GNSS data. Although they used the surface velocity data as GNSS data, the actual data which we can observe at GNSS station is the surface displacement data, not surface velocity data. In order to apply EnKF to the actual GNSS observational data, we conducted two numerical experiments, as follows.

i)We used the surface velocity data converted from the synthetic surface displacement data as observational data.

ii) We used the surface displacement data, not the surface velocity data as observational data.

We used the same model settings in above two numerical experiments as Hirahara and Nishikiori (2018) did. Firstly, we set a plane fault in homogeneous isotropic elastic body, whose angle of dip is 15 degrees. The frictional force on the plane fault follows a Rate and State Friction (RSF) law with an aging law [Dieterich,1979; Ruina,1983]. We set a velocity weakening (A-B<0) circular patch, whose radius R is 35 km, in the velocity strengthen (A-B>0) fault plane. We reproduced the observed L-SSEs in the Bungo Channel, using the frictional parameters in such a way that R is smaller than the critical nucleation size R_c [Rubin and Ampuero (2005), Chen and Lapusta (2009)]. Secondly, we considered the effect the seismogenic locked zones in the up-dip side of the L-SSEs zone. We set a locked zone at the up-dip of the L-SSE fault, whose back-slip rate is 6.0 cm/yr.

As the common analysis settings, we selected several pairs of frictional parameters in a wide range of parameter space which reproduce L-SSEs for the initial ensemble members of frictional parameters. We made the daily synthetic GNSS surface displacement data for 93 GEONET stations around the Bungo channel by calculating the surface displacements using true synthetic frictional parameters and adding random Gaussian noise. We set the assimilation interval to 10 days.

In experiment i), we calculated 31 day moving averages of the synthetic GNSS displacement data, and we obtained the surface velocities at GNSS stations from the derivatives of a 150-day cubic spline function fitting the moving averaged surface displacements. Then we applied EnKF to the obtained surface velocities and we successfully estimated slip evolution and frictional parameters. This result suggests this method for converting the surface displacement data into the surface velocity data at GNSS stations might be applicable.

©2019. Japan Geoscience Union. All Right Reserved.

In experiment ii), we applied EnKF to the synthetic GNSS displacement data directly. When we conducted experiment ii), we changed some analysis settings for stabilizing the assimilation. Firstly, when the slip velocity at the center of fault plane is low, we added larger random noise to the innovations artificially. Secondly, when the slip velocity at the center of fault plane is high, we reduced the assimilation interval to 1 day and introduced additive inflation to prevent the prediction errors from being too small. As a result, we also successfully estimated slip evolution and frictional parameters using the surface displacements, although the experiment sometime fails depending on the start timing of the analysis. Therefore, this method has not been fully stabilized yet, and we need to improve it for robust estimation.

Finally, we applied EnKF to the real GNSS data before the 2011 Tohoku-oki earthquake in the same settings as experiment i) and ii) respectively. We corrected offsets of major earthquakes and antenna changes in the GNSS data. However, both experiments stopped during the assimilation due to negative slip velocities. It manifests an importance of correction of GNSS data including removing annual and semiannual components for a stable assimilation of real GNSS data. Furthermore, we need to consider the realistic model settings including the geometry of the subducting Philippine Sea plate interface and distribution of both L-SSE and locked zones.

Acknowledgement: We used GNSS of GEONET provided by the Geospatial Information Authority of Japan (GSI).

Keywords: GNSS, Ensemble Kalman Filter (EnKF), Long-term SSEs, the Bungo channel

©2019. Japan Geoscience Union. All Right Reserved.

A data assimilation library with Python for parallel computing

*Shin ya Nakano[1], Yuya Ariyoshi[2], Tomoyuki Higuchi[1]

1. The Institute of Statistical Mathematics, 2. Faculty of Engineering, Nippon Bunri University

Parallel computing is essential to reduce the computational time in the ensemble-based data assimilation. However, it requires skills in parallel programming. It is sometimes a hard task to attain high computational efficiency with ensemble-based data assimilation. In particular, the particle filter (PF) algorithm, which is applicable to nonlinear and/or non-Gaussian problems, contains a procedure difficult to parallelize.
It is thus challenging to achieve high computational efficiency with the PF even for experienced users.

We have developed a Python library named P-cubed (Python Parallelized Particle Filter Library), that enables us to use parallel-ready PF algorithms with high parallel efficiency. Now we are also planning to attach a module of other data assimilation algorithms such as the ensemble Kalman filter to this library. In this presentation, we introduce the parallelized PF algorithms which are already available in P-cubed and explain the design and characteristics of the library. Future prospects of this library will also be discussed.

Keywords: data assimilation, particle filter, parallel computing, Python

©2019. Japan Geoscience Union. All Right Reserved.

[E] Oral | M (Multidisciplinary and Interdisciplinary)：M-GI General Geosciences, Information Geosciences & Simulations

Wed. May 29, 2019 1:45 PM - 3:15 PM JST | Wed. May 29, 2019 4:45 AM - 6:15 AM UTC | 104 1F

[M-GI30] Data assimilation: A fundamental approach in geosciences

convener:Shin ya Nakano(The Institute of Statistical Mathematics), Yosuke Fujii(Meteorological Research Institute, Japan Meteorological Agency), SHINICHI MIYAZAKI(Graduate School of Science, Kyoto University), Takemasa Miyoshi(RIKEN), Chairperson:Takemasa Miyoshi(RIKEN Advanced Institute for Computational Science), Shin'ya Nakano(情報・システム研究機構 統計数理研究所)

Data assimilation is an inversion approach to estimate the evolution of a system by utilizing a constraint given by a dynamical simulation model. Data assimilation is now widely used not only in meteorology and oceanography but also other fields of geosciences such as hydrology, solid earth science, and space science. This session aims at providing an opportunity for discussion on data assimilation studies among researchers of various field of geosciences. We encourage contributions addressing novel methods and theoretical developments of data assimilation. Contributions dealing with useful applications of data assimilation are also welcome.

1:45 PM - 2:00 PM JST | 4:45 AM - 5:00 AM UTC

[MGI30-01] Recent progresses and applications of geomagnetic data assimilation

★Invited Papers

*Julien Aubert[1], Vincent Lesur[1], Alexandre Fournier[1], Gauthier Hulot[1] (1.Institut de Physique du Globe de Paris, France)

2:00 PM - 2:15 PM JST | 5:00 AM - 5:15 AM UTC

[MGI30-02] Accounting for non-locality of vertical error correlation within ETKF through eigen-spectral localization

★Invited Papers

*Daisuke Hotta[1] (1.Meteorological Research Institute, Japan Meteorological Agency)

2:15 PM - 2:30 PM JST | 5:15 AM - 5:30 AM UTC

[MGI30-03] Data assimilation experiments with MODIS LAI observations and the dynamic global vegetation model SEIB-DGVM over Siberia

★Invited Papers

*Hazuki Arakida[1], Shunji Kotsuki[1], Shigenori Otsuka[1], Yohei Sawada[1,2], Takemasa Miyoshi[1] (1.RIKEN Center for Computational Science, 2.Meteorological Research Institute)

2:30 PM - 2:45 PM JST | 5:30 AM - 5:45 AM UTC

[MGI30-04] Inversion of the ocean vertical diffusivity from steady-state tracer distributions by using an adjoint method

★Invited Papers

*Akira Oka[1] (1.Atmosphere and Ocean Research Institute, The University of Tokyo)

2:45 PM - 3:00 PM JST | 5:45 AM - 6:00 AM UTC

[MGI30-05] Nonlinear data assimilation with 4DEnVar using iterative weather forecast model

*Sho Yokota[1], Ko Koizumi[1], Masaru Kunii[2,1], Kosuke Ito[3,1] (1.Meteorological Research Institute, Japan Meteorological Agency, 2.Numerical Prediction Division, Forecast Department, Japan Meteorological Agency, 3.University of the Ryukyus)

3:00 PM - 3:15 PM JST | 6:00 AM - 6:15 AM UTC

[MGI30-06] Development of Data Assimilation System for Atmospheric Density to Improve Satellite's Orbit Prediction Accuracy

*Hiroshi Kato[1], Hideaki Hinagawa[1], Kyohei Akiyama[1], Yuki Akiyama[1], Masaya Nakano[2], Daichi Obinata[2], Shinichi Nakamura[1] (1.Japan Aerospace Exploration Agency, 2.FUJITSU LIMITED)

Recent progresses and applications of geomagnetic data assimilation

*Julien Aubert[1], Vincent Lesur[1], Alexandre Fournier[1], Gauthier Hulot[1]

1. Institut de Physique du Globe de Paris, France

Over the past ten years, numerical simulations of Earth’ s core magnetohydrodynamics have advanced to a point where their output can be compared in detail to the geomagnetic field behaviour over time scales ranging from a few years to centuries. Motivated by this progress, geomagnetic data assimilation is an emerging discipline that aims at optimally combining the statistical output of such simulations with geomagnetic data. Among the many possible outcomes of this approach, the main goals are to infer the hidden dynamical properties of Earth’ s core from the surface observations, forecast the future evolution of the geomagnetic field in a dynamically consistent way and at horizons of a few years to a century, and improve the quality of source separation in analyses of the geomagnetic field. We will present a few examples to emphasize the value added by statistics extracted from Earth-like geodynamo simulations when attempting to tackle these underdetermined geophysical inverse problems. We will also put these works in context of forthcoming contributions to the 13th iteration of the International Reference Geomagnetic Field (IGRF 2020).

Keywords: Geomagnetism, Numerical Simulations, Earth's core, data assimilation

©2019. Japan Geoscience Union. All Right Reserved.

Accounting for non-locality of vertical error correlation within ETKF through eigen-spectral localization

*Daisuke Hotta[1]

1. Meteorological Research Institute, Japan Meteorological Agency

Covariance localization is an indispensable component of any EnKF and it is most straightforwardly formulated as tapering of the sampled background error covariance matrix by means of Schur product (B-loc). However, within most (L)ETKF implementations, this operation is substituted by artificial inflation of R-matrix for observations distant from the analyzed grid-point (R-loc) due to the computational the difficulty of B-loc approach. Recently studies (Bocquet et al. 2016; Bishop et al. 2017) have derived an efficient way to implement B-loc within an ETKF, so that B-loc within ETKF is now a feasible option.

The author's recent work has focused on clarifying the differences between B-loc and R-loc, and showed with idealized 1D models that B-loc can increase the effective rank of the background covariance while R-loc cannot and that B-loc can more faithfully reproduce canonical KF analysis than R-loc does when the observation operator is non-local, suggesting that B-loc is particularly advantageous in cases where the desired amount of assimilated observations are much larger than the affordable ensemble size and/or the observation operator is highly non-local.

This work extends the B-loc approach to accommodate situations where the true background error covariance is not well localized (i.e., the correlation between two grid-points is not given in terms of the physical distance between them). In the proposed scheme, the state vector of each background ensemble is first linearly transformed into the space spanned by the (truncated) eigenbasis of the climatological background error covariance prior to performing data assimilation. The transformed ensemble is then used to form sample covariance to which we apply localization (i.e., control on sampling noises) by neglecting all the off-diagonal components. This method reposes on two assumptions: (1) the true covariance, when expressed in its eigen-space, is diagonal, so that, in this space, any off-diagonal component present in the sample covariance from ensemble is a sign of sampling error, and (2) the eigenstructure of the true covariance is close to its climatological expectation.

In this presentation, I will show several preliminary verifications of this approach using an idealized 1-dimensional system and discuss its promise and limitations.

©2019. Japan Geoscience Union. All Right Reserved.

Keywords: data assimilation, covariance localization, EnKF

©2019. Japan Geoscience Union. All Right Reserved.

Data assimilation experiments with MODIS LAI observations and the dynamic global vegetation model SEIB-DGVM over Siberia

*Hazuki Arakida[1], Shunji Kotsuki[1], Shigenori Otsuka[1], Yohei Sawada[1,2], Takemasa Miyoshi[1]

1. RIKEN Center for Computational Science, 2. Meteorological Research Institute

In the previous study, Arakida et al. (2017) developed a data assimilation system with the SEIB-DGVM (Spatially Explicit Individual-Based Dynamic Global Vegetation Model, Sato et al. 2007) and assimilated satellite-observed Leaf Area Index (LAI) successfully at a flux measurement site in Siberia. In this study, we extend the experiment to a large domain in Siberia and estimate the vegetation functions and structures, and model parameters related to the phenology of the deciduous needle-leaved tree and the undergrowth. At the annual meeting in 2017, we presented the results of total LAI, tree LAI, above ground biomass, carbon flux, and the model parameters. This year, we present further comparisons with the previous studies: carbon flux (FLUXCOM: Tramontana et al., 2016, Jung et al., 2017) estimated by a machine learning method using in-situ flux measurements and various explanatory data, tree LAI (Delbart et al., 2005, Kobayashi et al., 2010) estimated by a radiative transfer model and satellite observations, and above ground biomass (Liu et al., 2015) estimated by satellite observations. The results showed high correlations between this study and the previous studies except for above ground biomass. This is probably because above ground biomass of Liu et al. [2015] is estimated from microwave-based observations, different from optical-based observations in this study, Kobayashi et al. [2010], and FLUXCOM. The results suggest that the type of the satellite sensor affect the estimation results. Most of the estimated variables by DA were highly correlated with the observed LAI and the previous studies, indicating that the DA system generally performed well over Siberia.

Arakida, H., T. Miyoshi, T. Ise, S. I. Shima, and S. Kotsuki (2017), Non-Gaussian data assimilation of satellite-based leaf area index observations with an individual-based dynamic global vegetation model, Nonlinear Proc. Geoph., 24, 553-567, doi:10.5194/npg-24-553-2017.

Delbart, N., L. Kergoat, T. L. Toan, J. Lhermitte, and G. Picard (2005), Determination of phenological dates in boreal regions using normalized difference water index, Remote Sens. Environ., 97, 26-38, doi:10.1016/j.rse.2005.03.011.

Jung, M., M. Reichstein, C. R. Schwalm, C. Huntingford, S. Sitch, A. Ahlström, A. Arneth, G. Camps-Valls, P. Ciais, P. Friedlingstein, F. Gans, K. Ichii, A. K. Jain, E. Kato, D. Papale, B. Poulter, B. Raduly, C. Rödenbeck, G. Tramontana, N. Viovy, Y. P. Wang, U. Weber, S. Zaehle and N. Zeng (2017), Compensatory water effects link yearly global land CO_2 sink changes to temperature, Nature, 541, 516-520, doi:10.1038/nature20780.

Kobayashi, H., N. Delbart, R. Suzuki, and K. Kushida (2010), A satellite-based method for monitoring seasonality in the overstory leaf area index of Siberian larch forest, J. Geophys. Res., 115, G01002, doi: 10.1029/2009JG000939.

Liu, Y. Y., A. I. J. M. van Dijk, R. A. M. de Jeu, J. G. Canadell, M. F. McCabe, J. P. Evans, and G. Wang (2015), Recent reversal in loss of global terrestrial biomass. Nat. Clim. Change, 5, 470-474, doi:10.1038/nclimate2581.

©2019. Japan Geoscience Union. All Right Reserved.

Sato, H., A. Itoh, and T. Kohyama (2007), SEIB–DGVM: A new Dynamic Global Vegetation Model using a spatially explicit individual-based approach, Ecol. Model., 200, 279–307, doi: 10.1016/j.ecolmodel.2006.09.006.

Tramontana, G., M. Jung, C. R. Schwalm, K. Ichii, G. Camps-Valls, B. Ráduly, M. Reichstein, M. A. Arain, A. Cescatti, G. Kiely, L. Merbold, P. Serrano-Ortiz, S. Sickert, S. Wolf, and D. Papale (2016), Predicting carbon dioxide and energy fluxes across global FLUXNET sites with regression algorithms, Biogeosciences, 13, 4291-4313, doi:10.5194/bg-13-4291-2016.

Keywords: data assimilation, vegetation model, satellite data

©2019. Japan Geoscience Union. All Right Reserved.

Inversion of the ocean vertical diffusivity from steady-state tracer distributions by using an adjoint method

*Akira Oka[1]

1. Atmosphere and Ocean Research Institute, The University of Tokyo

The ocean vertical diffusivity is important for controlling the distribution of various ocean tracer including the temperature and salinity. Recent studies clarified that its spatial distribution is very inhomogeneous but the global coverage of its direct measurements from turbulent mixing observations are not enough and its quantification is still difficult. On the other hand, recent observational data about the ocean tracer including temperature and salinity are increasing significantly and dataset covering the global ocean is available. The inversion of ocean velocity distribution from ocean tracer has been reported in the previous studies (e.g. Wunsch, 1996). In the same way as this velocity inversion, some studies tried the inversion of the ocean vertical diffusivity (e.g. Ganachaud and Wunsch, 2000) but there are few studies which discuss its detail 3-dimmensional distribution. In this presentation, I would like to report some attempts about the inversion of the ocean vertical diffusivity from the ocean tracer distribution; we focus on the temperature, salinity, and carbon isotope (C14) and discuss how their steady-state distribution is useful for obtaining the 3-dimmensional distribution of the ocean vertical diffusivity.

Keywords: ocean vertical diffusivity, adjoint method, ocean tracer model

©2019. Japan Geoscience Union. All Right Reserved.

Nonlinear data assimilation with 4DEnVar using iterative weather forecast model

*Sho Yokota[1], Ko Koizumi[1], Masaru Kunii[2,1], Kosuke Ito[3,1]

1. Meteorological Research Institute, Japan Meteorological Agency, 2. Numerical Prediction Division, Forecast Department, Japan Meteorological Agency, 3. University of the Ryukyus

En4DVar and 4DEnVar are two popular ensemble-based variational data assimilation methods for the numerical weather prediction. Although the ensemble-based forecast error covariance can be reflected in the analyses of both methods, En4DVar calculates the gradient of the cost function with the adjoint of tangent linear forecast model, which requires large development and computational costs. Such costs are generally not required in 4DEnVar because 4DEnVar does not use the tangent linear forecast model. However, 4DEnVar analyses are generally worse than those of adjoint-based En4DVar probably because 4DEnVar does not iteratively calculate the nonlinear forecast model. In this study, therefore, we developed 4DEnVar with iterative nonlinear forecast model (hereafter, 4DEnVar-IF). In 4DEnVar-IF, the nonlinear forecast model is iteratively calculated to gain the non-quadratic cost function and its gradient in each iteration. The 4DEnVar-IF applied to the Lorenz63 model showed that the 4DEnVar-IF analysis can be better than those of En4DVar and general 4DEnVar when nonlinearity is strong and ensemble perturbations are appropriate. Moreover, we also applied 4DEnVar-IF to JMA nonhydrostatic model-based 4DVar data assimilation (JNoVA) system. The single-observation assimilation experiments with JNoVA showed that 4DEnVar-IF can make the cost function smaller than En4DVar when the assimilated observation has the strong nonlinearity as like potential temperature associated with cloud microphysics. In the assimilation experiment of multiple real observations with 4DEnVar-IF of the small localization scale, however, the minimization of the cost function was not sufficiently succeeded. As a next step, we will develop the localization and hybrid of forecast error covariance matrix.

Keywords: data assimilation, ensemble forecast, nonlinear, 4DEnVar

©2019. Japan Geoscience Union. All Right Reserved.

Development of Data Assimilation System for Atmospheric Density to Improve Satellite's Orbit Prediction Accuracy

*Hiroshi Kato[1], Hideaki Hinagawa[1], Kyohei Akiyama[1], Yuki Akiyama[1], Masaya Nakano[2], Daichi Obinata[2], Shinichi Nakamura[1]

1. Japan Aerospace Exploration Agency, 2. FUJITSU LIMITED

Satellite's orbit prediction with high accuracy requires atmospheric drag prediction with high accuracy, because there is a slight atmosphere in a low-orbital environment. The atmospheric drag can be calculated from the atmospheric density, the ballistic coefficient (mass, cross-sectional area, drag coefficient) of each satellite, but the uncertainty of the atmospheric density is considered to occupy most of the uncertainty of atmospheric drag prediction.
Several atmospheric density models have been proposed so far. Although observation information in low orbit environments is very limited, the models are based on slight satellite observation information. However, it is difficult to predict the atmospheric density with high accuracy, and the satellite operator improves the accuracy of orbit prediction by estimating correction amount based on the orbit determination value.
Since 2018, JAXA has started to develop the atmospheric density reanalysis system (data assimilation system). This system realizes the reanalysis of the atmospheric density from the atmospheric density observation, which is averaged atmospheric density on the satellite locus, and atmospheric density models. The averaged atmospheric density on the satellite locus can be estimated based on orbit information of TLE (two-line element) of each satellite provided by NORAD in the United States. The atmospheric density model uses the NRLMSIS-00 model and the Jacchia-Bowman 2008 model usually used in the orbit field. As data assimilation methods, the ensemble Kalman filter and the ensemble transformed Kalman filter are implemented.
In this presentation, we introduce the details of the atmospheric density reanalysis system and show the results of the twin experiment (numerical experiment) being advanced as system verification.

Keywords: Satellite orbit prediction, Atmospheric density, Data assimilation

©2019. Japan Geoscience Union. All Right Reserved.

[E] Oral | M (Multidisciplinary and Interdisciplinary)：M-GI General Geosciences, Information Geosciences & Simulations

Wed. May 29, 2019 3:30 PM - 5:00 PM JST | Wed. May 29, 2019 6:30 AM - 8:00 AM UTC | 104 1F

[M-GI30] Data assimilation: A fundamental approach in geosciences

convener:Shin ya Nakano(The Institute of Statistical Mathematics), Yosuke Fujii(Meteorological Research Institute, Japan Meteorological Agency), SHINICHI MIYAZAKI(Graduate School of Science, Kyoto University), Takemasa Miyoshi(RIKEN), Chairperson:Shinichi Miyazaki(Kyoto University), Yosuke Fujii

Data assimilation is an inversion approach to estimate the evolution of a system by utilizing a constraint given by a dynamical simulation model. Data assimilation is now widely used not only in meteorology and oceanography but also other fields of geosciences such as hydrology, solid earth science, and space science. This session aims at providing an opportunity for discussion on data assimilation studies among researchers of various field of geosciences. We encourage contributions addressing novel methods and theoretical developments of data assimilation. Contributions dealing with useful applications of data assimilation are also welcome.

3:30 PM - 3:45 PM JST | 6:30 AM - 6:45 AM UTC

[MGI30-07] An LETKF-based ocean reanalysis for the Asia-Oceania region using Himawari-8 SSTs and SMOS/SMAP SSS

★Invited Papers

*Shun Ohishi[1], Tsutomu Hihara[2], Hidenori AIKI[1], Joji Ishizaka[1], Yasumasa Miyazawa[2], Misako Kachi[3] (1.Nagoya University, 2.JAMSTEC, 3.JAXA)

3:45 PM - 4:00 PM JST | 6:45 AM - 7:00 AM UTC

[MGI30-08] Validation of JCOPE-T DA ocean assimilation product

*Tsutomu Hihara[1], Sergey Varlamov[1], Yasumasa Miyazawa[1], Toru Miyama[1], Misako Kachi[2], Hiroshi Murakami[2] (1.Japan Agency for Marine-Earth Science and Technology, 2.Japan Aerospace Exploration Agency)

4:00 PM - 4:15 PM JST | 7:00 AM - 7:15 AM UTC

[MGI30-09] Do surface lateral flows matter for land data assimilation?: Implication for hyper-resolution land modeling and observation

*Yohei Sawada[1] (1.Meteorological Research Institute)

4:15 PM - 4:30 PM JST | 7:15 AM - 7:30 AM UTC

[MGI30-10] Geodynamo data assimilation for candidate models of IGRF13-SV from Japan team

*Takuto Minami[1], Shin ya Nakano[2], Futoshi Takahashi[3], Masaki Matsushima[4], Hisayoshi Shimizu[1], Hiroaki TOH[5] (1.Ocean Hemisphere Research Institute, Earthquake Research Institute,The University of Tokyo, 2.The Institute of Statistical Mathematics, 3.Faculty of Science, Kyushu University, 4.School of Science, Tokyo Institute of Technology, 5.Graduate School of Science, Kyoto University)

4:30 PM - 4:45 PM JST | 7:30 AM - 7:45 AM UTC

[MGI30-11] A pilot study of geomagnetic data assimilation into a geodynamo model

*Shin ya Nakano[1], Takuto Minami[2], Futoshi Takahashi[3], Masaki Matsushima[4], Hiroaki TOH[5], Hisayoshi Shimizu[2] (1.The Institute of Statistical Mathematics, 2.Earthquake Research Institute, the University of Tokyo, 3.Faculty of Science, Kyushu University, 4.School of Science, Tokyo Institute of Technology, 5.Data Analysis Center for Geomagnetism and Space Magnetism, Graduate School of Science, Kyoto University)

4:45 PM - 5:00 PM JST | 7:45 AM - 8:00 AM UTC

[MGI30-12] Bayesian parameter estimation of a physics-based model of postseismic crustal deformation

★Invited Papers

*Jun'ichi Fukuda[1], Kaj Johnson[2] (1.Earthquake Research Institute, University of Tokyo, 2.Department of Earth and Atmospheric Sciences, Indiana University)

An LETKF-based ocean reanalysis for the Asia-Oceania region using Himawari-8 SSTs and SMOS/SMAP SSS

*Shun Ohishi[1], Tsutomu Hihara[2], Hidenori AIKI[1], Joji Ishizaka[1], Yasumasa Miyazawa[2], Misako Kachi[3]

1. Nagoya University, 2. JAMSTEC, 3. JAXA

With the global spread of the Argo floats and development of high-resolution ocean models, global ocean reanalysis datasets have been released. Although regional high-resolution ocean reanalysis datasets also have been established around the North Pacific, most of their coverage area is limited to regions north of 10˚N. We suggest that reanalysis datasets for tropical-subtropical oceans are yet to be constructed for coastal environmental monitoring and typhoon researches around the Asia-Oceania region.
Since July 2015, a geostationary satellite “Himawari-8” has been measuring sea surface temperatures (SSTs) with a high spatial and temporal resolution of 2 km and 10 min. in the western Pacific region using an infrared sensor. Because of the high temporal resolution, daily composite map shows that coverage area of Himawari-8 exceeds that of an orbital satellite “GCOM-W” with a microwave sensor. The infrared sensor enables us to capture fine nearshore SST structure, such as localized cool SSTs induced by Ekman upwelling along the Vietnam coast during the southwesterly summer monsoon.
We have established a one-way nest high-resolution ocean data assimilation system based on LETKF (Hunt et al. 2007) with 20 ensemble members at 1-day interval. The southeast Asia coastal region [98˚–115˚E, 0˚–22˚N] has been modeled at a spatial resolution of 1/36˚ and 47 layers with an intent to be applied for fishery and marine environmental monitoring, while the large-scale western Pacific region [95˚E–165˚W, 50˚S–50˚N] has been constructed at a spatial resolution of 1/12˚ and 47 layers to make contributions to tropical cyclone studies. Himawari-8 SSTs and sea surface salinity (SSS) derived from SMOS and SMAP satellites as well as sea surface height, and temperature/salinity derived from GTSPP and AQC Argo dataset have been assimilated. To improve the salinity field, freshwater fluxes also have been incorporated. To avoid generation of spurious gravity waves, the Incremental analysis Update (IAU) filter (Bloom et al. 1996) have been implemented. We will introduce low salinity water transport from the Mekong river in the southeast Asia system and the SST cooling with the passage of tropical cyclones in the western Pacific system.

Keywords: southeast Asia, western Pacific, data assimilation, LETKF, Himawari-8, SMOS/SMAP

©2019. Japan Geoscience Union. All Right Reserved.

Validation of JCOPE-T DA ocean assimilation product

*Tsutomu Hihara[1], Sergey Varlamov[1], Yasumasa Miyazawa[1], Toru Miyama[1], Misako Kachi[2], Hiroshi Murakami[2]

1. Japan Agency for Marine-Earth Science and Technology, 2. Japan Aerospace Exploration Agency

We constructed the high resolution (3km, 1hour) ocean data assimilation system named as JCOPE-T DA which targets around Japan. This system is running operationally and that’ s outputs have been provided by JAXA through the Himawari Monitor website and P-Tree System since November 2018. One of the aims in this system is to make the useful ocean analysis and forecast data by assimilating satellite SST data provided by JAXA directly. We assimilate the satellite SST data observed by Himawari/AHI, GCOM-W/AMSR2, GPM main satellite/GMI, and Coriolis/WindSAT. Multi-3DVAR (Miyazawa et al. 2017) and IAU are applied in this system.

We will show the results of validation of JCOPE-T DA using independent in situ data observed by buoys and ship in this presentation. The results of comparison with CTD data observed by SHINSEI-MARU off the Kii Channel show that JCOPE-T DA ocean temperature data are good estimate in upper layer (Figure 1). Biases and RMS error are lower than ±0.2 deg.C and 0.7 deg.C in 2 –40m depth respectively. On the other hand, there are negative bias and large RMS difference (over 1 deg.C) in thermocline (5 –200 m depth). These mean that mixed layer of JCOPE-T DA is deeper than that of observation.
JCOPE-T DA clearly show the internal tide because the ocean model of JCOPE-T DA considers the tide effects. Especially, we find that the channel between Taiwan and Philippines causes strong internal tide which is made change of several degree Celsius at 500m depth in a day.

In the future plan, we are going to construct the higher resolution (1km grid) ocean model with CaMa-Flood river flow data. And also, we are going to assimilate the GCOM-C/SGLI SST data which have 250m resolution. Furthermore, we will construct a nest model for coastal area.

Keywords: Data assimilation, Satellite SST data, Regional ocean model

©2019. Japan Geoscience Union. All Right Reserved.

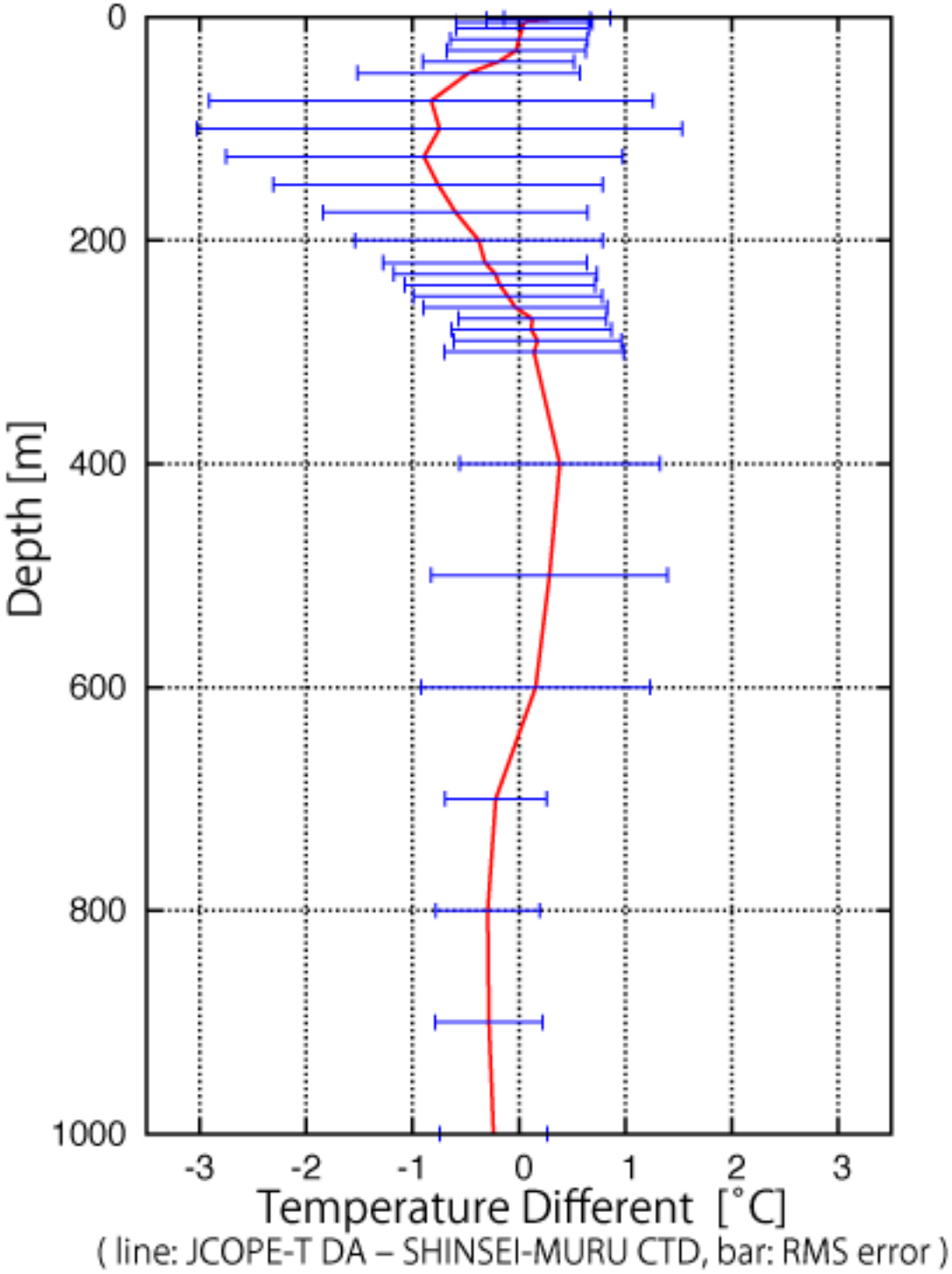

©2019. Japan Geoscience Union. All Right Reserved.

Do surface lateral flows matter for land data assimilation?: Implication for hyper-resolution land modeling and observation

*Yohei Sawada[1]

1. Meteorological Research Institute

Hyper-resolution land modeling is expected to innovate the simulation of terrestrial water, energy, and carbon cycles. One of the major advantages of existing hyper-resolution land models against conventional 1-demensional land surface models is that surface and subsurface lateral water flows can be explicitly simulated. Despite a lot of efforts on assimilating hydrological observations into the hyper-resolution integrated surface-groundwater land models, how and in what case topography-driven surface water flows matter for data assimilation of soil moisture observations has yet to be clarified. In this study, I perform a minimalist synthetic numerical experiment, in which shallow soil moisture observations are assimilated into an integrated surface-groundwater land model by an ensemble Kalman filter. Propagation of a background error due to surface lateral water flows is crucially important to adjust the unobserved model state and parameter variables by horizontally propagating the information of soil moisture observations. However, the non-Gaussianity of the background error induced by the nonlinear dynamics of topography-driven surface flows harms the performance of an ensemble Kalman filter and the efficiency of data assimilation strongly depends on soil characteristics. The new capability of data assimilation with the hyper-resolution land models found in this study may improve the monitoring and prediction of flash floods caused by local severe rainfalls.

Sawada, Y. (2018), Do surface lateral flows matter for data assimilation of soil moisture observations into hyperresolution land models?, *EarthArXiv,* https://doi.org/10.31223/osf.io/byguf

Keywords: land data assimilation

©2019. Japan Geoscience Union. All Right Reserved.

Geodynamo data assimilation for candidate models of IGRF13-SV from Japan team

*Takuto Minami[1], Shin ya Nakano[2], Futoshi Takahashi[3], Masaki Matsushima[4], Hisayoshi Shimizu[1], Hiroaki TOH[5]

1. Ocean Hemisphere Research Institute, Earthquake Research Institute,The University of Tokyo, 2. The Institute of Statistical Mathematics, 3. Faculty of Science, Kyushu University, 4. School of Science, Tokyo Institute of Technology, 5. Graduate School of Science, Kyoto University

International Geomagnetic Reference Field (IGRF) is a series of standard global geomagnetic field models that consist of Gauss coefficients to represent spatial distribution. International Association of Geomagnetism and Aeronomy (IAGA) produces IGRF every five years, the last version of which, the 12th generation of IGRF (IGRF-12), was released in December 2014 (Thebault et al., 2015). Each generation of IGRF comprises not only the main field part but secular variation (SV) part (first time derivative of the main field) to forecast evolution of the geomagnetic field for the next five years to come. The next generation, IGRF-13, will be published around December 2019, comprising the spatial distribution of the field at epoch 2020.0 and its secular variation in the period from 2020.0 to 2025.0. We plan to submit a candidate SV model to contribute for determining IGRF13-SV.
We employ data assimilation with geodynamo calculations to generate a SV candidate model for the period from 2020.0 to 2025.0. Although the two standard approaches, (1) adoption of SV at the IGRF release time and (2) spline extrapolation of the main field in the future, are common for generating SV candidates, they are not “physics-based” forecasts, and, intrinsically, cannot alleviate the effect of sudden changes in the SV field called “geomagnetic jerks” (Mandea et al., 2010). In this context, data assimilation is one of novel approach to obtain an appropriate initial condition for geodynamo calculations at the time of IGRF release time. Since the parameters used in geodynamo calculations are apart by some orders of magnitude from those for the Earth's core, it is not appropriate to take geodynamo solutions as they are for the predictions. Nevertheless, it is possible to rescale the time-axis of geodynamo calculations using the ratio of the so-called “secular-variation time-scale” (Chlistensen and Tilgner, 2004) between the geomagnetic field and geodynamo calculations. In this presentation, we are going to show candidate models of secular variation obtained by geodynamo data assimilation with discussions on the time-scales, the method of assimilation, and data-set employed for the assimilation.

Keywords: IGRF, Data assimilation, dynamo

©2019. Japan Geoscience Union. All Right Reserved.

A pilot study of geomagnetic data assimilation into a geodynamo model

*Shin ya Nakano[1], Takuto Minami[2], Futoshi Takahashi[3], Masaki Matsushima[4], Hiroaki TOH[5], Hisayoshi Shimizu[2]

1. The Institute of Statistical Mathematics, 2. Earthquake Research Institute, the University of Tokyo, 3. Faculty of Science, Kyushu University, 4. School of Science, Tokyo Institute of Technology, 5. Data Analysis Center for Geomagnetism and Space Magnetism, Graduate School of Science, Kyoto University

Geomagnetic secular variation is a long-term variation of the Earth's magnetic field. The magnetic field of the Earth is originated from a dynamo in the outer core. Modeling of geodynamo process is thus a straightforward approach for predicting geomagnetic secular variations. However, it is intrinsically difficult to resolve the current state of the geodynamo from observable magnetic field and to predict future evolution of geodynamo. We are developing a framework for estimating the current state of the geodynamo by using a data assimilation approach. As a preliminary study, we performed data assimilation experiments using synthetic geomagnetic data in order to evaluate if data assimilation methods are effective for estimating the state of the geodynamo. Some data assimilation schemes based on ensemble-based variational method were applied and compared. Preliminary results of the experiments will be demonstrated.

Keywords: ensemble-based data assimilation, geodynamo model, secular variation

©2019. Japan Geoscience Union. All Right Reserved.

Bayesian parameter estimation of a physics-based model of postseismic crustal deformation

*Jun'ichi Fukuda[1], Kaj Johnson[2]

1. Earthquake Research Institute, University of Tokyo, 2. Department of Earth and Atmospheric Sciences, Indiana University

Recent development GPS and other geodetic networks makes it possible to capture transient crustal deformation at high resolution in both space and time. A primary example of geodetically observed transient deformation in plate boundary zones is postseismic deformation following large earthquakes. Two primary processes that are responsible for observed postseismic deformation are viscoelastic relaxation of in the asthenosphere and afterslip on the plate interface surrounding the coseismic rupture. Both of the processes are triggered by stress changes induced by an earthquake and the evolution of the two processes is governed by rheological properties of the asthenosphere and frictional properties of the plate interface as well as coseismic stress perturbations.

In this study, we develop a physics-based model of postseismic deformation following the 2011 Mw9.0 Tohoku-oki earthquake that incorporates stress-driven afterslip and viscoelastic relaxation. In this model, the evolution of afterslip is assumed to be governed by a velocity-strengthening friction law that is characterized with a friction parameter. Viscoelastic relaxation of the asthenosphere is modeled with a biviscous Burgers rheology that is characterized with steady-state and transient viscosities. The evolution of afterslip and viscoelastic relaxation is calculated using coseismic slip distribution as an initial condition. We treat the friction parameters, viscosity parameters, coseismic slip distribution, and a smoothing parameter for coseismic slip distribution as unknown parameters and estimate them using coseismic and postseismic GPS and seafloor geodetic data.

In order to quantify uncertainties of the model, we adopt a Bayesian approach and estimate the posterior probability density function (PDF) of the model parameters. In principle, the Markov chain Monte Carlo (MCMC) methods can be used for this purpose. However, the MCMC methods require many forward calculations and the forward model employed in this study is computationally intensive. Therefore, it is difficult to sample the posterior PDF within a realistic computation time. We thus combine a surrogate modeling approach with the MCMC methods to efficiently sample the posterior PDF. In this approach, we first obtain a function approximation to the posterior PDF by fitting a surrogate function to the posterior probability densities calculated for sample points in the model parameter space. Then a MCMC method is used to sample the surrogate posterior PDF. By using this approach, we obtain the posterior PDFs of the model parameters that successfully reproduce the observed coseismic and time-dependent postseismic displacement fields. Our results suggest that such approaches may be useful for parameter estimation and uncertainty quantification of computationally intensive forward models.

Keywords: Bayesian inference, parameter estimation, GPS, postseismic crustal deformation

©2019. Japan Geoscience Union. All Right Reserved.

[J] Poster | M (Multidisciplinary and Interdisciplinary)：M-GI General Geosciences, Information Geosciences & Simulations

Wed. May 29, 2019 3:30 PM - 5:00 PM JST | Wed. May 29, 2019 6:30 AM - 8:00 AM UTC | Poster Hall International Exhibition Hall8, Makuhari Messe_22

[M-GI36] Social media and earth and planetary sciences

convener:Kazuo Amano(Department of Environmental Sciences,Ibaraki University), Takashi Oguchi(Center for Spatial Information Science, The University of Tokyo), Masaki Ito(Institute of Industrial Science, the University of Tokyo), Kayoko Yamamoto(University of Elctro-Communications)

The utilization of social media for earth and planetary sciences has been developed rapidly in recent years. We would like to call for papers on case studies, development of methods, reviews, application to environmental problems and disaster prevention/mitigation.

[MGI36-P01] Research and Development on Chatbot for Disaster Response

*Hiroki Azuma[1], Masatsugu Hangyo[2], Kiyonori Ohtake[3] (1.National Research Institute for Earth Science and Disaster Resilience, 2.Weathernews Inc., 3.National Institute of Information and Communications Technology)

[MGI36-P02] Collaboration between NIPR image platform service and social media

*Takeshi Terui[1], Yasuyuki Minamiyama[2], Masaki Hidano[3] (1.National Institute of Polar Research, 2.Tokyo Foundation for Policy Research, 3.Info Lounge Corporation)

[MGI36-P03] Twitter account of the Association of Japanese Geographers: History of establishment and operation

*Takashi Oguchi[1], Yuichiro Nishimura[2], Daichi Kohmoto[3], Atsuko Niina[4], Hitoshi Saito[5] (1.Center for Spatial Information Science, The University of Tokyo, 2.Division of Humanities and Social Sciences, Nara Women's University, 3.Nara University of Education, 4.Izu Peninsula Geopark Promotion Council, 5.College of Economics, Kanto Gakuin University)

[MGI36-P04] Utilization of SNS for the North-Ibaraki Geopark Plan after canceling the certification of JGC

*Kazuo Amano[1], Jun Hosoi[2] (1.The Institute of Natural Sciences, College of Humanities and Sciences, Nihon Univ., 2.Institute of Geology and Geoinformation, Geological Survey of Japan, AIST)

Research and Development on Chatbot for Disaster Response

*Hiroki Azuma[1], Masatsugu Hangyo[2], Kiyonori Ohtake[3]

1. National Research Institute for Earth Science and Disaster Resilience, 2. Weathernews Inc., 3. National Institute of Information and Communications Technology

Disaster response agencies always suffer from the human resource shortage under the disaster situation. To solve the problem, efficient disaster response applying ICT technology to the social media has been required. In this study, we are developing two systems helping disaster responses. The first system automatically collects and summarizes disaster damage reports through the interactions between a chatbot and a victim. The second system provides optimized information for each victim based on each situation estimated via the interaction. In this presentation, we introduce this study as a case study of social implementation of the social media with technical background.

Keywords: Disaster response, Chatbot, Social implementation

©2019. Japan Geoscience Union. All Right Reserved.

第2期SIP「国家レジリエンス（防災・減災）の強化」

共同研究開発機関：株式会社ウェザーニューズ
国立研究開発法人情報通信研究機構

対話型災害情報流通基盤の研究開発

2018年度～ 防災チャットボットをつくっています。

【研究の概要】
●個人が避難や活動に必要な情報をスマホ等での対話システムを介して入手・提供できるようにすることで、迅速・確実な避難を実現するとともに、その情報に基づいて災害対応機関の業務を効率化する情報流通基盤を研究開発する。
●①個人の状況・要望に応じて情報提供する技術（個人適応型対話技術）、②社会動態を観測する情報収集・要約技術（対話からの社会動態抽出技術）を開発し、個人との自動対話システムとして確立する。

●各種災害情報と発話情報の融合処理と、対話を介することで誤情報等を排除しながら効果的に情報収集を行い、社会動態として抽出

●LINE等、普段使いのメッセージングアプリ等で数十万人規模で実現

防災チャットボットはどんな課題を解決するの？

こんなことを実現する予定です。

- 国民一人ひとりに最適化された避難等の支援
- 逐次変化する状況/要望に合わせた最適な情報提供
- 従来のセンサーでは得られなかった情報の取得
- 大量の個別要望等を短時間に自動処理し、人的資源が不足する災害対応機関の業務効率化を支援

すでに始まっている取り組みを教えて

神戸市での実証実験（2018.12.21）をおこないました。

- SIP第2期で開発中の防災チャットボットのプロトタイプを用いてコンセプトを実証しました
- 防災チャットボットの有用性を確認しました
- 神戸の震災で救援の対応をされた経験のある危機管理室長から、「大変わかりやすく、阪神淡路大震災の時とは隔世の感がある」とコメントをいただきました

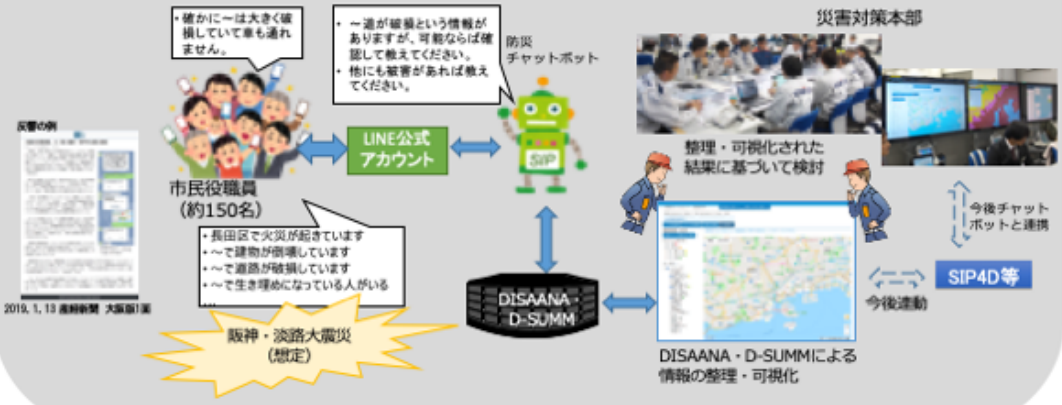

NIED 国立研究開発法人 防災科学技術研究所

©2019. Japan Geoscience Union. All Right Reserved.

Collaboration between NIPR image platform service and social media

*Takeshi Terui[1], Yasuyuki Minamiyama[2], Masaki Hidano[3]

1. National Institute of Polar Research, 2. Tokyo Foundation for Policy Research, 3. Info Lounge Corporation

NIPR is developing an open image archive platform with metadata that recorded the history of Antarctic / Arctic observation. This platform is now experimentally openned as NIPR Image Archive Web service as a following link.

https://image.nipr.ac.jp

Images to release on this platform are recorded pictures and videos in the Antarctic / Arctic. These images are data that recorded Japanese public activity in polar regions. In order to efficiently utilize data and distribute metadata, we are considering cooperation with various external Web services. For this reason, we are dealing with IIIF, Web API, JSON-LD, and we are testing the distribution on the Web. In the future we plan to respond to image retrieval and distribution enhancement on social media and various cloud services through image search engines. In this study, we will introduce the effect on data distribution expected to promote publication of image data by research institutions, and expectation to strengthen cooperation with social media and search engines.

Keywords: Image Search, Data Dissemination, Omeka, Polar Region, IIIF, Web API

©2019. Japan Geoscience Union. All Right Reserved.

Twitter account of the Association of Japanese Geographers: History of establishment and operation

*Takashi Oguchi[1], Yuichiro Nishimura[2], Daichi Kohmoto[3], Atsuko Niina[4], Hitoshi Saito[5]

1. Center for Spatial Information Science, The University of Tokyo, 2. Division of Humanities and Social Sciences, Nara Women's University, 3. Nara University of Education, 4. Izu Peninsula Geopark Promotion Council, 5. College of Economics, Kanto Gakuin University

The Twitter account of the Association of Japanese Geographers (AJG) with some 15,000 followers (@ajgeog) is widely recognized and has a certain level of social influence. Unlike most other accounts of academic societies, the AJG account often retweets geography-related tweets posted by various people, and refollows the majority of the followers. The account has been operated by the Public Relations Committee of the AJG for more than five years, to transfer information related to geography. This paper is presented by five AJG members who played a major role in creating the account and its operation at the early stage, to introduce background history.

Keywords: Association of Japanese Geographers, Twitter, History

©2019. Japan Geoscience Union. All Right Reserved.

Utilization of SNS for the North-Ibaraki Geopark Plan after canceling the certification of JGC

*Kazuo Amano[1], Jun Hosoi[2]

1. The Institute of Natural Sciences, College of Humanities and Sciences, Nihon Univ., 2. Institute of Geology and Geoinformation, Geological Survey of Japan, AIST

We would like to report the utilization of SNS in the North Ibaraki Geopark Plan after canceling the certification for the member of Japan Geopark Network(JGN). Toward recertification, strict opinions have been exchanged in the private Facebook about the North-Ibaraki Geopark and the geoparks in Japan. The whole concept of the geopark in Japan will be also argued based on the results of those discussions.

Keywords: SNS, North Ibaraki Geopark, Japan Gepark Network

©2019. Japan Geoscience Union. All Right Reserved.

[J] Poster | M (Multidisciplinary and Interdisciplinary)：M-GI General Geosciences, Information Geosciences & Simulations

Wed. May 29, 2019 5:15 PM - 6:30 PM JST | Wed. May 29, 2019 8:15 AM - 9:30 AM UTC | Poster Hall International Exhibition Hall8, Makuhari Messe_38

[M-GI36] Social media and earth and planetary sciences

convener:Kazuo Amano(Department of Environmental Sciences,Ibaraki University), Takashi Oguchi(Center for Spatial Information Science, The University of Tokyo), Masaki Ito(Institute of Industrial Science, the University of Tokyo), Kayoko Yamamoto(University of Elctro-Communications)

The utilization of social media for earth and planetary sciences has been developed rapidly in recent years. We would like to call for papers on case studies, development of methods, reviews, application to environmental problems and disaster prevention/mitigation.

[MGI36-P01] Research and Development on Chatbot for Disaster Response

*Hiroki Azuma[1], Masatsugu Hangyo[2], Kiyonori Ohtake[3] (1.National Research Institute for Earth Science and Disaster Resilience, 2.Weathernews Inc., 3.National Institute of Information and Communications Technology)

[MGI36-P02] Collaboration between NIPR image platform service and social media

*Takeshi Terui[1], Yasuyuki Minamiyama[2], Masaki Hidano[3] (1.National Institute of Polar Research, 2.Tokyo Foundation for Policy Research, 3.Info Lounge Corporation)

[MGI36-P03] Twitter account of the Association of Japanese Geographers: History of establishment and operation

*Takashi Oguchi[1], Yuichiro Nishimura[2], Daichi Kohmoto[3], Atsuko Niina[4], Hitoshi Saito[5] (1.Center for Spatial Information Science, The University of Tokyo, 2.Division of Humanities and Social Sciences, Nara Women's University, 3.Nara University of Education, 4.Izu Peninsula Geopark Promotion Council, 5.College of Economics, Kanto Gakuin University)

[MGI36-P04] Utilization of SNS for the North-Ibaraki Geopark Plan after canceling the certification of JGC

*Kazuo Amano[1], Jun Hosoi[2] (1.The Institute of Natural Sciences, College of Humanities and Sciences, Nihon Univ., 2.Institute of Geology and Geoinformation, Geological Survey of Japan, AIST)

Research and Development on Chatbot for Disaster Response

*Hiroki Azuma[1], Masatsugu Hangyo[2], Kiyonori Ohtake[3]

1. National Research Institute for Earth Science and Disaster Resilience, 2. Weathernews Inc., 3. National Institute of Information and Communications Technology

Disaster response agencies always suffer from the human resource shortage under the disaster situation. To solve the problem, efficient disaster response applying ICT technology to the social media has been required. In this study, we are developing two systems helping disaster responses. The first system automatically collects and summarizes disaster damage reports through the interactions between a chatbot and a victim. The second system provides optimized information for each victim based on each situation estimated via the interaction. In this presentation, we introduce this study as a case study of social implementation of the social media with technical background.

Keywords: Disaster response, Chatbot, Social implementation

©2019. Japan Geoscience Union. All Right Reserved.

第2期SIP「国家レジリエンス（防災・減災）の強化」

共同研究開発機関：株式会社ウェザーニューズ
国立研究開発法人情報通信研究機構

対話型災害情報流通基盤の研究開発

2018年度～ 防災チャットボットをつくっています。

【研究の概要】
●個人が避難や活動に必要な情報をスマホ等での対話システムを介して入手・提供できるようにすることで、迅速・確実な避難を実現するとともに、その情報に基づいて災害対応機関の業務を効率化する情報流通基盤を研究開発する。
●①個人の状況・要望に応じて情報提供する技術（個人適応型対話技術）、②社会動態を観測する情報収集・要約技術（対話からの社会動態抽出技術）を開発し、個人との自動対話システムとして確立する。

●各種災害情報と発話情報の融合処理と、対話を介することで誤情報等を排除しながら効果的に情報収集を行い、社会動態として抽出

●LINE等、普段使いのメッセージングアプリ等で数十万人規模で実現

防災チャットボットはどんな課題を解決するの？

こんなことを実現する予定です。

- 国民一人ひとりに最適化された避難等の支援
- 逐次変化する状況/要望に合わせた最適な情報提供
- 従来のセンサーでは得られなかった情報の取得
- 大量の個別要望等を短時間に自動処理し、人的資源が不足する災害対応機関の業務効率化を支援

すでに始まっている取り組みを教えて

神戸市での実証実験（2018.12.21）をおこないました。

- SIP第2期で開発中の防災チャットボットのプロトタイプを用いてコンセプトを実証しました
- 防災チャットボットの有用性を確認しました
- 神戸の震災で救援の対応をされた経験のある危機管理室長から、「大変わかりやすく、阪神淡路大震災の時とは隔世の感がある」とコメントをいただきました

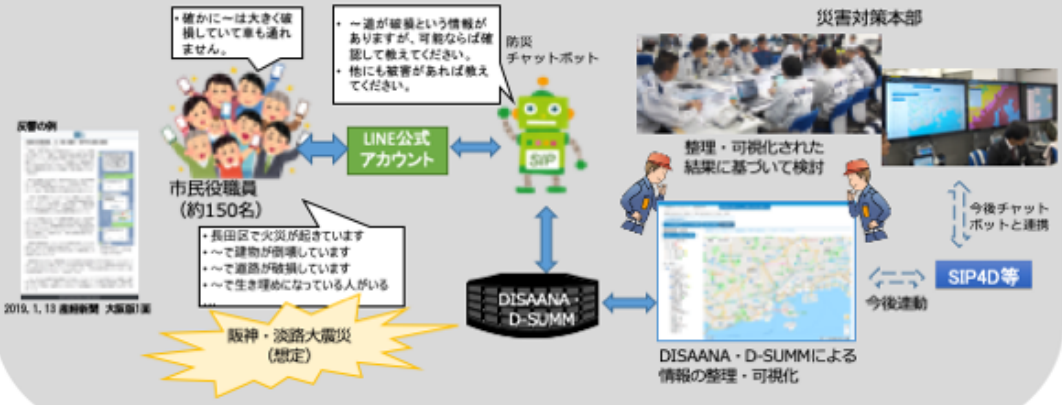

NIED 国立研究開発法人 防災科学技術研究所

©2019. Japan Geoscience Union. All Right Reserved.

Collaboration between NIPR image platform service and social media

*Takeshi Terui[1], Yasuyuki Minamiyama[2], Masaki Hidano[3]

1. National Institute of Polar Research, 2. Tokyo Foundation for Policy Research, 3. Info Lounge Corporation

NIPR is developing an open image archive platform with metadata that recorded the history of Antarctic / Arctic observation. This platform is now experimentally openned as NIPR Image Archive Web service as a following link.

https://image.nipr.ac.jp

Images to release on this platform are recorded pictures and videos in the Antarctic / Arctic. These images are data that recorded Japanese public activity in polar regions. In order to efficiently utilize data and distribute metadata, we are considering cooperation with various external Web services. For this reason, we are dealing with IIIF, Web API, JSON-LD, and we are testing the distribution on the Web. In the future we plan to respond to image retrieval and distribution enhancement on social media and various cloud services through image search engines. In this study, we will introduce the effect on data distribution expected to promote publication of image data by research institutions, and expectation to strengthen cooperation with social media and search engines.

Keywords: Image Search, Data Dissemination, Omeka, Polar Region, IIIF, Web API

©2019. Japan Geoscience Union. All Right Reserved.

Twitter account of the Association of Japanese Geographers: History of establishment and operation

*Takashi Oguchi[1], Yuichiro Nishimura[2], Daichi Kohmoto[3], Atsuko Niina[4], Hitoshi Saito[5]

1. Center for Spatial Information Science, The University of Tokyo, 2. Division of Humanities and Social Sciences, Nara Women's University, 3. Nara University of Education, 4. Izu Peninsula Geopark Promotion Council, 5. College of Economics, Kanto Gakuin University

The Twitter account of the Association of Japanese Geographers (AJG) with some 15,000 followers (@ajgeog) is widely recognized and has a certain level of social influence. Unlike most other accounts of academic societies, the AJG account often retweets geography-related tweets posted by various people, and refollows the majority of the followers. The account has been operated by the Public Relations Committee of the AJG for more than five years, to transfer information related to geography. This paper is presented by five AJG members who played a major role in creating the account and its operation at the early stage, to introduce background history.

Keywords: Association of Japanese Geographers, Twitter, History

©2019. Japan Geoscience Union. All Right Reserved.

Utilization of SNS for the North-Ibaraki Geopark Plan after canceling the certification of JGC

*Kazuo Amano[1], Jun Hosoi[2]

1. The Institute of Natural Sciences, College of Humanities and Sciences, Nihon Univ., 2. Institute of Geology and Geoinformation, Geological Survey of Japan, AIST

We would like to report the utilization of SNS in the North Ibaraki Geopark Plan after canceling the certification for the member of Japan Geopark Network(JGN). Toward recertification, strict opinions have been exchanged in the private Facebook about the North-Ibaraki Geopark and the geoparks in Japan. The whole concept of the geopark in Japan will be also argued based on the results of those discussions.

Keywords: SNS, North Ibaraki Geopark, Japan Gepark Network

©2019. Japan Geoscience Union. All Right Reserved.

[J] Oral | M (Multidisciplinary and Interdisciplinary)：M-SD Space Development & Earth Observation from Space

Wed. May 29, 2019 9:00 AM - 10:30 AM JST | Wed. May 29, 2019 12:00 AM - 1:30 AM UTC | 302 3F

[M-SD44] Future Missions of Satellite Earth Observation

convener:Yoshiaki HONDA(Center for Environmental Remote Sensing, Chiba University), Yukari Takayabu(Atmosphere and Ocean Research Institute, the University of Tokyo), Shinichi Sobue(Japan Aerospace Exploration Agency), Yuki Kaneko(Japan Aerospace Exploration Agency), Chairperson:Yoshiaki Honda

Satellite observation can be an effective tool in science and can be applied to the rapid global environmental change. Monitoring for a long term, advancing new ideas and developing technologies to support them are needed to solve social and scientific problems.
The Task Force on Future Space R&D System of the Subcommittee on Remote Sensing (TF) supported by 25 academic societies and affiliated organizations has formulated the ''Grand Design of Earth Observation'' in FY2017. From the academic point of view, it suggests earth observation missions that Japan should conduct within a decade. From September 2018 to December 2018, the TF calls for proposals of earth observation missions as a trial that aims to discover new ideas from the scientific and practical domains and refine those ideas through multidisciplinary discussion. The adopted proposals will be mentioned in the revised Grand Design, and the TF will work with the government on using it as a reference in updating the Implementation Plan of the Committee on National Space Policy.
This session consists of oral presentations of the proposals that passed the preliminary examination of documents and active discussions to expand and deepen the study. We welcome attendees from various backgrounds who are interested in earth observation.

9:00 AM - 9:05 AM JST | 12:00 AM - 12:05 AM UTC

Introduction

9:05 AM - 9:20 AM JST | 12:05 AM - 12:20 AM UTC

[MSD44-01] Experimental platform for design and advance evaluation of frequent satellite observations to innovate weather, ocean and land surface predictions

*Takemasa Miyoshi[1], Shunji Kotsuki[1], Koji Terasaki[1], Shigenori Otsuka[1], Takumi Honda[1], Atsushi Okazaki[1], Kohei Takatama[1] (1.RIKEN)

9:20 AM - 9:35 AM JST | 12:20 AM - 12:35 AM UTC

[MSD44-02] Technology demonstration mission for next generation precipitation observation radars

*Tomoo Ushio[1], Toshio Iguchi[2], Kenji Nakamura[4], Kinji Furukawa[3], Riko Oki[3], Daisuke Jodoi[3] (1.Tokyo Metropolitan University, 2.NICT, 3.JAXA, 4.Dokkyo University)

9:35 AM - 9:50 AM JST | 12:35 AM - 12:50 AM UTC

[MSD44-03] Mission of creating base maps as public infrastructures for disaster and monitoring

*ISHITSUKA Naoki[1] (1.The Remote Sensing Society of Japan)

9:50 AM - 10:05 AM JST | 12:50 AM - 1:05 AM UTC

[MSD44-04] Aerosol monitoring, forecasting and estimate of its impacts with multispectral imager data

*Keiya Yumimoto[1,2], Takashi Maki[2], Taichu Y Tanaka[2], Thomas Sekiyama[2], Toshihiko Takemura[1] (1.Kyushu University, 2.Meteorological Research Institute)

10:05 AM - 10:20 AM JST | 1:05 AM - 1:20 AM UTC

[MSD44-05] Global aerosol and cloud observation by space-borne multi-wavelength polarization high-spectral-resolution lidar

*Tomoaki Nishizawa[1], Hajime Okamoto[2], Syoken Ishii[3], Yoshitaka Jin[1] (1.National Institute for Environmental Studies, 2.Kyushu University, 3.National Institute of Information and Communication Technology)

10:20 AM - 10:30 AM JST | 1:20 AM - 1:30 AM UTC

Discussion

Experimental platform for design and advance evaluation of frequent satellite observations to innovate weather, ocean and land surface predictions

*Takemasa Miyoshi[1], Shunji Kotsuki[1], Koji Terasaki[1], Shigenori Otsuka[1], Takumi Honda[1], Atsushi Okazaki[1], Kohei Takatama[1]

1. RIKEN

We propose to develop a unique platform with an advanced data assimilation technology, realizing numerical simulation experiments for advance evaluation of future satellite missions in their design phase. This will provide a scientific, objective approach to an effective design of future satellite missions to maximize the benefit to practical applications such as hydrometeorological prediction and resource control of fisheries. The authors have been leading data assimilation research to explore the best mix of computer model simulations and real-world data for weather forecasting, taking advantage of new-generation technologies such as the K computer and Himawari-8 satellite. The authors' previous research revealed that every-10-minute Himawari-8 observations could lead to a large improvement of typhoon and heavy rainfall predictions, though every-30-minute observation was insufficient. We would expect that frequent observations would also be beneficial for ocean and land surface prediction. Therefore, we aim to develop a platform for numerical experimentation to evaluate potential future satellite missions such as quasi-zenith orbiters and small cube-sat constellations for frequent observation over Japan and its surrounding area. This platform will be useful for designing future satellite missions with high cost-benefit performance.

Keywords: satellite mission planning, numerical simulation experiment, data assimilation

©2019. Japan Geoscience Union. All Right Reserved.

Technology demonstration mission for next generation precipitation observation radars

*Tomoo Ushio[1], Toshio Iguchi[2], Kenji Nakamura[4], Kinji Furukawa[3], Riko Oki[3], Daisuke Jodoi[3]

1. Tokyo Metropolitan University, 2. NICT, 3. JAXA, 4. Dokkyo University

We have studied doppler velocity measurement for precipitation particles using a precipitation observation radar in a low Earth orbit as a post-mission of Dual-frequency Precipitation Radar (DPR) on the Global Precipitation Measurement (GPM) core satellite. Also, we have studied Geostationary Precipitation Radar (GPR) which can observe precipitation continuously and flexibly from a geostationary orbit as a future mission. In this study, we have studied the method which can separate precipitation echoes from ground/sea clutters by the doppler velocities in order to observe high latitude areas. Therefore, we need to verify the feasibility of the doppler velocity measurement for precipitation particles. Additionally, we need to improve antenna performance drastically in order to observe precipitation from a geostationary orbit which is far away from a low Earth orbit. Therefore, we need to verify the feasibility of upsizing an antenna for the GPR.

Based on the above background, the purpose of the proposed mission is to demonstrate that it is possible to measure the doppler velocity of precipitation particles from an orbit by a pulse compression radar using a planar antenna and to operate antenna deployment and connection mechanisms normally in an orbit. Also, we aim to get data regarding antenna deployment behavior and structural characteristics.

We consider the value of the proposed mission as follows. Firstly, the value of the doppler velocity measurement demonstration is as follows.
This demonstration contributes to realize post-GPM/DPR mission. If the doppler velocity measurement becomes possible in the mission, it is expected to understand the mechanical structure of a precipitation system globally and to improve the accuracy of weather and flood forecasts. This demonstration contributes to realize the GPR mission. If the GPR becomes possible, it is expected to identify the forming process of a typhoon and to improve the accuracy of weather and flood forecasts.
Next, the value of the antenna deployment and connection demonstration is as follows.
This demonstration contributes to improve the performance of satellite antennas for earth observation, communication, radio astronomy, disaster monitoring, national security, etc. because the deployment and connection mechanisms make it possible to enlarge planar antennas. This demonstration contributes to realize innovative missions like the GPR because the deployment and connection mechanisms make it possible to construct a 30-m-class large planar antenna. The deployment and connection mechanisms have the potential to construct super large space structures like Space Solar Power Systems (SSPS).
We consider the feasibility of the proposed mission as follows. When we assume that the size of a demonstration system is 1.2m x 2.2m x 0.7m in storage state and 1.2m x 2.2m x 4.4m in deployment state, we expect that the system meets the installation condition for HTV-X which has been developed as a post-KOUNOTORI (HTV) by JAXA. Also, as a result of thermal analysis for the system, we expect that the system meets the thermal condition for HTV-X. Furthermore, we demonstrated that it is possible to operate the half size deployment and connection mechanisms of the system normally by a ground experiment in FY2017.
As future works, we will study the feasibility of the doppler velocity measurement from the aspect of HTV-X attitude control performance. Also, we will improve the function and performance of the deployment and connection mechanisms.

©2019. Japan Geoscience Union. All Right Reserved.

Keywords: Precipitation Radar, Technology Demonstration, Doppler Velocity, Deployable Antenna, GPM/DPR Follow on

©2019. Japan Geoscience Union. All Right Reserved.

Mission of creating base maps as public infrastructures for disaster and monitoring

*ISHITSUKA Naoki[1]

1. The Remote Sensing Society of Japan

As a satellite earth observation mission to be realized as Japan, we propose a mission of creating base maps as public infrastructures for disaster and monitoring.

The purpose of the proposed mission, is the observation and the base map prepared, as well as the monitoring and elucidation of global resources from long-term and continuous quantitative monitoring of large-scale disasters. Optical and SAR sensors, which are the genealogy of ALOS, observe with high spatial resolution, so that it can be applied to basic information (land cover, topography), disaster prevention / reduction (change detection, flooding, illegal dumping) Actual utilization such as agriculture(precision farming, food security), forestry, fishery, energy (geology, reserves, resource management, pollution monitoring), climate change (glacier, drift ice, flood), environment (coastal environment, carbon stock) , To earth science, and so on.

High resolution earth observation data with a wide swath is necessary for detailed map creation which is limited in medium resolution satellite. The high-resolution base map created from the satellite data covering the whole earth will be developed as public infrastructures and become a data access hub and can contribute to social implementation of satellite images such as disaster and agriculture. Then, it will serve as a basis for use in policies to solve international and regional issues, and for use in providing services enriching our lives. In particular, agriculture, forestry and fisheries industry and land management, disaster prevention, social infrastructure is a leading application area. For example, it is difficult to predict when and where a disaster occurs, so it is necessary to maintain wide-area high-resolution images as a base map. In SIP the second phase by the Japanese Cabinet Office, "strengthening national resilience (disaster prevention and reduction)" is started, high-resolution satellite as public infrastructure, supposed to be the supply of data and information There. Also, for use in the map creation field, there are cases where ALOS data was used for updating maps at the Geographical Survey Institute, etc. and for field polygon production work at Ministry of Agriculture and Fisheries. Underlying data of these G space is necessary essential to the realization of data society called “Society 5.0” promoted by the government. In SAR, it is required to make observation of the ground change due to forest monitoring and interferometric SAR, making full use of the achievement of Japan 's L band. In addition, there is great expectation for high resolution monitoring of polar sea ice and glacier utilizing observational weatherability. It is desirable for both sensors to operate at the same time, since various effects such as complementation and improvement in accuracy can be obtained by using the optical sensor and the SAR sensor in an integrated fashion.

Thus, for optical, it is necessary capability to observe a wide range of several tens of km high resolution image having m ~ sub meter. In addition, it is regrettable that ALOS-3 could not install the all-time stereoscopic observation that was an advantage over other countries in ALOS, and it is desirable to have a resurrection by successor satellite. With regard to SAR, it is considered to adopt a new method by DBF in ALOS - 4, and it is considered that wide range high resolution observation such as several hundred kilometers at several m resolution by DBF technology can be continued for succeeding machines depending on the result.

©2019. Japan Geoscience Union. All Right Reserved.

However, since the data becomes extremely large in both optical and SAR, the part of downlinking this data becomes a bottleneck. It is important to continue to cooperate with the development of other data downlink environments including data transmission speed, data on board processing, data relay satellite, ground station and communication, basic research on data compression technology.

In addition, the observed frequency secure has become a real operational issues, this is a need for a solution to break, the number of satellites increases or the constellation, a wide swath, the study of technologies, such as the attitude maneuver. In addition, as an innovative solution, it is necessary to consider the high resolution observation from the geostationary orbiting satellite, etc.

Environmental changes caused by global warming, earth resources from the viewpoint of long-term monitoring of (mineral resources, biological resources, water resources, etc.), and continues without interrupted the ALOS Series with high resolution sensor is desired. We believe it will lead to a worldwide presence improvement of the ALOS series.

Keywords: High resolution, wide swath, ALOS series

©2019. Japan Geoscience Union. All Right Reserved.

Aerosol monitoring, forecasting and estimate of its impacts with multispectral imager data

*Keiya Yumimoto[1,2], Takashi Maki[2], Taichu Y Tanaka[2], Thomas Sekiyama[2], Toshihiko Takemura[1]

1. Kyushu University, 2. Meteorological Research Institute

Airborne aerosols are tiny particles that are globally distributed in the atmosphere from the troposphere to the stratosphere and that affect various aspects of human society and health and the Earth system including ocean biogeochemistry and climate. Our understanding of the aerosol lifecycle and aerosol impacts has been advanced by the following activities: (1) aerosol monitoring: observations of distributions of aerosol components and their radiative impacts, (2) assimilation/forecasting: aerosol (PM2.5) numerical prediction and early warning system to reduce effects on human society and health, and (3) climate data: long-term records including aerosol reanalysis product contributing climate and epidemiology studies. Multispectral imagers (from near UV to near infrared) onboard polar-orbiting and geostationary satellites have been providing essential data to those activities. In this presentation, we will make a brief review of those activities to show how multispectral imagers play the important role in aerosol studies and to provide an opportunity to consider their future plan.

Keywords: Aerosol, Satellite observation

©2019. Japan Geoscience Union. All Right Reserved.

Global aerosol and cloud observation by space-borne multi-wavelength polarization high-spectral-resolution lidar

*Tomoaki Nishizawa[1], Hajime Okamoto[2], Syoken Ishii[3], Yoshitaka Jin[1]

1. National Institute for Environmental Studies, 2. Kyushu University, 3. National Institute of Information and Communication Technology

We propose global satellite measurements of vertical distributions of aerosols and clouds (particles) by multi-wavelength polarization high-spectral-resolution lidar (HSRL) using both HSRL and polarization measurement techniques. This proposal realizes polarization HSRL measurements in ultraviolet, visible, and near-infrared spectral regions (355, 532, and 1064nm) and conducts multi-wavelength and multi-parameter measurements of particles simultaneously.
The proposed lidar, which has twice or larger measurement channels than the previous space lidars, measures global, three-dimensional (vertical and horizontal) distributions of particles; this enables to observe various optical and microphysical properties (e.g., extinction, size distribution, chemical components) simultaneously and to obtain more reliable particle information in quantitative and qualitative than the past. Observational studies using both these global, three-dimensional data of particles and numerical models (e.g., aerosol chemical transport model, and cloud resolving model) will lead to understating preprocess on aerosol-cloud interaction better, reducing uncertainties on evaluation the particle effects on climate change, and improving prediction accuracy of the climate change. Furthermore, this space lidar observation can be used to monitor and forecast transport and diffusion of aerosols getting air quality worse (e.g., volcanic ash, mineral dust, smoke, and air pollution) and to evaluate the aerosol effects on atmospheric environment (e.g., human health, vegetation, and air quality). These improvements of the scientific knowledges contribute to internationally consensus building to solve global warming issues and improving environmental measures both within and outside Japan.
The proposed lidar should have a role to be a succession sensor of space lidar mission to observe global particle distributions such as CALIPSO satellite lidar (CALIOP) launched in 2006 and EarthCARE satellite lidar (ATLID) launched in 2021 and lead internationally particle observation mission by space lidar after EarthCARE mission. More advanced techniques on laser and lidar in space by improving the laser and lidar techniques established in vegetation lidar mission MOLI as well as HSRL techniques developed for ground-based lidars are established in this proposal. The developed techniques are also key techniques for lidars to measure meteorological parameters such as temperature, wind speed, and water vapor. Thus, this proposal is also a bridge for the technical development of the space lidar to measure meteorological parameters.

Keywords: Space-borne lidar, Aerosols, Clouds, HSRL, multi-wavelength

©2019. Japan Geoscience Union. All Right Reserved.

[J] Oral | M (Multidisciplinary and Interdisciplinary)：M-SD Space Development & Earth Observation from Space

Wed. May 29, 2019 10:45 AM - 12:15 PM JST | Wed. May 29, 2019 1:45 AM - 3:15 AM UTC | 302 3F

[M-SD44] Future Missions of Satellite Earth Observation

convener:Yoshiaki HONDA(Center for Environmental Remote Sensing, Chiba University), Yukari Takayabu(Atmosphere and Ocean Research Institute, the University of Tokyo), Shinichi Sobue(Japan Aerospace Exploration Agency), Yuki Kaneko(Japan Aerospace Exploration Agency), Chairperson:Kazuhiro Asai(東北工業大学), Toshiyoshi Kimura(宇宙航空研究開発機構)

Satellite observation can be an effective tool in science and can be applied to the rapid global environmental change. Monitoring for a long term, advancing new ideas and developing technologies to support them are needed to solve social and scientific problems.
The Task Force on Future Space R&D System of the Subcommittee on Remote Sensing (TF) supported by 25 academic societies and affiliated organizations has formulated the ''Grand Design of Earth Observation'' in FY2017. From the academic point of view, it suggests earth observation missions that Japan should conduct within a decade. From September 2018 to December 2018, the TF calls for proposals of earth observation missions as a trial that aims to discover new ideas from the scientific and practical domains and refine those ideas through multidisciplinary discussion. The adopted proposals will be mentioned in the revised Grand Design, and the TF will work with the government on using it as a reference in updating the Implementation Plan of the Committee on National Space Policy.
This session consists of oral presentations of the proposals that passed the preliminary examination of documents and active discussions to expand and deepen the study. We welcome attendees from various backgrounds who are interested in earth observation.

10:45 AM - 11:00 AM JST | 1:45 AM - 2:00 AM UTC

[MSD44-06] Dual-Doppler-velocity-mission using cloud radar and lidar

*Okamoto Hajime[1], Kentaroh Suzuki[2], Tomoaki Nishizawa[3], Shoken Ishii[4] (1.Kyushu University, 2.The university of Tokyo, 3.National Instuitute for Environmental Studies, 4.National Institute of Information and Communications Technology)

11:00 AM - 11:15 AM JST | 2:00 AM - 2:15 AM UTC

[MSD44-07] Global wind profiling with space-based Doppler wind lidar for improvement of numerical weather prediction

*Shoken Ishii[1], Kozo Okaoto[2,1], Takuji Kubota[3], Atsushi Sato[4,1], Daisuke Sakaizaw[3], Tomoaki Nishizawa[5], Ayako Matsumoto[6], Tetsuya Tugami[6], Toshiyuki Ishibashi[2], Taichu Y Tanaka[2], Philippe Baron[1], Makoto Aoki[1], Riko Oki[3], Masaki Satoh[7], Toshiki Iwasaki[8] (1.National Institute of Information and Communications Technology, 2.JMA/MRI, 3.JAXA, 4.TIT, 5.NIES, 6.ANA, 7.University of Tokyo, 8.Tohoku University)

11:15 AM - 11:30 AM JST | 2:15 AM - 2:30 AM UTC

[MSD44-08] Technology demonstration of space-borne water vapor DIAL

*Makoto Abo[1], Chikao Nagasawa[1], Yasukuni Shibata[1], Osamu Uchino[2], Takashi Shibata[3] (1.Graduate School of System Design, Tokyo Metropolitan University, 2.National Institute for Environmental Studies, 3.Nagoya University)

11:30 AM - 12:00 PM JST | 2:30 AM - 3:00 AM UTC

[MSD44-09] Short presentation of poster session

*Yoshiaki HONDA[1] (1.Center for Environmental Remote Sensing, Chiba University)

12:00 PM - 12:15 PM JST | 3:00 AM - 3:15 AM UTC

Discussion

Dual-Doppler-velocity-mission using cloud radar and lidar

*Okamoto Hajime[1], Kentaroh Suzuki[2], Tomoaki Nishizawa[3], Shoken Ishii[4]

1. Kyushu University, 2. The university of Tokyo, 3. National Instuitute for Environmental Studies, 4. National Institute of Information and Communications Technology

Dual-Doppler velocity measuring mission from space-borne cloud radar and lidar is proposed. 94GHz cloud radar and lidar with Doppler function will measure three-dimensional air motion in clouds as well as in clear sky, respectively. High spectral resolution functions at 355nm and 532nm with polarization are planned to distinguish cloud particle type and aerosols. The lidar will have multiple field of views in order to penetrate relatively thick clouds. Since the radar will have capability to observe clouds and lidar will measure aerosols, it will be a successor mission to CloudSat and CALIPSO launched in 2006 and EarthCARE satellite in 2021. The mission will also serve to construct continuous records of clouds and aerosols for climate change studies.

Keywords: Doppler, cloud radar, lidar, clouds, wind

©2019. Japan Geoscience Union. All Right Reserved.

Global wind profiling with space-based Doppler wind lidar for improvement of numerical weather prediction

*Shoken Ishii[1], Kozo Okaoto[2,1], Takuji Kubota[3], Atsushi Sato[4,1], Daisuke Sakaizaw[3], Tomoaki Nishizawa[5], Ayako Matsumoto[6], Tetsuya Tugami[6], Toshiyuki Ishibashi[2], Taichu Y Tanaka[2], Philippe Baron[1], Makoto Aoki[1], Riko Oki[3], Masaki Satoh[7], Toshiki Iwasaki[8]

1. National Institute of Information and Communications Technology, 2. JMA/MRI, 3. JAXA, 4. TIT, 5. NIES, 6. ANA, 7. University of Tokyo, 8. Tohoku University

Wind is one of key meteorological elements describing the atmospheric state as well as pressure, temperature, and humidity. Global wind profile observation is important to significantly improve the initial conditions essential for numerical weather prediction (NWP) and other meteorological studies. Although space-based observation system is a very important role in NWP, current space-based wind observing system has a problem that it is biased to observation related to temperature and water vapor compared with wind observation. The World Meteorological Organization wants to develop a global wind profiling system. Space-based Doppler Wind Lidar (DWL) can provide global wind profiles, which is a promising technique to fill the current gap. Under the circumstance, ESA launched the first space-based DWL Aeolus in August 2018. Since target mission period of Aeolus is three years, many NWP and science communities want continuous global wind profile observation. The working group on Japanese space-based DWL has made feasibility study for the space-based DWL for future global wind profiling since 2011. In 2017, ANA Holdings Inc. proposed to apply for optimizing aviation route using wind data improved by the future space-based DWL wind measurement at the space business promotion event S-Booster 2017. The proposal won the grand prize at S-Booster 2017, and the space-based DWL for the space business has been spotlighted since the event. The proposal is based on the global wind profile observation with the space-based DWL. The purposes of the global wind profile observation are to improve the precision of NWP and to contribute to understandings of mechanism of natural disasters and climate change and to new applications of wind data use.

Keywords: Lidar, Doppler Wind Lidar, space-based observation, global wind profiling

©2019. Japan Geoscience Union. All Right Reserved.

Technology demonstration of space-borne water vapor DIAL

*Makoto Abo[1], Chikao Nagasawa[1], Yasukuni Shibata[1], Osamu Uchino[2], Takashi Shibata[3]

1. Graduate School of System Design, Tokyo Metropolitan University, 2. National Institute for Environmental Studies, 3. Nagoya University

We propose technology demonstration of space-borne water vapor differential absorption lidar (DIAL) for global high-resolution water vapor observations in the troposphere and lower stratosphere, to improve the understanding about the role of water in the global water and energy cycles and main physical processes (e.g., convection, emission, rainfall, the troposphere-stratosphere exchange of chemical species).

Keywords: DIAL, water vapor, space-borne

©2019. Japan Geoscience Union. All Right Reserved.

Short presentation of poster session

*Yoshiaki HONDA[1]

1. Center for Environmental Remote Sensing, Chiba University

The author will do a short presentation of the paper presented at the poster session of this session "M-SD44 Future Missions of Satellite Earth Observation".

Keywords: Global environmental, Satellite Earth Observation, Grand Design of Earth Observation

©2019. Japan Geoscience Union. All Right Reserved.

[J] Oral | M (Multidisciplinary and Interdisciplinary)：M-SD Space Development & Earth Observation from Space

Wed. May 29, 2019 1:45 PM - 3:15 PM JST | Wed. May 29, 2019 4:45 AM - 6:15 AM UTC | 302 3F

[M-SD44] Future Missions of Satellite Earth Observation

convener:Yoshiaki HONDA(Center for Environmental Remote Sensing, Chiba University), Yukari Takayabu(Atmosphere and Ocean Research Institute, the University of Tokyo), Shinichi Sobue(Japan Aerospace Exploration Agency), Yuki Kaneko(Japan Aerospace Exploration Agency), Chairperson:Riko Oki(宇宙航空研究開発機構)

Satellite observation can be an effective tool in science and can be applied to the rapid global environmental change. Monitoring for a long term, advancing new ideas and developing technologies to support them are needed to solve social and scientific problems.
The Task Force on Future Space R&D System of the Subcommittee on Remote Sensing (TF) supported by 25 academic societies and affiliated organizations has formulated the ''Grand Design of Earth Observation'' in FY2017. From the academic point of view, it suggests earth observation missions that Japan should conduct within a decade. From September 2018 to December 2018, the TF calls for proposals of earth observation missions as a trial that aims to discover new ideas from the scientific and practical domains and refine those ideas through multidisciplinary discussion. The adopted proposals will be mentioned in the revised Grand Design, and the TF will work with the government on using it as a reference in updating the Implementation Plan of the Committee on National Space Policy. This session consists of oral presentations of the proposals that passed the preliminary examination of documents and active discussions to expand and deepen the study. We welcome attendees from various backgrounds who are interested in earth observation.

1:45 PM - 2:00 PM JST | 4:45 AM - 5:00 AM UTC

[MSD44-10] **Himawari-8/9 follow-on satellites program**

*BESSHO Kotaro[1] (1.Japan Meteorological Agency)

2:00 PM - 2:15 PM JST | 5:00 AM - 5:15 AM UTC

[MSD44-11] Impact assessment of hyperspectral infrared sounders toward Himawari-8/9 follow-on satellites

*Kozo OKAMOTO[1], Hiromi Owada[2], Masahiro Kazumori[2], Michiko Otsuka[1], Yoshifumi Ota[2], Naotaka Uekiyo[1], Hiromu Seko[1], Akiyoshi Ando[2], Ryo Yoshida[2], Hiroshi Ishimoto[1], Masahiro Hayashi[1], Haruma Ishida[3], Yoshiaki Sato[2], Hiroshi Kunimatsu[2], Kotaro Bessho[2], Hironobu Yokota[2] (1.Meteorological Research Institute, 2.Japan Meteolological Agency, 3.Meteorological Satellite Center)

2:15 PM - 2:30 PM JST | 5:15 AM - 5:30 AM UTC

[MSD44-12] Observation system simulation experiments for a hyperspectral infrared sounder onboard geostationary satellite

*HIROMI OWADA[1], Kozo OKAMOTO[2], Masahiro Kazumori[1], NAOTAKA UEKIYO[2], Hiroshi Ishimoto[2], Masahiro Hayashi[2] (1.Japan Meteorological Agency, 2.Meteorological Research Institute)

2:30 PM - 2:45 PM JST | 5:30 AM - 5:45 AM UTC

[MSD44-13] Realization of pseudo high frequency high resolution observation by geostationary satellite and orbiting satellite combined observation

*Yoshiaki HONDA[1] (1.Center for Environmental Remote Sensing, Chiba University)

2:45 PM - 3:00 PM JST | 5:45 AM - 6:00 AM UTC

[MSD44-14] **Geostationary Optical Earth Observation Satellite**

*Kazuo Oki[1], Toshiyoshi Kimura[2], Tadahito Mizutani[2], Takeo Tadono[2] (1.The University of Tokyo, 2.JAXA)

3:00 PM - 3:15 PM JST | 6:00 AM - 6:15 AM UTC

Discussion

Himawari-8/9 follow-on satellites program

*BESSHO Kotaro[1]

1. Japan Meteorological Agency

This presentation will show the Himawari-8/9 follow-on satellites program.

Keywords: Satellite, Himawari, JMA

©2019. Japan Geoscience Union. All Right Reserved.

Impact assessment of hyperspectral infrared sounders toward Himawari-8/9 follow-on satellites

*Kozo OKAMOTO[1], Hiromi Owada[2], Masahiro Kazumori[2], Michiko Otsuka[1], Yoshifumi Ota[2], Naotaka Uekiyo[1], Hiromu Seko[1], Akiyoshi Ando[2], Ryo Yoshida[2], Hiroshi Ishimoto[1], Masahiro Hayashi[1], Haruma Ishida[3], Yoshiaki Sato[2], Hiroshi Kunimatsu[2], Kotaro Bessho[2], Hironobu Yokota[2]

1. Meteorological Research Institute, 2. Japan Meteolological Agency, 3. Meteorological Satellite Center

Japan Meteorological Agency has started the discussion on Himawari-8/9 follow-on satellites to be launched in 2028. We are investigating impacts on numerical weather prediction of a hyperspectral infrared sounder on the follow-on satellites using an observing system simulation experiment (OSSE) approach. We will present preliminary results of simulation and global and regional data assimilation experiments of the sounder.

Keywords: Himawari follow-on satellite, data assimilation, OSSE , hyperspectral infrared sounder

©2019. Japan Geoscience Union. All Right Reserved.

Observation system simulation experiments for a hyperspectral infrared sounder onboard geostationary satellite

*HIROMI OWADA[1], Kozo OKAMOTO[2], Masahiro Kazumori[1], NAOTAKA UEKIYO[2], Hiroshi Ishimoto[2], Masahiro Hayashi[2]

1. Japan Meteorological Agency, 2. Meteorological Research Institute

At the Japan Meteorological Agency, we started preparation for the Himawari-8/9 follow-on satellites. Hyperspectral infrared sounder (HSS) is one of the instruments to consider to be installed in the follow-on satellites. By installing HSS on a new geostationary satellite, it is possible to acquire information on highly accurate profiles of temperature and water vapor at high frequency, and it is expected that accuracy of numerical weather prediction is greatly improved by using this new data in data assimilation system. In order to confirm this assumption, we evaluate the impact on numerical weather prediction when we install HSS on the follow-on satellites and assimilate their data with observation system simulation experiment (OSSE).

In this presentation, we report on the generation of HSS pseudo observation data and the initial results of OSSE in JMA's current global data assimilation system.

Keywords: Himawari-8/9 follow-on satellites, Hyperspectral infrared sounder, Observation system simulation experiments

©2019. Japan Geoscience Union. All Right Reserved.

Realization of pseudo high frequency high resolution observation by geostationary satellite and orbiting satellite combined observation

*Yoshiaki HONDA[1]

1. Center for Environmental Remote Sensing, Chiba University

Observation data of the earth observation optical sensor data from both the earth science and the actual utilization is required more frequently and higher resolution. However, in order to realize this high frequency observation and high resolution observation at the same time, it is impossible with one satellite, and it is being realized by many operations of micro satellite. However, in general, micro satellites have problems such as short design life and no calibration system. On the other hand, satellites of medium size or more including geostationary satellites have a long design life and have a calibration system. However, in order to realize high frequency and high resolution with satellites of medium size or larger, if we try to secure the number of satellites, its budget is enormous and not realistic. This proposal is based on high frequency observation of geosynchronous satellites with relatively low resolution among satellites launched by Japan (assumed to be successors such as Himawari, GCOM - C, ALOS etc), and high resolution but low frequency orbiting satellite observations We aim to manufacture pseudo high frequency high resolution observation data through a model that adjusts part of sensor specifications of each satellite and adjusts the difference between observation geometries, and provides such a high quality long-term framework . This aims to expand the use of satellite optical sensor data in earth science and practical use fields, and to expand scientific progress and practical use. This framework is a planned budget size, one step to get bigger results, and expansion of the actual field of use will also contribute to the continuity of the Earth observation in Japan. Furthermore, by incorporating newly planned satellites of other countries into this framework, we aim to increase the presence of our Earth observation in the field of earth science and practical use.

Keywords: Geostationary satellite, Orbiting satellite combined observation, Pseudo High Frequency High Resolution Observation

©2019. Japan Geoscience Union. All Right Reserved.

Geostationary Optical Earth Observation Satellite

*Kazuo Oki[1], Toshiyoshi Kimura[2], Tadahito Mizutani[2], Takeo Tadono[2]

1. The University of Tokyo, 2. JAXA

Geostationary satellite is the most practical Earth Observation for its instantaneous observation and ability to choose target area on demand. Some kind of users, especially disaster monitoring, agriculture and national security users are demanding such unique character crucially. However, technical difficulties prevent from realization of the system, so far. Practical observation needs a certain fine ground resolution. But it means necessity for huge main mirror for the satellite optics. For an example, 5~7m resolution at Nadir position needs 3.6m diameter mirror. So far, 1~2m diameter one-piece mirrors were studied, in contrast. Recent optical technologies make it possible to have an extra large telescope using segmented mirrors for astronomical telescope on the ground, like Keck astronomy or TMT project. Using such technologies, we studied geostationary satellite telescope system with 3.6m diameter segmented telescope to materialize 7m ground resolution at Nadir position. Observation bands should have good correlation with ALOS-3 satellite on low Earth orbit, i.e. panchromatic, RGB, NIR and additional bands. To ensure the night observation, IR band is under consideration in addition. Such new Earth observation scheme improves time resolution dramatically, and it will make possible to observe movement of target like video camera. It will reveal many motile phenomena including Tsunami, Typhoon and human activities like car traffics. Also, it is expected that various social services unprecedented in cities, forests, agriculture, water (rivers and oceans), etc. are expected to be offered, and we believe that many users will appear in the field of science and practical use. The study started in 2018 and will end in 2020 to confirm the technical readiness level of required technologies, observation plan and algorithms for new earth observation data products.

Keywords: Geostationary Satellite, Extra large telescope, Geostationary satellite telescope system, ALOS-3, Social services, New earth observation data products

©2019. Japan Geoscience Union. All Right Reserved.

[J] Poster | M (Multidisciplinary and Interdisciplinary)：M-SD Space Development & Earth Observation from Space

Wed. May 29, 2019 5:15 PM - 6:30 PM JST | Wed. May 29, 2019 8:15 AM - 9:30 AM UTC | Poster Hall International Exhibition Hall8, Makuhari Messe_39

[M-SD44] Future Missions of Satellite Earth Observation

convener:Yoshiaki HONDA(Center for Environmental Remote Sensing, Chiba University), Yukari Takayabu(Atmosphere and Ocean Research Institute, the University of Tokyo), Shinichi Sobue(Japan Aerospace Exploration Agency), Yuki Kaneko(Japan Aerospace Exploration Agency)

Satellite observation can be an effective tool in science and can be applied to the rapid global environmental change. Monitoring for a long term, advancing new ideas and developing technologies to support them are needed to solve social and scientific problems.
The Task Force on Future Space R&D System of the Subcommittee on Remote Sensing (TF) supported by 25 academic societies and affiliated organizations has formulated the ''Grand Design of Earth Observation'' in FY2017. From the academic point of view, it suggests earth observation missions that Japan should conduct within a decade. From September 2018 to December 2018, the TF calls for proposals of earth observation missions as a trial that aims to discover new ideas from the scientific and practical domains and refine those ideas through multidisciplinary discussion. The adopted proposals will be mentioned in the revised Grand Design, and the TF will work with the government on using it as a reference in updating the Implementation Plan of the Committee on National Space Policy.
This session consists of oral presentations of the proposals that passed the preliminary examination of documents and active discussions to expand and deepen the study. We welcome attendees from various backgrounds who are interested in earth observation.

[MSD44-P01] Monitoring climate variability and global water cycle and understanding their mechanisms (AMSR3)

*Hirohiko Masunaga[1], Naoto Ebuchi[2], Takeshi Tamura[3], Kei Yoshimura[4], Kazumasa Aonashi[5], Masahiro Kazumori[6], Katsuya Saitoh[7] (1.Nagoya University, 2.Hokkaido University, 3.National Institute of Polar Research, 4.University of Tokyo, 5.Meteorological Research Institute, 6.Japan Meteorological Agency, 7.Japan Fisheries Information Service Center)

[MSD44-P02] Precipitation Measuring Mission by Active Sensors

*Nobuhiro Takahashi[1], Yukari Takayabu[2], Kinji Furukawa[3], Riko Oki[3], Kosuke Yamamoto[3], Yuki Kaneko[3] (1.Institute for Space-Earth Environmental Research, Nagoya University, 2.The Atmosphere and Ocean Research Institute (AORI) , 3.The Japan Aerospace Exploration Agency (JAXA))

[MSD44-P03] Asian Small Precipitation Radar Constellation (ASPRC)

*Kinji Furukawa[1], Toshiaki Ogawa[2], Riko Oki[1], Takuji Kubota[1], Moeka Yamaji[1] (1.Japan Aerospace Exploration Agency, 2.NEC Corporation)

[MSD44-P04] In-orbit Payload Demonstration of Circularly Polarized SAR

*Josaphat Tetuko Sri Sumantyo[1], Kuze Hiroaki[1], Nobuyoshi Imura[1] (1.Center for Environmental Remote Sensing, Chiba University)

[MSD44-P05] Global wind measurement system using Doppler Wind Lidar and Imaging FTS

*Okamoto Hajime[1], Toshiyoshi Kimura[2], Daisuke Sakaizawa[2], Shoken Ishii[3] (1.Kyushu University, 2.Japan Aerospace Exploration Agency, 3.National Institute of Information and Communications Technology)

[MSD44-P06] Mission regarding monitoring and elucidation of global environmental change (global radiation forcing and ecological change that affect global warming)

*Yoshiaki HONDA[1], Teruo AOKI[2], Takashi NAKAJIMA[3], Mitsuhiro TORATANI[4] (1.Center for Environmental Remote Sensing, Chiba University, 2.Graduate School of Natural Science and Technology, Okayama University, 3.Tokai University, Research & Information Center, 4.Tokai University, Earth and Environmental Systems)

[MSD44-P07] Proposal of satellite for observing large point sources of carbon dioxide

*Hirofumi Ohyama[1], Tsuneo Matsunaga[1], Isamu Morino[1], Yukio Yoshida[1], Makoto Saito[1] (1.National Institute for Environmental Studies)

[MSD44-P08] Earth's health diagnosis - Imaging spectrometer of SLCP for early verification of global warming countermeasure effect, and understanding of status of air pollution -

*YASUKO KASAI[1], Yugo Kanaya[2], Hiroshi Tanimoto[3], JSAC Satellite team[4] (1.NICT, 2.JAMSTEC, 3.NIES, 4.JSAC)

[MSD44-P09] Spaceborne Vegetation lidar (MOLI)

*Kazuhiro Asai[1], Yasumasa Hirata[2], Gen Takao[2], Haruhisa Shimoda[3], Yoshiaki HONDA[4], Koji Kajiwara[4], Yoshio Awaya[5], Junichi Susaki[9], Takahiro Endo[6], Tsuneo Matsunaga[7], Yoshito Sawada[7], Nobuo Sugimoto[7], Tomoaki Nishizawa[7], Kohei Mizutani[8], Shoken Ishii[8], Toshiyoshi Kimura[10], Tadashi Imai[10], Masato Hayashi[10], Daisuke Sakaizawa[10], Jyunpei Murooka[10], Rei Mituhashi[10] (1.Tohoku Institute of Technology, 2.Forestry and Forest Products Research Institute, 3.Tokai University, 4.Chiba University, 5.Gifu University, 6.The Remote Sensing Technology Center of Japan, 7.National Institute for Environmental Research, 8.National Institute of Information and Communications Technology, 9.Kyoto University, 10.Japan Aerospace Exploration Agency)

[MSD44-P10] Estimation of forest resources by a dual-wavelength imaging LiDAR system

*Ryuichi Hirata[1], Yoshito Sawada[1], Masato Hayashi[2], Hideki Saito[3], Tomoaki Takahashi[3], Tsuneo Matsunaga[1] (1.National Institute for Environmental Studies, 2.Japan Aerospace eXploration Agency, 3.Forestry and Forest Products Research Institute)

[MSD44-P11] Development of new satellite to monitor SIF and PRI of terrestrial vegetation with high spatial and wavelength resolutions

*Hibiki M Noda[1], Kenji Omasa[2], Kouki Hikosaka[3], Kazuhito Ichii[4], Hideki Kobayashi[5], Tomomichi Kato[6], Hiroyuki Muraoka[7] (1.NIES National Institute of Environmental Studies, 2.University of Tokyo, 3.Tohoku University, 4.Chiba University, 5.JAMSTEC, 6.Hokkaido University, 7.Gifu University)

[MSD44-P12] Satellite Observation of the Whole Atmosphere - Superconducting Submillimeter-Wave Limb-Emission Sounder (SMILES-2)

*Masato Shiotani[1], Akinori Saito[1], Takatoshi Sakazaki[1], Satoshi Ochiai[2], Philippe Baron[2], Toshiyuki Nishibori[3], Makoto Suzuki[3], Takumi Abe[3], Hiroyuki Maezawa[4], Shin-ichiro Oyama[5,6,7] (1.Kyoto University, 2.National Institute of Information and Communications Technology, 3.Japan Aerospace Exploration Agency, 4.Osaka Prefecture University, 5.Nagoya University, 6.University of Oulu, 7.National Institute of Polar Research)

[MSD44-P13] Simulation studies for Superconducting Submillimeter-Wave Limb-Emission Sounder-2 (SMILES-2)

*Philippe Baron[1], Satoshi Ochiai[1], Donal Murtagh[5], Hideo Sagawa[2], Akinori Saito[3], Masato Shiotani[3], Makoto Suzuki[4] (1.National Institute of Information and Communications Technology, 2.Kyoto Sangyo University, 3.Kyoto University, 4.Japan Aerospace Exploration Agency, 5.Chalmers University of Technology, Sweden)

[MSD44-P14] Feasibility of Superconducting Submillimeter-Wave Limb-Emission Sounder (SMILES-2) on an M-class satellite

*Satoshi Ochiai[1], Philippe Baron[1], Yoshihisa Irimajiri[1], Toshiyuki Nishibori[2], Makoto Suzuki[2], Yoshinori Uzawa[3], Hiroyuki Maezawa[4], Takeshi Manabe[4], Akinori Saito[5], Masato Shiotani[5] (1.National Institute of Information and Communications Technology, 2.Japan Aerospace Exploration Agency, 3.National Astronomical Observatory of Japan, 4.Osaka Prefecture University, 5.Kyoto University)

Monitoring climate variability and global water cycle and understanding their mechanisms (AMSR3)

*Hirohiko Masunaga[1], Naoto Ebuchi[2], Takeshi Tamura[3], Kei Yoshimura[4], Kazumasa Aonashi[5], Masahiro Kazumori[6], Katsuya Saitoh[7]

1. Nagoya University, 2. Hokkaido University, 3. National Institute of Polar Research, 4. University of Tokyo, 5. Meteorological Research Institute, 6. Japan Meteorological Agency, 7. Japan Fisheries Information Service Center

We propose an observational system by a spaceborne microwave radiometer (AMSR3) for long-term and continous high-frequency, high-resolution, all-sky observations aimed at the long-term monitoring and better understanding of global water cycle and climate variability with the measurements of sea-ice concentration, snow depth, sea surface temperature, precipitation, column water vapor, and soil moisture etc.

Keywords: Satellite Earth Observation, Climate variability, Global water cycle, Microwave remote sensing

©2019. Japan Geoscience Union. All Right Reserved.

Precipitation Measuring Mission by Active Sensors

*Nobuhiro Takahashi[1], Yukari Takayabu[2], Kinji Furukawa[3], Riko Oki[3], Kosuke Yamamoto[3], Yuki Kaneko[3]

1. Institute for Space-Earth Environmental Research, Nagoya University, 2. The Atmosphere and Ocean Research Institute (AORI) , 3. The Japan Aerospace Exploration Agency (JAXA)

We propose precipitation observation mission with DPR2, which is greatly improved performance of the dual-frequency precipitation radar (DPR) onboard the core satellite of Global Precipitation Measurement (GPM) mission in order to improve the understanding of cloud-precipitation mechanism and to monitor global precipitation. Based on the global precipitation observation heritages of more than 20 years by the precipitation radar (PR) onboard the tropical rainfall measuring mission (TRMM) satellite and GPM/DPR and new mission concept has been discussed by considering the current scientific issues regarding precipitation.

One of the urgent issues is the climate change (the global warming) issue. It is necessary to grasp phenomena of various scales to solve this issue, because it is necessary to evaluate not only the global climate (temperature) change but also the impact on the precipitation systems by global warming and it turns out the necessity of the accurate understanding of the earth's water circulation covering from the microphysical processes, cloud scale phenomena to the global scale precipitation and interactions among them. Considering the precipitation observation, we need better understanding of the cloud-precipitation processes, the global distribution of solid and liquid precipitation and the intense precipitation that affects the soil recharge and flooding. To implement these scientific purposes, observation (system) including cloud observation as well as observation specialized in precipitation in TRMM and GPM is necessary. Furthermore, in order to accurately grasp the precipitation formation mechanism from clouds, it is necessary to acquire dynamic information in the cloud. On the other hand, acquiring climatological information of global precipitation continued from TRMM and GPM is important as the long term record of precipitation. The improvement of the global precipitation map such as GSMaP are also necessary for practical use of precipitation information.

We need to consider the international cooperation such as the framework of TRMM and GPM that is Japan-US cooperative mission. In the United States, Cloud, Convection and Precipitation (CCP) and Aerosol (A) observations are listed as high priority observation in Decadal Survey report. The mission architecture study has been started focusing on aerosol, cloud and precipitation observation. The observation method exemplified in Decadal Survey is high sensitivity observation of cloud by scanning W-band cloud radar and Ka-band radar and Doppler velocity measurement with these radars. This observation concept is complementary to DPR2 concept.

DPR2 plans to improve the sensitivity from 10 times to 100 times (10 to 20 dB) of DPR by using advanced semiconductor devices such as GaN and introducing pulse compression technology, and also plans to introduce Doppler velocity measurement. Improvement in sensitivity is necessary to resolve that DPR has insufficient sensitivity to weak snowfall, as well as to sufficiently overlap the sensitivity range of cloud radar. Resources for improving the sensitivity can be utilized to the expansion of the scan width (but the sensitivity gets worse accordingly), for example, the data of the DPR2 observation can be directly input to the GSMaP to improve the accuracy. Regarding the utilization of this sensitivity resource as maximum, it is also consider the flexible radar operation. Theoretically, it is necessary to maintain correlation between

©2019. Japan Geoscience Union. All Right Reserved.

radar pulses for Doppler velocity measurement. Because of the very fast movement of satellite, sufficient correlation cannot be obtained with the antenna size of DPR, and at least double sized antenna is necessary. Technically, a deployable antenna should be introduced to realize the large antenna and it is a large development item for DPR2, the heritages from EarthCARE can be used for radar control and signal processing system on the Doppler velocity measurement.

Keywords: Precipitation, radar, Earth observing satellite

©2019. Japan Geoscience Union. All Right Reserved.

Asian Small Precipitation Radar Constellation (ASPRC)

*Kinji Furukawa[1], Toshiaki Ogawa[2], Riko Oki[1], Takuji Kubota[1], Moeka Yamaji[1]

1. Japan Aerospace Exploration Agency, 2. NEC Corporation

The Japan Aerospace Exploration Agency (JAXA) and NEC Corporation (NEC) have developed a Dual-frequency Precipitation Radar (DPR) equipped with a main satellite for the Global Precipitation Measurement (GPM) core observatory. GPM/DPR was launched in 2014, and its observation data is utilized in various ways such as being incorporated into the Global Satellite Mapping of Precipitation (GSMaP) provided by JAXA. GPM/DPR is superior to precipitation observation by microwave radiometer in that it can observe highly accurately without distinguishing between ocean and land, and it is possible to acquire vertical profile of rainfall etc. Meanwhile, GPM/DPR has a relatively narrow observation width and only one observatory is operated, so the problem is that the observation frequency at the same spot is small. In order to solve this problem, we propose Small Precipitation Radar Constellation based on the Ku band precipitation radar (KuPR) which constitutes GPM/DPR. It will decrease observation interval of the same spot about 6 hours. Note that this precipitation radar is supposed to be mounted on the small satellite bus NEXTAR-300L developed by NEC.
With the proposed Small Precipitation Radar Constellation, it is possible to greatly improve the observation frequency of the same spot with respect to GPM/DPR. Although the number of satellites will increase, both the precipitation radar and the satellite bus will utilize already developed products and it will be mounted on relatively inexpensive small satellite to reduce the cost of the overall system. Assuming that both the precipitation radar and the satellite bus utilize already developed products, we aim to target the development cost of the first observatory to 10 billion yen or less (excluding ground equipment, launch, operation cost).
As the application of the small precipitation radar constellation, it is assumed that utilization in disaster prevention such as improving the accuracy of weather forecast, predicting the occurrence of flood caused by typhoon and severe rainfall. Scientifically, it is useful for the study of the diurnal change of precipitation by high frequency observation in tropical zone. Observation data of this precipitation radar can also be used in Southeast Asian countries (Indonesia, the Philippines, Vietnam, etc.), and it is assumed that a satellite constellation will be constructed by countries which are interested in development and launch (Realized by ODA). As a technical development, we aim increase the number of constellation satellite for further high frequent precipitation obseravtion through further size down and cost reduction.

Keywords: Small Precipitation Radar, Constellation

©2019. Japan Geoscience Union. All Right Reserved.

In-orbit Payload Demonstration of Circularly Polarized SAR

*Josaphat Tetuko Sri Sumantyo[1], Kuze Hiroaki[1], Nobuyoshi Imura[1]

1. Center for Environmental Remote Sensing, Chiba University

Recently, we develop small circularly polarized SAR satellite, where the flight test of airborne circularly polarized SAR was success, and we plan to do the in-orbit payload demonstration of this circularly polarized SAR in the next step. Small circularly polarized SAR satellite is 100 kg microsatellite with circularly polarized synthetic aperture radar (CP-SAR) sensor onboard that is originally developed by Chiba University. This in-orbit satellite system has the objective to realize high level education and research on global environmental and disaster monitoring, i.e. active fault, landslide, earthquake, volcanic eruption etc, and data analysis.

Keywords: Synthetic Aperture Radar, Circular polarization, Remote sensing

©2019. Japan Geoscience Union. All Right Reserved.

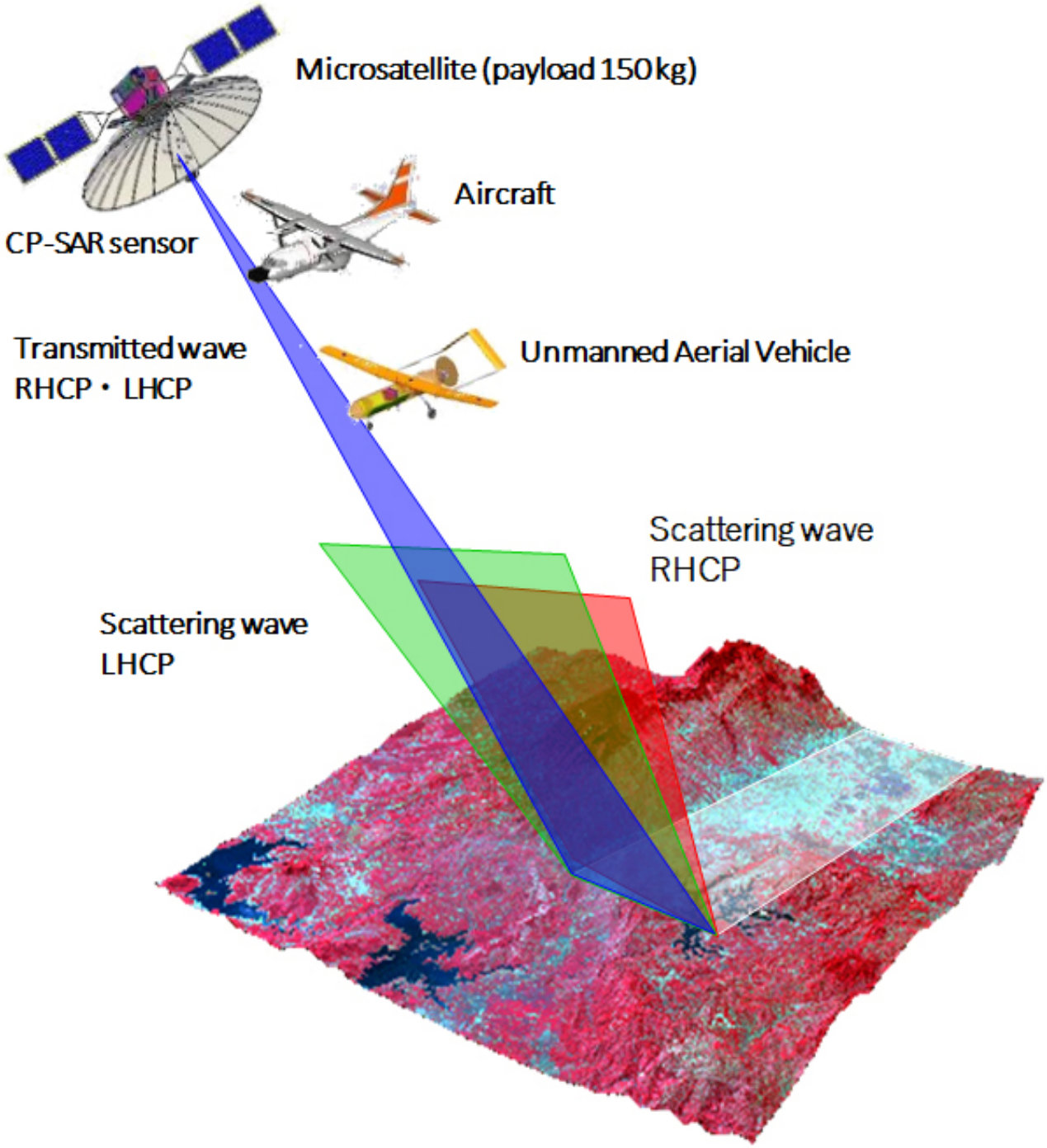

©2019. Japan Geoscience Union. All Right Reserved.

Global wind measurement system using Doppler Wind Lidar and Imaging FTS

*Okamoto Hajime[1], Toshiyoshi Kimura[2], Daisuke Sakaizawa[2], Shoken Ishii[3]

1. Kyushu University, 2. Japan Aerospace Exploration Agency, 3. National Institute of Information and Communications Technology

We propose global wind measurement system by using Doppler Wind Lidar (DWL) and FTS on Geostationary satellites. Wind as atmospheric circulation is the most important element in climate and weather studies. Air- and ship-traffic are also using wind information as most prioritized one to ensure their safe operation. Current systems cannot measure global distribution of winds. Recent progress of DWL technology made precise wind measurement possible in three-dimensional manner, limited to narrow swarth over its orbit. A DWL-satellite was already launched by European Space Agency, and NASA is also planning to launch. In Japan, NICT and JAXA are studying DWL. Also, recent geostationary weather satellite made possible to distinguish wind distribution by altitude using water vapor band imagery. Measurement error is still large. The basic concept is to combine DWL and FTS on Geostationary satellites to complement each other. To cover the globe using geostationary orbit, we need about four satellites at each region. Using current weather satellite network is the most demanded approach. NASA, ESA and JAXA/NICT can make a strong network to maintain data from spaceborne DWLs to calibrate the results of retrieved wind from imaging FTS on Geostationary satellite. The requirement of spacial resolution for the system is 1km horizontal resolution, 300m height distribution, <1m/s windspeed accuracy and wind vector.

Keywords: wind, Geostationary Satellite, lidar

©2019. Japan Geoscience Union. All Right Reserved.

Mission regarding monitoring and elucidation of global environmental change (global radiation forcing and ecological change that affect global warming)

*Yoshiaki HONDA[1], Teruo AOKI[2], Takashi NAKAJIMA[3], Mitsuhiro TORATANI[4]

1. Center for Environmental Remote Sensing, Chiba University, 2. Graduate School of Natural Science and Technology, Okayama University, 3. Tokai University, Research & Information Center, 4. Tokai University, Earth and Environmental Systems

The purpose of this proposal is to monitor and clarify global environmental change (long-term and ongoing quantitative monitoring) global environment change (global radiation forcing and global ecological change affecting global warming). The technology of optical (near ultraviolet to thermal infrared) imager is a fundamental technology that can develop into new optical sensors of the future and it is necessary to continue to maintain the world advantage.
Optical imagers, which are the genealogy of SGLI, can be monitored by a wide range of wavelengths, including current unexpected changes in climate system fluctuations that change with global warming. In addition, by being able to accurately grasp the predicted progress of climate change, it is possible to evaluate the effect of global warming control policy, and to develop adaptation measures for the future and to make a diagnostic orbit correction . By having its own information source as a sensor of its own country, it is possible to have Japan's unique judgment materials for grasping the situation of climate change and to disseminate it to the world as global standard information. And we can have an international strategy on climate change.

Keywords: Global environmental change

©2019. Japan Geoscience Union. All Right Reserved.

Proposal of satellite for observing large point sources of carbon dioxide

*Hirofumi Ohyama[1], Tsuneo Matsunaga[1], Isamu Morino[1], Yukio Yoshida[1], Makoto Saito[1]

1. National Institute for Environmental Studies

We propose an earth-observing satellite that aims to quantify amounts of atmospheric carbon dioxide (CO_2) emitted from large point sources (LPSs) such as thermal power plants and steel plants, which account for approximately 40% of energy-related CO_2 emissions in the world. In the Global Stocktake Process under the Paris Agreement, each country is required to report sources and sinks of greenhouse gases (inventory) with sufficient accuracy. However, there are large uncertainties in the CO_2 and methane (CH_4) emissions from the LPSs, especially for the developing countries. Space-borne observation could be useful for quantifying and verifying the emissions from the LPSs, given that it provides column abundances in and out a plume with high spatial resolution. With regard to the LPS observation of CH_4, several satellites with a footprint size of less than 1 km^2 are developed recently: GHGSat series (2016 and 2019, GHGSat Inc. in Canada), COOL (2020, Bluefield Technologies Inc. in the U.S.), and MethaneSAT (2021, Environmental Defense Fund in the U.S.). That kind of CO_2 satellite is, however, not planed. Our proposed satellite has an ability of measuring back-scattered solar spectra in the near-infrared region with a footprint size of less than 1 km x 1 km (if feasible, hundreds of meters by hundreds of meters) using an imaging grating spectrometer. Additionally, to increase the signal to noise ratio of the spectrum, the satellite is dedicated to a target observation mode that observe an area of ~50 km x ~50 km including the LPSs more than 2 min continuously by using a pointing mechanism as adopted for the Greenhouse gases Observing SATellite (GOSAT) series.

Keywords: Satellite, Carbon Dioxide, Large Point Source

©2019. Japan Geoscience Union. All Right Reserved.

Earth's health diagnosis - Imaging spectrometer of SLCP for early verification of global warming countermeasure effect, and understanding of status of air pollution -

*YASUKO KASAI[1], Yugo Kanaya[2], Hiroshi Tanimoto[3], JSAC Satellite team[4]

1. NICT, 2. JAMSTEC, 3. NIES, 4. JSAC

We propose a satellite constellation observation plan that understanting of inventory of short-lived climate pollutants (SLCP*) emitted by human activities. SLCP is related to both air pollution and climate change. As the reduction effect of SLCP is obtained in the short term compared with CO2, ministerial-level international efforts began in 2012 as a new method of countermeasures against global warming (CCAC). In addition, the number of deaths due to air pollution is around 3.7 million people worldwide (WHO Report 2012), which is about three times the number of traffic fatalities. Especially, the rate of early death in Japan is at the highest level in OECD countries and the situation is serious.
Also, the impact on agricultural crops can not be ignored. SLCP has local sources of emissions, and observation with a spatial resolution of 1 km class is necessary for grasping actual conditions, but it has not existed so far due to technical difficulties. The proposed SLCP imaging spectrometer (UV / VIS / SWIR) is installed in the low orbit satellite asynchronously realizing the world's first high horizontal resolution (target: horizontal resolution 1 to 2 km), day change observation. We propose detection of SLCP substances in the vicinity of the ground (especially oxidants affecting health damage) by MIR + MW spectroscopic observation synergy as an optional function. From the spatial resolution and observation local time (LT), this sensor has the function as "standard machine" for air pollution satellite observation around the world, and the existence of this machine enables constellation connecting world satellites. This will integrate satellite data around the world, obtain the highest standards of scientific knowledge and encourage evidence-based measures.

Keywords: Air pollution, Satellute, Imaging spectrometer

©2019. Japan Geoscience Union. All Right Reserved.

Spaceborne Vegetation lidar (MOLI)

*Kazuhiro Asai[1], Yasumasa Hirata[2], Gen Takao[2], Haruhisa Shimoda[3], Yoshiaki HONDA[4], Koji Kajiwara[4], Yoshio Awaya[5], Junichi Susaki[9], Takahiro Endo[6], Tsuneo Matsunaga[7], Yoshito Sawada[7], Nobuo Sugimoto[7], Tomoaki Nishizawa[7], Kohei Mizutani[8], Shoken Ishii[8], Toshiyoshi Kimura[10], Tadashi Imai[10], Masato Hayashi[10], Daisuke Sakaizawa[10], Jyunpei Murooka[10], Rei Mituhashi[10]

1. Tohoku Institute of Technology, 2. Forestry and Forest Products Research Institute, 3. Tokai University, 4. Chiba University, 5. Gifu University, 6. The Remote Sensing Technology Center of Japan, 7. National Institute for Environmental Research, 8. National Institute of Information and Communications Technology, 9. Kyoto University, 10. Japan Aerospace Exploration Agency

A lidar is a generic term for light wave radar using pulse laser for transmitter. The lidar on board satellite can precisely measure the ground level and the forest canopy height and three-dimensional forest structure by analyzing round trip time until a light pulse irradiated from orbit to the ground is reflected at the ground surface and returned to the lidar on orbit. This paper propose the Japan’ s first satellite-borne vegetation lidar (MOLI: Multi-footprint Observation Lidar and Imager) mission to investigate the above-ground ground forest biomass (AGB) on a global scale, which plays an important role for carbon cycle and climate change mechanism.
The main purpose of the MOLI mission on board ISS (International Space Station) -JEM (Japanese Experiment Module) is to successfully demonstrate the functional performance of the lidar in space for establishing a vegetation lidar that can acquire canopy height / three-dimensional forest structure information necessary for AGB evaluation with high accuracy. The second objective is to ultimately develop algorithms for highly accurate AGB estimation in high dense tropical forest zone that is inferior in reliability at the present time by merging MOLI data into L-band SAR (ALOS-2 / PALSAR-2 etc.) data and passive spectroscopic data such as GCOM-C / SGLI, and to obtain design guidelines for the practical space-borne lidar in future.
The MOLI proposed here has the function of self-determining the inclination angle and the azimuth angle for reducing the error in the canopy height measurement induced by the ground surface inclination. The output light of the pulse laser is split into two beams and then irradiated as a pair of foot prints on the ground surface. Each footprint diameter on the ground is 25 m, the footprint interval is about 50 m @ along - track, about 43 m @ cross - track. The inclination angle and the azimuth angle are determined from the difference between the trajectory-ground reciprocating time for three closest footprints among a large number of pairs of footprints appearing continuously in the along-track direction on each laser shot and on the ground. Transmission output is 20 mJ / pulse / foot print, repetition frequency 150 Hz, pulse width 7 nsec. The aperture diameter of the receiving optical system is 0.45 m, the detector is two-dimensional Si-APD, the A / D converter is bandwidth 500 MHz, 12 bit resolution. High resolution imager consists of R/G/NIR band, swath width 1000 m, ground resolution 5 m, and acquires information on the size, height, and field data of the canopy. Measurement accuracy of canopy height is <±3 m (<15 m forest height) or <±25% (> 15 m forest height) at ground level inclination angle <30 degrees. The target of AGB observation accuracy is <±20 t / ha (AGB<100 t / ha), <±25% (AGB> 100 t / ha) ,respectively. Field survey is an important work for forest management (forest register), but it comes across many difficulties especially in tropical forest areas. According to our estimate, by implementing MOLI data, a number of AGB field survey and survey costs are able to be reduced by 1/2 (ρ^2: coefficient of determination in two phase regression from ground survey to MOLI estimation) to 1/5 ($\rho^2 = 0.8$), there is a possibility of drastically reducing the maximum by 1/10 ($\rho^2 = 0.9$). A disadvantage of MOLI is strongly affected by weather conditions.

©2019. Japan Geoscience Union. All Right Reserved.

On the other hand, L-band SAR (ALOS-2 / PALSAR-2 etc.) is excellent not only for changes of AGB in real time because it can observe all weather, but also for measuring AGB even in steep mountain area because the method of correcting the distortion of data was recently improved very much. Since then, SAR observation is greatly been demanded. However, there is a big disadvantage for L-band SAR observation. Its backscattering signals easily saturate above AGB of 150 t/h in highly dense tropical forests, that is, in the South American Amazon basin, African Congo region, and Southeast Asia region. It will be able, therefore, to be achieved to improve the accuracy of AGB observation in the high dense rainforest region by complementing each other's advantage and disadvantage for MOLI and SAR with each other. Furthermore, realization of MOLI can be expected to work very effectively for JJ-FAST which is early warning system of deforestation using ALOS-2 / PALSAR-2. This logging detection system focuses on the measurement of deforestation area and does not have the function of AGB measurement. The fusion with MOLI data will also be able to precisely calculate the amount of carbon released at the logged place.

Keywords: Lidar, Canopy height , Forest structure, Forest biomass, L-band SAR, Imager

©2019. Japan Geoscience Union. All Right Reserved.

Estimation of forest resources by a dual-wavelength imaging LiDAR system

*Ryuichi Hirata[1], Yoshito Sawada[1], Masato Hayashi[2], Hideki Saito[3], Tomoaki Takahashi[3], Tsuneo Matsunaga[1]

1. National Institute for Environmental Studies, 2. Japan Aerospace eXploration Agency, 3. Forestry and Forest Products Research Institute

We propose a mission of a dual-wavelength imaging LiDAR system, which measure global forest resources such as canopy heights and forest biomass with high accuracy. The purpose of the mission is to clarify global carbon cycle, countermeasure climate change, and to protect biodiversity. They are useful to evaluate forest resources for REDD+ and MRV.

This system includes two new technologies. One is imaging LiDAR with modulating Laser light to measure spatial distribution of forest resource in a footprint. Another is dual-wavelength to detect ground surface with high accuracy. Measuring spatial distribution of forest in a footprint by modulating Laser Light gives us information about canopy height and biomass with high accuracy compared with the former sensor such as ICESat/GLAS. A dual-wavelength is able to detect forest surface and ground surface more correctly than the former sensor. This system can increase measurement accuracy for canopy height on a slope, which is difficult situation for evaluating canopy height by the former systems because the system is able to measure a shape of ground surface in the area of Laser irradiation. One of the objective of this mission is to evaluate canopy height with 1 m accuracy; the accuracy of canopy heitht of ICESat/GLAS was 5 m and that of MOLI will be 3 m.

©2019. Japan Geoscience Union. All Right Reserved.

Development of new satellite to monitor SIF and PRI of terrestrial vegetation with high spatial and wavelength resolutions

*Hibiki M Noda[1], Kenji Omasa[2], Kouki Hikosaka[3], Kazuhito Ichii[4], Hideki Kobayashi[5], Tomomichi Kato[6], Hiroyuki Muraoka[7]

1. NIES National Institute of Environmental Studies, 2. University of Tokyo, 3. Tohoku University, 4. Chiba University, 5. JAMSTEC, 6. Hokkaido University, 7. Gifu University

To deal effectively with global warming by mitigation and adaptation, it is necessary to monitor emission and sequestration of greenhouse gases with their underlying mechanisms including biogeochemical processes. The Earth-observation satellite is powerful tool to observe temporal and spatial variations in structure and function on ecosystem in regional to global scale. It has been conducted to estimate GPP (gross primary production) by using satellite-measured optical properties of vegetation canopy such as NDVI (normalized vegetation index). Those vegetation indices are related to greenness of the canopy but not reflect the photosynthetic activity, that are quite sensitive to climatic conditions. Thus, there are still large uncertainty in the estimation of GPP.
In recent years, advent of the Earth-observation satellite with high wavelength-resolution sensors enable us to observe SIF (Solar-Induced chlorophyll Fluorescence) emitted from terrestrial vegetation. Since the chlorophyll fluorescence is emitted in photochemical reaction, which is a part of photosynthetic process, SIF would be good indicator of photosynthetic activity. In the photochemical reaction, xanthophyll cycle is also play important roll to release extra energy and it is able to monitor its condition by using PRI (Photochemical Reflectance Index). In the recent study in single-leaf scale, it has been shown that simultaneously measured SIF and PRI help us to estimate accurate photosynthetic rate based on ecophysiological model (Hikosaka and Noda 2019). Similarly, simultaneous measurement of SIF and PRI with the Earth-observation satellite would be helpful to estimate GPP and understand the in regional to global scale. However, there are no satellite to measure SIF and PRI simultaneously to date. FLEX, which will be launched in 2022 is the only satellite mission to measure them.
In this talk, we will propose development of new satellite to observe SIF, PRI and other vegetation indices such as NDVI with high spatial and wavelength resolutions. This satellite would contribute accurate estimation of GPP and effective policy making against global warming.
In this talk we will suggest to develop new Earth-obsevation satellite to monitor SIF and PRI of terrestrail vegetation with high spatial and wavelength resolutions.

Keywords: vegetation remote sensing, solar-induced chlorophyll fluorescence, xanthophyll cycle

©2019. Japan Geoscience Union. All Right Reserved.

Satellite Observation of the Whole Atmosphere - Superconducting Submillimeter-Wave Limb-Emission Sounder (SMILES-2)

*Masato Shiotani[1], Akinori Saito[1], Takatoshi Sakazaki[1], Satoshi Ochiai[2], Philippe Baron[2], Toshiyuki Nishibori[3], Makoto Suzuki[3], Takumi Abe[3], Hiroyuki Maezawa[4], Shin-ichiro Oyama[5,6,7]

1. Kyoto University, 2. National Institute of Information and Communications Technology, 3. Japan Aerospace Exploration Agency, 4. Osaka Prefecture University, 5. Nagoya University, 6. University of Oulu, 7. National Institute of Polar Research

The Superconducting Submillimeter-Wave Limb-Emission Sounder (SMILES) launched by an H-IIB rocket with the H-II Transfer Vehicle (HTV) in September 2009 and attached to the Japanese Experiment Module (JEM) on the International Space Station (ISS) demonstrated high-sensitivity submillimeter limb-emission sounding of atmospheric observations. Though the observation period is limited to about 6 months (October 12, 2009- April 21, 2010) owing to the failure of a critical component, outstanding results have been achieved such as an identification of diurnal cycle of the stratospheric ozone, which had not been examined yet because of poor data quality in the previous satellite measurements. In addition by comparing SMILES data with existing observation data and results from the chemistry climate models, it has been recognized that we need a reference data for temperature, wind, and minor species with high precision to constrain the models. After the launch there has been discussions about the possibility to derive wind information from the Doppler shift of observed lines, and the necessity to have temperature information from adequate line selection. Thus we now recognize the potential of high-sensitivity observations about temperature and wind fields up to 150 km.

Based on the SMILES heritage, we propose a satellite mission to observe temperature and wind fields, and distributions of atmospheric minor species for the full diurnal cycle from the middle atmosphere (stratosphere and mesosphere) to the upper atmosphere (thermosphere and ionosphere) for a period of five years. SMILES-2 observations will enable us to obtain global information with unprecedented accuracy on the whole atmosphere including upper mesosphere and lower thermosphere where observation data have been lacking.

This mission has four science objectives:
(MO.1) To investigate the 4-D space-time structure of the diurnal variations (atmospheric tides) in view of dynamics, chemistry, and electromagnetic processes
(MO.2) To unveil the vertical propagation of synoptic-to-planetary scale disturbances from the middle atmosphere (non-migrating tides and stratospheric sudden warming events) to the upper atmosphere
(MO.3) To understand atmospheric variations due to energy inputs from the magnetosphere (particle precipitation and magnetic storm)
(MO.4) To provide benchmarks for whole atmosphere models and climate models with detailed description of the background thermal structure and distribution of minor species

Using observation data from the middle atmosphere to the upper atmosphere as a whole, we will be able to grasp the 4-D dynamical structure of diurnal variations (atmospheric tides) which are one of the most essential variabilities in the earth’ s atmosphere. For understanding climate change in view of chemical processes affecting the ozone layer, we will be able to utilize high-sensitivity measurements of the atmospheric minor species in a quantitative manner. In the upper atmosphere, a transition layer between the atmosphere and the outer space, we will be able to clarify a role of energy inputs from the

©2019. Japan Geoscience Union. All Right Reserved.

magnetosphere from the temperature and wind observations. These outcomes including the atmospheric trace gas data will greatly contribute to improvement in reliability of chemistry climate models for future projection and accuracy of prediction models for space weather.

Keywords: middle atmosphere, upper atmosphere, satellite observations, temperature, wind

©2019. Japan Geoscience Union. All Right Reserved.

Simulation studies for Superconducting Submillimeter-Wave Limb-Emission Sounder-2 (SMILES-2)

*Philippe Baron[1], Satoshi Ochiai[1], Donal Murtagh[5], Hideo Sagawa[2], Akinori Saito[3], Masato Shiotani[3], Makoto Suzuki[4]

1. National Institute of Information and Communications Technology, 2. Kyoto Sangyo University, 3. Kyoto University, 4. Japan Aerospace Exploration Agency, 5. Chalmers University of Technology, Sweden

SMILES-2 is a mission prepared for the next call-for-proposals for JAXA/ISAS M-class scientific satellite mission. It aims at scanning the atmospheric limb from 20 to 160 km above the surface at frequencies near 700 GHz and 2 THz. It could provide the temperature and composition as well as, for the first time, the horizontal wind vector above 30 km, the atomic oxygen in its ground state above 90 km, and the atmospheric density and the geomagnetic field vector near the mesopause. The measurement performances have been assessed from numerical simulations. We will present the results obtained for the 3 radiometers.

Keywords: middle and upper atmosphere, wind, geomagnetic field, atomic oxygen

©2019. Japan Geoscience Union. All Right Reserved.

Feasibility of Superconducting Submillimeter-Wave Limb-Emission Sounder (SMILES-2) on an M-class satellite

*Satoshi Ochiai[1], Philippe Baron[1], Yoshihisa Irimajiri[1], Toshiyuki Nishibori[2], Makoto Suzuki[2], Yoshinori Uzawa[3], Hiroyuki Maezawa[4], Takeshi Manabe[4], Akinori Saito[5], Masato Shiotani[5]

1. National Institute of Information and Communications Technology, 2. Japan Aerospace Exploration Agency, 3. National Astronomical Observatory of Japan, 4. Osaka Prefecture University, 5. Kyoto University

The Superconducting Submillimeter-Wave Limb-Emission Sounder-2 (SMILES-2) is a proposed mission for comprehensive observation of temperature, wind, and atmospheric compositions in the middle and upper atmospheres using limb observation technique at submillimeter-wave from an satellite on a non-sunsynchronous low Earth orbit. The proposal of SMILES-2 is assumed to be one of M-class missions of the Japan Aerospace Exploration Agency / the Institute of Space and Astronautical Science (JAXA/ISAS). SMILES-2 will enable us to observe temperature profile between the tropopause and the lower thermosphere below an altitude of 150 km, horizontal wind profile between the upper stratosphere above 30 km and the lower thermosphere, and atmospheric compositions including water vapor, ozone, and other minor species in the stratosphere and mesosphere and atomic oxygen in the lower thermosphere with a vertical resolution of 2.5 km or 5 km. Those observation will be daily and sampled at numerous positions spread in global scale. Diurnal cycles can be estimated. The local time of observing point will be shifted by 24 hours in about 3 months.
The observation of the diurnal cycles is one of the most important targets for the SMILES-2 science. To meet the scientific requirements, SMILES-2 shall have the superconducting receivers at bands of 638 GHz, 763 GHz, and 2 THz, and observe limb atmosphere from a satellite on an orbit at an altitude of 550 km and an inclination of 66 degree. Atmospheric vertical profiles are observed at every 690 km on the sun-shade side along the orbit. Each vertical profile is observed two times from different directions with a time interval of about 8 minutes so that horizontal wind vector can be retrieved. Approximately 830 vertical profiles will be observed in one day.Estimated precision of those measurements is summarized in another paper of this meeting. The wind measurement precision is estimated to be comparable or slightly better than a typical amplitude of diurnal cycle of the wind variation. The measurement precision depends on the receiver sensitivity and the spatial and time resolution of measurements. Because the average number of the wind observation can hardly increase, the receiver sensitivity is extremely important to keep a good measurement precision. Superconducting devices, which show the best performance among heterodyne receivers in the frequency range, are essential for the SMILES-2 receiver.
SMILES-2 will use a technological heritage of JEM/SMILES, which is a mission operated on the Japanese Experiment Module in the International Space Station for a half year from 2009 to 2010. JEM/SMILES successfully demonstrated submillimeter limb observation for the first time with superconducting heterodyne receivers cooled by spaceborne cryocooler. Although no cryocooler in Japan was demonstrated in space for much longer lifetime, an improved model of 4-K cryocooler for space has been tested on the ground and showed a lifetime of more than 4 years. The power consumption of the cryocooler for JEM/SMILES was measured about 153 W on the ground, and that of the JEM/SMILES payload was about 320 W. The power resource of an M-class satellite is very limited comparing to that of JEM missions. The available power for the mission is estimated about 323 W when the orbit comes at the maximum sun-shading ratio. That seems larger than the required power, but it is not enough because the SMILES-2 mission includes telecommunication systems and data recorders that are not in the JEM/SMILES payload. Moreover, the power consumption by the SMILES-2 cryocooler may be larger by increasing the number of frequency bands and requiring power margin for compensating the decrease of

©2019. Japan Geoscience Union. All Right Reserved.

cooling efficiency of the cryocooler for 3 or 5 year operation.
The design of power balance, as well as the cost evaluation, is the largest issue in judging the feasibility of SMILES-2 on M-class satellite. We are studying measures of reducing the cryocooler power consumption. For example, we are estimating power consumption with a detailed design of the cryostat for the receivers and cooling system. We are also developing a new receiver configuration that saves heat flow into the cooling stage, and designing the radiation cooling system to reduce the base temperature of cryocooling system. With additional reductions of the power consumption by the other mission components, we believe that the power consumption of the SMILES-2 mission can be kept within the available power.
The SMILES-2 mission will be proposed to JAXA/ISAS for the next opportunity of M-class mission, which is targeting a launch in 2026 or later.

Keywords: satellite observation, middle atmosphere, upper atmosphere, microwave observation, cryocooler, wind measurement

©2019. Japan Geoscience Union. All Right Reserved.

[E] Poster | M (Multidisciplinary and Interdisciplinary)：M-TT Technology & Techniques

Wed. May 29, 2019 1:45 PM - 3:15 PM JST | Wed. May 29, 2019 4:45 AM - 6:15 AM UTC | Poster Hall International Exhibition Hall8, Makuhari Messe_6

[M-TT45] Cryoseismology - a new proxy for detecting surface environmental variations of the Earth -

convener:Genti Toyokuni(Research Center for Prediction of Earthquakes and Volcanic Eruptions, Graduate School of Science, Tohoku University), Masaki Kanao(National Institute of Polar Research), Seiji Tsuboi(JAMSTEC, Center for Earth Information Science and Technology)

Several kinds of environmental signals associated with ocean - cryosphere - solid earth systems have recently been detected in bi-polar regions. Ice-related seismic motions for small magnitude events are generally named ice-quakes (ice-shocks) and can be generated by glacially related dynamics. Such kinds of cryoseismic sources are classified into the movements of ice sheets, sea-ice, oceanic tide-cracks, icebergs and the calving fronts of ice caps. Cryoseismic waves are likely to be influenced by variations in environmental conditions, and the continuous study of their time-space variability provides indirect evidence of climate change. As glacial earthquakes are the most prominent phenomena found recently in polar regions, in particular on the Greenland in this 21st century, the new innovative studies from seismology are expected by long-term monitoring under extreme conditions in the Earth's environment.

Taking these issues into account, the conveners are willing to invite many contributions to a special session on "Cryoseismology", which will cover the recent achievements on glacial related seismic events and associated phenomenon observed in polar regions. It is particularly encouraged to have contributions based on seismic signals involving the dynamics of ice sheets, sea-ice, and icebergs and glaciers. Although the glacial earthquakes are the most prominent evidence found recently in polar regions, all related topics involving polar seismology are welcome, such as studies of crust and mantle structure in the area, comparison of tectonic and glacier-related seismicity, recent triggered earthquakes and active volcanoes, glacial isostatic adjustment (GIA), harmonic tremor associated with cryoseismic events, etc. This session has been held every year since 2015, and was held as Union Session last year.

[MTT45-P01] Application of neural network and theoretical seismograms as training data to locate ice quakes

*Seiji Tsuboi[1], DAISUKE SUGIYAMA[1] (1.JAMSTEC, Center for Earth Information Science and Technology)

[MTT45-P02] **P-wave tomography beneath Greenland**

*Takaya Matsuno[1], Genti Toyokuni[1], Dapeng Zhao[1] (1.Research Center for Prediction of Earthquakes and Volcanic Eruptions, Graduate School of Science, Tohoku University)

[MTT45-P03] **Seismic observations in Greenland by a joint USA and Japanese GLISN team (2011–2018)**

*Genti Toyokuni[1], Masaki Kanao[2], Seiji Tsuboi[3], Yoko Tono[4] (1.RCPEVE, Tohoku Univ., 2.NIPR, 3.JAMSTEC, 4.ERI, Univ. Tokyo)

Application of neural network and theoretical seismograms as training data to locate ice quakes

*Seiji Tsuboi[1], DAISUKE SUGIYAMA[1]

1. JAMSTEC, Center for Earth Information Science and Technology

We have applied numerically computed theoretical seismograms and deep machine learning to locate earthquakes. We calculate theoretical seismograms for realistic three-dimensional Earth model and use these seismograms to create seismic wave propagation images at the surface of the Earth. Then we use these images as training dataset of convolutional neural network. We build neural networks for determination of hypocentral parameters, such as epicenter, depth, origin time and magnitude, and applied these networks to actual seismograms to examine if this procedure works to locate earthquake and determine magnitude. Although the number of earthquakes is small and the regional extent is quite limited, the results demonstrate that it is feasible to locate earthquakes by using this approach. Advantages of using this approach to locate earthquakes and determine magnitude are; accuracy of hypocenter parameters can be increased by accumulating theoretical seismograms for various earthquake location and size as learning dataset of deep machine learning; three dimensional Earth structure can be included without additional computational cost to locate earthquakes. Here we will discuss a possibility of applying this methodology to locate ice quakes, which happen in and near the ice sheet.

Keywords: icequakes, hypocenter determination, synthetic seismograms

©2019. Japan Geoscience Union. All Right Reserved.

P-wave tomography beneath Greenland

*Takaya Matsuno[1], Genti Toyokuni[1], Dapeng Zhao[1]

1. Research Center for Prediction of Earthquakes and Volcanic Eruptions, Graduate School of Science, Tohoku University

The Greenland landmass has a long and complex tectonic history (~4 billion years). However, most of the continent is covered by the extensive inland ice cap, so it was hard to access its geology and the underlying tectonics. The Greenland Ice Sheet Monitoring Network (GLISN) is an international project by 11 countries to establish a seismic network in and around Greenland (Toyokuni et al., 2014). The project was initiated in 2009, and now it provides broadband, continuous, and real-time seismic data recorded at 33 stations. In this study we aim to investigate the 3-D upper mantle structure beneath Greenland by using the GLISN data.

We inverted a number of P-wave arrival-time data of both local and teleseismic events, observed at 30 GLISN stations, to estimate a 3-D P-wave velocity (Vp) model beneath Greenland and surrounding regions. All of the GLISN arrival-time data are downloaded from the Bulletins of the International Seismological Centre. We used the seismic tomography method by Zhao et al. (2012).

In the polar region, if grid nodes are arranged on the basis of equatorial coordinates, distance between two adjacent nodes in the same latitude decreases as it gets closer to the pole. To overcome this problem, we converted our study region from the equatorial coordinates to the ecliptic coordinates. This scheme enables us to solve tomographic equations in quasi-Cartesian coordinates (e.g., Kobayashi & Zhao, 2004; Gupta et al., 2009; Takenaka et al., 2017). We set up a 3-D grid with a horizontal grid interval of 2° and a vertical grid interval of 15–30 km (at depths of 5–700 km).

The results of this study are summarized as follows.
(1) There is a prominent low-Vp anomaly beneath Iceland (depth < 500 km), which is related to the current Iceland plume.
(2) In the shallow mantle (40-250 km depths) beneath central and offshore eastern Greenland, Vp is relatively lower than those in the other inland areas of Greenland in the depth range, which may reflect the ancient motion path of the Iceland plume. This feature coincides with known basalt areas at central western and eastern coasts of Greenland.

References:
Kobayashi, R. & D. Zhao (2004) PEPI, 141, 167–181.
Gupta, S., D. Zhao & S. Rai (2009) Gondwana Res, 16, 109–118.
Takenaka, H. et al. (2017) EPS, 69, 67.
Toyokuni, G. et al. (2014) Antarctic Record, 58, 1–18.
Zhao, D. et al. (2012) GJI, 190, 816–828.

Keywords: Seismic tomography, Greenland, Iceland plume, GLISN project

©2019. Japan Geoscience Union. All Right Reserved.

Seismic observations in Greenland by a joint USA and Japanese GLISN team (2011–2018)

*Genti Toyokuni[1], Masaki Kanao[2], Seiji Tsuboi[3], Yoko Tono[4]

1. RCPEVE, Tohoku Univ., 2. NIPR, 3. JAMSTEC, 4. ERI, Univ. Tokyo

The Greenland Ice Sheet (GrIS) is a huge storehouse of water on Earth, and has the potential to raise the global sea level by approximately 7 m if completely melted. Although researchers have been mainly studying the GrIS surface snowmelt as a response to climate warming, recent progress in ice-core drilling, remote sensing, and theoretical analyses has turned a spotlight on its basal conditions. However, the traditional observation techniques, such as ice-core drilling and ice-penetrating radar, provide only discontinuous information in both time and space.

Seismic observation is now drawing widespread attention as an alternative method for monitoring the GrIS. The Greenland Ice Sheet Monitoring Network (GLISN), an international project between 11 countries that began in 2009, now provides broadband, continuous, and real-time seismic data from 33 stations in and around Greenland. Japan is a partner country from when the GLISN project was launched, and has been sending an expedition team every year since 2011. In 2011, a joint USA and Japanese GLISN team installed the dual seismic–GPS station ICESG-GLS2 in the middle of the GrIS. During 2012–2018, we conducted maintenance of three stations on the GrIS (station codes: ICESG-GLS2, DY2G-GLS1, and NEEM-GLS3), and three stations on bedrock in coastal areas (NUUK, DBG, and SOEG). We had succeeded in real-time transmission of broad-band and continuous seismic waveform data from the three ice stations. It was the first time in the world that the seismic data with such a high sampling rate are transferred from the ice sheet. The data is now open to public and available from the IRIS Data Management Center (http://www.iris.edu/ds/nodes/dmc/). This presentation will summarize our field activities for 2011–2018, and introduce the future field plans.

Acknowledgments: The Japanese GLISN team has been supported by research grants from JSPS (24403006).

Keywords: GLISN project, Seismic observation, Greenland Ice Sheet

©2019. Japan Geoscience Union. All Right Reserved.

[E] Poster | M (Multidisciplinary and Interdisciplinary)：M-TT Technology & Techniques

Wed. May 29, 2019 5:15 PM - 6:30 PM JST | Wed. May 29, 2019 8:15 AM - 9:30 AM UTC | Poster Hall International Exhibition Hall8, Makuhari Messe_40

[M-TT45] Cryoseismology - a new proxy for detecting surface environmental variations of the Earth -

convener:Genti Toyokuni(Research Center for Prediction of Earthquakes and Volcanic Eruptions, Graduate School of Science, Tohoku University), Masaki Kanao(National Institute of Polar Research), Seiji Tsuboi(JAMSTEC, Center for Earth Information Science and Technology)

Several kinds of environmental signals associated with ocean - cryosphere - solid earth systems have recently been detected in bi-polar regions. Ice-related seismic motions for small magnitude events are generally named ice-quakes (ice-shocks) and can be generated by glacially related dynamics. Such kinds of cryoseismic sources are classified into the movements of ice sheets, sea-ice, oceanic tide-cracks, icebergs and the calving fronts of ice caps. Cryoseismic waves are likely to be influenced by variations in environmental conditions, and the continuous study of their time-space variability provides indirect evidence of climate change. As glacial earthquakes are the most prominent phenomena found recently in polar regions, in particular on the Greenland in this 21st century, the new innovative studies from seismology are expected by long-term monitoring under extreme conditions in the Earth's environment.

Taking these issues into account, the conveners are willing to invite many contributions to a special session on "Cryoseismology", which will cover the recent achievements on glacial related seismic events and associated phenomenon observed in polar regions. It is particularly encouraged to have contributions based on seismic signals involving the dynamics of ice sheets, sea-ice, and icebergs and glaciers. Although the glacial earthquakes are the most prominent evidence found recently in polar regions, all related topics involving polar seismology are welcome, such as studies of crust and mantle structure in the area, comparison of tectonic and glacier-related seismicity, recent triggered earthquakes and active volcanoes, glacial isostatic adjustment (GIA), harmonic tremor associated with cryoseismic events, etc. This session has been held every year since 2015, and was held as Union Session last year.

[MTT45-P01] Application of neural network and theoretical seismograms as training data to locate ice quakes

*Seiji Tsuboi[1], DAISUKE SUGIYAMA[1] (1.JAMSTEC, Center for Earth Information Science and Technology)

[MTT45-P02] **P-wave tomography beneath Greenland**

*Takaya Matsuno[1], Genti Toyokuni[1], Dapeng Zhao[1] (1.Research Center for Prediction of Earthquakes and Volcanic Eruptions, Graduate School of Science, Tohoku University)

[MTT45-P03] **Seismic observations in Greenland by a joint USA and Japanese GLISN team (2011–2018)**

*Genti Toyokuni[1], Masaki Kanao[2], Seiji Tsuboi[3], Yoko Tono[4] (1.RCPEVE, Tohoku Univ., 2.NIPR, 3.JAMSTEC, 4.ERI, Univ. Tokyo)

Application of neural network and theoretical seismograms as training data to locate ice quakes

*Seiji Tsuboi[1], DAISUKE SUGIYAMA[1]

1. JAMSTEC, Center for Earth Information Science and Technology

We have applied numerically computed theoretical seismograms and deep machine learning to locate earthquakes. We calculate theoretical seismograms for realistic three-dimensional Earth model and use these seismograms to create seismic wave propagation images at the surface of the Earth. Then we use these images as training dataset of convolutional neural network. We build neural networks for determination of hypocentral parameters, such as epicenter, depth, origin time and magnitude, and applied these networks to actual seismograms to examine if this procedure works to locate earthquake and determine magnitude. Although the number of earthquakes is small and the regional extent is quite limited, the results demonstrate that it is feasible to locate earthquakes by using this approach. Advantages of using this approach to locate earthquakes and determine magnitude are; accuracy of hypocenter parameters can be increased by accumulating theoretical seismograms for various earthquake location and size as learning dataset of deep machine learning; three dimensional Earth structure can be included without additional computational cost to locate earthquakes. Here we will discuss a possibility of applying this methodology to locate ice quakes, which happen in and near the ice sheet.

Keywords: icequakes, hypocenter determination, synthetic seismograms

©2019. Japan Geoscience Union. All Right Reserved.

P-wave tomography beneath Greenland

*Takaya Matsuno[1], Genti Toyokuni[1], Dapeng Zhao[1]

1. Research Center for Prediction of Earthquakes and Volcanic Eruptions, Graduate School of Science, Tohoku University

The Greenland landmass has a long and complex tectonic history (~4 billion years). However, most of the continent is covered by the extensive inland ice cap, so it was hard to access its geology and the underlying tectonics. The Greenland Ice Sheet Monitoring Network (GLISN) is an international project by 11 countries to establish a seismic network in and around Greenland (Toyokuni et al., 2014). The project was initiated in 2009, and now it provides broadband, continuous, and real-time seismic data recorded at 33 stations. In this study we aim to investigate the 3-D upper mantle structure beneath Greenland by using the GLISN data.

We inverted a number of P-wave arrival-time data of both local and teleseismic events, observed at 30 GLISN stations, to estimate a 3-D P-wave velocity (Vp) model beneath Greenland and surrounding regions. All of the GLISN arrival-time data are downloaded from the Bulletins of the International Seismological Centre. We used the seismic tomography method by Zhao et al. (2012).

In the polar region, if grid nodes are arranged on the basis of equatorial coordinates, distance between two adjacent nodes in the same latitude decreases as it gets closer to the pole. To overcome this problem, we converted our study region from the equatorial coordinates to the ecliptic coordinates. This scheme enables us to solve tomographic equations in quasi-Cartesian coordinates (e.g., Kobayashi & Zhao, 2004; Gupta et al., 2009; Takenaka et al., 2017). We set up a 3-D grid with a horizontal grid interval of 2° and a vertical grid interval of 15–30 km (at depths of 5–700 km).

The results of this study are summarized as follows.
(1) There is a prominent low-Vp anomaly beneath Iceland (depth < 500 km), which is related to the current Iceland plume.
(2) In the shallow mantle (40-250 km depths) beneath central and offshore eastern Greenland, Vp is relatively lower than those in the other inland areas of Greenland in the depth range, which may reflect the ancient motion path of the Iceland plume. This feature coincides with known basalt areas at central western and eastern coasts of Greenland.

References:
Kobayashi, R. & D. Zhao (2004) PEPI, 141, 167–181.
Gupta, S., D. Zhao & S. Rai (2009) Gondwana Res, 16, 109–118.
Takenaka, H. et al. (2017) EPS, 69, 67.
Toyokuni, G. et al. (2014) Antarctic Record, 58, 1–18.
Zhao, D. et al. (2012) GJI, 190, 816–828.

Keywords: Seismic tomography, Greenland, Iceland plume, GLISN project

©2019. Japan Geoscience Union. All Right Reserved.

Seismic observations in Greenland by a joint USA and Japanese GLISN team (2011–2018)

*Genti Toyokuni[1], Masaki Kanao[2], Seiji Tsuboi[3], Yoko Tono[4]

1. RCPEVE, Tohoku Univ., 2. NIPR, 3. JAMSTEC, 4. ERI, Univ. Tokyo

The Greenland Ice Sheet (GrIS) is a huge storehouse of water on Earth, and has the potential to raise the global sea level by approximately 7 m if completely melted. Although researchers have been mainly studying the GrIS surface snowmelt as a response to climate warming, recent progress in ice-core drilling, remote sensing, and theoretical analyses has turned a spotlight on its basal conditions. However, the traditional observation techniques, such as ice-core drilling and ice-penetrating radar, provide only discontinuous information in both time and space.

Seismic observation is now drawing widespread attention as an alternative method for monitoring the GrIS. The Greenland Ice Sheet Monitoring Network (GLISN), an international project between 11 countries that began in 2009, now provides broadband, continuous, and real-time seismic data from 33 stations in and around Greenland. Japan is a partner country from when the GLISN project was launched, and has been sending an expedition team every year since 2011. In 2011, a joint USA and Japanese GLISN team installed the dual seismic–GPS station ICESG-GLS2 in the middle of the GrIS. During 2012–2018, we conducted maintenance of three stations on the GrIS (station codes: ICESG-GLS2, DY2G-GLS1, and NEEM-GLS3), and three stations on bedrock in coastal areas (NUUK, DBG, and SOEG). We had succeeded in real-time transmission of broad-band and continuous seismic waveform data from the three ice stations. It was the first time in the world that the seismic data with such a high sampling rate are transferred from the ice sheet. The data is now open to public and available from the IRIS Data Management Center (http://www.iris.edu/ds/nodes/dmc/). This presentation will summarize our field activities for 2011–2018, and introduce the future field plans.

Acknowledgments: The Japanese GLISN team has been supported by research grants from JSPS (24403006).

Keywords: GLISN project, Seismic observation, Greenland Ice Sheet

©2019. Japan Geoscience Union. All Right Reserved.